Scientific and Technical Aerospace Reports

STAR

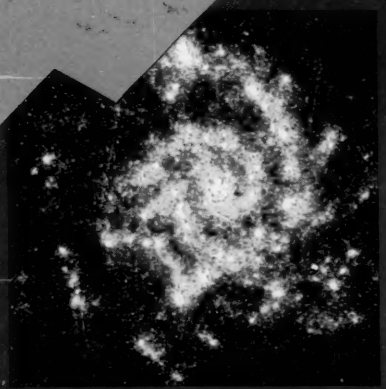

An Abstract Journal

NASA STI PROGRAM SCIENTIFIC & TECHNICAL INFORMATION

Volume 31, Number 4
April 1993
N93-14102 to N93-15658

Scientific and Technical Aerospace Reports (STAR) is an abstract journal that provides comprehensive coverage of worldwide aerospace-related reports. It is a major product of the International Aerospace Database managed by the NASA Scientific and Technical Information (STI) Program. The coverage includes reports on aeronautics, space, and supporting disciplines. *STAR* lists current, publicly available reports entered into the NASA STI Database during the 4-week period preceding publication. A typical citation and abstract appear on page viii. They explain how to read the items that are announced in this journal.

NASA sponsors a companion journal, *International Aerospace Abstracts (IAA) (NOVA* for internal NASA use) that lists abstracts of the open literature on aerospace subjects available worldwide. *IAA* is available for sale through the AIAA.

Entries found in *STAR* and *IAA* are available through NASA's online service, RECON, as the International Aerospace Database and through DIALOG as the Aerospace Database.

Information on aerospace and related subjects is gathered by the NASA STI Program through national and international agreements and exchanges and is made available to the NASA community as well as to the public in many forms through various outlets. The section on NASA STI Program Products and Services contains additional information.

For further information please contact:
NASA Center for AeroSpace Information (CASI)
800 Elkridge Landing Road
Linthicum Heights, MD 21090-2934
(301) 621-0390

US ISSN 0036-8741

This publication was prepared by the NASA Center for AeroSpace Information,
800 Elkridge Landing Road, Linthicum Heights, MD 21090-2934, (301) 621-0390.

Volume 31 Number 4 / April 1993

TABLE OF CONTENTS

AERONAUTICS For related information see also *Astronautics.*

01 AERONAUTICS (GENERAL) **777**

02 AERODYNAMICS **778**
Includes aerodynamics of bodies, combinations, wings, rotors, and control surfaces; and internal flow in ducts and turbomachinery. For related information see also *34 Fluid Mechanics and Heat Transfer.*

03 AIR TRANSPORTATION AND SAFETY **783**
Includes passenger and cargo air transport operations; and aircraft accidents. For related information see also *16 Space Transportation* and *85 Urban Technology and Transportation.*

04 AIRCRAFT COMMUNICATIONS AND NAVIGATION **788**
Includes digital and voice communication with aircraft; air navigation systems (satellite and ground based); and air traffic control. For related information see also *17 Space Communications, Spacecraft Communications, Command and Tracking* and *32 Communications and Radar.*

05 AIRCRAFT DESIGN, TESTING AND PERFORMANCE **790**
Includes aircraft simulation technology. For related information see also *18 Spacecraft Design, Testing and Performance* and *39 Structural Mechanics.* For land transportation vehicles see *85 Urban Technology and Transportation.*

06 AIRCRAFT INSTRUMENTATION **793**
Includes cockpit and cabin display devices; and flight instruments. For related information see also *19 Space craft Instrumentation* and *35 Instrumentation and Photography.*

07 AIRCRAFT PROPULSION AND POWER **798**
Includes prime propulsion systems and systems components, e.g., gas turbine engines and compressors; and onboard auxiliary power plants for aircraft. For related information see also *20 Spacecraft Propulsion and Power, 28 Propellants and Fuels,* and *44 Energy Production and Conversion.*

08 AIRCRAFT STABILITY AND CONTROL **802**
Includes aircraft handling qualities; piloting; flight controls; and autopilots. For related information see also *05 Aircraft Design, Testing and Performance.*

09 RESEARCH AND SUPPORT FACILITIES (AIR) **804**
Includes airports, hangars and runways; aircraft repair and overhaul facilities; wind tunnels; shock tubes; and aircraft engine test stands. For related information see also *14 Ground Support Systems and Facilities (Space).*

ASTRONAUTICS For related information see also *Aeronautics.*

12 ASTRONAUTICS (GENERAL) **804**
For extraterrestrial exploration see *91 Lunar and Planetary Exploration.*

13 ASTRODYNAMICS **813**
Includes powered and free-flight trajectories; and orbital and launching dynamics.

14 GROUND SUPPORT SYSTEMS AND FACILITIES (SPACE) **814**
Includes launch complexes, research and production facilities; ground support equipment, e.g., mobile transporters; and simulators. For related information see also *09 Research and Support Facilities (Air).*

15 LAUNCH VEHICLES AND SPACE VEHICLES **814**
Includes boosters; operating problems of launch/space vehicle systems; and reusable vehicles. For related information see also *20 Spacecraft Propulsion and Power.*

16 SPACE TRANSPORTATION **814**
Includes passenger and cargo space transportation, e.g., shuttle operations; and space rescue techniques. For related information see also *03 Air Transportation and Safety* and *18 Spacecraft Design, Testing and Performance.* For space suits see *54 Man/System Technology and Life Support.*

17 SPACE COMMUNICATIONS, SPACECRAFT COMMUNICATIONS, COMMAND AND TRACKING . **816**
Includes telemetry; space communications networks; astronavigation and guidance; and radio blackout. For related information see also *04 Aircraft Communications and Navigation* and *32 Communications and Radar.*

N.A.—no abstracts were assigned to this category for this issue.

18 SPACECRAFT DESIGN, TESTING AND PERFORMANCE **816**
Includes satellites; space platforms; space stations; spacecraft systems and components such as thermal and environmental controls; and attitude controls. For life support systems see *54 Man/System Technology and Life Support.* For related information see also *05 Aircraft Design, Testing and Performance, 39 Structural Mechanics,* and *16 Space Transportation.*

19 SPACECRAFT INSTRUMENTATION **825**
For related information see also *06 Aircraft Instrumentation* and *35 Instrumentation and Photography.*

20 SPACECRAFT PROPULSION AND POWER **826**
Includes main propulsion systems and components, e.g., rocket engines; and spacecraft auxiliary power sources. For related information see also *07 Aircraft Propulsion and Power, 28 Propellants and Fuels, 44 Energy Production and Conversion,* and *15 Launch Vehicles and Space Vehicles.*

CHEMISTRY AND MATERIALS

23 CHEMISTRY AND MATERIALS (GENERAL) **828**

24 COMPOSITE MATERIALS **828**
Includes physical, chemical, and mechanical properties of laminates and other composite materials. For ceramic materials see *27 Nonmetallic Materials.*

25 INORGANIC AND PHYSICAL CHEMISTRY **838**
Includes chemical analysis, e.g., chromatography; combustion theory; electrochemistry; and photochemistry. For related information see also *77 Thermodynamics and Statistical Physics.*

26 METALLIC MATERIALS **844**
Includes physical, chemical, and mechanical properties of metals, e.g., corrosion; and metallurgy.

27 NONMETALLIC MATERIALS **847**
Includes physical, chemical, and mechanical properties of plastics, elastomers, lubricants, polymers, textiles, adhesives, and ceramic materials. For composite materials see *24 Composite Materials.*

28 PROPELLANTS AND FUELS **854**
Includes rocket propellants, igniters and oxidizers; their storage and handling procedures; and aircraft fuels. For related information see also *07 Aircraft Propulsion and Power, 20 Spacecraft Propulsion and Power,* and *44 Energy Production and Conversion.*

29 MATERIALS PROCESSING **855**
Includes space-based development of products and processes for commercial application. For biological materials see *55 Space Biology.*

ENGINEERING For related information see also *Physics.*

31 ENGINEERING (GENERAL) **855**
Includes vacuum technology; control engineering; display engineering; cryogenics; and fire prevention.

32 COMMUNICATIONS AND RADAR **856**
Includes radar; land and global communications; communications theory; and optical communications. For related information see also *04 Aircraft Communications and Navigation* and *17 Space Communications, Spacecraft Communications, Command and Tracking.* For search and rescue see *03 Air Transportation and Safety,* and *16 Space Transportation.*

33 ELECTRONICS AND ELECTRICAL ENGINEERING **864**
Includes test equipment and maintainability; components, e.g., tunnel diodes and transistors; microminiaturization; and integrated circuitry. For related information see also *60 Computer Operations and Hardware* and *76 Solid-State Physics.*

34 FLUID MECHANICS AND HEAT TRANSFER **872**
Includes boundary layers; hydrodynamics; fluidics; mass transfer and ablation cooling. For related information see also *02 Aerodynamics* and *77 Thermodynamics and Statistical Physics.*

35 INSTRUMENTATION AND PHOTOGRAPHY **881**
Includes remote sensors; measuring instruments and gauges; detectors; cameras and photographic supplies; and holography. For aerial photography see *43 Earth Resources and Remote Sensing.* For related information see also *06 Aircraft Instrumentation* and *19 Spacecraft Instrumentation.*

36 LASERS AND MASERS **883**
Includes parametric amplifiers. For related information see also *76 Solid-State Physics.*

37 MECHANICAL ENGINEERING **888**
Includes auxiliary systems (nonpower); machine elements and processes; and mechanical equipment.

38 QUALITY ASSURANCE AND RELIABILITY **694**
Includes product sampling procedures and techniques; and quality control.

39 STRUCTURAL MECHANICS **695**
Includes structural element design and weight analysis; fatigue; and thermal stress. For applications see *05 Aircraft Design, Testing and Performance* and *18 Spacecraft Design, Testing and Performance.*

GEOSCIENCES For related information see also *Space Sciences.*

42 GEOSCIENCES (GENERAL) **903**

43 EARTH RESOURCES AND REMOTE SENSING **904**
Includes remote sensing of earth resources by aircraft and spacecraft; photogrammetry; and aerial photography. For instrumentation see *35 Instrumentation and Photography.*

44 ENERGY PRODUCTION AND CONVERSION **907**
Includes specific energy conversion systems, e.g., fuel cells; global sources of energy; geophysical conversion; and windpower. For related information see also *07 Aircraft Propulsion and Power, 20 Spacecraft Propulsion and Power,* and *28 Propellants and Fuels.*

45 ENVIRONMENT POLLUTION **909**
Includes atmospheric, noise, thermal, and water pollution.

46 GEOPHYSICS **912**
Includes aeronomy; upper and lower atmosphere studies; ionospheric and magnetospheric physics; and geomagnetism. For space radiation see *93 Space Radiation.*

47 METEOROLOGY AND CLIMATOLOGY **918**
Includes weather forecasting and modification.

48 OCEANOGRAPHY **925**
Includes biological, dynamic, and physical oceanography; and marine resources. For related information see also *43 Earth Resources and Remote Sensing.*

LIFE SCIENCES

51 LIFE SCIENCES (GENERAL) **932**

52 AEROSPACE MEDICINE **933**
Includes physiological factors; biological effects of radiation; and effects of weightlessness on man and animals.

53 BEHAVIORAL SCIENCES **936**
Includes psychological factors; individual and group behavior; crew training and evaluation; and psychiatric research.

54 MAN/SYSTEM TECHNOLOGY AND LIFE SUPPORT **938**
Includes human engineering; biotechnology; and space suits and protective clothing. For related information see also *16 Space Transportation.*

55 SPACE BIOLOGY ..... **N.A.**
Includes exobiology; planetary biology; and extraterrestrial life.

MATHEMATICAL AND COMPUTER SCIENCES

59 MATHEMATICAL AND COMPUTER SCIENCES (GENERAL) ..... **N.A.**

60 COMPUTER OPERATIONS AND HARDWARE **940**
Includes hardware for computer graphics, firmware, and data processing. For components see *33 Electronics and Electrical Engineering.*

61 COMPUTER PROGRAMMING AND SOFTWARE **942**
Includes computer programs, routines, algorithms, and specific applications, e.g., CAD/CAM.

62 COMPUTER SYSTEMS **958**
Includes computer networks and special application computer systems.

63 CYBERNETICS **960**
Includes feedback and control theory, artificial intelligence, robotics and expert systems. For related information see also *54 Man/System Technology and Life Support.*

64 NUMERICAL ANALYSIS **967**
Includes iteration, difference equations, and numerical approximation.

65 STATISTICS AND PROBABILITY **970**
Includes data sampling and smoothing; Monte Carlo method; and stochastic processes.

66 SYSTEMS ANALYSIS **971**
Includes mathematical modeling; network analysis; and operations research.

67 THEORETICAL MATHEMATICS ..... **N.A.**
Includes topology and number theory.

PHYSICS For related information see also *Engineering.*

70 PHYSICS (GENERAL) ..... **N.A.**
For precision time and time interval (PTTI) see *35 Instrumentation and Photography;* for geophysics, astrophysics or solar physics see *46 Geophysics, 90 Astrophysics,* or *92 Solar Physics.*

71 ACOUSTICS **972**
Includes sound generation, transmission, and attenuation. For noise pollution see *45 Environment Pollution.*

72 ATOMIC AND MOLECULAR PHYSICS **976**
Includes atomic structure, electron properties, and molecular spectra.

73 NUCLEAR AND HIGH-ENERGY PHYSICS **978**
Includes elementary and nuclear particles; and reactor theory. For space radiation see *93 Space Radiation.*

74 OPTICS **979**
Includes light phenomena and optical devices. For lasers see *36 Lasers and Masers.*

75 PLASMA PHYSICS **987**
Includes magnetohydrodynamics and plasma fusion. For ionospheric plasmas see *46 Geophysics.* For space plasmas see *90 Astrophysics.*

76 SOLID-STATE PHYSICS **989**
Includes superconductivity. For related information see also *33 Electronics and Electrical Engineering* and *36 Lasers and Masers.*

77 THERMODYNAMICS AND STATISTICAL PHYSICS **997**
Includes quantum mechanics; theoretical physics; and Bose and Fermi statistics. For related information see also *25 Inorganic and Physical Chemistry* and *34 Fluid Mechanics and Heat Transfer.*

SOCIAL SCIENCES

80 SOCIAL SCIENCES (GENERAL) **998**
Includes educational matters.

81 ADMINISTRATION AND MANAGEMENT **999**
Includes management planning and research.

82 DOCUMENTATION AND INFORMATION SCIENCE **999**
Includes information management; information storage and retrieval technology; technical writing; graphic arts; and micrography. For computer documentation see *61 Computer Programming and Software.*

83 ECONOMICS AND COST ANALYSIS **1010**
Includes cost effectiveness studies.

84 LAW, POLITICAL SCIENCE AND SPACE POLICY ..... **N.A.**
Includes NASA appropriation hearings; aviation law; space law and policy; international law; international cooperation; and patent policy.

85 URBAN TECHNOLOGY AND TRANSPORTATION ..... **N.A.**
Includes applications of space technology to urban problems; technology transfer; technology assessment; and surface and mass transportation. For related information see *03 Air Transportation and Safety, 16 Space Transportation,* and *44 Energy Production and Conversion.*

SPACE SCIENCES For related information see also *Geosciences.*

88 SPACE SCIENCES (GENERAL) ..... **N.A.**

89 ASTRONOMY **1010**
Includes radio, gamma-ray, and infrared astronomy; and astrometry.

90 ASTROPHYSICS **1014**
Includes cosmology; celestial mechanics; space plasmas; and interstellar and interplanetary gases and dust. For related information see also *75 Plasma Physics.*

91 LUNAR AND PLANETARY EXPLORATION **1022**
Includes planetology; and manned and unmanned flights. For spacecraft design or space stations see *18 Spacecraft Design, Testing and Performance.*

92 SOLAR PHYSICS **1048**
Includes solar activity, solar flares, solar radiation and sunspots. For related information see *93 Space Radiation.*

93 SPACE RADIATION **1049**
Includes cosmic radiation; and inner and outer earth's radiation belts. For biological effects of radiation see *52 Aerospace Medicine.* For theory see *73 Nuclear and High-Energy Physics.*

GENERAL

Includes aeronautical, astronautical, and space science related histories, biographies, and pertinent reports too broad for categorization; histories or broad overviews of NASA programs.

99 GENERAL **1051**

SUBJECT INDEX **I-1**

PERSONAL AUTHOR INDEX **I-105**

CORPORATE SOURCE INDEX **I-117**

CONTRACT NUMBER INDEX **I-137**

REPORT NUMBER INDEX **I-141**

APPENDIX **A-1**

TYPICAL CITATION AND ABSTRACT

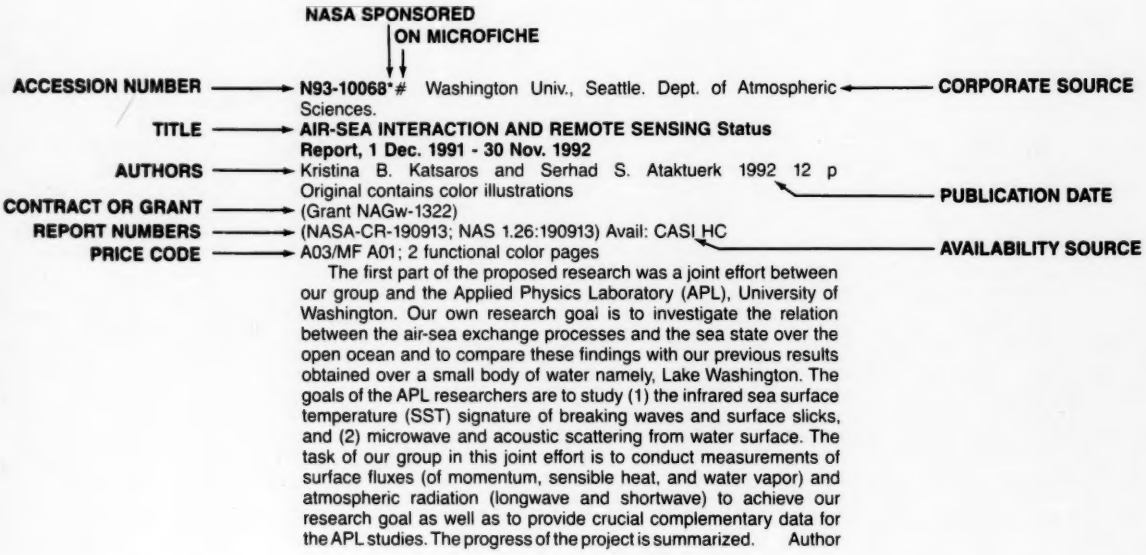
NASA SPONSORED
ON MICROFICHE
ACCESSION NUMBER
N93-10068* # Washington Univ., Seattle. Dept. of Atmospheric Sciences.
CORPORATE SOURCE
TITLE
AIR-SEA INTERACTION AND REMOTE SENSING Status Report, 1 Dec. 1991 - 30 Nov. 1992
AUTHORS
Kristina B. Katsaros and Serhad S. Ataktuerk 1992 12 p
Original contains color illustrations
PUBLICATION DATE
CONTRACT OR GRANT
(Grant NAGw-1322)
REPORT NUMBERS
(NASA-CR-190913; NAS 1.26:190913) Avail: CASI HC
AVAILABILITY SOURCE
PRICE CODE
A03/MF A01; 2 functional color pages

The first part of the proposed research was a joint effort between our group and the Applied Physics Laboratory (APL), University of Washington. Our own research goal is to investigate the relation between the air-sea exchange processes and the sea state over the open ocean and to compare these findings with our previous results obtained over a small body of water namely, Lake Washington. The goals of the APL researchers are to study (1) the infrared sea surface temperature (SST) signature of breaking waves and surface slicks, and (2) microwave and acoustic scattering from water surface. The task of our group in this joint effort is to conduct measurements of surface fluxes (of momentum, sensible heat, and water vapor) and atmospheric radiation (longwave and shortwave) to achieve our research goal as well as to provide crucial complementary data for the APL studies. The progress of the project is summarized. Author

VOLUME 31 NUMBER 4 / APRIL 1993

Scientific and Technical Aerospace Reports

A Monthly Publication of the National Aeronautics and Space Administration

01 AERONAUTICS (GENERAL)

N93-14102*# National Aeronautics and Space Administration. Lewis Research Center, Cleveland, OH.

AN ALGEBRAIC TURBULENCE MODEL FOR THREE-DIMENSIONAL VISCOUS FLOWS

R. V. Chima, P. W. Giel (Sverdrup Technology, Inc., Brook Park, OH.), and R. J. Boyle Jan. 1993 11 p Proposed for presentation at the 31st Aerospace Sciences Meeting and Exhibit, Reno, NV, 11-14 Jan. 1993; sponsored by AIAA

(RTOP 535-05-10)

(NASA-TM-105931; E-7442; NAS 1.15:105931) Copyright Avail: CASI HC A03/MF A01

An algebraic turbulence model is proposed for use with three-dimensional Navier-Stokes analyses. It incorporates features of both the Baldwin-Lomax and Cebeci-Smith models. The Baldwin-Lomax model uses the maximum of a function f(y) to determine length and velocity scales. An analysis of the Baldwin-Lomax model shows that f(y) can have a spurious maximum close to the wall, causing numerical problems and non-physical results. The proposed model uses integral relations to determine delta(*) u(sub e) and delta used in the Cebeci-Smith mode. It eliminates a constant in the Baldwin-Lomax model and determines the two remaining constants by comparison to the Cebeci-Smith formulation. Pressure gradient effects, a new wake model, and the implementation of these features in a three-dimensional Navier-Stokes code are also described. Results are shown for a flat plate boundary layer, an annular turbine cascade, and endwall heat transfer in a linear turbine cascade. The heat transfer results agree well with experimental data which shows large variations in endwall Stanton number contours with Reynolds number. Author

N93-14549# Wright Lab., Wright-Patterson AFB, OH.

PROCEEDINGS OF THE USAF STRUCTURAL INTEGRITY PROGRAM Final Report, 2-6 Dec. 1991

Thomas D. Cooper and John W. Lincoln Jul. 1992 787 p Conference held in San Antonio, TX, 2-6 December 1991

(AF Proj. 2418)

(AD-A255379; WL-TR-92-4045) Avail: CASI HC A99/MF A10

This report is a compilation of the papers presented at the 1991 USAF Structural Integrity Program Conference held at the Hyatt Regency, San Antonio, Texas on 2-6 December 1991. GRA

N93-14604* National Aeronautics and Space Administration, Washington, DC.

AERONAUTICAL ENGINEERING: A CONTINUING BIBLIOGRAPHY WITH INDEXES (SUPPLEMENT 282)

Sep. 1992 166 p

(NASA-SP-7037(282); NAS 1.21:7037(282)) Avail: CASI HC A08

This bibliography lists 623 reports, articles, and other documents introduced into the NASA scientific and technical information system in Aug. 1992. The coverage includes documents on the engineering and theoretical aspects of design, construction, evaluation, testing, operation, and performance of aircraft (including aircraft engines) and associated components, equipment, and systems. It also includes research and development in aerodynamics, aeronautics, and ground support equipment for aeronautical vehicles. Author

N93-14605* National Aeronautics and Space Administration, Washington, DC.

AERONAUTICAL ENGINEERING: A CONTINUING BIBLIOGRAPHY WITH INDEXES (SUPPLEMENT 284)

Nov. 1992 261 p

(NASA-SP-7037(284); NAS 1.21:7037(284)) Avail: CASI HC A12

This bibliography lists 974 reports, articles, and other documents introduced into the NASA scientific and technical information system in Oct. 1992. The coverage includes documents on design, construction, evaluation, testing, operation, and performance of aircraft (including aircraft engines) and associated components, equipment, and systems. It also includes research and development in aerodynamics, aeronautics, and ground support equipment for aeronautical vehicles. Author

N93-14613# National Aerospace Lab., Amsterdam (Netherlands).

SYMPOSIUM ON THE OCCASION OF THE FAREWELL OF PROF. DR. IR. O. H. GERLACH AS CHAIRMAN OF THE BOARD OF THE FOUNDATION NATIONAL AEROSPACE LABORATORY NLR, THE NETHERLANDS [SYMPOSIUM TER GELEGENHEID VAN HET AFSCHEID VAN PROF. DR. IR. O. H. GERLACH ALS VOORZITTER VAN HET BESTUUR VAN DE STICHTING NATIONAAL LUCHT- EN RUIMTEVAARTLABORATORIUM]

1991 85 p Symposium held in Amsterdam, Netherlands, 4 Oct. 1991

(ETN-92-92168) Avail: CASI HC A05/MF A01

A speech addressing the design of man machine systems for exploration of space beyond Earth orbit, in particular for the NASA manned Mars mission, from the human factors perspective, is presented. The history of 'aircraft parameter identification', and an attempt to project its effect on future developments in the theory and practice of dynamic flight test techniques, are presented. The technology of flight simulators is reviewed. For individual titles, see N93-14614 through N93-14616.

N93-14614*# National Aeronautics and Space Administration. Ames Research Center, Moffett Field, CA.

A VOYAGE TO MARS: A CHALLENGE TO COLLABORATION BETWEEN MAN AND MACHINES **c54**

Irving C. Statler *In* NAL, Symposium on the Occasion of the Farewell of Prof. Dr. Ir. O. H. Gerlach as Chairman of the Board of the Foundation National Aerospace Laboratory NLR, The Netherlands 1991 p 5-29

(For primary document see N93-14613 04-01)

Avail: CASI HC A03/MF A01

A speech addressing the design of man machine systems for exploration of space beyond Earth orbit from the human factors perspective is presented. Concerns relative to the design of automated and intelligent systems for the NASA Space Exploration Initiative (SEI) missions are largely based on experiences with integrating humans and comparable systems in aviation. The history, present status, and future prospect, of human factors in machine design are discussed in relation to a manned voyage to Mars. Three different cases for design philosophy are presented. The use of simulation is discussed. Recommendations for required research are given. ESA

N93-14615# Technische Univ., Delft (Netherlands). Faculty of Aerospace Engineering.

FLIGHT TESTING: PAST, PRESENT, AND FUTURE **c05**

J. A. Mulder *In* NAL, Symposium on the Occasion of the Farewell of Prof. Dr. Ir. O. H. Gerlach as Chairman of the Board of the Foundation National Aerospace Laboratory NLR, The Netherlands 1991 p 31-57

(For primary document see N93-14613 04-01)
Avail: CASI HC A03/MF A01

Ideas behind 'aircraft parameter identification' are presented in an historical context and an attempt is made to project their effect on future developments in the theory and practice of dynamic flight test techniques. In particular, the work of O.H. Gerlach in the analysis of a method for the measurement of performance and stability and control characteristics in unsteady symmetrical flight is discussed. Flight test maneuvers and instrumentation are described. ESA

N93-14616# Mooij and Associates, Oegstgeest (Netherlands).
FLIGHT SIMULATION LEAVES THE GROUND **c09**
H. A. Mooij *In* NAL, Symposium on the Occasion of the Farewell of Prof. Dr. Ir. O. H. Gerlach as Chairman of the Board of the Foundation National Aerospace Laboratory NLR, The Netherlands 1991 p 59-84
(For primary document see N93-14613 04-01)
Avail: CASI HC A03/MF A01

The technology of flight simulators is reviewed. Four examples demonstrating the 'art' of flight simulation are given. The visual subsystem, which directly impacts the usefulness of flight simulators, is addressed. The need for high fidelity reproduction of vehicle handling, full scenario flight operations, and the possibility of answering a multitude of questions related to crew-vehicle integration as a reason to improve simulation facilities are discussed. ESA

N93-14732* National Aeronautics and Space Administration, Washington, DC.
AERONAUTICAL ENGINEERING: A CONTINUING BIBLIOGRAPHY WITH INDEXES (SUPPLEMENT 283)
Oct. 1992 160 p
(NASA-SP-7037(283); NAS 1.21:7037(283)) Avail: CASI HC A08

This bibliography lists 615 reports, articles, and other documents introduced into the NASA scientific and technical information system in Sep. 1992. Subject coverage includes: design, construction and testing of aircraft and aircraft engines; aircraft components, equipment, and systems; ground support systems; and theoretical and applied aspects of aerodynamics and general fluid dynamics. Author

N93-15573*# National Aeronautics and Space Administration. Lewis Research Center, Cleveland, OH.
VIBRATION ISOLATION TECHNOLOGY: AN EXECUTIVE SUMMARY OF SYSTEMS DEVELOPMENT AND DEMONSTRATION
Carlos M. Grodsinsky, Kirk A. Logsdon, and Joseph F. Lubomski Jan. 1993 7 p Presented at the 31st Aerospace Sciences Meeting, Reno, NV, 11-14 Jan. 1993; sponsored by American Association of Aeronautics and Astronautics
(RTOP 694-03-0C)
(NASA-TM-105937; E-7454; NAS 1.15:105937) Avail: CASI HC A02/MF A01

A program was organized to develop the enabling technologies needed for the use of Space Station Freedom as a viable microgravity experimental platform. One of these development programs was the Vibration Isolation Technology (VIT). This technology development program grew because of increased awareness that the acceleration disturbances present on the Space Transportation System (STS) orbiter can and are detrimental to many microgravity experiments proposed for STS, and in the future, Space Station Freedom (SSF). Overall technological organization are covered of the VIT program. Emphasis is given to the results from development and demonstration of enabling technologies to achieve the acceleration requirements perceived as those most likely needed for a variety of microgravity science experiments. In so doing, a brief summary of general theoretical approaches to controlling the acceleration environment of an isolated space based payload and the design and/or performance of two prototype six degree of freedom active magnetic isolation systems is presented. Author

N93-15158# Societe Francaise d'Instruments de Mesure, Massy (France).
GROUND SUPPORT EQUIPMENT (GSE) FOR AIRCRAFT CONDITION MONITORING SYSTEM (ACMS) [DIE BODENSTATION (GSE) FUER DAS FLUGZEUGUEBERWACHUNGSSYSTEM (ACMS)]
A. Levionnois *In* DLR, Proceedings of the 16th Symposium on Aircraft Integrated Monitoring Systems Jan. 1992 p 115-128 (For primary document see N93-15152 04-06)
Avail: CASI HC A03/MF A06; DLR, Wissenschaftliches Berichtswesen, Postfach 90 60 58, Cologne, Germany, HC

N93-15181# Framasys A.G., Zurich (Switzerland).
FAILURE DIAGNOSTIC WITH MAINTEX BASED ON AIMS AT SWISSAIR [STOERUNGSDIAGNOSE MIT MAINTEX BASIEREND AUF AIMS BEI SWISSAIR]
R. Ottiger *In* DLR, Proceedings of the 16th Symposium on Aircraft Integrated Monitoring Systems Jan. 1992 p 557-566 (For primary document see N93-15152 04-06)
Avail: CASI HC A02/MF A06; DLR, Wissenschaftliches Berichtswesen, Postfach 90 60 58, Cologne, Germany, HC

N93-15185# MicroNet, Celle (Germany).
PERSONAL COMPUTER BASED TEST- AND EMULATION EQUIPMENT FOR MAINTENANCE AND GROUND SUPPORT [TESTGERAETE UND EMULATOREN AUF PERSONAL-COMPUTERBASIS FUER DIE WARTUNG UND DEN 'GROUND SUPPORT']
Anton Bader *In* DLR, Proceedings of the 16th Symposium on Aircraft Integrated Monitoring Systems Jan. 1992 p 629-646 (For primary document see N93-15152 04-06)
Avail: CASI HC A03/MF A06; DLR, Wissenschaftliches Berichtswesen, Postfach 90 60 58, Cologne, Germany, HC

02 AERODYNAMICS

Includes aerodynamics of bodies, combinations, wings, rotors, and control surfaces; and internal flow in ducts and turbomachinery.

For related information see also *34 Fluid Mechanics and Heat Transfer.*

N93-14160 Maryland Univ., College Park.
A STUDY OF VISCOUS INTERACTION EFFECTS ON HYPERSONIC WAVERIDERS Ph.D. Thesis
Jinhwa Chang 1991 220 p
Avail: Univ. Microfilms Order No. DA9222668

In a continuing effort to generate new and improved classes of viscous optimized hypersonic waveriders, the present work takes a step forward and examines the effects of viscous interaction in the waverider design and analysis process. Parametric runs are made to produce L/D, C(sub L), contour plots for Mach numbers 6.0 to 30.0 at an altitude 30.0 to 80.0 Km, for waverider designer's reference. This is the first work to examine the effects of viscous interactions on hypersonic waveriders, and to generate a new family of waveriders wherein viscous interaction effects are included within the optimization process. Corda's computer program is used to generate viscous optimized hypersonic waveriders from conical flowfields without viscous interaction. Each waverider is optimized for maximum L/D, and comparison studies are made between the cases with and without viscous interaction. Other results of the investigation agreed with viscous interaction theory in showing an increase in the surface pressure near the leading edge of a waverider, and also the tendency for it to approach the freestream value further downstream. This change in the surface pressure distribution as well as increases in the skin friction, resulted in a decrease in the maximum Lift/Drag for the waverider. The influence of viscous interactions on the surface pressure distribution and hence the maximum L/D were found to result in noticeably different viscous optimized waveriders generated without considering viscous interactions. Finally, the results show that aerodynamics performance of the viscous interaction waveriders are greatly reduced due mainly to a large increase in skin-friction drag associated with the viscous interaction phenomena that is increased with increasing the Mach number and altitude, but some of this loss can be recoupled by including viscous interactions within the optimization procedure. When the waverider is optimized for viscous interaction, the shape can change dramatically. The central conclusion of the present work delineates on a velocity-altitude map that region where viscous interaction effects are significant for modern hypersonic waveriders. In particular, viscous interaction effects become important at Mach numbers greater than sixteen and altitudes upwards of 140,000 feet. Dissert. Abstr.

N93-14173 Texas A&M Univ., College Station.
PARAMETRIC STUDY OF AIR SAMPLING CYCLONES Ph.D. Thesis
Murray Edward Moore 1991 159 p
Avail: Univ. Microfilms Order No. DA9216981

An improved method has been developed for the design of single and multiple inlet aerosol sampling cyclones. A single inlet design methodology allows aerodynamic particle (AED) cutpoint diameter predictions to be made for a standard Stairmand cyclone which has been an alteration in its outlet tube diameter. Three cyclone body diameters, 38.10 mm, 57.15 mm, 88.90 mm, were tested, while three different exhaust tubes sizes 26.7 mm, 42.9 mm, and 68.3 mm (inside diameter) were used to vary the exhaust tube diameter in the cyclone. Tested cyclone flowrates ranged from 16.3 LPM to 124 LPM. The measured particle AED cutpoints went from a minimum of 4.0 microns to a maximum of 18.8 microns. A functional relation using two nondimensional parameters, the cyclone flow Reynolds numbers and the ratio of the cutpoint particle diameter to the cyclone diameter. A multiple inlet cyclone was tested for two different length ratios, which allows for a degree of flexibility in the design of new systems. The size of the body diameter of the multiple inlet cyclones varied from 38.10 mm to 139.7 mm, where the two different lengths were twice and four times that of the cyclone body diameter. The minimum tested cyclone flowrate was 9.39 LPM, while the maximum tested flowrate was 1027 LPM. Particle AED cutpoints ranged from 3.9 microns to 17.1 microns. The data gathered were used to develop a technique for predicting the performance for a cyclone which had a length twice that of the cyclone diameter. The predicted flow rate for an 88.90 mm diameter cyclone differed by only 15 percent from the experimentally determined flowrate for a particle cutpoint of 10.0 microns AED diameter. Dissert. Abstr.

N93-14441# Wright Lab., Wright-Patterson AFB, OH.
A COMPILATION OF THE MATHEMATICS LEADING TO THE DOUBLET LATTICE METHOD Final Report, Jun. - Dec. 1991
Max Blair Mar. 1992 145 p
(AF Proj. 2401)
(AD-A256304; WL-TR-92-3028) Avail: CASI HC A07/MF A02

This report provides a theoretical development of the doublet lattice method, the method of choice for most subsonic unsteady aerodynamic modeling for over twenty years. This is a tutorial based on many-key mathematical developments provided in the references section. An example source code is provided in the appendix. GRA

N93-14451*# National Aeronautics and Space Administration. Hugh L. Dryden Flight Research Facility, Edwards, CA.
PRESSURE DISTRIBUTION FOR THE WING OF THE YAV-8B AIRPLANE; WITH AND WITHOUT PYLONS
Edwin J. Saltzman (PRC Kentron, Inc., Edwards, CA.), John H. DelFrate, Catherine M. Sabsay, and Jill M. Yarger Nov. 1992 139 p
(RTOP 505-59-53)
(NASA-TM-4429; H-1708; NAS 1.15:4429) Avail: CASI HC A07/MF A02

Pressure distribution data have been obtained in flight at four span stations on the wing panel of the YAV-8B airplane. Data obtained for the supercritical profiled wing, with and without pylons installed, ranged from Mach 0.46 to 0.88. The altitude ranged from approximately 20,000 to 40,000 ft and the resultant Reynolds numbers varied from approximately 7.2 million to 28.7 million based on the mean aerodynamic chord. Pressure distribution data and flow visualization results show that the full-scale flight wing performance is compromised because the lower surface cusp region experiences flow separation for some important transonic flight conditions. This condition is aggravated when local shocks occur on the lower surface of the wing (mostly between 20 and 35 percent chord) when the pylons are installed for Mach 0.8 and above. There is evidence that convex fairings, which cover the pylon attachment flanges, cause these local shocks. Pressure coefficients significantly more negative than those for sonic flow also occur farther aft on the lower surface (near 60 percent chord) whether or not the pylons are installed for Mach numbers greater than or equal to 0.8. These negative pressure coefficient peaks and associated local shocks would be expected to cause increasing wave and separation drag at transonic Mach number increases. Author

N93-14479 Cranfield Inst. of Tech., Bedford (England).
ROTATING STALL INCEPTION IN FANS OF LOW HUB-TIP RATIO Ph.D. Thesis
M. Soundranayagam 1991 257 p
Avail: Univ. Microfilms Order No. BRDX96883

An investigation was carried out to study the process of rotating stall inception in a low hub-tip ratio fan. Such fans are expected, based on an elementary analysis, to stall from the root. However, experimental evidence had led to the belief that the fans stalled from the tip. The effects of streamtube contraction were first studied and this was followed by an experimental investigation on an isolated rotor, with successive build modifications to increase the likelihood of rotating stall inception occurring at the root. A computer based streamline curvature method was used to study the effects of streamtube contraction and streamtube diffusion that commonly occur when a fan is operated at flows below its design flow rate. The results indicated a reduced expectation for the robot to stall first when compared to a simple 2-D flow analysis. Experimental measurements were then carried out to determine how the experimental local characteristics differed from the predicted characteristics. It was apparent that real fluid effects tended to steepen the root characteristic, thus enhancing the stability of the root. The tip characteristics tended to droop and become less stable. The enhancement of the root stability was also seen in the profiles of deviation angle. The axial velocity contours at the rotor exit supported the conclusion that the root stability enhancement was caused by 'centrifuging'. To determine the actual radial location of rotating stall inception, an array of hot wires was used to record events during the inception transient. Inception was first detectable at the tip. This tip stalling behavior persisted for all the build modifications. Measurements of unsteady pressure were also made to study the movement of the overall operating point since it was felt that this could continuously alternate between a pair of closely spaced characteristics. The results indicated that the fan operated along a unique characteristic. The overall conclusion was that a low hub-tip ratio fan shows a strong reluctance to stall at the root due to 'centrifuging' of the blade boundary layer. The inception process appears to be dominated by events in the tip region. Dissert. Abstr.

N93-14514 ESDU International Ltd., London (England).
PROGRAM FOR CALCULATION OF AILERON ROLLING MOMENT AND YAWING MOMENT COEFFICIENTS AT SUBSONIC SPEEDS
Oct. 1992 10 p
(ESDU-88040; ISBN-0-85679-832-0) Avail: Issuing Activity

ESDU 88040 describes the FORTRAN program ESDUpac A8840 that determines the aileron rolling and yawing moment coefficients for an aircraft. The program implements the empirical prediction methods of ESDU 88013 and 88029, accessing the graphical data in digitized form. Those documents must be consulted to establish the limitations of the program in terms of the geometries and flow conditions over which the methods were tested and the accuracy achieved. ESDU 88040 describes the input required by the program and illustrates the output through a worked example. The source code is provided on disc for use under MS DOS on personal computers. ESDU

N93-14515 ESDU International Ltd., London (England).
PRESSURE DRAG AND LIFT CONTRIBUTIONS FOR BLUNTED FOREBODIES OF FINENESS RATIO 2.0 IN TRANSONIC FLOW (M INFINITY LESS THAN OR EQUAL TO 1.4)
Jul. 1989 45 p
(ESDU-89033; ISBN-0-85679-850-9) Avail: Issuing Activity

ESDU 89033 presents axial and normal pressure force coefficient data obtained from a computed solution of the Euler equations for inviscid flow about spherically blunted tangent ogive and cone forebodies followed by a cylindrical afterbody in the Mach number range of 0.7 to 1.4. It is found that there is an optimum blunting ratio (ratio of the blunted nose diameter to the afterbody diameter) for which for a given Mach number and angle of attack the axial pressure force is a minimum. Charts show the variation of axial and normal pressure force coefficients around the optimum blunting for angles of attack up to 10 degrees, and axial pressure force coefficient (which is equivalent to the wave drag) at zero incidence. The derivation of the results is discussed, and examples compare forebody pressure distribution and force coefficients with those obtained in wind-tunnel tests so providing guidance on the expected accuracy of the calculations. ESDU

N93-14516 ESDU International Ltd., London (England).
DIRECT PREDICTION OF A SEPARATION BOUNDARY FOR AEROFOILS USING A VISCOUS-COUPLED CALCULATION METHOD
Apr. 1992 26 p
(ESDU-92008; ISBN-0-85679-813-4) Avail: Issuing Activity

ESDU 92008 describes the features of a viscous-coupled calculation method that are required to predict transonic flow over an aerofoil with some boundary layer separation. One particular method is considered in detail, its technical features are detailed, and the input and output are described together with the computer requirements. Its performance is compared with selected wind-tunnel data on pressure distribution, shock strength and location, trailing-edge pressure, and a separation boundary associated with trailing-edge pressure divergence together with the drag coefficient near that condition. The separation boundary was predicted to within about 0.08 in lift coefficient and the drag coefficient within 10 percent. Some details and trends were dealt with less satisfactorily; in particular, the often observed gradual increase in trailing-edge pressure prior to its rapid fall as separation becomes more extensive was not predicted and it seemed the extent and effects of shock-induced separation were underestimated. ESDU

N93-14595 Georgia Inst. of Tech., Atlanta.
THE EFFECT OF WAKE DYNAMICS ON ROTOR EIGENVALUES IN FORWARD FLIGHT Ph.D. Thesis
Yi-Ren Wang 1992 177 p
Avail: Univ. Microfilms Order No. DA9231760

An eigenvalue study can provide stability information for a system, and it is also an important part of aeroelastic analysis. In this work, a 2-D approximation to a set of 3-D generalized dynamic wake equations is studied first to obtain an overview of the characteristics of unsteady aerodynamics in forward flight. The generalized dynamic wake model employed is based on incompressible potential flow theory with an induced flow distribution expanded in a set of harmonic and radial shape functions, including undetermined time dependent coefficients as aerodynamic states. The second part of this work utilizes a 3-D wake eigen-analysis. Results with varying numbers of harmonies are computed, and the mode shapes of each eigenvalue are studied to understand the physical meaning of wake dynamics. The third part of this work is to investigate the damping of a blade-wake coupled system. The frequency response of this coupled model is also studied and compared with results from the 2-D approximation. A set of rigid-blade flapping equations is used to simplify the results. For this eigen-analysis, the blade-wake coupled system is represented by a set of periodic-coefficient differential equations in forward flight. Thus, Floquet Theory is applied to this stability problem. The eigenvalues of this matrix determine system characteristics. The flapping modes can be identified by the corresponding eigenvectors of each eigenvalue, and the stability of the whole aeroelastic system can be analyzed. This work gives us insight into the interaction of blade flapping and wake dynamics. The effect of wake dynamics on rotor eigenvalues in forward flight can be seen by comparison with the no inflow case. One can see from the results of this work that the inflow has a profound effect on blade dynamics even at high advance ratios. Dissert. Abstr.

N93-14631 Texas A&M Univ., College Station.
A FINITE ELEMENT MODEL FOR ANALYSIS OF THERMOVISCOPLASTIC BEHAVIOR OF HYPERSONIC LEADING EDGE STRUCTURES SUBJECT TO INTENSE AEROTHERMAL HEATING Ph.D. Thesis
Ted Gary Byrom 1992 144 p
Avail: Univ. Microfilms Order No. DA9232481

A finite element algorithm is formulated to model a hypersonic leading edge structure subject to severe localized aerothermal heating. The formulation contains nonlinear geometries, thermoviscoplastic material behavior, and inertial effects. The algorithm is tested against several exact solutions for simple test cases. The algorithm is then applied to two cases of a hypothetical leading edge structure with severe localized heating. Both quasistatic and dynamic results are obtained for each of the two cases. The results show that inclusion of the inertial effects are physically justified and also computationally beneficial. Dissert. Abstr.

N93-14661# Wright Lab., Wright-Patterson AFB, OH.
SUBSONIC AERODYNAMIC RESEARCH LABORATORY Interim Report, Jul. 1983 - May 1992
Aug. 1992 145 p
(AF Proj. 2404)
(AD-A256060; WL-TR-92-3053) Avail: CASI HC A07/MF A02

In July of 1983 Air Force Systems Command (AFSC) approved construction of the Subsonic Aerodynamic Research Laboratory (SARL). The SARL is designed to provide a low turbulence flow (less than 0.05 percent) for flow visualization and precision measurements. The test section walls are 80 percent optical quality plexiglass. The large viewing area lends the facility to flow measurement by laser velocimetry, a nonintrusive flow measurement technique. A computer system is available for force and pressure data. The octagonal test section is 7'w x 10'h making it possible to test large models at high angles-of-attack. The SARL is designed for efficient low cost operation. The flow conditioning section of the tunnel contains both screens and honeycomb material. The facility was designed to operate up to Mach 0.6. A natural frequency problem with the drive system presently limits top speed to Mach 0.5. The SARL construction project is somewhat unique, being an in-house effort not requiring an MCP. A significant cost savings was realized because several major components needed for the SARL, were available from other unused facilities. The fan was obtained from NASA Langley Research Center. The 20,000 hp drive system was supplied by Wright-Patterson AFB. GRA

N93-14737*# Barna (P. Stephen), Consultant, Norfolk, VA.
INVESTIGATIONS OF DETAIL DESIGN ISSUES FOR THE HIGH SPEED ACOUSTIC WIND TUNNEL USING A 60TH SCALE MODEL TUNNEL. PART 1: TESTS WITH OPEN CIRCUITS Final Report
P. Stephen Barna Jan. 1991 113 p
(NASA-CR-191671; NAS 1.26:191671) Avail: CASI HC A06/MF A02

This report summarizes the tests on the 1:60 scale model of the High Speed Acoustic Wind Tunnel (HSAWT) performed during the period of November 1989 to December 1990. Throughout the testing the tunnel was operated in the 'open circuit mode', that is when the airflow was induced by a powerful exhaust fan located outside the tunnel circuit. The tests were first performed with the closed test section and were subsequently repeated with the open test section. While operating with the open test section, a novel device, called the 'nozzle-diffuser,' was also tested in order to establish its usefulness of increasing pressure recovery in the first diffuser. The tests established the viability of the tunnel design. The flow distribution in each tunnel component was found acceptable and pressure recovery in the diffusers were found satisfactory. The diffusers appeared to operate without flow separation. All tests were performed at NASA LaRC. Author

N93-14738*# Barna (P. Stephen), Consultant, Norfolk, VA.
INVESTIGATIONS OF DETAIL DESIGN ISSUES FOR THE HIGH SPEED ACOUSTIC WIND TUNNEL USING A 60TH SCALE MODEL TUNNEL. PART 2: TESTS WITH THE CLOSED CIRCUIT Final Report
P. Stephen Barna Oct. 1991 65 p
(NASA-CR-191672; NAS 1.26:191672) Avail: CASI HC A04/MF A01

This report summarizes the tests on the 1:60 scale model of the High Speed Acoustic Wind Tunnel (HSAWT) performed during the period June - August 1991. Throughout the testing the tunnel was operated in the 'closed circuit mode,' that is when the airflow was set up by an axial flow fan, which was located inside the tunnel circuit and was directly driven by a motor. The tests were first performed with the closed test section and were subsequently repeated with the open test section, the latter operating with the nozzle-diffuser at its optimum setting. On this subject, reference is made to the report (1) issued January 1991, under contract 17-GFY900125, which summarizes the result obtained with the tunnel operating in the 'open circuit mode.' The tests confirmed the viability of the tunnel design, and the flow distributions in most of the tunnel components were considered acceptable. There were found, however, some locations where the flow distribution requires improvement. This applies to the flow upstream of the fan where the flow was found skewed, thus affecting the flow downstream. As a result of this, the flow appeared separated at the end of the large diffuser at the outer side. All tests were performed at NASA LaRC.

Author

N93-14767*# Oklahoma Univ., Norman. School of Aerospace and Mechanical Engineering.

COMPUTATIONAL ANALYSIS OF HYPERSONIC FLOWS PAST ELLIPTIC-CONE WAVERIDERS

Bok-Hyun Yoon and Maurice L. Rasmussen Jan. 1991 306 p (Grant NAG1-886)

(NASA-CR-191304; NAS 1.26:191304; OU-AME-91-2) Avail: CASI HC A14/MF A03

A comprehensive study for the inviscid numerical calculation of the hypersonic flow past a class of elliptic-cone derived waveriders is presented. The theoretical background associated with hypersonic small-disturbance theory (HSDT) is reviewed. Several approximation formulas for the waverider compression surface are established. A CFD algorithm is used to calculate flow fields for the on-design case and a variety of off-design cases. The results are compared with HSDT, experiment, and other available CFD results. For the waverider shape used in previous investigations, the bow shock for the on-design condition stands off from the leading-edge tip of the waverider. It was found that this occurs because the tip was too thick according to the approximating shape formula that was used to describe the compression surface. When this was corrected, the bow shock became closer to attached as it should be. At Mach numbers greater than the design condition, a lambda-shock configuration develops near the tip of the compression surface. At negative angles of attack, other complicated shock patterns occur near the leading-edge tip. These heretofore unknown flow patterns show the power and utility of CFD for investigating novel hypersonic configurations such as waveriders. Author

N93-14791*# National Aeronautics and Space Administration. Lewis Research Center, Cleveland, OH.

ESTIMATION OF UNSTEADY LIFT ON A PITCHING AIRFOIL FROM WAKE VELOCITY SURVEYS

K. B. M. Q. Zaman, J. Panda, and C. L. Rumsey (National Aeronautics and Space Administration. Langley Research Center, Hampton, VA.) Jan. 1993 16 p Presented at the 31st Aerospace Sciences Meeting and Exhibit, Reno, NV, 11-14 Jan. 1993

(RTOP 505-52-62)

(NASA-TM-105947; E-7465; NAS 1.15:105947) Avail: CASI HC A03/MF A01

The results of a joint experimental and computational study on the flowfield over a periodically pitched NACA0012 airfoil, and the resultant lift variation, are reported in this paper. The lift variation over a cycle of oscillation, and hence the lift hysteresis loop, is estimated from the velocity distribution in the wake measured or computed for successive phases of the cycle. Experimentally, the estimated lift hysteresis loops are compared with available data from the literature as well as with limited force balance measurements. Computationally, the estimated lift variations are compared with the corresponding variation obtained from the surface pressure distribution. Four analytical formulations for the lift estimation from wake surveys are considered and relative successes of the four are discussed. Author

N93-14836 State Univ. of New York, Buffalo.

MODELING VARIABLE BLOWING ON A SLENDER CONE IN HYPERSONIC FLOW Ph.D. Thesis

John Gary VanOsdol 1992 197 p

Avail: Univ. Microfilms Order No. DA9228100

A study of the effects of variable blowing in turbulent conical hypersonic boundary layers is presented. Numerical calculations of the skin friction and surface heat transfer rates are compared to the experimental measurements which were reported by Holden, VanOsdol and Rodrigues (1990) for a slender cone at zero angle of attack in steady flows at Mach numbers of 11 and 13. An analysis of the transpiration feed system of the cone model was performed and showed that the blowing rate could be variable along the cone surface. This effect is confirmed by internal pressure measurements which were taken inside the cone model. The blowing rates are re-calibrated using the internal gauge readings and used as the wall boundary condition for a compressible turbulent boundary layer calculation using the low Reynolds number k-epsilon model of Chien (1982). At low blowing rates the boundary layer calculations indicate that a situation where both the effects of suction and blowing are present within the same flow. The results show excellent qualitative prediction of the experimental data. These calculations are compared to earlier calculations made using the BLIMP code which assumed that the blowing rates were constant along the cone surface. Dissert. Abstr.

N93-14911*# National Aeronautics and Space Administration. Lewis Research Center, Cleveland, OH.

RESULTS OF LOW POWER DEICER TESTS ON A SWEPT INLET COMPONENT IN THE NASA LEWIS ICING RESEARCH TUNNEL

Thomas H. Bond and Jaiwon Shin Jan. 1993 21 p Presented at the 31st Aerospace Sciences Meeting and Exhibit, Reno, NV, 11-14 Jan. 1993; sponsored by AIAA

(RTOP 505-68-10)

(NASA-TM-105968; E-7495; NAS 1.15:105968; AIAA Paper 93-0032)

Avail: CASI HC A03/MF A01

Tests were conducted under a USAF/NASA Low Power Deicer program on two expulsive technologies to examine system performance on hardware representative of a modern aircraft part. The BF Goodrich Electro-Expulsive Deicing System and Pneumatic Impulse Ice Protection System were installed on a swept, compound curve, engine inlet component with varying leading edge radius, and tested through a range of icing and system operating conditions in the NASA Lewis Icing Research Tunnel. A description of the experimental procedure and results, including residual ice thickness, shed ice particle size, and changes in system energy/pressure characteristics are presented. Author

N93-15101 Notre Dame Univ., IN.

WAKE SIMILARITY AND VORTEX FORMATION FOR TWO-DIMENSIONAL BLUFF BODIES Ph.D. Thesis

Jose Luis Villafranc Nebres 1992 205 p

Avail: Univ. Microfilms Order No. DA9230042

An experimental study of the flow around a cylinder with a single straight perturbation was conducted in a wind tunnel. With this bluff body, positioned in a uniform crossflow, the vortex shedding frequency and other flow characteristics could be manipulated. The Strouhal number has been shown to be a function of the perturbation angular position, theta(p), as well as the perturbation size and Reynolds number. As much as a 50 percent change in Strouhal number could be achieved, simply by changing theta(p) by 1 deg. The perturbation size compared to the boundary-layer thickness, delta, was varied from approximately 1 delta to about 20 delta. The Reynolds number was varied from 10,000 to 40,000. A detailed investigation of the characteristic Strouhal number variations has shown that varying theta(p) had a significant influence on the boundary-layer separation and transition to turbulence. These significant changes occurring in the boundary-layer have been shown to cause variations in the spacing between the shear layers, base pressure, vortex formation length, drag, lift, and the longitudinal spacing between the vortices in the vortex street. The unique ability of the cylinder with a single straight perturbation to control the Strouhal number and other flow characteristics, was used to evaluate several previously proposed wake similarity concepts by Fage and Johansen (1927), Roshko (1955), Bearman (1967) and Griffin (1981). It was shown that these wake similarity concepts did not satisfactorily apply to the bluff body which was used in this study. The experimental results have shown that a wake similarity parameter, S(M) = kf(sub v)d*/U(infinity) has smaller variations from its mean values S(M sub 0) = 0.39, when compared to previously proposed wake similarity parameters. The quantity k is the base pressure parameter, f(sub v) is the vortex shedding frequency, d* is the spacing between the shear layers, and U(infinity) is the free stream velocity. The similarity parameter S(M), when applied to Fage and Johansen's measurements on a wide range of bluff bodies showed less variance and resulted in numbers near 0.39. The parameter, S(M), when used to evaluate the lateral-to-longitudinal stability of vortices in the vortex street was shown to favor von Karman's over Kronauer's wake stability criterion. Dissert. Abstr.

N93-15131# Max-Planck-Inst. fuer Stroemungsforschung, Goettingen (Germany).

AN EXPERIMENTAL INVESTIGATION OF BASE BLEED EFFECT ON THE WAKE TURBULENT STRUCTURE BEHIND A TWO-DIMENSIONAL BLUNT MODEL

V. L. Zhdanov and H. Eckelmann Nov. 1991 59 p Sponsored by Max-Planck-Inst. fuer Stroemungsforschung

(MPIS-9/1991; ETN-92-92731) Avail: CASI HC A04/MF A01

The flow pattern behind a two dimensional body with bleeding through a slot in its trailing edge was studied experimentally. Two bleeding modes were investigated. One with the maximum pressure at the body base and one with a zero excess momentum wake. In both cases the slot width, characterized by its width to trailing edge height ratio h/H, varied from 0.095 to 0.01875. Distributions of the mean velocity, longitudinal and transverse fluctuations in the wake were measured at nondimensional distances 3 less than or equal to x/H less than or equal to 30 from the body trailing edge. ESA

N93-15245# Naval Postgraduate School, Monterey, CA.
FLOWFIELD STUDY OF A CLOSE-COUPLED CANARD CONFIGURATION M.S. Thesis
John F. OLeary Jun. 1992 96 p
(AD-A256311) Avail: CASI HC A05/MF A01

A nulling five-hole pressure probe was used to complete a flowfield survey behind a close-coupled canard and wing model set at 22 degrees angle of attack. The canard and wing were both low-aspect-ratio, highly-swept, delta planforms with rounded leading edges. The model was set at the condition of maximum lift enhancement of the canard/wing configuration over a corresponding wing-alone configuration, based on previous force measurements. For comparison, the pressure measurements were made with the canard on and with the canard off. From the pressure measurements, flowfield velocity-vector, velocity-streamline and total-pressure-coefficient contours were plotted. These plots showed the dramatic effect of the canard vortex on the wing flowfield. The location and interaction of the canard and wing leading-edge vortices were analyzed. Large-scale reattachment of previously reversed flow over the wing was noted, as well as the re-establishment and strengthening of the wing leading-edge vortex. GRA

N93-15338*# National Aeronautics and Space Administration. Lewis Research Center, Cleveland, OH.
SURFACE ROUGHNESS DUE TO RESIDUAL ICE IN THE USE OF LOW POWER DEICING SYSTEMS
Jaiwon Shin and Thomas H. Bond Jan. 1993 16 p Presented at the 31st Aerospace Sciences Meeting and Exhibit, Reno, NV, 11-14 Jan. 1993; sponsored by AIAA
(RTOP 505-68-10)
(NASA-TM-105971; E-7494; NAS 1.15:105971; AIAA Paper 93-0031)
Avail: CASI HC A03/MF A01

Thicknesses of residual ice are presented to provide information on surface contamination and associated roughness during deicing events. Data was obtained from low power ice protection systems tests conducted in the Icing Research Tunnel at NASA Lewis Research Center (LeRC) with nine different deicing systems. Results show that roughness associated with residual ice is not characterized by uniformly distributed roughness. Results also show that deicing systems require a critical mass of ice to generate a sufficient expelling force to remove the ice. Author

N93-15404*# National Aeronautics and Space Administration. Lewis Research Center, Cleveland, OH.
AN OVERVIEW OF SHED ICE IMPACT IN THE NASA LEWIS ICING RESEARCH TUNNEL
Thomas H. Bond and Randall K. Britton (Sverdrup Technology, Inc., Brook Park, OH.) 14 Jan. 1993 14 p
(NASA-TM-105969; E-7492; NAS 1.15:105969; AIAA Paper 93-0301)
Avail: CASI HC A03/MF A01

One of the areas of active research in commercial and military rotorcraft is directed toward developing the capability of sustained flight in icing conditions. The emphasis to date has been on the accretion and subsequent shedding of ice in an icing environment, where the shedding may be natural or induced. Historically, shed-ice particles have been a problem for aircraft, particularly rotorcraft. Because of the high particle velocities involved, damage to a fuselage or other airframe component from a shed-ice impact can be significant. Design rules for damage tolerance from shed-ice impact are not well developed because of a lack of experimental data. Thus, NASA Lewis (LeRC) has begun an effort to develop a database of impact force and energy resulting from shed ice. This effort consisted of a test of NASA LeRC's Model Rotor Test Rig (MRTR) in the Icing Research Tunnel (IRT). Both natural shedding and forced shedding were investigated. Forced shedding was achieved by fitting the rotor blades with Small Tube Pneumatic (STP) deicer boots manufactured by BF Goodrich. A detailed description of the test is given as well as the design of a new impact sensor which measures the force-time history of an impacting ice fragment. A brief discussion of the procedure to infer impact energy from a force-time trace are required for the impact-energy calculations. Recommendations and future plans for this research area are also provided. Author

N93-15464# Lehigh Univ., Bethlehem, PA. Dept. of Mechanical Engineering and Mechanics.
WHITE PAPER ON THE AFOSR SUPERMANEUVERABILITY WORKSHOP Final Report, 1 Nov. 1991 - 31 Jul. 1992
Donald Rockwell 7 Sep. 1992 9 p Workshop held in Bethlehem, PA, 9-10 Apr. 1992
(Contract F49620-92-J-0065)
(AD-A256385; AFOSR-92-0878TR) Avail: CASI HC A02/MF A01

Tnis workshop promoted the exchange of information among researchers currently studying unsteady aerodynamics at high angle-of-attack and provided a basis for identification of the major, unresolved issues in this area. Detailed technical presentations were given covering AFOSR's 6.1 Trial in Unsteady Aerodynamics, namely Quasi-Two-Dimensional Unsteady Flows, Three-Dimensional Unsteady Flows and the Control of Unsteady Flows. GRA

N93-15483*# National Aeronautics and Space Administration. Ames Research Center, Moffett Field, CA.
THE APPLICAITON OF CFD TO ROTARY WING FLOW PROBLEMS
F. X. Caradonna (Army Aviation Research and Development Command, Moffett Field, CA.) Mar. 1992 75 p
(RTOP 505-61-51)
(NASA-TM-102803; A-90110; NAS 1.15:102803;
USAAVSCOM-TR-92-A-004) Avail: CASI HC A04/MF A01

This report is a review intended to serve as source and reference material for the CFD phase of a short course on rotorcraft aerodynamics. The review is mainly oriented toward engineering application methods. Therefore, emphasis is placed on potential methods and their various types and uses. However, the application of viscous codes is also discussed. These methods are discussed in the context of the various rotorcraft-specific problems including wake prediction, blade/vortex interactions, transonic problems, dynamic stall, and other separation problems. The exposition includes a discussion of the various flow equations and the physical approximations, which they embody. Basic methods of solving these are presented, especially integral and difference approaches to the various potential equations. The treatment of total rotor/wake problems by hybrid difference/integral schemes are discussed. These include both hover flow and forward flight methods requiring a consideration of trim. Unified schemes, which solve an entire rotor/wake flow on a single grid, are also treated. One of these, a vorticity convecting full-potential approach, is capable of predicting complete hover performance polars. Many comparisons are made with data from flight and model tests, to demonstrate the efficacy of the different flow treatments. Finally, advanced flow topics, requiring full viscous solutions, are shown in order to demonstrate the future possibilities and opportunities for CFD as newer methods mature and become practical. Author

N93-15489# Rolls-Royce Ltd., Derby (England).
TIME-DEPENDENT PREDICTIONS AND ANALYSIS OF TURBINE CASCADE DATA IN THE TRANSONIC FLOW REGION
A. Boelcs (Ecole Polytechnique Federale de Lausanne, Switzerland), A. Cargill, T. Fransson (Ecole Polytechnique Federale de Lausanne, Switzerland), A. Suddhoo, and K. Vogeler (Allmanna Svenska Elektriska A.B. Brown Boveri, Baden, Switzerland) 20 Oct. 1991 24 p
(PNR-90957; ETN-92-92230) Copyright Avail: CASI HC A03/MF A01

Experimentally determined steady state and time dependent blade surface pressures, obtained in an annular test facility, were compared to predictions by a finite element potential flow solver, FINSUP, for two model turbine cascade sections. The studied cascades are geometrically different (camber, thickness), but have a well defined interblade passage and are overlapped for about 35 percent of the chord. Most time dependent predictions were obtained with FINSUP in the two dimensional mode, and no special attempts was made to refine the computational mesh in the vicinity of the expected shock positions. It was concluded from the experimental results that an aerodynamic shock wave has a significant

influence on the unsteady pressures in the blade surface. The amplitude can become very large, and a phase shift can appear in the pressure. Results obtained in the traveling wave mode do not always, as they depend on the interblade phase angle, show this clearly. It is thus concluded that the physical understanding of shock influences may be found more easily if the influence coefficients are studied in detail, both as regards to the amplitude and the phase angle. ESA

N93-15588*# Washington Univ., Seattle.
INVESTIGATION OF THE AEROTHERMODYNAMICS OF HYPERVELOCITY REACTING FLOWS IN THE RAM ACCELERATOR Final Report, 17 Jul. 1989 - 30 Apr. 1992
A. Hertzberg, A. P. Bruckner, A. T. Mattick, and C. Knowlen 28 Dec. 1992 101 p
(Grant NAG3-1061)
(NASA-CR-191715; NAS 1.26:191715) Avail: CASI HC A06/MF A02

New diagnostic techniques for measuring the high pressure flow fields associated with high velocity ram accelerator propulsive modes was experimentally investigated. Individual propulsive modes are distinguished by their operating Mach number range and the manner in which the combustion process is initiated and stabilized. Operation of the thermally choked ram accelerator mode begins by injecting the projectile into the accelerator tube at a prescribed entrance velocity by means of a conventional light gas gun. A specially designed obturator, which is used to seal the bore of the gun, plays a key role in the ignition of the propellant gases in the subsonic combustion mode of the ram accelerator. Once ignited, the combustion process travels with the projectile and releases enough heat to thermally choke the flow within several tube diameters behind it, thereby stabilizing a high pressure zone on the rear of the projectile. When the accelerating projectile approaches the Chapman-Jouguet detonation speed of the propellant mixture, the combustion region is observed to move up onto the afterbody of the projectile as the pressure field evolves to a distinctively different form that implies the presence of supersonic combustion processes. Eventually, a high enough Mach number is reached that the ram effect is sufficient to cause the combustion process to occur entirely on the body. Propulsive cycles utilizing on-body heat release can be established either by continuously accelerating the projectile in a single propellant mixture from low initial in-tube Mach numbers (M less than 4) or by injecting the projectile at a speed above the propellant's Chapman-Jouguet detonation speed. The results of experimental and theoretical explorations of ram accelerator gas dynamic phenomena and the effectiveness of the new diagnostic techniques are presented in this report. Author

03 AIR TRANSPORTATION AND SAFETY

Includes passenger and cargo air transport operations; and aircraft accidents.

For related information see also *16 Space Transportation* and *85 Urban Technology and Transportation.*

N93-14277# Federal Aviation Administration, Washington, DC. Office of Aviation Medicine.
EFFECTS OF SEATING CONFIGURATION AND NUMBER OF TYPE 3 EXITS ON EMERGENCY AIRCRAFT EVACUATION Final Report
Garnet A. McLean, Charles B. Chittum, Gordon E. Funkhouser, Gregory W. Fairlie, and Earl W. Folk Aug. 1992 27 p
(AD-A256616; DOT/FAA/AM-92/27) Avail: CASI HC A03/MF A01

An increase in the required pathway width from aircraft center aisles to Type 3 overwing exits is being weighed by the FAA. To augment the analysis, an examination of seat/exit configuration effects on simulated emergency egress was conducted in the CAMI Evacuation Research Facility. Four subject groups traversed four different seat/exit configurations in a counter-balanced, repeated-measures design. Pathway width was modified by altering seat pitch. In single-exit trials the fastest times and highest flow-rates occurred with a 20 pathway between triple seats or a 10 inch pathway between double seats. Double exits produced 36 percent shorter egress times (p less than .007), although flow-rates declined 11 percent and exit plug removal times increased 32 percent, compared to single exits. Efficient egress requires optimization of the space around the exit. Generally, wider pathways and fewer obstructions enhance this process; however; when available space exceeds individual passenger needs, conflicts may be produced which inhibit egress. GRA

N93-14693 Columbia Univ., New York, NY.
AVIATION ACCIDENTS, INCIDENTS, AND VIOLATIONS: PSYCHOLOGICAL PREDICTORS AMONG US PILOTS Ph.D. Thesis
Maxine Esta Lubner 1992 509 p
Avail: Univ. Microfilms Order No. DA9232119

A retrospective case-control survey discovered candidate risk factors for pilots having aviation accidents, incidents and/or violations during 1987-1988. Risk factors included personal disposition, flight background, and demographic variables. A randomly selected sample from Federal Aviation Administration data bases of 1,049 civil aviation U.S. male pilots received anonymous questionnaires. Response rate was 46.3 percent. A check of threats to validity found negligible bias arising from non--response, exclusion of respondents, missing data, and power requirements. The final sample size was 394. Analyses were conducted by univariate inspection of variables, comparison of cases and controls using bivariate parametric and non-parametric tests on original and transformed data, and multivariate analyses of case-control status using selected variables. Logistic and multiple regressions tested predictors in tiered models: (1) personal disposition variables; (2) personal dispositions and demographics; and (3) personal dispositions, demographics, and flight backgrounds. Additional logistic regression tests were conducted within strata of three flight background variables: Experience, Exposure, and Skill. Within case bivariate and some multiple regression tests compared more severe with less severe cases. Severity of case status outcomes included: (1) type of concurrence; (2) Pilot-in-Command or not; (3) severity of accident/incident; (4) pilot- vs. other-caused occurrence; (5) number of occurrences ever had; and (6) rates of occurrences had, using experience and years flown as denominators. Environmental context predictors appeared in separate multiple regression models using occurrence rates outcomes. Certain variables consistently predicted case status offering a Risk Profile: high Thrill and Adventure Seeking, many ailments, not married, many years flown, many recent hours flown, and possibly, Eastern FAA Region. Stratified and within-cases analyses suggested several predictors of case status including low Superego, few safety behaviors, Private certificate, Personal flying, less education, and fewer pilot friends. The Five Hazardous Thoughts measure had little validity and requires refinement. Future research on theoretical and preventive issues should focus on risk-taking, conscientiousness, judgement, and learning. Methodological recommendations include using measures with improved psychometric properties and validity. Dissert. Abstr.

N93-14844*# National Aeronautics and Space Administration. Langley Research Center, Hampton, VA.
AIRBORNE WIND SHEAR DETECTION AND WARNING SYSTEMS. FOURTH COMBINED MANUFACTURERS' AND TECHNOLOGISTS' CONFERENCE, PART 2
Dan D. Vicroy, comp., Roland L. Bowles, comp., and Robert H. Passman, comp. (Federal Aviation Administration, Washington, DC.) Sep. 1992 416 p Conference held in Williamsburg, VA, 14-16 Apr. 1992; cosponsored by FAA Prepared in cooperation with FAA, Washington, DC
(RTOP 505-64-12-01)
(NASA-CP-10105-Pt-2; NAS 1.55:10105-Pt-2; DOT/FAA/RD-92/19-Pt-2)
Avail: CASI HC A18/MF A04

The Fourth Combined Manufacturers' and Technologists' Conference was hosted jointly by NASA Langley Research Center (LaRC) and the Federal Aviation Administration (FAA) in Williamsburg, Virginia, on April 14-16, 1992. The meeting was co-chaired by Dr. Roland Bowles of LaRC and Bob Passman of the FAA. The purpose of the meeting was to transfer significant ongoing results of the NASA/FAA Joint Airborne Wind Shear Program to the technical industry and to pose problems of current concern to the combined group. It also provided a forum for manufacturers to review forward-look technology concepts and for technologists to gain an understanding of the problems encountered by the manufacturers during the development of airborne equipment and the FAA certification requirements. The present document has been compiled to record the essence of the technology updates and discussions which follow each. For individual titles, see N93-14845 through N93-14858.

N93-14845*# National Aeronautics and Space Administration. Langley Research Center, Hampton, VA.

TWO MICRON LASER DEVELOPMENT FOR ATMOSPHERIC REMOTE SENSING AT NASA LANGLEY RESEARCH CENTER

Philip Brockman *In its* Airborne Wind Shear Detection and Warning Systems. Fourth Combined Manufacturers' and Technologists' Conference, Part 2 Sep. 1992 p 617-631 (For primary document see N93-14844 04-03)

Avail: CASI HC A03/MF A04

The topics addressed are: (1) eye safety revision of infrared MPE; (2) Tm:Ho dynamics characterization, which includes spectroscopy, laser experiments, and modeling; and (3) Q.M. model calculation, which includes energy levels, electric and magnetic dipole transition probabilities, lifetimes, branching ratios, absorption spectra, and emission spectra; (3) Q.M. model calculation; and (4) heat propagation in a laser rod. I.I.C.

N93-14846*# Lockheed Missiles and Space Co., Palo Alto, CA.

NASA/LMSC INSTRUMENT DESIGN AND FABRICATION

Russel Targ *In* NASA. Langley Research Center, Airborne Wind Shear Detection and Warning Systems. Fourth Combined Manufacturers' and Technologists' Conference, Part 2 Sep. 1992 p 633-657 (For primary document see N93-14844 04-03)

Avail: CASI HC A03/MF A04

The topics addressed are: (1) class-10 flight test program; (2) class system requirements; (3) Doppler wind velocity measurement; (4) systems specifications rational; (5) signal-to-noise equation for remote atmospheric sensing laser velocimeter; (6) variation of signal-to-noise ratios and true wind velocity with distance; (7) velocity error as a function of signal-to-noise ratio, with turbulence; and (8) final class optomechanical design on NASA B/737. I.I.C.

N93-14847*# Lockheed Missiles and Space Co., Palo Alto, CA.

NASA/LMSC COHERENT LIDAR AIRBORNE SHEAR SENSOR: SYSTEM CAPABILITIES AND FLIGHT TEST PLANS

Paul Robinson *In* NASA. Langley Research Center, Airborne Wind Shear Detection and Warning Systems. Fourth Combined Manufacturers' and Technologists' Conference, Part 2 Sep. 1992 p 659-671 (For primary document see N93-14844 04-03)

Avail: CASI HC A03/MF A04

The primary objective of the NASA/LMSC Coherent Lidar Airborne Shear Sensor (CLASS) system flight tests is to evaluate the capability of an airborne coherent lidar system to detect, measure, and predict hazardous wind shear ahead of the aircraft with a view to warning flight crew of any impending dangers. On NASA's Boeing 737 Transport Systems Research Vehicle, the CLASS system will be used to measure wind velocity fields and, by incorporating such measurements with real-time aircraft state parameters, identify regions of wind shear that may be detrimental to the aircraft's performance. Assessment is to be made through actual wind shear encounters in flight. Wind shear measurements made by the class system will be compared to those made by the aircraft's in situ wind shear detection system as well as by ground-based Terminal Doppler Weather Radar (TDWR) and airborne Doppler radar. By examining the aircraft performance loss (or gain) due to wind shear that the lidar predicts with that actually experienced by the aircraft, the performance of the CLASS system as a predictive wind shear detector will be assessed. Author

N93-14848*# Coherent Technologies, Inc., Boulder, CO.

SOLID-STATE COHERENT LASER RADAR WIND SHEAR MEASURING SYSTEMS

R. Milton Huffaker *In* NASA. Langley Research Center, Airborne Wind Shear Detection and Warning Systems. Fourth Combined Manufacturers' and Technologists' Conference, Part 2 Sep. 1992 p 673-684 (For primary document see N93-14844 04-03)

Avail: CASI HC A03/MF A04

Coherent Technologies, Inc. (CTI) was established in 1984 to engage in the development of coherent laser radar systems and subsystems with applications in atmospheric remote sensing, and in target tracking, ranging and imaging. CTI focuses its capabilities in three major areas: (1) theoretical performance and design of coherent laser radar system; (2) development of coherent laser radar systems for government agencies such as DoD and NASA; and (3) development of coherent laser radar systems for commercial markets. The topics addressed are: (1) 1.06 micron solid-state coherent laser radar system; (2) wind measurement using 1.06 micron system; and flashlamp-pumped 2.09 micron solid-state coherent laser radar system. I.I.C.

N93-14849*# Turbulence Prediction Systems, Boulder, CO.

DEVELOPMENT OF THE ADVANCE WARNING AIRBORNE SYSTEM(AWAS)

H. Patrick Adamson *In* NASA. Langley Research Center, Airborne Wind Shear Detection and Warning Systems. Fourth Combined Manufacturers' and Technologists' Conference, Part 2 Sep. 1992 p 687-780 (For primary document see N93-14844 04-03)

Avail: CASI HC A05/MF A04

The thermal characteristics of microbursts are utilized by the AWAS IR and OAT features to provide predictive warning of hazardous microbursts ahead of the aircraft during landing or take off. The AWAS was evaluated satisfactorily in 1990 on a Cessna Citation that was intentionally flown into a number of wind shear events. The events were detected, and both the IR and OAT thermal features were shown to be effective. In 1991, AWAS units were flown on three American Airline MD-80's and three Northwest Airlines DC-9's to study and to decrease the nuisance alert response of the system. The AWAS was also flown on the NASA B737 during the summer of 1991. The results of these flights were inconclusive and disappointing. The results were not as promising as before because NASA conducted research flights which were outside of the normal operating envelope for which the AWAS is designed to operate. In an attempt to compensate for these differences in airspeed and mounting location, the automatic features of the system were sometimes overridden by NASA personnel during the flight. Each of these critical factors is discussed in detail. The effect of rain on the OAT signals is presented as a function of the air speed. Use of a 4 pole 1/20 Hertz filter is demonstrated by both the IR and thermal data. Participation in the NASA 1992 program was discussed. FAA direction in the continuing Certification program requires the addition of a reactive feature to the AWAS predictive system. This combined system will not require flight guidance on newer aircraft. The features of AWAS-IV, with the NASA algorithm included, were presented. Expected completion of the FAA Certification plan was also described. Author

N93-14850*# Georgia Tech Research Inst., Atlanta.

A MILLIMETER-WAVE RADIOMETER FOR DETECTING MICROBURSTS

Robert McMillan *In* NASA. Langley Research Center, Airbourne Wind Shear Detection and Warning Systems. Fourth Combined Manufacturers' and Technologists' Conference, Part 2 Sep. 1992 p 781-803 (For primary document see N93-14844 04-03)

Avail: CASI HC A03/MF A04

This paper describes a millimeter-wave radiometer for the detection of wind shear from airborne platforms or at airport terminals. This proposed instrument will operate near the group of atmospheric oxygen absorptions centered near 60 GHz, which it will use to sense temperature from a distance. The instrument will use two channels to provide two different temperature measurements, providing the basis for solution of two equations in two unknowns, which are range to the wind shear plume and its temperature. A third channel will measure ambient atmospheric temperature. Depending on the temperature difference between the wind-shear plume and ambient, the standard deviation of range measurement accuracy is expected to be about 1 km at 5 km range, while the temperature measurement standard deviation will be about one-fourth the temperature difference between plume and ambient at this range. The instrument is expected to perform usefully at ranges up to 10 km, giving adequate warning of the presence of wind shear even for high performance jet aircraft. Other atmospheric hazards which might be detected by this radiometer include aircraft wakes and vortices, clear-air turbulence, and wind rotors, although the latter two phenomena would be detected by an airborne version of the instrument. A separate radiometer channel will be provided in the proposed instrument to detect aircraft wakes and vortices based on perturbation of the spectrum of microscopic atmospheric temperature fluctuations caused by the passage of large aircraft. Author

N93-14851*# Massachusetts Inst. of Tech., Cambridge.

THE ORLANDO TDWR TESTBED AND AIRBORNE WIND SHEAR DATE COMPARISON RESULTS

Steven Campbell, Anthony Berke, and Michael Matthews *In* NASA.

Langley Research Center, Airborne Wind Shear Detection and Warning Systems. Fourth Combined Manufacturers' and Technologists' Conference, Part 2 Sep. 1992 p 811-846 (For primary document see N93-14844 04-03)
Avail: CASI HC A03/MF A04

The focus of this talk is on comparing terminal Doppler Weather Radar (TDWR) and airborne wind shear data in computing a microburst hazard index called the F factor. The TDWR is a ground-based system for detecting wind shear hazards to aviation in the terminal area. The Federal Aviation Administration will begin deploying TDWR units near 45 airports in late 1992. As part of this development effort, M.I.T. Lincoln Laboratory operates under F.A.A. support a TDWR testbed radar in Orlando, FL. During the past two years, a series of flight tests has been conducted with instrumented aircraft penetrating microburst events while under testbed radar surveillance. These tests were carried out with a Cessna Citation 2 aircraft operated by the University of North Dakota (UND) Center for Aerospace Sciences in 1990, and a Boeing 737 operated by NASA Langley Research Center in 1991. A large data base of approximately 60 instrumented microburst penetrations has been obtained from these flights. Author

N93-14852*# National Center for Atmospheric Research, Boulder, CO.
TDWR 1991 PROGRAM REVIEW
Kim Elmore *In* NASA. Langley Research Center, Airborne Wind Shear Detection and Warning Systems. Fourth Combined Manufacturers' and Technologists' Conference, Part 2 Sep. 1992 p 847-875 (For primary document see N93-14844 04-03)
Avail: CASI HC A03/MF A04

The topics addressed are: (1) Terminal Doppler Weather Radar (TDWR) 1991 program review; (2) TDWR demonstrations notable results/events; (3) TDWR demonstration Denver chronology; (4) overview of generic integration concepts; (5) TDWR 1991 program review; (6) Denver operation 1991; and (7) FY-92 plans. I.I.C.

N93-14853*# Massachusetts Inst. of Tech., Cambridge.
EXPERIMENTAL EVALUATION OF CANDIDATE GRAPHICAL MICROBURST ALERT DISPLAYS
Craig Wanke and R. John Hansman *In* NASA. Langley Research Center, Airborne Wind Shear Detection and Warning Systems. Fourth Combined Manufacturers' and Technologists' Conference, Part 2 Sep. 1992 p 879-904 (For primary document see N93-14844 04-03)
Avail: CASI HC A03/MF A04

The topics addressed are: (1) experimental evaluation of candidate graphical microburst displays; (2) microburst detection and alerting; (3) previous part-task simulator experiment-comparison of presentation modes; (4) presentation mode comparison-results; (5) advantages of graphical mode of presentation; (6) graphical microburst alert experiment-objectives; and graphical microburst alert experiment-overview; and (7) candidate display design. I.I.C.

N93-14854*# Princeton Univ., NJ.
WIND SHEAR RELATED RESEARCH AT PRINCETON UNIVERSITY
Robert Stengel *In* NASA. Langley Research Center, Airborne Wind Shear Detection and Warning Systems. Fourth Combined Manufacturers' and Technologists' Conference, Part 2 Sep. 1992 p 905-955 (For primary document see N93-14844 04-03)
Avail: CASI HC A04/MF A04

The topics addressed are: (1) real-time decision aiding-aircraft guidance for wind shear avoidance; (2) reducing the thrust-manual recovery strategies; and (3) dynamic behaviour of and aircraft encountering a single axis vortex. I.I.C.

N93-14855*# Massachusetts Inst. of Tech., Cambridge.
SYSTEMS ISSUES IN AIRBORNE DOPPLER RADAR/LIDAR CERTIFICATION
James Evans *In* NASA. Langley Research Center, Airborne Wind Shear Detection and Warning Systems. Fourth Combined Manufacturers' and Technologists' Conference, Part 2 Sep. 1992 p 959-969 (For primary document see N93-14844 04-03)
Avail: CASI HC A03/MF A04

This report outlines: (1) thesis; (2) ground clutter challenge; (3) moving scatters (birds, bugs); (4) range ambiguities; and rain attenuation. I.I.C.

N93-14856*# Northwest Airlines, Inc., Saint Paul, MN.
RESULTS OF IN-SERVICE EVALUATION OF WIND SHEAR SYSTEMS
Todd Murr *In* NASA. Langley Research Center, Airborne Wind Shear Detection and Warning Systems. Fourth Combined Manufacturers' and Technologists' Conference, Part 2 Sep. 1992 p 977-995 (For primary document see N93-14844 04-03)
Avail: CASI HC A03/MF A04

The objective is to collect data in the operational environment to determine the capability of windshear systems and their effectiveness. I.I.C.

N93-14857*# Continental Airlines, Inc., Los Angeles, CA.
IN-SERVICE EVALUATION OF WIND SHEAR SYSTEMS
Sam Shirck *In* NASA. Langley Research Center, Airborne Wind Shear Detection and Warning Systems. Fourth Combined Manufacturers' and Technologists' Conference, Part 2 Sep. 1992 p 997-1005 (For primary document see N93-14844 04-03)
Avail: CASI HC A02/MF A04

A comprehensive study undertaken by Continental Airlines Flight Operations to establish procedures to prevent a re-occurrence of accident due to windshear is addressed. Some display and alerting scenarios that the predictive systems will provide is presented. I.I.C.

N93-14858*# American Airlines Flight Academy, Fort Worth, TX.
ADVANCED TECHNOLOGY WIND SHEAR PREDICTION SYSTEM EVALUATION
Greg Gering *In* NASA. Langley Research Center, Airborne Wind Shear Detection and Warning Systems. Fourth Combined Manufacturers' and Technologists' Conference, Part 2 Sep. 1992 p 1007-1015 (For primary document see N93-14844 04-03)
Avail: CASI HC A02/MF A04

The program overviews: (1) American Airline (AA)/Turbulence Prediction Systems (TPS), which have installed forward looking infrared predictive windshear system on 3 MD-80 aircraft; (2) AA/TPS AWAS III evaluation, which is a joint effort and is installed in the noise landing gear (NLG) area and a data recorder installed in the E/E compartment. I.I.C.

N93-15013# Advanced Aviation Concepts, Jupiter, FL.
WORKSHOP ON AERONAUTICAL DECISION MAKING (ADM). VOLUME 2: PLENARY SESSION WITH PRESENTATIONS AND PROPOSED ACTION PLAN Final Report
Richard J. Adams and Catherine A. Adams Aug. 1992 270 p Workshop held in Denver, CO, 6-7 May 1992
(Contract DTFA01-90-C-00042)
(DOT/FAA/RD-92/14-Vol-2) Avail: CASI HC A12/MF A03

This report analyzes the accomplishments and needs of ADM from the perspectives of the operators, researchers, the military and the FAA. Both the airplane and helicopter communitys' experiences are considered. The presentations and background material in this volume were a part of the Plenary Session conducted on the first day of the workshop. They were meant to provide a detailed understanding of the status and needs of ADM from both operational and research perspectives. Problem areas identified by the workshop participants which defined the need for basic research included: Can we define what constitutes a 'good decision'? Can we identify different decision 'nodes' during a flight? This volume presents the participants perspectives on the behavioral psychology and human factors work that has been done in these areas as well as in the area of new decision making models and concepts. For individual titles, see N93-15014 through N93-15026.

N93-15014# Air Force Inspection and Safety Center, Norton AFB, CA.
DOES COCKPIT MANAGEMENT TRAINING REDUCE AIRCREW ERROR?
Alan E. Diehl *In* Advanced Aviation Concepts, Workshop on Aeronautical Decision Making (ADM). Volume 2: Plenary Session With Presentations and Proposed Action Plan Aug. 1992 p 3-24 (For primary document see N93-15013 04-03)
Avail: CASI HC A03/MF A03

Human factors problems continue to be involved in majority of mishaps. Thus, the causes and cures for aircrew 'error' are widely discussed topics. Several experts have noted that labels like pilot 'error' are often misapplied in describing ergonomic, management, regulatory or systems design

shortcomings. This paper uses the generic term 'cockpit management' when referring to the wide variety of programs which are designed to reduce aircrew errors. In fact, recent evidence suggests Cockpit Resource Management (CRM) and Aeronautical Decision making (ADM) training may help reduce aircrew error accident rates by as much as 81 percent. These programs have only emerged in the last decade largely because of the fundamental problems associated with detecting and controlling human error. Many of us have lamented the greater difficulties of accurately documenting human vis-a-via mechanical failures, (e.g., mental fatigue is usually tougher to prove than metal fatigue). It is also often harder for us as air safety investigators to specify effective countermeasures in the human factors domain. Thus, some organizations unfortunately have assumed such errors are 'the price of doing business'. This paper addresses these issues by: (1) examining the prevalence of major types of contemporary errors and reviewing the traditional methods which have been used to improve human reliability; (2) discussing how innovative cockpit management training programs were developed and implemented; and (3) describing the current evidence on the effectiveness of such programs. Author

N93-15015# Air Force Inspection and Safety Center, Norton AFB, CA.
COCKPIT DECISION MAKING
Alan E. Diehl *In* Advanced Aviation Concepts, Workshop on Aeronautical Decision Making (ADM). Volume 2: Plenary Session With Presentations and Proposed Action Plan Aug. 1992 p 25-29 (For primary document see N93-15013 04-03)
Avail: CASI HC A01/MF A03

The categorical distinctions between Cockpit Resource Management (CRM) and Aeronautical Decision Making (ADM) training are becoming blurred. Most current versions of these programs have five common elements which deal with attention, crew, stress, attitude, and risk management issues. The results of six empirical and six operational evaluations provide strong evidence that these training programs can help reduce aircrew errors and thereby prevent accidents. While additional research and development continues, there is a growing realization that these programs ideally need to be introduced rarely in flight training, reinforced during upgrade training, and reviewed during recurrent training and accident prevention sessions. Author

N93-15016# Naval Safety Center, Norfolk, VA.
TRANS-COCKPIT AUTHORITY GRADIENT IN NAVY/MARINE AIRCRAFT MISHAPS
Robert A. Alkov, Michael S. Borowsky, Dana W. Williamson, and David W. Yacavone *In* Advanced Aviation Concepts, Workshop on Aeronautical Decision Making (ADM). Volume 2: Plenary Session With Presentations and Proposed Action Plan Aug. 1992 p 56-66 (For primary document see N93-15013 04-03)
Avail: CASI HC A03/MF A03

Navy and Marine Corps aircraft mishaps which have an aircrew causal factor assigned were analyzed to determine if the relative military rank of the pilot and copilot or Naval Flight Officer was associated with the rate of occurrence per 100,000 flight hours. All class A and B helicopter flight mishaps for the elevent calendar year period 1980-1990 were examined. Although statistically significant differences were not found, pairing helicopter pilots who were of equal rank yielded the lowest rate (2.81), seemingly refuting Elwyn Edward's notion that a flat 'trans-cockpit authority gradient' may lead to greater problems in the cockpit than his hypothetical 'optimum gradient'. When there was one rank difference in the cockpit the rate was 2.340. When copilots flew with pilots who differed by two or more ranks, the largest pilot error rate (3.45) was revealed. These findings seem to support Edward's hypothesis that a steeper 'trans-cockpit authority gradient' may be detrimental to helicopter flight safety. Data from fighter and attack jet aircraft, where there is only one pilot flying with a radar intercept officer or a bombardier/ navigator, were also studied for the calendar years 1986-91. It was discovered that the lowest aircrew error rate (1.80) occurred when the pilot and the other aircrew member differed by more than one rank. When the aircrew were of the same rank the rate was 3.51. For those crews in which there was a one rank difference the rate was 3.85. Reasons for these findings are discussed. Author

N93-15017# Advanced Aviation Concepts, Jupiter, FL.
HOW EXPERT PILOTS THINK
Richard J. Adams *In its* Workshop on Aeronautical Decision Making (ADM). Volume 2: Plenary Session With Presentations and Proposed Action Plan Aug. 1992 p 68-87 (For primary document see N93-15013 04-03)
Avail: CASI HC A03/MF A03

This paper provides an overview of the conceptual cognitive psychology research that defines and delineates the important characteristics of expertise. It is hoped that the understanding of the cognitive processes associated with 'experts', will increase the awareness of these processes in the pilot training community. The importance of the attainment of a higher level of cognitive skills by pilots is the opportunity to enhance performance and further reduce human error accidents through improved decision making training. Author

N93-15018# Colorado Univ., Boulder. Inst. of Cognitive Science.
METHODOLOGY FOR STUDYING AND TRAINING EXPERTISE
K. Anders Ericsson *In* Advanced Aviation Concepts, Workshop on Aeronautical Decision Making (ADM). Volume 2: Plenary Session With Presentations and Proposed Action Plan Aug. 1992 p 88-108 (For primary document see N93-15013 04-03)
Avail: CASI HC A03/MF A03

The topics addressed are: (1) brief historical background for the study of eminent people and experts-some approaches and issues; (2) the study of superior expert performance; and (3) sketch of a proposal for diagnosis and training of expert decision-making in pilots. I.I.C.

N93-15019# Advanced Aviation Concepts, Jupiter, FL.
ENHANCED AERONAUTICAL RESOURCE MANAGEMENT TRAINING ALTERNATIVES
Richard J. Adams *In its* Workshop on Aeronautical Decision Making (ADM). Volume 2: Plenary Session With Presentations and Proposed Action Plan Aug. 1992 p 109-128 (For primary document see N93-15013 04-03)
Avail: CASI HC A03/MF A03

Expert cognitive performance is characterized by rapid access to a well organized body of conceptual and procedural knowledge. This is a modifiable information structure based upon knowledge that is experienced. This experience allows the perception of large meaningful patterns in familiar and new situations which help the expert match goals to task demands. This means they can respond creatively or with opportunistic solutions when the situation requires such a response. Author

N93-15020# Klein Assoiciates, Inc., Fairborn, OH.
A COGNITIVE MODEL FOR TRAINING DECISION MAKING IN AIRCREWS
Gary A. Klein *In* Advanced Aviation Concepts, Workshop on Aeronautical Decision Making (ADM). Volume 2: Plenary Session With Presentations and Proposed Action Plan Aug. 1992 p 129-144 (For primary document see N93-15013 04-03)
Avail: CASI HC A03/MF A03

The topics addressed are: (1) prescriptions for effective decision making; (2) Recognition-Primed Decision (RPD) model; (3) key features of RPD model; (4) factors affecting the use of recognitional and analytical decisions; (5) team research and observations; (6) aspects of teamwork; (7) cognitive process of teams; (8) advanced team decision making- a development model; (9) key features and critical processes of decision making teams; (10) myths about team decision making; and (11) recommendations for team decision training. I.I.C.

N93-15021# Honeywell, Inc., Minneapolis, MN. Systems and Research Center.
ELEMENTS OF A THEORY OF NATURAL DECISION MAKING
John R. Bloomfield *In* Advanced Aviation Concepts, Workshop on Aeronautical Decision Making (ADM). Volume 2: Plenary Session With Presentations and Proposed Action Plan Aug. 1992 p 145-164 (For primary document see N93-15013 04-03)
Avail: CASI HC A03/MF A03

The preliminary theory provides a framework that can incorporate a broad range of decisions and decision situations: ranging from the tightly-defined situations investigated by classical decision theorists all the way to complex real-world situations, involving proficient decision-makers, under a great deal of stress, and/or time pressure. Author

N93-15022# Honeywell, Inc., Minneapolis, MN.
TAXONOMY OF FLIGHT VARIABLES
John R. Bloomfield, Lee Levitan, Barry Cooper (America West Airlines, Tempe, AZ.), Elizabeth A. Lyall (America West Airlines, Tempe, AZ.), and Eleana Edens (Federal Aviation Administration, Washington, DC.) *In* Advanced Aviation Concepts, Workshop on Aeronautical Decision Making (ADM). Volume 2: Plenary Session With Presentations and Proposed Action Plan Aug. 1992 p 165-171 (For primary document see N93-15013 04-03)
(Contract DTFA01-91-C-00040)
Avail: CASI HC A02/MF A03

Controlled Flight Into Terrain (CFIT) accidents and Controlled Flight Toward Terrain (CFTT) incidents, particularly those that occur when the flight crew believe that the autopilot, flight director, and/or flight management system is in use are investigated. The first step was to develop a taxonomy of flight variables. The taxonomy developed for CFIT accidents and incidents will also be of use in considering other air accidents and as a strawman taxonomy of flight of operations general. I.I.C.

N93-15023*# National Aeronautics and Space Administration. Ames Research Center, Moffett Field, CA.
SHARED MENTAL MODELS AND CREW DECISION MAKING
Judith Orasanu *In* Advanced Aviation Concepts, Workshop on Aeronautical Decision Making (ADM). Volume 2: Plenary Session With Presentations and Proposed Action Plan Aug. 1992 p 172-181 (For primary document see N93-15013 04-03)
Avail: CASI HC A02/MF A03

The topics addressed are: (1) structure of decisions tasks in the cockpit and their cognitive requirements; (2) what is known about effective crew decision making?; and (3) implications for training Aeronautical Decision Making (ADM). The model implies that effective crew decision making training would include different foci such as Situational Awareness, Planning, Communication, Resource Assessment and Prioritizing. I.I.C.

N93-15024# Textron Bell Helicopter, Fort Worth, TX.
EMBEDDED ADM REDUCES HELICOPTER HUMAN ERROR ACCIDENTS
Roy G. Fox *In* Advanced Aviation Concepts, Workshop on Aeronautical Decision Making (ADM). Volume 2: Plenary Session With Presentations and Proposed Action Plan Aug. 1992 p 182-229 (For primary document see N93-15013 04-03)
Avail: CASI HC A03/MF A03

The basic outlines are: (1) Who is responsible for safety?; (2) measuring risk; (3) means of reducing risk; and (4) crash survival; (5) accident causes (2/3 are Human); (6) judgement training; and heliprops effects on 206 human error accident rates. The conclusion made is that, Judgement Training has more safety improvement potential than the total elimination of all airworthiness failure causes (a primary goal since the start of aviation). I.I.C.

N93-15025# Textron Bell Helicopter, Fort Worth, TX.
MEASURING RISK IN SINGLE-ENGINE AND TWIN-ENGINE HELICOPTERS
Roy G. Fox *In* Advanced Aviation Concepts, Workshop on Aeronautical Decision Making (ADM). Volume 2: Plenary Session With Presentations and Proposed Action Plan Aug. 1992 p 230-253 (For primary document see N93-15013 04-03)
Avail: CASI HC A03/MF A03

Safety is the management of risk. Many decisions are made by businesses, government agencies and individuals using their perceptions of an aircraft's safety. Public perception of safety can deny the introduction of expansion of aviation in specific areas. Decisions to buy, use, repair, install improvements, insure, sell, and replace aircraft are all related to perceived safety. Likewise, governmental restrictions and rule-making are based on the perceived deterioration of safety, as in the proposed single-engine helicopter restrictions of ICAO Annex 6. Accurate aircraft safety measurements are thus essential to bring perceived and actual safety together. Such accuracy also provides realistic corrective actions for safety problems and evaluation of desirable and undesirable aspects of different aircraft configurations, as well as allowing individuals to determine their risk in flying in specific types of aircraft. Existing safety measuring methods are discussed, along with the advantages, disadvantages, and correctness of each method. Recent safety training and its effects are discussed, related to improved pilot judgment and significant reductions in accident rates--without any regulatory changes. Author

N93-15026# Advanced Aviation Concepts, Jupiter, FL.
PROPOSED ACTION PLAN TO IMPROVE ADM EFFECTIVENESS, PART 3: DEVELOPING A NEW ADM PARADIGM ON WHICH TO BUILD ADVANCED OR EXPERT DECISION MAKING TRAINING
In its Workshop on Aeronautical Decision Making (ADM). Volume 2: Plenary Session With Presentations and Proposed Action Plan Aug. 1992 p 254-267 (For primary document see N93-15013 04-03)
Avail: CASI HC A03/MF A03

Aeronautical Decision Making (ADM) training benefits in terms of reducing human error accident rates were documented during the presentations at the workshop. Basic research needs, training implementation problems and the need for additional modeling work were also identified. This document provides the aviation industry and the FAA with a suggested roadmap to assist in the development of improved ADM concepts and training methods. The basic questions that will be addressed are: (1) Can decision making tasks be identified and defined?; (2) What are the training objectives?; (3) What are the appropriate training strategies?; and (4) How can the training effectiveness be evaluated? Author

N93-15345*# National Aeronautics and Space Administration. Lewis Research Center, Cleveland, OH.
NUMERICAL MODELING OF ANTI-ICING SYSTEMS AND COMPARISON TO TEST RESULTS ON A NASA 0012 AIRFOIL
Kamel M. Al-Khalil and Mark G. Potapczuk Jan. 1993 14 p Presented at the 31st Aerospace Sciences Meeting and Exhibit, Reno, NV, 11-14 Jan. 1993; sponsored by AIAA
(RTOP 505-68-10)
(NASA-TM-105975; E-7498; NAS 1.15:105975; AIAA Paper 93-0170)
Avail: CASI HC A03/MF A01

A series of experimental tests were conducted in the NASA Lewis IRT on an electro-thermally heated NACA 0012 airfoil. Quantitative comparisons between the experimental results and those predicted by a computer simulation code were made to assess the validity of a recently developed anti-icing model. An infrared camera was utilized to scan the instantaneous temperature contours of the skin surface. Despite some experimental difficulties, good agreement between the numerical predictions and the experiment results were generally obtained for the surface temperature and the possibility for each runback to freeze. Some recommendations were given for an efficient operation of a thermal anti-icing system. Author

N93-15354*# National Aeronautics and Space Administration. Lewis Research Center, Cleveland, OH.
ICE ACCRETION AND PERFORMANCE DEGRADATION CALCULATIONS WITH LEWICE/NS
Mark G. Potapczuk, Kamel M. Al-Khalil (National Academy of Sciences - National Research Council, Washington, DC.), and Matthew T. Velazquez (Massachusetts Inst. of Tech., Cambridge.) Jan. 1993 22 p Presented at the 31st Aerospace Sciences Meeting and Exhibit, Reno, NV, 11-14 Jan. 1993; sponsored by AIAA
(RTOP 505-68-10)
(NASA-TM-105972; E-7497; NAS 1.15:105972; AIAA Paper 93-0173)
Avail: CASI HC A03/MF A01

The LEWICE ice accretion computer code has been extended to include the solution of the two-dimensional Navier-Stokes equations. The code is modular and contains separate stand-alone program elements that create a grid, calculate the flow field parameters, calculate the droplet trajectory paths, determine the amount of ice growth, calculate aeroperformance changes, and plot results. The new elements of the code are described. Calculated results are compared to experiment for several cases, including both ice shape and drag rise. Author

N93-15360*# National Aeronautics and Space Administration. Lewis Research Center, Cleveland, OH.
CLOSE-UP ANALYSIS OF AIRCRAFT ICE ACCRETION
R. John Hansman (Massachusetts Inst. of Tech., Cambridge.), Kenneth S. Breuer (Massachusetts Inst. of Tech., Cambridge.), Didier Hazan (Massachusetts Inst. of Tech., Cambridge.), Andrew Reehorst, and Mario

Vargas Jan. 1993 15 p Presented at the 31st Aerospace Sciences Meeting and Exhibit, Reno, NV, 11-14 Jan. 1993; sponsored by AIAA
(Grants NAG3-666; NGL-22-0069-640; RTOP 505-68-10)
(NASA-TM-105952; E-7473; NAS 1.15:105952; AIAA Paper 93-0029)
Avail: CASI HC A03/MF A01

Various types of ice formation have been studied by analysis of high magnification video observations. All testing was conducted in the NASA Lewis Icing Research Tunnel (IRT). A faired 8.9 cm (3.5 in.) diameter metal-clad cylinder and a 5.1 (2 in.) aluminum cylinder were observed by close-up and overview video cameras for several wind tunnel conditions. These included close-up grazing angle, close-up side view, as well as overhead and side overview cameras. Still photographs were taken at the end of each spray along with tracings of the subsequent ice shape. While in earlier tests only the stagnation region was observed, the entire area from the stagnation line to the horn region of glaze ice shapes was observed in this test. The modes or horn formation have been identified within the range of conditions observed. In the horn region, Horn Type A ice is formed by 'dry' feather growth into the flow direction and Horn Type B is formed by a 'wet' growth normal to the surface. The feather growth occurs when the freezing fraction is near unity and roughness elements exist to provide an initial growth site. Author

N93-15390# Federal Aviation Administration, Washington, DC. Office of Aviation Policy and Plans.
TERMINAL AREA FORECASTS FY 1992 - 2005
Jul. 1992 495 p
(AD-A255797) Avail: CASI HC A21/MF A04

This report contains forecasts of aviation activity of 869 airports in the United States for fiscal years 1992-2005. These include 400 airports with FAA air traffic control towers and radar approach control service and 26 FAA contract towers. For each airport, detailed forecasts are made for the four major users of the air traffic system: air carriers, air taxi/commuters, general aviation, and military. Summary tables contain national, FAA regional, and state aviation data and other airport specific highlights. The forecasts have been prepared to meet the budget and planning needs of the FAA and provide airport-specific information that can be used by state and local aviation authorities, the aviation industry, and the general public. GRA

N93-15522*# National Aeronautics and Space Administration. Lewis Research Center, Cleveland, OH.
ICE ACCRETION PREDICTION FOR A TYPICAL COMMERCIAL TRANSPORT AIRCRAFT
C. S. Bidwell Jan. 1993 23 p Presented at the 31st Aerospace Sciences Meeting and Exhibit, Reno, NV, 11-14 Jan. 1993; sponsored by AIAA
(RTOP 505-68-10)
(NASA-TM-105976; E-7499; NAS 1.15:105976; AIAA Paper 93-0174)
Avail: CASI HC A03/MF A01

Ice accretion calculations were made for a modern commercial transport using the NASA Lewis LEWICE3D ice accretion code. The ice accretion calculations were made for the wing and horizontal tail using both isolated flow models and flow models incorporating the entire airplane. The isolated flow model calculations were made to assess the validity of using these simplified models in lieu of the entire model in the ice accretion analysis of full aircraft. Ice shapes typifying a rime and a mixed ice shape were generated for a 30 minute hold condition. In general, the calculated ice shapes looked reasonable and appeared representative of a rime and a mixed ice conditions. The isolated flow model simplification was good for the main wing except at the root where it overpredicted the amount of accreted ice relative to the full aircraft flow model. For the horizontal tail the size and amount of predicted ice compared well for the two flow models, but the position of the accretions were more towards the upper surface for the aircraft flow model relative to the isolated flow model. This was attributed to downwash from the main wing which resulted in a lower effective angle of attack for the aircraft tail. Author

N93-15577# National Transportation Safety Board, Washington, DC.
SPECIAL INVESTIGATION REPORT: PIPER AIRCRAFT CORPORATION PA-46 MALIBU/MIRAGE ACCIDENTS/INCIDENT, 31 MAY 1989 - 17 MARCH 1991
21 Jul. 1992 101 p
(PB92-917007; NTSB/SIR-92/03) Avail: CASI HC A06/MF A02

Between May 31, 1989 and March 17, 1991, Piper PA-46 series Malibu and Mirage airplanes were involved in seven fatal accidents in the United States, Mexico, and Japan following departures from controlled flight. In addition to the seven accidents, another PA-46 airplane was involved in an incident that included substantial departures from controlled flight. In July 1990, following the fourth U.S. fatal accident, the Safety Board initiated a special investigation of the facts, conditions, and circumstances that led to the loss of the four Malibu/Mirage airplanes in the U.S. As other accidents occurred, they were included in the special investigation. Two of the seven fatal accidents occurred in Japan and Mexico, and the available information on the accidents was included in the special investigation. The special investigation included a review of the relevant design features of the Malibu and Mirage airplanes, including structural integrity, flight control systems, and operating limitations. The investigation also focused on the flight experience and training of the pilots of the airplanes, particularly as these factors related to flying the Malibu/Mirage airplanes in instrument meteorological conditions (IMC) at and above the freezing level with relatively sophisticated integrated flight guidance and control systems. As a consequence of the accidents, the Federal Aviation Administration, with the Safety Board's encouragement, conducted a special certification review of the airplanes, and the results are included in the report. GRA

N93-15164# Aeritalia S.p.A., Naples (Italy). Flight Safety.
THE FAIR (FLIGHT ANIMATED AND INTERACTIVE RECONSTRUCTION) TOOL [DIE INTERAKTIVE UND MIT HILFE VON TRICKFILMTECHNIKEN ARBEITENDE FLUGREKONSTRUKTION FAIR]
Silenzi Silvano *In* DLR, Proceedings of the 16th Symposium on Aircraft Integrated Monitoring Systems Jan. 1992 p 219-235 (For primary document see N93-15152 04-06)
Avail: CASI HC A03/MF A06; DLR, Wissenschaftliches Berichtswesen, Postfach 90 60 58, Cologne, Germany, HC

04 AIRCRAFT COMMUNICATIONS AND NAVIGATION

Includes digital and voice communication with aircraft; air navigation systems (satellite and ground based); and air traffic control.

For related information see also *17 Space Communications, Spacecraft Communications, Command and Tracking* and *Communications and Radar.*

N93-14275# Federal Aviation Administration, Washington, DC. Office of Aviation Medicine.
PERFORMANCE OF COLOR-DEPENDENT TASKS OF AIR TRAFFIC CONTROL SPECIALISTS AS A FUNCTION OF TYPE AND DEGREE OF COLOR VISION DEFICIENCY Final Report
Henry W. Mertens and Nelda J. Milburn Aug. 1992 18 p
(AD-A256614; DOT/FAA/AM-92/28) Avail: CASI HC A03/MF A01

This experiment was conducted to expand initial efforts to validate the requirement for normal color vision in Air Traffic Control Specialist (ATCS) personnel who work at en route center, terminal, and flight service station facilities. An enlarged data base was developed involving 121 individuals with normal color vision, 31 simple and 44 extreme anomalous trichromats, and 48 dichromats; both protans and duetans were included. The performance of subjects with normal color vision was compared with the performance of individuals in various classifications of color vision deficiency on a battery of color-dependent ATCS tasks. Simulations of the ATC color tasks concerned color coding in flight progress strips (at en route centers), aircraft lights and Aviation Signal Light indicator (in tower operations), and color weather radar (at flight service stations). Errors were rare among normal trichromats. Mean errors were significantly higher at every level (degree) of color vision deficiency than in normals. Approximately 6 percent of color deficient subjects were able to perform ATC color tasks without error. The six percent were all from the simple anomalous trichromat category; all extreme anomalous trichromats and dichromats were prone to error on ATC tasks. These findings provide support for the requirement of normal color vision in initial medical screening of ATCS personnel. GRA

N93-14276# Federal Aviation Administration, Washington, DC. Office of Aviation Medicine.

IDENTIFYING ABILITY REQUIREMENTS FOR OPERATORS OF FUTURE AUTOMATED AIR TRAFFIC CONTROL SYSTEMS Final Report

Carol A. Manning and Dana Broach Aug. 1992 27 p

(AD-A256615; DOT/FAA/AM-92/26) Avail: CASI HC A03/MF A01

This study was conducted to anticipate the impact on air traffic controller ability requirements that may result from implementation of a future stage of air traffic control automation. If important changes occur in ability requirements, it will be necessary to develop or modify selection procedures for future air traffic controllers. Accurate identification of ability requirements depends on knowledge of the job tasks to be performed, but only general information is currently available about the job tasks associated with later stages of air traffic control automation. In this study, nine air traffic controllers who had analyzed operational requirements for a future stage of automation described how controllers would perform four job tasks using the automation, assessed the degree to which nine specific abilities were likely to be required to perform the automated tasks, and assessed whether the amount of each ability required to perform the automated tasks would be different than the amount of the ability required to perform the equivalent tasks in the current system. The controllers thought that some changes will occur in the presentation of information, much of the requirement for verbal coordination will be removed, and much of the detailed information that the controller must be present will be supplanted by automation aids. At the same time, these controllers suggested that the future controller will have to have about the same levels as required today of the abilities discussed in the study to perform the tasks included in the study. GRA

N93-14501# Army Engineer Studies Center, Fort Belvoir, VA.

ESTABLISHMENT OF A TEST COURSE FOR HIGH ACCURACY DYNAMIC POSITIONING SYSTEMS Report No. 16, period ending 20 Sep. 1991

Peter J. Cervarich 20 Sep. 1992 7 p

(AD-A255407; ATEC-R-186) Avail: CASI HC A02/MF A01

The ability to use the Differential Global Positioning System (DGPS) to determine the position of a dynamic GPS receiver, such as would be found aboard a hydrographic survey boat, to an accuracy of one decimeter identified a related problem; e.g., the lack of a test range with instrumentation that could position a dynamic target to an accuracy of 1 cm. (An accepted rule-of-thumb is for the test instrumentation to be 10 times more accurate than the system being tested.) This paper will present the activities that lead to establishing a test course that could be used to test high accuracy dynamic positioning systems. The various alternatives that were considered and the factors that lead to selecting terrestrial photogrammetry will be presented, and the test course itself and the photogrammetric instrumentation will be described. GRA

N93-14517# Range Commanders Council, White Sands Missile Range, NM. Range Safety Group.

FLIGHT TERMINATION SYSTEMS COMMONALITY STANDARD

Aug. 1992 327 p

(AD-A255349; RSG-319-92) Avail: CASI HC A15/MF A03

This document is intended to provide technical specifications for the design, documentation, and test of all new and modified airborne FTSs or vehicles (including new programs) which will be acceptable for use on a specific flight vehicle at any Major Range and Test Facility Base (MRTFB). In this document, the MRTFB includes NASA launch facilities. GRA

N93-14574# Naval Command, Control and Ocean Surveillance Center, San Diego, CA. Research, Development, Test, and Evaluation Div.

A GENERAL OBSERVATION MATRIX FOR ATTITUDE ERROR ESTIMATION WITH AN OFFSET GPS ANTENNA Final Report

C. A. Bass, C. Karmokolias, and A. Khatri Jun. 1992 80 p

(AD-A255214; NRAD-TD-2311) Avail: CASI HC A05/MF A01

In conventional integrated Global Positioning System/Inertial Navigation System (GPS/INS) navigation systems, attitude errors are estimated through correlation to, primarily, velocity errors. This correlation develops due to the coupling of the attitude errors to the velocity errors via the presence of specific forces. Other GPS-based attitude measurement techniques typically employ multiple antennas and special receiver hardware. An alternate approach to attitude estimation is proposed. This report exploits the attitude (and attitude rate) information inherently present in pseudo-range and, particularly, delta-range measurements obtained when a GPS antenna is offset from the GPS/INS reference point of a platform undergoing attitude changes, independent of the value of specific forces. A more general observation matrix that captures this information is derived. The attitude information is recovered with standard recursive estimation techniques such as the Kalman Filter algorithms typically used in these systems. The proposed approach is ideally suited for applications where the antenna is mounted on a spinning platform, such as a spinning vehicle in exoatmospheric, free-fall conditions. Simulation results are provided to illustrate the attitude estimation capability in a free-falling vehicle application. The technique developed here has the advantage of being readily implementable through minor software modifications (i.e., there are no special hardware requirements). GRA

N93-14729# University of Technology, Leicester (England). Dept. of Transport Technology.

INFORMATION SYSTEMS FOR AIRPORT OPERATIONS

J. Shelton, D. Gillingwater, and N. J. Ashford May 1992 69 p

(TT-9202; ISBN-0-904747-37-8) Avail: CASI HC A04/MF A01

The aims of this research were threefold: (1) to undertake a systems analysis of the information requirements of a medium sized airport, serving between one and five million passengers per year; (2) to develop a generic model of airport information flows; and (3) to evaluate existing interactive software and hardware systems used at airports. The main product of the research is a report on the information requirements of an airport information system (APIS), using an approach based on 'structured systems analysis and design methods' (SSADM). It is divided into four sections: (1) an account of airport information system functions and system design objectives; (2) a case study of the information requirements of East Midlands International Airport (EMIA); (3) the definition and development of a generic model for an airport information system (APIS); and (4) the main conclusions arising from the research, together with recommendations for further development of the generic model towards a successful software implementation. Author

N93-15005# Army Topographic Engineering Center, Fort Belvoir, VA.

PROPOSED REVISIONS TO RTCM SC-104 RECOMMENDED STANDARDS FOR DIFFERENTIAL NAVSTAR/GPS SERVICE FOR CARRIER PHASE APPLICATIONS

Fred Gloeckler, A. J. VanDierendonck, and Ronald R. Hatch 18 Sep. 1992 11 p

(AD-A255276; TEC-R-191) Avail: CASI HC A03/MF A01

The Radio Technical Commission for Maritime Services (RTCM) Recommended Standards for Differential NAVSTAR/GPS Service have been widely adopted for code based differential GPS applications. To accommodate the present and expected future growth in use of differential carrier phase technology for high accuracy applications, it has been recognized that revisions to the RTCM standards are needed. A working group has been established to develop changes to the standards for carrier phase data. This is a report on the recommendations of the Carrier Phase Communications Working Group. GRA

N93-15186# Airbus Industrie, Toulouse (France).

AIRBUS INDUSTRIE TCAS EXPERIENCE

H. Ganz *In* DLR, Proceedings of the 16th Symposium on Aircraft Integrated Monitoring Systems Jan. 1992 p 647-674 (For primary document see N93-15152 04-06)

Avail: CASI HC A03/MF A06; DLR, Wissenschaftliches Berichtswesen, Postfach 90 60 58, Cologne, Germany, HC

05 AIRCRAFT DESIGN, TESTING AND PERFORMANCE

Includes aircraft simulation technology.

For related information see also *18 Spacecraft Design, Testing and Performance* and *39 Structural Mechanics*. For land transportation vehicles see *85 Urban Technology and Transportation*.

N93-14248# Naval Postgraduate School, Monterey, CA.
EXPERIMENTAL AND ANALYTICAL INVESTIGATION OF THE VIBRATION CHARACTERISTICS OF A REMOTELY PILOTED HELICOPTER M.S. Thesis
William T. Trainer Jun. 1992 145 p
(AD-A256131) Avail: CASI HC A07/MF A02

The Department of Aeronautics and Astronautics at the Naval Postgraduate School is involved in an ongoing program of Higher Harmonic Control (HHC) research using Remotely Piloted Helicopters (RPH). To date a host RPH has been acquired and a preliminary HHC design study completed. This thesis reports the results of a free vibration shake test conducted on the host RPH as well as efforts to construct a representative finite element model of the vehicle. Broadband noise was used to excite the structure both laterally and vertically from 10-200 Hz in and attempt to accurately document the airframe and rotor system dynamics. Primary airframe structural modes were identified in the tail boom and at frequencies well below the characteristic 4/rev (78.3 Hz) main rotor induced vibration frequency. These modes should not be of concern at normal operating rpm. Main rotor blade modes were documented under non-rotating conditions then extended to predict the modes at operating rpm. Finally, a finite element model of the structure was constructed. Difficulties in matching finite element predictions with experimental results, however, will require refinements to the computer model before it can become a useful design tool. GRA

N93-14432# Control Data Corp., Minneapolis, MN.
MIL-STD-1760 APPLICATION GUIDELINES Final Report, 1984 - 1987
Sep. 1991 408 p
(Contract N60530-82-R-0012)
(AD-A255714; Rept-182-80-18; ASD-TR-91-5009) Avail: CASI HC A18/MF A04

This report addresses those issues which are associated with the practical implementation of MIL-STD-1760, the Aircraft/Store Electrical Interconnection System, into both present and future aircraft and stores. The report provides practical guidance and associated rationale for implementors of MIL-STD-1760. The report consists of three parts: the Application Guidelines, Appendix A, and Appendix B. Avionics, aircraft/store electrical interface, MIL-STD-1760, MIL-STD-1553, stores management system, aircraft armament, weapons, stores. GRA

N93-14440# General Accounting Office, Washington, DC. National Security and International Affairs Div.
UNMANNED AERIAL VEHICLES: MORE TESTING NEEDED BEFORE PRODUCTION OF SHORT-RANGE SYSTEM
4 Sep. 1992 14 p
(AD-A256296; GAO/NSIAD-92-311) Avail: CASI HC A03/MF A01

UAV's are pilotless aircraft resembling small airplanes or helicopters that are remotely controlled or preprogrammed to be controlled by on-board equipment. The Department of Defense (DOD) initiated acquisition of the Short-Range UAV in fiscal year 1989 as a common-service system for use by the Army, Navy, and Marine Corps. The system is one of a family of UAV's being acquired by DOD to provide the capability to perform reconnaissance, surveillance, target acquisition, and intelligence collection. The UAV Joint Project Office (JPO), which manages acquisition of the Short-Range system, awarded contracts in September 1989 to two firms to provide candidate systems for competitive testing in fiscal year 1991. However, technical problems with the candidate systems delayed the program, and the competition continued into fiscal year 1992. In June 1992, one firm was unable to complete the competitive testing because it could not successfully certify military users to safely operate its system. The other firm completed the test program in July 1992 and was selected as the winning contractor. GRA

N93-14448 Cranfield Inst. of Tech., Bedford (England).
DESAID (THE DEVELOPMENT OF AN EXPERT SYSTEM FOR AIRCRAFT INITIAL DESIGN) Ph.D. Thesis
Seung-Hyeog Nah 1991 269 p
Avail: Univ. Microfilms Order No. BRDX96714

The tasks involved in designing an aircraft configuration show complex characteristics, considering the fact that aircraft configuration design means the integration of components such as lifting surfaces (wing), fuselage, power-plant, control surfaces (tail or canard), and undercarriage. The discrepancies and mismatches among the aircraft components make the configuration design iterative, repetitive, and thus time-consuming. The current research project is directed at the development of an expert system for aircraft design. This involves the use of Artificial Intelligence and its programming language called PROLOG (PROgramming in LOGic). The research started from a thorough analysis of the major component design areas and has constructed an EXPERT SYSTEM to find out the efficient Control Mechanism which can search intensively for the solutions to design problems for all types of aircraft: civil and military, subsonic and supersonic, conventional and unconventional, etc. In addition, users can have access to the explanations of important items such as a design process, terminology, equations, and results. The explanation facility is one of the most important functions of Expert Systems. Partly due to the limit of computer capacity and partly due to the magnitude of laborious program execution at this stage, the system implementation has focused on the high-subsonic, conventional and jet transport aircraft categories. The approach taken was to find an efficient and effective control mechanism (i.e. an Inference Engine), which integrated the PARAMETRIC STUDY, WING DESIGN, FUSELAGE DESIGN, ENGINE DESIGN, TAIL DESIGN, UNDERCARRIAGE DESIGN, WEIGHT ANALYSIS AND COST ANALYSIS into a whole configuration system. The comparison between Expert System results and existing aircraft such as Boeing 747, Airbus 300 series, BAe 146 series, McDonnell Douglas MD series, etc., showed the permissible ranges of error to be within about 10 percent. Such results enable the Expert System to claim that it can act as a useful design tool for the aircraft designer in the initial stage of aircraft configuration design. The author believes that the control mechanism devised for this Expert System can be used as a sound basis for extending the Expert System to include other types of aircraft and further to encompass spacecraft design, as the designer wishes. Dissert. Abstr.

N93-14462 Pennsylvania State Univ., University Park.
MULTI-POINT INVERSE DESIGN OF ISOLATED AIRFOILS AND AIRFOILS IN CASCADE IN INCOMPRESSIBLE FLOW Ph.D. Thesis
Michael Scott Selig 1992 239 p
Avail: Univ. Microfilms Order No. DA9226776

This thesis describes a multi-point inverse design method for airfoils and one for cascades. In the present sense, inverse design is taken to mean the problem of finding the shape which corresponds to the desired set of aerodynamic and geometric characteristics. These include the pitching moment, maximum thickness ratio, part of the velocity distribution or boundary-layer flow physics, for example, the shape-factor, skin-friction or linear stability amplification factor distribution. Specifically, the airfoil or cascade blade to be determined is divided into a desired number of segments along each of which either the desired velocity distribution or boundary-layer development is prescribed together with, if desired, the maximum thickness ratio, etc. The solution is formulated through the use of conformal mapping and a direct integral boundary-layer technique resulting in a system of nonlinear equations which are solved through multi-dimensional Newton iteration. It is shown that certain integral constraints, continuity constraints and stagnation point velocity distribution relations must be satisfied in order for the inverse problem to be well-posed. The satisfaction of these conditions may be handled conveniently. This makes the practical application of the method feasible. Several example airfoils and cascades are presented to illustrate the two inverse methods. A solution to the direct analysis problem for the velocity distributions about airfoils and cascades is also discussed. The current approach to both analysis problems differs significantly from the standard approaches such as those based on Theodorsen's method. The airfoil or cascade is mapped to the circle by one transformation that is expressed in derivative form so that the velocity distribution follows directly. Also, an exact solution to the flow through an infinite cascade is presented based on a mapping which has close ties to

the Joukowski transformation. As compared with Gostelow's method, exact solutions can be obtained in a straightforward way. Finally, extensions of the theory to the inverse design of radial cascades, semi-infinite bodies and channels are discussed briefly. Dissert. Abstr.

N93-14541 ESDU International Ltd., London (England).
ESTIMATION OF RATE OF CLIMB
Jun. 1992 14 p Supersedes ESDU Perf-EG3/1
(ESDU-92019; ISBN-0-85679-824-X) Avail: ESDU

ESDU 92019 presents the equations with various degrees of simplification for the calculation of rate of climb of jet-powered or propeller-driven aeroplanes. It is primarily concerned with 'steady-state climbs', that is with instantaneous climb rate, and does not treat the effect of acceleration introduced by a climb schedule. The general calculation procedure is illustrated by a worked example based on a jet-powered combat aircraft. For propeller-driven aeroplanes, approximate guidance is given graphically on maximum climb rate as a function of power/weight ratio. It is based on comparisons of computed data for a wide range of aircraft configurations, using typical propellers having a given variation of efficiency with speed, with published data for a large number of aircraft types with fixed- or variable-pitch propellers driven by piston or turbo-prop engines. Approximate guidance on the speed for best climb rate is also given, based on the computed results. A worked example shows how the data might be used at the preliminary project stage to assess maximum climb rate or, alternatively, installed power to achieve a given rate of climb. Author

N93-14571# Dayton Univ. Research Inst., OH.
DETERMINATION OF STRESSES ON LAMINATED AIRCRAFT TRANSPARENCIES BY THE STRAIN GAGE-HOLE DRILLING AND SECTIONING METHOD Final Report, Jan. 1989 - Sep. 1990
Thomas J. Whitney and Gregory J. Stenger Apr. 1992 205 p
(Contract F33615-84-C-3404)
(AD-A255548; UDR-TR-90-106; WL-TR-92-3025) Avail: CASI HC A10/MF A03

Reducing the incidence of transparency changeouts due to craze of the outer acrylic ply requires knowledge of stress levels in in-service aircraft transparencies. Laboratory and field craze data may then be correlated to predict craze onset. Experiments conducted during the first phase of this study verified that the strain gage-hole drilling method, with calibration modification, can measure biaxial stress states in laminated transparencies with an error of less than 10 percent for stresses over 500 psi. A device to apply this method to full-scale transparencies was then designed and fabricated. In the second phase, stresses due to three mechanisms (residual stress, installation, and cabin pressurizing) in full-scale transparencies were measured. For comparison purposes and to identify the contribution of particular mechanisms to the total stress state, the sectioning method was also used. The measurements made on full-scale transparencies removed from service due to craze indicate residual stresses are too low to cause crazing in a 'uniform' environment (one free from wide temperature variation and extended contact with crazing agents). Stresses due to transparency installation and cabin pressurizing were also low relative to the maximum principal stress criteria used in this study. Recommendations include examination of other craze criteria, examination of other stress inducing mechanisms such as moisture desorption from the surface, and examination of cyclic loading and chemical exposure on craze. GRA

N93-14601# Naval Postgraduate School, Monterey, CA.
THE V-22 OSPREY: A CASE ANALYSIS M.S. Thesis
Mark A. OBrien 1 Jun. 1992 93 p
(AD-A256445) Avail: CASI HC A05/MF A01

This thesis is a case analysis of the V-22 Osprey program. It examines the history of tilt-rotor technology, as well as the history of the program management. Congressional, OSD, and USMC/USN interplay is detailed chronologically from 1980 through to 1991 with particular reference to congressional action during this period. Various studies and simulations are analyzed with the objective of establishing the V-22 as an aircraft which is capable of fulfilling wide-ranging mission criteria established by the services much more effectively and efficiently than current or planned aircraft. The commercial and foreign military sales markets for the V-22 are also examined. This thesis concludes that the tilt-rotor concept has considerable worldwide potential for both military and civil applications. GRA

N93-14828 Georgia Inst. of Tech., Atlanta.
STABILITY OF ELASTICALLY TAILORED ROTOR BLADES Ph.D. Thesis
Mark Verner Fulton 1992 212 p
Avail: Univ. Microfilms Order No. DA9231728

A stability analysis has been developed for a hingeless, composite, isolated rotor in hover. The analysis is a finite element based solution of mixed, weak, intrinsic dynamic equations for a rotating beam. The aerodynamic forces were modeled with two-dimensional, quasi-steady strip theory, with inflow taken from momentum/blade element theory. The completely nonlinear analysis includes shear deformation, a mechanism for the inclusion of a complete 6 x 6 stiffness matrix (relating six generalized forces and moments to six generalized strains and elastic curvatures), and the effects of rotary inertia. In other words, the analysis can handle nonclassical couplings as well as shear deformation. In addition, no explicit restrictions on the magnitudes of the displacement and rotation components were made; the only implicit restriction was that the magnitudes of the strain components remain small compared to unity. The blade's equilibrium position was obtained by an iterative solution of the complete nonlinear equations using the Newton-Raphson method. The dynamic equations were linearized about this position and a small motion solution to the resulting eigen-problem was obtained. The eigenvalues give the damping and frequency of each eigenvector. The resultant FORTRAN program was thoroughly validated against analytical and existing experimental results for equilibrium, dynamic, and stability calculations. The validations encompassed both small and large equilibrium deflections. In addition, extensive correlations were performed against experimental composite results, including both static and dynamic cases. These studies indicate that the current approach accurately represents large deflections and linearized dynamics and is capable of predicting composite behavior quite well. The accuracy of the composite predictions was found to depend on the quality of the cross-sectional stiffnesses. The two-dimensional analyses used, however, gave nearly identical results for many cases because of their high quality. The performance of the 'classical' stiffnesses (which ignore shear deformation effects), however, was poor for several cases. The stability cases studied were not typically very sensitive to the nonclassical couplings. There was one stability case, however, for which a significant error appeared (especially at high thrust levels) when bending-shear coupling was neglected. Dissert. Abstr.

N93-14832 Georgia Inst. of Tech., Atlanta.
APPLICATION OF AN AEROELASTIC ANALYSIS METHOD FOR AERODYNAMIC IMPROVEMENT OF FIGHTER WINGS AT MANEUVER FLIGHT CONDITIONS Ph.D. Thesis
David Martin Schuster 1992 236 p
Avail: Univ. Microfilms Order No. DA9231750

Modern fighter aircraft must operate at a wide variety of flight conditions ranging from low-speed fight to transonic and supersonic cruise to transonic maneuver. The maneuvering characteristics of these aircraft is an important consideration when evaluating the overall effectiveness of the vehicle, but typically, these aircraft must be primarily designed to efficiently cruise, since this condition tends to consume the majority of the available fuel. Therefore, efficient design methods are required to optimize the aerodynamic performance of these aircraft at both cruise and maneuver flight conditions. An aeroelastic analysis method, based on three-dimensional Navier-Stokes equation aerodynamics, has been applied to improve the performance of fighter wings operating at sustained maneuver flight conditions. The scheme reduces the trimmed pressure drag of wings performing sustained high-g maneuvers through a simultaneous application of control surface deflection and aeroelastic twist. The aerodynamic and structural interactions are decoupled by assuming an aeroelastic twist mode shape and optimizing the performance based on this aeroelastic mode. The wing structural stiffness properties are then determined through an inverse scheme based on the aerodynamic loads and desired twist at the maneuver flight condition. The decoupled technique is verified by performing a fully coupled aeroelastic analysis using the maneuver flight conditions and the optimized structural stiffness distributions. This application uses a high-order numerical aerodynamic analysis method to efficiently define an aeroelastically deflected wing geometry with optimal aerodynamic performance at transonic maneuver

flight conditions. In addition, the aerodynamic performance of the wing at cruise conditions is in no way compromised by the application of this scheme. Thus, this method represents a multi-point wing design capability utilizing computational aerodynamics and aeroelastic tailoring.
Dissert. Abstr.

N93-15004# Naval Air Warfare Center, Warminster, PA. Air Vehicle and Crew Systems Technology Dept.
A NEURAL NETWORK PROTOTYPE FOR PREDICTING F-14B STRAINS AT THE B.L. 10 LONGERON Final Report, Mar. - May 1992
Margery E. Hoffman May 1992 48 p
(AD-A255272; NAWCADWAR-92042-60) Avail: CASI HC A03/MF A01

A neural network prototype was developed to predict strain from data obtained from an F-14 flight test program. Data from two flights were available: Flight 400 consisted of standard structural maneuvers, and Flight 401 consisted of maneuvers performed during typical fleet operations. Several variables were monitored during flight, including Nz, Mach number, altitude, wingsweep angle, roll rate, angle of attack, a weight-on-wheels indicator and the strain at B.L. 10 of the F-14B. The neural network was trained on Flight 400, and tested on Flight 401. A forward-stepwise-regression was also performed on Flight 400 and the selected model was tested on Flight 401, for comparison. Results were evaluated by comparing the correlation coefficients between the predicted and measured strains. The correlation coefficient obtained by the neural network was 0.93 and by the regression equation was 0.94. Based on these preliminary results, the conclusion is made that the neural network approach offers a viable alternative to standard regression analysis for predicting strains on airframes. GRA

N93-15126# Institut de Mecanique des Fluides de Lille (France).
AEROPLANE CRASHES ON THE RUNWAY: VALIDATION AND FINAL EVALUATION OF THE METHOD OF MODELING AN AIRFRAME STRUCTURE [CRASH DES AVIONS SUR PISTE: VALIDATION ET EVALUATION FINALE DE LA METHODOLOGIE DE MODELISATION D'UNE STRUCTURE DE CADRE AVION]
E. Deletombe and P. Geoffroy 30 Sep. 1991 58 p In FRENCH
(Contract DRET-88-003-01)
(IMFL-91-32; ETN-92-92721) Avail: CASI HC A04/MF A01

The validation and evaluation of a method of modeling an airframe structure subjected to a linear crushing is presented. The validation is based on the adjustment capacity of the model with respect to a criterion. The criterion, in this analysis, corresponds to the minimization of the difference, (in terms of absorbed energy, critical charge and post buckling rigidity), between the experimental force/displacement curve at the top of the cylindrical structure and the curve calculated with this macroelement method of modeling. During the evaluation the precision and cost of the model is compared to a classical model, of type 476 regular elements. The global benefit of this method in the complete modeling of the cylindrical structure of a commercial plane is assessed. ESA

N93-15227# Scientific-Atlantic, Inc., San Diego, CA. Signal Processing Systems.
ONBOARD SYSTEM EVALUATION OF ROTORS VIBRATION, ENGINES (OBSERVE) MONITORING SYSTEM Final Test Report, Aug. 1991 - Apr. 1992
J. A. Goodrich and K. M. Klepin Jul. 1992 22 p
(Contract DAAJ02-91-C-0030)
(AD-A255366) Avail: CASI HC A03/MF A01

The On Board System for the Evaluation of Rotors Engine and Vibration (OBSERVE) research and development (R and D) program was designed to investigate and demonstrate the benefits of onboard data recording/processing and rotor tuning equipment for monitoring and diagnosis of mechanical subsystems on the CH-47. The payoffs for such a concept include reduced aircraft vibration levels (with extended MTBF of electronics and mechanical system as well as reduced crew fatigue), reduced maintenance flights, and early warning of component failures. This program demonstrates an approach to a practical, automated system which monitors certain mechanical subsystems, provides inflight vibration and control system status, and prescribes corrective actions to the maintainer. Various monitoring components were developed and integrated to demonstrate this concept.
GRA

N93-15238# Naval Postgraduate School, Monterey, CA.
ANALYSIS OF IN-FLIGHT STRUCTURAL FAILURES OF P-3C WING LEADING EDGE SEGMENTS M.S. Thesis
Dennis A. Lott Jun. 1992 118 p
(AD-A256212) Avail: CASI HC A06/MF A02

A quantitative analysis was carried out to determine the stresses present in the leading-edge segment of a P-3C aircraft operating within and outside the normal operating envelope of the aircraft. The purpose of the analysis was to ascertain whether a specific weakness may exist in the leading-edge structure which might endanger future operating flight crews. A three-step process consisting of a static aeroelastic span-load analysis, an inviscid two-dimensional panel-method analysis, and finite-element analysis was employed in the course of the evaluation. Lift coefficient distributions from the wing span-load analyses were used in the two-dimensional panel method to determine the pressure distribution around the leading edge, which was then used as input to the finite-element analysis. Additionally, static aeroelastic-derived wing-twist effects were included in the structural model. The results of the analysis suggest that the leading edge segment studied may experience stress levels sufficient to cause failure within the normal operating envelope. GRA

N93-15314# Air Force Inst. of Tech., Wright-Patterson AFB, OH. School of Engineering.
WING ROCK PREDICTION METHOD FOR A HIGH PERFORMANCE FIGHTER AIRCRAFT M.S. Thesis
Robert C. Nolan, II May 1992 124 p
(AD-A256438; AFIT/GAE/ENY/92J-02) Avail: CASI HC A06/MF A02

This study is a limited investigation of the nonlinear aircraft behavior known as wing rock. An eight state F-15 model is analyzed using bifurcation theory. The wing rock onset point is identified and small perturbation analysis is used to linearize the equations of motion about this point. The eigenstructure of the model is analyzed and is used to identify the stability modes involved in this motion. A procedure is developed to predict wing rock onset and frequency and the critical stability derivatives involved in this motion are identified. The developed procedure is applied to existing F-4J data and a flight test involving RF-4C and T-38A aircraft is flown. The results show wing rock is an unstable dutch roll motion and the developed wing rock prediction parameter is accurate to within 1 degree of onset AOA. The frequency prediction parameter gives a fair estimate of wing rock motion but it may be adversely influenced by the type of flight test data. The slope of the prediction parameter versus AOA curve may be an indication of the severity of wing rock motion. GRA

N93-15328# Aeronautical Research Labs., Melbourne (Australia).
THE USE OF ULTRASONICS FOR OLEO COMPRESSION MEASUREMENTS ON A S-70B-2 (SEAHAWK) HELICOPTER
Jul. 1992 20 p
(AD-A256315; ARL-FLIGHT-MECH-TM-456; DODA-AR-006-670) Avail: CASI HC A03/MF A01

Dynamic measurements were conducted to acquire data for the development of a mathematical model of the undercarriage of a S-70B-2 (Seahawk) helicopter. The principal measuring instrumentation consisted of LVDT's and ultrasonic transducers. This memorandum discusses a Ranging Ultrasonic Transducer which was developed to overcome the inherent and excessive recovery time delay of the ultrasonic transducers when subjected to out-of-range distance operations during the flight trials. GRA

N93-15361# Naval Air Warfare Center, Patuxent River, MD. Aircraft Div.
STANDARDIZATION OF PRECIPITATION STATIC TEST METHODS AND EQUIPMENT FOR THE NAVY
Matthew R. Maier 1992 25 p
(AD-A257025) Avail: CASI HC A03/MF A01

The Naval Air Warfare Center Aircraft Division, Patuxent River, is currently the Navy's lead facility for Precipitation Static testing of aircraft. It was involved extensively with the design and production of standard Precipitation Static test methods and equipment. As part of tasking given by the Naval Air Systems Command, these methods are to be presented to other Navy facilities to provide additional test capability and overall fleet awareness of Precipitation Static. Further, this will provide standard procedures and equipment for Precipitation Static testing of aircraft Navy-wide. This paper presents an overview of the Precipitation Static test methods and equipment to be standardized, as well as the current plans

to distribute these to Navy facilities. Particular attention will be paid to test methodology, design of standard test equipment, and plans for distribution and training. GRA

N93-14615# Technische Univ., Delft (Netherlands). Faculty of Aerospace Engineering.
FLIGHT TESTING: PAST, PRESENT, AND FUTURE
J. A. Mulder *In* NAL, Symposium on the Occasion of the Farewell of Prof. Dr. Ir. O. H. Gerlach as Chairman of the Board of the Foundation National Aerospace Laboratory NLR, The Netherlands 1991 p 31-57 (For primary document see N93-14613 04-01)
Avail: CASI HC A03/MF A01

06 AIRCRAFT INSTRUMENTATION

Includes cockpit and cabin display devices; and flight instruments.

For related information see also *19 Spacecraft Instrumentation* and *35 Instrumentation and Photography.*

N93-14110# Air Force Occupational Measurement Center, Randolph AFB, TX.
F/FB-111 AVIONICS TEST STATION AND COMPONENT SPECIALIST/TECHNICIAN. AUTOMATIC TEST STATIONS MANUAL AND ELECTRONIC WARFARE TEST STATIONS. TRAINING REQUIREMENTS ANALYSIS (451X6), VOLUME 2
Nov. 1991 462 p
(AD-A252121) Avail: CASI HC A20/MF A01

Volume II of the training requirements analysis which includes the task analysis data for the F-111 Avionics Test Station and Component Specialty (AFSC 451X6) is included. This analysis encompasses tasks from the AFSC 451X6 USAF Job Inventory as well as additional tasks identified during interviews. The majority of the tasks analyzed were broad areas that covered many different pieces of equipment. To ensure complete coverage, every possible piece of equipment, tool, supply, activity, skill, and knowledge is listed. L.R.R.

N93-15152# Deutsche Forschungsanstalt fuer Luft- und Raumfahrt, Brunswick (Germany). Inst. fuer Flugfuehrung.
PROCEEDINGS OF THE 16TH SYMPOSIUM ON AIRCRAFT INTEGRATED MONITORING SYSTEMS [BEITRAEGE ZUM 16TH SYMPOSIUM BORDINTEGRIERTE UEBERWACHUNGSSYSTEME]
Jan. 1992 644 p Symposium held in Munich, Germany, 17-19 Sep. 1991
(DLR-Mitt-92-01; ETN-92-92162) Avail: CASI HC A99/MF A06; DLR, Wissenschaftliches Berichtswesen, Postfach 90 60 58, Cologne, Germany, HC

Reports on latest results achieved worldwide in Aircraft Integrated Monitoring Systems (AIMS) are presented. AIMS are utilized for many applications, such as aircaft performance monitoring, flight recording, pilot aircraft interaction, early fault detection in engine, airframe, and avionics, maintenance, improvement of aircraft operation, accident investigation, development of future requirements for design and operation of aircraft. Reports are presented under the following headings: AIMS developments, developments in recorders and read out, propulsion system monitoring techniques, helicopter health and usage monitoring, advanced monitoring tools, related systems, and techniques. For individual titles, see N93-15153 through N93-15186.

N93-15153# Japan Air Lines Co. Ltd., Tokyo.
DISCUSSION FOR THE IDEAL AIMS [BETRACHTUNGEN ZUM THEMA EINES IDEALEN AIMS]
F. Nagamatsu *In* DLR, Proceedings of the 16th Symposium on Aircraft Integrated Monitoring Systems Jan. 1992 p 19-36 (For primary document see N93-15152 04-06)
Avail: CASI HC A03/MF A06; DLR, Wissenschaftliches Berichtswesen, Postfach 90 60 58, Cologne, Germany, HC

Past experience with Aircraft Integrated Monitoring System (AIMS) is considered and its uses discussed: flight operations, aircraft maintenance, performance monitoring, ground proximity warning analysis, and engineering analysis. The present and future role of AIMS is discussed. More than 10 years ago, the AIMS was the only data system onboard the aircraft. But because of system integration and emergence of the other data systems on the newest aircraft models, the situation has changed. The question of whether AIMS can stay in the same position as it has been is considered. The need to review what is being done in the project of AIMS, and to find out what is involved in an ideal AIMS is discussed. ESA

N93-15154# Deutsche Airbus G.m.b.H., Munich (Germany).
SOFTWARE FLEXIBILITY AND CONFIGURATION CONTROL FOR THE A340/A330 AIRCRAFT CONDITION MONITORING SYSTEM (ACMS) [FLEXIBLE SOFTWARE UND DEREN KONFIGURATIONSKONTROLLE FUER DAS ZUSTANDSUEBERWACHUNGSSYSTEM (ACMS) FUER DIE FLUGZEUGTYPEN A340/A330]
Helmut Kalbe *In* DLR, Proceedings of the 16th Symposium on Aircraft Integrated Monitoring Systems Jan. 1992 p 37-56 (For primary document see N93-15152 04-06)
Avail: CASI HC A03/MF A06; DLR, Wissenschaftliches Berichtswesen, Postfach 90 60 58, Cologne, Germany, HC

The necessity of ACMS software changes onboard the aircraft are demonstrated. Problems with a flexible software and configuration control are discussed and a solution is presented. It is concluded that since the software is on the aircraft and the compatibility check includes the complete aircraft and airline ident, it is possible to have partially different functions in each aircraft of a fleet with always the same hardware. It is also possible to exchange data management units between customers with different ACMS functions as long as the same hardware configuration is used. This could be a way to reduce the effort for spare parts if appropriate cooperation between customers is established. All together it can be stated that the A340/A330 ACMS is a very flexible system which is open for customer modifications without moving around expensive hardware units. All programming work can be done in the personal computer based Ground Support Equipment (GSE) outside the aircraft. This means no hold up for aircraft in service for programming new monitoring tasks. The GSE enables also a comprehensive documentation of all modifications. Although the ACMS provides a high flexibility for reconfiguration the configuration control in and outside the aircraft will not be lost if the software part numbers are treated carefully. ESA

N93-15155# Teledyne Controls, Los Angeles, CA.
THE TELEDYNE CONTROLS AIRCRAFT CONDITION MONITORING SYSTEM [DAS ACMS-SYSTEM DER TELEDYNE CONTROLS]
A. Uythoven *In* DLR, Proceedings of the 16th Symposium on Aircraft Integrated Monitoring Systems Jan. 1992 p 57-68 (For primary document see N93-15152 04-06)
Avail: CASI HC A03/MF A06; DLR, Wissenschaftliches Berichtswesen, Postfach 90 60 58, Cologne, Germany, HC

An Aircraft Condition Monitoring System (ACMS) that is fully reprogrammable by airlines is considered. Salient features of the avionics and its associated ground support equipment are described. The system, which is now in operation with several airlines, provides airlines with a flexibility, which up until now was thought impossible. A number of benefits, which airlines using this system have realized, include improved operation, promotion of flight safety, extended warranties on engines, and more effective trouble shooting. ESA

N93-15156# Scandinavian Airlines System, Stockholm (Sweden).
FLIGHT DATA AND FLIGHT SAFETY IN SAS [FLUGDATEN UND FLUGSICHERHEIT BEI SAS]
Mads H. Brandt *In* DLR, Proceedings of the 16th Symposium on Aircraft Integrated Monitoring Systems Jan. 1992 p 69-85 (For primary document see N93-15152 04-06)
Avail: CASI HC A03/MF A06; DLR, Wissenschaftliches Berichtswesen, Postfach 90 60 58, Cologne, Germany, HC

The use of flight data as a tool for enhancement of flight safety and for internal audit, as well as for effective and timely maintenance is becoming part of our daily lives. It is no longer a question of whether to invest in airborne aircraft condition monitoring systems hardware or not. The question is rather how to make best use of the enormous amount of data collected during flight every second. The use of flight data has already proven itself as being cost effective for maintenance and flight operation. The SAS (Scandinavian Airline System) flight analysis and monitoring system, FLIDRAS, is considered and the following questions addressed: how should

raw data be retrieved?; how should reports triggered by data management units software be retrieved?; and where and when should this be done? ESA

N93-15157# Sundstrand Data Control, Inc., Redmond, WA.
FDAMS: AN EXTENDABLE AND RECONFIGURABLE SOLUTION FOR AVIONICS DATA MANAGEMENT SYSTEMS [FDAMS: EINE ERWEITERBARE LOESUNG FUER AVIONIKDATEN-VERARBEITUNGSSYSTEME]
Stephen B. Wilmot *In* DLR, Proceedings of the 16th Symposium on Aircraft Integrated Monitoring Systems Jan. 1992 p 87-114 (For primary document see N93-15152 04-06)
Avail: CASI HC A03/MF A06; DLR, Wissenschaftliches Berichtswesen, Postfach 90 60 58, Cologne, Germany, HC

The evolution of Aircraft Integrated Monitoring Systems (AIMS) has resulted in continued growth of monitoring and collecting aircraft information. It has become apparent that the users of AIMS require that the system be easily reconfigurable and extendable. A Flight Data Acquisition and Management System (FDAMS) is described. This was designed to satisfy the needs for information monitoring and storage requirements onboard modern aircraft, using a system which is both extendable and reconfigurable. ESA

N93-15158# Societe Francaise d'Instruments de Mesure, Massy (France).
GROUND SUPPORT EQUIPMENT (GSE) FOR AIRCRAFT CONDITION MONITORING SYSTEM (ACMS) [DIE BODENSTATION (GSE) FUER DAS FLUGZEUGUEBERWACHUNGSSYSTEM (ACMS)] **c01**
A. Levionnois *In* DLR, Proceedings of the 16th Symposium on Aircraft Integrated Monitoring Systems Jan. 1992 p 115-128 (For primary document see N93-15152 04-06)
Avail: CASI HC A03/MF A06; DLR, Wissenschaftliches Berichtswesen, Postfach 90 60 58, Cologne, Germany, HC

The purpose of the GSE (Ground Support Equipment) in aircraft and engine maintenance is outlined and a general description of Aircraft Condition Monitoring (ACM) systems is given. Information on the following is also given: GSE software, fleet management, programmation of the data management unit, smart access recorder data decompression ADEPT and APM interface, user management, hardware, and sofware requirements. ESA

N93-15159# Technical Univ. of Budapest (Hungary).
DETECTION OF TECHNICAL STATES WITH AIRCRAFT [ERMITTLUNG DES BETRIEBSZUSTANDES VON FLUGZEUGEN]
J. Rohacs *In* DLR, Proceedings of the 16th Symposium on Aircraft Integrated Monitoring Systems Jan. 1992 p 129-147 (For primary document see N93-15152 04-06)
Avail: CASI HC A03/MF A06; DLR, Wissenschaftliches Berichtswesen, Postfach 90 60 58, Cologne, Germany, HC

Experience gained in connection with the development of the onboard state monitoring and diagnostic systems for the technical systems with nonconstant parameters in aircraft is outlined. It is concluded that the technical conditions of aircraft can be detected through the deviations in their system parameters. The onboard integrated condition and failure detection systems can be designed for the detection of five states representing the real technical conditions (changing from the normal operation conditions to the operation with failure producing the accidents) and giving the more effective information for pilots. The information of technical state to the pilot is given if the system has identified a definite deviation from normal condition. ESA

N93-15160# Sundstrand Data Control, Inc., Redmond, WA.
REWRITABLE OPTICAL DISK: APPLICATION TO FLIGHT RECORDING [DER EINSATZ WIEDERBESCHREIBBARER OPTISCHER PLATTEN FUER DIE AUFZEICHNUNG VON FLUGDATEN] **c35**
Duane A. Teachout *In* DLR, Proceedings of the 16th Symposium on Aircraft Integrated Monitoring Systems Jan. 1992 p 149-168 (For primary document see N93-15152 04-06)
Avail: CASI HC A03/MF A06; DLR, Wissenschaftliches Berichtswesen, Postfach 90 60 58, Cologne, Germany, HC

As avionic systems have become more complex, the need for acquiring and storing flight data has increased. Historically, tape drives have filled the role of the recording systems. Emerging rewritable optical disk technology and its application as an alternative to tape based recording systems is discussed. The design for airborne use is described along with two application examples: a mass memory peripheral to the airborne computers, and a flight test recorder with an embedded acquisition system. ESA

N93-15161# National Aeronautical Lab., Bangalore (India).
INDIAN EXPERIENCE IN FLIGHT DATA READOUT AND ANALYSIS [INDISCHE ERFAHRUNGEN BEI DER FLUGDATEN-WWIEDERGABE UND -ANALYSE]
B. S. Adiga, S. J. Muralidhar, and S. Nagabhushana *In* DLR, Proceedings of the 16th Symposium on Aircraft Integrated Monitoring Systems Jan. 1992 p 169-183 (For primary document see N93-15152 04-06)
Avail: CASI HC A03/MF A06; DLR, Wissenschaftliches Berichtswesen, Postfach 90 60 58, Cologne, Germany, HC

The Digital Flight Data Recorder (DFDR) readout facility developed to read and analyze the raw digital from Lockheed Model 209F DFDR and other recorders is described. Three system configurations are considered: the first makes use of, as front end, the Lockheed FRIAR unit and a PDP-11 computer; the second uses direct memory access mode to directly transfer the raw data from the DFDR to the PDP-11; and the third unit is a stand-alone IBM compatible personal computer based DFDR readout system. Software was developed for channel selection, conversion to engineering units, time search, and graphic presentation. ESA

N93-15162# Ceskoslovenska Akademie Ved, Prague. Aeronautical Research and Test Inst.
CZECHOSLOVAK DEVELOPMENT AND EXPERIENCE IN FLIGHT DATA RECORDER READOUT AND ANALYSIS [ENTWICKLUNG UND ERFAHRUNGEN BEI DER FLUGSCHREIBERDATENAUS-LESUNG UND -AUSWERTUNG IN DER TSCHECHOSLOWAKEI]
J. Kozak *In* DLR, Proceedings of the 16th Symposium on Aircraft Integrated Monitoring Systems Jan. 1992 p 185-200 (For primary document see N93-15152 04-06)
Avail: CASI HC A03/MF A06; DLR, Wissenschaftliches Berichtswesen, Postfach 90 60 58, Cologne, Germany, HC

The development of an Automatic Test Mobile Equipment (AIME) intended for ground based performance testing of the jet trainer L 39 is addressed. The first step in development and production of ATE in Czechoslovakia was followed by a test and diagnostic system which is now being used for the L 39 MS jet trainer and for L 610 commuter aircraft. The onboard part of the system, the Digital Flight Data Recorder (DFDR) for combined accident and operational use, electronic unit and data entry panel, is intended for permanent record of maximum 200 parameters with the sampling rate 0.125 to 8 Hz. The ground evaluation equipment is personal computer based and equipped with programs for analysis from different points of view. Results of these developments together with other application examples and the future introduction of solid state memory are described. ESA

N93-15163# Deutsche Lufthansa A.G., Frankfurt am Main (Germany). Abt. Flugbetriebstechnik.
SOFTWARE FOR FLIGHT RECORDER DATA EVALUATION DEVELOPED BY LUFTHANSA [VON LUFTHANSA ENTWICKELTE EDV PROGRAMME ZUR AUSWERTUNG VON FLUGSCHREIBERN] **c61**
Matthias Kruedener *In* DLR, Proceedings of the 16th Symposium on Aircraft Integrated Monitoring Systems Jan. 1992 p 201-217 (For primary document see N93-15152 04-06)
Avail: CASI HC A03/MF A06; DLR, Wissenschaftliches Berichtswesen, Postfach 90 60 58, Cologne, Germany, HC

Since the introduction of aircraft equipped with analog or digital flight data recorder devices, computer software has been developed to evaluate the flight recorder data. Results of evaluations are applied to various investigations. The latest software developments, in particular video animation, are presented on the basis of an actual incident. ESA

N93-15164# Aeritalia S.p.A., Naples (Italy). Flight Safety.
THE FAIR (FLIGHT ANIMATED AND INTERACTIVE RECONSTRUCTION) TOOL [DIE INTERAKTIVE UND MIT HILFE VON TRICKFILMTECHNIKEN ARBEITENDE FLUGREKONSTRUKTION FAIR] **c03**
Silenzi Silvano *In* DLR, Proceedings of the 16th Symposium on Aircraft

Integrated Monitoring Systems Jan. 1992 p 219-235 (For primary document see N93-15152 04-06)
Avail: CASI HC A03/MF A06; DLR, Wissenschaftliches Berichtswesen, Postfach 90 60 58, Cologne, Germany, HC

Flight safety is an endless task, and its achievement calls for the use of every means possible. One of these is the flight data recorder system. The most important parameters are registered. Once they are processed with specific programs, they are listed in a long data sheet. It is important to be able to understand the relevant flight information and data. FAIR, an instrument capable of simplifying the analysis of an event, is considered. Details are given for the following: features, technical characteristics, visualization, animation, examples of satellite images, and power vision specifications. ESA

N93-15165# Aviatronic Ltd., Budapest (Hungary).
THE SIROM FLIGHT DATA RECORDER AND EVALUATION SYSTEM [DAS SYSTEM SIROM ZUR FLUGDATENERFASSUNG UND -AUSWERTUNG]
P. Giese *In* DLR, Proceedings of the 16th Symposium on Aircraft Integrated Monitoring Systems Jan. 1992 p 237-249 (For primary document see N93-15152 04-06)
Avail: CASI HC A03/MF A06; DLR, Wessenschaftliches Berichtswesen, Postfach 90 60 58, Cologne, Germany, HC

The SIROM solid state onboard data recorder for the acquisition of flight data and engine parameters is described. The SIROM replaces the optomechanical recorder of the type SARP12 used on MIG fighters and MI helicopters. The data memory unit has crash recorder quality. The ground based IBM personal computer compatible system performs automatic evaluation and has high resolution graphic and instrument panel displaying facilities. A modified variant of SIROM for the recording of the pilot's physiological parameters is discussed. ESA

N93-15166# Central Research Inst. for Physics, Budapest (Hungary).
DAR-2: ON-BOARD DATA ACQUISITION SYSTEM FOR AIRCRAFT ENGINES [DAR-2 - EIN BORDGESTUETZTES DATERNERFASSUNGSSYSTEM FUER FLUGTRIEBWERKE]
Istvan Apathy, Istvan Szemerey, Sandor Szendro, and Janos Farkas (Hungarian Airlines, Budapest.) *In* DLR, Proceedings of the 16th Symposium on Aircraft Integrated Monitoring Systems Jan. 1992 p 251-266 (For primary document see N93-15152 04-06)
Avail: CASI HC A03/MF A06; DLR, Wissenschaftliches Berichtswesen, Postfach 90 60 58, Cologne, Germany, HC

Details of the DAR-2 onboard data acquisition system for aircraft engines developed on Tupolyev TU-154 airliners are given. DAR-2, a reduced activity computer installed onboard the aircraft, collects and stores parameters describing the state of aircraft engines and ensures their processing by the airline ground processing center. As DAR-2 is based on the present service system, there is no need to invent new signal detectors. With only minor modifications it can be used on other aircraft types. ESA

N93-15167# Loral Data Systems, Sarasota, FL.
SOLID STATE FLIGHT DATA RECORDER WITH RAPID DATA ACCESS [FESTKOERPER-FLUGDATENSCHREIBER MIT SCHNELLEM DATENZUGRIFF] **c35**
Hans F. Napfel *In* DLR, Proceedings of the 16th Symposium on Aircraft Integrated Monitoring Systems Jan. 1992 p 267-286 (For primary document see N93-15152 04-06)
Avail: CASI HC A03/MF A06; DLR, Wissenschaftliches Berichtswesen, Postfach 90 60 58, Cologen, Germany, HC

Solid state recorders which have replaced magnetic tape recorders as airborne crash recorders are described. Processes for data retrieval are reviewed. Solid state recorders promise higher reliability and faster data access. However, the memory elements are more fragile. ESA

N93-15168# Dornier System G.m.b.H., Friedrichshafen (Germany).
INTEGRATED ENGINE CONTROL AND MONITORING WITH EXPERIENCES DERIVED FROM OLMOS [INTEGRIERTE TRIEBWERKSREGELUNG UND -UEBERWACHUNG MIT ERFAHRUNGEN AUS OLMOS] **c07**
Uwe Schulz and Julian Bott *In* DLR, Proceedings of the 16th Symposium on Aircraft Integrated Monitoring Systems Jan. 1992 p 287-310 (For primary document see N93-15152 04-06)
Avail: CASI HC A03/MF A06; DLR, Wissenschaftliches Berichtswesen, Postfach 90 60 58, Cologne, Germany, HC

A description of the Onboard Life Monitoring System (OLMOS) for a fighter aircraft is given. The experiences with the system in service and the modifications derived from this are presented. Based on these experiences and the technical requirements for engine control and monitoring, the advantages and disadvantages of an integrated concept are presented. Different requirements with respect to reliability and flight safety are considered. ESA

N93-15169*# National Aeronautics and Space Administration. Hugh L. Dryden Flight Research Facility, Edwards, CA.
REAL-TIME IN-FLIGHT ENGINE PERFORMANCE AND HEALTH MONITORING TECHNIQUES FOR FLIGHT RESEARCH APPLICATION [IN ECHTZEIT ARBEITENDE, BORDGESTUETZTE TRIEBWERKSLEISTUNGS- UND -ZUSTANDSUEBERWACHUNGSTECHNIKEN FUER ANWENDUNGEN IN DER FLUGFORSCHUNG]
Ronald J. Ray, John W. Hicks, and Keith D. Wichman *In* DLR, Proceedings of the 16th Symposium on Aircraft Integrated Monitoring Systems Jan. 1992 p 311-340 (For primary document see N93-15152 04-06)
Avail: CASI HC A03/MF A06; DLR, Wissenschaftliches Berichtswesen, Postfach 90 60 58, Cologne, Germany, HC

Various engine related performance and health monitoring techniques developed in support of flight research are described. Techniques used during flight to enhance safety and to increase flight test productivity are summarized. A description of the NASA range facility is given along with a discussion of the flight data processing. Examples of data processed and the flight data displays are shown. A discussion of current trends and future capabilities is also included. ESA

N93-15170# Ministry of Defence, London (England). Procurement Executive.
ROYAL AIR FORCE EXPERIENCE OF THE HARRIER INFORMATION MANAGEMENT SYSTEM [ERFAHRUNGEN DER ROYAL AIR FORCE MIT DEM INFORMATIONS-MANAGEMENT-SYSTEM DES HARRIER-FLUGZEUGES] **c82**
R. P. Bookham *In* DLR, Proceedings of the 16th Symposium on Aircraft Integrated Monitoring Systems Jan. 1992 p 341-360 (For primary document see N93-15152 04-06)
(Contract AE12A/159)
Avail: CASI HC A03/MF A06; DLR, Wissenschaftliches Berichtswesen, Postfach 90 60 58, Cologne, Germany, HC

The Harrier Information Management System (HIMS), part of the Harrier Engine Monitoring System (EMS), is considered. The EMS consists of a number of sensors and transducers feeding data into an Engine Monitoring Unit (EMU). The data is then passed from the EMU via an extraction unit, the Data Retrieval Unit (DRU), to the HIMS ground station, either directly or via a bulk data cassette recorder dependent upon whether the aircraft is on or off base. The data which is part processed in the EMU is further processed in the HIMS with the inclusion of external data about the aircraft flight fed into the system manually by aircraft tradesmen. Once fully processed the data has a number of outputs onto a VDU screen and a printer. The following are discussed: EMU functionality, HIMS functionality, HIMS deployment, system problems and solutions, HIMS performance, HIMS data analysis, possible system enhancements, and lessons learnt. ESA

N93-15171# Airbus Industrie, Blagnac (France).
MONITORING OF POWERPLANTS IN ADVANCED COMMERCIAL AIRCRAFT [TRIEBWERKSUEBERWACHUNG IN MODERNEN VERKEHRSFLUGZEUGEN] **c07**
Antoine Vieillard *In* DLR, Proceedings of the 16th Symposium on Aircraft Integrated Monitoring Systems Jan. 1992 p 361-372 (For primary document see N93-15152 04-06)
Avail: CASI HC A03/MF A06; DLR, Wissenschaftliches Berichtswesen, Postfach 90 60 58, Cologne, Germany, HC

Over the last decade, commercial aircraft design has evolved with a strong emphasis on the implementation of onboard computers. Solutions which have been taken for monitoring the powerplants in the current Airbus family (particularly A320) as well as those to be certified in the near future (A330, A340) are described. The powerplant control and monitoring have

changed by the introduction of digital engine control computers integrated with the aircraft system. The reliability requirements, highlighted by ETOPS, and the environmental conditions, such as vibration, reinforce the need for sophisticated monitoring and the definition of associated maintenance tasks. ESA

N93-15172# Motoren- und Turbinen-Union Muenchen G.m.b.H. (Germany).
EJ 200 ENGINE MONITORING SYSTEM: ON- AND OFF-BOARD DATA CAPTURE, ANALYSIS, AND MANAGEMENT SYSTEM [EJ 200 TRIEBWERKS-UEBERWACHUNGS-SYSTEM ON- UND OFF-BOARD DATENERFASSUNG, ANALSE, UND MANAGEMENT SYSTEM] **c07**
P. Stadlmeier *In* DLR, Proceedings of the 16th Symposium on Aircraft Integrated Monitoring Systems Jan. 1992 p 373-389 (For primary document see N93-15152 04-06)
Avail: CASI HC A03/MF A06; DLR, Wissenschaftliches Berichtswesen, Postfach 90 60 58, Cologne, Germany, HC

The EJ 200 engine monitoring system is part of the Integrated Monitoring and Recording System (IMRS) for the European Fighter Aircraft (EFA). The engine related part of the virtual system is considered. This includes the onboard data acquisition of engine data and subsequent onboard data analysis, the data transfer to the ground support system, and the remaining data analysis (not performed by the onboard system) and management of the ground support system. ESA

N93-15173# Motoren- und Turbinen-Union Muenchen G.m.b.H. (Germany).
RB199 ENGINE OIL SYSTEM FAILURE DIAGNOSTICS BY COMPARISON OF MEASURED AND CALCULATED OIL CONSUMPTION USING THE OLMOS ON-BOARD MONITORING SYSTEM [STOERUNGSDIAGNOSE FUER DAS RB199-OELSYSTEM DURCH VERGLEICH ZWISCHEN GEMESSENEN UND MIT DEM OLMOS ON-BOARD UEBERWACHUNGSSYSTEM GERECHNETEN OELVERBRAEUCHEN] **c07**
H. Pfoertner and H. Streifinger *In* DLR, Proceedings of the 16th Symposium on Aircraft Integrated Monitoring Systems Jan. 1992 p 391-414 Sponsored by Bundesministerium der Verteidigung (For primary document see N93-15152 04-06)
Avail: CASI HC A03/MF A06; DLR, Wissenschaftliches Berichtswesen, Postfach 90 60 58, Cologne, Germany, HC

The oil consumption of military aircraft engines varies, depending on the mission to be undertaken, throughout a flight. In order to detect oil system related failures and to reduce the number of engine ground runs required to check the oil consumption, a mathematical model was developed to calculate the expected oil consumption from available flight data. It was implemented in the engine monitoring function of OLMOS (Onboard Life Monitoring System). First flight test results and possible directions for the development of future systems are described. ESA

N93-15174# General Electric Co., Cincinnati, OH. Aircraft Engines.
A PHILOSOPHY FOR INTEGRATED MONITORING SYSTEM DESIGN [GRUNDSAEZLICHE UEBERLEGUNGEN ZUR ENTWICKLUNG INTEGRIERTER UEBERWACHUNGSSYSTEME] **c07**
David L. Doel *In* DLR, Proceedings of the 16th Symposium on Aircraft Integrated Monitoring Systems Jan. 1992 p 415-432 (For primary document see N93-15152 04-06)
Avail: CASI HC A03/MF A06; DLR, Wissenschaftliches Berichtswesen, Postfach 90 60 58, Cologne, Germany, HC

The use of a different philosophy for engine monitoring system design where diagnostic requirements are derived from goals for the aircraft is suggested and discussed. As an example jet engine gas path analysis is discussed. A better example, the Ground-based Engine Monitoring (GEM) software system to support the CF6-80A3 engines is disucssed. The software advances include automatic recognition of trends or step changes in the engine behavior, better integration of the system into the airline day to day activities, and earlier availability of results so problems are detected in near real time. Aims to build a better gas path algorithm are given. It is concluded that any fundamental improvement to engine monitoring systems will be preceded by a change in emphasis on the part of the designer. These changes are outlined. ESA

N93-15175# Universitaet der Bundeswehr, Hamburg (Germany).
SOME EXPERIMENTS AND IDEAS ON GPA BEFORE REACHING STEADY STATE OF ENGINE [EINIGE EXPERIMENTE UND UEBERLEGUNGEN UEBER GPA VOR ERREICHEN DES STATIONAEREN ZUSTANDES DES TRIEBWERKS] **c07**
K. Fiedler, R. Lunderstaedt, and K.-J. Schmidt *In* DLR, Proceedings of the 16th Symposium on Aircraft Integrated Monitoring Systems Jan. 1992 p 433-454 (For primary document see N93-15152 04-06)
Avail: CASI HC A03/MF A06; DLR, Wissenschaftliches Berichtswesen, Postfach 90 60 58, Cologne, Germany, HC

During normal operating conditions, often the steady state of jet engines and gas turbines is not reached. Nevertheless it is desirable to perform a Gas Path Analysis (GPA) even under these conditions. Therefore experimental and theoretical investigations were made concerning the time dependent reaction of a shaft power engine after changing the operating point. The time constants deduced from experimental results show good agreement with the theoretical values if somewhat sophisticated theories are applied. Concerning the GPA, it was found that the values for the capacity can be used after less than 10 s, but only after several minutes does the efficiency reach its steady state value, which is necessary for the existing GPA procedures. ESA

N93-15176# Technische Univ., Munich (Germany).
EXPERIMENTAL ANALYSIS OF STEADY-STATE AND DYNAMIC MONITORING OF POWER SHAFT TURBINES [ZUR EXPERIMENTELLEN ANALYSE DER STATIONAEREN UND DYNAMISCHEN ZUSTANDSUEBERWACHUNG VON WELLENLEISTUNGSTRIEBWERKEN] **c07**
S. Bogner, G. Kappler, and H. Rick *In* DLR, Proceedings of the 16th Symposium on Aircraft Integrated Monitoring Systems Jan. 1992 p 455-482 (For primary document see N93-15152 04-06)
Avail: CASI HC A03/MF A06; DLR, Wissenschaftliches Berichtswesen, Postfach 90 60 58, Cologne, Germany, HC

The increasing demand for safety and reliability of aircraft turbines, as well as the reduction of their life cycle costs, have led to intensive research of turbine monitoring systems. High accuracy engine models, which must be adapted to the present engine state by means of experimental modeling, are required for steady state and dynamic engine monitoring. Compressor disturbances are simulated in the steady and dynamic state and are calculated using engine monitoring models in order to identify engine failures. The tests are carried out on a helicopter engine situated on a computer controlled test stand which provides, among other things, extensive dynamic measuring techniques. ESA

N93-15177# Motoren- und Turbinen-Union Muenchen G.m.b.H. (Germany).
MODELLING THE ENGINE TEMPERATURE DISTRIBUTION BETWEEN SHUT DOWN AND RESTART FOR LIFE USAGE MONITORING [MODELLIERUNG DER TEMPERATURVERTEILUNG IM TRIEBWERK ZWISCHEN ABSCHALTEN UND NEUSTART FUER DIE LEBENSDAUERUEBERWACHUNG]
G. Dhondt and W. Moehres *In* DLR, Proceedings of the 16th Symposium on Aircraft Integrated Monitoring Systems Jan. 1992 p 493-498 (For primary document see N93-15152 04-06)
Avail: CASI HC A03/MF A06; DLR, Wissenschaftliches Berichtswesen, Postfach 90 60 58, Cologne, Germany, HC

The total life consumption during a flight depends on the initial temperature distribution in the engine. This definitely applies to helicopter systems, which often restart after a very short cooling time. An algorithm was developed to model these temperatures as a function of the temperature distribution at shutdown of the previous flight and the time elapsed. It is based on the same mathematical equations as the inflight temperature calculation and satisfies the severe constraints due to processor speed and storage size. Furthermore parts of the algorithm can be used to calculate the temperature at shutdown peaks. Examples show that the damage assessment can be significantly improved by using the modeled temperature distribution instead of ambient temperature, and by incorporating shutdown peaks. ESA

N93-15178# Teledyne Controls, Los Angeles, CA.
HELICOPTER FLIGHT DATA RECORDER AND HEALTH AND USAGE MONITORING SYSTEM [FLUGDATENAUFZEICHNUNGS- SOWIE ZUSTANDS- UND NUTZUNGSUEBERWACHUNGSSYTEM (FDR/HUMS) FUER HUBSCHRAUBER]
James E. Land and Grahame Daniels (British International Helicopters Ltd., Oxford, England) *In* DLR, Proceedings of the 16th Symposium on Aircraft Integrated Monitoring Systems Jan. 1992 p 499-518 (For primary document see N93-15152 04-06)
Avail: CASI HC A03/MF A06; DLR, Wissenschaftliches Berichtswesen, Postfach 90 60 58, Cologne, Germany, HC

In response to evolving user and regulatory requirements for improved helicopter monitoring, FDR/HUMS (Flight Data Recorder/Health and Usage Monitoring Systems) are now being installed on medium and large helicopters, starting with those which operate in the North Sea from bases in the United Kingdom and Europe. A summary of the technical requirements of these systems and the details of a particular implementation are presented. An overview of the regulatory and user requirements, the technical features of the avionics kit and ground systems as well as the operational features of the system is given. A summary of the system functions is presented. The details of the onboard processing approach in multiple, high speed digital processors are given. ESA

N93-15179# Stewart Hughes Ltd., Eastleigh (England).
HELICOPTER HEALTH MONITORING: CURRENT PRACTICE AND FUTURE TRENDS [ZUSTANDSUEBERWACHUNG BEI HUBSCHRAUBERN - DERZEITIGER EINSATZ UND ZUKUENFTIGE ENTWICKLUNGEN]
R. M. Stewart *In* DLR, Proceedings of the 16th Symposium on Aircraft Integrated Monitoring Systems Jan. 1992 p 519-538 (For primary document see N93-15152 04-06)
Avail: CASI HC A03/MF A06; DLR, Wissenschaftliches Berichtswesen, Postfach 90 60 58, Cologne, Germany, HC

The safety record of large passenger carrying helicopters and the way in which the United Kingdom Civil Aviation Authority is pressing owners of aircraft on its register to improve this, both in the medium and long term, are reviewed. Some of the theoretical weight penalties involved in achieving the new safety targets through both safe life and fail safe design practices are considered. Some of the design methodologies used to design the health and usage monitoring systems now being fitted to North Sea operating aircraft to improve safety through better monitoring of the aircraft's dynamic parts are reviewed. ESA

N93-15180# Vibro-Meter S.A., Fribourg (Switzerland).
NEW ROTOR TRIM AND BALANCE SYSTEM FOR HELICOPTER USAGE MONITORING [NEUARTIGES TRIMM- UND AUSWUCHTSYSTEM FUER DIE BETRIEBSUEBERWACHUNG VON HUBSCHRAUBERN]
T. A. Staub and C. S. Ventres (Technology International Corp., Bedford, MA.) *In* DLR, Proceedings of the 16th Symposium on Aircraft Integrated Monitoring Systems Jan. 1992 p 539-556 (For primary document see N93-15152 04-06)
Avail: CASI HC A03/MF A06; DLR, Wissenschaftliches Berichtswesen, Postfach 90 60 58, Cologne, Germany, HC

Conventional rotor trim and balance methods rely to some extent on the optical alignment of the blade tips. ROTABS (trademark for Rotor Trim and Balance System), a unique system that tackles the problem at its source by making a multiplane analysis of the airframe vibration characteristics using accelerometers, is described. The system is based on the philosophy that the rotor set up that produces the least vibration will be the best possible combination for performance, comfort and reduced structural fatigue. Vibration levels were significantly reduced from the levels previously achieved by helicopter operators and manufacturers in U.S. and Europe using conventional systems. Future developments are considered. ESA

N93-15181# Framasys A.G., Zurich (Switzerland).
FAILURE DIAGNOSTIC WITH MAINTEX BASED ON AIMS AT SWISSAIR [STOERUNGSDIAGNOSE MIT MAINTEX BASIEREND AUF AIMS BEI SWISSAIR] **c01**
R. Ottiger *In* DLR, Proceedings of the 16th Symposium on Aircraft Integrated Monitoring Systems Jan. 1992 p 557-566 (For primary document see N93-15152 04-06)
Avail: CASI HC A02/MF A06; DLR, Wissenschaftliches Berichtswesen, Postfach 90 60 58, Cologne, Germany, HC

Aircraft Integrated Monitoring Systems (AIMS) generate airborne data on system and component failure that often need to be interpreted by human experts as symptoms to localize and resolve the real cause of a superior problem. The adequate handling of the information requires great problem handling skills and experience. As trouble shooting experts are very rare and expensive, Swissair decided to build ground based diagnostic systems, as an essential complement to AIMS. MAINTEX diagnostic systems that use the information of AIMS according to the experience and knowhow of the best experts, guarantee good returns in investment: diagnosticians are more efficient, aircrafts spend less time on the ground and maintenance is optimized. ESA

N93-15182# Technische Univ., Brunswick (Germany). Inst. fuer Flugfuehrung.
SENSOR FAULT DETECTION USING NONLINEAR OBSERVER AND POLYNOMIAL CLASSIFIER [SENSORFEHLERERKENNUNG MIT NICHTLINEAREM BEOBACHTER UND POLYNOMKLASSIFIKATOR]
R. Brockhaus and J. J. Buchholz (Deutsche Forschungsanstalt fuer Luft- und Raumfahrt, Brunswick, Germany) *In* DLR, Proceedings of the 16th Symposium on Aircraft Integrated Monitoring Systems Jan. 1992 p 567-584 (For primary document see N93-15152 04-06)
Avail: CASI HC A03/MF A06; DLR, Wissenschaftliches Berichtswesen, Postfach 90 60 58, Cologne, Germany, HC

A sensor fault detection algorithm for the supervision of the aerodynamic states of an aircraft (airspeed, angle of attack and angle of sideslip) is presented. It consists of a Luenberger observer containing a three degree of freedom, nonlinear model of aircraft motion, and the implementation of a polynomial classifier on a transputer network. Results of state estimation and fault detection from flight measurements with a Dornier 128 research aircraft are presented, that prove the applicability of these methods as well as their limitations. ESA

N93-15183# Paderborn Univ. (Germany). Dept. of Electrical Engineering.
NEURAL NETWORK BASED CONDITION MONITORING [ZUSTANDSUEBERWACHUNG AUF DER BASIS NEURONALER NETZWERKE] **c63**
Dieter Barschdorff *In* DLR, Proceedings of the 16th Symposium on Aircraft Integrated Monitoring Systems Jan. 1992 p 585-606 (For primary document see N93-15152 04-06)
Avail: CASI HC A03/MF A06; DLR, Wissenschaftliches Berichtswesen, Postfach 90 60 58, Cologne, Germany, HC

In the case of impending failures in complex technical systems, only sophisticated real time methods of trend monitoring and fault prediction can avoid catastrophic situations. Neural network based adaptive diagnostic systems have demonstrated reliable results in various applications. The systems are trained by learning, but compute their diagnostic analysis within defined time intervals. Accepting even noisy or incomplete sensor input data, they show robust performance. A case study with aircraft flight data demonstrates the applicability of neural network based condition monitoring. ESA

N93-15184# Universitaet der Bundeswehr Muenchen, Neubiberg (Germany). Fakultaet fuer Systemdynamik und Flugmechanik.
MONITORING OF PILOT ACTIONS AS PART OF A KNOWLEDGE-BASED SYSTEM FOR PILOT ASSISTANCE [UEBERWACHUNG DER PILOTENAKTIONEN ALS TEILFUNKTION EINES WISSENSBASIERTEN PILOTEN-UNTERSTUETZUNGSSYSTEMS] **c53**
R. Onken, T. Wittig, and H.-L. Dudek (Dornier Luftfahrt G.m.b.H., Friedrichshafen, Germany) *In* DLR, Proceedings of the 16th Symposium on Aircraft Integrated Monitoring Systems Jan. 1992 p 607-627 (For primary document see N93-15152 04-06)
Avail: CASI HC A03/MF A06; DLR, Wissenschaftliches Berichtswesen, Postfach 90 60 58, Cologne, Germany, HC

A development of a knowledge based monitoring and warning system for human operators of vehicles, in particular aircraft pilots, is presented. This monitoring and warning system for aircraft pilots is part of an intelligent system assisting the pilot in instrument flight operation. Besides automatic

planning and plan execution aids, advice and warnings are delivered to the pilot on the basis of automatic situation assessment and monitoring of pilot actions, flight status, system status and environmental conditions. The development led to an implementation in a man-in the-loop-simulation. Some simulation test results are presented. ESA

N93-15185# MicroNet, Celle (Germany).
PERSONAL COMPUTER BASED TEST- AND EMULATION EQUIPMENT FOR MAINTENANCE AND GROUND SUPPORT [TESTGERAETE UND EMULATOREN AUF PERSONAL-COMPUTERBASIS FUER DIE WARTUNG UND DEN 'GROUND SUPPORT'] c01
Anton Bader *In* DLR, Proceedings of the 16th Symposium on Aircraft Integrated Monitoring Systems Jan. 1992 p 629-646 (For primary document see N93-15152 04-06)
Avail: CASI HC A03/MF A06; DLR, Wissenschaftliches Berichtswesen, Postfach 90 60 58, Cologne, Germany, HC

A modular, very powerful and versatile Aircraft Integrated Monitoring System (AIMS), based on a parallel and a personal computer, is described. Details of its requirements, architecture and hardware are given. The architecture and principles of the ARINC bus and data processing interfaces are shown plus the applied technique of ARINC data acquisition and simulation with the help of a simple personal computer. ESA

N93-15186# Airbus Industrie, Toulouse (France).
AIRBUS INDUSTRIE TCAS EXPERIENCE c04
H. Ganz *In* DLR, Proceedings of the 16th Symposium on Aircraft Integrated Monitoring Systems Jan. 1992 p 647-674 (For primary document see N93-15152 04-06)
Avail: CASI HC A03/MF A06; DLR, Wissenschaftliches Berichtswesen, Postfach 90 60 58, Cologne, Germany, HC

TCAS 2 equipment (Traffic Alert and Collisional Avoidance System) is viewed as a supplement to the pilot who, with the aid of air traffic control system, has the primary responsibility for avoiding mid air collisions. A description of the system is given. Installation principles and experience gained on several aircraft types before obtaining approval of TCAS 2 installation are provided. The integration of this system raised a lot of problems, ranging from European airworthiness/operational approval requirements, missing top level specification, a not mature system and integration/compatibility problems. ESA

N93-15235# Charles River Analytics, Inc., Cambridge, MA.
DESIGN FOR TACTICAL SITUATION AWARENESS DISPLAY Final Report
Greg L. Zacharias and Paul G. Gonsalves 15 Jun. 1992 93 p
(Contract DAAA15-90-C-0019)
(AD-A256194; R89351) Avail: CASI HC A05/MF A01

Because of continuing advances in on-board sensors, computers, and displays, we can expect to see significant growth in the amount of information presented to rotorcraft crews by next-generation tactical situation displays. If unchecked, this growth will easily exceed the crew's capability for dealing with the available on-board information base in a timely and effective fashion. A range of technologies are now being proposed to provide appropriate levels of information management and situation awareness, ranging from hardware upgrades like touch screen displays, to advanced computing horsepower to support multi-sensor data fusion, to new AI technologies including expert systems like Pilot's Associate. The problem, however, is not that there is a dearth of candidate technologies; rather it is that we have no reliable means for evaluating them in terms of the fundamental situation awareness they afford the crew. What is called for is an objective metric for evaluating the awareness level provided a crew by a new cockpit technology, and a rational means for using this metric in a structured methodology involving: (1) identification of mission-specific tactical informational requirements; (2) generation of candidate display formats and symbologies; and (3) metric-based evaluation of afforded situation awareness. GRA

07 AIRCRAFT PROPULSION AND POWER

Includes prime propulsion systems and systems components, e.g., gas turbine engines and compressors; and onboard auxilliary power plants for aircraft.

For related information see also *20 Spacecraft Propulsion and Power, 28 Propellants and Fuels,* and *44 Energy Production and Conversion.*

N93-14111# Quest Integrated, Inc., Kent, WA.
ACTIVE CONTROL OF COMBUSTION INSTABILITY IN A RAMJET USING LARGE-EDDY SIMULATIONS
S. Menon Sep. 1992 103 p LIMITED REPRODUCIBILITY; Availability; Document partially illegible
(Contract N00014-90-C-0089)
(AD-A255226; QUEST-TR-575) Avail: CASI HC A06/MF A02

Combustion instability in a ramjet engine is an extremely complex phenomenon involving nonlinear interactions among acoustic waves, vortex motion and unsteady heat release. Typically, the instability manifests itself as a large-amplitude pressure oscillation in the low-frequency range (100-800 Hz) and is very difficult to control. When the amplitude of the pressure oscillation reaches some critical limit, it can cause structural damage due to fatigue or can cause an engine 'unstart', which occurs when the shock in the inlet duct is expelled to form a bow shock ahead of the inlet. This phenomenon of engine unstart is one of the most serious technical problems encountered in developing an operational ramjet engine. Both experimental and numerical investigations have been conducted to determine the mechanism of the combustion instability. Attempts to control combustion instability using both passive and active control techniques have also been carried out in the past. Passive control methods that typically involve structural modifications have proven insufficient for controlling the low-frequency instability. Recent experimental studies suggest that active control techniques may be more effective in controlling the combustion instability in a ramjet. In parallel to the experimental studies, a numerical study of active control methods was carried out in the project. Earlier, the result of numerical studies of active control using acoustic feedback techniques was reported and it was shown that combustion instability can be successfully controlled using such techniques provided certain feedback criteria are satisfied. Although the results are in good agreement with experimental observations, it is well known that in realistic ramjet combustors, acoustic feedback control using loudspeakers as the controller may not be practical due to the prevailant hostile (hot) environment in the combustor. A numerical study of another type of active control technique which uses secondary injection of the premixed fuel as the controller was also carried out. Such a technique has been shown experimentally to be a more practical and effective control system. The results of the simulation carried out over the two year period from May 1990 to May 1992 are summarized. Papers that were written using the results of the study are included in Appendix A. L.R.R.

N93-14890# Advisory Group for Aerospace Research and Development, Neuilly-Sur-Seine (France). Propulsion and Energetics Panel.
PROPULSION AND ENERGETICS PANEL WORKING GROUP 20 ON TEST CASES FOR ENGINE LIFE ASSESSMENT TECHNOLOGY [CAS D'ESSAI POUR LA GESTION DE LA DUREE DE VIE DES MOTEURS]
Sep. 1992 232 p
(AGARD-AR-308; ISBN-92-835-0686-3) Copyright Avail: CASI HC A11/MF A03

This report presents a set of six test cases intended to provide support for the development and validation of structural analysis and life prediction codes applicable to gas turbine components. The test cases are based on actual engine simulation tests. The data bases comprising the test cases include geometric design information describing the component, rig interface information, material data, and test condition data including steady, dynamic, and thermal loading. Crack initiation and propagation data are also included. Hence, these test cases, for the first time, make available all of the component and loading information required to verify that existing codes or codes in development yield meaningful and consistent predictions. This Advisory Report was prepared at the request of the Propulsion and Energetics Panel of AGARD. For individual titles, see N93-14891 through N93-14898.

N93-14891# Army Aviation Systems Command, Cleveland, OH. Engine and Transmission Div.

[INTRODUCTION TO TEST CASES FOR ENGINE LIFE ASSESSMENT TECHNOLOGY]

Robert C. Bill *In* AGARD, Propulsion and Energetics Panel Working Group 20 on Test Cases for Engine Life Assessment Technology Sep. 1992 6 p (For primary document see N93-14890 04-07)

Copyright Avail: CASI HC A02/MF A03

The cost of maintaining fleet readiness and the trend toward higher power to weight ratio gas turbine engines has put increased importance on component structural analysis and life prediction. Over the past decade there has been considerable progress in the development of advanced structural analysis and life prediction codes for gas turbine engine components. The six test cases comprising this document include a collection of problems that consider crack initiation and crack propagation in hot section and cold section engine components. A broad range of component configurations and loading conditions are included as well as a detailed listing of test case attributes. Author

N93-14892# Societe Nationale d'Etudes et de Construction de Moteurs Aeronautiques, Moissy-Cramayel (France). Service YLEC.

LARZAC HP TURBINE DISK CRACK INITIATION AND PROPAGATION SPIN PIT TEST

Roland Krafft *In* AGARD, Propulsion and Energetics Panel Working Group 20 on Test Cases for Engine Life Assessment Technology Sep. 1992 13 p (For primary document see N93-14890 04-07)

Copyright Avail: CASI HC A03/MF A03

The component test of the LARZAC HP turbine disk proposed in this document provides the opportunity for validation of life prediction methodologies concerning crack initiation and propagation behavior on an area of a nickel-based refractory alloy turbine disk subjected to multi-axial loading. It should be noted, in particular, that this test, carried out under a partial vacuum at high temperature, proposes study of the natural initiation and propagation of a low-cycle fatigue crack. This test case offers the advantages of test analysis of a real turbine part, well defined test conditions, natural initiation of a crack in an area subjected to multi-axial loading leading to moderate plasticity, a well-known nickel-based material (INCONEL 718), and only two-dimensional test analysis, but requiring fine elastic-plastic modeling. The limitations of the test are that it is a component test carried out under isothermic conditions, with a simple load cycle (non-mission), and it involves a complex disk environment (recreating that of an engine) requiring modelling, of the adjacent parts to simulate realistic boundary conditions. From this study conducted by GE and RAE, it was concluded that the test case includes sufficient information to make analytic predictions of fatigue crack propagation behavior, and correlate life predictions with spin pit test results. Author

N93-14893# Motoren- und Turbinen-Union Muenchen G.m.b.H. (Germany).

RB 199 HIGH PRESSURE COMPRESSOR STAGE 3 SPIN PIT TESTS

Jurgen Broede *In* AGARD, Propulsion and Energetics Panel Working Group 20 on Test Cases for Engine Life Assessment Technology Sep. 1992 20 p (For primary document see N93-14890 04-07)

Copyright Avail: CASI HC A03/MF A03

The RB 199 test case presented here addresses areas with stress concentration to a stress level of local elastic-plastic material behavior. The material used is a corrosion resistant steel X8CrCoNiMo11. Information about component geometry, part processing, operating conditions and history, recommendations about stress analysis and relevant boundary and thermal conditions as well as materials data are presented. This test case deals with cyclic spin pit testing conducted on the 3rd stage HP compressor disk of the TURBO UNION RB 199 engine. The tests were performed to verify disk design and life prediction under a safe life LCF lifting concept. Addressed critical areas are Bolt Holes and Rim Slots. For Bolt Hole testing the original component geometry was modified slightly, for Rim testing significantly to ensure component failure to occur in the area under investigation and local stress distribution as under engine operating conditions. Following an independent analysis, it was concluded that the test case includes sufficient information to generate a viable stress analysis model, generate concentrated stress factors, and correlate life predictions with the spin pit test results. Analyses and the materials data provided in the test cases were used to predict the disk lives for the spin pit testing within 10 percent of the observed lives. Author

N93-14894# General Electric Co., Cincinnati, OH. Aircraft Engines.

CF6-6 HIGH PRESSURE COMPRESSOR STAGE 5 LOCKING SLOT CRACK PROPAGATION SPIN PIT TEST

Paul A. Domas *In* AGARD, Propulsion and Energetics Panel Working Group 20 on Test Cases for Engine Life Assessment Technology Sep. 1992 26 p (For primary document see N93-14890 04-07)

Copyright Avail: CASI HC A03/MF A03

The CF6-6 High Pressure Compressor Stage 5 Locking Slot Crack Propagation Spin Pit test case provides the opportunity for validation of stress analysis and crack propagation life prediction methodologies for a complex geometry, titanium material, gas turbine aircraft engine component. The case addresses crack growth from an artificial crack starter notch under isothermal, constant amplitude, continuous (no dwell period), cyclic testing in a partially evacuated spin pit test facility. The most outstanding attribute of the case in the comprehensive crack growth measurement data available in 200 cycle increments throughout the 7355 cycle test duration. The test case included use of actual hardware (field returned, titanium material, engine part); complex local part geometry involving a decaying stress gradient; an elastic-plastic stress level (local area yielding); realistic surface conditions (milled and shot peened surface), and assessment of a significant failure mode. To evaluate this test case, a two-dimensional axisymmetric finite element stress analysis of the compressor spool was completed followed by a two-dimensional finite element analysis of the concentration effect of the loading slot. These results were used to calculate the crack propagation behavior from the crack starter notches introduced at the loading slots. Factors to account for the effect of shot peening were derived empirically from the results given for the notched bend specimen. These factors were used in the component life calculation which resulted in a prediction within 13 percent of the observed life. The assessment confirmed the suitability of this test case. Author

N93-14895# Rolls-Royce Ltd., Bristol (England).

RB211-524B DISC AND DRIVE CONES HOT CYCLIC SPINNING TEST

Lawrence M. Jenkins and S. E. Crow *In* AGARD, Propulsion and Energetics Panel Working Group 20 on Test Cases for Engine Life Assessment Technology Sep. 1992 28 p (For primary document see N93-14890 04-07)

Copyright Avail: CASI HC A03/MF A03

The details of component dimensions, loading, material properties, and general arrangements required to perform a stress analysis on the RB211-524 HPT Disc and Drive Cones are presented. The experimental assembly was modelled using finite element stressing techniques at a temperature of 500 C, with the radial load being applied for the dummy blade weights. The test was halted after 3734 rig cycles due to LCF cracking at the runout of the bolt hole boss blend radius to the rear face diaphragm of the disc. Author

N93-14896# General Motors Corp., Indianapolis, IN. Allison Gas Turbine Div.

ENGINE LIFE ASSESSMENT TEST CASE TF41 LP COMPRESSOR SHAFT TORSIONAL FATIGUE

William H. Parker *In* AGARD, Propulsion and Energetics Panel Working Group 20 on Test Cases for Engine Life Assessment Technology Sep. 1992 63 p (For primary document see N93-14890 04-07)

Copyright Avail: CASI HC A04/MF A03

The test case presented here provides an example for crack initiation and crack growth of a shaft loaded with major, zero to maximum, torsional cycles with steady axial load and high cycle minor torsional cycles superimposed. The TF41 LP compressor drive shaft was tested as part of a U.S. Air Force Life Extension Program in the early to mid 1980s. This test program provided a controlled set of fatigue testing information and material characterization data which form the basis of the test case. Details of the engine shaft are presented along with pertinent processing information. The test setup and program are described in sufficient detail to permit users to model the component and predict the state of stress. Material data are presented with enough detail so that fatigue life models can be used to predict the shafting life and comparisons with test results can be made. Author

N93-14897# Pratt and Whitney Aircraft, West Palm Beach, FL. Government Engine Business.

F100 SECOND STAGE FAN DISK BOLTHOLE CRACK PROPAGATION FERRIS WHEEL TEST

Thomas E. Farmer *In* AGARD, Propulsion and Energetics Panel Working Group 20 on Test Cases for Engine Life Assessment Technology Sep. 1992 48 p (For primary document see N93-14890 04-07)

Copyright Avail: CASI HC A03/MF A03

This test case provides the opportunity for the evaluation of the overall stress state in a typical 'fracture critical' gas turbine engine rotor component and residual crack propagation life assessment at the bolthole for a simulated low cycle fatigue engine operation mission cycle. Ferris wheel testing provides the crack propagation data to which the prediction is correlated. In addition, an overload hot pre-spin treatment of the disk is evaluated as a means of establishing an induced beneficial near surface compressive residual stress at the bolthole to enhance the crack propagation life. The F100 2nd stage fan disk was tested as part of the U.S. Air Force Damage Tolerant Design for Cold-section Turbine Engine Disks Program AFWAL-TR-81-2045 in the late 70s. The component geometry, part processing, test rig set-up, operating conditions and environment, and materials data are presented in sufficient detail to allow users to model the component and predict the state of stress throughout the body of the disk with particular attention to the bolthole outer diameter location of interest. Solution of the stress state at the bolthole O.D. for the simulated mission cycle and use of crack propagation rate models allow prediction of the residual life from pre-cracks and make comparisons to actual test data. Author

N93-14898# Hawker Siddeley Canada Ltd., Toronto (Ontario). Orenda Div.

IN-SERVICE CONSIDERATIONS AFFECTING COMPONENT LIFE

Raj Thamburaj *In* AGARD, Propulsion and Energetics Panel Working Group 20 on Test Cases for Engine Life Assessment Technology Sep. 1992 16 p (For primary document see N93-14890 04-07)

Copyright Avail: CASI HC A03/MF A03

It is believed that the cases reported will be the forerunner of a number of future studies dealing with more complex combinations of factors that need to be considered to assess the life of a gas turbine component in actual service. Some of these considerations are discussed here, in relation to the test cases detailed in earlier chapters. While the focus is upon discs and spacers, to maintain a close relationship with the test cases presented earlier for other engines, blade life prediction is also discussed. Where appropriate, examples were drawn from experience in J85 and F404 engines operated in Canada. This paper considers various practical aspects of life prediction which merit further investigation. These are as follows: small crack behavior; the effect of loading conditions, multiaxial loading, HCF-LCF interactions, creep-fatigue and creep-fatigue-environment interactions; microstructural effects, long term service exposure effects, grain size, and grain shape effects, anisotropic behavior and single crystal turbine blades; coating effects; defects and damage tolerance; inspection sensitivity and reliability effects; residual stress effects; effects of repair; and usage monitoring. Author

N93-15143# Motoren- und Turbinen-Union Muenchen G.m.b.H. (Germany).

ENGINE TECHNOLOGIES FOR FUTURE SPACEPLANES

P. Krammer and R. R. Schwab 1991 10 p Presented at 10th ISABE, Nottingham, England, 1-6 Sep. 1991 Sponsored by BMFT and ESA

(ETN-92-92732) Avail: CASI HC A02/MF A01

The importance of propulsion generic technologies, in the successful design of an airbreathing hybrid propulsion system for hypersonic applications, is discussed. These technologies are put into perspective with regard to system performance and safety aspects. These technological requirements are discussed, and they include the following: aerothermodynamics of inlets and nozzles; hydrogen combustion and environmental effects; thermal management; and high temperature and hydrogen resistant materials and structures. ESA

N93-15337# Exotech, Inc., Fremont, CA.

AN EXPERIMENTAL AND ANALYTICAL STUDY OF TIP CLEARANCE EFFECTS IN AXIAL FLOW COMPRESSORS Ph.D. Thesis

Ian N. Moyle Dec. 1991 252 p

(AD-A256434; NPS-AA-92-001CR) Avail: CASI HC A12/MF A03

An analytical and experimental study of the performance changes and flow effects of rotor tip clearance variation in axial flow compressors is presented. The analyses demonstrate that previously unrecognized loss characteristics and flow behavior trends can be identified in a wide range of published tests of clearance effects. The performance and flow data are correlated at constant power conditions or nondimensionally in terms of the test compressor's geometry and wall flow conditions to observe the trends. Flow field changes caused by increasing the tip seal clearance of a low speed, large scale axial compressor having a symmetric velocity diagram were examined experimentally. The measurements were made at several clearances for one rotational speed. Synchronized blade-to-blade measurements of case wall static pressure and skin friction under the rotor tip of the second stage were collected. GRA

N93-15342*# National Aeronautics and Space Administration. Lewis Research Center, Cleveland, OH.

SUPERSONIC INVESTIGATION OF TWO DIMENSIONAL HYPERSONIC EXHAUST NOZZLES

Jeanne D. Carboni, Rickey J. Shyne, Laurence D. Leavitt (National Aeronautics and Space Administration. Langley Research Center, Hampton, VA.), John G. Taylor (National Aeronautics and Space Administration. Langley Research Center, Hampton, VA.), and Milton Lamb (National Aeronautics and Space Administration. Langley Research Center, Hampton, VA.) Oct. 1992 46 p

(RTOP 763-01-21)

(NASA-TM-105687; E-7067; NAS 1.15:105687) Avail: CASI HC A03/MF A01

An experimental investigation was conducted in the NASA Lewis 10 x 10 ft supersonic Wind Tunnel to determine the performance characteristics of 2D hypersonic exhaust nozzles/afterbodies at low supersonic conditions. Generally, this type of application requires a single expansion ramp nozzle (SERN) that is highly integrated with the airframe of the hypersonic vehicle. At design conditions (hypersonic speeds), the nozzle generally exhibits acceptable performance. At off-design conditions (transonic to mid-supersonic speeds), nozzle performance of a fixed geometry configuration is generally poor. Various 2-D nozzle configurations were tested at off-design conditions from Mach 2.0 to 3.5. Performance data is presented at nozzle pressure ratios from 1 to 35. Jet exhaust was simulated with high-pressure air. To study performance of different geometries, nozzle configurations were varied by interchanging the following model parts: internal upstream contour, expansion ramp, sidewalls, and cowl. Author

N93-15359*# National Aeronautics and Space Administration. Lewis Research Center, Cleveland, OH.

OPTIMIZATION OF CIRCULAR ORIFICE JETS MIXING INTO A HEATED CROSS FLOW IN A CYLINDRICAL DUCT

J. T. Kroll (California Univ., Irvine.), W. A. Sowa (California Univ., Irvine.), G. S. Samuelsen (California Univ., Irvine.), and J. D. Holdeman Dec. 1992 19 p Presented at the 31st Aerospace Sciences Meeting and Exhibit, Reno, NV, 11-14 Jan. 1993; sponsored by AIAA

(Grant NAG3-1110; RTOP 537-02-20)

(NASA-TM-105984; E-7508; NAS 1.15:105984; AIAA Paper 93-0249)

Avail: CASI HC A03/MF A01; 2 functional color pages

To examine the mixing characteristics of circular jets in an axisymmetric can geometry, temperature measurements were obtained downstream of a row of cold jet injected into a heated cross stream. The objective was to obtain uniform mixing within one duct radius downstream of the leading edge of the jet orifices. An area weighted standard deviation of the mixture fraction was used to help quantify the degree of mixedness at a given plane. Non-reacting experiments were conducted to determine the influence of the number of jets on the mixedness in a cylindrical configuration. Results show that the number of orifices significantly impacts the mixing characteristics of jets injected from round hole orifices in a can geometry. Optimum mixing occurs when the mean jet trajectory aligns with the radius which divides the cross sectional area of the can into two equal parts at one mixer radius downstream of the leading edge of the orifice. The optimum number of holes at momentum-flux ratios of 25 and 52 is 10 and 15 respectively. Author

N93-15403*# National Aeronautics and Space Administration. Lewis Research Center, Cleveland, OH.

ACOUSTIC MODE MEASUREMENTS IN THE INLET OF A MODEL TURBOFAN USING A CONTINUOUSLY ROTATING RAKE: DATA COLLECTION/ANALYSIS TECHNIQUES

David G. Hall (Sverdrup Technology, Inc., Brook Park, OH.), Laurence Heidelberg, and Kevin Konno Jan. 1993 14 p Presented at the 31st Aerospace Sciences Meeting, Reno, NV, 11-14 Jan. 1993; Sponsored by AIAA

(RTOP 535-03-10)

(NASA-TM-105936; E-7452; NAS 1.15:105936; AIAA Paper 93-0599)

Avail: CASI HC A03/MF A01

The rotating microphone measurement technique and data analysis procedures are documented which are used to determine circumferential and radial acoustic mode content in the inlet of the Advanced Ducted Propeller (ADP) model. Circumferential acoustic mode levels were measured at a series of radial locations using the Doppler frequency shift produced by a rotating inlet microphone probe. Radial mode content was then computed using a least squares curve fit with the measured radial distribution for each circumferential mode. The rotating microphone technique is superior to fixed-probe techniques because it results in minimal interference with the acoustic modes generated by rotor-stator interaction. This effort represents the first experimental implementation of a measuring technique developed by T. G. Sofrin. Testing was performed in the NASA Lewis Low Speed Anechoic Wind Tunnel at a simulated takeoff condition of Mach 0.2. The design is included of the data analysis software and the performance of the rotating rake apparatus. The effect of experiment errors is also discussed. Author

N93-15521*# National Aeronautics and Space Administration. Lewis Research Center, Cleveland, OH.

AN INTEGRAL EQUATION SOLUTION FOR MULTISTAGE TURBOMACHINERY DESIGN CALCULATIONS

Eric R. McFarland 1993 12 p Proposed for presentation at the 38th International Gas Turbine and Aeroengine Congress and Exposition, Cincinnati, OH, 24-27 May 1993; sponsored by ASME

(RTOP 505-62-52)

(NASA-TM-105970; E-7493; NAS 1.15:105970) Avail: CASI HC A03/MF A01

A method was developed to calculate flows in multistage turbomachinery. The method is an extension of quasi-three-dimensional blade-to-blade solution methods. Governing equations for steady compressible inviscid flow are linearized by introducing approximations. The linearized flow equations are solved using integral equation techniques. The flows through both stationary and rotating blade rows are determined in a single calculation. Multiple bodies can be modelled for each blade row, so that arbitrary blade counts can be analyzed. The method's benefits are its speed and versatility. Author

N93-15525*# National Aeronautics and Space Administration. Lewis Research Center, Cleveland, OH.

PROPULSION SYSTEM PERFORMANCE RESULTING FROM AN INTEGRATED FLIGHT/PROPULSION CONTROL DESIGN

Duane Mattern (Sverdrup Technology, Inc., Brook Park, OH.) and Sanjay Garg Oct. 1992 22 p Presented at the AIAA Guidance, Navigation, and Control Conference, Hilton Head, SC, 10-12 Aug. 1992; sponsored by AIAA Previously announced in IAA as A92-55281

(RTOP 505-62-50)

(NASA-TM-105874; E-7339; NAS 1.15:105874) Avail: CASI HC A03/MF A01

Propulsion-system-specific results are presented from the application of the integrated methodology for propulsion and airframe control (IMPAC) design approach to integrated flight/propulsion control design for a 'short takeoff and vertical landing' (STOVL) aircraft in transition flight. The IMPAC method is briefly discussed and the propulsion system specifications for the integrated control design are examined. The structure of a linear engine controller that results from partitioning a linear centralized controller is discussed. The details of a nonlinear propulsion control system are presented, including a scheme to protect the engine operational limits: the fan surge margin and the acceleration/deceleration schedule that limits the fuel flow. Also, a simple but effective multivariable integrator windup protection scheme is examined. Nonlinear closed-loop simulation results are presented for two typical pilot commands for transition flight: acceleration while maintaining flightpath angle and a change in flightpath angle while maintaining airspeed. The simulation nonlinearities include the airframe/engine coupling, the actuator and sensor dynamics and limits, the protection scheme for the engine operational limits, and the integrator windup protection. Satisfactory performance of the total airframe plus engine system for transition flight, as defined by the specifications, was maintained during the limit operation of the closed-loop engine subsystem. Author

N93-15168# Dornier System G.m.b.H., Friedrichshafen (Germany).

INTEGRATED ENGINE CONTROL AND MONITORING WITH EXPERIENCES DERIVED FROM OLMOS [INTEGRIERTE TRIEBWERKSREGELUNG UND -UEBERWACHUNG MIT ERFAHRUNGEN AUS OLMOS]

Uwe Schulz and Julian Bott *In* DLR, Proceedings of the 16th Symposium on Aircraft Integrated Monitoring Systems Jan. 1992 p 287-310 (For primary document see N93-15152 04-06)

Avail: CASI HC A03/MF A06; DLR, Wissenschaftliches Berichtswesen, Postfach 90 60 58, Cologne, Germany, HC

N93-15171# Airbus Industrie, Blagnac (France).

MONITORING OF POWERPLANTS IN ADVANCED COMMERCIAL AIRCRAFT [TRIEBWERKSUEBERWACHUNG IN MODERNEN VERKEHRSFLUGZEUGEN]

Antoine Vieillard *In* DLR, Proceedings of the 16th Symposium on Aircraft Integrated Monitoring Systems Jan. 1992 p 361-372 (For primary document see N93-15152 04-06)

Avail: CASI HC A03/MF A06; DLR, Wissenschaftliches Berichtswesen, Postfach 90 60 58, Cologne, Germany, HC

N93-15172# Motoren- und Turbinen-Union Muenchen G.m.b.H. (Germany).

EJ 200 ENGINE MONITORING SYSTEM: ON- AND OFF-BOARD DATA CAPTURE, ANALYSIS, AND MANAGEMENT SYSTEM [EJ 200 TRIEBWERKS-UEBERWACHUNGS-SYSTEM ON- UND OFF-BOARD DATENERFASSUNG, ANALSE, UND MANAGEMENT SYSTEM]

P. Stadlmeier *In* DLR, Proceedings of the 16th Symposium on Aircraft Integrated Monitoring Systems Jan. 1992 p 373-389 (For primary document see N93-15152 04-06)

Avail: CASI HC A03/MF A06; DLR, Wissenschaftliches Berichtswesen, Postfach 90 60 58, Cologne, Germany, HC

N93-15173# Motoren- und Turbinen-Union Muenchen G.m.b.H. (Germany).

RB199 ENGINE OIL SYSTEM FAILURE DIAGNOSTICS BY COMPARISON OF MEASURED AND CALCULATED OIL CONSUMPTION USING THE OLMOS ON-BOARD MONITORING SYSTEM [STOERUNGSDIAGNOSE FUER DAS RB199-OELSYSTEM DURCH VERGLEICH ZWISCHEN GEMESSENEN UND MIT DEM OLMOS ON-BOARD UEBERWACHUNGSSYSTEM GERECHNETEN OELVERBRAEUCHEN]

H. Pfoertner and H. Streifinger *In* DLR, Proceedings of the 16th Symposium on Aircraft Integrated Monitoring Systems Jan. 1992 p 391-414 Sponsored by Bundesministerium der Verteidigung (For primary document see N93-15152 04-06)

Avail: CASI HC A03/MF A06; DLR, Wissenschaftliches Berichtswesen, Postfach 90 60 58, Cologne, Germany, HC

N93-15174# General Electric Co., Cincinnati, OH. Aircraft Engines.

A PHILOSOPHY FOR INTEGRATED MONITORING SYSTEM DESIGN [GRUNDSAEZLICHE UEBERLEGUNGEN ZUR ENTWICKLUNG INTEGRIERTER UEBERWACHUNGSSYSTEME]

David L. Doel *In* DLR, Proceedings of the 16th Symposium on Aircraft Integrated Monitoring Systems Jan. 1992 p 415-432 (For primary document see N93-15152 04-06)

Avail: CASI HC A03/MF A06; DLR, Wissenschaftliches Berichtswesen, Postfach 90 60 58, Cologne, Germany, HC

N93-15175# Universitaet der Bundeswehr, Hamburg (Germany).
SOME EXPERIMENTS AND IDEAS ON GPA BEFORE REACHING STEADY STATE OF ENGINE [EINIGE EXPERIMENTE UND UEBERLEGUNGEN UEBER GPA VOR ERREICHEN DES STATIONAEREN ZUSTANDES DES TRIEBWERKS]
K. Fiedler, R. Lunderstaedt, and K.-J. Schmidt *In* DLR, Proceedings of the 16th Symposium on Aircraft Integrated Monitoring Systems Jan. 1992 p 433-454 (For primary document see N93-15152 04-06)
Avail: CASI HC A03/MF A06; DLR, Wissenschaftliches Berichtswesen, Postfach 90 60 58, Cologne, Germany, HC

N93-15176# Technische Univ., Munich (Germany).
EXPERIMENTAL ANALYSIS OF STEADY-STATE AND DYNAMIC MONITORING OF POWER SHAFT TURBINES [ZUR EXPERIMENTELLEN ANALYSE DER STATIONAEREN UND DYNAMISCHEN ZUSTANDSUEBERWACHUNG VON WELLENLEISTUNGSTRIEBWERKEN]
S. Bogner, G. Kappler, and H. Rick *In* DLR, Proceedings of the 16th Symposium on Aircraft Integrated Monitoring Systems Jan. 1992 p 455-482 (For primary document see N93-15152 04-06)
Avail: CASI HC A03/MF A06; DLR, Wissenschaftliches Berichtswesen, Postfach 90 60 58, Cologne, Germany, HC

08 AIRCRAFT STABILITY AND CONTROL

Includes aircraft handling qualities; piloting; flight controls; and autopilots.

For related information see also *05 Aircraft Design, Testing and Performance.*

N93-14252# Air Force Inst. of Tech., Wright-Patterson AFB, OH. School of Engineering.
AN EXAMINATION OF WING ROCK FOR THE F-15 M.S. Thesis
Michael T. Davison Feb. 1992 169 p
(AD-A256613; AFIT/GAE/ENY/92M-01) Avail: CASI HC A08/MF A02

Wing rock in the F-15 was examined both analytically and experimentally. Using a previously developed model for the F-15, bifurcation analysis and continuation techniques were used to map out the periodic wing rock solutions and the equilibrium solutions leading up to wing rock. This was done for four maneuvers: a 1 g stall, rudder sweeps, constant bank turns, and a symmetric pullup. To supplement this research, time history simulations were used to examine the time history of wing rock. A study of stability derivatives was also performed to determine the critical parameters in wing rock. Bifurcation was also used to study candidate feedback architectures used to suppress wing rock. It was found that feeding back roll rate was effective in delaying wing rock onset and suppressing the subsequent motion, but this made the aircraft more departure prone. The results of the 1 g stall, constant bank turns, and the symmetric pullup were experimentally tested through flight test. Wing rock onset differed 4 degrees AOA from that predicted in all maneuvers but the symmetric pullup, where the flight Mach number correlated with the computer model's flight condition/wing rock was found to be highly random and non periodic, directly contradicting computer predictions and prior research. GRA

N93-14447 Queens Univ., Belfast (Northern Ireland).
DIGITAL BANK-TO-TURN CONTROL AND GUIDANCE Ph.D. Thesis
George McConnell 1988 371 p
Avail: Univ. Microfilms Order No. BRDX96927

This thesis investigates the application of optimal digital control and estimation techniques to bank-to-turn (BTT), command to line-of-sight (CLOS) guidance. Initially it is assumed that the missile is ideal and thus responds instantaneously to the demands issued by the guidance law. In addition motion is restricted to a single-plane. Controllers are designed for both stationary and moving sightline engagements and discrete system tuning parameters derived. Subsequently these ideal missile designs are modified to take the actual missile dynamic lags into account and a full three dimensional control strategy proposed. These optimal digital controllers are then compared with those designed using classical frequency domain techniques and discrete pole placement. A multivariable BTT autopilot is developed which uses rudder action to reduce the level of roll induced cross coupling between the lateral dynamics. The autopilot contains integral action and uses a multivariable notch filter. Optimal multirate digital control theory is used to reduce the autopilot's computational requirements. The single-plane practical missile designs are repeated using optimal multirate estimation and control techniques to combine slow measurements generated by ground based tracking equipment with more frequent measurements obtained from missile based sensors. The potential benefits arising from the use of this technique are demonstrated. Classical and modern homing guidance laws are reviewed and then extended to take into account missile dynamic lags. The conditions under which the various homing guidance laws should be used are discussed. Finally the merger of CLOS and homing guidance laws to yield improved coverage boundaries and reduced miss distance is considered. Dissert. Abstr.

N93-14608# Air Force Inst. of Tech., Wright-Patterson AFB, OH. School of Engineering.
MULTIPLE MODEL ADAPTIVE ESTIMATION APPLIED TO THE VISTA F-16 WITH ACTUATOR AND SENSOR FAILURES M.S. Thesis
Timothy E. Menke 1 Jun. 1992 222 p
(AD-A256444; AFIT/GA/ENG/92J-01) Avail: CASI HC A10/MF A03

A Multiple Model Adaptive Estimation (MMAE) algorithm is applied to the Variable Stability In-flight Simulator Test Aircraft (VISTA) F-16 at a low dynamic pressure flight condition (0.4 Mach at 20,000 ft). A complete F-16 flight control system is modeled containing the longitudinal and lateral-directional axes. Single and dual actuator and sensor failures are simulated including: complete actuator failures, partial actuator failures, complete sensor failures, increased sensor noise, sensor biases, dual complete actuator failures, dual complete sensor failures, and combinations of actuator and sensor failures. Failure scenarios are examined in both maneuvering and straight and level flight conditions. Single scalar residual monitoring techniques are evaluated with suggestions for improved performance. A hierarchical moving bank structure is utilized for multiple failure scenarios. Simultaneous dual failures are included within the study. White Gaussian noise is included to simulate the effects of atmospheric disturbances, and white Gaussian noise is added to the measurements to simulate the effects of sensor noise. GRA

N93-14811*# McDonnell Aircraft Co., Saint Louis, MO.
ADVANCED AEROSERVOELASTIC STABILIZATION TECHNIQUES FOR HYPERSONIC FLIGHT VEHICLES
Samuel Y. Chan, Peter Y. Cheng, Thomas T. Myers (Systems Technology, Inc., Hawthorne, CA.), David H. Klyde (Systems Technology, Inc., Hawthorne, CA.), Raymond E. Magdaleno (Systems Technology, Inc., Hawthorne, CA.), and Duane T. McRuer (Systems Technology, Inc., Hawthorne, CA.) Nov. 1992 112 p
(Contract NAS1-18763; RTOP 505-70-64-01)
(NASA-CR-189702; NAS 1.26:189702) Avail: CASI HC A06/MF A02

Advanced high performance vehicles, including Single-Stage-To-Orbit (SSTO) hypersonic flight vehicles, that are statically unstable, require higher bandwidth flight control systems to compensate for the instability resulting in interactions between the flight control system, the engine/propulsion dynamics, and the low frequency structural modes. Military specifications, such as MIL-F-9490D and MIL-F-87242, tend to limit treatment of structural modes to conventional gain stabilization techniques. The conventional gain stabilization techniques, however, introduce low frequency effective time delays which can be troublesome from a flying qualities standpoint. These time delays can be alleviated by appropriate blending of gain and phase stabilization techniques (referred to as Hybrid Phase Stabilization or HPS) for the low frequency structural modes. The potential of using HPS for compensating structural mode interaction was previously explored. It was shown that effective time delay was significantly reduced with the use of HPS; however, the HPS design was seen to have greater residual response than a conventional gain stablized design. Additional work performed to advance and refine the HPS design procedure, to further develop residual response metrics as a basis for alternative structural stability specifications, and to develop strategies for validating HPS design and specification concepts in manned simulation is presented. Stabilization design sensitivity to structural uncertainties and aircraft-centered requirements are also assessed. Author

N93-14830 Georgia Inst. of Tech., Atlanta.
FINITE-STATE INFLOW APPLIED TO AEROELASTIC FLUTTER OF

FIXED AND ROTATING WINGS Ph.D. Thesis
Bruce David Nibbelink 1992 154 p
Avail: Univ. Microfilms Order No. DA9231746

A new p-type, finite-state, aerodynamic theory is used in the aeroelastic analysis of a fixed wing and a rotating wing in hover. The helicopter inflow theory is modified for application to a fixed-wing, or stopped-rotor configuration. The structural models are linear for both configurations, with elastic bending and torsion degrees of freedom. Results are compared with those using Theodorsen and Loewy theories, respectively, for the fixed and rotating wings. These results include steady and unsteady sectional lift distributions, as well as frequency and damping values as a function of the location of the centroidal axis. For the fixed wing, it is shown that dynamic inflow theory gives good qualitative behavior for the lift and aeroelastic properties of the limiting, stopped-rotor case. For the rotating wing, the results give new insight into the physics of the complex inflow/blade dynamics system. With the identification of both structural and aerodynamic modes, the involved frequency content of the flow is seen in a new, more detailed perspective. Dissert. Abstr.

N93-14831*# National Aeronautics and Space Administration. Lewis Research Center, Cleveland, OH.
ICING EFFECTS ON AIRCRAFT STABILITY AND CONTROL DETERMINED FROM FLIGHT DATA: PRELIMINARY RESULTS
T. P. Ratvasky and R. J. Ranaudo Jan. 1993 28 p Presented at the 31st Aerospace Sciences Meeting and Exhibit, Reno, NV, 11-14 Jan. 1993
(RTOP 505-68-10)
(NASA-TM-105977; E-7500; NAS 1.15:105977; AIAA Paper 93-0398)
Avail: CASI HC A03/MF A01

The effects of airframe icing on the stability and control characteristics of the NASA DH-6 Twin Otter icing research aircraft were investigated by flight test. The flight program was developed to obtain the stability and control parameters of the DH-6 in a baseline ('uniced') configuration and an 'artificially iced' configuration for specified thrust conditions. Stability and control parameter identification maneuvers were performed over a wide range of angles of attack for wing flaps retracted (0 deg) and wing flaps partially deflected (10 deg). Engine power was adjusted to hold thrust constant at one of three thrust coefficients (C(sub T) = 0.14, C(sub T) = 0.07, C(subT) = 0.00). This paper presents only the pitching- and yawing-moment results from the flight test program. Stability and control parameters were estimated for the uniced and artificially iced configurations using a modified stepwise regression algorithm. Comparisons of the uniced and iced stability and control parameters are presented for the majority of the flight envelope. The artificial ice reduced the elevator and rudder control effectiveness by 12 percent and 8 percent respectively for the 0 deg flap setting. The longitudinal static stability was also decreased substantially (approximately 10 percent) because of the tail ice. Further discussion is provided to explain some of the effects of ice on the stability and control parameters. Author

N93-14835 Princeton Univ., NJ.
ROBUST NONLINEAR FEEDBACK GUIDANCE FOR AN AEROSPACE PLANE: A GEOMETRIC APPROACH Ph.D. Thesis
Markus Antonius vanBuren 1992 250 p
Avail: Univ. Microfilms Order No. DA9230652

Single-stage-to-orbit vehicles using airbreathing propulsion -- referred to as aerospace planes -- hold promise for more economical delivery of payload to low Earth orbit. Feedback guidance logic is developed for efficiently and effectively steering such a vehicle through the atmosphere and into orbit. Accurate and robust regulation of the vehicle translational dynamics is considered first. A nonlinear design approach drawing from singular perturbations, feedback linearization, and variable structure control is employed to synthesize regulators which lead to similar dynamic behavior over the entire flight envelope. The design approach provides for a systematic way to counter disturbance effects as well as modeling uncertainties. Differential geometry provides a common framework for the three nonlinear feedback control methodologies. The two-time-scale behavior present in the vehicle translational dynamics allows the state space to be decomposed into an invariant slow manifold and an invariant foliation of fast manifolds. Feedback guidance logic with robust performance is obtained by synthesizing a composite feedback control from a slow control for the regulation of the nominal slow dynamics along the slow manifold and a fast control for robust tracking of the slow manifold in the presence of atmospheric disturbances and modeling errors. The tracking problem is solved as a family of stabilization problems along the fast foliation, using the feedback linearization methodology. In the presence of boundable disturbances, uniform ultimate boundedness of the exactly linearized fast dynamics can be ensured through application of a smoothed variable structure controller. The two-time-scale decomposition also provides the basis for developing feedback guidance logic for steering and accelerating an aerospace plane along the super- and hypersonic segments of a near-minimum fuel ascent trajectory. Accurate solutions of the minimum-fuel ascent problem show the effects of dynamic pressure, axial load, and heating rate constraints and establish a basis for the development and assessment of the guidance logic. The minimum-fuel ascent trajectories are found to track the ascent corridor constraints. This characterization permits the formulation of the robust near-minimum-fuel ascent guidance problem as a robust tracking problem, which is amenable to the geometric feedback synthesis approach. Dissert. Abstr.

N93-15366*# National Aeronautics and Space Administration. Langley Research Center, Hampton, VA.
SIMULATOR EVALUATION OF DISPLAYS FOR A REVISED TAKEOFF PERFORMANCE MONITORING SYSTEM
David B. Middleton, Raghavachari Srivatsan (Vigyan Research Associates, Inc., Hampton, VA.), and Lee H. Person, Jr Washington Dec. 1992 45 p
(RTOP 505-66-01-02)
(NASA-TP-3270; L-16761; NAS 1.60:3270) Avail: CASI HC A03/MF A01

Cockpit displays for a Takeoff Performance Monitoring System (TOPMS) to provide pilots with graphic and alphanumeric information pertinent to their decision to continue or abort a takeoff are evaluated. Revised head-down and newly developed head-up displays were implemented on electronic screens in the real-time Transport Systems Research Vehicle (TSRV) Simulator for the Boeing 737 airplane at the Langley Research Center and evaluated by 17 NASA, U.S. Air Force, airline, and industry pilots. Both types of displays were in color, but they were not dependent upon it. The TOPMS head-down display is composed of a runway graphic overlaid with symbolic status and advisory information related to both the expected takeoff point and the predicted stop point (in the event an abort becomes necessary). In addition, an overall Situation Advisory Flag indicates a preferred course of action based on analysis of the various elements of airplane performance and system status. A simpler head-up display conveys most of this same information and relates it to the visual scene. The evaluation pilots found the displays to be credible, easy to monitor, and appropriate for the task. In particular, the pilots said the head-up display was monitored with very little effort and did not obstruct or distract them from monitoring the simulated out-the-window runway scene. This report augments NASA TP-2908, 1989. Author

N93-15396# Naval Air Warfare Center, Patuxent River, MD. Aircraft Div.
F/A-18 CONTROLS RELEASED DEPARTURE RECOVERY FLIGHT TEST EVALUATION
David L. Prater, Marc G. Stevens, and James B. Lackey 1991 20 p
(AD-A256522) Avail: CASI HC A03/MF A01

The F/A-18 has had a history of numerous departures from controlled flight during operational fleet use. Several of these departures have resulted in mishaps. The current flight manual procedure requires the pilot to neutralize the control stick for departure recovery, however many F/A-18 departures are characterized by high lateral forces making it difficult to maintain neutral longitudinal and lateral control stick position. Recent mishap investigations have questioned the viability of releasing the control stick as a more effective way of maintaining neutral controls thereby reducing recovery times. The Naval Air Warfare Center--Aircraft Division was tasked by Naval Air Systems Command to determine if releasing the control stick during departure recovery would result in any airplane induced control inputs that would delay recovery. Additionally, from the desire to improve departure awareness of all F/A-18 pilots, an assessment was made of the suitability of the test maneuvers for inclusion into an airborne departure recognition and out-of-control flight training syllabus. Testing was conducted using a fleet representative F/A-18D which did not incorporate any non-production emergency recovery devices (i.e., no spin recovery chute). Test maneuvers included both high and low angle of attack departures up to 0.80 IMN. GRA

09 RESEARCH AND SUPPORT FACILITIES (AIR)

Includes airports, hangars and runways; aircraft repair and overhaul facilities; wind tunnels; shock tubes; and aircraft engine test stands.

For related information see also *14 Ground Support Systems and Facilities (Space).*

N93-14128# Army Engineer Waterways Experiment Station, Vicksburg, MS. Geotechnical Lab.

IN SITU MATERIAL CHARACTERIZATION FOR PAVEMENT EVALUATION BY THE SPECTRAL-ANALYSIS-OF-SURFACE-WAVES (SASW) METHOD Final Report

Don R. Alexander Jul. 1992 171 p

(AD-A255660; WES/TR/GL-92-10) Avail: CASI HC A08/MF A02

Spectral-analysis-of-surface-waves (SASW) is a method of nondestructive testing for material characterization of pavement systems. SASW is based on the theory of stress waves propagating in elastic media with the key elements being the generation and measurement of Rayleigh waves. From these measurements, shear wave velocity and modulus profiles can be obtained for multilayered elastic systems. SASW tests were conducted on six airfield pavement sites. Young's modulus profiles from SASW were compared with moduli backcalculated using falling weight deflectometer test results and with laboratory values. Results indicate that SASW is a viable method for in situ characterization of pavement materials. Automation of testing and analyses techniques is needed for routine pavement evaluations. Research is needed to evaluate low strain effects on the moduli for surface, base, and subgrade materials and the effect of reflected waves on SASW measurements. GRA

N93-14238# Army Engineer Waterways Experiment Station, Vicksburg, MS. Geotechnical Lab.

REANALYSIS OF MULTIPLE-WHEEL LANDING GEAR TRAFFIC TESTS Final Report

Richard G. Ahlvin and Jim W. Hall, Jr. Sep. 1992 35 p

(AD-A256593; WES/MP/GL-92-32) Avail: CASI HC A03/MF A01

Growth of aircraft to over a million pounds, with the need for many wheels to support such aircraft, has focused attention on the unduly conservative aspect of present equivalent single wheel load (ESWL) methods when applied to many grouped wheels. The assembly of all multiple-wheel accelerated traffic test data for use in reexamining ESWL methods provided an indication that the earliest multiple-wheel tests likely were treated extremely conservatively during their analysis some 40 years ago. Accordingly, these early tests (reported in TM 3-349) were subjected to a reexamination. The reexamination confirmed that the initial analysis was quite conservatively carried out. With the benefit of the added 40 years of research findings and experience with in-service pavements, a less conservative analysis can now be made and accepted with confidence. This report presents the reanalysis carried out and the revised pavement behavior indicated. GRA

N93-14559# Aerospace Medical Research Labs., Brooks AFB, TX.

ADVANTAGES OF USING A PROJECTED HEAD-UP DISPLAY IN A FLIGHT SIMULATOR Final Report, Jan. 1991 - Jun. 1992

Philipp W. Peppler Jul. 1992 14 p

(AF Proj. 1123)

(AD-A255332; AL-TR-1992-0042) Avail: CASI HC A03/MF A01

When viewing a real planar image through an aircraft head-up display (HUD) focused for 'infinity,' diplopia and other related problems render the HUD useless as a training device. Future flight simulator visual displays are being developed with real planar image projections; therefore, this problem must be resolved. Past research into decollimating aircraft HUD's for real planar visual displays presented several solutions, but major side effects limited the tasks that could be trained with a decollimated HUD. Recent advances in projector and graphics technology have made projecting a real planar HUD an attractive solution. Projected HUD technology at Armstrong Laboratory, Aircrew Training Research Division, Williams AFB, Arizona is described. The advantages of using a projected HUD were investigated and are discussed. Advantages of using projected HUDs in simulators with a real planar visual display are numerous. Projected HUD's are undoubtedly a technology for tomorrow. GRA

N93-14809*# MCAT Inst., San Jose, CA.

STUDY OF OPTICAL TECHNIQUES FOR THE AMES UNITARY WIND TUNNEL. PART 5: INFRARED IMAGERY Progress Report

George Lee Nov. 1992 32 p

(Contract NCC2-716)

(NASA-CR-191385; NAS 1.26:191385; MCAT-92-020) Avail: CASI HC A03/MF A01

A survey of infrared thermography for aerodynamics was made. Particular attention was paid to boundary layer transition detection. IR thermography flow visualization of 2-D and 3-D separation was surveyed. Heat transfer measurements and surface temperature measurements were also covered. Comparisons of several commercial IR cameras were made. The use of a recently purchased IR camera in the Ames Unitary Plan Wind Tunnels was studied. Optical access for these facilities and the methods to scan typical models was investigated. Author

N93-15498*# National Aeronautics and Space Administration. Lewis Research Center, Cleveland, OH.

USER MANUAL FOR NASA LEWIS 10 BY 10 FOOT SUPERSONIC WIND TUNNEL

Ronald H. Soeder 1992 54 p

(RTOP 505-62-84)

(NASA-TM-105626; E-6967; NAS 1.15:105626) Avail: CASI HC A04/MF A01

This manual describes the 10- by 10-Foot Supersonic Wind Tunnel at the NASA Lewis Research Center and provides information for users who wish to conduct experiments in this facility. Tunnel performance operating envelopes of altitude, dynamic pressure, Reynolds number, total pressure, and total temperature as a function of test section Mach number are presented. Operating envelopes are shown for both the aerodynamic (closed) cycle and the propulsion (open) cycle. The tunnel test section Mach number range is 2.0 to 3.5. General support systems, such as air systems, hydraulic system, hydrogen system, fuel system, and Schlieren system, are described. Instrumentation and data processing and acquisition systems are also described. Pretest meeting formats and schedules are outlined. Tunnel user responsibility and personnel safety are also discussed. Author

N93-14616# Mooij and Associates, Oegstgeest (Netherlands).

FLIGHT SIMULATION LEAVES THE GROUND

H. A. Mooij *In* NAL, Symposium on the Occasion of the Farewell of Prof. Dr. Ir. O. H. Gerlach as Chairman of the Board of the Foundation National Aerospace Laboratory NLR, The Netherlands 1991 p 59-84

(For primary document see N93-14613 04-01)

Avail: CASI HC A03/MF A01

12 ASTRONAUTICS (GENERAL)

For extraterrestrial exploration see *91 Lunar and Planetary Exploration.*

N93-14920# Canadian Space Agency, Ottawa (Ontario).

PROCEEDINGS OF THE SIXTH CASI CONFERENCE ON ASTRONAUTICS

Victor A. Wehrle, comp. Canadian Aeronautics and Space Inst. 1990 523 p Conference held in Ottawa, Ontario, 19-21 Nov. 1990

(CTN-92-60336) Avail: Canadian Aeronautics and Space Inst., 222 Somerset St. W., Suite 601, Ottawa, Ontario K2P 0J1 Canada

These proceedings comprise a compendium of scientific and technical work currently underway in industries, universities, and government concerning the Canadian space program. It also provides a perspective on the impact of education and human resource development on the future of space related research in Canada. Specific topics covered include robotics and automation, space electronics, spacecraft integration and testing, space technology, space physics and earth observation, satellite communications, science and technology issues in the exploration of space, and the development of education programs for space industries. For individual titles, see N93-14921 through N93-14963.

N93-14921# Canadian Space Society, Downsview (Ontario).

THE CANADIAN SOLAR SAIL PROJECT **c18**

Istvan Horvath, Kieran A. Carroll, and Andrew Williams *In* Canadian

Space Agency, Proceedings of the Sixth CASI Conference on Astronautics 1990 6 p Previously announced in IAA as A91-34927 (For primary document see N93-14920 04-12)
Avail: Canadian Aeronautics and Space Inst., 222 Somerset St. W., Suite 601, Ottawa, Ontario K2P 0J1 Canada

Details are provided of the design of the Canadian solar sail spacecraft which is to compete with other participating countries in a race to Mars. This competition is to be held in 1992 to commemorate the 500th anniversary of Columbus' historic voyage. The race is also intended to demonstrate and promote interest in solar sailing as a new propulsion technology. To be competitive in the race acceleration must be maximized. Maximum acceleration can be obtained by maximizing the area of the reflecting surface (the sail) while minimizing mass. The present configuration uses a spin stabilized sail composed of thirty radial vanes. Centripetal force will be used to aid vane deployment and to rigidize each vane. Three of the vanes will be variable pitch vanes which are used for spin control. The sail is made of aluminized kapton. The spacecraft will be launched with a spin about its main axis. The three variable pitch vanes will open first, reducing the spacecraft spin. This will permit the attitude sensing and control equipment to function. An offset mass is used to perform attitude control and sailing trim for the two axes of rotation within the plane of the sail. The third attitude control axis is controlled by the variable pitch vanes. A camera package will be placed on the spacecraft to observe spacecraft deployment. Author (CISTI)

N93-14922# Deputy Assistant Secretary of Defense (Environmental Quality), Washington, DC.
HUMAN EXPLORATION: MOON/MARS MISSION c91
Douglas A. OHandley *In* Canadian Space Agency, Proceedings of the Sixth CASI Conference on Astronautics 1990 9 p (For primary document see N93-14920 04-12)
Avail: Canadian Aeronautics and Space Inst., 222 Somerset St. W., Suite 601, Ottawa, Ontario K2P 0J1 Canada

With the initial launch of the elements of Space Station Freedom in 1992, America and her partners will become permanent residents of space. Establishment of the beginnings of what will become a permanent settlement on the moon is planned for early in the next century. Following that, extension of exploration and settlement to Mars is planned. This paper includes an outline of the early stages in the planning and development process. Currently, a group of senior specialists called the Synthesis group is soliciting ideas from the public, universities, and agencies of the US Government with a report expected in 1991. This group is establishing reference mission architectures, prioritizing a list of critical technologies, and identifying visible milestones on the way to the ultimate goal. In the near term, activities will include further analysis of the architectures developed in the Synthesis process. A wide array of system level studies will be performed at NASA and development of critical technologies will continue. Enabling technologies will be defined. The major priority in the near term will be the initiation of the long-lead development program required for a heavy-lift launch vehicle. Author (CISTI)

N93-14923# Victoria Univ. (British Columbia). Dept. of Mechanical Engineering.
COOPERATIVE CONTROL OF MULTIPLE SPACE MANIPULATORS c37
M. Nahon and J. Angeles (McGill Univ., Montreal, Quebec) *In* Canadian Space Agency, Proceedings of the Sixth CASI Conference on Astronautics 1990 10 p Previously announced in IAA as A91-34929 (For primary document see N93-14920 04-12)
Avail: Canadian Aeronautics and Space Inst., 222 Somerset St. W., Suite 601, Ottawa, Ontario K2P 0J1 Canada

The control of multi-armed robotic systems is inherently more complex than that of single-arm systems. Whereas a single manipulator can be controlled purely through positions or velocities, multiple manipulators handling a common payload must also be controlled in terms of forces. In this paper, the problem of finding force setpoints for the controller is formulated as a constrained optimization problem where the constraints are provided by the dynamics equations and the actuator capabilities. A number of potential objective functions which may be minimized are reviewed including the internal force, a norm of the vector of actuator torques and power losses in the system. These are then compared for a task in which the Special Purpose Dextrous Manipulator (SPDM) moves a payload in the absence of gravity. It is concluded that the actuator torque criterion appears to offer the worst compromise in performance, while the minimum internal force and minimum power loss criteria each have their advantages. Author (CISTI)

N93-14924# Spar Aerospace Ltd., Toronto (Ontario).
VISION SYSTEM REQUIREMENTS AND CONCEPT FOR THE SPECIAL PURPOSE DEXTEROUS MANIPULATOR SYSTEM (SPDM) c37
Leon Zucherman *In* Canadian Space Agency, Proceedings of the Sixth CASI Conference on Astronautics 1990 6 p Previously announced in IAA as A91-34930 (For primary document see N93-14920 04-12)
Avail: Canadian Aeronautics and Space Inst., 222 Somerset St. W., Suite 601, Ottawa, Ontario K2P 0J1 Canada

Artificial Vision System (AVS) requirements and concept for the Space Station Special Purpose Dexterous Manipulator (SPDM), currently under development for the Canadian Space Station Program, are discussed. The SPDM vision-related requirements are presented. The main purpose of the AVS is to support the SPDM and the Space Station Remote Manipulator System (SSRMS) operations, such as tracking, capturing, handling, berthing tools and Orbital Replacement Units (ORUSs), manipulation of tools, and Tool Change-out Mechanism (TCM) in maintenance and assembly operations. A comparison between the SPDM and the SSRMS vision-assisted operations is made. It is shown that the SPDM operations, in general, and the maintenance and assembly operations, in particular, are not just scaled-up SSRMS operations, but add an extra dimension to the task complexity, and thus introduce unique requirements for the vision system. In the initial implementation, the AVS under development for the SSRMS, is required also to support the SPDM operations. Consequently, the AVS data is to be used to support the operator during manual operation of the SSRMS and/or the SPDM. The AVS data are also provided to the SSRMS and SPDM computers and can be used for automatic tracking operations. The AVS is a distributed system. Its functional configuration and operation are briefly presented. Future work includes studies and trade-offs to be performed, possible improvements on the present solution, as well as alternate concepts in the field of SPDM-related vision. Author (CISTI)

N93-14925# Toronto Univ. (Ontario). Inst. for Aerospace Studies.
MOVE: A NEUTRAL NETWORK PARADIGM FOR ROBOTIC CONTROL c63
Darin P. W. Graham and Gabriele M. T. DeLeuterio *In* Canadian Space Agency, Proceedings of the Sixth CASI Conference on Astronautics 1990 14 p Previously announced in IAA as A91-34931 (For primary document see N93-14920 04-12)
Avail: Canadian Aeronautics and Space Inst., 222 Somerset St. W., Suite 601, Ottawa, Ontario K2P 0J1 Canada

Manipulator Operations using Value Encoding (MOVE) is an artificial neural network (ANN) paradigm for the control of manipulators. It attempts to encode simple knowledge about the dynamics of a robotic manipulator into a generic ANN structure. The MOVE architecture is based upon the Cerebellar Model Articulation Controller (CMAC) and includes several extensions. The improvements include a method that permits the combining of modules of neural networks in parallel and allow the role of each neuron to dynamically change and in doing so permit layering of finer-tuned networks. Such schemes have shown significant improvement in the overall network's performance. The CMAC is faster than typical back propagation networks by orders of magnitude. It is shown that the two enhancements of the MOVE ANN are faster and more efficient than the CMAC for control of a two-link, planar manipulator. Using MOVE for other control problems and the modeling of chaotic systems have shown similar results. Author (CISTI)

N93-14926# Ottawa Univ. (Ontario).
AN ACTIVE TACTILE PERCEPTION SYSTEM c37
E. Petriu, M. Greenspan, F. Gelinas, W. S. McMath (Canadian Space Agency, Ottawa, Ontario), and S. K. Yeung (Canadian Space Agency, Ottawa, Ontario) *In* Canadian Space Agency, Proceedings of the Sixth CASI Conference on Astronautics 1990 9 p Previously announced in IAA as A91-34932 (For primary document see N93-14920 04-12)
Avail: Canadian Aeronautics and Space Inst., 222 Somerset St. W., Suite 601, Ottawa, Ontario K2P 0J1 Canada

System development and application aspects are described for an experimental robotic system for the tactile perception of the global geometric profile of object surfaces which are larger than the dimensions of the

tactile sensor. Local cutaneous information provided by a tactile sensor is integrated with the kinesthetic position parameters of a robot arm, resulting in a 3D geometric model of the tactile sensor pose on the explored object surface. Currently available tactile sensors provide poor information on the geometric profile of 3D object surfaces. In order to maximize the information available for 3D analysis, an instrumented passive compliant wrist was used to attach a pressure measuring tactile probe to the robot arm carrier. Data was collected by a noncompliant planar sensing array in direct contact with an object surface. Information recorded includes the following: positional and orientation data on the robot arm manipulator, passive compliance kinesthetic data as measured by the kinematics of the wrist, and cutaneous tactile data represented by the binary image of the sensors pose on the object. The dimensions of the sensor array were found to be a critical factor in system performance. Use of a large array results in fewer touch poses being required to explore an object's surface, on the other hand a large planar array will touch fewer and higher peaks thus missing surface detail. To improve performance, there is a need to design tactile sensors specifically for geometric profile measuring. Author (CISTI)

N93-14927# Canadian Space Agency, Ottawa (Ontario).
MULTIPLE FAULT DIAGNOSIS OF SPACECRAFT ELECTRICAL POWER SYSTEMS **c33**
Peter Adamovits *In its* Proceedings of the Sixth CASI Conference on Astronautics 1990 9 p Previously announced in IAA as A91-34933 (For primary document see N93-14920 04-12)
Avail: Canadian Aeronautics and Space Inst., 222 Somerset St. W., Suite 601, Ottawa, Ontario K2P 0J1 Canada

The system described in this paper addresses the fault detection/diagnosis aspects of spacecraft electrical power system management. The Multiple Fault Diagnostic System (MFDS) project is a software implementation of actions performed at a typical ground segment operations center used to control and manage spacecraft subsystem operations. The MFDS software includes many concepts from the artificial intelligence research community including: model based reasoning, distributed knowledge bases, qualitative reasoning, and an assumption based truth maintenance system (ATMS). It is projected that software systems using techniques similar to those described herein will play an increasing role in spacecraft operations on future missions. It is expected that designs such as these will greatly enhance the reliability of ground operations decisions and operational availability of the controlled subsystems. The system is being implemented in Smalltalk/V on a PC clone platform. The model, fault detection system and user interface are now complete. The diagnostic system/ATMS and other MFDS components are now being implemented. Author (CISTI)

N93-14928# Spar Aerospace Ltd., Weston (Ontario).
CANADA'S ROLE IN PUSHING BACK THE FRONTIERS OF SPACE
Ian H. Rowe *In* Canadian Space Agency, Proceedings of the Sixth CASI Conference on Astronautics 1990 6 p Previously announced in IAA as A91-34934 (For primary document see N93-14920 04-12)
Avail: Canadian Aeronautics and Space Inst., 222 Somerset St. W., Suite 601, Ottawa, Ontario K2P 0J1 Canada

This paper outlines the history of Canada's involvement in space science. An early interest in upper atmosphere phenomena resulted from the influence of the north magnetic pole on long distance radio communication. With the launch of the ionospheric sounder, Alouette 1, in 1962, Canada became the third nation to have a spacecraft in space. Canada was the first country to provide domestic satellite service for commercial communications with the Anik series of satellites. The latest satellite, the M-SAT will provide two way voice and data services. (Primarily as a result of the work of the Canada Center for Remote Sensing, Canada has been a leader in airborne remote sensing. This interest has continued in the data acquisition and interpretation of space based remote sensing. Radarsat, a remote sensing satellite which will provide synthetic aperture radar imagery at 10 meter resolution is currently in the design stage. The final role has been in the development of STEM (extendable member) devices for manned space flights. The most notable contribution is the Shuttle Remote Manipulator System first flown on Columbia in 1981. Canada's contribution to Space Station Freedom will be the Mobile Servicing System. The current space science program involves study of the universe and solar system, of the near earth environment, and of physical and biological processes occurring in space. Author (CISTI)

N93-14929# Spar Aerospace Ltd., Weston (Ontario).
IN-SITU LUNAR OXYGEN EXTRACTION **c91**
Mark Lozowski *In* Canadian Space Agency, Proceedings of the Sixth CASI Conference on Astronautics 1990 6 p Previously announced in IAA as A91-34935 (For primary document see N93-14920 04-12)
Avail: Canadian Aeronautics and Space Inst., 222 Somerset St. W., Suite 601, Ottawa, Ontario K2P 0J1 Canada

An analysis is presented of a facility for extracting oxygen from lunar regolith for use in a manned space station. Available technologies for lunar oxygen (LUNOX) extraction are reviewed. The most promising involves the hydrogen reduction of ilmenite to iron, titanium oxide, and water followed by the electrolysis of the water to hydrogen and oxygen. It is concluded the best ore extraction and processing approach would involve the following: (1) a simple ballasted scoop regolith excavation; (2) batch ore preparation and benefication to extract the ilmenite ore; (3) ore hydrogenation; and (4) water electrolysis process. An economic analysis of the profitability of the venture indicates that production of oxygen for use in liquid hydrogen/liquid oxygen fuelled spacecraft would be profitable. A parametric analysis of the robustness of the economic analysis was performed in which development costs, launch costs, power requirements, the power to weight ratio of the power supply, and processing facility mass were varied. This analysis indicated that it was highly likely that manufacturing oxygen on the moon would be less costly than importing it from earth. Finally, a strategic analysis performed on the LUNOX facility indicated that Canada has the expertise and experience to undertake the development of such a facility. It is recommended that the project be investigated further. Author (CISTI)

N93-14930# Spar Aerospace Ltd., Weston (Ontario).
PHOTOVOLTAIC POWER SYSTEM FOR A LUNAR BASE **c44**
Kris Karia *In* Canadian Space Agency, Proceedings of the Sixth CASI Conference on Astronautics 1990 10 p Previously announced in IAA as A91-34936 (For primary document see N93-14920 04-12)
Avail: Canadian Aeronautics and Space Inst., 222 Somerset St. W., Suite 601, Ottawa, Ontario K2P 0J1 Canada

An assessment is provided of the viability of using photovoltaic power technology for lunar base application during the initial phase of the mission. The initial user power demands were assumed to be 25 kW (daytime) and 12.5 kW (night time). The effect of lunar adverse environmental conditions were also considered in deriving the photovoltaic power system concept. The solar cell array was found to impose no more design constraints than those solar arrays currently being designed for spacecraft and the Space Station Freedom. The long lunar night and the need to store sufficient energy to sustain a lunar facility during this period was found to be a major design driver. A photovoltaic power system concept was derived using high efficiency thin GaAs solar cells on a deployable flexible Kapton blanket. The solar array design was sized to generate sufficient power for daytime use and for a regenerative fuel cell (RFC) energy storage system to provide power during the night. Solar array sun-tracking is also proposed to maximize the array power output capability. The system launch mass was estimated to be approximately 10 metric tons. For mission application of photovoltaic technology other issues have to be addressed including the constraints imposed by launch vehicle, safety, and cost. For the initial phase of the mission a photovoltaic power system offers a safe option.
Author (CISTI)

N93-14931# Telesat Canada, Ottawa (Ontario).
NPR AND INTERMODULATION IN MOBILE SATELLITE SYSTEMS **c32**
Pat Amlekar *In* Canadian Space Agency, Proceedings of the Sixth CASI Conference on Astronautics 1990 15 p Previously announced in IAA as A91-34937 (For primary document see N93-14920 04-12)
Avail: Canadian Aeronautics and Space Inst., 222 Somerset St. W., Suite 601, Ottawa, Ontario K2P 0J1 Canada

Various topics related to noise power ratio (NPR) and intermodulation products are reviewed in connection with the design of a spacecraft payload. Findings of some of the basic studies carried out at Telesat Canada in connection with the mobile satellite program are presented. The close correlation between the software simulation and laboratory results indicate the usefulness of the software in the system design. The maximum improvement in carrier to noise ratio due to intermodulation noise over NPR value by voice activation and by bandwidth spreading is specified. It is shown that the optimum characteristic of a power amplifier is that of a piecewise linear limiter. Further improvements may be obtained by certain

payload configurations. The information provides useful design tools to a payload designer in selection of the power amplifier for the optimum utilization of the valuable spacecraft power. The results are applicable to spacecraft operating in any frequency band which operate in a multicarrier mode.
Author (CISTI)

N93-14932# Ecole Polytechnique, Montreal (Quebec). Lab. de Recherche en Hyperfrequences.
A NEW DEVICE TO AID IN THE CONCEPTION AND OPTIMIZATION OF MONOLITHIC MILLIMETER CIRCUITS: A DISTRIBUTED AND NONLINER MODEL OF A FIELD EFFECT TRANSISTOR [UN NOUVEL OUTIL D'AIDE A LA CONCEPTION ET A L'OPTIMISATION DES CIRCUITS MONOLITHIQUES AUX FREQUENCES MILLIMETRIQUES: LE MODELE DISTIBUE ET NON-LINEAIRE DE TRANSISTOR A EFFET DE CHAMP] **c33**
Eric Ongareau and Renato G. Bosisio *In* Canadian Space Agency, Proceedings of the Sixth CASI Conference on Astronautics 1990 10 p In FRENCH Previously announced in IAA as A91-34938 (For primary document see N93-14920 04-12)
Avail: Canadian Aeronautics and Space Inst., 222 Somerset St. W., Suite 601, Ottawa, Ontario K2P 0J1 Canada

The concept of monolithic nonlinear millimeter circuits necessitates the precise modeling of semiconducting devices. For high frequency applications, the effects distributed along the length and width of the component electrodes must be taken into account, particularly when harmonic frequencies are generated. This article presents a rigorous and systematic methodology for extracting a distributed and non-linear model of a field effect transistor, which can easily be applied to nonlinear simulators which employ harmonic balancing techniques. This new model is obtained from knowledge of the equivalent localized nonlinear circuit and from the geometric dimensions of the component. The circuit is then modeled by N identical sections, each of which include a nonlinear quadripole which simulates the field effect phenomena, placed between two linear octapoles which simulate inter-electrode coupling and the phase effects. Author (CISTI)

N93-14933# COM DEV Ltd., Cambridge (Ontario).
AN OVERVIEW OF RADARSAT PAYLOAD TECHNOLOGIES **c32**
Arunas Macikunas and Michael Pley *In* Canadian Space Agency, Proceedings of the Sixth CASI Conference on Astronautics 1990 11 p Previously announced in IAA as A91-34939 (For primary document see N93-14920 04-12)
Avail: Canadian Aeronautics and Space Inst., 222 Somerset St. W., Suite 601, Ottawa, Ontario K2P 0J1 Canada

The RADARSAT program incorporates a wide range of technologies in realizing a unique spaceborn synthetic aperture radar (SAR) system. Within the payload, the heart of the low power transmitter (LPT) is a digital code generator that allows for the selection of a number of different predefined transmit waveforms and the downloading of other waveforms that can be programmable in orbit. An I (in-phase) and Q (quadrature) upconversion technique for waveform generation is employed. The receiver portion of the payload has a high dynamic range to accommodate various imaging modes and ground reflectivities. A digital automatic gain control makes it possible to relay the data to earth with high transmission efficiency. The receiver noise figure is enhanced by the use of switchable surface acoustic wave filters that minimize the aliasing noise contribution for each of the predefined chirp waveforms. Extremely stable noise generators allow for the accurate on-board calibration of the receiver over the full mission life. Variable ferrite phase shifters allow for state of the art beam steering of the SAR beams. These payload features enable the system to image the earth's surface from a wide range of incidence angles and swath widths, as well as accounting for image areas with greatly differing reflectivity. The demanding requirements of the high power output circuits require the use of multipaction suppression techniques while maintaining system performance criteria for insertion loss and isolation of the transmit and receive signals.
Author (CISTI)

N93-14934# Ecole Polytechnique, Montreal (Quebec). Lab. de Recherche en Microondes.
CONCEPTUALIZATION OF A GaAs FIELD EFFECT TRANSISTOR FREQUENCY TRIPLER (2.5-7.5 GHz) FOR LOAD USE IN COMMUNICATION SATELLITES [CONCEPTION D'UN GAAS FET TRIPLEUR DE FREQUENCE (2.5-7.5 GHZ) POUR LA CHARGE UTILE DES SATELLITES DE COMMUNICATION] **c33**
Di-Luan Le, F. M. Ghannouchi, and R. G. Bosisio *In* Canadian Space Agency, Proceedings of the Sixth CASI Conference on Astronautics 1990 8 p In FRENCH Previously announced in IAA as A91-34940 (For primary document see N93-14920 04-12)
Avail: Canadian Aeronautics and Space Inst., 222 Somerset St. W., Suite 601, Ottawa, Ontario K2P 0J1 Canada

A conceptualization of a GaAs field effect transistor (FET) frequency multiplier is presented. The experimental results from a NE-71083 transistor measured by the harmonic load-pull technique were used to design a 2.5 to 7.5 GHz frequency tripler. The circuit adaptation on input and output as well as the optimal point of polarization were determined for maximum conversion gain and maximum efficacy. This technique can be used in the design of transistor frequency multipliers (when the multiplying factor is 4 or less) for microwaves and millimeter waves. Author (CISTI)

N93-14935# Canadian Astronautics Ltd., Ottawa (Ontario). Space Systems Group.
OPTIMIZED DESIGN OF A 5 kW CONSTANT FREQUENCY SERIES RESONANT CONVERTER FOR PULSED LOAD SPACE APPLICATIONS **c33**
Mehmet Celal Tanju *In* Canadian Space Agency, Proceedings of the Sixth CASI Conference on Astronautics 1990 10 p Previously announced in IAA as A91-34941 (For primary document see N93-14920 04-12)
Avail: Canadian Aeronautics and Space Inst., 222 Somerset St. W., Suite 601, Ottawa, Ontario K2P 0J1 Canada

The use of a static optimization algorithm that optimizes the design of a 10 kHz constant frequency 5 kW series resonant converter, to determine the minimum reactive component volt-ampere (VA) and energy storage ratings while all design requirements and constraints are met, is outlined. The static optimization algorithm is best suited for the search of a local extremum (maximum or minimum) of a multi variable function, the gradient of which is impossible or difficult to obtain directly. The function may include any number of variables and any number of inequality constraints on them or functions of them. The optimized design of a constant frequency series resonant converter for high power pulsed load space applications requires various design constraints to be satisfied in meeting a design objective that is a function of the design variables and design constants. The design objective is to minimize the VA and energy storage ratings of the reactive components of the converter and to minimize the converter losses. The optimized design of the double tuned resonant inverter minimizes the reactive power ratings of the converter resonant and output filter components and provides a very high inverter efficiency. Author (CISTI)

N93-14936# Ecole Polytechnique, Montreal (Quebec). Lab. de Recherche Microondes.
SIMULATION AND NONLINEAR MODELLING OF MICROWAVE TRANSISTORS [SIMULATION ET MODELISATION NON-LINEAIRE DES TRANSISTORS MICROONDES] **c33**
Rached Hajji, Fadhel M. Ghannouchi, and Renato G. Bosisio *In* Canadian Space Agency, Proceedings of the Sixth CASI Conference on Astronautics 1990 7 p In FRENCH Previously announced in IAA as A91-34942 (For primary document see N93-14920 04-12)
Avail: Canadian Aeronautics and Space Inst., 222 Somerset St. W., Suite 601, Ottawa, Ontario K2P 0J1 Canada

Two well known methods to simulate microwave and millimeter wave nonlinear circuits are presented. The steps required for a large signal microwave metal semiconductor field effect transistor (MESFET) modeling are described. The time domain method, which uses the solution of a system of differential equations to model the circuit, is presented. This method has a calculation time disadvantage as the circuit is strongly non-linear. Its advantage is that it permits transient state study. The second method, based on an harmonic balance technique (time and frequency domain), allows quick determination of the steady state regime of a nonlinear microwave circuit including the output power, the voltage, and current in

each branch of the circuit. Procedures required in MESFET modeling are described. The small signal measurements (S parameter) are used to obtain the intrinsic nonlinear parameters of the transistor allowing the nonlinear model to be deduced. Simulation and modeling results are presented.
Author (CISTI)

N93-14937# Impact Group (Canada).
SPACE EDUCATION: A SELF-PERSERVATION STRATEGY FOR THE CANADIAN SPACE INDUSTRY **c80**
Ron Freedman *In* Canadian Space Agency, Proceedings of the Sixth CASI Conference on Astronautics 1990 16 p Previously announced in IAA as A91-34943 (For primary document see N93-14920 04-12)
Avail: Canadian Aeronautics and Space Inst., 222 Somerset St. W., Suite 601, Ottawa, Ontario K2P 0J1 Canada

The growth and prosperity of Canada's space industry is closely tied to the nation's human resource potential. Future trends point to shortages in the supply of workers needed to fill critical space jobs in the private, public, and university sectors. The root of the problem is in our elementary and secondary schools, where fewer young people are electing to pursue careers in science, technology, mathematics, and engineering. Declining numbers of science graduates are coinciding with a growing requirement in all industries, which will lead to more intense competition for available workers. Falling European immigration is closing off Canada's traditional skill safety valve. While there is an inherent appeal to employment on the space industry, that will not be sufficient to overcome worker shortages. The space workers of the year 2000 are already in Canada's elementary and secondary schools. What is needed now is a national industry-led initiative designed to promote space and science careers to educators and students at a stage of their schooling where they still have options to pursue science and technology careers. The industry as a whole and individual organizations should take the next step and formalize their relationship with education.
Author (CISTI)

N93-14938# York Univ. (Ontario). Center for Research in Experimental Space Science.
INTERNATIONAL SPACE UNIVERSITY **c80**
J. Bird *In* Canadian Space Agency, Proceedings of the Sixth CASI Conference on Astronautics 1990 14 p Previously announced in IAA as A91-34944 (For primary document see N93-14920 04-12)
Avail: Canadian Aeronautics and Space Inst., 222 Somerset St. W., Suite 601, Ottawa, Ontario K2P 0J1 Canada

The goals and activities of the International Space University (ISU) are discussed. ISU is an international, multi-disciplinary program for graduate students. Three summer programs have been held, one at MIT, one in Strasbourg, and one at York University in Toronto in 1990. Lectures were presented on space architecture, business and management, engineering, life sciences, physical sciences, policy and law, resources and manufacturing, and satellite applications. Two design projects were carried out during the 1990 session. The International Program for Earth Observation project involved an assessment of the remote sensing requirements of the entire world and a comparison of the satellites available to meet those ends. The second study involved a feasibility study of an asteroid mining project. This study evaluated systems for allocating the contributions of various government agencies and industries plus the identification of policy and management arrangements.
Author (CISTI)

N93-14939# Telesat Canada, Ottawa (Ontario).
ANIK E SPACECRAFT INTEGRATION AND TEST **c18**
A. Kidd and E. Bertenyi *In* Canadian Space Agency, Proceedings of the Sixth CASI Conference on Astronautics 1990 15 p Previously announced in IAA as A91-34945 (For primary document see N93-14920 04-12)
Avail: Canadian Aeronautics and Space Inst., 222 Somerset St. W., Suite 601, Ottawa, Ontario K2P 0J1 Canada

In the spring of 1991 Telesat Canada plans to launch the first of its Anik E series of spacecraft. Since the existing C-band and Ku-band satellites will have to be replaced within a relatively short time, Telesat opted for a large capacity dual band satellite in order to replace both the current Anik C and Anik D satellite series. Anik E will provide enhanced performance in both frequency bands when compared to the existing space segment and will make possible the introduction of new services. The main features of the Anik E spacecraft are reviewed, and a summary of the integration and test experience with the spacecraft are given. Anik E will be among the first spacecraft to fly with a GE Astro 5000 bus, and will carry the first Spar Aerospace payload using C-band solid state power amplifiers. For those reasons, much of the integration and test program, while based on a protoflight approach, had many new units undergo qualification testing. Following an extensive series of in-orbit tests, the ANIK E spacecraft should be carrying traffic in 1991. The Anik E spacecraft platform was integrated at the GE Astro Space Facility in East Windsor, New Jersey, while the payload was developed and tested at the Spar Aerospace facility in Ste Anne de Bellevue, Quebec. The final spacecraft integration will be performed, by Spar, at the Canadian Government Facility, the David Florida Laboratories (DFL) in Ottawa, Ontario. Finally the launch plans and mission operations are described along with a summary of the in-orbit testing which is planned for the Anik E space segment.
Author (CISTI)

N93-14940# Canadian Space Agency, Ottawa (Ontario).
SPACECRAFT THERMAL DESIGN VERIFICATION IN CANADA **c18**
E. Choueiry and M. Donato (Spar Aerospace Ltd., Toronto, Ontario) *In its* Proceedings of the Sixth CASI Conference on Astronautics 1990 9 p Previously announced in IAA as A91-34946 (For primary document see N93-14920 04-12)
Avail: Canadian Aeronautics and Space Inst., 222 Somerset St. W., Suite 601, Ottawa, Ontario K2P 0J1 Canada

There are two types of space simulation techniques used in evaluation of spacecraft thermal design, differing in the preferred simulation of the effect of the sun (solar beam vs infrared simulator). This paper discusses the thermal design verification philosophy followed by Spar Aerospace and applied at the David Florida Laboratory (DFL). It also discusses the infrared development program conducted by Spar. Both the infrared (IRT) and solar simulation (SST) tests were performed successfully on the Olympus spacecraft thermal model. Infrared thermal tests were performed successfully on the Anik E satellite. Due to the inherent collimation of the beam, the solar simulation method continues to be more reliable for the verification of external view factors arising from multiple reflections or shadowing by complex structures. For simple structures the infrared technique has proven at least as reliable in correlating the internal network. This is due in part to the temperature measurement system accuracy. An additional advantage is the ability to perform consecutive thermal balance and thermal vacuum tests without breaking vacuum. In addition, the IR technique facilitates the simulation of end-of-life conditions, albedo and planetshine radiation. Such conditions cannot be easily recreated by solar simulation. The IR technique provides for a greater test flexibility on spacecraft whose orientation and movement are limited. The technique has proven to have significant cost advantages over the SST in terms of test and facility operational costs.
Author (CISTI)

N93-14941# Dynacon Enterprises Ltd., Downsview (Ontario).
SPACE BASED RADAR: TEST OF LARGE SPACE STRUCTURES **c32**
W. G. Sincarsin, D. J. McTavish, G. B. Sincarsin, and Y. Soucy (Communications Research Centre, Ottawa, Ontario) *In* Canadian Space Agency, Proceedings of the Sixth CASI Conference on Astronautics 1990 14 p Previously announced in IAA as A91-34947 (For primary document see N93-14920 04-12)
Avail: Canadian Aeronautics and Space Inst., 222 Somerset St. W., Suite 601, Ottawa, Ontario K2P 0J1 Canada

A general overview is provided of the main elements of space based radar (SBR) satellite design. Sixteen proposed SBR satellite designs were reviewed. Most fell into three main categories: space fed, corporate fed, and reactor feed. Included are descriptions of the major components incorporated into each design and their physical configuration, orbital information, and radar properties. The current status of deployment tests was assessed by considering the study of large or complex structures. For large structures ground based tests on reduced scale systems or substructures are recommended followed by identical tests in space. A similar approach is recommended for medium sized structures as well as full scale ground tests. Tests discussed in some detail include: deployed static structural tests, deployed dynamic structural tests, control structural interaction tests, stowed structural properties tests, and thermal tests. Canadian capabilities and facilities for meeting the needs of testing these large structures are identified.
Author (CISTI)

N93-14942# Canadian Space Agency, Ottawa (Ontario).
TECHNOLOGY DEVELOPMENT FOR NON-CONTACT MEASUREMENT IN MODAL TESTING OF LARGE SPACE STRUCTURES **c39**
Y. Soucy, W. B. Graham, A. K. Mitchell (Nova Scotia Technical Coll., Halifax.), and C. R. Hazell (Nova Scotia Technical Coll., Halifax.) *In* Canadian Space Agency, Proceedings of the Sixth CASI Conference on Astronautics 1990 15 p Previously announced in IAA as A91-34948 (For primary document see N93-14920 04-12)
Avail: Canadian Aeronautics and Space Inst., 222 Somerset St. W., Suite 601, Ottawa, Ontario K2P 0J1 Canada

This paper describes the Canadian Space Agency's technology development project, in cooperation with the Defence Research Establishment Ottawa, to develop non-contact measurement systems for ground-based modal testing of large space structures. The phases of the work are outlined, and the technical requirements and critical selection criteria for the systems are discussed. The two techniques of special interest which have emerged from the study to date are the projected grid and shadow moire methods, and the application of a laser vibrometer. The moire techniques are reviewed elsewhere. A description of the laser vibrometer is provided followed by a discussion of a new multi-channel system to be developed using the laser vibrometer. Modal tests of an epoxy test structure representative of a space structure are described and demonstrate the capabilities of the laser vibrometer system as well as the deficiencies of using accelerometers in testing lightweight structures.
Author (CISTI)

N93-14943# Canadian Space Agency, Ottawa (Ontario).
SPACE CRAFT VERIFICATION AT THE DAVID FLORIDA LABORATORY **c14**
Rolf Mamen *In its* Proceedings of the Sixth CASI Conference on Astronautics 1990 11 p Previously announced in IAA as A91-34949 (For primary document see N93-14920 04-12)
Avail: Canadian Aeronautics and Space Inst., 222 Somerset St. W., Suite 601, Ottawa, Ontario K2P 0J1 Canada

The David Florida Laboratory offers facilities and staff to support the integration and environmental testing of space subsystems and complete spacecraft. These capabilities encompass thermal verification and dynamic testing (vibration and modal analysis), as well as radio frequency (antenna pattern, RFI/EMC) measurements. Clean rooms are provided for the integration of solar arrays, antennas and spacecraft, and a range of ancillary support services facilitates the measurement of materials and mass properties and outgassing. These facilities, recently deployed in support of the Olympus program, are currently being exercised for the Anik-E satellites. Upgradings driven by the Olympus program encompass the thermal and dynamic domains and include an accurate, high capacity temperature measurement system and an additional support structure permitting vibration testing of very large and dynamically responsive test articles. Anik-E placed additional demands on laboratory capabilities but these upgradings are expected to be overshadowed by the test technology developments which may be mandatory to satisfy the requirements of MSAT, Radarsat and Space Station programs. These improvements could include an extended antenna measurement capability, improved deployment suspensions for large lightweight structures, materials testing for long duration, low earth orbit exposure and static load testing. Furthermore, the current trends toward enhanced capabilities are finding applications in a number of related disciplines such as radar.
Author (CISTI)

N93-14944# Spar Aerospace Ltd., Weston (Ontario). Advanced Technology Systems Div.
MISSION AND TECHNOLOGY ASSESSMENT OF HUMAN EXPLORATION TO THE MOON AND MARS **c91**
Moses Wong *In* Canadian Space Agency, Proceedings of the Sixth CASI Conference on Astronautics 1990 11 p Previously announced in IAA as A91-34950 (For primary document see N93-14920 04-12)
Avail: Canadian Aeronautics and Space Inst., 222 Somerset St. W., Suite 601, Ottawa, Ontario K2P 0J1 Canada

A comprehensive study has been undertaken by Spar Aerospace of a mission for human exploration to the moon and beyond based on the current U.S. Space Exploration Initiative. It offers a generalized scenario suitable for a range of missions and provides a basis for technology requirements and technology drivers assessment. A set of ten generalized mission phases with sub-level definition are presented. The mission phases provide a structured sequence of capability to place human explorers from the earth via a low orbit staging post to land on the moon and be productive on the lunar surface. Each phase is defined in sufficient detail to identify relevant technology requirements and operational activities. This set of mission phase definitions is applicable to the exploration of Mars with minor modifications. Technology drivers associated with the mission infrastructure are identified and assessed for two representative mission phases. Each technology area is examined in terms of its maturity status, including Canadian capabilities, and development effort needed to bring the technologies to fruition. An attempt is also made to identify priorities associated with the driver technologies which are defined as the enabling technologies to be developed prior to the others.
Author (CISTI)

N93-14945# University of Western Ontario, London.
CONTROL OF THERMOCAPILLARY CONVECTION IN A TWO-LAYER LIQUID SYSTEM **c34**
J. M. Floryan and C. Chen *In* Canadian Space Agency, Proceedings of the Sixth CASI Conference on Astronautics 1990 10 p Previously announced in IAA as A91-34951 (For primary document see N93-14920 04-12)
Avail: Canadian Aeronautics and Space Inst., 222 Somerset St. W., Suite 601, Ottawa, Ontario K2P 0J1 Canada

Thin liquid layers occur in many material deposition processes. Ability to control these processes depends on ability to control the dynamics of the liquid. The two technologically most important issues are prevention of rupture of the liquid layer and prevention of development of unsteady convection within the layer. In the absence of gravity, the dynamics of the liquid are dominated by thermocapillary effect. It has been shown that this effect always gives rise to convection in the case of a single layer and, furthermore, it tends to transform the configuration of the liquid from a layered form into a set of blobs. It is therefore important to identify means that could be used to stabilize the liquid. In this study we concentrate on a system consisting of a superposition of two liquid layers. The bottom layer is of interest from the material processing point of view, while the upper one can be used for stabilization purposes. Results show that the system preserves its topology only if the temperature field satisfies certain constraint conditions. The qualitative character of the flow occurring when the constraint conditions are satisfied is similar to the single layer case. The intensity of the convection can be significantly reduced by properly changing thickness and/or material properties of the top layer.
Author (CISTI)

N93-14946# Spar Aerospace Ltd., Weston (Ontario). Advanced Technology Systems Div.
APPLICATIONS OF THE MOBILE SERVICING SYSTEM TO THE SPACE EXPLORATION INITIATIVE **c18**
J. H. Dueckman *In* Canadian Space Agency, Proceedings of the Sixth CASI Conference on Astronautics 1990 10 p Previously announced in IAA as A91-34952 (For primary document see N93-14920 04-12)
Avail: Canadian Aeronautics and Space Inst., 222 Somerset St. W., Suite 601, Ottawa, Ontario K2P 0J1 Canada

This paper provides an analysis by Spar Aerospace of the potential application of the Mobile Servicing System (MSS), developed under the Canadian Space Station Program, to the Space Exploration Initiative (SEI). Initially, an overview of the MSS is provided which outlines the essential functions and elements of the MSS. An overview of the SEI is also provided which summarizes the overall goals and objectives of the initiative. This discussion also outlines the basic SEI missions and summarizes the infrastructure required to support them. The potential applications of the MSS to the SEI are summarized. For each application, the performance capability of the MSS is compared to the expected level of performance required to support the SEI missions. Any areas of potential performance increase are identified and design changes proposed. Finally, the growth capabilities of the MSS are compared to those which may be required to fully support the SEI. The MSS has the potential to play a significant role in the development and operational phases of the SEI. Additional growth capabilities could allow the MSS to play an even greater role, particularly in the areas of transportation and payload handling. MSS technologies are applicable to the systems required for surface operations. The MSS can play an important role in the areas of low earth orbit node construction and assembly, vehicle assembly, integration, and verification, servicing and maintenance, transportation, payload handling, and extra vehicular activity

support. The technologies currently being developed for the MSS are applicable for the development of surface robotic systems. In general, the performance capabilities of the MSS, in its baseline Space Station Freedom role, are sufficient to accommodate its potential role on the SEI. However, the expected increases in launch vehicle and spacecraft mass may exceed its payload handling and transportation capabilities. If the MSS is to be utilized on SEI to this extent, the required growth potential needs to be incorporated into its design now. Author (CISTI)

N93-14947# Spar Aerospace Ltd., Weston (Ontario). Advanced Technology Systems Div.

THE EVALUATION OF A CONCEPT FOR A CANADIAN-MADE AUTOMATED MULTIPURPOSE MATERIALS EXTRACTION FACILITY **c91**

H. Kleinberg *In* Canadian Space Agency, Proceedings of the Sixth CASI Conference on Astronautics 1990 9 p Previously announced in IAA as A91-34953 (For primary document see N93-14920 04-12)

Avail: Canadian Aeronautics and Space Inst., 222 Somerset St. W., Suite 601, Ottawa, Ontario K2P 0J1 Canada

Long-term habitation of space will eventually require use of off-Earth resources to reduce long-term program costs and risks to personnel and equipment due to launch from Earth. Extraction of oxygen from lunar soil is a prime example. Processes currently under study for such activities focus on the extraction of only one element / chemical from one type of soil on one world, and they produce large amounts of waste material. This paper presents the results of an examination by Spar Aerospace of a plasma separation concept as part of a materials extraction facility that might be used in space. Such a process has the far-reaching potential for extracting any or all of the elements available in soil samples, extraction of oxygen from lunar soil being the near-term application. Plasma separation has the potential for a 100 percent yield of extracted elements from input samples, and the versatility to be used on many non-terrestrial sites for the extraction of available elemental resources. The development of new materials extraction processes for each world would thus be eliminated. Such a facility could also reduce the generation of waste products by decomposing soil samples into pure, stable elements. Robotics, automation, and a plasma separation facility could be used to gather, prepare, process, separate, collect and ship the available chemical elements. The following topics are discussed: automated soil-gathering using robotics; automated soil pre-processing; plasma dissociation and separation of soil, and collection of sorted elements in an automated process; containment of gases, storage of pure elements, metals; and automated shipment of materials to a manned base, or pick-up site. Author (CISTI)

N93-14948# Spar Aerospace Ltd., Weston (Ontario).

VISION DEVELOPMENT TEST BED: THE CRADLE OF THE MSS ARTIFICIAL VISION SYSTEM **c74**

Leon Zucherman and John Stovman *In* Canadian Space Agency, Proceedings of the Sixth CASI Conference on Astronautics 1990 9 p Previously announced in IAA as A91-34954 (For primary document see N93-14920 04-12)

Avail: Canadian Aeronautics and Space Inst., 222 Somerset St. W., Suite 601, Ottawa, Ontario K2P 0J1 Canada

This paper presents the concept of the Vision Development Test-Bed (VDTB) developed at Spar Aerospace Ltd. in order to assist development work on the Artificial Vision System (AVS) for the Mobile Servicing System (MSS) of Space Station Freedom in providing reliable and robust target auto acquisition and robotic auto-tracking capabilities when operating in the extremely contrasty illumination of the space environment. The paper illustrates how the VDTB will be used to understand the problems and to evaluate the methods of solving them. The VDTB is based on the use of conventional but high speed image processing hardware and software. Auxiliary equipment, such as TV cameras, illumination sources, monitors, will be added to provide completeness and flexibility. A special feature will be the use of solar simulation so that the impact of the harsh illumination conditions in space on image quality can be evaluated. The VDTB will be used to assess the required techniques, algorithms, hardware and software characteristics, and to utilize this information in overcoming the target-recognition and false-target rejection problems. The problems associated with NTSC video processing and the use of color will also be investigated. The paper concludes with a review of applications for the VDTB work, such as AVS real-time simulations, application software development, evaluations, and trade-offs studies. Author (CISTI)

N93-14949# Alberta Research Council, Calgary.

A ROBOTIC PLANNING SYSTEM **c63**

Keith Chrystall, A. Dagnino, and P. Feighan *In* Canadian Space Agency, Proceedings of the Sixth CASI Conference on Astronautics 1990 9 p Previously announced in IAA as A91-34955 (For primary document see N93-14920 04-12)

Avail: Canadian Aeronautics and Space Inst., 222 Somerset St. W., Suite 601, Ottawa, Ontario K2P 0J1 Canada

Space station robots are expected to be viable substitutes to astronauts in the execution of space station assembly, repair and maintenance tasks. This paper presents a multi-level robotic planning system for the assembly of electronic components in a printed circuit board, employing surface-mount technology. The NASA/NBS Standard Reference Model (NASREM) control architecture was used as a model for this system. The NASREM architecture is hierarchically structured into multiple layers of decreasing complexity and horizontally partitioned into three sections: sensory processing, world modelling, and task decomposition. The approach followed in this project was to develop a knowledge based system to determine the activities and resources required to assemble components in a printed circuit board. Necessary activities are then decomposed into low level actions that can be executed by robotic workcells. By employing this system, robot programming is simplified as assembly tasks may be specified very concisely and all the required robot actions are automatically generated. The technology is adaptable to both space-based and terrestrial robot control systems. Author (CISTI)

N93-14950# Thomson-CSF, Ottawa (Ontario).

A CONCEPT FOR A SUPERVISED AUTONOMOUS ROBOT **c37**

S. Kalaycioglu *In* Canadian Space Agency, Proceedings of the Sixth CASI Conference on Astronautics 1990 17 p Previously announced in IAA as A91-34956 (For primary document see N93-14920 04-12)

Avail: Canadian Aeronautics and Space Inst., 222 Somerset St. W., Suite 601, Ottawa, Ontario K2P 0J1 Canada

The paper describes work in progress at Thomson-CSF Systems Canada Inc. on the Mobile Servicing System (MSS) Autonomous Robotics Program. The main objective of this program is to define and plan the development of technologies required to provide a supervised autonomous operation capability for the Special Purpose Dexterous Manipulator (SPDM) on the Mobile Servicing System (MSS). In this paper, a telerobotics system concept is introduced and a summary of the system requirements is given. The development methodology as well as the concept for a supervised autonomous robot (telerobotics) are briefly explained. The functional and physical architectures of the telerobotics system are also provided. This system will be responsible for carrying out operations such as assembly and maintenance of the Space Station Freedom; loading / unloading from the shuttle; and retrieval and deployment of the shuttle, etc. The paper also investigates an operational scenario for maintenance of the Space Station Freedom and briefly describes the operational scenario for changing an orbital replacement unit (ORU) on the Mobile Servicing System. The functional responsibilities of the system components in order to implement the ORU change are outlined. Author (CISTI)

N93-14951# Alberta Research Council, Edmonton.

A MONITORING AND CONTROL SYSTEM FOR COMPLEX MAN-MACHINE SYSTEMS: PRELIMINARY DESIGN **c54**

Maher Nessim, Lynn Sutherland, Breen Liblong, and Vickitt Lau *In* Canadian Space Agency, Proceedings of the Sixth CASI Conference on Astronautics 1990 13 p Previously announced in IAA as A91-34957 (For primary document see N93-14920 04-12)

Avail: Canadian Aeronautics and Space Inst., 222 Somerset St. W., Suite 601, Ottawa, Ontario K2P 0J1 Canada

Complex systems such as the Mobile Servicing System (MSS) consist of many highly interrelated components. Monitoring and control of these systems is an extremely complex task. A software design for the monitoring and control of complex systems is presented. The software uses artificial intelligence and probabilistic techniques to perform the monitoring and control functions. The system is designed to achieve independence between the generic functional modules and the domain specific knowledge modules so that the resulting software can be applied to a range of physical

systems by developing a knowledge base for each case. Candidate systems include the MSS, as well as offshore and marine transportation systems. The software design supports a number of important features, including real-time response, deep and shallow knowledge based reasoning, modelling of uncertainty and an intelligent user interface. The software is expected to interface with up to several hundred sensors and will maintain a performance history for updating and evaluation purposes. The main functional modules of the software system are a monitoring and control planner, a sensor data analyzer, a system status assessment module, a diagnosis module, a control action planner and an updating and reporting module. The approaches proposed to perform the functions of each of these modules are described. Author (CISTI)

N93-14952# Herzberg Inst. of Astrophysics, Ottawa (Ontario).
LISA: A LIMB IMAGING SPECTROGRAPH FOR AIRGLOW **c46**
F. R. Harris, R. L. Gattinger, F. Creutzberg, D. T. Bradley, F. Gauthier, J. W. Pygas, I. P. Powell (National Research Council of Canada, Ottawa, Ontario), and J. G. Rumbold (Canadian Space Agency, Ottawa, Ontario) *In* Canadian Space Agency, Proceedings of the Sixth CASI Conference on Astronautics 1990 11 p Previously announced in IAA as A91-34958 (For primary document see N93-14920 04-12)
Avail: Canadian Aeronautics and Space Inst., 222 Somerset St. W., Suite 601, Ottawa, Ontario K2P 0J1 Canada

In October 1992, three limb imaging spectrographs for airglow will be launched on a single sounding rocket from White Sands, New Mexico, with the objective of studying the chemistry of the lower nighttime thermosphere. The spectrographs are under development within a program named GEMINI (General Excitation Mechanisms In NIghtglow). The development is a collaborative effort between the National Research Council of Canada, participating university groups and the Canadian Space Agency. Two spectral ranges are covered: 255-400 nm and 540-780 nm. The imagers are required to have height resolutions of better than 1 km and spectral resolutions between 0.3 nm at 255 nm and 1 nm at 780 nm with signal to noise ratios adequate to deconvolve the atomic lines and molecular bands of interest. In this paper the optical, mechanical and detector designs and the theoretical specifications for the prototype imager (255-328 nm) are presented and details concerning the telemetry and pointing systems are also given. From a space station, atmospheric airglow emissions several orders of magnitude weaker than those measurable for GEMINI could be imaged. Author (CISTI)

N93-14953# Canadian Space Agency, Ottawa (Ontario).
EARTH ENVIRONMENT SPACE INITIATIVE **c43**
S. Parashar, H. H. Zwick (MacDonald, Dettwiler and Associates Ltd., Richmond, British Columbia), N. Hamilton (MacDonald, Dettwiler and Associates Ltd., Richmond, British Columbia), D. Thompson (INTERA Technologies Ltd., Ottawa, Ontario), R. Inkster (INTERA Technologies Ltd., Ottawa, Ontario), D. Epp (Royal Canadian Air Force, Toronto, Ontario), A. Stones (Bristol Aerospace Ltd., Winnipeg, Manitoba), and G. Tyc (Bristol Aerospace Ltd., Winnipeg, Manitoba) *In* Canadian Space Agency, Proceedings of the Sixth CASI Conference on Astronautics 1990 9 p Previously announced in IAA as A91-34959 (For primary document see N93-14920 04-12)
Avail: Canadian Aeronautics and Space Inst., 222 Somerset St. W., Suite 601, Ottawa, Ontario K2P 0J1 Canada

This paper provides a high level summary of work done by a team of four Canadian companies in the needs identification phase of a program definition study (PDS) for the Earth Environment Space Initiative (EESI). EESI is a proposed long-term program, aimed primarily at producing the earth observation information and the technology necessary to help protect the Canadian environment and resources and to help provide the contribution through which Canada can participate in international environment monitoring programs. EESI is to be an application specific series of key satellite missions. A number of areas where space-derived key information is needed have been identified. These areas were analyzed in terms of potential benefits. This resulted in the prioritized list of the top seven EESI opportunities being: deforestation, water pollution, greenhouse effect, soil degradation, acid rain, air pollution and environmental emergencies. The two leading mission candidates are given the tentative names, GREENSPACE and BLUESPACE. To implement these mission candidates in a cost effective manner requires several elements: instrument technology needs to be developed for the specific EESI missions; a flexible small satellite bus development for the instrument platform requires further study; an EESI information system to deliver products to the users needs to be developed; a Canadian mission control capability is needed; and user involvement and applications development is needed. Author (CISTI)

N93-14954# Telesat Canada, Ottawa (Ontario).
A LOW BIT RATE FSK TECHNIQUE FOR SCPC SATELLITE COMMUNICATION SYSTEMS **c32**
Vladimir Shpilka *In* Canadian Space Agency, Proceedings of the Sixth CASI Conference on Astronautics 1990 36 p Previously announced in IAA as A91-34960 (For primary document see N93-14920 04-12)
Avail: Canadian Aeronautics and Space Inst., 222 Somerset St. W., Suite 601, Ottawa, Ontario K2P 0J1 Canada

This paper concerns itself with the description and analysis of an application of FSK (frequency shift keying) communication system method, with which it is possible to eliminate the degrading effects of ground station as well as satellite contributed phase noise on very low bit rate communication systems. Typical transmitter and receiver block diagrams are provided. In situations where speed of information transmission is not of the greatest importance, but availability of DC power for the radio frequency transmitter is at premium, the above mentioned FSK technique would yield very low power communication systems, that could be used with the proposed MSAT satellite. Potential applications could include the development of handheld pocket sized messaging communicators and solar powered environmental data collection platforms. This class of earth terminals would operate at L-Band and would fall into the category of mobile earth terminals within the context of the MSAT system.
Author (CISTI)

N93-14955# Toronto Univ. (Ontario). Inst. for Aerospace Studies.
COMPOSITE MATERIALS IN SPACE: RESULTS FROM THE LDEF SATELLITE **c24**
R. C. Tennyson, J. S. Hansen, G. E. Mabson, W. D. Morison, and J. Kleiman *In* Canadian Space Agency, Proceedings of the Sixth CASI Conference on Astronautics 1990 15 p Previously announced in IAA as A91-34961 (For primary document see N93-14920 04-12)
Avail: Canadian Aeronautics and Space Inst., 222 Somerset St. W., Suite 601, Ottawa, Ontario K2P 0J1 Canada

Preliminary results are be presented on the behavior of a variety of fiber reinforced polymer matrix composites that comprised the University of Toronto Institute for Aerospace Studies (UTIAS) experiment on the Long Duration Exposure Facility (LDEF) satellite. LDEF was launched in April 1984, and retrieved in January 1990, thus providing a space exposure of about 70 months. The UTIAS experiment consisted of a variety of epoxy matrix composites with carbon, boron and aramid (Kevlar) reinforcements. A data acquisition system was incorporated to monitor 16 channels of strain and temperature every 16 hours for the first year in orbit. The following preliminary conclusions were made: (1) thermal model predictions are in excellent agreement with test data up to the first 300 days in orbit; (2) outgassing of the polymer matrix composites occurred over periods ranging from 40 to 120 days, depending on the material system; (3) significant permanent dimensional changes occurred in the samples due to outgassing, which must be factored into the design of low distortion composite laminates; (4) outgassing caused modest changes in the coefficient of thermal expansion (CTE), leading to asymptotic values that should be used in the design of zero CTE laminates for space applications; (5) low angle of incidence atomic oxygen eroded the composite materials which were located approximately 80 deg off the ram direction; and (6) reflected atomic oxygen caused erosion of the unexposed back surface of samples.
Author (CISTI)

N93-14956# MAYA Heat Transfer Technologies Ltd., Montreal (Quebec).
ADVANCES IN TMG **c34**
Kevin Duffy *In* Canadian Space Agency, Proceedings of the Sixth CASI Conference on Astronautics 1990 9 p Previously announced in IAA as A91-34962 (For primary document see N93-14920 04-12)
Avail: Canadian Aeronautics and Space Inst., 222 Somerset St. W., Suite 601, Ottawa, Ontario K2P 0J1 Canada

The Thermal Model Generator (TMG) modelling and analysis system continues to be enriched and expanded. The system is a comprehensive thermal modelling and analysis software package which can solve complex nonlinear and transient heat transfer problems using a geometry based

finite difference modelling approach. Several recent developments have significantly enhanced the product's functionality and scope. These have included the I-DEAS (TM) TMG interface and the Hydraulic Node capability for coupled thermal/fluid flow analysis. I-DEAS is a complete mechanical computer aided engineering system incorporating integrated modules for design, drafting, analysis, testing, and manufacturing. An overview of the current status of the TMG system is provided and the new features are described in detail. Author (CISTI)

N93-14957# Spar Aerospace Ltd., Weston (Ontario).
ON SOME KINEMATIC AND MASS CHARACTERISTICS OF FOLDABLE SOLAR ARRAYS **c44**
Thomas Szirtes *In* Canadian Space Agency, Proceedings of the Sixth CASI Conference on Astronautics 1990 22 p Previously announced in IAA as A91-34963 (For primary document see N93-14920 04-12)
Avail: Canadian Aeronautics and Space Inst., 222 Somerset St. W., Suite 601, Ottawa, Ontario K2P 0J1 Canada

Some kinematic and mass characteristics analyses of an unfolding solar array are presented. Considering the case where panels of an array are numbered from the base which is stationary, it its shown that the odd and even numbered panels behave differently. The even numbered panels move translationally and do not rotate; the odd numbered panels rotate but do not translate. At any instant all odd numbered panels rotate with identical angular speed, whereas the even numbered panels rotate with variable velocities. These latter velocities are always numerically equal to the product of the tangential speed of the tip of panel 1 and half the panel number. Resultant moment of inertia and equivalent mass values of the array are defined and analytically determined. These inertial parameters are what a motor (unfolding the array), placed at the hinge between any two adjacent panels, would work against. It is established that, despite the drastic change of the shape of the array during deployment, these quantities are independent of the array's deployment angle and hence they are time invariant constants of the structure. It is also demonstrated that these quantities vary, with good approximation, as the third power of the total number of panels in the array. Author (CISTI)

N93-14958# Defence Research Establishment, Ottawa (Ontario).
PROGRESS IN DND'S SPACE-BASED RADAR R/D PROJECT **c32**
Brian C. Eatock *In* Canadian Space Agency, Proceedings of the Sixth CASI Conference on Astronautics 1990 12 p Previously announced in IAA as A91-34964 (For primary document see N93-14920 04-12)
Avail: Canadian Aeronautics and Space Inst., 222 Somerset St. W., Suite 601, Ottawa, Ontario K2P 0J1 Canada

The Department of National Defense (Canada) has undertaken a program to study technology requirements of space based radar (SBR) because of its potential to provide wide area surveillance of the airspace over North America and its approaches. This project has reached the midpoint of its planned life; a series of technology definition contracts has been completed; and a series of technology development contracts has begun. This paper highlights the technical results of the contracts to date. The topics reviewed include antenna feeds, electric power systems, modelling and testing of large space structures, signal processing and target detection and tracking, monolithic microwave integrated circuit (MMIC) devices, communications links, and simulation of alternative SBR configurations. Author (CISTI)

N93-14959# Thomson and Nielsen Electronics, Ottawa (Ontario).
RADIATION MONITORING FOR LONG DURATION SPACE FLIGHTS **c93**
I. Thomson and G. Mackay *In* Canadian Space Agency, Proceedings of the Sixth CASI Conference on Astronautics 1990 12 p Previously announced in IAA as A91-34965 (For primary document see N93-14920 04-12)
Avail: Canadian Aeronautics and Space Inst., 222 Somerset St. W., Suite 601, Ottawa, Ontario K2P 0J1 Canada

Future space missions will require more detailed knowledge of radiation effects both on inherent electronics and on humans. Single event upsets due to cosmic rays have devastating effects on the former and all types of radiation will potentially damage the latter. The longer the flight duration, the greater the potential hazard. An astronaut, for example, can expect a dose of 9 rems for a 90 day mission in low earth orbit and 100 rems in a 1,000 day Mars mission. The recommended dose limits for radiation workers on earth are 5 rems/year and for the general public, 0.5 rem/year. This paper gives an overview of the space radiation environment and of the physical effects of radiation on electronic equipment and biological specimens. This is followed by a description of new, direct-reading electronic radiation monitoring techniques and their applications to problems in space. It is shown that the miniature silicon sensors can be used for the separate measurement of (1) trapped high energy protons and electrons and (2) comsmic rays. Two experimental applications of these technologies are described. One is a flight on a Soviet spacecraft and the other is the maiden flight of ESA's Ariane Technology Experiment Platform (ARTEP). ARTEP 1 is intended for real-time radiation monitoring in a wide range of space radiation environments. Future experiments and applications are discussed in terms of radiation monitoring and protection. Author (CISTI)

N93-14960# Telesat Mobile, Inc., Ottawa (Ontario).
PROGRESS TOWARD A FULL SCALE MOBILE SATELLITE SYSTEM FOR CANADA **c32**
Orest S. Roscoe *In* Canadian Space Agency, Proceedings of the Sixth CASI Conference on Astronautics 1990 11 p Previously announced in IAA as A91-34966 (For primary document see N93-14920 04-12)
Avail: Canadian Aeronautics and Space Inst., 222 Somerset St. W., Suite 601, Ottawa, Ontario K2P 0J1 Canada

The MSAT satellite, planned for launch in early 1994, will provide full scale, satellite based, mobile voice and data communication services to Canada. The MSAT system will provide mobile telephone, mobile radio and mobile data services to customers on the move in any part of North America. The Telesat Mobile Inc. (TMI) satellite will be backed up by a similar satellite to be operated by the American Mobile Satellite Corporation (AMSC) in the United States. An early entry mobile data service was inaugurated in the second quarter of 1990 using channels leased from INMARSAT on Marisat or Marecs-B. The baseline TMI system is described, beginning with the MSAT satellite under contract. The network architecture and the control system that are under development to support the mobile services are discussed. Since it is clearly desirable to have a North American system, such that customers may buy a mobile earth terminal (MET) from a number of qualified suppliers and be able to use it either in Canada or the U.S., TMI and AMSC are cooperating closely in the development of the space and ground segments of the system. The time scale for the procurement of all the elements of the systems is discussed.
Author (CISTI)

N93-14961# Spar Aerospace Ltd., Sainte-Anne-de-Bellevue (Quebec). Satellite and Communication Systems Div.
L-BAND ANTENNA DESIGN FOR MSAT MISSION **c32**
G. S. Gupta and Y. Patenaude *In* Canadian Space Agency, Proceedings of the Sixth CASI Conference on Astronautics 1990 6 p Previously announced in IAA as A91-34967 (For primary document see N93-14920 04-12)
Avail: Canadian Aeronautics and Space Inst., 222 Somerset St. W., Suite 601, Ottawa, Ontario K2P 0J1 Canada

The requirements and considerations peculiar to the design of satellite antennas for mobile communication satellites are described. Concepts considered for the MSAT satellite are discussed. The system must have maximum flexibility as the needs of the eventual users cannot be precisely determined until the system has been fully operational for a period of time. The system requirements include a high gain antenna, multiple high gain spot beams having low sidelobes, and high transmit power. These requirements place severe constraints on the design of radiators and beam forming network (BFN) components in regard to power handling capability and passive intermodulation (PIM). In addition, the system must be compact and of low mass while still providing high efficiency. The proposed system will feature a 6 by 5 m unfurlable reflector antenna fed by 24 circular cup dipole elements. Separate transmit and receive antennas will reduce system interference. Sidelobe nulling will improve isolation of the east and west beams. To minimize the risk of PIM generation in the feed array, an integrated cup dipole / BNF / filter assembly will be used. Author (CISTI)

N93-14962# Spar Aerospace Ltd., Toronto (Ontario).
NEXT GENERATION SATELLITE COMMUNICATIONS NETWORKS **c32**
P. J. Garland and F. J. Osborne (Department of Communications, Ottawa, Ontario) *In* Canadian Space Agency, Proceedings of the Sixth CASI Conference on Astronautics 1990 6 p Previously announced in IAA

as A91-34968 (For primary document see N93-14920 04-12)
Avail: Canadian Aeronautics and Space Inst., 222 Somerset St. W., Suite 601, Ottawa, Ontario K2P 0J1 Canada

Existing communication satellites are primarily bent pipe systems retransmitting unprocessed signals in a range of reserved frequency bands. Recent flown or planned space experiments employ a new generation of space hardware, involving a high level of signal handling and switching. The decoupling of up and down links through regeneration as well as advanced routing and switching, allow new markets and applications to be economically addressed, as well as enhancements to present services. Two possible services are highlighted in this paper, one an enhancement of current private business services offered in the Ku band. This allows full mesh T1 services to be offered on low cost very small aperture terminals (VSAT). The other utilizes similar on-board technologies, applying them to the Ka band in support of new personal / mobile services. These services require the development of a new generation of regenerative / switching satellites. A possible Canadian service and technology demonstration mission, projected for the 1997 timeframe is described.
Author (CISTI)

N93-14963# Spar Aerospace Ltd., Sainte-Anne-de-Bellevue (Quebec).
Ku-BAND ANTENNA DESIGN FOR MSAT MISSION **c32**
G. S. Gupta and P. Ilott *In* Canadian Space Agency, Proceedings of the Sixth CASI Conference on Astronautics 1990 13 p Previously announced in IAA as A91-34969 (For primary document see N93-14920 04-12)
Avail: Canadian Aeronautics and Space Inst., 222 Somerset St. W., Suite 601, Ottawa, Ontario K2P 0J1 Canada

The MSAT satellite is designed to provide communication links for remote or mobile transceivers to hook into regular communication networks. In this system the L-band will be used to both receive from and transmit signals to mobile units. The Ku band will be used to communicate with fixed ground stations only and the coverage beam does not need to be reconfigured. The Ku-band antenna offers a good vehicle for applications of shaped reflector technology. The antenna was optimized so that similar coverage was provided for both vertical and horizontal polarization modes. A corrugated horn reflector was designed using a computer software package which describes the surface in terms of Zernike polynomials. The final product of the computer program is a surface file which can be output to other programs. An antenna is being built to verify the performance predictions.
Author (CISTI)

N93-15646*# National Aeronautics and Space Administration. Langley Research Center, Hampton, VA.
LDEF: A BIBLIOGRAPHY WITH ABSTRACTS
H. Garland Gouger, ed. Nov. 1992 116 p
(NASA-TM-107705; NAS 1.15:107705) Avail: CASI HC A06/MF A02

The Long Duration Exposure Facility (LDEF) was a free-flying cylindrical structure that housed self-contained experiments in trays mounted on the exterior of the structure. Launched into orbit from the Space Shuttle Challenger in 1984, the LDEF spent almost six years in space before being recovered in 1990. The 57 experiments investigated the effects of the low earth orbit environment on materials, coatings, electronics, thermal systems, seeds, and optics. It also carried experiments that measured crystals growth, cosmic radiation, and micrometeoroids. This bibliography contains 435 selected records from the NASA aerospace database covering the years 1973 through June of 1992. The citations are arranged within subject categories by author and date of publication.
Author

13 ASTRODYNAMICS

Includes powered and free-flight trajectories; and orbital and launching dynamics.

N93-15103 Cincinnati Univ., OH.
OPTIMAL IMPULSIVE TRAJECTORIES FOR ORBITAL RENDEZVOUS BETWEEN ELLIPTIC ORBITS Ph.D. Thesis
Ching-Wei Cheng 1992 186 p
Avail: Univ. Microfilms Order No. DA9232332

This study uses and extends primer vector theory to obtain a minimum-fuel two or multiple impulse solution for co-planar and non co-planar elliptic-to-elliptic, time-fixed rendezvous. Lawden's conditions for an optimal impulsive trajectory and three additional methods to improve the non-optimal multiple impulse are introduced. To extend a 3-Impulse differential cost function provided by Jezewski and Rozendaal, the general differential cost function for an N-Impulse trajectory is developed. This approach defines the gradient vector for any set of boundary conditions. To determine the number of impulses, times, and locations for multiple-impulse optimal trajectories automatically, a computer program is developed. This software has been thoroughly tested in a wide variety of rendezvous situations. The singularity for a transfer angle of 180 degrees and the singular case of sin I = 0 are also accounted for in the program. Part of this work was accomplished using the Generalized Reduced Gradient method using its associated GRG2 computer code. The effects of inclination between the vehicle and target orbits, the initial positions of the vehicle and target, and the direction of the major axes are considered. Numerical results for several different orbit configurations are produced and discussed. The results are compared with the Hohmann/Hohmann type transfer and/or the optimal, finite, three-impulse transfer.
Dissert. Abstr.

N93-15367*# National Aeronautics and Space Administration. Langley Research Center, Hampton, VA.
ASPECTS OF PARKING ORBIT SELECTION IN A MANNED MARS MISSION
Prasun N. Desai, Robert D. Braun, and Richard W. Powell Washington Dec. 1992 30 p
(RTOP 506-49-11-01)
(NASA-TP-3256; L-17115; NAS 1.60:3256) Avail: CASI HC A03/MF A01

For any round-trip Mars mission, the selection of a parking orbit at Mars must consider the precession caused by the oblateness of the planet. This precession will affect the departure condition for Earth return and, therefore, the initial mass required in low Earth orbit (LEO). In this investigation, which considers precession effects, minimum initial LEO masses were obtained for parking orbits characterized by having near-equatorial inclinations, high eccentricities, and three-dimensional departure burns (i.e., a burn with an in-plane and an out-of-plane velocity increment component). However, because near-equatorial inclination orbits have poor planetary coverage characteristics, they are not desirable from a science viewpoint. To enhance the potential for satisfying science requirements along with landing site accessibility, a penalty in the initial LEO mass is required. This study shows that there are a set of orbits characterized by low to moderate essentricities (e = 0.2 to 0.5) and nonequatorial inclinations (i = 70 to 140 deg) that reduce this initial LEO mass penalty. Therefore, careful selection of a parking orbit at Mars can enhance the potential for satisfying science requirements with minimal mass penalties.
Author

N93-15392*# National Aeronautics and Space Administration. Marshall Space Flight Center, Huntsville, AL.
A PLAN FOR SPACECRAFT AUTOMATED RENDEZVOUS
A. W. Deaton, J. J. Lomas, and L. D. Mullins Oct. 1992 55 p
(NASA-TM-108385; NAS 1.15:108385) Avail: CASI HC A04/MF A01

An automated rendezvous approach has been developed that utilizes advances in technology to reduce real-time/near real-time flight operations support personnel to an acceptable level that is near the minimum without jeopardizing the success of the mission. The on-board flight targeting uses a rule-based system to select the pursuit vehicle phasing orbits and uses precise navigation updates from the pursuit/target spacecraft made possible by the global positioning system receivers/processors on both spacecraft to adjust the phasing orbits and achieve rendezvous. The ascent-to-orbit targeting for the pursuit vehicle has been successfully decoupled from the on-orbit orbit transfer phasing targeting. Typical launch window data have been developed for the heavy lift launch vehicle and cargo transfer vehicle for a Space Station Freedom rendezvous mission.
Author

N93-15000*# Technische Univ., Delft (Netherlands).
PRECISE ORBIT COMPUTATION AND SEA SURFACE MODELING
Karel F. Wakker, B. A. C. Ambrosius, R. Rummel, E. Vermaat, W. P. M. deRuijter (Utrecht State Univ., Netherlands), J. W. vanderMade (Rijkswaterstaat, Delft, Netherlands), and J. T. F. Zimmerman (Nederlands Inst. voor Onderzoek der Zee, Texel.) *In* JPL, TOPEX/Poseidon Science

Investigations Plan 1 Sep. 1991 p 161-168 Original contains color illustrations (For primary document see N93-14964 04-48)
Avail: CASI HC A02/MF A02; 22 functional color pages

14 GROUND SUPPORT SYSTEMS AND FACILITIES (SPACE)

Includes launch complexes, research and production facilities; ground support equipment, e.g., mobile transporters; and simulators.

For related information see also *09 Research and Support Facilities (Air).*

N93-14495*# National Aeronautics and Space Administration. Lyndon B. Johnson Space Center, Houston, TX.
FACILITIES AND CAPABILITIES CATALOG FOR LANDING AND ESCAPE SYSTEMS
Robert E. Meyerson, ed. Aug. 1992 232 p Prepared in cooperation with National Parachute Technology Council, Albuquerque, NM
(RTOP 906-11-00)
(NASA-RP-1282; S-682; NAS 1.61:1282) Avail: CASI HC A11/MF A03

This catalog serves as a single source reference for designers of landing and escape systems for spacecraft, aircraft, weapons, and airdrop system. It includes those facilities which may be required by a system designer in planning a development test program for many applications. The primary objective of this catalog is to provide a means for identifying critical facilities with the U.S. which can be used for the development of landing and escape systems. A secondary objective is to provide a useful tool to the system designer for picking and choosing facilities and capabilities. The six chapters in this volume include wind tunnels, drop zones, test aircraft, fabrication facilities, design tools, and other miscellaneous facilities. A different data sheet format is used for each of the chapters which provides information on performance, location, special capabilities, and a local point of contact. All inputs were solicited from the individual facilities and have not been independently verified for accuracy. Author

N93-14943# Canadian Space Agency, Ottawa (Ontario).
SPACE CRAFT VERIFICATION AT THE DAVID FLORIDA LABORATORY
Rolf Mamen *In its* Proceedings of the Sixth CASI Conference on Astronautics 1990 11 p Previously announced in IAA as A91-34949 (For primary document see N93-14920 04-12)
Avail: Canadian Aeronautics and Space Inst., 222 Somerset St. W., Suite 601, Ottawa, Ontario K2P 0J1 Canada

N93-15607*# Pittsburgh-Des Moines Steel Co., PA.
A NEW THERMAL VACUUM FACILITY AT THE MARTIN MARIETTA WATERTON PLANT
Robert N. Watson and John W. Bonn (CVI, Inc., Columbus, OH.) *In* NASA. Goddard Space Flight Center, The Seventeenth Space Simulation Conference. Terrestrial Test for Space Success Nov. 1992 p 165-182 (For primary document see N93-15593 04-18)
Avail: CASI HC A03/MF A03

N93-15610*# Space Systems/Loral, Palo Alto, CA.
THE EVOLUTION OF SPACE SIMULATION
Arthur A. Edwards *In* NASA. Goddard Space Flight Center, The Seventeenth Space Simulation Conference. Terrestrial Test for Space Success Nov. 1992 p 207-220 (For primary document see N93-15593 04-18)
Avail: CASI HC A03/MF A03

N93-15611*# NSI Technology Services Corp., Greenbelt, MD.
FROM DIFFUSION PUMPS TO CRYOPUMPS: THE CONVERSION OF GSFC'S SPACE ENVIRONMENT SIMULATOR
Ron Cary *In* NASA. Goddard Space Flight Center, The Seventeenth Space Simulation Conference. Terrestrial Test for Space Success Nov. 1992 p 221-227 (For primary document see N93-15593 04-18)
Avail: CASI HC A02/MF A03

N93-15612*# NSI Technology Services Corp., Greenbelt, MD.
CLEANING OF A THERMAL VACUUM CHAMBER WITH SHROUDS IN PLACE
William R. Bond *In* NASA. Goddard Space Flight Center, The Seventeenth Space Simulation Conference. Terrestrial Test for Space Success Nov. 1992 p 229-238 (For primary document see N93-15593 04-18)
Avail: CASI HC A02/MF A03

N93-15613*# Intespace, Toulouse (France).
INTESPACE'S NEW THERMAL-VACUUM TEST FACILITY: SIMMER
Raymond Duprat and Andre Mouton *In* NASA. Goddard Space Flight Center, The Seventeenth Space Simulation Conference. Terrestrial Test for Space Success Nov. 1992 p 239-250 (For primary document see N93-15593 04-18)
Avail: CASI HC A03/MF A03

15 LAUNCH VEHICLES AND SPACE VEHICLES

Includes boosters; operating problems of launch/space vehicle systems; and reusable vehicles.

For related information see also *20 Spacecraft Propulsion and Power.*

N93-14266# Prins Maurits Lab. TNO, Rijswijk (Netherlands).
VALIDATION OF THE FLUX LOOP DIAGNOSTIC FOR THE MEASUREMENT OF LAUNCH PACKAGE MOTION DURING ELECTROMAGNETIC LAUNCH Final Report
M. Koops Jul. 1992 30 p
(AD-A256547; PML-1992-42; TDCK-91-3641) Avail: CASI HC A03/MF A01

The development of diagnostics for studying the behavior and performance of armatures and rail accelerators is one of the subjects covered by the section EML-research of the PML-Pulse Physics Laboratory. Within that framework the development of data analysis software is in progress. This report describes a new data reduction technique to resolve armature motion from the measurement of the voltage induced in a flux loop diagnostic and the load current through the rail-armature circuit and/or its time derivative. Velocity and position of the armature as a function of time are calculated by the computer code developed. The recent improvements in data reduction are exemplified by the results of experiments performed with a 1m, 15mm square bore dipole rail accelerator. Validation of the flux loop diagnostic, in terms of accuracy, precision, range of operation, resolution, sensitivity and prospects is carried out. Suggestions to reduce the influence of the disadvantages observed are given. GRA

N93-15621*# General Dynamics Corp., Saint Louis, MO. Space Systems Div.
ACOUSTIC AND THERMAL TESTING OF THE TITAN/CENTAUR UPPER STAGE Abstract Only
Mark Gehringer, Chris Gibson, and Ron Janes *In* NASA. Goddard Space Flight Center, The Seventeenth Space Simulation Conference. Terrestrial Test for Space Success Nov. 1992 p 327 (For primary document see N93-15593 04-18)
Avail: CASI HC A01/MF A03

16 SPACE TRANSPORTATION

Includes passenger and cargo space transportation, e.g., shuttle operations; and space rescue techniques.

For related information see also *03 Air Transportation and Safety* and *18 Spacecraft Design, Testing and Performance.* For space suits see *54 Man/System Technology and Life Support.*

N93-14697# Arizona Univ., Tucson. Lunar and Planetary Lab.
SPECTRAL ANALYSIS OF THE SHUTTLE GLOW. SPA II/IBSS MISSION: AIS HARDWARE Final Report, Sep. 1986 - Sep. 1991
A. L. Broadfoot 23 Apr. 1992 54 p
(Contract F19628-86-K-0040; AF Proj. ST85)
(PL-TR-92-2148) Avail: CASI HC A04/MF A01

The experimental program was directed toward understanding the Shuttle

Glow phenomenon, shuttle/spacecraft contamination and associated problems. The Arizona Imager/Spectrograph experiment (AIS) was flown as part of the IBSS/SPAS 2 Mission. Several IBSS experiments were supported by the AIS. Much important data was gathered and is being analyzed at this time. The results from the successful mission will be used as the basis for further work on these important subjects. A second experiment using the same approach is being prepared as an attached shuttle experiment. The 'Shuttle Glow Experiment' (GLO) has been manifested on STS-53 as the next step in our study of the shuttle/spacecraft interaction with the earth's atmosphere. Author

N93-14698# Arizona Univ., Phoenix. Lunar and Planetary Lab.
SPECTRAL ANALYSIS OF THE SHUTTLE GLOW: AIS SCIENCE SUPPORT Final Report, Aug. 1988 - Nov. 1991
A. L. Broadfoot 23 Jun. 1992 75 p
(Contract F19628-88-K-0028; AF Proj. S321)
(PL-TR-92-2172) Avail: CASI HC A04/MF A01

The science support effort for the Arizona Imager/Spectrograph (AIS) included several aspects of shuttle and spacecraft interactions research. Software development, flight planning and analysis of related ground-based observations of the shuttle interaction were included. The AIS flight planning task continued from delivery of the experiment to the SPAS 2 as Messerschmitt-Bolkow-Blohm in Germany in May 1989 until flight of the experiment on STS-39 in April/May of 1991. Since the AIS was to provide supporting data for all of the experiments on the IBSS/SPAS 2 mission, special experiment sequences were developed for each of the six experiments. With various options, this amounted to about thirty templates or individual experiments. The AIS data were reviewed carefully to identify periods in which good data were received on the identified experiments. About 45 data sets were identified and work was begun on preparing them for analysis. A second scientific data set, which was a companion to the AIS, came from the AMOS observational program. The commonality between the data from the observations of thruster firings by the shuttle over AMOS and the AIS flight experiments joined these two scientific analysis programs. Author

N93-14730*# Martin Marietta Corp., Denver, CO. Space Launch Systems Co.
INTERPLANETARY PROGRAM TO OPTIMIZE SIMULATED TRAJECTORIES (IPOST). VOLUME 3: PROGRAMMER'S MANUAL Final Report
P. E. Hong, P. D. Kent, D. W. Olson, and C. A. Vallado Oct. 1992 72 p Revised
(Contract NAS1-18147; RTOP 506-49-11-02)
(NASA-CR-189653-Vol-3-Rev; NAS 1.26:189653-Vol-3-Rev) Avail: CASI HC A04/MF A01

The Interplanetary Program to Optimize Space Trajectories (IPOST) is intended to support many analysis phases, from early interplanetary feasibility studies through spacecraft development and operations. Here, information is given on the IPOST code. Author

N93-14736*# Lockheed Engineering and Sciences Co., Houston, TX. Flight Data Section.
STS-49: SPACE SHUTTLE MISSION REPORT
Robert W. Fricke Jul. 1992 47 p
(NASA-TM-108104; NAS 1.15:108104; NSTS-08276) Avail: CASI HC A03/MF A01

The STS-49 Space Shuttle Program Mission Report contains a summary of the Orbiter, External Tank (ET), Solid Rocket Booster/Redesigned Solid Rocket Motor (SRB/RSRM), and Space Shuttle main engine (SSME) subsystem performance during the forty-seventh flight of the Space Shuttle Program and the first flight of the Orbiter vehicle Endeavor (OV-105). In addition to the Endeavor vehicle, the flight vehicle consisted of an ET designated as ET-43 (LWT-36); three SSME's which were serial numbers 2030, 2015, and 2017 in positions 1, 2, and 3, respectively; and two SRB's designated as BI-050. The lightweight RSRM's installed in each SRB were designated as 360L022A for the left RSRM and 360L022B for the right RSRM. Author

N93-14768*# Martin Marietta Corp., Denver, CO. Space Launch Systems Group.
INTERPLANETARY PROGRAM TO OPTIMIZE SIMULATED TRAJECTORIES (IPOST). VOLUME 4: SAMPLE CASES Final Report
P. E. Hong, P. D Kent, D. W. Olson, and C. A. Vallado Oct. 1992 139 p
(Contract NAS1-18230; RTOP 506-49-11-02)
(NASA-CR-189653-Vol-4; NAS 1.26:189653-Vol-4) Avail: CASI HC A07/MF A02

The Interplanetary Program to Optimize Simulated Trajectories (IPOST) is intended to support many analysis phases, from early interplanetary feasibility studies through spacecraft development and operations. The IPOST output provides information for sizing and understanding mission impacts related to propulsion, guidance, communications, sensor/actuators, payload, and other dynamic and geometric environments. IPOST models three degree of freedom trajectory events, such as launch/ascent, orbital coast, propulsive maneuvering (impulsive and finite burn), gravity assist, and atmospheric entry. Trajectory propagation is performed using a choice of Cowell, Encke, Multiconic, Onestep, or Conic methods. The user identifies a desired sequence of trajectory events, and selects which parameters are independent (controls) and dependent (targets), as well as other constraints and the cost function. Targeting and optimization are performed using the Standard NPSOL algorithm. The IPOST structure allows sub-problems within a master optimization problem to aid in the general constrained parameter optimization solution. An alternate optimization method uses implicit simulation and collocation techniques. Author

N93-14794*# Martin Marietta Corp., Denver, CO. Space Launch Systems Co.
INTERPLANETARY PROGRAM TO OPTIMIZE SIMULATED TRAJECTORIES (IPOST). VOLUME 1: USER'S GUIDE Final Report
P. E. Hong, P. D. Kent, D. W. Olson, and C. A. Vallado Oct. 1992 213 p Revised
(Contract NAS1-18230; RTOP 506-49-11-02)
(NASA-CR-189653-Vol-1-Rev; NAS 1.26:189653-Vol-1-Rev) Avail: CASI HC A10/MF A03

IPOST is intended to support many analysis phases, from early interplanetary feasibility studies through spacecraft development and operations. The IPOST output provides information for sizing and understanding mission impacts related to propulsion, guidance, communications, sensor/actuators, payload, and other dynamic and geometric environments. IPOST models three degree of freedom trajectory events, such as launch/ascent, orbital coast, propulsive maneuvering (impulsive and finite burn), gravity assist, and atmospheric entry. Trajectory propagation is performed using a choice of Cowell, Encke, Multiconic, Onestep, or Conic methods. The user identifies a desired sequence fo trajectory events, and selects which parameters are independent (controls) and dependent (targets), as well as other constraints and the coat function. Targeting and optimization is performed using the Stanford NPSOL algorithm. IPOST structure allows sub-problems within a master optimization problem to aid in the general constrained parameter optimization solution. An alternate optimization method uses implicit simulation and collocation techniques. Author

N93-15474*# Rockwell International Corp., Pittsburgh, PA. Space Transportation Systems Div.
SPACE SHUTTLE ORBITER CREW HATCH JETTISON TEST USING A 0.0405-SCALE MODEL (16-0) IN THE TEXAS A/M LOW SPEED WIND TUNNEL (OA362). SPACE SHUTTLE AEROTHERMODYNAMIC DATA REPORT
C. E. Mitchell Jul. 1992 37 p Prepared in cooperation with Chrysler Technologies Airborne Systems, Inc., New Orleans, LA
(Contract NAS9-17840)
(NASA-CR-167698; NAS 1.26:167698; DMS-DR-2541) Avail: CASI HC A03/MF A01

This report contains post-test information for the Space Shuttle Orbiter Crew Hatch Jettison Test OA362 which was conducted in the Texas A&M Low Speed Wind Tunnel from 6/15/87 to 6/22/87. The test objective was to verify that the crew hatch, once jettisoned, would clear the orbiter under various simulated flight conditions. Several model hatches were used with the 0.0405-scale orbiter (Model 16-0). The model's angle of attack was set at 10, 15, and 20 degrees while the sideslip had values of minus

5, 0, and plus 5 degrees. The full scale Qbars that were simulated were 105, 128, 160, and 210 psf. In the hatch jettison mechanism itself, the plunger pressure was varied to achieve horizontal velocities of 3, 5, 7, and 20.1 feet per second model scale, and the plunger location was varied to achieve a variety of rotational velocities. The orbiter model was subjected to 122 runs with 13 different hatches. Of these, 60 were good runs.

Author

N93-15475*# Rockwell International Corp., Pittsburgh, PA. Space Transportation Systems Div.

RESULTS OF A FRSI MATERIAL TEST UNDER SPACE SHUTTLE ASCENT CONDITIONS IN THE AMES RESEARCH CENTER 9X7 FOOT SUPERSONIC WIND TUNNEL (OS13). SPACE SHUTTLE AEROTHERMODYNAMIC DATA REPORT

P. L. Lemoine and J. G. R. Collette Jul. 1992 131 p Prepared in cooperation with Chrysler Technologies Airborne Systems, Inc., New Orleans, LA

(Contract NAS9-17840)

(NASA-CR-167699; NAS 1.26:167699; DMS-DR-2287) Avail: CASI HC A07/MF A02

A test was conducted in the NASA/ARC 9 x 7 foot supersonic wind tunnel to verify the integrity of Felt Reusable Surface Insulation (FRSI) material in a panel flutter environment. A FRSI sample panel was subjected to the shocks, pressure gradients, and turbulence characteristics encountered at dynamic pressure 1.5 times the 3(sigma) dispersed trajectory flight conditions of the Space Shuttle. Static and fluctuating pressure data were obtained for Mach numbers ranging from 1.55 to 2.5 with dynamic pressures of 625 to 1250 psf. The FRSI panel suffered no appreciable damage as a result of the test. Author

17 SPACE COMM., SPACECRAFT COMM., COMMAND & TRACKING

Includes telemetry; space communications networks; astronavigation and guidance; and radio blackout.

For related information see also *04 Aircraft Communications and Navigation* and *32 Communications and Radar.*

N93-15477*# National Aeronautics and Space Administration. Ames Research Center, Moffett Field, CA.

SPACE STATION FREEDOM DATA MANAGEMENT SYSTEM GROWTH AND EVOLUTION REPORT

R. Bartlett (Digital Equipment Corp., Moffett Field, CA.), G. Davis, T. L. Grant, J. Gibson (RECOM Software, Inc., San Jose, CA.), R. Hedges, M. J. Johnson (Research Inst. for Advanced Computer Science, Moffett Field, CA.), Y. K. Liu, A. Patterson-Hine, N. Sliwa, and H. Sowizral et al Sep. 1992 66 p

(RTOP 488-51-01)

(NASA-TM-103869; A-91163; NAS 1.15:103869) Avail: CASI HC A04/MF A01

The Information Sciences Division at the NASA Ames Research Center has completed a 6-month study of portions of the Space Station Freedom Data Management System (DMS). This study looked at the present capabilities and future growth potential of the DMS, and the results are documented in this report. Issues have been raised that were discussed with the appropriate Johnson Space Center (JSC) management and Work Package-2 contractor organizations. Areas requiring additional study have been identified and suggestions for long-term upgrades have been proposed. This activity has allowed the Ames personnel to develop a rapport with the JSC civil service and contractor teams that does permit an independent check and balance technique for the DMS. Author

18 SPACECRAFT DESIGN, TESTING AND PERFORMANCE

Includes satellites; space platforms; space stations; spacecraft systems and components such as thermal and environmental controls; and attitude controls.

For life support systems see *54 Man/System Technology and Life Support.* For related information see also *05 Aircraft Design, Testing and Performance, 39 Structural Mechanics,* and *16 Space Transportation.*

N93-14253# Naval Postgraduate School, Monterey, CA.

PARALLELIZATION OF THE NAVY SPACE SURVEILLANCE CENTER (NAVSPASUR) SATELLITE MODEL M.S. Thesis

Warren E. Phipps, Jr. Jun. 1992 127 p

(AD-A256133) Avail: CASI HC A07/MF A02

The Naval Space Surveillance Center (NAVSPASUR) uses an analytic satellite motion model based on Brouwer-Lyddane theory to assist in tracking over 6000 objects in orbit around the Earth. The satellite motion model is implemented by a Fortran subroutine, PPT2. Due to the increasing number of objects required to be tracked, NAVSPASUR desires a method to reduce the computation time of this satellite motion model. Parallel computing offers one method to achieve this objective. This thesis investigates the parallel computing potential of the NAVSPASUR model using the Intel iPSC/2 hypercube multi-computer. The thesis develops several parallel algorithms for the NAVSPASUR satellite motion model using the various methods of parallelization, applies these algorithms to the hypercube, and reports on each algorithm's potential reduction in computation time. GRA

N93-14274 Michigan Univ., Ann Arbor.

DAMAGE LOCATION AND MODEL REFINEMENT FOR LARGE FLEXIBLE SPACE STRUCTURES USING A SENSITIVITY-BASED EIGENSTRUCTURE ASSIGNMENT METHOD Ph.D. Thesis

Thomas Anthony Lwang Kashangaki 1992 245 p

Avail: Univ. Microfilms Order No. DA9226935

The complexity and size of the next generation of spacecraft, along with the exceedingly high performance and pointing accuracy requirements, mandate that the load carrying capability of the structures be maintained at all times. This work describes a systematic method by which large structures, such as the Space Station Freedom, can be examined periodically to evaluate the integrity of the load carrying structures and determine the location and magnitude of damage to the structure if such damage exists. The Eigenstructure Assignment Damage Location method is developed and successfully demonstrated using modal data from a comprehensive set of tests on a hybrid scaled Space Station truss. The algorithm computes the distance between the measured eigenvectors and a subspace that is spanned by the columns of the damaged structure's system matrix. Damage is located when this distance is zero (for exact data). Once the damage has been located, a simple calculation provides the magnitude of the damage. The method has several unique features, including the ability to easily include loss of mass as well as the ability to filter noise from the measured data. The Model Sensitivity parameter, a scalar measure of each eigenpair's sensitivity to damage in a particular truss member, was developed to assist in pre-test determination of the ability to detect damage in different critical members. The modal strain energy distribution and the Modal Assurance Criterion are also shown to be useful indicators of the ability to detect damage. Dissert. Abstr.

N93-14536# Naval Postgraduate School, Monterey, CA.

COMPUTER BASED SATELLITE DESIGN M.S. Thesis

David D. Lashbrook Jun. 1992 235 p

(AD-A255315) Avail: CASI HC A11/MF A03

A computer program to design geosynchronous spacecraft has been developed. The program consists of four separate but interrelated executable computer programs. The programs are compiled to run on a DOS based personnel computer. The source code is written in DoD mandated Ada programming language. The thesis presents the design technique and design equations used in the program. Detailed analysis is performed in the following areas for both dual spin and three axis stabilized spacecraft configurations: (1) Mass Propellent Budget and Mass Summary; (2) Battery Cell and Solar

Cell Requirements for a Payload Power Requirement; and (3) Passive Thermal Control Requirements. A user's manual is included as Appendix A, and the source code for the computer programs as Appendix B. GRA

N93-14565# Synectics Corp., Rome, NY.
ARC DIGITAL RASTER IMAGERY EVALUATION Final Report, Aug. 1991 - Jan. 1992
Brad Rogers and Michael Wasilenko Jun. 1992 59 p
(Contract F30602-91-D-0003)
(AD-A255403; RL-TR-92-154) Avail: CASI HC A04/MF A01

The ARC Digital Raster Imagery (ADRI) evaluation process was an evaluation of the absolute horizontal and vertical accuracy of the ADRI product. Both absolute and relative horizontal evaluation activities employed the same statistical measures for the analysis, namely; the mean error in latitude and longitude; standard deviations of the errors in latitude and longitude; the root mean square of the errors for latitude and longitude; and the average error for latitude and longitude. The vertical accuracy analysis employed mean height error; standard deviation of the height errors; RMS of the height errors and average height error. GRA

N93-14585 Wisconsin Univ., Madison.
COMPARATIVE STUDY OF STABILITY OF FLEXIBLE SATELLITES WITH AND WITHOUT GUY-WIRE CONSTRAINTS Ph.D. Thesis
Andre Peter Mazzoleni 1992 121 p
Avail: Univ. Microfilms Order No. DA9221922

Stability criteria are obtained via Liapunov's direct method for gravity gradient and dual spin stabilized satellites with flexible appendages with and without guy-wire constraints. Examples show a significant difference in flexible appendage stiffness requirements between guy-wired and unconstrained satellites. Full field stability diagrams for guy-wired satellites are presented. While there may be design considerations that make the attachment of guy wires difficult for some satellite configurations, the results of this thesis show that there are significant advantages to be gained by using guy wires, and that their use should be strongly considered in satellite design. A nonlinear beam model is used in conjunction with Liapunov's direct method to obtain stability criteria for a satellite with flexible beams with three dimensional bodies attached to the ends of the beams. Previous studies in the literature using Liapunov's direct method to obtain stability criteria for satellites with flexible beams with attached masses restricted their analysis to a point mass at the end of each beam. Tests are developed to determine instability regions for general classes of systems in parameter space. Simplifications of the tests for even dimensional, Hamiltonian, second order, and damped systems are derived. These tests are used in conjunction with Liapunov's direct method to obtain exact stability boundaries in parameter space in cases where Liapunov methods give only sufficient conditions for stability. Dissert. Abstr.

N93-14586 Colorado Univ., Boulder.
PRECISION RADIATION FORCE MODELING FOR THE TOPEX/POSEIDON MISSION Ph.D. Thesis
Peter Garo Antreasian 1992 242 p
Avail: Univ. Microfilms Order No. DA9232659

The largest non-gravitational forces that will be acting on the Topex satellite will be those due to incident and emitted radiation on the spacecraft surfaces. In order to minimize the effects of these forces on orbit determination, a detailed model has been developed so that they may be accurately predicted. This model requires a precise description of the spacecraft shape and orientation, evaluation of the solar and Earth radiation impinging on the surfaces and a determination of the radiation being emitted from the surfaces as they heat and cool throughout the orbit. The TRASYS software system is used to evaluate the solar and Earth radiation (albedo and infrared) striking each surface of the spacecraft. this software has been modified to include a Earth radiation model which follows the seasonal variations in albedo and infrared radiation. The SINDA software system is then used to determine the transient temperatures of the spacecraft surfaces. Orbital thermal histories of significant features are given. These temperatures are used to determine the force exerted on each surface due to thermal emission. Especially unique to this area of research, is the detailed analysis of the thermal emissive force upon the spacecraft. The emission forces are combined with the incident radiation forces to determine the total force acting on the satellite. In addition, since TOPEX will employ active radiators such as the altimeter, an approximation of the recoil force from its transmission of radiation is given. Results are presented which show the accelerations induced on the spacecraft by these forces. The effects of solar radiation, albedo, infrared and surface emissions are given separately so that their relative importance may be clearly evaluated. A error analysis has been performed upon this computationally extensive model by incorporating upper and lower bounds of the various parameter definitions. The extent to which this 'Micro' model is being utilized to improve the orbit determination of TOPEX using simple 'Macro' models is also discussed. Dissert. Abstr.

N93-14606* National Aeronautics and Space Administration, Washington, DC.
LARGE SPACE STRUCTURES AND SYSTEMS IN THE SPACE STATION ERA: A BIBLIOGRAPHY WITH INDEXES (SUPPLEMENT 04)
Oct. 1992 329 p
(NASA-SP-7085(04); NAS 1.21:7085(04)) Avail: CASI HC A15

Bibliographies and abstracts are listed for 1211 reports, articles, and other documents introduced into the NASA scientific and technical information system between 1 Jul. and 30 Dec. 1991. Its purpose is to provide helpful information to the researcher, manager, and designer in technology development and mission design according to system, interactive analysis and design, structural concepts and control systems, electronics, advanced materials, assembly concepts, propulsion, and solar power satellite systems. Author

N93-14632 Texas A&M Univ., College Station.
DEVELOPMENT OF ENGINEERING METHODS FOR NONEQUILIBRIUM RADIATIVE PHENOMENA ABOUT AEROASSISTED ENTRY VEHICLES Ph.D. Thesis
Thomas Anthony Gally 1992 167 p
Avail: Univ. Microfilms Order No. DA9232502

A viscous shock layer analysis method has been developed which includes the effects of chemical nonequilibrium, multi-temperature effects, viscous effects, and radiative gasdynamic coupling. This flowfield analysis has been used to investigate a new multicomponent diffusion method and the effects of an existing thermodynamic nonequilibrium method. A new thermodynamic nonequilibrium model is developed based on a recent atomic excitation method for nitrogen and oxygen. Comparisons between the old and new thermodynamic models in part verify the assumptions used in the older model but indicate a possible over correction of the older method. Comparisons with flight test data show good agreement with the current methodology but show a need for improvement in the modeling of molecular nonequilibrium excitation. Dissert. Abstr.

N93-14725 Department of the Navy, Washington, DC.
SHAPE-STABLE REENTRY BODY NOSE TIP Patent Application
Walter K. Osaka, inventor (to Navy), Thomas T. Ngai, inventor (to Navy), and Anthony Wereta, Jr., inventor (to Navy) 28 Apr. 1992 12 p Filed 1 Feb. 1991
(AD-D015437; US-Patent-Appl-SN-660214) Avail: CASI HC A03/MF A01

A reentry body nose tip constructed from materials and produced by a process such that shape stability is maintained under ablative erosion occurring during atmospheric reentry is discussed. GRA

N93-14733*# Science Applications International Corp., Torrance, CA. Space and Defense Group.
REUSABLE REENTRY SATELLITE (RRS) SYSTEM DESIGN STUDY Final Report
Feb. 1991 392 p Prepared in cooperation with Fairchild Space Co., Germantown, MD
(Contract NAS9-18202)
(NASA-CR-187897; NAS 1.26:187897; RRS-037) Avail: CASI HC A17/MF A04

The Reusable Reentry Satellite (RRS) is intended to provide investigators in several biological disciplines with a relatively inexpensive method to access space for up to 60 days with eventual recovery on Earth. The RRS will permit totally intact, relatively soft, recovery of the vehicle, system refurbishment, and reflight with new and varied payloads. The RRS is to be capable of three reflights per year over a 10-year program lifetime. The RRS vehicle will have a large and readily accessible volume near the vehicle center of gravity for the Payload Module (PM) containing the

experiment hardware. The vehicle is configured to permit the experimenter late access to the PM prior to launch and rapid access following recovery. The RRS will operate in one of two modes: (1) as a free-flying spacecraft in orbit, and will be allowed to drift in attitude to provide an acceleration environment of less than 10(exp -5) g. the acceleration environment during orbital trim maneuvers will be less than 10(exp -3) g; and (2) as an artificial gravity system which spins at controlled rates to provide an artificial gravity of up to 1.5 Earth g. The RRS system will be designed to be rugged, easily maintained, and economically refurbishable for the next flight. Some systems may be designed to be replaced rather than refurbished, if cost effective and capable of meeting the specified turnaround time. The minimum time between recovery and reflight will be approximately 60 days. The PMs will be designed to be relatively autonomous, with experiments that require few commands and limited telemetry. Mass data storage will be accommodated in the PM. The hardware development and implementation phase is currently expected to start in 1991 with a first launch in late 1993. Author

N93-14837 Colorado Univ., Boulder.
THERMAL ELASTIC SHOCK AND ITS EFFECT ON SPACECRAFT ATTITUDE CONTROL Ph.D. Thesis
Darrell Frank Zimbelman 1990 208 p
Avail: Univ. Microfilms Order No. DA9232756

Thermal elastic shock (TES) is a twice per orbit impulsive disturbance torque experienced by low-Earth orbiting spacecraft. The disturbance is attributed to the vehicle passage in and out of the Earth's umbra. During penumbral transitions, large flexible appendages undergo thermally induced bending caused by rapidly changing thermal conditions. Flexible structures, in particular solar arrays, experience rapid cooling during entrance and rapid heating at exit. TES has been observed during normal on-orbit operations of the LANDSAT-4 spacecraft, the Communications Technology Satellite and the Hubble Space Telescope. The fundamental equations used to model the TES disturbance torque for typical spacecraft appendages (e.g. solar arrays and antenna booms) are derived in detail. The time rates of change of the thermal gradient are shown to be the driving force behind estimating the TES disturbance torque. In order to predict the thermal response of a typical satellite solar array, a detailed thermal model is developed. The TOPEX spacecraft, designed using LANDSAT heritage, is selected to demonstrate the extensive thermo-mechanical modeling of the TES disturbance. In particular, the attitude pointing performance of the TOPEX spacecraft, when subjected to the TES disturbance, is analyzed using a three-axis, non-linear, time-domain simulation. Results indicate that the TOPEX spacecraft will exceed its roll axis attitude control requirement during prenumbral transitions, and remain in violation for approximately 150 sec each orbit until the umbra collapses. Fortunately, the attitude deviations are not large enough to cause the primary science instrument, a radar altimeter, to break lock, which would result in temporary loss of data. A localized active control system is proposed as a solution to minimize and/or eliminate the degrading effects of the TES disturbance. The feasibility of the control system is demonstrated by including it as part of a TOPEX vehicle design and re-evaluating the attitude pointing performance using the numerical simulation. Results show that the roll axis control requirement violation period could be appreciably reduced, for a TOPEX vehicle, if the torque authority of the control system reaction wheel is about 0.6 N - m. Dissert. Abstr.

N93-14872*# Science Applications International Corp., Torrance, CA.
REUSABLE REENTRY SATELLITE (RRS) SYSTEM DESIGN STUDY: SYSTEM COST ESTIMATES DOCUMENT
Feb. 1991 341 p
(Contract NAS9-18202)
(NASA-CR-188480; NAS 1.26:188480; RRS-046) Avail: CASI HC A15/MF A03

The Reusable Reentry Satellite (RRS) program was initiated to provide life science investigators relatively inexpensive, frequent access to space for extended periods of time with eventual satellite recovery on earth. The RRS will provide an on-orbit laboratory for research on biological and material processes, be launched from a number of expendable launch vehicles, and operate in Low-Altitude Earth Orbit (LEO) as a free-flying unmanned laboratory. SAIC's design will provide independent atmospheric reentry and soft landing in the continental U.S., orbit for a maximum of 60 days, and will sustain three flights per year for 10 years. The Reusable Reentry Vehicle (RRV) will be 3-axis stabilized with artificial gravity up to 1.5g's, be rugged and easily maintainable, and have a modular design to accommodate a satellite bus and separate modular payloads (e.g., rodent module, general biological module, ESA microgravity botany facility, general botany module). The purpose of this System Cost Estimate Document is to provide a Life Cycle Cost Estimate (LCCE) for a NASA RRS Program using SAIC's RRS design. The estimate includes development, procurement, and 10 years of operations and support (O&S) costs for NASA's RRS program. The estimate does not include costs for other agencies which may track or interface with the RRS program (e.g., Air Force tracking agencies or individual RRS experimenters involved with special payload modules (PM's)). The life cycle cost estimate extends over the 10 year operation and support period FY99-2008. Author

N93-14904# Los Alamos National Lab., NM.
PREVIEW OF BLACKBEARD INTERFEROMETRY
M. J. Carter 1992 5 p Presented at the Beacon Satellite Symposium, Boston, MA, 5-12 Jul. 1992
(Contract W-7405-eng-36)
(DE92-040329; LA-UR-92-2609; CONF-9207118-4) Avail: CASI HC A01/MF A01

Blackbeard is a broadband VHF measurement satellite experiment designed and built by the Space Science and Technology Division of the Los Alamos National Laboratory. Blackbeard is a piggy-back experiment on the ALEXIS satellite to be launched into a 70 degree inclination orbit at an altitude of 750 km. The satellite experimental operation and data retrieval are controlled through a telemetry link from the Satellite Operations Center (SOC) located at Los Alamos, NM. The primary experimental objectives of Blackbeard are three-fold: (1) Study the dispersion of broad-band impulsive electromagnetic signals -- in particular, the higher-order amplitude and phase distortion due to propagation through the ionosphere. These depend on ionospheric conditions and irregularities. (2) Utilize RF interferometry and scintillation techniques in the low VHF-band to determine the size and extent of ionospheric irregularities and wave structure -- both natural and artificially induced. This narrow-band data will be used to categorize the ionospheric media as undisturbed, oscillatory, or turbulent. These parameters will then be input into transfer function simulations for broad-band propagation and compared with broad-band propagation data from Blackbeard. (3) Survey and characterize background noise in the VHF-band-consisting of (1) cataloging broadcast amplitudes and signatures and mapping their global pattern, and (2) cataloging the signatures of lightning events. Also, correlate emissions in the visible and VHF bands in an attempt to confirm broad-band RF emissions assumed to be associated with lightning. DOE

N93-15071# Aerospatiale, Cannes (France).
REGIONAL SATELLITES: THE EUROPEAN EXPERIENCE WITH EUTELSAT FOR TV, VOICE, DATA AND MOBILE TRANSMISSIONS
J. J. Bloch 1992 5 p
(Rept-921-440-106; ETN-92-92359) Avail: CASI HC A01/MF A01

The ten year old Eutelsat satellite network is described. The current generation and the initial satellites are compared. The capability to adjust to market demand is emphasized. Some teachings from the Eutelsat experience that can be used by designers and business planners of emerging satellite networks in Latin America are: keep flexibility in the payload, use transparent transponders, switchable coverages, and steerable beams; television (TV) is the backbone revenue making service; countries with liberal TV provision policies should be marketed heavily; worldwide TV networks should be a prime marketing target; do not expect telephony to take up much loading; and VSAT (Very Small Aperture Terminals) network using time division multiple access are not large bandwidth consumer--many private networks are needed to fill up a transponder. ESA

N93-15368*# National Aeronautics and Space Administration. Langley Research Center, Hampton, VA.
STRUCTURALLY ADAPTIVE SPACE CRANE CONCEPT FOR ASSEMBLING SPACE SYSTEMS ON ORBIT
John T. Dorsey, Thomas R. Sutter, and K. Chauncey Wu Washington Nov. 1992 20 p
(RTOP 506-43-41-02)
(NASA-TP-3307; L-17175; NAS 1.15:3307) Avail: CASI HC A03/MF A01

Many future human space exploration missions will probably require large vehicles that must be assembled on orbit. Thus, a device that can move, position, and assemble large and massive spacecraft components on orbit becomes essential for these missions. A concept is described for such a device: a space crane concept that uses erectable truss hardware to achieve high-stiffness and low-mass booms and uses articulating truss joints that can be assembled on orbit. The hardware has been tested and shown to have linear load-deflection response and to be structurally predictable. The hardware also permits the crane to be reconfigured into different geometries to satisfy future assembly requirements. A number of articulating and rotary joint concepts have been sized and analyzed, and the results are discussed. Two strategies were proposed to suppress motion-induced vibration: placing viscous dampers in selected truss struts and preshaping motion commands. Preliminary analyses indicate that these techniques have the potential to greatly enhance structural damping.

Author

N93-15593*# National Aeronautics and Space Administration. Goddard Space Flight Center, Greenbelt, MD.

THE SEVENTEENTH SPACE SIMULATION CONFERENCE. TERRESTRIAL TEST FOR SPACE SUCCESS

Joseph L. Stecher, III, comp. Washington Nov. 1992 346 p Conference held in Baltimore, MD, 9-12 Nov. 1992; cosponsored by AIAA, American Society for Testing and Materials, and Canadian Space Agency

(NASA-CP-3181; Rept-92B00118; NAS 1.55:3181) Avail: CASI HC A15/MF A03

The Institute of Environmental Sciences' Seventeenth Space Simulation Conference, 'Terrestrial Test for Space Success' provided participants with a forum to acquire and exchange information on the state of the art in space simulation, test technology, atomic oxygen, dynamics testing, contamination, and materials. The papers presented at this conference and the resulting discussions carried out the conference theme of 'terrestrial test for space success.' For individual titles, see N93-15594 through N93-15623.

N93-15594*# National Aeronautics and Space Administration. Lewis Research Center, Cleveland, OH.

LOW EARTH ORBIT ATOMIC OXYGEN SIMULATION FOR DURABILITY EVALUATION OF SOLAR REFLECTOR SURFACES

Kim K. deGroh and Bruce A. Banks *In* NASA. Goddard Space Flight Center, The Seventeenth Space Simulation Conference. Terrestrial Test for Space Success Nov. 1992 p 1-17 (For primary document see N93-15593 04-18)

Avail: CASI HC A03/MF A03

To evaluate the performance and durability of solar reflector surfaces in the atomic oxygen environment typical of low Earth orbit (LEO), one must expose the reflector surface either directly to LEO or to ground-laboratory atomic oxygen environments. Although actual LEO exposures are most desired, such opportunities are typically scarce, expensive, and of limited duration. As a result, ground-laboratory exposures must be relied upon as the most practical long-term durability evaluation technique. Plasma ashers are widely used as LEO simulation facilities by producing atomic oxygen environments for durability evaluation of potential spacecraft materials. Atomic oxygen arrival differs between ground and space exposure in that plasma asher exposure produces isotropic arrival and space solar tracking produces sweeping arrival. Differences in initial impact reaction probability occur, dependent upon the energy and species existing in these environments. Due to the variations in ground-laboratory and space atomic oxygen, quantification of in-space performance based on plasma asher testing is not straightforward. The various atomic oxygen interactions that can occur with reflector surfaces, such as undercutting in organic substrates at protective coating defect sites, ground-laboratory techniques recommended for evaluating the atomic oxygen durability of reflectors based on asher exposures, and computational techniques which make use of ground-laboratory atomic oxygen exposure to predict in-space LEO durability are addressed.

Author

N93-15595*# National Aeronautics and Space Administration. Lewis Research Center, Cleveland, OH.

SIMULATION OF THE SYNERGISTIC LOW EARTH ORBIT EFFECTS OF VACUUM THERMAL CYCLING, VACUUM UV RADIATION, AND ATOMIC OXYGEN

Joyce A. Dever, Kim K. deGroh, Curtis R. Stidham (Sverdrup Technology, Inc., Brook Park, OH.), Thomas J. Stueber (Sverdrup Technology, Inc., Brook Park, OH.), Therese M. Dever (Cleveland State Univ., OH.), Elvin Rodriguez (Cleveland State Univ., OH.), and Judith A. Terlep (Case Western Reserve Univ., Cleveland, OH.) *In* NASA. Goddard Space Flight Center, The Seventeenth Space Simulation Conference. Terrestrial Test for Space Success Nov. 1992 p 19-36 (For primary document see N93-15593 04-18)

Avail: CASI HC A03/MF A03

In order to assess the low Earth orbit (LEO) durability of candidate space materials, it is necessary to use ground laboratory facilities which provide LEO environmental effects. A facility combining vacuum thermal cycling and vacuum ultraviolet (VUV) radiation has been designed and constructed at NASA Lewis Research Center for this purpose. This facility can also be operated without the VUV lamps. An additional facility can be used to provide VUV exposure only. By utilizing these facilities, followed by atomic oxygen exposure in an RF plasma asher, the effects of the individual vacuum thermal cycling and VUV environments can be compared to the effect of the combined vacuum thermal cycling/VUV environment on the atomic oxygen durability of materials. The synergistic effects of simulated LEO environmental conditions on materials were evaluated by first exposing materials to vacuum thermal cycling, VUV, and vacuum thermal cycling/VUV environments followed by exposure to atomic oxygen in an RP plasma asher. Candidate space power materials such as atomic oxygen protected polyimides and solar concentrator mirrors were evaluated using these facilities. Characteristics of the Vacuum Thermal Cycling/VUV Exposure Facility which simulates the temperature sequences and solar ultraviolet radiation exposure that would be experienced by a spacecraft surface in LEO are discussed. Results of durability evaluations of some candidate space power materials to the simulated LEO environmental conditions will also be discussed. Such results have indicated that for some materials, atomic oxygen durability is affected by previous exposure to thermal cycling and/or VUV exposure.

Author

N93-15596*# National Aeronautics and Space Administration. Lewis Research Center, Cleveland, OH.

THE USE OF PLASMA ASHERS AND MONTE CARLO MODELING FOR THE PROJECTION OF ATOMIC OXYGEN DURABILITY OF PROTECTED POLYMERS IN LOW EARTH ORBIT

Bruce A. Banks, Bruce M. Auer, Sharon K. Rutledge, Kim K. deGroh, and Linda Gebauer (Cleveland State Univ., OH.) *In* NASA. Goddard Space Flight Center, The Seventeenth Space Simulation Conference. Terrestrial Test for Space Success Nov. 1992 p 37-48 (For primary document see N93-15593 04-18)

Avail: CASI HC A03/MF A03

The results of ground laboratory and in-space exposure of polymeric materials to atomic oxygen has enabled the development of a Monte Carlo computational model which simulates the oxidation processes of both environments. The cost effective projection of long-term low-Earth-orbital durability of protected polymeric materials such as SiO(x)-coated polyimide Kapton photovoltaic array blankets will require ground-based testing to assure power system reliability. Although silicon dioxide thin film protective coatings can greatly extend the useful life of polymeric materials in ground-based testing, the projection of in-space durability based on these results can be made more reliable through the use of modeling which simulates the mechanistic properties of atomic oxygen interaction, and replicates test results in both environments. Techniques to project long-term performance of protected materials, such as the Space Station Freedom solar array blankets, are developed based on ground laboratory experiments, in-space experiments, and computational modeling.

Author

N93-15597*# National Aeronautics and Space Administration. Lewis Research Center, Cleveland, OH.

LEVELING COATINGS FOR REDUCING THE ATOMIC OXYGEN DEFECT DENSITY IN PROTECTED GRAPHITE FIBER EPOXY COMPOSITES

D. A. Jaworske, Kim K. deGroh, G. Podojil (Cleveland State Univ., OH.), T. McCollum (Cleveland State Univ., OH.), and J. Anzic (Cleveland State Univ., OH.) *In* NASA. Goddard Space Flight Center, The Seventeenth Space Simulation Conference. Terrestrial Test for Space Success Nov.

1992 p 49-58 (For primary document see N93-15593 04-18)
Avail: CASI HC A02/MF A03

Pinholes or other defect sites in a protective oxide coating provide pathways for atomic oxygen in low Earth orbit to reach underlying material. One concept of enhancing the lifetime of materials in low Earth orbit is to apply a leveling coating to the material prior to applying any reflective and protective coatings. Using a surface tension leveling coating concept, a low viscosity epoxy was applied to the surface of several composite coupons. A protective layer of 1000 A of SiO2 was deposited on top of the leveling coating, and the coupons were exposed to an atomic oxygen environment in a plasma asher. Pinhole populations per unit area were estimated by counting the number of undercut sites observed by scanning electron microscopy. Defect density values of 180,000 defects/sq cm were reduced to about 1000 defects/sq cm as a result of the applied leveling coating. These improvements occur at a mass penalty of about 2.5 mg/sq cm.
Author

N93-15598*# Industrieanlagen-Betriebsgesellschaft m.b.H., Ottobrunn (Germany).

MULTI-AXIS TRANSIENT VIBRATION TESTING OF SPACE OBJECTS: TEST PHILOSOPHY, TEST FACILITY, AND CONTROL STRATEGY

Georg Lachenmayr *In* NASA. Goddard Space Flight Center, The Seventeenth Space Simulation Conference. Terrestrial Test for Space Success Nov. 1992 p 59-74 (For primary document see N93-15593 04-18)
Avail: CASI HC A03/MF A03

IABG has been using various servohydraulic test facilities for many years for the reproduction of service loads and environmental loads on all kinds of test objects. For more than 15 years, a multi-axis vibration test facility has been under service, originally designed for earthquake simulation but being upgraded to the demands of space testing. First tests with the DFS/STM showed good reproduction accuracy and demonstrated the feasibility of transient vibration testing of space objects on a multi-axis hydraulic shaker. An approach to structural qualification is possible by using this test philosophy. It will be outlined and its obvious advantages over the state-of-the-art single-axis test will be demonstrated by example results. The new test technique has some special requirements to the test facility exceeding those of earthquake testing. Most important is the high reproduction accuracy demanded for a sophisticated control system. The state-of-the-art approach of analog closed-loop control circuits for each actuator combined with a static decoupling network and an off-line iterative waveform control is not able to meet all the demands. Therefore, the future over-all control system is implemented as hierarchical full digital closed-loop system on a highly parallel transputer network. The innermost layer is the digital actuator controller, the second one is the MDOF-control of the table movement. The outermost layer would be the off-line iterative waveform control, which is dedicated only to deal with the interaction of test table and test object or non-linear effects. The outline of the system will be presented.
Author

N93-15599*# National Aeronautics and Space Administration. Goddard Space Flight Center, Greenbelt, MD.

VIBRATION AND ACOUSTIC TESTING OF TOPEX/POSEIDON SATELLITE

Dave Boatman (Jet Propulsion Lab., California Inst. of Tech., Pasadena.), Terry Scharton (Jet Propulsion Lab., California Inst. of Tech., Pasadena.), Donald Hershfeld, and Paul Larkin (Fairchild Space Co., Germantown, MD.) *In its* The Seventeenth Space Simulation Conference. Terrestrial Test for Space Success Nov. 1992 p 75-84 (For primary document see N93-15593 04-18)
Avail: CASI HC A02/MF A03

The satellite was subjected to a 1.5G swept sine vibration test and a 146 dB overall level acoustic test, in accordance with Ariane launch vehicle requirements, at the NASA Goddard Space Flight Center. Extensive pretest analysis of the sine test was conducted to plan the input notching and to justify vibration testing the satellite only in the longitudinal axis. A unique measurement system was utilized to determine the six components of interface force between the shaker and the satellite in the sine vibration test. The satellite was heavily instrumented in both the sine vibration and acoustic test in order to insure that the launch loads were enveloped with appropriate margin and that satellite responses did not exceed the compatibilities of the structure and equipment. The test specification, objectives, instrumentation, and test results are described herein.
Author

N93-15600*# European Space Agency. European Space Research and Technology Center, ESTEC, Noordwijk (Netherlands).

THE DESIGN CONCEPT OF THE 6-DEGREE-OF-FREEDOM HYDRAULIC SHAKER AT ESTEC

P.W. Brinkman and D. Kretz (Mannesmann-Rexroth, Lohr am Main, Germany) *In* NASA. Goddard Space Flight Center, The Seventeenth Space Simulation Conference. Terrestrial Test for Space Success Nov. 1992 p 85-107 Sponsored in part by AGE-Elektronik G.m.b.H.; SEREME; and ASAP (For primary document see N93-15593 04-18)
Avail: CASI HC A03/MF A03

The European Space Agency (ESA) has decided to extend its test facilities at the European Space and Technology Center (ESTEC) at Noordwijk, The Netherlands, by implementing a 6-degree-of-freedom hydraulic shaker. This shaker will permit vibration testing of large payloads in the frequency range from 0.1 Hz to 100 Hz. Conventional single axis sine and random vibration modes can be applied without the need for a configuration change of the test set-up for vertical and lateral excitations. Transients occurring during launch and/or landing of space vehicles can be accurately simulated in 6-degrees-of-freedom. The performance requirements of the shaker are outlined and the results of the various trade-offs, which are investigated during the initial phase of the design and engineering program are provided. Finally, the resulting baseline concept and the anticipated implementation plan of the new test facility are presented.
Author

N93-15601*# Rockwell International Corp., Canoga Park, CA. Rocketdyne Div.

AN ENVIRONMENTAL TESTING FACILITY FOR SPACE STATION FREEDOM POWER MANAGEMENT AND DISTRIBUTION HARDWARE Abstract Only

Arthur S. Jackola and Gary L. Hartjen *In* NASA. Goddard Space Flight Center, The Seventeenth Space Simulation Conference. Terrestrial Test for Space Success Nov. 1992 p 109 (For primary document see N93-15593 04-18)
Avail: CASI HC A01/MF A03

The plans for a new test facility, including new environmental test systems, which are presently under construction, and the major environmental Test Support Equipment (TSE) used therein are addressed. This all-new Rocketdyne facility will perform space simulation environmental tests on Power Management and Distribution (PMAD) hardware to Space Station Freedom (SSF) at the Engineering Model, Qualification Model, and Flight Model levels of fidelity. Testing will include Random Vibration in three axes - Thermal Vacuum, Thermal Cycling and Thermal Burn-in - as well as numerous electrical functional tests. The facility is designed to support a relatively high throughput of hardware under test, while maintaining the high standards required for a man-rated space program.
Author

N93-15602*# National Aeronautics and Space Administration. Lyndon B. Johnson Space Center, Houston, TX.

MANNED TESTING IN A SIMULATED SPACE ENVIRONMENT Abstract Only

Donna L. Fender *In* NASA. Goddard Space Flight Center, The Seventeenth Space Simulation Conference. Terrestrial Test for Space Success Nov. 1992 p 111 (For primary document see N93-15593 04-18)
Avail: CASI HC A01/MF A03

A view of the facility and operational requirements involved in performing a manned thermal vacuum test is presented. The requirements fall into two major categories. The first category deals with placing the suited crewmen in a hazardous environment and assuring their safety. The second category deals with the constraints and special requirements involved with a suited crewman operating flight hardware in a 1-G environment. Design areas that deal with man rating a chamber, including fire suppression, emergency repress, emergency power, backups, reliable instrumentation and data systems, communications, television monitoring, biomedical monitoring, material compatibilities, and equipment supporting the Extravehicular Mobility Unit (EMU) are discussed. The operational issues that are peculiar to manned testing such as test rules, test procedures, test protocol, emergency drills, availability of hyperbaric facilities, test team training and certification engineering concerns for a safe mechanical and

instrumentation buildup, hazard analysis, and Failure Modes and Effects Analysis are discussed. The constraints and special requirements involved with a suited crewman operating flight hardware in a 1-G environment are addressed. Author

N93-15603*# Electromagnetic Sciences, Inc., Norcross, GA.
ON-ORBIT DEPLOYMENT ANAMOLIES: WHAT CAN BE DONE?
Michael Freeman *In* NASA. Goddard Space Flight Center, The Seventeenth Space Simulation Conference. Terrestrial Test for Space Success Nov. 1992 p 113-136 (For primary document see N93-15593 04-18)
Avail: CASI HC A03/MF A03

Modern communications satellites rely heavily upon deployable appendage (i.e., solar arrays, communications antennas, etc.) to perform vital functions that enable the spacecraft to effectively conduct mission objectives. Communications and telemetry antennas provide the radio-frequency link between the spacecraft and the earth ground station, permitting data to be transmitted and received from the satellite. Solar arrays serve as the principle source of electrical energy to the satellite, and re-charge internal batteries during operation. However, since satellites cannot carry back-up systems, if a solar array fails to deploy, the mission is lost. The subject of on-orbit anomalies related to the deployment of spacecraft appendage, and possible causes of such failures are examined. Topics discussed include mechanical launch loading, on-orbit thermal and solar concerns, reliability of spacecraft pyrotechnics, and practical limitations of ground-based deployment testing. Of particular significance, the article features an in-depth look at the lessons learned from the successful recovery of the Telesat Canada Anik-E2 satellite in 1991. Author

N93-15604*# Computational Mechanics Consultants, Inc., Towson, MD.
HYPERVELOCITY IMPACT SIMULATIONS OF WHIPPLE SHIELDS
Steven B. Segletes and Jonas A. Zukas *In* NASA. Goddard Space Flight Center, The Seventeenth Space Simulation Conference. Terrestrial Test for Space Success Nov. 1992 p 137-149 (For primary document see N93-15593 04-18)
Avail: CASI HC A03/MF A03

The problem associated with protecting space vehicles from space debris impact is described. Numerical simulation is espoused as a useful complement to experimentation: as a means to help understand and describe the hypervelocity impact phenomena. The capabilities of a PC-based hydrocode, ZeuS, are described, for application to the problem of hypervelocity impact. Finally, results of ZeuS simulations, as applied to the problem of bumper shield impact, are presented and compared with experimental results. Author

N93-15605*# Spar Aerospace Ltd., Ottawa (Ontario). Satellite and Communications Systems Div.
OFFLOADING TECHNIQUES FOR LARGE DEPLOYABLE SPACE STRUCTURES Abstract Only
Levino Caravaggio and Alex Golob *In* NASA. Goddard Space Flight Center, The Seventeenth Space Simulation Conference. Terrestrial Test for Space Success Nov. 1992 p 151 (For primary document see N93-15593 04-18)
Avail: CASI HC A01/MF A03

The validation and verification of large deployable space structures are continual challenges which face the integration and test engineer today. Spar Aerospace Limited has worked on various programs in which such structure validation was required and faces similar tasks in the future. This testing is reported and the different offloading and deployment methods which were used, as well as the proposed methods which will be used on future programs, are described. Past programs discussed include the Olympus solar array ambient and thermal vacuum deployments, and the Anik-E array and reflector deployments. The proposed MSAT reflector and boom ambient deployment tests, as well as the proposed RADARSAT Synthetic Aperture Radar (SAR) ambient and thermal vacuum deployment tests will also be presented. A series of tests relating to various component parts of the offloading equipment systems was required. These tests included the characterization and understanding of linear bearings and large (180 in-lbf) constant force spring motors in a thermal vacuum environment, and the results from these tests are presented. Author

N93-15606*# Jet Propulsion Lab., California Inst. of Tech., Pasadena.
A NEW APPROACH FOR DATA ACQUISITION AT THE JPL SPACE SIMULATORS
Terry C. Fisher *In* NASA. Goddard Space Flight Center, The Seventeenth Space Simulation Conference. Terrestrial Test for Space Success Nov. 1992 p 153-164 (For primary document see N93-15593 04-18)
Avail: CASI HC A03/MF A03

In 1990, a personal computer based data acquisition system was put into service for the Space Simulators and Environmental Test Laboratory at the Jet Propulsion Laboratory (JPL) in Pasadena, California. The new system replaced an outdated minicomputer system which had been in use since 1980. This new data acquisition system was designed and built by JPL for the specific task of acquiring thermal test data in support of space simulation and thermal vacuum testing at JPL. The data acquisition system was designed using powerful personal computers and local-area-network (LAN) technology. Reliability, expandability, and maintainability were some of the most important criteria in the design of the data system and in the selection of hardware and software components. The data acquisition system is used to record both test chamber operational data and thermal data from the unit under test. Tests are conducted in numerous small thermal vacuum chambers and in the large solar simulator and range in size from individual components using only 2 or 3 thermocouples to entire planetary spacecraft requiring in excess of 1200 channels of test data. The system supports several of these tests running concurrently. The previous data system is described along with reasons for its replacement, the types of data acquired, the new data system, and the benefits obtained from the new system including information on tests performed to date. Author

N93-15607*# Pittsburgh-Des Moines Steel Co., PA.
A NEW THERMAL VACUUM FACILITY AT THE MARTIN MARIETTA WATERTON PLANT **c14**
Robert N. Watson and John W. Bonn (CVI, Inc., Columbus, OH.) *In* NASA. Goddard Space Flight Center, The Seventeenth Space Simulation Conference. Terrestrial Test for Space Success Nov. 1992 p 165-182 (For primary document see N93-15593 04-18)
Avail: CASI HC A03/MF A03

A new thermal-vacuum facility has been recently completed at the Martin Marietta Waterton plant near Denver, Colorado. The facility was designed, fabricated, installed, and tested as a turn-key project by Pitt-Des Moines Inc. and CVI Inc. The chamber has a 5.49 M by 6.10 M (18 ft by 20 ft) flat floor and a half-cylindrical roof with a diameter of 5.49 M (18 ft). Both ends of the chamber have full cross section doors, with one equipped with translating motors for horizontal motion. The chamber is provided with four 0.91 M (36 inches) cryopumps to obtain an ultimate pressure of 9 x 10(exp -8) Torr (Clean-Dry-Empty). The thermal shroud is designed to operate at a maximum of -179 C (-290 F) with an internal heat input of 316 MJ/Hr (300,000 BTU/Hr) using liquid nitrogen. The shroud is also designed to operate at any temperature between -156 C (-250 F) and 121 C (+250 F) using gaseous nitrogen, and heat or cool at a rate of 1.1 C (2 F) per minute. Author

N93-15608*# NSI Technology Services Corp., Greenbelt, MD.
APPLICATION OF PROGRAMMABLE LOGIC CONTROLLERS TO SPACE SIMULATION
Janet Sushon *In* NASA. Goddard Space Flight Center, The Seventeenth Space Simulation Conference. Terrestrial Test for Space Success Nov. 1992 p 183-195 (For primary document see N93-15593 04-18)
Avail: CASI HC A03/MF A03

Incorporating a state-of-the-art process control and instrumentation system into a complex system for thermal vacuum testing is discussed. The challenge was to connect several independent control systems provided by various vendors to a supervisory computer. This combination will sequentially control and monitor the process, collect the data, and transmit it to color a graphic system for subsequent manipulation. The vacuum system upgrade included: replacement of seventeen diffusion pumps with eight cryogenic pumps and one turbomolecular pump, replacing a relay based control system, replacing vacuum instrumentation, and upgrading the data acquisition system. Author

N93-15609*# Jet Propulsion Lab., California Inst. of Tech., Pasadena.
AN ALTERNATE METHOD FOR ACHIEVING TEMPERATURE CONTROL IN THE -130 C TO 75 C RANGE

Kenneth R. Johnson, Mark R. Anderson, Robert W. Lane, and Maximo G. Cortez *In* NASA. Goddard Space Flight Center, The Seventeenth Space Simulation Conference. Terrestrial Test for Space Success Nov. 1992 p 197-206 (For primary document see N93-15593 04-18)
Avail: CASI HC A02/MF A03

Thermal vacuum testing often requires temperature control of chamber shrouds and heat exchangers within the -130 C to 75 C range. There are two conventional methods which are normally employed to achieve control through this intermediate temperature range: (1) single-pass flow where control is achieved by alternately pulsing hot gaseous nitrogen (GN2) and cold LN2 into the feed line to yield the setpoint temperature; and (2) closed-loop circulation where control is achieved by either electrically heating or LN2 cooling the circulating GN2 to yield the setpoint temperature. A third method, using a mass flow ratio controller along with modulating control valves on GN2 and LN2 lines, provides excellent control but equipment for this method is expensive and cost-prohibitive for all but long-term continuous processes. The single-pass method provides marginal control and can result in unexpected overcooling of the test article from even a short pulse of LN2. The closed-loop circulation method provides excellent control but requires an expensive blower capable of operating at elevated pressures and cryogenic temperatures. Where precise control is needed (plus or minus 2 C), single-pass flow systems typically have not provided the precision required, primarily because of overcooling temperature excursions. Where several individual circuits are to be controlled at different temperatures, the use of expensive cryogenic blowers for each circuit is also cost-prohibitive, especially for short duration of one-of-a-kind tests. At JPL, a variant of the single-pass method was developed that was shown to provide precise temperature control in the -130 C to 75 C range while exhibiting minimal setpoint overshoot during temperature transitions. This alternate method uses a commercially available temperature controller along with a GN2/LN2 mixer to dampen the amplitude of cold temperature spikes caused by LN2 pulsing. The design of the GN2/LN2 mixer, the overall control system configuration, the operational procedure, and the prototype system test results are described. Author

N93-15610*# Space Systems/Loral, Palo Alto, CA.
THE EVOLUTION OF SPACE SIMULATION c14
Arthur A. Edwards *In* NASA. Goddard Space Flight Center, The Seventeenth Space Simulation Conference. Terrestrial Test for Space Success Nov. 1992 p 207-220 (For primary document see N93-15593 04-18)
Avail: CASI HC A03/MF A03

Thirty years have passed since the first large (more than 15 ft diameter) thermal vacuum space simulation chambers were built in this country. Many changes have been made since then, and the industry has learned a great deal as the designs have evolved in that time. I was fortunate to have been part of that beginning, and have participated in many of the changes that have occurred since. While talking with vacuum friends recently, I realized that many of the engineers working in the industry today may not be aware of the evolution of space simulation because they did not experience the changes that brought us today's technology. With that in mind, it seems to be appropriate to take a moment and review some of the events that were a big part of the past thirty years in the thermal vacuum business. Perhaps this review will help to understand a little of the 'why' as well as the 'how' of building and operating large thermal vacuum chambers. Author

N93-15611*# NSI Technology Services Corp., Greenbelt, MD.
FROM DIFFUSION PUMPS TO CRYOPUMPS: THE CONVERSION OF GSFC'S SPACE ENVIRONMENT SIMULATOR c14
Ron Cary *In* NASA. Goddard Space Flight Center, The Seventeenth Space Simulation Conference. Terrestrial Test for Space Success Nov. 1992 p 221-227 (For primary document see N93-15593 04-18)
Avail: CASI HC A02/MF A03

The SES (Space Environmental Simulator), largest of the Thermal Vacuum Facilities at The Goddard Space Flight Center, recently was converted from an oil diffusion pumped chamber to a Cryopumped chamber. This modification was driven by requirements of flight projects. The basic requirement was to retain or enhance the operational parameters of the chamber such as pumping speed, ultimate vacuum, pump down time, and thermal system performance. To accomplish this task, seventeen diffusion pumps were removed and replaced with eight 1.2 meter (48 inch) diameter cryopumps and one 0.5 meter (20 inch) turbomolecular pump. The conversion was accomplished with a combination of subcontracting and in-house efforts to maximize the efficiency of implementation. Author

N93-15612*# NSI Technology Services Corp., Greenbelt, MD.
CLEANING OF A THERMAL VACUUM CHAMBER WITH SHROUDS IN PLACE c14
William R. Bond *In* NASA. Goddard Space Flight Center, The Seventeenth Space Simulation Conference. Terrestrial Test for Space Success Nov. 1992 p 229-238 (For primary document see N93-15593 04-18)
Avail: CASI HC A02/MF A03

In February, 1991, a failure of a rotary booster pump caused the diffusion pumps to backstream into a 10 ft x 15 ft thermal vacuum chamber. Concerns existed about the difficulty of removing and reinstalling the shrouds without causing leaks. The time required for the shroud removal was also of concern. These concerns prompted us to attempt to clean the chamber without removing the shrouds. Author

N93-15613*# Intespace, Toulouse (France).
INTESPACE'S NEW THERMAL-VACUUM TEST FACILITY: SIMMER c14
Raymond Duprat and Andre Mouton *In* NASA. Goddard Space Flight Center, The Seventeenth Space Simulation Conference. Terrestrial Test for Space Success Nov. 1992 p 239-250 (For primary document see N93-15593 04-18)
Avail: CASI HC A03/MF A03

The development of an European satellite market over the last 10 years, the industrialization of space applications, and the new requirements from satellite prime contractors have led INTESPACE to increase the test center's environmental testing capacities through the addition of a new thermal-vacuum test facility of impressive dimensions referred to as the SIMMER. The SIMMER is a simulator specifically created for the purpose of conducting acceptance tests of satellites and of large structures of the double launching ARIANE IV or half ARIANE V classes. The chamber is 8.3 meters long with a diameter of 10 meters. The conceptual design of a chamber in the horizontal plane and at floor level is in a view to simplify test preparation and to permit final electrical checks of the spacecraft in its actual test configuration prior to the closing of the chamber. The characteristics of the SIMMER complies with the requirements being currently defined in terms of thermal-vacuum tests: (1) thermal regulation (temperatures cycling between 100 K and 360 K); (2) clean vacuum (10(exp -6) mbar); (3) 600 measurement channels; and (4) 100 000 cleanliness class. The SIMMER is located in INTESPACE's space vehicle test complex in which a large variety of environmental test facilities are made available for having a whole test program completed under one and a same roof. Author

N93-15614*# Science Applications International Corp., Glendora, CA.
OPERATIONAL STRATEGIES FOR CONTAMINATION CONTROL OF COMPOSITE MATERIALS Abstract Only c24
Patricia A. Hansen *In* NASA. Goddard Space Flight Center, The Seventeenth Space Simulation Conference. Terrestrial Test for Space Success Nov. 1992 p 251 (For primary document see N93-15593 04-18)
Avail: CASI HC A01/MF A03

Composite materials, used on many instruments, are a potential contamination source for sensitive sensors, especially for sensors or detectors cooled below -80 C. It is a well known fact that composite materials absorb water during fabrication, integration, test, and launch activities and desorb this water under vacuum conditions. Water absorption can be divided into two types: shallow water and deep water. Shallow water is generally about 500 A thick on a clean material surface and is easily desorbed under vacuum conditions. Deep water is a function of the material and is absorbed into the bulk of the material. Deep water can outgas for weeks, months, or years, depending on the vent path, the amount of absorbed water, and the temperature of the material. Several operational strategies have been successfully employed on the Wide Field Planetary Camera. The operational strategies include ultradry gaseous nitrogen purge, dew point of less than -80 C, and vacuum bake-out with verification of outgassing rates. The nitrogen purge is instituted during the fabrication phase and is continued through launch activities. Great care is taken to avoid extended periods of time that the material is exposed to the ambient environment (50 percent relative humidity). On-orbit operational

strategies include heat-up and cool-down scenarios which allow the deep water to be sufficiently outgassed before cooling the sensors or detectors. Author

N93-15615*# Jet Propulsion Lab., California Inst. of Tech., Pasadena.
ACCELERATED SIMULATION OF NEAR-EARTH-ORBIT POLYMER DEGRADATION **c27**
Eric Laue *In* NASA. Goddard Space Flight Center, The Seventeenth Space Simulation Conference. Terrestrial Test for Space Success Nov. 1992 p 253-274 (For primary document see N93-15593 04-18)
Avail: CASI HC A03/MF A03

There is a need to simulate the near-Earth-orbit environmental conditions, and it is useful to be able to monitor the changes in physical properties of spacecraft materials. Two different methods for simulating the vacuum-ultraviolet (VUV) and soft X-ray near-Earth-orbit flux are presented. Also, methods for monitoring the changes in optical ultraviolet transmission and mass loss are presented. The results of exposures to VUV photons and charged particles on these materials are discussed. Author

N93-15616*# National Aeronautics and Space Administration. Lewis Research Center, Cleveland, OH.
DEGRADATION OF RADIATOR PERFORMANCE ON MARS DUE TO DUST
James R. Gaier, Marla E. Perez-Davis, Sharon K. Rutledge, and Mark Forkapa (Cleveland State Univ., OH.) *In* NASA. Goddard Space Flight Center, The Seventeenth Space Simulation Conference. Terrestrial Test for Space Success Nov. 1992 p 275-288 (For primary document see N93-15593 04-18)
Avail: CASI HC A03/MF A03

An artificial mineral of the approximate elemental composition of Martian soil was manufactured, crushed, and sorted into four different size ranges. Dust particles from three of these size ranges were applied to arc-textured Nb-1 percent Zr and Cu radiator surfaces to assess their effect on radiator performance. Particles larger than 75 microns did not have sufficient adhesive forces to adhere to the samples at angles greater than about 27 deg. Pre-deposited dust layers were largely removed by clear wind velocities greater than 40 m/s, or by dust-laden wind velocities as low as 25 m/s. Smaller dust grains were more difficult to remove. Abrasion was found to be significant only in high velocity winds (89 m/s or greater). Dust-laden winds were found to be more abrasive than clear wind. Initially dusted samples abraded less than initially clear samples in dust laden wind. Smaller dust particles of the simulant proved to be more abrasive than large. This probably indicates that the larger particles were in fact agglomerates. Author

N93-15617*# Rockwell International Corp., Seal Beach, CA.
CONTROL OF ON-ORBIT CONTAMINATION FOR THE ARGOS (P91-1) SATELLITE
Joseph G. Kelley *In* NASA. Goddard Space Flight Center, The Seventeenth Space Simulation Conference. Terrestrial Test for Space Success Nov. 1992 p 289-301 (For primary document see N93-15593 04-18)
Avail: CASI HC A03/MF A03

The ARGOS (P91-1) satellite presents a challenging combination of on-orbit contamination concerns while mandating a low-cost approach. Several experiment payloads contain contamination sensitive optics, another contains large quantities of CO2 and Xe for release in orbit, and one contains an NH3 fueled arc jet thruster. The latter includes a suite of sensors to measure contamination; so prelaunch calculations will be tested. Planned contamination control techniques include: physical separation of sensitive surfaces from contamination sources; flight covers to protect sensitive surfaces during early outgassing on-orbit; gas release and thruster operation early in the flight, before flight covers are opened; and careful control of plumes and venting through a detailed analysis of each. Author

N93-15618*# Jet Propulsion Lab., California Inst. of Tech., Pasadena.
A NEW APPROACH FOR PERFORMING CONTAMINATION CONTROL BAKEOUTS IN JPL THERMAL VACUUM TEST CHAMBERS
Kenneth R. Johnson, Daniel M. Taylor, Robert W. Lane, Maximo G. Cortez, and Mark R. Anderson *In* NASA. Goddard Space Flight Center, The Seventeenth Space Simulation Conference. Terrestrial Test for Space Success Nov. 1992 p 303-312 (For primary document see N93-15593 04-18)
Avail: CASI HC A02/MF A03

Contamination control requirements for the Wide Field/Planetary Camera II (WF/PC II) are necessarily stringent to protect against post-launch contamination of the sensitive optical surfaces, particularly the cold charge coupled device (CCD) imaging surfaces. Typically, thermal vacuum test chambers have employed a liquid nitrogen (LN2) cold trap to collect outgassed contaminants. This approach has the disadvantage of risking recontamination of the test article from shroud offgassing during post-test warmup of the chamber or from any shroud warming of even a few degrees during the bakeout process. By using an enclave, essentially a chamber within a chamber, configured concentrically and internally within an LN2 shroud, a method was developed, based on a design concept by Taylor, for preventing recontamination of test articles during bakeouts and subsequent post-test warmup of the vacuum chamber. Enclaves for testing WF/PC II components were designed and fabricated, then installed in three of JPL's Environmental Test Lab chambers. The design concepts, operating procedures, and test results of this development are discussed. Author

N93-15619*# General Electric Co., Princeton, NJ. Astro Space Div.
MASS SPECTROMETER USE IN A LARGE CHAMBER Abstract Only
Tom Chuvala *In* NASA. Goddard Space Flight Center, The Seventeenth Space Simulation Conference. Terrestrial Test for Space Success Nov. 1992 p 313 (For primary document see N93-15593 04-18)
Avail: CASI HC A01/MF A03

The early satellites were somewhat insensitive to contamination produced during the construction and testing phases. The On-Orbit lifetime was such that contamination effects went either unnoticed or unrecognized. With today's On-Orbit lifetimes approaching 10+ years, contamination has become a paramount concern. The scientific payloads have increased in complexity and sensitivity. The ability to clean a contaminated sensor has greatly diminished. This requires better pumping systems and methods for improved monitoring. The conversion from diffusion pumped thermal vacuum chambers to cryo pumped chambers with the use of Misner traps and selective cold traps has reduced contamination. Witness samples supply a record of the condensates that remain after a testing cycle, but impart no knowledge of the contaminant migration during the cycle that may be a month in duration. Due to a customer's request that mass spectrometry be used during the testing of their spacecraft, a consultant was contracted to install a mass spectrometer to determine the feasibility of the instrument. The equipment and methodology described will start with the original system and its evolution to GE's present system. Author

N93-15620*# Martin Marietta Corp., Denver, CO. Astronautics Group.
TQM IN A TEST ENVIRONMENT **c38**
Gary D. Chambers, Elizabeth A. King, and Keith Oleson *In* NASA. Goddard Space Flight Center, The Seventeenth Space Simulation Conference. Terrestrial Test for Space Success Nov. 1992 p 315-326 (For primary document see N93-15593 04-18)
Avail: CASI HC A03/MF A03

In response to the changing aerospace economic climate, Martin Marietta Astronautics Group (MMAG) has adopted a Total Quality Management (TQM) philosophy to maintain a competitive edge. TQM emphasizes continuous improvement of processes, motivation to improve from within, cross-functional involvement, people empowerment, customer satisfaction, and modern process control techniques. The four major initiatives of TQM are Product Excellence, Manufacturing Resource Planning (MRP II), People Empowerment, and Subcontract Management. The Defense Space and Communications (DS&C) Test Lab's definition and implementation of the MRP II and people empowerment initiatives within TQM are discussed. The application of MRP II to environmental test planning and operations processes required a new and innovative approach. In an 18 month span, the test labs implemented MRP II and people empowerment and achieved a Class 'A' operational status. This resulted in numerous benefits, both tangible and intangible, including significant cost savings and improved quality of life. A detailed description of the implementation process and results are addressed. Author

N93-15621*# General Dynamics Corp., Saint Louis, MO. Space Systems Div.

ACOUSTIC AND THERMAL TESTING OF THE TITAN/CENTAUR UPPER STAGE Abstract Only **c15**

Mark Gehringer, Chris Gibson, and Ron Janes *In* NASA. Goddard Space Flight Center, The Seventeenth Space Simulation Conference. Terrestrial Test for Space Success Nov. 1992 p 327 (For primary document see N93-15593 04-18)

Avail: CASI HC A01/MF A03

A new version of the Centaur high-energy upper stage is being produced by General Dynamics for the USAF/Martin Marietta Titan launch vehicle. The Titan/Centaur upper stage is subject to consecutive acoustic and thermal testing in General Dynamics' Acoustic and Thermal Test Facility (ATTF). All data is acquired and processed digitally using the high-speed data acquisition system located in the ATTF. Processed data from over 250 sensors measuring acceleration, temperature, and sound pressure level is made available to the test team in minutes for use in making real-time test decisions. These tests represent the first consecutive large-scale environmental tests conducted on a complete, pressure stabilized, cryogenically tanked space launch vehicle. Some of the unique challenges involved in testing the Titan/Centaur and how these challenges were met using the ATTF are described. Author

N93-15622*# Alenia Spazio S.p.A., Turin (Italy).

SYSTEM TEST APPROACH FOR THE SAX SATELLITE

Pietro Giordano, Giacomo Raimondo, and Piero Messidoro *In* NASA. Goddard Space Flight Center, The Seventeenth Space Simulation Conference. Terrestrial Test for Space Success Nov. 1992 p 329-341 (For primary document see N93-15593 04-18)

Avail: CASI HC A03/MF A03

SAX satellite verification is based on a protoflight approach, in which only one system model is realized at flight standard level, taking into account the utilization of hardware already qualified for other space programs and the necessity to respect the schedule constraints for a scientific objective. In any case, this approach was tailored with some deviations in order to reduce risks inherent in such a choice. The protoflight approach was also pursued at subsystem/unit level in particular for those subsystems and units considered critical from the schedule point of view. Payload Instruments followed the same approach but complete spare units were developed to reduce the risks associated with such an approach. A description of the model philosophy is provided and then, at satellite level, the testing approach and rationale for each model is presented. Finally, a brief description of each test will be given, highlighting objectives, methodologies, and test configurations. Moreover, for the major tests, problems encountered and solutions applied in establishing a correct approach are described. Author

N93-15623*# Rockwell International Corp., Seal Beach, CA. Rocketdyne Div.

OVERVIEW OF ENVIRONMENTAL TEST PLANS FOR SPACE STATION FREEDOM WORK PACKAGE 4

Tom J. Peterson *In* NASA. Goddard Space Flight Center, The Seventeenth Space Simulation Conference. Terrestrial Test for Space Success Nov. 1992 p 343-351 (For primary document see N93-15593 04-18)

Avail: CASI HC A02/MF A03

The generation and distribution of electric power for Space Station Freedom (SSF) is critical to the station's success. Work Package 4 (WP-04) has the responsibility for the design, development, test, and delivery of the Electric Power System (EPS) for the SSF. During launch, assembly, and operation, the EPS will be subjected to various environments. A test and verification approach has been developed to assure that the EPS will function in these environments. An overview of that test program is presented with emphasis on environmental testing of hardware. Two key areas of the test program are highlighted in the overview. One area is the verification of the Solar Power Module (SPM) and associated cargo element hardware. This area includes detailing the plans for development and qualification testing of the SPM hardware. One series of tests, including modal and acoustic, has been completed on a development cargo element. Another area highlighted is the acceptance testing of high-power Orbital Replacement Units (ORU). The environmental test equipment plans are presented and reviewed in light of an aggressive production rate, which delivers ORU's to the WP-04 and other Space Station Work Packages. Through implementing the test program as outlined, the EPS hardware will be certified for flight and operation on the Space Station Freedom. Author

N93-15629*# Science Applications International Corp., Torrance, CA.

REUSABLE REENTRY SATELLITE (RRS): TELEMETRY, TRACKING, AND COMMAND (TT/C) COVERAGE TRADEOFF STUDY Summary Report

Feb. 1991 84 p

(Contract NAS9-18202)

(NASA-CR-188583; NAS 1.26:188583; RRS-025) Avail: CASI HC A05/MF A01

The Reusable Reentry Satellite (RRS) Telemetry, Tracking & Command (TT&C) Coverage Tradeoff Study described herein was performed during Part 1 of the RRS Phase B contract. This report is one of several that describes the results of various trade studies performed to arrive at a recommended design for the RRS satellite system. The overall RRS Phase B Study objective is to design a relatively inexpensive satellite to access space for extended periods of time, with eventual recovery of experiments on Earth. The RRS will be capable of: (1) being launched by a variety of expendable launch vehicles; (2) operating in low earth orbit as a free flying unmanned laboratory; and (3) executing an independent atmospheric reentry and soft landing. The RRS will be designed to be refurbished and reused up to three times a year for a period of 10 years. The expected principal use for such a system is research on the effects of variable gravity (0 to 1.5 g) and radiation on small animals, plants, lower life forms, tissue samples, and materials processes. This Summary Report provides a description of the RRS Telemetry, Tracking & Command Analysis performed to study the ground station coverage available to meet RRS requirements. Concepts were considered that used off-the-shelf technology, had generous margins of capability, and high reliability, were easily maintained, cost effective, and were compatible with existing support networks. From this study, a recommended RRS TT&C configuration will be developed.

Author

N93-15630*# Science Applications International Corp., Torrance, CA.

SEGMENT SPECIFICATION FOR THE PAYLOAD SEGMENT OF THE REUSABLE REENTRY SATELLITE: RODENT MODULE VERSION

Feb. 1991 44 p

(Contract NAS9-18202)

(NASA-CR-187884; NAS 1.26:187884; RRS-RM-200; SAIC-RRS-040)

Avail: CASI HC A03/MF A01

The Reusable Reentry Satellite (RRS) System is composed of the payload segment (PS), vehicle segment (VS), and mission support (MS) segments. This specification establishes the performance, design, development, and test requirements for the RRS Rodent Module (RM). Author

N93-15631*# Science Applications International Corp., Torrance, CA.

VEHICLE/PAYLOAD INTERFACE SPECIFICATION FOR THE REUSABLE REENTRY SATELLITE

Feb. 1991 22 p

(Contract NAS9-18202)

(NASA-CR-187883; NAS 1.26:187883; RRS-IFS-101; SAIC-RRS-044)

Avail: CASI HC A03/MF A01

This document describes the common interface requirements between the Vehicle Segment and the Payload Segment of the Reusable Reentry Satellite (RRS) system. The system consists of a single transport vehicle design that provides a uniform, unidirectional payload gravitational environment which is selectable during on-orbit operations over the range of 10(exp -5) (microgravity) to 1.5 g's. The initial Reusable Reentry Vehicle/Payload Module (RRV/PM) integration and checkout will occur at the launch base unless otherwise agreed to in a mission-unique addendum to this specification. Pre-integration interface qualification shall be done using emulators as described. Author

N93-15632*# Science Applications International Corp., Torrance, CA.

SYSTEM SPECIFICATION FOR THE REUSABLE REENTRY SATELLITE

Feb. 1991 72 p

(Contract NAS9-18202)

(NASA-CR-187882; NAS 1.26:187882; RRS-SS-100; SAIC-RRS-038)

Avail: CASI HC A04/MF A01

The RRS design shall provide a relatively inexpensive method of access

to micro and fractional gravity space environments for an extended period of time, with eventual intact recovery on the surface of the Earth. This specification establishes the performance, design, development, and test requirements for the Reusable Reentry Satellite (RRS) system. Author

N93-15633*# Ithaco, Inc., Ithaca, NY.
REUSABLE REENTRY SATELLITE (RRS) SYSTEM DESIGN STUDY. PHASE B, APPENDIX E: ATTITUDE CONTROL SYSTEM STUDY Final Report
Feb. 1991 46 p Prepared in cooperation with Science Applications International Corp., Torrance, CA
(Contracts NAS9-18202; SAIC-11-900286-39)
(NASA-CR-188578; NAS 1.26:188578; RRS-037-Phase-B-App-E; Rept-93851-Phase-B-App-E) Avail: CASI HC A03/MF A01

A study which consisted of a series of design analyses for an Attitude Control System (ACS) to be incorporated into the Re-usable Re-entry Satellite (RRS) was performed. The main thrust of the study was associated with defining the control laws and estimating the mass and power requirements of the ACS needed to meet the specified performance goals. The analyses concentrated on the different on-orbit control modes which start immediately after the separation of the RRS from the launch vehicle. The three distinct on-orbit modes considered for these analyses are as follows: (1) Mode 1 - A Gravity Gradient (GG) three-axis stabilized spacecraft with active magnetic control; (2) Mode 2 - A GG stabilized mode with a controlled yaw rotation rate ('rotisserie') using three-axis magnetic control and also incorporating a 10 N-m-s momentum wheel along the (Z) yaw axis; and (3) Mode 3 - A spin stabilized mode of operation with the spin about the pitch (Y) axis, incorporating a 20 N-m-s momentum wheel along the pitch (Y) axis and attitude control via thrusters. To investigate the capabilities of the different controllers in these various operational modes, a series of computer simulations and trade-off analyses have been made to evaluate the achievable performance levels, and the necessary mass and power requirements. Author

N93-15650*# National Aeronautics and Space Administration, Washington, DC.
SPACE STATION FREEDOM USER'S GUIDE
Aug. 1992 56 p
(NASA-TM-108105; NAS 1.15:108105) Avail: CASI HC A04/MF A01

This guide is intended to inform prospective users of the accommodations and resources provided by the Space Station Freedom program. Using this information, they can determine if Space Station Freedom is an appropriate laboratory or facility for their research objectives. The steps that users must follow to fly a payload on Freedom are described. This guide covers the accommodations and resources available on the Space Station during the Man-Tended Capability (MTC) period, scheduled to begin the end of 1996, and a Permanently Manned Capability (PMC) beginning in late 1999. Author

N93-15658*# Science Applications International Corp., Torrance, CA.
REUSABLE REENTRY SATELLITE (RRS): RECOVERY TRADEOFF STUDY Summary Report
Mar. 1990 98 p
(Contract NAS9-18202)
(NASA-CR-186396; NAS 1.26:186396; RRS-022) Avail: CASI HC A05/MF A02

The main objectives of the Recovery Tradeoff Study were as follows: (1) to determine whether a land or water recovery best suits RRS system requirements; (2) what type of terminal recovery system is best suited for the RRS; and (3) what are the recovery access timelines after system landing. Based on the trade parameters and evaluation criteria used in this study, the land-landing configuration has an advantage over the water-landing configuration. It is recommended that a land-landing configuration be developed assuming WSMR as the landing site. It is also recommended that natural orbits be used for low inclination missions and any orbit adjustments for landing site targeting be performed at the end of the mission. Near-integer orbits should be used for high inclination missions and allow orbital decay to precess the ground track over the landing site range. Author

N93-14921# Canadian Space Society, Downsview (Ontario).
THE CANADIAN SOLAR SAIL PROJECT
Istvan Horvath, Kieran A. Carroll, and Andrew Williams *In* Canadian Space Agency, Proceedings of the Sixth CASI Conference on Astronautics 1990 6 p Previously announced in IAA as A91-34927 (For primary document see N93-14920 04-12)
Avail: Canadian Aeronautics and Space Inst., 222 Somerset St. W., Suite 601, Ottawa, Ontario K2P 0J1 Canada

N93-14939# Telesat Canada, Ottawa (Ontario).
ANIK E SPACECRAFT INTEGRATION AND TEST
A. Kidd and E. Bertenyi *In* Canadian Space Agency, Proceedings of the Sixth CASI Conference on Astronautics 1990 15 p Previously announced in IAA as A91-34945 (For primary document see N93-14920 04-12)
Avail: Canadian Aeronautics and Space Inst., 222 Somerset St. W., Suite 601, Ottawa, Ontario K2P 0J1 Canada

N93-14940# Canadian Space Agency, Ottawa (Ontario).
SPACECRAFT THERMAL DESIGN VERIFICATION IN CANADA
E. Choueiry and M. Donato (Spar Aerospace Ltd., Toronto, Ontario) *In its* Proceedings of the Sixth CASI Conference on Astronautics 1990 9 p Previously announced in IAA as A91-34946 (For primary document see N93-14920 04-12)
Avail: Canadian Aeronautics and Space Inst., 222 Somerset St. W., Suite 601, Ottawa, Ontario K2P 0J1 Canada

N93-14946# Spar Aerospace Ltd., Weston (Ontario). Advanced Technology Systems Div.
APPLICATIONS OF THE MOBILE SERVICING SYSTEM TO THE SPACE EXPLORATION INITIATIVE
J. H. Dueckman *In* Canadian Space Agency, Proceedings of the Sixth CASI Conference on Astronautics 1990 10 p Previously announced in IAA as A91-34952 (For primary document see N93-14920 04-12)
Avail: Canadian Aeronautics and Space Inst., 222 Somerset St. W., Suite 601, Ottawa, Ontario K2P 0J1 Canada

19 SPACECRAFT INSTRUMENTATION

For related information see also *06 Aircraft Instrumentation* and *35 Instrumentation and Photography.*

N93-15140# Aerospatiale, Cannes (France).
ISOCAM EXPERIMENT CRYOGENIC TEST RESULTS
L. DeSa and B. Collaudin 1992 10 p
(Rept-921-440-104; ETN-92-92357) Avail: CASI HC A02/MF A01

ISOCAM is an infrared camera experiment to be mounted aboard the ISO (Infrared Space Observatory) satellite, to be launched in 1993. The mission of the satellite is to collect data in near infrared wavelength astronomy during its 18 months lifetime. The operating temperature is in the range 2.4 to 3.4 K. The main cryogenic test results and associated fundamental measurements are overviewed. Model fitting provided an evaluation of thermal conductances and of the heat distribution in the rotor and stator of a cryogenic stepper motor when functioning. Special phenomena, such as the 'chopped' functioning of motors, or the two time temperature rise after a continuous functioning of the motors, was evidenced. Model correlation with the test results ensures a high degree of confidence in the model. ESATAN software was the thermal modeling tool used. ESA

20 SPACECRAFT PROPULSION AND POWER

Includes main propulsion systems and components, e.g., rocket engines; and spacecraft auxilliary power sources.

For related information see also *07 Aircraft Propulsion and Power, 28 Propellants and Fuels, 44 Energy Production and Conversion,* and *15 Launch Vehicles and Space Vehicles.*

N93-14482*# National Aeronautics and Space Administration. Lewis Research Center, Cleveland, OH.

CLOSED BRAYTON CYCLE POWER SYSTEM WITH A HIGH TEMPERATURE PELLET BED REACTOR HEAT SOURCE FOR NEP APPLICATIONS

Albert J. Juhasz, Mohamed S. El-Genk (New Mexico Univ., Albuquerque.), and William B. Harper, Jr. (Allied-Signal Aerospace Co., Tempe, AZ.) Oct. 1992 12 p Presented at the 10th Symposium on Space Nuclear Power and Propulsion, Albuquerque, NM, 10-14 Jan. 1993

(RTOP 590-13-11)

(NASA-TM-105933; E-7446; NAS 1.15:105933) Avail: CASI HC A03/MF A01

Capitalizing on past and future development of high temperature gas reactor (HTGR) technology, a low mass 15 MWe closed gas turbine cycle power system using a pellet bed reactor heating helium working fluid is proposed for Nuclear Electric Propulsion (NEP) applications. Although the design of this directly coupled system architecture, comprising the reactor/power system/space radiator subsystems, is presented in conceptual form, sufficient detail is included to permit an assessment of overall system performance and mass. Furthermore, an attempt is made to show how tailoring of the main subsystem design characteristics can be utilized to achieve synergistic system level advantages that can lead to improved reliability and enhanced system life while reducing the number of parasitic load driven peripheral subsystems. Author

N93-14681*# Alabama Univ., Huntsville.

MACH 5 ELECTROFORMED NICKEL NOZZLE REFURBISHMENT FNAS INVESTIGATION OF ULTRA-SMOOTH SURFACES

Robert Rood, Charles Griffith, and Darell Engelhaupt 1992 12 p

(Contract NAS8-38609)

(NASA-CR-191416; NAS 1.26:191416; UAH-5-32937) Avail: CASI HC A03/MF A01

This task is in support of the Quiet Hypersonic Wind Tunnel effort currently in effect at NASA Langley Research Center, VA. A laminar flow wind tunnel nozzle has been previously fabricated by electroforming pure nickel over a machined and polished two piece stainless steel mandrel. The mandrel was removed leaving the replicate nozzle surface. The nozzle was then pressed into a heavy stainless steel jacket for mounting features and rigidity. The original nickel surface was a replication of the polished mandrel but had degraded due to oxidation. The inside surface requirements are very stringent in order to achieve laminar or quiet flow at the desired pressure and temperature for the specific design of Mach 5. The throat area of the axisymmetric device must have a surface finish with no defects greater than 16 microinches. This requires an rms average background of about four microinches or better for inspection purposes. A coating of nickel-phosphorous alloy was applied by catalytic deposition and then the inside of the nozzle was polished retaining dimensional and surface finish tolerances as specified per drawings supplied. Since the unit is not an optical component, conventional optical inspection methods for surface finish and figure are not readily achieved. Measurements were made using surface profilometry. Author

N93-14815# Sandia National Labs., Albuquerque, NM.

SAFSIM: A COMPUTER PROGRAM FOR ENGINEERING SIMULATIONS OF SPACE REACTOR SYSTEM PERFORMANCE

D. Dobranich 1992 7 p Presented at the Nuclear Technologies for Space Exploration, Jackson, WY, 16-19 Aug. 1992

(Contract DE-AC04-76DP-00789)

(DE92-016328; SAND-92-0746C; CONF-920803-11) Avail: CASI HC A02/MF A01

SAFSIM (System Analysis Flow SIMulator) is a FORTRAN computer program that provides engineering simulations of user-specified flow networks at the system level. It includes fluid mechanics, heat transfer, and reactor dynamics capabilities. SAFSIM provides sufficient versatility to allow the simulation of almost any flow system, from a backyard sprinkler system to a clustered nuclear reactor propulsion system. In addition to versatility, speed and robustness are primary goals of SAFSIM. The current capabilities of SAFSIM are summarized, and some illustrative example results are presented. DOE

N93-14883*# Toledo Univ., OH. Mechanical Engineering Dept.

NUMERICAL MODELING OF A VORTEX STABILIZED ARCJET Ph.D. Thesis, 1991 Final Report

Gary E. Pawlas Nov. 1992 154 p

(RTOP 506-42-31)

(NASA-CR-190797; E-7419; NAS 1.26:190797) Avail: CASI HC A08/MF A02

Arcjet thrusters are being actively considered for use in Earth orbit maneuvering applications. Experimental studies are currently the chief means of determining an optimal thruster configuration. Earlier numerical studies have failed to include all of the effects found in typical arcjets including complex geometries, viscosity, and swirling flow. Arcjet geometries are large area ratio converging nozzles with centerbodies in the subsonic portion of the nozzle. The nozzle walls serve as the anode while the centerbody functions as the cathode. Viscous effects are important because the Reynolds number, based on the throat radius, is typically less than 1,000. Experimental studies have shown that a swirl or circumferential velocity component stabilizes a constricted arc. This dissertation describes the equations governing flow through a constricted arcjet thruster. An assumption that the flowfield is in local thermodynamic equilibrium leads to a single fluid plasma temperature model. An order of magnitude analysis reveals the governing fluid mechanics equations are uncoupled from the electromagnetic field equations. A numerical method is developed to solve the governing fluid mechanics equations, the Thin Layer Navier-Stokes equations. A coordinate transformation is employed in deriving the governing equations to simplify the application of boundary conditions in complex geometries. An axisymmetric formulation is employed to include the swirl velocity component as well as the axial and radial velocity components. The numerical method is an implicit finite-volume technique and allows for large time steps to reach a converged steady-state solution. The inviscid fluxes are flux-split, and Gauss-Seidel line relaxation is used to accelerate convergence. Converging-diverging nozzles with exit-to-throat area ratios up to 100:1 and annular nozzles were examined. Quantities examined included Mach number and static wall pressure distributions, and oblique shock structures. As the level of swirl and viscosity in the flowfield increased the mass flow rate and thrust decreased. The technique was used to predict the flow through a typical arcjet thruster geometry. Results indicate swirl and viscosity play an important role in the complex geometry of an arcjet. Author

N93-15215# Argonne National Lab., IL.

EXPERIMENTAL DETERMINATION OF MAGNETOHYDRODYNAMIC SEAWATER THRUSTER PERFORMANCE IN A TWO TESLA TEST FACILITY

B. Picologlou, E. Doss, D. Black, and W. C. Sikes (Newport News Shipbuilding and Drydock Co., VA.) 1992 7 p Presented at the 27th Intersociety Energy Conversion Engineering Conference, San Diego, CA, 3-7 Aug. 1992

(Contract W-31-109-eng-38)

(DE92-019042; ANL/CP-76576; CONF-920801-22) Avail: CASI HC A02/MF A01

A two Tesla test facility was designed, built, and operated to investigate the performance of magnetohydrodynamic (MHD) seawater thrusters. The results of this investigation are used to validate MHD thruster performance computer models. The facility test loop, its components, and their design are presented in detail. Additionally, the test matrix and its rational are discussed. Finally, representative experimental results of the test program are presented, and are compared to pretest computer model predictions. Good agreement between predicted and measured data has served to validate the thruster performance computer models. DOE

N93-15370*# Sverdrup Technology, Inc., Brook Park, OH.

NUMERICAL STUDY OF CATHODE EMISSION CONSTRAINTS ON CYLINDRICAL SELF-FIELD MPD THRUSTER PERFORMANCE Final Report

Michael R. LaPointe Jan. 1993 14 p Presented at the 10th Symposium on Space Nuclear Power and Propulsion, Albuquerque, NM, 10-14 Jan.

1993
(Contract NAS3-25266; RTOP 506-42-31)
(NASA-CR-190795; E-7416; NAS 1.26:190795) Avail: CASI HC A03/MF A01

A stability equation relating thruster discharge current, argon propellant mass flow rate, and electrode geometry has been solved for a variety of cylindrical self-field MPD thruster configurations and discharge currents. Realistic values for cathode emission current densities were used to provide additional constraints on the thruster geometries. A two-dimensional MPD code was employed to provide better estimates of the maximum achievable specific impulse, thrust, and flow efficiency for cases of interest. The model results indicate that long life, cylindrical self-field MPD thrusters operated with argon propellant may not be able to provide specific impulse values in excess of 2100s. Alternate electrode geometries, applied magnetic fields, and/or low molecular weight propellants may be necessary to achieve higher values of specific impulse. Author

N93-15428*# National Aeronautics and Space Administration. Lewis Research Center, Cleveland, OH.

DEVELOPMENT OF NASA/DOE NTP SYSTEM PERFORMANCE MODELS

James T. Walton Dec. 1992 15 p Presented at the 10th Space Nuclear Power Symposium, Albuquerque, NM, 10-14 Jan. 1993; Sponsored by Univ. of New Mexico Inst. for Space Nuclear Power
(RTOP 593-00-71)
(NASA-TM-105982; E-7506; NAS 1.15:105982) Avail: CASI HC A03/MF A01

A critical enabling technology in the evolutionary development of Nuclear Thermal Propulsion (NTP) is the ability to predict the system performance under a variety of operating conditions. The ability to predict the system performance is critical for mission analysis and for control subsystem testing, as well as for the modeling of various failure modes. Performance must be accurately predicted during steady-state and transient operation, such as start-up, shut-down and after-cooling. The development and application of verified and validated system models has the potential to reduce testing, cost and time required for the technology to again reach flight-ready status. An integrated NASA/DOE team was formed in late 1991 to develop and implement a strategy for modeling NTP systems. It is the intent of the interagency team to develop several levels of computer programs, which vary in detail, to simulate NTP systems based on either prismatic, particle or advanced fuel forms. This paper presents an overview of the models under development by the interagency team. In addition, the status of the development and validation efforts for the Level 1 steady-state parametric model is discussed. Author

N93-15429*# National Aeronautics and Space Administration. Lewis Research Center, Cleveland, OH.

ION THRUSTER DEVELOPMENT AT NASA LEWIS RESEARCH CENTER

James S. Sovey, John A. Hamley, Michael J. Patterson, Vincent K. Rawlin, and Timothy R. Sarver-Verhey (Sverdrup Technology, Inc., Brook Park, OH.) Dec. 1992 10 p Presented at the 10th Symposium on Space Nuclear Power and Propulsion, Albuquerque, NM, 10-14 Jan. 1993; Sponsored by the Univ. of New Mexico Inst. for Space Nuclear Power
(RTOP 506-42-31)
(NASA-TM-105983; E-7507; NAS 1.15:105983) Avail: CASI HC A02/MF A01

Recent ion propulsion technology efforts at NASA's Lewis Research Center including development of kW-class xenon ion thrusters, high power xenon and krypton ion thrusters, and power processors are reviewed. Thruster physical characteristics, performance data, life projections, and power processor component technology are summarized. The ion propulsion technology program is structured to address a broad set of mission applications from satellite stationkeeping and repositioning to primary propulsion using solar or nuclear power systems. Author

N93-15526*# National Aeronautics and Space Administration. Lewis Research Center, Cleveland, OH.

SUMMARY OF THE NASA LEWIS COMPONENT TECHNOLOGY PROGRAM FOR STIRLING POWER CONVERTERS

Lanny G. Thieme and Diane M. Swec Oct. 1992 23 p Presented at the 27th Intersociety Energy Conversion Engineering Conference, San Diego, CA, 3-7 Aug. 1992; sponsored by the Society of Automotive Engineers
(RTOP 590-13-11)
(NASA-TM-105640; E-7070-1; NAS 1.15:105640) Avail: CASI HC A03/MF A01

An update is presented on the NASA Lewis Stirling component technology program. The component technology program has been organized as part of the NASA Lewis effort to develop Stirling converter technology for space power applications. The Stirling space power project is part of the High Capacity Power element of the NASA Civil Space Technology Initiative (CSTI). Lewis is also providing technical management of a DOE funded project to develop Stirling converter systems for distributed dish solar terrestrial power applications. The primary contractors for the space power and solar terrestrial projects develop component technologies directly related to their project goals. This Lewis component technology program, while coordinated with these main projects, is aimed at longer term issues, advanced technologies, and independent assessments. Topics to be discussed include bearings, linear alternators, controls and load interaction, materials/life assessment, and heat exchangers. Author

N93-15528*# National Aeronautics and Space Administration. Lewis Research Center, Cleveland, OH.

AEROTHERMODYNAMIC FLOW PHENOMENA OF THE AIRFRAME-INTEGRATED SUPERSONIC COMBUSTION RAMJET

James T. Walton Nov. 1992 24 p
(NASA-TM-4376; E-6751; NAS 1.15:4376) Avail: CASI HC A03/MF A01

The unique component flow phenomena is discussed of the airframe-integrated supersonic combustion ramjet (scramjet) in a format geared towards new players in the arena of hypersonic propulsion. After giving an overview of the scramjet aerothermodynamic cycle, the characteristics are then covered individually of the vehicle forebody, inlet, combustor, and vehicle afterbody/nozzle. Attention is given to phenomena such as inlet speeding, inlet starting, inlet spillage, fuel injection, thermal choking, and combustor-inlet interaction. Author

N93-15571*# National Aeronautics and Space Administration. Lewis Research Center, Cleveland, OH.

NUCLEAR THERMAL ROCKET NOZZLE TESTING AND EVALUATION PROGRAM

Kenneth O. Davidian and Kenneth J. Kacynski Jan. 1993 8 p Presented at the 10th Symposium on Space Nuclear Pwer and Propulsion, Albuquerque, NM, 10-13 Jan. 1993; sponsored by the Inst. for Space Nuclear Power Studies
(RTOP 506-42-72)
(NASA-TM-105962; E-7482; NAS 1.15:105962) Avail: CASI HC A02/MF A01

Performance characteristics of the Nuclear Thermal Rocket can be enhanced through the use of unconventional nozzles as part of the propulsion system. The Nuclear Thermal Rocket nozzle testing and evaluation program being conducted at the NASA Lewis is outlined and the advantages of a plug nozzle are described. A facility description, experimental designs and schematics are given. Results of pretest performance analyses show that high nozzle performance can be attained despite substantial nozzle length reduction through the use of plug nozzles as compared to a convergent-divergent nozzle. Pretest measurement uncertainty analyses indicate that specific impulse values are expected to be within + or - 1.17 pct. Author

N93-15572*# National Aeronautics and Space Administration. Lewis Research Center, Cleveland, OH.

LOW THRUST CHEMICAL ROCKET TECHNOLOGY

Steven J. Schneider Nov. 1992 32 p Presented at the 43rd Congress of the International Astronautical Federation, Washington, DC, 28 Aug. - 5 Sep. 1992
(RTOP 506-42-31)
(NASA-TM-105927; E-7434; NAS 1.15:105927; IAF-92-0669) Avail: CASI HC A03/MF A01

An on-going technology program to improve the performance of low thrust chemical rockets for spacecraft on-board propulsion applications is reviewed. Improved performance and lifetime is sought by the development of new predictive tools to understand the combustion and flow physics, introduction of high temperature materials and improved component designs to optimize performance, and use of higher performance propellants.

Improved predictive technology is sought through the comparison of both local and global predictions with experimental data. Predictions are based on both the RPLUS Navier-Stokes code with finite rate kinetics and the JANNAF methodology. Data were obtained with laser-based diagnostics along with global performance measurements. Results indicate that the modeling of the injector and the combustion process needs improvement in these codes and flow visualization with a technique such as 2-D laser induced fluorescence (LIF) would aid in resolving issues of flow symmetry and shear layer combustion processes. High temperature material fabrication processes are under development and small rockets are being designed, fabricated, and tested using these new materials. Rhenium coated with iridium for oxidation protection was produced by the Chemical Vapor Deposition (CVD) process and enabled an 800 K increase in rocket operating temperature. Performance gains with this material in rockets using Earth storable propellants (nitrogen tetroxide and monomethylhydrazine or hydrazine) were obtained through component redesign to eliminate fuel film cooling and its associated combustion inefficiency while managing head end thermal soakback. Material interdiffusion and oxidation characteristics indicated that the requisite lifetimes of tens of hours were available for thruster applications. Rockets were designed, fabricated, and tested with thrusts of 22, 62, 440 and 550 N. Performance improvements of 10 to 20 seconds specific impulse were demonstrated. Higher performance propellants were evaluated: Space storable propellants, including liquid oxygen (LOX) as the oxidizer with nitrogen hydrides or hydrocarbon as fuels. Specifically, a LOX/hydrazine engine was designed, fabricated, and shown to have a 95 pct theoretical c-star which translates into a projected vacuum specific impulse of 345 seconds at an area ratio of 204:1. Further performance improvment can be obtained by the use of LOX/hydrogen propellants, especially for manned spacecraft applications, and specific designs must be developed and advanced through flight qualification.

Author

N93-15584*# Sverdrup Technology, Inc., Brook Park, OH.

COMBINED HIGH AND LOW THRUST PROPULSION FOR FAST PILOTED MARS MISSIONS Final Report

James H. Gilland and Steven R. Oleson Nov. 1992 12 p

(RTOP 539-72-00)

(NASA-CR-190788; E-7423; NAS 1.26:190788) Avail: CASI HC A03/MF A01

The mission benefits of using both high thrust nuclear thermal propulsion (NTP) and low acceleration, high specific impulse nuclear electric propulsion (NEP) to reduce piloted trip times to Mars with reasonable initial mass are assessed. Recent updates in mission design, such as the Earth fly-by return, are assessed for their impact on previous studies. In addition, the Synthesis Commission split mission to Mars in 2014 is also assessed using combined propulsion. Results show an 80 to 100 day reduction in trip time over the reference NTP or NEP systems and missions, with comparable or reduced vehicle initial masses. The impacts of the mission and system analyses upon technology planning and design are discussed.

Author

23 CHEMISTRY AND MATERIALS (GENERAL)

N93-14459*# National Aeronautics and Space Administration. Langley Research Center, Hampton, VA.

THE PRELIMINARY LONG DURATION EXPOSURE FACILITY (LDEF) MATERIALS DATA BASE

Joan G. Funk, John W. Strickland (BAMSI, Inc., Huntsville, AL.), and John M. Davis (National Aeronautics and Space Administration. Marshall Space Flight Center, Huntsville, AL.) Oct. 1992 25 p

(RTOP 506-48-91)

(NASA-TM-107692; NAS 1.15:107692) Avail: CASI HC A03/MF A01

A preliminary Long Duration Exposure Facility (LDEF) Materials Data Base was developed by the LDEF Materials Special Investigation Group (MSIG). The LDEF Materials Data Base is envisioned to eventually contain the wide variety and vast quantity of materials data generated for LDEF. The data is searchable by optical, thermal, and mechanical properties, exposure parameters (such as atomic oxygen flux), and author(s) or principal investigator(s). The LDEF Materials Data Base was incorporated into the Materials and Processes Technical Information System (MAPTIS). MAPTIS is a collection of materials data which was computerized and is available to engineers, designers, and researchers in the aerospace community involved in the design and development of spacecraft and related hardware. This paper describes the LDEF Materials Data Base and includes step-by-step example searches using the data base. Information on how to become an authorized user of the system is included.

Author

N93-14718 Westinghouse Savannah River Co., Aiken, SC.

ELECTROCHEMICAL OXIDATION OF ORGANIC MATERIALS Patent Application

A. C. Almon, inventor (to DOE) 1991 13 p

(Contract DE-AC09-89SR-18035)

(DE92-019822; US-Patent-Appl-SN-641823; Patents-US-A-7641823) Avail: CASI HC A03/MF A01

This invention is a method and apparatus for the direct oxidation of organic materials, especially organic wastes, in an electrochemical cell. It fulfills the need for a simple, cost-effective way for generators of small quantities of waste to deal with that waste. It does not use an electron transfer agent, which may be a source of additional hazardous waste. The anode is made of carbon felt; the cathode is platinum; and the electrolyte is a strong oxidizer, preferably nitric acid. The potential difference is 2 to 3 volts; the current density is 0.15 to 0.25 A/sq cm. The porous barrier is a medium grade alumina frit or an ion exchange membrane. The organic materials are fed to the anode compartment; the resulting oxygen bubbling circumvents the need for stirring or circulating the waste. Many different types of waste (e.g. rubber gloves, TBP, process solutions, etc.) can be fed to the anode compartment without the need to process or store it.

DOE

N93-15576*# National Aeronautics and Space Administration. Lewis Research Center, Cleveland, OH.

THE EFFECT OF PROCESSING AND COMPOSITIONAL CHANGES ON THE TRIBOLOGY OF PM212 IN AIR

Michael S. Bogdanski (Case Western Reserve Univ., Cleveland, OH.), Harold E. Sliney, and Christopher DellaCorte 1993 16 p Preposed for presentation at the 1993 STLE Annual Meeting, Calgary, Alberta, 17-20 May 1993; sponsored by the Society of Tribologists and Lubrication Engineers

(RTOP 505-63-5A)

(NASA-TM-105945; E-7462; NAS 1.15:105945) Avail: CASI HC A03/MF A01

The effects of processing and compositional variations on the tribological performance of PM212 were studied. PM212 is a self lubricating powder metallurgy composite, comprised of a wear resistant metal bonded chromium carbide matrix, containing the solid lubricants barium fluoride/calcium fluoride eutectic and silver. Several composites were formulated which had lubricant, matrix, and processing variations. Processing variations included sintering and hot isostatic pressing. Pins fabricated from the composites were slid against superalloys disks in a pin-on-disk tribometer to study the tribological properties. Several composites exhibited low friction and wear in sliding against a nickel based superalloy. The tribological performance by several different composites showed that the composition of PM212 can be altered without dramatically affecting performance.

Author

24 COMPOSITE MATERIALS

Includes physical, chemical, and mechanical properties of laminates and other composite materials.

For ceramic materials see *27 Nonmetallic Materials.*

N93-14142 Missouri Univ., Rolla.

CHARACTERIZATION OF FIBER REINFORCED PHENOLIC COMPOSITES Ph.D. Thesis

Subramaniam Narayan 1992 157 p

Avail: Univ. Microfilms Order No. DA9224677

Phenolic resins of the straight and modified type were reinforced with short fibers that are potential substitutes for asbestos used in friction materials, to yield composite materials. These composites were tested for several mechanical properties and the Young's modulus was predicted based on the Halpin-Tsai model for random short fiber composites. The

study was extended to friction materials containing glass fibers of varying length and diameter. Fiber sizing, length, and diameter were found to play a significant role in affecting the mechanical properties. The role of chemical species such as water, salt water, isooctane, ethylene glycol, and other liquids on phenolic resins and its composites were investigated. The sorption and diffusion of these small molecules in these materials were studied using Fick's laws. The maximum solvent uptake and the diffusion coefficient of the solvent in these systems were determined and the experimental data fitted to a model. After exposure to these contaminants, the mechanical properties of all the systems were determined and a general degradation in properties was found. The dynamics of water in the resin and composite was investigated using deuterium NMR. The relaxation times of the mobile components of the spectra was calculated for the resin and the composite as a function of temperature. In order to characterize the fiber-matrix interface, the interfacial shear strength of Kevlar reinforced phenolics was determined using the single strand pull out technique. Dissert. Abstr.

N93-14192 Georgia Inst. of Tech., Atlanta.
NONDESTRUCTIVE EVALUATION OF DAMAGE IN SiC/Al METAL MATRIX COMPOSITE USING X RAY TOMOGRAPHIC MICROSCOPY Ph.D. Thesis
Thomas M. Breunig 1992 218 p
Avail: Univ. Microfilms Order No. DA9223769

A fundamental understanding of damage evolution will be required before metal matrix composites (MMC) can be utilized safely for structural applications. Although macroscopic mechanical response to cyclic loading has been monitored in many mechanical and thermal test programs, little is known about the nucleation and growth of damage in MMC's. The goal of the present work is to improve the understanding of damage accumulation in SiC/Al using a new microscopic non-destructive volume-imaging technique, X-ray Tomographic Microscopy (XTM), which has resolution comparable to optical microscopy. Correlation of damage initiation and accumulation mechanisms and the macroscopic mechanical response of samples are discussed for continuous fiber SiC/Al MMC's. A series of mechanical tests were performed on a continuous, aligned fiber SiC/Al MMC, and the ensuing three-dimensional damage state was nondestructively characterized using XTM to map the x-ray absorptivity within the sample. The types of damage detected include: fiber fracture (SiC sheath, and C core), fiber-matrix interface microcracking, intra-ply matrix voids, and cracks. Quantitative three-dimensional measurements of damage are reported in as-fabricated, monotonically loaded and mechanically fatigue loaded SiC/Al. The XTM results indicate that increases in observed macroscopic structural stiffness during monotonic loading and the first few fatigue cycles of an MMC coupon correspond to elimination of processing-related matrix porosity and to displacement of the fibers from a somewhat irregular arrangement into a more nearly hexagonal array. The XTM of monotonically loaded samples also show that the carbon cores begin to fracture at or below 828 MPa, that is, at loads far less than those for fracture of the entire fiber. The fracture of the SiC sheath appears to be significantly affected by the fracture of the C cores. The fiber fracture surface topography and sub-surface damage modes observed provide insight into the overall monotonic loading fracture process of this MMC. Structural changes due to the high and low cycle fatigue processes are illustrated. The implication of these results and the use of in situ loading for damage quantification are discussed for mechanical modeling. Dissert. Abstr.

N93-14193 Virginia Polytechnic Inst. and State Univ., Blacksburg.
THE EFFECT OF THE INTERPHASE/INTERFACE REGION ON CREEP AND CREEP RUPTURE OF THERMOPLASTIC COMPOSITES Ph.D. Thesis
Yeou Shin Chang 1992 164 p
Avail: Univ. Microfilms Order No. DA9224533

The effect of the interphase/interface region on the static mechanical properties, creep and creep rupture behavior of thermoplastic (J2) composites was investigated. The mechanical properties of the J2 composites were altered by systematic changes in fiber surface chemistry. Four fiber systems were used including the AU4, AS4(1) & (2), and AS4CGP fibers. (AS4(1) and AS4(2) represent different batch numbers.) Surface energies and chemistry of carbon fibers were examined using the Dynamic Contact Angle (DCA) method and X-ray Photoelectron Spectroscopy (XPS), respectively. The mesoindentation technique was used to measure the interfacial shear strengths (ISS) of the composites. For the same batch of the composites, the ISS ratios for AS4(2)/J2 to AU4/J2 and AS4CGP/J2 to AU4/J2 were 1.22 and 1.24, respectively. The mechanical properties of these composites in the fiber direction were insensitive to the ISS. The transverse and shear moduli of the J2 composites were also not affected by the ISS. The static strengths, in general, ordered themselves from strong to weak as follows: AS4(2)/J2 greater than AS4CGP/J2 is greater than AU4/J2. However, the creep rupture strength revealed a different ordering: AS4CGP/J2 is greater than AS4(2)/J2 is greater than AU4/J2. This suggests that static mechanical properties may not be a good indicator for long term mechanical performance. Experimental results showed that the interphase/interface region did not affect the degradation rates of the creep rupture strength of the J2 composites. DMA creep tests were performed at elevated temperatures for J2 composites. A master curve of each composite was generated. The shift factors obeyed the Arrhenius type equation. The activation energies of composites were approximately the same. The creep response of the AU4/J2, AS4(2)/J2, and AS4CGP/J2 composites were not dependent upon the ISS. Severe delaminations were observed in the AS4(1)/J2 composite laminates. The (plus or minus 45/90-2 sub s) in laminate tensile strength of AS4(1)/J2 composite was less than that of AS4(2)/J2 and AS4CGP/J2 composite. The creep rupture strength of the AS4(1)/J2 composite laminates degraded about two times faster than that of the other three composite systems. Dissert. Abstr.

N93-14221 Virginia Polytechnic Inst. and State Univ., Blacksburg.
MODAL INTERACTIONS IN THE DYNAMIC RESPONSE OF ISOTROPIC AND COMPOSITE PLATES Ph.D. Thesis
Mohammad Jafar Hadian 1992 175 p
Avail: Univ. Microfilms Order No. DA9223448

Generalized Levy-type solutions are obtained for the problem of linear free vibrations and linear stability of shear-deformable cross-ply laminated plates. The governing equations are transformed into a set of first-order linear ordinary-differential equations with constant coefficients. The general solution of these equations is obtained by using the state-space concept. Then, the application of the boundary conditions yields equations for the natural frequencies and critical loads. However, a straightforward application of the state-space concept yields numerically ill-conditioned problems as the plate thickness is reduced. Various methods for overcoming this problem are discussed. An initial value method with orthonormalization is selected. It is shown that this method not only yields results that are in excellent agreement with the results in the literature, but it also converges fast and gives all the frequencies and buckling loads regardless of the plate thickness. Further, it is shown that the application of classical plate theory to thick plates yields inaccurate results. The influence of modal interactions on the response of harmonically excited plates is investigated in detail. The case of a two-to-one autoparametric resonance in shear-deformable composite laminated plates is considered. Four first-order ordinary-differential equations describing the modulation of the amplitudes and phases of the internally resonant modes are derived using the averaged Lagrangian when the higher mode is excited by a primary resonance. The fixed-point solutions are determined using a homotopy algorithm and their stability is analyzed. It is shown that besides the single-mode solution, two-mode solutions exist for a certain range of parameters. It is further shown that in the multi-mode case the lower mode, which is indirectly excited through the internal resonance may dominate the response. For a certain range of parameters, the fixed points lose stability via a Hopf bifurcation, thereby giving rise to limit cycle solutions. It is shown that these limit-cycles undergo a series of period-doubling bifurcations, culminating in chaos. Finally, the case of a combination resonance involving the first three modes of axisymmetric circular plates is studied. Dissert. Abstr.

N93-14224 Pennsylvania State Univ., University Park.
ELASTIC WAVE SCATTERING BY PARTIALLY DEBONDED OR PARTIALLY COATED FIBERS Ph.D. Thesis
Yong Woo Kim 1992 229 p
Avail: Univ. Microfilms Order No. DA9226720

The prediction and quantitative assessment of composite material behavior remains difficult since the macromechanical behavior of composite materials depends not only on the microstructure but also on the way in which damage occurs. The damage may be accumulated from delamination, debonding, initiation and growth of cracks in the fiber and matrix and at the interface. This accumulation can affect the structural or mechanical performance of the advanced composite material. Thus, the prevention of

structural or mechanical failure is an important requirement in designing the advanced composite material, which is very difficult to achieve employing the classical theories of mechanics that are not useful for analyzing the inhomogeneity arising from the material microstructure and nonuniform damage. To examine such problems, we have developed a modification of the null field method to study the effects of debonding at the interface between the reinforcing fiber and matrix medium on the dynamic response of a composite material. The modification of null field approach is achieved by the introduction of a mathematical surface as well as by field expansions inside the cylinder in terms of regular waves and the field outside the cylinder as a sum of the incident field and the scattered field. The scattering cross section and the farfield amplitude are calculated as a function of frequency, fiber properties and debonding area. Another practical application of such a study is nondestructive evaluation and fracture characterization of composite materials. By ultrasonic testing and inverse analysis, one can represent the geometrical and relevant fracture parameters of the material. Also, an alternative null field approach has been developed to study elastic wave scattering from a partially coated fiber corresponding to a thin coating on a curved surface which is typically referred to as concavo-convex. The validity of the numerical results is ensured by checking the symmetry and unitarity condition on the T-matrix as well as making comparisons with known results. Dissert. Abstr.

N93-14232# Naval Surface Warfare Center, Bethesda, MD.
THE EFFECT OF A SEAWATER ENVIRONMENT ON THE GALVANIC CORROSION BEHAVIOR OF GRAPHITE/EPOXY COMPOSITES COUPLED TO METALS
D. M. Aylor and J. N. Murray Jul. 1992 61 p
(AD-A256072; SME/92-32) Avail: CASI HC A04/MF A01

Galvanic compatibility between graphite/epoxy (Gr/epoxy) composites and metals (HY80 steel and nickel aluminum bronze (NAB)) was evaluated in 180-day seawater galvanic couple tests and laboratory electrochemical tests. Results indicate that significant galvanic corrosion of NAB and HY80 can occur when each material is coupled to a Gr/epoxy composite containing exposed graphite fibers, with the rate of the metallic corrosion increasing as the exposed graphite fiber area in the composite is increased. Galvanic corrosion can also occur between Gr/epoxy composites with no graphite fibers initially exposed to the environment and a metal as a result of moisture absorption through the epoxy outerlayer to the graphite fibers. The electrochemical impedance spectroscopy evaluation demonstrated that Gr/epoxy composites with no graphite fibers initially exposed to the environment can act as an effective cathode for oxygen reduction in seawater. It was estimated that after a 200 day seawater exposure, 15 percent of the planar area of this Gr/epoxy composite contained seawater-exposed graphite fibers. The potentiodynamic polarization results suggest that short-term electrochemical testing is not a reliable method for assessing long-term galvanic corrosion behavior of Gr/epoxy-metal couples but does indicate a sensitivity to graphite fiber area effects. GRA

N93-14436# Sabbagh Associates, Inc., Bloomington, IN.
EFFICIENT ASYMPTOTIC CLOSED FORM APPROXIMATION FOR DYADIC GREEN'S FUNCTION FOR ANISOTROPIC SUBSTRATES, PHASE 1 Final Report
Sina Barkeshli 15 Aug. 1992 97 p
(Contract DAAL02-91-C-0020)
(AD-A256258; SA/TR-5/91) Avail: CASI HC A05/MF A02

An efficient closed form asymptotic representation for a grounded double-layered anisotropic uniaxial geometry is developed. The large parameter of this asymptotic development is directly proportional to the lateral separation between the source and observation point. However the asymptotic solution remains accurate even for very small (a few tenths of a wavelength) lateral separation of the source and field points. the asymptotic closed form dyadic Green's function was cast in such a form that the physical behavior of the electromagnetic fields due to anisotropy of the medium reveals itself through a simple mathematical parameters. Thus, the physical understanding of the interaction of the spatially confined source with an anisotropic (uniaxial) double-layered grounded slab is greatly enhanced through the newly developed asymptotic closed form representation of the dyadic Green's function. Also, this efficient representation is very useful in the moment method (MM) solution of the current excited on the microstrip antennas and arrays in a grounded double-layered uniaxial geometry, as well as the volumetric current excited within a dielectric scatterer buried in a grounded double layered anisotropic uniaxial slab. The MM analysis, especially for microstrip arrays and guided wave structures, requires a very large number of computations where the lateral distance between the source and the field points in the dyadic Green's function can range from extremely small to very large values. GRA

N93-14466 Michigan Univ., Ann Arbor.
MODELING OF THE THERMAL ELASTO-PLASTIC BEHAVIOR FOR COMPOSITE MATERIALS USING THE HOMOGENIZATION METHOD Ph.D. Thesis
Chao-Hsien Cheng 1992 226 p
Avail: Univ. Microfilms Order No. DA9226865

In this dissertation, the homogenization method is used to investigate the thermo-mechanical behavior of composite materials. Assuming the characteristic microstructure in a composite material is spatially repeating, the equivalent material properties in one unit cell are calculated. These equivalent material properties represent the microscopic information. Using this approach, three research topics, in particular, stationary heat conduction, thermoelasticity and thermal elastoplasticity in composite materials are studied in order to determine the global behavior and the local response at the microscopic level. For heat conduction in composite materials, the well-known homogenization method is used to solve for the homogenized conductivity and the local heat flux field. Two boundary value problems, one, a local problem, the other, a global problem, are derived in order to obtain the characteristic temperature field in the microstructure and the equivalent thermal conductivity. Overall and local thermal response of the composite material is then determined. This rigorous method is extended to inquire into the stress mismatch in the microstructure and the effective stress field in macrostructure for the thermal stresses in composites. The global thermal expansion behavior as well as the microscopic thermal stress analysis is studied theoretically by employing the homogenization method. It is found that this method provides good results in comparison with other analytical theories. From the examples, it is interesting to note that the thermal effect causes severe stress concentrations at the interface between the constituents, due to the mismatch in their thermal expansion coefficients. The homogenization method is not limited by its assumption of periodicity in the microstructure. It can be used to deal with both geometrically and materially nonlinear problems such as thermal elastoplasticity in composite materials. In association with the total Lagrangian update scheme, the proposed method can be used to model both globally and locally the thermophysical behavior of composites undergoing plastic deformation. Dissert. Abstr.

N93-14484*# California Univ., Santa Barbara. Dept. of Mechanical and Environmental Engineering.
ON THE STRUCTURE OF NONLINEAR CONSTITUTIVE EQUATIONS FOR FIBER REINFORCED COMPOSITES
Stefan Jansson Cleveland, OH NASA. Lewis Research Center Sep. 1992 32 p
(Grant NAG3-894; RTOP 510-01-50)
(NASA-CR-191024; E-7461; NAS 1.26:191024) Avail: CASI HC A03/MF A01

The structure of constitutive equations for nonlinear multiaxial behavior of transversely isotropic fiber reinforced metal matrix composites subject to proportional loading was investigated. Results from an experimental program were combined with numerical simulations of the composite behavior for complex stress to reveal the full structure of the equations. It was found that the nonlinear response can be described by a quadratic flow-potential, based on the polynomial stress invariants, together with a hardening rule that is dominated by two different hardening mechanisms. Author

N93-14493# Stanford Univ., CA. Dept. of Aeronautics and Astronautics.
DELAMINATION GROWTH BEHAVIOR IN CROSS-PLY LAMINATED COMPOSITES DUE TO TRANSVERSE CONCENTRATED LOADING Annual Progress Report, 1 Oct. 1990 - 30 Sep. 1991
Sheng Liu and Fu-Kuo Chang 30 Sep. 1991 28 p
(Grant AF-AFOSR-0554-89)
(AD-A255974; AFOSR-92-0891TR) Avail: CASI HC A03/MF A01

An analytical model was developed to study the delamination growth behavior of graphite/epoxy cross-ply laminated composites resulting from quasi-static transverse concentrated loads. The objective of the study was

to fundamentally understand the interaction between the initial matrix cracking and the delamination initiation and growth in laminated composites due to transverse concentrated loads. During this period of the investigation, attention is given to the growth of the surface matrix crack-induced delamination in cross-ply composites and the interaction between the matrix cracking and the delamination initiation and propagation inside the laminates. Based on the study, it shows that delamination growth in laminated composites due to transverse loads is strongly affected by the initial matrix cracks. Delamination induced by a bending crack (surface) would grow into a slender shape with its major axis parallel to the direction of the surface cracks. Mode 1 fracture toughness dominates the initiation and growth of the delamination induced by the bending cracks. Also, bending crack-imposed delamination is stable in laminated composites. GRA

N93-14509# Naval Surface Warfare Center, Bethesda, MD. Ship Materials Engineering Dept.

KIND-BAND FAILURE ANALYSIS OF THICK COMPOSITES IN COMPRESSION

E. T. Camponeschi, Jr., J. W. Gillespie, Jr., and D. J. Wilkins Apr. 1992 42 p

(AD-A255431; CARDEROCKDIV-SME-92/29) Avail: CASI HC A03/MF A01

This paper describes an analysis of 6.4 to 25.4 mm (0.25 to 1.0 in.) thick composite laminates subjected to uniaxial compressive loading that experimentally showed a decrease in strength with increasing thickness. The analysis was performed to determine if the reduction in strength was an intrinsic thickness material effect or if it could be attributed to through-thickness restraint on the specimen caused by the test fixture. The analysis was based on closed form solutions for the formation of kink-band failures in the presence of fibers misaligned with the principal axis of compression loading. The fiber misalignment was determined by a finite element analysis that accounted for the displacement of the laminate outer plies where the laminate exited the compression test fixture. The correlation between the experimental results and the theoretical analysis showed the compression strength of the AS4/3501-6 and S2/3501-6 laminates to be independent of thickness and directly proportional to the through-thickness fixture restraint on through-thickness Poisson expansion. This theoretical and experimental comparison also demonstrated a strong correlation between fiber misalignment, its resulting shear stress state, and the kink-band compression failure mechanism. GRA

N93-14550# Rensselaer Polytechnic Inst., Troy, NY.

MECHANICS OF COMPOSITE MATERIALS FOR SPACECRAFT Final Report, 1 Jun. - 31 Dec. 1991

George J. Dvorak and Mark S. Shephard Aug. 1992 156 p

(AD-A255380) Avail: CASI HC A08/MF A02

During this seven month project efforts continued on the development of advanced analytical and numerical techniques which can be effectively combined to provide advanced thermomechanical modeling of composite materials with nonlinear constituents. The areas of emphasis during this period were: development of thermoplastic and thermoviscoplastic models of composite materials using transformation strains; finite element formulation of bimodal plasticity model in combination with various forms of dimensional reduction; and idealization control for composite materials. GRA

N93-14597 Strathclyde Univ., Glasgow (Scotland).

THE EFFECT OF GEOMETRY AND PRESCRIBED DELAMINATIONS ON THE POSTBUCKLING BEHAVIOUR OF LAMINATED CARBON-FIBRE REINFORCED PLASTIC PANELS Ph.D. Thesis

Gin Boay Chai 1988 520 p

Avail: Univ. Microfilms Order No. BRD-97064

The instability behavior of carbon-fiber reinforced plastics laminated panels is investigated both theoretically and experimentally in this thesis. The effect of geometry and delaminations on the postbuckling behavior is also studied both analytically and experimentally. Theoretical analyses for the buckling and postbuckling behavior are presented. A four-term polynomial function is used to postulate the out-of-plane deflection form of the panel. The effect of the coupling terms is investigated and some of these terms are allowed for in the theoretical approach. A one-term postbuckling function is used in conjunction with the semi-energy method of analysis. The effect of initial imperfections is also covered in the study. The theoretical study of prescribed interply delaminations on the postbuckling behavior is based on the instability behavior of the sublaminate (delaminated region). A failure approach is also adopted to describe failure based on existing failure criteria. Details are given of an extensive experimental investigation which is undertaken to ascertain the validity and accuracy of the theoretical approaches. The equipment, instrumentation and testing setups are appropriately discussed. Extensive strain gauging is involved to obtain a thorough investigation of the behavior of the distribution of the strains on the surface of the panel. Results of the experimental investigation are compared with the theoretical prediction. The correlation between theory and experiment is on the whole reasonably good. Dissert. Abstr.

N93-14607 Utah Univ., Salt Lake City.

CHARACTERIZING LONGITUDINAL SPLITTING AND DELAMINATION FRACTURE TOUGHNESS OF COMPOSITES Ph.D. Thesis

Hsichieh Chen 1992 231 p

Avail: Univ. Microfilms Order No. DA9233326

The testing methods currently used to characterize the toughness of new composites give limited information concerning matrix-dominated failure modes. This study focuses on matrix-dominated fracture problems and on mathematical modelling of failure. An improved shear-lag analysis including fiber bridging effects was applied to unidirectional longitudinal split fracture. Graphite/epoxy, graphite/K-polymer, and graphite/PEEK composites were studied. Interlaminar delamination fracture of K-polymer composites was studied. Fracture toughnesses were determined using a large displacement beam theory and an area method. Damage zone and fiber bridging effects for fracture toughnesses were investigated. The results of delamination tests and longitudinal split tests were compared to each other. Mixed mode intralaminar fracture was studied. Three test methods were used to determine a failure criterion for mixed mode fracture. It was concluded that the asymmetric four-point bending test results gave the most reliable results. This study also found that some previous literature results should be re-evaluated. Dissert. Abstr.

N93-14665# Florida Univ., Alachua. Advanced Materials Research Center.

ULTRASTRUCTURE PROCESSING AND ENVIRONMENTAL STABILITY OF ADVANCED STRUCTURAL AND ELECTRONIC MATERIALS Final Report, 1 Apr. 1988 - 31 Jul. 1992

Larry L. Hench 31 Aug. 1992 119 p

(Contract F49620-88-C-0073)

(AD-A256153; AFOSR-92-0853TR) Avail: CASI HC A06/MF A02

The goals of this Multi-Investigator Research Program (MIRP) are: (1) achieve an understanding of the science of ultrastructure processing; and (2) apply the science of ultrastructure processing to produce new optical, electronic, optoelectronic, and structural materials. Ultrastructure processing refers to the manipulation and control of chemistry based processes to attain a new generation of high performance materials. Problem areas to benefit from ultrastructure processing include: advanced optical and opto-electronic systems, non-linear optical matrices, laser hosts, controlled particulates, transpiration cooled optics, effects of energetic particle beams, electronic behavior of high band gap semiconductors. Six projects are pursued. A cumulative list of the 60 papers published and 11 patents submitted during this contract is presented. A few papers from each project published during 1991-92 are presented. Project A: Sol-Gel Processing Science. Three papers describe the physical chemical factors and structural evolution and characterization of the sol-gel processing of large SiO_2 monoliths. Real time monitoring of the drying behavior of large silica gels is reported. A third paper reports on sol-gel derived titania-silica glasses with FTIR and structural characterization. GRA

N93-14672# Naval Air Development Center, Warminster, PA. Air Vehicle and Crew Systems Technology Dept.

THERMAL FATIGUE ANALYSIS OF METAL MATRIX COMPOSITE WITH SPHERICAL REINFORCEMENTS Final Report

Eun U. Lee 1 Oct. 1991 34 p

(AD-A255313; NADC-91059-60) Avail: CASI HC A03/MF A01

The stresses and strains, induced by coefficient of thermal expansion (CTE) mismatch, are analyzed for a metal matrix composite with a spherical reinforcement particle. The spherical reinforcement particle is found to be in a hydrostatic stress state and remains in the elastic state. The stresses and strains are largest, and plastic deformation occurs in the matrix adjacent to the reinforcement particle. Accordingly, the reinforcement particle/matrix

interface becomes a potential crack initiation site under thermal cycling. The critical internal pressure for plastic deformation is less than 2/3 of the yield stress of the matrix material and it decreases with increasing range of thermal cycle. From the analytically determined strains, the thermal fatigue life can be estimated. GRA

N93-14675# Naval Surface Warfare Center, Dahlgren, VA.
EVALUATION OF CORROSION PROTECTION METHODS FOR ALUMINUM METAL MATRIX COMPOSITES Final Report
Harold J. Greene 9 Jul. 1992 289 p
(AD-A255375) Avail: CASI HC A13/MF A03

Corrosion protection of Aluminum Metal Matrix Composites (MMC) using anodizing, chromate conversion coating and polymer coatings was investigated. Electrochemical Impedance Spectroscopy, DC polarization measurements, and Scanning Electron Microscopy (SEM) with Energy Dispersive X-ray Spectroscopy (EDS) were used. The materials studied included 606 1/SiC, A356/SiC, 2009/SiC, 2014/Al2O3 and 6061/Al2O3 in various reinforcement concentrations. The electrochemical behavior of the MMC's without protection was also investigated. MMC's were found to have similar corrosion and pitting potentials as the matrix alloy. The cathodic current density were found to be higher for MMC's with the current density increasing with reinforcement concentration. The increased current density is attributed to the interface between the matrix and the reinforcement particles which increases the corrosion rate. Anodizing was performed on both Al alloys and MMC's. A new model is proposed for Al alloys. Anodizing and hot water sealing on MMC's was less effective than on Al. Improved results were noted for dichromate sealing. GRA

N93-14700* National Aeronautics and Space Administration. Pasadena Office, CA.
CORE DESIGN FOR USE WITH PRECISION COMPOSITE REFLECTORS Patent
Christopher C. Porter, inventor (to NASA), Paul J. Jacoy, inventor (to NASA), and Wesley P. Schmitigal, inventor (to NASA) 10 Nov. 1992 11 p Filed 30 Mar. 1990 Supersedes N90-26880 (28 - 21, p 2970)
(Contract NAS7-918)
(NASA-Case-NPO-17858-1-CU; US-Patent-5,162,143; US-Patent-Appl-SN-503487; US-Patent-Class-428-179; US-Patent-Class-428-105; US-Patent-Class-428-182; US-Patent-Class-428-184; US-Patent-Class-428-185; US-Patent-Class-428-186; US-Patent-Class-428-213) Avail: US Patent and Trademark Office

A uniformly flexible core, and method for manufacturing the same, is disclosed for use between the face plates of a sandwich structure. The core is made of a plurality of thin corrugated strips, the corrugations being defined by a plurality of peaks and valleys connected to one another by a plurality of diagonal risers. The corrugated strips are orthogonally criss-crossed to form the core. The core is particularly suitable for use with high accuracy spherically curved sandwich structures because undesirable stresses in the curved face plates are minimized due to the uniform flexibility characteristics of the core in both the X and Y directions. The core is self venting because of the open geometry of the corrugations. The core can be made from any suitable composite, metal, or polymer. Thermal expansion problems in sandwich structures may be minimized by making the core from the same composite materials that are selected in the manufacture of the curved face plates because of their low coefficients of thermal expansion. Where the strips are made of a composite material, the core may be constructed by first cutting an already cured corrugated sheet into a plurality of corrugated strips and then secondarily bonding the strips to one another or, alternatively, by lying a plurality of uncured strips orthogonally over one another in a suitable jig and then curing and bonding the entire plurality of strips to one another in a single operation.
Official Gazette of the U.S. Patent and Trademark Office

N93-14706* National Aeronautics and Space Administration. Lewis Research Center, Cleveland, OH.
METHOD OF APPLYING A THERMAL BARRIER COATING SYSTEM TO A SUBSTRATE Patent
Robert A. Miller, inventor (to NASA) 8 Dec. 1992 5 p Filed 23 May 1991 Supersedes N91-25202 (29 - 17, p 2747) Division of abandoned US-Patent-Appl-SN-601957, filed 23 Oct. 1990
(NASA-Case-LEW-15020-2; US-Patent-5,169,674; US-Patent-Appl-SN-708255; US-Patent-Appl-SN-601957; US-Patent-Class-427-456; US-Patent-Class-427-367; US-Patent-Class-427-404; US-Patent-Class-427-419.2; Int-Patent-Class-B05D-1/02; Int-Patent-Class-B05D-3/12) Avail: US Patent and Trademark Office

A metallic close-out layer is applied to the surface of a thermal barrier coating system to seal the ceramic material in the coating. The close-out layer is glass-bead preened to densify the surface.
Official Gazette of the U.S. Patent and Trademark Office

N93-14744*# National Aeronautics and Space Administration. Langley Research Center, Hampton, VA.
FIBER-TEX 1991: THE FIFTH CONFERENCE ON ADVANCED ENGINEERING FIBERS AND TEXTILE STRUCTURES FOR COMPOSITES
John D. Buckley, ed. Washington Oct. 1992 183 p Conference held in Raleigh, NC, 15-17 Oct. 1991; cosponsored by DoD, North Carolina State Univ., Clemson Univ., and Drexel Univ.
(RTOP 505-63-50-05)
(NASA-CP-3176; L-17173; NAS 1.55:3176) Avail: CASI HC A09/MF A02

This document is a compilation of papers presented at a joint NASA/North Carolina State University/DoD/Clemson University/Drexel University conference on Fibers, Textile Technology, and Composites Structures held at the College of Textiles Building on Centennial Campus of North Carolina State University, Raleigh, North Carolina on October 15-17, 1991. Conference papers presented information on advanced engineering fibers, textile processes and structures, structural fabric production, mechanics and characteristics of woven composites, pultruded composites, and the latest requirements for the use of textiles in the production of composite materials and structures. For individual titles, see N93-14745 through N93-14757.

N93-14745*# BASF Structural Materials, Inc., Charlotte, NC.
AN EVALUATION OF COMPOSITES FABRICATED FROM POWDER EPOXY TOWPREG
J. Timothy Hartness and Tim Greene *In* NASA. Langley Research Center, FIBER-TEX 1991: The Fifth Conference on Advanced Engineering Fibers and Textile Structures for Composites Oct. 1992 p 1-9 (For primary document see N93-14744 04-24)
(Contract NAS1-18834)
Avail: CASI HC A02/MF A02

BASF has developed a unique process for applying powdered resin systems to continuous reinforcement fibers in order to produce flexible towpreg material. Evaluation of three powder epoxy resins using this towpregging process is in progress under NASA contract NAS1-18834. Shell RSS-1952, Dow CET-3, and 3M PR 500 powder epoxy systems have been successfully towpregged with G30-500 6K carbon fiber. Both neat resin and basic unidirectional composite properties have been developed to compare performance. Cure cycles for each system have also been developed for repeatable fabrication of high-quality composite laminates. Evaluations of the powder towpreg material for use in textiles processes such as weaving and braiding are underway. Traditional 8-harness weaving has been successfully performed with one system (PR500/G30-500) to date, with some basic composite properties generated. Ongoing work will demonstrate scaleup of the towpregging process for higher throughput, as well as evaluation of the powder towpreg material in advanced preforming processes such as 3-D braiding and weaving. An outline and figures summarize the research results. Author

N93-14746*# Philadelphia Coll. of Textiles and Science, PA.
ADVANCED STITCHING TECHNOLOGY
Frank L. Scardino *In* NASA. Langley Research Center, FIBER-TEX 1991: The Fifth Conference on Advanced Engineering Fibers and Textile Structures for Composites Oct. 1992 p 11-22 (For primary document see N93-14744 04-24)
Avail: CASI HC A03/MF A02

In the design of textile composites, the selection of materials and constructional techniques must be matched with product performance, productivity, and cost requirements. Constructional techniques vary. A classification of various textile composite systems is given. In general, the chopped fiber system is not suitable for structural composite applications because of fiber discontinuity, uncontrolled fiber orientation and a lack of

fiber integration or entanglement. Linear filament yarn systems are acceptable for structural components which are exposed to simple tension in their applications. To qualify for more general use as structural components, filament yarn systems must be multi-directionally positioned. With the most sophisticated filament winding and laying techniques, however, the Type 2 systems have limited potential for general load-bearing applications because of a lack of filament integration or entanglement, which means vulnerability to splitting and delamination among filament layers. The laminar systems (Type 3) represented by a variety of simple fabrics (woven, knitted, braided and nonwoven) are especially suitable for load-bearing panels in flat form and for beams in a roled up to wound form. The totally integrated, advanced fabric system (Type 4) are thought to be the most reliable for general load-bearing applications because of fiber continuity and because of controlled multiaxial fiber orientation and entanglement. Consequently, the risk of splitting and delamination is minimized and practically omitted. Type 4 systems can be woven, knitted, braided or stitched through with very special equipment. Multiaxial fabric technologies are discussed. Author

N93-14747*# National Inst. of Standards and Technology, Gaithersburg, MD. Polymers Div.

FLOW BEHAVIOR IN LIQUID MOLDING c34

D. Hunston, F. Phelan, and R. Parnas *In* NASA. Langley Research Center, FIBER-TEX 1991: The Fifth Conference on Advanced Engineering Fibers and Textile Structures for Composites Oct. 1992 p 23-42 (For primary document see N93-14744 04-24)

Avail: CASI HC A03/MF A02

The liquid molding (LM) process for manufacturing polymer composites with structural properties has the potential to significantly lower fabrication costs and increase production rates. LM includes both resin transfer molding and structural reaction injection molding. To achieve this potential, however, the underlying science base must be improved to facilitate effective process optimization and implementation of on-line process control. The National Institute of Standards and Technology (NIST) has a major program in LM that includes materials characterization, process simulation models, on-line process monitoring and control, and the fabrication of test specimens. The results of this program are applied to real parts through cooperative projects with industry. The key feature in the effort is a comprehensive and integrated approach to the processing science aspects of LM. This paper briefly outlines the NIST program and uses several examples to illustrate the work. Author

N93-14748*# North Carolina State Univ., Raleigh. Mars Mission Research Center.

ADVANCES IN 3-DIMENSIONAL BRAIDING c31

Cirrelia Thaxton, Rona Reid, and Aly El-Shiekh *In* NASA. Langley Research Center, FIBER-TEX 1991: The Fifth Conference on Advanced Engineering Fibers and Textile Structures for Composites Oct. 1992 p 43-65 (For primary document see N93-14744 04-24)

Avail: CASI HC A03/MF A02

This paper encompasses an overview of the history of 3-D braiding and an in-depth survey of the most recent, technological advances in machine design and implementation. Its purpose is to review the major efforts of university and industry research and development into the successful machining of this textile process. Author

N93-14749*# National Aeronautics and Space Administration. Langley Research Center, Hampton, VA.

DEVELOPMENT OF GENERALIZED 3-D BRAIDING MACHINES FOR COMPOSITE PREFORMS c31

Cecil O. Huey, Jr. (Clemson Univ., SC.) and Gary L. Farley *In its* FIBER-TEX 1991: The Fifth Conference on Advanced Engineering Fibers and Textile Structures for Composites Oct. 1992 p 67-76 (For primary document see N93-14744 04-24)

Avail: CASI HC A02/MF A02

The development of prototype braiding machines for the production of generalized braid patterns is described. Mechanical operating principles and control strategies are presented for two prototype machines which have been fabricated and evaluated. Both machines represent advances over current fabrication techniques for composite materials by enabling nearly ideal control of fiber orientations within preform structures. They permit optimum design of parts that might be subjected to complex loads or that have complex forms. Further, they overcome both the lack of general control of produced fiber architectures and the complexity of other weaving processes that have been proposed for the same purpose. One prototype, the Farley braider, consists of an array of turntables that can be made to oscillate in 90 degree steps. Yarn ends are transported about the surface formed by the turntables by motorized tractors which are controlled through an optical link with the turntables and powered through electrical contact with the turntables. The necessary relative motions are produced by a series of linear tractor moves combined with a series of turntable rotations. As the tractors move about, they weave the yarn ends into the desired pattern. The second device, the shuttle plate braider, consists of a braiding surface formed by an array of stationary square sections, each separated from its neighbors by a gap. A plate beneath this surface is caused to reciprocate in two perpendicular directions, first in one direction and then in the other. This movement is made possibly by openings in the plate that clear short columns supporting the surface segments. Yarn ends are moved about the surface and interwoven by shuttles which engage the reciprocating plate as needed to yield the desired movements. Power and control signals are transmitted to the shuttles through electrical contact with the braiding surface. The shuttle plate is a passively driven prime mover that supplies the power to move all shuttles and the shuttles are simple devices that employ only a solenoid to engage the shuttle plate on command. Each shuttle is assigned a unique identity and is controlled independently. When compared to each other, the Farley braider is felt to have the advantage of speed and the shuttle plate braider, the advantage of simplicity. Author

N93-14750*# Hoechst Celanese Corp., Charlotte, NC. Technical Fibers Div.

INDUSTRIAL APPLICATIONS OF MULTIAXIAL WARP KNIT COMPOSITES

James R. Kaufmann *In* NASA. Langley Research Center, FIBER-TEX 1991: The Fifth Conference on Advanced Engineering Fibers and Textile Structures for Composites Oct. 1992 p 77-86 (For primary document see N93-14744 04-24)

Avail: CASI HC A02/MF A02

Over the past few years, multiaxial warp knit (MWK) fabrics have made significant inroads into the industrial composites arena. This paper examines the use of MWK fabrics in industrial composite applications. Although the focus is on current applications of MWK fabrics in composites, this paper also discusses the physical properties, advantages and disadvantages of MWK fabrics. The author also offers possibilities for the future of MWK fabrics in the industrial composites arena. Author

N93-14751*# Dow Corning Corp., Midland, MI.

PROPERTIES OF TEXTILE GRADE CERAMIC FIBERS c27

Eric Pudnos *In* NASA. Langley Research Center, FIBER-TEX 1991: The Fifth Conference on Advanced Engineering Fibers and Textile Structures for Composites Oct. 1992 p 87-100 (For primary document see N93-14744 04-24)

Avail: CASI HC A03/MF A02

The availability of textile grade ceramic fibers has sparked great interest for applications in composite reinforcement and high temperature insulation. This paper summarizes the properties of various small diameter textile grade ceramic fibers currently available. Room temperature mechanical and electrical properties of the fibers are discussed for three cases: ambient conditions, after heat aging in argon, and after heat aging in wet air. Dow Corning (R) HPZ Ceramic Fiber, a silicon nitride type fiber, is shown to have improved retention of mechanical and electrical properties above 1200 C. Author

N93-14752*# California Univ., Davis. Div. of Textiles and Clothing.

THE OPTIMAL FIBER VOLUME FRACTION AND FIBER-MATRIX PROPERTY COMPATIBILITY IN FIBER REINFORCED COMPOSITES

Ning Pan *In* NASA. Langley Research Center, FIBER-TEX 1991: The Fifth Conference on Advanced Engineering Fibers and Textile Structures for Composites Oct. 1992 p 101-122 (For primary document see N93-14744 04-24)

Avail: CASI HC A03/MF A02

Although the question of minimum or critical fiber volume fraction beyond which a composite can then be strengthened due to addition of fibers has been dealt with by several investigators for both continuous and

short fiber composites, a study of maximum or optimal fiber volume fraction at which the composite reaches its highest strength has not been reported yet. The present analysis has investigated this issue for short fiber case based on the well-known shear lag (the elastic stress transfer) theory as the first step. Using the relationships obtained, the minimum spacing between fibers is determined upon which the maximum fiber volume fraction can be calculated, depending on the fiber packing forms within the composites. The effects on the value of this maximum fiber volume fraction due to such factors as fiber and matrix properties, fiber aspect ratio and fiber packing forms are discussed. Furthermore, combined with the previous analysis on the minimum fiber volume fraction, this maximum fiber volume fraction can be used to examine the property compatibility of fiber and matrix in forming a composite. This is deemed to be useful for composite design. Finally some examples are provided to illustrate the results.
Author

N93-14753*# Army Aerostructures Directorate, Hampton, VA.
MECHANICAL RESPONSE OF COMPOSITE MATERIALS WITH THROUGH-THE-THICKNESS REINFORCEMENT
Gary L. Farley and Larry C. Dickinson (Lockheed Engineering and Sciences Co., Hampton, VA.) *In* NASA. Langley Research Center, FIBER-TEX 1991: The Fifth Conference on Advanced Engineering Fibers and Textile Structures for Composites Oct. 1992 p 123-143 (For primary document see N93-14744 04-24)
Avail: CASI HC A03/MF A02

An experimental investigation was conducted to identify the key geometrical parameters and quantify their influence on the mechanical response of through-the-thickness (TTT) reinforced composite materials. Composite laminates with TTT reinforcement fibers were fabricated using different TTT reinforcement materials and reinforcement methods and laminates were also fabricated of similar construction but without TTT reinforcement fibers. Coupon specimens were machined from these laminates and were destructively tested. TTT reinforcement yarns enhance damage tolerance and improve interlaminar strength. Thick-layer composites with TTT reinforcement yarns have equal or superior mechanical properties to thin-layer composites without TTT reinforcement yarns. A significant potential exists for fabrication cost reduction by using thick-layer composites with TTT reinforcement yarns. Removal of the surface loop of the TTT reinforcement improves compression strength. Stitching provides somewhat higher mechanical properties than integral weaving. Author

N93-14754*# North Carolina Agricultural and Technical State Univ., Greensboro. Mars Mission Research Center.
TENSILE PROPERTIES OF TEXTILE COMPOSITES
V. Sarma Avva, Robert L. Sadler, and Malcolm Lyon *In* NASA. Langley Research Center, FIBER-TEX 1991: The Fifth Conference on Advanced Engineering Fibers and Textile Structures for Composites Oct. 1992 p 145-151 (For primary document see N93-14744 04-24)
(Grant NAGw-1331)
Avail: CASI HC A02/MF A02

The importance of textile composite materials in aerospace structural applications has been gaining momentum in recent years. With a view to better understand the suitability of these materials in aerospace applications, an experimental program was undertaken to assess the mechanical properties of these materials. Specifically, the braided textile preforms were infiltrated with suitable polymeric matrices leading to the fabrication of composite test coupons. Evaluation of the tensile properties and the analyses of the results in the form of strength moduli, Poisson's ratio, etc., for the braided composites are presented. Based on our past experience with the textile coupons, the fabrication techniques have been modified (by incorporating glass microballoons in the matrix and/or by stabilizing the braid angle along the length of the specimen with axial fibers) to achieve enhanced mechanical properties of the textile composites. This paper outlines the preliminary experimental results obtained from testing these composites. Author

N93-14755*# Naval Air Development Center, Warminster, PA.
MODELING OF EUCLIDEAN BRAIDED FIBER ARCHITECTURES TO OPTIMIZE COMPOSITE PROPERTIES
E. Armstrong-Carroll, C. Pastore (North Carolina State Univ., Raleigh.), and F. K. Ko (Drexel Univ., Philadelphia, PA.) *In* NASA. Langley Research Center, FIBER-TEX 1991: The Fifth Conference on Advanced Engineering Fibers and Textile Structures for Composites Oct. 1992 p 153-156 (For primary document see N93-14744 04-24)
Avail: CASI HC A01/MF A02

Three-dimensional braided fiber reinforcements are a very effective toughening mechanism for composite materials. The integral yarn path inherent to this fiber architecture allows for effective multidirectional dispersion of strain energy and negates delamination problems. In this paper a geometric model of Euclidean braid fiber architectures is presented. This information is used to determine the degree of geometric isotropy in the braids. This information, when combined with candidate material properties, can be used to quickly generate an estimate of the available load-carrying capacity of Euclidean braids at any arbitrary angle. Author

N93-14756*# North Carolina Agricultural and Technical State Univ., Greensboro. Mars Mission Research Center.
MICROSTRUCTURE-FAILURE MODE CORRELATIONS IN BRAIDED COMPOSITES
G. J. Filatovs, Robert L. Sadler, and Aly El-Shiekh (North Carolina State Univ., Raleigh.) *In* NASA. Langley Research Center, FIBER-TEX 1991: The Fifth Conference on Advanced Engineering Fibers and Textile Structures for Composites Oct. 1992 p 157-169 Sponsored in part by ONR (For primary document see N93-14744 04-24)
(Grant NAGw-1331)
Avail: CASI HC A03/MF A02

Explication of the fracture processes of braided composites is needed for modeling their behavior. Described is a systematic exploration of the relationship between microstructure, loading mode, and micro-failure mechanisms in carbon/epoxy braided composites. The study involved compression and fracture toughness tests and optical and scanning electron fractography, including dynamic in-situ testing. Principal failure mechanisms of low sliding, buckling, and unstable crack growth are correlated to microstructural parameters and loading modes; these are used for defining those microstructural conditions which are strength limiting. Author

N93-14757*# North Carolina Agricultural and Technical State Univ., Greensboro.
IMPROVED INHOMOGENEOUS FINITE ELEMENTS FOR FABRIC REINFORCED COMPOSITE MECHANICS ANALYSIS
R. L. Foye *In* NASA. Langley Research Center, FIBER-TEX 1991: The Fifth Conference on Advanced Engineering Fibers and Textile Structures for Composites Oct. 1992 p 171-183 Prepared in cooperation with Lockheed Engineering and Sciences Co., Hampton, VA (For primary document see N93-14744 04-24)
Avail: CASI HC A03/MF A02

There is a need to do routine stress/failure analysis of fabric reinforced composite microstructures to provide additional confidence in critical applications and guide materials development. Conventional methods of 3-D stress analysis are time consuming to set up, run and interpret. A need exists for simpler methods of modeling these structures and analyzing the models. The principal difficulty is the discrete element mesh generation problem. Inhomogeneous finite elements are worth investigating for application to these problems because they eliminate the mesh generation problem. However, there are penalties associated with these elements. Their convergence rates can be slow compared to homogeneous elements. Also, there is no accepted method for obtaining detailed stresses in the constituent materials of each element. This paper shows that the convergence rate can be significantly improved by a simple device which substitutes homogeneous elements for the inhomogeneous ones. The device is shown to work well in simple one and two dimensional problems. However, demonstration of the application to more complex two and three dimensional problems remains to be done. Work is also progressing toward more realistic fabric microstructural geometries. Author

N93-14819 EG and G Energy Measurements, Inc., Idaho Falls.
FABRICATION OF HIGH TEMPERATURE MATERIALS BY EXOTHERMIC SYNTHESIS AND SUBSEQUENT DYNAMIC CONSOLIDATION Patent Application
B. H. Rabin, inventor (to DOE), G. E. Korth, inventor (to DOE), R. N. Wright, inventor (to DOE), and R. L. Williamson, inventor (to DOE) 1991 20 p
(Contract DE-AC07-76ID-01570)

(DE92-019836; US-Patent-Appl-SN-641945; Patents-US-A-7641945) Avail: CASI HC A03/MF A01

An apparatus and method for synthesizing a composite material such as titanium carbide and alumina from exothermic reaction of a sample followed by explosive induced consolidation of the reacted sample. The apparatus includes a lower base for holding a powdered composite sample, an igniter and igniter powder for igniting the sample to initiate an exothermic reaction and a piston for dynamically compressing the sample utilizing an explosive reaction. DOE

N93-15075# Deutsche Forschungsanstalt fuer Luft- und Raumfahrt, Brunswick (Germany). Inst. fuer Strukturmechanik.

FRACTURE/DAMAGE MECHANICS OF COMPOSITES: STATIC AND FATIGUE PROPERTIES Final Report

Heinrich W. Bergmann, ed., Joachim Block, ed., R. Prinz, A. Pabsch, B. Geier, M. Gaedke, H. C. Goetting, L. Kirschke, W. Hartung, and H. Eggers et al Jan. 1992 329 p

(Contract ESTEC-8219/89/NL/PH(SC))

(DLR-Mitt-92-03; ETN-92-92405) Avail: CASI HC A15/MF A03; DLR, VB-PL-DO, Wissenschaftlisches Berichtswesen, Postfach 90 60 58, 5000 Cologne, Germany, HC

Research on damage mechanisms of carbon fiber reinforced materials under tension and compression loads is reported. Investigations which include the effects of inhomogeneities in laminates for strength critical applications are presented. Specimens with and without circular holes and sharp notches, with different stacking orders and different aspect ratios, were investigated. Static and cyclic loads were applied to assess size effects. The experimental results obtained with T300/914C epoxy material were complemented by test specimens prepared from a T800/Narmco 5250-2 (bismaleimide) and a T800/CPI2274 (polyimide) material system. The specimens were subjected to thermal conditions representative of typical Hermes flights. Analytical investigations to develop predictive tools for the forecast of damage patterns were performed. ESA

N93-15076# Deutsche Forschungsanstalt fuer Luft- und Raumfahrt, Stuttgart (Germany). Gruppe Konstruktionssystematik.

PRELIMINARY DESIGN OF COMPOSITE JOINTS

Kuno Stellbrink Apr. 1992 53 p

(DLR-Mitt-92-05; ETN-92-92407) Avail: CASI HC A04/MF A01; DLR, VB-PL-DO, Wissenschaftlisches Berichtswesen, Postfach 90 60 58, 5000 Cologne, Germany, HC

Procedures for designing the basic methods for joining thin walled composite structures, bonding, riveting and loops are presented. The aim of the study is the derivation of simple and handy analytical procedures for solving structural load transfer and load introduction problems. Approximate formulae and the derivation of the analysis of bonded joints using linear elastic/perfectly plastic adhesives are included. Loop shaped load introduction elements in solid composite bars are considered to sustain stress states similar to those which are generated in pressure loaded thick walled tubes. Distinction between plane stress state and plane strain state is made. The most effective parameter besides bolt diameter and laminate properties, the washer clamp-up pressure, is investigated. For many mechanical engineering tasks the approximate results of these analyses are adequate. High performance apparatuses, machines and vehicles with high reliability and mass requirements, need more sophisticated tools like finite element analysis and/or experimental proof tests. Prominent examples are manned aircraft and aerospace structures. ESA

N93-15144 Tel-Aviv Univ. (Israel). Dept. of Solid Mechanics, Materials and Structures.

ELASTIC WAVE PROPAGATION IN LAMINATED COMPOSITES M.S. Thesis

Iris Hevroni Jul. 1990 161 p In HEBREW

(ITN-93-85186) Copyright Avail: Tel-Aviv Univ., Exact Sciences Library, Ramat Aviv 69978, Israel

The dynamic response of laminated composites for propagation of elastic harmonic waves is affected by many parameters such as: the propagation direction with respect to the layering, the wavelength, the thickness of the layers, anisotropy of the layers, etc. This thesis presents a continuum model in the form of dynamic equations of motion which describe the time-dependent response of the laminated composite. For harmonic waves, these equations provide the dispersion relation of the laminated medium, for a given direction of propagation. The model is applied to study harmonic waves propagating in various directions in periodically bilaminated composites. In each case, a dispersion equation which relates the wave length to the phase velocity was derived. The dispersion curves obtained from the model were compared with those generated using other methods, and good agreement was obtained. Author (ISA)

N93-15145# Queens Univ., Kingston (Ontario). Dept. of Metallurgical Engineering.

A STUDY FOR THE DEVELOPMENT OF PRACTICES TO PROTECTIVELY COAT AND JOIN FIBRE EPOXY COMPOSITES FOR USE IN THE SPACE STATION PROGRAMME Final Report

Reginald Smith 31 Mar. 1988 121 p

(CTN-93-60626) Avail: CASI HC A06/MF A02

A study was undertaken to develop within Canada a suitable knowledge base and technological capability in space station component construction and repair. As part of an exploratory investigation to help define some of the problems involved, a selection of polymeric monoliths and composites were coated in several ways with various materials. The choice material to resist atomic oxygen degradation appears to be aluminum and this material was examined extensively. Experiments were conducted to determine the conditions for obtaining a highly adherent aluminum film free from perforations. The attachment forces of such films to the polymeric matrices were determined as a function of pretreatment and coating conditions. Potential joining techniques to attach one metallized component to another in low earth orbit were reviewed and soldering was selected as the simplest effective technique. A test of the technique was devised for a KC-135 flight. A simulation of the possible degradation of polymeric and aluminum-coated materials was attempted. A review of relevant literature shows that a closely accurate simulation is rather costly. A detailed proposal for a more definitive study is included. Author (CISTI)

N93-15146 Washington Univ., Seattle.

THERMAL, MECHANICAL, AND ELECTROELASTIC BEHAVIOR OF COMPOSITE MATERIALS Ph.D. Thesis

Martin Leonard Dunn 1992 310 p

Avail: Univ. Microfilms Order No. DA9230355

A unified analytical approach is developed to predict the effective behavior of composite materials for electronic applications. The target applications are materials for electronic packaging and electromechanical transducers where the material properties of interest are the effective thermal expansion coefficients, thermal conductivity, dielectric constant, and the couples electroelastic behavior. The analytical approach that is forwarded is based on the equivalent inclusion method of Eshelby (1957) extended to finite reinforcement concentrations through the Mori-Tanaka (1973) mean field approach. In addition to the effects of the material properties of the constituents, the effects of the volume fraction, shape, and orientation distribution of the reinforcing phase are considered. Through this approach, internal stresses generated due to the mismatch in thermal expansion coefficients of the constituents of a composite material are studied. Thermal expansion coefficients and time dependent creep deformations under a constant applied stress are analyzed. Analytical predictions of the proposed model are seen to be in good agreement with measured results of a multiphase Al2O3/Si3N4/Kerimid composite. The Mori-Tanaka mean field approach is also utilized to study the effective physical properties, modeled by Laplace's equation, of composite materials. Particular attention is devoted to microdamaged composites containing porosity or microcracks in the matrix and composites with coated reinforcement. Analytical predictions are shown to be in good agreement with measured results of the effective thermal conductivity for a multiphase Al2O3/Si3N4/Kerimid composite. Finally, the rigorous analytical solution for the couples electroelastic behavior of piezoelectric inclusions (Deeg, 1980) is utilized to derive the constraint tensors for an ellipsoidal piezoelectric inclusion in a infinite matrix. These tensors are analogous to Eshelby's tensor. A micromechanics model is developed to predict the effective electroelastic properties of particle and fiber reinforced piezoelectric composites. The model is applicable to a much wider range of composite microstructural geometry than existing models. As a byproduct of the proposed analytical approach, expressions for stress concentrations in and around ellipsoidal piezoelectric particles embedded in a piezoelectric matrix are obtained. In the dilute limit these expressions are new exact results. A matrix formulation is then proposed from which the predictions of other micromechanics approaches are readily

obtained. Analytical predictions are seen to be in good agreement with experimental data obtained from the literature for piezoelectric composites of a variety of microstructural geometry. Dissert. Abstr.

N93-15193# Army Armament Research, Development and Engineering Center, Watervliet, NY.
DEGRADATION AND FAILURE MODES OF CARBON/BISMALEIMIDE LAMINATES SUBJECTED TO A TROPICAL EXPOSURE Final Report
J. H. Underwood and A. A. Kapusta Aug. 1992 17 p
(AD-A256328; ARCCB-TR-92036) Avail: CASI HC A03/MF A01

A scanning electron microscope (SEM) was used to characterize the degradation of the outermost layers of carbon/bismaleimide laminates as the result of exposure to a natural tropical environment. The surface that was exposed to the sun for 4000 hours suffered complete degradation of the bismaleimide matrix to a shallow depth. SEM fractography showed little difference in the appearance of the fibers in a carbon/bismaleimide laminate, which displayed considerable fiber pullout compared to fibers in a carbon/epoxy laminate, which displayed little pullout. GRA

N93-15218# Quantum Consultants, Inc., East Lansing, MI.
SMART MATERIALS FOR ARMY STRUCTURES Final Report, Jul. 1991 - Feb. 1992
Subramaniam Ramamurthy, Mukesh V. Gandhi, and Brian S. Thompson Apr. 1992 206 p
(Contract DAAL04-91-C-0033)
(AD-A254925; MTL-TR-92-29) Avail: CASI HC A10/MF A03

This final report documents the results of the research and development activities focused on the development of a new generation of smart structures incorporating embedded hybrid multiple actuation systems which capitalize on the diverse strengths of both electrorheological fluids and piezoelectric materials, and employ fiber-optic sensing systems. A state-of-the-art review of smart materials and structures technologies has been undertaken, and an in-depth critique of the current generation of actuators and sensors for smart structures applications has also been presented. An in-depth review of analytical, computational and experimental investigations on controlling the vibrational characteristics of beams, plates and a variety of prototype structural systems has also been undertaken. Furthermore, variational formulations for predicting the performance characteristics of smart structures featuring hybrid embedded piezoelectric and electrorheological domains have been successfully developed. These formulations will form viable bases for the development of finite element design tools of phase 2. GRA

N93-15236# Naval Postgraduate School, Monterey, CA.
EFFECT OF THERMOMECHANICAL TREATMENTS ON THE AGING RESPONSE OF CENTRIFUGALLY CAST SILICON CARBIDE/ALUMINUM COMPOSITES M.S. Thesis
Christopher W. May Jun. 1992 43 p
(AD-A256204) Avail: CASI HC A03/MF A01

Differential scanning calorimetry was conducted using centrifugally cast monolithic A356 aluminum material and 26 volume percent silicon carbide (SiC) particle reinforced A356 aluminum matrix composite material in as-cast, cast and rolled, and cast and extruded conditions. Electrical resistivity and matrix micro-hardness measurements during isothermal aging treatments were also conducted. The effects of thermomechanical processing and SiC particle additions on the mechanical properties and aging kinetics of the metastable phases in each material were studied. GRA

N93-15246# Department of the Navy, Washington, DC.
SUPERSTRENGTH METAL COMPOSITE MATERIAL AND PROCESS FOR MAKING THE SAME Patent Application
N. P. Louat, inventor (to Navy), V. Provenzano, inventor (to Navy), M. A. Imam, inventor (to Navy), and K. Sadananda, inventor (to Navy) 31 Jan. 1992 20 p Filed 31 Jan. 1992
(AD-D015379; US-Patent-Appl-SN-828630) Avail: CASI HC A03/MF A01

A metal composite material provides improved strength at all temperatures, in particular at those temperatures greater half the melting point of its matrix. The metal composite material is at least 50 volume percent hard particulate material in a matrix which is significantly more ductile than the hard particulate material. At or above 50 volume percent hard particulate material, each particle is surrounded by a thin film of the matrix material. This thin film resists deformation by converting sliding motion between particles into the rotational motion of the particles about each other. The matrix may be made by infiltrating a powder of the particulate material with a charge of the matrix material, for example, by hot isostatically pressing the matrix material into the powder or by melting a block of matrix material on top of the powder and thus infiltrating the powder by gravitational flow of the melted matrix material into the powder. GRA

N93-15253# Office National d'Etudes et de Recherches Aerospatiales, Paris (France). Direction Scientifique des Materiaux.
STRUCTURAL STUDY OF THERMOHARDENING MATRICES: DEFORMATION OF COMPOSITE MATRICES IN RELATION TO THEIR MOLECULAR STRUCTURE [ETUDE STRUCTURALE DES MATRICES THERMODURCISSABLES: PROCESSUS DE DEFORMATION DES MATRICES DE COMPOSITES EN RELATION AVEC LEUR STRUCTURE MOLECULAIRE]
P. Sigety, B. Bloch, and J. C. Laizet Dec. 1990 25 p In FRENCH
(Contract DRET-88-34-001-BC-35)
(ONERA-RT-12/3521-M; ETN-92-92725) Avail: CASI HC A03/MF A01

Two methods to measure the structural hardening coefficient were applied to composite materials and compared. Trials were performed on thermoplastic and thermohardening matrix composite materials, and an epoxy model matrix composites. The results conformed with expectations but it is difficult to connect the obtained values with real modes of in situ resin deformation. ESA

N93-15373# Lehigh Univ., Bethlehem, PA.
DIFFUSION PROBLEMS IN BONDED NONHOMOGENEOUS MATERIALS WITH AN INTERFACE CUT Final Report
Fazil Erdogan and Murat Ozturk Aug. 1992 37 p
(Contract N00014-89-C-3188)
(AD-A256470) Avail: CASI HC A03/MF A01

The mixed boundary value problem for a nonhomogeneous medium bonded to a rigid subspace is considered. The main objective is to investigate the techniques that would lead to analytically tractable solutions and to provide examples comparing the results of various kinds of material nonhomogeneities. The problem studied is a two dimensional diffusion problem in which the interface contains a plane crack. An elastic medium under antiplane shear loading is used to formulate the problem. However, the results may be interpreted in terms of any number of steady-state diffusion phenomena. The method used is essentially an inverse method in the sense that it provides the material constitutive behavior for which the mixed boundary value problem can be solved rather than solving the problem for a given material. Two different methods are described and some numerical examples are given. GRA

N93-15387# Allied-Signal Aerospace Co., Torrance, CA.
DEVELOPMENT OF CERAMIC MATRIX COMPOSITES FOR APPLICATION IN CERAMIC TECHNOLOGY FOR ADVANCED HEAT ENGINES PROJECT, PHASE 2 Final Report, Apr. 1988 - Apr. 1991
H. Yeh, E. Solidum, K. Karasek, G. Stranford, D. Yuhas, J. Schienle, and S. Bradley Apr. 1992 103 p Prepared in cooperation with Oak Ridge National Lab, TN
(Contract DE-AC05-84OR-21400)
(DE92-041379; ORNL/Sub-85-22011/2) Avail: CASI HC A06/MF A02

The objectives of the program are to develop an advanced toughened silicon nitride composite and a process for near net shape part fabrication. This program was initiated in 1985. The initial phase of the program considered particulate and whisker-reinforced composites and examined the effect of TiC and SiC dispersoids on fracture toughness of Si3N4. The best results were obtained with whisker reinforcements. Silicon carbide whisker-reinforced Si3N4 was selected for further development. A predictive model that relates microstructure-fracture toughness dependence developed and scrutinized in the course of these studies has shown that fracture toughness of polycrystalline ceramics could be affected by changes of grain size and shape as well as strength of intergranular bond. Accordingly, it was shown that a deflection/debonding mechanism could utilize Si3N4 whiskers to toughen Si3N4 body. Si3N4-SiC composites offer a number of distinct advantages over 'monolith', which in addition to their improved thermal shock and wear resistance (due particularly to improved conductivity and hardness), Si3N4-SiC composites are tailorable with respect to high-temperature properties. It was considered that in heat engine

applications, Si3N4-SiC whisker composites, due to their higher hardness, thermal conductivity, thermal shock, and wear resistance, have a definite advantage and warrant further development. In the current program, 1987-1989, the properties were further improved to achieve nearly two times higher fracture toughness and considerably improved elevated temperature (1400 C) strength of the composite. These improvements were obtained through optimization of processing and modifications of composite phase assembly, primarily intergranular phase. DOE

N93-15388# Norton Co., Northboro, MA.
MATERIAL DEVELOPMENT IN THE Si3N4 SYSTEM USING GLASS ENCAPSULATED HIP'ING
N. D. Corbin, G. J. Sundberg, K. N. Siebein, C. A. Willkens, V. K. Pujari, G. A. Rossi, J. S. Hansen, C. L. Chang, and J. L. Hammarstrom Apr. 1992 115 p Prepared in cooperation with Norton Co., Northboro, MA
(Contract DE-AC05-84OR-21400)
(DE92-041381; ORNL/Sub-86-95906/2) Avail: CASI HC A06/MF A02

This report covers a two-year program to develop fully dense Si3N4 matrix SiC whisker composites with enhanced properties over monolithic Si3N4 materials. The primary goal was to develop a composite with a fracture toughness greater than 10 MPa(sq. root of m) capable of using high pressure glass encapsulated HIP'ing. Coating methods were developed to apply thin (less than 150 nm) stoichiometric BN layers to SiC whiskers and also to apply a dual coating of SiC over carbon to the whiskers. Fracture toughness of the composites was determined to increase as the quantity of whiskers (or elongated grains) with their axis perpendicular to the crack plane increased. Of the interface compositions evaluated in this effort, carbon was determined to be the most effective for increasing toughness. The highest toughnesses (6.8-7.0 MPa(sq. root of m)) were obtained with uniaxially aligned carbon coated whiskers. There was no evidence of the carbon coating compromising the oxidation resistance of the composites at 1370 C. DOE

N93-15401*# Battelle Columbus Labs., OH.
INELASTIC DEFORMATION OF METAL MATRIX COMPOSITES: PLASTICITY AND DAMAGE MECHANISMS, PART 2 Final Report
B. S. Majumdar and G. M. Newaz National Aeronautics and Space Administration, Lewis Oct. 1992 50 p
(RTOP 510-01-50)
(NASA-CR-189096-Pt-2; E-7412-Pt-2; NAS 1.26:189096-Pt-2) Avail: CASI HC A03/MF A01

The inelastic deformation mechanisms for the SiC (SCS-6)/Ti-15-3 system were studied at 538 C (1000 F) using a combination of mechanical measurements and detailed microstructural examinations. The objectives were to evaluate the contributions of plasticity and damage to the overall MMC response, and to compare the room temperature and elevated temperature deformation behaviors. Four different laminates were studied: (0)8, (90)8,(+ or -45)2s, and (0/90)2s, with the primary emphasis on the unidirectional (0)8, and (90)8 systems. The elevated temperature responses were similar to those at room temperature, involving a two-stage elastic-plastic type of response for the (0)8 system, and a characteristic three-stage deformation response for the (90)8 and (+ or -45)2s systems. The primary effects of elevated temperatures included: (1) reduction in the 'yield' and failure strengths; (2) plasticity through diffused slip rather than concentrated planar slip (which occurred at room temperature); and (3) time-dependent deformation. The inelastic deformation mechanism for the (0)8 MMC was dominated by plasticity at both temperatures. For the (90)8 and (+ or -45)2s MMCs, a combination of damage and plasticity contributed to the deformation at both temperatures. Author

N93-15426# Los Alamos National Lab., NM.
SPUTTER DEPOSITION AND CHARACTERIZATION OF MoSi2/SiC COMPOSITE COATINGS
J.-P. Hirvonen (Technical Research Centre of Finland, Espoo.), H. Kattelus (Technical Research Centre of Finland, Espoo.), I. Suni (Technical Research Centre of Finland, Espoo.), J. Likonen (Technical Research Centre of Finland, Espoo.), T. R. Jervis, and M. Nastasi 1992 7 p Presented at the NATO Advanced Study Institute on Mechanical Properties of Materials Having Ultra-Fine Microstructure, Porto Novo, Portugal, 17 Jun. 1 Jul. 1992
(Contract W-7405-eng-36)
(DE92-040326; LA-UR-92-2604; CONF-9206271-1) Avail: CASI HC A02/MF A01

We have deposited layered structures of MoSi2/SiC composite coatings on different substrates by using a sputtering technique. SiC was used for a constituent of this structure because of the thermodynamic stability of the MoSi2/SiC system. DC-magnetron and rf-diode systems were used to sputter MoSi2 and SiC, respectively. The substrates were mounted on a rotating holder allowing successive deposition of MoSi2 and SiC layers. The total number of sublayers of each kind was 90. The thickness of the MoSi2 sublayers was 10 nm and that of the SiC 3 nm. The coatings were characterized in terms of a composition and microstructure by Rutherford backscattering (RBS), secondary ion mass spectrometry (SIMS), x-ray diffraction, indentation fracture, and nanoindentation. The layered structure was still observed after the coating was annealed at 500 C for 1 h, which recrystallized the MoSi2 layer. However, hardness and indentation modulus were increased from 11.6 plus minus 0.8 and 220 plus minus 20 GPa to 20.8 plus minus 1.2 and 290 plus minus 30 GPa, respectively. Preliminary indentation fracture measurements indicate that the layered structure is more brittle than a single, amorphous as-deposited MoSi2 layer. Although no improvement in the room teruperature toughness was obtained, the hardness of the recrystallized composite coating was significantly higher than reported previously for a MoSi2/SiC composite. DOE

N93-15454# Norton Co., Northboro, MA.
ANALYTICAL AND EXPERIMENTAL EVALUATION OF JOINING SILICON CARBIDE TO SILICON CARBIDE AND SILICON NITRIDE TO SILICON NITRIDE FOR HEAT ENGINE APPLICATIONS
M. R. Foley, G. A. Rossi, G. J. Sundberg, J. A. Wade, and F. J. Wu Apr. 1992 197 p Prepared for Oak Ridge National Lab., TN
(Contract DE-AC05-84OR-21400)
(DE92-041376; ORNL/Sub-87-SB045/1) Avail: CASI HC A09/MF A03

Techniques were developed to produce reliable ceramic-ceramic joins and analytical models were developed to predict the mechanical performance of the joins at room and elevated temperatures. Si3N4 - 4 percent Y2O3 (Norton NCX-5100) and (beta)-SiC (Norton NCX-4500) were joined to themselves in the green state prior to final densification. The joins and controls were chemically and mechanically characterized at room and elevated temperatures to prepare the data banks for analytical modeling. Analytical models combining finite element and probabilistic software were developed that are capable of predicting the reliability of the joined components under fast fracture and creep. DOE

N93-15455# Allied-Signal Aerospace Co., Torrance, CA. Garrett Ceramic Components Div.
DEVELOPMENT OF CERAMIC MATRIX COMPOSITES FOR APPLICATION IN THE CERAMIC TECHNOLOGY FOR ADVANCED HEAT ENGINES PROJECT
H. Yeh, E. Solidum, K. Karasek, G. Stranford, D. Yuhas, J. Schienle, and S. Bradley Apr. 1992 200 p Prepared for Oak Ridge National Lab., TN
(Contract DE-AC05-84OR-21400)
(DE92-041378; ORNL/Sub-85-22008/2) Avail: CASI HC A09/MF A03

The objective of this effort (Phase 2 of a multi-phase program) was to maximize the toughness of a high-temperature Si3N4 (GN-10) by the near-net-shape fabrication technology established previously (Phase 1). Acid-etched American Matrix SiC whiskers were selected as the reinforcement. Extensive green forming and densification process optimizations were conducted. The results showed that whisker addition increased the toughness slightly, but decreased the strength of the material. It has been recommended to discontinue the whisker reinforcement approach, and to instead pursue the in-situ grown-whisker reinforcement approach. To address future needs for the composite technology, two supplemental efforts were conducted using monolithic GN-10 Si3N4. These were nanometer deposition of sintering aids and ultrasonic characterization of drying. Spray drying, polymerization, basic precipitation, and evaporation yielded more uniform sintering aid distributions than conventional ball milling. Spray drying was selected for scale-up study. Improved mechanical properties were demonstrated. The results of the ultrasonic study showed that variations in ultrasonic compressional velocity in slip-cast components are more complex than anticipated. Specifically, it was found that the sonic velocity, as a function of moisture content, was double-valued. This behavior, together with the problems associated with maintaining uniform couplant, precludes the use of ultrasonics as a routine means of monitoring moisture content. DOE

N93-15490# Aerospatiale Aquitaine, Saint-Medard en Jalles (France).
FIBER REINFORCED COMPOSITES: A NEW CLASS OF GLASS AND GLASS CERAMIC MATERIALS FOR THERMOMECHANICAL APPLICATIONS
P. Lespade, G. Larnac, P. Peres, J. M. Donzac, C. Drouet (Ceramiques et Composites, Bazet, France), E. Menessier (Ceramiques et Composites, Bazet, France), T. Grenier (Office National d'Etudes et de Recherches Aerospatiales, Paris, France), M. Parlier (Office National d'Etudes et de Recherches Aerospatiales, Paris, France), and Y. Montardi (Rhone-Poulenc Industries, Paris, France) 1992 7 p Sponsored by Direction des Recherches, Etudes et Techniques
(Rept-921-430-104; ETN-92-92352) Avail: CASI HC A02/MF A01

Silicon carbide (SiC) fiber reinforced MAS glass and glass ceramic type matrix composites were investigated as potential materials for advanced structural applications. Results on microstructural studies and mechanical properties of these composites fabricated by hot pressing are presented. The need for such strong and tough ceramic matrix composites is due to the merging needs of future aeronautic and space applications such as thermomechanical parts and structures and high dimensional stability frames. The starting materials and the fabrication techniques are presented. The mechanical properties of the materials at room temperature and the effect of temperature changes are analyzed. From the results of this investigation of the SiC fiber reinforced MAS type matrix composites system, it is demonstrated that these materials can be fabricated to give a glass MAS-Zr matrix composite and a family of glass ceramic matrix composites with high strength and good toughness properties. ESA

N93-15625# Pennsylvania State Univ., University Park. Applied Research Lab.
NONLINEAR FINITE ELEMENT ANALYSIS OF METALS AND METAL MATRIX COMPOSITES: A LOCAL-GLOBAL INVESTIGATION
M. B. House and R. B. Bhagat Oct. 1992 105 p
(Contract N00039-88-C-0051)
(AD-A256782; TR-92-01) Avail: CASI HC A06/MF A02

A computational investigation of the fracture mechanics of metals and metal matrix composites was performed. The ductile fracture of structural alloys was analyzed through a two dimensional nonlinear finite element approach, while the mechanics of load transfer in silicon carbide (SCS-6) fiber reinforced titanium alloy (Ti-15V-3Cr-3Al-3Sn) were studied using a local-global finite element analysis procedure. The computed values of the J-Integral for compact tension specimens of steel and aluminum alloys (0.533 less than or = a/W less than or = 0.884) remain path independent up to a certain load which is attributed to crack initiation, and then diverge. There is a unique signature of the strain energy density (dW/dV) ahead of the crack in the 0 deg direction: the strain energy first decreases, reaches a minimum, and then increases with increasing distance from the crack tip. The minimum strain energy shows a unique dependence on the applied load. This leads to the prediction of the fracture loads for the cracked specimens. A novel coordinate system rotation was employed in extracting the boundary conditions from the two-dimensional global model to the three-dimensional local model for the local-global finite element analysis of the unidirectional composite. GRA

N93-14955# Toronto Univ. (Ontario). Inst. for Aerospace Studies.
COMPOSITE MATERIALS IN SPACE: RESULTS FROM THE LDEF SATELLITE
R. C. Tennyson, J. S. Hansen, G. E. Mabson, W. D. Morison, and J. Kleiman *In* Canadian Space Agency, Proceedings of the Sixth CASI Conference on Astronautics 1990 15 p Previously announced in IAA as A91-34961 (For primary document see N93-14920 04-12)
Avail: Canadian Aeronautics and Space Inst., 222 Somerset St. W., Suite 601, Ottawa, Ontario K2P 0J1 Canada

N93-15614*# Science Applications International Corp., Glendora, CA.
OPERATIONAL STRATEGIES FOR CONTAMINATION CONTROL OF COMPOSITE MATERIALS Abstract Only
Patricia A. Hansen *In* NASA. Goddard Space Flight Center, The Seventeenth Space Simulation Conference. Terrestrial Test for Space Success Nov. 1992 p 251 (For primary document see N93-15593 04-18)
Avail: CASI HC A01/MF A03

25 INORGANIC AND PHYSICAL CHEMISTRY

Includes chemical analysis, e.g., chromatography; combustion theory; electrochemistry; and photochemistry.

For related information see also *77 Thermodynamics and Statistical Physics.*.

N93-14418# Yale Univ., New Haven, CT. Dept. of Chemical Engineering.
TRANSPORT PHENOMENA AND INTERFACIAL KINETICS IN MULTIPHASE COMBUSTION SYSTEMS. Annual Technical Report, 15 Feb. 1991 - 14 Feb. 1992
Daniel E. Rosner Aug. 1992 68 p Revised
(Grant AF-AFOSR-0170-91)
(AD-A255999; AFOSR-92-0890TR) Avail: CASI HC A04/MF A01

This annual technical report summarizes Yale High Temperature Chemical Reaction Engineering Laboratory research activities (under Grant AFOSR 91-0170) for the one-year period ending 14 February 1992. Among our research results described in detail in the cited references, the most noteworthy are the development of: rational correction factors to account for the effects of suspended particle morphology on convective diffusion mass deposition rate's; quantitative criteria for influence of particle thermophoresis on the structure of two-phase laminar counterflow diffusion flames (potentially useful to predict IR radiation from such flames and optimize particle properties in synthesis applications); and quantitative methods for predicting/correlating the effects of particle inertia on thermophoretic deposition across laminar boundary layers on targets with streamwise curvature (experimentally verified by our seeded micro-combustor experiments on concave ribbon targets). Fifteen presentations and two PhD dissertations have resulted from this research program. Copies of three reprints appearing during this period are included in the appendices. GRA

N93-14435# Army Belvoir Research and Development Center, Fort Belvoir, VA.
APPLICATION OF FOURIER TRANSFORM-INFRARED SPECTROSCOPY (FT-IR) FOR MATERIALS ANALYSIS Final Report, Jan. 1989 - Dec. 1991
Philip Patterson and William Lum Aug. 1992 26 p
(AD-A255727; BRDEC-TR-2529) Avail: CASI HC A03/MF A01

In the past, a number of Mission Related Requests were made of the Coatings, Corrosion, and Packaging Team, Advanced Technology Division at BRDEC to analyze a variety of materials for chemical composition. This technical report presents an overview of one approach, Fourier Transform-Infrared Spectroscopy (FT-IR), that the Laboratory Analyst utilizes to support such requests. GRA

N93-14454# Army Belvoir Research and Development Center, Fort Belvoir, VA.
SURFACE PREPARATION OF STAINLESS STEEL PRIOR TO PAINTING Final Report, Jan. - Sep. 1992
Dario A. Emeric and Christopher E. Miller Sep. 1992 23 p
(AD-A256253; BRDEC-TR-2534) Avail: CASI HC A02/MF A01

Military specification MIL-T-704, Treatment and paint of materiel, requires the passivation of corrosion-resisting steel surfaces before painting. It also states surfaces to be painted shall be treated with wash primer conforming to DOD-P-15328, Primer (wash) pretreatment (Formula No. 117 for metals), metric, or MIL-C-8514, Coating compound, metal pretreatment, resin-acid. Federal, state and city environmental and/or health regulations may prohibit the use of hexavalent chromium-one of the components of the passivating formulation used for the treatment of corrosion-resisting steels. Many companies are not passivating the corrosion-resisting steels before the application of wash primer. Based on the above, we started a laboratory investigation to determine if the elimination of the passivating procedure will have an adverse effect on the camouflage paint system. From the information obtained, it is recommended that consideration be given to the elimination of the passivation requirement for stainless steel. It is also recommended that more extensive work be conducted to verify these findings. GRA

N93-14463 Michigan Univ., Ann Arbor.
DYNAMIC BEHAVIOR OF A DENSE SPRAY DIFFUSION FLAME IN A POTENTIAL VORTEX Ph.D. Thesis
Sheau-Ming Shiah 1992 191 p
Avail: Univ. Microfilms Order No. DA9227002

The interaction of a dense spray diffusion flame and a plane potential vortex is analytically investigated assuming constant property, sheath spray combustion, the flame sheet approximation, and the locally one-dimensional approximation. The problem is a modification of the original Marble problem with the gaseous fuel and the viscously decaying vortex replaced by a liquid fuel spray and a non-decaying potential vortex. The study is divided into three stages: (1) the interaction of a nonsteady gaseous diffusion flame and a potential vortex; (2) the time-dependent sheath combustion of a planar fuel droplet cloud; and (3) the interaction of a dense spray diffusion flame and a potential vortex. In state (1) the validity of a proposed patching method as applied to an unsteady gaseous diffusion flame scope is justified for application in subsequent stages. State (2) considers the plane case of stage (3) and provides a basis for evaluating the vortex effect on a spray diffusion flame. The final stage investigates the dynamic behavior of the vortex interaction with a spray diffusion flame and its influence on the global fuel consumption rate and the growth of a core-like reacted region. Subject to the approximations made in this study, the diffusion layer structure of the spray flame is shown to be self similar in time and space. The global flame is also self similar, and is governed by the ratio of the vortex strength to the diffusion coefficient, gamma/D. The radius of the reacted core normalized by the square root of Dt is proportional to (gamma/D)(exp 1/3). The augmentation in fuel consumption rate normalized by D is proportional to (gamma/D)(exp 2/3). Criteria for approximation of a viscous vortex by a potential vortex are also developed. It is concluded that analytical solutions for the interaction of a dense spray diffusion flame with a potential vortex can be determined, provided the spray undergoes sheath combustion, and that the results can be related to those of the original Marble problem. Dissert. Abstr.

N93-14530# Aerospace Corp., El Segundo, CA. Technology Operations.
HIGH RESOLUTION ABSOLUTE ABSORPTION CROSS SECTIONS OF NO2 AT 295, 573, AND 673 K AT VISIBLE WAVELENGTHS: COMPREHENSIVE DATA TABLES
Timothy C. Corcoran, Edward J. Beiting, and Mark O. Mitchell 30 Jun. 1992 359 p
(Contract F04701-88-C-0089)
(AD-A255261; TR-0091(6935-18)-1; SSD-TR-92-26) Avail: CASI HC A16/MF A03

Absolute absorption cross sections of nitrogen dioxide were measured with a resolution of 0.008 nm in 470 to 490, 520 to 534, 588 to 601, and 603 to 616 nm spectral regions at temperatures of 295, 573, and 673 K. An absolute error of +/- 10 pct. is due principally to uncertainty in the NO2 concentration. Absorption cross sections were also measured at these temperatures in the 450 to 650 nm spectral region with a resolution of 0.075 nm with an error of +/- 10 pct. All data were corrected for thermal decomposition of NO2 at the elevated temperatures. The spectral features show broadening at elevated temperatures consistent with the breakdown of delta K selection rules for higher rotational levels. GRA

N93-14539 ESDU International Ltd., London (England).
VISCOSITY OF LIQUIDS. HALOGENATED METHANES
Oct. 1992 32 p
(ESDU-92028; ISBN-0-85679-834-7) Avail: ESDU

ESDU 92028 tabulates the viscosity of 25 halogenated methanes at saturation pressure for temperatures from just above the melting point to approximately 0.9 of the critical temperature. Experimental data extracted from the literature were fitted by an equation for the logarithm of dynamic viscosity as a function of reduced temperature. The equation contains four constants and the values determined for them from the correlation are tabulated for each compound. Viscosities are given at 10 K and 10 C intervals, together with an assessment of the uncertainty in each value. The sources of the data for each compound are listed, and the critical temperature is given. It is noted that viscosity increases by 1 percent for a pressure increase of 10 bar, and an equation is suggested for calculating the effect of pressure up to 500 bar. Author

N93-14540 ESDU International Ltd., London (England).
ORTHOBARIC DENSITIES AND MOLAR VOLUMES OF LIQUIDS. HALOGENATED ETHYLENES
Aug. 1992 26 p
(ESDU-92018; ISBN-0-85679-822-3) Avail: ESDU

ESDU 92018 tabulates density and molar volumes for 10 haloethylenes. The tables are in units of kg/cu m and cu cm/mol respectively from near the melting point to within a few degrees of the critical point. The temperature interval chosen is varied from 10 K to 1 K to keep the increments in density reasonably small. Although the Rackett equation does not represent the variation of density over the full temperature range so well as the equation used in ESDU 92018 (log reduced density as a polynomial function of reduced temperature), it was used to estimate the critical density. The estimated values were slightly adjusted to give a smooth variation between compounds. The log/polynomial equation was then fitted to the experimental data for density for each compound taken from a wide range of sources in the literature; values established for the coefficients in the equation for each compound are also tabulated. Estimates of the accuracy of the predictions are included, as is a list of the sources of data actually used for each compound. Values at the critical point are provided together with normal boiling and melting points. Author

N93-14542 ESDU International Ltd., London (England).
THERMAL CONDUCTIVITY OF LIQUID ALIPHATIC HYDROCARBONS. PART 2: ALKENES, DIENES AND TRIENES
Apr. 1992 85 p Supersedes ESDU-75009
(ESDU-92025; ISBN-0-85679-830-4) Avail: ESDU

ESDU 92025 gives data for 61 alkenes, 15 dienes and Hexa-1, cis-3, 5-triene. Experimental results drawn from the literature for each compound were fitted with a four-term polynomial equation in reduced temperature. The coefficients were also faired with changing molecular structure to ensure the best correlation not only for the individual compounds but also as members of their chemical series. The coefficient correlations also allowed values to be predicted for compounds for which no measured data exist. The equations were used to tabulate thermal conductivity values from the melting point to about 0.9 critical temperature in SI units at 10 K and 10 C intervals. The critical points, coefficients and sources of the data are given for each compound. Conversion factors are provided for common British units, the effect of pressure is briefly considered and the likely accuracy of the tabulated values is discussed. Author

N93-14544 ESDU International Ltd., London (England).
THERMOPHYSICAL PROPERTIES OF NITRIC OXIDE
Oct. 1992 17 p
(ESDU-92027; ISBN-0-85679-833-9) Avail: ESDU

ESDU 92027 gives equations obtained from a critical evaluation of experimental data in the literature for the variation along the saturation line with temperature, for both the liquid and the vapour, of: density, enthalpy, heat capacity at constant pressure, dynamic viscosity and thermal conductivity. Also given are equations for the variation with temperature along the saturation line of the vapour pressure, latent heat of vaporization and surface tension, together with equations for the variation with temperature for the ideal gas of specific heat capacity at constant pressure, enthalpy, dynamic viscosity and thermal conductivity. Results on the saturation line evaluated in SI units using the equations are tabulated at 2 K intervals and at 2 C intervals from the melting point to the critical point, or as close to it as possible for some properties. Results for the ideal gas evaluated also in SI units using the equations are tabulated at 20 K and at 20 C intervals from the melting point to 1000 K. In the absence of experimental values some of these results involve extrapolation and they are indicated in the tables. Conversion factors to facilitate use of the data in British units are included. Author

N93-14617# Von Karman Inst. for Fluid Dynamics, Rhode-Saint-Genese (Belgium).
MODELING OF COMBUSTION AND TURBULENCE
1992 599 p Lecture series held in Rhode-Saint-Genese, Belgium, 9-13 Mar. 1992
(VKI-LS-1992-03; ETN-92-92360) Copyright Avail: CASI HC A25/MF A06

The state of the art of modeling combustion phenomena is reviewed. Advances in both numerical modeling and experimental techniques gave a

better understanding of the fundamental aspects of the combustion phenomenon and increased the reliability of the design phase for practical applications. The remaining problems to be solved and the advances to be expected in the near future are considered. The physics of combustion, the most recent advances in modeling and numerical simulations, and specific problems of relevant practical interest such as droplet combustion, supersonic combustion, and pollutant formation, are studied. For individual titles, see N93-14618 through N93-14627.

N93-14618# Provence Univ., Marseille (France). Lab. de Recherche en Combustion.

FUNDAMENTALS OF COMBUSTION OF PREMIXED GASES

Paul Clavin *In* VKI, Modeling of Combustion and Turbulence 46 p(SEE N93-14617 04-25) 1992 (For primary document see N93-14617 04-25)

Copyright Avail: CASI HC A03/MF A06

Some results concerning the application of a singular perturbation method, based on an asymptotic expansion, to describe the propagation of premixed flames, extinction phenomena, and kinetic effects in the dynamic behavior of flame fronts, are reviewed. The concepts and theories of turbulence flames are summarized. Despite some progress in this field, there are not yet satisfactory theories of turbulent combustion to support the engineering models used in industrial computations. A large number of new approaches are now available but in the absence of pertinent experimental data in sufficient quantity, most of these approaches are not sufficiently firmly based. The main objectives of this lecture are as follows: to provide the nonspecialists with an introduction to the field of turbulent premixed flames; to identify some simplified problems whose solutions may be useful in turbulent combustion; to present new insights based on semi-phenomenological analysis concerning both the limiting cases of low and high intensity turbulent flows. ESA

N93-14619# Stuttgart Univ. (Germany). Inst. fuer Technische Verbrennung.

CHEMICAL KINETICS FOR COMBUSTION

J. Warnatz *In* VKI, Modeling of Combustion and Turbulence 1992 155 p Sponsored by BMFT, EEC, Fonds der Chemischen Industrie, and Max-Buchner-Stiftung (For primary document see N93-14617 04-25)

Copyright Avail: CASI HC A08/MF A06

A quantitative description of typical combustion processes are reviewed. The understanding of combustion processes needs extreme computational efforts, but a rather simplified treatment can give a lot of insight into combustion processes. Homogeneous reaction systems, which involve processes like transport phenomena, thermodynamics, and chemistry in spatially homogeneous systems are overviewed. The usual methods applied to solve turbulent flame problems are discussed. The structure of stationary laminar flame fronts as the result of the interaction of transport, chemistry, and flow is considered for simple hydrocarbon fuels. The instationary behavior which plays an important role in ignition processes for phenomena like quenching of turbulent flames, and noise generation, is included. The chemistry of combustion necessary to describe and understand pollutant formation is discussed. Different methods to include detailed chemistry in terms of the set of elementary reactions into turbulent combustion modeling are described. ESA

N93-14620# Imperial Coll. of Science and Technology, London (England).

TURBULENCE MODELING FOR COMBUSTION FLOWS

W. P. Jones *In* VKI, Modeling of Combustion and Turbulence 34 p(SEE N93-14617 04-25) 1992 (For primary document see N93-14617 04-25)

Copyright Avail: CASI HC A03/MF A06

Computations of constant density flows carried out over the past five years demonstrated that second moment closures, even with quite simple closure approximations, present a much more accurate method of calculating complex flows than is provided by eddy viscosity k-epsilon type models. The progress made in devising second moment closures for the Reynolds stress and scalar flux and their extension to combustion flows through the use of Favre averaging is summarized. The approximations range from the relatively simple and widely used, to current developments aimed at devising closure approximations which behave properly in the limit of the turbulence becoming two dimensional. Attention is focused on high turbulence Reynolds numbers and flow near solid surfaces is excluded. Second moment closures are likely to have a limited but sufficiently wide range of applicability to be of practical value. The extent of their applicability can only be determined by a careful and detailed comparison between computation and experiment. ESA

N93-14621# British Gas Corp., Solihull (England).

RADIATIVE HEAT TRANSFER IN COMBUSTION SYSTEMS

P. Docherty and M. Fairweather *In* VKI, Modeling of Combustion and Turbulence 47 p(SEE N93-14617 04-25) 1992 (For primary document see N93-14617 04-25)

Copyright Avail: CASI HC A03/MF A06

Current models for predicting radiative heat transfer in combustion systems are reviewed. In order to accurately calculate radiative heat transfer in practical, inhomogeneous combustion systems, it is necessary to include scattering effects and the spectral variation of radiative properties in the solution method. Gas radiation, is discussed, starting from a description of the spectra associated with radiating gases through simplified methods of predicting total properties. In a second step, particle radiation effects are introduced in the gas radiation analysis. Despite the large volume of work relevant to radiative heat transfer calculations, a number of problem areas remain. In particular, theoretical modeling of, and experimental data on, the radiative properties of a number of types of gaseous molecules and particulates is required. The effects of turbulent flow in radiative transfer calculations should be taken into account by the model. ESA

N93-14622# Centre National de la Recherche Scientifique, Paris (France). Lab. d'Energetique Moleculaire et Macroscopique-Combustfion.

DIRECT SIMULATION OF TURBULENT COMBUSTION

Thierry J. Poinsot *In* VKI, Modeling of Combustion and Turbulence 94 p(SEE N93-14617 04-25) 1992 (For primary document see N93-14617 04-25)

Copyright Avail: CASI HC A05/MF A06

Direct Numerical Simulation (DNS) results obtained for premixed turbulent flames are presented and discussed to provide a description of the DNS possibilities and limitations. Numerical issues and boundary conditions are discussed. The basis of flamelet models is given. This classical theory is the framework in which most DNS of premixed flames take place and need to be described before DNS results are presented the DNS of flame-vortex interactions and the DNS of flame-turbulence interactions are summarized. Through some examples of DNS of premixed flame vortex interactions and of turbulent flames, the impact of such computations in understanding and modeling of turbulent combustion is shown. DNS of turbulent reacting flows is a fast growing domain of study and applications should be mentioned. ESA

N93-14623# California Univ., Davis. Dept. of MAME.

PDF TRANSPORT MODELLING

W. Kollmann *In* VKI, Modeling of Combustion and Turbulence 71 p(SEE N93-14617 04-25) 1992 (For primary document see N93-14617 04-25)

Copyright Avail: CASI HC A04/MF A06

The basic theory, the properties, and the characteristic function of Probability Density Functions (PDF's) are reviewed. The closure of the PDF equation, and the numerical solution of moment equations and the PDF equation are outlined. Finite difference methods are considered for moment equations and stochastic simulation techniques for the PDF equation. PDF methods are applied to a variety of reacting and nonreacting turbulent flows. The simulation of combustion in maintained homogeneous turbulence and several turbulent nonpremixed flames is presented. The results are evaluated by comparison with available experimental data. PDF methods were derived and shown to lead to a closure problem distinctly different from the moment approach to turbulence. The following conclusions can be drawn: convection appears as closed term in the equation for the velocity scalar PDF and has the same form as the convection term in the basic balance equations for mass momentum and scalars; chemical source terms arising in combustion flows have a highly nonlinear structure but are local in the sense that they do not contain derivatives or integrals with respect to time and location; molecular transport leads to nonclosed terms in the PDF equation and can be shown to depend in two point PDF's or, equivalently, on conditional expectations of the instantaneous viscous/diffusive fluxes; the numerical solution of PDF equations has to rely on stochastic simulation techniques since classical methods are too expensive; and PDF methods were applied to a variety of homogeneous

and nonhomogeneous flows. Results, including methane-air nonpremixed flames and sooting ethylene flames, illustrated the properties and advantage of PDF methods. ESA

N93-14624# Institut National des Sciences Appliquees, Routen (France).
APPLICATIONS OF PDF TURBULENT COMBUSTION MODELS TO REAL NON PREMIXED FLAME CALCULATIONS
L. Vervisch *In* VKI, Modeling of Combustion and Turbulence 56 p(SEE N93-14617 04-25) 1992 (For primary document see N93-14617 04-25)
Copyright Avail: CASI HC A04/MF A06

Two Probability Density Function (PDF) methods are presented: an approximated Peul method and a classical Monte carlo method. In these methods, basic mixing models can be used in the case of nonpremixed combustion. It is shown that the competition between the turbulent and the chemical processes is correctly represented. For both methods, the agreement with measurements in this flow configuration is quite good. The computations show that the simplified PDF approach is an interesting compromise for industrial problems; in counterpart, the Montecarlo method is able to manage a four step reduced kinetics scheme and to reproduce mean temperature fluctuations. The following points are to be improved in these methods: the most important is the mixing model, which does not satisfy all the physical properties of the mixing process; and the second is the approximation of the mean integral time scale. More information is needed to improve the PDF description, information related to the joint PDF of a scalar, and also to its gradient. The representation of the chemical phenomena also needs improvement. ESA

N93-14625# Cambridge Univ. (England).
CALCULATION OF CHEMICAL REACTION RATES IN TURBULENT COMBUSTION
K. N. C. Bray *In* VKI, Modeling of Combustion and Turbulence 27 p(SEE N93-14617 04-25) 1992 (For primary document see N93-14617 04-25)
Copyright Avail: CASI HC A03/MF A06

Some modeling techniques to predict mean rates of chemical reaction, for use in theoretical models of turbulent combustion, are presented. Emphasis is placed on laminar flamelet models for combustion of premixed reactants. Descriptions of some other models are included. Laminar flamelet models can, in principle, incorporate chemical kinetic information of arbitrary complexity which are then stored and interpolated in subsequent turbulent flame computations. However, the accuracy of current models is limited by factors other than the chemical kinetic input to their flamelet submodels, and flamelet models do not meet the requirement of applicability in all combustion regimes. Models based on the solution of a probability density function transport equation come closest to meeting the requirement for wide applicability and capacity to include realistic chemical kinetics. Available models are applicable to either flamelet or nonflamelet combustion but not both. Advantages are found in analyzing the whole flow and combustion problem in a Lagrangian Monte Carlo simulation. Further development of all these models is still required. Direct numerical simulations of idealized turbulent reacting flows are important in the development and testing of modeling assumptions. ESA

N93-14626# Rouen Univ. (France). Faculte des Sciences.
INTRODUCTION TO SPRAY COMBUSTION MODELLING
R. Borghi *In* VKI, Modeling of Combustion and Turbulence 26 p(SEE N93-14617 04-25) 1992 Sponsored by SEP, CNES, and CNRS (For primary document see N93-14617 04-25)
Copyright Avail: CASI HC A03/MF A06

The combustion of a single droplet of fuel in an ambient oxidizing atmosphere is presented. The simple quasi-steady theory is given, and corrections to this theory are described. A physical description of the fine structure of flames in sprays, either for a 'premixed spray' or for a 'nonpremixed spray flame', is given. The basic equations for ths spray, in the Eulerian form for a 'two velocities approach' or in Eulerian-Lagrangian form, are included. The problems due to the interaction terms are emphasized. References are given, but no detailed discussion of the existing models is included. Some emphasis is put on the reaction term that gives the volumetric rate of consumption of droplets in a given volume of spray. Some typical results of calculations, showing the most advanced capabilities available, are presented. ESA

N93-14627# Ecole Nationale Superieure de Mecanique et d'Aerotechnique, Poitiers (France).
COMBUSTION IN SUPERSONIC FLOWS
B. Deshaies and M. Champion *In* VKI, Modeling of Combustion and Turbulence 38 p(SEE N93-14617 04-25) 1992 (For primary document see N93-14617 04-25)
Copyright Avail: CASI HC A03/MF A06

The main features of some basic elementary problems relevant to combustion in supersonic 1-D and 2-D flows involving premixed and nonpremixed configurations are presented. The flows are analyzed from a laminar stationary point of view. However, problems remain to be solved before designing and developing practical systems using supersonic combustion as a propulsion mechanism, and three different fields of investigation can be clearly identified: the influence of turbulence on combustion in a supersonic flow; special geometrical configurations have to be studied and developed to improve the mixing between oxidizer and combustible; and the stability of complex systems involving simultaneously, turbulence, combustion, shock waves, mixing, and boundary layers. ESA

N93-14652# Chicago Univ., IL. Dept. of Chemistry.
GAS-SURFACE INTERACTIONS Final Technical Report, 1 Oct. 1988 - 30 Sep. 1991
Steven J. Sibener 20 Aug. 1992 15 p
(Contract N00014-89-J-1061)
(AD-A255390) Avail: CASI HC A03/MF A01

Molecular beam scattering techniques have firmly established themselves among the major tools for studying the kinetics and dynamics of gas-surface interactions. They have also proven themselves to be of great use in materials synthesis, most notably being used for the molecular beam epitaxial (MBE) growth of semiconductor substrates and superlattices. During the past few years our research group has been very active in developing new and quite general molecular beam techniques for studying the kinetic mechanisms of surface chemical reactions. We have, in particular, focussed much of our attention on extending traditional molecular beam measurements to allow us to routinely explore coverage dependent kinetic mechanisms under essentially linearized conditions. These efforts have been quite successful. Our three molecular beam scattering arrangement is unique in the world, and significantly expands the range and power of modulated beam reactive scattering for studying complex kinetics at surfaces. The experimental methodology we have developed utilizes two continuous, independently adjustable beams to establish a desired steady state surface concentration, while a weaker modulated third beam induces small concentration perturbations around the selected steady state. This linearized approach permits the coupled differential equations which represent the overall surface reaction mechanism to be solved perturbatively, yielding quantitative information about the various kinetic steps which comprise overall reaction mechanisms. GRA

N93-14658# Arkansas Univ. for Medical Sciences, Little Rock.
NMR IMAGING OF ELASTOMERIC MATERIALS Final Report, 1 Jul. 1989 - 30 Jun. 1992
Richard A. Komoroski, Subhendra N. Sarkar, and E. W. Wooten 31 Aug. 1992 43 p
(Grant AF-AFOSR-0418-89)
(AD-A256034; AFOSR-92-0865TR) Avail: CASI HC A03/MF A01

NMR imaging has been applied to elastomeric materials of industrial and military interest. The T2 spin-spin relaxation times of common elastomers, particularly after filling and curing, are sufficiently short that spin-echo sequences at submillisecond echo times cannot produce T2-independent images. The sensitivity to T2 makes spin echo imaging a good probe of elastomer blend composition, as demonstrated for a series of filled, cured cis-polybutadiene, styrene-butadiene rubber blends. The technique can distinguish good and bad carbon black dispersion in actual tire tread samples. The configuration of non-metallic tire cord, voids, rubber layer boundaries, apparent migration of additives, and other inhomogeneities can be detected in end-product tire samples. Arrowhead patterns, arising from magnetic susceptibility differences for defects in carbon-black-filled elastomers, were attributed to graphitized 'coke' particles from the carbon black. NMR images were obtained for porous glass disks of different porosities as models of materials such as oil cores. The mottled appearance often seen for such images is attributed largely to insufficient signal-to-noise ratio, and not pore structures. Comparison of spin-echo and gradient-echo

images demonstrates the defect-magnification effect of the gradient-echo sequence seen previously for elastomers. The advantages of volume imaging, isotropic voxels in thin slices, and higher resolution are demonstrated for porous materials. GRA

N93-14664# State Univ. Coll. of New York, Buffalo. Dept. of Chemistry.
STUDIES OF COMPONENTS FOR THERMALLY REGENERATIVE ELECTROCHEMICAL SYSTEMS Final Report, 1 Aug. 1985 - 31 Dec. 1987
Robert A. Osteryoung 1 Sep. 1991 5 p
(Contract N00014-85-K-0789)
(AD-A256124) Avail: CASI HC A01/MF A01

Electrochemical studies on the reduction of AlCl(4-) ion and the anodization of Al(0) in basic 1-methyl-3-ethylimidazolium chloride (ImCl) mixed with aluminum chloride (AlCl3) were carried out; a basic melt is one containing excess ImCl. It was not found possible to reduce the AlCl4 ion at temperatures as high as 250 C. The anodization of aluminum was found to be controlled by the diffusion of chloride ion to the electrode. The disposition of Li and Bi were studied at tungsten microelectrodes in LiCl-KCl eutectic molten salt at 450 C. GRA

N93-14669# Emory Univ., Atlanta, GA. Dept. of Chemistry.
SPECTROSCOPY AND REACTIONS OF HYDRAZOIC ACID ON SILICON SINGLE CRYSTAL SURFACES (III). HN3 AND DN3 ON Si(111)-7 X 7
Jason C. Chu, Y. Bu, and M. C. Lin 1992 32 p
(Contract N00014-89-J-1235)
(AD-A255241; TR-11) Avail: CASI HC A03/MF A01

We have studied the thermal stability and spectroscopy of HN3 on Si(111)-7x7 in the temperature range from 120 to 1350 K. The results are similar to those observed on other two low-index Si surfaces. HN3 was found to molecularly adsorb on Si(111)-7x7 at 120 K, with the formation of dimers at higher dosages (less then or equal to 2.0 L). At 270 K, HN3 began to decompose into HN and N2 species as indicated by the changes in the NH vibration mode in HREELS and the chemical shift of N 1s XPS peak. Between 300 and 800 K, the NH species further decomposed into H and N on the surface, while N2 desorbed molecularly. In this temperature range, the steady increase of the SiN(x) and Si-H peaks were noted and LEED exhibited a weak (1x1) pattern. GRA

N93-14671# California Univ., Berkeley. Dept. of Chemistry.
THRESHOLD PHOTODETACHMENT SPECTROSCOPY Final Report, 1 Jul. 1987 - 30 Sep. 1992
Daniel M. Neumark 3 Sep. 1992 5 p
(Contract N00014-87-K-0495)
(AD-A255278) Avail: CASI HC A01/MF A01

The goal of this project is to learn about the electronic and vibrational spectroscopy of size-selected clusters. This is done using high resolution negative ion photodetachment techniques developed in our laboratory during the last four years. In our experiments, a beam of cluster anions (typically C(n)- or Si(n)-) is generated using a laser vaporization source, mass-selected, and photodetached with a fixed frequency or tunable laser. In the fixed-frequency experiments, we measure the electron kinetic energy distribution, thereby obtaining the anion photoelectron spectrum. This enables us to map out the electronic and vibrational states of the neutral cluster with about 10 meV resolution. For higher (0.4 meV) resolution studies, we use a technique called threshold photodetachment spectroscopy. Here, the cluster anions are detached with a tunable laser, and only those photoelectrons produced with nearly zero kinetic energy are collected. In principle, this yields the same information as the photoelectron spectrum, but the considerably higher resolution allows us to make much more definite assignments of the spectral features. GRA

N93-14678# Army Lab. Command, Fort Monmouth, NJ. Electronics Technology and Devices Lab.
ULTRAVIOLET-OZONE CLEANING OF SEMICONDUCTOR SURFACES, REVISION 1
John R. Vig Oct. 1992 48 p
(DA Proj. 1L1-62705-AH-94)
(AD-A256158; SLCET-TR-91-33-Rev-1) Avail: CASI HC A03/MF A01

The ultraviolet (UV)/ozone surface-cleaning method, which is reviewed in this report, is an effective method of removing a variety of contaminants from silicon (as well as many other) surfaces. It is a simple-to-use dry process which is inexpensive to set up and operate. It can rapidly produce clean surfaces, in air or in a vacuum system, at ambient temperatures. In combination with a dry method for removing inorganic contamination, the method may meet the requirements for the all-dry cleaning methods that will be necessary for future generations of semiconductor devices. Placing properly precleaned surfaces within a few millimeters of an ozone-producing UV source can produce clean surfaces in less than one minute. The technique can produce near-atomically clean surfaces, as evidenced by Auger electron spectroscopy, ESCA, and ISS/SIMS studies. Topics discussed include the variables of the process, the types of surfaces which have been cleaned successfully, the contaminants that can be removed, the construction of an UV/ozone cleaning facility, the mechanism of the process, UV/ozone cleaning in vacuum systems, rate-enhancement techniques, safety considerations, effects of UV/ozone other than cleaning, and applications. GRA

N93-14824 Department of the Navy, Washington, DC.
APPARATUS AND PROCESS FOR DESALINATION OF SEAWATER Patent Application
Joseph F. Pizzino, inventor (to Navy) and David B. Patchett, inventor (to Navy) 7 Apr. 1992 12 p Filed 1 Nov. 1990
(AD-D015428; US-Patent-Appl-SN-607936; US-Patent-Class-210-640)
Avail: CASI HC A03/MF A01

An apparatus and process for desalination of seawater using a hydrophobic vapor permeable membrane. Heated seawater is passed across one surface of a membrane at rates which cause the flow to be turbid such that its turbidity is characterized by Reynolds numbers in excess of 1000. Fresh water is passed across the other surface of the membrane to act as a condenser and collector of vapor which passes through the membrane. GRA

N93-14908# Minnesota Univ., Minneapolis. Dept. of Chemistry.
VARIATIONAL TRANSITION STATE THEORY
D. G. Truhlar 20 Dec. 1991 25 p
(Contract DE-FG02-86ER-13579)
(DE92-040498; DOE/ER-13579/6) Avail: CASI HC A03/MF A01

This project is concerned with the development and use of variational transition state theory to calculate reaction rates of gas-phase chemical reactions. Potential energy surfaces were modeled for specific reactions such as Cl + H2, HCl + H, Cl(-) + CH3*Cl, Cl(-)(H2O) + CH3*Cl, and F + H2. New methods for interfacing electronic structure theory with dynamics were worked on; semiempirical molecular orbital theory is used to carry out direct dynamics calculations. Interpolated variational transition state theory is also used to carry out dynamics calculations without fitting a global potential energy surface. New theoretical approximations are under study, such as large-curvature tunneling including excited states, correlation of quantized transition state structure , optimization of stationary points on potential energy surfaces, calculation of quantal partition functions for hindered internal rotators, mode-mode coupling in quantum partition functions, and definition of reaction-path coordinates. Kinetic isotope effects are studied. Several enhancements have been made to the POLYRATE code. DOE

N93-15114# California Inst. of Tech., Pasadena. Graduate Aeronautical Labs.
CHEMICAL REACTIONS IN TURBULENT MIXING FLOWS Final Report, period ending 14 May 1992
Paul E. Dimotakis, James E. Broadwell, and Anthony Leonard 15 Jul. 1992 81 p
(Grant AF-AFOSR-0304-90)
(AD-A256004; AFOSR-92-0874TR) Avail: CASI HC A05/MF A01

The purpose of this research is to conduct fundamental investigations of turbulent mixing, chemical reaction and combustion processes in turbulent, subsonic and supersonic flows. Our approach has been to carry out a series of detailed theoretical and experimental studies of turbulent mixing in both free shear layers and axisymmetric jets. To elucidate molecular transport effects, experiments and theory concern themselves with both reacting and non-reacting flows of liquids and gases, in fully-developed turbulent flows, i.e., in moderate to high Reynolds number flows. The computational studies are, at present, focused at fundamental issues pertaining to the computational simulation of both compressible and incompressible flows. Modeling has been focused on both shear layers

and turbulent jets, with an effort to include the physics of the molecular transport processes, as well as formulations of models that permit the full chemical kinetics of the combustion process to be incorporated. Our primary diagnostic development efforts are currently focused on data-acquisition electronics to meet very high-speed, high-volume data requirements, the acquisition of single, or a sequence, of two-dimensional images, and the acquisition of data from arrays of supersonic flow sensors. Progress has also been made in the development of a dual-beam laser interferometer/correlator to measure convection velocities of large scale structures in supersonic shear layers and in a new method to acquire velocity field data using pairs of scalar images closely spaced in time. GRA

N93-15200# Northwestern Univ., Evanston, IL. Dept. of Chemistry.
EXPERIMENTAL AND THEORETICAL INVESTIGATION OF SURFACE CHEMISTRY INDUCED BY DIRECT AND INDIRECT ELECTRONIC EXCITATION Final Report, Aug. 1988 - Jan. 1992
S. J. Garrett, Peter C. Stair, and Eric Weitz 1 Aug. 1992 66 p
(Grant AF-AFOSR-0297-88)
(AD-A256342; AFOSR-92-0898TR) Avail: CASI HC A04/MF A01

A combined theoretical and experimental investigation of the photochemistry of methyl iodide on rutile at 100-110 K was attempted in order to assess the importance of each of the possible direct or indirect photon absorption processes. We have used x-ray photoelectron spectroscopy (XPS), temperature programmed desorption (TPD), and a UHV chamber designed for 257-351 nm laser irradiation of the adlayer followed by time-of-flight mass spectrometry (TOF-MS). We have observed that following irradiation, methyl photofragments are ejected into the vacuum. These photofragments possess a characteristic translational energy distribution extending up to 1.9 eV in the case of 257 nm radiation, which varies somewhat with photodissociation wavelength and methyl iodide coverage. Two broad peaks are visible in the translational energy distribution corresponding to methyl fragments with energies of 1.1 and 0.03 eV. The higher energy fragments are produced with a relatively narrow angular distribution and some vibrational excitation in the v' = 1 and 2 'umbrella' modes of the methyl radical, whilst those of low translational energy are produced with a much broader angular distribution and almost no population in either of the v'' vibrational mode v'' = 1 and 2. GRA

N93-15283# Los Alamos National Lab., NM.
INFRARED LABORATORY SPECTRA AND COMPOSITION CHANGES OF SYNTHETIC AMORPHOUS SILICATE GRAINS
A. Blanco, S. Fonti, M. Martino (Lecce Univ., Italy), E. Bussoletti, V. Mennella, L. Colangeli (Cassino Univ., Italy), and J. R. Stephens 1992 3 p Presented at the Astronomical Infrared Spectroscopy Conference, Calgar, Ontario, 16-19 Jun. 1992
(Contract W-7405-eng-36)
(DE92-040211; LA-UR-92-2477; CONF-9206278-1) Avail: CASI HC A01/MF A01

We present infrared laboratory spectra of some amorphous silicates of olivine composition. By changing the metal to silicon ratio as well as the content of iron relative to magnesium, we investigate the spectroscopic effects of chemical fractionation during formation and processing of grains materials in astronomical environments. DOE

N93-15356*# Eloret Corp., Sunnyvale, CA.
COMPUTED POTENTIAL ENERGY SURFACES FOR CHEMICAL REACTIONS Semiannual Report, 1 Jan. - 30 Jun. 1992
K. Heinemann and Stephen P. Walch 25 Aug. 1992 52 p
(Contract NCC2-478)
(NASA-CR-190741; NAS 1.26:190741) Avail: CASI HC A04/MF A01

The work on the NH + NO system which was described in the last progress report was written up and a draft of the manuscript is included in the appendix. The appendix also contains a draft of a manuscript on an Ar + H + H surface. New work which was completed in the last six months includes the following: (1) calculations on the (1)CH2 + H2O, H2 + HCOH, and H2 + H2CO product channels in the CH3 + OH reaction; (2) calculations for the NH2 + O reaction; (3) calculations for the CH3 + O2 reaction; and (4) calculations for CH3O and the two decomposition channels--CH2OH and H + H2CO. Detailed descriptions of this work will be given in manuscripts; however, brief descriptions of the CH3 + OH and CH3 + O2 projects are given. For individual titles, see N93-15357 through N93-15358.

N93-15357*# Eloret Corp., Palo Alto, CA.
THEORETICAL CHARACTERIZATION OF THE POTENTIAL ENERGY SURFACE FOR NH + NO
Stephen P. Walch *In its* Computed Potential Energy Surfaces for Chemical Reactions 25 Aug. 1992 30 p (For primary document see N93-15356 04-25)
(Contract NCC2-478)
(NASA-CR-190741) Avail: CASI HC A03/MF A01

The potential energy surface (PES) for NH + NO was characterized using complete active space self-consistent field (CASSCF) gradient calculations to determine the stationary point geometries and frequencies followed by CASSCF/internally contracted configuration interaction (CCI) calculations to refine the energetics. The present results are in qualitative accord with the BAC-MP4 calculations, but there are differences as large as 8 kcal/mol in the detailed energetics. Addition of NH to NO on a (2)A' surface, which correlated with N2 + OH or H + N2O products, involves barriers of 3.2 kcal/mol (trans) and 6.3 kcal/mol (cis). Experimental evidence for these barriers is found in earlier works. The (2)A' surface has no barrier to addition, but does not correlate with products. Surface crossings between the barrierless (2)A' surface and the (2)A' surface may be important. Production of N2 + OH products is predicted to occur via a planar saddle point of (2)A' symmetry. This is in accord with the preferential formation of II(A') lambda doublet levels of OH in earlier experiments. Addition of NH (1)delta to NO is found to occur on an excited state surface and is predicted to lead to N2O product as observed in earlier works. Author

N93-15358*# National Aeronautics and Space Administration. Ames Research Center, Moffett Field, CA.
A GLOBAL POTENTIAL ENERGY SURFACE FOR ArH2
David W. Schwenke (National Aeronautics and Space Administration. Ames Research Center, Moffett Field, CA.), Stephen P. Walch (Eloret Corp., Palo Alto, CA.), and Peter R. Taylor (Eloret Corp., Palo Alto, CA.) *In* Eloret Corp., Computed Potential Energy Surfaces for Chemical Reactions 25 Aug. 1992 18 p Submitted for publication Prepared in cooperation with Eloret Corp., Palo Alto, CA (For primary document see N93-15356 04-25)
(Contracts NCC2-478; NCC2-371)
(NASA-CR-190741) Avail: CASI HC A03/MF A01

We describe a simple analytic representation of the ArH2 potential energy surface which well reproduces the results of extensive ab initio electronic structure calculations. The analytic representation smoothly interpolates between the dissociated H2 and strong bonding limits. In the fitting process, emphasis is made on accurately reproducing regions of the potential expected to be important for high temperature (ca. 3000 K) collision processes. Overall, the anisotropy and H2 bond length dependence of the analytic representation well reproduce the input data. Author

N93-15414# Cornell Univ., Ithaca, NY.
ADSORPTION AND DIFFUSION OF FLUIDS IN WELL-CHARACTERIZED ADSORBENT MATERIALS
1991 8 p
(Contract DE-FG02-88ER-13974)
(DE92-040160; DOE/ER-13974/3) Avail: CASI HC A02/MF A01

This grant covers theoretical and molecular simulation studies in two areas: the thermodynamic behavior of associating liquids and their mixtures in the bulk phase, and the behavior of fluids in narrow pores. Fluids of longer chains are being simulated to test the perturbation theory. The Helmholtz free energy equation with the first order theory for association was applied to a wide variety of pure and mixed fluids; good agreement with experiment was found. In the second area, the nonlocal form of density functional theory was used together with molecular simulation (grand canonical Monte Carlo and molecular dynamics methods) to study pure and mixed fluids in pores. The fluids were organic compounds and argon; the porous materials were graphite, aluminophosphates, molecular sieves, and clays. DOE

N93-15497# Harvard Univ., Cambridge, MA. Dept. of Physics.
EXPERIMENTAL ATTEMPT TO METALLIZE HYDROGEN AT VERY HIGH PRESSURES Final Report, 3 Mar. 1989 - 2 Mar. 1992

Issac F. Silvera Aug. 1992 35 p
(Contract F04611-89-K-0003)
(AD-A257086; Rept-33-518; Rept-7415-2; PL-TR-92-3016; AD-E201186)
Avail: CASI HC A03/MF A01

Metallic hydrogen is a potential candidate as a high energy density material. The possibility of metallizing hydrogen by submitting it to very high pressures has been experimentally investigated. Great advances have been made in this study. Pressures as high as 2.3 megabar on hydrogen have been obtained in diamond anvil cells (DAC's). Several new phase transitions have been observed in the megabar pressure region. One of these, called the hydrogen-A (H-A) phase is believed to be the metallic molecular phase of hydrogen. However, current limitations on the optical techniques available to diamond anvil cell research have prevented direct determination of the conductive state and techniques for the direct measurement of the dc electrical conductivity are still under development. Band structure calculations have shown that metallization may be profoundly affected by molecular orientational order. Other observed phase transitions are believed to be associated with orientational order and fundamental changes in the molecular symmetry at high densities. A pulsed NMR system for studying very small samples of hydrogen has been constructed and will be useful in analyzing the nature of high density hydrogen. GRA

N93-15504*# National Aeronautics and Space Administration. Lewis Research Center, Cleveland, OH.
SIMPLIFIED JET-A KINETIC MECHANISM FOR COMBUSTOR APPLICATION
Chi-Ming Lee, Krishna Kundu, and Bahman Ghorashi (Cleveland State Univ., OH.) Jan. 1993 11 p Presented at the 31st Aerospace Sciences Meeting, Reno, NV, 11-14 Jan. 1993; sponsored by AIAA Original contains color illustrations
(RTOP 537-01-11)
(NASA-TM-105940; E-7457; NAS 1.15:105940; AIAA Paper 93-0021)
Avail: CASI HC A03/MF A01; 1 functional color page

Successful modeling of combustion and emissions in gas turbine engine combustors requires an adequate description of the reaction mechanism. For hydrocarbon oxidation, detailed mechanisms are only available for the simplest types of hydrocarbons such as methane, ethane, acetylene, and propane. These detailed mechanisms contain a large number of chemical species participating simultaneously in many elementary kinetic steps. Current computational fluid dynamic (CFD) models must include fuel vaporization, fuel-air mixing, chemical reactions, and complicated boundary geometries. To simulate these conditions a very sophisticated computer model is required, which requires large computer memory capacity and long run times. Therefore, gas turbine combustion modeling has frequently been simplified by using global reaction mechanisms, which can predict only the quantities of interest: heat release rates, flame temperature, and emissions. Jet fuels are wide-boiling-range hydrocarbons with ranges extending through those of gasoline and kerosene. These fuels are chemically complex, often containing more than 300 components. Jet fuel typically can be characterized as containing 70 vol pct paraffin compounds and 25 vol pct aromatic compounds. A five-step Jet-A fuel mechanism which involves pyrolysis and subsequent oxidation of paraffin and aromatic compounds is presented here. This mechanism is verified by comparing with Jet-A fuel ignition delay time experimental data, and species concentrations obtained from flametube experiments. This five-step mechanism appears to be better than the current one- and two-step mechanisms. Author

26 METALLIC MATERIALS

Includes physical, chemical, and mechanical properties of metals, e.g., corrosion; and metallurgy.

N93-14132# Howmet Turbine Components Corp., White Hall, MI.
THE 7TH WORLD CONFERENCE ON TITANIUM Final Report
Neil Paton and F. H. Froes (Idaho Univ., Moscow.) 2 Jul. 1992 5 p Conference held in San Diego, CA, 28 Jun. - 2 Jul. 1992
(Grant AF-AFOSR-0090-91)
(AD-A255674; AFOSR-92-0871TR) Avail: CASI HC A01/MF A01

This report covers the 7th World Conference on Titanium held in San Diego California, June 28 to July 2 1992. The purpose of the conference was to exchange information on advances in technology in titanium alloys, titanium processing, and applications of titanium alloys. Over 300 oral and 180 poster presentations were made by attendees from over 40 different countries including the former Soviet Union, Japan, China, and Europe. Total attendence was over-700, which exceeded conference expectations. GRA

N93-14264# Pratt and Whitney Aircraft, West Palm Beach, FL. Government Engines and Space Propulsion.
FATIGUE IN SINGLE CRYSTAL NICKEL SUPERALLOYS
Daniel P. DeLuca and Charles Ann 15 Sep. 1992 9 p
(Contract N00014-91-C-0124)
(AD-A256095; PWA-FR21998-11) Avail: CASI HC A02/MF A01

This program investigates the seemingly unusual behavior of single crystal airfoil materials. The fatigue initiation processes in single crystal (SC) materials are significantly more complicated and involved than fatigue initiation and subsequently behavior of a (single) macrocrack in conventional, isotropic, materials. To understand these differences is the major goal of this project. GRA

N93-14472 California Univ., Berkeley.
DEFORMATION CHARACTERIZATION OF POWDERED METALS IN COMPACTION AND APPLICATION OF THE FINITE ELEMENT METHOD TO COMPACTION PROCESSES Ph.D. Thesis
Beong-Bok Hwang 1991 286 p
Avail: Univ. Microfilms Order No. DA9228690

A plasticity theory is developed for a powdered metal compact. The yield criterion used for sintered powdered metals is modified for describing asymmetric behavior of powdered metal compacts in tension and compression. Three parameters are involved in the yield function. Two parameters are determined from the behavior of sintered powdered compacts as functions of relative density. The third parameter was determined from green strength vs relative density relationship for powdered metal compacts and the yield function was completely defined with the effect of relative density. Yield surfaces for various density levels are compared with the experimental data for copper powders. The constitutive equation is applied to the variational principle and its discretization is developed. The discretized formulation has been implemented into a finite code and the program has been tested and applied to simulations of axisymmetric die pressings with copper powders. The simulation includes single-action and double-action pressings of solid cylinders as well as cylindrical rings. It was found that the results from the finite element analysis, in general, agree well with the experimental observations. Flange and flange-hub type axisymmetric rigid-die compactions with three different pin lengths are taken as an example of designing compaction process which produce a compact with relatively uniform density. Three different initial mold shapes are tested to produce the same compact in final shape. From the simulation result, the best process is selected by considering uniformity in density of the compact and the stresses exerted on tooling devices. A process is tested by changing the initial mold geometries. Three-level axisymmetric parts are taken as specimens to simulate the compaction processes with a combined operational press. Two different compaction methods are employed in the simulation. The main objective of this simulation is to obtain primary information on the proper compaction process of multi-level parts. From the simulation result, it is found that the synchronization of each individual punch speed is crucial in designing the compaction process to produce a compact with relatively uniform density. In the case of the severely localized distortion encountered during simulations, a remeshing scheme based on the bilinear interpolation method is employed to overcome the computational difficulties. Dissert. Abstr.

N93-14508# Southwest Research Inst., San Antonio, TX.
STRAIN-RATE EFFECTS IN REPLICA SCALE MODEL PENETRATION EXPERIMENTS Interim Report, Jul. 1991 - Apr. 1992
Charles E. Anderson, Jr., Scott A. Mullin, and Chris J. Kuhlman 17 Aug. 1992 38 p
(Contracts DAAL03-91-C-0021; DE-AC04-90A1-58770)
(AD-A255426; SWRI-3593-002) Avail: CASI HC A03/MF A01

A computational study was performed to quantify the effects of strain rate on replica-model (scaled) experiments of penetration and perforation. The impact of a tungsten-alloy long-rod projectile into an armor steel target at 1.5 km/s was investigated. It was found that over a scale factor of 10, strain-rate effects change the depth of penetration, for semi-infinite

targets, and the residual velocity and length of the projectile, for finite-thickness targets, on the order of 5 percent. Although not modeled explicitly in the present study, the time-dependence of damage was examined. Damage accumulation is a strong function of absolute time, not scaled time. At homologous times, a smaller scale will have less accumulated damage than a larger scale; therefore, the smaller scale will appear stronger, particularly in situations where the details of damage evolution are important. GRA

N93-14705* National Aeronautics and Space Administration. Langley Research Center, Hampton, VA.
METHOD OF CHARACTERIZING RESIDUAL STRESS IN FERROMAGNETIC MATERIALS USING A PULSE HISTOGRAM OF ACOUSTIC EMISSION SIGNALS Patent
Min Namkung, inventor (to NASA), William T. Yost, inventor (to NASA), Peter W. Kushnick, inventor (to NASA), and John L. Grainger, inventor (to NASA) 17 Nov. 1992 14 p Filed 23 Jul. 1990 Supersedes N91-13527 (29 - 5, p 636)
(NASA-Case-LAR-14239-1; US-Patent-5,164-669;
US-Patent-Appl-SN-555864; US-Patent-Class-324-209;
US-Patent-Class-73-598; US-Patent-Class-73-801; US-Patent-Class-324-227;
US-Patent-Class-324-232; Int-Patent-Class-G01B-33/12;
Int-Patent-Class-G01B-7/24) Avail: US Patent and Trademark Office

The invention is a method and apparatus for characterizing residual uniaxial stress in a ferromagnetic test member by distinguishing between residual stresses resulting from positive (tension) forces and negative (compression) forces by using the distinct and known magnetoacoustic (MAC) and a magnetoacoustic emission (MAE) measurement circuit means. A switch permits the selective operation of the respective circuit means.
Official Gazette of the U.S. Patent and Trademark Office

N93-14717 Oak Ridge National Lab., TN.
CESIUM IODIDE ALLOYS Patent Application
Hyoun-Ee Kim, inventor (to DOE) and A. J. Moorhead, inventor (to DOE) 1991 20 p
(Contract DE-AC05-84OR-21400)
(DE92-019818; US-Patent-Appl-SN-645448; Patents-US-A-7645448) Avail: CASI HC A03/MF A01

This invention relates to a CsI composition with improved mechanical strength and outstanding multispectral infrared transmittance, for window use. The additive is a monovalent iodide, other than CsI, added in amounts sufficient to maximize fracture strength from 16 to 40 MPa, while maintaining at least 10 percent transparency in the 4 to 50 micrometer wavelength range. The preferred additive is AgI, although RbI or CuI can be used.
DOE

N93-14723# EG and G Rocky Flats, Inc., Golden, CO.
PLUTONIUM PYROPHORICITY
J. L. Stakebake 2 Jun. 1992 11 p
(Contract DE-AC04-90DE-62349)
(RFP-4517) Avail: CASI HC A03/MF A01

A review of the published literature on ignition and burning of plutonium metal was conducted in order to better define the characteristics of pyrophoric plutonium. The major parameter affecting ignition is the surface area/mass ratio of the sample. Based on this parameter, plutonium metal can be classified into four categories: (1) bulk metal; (2) film and foils; (3) chips and turnings; and (4) powder. Other parameters that can alter the ignition of the metal include experimental, chemical, physical, and environmental effects. These effects are reviewed in this report. It was concluded from this review that pyrophoric plutonium can be conservatively defined as: Plutonium metal that will ignite spontaneously in air at a temperature of 150 C or below in the absence of external heat, shock, or friction. The 150 C temperature was used to compensate for the self-heating of plutonium metal. For a practical definition of whether any given metal is pyrophoric, all of the factors affecting ignition must be considered. Author

N93-14726# Naval Air Warfare Center, Warminster, PA. Air Vehicle and Crew Systems Technology Dept.
HIP CONSOLIDATION OF ALUMINUM-RICH INTERMETALLIC ALLOYS AND THEIR COMPOSITES Final Report, Sep. 1990 - Sep. 1991
William E. Frazier and Mary E. Donnellan 3 Feb. 1992 18 p
(NAWCADWAR-92003-60) Avail: CASI HC A03/MF A01

The near-net-shape processing of structural materials for application in advanced airframes and propulsion systems is of significant technological interest. The hot isostatic press (HIP) is considered an enabling technology for consolidating costly and difficult to melt-process intermetallics and intermetallic matrix composites (IMC). Concomitant with the development of HIP technology for IMC's is the formulation of intelligent processing of materials (IPM) concepts and technology. There has been significant research and development activity in the area of light weight, high temperature intermetallic alloys, e.g., alpha-two and gamma titanium aluminides. However, Al3Ti, an intermetallic which has a low density (3.35 gcm(exp -3)), a high elastic modulus (170 GPa), and a high melting point (1350 C) has received little scientific scrutiny, principally because of its intrinsically low ductility (1.2). Currently, research efforts are in progress examining the affects of rapid solidification, alloy chemistry, and consolidation processing on toughening. Rapid solidification enhances chemical uniformity and the addition of copper transforms the structure of Al3Ti from tetragonal DO(exp 22) into cubic L1(exp 2), a structure with a higher crystallographic symmetry. This paper describes preliminary work directed towards utilizing HIP technology to consolidate aluminum-rich intermetallics and aluminum-rich IMC's. Author

N93-14740# Massachusetts Inst. of Tech., Cambridge.
MECHANISMS OF FORMING INTERGRANULAR MICROCRACKS AND MICROSCOPIC SURFACE DISCONTINUITIES IN WELDS M.S. Thesis
Stephanie A. Douglas Jun. 1992 161 p
(Contract N00014-86-J-1218)
(AD-A255371) Avail: CASI HC A08/MF A02

Surface microstructures of various materials and weld types were observed using confocal laser microscopy to determine their effects on the formation of microscopic surface formations and microcracks in an attempt to classify the possible sensitivity to fracture in service. The general appearance of the weld, HAZ, and base metal were observed through the use of the confocal scanning laser microscope in order to categorize the presence of surface discontinuities and microcracks according to weld process and material type. The effects of welding conditions such as heat input and welding speed were considered along with the effects of specimen thickness. The materials investigated were mild steel, aluminum, 304 stainless steel, titanium, and high strength steels, including HY-100, HY-130, and HSLA 100. The welding processes considered were electron beam (EB) welding, gas metal arc (GMA) welding, gas tungsten arc (GTA) welding, and laser beam (LB) welding. The specific heat input and welding speed was varied for the electron beam welding and several of the thin plate samples. The surface microstructure was examined with a Nikon Optiphot confocal He-Ne scanning laser microscope. This microscope allows surface visualization for magnifications with a resolution limit of 0.25 microns. The image monitoring equipment associated with the microscope provides for the slow scanning of specimens for measuring surface contours, superimposing layers of images, and producing a single clear image in memory of a highly textured surface. GRA

N93-14888# Department of the Navy, Washington, DC.
METHOD OF BONDING MOLYBDENUM TO STEEL Patent Application
William A. Ferrando, inventor (to Navy), Subhash D. Karmarkar, inventor (to Navy), Scott M. Hoover, inventor (to Navy), and Amarnath P. Divecha, inventor (to Navy) 21 Jul. 1992 14 p
(AD-D015410; US-Patent-Appl-SN-916428) Avail: CASI HC A03/MF A01

A thin layer of silver metal is formed between a molybdenum surface and a steel surface. The silver metal layer is diffusion bonded to the molybdenum surface and diffusion bonded to the steel surface, thus bonding the molybdenum and steel surfaces together. A steel gun barrel is reinforced by a molybdenum tube placed over the outside surface of the barrel. The outer surface of the molybdenum tube is covered with a protective steel jacket. The silver metal diffusion bonding technique is used to bond the molybdenum tube to the steel gun barrel and to bond the steel jacket to the molybdenum tube. GRA

N93-14900# Welding Consultants, Inc., Columbus, OH.
THE META-LAX METHOD OF STRESS REDUCTION IN WELDS
S. M. Smith 31 Jul. 1992 14 p
(Contract DE-FG01-91CE-15978)
(DE92-018477; DOE/CE-15978/T1) Avail: CASI HC A03/MF A01

This study is the second phase of ongoing research into the mechanics and feasibility of using the Meta-Lax method of vibratory stress relief in place of thermal methods of stress relief. The first phase of this research revealed results that were similar to, and even superior to those achieved using thermal methods. The testing here was designed to eliminate the effects of interbead tempering by utilizing single pass bead-on-plate welds only. A metallurgical explanation for the success of the Meta-Lax method was not found. No significant structure or chemical changes were noted when used with ASTM A36 or AISI 4140 materials, and the phenomena noted in phase 1 was apparently due to interbead tempering. The theory of accelerated aging has been proposed and studies exist which observed dislocation motion as a result of vibratory treatment. It is evident that the vibratory stress relief system does not impart sufficient energy to bring about the magnitude of change seen with thermal methods. However the physical improvement is a reality, and vibratory methods should be evaluated further. DOE

N93-15056# Naval Command, Control and Ocean Surveillance Center, San Diego, CA. Structural Materials Science Branch.

ANALYSIS OF OSPREY PROCESSES AND CONVENTIONAL POWER ALUMINUM ALLOYS Final Report

G. G. Chase and W. E. Glad Apr. 1992 32 p

(AD-A255764; NRAD-TR-1500) Avail: CASI HC A03/MF A01

The materials laboratory analyzed samples of nonstandard 7000 series aluminum alloy made by the OSPREY process and by a conventional powder process. GRA

N93-15059# Oak Ridge National Lab., TN.

Fe3Al-TYPE IRON ALUMINIDES: AQUEOUS CORROSION PROPERTIES IN A RANGE OF ELECTROLYTES AND SLOW-STRAIN RATE DUCTILITIES DURING AQUEOUS CORROSION

R. A. Buchanan and J. G. Kim Aug. 1992 49 p Prepared in cooperation with Tennessee Univ., Knoxville, TN

(Contract DE-AC05-84OR-21400)

(DE92-040520; ORNL/SUB-88-07685CT92/02) Avail: CASI HC A03/MF A01

The Fe3Al-type iron aluminides have undergone continued development at the Oak Ridge National Laboratory for enhancement of mechanical and corrosion properties. Improved alloys and thermomechanical processing methods have evolved. The overall purpose of the project herein described was to evaluate the aqueous corrosion properties of the most recent alloy compositions in a wide range of possibly-aggressive solutions and under several different types of corrosion-test conditions. The work supplements previous aqueous-corrosion studies on iron aluminides by the present authors. Four stages of this one-year aqueous-corrosion investigation are described. First the corrosion properties of selected iron aluminides were evaluated by means of electrochemical tests and longer-time immersion tests in a range of acidic, basic and chloride solutions. These tests were performed under non-crevice conditions, i.e., the specimens were not designed to contain crevice geometries. Second, the iron-aluminide alloy that proved most resistance to chloride-induced localized corrosion under non-crevice conditions was further evaluated under more-severe crevice conditions by electrochemical and immersion testing. Third, in order to study the relative roles of Fe, Al, Cr and Mo in the formation of passive films, the chemical compositions of passive films were determined by x-ray photoelectron spectroscopy (XPS). And fourth, in order to study aqueous-corrosion effects on the ductilities of iron aluminides as related to hydrogen embrittlement and/or stress-corrosion cracking, slow-strain-rate corrosion (SSRC) tests were conducted over a range of electrochemical potentials. DOE

N93-15138# Pacific Northwest Lab., Richland, WA.

THE RESPONSE OF DISPERSION-STRENGTHENED COPPER ALLOYS TO HIGH FLUENCE NEUTRON IRRADIATION AT 415 C

D. J. Edwards, J. W. Newkirk (Missouri Univ., Rolla.), F. A. Garner, M. L. Hamilton, A. Nadkarny, and P. Samal (SCM Metal Products, Bradfordwoods, PA.) Jun. 1992 41 p Presented at the 16th Annual Symposium of American Society of Testing and Materials, Denver, CO, 21-22 Jun. 1992

(Contract DE-AC06-76RL-01830)

(DE92-019434; PNL-SA-19956; CONF-920673-9) Avail: CASI HC A03/MF A01

Various oxide-dispersion-strengthened copper alloys have been irradiated to 150 dpa at 415 C in the Fast Flux Test Facility (FFTF). The Al2O3-strengthened GlidCop(trademark) alloys, followed closely by a HfO2-strengthened alloy, displayed the best swelling resistance, electrical conductivity, and tensile properties. The conductivity of the HfO2-strengthened alloy reached a plateau at the higher levels of irradiation, instead of exhibiting the steady decrease in conductivity observed in the other alloys. A high initial oxygen content resulted in significantly higher swelling for a series of castable oxide-dispersion-strengthened alloys, while a Cr2O3-strengthened alloy showed poor resistance to radiation. DOE

N93-15189# Naval Air Warfare Center, Warminster, PA. Air Vehicle and Crew Systems Technology Dept.

STRESS CORROSION SUSCEPTIBILITY OF ULTRA-HIGH STRENGTH STEELS FOR NAVAL AIRCRAFT APPLICATIONS Final Report

Joseph Kozol and Charles E. Neu 10 Jan. 1992 48 p LIMITED REPRODUCIBILITY: Availability: Document partially illegible

(AD-A256126; NAWCADWAR-92018-60) Avail: CASI HC A03/MF A01

Low alloy quenched and tempered steels used in current Naval aircraft applications, particularly the ultrahigh strength steels used in landing gear, have characteristically small critical flaw sizes and extreme susceptibility to stress corrosion cracking in a shipboard environment. Newly developed steels which develop ultrahigh strengths with secondary hardening based on precipitation of M2C carbides offer significantly larger critical flaw sizes; and while susceptible to stress corrosion cracking, their susceptibility is substantially less than that of low alloy steels. A long term test program conducted by the Naval Air Warfare Center Aircraft Division Warminster has characterized the stress corrosion cracking susceptibility of the newly developed steels. Results of the program have shown that, compared to low alloy steels, the newly developed steels show substantially reduced susceptibility to stress corrosion at short exposure times and maintain their advantage to a lesser extent at exposure times up to 1 0,000 hours. The test program has demonstrated also that 1,000 hour exposure times, characteristically used for stress corrosion tests of steels, are insufficient to establish stress corrosion thresholds (Klscc), as numerous failures were observed at exposure times between 1,000 and 10,000 hours. Fracture characteristics of the stress corrosion failures are shown. GRA

N93-15231# Department of the Navy, Washington, DC.

MULTIFILAMENTARY SUPERCONDUCTING CABLE AND A METHOD OF MANUFACTURING IT Patent Application

William A. Ferrando, inventor (to Navy), Amarnath P. Divecha, inventor (to Navy), and James Kerr, inventor (to Navy) 7 Jul. 1992 12 p Filed 7 Jul. 1992

(AD-D015391; US-Patent-Appl-SN-914669) Avail: CASI HC A03/MF A01

A Nb-Ti or Nb-Zr low temperature superconducting (LTS) wire is coated with molten AgNO3 which is then decomposed to form a uniform silver metal (Ag) coating on the LTS wire. A uniform coating of molten Al or Al alloy is formed on the Ag coated LTS wire and then solidified. A bundle of the coated LTS wires is inserted into an Al or Al alloy tube and cold worked to form a multifilamentary LTS cable comprising the Ag coated LTS wires each surrounded by an Al or Al alloy matrix. GRA

N93-15348# Brookhaven National Lab., Upton, NY.

EFFECTS OF HIGH THERMAL NEUTRON FLUENCES ON TYPE 6061 ALUMINUM

J. R. Weeks, C. J. Czajkowski, and K. Farrell (Oak Ridge National Lab., TN.) 1992 16 p Presented at the 16th International Symposium on the Effects of Radiation on Materials, Aurora, CO, 23-25 Jun. 1992

(Contract DE-AC02-76CH-00016)

(DE92-040569; BNL-46330; CONF-9206282-1) Avail: CASI HC A03/MF A01

The control rod drive follower tubes of the High Flux Beam Reactor are contructed from precipitation-hardened 6061-T6 aluminum alloy and they operate in the high thermal neutron flux regions of the core. It is shown that large thermal neutron fluences up to approximately 4 x 10(exp 23) n/cm(exp 2) at 333 K cause large increases in tensile strength and relatively modest decreases in tensile elongation while significantly reducing the notch impact toughness at room temperature. These changes are attributed to the development of a fine distribution of precipitates of amorphous silicon of which about 8 percent is produced radiogenically. A proposed role of thermal-to-fast flux ratio is discussed. DOE

N93-15382# Sandia National Labs., Albuquerque, NM.
APPLICATION OF THE SQUARE ROOT DIFFUSIVITY ANALYSIS TO MEASURING THE DIFFUSIVITY OF MULTICOMPONENT ALLOYS
Yoon-Ho Son, J. E. Morral, M. S. Thompson (United Technologies Research Center, East Hartford, CT.), and A. D. Romig, Jr. 1992 7 p Presented at the 2nd Iketani International Conference on Diffusion in Materials (DIMAT-92), Kyoto, Japan, 7-11 Sep. 1992
(Contract DE-AC04-76DP-00789)
(DE92-040978; SAND-92-2001C; CONF-9209179-3) Avail: CASI HC A02/MF A01

The well known 'Boltzmann-Matano analysis' can be used in general to measure the diffusivity of binary and ternary alloys. However for alloys containing four or more components, the analysis requires making assumptions, for example that the diffusivity is constant. Conversely, it can be shown that the 'square root diffusivity analysis' applies to measuring diffusivities that vary with concentration, as long as the variation is linear with concentration. Methods of designing samples and evaluating data for the square root diffusivity analysis are discussed. DOE

N93-15383# Sandia National Labs., Albuquerque, NM.
EXCEPTIONALLY HIGH-STRENGTH (APPROXIMATELY 3 GPa) ALUMINUM ALLOYS DEMONSTRATED BY OXYGEN ION IMPLANTATION
D. M. Follstaedt, S. M. Myers, R. J. Bourcier, and M. T. Dugger 1992 11 p Presented at the 8th International Conference on TMS Beam Processing of Advanced Materials, Chicago, IL, 5 Nov. 1992
(Contract DE-AC04-76DP-00789)
(DE92-040980; SAND-92-0213C; CONF-921183-3) Avail: CASI HC A03/MF A01

Oxygen-implanted Al surface layers are shown to have exceptional flow stresses, with values up to 2.9 GPa for 20 at. percent O. Quantitative evaluations are obtained by probing the hardness with low-load indentation and evaluating the combined response of the layer and substrate with finite element modeling. The high densities of nanometer-size oxide precipitates observed with TEM account for the high strengths through conventional dispersion hardening theory. High strength is found even after the 20 percent alloy is annealed at 550 C (1.2 GPa). Relatively high strengths are also found for unannealed Al implanted with as little as 5 at. percent O (1.4 GPa). In addition, the coefficient of friction of Al and associated stick-slip adhesion are greatly reduced by O implantation. This work indicates that the fcc Al matrix can be precipitation hardened far beyond the strengths of current aerospace alloys (approximately 0.5 GPa), and that conventional hardening theories can be applied to high volume fractions of nanometer-size precipitates to aid in designing new high-strength alloys. Aluminum oxide precipitates should be considered for strengthening Al alloys because of their effectiveness in blocking dislocation motion at small sizes and their relatively high thermal stability. Oxygen implantation should be evaluated for treatment of Al-alloy engineering components in sliding contact to improve their tribological performance. DOE

N93-15524*# National Aeronautics and Space Administration. Lewis Research Center, Cleveland, OH.
PROCESSING AND MICROSTRUCTURE OF Nb-1 PERCENT Zr-0.1 PERCENT C ALLOY SHEET
Mehmet Uz (Lafayette Coll., Easton, PA.) and Robert H. Titran Oct. 1992 17 p Presented at the Tenth Symposium on Space Nuclear Power and Propulsion, Albuquerque, NM, 10-14 Jan. 1993; sponsored by the Inst. for Space Nuclear Power Studies
(Contract DE-AI03-86SF-16310; RTOP 590-13-11)
(NASA-TM-105921; E-7414; NAS 1.15:105921) Avail: CASI HC A03/MF A01

A systematic study was carried out to evaluate the effects of processing on the microstructure of Nb-1 wt. pct. Zr-0.1 wt. pct. C alloy sheet. The samples were fabricated by cold rolling different sheet bars that were single-, double- or triple-extruded at 1900 K. Heat treatment consisted on one- or two-step annealing of different samples at temperatures ranging from 1350 to 1850 K. The assessment of the effects of processing on microstructure involved characterization of the precipitates including the type, crystal structure, chemistry and distribution within the material as well as an examination of the grain structure. A combination of various analytical and metallographic techniques were used on both the sheet samples and the residue extracted from them. The results show that the relatively coarse orthorhombic Nb2C carbides in the as-rolled samples transformed to rather fine cubic monocarbides of Nb and Zr with varying Zr/Nb ratios upon subsequent heat treatment. The relative amount of the cubic carbides and the Zr/Nb ratio increased with increasing number of extrusions prior to cold rolling. Furthermore, the size and the aspect ratio of the grains appear to be strong functions of the processing history of the material. These and other results obtained will be presented with the emphasis on a possible relationship between processing and microstructure. Author

N93-15586*# National Aeronautics and Space Administration. Lewis Research Center, Cleveland, OH.
PROGRESS TOWARD A TUNGSTEN ALLOY WIRE/HIGH TEMPERATURE ALLOY COMPOSITE TURBINE BLADE
F. J. Ritzert and R. L. Dreshfield Nov. 1992 10 p Presented at the International Conference on Tungsten and Tungsten Alloys, Washington, DC, 16-18 Nov. 1992; sponsored by the Metal Powder Industries Federation
(RTOP 590-21-11)
(NASA-TM-105901; E-7368; NAS 1.15:105901) Avail: CASI HC A02/MF A01

A tungsten alloy wire reinforced high temperature alloy composite is being developed for potential application as a hollow turbine blade for advanced rocket engine turbopumps. The W-24Re-HfC alloy wire used for these composite blades provides an excellent balance of strength and wire ductility. Preliminary fabrication, specimen design, and characterization studies were conducted by using commercially available W218 tungsten wire in place of the W-24Re-Hfc wire. Subsequently, two-ply, 50 vol pct composite panels using the W-24Re-HfC wire were fabricated. Tensile tests and metallographic studies were performed to determine the material viability. Tensile strengths of a Waspaloy matrix composite at 870 C were 90 pct of the value expected from rule-of-mixtures calculations. During processing of this Waspaloy matrix composite, a brittle phase was formed at the wire/matrix interface. Circumferential wire cracks were found in this phase. Wire coating and process evaluation efforts were performed in an attempt to solve the reaction problem. Although problems were encountered in this study, wire reinforced high temperature alloy composites continue to show promise for turbopump turbine blade material improvement. Author

27 NONMETALLIC MATERIALS

Includes physical, chemical, and mechanical properties of plastics, elastomers, lubricants, polymers, textiles, adhesives, and ceramic materials.

For composite materials see *24 Composite Materials.*

N93-14166# Illinois Univ., Urbana. Dept. of Chemistry.
FLUIDS, GELS, AND GLASSES UNDER EXTREME CONDITIONS OF PRESSURE AND TEMPERATURE Final Report, 1 Oct. 1988 - 30 Jun. 1992
J. Jonas 2 Sep. 1992 13 p
(Grant AF-AFOSR-0099-89)
(AD-A255675; AFOSR-92-0872TR) Avail: CASI HC A03/MF A01

An improved molecular level understanding of the fundamental relationship between molecular properties and macroscopic properties of highly viscous liquids and sol-gel prepared glasses represented the main goal of research supported by this grant. In addition, the behavior of fluids in confined geometries was investigated. Further development of unique NMR and laser Raman scattering instrumentation for experiments under extreme conditions of high pressure continued to represent an important part of our research. In the project dealing with liquids confined to porous glasses, we succeeded, for the first time, in investigating the effect of pressure on the dynamics of liquids confined to porous glasses, and also in recording a high-resolution NMR spectrum of a model lubricant in confined geometries. These unique experiments not only open new directions in the research on liquids in confined geometries but have important implications for the applied field of lubrication. GRA

N93-14170 Maryland Univ., College Park.
ELECTRONIC, VIBRATIONAL, AND TRANSPORT PROPERTIES OF CONDUCTING POLYMERS Ph.D. Thesis

Richard Jonathan Cohen 1991 205 p
Avail: Univ. Microfilms Order No. DA9222670

The Su-Schrieffer-Heeger model for conducting polymers is extended to include both the Coulomb field of the donor or acceptor impurities as well as electron-electron interactions treated in mean-field theory. The emphasis is on obtaining the optical and infrared properties of charged solitons in the presence of these interactions to ascertain the role of solitons in understanding the experiments on both lightly doped and photoexcited samples of polyacetylene. In this regard, we include a review of the optical and infrared properties of charged solitons in the standard Su-Schrieffer-Heeger model and point out the discrepancies with experiment that have led to our work. The ground state and infrared properties of a chain of transpolyacetylene in the presence of multiple impurities is investigated with emphasis on the existence and nature of the proposed many-soliton state for intermediate doping levels. The infrared spectrum is shown to be a useful tool for probing properties of the spatial distribution of the impurities adjacent to the polymer chain. The infrared properties of solitons produced in the final state of an x-ray absorption event are calculated. Results show that future experiments on such systems may find infrared structure quite different from that found in chemically doped and photoexcited samples. Finally the physics of the heavily doped 'metallic' state of polyacetylene is investigated along two lines. The first line of research is to calculate the effect of the Coulomb field of the dopants on both interchain and on-chain electronic hopping as an initial step towards a better understanding of the electronic structure in the heavily doped state. The second investigation is aimed at developing tools for understanding microscopic structures that may give rise to the anomalous temperature dependence of the conductance in the 'metallic' state. Techniques are developed for such studies and applied to both a model of bonding defects and finite-sized semiconducting regions embedded in otherwise conducting channels. Dissert. Abstr.

N93-14222 Michigan Univ., Ann Arbor.
APPLICATIONS OF A CONSTITUTIVE EQUATION FOR MICROSTRUCTURAL CHANGE IN POLYMERS Ph.D. Thesis
Hugh Edgar Huntley 1992 234 p
Avail: Univ. Microfilms Order No. DA9226924

Constitutive equations currently available in non-linear elasticity and for non-linear viscoelastic solids fail to capture permanent set upon release of loading, observed experimentally in polymers under large deformation. In order to address this phenomenon and to incorporate softening and 'yield' behavior also observed, the implications of a constitutive equation assuming deformation-dependent microstructural transformation are studied. The constitutive equation assumes the action of two separate micro-mechanisms for the generation of stress: the elastic distortion of cross-link networks and the simultaneous rupture of existing networks and their replacement with networks having new reference configuration. Throughout the study, materials are assumed isotropic and incompressible and the constituent networks are assumed to respond elastically. Analytical results applicable to the general statement of the constitutive equation are obtained when possible. Analytical and numerical studies assuming neo-Hookean response of the constituent networks supplement these results. The constitutive equation is studied in the contexts of homogeneous simple shear and equal biaxial extension. Numerical examples demonstrate softening, dependent on both the parameters controlling microstructural transformation and the responses of the constituent networks. It is shown that the equation may imply a local maximum in the stress-deformation relations for any constituent network materials, possibly indicating 'yield'. The existence of permanent set is established analytically for the general case. It is also shown that a deformation cycle is a dissipative process regardless of the constituent network responses. The constitutive equation is applied to two boundary-value problems. Results from these problems may form a basis for experimental verification of the equation. Numerical examples of the circumferential shear of a hollow cylinder show that the constitutive equation can imply the formation of a boundary layer of high shear at the inner surface. Numerical studies of a hollow sphere subjected to radial tensile tractions demonstrate that the equation can imply redistribution of normal stresses; in particular, an inner boundary layer of high residual circumferential compressive stress remains after release of external tractions. It is shown analytically that the process of microstructural transformation can affect the emergence of a local maximum in the traction-deformation relation; this result is demonstrated numerically. Dissert. Abstr.

N93-14287 Pennsylvania State Univ., University Park.
A GEOMETRICALLY NONLINEAR STRESS-DEFLECTION RELATION FOR THIN FILM/SUBSTRATE SYSTEMS Ph.D. Thesis
Christine Beisler Masters 1992 161 p
Avail: Univ. Microfilms Order No. DA9226743

Most thin films develop some type of intrinsic stress as they are deposited onto a substrate. If the substrate is flexible, this stress will cause the system to deflect. In the beam or plate bending technique for measuring intrinsic film stress, this deflection is measured and typically, a linear relation is used to relate the deflection back to the intrinsic stress in the film. However, as deflections become large, geometrically nonlinear effects become significant and a nonlinear relation must be used to calculate intrinsic film stress. In this research, the film/substrate is modeled as a composite plate, using several polynomials with unknown coefficients to approximate the out-of-plane deflections and midplane normal strains. Using these approximations with the partially nonlinear strain-displacement relations produces an algebraic equation for the strain energy in the composite film/substrate system. Minimizing this strain energy produces several plate deflection configurations. In an isotropic system, at very low intrinsic film stresses, a single, stable, spherical plate configuration is predicted. However, as the intrinsic film stress increases the theoretical solution bifurcates, predicting one unstable spherical shape and two stable ellipsoidal shapes. In the limit as the intrinsic film stress approaches infinity, the ellipsoidal configurations develop into cylindrical plate curvatures about either one of the two axes. When deflections become larger than half the thickness of the combined film and substrate, the relative error between the linear and nonlinear stress calculation excees 10 percent and this error continues to increase as deflections increase. Approximating the out-of-plane deflections with a 2nd order polynomial and each of the midplane normal strains with a 6th order polynomial while applying the constraint (based on conventional plate theory boundary conditions) that the midplane shear strain be zero at the free edges, plate deflections are predicted which show good correlation with a fully nonlinear finite element analysis of the film/substrate system. This indicates that, although simplifying assumptions were made in the theoretical development, the final nonlinear stress deflection relation can confidently be used to model the nonlinear behavior occurring in thin film/substrate systems when deflections are large. Dissert. Abstr.

N93-14401# California Univ., Santa Barbara. Inst. for Polymers and Organic Solids.
ORIENTED ELECTRO/OPTICAL POLYMERS THROUGH IN-SITU CHEMISTRY DURING GEL PROCESSING: A RESEARCH OPPORTUNITY Final Report, 15 Sep. 1988 - 31 Dec. 1991
Alan J. Heeger, Paul Smith, and Fred Wudl 4 Sep. 1992 13 p
(Contract F49620-88-C-0138)
(AD-A255968; AFOSR-92-0867TR) Avail: CASI HC A02/MF A01

The focus of the research was to obtain high performance properties (electrical and/or optical) from conjugated polymers by improving the structural order through polymer processing. The success of the approach is quantified by the demonstration of third order optical susceptibility values in excess of 10 exp 8 and 10 exp -7 esu for high quality, oriented trans-polyacetylene at frequencies in the infrared (frequencies which are relevant to optical communications). Equally important, we have identified a structure/property relationship that can be used to direct synthesis of new conjugated polymers with comparably large NLO coefficients: in conjugated polymers with degenerate ground state, the dominant NLO mechanism results from the neutral soliton Ag intermediate state mechanism. In a parallel effort, high performance electrical and mechanical properties were demonstrated in fibers made from conducting polymers. GRA

N93-14486# Army Cold Regions Research and Engineering Lab., Hanover, NH.
SOFTENING OF RIGID POLYVINYL CHLORIDE BY HIGH CONCENTRATIONS OF AQUEOUS SOLUTIONS OF METHYLENE CHLORIDE
Louise V. Parker, Thomas A. Ranney, and Susan Taylor May 1992 44 p
(AD-A255453; CRREL-SR-92-12) Avail: CASI HC A03/MF A01

In this experiment, small pieces of rigid PVC pipe were exposed to

high aqueous concentrations of methylene chloride corresponding to 0.2, 0.4, 0.6, 0.8, and 1.0 activity solutions. Samples were exposed to the test solutions for 4, 8, 15, 22, and 33 days. Samples exposed to the highest activity solution (1.0) softened within the first 4 days, while samples exposed to the 0.8 activity solution took 22 days to soften. Samples exposed to the lowest activity solution (0.2) showed no signs of softening, while the results for the samples exposed to the 0.4 and 0.6 activity solutions showed some slight changes, indicating some softening. These results reveal that concentrations of methylene chloride below 3340 mg/L (0.2 activity) will not cause softening or serious swelling of rigid PVC. GRA

N93-14489# Connecticut Univ., Storrs. Dept. of Chemistry.
PRELIMINARY INVESTIGATIONS OF METAL LIQUID-LIKE FILMS AND COATINGS DERIVED FROM THEM Final Report, 19 Mar. 1990 - 18 Mar. 1992
Michael S. Bradley 24 Jun. 1992 13 p
(Contract DAAL03-90-G-0060)
(AD-A255477; ARO-27759.CH) Avail: CASI HC A03/MF A01

Metal liquid-like films consist of a layer of metal deposited between two immiscible liquids. The films are glossy, and have rheological properties similar to a liquid, but are not conductive. We have carried out studies on these films under high pressure, to alter their structure, and after the film has dried, to study their use as coatings. Pressure does not severely alter the form of the MELLF, though temperature and pressure may combine to affect their long term stability. Coatings on silica gels successfully maintain the properties of reflectivity and non-conductivity; spectra indicate no change in the chemical properties occurred. Further work will include long term stability measurements and more work on the coating procedures. GRA

N93-14527# TRW Space and Defense Sector, Redondo Beach, CA.
HIGH TEMPERATURE POLYMER DIELECTRIC FILM INSULATION Final Report, Aug. 1988 - May 1991
Robert J. Jones and Ward F. Wright Feb. 1992 110 p
(Contract F33615-88-C-2902)
(AD-A255243; WL-TR-91-2105) Avail: CASI HC A06/MF A02

The overall objective of this program was to identify and evaluate advanced aromatic and/or heterocyclic film forming polymers having improved electrical and thermal properties over Kapton R for wire insulation applications in future spacecraft. Five polymeric candidates were screened for high (300 C) and low temperature (-269 C) behavior, initial electrical properties and oxidative/solvent resistance versus Kapton R film as the control material for R which a replacement was sought. It was experimentally determined that EYMYD L-30N, IP-200 PPQ and UPILE XR S films possessed a very promising initial combination of properties versus Kapton R indicative of high promise for 300 C insulation service. GRA

N93-14531# Army Biomedical Research and Development Lab., Fort Detrick, MD.
ABSORPTION OF PROPELLANT VAPORS INTO POLYMER FILMS Final Technical Report, Jan. 1987 - Sep. 1991
Steven H. Hoke and Charles O. Buffington 1 Aug. 1992 36 p
(AD-A255274; USABRDL-TR-9117) Avail: CASI HC A03/MF A01

A preliminary study of the absorption and desorption of methylethyl ketone and nitrobenzene on various commercial and laboratory prepared polymer films was performed. The development of film exposure techniques along with the evaluation of the feasibility of using FTIR detection of the absorbed vapors was completed. The techniques were tested with 2,4-dinitrotoluene and 2,4,6-trinitrotoluene. DNT and TNT desorption studies for ethyl cellulose and Tedlar were performed. GRA

N93-14561# Total Army Personnel Agency (Provisional), Alexandria, VA.
THE ROLE OF ENTANGLEMENTS IN THE SWELLING OF POLY(DIMETHYLSILOXANE) NETWORKS M.S. Thesis Final Report
Shawn P. Malone Aug. 1992 122 p
(AD-A255359) Avail: CASI HC A06/MF A02

The swelling of model and imperfect polydimethylsiloxane (PDMS) networks in solvents and polymer chains was studied to see how the role of entanglements affects the predictions of the Flory-Rehner swelling model. The model networks were prepared by end-linking difunctional PDMS (B2) with a given amount of tetrafunctional crosslinker (A4) to obtain networks with a minimum amount of elastically ineffective chains. The imperfect networks were prepared by end-linking mixtures of monofunctional PDMS (B1), B2, and A4 to obtain networks containing pendant chains and branched structures. The equilibrium elastic moduli, Ge, of the networks were determined from dynamic mechanical experiments and were found to be greater than the values predicted from the affine and phantom network theories when using a branching model of nonlinear polymerization (Macosko-Miller model) to characterize the networks. GRA

N93-14573# Cape Cod Research, Buzzards Bay, MA.
WATERBORNE POLYURETHANE BINDER RESINS FOR COMPLIANT AIRCRAFT COATINGS Final Report, 30 Aug. 1991 - 29 Feb. 1992
Francis L. Koehan, Regina M. Stewart, and Wendy M. Gomes Feb. 1992 32 p
(Contract N62269-91-C-0249)
(AD-A256246; NAWCADWAR-92060-60) Avail: CASI HC A03/MF A01

This Small Business Innovation Research (SBIR), Phase 1 research project investigated the feasibility of producing a one-component, water-borne, low volatile organic compounds (VOC) coating for the protection of naval aircraft and ground support equipment. Novel silane-terminated, silicone-modified, polyurethane copolymers were prepared and evaluated. GRA

N93-14668# Arizona State Univ., Tempe.
RELIABILITY OF SOL-GEL DERIVED FERROELECTRIC MEMORIES Final Report, Jan. 1989 - 31 May 1992
Sandwip K. Dey Jul. 1992 8 p
(Contract DAAL03-89-K-0104)
(AD-A255240; ARO-26827.7-PH) Avail: CASI HC A02/MF A01

A process was developed to prepare PZT(52/48) precursor solutions. Five spin-on depositions of this solution (0.5 M) were necessary to grow 0.5 micron thin films of polycrystalline PZT onto PT passivated silicon wafers. An addition of 15 percent excess PbO aided the densification process. Films derived from 1.5M solutions resulted in PZT films of equivalent thickness in only two depositions. Dielectric constant and tan Sigma were 800 and 2 percent respectively, at 1 kHz. Remnant and saturation polarizations were 12 and 25 micron C/cm(exp 2), respectively. Coercive fields of 36-48 kv/cm were measured. From retention experiments, a polarization loss of 11.2 percent after 3.2 years was estimated (i.e., the switched charge would diminish from 5.8 to 5.2 AC/CM2). High frequency pulse fatigue data on Nb and Sn modified PZT showed a reduction of the switched charge of 26 percent after 4x, 10 12 polarization reversals. GRA

N93-14709* National Aeronautics and Space Administration. Langley Research Center, Hampton, VA.
LOW TOXICITY HIGH TEMPERATURE PMR POLYIMIDE Patent
Ruth H. Pater, inventor (to NASA) 15 Dec. 1992 18 p Filed 5 Feb. 1991 Supersedes N92-11199 (30 - 2, p 218)
(NASA-Case-LAR-14639-1; US-Patent-5,171,822;
US-Patent-Appl-SN-651062; US-Patent-Class-528-188;
US-Patent-Class-528-125; US-Patent-Class-528-126;
US-Patent-Class-528-128; US-Patent-Class-528-170;
US-Patent-Class-528-172; US-Patent-Class-528-173) Avail: US Patent and Trademark Office

In-situ polymerization of monomer reactants (PMR) type polyimides constitute an important class of ultra high performance composite matrix resins. PMR-15 is the best known and most widely used PMR polyimide. An object of the present invention is to provide a substantially improved high temperature PMR-15 system that exhibits better processability, toughness, and thermo-oxidative stability than PMR-15, as well as having a low toxicity. Another object is to provide new PMR polyimides that are useful as adhesives, moldings, and composite matrices. By the present invention, a new PMR polyimide comprises a mixture of the following compounds: 3,4'-oxydianiline (3,4'-ODA), NE, and BTDE which are then treated with heat. This PMR was designated LaRC-RP46 and has a broader processing window, better reproducibility of high quality composite parts, better elevated temperature mechanical properties, and higher retention of mechanical properties at an elevated temperature, particularly, at 371 C.
Official Gazette of the U.S. Patent and Trademark Office

N93-14743 Department of the Navy, Washington, DC.
METHOD OF MAKING SUBSTANTIALLY SINGLE PHASE SUPERCONDUCTING OXIDE CERAMICS HAVING A TC ABOVE 85 DEGREES Patent
Syed B. Quadri, inventor (to Navy), Louis E. Toth, inventor (to Navy), Michael S. Osofsky, inventor (to Navy), Steven H. Lawrence, inventor (to Navy), and Donald U. Gubser, inventor (to Navy) 21 Apr. 1992 7 p Filed 19 Sep. 1990
(AD-D015422; US-Patent-5,106,829; US-Patent-Appl-SN-587466) Avail: CASI HC A02/MF A01

A substantially single phase superconducting composition is formed from a of 1:2:3 molar ratio of fine powders of a superconducting rare earth oxide, CuO, and BaCO3. The mixed powders and shaped articles formed from the mixed powders are calcined, sintered, and cooled in an oxygen containing atmosphere. The cooling step is done slowly to convert the sample to the orthorhombic structure and to improve the superconducting properties. The article formed is a substantially single phase superconducting composition. GRA

N93-14802# Department of the Navy, Washington, DC.
SPIROBISLACTONE ACRYLATE POLYMERS Patent Application
Allison M. Sikes, inventor (to Navy) and Robert F. Brady, inventor (to Navy) 25 Jun. 1992 18 p Filed 25 Jun. 1992
(AD-D015443; US-Patent-Appl-SN-904096) Avail: CASI HC A02/MF A01

This invention is directed to a thermoplastic polymer that is solid at room temperature and which expands on further polymerization, to form a crosslinked polymer, and to a process for preparing the polymer and the crosslinked polymer. In a preferred embodiment the polymer is prepared by polymerizing 10-90 but preferably 20-80 mole percent of a lower alkyl acrylic monomer containing a spirobislactone moiety, 10-90 but preferably 20-80 mole percent of a lower alkyl acrylic monomer containing an epoxide moiety, and 0.1-5 but preferably 0.5-1 mole percent of a lower alkyl acrylic monomer containing a functional moiety chosen from primary amino, secondary amino, mercaptan, and hydroxyl groups which can initiate crosslinking with the spirobislactone moiety. The crosslinked polymer is devoid of a spirobislactone carbonyl absorption band and is insoluble in conventional organic solvents. GRA

N93-14825 Department of the Navy, Washington, DC.
METHOD FOR FABRICATING OHMIC CONTACTS ON SEMICONDUCTING DIAMOND Patent Application
James R. Zeidler, inventor (to Navy) and Khosrow L. Moazed, inventor (to Navy) 8 Oct. 1991 9 p Filed 29 Jun. 1989
(AD-D015432; US-Patent-Appl-SN-374498; US-Patent-Class-437-188)
Avail: CASI HC A02/MF A01

A method is disclosed for fabricating ohmic contacts on semiconducting diamond. A carbide forming metal is deposited over a surface of the semiconducting diamond. In some applications, one or more layers of an intermediate metal are deposited over the carbide forming metal. A corrosion resistant metal is then deposited over the intermediate metal, if present, or the carbide forming metal. The semiconducting diamond and metals are heated in an inert environment at a temperature anywhere from 350 to 1200 degrees Celsius. GRA

N93-14886*# National Aeronautics and Space Administration. Lewis Research Center, Cleveland, OH.
COMMENTS ON 'KINETIC STUDY ON THE HEXACELSIAN-CELSIAN PHASE TRANSFORMATION'
Narottam P. Bansal and Charles H. Drummond, III (Ohio State Univ., Columbus.) Nov. 1992 9 p
(RTOP 510-01-50)
(NASA-TM-105917; E-7408; NAS 1.15:105917) Avail: CASI HC A02/MF A01

A value of 20.1 +/- 4 kcal/mole for the activation energy (E) for the hexacelsian to celsian phase transformation in BaAl2Si2O8 was reported in an earlier work. In the present work, the earlier experimental data were reanalyzed and a much higher value of E was obtained. This revised E value is consistent with the transformation mechanism of a layered hexacelsian structure into a three-dimensional feldspar structure of celsian which would necessitate the breaking of the Si-O and/or the Al-O bonds. Author

N93-14903# Oregon State Univ., Corvallis.
HYPERFINE EXPERIMENTAL INVESTIGATION OF ZIRCONIA CERAMICS
1992 16 p
(Contract DE-FG06-85ER-45191)
(DE92-040301; DOE/ER-45191/20) Avail: CASI HC A03/MF A01

This research program has encompassed a broad investigation of microscopic structure and point defect properties in insulating materials and some recent exploratory work on semiconductors. The major experimental technique is perturbed angular correlation (PAC) spectroscopy. Our research provides information about the microscopic structure, nucleation, and equilibrium of structural phases in materials under investigation. We have studied phase equilibria in monoclinic, tetragonal, and cubic zirconia in the past and have recently begun a more detailed investigation of high-temperature anomalies in monoclinic zirconia and tetragonal stabilized zirconia. We also have found a number of instances where the indium PAC probe has detected subtle phase changes, small precipitate formation, and other phase behavior that are difficult to detect by conventional diffraction methods. The PAC experimental technique is described briefly in section 2, and recent research is reviewed in section 3. DOE

N93-15049# National Inst. of Standards and Technology, Gaithersburg, MD. Ceramics Div.
A FUNDAMENTAL UNDERSTANDING OF THE EFFECTS OF CERAMIC PROCESSING ON PRODUCT MICROSTRUCTURE Final Report
G. G. Long, J. P. Cline, and J. J. Ritter 15 Feb. 1992 57 p
(Contracts MIPR-120-89; MIPR-102-90)
(AD-A255729) Avail: CASI HC A04/MF A01

This is the final report arising from our research program involving the investigation of processing/microstructure relationships in selected ceramic systems. The first year of this program was dedicated to the development and detailed assessment of the novel neutron scattering and x-ray diffraction techniques required for the measurement of ceramic microstructure evolution as a function of sintering and chemistry. The next two years of the program were used to study several systems in detail, and has led to some remarkable conclusions which have changed the way in which the sintering stages in different systems are understood. The sintering behavior of a ceramic body and the properties of the ceramic product depend directly on the internal microstructure. The goal of our research program has been to investigate well-characterized systems and to measure microstructure evolution during ceramic processing in order to obtain an improved understanding of the relationships between processing and microstructure. This approach has led to progress in improving process models and to improved predictability of product microstructure. GRA

N93-15064# Chemical Research and Development Center, Aberdeen Proving Ground, MD.
REMOVAL OF THD FROM PAINTED TEST PANELS BY LIQUID SYSTEMS Final Report, Aug. 1990 - Apr. 1991
Yu-Chu Yang, Kurt Goergens, and Manfred Zillmer Aug. 1992 25 p
(DA Proj. 1N4-64806-DF-97)
(AD-A255624; CRDEC-TR-392) Avail: CASI HC A03/MF A01

More than 40 nonreactive liquid systems were systematically evaluated against the removal of THD (thicked mustard, 2,2'-dichlorodiethyl sulfide). On panels with nonsorptive paint, high decontamination efficacy was achieved by nonreactive systems, which rapidly solubilized the THD. Adding reactants to these-systems did not change the results. Chemical reaction alone could not remove the THD when the solvent failed to solubilize it rapidly. Consequently, solubilization was sufficient and necessary for achieving high efficancy. The following exception was noted: high efficancies were measured for aqueous bleach solutions via vigorous reactions only at the HD-water interface. However, on panels with sorptive paint into which HD had penetrated, a better decontamination efficacy was obtained by adding a reactant. GRA

N93-15111# Worcester Polytechnic Inst., MA. Dept. of Chemistry.
RADICAL ION FORMATION IN POLYMERS AS A MECHANISM FOR LASER EYE PROTECTION Final Report, Apr. 1991 - Apr. 1992
W. G. McGimpsey and S. J. Weininger 31 Aug. 1992 30 p
(Contract DAAK60-91-K-0002)
(AD-A255992) Avail: CASI HC A03/MF A01

Phase 1 of this contract involved the synthesis of several representative compounds containing organic chromophores which are capable of donating and accepting a single electron after two-photo excitation. The selection of suitable chromophores was based on a set preset criteria which is listed in the contract proposal. The suitability of these chromophores for the stated application was determined first by studying their spectroscopic and electron transfer properties as separate molecules in solution (i.e., intermolecular). Once the intermolecular behavior of these chromophores was evaluated, synthesis of molecules incorporating both the donating and accepting chromophores was carried out. This report describes the following work: (1) spectroscopic evaluation of the two-photon-induced intermolecular electron donor/acceptor abilities of the chosen chromophores; (2) synthesis of molecules incorporating both the electron donating and accepting chromophores; and (3) preliminary spectroscopic investigation in solution of the synthesized molecules. GRA

N93-15127# Ecole Nationale Superieure du Petrole et des Monteurs, Rueil-Malmaison (France). Centre de Materiaux Pierre Marie Fourt.
DAMAGE AND RUPTURE OF CERAMIC COMPOSITES Final Report [ENDOMMAGEMENT ET RUPTURE DES COMPOSITES CERAMIQUES]
N. Frety and M. Boussuge Oct. 1991 124 p In FRENCH
(Contract DRET/ARMINES-89-250)
(ETN-92-92722) Avail: CASI HC A06/MF A02

The mechanical characteristics of the basic elements of SiC/SiC unprotected long fiber material composites, is considered. The mesoscopic scale is studied by performing traction trials on strands and woven layers of densified SiC/SiC. The aim of the trials is to predict the mechanical behavior of an elementary material cell, from which will be deduced that of bidirectional SiC/SiC materials, made up from layers of woven layers. ESA

N93-15222# Jet Process Corp., New Haven, CT.
JET VAPOR DEPOSITION OF THIN FILMS FOR SOLID OXIDE AND OTHER FUEL CELL APPLICATIONS
B. L. Halpern, J. J. Schmitt, J. W. Golz, and Y. Di 1992 9 p Presented at the US Department of Energy Contractors Review Meeting on Fuel Cells, Morgantown, WV, 14-15 Jul. 1992
(Contract DE-FG05-91ER-81156)
(DE92-019980; DOE/ER-81156/92/C0059; CONF-920748-6) Avail: CASI HC A02/MF A01

JVD has demonstrated promise for thin film SOFC research and fabrication. Micron scale YSZ films made via JVD are dense and pinhole free; they seal highly porous electrode surfaces and are gas tight. There is little chance for impurity incorporation in JVD, and the evidence points to oxygen ion conductivity. DOE

N93-15242# Aerospace Corp., El Segundo, CA. Mechanics and Materials Technology Center.
THE INFLUENCE OF STEEL SURFACE CHEMISTRY ON THE BONDING OF LUBRICANT FILMS
S. V. Didziulis, M. R. Hilton, and P. D. Fleischauer 1 Sep. 1992 26 p
(Contract F04701-88-C-0089)
(AD-A256231; TR-0091(6945-03)-5; SMC-TR-92-38) Avail: CASI HC A03/MF A01

Virtually all moving mechanical assemblies on spacecraft contain steel components that must be effectively lubricated to ensure optimum performance and long life. This report details the surface chemical composition of 440C stainless steel and its interaction with two lubricant species: the solid lubricant MoS2 and the liquid lubricant extreme pressure (EP) additive, lead naphthenate (Pbnp). X-ray photoelectron spectroscopy (XPS) studies show that the 440C surface has a layered oxide structure following polishing and solvent cleaning; a 2.5 nm thick iron oxide layer exists on top of a thinner 1.5 nm chromium oxide underlayer. A region of high metal carbide concentration is present at the chromium oxide-bulk steel interface. Therefore, a layer of iron oxide (not the corrosion barrier formed by the chromium oxide layer) is the top surface layer with which lubricant species interact under conditions of low stress. The surface chemical composition of 440C can be altered by chemical or physical means. Chemical treatments such as acidic and alkaline etches selectively remove the iron oxide overlayer, leaving behind a surface enriched in chromium oxide. Furthermore, the alkaline treatment proved to be more controllable, while the acid treatment can cause surface damage by breaking through the corrosion barrier and severely oxidizing the bulk steel. GRA

N93-15282# Argonne National Lab., IL.
THREE-DIMENSIONAL NUCLEAR MAGNETIC RESONANCE IMAGING OF GREEN-STATE CERAMICS
S. L. Dieckman, N. Gopalsami, J. M. Ford, A. C. Raptis, W. A. Ellingson, and P. Rizo Sep. 1991 36 p Prepared in cooperation with Norton Co., Northboro, MA
(Contract W-31-109-eng-38)
(DE93-000930; ANL-91/39) Avail: CASI HC A03/MF A01

Objective is the development of nuclear magnetic resonance imaging techniques and technology applicable to the nondestructive characterization of green-state ceramics. To this end, a three-dimensional (3-D) NMR imaging technique has been developed, based on a back-projection acquisition protocol in combination with image reconstruction techniques that are based on 3-D Radon transform inversion. The method incorporates the experimental flexibility to overcome many of the difficulties associated with imaging of solid and semisolid broad-line materials, and also provides contiguously sampled data in three dimensions. This technique has been evaluated as a nondestructive characterization method for determining the spatial distribution of organic additives in green-state injection-molded cylindrical Si3N4 tensile specimens. The technique has been evaluated on the basis of providing moderate image resolution over large sample volumes, high resolution over smaller specimen volumes, and sensitivity to variations in the concentration of organics. Resolution of 200 microns has been obtained with excellent sensitivity to concentration. A detailed account of the 3-D imaging results obtained from the study, a discussion of the difficulties and limitations of the imaging technique, and suggestions for technique and system improvements are included. DOE

N93-15294# Battelle Columbus Labs., OH.
ANALYTICAL AND EXPERIMENTAL EVALUATION OF JOINING CERAMIC OXIDES TO CERAMIC OXIDES AND CERAMIC OXIDES TO METAL FOR ADVANCED HEAT ENGINE APPLICATIONS
J. Ahmad, B. Majumdar, A. R. Rosenfield, S. L. Swartz, J. Cawley, E. Park, D. Hauser, and A. T. Hopper Apr. 1992 133 p Prepared for Oak Ridge National Lab., TN
(Contract DE-AC05-84OR-21400)
(DE92-041383; ORNL/Sub-87-SB046/1) Avail: CASI HC A07/MF A02

The problem of designing reliable, high strength zirconia-to-zirconia and zirconia-to-nodular cast iron joints is addressed by developing a general joint design and assessment methodology. A joint's load carrying capability is predicted in terms of its material strength and fracture toughness characteristics. The effects of joint constituent properties and joining process variables are included. The methodology is verified in a two step process by applying it first to notched bend bars and then to a notched disk specimen loaded in compression. Key technical accomplishments in the program include the development of a joint design and assessment methodology which predicts failure based on a combination of strength and toughness, the development of a new method of hot forging magnesia partially stabilized zirconia to itself, and the development of a bimaterial disk-shaped specimen notched along the diametral bond line and compressively loaded to generate both shear and tensile loadings on the bond line. Mechanical and thermal characterization of joints, adherents, and interlayer materials were performed to provide data for input to the design methodology. Results from over 150 room temperature tests and 30 high temperature tests are reported. Extensive comparisons of experimental results are made with model predictions of failure load. The joint design and assessment model, as applied to the materials and test specimens of this program, has been programmed for a PC and is available to interested researchers. DOE

N93-15295# Norton Co., Northboro, MA.
TRIBOLOGY OF IMPROVED TRANSFORMATION-TOUGHENED CERAMICS-HEAT ENGINE TEST
E. Lilley, G. A. Rossi, and P. J. Pelletier Apr. 1992 101 p Prepared for Oak Ridge National Lab., TN
(Contract DE-AC05-84OR-21400)
(DE92-041385; ORNL/Sub-90-SG372/1) Avail: CASI HC A06/MF A02

A short term study has been carried out to evaluate the suitability as cam roller followers of three ceria zirconia toughened aluminas and two

yttria stabilized tetragonal zirconias (YTZP's) previously enhanced in programs supported by ORNL. Norton Si3N4 (NBD-100) was also included in this study as a reference material, because it was known from work at Northwestern University that Si3N4 to experienced little or no wear in this application, and NBD-100 is currently a successful commercial bearing material. The tribological studies were subcontracted to the Torrington Company. They found that in cam roller follower simulated tests that there was essentially no wear after 1 hour and 5 hours of testing detectable by weighing and concluded that all of these ceramics are, therefore, candidate materials. Because of the minute amounts of wear it was not possible to identify the wear mechanism or to make any correlations with the other physical properties which were evaluated such as MOR, K(sub IC) hardness, density, and grain size. Phase transformation during rolling has been of interest in the tribology of zirconia contain materials. The least stable of the ceria zirconia toughened aluminas resulted in as much as 33 monoclinic phase after testing whereas the yttria stabilized (TTZ) contained very little of this transformed phase. The results of this study show that oxide materials can now be considered as candidates for cam roller followers in heat engines. DOE

N93-15320# Los Alamos National Lab., NM.
COMPACTION OF SUBMICRON AND NANOCRYSTALLINE Al2O3-ZrO2 CERAMICS
J. McKittrick, B. Tunaboylu (California Univ., San Diego.), and J. Katz 1992 7 p Presented at the NATO Advanced Study Institute Meeting on Mechanical Properties and Deformation Behavior of Materials Having Ultra-Fine Microstructures, Porto Novo, Portugal, Jul. 1992
(Contract W-7405-eng-36)
(DE92-040233; LA-UR-92-2721; CONF-9207146-1) Avail: CASI HC A02/MF A01

The eutectic in the Al2O3-ZrO2 system was rapidly solidified by heating with an O2-H2 torch and then quenching the melt with a twin roller device. The as-quenched material, which was amorphous or nanocrystalline, was milled with B4C or Al2O3 media and pressed into pellets which were sintered conventionally or with microwaves. Samples contaminated with boron carbide resulted in compacts with substantially reduced porosity and a lower fraction of tetragonal ZrO2. Conventional sintering at low temperatures resulted in the formation of 'rods' of an Al2O3 rich phase which grew from the presence of a low melting B2O3-rich liquid. Conventional and microwave sintering at temperatures up to 1600 C resulted in a microstructure where 100-200 nm ZrO2 grains were present intragranularly in the alpha-Al2O3 grains. Larger ZrO2 grains (approximately 1 micron) were found intergranularly. As-quenched lamellar microstructures were preserved at low temperatures but spheroidized at sintering temperatures greater than 1600 C. DOE

N93-15344*# National Aeronautics and Space Administration. Lewis Research Center, Cleveland, OH.
LEVELING COATINGS FOR REDUCING THE ATOMIC OXYGEN DEFECT DENSITY IN PROTECTED GRAPHITE FIBER EPOXY COMPOSITES
D. A. Jaworske, K. K. deGroh, G. Podojil (Cleveland State Univ., OH.), T. McCollum (Cleveland State Univ., OH.), and J. Anzic (Cleveland State Univ., OH.) Nov. 1992 12 p Presented at the 17th Space Simulation Conference, Baltimore, MD, 9-12 Nov. 1992; sponsored by the Inst. of Environmental Sciences
(RTOP 506-41-41)
(NASA-TM-105732; E-7136; NAS 1.15:105732) Avail: CASI HC A03/MF A01

Pinholes or other defect sites in a protective oxide coating provide pathways for atomic oxygen in low Earth orbit to reach underlying material. One concept for enhancing the lifetime of materials in low Earth orbits is to apply a leveling coating to the material prior to applying any reflective and protective coatings. Using a surface tension leveling coating concept, a low viscosity epoxy was applied to the surface of several composite coupons. A protective layer of 1000 A of SiO2 was deposited on top of the leveling coating, and the coupons were exposed to an atomic oxygen environment in a plasma asher. Pinhole populations per unit area were estimated by counting the number of undercut sites observed by scanning electron microscopy. Defect density values of 180,000 defects/sq cm were reduced to about 1000 defects/sq cm as a result of the applied leveling coating. These improvements occur at a mass penalty of about 2.5 mg/sq cm. Author

N93-15394# California Univ., San Diego. Dept. of Applied Mechanics and Engineering Sciences.
AN INVESTIGATION OF THE PROCESSING, HIGH TEMPERATURE DEFORMATION AND FRACTURE CHARACTERISTICS OF SUPERPLASTIC CERAMICS Final Report, 15 Sep. 1989 - 14 Sep. 1990
Atul H. Chokshi and Joanna McKittrick 11 Sep. 1992 2 p
(Contract DAAL03-89-K-0145)
(AD-A256519; ARO-26852.10-MS-A) Avail: CASI HC A02/MF A01

The considerable interest in using ceramics for structural applications is constrained in large part by the difficulty in forming ceramics in useful component shapes. Superplasticity, a term referring to the ability of some fine grained crystalline materials to deform extensively, is being used commercially to form metallic components with complex shapes. It may be possible to use this phenomenon to form structural ceramics. This proposal outlines a three year, detailed, fundamental research program to investigate processing and mechanical properties of fine grained structural superplastic ceramics with the appropriate characterization. We will use an alkoxide synthesis technique to process the structural ceramics, and evaluate the high temperature mechanical properties in both tension and compression. The microstructural aspects of superplastic deformation and cavitation failure will be examined using x ray diffraction, optical, scanning electron and transmission electron microscopy. It is anticipated that the present experimental study will substantially improve the understanding of superplasticity in structural ceramics, and this is likely to enhance the prospects of using this phenomenon for forming ceramics. GRA

N93-15415# Wisconsin Univ., Madison.
MORPHOLOGICAL ANALYSIS OF IONOMERS
1991 7 p
(Contract DE-FG02-88ER-45370)
(DE92-040162; DOE/ER-45370/4) Avail: CASI HC A02/MF A01

Anomalous small-angle x-ray scattering (SAXS) investigations were carried out on amorphous and semi-crystalline ionomers (Ni- neutralized sulfonated polystyrene ionomers, polyurethane ionomer). Ionomers with semicrystalline matrices (three-phase materials) were also studied with SAXS (poly(ethylene-co-methacrylic acid) ionomer). Ethylene oxide units were incorporated into the backbone of sulfonated polyurethane ionomers in an attempt to induce aggregate dissociation. Small-angle neutron scattering was used to study the effect of ionic aggregation on ionomer chain dimensions in telechelic and model polyurethane ionomers. Studies have been completed on carboxylated and sulfonated model polyurethane ionomers in order to determine the effect of the pendant ionic group on ionomer structure-property relationships (mechanical properties). DOE

N93-15431*# Old Dominion Univ., Norfolk, VA. Dept. of Civil Engineering.
POLYMER INFILTRATION STUDIES Final Report, 1 Oct. - 31 Dec. 1992
Joseph M. Marchello Dec. 1992 35 p
(Grant NAG1-1067)
(NASA-CR-191652; NAS 1.26:191652) Avail: CASI HC A03/MF A01

Significant progress has been made during the past three months on the preparation of carbon fiber composites using advanced polymer resins. The results are set forth in recent reports and publications, and will be presented at forthcoming national and international meetings. Current and ongoing research activities reported herein include: powdered tow ribbonizing; unitape from powdered tow; customized towpreg for textiles and ATP; and textile composite research. During the period ahead research will be directed toward further development of the new powder curtain prepregging method and on ways to customize dry powder towpreg for textile and robotic applications in aircraft part fabrication. Studies of multi-tow powder prepregging and ribbon preparation will be initiated in conjunction with continued development of prepregging technology and the various aspects of composite part fabrication using customized towpreg. Also, a major effort during the coming months will be participating in the analysis of the performance of the new solution prepregger. Author

N93-15437# GTE Labs., Inc., Waltham, MA.
DEVELOPMENT OF ADHERENT CERAMIC COATINGS TO REDUCE CONTACT STRESS DAMAGE OF CERAMICS

C. DAngelo, H. J. Kim, D. W. Oblas, H. E. Rebenne, and V. K. Sarin Apr. 1992 113 p Prepared for Oak Ridge National Lab., TN
(Contract DE-AC05-84OR-21400)
(DE92-041373; ORNL/Sub-86-95915/1) Avail: CASI HC A06/MF A02

High-strength, oxidation-resistant materials for advanced heat engine applications are susceptible to contact stress damage at ceramic/ceramic interfaces. It has been observed that surface damage and strength loss under sliding contact can be substantially reduced by applying a thin ceramic coating. In this program, a multilayered, compositionally graded coating was designed for ceramic components in advanced heat engines. A chemical vapor deposition process was developed for applying coatings in the thickness range of 2 - 20 micron 2 in. x 1/4 in. x 1/8 in. bars. Strongly adherent coatings were grown on the three substrates of interest -- reaction bonded silicon nitride, hot isostatically pressed silicon nitride, and sintered silicon carbide. The effect of the coating on relevant mechanical properties of the substrate materials was evaluated. Performance of the coated material was assessed by conducting long-term high-temperature oxidation and thermal shock tests at 1000 C and 1200 C. Some oxidation tests were also performed at 1375 C. Coated material was prepared for contact stress testing at 1000 C and 1200 C. Results indicate that with the present coating configuration, potential exists for commercial application at temperatures of up to 1200 C. Increases in the use temperature appear possible by modifying the coating properties. DOE

N93-15438# Virginia Polytechnic Inst. and State Univ., Blacksburg. Center for Advanced Ceramic Materials.
DEVELOPMENT OF LOW-EXPANSION CERAMICS FOR DIESEL ENGINE APPLICATIONS
J. J. Brown, Jr. Apr. 1992 97 p Prepared for Oak Ridge National Lab., TN
(Contract DE-AC05-84OR-21400)
(DE92-041380; ORNL/Sub-86-22049/1) Avail: CASI HC A05/MF A02

The need for stable fabricable low thermal expansion ceramics for use in advanced heat engines was first recognized in the Department of Energy Advanced Gas Turbine (AGT) technology programs. More recently, the need for ceramic materials having low thermal expansion for use in components of advanced low heat rejection diesel engines has also been recognized. This investigation concentrated on; (1) synthesis; (2) property characterization; and (3) fabrication of candidate low thermal expansion ceramics from four systems based upon aluminum phosphate, silica, mullite, and zircon. The NZP(zircon - NaZr2(PO4)3) structures clearly represent a new class of high melting, thermal shock-resistant ceramics. DOE

N93-15439# Cummins Engine Co., Inc., Columbus, IN.
DEVELOPMENT OF WEAR-RESISTANT CERAMIC COATINGS FOR DIESEL ENGINE COMPONENTS
M. G. S. Naylor Jun. 1992 195 p Prepared for Oak Ridge National Lab., TN
(Contract DE-AC05-84OR-21400)
(DE92-041382; ORNL/Sub-87-SA581/1) Avail: CASI HC A09/MF A03

The tribological properties of a variety of advanced coating materials have been evaluated under conditions which simulate the piston ring -- cylinder liner environment near top ring reversal in a heavy duty diesel engine. Coated 'ring' samples were tested against a conventional pearlitic grey cast iron liner material using a high temperature reciprocating wear test rig. Tests were run with a fresh CE/SF 15W40lubricant at 200 and 350 C, with a high-soot, engine-tested oil at 200 C and with no lubrication at 200 C. For lowest wear under boundary lubricated conditions, the most promising candidates to emerge from this study were high velocity oxy-fuel (HVOF) Cr3C2 - 20 percent NiCr and WC - 12 percent Co cermets, low temperature arc vapor deposited (LTAVD) CrN and plasma sprayed chromium oxides. Also, plasma sprayed Cr2O3 and Al2O3-ZrO2 materials were found to give excellent wear resistance in unlubricated tests and at extremely high temperatures (450 C) with a syntheticoil. All of these materials would offer substantial wear reductions compared to the conventional electroplated hard chromium ring facing and thermally sprayed metallic coatings, especially at high temperatures and with high-soot oils subjected to degradation in diesel environments. The LTAVD CrN coating provided the lowest lubricated wear rates of all the materials evaluated, but may be too thin (4 micron) for use as a top ring facing. Most of the coatings evaluated showed higher wear rates with high-soot, engine-tested oil than with fresh oil, with increases of more than a factor of ten in some cases. Generally, metallic materials were found to be much more sensitive to soot/oil degradation than ceramic and cermet coatings. Thus, decreased 'soot sensitivity' is a significant driving force for utilizing ceramic or cermet coatings in diesel engine wear applications. DOE

N93-15452# Allied-Signal Aerospace Co., Torrance, CA. Garrett Ceramic Components Div.
DEVELOPMENT OF CERAMIC MATRIX COMPOSITES FOR APPLICATION IN THE CERAMIC TECHNOLOGY FOR ADVANCED HEAT ENGINES PROJECT. PHASE 2A: DEVELOPMENT OF IN-SITU TOUGHENED SILICON NITRIDE
J. Pollinger, D. Newson, H. Yeh, E. Solidum, J. Yamanis (Allied-Signal Corp., Morristown, NJ.), M. Behi (Allied-Signal Corp., Morristown, NJ.), C. W. Li (Allied-Signal Corp., Morristown, NJ.), and P. Whalen (Allied-Signal Corp., Morristown, NJ.) Jun. 1992 81 p Prepared for Oak Ridge National Lab., TN
(Contract DE-AC05-84OR-21400)
(DE92-041371; ORNL/Sub-85-22008/3-Phase-2A) Avail: CASI HC A05/MF A01

The objective of this program was to develop a net shape forming process for an in-situ reinforced Si3N4 (AS-700). AS-700 was initially developed using cold isostatic pressing (CIP) of alcohol milled powders. The CIP'ed AS-700 material exhibited a moderate strength (690 MPa) and high toughness (9 MPa(radical)m) at room temperature. In addition to net-shape process development, optimization of AS-700 properties was also investigated through the refinement of densification processes, and evaluation of the effect of Si3N4 powder properties on resulting microstructure and mechanical properties. Slip casting was chosen as the net-shape forming process. A slip casting process was successfully developed for forming green parts ranging from thin plates to thick cylinders, and to large complex shaped turbine rotors. The densification cycle was optimized to achieve full density parts without any cracks or warpage, and with comparable properties and microstructure to the CIP'ed baseline AS-700 material. The evaluation of six (6) alternate Si3N4 powders indicated that Si3N4 powders have a very strong influence on the development of resulting AS-700 in-situ microstructures and mechanical properties. The AS-700 slip casting process and optimized densification process were then combined and a number of test specimens were fabricated. The mechanical properties and microstructure of the optimized slip cast AS-700 Si3N4 were then fully characterized. The key property values are: 695 MPa at room temperature, 446 MPa at 1370 C flexural strengths and 8.25 MPa/sq m toughness. DOE

N93-15453# Norton Co., Northboro, MA.
PROCESSING OF SINTERABLE TRANSFORMATION TOUGHENED CERAMICS FOR APPLICATION IN CERAMIC TECHNOLOGY FOR ADVANCED HEAT ENGINES PROJECT
E. Lilley and G. A. Rossi Apr. 1992 125 p Prepared for Oak Ridge National Lab., TN
(Contract DE-AC05-84OR-21400)
(DE92-041372; ORNL/Sub-85-22031/2) Avail: CASI HC A06/MF A02

The Y-TZP material developed in Phase 1 of this ORNL/DOE contract was modified in its composition to give improved resistance to low temperature degradation without loss of strength and toughness. The variations in yttria between 4.69 and 5.52 w percent produced little difference in strength in the ceramics measured between RT and 700 C, nor was there any clear influence on toughness. The addition of 4.0 w percent ceria together with 4.49 w percent yttria, however did reduce the strength. No correlation between grain size and toughness was found although there was a strong correlation between either yttria concentration or grain size and the fracture surface monoclinic phase percent. These results suggest that there may be another toughening mechanism in operation in addition to irreversible transformation toughening. DOE

N93-15462# Lawrence Livermore National Lab., CA.
CHARACTERISTICS OF THE NOVA LASER DISK EDGE CLADDING EPOXY
C. R. Wolfe 20 Aug. 1992 25 p
(Contract W-7405-eng-48)
(DE92-041046; UCRL-ID-111521) Avail: CASI HC A03/MF A01

The technical characteristics of the optical epoxy used to edge clad laser disks are described. Incoming QA of this material is required to

account for variation of the commercial supply over time and to ensure optimal performance of the material in high power laser applications. Characteristics of the epoxy starting components and the cured polymer are described. Testing of four batches of commercially supplied materials used over a period of five years is reported. DOE

N93-15640# Chemical Research and Development Center, Aberdeen Proving Ground, MD.
PREDICTING POLYMER PROPERTIES BY COMPUTATIONAL METHODS 2: A COMPARISON OF SEMI-EMPIRICAL METHODS Final Report, Jun. - Sep. 1989
A. Birenzvige, L. M. Sturdivan, G. R. Famini, P. N. Krishnan, and R. E. Morris Sep. 1992 37 p
(DA Proj. 1L1-62622-A-553)
(AD-A256856; CRDEC-TR-361) Avail: CASI HC A03/MF A01

The physical properties of various molecules calculated by MNDO, AM1, and PM3 methods are compared to experimental values using rigorous statistical analysis. The results show the best methods for calculating physical properties will depend on the property and that no one method is adequate to calculate all the physical properties. Furthermore, the results show the value of employing statistical methods in the area of computational chemistry. GRA

N93-14751*# Dow Corning Corp., Midland, MI.
PROPERTIES OF TEXTILE GRADE CERAMIC FIBERS
Eric Pudnos *In* NASA. Langley Research Center, FIBER-TEX 1991: The Fifth Conference on Advanced Engineering Fibers and Textile Structures for Composites Oct. 1992 p 87-100 (For primary document see N93-14744 04-24)
Avail: CASI HC A03/MF A02

N93-15615*# Jet Propulsion Lab., California Inst. of Tech., Pasadena.
ACCELERATED SIMULATION OF NEAR-EARTH-ORBIT POLYMER DEGRADATION
Eric Laue *In* NASA. Goddard Space Flight Center, The Seventeenth Space Simulation Conference. Terrestrial Test for Space Success Nov. 1992 p 253-274 (For primary document see N93-15593 04-18)
Avail: CASI HC A03/MF A03

28 PROPELLANTS AND FUELS

Includes rocket propellants, igniters, and oxidizers; their storage and handling procedures; and aircraft fuels.

For related information see also *07 Aircraft Propulsion and Power*, *20 Spacecraft Propulsion and Power*, and *44 Energy Production and Conversion*.

N93-14630 Florida Inst. of Tech., Melbourne.
PHYSICS OF HYDROGEN STORAGE IN METAL-HYDRIDES Ph.D. Thesis
Ragaiy Abdelfattah-Zidan 1992 99 p
Avail: Univ. Microfilms Order No. DA9228377

Physical aspects of the hydrogenation-dehydrogenation mechanisms of metal-metal hydride systems were examined. Experimental investigation was conducted for magnesium hydride as a case study. Theoretical analysis and computational study were carried out. The kinetics of hydrogenation-dehydrogenation of traditionally prepared Mg-MgH2 and chemically synthesized Mg-MgH2 were experimentally investigated. A detailed investigation was carried out to determine the reasons for the improved performance of a chemically synthesized Mg-MgH2 previously reported by Bogdanovic and co-workers. A scanning electron microscope was used to examine the surface morphology of the samples. The surface of chemically prepared samples appeared to be covered with micro-spheroidal beads ranging in radius between 0.5 microns and 0.05 microns formed in a fractal-like configuration. Theoretical analysis indicated that the unusual surface structure of the chemically prepared samples could be responsible for the rapid uptake and release of hydrogen. The uptake and release enhancement is believed to be partially due to the substantial increase in the surface area and partially due to the fast diffusion into the smaller particles. The effect of the addition of nickel to the surface was also investigated. Theoretical analysis was carried out. Models for the process at the surface as well as in the bulk were developed. Diffusion equation was examined taking into account the diffusion coefficient being a function of concentration. A non-linear differential equation resulted for this case. The differential equation was numerically solved. Dissert. Abstr.

N93-14801 Department of the Navy, Washington, DC.
PROPELLANT GRAIN ASSEMBLY FOR A GAS GENERATOR Patent Application
Kenneth E. Adams, inventor (to Navy) 7 Apr. 1992 13 p Filed 30 Nov. 1990
(AD-D015439; US-Patent-Appl-SN-621103; US-Patent-Class-102-290)
Avail: CASI HC A03/MF A01

A gas generator for a long range missile is driven by a solid propellant grain assembly which includes a cylindrical inhibitor, a forward closure assembly that is attached to one end of the inhibitor and a propellant grain that is cast into the cylindrical cavity formed by the interior surface of the cylindrical inhibitor. Between the grain and inhibitor and between the grain and forward closure assembly is an adhesive bonding system for attaching the grain to the inhibitor and forward closure assembly. The exposed or aft end of the grain is the initial burning surface and includes a plurality of annular concentric grooves and a configuration that provides optimum burn progression that results in a complete high pressure burn. The external surface of the inhibitor is machined so that the solid propellant grain assembly may be readily inserted and removed from the gas generator. GRA

N93-14834*# National Aeronautics and Space Administration. Lewis Research Center, Cleveland, OH.
ENERGY LOSS ANALYSIS OF AN INTEGRATED SPACE POWER DISTRIBUTION SYSTEM
M. David Kankam and P. F. Ribeiro (Dordt Coll., Sioux Center, IA.) Aug. 1992 8 p Presented at the 27th Intersociety Energy Conversion Engineering Conference, San Diego, CA, 3-7 Aug., 1992; cosponsored by ANS, SAE, ASC, AIAA, IEEE, and AIChE
(RTOP 506-41-41)
(NASA-TM-105772; E-7055; NAS 1.15:105772) Avail: CASI HC A02/MF A01

The results of studies related to conceptual topologies of an integrated utility-like space power system are described. The system topologies are comparatively analyzed by considering their transmission energy losses as functions of mainly distribution voltage level and load composition. The analysis is expedited by use of a Distribution System Analysis and Simulation (DSAS) software. This recently developed computer program by the Electric Power Research Institute (EPRI) uses improved load models to solve the power flow within the system. However, present shortcomings of the software with regard to space applications, and incompletely defined characteristics of a space power system make the results applicable to only the fundamental trends of energy losses of the topologies studied. Accountability, such as included, for the effects of the various parameters on the system performance can constitute part of a planning tool for a space power distribution system. Author

N93-15011# Army Chemical Research and Development Center, Aberdeen Proving Ground, MD. Ballistic Research Lab.
THERMAL DECOMPOSITION OF HNIW AND HNIW-BASED FORMULATIONS Final Report, Aug. - Nov. 1991
Rose A. Pesce-Rodriguez, Robert A. Fifer, Kevin L. McNesby, Jeffrey B. Morris, and Michael A. Schroeder Sep. 1992 42 p
(DA Proj. 1L1-61102-AH-43)
(AD-A255613; BRL-TR-3402) Avail: CASI HC A03/MF A01

The pyrolytic decomposition of hexanitrohexazaisowurtzitane (HNIW) and a HNIW-based propellant formulation were investigated using several infrared and mass spectrometric techniques. The pyrolysis produce distributions of HNIW (500 C and 1000 C pyrolysis) were compared to those of HMX and RDX. At both temperatures, HNIW produced a higher CO2:N2O ratio than did HMX or RDX. Several products were generated by all three nitramines, while others were unique to HNIW. When heated under vacuum conditions, HMX appears to undergo both vaporization and decomposition, while HNIW appears to remain in the condensed phased prior to rapid decomposition. Investigation of the effect of propellant ingredients (i.e., nitrate ester, plasticizers and a modified DuPont HYCAR thermoplastic elastomer) on the pyrolysis product distribution of a HNIW-based propellant indicates the

removal of several HNIW decomposition products by those ingredients. Observed variations in the pyrolysis product distribution as a function of sample size are attributed to as yet unidentified secondary reactions.
GRA

N93-15478# Mound Lab., Miamisburg, OH.
THE SENSITIVITY OF ENERGETIC MATERIALS TO FRICTION, IMPACT, AND ELECTROSTATIC STIMULI
M. D. Vannet 24 Sep. 1992 25 p
(Contract DE-AC04-88DP-43495)
(DE92-041227; MLM-3762) Avail: CASI HC A03/MF A01

Friction, impact, and electrostatic tests were conducted on materials that had not previously been tested at Mound, including PETN, BTF, HNS-IV, and pyrotechnic and thermite powders. Results are presented. Tables and charts including previous results are also included. DOE

29 MATERIALS PROCESSING

Includes space-based development of products and processes for commercial applications.

For biological materials see *55 Space Biology*.

N93-14793*# Alabama Univ., Huntsville. Materials Processing Lab.
STUDY OF FLUID EXPERIMENT SYSTEM (FES)/CAST/HOLOGRAPHIC GROUND SYSTEM (HGS)
Gary L. Workman, Rick Cummings, and Brian Jones 20 Oct. 1992 19 p
(Contract NAS8-38609)
(NASA-CR-184483; NAS 1.26:184483) Avail: CASI HC A03/MF A01

The use of holographic and schlieren optical techniques for studying the concentration gradients in solidification processes has been used by several investigators over the years. The HGS facility at MSFC has been primary resource in researching this capability. Consequently, scientific personnel have been able to utilize these techniques in both ground based research and in space experiments. An important event in the scientific utilization of the HGS facilities was the TGS Crystal Growth and the casting and solidification technology (CAST) experiments that were flown on the International Microgravity Laboratory (IML) mission in March of this year. The preparation and processing of these space observations are the primary experiments reported in this work. This project provides some ground-based studies to optimize on the holographic techniques used to acquire information about the crystal growth processes flown on IML. Since the ground-based studies will be compared with the space-based experimental results, it is necessary to conduct sufficient ground based studies to best determine how the experiment worked in space. The current capabilities in computer based systems for image processing and numerical computation have certainly assisted in those efforts. As anticipated, this study has certainly shown that these advanced computing capabilities are helpful in the data analysis of such experiments. Author

N93-15201# Victoria Univ. (British Columbia). Dept. of Mechanical Engineering.
STUDY OF THE MATHEMATICAL MODELLING AND COMPUTER SIMULATION OF CRYSTAL GROWTH FROM LIQUID PHASE UNDER MICROGRAVITY CONDITIONS Final Report
Sadik Dost 31 Mar. 1991 118 p
(CTN-93-60619) Avail: CASI HC A06/MF A02

The general governing equations for the LPEE (liquid phase electroepitaxy) growth process, and the relevant governing equations and appropriate boundary conditions for LPEE growth of binary compounds, are presented. Elucidation of the role of convection, together with other phenomena, is one of the main objectives of the work. Experimental and theoretical studies on LPEE are reviewed along with existing theoretical models and their contributions to LPEE research. The basic equations of a proposed model for LPEE growth of GaAs are derived using the fundamental principles of electrodynamics, mechanics, and thermodynamics. The constitutive equations of the solid and liquid phases are obtained via an irreversible thermodynamic theory. The fundamental equations and interface conditions of a model of LPEE growth of binary compounds are used for formulating the governing equations and the related boundary and interface conditions of the liquid phase epitaxial growth of Si from an In solution in a sandwich system. These equations and conditions are also given for a two-dimensional model. The problem of the growth of triglycerine sulfate crystals from an aqueous solution is briefly discussed and its basic equations are presented. After verification of these models a computer simulation to predict the growth process under microgravity can be carried out.
Author (CISTI)

N93-15420*# National Aeronautics and Space Administration. Lewis Research Center, Cleveland, OH.
NUCLEATE POOL BOILING IN THE LONG DURATION LOW GRAVITY ENVIRONMENT OF THE SPACE SHUTTLE
M. M. Hasan, C. S. Lin, R. H. Knoll, M. D. Bentz (Boeing Co., Seattle, WA.), and J. S. Meserole (Boeing Co., Seattle, WA.) Jan. 1993 11 p Presented at the 31st Aerospace Sciences Meeting and Exhibit, Reno, NV, 11-14 Jan. 1993; Sponsored by AIAA
(RTOP 589-01-2C)
(NASA-TM-105973; E-7485; NAS 1.15:105973; AIAA Paper 93-0465)
Avail: CASI HC A03/MF A01

The results are presented of an experimental study of nucleate pool boiling performed in the low gravity environment of the space shuttle. Photographic observations of pool boiling in Freon 113 were obtained during the 'Tank Pressure Control Experiment,' flown on the Space Transportation System, STS-43 in August 1991. Nucleate boiling data from large (relative to bubble size) flat heating surfaces (0.1046 by 0.0742 m) was obtained at very low heat fluxes (0.22 to 1.19 kW/sq m). The system pressure and the bulk liquid subcooling varied in the range of 40 to 60 kPa and 3 to 5 C respectively. Thirty-eight boiling tests, each of 10-min duration for a given heat flux, were conducted. Measurements included the heater power, heater surface temperature, the liquid temperature and the system pressure as functions of heating time. Video data of the first 2 min of heating was recorded for each test. In some tests the video clearly shows the inception of boiling and the growth and departure of bubbles from the surface during the first 2 min of heating. In the absence of video data, the heater temperature variation during heating shows the inception of boiling and stable nucleate boiling. During the stable nucleate boiling, the wall superheat varied between 2.8 to 3.8 C for heat fluxes in the range of 0.95 to 1.19 kW/sq m. The wall superheat at the inception of boiling varied between 2 to 13 C. Author

31 ENGINEERING (GENERAL)

Includes vacuum technology; control engineering; display engineering; cryogenics; and fire prevention.

N93-14467 Michigan Univ., Ann Arbor.
AN INTEGRATED OPTIMIZATION ENVIRONMENT FOR STRUCTURAL CONFIGURATION DESIGN Ph.D. Thesis
Mehran Chirehdast 1992 212 p
Avail: Univ. Microfilms Order No. DA9226871

The relatively recent efforts for designing lightweight structures have motivated increasing use of formal mathematical optimization techniques for selecting the shape and sizes of structural members. How to obtain rigorous optimal topologies has been an elusive goal until the very recent introduction of the homogenization method. This dissertation describes a system for designing complete structures starting only with an available space and loading and boundary specifications. A three-phase design process is followed: generate an approximate topological image with homogenization (Phase 1), process the image to obtain a practical realistic structure (Phase 2), and refine the final topology by detailed shape and size optimization (Phase 3). An overview of the system is given together with several practical examples. The emphasis of this dissertation is on the appropriate design and implementation of the image interpretation module in Phase 2. Image processing and computer vision techniques are used in conjunction with insights from mechanics and knowledge about fabrication processes to implement the system. The main concentration of this dissertation is on two-dimensional structures. In Phase 2, two types of models are distinguished for two-dimensional structures, namely, skeletal and plain stress/plain strain models. Different approaches are taken for the treatment of both models in Phase 2. For skeletal structures their skeleton is useful, whereas for solid structures the information on their boundaries is pertinent. Techniques to extract and process this information

are described. For each type of structure a fabrication domain is chosen, and rules are devised whose application to the representations in Phase 2 generates designs that are more easily manufacturable. For solid structures casting is chosen as the fabrication domain and, for skeletal structures weldments of trusses are explored. Extraction of other useful properties, such as symmetry and immobility for two-dimensional structures, is discussed. Interpretation of three-dimensional images is more challenging, and the techniques described for two-dimensional structures cannot easily be extended to apply to three-dimensional structures. A novel algorithm is devised that converts the spatial enumeration scheme generated in Phase 1 into a constructive solid geometry (CSG) scheme. The CSG representation is at a higher level of abstraction and can be used for further manipulation of the design. Dissert. Abstr.

N93-15105# Air Force Inst. of Tech., Wright-Patterson AFB, OH. Foreign Aerospace Science and Technology Center.

METHOD OF LOCAL SHAPING OF THERMOPLASTICS

V. I. Tseyler and A. T. Kutserubov 6 Aug. 1992 6 p Transl. into ENGLISH of Russian Patent No. 379402 (20 Apr. 1973) 1 p

(AD-A255913; FASTC-ID(RS)T-0571-92) Avail: CASI HC A02/MF A01

A method for local shaping of thermoplastics with a rigid punch which is characterized by the fact that for the purpose of simplifying it when shaping in places on parts which are not easily accessible the heated thermoplastic material is shaped with a ferromagnetic punch which interacts with the magnetized matrix. GRA

N93-15234# Naval Postgraduate School, Monterey, CA. Dept. of Administrative Sciences.

A PROPOSAL TO APPLY TAGUCHI-INSPIRED METHODS TO THE REDUCTION OF MACHINING VARIANCE Technical Report, period ending 1992

Dan Trietsch 16 Sep. 1992 37 p

(AD-A256129; NPS-AS-92-021) Avail: CASI HC A03/MF A01

The probability that a machined part will be defective increases with the variance of the machined dimensions. Even for parts within tolerance, the quality decreases with the variance. By reducing the variance of these dimensions better parts will be produced. Several factors, some of which are controllable, impact this variance, and they may also interact with each other. By choosing an appropriate level for each controllable factor we can minimize the variance. Since factors may interact with each other, a factorial experimental design is appropriate to optimize the levels of the factors; optimizing one factor at a time is not likely to yield the global optimum in the presence of interactions. The designed experiments must be conducted in stages: (1) at the preliminary stage one determines which factors and interactions are likely to be important; (2) at the exploratory stage one runs a fractional design to identify the factors that are really important and to verify/update the preliminary hypotheses about the interactions; (3) at the search stage one uses a sequence of experiments with varying levels of the factors that were identified as important to optimize their levels; finally, (4) at the verification stage one runs the process under the levels deemed to be optimal, to check if the process behaves according to the predictions. At any stage, after analyzing the current data, one may have to go back to a previous stage. This report presents a list of factors and interactions (preliminary stage output), and a design for the exploratory stage. We also discuss how to interpret the results and conduct the search stage. The plan is designed as a generic blueprint that can be used at any machine shop. GRA

N93-15353*# Applied Technology Associates, Inc., Albuquerque, NM.

DIGITAL ACTIVE MATERIAL PROCESSING PLATFORM EFFORT (DAMPER), SBIR PHASE 2 Final Report

John Blackburn and Dennis Smith NASA Nov. 1992 60 p

(RTOP 694-03-0C)

(NASA-CR-190798; E-7421; NAS 1.26:190798) Avail: CASI HC A04/MF A01

Applied Technology Associates, Inc., (ATA) has demonstrated that inertial actuation can be employed effectively in digital, active vibration isolation systems. Inertial actuation involves the use of momentum exchange to produce corrective forces which act directly on the payload being actively isolated. In a typical active vibration isolation system, accelerometers are used to measure the inertial motion of the payload. The signals from the accelerometers are then used to calculate the corrective forces required to counteract, or 'cancel out' the payload motion. Active vibration isolation is common technology, but the use of inertial actuation in such systems is novel, and is the focus of the DAMPER project. A May 1991 report was completed which documented the successful demonstration of inertial actuation, employed in the control of vibration in a single axis. In the 1 degree-of-freedom (1DOF) experiment a set of air bearing rails was used to suspend the payload, simulating a microgravity environment in a single horizontal axis. Digital Signal Processor (DSP) technology was used to calculate in real time, the control law between the accelerometer signals and the inertial actuators. The data obtained from this experiment verified that as much as 20 dB of rejection could be realized by this type of system. A discussion is included of recent tests performed in which vibrations were actively controlled in three axes simultaneously. In the three degree-of-freedom (3DOF) system, the air bearings were designed in such a way that the payload is free to rotate about the azimuth axis, as well as translate in the two horizontal directions. The actuator developed for the DAMPER project has applications beyond payload isolation, including structural damping and source vibration isolation. This report includes a brief discussion of these applications, as well as a commercialization plan for the actuator. Author

N93-14748*# North Carolina State Univ., Raleigh. Mars Mission Research Center.

ADVANCES IN 3-DIMENSIONAL BRAIDING

Cirrelia Thaxton, Rona Reid, and Aly El-Shiekh *In* NASA. Langley Research Center, FIBER-TEX 1991: The Fifth Conference on Advanced Engineering Fibers and Textile Structures for Composites Oct. 1992 p 43-65 (For primary document see N93-14744 04-24)

Avail: CASI HC A03/MF A02

N93-14749*# National Aeronautics and Space Administration. Langley Research Center, Hampton, VA.

DEVELOPMENT OF GENERALIZED 3-D BRAIDING MACHINES FOR COMPOSITE PREFORMS

Cecil O. Huey, Jr. (Clemson Univ., SC.) and Gary L. Farley *In its* FIBER-TEX 1991: The Fifth Conference on Advanced Engineering Fibers and Textile Structures for Composites Oct. 1992 p 67-76 (For primary document see N93-14744 04-24)

Avail: CASI HC A02/MF A02

32 COMMUNICATIONS AND RADAR

Includes radar; land and global communications; communications theory; and optical communications.

For related information see also *04 Aircraft Communications and Navigation* and *17 Space Communications, Spacecraft Communications, Command and Tracking.* For search and rescue see *03 Air Transportation and Safety,* and *16 Space Transportation.*

N93-14107# Ohio State Univ., Columbus. Electroscience Lab.

SCATTERER MODELING/CALIBRATION STUDY Final Report

R. J. Marhefka, J. D. Young, N. Akhter, T. J. Brinkley, and L. P. Ivrissimtzis Jun. 1992 100 p

(Contract F33615-88-C-1792)

(AD-A255855; TR-721198-6; WL-TR-92-1006) Avail: CASI HC A05/MF A02

This is the final report on Contract No. F33615-88-C-1792 for Wright-Patterson Air Force Base over the period August 1988 through May 1991. The overall goals and accomplishments are summarized. The goal of this contract is the investigation of monostatic and bistatic polarization and electromagnetic phenomenology at various low and high frequencies such as L, X and Ka bands for the purpose of enhancing the performance of synthetic aperture ground imaging radars for automatic target detection/classification. This is accomplished via measurements and analytic modeling of simple scatterers and complex targets comprising an ensemble of simple scatterers. Specific radar scattering data are obtained in the frequency range 2-18 GHZ on scale model targets and at frequencies below 2 GHz for full size targets. In both cases, coherent magnitude and phase signal versus target orientation, frequency and polarization are collected. GRA

N93-14126 Montana State Univ., Bozeman.
QUANTUM FLUCTUATIONS IN STIMULATED RAMAN SCATTERING Ph.D. Thesis
Rand Curtis Swanson 1991 117 p
Avail: Univ. Microfilms Order No. DA9216658

Results from a study of quantum noise and its macroscopic manifestations in stimulated Raman scattering are presented. Shot to shot fluctuations in quantrum noise initiated Stokes spectra are considered. The strokes spectra were recorded experimentally using a Fabry-Perot interferometer. For comparison, numerically generated Stokes spectra were produced using the semi-classic model of stimulated Raman scattering with a numerically generated 'vacuum' input field. The amount of structure on each spectrum was quantified by calculating the spectrum's standard deviation from its mean frequency. It was found that ensembles with the noisy spectra removed had narrower distributions of mean frequencies than ensembles that included noisy spectra. The effect of these shot to shot spectral fluctuations on soliton formation in simulated Raman scattering are presented next. Experimentally, the solitons were formed by using a Pockels cell to put a pi phase shift on the input Stokes pulse to a Raman amplifier. Theoretical solitons were produced by numerically placing a pi phase shift in a Stokes field that was amplified using the semi-classical model of simulated Raman scattering. Experimentally, noisy input spectra were discarded to insure the pi phase shift was the dominant phase structure. Good agreement was found with the numerical model when the noisy spectra were removed from the ensemble. These results indicate that soliton decay is directly related to quantum noise are presented. The amount of noise added to a signal during amplification was studied by placing an amplifier in each leg of an interferometer. The noise added by the amplifier was deduced from the degradation of the output fringe pattern from the interferometer. This was done experimentally using Raman amplifiers and numerically using ideal, single mode amplifiers and Raman amplifiers. The results indicate that the amount of noise added by the Raman amplifiers corresponds to 1 photon per mode input to a noiseless amplifier. This is the lowest amount of noise allowed by quantum mechanics. Dissert. Abstr.

N93-14155*# New Mexico State Univ., Las Cruces. Center for Space Telemetering and Telecommunications Systems.
ON THE PERFORMANCE OF TRELLIS CODED MODULATION WITH OCTAL PHASE SHIFT KEYING OVER THE TDRSS CHANNEL Semiannual Report, Jul. 1992 - Jan. 1993
William P. Osborne, Ted J. Wolcott, Brian T. Kopp, and Michael Ross Jan. 1993 73 p
(Grant NAG5-1491)
(NASA-CR-191366; NAS 1.26:191366) Avail: CASI HC A04/MF A01

As the National Aeronautics and Space Administration moves into the 21st century with programs like Space Station Freedom, a manned mission to Mars, and the new Landsat mission, transmission demands on the Tracking and Data Relay Satellite System (TDRSS) will very likely exceed the available bandwidth. The Manual Lujan, Jr. Center for Space Telemetering and Telecommunications Systems (CSTTS) at New Mexico State University (NMSU) is studying techniques for increasing the data rate capabilities of TDRSS. These techniques include the use of advanced bandwidth efficient modulation formats to increase the data rate that can be sustained in a TDRSS transponder and the use of lossless bandwidth compression of the data to be transmitted to lower the data rate required from the user spacecraft. Based upon current technology the most promising bandwidth efficient modulation technique is Trellis Coded Modulation (TCM) operating with Octal Phase shift Keying (8PSK). Trellis Coded Modulation coding with 8PSK carrier modulation has the capability to increase the data rate which can be transmitted through the TDRSS spacecraft by a factor of 2 to 2.5 times that available with todays coded QPSK systems with only a small penalty in link performance relative to the existing systems. However, before NASA can safely employ TCM coding it is necessary to prove that this complex format can perform on the real TDRSS link as it does in labs and simulation studies. This proof-of-concept test over a live satellite channel was the objective of the construction and testing performed under this task of the NMSU NASA grant referenced above. In conjunction with NASA, NMSU's CSTTS has constructed a system to test a new candidate TDRSS modulation scheme, TCM 8PSK, that can enhance the information throughput of the TDRSS spacecraft. The test system for this project which was constructed over a period of 18 months by NMSU consisted of two racks of commercial and univeristy-designed and -built equipment. This project has included modifications of an existing White Sands Ground Terminal (WSGT) High Rate QPSK Demodulator to demodulate 8PSK as well as the construction of other support hardware. Also, two TCM codecs (coder/decoders) have been constructed to implement two levels of bandwidth efficiency. One was designed and built by the research team at NMSU while the other was created by the University of Notre Dame with the University of South Australia. The NMSU codec achieves a 2-to-1 increase in data rate per unit bandwidth with a coding gain relative to QPSK of about 3dB. The Notre Dame/South Australia codec achieves a 2.5-to-1 increase in data rate per unit of occupied bandwidth and a coding gain of about 2dB. Author

N93-14181# Naval Research Lab., Washington, DC.
MULTI-ACCESS STRATEGIES FOR VOICE/DATA INTEGRATION IN HETEROGENEOUS MIXED-MEDIA PACKET RADIO NETWORKS Interim Report, Mar. - Nov. 1991
Evaggelos Geraniotis and Mohsen Soroushnejad 8 Sep. 1992 55 p
(DA Proj. RR0-1509)
(AD-A255636; NRL/MR/5521-92-7107) Avail: CASI HC A04/MF A01

The problem of voice/data integration in a mixed-media packet radio network employing both ground radio links and SATCOM radio links is investigated. Multi-access strategies are devised to take advantage of different characteristics of both radio channels to better serve the requirements of both traffic types. Code-division multiple-access with movable boundary in the code domain is used in the ground subnetwork to serve the voice traffic and the retransmitted data traffic while framed ALOHA with movable boundary is used on the satellite subnetwork for both data and voice. Based on a Markovian model of the system, a complete analysis of the channel access protocols for both traffic types is given. The performance of the multiple-access schemes used in this mixed-media network is evaluated in terms of voice and data throughput, voice blocking probability, and data delay. It is observed that splitting of retransmission traffic between the satellite and ground subnet may increase the overall data throughput when the voice load is high. GRA

N93-14189 Illinois Univ., Chicago.
INVESTIGATION OF THE ON-SURFACE BOUNDARY OPERATORS FOR ELECTROMAGNETIC SCATTERING BY CONDUCTING OBJECT Ph.D. Thesis
Wan Jong Chun 1992 295 p
Avail: Univ. Microfilms Order No. DA9226233

This research investigation presents an approach to obtain simple analytical solution for the electromagnetic scattering and interaction by the perfectly conducting two and three dimensional arbitrary shaped objects. This has been attempted by examining the basic physics of wave propagation, and scattering in the complex near field region and the near-field radiation boundary conditions. The dissertation addresses various unresolved issues and take up a study of near-field boundary operators to demonstrate the question of accounting the relevant physics of electromagnetic scattering and interaction. The evaluation of the near-field higher order radiation boundary operators is initially studied using a canonical geometry in a two dimensional case to predict behavior of the fields in the illuminated region and low level field distributions and the critical creeping wave field effects in the shadow region. Approaches are formulated to include the nonuniform edge currents at the corners based on the electromagnetic equivalences so that arbitrary cross sectional convex geometries consisting of arbitrary edges and corners can be analyzed. Number of two dimensional canonical conducting scattering objects, such as a circular scatterer, a triangular scatterer and a thin strip scatterer, are analyzed for plane wave excitation to demonstrate applicability of the On-Surface Radiation Condition theory which is developed in this dissertation. Further implementation of the OSRC theory for the study of scattering by a three dimensional object, is also considered. In the initial study, the scalar type three dimensional boundary operators are utilized to construct the three dimensional vector fields associated with a conducting sphere. Further, the various orders of three dimensional scalar boundary operators are evaluated in detail. To show applicability and limitation of the OSRC theory for the case of three dimensional scatterer, the perfectly conducting sphere is investigated using higher order radiation boundary operators using spherical wave functions.

Results of the induced surface electric current and the radar cross section are reported for the case of perfectly conducting sphere in free space medium. Dissert. Abstr.

N93-14233# Naval Research Lab., Washington, DC.
ON THE DETECTION OF ULTRAWIDEBAND RADAR SIGNALS Interim Report
M. Steiner 11 Sep. 1992 20 p
(AD-A256075; NRL/FR/5340-92-9517) Avail: CASI HC A02/MF A01

The detection of ultra-wide-band (UWB) radar signals is considered. Conventional radar theory is examined in the context of ultrawideband signals and extended when necessary. Point target detectors are found for the cases when the additive interference is white Gaussian noise and correlated Gaussian noise or clutter. A conventional moving target indicator (MTI) design is generalized for UWB radar. The effects of bandwidth on the resolution of clutter and target are examined. Optimal and conventional processing are compared for single echo detection. An optimal detector is found for a distributed target with a known target profile. Additionally, optimal detectors are found under two models where only second-order statistics of the target profile are assumed known. Future work areas are suggested. GRA

N93-14250# Air Force Inst. of Tech., Wright-Patterson AFB, OH. School of Engineering.
THE DETECTION AND CORRELATION MODELING OF RAYLEIGH DISTRIBUTED RADAR SIGNALS M.S. Thesis
Alan L. Buterbaugh Sep. 1992 78 p
(AD-A256612; AFIT/GE/ENG/92S-03) Avail: CASI HC A05/MF A01

This thesis provides a method for determining the detection of partially correlated Rayleigh distributed radar returns by a pulsed search radar. The receiver consists of a quadrature demodulator receiver, followed by a square law envelope detector and a linear post-detection integrator. In addition, a technique for determining the pulse-to-pulse correlation of a complex target is given using inverse Fourier transforms of the target scattering centers. An AIM-9 missile is used to illustrate how the partially correlated detection techniques and the pulse-to-pulse correlation predictions can be used to determine the probability of detection. GRA

N93-14259# Naval Research Lab., Washington, DC.
NONLINEAR MODELING OF GATED RANGE TRACKER DYNAMICS WITH APPLICATION TO RADAR RANGE RESOLUTION, PHASE 1 Report, 1 Oct. 1988 - 30 Sep. 1989
Eyad H. Abed, Allen J. Goldberg, and Robert E. Gover 22 Sep. 1992 32 p
(AD-A256074; NRL/FR/5753-92-9371) Avail: CASI HC A03/MF A01

Nonlinear dynamic models for gated radar range trackers are developed and applied to the range resolution problem. Two common types of tracking loop dynamics, as well as the automated gain control (AGC), are accounted for in the models. The null detector is formulated in a general way that encompasses many important error detector laws, including centroid and leading-edge. Both discrete-time and continuous-time dynamic models are presented for each class of tracking loop. The discrete-time models are derived by using an analytical description of the pulse-to-pulse dynamics of the tracker. The continuous time models are approximations of their discrete-time counterparts for sufficiently small values of the pulse repetition interval. Each of the models is analyzed for a deterministic target return condition. General criteria for asymptotic stability of equilibrium points of the models are studied. The most striking of the stability criteria is a sign requirement on the slope of a range error curve. These criteria are used in a two-target example to evaluate conclusions on a tracker's resolution capability as a function of target separation. These conclusions are compared with those obtained previously using Woodward's ambiguity function approach to resolvability. GRA

N93-14408# Michigan Univ., Ann Arbor. Ultrafast Science Lab.
TRANSPORT IN HETEROSTRUCTURES AND DEVICE IN MICROWAVE AND MILLIMETER WAVE REGIMES Annual Report, 1 Apr. 1991 - 31 Mar. 1992
Gerard Mourou, Theodore Norris, and John Whitaker 31 Mar. 1992 13 p
(Grant AF-AFOSR-0214-90)
(AD-A255975; AFOSR-92-0888TR) Avail: CASI HC A02/MF A01

All modern high speed devices deal with small structures (nanometers) and high-fields (several hundred kilovolt/cm). The relevant time constants involved in, the carrier transport are typically in the subpicosecond domain. Under the URI contract, with techniques based on ultrashort laser pulses, we have studied the dynamics of carriers in the 100-1000 GHz regime in bulk, low-temperature grown, and quantum-size semiconductors. In addition, because of the relevance of high-speed electronics, we have studied the carrier dynamics in high T(c) superconductors in the same frequency regime. During the course of the URI a number of technological innovations have been demonstrated and have found their way to the commercial world. The URI is at the origin of two spin-off companies, Medox Research and Picotronix, now selling products first demonstrated in our laboratories. Also a license is being granted to a laser company to develop a laser amplifier product demonstrated during the course of the URI last year. It is important to note that the URI has helped to originate a large grant from NSF that was awarded to our group to pursue and expand our activity in the ultrafast science and technology domain. GRA

N93-14415# Naval Surface Warfare Center, Dahlgren, VA.
USE OF KINEMATIC CONSTRAINT IN TRACKING CONSTANT SPEED MANEUVERING TARGETS
W. D. Blair, G. A. Watson, and A. T. Alouani Nov. 1991 68 p
(AD-A255988; NAVSWC-TR-91-561) Avail: CASI HC A04/MF A01

The use of a kinematic constraint as a pseudomeasurement in the tracking of constant speed maneuvering targets is considered in this report. The kinematic constraint provides additional information about the target motion that can be processed as a pseudomeasurement to improve tracking performance. The kinematic constraint for constant speed targets is A - V = 0, where A and V are the target acceleration and velocity vectors, respectively. In previous publications, the measurement equation for processing the kinematic constraint as a pseudomeasurement was derived by a direct application of Taylor's theorem for a first order linearization of that pseudomeasurement equation. A new formulation of the constraint equation that provides significantly better tracking performance than the previous formulation is presented, and the rationale for the new formulation is discussed. The filter using the kinematic constraint for constant speed targets is shown to be unbiased and stochastically stable. Simulated tracking results are given to show the potential for further improving the performance of a track filter through the use of the proposed kinematic constraint. Simulation studies are presented for various data rates, levels of measurement errors, and deviations in speed. GRA

N93-14426# Massachusetts Inst. of Tech., Lexington.
A MULTIPLE-APERTURE MULTIPLE-BEAM EHF ANTENNA FOR SATELLITE COMMUNICATIONS
Lawrence W. Rispin and David S. Besse 13 Aug. 1992 36 p
(Contract F19628-90-0002)
(AD-A256020; MIT-TR-957; ESC-TR-92-072) Avail: CASI HC A03/MF A01

Measurements on an experimental model of a 127-beam multiple-aperture EHF antenna are reported. Featuring a hexagonal arrangement of seven individual multiple-beam lens antennas, the 44-GHz antenna array was designed for adaptive nulling applications in which 14 beams could be accessed to simultaneously provide 1.50 theater coverage and two independent agile beams. Antenna pattern and gain measurements for all 127 beams and results from simulated nulling experiments using a simple mechanically driven weighting network are discussed. Null depths of 30 dB and nulling resolutions of 0.1 deg are shown. The measurement results support the viability of this type of adaptive antenna system. GRA

N93-14437# Minnesota Univ., Minneapolis. Dept. of Electrical Engineering.
OPTICAL SIGNAL DISTRIBUTION SCHEMES FOR MILLIMETER PHASED ARRAY RADAR Final Report
Ali Ghiasi and Anand Gopinath May 1992 145 p
(Contract F19628-88-K-0007)
(AD-A256262; RL-TR-92-104) Avail: CASI HC A07/MF A02

The goal is the modulation of lasers above the -3dB modulation bandwidth. The approach is to coat one laser facet with an anti-reflection coating and form an external cavity. The external cavity laser was built and characterized theoretically. An impedance-matching microstrip was designed and measured. An 8 GHz oscillator was built using a 0.3 micron

MESFET. It was found that the optical feedback increases the light modulation depth by 25 dB on the first harmonic and 34dB on the second harmonic in external cavity laser diodes. The model, which has proven accurate thus far, indicates that diode parasitics make it preferable to use the second harmonic generated by a 30 GHz cavity, rather than the first harmonic from a 60 GHz cavity. GRA

N93-14442# Naval Postgraduate School, Monterey, CA.
A COMPLETE-TIME APPROACH FOR CHAINING AND EXECUTION CONTROL IN THE AN/UYS-2 PARALLEL SIGNAL PROCESSOR M.S. Thesis
Harold A. Bell Jun. 1992 78 p
(AD-A256306) Avail: CASI HC A05/MF A01

The AN/UYS-2 represents the US Navy's effort to meet the signal processing demands of the 21st century. It is programmed using the Processing Graph Methodology (PGM), where signal processing applications are represented as graphs and the nodes specify library primitives. Presently the AN/UYS-2 incorporates a first-come-first-serve run-time technique to allocate system resources to support large-grain data-flow execution. While this technique results in low run-time overhead, the system throughput degrades rapidly under high system load. To provide uniform output even under high load, a compile-time technique, called Revolving Cylinder (RC) Analysis, is developed further to identify optimal chains and restructure the graph. It is shown by simulation that such chaining and restructuring improve the overall system performance. GRA

N93-14453# Tetra Corp., Albuquerque, NM.
A QUASI-EQUILIBRIUM KINETIC MODEL OF HF AIR BREAKDOWN Final Report, Feb. - Sep. 1991
A. E. Rodriguez and M. G. White Sep. 1991 81 p
(Contract DAAL02-91-C-0025)
(AD-A256240; TETRA-TR91-17) Avail: CASI HC A05/MF A01

In Phase 1 of the program, we developed the basic tools needed to build a high-frequency air breakdown model. We developed a Quasi-Equilibrium Methodology (QEM) for extending fluid electron transport models to the nonequilibrium regime, based on assuming that the transport coefficients relax toward their equilibrium values on time scales quantified by time-dependent Boltzmann equation solutions. Our analysis of nonequilibrium electron transport discovered and explained a velocity overshoot effect that is not generally known. That tendency of the electrons to overshoot the equilibrium drift velocity is shown to have a profound effect on streamer behavior. We examined the extent of possible simplifications to our kinetic air breakdown model, concluding that factors of 2 to 5 speed-up are possible. We have identified the major phenomenological issues in a modeling strategy, and examined nonequilibrium effects on ionization waves. Finally, we present a plan to complete development of a computational model of High Frequency air breakdown suitable for incorporation into EMP coupling codes, including model verification experiments and implementation of the computer module in an existing EMP coupling code. GRA

N93-14488# Mitre Corp., Bedford, MA.
AIRBORNE RADAR SIMULATION WITH ADAPTIVE ANTENNA TECHNIQUES
B. N. SureshBabu and J. A. Torres Jul. 1992 12 p
(AD-A255460; M92B0000083) Avail: CASI HC A03/MF A01

This document presents a reprint of a conference paper given at the Summer Computer Simulation Conference (SCSC) held in Reno, Nevada. It describes a flexible general airborne radar simulation with adaptive space-time processing (STP) antenna techniques for clutter and jammer suppression. This paper presents parametric performance curves for different array configurations and different suboptimal STP architectures. GRA

N93-14490# Naval Oceanographic and Atmospheric Research Lab., Bay Saint Louis, MS.
INVESTIGATION OF THE USE OF SURFACE ELECTRICAL CURRENTS FOR SHORT-RANGE SHIPBOARD DATA COMMUNICATIONS Final Report
F. B. Grosz, R. T. Miles, S. R. Griffin, and C. R. Holland Jun. 1992 14 p
(AD-A256197; NOARL-TN-268) Avail: CASI HC A02/MF A01

In January 1991, the Naval Oceanographic and Atmospheric Research Laboratory (NOARL) Code 252 undertook to investigate for NAVSEA PMS 400D52 the possibility of communicating data through a ship's bulkhead without penetrating the bulkhead physically. Four possible methods of transmission were identified: ultrasonic, electric current injection, magnetic coupling, and current carrier. Of these, the electric current injection method was selected as the most promising, and a device using this technique was developed. GRA

N93-14610# Naval Postgraduate School, Monterey, CA.
MODELING AND CONTROL OF A TRAILING WIRE ANTENNA TOWED BY AN ORBITING AIRCRAFT Ph.D. Thesis
James M. Clifton Sep. 1992 244 p
(AD-A256450) Avail: CASI HC A11/MF A03

A model of the dynamics of a long trailing-wire antenna towed behind an orbiting aircraft was developed and then an investigation was made of several candidate schemes to control the wire's steady-state shape and oscillations due to wind gradients. A computer simulation was developed using the classic vibrating chain with free/fixed boundary conditions superimposed upon the wire's steady-state shape and tension distribution. Several forms of restorative and dissipative forces were considered in the analysis. The validity of the superposition approach was demonstrated for a wide operating range. A control law was developed which modulated the towplane orbit radius and demonstrated a potential for a 50 percent or better reduction in all oscillations. A second scheme using a controllable drogue at the trailing end of the wire was investigated. The controllable drogue had a limited success in oscillation reduction, but was found useful in tailoring the steady state shape of the wire. GRA

N93-14649# Air Force Inst. of Tech., Wright-Patterson AFB, OH. School of Engineering.
AFIT/AFOSR WORKSHOP ON THE ROLE OF WAVELETS IN SIGNAL PROCESSING APPLICATIONS Final Report, 1 Oct. 1991 - 15 Sep. 1992
Bruce W. Suter, Mark E. Oxley, and Gregory T. Warhola 28 Aug. 1992 474 p Workshop held in Wright-Patterson AFB, OH, 12-13 Mar. 1992
(Grant AF-AFOSR-0019-92)
(AD-A256172; AFIT/EN-TR-92-3) Avail: CASI HC A20/MF A04

The Air Force Institute of Technology (AFIT) hosted a workshop on the Role of Wavelets in Signal Processing Applications on 12-13 Mar. 1992 at the AFIT Science and Research Center, Wright-Patterson AFB, OH. The workshop was sponsored by the Air Force Office of Scientific Research (AFOSR), Bolling AFB, DC. The major technical themes were as follows: (1) time/scale analysis versus frequency analysis of signals; and (2) filter bank structures versus discrete wavelet expansions. GRA

N93-14663# Naval Research Lab., Washington, DC.
SYSTEM DESIGN AND DEVELOPMENT OF A LOW DATA RATE VOICE (1200 BPS) RATE CONVERTER Interim Report, Jul. 1991 - Jun. 1992
J. P. Hauser 30 Sep. 1992 44 p
(DA Proj. RC3-2-A-13)
(AD-A256071; NRL/MR/5520-92-7136) Avail: CASI HC A03/MF A01

This report presents both a high level and a detailed design for a low data rate voice Rate Converter (RC). On the transmit side, converter reduces 2400 bps voice generated by an Advanced Narrowband Digital Voice Terminal (ANDVT) to a 1200 bps bit stream. On the receive Bide it converts the 1200 bps bit stream back to a 2400 bps stream in ANDVT format. Rate reduction is accomplished with little degradation to the inherent voice quality of the ANDVT. This primary focus is upon the real-time software design which is implemented using VxWorks, a real-time, multi-tasking operating system and development environment. The high level design defines four tasks, each having its own execution thread and its own pipe to facilitate inter-task communication. The Supervisor Task performs initialization and managers input of commands and data to the RC. The Compressor Task reduces a 2400 bps bit stream to 1200 bps while the Decompressor Task converts from 1200 bps back to 2400 bps. The Output Task manages the output of data from the RC. Latter sections of this report describe the software in detail. GRA

N93-14728# Dayton Univ., OH.
DIRECT OPTICAL TO MICROWAVE CONVERSION Final Report, Apr. 1990- Jul. 1991
Henry F. Taylor (Texas A&M Univ., College Station.) Dec. 1991 19 p

(Contract F30602-88-D-0028; AF Proj. 2853)
(RL-TR-91-375) Avail: CASI HC A03/MF A01

A traveling wave (TM) photodetector with a coplanar stripline structure was designed and fabricated in semiinsulating GaAs. Ohmic Au/Ge/Ni contacts were formed by a thermal annealing process. Testing was accomplished using an optical delay line arrangement to achieve either matching or mismatching of the microwave phases of the optical inputs and the microwave output signal. For the phase-matched case, the optical inputs are coherently combined to produce the TW photodetector output. The observed average microwave output power over the frequency range 0.5-5 GHz was 11 dB greater for four identical inputs than for a single input. This compares with an ideal value of 12 dB for the power increase. For the unmatched case, the TW photodetector operates as transversal filter, with the fundamental frequency determined by the optical/microwave time-delay mismatch. Experimentally, a fundamental frequency of 4.3 GHz was observed for two, three, or four optical inputs. The expected sidelobe pattern was seen in each case. Author

N93-14742 Department of the Navy, Washington, DC.
METHOD AND APPARATUS FOR INCREASING A RADAR'S RANGE WITH IMPROVED SCAN-TO-SCAN INTEGRATION OF DOPPLER FILTERED SIGNALS Patent
William M. Waters, inventor (to Navy) 21 Apr. 1992 14 p Filed 22 Jun. 1990
(AD-D015421; US-Patent-5,107,270; US-Patent-Appl-SN-541991; US-Patent-Class-342-111) Avail: CASI HC A03/MF A01

Method and apparatus for improving detection ranges of a pulsed radar system wherein electromagnetic return signal data in range cell order is Doppler filtered, digitized, and stored in Doppler memory channels over multiple scans of an azimuth. The digital doppler data in each Doppler memory channel is scan-to-scan integrated over a predetermined number of scans to produce target displays for each possible velocity. The target displays are stored in a velocity memory, which is partitioned into velocity channels, each velocity channel corresponding to one possible velocity. A selector selects the target display having the largest total magnitude as a display signal. The scan-to-scan integrated target displays are not subject to collapsing losses since only target signals plus noise signals will be stored in the doppler memory channel corresponding to the target's velocity. GRA

N93-14805# Physics and Electronics Lab. TNO, The Hague (Netherlands).
DEFINITION STUDY PHARUS Final Report
P. Hoogeboom, P. J. Koomen, W. P. Keizer, M. P. Otten, and M. H. Paquay Nov. 1991 108 p
(AD-A256560; FEL-91-A375; TDCK-91-3982) Avail: CASI HC A06/MF A02

This report describes the results of the PHARUS definition stage which can be distinguished in three main parts: antenna technology study, motion compensation study, realization of a SAR. The antenna technology study was mainly focussed on the theory and design of patch antennae. Further the study included the theory of internal calibration of SAR systems, microwave components under pulsed conditions and measurements of phased arrays under operational conditions. The second study was focussed on finding a solution for the motion compensation in PHARUS. The study included the development of a SAR data simulator to evaluate the degradation of the SAR image by the motion of the aircraft. A motion sensor package for PHARUS was proposed. For verification, this motion sensor package was used in the SAR testbed. GRA

N93-14806# Physics and Electronics Lab. TNO, The Hague (Netherlands).
SHORT RANGE PROPAGATION MEASUREMENTS AT 2.4, 4.5, AND 11.5 GHz IN INDOOR AND OUTDOOR ENVIRONMENTS
G. J. Janssen May 1992 106 p
(AD-A256563; FEL-92-B154; TDCK-92-1439) Avail: CASI HC A06/MF A02

This report concerns the project SHF Indoor/Outdoor Propagation Measurements, which has been carried out in cooperation with the Technical University of Delft. Within this project a measurement system has been developed at FEL for wideband coherent propagation measurements (complex frequency response/channel impulse response). Measurements have been carried out at 2.4, 4.75 and 11.5 GHz in indoor (office and conference rooms) and outdoor (forest and open terrain) environments at distances within pico-cellular dimensions (less than 50 m). For the outdoor measurements a special technique has been applied to extend the range to distances greater than 30 m. In total over 1000 measurements have been performed under different conditions. In this report details on the measurement system that was used, and measurement results on path-loss, delay time spread RRMS and the influence of people on the channel (indoor situation), are presented. The measurement results that are available now, form a good basis for further theoretical research and validation of this work, as well as for practical application research. GRA

N93-14879# Department of the Navy, Washington, DC.
LAYERED PARALLEL INTERFACE FOR AN ACTIVE ANTENNA ARRAY Patent Application
William M. Waters, inventor (to Navy) 24 Jul. 1992 30 p
(AD-D015411; US-Patent-Appl-SN-903316) Avail: CASI HC A03/MF A01

A transmit/receive layer is provided adjacent to an array of antenna elements. The transmit/receive layer has an array of transmit receive modules, each module associated with one of the antenna elements. An analog to digital converter and a digital to optical converter of one of the modules couple an RF signal from the associated antenna element to optical fibers. An optical to RF converter in each of the modules converts an amplitude modulated optical transmit signal from an optical fiber to an RF transmit signal for transmission by the associated antenna element. Frequency down and up converters can be added to perform super heterodyne frequency conversion based on a reference frequency control signal transmitted over the optical fibers. At the ends of the optical fibers opposite to the transmit/receive layer, a receive layer, a transmit layer, transmit and receive beamforming layers, dedicated signal synthesizer, control signals, and amplitude modulated optical diode lasers and photodiodes are provided. GRA

N93-14889# Department of the Navy, Washington, DC.
MECHANICAL SHIELDING FOR ELECTRIC PRIMER Patent Application
Raymond J. Goetz, inventor (to Navy) 27 Apr. 1992 19 p
(AD-D015417; US-Patent-Appl-SN-874156) Avail: CASI HC A03/MF A01

An electric primer for cartridge ammunition (e.g., Phalanx 20 mm cartridges) is designed to minimize antenna coupling, capacitive coupling, and aperture coupling of stray electromagnetic radiation thereinto for avoiding accidental primer detonation with resulting ignition of cartridge propellant. The primer is provided with a button electrode which is deeply recessed totally behind a small diameter access aperture which physically guards the button electrode from antenna and capacitive coupling. Furthermore, the small opening channels stray radiation about its periphery rather than admitting it to the button. GRA

N93-15095# Universiteit Twente, Enschede (Netherlands). Tele-Informatics and Open Systems Group.
THE EVOLUTION OF SIGNALLING FROM ISDN TO B-ISDN
I. G. Niemegeers and G. J. Heijenk Apr. 1992 13 p Presented at America's Telecom Technical Symposium, Acapulco, Mexico, 4-6 Apr. 1992 Submitted for publication
(Memo-INF-92-30; TIOS-92/13; ETN-92-92443) Copyright Avail: CASI HC A03/MF A01

Issues in B-ISDN (Broadband-Integrated Services Digital Network) signaling are clarified and directions for solutions are discussed. Signaling is one of the key elements in the provision of services by modern telecommunication systems. Where the introduction of ISDN can still be regarded as a straightforward evolution from the world of telephony, B-ISDN, represents a radical departure. The scope of the services to be offered in the target B-ISDN is much wider, and the underlying technology, such as ATM (Asynchronous Transfer Mode), is vastly different. This results in requirements for signaling which cannot be met by the present systems such as SS7 (common channel Signaling System) and DSS1 (Digital Subscriber Signaling). The new requirements are examined and some of the directions presently being investigated for supporting the target B-ISDN are analyzed. ESA

N93-15097# Ecole Nationale Superieure des Telecommunications, Paris (France). Groupe de Recherches et d'Etudes en Telecommunication et Systemes Aerospatiaux.

INTEGRATION OF SATELLITE LINKS INTO AN ATM MODE BROADBAND ISDN Ph.D. Thesis [INTEGRATION DES LIAISONS PAR SATELLITES DANS UN RNIS LARGE BANDE FONCTIONNANT EN MODE ATM]

Tarif ZeinalAbedeen 1991 166 p In FRENCH

(TELECOM-Paris-91-E-022; ETN-92-92551) Copyright Avail: CASI HC A08/MF A02

The role that can be played by satellites in European Broadband Integrated Services Digital Network (B-ISDN) development is analyzed. In particular, the future use of satellites is shown to be indispensable during the transition phase since they will allow the targeted network a sufficient connectivity level in a relatively short delay. Satellites are also particularly adaptable to such services as broadcasting or mobile communications. Nevertheless, to integrate satellites into the broadband network, high output digital links and adaptation to multiple access ATM (Asynchronous Transfer Mode) are necessary. Existing satellites are shown to be well adapted to the output problem and solutions for the next generation of satellites to allow them to offer higher output at lower cost are proposed. A new multiple access technique called anticipated reservation access which reduces transmission delay and the impact of the satellite in the ground network is proposed. A connection acceptance algorithm which guarantees performance threshold is also proposed. ESA

N93-15098# Ecole Nationale Superieure des Telecommunications, Paris (France).

ON THE THEORY OF CODED MODULATION SYSTEMS FOR HIGH OUTPUT DIGITAL TRANSMISSION Ph.D. Thesis [SUR LA THEORIE DES SYSTEMES DE MODULATION CODEE POUR LA TRANSMISSION NUMERIQUE A DEBIT ELEVE]

Helio MagalhaesdeOliveira 1992 243 p In ENGLISH and FRENCH Sponsored by Univ. Federale de Pernambouc, Brazil and ARECOM

(TELECOM-Paris-92-E-001; ETN-92-92552) Copyright Avail: CASI HC A11/MF A03

The problem of carrier phase recovery is addressed in the case of Trellis Coded Modulation (TCM), resulting in a differentially coherent TCM. An optimum binary labeling of the symbols in square constellations is introduced and a family of generalized cross constellations is studied. Tight bounds on their performance are developed and their spectral efficiency is evaluated. By means of the Minkowski-Hlawska theorem of the geometry of numbers, a capacity theorem for lattice codes over the additive white Gaussian noise channel, including its negative statement (strong converse), is proved, establishing the existence of deterministic means (highly structured codes) to approach capacity. Bounds in the performance of lattice codes are obtained. An improvement of Forney's continuous approximation used in order to estimate the mean normalized two dimensional power is suggested. In particular the behavior of these bounds is analyzed for high dimensionalities, leading to the conjecture that the problem of approaching capacity is connected with searching for good coverings rather than for dense packings. Emphasis is then put on coding modulation for a finite number of dimensions. Shannon's random coding argument and Battail's criticism of the minimum distance criterion are applied. Euclidean distance spectra of several coding modulation schemes are evaluated. A phenomenon of normalized distance 'hardening' is found when the dimensionality increases, which can be interpreted as a kind of Varshamov-Gilbert bound on the Euclidean distance. The statement 'all codes are good' is shown to still hold for the coded constellations. The investigations result in proposing a better overview on the asymptotic behavior of coded modulation. ESA

N93-15106# Air Force Inst. of Tech., Wright-Patterson AFB, OH. Foreign Aerospace Science and Technology Center.

A NEW MULTIPLIER-FREE STRUCTURE FOR DFT BASED ON DELTA MODULATION

Tang Kaijun, Siang Jingcheng, and Huang Shunji 29 Aug. 1992 26 p Transl. into ENGLISH from Dianzi Xuebao (China), v. 9, no. 1, Jan. 1987 p 1-10

(AD-A255927; FASTC-ID(RS)T-1060-91) Avail: CASI HC A03/MF A01

A new implementation of the DFT based on delta modulation (DM) is proposed. It is different from the conventional implementation based on PCM. The hardware structure of the method is constructed without A/D converter and multiplier, so it is simpler and of lower cost. Its SNR can approach that of the conventional one, such as FFT. Computer simulations demonstrate that for deterministic signals, results obtained agree well with theoretical analyses, for band-limited Gaussian signals; if step size is suitably selected, results similar to the conventional DFT can still be obtained. Because of the limitation of the working speed of the device, this method will be suitable for processing speech and seismic signals. Finally, the hardware structure which simply consists of a ROM, an adder, and some other auxiliary circuits is given. GRA

N93-15220# Office of Radiation Programs, Montgomery, AL. National Air and Radiation Environmental Lab.

MEASUREMENTS OF ELECTRIC AND MAGNETIC FIELDS IN THE WAIANAE, HAWAII AREA

Edwin D. Mantiply Jul. 1992 47 p

(DE92-019891; EPA-400R-92-009) Avail: CASI HC A03/MF A01

During November 27 to 30, 1990, the U.S. EPA conducted a measurement survey of electric and magnetic field levels along the southwest coast of Oahu, Hawaii. These measurements were requested by the State of Hawaii to determine the levels of radiofrequency (RF) electric and magnetic fields near Naval radio transmitters at Lualualei. The objective was to determine maximum fields in residential areas. This report documents the measurement results. Also, a few measurements were made of extremely-low-frequency (ELF) electric and magnetic fields at 60 hertz, the frequency used for electrical power. DOE

N93-15237# Naval Postgraduate School, Monterey, CA.

RADAR DATA PROCESSING USING A DISTRIBUTED COMPUTATIONAL SYSTEM Ph.D. Thesis

Gilberto F. Mota Jun. 1992 227 p

(AD-A256209) Avail: CASI HC A11/MF A03

This research specifies and validates a new concurrent decomposition scheme, called Confined Space Search Decomposition (CSSD), to exploit parallelism of Radar Data Processing algorithms using a Distributed Computational System. To formalize the specification, we propose and apply an object-oriented methodology called Decomposition Cost Evaluation Model (DCEM). To reduce the penalties of load imbalance, we propose a distributed dynamic load balance heuristic called Object Reincarnation (OR). To validate the research, we first compare our decomposition with an identified alternative using the proposed DCEM model and then develop a theoretical prediction of selected parameters. We also develop a simulation to check the Object Reincarnation Concept. GRA

N93-15316# Air Force Inst. of Tech., Wright-Patterson AFB, OH. School of Engineering.

COMPARISON OF SYNCHRONIZATION TECHNIQUES FOR THE AFIT DIRECT SEQUENCE SPREAD SPECTRUM SYSTEM Final Report

Edward A. Bednar 21 Apr. 1992 82 p

(AD-A256440; AFIT/GE/ENG/92J-01) Avail: CASI HC A05/MF A01

The performance was analyzed and evaluated of several code synchronization methods that could be used in the Air Force Institute of Technology's (AFIT) Direct-Sequence Spread Spectrum (DSSS) communication system. These methods include the sliding correlator, transmitted reference, sequential estimation, and three types of matched filters. The matched filters are the baseband matched filter, delay line matched filter, and the convolver. The criteria used for the evaluation of these synchronization methods are theoretical synchronization times and probability of bit-error. Advantages and disadvantages of each synchronization method are described and a method is recommended to be tested in the existing AFIT DSS system prototype. The effect of adding a PLL circuit to the AFIT system needs to be studied, especially the effect on the bit-error curve measured by James Stephens when he built the AFIT system. A matched filter convolver should be added in place of the synchronous oscillator. GRA

N93-15317# Air Force Inst. of Tech., Wright-Patterson AFB, OH. School of Engineering.

CO-CHANNEL SPEAKER SEPARATION M.S. Thesis

Thomas S. Andrews Sep. 1992 100 p

(AD-A256443; AFIT/GE/ENG/92S-07) Avail: CASI HC A05/MF A02

In the co-channel speaker separation problem, the goal is to recover two separate speech signals from a monaural channel which contains the

sum of the two speech signals. A new methodology is developed that if given that a segment of co-channel speech is separated into a stronger and weaker segment, the correct assignment of these separated segments to the appropriate talker can be made using a Linear Predictive Coding (LPC) based minimum-prediction residual computation. The uniqueness of the developed technique is that no a priori information is required of the co-channel speech signal. The information needed to appropriately assign these separated segments from the co-channel speech signal are clean speech that is separate from the co-channel speech signal that are used to compute model LPC vectors. This clean speech is derived from the same channel that the co-channel speech signal is derived from. This technique has shown the ability to correctly assign the given stronger and weaker segments to the appropriate talker at signal-to-signal ratios down to equal power levels. The resulting separated speech is clearly understandable, and the interfering talker's speech signal is effectively eliminated. GRA

N93-15334# Northwest Research Associates, Inc., Bellevue, WA.
NEW METHODS FOR NONLINEAR TRACKING AND NONLINEAR CHAOTIC SIGNAL PROCESSING Progress Report No. 1, 26 Jul. - 25 Aug. 1992
Jon A. Wright 11 Sep. 1992 8 p
(Contract N00014-92-C-0043)
(AD-A256421) Avail: CASI HC A02/MF A01

The aim was to identify and/or classify the individual signals that make up the total signal. The algorithm can function either as a detection algorithm or as an algorithm for preliminary processing leading to actual separation and cleaning of signals. It is not currently possible to do this latter task, even in the simplest situation, without first determining what signals are to be separated. We imagine that we have a library of samples of signals from sources of interest. An incoming signal is received that is a sum of one or more of the signals in the library plus noise, and we wish to determine which signals are actually present (i.e., we want to identify the source of the signal) and what are the relative amplitudes of the signals. We assume that some, perhaps all, of the signals have a broad frequency spectrum so that conventional linear filtering is inadequate. It is further assumed that we have samples of the individual signals in a library, although if they are broadband chaotic, the signals will not be identical. One or more of the signals may be noise with its own characteristics. To illustrate that we can actually accomplish this, results are presented of some simulations. In the figures are some samples of the signals we have been working with. GRA

N93-15339*# Cornell Univ., Ithaca, NY. Dept. of Computer Science.
NONBLOCKING AND ORPHAN FREE MESSAGE LOGGING PROTOCOLS
Lorenzo Alvisi, Bruce Hoppe, and Keith Marzullo Dec. 1992 24 p
(Grant NAG2-593)
(NASA-CR-191631; NAS 1.26:191631; TR-92-1317) Avail: CASI HC A03/MF A01

Currently existing message logging protocols demonstrate a classic pessimistic vs. optimistic tradeoff. We show that the optimistic-pessimistic tradeoff is not inherent to the problem of message logging. We construct a message-logging protocol that has the positive features of both optimistic and pessimistic protocol: our protocol prevents orphans and allows simple failure recovery; however, it requires no blocking in failure-free runs. Furthermore, this protocol does not introduce any additional message overhead as compared to one implemented for a system in which messages may be lost but processes do not crash. Author

N93-15376# Army Communications-Electronics Command, Fort Monmouth, NJ.
TACTICAL LINE-OF-SIGHT PATH RELIABILITY: IMPROVED MSE SYSTEM PROCEDURES
Kenneth D. Chaney, Kenneth H. Brockel, William T. Barnett, Joseph R. Inserra, and Robert J. Locher Apr. 1992 83 p
(AD-A256504; CECOM-TR-92-1) Avail: CASI HC A05/MF A01

Mobile Subscriber Equipment (MSE) provides digital voice, data, and packet-switched tactical communications for Army corps and division areas of coverage deployed anywhere in the world. Line-of-sight (LOS) links in MSE must operate satisfactorily in all climates and terrains; however, difficult propagation environments (e.g., that encountered in Southwest Asia) can diminish link reliability. This report describes enhancements to MSE operating procedures to address this problem. The enhanced procedures call for the user to specify the propagation reliability desired on a link, e.g., 99.9 percent. The corresponding required margin is then calculated as a function of link parameters such as path length and climate. The margin achieved during link initialization is measured, reported, and compared to the required margin as the basis for link acceptance. Also, since propagation-caused problems can not be cured by the current practice of replacing equipment, enhanced troubleshooting procedures are described. Although this report utilizes the MSE framework and terminology, the methodology and recommendations are applicable to any LOS digital radio system. GRA

N93-15397# Rome Lab., Hanscom AFB, MA.
ANALYTICAL CHARACTERIZATION OF BISTATIC SCATTERING FROM ROUGH SURFACES: DEPENDENCE ON SURFACE CORRELATION FUNCTION Report, period ending 31 Mar. 1992
Lisa M. Sharpe Jun. 1992 56 p
(AF Proj. 2305)
(AD-A256525; RL-TR-92-134) Avail: CASI HC A04/MF A01

Analyses of the statistical properties of electromagnetic scattering from random rough surfaces for finite clutter cells have assumed that the rough surface can be modeled by a Gaussian correlation function. However, some real surfaces are more accurately described by correlation functions other than Gaussian. In this study, the effect of decreasing the clutter cell size is examined for power law and exponential, as well as Gaussian correlation functions for a one dimensionally rough surface. Results show that for a Gaussian correlated surface and a surface described by a power law correlation the scattering statistics are similar and deviate significantly from Rayleigh with decreasing cell size, particularly in the backscatter region. For exponentially correlated surfaces, however, the statistics of the scattering are not changed when the cell size is decreased. This is important because urban areas are described by an exponential correlation function. GRA

N93-15427# Los Alamos National Lab., NM.
DETERMINISTIC TRANSFER FUNCTION FOR TRANSIONOSPHERIC PROPAGATION
R. Roussel-Dupre and P. Argo 1992 7 p Presented at the Beacon Satellite Symposium, Boston, MA, 5-12 Jul. 1992
(Contract W-7405-eng-36)
(DE92-040327; LA-UR-92-2607; CONF-9207118-2) Avail: CASI HC A02/MF A01

Recent interest in ground-to-satellite propagation of broadband signals has prompted investigation into the development of a transfer function for the ionosphere that includes effects such as dispersion, refraction, changes in polarization, reflection, absorption, and scattering. Depending on the application (e.g. geolocation), it may be necessary to incorporate all of these processes in order to extract the information of interest from the measured transionospheric signal. A transfer function for midlatitudes at VBF from 25 - 175 MHz is one of the goals of the BLACKBEARD program in characterizing propagation distortion. In support of this program we discuss in this paper an analytic model for the deterministic transfer function of the ionosphere that includes the effects of dispersion, refraction, and changes in polarization to second order in the parameter X = omega(sub pe)(exp 2)/(omega)(exp 2) where X is assumed to be small compared to one, (omega)(sub pe) is the peak plasma frequency of the ionosphere, and omega is the wave frequency. Analytic expressions for the total phase change, group delay, and polarization change in a spherical geometry assuming a radial, electron density profile are presented. A computer code ITF (Ionospheric Transfer Function) that makes use of the ICED (Ionospheric Conductivity and Electron Density) model to, venerate electron density profiles was developed to calculate the ionospheric transfer function along a specified transmitter-to-receiver path. Details of this code will be presented as well as comparisons made between ITF analytic results and ray-tracing calculations. DOE

N93-15435# Los Alamos National Lab., NM.
SATELLITE MEASUREMENT OF IONOSPHERIC-INDUCED VHF DISTORTION
W. T. Armstrong, T. Murphy, R. Roussel-Dupre, M. J. Carter, and B. Blevins 1992 5 p Presented at the Beacon Satellite Symposium, Boston, MA, 5-12 Jul. 1992

(Contract W-7405-eng-36)
(DE92-040328; LA-UR-92-2608; CONF-9207118-3) Avail: CASI HC A01/MF A01

BLACKBEARD is a satellite RF experiment designed to study distortion and interference effects on transient transionospheric VHF signals. RF distortion will be characterized by a frequency-coherence bandwidth for different ionospheric conditions. Limitations of broad-band measurements from the frequency-coherence bandwidth of the ionosphere and broadcast interference signals will be established through these studies. Distinction between multi-path distortion resulting from large scale, coherent perturbations and small scale, random perturbations to the ionosphere will be emphasized. Ionospheric transfer function models, trans-ionospheric signal predictions, and coherence bandwidth predictions will be tested and optimized with these measurements. A global data base for both broadcast and lightning interference will also derive from these studies. This database will form the basis for interference feature extraction, signal typing, and possible neural network cataloging. The specific missions of the BLACKBEARD experiment include: perform broad-band VHF measurements of transient signals originating from a controlled pulsed ground beacon, to characterize broad-band ionospheric distortion, perform narrow-band VHF measurements of cw signals from a multi-chord interferometry ground beacon array, to characterize ionospheric structure contributing to transmission distortion, and survey power envelopes of lightning and man-made interference in selectable VHF bands, for background rejection purposes. BLACKBEARD is part of the ALEMS soft x-ray measurement satellite, a small satellite system designed for a PEGASUS launch into a 70 deg inclination, low earth orbit in late 1992. DOE

N93-15440# Oak Ridge National Lab., TN.
A POWER COMPENSATION SYSTEM FOR PHASED OPERATION OF THE JET A2 ANTENNA ARRAYS
R. H. Goulding, D. J. Hoffman, P. M. Ryan, V. Bhatnagar, G. Bosia, and T. J. Wade 1992 4 p Presented at the 17th Symposium on Fusion Technology, Rome, Italy, 14-18 Sep. 1992
(Contract DE-AC05-84OR-21400)
(DE92-041020; CONF-920930-1) Avail: CASI HC A01/MF A01

A large power transfer can occur between the coupled elements of the four-strap JET A(sub 2) antennas during operation with the elements phases at other than 0 or mu. This transfer reduces the effective input resistance R(sub c) of the element most lagging in phase and can even drive it negative, making matching to the transmitter impedance difficult or impossible. Large inequalities in the input powers to the four straps are also required if nearly equal current amplitudes on the radiating sections are to be obtained. A system for power compensation has been devised to counter this effect, which circulates power in the direction opposite to that occurring at the antennas. It is designed to work with the present RF control system, which provides automatic matching and continuous control of phase and amplitude of the antenna element currents. Cascades coupled transmission line models of the A(sub 2) antenna array and feed circuits have been developed, including the power compensation system. The design of this system is discussed, together with predicted performance based on modeling results. DOE

N93-15470# Georgia Inst. of Tech., Atlanta. School of Electrical Engineering.
JSEP FELLOWSHIP Final Report, 1 Jul. 1989 - 30 Jun. 1992
James G. Maloney 17 Sep. 1992 6 p
(Contract DAAL03-89-G-0078)
(AD-A257021; T-87-109; ARO-27006.2-EL-F) Avail: CASI HC A02/MF A01

The objective of this research was to study the mechanisms of transient radiation by various antenna structures, and to apply to understanding gained to the design of new, better transient antennas. The approach chosen for this research program was to extend the finite-difference time-domain (FDTD) numerical method to antenna analysis and to use the developed methodology to study/design transient antennas. GRA

N93-15487# Messerschmitt-Boelkow-Blohm G.m.b.H., Munich (Germany).
MODELING LIMITS OF THE EMV ANALYSIS PROGRAM CONCEPT BY EXAMPLE OF THE INFLUENCE OF A HELICOPTER STRUCTURE ON A FRAME ANTENNA [MODELLIERUNGSGRENZEN DES EMV-ANALYSEPROGRAMMS CONCEPT AM BEISPIEL DES EINFLUSSES EINER HUBSCHRAUBERSTRUKTUR AUF EINE RAHMENANTENNE]
Wolfgang Tauber (Eurocopter G.m.b.H., Ottobrunn, Germany) 1992 15 p In GERMAN Presented at the 3rd Internationale Fachmesse und Kongress fuer Elektromagnetische Vertraeglichkeit, Karlsruhe, Germany, 25-27 Feb. 1992
(MBB-UD-0614-92-PUB; ETN-92-92109) Avail: CASI HC A03/MF A01

Examinations showed that the EMV (German acronym for electromagnetic compatibility) program CONCEPT can be perfectly used for solutions where wavelengths are much greater than helicopter dimensions. The emphasis is put on the necessity of carrying out the right model in the case of ill conducting helicopter structure modeling. The selection of rod radius is shown to be difficult. It is made easier by using alternating current resistance, in particular for good conducting structures. For complex arrangements, a large computer is to be used for the verification and the determination of exact values. ESA

N93-15495# Massachusetts Inst. of Tech., Cambridge. Research Lab. of Electronics.
RADAR SCENE GENERATION FOR TACTICAL DECISION AIDS Final Report, 1 May 1987 - 31 Jul. 1992
J. A. Kong 5 Oct. 1992 108 p
(Contract DACA39-87-K-0022)
(AD-A257069) Avail: CASI HC A06/MF A02

EMSARS (Electomagnetic Model of Scattering Applied to Remote Sensing) is an electromagnetic background scattering model developed at the Massachusetts Institute of Technology. The physical characterization of the terrain background is in terms of layered continuous random media and discrete scatterer models. Various theories and mathematical techniques such as the analytical Wave Theory with the Born Approximation and the Radiative Transfer Theory are used to solve the integral equations characterizing the electromagnetic scattering effects. We recently presented applications of the EMSARS model to millimeter wave scattering by vegetation. Tree is modeled as discrete scatterers with multiple size for the trunk, the branches and leaves, respectively. The leaves of coniferous trees, the branches, and the trunks are modeled as circular cylinders. For deciduous trees, the leaves are modeled as thin circular disks. The physical optics approximation is used to calculate the millimeter wave returns from circular disks while finite cylinder approximation is used for circular cylinders. Then, the branching structure and their orientation distributions are applied to obtain the radar returns from vegetation. The trunk is model as a circular cylinder with random surface roughness where geometrical optics approximation is used to calculate the radar return from the surface of trunk. Except the case in which the ground is illuminated, we only consider single scattering returns. Transmission loss factors, due to absorption and scattering, are included when computing the contribution from interior branches and leaves. Theoretical predictions are compared with the measurement data collected in Bend, Oregon by NVEOD using a 94 GHz radar. I.I.C.

N93-15624# Pennsylvania State Univ., University Park. Applied Research Lab.
THE INTELLIGIBILITY OF WORDS, SENTENCES, AND CONTINUOUS DISCOURSE USING THE ARTICULATION INDEX
R. A. DePaolis Oct. 1992 150 p
(Contract N00038-88-C-0051)
(AD-A256781; TR-92-04) Avail: CASI HC A07/MF A02

The purpose of this research was to investigate the effect of message redundancy upon intelligibility. The original methodology for the Articulation Index (AI) French and Steinberg, J. Acoust. Soc. Am., 19, 90-119, 1947 was used to examine the relation between words, meaningful sentences, and continuous discourse (CD). One primary consideration was to derive the relations between the three speech types with tightly controlled, highly repeatable experimental conditions such that any difference between them could be attributed solely to inherent contextual differences. One male speaker recorded 616 monosyllabic words, 176 meaningful speech perception in noise (SPIN) sentences, and 44 seventh-grade reading level

CD passages. Twenty-four normal hearing subjects made intelligibility estimates of the CD and sentences and identified words at each of 44 conditions of filtering and signal-to-noise ratio. The sentence intelligibility scores and continuous discourse intelligibility scores plotted versus the AI (transfer function) were within 0.05 AI of each other. The word recognition scores were considerably lower for equivalent AI values of both sentences and CD. GRA

N93-15636# Naval Postgraduate School, Monterey, CA.
A MIXED EXCITATION VOCODER WITH FUZZY LOGIC CLASSIFIER M.S. Thesis
James T. Moore Jun. 1992 93 p
(AD-A256834) Avail: CASI HC A05/MF A01

The aim of this thesis work is to explore the use of fuzzy systems in a speech coding and classification application. A mixed excitation LPC based speech coder is developed. The excitation classifier for the speech coder is then implemented using a fuzzy system. The fuzzy logic based classifier determines the type of excitation to be used in constructing the synthetic speech. The results of various implementations of this speech coder are presented for comparison. This work demonstrates that a fuzzy system can be developed and implemented for a classification problem. GRA

N93-15638*# Office of Space Science and Applications, Washington, DC.
DIRECTORY OF RESEARCH PROJECTS: PLANETARY GEOLOGY AND GEOPHYSICS PROGRAM
Henry Holt, ed. Dec. 1992 152 p
(NASA-TM-4428; NAS 1.15:4428) Avail: CASI HC A08/MF A02

Information about currently funded scientific research within the Planetary Geology and Geophysics Program is provided. The directory consists of the proposal summary sheet from each proposal funded under the program during Fiscal Year 1992. The sheets provide information about the research project, including title, principal investigator, institution, summary of research objectives, past accomplishments, and proposed new investigations. Author

N93-14931# Telesat Canada, Ottawa (Ontario).
NPR AND INTERMODULATION IN MOBILE SATELLITE SYSTEMS
Pat Amlekar *In* Canadian Space Agency, Proceedings of the Sixth CASI Conference on Astronautics 1990 15 p Previously announced in IAA as A91-34937 (For primary document see N93-14920 04-12)
Avail: Canadian Aeronautics and Space Inst., 222 Somerset St. W., Suite 601, Ottawa, Ontario K2P 0J1 Canada

N93-14933# COM DEV Ltd., Cambridge (Ontario).
AN OVERVIEW OF RADARSAT PAYLOAD TECHNOLOGIES
Arunas Macikunas and Michael Pley *In* Canadian Space Agency, Proceedings of the Sixth CASI Conference on Astronautics 1990 11 p Previously announced in IAA as A91-34939 (For primary document see N93-14920 04-12)
Avail: Canadian Aeronautics and Space Inst., 222 Somerset St. W., Suite 601, Ottawa, Ontario K2P 0J1 Canada

N93-14941# Dynacon Enterprises Ltd., Downsview (Ontario).
SPACE BASED RADAR: TEST OF LARGE SPACE STRUCTURES
W. G. Sincarsin, D. J. McTavish, G. B. Sincarsin, and Y. Soucy (Communications Research Centre, Ottawa, Ontario) *In* Canadian Space Agency, Proceedings of the Sixth CASI Conference on Astronautics 1990 14 p Previously announced in IAA as A91-34947 (For primary document see N93-14920 04-12)
Avail: Canadian Aeronautics and Space Inst., 222 Somerset St. W., Suite 601, Ottawa, Ontario K2P 0J1 Canada

N93-14954# Telesat Canada, Ottawa (Ontario).
A LOW BIT RATE FSK TECHNIQUE FOR SCPC SATELLITE COMMUNICATION SYSTEMS
Vladimir Shpilka *In* Canadian Space Agency, Proceedings of the Sixth CASI Conference on Astronautics 1990 36 p Previously announced in IAA as A91-34960 (For primary document see N93-14920 04-12)
Avail: Canadian Aeronautics and Space Inst., 222 Somerset St. W., Suite 601, Ottawa, Ontario K2P 0J1 Canada

N93-14958# Defence Research Establishment, Ottawa (Ontario).
PROGRESS IN DND'S SPACE-BASED RADAR R/D PROJECT
Brian C. Eatock *In* Canadian Space Agency, Proceedings of the Sixth CASI Conference on Astronautics 1990 12 p Previously announced in IAA as A91-34964 (For primary document see N93-14920 04-12)
Avail: Canadian Aeronautics and Space Inst., 222 Somerset St. W., Suite 601, Ottawa, Ontario K2P 0J1 Canada

N93-14960# Telesat Mobile, Inc., Ottawa (Ontario).
PROGRESS TOWARD A FULL SCALE MOBILE SATELLITE SYSTEM FOR CANADA
Orest S. Roscoe *In* Canadian Space Agency, Proceedings of the Sixth CASI Conference on Astronautics 1990 11 p Previously announced in IAA as A91-34966 (For primary document see N93-14920 04-12)
Avail: Canadian Aeronautics and Space Inst., 222 Somerset St. W., Suite 601, Ottawa, Ontario K2P 0J1 Canada

N93-14961# Spar Aerospace Ltd., Sainte-Anne-de-Bellevue (Quebec). Satellite and Communication Systems Div.
L-BAND ANTENNA DESIGN FOR MSAT MISSION
G. S. Gupta and Y. Patenaude *In* Canadian Space Agency, Proceedings of the Sixth CASI Conference on Astronautics 1990 6 p Previously announced in IAA as A91-34967 (For primary document see N93-14920 04-12)
Avail: Canadian Aeronautics and Space Inst., 222 Somerset St. W., Suite 601, Ottawa, Ontario K2P 0J1 Canada

N93-14962# Spar Aerospace Ltd., Toronto (Ontario).
NEXT GENERATION SATELLITE COMMUNICATIONS NETWORKS
P. J. Garland and F. J. Osborne (Department of Communications, Ottawa, Ontario) *In* Canadian Space Agency, Proceedings of the Sixth CASI Conference on Astronautics 1990 6 p Previously announced in IAA as A91-34968 (For primary document see N93-14920 04-12)
Avail: Canadian Aeronautics and Space Inst., 222 Somerset St. W., Suite 601, Ottawa, Ontario K2P 0J1 Canada

N93-14963# Spar Aerospace Ltd., Sainte-Anne-de-Bellevue (Quebec).
Ku-BAND ANTENNA DESIGN FOR MSAT MISSION
G. S. Gupta and P. Ilott *In* Canadian Space Agency, Proceedings of the Sixth CASI Conference on Astronautics 1990 13 p Previously announced in IAA as A91-34969 (For primary document see N93-14920 04-12)
Avail: Canadian Aeronautics and Space Inst., 222 Somerset St. W., Suite 601, Ottawa, Ontario K2P 0J1 Canada

33 ELECTRONICS AND ELECTRICAL ENGINEERING

Includes test equipment and maintainability; components, e.g., tunnel diodes and transistors; microminiaturization; and integrated circuitry.

For related information see also *60 Computer Operations and Hardware* and *76 Solid-State Physics.*

N93-14190 Virginia Polytechnic Inst. and State Univ., Blacksburg.
EFFECT OF INTERFACIAL THERMAL CONDUCTANCE AND FIBER ORIENTATION ON THE THERMAL DIFFUSIVITY/CONDUCTIVITY OF UNIDIRECTIONAL FIBER-REINFORCED CERAMIC MATRIX COMPOSITES Ph.D. Thesis
Hemanshu Devshankar Bhatt 1992 157 p
Avail: Univ. Microfilms Order No. DA9218503

The role of an interfacial barrier at the fiber-matrix interface in the heat conduction behavior of a uniaxial silicon nitride and the effect of fiber orientation on the heat conduction characteristics of carbon fiber-reinforced borosilicate glass was investigated. A composite with fibers having a carbon-rich coating of about 3 microns was chosen as the reference material. The fiber-matrix interface was then modified using fibers with no carbon coating and using hot-isostatic-pressure (HIP) after nitridation. The formation of an interfacial gap at the interface resulted in the dependence of thermal diffusivity/conductivity on the surrounding atmosphere. However, no

atmospheric effects were observed for composites with fibers without the carbon coating. HIP'ing increased the thermal diffusivity/conductivity of the composites due to densification of the matrix, crystallization of the fibers and increased physical contact at the interface. Removal of the interfacial carbon layer lowered the interfacial conductance considerably, due to decrease in the direct thermal contact between the fibers and the matrix. Interfacial contact conductance increased rapidly with increasing temperature in accordance with interfacial gap closure. These observations indicate that the heat conduction behavior was strongly affected by the existence of an interfacial thermal barrier. An analysis was conducted to determine the expression for the effective thermal conductivity of a uniaxially reinforced finite composite strip with insulated edges as a function of the angle between the fiber direction and the temperature gradient. Three carbon fiber-reinforced aluminoborosilicate glass composite specimens were used: thin, angled and thick rectangular. The thin specimens and the angled specimens represented the case of a composite infinite in extent. The thick rectangular specimens were expected to behave like a finite composite strip. For thin and angled specimens, the thermal conductivity dependence on fiber orientation showed excellent agreement with theoretical behavior predicted from the analysis of a semi-infinite plate. However, for thick specimens the thermal conductivity turned out to be much lower than for thin and angled specimens, especially for small fiber angles below 45 deg. Thermal conductivity values agreed very well with experimental values for the thick rectangular specimens for high fiber angles greater than 45 deg. Dissert. Abstr.

N93-14191 Keele Univ. (England).
ELECTRICAL CONDUCTIVITY MEASUREMENTS IN EVAPORATED CADMIUM TELLURIDE THIN FILMS Ph.D. Thesis
Bakar Binlsmail 1990 251 p
Avail: Univ. Microfilms Order No. BRDX96585

An investigation has been made into the electrical, optical, and structural properties of CdTe thin films. Capacitance measurements indicate that the films have a relative permittivity of 9.6 (Merck Patinal) and 10.68 (Balzers). The dark resistivity was found to be of the order of 10(exp 4) Ohm-m, with its precise value depending on the deposition conditions. From dc J-V measurements, at low fields hopping conduction has been observed particularly at low temperature, while at high fields space-charge-limited current and, for doped material, the Poole-Frenkel effect have been observed. In the space-charge limited region both a discrete level and an exponential trap distribution have been identified in evaporated CdTe thin films. The ac conductivity of these samples is proportional to omega(exp 5) where omega is the angular frequency and zeta is a temperature-dependent quantity; the value of zeta decreases with increase in temperature. An analysis of the low temperature results indicates that the mechanism of conduction is via hopping. The ac capacitance was dependent both on temperature and frequency, but became constant for all frequencies at low temperature and can be satisfactorily explained in terms of the model of Goswami and Goswami. Optical absorption studies have also been performed on CdTe thin films, and it has been shown that the optical band gap increases with the thickness of the films. X-ray diffraction studies showed that the films are microcrystalline with typical grain size 74 nm and with preferred orientation in the zone axes (111) direction. The micro-strain and the grain size of CdTe thin films depend on deposition parameters such as rate of evaporation, thickness and the substrate temperature. Dissert. Abstr.

N93-14246# Westinghouse Science and Technology Center, Pittsburgh, PA.
PROCESSING, FABRICATION, AND DEMONSTRATION OF HTS INTEGRATED MICROWAVE CIRCUITS Status Report Nos. 1 thru 4, 24 Jul. 1991 - 26 Jul. 1992
G. R. Wagner 26 Jul. 1992 13 p
(Contract N00014-91-C-0112; ARPA Order 7932)
(AD-A256109) Avail: CASI HC A03/MF A01

Volume comparisons were made between HTS microstrip transmission lines and other high Q electromagnetic structures and between HTS microstrip and high-performance multimode coupled dielectric resonator filterbanks. An assessment was made of the potential performance of HTS filterbanks for EW systems as compared with measured results to date using magnetostatic-wave (MSW) filterbanks. Assuming pulsed input signals centered at next-to-adjacent channels, we compared their rejection and the time-lapse required to attain this rejection. MSW filterbanks achieve a 55 dB rejection after about 400 nS. GRA

N93-14254# Naval Postgraduate School, Monterey, CA.
EXTENDED SURFACE HEAT SINKS FOR ELECTRONIC COMPONENTS: A COMPUTER OPTIMIZATION M.S. Thesis
John R. Gensure Jun. 1992 117 p
(AD-A256134) Avail: CASI HC A06/MF A02

Heat sinks consisting of individual fins and arrays of fins are used extensively throughout the Navy and industry. The fins serve to increase the surface area through which heat is transferred to the surrounding environment by natural convection. Extended surfaces or fins are commonly found on electronic components ranging from power supplies to transformers. The dissipation and subsequent rejection of potentially destructive self produced heat is an important aspect of electronic equipment design. Fin design theory is examined starting with the optimization of individual fin dimensions. The insights obtained are utilized in an investigation of the optimal number and spacing of elements in an array of fins. The results are implemented in a computer program written in ADA and compiled for use on IBM compatible machines. The program takes as inputs thermal and physical data and outputs an optimized fin configuration. GRA

N93-14410# Massachusetts Inst. of Tech., Cambridge. Research Lab. of Electronics.
ORGANIZATION OF WORKSHOP ON EMERGING TECHNOLOGIES FOR IN-SITU PROCESSING Final Report, 15 Mar. - 31 Aug. 1992
John Melngailis 31 Aug. 1992 78 p
(Contract F49620-92-J-0233)
(AD-A255977; AFOSR-92-0862TR) Avail: CASI HC A05/MF A01

The goal of the workshop was to bring together government, industrial and university representatives to assess the progress and future direction of in situ processing of semiconductors. Since the first NATO Workshop in this topic area (Cargese, Corsica in 1987) there has been surprising progress toward the industrial applications, particularly as exemplified by cluster tools and laser/ion beam real-time fabrication machines. The consensus of the workshop was that the economic implications of in situ processing are accelerating strongly, particularly for smaller countries (or even larger ones) where the costs of traditional semiconductor factories are growing at unacceptable rates. This problem and the potential solutions were the central themes of the conference. The talks by Larrabee, Saraswat and Prabhakar pointed to the need for future factories that are smaller and use flexible intelligent manufacturing. In semiconductor device manufacturing, in particular, smaller lots, cluster tools (i.e., in-situ processing), and tight process control will result in better contamination control and lower cost. The other talks of the conference provided specified examples of advances in in-situ processing that will contribute to making this vision of intelligent flexible manufacturing a reality. GRA

N93-14425# Columbia Univ., New York, NY. Microelectronics Science Lab.
ADVANCED LASER CHEMICAL PROCESSING FOR MICROELECTRONICS AND INTEGRATED OPTICS Final Report, 15 Jun. 1989 - 15 Jun. 1992
Richard M. Osgood, Jr. and Robert Scarmozzino 15 Aug. 1992 23 p
(Contract F49620-89-C-0088)
(AD-A255980; AFOSR-92-0866TR) Avail: CASI HC A02/MF A01

This report summarizes a three-year research effort to explore advanced laser-chemical processing for microelectronics and integrated optics. The main goals of the work have been: (1) to develop techniques for fabrication of integrated optical devices in GaAs multilayer and quantum well structures, and (2) to explore new and novel techniques of advanced semiconductor processing for microelectronics and optoelectronics. GRA

N93-14457# Virginia Univ., Charlottesville.
ELECTRONICALLY ACTIVE CYCLOCARBORANE-METAL-ARENE ASSEMBLIES Final Report
Russell N. Grimes 31 Jul. 1992 8 p
(Contract DAAL03-89-K-0105)
(AD-A256288) Avail: CASI HC A02/MF A01

The designed synthesis of stable, soluble macromolecular complexes incorporating MC2B3 subunits (in which M is a transition metal) was explored

in detail, with emphasis on the following: (1) the efficient preparation of viable building-block molecules such as Cp*Co(Et2C2B3H5) (Cp* = eta5-C5Me5); (2) the derivatization and tailoring of these via attachment of substituents (including organic functional groups) to the carborane rings; (3) the construction of multidecker stacks via a novel metal-promoted stacking process; (4) the linkage of stacked sandwiches via coupling, fusion, and other methods; and (5) initial studies on the preparation of electroactive or magnetoactive solid state materials from metallacarborane precursors. The synthesis of novel metallacarborane sandwiches that are direct structural analogues of metallocenes, and mixed-sandwich salts of the type Cp2M(+)(Et2C2Bn)2M' in which M and M' are transition metals was also achieved. Detailed studies of the molecular and electronic structures of many of the above systems were conducted via NMR, ESR, X-ray crystallography, and electrochemical methods. GRA

N93-14504# Naval Research Lab., Washington, DC.
BEAM TRAPPING IN A MODIFIED BETATRON WITH A LOCALIZED BIPOLAR ELECTRIC FIELD PULSE Interim Report
J. Mathew, C. A. Kapetanakos, S. J. Marsh, and D. Dialetis 24 Aug. 1992 51 p
(AD-A255414; NRL/MR/4795-92-7114; NRL/FR-4795-92-7114) Avail: CASI HC A04/MF A01

This paper describes a scheme for trapping the injected beam in a modified betatron accelerator using a localized inductive electric field pulse generated by a charged coaxial pulseline. The average canonical angular momentum (P(sub theta)) is not conserved in this scheme. Numerical simulations demonstrate trapping over a wide range of operating parameters. A 0.84-ohm, 45-ns water dielectric pulseline was built for testing the trapping concept. The pulseline is switched using triggered vacuum surface switches. By crowbarring the pulseline, its output is limited to a single bipolar pulse that has an approximately 22-ns rise time. GRA

N93-14534# Interuniversity Micro-Electronics Center, Leuven (Belgium).
GATE-ALL-AROUND DEVICE Final Technical Report, 5 Jul. 1991 - 4 Jul. 1992
P. Smeys and J. P. Colinge 4 Sep. 1992 65 p
(Grant AF-AFOSR-0360-90)
(AD-A255287; RHD-04) Avail: CASI HC A04/MF A01

The gate-all-around device is an SOI MOS field-effect transistor. The gate electrode and the thin gate oxide are wrapped around the active channel region. No other insulator (field oxide or buried oxide) is in contact with the active region of the device. The gate-all-around device exhibits a high transconductance (up to 4 times that of a normal SOI transistor), an ideally sharp subthreshold slope, and demonstrates the concept of volume inversion in thin SOI films. Both n-channel and p-channel devices have been fabricated. GRA

N93-14552# Army Lab. Command, Fort Monmouth, NJ. Electronics Technology and Devices Lab.
LITHIUM RECHARGEABLE CELL WITH A POLY 3-METHYLTHIOPHENE CATHODE
Charles W. Walker, Jr. and Steven M. Slane Aug. 1992 15 p
(AD-A255436; SLCET-TR-91-31) Avail: CASI HC A03/MF A01

A poly 3-methylthiophene (PMT) cathode showed excellent coulombic efficiency during cycling in a lithium rechargeable cell. An electrolyte containing dimethyl carbonate was used since it is stable at the high anodic potentials reached during cell charging. The polymer cathode tolerated modest overcharge and was able to continue cycling after a severe short-circuit with minimal loss of capacity. GRA

N93-14555# Booz-Allen and Hamilton, Inc., Arlington, VA.
SETA SUPPORT FOR THE DARPA MICROELECTRONICS TECHNOLOGY INSERTION PROGRAM OF THE MICROELECTRONICS TECHNOLOGY OFFICE Quarterly Technical Report No. 2, 1 May - 31 Jul. 1992
Daniel H. Butler, Jr. 17 Aug. 1992 74 p
(Contract MDA972-92-C-0029)
(AD-A255551) Avail: CASI HC A04/MF A01

Booz-Allen and Hamilton provides DARPA's Microelectronics Technology Office with a broad range of SETA support under contract MDA972-92-C-0029. This report describes activities during the first quarter of this contract. The main programs supported were: the Digital Gallium Arsenide Insertion Program, the Transition of Optical Processors to Systems (TOPS), the Microelectronics Manufacturing Strategy (MMST) Program, the Flexible, Intelligent Microelectronics Manufacturing Program (FIMM), and the Artificial Neural Networks Technology Program (ANNT). This report is organized by subtask areas in the statement of work, indicating for each subtask the Task Objectives, General Methodology, Technical Results, and Important Findings and Conclusions. The final section of this report presents a summary and conclusions, and appendices present deliverables from Booz-Allen and special consultants providing MTO Support via this contract. GRA

N93-14562# Illinois Univ., Urbana.
NOVEL ENGINEERED COMPOUND SEMICONDUCTOR HETEROSTRUCTURES FOR ADVANCED ELECTRONICS APPLICATIONS Final Report, 1 Apr. 1989 - 31 Mar. 1992
Gregory E. Stillman, Nick Holonyak, Jr., and James J. Coleman 22 Jun. 1992 77 p
(Contract DAAL03-89-K-0080)
(AD-A255363; ARO-26923.1-EL-SDI) Avail: CASI HC A05/MF A01

To provide the technology base that will enable SDIO capitalization on the performance advantages offered through novel engineered multiple-lavered compound semiconductor structures, this project has focussed on three specific areas: (1) carbon doping of AlGaAs/GaAs and InP/InGaAs materials for reliable high frequency heterojunction bipolar transistors; (2) impurity induced layer disordering and the environmental degradation of AlxGal-xAs-GaAs quantum-well heterostructures and the native oxide stabilization of AlxGal-xAs-GaAs quantum well heterostructure lasers; and (3) non-planar and strained-layer quantum well heterostructure lasers and laser arrays. The accomplishments in this three year research are reported in fifty-six publications and the abstracts included in this report. GRA

N93-14577# Pennsylvania Univ., Philadelphia. School of Medicine.
DESIGN AND HARDWARE IMPLEMENTATION OF NEURAL SYSTEMS Final Report, 1 Oct. 1988 - 30 Sep. 1991
Paul Mueller 15 Dec. 1991 7 p
(Contract N00014-89-J-1249)
(AD-A256040) Avail: CASI HC A02/MF A01

This project had two major aims. One was the design and computer simulation of specific neural circuits modeled after the early vision system of higher vertebrates. The second aim was the design and construction of electronic analog neural systems that could be used for implementing such a vision system and possibly other neural systems. Our initial approach to the hardware implementation was to build an entirely hardwired system using VLSI assemblies of electronic neurons and separate resistive synapse connection matrices fabricated by CVD deposition of amorphous silicon. During further simulation studies of the vision system, it became clear that at this early state of development a completely hardwired system would be too restrictive and for this reason we felt that we needed a system that would incorporate modifiable synapses and a programmable connection architecture. GRA

N93-14583# EIC, Inc., Norwood, MA.
PHOTOELECTROCHEMISTRY OF ELECTRONIC AND ELECTRO-OPTICAL MATERIALS Final Report, 1 Mar. 1987 - 30 Sep. 1989
R. D. Rauh 24 Sep. 1992 5 p
(Contract N00014-87-C-0408)
(AD-A256239; C912F) Avail: CASI HC A01/MF A01

The broad objective of this work is to investigate applications of photoelectrochemistry to semiconductor and electro-optical technology. Experiments are being undertaken to understand the functions of reaction velocity and crystallographic orientation in determining profiles and morphologies of photoelectrochemically etched features in Si, SiC, and III-V compounds. Work was also conducted to determine the relationship between liquid junction response and solid state diode electrical characteristics of the polar faces of III-V crystals and to develop chemical surface passivants for compound semiconductor device electronics. GRA

N93-14642# Army Lab. Command, Fort Monmouth, NJ. Electronics Technology and Devices Lab.

SMART BATTERY CONTROLLER FOR LITHIUM SULFUR DIOXIDE BATTERIES

Terrill Atwater, Arnold Bard, Bruce Testa, and William Shader Aug. 1992 19 p

(AD-A255490; SLCET-TR-91-36) Avail: CASI HC A03/MF A01

Each year, the U.S. Army purchases millions of lithium sulfur dioxide batteries for use in portable electronics equipment. Because of their superior rate capability and service life over a wide variety of conditions, lithium batteries are the power source of choice for military equipment. There is no convenient method of determining the available energy remaining in partially used lithium batteries; hence, users do not take full advantage of all the available battery energy. Currently, users replace batteries before each mission, which leads to premature disposal, and results in the waste of millions of dollars in battery energy every year. Another problem of the lithium battery is that it is necessary to ensure complete discharge of the cells when the useful life of the battery has been expended, or when a hazardous condition exists; a hazardous condition may result in one or more of the cells venting. The Electronics Technology and Devices Laboratory has developed a working prototype of a smart battery controller (SBC) that addresses these problems. GRA

N93-14666# Trymer Co., Leander, TX.

A NOVEL, HIGH ENERGY-DENSITY ELECTRICAL STORAGE DEVICE FOR ELECTRIC WEAPONS Final Report, 26 Feb. - 25 Aug. 1992

Jon M. Schroeder 25 Aug. 1992 20 p

(Contract DASG60-92-C-0049)

(AD-A255205) Avail: CASI HC A03/MF A01

Three different energy storage variants were developed and tested during Phase 1. Each was based on the close-coupled, thermopile storage principle. First, direct current was stored in a thermopile ring, which was open-switched into a dummy load to measure the energy release. In the second variant, alternating magnetic energy was stored in a split ring. Energy storage was caused by pumping alternating current in the thermopile circuit, connected as an LC oscillator. Both methods were found to store energy and each delivered pulse power, resulting in a twenty-to-one pulse-power advantage between energy released from the store and energy available from the power supply at the input. Power was drawn from these systems in a millisecond, making use of a specially developed, sequentially opening switch that takes full advantage of the MOSFET's nanosecond hyper-operating speed, the intermediate switching speed of a silicon controlled rectifier (SCR), and a slower speed electro-mechanical switch. Further work with modifications of these two storage methods led then to the development of an inductor-to-inductor (L(sup 2)) electromagnetic storage system. This new type storage device seems to out perform the first two methods by roughly two orders of magnitude in storage capacity. During flux pump experiments, we also found that the L(sup 2) prototype system could be tuned to operate efficiently at certain particular frequencies depending on the value of capacitor chosen, placed across the two conductors, to tune in steps between 50 Hz and 50 MHz, possibly operating efficiently in the GHz range. GRA

N93-14699# Raytheon Co., Marlborough, MA. Equipment Div.

TESTABILITY DESIGN RATING SYSTEM: TESTABILITY HANDBOOK, VOLUME 1 Final Report, Jun. 1989 - Feb. 1991

Ronald Press, Michael E. Keller, and Gregory J. Maguire Feb. 1992 411 p

(Contract F30602-89-C-0121; AF Proj. 2338)

(RL-TR-92-12-Vol-1) Avail: CASI HC A18/MF A04

This effort provides a means of rating the testability of an electronic design at any stage in the design life. Volume 1, Testability Handbook, discusses the particulars of the circuit design and how they relate to testability. It also discusses the software developed in this program and how to obtain the software. The software, which will run on any IBM compatible PC having 512 k of available memory and a hard disk, asks a number of questions, and based on the answers, will provide a testability rating and a credibility rating. Volume 2 provides means of doing the testability analysis without the computer. Author

N93-14721*# Minnesota Univ., Minneapolis. High Temperature Lab.

ARC-CATHODE INTERACTION STUDY Final Report

X. Zhou and J. Heberlein 4 Dec. 1992 13 p Original contains color illustrations

(Grant NAG3-1332)

(NASA-CR-191356; NAS 1.26:191356) Avail: CASI HC A03/MF A01; 1 functional color page

Insufficient electrode life and uncertainties in that life are major problems hampering the development in many plasma application areas which make use of plasma torches, arc heaters, and arc jet thrusters. In spite of a considerable amount of work published dealing with arc-cathode phenomena, our present understanding is still incomplete because different physical phenomena dominate for different combinations of experimental parameters. The objective of our present research project is to gain a better understanding of the behavior of arc-cathode surface interaction over a wide range of parameters, and furthermore to develop guidelines for better thermal design of the electrode and the selection of materials. This report will present the research results and progress obtained on the arc-cathode interaction studies at the University of Minnesota. It includes results which have been obtained under programs other than the NASA funded program. Some of the results have been submitted in an informal interim progress report, and all of the results have been presented in a seminar during a visit to the NASA Lewis Research Center on October 16, 1992. Author

N93-14798*# Sverdrup Technology, Inc., Brook Park, OH. Research Center Group.

AUTONOMOUS POWER SYSTEM BRASSBOARD Final Report

Anthony Merolla Oct. 1992 12 p

(Contract NAS3-25266; RTOP 590-12-33)

(NASA-CR-189115; E-6822; NAS 1.26:189115) Avail: CASI HC A03/MF A01

The Autonomous Power System (APS) brassboard is a 20 kHz power distribution system which has been developed at NASA Lewis Research Center, Cleveland, Ohio. The brassboard exists to provide a realistic hardware platform capable of testing artificially intelligent (AI) software. The brassboard's power circuit topology is based upon a Power Distribution Control Unit (PDCU), which is a subset of an advanced development 20 kHz electrical power system (EPS) testbed, originally designed for Space Station Freedom (SSF). The APS program is designed to demonstrate the application of intelligent software as a fault detection, isolation, and recovery methodology for space power systems. This report discusses both the hardware and software elements used to construct the present configuration of the brassboard. The brassboard power components are described. These include the solid-state switches (herein referred to as switchgear), transformers, sources, and loads. Closely linked to this power portion of the brassboard is the first level of embedded control. Hardware used to implement this control and its associated software is discussed. An Ada software program, developed by Lewis Research Center's Space Station Freedom Directorate for their 20 kHz testbed, is used to control the brassboard's switchgear, as well as monitor key brassboard parameters through sensors located within these switches. The Ada code is downloaded from a PC/AT, and is resident within the 8086 microprocessor-based embedded controllers. The PC/AT is also used for smart terminal emulation, capable of controlling the switchgear as well as displaying data from them. Intelligent control is provided through use of a T1 Explorer and the Autonomous Power Expert (APEX) LISP software. Real-time load scheduling is implemented through use of a 'C' program-based scheduling engine. The methods of communication between these computers and the brassboard are explored. In order to evaluate the features of both the brassboard hardware and intelligent controlling software, fault circuits have been developed and integrated as part of the brassboard. A description of these fault circuits and their function is included. The brassboard has become an extremely useful test facility, promoting artificial intelligence (AI) applications for power distribution systems. However, there are elements of the brassboard which could be enhanced, thus improving system performance. Modifications and enhancements to improve the brassboard's operation are discussed. Author

N93-14803# Physics and Electronics Lab. TNO, The Hague (Netherlands).

HIGH POWER MILLIMETRE-WAVE POLARIZERS Final Report

F. A. Nennie Apr. 1992 42 p

(AD-A256558; FEL-91-A324; TDCK-91-3693) Avail: CASI HC A03/MF A01

The operation and realization of 4 high-power polarizers at 35.0 GHz and 94.0 GHz are described in this report. Results of calculations and measurements are discussed. The realized polarizers make use of an elliptical waveguide to convert the linearly polarized incident wave into an outward left or right-hand circularly polarized wave. Main measurement results are: the axial ratio at 35.0 GHz is less than 1.0 dB over 5 percent bandwidth. The return loss is better than 21 dB (VSWR less than 1.2) over more than 30 percent bandwidth. The insertion loss is less than 0.3 dB over more than 30 percent bandwidth. The isolation is more than 18 dB over 5 percent bandwidth. The maximum peak-power is 63 kW. The axial ratio at 94.0 GHz is less than 1.0 dB over 5 percent bandwidth. The return loss is better than 26 dB (VSWR less than 1.1) over more than 3 percent bandwidth. The insertion loss is less than 0.75 dB over more than 3 percent bandwidth. The isolation is more than 20 dB over 3 percent bandwidth. The maximum peak-power is 9.5 kW. All polarizers have been made waterproof and dust-proof. GRA

N93-14826 Department of the Navy, Washington, DC.
INTERNAL GROUNDING ARRANGEMENT IN A SWITCHING POWER CONVERTER Patent Application
George A. Banura, inventor (to Navy) 26 Nov. 1991 12 p Filed 19 Nov. 1990
(AD-D015435; US-Patent-Appl-SN-618323; US-Patent-Class-323-351)
Avail: CASI HC A03/MF A01

An internal grounding arrangement which minimizes output of current spikes by isolating the switching spikes from the input and output includes an arrangement of separate grounding planes for different functional groups of components, such as high current switching, low current switching and input/output components, with RF chokes and a single conductor line. The RF chokes and single conductor provide electrical isolation between the grounding planes of these different functional groups of components. GRA

N93-14887# Department of the Navy, Washington, DC.
POWER CONVERSION SYSTEM MODIFICATION TO PERMIT USE OF DC POWER SOURCE Patent Application
Thomas A. Frank, inventor (to Navy) and Claude D. Michel, inventor (to Navy) 7 Aug. 1992 12 p
(AD-D015409; US-Patent-Appl-SN-926112) Avail: CASI HC A03/MF A01

The patent application discloses an electrical power conversion system designed to operate on 115 volt, three-phase AC voltage generated by a motor generator. A modification is provided to also permit the use of a DC power source. The power conversion system has a plurality of AC-to-DC conversion means for converting the generated three-phase AC voltages. The first specified DC voltage is supplied to a voltage reduction means and the second specified DC voltage is supplied to a control logic circuit of the power source and means, utilizing power from said DC power source, for supplying DC voltages equivalent to the first and second specified DC voltages. The supplying means is isolated from the generated three-phase voltage such that the power conversion system can operate on: (1) three-phase AC voltage generated by the motor generator; (2) DC voltages equivalent to the first and second specified DC voltages from the supplying means; or (3) a combination of the three-phase AC voltage generated by the motor generator and the DC voltages from the supplying means. GRA

N93-14915*# Lockheed Missiles and Space Co., Palo Alto, CA.
PERFORMANCE CHARACTERISTICS OF STIS DETECTORS Final Report, 1 Sep. 1988 - 31 Dec. 1992
Robert A. Stern 31 Dec. 1992 50 p
(Contract NAS5-30435)
(NASA-CR-191636; NAS 1.26:191636) Avail: CASI HC A03/MF A01

We report quantum efficiency measurements of back-illuminated, ion-implanted, laser-annealed charge coupled devices (CCD's) in the wavelength range 13-10,000 A. The equivalent quantum efficiency (EQE = effective photons detected per incident photon) ranges from a minimum of 5 percent as 1216 A to a maximum of 87 percent at 135 A. Using a simple relationship for the charge collection efficiency of the CCD pixels as a function of depth, we present a semi-empirical model with few parameters which reproduces our measurements with a fair degree of accuracy. The advantage of this model is that is can be used to predict CCD QE performance for shallow backside implanted devices without detailed solution of a system of differential equations, as in conventional approaches, and yields a simple analytic form for the charge collection efficiency which is adequate for detector calibration purposes. Making detailed assumptions about the dopant profile, we also solve the carrier density and continuity equations in order to relate our semi-empirical model parameters to surface and bulk device properties. The latter procedure helps to better establish device processing parameters for a given level of CCD QE performance. Author

N93-15010# Brown Univ., Providence, RI. Dept. of Chemistry.
NEW ELECTRONIC MATERIALS Final Report, 1-31 May 1992
Aaron Wold 9 Oct. 1992 6 p
(Contract N00014-89-J-1849)
(AD-A255612) Avail: CASI HC A02/MF A01

The work on the synthesis of metal oxide and sulfide thin films was started. This program centered around the development of new methods for the preparation and characterization of oxide and sulfide thin films, as well as the investigation of materials which transmit in the far infrared. An effort was also started on the preparation of diamond films because of its potential as a material for infrared transmission. All of the materials prepared were characterized as to their electronic and optical properties, stability toward decomposition and hardness. Several special transparent gold furnaces were designed and built so the entire growth process could be seen. During this year we used the novel spray pyrolysis technique developed in this lab to prepare metal oxide and metal sulfide thin films. GRA

N93-15107# Department of the Navy, Washington, DC.
METHOD AND APPARATUS FOR A HIGH RESOLUTION, FLAT PANEL CATHODOLUMINESCENT DISPLAY SCREEN Patent Application
Ronald R. Price, inventor (to Navy) and Henry F. Gray, inventor (to Navy) 29 May 1992 30 p
(AD-D015400; US-Patent-Appl-SN-889885) Avail: CASI HC A03/MF A01

A high resolution, cathodoluminescent display screen or device and a method of producing such a display device is disclosed. The display screen includes a plurality of channel structures having longitudinal ends, a transparent medium formed in a plane to which the channel structures are fixed with one longitudinal end thereof oriented toward the plane of the transparent medium, and a cathodoluminescent material deposited on the channel structures whereby incident electrons and light generated by the incident electrons are directed along the channel structures. Preferably, the display screen also includes a mechanism for removing built up charge from the display screen, such as conductive channel structures and/or a conductive transparent medium. The cathodoluminescent material can include phosphors, and for producing a color display, different materials producing different colors would be used. In one preferred embodiment, the channel structures are tubules. Alternately, the channel structures can be channel plates or other structures providing channeling structures. GRA

N93-15108# Santa Barbara Focalplane, Goleta, CA.
ORGANIC/IR-SEMICONDUCTOR HETEROJUNCTIONS FOR LOW-COST, HIGH TEMPERATURE IR ARRAYS Final Report, 31 Dec. 1991 - 31 Jun. 1992
Colin E. Jones 30 Aug. 1992 42 p
(Contract F49620-92-C-0014)
(AD-A255971; OR-SBIR-92-6; AFOSR-92-0896TR) Avail: CASI HC A03/MF A01

This program evaluated a new technology for producing infrared photo-diodes in HgCdTe and InSb using evaporated organic heterojunctions. High quantum-efficiency IR detectors were demonstrated with the organic process comparable to commercial IR detectors. The organic photodiodes at room temperature were better than commercial detectors. They had lower leakage currents and higher resistance-area products (RoAs). Detector arrays made with the organics can operate at higher temperatures than the current detectors. Initial data at low temperatures were poorer than commercial detectors with lower RoAs and slightly higher 1/f noise. This comparison at low temperature may change with further optimization of the organic process. The organic diode process is very simple, low cost and non-damaging to the HgCdTe or InSb. It involves thermal evaporation of the organic onto the HgCdTe or InSb followed by evaporation of metal

contacts through a shadow mask. Phase 1 demonstrated organic/HaCdTe IR detectors with quantum efficiencies similar to commercial devices operating at higher temperatures. The technology is ready for a Phase 2 to further optimize the processing for IR arrays and to increase yields.
GRA

N93-15133# Radiation Experiments and Monitors, Oxford (England).
IMPROVEMENT AND ANALYSIS OF THE RADIATION RESPONSE OF RADFET DOSIMETERS Final Report, 17 Aug. 1990 - 15 Jun. 1992
Andrew G. Holmes-Siedle 15 Jun. 1992 62 p
(Contract DAJA45-90-C-0042; DA Proj. 1L1-61102-BH-57)
(AD-A254115; REM-AR-92-2R; R/D-6474-CH-01) Avail: CASI HC A04/MF A01

This is the Final Report on the preparation of three lots of improved RADFET dosimeter devices with the partial support U.S. Army Contract No. DAJA45-90-C-0042 and scientific collaboration from CECOM personnel visiting the UK, including radiation testing of RADFET samples. A silicon RADFET wafer fabrication run was made and tests of performance under irradiation were made, including a pulsed x-ray test as guests of the UK Ministry of Defence, correlated with tests on a Co-60 gamma therapy source and copper tube x-rays. A new design of chip carrier was evaluated and found to be a useful advance in dosimeter packaging technique. The thickest oxide grown was 1.24 micro-meters. This had high responsivity and was very stable. The Army decided to have chips from these wafers packaged for the second and third deliveries. GRA

N93-15188# Southampton Univ. (England).
ABSTRACTS BOOKLET
Jul. 1992 163 p International Conference on Narrow Gap Semiconductors held in Southampton, England, 19-23 Jul. 1992
(Contract DAJA45-92-M-0334)
(AD-A256115; R/D-6971-EE-02) Avail: CASI HC A08/MF A02

We have performed the first experiment on the Free-Electron Laser (CLIO) at the Laboratoire pour l'Utilisation du Rayonnement Electromagnetique (LURE). Strong power limiting has been observed in a transmission experiment on InSb at wavelengths longer than the absorption edge. This is associated with induced free-carrier absorption produced by direct interband two-photon transitions. We have estimated the Two-Photon Absorption (TPA) Coefficient (Beta) of InSb to be 2 cm/MW at 8.9 microns (utilizing the tunability of the FEL for wavelengths other than hitherto available with CO2 lasers), by fitting the power-limiting effect to a simple theory. The result distinguishes between different theoretical models for the process. GRA

N93-15194# Army Lab. Command, Fort Monmouth, NJ. Electronics Technology and Devices Lab.
PROCESSING AND CHARACTERIZATION OF ELECTROPHORETICALLY DEPOSITED HOLMIUM BARIUM COPPER OXIDE SUPERCONDUCTOR FILMS Technical Report, period ending 1991
Michelle A. Dornath-Mohr, Donald W. Eckart, Robert D. Finnegan, Ernest Potenziani, II, and William Wilber Sep. 1992 15 p
(DA Proj. 1L1-61102-AH-47)
(AD-A256329; SLCET-TR-92-12) Avail: CASI HC A03/MF A01

Thick films of HoBa2Cu3O(7-x) (HBCO) were electrophoretically deposited on bulk YBa2Cu3O(7-x) (YBCO) pellets in magnetic fields of 0 and 2 T. X-ray diffraction patterns indicated no preferred orientation for the films. Scanning electron microscopy revealed that the films averaged 7 microns thick, have an open pore structure with microbridges between particles, and a minimal amount of grain growth. Some microcracking of the films was observed. The surface resistivities (Rs) of the films were measured from 5 to 140K using a resonant cavity at 35 GHz. The best films had a Rs of 30 milliohms at 10 K. The transition temperature (Tc) of the films ranged from 85 to 90 K as measured by the four-point probe method.
GRA

N93-15196# Tetra Corp., Albuquerque, NM.
MICROSTACK INSULATOR FOR FLASHOVER INHIBITION, PHASE 2 Technical Report, 27 Mar. 1989 - 31 Mar. 1991
Juan M. Elizondo and William M. Moeny Oct. 1992 161 p
(Contract DNA001-89-C-0025)
(AD-A256338; DNA-TR-91-86) Avail: CASI HC A08/MF A02

The program achieved results that represent a breakthrough in vacuum surface flashover insulation. The samples designed as the optimum configuration failed through the dielectric bulk before surface flashover was observed. In fact, the ultimate limitation is the vacuum breakdown of the anode-cathode electrode system. As shown later, we determine that for 100-nsec-long pulses the vacuum breakdown voltage of the electrode system was above 350 kV/cm, with some pulses as high as 450 kv/cm. Typical microstacks will sustain voltages above 280 kv/cm, with optimized samples failing typically at average fields above 400 kv/cm and not because of surface flashover but through the bulk of the sample. These numbers are excellent considering that the fitted data corresponds to 1 failure out of 15 pulses. The scaling equation from J. C. Martin is used for a 50 percent probability of failure. The scaling equation produced by the microstack insulator comes from better than 10 percent (6.6 percent) probability of failure, or 94 percent reliability at the calculated voltage.
GRA

N93-15214# Martin Marietta Energy Systems, Inc., Oak Ridge, TN.
MICROWAVE PROCESSING OF TANTALUM CAPACITOR ANODES
R. J. Lauf, C. Hamby, C. E. Holcombe, and W. F. Vierow (AVX-Tantalum Corp., Biddeford, ME.) 1992 6 p Presented at the Material Research Society Spring Meeting, San Francisco, CA, 27 Apr. - 2 May 1992
(Contract DE-AC05-84OR-21400)
(DE92-017829; CONF-920402-45) Avail: CASI HC A02/MF A01

Porous tantalum anodes were sintered from 1600 to 1900 C using a conventional high vacuum furnace as well as both 2.45 GHz fixed-frequency and 4 to 8 GHz variable frequency microwave furnaces. Various insulation and casketing techniques were used to couple the microwave power to the tantalum compacts. Several types of tantalum powder were used to assess the effect of microwave processing on sintered surface area and impurity levels. Some microwave sintered anodes have an unusual surface rippling not seen on conventionally fired parts. The rippling suggests that a microscopic arcing or plasma might have been generated. Two important effects could be exploited if this phenomenon can be controlled. First, the effective tantalum surface area could be increased, yielding higher capacitance per volume. Second, surface impurities might be cleaned away, allowing the formation of a better dielectric film during the anodization process and, ultimately, higher working voltage. DOE

N93-15226# Northest Sustainable Energy Association, Greenfield, MA.
S/EV 1991: SOLAR AND ELECTRIC VEHICLE SYMPOSIUM, CAR AND TRADE SHOW
1991 216 p Symposium held in Boxborough, MA, 25-26 Oct. 1991 Sponsored by DOE
(DE92-019890; CONF-911094) Avail: CASI HC A10/MF A03

These proceedings cover the fundamentals of electric vehicles. Papers on the design, testing and performance of the power supplies, drive trains, and bodies of solar and non-solar powered electric vehicles are presented. Results from demonstrations and races are described. Public policy on the economics and environmental impacts of using electric powered vehicles is also presented. DOE

N93-15257# Polytechnic Inst. of New York, Farmingdale.
BASIC RESEARCH IN ELECTRONICS (JSEP) Final Technical Report
Erich Kunhardt 31 Dec. 1991 54 p
(Contract F49629-88-C-0075)
(AD-A256016; POLY-WRI-1600-91; AFOSR-92-0895TR) Avail: CASI HC A04/MF A01

This Final Technical Report presents the work accomplished for the Joint Services Electronics Program (JSEP) under the contract no. F49620-88-C-0075. The Joint Services Electronics Program at Polytechnic University is the core of interdisciplinary research in electronics encompassing programs in the Department of Electrical Engineering, Physics, and Chemistry under the aegis of the Weber Research Institute. The research encompassed by this program is grouped into two broad categories: Interactions of Wide-Band Electromagnetic Radiation with Complex Macro- and Micro-Structures (EM) and Field-Particle Interactions in Matter: Single Particle, Collective and Cooperative Phenomena (FP). The detailed projects (research units) comprising the complete program are listed in the Table of Contents. GRA

N93-15269# Department of the Navy, Arlington, VA.
HIGH PERFORMANCE PULSE GENERATOR Patent Application

Michael G. Grothaus, inventor (to Navy), Stuart L. Moran, inventor (to Navy), and Leonard W. Hardesty, inventor (to Navy) 15 Jun. 1992 22 p Filed 15 Jun. 1992
(AD-D015378; US-Patent-Appl-SN-898591) Avail: CASI HC A03/MF A01

The device is a compact Marx-type generator capable of producing a high-voltage burst of pulses having risetimes less than 10 nanoseconds at repetition rates up to 10 kHz. High-pressure hydrogen switches are used as the switching elements to achieve high rep-rate. A small coaxial design provides low inductance and a fast risetime. The device may be used as a high-rep-rate high-voltage trigger generator, or as a high-voltage pulse source capable of producing up to 1 MV pulses at high repetition rates. GRA

N93-15276# Westinghouse Idaho Nuclear Co., Inc., Idaho Falls.
DESIGN AND IMPLEMENTATION OF A DC-BASED MAGNETIC FIELD CONTROLLER WITH ELECTRONIC TEMPERATURE STABILIZED HALL GENERATOR
T. C. Piper and J. P. Morgan Jul. 1992 40 p
(Contract DE-AC07-84ID-12435)
(DE92-019796; WINCO-1100) Avail: CASI HC A03/MF A01

The document provides information on a dc-based magnetic field controller and Hall generator temperature-stabilization circuitry used as integral part of mass spectrometer magnet systems at the Idaho Chemical processing Plant. Sections are divided into general operation, theory of operation, calibration and service. DOE

N93-15330# Army Lab. Command, Fort Monmouth, NJ. Electronics Technology and Devices Lab.
INTRODUCTION TO QUARTZ FREQUENCY STANDARDS, REVISION 1
John R. Vig Oct. 1992 56 p
(AD-A256373; SLCET-TR-92-1-Rev-1) Avail: CASI HC A04/MF A01

The fundamentals of quartz frequency standards are reviewed. The subjects discussed include: crystal resonators and oscillators, oscillator types, and the characteristics and limitations of temperature compensated crystal oscillators (TCXO) and oven controlled crystal oscillators (OCXO). The oscillator instabilities discussed include: aging, noise, frequency vs. temperature, warmup, acceleration effects, magnetic field effects, atmospheric pressure effects, radiation effects, and interactions among the various effects. Guidelines are provided for oscillator comparison and selection. Discussions of specifications are also included, as are references and suggestions for further reading. GRA

N93-15389# Lawrence Livermore National Lab., CA.
THERMAL ANALYSIS OF MAGNETRON SPUTTERING DESIGNS
Sang-Wook Kang, D. M. Makowiecki, and P. B. Ramsey 12 Aug. 1992 29 p
(Contract W-7405-eng-48)
(DE93-000348; UCRL-ID-110831) Avail: CASI HC A03/MF A01

Thermal flow characteristics of a new type of magnetron sputtering source design have been analyzed for various materials, heat rates and geometries using TOPAZ2D code. Thermal conduction has been assumed to be the only mechanism for transporting heat through the apparatus. Solutions compare well with experiments and demonstrate the usefulness (and cost savings) of performing experimental parameter variations with the model rather than the hardware. Optimal designs based on the present analysis are also discussed. DOE

N93-15412# National Inst. of Standards and Technology, Gaithersburg, MD. Electricity Div.
RESEARCH FOR ELECTRIC ENERGY SYSTEMS Annual Report
W. E. Anderson, ed. Jun. 1992 79 p
(Contract DE-AI01-87CE-34011)
(DE92-040076; NISTIR-4931) Avail: CASI HC A05/MF A01

This report documents the technical progress in the four investigations which make up the project 'Support of Research Projects for Electrical Energy Systems', Department of Energy Task Order Number 137, funded by the US Department of Energy and performed by the Electricity Division of the National Institute of Standards and Technology (NIST). The first investigation is concerned with the measurement of magnetic fields in support of epidemiogical and in vitro studies of biological field effects. The second investigation is concerned with two different activities: the production of S2F10 in negative corona in SF6 and the measurement of electron scattering and dissociative electron attachment cross sections for SF6 and its electrical by-products. The third investigation is also concerned with tvo different activities: several liquids that are currently used or have potential for use as high voltage dielectrics are studied using conventional impulse breakdown measurement techniques and high-speed photography and advances in partial discharge measurement techniques are presented. The last investigation is concerned with the evaluation and improvement of methods for measuring fast transients in electrical power systems such as might be associated with an electromagnetic impulse. DOE

N93-15421# Los Alamos National Lab., NM.
SCRUNCHER PHASE AND AMPLITUDE CONTROL
R. A. DeHaven, C. L. Morris, R. Johnson, J. Davis, and J. M. ODonnell 1992 4 p Presented at the 16th International LINAC Conference, Ottawa, Ontario, 23-28 Aug. 1992
(Contract W-7405-eng-36)
(DE92-040225; LA-UR-92-2746; CONF-9208109-29) Avail: CASI HC A01/MF A01

The analog controller for phase and amplitude control of a 402.5 MHz super conducting cavity is described in this paper. The cavity is a single cell with niobium explosively bonded to a copper cavity. It is used as an energy compressor for pions at the Clinton P. Anderson Meson Physics Facility (LAMPF). The controller maintains cavity frequency to within 4 degrees in phase of the LAMPF beam frequency. Field amplitude is maintained to within 2 percent. This control is accomplished at critical coupling (Q loaded of 1 x 10(exp 9)) with the use of only a 30 watt RF amplifier for accelerating fields of 6 MV/m. The design includes the use of piezoelectric crystals for fast resonance control. Three types of control, self excited VCO, and a reference frequency driven, were tried on this cavity and we present a comparison of their performance. DOE

N93-15424# Los Alamos National Lab., NM.
DESIGN FEATURES OF A SEVEN-CELL HIGH-GRADIENT SUPERCONDUCTING CAVITY
D. J. Liska, J. Ledford, S. Black, G. Spalek, and J. N. DiMarco 1992 4 p Presented at the 16th International LINAC Conference, Ottawa, Ontario, 23-28 Aug. 1992
(Contract W-7405-eng-36)
(DE92-040229; LA-UR-92-2734; CONF-9208109-34) Avail: CASI HC A01/MF A01

A cavity development program is in place at Los Alamos National Laboratory to evaluate structures that could be used to accelerate pions. The work is being guided by the conceptual design of PILAC, a high-gradient superconducting linac for raising the energy of rapidly decaying intense pion beams generated by Los Alamos Meson Physics Facility (LAMPF) to 1 GeV. The specification requires a cavity gradient of 12.5 MV/m at 805 MHz. The design of a seven-cell prototype cavity to achieve these high gradients has been completed by the Accelerator Technology division. The cavity is presently under procurement for high power testing a 2.0 K in 1993. DOE

N93-15441# Argonne National Lab., IL.
DUAL ROLE OF NICKEL IN SODIUM/NICKEL CHLORIDE BATTERIES
J. Prakash, L. Redey, R. Skocypec, R. Lowrey, and D. Vissers 1992 2 p Presented at the 182d Meeting of the Electrochemical Society, Toronto (Canada), 11-16 Oct. 1992
(Contract W-31-109-eng-38)
(DE92-041102; ANL/CP-76155; CONF-921036-8) Avail: CASI HC A01/MF A01

Corrosion of Ni metal in chloroaluminate melts containing sulfur additive was investigated in order to see whether Ni could be used not only as active material but also as current collector and cell- case material. Three layers were found after three days; they comprised NiCl2, Ni sulfide, and NaAlCl4. Ni-200 wires were also tested under tension in NaAlCl4 + 2 wt percent S at 300 C; no stress corrosion was observed. Results show that Ni metal is very stable even under severe cell conditions with respect to corrosion or electochemical dissolution. The nickel metal, therefore, can serve the dial role of active material for the positive electode and material for the current-collector and cell-case assembly in the Na/NiCl2 cell with sulfur additive in the positive electrode. DOE

N93-15456# Michigan Univ., Ann Arbor. Ultrafast Science Lab.
DEVELOPMENT OF A 500 GHz OPTOELECTRONIC MODULATOR USING SUPERCONDUCTING TRANSMISSION LINES Final Report, 15 Apr. 1989 - 14 Oct. 1991
Steven L. Williamson, John A. Nees, and Gerard Mourou 31 Aug. 1992 29 p
(Contract DAAL03-89-K-0071)
(AD-A257062; ARO-26760.3-EL) Avail: CASI HC A03/MF A01

This contract was set in place to investigate the technologies necessary to demonstrate multi-hundred-GHz modulation of optical signals. Techniques for eliminating velocity mismatch and modal dispersion, the two major limitations on state-of-the-art modulators, are presented. Further work to reduce signal distortion due to skin effect losses in normal conductors is detailed. Associated problems of interconnects and test instrumentation are also treated. GRA

N93-15479# Pacific Northwest Lab., Richland, WA.
RESULTS FROM A PILOT CELL TEST OF CERMET ANODES
C. F. Windisch, Jr., D. M. Strachan, C. H. Henager, Jr., E. N. Greenwell, and T. R. Alcorn (Reynolds Metals Co., Muscle Shoals, AL.) Aug. 1992 209 p
(Contract DE-AC06-76RL-01830)
(DE92-041357; PNL-8269) Avail: CASI HC A10/MF A03

The goal was to develop long-lasting, energy-efficient anodes for Hall-Heroult cells used to produce Al metal. The anodes were made from a ceramic/metal composite consisting of NiO and NiFe2O4 and a Cu/Ni metal phase. Thirteen cermet anodes were tested at Reynolds Metals Co., Muscle Shoals, AL. All anodes corroded severely during the pilot test. Electrolyte components were found deep within the anodes. However, there were many deficiencies in the pilot cell test, mainly the failure to maintain optimal operating conditions. It is concluded that there is a variety of fabrication and operational considerations that need to be addressed carefully in any future testing. DOE

N93-15485# SRI International Corp., Menlo Park, CA.
SOLID POLYMER ELECTROLYTES FOR RECHARGEABLE BATTERIES
Subhash C. Narang and Susanna C. Ventura Feb. 1992 20 p Prepared in cooperation with California Univ., Berkeley, Lawrence Berkeley Lab.
(Contract DE-AC03-76SF-00098)
(DE93-001603; LBL-32059) Avail: CASI HC A03/MF A01

SRI International has synthesized and tested new, dimensionally stable polymer electrolytes for high energy density rechargeable lithium batteries. We have prepared semi-interpenetrating networks of sulfur-substituted polyethyleneoxide with tetraethylorthosilicate (TEOS). The in situ hydrolysis of TEOS produces a mechanically stable three-dimensional network that entangles the polymer electrolytes and makes the film dimensionally flexible and stable. With this approach, the best dimensionally stable polymer electrolyte of this type produced so far, has a room temperature lithium ion conductivity of 7.5 x 10(exp -4) S cm(exp -1). Another type of solid polymer electrolytes, polydiacetylene-based single-ion conductors with high room temperature proton conductivity were also developed. The best conductivity of these polymers is two orders of magnitude higher than that of Nafion under comparable experimental conditions. With further appropriate chemical modification, the new polymers could be used in fuel cells. DOE

N93-15503*# National Aeronautics and Space Administration. Lewis Research Center, Cleveland, OH.
EMTP BASED STABILITY ANALYSIS OF SPACE STATION ELECTRIC POWER SYSTEM IN A TEST BED ENVIRONMENT
Narayan V. Dravid, Thomas J. Kacpura (Sverdrup Technology, Inc., Brook Park, OH.), and Andrew M. OConnor (Analytical Engineering Corp., North Olmsted, OH.) Aug. 1992 9 p Presented at the 27th Intersociety Energy Conversion Engineering Conference, San Diego, CA, 3-7 Aug. 1992; cosponsored by ANS, SAE, ACS, AIAA, ASME, and IEEE
(RTOP 474-42-10)
(NASA-TM-105845; E-7288; NAS 1.15:105845) Avail: CASI HC A02/MF A01

The Space Station Freedom Electric Power System (EPS) will convert solar energy into electric energy and distribute the same using an 'all dc', Power Management and Distribution (PMAD) System. Power conditioning devices (dc to dc converters) are needed to interconnect parts of this system operating at different nominal voltage levels. Operation of such devices could generate under damped oscillations (instability) under certain conditions. Criteria for instability are examined and verified for a single device. Suggested extension of the criteria to a system operation is examined by using the EMTP model of the PMAD DC test bed. Wherever possible, data from the test bed is compared with the modeling results. Author

N93-15529*# National Aeronautics and Space Administration. Goddard Space Flight Center, Greenbelt, MD.
OUTPUT DATA FORMATTER FOR THE ELECTRONICALLY SCANNED THINNED ARRAY RADIOMETER (ESTAR) INSTRUMENT
William A. Chren, Jr. Jan. 1993 16 p
(NASA-TM-4432; NAS 1.15:4432; Rept-93B00007) Avail: CASI HC A03/MF A01

A prototype Output Data Formatter (ODF) for the ESTAR (Electronically Scanned Thinned Array Radiometer) instrument has been designed and tested. It employs programmable logic devices to format and tag correlator data for transmission to Earth. After accepting 170 bits or correlator and error data in parallel, it appends an identification word and then serially passes the data to the Small Explorer Data System (SEDS) for transmission at a maximum rate of greater than 15 Mb/sec. Implemented with two reprogrammable field programmable gate arrays (FPGA's), each contained in a 132-pin plastic pin grid array (PGA) package, the design is cascadeable, fully testable, and low-power. Author

N93-15531*# National Aeronautics and Space Administration. Lewis Research Center, Cleveland, OH.
USER'S GUIDE FOR A LARGE SIGNAL COMPUTER MODEL OF THE HELICAL TRAVELING WAVE TUBE
Raymond W. Palmer Washington Dec. 1992 27 p
(RTOP 506-72-00)
(NASA-TP-3251; E-6804; NAS 1.60:3251) Avail: CASI HC A03/MF A01

The use is described of a successful large-signal, two-dimensional (axisymmetric), deformable disk computer model of the helical traveling wave tube amplifier, an extensively revised and operationally simplified version. We also discuss program input and output and the auxiliary files necessary for operation. Included is a sample problem and its input data and output results. Interested parties may now obtain from the author the FORTRAN source code, auxiliary files, and sample input data on a standard floppy diskette, the contents of which are described herein. Author

N93-14927# Canadian Space Agency, Ottawa (Ontario).
MULTIPLE FAULT DIAGNOSIS OF SPACECRAFT ELECTRICAL POWER SYSTEMS
Peter Adamovits *In its* Proceedings of the Sixth CASI Conference on Astronautics 1990 9 p Previously announced in IAA as A91-34933 (For primary document see N93-14920 04-12)
Avail: Canadian Aeronautics and Space Inst., 222 Somerset St. W., Suite 601, Ottawa, Ontario K2P 0J1 Canada

N93-14932# Ecole Polytechnique, Montreal (Quebec). Lab. de Recherche en Hyperfrequences.
A NEW DEVICE TO AID IN THE CONCEPTION AND OPTIMIZATION OF MONOLITHIC MILLIMETER CIRCUITS: A DISTRIBUTED AND NONLINER MODEL OF A FIELD EFFECT TRANSISTOR [UN NOUVEL OUTIL D'AIDE A LA CONCEPTION ET A L'OPTIMISATION DES CIRCUITS MONOLITHIQUES AUX FREQUENCES MILLIMETRIQUES: LE MODELE DISTIBUE ET NON-LINEAIRE DE TRANSISTOR A EFFET DE CHAMP]
Eric Ongareau and Renato G. Bosisio *In* Canadian Space Agency, Proceedings of the Sixth CASI Conference on Astronautics 1990 10 p In FRENCH Previously announced in IAA as A91-34938 (For primary document see N93-14920 04-12)
Avail: Canadian Aeronautics and Space Inst., 222 Somerset St. W., Suite 601, Ottawa, Ontario K2P 0J1 Canada

N93-14934# Ecole Polytechnique, Montreal (Quebec). Lab. de Recherche en Microondes.
CONCEPTUALIZATION OF A GaAs FIELD EFFECT TRANSISTOR FREQUENCY TRIPLER (2.5-7.5 GHz) FOR LOAD USE IN COMMUNICATION SATELLITES [CONCEPTION D'UN GAAS FET TRIPLEUR DE FREQUENCE (2.5-7.5 GHZ) POUR LA CHARGE UTILE DES SATELLITES DE COMMUNICATION]
Di-Luan Le, F. M. Ghannouchi, and R. G. Bosisio *In* Canadian Space Agency, Proceedings of the Sixth CASI Conference on Astronautics 1990 8 p In FRENCH Previously announced in IAA as A91-34940 (For primary document see N93-14920 04-12)
Avail: Canadian Aeronautics and Space Inst., 222 Somerset St. W., Suite 601, Ottawa, Ontario K2P 0J1 Canada

N93-14935# Canadian Astronautics Ltd., Ottawa (Ontario). Space Systems Group.
OPTIMIZED DESIGN OF A 5 kW CONSTANT FREQUENCY SERIES RESONANT CONVERTER FOR PULSED LOAD SPACE APPLICATIONS
Mehmet Celal Tanju *In* Canadian Space Agency, Proceedings of the Sixth CASI Conference on Astronautics 1990 10 p Previously announced in IAA as A91-34941 (For primary document see N93-14920 04-12)
Avail: Canadian Aeronautics and Space Inst., 222 Somerset St. W., Suite 601, Ottawa, Ontario K2P 0J1 Canada

N93-14936# Ecole Polytechnique, Montreal (Quebec). Lab. de Recherche Microondes.
SIMULATION AND NONLINEAR MODELLING OF MICROWAVE TRANSISTORS [SIMULATION ET MODELISATION NON-LINEAIRE DES TRANSISTORS MICROONDES]
Rached Hajji, Fadhel M. Ghannouchi, and Renato G. Bosisio *In* Canadian Space Agency, Proceedings of the Sixth CASI Conference on Astronautics 1990 7 p In FRENCH Previously announced in IAA as A91-34942 (For primary document see N93-14920 04-12)
Avail: Canadian Aeronautics and Space Inst., 222 Somerset St. W., Suite 601, Ottawa, Ontario K2P 0J1 Canada

34 FLUID MECHANICS AND HEAT TRANSFER

Includes boundary layers; hydrodynamics; fluidics; mass transfer; and ablation cooling.

For related information see also *02 Aerodynamics* and *77 Thermodynamics and Statistical Physics.*

N93-14119 Texas Univ., Austin.
TURBULENT DRAG AND TRANSPORT IN HIGH REYNOLDS NUMBER COUETTE-TAYLOR FLOW Ph.D. Thesis
Daniel Perry Lathrop 1992 149 p
Avail: Univ. Microfilms Order No. DA9225642

A new scientific instrument was designed to study turbulent flow between concentric cylinders for Reynolds numbers 800 is less than or equal to R is less than or equal to 1.23 x 10(exp 6). Despite predictions for the torque scaling as a power law of the Reynolds number, high precision torque measurements reveal no Reynolds number range with a fixed power law. A well-defined nonhysteretic transition is observed at R = 1.3 x 10(exp 4) to wall-bounded shear driven turbulence. Above the transition, the torque measurements and observed time scales indicate a close correspondence between this closed flow system and open wall-bounded shear flows such as pipe flow and flow over a flat plate. Flow quantities such as the axial turbulent diffusivity, the time scales associated with the fluctuations of the wall shear stress, and the rms fluctuations of the wall shear stress and its time derivative are all shown to be simply related to the global torque measurements. Dissert. Abstr.

N93-14150*# National Aeronautics and Space Administration. Lewis Research Center, Cleveland, OH.
CURRENT STATUS OF LIQUID SHEET RADIATOR RESEARCH
Donald L. Chubb, Frederick D. Calfo, and Matthew S. McMaster (Toledo Univ., OH.) 1993 15 p Proposed for presentation at the First International Conference on Aerospace Heat Exchanger Technology, Palo Alto, CA, 15-17 Feb. 1993; sponsored by AIAA and ASME
(RTOP 506-41-11)
(NASA-TM-105764; E-7181; NAS 1.15:105764) Avail: CASI HC A03/MF A01

Initial research on the external flow, low mass liquid sheet radiator (LSR), has been concentrated on understanding its fluid mechanics. The surface tension forces acting at the edges of the sheet produce a triangular planform for the radiating surface of width, W, and length, L. It has been experimentally verified that (exp L)/W agrees with the theoretical result, L/W = (We/8)exp 1/2, where We is the Weber number. Instability can cause holes to form in regions of large curvature such as where the edge cylinders join the sheet of thickness, tau. The W/tau limit that will cause hole formation with subsequent destruction of the sheet has yet to be reached experimentally. Although experimental measurements of sheet emissivity have not yet been performed because of limited program scope, calculations of the emissivity and sheet lifetime is determined by evaporation losses were made for two silicon based oils; Dow Corning 705 and Me(sub 2). Emissivities greater than 0.75 are calculated for tau greater than or equal to 200 microns for both oils. Lifetimes for Me(sub 2) are much longer than lifetimes for 705. Therefore, Me(sub 2) is the more attractive working fluid for higher temperatures (T greater than or equal to 400 K). Author

N93-14200 Maryland Univ., College Park.
SIMULATION OF VAPOR COMPRESSION HEAT PUMPS WITH SOLUTION CIRCUITS Ph.D. Thesis
Karim Amrane 1991 360 p
Avail: Univ. Microfilms Order No. DA9222649

Vapor compression heat pumps with solution circuits (VCHSC) offer two main advantages compared to conventional heat pumps: capacity control by adjustment of the circulating mixture composition and performance improvement by approximating the Lorenz process. The objective of this work is two fold: (1) Development and verification of computer models simulating single and two-stage VCHSC. (2) Investigation of the performance potentials of VCHSC using the models and second law analysis. Steady state model for the single and two-stage VCHSC are developed based on energy and mass balances and heat transfer relationships for components of the cycles. The heat exchangers are described by their UA values. Comparisons between experimental and simulated data are good, validating the models, although pointing out several needed refinements such as the assumptions of negligible pressure drops and heat losses to the surroundings. Performance curves a single-state VCHSC and two of its modified versions are generated and are compared based on the same total UA value based on the same total UA value including all heat exchangers. The parameters studied are the COP, the solution heat exchanger effectiveness, the pressure ratio, the temperature glides in the desorber and absorber, the cooling capacity and the distribution of the UA values. The principle of capacity control is clearly demonstrated as the cooling load is changed by up to a factor of ten by varying the concentration. Improvement in COP by as much as 23 percent is obtained by incorporating a preheater and an additional desorber. By staging the solution circuits in parallel, the effective vapor pressure curve of the refrigerant is manipulated leading to a two-stage cycle capable of very high temperature lifts (over 100 C) with very low pressure ratios (as low as 7). Simulation results show that the absorbent balance in the cycle is more efficiently done by using a bleed line instead of rectifying the refrigerant vapor. The cycles show an increase of up to 20 percent in the cooling COP and capacity by adding a desuperheater. A second law analysis is then conducted and the location and magnitude of the irreversibilities in the cycles determined. Based on this analysis system improvements are identified. Dissert. Abstr.

N93-14257# Cornell Univ., Ithaca, NY.
WALL LAYERS Final Report, 15 Jan. 1989 - 14 Jan. 1992
John L. Lumley, Sidney Leibovich, Philip Holmes, and John Guckenheimer 14 Jan. 1992 36 p
(Grant AF-AFOSR-0226-89)
(AD-A256152; AFOSR-92-0857TR) Avail: CASI HC A03/MF A01

Narrative reports of progress made during each of the three contract years are presented. These reports are given together with lists for each year of publications and reports, presentations, and various professional responsibilities of the principal investigators. GRA

N93-14273 Michigan Univ., Ann Arbor.
SIMULATION OF UNSTEADY INVISCID FLOW ON AN ADAPTIVELY REFINED CARTESIAN GRID Ph.D. Thesis
Yu-Liang Chiang 1992 195 p
Avail: Univ. Microfilms Order No. DA9226868

A numerical method for the solution of the unsteady Euler equations is presented. The grid used in this method results from the self-adaptive refinement of a Cartesian mesh. The refinement process automatically adapts the computational grid to those flow features that require high resolution. In order to make this technique efficient, a corresponding time-step adaptation method is included. The strategy of time-step adaptation is to use many small time-steps in fine cells, while taking one large step in the coarsest cells. In order to obtain second-order spatial accuracy a version of Van Leer's MUSCL algorithm, based on upwind-biased differencing is implemented. This means: linear reconstruction of distributions inside cells, and use of Roe's approximate Riemann solver for computing interface fluxes. As a temporal discretization, explicit two-stage marching is implemented. Correspondingly, a quadratic temporal interpolation is used in the coarse cells abutting on any refinement boundary. A significant aspect of the present methodology is that the wave strengths and wave speeds needed for the flux calculation are reused in various ways. In particular, the curvature of one-dimensional wave strength distributions is introduced as the key quantity in refinement and recoarsening criteria. Furthermore, wave speed and wave directions are used to predict the region traversed by strong waves; these are then flagged for refinement. In this way, important flow features are kept from leaving the fine-cell region during one global time step, which could happen because of the great disparity between the fine-cell and coarse-cell time-steps. The numerical results presented show that this method can achieve the same accuracy on the adaptive grid as on a uniform grid with cells as fine as the finest cells of the adaptive grid, at a large savings of computing time. Dissert. Abstr.

N93-14278 Michigan Univ., Ann Arbor.
THE NUMERICAL STABILITY OF NONLINEAR FLOATING BODY CALCULATIONS Ph.D. Thesis
Jong-Hwan Park 1992 179 p
Avail: Univ. Microfilms Order No. DA9226979

The numerical stability of nonlinear body-wave interaction problems is investigated by applying potential flow assumptions to oscillating, non-wallsided two-dimensional and three-dimensional axisymmetric bodies. This body-wave interaction problem is solved using a mixed two-step Eulerian-Lagrangian method. In the first step, Laplace's equation is solved to determine the unknown potential values on the body and the unknown derivatives of the potentials on the free surface. In the second step, free surface boundary conditions are applied using the results of the first step to find the evolved free surface location and new potential values on the new location. Each step has particular mathematical characteristics (elliptic or parabolic-like), so that each step requires different numerical schemes. Consequently, the numerical stability of this body-wave interaction problem contains the characteristics of both of these two steps. The major contributions made to this body-wave interaction problem are the effects of the various parameters (i.e. time increments, panel length, etc.) and the different forms of the Boundary Integral Method (BIM) on numerical stability and accuracy. The far-field truncation requirement is met by matching the linear outer solution to the nonlinear inner solution at the truncation boundary. The intersection point is traced by the extrapolation method with a special boundary condition at the intersection point. To determine the evolution of the free surface according to a Lagrangian model, a regridding scheme is utilized to prevent the concentration of the Lagrangian markers in the vicinity of high gradients. A parameter for the numerical stability of free surface waves, the Free Surface Stability (FSS) number, is defined as a function of the time step size and the discretized panel length. The various stability regions are investigated by changing the FSS number, Green's function constant c, and numerical schemes. A nonlinear stability analysis is also compared to the results of the linear stability analysis for a number of specific conditions to study the effect of nonlinear boundary conditions. Dissert. Abstr.

N93-14400# University of Southern California, Los Angeles. Dept. of Aerospace Engineering.
CONTROL OF ASYMMETRIC JET Final Technical Report, 1 May 1990 - 30 Apr. 1992
Chih-Ming Ho 30 Jun. 1992 127 p
(Grant AF-AFOSR-0301-90)
(AD-A255967; AFOSR-92-0864TR) Avail: CASI HC A07/MF A01

A passive method of enhancing the rate of entrainment by as much as 500 percent in subsonic open nozzle flows has been obtained by modifying axisymmetric nozzle geometry to a 2:1 aspect-ratio elliptic nozzle. Small aspect-ratio elliptical nozzles have been demonstrated to more efficiently control mixing processes and to exhibit increased rates of spreading, entrainment, and fine-scale mixing than axisymmetric nozzles at subsonic and supersonic conditions in a confined dump combustor and in high-temperature ramjets. Vortex self-induction is the principle mechanism controlling mixing processes in asymmetric jet nozzles. GRA

N93-14421# Arnold Engineering Development Center, Arnold AFS, TN.
TRANSONIC FLOW CALCULATIONS FOR A CAVITY WITH AND WITHOUT A STORE Final Report, Oct. 1988 - Jan. 1992
N. E. Suhs Sep. 1992 134 p
(AD-A255954) Avail: CASI HC A07/MF A02

A computational fluid dynamics capability was developed to support weapons bay (cavity) and internal store separation testing. Specifically, a computational capability that can be used to improve the ability to predict store trajectories and strut or sting interference was targeted by this effort. The chimera embedded grid scheme, a domain decomposition technique, was used to divide the cavity, store, and support hardware into simpler overlapping regions for which grids were more easily generated. The flow field was solved using an implicit Navier-Stokes code based on the Pulliam-Steger algorithm with thin-layer approximations to the viscous terms. Unsteady flow calculations were made for an empty cavity at Mach numbers of 0.60, 0.95, and 1.20 for a cavity length-to-height ratio of 4.5. Computations were also made for an ogive-cylinder-ogive store supported by a sting and positioned both in a free-stream flow and in the plane of the cavity opening at Mach numbers of 0.60, 0.95, and 1.20. Additional flow-field computations were made for the store supported by the sting at other positions within and outside the cavity at a Mach number of 1.20. Comparisons of the computations with experimental data were made for the time-averaged and fluctuating static pressures along the walls of the cavity for all of the above calculations. Comparisons were also made for the computed and measured time-averaged static pressures located axially along two opposing sides of the store. The evaluation of sting interference was achieved by removing the sting grid, calculating the flow field for this new configuration, and assessing differences between the store pressures and loads with and without the sting. GRA

N93-14464 Illinois Inst. of Tech., Chicago.
FEEDBACK CONTROL OF FLOW SEPARATION AND TRANSITION TO TURBULENCE IN UNSTEADY BOUNDARY LAYERS Ph.D. Thesis
Scott Richard Anderson 1992 202 p
Avail: Univ. Microfilms Order No. DA9231110

The model used in an analytical study should represent the primary characteristics of the system. A significant number of practical systems are distributed in nature and must be described by nonlinear partial differential equations in the independent time and spatial variables. Fluid flow is an example of such a system. Control of systems described by nonlinear partial differential equations is complicated, since no systematic procedures are developed as for lumped parameter systems. In the current study, a feedback control system is developed to prevent separation and transition to turbulence in unsteady boundary layer flow over aerodynamic surfaces. A feedback control system is required since the unsteady external flow is not known a priori. The flow is described by the nonlinear Prandtl boundary layer and continuity equations. A technique is developed based on Lyapunov's second method to formulate a control law which guarantees asymptotic stability of a controllable desired profile when the control law is calculated using the actual velocity in the boundary layer. For distributed parameter systems it is not practical to measure the actual system state, since an infinite number of sensors are required. In this study a nonlinear observer estimator is used to formulate an estimate of the velocity in the boundary layer from several discrete sensors in the boundary flow. Simulation of the boundary layer equations indicate that the observer estimator and resulting feedback control system are stable and drive the velocity in the boundary layer to the desired profile. Simulation results are given for flat plate at zero incidence to the exterior flow and for a flat plate at an angle of attack. The asymptotically stable system requires that a controllable

profile be determined by solving a partial differential equation on-line. In a practical implementation, the desired profile should be determined in a simpler manner. The resulting desired profile may not be controllable. Simplified control laws are also formulated which, while not asymptotically stable, give good performance for arbitrary desired velocity profiles. Simulation results for a flat plate at zero incidence are given for these simplified control laws. Dissert. Abstr.

N93-14465 Delaware Univ., Newark.
NUMERICAL AND EXPERIMENTAL STUDY OF BUBBLE GROWTH IN HIGHLY VISCOUS FLUIDS Ph.D. Thesis
Ali Arefmanesh 1991 214 p
Avail: Univ. Microfilms Order No. DA9223698

The phenomenon of bubble growth in viscous fluids plays an important role in many diverse fields such as composite manufacturing, glassmaking and polymer processing. In the first part, a fundamental analysis on the diffusion-induced growth of a gas bubble in Newtonian and viscoelastic fluids is performed. A method is developed to predict the bubble growth in a shell of fluid with finite thickness and limited dissolved gas. The predicted bubble growth is compared with the results obtained using the approximate polynomial profiles for the gas concentration. It is shown that the approximate polynomial solutions do not depict the correct physics of the bubble growth in a finite medium as they overpredict the equilibrium bubble radius by three to four orders of magnitude. To investigate the impact of the fluid elasticity, the upper-convected Maxwell model is used. The system of equations governing the bubble growth in the viscoelastic fluid is non-dimensionalized and a parametric study is conducted. This study reveals that the fluid elasticity has a significant impact on the growth-rate only at the early stages of the bubble growth. However, bubbles attain the same steady-state configuration in Newtonian and viscoelastic fluids. The second part of this study focuses on the simultaneous growth and motion of a system of bubbles during the foam molding process. The equations governing the growth of a single bubble in a shell of polymeric liquid are coupled with the continuity and the momentum equations for the flow of the polymeric foam in a mold under non-isothermal conditions. To model the physics of the foam molding process, a numerical simulation is developed. The results indicate a significant bubble size distribution along the axial direction in the mold with larger bubbles close to the melt front and smaller bubbles close to the mold gate. The outcome of a parametric study on the bubble density in the melt reveals that increase in the bubble density beyond a certain limit will not have a significant impact on the bulk foam density. Experimental studies on the structural foam molding under non-isothermal conditions are performed and the transient bulk foam density is measured. Dissert. Abstr.

N93-14475 Old Dominion Univ., Norfolk, VA.
CONTROL OF LOW-SPEED TURBULENT SEPARATED FLOW OVER A BACKWARD-FACING RAMP Ph.D. Thesis
John Ching-Nien Lin 1992 204 p
Avail: Univ. Microfilms Order No. DA9222141

The relative performance and flow phenomena associated with several devices for controlling turbulent separated flow were investigated at low speeds. Relative performance of the devices was examined for flow over a curved, backward-facing ramp in a wind tunnel, and the flow phenomena were examined in a water tunnel using dye-flow visualization. Surface static pressure measurements and oil-flow visualization results from the wind tunnel tests indicated that transverse grooves, longitudinal grooves, submerged vortex generators, vortex generator jets (VGJ's), Viets' fluidic flappers, elongated arches at (+)alpha (positive angle of attack), and large-eddy breakup devices (LEBUS's) at (+)alpha placed near the baseline separation location reduce flow separation and increase pressure recovery. Spanwise cylinders reduce flow separation but decrease pressure recovery downstream. Riblets, passive porous surfaces, swept grooves, Helmholtz resonators, and arches and LEBU's with alpha less than or equal to 0 deg had no significant effect in reducing the extent of the separation region. Wall-cooling computations indicated that separation delay on partially-cooled ramp is nearly the same as on a fully-cooled ramp, while minimizing the frictional drag increase associated with the wall cooling process. Dye-flow visualization tests in the water tunnel indicated that wishbone vortex generators in the forward orientation shed horseshoe vortices; wishbone vortex generators oriented in the reverse direction and doublet vortex generators shed streamwise counterrotating vortices; a spanwise cylinder located near the wall and LEBU's at alpha = -10 deg produced eddies or transverse vortices which rotated with the same sign as the mean vorticity in a turbulent boundary layer; and the most effective VGJ's produced streamwise co-rotating vortices. Comparative wind-tunnel test results indicated that transferring momentum from the outer region of a turbulent boundary layer through the action of embedded streamwise vortices is more effective than by transverse vortices for the separation control application studied herein. Dissert. Abstr.

N93-14476 Illinois Inst. of Tech., Chicago.
ANALYTICAL AND EXPERIMENTAL INVESTIGATION OF CLOSED-CYCLE SORPTION COOLING SYSTEMS Ph.D. Thesis
Lianquan Liu 1992 205 p
Avail: Univ. Microfilms Order No. DA9231123

The first part of the present thesis concerns the Coefficient of Performance (COP) of two types of closed-cycle sorption cooling systems: the Single Effect Liquid (SEL) absorption system and the Regenerative Solid (RS) adsorption system. When specific cycle configurations are considered, the COP is always less than that allowed by the second law. The potential of the two systems to approach the second law limit is considered in this work. The analysis shows that COP of a SEL system using LiBr-H2O is not limited by one, as believed before, and that the COP of a RS cooling system using zeolite-water is considerably larger than that of the SEL system. This is due to recovery of the heat of adsorption which is made possible by capturing the thermal wave in the solid adsorbent. In the second part, a one dimensional model has been developed for a real RS cooling system featured by finite heat transfer coefficients. The problem is solved numerically to yield the temperature and uptake profiles, COP, and cooling capacity and cooling rates. The effects of various design and operating parameters on system performance have been investigated by using the model. The convective heat transfer coefficient at the inner wall of the fluid channel passing through the zeolite columns, the flow rate of the heat transfer fluid, the condenser and evaporator temperature are identified as the most significant factors. A new correlation of adsorption equilibrium has been derived in this thesis. The derivation is based on established thermodynamic relationships and is shown to be able to well represent the data of three adsorption pairs widely used in sorption cooling applications: zeolite-water, silica gel-water and activated carbon-methanol. Finally, in the experimental part of the present work a test set-up of a zeolite-water heat and mass regenerator was designed, instrumented and built. Temperature profiles at various operating conditions were measured. The data of a 'single blow' mode are compared with the numerical predictions. Dissert. Abstr.

N93-14477 George Washington Univ., Washington, DC.
BOUNDARY LAYER TRANSITION MEASUREMENTS BY OPTICAL ANEMOMETRY Ph.D. Thesis
Carlos Alberto Lopez 1992 219 p
Avail: Univ. Microfilms Order No. DA9222635

A shadowgraph optical anemometry system capable of the quantitative detection and measurement of the complete boundary layer transition process was developed. The capability of the optical system is demonstrated by the detection of instability waves and turbulent bursting on a heated tangent-ogive model configuration. The unique capability of non-instrusive quantitative detection of the complete transition process by an optical system--from the initiation of instability waves to fully turbulent flow--which is presented here, has not been previously reported in the literature. The optical system developed here provides versatility, high resolution and a means of efficient boundary layer transition detection and measurement. As part of the verification process for the optical anemometry system, the optical and hot-film probe anemometers were compared in simultaneous measurements for different phases of transition. In the simultaneous measurements of instability waves, excellent agreement was observed between the two methods in the output signal time traces. Both methods responded similarly to the amplification and decay of instability waves and both measured the same wavelengths. In the case of turbulent bursting, the optical and hot-film anemometers also compared exceptionally well. Differences displayed in the time traces recorded by the optical and hot-film techniques were attributed to the basic nature of each method. The hot-film technique measures localized properties while the optical technique measures properties integrated along the path of the light beam. The optical anemometer responded well to all turbulent bursts detected by the

hot-film probe. In addition, the optical anemometer responded to turbulent bursts not detected by the hot-film probe located along the optical line of sight. This unique property of the optical system, not shared by the hot-film probe, provides a simple and accurate method for locating the boundary for fully turbulent flow or simply, the point of transition. Dissert. Abstr.

N93-14481*# North Carolina State Univ., Raleigh. Dept. of Mechanical and Aerospace Engineering.

EXPLOITING SIMILARITY IN TURBULENT SHEAR FLOWS FOR TURBULENCE MODELING Progress Report No. 27, 15 Jun. - 14 Dec. 1992

David F. Robinson, Julius E. Harris (National Aeronautics and Space Administration. Langley Research Center, Hampton, VA.), and H. A. Hassan 14 Dec. 1992 13 p Proposed for presentation to the 24th AIAA Fluid Dynamics Conference, Orlando, FL, 6-9 Jul. 1993 Submitted for publication

(Contract NCC1-22; NAGw-1331)

(NASA-CR-191621; NAS 1.26:191621) Avail: CASI HC A03/MF A01

It is well known that current k-epsilon models cannot predict the flow over a flat plate and its wake. In an effort to address this issue and other issues associated with turbulence closure, a new approach for turbulence modeling is proposed which exploits similarities in the flow field. Thus, if we consider the flow over a flat plate and its wake, then in addition to taking advantage of the log-law region, we can exploit the fact that the flow becomes self-similar in the far wake. This latter behavior makes it possible to cast the governing equations as a set of total differential equations. Solutions of this set and comparison with measured shear stress and velocity profiles yields the desired set of model constants. Such a set is, in general, different from other sets of model constants. The rational for such an approach is that if we can correctly model the flow over a flat plate and its far wake, then we can have a better chance of predicting the behavior in between. It is to be noted that the approach does not appeal, in any way, to the decay of homogeneous turbulence. This is because the asymptotic behavior of the flow under consideration is not representative of the decay of homogeneous turbulence. Author

N93-14677# Illinois Univ., Urbana. Dept. of Mechanical and Industrial Engineering.

A PLUME-INDUCED BOUNDARY LAYER SEPARATION EXPERIMENT Report, 1 Jan. - 30 Jun. 1992

Russell J. Shaw and J. C. Dutton 30 Jun. 1992 18 p

(Contract DAAL03-90-G-0021)

(AD-A255397; ARO-27558.9-EG) Avail: CASI HC A03/MF A01

The current paper describes an experimental investigation of a PIBLS flowfield produced by the interaction between two nonparallel, supersonic streams in the presence of a finite thickness base. The purpose of the study is to gain a better understanding of., the extent to which the fluid dynamic mechanisms and interactions present in the PIBLS flowfield influence the turbulence properties of the flow. A two-stream, supersonic wind tunnel, incorporating a two-dimensional planar geometry and operating in the blowdown mode, was specifically designed to produce a PIBLS flowfield. Preliminary experiments have demonstrated that the wind tunnel is capable of producing a wide range of PIBLS flowfields by simply regulating the stagnation pressure of the lower stream (jet flow) relative to the upper stream (freestream flow). One PIBLS flowfield has been chosen in which to conduct a detailed set of measurements. This flowfield has its separation point located about 6 delta 0 upstream of the base corner. A detailed study of this PIBLS flowfield is under way using schlieren photography and shadowgraph pictures, surface streakline visualization, surface static pressure measurements, and two-component, coincident LDV measurements. GRA

N93-14687*# Old Dominion Univ., Norfolk, VA. Dept. of Mechanical Engineering and Mechanics.

ANALYSIS AND CONTROL OF ASYMMETRIC VORTEX FLOWS AND SUPERSONIC VORTEX BREAKDOWN Final Report, 1 Dec. 1991 - 30 Nov. 1992

Osama A. Kandil Nov. 1992 127 p

(Grant NAG1-994)

(NASA-CR-191264; NAS 1.26:191264) Avail: CASI HC A07/MF A02

The acccmplishments which have been achieved in the present year covering the period from Dec. 1, 1991 until Nov. 30, 1992 are given. These accomplishments include publications, national and international presentations, NASA Research Highlights and presentations, and the research group supported under this grant. For individual titles, see N93-14688 through N93-14692.

N93-14688*# National Aeronautics and Space Administration. Langley Research Center, Hampton, VA.

RECENT ADVANCES IN NUMERICAL SIMULATION AND CONTROL OF ASYMMETRIC FLOWS AROUND SLENDER BODIES

Osama A. Kandil (Old Dominion Univ., Norfolk, VA.), Tin-Chee Wong (Old Dominion Univ., Norfolk, VA.), Hazem H. Sharaf (Old Dominion Univ., Norfolk, VA.), and C. H. Liu *In* Old Dominion Univ., Analysis and Control of Asymmetric Vortex Flows and Supersonic Vortex Breakdown Nov. 1992 13 p Presented at the IUTAM Symposium on Fluid Dynamics of High Angle of Attack, Tokyo, Japan, 13-17 Sep. 1992 (For primary document see N93-14687 04-34)

(Grant NAG1-994)

(Paper-W.1.2) Avail: CASI HC A03/MF A02

The problems of asymmetric flow around slender bodies and its control are formulated using the unsteady, compressible, thin-layer or full Navier-Stokes equations which are solved using an implicit, flux-difference splitting, finite-volume scheme. The problem is numerically simulated for both locally-conical and three-dimensional flows. The numerical applications include studies of the effects of relative incidence, Mach number and Reynolds number on the flow asymmetry. For the control of flow asymmetry, the numerical simulation cover passive and active control methods. For the passive control, the effectiveness of vertical fins placed in the leeward plane of geometric symmetry and side strakes with different orientations is studied. For the active control, the effectiveness of normal and tangential flow injection and surface heating and a combination of these methods is studied. Author

N93-14689*# National Aeronautics and Space Administration. Langley Research Center, Hampton, VA.

SHOCK/VORTEX INTERACTION AND VORTEX-BREAKDOWN MODES

Osama A. Kandil (Old Dominion Univ., Norfolk, VA.), H. A. Kandil (Old Dominion Univ., Norfolk, VA.), and C. H. Liu *In* Old Dominion Univ., Analysis and Control of Asymmetric Vortex Flows and Supersonic Vortex Breakdown Nov. 1992 13 p Presented at the IUTAM Symposium of Fluid Dynamics of High Angle of Attack, Tokyo, Japan, 13-17 Sep. 1992 (For primary document see N93-14687 04-34)

(Grant NAG1-994)

(Paper-T.1.3) Avail: CASI HC A03/MF A02

Computational simulation and study of shock/vortex interaction and vortex-breakdown modes are considered for bound (internal) and unbound (external) flow domains. The problem is formulated using the unsteady, compressible, full Navier-Stokes (NS) equations which are solved using an implicit, flux-difference splitting, finite-volume scheme. For the bound flow domain, a supersonic swirling flow is considered in a configured circular duct and the problem is solved for quasi-axisymmetric and three-dimensional flows. For the unbound domain, a supersonic swirling flow issued from a nozzle into a uniform supersonic flow of lower Mach number is considered for quasi-axisymmetric and three-dimensional flows. The results show several modes of breakdown; e.g., no-breakdown, transient single-bubble breakdown, transient multi-bubble breakdown, periodic multi-bubble multi-frequency breakdown and helical breakdown. Author

N93-14690*# National Aeronautics and Space Administration. Langley Research Center, Hampton, VA.

THREE-DIMENSIONAL COMPUTATIONAL STUDY OF ASYMMETRIC FLOWS USING NAVIER-STOKES EQUATIONS

Y. K. Cheung, ed. (Hong Kong Univ.), J. H. W. Lee, ed. (Hong Kong Univ.), A. Y. T. Leung, ed. (Hong Kong Univ.), Tin-Chee Wong (Old Dominion Univ., Norfolk, VA.), Osama A. Kandil (Old Dominion Univ., Norfolk, VA.), and C. H. Liu *In* Old Dominion Univ., Analysis and Control of Asymmetric Vortex Flows and Supersonic Vortex Breakdown Nov. 1992 8 p Repr. from Computational Mechanics (Balkema, Rotterdam), 1991 p 1365-1371 Presented at the Asian Pacific Conference on Computational Mechanics, Hong Kong, 11-13 Dec. 1991 (For primary document see N93-14687 04-34)

(Grant NAG1-994)

(ISBN-90-5410-029-X) Avail: CASI HC A02/MF A02

The unsteady, compressible, thin-layer Navier-Stokes equations are used

to obtain three-dimensional, asymmetric, vortex-flow solutions around cones and cone-cylinder configurations. The equations are solved using an implicit, upwind, flux-difference splitting, finite-volume scheme. The computational applications cover asymmetric flows around a 5 semi-apex angle cone of unit length at various Reynolds number. Next, a cylindrical afterbody of various length is added to the conical forebody to study the effect of the length of cylindrical afterbody on the flow asymmetry. All the asymmetric flow solutions are obtained by using a short-duration side-slip disturbance. Author

N93-14691*# National Aeronautics and Space Administration. Langley Research Center, Hampton, VA.

NUMERICAL SIMULATION OF STEADY AND UNSTEADY ASYMMETRIC VORTICAL FLOW

Osama A. Kandil (Old Dominion Univ., Norfolk, VA.), Tin-Chee Wong (Old Dominion Univ., Norfolk, VA.), and C. H. Liu *In* Old Dominion Univ., Analysis and Control of Asymmetric Vortex Flows and Supersonic Vortex Breakdown Nov. 1992 18 p Repr. from Journal of Fluids and Structures, v. 6, 1992 p 249-265 (For primary document see N93-14687 04-34)

(Contract NAS1-18584; NAG1-994)

Avail: CASI HC A03/MF A02

The unsteady, compressible, thin-layer, Navier-Stokes (NS) equations are solved to simulate steady and unsteady, asymmetric, vortical laminar flow around cones at high incidences and supersonic Mach numbers. The equations are solved by using an implicit, upwind, flux-difference splitting (FDS), finite-volume scheme. The locally conical flow assumption is used and the solutions are obtained by forcing the conserved components of the flowfield vector to be equal at two axial stations located at 0.95 and 1.0. Computational examples cover steady and unsteady asymmetric flows around a circular cone and its control using side strakes. The unsteady asymmetric flow solution around the circular cone has also been validated using the upwind, flux-vector splitting (FVS) scheme with the thin-layer NS equations and the upwind FDS with the full NS equations. The results are in excellent agreement with each other. Unsteady asymmetric flows are also presented for elliptic- and diamond-section cones, which model asymmetric vortex shedding around round- and sharp-edged delta winds. Author

N93-14692*# National Aeronautics and Space Administration. Langley Research Center, Hampton, VA.

PASSIVE CONTROL OF SUPERSONIC ASYMMETRIC VORTICAL FLOWS AROUND CONES

C. H. Liu, Osama A. Kandil (Old Dominion Univ., Norfolk, VA.), and Tin-Chee Wong (Old Dominion Univ., Norfolk, VA.) *In* Old Dominion Univ., Analysis and Control of Asymmetric Vortex Flows and Supersonic Vortex Breakdown Nov. 1992 17 p Repr. from Impact of Computing in Science and Engineering, v. 4, 1992 p 80-96 (For primary document see N93-14687 04-34)

(Contract NAS1-18584)

Avail: CASI HC A03/MF A02

The unsteady, compressible, thin-layer Navier-Stokes equations are used to numerically study the passive control of steady and unsteady supersonic asymmetric flows around circular and noncircular cones. The main computational scheme of the present study is an implicit upwind, flux-difference splitting, finite-volume scheme. Passive control of flow asymmetry is studied by using a vertical fin in the leeward plane of geometric symmetry and side strakes with and without thickness at different orientations. The study focuses on circular-section cones since they are the most likely section-shapes for strong flow asymmetry. Side-strake passive control is shown to be more efficient and practical than vertical-fin passive control. Author

N93-14694 Texas Univ., Arlington.

AN INVESTIGATION OF GENUINELY MULTIDIMENSIONAL SCHEMES FOR THE EULER EQUATIONS Ph.D. Thesis

Donna Jean Michalek 1992 110 p

Avail: Univ. Microfilms Order No. DA9231252

Efforts to improve algorithms which are used to obtain solutions to the Euler equations have resulted in the development of genuinely multidimensional schemes. These differ from classical operator-split schemes by allowing the wave components of the numerical model to propagate independently of the underlying grid geometry. While genuinely multidimensional solvers show high resolution of flowfield features, they lack the robustness of the classical methods. This work has sought to develop a more robust genuinely multidimensional scheme. The result of this investigation is a new genuinely multidimensional scheme which makes use of gradient data taken from the flowfield. The numerical model consists of five waves which are elementary solutions to the Euler equations. These waves are used with a newly developed flux formulation which models the effect of the passage of the waves over a portion of the domain. It is these flux values which are used to obtain the flowfield solution. An evaluation of the method was conducted by using it to solve a wide variety of two dimensional flow problems and then comparing the results to those obtained using a classical solution technique. This comparison showed that the present scheme always improved resolution of flowfield features for supersonic flows while maintaining nearly-monotone strong shock transitions. The method displayed no such improvements for the subsonic and transonic flow cases investigated. While the present method did exhibit an improvement in convergence to steady state over that seen by similar methods, it still does not meet a rigorous convergence criterion. Recommendations are made for continuing research with the present method together with suggestions for possible improvements to it. Dissert. Abstr.

N93-14695 Rutgers - The State Univ., New Brunswick, NJ.

A NUMERICAL INVESTIGATION OF THE INTERACTION BETWEEN CROSSING OBLIQUE SHOCKS AND A TURBULENT BOUNDARY LAYER Ph.D. Thesis

Natraj Narayanswami 1992 264 p

Avail: Univ. Microfilms Order No. DA9232939

A numerical investigation of the 3-D interaction between crossing oblique shock waves and a turbulent boundary layer is described. The flow geometry is a simplified representation of a high speed inlet and consists of a pair of symmetric, opposing sharp find mounted on a flat plate. The focus of the research is the flowfield associated with the interaction between the crossing oblique shocks generated by supersonic flow past the fins and the turbulent boudary layer on the plate. The theoretical model is the full 3-D mean compressible Reynolds-averaged Navier-Stokes equations incorporating the Baldwin-Lomax algebraic turbulent eddy viscosity model. Two sets of computations are presented. The first involves supersonic flow past (9 deg, 9 deg) and (11 deg, 11 deg) fins for M(sub infinity) = 8.2, Re(sub delta(sub infinity)) = 1.6(10)(exp 5) and cooled walls. The incoming boundary layer is 'thick', (sigma infinity is approximately find separation distance). Computed results show very good agreement with experiment for surface pressure and surface streamline patterns. The peak heat transfer on the plate (off the centerline) is overestimated by almost a factor of two. The surface flow pattern indicates separation in the sense of Lighthill. A low energy jet forms downstream of the crossed shocks, similar to that observed at Mach 2.95, occupying a significant portion of the outflow. This flow structure appears to be a fundamental feature of crossing shock interactions. A preliminary picture of the wave structure of the interaction is derived. Dissert. Abstr.

N93-14715 Lawrence Livermore National Lab., CA.

OPTICAL MONITOR FOR OBSERVING TURBULENT FLOW Patent Application

G. F. Albrecht, inventor (to DOE) and T. R. Moore, inventor (to DOE) 1991 24 p

(Contract W-7405-eng-48)

(DE92-019831; US-Patent-Appl-SN-642577; Patents-US-A-7642577) Avail: CASI HC A03/MF A01

The present invention provides an apparatus and method for non-invasively monitoring turbulent fluid flows including anisotropic flows. The present invention uses an optical technique to filter out the rays travelling in a straight line, while transmitting rays with turbulence induced fluctuations in time. The output is two dimensional, and can provide data regarding the spectral intensity distribution, or a view of the turbulence in real time. The optical monitor of the present invention comprises a laser that produces a coherent output beam that is directed through a fluid flow, which phase-modulates the beam. The beam is applied to a temporal filter that filters out the rays in the beam that are straight, while substantially transmitting the fluctuating, turbulence-induced rays. The temporal filter includes a lens and a photorefractive crystal such as BaTiO3 that is positioned in the converging section of the beam near the focal plane. An

imaging system is used to observe the filtered beam. The imaging system may take a photograph, or it may include a real time camera that is connected to a computer. The present invention may be used for many purposes including research and design in aeronautics, hydrodynamics, and combustion. DOE

N93-14758*# National Aeronautics and Space Administration. Lewis Research Center, Cleveland, OH.

SUPERSONIC BOUNDARY-LAYER FLOW TURBULENCE MODELING

Chi-Rong Wang Mar. 1993 12 p Proposed for presentation at the International Conference on Near-Wall Turbulence Flows, Tempe, AZ, 15-18 Mar. 1993

(RTOP 505-62-52)

(NASA-TM-105893; E-7360; NAS 1.15:105893) Avail: CASI HC A03/MF A01

Baldwin-Lomax and kappa-epsilon turbulence models were modified for use in Navier-Stokes numerical computations of Mach 2.9 supersonic turbulent boundary layer flows along compression ramps. The computational results of Reynolds shear stress profiles were compared with experimental data. The Baldwin-Lomax model was modified to account for the Reynolds shear stress amplification within the flow field. A hybrid kappa-epsilon model with viscous sublayer turbulence treatment was constructed to predict the Reynolds shear stress profiles within the entire flow field. These modified turbulence models were effective for the computations of the surface pressure and the skin friction factor variations along an 8 deg ramp surface. The hybrid kappa-epsilon model could improve the predictions of the Reynolds shear stress profile and the skin friction factor near the corner of a 16 deg ramp. Author

N93-14797*# High Technology Corp., Hampton, VA.

BLSTA: A BOUNDARY LAYER CODE FOR STABILITY ANALYSIS Final Report

Yong-Sun Wie Dec. 1992 114 p

(Contract NAS1-19299; RTOP 505-59-10)

(NASA-CR-4481; HTC-9204; NAS 1.26:4481) Avail: CASI HC A06/MF A02

A computer program is developed to solve the compressible, laminar boundary-layer equations for two-dimensional flow, axisymmetric flow, and quasi-three-dimensional flows including the flow along the plane of symmetry, flow along the leading-edge attachment line, and swept-wing flows with a conical flow approximation. The finite-difference numerical procedure used to solve the governing equations is second-order accurate. The flow over a wide range of speed, from subsonic to hypersonic speed with perfect gas assumption, can be calculated. Various wall boundary conditions, such as wall suction or blowing and hot or cold walls, can be applied. The results indicate that this boundary-layer code gives velocity and temperature profiles which are accurate, smooth, and continuous through the first and second normal derivatives. The code presented herein can be coupled with a stability analysis code and used to predict the onset of the boundary-layer transition which enables the assessment of the laminar flow control techniques. A user's manual is also included. Author

N93-14816# General Electric Co., Schenectady, NY. Knolls Atomic Power Lab.

ADIABATIC TWO-PHASE FLOW IN A TEST SECTION WITH PARTIAL FLOW BLOCKAGES

P. D. Symolon, W. E. Moore, and W. O. Morris Apr. 1992 47 p Presented at the American Society of Mechanical Engineers National Heat Transfer Conference and Exposition, San Diego, CA, 9-12 Aug. 1992

(Contract DE-AC12-76SN-00052)

(DE92-016360; KAPL-4733; CONF-920804-23) Avail: CASI HC A03/MF A01

An experiment has been performed to study vertical two-phase flow behavior in the vicinity of partial flow blockages, where complex phenomena such as phase separation, droplet entrainment and flow stratification are occurring. Freon-114 was used to simulate a high pressure steam/water mixture to permit low pressure testing with full visual access. Detailed void fraction scans were taken with a gamma densitometer. Flowing quality was obtained from inlet temperatures and the known heat input. Data were taken over a mass flux range of 75 to 600 Kg/sq M-sec (55,000 to 440,000 lbm/Hr-sq ft), and an inlet void fraction range of 4 to 60 percent, at a pressure of 0.275 MPa (40 psia). The objective of this work is to provide data for two-phase flow model assessment and code qualification. Comparisons of the test data with the TRACE and FLOW-3D codes were made, using constitutive models from the open literature. The flow blockages divert the mixed phases laterally, and a liquid recirculation zone with some entrained bubbles is produced downstream of the flow blockage. For higher inlet void fraction and low flow rates, the flow is more chaotic and at times exhibits oscillatory behavior. For higher flow rates increased phase separation occurs due to acceleration around the blockage. For example, at 60 percent inlet void fraction there is a liquid layer above the first flow blockage followed by a vapor pocket. Entrained liquid drops are present in this voided pocket, which fall downward, replenishing the liquid rich layer on top of the flow blockage. The vapor pocket becomes more pronounced and the liquid rich layer becomes more shallow at increased mass flow. DOE

N93-14829*# National Aeronautics and Space Administration. Lewis Research Center, Cleveland, OH.

SECOND ORDER CLOSURE MODELING OF TURBULENT BUOYANT WALL PLUMES

Gang Zhu (Wayne State Univ., Detroit, MI.), Ming-Chia Lai (Wayne State Univ., Detroit, MI.), and Tsan-Hsing Shih Dec. 1992 14 p

(RTOP 505-62-21)

(NASA-TM-105956; E-7476; NAS 1.15:105956; ICOMP-92-23; CMOTT-92-11) Avail: CASI HC A03/MF A01

Non-intrusive measurements of scalar and momentum transport in turbulent wall plumes, using a combined technique of laser Doppler anemometry and laser-induced fluorescence, has shown some interesting features not present in the free jet or plumes. First, buoyancy-generation of turbulence is shown to be important throughout the flow field. Combined with low-Reynolds-number turbulence and near-wall effect, this may raise the anisotropic turbulence structure beyond the prediction of eddy-viscosity models. Second, the transverse scalar fluxes do not correspond only to the mean scalar gradients, as would be expected from gradient-diffusion modeling. Third, higher-order velocity-scalar correlations which describe turbulent transport phenomena could not be predicted using simple turbulence models. A second-order closure simulation of turbulent adiabatic wall plumes, taking into account the recent progress in scalar transport, near-wall effect and buoyancy, is reported in the current study to compare with the non-intrusive measurements. In spite of the small velocity scale of the wall plumes, the results showed that low-Reynolds-number correction is not critically important to predict the adiabatic cases tested and cannot be applied beyond the maximum velocity location. The mean and turbulent velocity profiles are very closely predicted by the second-order closure models. but the scalar field is less satisfactory, with the scalar fluctuation level underpredicted. Strong intermittency of the low-Reynolds-number flow field is suspected of these discrepancies. The trends in second- and third-order velocity-scalar correlations, which describe turbulent transport phenomena, are also predicted in general, with the cross-streamwise correlations better than the streamwise one. Buoyancy terms modeling the pressure-correlation are shown to improve the prediction slightly. The effects of equilibrium time-scale ratio and boundary condition are also discussed. Author

N93-14885*# National Aeronautics and Space Administration. Lewis Research Center, Cleveland, OH.

PRECONDITIONED CONJUGATE-GRADIENT METHODS FOR LOW-SPEED FLOW CALCULATIONS

Kumud Ajmani, Wing-Fai Ng (Virginia Polytechnic Inst. and State Univ., Blacksburg.), and Meng-Sing Liou Jan. 1993 13 p Presented at the 31st Aerospace Sciences Meeting and Exhibit, Reno, NV, 11-14 Jan. 1993

(RTOP 505-62-21)

(NASA-TM-105929; E-7438; NAS 1.15:105929) Avail: CASI HC A03/MF A01

An investigation is conducted into the viability of using a generalized Conjugate Gradient-like method as an iterative solver to obtain steady-state solutions of very low-speed fluid flow problems. Low-speed flow at Mach 0.1 over a backward-facing step is chosen as a representative test problem. The unsteady form of the two dimensional, compressible Navier-Stokes equations is integrated in time using discrete time-steps. The Navier-Stokes equations are cast in an implicit, upwind finite-volume, flux split formulation. The new iterative solver is used to solve a linear system of equations at each step of the time-integration. Preconditioning techniques are used with

the new solver to enhance the stability and convergence rate of the solver and are found to be critical to the overall success of the solver. A study of various preconditioners reveals that a preconditioner based on the Lower-Upper Successive Symmetric Over-Relaxation iterative scheme is more efficient than a preconditioner based on Incomplete L-U factorizations of the iteration matrix. The performance of the new preconditioned solver is compared with a conventional Line Gauss-Seidel Relaxation (LGSR) solver. Overall speed-up factors of 28 (in terms of global time-steps required to converge to a steady-state solution) and 20 (in terms of total CPU time on one processor of a CRAY-YMP) are found in favor of the new preconditioned solver, when compared with the LGSR solver. Author

N93-14914*# National Aeronautics and Space Administration. Lewis Research Center, Cleveland, OH.

NUMERICAL STUDY OF MIXING OF TWO FLUIDS UNDER LOW GRAVITY

Walter M. B. Duval Oct. 1992 45 p

(RTOP 674-21-05)

(NASA-TM-105865; E-7326; NAS 1.15:105865) Avail: CASI HC A03/MF A01

The mixing characteristics of two fluids inside a cavity due to buoyancy driven flow fields for low gravity conditions is investigated via numerical experiments. The buoyancy driven flow, depending on the parametric region, stretches and deforms the material interface into a wave morphological pattern. The morphological pattern affects the resulting stratification thickness of the mixed region. Three basic mixing regimes occur: convective, diffusive, and chaotic. In the convective regime, an overturning motion occurs which gives rise to a stable wave formation. This wave oscillates and its decay leads to a stable stratification. Whereas, in the diffusive regime, the length of the interface remains constant while mixing occurs. This limiting behavior is very important to materials processing in space, and it admits a closed form solution corresponding to vanishing convective terms which agrees with computational results. Finally, in the chaotic regime, the material interface continuously stretches and folds on itself similar to a horseshoe map. The length of stretch of the interface increases exponentially. Internal wavebreaking occurs for this case. This wavebreaking generates local turbulence, and provides an effective mechanism for mixing. Author

N93-15065# Cincinnati Univ., OH. Dept. of Aerospace Engineering and Engineering Mechanics.

L.D.V. MEASUREMENTS OF UNSTEADY FLOW FIELDS IN RADIAL TURBINE Final Report

W. Tabakoff and M. Pasin Jul. 1992 164 p

(Contract DAAL03-90-G-0129)

(AD-A255728; Rept-92-105) Avail: CASI HC A08/MF A02

Detailed measurements of an unsteady flow field within the inlet guide vanes (IGV) and the rotor of a radial inflow turbine were performed using a three component Laser Doppler Velocimeter (LDV) system together with a rotary encoder. The mean velocity, the flow angle and the turbulence contours for IGV passages are presented at four blade-to-blade planes for different rotor positions to give three dimensional, unsteady behavior of the IGV flow field. These results are compared with the measurements obtained in the same passage in the absence of the rotor. The flow field of the IGV passage was found to be affected by the presence of the rotor. The ratio of the tangential normal stresses to the radial normal stresses at the exit of the IGV was found to be more than doubled when compared to the case without the rotor. The rotor flow field measurements are presented as relative mean velocity and turbulence stress contours at various cross section planes throughout the rotor. The cross flow and turbulence stress levels were found to be influenced by the incidence angle. Transportation of the high turbulence fluid by the cross flow was observed downstream in the rotor blade passages. GRA

N93-15120# Universitaet der Bundeswehr Muenchen, Neubiberg (Germany). Inst. fuer Raumfahrttechnik.

ASYMMETRIC NATURAL DAMPED FREQUENCIES OF A ROTATING INFINITELY LONG VISCOUS LIQUID COLUMN

Helmut F. Bauer 1991 43 p

(LRT-WE-9-FB-23-1991; ETN-92-92734) Avail: CASI HC A03/MF A01

The natural damped frequencies were determined for the asymmetric motion of an infinitely long liquid column consisting of incompressible and viscous liquid. Instability of the column appears, if the axial wave length satisfies with the Weber number. This includes the axisymmetric m = 0 instability, the C-mode (m = 1) instability and also those of high angular modes. Stability is independent of viscosity. The result is also valid for the nonrotating liquid column. ESA

N93-15122# Paris-Sud Univ., Orsay (France). Lab. d'Analyse Numerique.

DYNAMICS SYSTEMS APPLIED TO NAVIER-STOKES EQUATIONS FOR THE STUDY OF TURBULENCE Final Summary Report [APPROACHE SYSTEMES DYNAMIQUES APPLIQUEE AUX EQUATIONS DE NAVIER-STOKES POUR L'ETUDE DE LA TURBULENCE]

R. Temam, T. Dubois, F. Jauberteau, F. Pascal, C. Rosier, J. Laminie, and M. Marion 17 Mar. 1991 38 p In FRENCH

(Contract DRET-88-164)

(ETN-92-92553) Avail: CASI HC A03/MF A01

Implementation of the nonlinear Galerkin method for two dimensional numerical simulation of Navier-Stokes equations is considered. Discretization of this method by finite element method is explored. Turbulent flows are mathematically described by a compact attractor in the phase space. The approximation of this attractor, which is very likely fractal, by smooth manifolds, the approximated inertial manifolds, may lead to a better understanding of the physics of turbulence. It leads already to the development of new algorithms, similar to subgrid modeling in fluid mechanics, which seem well adapted to the numerical integration of the Navier-Stokes equations in large intervals of time. The nonlinear Galerkin method that was studied is stable and easy to implement; and by saving a significant amount of computing time it pushes slightly the edges of what can be done with the present computers. ESA

N93-15132# Universitaet der Bundeswehr Muenchen, Neubiberg (Germany). Inst. fuer Raumfahrttechnik.

TRANSIENT RESPONSE OF A VISCOUS LIQUID BRIDGE OF FINITE LENGTH AND ANCHORED EDGES

Helmut F. Bauer 1991 46 p

(LRT-WE-9-FB-25-1991; ETN-92-92735) Avail: CASI HC A03/MF A01

The dynamic response of an axially excited viscous liquid bridge with anchored edges due to sudden change of excitation amplitude and forcing frequency is investigated analytically. The transient behavior of the free liquid surface displacement was evaluated numerically for various excitation changes. It depends on the surface tension parameter, the aspect ratio and is presented as a function of the dimensionless time. The result is of importance for sweeping experiments to find the proper sweeping speed, in order to really measure steady state oscillations. ESA

N93-15187# Amtec Engineering, Inc., Bellevue, WA.

THE 3D NAVIER-STOKES FLOW ANALYSIS FOR SHARED AND DISTRIBUTED MEMORY MIMD COMPUTERS Final Report, 15 May 1990 - 30 Jul. 1992

Scott T. Imlay and Moeljo Soetrisno 15 Sep. 1992 119 p

(Contract DAAH01-90-C-0373; ARPA Order 6685)

(AD-A256038) Avail: CASI HC A06/MF A02

Multiple instruction multiple data (MIMD) parallel computers were investigated as a means of obtaining the immense computer power required to analyze the flow about a complete aircraft configuration. A computational fluid dynamics computer program for solving the Navier-Stokes equations, with coupled nonequilibrium chemistry, was parallelized on three MIMD computers: the Intel Touchstone distributed memory computer, the Cray Y/MP supercomputer, and the Silicon Graphics IRIS 4-D/380 shared memory computer. The program used an LU-SGS implicit algorithm. The parallelization was performed using permanent domain decomposition. The parallel efficiency and the main limitations to efficient parallelization were evaluated for a series of real life engineering problems. On the Intel Touchstone, the parallel efficiency decreased slowly as the number of processors was increased. The main deterrent to parallel performance was the latency time for interprocessor communication. On the Cray Y/MP, the parallel efficiency dropped rapidly as the number of processors was increased. The main deterrent to parallel performance was the reduction in vector length during domain decomposition. GRA

N93-15285# Lawrence Livermore National Lab., CA.

ALPHA MIGRATION THROUGH AIR FILTERS: A NUMERICAL SIMULATION

Arthur H. Biermann, Robert A. daRoza, and Yun Chang 11 Dec. 1991 33 p
(Contract W-7405-eng-48)
(UCRL-LR-109866) Avail: CASI HC A03/MF A01

This theoretical study investigates the migration of alpha-emitting particles through high-efficiency particulate air (HEPA) filters. As part of the study, a review of previous research relating to the alpha-migration phenomena was conducted. As a result of the literature review, a numerical model was developed to simulate the migration of alpha-emitting radionuclide aerosols through HEPA filters. This model predicts the filter performance with regard to particle penetration. It can be used to better estimate the penetration of alpha radioactive species through filter systems for environmental concerns, to aid in the use of current filter systems, and to design new filter systems. Author

N93-15332# Wright Lab., Eglin AFB, FL.
A MULTIGRID APPROACH TO EMBEDDED-GRID SOLVERS Interim Report, Jan. 1991 - Apr. 1992
Rudy A. Johnson Aug. 1992 84 p
(AF Proj. 2567)
(AD-A256405; WL-TR-92-7039) Avail: CASI HC A05/MF A01

The explicit first order flux difference splitting (FDS) is used to solve the equations governing inviscid fluid flow on a single grid for the 5 degree ramp and the 5 degree ramp near a flat plate. Calculations were made for the Mach 2 case using local time stepping at a Courant number of 0.96. The multigrid full approximation scheme (FAS) is applied to this non-linear problem to provide increased convergence rates and reduced central processing unit (CPU) time requirements. Several systems of embedded grids are implemented to provide increased accuracy near shock waves. Embedded grids were aligned with the shocks to take advantage of the excellent shock capturing capability of the FDS scheme. The nonaligned multigrid is introduced to provide increased convergence for the embedded grid systems by treating the individual grids as levels in the multigrid solution procedure. This technique is able to converge 69 pct. faster than the embedded grid procedure for the 5 degree ramp, and 28 pct. faster for a more complex reflected shock case. GRA

N93-15355*# National Aeronautics and Space Administration. Lewis Research Center, Cleveland, OH.
USE OF SURFACE HEAT TRANSFER MEASUREMENTS AS A FLOW SEPARATION DIAGNOSTIC IN A TWO DIMENSIONAL REFLECTED OBLIQUE SHOCK/TURBULENT BOUNDARY LAYER INTERACTION
A. Robert Porro and Warren R. Hingst Jan. 1993 18 p Presented at the 31st Aerospace Sciences Meeting and Exhibit, Reno, NV, 11-14 Jan. 1993; sponsored by AIAA
(RTOP 505-62-52)
(NASA-TM-105981; E-7505; NAS 1.15:105981; AIAA Paper 93-0775)
Avail: CASI HC A03/MF A01

The feasibility of using streamwise surface heat transfer measurements to detect the presence of flow separation in a two-dimensional reflected oblique shock/turbulent boundary layer interaction is reported. Surface heat transfer and static pressure data are presented for attached and separated flows for a free stream nominal Mach number range of 2.5 to 3.5 and shock generator angles of 2 to 8 degrees. The static pressure data do show the characteristic triple inflection point distribution for the strongly separated flow cases. The corresponding surface heat transfer data show unique trends that correlate well with the static pressure determination of the extent of the separated flow region. For the incipient or weakly separated flow cases, the static pressure data do not exhibit the characteristic triple inflection point distribution. However, the same trends in the heat transfer data that are seen for the strongly separated flow cases are evident for the weakly separated flows. Hence, the heat transfer data can be used to determine the extent of weakly separated flows when the surface static pressure distributions often can not. Author

N93-15402*# Sverdrup Technology, Inc., Brook Park, OH.
ADVANCEMENTS IN THE LEWICE ICE ACCRETION MODEL Final Report
William B. Wright NASA Jan. 1993 18 p Presented at the 31st Aerospace Sciences Meeting and Exhibit, Reno, NV, 11-14 Jan. 1993; Sponsored by AIAA
(Contract NAS3-25266; RTOP 505-68-10)
(NASA-CR-191019; E-7523; NAS 1.26:191019; AIAA Paper 93-0171)
Avail: CASI HC A03/MF A01

Recent evidence has shown that the NASA/Lewis Ice Accretion Model, LEWICE, does not predict accurate ice shapes for certain glaze ice conditions. This paper will present the methodology used to make a first attempt at improving the ice accretion prediction in these regimes. Importance is given to the correlations for heat transfer coefficient and ice density, as well as runback flow, selection of the transition point, flow field resolution, and droplet trajectory models. Further improvements and refinement of these modules will be performed once tests in NASA's Icing Research Tunnel, scheduled for 1993, are completed. Author

N93-15434*# National Aeronautics and Space Administration. Langley Research Center, Hampton, VA.
FINITE-DIFFERENCE SOLUTION FOR LAMINAR OR TURBULENT BOUNDARY LAYER FLOW OVER AXISYMMETRIC BODIES WITH IDEAL GAS, CF4, OR EQUILIBRIUM AIR CHEMISTRY
H. Harris Hamilton, II, Daniel R. Millman (George Washington Univ., Hampton, VA.), and Robert B. Greendyke (Vigyan Research Associates, Inc., Hampton, VA.) Washington Dec. 1992 23 p
(RTOP 506-40-91-01)
(NASA-TP-3271; L-17102; NAS 1.60:3271) Avail: CASI HC A03/MF A01

A computer code was developed that uses an implicit finite-difference technique to solve nonsimilar, axisymmetric boundary layer equations for both laminar and turbulent flow. The code can treat ideal gases, air in chemical equilibrium, and carbon tetrafluoride (CF4), which is a useful gas for hypersonic blunt-body simulations. This is the only known boundary layer code that can treat CF4. Comparisons with experimental data have demonstrated that accurate solutions are obtained. The method should prove useful as an analysis tool for comparing calculations with wind tunnel experiments and for making calculations about flight vehicles where equilibrium air chemistry assumptions are valid. Author

N93-15473# Rolls-Royce Ltd., Derby (England).
THE USE OF A NOVEL MANUFACTURING PROCESS FOR HIGH PERFORMANCE TITANIUM PLATE FIN HEAT EXCHANGERS
C. I. Adderley (Rolls-Royce and Associates Ltd., Derby, England) and J. O. Fowler 2 Aug. 1991 10 p Presented at the I.Chem.E/EEO International Conference on Heat Exchanger Technology: Current Practice and Future Developments, Leeds, England, Jul. 1991
(PNR-90934; ETN-92-92214) Copyright Avail: CASI HC A02/MF A01

The titanium Superplastic Forming/Diffusion Bonding (SPF/DB) process developed for the cost effective manufacture of critical aeroengine components is applied to the manufacture of Plate Fin Heat Exchangers (PFHEs). Using this process, the primary and secondary heat transfer surfaces are joined by solid state diffusion bonds. This results in a high integrity exchanger which can operate at pressures in excess of 200 bar and at temperatures up to 300 C. The SPF/DB process, together with the excellent corrosion resistance of titanium, greatly extends the range of application of the PFHE. The SPF/DB process and its application to the design of a PFHE for a typical offshore duty is described. ESA

N93-15481*# National Aeronautics and Space Administration. Langley Research Center, Hampton, VA.
ON EXPLICIT ALGEBRAIC STRESS MODELS FOR COMPLEX TURBULENT FLOWS
T. B. Gatski and C. G. Speziale (Institute for Computer Applications in Science and Engineering, Hampton, VA.) Nov. 1992 35 p
(Contracts NAS1-18605; NAS1-19480; RTOP 505-90-52-01)
(NASA-CR-189725; NAS 1.26:189725; ICASE-92-58) Avail: CASI HC A03/MF A01

Explicit algebraic stress models that are valid for three-dimensional turbulent flows in noninertial frames are systematically derived from a hierarchy of second-order closure models. This represents a generalization of the model derived by Pope who based his analysis on the Launder, Reece, and Rodi model restricted to two-dimensional turbulent flows in an inertial frame. The relationship between the new models and traditional algebraic stress models -- as well as anistropic eddy visosity models -- is theoretically established. The need for regularization is demonstrated in an effort to explain why traditional algebraic stress models have failed in

complex flows. It is also shown that these explicit algebraic stress models can shed new light on what second-order closure models predict for the equilibrium states of homogeneous turbulent flows and can serve as a useful alternative in practical computations. Author

N93-15488# Rolls-Royce Ltd., Derby (England).
HIGH PERFORMANCE TITANIUM PLATE FIN HEAT EXCHANGER USING A NOVEL MANUFACTURING PROCESS
C. I. Adderley (Rolls-Royce and Associates Ltd., Derby, England) and J. O. Fowler 2 Mar. 1991 14 p Presented at the 18th Eurotherm Seminar on Design and Operation of Heat Exchangers, Hamburg, Germany, Feb. 1991
(PNR-90933; ETN-92-92213) Copyright Avail: CASI HC A03/MF A01

The Plate Fin Heat Exchanger (PFHE), a compact heat exchanger which offers significant advantages over shell and tube exchangers in terms of weight, volume, and thermal effectivenesss, is described. It has a multistream capability and consequently a single unit can replace several shell and tube exchangers. The superplastic forming/diffusion bonding manufacturing process, which overcomes the limitations imposed by the conventional PFHE manufacturing route and allows greater flexibility in the design of PFHE's, is described. ESA

N93-15499*# National Aeronautics and Space Administration. Lewis Research Center, Cleveland, OH.
ON THE NONLINEAR THREE DIMENSIONAL INSTABILITY OF STOKES LAYERS AND OTHER SHEAR LAYERS TO PAIRS OF OBLIQUE WAVES
Xuesong Wu (Imperial Coll. of Science and Technology, London, England), Sang Soo Lee (Sverdrup Technology, Inc., Brook Park, OH.), and Stephen J. Cowley (Cambridge Univ., England) Dec. 1992 51 p
(RTOP 505-62-21)
(NASA-TM-105918; E-7410; ICOMP-92-20; NAS 1.15:105918) Avail: CASI HC A04/MF A01

The nonlinear evolution of a pair of initially oblique waves in a high Reynolds Number Stokes layer is studied. Attention is focused on times when disturbances of amplitude epsilon have O(epsilon(exp 1/3)R) growth rates, where R is the Reynolds number. The development of a pair of oblique waves is then controlled by nonlinear critical-layer effects. Viscous effects are included by studying the distinguished scaling epsilon = O(R(exp -1)). This leads to a complicated modification of the kernel function in the integro-differential amplitude equation. When viscosity is not too large, solutions to the amplitude equation develop a finite-time singularity, indicating that an explosive growth can be introduced by nonlinear effects; we suggest that such explosive growth can lead to the bursts observed in experiments. Increasing the importance of viscosity generally delays the occurrence of the finite-time singularity, and sufficiently large viscosity may lead to the disturbance decaying exponentially. For the special case when the streamwise and spanwise wavenumbers are equal, the solution can evolve into a periodic oscillation. A link between the unsteady critical-layer approach to high-Reynolds-number flow instability, and the wave vortex approach is identified. Author

N93-15527*# Sverdrup Technology, Inc., Brook Park, OH.
UNSTEADY SHEAR DISTURBANCES WITHIN A TWO DIMENSIONAL STRATIFIED FLOW Final Report
Jeffrey W. Yokota Oct. 1992 59 p
(Contract NAS3-25266)
(NASA-CR-189121; NAS 1.26:189121) Avail: CASI HC A04/MF A01

The origin and evolution of shear disturbances within a stratified, inviscid, incompressible flow are investigated numerically by a Clebsch/Weber decomposition based scheme. In contrast to homogeneous flows, within which vorticity can be redistributed but not generated, the presence of a density stratification can render an otherwise irrotational flow vortical. In this work, a kinematic decomposition of the unsteady Euler equations separates the unsteady velocity field into rotational and irrotational components. The subsequent evolution of these components is used to study the influence various velocity disturbances have on both stratified and homogeneous flows. In particular, the flow within a two-dimensional channel is used to investigate the evolution of rotational disturbances, generated or convected, downstream from an unsteady inflow condition. Contrasting simulations of both stratified and homogeneous flows are used to distinguish between redistributed inflow vorticity and that which is generated by a density stratification. Author

N93-15585*# National Aeronautics and Space Administration. Lewis Research Center, Cleveland, OH.
TURBULENT FLUID MOTION IV-AVERAGES, REYNOLDS DECOMPOSITION, AND THE CLOSURE PROBLEM
Robert G. Deissler Sep. 1992 67 p
(RTOP 505-90-53)
(NASA-TM-105822; E-7253; NAS 1.15:105822) Avail: CASI HC A04/MF A01

Ensemble, time, and space averages as applied to turbulent quantities are discussed, and pertinent properties of the averages are obtained. Those properties, together with Reynolds decomposition, are used to derive the averaged equations of motion and the one- and two-point moment or correlation equations. The terms in the various equations are interpreted. The closure problem of the averaged equations is discussed, and possible closure schemes are considered. Those schemes usually require an input of supplemental information unless the averaged equations are closed by calculating their terms by a numerical solution of the original unaveraged equations. The law of the wall for velocities and temperatures, the velocity- and temperature-defect laws, and the logarithmic laws for velocities and temperatures are derived. Various notions of randomness and their relation to turbulence are considered in light of ergodic theory. Author

N93-15635# Naval Postgraduate School, Monterey, CA.
PREDICTION OF TURBINE CASCADE FLOWS WITH A QUASI-THREE-DIMENSIONAL ROTOR VISCOUS CODE AND THE EXTENSION OF THE ALGEBRAIC TURBULENCE MODEL M.S. Thesis
Chun-Wei Wang Jun. 1992 69 p
(AD-A256831) Avail: CASI HC A04/MF A01

A quasi-three-dimensional rotor viscous code is used to predict high subsonic flow through an annular cascade of turbine blades. The well known Baldwin-Lomax turbulence model is used in the program. An attempt was made to implement a new turbulence model based on renorminalization group theory. This was done to improve the prediction of the boundary layer transition on the blade surfaces and subsequent wake development. The comparison of these two turbulence models with experimental data are presented. Pressure, velocity ratio, flow angle distributions, and downstream wake predictions were studied using results from RVCQ3D (Rotor Viscous Code Quasi-Three-Dimensional) code. The computed results showed good agreement with experiment when comparing the blade surface local static pressure to inlet total pressure ratio at the midspan position of the annular turbine cascade. The computational approach used to implement the turbulence model is also described. GRA

N93-15643*# Creare, Inc., Hanover, NH.
NUMERICAL MODELING TOOLS FOR CHEMICAL VAPOR DEPOSITION Progress Report, 5 May 1988 - 31 May 1991
Thomas J. Jasinski and Edward P. Childs Washington National Aeronautics and Space Administration Dec. 1992 100 p
(Contract NAS1-18648; RTOP 324-02-00)
(NASA-CR-4480; NAS 1.26:4480; TM-1504) Avail: CASI HC A05/MF A02

Development of general numerical simulation tools for chemical vapor deposition (CVD) was the objective of this study. Physical models of important CVD phenomena were developed and implemented into the commercial computational fluid dynamics software FLUENT. The resulting software can address general geometries as well as the most important phenomena occurring with CVD reactors: fluid flow patterns, temperature and chemical species distribution, gas phase and surface deposition. The physical models are documented which are available and examples are provided of CVD simulation capabilities. Author

N93-15652# Lehigh Univ., Bethlehem, PA. Dept. of Mechanical Engineering and Mechanics.
UNSTEADY FLOW DISTORTION PAST BLADES: SOURCES OF NOISE GENERATION IN ROTATING FLOWS
D. O. Rockwell, O. Akin, J. H. Kim, S. Konak, and J. Kuryla 26 Aug. 1992 58 p
(Contract N00014-89-J-1799)
(AD-A255496) Avail: CASI HC A04/MF A01

The objectives of this research were to determine th flow structure and leading- and trailing-edges of blading tin terms of velocity gradients representing pressure sources and to employ active and passive control techniques to manipulate crucial phase shifts of vorticity fields past blading. The topics covered include the following: principal physical and theoretical concepts; experimental techniques, generic classes of edge/surface interaction; experimental systems; and flow structure in actively-controlled radial-flow machines. Author

N93-14747*# National Inst. of Standards and Technology, Gaithersburg, MD. Polymers Div.
FLOW BEHAVIOR IN LIQUID MOLDING
D. Hunston, F. Phelan, and R. Parnas *In* NASA. Langley Research Center, FIBER-TEX 1991: The Fifth Conference on Advanced Engineering Fibers and Textile Structures for Composites Oct. 1992 p 23-42 (For primary document see N93-14744 04-24)
Avail: CASI HC A03/MF A02

N93-14945# University of Western Ontario, London.
CONTROL OF THERMOCAPILLARY CONVECTION IN A TWO-LAYER LIQUID SYSTEM
J. M. Floryan and C. Chen *In* Canadian Space Agency, Proceedings of the Sixth CASI Conference on Astronautics 1990 10 p Previously announced in IAA as A91-34951 (For primary document see N93-14920 04-12)
Avail: Canadian Aeronautics and Space Inst., 222 Somerset St. W., Suite 601, Ottawa, Ontario K2P 0J1 Canada

N93-14956# MAYA Heat Transfer Technologies Ltd., Montreal (Quebec).
ADVANCES IN TMG
Kevin Duffy *In* Canadian Space Agency, Proceedings of the Sixth CASI Conference on Astronautics 1990 9 p Previously announced in IAA as A91-34962 (For primary document see N93-14920 04-12)
Avail: Canadian Aeronautics and Space Inst., 222 Somerset St. W., Suite 601, Ottawa, Ontario K2P 0J1 Canada

35 INSTRUMENTATION AND PHOTOGRAPHY

Includes remote sensors; measuring instruments and gages; detectors; cameras and photographic supplies; and holography.

For aerial photography see *43 Earth Resources and Remote Sensing*. For related information see also *06 Aircraft Instrumentation*, and *19 Spacecraft Instrumentation*.

N93-14105# Army Aeromedical Research Lab., Fort Rucker, AL.
TEST AND EVALUATION REPORT OF THE CATALYST RESEARCH OXYGEN MONITOR, MODEL MINIOX 3 Test Report
James E. Bruckart, Martin Quattlebaum, Joseph R. Licina, and Bill Olding (Universal Energy Systems, Inc., Dayton, OH.) Jul. 1992 66 p
(DA Proj. 3M4-63807-D-836)
(AD-A255849; USAARL-92-29) Avail: CASI HC A04/MF A01

The Catalyst Research Oxygen Monitor, Model Miniox 3, was tested for electromagnetic interference/compatibility in the UH-60A helicopter under the U.S. Army Program for Testing and Evaluation of Equipment for Aeromedical Operations. The tests were conducted using current military and industrial standards and procedures for electromagnetic interference/compatibility and human factors. The Catalyst Research Oxygen Monitor, Model Miniox III, was found to be compatible with U.S. Army MEDEVAC UH-60 Black Hawk. GRA

N93-14494*# Lovelace Scientific Resources, Inc., Albuquerque, NM.
ADVANCED SENSORS TECHNOLOGY SURVEY Final Report
Tommy G. Cooper, David J. Costello, Jerry G. Davis (Lovelace Scientific Resources, Inc., Albuquerque, NM.), Richard L. Horst (Man-Made Systems Corp., Ellicott City, MD.), Charles S. Lessard (Texas A&M Univ., College Station.), H. Herbert Peel (Southwest Research Inst., San Antonio, TX.), and Robert Tolliver (Lovelace Scientific Resources, Inc., Albuquerque, NM.) 10 Feb. 1992 159 p Prepared in cooperation with General Electric Co., Houston, TX
(Contract NAS9-17884)
(NASA-CR-185691; NAS 1.26:185691) Avail: CASI HC A08/MF A02

This project assesses the state-of-the-art in advanced or 'smart' sensors technology for NASA Life Sciences research applications with an emphasis on those sensors with potential applications on the space station freedom (SSF). The objectives are: (1) to conduct literature reviews on relevant advanced sensor technology; (2) to interview various scientists and engineers in industry, academia, and government who are knowledgeable on this topic; (3) to provide viewpoints and opinions regarding the potential applications of this technology on the SSF; and (4) to provide summary charts of relevant technologies and centers where these technologies are being developed. I.I.C.

N93-14653# Sea Tech, Inc., Corvallis, OR.
DEVELOPMENT OF AN EXPENDABLE PARTICLE SENSOR Progress Report, Apr. - Jul. 1992
Robert Bartz 3 Sep. 1992 10 p
(Contract N00014-90-C-0123)
(AD-A255702) Avail: CASI HC A02/MF A01

This report addresses progress on the Phase 2 Development of the Expendable Particle Sensor (EPS) over the time period of April through July 1992. Significant technical progress has been made during this time related to the study and measurement of the XOTD transmission line characteristics. The results of the study and measurement allowed Sea Tech to design the telemetry system line receiver to interface with the Sparton transmission line. The new telemetry system was then tested in both the laboratory and the field with excellent results. Determining the characteristics of the two wire transmission line for both air and water consumed a significant amount of time during this period. An understanding of transmission line characteristics is essential if the transmission line receiver is to be designed with optimum performance. The resistance, inductance and capacitance are the fundamental electrical characteristics of the transmission line. The resistance of the wire is given by the manufacturer. The transmission line inductance has no effect because a differential source is used to drive the transmission line, and therefore it is ignored. The capacitance of the transmission wire is not given by the manufacturer, so it was necessary to calculate and measure the bifilar wire capacitance for both air and water environments. GRA

N93-14714* National Aeronautics and Space Administration. Langley Research Center, Hampton, VA.
METHOD OF FORMING A MULTIPLE LAYER DIELECTRIC AND A HOT FILM SENSOR THEREWITH Patent
Purnell Hopson, Jr., inventor (to NASA) and Sang Q. Tran, inventor (to NASA) 27 Oct. 1992 8 p Continuation-in-part of abandoned US-Patent-Appl-SN-458214, filed 28 Dec. 1989 Division of US-Patent-Appl-SN-176547, filed 1 Apr. 1988
(NASA-Case-LAR-13678-3; US-Patent-5,158,801;
US-Patent-Appl-SN-688361; US-Patent-Class-427-58;
US-Patent-Class-427-255; US-Patent-Class-427-344;
US-Patent-Class-427-527; US-Patent-Class-427-255.7;
US-Patent-Class-427-248.1; US-Patent-Class-427-255.6) US Patent and Trademark Office

The invention is a method of forming a multiple layer dielectric for use in a hot-film laminar separation sensor. The multiple layer dielectric substrate is formed by depositing a first layer of a thermoplastic polymer such as on an electrically conductive substrate such as the metal surface of a model to be tested under cryogenic conditions and high Reynolds numbers. Next, a second dielectric layer of fused silica is formed on the first dielectric layer of thermoplastic polymer. A resistive metal film is deposited on selected areas of the multiple layer dielectric substrate to form one or more hot-film sensor elements to which aluminum electrical circuits deposited upon the multiple layered dielectric substrate are connected.
Official Gazette of the U.S. Patent and Trademark Office

N93-14716 Westinghouse Savannah River Co., Aiken, SC.
VARIABLE PATH LENGTH SPECTROPHOTOMETRIC PROBE Patent Application
P. E. ORourke, inventor (to DOE), J. E. McCarty, inventor (to DOE), and R. A. Haggard, inventor (to DOE) 1991 11 p
(Contract DE-AC09-89SR-18035)
(DE92-019834; US-Patent-Appl-SN-641978; Patents-US-A-7641978) Avail: CASI HC A03/MF A01

This invention consists of a compact, variable pathlength, fiber optic

probe for spectrophotometric measurements of fluids in situ. The probe comprises a probe body with a shaft having a polished end penetrating one side of the probe; a pair of optic fibers, parallel and coterminous, entering the probe opposite the reflecting shaft; and a collimating lens to direct light from one of the fibers to the reflecting surface of the shaft and to direct the reflected light to the second optic fiber. The probe body has an inlet and an outlet port to allow the liquid to enter the probe body and pass between the lens and the reflecting surface of the shaft. A linear stepper motor is connected to the shaft to cause the shaft to advance toward or away from the lens in increments so that absorption measurements can be made at each of the incremental steps. The shaft is sealed to the probe body by a bellows seal to allow freedom of movement of the shaft and yet avoid leakage from the interior of the probe. DOE

N93-14810*# Georgia Inst. of Tech., Atlanta.
DEVELOPMENT OF A FIBER OPTIC HIGH TEMPERATURE STRAIN SENSOR Progress Report, 1 Apr. 1991 - 31 Aug. 1992
E. O. Rausch, K. E. Murphy, and S. P. Brookshire Nov. 1992 102 p
(Grant NAG8-869)
(NASA-CR-191316; NAS 1.26:191316) Avail: CASI HC A06/MF A02

From 1 Apr. 1991 to 31 Aug. 1992, the Georgia Tech Research Institute conducted a research program to develop a high temperature fiber optic strain sensor as part of a measurement program for the space shuttle booster rocket motor. The major objectives of this program were divided into four tasks. Under Task 1, the literature on high-temperature fiber optic strain sensors was reviewed. Task 2 addressed the design and fabrication of the strain sensor. Tests and calibration were conducted under Task 3, and Task 4 was to generate recommendations for a follow-on study of a distributed strain sensor. Task 4 was submitted to NASA as a separate proposal. Author

N93-14840*# National Aeronautics and Space Administration. Lewis Research Center, Cleveland, OH.
APPARATUS FOR CHECKING THREADED HOLE PERPENDICULARITY Patent Application
August R. Scarpelli, inventor (to NASA) 21 Sep. 1992 9 p
(NASA-Case-LEW-15444-1; US-Patent-Appl-SN-947597) Avail: CASI HC A02/MF A01

A simple assembly for checking the perpendicularity of a hole relative to a datum surface is described. A 'go' plug is inserted into the hole and serves as a mounting stand for a cylindrical disk which houses an indicator. The indicator is then rotated 360 deg while checking for any deflection of the indicator that would signal the hole is not perpendicular. NASA

N93-14841*# National Aeronautics and Space Administration. Lyndon B. Johnson Space Center, Houston, TX.
SYSTEM FOR MEMORIZING MAXIMUM VALUES Patent Application
Richard J. Bozeman, Jr., inventor (to NASA) 3 Aug. 1992 15 p
(NASA-Case-MSC-21922-1; US-Patent-Appl-SN-924213) Avail: CASI HC A03/MF A01

The invention discloses a system capable of memorizing maximum sensed values. The system includes conditioning circuitry which receives the analog output signal from a sensor transducer. The conditioning circuitry rectifies and filters the analog signal and provides an input signal to a digital driver, which may be either linear or logarithmic. The driver converts the analog signal to discrete digital values, which in turn triggers an output signal on one of a plurality of driver output lines n. The particular output lines selected is dependent on the converted digital value. A microfuse memory device connects across the driver output lines, with n segments. Each segment is associated with one driver output line, and includes a microfuse that is blown when a signal appears on the associated driver output line. NASA

N93-14878# Department of the Navy, Washington, DC.
STATISTICALLY CALIBRATED TRANSDUCER Patent Application
Edmund J. Sullivan, inventor (to Navy) 13 Aug. 1992 13 p
(AD-D015408; US-Patent-Appl-SN-929215) Avail: CASI HC A03/MF A01

An apparatus and method for determining the direction of an incoming sonar signal using a towed array having at least two auxiliary transducers positioned along the array is disclosed. Each auxiliary transducer contains a plurality of small transducers. By summing the output from each of the small transducers, thereby forming the outputs of the auxiliary transducers with the output of the towed array, the direction of arrival of a sonar signal impinging upon the towed array is determined. GRA

N93-15096# Ecole Nationale Superieure des Telecommunications, Paris (France).
OFF-AXIS CONOSCOPIC HOLOGRAPHY: OPTICAL AND DIGITAL RECONSTRUCTION Ph.D. Thesis [L'HOLOGRAPHIE CONOSCOPIQUE HORS DE L'AXE: RECONSTRUCTIONS OPTIQUES ET NUMERIQUES]
Eric Dufresne 1990 261 p In FRENCH
(TELECOM-Paris-90-E-023; ETN-92-92550) Copyright Avail: CASI HC A12/MF A03

The possibility of obtaining off-axis conoscopic holograms is discussed. Conoscopic holography is a new technique used to record incoherent holograms by means of a birefringent crystal. The effective separation of the twin images and the DC component in the Fourier space can be performed without loss of information by tilting the optical axis of the crystal and using a space invariant limiting aperture device. Different operational solutions are presented. The recording system using a Charged Coupled Device (CCD) camera is described, pointing out the differences with the on-axis setup. The sampling requirement to perform the spectra separation without having aliasing effects and its consequence on the resolution in the z direction are emphasized. The off-axis holograms can be reconstructed optically. The digital output of the CCD camera, after being stored in a personal computer, is coded on a photographic plate. The reconstruction is performed by using a collimated laser beam and a spatial filter in the Fourier plane to block the unwanted frequential components. If the sampling is done properly, the hologram can be seen as a convolution. Thus, these holograms can be reconstructed numerically. The reconstruction algorithm simulated the inverse propagation of the light through a crystal whose optical axis is tilted at the opposite angle of the one used for the recording. This gives a transfer function that is complex conjugate of the initial recording one. Both optical and numerical results in three and two dimensional objects are presented. ESA

N93-15247# Department of the Navy, Arlington, VA.
THERMAL FIXTURE FOR TESTING AN INTEGRATED CIRCUIT Patent Application
Walter T. Schneider, inventor (to Navy) 10 Apr. 1992 17 p Filed 10 Apr. 1992
(AD-D015380; US-Patent-Appl-SN-866920) Avail: CASI HC A03/MF A01

Apparatus for controlling the temperature of an integrated circuit is discussed. A thermally conductive block has a vacuum passage connected to a vacuum pump for clamping the block to the top of an integrated circuit housing without mechanical clamping structures. A closed fluid loop including a circulating pump, heater and chiller modulate the temperature of a fluid passing through the conductive block thereby to control its temperature and the temperature of the integrated circuit independently of any other integrated circuit. GRA

N93-15381# Sandia National Labs., Albuquerque, NM.
HIGH SPEED IMAGING FOR FLASH RADIOGRAPHY USING PIN DIODES
G. J. Lockwood, L. B. Bishop, and M. M. Selph 1992 9 p Presented at the 20th International Congress on High Speed Photography and Photonics, Victoria, Ontario, 25-26 Sep. 1992
(Contract DE-AC04-76DP-00789)
(DE92-040959; SAND-92-1845C; CONF-9209188-3) Avail: CASI HC A02/MF A01

A high speed readout imaging system utilizing a commercial flash x-ray machine and miniature x-ray detectors has been developed. This system was designed to operate in the environment near a nuclear detonation where film or camera imaging cannot be used. The temporal resolution of the system is set by the 20 nanosecond FWHM of the x-ray pulse. The spatial resolution of the system was determined by the size and close packing of the PIN diodes used as the x-ray detectors. In the array used here, the PIN diodes have an active area of 2 mm in diameter and were placed 3.8 mm center to center. Computer-generated images using algorithms developed for this system are presented and compared with an image captured on film in the laboratory. DOE

N93-15411# Argonne National Lab., IL.
ADVANCED RESEARCH IN INSTRUMENTATION AND DIAGNOSTICS TECHNOLOGY
S. H. Sheen, W. P. Lawrence, and A. C. Raptis Sep. 1992 18 p Presented at the US DOE Contractors Review Meeting on Gasification and Gas Stream Cleanup Systems, Morgantown, WV, 15-17 Sep. 1992
(Contract W-31-109-eng-38)
(DE92-041121; ANL/CP-76750; CONF-920951-1) Avail: CASI HC A03/MF A01

This research project will develop an ultrasonic flow imaging system based on tomographic technique. Initially, we will demonstrate both the reflection and diffraction tomographic applied to flow imaging. Then, the direct inversion problem will be examined. In this paper, we present the initial assessment of the feasibility and the evaluation of practical wedge designs. Major tasks of the project include (1) a feasibility study, (2) evaluation of sensing geometry and wedge design, (3) development of image reconstruction algorithm, and (4) flow tests of the imaging system. Presently, we have completed the feasibility study and are in the process of evaluating wedge design. DOE

N93-15039*# Advanced Development Corp., Burlington, MA.
CORROSION OF METAL PARTICLE AND METAL EVAPORATED TAPES
Dennis E. Speliotis *In* NASA. Goddard Space Flight Center, Proceedings of the NSSDC Conference on Mass Storage Systems and Technologies for Space and Earth Science Applications 1991 p 173-185 (For primary document see N93-15027 04-82)
Avail: CASI HC A03/MF A03

N93-15042*# Ampex Corp., Redwood City, CA.
THE 19 mm DATE RECORDERS: SIMILARITIES AND DIFFERENCES
Steve Atkinson *In* NASA. Goddard Space Flight Center, Proceedings of the NSSDC Conference on Mass Storage Systems and Technologies for Space and Earth Science Applications 1991 p 215-219 (For primary document see N93-15027 04-82)
Avail: CASI HC A01/MF A03

N93-15043*# Ampex Corp., Redwood City, CA.
AN EMPIRICAL APPROACH TO PREDICTING LONG TERM BEHAVIOR OF METAL PARTICLE BASED RECORDING MEDIA
Allan S. Hadad *In* NASA. Goddard Space Flight Center, Proceedings of the NSSDC Conference on Mass Storage Systems and Technologies for Space and Earth Science Applications 1991 p 220-236 (For primary document see N93-15027 04-82)
Avail: CASI HC A03/MF A03

N93-15160# Sundstrand Data Control, Inc., Redmond, WA.
REWRITABLE OPTICAL DISK: APPLICATION TO FLIGHT RECORDING [DER EINSATZ WIEDERBESCHREIBBARER OPTISCHER PLATTEN FUER DIE AUFZEICHNUNG VON FLUGDATEN]
Duane A. Teachout *In* DLR, Proceedings of the 16th Symposium on Aircraft Integrated Monitoring Systems Jan. 1992 p 149-168 (For primary document see N93-15152 04-06)
Avail: CASI HC A03/MF A06; DLR, Wissenschaftliches Berichtswesen, Postfach 90 60 58, Cologne, Germany, HC

N93-15167# Loral Data Systems, Sarasota, FL.
SOLID STATE FLIGHT DATA RECORDER WITH RAPID DATA ACCESS [FESTKOERPER-FLUGDATENSCHREIBER MIT SCHNELLEM DATENZUGRIFF]
Hans F. Napfel *In* DLR, Proceedings of the 16th Symposium on Aircraft Integrated Monitoring Systems Jan. 1992 p 267-286 (For primary document see N93-15152 04-06)
Avail: CASI HC A03/MF A06; DLR, Wissenschaftliches Berichtswesen, Postfach 90 60 58, Cologen, Germany, HC

36 LASERS AND MASERS

Includes parametric amplifiers.
For related information see also *76 Solid-State Physics.*

N93-14123 Drexel Univ., Philadelphia, PA.
THE DYNAMICS OF SPATIALLY EXTENDED LASERS Ph.D. Thesis
Charles Kenneth Green 1991 176 p
Avail: Univ. Microfilms Order No. DA9213864

The dynamics of spatially extended lasers is studied both experimentally and theoretically in order to understand instabilities and losses of spatial coherence in the output intensity. Analysis first begins with small bore CO2 lasers in which experimental evidence of time-dependent and stationary complex spatial structures is shown. A comparison of the data with a theoretical model supports the notion that the observed phenomena result from the nonlinear interaction of transverse cavity modes with the active medium. The sequence of events in which going from a simple pattern (symmetric pattern) to a complex pattern is studied in a large bore CO2, laser by considering a qualitative theory of bifurcations. In particular demonstrated is that the spatiotemporal behavior of lasers can be characterized by group theory, that structures experimentally observed are created from the symmetry breaking of the O(2)XT(exp 2) group, and that spontaneous symmetry breaking is at the origin of a gradual increase of complexity in space and time. After each bifurcation a new frequency is added until two or three frequencies in the intensity usually produce local chaotic behavior. At that point almost any degree of spatial symmetry is lost. Numerical integration of the laser equations is carried out to make a further analysis. In particular the numerical code shows the appearance of defects. As a measure of complexity (turbulence) a function to indicate loss of spatial coherence (correlation function) is introduced. The presence of defects on the correlation function is to produce a loss of coherence. Dissert. Abstr.

N93-14125 Stanford Univ., CA.
THREE-DIMENSIONAL GUIDING EFFECTS IN A FREE-ELECTRON LASER Ph.D. Thesis
Bruce Aram Richman 1991 133 p
Avail: Univ. Microfilms Order No. DA9205710

The use of free-electron lasers (FEL's) is quickly expanding in electro-optics and other fields. FEL applications include nonlinear optics, photochemistry, and multiple stage amplification. These applications require a laser beam of known spatial characteristics. Previous theory and experiments have shown that gain amplitude guiding and refractive optical guiding of the laser beam by a narrower electron beam within the laser resonator is significant. Those experiments averaged over the longitudinal extent of the laser beam and were not designed to observe longitudinal effect. The results are reported of a full spatial and temporal free-electron laser computer simulation code, FELEX, which was used to predict the behavior of the MKIII FEL at the Stanford Photon Research Laboratory. These results show that the optical guiding in short pulses has a monotonic dependence on longitudinal position, which is strongest at the trailing edge of the pulses. Second, the autocorrelation measurements performed on the MKIII are described. This was the first experiment designed to detect longitudinally dependent guiding within the picosecond optical pulses. The measurements were performed using a variable aperture in the far field of the laser beam. The dependence on electron beam parameters (pulse length) and resonator length detuning was studied. The results of this experiment were inconclusive because laser instability and drift was as significant as any observed effect. Nevertheless, an upper limit of a 5 percent difference in the peak value of the normalized autocorrelation functions with and without the aperture was measured. Third, the development of sidebands, or optical spikes, was studied, and the autocorrelation results are presented showing the growth of spikes. The experimental data agrees with the FELEX predictions. These autocorrelation results are the first observation of the spiking behavior in the time domain. Dissert. Abstr.

N93-14131# Loughborough Univ. of Technology (England). Dept. of Physics.
APPLICATION OF GEL-SILICA OPTICS TO LASER TECHNOLOGY AND OPTICAL ELEMENT FABRICATION Final Report, 1 Aug. 1991 - 31 Jul. 1992

Nicholas J. Phillips Sep. 1992 19 p
(Grant AF-AFOSR-0300-91)
(AD-A255666; AFOSR-92-0870TR) Avail: CASI HC A03/MF A01

Three main areas of activity are summarized in this report: (1) The creation of novel optical materials i.e., composites of gel-silica with materials such as pm.m.ma. (acrylic) so as to achieve invariance of the refractive index or optical path during thermal expansion -- a new class of optical materials for worldwide use. (2) The impregnation of porous gel-silica with anthracene, for example, to create a solid composite material capable of emitting blue light by electro-luminescence. This area of activity is aimed at the fabrication of solid state devices that can fill the gap not currently filled by semiconducting devices. Porous gel-silica anthracene complexes may provide at least an intermediate class of devices capable of providing reasonably pure blue light emission under electrical excitation. (3) The impregnation of porous gel-silica with imaging monomer to create thick volume optical elements for optical systems. The methodology is reasonably straightforward and leads to the formation of lenses or gratings in the volume of thick silica layers. Such materials are optically useful for beam steering, head up displays, and other applications. GRA

N93-14141 Keele Univ. (England).
A STUDY OF AN OPTICALLY PUMPED FREE-JET MOLECULAR IODINE LASER OPERATING IN THE VISIBLE SPECTRUM Ph.D. Thesis
David Jones 1990 259 p
Avail: Univ. Microfilms Order No. BRDX96575

The spectroscopic and oscillation properties of an optically pumped free-jet molecular iodine laser, employing a ring resonator system, are investigated in the visible spectrum. The laser properties of the free-jet are shown to be greatly superior to those of the bulk gas cell. This includes lower threshold levels, higher output powers and many new oscillating lines. The theoretical discussion reveals that unidirectional laser operation is due to both Raman gain and the direction-dependent overlap of the hyperfine gain profiles. Numerical gain calculations further reveal that the superior laser properties of the free-jet are a consequence of two factors. First, greater overlap of the narrow Raman gain profiles due to increased collision broadening. Second, more efficient pumping of the hyperfine structure due to the reduced widths of the Doppler profiles present in supersonic free-jet expansions. The absorption loss mechanisms are examined. Broadband single-step continuum absorption from the X ground electronic state to higher dissociating states is not detected - contrary to previous authors. Correct interpretation of the two-step continuum absorption explains how, in the visible spectrum, the free-jet regime enables laser oscillation to be secured on the weak v''-even transitions. Finally, a new and lower value for the B = X electronic transition strength in molecular iodine is determined from a simple absorption experiment. A simple positive-step alignment technique for ring resonator systems is presented that reduces alignment of a ring laser to a trivial operation.
Dissert. Abstr.

N93-14175 York Univ. (Ontario).
EXCIMER LASER IRRADIATION OF METAL SURFACES Ph.D. Thesis
Grant Kinsman 1991 248 p
Avail: Univ. Microfilms Order No. DANN65684

In this work a new method of enhancing CO2 laser processing by modifying the radiative properties of a metal surface is studied. In this procedure, an excimer laser (XeCl) or KrF) exposes the metal surface to overlapping pulses of high intensity, 10(exp 8) - 10(exp 9) W cm(exp -2), and short pulse duration, 30 nsec FWHM (Full Width Half Maximum), to promote structural and chemical change. The major processing effect at these intensities is the production of a surface plasma which can lead to the formation of a laser supported detonation wave (LSD wave). This shock wave can interact with the thin molten layer on the metal surface influencing to a varying degree surface oxidation and roughness features. The possibility of the expulsion, oxidation and redeposition of molten droplets, leading to the formation of micron thick oxide layers, is related to bulk metal properties and the incident laser intensity. A correlation is found between the expulsion of molten droplets and a Reynolds number, showing the interaction is turbulent. The permanent effects of these interactions on metal surfaces are observed through scanning electron microscopy (SEM), transient calorimetric measurements and Fourier transform infrared (FTIR) spectroscopy. Observed surface textures are related to the scanning procedures used to irradiate the metal surface. Fundamental radiative properties of a metal surface, the total hemispherical emissivity, the near-normal spectral absorptivity, and others are examined in this study as they are affected by excimer laser radiation. It is determined that for heavily exposed Al surface, alpha' (10.6 microns) can be increased to values close to unity. Data relating to material removal rates and chemical surface modification for excimer laser radiation is also discussed. The resultant reduction in the near-normal reflectivity solves the fundamental problem of coupling laser radiation into highly reflective and conductive metals such as copper and aluminum. The increased absorption at 10.6 microns enables enhanced CO2 laser drilling and cutting rates in electrolytic Cu at incident intensities, I(0) of approximately 10(exp 6) W cm(exp -2). Data showing enhanced drilling rates in Al 1100-H14 is also presented. In these regimes the majority of material is removed in the liquid state. The amount of molten material formed can be directly attributed to the enhanced initial coupling of the excimer laser irradiated surface. Previously, to process Cu and Al it has been required to increase I(0) until material removal occurs through vaporization. This fundamental data and analysis provides a basic framework for further work in this new field of study. In the field of surface modification technology, interest in the use of excimer lasers is growing. It is expected that applications beyond those described here will soon be explored. Dissert. Abstr.

N93-14284# Massachusetts General Hospital, Boston. Labs. of Photomedicine.
OPTICAL PROBES FOR LASER INDUCED SHOCKS Final Report, 15 Mar. 1990 - 14 Mar. 1992
T. F. Deutsch 14 Mar. 1992 39 p
(Grant AF-AFOSR-0210-90)
(AD-A256092; AFOSR-92-0893TR) Avail: CASI HC A03/MF A01

The support provided by the grant AFOSR-90-0210 has resulted in the publication of four papers and three conference proceedings. Our research covered three topics. GRA

N93-14402# State Univ. of New York, Stony Brook. Dept. of Physics.
ADVANCES IN LASER COOLING Annual Technical Report, Aug. 1991 - Jul. 1992
Harold Metcalf 1 Sep. 1992 22 p
(Grant AF-AFOSR-0305-91)
(AD-A255969; TR-1; AFOSR-92-0889TR) Avail: CASI HC A02/MF A01

We have made important progress in experiments and theory of laser cooling of neutral atoms. In addition, our understanding of quantum effects in laser cooling is evolving very rapidly, and this has enormous influence on how we view the subject. This change has impacted on both experimental and theoretical work. GRA

N93-14414# Q-Source, Inc., East Hartford, CT.
COMPACT HIGH PRF CO2 TRANSMITTER Final Report
1991 19 p
(Contract N00014-91-C-0154)
(AD-A255985) Avail: CASI HC A02/MF A01

The Phase 1 program explored the generation of submicrosecond wide CO2 laser pulsewidths using a completely sealed-off, non-recirculating pulsed discharge gain medium. Two sealed-off devices with nominal gain volumes of 1.5 mL and 35 mL were utilized in the Phase 1 program to generate pulses as short as several microseconds at atmospheric pressure and as long as 10 to 20 microseconds at pressures in the 60 to 100 torr region. Sealed-off PRF's from 50 to 500 Hz were used and single-fill lifetimes in excess of 4.4 x 10 to the 6th power pulses were achieved in preliminary experiments. Using the above sealed-off devices, pulsewidths as short as 500 nsec were shown to be possible using an intracavity gas modulator in conjunction with high level discharge pulsing. The function of the passive Q-switching modulator was to delay the onset of lasing until a higher inversion could accumulate and prevent the re-emergence of a second Q-switching laser pulse when the upper CO2 laser level re-equilibrates. Q-switching under an enhanced gain-switched envelope produced output pulses with energies up to several mJ/pulse with peak power in the several KW range. In addition to generating pulsewidths meeting the Phase I goals, the pressure at which the above devices operated was shown to be generally compatible with a single laser that could operate with a cw and energetic short pulse output format. GRA

N93-14497# Wisconsin Univ., Madison. Dept. of Meteorology.
UPGRADE THE UNIVERSITY OF WISCONSIN VOLUME IMAGING LIDAR Final Report
E. W. Eloranta 1 May 1992 25 p
(Contract DAAL03-91-G-0222)
(AD-A255476; ARO-29204.3-GS-EQ) Avail: CASI HC A03/MF A01

This grant provided funds to upgrade the University of Wisconsin Volume Imaging Lidar. A new computer system was purchased to increase data acquisition and data processing rates. Lidar data algorithms execute 20 to 50 times faster on the new IBM RS/6000 model 550 than on the old Digital Equipment Corp. VAX 750. The new computer has allowed us to begin systematically processing all of the 20 Gbyte data set acquired in the 1989 FIFE program. This report describes applications of the new computer. GRA

N93-14568# Carnegie-Mellon Univ., Pittsburgh, PA. Robotics Inst.
AN ICONIC POSITION ESTIMATOR FOR A 2-D LASER RANGEFINDER
Javier Gonzalez, Anthony Stentz, and Anibal Ollero May 1992 21 p
(AD-A255523; CMU-RI-TR-92-04) Avail: CASI HC A03/MF A01

Position determination for a mobile robot is an important part of autonomous navigation. In many cases, dead reckoning is insufficient because it leads to large inaccuracies over time. Beacon- and landmark-based estimators require the emplacement of beacons and the presence of natural or man-made structure respectively in the environment. In this paper we present a new algorithm for efficiently computing accurate position estimates based on a radially-scanning laser rangefinder that requires minimal structure in the environment. The algorithm employs a connected set of short lie segments to approximate the shape of any environment and can easily be constructed by the rangefinder itself. We describe techniques for efficiently managing the environment map, matching the sensor data to the map, and computing the robot's position. We present accuracy and runtime results for our implementation. GRA

N93-14599# Massachusetts Inst. of Tech., Cambridge. Research Lab. of Electronics.
COMPACT FREE ELECTRON LASER FOR MEDICAL APPLICATIONS Annual Technical Report, 30 Sep. 1991 - 29 Sep. 1992
George Bekefi 30 Sep. 1992 8 p
(Contract N00014-90-J-4130)
(AD-A256236) Avail: CASI HC A02/MF A01

The 70-period microwiggler has been tuned. A novel iterative tuning regimen was employed which involves perturbing the tuning profile at selected points in order to produce an empirical Taylor expansion matrix relating the magnetic field profile (described as a 140-dimensional vector consisting of the peak amplitude of each half-period) to the tuning resistor profile (described as a 140-dimensional vector consisting of the length of the tuning resistor of each half-period). The resulting matrix equation is then numerically inverted to produce a list of resistor adjustments which to first order will produce a flat field amplitude profile. Some field error invariably will remain, however, due to non-linear saturation effects and measurement error in the matrix entries. The process is then repeated until the errors in the field profile are of the same magnitude as the errors inherent in the field measurement system. Experience has shown that this regimen converges very rapidly, with 3-4 iteration required to reduce field errors from 2.5 percent RMS (untuned) to 0.08 percent RMS. Tuning, therefore can be accomplished in 3-4 working days during most of which time the Microwiggler System runs unattended under computer control. GRA

N93-14647# Cincinnati Univ., OH. Dept. of Electrical and Computer Engineering.
LEVEL-MIXING ASSISTED TUNABILITY OF NUCLEAR RESONANCE LINEWIDTHS FOR GAMMA RAY LASERS Final Report
P. Boolchand and R. Coussement 1992 106 p
(Contract N00014-88-2035)
(AD-A255791) Avail: CASI HC A06/MF A02

The present approach to a gamma-ray laser is based on the use of a long-lived nuclear state acting both as the storage and lasing level. The present approach requires that nuclear resonant emission occur from long-lived states. We have examined the issue both theoretically and experimentally. Theoretically, as discussed in a recent paper, there are reasons to believe that for long lived states the controlling width for nuclear resonance is not the natural linewidth but the homogeneously broadened relaxation width. This would make observation of the Mossbauer effect from long-lived states less stringent than previously believed. Experimentally, our efforts have continued to focus on observing the Mossbauer effect with the 88 keV level in Ag-109 possessing a meanlife of 57.14 seconds. A facility dedicated to these experiments and based on a vibration-free He-closed cycle cryostat which can provide for T-variation and control at cryogenic temperatures was developed during the course of this grant. The first results on the resonant self absorption experiments on this facility are now available and are discussed in section 2 of the report. GRA

N93-14667# Illinois Univ., Urbana. Dept. of Electrical and Computer Engineering.
THE III-V SEMICONDUCTOR QUANTUM WELL LASERS AND RELATED OPTOELECTRONIC DEVICES (ON SILICON). OXIDE-DEFINED SEMICONDUCTOR QUANTUM WELL LASERS AND OPTOELECTRONIC DEVICES: Al-BASED III-V NATIVEOXIDE S Final Report
N. Holonyak, Jr., K. C. Hsieh, and G. E. Stillman May 1992 37 p
(Contract DAAL03-89-K-0008)
(AD-A255239) Avail: CASI HC A03/MF A01

Measurements of the hole density in heavily carbon-doped GaAs and Al(x)Ga(1-x)As as a function of the annealing temperature are presented. It is shown that the hole density increases and the hole mobility decreases after annealing at low temperatures (T less than 550 C). However, higher annealing temperatures (T greater than 600 C) result in a reduction of the hole concentration reaching a maximum carrier concentration of 5 x 10(exp 19) cm(exp -3). These changes observed in the electrical properties can be explained by two mechanisms: (1) the passivation of carbon acceptors by hydrogen incorporated during growth; and (2) the change in the lattice site location of carbon atoms, which is dependent on the total carbon concentration. GRA

N93-14703* National Aeronautics and Space Administration. Pasadena Office, CA.
MULTIPERIOD-GRATING SURFACE-EMITTING LASERS Patent
Robert J. Lang, inventor (to NASA) 17 Nov. 1992 12 p Filed 21 Oct. 1991 Supersedes N92-17862 (30 - 8, p 1305) Prepared in cooperation with Jet Propulsion Lab., California Inst. of Tech., Pasadena.
(NASA-Case-NPO-17763-1-CU; US-Patent-5,164,956;
US-Patent-Appl-SN-782009; US-Patent-Class-372-96;
US-Patent-Class-372-20; US-Patent-Class-372-108;
Int-Patent-Class-H01S-3/19) US Patent and Trademark Office

Surface-emitting distributed feedback (DFB) lasers are disclosed with hybrid gratings. A first-order grating is provided at one or both ends of the active region of the laser for retroreflection of light back into the active region, and a second-order or nonresonant grating is provided at the opposite end for coupling light out perpendicular to the surfaces of the laser or in some other selected direction. The gratings may be curved to focus light retroreflected into the active region and to focus light coupled out to a point. When so focused to a point, the DFB laser may be part of a monolithic read head for a laser recorded disk, or an optical coupler into an optical fiber. Official Gazette of the U.S. Patent and Trademark Office

N93-14722 Department of the Navy, Washington, DC.
OPTICS FOR DIODE ARRAY TRANSVERSE PUMPED LASER ROD Patent Application
Frank Hanson, inventor (to Navy) 26 May 1992 4 p Filed 29 Mar. 1990
(AD-D015436; US-Patent-Appl-SN-502001) Avail: CASI HC A01/MF A01

A solid state laser rod of an anisotropic material is more efficiently side pumped by using cylindrical lenses and a half-wave plate with linear laser diode arrays disposed along the length of the solid state laser rod such that the polarization of the diode array light is rotated to achieve a maximum absorption coefficient in the laser rod material. In addition, Fresnel reflection losses at the lens and laser rod surfaces are reduced by 90 deg. GRA

N93-14821 Department of the Navy, Washington, DC.
METHOD FOR DETECTING CHEMICAL VAPORS USING A LASING DYE SENSOR Patent
Terence W. Barrett, inventor (to Navy) and John F. Giuliani, inventor (to Navy) 28 Apr. 1992 7 p Filed 16 Sep. 1988

(AD-D015424; US-Patent-5,108,931; US-Patent-Appl-SN-245421; US-Patent-Class-436-113) Avail: CASI HC A02/MF A01

In a lasing dye sensor system, a stream of lasing dye free-flows across an area open to the atmosphere. A chemical reaction between contaminants in the atmosphere and the lasing dye result in the change of emission spectra of the lasing dye. The change in emission spectra is detected and provides an improved apparatus and method for detecting low concentrations of chemical vapors in the atmosphere. GRA

N93-14906# Lawrence Livermore National Lab., CA.
OPTICAL GLASSES FOR HIGH-PEAK-POWER LASER APPLICATIONS
J. H. Campbell and F. Rainer 31 Jul. 1992 12 p Presented at the SPIE International Symposium on Optical Applied Science and Engineering, San Diego, CA, 19-24 Jul. 1992
(Contract W-7405-eng-48)
(DE92-040403; UCRL-JC-109255; CONF-920792-31) Avail: CASI HC A03/MF A01

Only a limited number of optical glasses are commercially available that can be used in high-fluence laser applications between 0.35 and 1.05 microns. These include primarily certain phosphate glasses and fused silica. Phosphate glasses can now be made free of Pt-inclusions; the technology leading to this improvement is briefly discussed. In addition, inclusion-free fused silica can be made by a high temperature, chemical-vapor-deposition (CVD) process. Measured damage thresholds over a range of wavelengths and pulse lengths are reported for these materials. In addition, the use of doped layers of plasma CVD fused silica as a means of making high damage-threshold rugate filters is presented. The impact of a high nonlinear refractive index n(sub 2) on the spatial profile of the laser beam is discussed. Dramatic improvements in laser performance are possible if an inclusion-free, low-n(sub 2) glass (such as fluorophosphate) could be made. Multiphoton absorption and solarization of fused silica at 351 nm are also reviewed; fused silica continues to be the preferred material for high fluence applications at this wavelength. DOE

N93-14907# Department of Energy, Washington, DC.
ENVIRONMENTAL ASSESSMENT: OMEGA UPGRADE PROJECT AT THE LABORATORY FOR LASER ENERGETICS, UNIVERSITY OF ROCHESTER
May 1992 49 p
(DE92-040410; DOE/EA-0548) Avail: CASI HC A03/MF A01

The OMEGA laser system at the University of Rochester's Laboratory for Laser Energetics (UR/LLE) is the only major facility in the United States capable of conducting fully diagnosed direct-drive, spherical-implosion Inertial Confinement Fusion (ICF) experiments. The LLE also serves as the National Laser Users Facility, available to scientists throughout the country for high energy density laser-matter interaction experiments. In the mid-1980s, the University initiated a request to begin investigations to upgrade the OMEGA laser system. The purpose of the OMEGA Upgrade will provide a unique national resource capable of achieving sufficient thermonuclear yield to address ignition-scaling physics issues for the Inertial Fusion Research Program. Multi-laboratory collaborative experiments to investigate a number of important ICF issues (ignition scaling, fuel-pusher interface mix, preheat, long-scale-length plasma physics, and hydrodynamic instabilities) will be carried out on the upgraded facility. These experiments will increase the confidence associated with the success of a national high-gain laboratory facility. DOE

N93-15058# Texas A&M Univ., College Station. Dept. of Chemistry.
DEVELOPMENT OF LASER-ION BEAM PHOTODISSOCIATION METHODS
D. H. Russell Aug. 1992 9 p
(Contract DE-FG05-85ER-13434)
(DE92-040512; DOE/ER-13434/7) Avail: CASI HC A02/MF A01

During this report period our research efforts have concentrated on the continued development of the tandem magnetic sector (EB)/reflectron-time-of-flight (TOF) instrument, preliminary experiments with the tandem TOF/TOF E/R-TOF instrument, developing the methodology for performing photodissociation with pulsed lasers on the EB/R-TOF instrument, preliminary experiments with laser ionization on the aerosol-particle beam apparatus, development of a vacuum ultraviolet laser for photoionization/photoexcitation of gas phase ions, and fundamental studies on matrix-assisted laser desorption ionization (MALDI). DOE

N93-15069# New Mexico Univ., Albuquerque.
FAST OPTOELECTRONIC SWITCHING PROCESSES IN SURFACE-EMITTING SEMICONDUCTOR LASERS AND NONLINEAR ETALONS Final Technical Report, Sep. 1989 - Sep. 1991
John G. McInerney May 1992 47 p
(Contract F19628-89-K-0037)
(AD-A255802; RL-TR-92-50) Avail: CASI HC A03/MF A01

We describe theoretical and experimental research on optoelectronic switching processes in GaAs/AlGaAs multiple quantum well etalons, where the quantum wells are spaced by one half the optical wavelength at which the structure is designed to operate. Results have been obtained with the quantum wells pumped above threshold (i.e., the structure behaves as a surface-emitting laser) and below threshold (when it behaves as a saturable absorber with feedback). In the former case, high-speed (10 ps impulse response) switching has been demonstrated, but the threshold is relatively high. Some suggestions for more efficient switching are made. In the latter case, a detailed theoretical model has been developed which demonstrates the potential advantages and disadvantages of absorptive bistable optical switching in half-wave-periodic MQW etalons over the conventional non-resonant MQW or bulk structures. The initial experiments were promising but hampered by materials growth and uniformity problems. We include several specific recommendations for additional experiments to complete our investigations of the below threshold switching regime, as well as extension to 2-D switch arrays, new research directions and applications such as time-division multiplexing. GRA

N93-15115# New Mexico Univ., Albuquerque. Center for High Technology Materials.
OPTOELECTRONICS MATERIAL CENTER: A COLLABORATIVE PROGRAM INCLUDING CENTER FOR HIGH TECHNOLOGY MATERIALS OF THE UNIVERSITY OF NEW MEXICO, STANFORD UNIVERSITY, CALIFORNIA INSTITUTE OF TECHNOLOGY Quarterly Report, 30 Sep. - 31 Dec. 1991
S. R. Brueck 11 Sep. 1992 16 p
(Contract MDA972-90-C-0046; ARPA Order 7526)
(AD-A256005) Avail: CASI HC A03/MF A01

The Optoelectronic Materials Center is a collaborative program involving the University of New Mexico, Stanford University, and the California Institute of Technology. Sandia National Laboratories and MIT Lincoln Laboratory are also involved in this program under separate contract vehicles. This program emphasizes three main areas: diode-based visible sources two-dimensional optical interconnects, and high-speed optoelectronics. Progress on individual tasks is very briefly discussed below. Several of the tasks will impact more than one of the above areas. For simplicity, the tasks are arranged by institution in an order roughly determined by the above areas. GRA

N93-15128# Direction des Recherches, Etudes et Techniques, Paris (France).
PRECISE MEASUREMENTS MADE FROM A DISTANCE OF LOCAL DEFORMATIONS INDEPENDENT OF SMALL OBJECT MOVEMENTS Final Report [MESURE PRECISE ET A DISTANCE DE DEFORMATIONS LOCALES INDEPENDAMMENT DES PETITS MOUVEMENTS DE L'OBJET]
J. C. Dupre and A. Lagarde 1992 66 p In FRENCH
(Contract DRET-90-1625-A000)
(ETN-92-92723) Avail: CASI HC A04/MF A01

A study whose aim was to make a deformation measurement operational is reported. The method is based on the diffraction of a laser beam by a mesh at the surface of the object. It was hoped to increase the accuracy of the method (to an order of 0.00001) and to make the measurements independent of small, and often inevitable movements, of the object. In order to be able to notice all possible movements, the relation between valid diffraction of oblique incident laser beam and for any tilt of the array, was formulated. The assembly which brings back the measurement by optical diffraction (measurement at distance) to an analysis by a parallel processing network (most sensitive method) is described. The application of a quasi-heterodyning technique to improve the sensitivity and precision of the measurement is reported. ESA

N93-15135# Los Alamos National Lab., NM.
LASER-BASED STUDIES WITH AN ION-TRAP MASS SPECTROMETER: ION TOMOGRAPHY AND ANALYTICAL APPLICATIONS
M. L. Alexander, M. E. Cisper, P. H. Hemberger, N. S. Nogar, J. D. Williams (Purdue Univ., West Lafayette, IN.), and J. E. P. Syka (Finnigan MAT, San Jose, CA.) 1992 5 p Presented at the 6th International Symposium on Resonance Ionization Spectroscopy and its Applications, Santa Fe, NM, 24-29 May 1992
(Contract W-7405-eng-36)
(DE92-017529; LA-UR-92-1862; CONF-920574-10) Avail: CASI HC A01/MF A01

The iron trap mass spectrometer (ITMS) is an ion storage device which consists of two hyperbolic endcaps and a hyperbolic ring electrode. This forms a trapping cavity having a volume of several cm(sup 3). An RF potential applied to the ring electrode produces a time-varying potential which can be used to trap and/or manipulate ions under controlled conditions. This device has been used in ion trapping studies for a number of years. More recently, a commercial version has been produced and sold which allows for mass-selective ejection of trapped ions, with subsequent detection by an electron multiplier. In this mode, it operates as a compact, high efficiency, high resolution mass spectrometer. The instrument has found applications in GC/MS, in tandem mass spectroscopy and in portable mass spectral analysis. In this manuscript, we present a survey of recent results incorporating laser desorption, ionization, or photodissociation with ITMS. In one instance, we describe the use of laser photodissociation to map the spatial distribution of trapped ions in the ITMS. In this tomographic study, we have parameterized the effects of trapping potential, buffer gas pressure, supplementary RF-potential, and laser intensity. In separate studies, laser desorption was used to generate gas phase ions in the ITMS from a solid probe, by irradiation of both neat and matrix-dissolved samples. The latter experiment produced both high molecular weight ions and significant numbers of negative ions. DOE

N93-15250# Department of the Navy, Washington, DC.
COLOR CENTER LASER WITH TRANSVERSE AUXILIARY ILLUMINATION Patent Application
Irwin Schneider, inventor (to Navy) and Robert S. Afzal, inventor (to Navy) 15 Apr. 1992 32 p Filed 15 Apr. 1992
(AD-D015387; US-Patent-Appl-SN-868806) Avail: CASI HC A03/MF A01

A color center laser is provided with a crystal disposed within a longitudinally pumped cavity. Optics are provided to transversely excite the crystal. Both a circular lens and a cylindrical lens-focus an auxiliary beam into the crystal of the color center laser to produce (F2+)A color centers for lasing. The cylindrical lens is used to focus the auxiliary beam to a narrow focal line. The circular lens is used to adjust the length of the focal line. By adjusting the length of the focal line, an entirety of the pump beam is used for excitation. The lenses thus collimate and focus the focal line to a length within an active volume in the crystal of the color center laser essentially equal to a length of the crystal. GRA

N93-15296# Nagoya Univ. (Japan). Plasma Science Center.
ELECTRON ACCELERATION BY LONGITUDINAL ELECTRIC FIELD OF A GAUSSIAN LASER BEAM
Satoshi Takeuchi (Yamanashi Univ., Kofu, Japan), Ryo Sugihara, and Koichi Shimoda Nov. 1991 21 p
(DE92-526947; PSC-16) Avail: CASI HC A03/MF A01

It is shown that the longitudinal electric field of a transverse magnetic mode of a Gaussian laser beam accelerates an electron to an ultra-relativistic energy. The electron is captured and accelerated in a length of the order of the Rayleigh range. The ultimate energy increment of the electron with a single laser beam is given by the product of transverse field intensity and the beam waist, and can be of the order of 100 MeV. This fact implies that a multi-stage acceleration enables TeV-order-acceleration in a length of a few kilometers with the present state of the art. DOE

N93-15325# California Univ., Berkeley. Lawrence Berkeley Lab.
SIMPLE FORMULAE FOR THE OPTIMIZATION OF THE FEL GAIN LENGTH INCLUDING THE EFFECTS OF EMITTANCE, BETATRON OSCILLATIONS, AND ENERGY SPREAD
Y. H. Chin Aug. 1992 10 p Presented at the 14th International Free Electron Laser Conference, Kobe, Japan, 23-28 Aug. 1992
(Contract DE-AC03-76SF-00098)
(DE92-040378; LBL-32249; ESG-179; CONF-9208142-1) Avail: CASI HC A02/MF A01

Simple analytical formulae are presented for a quick optimization of the Free Electron Laser (FEL) gain length for given values of radiation wavelength, electron beam current, normalized transverse emittance, and energy spread. The optimization parameters include the gap size of the wiggler, the wiggler period, and the betatron wavelength (in the case of external focusing). The method is based on the handy formulae for the FEL gain of a Gaussian beam including the effects of energy spread, emittance, and betatron oscillations of the electron beam. We have found a simple relation between the minimum FEL gain length and the optimum betatron wavelength for given energy spread, emittance, and gap size of the wiggler. When the emittance is about the radiation wavelength divided by 4(rho) and the energy spread is negligible, this relation shows that the gain length is optimized if the betatron wavelength is chosen so that the betatron phase advances by a half radian in the gain length. DOE

N93-15347# California Univ., Santa Barbara.
CONDENSED MATTER RESEARCH USING THE UCSB FEL
1992 13 p
(Contract DE-FG03-84ER-45089)
(DE92-040560; DOE/ER-45089/T1) Avail: CASI HC A03/MF A01

The University of California, Santa Barbara (UCSB) Free Electron Laser (FEL) project was initiated in 1981 to test the idea of using an electrostatic accelerator in a recirculating beam mode to produce high-power, continuously tunable, coherent far infrared radiation. The development and application of this device to condensed matter research are briefly recounted. Emphasis was on semiconductor research and two-photon experiments. DOE

N93-15417# Los Alamos National Lab., NM.
HIGH-BRIGHTNESS LINAC FOR THE ADVANCED FREE-ELECTRON LASER INITIATIVE AT LOS ALAMOS
R. L. Sheffield, B. E. Carlsten, and L. M. Young 1992 4 p Presented at the 16th International LINAC Conference, Ottawa, Ontario, 23-28 Aug. 1992
(Contract W-7405-eng-36)
(DE92-040213; LA-UR-92-2804; CONF-9208109-26) Avail: CASI HC A01/MF A01

This paper describes the design of an accelerator that can produce beams of greater than 1 x 10(exp 13) A/m(exp 2) (brightness = 2xI/epsilon(exp 2), where epsilon is the rms emittance). The beam emittance growth in the accelerator is minimized by: producing a short-electron bunch in a high-gradient rf cavity, using a focusing solenoid to correct the emittance growth caused by space charge, and designing the coupling slots between accelerator cavities to minimize quadrupole effects. The results from simulations are, at 2.3 nC, a peak current of 180 A and an emittance of 1.6 pi mm-mrad, and, at 4.6 nC a peak current of 300 A and an emittance of 2.4 pi mm-mrad. The exit energy from the linac is 20 MeV for both cases. DOE

N93-15472# Krug Life Sciences, Inc., San Antonio, TX.
ULTRASHORT-PULSE LASER SYSTEM: THEORY OF OPERATION AND OPERATING PROCEDURES Final Report, Nov. 1989 - Jul. 1992
Clarence P. Cain Jul. 1992 37 p
(Contract F33615-88-C-0631)
(AD-A257023; AL-TR-1991-0146) Avail: CASI HC A03/MF A01

This report describes the ultrashort-pulse laser system manufactured by Spectra-Physics, Inc., in detail so the system operator can turn on the system, bring it up to operating specifications, and fine-tune the system to give optimum pulsewidth and energy/pulse output. This report also incorporates the system turn-on procedures developed for the system license and includes greatly expanded optimizing procedures in addition to the theory of operation of each component instrument. The basic system has been configured to operate on a single 4- by 12-ft optical bench. Some diagnostic instruments are also permanently mounted on the bench. Each system component is described in the same order as required to turn on the system and reach stabilized pulses. The theory of operation will be incorporated into this turn-on procedure along with optimizing procedures. Much of the theory of operation was copied verbatim from the instrument manuals provided by Spectra-Physics. GRA

37 MECHANICAL ENGINEERING

Includes auxiliary systems (nonpower); machine elements and processes; and mechanical equipment.

N93-14202 Georgia Inst. of Tech., Atlanta.
ROBUST CONTROL OF A FLEXIBLE LINK ROBOT AND RIGID LINK ROBOT: THEORY, SIMULATION, AND EXPERIMENT Ph.D. Thesis
Soo Han Lee 1992 204 p
Avail: Univ. Microfilms Order No. DA9223783

The goal is to design a controller for multi-link flexible robots that ensures accurate joint trajectory tracking and fast vibration damping. Two methods are followed, theoretical and experimental. The theoretical approach comprises derivation of dynamic model, design of a robust controller, stability analysis of the designed controller, and computer simulations. The experimental approach includes verifications of the dynamic model and real time implementations of the controller. Dynamic equations are derived using Hamilton's principle and Lagrange's equations. From the dynamic equations derived by Lagrange's equation, it is found that the flexible motion significantly influences nonlinear terms, centrifugal and Coriolis terms, rather than the inertia matrix. Discrepancies were found between the model and the physical robot become smaller when the actuator's dynamics are included in the model. Two submodels, one slow and one fast submodel, are derived applying singular perturbation technique to the model. A robust controller is developed for the slow submodel that represents the rigid link robot. A velocity feedback controller is developed for the fast submodel that represents the flexible motion. The stability of the composite controller consisting of a robust controller for the slow submodel and a velocity feedback controller for the fast submodel is analyzed by a composite Lyapunov function. From the analysis, it is shown that the composite controller stabilizes a flexible robot and guarantees trajectory tracking of the joint motion and the suppression of the flexible motion if the perturbation parameter is less than a value whose bound is obtained analytically. Experiments on SAM, RALF, and RALF with SAM at its tip are performed to verify the mathematical analysis. Experimental results show excellent trajectory tracking of joint motion and fast suppression of flexible motion. The effectiveness of the inertial forces of SAM on the control of the flexible motion of RALF is demonstrated by simulations and experiments, where SAM is mounted at the tip of RALF. Dissert. Abstr.

N93-14226 Michigan Univ., Ann Arbor.
FINITE ELEMENT MODELS OF LASER WELDING Ph.D. Thesis
Jinhee Lee 1992 168 p
Avail: Univ. Microfilms Order No. DA9226952

A numerical study was undertaken in an effort to understand the complex heat and fluid flow during the laser beam welding process. The finite element method was applied, and a horizontal cross sectional model and a vertical cross sectional model have been suggested. In the horizontal cross sectional model, heat transfer in the deep penetration mode laser welding was discussed with the assumption that a keyhole has been formed and heat and fluid flow are two dimensional. Even though the driving forces of the weld convection are missing in the horizontal cross sectional model and the heat and fluid flow in the weld pool are more complicated than can be explained by it, the model included the penetration mode concept of the keyhole and is a helpful conceptual stepping stone toward the understanding of laser welding. It also served as a point of introduction for the enthalpy method in finite element analysis. The weld pool convection induced by the surface tension gradient in the conduction mode laser welding has been discussed in the vertical cross sectional model with and without a flat free surface assumption. It was found that a typical surface tension gradient during welding created violent convection in the weld pool. This model explains the elements of weld pool convection in conduction mode laser welding. Free surface problems with kinematic boundary conditions were also introduced as a part of the vertical cross sectional model. It was found that the presence of normal stress on the free surface places a severe restriction on the time step in the computations of time dependent problems. An enthalpy method has been shown to be useful in solving the Stefan problems with moving multi-phase interfaces. The presence of latent heat in the simulations of welding influences heat and fluid flow such that the weld pool is stretched in the direction of welding when the latent heat is included in the model. Dissert. Abstr.

N93-14434# Stanford Univ., CA. Center for Design Research.
UTILIZING SENSED INCIPIENT SLIP SIGNALS FOR GRASP FORCE CONTROL
M. R. Tremblay, W. J. Packard, and M. R. Cutkosky 15 Jul. 1992 7 p
(Contract N00014-90-J-4014)
(AD-A255725) Avail: CASI HC A02/MF A01

We present a scheme by which a manipulator can identify when it is about to lose hold of a grasped object so that it can take preventive measures to maintain the grasp before slipping occurs. By detecting localized slips which precede gross slip between the gripping surface and a grasped object, a controller can reliably modify the grasp force and prevent the object from slipping. The motivation behind our sensor design comes from current physiological research which reveals the importance of a textured gripping surface in detecting these localized, or incipient, slips and provides us with insight into human grasping and manipulation strategies. By using our sensor as an active gripping surface on a simple manipulator and modeling our control strategy after humans, we are able to dynamically control the amount of force used to grasp objects, while preventing them from slipping. Our results show that the sensor is not greatly affected by variations in the material properties of the grasped object and indicate that the force control strategy is adequately immune to mechanical vibrations in the manipulator. GRA

N93-14473 California Univ., Berkeley.
FORCE AND POSITION CONTROL OF ROBOT MANIPULATORS: LEARNING AND REPETITIVE CONTROL APPROACH Ph.D. Thesis
Doyoung Jeon 1991 150 p
Avail: Univ. Microfilms Order No. DA9228696

When a robot performs the same task repeatedly, a learning or repetitive controller can enhance the performance of the system significantly. Learning or repetitive control, however, has not been studied in the force control of a robot manipulator as extensively as in the position control of a robot manipulator. In this dissertation, learning control is applied to hybrid force and position control of robot manipulators. Also, repetitive control is applied to the control of a spring loaded end effector. When the geometry and position of the constraint surface is known, the hybrid force and position controller and the feedforward compensator can be designed in the constraint coordinates. When the operation is periodic, the learning hybrid force and position control enhances the control performance as the feedforward compensator is updated in each cycle by the force and position error in the preceding trials. This scheme is proved to be stable in the sense of Lyapunov. In the experiments, a two degree of freedom SCARA-type direct-drive robot manipulator is used to test the feasibility of the learning hybrid force and position control. The deburring tool mounted on the upper link of the robot could follow a flat, tilted flat, and curved 1/4 inch aluminum plate with a desired contact force of 10 N (within the robot-mean-square force error of 1.95 N) and with desired tangential velocity. Considering the loss of contact observed at the initial trial, the performance of the system improved significantly. A spring loaded end effector is useful in assembly operations such as mounting an electronics package on a board. With the known stiffness of the spring, the desired contact force tracking is accomplished by controlling the spring displacement. Uncertainties in the environment such as the stiffness of the board make it difficult to program the required control force. As the operation repeats, the tracking errors for the spring displacement, i.e., the contact force, are compensated by the repetitive control. Repetitive control is robust under the presence of parametric uncertainties. Unmodeled dynamics make it necessary to modify the repetitive controller to gain stability robustness at the expense of tracking performance at high frequencies. The compliance of the contact mechanism plays an important role in the stability of the force control. When the compliance is known in advance, the lumped stiffness is estimated, and the feedback controller gains change according to the stiffness estimation. When the position of the constraint surface has uncertainty, a method of estimating both the stiffness and the position of the constraint surface is suggested. Dissert. Abstr.

N93-14478*# National Aeronautics and Space Administration. Lewis Research Center, Cleveland, OH.
DEVELOPMENT OF BRAIDED ROPE SEALS FOR HYPERSONIC ENGINE APPLICATIONS: FLOW MODELING
Rajakkannu Mutharasan (Drexel Univ., Philadelphia, PA.), Bruce M. Steinetz, Xiaoming Tao (Drexel Univ., Philadelphia, PA.), Guang-Wu Du (Drexel Univ.,

Philadelphia, PA.), and Frank Ko (Drexel Univ., Philadelphia, PA.) Dec. 1992 22 p Submitted for publication
(RTOP 505-63-5B)
(NASA-TM-105942; E-6166-1; NAS 1.15:105942) Avail: CASI HC A03/MF A01

A new type of engine seal is being developed to meet the needs of advanced hypersonic engines. A seal braided of emerging high temperature ceramic fibers comprised of a sheath-core construction was selected for study based on its low leakage rates. Flexible, low-leakage, high temperature seals are required to seal the movable engine panels of advanced ramjet-scramjet engines either preventing potentially dangerous leakage into backside engine cavities or limiting the purge coolant flow rates through the seals. To predict the leakage through these flexible, porous seal structures new analytical flow models are required. Two such models based on the Kozeny-Carman equations are developed herein and are compared to experimental leakage measurements for simulated pressure and seal gap conditions. The models developed allow prediction of the gas leakage rate as a function of fiber diameter, fiber packing density, gas properties, and pressure drop across the seal. The first model treats the seal as a homogeneous fiber bed. The second model divides the seal into two homogeneous fiber beds identified as the core and the sheath of the seal. Flow resistances of each of the main seal elements are combined to determine the total flow resistance. Comparisons between measured leakage rates and model predictions for seal structures covering a wide range of braid architectures show good agreement. Within the experimental range, the second model provides a prediction within 6 to 13 percent of the flow for many of the cases examined. Areas where future model refinements are required are identified. Author

N93-14499# Naval Postgraduate School, Monterey, CA.
AN ENERGY ANALYSIS OF THE PSEUDO WIGNER-VILLE DISTRIBUTION IN SUPPORT OF MACHINERY MONITORING AND DIAGNOSTICS M.S. Thesis
Scott G. Spooner Jun. 1992 98 p
(AD-A256202) Avail: CASI HC A05/MF A02

The Pseudo Wigner-Ville Distribution is a signal transformation of an input time signal into a joint time-frequency domain that provides an excellent characterization of an input signal as well as it's respective energy content. A smoothing window and energy sensitivity analysis of the discretized Pseudo Wigner-Ville Distribution is presented along with a machinery monitoring application using the resulting Wigner-Ville Distribution energy of the sampled signal. The ability to apply the Pseudo Wigner-Ville Distribution to both steady-state and transient machinery may enable the monitoring and diagnostics of virtually any piece of equipment. GRA

N93-14528# Carnegie-Mellon Univ., Pittsburgh, PA. Robotics Inst.
MODEL REDUCTION OF FLEXIBLE MANIPULATORS
Jie Yang, Yangsheng Xu, and C. S. Chen Jun. 1992 23 p
(AD-A255251; CMU-RI-TR-92-08) Avail: CASI HC A03/MF A01

Flexible manipulators can be characterized by a dynamic model with a large number of vibration modes, and the use of the model in the model-based control schemes requires reduction of model order. Balanced truncation is an effective method for model reduction of asymptotically stable systems by transforming the states to a coordinate system in which the controllability and observability Gramians are equal and diagonal, and eliminating the states which contribute weakly to the input-output map. An elastic flexible manipulator, however, is a marginally stable system and thus the balanced truncation method can not be directly applied. Herein, a method is presented of reducing the order of a marginally stable system based on the fact that translation transformations in the frequency domain preserve input-output properties of the system. The successful application is addressed of the method to model reduction of flexible manipulators with infinite-dimensional for finite-dimensional model. The method is also applicable for any other marginally stable model, such as elastic space trusswork and multi-dimensional space vehicle structure. GRA

N93-14529# Carnegie-Mellon Univ., Pittsburgh, PA. Robotics Inst.
AN ACTIVE Z GRAVITY COMPENSATION SYSTEM
Greg White and Yangsheng Xu Jul. 1992 29 p
(AD-A255258; CMU-RI-TR-92-09) Avail: CASI HC A03/MF A01

To perform simulations of partial or microgravity environments on earth requires some method of compensation for the earth's gravitational field. This paper discusses an active compensation system that modulates the tension in a counterweight support cable in order to minimize state deviation between the compensated body and the ideal weightless body. The system effectively compensates for inertial effects of the counterweight mass, viscous damping of all pulleys, and static friction in all parts of the GC system using a hybrid PI/fuzzy control algorithm. The dynamic compensation of inertia and viscous damping is performed by PI control, while static friction compensation is performed by the fuzzy system. The system provides very precise gravity compensation force, and is capable of non-constant gravity force compensation in the case that the payload mass is not constant. The only additional hardware requirements needed for the implementation of this system on a passive counterweight balance system are: a strain gauge tension sensor, and a torque motor with encoder. GRA

N93-14543 ESDU International Ltd., London (England).
CALCULATION METHODS FOR EXTERNALLY PRESSURISED (HYDROSTATIC) JOURNAL BEARINGS WITH CAPILLARY RESTRICTOR CONTROL
Sep. 1992 33 p
(ESDU-92026; ISBN-0-85679-831-2) Avail: ESDU

ESDU 92026 provides a procedure for the design and performance analysis of the bearings with five or more identical equally-spaced rectangular recesses (or pockets) fed by identical capillary restrictors from a constant pressure supply. The method takes account of stiffness and overload capacity requirements and determines the bearing overall size and proportions from the required load, speed and shaft diameter, recommends the clearance and supply pressure, and defines the recess dimensions and capillary restrictor size from the properties of the chosen lubricant. Equations and charts allow prediction of the journal displacement under load, the power loss, the lubricant flow rate, and the bearing and lubricant temperatures. The method applies to laminar flow and guidance is given for assessing the onset of non-laminar flow in the bearing and restrictors. Guidance is also given on the likelihood of bearing-induced instability. The user is assisted by flowcharts in applying the method, and two practical worked examples illustrate the procedure. ESDU 92037 introduces a FORTRAN program that implements the method, and magnetic media are available in ESDUpac A9237. Author

N93-14545# Carnegie-Mellon Univ., Pittsburgh, PA. Robotics Inst.
GLOBAL OPTIMUM PATH PLANNING FOR A REDUNDANT SPACE ROBOT
Om P. Agrawal and Yangsheng Xu Dec. 1991 45 p
(AD-A255316; CMU-RI-TR-91-15) Avail: CASI HC A03/MF A01

Robotic manipulators will play a significant role in the maintenance and repair of space stations and satellites, and other future space missions. Robot path planning and control for the above applications should be optimum, since any inefficiency in the planning may considerably risk the success of the space mission. This paper presents a global optimum path planning scheme for redundant space robotic manipulators to be used in such missions. In this formulation, a variational approach is used to minimize the objective functional. Two optimum path planning problems are considered: first, given the end-effector trajectory, find the optimum trajectories of the joints, and second, given the terminal conditions of the end-effector, find the optimum trajectories for the end-effector and the joints. It is explicitly assumed that the gravity is zero in, and the robotic manipulator is mounted on a completely free-flying base (spacecraft) and the attitude control (reaction wheels or thrust jets) is off. Linear and angular momentum conditions for this system lead to a set of mixed holonomic an nonholonomic constraints. These equations are adjoined to the objective functional using a Lagrange multiplier technique. The formulation leads to a system of Differential and Algebraic Equations (DAEs) and a set of terminal conditions. A numerical scheme is presented for forward integration of the above system of DAEs, and an iterative shooting method is used to satisfy the terminal conditions. This approach is significant since most space robots that have been developed so far are redundant. The kinematic redundancy of space robots offers efficient control and provides the necessary dexterity for extra-vehicular activity or avoidance of potential obstacles in space stations. GRA

N93-14567*# Carnegie-Mellon Univ., Pittsburgh, PA. Robotics Inst.
A MINIMUM-SLIP ATTITUDE CONTROL METHOD FOR THE EREBUS WALKING ROBOT
Peter V. Nagy May 1992 34 p
(Grant NAGw-2998)
(NASA-CR-191646; NAS 1.26:191646; AD-A255522; CMU-RI-TR-92-07)
Avail: CASI HC A03/MF A01

In this report, a method for attitude control of statically-stable walking robots is developed such that slip is minimized when the body is leveled by using only the actuators which cause vertical link motions. If all legs of a walker have three independent translational degrees of freedom, then an attitude control method that uses all actuators may be used to level the body with no foot slippage. However, there are some advantages in reducing the number of controllable degrees-of-freedom, as with the Erebus walker. The task is then to determine the best method to adjust the attitude of the walker body such that foot slippage and the build-up of internal link forces is minimized. The method that does this--the minimum-slip z-axes attitude control method--is developed in this technical report for that purpose. GRA

N93-14684 Oregon State Univ., Newport.
DYNAMICS AND CONTROL OF A RIGID/FLEXIBLE MANIPULATOR Ph.D. Thesis
Chun-Tien Yeh 1992 151 p
Avail: Univ. Microfilms Order No. DA9229776

Control of high-speed, light-weight robotic manipulators is a challenge because of their special dynamic characteristics. A two-stage control algorithm for the position control of flexible manipulators is proposed. First, the more complex, flexible robot system is replaced by a simplified hypothetical rigid body system (HRRA) with offline trajectory planning. This reduces the complexity of the controller design for the flexible robotic arm. A parameter-optimization approach was adopted to minimize the difference between these two models in this stage. Also, a comparison of computational efficiency is made among the methods of calculus-of-variations, dynamic-programming, and the proposed parameter-optimization. At the second stage, simple linear state feedback controllers, based on the simplified hypothetical rigid body model, are proposed to control the actual robotic system. With the feedback gains selected properly by the pole-placement and linear quadratic methods, the results show satisfactory achievement of the motion objectives. The algorithm is implemented for a two-link rigid/flexible robotic arm, and the results indicate that the procedure is capable of providing effective control with much simpler computational requirements than those of procedures published previously.
Dissert. Abstr.

N93-14685 Clemson Univ., SC.
OPTIMAL AND ROBUST CONTROL OF ROBOT MANIPULATORS Ph.D. Thesis
Michael Thomas Grabbe 1992 113 p
Avail: Univ. Microfilms Order No. DA9233385

The problem of controlling a robot manipulator typically requires determining the actuating torques at each joint, in the form of a feedback control law, which force the manipulator joint angles to follow a prescribed trajectory. This problem is often referred to as the trajectory tracking problem, and is difficult to solve due to the highly nonlinear dynamics associated with the robot manipulator and the time variance of the system induced by the prescribed trajectory. The complexity of the problem is compounded in cases where the manipulator end effector is constrained by contact with a surface, there are modeling or parametric uncertainties in the manipulator dynamics, or there are disturbances to the system. The trajectory tracking problem is addressed in two distinct cases. The first case involves the ideal situation in which the manipulator is unconstrained in its motion and there are no uncertainties or disturbances in the system. Optimal control theory is used to develop a class of feedback control laws which produce a globally uniformly asymptotically stable (GUAS) system. The second case involves both constrained motion and the possibilities of uncertainties and disturbances in the system. Two feedback control laws are developed which are robust with respect to uncertainties and disturbances, provide globally exponentially stable (GES) position tracking error, and provide a means of regulating the force applied. Dissert. Abstr.

N93-14702* National Aeronautics and Space Administration. Lyndon B. Johnson Space Center, Houston, TX.
THRUSTER SEALING SYSTEM AND APPARATUS Patent
Paul A. Svejkovsky, inventor (to NASA) 24 Nov. 1992 10 p Filed 22 Oct. 1991 Supersedes N92-17872 (30 - 8, p 1307)
(NASA-Case-MSC-21898-1; US-Patent-5,165,229;
US-Patent-Appl-SN-780512; US-Patent-Class-60-271;
US-Patent-Class-60-223; US-Patent-Class-60-259;
US-Patent-Class-60-39.091; Int-Patent-Class-F02K-9/96;
Int-Patent-Class-B65D-39/12) Avail: US Patent and Trademark Office

A thruster nozzle sealing system and apparatus is provided for protection of spacecraft thruster motors. The system includes a sealing plug, a sealing plug insertion tool, an outer cover, an outer cover attachment, and a ferry flight attachment. The sealing plug prevents moisture from entering the thruster engine so as to prevent valve failure. The attachments are interchangeably connectable with the sealing plug. The ferry flight attachment is used during air transportation of the spacecraft, and the outer cover attachment is used during storage and service of the spacecraft. The outer cover provides protection to the thruster nozzle from mechanical damage. Official Gazette of the U.S. Patent and Trademark Office

N93-14710* National Aeronautics and Space Administration. Goddard Space Flight Center, Greenbelt, MD.
RETRACTABLE TOOL BIT HAVING SLIDER TYPE CATCH MECHANISM Patent
George M. Voellmer, inventor (to NASA) 29 Dec. 1992 8 p Filed 24 Sep. 1991 Supersedes N92-24058 (29 - 14, p 2385)
(NASA-Case-GSC-13358-1; US-Patent-5,174,694;
US-Patent-Appl-SN-765069; US-Patent-Class-408-124;
US-Patent-Class-279-79; US-Patent-Class-279-89;
US-Patent-Class-408-239R; US-Patent-Class-408-241R;
US-Patent-Class-901-41; Int-Patent-Class-B23B-31/10) Avail: US Patent and Trademark Office

A retractable tool bit assembly utilized in connection with a robotic gripper type end-effector is presented. The apparatus includes one or more spring loaded nestable or telescoping tubular sections together with a catch mechanism for capturing and holding the toll, such as an allen key, in its retracted position. The innermost tubular section includes a threshold cap and engages and holds the tool. The catch mechanism consists of a slider type mechanism located adjacent a relatively larger outer base section and includes means for engaging a conically or mushroom shaped rear end portion of the tool when the telescoping sections are moved to a retracted or parked position. The catch mechanism is released upon actuation of a rotary tool drive motor coupled to a circular mount and which holds the base section. When released all the telescoping sections including the tool extends fully outward to a use position.
Official Gazette of the U.S. Patent and Trademark Office

N93-14712* National Aeronautics and Space Administration, Washington, DC.
WORK ATTACHMENT MECHANISM/WORK ATTACHMENT FIXTURE Patent
John M. Vranish, inventor (to NASA) 29 Dec. 1992 10 p
(NASA-Case-GSC-13430-1; US-Patent-5,174,772;
US-Patent-Appl-SN-824126; US-Patent-Class-439-131;
US-Patent-Class-439-139; US-Patent-Class-439-310;
Int-Patent-Class-H01R-13/54) Avail: US Patent and Trademark Office

A mechanical coupling system is described wherein a spline screw system is used to connect two bodies, a work attachment mechanism and a work attachment fixture. A kinematic clamp first guides and mates the attachment mechanism to the attachment fixture. The kinematic clamp includes three round roller members equidistantly located around the periphery of the bodies and three correspondingly located V-shaped grooves located on the periphery of the other body. A motor driven spline screw in the attachment mechanism then engages a spline bolt head in the attachment fixture and includes a threaded shank upon which is mounted a translatable nut which is adapted to translate up and down the shank but not rotate. The nut carries one or more electrical connectors which travel upwardly during a connecting sequence and cams open a set of dust covers which operate to engage an opposing set of dust covers adjacent complementary type electrical connectors on the attachment

mechanism. A mechanical and electrical interconnection process between the bodies occurs sequentially.
Official Gazette of the U.S. Patent and Trademark Office

N93-14735# Army Materials Technology Lab., Watertown, MA. Mechanics and Structures Branch.
TESTING AND ANALYSIS OF MODIFIED HMMWV FRONT LIFT PROVISIONS Final Report
Christopher Cavallaro, Robert B. Dooley, Kristen D. Weight, and Paul V. Cavallaro May 1992 45 p
(DA Proj. 1L1-62105-AH-84)
(MTL-TR-92-31) Avail: CASI HC A03/MF A01

The U.S. Army Materials Technology Laboratory (MTL) was requested by the Tank and Automotive Command (TACOM) and the Military Traffic Management Command (MTMC) to investigate the performance of the modified front lift provisions on the high mobility, multipurpose, wheeled vehicle (HMMWV). In order to evaluate the front lift provisions, a series of simulated air lift, ultimate pull, and fatigue tests were performed. Each type of test was performed for two different load magnitudes and angles. In addition to the mechanical tests performed, nondestructive testing procedures were utilized to inspect the provisions for imperfections and cracks before and after testing. A finite element analysis (FEA) was also conducted to analyze the hook and the provision bracket for each of the two load configurations. Author

N93-14763*# Alabama Univ., Huntsville. Materials Processing Lab.
FIBER PULLING APPARATUS MODIFICATION Final Report
Guy A. Smith and Gary L. Workman Nov. 1992 14 p
(Contract NAS8-38609)
(NASA-CR-184498; NAS 1.26:184498) Avail: CASI HC A03/MF A01

A reduced gravity fiber pulling apparatus (FPA) was constructed in order to study the effects of gravity on glass fiber formation. The apparatus was specifically designed and built for use on NASA's KC-135 aircraft. Four flights have been completed to date during which E-glass fiber was successfully produced in simulated zero, high, and lunar gravity environments. In addition simulated lunar soil samples were tested for their fiber producing properties using the FPA. Author

N93-14822 Department of the Navy, Washington, DC.
CABLE-LINE SHORTENING DEVICE Patent Application
Michael B. Young, inventor (to Navy) 5 May 1992 6 p Filed 19 Jul. 1990
(AD-D015427; US-Patent-Appl-SN-557450; US-Patent-Class-24-71.2)
Avail: CASI HC A02/MF A01

A device and method for shortening a cable or line includes a winding member having a winding surface for forming one or more transverse windings of an otherwise longitudinally oriented cable or line. The device includes elements located on the winding surface for redirecting the cable or line from its original longitudinal orientation to a transverse winding orientation. There may further be included an element for preventing the cable or line windings from overlapping one another. GRA

N93-14842*# National Aeronautics and Space Administration. Lyndon B. Johnson Space Center, Houston, TX.
EXTRA-VEHICULAR ACTIVITY TRANSLATION TOOL Patent Application
Leslie S. Hartz, inventor (to NASA) 21 Aug. 1992 20 p
(NASA-Case-MSC-21955-1; US-Patent-Appl-SN-931468) Avail: CASI HC A03/MF A01

A portable hand-grip device for use during extravehicular activity is described. The device has a base member overlaid by a flexible pad having its opposite end releasably secured to the base. The pad includes an adhesive-covered surface which may be attached to a flat surface. A plurality of closely-spaced elongated rigid members are arranged side-by-side across the back of the flexible sheet to reinforce the flexible pad. The ends of these reinforcing members project beyond the opposite sides of the base and flexible pad. A selectively-operable mechanism on the base member releasably captures the outer end of the reinforcing members and secures them when the pad member is attached to a flat surface and provides a load path between a handle on the base and the flexible pad. The selectively-operable mechanism is further arranged to selectively release the reinforcing members so that the device may be progressively peeled away from a wall surface. NASA

N93-14843*# National Aeronautics and Space Administration. Lyndon B. Johnson Space Center, Houston, TX.
HIGH-TEMPERATURE, HIGH-PRESSURE OXYGEN METERING VALVE Patent Application
Rollin C. Christianson, inventor (to NASA), Peter P. Lycou, inventor (to NASA), and James A. Daniel, inventor (to NASA) 14 Aug. 1992 21 p
(NASA-Case-MSC-21823-1; US-Patent-Appl-SN-929552) Avail: CASI HC A03/MF A01

A control valve includes a body defining a central cavity arranged between a fluid inlet and outwardly-diverging first and second fluid outlets respectively disposed in a common transverse plane. A valve member is arranged in the cavity for rotation between first and second operating positions where a transverse fluid passage through the valve member alternatively communicates the fluid inlet with one or the other of the fluid outlets. To minimize fluid turbulence when the valve member is rotated to an alternate operating position, the fluid passage has a convergent entrance for maintaining the passage in permanent communication with the fluid inlet as well as an oblong exit opening with spaced side walls for enabling the exit opening to temporarily span the first and second fluid outlets as the valve member is turned between its respective operating positions.
NASA

N93-14871* National Aeronautics and Space Administration. Lyndon B. Johnson Space Center, Houston, TX.
BEARING SERVICING TOOL Patent
Rex A. Boyce, inventor (to NASA) 24 Nov. 1992 8 p Filed 31 Oct. 1991
(NASA-Case-MSC-21881-1; US-Patent-5,165,169;
US-Patent-Appl-SN-785637; US-Patent-Class-29-898.08;
US-Patent-Class-29-898.01; US-Patent-Class-29-898.07;
US-Patent-Class-29-426.5; US-Patent-Class-29-263;
Int-Patent-Class-B23P-19/00) Avail: US Patent and Trademark Office

A tool for removing and/or replacing bearings in situ is presented. The tool is comprised of a brace having a first end adapted to engage a first end of the bearing housing, and a second end adapted to engage a second end of the bearing housing. If the two ends of the bearing housing are different in configuration, then the respective ends of the brace are configured accordingly. An elongate guide member integral with the brace has two parts, each projecting endwise from a respective end of the brace. A removable pressure plate can be mounted on either part of the guide member for longitudinal movement therealong and has first and second ends of different configurations adapted to engage the first and second ends of the bearing. A threaded-type drive is cooperative between the guide and the pressure plate to move the pressure plate longitudinally along the guide and apply a force to the bearing, either to remove the bearing from its housing, or to emplace a new bearing in the housing.
Official Gazette of the U.S. Patent and Trademark Office

N93-14881# Department of the Navy, Washington, DC.
METHOD AND DEVICES FOR THE IN SITU REPAIR OF DAMAGED THREADS Patent Application
Robert V. Belenger, inventor (to Navy) 29 Jun. 1992 15 p
(AD-D015416; US-Patent-Appl-SN-905702) Avail: CASI HC A03/MF A01

A method and device for rehabilitating damaged threaded connections in situ is disclosed. After the threaded connection is separated, a thin metal strip having a hardness that is less than or equal to the hardness of the threads is inserted into and against internal threads. The threaded connection is then reassembled. As the external threads advance along the internal threads, the metal strip deforms into gaps between the threads particularly in any area of damage thereby to rehabilitate the threaded connection. GRA

N93-14916*# Mechanical Technology, Inc., Latham, NY.
A FEASIBILITY ASSESSMENT OF MAGNETIC BEARINGS FOR FREE-PISTON STIRLING SPACE POWER CONVERTERS Final Report, Jul. 1990 - Aug. 1991
Peter W. Curwen, Dantam K. Rao, and Donald R. Wilson Jun. 1992 90 p

(Contract NAS3-26061)
(NASA-CR-189135; E-7440; NAS 1.26:189135; MTI91-TR-53) Avail: CASI HC A05/MF A01

This report describes a design and analysis study performed by Mechanical Technology Incorporated (MTI) under NASA Contract NAS3-26061. The objective of the study was to assess the feasibility and efficacy of applying magnetic bearings to free-piston Stirling-cycle power conversion machinery of the type currently being evaluated for possible use in long-term space missions. The study was performed for a 50-kWe Reference Stirling Space Power Converter (RSSPC) system consisting of two 25-kWe free-piston Stirling engine modules. Two different versions of the RSSPC engine modules have been defined under NASA Contract NAS3-25463. These modules currently use hydrostatic gas bearings to support the reciprocating displacer and power piston assemblies. Results of this study show that active magnetic bearings of the attractive electromagnetic type are technically feasible for RSSPC application provided that wire insulation with 60,000-hr life capability at 300 C can be developed for the bearing coils. From a design integration standpoint, both versions of the RSSPC were found to be conceptually amenable to magnetic support of the power piston assembly. However, only one version of the RSSPC was found to be amendable to magnetic support of the displacer assembly. Unacceptable changes to the basic engine design would be required to incorporate magnetic displacer bearings into the second version. Complete magnetic suspension of the RSSPC can potentially increase overall efficiency of the Stirling cycle power converter by 0.53 to 1.4 percent (0.15 to 0.4 efficiency points). Magnetic bearings will also overcome several operational concerns associated with hydrostatic gas bearing systems. However, these advantages are accompanied by a 5 to 8 percent increase in specific mass of the RSSPC, depending on the RSSPC version employed. Additionally, magnetic bearings are much more complex, both mechanically and particularly electronically, than hydrostatic bearings. Accordingly, long-term stability and reliability represent areas of uncertainty for magnetic bearings. Considerable development effort will be required to establish the long-term suitability of these bearings for Stirling space power applications.
Author

N93-15102 Virginia Polytechnic Inst. and State Univ., Blacksburg.
POSITION AND VIBRATION CONTROL OF FLEXIBLE SPACE ROBOTS Ph.D. Thesis
Seungchul Lim 1992 139 p
Avail: Univ. Mircofilms Order No. DA9226035

This dissertation is concerned with the position and vibration control of flexible articulated space robots consisting of a rigid platform, two flexible arms, and a rigid end-effector carrying a payload, all components being serially connected through revolute joints. The mission is to carry a payload over a prescribed trajectory in the inertial space, while suppressing the elastic vibration of the arms and the rigid-body perturbations. The equations of motion governing the robot dynamics are derived by means of Lagrangian mechanics and they include actuator dynamics. Based on the assumption that the elastic deformations and the rigid-body perturbations are small relative to the nominal trajectory-following rigid-body motions, a perturbation approach is adopted to separate the equations into nonlinear rigid-body equations and linear perturbation equations. The nominal trajectory is planned to conserve the limited actuator resources and keep the platform attitude stationary, by eliminating the inherent kinematic redundancy of the manipulator. By assuming perfect sensing, i.e., all the states are completely accessible, two kinds of controls are designed in discrete time. First, a feedforward control is designed to minimize the persistent disturbance resulting from the nominal motions. Next, a feedback control is synthesized based on the Linear Quadratic Regulator (LQR) theory with a prescribed degree of stability to make the system stable and further enhance the disturbance-rejection performances. These controls are subsequently applied to the case in which only the sensor outputs are available, and they are noisy. A finite number of sensors is assumed. A Kalman filter is designed to estimate the state on the assumption of zero-mean Gaussian white plant and measurement noise. In the real situation, controls are applied to the original plant rather than the linearized model, so that the Linear Quadratic Gaussian (LQG) control combined with robustness recovery methods is tested on the plant. Due to difficulties in implementing a Kalman Filter, a Maximum Likelihood Estimator (MLE) is proposed. A numerical example illustrates the approach. Dissert. Abstr.

N93-15104 California Inst. of Tech., Pasadena.
THEORY AND APPLICATIONS OF HYPER-REDUNDANT ROBOTIC MANIPULATORS Ph.D. Thesis
Gregory Scott Chirikjian 1992 211 p
Avail: Univ. Microfilms Order No. DA9232167

The term 'hyper-redundant' refers to robotic manipulators and mobile robots with a very large, possibly infinite, number of actuatable degrees of freedom. These robots are analogous in morphology and operation to snakes, worms, elephant trunks, and tentacles. This thesis presents a novel kinematic framework for hyper-redundant manipulator motion planning and a task implementation. The basis of this formulation is the use of a 'backbone reference set' which captures the essential macroscopic geometric features of hyper-redundant robots. In the analytical part of this work, the backbone representation is developed and used to solve problems in obstacle avoidance, locomotion, grasping, and 'optimal' end effector placement. The latter part of this thesis deals with the design and implementation of a thirty-degree-of-freedom planar hyper-redundant manipulator which is used to demonstrate these novel kinematic and motion planning techniques. Design issues such as robustness with respect to mechanical failure, and design for easy assembly and repair are also addressed. The analytical and design concepts are combined to illustrate tasks for which hyper-redundant robotic mechanisms are well suited.
Dissert. Abstr.

N93-15117*# Alabama Univ., Huntsville. Center for Automation and Robotics.
DEVELOPMENT OF ADVANCED SEAL VERIFICATION Final Report
Gary L. Workman, Susan E. Kosten, and Mustafa A. Abushagur 18 Sep. 1992 42 p
(Contract NAS8-36955)
(NASA-CR-184502; NAS 1.26:184502) Avail: CASI HC A03/MF A01

The purpose of this research is to develop a technique to monitor and insure seal integrity with a sensor that has no active elements to burn-out during a long duration activity, such as a leakage test or especially during a mission in space. The original concept proposed is that by implementing fiber optic sensors, changes in the integrity of a seal can be monitored in real time and at no time should the optical fiber sensor fail. The electrical components which provide optical excitation and detection through the fiber are not part of the seal; hence, if these electrical components fail, they can be easily changed without breaking the seal. The optical connections required for the concept to work does present a functional problem to work out. The utility of the optical fiber sensor for seal monitoring should be general enough that the degradation of a seal can be determined before catastrophic failure occurs and appropriate action taken. Two parallel efforts were performed in determining the feasibility of using optical fiber sensors for seal verification. In one study, research on interferometric measurements of the mechanical response of the optical fiber sensors to seal integrity was studied. In a second study, the implementation of the optical fiber to a typical vacuum chamber was implemented and feasibility studies on microbend experiments in the vacuum chamber were performed. Also, an attempt was made to quantify the amount of pressure actually being applied to the optical fiber using finite element analysis software by Algor.
Author

N93-15150 Waterloo Univ. (Ontario).
DYNAMICS AND CONTROL OF FLEXIBLE ARM ROBOTS Ph.D. Thesis
Tarun-Raj Singh 1991 309 p
(ISBN-0-315-69011-9) Avail: Univ. Microfilms Order No. DANN69011

This thesis describes an experimental and analytical investigation into the dynamics and control of flexible link robots. The author has attempted to provide a comprehensive exposition of the modelling, control and dynamics of flexible arm robots. Flexible arm robots are represented by partial differential equations reflecting the distributed nature of mass and stiffness. Hamilton's principle is used to model the system and the sliding mode and shaped input concepts are used to design controllers. Perturbation analysis is used to study the nonlinear dynamics of a flexible arm robot. A generalized technique to arrive at equations of motion of distributed parameter systems is discussed. The assumed mode method is used to reduce the partial differential equations into a set of ordinary differential equations. A MAPLE (symbolic manipulator) program has been developed to derive the equations of motion of any rigid/flexible link robot. The input to this program are the radius vectors of typical points on the links and

eigenfunctions for the flexible links. The MAPLE program has been used to derive the equations of motion of a single-link flexible arm robot, a two link, rigid robot and a two link flexible arm robot. These equations were used later in the design of controllers. Control of rigid multi-link robots is a fairly complex topic as it falls into the realm of nonlinear control. Addition of flexibility to the links add another dimension to the problem. A generalized scheme is proposed for the tip control of flexible/rigid link robots. The proposed scheme includes two exotic concepts: sliding mode control and shaped input control. These two techniques are used in conjunction with each other, the sliding mode controller caters to the rigid body motion, while the shaped input controller modifies the reference input to eliminate any vibratory motion due to the link flexibility. An experimental two-link flexible arm robot is designed and fabricated to corroborate the proposed controllers. Data acquisition and control, software and hardware is developed to communicate with the plant. The experimental sliding mode and sliding mode/shapes input controllers authenticate the analytical predicitions. The governing equations of multi-link robots are nonlinear in nature. Perturbation analysis is used to arrive at approximately closed form solutions to better understand the behavior of these systems at resonance, when flexibility is introduced into the links. A model is chosen which includes a flexible link and a flexible joint to study the effects of nonlinearities. MAPLE is used in this study to arrive at the approximate solution of the equations of motion of the robot in question. The two variable expansion method is used, where the variables are expanded in a power series and the terms of this series are solved recursively. The study reveals that the system behaves like one with quadratic nonlinearities, and predicts saturation at internal resonance and the pump resonance phenomenon. Dissert. Abstr.

N93-15232# Department of the Navy, Washington, DC.
LIQUID FLOW REACTOR AND METHOD OF USING Patent Application
Dennis R. Hardy, inventor (to Navy), Erna J. Beal, inventor (to Navy), and Jack C. Burnett, inventor (to Navy) 30 Apr. 1992 12 p Filed 30 Apr. 1992
(AD-D015392; US-Patent-Appl-SN-875955) Avail: CASI HC A03/MF A01

The tendency of liquid hydrocarbon-based fuels, such as kerosene, diesel fuel, and jet fuel toward the formation of fuel-insoluble solids during thermal stress in an aircraft fuel system is assessed by an accelerated test method comprising passing a predetermined quantity of a sample of fuel through a heated test section maintained at a predetermined temperature, at a predetermined fuel flow rate. A metal test strip, weighed before the test, is clamped in the heated test section during the test. It is weighed again after the test and the weight of solids buildup during the test is determined. It is related directly to the tendency of the fuel to form fuel-insoluble solids during thermal stress. A filter is weighed before the test. It is then connected to the outlet of the test section, and liquid fuel leaving the test section during the test is passed through it. The filter is then weighed a second time and the weight increase of the filter due to its capture of fuel-insoluble solids is calculated. It also is directly related to the tendency of the fuel to form fuel-insoluble solids during thermal stress. GRA

N93-15248# Department of the Army, Washington, DC.
JOINTED ASSEMBLY ACTUATED BY FLUID PRESSURE Patent Application
John W. Monroe, inventor (to Army) 5 Aug. 1992 23 p Filed 5 Aug. 1992
(AD-D015383; US-Patent-Appl-SN-925048) Avail: CASI HC A03/MF A01

The invention is an assembly of a plurality of relatively movable jointed members such as robotic arm segments and a mechanical muscle connected between two of the segments. The muscle has a longitudinally inflexible, radially expandable sleeve containing a pressurizable bladder of elastic material. The bladder enlarges diametrically when pressurized and bulges the wall of the sleeve outward. The sleeve thereupon contracts axially to compensate for length taken up by the sleeve's outward bulge. Terminus at either end of the sleeve connects the sleeve to different segments of a jointed arm, that the sleeve's axial contraction effects movement of one segment relative to the other. GRA

N93-15251# Department of the Army, Washington, DC.
REMOTE VEHICLE CONTROLLER Patent Application
John J. Schmitz, inventor (to Army) 22 Jun. 1992 17 p Filed 22 Jun. 1992
(AD-D015389; US-Patent-Appl-SN-902264) Avail: CASI HC A03/MF A01

A remote control system is disclosed for use with vehicles having radios. A first vehicle has a controller attached to the radio for use in sending signals to a second vehicle. The second, remotely controlled, vehicle has a receiver connected to the vehicle radio which receives commands from the first radio to effect the desired motion and action of the second vehicle. The receiver and controller have circuitry which allows them to be reprogrammed to function on various military vehicles and also be attached to the different radio systems in use by the U.S. Military. GRA

N93-15278# Oak Ridge National Lab., TN.
VARIABLE SPEED ROTARY COMPRESSOR AND ADJUSTABLE SPEED DRIVE EFFICIENCIES MEASURED IN THE LABORATORY
W. A. Miller 1992 8 p Presented at the Winter Annual Meeting of the American Society of Mechanical Engineers, Anaheim, CA, 8-13 Nov. 1992
(Contract DE-AC05-84OR-21400)
(DE92-040026; CONF-921110-26) Avail: CASI HC A02/MF A01

Two state-of-the-art variable-speed rotary compressors, of nominal one ton cooling capacity, were instrumented and tested in the laboratory. Both compressors were identical except for their respective variable-speed drive systems (i.e., motor and inverter). One compressor had an inverter driven induction motor (IDIM) drive, and the other had a permanent magnet electronically commutated motor drive (PM-ECM). The laboratory study evaluated the compressor's efficiency under representative variable-speed conditions. Testing was conducted as a function of compressor drive frequency and of refrigerant condensing and evaporating conditions. Saturated refrigerant conditions, inlet superheat, and subcooling were controlled using a secondary refrigerant calorimeter. Spectrum analysis was conducted on the current input to one phase of the three-phase drive systems to measure motor speed and characterize harmonic content of the inverters. An optimal volt per Hz ratio was determined at 120-, 90-, 60-, and 30-Hz drive frequencies and at different load conditions for the rotary with induction motor as driven by a PWM inverter and also by a motor generator set (ideal induction motor drive). Variation of voltage input to the compressor had the largest effect at the lowest drive frequency (30Hz). A 5 percent variation about the optimal voltage at 30 Hz frequency caused a roughly 5 percent drop in compressor isentropic efficiency. Calorimeter data were used to develop modulating compressor and drive system performance maps. Performances of the two compressors were compared and the rotary with PM-ECM drive showed better efficiency trends at 30-Hz drive frequency. Above the 30-Hz drive frequency no clear advantage was observed for the PM-ECM vs the IDIM, possibly due to oversizing of the PM-ECM inverter. DOE

N93-15380# Maryland Univ., College Park.
THE TRAJECTORY ANALYSIS OF BEVEL PLANETARY GEAR TRAINS
Chen-Chou Lin and Lung-Wen Tsai 1991 8 p Presented at the 17th ASME Design Automation Conference, Miami, FL, 22-25 Sep. 1991
(Contract DE-FG05-88ER-13977)
(DE92-040898; CONF-910957-4) Avail: CASI HC A02/MF A01

In this paper, the trajectory of bevel planetary wear trains has been studied. The parametric equations of trajectory are derived. It is shown that the trajectory generated by a tracer point on the planet of a bevel planetary gear train is analogous to that of a spur planetary gear train. Two cases, gear ratio equal to one and two, are presented in detail including the geometric description, plane of symmetry, extent of trajectory, number of nodes (cusps), and their locations. The criteria for the existence of cusps are verified algebraically, and interpreted from geometrical point of view. DOE

N93-15410# Wisconsin Univ., Madison. Engine Research Center.
CENTER FOR ADVANCED PROPULSION SYSTEMS (RESEARCH) Final Report
G. L. Borman 31 Aug. 1992 44 p
(Contracts DAAL03-86-K-0174; DAAL03-86-G-0200)
(AD-A256628; ARO-24623.111-EG-UIR) Avail: CASI HC A03/MF A01

A brief description is given for sixteen fellows that studied at the ERC

with the support of this grant. The individual research summaries are followed by a listing of the Ph.D. theses and publications for each fellow.
GRA

N93-15416# Edgerton, Germeshausen and Grier, Inc., Idaho Falls, ID.
DUAL-SHAFT ELECTRIC PROPULSION (DSEP) TECHNOLOGY DEVELOPMENT PROGRAM
Aug. 1992 466 p Prepared in cooperation with Department of Energy, Idaho Falls, ID
(Contract DE-AC07-84NV-10366)
(DE92-040189; DOE/NV-10366/21) Avail: CASI HC A20/MF A04

The background, progress, and current state of the DOE-sponsored Advanced Dual-Shaft Electric Propulsion Technology Development are presented. Three electric-drive vehicles were build as conversions of a commercial gasoline-powered van, using program-designed components and systems as required. The vehicles were tested primarily on dynamometer or test tract. Component and system testing represented a major portion of the development effort. Test data are summarized in this report, and an Appendix contains the final component design specifications. This major programmatic concerns were the traction battery, the battery management system, the dc-to-ac inverter, the drive motor, the transaxle and its ancillary equipment, and the vehicle controller. Additional effort was devoted to vehicle-related equipment: gear selector, power steering, power brakes, accelerator, dashboard instrumentation, and heater. Design, development, and test activities are reported for each of these items, together with an appraisal (lessons learned) and recommendations for possible further work. Other programmatic results include a Cost and Commercialization Analysis, a Reliability and Hazards Analysis Study, Technical Recommendations for Next-Generation Development, and an assessment of overall program efforts. DOE

N93-15461# Department of the Navy, Washington, DC.
THREE POSITION POWER CYLINDER Patent Application
Paul Moody, inventor (to Navy) 22 Jun. 1992 17 p
(AD-D015393; US-Patent-Appl-SN-902262) Avail: CASI HC A03/MF A01

An assembly for moving objects by mechanical linkages has a power cylinder with a shoulder at the juncture of a small bore and a large bore and with ports adjacent to each end and one adjacent to the shoulder. A shaft extends through the cylinder with a larger diameter portion in the smaller bore with a piston thereon sealing against the surface of the smaller bore. A second piston slidably seals on the small diameter of the shaft and against the larger bore, being biased towards the shoulder by a spring. A lost motion device on the end of the shaft projects outwardly of the smaller bore end of the power cylinder and has a housing with a chamber in which the end of the shaft is slidable against a spring which biases it outwardly of the housing. Pressurized fluid when supplied to the ports in the large portion of the power cylinder moves the shaft within the lost motion device against the spring to move the lost motion device, and when supplied to the ports at the ends of the power cylinder, permits the spring of the lost motion device to bias the piston shaft in the direction of the large bore. When supplied only to the port in the smaller diameter bore, the shoulder on the piston shaft will move the slidable piston against its spring and the piston shaft is moved still further in the direction of the large bore. GRA

N93-14923# Victoria Univ. (British Columbia). Dept. of Mechanical Engineering.
COOPERATIVE CONTROL OF MULTIPLE SPACE MANIPULATORS
M. Nahon and J. Angeles (McGill Univ., Montreal, Quebec) *In* Canadian Space Agency, Proceedings of the Sixth CASI Conference on Astronautics 1990 10 p Previously announced in IAA as A91-34929 (For primary document see N93-14920 04-12)
Avail: Canadian Aeronautics and Space Inst., 222 Somerset St. W., Suite 601, Ottawa, Ontario K2P 0J1 Canada

N93-14924# Spar Aerospace Ltd., Toronto (Ontario).
VISION SYSTEM REQUIREMENTS AND CONCEPT FOR THE SPECIAL PURPOSE DEXTEROUS MANIPULATOR SYSTEM (SPDM)
Leon Zucherman *In* Canadian Space Agency, Proceedings of the Sixth CASI Conference on Astronautics 1990 6 p Previously announced in IAA as A91-34930 (For primary document see N93-14920 04-12)
Avail: Canadian Aeronautics and Space Inst., 222 Somerset St. W., Suite 601, Ottawa, Ontario K2P 0J1 Canada

N93-14926# Ottawa Univ. (Ontario).
AN ACTIVE TACTILE PERCEPTION SYSTEM
E. Petriu, M. Greenspan, F. Gelinas, W. S. McMath (Canadian Space Agency, Ottawa, Ontario), and S. K. Yeung (Canadian Space Agency, Ottawa, Ontario) *In* Canadian Space Agency, Proceedings of the Sixth CASI Conference on Astronautics 1990 9 p Previously announced in IAA as A91-34932 (For primary document see N93-14920 04-12)
Avail: Canadian Aeronautics and Space Inst., 222 Somerset St. W., Suite 601, Ottawa, Ontario K2P 0J1 Canada

N93-14950# Thomson-CSF, Ottawa (Ontario).
A CONCEPT FOR A SUPERVISED AUTONOMOUS ROBOT
S. Kalaycioglu *In* Canadian Space Agency, Proceedings of the Sixth CASI Conference on Astronautics 1990 17 p Previously announced in IAA as A91-34956 (For primary document see N93-14920 04-12)
Avail: Canadian Aeronautics and Space Inst., 222 Somerset St. W., Suite 601, Ottawa, Ontario K2P 0J1 Canada

38 QUALITY ASSURANCE AND RELIABILITY

Includes product sampling procedures and techniques; and quality control.

N93-14104# Hughes Aircraft Co., El Segundo, CA.
ELECTRONICS RELIABILITY FRACTURE MECHANICS. VOLUME 1: CAUSES OF FAILURES OF SHOP REPLACEABLE UNITS AND HYBRID MICROCIRCUITS Final Report, May 1987 - Sep. 1991
J. Kallis, D. Buechler, J. Erickson, D. V. Westerhuyzen, and R. Strokes May 1992 577 p
(Contract F33615-87-C-3402)
(AD-A255836; EDFG-R-160309-Vol-1; WL-TR-92-3015-Vol-1) Avail: CASI HC A25/MF A05

This is the first of two volumes. The other volume (WL-TR-91-3119) is 'Fracture Mechanics'. The objective of the Electronics Reliability Fracture Mechanics (ERFM) program was to develop and demonstrate a life prediction technique for electronic assemblies, when subjected to environmental stress of vibration and thermal cycling, based upon the mechanical properties of the materials and packaging configurations which make up an electronic system. A detailed investigation was performed of the following two shop replaceable units (SRUs): Timing and Control Module (P/N 3562102) and Linear Regulator Module (P/N 3569800). The SRUs are in the Programmable Signal Processor (3137042) Line Replaceable Unit (LRU) of the Hughes AN/APG-63 Radar for the F-15 Aircraft. GRA

N93-14500# Naval Postgraduate School, Monterey, CA.
THE USE OF INTERNATIONAL STANDARDS ORGANIZATION ISO 9000 QUALITY ASSURANCE STANDARDS IN PLACE OF MILITARY STANDARDS M.S. Thesis
Stanley M. Beckerdite Jun. 1992 149 p
(AD-A256203) Avail: CASI HC A07/MF A02

The implementation of quality standards within the European Community by the creation of International Quality Standards 9000 is another step toward development of a global marketplace. It is in the interests of DoD to support this trend in order to help maintain the defense industrial base. The first part of this study performs a comparison of DoD quality standards to the ISO 9000 Standards. The second part of the study consists of a survey of U.S. firms that have become ISO 9000 registered. This survey is intended to provide an assessment of the current movement within the defense industrial base toward adoption of ISO 9000 Standards. The survey also attempts to identify potential implementation issues relating to adoption of ISO 9000 Standards in place of military standards. It is concluded that DoD should implement ISO 9000 and that the impact of this implementation will be favorable. GRA

N93-15139# Aerospatiale, Cannes (France).
RELIABILITY MODELLING FOR NON-ELECTRONIC SYSTEMS
N. Valisena (European Space Agency. European Space Research and

Technology Center, ESTEC, Noordwijk, Netherlands) and T. deMollerat 1992 6 p
(Rept-921-440-103; ETN-92-92356) Avail: CASI HC A02/MF A01

An approach for reliability modeling of nonelectronic systems is presented. The need for a specific methodology to be applied in the nonelectronic area is justified because nonelectronic items are generally single point failure of the system, and the classical approach used in electronics cannot be realistically applied to nonelectronic items, due to their particularities. Specific models, depending on both design margins and provisions for realization aspects, are proposed. Examples of such models and rules of combination of the models at system level are given. The results of research conducted on typical probabilities in the space area for human errors and inspection efficiencies are presented. ESA

N93-15204# Hughes Aircraft Co., Fullerton, CA. Ground Systems Group.
RELIABILITY TECHNIQUES FOR COMBINED HARDWARE AND SOFTWARE SYSTEMS Final Report, Jan. 1989 - Jan. 1991
M. A. Friedman, P. Y. Tran, and P. L. Goddard Feb. 1992 300 p
(Contract F30602-89-C-0111)
(AD-A256347; RL-TR-92-15) Avail: CASI HC A13/MF A03

Techniques were developed for reliability prediction, allocation, growth and demonstration testing of systems that contain both hardware and software. The techniques are compatible with existing hardware reliability concepts, standards and procedures. A draft DOD-HDBK containing the various reliability techniques was also prepared as a part of this study effort. It is intended that the study results and handbook will form the basis for an approved DOD Handbook on software reliability assessment. GRA

N93-15413# Los Alamos National Lab., NM.
ACOUSTIC RESONANCE TECHNIQUES FOR QUALITY CONTROL
D. N. Sinha 1992 16 p Presented at the American Society of Mechanical Engineers (ASME) Annual Winter Meeting, Richland, WA, 12 Nov. 1992
(Contract W-7405-eng-36)
(DE92-040150; LA-UR-92-3044; CONF-921199-1) Avail: CASI HC A03/MF A01

Acoustic resonance based nondestructive techniques are described that can be used for both process and quality control in manufacturing. The Acoustic Resonance Spectroscopy (AS) technique is highlighted for its capability in fluid property (flow, density, viscosity, and speed of sound) monitoring. Possible applications of these noninvasive techniques for textile manufacturing are pointed out. DOE

N93-15433*# National Aeronautics and Space Administration. Marshall Space Flight Center, Huntsville, AL.
AN OVERVIEW OF RELIABILITY GROWTH MODELS AND THEIR POTENTIAL USE FOR NASA APPLICATIONS
V. S. Taneja and F. M. Safie Washington Dec. 1992 28 p
(NASA-TP-3309; M-705; NAS 1.60:3309) Avail: CASI HC A03/MF A01

An overview is provided of reliability growth literature over the past 25 years. This includes a thorough literature review of different areas of the application of reliability growth such as design, prediction, tracking/management, and demonstration. Various reliability growth models use different bases on how they characterize growth. Different models are discussed. Also, the use is addressed of reliability growth models to NASA applications. This includes the application of these models to the space shuttle main engine. For potential NASA applications, we classify growth models in two groups, which are characterized. Author

N93-15582*# Sverdrup Technology, Inc., Brook Park, OH. Lewis Research Center Group.
ENVIRONMENTAL QUALIFICATION TESTING OF THE PROTOTYPE POOL BOILING EXPERIMENT Final Report
J. Andrew Sexton NASA Nov. 1992 11 p
(Contract NAS3-25266; RTOP 694-03-03)
(NASA-CR-190774; E-7385; NAS 1.26:190774) Avail: CASI HC A03/MF A01

The prototype Pool Boiling Experiment (PBE) flew on the STS-47 mission in September 1992. This report describes the purpose of the experiment and the environmental qualification testing program that was used to prove the integrity of the prototype hardware. Component and box level vibration and thermal cycling tests were performed to give an early level of confidence in the hardware designs. At the system level, vibration, thermal extreme soaks, and thermal vacuum cycling tests were performed to qualify the complete design for the expected shuttle environment. The system level vibration testing included three axis sine sweeps and random inputs. The system level hot and cold soak tests demonstrated the hardware's capability to operate over a wide range of temperatures and gave the project team a wider latitude in determining which shuttle thermal altitudes were compatible with the experiment. The system level thermal vacuum cycling tests demonstrated the hardware's capability to operate in a convection free environment. A unique environmental chamber was designed and fabricated by the PBE team and allowed most of the environmental testing to be performed within the project's laboratory. The completion of the test program gave the project team high confidence in the hardware's ability to function as designed during flight. Author

N93-15620*# Martin Marietta Corp., Denver, CO. Astronautics Group.
TQM IN A TEST ENVIRONMENT
Gary D. Chambers, Elizabeth A. King, and Keith Oleson *In* NASA. Goddard Space Flight Center, The Seventeenth Space Simulation Conference. Terrestrial Test for Space Success Nov. 1992 p 315-326
(For primary document see N93-15593 04-18)
Avail: CASI HC A03/MF A03

39 STRUCTURAL MECHANICS

Includes structural element design and weight analysis; fatigue; and thermal stress.

For applications see *05 Aircraft Design, Testing and Performance* and *18 Spacecraft Design, Testing and Performance.*

N93-14158 Georgia Inst. of Tech., Atlanta.
ANALYSIS OF ADVANCED THIN-WALLED COMPOSITE STRUCTURES Ph.D. Thesis
Ashraf M. Badir 1992 146 p
Avail: Univ. Microfilms Order No. DA9223766

The use of fiber reinforced composites is increasing in engineering applications. One of the major issues is composite structures in the understanding of the role of the material's anisotropy on the deformation modes, damage modes and failure mechanisms. This research work addresses these stiffness and strength related issues by developing analytical models for the prediction of deformation modes and their coupling effects and damage onset and growth in laminated composites. Accurate prediction of stiffness, response, damage modes and failure mechanisms is bound to lead to the design of efficient and damage tolerant composite structures. In the first part of this work shear deformation models including hygrothermal effects are developed for the analysis of mid-plane edge delamination and local delamination originating from transverse cracks in 90 degree plies. The results of these models are combined with a previously developed shear deformation model for mixed-mode edge delamination to yield a unified analysis of delamination and the ability to identify the critical failure modes and loads. In the second part, a variationally and asymptotically consistent theory for thin-walled beams that incorporates the anisotropy associated with laminated composites is developed. The theory is based on an asymptotical analysis of 2D shell energy. Dissert. Abstr.

N93-14185 Virginia Polytechnic Inst. and State Univ., Blacksburg.
INTEGRATION AND PROCESSING OF HIGH-RESOLUTION MOIRE-INTERFEROMETRY DATA Ph.D. Thesis
Shih-Yung Lin 1992 118 p
Avail: Univ. Microfilms Order No. DA9224544

A new hybrid method combining moire interferometry, high-resolution data-reduction technique, two-dimensional data-smoothing method, and Finite Element Method (FEM) has been successfully developed. This hybrid method has been applied to residual strain analyses of composite panels, strain concentrations around optical fibers embedded in composites, and cruciform composite shear test. This hybrid method allows moire data to be collected with higher precision and accuracy by digitizing overexposed moire patterns. (U & V fields) with appropriate carrier fringes. The resolution of the data is plus or minus 20 nm. The data extracted from the moire patterns are

interfaced to an FEM package through an automatic mesh generator. This mesh generator produces a non-uniform FEM mesh by connecting the digitized data points into triangles. The mesh, which uses digitized displacement data as boundary conditions, is then fed to and processed by a commercial FEM package. Due to the natural scatter of the displacement data digitized from moire patterns, the accuracy of strain values is significantly affected. A modified finite-element model with linear spring elements is introduced so data-smoothing can be done easily in two-dimensional space. The results of the data smoothing are controlled by limiting the stretch of those springs to be less than the resolution of the experimental method. With the full-field hybrid method, the strain contours from moire interferometry can be easily obtained with good accuracy. If the properties of the material are known, the stress patterns can also be obtained. In addition, this method can be used to analyze any two-dimensional displacement data, including the grid method and holography. The application of this method will be demonstrated with a composite residual strain test and a cruciform composite shear test. The latter case is also compared with the localized hybrid method (1,2) which uses only the boundary conditions defined on the perimeter of the region of interest. The precision of the full-field hybrid method will also be investigated by using a numerical model. Dissert. Abstr.

N93-14186 Georgia Inst. of Tech., Atlanta.
NON-LINEAR ANALYSIS OF WAVE PROGAGATION USING TRANSFORM METHODS AND PLATES AND SHELLS USING INTEGRAL EQUATIONS Ph.D. Thesis
Daniel Scott Pipkins 1992 233 p
Avail: Univ. Microfilms Order No. DA9223793

Two diverse topics of relevance in modern computational mechanics are treated. The first involves the modeling of linear and non-linear wave propagation in flexible, lattice structures. The technique used combines the Laplace Transform with the Finite Element Method (FEM). The procedure is to transform the governing differential equations and boundary conditions into the transform domain where the FEM formulation is carried out. For linear problems, the transformed differential equations can be solved exactly, hence the method is exact. As a result, each member of the lattice structure is modeled using only one element. In the non-linear problem, the method is no longer exact. The approximation introduced is a spatial discretization of the transformed non-linear terms. The non-linear terms are represented in the transform domain by making use of the complex convolution theorem. A weak formulation of the resulting transformed non-linear equations yields a set of element level matrix equations. The trial and test functions used in the weak formulation correspond to the exact solution of the linear part of the transformed governing differential equation. Numerical results are presented for both linear and non-linear systems. The linear systems modeled are longitudinal and torsional rods and Bernoulli-Euler and Timoshenko beams. For non-linear systems, a viscoelastic rod and Von Karman type beam are modeled. The second topic is the analysis of plates and shallow shells under-going finite deflections by the Field/Boundary Element Method. Numerical results are presented for two plate problems. The first is the bifurcation problem associated with a square plate having free boundaries which is loaded by four, self equilibrating corner forces. The results are compared to two existing numerical solutions of the problem which differ substantially. The second problem involves a simply supported rhombic plate. The bending moments in the non-linear model are compared to those in the linear model. The intent being to study the effect the non-linearity and in-plane boundary conditions have on the singular bending moments known to occur in the linear problem. Dissert. Abstr.

N93-14187 Missouri Univ., Rolla.
AN INVESTIGATION OF CRACK GROWTH AT INTERFACES IN BIMATERIALS AND COMPOSITES USING A CONSISTENT SHEAR-LAG MODEL Ph.D. Thesis
David Brian Popejoy 1992 68 p
Avail: Univ. Microfilms Order No. DA9224679

The problem of a crack impinging upon an interface between dissimilar materials is investigated using a Consistent Shear-Lag (COSL) model. The goal is to determine whether the crack will penetrate the interface or be deflected into it. Since the stress and displacement fields in the vicinity of the interface usually create computational difficulties, especially when the elastic moduli very greatly, the COSL model is modified to include an interlayer region at the interface to act as a buffer. The energy release rates for both doubly-deflected and penetrating cracks are determined. The ratio of these two quantities is then compared to that of debond and Mode 1 toughnesses to investigate the two scenarios for crack extension. The effect of elastic mismatch on the energy release rates, and hence on the mode of crack extension, is investigated. These results compare favorably with analytical solutions for similar bimaterial problems. Since the computed energy release rates depend to a large extent on the initial crack length and debond length, their effects on crack growth is studied. The effect of anisotropy is investigated to determine the relative importance of the elastic constants on the energy release rate ratio. It is shown that of these, the longitudinal and transverse elastic moduli are of greater significance. When applied to composite materials, this model shows that the fiber volume fraction has little effect on the ratio of energy release rates. To account for the possibility of flaws and imperfections within composites, the previous formulation is modified to include a crack impinging upon an initially debonded zone. It is shown that proximity of the crack tip to the debond is very important in predicting the mode of crack growth. Finally, the effects of fiber coatings and thermal residual stresses are investigated to show their influence on crack growth. Dissert. Abstr.

N93-14188 Alabama Univ., University.
APPLICATION OF PARTITION MATRIX METHODS TO SOLVE LARGE EIGENPROBLEMS IN STRUCTURAL DYNAMICS Ph.D. Thesis
Louis Harvie Turcotte 1992 340 p
Avail: Univ. Microfilms Order No. DA9225858

Eigenvalue and eigenvector problems are addressed for large, sparse matrices resulting from the vibration analysis of complex structures. Problems of this type are computationally intensive and have traditionally been solved using supercomputers. Partitioned matrices are employed, herein, to produce a set of out-of-core algorithms which can be used for eigenproblems with several thousand degrees-of-freedom. The efficiency of a Rayleigh-Ritz iterative procedure, based on partitioned matrices, is compared with competing out-of-core eigensolution strategies. These results demonstrate that partition matrix algorithms are computationally competitive and may be implemented successfully across a wide range of computers to solve large eigenproblems. The partition matrix routines are implemented as extensions of the widely used commercial software system MATLAB. These extensions employ compiled FORTRAN routines which are linked into MATLAB and provide a set of user friendly analysis tools that are easily employed to solve eigenproblems which were previously too large for this environment. Both workstations and supercomputers were used to evaluate the efficiency of the partition matrix algorithms. Additionally, a parallelized version of the software was implemented across a cluster of workstations. The parallelized code demonstrates the practicality of using a cluster of workstations to efficiently solve large eigenproblems typically requiring the use of a supercomputer. Dissert. Abstr.

N93-14214 Harvard Univ., Cambridge, MA.
THE MECHANICS OF DISLOCATION NUCLEATION AT A CRACK TIP Ph.D. Thesis
Glenn Edward Beltz 1992 149 p
Avail: Univ. Microfilms Order No. DA9228162

This thesis presents analyses of several problems related to an atomistic description of the ductile versus brittle behavior of crystal, with emphasis on a new approach to the analysis of dislocation nucleation which makes use of Peierls-type stress versus displacement relation on a slip plan ahead of the tip. As in later versions of the Rice-Thomson model, the ductile-brittle competition may be evaluated in terms of the parameters G(sub cleave), the energy release rate for cleavage, and G(sub disl), the energy release rate associated with the emission of a single dislocation from the crack tip. The advantage of the Peierls-framework is that it allows for the existence of an extended dislocation core during nucleation, eliminating the need for a core cutoff radius. In Chapter 1, analysis of dislocation nucleation is carried out for situations where the slip plane may be inclined with respect to the crack plane. Also, the effect of mixed-mode loadings are considered. It is found that tension across the slip plane reduces the critical load for dislocation emission. In Chapter 3, the analysis is generalized to include bimaterial interfaces, and results are presented for the nucleation of dislocations from a copper/sapphire interfacial crack, loaded with a substantial negative mode II component. The specific case of a copper crystal bonded on a (221) face to sapphire is analyzed, and

the results are used to interpret experimental observations of directional toughness along this type of interface, which are discussed in detail in Chapter 4. The directional toughness arises from the difference in load to nucleate a dislocation, when evaluated for a slip plane inclination of 125.3 versus 164.2 deg. The activation energy for dislocation nucleation from a crack tip is calculated in Chapter 5. The analyses carried out thus far are rigorous at zero Kelvin and take thermal effects into account only via the weak temperature dependence of the elastic constants. The energy required to activate a stable, incipient dislocation into its unstable 'saddle-point' configuration is directly calculated for loads less than the critical value. Implications for the emission of dislocations in copper and alpha-iron at elevated temperature are discussed. Furthermore, the activation energy for dislocation nucleation in silicon loaded to the point of Griffith cleavage is calculated; the number is consistent with the thermal activation of dislocations at its ductile-to-brittle transition temperature. Dissert. Abstr.

N93-14215 Harvard Univ., Cambridge, MA.
FRACTURE ANALYSES OF THIN FILMS, INTERFACES, AND JOINTS Ph.D. Thesis
Jack Lee Beuth, Jr. 1992 136 p
Avail: Univ. Microfilms Order No. DA9228164

This thesis presents fracture analyses related to three practical problems. Chapter 2 and 3 both address the problem of cracking of thin bonded films in tension. In Chapter 2, solutions are obtained for two plan strain problems relevant to the cracking of a thin elastic film bonded to a dissimilar, thick elastic substrate material. Complete results from the solution of each problem are given over the full range of practical elastic mismatches. Dimensionless quantities important in describing the cracking of thin films are introduced and accurate approximate formulas based on the solution results are given for them. Applications are discussed, including criteria for avoiding thin film crack extension and a formula for the curvature change induced by the cracking of a thin film bonded to a substrate of finite thickness. In Chapter 3, a numerical analysis is made extending some of the results from Chapter 2 so that plastic yielding of the substrate is allowed. A simple shear-lag model of the problem is also presented which gives reasonable predictions for the dependence of the dimensionless fracture quantities on the normalized loading over a wide range of material mismatches. In Chapter 4, a recently-developed interfacial fracture toughness specimen is analyzed to allow the determination of interfacial fracture toughness values as a function of mode mixity for any two bonded materials. An analytic steady-state formula for the complex stress intensity factor for the specimen is presented. All parameters in the formula are known except for a single parameter, omega, which can be interpreted as the difference in phase between the far-field applied displacements and the near-tip crack face displacements. The parameter w is solved for numerically and presented as a function of the problem parameters. Also, some work is presented on the role of crack face interpenetration or contact in the analysis and use of the specimen. In Chapter 5, an analysis is presented of MSD or multi-site damage (multiple small fatigue cracks emerging from rivet holes along a single line of rivets) in the lap joints of the skins of aging aircraft. Stress intensity factors are plotted as a function of normalized crack length for two types of rivet contact conditions. The roles of transverse stresses and residual stresses induced by the riveting process are explored. The underlying cause of MSD cracking is investigated, including the potential influence of the shedding of load from one cracked rivet hole to a lesser cracked neighbor. Dissert. Abstr.

N93-14217 National Tsing Hua Univ., Hsinchu (Taiwan).
DIGITAL CAUSTIC INVESTIGATION OF NEAR SURFACE CRACKS UNDER TRANSIENT THERMAL LOADING Ph.D. Thesis
Tsai-Lin Chen 1991 171 p
Avail: Univ. Microfilms Order No. DA9218818

In this dissertation, the digital caustics technique was used to determine the transient thermal stress intensity factors of near-surface internal cracks in a semi-infinite thin plate, when the plate edge experiences a rapid temperature change. The internal cracks of different crack lengths and different crack orientations were studied. A series of computer programs were developed on the digital caustic system to analyze the caustics patterns. Then, the variations of transient thermal stress intensity factors with time were discussed. Finally, the correlation expressions between the variations of transient thermal stress intensity factors with the time, temperature difference and geometrical parameters of cracks were obtained by the regression procedure. Dissert. Abstr.

N93-14219 Drexel Univ., Philadelphia, PA.
SOME THEORETICAL AND EXPERIMENTAL ASPECTS OF THE GENERATION OF GUIDED ELASTIC WAVES USING FINITE SOURCES Ph.D. Thesis
John Joseph Ditri 1992 140 p
Avail: Univ. Microfilms Order No. DA9227953

In this thesis, the problem of the excitation of linearly elastic waveguides by applied surface tractions is examined. Attention is focussed on flat layer waveguides of arbitrary anisotropy, and isotropic hollow circular cylinder waveguides. In the first two sections, the applied tractions are assumed to be time harmonic, and the Normal Mode Expansion Technique is used to determine the field inside the waveguide due to the loading. In this technique, the fields in the loaded waveguide are expanded in terms of the normal modes permissible in the free waveguide multiplied by unknown expansion coefficients. Use of the complex reciprocity relation and an orthogonality relationship between free waveguide modes enables the determination of the expansion amplitudes, hence the fields in the loaded waveguide. Expressions are given for the amplitude with which any propagating mode of the structure is generated due to the applied surface tractions. The principle of linear superposition is then employed to determine the field generated by a transducer producing finite time duration loading, by superimposing time harmonic solutions via an integration over the dispersion curves of the structure. Finally several experiments are performed to verify the analysis. Dissert. Abstr.

N93-14236# Naval Postgraduate School, Monterey, CA.
WEIGHT OPTIMUM ARCH STRUCTURES M.S. Thesis
Thomas J. Williamson Jun. 1992 117 p
(AD-A256080) Avail: CASI HC A06/MF A01

The goal of this investigation is to design minimum weight arch structures which span the distance between two points in two-dimensional space. An arch of unknown shape and variable cross-sectional width is modeled as a series of straight bar-beam elements. Finite element methods are used to compute the stresses in each element. Automated Design Synthesis (ADS) software is then used to vary the slope of each element and the cross-sectional width to prevent the yield stress of the material from being exceeded as ADS minimizes the volume of the arch to arrive at the minimum weight structure. Results are presented for a number of different loadings and boundary conditions. GRA

N93-14251 Virginia Polytechnic Inst. and State Univ., Blacksburg.
ANALYSIS AND OPTIMAL DESIGN OF PRESSURIZED, IMPERFECT, ANISOTROPIC RING-STIFFENED CYLINDERS Ph.D. Thesis
Robert Paul Ley 1992 261 p
Avail: Univ. Microfilms Order No. DA9229607

Development of an algorithm to perform the structural analysis and optimal sizing of buckling resistant, imperfect, anisotropic ring stiffened cylinders subjected to axial compression, torsion, and internal pressure is presented. The structure is modeled as a branched shell. A nonlinear axisymmetric prebuckling equilibrium state is assumed which is amenable to exact solution within each branch. Buckling displacements are represented by a Fourier series in the circumferential coordinate and finite elements in the axial or radical coordinate. A separate, more detailed analytical model is employed to predict prebuckling stresses in the flange/skin interface region. Results of case studies indicate that a nonlinear prebuckling analysis is needed to accurately predict buckling loads and mode shapes of these cylinders, that the rings have a greater influence on the buckling resistance as the relative magnitude of the torsional loading to axial compression loading is increased, but that this ring effectiveness decreases somewhat when internal pressure is added. The enforcement of stability constraints is treated in a way that does not require any eigenvalue analysis. Case studies performed using a combination of penalty function and feasible direction optimization methods indicate that the presence of the axisymmetric initial imperfection in the cylinder wall can significantly affect the optimal designs. Weight savings associated with the addition of two rings to the unstiffened cylinder and/or the addition of internal pressure is substantial when torsion makes up a significant fraction of the combined load state. Assumption of criticality of the stability constraints and neglect of the stress constraints during the optimal sizing of the cylinders produced designs

that nevertheless satisfied all of the stress constraints, in general, as well as the stability constraints. Subsequent re-sizing of one cylinder to satisfy a violated in-plane matrix cracking constraint resulted in an optimal design that was 49 percent heavier than the optimal design produced when this constraint was ignored. The additional internal pressure necessary to produce a violation of a stress constraint for each optimal design was calculated. Using an unsymmetrically laminated ring flange, a substantial increase in the strength of the flange/skin joint was observed. Dissert. Abstr.

N93-14272# Georgia Inst. of Tech., Atlanta.
A STUDY OF THE RELATIONSHIP BETWEEN MACROSCOPIC MEASURES AND PHYSICAL PROCESSES OCCURRING DURING CRACK CLOSURE Annual Report
Stephen D. Antolovich and Stuart R. Stock 8 Oct. 1991 31 p
(Contract N00014-89-J-1708)
(AD-A256587) Avail: CASI HC A03/MF A01

Activity centered on the development and implementation of robust methods for measuring crack opening in the samples studied with X-ray Tomographic Microscopy (XTM). The existing XTM data of notched tensile (NT) samples consists of a three-dimensional stack of several hundred two-dimensional slices, each containing between 400x400 and 600x600 pixels. Analysis of the three-dimensional crack wandering through this volume is done in several steps. The first step is to determine the separation between crack faces using cuts perpendicular to the stack of slices. Separation will be measured as a function of position for the different applied loads. Cuts parallel to the load axis are expected to give a more precise measure of crack opening than measurements within planes parallel to the slices, especially when the openings are on the order of one or two pixels in size. GRA

N93-14279 Ohio State Univ., Columbus.
THEORETICAL AND EXPERIMENTAL ANALYSIS OF RESIDUAL STRESS FORMATION AFTER IMPLANT RESISTANCE WELDING OF POLYCARBONATE Ph.D. Thesis
Joon Boo Park 1992 212 p
Avail: Univ. Microfilms Order No. DA9227352

Formation of residual stress during thermoplastic welding causes detrimental effects to the joint quality under both dynamic and static loading conditions. Residual stress can reduce the solvent resistance of polymers as well as the tensile strength and fatigue life of the joint. Therefore, it is vital to predict and measure the level of residual stresses. Here, the formation of thermal and residual stresses during implant resistance welding of polycarbonate was studied. Thermocouples and an infrared temperature sensor were used to measure the temperature history and temperature distribution in the parts during welding. Heat flow analysis during implant resistance welding was done using Finite Element Method (FEM) and Finite Difference Method (FDM) which are connected with FEM and a simplified modeling analysis so-called 'multi-bar analogy' respectively for stress analysis. FEM and FDM predictions of heat flow analysis were in good agreement with experimental measurements. The formation of thermal and residual stress was predicted using 2-D finite element analysis and multi-bar analogy in conjunction with non-isothermal linear viscoelasticity for a thermorheologically simple material. The residual stresses in the parts were measured using both photoelasticity and moire interferometry. Sectioning method utilizing moire interferometry was used to measure residual stress. FEM prediction of residual stress was in good agreement with photoelasticity measurement and moire interferometry measurement. Residual stress formation in the weld was predicted by multi-bar analogy modeling analysis and multi-bar analogy prediction was in good agreement with FEM prediction. Heat treatment to reduce residual stress after welding was performed. Residual stress distribution after heat treatment was predicted using FEM. The FEM prediction was in good agreement with photoelasticity measurement and moire interferometry measurement. This methodology for prediction, measurement and reduction of residual stress can be incorporated into the design analysis and welding procedures for plastic and composite joints. This will result in stronger and more reliable welds. Dissert. Abstr.

N93-14282 Purdue Univ., West Lafayette, IN.
NONLINEAR DYNAMIC RESPONSE OF SHALLOW ARCHES TO HARMONIC FORCING Ph.D. Thesis
Kim Billy Blair 1992 96 p
Avail: Univ. Microfilms Order No. DA9229087

Buckled beams and shallow arches exhibit nonlinear force-deflection curves as a result of their geometric shape. These structural components share the common characteristic of nonlinear load-deflection curves, exhibiting both stable and unstable equilibrium states. Previous work has shown that with the application of sufficiently large static or dynamic loads, snap-buckling can occur, in which the structure suddenly jumps from one stable equilibrium configuration to another. The dynamic response due to harmonic forcing has been shown to contain orbits encompassing either of the stable equilibrium positions, or orbits encompassing both the stable and unstable equilibrium positions. The investigation of the dynamic response of a shallow arch is undertaken using a two rigid-link, single degree of freedom (SDOF) model. The method of harmonic balance, coupled with a continuation scheme, is used to find the solutions for an entire range of externally applied loading. Floquet analysis provides the requisite stability information, as well as information about the bifurcation points encountered in the solution. The dynamic response of the arch to harmonic forcing is shown to exhibit both symmetric and asymmetric solutions. Additionally, stable solutions are found that have a fundamental period of an integer multiple of the excitation period. Finally, regions of chaotic motion are found. Results are presented for three cases of varying the magnitude of the applied harmonic loading for a constant execution frequency, and for the three cases of varying the excitation frequency of the applied harmonic loading for constant magnitude. The investigation is extended to the case of a four-link, three degree of freedom model. It is shown that for loading cases away from combination and internal resonances, the above SDOF model provides an accurate representation of the dynamic response. The dynamic response to the model to antisymmetric loading is investigated. A hardening type response is observed, and the symmetric and asymmetric response curves are traced for three levels of damping. Additionally, the birth of the bifurcation point connecting the symmetric and asymmetric branches of the response is shown. Dissert. Abstr.

N93-14419# Wright Lab., Wright-Patterson AFB, OH.
A PRELIMINARY INVESTIGATION OF DUAL MODE FRACTURE SUSTAINED BY GRAPHITE/EPOXY LAMINATES IMPACTED BY HIGH-VELOCITY SPHERICAL METALLIC PROJECTILES Final Report, 1 Jan. 1990 - 15 Dec. 1991
Gregory J. Czarnecki Apr. 1992 106 p
(AF Proj. 2402)
(AD-A255790; WL-TR-92-3094) Avail: CASI HC A06/MF A02

The basis for delamination initiation and propagation within an impacted laminate is studied. The work provides an explanation for fracture mode transformation along the projectile's path. Post-impact observations of graphite/epoxy (AS4/3501-6) laminates penetrated by steel spheres (0.5-inch diameter) reveal a fracture mode, similar to shear plugging, adjacent to the impacted surface. This fracture mode is contrasted with that of delamination adjacent to the rear surface. The sudden transition from shear plugging to delamination occurs when the projectile interacts with the returning impact-generated tensile wave. To demonstrate the transition, results are presented from ballistically impacted laminates containing a series of embedded carbon stress and constantan strain gages. Results are based on impact velocities of 1825 and 2380 f/s. Transverse stress waves are shown capable of creating delamination until attenuated by a localized compression front associated with the on-coming projectile. GRA

N93-14446 Purdue Univ., West Lafayette, IN.
MULTIOBJECTIVE CONTROL/STRUCTURE DESIGN OPTIMIZATION IN THE PRESENCE OF PRACTICAL CONSTRAINTS Ph.D. Thesis
Jeffrey Boese Layton 1992 281 p
Avail: Univ. Microfilms Order No. DA9229150

The purpose of this research is to examine true multiobjective control/structure pareto optimization in the presence of practical constraints. The practical constraints that are addressed in this thesis are: (1) limiting the maximum time response of the output, and (2) reduced order controllers. The purpose is also to examine the benefits of combined optimization when these practical constraints are included in the control synthesis. To perform the investigation, a new methodology was developed for combined optimization. This uses a new control law parameterization which chooses the closed loop covariance matrix as controller design variables. This

parameterization allows the control design to be cast in the same form as the structural optimization design problem, i.e., a nonlinear constrained optimization problem. A number of independent design constraints are closed form and gradients can be found analytically to aid the nonlinear minimization. Two sets of design examples were used in this study. The first series minimizes control effort with the structure fixed. The second set of studies minimizes both control effort and total structural mass to find a pareto optimal solution. For all of the examples examined, the controller objectives are much more sensitive to the control variables than to the structural variables. Also, including the structural optimization in the combined problems does not substantially change the structural mass. This suggests that any benefit of simultaneous optimization of the controller and the structure may be mitigated by local minima in the numerical search. It was also found that minimizing control effort without constraining the closed loop eigenvalues or damping ratios can cause the resulting closed loop system to have substantially less damping than the initial closed loop system. Dissert. Abstr.

N93-14468 Strathclyde Univ., Glasgow (Scotland).
ONLINE VIBRATION CONTROL OF A FLEXIBLE ROTOR/BEARING SYSTEM Ph.D. Thesis
Shaun Clements 1987 260 p
Avail: Univ. Microfilms Order No. BRD-96808

An electromagnetic controller was located between two conventional, 100 mm diameter oil film bearings in order to investigate the adoption of an open loop control strategy for synchronous vibration control of a flexible rotor/bearing system. Application of control in an open loop manner removes practical constraints previously imposed due to the adoption of a closed loop strategy. Consideration of the 'closed loop system' stability restricted attention to positive non-adaptive controller stiffness and damping coefficients only. Use of an efficient least squares algorithm and real time software enabled open loop control forces to be determined on-line using the control element as a force actuator. Thus the frequency dependent control forces could be determined without prior knowledge of the rotor/bearing system characteristics. A method is presented which aids in the identification of suitable measurement locations (sparse models) for control force estimation. Three sparse model cases were experimentally investigated, namely measurement of (1) Bearing locations only; (2) Bearing and one mid-span station only; and (3) Two mid-span stations only. Experimental behavior of the control forces and controlled responses for the three sparse model cases considered were in good agreement with simulated results. In all cases, controlled vibration levels were maintained at extremely low levels, effectively eliminating the characteristic resonance peak at the first flexural critical speed. However, results for journal bearing response showed that there was little advantage in the use of sparse model (1) over that of models (2) or (3). Alternatively mid span controlled response was significantly degraded by the use of sparse model (1). Interpretation of statistical data resulting from the use of the LSE indicated that for this rotor/bearing system at least, adequate control may be achievable by measuring at the controller location only. Dissert. Abstr.

N93-14469 Stevens Inst. of Tech., Hoboken, NJ.
FINITE ELEMENT ANALYSIS OF ELASTIC FRACTURE UNDER UNSTEADY TRANSLATIONAL AND ROTATIONAL LOADING Ph.D. Thesis
Chung-Yun Gau 1992 133 p
Avail: Univ. Microfilms Order No. DA9227877

The broad objective of the investigations described in this dissertation is the accurate finite element computation of stress intensity factors in cracked elastic bodies under steady or unsteady translational and rotational loads. Applications of interest include fatigue under adverse environments, such as stall in turbomachinery and critical speeds in elastic mechanisms. The enriched element formulation of Gifford and Hilton has been extended to include inertial, centrifugal, Coriolis and angular acceleration effects, and to include Mode III (tearing), which is coupled to Modes I and II under unsteady rotation. The extension is based on the fact, which does not appear to be widely appreciated, that inertial effects near the crack tip are completely accounted for by the time dependence of the stress intensity factors. For Mode III, the Mindlin formulation for a plate in bending has been adopted in order to extend the enriched element formulation to torsion and bending effects. The centrifugal and angular acceleration effects are fully coupled to the displacements, which for example permits calculation of critical speeds in cracked elastic bodies. A finite element code by Gifford and Hilton for static problems in Modes I and II has been thoroughly rewritten and expanded to implement the dynamic features and Mode III, leading to an essentially new code called DFRAC (after Dynamic FRACture). The code incorporates matrices and vectors representing translational, Coriolis, centrifugal and angular acceleration effects. It implements the Newmark method for time integration, and a non-symmetric 'wave front' solver. First, DFRAC is validated for static and steady rotational loads, giving errors compared to benchmark solutions of less than 7 percent. Second, validating computations are presented for a rotating beam-column (no crack), showing good agreement both in 1-D and 3-D: centrifugal, Coriolis and angular acceleration effects are exerted both through the force vector and through the stiffness matrix. Third, applications to wave propagation and to mixed-mode fatigue growth are developed, including some validating calculations. Finally, simulations are detailed for a configuration relevant to turbine blades. Dissert. Abstr.

N93-14471 Michigan Univ., Ann Arbor.
LARGE PLASTIC DEFORMATIONS BY SEQUENTIAL LIMIT ANALYSIS: A FINITE ELEMENT APPROACH WITH APPLICATIONS IN METAL FORMING Ph.D. Thesis
Chung-Li Hwan 1992 128 p
Avail: Univ. Microfilms Order No. DA9226925

A new method, Sequential Limit Analysis, has been developed for solving large plastic deformation problems of metal both in plane strain and axisymmetric conditions. This method is a modern limit analysis that employs duality theorem to equate the least upper bound to the greatest lower bound and uses mathematical programming techniques to search for optimal solutions. It involves no complex stress calculations. It can treat material property nonlinearly by updating local yield criteria step by step and has the advantage of global stability of computation even in the case of increasing deformation under decreasing load. It can also treat frictional contact phenomena easily because this method is explicit in nature. Moreover, it is mathematically concise and computationally easy to implement. To verify the capability of this new method, extensive numerical experiments have been done. These numerical experiments include strip tension, block compression and extrusion through a wedge die in the plane strain condition, and bar/tube tension, heading, and ball indentation in the axisymmetric condition. The computed results have been compared in good agreement with existing analytical and/or experimental solutions. Because of its success and efficiency in solving the above problems, Sequential Limit Analysis is ready for studying more complex industrial forming problems. Although Sequential Limit Analysis is a powerful method and has been successfully employed to solve metal forming problems, it also exhibits limitations at present. First, it cannot predict unloading behavior due to the neglect of elastic behavior. Second, it is unable to treat rate-dependent problems, and thus cannot explore both impact and thermomechanical coupling phenomena in dynamic indentation and hot forming processes. Third, it may encounter slow or even difficult convergence of solution for problems having an almost flat functional which admits nonunique solutions. To extend the capability of Sequential Limit Analysis, adequate methodologies to overcome these limitations have to be proposed and studied. Dissert. Abstr.

N93-14474 California Univ., Berkeley.
FRACTURE MECHANISMS AND FRACTURE CONTROL IN COMPOSITE STRUCTURES Ph.D. Thesis
Wone-Chul Kim 1991 162 p
Avail: Univ. Microfilms Order No. DA9228716

Four basic failure modes--delamination, delamination buckling of composite sandwich panels, first-ply failure in cross-ply laminates, and compression failure--are analyzed using linear elastic fracture mechanics (LEFM) and the J-integral method. Structural failures, including those at the micromechanical level, are investigated with the aid of the models developed, and the critical strains for crack propagation for each mode are obtained. In the structural fracture analyses area, the fracture control schemes for delamination in a composite rib stiffener and delamination buckling in composite sandwich panels subjected to in-plane compression are determined. The critical fracture strains were predicted with the aid of LEFM for delamination and the J-integral method for delamination buckling. The use of toughened matrix systems has been recommended for improved damage tolerant design for delamination crack propagation. An experimental

study was conducted to determine the onset of delamination buckling in composite sandwich panel containing flaws. The critical fracture loads computed using the proposed theoretical model and a numerical computational scheme closely followed the experimental measurements made on sandwich panel specimens of graphite/epoxy faceskins and aluminum honeycomb core with varying faceskin thicknesses and core sizes. Micromechanical models of fracture in composites are explored to predict transverse cracking of cross-ply laminates and compression fracture of unidirectional composites. A modified shear lag model which takes into account the important role of interlaminar shear zones between the 0 degree and 90 degree piles in cross-ply laminate is proposed and criteria for transverse cracking have been developed. For compressive failure of unidirectional composites, pre-existing defects play an important role. Using anisotropic elasticity, the stress state around a defect under a remotely applied compressive load is obtained. The experimentally observed complex compressive failure modes, such as shear crippling and pure compressive fiber failure of fibers are explained by the predicted stress distributions calculated in this work. These fracture analyses can be damage tolerant design methodology for composite structures. The proposed fracture criteria and the corresponding critical fracture strains provide the designer with quantitative guidelines for safe-life design. These have been incorporated into a fracture control plan for composite structures, which is also described. Currently, fracture control plans do not exist for composite structures; the proposed plan is a first step towards establishing fracture control and damage tolerant design methodology for this important class of materials.
Dissert. Abstr.

N93-14480 Johns Hopkins Univ., Baltimore, MD.
THE INFLUENCE OF GEOMETRICAL CONSTRAINT ON CYCLIC, ELASTOPLASTIC, NOTCH ROOT BEHAVIOR, AND FATIGUE MICROCRACK INITIATION Ph.D. Thesis
Robert Lee Tregoning 1992 412 p
Avail: Univ. Microfilms Order No. DA9229417

Fatigue failures are typically caused by unstable crack growth from some geometrical stress raiser such as a notch. The fatal flaw usually initiates at the stress raiser's surface, near the mid-thickness plane, where geometrical constraint is the largest. Unfortunately, the fatigue characteristics at this location are not completely known due to the inherent limitations of classical and experimental techniques. The purpose of this study is to independently characterize both the local biaxial strain/stress behavior and the onset of fatigue crack formation at a notch root's center over a range of constraints. This information is then used to examine the influence of the deformation state on the qualitative and quantitative characteristics of grain-sized microcrack initiation. Three separate approaches were used in this research to study the overall fatigue characteristics of notched specimens. First, experiments were conducted on fine-grained, isotropic, HY-80 steel specimens to +/- 1 percent axial strain. Four different levels of constraint were produced in the double-notched specimens simply by varying the thickness-to-notch-radius ratio. Experimentally, the biaxial strains at the notch root were then determined using an interferometric based technique which accurately measured real-time strains over small gage lengths (150-200 micron). Next, a three-dimensional, elastoplastic, finite element study simulated the actual tests so that the results can be compared with the experimental data. The finite element study also obtains full-field stress-strain information and is used to evaluate the underlying assumptions which constitute two approximate notch root models: the Neuber and Glinka relations. Finally, microcrack initiation was examined on identical double-notched specimens using an acetylcellulose replication technique. These results were then compared with predictions from three different crack initiation models: the Coffin-Manson relation, a plastic work theory, and a micromechanical model. The results of this study indicate that while constraint does greatly influence notch fatigue behavior, the notch shape and specimen thickness are also important. The notch root strain experiments show that the severity of the biaxial, maximum and residual strains decreases as the amount of constraint increases. The three-dimensional finite element results confirm these trends for both the local strains and stresses. These results also show that constraint and the notch shape define the full-field distribution and delineate the regions where the Neuber and Glinka models are most effective. The microcrack initiation tests indicate that initiation is governed not only by the geometrical constraint and notch shape, but by the specimen thickness. The Coffin-Manson and plastic work crack initiation theories do not significantly account for constraint effects and consequently do not predict the differences in microcrack initiation evident in these results. The micromechanical model, however, does predict initiation more accurately.
Dissert. Abstr.

N93-14483*# National Aeronautics and Space Administration. Langley Research Center, Hampton, VA.
RELIABILITY OF STIFFENED STRUCTURAL PANELS: TWO EXAMPLES
W. Jefferson Stroud, D. Dale Davis, Jr. (Army Aerostructures Directorate, Hampton, VA.), Lise D. Maring (Lockheed Engineering and Sciences Co., Hampton, VA.), Thiagaraja Krishnamurthy (Analytical Services and Materials, Inc., Hampton, VA.), and Isaac Elishakoff (Florida Atlantic Univ., Boca Raton.) Dec. 1992 20 p Presented at the ASME Winter Annual Meeting: Symposium on Reliability Technology, Anaheim, CA, 8-13 Nov. 1992
(RTOP 505-63-53-01)
(NASA-TM-107687; NAS 1.15:107687; ATCOM-TR-92-B-015) Avail: CASI HC A03/MF A01

The reliability of two graphite-epoxy stiffened panels that contain uncertainties is examined. For one panel, the effect of an overall bow-type initial imperfection is studied. The size of the bow is assumed to be a random variable. The failure mode is buckling. The benefits of quality control are explored by using truncated distributions. For the other panel, the effect of uncertainties in a strain-based failure criterion is studied. The allowable strains are assumed to be random variables. A geometrically nonlinear analysis is used to calculate a detailed strain distribution near an elliptical access hole in a wing panel that was tested to failure. Calculated strains are used to predict failure. Results are compared with the experimental failure load of the panel.
Author

N93-14498# Hughes Aircraft Co., El Segundo, CA. Electro-Optical and Data Systems Group.
ELECTRONICS RELIABILITY FRACTURE MECHANICS. VOLUME 2: FRACTURE MECHANICS Final Report, May 1987 - Sep. 1991
J. Kallis, L. Duncan, D. Buechler, P. Backes, and D. Sandkulla May 1992 367 p Prepared in cooperation with Southwest Research Inst., San Antonio, TX and Failure Analysis Associates, Inc., Menlo Park, CA
(Contract F33615-87-C-3403)
(AD-A256200; HAC/EDSG-R160309; WL-TR-91-3119) Avail: CASI HC A16/MF A03

This is the second of two volumes. The other volume (WL-TR-92-3015) is 'Causes of Failures of Shop Replaceable Units and Hybrid Microcircuits.' The objective of the Electronics Reliability Fracture Mechanics (ERFM) program was to develop and demonstrate a life prediction technique for electronic assemblies, when subjected to environmental stresses of vibration and thermal cycling, based upon the mechanical properties of the materials and packaging configurations which make up an electronic system. The application of fracture mechanics to microscale phenomena in electronic assemblies was a pioneering research effort. The small scale made the experiments very difficult; for example, the 1-mil-diameter bond wires in microelectronic devices are 1/3 the diameter of a human hair. A number of issues had to be resolved to determine whether a fracture mechanics modelling approach is correct for the selected failures; specifically, the following two issues had to be resolved: What fraction of the lifetime is spent in crack initiation? Are macro fracture mechanics techniques, used in large structures such as bridges, applicable to the tiny structures in electronic equipment? The following structural failure mechanisms were selected for modelling: bondwire fracture from mechanical cycling; bondwire fracture from thermal (power) cycling; plated through hole (PTH) fracture from thermal cycling. The bondwire fracture test specimens were A1-1 percent Si wires, representative of wires used in the parts in the modules selected for detailed investigation in this program (see Vol. 1 of this report); 1-mil-diameter wires were tested in this program. The PTH test specimens were sections of 14-layer printed wiring boards of the type used.
GRA

N93-14553 ESDU International Ltd., London (England).
FATIGUE STRENGTH OF CRUCIFORM AND OTHER FILLET WELDED JOINTS IN ALUMINUM ALLOYS
Aug. 1992 51 p
(ESDU-92017; ISBN-0-85679-821-5) Avail: ESDU

ESDU 92017 presents the results extracted from the literature of nearly 850 constant amplitude loading fatigue tests. Joints were load-carrying

and non load-carrying transverse cruciform, load-carrying and non load-carrying transverse and longitudinal cover plate, and single- and double-fillet lap under axial loading. Data are included on fillet welded attachments under axial loading and tee fillet welded joints under either axial or bending loading. The effect of mean stress is shown for cruciform and cover plate joints, and the effect of post-weld treatments (shot peening and tungsten-inert-gas dressing) is shown for some cover plate joints. The joints were in twelve alloys in the 5000, 6000, or 7000 series with fillers in the 5000 series. All welding process variables and geometries are detailed and the location of failure is indicated. A table summarizes fatigue strengths at lives of a million and 10 million cycles for stress ratios of zero and -1. Summary graphs compare the scatter bands for all joint types in all materials and also mean fatigue strength curves for all types in alloy 5083. A graph also shows the influence of parent alloy tensile strength on welded joint fatigue strength. Author

N93-14587 California Inst. of Tech., Pasadena.
ON THE DEVELOPMENT AND APPLICATION OF A MODIFIED BOUNDARY ELEMENT METHOD FOR THE ANALYSIS OF THREE DIMENSIONAL ELASTOSTATIC PROBLEMS IN THICK PLATES
Lingyun Lu 1992 186 p
Avail: Univ. Microfilms Order No. DA9232197

A modified three-dimensional boundary element method (BEM) is developed. This method is specially tailored towards applications in three-dimensional elasticity, involving regions containing two parallel planar surfaces. Typical structures are the three-dimensional plate structures. The formulation makes use of the three-dimensional fundamental solution of a concentrated load applied in an infinite three-dimensional plate of uniform finite thickness (obtained by Benitez and Rosakis in 1985). The most attractive feature of this modified BEM is that, for the class of problems involving structures described above subjected to traction-free boundary conditions on the planar surfaces, discretization is only required on the lateral surfaces of the plate and the surfaces of the cavities, holes, and cracks in the plate. No discretization is needed on the planar surfaces of the plate. In this initial study, three problems involving a pressurized hole in an infinite three-dimensional plate are analyzed. The shapes of the holes include a circular hole and two elliptical holes with the aspect ratios of 4 and 10, respectively. In all the cases, the accuracy of the modified BEM is established by direct comparison of its results with those of finite element calculations. The results of the modified BEM are also compared with the plane-stress and plane-strain approximations of the problems under consideration. This comparison makes it possible to access the important three-dimensioanl effects near the surface of the elliptical hole.
Dissert. Abstr.

N93-14766*# Technion Research and Development Foundation Ltd., Haifa (Israel). Faculty of Aerospace Engineering.
MULTI-DISCIPLINARY OPTIMIZATION OF AEROSERVOELASTIC SYSTEMS Annual Report, 1 Oct. 1991 - 30 Sep. 1992
Mardechay Karpel (National Aeronautics and Space Administration. Langley Research Center, Hampton, VA.) 15 Nov. 1992 24 p
(Grant NAGw-1708)
(NASA-CR-191255; NAS 1.26:191255; Rept-160-573) Avail: CASI HC A03/MF A01

The purpose of the research project was to continue the development of new methods for efficient aeroservoelastic analysis and optimization. The main targets were as follows: to complete the development of analytical tools for the investigation of flutter with large stiffness changes; to continue the work on efficient continuous gust response and sensitivity derivatives; and to advance the techniques of calculating dynamic loads with control and unsteady aerodynamic effects. An efficient and highly accurate mathematical model for time-domain analysis of flutter during which large structural changes occur was developed in cooperation with Carol D. Wieseman of NASA LaRC. The model was based on the second-year work 'Modal Coordinates for Aeroelastic Analysis with Large Local Structural Variations'. The work on continuous gust response was completed. An abstract of the paper 'Continuous Gust Response and Sensitivity Derivatives Using State-Space Models' was submitted for presentation in the 33rd Israel Annual Conference on Aviation and Astronautics, Feb. 1993. The abstract is given in Appendix A. The work extends the optimization model to deal with continuous gust objectives in a way that facilitates their inclusion in the efficient multi-disciplinary optimization scheme. Currently under development is a work designed to extend the analysis and optimization capabilities to loads and stress considerations. The work is on aircraft dynamic loads in response to impulsive and non-impulsive excitation. The work extends the formulations of the mode-displacement and summation-of-forces methods to include modes with significant local distortions, and load modes. An abstract of the paper,'Structural Dynamic Loads in Response to Impulsive Excitation' is given in appendix B. Another work performed this year under the Grant was 'Size-Reduction Techniques for the Determination of Efficient Aeroservoelastic Models' given in Appendix C. Author

N93-14790# Army Materials Technology Lab., Watertown, MA.
USE OF THE THIN-WALLED TORSION SPECIMEN Final Report
Charles S. White Aug. 1992 29 p
(AD-A255593; MTL-TR-92-49) Avail: CASI HC A03/MF A01

The thin-walled torsion specimen was analyzed by the finite element method to determine its usefulness in material testing. A particular geometry, having a short gauge section and thick shoulder regions, was examined using material constants for 316 stainless steel. The specimen was analyzed with an eye toward determining its usefulness in approximating simple shear deformation. Both forward and single reverse behavior were examined. Classical isotropic and Prager-Ziegler kinematic hardening (using Jaumann stress rates) were used in the analyses. The gauge section did not contain uniform stress components throughout, but nevertheless, the macroscopic response of the specimen compared favorably with simple shear results. Plastic deformation was not entirely constrained to the gauge section but it extended some distance into the shoulder region. Consequently, the shear strain in the gauge section must be directly measured with an extensometer or a correction factor used when converting the applied machine rotation to gauge shear strain. This correction factor was determined from the finite element calculations. In reverse twisting, the macroscopic response of the specimen again matched well with simple shear results but neither material law provided even a qualitative match with experiment. The limitations of the thin-wall specimen are described and quantified in this report. GRA

N93-14799*# Georgia Inst. of Tech., Atlanta. School of Aerospace Engineering.
SAPNEW: PARALLEL FINITE ELEMENT CODE FOR THIN SHELL STRUCTURES ON THE ALLIANT FX-80 Final Report
Manohar P. Kamat and Brian C. Watson Nov. 1992 42 p
(Grant NAG3-895; RTOP 505-63-1B)
(NASA-CR-189212; E-7422; NAS 1.26:189212) Avail: CASI HC A03/MF A01

The finite element method has proven to be an invaluable tool for analysis and design of complex, high performance systems, such as bladed-disk assemblies in aircraft turbofan engines. However, as the problem size increase, the computation time required by conventional computers can be prohibitively high. Parallel processing computers provide the means to overcome these computation time limits. This report summarizes the results of a research activity aimed at providing a finite element capability for analyzing turbomachinery bladed-disk assemblies in a vector/parallel processing environment. A special purpose code, named with the acronym SAPNEW, has been developed to perform static and eigen analysis of multi-degree-of-freedom blade models built-up from flat thin shell elements. SAPNEW provides a stand alone capability for static and eigen analysis on the Alliant FX/80, a parallel processing computer. A preprocessor, named with the acronym NTOS, has been developed to accept NASTRAN input decks and convert them to the SAPNEW format to make SAPNEW more readily used by researchers at NASA Lewis Research Center.
Author

N93-15066# Pennsylvania State Univ., University Park. Dept. of Engineering Science and Mechanics.
THE STRESS DEVELOPMENT DURING FILAMENT WINDING OF THICK CYLINDERS
H. T. Hahn and S. S. Lee Aug. 1992 34 p
(Contract N00014-91-J-4103)
(AD-A255765) Avail: CASI HC A03/MF A01

The stress development during filament winding of thick composite cylinders has been studied using dry glass fiber tows. The thicknesses of the wound cylinders were more than 38 mm while the aluminum mandrel

used had an outside diameter of 58 mm. Circumferential winding was used and the winding tension was varied between 4 and 23 N. The radial pressure measured at the mandrel surface using foil gages increased over the first 6 layers or so of winding, and then stayed constant or even decreased slightly with subsequent winding. Predictions based on elastic analyses were fitted to the data by varying the effective radial modulus. The resulting values of the radial modulus were much less than the circumferential modulus, the latter being more than ten-thousand times greater than the former. Such high anisotropy was responsible for the asymptotic increase of the mandrel pressure with winding. The calculated circumferential stress in the fibers was compressive throughout most of the inner part of the wound cylinder however, its magnitude was rather small. A higher winding tension resulted in a better compaction, and therefore, a smaller effective layer thickness, a higher radial modulus, and higher internal stresses. Under the winding conditions studied in the present work, fiber buckling due to the development of compressive circumferential stress does not appear possible. GRA

N93-15070# Air Force Inst. of Tech., Wright-Patterson AFB, OH. Foreign Aerospace Science and Technology Center.

A SIMULATION STUDY OF PLANAR SWAGING DEFORMATION

Cheng-Gen Zhang, Gwang-Shen Jen, and Gwang-Huei Su 28 Aug. 1992 20 p Transl. into ENGLISH from Jixie Gongcheng Xuebao (China), v. 25, no. 3, Sep. 1989 p 72-77

(AD-A255908; FASTC-ID(RS)T-1065-91) Avail: CASI HC A03/MF A01

Planar swaging deformation was studied with a photoplastic method. The domestic polycarbonate was used as a simulation material. The full-field strain distribution for planar swaging deformation was obtained. The average error of the calculated strain was less than 7 percent. The deformation area and the effect of friction on deformation area were studied with the characteristics of photoplasticity. This paper points out the special features of planar swaging deformation and the effect of lubrication on deformation flow. GRA

N93-15202*# National Aeronautics and Space Administration. Langley Research Center, Hampton, VA.

OPTIMAL ACTIVE VIBRATION ABSORBER: DESIGN AND EXPERIMENTAL RESULTS

Gina Lee-Glauser (Clarkson Univ., Potsdam, NY.), Jer-Nan Juang, and Jeffrey L. Sulla (Lockheed Engineering and Sciences Co., Hampton, VA.) Dec. 1992 81 p

(RTOP 590-14-21-01)

(NASA-TM-107709; NAS 1.15:107709) Avail: CASI HC A05/MF A01

An optimal active vibration absorber can provide guaranteed closed-loop stability and control for large flexible space structures with collocated sensors/actuators. The active vibration absorber is a second-order dynamic system which is designed to suppress any unwanted structural vibration. This can be designed with minimum knowledge of the controlled system. Two methods for optimizing the active vibration absorber parameters are illustrated: minimum resonant amplitude and frequency matched active controllers. The Controls-Structures Interaction Phase-1 Evolutionary Model at NASA LaRC is used to demonstrate the effectiveness of the active vibration absorber for vibration suppression. Performance is compared numerically and experimentally using acceleration feedback. Author

N93-15210# Sandia National Labs., Albuquerque, NM.

CHARACTERIZATION OF IMPACT-LIMITING MATERIAL

T. A. Duffey (Spectra Research Inst., Albuquerque, NM.), R. E. Glass, and P. McConnel (GRAM, Inc., Albuquerque, NM.) May 1992 161 p

(Contract DE-AC04-76DP-00789)

(DE92-016767; SAND-92-0773; TTC-1207) Avail: CASI HC A08/MF A02

Methods of mechanical and thermal testing specifically directed toward evaluation of impact-limiting materials for radioactive material transportation containers are presented. Associated figures of merit and procedures for rank-ordering the materials are also developed. Based on testing and evaluation procedures developed herein, thermal and mechanical results are presented for high- and low-density aluminum honeycombs, polyurethane foams, and aluminum foams. On a minimum mass basis, the high-density aluminum honeycomb is found to be a superior impact energy absorber up to the point of lock up. On a minimum volume basis, the high-density polyurethane foam is far superior, however. Based on the thermal figures of merit, the high-density polyurethane foam was found to be the most favorable material. DOE

N93-15260# Georgia Inst. of Tech., Atlanta. School of Civil Engineering.

VALIDATION OF AN AUTOMATED TORSIONAL AND WARPING STRESS ANALYSIS PROGRAM M.S. Thesis

Stephen M. Azzinari 19 Aug. 1992 358 p

(AD-A256035) Avail: CASI HC A16/MF A03

An automated procedure for determining warping and torsional stresses in open steel members was developed by Joseph Palacak, Jr. in 1985. His FORTRAN program, called 'TORSION', determined stresses in wide flange, channel, and single angle members under various longitudinal bending and torsional loadings. In order to validate the 'TORSION' program, twelve test cases were run and compared to the same cases analyzed using a commonly used manual technique. For this manual technique, the Torsional Analysis Case Charts, developed by Bethlehem Steel were used to compute warping and torsional stresses. Tables comparing the calculated stresses by the 'TORSION' program and the torsion tables were developed. In addition, stress values from the hand-calculated problems were compared to values from GTSTRUDL output. Comparison tables between GTSTRUDL and the hand-calculated values are also presented. GRA

N93-15343*# National Aeronautics and Space Administration. Lewis Research Center, Cleveland, OH.

ROOT DAMAGE ANALYSIS OF AIRCRAFT ENGINE BLADE SUBJECT TO ICE IMPACT

E. S. Reddy (Sverdrup Technology, Inc., Brook Park, OH.), G. H. Abumeri (Sverdrup Technology, Inc., Brook Park, OH.), C. C. Chamis, and P. L. N. Murthy Aug. 1992 16 p

(RTOP 505-62-0K)

(NASA-TM-105779; E-7206; NAS 1.15:105779) Avail: CASI HC A03/MF A01

The blade root response due to ice impact on an engine blade is simulated using the NASA in-house code BLASIM. The ice piece is modeled as an equivalent spherical object impacting on the leading edge of the blade and has the velocity opposite to that of the aircraft with direction parallel to the engine axis. The effect of ice impact is considered to be an impulse load on the blade with its amplitude computed based on the momentum transfer principle. The blade response due to the impact is carried out by modal superposition using the first three modes. The maximum dynamic stresses at the blade root are computed at the quarter cycle of the first natural frequency. A combined stress failure function based on modified distortion energy is used to study the spanwise bending damage response at the blade root. That damage function reaches maximum value for very low ice speeds and increases steeply with increases in engine speed. Author

N93-15369*# National Aeronautics and Space Administration. Lewis Research Center, Cleveland, OH.

CLOSED FORM EXPRESSIONS FOR CRACK MOUTH DISPLACEMENTS AND STRESS INTENSITY FACTORS FOR CHEVRON NOTCHED SHORT BAR AND SHORT ROD SPECIMENS BASED ON EXPERIMENTAL COMPLIANCE MEASUREMENTS

R. T. Bubsey, T. W. Orange, W. S. Pierce, and J. L. Shannon, Jr. Oct. 1992 32 p

(RTOP 505-63-5B)

(NASA-TM-83796; E-2293; NAS 1.15:83796) Avail: CASI HC A03/MF A01

A set of equations are presented describing certain fracture mechanics parameters for chevron notch bar and rod specimens. They are developed by fitting compliance calibration data reported earlier. The equations present the various parameters in their most useful forms. The data encompass the entire range of the specimen geometries most commonly used. Their use will facilitate the testing and analysis of brittle metals, ceramics, and glasses. Author

N93-15372# Lehigh Univ., Bethlehem, PA.

THE MIXED MODE CRACK PROBLEM IN A NONHOMOGENEOUS ELASTIC PLANE Final Report

Noboru Konda and F. Erdogan Aug. 1992 30 p

(Contract N00014-89-C-3188)
(AD-A256469) Avail: CASI HC A03/MF A01

In this paper, a nonhomogeneous elastic medium containing a crack arbitrarily oriented with respect to the direction of property gradient is considered. The problem is solved under plane strain or generalized plane stress conditions. This is a highly simplified version of a class of physical problems that may arise in fracture mechanics studies of ceramic coatings, metal/ceramic composites, and interfacial zones with continuously varying volume fractions or graded properties. The main results of the paper are the calculated modes 1 and 2 stress intensity factors. Among the questions studied are the effects of the material nonhomogeneity constant, the crack orientation, the loading conditions, and the Poisson's ratio on the stress intensity factors. Briefly discussed are also the stress state near the crack tip and the crack opening displacement. GRA

N93-15374# Lehigh Univ., Bethlehem, PA.
THE CRACK PROBLEM FOR AN ORTHOTROPIC HALF PLANE STIFFENED BY ELASTIC FILMS Final Report
R. Mahajan, F. Erdogan, and Y. T. Chou Aug. 1992 48 p
(Contract N00014-89-C-3188)
(AD-A256471) Avail: CASI HC A03/MF A01

In this paper, various contact and crack problems for an orthotropic substrate, stiffened by elastic films are considered. The film is modeled as a membrane and the substrate as an orthotropic half-plane with the principal axes of orthotropy parallel and perpendicular to the boundary. The problem is formulated in terms of a system of singular integral equations. Various asymptotic analyses are carried out in order to determine the nature of the stress singularities. The special cases for which the solution is obtained and results are provided include the stiffened half-plane without the crack, the cracked half-plane without any stiffeners, the orthotropic half-plane with a single stiffener and a crack emanating from the endpoint of the stiffener, and a broken stiffener on a cracked half-plane. In each case the influence of the relative crack/stiffener dimensions, the film/substrate stiffness ratios, and the material orthotropy on the stress intensity factors is studied and some sample results are given. GRA

N93-15423# Los Alamos National Lab., NM.
CALCULATION OF MECHANICAL VIBRATION FREQUENCIES OF STIFFENED SUPERCONDUCTING CAVITIES
S. J. Black and G. Spalek 1992 4 p Presented at the 16th International LINAC Conference, Ottawa, Ontario, 23-28 Aug. 1992
(Contract W-7405-eng-36)
(DE92-040228; LA-UR-92-2735; CONF-9208109-31) Avail: CASI HC A01/MF A01

We calculated the frequencies of transverse and longitudinal mechanical-vibration modes of the HEPL- modified, CERN/DESY four-cell superconducting cavity, using finite-element techniques. We compared the results of these calculations, including the stiffening of the cavity with rods, with mode frequencies measured at HEPL. The correlation between data was significant. The same techniques were also used to design and optimize the stiffening scheme for the seven-cell 805-MHz superconducting cavity being developed at Los Alamos. In this report, we describe the final stiffening scheme and the results of our calculations. DOE

N93-15530*# National Aeronautics and Space Administration. Lyndon B. Johnson Space Center, Houston, TX.
EMITTANCE MEASUREMENTS OF SPACE SHUTTLE ORBITER REINFORCED CARBON-CARBON
Jose M. Caram, Stanley A. Bouslog (Lockheed Engineering and Sciences Co., Houston, TX.), and George R. Cunnington, Jr. (Lockheed Missiles and Space Co., Palo Alto, CA.) Dec. 1992 29 p
(NASA-TP-3293; S-691; NAS 1.60:3293) Avail: CASI HC A03/MF A01

The spectral and total normal emittance of the Reinforced Carbon-Carbon (RCC) used on Space Shuttle nose cap and wing leading edges has been measured at room temperature and at surface temperatures of 1200 to 2100 K. These measurements were made on virgin and two flown RCC samples. Room temperature directional emittance data were also obtained and were used to determine the total hemispherical emittance of RCC as a function of temperature. Results of the total normal emittance for the virgin samples showed good agreement with the current RCC emittance design curve; however, the data from the flown samples showed an increase in the emittance at high temperature possibly due to exposure from flight environments. Author

N93-15653*# Michigan Univ., Ann Arbor. Dept. of Aerospace Engineering.
FAILURE OF COMPOSITE PLATES UNDER STATIC BIAXIAL PLANAR LOADING Final Report
Anthony M. Waas and Amir R. Khamseh 18 Dec. 1992 28 p Original contains color illustrations
(Grant NAG1-1040)
(NASA-CR-191391; NAS 1.26:191391) Avail: CASI HC A03/MF A01; 1 functional color page

The project involved detailed investigations into the failure mechanisms in composite plates as a function of hole size (holes centrally located in the plates) under static loading. There were two phases to the project, the first dealing with uniaxial loads along the fiber direction, and the second dealing with coplanar biaxial loading. Results for the uniaxial tests have been reported and published previously, thus this report will place emphasis on the second phase of the project, namely the biaxial tests. The composite plates used in the biaxial loading experiments, as well as the uniaxial, were composed of a single ply unidirectional graphite/epoxy prepreg sandwiched between two layers of transparent thermoplastic. This setup enabled us to examine the failure initiation and propagation modes nondestructively, during the test. Currently, similar tests and analysis of results are in progress for graphite/epoxy cruciform shaped flat laminates. The results obtained from these tests will be available at a later time. Author

N93-14942# Canadian Space Agency, Ottawa (Ontario).
TECHNOLOGY DEVELOPMENT FOR NON-CONTACT MEASUREMENT IN MODAL TESTING OF LARGE SPACE STRUCTURES
Y. Soucy, W. B. Graham, A. K. Mitchell (Nova Scotia Technical Coll., Halifax.), and C. R. Hazell (Nova Scotia Technical Coll., Halifax.) *In* Canadian Space Agency, Proceedings of the Sixth CASI Conference on Astronautics 1990 15 p Previously announced in IAA as A91-34948
(For primary document see N93-14920 04-12)
Avail: Canadian Aeronautics and Space Inst., 222 Somerset St. W., Suite 601, Ottawa, Ontario K2P 0J1 Canada

42 GEOSCIENCES (GENERAL)

N93-15496# City Coll. of the City Univ. of New York, NY. Dept. of Earth and Atmospheric Sciences.
MODERN METHODS IN METEOROLOGICAL AND OCEANOGRAPHIC DATA ANALYSIS Final Report
Edward E. Hindman 9 Oct. 1992 33 p
(Contract N00014-09-J-1777)
(AD-A257080) Avail: CASI HC A03/MF A01

A two-dimensional, parameterized kinematic cloud microphysics model is described and used to simulate the form of cyclonic precipitation and its thermal impact in three idealized situations. The first situation represents a strong warm or stationary front with a zone of freezing rain and ice pellets separating regions of rain and snow. The second represents a storm with initial surface temperatures slightly above 0 C, and in which precipitation at the ground changes from rain to snow as a result of cooling by melting and evaporation of hydrometeors. The third represents a shallow cloud in a sounding with all temperatures below 0 C that initially produces freezing drizzle before a change to snow or ice pellets. GRA

43 EARTH RESOURCES AND REMOTE SENSING

Includes remote sensing of earth resources by aircraft and spacecraft; photogrammetry; and aerial photography.

For instrumentation see *35 Instrumentation and Photography.*

N93-14174 Iowa Univ., Iowa City.
A GENERAL PURPOSE RADIATIVE TRANSFER MODEL FOR APPLICATION TO REMOTE SENSING IN MULTIDIMENSIONAL SYSTEMS Ph.D. Thesis
Alejo Sanchez-Alias 1991 296 p
Avail: Univ. Microfilms Order No. DA9217205

The objective is the development, implementation, and validation of a radiation transfer model with applicability to one-, two-, and three-dimensional rectangular domains. The formulation and implementation of the discrete ordinates method, selected as the method to be used in the development of the model, is discussed in detail. The discussion includes: quadrature selection; scattering phase function modeling; spatial and directional discretization of the governing equations; modeling of lesser dimensionality domains by means of a three-dimensional code; implementation of a collimated source; and evaluation of output intensities in any desired direction, among others. The resulting algorithm is capable of accounting for: black, gray, specularly reflecting, and spectrally emitting boundaries with any given temperature distribution; symmetric and/or periodic boundaries; spectral and spatial variations of radiatively participating gases and polydispersions (absorbing, emitting, and anisotropically scattering media) under optically thin or optically thick conditions; non-homogeneous media; radiative equilibrium on a gray or spectral basis; internal energy sources; isotropic background radiation source; incoming collimated source from any direction and acting on any set of boundaries; output intensity toward an instrument placed in any desired direction; and easy coupling with other models performing fluid flow calculations. Two computer programs capable of solving for all of the above are presented and are complemented with the ability to perform radiative properties calculations for polydispersions with renormalized phase functions according to any desired order of quadrature. The computer package is specially designed for easy use, computational efficiency; accuracy, stability, and the potential to take advantage of modern parallel and vector machines. The model is particularly suited, but not limited, to remote sensing applications. Dissert. Abstr.

N93-14220 Maine Univ., Orono.
MEASUREMENT-BASED MULTIPURPOSE CADASTRAL SYSTEMS Ph.D. Thesis
Taher Bin Buyong 1992 188 p
Avail: Univ. Microfilms Order No. DA9227977

Multipurpose cadastral systems are required by local governments to improve land-conveyance procedures, furnish a basis for equitable taxation, and provide information for resource management and environmental planning. Several problems inherent in present coordinate-based implementations, however, slow the rate of introduction of multipurpose cadastral systems in many potential local governments. This thesis investigates multipurpose cadastral systems that are based on measurements. The fundamental concepts of measurement-based multipurpose cadastral systems are that measurements are first class objects and are the primary carriers of metric information. Coordinate values that are required to answer metric queries are computed from the stored measurements as needed. Coordinate computations by local least squares adjustments consider measurements around the neighborhood of query areas only. To update a system with new measurements only requires the addition of the measurements to the database. The information on the quality of measurements available in a measurement-based system is useful when assessment about the reliability of measurements and derived metric values must be made. Preserving original measurements as opposed to calculated coordinates is the foundation for building a legally supported multipurpose cadastral system. The investigation reveals that measurement-based concepts can serve as the foundation for a cadastral system. An implementation can start without prior establishment of a network of control points. Existing cadastral measurements are used as a basis of a system. With precise instruments available to surveyors, good quality measurements from standard daily operations are added to the system without extra cost. Control measurements are integrated into the system the same way as cadastral measurements. The addition of measurements increases the accuracy of the system over time. An implementation of a measurement-based system is feasible in a very near future with the rapid development of computers. The hardware issues are resolved: the storage of redundant measurements is no longer a problem because storage media like hard disk are now afforable. Various database management software allows easy management of measurements. The processing speed of workstations in the mid 1990's will permit local adjustments to be performed of the order of seconds. Dissert. Abstr.

N93-14223 Ohio State Univ., Columbus.
A FEASIBILITY STUDY OF SPACE VLBI FOR GEODESY AND GEODYNAMICS Ph.D. Thesis
Madhav Narayan Kulkarni 1992 231 p
Avail: Univ. Microfilms Order No. DA9227312

Space Very Long Baseline Interferometry (VLBI) is an extension of the ground based VLBI to space. With the launching of two or more Space VLBI satellites in the future, Space VLBI observations will be available for astrometric, geodetic and geodynamic applications. This new technique holds potential for various important applications including monitoring Earth rotation and interconnection of the reference frames used in geodesy and geodynamics. The aim of this feasibility study has been to investigate the possibility of precise estimation of geodetic parameters, with emphasis on the Earth rotation parameters (ERP's) from Space VLBI observations. A brief description of the Space VLBI technique, it's possible applications, and the Space VLBI missions being planned has been given. Estimability analysis to investigate the estimability of geodetic parameters from Space VLBI observations has been carried out and a simplifield of sensitivity analysis carried out to study the sensitivity of the Space VLBI observables to the geodetic parameters of interest, including the number of these parameters and random errors in their a priori values, have been presented. Some of the dominant systematic effects including atmospheric refraction, solar radiation pressure and relativistic effects have also been investigated. Simulation studies have been carried out to study the influence of these systematic effects and a priori information on the estimation of the Earth rotation parameters. The results from the simulation studies indicate that it may be possible to use the Space VLBI technique for monitoring Earth rotation and polar motion, only if the orbital systematic effects can be modeled to a high degree of accuracy (or the satellites can be tracked, with high accuracy, independently), and precise a priori information on station coordinates from other sources is used. A brief description of the Space VLBI software developed during this study has been presented, along with conclusions from this study and recommendations for further work in this area. Dissert. Abstr.

N93-14262# Naval Postgraduate School, Monterey, CA.
EFFECTS OF WATER VAPOR AND ANISOTROPIC SCATTERING ON AEROSOL OPTICAL DEPTH RETRIEVAL M.S. Thesis
Mary B. Clifford Dec. 1991 47 p
(AD-A256087) Avail: CASI HC A03/MF A01

NOAA-7 AVHRR data from April 1982 was used to perform global-scale analysis of aerosol particle characteristics. Mahony's (1991) water vapor correction was incorporated into the AVHRR multichannel satellite data processing technique used by Frost (1988). Channel 4/ Channel 5 brightness temperature difference was used as an estimate of water vapor content in an air column. Greatest measured water vapor content was at the equator, decreasing toward the poles. Applying the correction reduced the aerosol particle size index, resulting in an increase in aerosol optical depths. In addition, the high particle size index over the low latitudes in the Southern Hemisphere noted by Frost, was reduced significantly after applying the correction. A comparison was made between Frost's values for the variable two-term Henyey-Greenstein phase function and those derived with the water vapor correction. The basic shape of the curve is similar to that determined by Frost. GRA

N93-14263# Naval Postgraduate School, Monterey, CA.
IMPROVED AEROSOL OPTICAL DEPTH AND PARTICLE SIZE INDEX FROM SATELLITE DETECTED RADIANCE M.S. Thesis
Brian H. Miller Dec. 1991 57 p
(AD-A256089) Avail: CASI HC A04/MF A01

An algorithm that extracts aerosol optical depth and particle size index from satellite observations of upwelling radiance over clear ocean areas was modified and studied. In order to examine the algorithm's performance

on a regional scale, a previously analyzed data set, retrieved by the NOAA-9 AVHRR sensor, was reprocessed. The area of the study was in the central Pacific Ocean during the RITS-88 cruise from 7 April to 5 May 1988. The results were compared to those of the earlier study and used to investigate changes caused by modifications to the algorithm. One significant modification was to account for the absorption of column water vapor in the calculations. In addition, the correlation between aerosol optical depth and the two-term Henyey-Greenstein phase function was investigated by normalizing measured radiance values. The results compared well with the earlier study and supported the modifications to the algorithm. Based on this study, aerosol optical depth was shown to be correlated to the Henyey-Greenstein phase function. This knowledge helped in formulating improvements to the phase function. It was concluded that satellite imaging and processing on a regional scale is a useful way to study marine aerosols, that results can be improved by considering the effects of atmospheric water vapor absorption and other modifications to the calculations, and that there is room for improvement to the two-term Henyey-Greenstein phase function. GRA

N93-14430# Loral Defense Systems, Akron, OH.
TERRAIN VISUALIZATION FOR THE PORTABLE ALL-SOURCE ANALYSIS WORK STATION Technical Report, Jun. 1990 - Oct. 1991
Oct. 1991 70 p
(Contract DACA76-90-C-0018)
(AD-A255708; TEC-0011) Avail: CASI HC A04/MF A01

This report for the Terrain Visualization program was written to document significant program design elements. It reflects the successful achievement of the principal objective of the program--the implementation of sophisticated visualization capabilities using a low to medium performance computing platform. By requiring that this platform be the same as that used in the Digital Topographic Support System (DTSS), this program also advanced the potential use of terrain visualization technology in terrain analysis. GRA

N93-14450 Instituto de Pesquisas Espaciais, Sao Jose dos Campos (Brazil).
THE REGIONAL LAND USE OF PARAIBA VALLEY AND THE NORTH COAST OF SAO PAULO STATE, BRAZIL [MACROZONEAMENTO DA REGIAO DO VALE DO PARAIBA E LITORAL NORTE DO ESTADO DE SAO PAULO]
1992 246 p In BURMESE Original contains color illustrations
Avail: Issuing Activity

The regional land use planning of Paraiba Valley and the North Coast of Sao Paulo State - Brazil, was done using mainly orbital remote sensing data. The area of this region is approximately 18,000 km(exp 2). Emphasis was given on photointerpretation of satellite images to produce geological, geomorphological, ground water and land use maps. Geological engineering and agricultural land use suitability maps were elaborated by integrating different maps. All of them were presented at the scale of 1:250,000. In order to have a comprehensive view of the region, socioeconomic data and official information related to environmental protected areas, as well as mining activities in the region were considered. Finally, economical alternatives were proposed and different land use arrangements were indicated to promote the self-sustainable regional development. Author

N93-14522# Superconducting Super Collider Lab., Dallas, TX.
DATA MANAGEMENT AND PROCESSING PLAN, DEPARTMENT OF APPLIED GEODESY
Aug. 1992 15 p
(Contract DE-AC35-89ER-40486)
(DE93-000774; SSCL-595) Avail: CASI HC A03/MF A01

Data Management and Data Processing requirements of the Department of Applied Geodesy (DAG) are outlined in this plan and the plan to meet these requirements is outlined. These requirements are derived from the functional needs of the Department to meet the Superconducting Super Collider Laboratory (SSCL) alignment tolerances and schedules. In addition, this document presents a schedule for the implementation of this plan. This document is an integral part of the Alignment Plan of the SSCL. DOE

N93-14676# Army Topographic Engineering Center, Fort Belvoir, VA.
USING DIGITAL SCANNED AERIAL PHOTOGRAPHY FOR WETLANDS DELINEATION Report, 2-5 Apr. 1992
John Anderson and Maurits Roos 5 Apr. 1992 8 p
(AD-A255392; TEC-R-187) Avail: CASI HC A02/MF A01

The Corps of Engineers. U.S. Fish and Wildlife Service and the Environmental Protection Agency are charged the responsibility to jointly manage the nation's wetlands in accordance with the Clean Water Act and the Rivers and Harbors Act. The Corps' role is enforcement of regulations concerning dredging and filling of specific types and areas of wetlands that fall within jurisdictional boundaries. Current research is being conducted to enhance the field scientist's ability to manage these ecosystems using digital aerial photography, image processing and photo interpretation logic. This paper presents techniques used to scan (digitize), archive and use digital aerial photography for environmental resource management using a photogrammetrically accurate, CCD-based scanner. Spectral characteristics of the imagery and useful image processing routines to enhance the resulting raster file(s) for interpretation will be discussed. GRA

N93-14792*# Georgia Inst. of Tech., Atlanta. School of Electrical Engineering.
INVESTIGATION OF ANTENNA PATTERN CONSTRAINTS FOR PASSIVE GEOSYNCHRONOUS MICROWAVE IMAGING RADIOMETERS Final Report
A. J. Gasiewski and G. M. Skofronick Dec. 1992 75 p Prepared for Research Triangle Inst., Research Triangle Park, NC
(Contract NAS1-18925; RTOP 506-49-64-01)
(NASA-CR-189728; RTI/4500/017-02F; NAS 1.26:189728) Avail: CASI HC A04/MF A01

Progress by investigators at Georgia Tech in defining the requirements for large space antennas for passive microwave Earth imaging systems is reviewed. In order to determine antenna constraints (e.g., the aperture size, illumination taper, and gain uncertainty limits) necessary for the retrieval of geophysical parameters (e.g., rain rate) with adequate spatial resolution and accuracy, a numerical simulation of the passive microwave observation and retrieval process is being developed. Due to the small spatial scale of precipitation and the nonlinear relationships between precipitation parameters (e.g., rain rate, water density profile) and observed brightness temperatures, the retrieval of precipitation parameters are of primary interest in the simulation studies. Major components of the simulation are described as well as progress and plans for completion. The overall goal of providing quantitative assessments of the accuracy of candidate geosynchronous and low-Earth orbiting imaging systems will continue under a separate grant. Author

N93-14823 Waterloo Univ. (Ontario).
INTEGRATING SATELLITE IMAGERY INTO A GEOGRAPHIC INFORMATION SYSTEM FOR MONITORING THE DOWNSTREAM IMPACTS OF DAM CONSTRUCTION ON FLOODPLAIN AGRICULTURE IN SOKOTO STATE, NIGERIA Ph.D. Thesis
Paul Gilles Pilon 1991 215 p
Avail: Univ. Microfilms Order No. DANN69108

In developing countries, such as Nigeria, large-scale resource development often proceeds without adequate attention being given to the consequential effects of development on natural resources and the environment. In northern Nigeria, environmental change associated with the construction of two large-scale dams has had a negative impact on traditional agricultural activities in floodplain areas downstream of the dams. Although the negative effects of these dams have been acknowledged by local government agencies for some time, the exact extent, location and nature of downstream impacts have remained largely unknown. This can be attributed, in part, to a failure to acquire and examine relevant resource and environmental information on the consequential effects of such large-scale development prior to project implementation. Post-development attempts to monitor the impacts of dam construction are hampered by a lack of relevant information describing pre-dam and post-dam conditions, and the difficulty of comparing diverse data sources in such a way that they can be effectively utilized for integrated resource monitoring. The research reported in this thesis utilizes satellite imagery as the primary multitemporal data source and incorporates this imagery with other available spatial data in a geographic database. Spatial data sets acquired for a

floodplain area in northern Nigeria are compiled and co-registered using a TYDAC SPANS Geographic Information System. The data sets include: soil, topographic and relief information obtained from existing maps and aerial photographs; land cover and land use information; and change information derived from multitemporal satellite imagery, and questionnaire and field observation data. Comparative analysis of the data sets indicates that the effects of dam construction are not equally distributed in downstream areas. Farmers who have fields adjacent to the main river courses are more likely to benefit positively from regulated water flow associated with dam construction. In areas farther from the main river courses, where the availability of water has been reduced, impacts are more detrimental. Such information on the precise nature, magnitude and location of impacts can help identify specific sites where remedial measures such as diversion canals, new wells or the installation of pumps can be most effectively located to assist local farmers. Dissert. Abstr.

N93-14839 Colorado Univ., Boulder.
OCEAN WAVE DETECTION USING SATELLITE ALTIMETRY Ph.D. Thesis
Mohammad Basel Dayyani 1992 182 p
Avail: Univ. Microfilms Order No. DA9232679

The principal objective of this study is to develop a new method to detect wave motion from satellite altimetric measurements of sea surface height. The essence of the approach is to construct a two-dimensional Fourier series representation of the amplitude field in wavenumber space within a pre-specified oceanic region. The method uses an iterative, nonlinear least-squares technique based on the Marquardt-Levenberg algorithm to solve for model parameters describing the position, shape, direction of propagation and dispersion characteristics of the wave system. The Marquardt-Levenberg Fourier Series (MLFS) algorithm was used to detect two prominent wave systems in the equatorial Pacific Ocean using GEOSAT Exact Repeat Mission altimetry data during the two year period November, 1986 to January, 1989. Kelvin waves associated with the 1986-87 El Nino were investigated and its detected wave characteristics were found to be in accord with linear theory for baroclinic wave motion, earlier field measurements, and another set of satellite observations that employed a time series method of wave field detection. Shear-driven Legeckis waves were also investigated during their time of high activity in the fall of 1988 and characteristics for these eddies were found to be in accord with both linear stability theory and other independent field and satellite observations. The advantage of the present detection scheme over previous methods lies in its ability to determine modal phase speeds which give the dispersion relation over a finite range of wavenumbers. The group velocity which determines the direction of wave energy transport may then be calculated from the dispersion relation. The variable phase speed decomposition allows reconstruction of the instantaneous spatial structure of the wave system thereby yielding a direct view of amplitude modulations between neighboring waves and structural changes such as the fusion and fission of individual waves. Dissert. Abstr.

N93-15007# Army Topographic Engineering Center, Fort Belvoir, VA.
ADAPTIVE MESH IN VISUALIZATION OF TERRAIN ELEVATION DATA
J. J. Kim 7 Aug. 1992 7 p
(AD-A255481; TEC-R-182) Avail: CASI HC A02/MF A01

The initial step in terrain visualization is to utilize terrain elevation data to portray the earths surface. After that, features are overlaid as terrain colors, textures, or models on the visualized elevation data. Terrain elevation data are often visualized in a wire-frame mesh where grid posts represent the elevations of corresponding points in the terrain. When terrain is displayed in a perspective view, the grid sizes in the wire-frame mesh must be varied adaptively according to the distance between the viewpoint and the terrain so that the area nearest to the viewer is more densely sampled than the area further from the viewer. A wire-frame mesh with such varying grid sizes is called an adaptive mesh in this paper. A loosely defined adaptive mesh often creates anomalies between two areas with different grid sizes. This paper presents a few schemes for adaptive meshes that do not create anomalies. GRA

N93-15364# Army Signals Warfare Lab., Vint Hill Farms Station, VA.
AUTOMATED INTERPRETATION OF TOPOGRAPHIC MAPS
T. M. Cronin Aug. 1992 23 p
(AD-A257040; CSWD-92-TRF-0041) Avail: CASI HC A03/MF A01

Some new results which impact favorably upon the issue of automated topographic map interpretation are presented. Actually, the 'new' results consist of heretofore undiscovered applications of two concepts known to mathematicians and computer scientists for many years: binary search, and the normal vector. Binary search is extended by the technique from not only one to two dimensions, but arguably to three dimensions, since topographical maps are two-dimensional representations of three dimensional surfaces. Such maps are essentially sorted hierarchies of nested contours, which form a multiply-connected subdivision of the plane. The perimeter of a subdivision element is defined by a set of contours of extremal elevation and the edges of the map; a naming convention attaches a label to each element of the planar subdivision. Whenever one is afforded the luxury of dealing with a sorted data structure, one may invoke the power of binary search to achieve O(log n) time complexity during processing of a topographical query, where n is the number of contours which comprise a specific element of the planar subdivision. A topographical query is a request by a user to interpret the position of an arbitrary map coordinate, called query point, topographic map background. GRA

N93-15442# Argonne National Lab., IL.
INFORMATION TECHNOLOGIES FOR GLOBAL RESOURCES MANAGEMENT AND ENVIRONMENTAL ASSESSMENT
A. P. Campbell and Hua Wang 1992 8 p Presented at the International Symposium on Energy, Environment and Information Management, Argonne, IL, 15-28 Sep. 1992
(Contract W-31-109-eng-38)
(DE92-041107; ANL/CP-77152; CONF-9209160-17) Avail: CASI HC A02/MF A01

Recent advances in computer and communications technologies offer unprecedented opportunities to develop sophisticated information resources management systems for global resources management and environment assessment in an efficient, effective, and systematic manner. In this paper, the emerging global energy and environmental issues are identified. Since satellite-based remote sensing systems are becoming increasingly available and produce massive data collections, the utilization of imaging processing techniques and their applications for regional and global resources management and environmental studies are described. Interoperability and interconnectivity among heterogeneous computer systems are major issues in designing a totally integrated, multimedia-based, information resources management system that operates in a networking environment. Discussions of the future technology trends are focused on as are a number of emerging information management technologies and communications standards which will aid in achieving seamless system integration and offer user-friendly operations. It can be foreseen that advances in computer and communications technologies, increasingly sophisticated image processing techniques and Geographical Information Systems (GIS), and the development of globally comprehensive data bases will bring 'global visualization' onto multimedia desktop computers before the end of this decade. DOE

N93-14953# Canadian Space Agency, Ottawa (Ontario).
EARTH ENVIRONMENT SPACE INITIATIVE
S. Parashar, H. H. Zwick (MacDonald, Dettwiler and Associates Ltd., Richmond, British Columbia), N. Hamilton (MacDonald, Dettwiler and Associates Ltd., Richmond, British Columbia), D. Thompson (INTERA Technologies Ltd., Ottawa, Ontario), R. Inkster (INTERA Technologies Ltd., Ottawa, Ontario), D. Epp (Royal Canadian Air Force, Toronto, Ontario), A. Stones (Bristol Aerospace Ltd., Winnipeg, Manitoba), and G. Tyc (Bristol Aerospace Ltd., Winnipeg, Manitoba) *In* Canadian Space Agency, Proceedings of the Sixth CASI Conference on Astronautics 1990 9 p Previously announced in IAA as A91-34959 (For primary document see N93-14920 04-12)
Avail: Canadian Aeronautics and Space Inst., 222 Somerset St. W., Suite 601, Ottawa, Ontario K2P 0J1 Canada

N93-14967*# Institut Geographique National, Paris (France).
TERRESTRIAL REFERENCE SYSTEMS RELATED TO THE TOPEX/POSEIDON PROJECT
Claude Boucher, P. Willis, Francois Barlier (Centre d'Etudes et de Recherches Geodynamiques et Astronomiques, Grasse, France), and P. Mazzega (Centre National d'Etudes Spatiales, Toulouse, France) *In*

JPL, TOPEX/Poseidon Science Investigations Plan 1 Sep. 1991 p 27-28 (For primary document see N93-14964 04-48)
Avail: CASI HC A01/MF A02; 22 functional color pages

N93-14992*# Tokyo Univ. (Japan).
APPLICATION OF PRECISE ALTIMETRY TO THE STUDY OF PRECISE LEVELING OF THE SEA SURFACE, THE EARTH'S GRAVITY FIELD, AND THE ROTATION OF THE EARTH
J. Segawa, Y. Ganeko (Maritime Safety Agency, Tokyo, Japan), M. Sasaki (Maritime Safety Agency, Tokyo, Japan), T. Mori (Maritime Safety Agency, Tokyo, Japan), M. Ooe (Mizusawa International Latitude Observatory, Japan), I. Nakagawa (Kyoto Univ., Japan), H. Ishii, and Y. Hagiwara *In* JPL, TOPEX/Poseidon Science Investigations Plan 1 Sep. 1991 p 126-130 Original contains color illustrations (For primary document see N93-14964 04-48)
Avail: CASI HC A01/MF A02; 22 functional color pages

44 ENERGY PRODUCTION AND CONVERSION

Includes specific energy conversion systems, e.g., fuel cells; global sources of energy; geophysical conversion; and windpower.

For related information see also *07 Aircraft Propulsion and Power, 20 Spacecraft Propulsion and Power,* and *28 Propellants and Fuels.*

N93-14817# Midwest Research Inst., Golden, CO.
NREL PHOTOVOLTAIC SUBCONTRACT REPORTS: ABSTRACTS AND DOCUMENT CONTROL INFORMATION Report, 1 Aug. 1991 - 31 Jul. 1992
Aug. 1992 56 p
(Contract DE-AC02-83CH-10093)
(DE92-016408; NREL/TP-410-5008) Avail: CASI HC A04/MF A01

This report contains document control information and abstracts for the National Renewable Energy Laboratory (NREL) subcontracted photovoltaic program publications. It also lists source information on additional publications that describe U.S. Department of Energy (DOE) PV research activities. It is not totally exhaustive, so it lists NREL contacts for requesting further information on the DOE and NREL PV programs. This report covers the period from August 1, 1991, through July 31, 1992. The purpose of continuing this type of publication is to help people keep abreast of specific PV interests, while maintaining a balance on the costs to the PV program. The information in this report is organized under PV technology areas: Amorphous silicon research; polycrystalline thin films (including copper indium diselenide, cadmium telluride, and thin-film silicon); crystalline materials and advanced concepts (including silicon, gallium arsenide, and other group III-V materials); and PV manufacturing technology development (which may include manufacturing information for various types of PV materials). DOE

N93-15061# Los Alamos National Lab., NM.
COMPONENTS AND MATERIALS ISSUES IN POLYMER ELECTROLYTE FUEL CELLS FOR TRANSPORTATION APPLICATIONS
C. R. Derouin, T. E. Springer, F. A. Uribe, J. A. Valerio, M. S. Wilson, T. A. Zawodzinski, and S. Gottesfeld 1992 21 p Presented at the 182nd Meeting of the Electrochemical Society, Toronto, Ontario, 11-16 Oct. 1992
(Contract W-7405-eng-36)
(DE92-013384; LA-UR-92-1434; CONF-921036-1) Avail: CASI HC A03/MF A01

Recent research work on the polymer electrolyte fuel cell (PEFC) is described. This research work addresses the goal of bringing the PEFC technology to the performance and the cost levels required for its wide spread use in transportation. The main topics are (1) a new approach to the fabrication of Pt/C catalyst layers of high performance, employing loadings as low as 0.1 mgPt/cm(sup 2); (2) measurements and modeling of membrane, cathode catalyst and cathode backing contributions to cell loses in the PEFC; and (3) carbon monoxide poisoning of anode electrocatalysts in the PEFC -- the problem and possible solutions. DOE

N93-15134# Sandia National Labs., Albuquerque, NM.
THE CPG 5-kW(e) DISH-STIRLING DEVELOPMENT PROGRAM
J. R. Bean (Cummins Power Generation, Inc., Columbus, IN.) and R. B. Diver 1991 21 p Presented at the 27th Intersociety Energy Conversion Engineering Conference, San Diego, CA, 3-7 Aug. 1992
(Contract DE-AC04-76DP-00789)
(DE92-017050; SAND-91-2813C; CONF-920801-16) Avail: CASI HC A03/MF A01

Through a program sponsored by the US Department of Energy (DOE), Cummins Power Generation, Inc. (CPG) and Sandia National Laboratories (SNL) have entered into a joint venture to develop and commercialize economically competitive dish-Stirling systems for remote power applications. CPG plans to commercialize 5-kW(sub e) systems that can be used in remote locations for water pumping and village electrification or connected to an existing utility grid. The $14 million Dish-Stirling Joint Venture Program (JVP) is being conducted in three phases over a 3 1/2-year period in accordance with the Cummins Total Quality System (TQS) for new product development. Sixteen systems representing three generations of technology will be fielded and tested. The JVP is being funded equally by CPG, including its industrial partners, and the DOE. Following completion of the program, CPG's commercialization effort will continue with limited production expected to start about 1995. In this paper, the program plan and technical approach for the JVP is presented. A technical description and current status of the key components and discussions of the key technical issues are also provided. DOE

N93-15213# Booz-Allen and Hamilton, Inc., Bethesda, MD.
TECHNOLOGY COMMERCIALIZATION COST MODEL AND COMPONENT CASE STUDY
Dec. 1991 48 p Prepared in cooperation with Cobb (Michael A.) and Co., Akron, OH
(Contract DE-AC21-86MC-25104)
(DE92-001280; DOE/MC-25104/3092) Avail: CASI HC A03/MF A01

Fuel cells seem poised to emerge as a clean, efficient, and cost competitive source of fossil fuel based electric power and thermal energy. Sponsors of fuel cell technology development need to determine the validity and the attractiveness of a technology to the market in terms of meeting requirements and providing value which exceeds the total cost of ownership. Sponsors of fuel cell development have addressed this issue by requiring the developers to prepare projections of the future production cost of their fuel cells in commercial quantities. These projected costs, together with performance and life projections, provide a preliminary measure of the total value and cost of the product to the customer. Booz-Allen & Hamilton Inc. and Michael A. Cobb & Company have been retained in several assignments over the years to audit these cost projections. The audits have gone well beyond a simple review of the numbers. They have probed the underlying technical and financial assumptions, the sources of data on material and equipment costs, and explored issues such as the realistic manufacturing yields which can be expected in various processes. Based on the experience gained from these audits, DOE gave Booz-Allen and Michael A. Cobb & company the task to develop a criteria to be used in the execution of future fuel cell manufacturing cost studies. It was thought that such a criteria would make it easier to execute such studies in the future as well as to cause such studies to be more understandable and comparable. DOE

N93-15219# Oak Ridge National Lab., TN.
LATENT HEAT THERMAL ENERGY STORAGE FOR LUNAR OXYGEN PRODUCTION
A. D. Solomon (Solomon, A. D., Omer, Israel), V. Alexiades, G. Jacobs, M. Naney, and M. Olszewski 1992 13 p Presented at the Winter Annual Meeting of the American Society of Mechanical Engineers, Anaheim, CA, 8-13 Nov. 1992
(Contract DE-AC05-84OR-21400)
(DE92-017817; CONF-921110-9) Avail: CASI HC A03/MF A01

A necessary component of a solar-based lunar oxygen production system is a thermal energy storage module. We discuss some of the heat transfer and phase change problems associated with the design and operation of such a module based on the latent heat of melting of lunar rock. DOE

N93-15224# High Intensity Photovoltaics, Inc., Olmstead Falls, OH.
A HIGH INTENSITY SOLAR CELL INVENTION: THE EDGE-ILLUMINATED VERTICAL MULTI-JUNCTION (VMJ) SOLAR CELL

Bernard L. Sater Aug. 1992 14 p
(Contract DE-FG01-87CE-15337)
(DE92-019015; DOE/CE-15337/T15) Avail: CASI HC A03/MF A01

A summary is presented of a High Intensity Solar Cell (HI Cell) development carried out under the NIST/DOE Energy-Related Invention Program. The HI Cell, or Edge-Illuminated Vertical Multi-junction Solar Cell, eliminates most major problems encountered with other concentrator solar cell designs. Its high voltage and low series resistance features make it ideally suited for efficient operation at high intensities. Computer modeling shows efficiencies near 30 pct. at 500 suns intensity are possible with state-of-the-art processing. Development of a working model was largely successful before encountering an unexpected problem during the last fabrication step with the anti-reflection coating. Unfortunately, funding was exhausted before its resolution. Recommendations are made to resolve the AR coating problem and to integrate all the knowledge gained during this development into a viable prototype model. The invention will provide the technical and economic performance needed to make photovoltaic systems cost-effective for wide use. DOE

N93-15271# Department of Energy, Washington, DC. Geothermal Div.
GEOTHERMAL ENERGY AND THE UTILITY MARKET: THE OPPORTUNITIES AND CHALLENGES FOR EXPANDING GEOTHERMAL ENERGY IN A COMPETITIVE SUPPLY MARKET: PROCEEDINGS
1992 230 p Conference held in San Francisco, CA, 24-26 Mar. 1992
(DE92-019090; CONF-920378) Avail: CASI HC A11/MF A03

Each year the Geothermal Division of the US Department of Energy conducts an in-depth review of its entire geothermal R&D program. The conference serves several purposes: a status report on current R&D activities, an assessment of progress and problems, a review of management issues, and a technology transfer opportunity between DOE and the US geothermal city. This year's conference, Program Review X, was held in San Francisco on March 24 - 26, 1992. The theme of the review, 'Geothermal Energy and the Utility Market - The Opportunities and Challenges for Expanding Geothermal Energy in a Competitive Supply Market', focused on the needs of the electric utility sector. Geothermal energy, with its power capacity potential of 10 GWe by the year 2010, can provide reliable, enviromentally clean electricity which can help offset the projected increase in demand. Program Review X consisted of seven sessions including an opening session with presentations by Mr. Vikram Budhraja, Vice President of System Planning and Operations, Southern California Edison Company, and Mr. Richard Jaros, President and Chief Operating Officer, California Energy Company. The six technical sessions included presentations by the relevant field researchers covering DOE-sponsored R&D in hydrothermal, hot dry rock, and geopressured energy. Individual projects are processed separately for the data bases. DOE

N93-15322# Westinghouse Electric Corp., Pittsburgh, PA.
HIGH TEMPERATURE TUBULAR SOLID OXIDE FUEL CELL DEVELOPMENT
E. R. Ray 1992 8 p Presented at the US DOE Contractors Review Meeting on Fuel Cells, Morgantown, WV, 14-15 Jul. 1992
(Contract DE-FC21-91MC-28055)
(DE92-040253; DOE/MC-28055/92/C0065; CONF-920748-20) Avail: CASI HC A02/MF A01

Important to the development commercialization of any new technology is a field test program. This is a mutually beneficial program for both the developer and the prospective user. The developer is able to acquire valuable field operating experience that is not available in a laboratory while the user has the opportunity to become familiar with the new technology and gains a working knowledge of it through hands-on experience. Westinghouse, recognizing these benefits, initiated a program in 1986 by supplying a 400 W SOFC generator to Tennessee Valley Authority. This generator operated for approximately 1,760 hours and was constructed of twenty-four 30 cm thick-wall PST cells. In 1987, three, 3 kW SOFC generators were installed and operated at the facilities of the Tokyo Gas Company and the Osaka Gas Company. At Osaka Gas, two generators were used. First a training generator, operated for 2900 hours before it was replaced on a preplanned schedule with the second generator. The second generator operated for 3,600 hours. Tokyo Gas generator was operated for 4,900 hours. These generators had a 98 percent availability and measured NO(x) levels of less than 1.3 ppm. The 3 kW SOFC generators were constructed of 144 36 cm thick-wall PST cells. The 3 kW generators, as was the TVA generator, were fueled with hydrogen and carbon monoxide. The next major milestone in the field unit program was reached in early 1992 with the delivery to the UTILITIES, a consortium of the Kansai Electric Power company, the Tokyo Gas Company, and the Osaka Gas Company, of a natural gas fueled all electric SOFC system. This system is rated at a nominal 25 kW dc with a peak capacity of 40 kW dc. The NO(x) was measured at less than 0.3 ppM (corrected to 15 percent oxygen). The system consists of 1152 cells (thin-wall PST) of 50 cm active length, manufactured at the PPMF. Cells are contained in two independently controlled and operated generators. The 2,300 hours of stable operation has been obtained on the first unit. DOE

N93-15323# Westinghouse Electric Corp., Pittsburgh, PA. Science and Technology Center.
CONTAMINANT EFFECTS IN SOLID OXIDE FUEL CELLS
N. J. Maskalisk and E. R. Ray 1992 12 p Presented at the US DOE Contractors Review Meeting on Fuel Cells, Morgantown, WV, 14-15 Jul. 1992
(Contract DE-AC21-89MC-26355)
(DE92-040255; DOE/MC-26355/92/C0062; CONF-920748-18) Avail: CASI HC A03/MF A01

Two full scale (50-cm length) SOFCS, each representative of generator cells in the field, were electrically connected in series; then operated at 1000 C and 350 mA/sq. cm. An initial run of approximately 150 hours served to establish baseline performance in 89 percent H2, 11 percent H2O fuel at 85 percent fuel utilization and 4 stoichs, air. Then, for approximately 200 hours, a similar base-line was established for operation in simulated coal gas fuel. Finally, the fuel impurity components were sequentially added. The cumulative effect on performance are shown in table 3. These data reveal no strong association of cell resistance with cell performance change in the cases of NH3 and HCl. When H2S is added, resistance increases account for a minor part of the 0.06 V decline observed for each cell over the first 24 hours. However, cell resistances thereafter change linearly, along with linearly declining voltages. In this latter phase, resistance accounts for a major part of each observed cell voltage decline. The same two SOFC'swere subsequently continued in operation, but at a moderately higher temperature, 1025 C. As Figure 2 demonstrates, No. 1 cell tended to decline more slowly, and No. 2 cell continued to decline at the same rate as before, when it was operating at 1000 C. Later operation, without impurities, at 1025 C for 450 hours served to improve performance and stabilize the cells. When operation at 1000 C resumed, the cell resistance trend lines returned to approximately the original R vs. t slopes observed during 0-500 hours on test, signifying cessation of impurity-related voltage degradation. DOE

N93-15384# Sandia National Labs., Albuquerque, NM.
FREQUENCY-DOMAIN SYNTHESIS OF THE FATIGUE LOAD SPECTRUM FOR THE NPS 100-kW WIND TURBINE
H. J. Sutherland and R. M. Osgood 28 Aug. 1992 19 p Presented at the Windpower 1992, Seattle, WA, 19-23 Oct. 1992
(Contracts DE-AC04-76DP-00789; DE-FC02-86CH-10311)
(DE92-040984; SAND-92-0611C; CONF-921049-1) Avail: CASI HC A03/MF A01

The LIFE2 code is a fatigue/fracture mechanics code that is specialized to the analysis of wind turbine components. This code permits the analysis of both time series and frequency domain data. Two frequency-domain stress spectra techniques contained in this code are used to analyze the measured frequency loads spectra from the Northern Power Systems 100-kW turbine. In the first, the cycle content is determined using the entire stress spectrum, an FFT, and a rainflow counter. In the second technique, the cycle content is determined using time series data for the deterministic (azimuth average) loads and frequency spectra data for the non-deterministic (random) loads. Results of the two techniques are compared to cycle counts obtained directly from time series data. These results provide the wind turbine designer with two techniques for determining the cycle-counts from frequency data and illustrate the accuracy that the designer can expect from various cycle-counting techniques. Moreover, these results illustrate the importance of relatively long time series data on the determination of the high-stress tail in the distribution of the stress cycles. DOE

N93-15467# California Univ., Berkeley. Lawrence Berkeley Lab.
WORLD ENERGY: BUILDING A SUSTAINABLE FUTURE
L. Schipper and S. Meyers Apr. 1992 118 p
(Contract DE-AC03-76SF-00098)
(DE93-001598; LBL-32385) Avail: CASI HC A06/MF A02

As the 20th century draws to a close, both individual countries and the world community face challenging problems related to the supply and use energy. These include local and regional environmental impacts, the prospect of global climate and sea level change associated with the greenhouse effect, and threats to international relations in connection with oil supply or nuclear proliferation. For developing countries, the financial cost of providing energy to provide basic needs and fuel economic development pose an additional burden. To assess the magnitude of future problems and the potential effectiveness of response strategies, it is important to understand how and why energy use has changed in the post and where it is heading. This requires study of the activities for which energy is used, and of how people and technology interact to provide the energy services that are desired. The authors and their colleagues have analyzed trends in energy use by sector for most of the world's major energy-consuming countries. The approach we use considers three key elements in each sector: the level of activity, structural change, and energy intensity, which expresses the amount of energy used for various activities. At a disaggregated level, energy intensity is indicative of energy efficiency. But other factors besides technical efficiency also shape intensity. DOE

N93-15484# California Univ., Berkeley. Lawrence Berkeley Lab.
EXPLORATORY TECHNOLOGY RESEARCH PROGRAM FOR ELECTROCHEMICAL ENERGY STORAGE
K. Kinoshita, ed. Jun. 1992 49 p
(Contract DE-AC03-76SF-00098)
(DE93-001595; LBL-32212) Avail: CASI HC A03/MF A01

The U.S. Department of Energy's Office of Propulsion Systems provides support for an electrochemical energy storage program, that includes research and development (R&D) on advanced rechargeable batteries and fuel cells. A major goal of this program is to develop electrochemical power sources suitable for application in electric vehicles. The program centers on advanced systems that offer the potential for high performance and low life-cycle costs. The DOE Electrochemical Energy Storage Program is divided into two projects: the Electric Vehicle Advanced Battery Systems Development (EVABS) Program and the Exploratory Technology Research (ETR) Program. The EVABS Program management responsibility has been assigned to Sandia National Laboratory, and the Lawrence Berkeley Laboratory is responsible for management of the ETR Program. The EVABS and ETR Programs include an integrated matrix of R&D efforts designed to advance progress on several candidate electrochemical systems. The United States Advanced Battery Consortium (USABC), a tripartite undertaking between DOE, the U.S. automobile manufacturers and the Electric Power Research Institute (EPRI), was formed in 1991 to accelerate the development of advanced batteries for consumer EVs. The role of the ETR Program is to perform supporting research on the advanced battery systems under development by the USABC and EVABS Program, and to evaluate new systems with potentially superior performance, durability and/or cost characteristics. The specific goal of the ETR Program is to identify the most promising electrochemical technologies and transfer them to the USABC, the battery industry and/or the EVABS Program for further development and scaleup. This report summarizes the research, financial and management activities relevant to the ETR Program in FY 1991. DOE

N93-15523*# National Aeronautics and Space Administration. Lewis Research Center, Cleveland, OH.
POWER REQUIREMENTS FOR THE FIRST LUNAR OUTPOST (FLO)
Robert L. Cataldo and John M. Bozek Jan. 1993 11 p Presented at the Tenth Symposium on Space Power and Propulsion, Albuquerque, NM, 10-14 Jan. 1993; sponsored by New Mexico University
(RTOP 590-49-00)
(NASA-TM-105925; E-7427; NAS 1.15:105925) Avail: CASI HC A03/MF A01

NASA's Exploration Program Office is currently developing a preliminary reference mission description that lays the framework from which the nation can return to the Moon by the end of the decade. The First Lunar Outpost is the initial phase of establishing a permanent presence on the Moon and the next step of sending humans to Mars. Many systems required for missions to Mars will be verified on the Moon, while still accomplishing valuable lunar science and in-situ resource utilization (ISRU). Some of FLO's major accomplishments will be long duration habitation, extended surface roving (both piloted and teleoperated) and a suite of science experiments, including lunar resources extraction. Of equal challenge will be to provide long life, reliable power sources to meet the needs of a lunar mission. Author

N93-14930# Spar Aerospace Ltd., Weston (Ontario).
PHOTOVOLTAIC POWER SYSTEM FOR A LUNAR BASE
Kris Karia *In* Canadian Space Agency, Proceedings of the Sixth CASI Conference on Astronautics 1990 10 p Previously announced in IAA as A91-34936 (For primary document see N93-14920 04-12)
Avail: Canadian Aeronautics and Space Inst., 222 Somerset St. W., Suite 601, Ottawa, Ontario K2P 0J1 Canada

N93-14957# Spar Aerospace Ltd., Weston (Ontario).
ON SOME KINEMATIC AND MASS CHARACTERISTICS OF FOLDABLE SOLAR ARRAYS
Thomas Szirtes *In* Canadian Space Agency, Proceedings of the Sixth CASI Conference on Astronautics 1990 22 p Previously announced in IAA as A91-34963 (For primary document see N93-14920 04-12)
Avail: Canadian Aeronautics and Space Inst., 222 Somerset St. W., Suite 601, Ottawa, Ontario K2P 0J1 Canada

45 ENVIRONMENT POLLUTION

Includes atmospheric, noise, thermal, and water pollution.

N93-14118 Carnegie-Mellon Univ., Pittsburgh, PA.
MULTISCALE MODELING OF THE LONG-RANGE TRANSPORT AND FATE OF POLLUTANTS EMITTED FROM URBAN AREAS Ph.D. Thesis
Mehmet Talat Odman 1992 124 p
Avail: Univ. Microfilms Order No. DA9224212

Air quality models relate future air quality to changes in pollutant emissions. Though many aspects of current models have matured, there is a well acknowledged gap in capturing the effects of urban emissions onto regional pollutant dynamics. This work focuses on several modeling issues concerning the long-range transport and chemistry of pollutants emitted from urban and industrial sources. A multiscale model was developed that increases horizontal resolution in areas where pollutant concentration gradients are large. This enables detailed and accurate treatment of the transport from urban to regional areas. The model also uses coarse resolution over rural areas, hence enables modeling of large regions efficiently. The central component of the multiscale model is the horizontal transport scheme. The scheme solves the advection-diffusion equation using the linear Petrov-Galerkin method. This method yields high-order accurate solutions. Any spurious waves that are generated near sharp gradients are eliminated by applying a nonlinear smoothing filter. The resolution of this scheme is increased in areas of interest by using local finite element refinements. One major task in this research has been the investigation of simple test cases that would reveal the performance characteristics of model components. It was shown that the more popular tests may not always be reliable and new test problems were proposed. The model was applied to a 3-day period over Southern California. A fine-scaled uniform grid and a multiscale grid were used in the simulations. The results obtained from both grid systems were very similar within the fine-resolution portion of the multiscale domain. This shows that the multiscale model is able to approach fine-grid accuracy while considerably improving efficiency through the incorporation of coarser grids. The model predictions compared favorably with the observed air quality fields. Multiscale modeling will lead to much improved understanding of pollutant dynamics in regions with dense urban-to-rural transitions. Dissert. Abstr.

N93-14261# Naval Postgraduate School, Monterey, CA.
SATELLITE DETECTION OF COMPLEX AEROSOLS OVER THE ARABIAN PENINSULA/GULF M.S. Thesis
William P. Morgan Mar. 1992 118 p
(AD-A256085) Avail: CASI HC A06/MF A02

Satellite detection of complex aerosols, in particular, oil smoke over

water and dust over land, is generally difficult. On 1 March 1991, a smoke plume generated by burning Kuwaiti oil wells and a dust storm over the southwestern Arabian Peninsula, provide the opportunity to study both of these effects. Utilizing NOAA-11 AVHRR data, a two dimensional scatter plot analysis technique was employed to determine and classify the radiative signatures of the smoke and dust. A two dimensional mask routine was then used to assess the reliability of the scatter plot analyses and spatially display the results. A channel 1 to channel 2 radiance ratio and a channel 4 brightness temperature combination provided the best separation of the smoke signature from water. The dust plume was unambiguously represented by a channel 5 brightness temperature minus channel 4 brightness temperature image and a channel 4 brightness temperature combination. Together the 2D scatter plot technique and 2D mask form the groundwork for a possible detection algorithm. GRA

N93-14655# Wyle Labs., Inc., El Segundo, CA.
AIR FORCE PROCEDURE FOR PREDICTING NOISE AROUND AIRBASES: NOISE EXPOSURE MODEL (NOISEMAP) Technical Report, Jan. 1989 - Mar. 1992
Carey L. Moulton May 1992 167 p
(AF Proj. 622-02-F-7231)
(AD-A255769; AL-TR-1992-0059) Avail: CASI HC A08/MF A02

NOISEMAP was the name given to the original Fortran program, developed for the USAF in the mid 1970's to calculate total noise exposure around military airbases. NOISEMAP now refers to a suite of programs that automate the noise exposure calculation process from operations data collection to final contour plotting. The noise calculation part of this suite of programs is now called NMAP 6.1 (the 6.1 being the current version number). New algorithms for calculating lateral attenuation and an expanded database are included in this version 6.1. NOISEMAP has also been rehosted from operation on a CDC mainframe computer to run on a desktop microcomputer (IBM compatible). This report is a technical overview of the algorithms used in NMAP 6.1. Most of these algorithms were originally outlined by Dr William Galloway in the report 'Community Noise Exposure Resulting from Aircraft Operations: Technical Review' published in November 1974. This report covers all the current algorithms used in NMAP 6.1 and includes an example computation for a single aircraft takeoff and ground runup operation. GRA

N93-14739# Mason and Hanger-Silas Mason Co., Inc., Amarillo, TX.
MANAGEMENT AND MINIMIZATION OF PHOTOGRAPHIC WASTES AT PANTEX PLANT
J. Greg Locke Jan. 1992 10 p
(Contract DE-AC04-91AL-65030)
(MHSMP-92-01; UC-602) Avail: CASI HC A02/MF A01

There are a variety of photographic processes in use at Pantex Plant. This report describes our approach to minimization of these various waste streams. The wastewater discharge from the Photo Lab has been reduced from 17,400 to 2,400 gallons/month by the use of wash water recirculation. Use of an evaporation system has reduced liquid effluents by 90 percent. When installed, the water recirculation systems in X-ray will reduce wastewater discharge from 112,500 to 5,600 gallons/month. Author

N93-14764*# Alabama Univ., Huntsville. Center for Applied Optics.
SURFACE EVALUATION OF UV-DEGRADED CONTAMINATION Final Report
Robert Connatser and James B. Hadaway Sep. 1992 12 p
(Contract NAS8-36955)
(NASA-CR-184500; NAS 1.26:184500) Avail: CASI HC A03/MF A01

Three different areas of work were accomplished under this contract: (1) contamination testing and evaluation; (2) UV irradiation testing; and (3) surface evaluation testing. Contamination testing was generally performed in the In-Situ Contamination Effects Facility at Marshall Space Flight Center (MSFC). UV irradiation testing was also performed primarily at MSFC, utilizing facilities there. Finally, the surface evaluation was done at facilities at UAH Center for Applied Optics. Author

N93-15063# Westinghouse Savannah River Co., Aiken, SC.
PERFORMING WIND-TUNNEL MODELING FOR BETTER MANAGEMENT OF NEAR-FIELD RISKS
Ju-Chrong Huang and A. H. Weber 1992 21 p Presented at the 1992 Energy Facility Contractors Group Analysis Workshop, Salt Lake City, UT, 11-13 Aug. 1992
(Contract DE-AC09-89SR-18035)
(DE92-040205; WSRC-MS-92-211; CONF-9208117-12) Avail: CASI HC A03/MF A01

All industrial complexes must be able to demonstrate that air pollutant concentrations from normal and accidental releases are within the bounds of stringent acceptance criteria. The offsite concentrations are comparatively easy to compute with the standard Gaussian models. By contrast, the onsite (in particular, near-field) concentrations can be more complex since the wind flows can interact with various structures in complex ways to create regions of relatively high local concentrations. Three methods can be used to predict the air pollutant concentrations: (1) mathematical models, (2) field experiments, and (3) fluid models (wind-tunnel testing). The complex flow in the vicinity of buildings is not amenable to simple mathematical generalizations. Field experiments cannot encompass the wind spectrum of meteorological conditions in the time generally allotted. Wind tunnel testing works best where numerical models fail and field testing is not applicable. This paper covers the following aspects related to the wind-tunnel modeling studies: (1) planning strategies; (2) types of wind-tunnel modeling studies -- flow visualization and concentration measurement experiments; (3) highlights (video tape show) of the wind tunnel experiments; (4) technical challenges; and (5) various applications. DOE

N93-15209# Argonne National Lab., IL.
COMPARISON OF THE PREVALENCE INDEX AND AVERAGE WETLAND VALUES FOR IDENTIFICATION OF WETLAND VEGETATION
R. E. Zimmerman, L. M. Shem, M. J. Gowdy, G. D. VanDyke (Trinity Christian Coll., Palos Heights, IL.), and C. T. Hackney (North Carolina Univ., Wilmington.) 1992 6 p Presented at the 13th Annual Meeting of the Society of Wetlands Scientists (SWS), New Orleans, LA, 31 May - 6 Jun. 1992
(Contract W-31-109-eng-38)
(DE92-016701; ANL/CP-75445; CONF-9205204-2) Avail: CASI HC A02/MF A01

Prevalence index values (FICWD, 1989) and average wetland values for all species present were compared for three wetland gas pipeline rights-of-way (ROWS) and adjacent natural areas. The similarities in results using these two indicator values suggest that an average wetland value may offer a simpler, less time-consuming method of evaluating the vegetation of a study site as an indication of wetness. Both PIVs and AWVs, are presented for the ROWs and the adjacent natural area at each site. DOE

N93-15217# Planning Research Corp., Cincinnati, OH.
TECHNOLOGY EVALUATION REPORT: THE CARVER-GREENFIELD PROCESS, DEHYDRO-TECH CORPORATION
Aug. 1992 230 p
(Contract EPA-68-CO-0047)
(PB92-217462; EPA/450/R-92/002) Avail: CASI HC A11/MF A03

The ability was evaluated of Dehydro-Tech Corp. (DTC) Carver-Greenfield Process to separate oil contaminated waste drilling muds to their constituent solids, oil and water fractions. The C-G was developed by DTC and is licensed. The technology is designed to separate solid-liquid mixtures into three product streams: a clean, dry solid; a water product substantially free of solids and organics; and a concentrated mixture of extracted organics. A mobile pilot plant was used for the demonstration. The C-G process demonstrated using waste drilling muds from the PAB Oil and Chemical Services, Inc. site in Vermilion Parish, LA. PAB Oil operated three oil drilling mud separation pits from which the waste material used in the demonstration was collected. GRA

N93-15270# Oak Ridge National Lab., TN.
DATA ANALYSIS AND INTERPRETATION FOR ENVIRONMENTAL SURVEILLANCE
Jun. 1992 149 p Presented at the Data Analysis and Interpretation for Environmental Surveillance Conference, Lexington, KY, 5-7 Feb. 1990
(Contract DE-AC05-84OR-21400)
(DE92-019009; CONF-9002111) Avail: CASI HC A07/MF A02

The Data Analysis and Interpretation for Environmental Surveillance Conference was held in Lexington, Kentucky, February 5 to 7, 1990. The conference was sponsored by what is now the Office of Environmental Compliance and Documentation, Oak Ridge National Laboratory. Participants included technical professionals from all Martin Marietta Energy Systems

facilities, Westinghouse Materials Company of Ohio, Pacific Northwest Laboratory, and several technical support contractors. Presentations at the conference ranged the full spectrum of issues that effect the analysis and interpretation of environmental data. Topics included tracking systems for samples and schedules associated with ongoing programs; coalescing data from a variety of sources and pedigrees into integrated data bases; methods for evaluating the quality of environmental data through empirical estimates of parameters such as charge balance, pH, and specific conductance; statistical applications to the interpretation of environmental information; and uses of environmental information in risk and dose assessments. Hearing about and discussing this wide variety of topics provided an opportunity to capture the subtlety of each discipline and to appreciate the continuity that is required among the disciplines in order to perform high-quality environmental information analysis. DOE

N93-15272# State Univ. of New York, Albany.
SPATIAL AND TEMPORAL PATTERNS OF BIOTIC EXCHANGES OF CO2 BETWEEN THE ATMOSPHERE AND TROPICAL LANDSCAPES AND THEIR ROLE IN THE GLOBAL CARBON BALANCE
1992 10 p
(Contract DE-FG02-90ER-61080)
(DE92-019170; DOE/ER-61080/2) Avail: CASI HC A02/MF A01

At SUNY ESF, our overall objective for this year was to finish refining the methods used to convert our previous models of global carbon flux and land use change into a GIS-compatible format. We now have the ability to obtain, convert, and incorporate geographic data into spatial simulation models that describe past carbon exchange patterns, as well as predict future land use change and carbon exchange. Our initial tests of this model in Peninsula Malaysia have been very promising, in that we are able to successfully predict land use from 1972 to 1982 and even from 1870 to 1970. In this context 'successful' means that we classify in the model from 80 to 95 percent of the cells correctly, depending upon the number of land use types we try to predict. We are now preparing to apply this model to the entire continent of Africa and to Central America. DOE

N93-15273# Oak Ridge National Lab., TN.
ECOLOGICAL IMPLICATIONS OF LANDSCAPE FRAGMENTATION
R. H. Gardner, R. V. ONeill, and M. G. Turner 1991 28 p Presented at the 1991 Cary Conference on Humans As Components of Ecosystems, Millbrook, NY, 4-8 May 1991
(Contract DE-AC05-84OR-21400)
(DE92-019186; CONF-9105365-1) Avail: CASI HC A03/MF A01

The effects of scale-dependent changes in habitat patterns were investigated by simulating two consumer populations on random and hierarchically random landscapes. The first consumer depleted resources as it randomly walked across the landscape, while the second consumer spread outwards to suitable sites from an initial point. Simple random landscapes were generated by randomly selecting the habitat suitability of each site, while hierarchically random maps were generated by a nested series of rules which changed the probabilities with spatial scale. These two map types were compared to digitized land-use data. Three effects were observed: (1) the reduction of available habitat always reduced population abundance and spread; (2) small changes in landscape pattern produced sudden changes in abundance which could be predicted from the interaction between landscape characteristics and population specific life history parameters; and (3) the hierarchically structured landscapes affected abundances most when habitat fragmentation coincided with the scales at which the consumer populations utilized spatial resources. DOE

N93-15280# Lawrence Livermore National Lab., CA.
A CORRELATED k-DISTRIBUTION MODEL OF THE HEATING RATES FOR CO2 AND O3 IN THE ATMOSPHERE BETWEEN 0 AND 60 km
A. S. Grossman and K. Grant 25 Jul. 1992 15 p
(Contract W-7405-eng-48)
(DE93-000889; UCRL-ID-111805) Avail: CASI HC A03/MF A01

A prototype infrared radiative transfer model using a correlated k-distribution technique to calculate the transmission between atmospheric levels has been used to calculate the radiative fluxes and heating rates for CO2 and O3 in the atmosphere between 0 and 60 km. For CO2 the 15, 10, and 4.3 micron bands are included and for O3 the 9.6 and 14 micron bands are included. The major heating/cooling effects are due to the 15 micron band of CO2 and the 9.6 micron band of O3. The computational efficiency of the k-distribution technique allows 50 cm(exp -1) wave number bins to produce fluxes and heating rates which are within ten percent of the results of detailed line by line calculations. DOE

N93-15281# Lawrence Livermore National Lab., CA.
A CORRELATED k-DISTRIBUTION MODEL OF THE ATMOSPHERIC HEATING RATES FOR OVERLAPPING SPECTRA OF CH4 AND N2O
K. E. Grant and A. S. Grossman 25 Jul. 1992 13 p
(Contract W-7405-eng-48)
(DE93-000890; UCRL-ID-111804) Avail: CASI HC A03/MF A01

The problem of overlapping the spectra of CH4 and N2O in the 7-9 micron wavelength band has been considered using a correlated K-distribution model for the transmission in the atmosphere between 0 and 60 km. Individual k-distributions for the two gases have been combined using an overlap model to produce k-distributions for the mixture of CH4 plus N2O. A prototype radiative transfer model has been used to calculate atmospheric heating rates and fluxes. The results of the overlap model have been compared to detailed line-by-line calculations, as well as the results of a correlated k-distribution model of the combined mixture. The heating rates for the overlap model agree to about 1 percent with the combined mixture values and the line-by-line values. DOE

N93-15460 Institut d'Aeronomie Spatiale de Belgique, Brussels.
GEOGRAPHICAL DISTRIBUTION AND SEASONAL VARIATION OF SURFACE EMISSIONS AND DEPOSITION VELOCITIES OF ATMOSPHERIC TRACE GASES
Jean-Francois Mueller (Belgian National Foundation for Scientific Research, Brussels.) 1991 74 p Submitted for publication
(Aeronomica-Acta-A-361-1991; ETN-92-92269) Copyright Avail: Institut d'Aeronomie Spatiale de Belgique, 3 Avenue Circulaire, B-1180 Brussels, Belgium

The geographical distributions on the global scale of trace gas surface emission and deposition are established on the basis of a variety of technical, geographic and climatic data. Five by five deg resolution maps of the sources and deposition velocities are constructed, which can be used as surface boundary conditions in the three dimensional chemical/transport model of the troposphere. Special attention is devoted to emissions of CO, NO(x), and several non-methane hydrocarbons, and to the fossil fuel emissions of methane. Anthropogenic sources, i.e. the emissions produced or controlled by human activities, represent about 75 percent or more of the total surface emissions of CO, CH4, SO(x) and NO(x), and about two thirds of the total production of atmospheric CO (from surface sources and atmospheric oxidation of hydrocarbons). The possibility arises that methane releases from natural gas exploitation in the USSR are substantially larger than accounted for in previous studies, implying possible important consequences for the methane budget. ESA

N93-15480*# Colorado State Univ., Fort Collins. Metabolic Lab.
MODELLING GLOBAL METHANE EMISSIONS FROM LIVESTOCK: BIOLOGICAL AND NUTRITIONAL CONTROLS Final Report, 1 Jul. 1989 - 30 Jun. 1992
Donald E. Johnson 15 Oct. 1992 80 p
(Grant NAGw-1829)
(NASA-CR-191354; NAS 1.26:191354) Avail: CASI HC A05/MF A01

The available observations of methane production from the literature have been compiled into a ruminant methane data base. This data base includes 400 treatment mean observations of methane losses from cattle and sheep, and minor numbers of measurements from other species. Methane loss varied from 2.0 to 11.6 percent of dietary gross energy. Measurements included describe the many different weights and physiological states of the animals fed and diets ranging from all forage to all concentrate diets or mixtures. An auxiliary spreadsheet lists approximately 1000 individual animal observations. Many important concepts have emerged from our query and analysis of this data set. The majority of the world's cattle, sheep, and goats under normal husbandry circumstances likely produce methane very close to 6 percent of their daily diets gross energy (2 percent of the diet by weight). Although individual animals or losses from specific dietary research circumstances can vary considerably, the average for the vast majority of groups of ruminant livestock are likely to fall between 5.5 to 6.5 percent. We must caution, however, that little experimental data is available for two-thirds of the world's ruminants in

developing countries. Available evidence suggests similar percentage of emissions, but this supposition needs confirmation. More importantly, data is skimpy or unavailable to describe diet consumption, animal weight, and class distribution. Author

46 GEOPHYSICS

Includes aeronomy; upper and lower atmosphere studies; ionospheric and magnetospheric physics; and geomagnetism.

For space radiation see *93 Space Radiation.*

N93-14117 Georgia Inst. of Tech., Atlanta.
AN INVESTIGATION OF TRANSIENT ATMOSPHERIC INORGANIC PEROXIDES: A THEORETICAL AND EXPERIMENTAL STUDY Ph.D. Thesis
Vernon Robinson Morris 1991 144 p
Avail: Univ. Microfilms Order No. DA9223788

A combined theoretical and experimental study has been performed to characterize the peroxy isomers of NO3 and ClO2. Inorganic peroxy radicals are known to play key roles in chemical cycles controlling ozone in both the urban and remote troposphere as well as in the midlatitude and polar stratosphere. They may also be important in heterogeneous processes in the atmosphere. Until recently, because of their inherent lability and/or rapid dissociation, structural, spectroscopic, and thermodynamic information on the peroxy isomers of free radicals and intermediates involved in the NO(X) and ClO(X) cycles were virtually unknown. Despite the recent advances in obtaining detailed thermodynamic information for the symmetric forms of these free radicals (sym-NO3 and OClO), there remain significant uncertainties regarding their structural isomers, bonding patterns, relative stabilities, electronic states, and spectroscopic constants. This thesis presents the results of ab-initio Self-Consistent Field (SCF) calculations performed at the Hartree-Fock and Mfller-Plesset levels of theory for the electronic structure, equilibrium geometries, harmonic frequencies, and relevant thermodynamic parameters for transient peroxy isomers of NO3 and ClO2. Harmonic frequency analysis and calculation of isotopic shifts for several isomers of sym-NO3 suggest a C(2u) equilibrium geometry. Energy and thermochemical analysis of the C(s) peroxy isomers of NO3 indicate that its formation is favorable in the NO2 plus O3 reaction. Frequency analysis of cis and trans-OONO identify intense absorptions for the NO2 asymmetric stretching and rocking modes in addition to the N = O stretching. The isomerization of OClO to ClOO has also been investigated. The results indicate that the isomerization may be favorable as an adiabatic process rather than the Herzberg-Teller allowed mechanism previously suggested. Calculated thermochemical constants for ClOO are in good agreement with experiment but extensive frequency analysis indicates strong electron correlation in the bonding of this molecule. In addition to the theoretical analysis, experimental studies employing the matrix-isolation technique coupled with infrared spectroscopy have also been performed. Spectral analysis of the product spectra indicate that both symmetrical nitrate and peroxynitrite are formed in the NO2 plus O3 reaction. The observed product distribution suggests that OONO reactivity is dominated by rapid dissociation to NO and O2 and reaction with NO2. Dissert. Abstr.

N93-14121 New Hampshire Univ., Durham.
FINE STRUCTURE OF AURORAL PARTICLE ACCELERATION Ph.D. Thesis
Kristina Anne Lynch 1992 204 p
Avail: Univ. Microfilms Order No. DA9225256

A mass-analyzing capped hemispherical electrostatic analyzer was developed for the purpose of resolving the mass, energy, and pitch angle distributions of auroral ions. The instrument, the B-field Hemispherical Electrostatic Energy and Pitch Angle Spectrometer (BEEPS), is an extension of the HEEPS instrument, which uses a hemispherical analyzer and microchannel plates to measure the angular and energy distribution of ions. BEEPS uses a toroidal magnetic field constructed from rare-earth permanent magnets to separate ion measurements into two groups, protons and heavier ions. BEEPS was flown in February, 1991, from Poker Flat, Alaska, on the TOPAZ3 sounding rocket. This sounding rocket mission carried a full array of particle and field instrumentation to an altitude of over 1000 km. Electron data from the flight are presented and discussed in detail, and are shown in light of both ion and wave data taken during the same flight. Correspondences between the various data sets are presented. Particular note is made of the observation that ion heating seems to correspond with a field-aligned plateau in the electron distribution function below the peak electron energy. The growth rate of the n = -1 anomalous Doppler resonance of medium energy electrons with lower hybrid waves is discussed, and proposed as a mechanism for converting energy from the auroral electrons, the driver of the auroral activity, to the ion heating events. Dissert. Abstr.

N93-14177 Minnesota Univ., Minneapolis.
AN ANALYSIS OF THE SCEX 3 IONOSPHERIC ELECTRON BEAM INJECTION EXPERIMENT Ph.D. Thesis
Roger Theodore Goerke 1992 255 p
Avail: Univ. Microfilms Order No. DA9217664

The SCEX 3 experiment (Several Compatible EXperiments using a rocket-borne accelerator) was carried to ionospheric altitudes (375 km) by a Black Brant 11 rocket on February 1, 1990. The experiment was launched from Poker Flat Research Range (65.1 degree N, 147.5 degree W) at 1207 UT. The payload split into two parts (hereafter forward and aft payloads) 116 seconds after launch. The aft payload carried two electron accelerators as well as several diagnostic instruments. The forward payload was ejected at an angle of 6 degree with the magnetic field in a northwesterly direction. This payload carried a multiband plasma wave receiver and various particle detectors to make in situ measurements of the Beam Plasma Interaction (BPI) region. Two Throw Away Detectors (TAD's 1 and 2) were also ejected from the aft payload in the east and west directions respectively. TAD 1 also carried a multiband plasma wave receiver. Preceding the launch an auroral arch along the southern boundary of a diffuse auroral patch suddenly brightened, split into two separate arcs and moved to a position north of the rocket's trajectory. SCEX 3 was launched into an active breakup aurora consisting of tall rays and diffuse patches. The purpose of this experiment were (1) to observe injected electrons reflected from the naturally occurring parallel electric field structures which are thought to accelerate the auroral electron, (2) to observe a variety of plasma effects caused by the artificial electron beam and the associated spacecraft charging, and (3) study the natural phenomena associated with auroral activity. This work is a summary of the interesting observations made by the SCEX 3 experiment. These observations include VHF emissions produced by the electron beam via the Beam Plasma Discharge (BPD), Diffuse resonance emissions by the hot plasma region surrounding the electron beam and auroral Z-mode emissions. The response of the plasma to the initiation of the electron beam injection will also be discussed.

Dissert. Abstr.

N93-14178 Illinois Univ. at Urbana-Champaign, Savoy.
CARBON DIOXIDE INDUCED OCEAN CLIMATIC CHANGE AND TRACER EXPERIMENT WITH AN ATMOSPHERE-OCEAN GENERAL CIRCULATION MODEL Ph.D. Thesis
Xingjian Jiang 1991 313 p
Avail: Univ. Microfilms Order No. DA9210851

The principal objective of this study is to determine whether or not the penetration of a passive tracer is analogous to the penetration of a greenhouse-gas-induced heating. The Atmosphere Ocean General Circulation Model (A-O GCM) has been used to study CO2-induced climate change and the penetration of passive tracers into the world ocean. The present climate and a 2 x CO2 climate have been simulated. The passive tracers tritium, CFC-11, CFC-12 and a 'passive CO2- induced heating' are simulated. The CO2-induced active and passive warmings are larger in the subtropics and high latitudes than in the tropics. The largest difference between the active and passive CO2-induced heatings occur in the North Atlantic deep ocean, with maximum cooling about -1.5C for the active case in layer four of the ocean (1150m). There is no hemispherically asymmetric warming as that found by Manabe et al. (1990) and Stouffer et al. (1990). The convective overturning and large-scale sinking motion are responsible for the large penetration of CO2-induced warming in high latitudes. The CO2-induced circulation changes show that the North Atlantic thermohaline circulation is significantly weakened due to the penetration of CO2-induced heating. Associated with this change, the strength of North Atlantic conveyor belt is reduced, which results in a large warming in the upper ocean and cooling in the deep layers. The characteristic response time ranges from 40-50 years for the active CO2-induced climate change, and 70-160 years for passive CO2-induced climate change. The physical processes controlling

the geochemical tracer penetration are very similar to those for the CO2-induced heating. There is not a single tracer which penetrates into the ocean exactly like the active CO2-induced heating in terms of distribution, transport or physical process. CFC's may be the best candidate as a surrogate for the CO2-induced oceanic climate study. The model is capable of simulating the observed ocean-atmosphere pCO2 difference (delta-pCO2) in most areas. However, the model cannot simulate the observed magnitude and detailed geographical distribution of delta-pCO2 because they are also determined by the organic and biological processes which are neglected in the present study. Dissert. Abstr.

N93-14199 Michigan Univ., Ann Arbor.
A STUDY OF MID-LATITUDE 5577 A OI DAYGLOW EMISSIONS Ph.D. Thesis
Edward Eugene Hume, Jr. 1992 272 p
Avail. Univ. Microfilms Order No. DA9226922

The green line (5577 A) is a bright, persistent component of the visible airglow that is produced by an electric quadrupole transition from the meta-stable second excited state (S0-1) to the first excited state (D2-1) of atomic oxygen. In this thesis, production and loss mechanisms important to the F-region dayglow 5577 A emission are investigated. Four major source reactions need to be incorporated in the modeling of the emission profile, photoelectron impact on atomic oxygen, dissociative recombination of O2(+), quenching of N2(A3 Sigma u +) by atomic oxygen, and photo-dissociation of O2 which becomes more important below the emission peak. For some of the reactions, the properties of the rate coefficients, branching ratios, and cross sections are not well known. Models are used to determine the rate coefficient, branching ratios, and cross sections for these reactions based on observations. The impact of photoelectrons on atomic oxygen is the primary source of 5577 A dayglow emission in the thermosphere. The observed profiles of 5577 A emission are best reproduced by the impact cross sections of Henry et al. (1969). This is in a good agreement with the latest theoretical cross sections of Berrington and Burke (1991, Personal Communication) but about a factor of two smaller than the cross sections measured by Shyn et al. (1986). The quenching of N2 (A) by atomic oxygen is an important source of the 5577 A emission at the peak in the layer. The total quenching rate was determined using a vibrational model and a band model for N2 to study emissions at 3371 A from the Atmosphere Explorer satellite. The value of the rate coefficient deduced here agrees well with experimental values by Piper and Caledonia (1981) and Thomas and Kaufman (1985). The effective branching ratio determined by this study tends to support the results from Piper (1982) and De Souza et al (1985). The effect of the distribution of the vibrational population of the N2(A3 Sigma u +) state on the branching ratio is also discussed. The extension of the dayglow photochemistry into the twilight is also investigated. The model developed for the dayglow can reasonably reproduce the rapidly changing twilight emissions. Dissert. Abstr.

N93-14207 California Univ., San Diego.
THE ISOTOPES OF CARBON MONOXIDE IN THE FREE TROPOSPHERE AND THEIR IMPLICATIONS TO ATMOSPHERIC CHEMISTRY Ph.D. Thesis
John Eugene Mak 1992 117 p
Avail: Univ. Microfilms Order No. DA9227866

My thesis project was designed to provide information for answering the following questions: What is the oxidative capacity of the troposphere, and how are the source strengths of carbon monoxide partitioned? Because of its active role in tropospheric chemistry, carbon monoxide is important in determining the fate of a number of species, including hydroxyl radicals. OH is responsible for the oxidation of most hydrocarbons and many other reduced trace gas species, including carbon monoxide C-14O in atmospheric CO serves as a natural tracer for its destruction, as the source function can be well constrained. By determining the tropospheric inventory of C-14O and calculating its source strength, one may realize the rate of destruction. Similarly, because certain sources have unique stable isotope signatures, an analysis of the stable isotopes provides information on the relative strengths of those sources. This enables the partitioning of anthropogenic sources (such as biomass burning and fossil fuel combustion) from natural pathways (e.g., hydrocarbon oxidation). The airborne sampling system which has been built for the collection of large (1000 liters) air samples is discussed, with particular attention given to the modifications necessary to ensure the integrity of the samples. The methodology for extraction and analysis of carbon monoxide is also discussed. C-14O, C-13O, CO-18, and CO concentration results are presented and interpreted. For the C-14O data, a two dimensional transport model has been used to help relate C-14O to OH. Based on this analysis there exists a possibility of a sink for carbon monoxide which may be as large as 35 percent of the presently known sink strength. The stable isotopes are used to constrain the relative contributions from various sources between the two hemispheres. Dissert. Abstr.

N93-14211 Johns Hopkins Univ., Baltimore, MD.
REVELATIONS OF A STRATOSPHERIC CIRCULATION: THE DYNAMICAL TRANSPORT OF HYDROCARBONS IN THE STRATOSPHERE OF URANUS Ph.D. Thesis
William Wallace McMillan 1992 301 p
Avail: Univ. Microfilms Order No. DA9229368

Observations by the Ultraviolet Spectrometer (UVS) onboard the Voyager 2 spacecraft revealed that above the 1 mb level, the mixing ratios of CH4, C2H2, and C2H6 are at least 10-100 times larger at the equator than at the south pole. In addition, the Voyager 2 Infrared Interferometric Spectrometer (IRIS) measured small meridional temperature gradients at the tropopause (60-200 mb) and in the upper troposphere (200-1000 mb) of Uranus. These temperature gradients result from a weak meridional circulation in the Uranian troposphere which penetrates into the stratosphere with upwelling at low southern latitudes and polar subsidence (vertical velocities approximately 10(exp -6) m/s, meridional velocities approximately 10(exp -3) m/s). The role of the zonally-averaged, meridional stratospheric circulation in determining the distribution of hydrocarbons in the stratosphere (0.1-100 mb) of Uranus is investigated with a 2-dimensional photo-chemical transport model. The stratospheric circulation is calculated with a linear, zonally-symmetric model with Newtonian cooling and Rayleigh friction similar to that used by Flasar et al. (1987). Operator-splitting is utilized to numerically solve the continuity equations for trace species in the stratosphere of Uranus. It is determined that advective transport by the stratospheric circulation can account for the essential observed meridional variation of stratospheric hydrocarbon abundances. However, vertical transport by eddy and molecular diffusion is required to fit the inferred vertical distribution of hydrocarbons. The uniform eddy diffusion coefficient is constrained to 10 sq cm/s less than K less than 100 sq cm/s (i.e. constant in both altitude and latitude). The best fit model has a meridional circulation three times stronger than the circulation of Flasar et al. and a weak uniform eddy diffusion coefficient, K = 100 sq cm/s. Dissert. Abstr.

N93-14225 California Univ., Berkeley.
IMAGING EARTH'S INTERIOR: TOMOGRAPHIC INVERSIONS FOR MANTLE P-WAVE VELOCITY STRUCTURE Ph.D. Thesis
Robert Jay Pulliam 1991 277 p
Avail: Univ. Microfilms Order No. DA9228820

A formalism is developed for the tomographic inversion of seismic travel time residuals. The travel time equations are solved both simultaneously, for velocity model terms and corrections to the source locations, a progressively, for each set of terms in succession. The methods differ primarily in their treatment of source mislocation terms. Additionally, the system of equations is solved directly, neglecting source terms. The efficacy of the algorithms is explored with synthetic data as we perform simulations of the general procedure used to produce tomographic images of Earth's mantle from global earthquake data. The patterns of seismic heterogeneity in the mantle that would be returned reliably by a tomographic inversion are investigated. We construct synthetic data sets based on real ray sampling of the mantle by introducing spherical harmonic patterns of velocity heterogeneity and perform inversions of the synthetic data. Inversions of real data, supplied by the ISC, are also performed. We use P arrival data from January 1964 through January 1987 and our inversion algorithms to solve for three-dimensional P velocity models of the mantle and source mislocations. The three-dimensional velocity model is presented in conjunction with the resolution estimates produced by an inversion for a checkboard test pattern. Covariance is estimated by averaging results from inversions of realistic errors and by a jacknife procedure. The three-dimensional velocity model shows a fast anomaly in the lower mantle beneath the Tonga-New Hebrides subduction zone to a depth of 1670 km and another fast anomaly beneath the Japanese Island arc and eastern Asia reaching nearly to the core-mantle boundary. Continuity between these anomalies and shallower anomalies is not clear. A fast anomaly extending

from 670 km to 2070 km depend appears beneath the eastern United States, Caribbean Sea, and Central South America. In addition, a number of slow anomalies associated with hotspots extend through the upper mantle but are extinguished in the lower mantle by our resolution weighting. Mid-ocean ridges are associated with moderately slow anomalies in the top 400 km of our model. The transition zone between depths of 400 and 670 km shows large l = 1, 2, and 3 spheical harmonic components. Dissert. Abstr.

N93-14511# Air Force Inst. of Tech., Wright-Patterson AFB, OH.
A STUDY OF MID-LATITUDE 5577A CI DAYGLOW EMISSIONS Ph.D. Thesis
Edward E. Hume, Jr. 1992 252 p
(AD-A255444; AFIT/CI/CIA-92-012D) Avail: CASI HC A12/MF A03

The green line (5577 A) is a bright, persistent component of the visible airglow. It is produced by an electric quadrupole transition from the metastable second excited state (1)S(sub 0) to the first excited state (1)D(sub 2) of atomic oxygen. These two excited states all lie in the same electron shell of the atom and have the same electron configuration as the ground state of 1s(sup 2)2s(sup 2)2p(sup 4), which is the (3)P(sub 2,1,0). This emission is present in both the daytime and night airglow and in the aurora, and despite a long history of study it is still not fully understood. The emission in the dayglow and the nightglow is relatively homogeneous spatially and global in coverage. In the aurora, the emission is much brighter than the airglow, high structured and very localized being restricted to higher latitudes. The structure of the 5577 A emission with altitude and the chemistry responsible for the production of the emission are complex. The vertical structure for the emission has two distinct layers in the airglow each with its own set of production and loss mechanisms. The chemistry for either of these layers is not completely known. The auroral emission is not understood either since it overlaps the upper and lower layer altitudes and it tends to contain some parts of the chemistry of both layers as sources and losses. GRA

N93-14589 Colorado Univ., Boulder.
PRECISION TESTS OF GRAVITATION: LIQUID-SUPPORTED TORSION BALANCE EXPERIMENTS AND A TOWER EXPERIMENT Ph.D. Thesis
Martin Patrick McHugh 1992 143 p
Avail: Univ. Microfilms Order No. DA9232712

The use of a liquid-supported torsion balance (LSTB) in precision tests of gravity is explored. The LSTB uses water at its maximum density point of 4 C for support, and an electrostatic array for the centering force and the linear restoring torque. An optical detection system is used to measure the angular displacement. The LSTB holds 12 test masses arranged in a ring--6 made of copper, 6 made of lead. A proposed new intermediate-range (10 m-1000 m) composition-dependent force was tested using the local mass inhomogeneity of the sub-basement laboratory as the source. Attempts at improving the limits of a possible breakdown of the weak equivalence principle (universal free fall) at longer ranges, using the gravitational field of the sun as the source, were also made using two approaches. One approach was to look for a 24 h period in the torque on the balance due to a differing free fall rate between lead and copper. The other approach is similar except that the balance was rotated with period of 6 h in an attempt to remove the effect of other 24 h period disturbances on the balance. All results were consistent with Newtonian gravity with the accuracy limited by gravity multipole couplings, tilts, and temperature effects. A test of the inverse-square law of gravity was also undertaken on a 300 m tower at Erie, CO. This test is sensitive to the strength and range of a finite-range (Yukawa) force. Surface gravity data was used to predict the Newtonian gravity at eight heights on the tower. The measurements of gravity on the tower were done with LaCoste and Romberg relative gravimeters. The differences between the measured and the predicted values had an rms value of 10 microGal with the value at the 300 m height being 10 plus or minus microGal. Dissert. Abstr.

N93-14641 Colorado State Univ., Fort Collins.
VERTICAL PATH ATMOSPHERIC TURBULENCE: TEMPORAL SPECTRA AND DIFFERENTIAL IMAGE MOTION MEASUREMENTS Ph.D. Thesis
David Brian Soules 1992 172 p
Avail: Univ. Microfilms Order No. DA9231830

The familiar 'twinkling' of starlight is caused by atmospheric turbulence, which is characterized by variations in the index of refraction of the atmosphere from one turbulent cell to the next. As emerging fields such as adaptive optics and high resolution digital imaging continue to progress, there is a strong interest in quantifying the turbulent effects. Lacking the ability to measure fundamental quantities such as the index of refraction in situ over vertical propagation paths, we turn to a parameter known as the transverse coherence length, or r(sub o), to quantify the turbulent effects. A means of determining r(sub o), (which in a rough sense is a measure of the quality of the atmosphere as an optical transmission medium) by measuring differential stellar image motion is presented. Particular attention is paid to the effects of varying the sampling parameters of the detection system used to acquire the data (particularly the frame rate and exposure time) in order to establish suitable bounds for these data acquisition parameters. In addition, the measurements are presented in the form of power spectral density plots, which provide crucial temporal frequency content information for adaptive optics system designers. The power spectral density analysis also suggests that numerous layers within the atmosphere are contributing to the overall image degradation encountered with ground based imaging systems. Dissert. Abstr.

N93-14724# Los Alamos National Lab., NM.
WORKSHOP ON NONINVASIVE GEOPHYSICAL SITE CHARACTERIZATION
Edward VanEeckhout, comp. and Charles Calef, comp. Jul. 1992 37 p
Proceedings of Workshop in Dallas, TX, 29-30 Aug. 1991
(Contract W-7405-eng-36)
(LA-12311-C; UC-903) Avail: CASI HC A03/MF A01

Workshop participants were asked to discuss DOE's needs for waste site characterization and the current status of noninvasive geophysical technology available to satisfy these needs. The initial discussions focused on electromagnetic, ground-penetrating radar, seismic, gravity, and magnetic methods. However, an additional technology, 'data fusion' arose and was added to the list. The ultimate ranking of these technologies (i.e., in the order they would provide the most benefit to the DOE at the most sites, for the least cost, from top down) was as follows: (1) data fusion; (2) electromagnetic; (3) ground penetrating radar; (4) seismic; (5) gravity; and (6) magnetic. Author

N93-14727# SRI International Corp., Menlo Park, CA.
COMPARISON BETWEEN IRREGULARITY MOTION AND BULK PLASMA DRIFTS AT HIGH LATITUDES Final Report, 28 Jul. 1988 - 29 Oct. 1991
Robert C. Livingston and Mary C. McCready Oct. 1991 53 p
(Contract F19628-88-K-0031; AF Proj. 4643)
(PL-TR-91-2292) Avail: CASI HC A04/MF A01

Coincident measurements of ionospheric motion, derived from two different techniques, are compared. This first technique is incoherent-scatter radar measurement of bulk plasma drift; if the plasma flow is uniform within its field of view, the radar provides precise measurements of motion resolved form multiple line-of-sight velocity samples. The second technique is spaced-receiver measurement of kilometer-scale irregularity motion; the velocity is extracted from the diffraction pattern produced by integrated propagation effects along the radio raypath. Detailed comparisons of coincident measurements are made for five experiments in Alaska and Greenland, under a variety of background conditions. When the ionospheric drifts are uniform, the agreement between the two techniques is good. When this is not the case, as is typical near the polar cap boundary, the superior time and spatial resolution of the scintillation technique reveals small-scale flow patterns which are difficult to derive from the radar data. Author

N93-14861 Washington Univ., Seattle.
OPTIMIZATION OF A COUNTERFLOW VIRTUAL IMPACTOR (CVI) FOR STUDYING AEROSOL EFFECTS ON CLOUD DROPLET NUMBER Ph.D. Thesis
Theodore Lynde Anderson 1992 246 p
Avail. Univ. Microfilms Order No. DA9230323

This dissertation considers the problem of collecting cloud droplets in order to study the relationship between droplet-nucleating particles and cloud droplet number concentration. Aerosol-induced modulation of cloud droplet number is potentially significant to global climate. The key activity was optimized of a Counterflow Virtual Impactor (CVI) for performing the cloud droplet collection. This involved numerical modeling of the collection

process, construction and calibration of a new version of the CVI, and deployment of the new CVI in a field experiment. Numerical modeling revealed, with one caveat, the CVI measurements will not be significantly distorted either by droplet evaporation ahead of the collection plane or by droplet collisions during collection. The caveat is that if large (drizzle-size) droplets shatter upon collision with smaller droplets, the measurement of droplet number could be distorted upwards. Laboratory calibration activities showed the new version to perform its size selection as predicted by theory and to have excellent cut sharpness. In addition, evidence of droplet shattering in the presence of large droplets was obtained. Thus, both laboratory and modeling evidence regarding large droplets lead to the suggestion that these be excluded from the inlet in field applications. The field experiment studying coastal stratiform clouds showed the CVI to perform well and to provide a large and unique data set relevant to examining the relationship between aerosol loading (number or volume) and cloud droplet number. Key results were (1) the majority of cloud droplet residue particles were smaller than one-tenth micrometer (diameter) in both clean and continentally influenced conditions, (2) total particle number variations were not correlated to cloud droplet number variations on any time scale, and (3) dominant sources of cloud variation, which tended to obscure the detection of aerosol effects, were meteorology and cloud patchiness.
Dissert. Abstr.

N93-14873 Nevada Univ., Reno.
WAVE DRAG IN THE ATMOSPHERIC BOUNDARY LAYER Ph.D. Thesis
Branko Grisogono 1992 125 p
Avail: Univ. Microfilms Order No. DA9230127

The Reynolds stress caused by surface-generated waves in the atmospheric boundary layer (ABL) can have the same order of magnitude as that conventionally associated with turbulence. A simple implementation of turbulence in an analytical study of wave drag (WD) is based upon suitably modified governing equations (linearized, adiabatic, dry Boussinesq flow, two-dimensionality). In spite of simplifications, it is shown that WD strongly depends on the vertical profiles of the mean wind and temperature, the shape of the orographic disturbances, and eddy diffusivity (a parameterization for turbulence). Since eddy diffusivity is present, WD is not constant with height but continuously dissipated in the ABL. Under typical conditions this dissipation can remove up to 30 percent of WD at the surface. It is qualitatively revealed that WD supports turbulence. Conditions when gravity waves and associated WD can govern dynamics of the ABL and determine the air-transport are identified. Results can be useful for an improvement of mesoscale models and observational analyses.
Dissert. Abstr.

N93-14874 Colorado State Univ., Fort Collins.
LOW-FREQUENCY OSCILLATIONS IN RADIATIVE-CONVECTIVE MODELS Ph.D. Thesis
Qi Hu 1992 209 p
Avail: Univ. Microfilms Order No. DA9231788

Although slow eastward propagation has long been considered one of the essential features of the 30-60 day oscillations in the tropical atmosphere, recent observations have shown the presence of a stationary or quasi-stationary component in the oscillations. This stationary component is significant especially in the thermodynamic fields, e.g., the diabatic heating and the geopotential height. The theories for the low frequency oscillations, derived from the wave-CISK concept, generally have difficulties in explanation of the period and the vertical structure of these oscillations. On the other hand, numerical experiments are providing more and more evidence showing that low frequency waves in the atmosphere are very likely to be excited by cumulus convection which itself varies on long time scales. These numerical results are supported by the observations. In this study our hypothesis is that the low frequency oscillations are forced by a stationary oscillating heat source. Moreover, we propose that the low-frequency oscillating heat source can result from nonlinear interactions among radiation, cumulus convection, and surface moisture flux. Three one-dimensional models, two numerical and one conceptual, are developed to test our hypothesis. The physical processes included in these models are the same, i.e., the atmospheric radiation, cumulus convection, and the surface moisture flux. Results from all three models show the presence of low-frequency oscillations in cumulus convection and latent heat release. In addition, the oscillations disappear from the results when the interactions between radiation and cumulus convection are removed artificially from the models. No oscillations are obtained for the case of a dry atmosphere. The stationary low-frequency oscillating heat source associated with the oscillating cumulus convection can force low frequency oscillations in the winds, and so can excite the observed 30-60 day oscillations in the tropics.
Dissert. Abstr.

N93-14877# Lawrence Livermore National Lab., CA.
EVALUATION OF A SOIL FIXATIVE TO RETARD PARTICLE ENTRAINMENT: A LABORATORY STUDY
A. Biermann, S. Sawyer, and R. Cappabianca 26 Dec. 1991 27 p
(Contract W-7405-eng-48)
(UCRL-LR-109806) Avail: CASI HC A03/MF A01

We evaluated the effectiveness of liquid spray treatments to reduce particle entrainment and migration from soil surfaces. To simulate particle entrainment from a solid surface, we performed controlled experiments in a laboratory wind tunnel using artificially prepared soil surfaces. The experimental testing included three soil treatments, three soil types, and four wind speeds. The soil treatments were a spray application of a 4 percent water-based flour formulation, a spray application of water only, and no spray treatment. The water-only spray and no spray conditions served as controls for evaluating the treatment with the flour formulation. We also investigated the effect of aging the soil surfaces under hot and dry conditions. In addition, we evaluated a quantitative assessment of the treatment's effectiveness to retard particle movement from the soil surface for both respirable particles from 0.3- to 8.0-microns-in. diameter and larger nonrespirable particles. We varied wind velocities from 2 to 16 m/s. In the wind-tunnel testing, we used three soils--54 percent clay, 72 percent silt, and 78 percent sand. Preparation of the soil surfaces simulated the behavior of an unpacked soil whose surface is exposed to a gust of wind. Spray applications of the treatments to the soil surfaces were typically 8 - 15 mg/sq cm. For wind velocities less than or equal to 22 mph, both treatments were effective in preventing entrainment of respirable particles. Based on aerosol concentration measurements, the effectiveness of the treatments averaged 98 percent over all conditions and soil types (i.e., 50 times less entrainment than for untreated soil surfaces). At the highest wind-velocity condition, 35 mph, the flour-formulation treatment was significantly more effective than the water-only treatment. In general, aerosol results paralleled the surface collection measurements, which indicate the movement of particles too large to be considered respirable. Soil surface treated with the flour formulation continued to be effective in preventing particle entrainment even after aging periods up to 20 days. In contrast, surfaces treated with water only indicated marked deterioration in performance under certain aging conditions.
Author

N93-14884 California Inst. of Tech., Pasadena.
MULTIPLY CONNECTED SPACETIMES AND CLOSED TIMELIKE CURVES IN SEMICLASSICAL GRAVITY Ph.D. Thesis
Gunnar Ulrich Klinkhammer 1992 72 p
Avail: Univ. Microfilms Order No. DA9232192

In this thesis, we present three studies motivated by the recent interest in spacetimes with closed timelike curves (CTC's). First, it was shown that certain energy conditions must be violated if spacetime is to develop CTC's. We initiate a study of whether quantum field theory permits such violations by proving that, in Minkowski spacetime, a free scalar field will satisfy the weak and strong energy conditions averaged along any complete null or timelike geodesic. We remark that in flat, but topologically nontrivial spacetimes, the averaged weak energy condition can be violated. Second, it was argued that the most likely way by which Nature might prevent the creation of CTC's is a divergent vacuum polarization at the chronology horizon where such CTC's first arise. We derive the form of the vacuum polarization of a conformal scalar field and of a spin-1/2 field near a closed null geodesic from which the null generators of a generic compactly generated chronology horizon spring forth. We show that the tensorial structure of the polarization and its degree of divergence are the same for scalar and for spin-1/2 fields and are independent of the details of the spacetime geometry. We also show that in generic cases, there will be no cancellation of this divergence for a combination of scalar and spin-1/2 fields that has equal numbers of Fermi and Bose degrees of freedom. Third, in anticipation of the possibility that Nature might permit CTC's, we demonstrate that for a classical body with a hard-sphere potential and no internal degrees of freedom (a 'billiard ball') traveling nonrelativistically in a wormhole spacetime with CTC's, the Cauchy problem is ill-posed in a peculiar way. For certain (dangerous) initial data, there would appear to be

no self-consistent solution to the equations of motion because the ball collides with its younger self after having traversed the wormhole. However, we show that for a wide range of dangerous and non-dangerous initial data, there is an infinity of self-consistent solutions, each involving one self-collision. No initial data are found for which there is no self-consistent solution. Dissert. Abstr.

N93-14899# Lockheed Missiles and Space Co., Palo Alto, CA. Space Sciences Lab.

RADIATION BELT DYNAMIC AND QUASI-STATIC MODELING BASED ON CRRES DATA: OUTER-BELT SHORT-TERM RESPONSE DATA BASE

Y. T. Chiu, M. A. Rinaldi, W. E. Francis, R. M. Robinson, and R. W. Nightingale 15 Jun. 1992 44 p

(Contract F19628-90-C-0097)

(AD-A256483; PL-TR-92-2160; AD-E201218; SR-2) Avail: CASI HC A03/MF A01

New features of the outer radiation belt dynamic response to geomagnetic storms are characterized using CRRES data. The response is found to have an intermediate (10-20 days) time scale and an intense short time scale (1-2 days). The intermediate time scale changes are characterized as invariant-violating diffusion, as has been developed by us for SCATHA data. The short time scale decreases of flux are characterized as adiabatic (reversible) dynamics, conserving the first variant under trapping volume change. GRA

N93-14913*# Miami Univ., FL. Rosenstiel School of Marine and Atmospheric Science.

PLATE TECTONICS FROM VLBI AND SLR GLOBAL DATA Final Report

Christopher G. A. Harrison and Stefano Robaudo May 1992 16 p

(Grant NAG5-741)

(NASA-CR-191319; NAS 1.26:191319) Avail: CASI HC A03/MF A01

This study is based on data derived from fifteen years of observations of the SLR (side-looking radar) network and six years of the VLBI (very long baseline interferometry) network. In order to use all available information VLBI and SLR global data sets were combined in a least squares fashion to calculate station horizontal velocities. All significant data pertaining to a single site contribute to the station horizontal motion. The only constraint on the solution is that no vertical motion is allowed. This restriction does not greatly affect the precision of the overall solution given the fact that the expected vertical motion for most stations, even those experiencing post glacial uplift, is well under 1 cm/yr. Since the average baseline is under 4,000 km, only a small fraction of the station vertical velocity is translated into baseline rates so that the error introduced in the solution by restricting up-down station movement is minimal. As a reference, station velocities were then compared to the ones predicted by the NUVEL-1 geological model of DeMets et al. (1990). The focus of the study is on analyzing these discrepancies for global plate tectonics as well as regional tectonic settings. The method used also allows us not only to derive horizontal motion for individual stations but also to calculate Euler vectors for those plates that have enough stations located on the stable interior like North America, Pacific, Eurasia, and Australia. Author

N93-15080# National Science Foundation, Washington, DC.

ANTARCTIC NEWS CLIPS - 1992

Jul. 1992 268 p

(NSF-92-83) Avail: CASI HC A12/MF A03

The newspaper and magazine stories selected for this book present only a sampling of one year's (July 1991 to July 1992) news coverage of Antarctica. The only requirement for inclusion in this publication is that the article's subject matter pertains or refers to Antarctica in some way - whether it is focused on the science done there, or on the people who play such a large part in the work accomplished, or on the issues related to it. No attempt has been made to correlate the number of articles, or their length, with the importance of the subjects treated. Clippings are provided to the Foundation by a service that searches for items containing the phrase 'National Science Foundation'. Identical versions of many stories, especially those written and distributed by wire services such as the Associated Press and United Press International, and by syndicated columnists, are published in numerous papers across the United States. Other articles are submitted from a variety of sources, including interested readers across the United States and in New Zealand. Author

N93-15136# EG and G Energy Measurements, Inc., Idaho Falls.

ADDRESSING EARTHQUAKE STRONG GROUND MOTION ISSUES AT THE IDAHO NATIONAL ENGINEERING LABORATORY

Ivan G. Wong (Woodward-Clyde Consultants, Oakland, CA.), Walter J. Silva, Cathy L. Stark (Pacific Engineering and Analysis, El Cerrito, CA.), Suzette Jackson, and Richard P. Smith 1991 10 p Presented at the Natural Phenomena Hazards Mitigation Conference, St. Louis, MO, 15-18 Oct. 1992

(Contract DE-AC07-76ID-01570)

(DE92-017841; EGG-M-91365; CONF-9110122-29) Avail: CASI HC A02/MF A01

In the course of reassessing seismic hazards at the Idaho National Engineering Laboratory (INEL), several key issues have been raised concerning the effects of the earthquake source and site geology on potential strong ground motions that might be generated by a large earthquake. The design earthquake for the INEL is an approximate moment magnitude (M(sub w)) 7 event that may occur on the southern portion of the Lemhi fault, a Basin and Range normal fault that is located on the northwestern boundary of the eastern Snake River Plain and the INEL, within 10 to 27 km of several major facilities. Because the locations of these facilities place them at close distances to a large earthquake and generally along strike of the causative fault, the effects of source rupture dynamics (e.g., directivity) could be critical in enhancing potential ground shaking at the INEL. An additional source issue that has been addressed is the value of stress drop to use in ground motions predictions. In terms of site geology, it has been questioned whether the interbedded volcanic stratigraphy beneath the ESRP and the INEL attenuates ground motions to a greater degree than a typical rock site in the western US. These three issues have been investigated employing a stochastic ground motion methodology which incorporates the Band-Limited-White-Noise Source Model for both a point source and finite fault, random vibration theory, and an equivalent linear approach to model soil response. DOE

N93-15252# Royal Inst. of Tech., Stockholm (Sweden). Alfven Lab.

A NUMERICAL MODEL OF IONOSPHERIC CONVECTION DERIVED FROM FIELD-ALIGNMENT CURRENTS AND THE CORRESPONDING CONDUCTIVITY

L. G. Blomberg and G. T. Marklund Aug. 1991 32 p Revised

(TRITA-EPP-91-03-Rev; TRITA-EPP-88-03-Rev; ETN-92-92624) Avail: CASI HC A03/MF A01

A numerical model for the calculation of ionospheric convection patterns from given distributions of field aligned current and ionospheric conductivity is described. The model includes a coupling between the conductivity and the field aligned current. The input contributions, the field aligned current and the conductivity, are parametrized. From the primary model output a number of other quantities can be computed: the potential in the inertial frame, the potential in the magnetospheric equatorial plane, the distribution of ionosheric current, and the Joule heating in the ionosphere. This model was used together with a technique to caculate the high latitude potential distribution prevailing during a particular event by combining information from global auroral images and local measurements of fields and particles. The model potential variation along the satellite orbit was found to be in agreement with that calculated from the measured electric field. The model was also used to study some fundamental properties of the electrodynamics of the high latitude ionosphere. ESA

N93-15375# Scripps Institution of Oceanography, La Jolla, CA.

SURFACE GRAVITY WAVES AND AMBIENT MICROSEISMIC NOISE Final Technical Report

R. T. Guza 15 Sep. 1992 6 p

(Contract N00014-90-J-1113)

(AD-A256498) Avail: CASI HC A02/MF A01

A coherent array of 24 pressure transducers was deployed on the sea bed in 13 m depth, approximately 2 km from shore, at Duck, North Carolina. The objective of this experiment was to examine the generation of low frequency (0.005-0.05 Hz) and high frequency (0.25-1.0 Hz) pressure fluctuations on the sea floor through nonlinear interactions of sea and swell. The pressure transducers were carefully positioned and buried about 10 cm within the sandy sea bed to reduce flow noise. The sample frequency

is 4 Hz. Data was collected nearly continuously between 3 September and 1 December 1990. During this period, a 170 minutes long data run was acquired every 3 hours. The sea floor pressure measurements collected in 13 m depth are unique in terms of the array aperture, number of sensors deployed, sensor placement accuracy, the wide range of wave conditions encountered, and the available environmental data (extensive bathymetry and wind data were collected by the Army Corps of Engineers Field Research Facility). GRA

N93-15395# Boston Univ., MA. Center for Space Physics.
THE EFFECTS OF MAGNETIC STORM PHASES ON F-LAYER IRREGULARITIES FROM AURORAL TO EQUATORIAL LATITUDES Quarterly Report, 1 Jul. - 30 Sep. 1992
Jules Aarons and Michael Mendillo 30 Sep. 1992 3 p
(Contract N00014-89-J-1754)
(AD-A256520) Avail: CASI HC A01/MF A01

The review of equatorial data relative to F-layer irregularities continued during this period with an emphasis in this quarter on determining the effects of localized effects on the generation of F-region irregularities. The study compares initially for one month TEC and scintillation data for Manila, the Philippines, Palehua, Hawaii Tepei, Taiwan, and Osan, Korea all in the Pacific Sector. For some periods in 1980 and 1981, all the data are available. The initial study will be the data set for July 1980. GRA

N93-15459# Army Engineer Waterways Experiment Station, Vicksburg, MS. Geotechnical Lab.
USACE GEOTECHNICAL EARTHQUAKE ENGINEERING SOFTWARE, REPORT 1 WESHAKE FOR PERSONAL COMPUTERS (VERSION 1.0) Instruction Report
David W. Sykora, Ronald E. Wahl, and David C. Wallace Sep. 1992 218 p
(AD-A257068; WES/IR/GL-92-4) Avail: CASI HC A10/MF A03

One of the basic problems to be solved by geotechnical engineers in regions where earthquake hazards exist is to estimate the site-specific dynamic response of a layered soil deposit under a level ground surface. This problem is commonly referred to as a site-specific response analysis or soil amplification study (although motions may be deamplified). The solution of this problem allows the geotechnical engineer to evaluate the potential for liquefaction, to conduct the first analytical phase of seismic stability evaluations for slopes and embankments, to calculate site natural periods, to assess ground motion amplification, and to provide structural engineers with various parameters, primarily response spectra, for design and safety evaluations of structures. The computer program described and provided in this report, WESHAKE, may be used to accomplish this task. WESHAKE is an adaptation of the original computer program, SHAKE, written at the University of California at Berkeley by Schnabel, Lysmer, and Seed (1972). WESHAKE was created and has been continually modified by WES to keep pace with state-of-the-art technology and provide a user-friendly interface. GRA

N93-15463# California Univ., Santa Barbara. Dept. of Chemistry.
PHOTODISSOCIATION DYNAMICS OF CLUSTER IONS Final Report, 15 Nov. 1988 - 14 Nov. 1991
Michael T. Bowers 18 Sep. 1992 6 p
(Grant AF-AFOSR-0102-89)
(AD-A256375; AFOSR-92-0899TR) Avail: CASI HC A02/MF A01

There are two somewhat different objectives of this grant, unified by their common interest in clusters. We have made substantial progress both in photodissociation of atmospheric clusters (11 papers) and in the generation and reactivity of semiconductor and metallic clusters (7 papers). Of particular interest is our development of a new ion chromatography technique that allows determination of the shape of clusters, or other species, in the gas phase. GRA

N93-15466# Arkansas Univ., Pine Bluff. Space and Environment Studies Lab.
GLOBAL ZONES OF PARTICLE PRECIPITATION AS OBSERVED BY EXOS-C Annual Report, 1 Jul. 1991 - 30 Jun. 1992
M. A. Miah 27 Sep. 1992 34 p
(Contract F49620-89-C-0071)
(AD-A256397; SESC-UAPB-01-92; AFOSR-92-0897TR) Avail: CASI HC A03/MF A01

A study of the temporal variation of quasi-trapped proton population near the geomagnetic equator reveals that the peak value of the equatorially mirroring component may increase by a factor of 50 or more between a solar maximum and a minimum condition. During a solar maximum condition more hydrogen escapes to outer space than during a minimum condition. The escaping light gas may cause more neutral generation by charge exchange interaction with the radiation belt/ring current protons, thereby enhancing the quasitrapped proton population at equatorial thermospheric altitude. This reported result is based on the observation of quasitrapped proton population in 1969-70, 1982, and 1984-86 by AZUR, S81-1, and EXOS-C missions. Also, a study based on EXOS-C mission alone shows that the peak flux profile of protons precipitate in the equatorial, and low-latitude, midlatitude, and auroral zones lying to the north of the equator, exist in parallel with the minimum magnetic field equator. Further, proton (0.64-35 MeV) and electron (0.19 - 3.2 MeV) population in the said midlatitude zone show longitude and altitude dependences. Contrary to previous observations, the locations of the peak flux profiles in all the three zones in L space depend upon the pitch of the particles. GRA

N93-15574*# Aerospace Corp., El Segundo, CA. Engineering and Technology Group.
ENERGETIC AND MAGNETOSHEATH ENERGY PARTICLE SIGNATURES OF THE LOW-LATITUDE BOUNDARY LAYER AT LOW ALTITUDES NEAR NOON
J. L. Roeder and L. R. Lyons 15 Nov. 1992 17 p Repr. from Journal of Geophysical Research, v. 97, no. A9, 1 Sep. 1992 p 13,817-13,828 Previously announced in IAA as A92-55116
(Grant NAGw-1613)
(NASA-CR-191388; NAS 1.26:191388; ATR-91(7190)-2) Avail: CASI HC A03/MF A01

The low-latitude boundary layer (LBL) and its separation from the cusp have previously been identified using observations of particle precipitation at magnetosheath energies. Using S3-3 satellite observations, we have determined that these identifications can also be made from energetic particle observations on polar-orbiting satellites. It is found that the equatorward boundary of the LBL is identifiable as an approximately discontinuous decrease in 33-keV electron fluxes from low to high latitudes. Both the energetic ion and electron fluxes decrease discontinuously at the boundary between the LBL and the cusp or polar cap. A distinct LBL is nearly always identifiable in energetic particle measurements in the 10-14 MLT region when counting rates are statistically significant. The identifications obtained using the energetic particle measurements have been compared to those obtained using criteria developed by Newell and Meng (1988, 1989) for magnetosheath energy particle precipitation. In this way, we have evaluated the accuracy of both techniques and used the energetic particle measurements to supplement the identifications obtained using the Newell and Meng criteria. We propose that the Newell and Meng threshold on ion energy flux can be reduced by a factor of 6. This modification provides identification of the LBL for lower ion intensity levels than has previously been thought possible. Source, acceleration, and scattering processes have also been studied within and in the vicinity of the LBL. Observed trapped pitch angle distributions of energetic electrons imply that the LBL is at least partially on closed field lines. Strong scattering of energetic protons is found within and equatorward of the LBL and thus must occur at least partially along closed field lines. Field-aligned electron acceleration by parallel electric fields can be discerned within and poleward of the LBL, but a more detailed analysis is necessary for a statistical study. Conical ion acceleration was seen relatively frequently within the LBL and about half as often poleward of the LBL. Neither acceleration process could be identified anywhere equatorward of the LBL. Author

N93-14952# Herzberg Inst. of Astrophysics, Ottawa (Ontario).
LISA: A LIMB IMAGING SPECTROGRAPH FOR AIRGLOW
F. R. Harris, R. L. Gattinger, F. Creutzberg, D. T. Bradley, F. Gauthier, J. W. Pygas, I. P. Powell (National Research Council of Canada, Ottawa, Ontario), and J. G. Rumbold (Canadian Space Agency, Ottawa, Ontario) *In* Canadian Space Agency, Proceedings of the Sixth CASI Conference on Astronautics 1990 11 p Previously announced in IAA as A91-34958 (For primary document see N93-14920 04-12)
Avail: Canadian Aeronautics and Space Inst., 222 Somerset St. W., Suite 601, Ottawa, Ontario K2P 0J1 Canada

N93-14969*# Centre National d'Etudes Spatiales, Toulouse (France).
GEOPHYSICAL INVESTIGATIONS WITH TOPEX/POSEIDON ALTIMETRY DATA
Anny Cazenave, G. Balmino, K. Dominh, B. Lago, M. Rabinowicz, R. Biancale, S. Houry, E. B. Okal (Northwestern Univ., Chicago, IL.), M. Diament (Institut de Physique du Globe, Paris, France), and B. Parsons (Oxford Univ., England) et al *In* JPL, TOPEX/Poseidon Science Investigations Plan 1 Sep. 1991 p 34-35 (For primary document see N93-14964 04-48)
Avail: CASI HC A01/MF A02; 22 functional color pages

N93-14982*# Centre National d'Etudes Spatiales, Toulouse (France).
GEOPHYSICAL VALIDATION OF TOPEX/POSEIDON ALTIMETRY PRODUCTS
Yves Menard, A. Guillaume (Direction de la Meteorologie Nationale, Paris, France), V. Casse (Direction de la Meteorologie Nationale, Paris, France), Jean-Francois Minster, B. Lago, C. Brossier, S. Arnault (Laboratoire d'Oceanographie Dynamique et de Climatologie, Paris, France), Jacques Merle (Laboratoire d'Oceanographie Dynamique et de Climatologie, Paris, France), F. Ramamonjiarisoa (Aix-Marseilles Univ., France), and N. Mognard (Puget Sound Univ., Tacoma, WA.) *In* JPL, TOPEX/Poseidon Science Investigations Plan 1 Sep. 1991 p 82-88 (For primary document see N93-14964 04-48)
Avail: CASI HC A02/MF A02; 22 functional color pages

N93-14993*# Centre National d'Etudes Spatiales, Toulouse (France).
PRESENT-DAY PLATE MOTIONS: RETRIEVAL FROM THE TOPEX/POSEIDON ORBITOGRAPHY NETWORK (DORIS SYSTEM)
Annie Souriau, Anny Cazenave, R. Biancale, G. Balmino, K. Dominh, P. Mazzega, J.-M. Lemoine, Claude Boucher (Institut Geographique National, Paris, France), P. Willis (Institut Geographique National, Paris, France), and M. Kasser (Institut Geographique National, Paris, France) et al *In* JPL, TOPEX/Poseidon Science Investigations Plan 1 Sep. 1991 p 131-136 (For primary document see N93-14964 04-48)
Avail: CASI HC A02/MF A02; 22 functional color pages

N93-14999*# Colorado Univ., Boulder.
A TOPEX/POSEIDON STUDY OF OCEANIC EFFECTS ON OBSERVATIONS OF THE EARTH'S INTERIOR
John Wahr and N. Benton *In* JPL, TOPEX/Poseidon Science Investigations Plan 1 Sep. 1991 p 159-160 (For primary document see N93-14964 04-48)
Avail: CASI HC A01/MF A02; 22 functional color pages

47 METEOROLOGY AND CLIMATOLOGY

Includes weather forecasting and modification.

N93-14114 Rutgers - The State Univ., New Brunswick, NJ.
TECHNOLOGY RECONCILIATION IN THE REMOTE SENSING ERA OF US CIVILIAN WEATHER FORCASTING: 1957 - 1987 Ph.D. Thesis
Margaret Eileen Courain 1991 964 p
Avail: Univ. Microfilms Order No. DA9211420

An understanding is sought of the management of a major technological change in meteorology. The study examines the connection between changes in production and real-time use of data products derived from remote sensing data collection and the evolution of U.S. civilian weather forecasting 1957-1987. The role of data collection in weather forecasting throughout history is examined, giving most attention to the 1957-1987 period. Critical to the real-time use of remote sensing data was technology reconciliation. It is defined as the function or process by which data products and information derived from a new technology are made consistent or congruent with the existing data representations of a science in order to be used effectively. No model had been developed for a technology reconciliation process, or definition of the major role technology reconciliators played in the 30-year evolution of the science of weather forecasting. In order to assess the new remote sensing data resources and its use in U.S. civilian weather forecasting, a Data Accountability and Review Technique (DART) was developed. This technique was used to identify 16 of the technology reconciliators who developed and reconciled 25 new remote sensing data products with the weather charts, maps and computer models of the National Weather Service. In five separate program teams, they were responsible for 15 improvements in the products (forecasts) and 18 improvements in the process of weather forecasting. A model of the technology reconciliation is proposed which can be applied to understanding the contemporary history of other sciences. The model, as well as the methods developed by the author to recognize the process of technology reconciliation has a much more general applicability beyond the sciences. Any field implementing new technology that promises to improve its whole way of working will be faced with the task of technology reconciliation. Scientists, engineers, R & D managers, and science/technology policy-makers should find the case study, the methodology, and the generalized model helpful in guiding them through the complex process of interpreting new data from new technology. Dissert. Abstr.

N93-14115 Wisconsin Univ., Madison.
EXTREME CLIMATIC EVENTS IN THE AMAZON BASIN AND THEIR ASSOCIATIONS WITH THE CIRCULATION OF THE GLOBAL TROPICS Ph.D. Thesis
Jose Antonio MarengoOrsini 1991 165 p
Avail: Univ. Microfilms Order No. DA9135479

The mechanisms of climate anomalies in the Amazon Basin were explored in three complementary lines of investigations, drawing on surface climatological and hydrological series, upper-air and satellite observations, as well as the general circulation model (GCM) of the Goddard Institute for Space Studies (GISS). Work focused on the March-April rainy season peak in the northern portion of the Amazon Basin (NA). Correlation analyses indicate that rainfall in NA tends to be more abundant with a stronger North Atlantic high, accelerated Northeast trades, colder North and warmer South Atlantic waters, and during the high phase of the Southern Oscillation (SO; defined by anomalously high/low pressure at Tahiti/Darwin). GISS GCM simulations using globally observed sea surface temperature (SST) during 1979-86 reproduced major features of circulation and rainfall over tropical South America, but most satisfactorily for years with extreme SST conditions. Detailed case studies for the moderately WET year 1986 and the extremely DRY year 1983 showed during WET pronounced subsidence off the West coast of South America, contrasting with strong ascending motion and vigorous convection to the East of the Andes, and weak STWJ's in both hemispheres; while DRY featured ascending motion and convective rainfall over the Pacific coast of South America, subsidence over the Amazon Basin, and strong STWJ's. In synthesis from these three lines of investigations, some major mechanisms of extreme rainfall events over NA stand out, but only for the late austral summer. The near-equatorial low pressure trough and embedded Intertropical Convergence Zone (ITCZ) attain their southernmost position, the intense summertime convection over Amazonia being an important component of the ITCZ. Thus, ascending motion over the northern part of the Amazon Basin with an anomalously far southward displaced ITCZ appears compatible with subsidence to the West of the Andes, during the high SO phase. By contrast, ascending motion and convection over the easternmost equatorial Pacific, as common during extreme events of the low SO phase, require compensatory subsidence, and this may interfere with convection to the East of the Andes. Finally, the study indicates that hydrometeorological anomalies in Amazonia are not prevailingly related to the SO. Dissert. Abstr.

N93-14153# Massachusetts Univ., Lowell. Dept. of Earth Sciences.
SUPER-MICRO COMPUTER WEATHER PREDICTION MODEL Final Report, 17 May 1988 - 30 Nov. 1991
Keith L. Seitter and Frank P. Colby, Jr. Jan. 1992 78 p
(Contract F19628-88-K-0016)
(AD-A255668; PL-TR-92-2023; AD-E201155) Avail: CASI HC A05/MF A01

A meso-beta scale numerical model is described that is designed specifically for operational use on relatively small computers. A major aspect of the model is that it treats the boundary layer as a single model layer of known structure whose depth can evolve during the integration. The model equations are recast in a coordinate system, referred to as boundary-layer coordinates, based on the depth of the evolving boundary layer. The model described here does not include condensation processes, but it does include a radiation parameterization, schemes governing the structure of the stable and unstable boundary layers and the transitions between these regimes, and parameterizations for the fluxes of heat and moisture between the boundary layer and the earth's surface. Simulations have been carried out with a prototype model that has five layers and 20 km resolution in the

fine grid mesh of its nested domain. The results of these simulations show that the model is capable of reproducing such mesoscale phenomena as mountain lee waves and the Florida sea-breeze circulation fairly well. Results are also presented of some preliminary simulations for the complex terrain of southern New England that demonstrate the need for carefully prepared terrain fields in numerical models. GRA

N93-14180 California Univ., Davis.
CLOUD-RADIATIVE FEEDBACKS IN TROPICAL CONVECTION Ph.D. Thesis
Lorraine Ann Remer 1991 145 p
Avail: Univ. Microfilms Order No. DA9217597

This study of cloud-radiation feedbacks on tropical convection has two parts. First, we use the International Satellite Cloud Climatology Project (ISCCP) data sets to characterize the clouds and convection in a specific tropical region. Second, we employ a simple radiative transfer model, initialized with the results of the satellite data analysis, to test several hypotheses on the nature of the radiative feedbacks. Time series analyses are performed on the outgoing longwave radiation of the B3 ISCCP data set. The results show that the diurnal cycle is prominent over most land areas and weaker but still discernible over convectively active ocean areas. Analysis of the cloud fraction data from the ISCCP C1 data set for clouds with various cloud top heights allow us to better characterize the diurnal cycle of the convection. We find that the towers representing deep convection are most numerous in the morning hours for convection over the western tropical Pacific, while the anvils are most numerous in the afternoons. We also find that the mean fractional cloudiness is the same for the towers over both the southeast Asia continent and the western tropical Pacific ocean, but that these two regions differ in the phase of their diurnal cycles. The diurnal cycles of the cloud fractions of clouds with differing heights are used in conjunction with a simple radiative transfer model to test three theoretical feedback hypotheses. One of these, involving radiatively forced subsidence leading to an enhancement of low level convergence, is found to be inconsistent with the observed data. Both differential vertical heating, leading to destabilization of the column, and differential horizontal heating, leading to low level convergence, however, are found to be consistent with the observed data. The magnitudes of the differential vertical and horizontal heating components are found to be sufficiently large to explain diurnal variation of oceanic convection.
Dissert. Abstr.

N93-14196 Oxford Univ. (England).
INFRARED RADIATIVE PROPERTIES OF CLOUDS Ph.D. Thesis
Peter N. Francis 1991 260 p
Avail: Univ. Microfilms Order No. BRD-96786

Cloud-radiation interaction is one of the most important processes in climate and weather prediction, with the presence of clouds greatly modifying the distribution of radiative heating and cooling in the troposphere. It is therefore of great importance to be able to understand the fundamental physical processes involved in cloud radiative transfer, and to be able to model them accurately. The development of a cloud-radiation model is described. The effects of multiple scattering are included using a matrix operator algorithm, which has been improved from a previous version via the implementation of a superior initialization technique, and by the introduction of the delta-M method, whereby flux conservation and phase function renormalization are performed automatically. Continuum absorption for both water vapor and carbon dioxide is included. The effect of the line cores is included using the correlated-k method. The spectrum of the scattered radiance can be convolved over detector response functions, to produce readily comparable brightness temperatures. Five experimental aircraft flights are reported, in which meteorological, microphysical and radiometric data were taken from various different types of water clouds. Model clouds are constructed using the data collected from these flights, and used as input to the cloud-radiation model. The results are compared with radiances measured by a Multi-Channel Radiometer, mounted in the port wing-pod of the aircraft. Agreement is generally good; discrepancies are attributed to variability of the cloud structure. Broad-band long-wave and short-wave data are also reported from four of the flights, and are compared with radiation schemes currently employed in the Meteorological Office's unified model. Data measured during some of the flights are used to validate a cloud-top temperature satellites imagery product, which is found to be accurate to well within 1 K. Dissert. Abstr.

N93-14197 Utah Univ., Salt Lake City.
SIMULATIONS OF THE AMAZON BASIN CIRCULATION USING THE PENNSYLVANIA STATE UNIVERSITY/NATIONAL CENTER FOR ATMOSPHERIC RESEARCH MESOSCALE MODEL Ph.D. Thesis
Andrea Noemi Hahmann 1992 125 p
Avail: Univ. Microfilms Order No. DA9227935

A regional model has been used to investigate the dynamical processes that control the circulation features over the Amazon Basin. The application of a regional model to the Amazon Basin is unique and the method in which the model output is diagnosed is also distinct from other regional model studies. Two synoptic cases are chosen to describe the ability of the regional model to simulate the circulation over the Amazon Basin. The first case, which occurs during 15-17 April 1990, represents a good example of the dominant circulation over the basin during the summer season. The second case study occurs during the period 27 February-1 March 1990. At the onset of this period, a vigorous trough is located in the subtropical westerlies of the Southern Hemisphere, which promotes advection of drier air by the low-level southerly flow into the southern part of the Basin. There is limited agreement between the observed circulation and the model simulations for the two studies, except in the largest-scale features. The model does appear to simulate a number of dynamical processes that are known to take place in this environment. However, the timing of individual rain bands and their locations differ significantly from those observed. The sensitivity of the model simulation to the size of the grid spacing and the domain reveal that the regional circulation is most economically simulated with a nested domain and 60 km grid spacing. Larger grid spacings lead to excessive rainfall totals near the Andes Mountains and circulations that are unrealistic. Restricted domains, which cover the Amazon Basin only, produce excessive precipitation along the horizontal boundaries. Model simulations using several different combinations of convective and explicit precipitation parameterizations are performed. Experiments using the explicit moisture scheme without a cumulus parameterization scheme show the development of grid point instabilities. These instabilities result from interaction processes among latent heat release, large-scale moisture convergence, and surface pressure. When the Kuo-Anthes cumulus parameterization is included, grid point instabilities are substantially reduced. Dissert. Abstr.

N93-14198 North Carolina State Univ., Raleigh.
FOUR-DIMENSIONAL DATA ASSIMILATION OF GALE DATA USING A MULTIVARIATE ANALYSIS SCHEME AND A MESOSCALE MODEL WITH DIABATIC INITIALIZATION Ph.D. Thesis
Dewey Elvin Harms 1992 238 p
Avail: Univ. Microfilms Order No. DA9226384

A method of assimilating 3-hourly sounding data is developed and successfully tested in this study. First, the successive corrections scheme of Bratseth (1986), which converges to optimum interpolation, is applied for the numerical analysis of data collected during the Genesis of Atlantic Lows Experiment (GALE). Univariate analyses of the mass and wind field are produced. The coupling of the mass and wind field is achieved by further iterations of the geopotential utilizing improving estimates of the geostrophic wind to extrapolate the geopotential to the grid points. The univariate wind analysis is then corrected for the new geostrophic wind. Next, diabatic forcing is incorporated into a vertical mode initialization scheme to provide more realistic initial conditions and to shorten the spinup time of the Naval Research Laboratory/North Carolina State University (NRL/NCSU) mesoscale model. Latent-heating profiles are computed from 'spun-up' model-generated and observed rainfall. The latent heating is distributed in the vertical according to the cumulus convective parameterization scheme (Kuo scheme) of the model. Compatibility between the specified heating during initialization and the heating during early model integration is retained by merging the model integrated rainfall and heating rates with those rates from the initialization. Finally, the multivariate, successive correction analysis scheme and the diabatic initialization procedure are combined with the NRL/NCSU model to form an intermittent data-assimilation system. Assimilations of the GALE data over a 2 1/2-day period were performed with differing update cycles of 3, 6, and 12 h. Twelve-hour NMC hemispheric analyses served as the 'no assimilation' control case for comparison. The assimilation of 3-hourly GALE data led to large decreases in background forecast rms errors and smaller decreases in analysis rms error. Better consistency in time was achieved between

forecasts and analyses in the assimilation experiments. Rainfall prognoses from the assimilated state verified reasonably well with the observed rainfall and showed much more rapid spinup and better overall patterns than did the 'no assimilation' precipitation forecasts. Dissert. Abstr.

N93-14213 California Univ., San Diego.
THE PREFERRED LATITUDES OF THE INTERTROPICAL CONVERGENCE ZONE: OBSERVATIONS AND THEORY Ph.D. Thesis
Duane Edward Waliser 1992 186 p
Avail: Univ. Microfilms Order No. DA9227856

The latitude preference of the Intertropical Convergence Zone (ITCZ) is examined on the basis of observations, theory, and a modeling analysis. Observational analysis indicates that a dynamical mechanism in the atmosphere is acting to position the ITCZ(s) away from the equator to latitudes of about 4-10 deg, even in regions where the SST is maximum on the equator. Earlier theories for this off-equatorial preference of the ITCZ are reviewed and a new explanation is presented based on analogous results from a forced, linear shallow-water model and a moist primitive equation model. The results from the simplified model show that finite-width mid-level tropospheric heating (i.e., an ITCZ) induces the greatest low-level convergence when the heating is placed a finite distance away from the equator. The results from the primitive equation model show that when the latent heating field is not specified but is determined internally, the above phenomena leads to a positive feedback between the heating field and the induced low-level convergence that favors ITCZ development at latitudes of about 4-10. The relationship between this mechanism and earlier theories is discussed, as are implications concerning the roles played by mid-level latent heating and SST-gradients in forcing the low-level atmospheric circulation, as well as other implications on related aspects of tropical meteorology and oceanography. In addition to the above results, comparative analyses of long-record satellite indices of tropical convection reveal that the highly Reflective Cloud (HRC) data set is generally superior to the Outgoing Longwave Radiation data set for studies of tropical deep convection. Further, analysis of the relationship between these two data sets and local SST reveals that monthly SSTs in excess of about 29.5 C tend to occur only under conditions of diminished local convection. This new and important finding helps to further define the complex relationship between SST and tropical deep convection and demonstrates the importance of the cooling mechanisms associated with deep convection in limiting tropical SSTs. Additionally, the features of the HRC data set are exploited to present a new and unique long-term, global climatology of the ITCZ. Dissert. Abstr.

N93-14256# Institute for Naval Oceanography, Bay Saint Louis, MS.
WIND STRESS ANALYSIS OVER THE WESTERN EQUATORIAL PACIFIC AND NORTH ATLANTIC OCEANS BASED ON ECMWF OPERATIONAL WIND PRODUCTS, 1985-1989
L. N. Ly, John C. Kindle, J. D. Thompson, and Wesley J. Youtsey Aug. 1992 117 p
(AD-A256147; INO-TR-3) Avail: CASI HC A06/MF A02

The mean annual and monthly mean wind stress and wind stress curl over the ocean were computed for 1985-1989 from European Center for Medium-Range Weather Forecasting (ECMWF) 12-hourly operational 1000 mb, 10 m winds, and direct surface stresses. Both linear and non-linear drag coefficient formulations were employed. The analyses focused on wind stress and curl fields over the Western Equatorial Pacific and the North Atlantic Basin. The wind stress and curl fields of the various ECMWF and Hellerman and Rosenstein wind products are compared. GRA

N93-14258# Nevada Univ., Reno. Desert Research Inst.
CCN SPECTRA MEASUREMENTS AS AN ACTIVE TRACER OF STRATOCUMULUS MECHANISMS Annual Report
James G. Hudson Oct. 1992 3 p Sponsored by ONR
(AD-A255678) Avail: CASI HC A01/MF A01

Papers submitted for publication are briefly described. The papers address cloud condensation nuclei (CCN) near marine cumulus and a comparison of CCN and cloud droplet concentrations in FIRE. Data acquisition using the DRI CCN spectrometer is also reported. GRA

N93-14547# Massachusetts Inst. of Tech., Lexington. Lincoln Lab.
TERMINAL DOPPLER WEATHER RADAR/LOW-LEVEL WIND SHEAR ALERT SYSTEM INTEGRATION ALGORITHM SPECIFICATION, VERSION 1.1
Rodney E. Cole 24 Feb. 1992 33 p
(Contracts DTFA01-89-Z-02033; F19628-90-C-0002)
(AD-A255319; MIT-ATC-187; DOT/FAA/NR-92/3) Avail: CASI HC A03/MF A01

There will be a number of airports that receive both a Terminal Doppler Weather Radar (TDWR) windshear detection system and a phase 3 Low-Level Wind Shear Alert System (LLWAS). At those airports, the two systems will need to be combined into a single windshear detection system. This report specifies the algorithm to be used to integrate the two subsystems. The algorithm takes in the alphanumeric runway alert messages generated by each subsystem and joins them into integrated alert messages. The design goals of this windshear detection system are (1) to maintain the probability of detection for hazardous events while reducing the number of false alerts and microburst overwarnings and (2) to increase the accuracy of the loss/gain estimates. The first design goal is accomplished by issuing an integrated alert for an operational runway whenever either subsystem issues a 'strong' alert for that runway; by canceling a 'weak' windshear alert on an operational runway if only one subsystem is making the declaration; and by reducing a 'weak' microburst alert on an operational runway to a 'strong' windshear alert if only one subsystem is making the declaration. The second design goal is accomplished by using the average of the two loss/gain values, when appropriate. GRA

N93-14588 Georgia Inst. of Tech., Atlanta.
A SIMULATION MODEL OF ATMOSPHERIC TURBULENCE FOR ROTORCRAFT APPLICATIONS Ph.D. Thesis
Jamshed Riaz 1992 137 p
Avail: Univ. Microfilms Order No. DA9231747

Stochastic description of atmospheric turbulence for rotorcraft applications is a complex cyclostationary process. Due to its nonstationary structure, this process is not amenable to conventional filtering techniques; consequently, researchers have found it difficult to construct turbulence sample functions for rotorcraft simulation studies. The present study addresses this need and presents a method for generating turbulence sample functions suitable for rotorcraft applications. In this method, the cyclostationary process is expanded into a series of multi-dimensional cosine functions with rotational sampling embedded into the parameters. It is shown that this simulation technique generates turbulence sample functions containing appropriate second-order statistics in terms of mean and covariance. The simulation method takes into account the cross-correlation between elements of the rotor blades--a consideration that has been neglected in the past. The method avoids complicated filter designs, and can easily be integrated into rotorcraft simulation programs that are based on blade element analysis. The simulation method is used to investigate the effect of atmospheric turbulence on the flapping response of an isolated blade. Using the concept of 'phase-randomization', the response statistics of blade flapping are explained in physically meaningful terms. Finally, the turbulence simulation method is used to predict the response of the UH-60A Black Hawk helicopter to atmospheric turbulence. Dissert. Abstr.

N93-14640 Princeton Univ., NJ.
A NUMERICAL STUDY OF THE MIDDLE ATMOSPHERE RESPONSE TO TROPICAL AND SUBTROPICAL TROPOSPHERIC HEAT SOURCES Ph.D. Thesis
Elisa Manzini 1992 179 p
Avail: Univ. Microfilms Order No. DA9230635

The excitation and propagation of planetary and gravity waves in the atmosphere are studied by comparing solutions from a numerical model based on the linear primitive equations and from the comprehensive Geophysical Fluid Dynamics Laboratory (GFDL) SKYHI general circulation model (GCM) for the troposphere, stratosphere, and mesosphere. The basic state of the linear model is time dependent and derived from the mean zonal wind and temperature given by a 78-day simulation with the SKYHI model. The latent and convective heating fields of this SKYHI simulation provide the forcing for the linear model in the tropical and subtropical troposphere. The phase characteristics of the vertically propagating equatorial Kelvin waves and gravity waves exhibited in calculations with the linear model and the GCM are found to be remarkably

similar, indicating that the latent and convective heating is the main mechanism producing wave activity in the tropical atmosphere of the GCM. The results also show that gravity waves generated in the equatorial troposphere can reach the midlatitude mesosphere when strong mean flows exist whose direction is opposite the phase speed. In both models the vertical extent of the thermal forcing appears to control the dominant phase characteristics of the Kelvin and gravity waves. However, the amplitudes of the vertically propagating waves in the SKYHI model, particularly in the mesosphere, are somewhat smaller than those of linear model, which has only radiative damping and horizontal diffusion. This difference indicates that vertical diffusion is important in the full GCM. The global scale Rossby normal modes seen in observations are also identified in the analyses of easterly propagating planetary waves in both models. They are of realistic amplitude in the SKYHI simulation but are much weaker in the linear model. Thus it appears that latent and convective heating is not the main source of excitation for the Rossby normal modes.
Dissert. Abstr.

N93-14680# Naval Research Lab., Washington, DC.
FOUR-DIMENSIONAL DATA ASSIMILATION OF GALE DATA USING A MULTIVARIATE ANALYSIS SCHEME AND A MESOSCALE MODEL WITH DIABATIC INITIALIZATION
Dewey E. Harms, Keith D. Sashegyi, Rao V. Madala, and Sethu Raman 6 Oct. 1992 235 p
(AD-A256063; NRL/MR/4223-92-7147) Avail: CASI HC A11/MF A03

A method of assimilating 3-hourly sounding data is developed and successfully tested in this study. First, the successive corrections scheme of Bratseth (1986) which converges to optimum interpolation, is applied for the numerical analysis of data collected during the Genesis of Atlantic Lows Experiment (GALE). Next, diabatic forcing is incorporated into a vertical mode initialization scheme to provide more realistic initial conditions and to shorten the spinup time of the Naval Research Laboratory/North Carolina State University (NRL/NCSU) mesoscale mode. Latent-heating profiles are computed from 'spun-up' model-generated and observed rainfall. Finally, the multivariate, successive correction analysis scheme correction analysis scheme and the diabatic initialization procedure are combined with the NRL/NCSU model to form an intermittent data-assimilation system. Assimilations of the GALE data over a 2 1/2-day period were performed with differing update cycles of 3, 6, and 12 h. Twelve-hour NMC hemispheric analyses served as the 'no assimilation' control case for comparison. The assimilation of 3-hourly GALE data led to large decreases in background forecast rms errors and smaller decreases in analysis rms error. Rainfall prognoses from the assimilated states showed mucn more rapid spinup and better overall patterns than did the 'no assimilation' precipitation forecasts.
GRA

N93-14682 Colorado State Univ., Fort Collins.
AN OBSERVATIONAL AND THEORETICAL STUDY OF SQUALL LINE EVOLUTION Ph.D. Thesis
Erik Nels Rasmussen 1992 125 p
Avail: Univ. Microfilms Order No. DA9231822

By utilizing a number of Doppler radar observations of ten squall lines, a certain class of squall lines is documented that is quasi-two-dimensional and has a solid leading edge at some time during the life cycle. It is found that the kinematic structure of these systems can be described as being due to a sloping zone of negative horizontal vorticity which extends across the entire squall line. Further, the evolution of these systems can be characterized by the sloping of this vorticity zone from erect to more horizontal orientations. The existence of the vorticity zone appears to be due to buoyancy gradients extending across the system. The primary difference between the system studied is the rate at which tilting occurs. Motivated by the observations, a new theory is developed for squall line evolution. The theory allows for an environment with two layers characterized by differing shear values, and the squall line is characterized by a sloping region with a specified average vorticity. Using a circulation tendency approach, the rate of change of squall line slope is predicted based on environmental shear and cold pool strength. The predictions of the theory compare well with observations, and previously published theoretical and modeling results.
Dissert. Abstr.

N93-14683 Oklahoma Univ., Norman.
CONVECTIVE SCALE 4-D DATA ASSIMILATION USING SIMULATED SINGLE-DOPPLER RADAR OBSERVATIONS Ph.D. Thesis
Juanzhen Sun 1992 188 p
Avail: Univ. Microfilms Order No. DA9230149

The adjoint method of variational data assimilation is used to retrieve the 3-dimensional wind and thermal dynamic variables from simulated single-Doppler radar data. The constraining numerical model simulates dry thermal convection with incompressible Boussinesq dynamics. This technique attempts to determine all the control parameters of the model, i.e., the initial and boundary conditions of the model and the mean profiles, by iteratively minimizing the difference between the observations and the model predictions of the radial velocity and the reflectivity. The three-dimensional wind and temperature are recovered when the predictions best match the observations. The minimization algorithm requires the calculation of the gradient of the cost function with respect to the control parameters. A set of adjoint equations is therefore constructed to determine this gradient. It is demonstrated that this method is able to determine satisfactorily the initial state of the unobserved velocity components and temperature as well as the mean profiles in less than 100 iterations. The retrieval of the boundary conditions, however, is not as successful. It is demonstrated that the algorithm is robust to data increments and random observational errors. The effects of the model errors are tested by leaving out certain terms in the governing equations. It is shown that the algorithm is also fairly robust to such model errors. Studies on the behavior of cost function with respect to length of assimilation indicate that the width of the global minimum is large enough to allow the algorithm to start from a rough first guess as long as the assimilation period is shorter than the initial error doubling time. Proper use of penalty functions improves the conditioning of the cost function, so the convergence of the retrieval takes less time.
Dissert. Abstr.

N93-14827 Washington Univ., Seattle.
STRUCTURE AND PROPAGATION OF FRONTS EAST OF THE ROCKY MOUNTAINS AND THEIR RELATIONSHIP TO PRECIPITATION Ph.D. Thesis
Jonathan Edward Martin 1992 304 p
Avail: Univ. Microfilms Order No. DA9230405

The role of frontogenetic processes in generating and distributing precipitation east of the Rocky Mountains in the United States is examined using data collected during the Genesis of Atlantic Lows Experiment (GALE). A set of mid-tropospheric, frontogenetic, precipitation-producing features are discussed. A recurrent, non-classical, synoptic scale structure characterized these cases. Based on observations from four cases, a conceptual model is proposed for these structures; the cold frontogenesis aloft (CFA) model. In one case study, the secondary circulation about an upper-level front, in a region of conditional symmetric instability (CSI), produced a rainband of moderate intensity. The potential influence of upper-level frontogenesis processes on the evolution of the CSI is explored through Lagrangian, adiabatic changes in the equivalent potential vorticity. The interactions between a surface cold front and an upper-level front that resulted in the production of a deep, precipitating frontal structure is examined. An increase in the vigor of the frontal convention is attributed to favorable vertical superposition of the surface cold front and the upper-level front. Mid-level latent heat release was likely responsible for the diabatic steepening of the dynamic tropopause. This steepening contributed to the subsequent rapid development of a surface cyclone on the East Coast. The mesoscale structure and distribution of precipitation along a surface cold front is investigated. The precipitation cores in a narrow cold-frontal rainband (NCFR) showed some differences, as well as similarities, to previously observed NCFRs. A correspondence between precipitation intensity and the slope of the frontal surface was observed for a wide cold-frontal rainband (WCFR) associated with this cold front. The nature of this correspondence is investigated and some possible mechanisms for changing the slope of the frontal topography are examined.
Dissert. Abstr.

N93-14862 Columbia Univ., New York, NY.
GLOBAL SURVEY OF EFFECTIVE PARTICLE SIZE IN LIQUID WATER CLOUDS BY SATELLITE OBSERVATIONS Ph.D. Thesis
Qingyuan Han 1992 219 p
Avail: Univ. Microfilms Order No. DA9232016

A global survey of cloud particle size is needed for climate change studies. This can supply crucial information for parameterizing cloud optical properties on a global scale as well as to estimate variation in cloud liquid water content with environmental temperature, a relationship that has been suggested as being important for climate feedback. Cloud particle size is also helpful in evaluating the effect of aerosol variations (both anthropogenic and natural), which represents another major uncertainty in climate change studies. In this dissertation, a method for retrieving cloud particle size information on a global scale, using currently available satellite data from ISCCP (International Satellite Cloud Climatology Program), is described. Four months of data for the satellites NOAA-9 and NOAA-10 have been processed. A radiative transfer model is used to retrieve cloud particle size. The model includes the major absorbing gases as well as scattering, absorption and emission by clouds in the computation of synthetic radiances for specified satellite viewing geometry. The model results have been validated against clear sky observations and are consistent with the observed radiance range under cloudy conditions. A method has been developed for estimating instrument noise and accounting for its effects on the analysis. Surface reflectance at 3.7 microns has been retrieved globally, and its effect on cloud particle size has been considered. Error sources and the range of their contributions are included for each retrieved cloud particle size. The results of this global survey reveal continental and maritime differences, hemispheric contrasts, seasonal and diurnal variations effective droplet radii as well as existence of a relationship between cloud optical thickness and droplet size. The hemispheric contrasts are indicative of some impact of anthropogenic aerosols. However, the cloud droplet size variation with sea surface temperature in remote ocean areas suggest little effect of DMS (dimethylsulfide) aerosols. The average liquid water path retrieved by this method is consistent with microwave measurement analyzed by other authors over ocean areas. The present survey makes it possible to retrieve cloud liquid water path information over land. Dissert. Abstr.

N93-14864 Hawaii Univ., Honolulu.
SENSITIVITY OF THE YOSHIDA JET TO THE PARAMETERIZATION OF VERTICAL MIXING: DO EASTERLY WINDS IMPLY EQUATORIAL UPWELLING? Ph.D. Thesis
Niklas Schneider 1992 113 p
Avail: Univ. Microfilms Order No. DA9230519

This study investigates the sensitivity of the dynamics of the equatorial ocean to the parameterization of vertical mixing and focuses on the circulation in the meridional-vertical plane driven by easterly winds: the Yoshida jet. A new high resolution, numerical model of a zonally independent, equatorial channel helps explore this question and includes three parameterizations, all of which increase mixing for decreasing Richardson numbers. It compares the smooth increase of eddy coefficients traditionally used in general circulation models, the dramatic increase of the eddy coefficients for small Richardson numbers recently observed in the equatorial Pacific, and a combination of a mixing mechanism based on the diagnostic adjustment of the water column to noncritical Richardson numbers and a bulk mixed-layer model. The main numerical result is that the meridional and vertical velocity fields in the surface layer are very sensitive to the strength of mixing implied by the different parameterizations. For the smooth Richardson number dependence of the eddy coefficients, equatorial upwelling due to easterly winds reaches the surface. The dramatically increasing eddy coefficients for small Richardson numbers yield reduced equatorial upwelling rates in the surface layer. The diagnostic adjustment of the Richardson number shows downwelling in response to easterly winds! A simple model explains the wind drift at the equator in the presence of a meridional density gradient and reproduces this reversal of the meridional and vertical flows. The density gradient causes a vertically dependent pressure gradient force which is partially balanced by the meridional component of the Coriolis force, indicating that the zonal flow and the density are nearly in geostrophic balance. The residual of this balance determines the sign of the meridional shear and depends critically on the size of the eddy coefficient. A critical value at which the residual and the vertical velocity change signs of the order of 10(exp -3) m(exp 2) s(exp -1). This value is of the same order as measured in the surface equatorial Pacific and used in general circulation models. The physics of the reversal of the meridional circulation are so basic it is likely they are active in the ocean and three dimensional circulation models. Dissert. Abstr.

N93-14875 Nevada Univ., Reno.
ON THE ROLE OF WATER GROWTH IN ATMOSPHERIC AEROSOL Ph.D. Thesis
Marc Lynn Pitchford 1992 203 p
Avail: Univ. Microfilms Order No. DA9230121

Atmospheric particle growth by condensation of water vapor was investigated using sophisticated particle growth and compositional measurements made during the Winter of 1990 at Grand Canyon National Park, AZ. Growth measurements by the Tandem Differential Mobility Analyzer (TDMA) and fine particle compositional analysis data were examined to assess the nature of the particles and the applicability of certain growth and composition models. A model was developed to estimate the sulfate to ammonium ion concentration ratio by apportioning measured hydrogen concentrations between organic and sulfate aerosol components. The model had insufficient resolution for this data to determine the ion ratio. The overall volume fraction of soluble material as determined by chemical analysis of particle samples was apportioned between high growth and low growth particles by a model based upon TDMA measured growth data. Growth data indicate the simultaneous presence of two, and occasionally three, types of particles. At relative humidities above about 78 percent, particles split into two distinguishable growth categories. Most of the particles grew considerably (categorized as more hygroscopic), while a small fraction of the particles grew slightly (categorized as less hygroscopic). On a few days, particles separated by growth at relative humidities in the mid 60 percent range, with a small fraction of the particles having high growth. At higher relative humidities these particles became indistinguishable from the more hygroscopic particles. Sulfate species dominate the soluble fraction most days, with nitrates occasionally in comparable concentrations. The model to estimate the soluble fraction of the particles in the more and less hygroscopic growth categories also determines the soluble material growth characteristic, which is assumed to be the same for all particles in any individual TDMA measurement. The predicted growth characteristics for the soluble material is in good agreement with laboratory measured values for most days. On average, the composition of the more hygroscopic particles are half soluble and half insoluble material. The less hygroscopic fraction is dominated by insoluble material (about 85 percent). Assuming spherical symmetry, a less hygroscopic particle's soluble layer surrounding its insoluble core is about 50A thick regardless of dry particle size.
Dissert. Abstr.

N93-14901# Colorado State Univ., Fort Collins. Dept. of Atmospheric Science.
LOW-FREQUENCY OSCILLATIONS IN RADIATIVE-CONVECTIVE MODELS
Qi Hu and D. A. Randall 1991 4 p Presented at the 5th American Meteorological Society (AMS) Conference on Climate Variations, Denver, CO, 14-18 Oct. 1991
(Contract DE-FG02-89ER-69027)
(DE92-018779; CONF-9110161-6) Avail: CASI HC A01/MF A01

Although eastward propagation is usually regarded as an essential feature of the low-frequency 'Madden-Julian oscillation' observed in the tropical atmosphere, many observations indicate that there is an important stationary or quasi-stationary component of the oscillation. Yasunari (1979), for example, investigated the stationary 30-60 day variation in upper tropospheric cloudiness in the Asian summer monsoon region. In a case study of the 30-60 day oscillation, Hsu et al. (1990) found a strong stationary oscillation of the divergence, outgoing longwave radiation and other fields. A recent observational study by Weickmann and Khalsa (1990) offers further evidence that the Madden-Julian oscillation has an important stationary component. In this paper, we present evidence that intraseasonal oscillations can be produced by local radiative and convective processes. This suggests that the observed propagating Madden-Julian wave is produced by interactions between these local processes and the large scale motion field, and is not essential for the existence of the observed oscillation. DOE

N93-14910*# Stanford Univ., CA. STAR Lab.
THUNDERSTORM COUPLING TO THE MAGNETOSPHERE AND ASSOCIATED IONOSPHERIC EFFECTS Semiannual Report, 1 Nov. 1991 - 30 Apr. 1992
Umran S. Inan 1992 7 p

(Grant NAG5-1549)
(NASA-CR-191383; NAS 1.26:191383) Avail: CASI HC A02/MF A01

This project deals with the coupling of electromagnetic energy released during a thunderstorm to the magnetosphere and the ionosphere. Both the effects of an individual lightning event as well the aggregate of all the lightning events during a thunderstorm are considered. Energy in the very low frequency (VLF) band can play a variety of roles in the magnetospheric and ionospheric physics: generation of plasmaspheric hiss believed to be responsible for the slot region in the radiation belts, generation of lower hybrid waves that can heat ions in the auroral and subauroral regions, precipitation of energetic electrons, ionospheric heating etc. While these phenomena have been identified, and characterized to some extent, the influence and role of thunderstorm energy on the magnetosphere and ionosphere at a global scale is not known. Only recently, simultaneous high resolution (temporal and spatial) data sets from ground based lightning detectors and space and ground based VLF detectors have become available, and thus it has become possible to raise a question of the kind mentioned above and try to answer it quantitatively. Work on the correlation between individual lightning discharges in a thunderstorm as detected by the lightning network and the whistlers observed on the DE-1 satellite continued during this period. Results are summarized. Author

N93-14919 Delaware Univ., Newark.
SYNOPTIC SCALE STRUCTURE OF SUMMERTIME WET AND DRY SPELLS IN NORTHEASTERN KANSAS Ph.D. Thesis
Jonathan Anders Skindlov 1992 304 p
Avail: Univ. Microfilms Order No. DA9232604

An integrated automated synoptic index, incorporating both surface and upper air weather observations at Topeka, KS, was constructed for summers (June, July, and August) from 1957 through 1984. Principal components analysis generated 62 orthogonal components from the 62 meteorological variables. Average linkage (hierarchical) clustering of the first seven components produced 12 synoptic type seeds which were used by a k-means (non-hierarchical) clustering procedure to reclassify all 2576 days into the 12 distinct synoptic types. These types were matched with six-hourly Topeka precipitation totals for evaluation of temporal variance and, for 1978-84, with manually digitized radar (MDR) data from a 120 by 120 km area for analysis of spatial variation. Differences in diurnal preferences (noctural versus daytime storms), amount of rainfall per storm, and duration and frequency of storms were noted. Links between the synoptic types (i.e., their mean meteorological conditions) and rainfall and radar echo variations, wet and dry spells, and the eventual temperature and rainfall character each summer were ascertained. Long- and short-term precipitation trends provided a context for interpreting the synoptic climatology. Topeka monthly precipitation records from 1878 through 1987 revealed inter-annual variation of wet and dry periods. Summer precipitation - monthly, daily, and six-hourly - from 1957 through 1984 revealed short-term, intra-seasonal variations. Both wet and dry as well as hot and cool weather were uniquely captured by the 12 synoptic types. Temporal difference in Topeka rainfall - both intra-seasonally and inter-seasonally - were explained well by differences in the frequency of occurrence of the 12 synoptic types. Spatial differences in the MDR data were reasonably accounted for by synoptic type characteristics; temporal differences were less clear. A few of the dry synoptic types were associated with rare but intense rainfall and radar echoes. The temperature character of summer, dependent on synoptic scale weather features, is very well modeled using synoptic type frequencies. The rainfall character of summer, which is more dependent on mesobeta scale phenomena, was well modeled by regression with wet and dry spell characteristics and only adequately modeled using synoptic type frequencies. Dissert. Abstr.

N93-15087 Georgia Inst. of Tech., Atlanta.
AN INVESTIGATION INTO THE ROLE OF MOIST, VERTICAL DRAFTS IN THE ROTATIONAL DEVELOPMENT OF STORMS Ph.D. Thesis
John Victor Cortinas, Jr. 1992 154 p
Avail: Univ. Microfilms Order No. DA9231727

A simple two-dimensional, quasi-steady-state model is used to investigate the effect of various parameters on producing convergence at the top of downdrafts. The result from this model indicate that convergence occurs within a narrow region of the storm cloud at the top of strong downdrafts within certain environments. The inflow region consistently occurred over a thickness of 1-2 km. This convergence roughly doubled the tangential velocities of a mesocyclone within one hour. The environment that produced the strongest downdraft convergence was characterized by low relative humidity, a dry-adiabatic lapse rate, a large concentration of small droplets and minimal horizontal airflow. This paper details a sensitivity study that examined the effect of initial droplet size, initial relative humidity, environmental lapse rate, droplet drag, initial liquid water content and non-hydrostatic pressure gradients on downdraft convergence. The results show initial droplet size is a particularly important consideration followed by relative humidity, environmental lapse rates and droplet concentration. Non-hydrostatic pressure gradients accelerated the downdraft above the maximum inflow and decelerated it below. This model is unlike other downdraft studies that have assumed a developed rain distribution and vertical velocity structure at the top of the downdraft. This study concentrates on the top of the downdraft where the vertical velocity is zero and droplet sizes are small. These conditions are representative of the cloud region within many large convective systems. Using a monodispersion of cloud-size droplets, a neutral stability atmosphere and an initial vertical velocity of -0.5 m/s, the model produced a horizontal inflow velocity 2-32 m/s at a radius of 5 km. Several results showed the sensitivity and the limitations of the model. The results indicate that the model was sensitive to the assumed downdraft radial velocity profile. The inflow thickness was related to the type of radial profile of vertical velocity assumed. The inflow thickness was a minimum using a top-hat velocity profile and a maximum with a triangular velocity profile. Droplets with radii larger than 0.5 mm were found to be too large to be moved horizontally by a 2-3 m/s wind and represented the limiting droplet size. The results from this study provide a better understanding of downdraft inflow structure and the role of downdrafts in the rotational development of storms. Dissert. Abstr.

N93-15088 Nevada Univ., Reno.
SIERRA NEVADA WINTER STORMS: A STUDY USING MICROWAVE RADIOMETRY, ICE CRYSTAL, AND ISOTOPIC ANALYSIS TECHNIQUE Ph.D. Thesis
Belay Berhane Demoz 1992 174 p
Avail: Univ. Microfilms Order No. DA9230122

An observational study has been made of ice-phase storm clouds over the Sierra Nevada mountains. In Part 1, two microwave radiometers, one designed with a spinning reflector to shed precipitation particles while the other radiometer's reflector was fixed are compared. The absence/presence of contaminated periods in the data was attributed to difference in design. These apparent contaminated periods led to lower correlation coefficients between the radiometers. Comparison of radiometer and rawinsonde resulted in a correlation coefficient of 0.97 for the spinning reflector as opposed to 0.8 for the fixed reflector radiometer. In Part 2, stable water isotopes were used to study mesoscale and microscale storm modifications by the Sierra Nevada. Initially, a low level warm front lay across the region and its elevation lowered with time from 2.5 km to 1.7 km. This decrease of frontal surface height was accompanied by a steady increase in the delta O-18 values. In the pre-cold frontal period, the delta O-18 values at the upwind site signified warmer origin ice crystals than the downwind site. This is explained by orographic effects and the production of supercooled liquid water at low elevations on the upslope side. The delta O-18 value peaked around -13 0/00 which translates to an 'equivalent temperature' of -10.7 C for ice phase water capture at the upwind site. At the downwind site, this was some 5 to 6 centigrade degrees colder. During surface cold front passage, the differences in delta O-18 at the two sites are small probably because, during frontal passage, the orography plays a less significant role in the precipitation production process. In Part 3, observations of precipitation rates, ice crystals, wind and supercooled liquid water (SLW) upwind and downwind of the Sierra Nevada are presented. Observations show that the stage of development of the storms was important in the liquid and vapor development. High SLW, and increased riming were located before the frontal passage. Duration of SLW as observed by the radiometers, was always shorter over the downwind station. Heavy riming was associated with precipitation decrease while high precipitation rates were correlated with high number fraction of aggregate crystals. Aggregation was found to be an important process for precipitation development over the downwind station. Dissert. Abstr.

N93-15099 Colorado State Univ., Fort Collins.
THE INFLUENCE OF BAROCLINIC PROCESSES ON TROPICAL

CYCLONE MOTION Ph.D. Thesis
Maria Flatau 1992 154 p
Avail: Univ. Microfilms Order No. DA9231778

The numerical study presented here has focused on baroclinic processes which contribute to tropical cyclone propagation. Two numerical models were used in this work. A linear one-layer shallow water model was used to analyze the development of instabilities in the hurricane outflow layer. A three-dimensional, semi-spectral, primitive equation model of baroclinic vortex was developed to study TC motion. We have investigated how vortex motion is affected by (1) the interaction between upper and lower potential vorticity anomalies in a tilted vortex, (2) asymmetric distribution of diabatic heating, and (3) the presence of dynamic instabilities in a cyclone outflow layer. When a vortex is tilted, interaction between upper and lower level vorticity anomalies leads to vortex propagation relative to the steering flow. On a beta-plane, with no environment flow, the vortex is slightly tilted toward the south and the interaction between the layers reduces the westward movement of the vortex. The vortex tilting can also occur due to the vertical shear in the environmental wind. On an f-plane, the interaction between the layers causes the northward movement of the vortex in westerly linear shear, and the southward movement in easterly linear shear, with a meridional velocity of about 1 m/s. This velocity increases with increasing vortex intensity and vertical motion. The magnitude of the meridional vortex velocity caused by this effect is comparable with the motion resulting from advection of planetary vorticity. The response of baroclinic vortex motion to asymmetric heat sources show that asymmetries placed at larger radii create potential vorticity anomalies similar to 'beta gyres'. The response of baroclinic vortex motion to asymmetric heat sources show that asymmetries placed at larger radii create potential vorticity anomalies similar to 'beta gyres'. Circulation associated with these anomalies advects the vortex. Diabatic heating anomalies located in the southern and southeastern part of a vortex significantly reduce the motion due to the beta effect. The results of a shallow water, linear model show that dynamically unstable modes can develop in the cyclone outflow layer even in the absence of environmental forcing. Development of both barotropic and inertial instability is possible. In a three-dimensional model, vortices with different intensities respond differently to identical environmental forcing. In strong vortices, slow looping motion with period of few days can be observed. Since the period of this slow oscillation corresponds to the frequency of barotropically unstable modes, we attribute this type of motion to development of barotropic instability in the outflow layer of a baroclinic vortex. Dissert. Abstr.

N93-15100 Colorado State Univ., Fort Collins.
FITTING MICROPHYSICAL OBSERVATIONS TO A NUMERICAL MODEL THROUGH AN OPTIMAL CONTROL THEORY TECHNIQUE Ph.D. Thesis
Johannes Verlinde 1992 93 p
Avail: Univ. Microfilms Order No. DA9231833

Rapid advances in the quality and quantity of atmospheric observations have placed a demand for the development of techniques to assimilate these data sources into numerical forecasting models. Four-dimensional variational assimilation is a promising technique that has been applied to atmospheric and oceanic dynamical models, and also to the retrieval of three-dimensional wind fields from single Doppler radar observations. This study investigates the feasibility of using four-dimensional variational assimilation for a complex discontinuous numerical model. Three test models were developed, a positive definite advection scheme, a one-dimensional liquid physics kinematic microphysical model with a positive definite advection scheme, and a two-dimensional liquid physics kinematic microphysical model. These models were used in identical twin experiments, with observations taken intermittently. Small random errors were introduced into the observations. The retrieval runs were initialized with a large perturbation of the observation run initial conditions. All the models were able to retrieve the original initial conditions to a satisfactory degree when observations of all the model prognostic variables were used. Greater overdetermination of the degrees of freedom (the initial condition being retrieved) resulted in greater improvement of the errors in the observations of the initial conditions, but at a rapid increase in computational cost. Experiments where only some of the prognostic variables were observed also improved the initial conditions, but at a greater cost. To substantially improve the first guess of the field not observed, some spot observations are needed. The proper scaling of the variables was found to be important for the rate of convergence. This study suggests that scaling factors related to the error variance of the observations give good convergence rates. To show how this technique can be used when observations are general functions of the prognostic variables of the model (e.g., reflectivity or liquid water path), a form is derived which shows that this can be accomplished. This is considered to be an advantage of this technique over others, since it is particulary suitable to remote sensing systems where only integral parameteres of derivatives of model prognostic variables are observed. Dissert. Abstr.

N93-15331# Augsburg Coll., Minneapolis, MN. Center for Atmospheric and Space Sciences.
A SINGLE-STATION FORECASTING MODEL Final Report, 15 Dec. 1988 - 15 Jan. 1992
William H. Jasperson, David E. Venne, and Miriam R. Peterson 1 Apr. 1992 31 p
(Contract F19628-89-C-0015)
(AD-A256403; PL-TR-92-2097) Avail: CASI HC A03/MF A01

The development is described of an advanced prototype expert system, named Itasca, for the classical single-station weather forecasting problem. The forecasting skills necessary to produce forecasts from limited data are being lost though they continue to have application to certain military scenarios which include communications interruptions. Itasca is intended for use at an arbitrary mid-latitude station, and utilizes physical relationships between the synoptic weather and variables that affect the local weather rather than station specific rules. Itasca is designed as an embedded expert system where the user has control over the operation of the system through a user interface. Rule bases are loaded and used as appropriate to the task at hand. The rule bases and the class/object structure used in the expert system were developed using the NEXPERT-object development system. Testing of the system during development was limited by the lack of suitable datasets, but a plan is in place for further independent testing and evaluation. GRA

N93-15501*# National Aeronautics and Space Administration. Langley Research Center, Hampton, VA.
CLOUD FRACTION, LAYER, AND DIRECTION OF MOVEMENT RESULTS FROM SKY CAMERAS DURING THE FIRE IFO, COFFEYVILLE, KANSAS, EXPERIMENT FOR THE PERIOD NOV. 12 THROUGH DEC. 9, 1991
Gerald C. Purgold, Robert J. Wheeler (Lockheed Engineering and Sciences Co., Hampton, VA.), and Charles H. Whitlock Dec. 1992 32 p
(RTOP 578-12-23-70)
(NASA-TM-107647; NAS 1.15:107647) Avail: CASI HC A03/MF A01

Tables and figures are presented which show local site observations of cloud fractions, the number of cloud layers, direction of movement, and precipitation data collected during the FIRE (First ISCCP Regional Experiment) Phase 2 Cirrus Intensive Field Observations (IFO) conducted in Coffeyville, Kansas during November and December, 1991. Selected data are also presented at the times of the TIROS Operational Vertical Sounder (TOVS) satellite overpass. Several major scientific projects have used surface-based observations of clouds to compare directly with those being observed from satellites. Characterizing the physical properties of clouds is extremely useful in obtaining a more accurate analysis of the effect of clouds and their movements on weather and climate. It is the purpose of this paper to report data collected during the FIRE Phase 2 IFO experiment and to provide a brief history of such a surface-based system and the technical information required for recording local cloud parameters. Author

N93-15581*# Pennsylvania State Univ., University Park. Dept. of Meteorology.
DEVELOPMENT AND APPLICATION OF A TIME-SPACE CONVERSION TECHNIQUE FOR ANALYSIS OF WEATHER SYSTEMS PASSING OVER THE KENNEDY SPACE CENTER Final Report
Gregory S. Forbes NASA Nov. 1992 121 p
(Contracts NAG8-754; F19628-86-C-0092; N00014-86-K-0688; N00014-84-C-0717; NSF ATM-86-01405)
(NASA-CR-4474; M-703; NAS 1.26:4474) Avail: CASI HC A06/MF A02

A procedure for using asynchronous data to generate spatial analyses for a single time is described. This procedure, called a time-space conversion scheme, involves a separation of an individual observation into a perturbation component and mean component. The mean component is readily estimated

by averaging temporally over a series of observations taken at the same spatial location. The perturbation component at an individual time is then computed by taking the difference between the observation at that time and the temporal average at that location. When this separation is done for numerous sites and the data are plotted on a map and analyzed, it can be seen that the temporal-mean data relate to the large scale conditions over the region. The perturbation data depict much smaller scales, indicative of mesoscale systems or substructures travelling through (and 'steered' by) the larger scale system. Accordingly, the perturbation component observed at a site at a particular time is displaced to the appropriate position at the analysis time, where it is added to the mean value at that location. The displacement is performed in a manner that preserves the position of the perturbation value with respect to the travelling mesoscale feature. Data from conventional National Weather Service (NWS) and Department of Defense (DOD) rawinsonde releases, special rawinsonde ascents, serial rawinsonde and jimsphere launches at Kennedy Space Center (KSC), and from a wind profiler at KSC have been used in the time-space conversion scheme to perform analyses in a case study of a weather system passing over KSC. Because some of the perturbations measured over Florida and near the Gulf Coast and East Coast States become displaced over data-sparse oceanic regions, it became necessary to devise a method for determining temporal means over the offshore areas. This was done by using analyses from the Nested Grid Model (NGM) run twice daily. Pseudo-soundings were constructed from these analyses at an array of oceanic locations and used to construct the temporal mean fields offshore. The analyses reveal that a jet stream and front were detected over KSC at the launch of STS-27, including wind shear. Author

48 OCEANOGRAPHY

Includes biological, dynamic, and physical oceanography; and marine resources.

For related information see also *43 Earth Resources and Remote Sensing.*

N93-14428# Nova Univ., Dania, FL. Oceanographic Center.
MIXED-LAYER PARAMETERIZATION IN MODELS OF THE INDIAN OCEAN Final Report
Julian P. McCreary, Jr. 18 Sep. 1992 2 p
(Contract N00014-91-J-4008)
(AD-A255937) Avail: CASI HC A01/MF A01

A 2 1/2-layer, thermodynamic numerical model is used to study the dynamics, thermodynamics, and mixed-layer physics of Indian-Ocean circulation. A surface mixed layer of temperature T(sub m) is imbedded in the upper layer of the model, and entrainment and detrainment in the mixed layer are determined by wind stirring and surface cooling. There is also detrainment w(sub d) through the base of the upper layer that models subduction. Monthly climatological data, including air temperature T(sub a) and specific humidity q(sub a), are used to force the model, but model sea surface temperature (SST), T(sub m), is used to determine the sensible and latent heat fluxes. With a few notable exceptions, our main-run solution compares well with observed current and SST data; this is particularly true for T(sub m), which typically differs from observed SST by less than 0.5 - 1.0 C. Our analysis focuses on three topics: the relative importance of remote versus local forcing, the thermodynamic processes, that determine the model SST field, and the development of meridional circulation cells. GRA

N93-14452# Coast Guard, Washington, DC.
REPORT OF THE INTERNATIONAL ICE PATROL IN THE NORTH ATLANTIC, BULLETIN NO. 77 Annual Report
1991 51 p
(AD-A256162; USCG-188-46) Avail: CASI HC A04/MF A01

This is the 77th annual report of the International Ice Patrol (IIP). It contains information on Ice Patrol operations, environmental conditions, and ice conditions for the 1991 IIP season. Commander, International Ice Patrol, working under Commander, Coast Guard Atlantic Area, directs the IIP from offices located in Groton, Connecticut. IIP analyzes ice and environmental data, prepares daily ice bulletins and facsimile charts, and replies to requests for ice information. IIP uses aerial Ice Reconnaissance Detachments and, when necessary, surface patrol cutters to survey the southeastern, southern, and southwestern regions of the Grand Banks of Newfoundland for icebergs. IIP makes twice-daily radio broadcasts to warn mariners of the limits of all known ice. GRA

N93-14503# Institute for Naval Oceanography, Bay Saint Louis, MS.
PROCEEDINGS OF THE DATA ASSIMILATION IN COUPLED AIR-SEA NOWCAST/FORECAST SYSTEMS WORKSHOP
A. L. Perkins Jul. 1992 180 p Workshop held in Diamond Head, MS, 27-28 Feb. 1992
(DA Proj. R31-030)
(AD-A255409; INO-SP-8) Avail: CASI HC A09/MF A02

The Institute for Naval Oceanography (INO) sponsored a Workshop on Data Assimilation in Coupled Air-Sea Nowcast/Forecast Systems that was held 27-28 Feb. 1992, to promote discussions and develop a strategy for research and development of data assimilation techniques in coupled atmospheric/ocean nowcast/forecast modeling systems for the Mediterranean Sea. The motivation for the workshop, in terms of INO's program, is the changing priority of Navy program sponsors to an emphasis in coastal and semi-enclosed seas research and development efforts. Within this area, the Mediterranean Sea was specifically identified by the Navy as a priority. GRA

N93-14512# Defence Research Establishment Atlantic, Dartmouth (Nova Scotia).
ACOUSTIC PROPAGATION LOSS PREDICTIONS FOR A SITE ON THE BERMUDA RISE AT LOW AND VERY LOW FREQUENCIES
Frederick D. Cotaras and James A. Theriault Jun. 1992 45 p
(AD-A255445; DREA-TM-92/215) Avail: CASI HC A03/MF A01

Low (10 - 100 Hz) and very low (1 - 10 Hz) frequency acoustic propagation loss is predicted for a site on the Bermuda Rise near 30 deg N 69 deg W. An extensive survey of the open literature is reported, and a geo-acoustic model of the acoustic environment at the site is developed. The results of a brief numerical investigation of the effect of shear waves and detailed sub-bottom layering on the acoustic propagation-loss predictions are discussed. The acoustic propagation-loss model used is SAFARI, which accounts for shear waves in the sediment but assumes a range-invariant environment. The propagation-loss predictions for 5, 10, 20, and 50 Hz are then presented. Also presented are predictions of the reflection loss in the form of grey-scale plots as a function of frequency and grazing angle. No comparison with experimental data is attempted. GRA

N93-14769*# Purdue Univ., West Lafayette, IN. Dept. of Earth and Atmospheric Sciences.
SYNOPTIC/PLANETARY-SCALE INTERACTIONS AND BLOCKING OVER THE NORTH ATLANTIC OCEAN Final Report, 21 Feb. 1989 - 7 Dec. 1992
Phillip J. Smith 15 Dec. 1992 12 p
(Grant NAG8-764)
(NASA-CR-191376; NAS 1.26:191376) Avail: CASI HC A03/MF A01

The work completed under this grant represents a continuing investigation of synoptic/planetary-scale interactions over the North Atlantic Ocean in late Jan. 1979. The focus of attention was a blocking episode that developed over southern Greenland on 21 Jan. However, the diagnosis also extended to antecedent cyclone activity and the role of moist processes during wave development. In all, the project was partitioned into two phases: (1) an extension of diagnoses that were already in progress of the 21 Jan. blocking episode and its antecedent cyclone activity using satellite-enhanced level 3-b NASA/Goddard Laboratory for Atmospheres (GLA) analyses; and (2) an analysis of the extent to which the results of Phase 1 are sensitive to the presence of satellite information. Author

N93-14964*# Jet Propulsion Lab., California Inst. of Tech., Pasadena.
TOPEX/POSEIDON SCIENCE INVESTIGATIONS PLAN
David Fulton, ed. 1 Sep. 1991 186 p Original contains color illustrations
(NASA-CR-190616; JPL-Publ-91-27; NAS 1.26:190616) Avail: CASI HC A09/MF A02; 22 functional color pages

TOPEX/POSEIDON is a satellite mission that will use the technique of radar altimetry to make precise measurement of sea level with a primary goal of studying the global ocean circulation. The mission represents the culmination of the development of satellite altimetry over the past two decades. The major thrust of the mission is a commitment to measuring

seal level with an unprecedented accuracy such that the small-amplitude, basinwide sea level changes that bear significant effects on global change can be detected. The mission will be conducted jointly by the United States National Aeronautics and Space Administration and the French space agency, Centre National d'Etudes Spatiales. The 3- to 5-year mission will study the long-term mean and variability of ocean circulation. This document provides brief descriptions of the planned investigations as well as a summary of the major elements of the mission. For individual titles, see N93-14965 through N93-15002.

N93-14965*# Groupe de Recherche de Geodesie Spatiale, Grasse (France).

THE WESTERN MEDITERRANEAN SEA: AN AREA FOR A REGIONAL VALIDATION FOR TOPEX/POSEIDON AND A FIELD FOR GEOPHYSICAL AND OCEANOGRAPHIC STUDIES

Francois Barlier, G. Balmino (Bureau Gravimetrique International, Toulouse, France), Claude Boucher (Institut Geographique National, Paris, France), P. Willis (Institut Geographique National, Paris, France), R. Biancale (Observatoire de Midi-Pyresnees, Toulouse, France), Yves Menard (Observatoire de Midi-Pyresnees, Toulouse, France), P. Vincent (Observatoire de Midi-Pyresnees, Toulouse, France), J. P. Bethoux (Centre de Recherches Oceanographiques, Villefranche-sur-Mer, France), P. Exertier, and F. Pierron et al *In* JPL, TOPEX/Poseidon Science Investigations Plan 1 Sep. 1991 p 18-22 (For primary document see N93-14964 04-48)

Avail: CASI HC A01/MF A02; 22 functional color pages

The research project has two kinds of objectives. The first is focused on the regional validation of the altimeter, orbit, and mean sea surface; it will be performed in close cooperation with the local validation performed at Lampedusa/Lampione (Italy). The second deals with the geophysical and oceanographic research of interest in this area. Author

N93-14966*# Colorado Univ., Boulder. Center for Astrodynamics Research.

THE USE OF SATELLITE ALTIMETRY IN THE STUDY OF WEAKLY DEFINED AND VARIABLE OCEANIC GYRES

George H. Born, W. Emery, G. Rosborough, and R. Leben *In* JPL, TOPEX/Poseidon Science Investigations Plan 1 Sep. 1991 p 23-26 Original contains color illustrations (For primary document see N93-14964 04-48)

Avail: CASI HC A01/MF A02; 22 functional color pages

Most of what is known about oceanic gyres comes from studies of the two main Northern Hemisphere subtropical gyres. Also important in the overall circulation of the world's oceans are the Southern Hemisphere subtropical gyres and the cyclonic Alaskan Gyre in the northern Pacific. Due in part to their weaker surface topography signatures and their variable character, these gyres have not been observed and studied as well as the northern subtropical gyres. The combination of satellite altimetry with in situ ocean measurements will lead to improved resolution of the interannual and seasonal change in the circulation of these ocean gyres. Also, it will provide initialization input and verification for numerical modeling work designed to better understand internal gyre dynamics. The objective of this proposal is to combine satellite and in situ data in a study dedicated to a better understanding of the basic structure and dynamics of the weakly defined Southern Hemisphere gyres and the Alaskan Gyre and their roles in oceanic heat and mass transport of the world ocean. Emphasis will be on description of the Alaskan Gyre. Author

N93-14967*# Institut Geographique National, Paris (France).

TERRESTRIAL REFERENCE SYSTEMS RELATED TO THE TOPEX/POSEIDON PROJECT **c43**

Claude Boucher, P. Willis, Francois Barlier (Centre d'Etudes et de Recherches Geodynamiques et Astronomiques, Grasse, France), and P. Mazzega (Centre National d'Etudes Spatiales, Toulouse, France) *In* JPL, TOPEX/Poseidon Science Investigations Plan 1 Sep. 1991 p 27-28 (For primary document see N93-14964 04-48)

Avail: CASI HC A01/MF A02; 22 functional color pages

In the TOPEX/POSEIDON project, several satellite positioning systems, such as Laser, Doppler Orbitography and Radiopositioning Integrated by Satellite (DORIS), and Global Positioning Satellite (GPS) (on an experimental basis), will be used to track the satellite and to provide accurate orbits. Unfortunately, these systems will provide their dedicated tracking-station coordinates and the satellite orbits in different reference frames. Each technique will use, de facto, a different reference frame. In fact, even for the same technique, each group, depending on the hypothesis used in its computation, will use a different reference frame. This problem is not new for geodesists and can be overcome, in large part, but could create trouble for other scientists when they compare or combine different coordinate data sets. The main purpose of this investigation is to determine a consistent terrestrial system for TOPEX/POSEIDON in which all the tracking-station coordinates, all the orbit ephemerides, and all the other station coordinates of specific interest (such as tide gauges) could be expressed. Another issue of this investigation is the provision of reliable information concerning the relationships between all the possible reference frames of interest for th TOPEX/POSEIDON project. To be more explicit, we plan to provide the possible transformation formula between the TOPEX/POSEIDON terrestrial reference frame and the Laser, DORIS, GPS, and other internationally recognized frames such as the International Terrestrial Reference Frame (ITRF). Author

N93-14968*# Australian Inst. of Marine Science, Queensland.

NORTH-AUSTRALIAN TROPICAL SEAS CIRCULATION STUDY

Derek Burrage, R. Coleman (Sydney Univ., Australia), L. Bode (James Cook Univ. of North Queensland, Townsville, Australia), and M. Inoue (Louisiana State Univ., Baton Rouge.) *In* JPL, TOPEX/Poseidon Science Investigations Plan 1 Sep. 1991 p 29-33 (For primary document see N93-14964 04-48)

Avail: CASI HC A01/MF A02; 22 functional color pages

This investigation is intended to fully address the stated objective of the TOPEX/POSEIDON mission (National Aeronautics and Space Administration, 1986). Hence, we intend to use TOPEX/POSEIDON altimetry data to study the large-scale circulation of the Coral Sea Basin and the Arafura Sea and the mass exchange between these and adjoining basins. We will obtain data from two such cruises in 1993 and 1994 and combine them with TOPEX/POSEIDON radar altimetry data to identify interannual and seasonal changes in: (1) the location of the major ocean currents and the South Equatorial Current bifurcation in the Coral Sea; (2) the source region of the South Tropical Counter Current (STCC); and (3) the water exchange between the Coral Sea and the adjoining seas. We will also estimate seasonal and interannual variations in the horizontal transport of mass and heat associated with near-surface geostrophic and wind-driven currents. In addition, the tidal components of the Coral Sea will be studied to provide a correction for altimetry subtidal sea level changes and to develop a regional numerical model for tidal forcing in the Great Barrier Reef (GBR) and Papua New Guinea Reef regions. I.I.C.

N93-14969*# Centre National d'Etudes Spatiales, Toulouse (France).

GEOPHYSICAL INVESTIGATIONS WITH TOPEX/POSEIDON ALTIMETRY DATA **c46**

Anny Cazenave, G. Balmino, K. Dominh, B. Lago, M. Rabinowicz, R. Biancale, S. Houry, E. B. Okal (Northwestern Univ., Chicago, IL.), M. Diament (Institut de Physique du Globe, Paris, France), and B. Parsons (Oxford Univ., England) et al *In* JPL, TOPEX/Poseidon Science Investigations Plan 1 Sep. 1991 p 34-35 (For primary document see N93-14964 04-48)

Avail: CASI HC A01/MF A02; 22 functional color pages

In the proposed research, TOPEX/POSEIDON altimeter data will be used with Geosat and European Remote Sensing satellite (ERS-1) data to compute global, region, and local oceanic geoid surfaces. These observations will then be analyzed to conduct geophysical studies relative to the structure of the oceanic lithosphere and mantle. Author

N93-14970*# Oregon State Univ., Corvallis.

MESOSCALE AND LARGE-SCALE VARIABILITY OF THE ANTARCTIC CIRCUMPOLAR CURRENT

Dudley B. Chelton, A. F. Bennett, R. A. deSzoeke, R. N. Miller, and Lee-Lueng Fu (Jet Propulsion Lab., California Inst. of Tech., Pasadena.) *In* JPL, TOPEX/Poseidon Science Investigation Plan 1 Sep. 1991 p 36-39 Original contains color illustrations (For primary document see N93-14964 04-48)

Avail: CASI HC A01/MF A02; 22 functional color pages

This investigation of the physical oceanography of the Southern Ocean will carry out two parallel efforts during the years preceding the launch of TOPEX/POSEIDON. First, the Geosat data will be used to develop a preliminary descriptive picture of the mesoscale and large-scale,

low-frequency surface circulation of the Southern Ocean. Some of this analysis of Geosat data has already begun. For example, as a measure of the geographical distribution of mesoscale variability, a color-coded map of the standard deviation of sea level from two years of Geosat data is shown. Efforts are presently under way to investigate the seasonal and year-to-year variability of this mesoscale energy. The data are also being used to generate low-pass filtered fields of sea level from which the temporal evolution of large-scale variability in the Southern Ocean may be investigated. The second parallel effort is the development and test of modeling and data assimilation techniques that will later be applied to TOPEX/POSEIDON data during the postlaunch phase. One objective of the modeling and data assimilation is to investigate the relation between mesoscale sea level variations and eddy flux in the Southern Ocean. Uncertainties in present estimates of the various components of meridional oceanic heat transport are large. The evidence presented indicates that the very energetic mesoscale variability in the ACC apparently accounts for much of the estimated 0.45x10(exp 15) watts of poleward heat transport across the ACC required to balance the heat budget. Eddy variability is strongly coherent vertically in the ACC, at least in the vicinity of Drake Passage where nearly all of the historical in situ data have been collected. Author

N93-14971*# Commonwealth Scientific and Industrial Research Organization, Hobart (Australia). Marine Labs.

OCEAN TRANSPORT AND VARIABILITY STUDIES OF THE SOUTH PACIFIC, SOUTHERN, AND INDIAN OCEANS

John A. Church, G. R. Cresswell, C. S. Nilsson, T. J. McDougall, R. Coleman (Sydney Univ., Broadway, Australia), C. Rizos (New South Wales Univ., Kensington, Australia), J. Penrose (Western Australian Inst. of Tech., Bentley.), J. R. Hunter (Western Australian Inst. of Tech., Bentley.), and M. J. Lynch (Western Australian Inst. of Tech., Bentley.) *In* JPL, TOPEX/Poseidon Science Investigations Plan 1 Sep. 1991 p 40-42 (For primary document see N93-14964 04-48)

Avail: CASI HC A01/MF A02; 22 functional color pages

The objectives of this study are to analyze ocean dynamics in the western South Pacific and the adjacent Southern Ocean and the eastern Indian Ocean. Specifically, our objectives for these three regions are, for the South Pacific Ocean: (1) To estimate the volume transport of the east Australian Current (EAC) along the Australian coast and in the Tasman Front, and to estimate the time variability (on seasonal and interannual time scales) of this transport. (2) To contribute to estimating the meridional heat and freshwater fluxes (and their variability) at about 30 deg S. Good estimates of the transport in the western boundary current are essential for accurate estimates of these fluxes. (3) To determine how the EAC transport (and its extension, the Tasman Front and the East Auckland Current) closes the subtropical gyre of the South Pacific and to better determine the structure at the confluence of this current and the Antarctic Circumpolar Current. (4) To examine the structure and time variability of the circulation in the western South Pacific and the adjacent Southern Ocean, particularly at the Tasman Front. For the Indian Ocean: (5) To study the seasonal interannual variations in the strength of the Leeuwin Current. (6) To monitor the Pacific-Indian Ocean throughflow and the South Equatorial and the South Java Currents between northwest Australia and Indonesia. (7) To study the processes that form the water of the permanent oceanic thermocline and, in particular, the way in which new thermocline water enters the permanent thermocline in late winter and early spring as the mixed layer restratifies. For the Southern Ocean: (8) To study the mesoscale and meridional structure of the Southern Ocean between 150 deg E and 170 deg E; in particular, to describe the Antarctic frontal system south of Tasmania and determine its interannual variability; to estimate the exchanges of heat, salt, and other properties between the Indian and Pacific Oceans; and to investigate the annual ventilation of the Antarctic Intermediate Water and Subantarctic Mode Water Masses. Author

N93-14972*# Centre National d'Etudes Spatiales, Toulouse (France). Groupe de Recherche de Geodesie Spatiale.

ASSIMILATION OF ALTIMETER TOPOGRAPHY INTO OCEANIC MODELS

Pierre DeMey, Yves Menard, Nadia Pinardi (Istituto per lo Studio delle Metodologie Geofische Ambientali, Modena, Italy), J. Schroeter (Alfred-Wegener-Inst. for Polar Research, Bremerhaven, Germany), and J. Verron (Institut de Mecanique de Grenoble, France) *In* JPL, TOPEX/Poseidon Science Investigations Plan 1 Sep. 1991 p 43-51 Original contains color illustrations (For primary document see N93-14964 04-48)

Avail: CASI HC A02/MF A02; 22 functional color pages

The primary goals of the authors are to build an intuition for assimilation techniques and to investigate the impact of variable altimeter topography on simple or complex oceanic models. In particular, applying various techniques and sensitivity studies to model and data constraints plays a key role. We are starting to use quasi-geostrophic, semigeostrophic, and primitive-equation (PE) models and to test the schemes in regions of interest to the World Ocean Circulation Experiment (WOCE), as well as in the northeast Atlantic and the Mediterranean. The impact of scatterometer wind forcing on the results is also investigated. The use of Geosat, European Remote Sensing satellite (ERS-1), and TOPEX/POSEIDON altimetry data is crucial in fine tuning the models and schemes to the selected areas of interest. Author

N93-14973*# Institut Francais de Recherche pour l'Exploitation de la Mer, Brest (France).

STUDIES OF THE INTERMEDIATE AND DEEP CIRCULATION IN THE WESTERN EQUATORIAL ATLANTIC

Yves Desaubies, C. Frankignoul (Paris VI Univ., France), and Jacques Merle (Paris VI Univ., France) *In* JPL, TOPEX/Poseidon Science Investigations Plan 1 Sep. 1991 p 52 (For primary document see N93-14964 04-48)

Avail: CASI HC A01/MF A02; 22 functional color pages

This proposal concerns the preparation and design of an experiment, the objective of which is to improve our knowledge of the intermediate and deep circulation in the western equatorial Atlantic Ocean. We shall focus on the description of the western boundary currents, of their crossing with the equator, on the estimation of their mass and heat fluxes, and their seasonal and interannual variations. We will use satellite altimetric data, tomographic measurements, and in situ observations (current measurements, hydrology, and floaters). We propose a feasibility study and the definition of a strategy based on a high-resolution Geophysical Fluid Dynamics Laboratory (GFDL) numerical model to define which in situ measurements are necessary to optimally complete the altimetric observations. Author

N93-14974*# National Aeronautics and Space Administration. Goddard Space Flight Center, Greenbelt, MD.

APPLICATION OF TOPEX/POSEIDON ALTIMETRY TO OCEAN DYNAMICS AND GEOPHYSICS

Bruce Douglas (National Ocean Service, Rockville, MD.), R. Cheney (National Ocean Service, Rockville, MD.), L. Miller (National Ocean Service, Rockville, MD.), D. McAdoo (National Ocean Service, Rockville, MD.), A. Leetmaa (National Weather Service, Washington, DC.), P. Schopf, and E. W. Schwiderski (Naval Surface Weapons Center, Dahlgren, VA.) *In* JPL, TOPEX/Poseidon Science Investigations Plan 1 Sep. 1991 p 53-54 (For primary document see N93-14964 04-48)

Avail: CASI HC A01/MF A02; 22 functional color pages

We will analyze the TOPEX/POSEIDON data using techniques developed for Geosat, although the more accurate TOPEX/POSEIDON data will enable a wider range of problems to be addressed. Our proposed investigations will have five distinct areas: (1) a description of global sea level variability; (2) tropical ocean dynamics; (3) coupled models for El Nino prediction; (4) structure of the lithosphere; and (5) global tide model improvement. I.I.C.

N93-14975*# Jet Propulsion Lab., California Inst. of Tech., Pasadena.

CIRCULATION OF THE GYRES OF THE WORLD OCEAN: OBSERVATION MODELING USING TOPEX/POSEIDON ALTIMETER DATA

Lee-Lueng Fu, V. Zlotnicki, W. R. Holland (National Center for Atmospheric Research, Boulder, CO.), and P. Malanotte-Rizzoli (Massachusetts Inst. of Tech., Cambridge.) *In its* TOPEX/Poseidon Science Investigations Plan 1 Sep. 1991 p 55-57 Original contains color illustrations (For primary document see N93-14964 04-48)

Avail: CASI HC A01/MF A02; 22 functional color pages

The overall objectives of the proposed investigation are to study the dynamics of the large-scale recirculating cells of water in the ocean, which are loosely defined as 'gyres' in this study. A gyre is normally composed

of a swift western boundary current (e.g., the Gulf Stream and the Kuroshio), a tight recirculating cell attached to the current, and a large-scale sluggish return flow. The water, of course, is not entirely recirculating within a gyre. The exchange of water among gyres is an important process in maintaining the meridional heat transport of the ocean. The gyres constitute a major mode of water movement in the ocean and play significant roles in the global climate system. Author

N93-14976*# National Research Inst. for Oceanology, Stellenbosch (South Africa).

SOUTH AFRICAN TOPEX/POSEIDON ALTIMETER EXPERIMENT

Marten L. Gruendlingh, L. V. Shannon (Sea Fisheries Research Inst., Cape Town, South Africa), and J. R. Lutjeharms (Cape Town Univ., South Africa) *In* JPL, TOPEX/Poseidon Science Investigations Plan 1 Sep. 1991 p 58-62 (For primary document see N93-14964 04-48)

Avail: CASI HC A01/MF A02; 22 functional color pages

The area surrounding the southern tip of Africa contains a juxtaposition of a variety of interesting and climatically relevant features. On the Indian Ocean side, the Agulhas Current with its tributaries form a conduit through which much of the southern Indian Ocean surface flow is focused. South of the continent, this flow is fragmented and partially injected into the Atlantic Ocean and across the Subtropical Convergence into the Southern Ocean. To the west of the subcontinent, the circulation of the South Atlantic subtropical gyre in the Cape Basin interacts with the vigorous Benguela upwelling regime. The creation, transformation, and transport of water masses and the intra-annual and climatic importance of all these processes have been specifically recognized by the World Ocean Circulation Experiment (WOCE). The South African TOPEX/POSEIDON Altimeter Experiment addresses many of these issues through four mutually complementary and interrelated subprojects. Author

N93-14977*# National Aeronautics and Space Administration. Goddard Space Flight Center, Greenbelt, MD.

SEA LEVEL RESPONSE TO WIND FORCING IN THE TROPICAL ATLANTIC

Eli Joel Katz (Columbia Univ., New York, NY.), A. J. Busalacchi, Jr., M. Cane (Lamont-Doherty Geological Observatory, Palisades, NY.), J. Carton (Maryland Univ., College Park.), and R. Miller (Woods Hole Oceanographic Inst., MA.) *In* JPL, TOPEX/Poseidon Science Investigations Plan 1 Sep. 1991 p 63-64 (For primary document see N93-14964 04-48)

Avail: CASI HC A01/MF A02; 22 functional color pages

. The circulation of the warm-water layer of the tropical Atlantic varies seasonally. This predominant signal is imposed by the annual migration of the Intertropical Covergence Zone separating two trade-wind regimes. As the migration varies interannually, so does the ocean circulation. A long-time objective of climate studies is to understand this interannual variability: to define its range, to fully explain the causal relationship between wind and ocean response, and eventually to understand how the resulting changes in sea surface temperature affect the wind field itself. Our initial objective is to observe and model the oceanic response. Author

N93-14978*# Institut de Mecanique de Grenoble (France).

GLOBAL OCEAN TIDES THROUGH ASSIMILATION OF OCEANOGRAPHIC AND ALTIMETER SATELLITE DATA IN A HYDRODYNAMIC MODEL

Christian LeProvost, P. Mazzega (Centre National d'Etudes Spatiales, Toulouse, France), and P. Vincent (Centre National d'Etudes Spatiales, Toulouse, France) *In* JPL, TOPEX/Poseidon Science Investigations Plan 1 Sep. 1991 p 65-69 (For primary document see N93-14964 04-48)

Avail: CASI HC A01/MF A02; 22 functional color pages

Ocean tides must be considered in many scientific disciplines: astronomy, oceanography, geodesy, geophysics, meteorology, and space technologies. Progress in each of these disciplines leads to the need for greater knowledge and more precise predictions of the ocean tide contribution. This is particularly true of satellite altimetry. On one side, the present and future satellite altimetry missions provide and will supply new data that will contribute to the improvement of the present ocean tide solutions. On the other side, tidal corrections included in the Geophysical Data Records must be determined with the maximum possible accuracy. The valuable results obtained with satellite altimeter data thus far have not been penalized by the insufficiencies of the present ocean tide predictions included in the geophysical data records (GDR's) because the oceanic processes investigated have shorter wavelengths than the error field of the tidal predictions, so that the residual errors of the tidal corrections are absorbed in the empirical tilt and bias corrections of the satellite orbit. For future applications to large-scale oceanic phenomena, however, it will no longer be possible to ignore these insufficiencies. Author

N93-14979*# Jet Propulsion Lab., California Inst. of Tech., Pasadena.

LOW-FREQUENCY VARIABILITY OF SEA LEVEL AS RELATED TO THE HEAT BALANCE OF GLOBAL OCEANS

W. Timothy Liu, P. Niiler (Scripps Institution of Oceanography, San Diego, CA.), and W. Patzert *In its* TOPEX/Poseidon Science Investigations Plan 1 Sep. 1991 p 70-71 (For primary document see N93-14964 04-48)

Avail: CASI HC A01/MF A02; 22 functional color pages

The TOPEX/POSEIDON mission will determine global changes of sea level with unprecedented accuracy. Our main objective is the use TOPEX/POSEIDON data, concurrent in situ ocean measurements, and other satellite observations to document and diagnose physical processes by which heat is exchanged with the atmosphere, stored in the ocean, or transported by ocean circulation. During the prelaunch period, our objectives are to advise the project on an improved method of retrieving sea level data and prepare for the application of TOPEX/POSEIDON data by developing a diagnostic model using in situ measurements and altimeter observations from Geosat and the European Remote Sensing satellite. Author

N93-14980*# National Aeronautics and Space Administration. Goddard Space Flight Center, Greenbelt, MD.

STUDIES OF TROPICAL OCEAN DYNAMICS USING THE TOPEX/POSEIDON ALTIMETER-DERIVED SEA SURFACE TOPOGRAPHY

Roger Lukas (Hawaii Univ., Honolulu.), A. J. Busalacchi, Jr., G. T. Mitchum (Hawaii Univ., Honolulu.), and K. Wyrtki (Hawaii Univ., Honolulu.) *In* JPL, TOPEX/Poseidon Science Investigations Plan 1 Sep. 1991 p 72-75 (For primary document see N93-14964 04-48)

Avail: CASI HC A01/MF A02; 22 functional color pages

Our primary objective is to carry out studies of tropical ocean dynamics using the TOPEX/POSEIDON altimeter-derived sea level data set in conjunction with the large in situ sea level data set available at the Tropical Ocean Global Atmosphere (TOGA) Sea Level Center. These studies will be supported by an interaction with numerical model simulations of tropical ocean variability. Five specific objectives can be identified: (1) research products; (2) short-term climate variations; (3) tropical-current variations; (4) synoptic-scale variability; and (5) model simulations. I.I.C.

N93-14981*# National Aeronautics and Space Administration. Goddard Space Flight Center, Greenbelt, MD.

OCEAN TOPOGRAPHY MAPPING, IMPROVEMENT OF THE MARINE GEOID, AND GLOBAL PERMANENT OCEAN CIRCULATION STUDIES FROM TOPEX/POSEIDON ALTIMETER DATA

James G. Marsh, F. J. Lerch, C. J. Koblinsky, R. S. Nerem, S. M. Klosko (ST Systems Corp., Lanham, MD.), and R. G. Williamson (ST Systems Corp., Lanham, MD.) *In* JPL, TOPEX/Poseidon Science Investigations Plan 1 Sep. 1991 p 76-81 Original contains color illustrations (For primary document see N93-14964 04-48)

Avail: CASI HC A02/MF A02; 22 functional color pages

The TOPEX/POSEIDON altimeter measurements will be the first global observations of the sea surface with accuracy sufficient to make quantitative determinations of the ocean's general circulation and its variations. These measurements are an important step to understanding global change in the ocean and its impact on the climate. Our investigation will focus on the examination of features in the sea surface elevation at the largest spatial and temporal scales. TOPEX/POSEIDON altimeter measurements will be used in conjunction with observations from past satellite-altimeter missions, such as NASA's GEOS-3 and Seasat, the U.S. Navy's Geosat and SALT, and the European Remote Sensing satellite in order to address the following issues: (1) Improve models of the marine geoid, especially at wavelengths needed to understand the basin-scale ocean dynamic topograpy. (2) Measure directly from the altimeter data the expression of the mean global ocean circulation in the sea surface at the largest scales through a simultaneous solution for gravity, orbital, and oceanographic

parameters. (3) Examine the sea surface measurements for changes in global ocean mass or volume, interannual variations in the basin-scale ocean circulation, and annual changes in the heating and cooling of the upper ocean. Author

N93-14982*# Centre National d'Etudes Spatiales, Toulouse (France).
GEOPHYSICAL VALIDATION OF TOPEX/POSEIDON ALTIMETRY PRODUCTS **c46**

Yves Menard, A. Guillaume (Direction de la Meteorologie Nationale, Paris, France), V. Casse (Direction de la Meteorologie Nationale, Paris, France), Jean-Francois Minster, B. Lago, C. Brossier, S. Arnault (Laboratoire d'Oceanographie Dynamique et de Climatologie, Paris, France), Jacques Merle (Laboratoire d'Oceanographie Dynamique et de Climatologie, Paris, France), F. Ramamonjiarisoa (Aix-Marseilles Univ., France), and N. Mognard (Puget Sound Univ., Tacoma, WA.) *In* JPL, TOPEX/Poseidon Science Investigations Plan 1 Sep. 1991 p 82-88 (For primary document see N93-14964 04-48)

Avail: CASI HC A02/MF A02; 22 functional color pages

The objectives of this study are the following: (1) to assess the quality of the sea level observed by altimetry on a global scale, especially in tropical regions where the atmospheric effects are the most critical, and to prepare the altimeter data for their assimilation into tropical Oceanic General Circulation Models; and (2) to validate and calibrate the altimeter-derived sea state parameters, to assimilate these parameters into numerical models, and to estimate the altimeter's sea state and electromagnetic biases. I.I.C.

N93-14983*# Laboratoire d'Oceanographie Dynamique et de Climatologie, Paris (France).
STUDY OF MASS AND HEAT TRANSPORT OF THE TROPICAL ATLANTIC OCEAN USING MODELS AND ALTIMETER DATA

Jacques Merle, S. Arnault, A. Morliere, J. M. Verstraete, Yves Menard (Centre National d'Etudes Spatiales, Toulouse, France), and L. Gourdeau (Centre National d'Etudes Spatiales, Toulouse, France) *In* JPL, TOPEX/Poseidon Science Investigations Plan 1 Sep. 1991 p 89-92 (For primary document see N93-14964 04-48)

Avail: CASI HC A01/MF A02; 22 functional color pages

The specific objectives of this proposal are: (1) to assess the quality of the TOPEX/POSEIDON surface altimeter data in regard to its use for a large, low-frequency monitoring of the surface topography of the tropical Atlantic Ocean; (2) to develop a method, on a demonstration basis, to derive from the tropical Atlantic the depth of the thermocline and the heat content changes from the surface altimeter data field; (3) to develop a method of assimilation of altimeter data into Oceanic General Circulation Models (OGCM's) for the purpose of preparing an operational, permanent, three-dimensional now casting of the tropical Atlantic Ocean (a TOGA objective); and (4) to derive from these models global circulation fields and a time series of mass and meridional heat transports across the tropical Atlantic region (a WOCE objective). Author

N93-14984*# Centre National d'Etudes Spatiales, Toulouse (France).
OCEAN CIRCULATION USING ALTIMETRY

Jean-Francois Minster, C. Brossier, M. C. Gennero, P. Mazzega, F. Remy, P. Y. LeTraon, and F. Blanc *In* JPL, TOPEX/Poseidon Science Investigations Plan 1 Sep. 1991 p 93-94 (For primary document see N93-14964 04-48)

Avail: CASI HC A01/MF A02; 22 functional color pages

Our group has been very actively involved in promoting satellite altimetry as a unique tool for observing ocean circulation and its variability. TOPEX/POSEIDON is particularly interesting as it is optimized for this purpose. It will probably be the first instrument really capable of observing the seasonal and interannual variability of subtropical and polar gyres and the first to eventually document the corresponding variability of their heat flux transport. The studies of these phenomena require data of the best quality, unbiased extraction of the signal, mixing of these satellite data with in situ measurements, and assimilation of the whole set into a dynamic description of ocean circulation. Our group intends to develop responses to all these requirements. We will concentrate mostly on the circulation of the South Atlantic and Indian Oceans: This will be done in close connection with other groups involved in the study of circulation of the tropical Atlantic Ocean, in the altimetry measurements (in particular, those of the tidal issue), and in the techniques of data assimilation in ocean circulation models. Author

N93-14985*# National Aeronautics and Space Administration. John C. Stennis Space Center, Bay Saint Louis, MS.
THE DYNAMICS AND ENERGETICS OF MIDLATITUDE WESTERN BOUNDARY CURRENTS: A COMPARISON OF THE KUROSHIO EXTENSION AND THE GULF STREAM

James L. Mitchell, Z. R. Hallock, H. E. Hurlburt, D. R. Johnson, J. C. Kindle, W. J. Teague, J. D. Thompson, and W. J. Schmitz (Woods Hole Oceanographic Inst., MA.) *In* JPL, TOPEX/Poseidon Science Investigations Plan 1 Sep. 1991 p 95-102 Original contains color illustrations (For primary document see N93-14964 04-48)

Avail: CASI HC A02/MF A02; 22 functional color pages

We will use TOPEX/POSEIDON altimetry in combination with ongoing and planned efforts, including data from the European Remote Sensing satellite (ERS-1), in situ measurements designed specifically to complement satellite altimetry, and assimilation of these several data types into eddy-resolving numerical models in order to understand the dynamics and energetics of midlatitude western boundary currents (specifically, the Gulf Stream and the Kuroshio Extension). A better understanding of the recirculation of midlatitude gyres can best be undertaken in the format of such regional, eddy-resolving experiments. Such regional programs will enhance and be enhanced by the larger scale circulation studies of the World Ocean Circulation Experiment (WOCE) as well as by global-scale eddy-resolving models that we will develop prior to the TOPEX/POSEIDON mission. This effort includes participation on the TOPEDX/POSEIDON Science Team. Author

N93-14986*# Alfred-Wegener-Inst. for Polar Research, Bremerhaven (Germany).
OCEAN CIRCULATION MODELING BY USE OF RADAR ALTIMETER DATA

Dirk Olbers, W. Alpers (Bremen Univ., Germany), K. Hasselmann (Max-Planck-Inst. fuer Meteorologie, Hamburg, Germany), E. Maier-Reimer (Max-Planck-Inst. fuer Meteorologie, Hamburg, Germany), R. Kase (Kiel Univ., Germany), W. Krauss (Kiel Univ., Germany), G. Siedler (Kiel Univ., Germany), J. Willebrand (Kiel Univ., Germany), and W. Zahel (Hamburg Univ., Germany) *In* JPL, TOPEX/Poseidon Science Investigations Plan 1 Sep. 1991 p 103-104 (For primary document see N93-14964 04-48)

Avail: CASI HC A01/MF A02; 22 functional color pages

The project will investigate the use of radar altimetry (RA) data in the determination of the ocean circulation models. RA data will be used to verify prognostic experiments of the steady state and seasonal cycle of large-scale circulation models and the statistical steady state of eddy-resolving models. The data will serve as initial and update conditions in data assimilation experiments and as constraints in inverse calculations. The aim of the project is a better understanding of ocean physics, the determination and mapping of ocean currents, and a contribution to the establishment of ocean circulation models for climate studies. The goal of the project is to use satellite radar altimetry data for improving our knowledge of ocean circulation both in a descriptive sense and through the physics that govern the circulation state. The basic tool is a series of ocean circulation models. Depending on the model, different techniques will be applied to incorporate the RA data. Author

N93-14987*# Institut Francais de Recherche pour l'Exploitation de la Mer, Brest (France).
GENERAL CIRCULATION OF THE SOUTH ATLANTIC BETWEEN 5 DEG N AND 35 DEG S

Michel Ollitrault, H. Mercier, F. Blanc (Centre National d'Etudes Spatiales, Toulouse, France), and L. Y. LeTraon (Centre National d'Etudes Spatiales, Toulouse, France) *In* JPL, TOPEX/Poseidon Science Investigations Plan 1 Sep. 1991 p 105-107 (For primary document see N93-14964 04-48)

Avail: CASI HC A01/MF A02; 22 functional color pages

The TOPEX/POSEIDON altimeter will provide the temporal mean seal level. So, secondly, we propose to compute the difference between these two surfaces (mean sea level minus general circulation dynamic topography). The result will be an estimate of the marine geoid, which is time invariant for the 5-year period under consideration. If this geoid is precise enough, it will permit a description of seasonal variability of the large-scale surface

circulation. If there happens to be enough float data, it may be possible to infer the first vertical modes of this variability. Thus the main goal of our investigation is to determine the 3-D general circulation of the South Atlantic and the large-scale seasonal fluctuations. This last objective, however, may be restricted to the western part of the South Atlantic because float deployments have been scheduled only in the Brasil basin. Author

N93-14988*# Nansen Ocean and Remote Sensing Center, Solheimsvik (Norway).

OCEAN DYNAMICS IN THE NORDIC SEAS USING SATELLITE ALTIMETRY

Lasse H. Pettersson, O. M. Johannessen, and T. I. Olaussen *In* JPL, TOPEX/Poseidon Science Investigations Plan 1 Sep. 1991 p 108-113 Original contains color illustrations (For primary document see N93-14964 04-48)

Avail: CASI HC A02/MF A02; 22 functional color pages

The main objective of this TOPEX/POSEIDON project is to integrate the accurately measured sea surface topography, as resolved by both TOPEX/POSEIDON radar altimeters, into the above-mentioned quantitative studies of the short- and long-term variations in the mesoscale ocean dynamics of the Nordic Seas south of 66 deg N. This implies: (1) comparison and validation of the capability to resolve the general basin-scale circulation and the mesoscale variability by, respectively, radar altimeters and numerical ocean circulation models; (2) calibration and validation of the altimeter-derived sea surface topography against in situ measurements from research vessels and moorings, particularly under extreme wind and wave conditions; and (3) improved monitoring and understanding of the flux variations between the North Atlantic and the Nordic Seas, both on the short and seasonal time scales. Author

N93-14989*# National Aeronautics and Space Administration. Goddard Space Flight Center, Greenbelt, MD.

APPLICATION OF TOPEX/POSEIDON ALTIMETRY MEASUREMENTS TO OBSERVATIONAL AND MODELING STUDIES OF THE LOW-FREQUENCY UPPER OCEAN MASS AND HEAT CIRCULATION IN THE TROPICAL PACIFIC

Joel Picaut (Institut Francais de Recherche Scientifique pour le Developpement en Cooperation, Paris, France), T. Delcroix (Institut Francais de Recherche Scientifique pour le Developpement en Cooperation, Paris, France), Y. duPenhoat (Institut Francais de Recherche Scientifique pour le Developpement en Cooperation, Paris, France), A. J. Busalacchi, Jr., G. Gautier (California Univ., Santa Barbara.), S. P. Hayes (National Oceanic and Atmospheric Administration, Seattle, WA.), and M. J. McPhaden (National Oceanic and Atmospheric Administration, Seattle, WA.) *In* JPL, TOPEX/Poseidon Science Investigations Plan 1 Sep. 1991 p 114-117 (For primary document see N93-14964 04-48)

Avail: CASI HC A01/MF A02; 22 functional color pages

The main purpose of the proposed work is to describe the seasonal and interannual variability of the upper ocean mass and heat transport in the tropical Pacific and to understand the mechanisms responsible for these transports. This will be done through a combination of experimental and modeling approaches. Remotely sensed sea level and derived current, observed on the basin scale, will be compared, analyzed, and combined with routine and enhanced in situ measurements of thermal and current field, as well as with model solutions forced by satellite-derived estimates of momentum and heat fluxes. The practical scientific rationale for this work stems from the unique data sets collected by (or easily available to) the investigator's team and from the team members' complementary backgrounds (physical oceanography and meteorology) and expertise (in situ and satellite-observation analysis and numerical ocean modeling).

Author

N93-14990*# Ohio State Univ., Columbus.

MEAN SEA SURFACE AND GRAVITY INVESTIGATIONS USING TOPEX/POSEIDON ALTIMETER DATA

Richard H. Rapp *In* JPL, TOPEX/Poseidon Science Investigations Plan 1 Sep. 1991 p 118-120 (For primary document see N93-14964 04-48)

Avail: CASI HC A01/MF A02; 22 functional color pages

From a broad point of view, we will be concerned with studying global ocean circulation patterns on the basis of ocean surface determinations with geoid undulation information. In addition, we will study local variations of the gravity field implied by the altimeter data. These general goals are reflected in the title of our investigation. To meet our general goal, we have defined a number of specific objectives: (1) sea surface topography representation; (2) mean sea surface determination; (3) development of local geoid models; (4) mean sea surface comparisons; (5) sea surface topographic files; and (6) gravity anomaly determination. I.I.C.

N93-14991*# National Aeronautics and Space Administration. Goddard Space Flight Center, Greenbelt, MD.

GLOBAL OCEAN TIDE MAPPING USING TOPEX/POSEIDON ALTIMETRY

Braulio V. Sanchez, D. E. Cartwright (ST Systems Corp., Lanham, MD.), R. H. Estes (ST Systems Corp., Lanham, MD.), R. G. Williamson (ST Systems Corp., Lanham, MD.), and O. L. Colombo (Maryland Univ., College Park.) *In* JPL, TOPEX/Poseidon Science Investigations Plan 1 Sep. 1991 p 121-125 (For primary document see N93-14964 04-48)

Avail: CASI HC A01/MF A02; 22 functional color pages

The investigation's main goals are to produce accurate tidal maps of the main diurnal, semidiurnal, and long-period tidal components in the world's deep oceans. This will be done by the application of statistical estimation techniques to long time series of altimeter data provided by the TOPEX/POSEIDON mission, with additional information provided by satellite tracking data. In the prelaunch phase, we will use in our simulations and preliminary work data supplied by previous oceanographic missions, such as Seasat and Geosat. These results will be of scientific interest in themselves. The investigation will also be concerned with the estimation of new values, and their uncertainties, for tidal currents and for the physical parameters appearing in the Laplace tidal equations, such as bottom friction coefficients and eddy viscosity coefficients. This will be done by incorporating the altimetry-derived charts of vertical tides as boundary conditions in the integration of those equations. The methodology of the tidal representation will include the use of appropriate series expansions such as ocean-basin normal modes and spherical harmonics. The results of the investigation will be space-determined tidal models of coverage and accuracy superior to that of the present numerical models of the ocean tides, with the concomitant benefits to oceanography and associated disciplinary fields.

Author

N93-14992*# Tokyo Univ. (Japan).

APPLICATION OF PRECISE ALTIMETRY TO THE STUDY OF PRECISE LEVELING OF THE SEA SURFACE, THE EARTH'S GRAVITY FIELD, AND THE ROTATION OF THE EARTH **c43**

J. Segawa, Y. Ganeko (Maritime Safety Agency, Tokyo, Japan), M. Sasaki (Maritime Safety Agency, Tokyo, Japan), T. Mori (Maritime Safety Agency, Tokyo, Japan), M. Ooe (Mizusawa International Latitude Observatory, Japan), I. Nakagawa (Kyoto Univ., Japan), H. Ishii, and Y. Hagiwara *In* JPL, TOPEX/Poseidon Science Investigations Plan 1 Sep. 1991 p 126-130 Original contains color illustrations (For primary document see N93-14964 04-48)

Avail: CASI HC A01/MF A02; 22 functional color pages

Our program includes five research items: (1) determination of a precision geoid and gravity anomaly field; (2) precise leveling and detection of tidal changes of the sea surface and study of the role of the tide in the global energy exchange; (3) oceanic effect on the Earth's rotation and polar motion; (4) geological and geophysical interpretation of the altimetry gravity field; and (5) evaluation of the effectiveness of local tracking of TOPEX/POSEIDON by use of a laser tracker. Author

N93-14993*# Centre National d'Etudes Spatiales, Toulouse (France).

PRESENT-DAY PLATE MOTIONS: RETRIEVAL FROM THE TOPEX/POSEIDON ORBITOGRAPHY NETWORK (DORIS SYSTEM) **c46**

Annie Souriau, Anny Cazenave, R. Biancale, G. Balmino, K. Dominh, P. Mazzega, J.-M. Lemoine, Claude Boucher (Institut Geographique National, Paris, France), P. Willis (Institut Geographique National, Paris, France), and M. Kasser (Institut Geographique National, Paris, France) et al *In* JPL, TOPEX/Poseidon Science Investigations Plan 1 Sep. 1991 p 131-136 (For primary document see N93-14964 04-48)

Avail: CASI HC A02/MF A02; 22 functional color pages

The goal of the proposal is to determine the present motion of the main tectonic plates from the Doppler data of the Doppler Orbitography and Radiopositioning Integrated by Satellite (DORIS) orbitography system, which includes in its final configuration about 50 tracking stations with a world-wide distribution. Author

N93-14994*# Oregon State Univ., Corvallis.
EQUATORIAL AND EASTERN BOUNDARY CURRENT VARIABILITY IN THE NORTH AND SOUTH PACIFIC OCEANS
P. Ted Strub, M. D. Levine, and D. B. Enfield (National Oceanic and Atmospheric Administration, Miami, FL.) *In* JPL, TOPEX/Poseidon Science Investigations Plan 1 Sep. 1991 p 137-140 (For primary document see N93-14964 04-48)
Avail: CASI HC A01/MF A02; 22 functional color pages

The overall objective of our investigation within the TOPEX/POSEIDON project is to describe the large-scale and mesoscale circulation of the upper ocean in the eastern North and South Pacific Oceans. We also wish to understand the relation between these currents and local and distant wind forcing. In this contest, 'large scale' refers to basin-scale fluctuations at annual and interannual time scales; 'mesoscale' refers to variability with periods less than 60 days, regardless of the spatial scale. Author

N93-14995*# Scripps Institution of Oceanography, La Jolla, CA.
AN INTEGRATED RESEARCH PROGRAM FOR TOPEX/POSEIDON WITH EMPHASIS ON THE PACIFIC OCEAN
Chang-Kou Tai and W. B. White *In* JPL, TOPEX/Poseidon Science Investigations Plan 1 Sep. 1991 p 141-142 (For primary document see N93-14964 04-48)
Avail: CASI HC A01/MF A02; 22 functional color pages

There are four distinct but related tasks in this investigation. First, we want to combine estimates of the surface dynamic topography derived independently from altimetry and from hydrography in an optimal way (weighted least squares with a priori estimates) to produce an optimal estimate (with error bounds) of the large-scale circulation. Second, we want to study the large-scale (as opposed to the mesoscale) variability using crossover differences as well as exact repeat tracks. The third task involves the study of mesoscale variability in the Kuroshio Extension, the California Current, and eventually the Pacific Ocean and the whole globe, wherein surface transport estimates are provided for both the Kuroshio Extension and the Gulf Stream. The final task is a study of how altimeter data and other data can be assimilated into numerical models. I.I.C.

N93-14996*# Tokyo Univ. (Japan).
OCEANIC TRANSPORTS OF MASS, HEAT, AND SALT IN THE WESTERN NORTH PACIFIC
K. Taira, T. Mori (Japan Oceanographic Data Center, Tokyo.), M. Saiki (Japan Meteorological Agency, Tokyo.), H. Nishida (Maritime Safety Agency, Tokyo, Japan), and S. Matsumura (Japan Oceanographic Data Center, Tokyo.) *In* JPL, TOPEX/Poseidon Science Investigations Plan 1 Sep. 1991 p 143-144 (For primary document see N93-14964 04-48)
Avail: CASI HC A01/MF A02; 22 functional color pages

An optimum orbit of the satellite will be presented for confirmation of estimates of tides and interpolation errors. Hydrographic surveys complementary to the routine surveys will be planned in Phase 1 by using research vessels belonging to Japanese universities. Direction measurements of oceanic transports with moored current meters and shipborne acoustic Doppler velocimeters will be planned for selected sections as an activity of the Japan-WOCE (World Ocean Circulation Experiment) Project. In the operational phase of TOPEX/POSEIDON, the delivered altimeter data will be used for the computation of surface geostrophic velocities to be applied in the hydrographic sections of the Japan Meteorological Agency, Hydrographic Department, Japan Fisheries Agency, and the universities. The estimates of transports are made by the co-investigators of each agency. The composite of the transports in the circulations will be made at the Japan Oceanographic Data Center. The direct measurements of current velocity and transports will be made mainly by the principal investigator. Author

N93-14997*# Texas Univ., Austin.
THE DETERMINATION AND INTERPRETATION OF OCEAN SURFACE TOPOGRAPHY USING TOPEX/POSEIDON ALTIMETER DATA
Byron D. Tapley, B. E. Schutz, C. K. Shum, D. T. Sandwell (Scripps Institution of Oceanography, San Diego, CA.), and R. H. Stewart (Texas A&M Univ., College Station.) *In* JPL, TOPEX/Poseidon Science Investigations Plan 1 Sep. 1991 p 145-152 Original contains color illustrations (For primary document see N93-14964 04-48)
Avail: CASI HC A02/MF A02; 22 functional color pages

The objectives of this investigation are to use the complete set of TOPEX/POSEIDON altimeter and tracking data, in combination with altimeter and tracking data from ERS-1 and other satellites, to perform scientific research in the areas of oceanography, geodynamics, and geophysics. The following specific objectives will be addressed: (1) in oceanography, to create a dynamically consistent global mean sea surface and to separate and study the constant and time-varying components of the ocean surface topography; (2) in geodynamics, to improve the global marine geoid and the global ocean tide model to support studies in basin-scale ocean circulation; and (3) in geophysics, to improve the detail and accuracy of the global sea surface topography to support marine geophysical studies, to use the improved surface to obtain further understanding of the remote ocean basins, and to study thermal and mechanical features such as spreading ridges, fracture zones, and trenches. Author

N93-14998*# Institut de Physique du Globe, Paris (France).
ANALYSIS OF ALTIMETER DATA JOINTLY WITH SEAFLOOR ELECTRIC DATA (VERTICALLY INTEGRATED VELOCITY) AND VCTD-YOYO DATA (DETAILED PROFILES OF VCTD)
Pascal D. Tarits, M. Menvielle (Centre National de la Recherche Scientifique, Paris, France), C. Provost (Paris VI Univ., France), and J. H. Filloux (Scripps Institution of Oceanography, La Jolla, CA.) *In* JPL, TOPEX/Poseidon Science Investigations Plan 1 Sep. 1991 p 153-158 (For primary document see N93-14964 04-48)
Avail: CASI HC A02/MF A02; 22 functional color pages

We propose simultaneous analyses of the TOPEX/POSEIDON altimetry data, in situ data--mainly permanent seafloor electric recordings--and velocity, conductivity, temperature, density (VCTD)-yoyo data at several stations in areas of scientific interest. We are planning experiments in various areas of low and high energy levels. Several complementary and redundant methods will be used to characterize the ocean circulation and its short- and long-term variability. We shall emphasize long-term measurement using permanent stations. Our major initial objectives with the TOPEX/POSEIDON mission are the Confluence area in the Argentine Basin and the Circumpolar Antarctic Current. An early experiment was carried out in the Confluence zone in 1988 and 1990 (Confluence Principal Investigators, 1990) to prepare for an intensive phase later one. This intensive phase will include new types of instrumentation. Preliminary experiments will be carried out in the Mediterranean Sea (in 1991) and in the North Atlantic Ocean (in 1992, north of the Canary Islands) to test the new instrumentation. Author

N93-14999*# Colorado Univ., Boulder.
A TOPEX/POSEIDON STUDY OF OCEANIC EFFECTS ON OBSERVATIONS OF THE EARTH'S INTERIOR **c46**
John Wahr and N. Benton *In* JPL, TOPEX/Poseidon Science Investigations Plan 1 Sep. 1991 p 159-160 (For primary document see N93-14964 04-48)
Avail: CASI HC A01/MF A02; 22 functional color pages

The primary objective of our research program is the application of TOPEX/POSEIDON oceanic data to the study of various geophysical observations, thereby improving our knowledge of the Earth's interior. Observations of the Earth's solid tides, rotation, time-dependent gravity, and crustal deformation provide potentially useful constraints on properties of the solid Earth and its liquid core, but all these parameters are also sensitive to oceanic effects. Depending on the type of observation, those effects are usually either removed by modeling (often using particularly simple assumptions about the dynamics of the ocean) or ignored entirely. Useful oceanic data are rarely available. In many cases, the uncertainty in the oceanic correction is the main source of error in the geophysical interpretation of the results. We describe, below several of these geophysical observations, how their interpretation in terms of the Earth's interior is affected by the oceans, and how data from the TOPEX/POSEIDON mission can be used to improve this situation. Author

N93-15000*# Technische Univ., Delft (Netherlands).
PRECISE ORBIT COMPUTATION AND SEA SURFACE MODELING **c13**
Karel F. Wakker, B. A. C. Ambrosius, R. Rummel, E. Vermaat, W. P. M. deRuijter (Utrecht State Univ., Netherlands), J. W. vanderMade (Rijkswaterstaat, Delft, Netherlands), and J. T. F. Zimmerman (Nederlands Inst. voor Onderzoek der Zee, Texel.) *In* JPL, TOPEX/Poseidon Science Investigations Plan 1 Sep. 1991 p 161-168 Original contains color

illustrations (For primary document see N93-14964 04-48)
Avail: CASI HC A02/MF A02; 22 functional color pages

The research project described below is part of a long-term program at Delft University of Technology aiming at the application of European Remote Sensing satellite (ERS-1) and TOPEX/POSEIDON altimeter measurements for geophysical purposes. This program started in 1980 with the processing of Seasat laser range and altimeter height measurements and concentrates today on the analysis of Geosat altimeter data. The objectives of the TOPEX/POSEIDON research project are the tracking of the satellite by the Dutch mobile laser tracking system MTLRS-2, the computation of precise TOPEX/POSEIDON orbits, the analysis of the spatial and temporal distribution of the orbit errors, the improvement of ERS-1 orbits through the information obtained from the altimeter crossover difference residuals for crossing ERS-1 and TOPEX/POSEIDON tracks, the combination of ERS-1 and TOPEX/POSEIDON altimeter data into a single high-precision data set, and the application of this data set to model the sea surface. The latter application will focus on the determination of detailed regional mean sea surfaces, sea surface variability, ocean topography, and ocean currents in the North Atlantic, the North Sea, the seas around Indonesia, the West Pacific, and the oceans around South Africa. Author

N93-15001*# Proudman Oceanographic Lab., Birkenhead (England).
MARINE RESEARCH USING DATA FROM TOPEX/POSEIDON
Philip L. Woodworth, T. F. Baker, J. M. Huthnance, J. M. Vassie, M. Srokosz (British National Space Centre, Wormley, England), P. Challenor (Institute of Oceanographic Sciences, Wormley, England), T. H. Guymer (Institute of Oceanographic Sciences, Wormley, England), and D. J. Webb (Institute of Oceanographic Sciences, Wormley, England) *In* JPL, TOPEX/Poseidon Science Investigations Plan 1 Sep. 1991 p 169-173 (For primary document see N93-14964 04-48)
Avail: CASI HC A01/MF A02; 22 functional color pages

The Proudman Oceanographic Laboratory (POL), the Institute of Oceanographic Sciences Deacon Laboratory (IOSDL), and the British National Space Centre (BNSC) plan to use radar altimeter data from the TOPEX/POSEIDON mission in five main areas of research. These are: (1) investigation of variations in Southern Ocean sea levels and circulation; (2) related numerical modeling and data assimilation; (3) global and regional ocean tides; (4) North Sea and northeast Atlantic studies; and (5) winds and waves. Each one of these topics is described briefly below while more information can be extracted from the United Kingdom response to the TOPEX/POSEIDON Announcement of Opportunity. Author

N93-15002*# Massachusetts Inst. of Tech., Cambridge.
GLOBAL OCEAN CIRCULATION BY ALTIMETRY
Carl Wunsch and D. Haidvogel (Johns Hopkins Univ., Baltimore, MD.) *In* JPL, TOPEX/Poseidon Science Investigations Plan 1 Sep. 1991 p 174-176 (For primary document see N93-14964 04-48)
Avail: CASI HC A01/MF A02; 22 functional color pages

The overall objectives of this project are to determine the general circulation of the oceans and many of its climate and biochemical consequences through the optimum use of altimetry data from TOPEX/POSEIDON and related missions. Emphasis is on the global-scale circulation, as opposed to the regional scale, but some more local studies will be carried out. Because of funding limitations, the primary initial focus will be on the time-dependent global-scale circulation rather than the mean; eventually, the mean circulation must be dealt with as well. Author

N93-15113# Coastal Engineering Research Center, Vicksburg, MS.
EVALUATION OF METHODS FOR ESTIMATING WIND WAVE GROWTH ON NARROW IRREGULAR FETCHES Final Report
Kenneth J. Eisses Aug. 1992 50 p
(AD-A256002; CERC-TR-92-8) Avail: CASI HC A03/MF A01

The purpose of this study was to compare three different methods for generating wave heights and periods on a narrow irregular fetch with data from a typical Alaskan site. Kodiak, Alaska, was selected because concurrent wind and wave measurements were available for a period of 3 years. Based on wind direction blowing down the narrow fetch to the wave buoy, 79 cases for comparison were chosen. Swell was removed from the buoy data so that only wind waves generated down the narrow fetch were compared. Comparisons were made against the JONSWAP wave growth equations as found in the Shore Protection Manual (1984) or Water Levels and Wave Heights for Coastal Engineering Design (1989), NARFET, a wind-wave generation on restricted fetches analytical model, and STWAVE, a gridded steady-state spectral model. Results of the study showed that STWAVE matched the buoy wave heights within 0.1 ft based on the mean and that NARFET matched the buoy wave periods within 0.2 sec, based on the mean. This limited study suggests that STWAVE and NARFET, respectively, should be used for determining wave heights and periods for narrow irregular fetches. GRA

N93-15645*# National Aeronautics and Space Administration. Goddard Space Flight Center, Greenbelt, MD.
SeaWiFS TECHNICAL REPORT SERIES. CLOUD SCREENING FOR POLAR ORBITING VISIBLE AND INFRARED (IR) SATELLITE SENSORS, VOLUME 7
Michael Darzi, Stanford B. Hooker, ed., and Elaine R. Firestone, ed. (General Sciences Corp., Laurel, MD.) Washington Nov. 1992 10 p
(NASA-TM-104566; Rept-93B00016-Vol-7; NAS 1.15:104566) Avail: CASI HC A02/MF A01

Methods for detecting and screening cloud contamination from satellite derived visible and infrared data are reviewed in this document. The methods are applicable to past, present, and future polar orbiting satellite radiometers. Such instruments include the Coastal Zone Color Scanner (CZCS), operational from 1978 through 1986; the Advanced Very High Resolution Radiometer (AVHRR); the Sea-viewing Wide Field-of-view Sensor (SeaWiFS), scheduled for launch in August 1993; and the Moderate Resolution Imaging Spectrometer (IMODIS). Constant threshold methods are the least demanding computationally, and often provide adequate results. An improvement to these methods are the least demanding computationally, and often provide adequate results. An improvement to these methods is to determine the thresholds dynamically by adjusting them according to the areal and temporal distributions of the surrounding pixels. Spatial coherence methods set thresholds based on the expected spatial variability of the data. Other statistically derived methods and various combinations of basic methods are also reviewed. The complexity of the methods is ultimately limited by the computing resources. Finally, some criteria for evaluating cloud screening methods are discussed. Author

51 LIFE SCIENCES (GENERAL)

N93-14532# Tennessee Univ., Knoxville.
BIOFILM ECOLOGY OF BIOLUMINESCENT BACTERIA Final Report, 1 Apr. 1991 - 30 May 1992
Marc W. Mittelman and David C. White 10 Aug. 1992 28 p
(Contract N00014-91-J-1598)
(AD-A255282) Avail: CASI HC A03/MF A01

Test systems have been developed which enable the evaluation of bacterial biofilm formation and metabolic activity under conditions simulating those of the in situ environment. A series of laminar-flow adhesion cells were constructed with provisions for on-line, nondestructive measurements of bioluminescence, fluorescence, open circuit potential, and po2 for monitoring colonization and succession as influenced by a systematic change in bulk-phase and substratum conditions. Bioluminescence and fluorescence by biofilms of the bioluminescent, marine bacterium, Vibrio harveyi were utilized as endpoints for adhesion in evaluations of antifouling (AF) ship hull coatings. Resistance to colonization of V. harveyi was noted in the order of F-121 (Navy) greater than BRA 640 (IP) greater than 15 pct. DNP. Future work will evaluate changes in cellular lipid biomarkers associated with biofilms and planktonic cultures exposed to copper contained in AF coatings and in bulk-phase chemostats, respectively. The test systems and procedures developed under ONR funding will enable studies of materials compatibility, antifouling efficacy, and biocide toxicity in diverse ecosystems. GRA

N93-14557# Stanford Univ., CA. Dept. of Civil Engineering.
ANAEROBIC MICROBIAL TRANSFORMATION OF AROMATIC HYDROCARBONS AND MIXTURES OF AROMATIC HYDROCARBONS AND HALOGENATED SOLVENTS Final Report, 30 Sep. 1988 - 31 Mar. 1992
Elizabeth A. Edwards, Li-Nuo Liang, and Dunia Grbic-Galic 25 Aug. 1992

169 p
(Grant AF-AFOSR-0351-88)
(AD-A255696; AFOSR-92-0875TR) Avail: CASI HC A08/MF A02

Anaerobic microbial transformation of monoaromatic hydrocarbons (MAH), chlorinated benzenes (CB), and mixtures of MAH and CB, as well as MAH and chlorinated aliphatic solvents (tetrachloroethylene -- PCE, and carbon tetrachloride --CT) was studied in laboratory microcosms derived from hydrocarbon-contaminated groundwater aquifers. Some MAH, such as toluene and o-xylene, were completely degraded to CO2 and CH4 by mixed methanogenic cultures from a creosote-contaminated aquifer. This degradation was inhibited by the addition of accessory electron acceptors (oxygen, nitrate, sulfate), indicating acclimation of the micrcbial community to methanogenic conditions. The addition of preferred substrates, such as acetate, propionate, methanol, fatty acids, glucose, casamino acids, pepton, yeast extract, or acetone also inhibited MAH degradation, indicating that the presence of natural organic substrates may preclude anaerobic biodegradation of MAH in situ. Cyclohexane, CT, and high concentrations of toluene and o-xylene had a toxic effect under sulfate-reducing conditions. Several MAH -toluene, all three xylene isomers, and benzene were mineralized to CO2, by microorganisms from a petroleum-contaminated, sulfidogenic aquifer. Whereas-toluene and xylenes were sequentially degraded in a mixture, benzene was degraded only if alone, or slowly transformed in a mixture with toluene. This explains previously reported recalcitrance of benzene under anaerobic conditions. GRA

N93-14648# Catholic Univ. of America, Washington, DC. Vitreous State Lab.
MECHANISMS OF MICROWAVE INDUCED DAMAGE IN BIOLOGIC MATERIALS Annual Report, 22 Sep. 1990 - 21 Sep. 1991
T. A. Litovitz, J. J. Greene, D. Krause, R. Meister, and R. K. Mohr Jan. 1992 59 p
(Contract DAMD17-86-C-6260)
(AD-A255799) Avail: CASI HC A04/MF A01

The results of research directed at several of the very fundamental issues concerning cellular effects of weak electromagnetic fields is described. Despite their importance, these issues have not been satisfactorily addressed by the scientific community. They include the following issues: (1) replication of experimental effects; (2) how weak electromagnetic fields can affect cells that exist in an electrically noisy environment; and (3) the explanation of complex dose-response relationships. GRA

N93-15208# Florida Sea Grant Coll., Gainesville.
THE PRODUCTION AND USE OF AEROPONICALLY GROWN INOCULA OF VAM FUNGI IN THE NATIVE PLANT NURSERY
Amiel G. Jarstfer and David M. Sylvia (Florida Univ., Gainesville.) Jun. 1992 18 p Submitted for publication
(Grant NA89AA-D-SG-053; Proj. R/C-S-27; Proj. IR-90-2)
(PB92-204973; SGEB-22) Avail: CASI HC A03/MF A01

Selected vesicular-arbuscular mycorrhizal (VAM) fungi have been shown to enhance the growth of numerous plants of economic importance, including native plants used for revegetation of disturbed sites such as renourished coastal beaches and strip mined lands. Major benefits for the plants are increased uptake of phosphorous and other poorly mobile nutrients and tolerance of water stress. Nonetheless, VAM fungi are not used widely in plant production systems because inoculum sources are limited and application technologies are not well developed. GRA

N93-15211# Oregon Regional Primate Research Center, Beaverton.
JOINT HVAC TRANSMISSION EMF ENVIRONMENTAL STUDY
F. Stormshak and J. Thompson May 1992 191 p Prepared in cooperation with Portland State Univ., OR; Oregon Health Sciences Univ., Portland Prepared for Bonneville Power Administration, Portland. OR
(Contract DE-BI79-90BP-04293)
(DE92-017863; DOE/BP-1792) Avail: CASI HC A09/MF A02

This document describes the rationale, procedures, and results of a carefully controlled study conducted to establish whether chronic exposure of female (ewe) Suffolk lambs to the environment of a 500-kV 60-Hz transmission line would affect various characteristics of growth, endocrine function, and reproductive development. This experiment used identical housing and management schemes for control and line-exposed ewes, thus minimizing these factors as contributors to between-group experimental error. Further, throughout the 10-month duration of this study, changes in electric and magnetic fields, audible noise, and weather conditions were monitored continuously by a computerized system. Such measurements provided the opportunity to identify any relationship between environmental factors and biological responses. Because of reports in the literature that electric and magnetic fields alter concentrations of melatonin in laboratory animals, the primary objective of this study was to ascertain whether a similar effect occurs in lambs exposed to a 500-kV a-c line in a natural setting. In addition, onset of puberty, changes in body weight, wool growth, and behavior were monitored. To determine whether the environment of a 500-kV line caused stress in the study animals, serum levels of cortisol were measured. The study was conducted at Bonneville Power Administration's Ostrander Substation near Estacada, Oregon. DOE

52 AEROSPACE MEDICINE

Includes physiological factors; biological effects of radiation; and effects of weightlessness on man and animals.

N93-14103# Army Aeromedical Research Lab., Fort Rucker, AL.
TEST AND EVALUATION REPORT OF THE PHYSIO CONTROL DEFIBRILLATOR/MONITOR, MODEL LifePak(tm) 6s Final Report
James E. Bruckart, Martin Quattlebaum, Joseph R. Licina, and Bill Olding Jul. 1992 78 p
(DA Proj. 3M4-63807-D-836)
(AD-A255691; AARL-92-27) Avail: CASI HC A05/MF A01

The Physio Control Defibrillator/Monitor, Model LifePak 6s, was tested for electromagnetic interference/compatibility in the UH-60A helicopter under the U.S. Army Program for Testing and Evaluation of Equipment for Aeromedical Operations. The tests were conducted using current military and industrial standards and procedures for electromagnetic interference/compatibility and human factors. The Physio Control Defibrillator/Monitor, Model LifePak 6s was found to be compatible with U.S. Army aeromedical aircraft. GRA

N93-14109# Educational Testing Service, Princeton, NJ.
A PSYCHOMETRICALLY SOUND COGNITIVE DIAGNOSTIC MODEL: EFFECT OF REMEDIATION AS EMPIRICAL VALIDITY Interim Report, Apr. 1989 - Aug. 1992
Kikumi K. Tatsuoka and Maurice M. Tatsuoka 10 Jul. 1992 65 p
(Contract N00014-90-J-1307; NR Proj. RR0-4204)
(AD-A255926; ETS-RR-92-38-0N4) Avail: CASI HC A04/MF A01

The purpose of this study was to validate the results of cognitive diagnoses using the rule-space model and to demonstrate the usefulness of cognitive diagnoses for instruction. The results of the study strongly indicated that the rule-space model can effectively diagnose students' knowledge states and can point out ways for remediating their errors quickly with minimum effort. It was also found that the designing of instructional units for remediation can be effectively guided by the rule-space patterns, given an incidence matrix, and is based on a tree structure of cognitive attributes, knowledge, states, and items. GRA

N93-14162# Walter Reed Army Inst. of Research, Washington, DC.
WALTER REED ARMY INSTITUTE OF RESEARCH BIANNUAL REPORT Final Report, FY 1990 - FY 1991
J. D. Berman Jan. 1992 93 p
(AD-A255630; WRAIR-92-001) Avail: CASI HC A05/MF A01

This annual report is intended to convey WRAIR's ability to perform basic research and development in three major threat areas: biologically active substances, high energy and trauma, and stress and performance. In general, the resources of several disciplines and divisions are used to counter a threat. Each chapter describes one threat and WRAIR's response. A summary of FY 90-91 accomplishments begins each chapter. An introduction follows, which details the scientific and military significance of the threat being studied. An accomplishments section describes the recent work in detail. The organizational units that contributed to the work are then listed, followed by FY 91 personnel involved in the effort. GRA

N93-14163# Ohio Wesleyan Univ., Delaware.
ANALYSIS OF RETINAL FUNCTION FOLLOWING LASER IRRADIATION Final Report, 1 Aug. 1983 - 29 May 1992
David O. Robbins 26 Jun. 1992 38 p

(Contracts DAMD17-83-C-3172; DAMD17-88-C-8032; DA Proj. 3M1-62787-A-878)
(AD-A255649) Avail: CASI HC A03/MF A01

Exposure of the fovea to single or multiple pulses of coherent light (532 nm) can produce both transient and permanent changes in the eye's ability to resolve fine spatial detail. The immediate effects for extended duration exposures (greater than 50 msec) are often large, producing acuity deficits as great as 90 percent of its pre-exposure level. The size of these deficits often reflect a total loss of foveal functioning although, depending upon the energy and duration of the exposure, these changes are reversible. Permanent changes in acuity can be noted in the absence of gross morphological damage and at power densities below the ED50 level provided the area of involvement is large. On the other hand, at power densities above the ED50 level, little if any permanent or consistent visual deficits are noted if the damage is restricted to relatively isolated areas within either the foveal or parafovea. Multiple pulses which increase the area of total involvement are more effective in permanently shifting postexposure acuity than are the single pulse conditions. Cumulative effects of repetitive exposures separate in time by as much as several days are possible. The exact parameters of any observed loss in visual performance is dependent upon the discrimination task and its ability to depict subtle changes in the retina mosiac. GRA

N93-14210# Hecht-Nielsen Neurocomputer Corp., Inc., San Diego, CA.
NEURAL NETWORK RETINAL MODEL REAL TIME IMPLEMENTATION Final Report, 14 Aug. 1991 - 31 Aug. 1992
Robert W. Means 2 Sep. 1992 24 p
(Contract DAAH01-91-C-R240)
(AD-A255652; Rept-3405-F-92) Avail: CASI HC A03/MF A01

The solution of complex image processing problems, both military and commercial are expected to benefit significantly from research onto biological vision systems. However, current development of biological models of vision are hampered by lack of low-cost, high-performance, computing hardware that addresses the specific needs of vision processing. The goal of this SBIR Phase 1 project has been to take a significant neural network vision application and to map it onto dedicated hardware for real time implementation. The neural network was already demonstrated using software simulation on a general purpose computer. During Phase 1, HNC took a neural network model of the retina and, using HNC's Vision Processor (ViP) prototype hardware, achieved a speedup factor of 200 over the retina algorithm executed on the Sun SPARCstation. A performance enhancement of this magnitude on a very general model demonstrates that the door is open to a new generation of vision research and applications. The model is described along with the digital hardware implementation of the algorithm using the new ViP chip set. GRA

N93-14240# Naval Health Research Center, San Diego, CA.
SLEEP INERTIA: IS THERE A WORST TIME TO WAKE UP? Interim Report, May 1989 - Sep. 1991
Paul Naitoh, Tamsin Kelly, and Harvey Babkoff 7 Jul. 1992 29 p
Sponsored by Naval Medical Research and Development Command
(AD-A256602; NHRC-91-45) Avail: CASI HC A03/MF A01

Sleep inertia, a brief period of inferior task performance and/or disorientation immediately after awakening from sleep could impact on military personnel required to work soon after awakening. The objective of this study was to determine whether severity of sleep inertia showed a circadian rhythm. Subjects underwent either 64-hr without sleep or 64-hr with a 20-min nap period every 6-hr. Sleep inertia was measured by performance scores of Baddeley's logical reasoning task. The effects of sleep inertia were additive to those of sleep deprivation. Overall, effects of naps are beneficial, but naps have the side-effect of introducing a short period of performance degradation. GRA

N93-14535# Indiana Univ., Bloomington. School of Medicine.
NERVES AND TISSUE REPAIR Midterm Report, 10 Dec. 1990 - 9 May 1992
Anthony L. Mescher 21 May 1992 24 p
(Contract DAMD17-91-Z-1002; DA Proj. 3M1-62787-A-874)
(AD-A255299) Avail: CASI HC A03/MF A01

Studies have been conducted with regenerating amphibian sciatic nerves in organ culture to characterize further transport and release of transferrin in growing axons of peripheral nerves. The hypothesis under investigation is that transferrin, the iron-transport protein which is required as a permissive factor for cell growth, is delivered axonally to target cells and is involved in the nerve-dependence of cell proliferation during repair in avascular tissues lacking an adequate supply of transferrin from capillaries. Amphibian (axolotl) limb regeneration is a well-characterized model system in which the early period of growth shows complete dependence on nerves. Organ culture of sciatic nerves, combined with an assay for axolotl transferrin developed earlier, allows quantitative study of the release of this factor as well as its transport. As reported elsewhere for regenerating nerves in vivo, distal delivery of transferrin by fast axonal transport was found in cultured nerves. Moreover, transferrin was secreted and released to the medium in significant quantities at the axonal growth cones. These results have important implications for understanding the trophic effect of regenerating nerves on cell proliferation during tissue repair. GRA

N93-14556# Army Command and General Staff Coll., Fort Leavenworth, KS.
A PROGRESSIVE RESISTANCE WEIGHT TRAINING PROGRAM DESIGNED TO IMPROVE THE ARMOR CREWMAN'S STRENGTH M.S. Thesis
Bradley W. May 5 Jun. 1992 166 p
(AD-A255553) Avail: CASI HC A08/MF A02

The duties of a tank crewman are physically demanding. If a tank crewman is stronger, he will preform his job better, easier, quicker, and safer. Therefore, the focus of this thesis is the design of a weight training program to improve individual strength which will result in enhanced performance. While U.S. Army physical fitness manuals contain substantial information on weight training and principles of strength training, current doctrine does not address the specific needs of armor crewmen in the performance of their tasks. Because there is no standardized or sample weight training program, each soldier must design his own plan by selecting exercises from the manuals. The goal of my research is to bridge this gap by synthesizing this information into a prototype program. GRA

N93-14603* National Aeronautics and Space Administration, Washington, DC.
AEROSPACE MEDICINE AND BIOLOGY: A CONTINUING BIBLIOGRAPHY WITH INDEXES (SUPPLEMENT 368)
Nov. 1992 93 p
(NASA-SP-7011(368); NAS 1.21:7011(368)) Avail: CASI HC A05

This bibliography lists 305 reports, articles, and other documents introduced into the NASA Scientific and Technical Information System during Sep. 1992. The subject coverage concentrates on the biological, physiological, psychological, and environmental effects to which humans are subjected during and following simulated or actual flight in the Earth's atmosphere or in interplanetary space. References describing similar effects on biological organisms of lower order are also included. Such related topics as sanitary problems, pharmacology, toxicology, safety and survival, life support systems, exobiology, and personnel factors receive appropriate attention. Applied research receives the most emphasis, but references to fundamental studies and theoretical principles related to experimental development also qualify for inclusion. Author

N93-14708* National Aeronautics and Space Administration. Goddard Space Flight Center, Greenbelt, MD.
COMPLIANT WALKER Patent
James J. Kerley, inventor (to NASA), Wayne D. Eklund, inventor (to NASA), and J. Allen Crane, inventor (to NASA) 29 Dec. 1992 12 p Filed 3 Jul. 1991 Supersedes N91-29714 (29 - 21, p 3548)
(NASA-Case-GSC-13348-2; US-Patent-5,174,590;
US-Patent-Appl-SN-725111; US-Patent-Class-280-1.5;
US-Patent-Class-280-290; US-Patent-Class-280-87.051;
US-Patent-Class-482-69; US-Patent-Class-482-68;
Int-Patent-Class-B62D-51/04) Avail: US Patent and Trademark Office

A compliant walker is provided for humans having limited use of their legs and lower back. It includes an upright wheel frame which at least partially surrounds an upright user wearing a partial body harness. It is attached to the frame by means of cable compliant apparatus consisting of sets of cable segments and angle bracket members connected between opposite side members of the frame and adjacent side portions of the harness. Novelty is believed to exist in the combination of a wheeled frame including a side support structure, a body harness, and compliance

means connecting the body harness to the side support structure for flexibility holding and supporting a person in a substantially upright position when the user sags in the frame when taking weight off the lower extremities. Official Gazette of the U.S. Patent and Trademark Office

N93-14731* National Aeronautics and Space Administration, Washington, DC.
AEROSPACE MEDICINE AND BIOLOGY: A CONTINUING BIBLIOGRAPHY WITH INDEXES (SUPPLEMENT 369)
Dec. 1992 77 p
(NASA-SP-7011(369); NAS 1.21:7011(369)) Avail: CASI HC A05

This bibliography lists 209 reports, articles and other documents introduced into the NASA Scientific and Technical Information System during Nov. 1992. Subject coverage includes: aerospace medicine and physiology, life support systems and man/system technology, protective clothing, exobiology and extraterrestrial life, planetary biology, and flight crew behavior and performance. Author

N93-14782# California Univ., San Diego, La Jolla. Dept. of Psychiatry.
EXTRATHALMIC MODULATION OF CORTICAL FUNCTION Annual Report, 1 Jul. 1991 - 30 Jun. 1992
Stephen L. Foote and Jaime A. Pineda 15 Aug. 1992 8 p
(Grant AF-AFOSR-0325-90)
(AD-A255440; AFOSR-92-8841TR) Avail: CASI HC A02/MF A01

The goal of the proposed studies is to characterize the effects of noradrenergic (NA) afferents on cortical information processing. Our previous studies indicate that the primate locus coeruleus (LC) system, originating in the pontine brainstem, innervates the neocortex more densely than previously thought, exhibiting highly specific patterns in terms of the regional and laminar distribution of its axons. Our previous neurophysiological observations suggest that this system imposes state-related modulatory effects on thalamo-cortical and cortico-cortical systems. The proposed studies have the following Specific Aims: (1) to examine, in monkeys, the effects of manipulating the LC-NA system on ERPs, EEG characteristics, and associated behaviors in operant paradigms that utilize visual or auditory cues; (2) to correlate the activities of individual monkey LC-NA neurons with cortical neuronal activity and the measures utilized in Aim 1; (3) to extend our preliminary observation that activation of the LC by local drug infusion, in halothane-anesthetized rats, produces EEG signs of cortical and hippocampal activation; and (4) to examine the relationship between the intensity of LC neuronal activity and rates of norepinephrine release in neocortex and hippocampus by performing microdialysis in these forebrain terminal regions in anesthetized rats during manipulation of LC activity. GRA

N93-14789# Naval Air Warfare Center, Warminster, PA. Air Vehicle and Crew Systems Technology Dept.
STATISTICAL ANALYSIS OF THE HUMAN STRANGULATION EXPERIMENTS: COMPARISON TO +Gz-INDUCED LOSS OF CONSCIOUSNESS Final Report, Feb. 1991 - Feb. 1992
Estrelle M. Forster and James E. Whinnery 18 Feb. 1992 31 p
(AD-A255485; NAWCADWAR-92026-60) Avail: CASI HC A03/MF A01

In 1943, Rossen, Kabat, and Anderson (RKA), published the results of their investigations involving acute arrest of the cerebral circulation in man. Their studies on the effects of brief periods of cerebral ischemia have become a classic reference in a wide variety of scientific publications including those related to acceleration induced loss of consciousness (G-LOC). An accurate quantitative kinetic comparison of the RKA data and data from G-LOC could provide information concerning the possible similarities and/or differences in the mechanisms of the two phenomena. To this end, we attempted to relate the RKA work with current G-LOC theory by re-analyzing the RKA data in such a way that quantitative comparisons could be accomplished. The induction time for RKA loss of consciousness (LOC) was 6.4 to 6.9 s and found to be similar to both the equivalent parameter in G-LOC research of 8.8 s, and the time at maximum +Gz prior to LOC of 7.3 s. The RKA time from LOC to recovery was 5.9 to 6.4 s and shorter than the equivalent G-LOC parameter of 23.7 s. However, the predicted minimum G-LOC recovery time is 6.8 s. Further, the loss of consciousness syndrome encompassing numerous psychophysiologic symptoms are essentially equivalent for both types of insults. The results seem to suggest an analogous mechanism for LOC induction and recovery caused by strangulation (RKA) and +Gz stress. GRA

N93-15006# State Univ. of New York, Stony Brook. Health Sciences Center.
TRAINING, MUSCLE FATIGUE AND STRESS FRACTURES Final Report, 28 Sep. 1990 - 29 Dec. 1991
Clinton T. Rubin 29 Jul. 1992 49 p
(Contract DAMD17-90-Z-0054; DA Proj. 301-61102-BS-15)
(AD-A255277) Avail: CASI HC A03/MF A01

The objective of this twenty month contract has been to identify the causative mechanical factors responsible for the stress fracture lesion. Over this period, the research has focussed exclusively on an animal model developed specifically for this work, the functionally isolated avian ulna. The stress fracture protocols have exploited this model's ability to withstand, in vivo, high cyclic loading, applied both axially and torsionally, with the aim of identifying that specific mechanical agent within the physical regimen which stimulates this debilitating condition. Previous work from our group suggests that the lesion is a product of tissue remodeling (intracortical porosis), not material microdamage. As importantly, the site of the lesion, when correlated to the mechanical environment to which the bone is subjected, emphasizes that the pathology predominates in areas of least normal strain, not those areas subject to greatest deformation. Finally, the pathology observed in this animal model is identical to that which occurs in humans, demonstrating the appropriateness of using these studies to better understand the etiology of the human condition. From these developments, we proposed that the stress fracture lesions, or rather elevated intracortical remodeling, was not intensity dependent, but instead was a product of redundant, cyclic activity. GRA

N93-15009# London Univ. (England). Dept. of Pharmacology.
AUTORADIOGRAPHIC DISTRIBUTION AND APPLIED PHARMACOLOGICAL CHARACTERISTICS OF DEXTROMETHORPHAN AND RELATED ANTITISSUE/ANTICONVULSANT DRUGS AND NOVEL ANALOGS Annual Report, 15 Jul. 1991 - 14 Jul. 1992
Norman G. Bowery 1 Aug. 1992 12 p
(Contract DAMD17-90-C-0124; DA Proj. 3M1-61102-BS-11)
(AD-A255607) Avail: CASI HC A03/MF A01

Binding of dextromethorphan and its analogues to the dextromethorphan binding site and to the PCP and glycine binding sites associated with the N-methyl-D-aspartate receptor-channel complex was investigated using 3H-DM, H-TCP and 3H-glycine as radioligands. The experiments were carried out in 1 ml tubes (miniblocks), in a final incubation volume of 0.5 ml. All reagents were diluted and dispensed using a TECAN and filtering was done using a Brandel M-48R. Samples were counted in 5 ml of Esoscint A. after an extraction period of at least 6 hours, using a Beckman LS1701 liquid scintillation counter. All compounds were dissolved in distilled water except compound 3 which was dissolved in DMSO/lactic acid and diluted with distilled water. Standards were obtained from commercial sources except dichlorokynurenic acid (DCK) which was a gift from Pfizer Central Research, Sandwich, Kent. GRA

N93-15053# Ohio State Univ., Columbus.
DEMODULATION PROCESSES IN AUDITORY PERCEPTION Final Report, 1 Dec. 1988 - 31 May 1992
Lawrence L. Feth 15 Aug. 1992 191 p
(Grant AF-AFOSR-0227-89)
(AD-A255748; AFOSR-92-0837TR) Avail: CASI HC A09/MF A02

This document reports the accomplishments of a project on the application of the Envelope-Weighted Average of Instantaneous Frequency (EWAIF) model to the processing of complex, time-varying sounds. We consider the task of human listeners to be one of recovering information imposed on the sound stream by a variety of sources. These include speech, music and other environmentally-important signals. Information is encoded in amplitude (envelope) and angle (frequency or phase) modulations of the sound stream carrier. The human listener must demodulate the stream to recover the information. EWAIF first demonstrated that these modulations interact and could provide discrimination cues even for steady-state signals such as those used in profile analysis or co-modulation masking. This project revised the EWAIF model into the IWAIF version Intensity (envelope-squared) weighting leads to greater computational efficiency (via the FFT) and to an intuitively appealing representation. The

IWAIF calculation leads to the center-of-gravity of the spectrum. Tracking frequency modulations imposed on a narrow bandwidth carrier, then may be thought of as tracking the spectral center of gravity. Work continues on the extension of the IWAIF model to handle processing of signals with multiple modulation sources and to refining the short-term tracking abilities of the model. GRA

N93-15192# Biotronics Technologies, Inc., Waukesha, WI.
TRANSCUTANEOUS ANALYTE MEASURING METHODS (TAMM), PHASE 2 Quarterly Progress Report No. 4
Kenneth J. Schlager 12 Oct. 1992 7 p
(Contract N00014-91-C-0190)
(AD-A256327) Avail: CASI HC A02/MF A01

The major objective of this extended quarter was to complete the analysis of pre-clinical data collected at the National Naval Medical Center (NNMC) in Bethesda, Maryland for the purposes of accuracy evaluation and algorithm development so as to allow for the initiation of field instrument development. Data on the first 250 patients were collected at the Bethesda NNMC beginning on June 23, 1992 during two separate time periods. Testing was completed on August 4th. All patients were military personnel undergoing physical examinations. This patient group was selected to be representative of combat age military personnel. Meanwhile, testing of the second group of 250 patients began at Froedtert Lutheran Memorial Hospital in Milwaukee on September 9, 1992 in conjunction with the Department of Endocrinology and the Shared Clinic of the Medical College of Wisconsin. Patients tested are people with various medical problems that were being treated on an out-patient basis. Testing will be completed on or about November 30th. GRA

N93-15198# New York Univ., New York. Dept. of Physiology and Biophysics.
BIOPHYSICAL AND BIOCHEMICAL MECHANISMS IN SYNAPTIC TRANSMITTER RELEASE Final Report, 1 Feb. 1989 - 31 Jan. 1992
Rodolfo R. Llinas 31 Jan. 1992 71 p
(Grant AF-AFOSR-0270-89)
(AD-A256340; AFOSR-92-0901TR) Avail: CASI HC A04/MF A01

The initial question addressed in 1989 was that of synaptic vesicle movement as determined by direct microscopic visualization. This research demonstrated that vesicles were actually mobilized from the point of injection in the axon to the active zones, i.e. the place where synaptic transmitter is released. It was also found that a change in either oxygenation or the surface properties of vesicles can lead to no movement or, to change in movement direction. The second aspect of synapse work performed that year was a demonstration of the category of calcium channel that is responsible for transmitter release. The work in 1990 demonstrated that miniature potentials could be modulated in the squid synapse by injection of Synapsin 1 and of protein kinase 2. In the third year of the grant, 1991, the first demonstration of calcium microdomains in synaptic transmission was performed. GRA

N93-15249# Department of the Army, Washington, DC.
IMPROVED HEAD SUPPORT STAND ADJUSTABLE BY COMPOUNDTURNBUCKLE Patent Application
Bruce E. Amrein, inventor (to Army) and Jeffery D. Nickel, inventor (to Army) 22 Jun. 1992 18 p Filed 22 Jun. 1992
(AD-D015384; US-Patent-Appl-SN-902166) Avail: CASI HC A03/MF A01

The invention is an improved head support stand used to smoothly and accurately position a patient's head when imaging the patient's upper spinal area. The improved stand includes a compound turnbuckle mounted between a base of the stand and a head cradle or face plate mounted to the base. The compound turnbuckle includes two rods threadingly engaged to a turnbuckle body so that the rods translate with respect to the body when it rotates. When the compound turnbuckle is in a fully retracted position, the rods are in a telescoped configuration within the turnbuckle body. When the compound turnbuckle is in a fully extended position, the rods are axially remote from each other and project substantially all the way out of the turnbuckle body. GRA

N93-15583*# George Washington Univ., Washington, DC. Science Communications Studies Dept.
PUBLICATIONS OF THE SPACE PHYSIOLOGY AND COUNTERMEASURES PROGRAM, NEUROSCIENCE DISCIPLINE: 1980-1990
Katherine J. Dickson, Janice Wallace-Robinson, Janet V. Powers, and Elizabeth Hess NASA Dec. 1992 117 p
(Contract NASw-4324)
(NASA-CR-4476; NAS 1.26:4476) Avail: CASI HC A06/MF A02

A 10-year cumulative bibliography of publications resulting from research supported by the neuroscience discipline of the space physiology and countermeasures program of NASA's Life Sciences Division is provided. Primary subjects included in this bibliography are space motion sickness; vestibular performance, posture, and motor coordination; vestibular physiology; central and peripheral nervous system physiology; and general performance and methodologies. General physiology references are also included. Author

53 BEHAVIORAL SCIENCES

Includes psychological factors; individual and group behavior; crew training and evaluation; and psychiatric research.

N93-14267# Institute for Perception RVO-TNO, Soesterberg (Netherlands).
A SPURIOUS POP-OUT IN VISUAL SEARCH Final Report
J. Theeuwes and M. P. Lucassen Sep. 1992 17 p
(AD-A256548; IZF-1992-B-8; TDCK-92-2288) Avail: CASI HC A03/MF A01

The present study demonstrates that an object embedded in an array of identical objects can pop-out. Dependent on the stimuli preceding the search display, local (chromatic) adaptation causes an identical object to pop-out because it appears to have a color (Experiment 1) or brightness (Experiment 2) that is slightly different from the color and brightness of the other objects in the display. Experiment 3 shows that this pop-out even occurs when the stimulus preceding the search display is presented for 100 Ms. The present findings have severe implications on the design of experiments in which no eye movements are allowed involving multiple displays presented in successive order. GRA

N93-14416# Human Engineering Labs., Aberdeen Proving Ground, MD.
EFFECTS OF SPATIAL LUMINANCE NONUNIFORMITIES ON VISUAL-TASK PERFORMANCE AND SUBJECTIVE UNIFORMITY Final Report
J. J. Gallimore and W. W. Farley Jul. 1992 17 p
(DA Proj. 1L1-62716-AH-70)
(AD-A255989; HEL-TM-5-92) Avail: CASI HC A02/MF A01

The objectives of the experiment described in the paper were the determination of the effects of nonuniformities on operator performance and perception, and the validation of current recommended standards. Subjects performed two tasks in the presence of nonuniformities: an objective visual search task and a subjective magnitude-estimation task for the determination of perceived uniformity. The results indicated that the nonuniformities did not appreciably affect search performance, and that current recommendations are appropriate, although the magnitude-estimation task results indicated that the subjects were sensitive to the nonuniformities. The subject impressions of perceived uniformity results follow the contrast threshold function of the visual system. GRA

N93-14510# Minnesota Univ., Minneapolis. Dept. of Psychology.
PSYCHOPHYSICAL ANALYSES OF PERCEPTUAL REPRESENTATIONS Annual Report, 15 Apr. 1991 - 14 Apr. 1992
Irving Biederman and Gordon E. Legge 18 Aug. 1992 12 p
(Grant AF-AFOSR-0274-90)
(AD-A255432; AFOSR-92-0834TR) Avail: CASI HC A03/MF A01

Research during the past year was divided between studies at USC (Biederman and students) and Minnesota. Our research continues to focus on linking early sensory representations to higher-level perceptual representations. Studies outlined below have examined the sensory/perceptual middle ground in object recognition, depth perception, reading, and auditory perception. Several of our studies have used

ideal-observer analysis. The ideal-observer approach provides a means for quantifying the information available to perception and for evaluating the effectiveness with which humans use that information. GRA

N93-14580# Massachusetts Inst. of Tech., Lexington.
PARAMETRIC STUDY OF DIFFUSION-ENHANCEMENT NETWORKS FOR SPATIOTEMPORAL GROUPING IN REAL-TIME ARTIFICIAL VISION Annual Technical Report, Apr. 1991 - Jun. 1992
Robert K. Cunningham and Allen M. Waxman 24 Jul. 1992 41 p
(Contract F19628-90-C-0002)
(AD-A256059; ESC-TR-92-121) Avail: CASI HC A03/MF A01

This is the second Annual Technical Summary of the MIT Lincoln Laboratory parametric study of diffusion-enhancement networks for spatiotemporal grouping in real-time artificial vision. Spatiotemporal grouping phenomena are examined in the context of static and time-varying imagery. Dynamics that exhibit static feature grouping on multiple scales as a function of time, and long-range apparent motion between time-varying inputs, are developed for a biologically plausible diffusion-enhancement layer coupled by feedforward and feedback connections; input is provided by a separate feature-extracting layer. The model is cast as an analog circuit that is realizable in VLSI, the parameters of which are selected to satisfy a psychophysical data base on apparent motion. GRA

N93-14600# Army Aeromedical Research Lab., Fort Rucker, AL.
THE RELATIONSHIP BETWEEN COMPUTER SCORING AND SAFETY-PILOT GRADING OF FLIGHT PERFORMANCE
John A. Caldwell, Heber D. Jones, David J. Carter, and J. L. Caldwell Jul. 1992 44 p
(DA Proj. 3M2-63002-F-995)
(AD-A256245; AARL-92-30) Avail: CASI HC A03/MF A01

Three different measures of helicopter pilot performance were correlated: two types of computer scores and one type of safety/instructor pilot grades. Results indicated the two types of computer scores were basically interchangeable. The direction of the relationship between the different types of computer and safety-pilot measures was as expected for 76 percent of the measures examined, but statistical significance was attained in fewer cases (approximately 50 percent of the total). Reasons for any noted discrepancies are discussed along with findings about the most strongly associated measures. The computer scores and safety-pilot grades were related strongly enough to conclude that they were both accurately measuring the sample type of performance. GRA

N93-14602# Institute for Perception RVO-TNO, Soesterberg (Netherlands).
DECISION MAKING IN A DYNAMIC TASK ENVIRONMENT: THE EFFECT OF TIME PRESSURE Final Report
J. H. Kerstholt 23 Jan. 1992 23 p
(AD-A256557; IZF-1992-B-1; TDCK-92-0240) Avail: CASI HC A03/MF A01

Two experiments were conducted to investigate time pressure effects on both the selected decision strategy and the quality of task performance. A dynamic task environment was used. Subjects were required to monitor the continuously changing fitness level of an athlete, and to recover the athlete whenever fitness decline had a physiological cause. Time pressure was defined by the rate at which the fitness level changed over time. The major decision problem of the subjects was to trade-off the costs of requesting information against the increasing risk of a costly consequence. The experiments differed in the incentive scheme that was used: in the first experiment, the subjects increased their chance on a bonus by saving time, whereas in the second experiment they could directly save on money. Both experiments showed a speed-up of information processing as time pressure increased. In the first experiment, subjects started to request information at the saw fitness levels in all time pressure conditions, whereas in second experiment subjects started to request information at higher fitness levels when time pressure increased. However, in both experiments performance equally deteriorated under time pressure, as indicated by the number of athlete collapses. It is concluded that even though the subjects changed their strategy and increased their speed of information processing under time pressure, performance declined more than predicted by time constraints alone. This extra effect is ascribed to the characteristics of the task environment. GRA

N93-14646# New York Univ., New York.
NEUROMAGNETIC INVESTIGATIONS OF CORTICAL REGIONS UNDERLYING SHORT-TERM MEMORY Final Report, 1 Jul. 1991 - 30 Jun. 1992
Samuel J. Williamson and Lloyd Kaufman 18 Aug. 1992 45 p
(Grant AF-AFOSR-0401-91)
(AD-A255788) Avail: CASI HC A03/MF A01

Spontaneous neuronal activity of the brain within the alpha frequency bandwidth is found to be suppressed in the visual cortex when comparing a rotated, and possibly inverted object with an object previously seen to determine whether they are identical. Moreover, the pattern of suppression adjusts to task demands. Thus, the visual cortex participates in the processes of mental imagery. A mathematical solution for the magnetic inverse problem was developed to determine the locations of alpha suppression within the brain based on magnetic field measurements of the magnetic field power across the scalp. Behavioral studies of a person's loss of memory for the loudness of a tone can be characterized by a decaying exponential dependence on time. The characteristic lifetime is found to match to within 0.2 sec the individual's lifetime for the decay of the neuronal activation trace in primary determined neuromagnetically. GRA

N93-14660# Rochester Univ., NY. Dept. of Computer Science.
THE PERCEPTION OF ARTICULATED MOTION: RECOGNIZING MOVING LIGHT DISPLAYS Ph.D. Thesis
Nigel H. Goddard Jun. 1992 186 p
(AD-A256046; TR-405) Avail: CASI HC A10/MF A02

Recognition of motion sequences is a crucial ability for biological and robot vision systems. We present an architecture for the higher level processes involved in recognition of complex structured motion. The work is focused on modeling human recognition of Moving Light Displays. MLD's are image sequences that contain only motion information at a small number of locations. Despite the extreme paucity of information in these displays, humans can recognize MLD's generated from a variety of common human movements. This dissertation explores the high level representations and computational processes required for the recognition task. The structures and algorithms are articulated in the language of structured connectionist models. The implemented network can discriminate three human gaits from data generated by several actors. Recognition of any motion involves indexing into stored models of movement. We present a representation for such models, called scenarios, based on coordinated sequences of discrete motion events. A method for indexing into this representation is described. We develop a parallel model of spatial and conceptual attention that is essential for disambiguating the spatially and temporally diffuse MLD data. The major computational problems addressed are: (1) representation of time varying visual models; (2) integration of visual stimuli over time; (3) gestalt formation in and between spatially-localized feature maps and central movement representations; (4) contextual feedback to lower levels; and (5) the use of attention to focus processing on particular spatial locations and particular high level representations. Several novel connectionist mechanisms are developed and used in the implementation. GRA

N93-14788# New York Univ., New York.
COGNITION AND THE BRAIN Annual Technical Report, 15 Feb. 1991 - 14 Feb. 1992
S. J. Williamson and L. Kaufman 25 May 1992 119 p
(Grant AF-AFOSR-0221-90)
(AD-A255483; AFOSR-92-05446TR) Avail: CASI HC A06/MF A02

Magnetic fields associated with spontaneous neuronal activity of the cerebral cortex are shown to be locally suppressed when an area of the brain engages in a cognitive function. Suppression occurs in visual cortex when the image of an object is compared with a memory set of objects previously seen, or with the same object rotated. Suppression occurs in auditory cortex when memory of a tone is compared with a memory set of tones. Suppression occurs first over a visual cortex and subsequently over the anterior temporal area when a subject responds to a displayed word by seeking a word that rhymes with it. Significant correlations are found between the timing of cortical suppression and classic behavioral studies of reaction times. It is concluded that regional changes in cortical spontaneous activity are meaningfully related to memory scanning, image transformations, and silent speech. A computational procedure, called the minimum-norm least-square (MNLS) estimate, was developed to provide a unique solution for the magnetic inverse problem. With this algorithm, the

distribution of intracellular current across the surface of cerebral cortex can be deduced from the magnetic field pattern that it produces across the scalp. This approach was generalized to provide a unique estimate for the distribution of time-average current power, obtained from the average field power. It can also be applied to determine the pattern of current power suppression when the subject is engaged in a cognitive task. GRA

N93-15067# Dartmouth Coll., Hanover, NH. Dept. of Psychiatry.
MULTIMODAL INTERACTIONS IN SENSORY-MOTOR PROCESSING Final Report, 1 Jul. 1989 - 30 Jun. 1992
Michael S. Gazzaniga 30 Jun. 1992 114 p
(Grant AF-AFOSR-0437-89)
(AD-A255780; AFOSR-92-0883TR) Avail: CASI HC A06/MF A02

Intersensory (visual/auditory) facilitation of reaction times (RT's) was examined using three different response systems: saccadic eye movements, directed manual responses (deflections of a joystick towards the target location) and simple manual responses. The data were examined in the context of race models (in which facilitation is attributed to the minimum of two random variables representing the detection times associated with the visual and auditory targets) versus neural summation coactivation models (where the facilitation is attributed to a combination of the activities within the visual and auditory channels prior to detection). The first experiment provides evidence for neural summation coactivation in all three response model. The effects of varying combinations of auditory and visual stimulus intensity were examined in the second experiment. Intensity-dependent mismatches in the auditory and visual RT's had little effect on the magnitude of the redundant targets effect, indicating that visual-auditory integration occurs over temporal intervals of at least 40 msecs. The effects of spatial correspondence (auditory and visual targets presented in spatial register or in opposite hemifields) was examined in the third experiment. Coactivation depends upon the spatial alignment of the targets for directed responses (both saccades and directed manual responses) but not simple manual RT's. GRA

N93-15216# Technico Southwest, Inc., Los Alamos, NM.
THE EFFECT OF PAIN ON TASK PERFORMANCE: A REVIEW OF THE LITERATURE
Gerald L. Gamache and Albert S. Glickman Jul. 1992 35 p
(Contract DNA001-88-C-0207)
(AD-A254336; DNA-TR-91-178) Avail: CASI HC A03/MF A01

The authors reviewed 273 abstracts relating to pain and 36 abstracts relating to pain and task performance. Of the 309 abstracts reviewed, 93 articles were pertinent to elements of the problem and are the basis of this report; however none specifically related burn pain to task performance. Two simple five-point scales were found that can be used to measure pain severity resulting from burns. The first is the McGill Pain Questionnaire that has been widely used, and the second is the Visual Analogue Scale which is often used together with a Verbal Rating Scale developed by Banos. Some alternatives to a five-point scale to relate pain severity to performance are presented as offering potential for further development. GRA

N93-15329# New York Univ., New York. Center for Neural Science.
HIGHER ORDER MECHANISMS OF COLOR VISION Final Report, 15 Jun. 1989 - 14 Jun. 1992
John Krauskopf 9 Sep. 1992 12 p
(Grant AF-AFOSR-0429-89)
(AD-A256369; TR-2; AFOSR-92-0877TR) Avail: CASI HC A03/MF A01

The main accomplishments have been: (1) Completion and publication of a comprehensive study of the effects of chromatic content, blur and contrast of targets on vernier acuity and on stereo acuity; (2) The use of a new method of measuring chromatic discrimination under conditions of constant adaptation and the publication of reports on this work; (3) Experiments on the significance of color in the perception of motion; (4) Experiments on the effects of chromatic adaptation on color matching; (5) The effects of noise masks on the detection of chromatic and luminance pulses; (6) Continuation of the study of the chromatic properties of single cells in the monkey cortex extending our experiments to Area V2; (7) Experiments on the effects of chromatic adaptation on the responses of single neurons in monkey LGN to chromatic stimuli; and (8) The development of a new system for making displays for visual experiments on TV monitors which allows at least 12 bits of accuracy in the specification of the intensity of each of the three primaries. GRA

N93-15400# Institute for Perception RVO-TNO, Soesterberg (Netherlands).
HIGH-RESOLUTION CONTRAST CONTROL ON A VIDEO DISPLAY: METHOD AND CALIBRATION Final Report
J. M. Valeton and A. J. deReus 25 Aug. 1992 31 p
(AD-A256552; IZF-1992-B-7; TDCK-92-2282) Avail: CASI HC A03/MF A01

In visual psychophysics it is sometimes necessary to be able to display Luminances with 12 bit precision. This report describes a method where two 8 bit color outputs of a DeAnza IP8400 image processor are combined into a monochrome signal with an effective resolution of 12 bits. The implementation in hardware and software, and the calibration of the system are described. Measurements show that the system meets the desired specifications. GRA

N93-15184# Universitaet der Bundeswehr Muenchen, Neubiberg (Germany). Fakultaet fuer Systemdynamik und Flugmechanik.
MONITORING OF PILOT ACTIONS AS PART OF A KNOWLEDGE-BASED SYSTEM FOR PILOT ASSISTANCE [UEBERWACHUNG DER PILOTENAKTIONEN ALS TEILFUNKTION EINES WISSENSBASIERTEN PILOTEN-UNTERSTUETZUNGSSYSTEMS]
R. Onken, T. Wittig, and H.-L. Dudek (Dornier Luftfahrt G.m.b.H., Friedrichshafen, Germany) *In* DLR, Proceedings of the 16th Symposium on Aircraft Integrated Monitoring Systems Jan. 1992 p 607-627 (For primary document see N93-15152 04-06)
Avail: CASI HC A03/MF A06; DLR, Wissenschaftliches Berichtswesen, Postfach 90 60 58, Cologne, Germany, HC

54 MAN/SYSTEM TECHNOLOGY AND LIFE SUPPORT

Includes human engineering; biotechnology; and space suits and protective clothing.

For related information see also *16 Space Transportation.*

N93-14161# National Academy of Sciences - National Research Council, Washington, DC.
BODY COMPOSITION AND PHYSICAL PERFORMANCE
Bernadette M. Marriott and Judith Grumstrup-Scott 1 Aug. 1992 372 p
(Contract DAMD17-92-J-2003; DA Proj. 3M1-61102-BS-15)
(AD-A255627) Avail: CASI HC A16/MF A03

The relationship of body composition to performance of physical tasks is of major interest to the military. Not only is it important in the decisions of acceptance or rejection of recruits for military service, but it also has significant implications for the individual relating to retention and advancement while in the services. There are financial implications as well for the military services, due to the high cost of training replacements, when individuals are discharged for failure to meet the established standards. The discharge of highly trained and experienced specialists has significant additional implications concerning unit readiness and performance. The application of body composition standards in the military on a rational and equitable basis based on ethnicity, gender, and age is therefore an important issue. GRA

N93-14427# Indiana Univ., Bloomington. Poplars Research and Conference Center.
INSTITUTE FOR THE STUDY OF HUMAN CAPABILITIES Annual Technical Report, 1 Jun. 1991 - 31 May 1992
Charles S. Watson 31 Aug. 1992 74 p
(Grant AF-AFOSR-0215-90)
(AD-A256091; AFOSR-92-0852TR) Avail: CASI HC A04/MF A01

We continue to make significant progress toward our long-term goals. The Institute maintains an inter-laboratory, work-station based computer network. A third conference was held during this funding period, on March 25-27, 1992, again on the subject of Human Error. During the funding period, the university completed rehabilitation of three buildings for use in Institute-related research. Andrew Dillon, from the Human Sciences and

Advanced Technology Research Institute in Loughborough, England, collaborated with several groups at the university on human-computer interactions. The institute has provided partial support of research leading to the publication, during the past year, of 46 journal articles and book chapters, and the presentation of 28 papers at meetings of scientific societies, described in this report. GRA

N93-14520# Wright Lab., Wright-Patterson AFB, OH.
THE HUMAN-ELECTRONIC CREW: IS THE TEAM MATURING? THE 2ND JOINT GAF/RAF/USAF WORKSHOP ON HUMAN-ELECTRONIC CREW TEAMWORK
Terry Emerson, Michael Reinecke, John Reising, and Robert Taylor 10 Jul. 1992 184 p Workshop held in Ingolstadt, Germany, 25-28 Sep. 1990
(AF Proj. 2403)
(AD-A256192; WL-TR-92-3078) Avail: CASI HC A09/MF A02

Advances in artificial intelligence (AI) will enable future fighter/attack aircraft to have a rather unique crew -- one human and one electronic. The objective of the workshop was to bring together AI specialists, aircrew, and cockpit designers in order to exchange ideas relative to (1) the state of the art in aircraft applications of AI technology and (2) the impact on the cockpit of the human/electronic crew. This meeting provided a valuable forum for the experts of several countries to exchange ideas, concepts, and data relative to hardware and software capabilities that can be included in an aircraft system design to aid the human operator in performing the mission. GRA

N93-14548# George Mason Univ., Fairfax, VA. Center for Computational Statistics.
EVALUATION AND ESTIMATION OF HANDLING QUALITIES VIA STATISTICAL MODELING OF PILOT RESPONSE DATA Final Report, 15 Jul. 1989 - 28 Feb. 1991
Donald T. Gantz, Lawrence C. Baldwin, and Linda J. Davis Nov. 1991 105 p
(Contract N00014-89-J-3146)
(AD-A255324) Avail: CASI HC A06/MF A02

This report describes a research project which measured pilot response to seven control systems simulating different handling qualities, quantitatively evaluated and compared the systems based on these measurements, and compared the quantitative system evaluation based on measured pilot performance with a qualitative evaluation using the Cooper-Harper technique. The objective of the project is implementation of a methodology for system evaluation via pilot performance to complement the current evaluation technique based on subjective ratings by test pilots. Pilot performance is determined through analysis of objective dynamic measurements of pilot response typical of flight test environments. In short, the methodology specifies a general approach for condensing the typically huge mound of measured test data accumulated during flight simulation experiments into meaningful quantities for system evaluation. The key element in the methodology is statistical modeling of a law for pilot control. Statistical modeling of pilot control provides an assessment of pilot performance in terms of standard statistical estimation parameters. The methodology requires that this control model be used to compute control input in a closed loop tracking task; the accuracy of the control model in performing this task is an important measure of pilot performance relevant to system evaluation. In addition, these parameters computed from the dynamic measurements of pilot performance are shown to enhance understanding of the aspects of the handling qualities underlying subjective rating techniques such as Cooper-Harper. GRA

N93-14554# Coast Guard Research and Development Center, Groton, CT.
EVALUATION OF NIGHT VISION GOGGLES (NVG) FOR MARITIME SEARCH AND RESCUE (JOINT CANADIAN/US COAST GUARD EXPERIMENT) Interim Report, Mar. 1989 - Feb. 1991
R. Q. Robe, J. V. Plourde, and R. L. Marsee Nov. 1991 67 p Prepared in cooperation with Analysis and Technology, Inc., New London, CT
(AD-A255525; USCG-D-13-92; USCG-R&DC-03/92) Avail: CASI HC A04/MF A01

Three experiments were conducted in 1989 and three more were conducted in 1990 by the U.S. Coast Guard Research and Development (R&D) Center to evaluate night vision goggles (NVGs) for their effectiveness in detecting small targets at night. Three types of NVGs have been evaluated: the AN/AVS-6 Aviators Night Vision Imaging System (ANVIS) NVG has been tested onboard U.S. Coast Guard HH-3 and CH-3 helicopters, and the AN/PVS-5C and AN/PVS-7A NVGs have been tested onboard U.S. Coast Guard 41-foot utility boats (UTBs) and a U.S. Coast Guard 210-foot medium endurance cutter and a Canadian Coast Guard 234-foot (71.5-meter) ship. During the fall 1990 experiment in the waters of Canso Bank off the coast of Nova Scotia, the medium endurance cutter and Canadian Coast Guard ship were employed in realistically-simulated search missions for 4- and 6-person lighted and unlighted life rafts with retroreflective tape. This interim report discusses the results of the Canso Bank experiment. GRA

N93-14651# Dynamics Research Corp., Wilmington, MA. Systems Div.
DEVELOPMENT OF MEASURES OF CREW COORDINATION Final Report, Jan. - Sep. 1990
Robert Simon, Daniel T. Riser, and Eugene A. Pawlik, Sr. Jul. 1992 137 p
(Contract DAHC35-89-D-0030)
(AD-A255384; ARI-RN-92-68) Avail: CASI HC A07/MF A02

This report describes the development of a reliable, objective, and quantitative set of metrics for measuring and assessing aircrew coordination in terms of aviator performance and safety. Based on a review of programs to evaluate aircrew coordination in the commercial and military sectors, three rating instruments were developed for specific application to UH-60 helicopter aircrews. These instruments included a military adaptation of the Cockpit Management Attitudes Questionnaire (CMAQ), the Aircrew Coordination Evaluation Checklist, and a revised set of Aircrew Training Manual (ATM) maneuver standards. All three instruments were used by the U.S. Army Research Institute for the Behavioral and Social Sciences (ARI) to evaluate UH-60 aircrews in May 1990 at Fort Campbell, Kentucky. Data from this experiment are being analyzed by ARI and will provide a basis for developing training standards and methods in this area. GRA

N93-14713* National Aeronautics and Space Administration. Ames Research Center, Moffett Field, CA.
PASSIVE ZERO-GRAVITY LEG RESTRAINT Patent
Christopher R. Miller, inventor (to NASA) 12 Sep. 1989 9 p
(NASA-Case-ARC-11882-1-CU; US-Patent-4,865,270;
US-Patent-Appl-SN-254052; US-Patent-Class-244-118.5;
US-Patent-Class-244-158R; US Patent-Class-244-162;
US-Patent-Class-297-423; US-Patent-Class-272-145;
Int-Patent-Class-B64G-1/60) Avail: US Patent and Trademark Office

A passive zero or microgravity leg restraint is described which includes a central support post with a top and a bottom. Extending from the central support post are a calf pad tab, to which calf pad is attached, and a foot pad tab, to which foot tab is attached. Also extending from central support post are knee pads. When the restraint is in use the user's legs are forced between pads by a user imposed scissors action of the legs. The user's body is then supported in a zero or microgravity neutral body posture by the leg restraint. The calf pad has semi-ridig elastic padding material covering structural stiffener. The foot pad has padding material and a structural stiffener. Knee pads have s structural tube stiffener at their core. Official Gazette of the U.S. Patent and Trademark Office

N93-14870* National Aeronautics and Space Administration. Marshall Space Flight Center, Huntsville, AL.
BAR-HOLDING PROSTHETIC LIMB Patent
Thomas W. Vest, inventor (to NASA), William E. Norton, inventor (to NASA), Jewell G. Belcher, inventor (to NASA), and James R. Carden, inventor (to NASA) 17 Nov. 1992 7 p Filed 15 Apr. 1992 Sponsored by NASA
(NASA-Case-MFS-28481-1; US-Patent-5,163,966;
US-Patent-Appl-SN-873931; US-Patent-Class-623-65;
US-Patent-Class-623-57; Int-Patent-Class-A61F-2/54) Avail: US Patent and Trademark Office

A prosthetic device for below-the-elbow amputees is disclosed. The device has a removable effector, which is attached to the end of an arm cuff. The effector is comprised of a pair of C-shaped members that are oriented so as to face each other. Working in concert, the C-shaped members are able to hold a bar such as a chainsaw handle. A flat spring is fitted around the C-shaped members to hold them together.
Official Gazette of the U.S. Patent and Trademark Office

N93-15363# Pennsylvania Univ., Philadelphia. Dept. of Computer and Information Sciences.
MODELING CLOTHED FIGURES Final Report, 1 Aug. 1990 - 30 Jun. 1991
Norman I. Badler 31 Aug. 1992 10 p
(Contract DAAL03-90-G-0191)
(AD-A257037; ARO-28066.1-MA) Avail: CASI HC A02/MF A01

In most workplace environments we have encountered, clothed figures are the norm and would be expected by the designer. Adding clothing to a human figure improves its graphical appearance and realism. Clothes modeling can be done in many ways ranging from very simple to more realistic but complicated. The simplest technique is to change the attributes of certain segments of the body figure; for example, by modifying the colors of the lower legs we get the effect of a body wearing short pants. This is not quite as silly as it sounds, because the body segment geometry can be created with a clothed rather than bare-skinned shape. The best but more complicated approach is to drape and attach clothing over a body to simulate the intricate properties of garments. Besides improving realism, there is a practical human factors aspect to clothing. Clothing constrains movement by restricting the joint angle limits. An approach to analyzing this problem has been developed by using collision detection for a geometric clothes model. GRA

N93-14614*# National Aeronautics and Space Administration. Ames Research Center, Moffett Field, CA.
A VOYAGE TO MARS: A CHALLENGE TO COLLABORATION BETWEEN MAN AND MACHINES
Irving C. Statler *In* NAL, Symposium on the Occasion of the Farewell of Prof. Dr. Ir. O. H. Gerlach as Chairman of the Board of the Foundation National Aerospace Laboratory NLR, The Netherlands 1991 p 5-29 (For primary document see N93-14613 04-01)
Avail: CASI HC A03/MF A01

N93-14951# Alberta Research Council, Edmonton.
A MONITORING AND CONTROL SYSTEM FOR COMPLEX MAN-MACHINE SYSTEMS: PRELIMINARY DESIGN
Maher Nessim, Lynn Sutherland, Breen Liblong, and Vickitt Lau *In* Canadian Space Agency, Proceedings of the Sixth CASI Conference on Astronautics 1990 13 p Previously announced in IAA as A91-34957 (For primary document see N93-14920 04-12)
Avail: Canadian Aeronautics and Space Inst., 222 Somerset St. W., Suite 601, Ottawa, Ontario K2P 0J1 Canada

55 SPACE BIOLOGY

Includes exobiology; planetary biology; and extraterrestrial life.

No abstracts in this category.

59 MATHEMATICAL AND COMPUTER SCIENCES (GENERAL)

No abstracts in this category.

60 COMPUTER OPERATIONS AND HARDWARE

Includes hardware for computer graphics, firmware, and data processing.

For components see *33 Electronics and Electrical Engineering.*

N93-14491# Carnegie-Mellon Univ., Pittsburgh, PA. School of Computer Science.
A SPECIFICATION OF THE SOAR COGNITIVE ARCHITECTURE IN Z
Garrett Pelton, Robert Doorenbos, Mike Hucka, John Laird, and Paul Rosenbloom 31 Aug. 1992 243 p
(Contract F33615-90-C-1465; ARPA Order 7597)
(AD-A256198; CMU-CS-92-169) Avail: CASI HC A11/MF A03

A formal specification of the sixth revision of the Soar architecture in the Z notation was constructed to elucidate and clarify the definition of Soar and to guide its implementation. Soar is a cognitive architecture that has been successfully applied to many domains and has been proposed as an exemplar unified theory of cognition. Z is a model theoretic specification language based in set theory that has syntax and type checking programs available. The specification has a complete coverage of the architecture, a low level of abstraction and a considerable implementation bias. GRA

N93-14644# Naval Surface Warfare Center, Silver Spring, MD.
MISSION CRITICAL SYSTEM DEVELOPMENT: DESIGN VIEWS AND THEIR INTEGRATION
Ngocdung Hoang, Steve Howell, and Nicholas Karangelen Oct. 1991 74 p
(NR Proj. RS3-4-P-11)
(AD-A255498; NAVSWC-TR-91-586) Avail: CASI HC A04/MF A01

The purpose of this document is to describe a formalism that allows for the capture and analysis of very large, computer-based, real-time, mission critical computer resource (MCCR) systems. The formalism covers all aspects of the system including functional (the functions a system performs) and nonfunctional (characteristics of system performance) attributes. Nonfunctional attributes of the systems, such as timing, dependability, security, and reliability should be captured and analyzed at the early stage of the system development process to guarantee the correctness of a system's performance. The current proposed formalism captures the system design in five different views such that analysis can be correctly performed. The views are Informational, Functional, Behavioral, Implementation, and Environmental. Each view explores different aspects of the system and all five in total provide a more complete understanding of the system. Even though the ultimate goal is to capture all aspects of the system in the five views, at this time there is no perfect vehicle for analyzing system attributes such as hard real-time, security, reliability, and dependability. However, as the formalism matures, all aspects that affect the system will be covered in detail. GRA

N93-14704* National Aeronautics and Space Administration. Pasadena Office, CA.
HIGH SPEED MAGNETO-RESISTIVE RANDOM ACCESS MEMORY
Patent
Jiin-Chuan Wu, inventor (to NASA) (Jet Propulsion Lab., California Inst. of Tech., Pasadena.), Henry L. Stadler, inventor (to NASA) (Jet Propulsion Lab., California Inst. of Tech., Pasadena.), and Romney R. Katti, inventor (to NASA) (Jet Propulsion Lab., California Inst. of Tech., Pasadena.) 22 Dec. 1992 11 p Filed 28 Jun. 1990 Supersedes N90-26519 (28 - 20, p 2904)
(NASA-Case-NPO-17954-1-CU; US-Patent-5,173,873;
US-Patent-Appl-SN-545019; US-Patent-Class-365-173;
US-Patent-Class-365-158; Int-Patent-Class-G11C-11/15) Avail: US Patent and Trademark Office

A high speed read MRAM memory element is configured from a sandwich of magnetizable, ferromagnetic film surrounding a magneto-resistive film which may be ferromagnetic or not. One outer ferromagnetic film has a higher coercive force than the other and therefore remains magnetized in one sense while the other may be switched in sense by a switching magnetic field. The magneto-resistive film is therefore sensitive to the amplitude of the resultant field between the outer ferromagnetic films and may be constructed of a high resistivity, high magneto-resistive material capable of higher sensing currents. This permits higher read voltages and therefore faster read operations. Alternate embodiments with perpendicular

anisotropy, and in-plane anisotropy are shown, including an embodiment which uses high permeability guides to direct the closing flux path through the magneto-resistive material. High density, high speed, radiation hard, memory matrices may be constructed from these memory elements.
Official Gazette of the U.S. Patent and Trademark Office

N93-14770*# New Mexico State Univ., Las Cruces. Dept. of Electrical and Computer Engineering.
HIGH-SPEED ARCHITECTURE FOR THE DECODING OF TRELLIS-CODED MODULATION Semiannual Report, Jan. - Jul. 1992
William P. Osborne 1992 214 p
(Grant NAG5-1491)
(NASA-CR-191374; NAS 1.26:191374) Avail: CASI HC A10/MF A03

Since 1971, when the Viterbi Algorithm was introduced as the optimal method of decoding convolutional codes, improvements in circuit technology, especially VLSI, have steadily increased its speed and practicality. Trellis-Coded Modulation (TCM) combines convolutional coding with higher level modulation (non-binary source alphabet) to provide forward error correction and spectral efficiency. For binary codes, the current stare-of-the-art is a 64-state Viterbi decoder on a single CMOS chip, operating at a data rate of 25 Mbps. Recently, there has been an interest in increasing the speed of the Viterbi Algorithm by improving the decoder architecture, or by reducing the algorithm itself. Designs employing new architectural techniques are now in existence, however these techniques are currently applied to simpler binary codes, not to TCM. The purpose of this report is to discuss TCM architectural considerations in general, and to present the design, at the logic gate level, or a specific TCM decoder which applies these considerations to achieve high-speed decoding. Author

N93-15089# Universiteit Twente, Enschede (Netherlands). Dept. of Computer Science.
ARCHITECTURE OF LOW COST, LARGE SCALE NEURAL NETWORKS
Stef Joosten 25 Feb. 1992 9 p
(Memo-INF-92-16; ETN-92-92434) Copyright Avail: CASI HC A02/MF A01

Ideas about implementing a neurocomputer are presented. The architecture can cope with large amounts of neurons (in the range of 1000 to 1,000,000), with a large number of inputs per neuron (about 1000 to 10,000). The architecture exploits wafer scale integration and integrated optics. The architecture and its feasibility are qualitatively discussed. ESA

N93-15090# Universiteit Twente, Enschede (Netherlands). Tele-Informatics and Open Systems Group.
SENSITIVITY AND UNCERTAINTY ANALYSIS IN PERFORMABILITY MODELLING
Boudewijn R. Haverkort and Adrianus M. H. Meeuwissen (Technische Univ., Delft, Netherlands) Mar. 1992 29 p
(Memo-INF-92-18; TIOS-92/09; ETN-92-92436) Copyright Avail: CASI HC A03/MF A01

The issue of sensitivity analysis of performability measures is addressed. An exact Taylor series of the steady state performability measures is presented and the validity region of this approximation is discussed. An uncertainty analysis approach based on Monte Carlo simulation is described. For a small performability model (described as a Markov reward model), both approaches are applied and their relative merits are discussed. For a much larger model (described as a dynamic queueing network), an uncertainty analysis is carried out. The dependencies between model parameters are varied and their influence is discussed. ESA

N93-15123# Institut National Polytechnique, Grenoble (France). Lab. Conception de Systemes Integres.
AUTOMATED CODING AND INTERSECTING CUBE THEORY Ph.D. Thesis [CODAGE D'AUTOMATES ET THEORIE DES CUBES INTERSECTANTS]
Christopher Duff 1991 175 p In FRENCH
(ETN-92-92675) Avail: CASI HC A08/MF A02

A state assignment method for finite state machines, based on an embedding theory called intersecting cube theory, is proposed. Predictive minimization situations are looked for in the control flow graph. The research is based on the partition pair theory, aiming at reduced dependency of the output and next state equations towards inputs and present state variables. This leads to the definition of encoding constraints in terms of adjacency groups, defined as sets of states to be put bijectively on faces or cubes of the hypercube. These sets of states are generally intersecting ones. A solution of the generalized intersecting face or cube embedding problem is proposed. The hypercube is viewed as the lattice of the parts of a set of N elements. The intersecting cube embedding problem is processed within the frame of the corresponding theory. This approach was implemented by a software in the ASYL system. The gain in silicon area, critical path, and routing factor with respect to random assignment, appears to be one of the best presently known. ESA

N93-15239# Carnegie-Mellon Univ., Pittsburgh, PA. School of Computer Science.
EXPERIENCE WITH A COURSE ON ARCHITECTURES FOR SOFTWARE SYSTEMS. PART 1: COURSE DESCRIPTION
David Garlan, Mary Shaw, Chris Okasaki, Curtis M. Scott, and Roy F. Swonger Aug. 1992 33 p
(AD-A256221; CMU-CS-92-176) Avail: CASI HC A03/MF A01

As software systems grow in size and complexity their design problem extends beyond algorithms and data structures to issues of system design. This area receives little or no treatment in existing computer science curricula. Although courses about specific systems are usually available, there is no systematic treatment of the organizations used to assemble components into systems. These issues - the software architecture level of software design - are the subject of a new course that we taught for the first time in Spring 1992. In this pair of reports, Part 1 presents the motivation for the course, the content and structure of the current version, and our plans for improving the next version. Part 2 consists of teaching materials from the first offering, including assignments and overheads for lectures. GRA

N93-15240# Carnegie-Mellon Univ., Pittsburgh, PA. School of Computer Science.
TRANSACTIONAL DISTRIBUTED SHARED MEMORY
Andrew B. Hastings Jul. 1992 187 p
(Contract MDA972-90-C-0035; ARPA Order 7330)
(AD-A256222; CMU-CS-92-167) Avail: CASI HC A09/MF A02

Atomic transactions have proven to be an important technique for constructing reliable applications. Traditionally, transactions have been extended to distributed environments through the use of function shipping, a technique in which message passing or remote procedure calls are used to invoke computational requests on remote nodes. Recently, the data sharing approach to constructing distributed applications has received attention in the form of distributed file systems and distributed memory. Applying the data sharing approach to transactions produces transactional distributed memory (TDSM) which yield benefits for a certain class of distributed application. The union of transactions and distributed shared memory offers synergies in transaction recovery, concurrency control, and coherency control, but introduces challenges in transaction recovery. In this dissertation, I describe the design of a system that provides TDSM in the form of distributed recovery virtual memory. Using the external pager interface of the Mach operating system, I implemented a prototype based on the Camelot distributed transaction facility. I analyze the prototype and its performance, offer techniques for improving the design of future TDSM systems, and characterize the applications for which TDSM is useful.
GRA

N93-15628# Massachusetts Inst. of Tech., Cambridge. Lab. for Computer Science.
ASPECTS OF A PARALLEL-ARCHITECTURE SIMULATOR
Eric A. Brewer Feb. 1992 74 p
(Contract N00014-89-J-1988; NSF CCR-87-16884)
(AD-A256872; MIT/LCS/TR-527) Avail: CASI HC A04/MF A01

This thesis discusses the use of code augmentation in PROTEUS, a high-performance parallel-architecture simulator. PROTEUS multiplexes a single processor among the various activities in a simulated parallel machine to provide accurate information about the timing and behavior of an application and the underlying simulated architecture. PROTEUS is fast, accurate, and flexible: it is one to two orders of magnitude faster than comparable simulators, it can reproduce results from real multiprocessors, and it is easily configured to simulate a wide range of MIMD architectures. Traditional multiprocessor simulators simulate the machine cycle by cycle, interpreting each instruction. The high overhead of instruction interpretation makes these simulators too slow for research in the area of parallel systems.

PROTEUS simulates most instructions via a combination of direct execution and code augmentation, which reduces the simulation overhead for these instructions by roughly a factor of one hundred. In addition to performance, code augmentation offers several other benefits for multiprocessor simulators, such as nonintrusive profiling and stack overflow detection. Primary among these benefits is precise control of the cost in machine cycles of a piece of code. The ability to assign code a cost of zero cycles allows users to generate nonintrusive monitoring and debugging code. Because the monitoring code costs zero cycles, it has no effect on the timing of the simulation. Thus, users can add arbitrary monitoring and debugging code without interfering with the simulation. The ability to assign costs also allows users to tune costs to match a particular architecture, thus increasing the accuracy of the simulation. GRA

61 COMPUTER PROGRAMMING AND SOFTWARE

Includes computer programs, routines, alogorithms, and specific applications, e.g., CAD/CAM.

N93-14164# Naval Surface Warfare Center, Dahlgren, VA.
Ada-BASED MULTITASKING TERMINAL I/O
John C. Chalkley and Michael W. Masters Feb. 1992 129 p
(AD-A255656; NAVSWC-TR-91-783) Avail: CASI HC A07/MF A02

This report describes ANSI Terminal Services, a reusable Ada-based layered approach to providing protected asynchronous terminal I/O in a multitasking environment. The traditional single-threaded, sequential programming model is inadequate for Ada multitask programs, particularly for real-time applications. An application is likely to contain several tasks needing to perform output concurrently. Any shared resources contained in the I/O software must, therefore, be protected through some form of mutual exclusion. Also, an application will likely need to support input operations concurrently with outputs. This requirement is especially important since Ada implementations on most current operating systems are process synchronous, rather than task synchronous/process asynchronous. As a result, they cause the entire user process to block on an input request. Thus, other program tasks that may be performing critical functions are suspended until user input is complete. Such a result is clearly inappropriate in a real-time environment. ANSI Terminal Services solves these problems and provides both a standard programmer interface and the necessary multitasking concurrency control. GRA

N93-14237# Massachusetts Inst. of Tech., Cambridge. Dept. of Mathematics.
GOALS VERSUS ALGORITHMS Final Report, 1 Jul. 1989 - 30 Jun. 1992
Peter J. Huber 30 Jun. 1992 13 p
(Grant AF-AFOSR-0412-89)
(AD-A256106; PHJ-91-2; AFOSR-92-0860TR) Avail: CASI HC A03/MF A01

Computational methods in statistics often are defined through an algorithm. It is argued that a precise finite sample specification of the goals to be achieved by the algorithm is at least equally important. The issues are discussed in the special case of Projection Pursuit Regression. An interesting initial result of this work, which is still in progress, is that the Friedman-Stuetzle algorithm appears to be systematically biased toward overfitting. GRA

N93-14241# Air Force Inst. of Tech., Wright-Patterson AFB, OH. School of Engineering.
DEVELOPMENT OF AN ENVIRONMENT FOR SOFTWARE RELIABILITY MODEL SELECTION Ph.D. Thesis
Salah A. Elewa Sep. 1992 225 p
(AD-A256609; AFIT/DS/ENC/92-1) Avail: CASI HC A10/MF A03

An environment was developed for solving the problem of selecting a proper software reliability model for a given set of software failures. The idea behind the environment developed in this dissertation was to liken a collected set of software failure data to a previous one that proved to fit well with a specified software reliability model. Software failures were assumed to have a two-Parameter exponential distribution with unequal type 2 censoring. A test criterion was derived for testing ratio criterion. The exact distribution of the test criterion was derived. An asymptotic approximation was also obtained and was found to be very close to the exact distribution when the number of failures were more than twenty. Software failure data, available from the Data and Analysis Center for Software (DACS), were used as the initial group of software failure sets. The environment was then applied for testing the quality of several software failure sets. GRA

N93-14247# Naval Postgraduate School, Monterey, CA.
DEVELOPMENT OF A MATLAB TOOLBOX FOR IMAGE PROCESSING M.S. Thesis
Dorothy J. Freer Jun. 1992 49 p
(AD-A256130) Avail: CASI HC A03/MF A01

This thesis provides an Image Processing Toolbox for use with MATLAB which contains ready-made tools for students and faculty who wish to continue research in image processing and related areas. The Toolbox is available for several computer environments. The documentation provided with the distribution diskette contains both a tutorial and reference section in the MATLAB style. This thesis report provides information needed to write and compile C language programs for use as MEX-files, an overview of the Toolbox, and a case study which illustrates the use of some of the functions in the Toolbox. GRA

N93-14268# Carnegie-Mellon Univ., Pittsburgh, PA. Dept. of Computer Science.
A PROOF OF THE CHURCH-ROSSER THEOREM AND ITS REPRESENTATION IN A LOGICAL FRAMEWORK
Frank Pfenning Sep. 1992 48 p
(Contract F33615-90-C-1465; ARPA Order 7597)
(AD-A256574; CMU-CS-92-186) Avail: CASI HC A03/MF A01

We give a detailed, informal proof of the Church-Rosser property for the untyped lambda-calculus and show its representation in LF. The proof is due to Tait and Martin-Lof and is based on the notion of parallel reduction. The representation employs higher-order abstract syntax and the judgments-as-types principle and takes advantage of term reconstruction as it is provided in the Elf implementation of LF. Proofs of meta-theorems are represented as higher-level judgments which relate sequences of reductions and conversions. GRA

N93-14285# Harvard Univ., Cambridge, MA. Dept. of Statistics.
ITERATIVE ALGORITHMS FOR INTEGRAL EQUATIONS OF THE FIRST KIND WITH APPLICATIONS TO STATISTICS
Mark Vangel Oct. 1992 185 p
(Contract N00014-91-J-1005)
(AD-A256529; TR-ONR-C-12) Avail: CASI HC A09/MF A02

The use of a preconditioned Richardson iterative algorithm for the solution of linear and nonlinear ill-posed integral equations of the first kind is discussed. The discussion consists of three parts, which can be roughly categorized as follows: numerical analysis, applications to statistical methodology, and an application to an inverse problem. In the first part, singular matrix equations that result from discretizing ill-posed integral equations of the first kind are considered. Sufficient conditions for the convergence of Richardson's algorithm to a solution are established, and necessary and sufficient conditions are proven for special cases. The inconsistent case is also discussed. A preconditioning for equations with positive kernels leads to the Conditional Expectation algorithm, which is discussed in detail. A notion of 'iterative regularization' is introduced and related to the more usual penalized least squares approach to regularization. GRA

N93-14405# IBM Federal Systems Div., Gaithersburg, MD.
SOFTWARE TECHNOLOGY FOR ADAPTABLE, RELIABLE SYSTEMS (STARS) PROGRAM. SOFTWARE PROCESS TOOLS AND TECHNIQUES EVALUATION REPORT, VERSION 1.0. TASK IS15: SOFTWARE PROCESS MANAGEMENT
William H. Ett 30 Sep. 1991 173 p
(Contract F19628-88-D-0032)
(AD-A255945; Rept-03705-001) Avail: CASI HC A08/MF A02

This document describes the tools and technology examined on STARS Task IS15. This report summarizes the IBM team's examination of software

process representation tools and techniques. It also summarizes the examination of software process enactment tools, and techniques for implementing a process system from a well-defined system of processes such as the Cleanroom Engineering Software Development Process . The software process definition tools and techniques sections of the document are organized to accomplish the following: (1) to examine the feasibility of porting the Software Process Management System (SPMS) from the Apple Macintosh to the IBM STARS SEE; (2) to provide a SPMS Port plan; and (3) to discuss the use of box structures as a notation for recording aspects of software processes. The software process enactment tools and techniques sections of the document are organized to accomplish the following: (1) describe the KI Shell tool selected for supporting the IBM STARS Cleanroom Software Process Case Study; (2) describe the specification, design, and implementation of the Cleanroom Engineering Process Assistant prototype; and (3) provides lessons learned from performing the Cleanroom Software Process Case Study. Finally the document makes recommendations for the selection of software process definition and enactment support capabilities for the IBM ST ARS SEE. GRA

N93-14420# Naval Postgraduate School, Monterey, CA. Dept. of Computer Science.

ITERATIVE SOFTWARE TESTING Progress Report, Oct. 1991 - Jun. 1992

Timothy J. Shimeall and Stephen C. Shimeall 4 Jun. 1992 26 p

(AD-A255953; NPSCS-92-008) Avail: CASI HC A03/MF A01

Software is often developed via a series of modifications and releases. This sort of development implies that the testing often takes place in an increasingly familiar structure, rather than a unique or unfamiliar structure. This paper discusses how to exploit this type of development in test planning and execution, by presenting a motivational example, a formal model of test iteration and a discussion of tools to enhance the efficiency of testing when an iterative approach is used. GRA

N93-14423# Carnegie-Mellon Univ., Pittsburgh, PA. School of Computer Science.

WAIT-FREE CONSENSUS Ph.D. Thesis

James Aspnes 24 Jul. 1992 79 p Sponsored in cooperation with IBM, and NSF

(AD-A255978; CMU-CS-92-164) Avail: CASI HC A05/MF A01

Consensus is a decision problem in which n processors, each starting with a value not known to the others, must collectively agree on a single value. If the initial values are equal, the processors must agree on that common value-: this is the validity condition. A consensus protocol is wait-free if every processor finishes in a finite number of its own steps regardless of the relative speeds of the other processors, a condition that precludes the use of traditional synchronization techniques such as critical sections, locking, or leader election. Wait-free consensus is fundamental to synchronization without mutual exclusion, as it can be used to construct wait-free implementations of arbitrary concurrent data structures. It is known that no deterministic algorithm for wait -free consensus is possible, although many randomized algorithms have been proposed. I present two algorithms for solving the wait-free consensus problem in the standard asynchronous shared-memory model. The first is a very simple, protocol based on a random walk. The second is a protocol based on weighted voting, in which each processor executes 0(n log squared n) expected operations This bound is close to the trivial lower bound of Omega(n), and it substantially improves on the best previously-known bound of 0(n squared log n) due to Bracha and Rachman. GRA

N93-14502# Electronics Research Lab., Adelaide (Australia).

PROGRAM VERIFICATION USING HIGHER ORDER LOGIC

A. Cant Jan. 1992 91 p

(AD-A255408; ERL-0600-RR; DODA-AR-006-933) Avail: CASI HC A05/MF A01

This paper describes a number of experiments in program verification carried out within two automated proof assistants, namely the HOL (High Order Logic) system and Isabelle. Various approaches to programming language semantics are described. Theories and tactics for proving the correctness of programs written in small functional and imperative languages are then constructed within HOL and Isabelle. GRA

N93-14505# Army Construction Engineering Research Lab., Champaign, IL.

A METHODOLOGY FOR THE EVALUATION OF STRUCTURAL DESIGN SOFTWARE FOR DOS-BASED MICROCOMPUTERS Final Report

Hojjat Adeli, James Wilcoski, and John R. Hayes, Jr. Jul. 1992 25 p

(AD-A255421; CERL-TR-FM-92/02) Avail: CASI HC A03/MF A01

The missions of the U.S. Army Corps of Engineers and Installation Directorates of Engineering and Housing require structural design engineers to produce high-quality designs with efficiency and accuracy. Therefore, the Army has an interest in the productivity and quality enhancements offered by structural design computer software. This report presents a methodology for evaluating the performance of commercially available structural design software for DOS-based microcomputers. Careful evaluation of such software is necessary because the quality of these products varies widely, and these differences may not be apparent without systematic evaluation by the potential user. Significant savings in the design process can be realized if a high-quality software program is used for its intended purpose. GRA

N93-14546# Maryland Univ., College Park. Center for Automation Research.

GEOMETRIC INVARIANTS AND OBJECT RECOGNITION

Isaac Weiss Aug. 1992 46 p

(Contracts N00014-91-J-1222; DACA76-92-C-0009; ARPA Order 8459)

(AD-A255317; CAR-TR-632; CS-TR-2942) Avail: CASI HC A03/MF A01

In this paper we discuss the role of the general invariance concept in object recognition, and review the classical and recent literature on projective invariance. Invariants help solve major problems of object recognition. For instance, different images of the same object often differ from each other, because of the different viewpoint from which they were taken. To match the two images, common methods thus need to find the correct viewpoint, a difficult problem that can involve search in a large parameter space of all possible points of view and/or finding point correspondences. Geometric invariants are shape descriptors, computed from the geometry of the shape, that remain unchanged under geometric transformations such as changing the viewpoint. Thus they can be matched without search. Deformations of objects are another important class of changes for which invariance is useful. GRA

N93-14558# Carnegie-Mellon Univ., Pittsburgh, PA. School of Computer Science.

DESIGN AND IMPLEMENTATION OF PRACTICAL CONSTRAINT LOGIC PROGRAMMING SYSTEMS Ph.D. Thesis

Spiro Michaylov 24 Aug. 1992 240 p

(Contract F33615-90-C-1465; ARPA Order 7597)

(AD-A256191; CMU-CS-92-168) Avail: CASI HC A11/MF A03

The Constraint Logic Programming (CLP) scheme, developed by Jaffar and Lassez, defines a class of rule-based constraint programming languages. These generalize traditional logic programming languages (like Prolog) by replacing the basic operational step, unification, with constraint solving. While CLP languages have a tremendous advantage in terms of expressive power, they must be shown to be amenable to practical implementations. This thesis describes a systematic approach to the design and implementation of practical CLP systems. The approach is evaluated with respect to two major objectives. First, the Prolog subset of the languages must be executed with essentially the efficiency of an equivalent Prolog system. Second, the cost of constraint solving must be commensurate with the complexity of the constraints arising. The language CLP(R), whose domain is uninterpreted functors over real numbers, is the central case study. First, the design of CLP(R) is discussed in relation to programming methodology. The discussion of implementation begins with an interpreter that achieves the efficiency of equivalent Prolog interpreters, and meets many of the basic efficiency requirements for constraint solving. Many of the principles applied in the interpreter are then used to develop an abstract machine for CLP(R), leading to a compiler-based system achieving performance comparable to modern Prolog compilers. Furthermore, it is shown how this technology can be extended so that the efficiency of CLP(R) approaches that of imperative programming languages. GRA

N93-14563# Carnegie-Mellon Univ., Pittsburgh, PA. Software Engineering Inst.

FAULT TOLERANT SYSTEMS PRACTITIONER'S WORKSHOP Final Report

Walter L. Heimerdinger and Charles B. Weinstock Oct. 1991 22 p Workshop held in Pittsburgh, PA, 10-11 Jun. 1991

(Contract F19628-90-C-0003)

(AD-A255376; CMU/SEI-91-SR-13) Avail: CASI HC A03/MF A01

On June 10-11, 1991, a Fault Tolerant Systems Practitioner's Workshop was held at the Software Engineering Institute. The purpose of the workshop was to attempt to identify how fault tolerance is being applied today, why fault tolerance is under used, and what can be done to bring fault tolerant practices into wider use. Attendence at the workshop was limited to a small number of practitioners who had successfully applied fault tolerance in a systems context. This report summarizes the proceedings of the workshop which included a discussion of barriers to the deployment of fault tolerant systems, a summary of the state of the practice, and a discussion of the technology needs of fault tolerance. The report concludes with a discussion of ways the Software Engineering Institute may be able to help bring fault tolerant practices into wider use. GRA

N93-14564# Rutgers - The State Univ., New Brunswick, NJ. Dept. of Computer Science.

COMPUTER-AIDED DESIGN PACKAGE FOR DESIGNERS OF DIGITAL OPTICAL COMPUTERS Annual Report, 1 May 1991 - 30 Apr. 1992

Miles Murdocca May 1992 21 p

(Contract N00014-90-J-4018)

(AD-A255381) Avail: CASI HC A03/MF A01

This report covers progress for the period 5/1/91 4/30/92 on a jointly sponsored AFOSR/ONR grant to Rutgers University that supports research in architecture and design of digital optical computers. Progress for this reporting period includes the development of an interactive design tool for digital optical circuits, the development of optical interconnection methods, and an investigation into the architectural implications of reconfigurable optical interconnects. Prior to this reporting period, an emphasis had been placed on the Bell Labs style of digital optical processor, in which arrays of optical logic gates are interconnected in free space with regular patterns at the gate level. The computer-aided design (CAD) tools and the optical interconnection methods that we have been developing allow us to characterize tradeoffs between the complexity of the optical interconnects and the complexity of the computer architecture. We plan to spend the final year of the effort engaged in characterizing these tradeoffs, a few of which are described below in the Micro vs. Macro-Optics section. One tradeoff that is of particular interest is in how the regularity of the interconnects affect the complexity of the optics, and how the regularity affects the depth and breadth of the resulting circuits. GRA

N93-14566# Carnegie-Mellon Univ., Pittsburgh, PA. Robotics Inst.

VANTAGE: A FRAME-BASED GEOMETRIC MODELING SYSTEM PROGRAMMER/USER'S MANUAL, V2.0

B. Kumar, J. C. Robert, R. Hoffman, K. Ikeuchi, and T. Kanade Dec. 1991 81 p

(AD-A255434; CMU-RI-TR-91-31) Avail: CASI HC A05/MF A01

Geometric modeling systems allow users to create, store, and manipulate models of three-dimensional (3-D) solid objects. These geometric modeling systems have found many applications in CAD/CAM and robotics areas. Graphic display capability which rivals photographic techniques allows realistic visualization of design and simulation. Capabilities to compute spatial and physical properties of objects, such as mass property calculation and static interference check, are used in the design and analysis of mechanical parts and assembly. Output from the geometric modelers can be used for automatic programming of NC machines and robots. These geometric modeling systems are powerful in many application domains, but have severe limitations to be used for tasks such as model-based computer vision. Among others, (1) there is no explicit symbolic representation of the two-dimensional information obtained by the projection of the 3-D model. The output image displayed on the screen is a set of pixel intensity values, with no knowledge of the logical grouping of points, lines and polygons. Also, the relationship between 3-D and 2-D information is not maintained properly. (2) Most of the current 3-D geometric modeling systems are designed with a closed architecture, with a minimum of documentation describing the internal data structures. Moreover, some of the data structures are packed into bit-fields, making understanding and modification difficult. (3) They run as stand-alone interactive systems and cannot easily be interfaced to other programs. GRA

N93-14569# Carnegie-Mellon Univ., Pittsburgh, PA. Robotics Inst.

IMPLEMENTATION OF THE PURE PURSUIT PATH TRACKING ALGORITHM

R. C. Coulter Jan. 1992 13 p

(AD-A255524; CMU-RI-TR-92-01) Avail: CASI HC A03/MF A01

The main purpose of this technical report is to describe in detail the implementation of the pure pursuit path tracking algorithm. Given the general success of the algorithm over the past few years, it seems likely that it will be used again in land-based navigation problems. This report also includes a geometric derivation of the method, and presents some insights into the performance of the algorithm as a function of its parameters. GRA

N93-14572# Science Applications International Corp., San Diego, CA.

SOFTWARE RELIABILITY, MEASUREMENT, AND TESTING SOFTWARE RELIABILITY AND TEST INTEGRATION, VOLUME 1 Final Report, Sep. 1986 - Dec. 1989

James A. McCall, William Randell, Janet Dunham, and Linda Lauterbach Apr. 1992 255 p

(Contract F30602-86-C-0269)

(AD-A256242; RL-TR-92-52-Vol-1) Avail: CASI HC A12/MF A03

This effort integrated software reliability, measurement, and test techniques in terms of prediction, estimation, and assessment. Experiments were conducted to compare six testing techniques and to measure the effect of software product and process variables on software reliability. A guidebook was produced to help program managers control and manage software reliability and testing. Error/anomaly and code reviews were the test techniques found to be the most effective at the unit level; branch testing and code reviews were the most effective at the CSC level. GRA

N93-14575# Naval Surface Warfare Center, Silver Spring, MD.

SYSTEMS MODELING

Dong Choi, Janet Youngblood, Steve Howell, and Phil Hwang 2 Feb. 1992 46 p

(NR Proj. RS3-4-P-12)

(AD-A255215; NAVSWC-TR-91-592) Avail: CASI HC A03/MF A01

The evaluation and assessment techniques that may be applied to the different phases of the system life cycle--from requirements specification to implementation and reengineering --are explored. At each stage of the system life cycle, there are suitable techniques that may be applied to predict the behavior of the system, some more appropriate than others. Currently, however, there is no formal method for applying this evaluation information to the forward or reverse engineering process. Consequently, maximum use of the information available to the system developers rarely occurs. In addition, this report investigates the issues relevant to the integration of evaluation methods to the system development process. GRA

N93-14581# Science Applications International Corp., San Diego, CA.

SOFTWARE RELIABILITY, MEASUREMENT, AND TESTING. VOLUME 2: GUIDEBOOK FOR SOFTWARE RELIABILITY MEASUREMENT AND TESTING Final Report, Sep. 1986 - Dec. 1989

James A. McCall, William Randell, Janet Dunham, and Linda Lauterbach Apr. 1992 265 p

(Contract F30602-86-C-0269)

(AD-A256164; RL-TR-92-52-Vol-2) Avail: CASI HC A12/MF A03

This effort integrated software reliability, measurement, and test techniques in terms of prediction, estimation, and assessment. Experiments were conducted to compare six testing techniques and to measure the effect of software product and process variables on software reliability. A guidebook was produced to help program managers control and manage software reliability and testing. Error/anomaly and code reviews were the test techniques found to be the most effective at the unit level; branch testing and code reviews were the most effective at the CSC level. GRA

N93-14654# Rochester Univ., NY. Dept. of Computer Science.
A PROBABILISTIC APPROACH TO ANYTIME ALGORITHM FOR INTELLIGENT REAL-TIME PROBLEM SOLVING Final Report, 1 Dec. 1990 - 31 May 1992
Josh Tenenberg and James Allen 4 Aug. 1992 38 p
(Grant AF-AFOSR-0108-91)
(AD-A255709; AFOSR-92-0828TR) Avail: CASI HC A03/MF A01

Our work on real time intelligent problem solving has focussed on the tradeoff between deliberation and activity. Such a tradeoff is required, since an excess of deliberation will be defeated by the dynamical nature of the world and by errors in the predictive model, and a lack of deliberation will not provide the agent with sufficient flexibility to perform well in novel situations. Our framework for evaluating this tradeoff includes both an explicit and an implicit component. In the explicit work, we represent the uncertainties associated with inaccuracies in the model and the inability to completely monitor changes in the world by expanding our language to include probabilities, and making choices about when to act and when to deliberate further based upon these explicit uncertainty measures. In the implicit approach, we use reinforcement learning of a Markov Decision Process to place a strict bound on deliberation. The agent's knowledge is obtained through an active sensory system having limited bandwidth, overcoming the standard limitations of assuming complete knowledge, but requiring modifications to the standard learning algorithm. Learning time is decreased by the use of social learning mechanisms as well as task decomposition and dynamic policy merging. GRA

N93-14659# Rensselaer Polytechnic Inst., Troy, NY. Dept. of Mathematical Sciences.
USING AN INTERIOR POINT CUTTING PLANE METHOD TO SOLVE INTEGER PROGRAMMING PROBLEMS Final Report
John E. Mitchell 30 Sep. 1992 13 p
(Contract N00014-91-3-1714)
(AD-A256041) Avail: CASI HC A03/MF A01

There were several accomplishments of this research, both theoretical and computational. In joint work with Todd, we presented a cutting plane primal projective interior point method which we applied to matching problems, with encouraging computational results. Primal projective methods require a method to update the dual; we showed how various dual updates are related to each other and we also derived a dual projective algorithm. We derived a polynomial-time shifted barrier warm start algorithm which can be used in a cutting plane method; we showed that the directions obtained are strongly related to the directions derived in the work with Todd; computational results showed that the algorithm can be useful in some situations. The grant partially supported a Ph.D. student, Brian Borchers, who received his degree in August, 1992. His thesis concerned the use of branch-and-bound methods and contained good computational results as well as interesting theoretical observations. One paper from this thesis describes how the primal-dual interior point method can be used efficiently in a branch-and-bound method for solving mixed integer linear programming problem. Another paper describes how branch and bound algorithms for nonlinear integer programming problems can be improved. Borchers and I also developed a primal-dual interior point cutting plane method for solving linear ordering problems; the computational results for this algorithm were very encouraging, with run times comparable to those required by a simplex based cutting plane algorithm. GRA

N93-14696# Sparta, Inc., Lexington, MA.
DEVELOPMENT OF AN INTEGRATED PACKAGE OF PHYSICS MODELS FOR SCENE SIMULATION STUDIES TO SUPPORT SMART WEAPONS DESIGN STUDIES
J. R. Hummel, N. L. DePiero, D. R. Longtin, and J. R. Jones 17 Mar. 1992 117 p
(Contract F19628-91-C-0093; AF Proj. 5321)
(LTR92-004; PL-TR-92-2081; SR-1) Avail: CASI HC A06/MF A02

The Balanced Technology Initiative (BTI) on Smart Weapons Operability Enhancement (SWOE) has as a goal to model the radiant field from complex natural backgrounds. During the three years of the program, the calculation of these radiant fields has evolved to produce a process, known as the SWOE Process, that will enable a smart weapons designer or tester to specify and obtain the data required to describe the physical characteristics and the environmental conditions of a scene, model the physical processes controlling the generation of the radiant field, and display and analyze the results of the simulated scene. In this, the last year of the BTI/SWOE program, the emphasis was on the delivery of a package of models on a computer platform for use in performing scene simulations for smart weapons design and testing applications. The efforts reported on here consisted of making enhancements to the SWOE thermal models and the design of a new Command Interface System and User Interface System. Author

N93-14807*# Ohio State Univ., Columbus. Electroscience Lab.
A VERY EFFICIENT RCS DATA COMPRESSION AND RECONSTRUCTION TECHNIQUE, VOLUME 4 Final Report
N. Y. Tseng and W. D. Burnside Nov. 1992 130 p
(Grant NAG2-542)
(NASA-CR-191378-Vol-4; NAS 1.26:191378-Vol-4; OSU-722780-4-Suppl-2)
Avail: CASI HC A07/MF A02

A very efficient compression and reconstruction scheme for RCS measurement data was developed. The compression is done by isolating the scattering mechanisms on the target and recording their individual responses in the frequency and azimuth scans, respectively. The reconstruction, which is an inverse process of the compression, is granted by the sampling theorem. Two sets of data, the corner reflectors and the F-117 fighter model, were processed and the results were shown to be convincing. The compression ratio can be as large as several hundred, depending on the target's geometry and scattering characteristics. Author

N93-14876# Allied-Signal Aerospace Co., Kansas City, MO.
PERSONAL COMPUTER BASED COMPUTED TOMOGRAPHY SYSTEM
J. W. Ekis Jun. 1992 17 p Original contains color illustrations
(Contract DE-AC04-76DP-00613)
(KCP-613-4806) Avail: CASI HC A03/MF A01; 2 functional color pages

The purpose of this project was to construct a personal computer (PC) based computed tomography (CT) system. The average industrial CT system ranges in price from $1,000,000 to $2,500,000. The entire PC based system at KCD totaled around $300,000 to build. The system consists of a 80386 computer, a 320 kV industrial x-ray source, and a four-axis positioning stage with 1 micron resolution. The system is capable of testing objects that are less than 30 inches tall, less than 14 in. diameter, and weigh less than 50 pounds. Because the system uses only a single 80386 PC and the detector assembly was manufactured from cadmium tungstate, data collection is the greatest limitation of the system. A typical scan for a single slice requires 4 hours and 45 minutes. Author

N93-14882* National Aeronautics and Space Administration. Pasadena Office, CA.
MODIFIED FAST FREQUENCY ACQUISITION VIA ADAPTIVE LEAST SQUARES ALGORITHM Patent
Rajendra Kumar, inventor (to NASA) 17 Nov. 1992 10 p
Continuation-in-part of abandoned US-Patent-Appl-SN-523692, filed 15 May 1990
(NASA-Case-NPO-17845-2-CU; US-Patent-5,165,051;
US-Patent-Appl-SN-799857; US-Patent-Class-324-79D;
US-Patent-Class-324-79R; US-Patent-Class-324-83Q;
US-Patent-Class-364-724.06; US-Patent-Class-364-724.07;
US-Patent-Class-364-724.08; US-Patent-Class-342-100) US Patent and Trademark Office

A method and the associated apparatus for estimating the amplitude, frequency, and phase of a signal of interest are presented. The method comprises the following steps: (1) inputting the signal of interest; (2) generating a reference signal with adjustable amplitude, frequency and phase at an output thereof; (3) mixing the signal of interest with the reference signal and a signal 90 deg out of phase with the reference signal to provide a pair of quadrature sample signals comprising respectively a difference between the signal of interest and the reference signal and a difference between the signal of interest and the signal 90 deg out of phase with the reference signal; (4) using the pair of quadrature sample signals to compute estimates of the amplitude, frequency, and phase of an error signal comprising the difference between the signal of interest and the reference signal employing a least squares estimation; (5) adjusting the amplitude, frequency, and phase of the reference signal from the numerically controlled oscillator in a manner which drives the error signal towards zero; and (6) outputting the estimates of the amplitude, frequency, and phase of the error signal in combination with the reference signal to

produce a best estimate of the amplitude, frequency, and phase of the signal of interest. The preferred method includes the step of providing the error signal as a real time confidence measure as to the accuracy of the estimates wherein the closer the error signal is to zero, the higher the probability that the estimates are accurate. A matrix in the estimation algorithm provides an estimate of the variance of the estimation error.
Official Gazette of the U.S. Patent and Trademark Office

N93-14902# Oak Ridge National Lab., TN.
A UNIX PRINT FILTER FOR CONTROLLING AN HP LASERJET PRINTER
F. M. Hoffman Sep. 1992 21 p
(Contract DE-AC05-84OR-21400)
(DE92-041350; ORNL/TM-12190) Avail: CASI HC A03/MF A01

This report describes a Unix print filter designed to control an Hewlett Packard Laserjet or other printer that uses Hewlett Packard's Printer Control Language (HP-PCL). The filter gives users the ability to control print pitch, orientation, and indentation by using standard flags to the Unix 1pr. command or multiple entries in the /etc/printcap file and allows both ascii and binary (i.e., graphics and down-loadable fonts) files to be printed. Additionally, the filter provides some accounting capability. The supported print pitch and orientation options are described, as are the different configuration options. The code for the filter and sample entries for the /etc/printcap file are included. DOE

N93-15003# Oak Ridge K-25 Site, TN.
AUTOMATED ESTIMATING SYSTEM (AES), VERSION 5.1. USER'S MANUAL
R. K. Schwarz, ed. Aug. 1992 174 p
(Contract DE-AC05-84OT-21400)
(DE93-000380; K/CSD/TM-64-Rev-4) Avail: CASI HC A08/MF A02

This document describes Version 5.1 of the Automated Estimating System (AES), a personal computer-based software package. The AES is designed to aid in the creation, updating, and reporting of project cost estimates for the Estimating and Scheduling Department of the Martin Marietta Energy Systems, Inc., Engineering Division. AES provides formatted input screens to guide the user though the estimate creation/update process and provides several standardized reports that allow cost to be sorted and summarized in many different formats and at several levels of aggregation. DOE

N93-15052# Naval Research Lab., Washington, DC.
SOFTWARE REQUIREMENTS FOR THE A-7E AIRCRAFT Final Report
Thomas A. Alspaugh, Stuart R. Faulk, Kathryn H. Britton, R. A. Parker, and David L. Parnas 31 Aug. 1992 435 p Revised
(AD-A255746; NRL/FR/5530-92-9194) Avail: CASI HC A19/MF A04

The Software Cost Reduction (SCR) research project introduced a new approach to specifying requirements for real-time embedded systems. The principles were applied in the development of the Software Requirements of the A-7E Aircraft, as an example of the use of the approach. The system software requirements specification document comprises the first product in a series of products which the SCR methodology produces. The methodology is intended to be adaptable for various types of systems. Specification properties which it supports include: (1) conciseness; (2) preciseness; (3) aids to completeness; (4) avoidance of redundancy; (5) descriptions of all externally visible behavior; (6) ease of change; (7) good reference tool; (8) record of fundamental assumptions which might otherwise be only implicit; (9) record of responses to error conditions; (10) specification of constraints on the system; and (11) separation of concerns; that is, a division of the information into distinct, independent parts. GRA

N93-15068# Vector Research, Inc., Ann Arbor, MI.
SIDR RELATIVE WEIGHTED PRODUCT (RWP) ASSIGNMENT PROCESS Draft Report
Stuart W. Baker 15 Jul. 1992 105 p
(Contract MDA903-88-C-0147)
(AD-A255801; VRI-DMIS-2.60-WP92-10) Avail: CASI HC A06/MF A02

This report serves as documentation of the Defense Medical Information System (DMIS) Relative Weighted Product (RWP) computation and assignment process. Included are an overview of the process, detailed step-by-step guidelines for running the computer programs, and discussion of Quality Control (QC) and information reports used to validate the data and summarize the results. GRA

N93-15072 National Physical Lab., Teddington (England). Div. of Information, Technology and Computing.
SOFTWARE STAMPING
Fiona Williams and Samantha Green Apr. 1992 15 p Sponsored by Dept. of Trade and Industry, London, England
(NPL-DITC-198/92; ETN-92-92376) Copyright Avail: National Physical Lab., Teddington, Middlesex, TW11 0LW, England

The application of a checkable digital stamp to a piece of software to prove its integrity at a later time is considered. The criteria for such a stamp are developed and available techniques that could be used are analyzed. A methodology for stamping, using current cryptographic and hashing techniques, is proposed. Some of the practical problems that might be encountered if this methodology were implemented are given.
ESA

N93-15077# Universiteit Twente, Enschede (Netherlands). Tele-Informatics and Open Systems Group.
FROM DATA STRUCTURE TO PROCESS STRUCTURE
Ed Brinksma and Pim Kars 1991 35 p Sponsored in part by EEC
(Memo-INF-91-38; TIOS-91/11; ETN-92-92426) Copyright Avail: CASI HC A03/MF A01

Transformations in a process algebraic formalism extended with an abstract data type language for the representation of value expressions are addressed. These can be used to instantiate value parameters of behavior expressions that parameterize communication and control structures, as well as process definitions. The stepwise transformation of a well known class of process (bags, queues, stacks, etc.) descriptions, in terms of simple process definitions and complex parameters, into equivalent systems of interacting processes with state parameters of reduced complexity is shown. The key to the derivation of such transformations is the solution of related complex equations in which the context is the unknown entity.
ESA

N93-15078# Universiteit Twente, Enschede (Netherlands). Tele-Informatics and Open Systems Group.
IMPLEMENTATION ISSUES CONCERNING INJECTION SIMULATION. PART 1: THE BACKBONE IMPLEMENTATION
Aad P. A. vanMoorsel 1991 56 p
(Memo-INF-91-57-Pt-1; TIOS-91/37-Pt-1; ETN-92-92427) Copyright Avail: CASI HC A04/MF A01

Implementation issues of the fast simulation technique Injection Simulation (IS) are discussed. Bias and variance reduction properties of IS estimators and other characteristics such as the extrapolative nature of the estimators, possible hybrid use, and backbone implementation are studied. A natural way of applying the technique, the so called backbone implementation, is addressed. Alternatives for several choices in the backbone implementation are discussed. Throughout the study, results for an M/M/1 queueing system with server breakdowns are used to demonstrate the derived characteristics of IS.
ESA

N93-15084# Universiteit Twente, Enschede (Netherlands). Dept. of Computer Science.
OBSTACLES IN OBJECT-ORIENTED SOFTWARE DEVELOPMENT
Mehmet Aksit and Lodewijk Bergmans Feb. 1992 34 p
(Memo-INF-92-15; ETN-92-92433) Copyright Avail: CASI HC A03/MF A01

Obstacles in Object Oriented (OO) software development, with respect to pilot applications, are summarized. The aim is to make software engineers aware of problems they may encounter during object oriented development and to inspire researchers to initiate new research activities. Background information, the basic characteristics, and the principles of OO software development are covered. Problems encountered and related research activities are outlined.
ESA

N93-15091# Universiteit Twente, Enschede (Netherlands). Dept. of Computer Science.
A NON-DETERMINISTIC RECOGNISER GENERATOR
Albert Nymeyer Mar. 1992 25 p
(Memo-INF-92-21; ETN-92-92437) Copyright Avail: CASI HC A03/MF A01

A construction method to generate a nondeterministic finite automaton is addressed. Nondeterministic finite automata are used in applications,

like scanners and editors, that use pattern matching. Thomson's construction is an algorithm that will generate a nondeterministic finite automaton given a regular expression. This construction is specified and implemented using an attribute grammer, and using a scanner and parser generator, recognizer generators that can generate a recognizer for a given regular expression are built. The recognizer uses a backtracking algorithm to determine whether a string matches the regular expression. The problem of regular expressions that cause the recognizer to loop is solved. ESA

N93-15092# Universiteit Twente, Enschede (Netherlands). Dept. of Computer Science.
A PARA-FUNCTIONAL VERSION OF WARSHALL'S ALGORITHM
Duco Fijma 9 Mar. 1992 19 p
(Memo-INF-92-23; ETN-92-92438) Copyright Avail: CASI HC A03/MF A01

The development of a parallel version of Warshall's algorithm is used to illustrate the development of parallel programs using functional programming languages. Functional programs carry much less overspecification of evaluation order than the equivalent imperative programs. Therefore, detecting and using parallelism is much easier. The extension of functional languages in order to be able to express the resulting parallel algorithm is discussed. A method of annotating subexpressions for parallel execution is introduced. Adding these annotations to programs is illustrated as not being enough to exploit the potential parallelism. In the study case, some program transformations were needed to be applied to reduce the conflicts between the various subexpressions. Using functional programming, these conflicts are easy to spot and remove or minimize. ESA

N93-15125# Institut National Polytechnique, Grenoble (France). Lab. de Conception de Systemes Integres.
OPTIMAL SYNTHESIS METHODS FOR SILICON COMPILERS Ph.D. Thesis [METHODES DE SYNTHESE OPTIMISEE POUR COMPILATEURS DE SILICIUM]
Franck Poirot 1990 184 p In FRENCH
(ETN-92-92677) Avail: CASI HC A09/MF A02

The logic synthesis of silicon compilers is considered. The state of the art of multilayer synthesis is still an open problem. The purpose of the investigation is to present methods for controller synthesis and combinatory systems in order to implement multilayers based on library cells. The silicon compilation concept and the logic synthesis are presented. The importance of the logic synthesis market and the influence on the design of integrated circuits are included. The coding of turing machines and a method based on the immersion intersecting cubes in a boolean hypercube are presented. A synthesis of combinatorial circuits and a time optimization method for such devices are included. ESA

N93-15199# Maryland Univ., College Park. Dept. of Computer Science.
RESEARCH IN PROGRAMMING LANGUAGES AND SOFTWARE ENGINEERING Final Report, 1 Nov. 1989 - 30 Jun. 1992
Victor R. Basili, John D. Gannon, and Marvin V. Zelkowitz 10 Sep. 1992 13 p
(Grant AF-AFOSR-0031-90)
(AD-A256341; AFOSR-92-0900TR) Avail: CASI HC A03/MF A01

This report summarizes the activities during the period 1 May 1991 - 30 June 1992. The following three sections describe results from three major activities: a risk-based model of software decision making, construction of models for software development processes, and verification of safety properties of software requirements specifications. GRA

N93-15206# Carnegie-Mellon Univ., Pittsburgh, PA. School of Computer Science.
GRAMMATICAL TRIGRAMS: A PROBABILISTIC MODEL OF LINK GRAMMAR
John Lafferty, Daniel Sleator, and Davy Temperley Sep. 1992 11 p
(AD-A256365; CMU-CS-92-181) Avail: CASI HC A03/MF A01

In this paper we present a new class of language models. This class derives from link grammar a context-free formalism for the description of natural language. We describe an algorithm for determining maximum-likelihood estimates of the parameters of these models. The language models which we present differ from previous models based on stochastic context-free grammars in that they are highly lexical. In particular they include the familiar n-gram models as a natural subclass. The motivation for considering this class is to estimate the contribution which grammar can make to reducing the relative entropy of natural language. GRA

N93-15225# Martin Marietta Energy Systems, Inc., Piketon, OH.
CONTINUING ENGINEERING EDUCATION FOR SOFTWARE ENGINEERING PROFESSIONALS
Paul I. Davis 19 Feb. 1992 17 p Presented at the 5th World Conference on Continuing Engineering Education, Espoo, Finland, 2-5 Jun. 1992
(Contract DE-AC05-76OR-00001)
(DE92-019888; POEF-T-3559B; CONF-9206267-1) Avail: CASI HC A03/MF A01

Designers of software for safety-critical applications are impelled to supplement their education through continuing engineering studies in the areas of requirements analysis, hazard identification, risk analysis, fault tolerance, failure modes, and psychology. Today's complex level of design is contributing to opportunities for catastrophic design errors in computer functions where failure of such functions is capable of causing injury and death. A syllabus of post-graduate, core studies within the curricula of five engineering specialties is suggested. Software Engineers are exhorted to undertake a professional, responsible role in safety-critical software design. DOE

N93-15228# Hurd (Harry L.) Associates, Inc., Raleigh, NC.
WORKSTATION TOOLS FOR FEATURE EXTRACTION AND CLASSIFICATION FOR NONSTATIONARY AND TRANSIENT SIGNALS Final Report, 1 Oct. 1989 - 31 May 1992
Harry L. Hurd 30 Jul. 1992 16 p
(Contract N00014-89-C-0310)
(AD-A255389) Avail: CASI HC A03/MF A01

This work was motivated by the recognition that the solution of technical problems involving nonstationary processes will require a body of theory and practical tools that facilitate serving and characterizing various types of nonstationary processes. This report contains a sketch of the theoretical background that motivate the experimental methodology, a summary of new theoretical results and a high-level description of the workstation software package that was developed under this contract. GRA

N93-15261# CASA-RI/SME, Tel Aviv (Israel).
PROCEEDINGS OF THE INTERNATIONAL CONFERENCE ON CAD/CAM AND AMT. VOLUME 4: VHDL (VHSIC HARDWARE DESCRIPTION LANGUAGE) SEMINAR
14 Dec. 1989 51 p Conference held in Jerusalem, Israel, December 11-14, 1989 Sponsored by Israel Ministry of Defense; Israel Ministry of Science and Technology; Rafael; and Dazix Prepared in cooperation with Israel Society for CAD/CAM, Tel Aviv; International Federation for Information Processing, Geneva, Switzerland; International Inst. for Production Engineering Research, Paris, France; International Federation of Associations of Computer Users in Engineering and Architecture; IEEE, New York, NY; and National Computer Graphics Association, Fairfax, VA
(ITN-92-85130) Avail: CASI HC A04/MF A01

This is the fourth of four volumes of papers presented at the conference on CAD/CAM. The included papers cover the history and current status of VHDL, and its applications, including the following: US defense procurement; the VHDL design environment; system design; the test environment; design of a virtual system; integration with existing EDA tools; and simulation tools. For individual titles, see N93-15262 through N93-15268.

N93-15262# Virginia Univ., Charlottesville. Center for Semicustom Integrated Systems.
VHDL (VHSIC HARDWARE DESCRIPTION LANGUAGE): ORIGINS, STATUS, CAPABILITIES, AND WORLD ENVIRONMENT
Ronald Waxman and Larry Saunders (International Business Machines Corp., Rochester, MN.) *In* CASA-RI/SME, Proceedings of the International Conference on CAD/CAM and AMT. Volume 4: VHDL Seminar 14 Dec. 1989 9 p (For primary document see N93-15261 04-61)
(VH-1) Avail: CASI HC A02/MF A01

This paper addresses the origin and evolution of the VHSIC Hardware Description Language (VHDL - IEEE Standard 1076-1987). The motivating forces that fostered its development, the characteristics of the language, how VHDL may be applied, the development and standardization process,

and the experience undergone in maintaining the language are reviewed. The application tool base that has developed during the first several months that VHDL was a standard is described. Finally, the international standards environment in which VHDL exists is discussed. ISA

N93-15263# CADonomist, San Francisco, CA.
VHDL (VHSIC HARDWARE DESCRIPTION LANGUAGE) USE IN THE US DEFENSE PROCUREMENT PROCESS
Randolph E. Harr *In* CASA-RI/SME, Proceedings of the International Conference on CAD/CAM and AMT. Volume 4: VHDL Seminar 14 Dec. 1989 11 p (For primary document see N93-15261 04-61)
(VH-2) Avail: CASI HC A03/MF A01

The motivations and concepts which are leading to the creation, adoption, and use of a standard hardware description language (HDL) in the defense procurement process are detailed. Introduced are the source of needs for a standard HDL and the key changes which are initiating the use of an HDL. A key milestone in incorporation of an HDL is the creation, within the defense system infrastructure, of contract specifications and standards which require the use of a standard language. The programs funding such development are introduced along with (where feasible) the actual text of the standards documents. Related industry standards efforts are covered also. Finally, to show the reality of it all, the programs which are using VHDL and the vendors supplying VHDL are briefly touched upon. ISA

N93-15264# Virginia Univ., Charlottesville. Center for Semicustom Integrated Systems.
THE EXTENDED VHDL (VHSIC HARDWARE DESCRIPTION LANGUAGE) DESIGN ENVIRONMENT: AN UNIQUE INTEGRATED SYSTEM AND HARDWARE DESIGN ENVIRONMENT
Ronald Waxman and James H. Aylor *In* CASA-RI/SME, Proceedings of the International Conference on CAD/CAM and AMT. Volume 4: VHDL Seminar 14 Dec. 1989 5 p Sponsored by Virginia Center for Innovative Technology; IBM; and Hughes Aircraft Corp. (For primary document see N93-15261 04-61)
(VH-3) Avail: CASI HC A01/MF A01

The objective of the research project discussed in this paper is to develop a single-path design environment to support the digital design process from concept to implementation. A new methodololgy for modeling and simulation of digital systems is presented. The technique allows one to use a single hardware description language (VHDL) to specify a design using token-passing specification models and to refine the design successively adding function in a step-wise fashion until the design is fully described. The design, as it progresses, can be simulated in a single (VHDL) simulation environment, though the model is composed of elements with undefined function (Uninterpreted Models) intermixed with defined function (Interpreted Models). ISA

N93-15265# International Business Machines Corp., Poughkeepsie, NY.
SYSTEM DESIGN IN A LARGE CORPORATION, USING VHDL (VHSIC HARDWARE DESCRIPTION LANGUAGE)
Leon Maissel *In* CASA-RI/SME, Proceedings of the International Conference on CAD/CAM and AMT. Volume 4: VHDL Seminar 14 Dec. 1989 3 p (For primary document see N93-15261 04-61)
(VH-4) Avail: CASI HC A01/MF A01

The experience of the various groups within IBM, in adapting one another's hardware design languages to their own use, is considered as a microcosm of the whole computer industry. Adoption of VHDL as a standard largely eliminates difficulties inherent in using design systems based on different, internally developed languages. Switching to VHDL presents almost no problems in design entry. Its use in simulation entails ensuring that the simulator receives only a predefined subset of the VHDL language. For logic synthesis, VHDL requires preprocessing, to remove statements relating only to simulation. VHDL can handle hierarchial design and eliminates the need for separate hierachies for function design and physical design. ISA

N93-15266# Cincinnati Univ., OH. Center for Digital Systems Engineering.
SYNTHESIS AND SIMULATION WITH VHDL (VHSIC HARDWARE DESCRIPTION LANGUAGE)
Harold W. Carter *In* CASA-RI/SME, Proceedings of the International Conference on CAD/CAM and AMT. Volume 4: VHDL Seminar 14 Dec. 1989 5 p Sponsored by the DARPA (For primary document see N93-15261 04-61)
(VH-5) Avail: CASI HC A01/MF A01

Methods for efficiently simulating and synthesizing digital electronic components and systems using VHDL descriptions are presented. Both uniprocessor and distributed processing approaches are explored. Using a subject-oriented approach to simulator design promises a unified approach to VHDL simulation on either uniprocessors or distributed processors. Methods for synthesizing realizable and efficient digital circuits from VHDL constructs are allowed. A design methodology using VHDL is also presented which shows promise owing to the integration of design and simulation at each step of the design decomposition process. ISA

N93-15267# Institute for Defense Analyses, Alexandria, VA.
VHDL (VHSIC HARDWARE DESCRIPTION LANGUAGE) IN THE TEST ENVIRONMENT
Robert M. Rolfe *In* CASA-RI/SME, Proceedings of the International Conference on CAD/CAM and AMT. Volume 4: VHDL Seminar 14 Dec. 1989 5 p (For primary document see N93-15261 04-61)
(VH-6) Avail: CASI HC A01/MF A01

The Institute of Electrical and Electronic Engineers, Inc. (IEEE) 1076 VHDL information standard may be used to improve the test development process during product development, manufacturing and support phases. The ability of a single representation to cover product design and test development throughout the product life cycle allows shorter engineering lead times, improved product and test quality and provides the opportunity for concurrent development of product design and test information. This paper describes the issues associated with product test information standards, a system developed to demonstrate these standards, and some characteristics of one standard being developed upon VHDL for digital test waveform and vector specification. ISA

N93-15268# Daisy/Cadnetix Israel Ltd., Herzliya.
INTEGRATING VHDL (VHSIC HARDWARE DESCRIPTION LANGUAGE) WITH EXISTING EDA TOOLS
Baruch Deutsch *In* CASA-RI/SME, Proceedings of the International Conference on CAD/CAM and AMT. Volume 4: VHDL Seminar 14 Dec. 1989 4 p (For primary document see N93-15261 04-61)
(VH-8) Avail: CASI HC A01/MF A01

This paper presents some of the basic issues involved in the integration of VHDL into existing EDA systems. It presents important aspects of the design process, including component modeling, the design cycle, simulation, debugging, and layout and manufacturing. The author shows why VHDL should not replace existing EDA tools, but rather should complement and expand their capabilities. The paper is based on the experience gained during the integration of VHDL into a specific set of EDA tools. The conclusions, however, apply to other EDA systems also. ISA

N93-15274# Washington State Univ., Pullman. Dept. of Mechanical and Materials Engineering.
INDEPENDENT VALIDATION TESTING OF THE FLAME COMPUTER CODE, VERSION 1.0
P. Martian and J. N. Chung Jul. 1992 30 p Prepared for Edgerton, Germeshausen and Grier, Inc., Idaho Falls, ID
(Contract DE-AC07-76ID-01570)
(DE92-019691; EGG-GEO-10368) Avail: CASI HC A03/MF A01

Independent testing of the FLAME computer code, Version 1.0, was conducted to determine if the code is ready for use in hydrological and environmental studies at Department of Energy sites. This report describes the technical basis, approach, and results of this testing. Validation tests, (i.e., tests which compare field data to the computer generated solutions) were used to determine the operational status of the FLAME computer code and were done on a qualitative basis through graphical comparisons of the experimental and numerical data. These tests were specifically designed to check: (1) correctness of the FORTRAN coding; (2) computational accuracy; and (3) suitability to simulating actual hydrologic conditions. This testing was performed using a structured evaluation protocol which consisted of: (1) independent applications; and (2) graduated difficulty of test cases. Three tests ranging in complexity from simple one-dimensional steady-state flow field problems under near-saturated conditions to two-dimensional transient flow problems with very dry initial conditions. DOE

N93-15298# CASA-RI/SME, Tel Aviv (Israel).
PROCEEDINGS OF THE INTERNATIONAL CONFERENCE ON CAD/CAM AND AMT. VOLUME 3: IFIP (INTERNATIONAL FEDERATION OF INFORMATION PROCESSING)/ROBOTICS: INTERNATIONAL SESSIONS ON ROBOTS AND ASSEMBLY
14 Dec. 1989 98 p Conference held in Jerusalem, Israel, December 11-14, 1989 Sponsored by Israel Ministry of Defense; Israel Ministry of Science and Technology; Rafael; and Dazix Prepared in cooperation with Israel Society for CAD/CAM, Tel Aviv; International Federation for Information Processing, Geneva, Switzerland; International Inst. for Production Engineering Research, Paris, France; International Federation of Associations of Computer Users in Engineering and Architecture; IEEE, New York, NY; and National Computer Graphics Association, Fairfax, VA
(ITN-92-85129) Avail: CASI HC A05/MF A02

This is the third of four volumes of papers presented at the conference on CAD/CAM. The included papers cover aspects of robotics including programming, signal processing, task-learning, motion planning, control, and optimization For individual titles, see N93-15299 through N93-15308.

N93-15299# Hungarian Academy of Sciences, Budapest. Computer and Automation Inst.
CAD-BASED OFF-LINE PROGRAMMING AND SENSOR SIGNAL PROCESSING IN ROBOTICS
Andras Siegler and Miklos Bathor *In* CASA-RI/SME, Proceedings of the International Conference on CAD/CAM and AMT. Volume 3: IFIP/Robotics: International Sessions on Robots and Assembly 14 Dec. 1989 8 p (For primary document see N93-15298 04-61)
(F-2-2) Avail: CASI HC A02/MF A02

The first part of the paper describes a three-dimensional computer animation system to be used for creating motion programs for a set of actors. The animation package includes a language for describing spatial motion of bodies as well as an interactive tool to be used for assigning geometrical attributes to them and for guiding and visualizing the play-back of motion programs. One of the main uses of the package is robot programming and motion simulation. A geometrical modeller, which is an aid in creating the models of animated bodies, is also described. The second part of the paper gives an overview on computer vision and force torque measurement and processing units developed for robotics and other automation purposes. ISA

N93-15300# Technion - Israel Inst. of Tech., Haifa. Faculty of Industrial and Management Engineering.
METHODOLOGY FOR ROBOT CAPABILITY AND PERFORMANCE CHARACTERIZATION: THE BASIS FOR ROBOT TASK PLANNINGG
Jacob Rubinovitz and Richard A. Wysk (Pennsylvania State Univ., University Park.) *In* CASA-RI/SME, Proceedings of the International Conference on CAD/CAM and AMT. Volume 3: IFIP/Robotics: International Sessions on Robots and Assembly 14 Dec. 1989 9 p (For primary document see N93-15298 04-61)
(F-2-3) Avail: CASI HC A02/MF A02

The motion capabilities and limitations of ASAE's IRB/L6 welding robot were studied, including timing of its motion along nine different straight line segments, ranging in length from 10-300 mm. Data collection and analysis were performed automatically by a personal computer linked to the robot. Indirect time and motion study was performed by measuring accelerations at the tool center point. The programmed motion velocities ranged from 100-1100 mm/sec. A model for determining programmed robot velocities and for estimating times of motion, while taking full advantage of the robot's capabilities was developed. The model and the data collected during the measurements were integrated into a database of robot capabilities which was implemented in an off-line task-planning and programming system for robotic welding. Alternative motion paths between seams were evaluated, and motion velocities were assigned to these paths. Similar methodology can be applied to different robots by implementing the established database for automated task planning. ISA

N93-15301# Paris VI Univ. (France). Lab. de Robotique.
COORDINATED MOTION CONTROL OF A TWO-HAND ASSEMBLY SYSTEM
P. Bidaud, D. Fontaine, F. Boudin, and J. C. Guinot *In* CASA-RI/SME, Proceedings of the International Conference on CAD/CAM and AMT. Volume 3: IFIP/Robotics: International Sessions on Robots and Assembly 14 Dec. 1989 4 p (For primary document see N93-15298 04-61)
(F-2-8) Avail: CASI HC A01/MF A02

This paper presents the implementation of an original cooperating system for precise assembly operations. The whole mechanical architecture consists of a conventional manipulator robot and a micro-manipulator setting in parallel. The micro-manipulator used is a manipulator-gripper in a left-hand configuration. The mechanism of the manipulator-gripper was designed to perform active or passive fine compliant motions. A hybrid force/position control structure is used to control the grasped object motions in operational space. A real-time distributed computer system has been developed for coordinated-motion control. For complex assembly tasks, automatic fine motion strategies are obtained by a rule-based expert system. ISA

N93-15302# Johannes Kepler Univ., Linz (Austria). Research Inst. for Symbolic Computation.
OFF-LINE GENERATION OF ERROR-FREE ROBOT/NC (NUMERICAL CONTROL) CODE USING SIMULATION AND AUTOMATIC PROGRAMMING TECHNIQUES
Herwig Mayr and Sabine Stifter *In* CASA-RI/SME, Proceedings of the International Conference on CAD/CAM and AMT. Volume 3: IFIP/Robotics: International Sessions on Robots and Assembly 14 Dec. 1989 6 p Sponsored in part by AIS (For primary document see N93-15298 04-61)
(BWF Proj. 609.506/1-26/88)
(F-3-1) Avail: CASI HC A02/MF A02

We present simulation and automatic programming tools for robotics and NC (numerical control) machining that have been developed at RISC-Linz in cooperation with AIS Linz, Austria. These tools constitute a new era in off-line programming: our software packages support or even guarantee correct (i.e., error-free) robot/NC code. Thus, it is possible to start the desired production process immediately after designing the concept with computer assistance - no human verification is necessary. This goal is achieved by two steps: (1) verification of manually coded robot/NC programs by graphic simulation, together with algorithmic collision checking and program transformation algorithms; and (2) fully automatic generation of robot/NC code by supplying application adapted machining algorithms covering both geometrical and technological aspects. Our research and development work resulted in products for both steps. Universal machining and manufacturing simulation systems can be used for modeling, simulating, and programming of arbitrarily designed work cells (SMART) as well as arbitrary machining processes (SAVE). FAAST and GeoPocket are program packages for fully automatic programming of stamping presses and milling machines, respectively. In this paper, we show the benefits of applying methods of computational geometry as well as modern data structure concepts for the efficiency of simulating and programming robotics and NC tasks. We give details of our universal approaches to algorithmic task generation and task verification and their application to flexible manufacturing and low quantity production. Open problems like verification strategies for very complex tasks, or optimal modeling structures, are also discussed. ISA

N93-15303# Weizmann Inst. of Science, Rehovoth (Israel). Dept. of Applied Mathematics and Computer Science.
ROBOT LEARNING OF CONTACT TASKS **c63**
M. Benady, T. Flash, and D. Gershon *In* CASA-RI/SME, Proceedings of the International Conference on CAD/CAM and AMT. Volume 3: IFIP/Robotics: International Sessions on Robots and Assembly 14 Dec. 1989 6 p (For primary document see N93-15298 04-61)
(F-3-2) Avail: CASI HC A02/MF A02

This paper describes a learning scheme for an impedance-controlled robot performing manipulation tasks. An impedance controller was developed in which an outer impedance control loop is closed around an inner position control loop. This approach requires force feedback from a wrist force sensor mounted between the robot flange and the tool. Optimal impedance parameters are learned using an associative search network (ASN). The network solves an optimization problem to minimize the deviation of the manipulator tip from specified criteria (e.g., force and velocity profiles). During the learning process, the inner variables of the network are modified to implicitly represent acquired knowledge of the system. The learning scheme does not use a model of the robot and its environment. It is a stochastic scheme which uses a single scalar value as a measure of the system performance. The learning scheme was implemented for a surface-following task on the AdeptOne manipulator. ISA

N93-15304# Ben Gurion Univ. of the Negev, Beersheva (Israel). Dept. of Industrial Engineering and Management.

MULTIPLE ROBOT PROGRAMMING USING CONCURRENT LOGIC LANGUAGE

D. Ben-Arieh and O. Maimon *In* CASA-RI/SME, Proceedings of the International Conference on CAD/CAM and AMT. Volume 3: IFIP/Robotics: International Sessions on Robots and Assembly 14 Dec. 1989 5 p Sponsored by the Paul Ivanier Center for Research in Robots and Production Management Prepared in cooperation with Tel-Aviv Univ., Israel (For primary document see N93-15298 04-61)

(F-3-3) Avail: CASI HC A01/MF A02

Advances in robotics lead to cooperation of multiple robots among themselves and with their industrial automation environment. Efficient interaction with industrial robots thus becomes one of the key factors in successful utilization of this modern equipment. When multiple manipulators have to be coordinated there is a need for a new programming approach that facilitates and encompasses the needs of concurrency, synchronization, timing, and communication. Most robot languages have been developed with little attention given to the integration of the robot with its environment. Currently there is a gap between the robot capabilities, the task definition environment, and language facilities supplied to users of robots. This paper analyses the needs and then establishes that a concurrent logic programming approach is a step towards achieving a multi-robot knowledgeable task programming. In particular, the FCP dialect of concurrent Prolog is demonstrated and analyzed. ISA

N93-15305# Tel-Aviv Univ. (Israel). Faculty of Engineering.

PLANNING OF CONTINUOUS PATH ROBOTIC MOTIONS BY DISCRETE TIME OPTIMIZATION **c63**

V. Netzer *In* CASA-RI/SME, Proceedings of the International Conference on CAD/CAM and AMT. Volume 3: IFIP/Robotics: International Sessions on Robots and Assembly 14 Dec. 1989 6 p (For primary document see N93-15298 04-61)

(F-3-5) Avail: CASI HC A02/MF A02

This paper presents a near-optimal solution to the problem of moving a manipulator in minimum time along a specified path, subject to actuators torque/force constraints. The proposed method is based on a combination of a nonlinear optimization algorithm with a path discretization scheme and provides the end-effector position, velocity, acceleration, and torques that minimize the traversal time from the initial to the final configuration. To illustrate the method, two trajectories are simulated for a three-degrees-of-freedom manipulator and the results are compared with those obtained by true optimal solutions. ISA

N93-15306# Tel-Aviv Univ. (Israel). Faculty of Engineering.

TIME-OPTIMIZATION OF POINT-TO-POINT ROBOTIC MOTIONS **c63**

L. Beiner *In* CASA-RI/SME, Proceedings of the International Conference on CAD/CAM and AMT. Volume 3: IFIP/Robotics: International Sessions on Robots and Assembly 14 Dec. 1989 6 p (For primary document see N93-15298 04-61)

(F-3-6) Avail: CASI HC A02/MF A02

A nonlinear programming approach to minimum-time point-to-point robotic motions is presented for the case when all joints move synchronously according to trapezoidal velocity profiles. Full robot dynamics is combined with the joint kinematics in order to transform the differential equations of motion into algebraic relations and cast the problem into a constrained parameter optimization form. Optimal joint velocity profiles and the required torques/forces are obtained via a direct search algorithm which is fast and guarantees a global optimum without resorting to optimization techniques or numerical integrations. Three examples of time-optimized point-to-point robotic motions are presented. ISA

N93-15307# Weizmann Inst. of Science, Rehovoth (Israel). Dept. of Applied Mathematics.

REDUNDANCY CONTROL OF ROBOTS BY CONSTRAINED OPTIMIZATION **c63**

Tzila Shamir *In* CASA-RI/SME, Proceedings of the International Conference on CAD/CAM and AMT. Volume 3: IFIP/Robotics: International Sessions on Robots and Assembly 14 Dec. 1989 4 p (For primary document see N93-15298 04-61)

(F-3-7) Avail: CASI HC A01/MF A02

The motion planning problem for kinematically redundant manipulators involves not only the motion of the end effector, but of the whole arm. The versatility gained by the redundancy must be utilized in an effective, predictable, and stable way. This paper presents a method for incorporating the optimization of a posture-dependent objective function into the actual motion control of the arm, while keeping the configuration stable and predictable. This yields an algorithmic method that guides the arm to track given paths with the hand while remaining at the optimal configurations. It is also shown, however, that there may be some difficulties in actual implementation due to the existence of bifurcations that cause sudden switching from maxima to minima of the objective function. ISA

N93-15308# Indian Inst. of Tech., Madras. Dept. of Mechanical Engineering.

ADAPTIVE CONTROL OF A MANIPULATOR IN CARTESIAN SPACE **c63**

Venkataesh V. Murty and M. S. Shunmugam *In* CASA-RI/SME, Proceedings of the International Conference on CAD/CAM and AMT. Volume 3: IFIP/Robotics: International Sessions on Robots and Assembly 14 Dec. 1989 5 p (For primary document see N93-15298 04-61)

(F-4-2) Avail: CASI HC A01/MF A02

A cartesian based nonlinear adaptive controller is presented for the trajectory control of a robot manipulator. The stability of the control formulation is proved using Lyapunov's second method. The unknown parameters of the system, as well as the variable payload are estimated on-line, tending the system errors to zero. This formulation, unlike other adaptive controllers present in the literature, neither makes any ad hoc linearization of the nonlinear equations nor requires the inversion of the inertia matrix. It also does not require the measurement of acceleration and the conversion of path planning specifications from cartesian space to joint space. Trajectory tracking, with unknown parameter values and variable payload, is simulated to show the effectiveness of the proposed adaptive control algorithm. ISA

N93-15313# Air Force Inst. of Tech., Wright-Patterson AFB, OH. School of Engineering.

DEVELOPMENT OF AN ANALOG MIMO QUANTITATIVE FEEDBACK THEORY (QFT) CAD PACKAGE M.S. Thesis

Richard R. Sating Jun. 1992 245 p

(AD-A256435; AFIT/GE/ENG/92J-04) Avail: CASI HC A11/MF A03

The development is described of an analog MIMO Quantitative Feedback Theory (QFT) CAD package for the automation of the multivariable control design process. The CAD package is capable of carrying a design from problem setup through the design process to a frequency domain analysis of the compensated MIMO system. The package automates the selection of the weighting matrix, formation of the square effective plants, the polynomial matrix inverse required to form the equivalent plants, generation of stability, tracking, disturbance, gamma, and composite bounds, loop shaping, design of the prefilter elements, and the frequency domain analysis of the completed design. Disturbance allocation is automatically performed while generating tracking bounds. The package allows gain scheduling to be used in the weighting matrix. The improved method may be applied for the case of 2x2 effective plant. The package is implemented using Mathematica for use on the Sun Workstations. GRA

N93-15336# Carnegie-Mellon Univ., Pittsburgh, PA. School of Computer Science.

CMU COMMON LISP USER'S MANUAL

Robert A. MacLachlan Jul. 1992 144 p

(Contract MDA972-90-C-0035; ARPA Order 7330)

(AD-A256431; CMU-CS-92-161) Avail: CASI HC A07/MF A02

CMU Common Lisp is an implementation of that Common Lisp which is currently supported on MIPS-processor DECstations, Sparc-based workstations from Sun and the IBM RT PC, and other ports are planned. All architectures are supported under Mach, a Berkeley Unix 4.3 binary compatible operating system. The Sparc is also supported under SunOS. The largest single part of this document describes the Python compiler and the programming styles and techniques that the compiler encourages. The rest of the document describes extensions and the implementation dependent choices made in developing this implementation of Common Lisp. We have added several extensions, including a source level debugger, an interface to Unix system calls, a foreign function call interface, support

for interprocess communication and remote procedure call, and other features that a good environment for developing Lisp code. GRA

N93-15386# Rolls-Royce Ltd., Derby (England).
A METHOD OF REPRESENTATING DIMENSIONS AND TOLERANCES IN SOLID BASED FREEFORM SURFACES
M. J. Cardew-Hall, T. Labans (Curtin Univ. of Technology, Perth, Australia), G. West (Curtin Univ. of Technology, Perth, Australia), and P. Dench (Curtin Univ. of Technology, Perth, Australia) 15 Nov. 1991 49 p
(PNR-90998; ETN-92-92252) Copyright Avail: CASI HC A03/MF A01

A mathematical model of representing tolerances and dimensions (integral parts of the product definition of any component controlling its functionality and manufacturability) on a boundary representation (BREP) solid modeller is put forward. The mode enables tolerances to be applied to a general free form surface, in particular, an airfoil geometry. The method is based on three tolerance formats: a position tolerance, a form tolerance and a datum tolerance. It combines a matrix method for the representation of geometric positioning and tolerancing with a graph theoretic approach for spatial analysis. Application with a BREP modeling system and within inspection analysis are discussed. ESA

N93-15405# Air Force Inst. of Tech., Wright-Patterson AFB, OH. School of Engineering.
IMPLEMENTATION AND ANALYSIS OF NP-COMPLETE ALGORITHMS ON A DISTRIBUTED MEMORY COMPUTER M.S. Thesis
Joel S. Garmon Mar. 1992 188 p
(AD-A256564; AFIT/GE/ENG/92-M)

The purpose of this research is to explore methods used to parallelize NP-complete problems and the degree of improvement that can be realized using different methods of load balancing. A serial and four parallel A* branch and bound algorithms were implemented and executed on an Intel iPSC/2 hypercube computer. One parallel algorithm used a global, or centralized, list to store unfinished work and the other three parallel algorithms used a distributed list to store unfinished work locally on each processor. The three distributed list algorithms are: without load balancing, with load balancing, and with load balancing and work distribution. The difference between load balancing and work distribution is load balancing only occurs when a processor becomes idle and work distribution attempts to emulate the global list of unfinished work by sharing work throughout the algorithm, not just at the end. Factors which effect when and how often to load balance are also investigated. Which algorithm performed best depended on how many processors were used to solve the problem. For a small number of processors, 16 or less, the centralized list algorithm easily outperformed all others. However, after 16 processors, the overhead of all processors trying to communicate and request work from the same centralized list began to outweigh any benefits of having a global list. Now the distributed list algorithms began to perform best. When using 32 processors, the distributed list with load balancing and work distribution out performed the other algorithms. GRA

N93-15432*# Institute for Computer Applications in Science and Engineering, Hampton, VA.
PARALLEL SIMULATION TODAY Final Report
David Nicol (College of William and Mary, Williamsburg, VA.) and Richard Fujimoto (Georgia Inst. of Tech., Atlanta.) Washington Nov. 1992 37 p Submitted for publication
(Contracts NAS1-18605; NAS1-19480; NAG1-1060; NAG1-995; DASG60-90-C-0147; NSF ASC-88-19373; NSF CCR-92-01195; NSF CCR-89-02362; RTOP 505-90-52-01)
(NASA-CR-189733; NAS 1.26:189733; ICASE-92-62) Avail: CASI HC A03/MF A01

This paper surveys topics that presently define the state of the art in parallel simulation. Included in the tutorial are discussions on new protocols, mathematical performance analysis, time parallelism, hardware support for parallel simulation, load balancing algorithms, and dynamic memory management for optimistic synchronization. Author

N93-15445# Science Applications International Corp., McLean, VA.
CREW REQUIREMENTS DEFINITION SYSTEM USER'S GUIDE Final Report, Sep. 1985 - Mar. 1991
Arthur J. Kellner and Richard E. Christ Jul. 1992 106 p
(Contract MDA903-85-C-0440; DA Proj. 2Q2-63007-A-793)
(AD-A257052; ARI-RP-92-07) Avail: CASI HC A06/MF A02

The Crew Requirements Definition System (CRDS) permits analysts and researchers to develop, examine, and modify crew designs in a timely, cost-effective manner. Designs may vary in terms of the number and types of tasks to be performed, the number and types of personnel assigned to perform the tasks, the time-based task network, and the time required to perform each task. Since the CRDS is a fully computer-assisted task performance analysis tool, the effects of these variables can be examined without conducting field studies for each design alternative. This User's Guide begins with an overview of the CRDS. After providing instructions on how to install the CRDS on a personal computer and information on the user-software interface, the User's Guide describes the underlying rationale, capabilities, and features of the CRDS and gives annotated instructions for its use. To facilitate the user's understanding of the capabilities of the CRDS, the Guide assists the user in developing, examining, and modifying one example problem and then thoroughly describes two additional sample problems. GRA

N93-15450# Oak Ridge K-25 Site, TN.
AUTOMATED ESTIMATED SYSTEM (AES) STANDARD VALUE AND GUIDELINES PROGRAMS USER'S MANUAL
R. K. Schwarz, ed. Aug. 1992 54 p
(Contract DE-AC05-84OT-21400)
(DE92-041243; K/CSD/TM-102) Avail: CASI HC A04/MF A01

This manual contains instructions for operating two administrative programs: the Standard Value program and the Guidelines program. These programs are operated and controlled by a selected individual in the Estimating. and Scheduling Department of the Martin Marietta Energy Systems, Inc., Engineering Division. They are used to control and standardize input into the Automated Estimating System (AES) Estimating program, a personal computer-based software package designed to aid in the creation, updating, and reporting of project cost estimates. The AES Estimating program is documented in a separate user's manual. DOE

N93-15451# Stanford Linear Accelerator Center, CA.
PROCEEDINGS OF THE REXX SYMPOSIUM FOR DEVELOPERS AND USERS
Sep. 1992 401 p Symposium held in Annapolis, MD, 3-5 May 1992
(Contract DE-AC03-76SF-00515)
(DE92-041359; SU-SLAC-401; CONF-9205149) Avail: CASI HC A18/MF A04

The third annual REXX Symposium for Developers and Users was held on May 3-5, 1992 in Annapolis, Maryland. Ninety-one people attended, representing eight countries and nineteen American States. There was a great deal of interest regarding REXX in the UNIX world. Alberto Villarica and Anders Christensen announced two free versions of REXX for UNIX. Also, the Workstation Group announced a free run-time version of their Uni-REXX available to any educational institution. Two flavors of REXX under MS/Windows were presented by Edc Giguere and Charles Daney. Both implementations demonstrated the ease in which REXX was able to create GUI applications. This prompted some discussion of REXX under the Macintosh, probably the last frontier for REXX. Along with his usual informed opinions, Mike Cowlishaw described some of his current research efforts. He also wowed us with some statistics demonstrating the incredible penetration REXX has made internationally as measured by the number of books published about it and the millions of users with access to it. Prompted, in part, by Lotus' announcement of a REXX interface to 1-2-3, there was much discussion of ways that REXX could be promoted as a universal scripting and macro language. In this context, REXX was compared both to PERL and to Visual BASIC, which appears to be Microsoft's attempt to cover some of the deficiencies of BASIC. DOE

N93-15457# Paramax Systems Corp., Reston, VA. Tactical Systems Div.
USER MANUAL FOR THE SOFTWARE TECHNOLOGY FOR ADAPTABLE, RELIABLE SYSTEMS (STARS). PCTE BROWSER TOOL (PBT) VERSION 0.1 SunOS IMPLEMENTATION Informal Technical Data
Michael J. Horton 12 Jun. 1992 37 p
(Contract F19628-88-D-0031)
(AD-A257064; STARS-TC-04014/003/00) Avail: CASI HC A03/MF A01

The PCTE Browser Tool (PBT) is an instance of the Paramax STARS

Reusable Graphical Browser (RGB), a generic graphical browser for the display of networks of nodes and arcs. In the case of the PBT, the nodes displayed by the RGB are PCTE objects, and the arcs are PCTE links. The PBT is an X Window System application, and as such makes use of the Paramax STARS implementation of Ada/Xt and the Ada implementation of some MIT Athena and Hewlett Packard widgets. GRA

N93-15471# Paramax Systems Corp., Reston, VA.
SOFTWARE TECHNOLOGY FOR ADAPTABLE, RELIABLE SYSTEMS (STARS)
25 Aug. 1992 50 p
(Contract F19628-88-D-0031)
(AD-A257022; STARS-AC-04107A/001/00) Avail: CASI HC A03/MF A01

The purpose of this document is to describe the technical concepts of the command center (CC) library, including library modelling, the library software infrastructure, security, and interoperability. This document will baseline the technical foundation for the CC library and for other domain-specific libraries to be implemented by the Central Archive for Reusable Defense Software (CARDS) program. This document supersedes the Technical Concept Document dated 15 July 1991, and reflects the most current concepts being employed by CARDS. The next periodic update to this document should occur in February 1993. GRA

N93-15476# Rolls-Royce Ltd., Derby (England).
INTEGRATED SUPPORT FOR REAL-TIME CONTROL SYSTEMS
Martin Beeby (NEI Control Systems Ltd., Gateshead, England), J. S. Parkinson (Rolls-Royce and Associates Ltd., Derby, England), and Vivien Hamilton 28 Apr. 1992 13 p
(PNR-90994; ETN-92-92250) Copyright Avail: CASI HC A03/MF A01

A project to investigate CASE tool integration with a view to producing, or recommending, an integrated project support environment is described. The integration of tools is limited to those which primarily support software development. The aim was to build an environment through integrating tools, but it was found that the process model was of far greater importance: the current integration technology not sufficiently mature for users to be able to create their own environments. It is concluded that it is essential to have a process model to specify the functionality of any environment. Many people believe that written procedures are sufficient, but they are not. A process model should embody the concept of methods and roles; accommodate decision making by users; and be based around a critical feature of the development process. A process model provides the best media for evaluating changes to a development process and providing the feedback to allow continuous process improvement. This is necessary to increase process maturity. A high level process model can contribute to the understanding of the whole development process by those involved in the execution of parts of the process. By providing a consistent view it can serve as a useful training aid for all involved: project managers, engineers, testers, etc. ESA

N93-15493# Lawrence Livermore National Lab., CA.
MATHEMATICAL SOFTWARE UNDER UNICOS AT LCC
F. N. Fritsch 1 Sep. 1992 20 p
(Contract W-7405-eng-48)
(DE93-001828; UCRL-ID-111810) Avail: CASI HC A03/MF A01

Mathematical libraries provide computer users access to pre-programmed routines to solve general mathematical problems or evaluate commonly occurring functions. Such libraries provide a cost-effective means of delivering the results of numerical algorithms research to applications. By using standard libraries that are available on a wide range of platforms, the numerical kernel of application codes can be ported to new environments with a minimum of effort. We describe here the mathematical utilities and libraries currently available to Livermore Computer Center (LCC) Cray users under UNICOS. (Only FORTRAN libraries are currently available.) Author

N93-15502*# National Aeronautics and Space Administration. Goddard Space Flight Center, Greenbelt, MD.
FLIGHT DYNAMICS SYSTEM SOFTWARE DEVELOPMENT ENVIRONMENT (FDS/SDE) TUTORIAL
John Buell and Philip Myers Jul. 1986 135 p
(NASA-TM-108580; NAS 1.15:108580; SEL-86-003) Avail: CASI HC A07/MF A02

A sample development scenario using the Flight Dynamics System Software Development Environment (FDS/SDE) is presented. The SDE uses a menu-driven, fill-in-the-blanks format that provides online help at all steps, thus eliminating lengthy training and allowing immediate use of this new software development tool. Author

N93-15533 Canadian Human-Computer Communications Society, Toronto (Ontario).
PROCEEDINGS: GRAPHICS INTERFACE 1992 [COMPTE RENDU: GRAPHICS INTERFACE 1992]
Canadian Information Processing Society 1992 340 p In ENGLISH and FRENCH Conference held in Vancouver, British Columbia, 11-15 May 1992; sponsored by Canadian Human-Computer Communications Society, Association for Computing Machinery, Natural Sciences and Engineering Research Council of Canada, and National Research Counc Original contains color illustrations
(ISBN-0-9695338-1-0) Copyright Avail: Issuing Activity

This Graphics Interface is part of the combined AI/GI/VI 1992 Conference held at the University of British Columbia in Vancouver, British Columbia. This year's technical program consists of 36 carefully selected papers. This technical program contains original work covering a wide area of computer graphics and human-computer interaction. For individual titles, see N93-15534 through N93-15570.

N93-15534 Waterloo Univ. (Ontario). Computer Graphics Lab.
AN IMPLEMENTATION OF MULTIVARIATE B-SPLINE SURFACES OVER ARBITRARY TRIANGULATIONS
Philip Fong and Hans-Peter Seidel *In* Canadian Human-Computer Communications Society, Proceedings: Graphics Interface 1992 1992 p 1-10 Sponsored in part by Natural Sciences and Engineering Research Council of Canada (For primary document see N93-15533 04-61)
Copyright Avail: Issuing Activity

Recently a new multivariate B-spline scheme based on blending functions and control vertices was developed. This surface scheme allows C(exp k-1) continuous piecewise polynomial surfaces of degree k over arbitrary triangulations to be modelled. Actually, piecewise polynomial surfaces over a refined triangulation are produced given an arbitrary triangulation. The scheme exhibts both affine invariance and the convex hull property, and the control points can be used to manipulate the shape of the surface locally. This paper describes a test implementation of the scheme for quadratic and cubic surfaces. Issues such as evaluating points on the surface, evaluating derivatives on the surface and representing piecewise polynomial surfaces as linear combinations of B-splines will be discussed. Several examples illustrate the implementation. The work is incorporated into a surface editor which is currently being developed at the University of Waterloo. Author

N93-15535 Bell Telephone Labs., Inc., Murray Hill, NJ.
INTERACTIVE SOLID GEOMETRY VIA PARTITIONING TREES
Bruce F. Naylor *In* Canadian Human-Computer Communications Society, Proceedings: Graphics Interface 1992 1992 p 11-18 (For primary document see N93-15533 04-61)
Copyright Avail: Issuing Activity

The extension from interactive 2D wireframe geometry to interactive solid geometry has for some time been one of the goals of computer graphics. Our approach to this objective is the utilization of a computational representation of geometric sets that we believe is better suited to geometric computation than alternatives inherited from mathematics. This representation is the binary space partitioning tree. Employing such a representation leads to simpler and faster algorithms and has enabled us to construct an elementary interactive solid geometry system which can execute effectively on workstations with no graphics acceleration hardware. Interactive manipulation of a collection of polyhedral objects is provided utilizing set operations, affine transformations, collision detection, picking and dragging, calculation of metric properties, rendering of transparent objects, and solid clipping to an arbitrary polygonal view volume. This is the first such system based on partitioning trees, and as a consequence, is the first interactive system that fully supports set operations, collision detection, and transparency for arbitrary polyhedral objects. Author

N93-15536 Georgia Inst. of Tech., Atlanta. Graphics, Visualization, and Usability Center.

FAST ALGORITHMS FOR RENDERING CUBIC CURVES

Benjamin Watson and Larry F. Hodges *In* Canadian Human-Computer Communications Society, Proceedings: Graphics Interface 1992 1992 p 19-28 (For primary document see N93-15533 04-61)

Copyright Avail: Issuing Activity

We present two integer-only algorithms to be used in tandem for rendering cubic functions and parametric cubic curves with rational coefficients. Analysis of execution speed of existing algorithms shows that our algorithms will match or outperform other current algorithms. Furthermore, while other existing algorithms can only handle curves shaped by rational coefficients by introducing some approximation error, our algorithms always choose the best approximation. Curves may have to be split before rendering, because each algorithm only handles curves with slope in a certain range. When plotting parametric curves, our algorithms may require more bits of representation for some integer variables than other existing algorithms. Author

N93-15537 Purdue Univ., West Lafayette, IN. Dept. of Computer Sciences.

PARAMETERIZATION IN FINITE PRECISION

Chandrajit Bajaj and Andrew V. Royappa *In* Canadian Human-Computer Communications Society, Proceedings: Graphics Interface 1992 1992 p 29-36 (For primary document see N93-15533 04-61)

(Grants AF-AFOSR-0276-91; NSF CCR-90-00028; NSF DMS-91-01424)

Copyright Avail: Issuing Activity

Certain classes of algebraic curves and surfaces admit both parametric and implicit representations. Such dual forms are highly useful in geometric modeling since they combine the strengths of the two representations. We consider the problem of computing the rational parameterization of an implicit curve or surface in a finite precision domain. Known algorithms for this problem are based on classical algebraic geometry, and assume exact arithmetic involving algebraic numbers. In this work, we investigate the behavior of published parameterization algorithms in a finite precision domain and derive succinct algebraic and geometric error characterizations. We then indicate numerically robust methods for parameterizing curves and surfaces which yield no error in extended finite precision arithmetic and alternatively, minimize the output error under fixed finite precision calculations. Author

N93-15538 Freie Univ., Berlin (Germany). Dept. of Computer Science.

HYPER-RENDERING

Juergen Emhardt and Thomas Strothotte *In* Canadian Human-Computer Communications Society, Proceedings: Graphics Interface 1992 1992 p 37-43 Original contains color illustrations (For primary document see N93-15533 04-61)

Copyright Avail: Issuing Activity

Current systems for the automatic generation of information presentation or the automatic illustration of objects are mainly generation-oriented, i.e. they generate solutions to a user who in turn has only few possibilities to lead a dialogue with the generation system. By contrast, systems which emphasize dialogues tend to be weak in graphical interaction. In order to build systems which are both generation- and dialogue-oriented, we present a new software architecture for computer graphics applications. We develop the concept of hyper-rendering which produces a formal description of the scene as viewed by the user and can either be carried out within a renderer or in a separate program. The output of the hyper-rendering program is an image description which consists of information which conventional renderers usually compute but typically throw away. We describe two broad categories of applications of hyper-rendering and a prototypical implementation. Examples of the pictures produced as well as a sample session with an application are included. Author

N93-15539 Toronto Univ. (Ontario). Dept. of Computer Science.

PROGRAM AURALIZATION: SOUND ENHANCEMENTS TO THE PROGRAMMING ENVIRONMENT

Christopher J. DiGiano and Ronald M. Baecker *In* Canadian Human-Computer Communications Society, Proceedings: Graphics Interface 1992 1992 p 44-52 (For primary document see N93-15533 04-61)

Copyright Avail: Issuing Activity

Sound has the potential to improve our understanding of a programs's function, structure, and behavior. In this paper we identify classes of program information suitable for mapping to sound and suggest how to add auralization capabilities to programming environments. We describe LogoMedia, a sound-enhanced programming system which illustrates these concepts. Author

N93-15540 Open Univ., Milton (England). Human Cognition Research Lab.

A FRAMEWORK FOR DESCRIBING AND IMPLEMENTING SOFTWARE VISUALIZATION SYSTEMS

John Domingue, Blaine A. Price, and Marc Eisenstadt *In* Canadian Human-Computer Communications Society, Proceedings: Graphics Interface 1992 1992 p 53-60 (For primary document see N93-15533 04-61)

Copyright Avail: Issuing Activity

In recent years many prototype systems have been developed for graphically visualizing program execution in an attempt to create a better interface between software engineers and their programs. Several classification-based taxonomies have been proposed to describe computer program visualization systems and general frameworks have been suggested for implementation. In this paper we provide a framework for both describing existing systems and implementing new ones. We demonstrate the utility of automatic program visualization by re-implementing a number of classic systems using this framework. Author

N93-15541 Stanford Univ., CA. Computer Science Dept.

VOLUME RENDERING USING THE FOURIER PROJECTION-SLICE THEOREM

Marc Levoy *In* Canadian Human-Computer Communications Society, Proceedings: Graphics Interface 1992 1992 p 61-69 Original contains color illustrations (For primary document see N93-15533 04-61)

Copyright Avail: Issuing Activity

The Fourier projection-slice theorem states that the inverse transform of a slice extracted from the frequency domain representation of a volume yields a projection of the volume in a direction perpendicular to the slice. This theorem allows the generation of attenuation-only renderings of volume data in O(N(exp 2)log N) time for a volume of size N(exp 3). We show how more realistic renderings can be generated using a class of shading models whose terms are Fourier projections. Models are derived for rendering depth cueing by linear attenuation of variable energy emitters and for rendering directional shading by Lambertian reflection with hemispherical illumination. While the resulting images do not exhibit the occlusion that is characteristic of conventional volume rendering, they provide sufficient depth and shape cues to give a strong illusion that occlusion exists. Author

N93-15542 Alberta Univ., Edmonton. Dept. of Computing Science.

AN EXTENDED CUBERILLE MODEL FOR IDENTIFICATION AND DISPLAY OF 3D OBJECTS FROM 3D GRAY VALUE DATA

Xiaoqing Qu and Wayne Davis *In* Canadian Human-Computer Communications Society, Proceedings: Graphics Interface 1992 1992 p 70-77 (For primary document see N93-15533 04-61)

Copyright Avail: Issuing Activity

This paper presents an extended cuberille model for the identification, reconstruction, and display of 3D objects from 3D gray value data. 3D edge elements are gradients detected at voxels, and the orientations of gradients are quantized to 26 directions. The edge elements are then converted to the extended cuberille model. The model has four volume primitives. Besides a cube, voxels are extended to include three other polyhedra so that voxel faces are compatible with 26 gradient orientations. The merits of the three representation schemes--space occupancy enumeration, octree, and surface representation by the extended cuberille model--are briefly discussed. To identify border voxels, asymmetric Gaussian filters are applied to compute second derivatives at each voxel. Conditions are defined for identifying border voxels based on the sign of the second derivative. From these conditions, there exists exactly one layer of border voxels, and subsequent surface tracking is therefore straightforward. Experimental results of 3D surface identification, tracking, and display by the extended cuberille model on test data and medical data are given. Because there are only four types of external voxel faces in the model, a surface of any object consists of only the four types of external voxed faces. Author

N93-15543 Columbia Univ., New York, NY. Dept. of Computer Science.
ANNOTATING THE REAL WORLD WITH KNOWLEDGE-BASED GRAPHICS ON A SEE-THROUGH HEAD-MOUNTED DISPLAY
Steven Feiner, Blair MacIntyre, and Doree Seligmann *In* Canadian Human-Computer Communications Society, Proceedings: Graphics Interface 1992 1992 p 78-85 (For primary document see N93-15533 04-61)
(Contracts N00014-91-J-1872; N00039-84-C-0165; NSF ECD-88-11111; NSF CDA-90-22123)
Copyright Avail: Issuing Activity

We describe an experimental, knowledge-based, virtual-world system that uses a monocular 'see-through' head-mounted display to overlay graphics on the user's view of the real world. In a simple equipment maintenance domain that we have developed, the overlaid graphics include 3D representations of actual physical objects, textual annotations and callouts, and virtual meta-objects, such as arrows. A set of 3D position and orientation sensors monitor the user's head and several of the objects in the world. Our system includes a knowledge-based graphics component that determines what information to present, a display-list-based display server that represents the models to be displayed, and a set of sensor servers that track the user and selected objects. The sensor servers directly modify the object transformations and viewing specification in the display list. The knowledge-based graphics component also receives the sensor data and uses it to redesign the information being presented. Author

N93-15544 York Univ. (Ontario). Dept. of Computer Science.
ALGORITHMS FOR THE DETECTION AND ELIMINATION OF SPECULAR ALIASING
John Amanatides *In* Canadian Human-Computer Communications Society, Proceedings: Graphics Interface 1992 1992 p 86-93 (For primary document see N93-15533 04-61)
Copyright Avail: Issuing Activity

This paper introduces an algorithm that, given the geometry and surface characteristics of an object (the Phong highlight model is assumed), detects when specular or highlight aliasing is expected and indicates the correct sampling rate to eliminate it. This is accomplished by noting the geometric properties of the surface, the direction and distances to the eye and light sources, and the specular shading parameters. Also, an auxiliary algorithm is presented that eliminates the specular aliasing without increasing the sampling rate. It accomplishes this by clamping the specular function parameters to values that will not introduce significant high frequency components. Author

N93-15545 Toronto Univ. (Ontario).
HIERARCHICAL POISSON DISK SAMPLING DISTRIBUTIONS
Michael McCool and Eugene Fiume *In* Canadian Human-Computer Communications Society, Proceedings: Graphics Interface 1992 1992 p 94-105 (For primary document see N93-15533 04-61)
Copyright Avail: Issuing Activity

A relaxation method is presented that generates a series of spatially distributed stochastic samples following the Poisson disk distribution over a range of scales. The series is structured so that a prefix subsequence forms a lower frequency sampling pattern that is also Poisson disk distributed. Unlike strict dart-throwing, the relaxation procedure is guaranteed to terminate. The hierarchical structure allows straightforward adaptive sampling, using techniques analogous to ordered dithering. Also presented is an efficient method to optimize the location of samples under a minimum root mean square quantization error criterion. Author

N93-15546 Xerox Palo Alto Research Center, CA.
PERFORMING IN-PLACE AFFINE TRANSFORMATIONS IN CONSTANT SPACE
Ken Fishkin *In* Canadian Human-Computer Communications Society, Proceedings: Graphics Interface 1992 1992 p 106-114 (For primary document see N93-15533 04-61)
Copyright Avail: Issuing Activity

Affine transformations of 2-D frame buffer images are a common computer graphics operation. Such transformations take a rectangular raster of image memory, perform some affine transformation (e.g. scale, shift, shear, rotate) upon it, and write the result into some other rectangular raster of image memory. If the source and destination share the same memory, the operation is termed in-place. Previous in-place affine transformation algorithms on an m by n region required O(max(m,n)) space for internal buffers. The algorithm presented here requires O(1) (constant) space: this allows in-place affine transformations to be performed on large images on processors with small memory. Author

N93-15547 Toronto Univ. (Ontario). Dept. of Computer Science.
WORKING TOGETHER, VIRTUALLY
Jin Li and Marilyn Mantei *In* Canadian Human-Computer Communications Society, Proceedings: Graphics Interface 1992 1992 p 115-122 (For primary document see N93-15533 04-61)
Copyright Avail: Issuing Activity

Although technologies such as media spaces have been designed to facilitate collaborative work at a distance, the existing systems have primarily focused on the use of computer managed audio and video as mechanisms to support meetings and video phone calls. Research has shown that frequent and spontaneous informal communication is crucial for project coordination and work progress. It has also found that the amount of collaboration that occurs varies directly with the proximity of co-workers. However, proximity is not always possible or desirable in today's work world. In this paper, we introduce the concept of a virtual open office, a simulated shared open office environment which creates proximity without its inherent disadvantages. We suggest that a large amount of communication among co-workers is not from actual intentional communication contact but from opportunistic contact and environmental scanning in which each individual is picking up valuable coordination information. We propose that it is this aspect of the constant contact of an open office environment which provides the closeness and cohesion necessary for effective work coordination. Based on this premise, we argue for a set of unique user requirements for the virtual open office and demonstrate an instantiation of these requirements in a working prototype, called VOODOO. Author

N93-15548 Toronto Univ. (Ontario).
TELEPRESENCE: INTEGRATING SHARED TASK AND PERSON SPACES
William A. A. Buxton *In* Canadian Human-Computer Communications Society, Proceedings: Graphics Interface 1992 1992 p 123-129 (For primary document see N93-15533 04-61)
Copyright Avail: Issuing Activity

From a technological and human perspective, shared space in remote collaboration has tended to focus on shared space of either the people or the task. The former would be characterized by traditional video-teleconferencing or videophones. The latter could be characterized by synchronous computer conferencing or groupware. The focus of this presentation is the area where these two spaces meet and are integrated into what could be characterized as video-enhanced computer conferencing or computer-enhanced video conferencing. From the behavioral perspective, the interest lies in how--in collaborative work--we make transitions between these two spaces. For example, in negotiating, the activity is mainly in the shared space of the participants themselves, where we are 'reading' each other for information about trust and confidence. On the other hand, in preparing a budget using a shared electronic spreadsheet, for example, the visual channel is dominated by the task space. How well systems afford natural transitions between these spaces will have a large impact on their usability, usefulness, and acceptance. Consequently, we investigate the design space and some of the issues affecting it. Author

N93-15549 Toronto Univ. (Ontario). Dept. of Computer Science.
CSCW - WCSC: COMPUTER-SUPPORTED COOPERATIVE WORK. WHAT CHANGES FOR THE SCIENCE OF COMPUTING
Marilyn M. Mantei *In* Canadian Human-Computer Communications Society, Proceedings: Graphics Interface 1992 1992 p 130-139 (For primary document see N93-15533 04-61)
Copyright Avail: Issuing Activity

Computer-supported cooperative work environments change some of the underlying beliefs about solutions that have been built for distributed computing. Electronic mail and file transfers have worked efficiently and effectively by breaking the information to be transferred into packets and reassembling the packets at the destination. This is not a viable solution for handling shared real time drawing or writing. Integrity has been maintained by locking out portions of a database until an update is completed. Such lockout is not always suitable in a groupware interface. Other solutions are necessary for resolving conflicts. Client-server architectures have worked well for managing distributed processing but replicated architectures, coupled

with their fragility and synchronization problems are needed for groupware products in order to preserve acceptable local response time. The addition of multi-media to the environment complicates the problem more. Control of analog video requires a client-server environment which can build in intolerable delays as distances between communicating parties increase. This paper approaches design criteria for shared software from the human side and points out profound architectural problems that need to be solved if multi-media cooperative work environments are to function effectively.
Author

N93-15550 Guelph Univ. (Ontario). Dept. of Computing and Information Science.
MOVEMENT TIME PREDICTION IN HUMAN-COMPUTER INTERFACES
I. Scott MacKenzie *In* Canadian Human-Computer Communications Society, Proceedings: Graphics Interface 1992 1992 p 140-150 (For primary document see N93-15533 04-61)
Copyright Avail: Issuing Activity

The prediction of movement time in human-computer interfaces as undertaken using Fitts' law is reviewed. Techniques for model building are summarized and three refinements to improve the theoretical and empirical accuracy of the law are presented. Refinements include the following: (1) the Shannon formulation for the index of task difficulty; (2) new interpretations of 'target width' for two- and three-dimensional tasks; and (3) a technique for normalizing error rates across experimental factors. Finally, a detailed application example is developed showing the potential of Fitts' law to predict and compare the performance of user interfaces before designs are finalized.
Author

N93-15551 Pennsylvania Univ., Philadelphia. Computer Graphics Lab.
ARCBALL: A USER INTERFACE FOR SPECIFYING THREE-DIMENSIONAL ORIENTATION USING A MOUSE
Ken Shoemake *In* Canadian Human-Computer Communications Society, Proceedings: Graphics Interface 1992 1992 p 151-156 (For primary document see N93-15533 04-61)
Copyright Avail: Issuing Activity

Arcball is an input technique for 3-D computer graphics, using a mouse to adjust the spatial orientation of an object. In Arcball, human factors and mathematical fundamentals come together exceptionally well. Arcball provides consistency between free and constrained rotations using any direction as an axis; consistent visual input and feedback; kinesthetic agreement between mouse motion and object rotation; and consistent interpretation of mouse position. Attention to mathematical detail facilitates the tasks of users and implementors. Users say that as a general-purpose rotation controller Arcball is easier to use than its nearest rival, the Virtual Sphere. It is also more powerful and simpler to implement.
Author

N93-15552 Toronto Univ. (Ontario). Dept. of Industrial Engineering.
DESIGNING VIDEO ANNOTATION AND ANALYSIS SYSTEMS
Beverly L. Harrison and Ronald M. Baecker *In* Canadian Human-Computer Communications Society, Proceedings: Graphics Interface 1992 1992 p 157-166 (For primary document see N93-15533 04-61)
Copyright Avail: Issuing Activity

Although video has been used for many years to record data, few tools have been developed to help analyze video data. Current multimedia interfaces have severe cognitive and attentional limitations, reflecting technology-centered designs which have not profited from human factors theory and user-centered design. This paper discusses user requirements for video analysis, from which we derive a set of functional specifications. These specifications are useful for evaluating existing systems and for guiding the development of new systems. A number of existing systems are briefly described, as is the VANNA (Video ANNotation and Analysis) system, which integrates video, non-speech audio, voice, textual and graphical data, and which incorporates emerging technology, user-centered design and human factors theory.
Author

N93-15553 Thinking Machines Corp., Cambridge, MA.
A DATA PARALLEL ALGORITHM FOR RAYTRACING OF HETEROGENEOUS DATABASES
Peter Schroeder (Princeton Univ., NJ.) and Steven M. Drucker (Massachusetts Inst. of Tech., Cambridge.) *In* Canadian Human-Computer Communications Society, Proceedings: Graphics Interface 1992 1992 p 167-175 (For primary document see N93-15533 04-61)
Copyright Avail: Issuing Activity

We describe a new data parallel algorithm for raytracing. Load balancing is achieved through the use of processor allocation, which continually remaps available resources. In this manner heterogeneous data bases are handled without the usual problems of low resource usage. The proposed approach adapts well to both extremes: a small number of rays and a large database; a large number of rays and a small database. The algorithm scales linearly--over a wide range--in the number of rays and available processors. We present an implementation on the Connection Machine CM2 system and provide timings.
Author

N93-15554 Apple Computer, Inc., Cupertino, CA.
OBJECT SPACE TEMPORAL COHERENCE FOR RAY TRACING
David A. Jevans *In* Canadian Human-Computer Communications Society, Proceedings: Graphics Interface 1992 1992 p 176-183 Original contains color illustrations (For primary document see N93-15533 04-61)
Copyright Avail: Issuing Activity

A method is presented for exploiting object space temporal coherence to speed up ray tracing of animation sequences where the camera remains static. The object space is subdivided with a hierarchical voxel grid structure. Each voxel keeps a list of the rays that pass through it when the first frame of a sequence is rendered. To render a successive frame, only rays that passed through voxels in which an object has moved are retraced. The method speeds up ray tracing of a test animation sequence by nearly a factor of four.
Author

N93-15555 Alias Research Corp., Toronto (Ontario).
RAY TRACING POLYGONS USING SPATIAL SUBDIVISION
Andrew Woo *In* Canadian Human-Computer Communications Society, Proceedings: Graphics Interface 1992 1992 p 184-191 Original contains color illustrations (For primary document see N93-15533 04-61)
Copyright Avail: Issuing Activity

Ray tracing consumes a lot of computational resources to render images. This expense usually lies in the ray-surface intersection tests. If the surfaces were polygonal, then we should be able to apply more polygon-specific optimizations to partially cull intersections. Our ray tracer uses a non-memory intensive, voxel traversal intersection culler to assist in such optimizations.
Author

N93-15556 Loral Western Development Labs., San Jose, CA.
PARAMETRIC HEIGHT FIELD RAY TRACING
David W. Paglieroni and Sidney M. Petersen *In* Canadian Human-Computer Communications Society, Proceedings: Graphics Interface 1992 1992 p 192-200 (For primary document see N93-15533 04-61)
Copyright Avail: Issuing Activity

Height field ray tracing is one approach to photo-realistic visualization of terrain. Parametric methods, which fall into a new class of height field ray trace methods, are introduced. The height field is horizontally sliced into evenly spaced cross-sections. For each cross-section, the Euclidean distance from each point to the nearest point where the slice cuts through terrain is computed off-line. These planes of distance values are condensed into parameter planes that encode cones of empty space above each height field cell, where cone width is bounded by the terrain relief. Parametric ray tracing occurs along intersections between rays and these cones. Parametric methods are shown to be memory efficient and often much faster than the other popular height field ray trace methods.
Author

N93-15557 Bell Telephone Labs., Inc., Murray Hill, NJ.
PARTITIONING TREE IMAGE REPRESENTATION AND GENERATION FROM 3D GEOMETRIC MODELS
Bruce F. Naylor *In* Canadian Human-Computer Communications Society, Proceedings: Graphics Interface 1992 1992 p 201-212 Original contains color illustrations (For primary document see N93-15533 04-61)
Copyright Avail: Issuing Activity

While almost all research on image representation has assumed an underlying discrete space, the most common sources of images have the structure of the continuum. Although employing discrete space representations leads to simple algorithms, among its costs are quantization

errors, significant verbosity, and lack of structural information. A neglected alternative is the use of continuous space representations. In this paper we discuss one such representation and algorithms for its generation from views of 3D continuous space geometric models. For this we use binary space partitioning trees for representing both the model and the image. Our approach falls under the general rubric of visible surface algorithms, providing an object-space algorithm which under certain conditions requires only sub-linear time for a partitioning tree represented model, and in general exploits occlusion so that the computational cost converges toward the complexity of the image as the depth complexity increases. Visible edges can also be generated as a step following visible surface determination. However, an important contextual difference is that the resulting image trees are used in subsequent continuous space operations. These include affine transformations, set operations, and metric calculations, which can be used to provide image compositing, incremental image modification in a sequence of frames, and facilitating matching for computer vision/robotics. Image trees can also be used with the hemicube and light buffer illumination methods as a replacement for regular grids, thereby providing exact rather than approximate visibility. Author

N93-15558 Calgary Univ. (Alberta). Dept. of Computer Science.

ESCAPE-TIME VISUALIZATION METHOD FOR LANGUAGE-RESTRICTED ITERATED FUNCTION SYSTEMS

Przemyslaw Prusinkiewicz and Mark S. Hammel *In* Canadian Human-Computer Communications Society, Proceedings: Graphics Interface 1992 1992 p 213-223 (For primary document see N93-15533 04-61)

Copyright Avail: Issuing Activity

The escape-time method was introduced to generate images of Julia and Mandelbrot sets, then applied to visualize attractors of iterated function systems. This paper extends it further to language-restricted iterated function systems (LRIFS's). They generalize the original definition of IFS's by providing means for restricting the sequences of applicable transformations. The resulting attractors include sets that cannot be generated using ordinary IFS's. The concepts of this paper are expressed using the terminology of formal languages and finite automata. Author

N93-15559 Illinois Univ., Chicago. Electronic Visualization Lab.

THE OBJECT INSTANCING PARADIGM FOR LINEAR FRACTAL MODELING

John C. Hart *In* Canadian Human-Computer Communications Society, Proceedings: Graphics Interface 1992 1992 p 224-231 (For primary document see N93-15533 04-61)

Copyright Avail: Issuing Activity

The recurrent iterated function system and the L-system are two powerful linear fractal models. The main drawback of recurrent iterated function systems is a difficulty in modeling whereas the main drawback of L-systems is inefficient geometry specification. Iterative and recursive structures extend the object instancing paradigm, allowing it to model linear fractals. Instancing models render faster and are more intuitive to the computer graphics community. A preliminary section briefly introduces the object instancing paradigm and illustrates its ability to model linear fractals. Two main sections summarize recurrent iterated function systems and L-systems and provide methods with examples for converting such models to the object instancing paradigm. Finally, a short epilogue describes a particular use of color in the instancing paradigm and the conclusion outlines directions for further research. Author

N93-15560 California Univ., Berkeley.

ALGORITHMS FOR INTERSECTING PARAMETRIC AND ALGEBRAIC CURVES

Dinesh Manocha and James Demmel *In* Canadian Human-Computer Communications Society, Proceedings: Graphics Interface 1992 1992 p 232-241 (For primary document see N93-15533 04-61)

(Grants NSF ASC-90-05933; NSF ASC-87-15728; NSF DCR-85-52474)

Copyright Avail: Issuing Activity

The problem of computing the intersection of parametric and algebraic curves arises in many applications of computer graphics, geometric, and solid modeling. Earlier algorithms are based on techniques from Elimination theory of subdivision and iteration. The former is however, restricted to low degree curves. This is mainly due to issues of efficiency and numerical stability. In this paper we use Elimination theory and express the resultant of the equations of intersection as a matrix determinant. The matrix itself rather than its symbolic determinant, a polynomial, is used as the representation. The algorithm for intersection corresponds to substituting the other equation to construct an equivalent matrix such that the intersection points can be extracted from the eigenvalues and eigenvectors of the latter. Moreover, the algebraic and geometric multiplicities of the eigenvalues give us information about the intersection (multiplicity, tangential intersection, etc.). As a result we are able to accurately compute higher order intersections. The main advantage of this approach lies in its efficiency and robustness. Moreover, the numerical accuracy of these operations is well understood. For almost all cases we are able to compute accurate answers in 64 bit IEEE floating point arithmetic. Author

N93-15561 Carnegie-Mellon Univ., Pittsburgh, PA. School of Computer Science.

AN INTERVAL REFINEMENT TECHNIQUE FOR SURFACE INTERSECTION

Michael Gleicher and Michael Kass (Apple Computer, Inc., Cupertino, CA.) *In* Canadian Human-Computer Communications Society, Proceedings: Graphics Interface 1992 1992 p 242-249 Original contains color illustrations (For primary document see N93-15533 04-61)

Copyright Avail: Issuing Activity

A technique for computing the intersections of two parametric surfaces based on interval arithmetic is described. The algorithm, which can be stopped and restarted at any point, uses search techniques to refine its description of the intersections progressively. Interval arithmetic provides guaranteed points on the intersection curves to within a user-specified tolerance. These points are connected into polygons and used to triangulate the trimmed surfaces. We provide details of an implementation and give examples of the algorithm's use. Author

N93-15562 Instituto de Matematica Pura e Aplicada, Rio de Janeiro (Brazil).

PHYSICALLY-BASED METHODS FOR POLYGONIZATION OF IMPLICIT SURFACES

Luiz Henrique deFigueiredo, Jonas deMirandaGomes (Toronto Univ., Ontario), Demetri Terzopoulos (Toronto Univ., Ontario), and Luiz Velho (Toronto Univ., Ontario) *In* Canadian Human-Computer Communications Society, Proceedings: Graphics Interface 1992 1992 p 250-257 (For primary document see N93-15533 04-61)

Copyright Avail: Issuing Activity

We present discrete physically-based methods for generating polygonal approximations of implicit surfaces. These methods not only generate a combinatorial manifold approximating the surface, but also produce a structure that is well suited to numerical simulations in physically-based modeling and animation systems. Author

N93-15563 Pennsylvania Univ., Philadelphia. Computer Graphics Lab.

MATRIX ANIMATION AND POLAR DECOMPOSITION

Ken Shoemake and Tom Duff (Bell Telephone Labs., Inc., Murray Hill, NJ.) *In* Canadian Human-Computer Communications Society, Proceedings: Graphics Interface 1992 1992 p 258-264 (For primary document see N93-15533 04-61)

Copyright Avail: Issuing Activity

General 3x3 linear or 4x4 homogenous matrices can be formed by composing primitive matrices for translation, rotation, scale, shear, and perspective. Current 3-D computer graphics systems manipulate and interpolate parametric forms of these primitives to generate scenes and motion. For this and other reasons, decomposing a composite matrix in a meaningful way has been a long standing challenge. This paper presents a theory and method for doing so, proposing that the central issue is rotation extraction, and that the best way to do that is Polar Decomposition. This method also is useful for renormalizing a rotation matrix containing excessive error. Author

N93-15564 IBM Watson Research Center, Yorktown Heights, NY.

GENERATING NATURAL-LOOKING MOTION FOR COMPUTER ANIMATION

Jessica K. Hodgins, Paula K. Sweeney, and David G. Lawrence *In* Canadian Human-Computer Communications Society, Proceedings: Graphics Interface 1992 1992 p 265-272 (For primary document see N93-15533 04-61)

Copyright Avail: Issuing Activity

The automatic generation of motion for animation remains an unsolved problem in computer graphics. One approach to the problem is to combine physically accurate models with control systems. The user specifies high-level goals and the control system computes the forces and torques that the simulated muscles or motors should exert to cause the model to perform the desired task. In this paper we describe control systems for rigid-body models of humans performing four tasks: pumping a swing, riding a seesaw, juggling, and pedaling a unicycle. We designed the control systems with the goal of producing natural-looking motion, and we discuss the techniques that we used to achieve this goal. Author

N93-15565 Toronto Univ. (Ontario). Dept. of Computer Science.
BEYOND KEYFRAMING: AN ALGORITHMIC APPROACH TO ANIMATION
A. James Stewart and James F. Cremer *In* Canadian Human-Computer Communications Society, Proceedings: Graphics Interface 1992 1992 p 273-281 (For primary document see N93-15533 04-61)
Copyright Avail: Issuing Activity

The use of physical system simulation has led to realistic animation of passive objects, such as sliding blocks or bouncing balls. However, complex active objects like human figures and insects need a control mechanism to direct their movements. We present a paradigm that combines the advantages of both physical simulation and algorithmic specification of movement. The animator writes an algorithm to control the object and runs this algorithm on a physical simulator to produce the animation. Algorithms can be reused or combined to produce complex sequences of movements, eliminating the need for keyframing. We have applied this paradigm to control a biped which can walk and can climb stairs. The walking algorithm is presented along with the results from testing with the Newton simulation system. Author

N93-15566 Bell Telephone Labs., Inc., Murray Hill, NJ.
A MINIMALIST GLOBAL USER INTERFACE
Rob Pike *In* Canadian Human-Computer Communications Society, Proceedings: Graphics Interface 1992 1992 p 282-293 (For primary document see N93-15533 04-61)
Copyright Avail: Issuing Activity

Help is a combination of editor, window system, shell, and user interface that provides a novel environment for the construction of textual applications such as browsers, debuggers, mailers, and so on. It combines an extremely lean user interface with some automatic heuristics and defaults to achieve significant effects with minimal mouse and keyboard activity. The user interface is driven by a file-oriented programming interface that may be controlled from programs or even shell scripts. By taking care of user interface issues in a central utility, help simplifies the job of programming applications that make use of a bitmap display and mouse. Author

N93-15567 Paris-Sud Univ., Orsay (France).
A MULTI-LAYER GRAPHIC MODEL FOR BUILDING INTERACTIVE GRAPHICAL APPLICATIONS
Jean-Daniel Fekete *In* Canadian Human-Computer Communications Society, Proceedings: Graphics Interface 1992 1992 p 294-300 (For primary document see N93-15533 04-61)
Copyright Avail: Issuing Activity

In this article, we present a model for building interactive graphical applications based on multi-layer graphics. With this model, a variety of components of an interactive graphical editor (transient objects like the selection rectangle, selected objects, grids, cursors), as well as the handling of input events, are realized in a more straightforward way. We show how an interactive graphical application can use layered graphics in a simple and effective way to represent direct manipulation, some graphic constraints and event handling using various input devices. By clarifying the status of abstract elements of an interactive application, the model encompasses a significant part of the dynamic aspect of the interaction. Author

N93-15568 IBM Watson Research Center, Yorktown Heights, NY.
A LINEAR CONSTRAINT TECHNOLOGY FOR INTERACTIVE GRAPHIC SYSTEMS
Richard Helm, Tien Huynh, Catherine Lassez, and Kim Marriott *In* Canadian Human-Computer Communications Society, Proceedings: Graphics Interface 1992 1992 p 301-309 (For primary document see N93-15533 04-61)
Copyright Avail: Issuing Activity

Constraints provide a natural formalism for user-interface design and graphical layout. Recent results and algorithms from symbolic computation and geometry provide new techniques to manipulate linear arithmetic constraints. We show how these results can be applied to interactive graphical user-interfaces and how they extend the capabilities of previous interactive constraint-based user interface systems. We propose an architecture for such systems based on these techniques. Author

N93-15569 Texas Univ., Austin. Balcones Research Center.
NON-UNIFORM PATCH LUMINANCE FOR GLOBAL ILLUMINATION
Burning Bian, Norman Wittels (Worcester Polytechnic Inst., MA.), and Donald S. Fussell *In* Canadian Human-Computer Communications Society, Proceedings: Graphics Interface 1992 1992 p 310-318 (For primary document see N93-15533 04-61)
Copyright Avail: Issuing Activity

A new radiosity model is presented in which all patches are represented as isoparametric elements and the patch luminances change bilinearly. The surfaces are tessellated into planar quadrilaterals and continuous surface luminance is maintained where patches meet. A new form factor, accounting for the luminance contributions between patches, is derived and calculated using hemisphere projections and Gaussian quadrature. Images generated from the new approach were tested by pixel-level comparison with real images acquired by a calibrated imaging system, and compared with the images generated by the uniform patch luminance radiosity. The comparison results indicate that fewer bilinear patches are required to achieve comparable luminance accuracy. Author

N93-15570 Institut de Recherche en Informatique et Systemes Aleatoires, Rennes (France).
A TWO-PASS PHYSICS-BASED GLOBAL LIGHTING MODEL
Kadi Bouatouch and Pierre Tellier *In* Canadian Human-Computer Communications Society, Proceedings: Graphics Interface 1992 1992 p 319-328 Original contains color illustrations (For primary document see N93-15533 04-61)
Copyright Avail: Issuing Activity

A two-pass implementation of a physics-based global lighting model is presented. This latter uses a physics-based reflection model, spectral distribution of light powers, and does not make any assumption on the specular behavior of materials. The scenes are discretized into points instead of patches. Hence, any kind of surface can be used without having to break it down into small planar patches. A data structure, named visibility graph, is built to efficiently evaluate the visibility between the sample points of the scene. Even though the photometric properties of surfaces (reflection, transmission, roughness, emitted powers, etc.) are modified, this graph does not change, which makes it easy to produce very quickly several images. Methods for computing the Fresnel factor are given in appendix. Author

N93-15578*# National Aeronautics and Space Administration. Goddard Space Flight Center, Greenbelt, MD.
SOFTWARE MANAGEMENT ENVIRONMENT (SME) INSTALLATION GUIDE
David Kistler and Kellyann Jeletic Jan. 1992 35 p
(NASA-TM-108578; NAS 1.15:108578; SEL-92-001) Avail: CASI HC A03/MF A01

This document contains installation information for the Software Management Environment (SME), developed for the Systems Development Branch (Code 552) of the Flight Dynamics Division of Goddard Space Flight Center (GSFC). The SME provides an integrated set of management tools that can be used by software development managers in their day-to-day management and planning activities. This document provides a list of hardware and software requirements as well as detailed installation instructions and trouble-shooting information. Author

N93-15579*# National Aeronautics and Space Administration. Goddard Space Flight Center, Greenbelt, MD.
DATA COLLECTION PROCEDURES FOR THE SOFTWARE ENGINEERING LABORATORY (SEL) DATABASE
Gerard Heller, Jon Valett, and Mary Wild Mar. 1992 143 p
(NASA-TM-108579; NAS 1.15:108579; SEL-92-002) Avail: CASI HC A07/MF A02

This document is a guidebook to collecting software engineering data

on software development and maintenance efforts, as practiced in the Software Engineering Laboratory (SEL). It supersedes the document entitled Data Collection Procedures for the Rehosted SEL Database, number SEL-87-008 in the SEL series, which was published in October 1987. It presents procedures to be followed on software development and maintenance projects in the Flight Dynamics Division (FDD) of Goddard Space Flight Center (GSFC) for collecting data in support of SEL software engineering research activities. These procedures include detailed instructions for the completion and submission of SEL data collection forms. Author

N93-15163# Deutsche Lufthansa A.G., Frankfurt am Main (Germany). Abt. Flugbetriebstechnik.
SOFTWARE FOR FLIGHT RECORDER DATA EVALUATION DEVELOPED BY LUFTHANSA [VON LUFTHANSA ENTWICKELTE EDV PROGRAMME ZUR AUSWERTUNG VON FLUGSCHREIBERN]
Matthias Kruedener *In* DLR, Proceedings of the 16th Symposium on Aircraft Integrated Monitoring Systems Jan. 1992 p 201-217 (For primary document see N93-15152 04-06)
Avail: CASI HC A03/MF A06; DLR, Wissenschaftliches Berichtswesen, Postfach 90 60 58, Cologne, Germany, HC

62 COMPUTER SYSTEMS

Includes computer networks and special application computer systems.

N93-14151# Carnegie-Mellon Univ., Pittsburgh, PA. School of Computer Science.
A PORTABLE MULTIPROCESSOR INTERFACE FOR STANDARD ML OF NEW JERSEY
J. Gregory Morrisett and Andrew Tolmach Jun. 1992 33 p
(Contract F19628-91-C-0168; ARPA Order 8313)
(AD-A255639; CMU-CS-92-155) Avail: CASI HC A03/MF A01

A portable interface between shared-memory multiprocessors and Standard ML of New Jersey was designed. The interface is based on the conventional kernel thread model and provides facilities that can be used to implement user-level thread packages. The interface supports experimentation with different thread scheduling policies and synchronization constructs. It has been ported to three different multiprocessors and used to construct a general purpose, user-level thread-package. In this paper, we discuss the interface and its implementation and performance, with emphasis on the Silicon Graphics 4D/380S multiprocessor. GRA

N93-14645# Naval Surface Warfare Center, Silver Spring, MD.
ENGINEERING OF MASSIVELY INTERCONNECTED COMPUTER SYSTEMS
Michael Jenkins, Charles Yeh, and Steven Howell 1 Oct. 1991 38 p
(NR Proj. RS3-4-P-11)
(AD-A255501; NAVSWC-TR-91-588) Avail: CASI HC A03/MF A01

This document provides an analysis of design elements whose implementation involves algorithmic tasks and hardware resources which must handle large amounts of data or which otherwise present communication (data flow) impasses to the timely (or functional) fulfillment of a design. It proposes a methodology for evaluating candidate resources and selecting those which reduce communication complexity and meet system requirements. The techniques of this methodology should integrate with other steps in the design process so that necessary information is not ignored or lost. They should also be easily automated, since the number of combinations involved may be intractable if attempted by hand. As an indication of future research, it presents background information on resources used in the design of such systems and addresses the implications of introducing physical constraints on these design elements. GRA

N93-14808*# SRI International Corp., Menlo Park, CA.
FORMAL VERIFICATION OF AN ORAL MESSAGES ALGORITHM FOR INTERACTIVE CONSISTENCY
John Rushby Oct. 1992 51 p
(Contract NAS1-18969)
(NASA-CR-189704; NAS 1.26:189704) Avail: CASI HC A04/MF A01

The formal specification and verification of an algorithm for Interactive Consistency based on the Oral Messages algorithm for Byzantine Agreement is described. We compare our treatment with that of Bevier and Young, who presented a formal specification and verification for a very similar algorithm. Unlike Bevier and Young, who observed that 'the invariant maintained in the recursive subcases of the algorithm is significantly more complicated than is suggested by the published proof' and who found its formal verification 'a fairly difficult exercise in mechanical theorem proving,' our treatment is very close to the previously published analysis of the algorithm, and our formal specification and verification are straightforward. This example illustrates how delicate choices in the formulation of the problem can have significant impact on the readability of its formal specification and on the tractability of its formal verification. Author

N93-15082# Universiteit Twente, Enschede (Netherlands). Dept. of Computer Science.
PARALLEL ON-LINE PARSING IN CONSTANT TIME
Klaas Sikkel Aug. 1991 13 p
(Memo-INF-91-64; ETN-92-92428) Avail: CASI HC A03/MF A01

The parallelization of online parsers is considered. An online parser processes each word as soon as it is typed by the user, without waiting for the end of the sentence. Thus, in an interactive system, a sentence will be parsed almost immediately after the last word is presented. The complexity of an online parser is determined by the resources needed for the analysis of a single word, as it is assumed that previous words are already processed. Traditional parsing algorithms like Cocke Younger Kasami or Earley need O(n squared) time for the nth word of a sentence. A parallel implementation in O(n) time on O(n) processors is straightforward. A parallel online parser that needs O(1) time on O(n squared) processors is presented. ESA

N93-15093# Universiteit Twente, Enschede (Netherlands). Dept. of Computer Science.
PARALLELISM IN A MAIN-MEMORY DBMS: THE PERFORMANCE OF PRISMA/DB
Annita N. Wilschut, Jan Flokstra, and Peter M. G. Apers Feb. 1992 21 p
(Memo-INF-92-25; ETN-92-92439) Copyright Avail: CASI HC A03/MF A01

The performance of the parallel, main memory DBMS (Data Base Management System) PRISMA/DB is evaluated. An abstract architecture for parallel query execution is presented. A performance model for the execution of simple relational operations on this architecture is developed. The parameters in the model are set using experiments on PRISMA/DB, and the performance of PRISMA/DB is analyzed in the context of the model. Several conclusions can be drawn from the model combined with the results of the performance experiments: the performance of PRISMA/DB appears to be competitive with respect to the systems; the developed model can explain the results from the performance experiments to a large extent; the observed linear speedup for small numbers of processors cannot always be extrapolated to larger numbers of processors; the optimal number of processors for the parallel execution of an operation is smaller for a main memory system than a disk based system. The results of this study can be used to design data fragmentation strategies for large parallel machines. ESA

N93-15124# Institut National Polytechnique, Grenoble (France). Lab. de Genie Informatique.
PROGAMMABLE CONNECTION PARALLEL ARCHITECTURE: DESIGN AND ROUTING Ph.D. Thesis [ARCHITECTURES PARALLELES A CONNECTIQUE PROGRAMMABLE: RECONFIGURATION ET ROUTAGE]
Philippe Waille 1991 180 p In FRENCH
(ETN-92-92676) Avail: CASI HC A09/MF A02

In a machine without a common memory, messages between processors are exchanged by means of point by point links. In fixed connection machines, permanent bindings occur under regular interconnections such as grid or hypercube. Messages without direct links are routed from neighbor to neighbor until reaching the target. The performances of these machines depend on the tributary adequacy between the communications graph between tasks and the physical interconnection graph between the processors. Programmable interconnection machine networks and two operating modes are discussed. The interconnection processes are run

only once before an application. The network can be systematically reprogrammed for each message. Such a configuration is named synchronous. ESA

N93-15141# Universiteit Twente, Enschede (Netherlands). Dept. of Computer Science.

PRISMA/DB: A PARALLEL, MAIN-MEMORY RELATIONAL DBMS

Peter M. G. Apers, Carel A. vandenBerg, Jan Flokstra (Center for Mathematics and Computer Science, Amsterdam, Netherlands), Paul W. P. J. Grefen, Martin L. Kersten (Center for Mathematics and Computer Science, Amsterdam, Netherlands), and Annita N. Wilschut Feb. 1992 27 p

(Memo-INF-92-12; ETN-92-92432) Copyright Avail: CASI HC A03/MF A01

PRISMA/DB is a full fledged parallel, main memory relational Data Base Management System (DBMS), the design of which is characterized by two main ideas: high performance is obtained by the use of parallelism for query processing and main memory storage of the entire database; a flexible architecture for experimentating with functionality and performance is obtained via a modular implementation of the system in an object oriented programming language. The design and implementation of PRISMA/DB are detailed. A performance evaluation of the system shows that the system is comparable to other state of the art database machines. The prototype implementation of the system is ready, and runs in a 100 node parallel multiprocessor. The achieved flexibility of the system makes it a valuable platform for research in various directions. ESA

N93-15142# Universiteit Twente, Enschede (Netherlands). Dept. of Computer Science.

DATA FRAGMENTATION FOR PARALLEL TRANSITIVE CLOSURE STRATEGIES

Maurice A. W. Houtsma, Peter M. G. Apers, and Gideon L. V. Schipper Feb. 1992 24 p Sponsored in part by Royal Netherlands Academy of Arts and Sciences

(Memo-INF-92-17; ETN-92-92435) Copyright Avail: CASI HC A03/MF A01

The topic of parallel (distributed) computation of transitive closure queries is addressed. In particular, the issues that influence data fragmentation are discussed. A number of algorithms, each focusing on one of the important issues, are presented. The pros and cons of the algorithms are discussed and some results of applying the algorithms to different types of graphs are given. This last aspects shows to what respect the algorithms indeed conform to the goals set out. ESA

N93-15205# Carnegie-Mellon Univ., Pittsburgh, PA. School of Computer Science.

WORK EFFICIENT HASHING ON PARALLEL AND VECTOR COMPUTERS

Thomas J. Sheffler and Randal E. Bryant 18 Aug. 1992 15 p

(Contract F33615-90-C-1465; ARPA Order 7597)

(AD-A256355; CMU-CS-92-172) Avail: CASI HC A03/MF A01

Hashing techniques have long been used to efficiently store and locate data indexed by key. Recently, parallel hashing algorithms were developed that allow table insertion of many keys in a few parallel steps. The analyses of these algorithms have focused on the expected number of steps required, ignoring the issue of work complexity. As a result, these algorithms have not been work efficient. In this paper, we present a parallel hashing algorithm that is shown to be work efficient because it performs no more work than its serial counterpart. An analysis of its behavior shows that it performs S = O(log n) expected parallel steps and W = O(n) expected work. Many parallel algorithms can make use of hashing as a core step. Procedures such as histogramming, set difference, keyed reduction, and dictionary lookup can be formulated using a general hash routine. Thus, parallel hashing is an important fundamental parallel operation. The above applications may also be implemented using sorting as the core step. While the use of parallel hashing has been generally accepted in the folklore of parallel computing, a dearth of literature about the expected performance of such algorithms has led many to favor the use of sorting. This paper sheds light on the performance that may be achieved using parallel hashing algorithms and should lend credibility to their use. GRA

N93-15207# Carnegie-Mellon Univ., Pittsburgh, PA. School of Computer Science.

IMPLEMENTING THE MULTIPREFIX OPERATION ON PARALLEL AND VECTOR COMPUTERS

Thomas J. Sheffler 18 Aug. 1992 26 p

(Contract F33615-90-C-1465; ARPA Order 7597)

(AD-A256367; CMU-CS-92-173) Avail: CASI HC A03/MF A01

For an ordered set of n values, each with an associated integer label, the multiprefix operation calculates a partial sum for each value that is the sum of all preceding values with the same label. The multiprefix operation was proposed as a parallel primitive because of its power for expressing many data parallel algorithms succinctly. However, most approaches to implementing this operation have used integer sorting to gather elements with the same label together or have suggested special hardware. In this paper we present a work efficient algorithm for the multiprefix operation on n elements that runs in S = O(the square root of n) parallel steps on a p = the square root of n processor CRCW-ARB PRAM. The CRCW-ARB model ensures only that of multiple processors writing to the same location, an arbitrary one succeeds. We make use of this feature to resolve data dependencies in the first phase of the algorithm only so that all later steps guarantee EREW memory access. A fully vectorized version of our algorithm was designed for the CRAY Y-MP and provides good performance for a number of important algorithms. For the integer sorting test of the NAS benchmarks, our multiprefix operation was used to create an algorithm that is competitive in performance with the current best algorithms for that machine. As another example, we show that by using the multiprefix operator for sparse-matrix dense-vector multiplication, we obtain performance exceeding traditional FORTRAN-based approaches. Finally, our algorithm also makes possible the simulation of a CRCW-PLUS PRAM on a p processor CRCW-ARB PRAM with only constant slowdown for problem sizes n greater than p(exp 2). GRA

N93-15319# Physics and Electronics Lab. TNO, The Hague (Netherlands).

A DEADLOCK-FREE COMMUNICATION SYSTEM FOR A TRANSPUTER NETWORK [EEN DEADLOCK-FREE COMMUNICATIESYSTEEM VOOR EEN TRANSPUTER NETWERK]

P. P. Meiler Feb. 1992 96 p In DUTCH

(AD-A256473; FEL-90-B370) Avail: CASI HC A05/MF A01

Real-time applications using a network of transputers require that the communication between the transputers is flexible and deadlock-free. Two problems are encountered when implementing such a communication system. A transputer has four links to communicate directly with four other transputers. Often there are more than four processes on one transputer that need to communicate with a process on another transputer. The messages of several processes must then be multiplexed on one link. Processes on different transputers communicate using a path of connections between in transputers in the network. This path must be set for each message. The deadlock-free communication system presented in this report is a solution to these problem. It is a software interface between the application processes running on the transputers in the networks. It provides the applications programmer with an unlimited number of virtual channels. A virtual channel is deadlock-free and can connect any two processes in the network. The system is implemented as a kernel process. Each transputer in the network must run one such process in parallel with the application processes. GRA

N93-15407# Carnegie-Mellon Univ., Pittsburgh, PA. Dept. of Computer Science.

A MASSIVELY DISTRIBUTED PARALLEL GENETIC ALGORITHM Final Report

Shumeet Baluja 13 Oct. 1992 20 p

(AD-A256617; CMU-CS-92-196) Avail: CASI HC A03/MF A01

The effectiveness of combinatorial search heuristics, such as Genetic Algorithms (GA), is limited by their ability to balance the need for a diverse set of sampling points with the desire to quickly focus search upon potential solutions. One of the method often used to address this problem is to simulate the theory of punctuated equilibria in the GA. The GA introduced here uses the basic premises derived from punctuated equilibria, but hopes to remedy the problems associated with sudden introduction of new genetic material by relying upon a much greater degree of distribution and an overlap population architecture. Presented here is a description and

preliminary empirical test results of a massively distributed genetic algorithm. On the seventeen test problems attempted, the mdpGA did significantly better than a simple parallel GA. The massive distribution of the GA and the modified population topology yield improvements in speed, and also prove to be far less vulnerable than other genetic algorithms to biases in the function space which lead away from global optima. GRA

N93-15494# Carnegie-Mellon Univ., Pittsburgh, PA. School of Computer Science.
AN AXIOMATIC TREATMENT OF PARTIAL CORRECTNESS AND DEADLOCK IN A SHARED VARIABLE PARALLEL LANGUAGE
Stephen Brookes Jun. 1992 41 p
(Contract F33615-90-C-1465; DARPA Order 7597)
(AD-A256234; CMU-CS-92-154) Avail: CASI HC A03/MF A01

We give a semantically based axiomatic treatment of partial correctness and deadlock for an imperative shared variable parallel programming language. The Owicki-Gries proof methodology for this language proves conventional Hoare-style partial correctness assertions and involves the notion of interference-freedom of proofs (to guarantee soundness), auxiliary variables (to guarantee relative completeness), and global invariants (to permit reasoning about deadlock-freedom). Our axiomatic proof system is based more explicitly on the underlying operational semantics, using assertions whose syntactic structure directly reflects the operational behavior of parallel programs at an appropriate level of abstraction. We build a proof system that requires neither interference freedom nor auxiliary variables. Novel features include the use of a syntactic form of parallel composition of assertions, and the use of conjunction and implication as connectives on assertions. It is possible simultaneously to reason about partial correctness and deadlock-freedom using our proof system, without recourse to global variants. We discuss some non-trivial examples, and compare our proof methodology with some other proof methods from the literature. Author

N93-15510*# Arizona Univ., Tucson.
PROPOSAL FOR MASSIVELY PARALLEL DATA STORAGE SYSTEM
M. Mansuripur *In its* Research Studies on Advanced Optical Module/Head Designs for Optical Data Storage 15 Mar. 1992 p 89-103 (For primary document see N93-15505 04-74)
Avail: CASI HC A03/MF A03

63 CYBERNETICS

Includes feedback and control theory, artificial intelligence, robotics and expert systems.

For related information see also *54 Man/System Technology and Life Support.*

N93-14201 Texas Univ., Austin.
DECISION-MAKING FOR INTELLIGENT CONTROL OF DUAL-ARM ROBOTIC OPERATIONS Ph.D. Thesis
Daniel Joseph Cox 1992 421 p
Avail: Univ. Microfilms Order No. DA9225556

Cooperating manipulators in dual-arm robots usually result in an overconstrained system having more actuated inputs than freedom of motion, or an excess of actuator inputs. This redundancy in drivability condition provides the opportunity for choice, or decision, the fundamental quality of an intelligent machine. In general, an infinite number of selections are possible for actuator inputs and resultant internal load states to satisfy a specified output load state and motion trajectory in a dual-arm robot with cooperating manipulators. In this work, decision making criteria for cooperative modes of operation in dual-arm robots are investigated in order to use the criteria as a basis for intelligent control decisions. Decision making criteria are necessary to make effective use of dual-arm robotic system resources, as well as to enhance performance. The criteria are based on a full geometric description of the system. The decision making criteria are based on parameters inherent to the two cooperating manipulators, and parameters intrinsic to cooperative modes of operation in dual-arm robots. The effects of criteria selection on system performance and the influence of the decision making criteria selections within the dual-arm robotic system are examined through the use of interactive computer graphics. A command architecture for dual-arm robots is established to associate the decision making criteria with dual-arm robotic modes of operation. Within the architecture, a geometric operation descriptor provides the fundamental geometric relationships for motion and constraint in cooperative dual-arm robotic operations. The architecture makes use of the decision making criteria to evaluate spatial motion and load-state information for cooperative dual-arm robotic operations. The goal is to significantly expand the range of operational conditions that can be satisfied by studying decision making criteria considering dual-arm robotic operations, and to examine how these criteria can be used to enhance the operation of dual-arm robots. Dissert. Abstr.

N93-14203 Illinois Univ., Chicago.
MANIPULATION STRATEGIES FOR REDUNDANT MANIPULATORS Ph.D. Thesis
Vinod Kumar Singh 1992 229 p
Avail: Univ. Microfilms Order No. DA9226271

Some aspects of iterative inverse kinematics of redundant manipulators are examined. The joints are divided into two groups: active (or basic) and inactive (on non-basic) groups. The inactive joints are either locked or undergo predetermined smooth transitional motions. The inactive joints are initially frozen (or locked); however, the starting robot configuration can be improved by optimizing the locked values of the inactive joints. If the manipulator approaches a singularity, the algorithm detects this situation in advance and the manipulator motion is stopped. An optimization scheme is then used to adjust the inactive joints in order to improve the robot configuration at this trajectory station. The trajectory motion is then resumed in a smooth way. To avoid the problems of joint limits predetermined joint exchanges with smooth transitional motions can be utilized to alter the active and inactive joint groups. The attractive features of the proposed iterative inverse algorithm are that the initial guess need not be accurate, accuracy of solution at any trajectory station is independent of the accuracy of solution at previous trajectory stations, and the algorithm can converge even with large discretization time steps and tight convergence criterion. Dissert. Abstr.

N93-14239# Naval Oceanographic and Atmospheric Research Lab., Bay Saint Louis, MS.
ALTIMETER AND OCEANOGRAPHIC IN SITU MEASUREMENTS IN THE AREA OF THE GREENLAND-ICELAND-NORWEGIAN SEA, 1987-1988 Final Report
Pavel Pistek Jun. 1992 77 p
(AD-A256598; NOARL-14) Avail: CASI HC A05/MF A01

A multidisciplinary oceanographic study was performed in the area of the Greenland-Iceland-Norwegian Sea (GIN Sea). To assess the usefulness and the potential of altimetry in this region, the GEOSAT data, the satellite infrared images, and simultaneous in situ measurements of (1) airborne expendable bathythermographs deployed from P-3 aircraft, and (2) ship measurements of conductivity-temperature-depth (CTD). Thermistor chain data along the altimeter tracks were collected. In addition, the historical CTD data base, Generalized Digital Environmental Model (GDEM), was studied and used with altimetry. It was found that the variation in the signal amplitude of altimetric residuals corresponding to mesoscale variability is between 5 and 15 cm. In spite of this small amplitude, the signal is correlated with the oceanographic structure. Dynamic heights computed from CTD cross sections taken along the altimeter ground tracks were used to improve the empirical geoid. The altimetric signal results, namely, across the Norwegian current and the Faeroe-Shetland inflow, indicate the possibility of monitoring the inflow by altimetery. In analogy to the CTD method discussed, dynamic height was computed from GDEM data and was used for correcting the altimeter data. This method can be useful in some areas as a first approximation in the improvement of the geoid. In spite of the detection by altimeter of the stronger and larger mesoscale features south of the Iceland-Faeroe front, the front itself was not easily detected because of tidal contamination. Statistical results (namely variance) derived from altimetry indicate the larger variability to be near the frontal regions. GRA

N93-14281 Stevens Inst. of Tech., Hoboken, NJ.
A CONCURRENT REAL-TIME AUTONOMOUS MOBILE ROBOT PROGRAMMING SYSTEM Ph.D. Thesis
Huiming Yu 1992 189 p
Avail: Univ. Microfilms Order No. DA9227899

Autonomous Mobile Robots (AMRs) often operate in unknown environments and their control program execution sequence depends on unpredictable external events. Many action sequences may be required simultaneously such as camera panning, curve-linear motion and manipulator retraction. AMRs therefore require a Concurrent Real-time autonomous mobile Robot Programming System (CRRPS) with a high degree of concurrency and real-time response in order to efficiently specify the robot's actions and responses to external stimuli. An intial design and implementation of such a CRRPS is presented in this dissertation. A unique feature of the CRRPS is that it treats the AMR's hardware actions and software processes in a homogeneous manner. A concurrent module is proposed that offers the means for parallel programming. The COMBINATION communication model sets up a unified communication protocol for hardware devices and concurrent software processes. A new language structure, the SYSTEM DESCRIPTOR, is presented that exhibits powerful functionality--namely making the application program independent from hardware. Therefore, the CRRPS allows for changes in the robot's hardware configuration without a need to modify the users' programs. An efficient scheduling policy, the Reexecutive Scheduling Algorithm, is presented for scheduling multi-processes with varying priorities. The developed Real-Time Executive includes a Preemptive Priority algorithm which allows the system to respond to urgent events within specified requirement times. An Optimal Obstacle Avoidance algorithm has been developed and incorporated in a Dynamic Path Planning algorithm and has been implemented to verify the characteristic features of CRRPS. Dissert. Abstr.

N93-14399 Purdue Univ., West Lafayette, IN.
L2 AND L-INFINITY MULTIOBJECTIVE CONTROL FOR LINEAR SYSTEMS Ph.D. Thesis
Guoming Zhu 1992 172 p
Avail: Univ. Microfilms Order No. DA9229216

In this research the Block diagonal Output Covariance Constraint (BOCC) problem is addressed for both continuous and discrete periodic systems. The stochastic BOCC problem is defined for white noise inputs, and the deterministic BOCC for L2 inputs. The L2 to L-infinity gains of continuous and discrete periodic systems pave the way to equate stochastic and deterministic BOCC problems. The BOCC algorithm developed in this research has been applied to design controllers for the JPL's Control Technology Experiment Facility. The covariance control theory has been extended to the discrete periodic case. New and less conservative bounds are derived for six different robustness problems of continuous and discrete periodic systems: L2 to L-infinity gains, time-varying structured and unstructured parameter variations. This is the first treatment for the discrete periodic case. All of the new bounds are shown to be directly related to the properties of the closed loop covariance of a related system driven by white noise. The BOCC controllers minimize the control power subject to output covariance inequality constraints on each output group. The theoretical contribution of this research is an iterative controller design algorithm to solve the BOCC problem with the proof of feasibility. Due to the equivalence of the stochastic and deterministic BOCC problems, the algorithm can also be applied to satisfy L-infinity constraints on multiple outputs. The OBCC problem is addressed for both continuous and discrete periodic systems. The BOCC algorithm can be also applied to design multirate controllers guaranteeing the output covariance or L-infinity bounds, because a multirate sampling system can be put into a discrete periodic model. Psuedo-decentralized multirate controllers can be designed by the algorithm to reduce the amount of real time computation. A design strategy is proposed which integrates both model reduction and BOCC controller synthesis. The corresponding software has been well developed for this strategy, which has been applied to the JPL LSCL Experiment Facility, a large flexible structure. The covariance control theory characterizes the set of all positive definite covariance functions that a linear discrete periodic system with a fixed order controller may process. The controller assigning such covariance function to any linear discrete periodic system is explicitly in the closed form. Dissert. Abstr.

N93-14409# Carnegie-Mellon Univ., Pittsburgh, PA. Dept. of Electrical and Computer Engineering.
NEURAL NETS FOR SCENE ANALYSIS Final Report, 31 Mar. 1989 - 30 Sep. 1992
David Casasent Sep. 1992 64 p
(Contract DAAH01-89-C-0418; ARPA Order 6671)
(AD-A255976; DARPA-RD/0992) Avail: CASI HC A04/MF A01

This project involved various new optical and digital neural net techniques for scene analysis. The original neural net concept was the adaptive clustering neural net (ACNN). This is detailed in Chapter 2. Our original associative processor concept was the Ho-Kashyap neural net. This is detailed in Chapter 3. Our overview of how neural nets should be used in scene analysis is detailed in Chapter 4. This also includes an overview of our two new higher order neural nets. Our new PQNN neural net (which produces higher-order decision surfaces much more efficiently than other neural nets) is noted in Chapter 5. To achieve high performance on systems with components with analog accuracy and various nonidealities, we developed a new algorithm and technique discussed in Chapter 6. We have fabricated our optical laboratory neural net and tested it on several different case studies and achieved excellent results as noted in Chapter 7. GRA

N93-14445 Purdue Univ., West Lafayette, IN.
INTELLIGENT PATH PREDICTION FOR VEHICULAR TRAVEL Ph.D. Thesis
James Alan Krozel 1992 102 p
Avail: Univ. Microfilms Order No. DA9229147

This thesis presents a methodology for intelligent path prediction, predicting the motion of an observed vehicle by reasoning about the actions taken by the operator of the vehicle. The thesis considers only the problem of tracking a vehicle performing a transit mission, a mission that proceeds from a start location to a goal location guided by an intelligent planning criterion. Intelligent planning criteria are modeled by generalized cost criteria, which allow for basis cost criterion, for example, distance, visibility, or safety, to be considered, or convex combinations of such basis cost criteria to be considered. Two main investigations are addressed. The first investigation is to develop a method for identifying a decision-making strategy that seemingly explains the observed vehicle's motion. The start location is assumed to be known, the goal location is assumed to be in a given set of candidate goal locations, and an intelligent planning criterion is assumed to be guiding the vehicle. Given the history of the observed vehicle's path, the objectives are to (1) select the cost criterion that best explains the observed motion, (2) predict the goal location of the vehicle, and (3) predict the future path leading to the goal location. In solving this problem, search pointer information provided by reverse graph searches is exploited. Best fitting a goal location and cost criterion pair to explain the decision-making strategy of the vehicle is accomplished through a path similarity correlation measure comparing the observed path data to search gradient direction information. The second investigation is to develop a method of automatically proposing a candidate goal location for the observed vehicle. Given the cost criteria that best explains the history of the observed vehicle's path, the objectives are to (1) propose a region of plausible goal locations and (2) rank the locations in the set of plausible goal locations based on some heuristic merit. In solving this problem, search pointer information provided by forward graph searches is exploited. Establishing the region of plausible goal locations is accomplished using search tree results. Finally, the region of plausible goal location is analyzed to rank the locations based on heuristic merit. Dissert. Abstr.

N93-14470 California Univ., Berkeley.
ADAPTIVE CONTROL OF NONLINEAR NONMINIMUM PHASE SYSTEMS Ph.D. Thesis
Swaminathan Gopalswamy 1991 130 p
Avail: Univ. Microfilms Order No. DA9228668

We consider square, nonlinear systems, affine in the input. Furthermore, we assume that the systems have a (locally) well defined relative degree (i.e., in a sense, the input output dynamics is invertible). Then, using standard techniques, it is possible to make y track y(sub d) asymptotically, where y(sub d) is any smooth desired trajectory. Two issues involved in tracking such systems, using the input-output invertibility, are addressed in this dissertation: (1) The dynamics of the output reflects only a part of the dynamics of the entire system. The remaining part of the system dynamics is called the internal dynamics (when the output is held identically zero, it is the zerodynamics). If this internal dynamics is unstable, the system is said to be non-minimum phase (analogous to right half plane transmission zeros in linear system). In this dissertation, a methodology is proposed to deal with systems that have unstable, or unacceptable zero dynamics. For

a class of such systems and trajectories an ideal internal dynamics, i.e., a particular solution of the internal dynamics that is acceptable, is identified. Then, the ideal internal dynamics is made attractive by an appropriate output redefinition. (2) Tracking is made robust to uncertainties satisfying some conditions, by either using increased control gains or through adaptive estimation techniques. In this dissertation, a robust adaptive control methodology is presented for MIMO systems, where all constant uncertainties that appear linearly in the input output dynamics are adaptively estimated, while other uncertainties and disturbances satisfying a matching condition are accounted for by using appropriate control gains. The development of the two issues enable one to combine the techniques to apply adaptive control to non-minimum phase systems. The theory developed is illustrated through numerical simulations on the pitch axis dynamics of an AFTI-F16, a high performance aircraft. The pitch axis dynamics of the AFTI-F16 suffers from undesirable internal dynamics (zerodynamics), and the simulations demonstrate the effectiveness of the output-redefinition approach. Further, we present simulations where the aerodynamic coefficients related to the control surfaces are adaptively estimated, and improved tracking is achieved. Dissert. Abstr.

N93-14519# Mitre Corp., Bedford, MA.
THE 1992 SUMMER SIGAda AIWG WORKSHOP APPLICATIONS EXPERIENCES AND LESSONS LEARNED PANEL MESSAGE FROM THE PANEL CHAIR
Janet F. Johns Sep. 1992 43 p Workshop held 24-27 Jun. 1992
(AD-A256188; Mitre-92-103) Avail: CASI HC A03/MF A01

On 24-27 June 1992, the Association for Computing Machinery (ACM) Special Interest Group for Ada (SIGAda) Artificial Intelligence Working Group (AIWG) held a workshop to discuss Ada real-time and AI issues. Panels organized for the workshop focused on blackboard architectures, experiences and lessons learned, real-time development approaches and issues, and Ada 9X issues for AI systems. This paper assesses the state-of-the-art for AI development processes and provides a summary of the related workshop discussions from the experiences and lessons learned panel. Issues associated with requirements analysis, design methodologies, development techniques, test and validation, and maintainability are discussed for AI applications and for AI with Ada applications. GRA

N93-14525# Army Command and General Staff Coll., Fort Leavenworth, KS.
THE EVOLUTION OF ARTIFICIAL INTELLIGENCE AND EXPERT COMPUTER SYSTEMS IN THE ARMY M.S. Thesis
Rickey L. Hanson 5 Jun. 1992 143 p
(AD-A255221) Avail: CASI HC A07/MF A02

This study is an analysis of the evolution of artificial intelligence and expert computer systems in the U.S. Army and the role the Army should play in the future evolution of these technologies. This study investigates the Army's approach to the development and use of these computer systems. It will assess whether the Army should play a leadership or a follower role in the development of these systems. The Army's decision to either lead or follow in these technologies will have significant effects on the limited resources of tomorrows smaller and less resourced force. This study will examine these issues given the trend in reduced fiscal resources and personnel. The civilian sector's development and use of these systems are evaluated to determine benefits to the Army through the use of these systems. The adaptability of these systems to various Army requirements are evaluated as are the near and far term costs of these systems. This study concludes that the U.S. Army should play a follower role in the future evolution of both expert computer systems and artificial intelligence. The Army should exploit current technologies and help guide the civilian community in the research and development of military applications. GRA

N93-14533# Army Armament Research, Development and Engineering Center, Watervliet, NY. Benet Lab.
MACHINE INTELLIGENCE, A FOREWORD: THE BRAIN AS ELECTRONIC CIRCUITRY; ELECTRONIC CIRCUITRY AS A BRAIN Final Report
Mark Johnson and Raymond Scanlon Jun. 1992 15 p
(AD-A255283; ARCCB-TR-92030) Avail: CASI HC A03/MF A01

We introduce a series of reports that attempt to resolve the conflict between the desire to build a thinking machine and the claimed impossibility of discussing the general design in rational language. We present the basic structure of our investigation and its position in current controversy without supporting arguments. We look at nonliving intelligence and the biological brain through a smoky glass and see--electronic circuitry. This is the electronic age. We approach the design of a machine brain as a problem in reverse engineering. GRA

N93-14551# Boston Univ., MA. Center for Adaptive Systems.
DEVELOPMENT OF NEURAL NETWORK ARCHITECTURES FOR SELF-ORGANIZING PATTERN RECOGNITION AND ROBOTICS Annual Technical Report No. 2, 15 Dec. 1990 - 14 Feb. 1992
Gail A. Carpenter and Stephen Grossberg Jul. 1992 14 p
(Grant AF-AFOSR-0083-90)
(AD-A255433; AFOSR-92-0835TR) Avail: CASI HC A03/MF A01

During the second year of the DARPA ANNT Program contract, new neural network architectures were developed to carry out autonomous real-time preprocessing, segmentation, recognition, timing, and control of both spatial and temporal inputs. These architectures contribute to: (1) preprocessing of visual form and motion signals; (2) preprocessing of acoustic signals; (3) adaptive pattern recognition and categorization in an unsupervised learning context; (4) adaptive pattern recognition and prediction in a supervised learning context; (5) processing of temporal patterns using working memory networks, with applications to 3-D object recognition; (6) adaptive timing for task scheduling; and (7) adaptive sensory-motor control using head-centered spatial representations of 3-D target position. GRA

N93-14598# University of Southern California, Los Angeles. Dept. of Electrical Engineering.
STABILITY AND ADAPTATION OF NEURAL NETWORKS Final Report, 1 Aug. 1988 - 31 Dec. 1991
Bart Kosko 23 Sep. 1992 120 p
(Grant AF-AFOSR-0236-88)
(AD-A256227; AFOSR-92-0885TR) Avail: CASI HC A06/MF A02

This research studied the stability, adaptation, and robustness of neural networks and fuzzy systems. Key results include the stability of random adaptive bidirectional associative memories (RABAM's) and neural-fuzzy competitive and differential-Hebbian ABAM's; the introduction, analysis, and testing of the differential competitive learning law; new theorems on the stochastic convergence of competitive learning for vector quantization; a universal approximation theorem for fuzzy systems; unsupervised schemes for Teaming fuzzy rules with neural networks with tests on truck-and-trailer control systems; and coding and compression of still images and image sequences. GRA

N93-14656# Pittsburgh Univ., PA. Learning Research and Development Center.
ANALYSIS OF SYMBOLIC MODELS OF COGNITION PROJECT (ASPM-PITT) Quarterly Progress Report, Apr. - Jun. 1992
Kurt VanLehn 11 Sep. 1992 2 p
(Contract N00014-91-J-1529)
(AD-A255929) Avail: CASI HC A01/MF A01

This letter is a quarterly progress report for the University of Pittsburgh part of the Analysis of Symbolic Nodels of Congnition project (ASPM-Pitt), grant number N00014-91-J-1529. It covers the period April, 1992 to June, 1992. GRA

N93-14701* National Aeronautics and Space Administration. Goddard Space Flight Center, Greenbelt, MD.
DRIVEN SHIELDING CAPACITIVE PROXIMITY SENSOR Patent
John M. Vranish, inventor (to NASA) and Robert L. McConnell, inventor (to NASA) 24 Nov. 1992 5 p Filed 6 Jun. 1991 Supersedes N91-28785 (29 - 20, p 3390)
(NASA-Case-GSC-13377-1; US-Patent-5,166,679;
US-Patent-Appl-SN-710845; US-Patent-Class-340-870.37;
US-Patent-Class-324-687; US-Patent-Class-340-562;
Int-Patent-Class-G08C-19/10; Int-Patent-Class-G08B-13/26) US Patent and Trademark Office

A capacitive proximity sensing element, backed by a reflector driven at the same voltage as and in phase with the sensor, is used to reflect the field lines away from a grounded robot arm towards an intruding object, thus dramatically increasing the senors's range and sensitivity.
Official Gazette of the U.S. Patent and Trademark Office

N93-14765*# National Aeronautics and Space Administration. Ames Research Center, Moffett Field, CA.
PURPOSIVE DISCOVERY OF OPERATIONS
Michael H. Sims and John L. Bresina (Sterling Federal Systems, Inc., Moffett Field, CA.) 21 Jul. 1992 38 p
(NASA-TM-108116; FIA-92-27; NAS 1.15:108116) Avail: CASI HC A03/MF A01

The Generate, Prune & Prove (GPP) methodology for discovering definitions of mathematical operators is introduced. GPP is a task within the IL exploration discovery system. We developed GPP for use in the discovery of mathematical operators with a wider class of representations than was possible with the previous methods by Lenat and by Shen. GPP utilizes the purpose for which an operator is created to prune the possible definitions. The relevant search spaces are immense and there exists insufficient information for a complete evaluation of the purpose constraint, so it is necessary to perform a partial evaluation of the purpose (i.e., pruning) constraint. The constraint is first transformed so that it is operational with respect to the partial information, and then it is applied to examples in order to test the generated candidates for an operator's definition. In the GPP process, once a candidate definition survives this empirical prune, it is passed on to a theorem prover for formal verification. We describe the application of this methodology to the (re)discovery of the definition of multiplication for Conway numbers, a discovery which is difficult for human mathematicians. We successfully model this discovery process utilizing information which was reasonably available at the time of Conway's original discovery. As part of this discovery process, we reduce the size of the search space from a computationally intractable size to 3468 elements.
Author

N93-14783# Yale Univ., New Haven, CT. Dept. of Computer Science.
RECURSIVELY GENERATED NETWORKS AND DYNAMICAL LEARNING Final Report
Eric Mjolsness 31 Dec. 1991 50 p
(Grant AF-AFOSR-0240-88)
(AD-A255441; AFOSR-92-0831TR) Avail: CASI HC A03/MF A01

Much of the research was based on the premise that mathematical methods and notation associated with constrained optimization should be used to specify a neural net, which can then be compiled to diverse implementations. But where do they get such a compiler? And what are the details of this mathematical notation? We have made substantial progress on these research questions. We have developed mathematical methods that can transform one algebraic NN description into another, more implementable one. These developments were attained by serious work in the applied mathematics of neural nets. They can form the basis of a neural compiler because they address most of the major NN compilation and implementation issues. But they do not yet suffice. We are accumulating the research in a neural simulator. It can be expanded into a semi-automatic compiler: a neural net design and implementation environment based on mathematical methods. We have developed a mathematical notation (not yet a formal language) for describing complex problem domains in terms of constrained optimization problems. The optimization problems can be solved by neural nets.
GRA

N93-14786# Rochester Univ., NY. Dept. of Philosophy.
PROBABILISTIC INFERENCE
Henry E. Kyburg, Jr. 1992 11 p
(Contract DAAB10-86-C-0567)
(AD-A255471; CSWD-92-TRF-0050) Avail: CASI HC A03/MF A01

It is important to distinguish probabilistic reasoning from probabilistic inference. Probabilistic reasoning may concern the manipulation of knowledge of probabilities in the context of decision theory, or it may involve the updating of probabilities in the light of new evidence via Bayes' theorem or some other procedure. Both of these operations are essentially deductive in character. Contrasted with these procedures of manipulating or computing with probabilities, is the use of probabilistic rules of inference: rules that lead from one sentence (or a set of sentences) to another sentence, but do so in a way that need not be truth preserving. One could attempt to get along without probabilistic inference in AI, but it would be very difficult and unnatural. Instances of such rules are several classes of inference rules associated with statistics, and some rules discussed by philosophers. In artificial intelligence the rules that fall into this category are (mainly) default rules; these are not generally construed probabilistic, but obviously default rules that more often lead you astray than to the truth would be poor ones.
GRA

N93-14818# Oak Ridge National Lab., TN.
SENSOR-BASED DRIVING OF A CAR WITH FUZZY INFERENCING VLSI CHIPS AND BOARDS
F. G. Pin and Y. Watanabe 1992 8 p Presented at the ISRAM 1992: 4th International Symposium on Robotics and Manufacturing, Sante Fe, NM , 11-13 Nov. 1992
(Contract DE-AC05-84OR-21400)
(DE92-017819; CONF-921181-1) Avail: CASI HC A02/MF A01

This paper discusses the sensor-based driving of a car in a-priori unknown environments using 'human-like' reasoning schemes. The schemes are implemented on custom-designed VLSI fuzzy inferencing boards and are used to investigate two control modes for driving a car on the basis of very sparse and imprecise range data. In the first mode, the car navigates fully autonomously, while in the second mode, the system acts as a driver's aid providing the driver with linguistic (fuzzy) commands to turn left or right and speed up, slow down, stop, or back up depending on the obstacles perceived by the sensors. Experiments with both modes of control are described in which the system uses only three acoustic range (sonar) sensor channels to perceive the environment. Sample results are presented which illustrate the feasibility of developing autonomous navigation systems and robust safety enhancing driver's aid using the new fuzzy inferencing VLSI hardware and 'human-like' reasoning schemes.
DOE

N93-15083# Universiteit Twente, Enschede (Netherlands). Dept. of Computer Science.
PROCESSOR CONTROLPATH MICROARCHITECTURE SYNTHESIS BASED ON THE A(ASTERISK) ALGORITHM
A. J. W. M. tenBerg Feb. 1992 24 p
(Memo-INF-92-10; ETN-92-92430) Copyright Avail: CASI HC A03/MF A01

The integration of methods from artificial intelligence in the synthesis of microarchitectures for processor control paths is described. For control path and finite state machine synthesis many algorithms are known. Unfortunately all these algorithms perform an optimization or decomposition of a specific microarchitecture. A general synthesis method, however, requires exploration of the design space for optical microarchitectures. Because existing algorithms are all bound to specific microarchitectures, their actions are local from a design space point of view. Therefore, it is very difficult to merge these algorithms to one global synthesis algorithm. However, with the introduction of a design state abstraction for a microarchitecture, the synthesis problem can be formulated as a search problem in a design state space. In this space, existing synthesis algorithms act as design actions and perform local design state transitions. Artificial intelligence provides the global synthesis process with tools for state space search and action planning. These obtain the shortest path of design actions to a user defined target design state. For this design state space search the A(star) algorithm is implemented. The prototype system implements only a limited number of design actions, but demonstrates the power and large flexibility of this approach.
ESA

N93-15147 Georgia Inst. of Tech., Atlanta.
LEARNING POSITION AND FORCE CONTROL FOR MECHANICAL MANIPULATORS Ph.D. Thesis
Kennon Hardy Guglielmo 1992 109 p
Avail: Univ. Microfilms Order No. DA9231729

This dissertation addresses the application of 'learning' control to robotic manipulators. Learning control attempts to estimate the feed-forward input necessary to force the robot to perform some desired task with zero error. This feedforward signal is estimated in a general way so that very little modeling or identification of the system is involved. The tasks may be position control described in either the joint or Cartesian space of the manipulator, or force control as the robot interacts with an object. Two basic forms of the learning control law are developed. This first is a 'repetitive' controller which requires the desired trajectory to be cyclic with a finite period. The second is a 'non-repetitive' scheme which relaxes the restriction of periodicity of the task, but requires some very general modeling of the system. Stability of the learning algorithms is proven using the Lyapunov approach, and all of the controllers are implemented on an

actual IBM 7545 robot. Performance comparisons to simple classical feedback algorithms as well as some high performance 'computed-torque' and adaptive controllers show that the learning schemes are capable of obtaining significantly better tracking in all cases. All of the new learning controllers presented are computationally and memory efficient, and are easily implemented on today's digital hardware. In fact, one of the 'non-repetitive' schemes can be viewed as an efficient form of a 'neural network' capable of being implemented in real-time on a low cost microcomputer. Although a robotic manipulator was chosen as the test bed for implementation studies of these learning controllers, many other nonlinear systems may benefit from application of these algorithms. In fact, the extension of the basic topology of the learning scheme to these different areas of robotic control demonstrates the algorithm's easy applicability. The work presented in formulating the controllers in terms of the nonlinear equations of motion of a mechanical manipulator provides an outline for extension to other systems. Dissert. Abstr.

N93-15148 Georgia Inst. of Tech., Atlanta.
ROBUST CONTROL DESIGN FOR UNCERTAIN NONLINEAR DYNAMIC SYSTEMS Ph.D. Thesis
Myung-Chul Han 1992 168 p
Avail: Univ. Microfilms Order No. DA9231730

The class of uncertain systems considered in this thesis is nonlinear, with non-autonomous nominal portion, and with (possibly past) time-varying uncertainties. The uncertainties are assumed to lie within prescribed bounded sets, whose bounds are known or unknown. No statistical information of the uncertainties is imposed. Only the deterministic information of the uncertainties (e.g., their possible bounds) is utilized for the control design and the resulting system performance is described in a deterministic manner (e.g., practical stability). The major contribution of this thesis can be divided in five parts. First, a new controller design which invokes a polynomial state dependent gain is proposed. As compared with the previous work, more design flexibility and other advantages of the new control emerged. Second, two classes of decentralized robust controls, namely, non-adaptive and adaptive, are constructed for interconnected uncertain nonlinear systems with cone-bounded interconnections. In the non-adaptive robust control, only the possible bound of the uncertainty is assumed to be known. In the adaptive robust control, the designer does not need to know this bound a priori. Third, a new decentralized control design is introduced for interconnected uncertain large-scale systems where the interconnections as well as the nominal parts of the subsystems are nonlinear. This setting renders the previous work in this area as special cases. The new control design explicitly takes this arbitrary interconnection structure into account. Fourth, the combination of two control techniques is explored. The first is feedback linearization control which addresses a known nonlinear system. The second is the robust control which is especially suitable if any uncertainty and/or time-varying factors are involved in the nonlinear dynamics. We show how to combine these two controllers to stabilize a class of large-scale nonlinear uncertain systems. Fifth, two classes of robust composite control schemes, position and hybrid, are proposed for flexible-joint manipulators. Two classes of robust control schemes are first constructed for the rigid counterpart of the flexible-joint robots and then velocity control terms are added to the robust control law to stabilize the elastic vibrations at the joint. A singular perturbation approach for the stability study is adopted.
Dissert. Abstr.

N93-15149 Florida Inst. of Tech., Melbourne.
SAMPLED-DATA CONTROL AND ROBUST CONTROL FOR DISCRETE-TIME SYSTEMS Ph.D. Thesis
Hsing-Hsin Huang 1992 129 p
Avail: Univ. Microfilms Order No. DA9231104

Recently, research in optimal robust control theory is being extensively explored. In this dissertation, optimal robust control system design methods are developed in two specific areas: (1) robust analysis and synthesis of discrete-time dynamic and static output feedback controllers. For the sampled-data Kalman filter and Linear Quadratic Gaussian (LQG) problems, equivalent discrete-time estimation and control problems are derived based upon conversions of the continuous-time systems. An averaging A/D device is used to account for noisy measurements. This results in averaged measurements that depend on the delayed samples of the state. An augmented model is developed to include the discretized states as well as the averaged measurements so that the delay effect can be explicitly eliminated. In this manner, the equivalent discrete-time problems are shown to be of increased dimension. The fixed-structure optimal projection approach for reduced-order, discrete-time estimation and control is applied to the equivalent discrete-time problems in order to characterize fixed-order (i.e., reduced- and full-order) estimators and controllers. Two properties of sampled-data estimation and control are addressed. First, for the sampled-data estimation problem involving unstable dynamics, a generalized-hold architecture framework is shown to be essential for assuring that the least-squares state-estimation error criterion is bounded. Two examples are presented to illustrate that a zero-order-hold reconstruction architecture may lead to an unbounded state-estimation error criterion. Next, the duality between sampled-data control and estimation is investigated. It is shown that there is no duality between the sampled-data full-state feedback control and the full-order sampled-data estimation. In the second part of this dissertation, we consider the robust analysis and synthesis problems via fixed-order dynamic compensation. Two distinct frameworks suggested by recent work on continuous-time and discrete-time robust stability are exploited to construct fixed and parameter dependent quadratic Lyapunov bounds for uncertain discrete-time systems. These bounds are utilized in conjunction with the guaranteed cost approach to guarantee robust stability with a robust performance bound. The principal results involve sufficient conditions for characterizing robust full- and reduced-order controllers with worst case performance bounds.
Dissert. Abstr.

N93-15258# Massachusetts Inst. of Tech., Lexington.
NEURAL NETWORK ARCHITECTURES FOR GENERAL IMAGE RECOGNITION
Robert L. Harvey, Paul N. DiCaprio, and Karl G. Heinemann 21 Jul. 1992 129 p
(Contract F19628-90-C-0002)
(AD-A256017; MIT-TR-92-100; ESC-TR-92-100) Avail: CASI HC A07/MF A02

As part of Lincoln Laboratory's research on neural network technology, a general-purpose machine vision system was designed that can learn to recognize diverse objects. This system models human vision, primarily with neural networks, and the learning is by example. The system was tested on two disparate classes of objects, military vehicles and human cells, with video images of natural scenes. These objects were chosen because large databases are available and because most researchers judge them to be unrelated. The system was trained and tested with 40 images of military vehicles. After training with 18 images, the system was able to recognize the tanks, howitzers, and armored personnel carriers of the remaining images without error. Pathologists at Lahey Clinic Medical Center collaborated in the cytology study where the system was trained and tested on 156 cell images from human cervical Pap smears. After training with 118 images, the system correctly classified all of the other cells as normal or abnormal (that is, precancer). These results are preliminary because the number of military vehicles and Pap smear samples was small. Nonetheless, the results are extremely encouraging and clearly indicate that additional development of the system is warranted. We note that the architecture of the system is applicable to many civilian and military tasks. The application of the system to a specific task requires appropriate training. GRA

N93-15286*# National Aeronautics and Space Administration. Ames Research Center, Moffett Field, CA.
MINIMIZING CONFLICTS: A HEURISTIC REPAIR METHOD FOR CONSTRAINT-SATISFACTION AND SCHEDULING PROBLEMS
Steve Minton (Sterling Federal Systems, Inc., Moffett Field, CA.), Mark Johnston (Space Telescope Science Inst., Baltimore, MD.), Andrew Philips (Sterling Federal Systems, Inc., Moffett Field, CA.), and Phil Laird Jun. 1992 34 p
(NASA-TM-108121; FIA-92-21; NAS 1.15:108121) Avail: CASI HC A03/MF A01

This paper describes a simple heuristic approach to solving large-scale constraint satisfaction and scheduling problems. In this approach one starts with an inconsistent assignment for a set of variables and searches through the space of possible repairs. The search can be guided by a value-ordering heuristic, the min-conflicts heuristic, that attempts to minimize the number of constraint violations after each step. The heuristic can be used with a variety of different search strategies. We demonstrate empirically that on

the n-queens problem, a technique based on this approach performs orders of magnitude better than traditional backtracking techniques. We also describe a scheduling application where the approach has been used successfully. A theoretical analysis is presented both to explain why this method works well on certain types of problems and to predict when it is likely to be most effective. Author

N93-15287*# National Aeronautics and Space Administration. Ames Research Center, Moffett Field, CA.

SCHEDULING AND RESCHEDULING WITH ITERATIVE REPAIR

Monte Zweben, Eugene Davis (RECOM Technologies, Inc., Moffett Field, CA.), Brian Daun (RECOM Technologies, Inc., Moffett Field, CA.), and Michael Deale (Lockheed Space Operations Co., Washington, DC.) Apr. 1992 30 p

(NASA-TM-108120; FIA-92-16; NAS 1.15:108120) Avail: CASI HC A03/MF A01

This paper describes the GERRY scheduling and rescheduling system being applied to coordinate Space Shuttle Ground Processing. The system uses constraint-based iterative repair, a technique that starts with a complete but possibly flawed schedule and iteratively improves it by using constraint knowledge within repair heuristics. In this paper we explore the tradeoff between the informedness and the computational cost of several repair heuristics. We show empirically that some knowledge can greatly improve the convergence speed of a repair-based system, but that too much knowledge, such as the knowledge embodied within the MIN-CONFLICTS lookahead heuristic, can overwhelm a system and result in degraded performance. Author

N93-15288*# National Aeronautics and Space Administration. Ames Research Center, Moffett Field, CA.

RESCHEDULING WITH ITERATIVE REPAIR

Monte Zweben, Eugene Davis (RECOM Technologies, Inc., Moffett Field, CA.), Brian Daun (Lockheed Space Operations Co., Washington, DC.), and Michael Deale (Lockheed Space Operations Co., Washington, DC.) Apr. 1992 17 p

(NASA-TM-108119; FIA-92-15; NAS 1.15:108119) Avail: CASI HC A03/MF A01

This paper presents a new approach to rescheduling called constraint-based iterative repair. This approach gives our system the ability to satisfy domain constraints, address optimization concerns, minimize perturbation to the original schedule, produce modified schedules, quickly, and exhibits 'anytime' behavior. The system begins with an initial, flawed schedule and then iteratively repairs constraint violations until a conflict-free schedule is produced. In an empirical demonstration, we vary the importance of minimizing perturbation and report how fast the system is able to resolve conflicts in a given time bound. We also show the anytime characteristics of the system. These experiments were performed within the domain of Space Shuttle ground processing. Author

N93-15289*# National Aeronautics and Space Administration. Ames Research Center, Moffett Field, CA.

LEARNING TO IMPROVE ITERATIVE REPAIR SCHEDULING

Monte Zweben and Eugene Davis (RECOM Technologies, Inc., Moffett Field, CA.) Jan. 1992 17 p

(NASA-TM-108118; FIA-92-14; NAS 1.15:108118) Avail: CASI HC A03/MF A01

This paper presents a general learning method for dynamically selecting between repair heuristics in an iterative repair scheduling system. The system employs a version of explanation-based learning called Plausible Explanation-Based Learning (PEBL) that uses multiple examples to confirm conjectured explanations. The basic approach is to conjecture contradictions between a heuristic and statistics that measure the quality of the heuristic. When these contradictions are confirmed, a different heuristic is selected. To motivate the utility of this approach we present an empirical evaluation of the performance of a scheduling system with respect to two different repair strategies. We show that the scheduler that learns to choose between the heuristics outperforms the same scheduler with any one of two heuristics alone. Author

N93-15290*# National Aeronautics and Space Administration. Ames Research Center, Moffett Field, CA.

A BEGINNER'S GUIDE TO BELIEF REVISION AND TRUTH MAINTENANCE SYSTEMS

Cindy L. Mason Oct. 1992 19 p

(NASA-TM-108117; FIA-92-33; NAS 1.15:108117) Avail: CASI HC A03/MF A01

This brief note is intended to familiarize the non-TMS audience with some of the basic ideas surrounding classic TMS's (truth maintenance systems), namely the justification-based TMS and the assumption-based TMS. Topics of further interest include the relation between non-monotonic logics and TMS's, efficiency and search issues, complexity concerns, as well as the variety of TMS systems that have surfaced in the past decade or so. These include probabilistic-based TMS systems, fuzzy TMS systems, tri-valued belief systems, and so on. Author

N93-15291*# National Aeronautics and Space Administration. Ames Research Center, Moffett Field, CA.

AN APPLICATION OF ARTIFICIAL INTELLIGENCE TO AUTOMATIC TELESCOPES

Keith Swanson, Mark Drummond (Sterling Software, Moffett Field, CA.), and John Bresina (Sterling Software, Moffett Field, CA.) Jul. 1992 12 p Repr. from Proceedings of the Remote Observing Workshop, Tuscon, AZ, Apr. 1992 and Proceedings of the Steerable Automatic Lunar Ultraviolet Telescope Explorer (SALUTE) Workshop, NASA-Ames, Moffett Field, CA, May 1992

(NASA-TM-108115; FIA-92-26; NAS 1.15:108115) Avail: CASI HC A03/MF A01

Automatic Photoelectric Telescopes (APT's) allow an astronomer to be removed form the telescope site in both time and space. APT's 'execute' an observation program (a set of observation requests) expressed in an ASCII-based language (ATIS) and collect observation results expressed in this same language. The observation program is currently constructed by a Principal Astronomer from the requests of multiple users; the execution is currently controlled by a simple heuristic dispatch scheduler. Research aimed at improving the use of APT's is being carried out by the Entropy Reduction Engine (ERE) project at NASA Ames. The overall goal of the ERE project is the study and construction of systems that integrate planning, scheduling, and control. This paper discusses the application of some ERE technical results to the improvement of both the scheduling and the operation of APT's. Author

N93-15292*# National Aeronautics and Space Administration. Ames Research Center, Moffett Field, CA.

MATE: THE MULTI-AGENT TEST ENVIRONMENT

Cindy L. Mason Jun. 1992 12 p

(NASA-TM-108114; FIA-92-25; NAS 1.15:108114) Avail: CASI HC A03/MF A01

In this report we present the Multi-Agent Test Environment, MATE. MATE is a collection of experiment management tools for assisting in the design, testing, and evaluation of distributed problem-solvers. It provides the experimenter with an automated tool for executing and monitoring experiments choosing among rule bases, number of agents, communication strategies, and inference engines. Using MATE the experimenter can run a series of distributed problem-solving experiments without human intervention. Author

N93-15293*# National Aeronautics and Space Administration. Ames Research Center, Moffett Field, CA.

KNOWLEDGE AND REGULARITY IN PLANNING

John A. Allen (California Univ., Irvine.), Pat Langley, and Stan Matwin (Ottawa Univ., Ontario) Jul. 1992 13 p

(NASA-TM-108113; FIA-92-24; NAS 1.15:108113) Avail: CASI HC A03/MF A01

The field of planning has focused on several methods of using domain-specific knowledge. The three most common methods, use of search control, use of macro-operators, and analogy, are part of a continuum of techniques differing in the amount of reused plan information. This paper describes TALUS, a planner that exploits this continuum, and is used for comparing the relative utility of these methods. We present results showing how search control, macro-operators, and analogy are affected by domain regularity and the amount of stored knowledge. Author

N93-15352# Harvard Univ., Cambridge, MA.
DYNAMICS OF ANALOG ELECTRONIC NEURAL NETWORKS Final Report, Jun. 1989 - Jun. 1992
Frederick R. Waugh 31 Aug. 1992 11 p
(Contract DAAL03-89-G-0076)
(AD-A257019; ARO-27007.8-EL-F) Avail: CASI HC A03/MF A01

We review recent results on dynamics and stability of analog neural networks and discuss their application to associative memory and visual processing. Stability criteria for these networks, guarantee convergence to fixed-point attractors under continuous-time and discrete-time, parallel updating. For associative memory, phase diagrams describing different attractor types are discussed, and it is shown that reducing analog transfer function steepness improves network performance. For visual processing, a two-dimensional, translation-invariant network is described. The network detects image features using a novel architecture that greatly reduces network wiring. GRA

N93-15385# Sandia National Labs., Albuquerque, NM.
SMART: A MODULAR ARCHITECTURE FOR ROBOTICS AND TELEOPERATION
R. J. Anderson 1992 8 p Presented at the ISRAM 1992: Fourth International Symposium on Robotics and Manufacturing, Santa Fe, NM, 11-13 Nov. 1992
(Contract DE-AC04-76DP-00789)
(DE92-040985; SAND-92-1632C; CONF-921181-3) Avail: CASI HC A02/MF A01

This paper introduces SMART: Sandia National Laboratory's Modular Architecture for Robotics and Teleoperation. SMART is designed to integrate the different slave devices (e.g., large hydraulic arms, mobile manipulators, and gantry robots), sensors (e.g., ultra-sonic sensors and force sensors), and input devices, (e.g., track ball, force-reflecting master, and autonomous trajectory generators) required for waste management and environmental restoration tasks. The modular architecture allows for rapid synthesis of complex telerobotic systems. This paper introduces some sample modules and illustrates how the modules can be connected to achieve telerobotic behaviors. Examples include autonomous control, impedance control, and enhanced bilateral teleoperation. DOE

N93-15406# Air Force Inst. of Tech., Wright-Patterson AFB, OH. School of Engineering.
DESIGN OF AN ARTIFICIAL NEURAL NETWORK BASED TACTILE SENSOR FOR THE UTAH/MIT DEXTEROUS HAND M.S. Thesis
Jeffery D. Nering Sep. 1992 85 p
(AD-A256565; AFIT/GE/ENG/92S-04) Avail: CASI HC A05/MF A01

The Neural Tactile Sensor (NTS) is a high resolution, easily manufactured tactile sensor consisting of electrodes, a thin resistive 'skin', and pattern recognition circuitry that is capable of resolving dynamic and static contact location, force, and slip throughout the continuum of the sensor's active region. The sensor operates by means of a resistive 'skin' harboring the electric field generated when a current is injected into it, and a plurality of electrodes for taking measurements of said electric field. When current flows through the resistive medium from the location of tactile contact, an electric field within the resistive medium is established, with a voltage distribution pattern dependent on where the contact was made. The contact generated electric field is measured at a plurality of locations on or in the resistive medium by the electrodes. The outputs of these electrodes can be interpreted as a continuum of field representing voltage patterns that are unique, repeatable, and dependent upon the location that field establishing contact was made. The dynamics of said voltage patterns are related to contact trajectory and slip. These voltage patterns are then used as input to appropriate pattern recognizer circuitry, such as the multilayer perceptron Artificial Neural Network (ANN). GRA

N93-15408# Rome Lab., Griffiss AFB, NY.
ANALOG VERY LARGE SCALE INTEGRATION (VLSI) IMPLEMENTATIONS OF ARTIFICIAL NEURAL NETWORKS Report, Oct. 1991 - Apr. 1992
Michael L. Hinman Sep. 1992 39 p
(AF Proj. 4594)
(AD-A256621; RL-TR-92-149) Avail: CASI HC A03/MF A01

There has been a recent resurgence of interest in the multi-disciplinary field of artificial neural networks. Artificial neural networks, originally inspired by the computational capabilities of the human brain, refer to a variety of computing architectures that consist of massively parallel interconnections of simple processing elements. Currently, there exist two promising advanced technologies for implementing neural networks: Very Large Scale Integrated (VLSI) circuits and optical. The use is described of VLSI circuits for implementing various neural networks, with an emphasis on analog VLSI. A comparison of the different implementation techniques is provided, as is the type of paradigm implemented (e.g., backpropagation, hopfield, bidirectional associative memories, etc.). GRA

N93-15491# Universiteit Twente, Enschede (Netherlands). Tele-Informatics and Open Systems Group.
A QUEUE MODEL RELATING SYNCHRONOUS AND ASYNCHRONOUS COMMUNICATION
Jan Tretmans and Louis Verhaard (TFL, Hoersholm, Denmark) 1992 51 p Sponsored in part by EEC
(Memo-INF-92-04; TIOS-92/02; TFL-RR-1992-1; ETN-92-92429) Copyright Avail: CASI HC A04/MF A01

The problem of comparing specifications that use asynchronous communication (for example ESTELLE, SDL (specification and description language)) with specifications that use synchronous communication (for example LOTOS) is approached by modeling asynchronous communication in the realm of labeled transition systems using a context. A particular context consisting of two queues, one for input and one for output, is investigated. This queue context is modeled by a queue operator on labeled transition systems. A new equivalence, queue equivalence, is introduced as testing equivalence in a queue context. It turns out that this equivalence can be characterized by sets of traces instead of by failure pairs, as in the case of conventional testing equivalence on labeled transition systems. A few nonequivalence relations for queue contexts are introduced that can serve as implementation relations. They are related to the implementation relations of failure preorder, trace preorder, and conformance. ESA

N93-14925# Toronto Univ. (Ontario). Inst. for Aerospace Studies.
MOVE: A NEUTRAL NETWORK PARADIGM FOR ROBOTIC CONTROL
Darin P. W. Graham and Gabriele M. T. DeLeuterio *In* Canadian Space Agency, Proceedings of the Sixth CASI Conference on Astronautics 1990 14 p Previously announced in IAA as A91-34931 (For primary document see N93-14920 04-12)
Avail: Canadian Aeronautics and Space Inst., 222 Somerset St. W., Suite 601, Ottawa, Ontario K2P 0J1 Canada

N93-14949# Alberta Research Council, Calgary.
A ROBOTIC PLANNING SYSTEM
Keith Chrystall, A. Dagnino, and P. Feighan *In* Canadian Space Agency, Proceedings of the Sixth CASI Conference on Astronautics 1990 9 p Previously announced in IAA as A91-34955 (For primary document see N93-14920 04-12)
Avail: Canadian Aeronautics and Space Inst., 222 Somerset St. W., Suite 601, Ottawa, Ontario K2P 0J1 Canada

N93-15183# Paderborn Univ. (Germany). Dept. of Electrical Engineering.
NEURAL NETWORK BASED CONDITION MONITORING [ZUSTANDSUEBERWACHUNG AUF DER BASIS NEURONALER NETZWERKE]
Dieter Barschdorff *In* DLR, Proceedings of the 16th Symposium on Aircraft Integrated Monitoring Systems Jan. 1992 p 585-606 (For primary document see N93-15152 04-06)
Avail: CASI HC A03/MF A06; DLR, Wissenschaftliches Berichtswesen, Postfach 90 60 58, Cologne, Germany, HC

N93-15303# Weizmann Inst. of Science, Rehovoth (Israel). Dept. of Applied Mathematics and Computer Science.
ROBOT LEARNING OF CONTACT TASKS
M. Benady, T. Flash, and D. Gershon *In* CASA-RI/SME, Proceedings of the International Conference on CAD/CAM and AMT. Volume 3: IFIP/Robotics: International Sessions on Robots and Assembly 14 Dec. 1989 6 p (For primary document see N93-15298 04-61)
(F-3-2) Avail: CASI HC A02/MF A02

N93-15305# Tel-Aviv Univ. (Israel). Faculty of Engineering.
PLANNING OF CONTINUOUS PATH ROBOTIC MOTIONS BY DISCRETE TIME OPTIMIZATION
V. Netzer *In* CASA-RI/SME, Proceedings of the International Conference on CAD/CAM and AMT. Volume 3: IFIP/Robotics: International Sessions on Robots and Assembly 14 Dec. 1989 6 p (For primary document see N93-15298 04-61)
(F-3-5) Avail: CASI HC A02/MF A02

N93-15306# Tel-Aviv Univ. (Israel). Faculty of Engineering.
TIME-OPTIMIZATION OF POINT-TO-POINT ROBOTIC MOTIONS
L. Beiner *In* CASA-RI/SME, Proceedings of the International Conference on CAD/CAM and AMT. Volume 3: IFIP/Robotics: International Sessions on Robots and Assembly 14 Dec. 1989 6 p (For primary document see N93-15298 04-61)
(F-3-6) Avail: CASI HC A02/MF A02

N93-15307# Weizmann Inst. of Science, Rehovoth (Israel). Dept. of Applied Mathematics.
REDUNDANCY CONTROL OF ROBOTS BY CONSTRAINED OPTIMIZATION
Tzila Shamir *In* CASA-RI/SME, Proceedings of the International Conference on CAD/CAM and AMT. Volume 3: IFIP/Robotics: International Sessions on Robots and Assembly 14 Dec. 1989 4 p (For primary document see N93-15298 04-61)
(F-3-7) Avail: CASI HC A01/MF A02

N93-15308# Indian Inst. of Tech., Madras. Dept. of Mechanical Engineering.
ADAPTIVE CONTROL OF A MANIPULATOR IN CARTESIAN SPACE
Venkataesh V. Murty and M. S. Shunmugam *In* CASA-RI/SME, Proceedings of the International Conference on CAD/CAM and AMT. Volume 3: IFIP/Robotics: International Sessions on Robots and Assembly 14 Dec. 1989 5 p (For primary document see N93-15298 04-61)
(F-4-2) Avail: CASI HC A01/MF A02

64 NUMERICAL ANALYSIS

Includes iteration, difference equations, and numerical approximation.

N93-14235# Carnegie-Mellon Univ., Pittsburgh, PA. Dept. of Computer Science.
REPRESENTATION AND MANIPULATION OF INDUCTIVE BOOLEAN FUNCTIONS
Aarti Gupta and Allan L. Fisher Apr. 1992 23 p
(Contract F33615-90-C-1465; DARPA Order 7597)
(AD-A256078; CMU-CS-92-129) Avail: CASI HC A02/MF A01

TV high level of complexity of current hardware systems has led to an interest in formal methods for proving their correctness. Reasoning by induction is a powerful formal proof method with the advantages that a single proof establishes the correctness of an entire family of circuits varying according to some size parameter, and the size of this proof is independent of the size of the circuit. Tautology-checking of symbolic Boolean functions is another method that has been successfully used in formal verification, both for checking equivalence/satisfaction with respect to a functional specification and as a basis for modelchecking. In this paper, we present a representation and algorithms for symbolic manipulation of inductive Boolean functions, based on extensions of Binary Decision Diagrams. Our approach allows us to combine reasoning by induction with efficient tautology-checking in an automatic way. GRA

N93-14255# Naval Postgraduate School, Monterey, CA.
THE USE OF CHAOS METRICS TO ANALYZE LAGRANGIAN PARTICLE DIFFUSION MODELS M.S. Thesis
Korey V. Jackson Jun. 1992 162 p
(AD-A256142) Avail: CASI HC A08/MF A02

Chaos metrics are examined as a tool to analyze atmospheric three-dimensional dispersion models at the individual particle rather than the aggregate level. These include the self-affine fractal dimension--DA, Shannon entropy--S, and Lyapunov exponent--lambda. Intercomparison of these metrics is first performed with the one-dimensional logistics difference equation and the two-dimensional Henon systems of equations. The fractal dimension and Shannon entropy are then measured as a function of the inverse Monin-Obukhov length (1/L) for two three-dimensional Lagrangian particle dispersion models: the McNider particle dispersion model and the NPS particle dispersion model now under development. The fractal dimension and Shannon entropy uncover weaknesses in both models which are not obvious with standard geophysical measures. They also reveal similarities and difference between the atmospheric models and simple chaos systems. Combined, these chaos measures may lend detailed insight into the behavior of Lagrangian Monte Carlo dispersion models in general. GRA

N93-14270# California Univ., Berkeley. Center for Pure and Applied Mathematics.
THE METHOD OF MINIMAL REPRESENTATIONS IN 2D ISING MODEL CALCULATIONS
Beresford Parlett and Wee-Liang Heng May 1992 26 p
(Contract N00014-90-J-1372)
(AD-A256581; PAM-549) Avail: CASI HC A03/MF A01

The Ising model was proposed to explain properties of ferromagnets but since then it has found application to topics in Chemistry and Biology as well as in Physics. For any reader unfamiliar with the model an excellent introduction targeted at a general audience is Cip87. The remainder of this section assumes some knowledge of the so called transfer matrix. This paper presents a numerical method for computing properties of the 2D Ising model for given parameter values such as magnetic field strength B, temperature T and coupling constants J. There are two avenues leading to such calculations: combinatorial and algebraic. Our method is in the second category. GRA

N93-14271# California Univ., Berkeley. Center for Pure and Applied Mathematics.
ANALYSIS OF PROJECTIONS OF THE TRANSFER MATRIX IN 2D ISING MODELS
Wee-Liang Heng Jan. 1992 58 p
(Contract N00014-90-J-1372)
(AD-A256583; PAM-545) Avail: CASI HC A04/MF A01

The Ising model, originally proposed to explain properties of ferromagnets, consists of a regular lattice whose vertices are considered to be 'sites' that can be in exactly one of two possible states. Of interest is the partition function, which is the sum of the energy of the lattice over all possible configurations. There are two main approaches to computing the partition function: the combinatorial method uses an expansion whose coefficients are the number of subgraphs satisfying certain criteria; the algebraic approach introduces a transfer matrix whose spectral radius is the partition function per spin. In the semi-infinite 2D model with n rows, the associated transfer matrix M(n) is duodiagonal of order 2n. This thesis introduces a special class of subspaces for approximating the dominant eigenvectors of M(n), and analyzes the projections of Mn, and its adjoint onto these subspaces. We shall show that the projections are sparse (with 2 or 4 nonzero entries per column), and are of order 0(n(sup 2) 2(sup l-1)) where l is a parameter of the subspaces. Some optimal properties of these subspaces are established. GRA

N93-14412# Howard Univ., Washington, DC.
THE CENTER FOR NONLINEAR PHENOMENA AND MAGNETIC MATERIALS Final Report, 1 Jul. 1989 - 30 Sep. 1992
Tepper L. Gill 30 Sep. 1992 33 p
(Contract F49620-89-C-0079)
(AD-A255983; AFOSR-92-0854TR) Avail: CASI HC A03/MF A01

We have proved existence and obtained estimates for the (finite) Hausdorff and fractal dimensions of global (maximal compact) attractors for the Landau-Lifschitz equations. These are the fundamental equations of the classical theory of ferromagnetism. In order to obtain more detailed information about these attractors, we are currently developing approximation methods based on the theory of inertial manifolds. Inertial manifolds are finite dimensional manifolds which attract all solutions at an exponential rate. They contain the global attractor and have the advantage that they are manifolds whereas the attractors generally are not (they can be complicated fractal sets). The equations reduce to a finite-dimensional system of ordinary differential equations (O.D.E.'s) on the inertial manifolds. There is a class of calculational methods that have been developed in recent

years, called nonlinear or modified Galerkin methods, which are closely related to the concept of inertial manifold and which are especially useful for the long-time integration of nonlinear differential equations. In the usual Galerkin approach, solutions of the nonlinear equation are sought in linear manifolds P(mu)H which are spanned by the eigenfunctions of a linear operator which occurs in the problem. In the case of the Landau-Lifschitz equations, this is the Laplacian. GRA

N93-14431# Defence Research Agency, Malvern (England).
PROOF OF THEOREMS IN Z
A. Smith Mar. 1992 26 p
(AD-A255711; DRA-92006) Avail: CASI HC A03/MF A01

This paper is concerned with user aspects of proof in the specification language Z. A number of techniques for proving theorems in Z are presented. Some of the techniques are not new, being drawn from the area of general mathematical theorem proving, but are brought together in one place and applied specifically to Z. The techniques were written so that they can be understood and applied by a person carrying out a pen and paper proof. Some of the techniques may be automated, and would result in a proof tool tailored to the needs of the user; currently a user has to tailor a proof to fit a tool. GRA

N93-14492# Carnegie-Mellon Univ., Pittsburgh, PA. School of Computer Science.
TRACE ALGEBRA FOR AUTOMATIC VERIFICATION OF REAL-TIME CONCURRENT SYSTEMS
Jerry R. Burch Aug. 1992 167 p
(Contract F33615-90-C-1465; ARPA Order 7597)
(AD-A256199; CMU-CS-92-179) Avail: CASI HC A08/MF A02

Verification methodologies for real-time systems can be classified according to whether they are based on a continuous time model or a discrete time model. Continuous time often provides a more accurate model of physical reality, while discrete time can be more efficient to implement in an automatic verifier based on state exploration techniques. Choosing a model appears to require a compromise between efficiency and accuracy. We avoid this compromise by constructing discrete time models that are conservative approximations of appropriate continuous time models. Thus, if a system is verified to be correct in discrete time, then it is guaranteed to also be correct in continuous time. We also show that models with explicit simultaneity can be conservatively approximated by models with interleaving semantics. GRA

N93-14609# Naval Postgraduate School, Monterey, CA.
INTRODUCTION TO REAL ORTHOGONAL POLYNOMIALS M.S. Thesis
William H. Thomas, III Jun. 1992 113 p
(AD-A256448) Avail: CASI HC A06/MF A02

The fundamental concept of orthogonality of mathematical objects occurs in a wide variety of physical and engineering disciplines. The theory of orthogonal functions, for example, is central to the development of Fourier series and wavelets, essential for signal processing. In particular, various families of classical orthogonal polynomials have traditionally been applied to fields such as electrostatics, numerical analysis, and many others. This thesis develops the main ideas necessary for understanding the classical theory of orthogonal polynomials. Special emphasis is given to the Jacobi polynomials and to certain important subclasses and generalizations, some recently discovered. Using the theory of hypergeometric power series and their q-extensions, various structural properties and relations between these classes are systematically investigated. Recently, these classes have found significant applications in coding theory and the study of angular momentum, and hold much promise for future applications. GRA

N93-14787# National Academy of Sciences - National Research Council, Washington, DC. Board on Mathematical Sciences.
CORE SUPPORT OF THE BOARD ON MATHEMATICAL SCIENCES Final Report
11 Aug. 1992 8 p
(Contracts MIPR-ARO-145-89; MIPR-ARO-137-90)
(AD-A255482; ARO-27058.1-MA) Avail: CASI HC A02/MF A01

The Board on Mathematical Sciences (BMS), National Research Council was established in 1984. The Board has one standing committee, the Committee on Applied and Theoretical Statistics (CATS). The Board, CAT'S, and other ad hoc committees, panels, and working groups established by the Board typically comprise at any one time over 200 mathematical scientists, other scientists, engineers, and medical personnel. The major activities of the Board involve the following: annual mathematical sciences department chairs colloquium, annual national science and technology symposium, health of the mathematical sciences, articulating emerging research directions, mathematical sciences interacting with other areas, mathematical sciences education, recommendations to federal agencies on research directions, and international representation. The BMS is a catalyst, convener, coordinator, and consensus builder for the mathematical sciences on the national level. It follows a policy of inclusion. It undertakes to do those activities that are necessary for nationwide reform and revitalization but are unlikely to be carried out effectively by other organizations. GRA

N93-14804# Physics and Electronics Lab. TNO, The Hague (Netherlands).
THEORY AND APPLICATIONS OF THE 3-DIMENSIONAL FINITE-DIFFERENCE TIME-DOMAIN METHOD Final Report
G. J. VanGennip Jun. 1992 36 p
(AD-A256559; FEL-92-B190; TDCK-92-1762) Avail: CASI HC A03/MF A01

The 3-dimensional finite-difference time-domain method is a numerical method for solving electromagnetic penetration and scattering problems. It uses a finite difference representation of the time dependent Maxwell equations. The object of interest is embedded in a lattice and the time is divided in discrete intervals. By applying the finite-difference equations for every time step the propagation and scattering of waves is simulated. In this report the 3-dimensional FD-TD method and its algorithms are explained. Results are presented for a perfectly conducting plate, cube and wedge and for a dielectric layered sphere. The calculated results agree with experimental and exact theoretical results. GRA

N93-15094# Universiteit Twente, Enschede (Netherlands). Tele-Informatics and Open Systems Group.
COMPACTNESS AND LOEWENHEIM-SKOLEM PROPERTIES IN PRE-INSTITUTION CATEGORIES
Antonino Salibra (Pisa Univ., Italy) and Giuseppe Scollo (Ecole Normale Superieure, Paris, France) 18 Mar. 1992 26 p
(Memo-INF-92-27; TIOS-92/12; ETN-92-92441) Copyright Avail: CASI HC A03/MF A01

The abstract model theoretic concepts of compactness and Loewenheim-Skolem poroperties are investigated in the 'softer' framework of pre-institution categories. Two compactness results are presented; a more informative reformulation of the compactness theorem for pre-institution transformations, and a theorem on natural equivalences with an abstract form of first order pre-institutions. These results rely on notions of compact transformation, which are introduced as arrow oriented generalizations of the classical, object oriented notions of compactness. A notion of cardinal pre-institution is introduced, and a Loewenheim-Skolem preservation theorem for cardinal pre-institutions is presented. ESA

N93-15121# Universiteit Twente, Enschede (Netherlands). Dept. of Computer Science.
GRAPH REWRITING USING A SINGLE PUSHOUT; A COMPARISON
P. M. vandenBroek and J. Kuper Apr. 1992 15 p
(Memo-INF-92-28; ETN-92-92442) Copyright Avail: CASI HC A03/MF A01

Two algebraic approaches to graph rewriting which use only single pushouts are compared. The first approach uses the category of Graphs and Partial Morphisms (GPaM) and the second uses the category of Marked Graphs (MG). They are shown to be almost the same, the only difference being the way dangling arcs are treated. From the point of view of graph rewriting, GPaM is equivalent to a subcategory of Proper Marked Graphs (PrMG). The difference between the MG approach and the PrMG approach is that where in the MG approach, given a rule and an occurrence, a rewriting may not exist due to dangling arcs in the pushout of the rule and the occurrence, the rewriting in the PrMG approach does always exist since in the pushout on PrMG those dangling arcs are removed. ESA

N93-15195# National Academy of Sciences - National Research Council, Washington, DC.
CORE SUPPORT FOR THE BOARD ON MATHEMATICAL SCIENCES

Final Report
11 Aug. 1992 8 p
(AD-A256333) Avail: CASI HC A02/MF A01

The Board on Mathematical Sciences (BMS), National Research Council was established in 1984. The BMS has one standing committee, the Committee on Applied and Theoretical Statistics (CAT'S). The BMS, CAT'S, and other ad hoc committees, panels, and working groups established by the BMS typically comprise at any one time over 200 mathematical scientists, other scientists, engineers, and medical personnel. The major activities of the BMS involve annual mathematical sciences department chairs colloquium, annual national science and technology symposium, health of the mathematical sciences, articulating emerging research directions, mathematical sciences interacting with other areas, mathematical sciences education, recommendations to federal agencies on research directions, and international representation. The BMS is a catalyst, convener, coordinator, and consensus builder for the mathematical sciences on the national level. It follows a policy of inclusion. It undertakes to do those activities that are necessary for nationwide reform and revitalization but are unlikely to be carried out effectively by other organizations. GRA

N93-15212# Oak Ridge National Lab., TN.
THE COVARIANCE MATRIX OF DERIVED QUANTITIES AND THEIR COMBINATION
Z. Zhao (Chinese Nuclear Data Center, Beijing.) and F. G. Perey Jun. 1992 52 p
(Contract DE-AC05-84OR-21400)
(DE92-019066; ORNL/TM-12106) Avail: CASI HC A04/MF A01

The covariance matrix of quantities derived from measured data via nonlinear relations are only approximate since they are functions of the measured data taken as estimates for the true values of the measured quantities. The evaluation of such derived quantities entails new estimates for the true values of the measured quantities and consequently implies a modification of the covariance matrix of the derived quantities that was used in the evaluation process. Failure to recognize such an implication can lead to inconsistencies between the results of different evaluation strategies. In this report we show that an iterative procedure can eliminate such inconsistencies. DOE

N93-15256# Texas A&M Univ., College Station.
UNDETERMINED COEFFICIENT PROBLEMS FOR QUASI-LINEAR PARABOLIC EQUATIONS Final Report, 1 Jan. 1989 - 30 Sep. 1992
William Rundell and Michael S. Pilant 30 Sep. 1992 9 p
(Contract N00014-89-J-1008)
(AD-A256012) Avail: CASI HC A02/MF A01

Our research efforts during the grant period were concerned with undetermined coefficient problems in partial differential equations focusing on three distinct areas: problems where the unknown coefficients depend only on the dependent variables; problems giving rise to first order equations where the boundary conditions and the coefficients in the equations have a nonlocal dependence on the variables; and inverse spectral problems, in which unknown coefficients have to be determined from eigenvalue data. These problems originate from situations where one wants to recover unknown material properties, or to determine the nature of an unknown physical law. A number of theoretical results (existence as well as uniqueness) as well as computational algorithms were derived for model elliptic, parabolic and hyperbolic equations. During the period of the grant, two major conferences were organized by the principal investigators, 1 Ph.D. thesis was completed, 17 publications appeared, and an additional 5 manuscripts were submitted. GRA

N93-15341*# National Aeronautics and Space Administration. Lewis Research Center, Cleveland, OH.
ENO-OSHER SCHEMES FOR EULER EQUATIONS
Jacobus J. VanDerVegt (Stanford Univ., CA.) Nov. 1992 13 p Presented at the 31st Aerospace Science Meeting and Exhibit, Reno, NV, 11-14 Jan. 1993; sponsored by AIAA
(NASA Order C-99066-G; RTOP 505-62-21)
(NASA-TM-105928; E-7435; NAS 1.15:105928; ICOMP-92-21; CMOTT-92-10; AIAA Paper 92-0335) Avail: CASI HC A03/MF A01

The combination of the Osher approximate Riemann solver for the Euler equations and various ENO schemes is discussed for one-dimensional flow. The three basic approaches, viz. the ENO scheme using primitive variable reconstruction, either with Cauchy-Kowalewski procedure for time integration or the TVD Runge-Kutta scheme, and the flux-ENO method are tested on different shock tube cases. The shock tube cases were chosen to present a serious challenge to the ENO schemes in order to test their ability to capture flow discontinuities, such as shocks. Also the effect of the ordering of the eigen values, viz. natural or reversed ordering, in the Osher scheme is investigated. The ENO schemes are tested up to fifth order accuracy in space and time. The ENO-Osher scheme using the Cauchy-Kowalewski procedure for time integration is found to be the most accurate and robust compared with the other methods and is also computationally efficient. The tests showed that the ENO schemes perform reasonably well, but have problems in cases where two discontinuities are close together. In that case there are not enough points in the smooth part of the flow to create a non-oscillatory interpolation. Author

N93-15379# Florida Univ., Gainesville. Dept. of Physics.
THE SINE-GORDON MODEL AND THE SMALL (KAPPA)(SUP +) REGION OF LIGHT-CONE PERTURBATION THEORY
P. A. Griffin 1992 13 p
(Contract DE-FG05-86ER-40272)
(DE92-040506; DOE/ER-40272/165; UFIFT-HEP-92-17) Avail: CASI HC A03/MF A01

The non-perturbative ultraviolet divergence of the sine-Gordon model is used to study the k(sup +) = 0 region of light-cone perturbation theory. The light-cone vacuum is shown to be unstable at the non-perturbative beta(sup 2) = 8(pi) critical point by a light-cone version of Coleman's variational method. Vacuum bubbles, which are k(sup +) = 0 diagram in light-cone field theory and are individually finite and non-vanishing for all beta, conspire to generate ultraviolet divergences of the light-cone energy density. The k(sup +) = 0 region of momentum also contributed to connected Green's functions: the connected two point function will not diverge, as it should, at the critical point unless diagrams which contribute only at k (sup +) = 0 are properly included. This analysis shows in a simple way how the k (sup +) = 0 region cannot be ignored even for connected diagrams. This phenomenon is expected to occur in higher dimensional gauge theories starting at two loop order in light-cone perturbation theory. DOE

N93-15398# Wisconsin Univ., Madison. Center for Mathematical Sciences.
MULTIRESOLUTION ANALYSIS BY INFINITELY DIFFERENTIABLE COMPACTLY SUPPORTED FUNCTIONS Summary Report
N. Dyn and A. Ron Sep. 1992 12 p
(Contract DAAL03-G-90-0090; NSF DMS-90-00053)
(AD-A256526; CMS-TSR-93-4) Avail: CASI HC A03/MF A01

The paper is concerned with the introduction and study of multiresolution analysis based on the up function, which is an infinitely differentiable function supported on (0,2). Such analysis is, necessarily, nonstationary. It is shown that the approximation orders associated with the corresponding spaces are spectral, thus making the spaces attractive for the approximation of very smooth functions. GRA

N93-15399# Wisconsin Univ., Madison. Center for Mathematical Sciences.
CHARACTERIZATIONS OF LINEAR INDEPENDENCE AND STABILITY OF THE SHIFTS OF A UNIVARIATE REFINABLE FUNCTION IN TERMS OF ITS REFINEMENT MASK Summary Report
Amos Ron Sep. 1992 18 p
(Contract DAAL03-G-90-0090; NSF DMS-90-00053)
(AD-A256527; CMS-TSR-93-3) Avail: CASI HC A03/MF A01

Characterizations of the linear independence and stability properties of the integer translates of a compactly supported univariate refinable function in terms of its mask are established. The results extend analogous ones of Jia and Wang which were derived for dyadic refinements and finite masks. GRA

N93-15656# Oak Ridge National Lab., TN.
THE SPATIAL CORRELATION FUNCTION APPROACH TO RESPONSE SURFACE EMISSION
T. J. Mitchell and M. D. Morris 1992 8 p Presented at the 1992 Winter Simulation Conference, Arlington, VA, 13-16 Dec. 1992

(Contract DE-AC05-84OR-21400)
(DE92-040875; CONF-921219-2) Avail: CASI HC A02/MF A01

This is an expository paper which discusses an alternative to conventional response surface methodology for use in simulation experiments where the objective is to express an output variable (response) as a function of several input variables. The method is Bayesian in the sense that uncertainty about the true response function y is expressed by the random function Y, defined on the region of interest X in the space of the input parameters. If Y is Gaussian, straightforward formulas exist for updating y given observations of y(x(sup 1)), y(x(sup 2)), ..., Y(x(sup n)), which are available from n simulation runs at different settings of the input parameters. The posterior mean of Y(x), viewed as a function of x, serves as the estimated response function (cflx y). The method is driven primarily by means of a chosen spatial correlation function (SCF), which defines the prior correlation between the responses at any two points in the space of the input parameters. Once the SCF is chosen, the method is naturally adaptive -- (cflx y) becomes more subtle and complex as more simulation runs are made, with no intervention required to add terms to a parametric model. Although much of the focus of this paper is on deterministic simulations, where we have had most of our experience, we shall show how modifications can be made to handle 'random' responses. Some examples are discussed to illustrate the ideas and the nature of the results. DOE

65 STATISTICS AND PROBABILITY

Includes data sampling and smoothing; Monte Carlo method; and stochastic processes.

N93-14443# Naval Postgraduate School, Monterey, CA.
OPTIMUM POSE MEASUREMENTS FOR KINEMATIC PARAMETERS IDENTIFICATION M.S. Thesis
Ronald L. Edwards Jun. 1992 65 p
(AD-A256307) Avail: CASI HC A04/MF A01

A six degree of freedom manipulator arm, a PUMA 560, is calibrated using random subsets of available experimental calibration data. Some of these subsets produce good results motivating the search for an optimum procedure which will use a small number of poses. Statistical analysis of the joint excursions and end effector position variation in both 'good' and 'bad' subsets of poses were conducted. No significant statistical differences between them was discovered. The condition number of the Jacobian matrix is investigated as a potential measure of the accuracy which may be obtained from the subset under consideration. The obtained condition number contained too much variability to be a reliable predictor of accuracy. A computer simulation was conducted using a numerical optimizer to select the joint angles to be used for calibration. The optimizer studies failed to find an optimum set of poses for calibration. The conclusion of these studies is that there is no optimum set of poses to be used for calibration. An alternative hypothesis, that the resultant calibration accuracy depends only upon the accuracy of the measurements taken, seems to be proven. GRA

N93-14455# Illinois Univ., Urbana. Dept. of Statistics.
SIMULTANEOUS DIF AMPLIFICATION AND CANCELLATION: SHEALY-STOUT TEST FOR DIF
Ratna Nandakumar 15 Aug. 1992 38 p
(Contract N00014-90-J-1940)
(AD-A256284; TR-1992-4) Avail: CASI HC A03/MF A01

The present study investigates the phenomena of simultaneous DIF (differential item functioning) amplification and cancellation and SIBTEST's role in detecting such. A variety of simulated test data were generated for this purpose. In addition, real test data from various sources were used. The results from both simulated as well as real test data, as Shealy and Stout's theory suggests, show that the SIBTEST is effective in assessing the DIF amplification and cancellation (partially or fully) at the test score level. Finally, methodological and substantive implications of DIF amplification and cancellation are discussed. GRA

N93-14456# Wisconsin Univ., Madison. Dept. of Electrical and Computer Engineering.
COMPUTATION AND COMMUNICATION CONSTRAINTS FOR DISTRIBUTED ESTIMATION SYSTEMS Final Technical Report, 1 May 1990 - 30 Jun. 1992
John A. Gubner 30 Jun. 1992 66 p
(Grant AF-AFOSR-0181-90)
(AD-A256287; AFOSR-92-0875TR) Avail: CASI HC A04/MF A01

Research performed under this grant fall into four areas which are reflected in published papers: (1) J.A. Gubner, 'Random Coding for the Constrained Multiple-Access Arbitrarily Varying Channel.' Proc. Twenty-Eighth Annual Allerton Conf. Commun. Contr. Comput., Univ of Illinois, Urbana, IL, pp. 684-690, Oct. 1990. 'The Capacity Region of the Additive Multiple-Access Arbitrarily Varying Channel,' Proc. 1991 IEEE Int. Symp. Inform. Theory, Budapest, Hungary, P. 218, June 1991. 'On the Capacity Region of the Discrete Additive Multiple-Access Arbitrarily Varying Channel,' IEEE Trans. Inform. Theory, vol 38, no. 4, pp. 1344-1347, July 1991 - concerned arbitrarily varying channels. (2) 'Distributed Estimation and Quantization,' IEEE Trans. Inform. Theory, submitted 1992, and W.H. Wehbo, 'Quantization for Distributed Estimation Systems,' M.S. report, Dep, Elect. Comp. Eng., University of Wisconsin, Madison, 1992 focussed on the design of distributed estimation systems subject to communication and computation constraints (3) 'On the Computation of Shot-Noise Probability Distributions,' Transform. Theory, submitted 1992. and R.E. Sequeira, J.A. Gubner and B.E.A. Saleh. 'Image Detection Under Low-Level Illumination.' IEEE Trans. Image Proc., in press, concerned the computation of shot-noise probability distributions and image detection based on shot-noise observations. (4) J.A. Gubner and W.B. Chang. 'Wavelet Transforms for Discrate-Time Periodic Signals,' IEEE Trans. Signal Proc., submitted 1992 is a tutorial paper on wavelet transforms for discrate-time periodic signals. GRA

N93-14487# Florida State Univ., Tallahassee. Dept. of Statistics.
A PROOF OF CONVERGENCE OF THE MARKOV CHAIN SIMULATION METHOD
Krishna B. Athreya, Hani Ddoss, and Jayaram Sethuraman Jul. 1992 32 p
(Contract DAAL03-90-G-0103)
(AD-A255456; FSU-M-868; ARO-27868.16-MA) Avail: CASI HC A03/MF A01

The Markov chain simulation method has been successfully used in many problems, including some that arise in Bayesian statistics. We give a self-contained proof of the convergence of this method in general state spaces under conditions that are easy to verify. We also provide a result giving a geometric rate of convergence. GRA

N93-14538# Florida State Univ., Tallahassee. Dept. of Statistics.
WAVELET METHODS FOR CURVE ESTIMATION
A. Antoniadis, G. Gregoire, and I. W. McKeague Jul. 1992 33 p
(Contract DAAL03-90-G-0103; AF-AFOSR-0048-91)
(AD-A255357; FSU-M-869; ARO-D-126; ARO-27868.18-MA) Avail: CASI HC A03/MF A01

The theory of wavelets is a developing branch of mathematics with a wide range of potential applications. Compactly supported wavelets are particularly interesting because of their natural ability to represent data with intrinsically local properties. They are useful for the detection of edges and singularities in image and sound analysis, and for data compression. However, most of the wavelet based procedures currently available do not explicitly account for the presence of noise in the data. A discussion of how this can be done in the setting of some simple nonparametric curve estimation problems is given. Wavelet analogues of some familiar kernel and orthogonal series estimators are introduced and their finite sample and asymptotic properties are studied. We discover that there is a fundamental instability in the asymptotic variance of wavelet estimators caused by the lack of translation invariance of the wavelet transform. This is related to the properties of certain lacunary sequences. The practical consequences of this instability are assessed. GRA

N93-15109# Stanford Univ., CA. Dept. of Statistics.
NONPARAMETRIC BAYESIAN BIOASSAY INCLUDING ORDERED POLYTOMOUS RESPONSE
Alan E. Gelfand and Lynn Kuo 14 Sep. 1992 29 p

(Contracts N00014-92-J-1254; N00025-92-J-1264)
(AD-A255990; TR-458-ONR) Avail: CASI HC A03/MF A01

Previous attempts at implementing fully Bayesian nonparametric bioassay have enjoyed limited success due to computational difficulties. We show here how this problem may be generally handled using a sampling based approach to develop desired marginal posterior distributions and their features. A useful extension is presented which treats the case of ordered polytomous response. Illustrative examples are provided. GRA

N93-15110# Stanford Univ., CA. Dept. of Statistics.
AN ITERATIVE MONTE CARLO METHOD FOR NONCONJUGATE BAYESIAN ANALYSIS
Bradley P. Carlin and Alan E. Gelfand 7 Sep. 1992 28 p
(Contracts N00014-92-J-1254; N00025-92-J-1264)
(AD-A255991; SU-TR-457-ONR) Avail: CASI HC A03/MF A01

The Gibbs sampler has been proposed as a general method for Bayesian calculation in Gelfand and Smith (1990). However experience to date is almost exclusively in applications assuming conjugacy where implementation is reasonably straightforward. This paper describes a tailored rejection method approach for implementation of the Gibbs sampler when nonconjugate structure is present. Several challenging applications are presented for illustration. GRA

N93-15119# Universiteit Twente, Enschede (Netherlands). Tele-Informatics and Open Systems Group.
APPROXIMATE PERFORMABILITY ANALYSIS USING GENERALIZED STOCHASTIC PETRI NETS
Boudewijn R. Haverkort Feb. 1992 24 p
(Memo-INF-92-11; TIOS-92/07; ETN-92-92431) Copyright Avail: CASI HC A03/MF A01

The use of generalized stochastic Petri nets for the description of dependability of performance models is addressed. Two heuristic state space truncation techniques that allow very good approximations for the steady state performability while only assessing a few percent of the states of the untruncated model are discussed. For a class of reversible performability models, explicit lower and upper bounds in the exact steady state performability are derived. For a much wider class, a truncation theorem exists that allows bounds to be obtained for the error made in the truncation. This theorem is discussed in the context of approximate performability models, and comments on its applicability are given. ESA

66 SYSTEMS ANALYSIS

Includes mathematical modeling; network analysis; and operations research.

N93-15626# General Accounting Office, Washington, DC. Information Management and Technology Div.
MILITARY SPACE OPERATIONS: SATELLITE CONTROL SYSTEM IMPROVED, BUT SERIOUS PROBLEMS REMAIN
Dec. 1991 49 p
(AD-A256809; GAO/IMTEC-92-3) Avail: CASI HC A03/MF A01

The Department of Defense's (DOD) satellites perform a wide variety of missions to support national security interests and pursue advances in research and development. The missions include communications, navigation, strategic defense, tactical warning and attack assessment, and other classified missions. The Air Force's Satellite Control Network controls satellite launches, maintains satellites, and keeps them in orbit. Since 1980, Air Force Systems Command has been upgrading its satellite command and control system, called the Command and Control Segment (CCS). The Chairman, Subcommittee on Strategic Forces and Nuclear Deterrence, Senate Committee on Armed Services, concerned about the program's shifting requirements, continuing schedule delays, technical problems, and increasing costs, asked GAO to review the Air Force's actions to complete the command and control system upgrade and turn it over to Air Force Space Command in 1993. GRA

67 THEORETICAL MATHEMATICS

Includes topology and number theory.

No abstracts in this category.

70 PHYSICS (GENERAL)

For precision time and time interval (PTTI) see *35 Instrumentation and Photography;* for geophysics, astrophysics or solar physics see *46 Geophysics, 90 Astrophysics,* or *92 Solar Physics.*

N93-14108# Aerospace Corp., El Segundo, CA. Engineering and Technology Group.
DETERMINING OPTIMUM C-FIELD SETTINGS THAT MINIMIZE OUTPUT FREQUENCY VARIATIONS IN CESIUM ATOMIC FREQUENCY STANDARDS
S. K. Karuza, W. A. Johnson, F. J. Voit, and J. P. Hurrell 15 Dec. 1991 29 p
(Contract F04701-88-C-0089)
(AD-A255902; TR-0091(6925-08)-4; SMC-TR-92-49) Avail: CASI HC A03/MF A01

De Marchi at the National Institute of Standards and Technology (NIST) performed an experiment on Hewlett-Packard cesium (Cs) frequency standards, in which he showed that there exist optimum values of the C-field that make the output frequency insensitive to variations in microwave power. Moreover, and most important, De Marchi demonstrated that the long-term stability of the Cs standard was improved at these optimum values of the C-field. To see if these results could be obtained with standards made by different manufacturers and having different modulation schemes and Cs tube designs, we performed a similar study using a completely automated measurement system on four Cs standards made by two other manufacturers. Our results, similar to those of De Marchi, showed that there are similar optimum C-field settings in these standards; furthermore, they showed that it may be more important to tune the microwave cavity precisely to the center Cs resonance frequency (fo) than it is to set the C-field at an optimum value. The best procedure, of course, is to do both, i.e., tune the cavity to the Cs resonance frequency as well as set an optimum C-field. GRA

N93-14245# Rome Lab., Griffiss AFB, NY.
RELATIVISTIC DYNAMICS OF A CHARGED SPHERE: UPDATING THE LORENTZ-ABRAHAM MODEL Interim Report
Arthur D. Yaghjian Feb. 1992 110 p
(AD-A256107; RL-TR-92-46) Avail: CASI HC A06/MF A02

The primary purpose of this work is to determine an equation of motion for the classical Lorentz model of the electron that is consistent with causal solutions to the Maxwell-Lorentz equations, the relativistic generalization of Newton's second law of motion, and Einstein's mass-energy relation. The work begins by reviewing the contributions of Lorentz, Abraham, Poincare, and Schott to this century-old problem of finding the equation of motion of an extended electron. Their original derivations, which were based on the Maxwell-Lorentz equations and assumed a zero bare mass, are modified and generalized to obtain a nonzero bare mass and consistent force and power equations of motion. By looking at the Lorentz model of the electron as a charged insulator, general expressions are derived for the binding forces that Poincare postulated to hold the charge distribution together. A careful examination of the classic Lorentz-Abraham derivation reveals that the self electromagnetic force must be modified during the short time interval after the external force is first applied. The resulting modification to the equation of motion, although slight, eliminates the noncausal pre-acceleration that has plagued the solution to the Lorentz-Abraham equation of motion. As part of the analysis, general momentum and energy relations are derived and interpreted physically for the solutions to the equation of motion, including hyperbolic and runaway solutions. GRA

N93-14280 Ohio State Univ., Columbus.
NONLINEAR FREE VIBRATION ANALYSIS OF STRINGS BY THE GALERKIN METHOD Ph.D. Thesis
Ahmed Moustafa Saad 1992 197 p
Avail: Univ. Microfilms Order No. DA9227370

A new, more accurate, system of coupled, nonlinear partial differential equations of motion describing the large-amplitude, planar, free vibration of the elastic stretched string is carefully developed taking into account the nonlinear coupling between the transverse and the longitudinal motions. The only assumption made in the derivation is that the string material remains linearly elastic during the motion so that it always obeys Hooke's law. The developed equations are then solved numerically by applying the Galerkin method both in space and time using an incremental approach to march in time. The assumed solution is written in terms of a series of coordinate functions which are sinusoidal in space and polynomial in time. Over each time step, the assumed solution satisfies the boundary conditions all the time and initial conditions at the beginning of the time step. The validity of the method is established by comparison with exact solutions for three classical problems: (1) damped free vibration of a particle, (2) large (nonlinear) oscillation of a pendulum, and (3) hard spring, nonlinear vibration governed by the Duffing equation. Numerical results of applying the incremental Galerkin method to the developed equations are presented in detail for three example problems: (1) a string subjected to moderate initial tension and moderate amplitude, (2) a string subjected to moderate initial tension and large amplitude, and (3) a string subjected to very small initial tension and moderate amplitude. Up to three transverse and five longitudinal symmetrical modes are included in the analysis. For the last two problems, the results are found to be significantly different from those of the Carrier integro-differential equation. A parametric study is presented showing the effect of varying the initial tension and the amplitude of the motion on the fundamental frequency of the string. The effect of varying the initial longitudinal displacement, and the generation of (typically higher) modes absent from the initial configuration are also demonstrated. Validity of results is verified by independent finite difference solutions.
Dissert. Abstr.

N93-14496# Army Lab. Command, Fort Monmouth, NJ. Electronics Technology and Devices Lab.
THE EFFECTS OF ACCELERATION ON PRECISION FREQUENCY SOURCES
John R. Vig, Claude Audoin, Leonard S. Cutler, Michael M. Driscoll, and Errol P. EerNisse Jul. 1992 64 p Supersedes AD-A235470
(AD-A255465; SLCET-TR-91-3-Rev-1) Avail: CASI HC A04/MF A01

The effects of acceleration on quartz and atomic frequency sources are reviewed. Guidelines are provided for the specification and testing of oscillator acceleration sensitivities. The discussion includes: steady-state acceleration effects, gravity change effects, shock effects, and vibration effects. The vibration effects section includes: sinusoidal vibration, random vibration, acoustic noise, the effects on short term stability, and spectral responses at other than the vibration frequency." GRA

N93-14679# Queens Coll., Flushing, NY. Dept. of Physics.
THIN-FILM PERMANENT MAGNETS FOR INTEGRATED ELECTROMAGNETIC COMPONENTS Final Report, Apr. 1988 - Sep. 1991
F. J. Cadieu Jun. 1992 50 p
(Contract F19628-88-K-0021)
(AD-A256175; RL-TR-92-184) Avail: CASI HC A03/MF A01

Methods were developed under this program that allow the deposition and photo-patterning of relatively thick (up to 100 microns) high-energy product (15-25 MgOe) highly oriented films of Sm-Co based permanent magnet materials onto various substrate materials, including GaAs and sapphire. The deposition process allows the magnetization to be in any direction desired in the plane of the film. The films have a Curie point of 700 C and are stable. NdFeB films, with magnetization perpendicular to the plane of the film, were also deposited. Methods developed included: Direct crystallization, in the presence of a magnetic field, of the sputtered materials onto heated substrates; the use of an Aluminum oxide boundary layer to promote adhesion and allow the growth of thick films; and the use of Ar and Xe as a sputtering gas to thermalize the sputtered atoms. Magnets such as those developed under this contract are a significant advance towards providing thin-film bias magnets for planar nonreciprocal microwave devices such as circulators and isolators. GRA

N93-15057# Florida Univ., Gainesville. Dept. of Physics.
EXPLAINING CLOUD CHAMBER TRACKS
A. A. Broyles 16 Jun. 1992 6 p
(Contract DE-FG05-86ER-40272)
(DE92-040502; DOE/ER-40272/168; UFIFT-HEP-92-21) Avail: CASI HC A02/MF A01

The operation of many detection devices is usually explained in terms of the ionization tracks produced by particles despite the fact that the corresponding incident wave functions extended over the entire sensitive regions of the detectors. The mechanisms by which the wave function appears to collapse to a track are analyzed. DOE

N93-15243# Aerospace Corp., El Segundo, CA. Electronics Technology Center.
FREQUENCY SHIFTS IN A RUBIDIUM FREQUENCY STANDARD DUE TO COUPLING TO ANOTHER STANDARD
B. Jaduszliwer, R. A. Cook, and R. P. Frueholz 15 Oct. 1991 15 p
(Contract F04701-88-C-0089)
(AD-A256232; TR-0091(6470-03)-1; SMC-TR-92-48) Avail: CASI HC A03/MF A01

Highly reliable timing systems, such as used on board satellites, may incorporate a hot standby atomic clock besides the active one. RF couplings between them may affect the performance of the active clock. We have investigated the effect of such couplings between two rubidium atomic clocks and found that they will add an oscillatory term to the Allan Variance of the active clock, degrading its frequency stability, and that under certain circumstances they may also shift the active clock's operating frequency. We discuss these two effects in detail, and establish the level of isolation required to render them negligible. GRA

71 ACOUSTICS

Includes sound generation, transmission and attenuation.
For noise pollution see *45 Environmental Pollution.*

N93-14144 California Univ., Los Angeles.
TURBULENCE AND CHAOS IN CLASSICAL AND QUANTUM SYSTEMS Ph.D. Thesis
Mitchell Behjan Haeri 1992 98 p
Avail: Univ. Microfilms Order No. DA9224112

The nonlinear quantum kinetic equation for the interaction of sound waves and Liouville's equation for the kicked rotor are solved via analytic and numerical techniques. In the classical regime sound wave energy cascades to higher frequency (omega) according to the steady state power law omega(exp -3/2). In the quantum limit, the system prefers a reverse cascade of energy which follows the steady state power law omega(exp -6). Above a critical flux, a new type of spectrum appears for the interaction of sound waves which is neither self-similar nor close to equilibrium. This state of nonlinear quantum wave turbulence represents a flow of energy directly from the classical source to the quantum degrees of freedom. The classical kinetic equation is used to examine the locality issue associated with turbulence. In contrast to the Kolmogorov picture of vortex turbulence, we find that the time development of each mode is governed by a nonlocal interaction with the source where energy is injected. The local equations for wave turbulence are used to derive analytically an expression for the minimum flux required to overcome viscous damping and generate a turbulent spectrum. A map of the probability distribution function for the kicked classical rotor is generated by exactly solving Liouville's equation for any arbitrary initial condition and kicking strength. This solution is compared to the analogous quantum mechanical map in an attempt to define chaos in the quantum rotor. In this way we compare two linear partial differential equations. Unlike the standard map generated from the canonical equations of motion, the map of the classical probability distribution function is 'practically' reversible for large values of the kicking potential. In fact, the conditions for reversibility of Liouville's equation are similar to those for Schroedinger's. In all other respects, the solution to Liouville's equation is similar to the standard map. However, there is no metric like Liapunov

exponents to quantify chaos in Liouville's equation. Any method used to define chaos in Liouville's equation can be applied to Schroedinger's equation. Dissert. Abstr.

N93-14145 Texas Univ., Austin.
SCATTERING OF SOUND BY SOUND: NONLINEAR INTERACTION OF COLLINEAR AND NONCOLLINEAR SOUND BEAMS Ph.D. Thesis
James Alan TenCate 1992 135 p
Avail: Univ. Microfilms Order No. DA9225741

An experimental investigation of the scattering of sound by sound, a classic yet controversial problem in nonlinear acoustics, is presented. When intense sound beams interact, scattered sound is produced in the region where the interaction occurs. Our experiments show that, contrary to what early researchers thought, scattered sound can be radiated outside the interaction region. All measurements were performed in water. The transducers were uniform pistons (source radii 3.2 mm to 19 mm, frequencies 0.5 MHz to 5 MHz) and nearly Gaussian source (effective radius 5.2 mm, frequency 2 MHz). Measurements were completely automated. Dynamic range obtained was about 70 dB; signal-to-noise ratios achieved in beam patterns were nearly 100 dB. Two types of experiments were performed: (1) measurements of scattered sound (so-called fingers) in higher harmonic beam patterns produced by a single uniform source, and (2) measurements of scattered sound produced by the interaction of two noncollinear sound beams of different frequencies. Although fingers have been observed in the past, we are the first to demonstrate that they are scattered sound. Fingers were measured in beam patterns of several uniform pistons. Careful comparison of theory with data was made for one of the sources, a 1 MHz, 12 mm radius uniform piston with source level of 223 dB (re 1 microPa). Beam patterns of the first four harmonics compare exceedingly well with theory. Propagation curves of a 2.2 MHz, 3.2 mm radius uniform piston with source level of 217 dB (re 1 microPa) were also measured. As predicted, fingers decay as 1/r, and the other lobes decay more slowly. Noncollinear scattering of sound by sound experiments were also performed. The most interesting results were obtained from experiments with a 5 MHz, 9.5 mm radius piston and 0.5 MHz, 12 mm radius piston interacting at angles of 3-6 deg. Although theoretical calculations were not possible, the results do show evidence of scattered sound. Dissert. Abstr.

N93-14159# Iowa State Univ. of Science and Technology, Ames.
A TIME-DOMAIN STUDY OF THE RELATIONSHIP BETWEEN DRIVE FORCE TIME BANDWIDTH AND FARFIELD ACOUSTIC RADIATION Final Technical Report
J. Adin Mann Aug. 1992 91 p
(Contract N00014-91-J-2002)
(AD-A255616) Avail: CASI HC A05/MF A01

Interaction between a vibrating cylindrical shell and a surrounding fluid is of keen interest to many acousticians working in structural acoustics. Much analysis has been done on the scattering and radiation properties of such a system in the frequency domain. Hence, the main objective of this thesis is to examine energy radiated by a fluid loaded, point driven, finite cylindrical shell in the time domain. GRA

N93-14227 California Univ., Berkeley.
THE TIME VARIABILITY OF JUPITER'S SYNCHROTRON RADIATION Ph.D. Thesis
Scott Jay Bolton 1991 160 p
Avail: Univ. Microfilms Order No. DA9228579

The time variability of the Jovian synchrotron emission is investigated by analyzing radio observations of Jupiter at decimetric wavelengths. The observations are composed from two distinct sets of measurements addressing both short term (days to weeks) and long term (months to years) variability. The study of long term variations utilizes a set of measurements made several times each month with the NASA Deep Space Network (DNS) antennas operating at 2295 MHz (13.1 cm). The DSN data set, covering 1971 through 1985, is compared with a set of measurements of the solar wind from a number of Earth orbiting spacecraft. The analysis indicates a maximum correlation between the synchrotron emission and the solar wind ram pressure with a two year time lag. Physical mechanisms affecting the synchrotron emission are discussed with an emphasis on radial diffusion. Calculations are performed that suggest the correlation is consistent with inward adiabatic diffusion of solar wind particles driven by Brice's model of ionospheric neutral wind convection (Brice 1972). The implication is that the solar wind could be a source of particles of Jupiter's radiation belts. The investigation of short term variability focuses on a three year Jupiter observing program using the University of California's Hat Creek radio telescope operating at 1400 MHz (21 cm). Measurements are made every two days during the months surrounding opposition. Results from the three year program suggest short term variability near the 10-20 percent level but should be considered inconclusive due to scheduling and observational limitations. A discussion of magneto-spheric processes on short term timescales identifies wave-particle interactions as a candidate source. Further analysis finds that the short term variations could be related to whistler mode wave-particles interactions in the radiation belts associated with atmospheric lightning on Jupiter. However, theoretical calculations on wave particle interactions imply thought if whistler mode waves are to interact with the synchrotron emitting electrons. Dissert. Abstr.

N93-14234# Naval Postgraduate School, Monterey, CA. Mathematics Dept.
AUDIO DETECTION ALGORITHMS Technical Report, 10 Jan. - 31 Jul. 1992
B. Neta and B. Mansager 10 Aug. 1992 11 p
(AD-A256076; NPS-MA-92-008) Avail: CASI HC A02/MF A01

Audio information concerning targets generally includes direction, frequencies, and energy levels. One use of audio cueing is to use direction information to help determine where more sensitive visual direction and acquisition sensors should be directed. Generally, use of audio cueing will shorten times required for visual detection, although there could be circumstances where the audio information is misleading and degrades visual performance. Audio signatures can also be useful for helping classify the emanating platform, as well as to provide estimates of its velocity. The Janus combat simulation is the premier high resolution model used by the Army and other agencies to conduct research. This model has a visual detection model which essentially incorporates algorithms as described by Hartman(1985). The model in its current form does not have any sound cueing capability. This report is part of a research effort to investigate the utility of developing such a capability. GRA

N93-14269# Electronics Research Lab., Adelaide (Australia).
AN ANALYSIS OF THE EFFECT OF ACOUSTIC NON-LINEARITIES IN WIDE BANDWIDTH ACOUSTO-OPTIC BRAGG CELLS
Anthony C. Lindsay, Ian G. Fuss, and Shaun C. Troedson Aug. 1992 32 p
(AD-A256579; ERL-0643-RR; DODA-AR-006-986) Avail: CASI HC A03/MF A01

In this report an extension of the theory of acoustic non-linearities accurate to fourth order is derived. A new fundamental limitation on the high frequency operation of acousto-optic signal processing architectures is demonstrated. GRA

N93-14406# Aerospace Medical Research Labs., Wright-Patterson AFB, OH.
EVALUATION OF THREE MODELS USED FOR PREDICTING NOISE PROPAGATED LONG DISTANCES OVERGROUND Interim Report, Aug. 1990 - Sep. 1991
W. R. Lundberg Sep. 1991 44 p
(AF Proj. 7321)
(AD-A255963; AL-TR-1991-0126) Avail: CASI HC A03/MF A01

Pershing 2 missile elimination noise measurements were used as the basis for comparing three noise prediction programs' ground-to-ground propagation modeling approaches. The effects of atmospheric refraction, atmospheric absorption, and ground impedance are considered. The noise models were compared because they are currently in use, in different venues, for environmental noise propagation modeling. The respective strong points of each model are emphasized. The results are used to delineate the needs for development of a model which produces both rapid and physically detailed predictions. GRA

N93-14458# Texas Univ., Austin. Dept. of Mechanical Engineering.
PROBLEMS IN NONLINEAR ACOUSTICS: RAYLEIGH WAVES, PULSED SOUND BEAMS, REFLECTION OF FOCUSED BEAMS, WAVEGUIDES, COOPERATIVE RADIATION OF SOUND BY BUGGLES, ACOUSTIC STREAMING EFFECTS IN STANDING WAVES, AND SPARK-SOURCE LITHOTRIPTER PULSES Annual Summary Report, 1 Aug. 1991 - 14 Aug. 1992
Mark F. Hamilton 14 Aug. 1992 29 p
(Contract N00014-89-J-1003)
(AD-A256289; ASR-4) Avail: CASI HC A03/MF A01

Nine projects are discussed in this annual summary report, all of which involve basic research in physical acoustics, mainly nonlinear acoustics: (1) Nonlinear Rayleigh Waves, (2) Finite Amplitude Pulses in Liquids with Strong Absorption, (3) Reflection of a Focused Beam from a Curved Target, (4) Finite Amplitude Propagation in a Sound Velocity Channel, (5) Second Harmonic Generation in Pekeris Waveguides, (6) Finite Amplitude Propagation in Multiple Waveguide Modes, (7) Cooperative Radiation and Scattering of Sound by Bubbles, (8) Water Fountains Produced by Intense Standing Waves in Air, and (9) Spark-Source Lithotripter Pulses. GRA

N93-14734 Institute of Sound and Vibration Research, Southampton (England). Signal Processing and Control Group.
ADAPTIVE ACTIVE NOISE CONTROL USING MULTIPLE-MODEL APPROACHES
H. D. Nam and S. J. Elliott Oct. 1992 33 p
(ISVR-TR-210) Copyright Avail: Issuing Activity

The adaptive active noise control problem is considered, in which the response of the system under control varies with time. A new algorithm for system identification in such circumstances, using multiple models of the secondary path transfer function is presented. The computational burden of the proposed algorithm is much smaller than the existing methods, so it could be applied to the multi-channel cases. An IIR structure is assumed for the control filter, and the recursive least mean squares algorithm introduced by Feintuch is used to adjust the filter coefficients. Combining the proposed identification technique and the filter-x recursive least mean squares algorithm, the multiple model adaptive controller (MMAC) for active noise control problems is presented. This method requires a priori information about the plant to select models of the secondary path transfer function, so it can be used when we have some information on the plant and operating situations. Computer simulations was performed to show the effectiveness of the proposed algorithm in a simple duct problem. Author

N93-14912# Systems Control Technology, Inc., Arlington, VA.
TILTROTOR AIRCRAFT NOISE: A SUMMARY OF THE PRESENTATIONS AND DISCUSSIONS AT THE 1991 FAA/GEORGIA TECH WORKSHOP Final Report
K. K. Ahuja (Georgia Inst. of Tech., Atlanta.) Jan. 1992 53 p
(Contract DTFA01-87-C-00014)
(DOT/FAA/RD-91/23; SCT-A8924-1) Avail: CASI HC A04/MF A01

Georgia Institute of Technology hosted a workshop in Atlanta on 28 and 29 March 1991 on the noise problems associated with tiltrotors. The workshop had two major objectives: (1) to review the status of research and development in predicting and reducing tiltrotor noise; and, (2) to identify key technical and operational issues and methods to address them. The second objective had both near term and far term implications. In the near term, the goal is to arrive at a level of technical credibility that can support decisions to develop urban and inner city markets. The long term goal is to target resources and actions which will lead to tiltrotor noise abatement and effective control. The opening session of this workshop consisted of an overview and a discussion of the physics of tiltrotor noise mechanisms. A review of the available experimental data followed. A discourse on potential flight operational procedures to minimize noise impacts, and a general presentation of industry and government perspectives concluded the workshop. Subsequent sessions were available for participants to present observations on and experiences with the XV-15 and V-22. Operational experiences included flight tests, wind tunnel tests, and other simulations. Experiences with computational fluid dynamics codes, small-scale model testing, and other related research were shared. This document provides a summary of the presentations and discussions that took place during the workshop. Author

N93-15012# Naval Oceanographic and Atmospheric Research Lab., Bay Saint Louis, MS.
ADVANCED DEVELOPMENT ACTIVE MODEL: A USERS GUIDE Final Report
J. K. Fulford Aug. 1992 35 p
(AD-A255614; NOARL-TN-290) Avail: CASI HC A03/MF A01

The Naval Oceanographic and Atmospheric Research Laboratory has developed a numeric model for the prediction of boundary and volume reverberation in shallow-water environments for midfrequency regimes. The model's theoretic foundation is that of the (Naval Research Laboratory) Range Dependent Active System Performance Model. While retaining the theoretic foundation of the NRL model, it was necessary to introduce new algorithms for the computation of the acoustic ray trajectories, and the calculation of the elemental scattering areas used in the prediction of boundary reverberation. The changes were required to implement range-dependent bistatic reverberation and to account for the possibility of strong sound speed gradients in the upper regions of the water column. This technical note serves as a users guide for the Advanced Development Active Model. While the model usually performs without major malfunctions, users should remember that this model is a research and development model. GRA

N93-15073# Loughborough Univ. of Technology (England). Dept. of Mathematical Sciences.
BOUNDARY ELEMENT ANALYSIS OF LOW FREQUENCY CAVITY ACOUSTICAL PROBLEMS
K. A. Hussain (Motor Industry Research Association, Lindley, England) and K. S. Peat Apr. 1992 25 p Sponsored by Dept. of Trade and Industry, London, England
(MATHS-Rept-A-158; ETN-92-92381) Avail: CASI HC A03/MF A01

The conventional boundary element method of analysis of noise problems inside cavities is inaccurate at very low frequencies. A new low frequency boundary element formulation based upon a series solution in terms of the wave number is presented. The new formulation gives accurate results and requires only a single point quadrature scheme. The wave number is decoupled from the boundary integrals, such that only one matrix assembly and solution is needed for the entire frequency range of analysis. The formulation is similar to that developed for eigenvalue extraction of cavity modes. Both formulations result in a boundary integral analysis of Laplace's equation rather than Helmholtz's equation, with a consequent decoupling of the wavenumber. The formulation presented addresses the accurate low frequency analysis of forced problems by a series solution in terms of the wavenumber. The eigenvalue extraction formulation covers free vibration problems across the frequency spectrum by a pseudosource technique. ESA

N93-15074# Norwegian Defence Research Establishment, Kjeller.
SONAR PROCESSING ON CESAR
Halvor Bjordal 20 Mar. 1992 39 p In NORWEGIAN
(FFI-92/7007; ETN-92-92392) Avail: CASI HC A03/MF A01

An implementation of data processing from an active low frequency sonar on a CESAR computer system is described. CESAR is a powerful vector computer developed for fast delivery SAR (Synthetic Aperture Radar) processing. Data input, resampling, beamforming, and correlation are covered. The parallelization process is shown. ESA

N93-15129# Office National d'Etudes et de Recherches Aerospatiales, Paris (France). Direction Scientifique des Structures.
BROADBAND VIBROACOUSTIC FREQUENCY CONTROL VIA PIEZOELECTRIC FILMS [CONTROLABILITE PAR LARGES BANDES DE FREQUENCES DANS LE DOMAINE VIBROACOUSTIQUE VIA LA TECHNIQUE DES FILMS PIEZOELECTRIQUES]
N. Meidinger Jan. 1992 41 p In FRENCH
(Contract DRET-89-34-001)
(ONERA-RT-8/3654-RY-010-R; ETN-92-92724) Avail: CASI HC A03/MF A01

The vibroacoustic optimal control on beta broadband frequencies, called beta optimal control, is presented. The source of the noise is a plate excited by a local force. Control is through piezoelectric patches situated on the plate. The numerical resolution of the optimal control is presented. Illustrations for optimal beta control for a thin plate, in two boundary condition configurations, are given: fre-free and embedded. The realization

of optimal control is considered. The state of the art in active and noise adaptive control is outlined. Differential experimental schemas of vibroacoustic control is described. ESA

N93-15130# Office National d'Etudes et de Recherches Aerospatiales, Paris (France). Direction de la Physique Generale.

DEVELOPMENT OF A TDS MEASUREMENT SYSTEM. APPLICATION TO ACOUSTIC PROPAGATION MEASUREMENT IN A NON ANECHOIC ENVIRONMENT [DEVELOPPEMENT D'UN SYSTEME DE MESURE TDS. APPLICATION A DES MESURES DE PROPAGATION ACOUSTIQUE DANS UN ENVIRONNEMENT NON ANECHOIQUE]

S. Canard-Caruana Nov. 1991 45 p In FRENCH

(Contract DRET-89-001-218)

(ONERA-RT-18/3641-PY; ETN-92-92726) Avail: CASI HC A03/MF A01

The development of a Time Delay Spectrometry (TDS) system which enables separation, in one point of measure, of different acoustic paths coming from a point source is described. This method was developed with the aim of analyzing acoustic propagation test in a non-anechoic wind tunnel. This method was validated successfully by measurements performed in anechoic chambers, where several acoustic paths were realized using a reflecting panel. It could be used to make acoustic measurements in nonanechoic surroundings. ESA

N93-15259# Woods Hole Oceanographic Inst., MA.

EXPERIMENTAL INVESTIGATION OF SCATTERING FROM RANDOMLY ROUGH PLASTIC CYLINDERS M.S. Thesis

John V. Gurley Sep. 1992 115 p

(AD-A256018) Avail: CASI HC A06/MF A02

Acoustical backscattering from randomly rough infinitely long elastic cylinders surrounded by a fluid medium is examined. The cylinder radius is allowed to vary along its lengthwise axis creating one-dimensional rotationally symmetric roughness. Using recently published rough cylinder formulations T.K. Stanton, J. Acoust. Soc. Am., 92, 1641-1664 (1992) and T.K. Stanton and D. Chu, J. Acoust. Soc. Am., 92, 1665-1678 (1992), explicit expressions are derived for the backscattered field for a laboratory pulse-echo environment: spherically spreading directional source and receiver with arbitrary beam patterns. Efficient numerical integration algorithms are developed to solve for the backscattered field from a specified surface profile. Experimental measurements from dense elastic (stainless steel) cylinders immersed in water are presented to quantitatively illustrate the effects of small scale surface roughness (sigma/a = 0.0131 where sigma, is the surface rms roughness and a is the mean cylinder radius) for 4.5 less than ka less than 70 where k is the acoustic wavenumber. The actual target surface profile is well described and used as an input in the numerical simulations. Agreement is found between measurements and simulation predictions both in the mean field levels and the field fluctuations over a wide range of frequencies. GRA

N93-15391*# National Aeronautics and Space Administration. Langley Research Center, Hampton, VA.

UNSTEADY PRESSURE LOADS IN A GENERIC HIGH SPEED ENGINE MODEL

Tony L. Parrott, Michael G. Jones (Lockheed Engineering and Sciences Co., Hampton, VA.), and Ernie M. Thurlow (Lockheed Engineering and Sciences Co., Hampton, VA.) Dec. 1992 77 p

(RTOP 763-01-41-27)

(NASA-TP-3189; L-16912; NAS 1.60:3189) Avail: CASI HC A05/MF A01

Unsteady pressure loads were measured along the top interior wall of a generic high-speed engine (GHSE) model undergoing performance tests in the combustion-Heated Scramjet Test Facility at the Langley Research Center. Flow to the model inlet was simulated at 72000 ft and a flight Mach number of 4. The inlet Mach number was 3.5 with a total temperature and pressure of 1640 R and 92 psia. The unsteady pressure loads were measured with 5 piezoresistive gages, recessed into the wall 4 to 12 gage diameters to reduce incident heat flux to the diaphragms, and distributed from the inlet to the combustor. Contributors to the unsteady pressure loads included boundary layer turbulence, combustion noise, and transients generated by unstart loads. Typical turbulent boundary layer rms pressures in the inlet ranged from 133 dB in the inlet to 181 dB in the combustor over the frequency range from 0 to 5 kHz. Downstream of the inlet exist, combustion noise was shown to dominate boundary layer turbulence noise at increased heat release rates. Noise levels in the isolator section increased by 15 dB when the fuel-air ratio was increased from 0.37 to 0.57 of the stoichiometric ratio. Transient pressure disturbances associated with engine unstarts were measured in the inlet and have an upstream propagation speed of about 7 ft/sec and pressure jumps of at least 3 psia. Author

N93-15430*# National Aeronautics and Space Administration. Lewis Research Center, Cleveland, OH.

COMPUTATION OF SUPERSONIC JET NOISE UNDER IMPERFECTLY EXPANDED CONDITIONS

Chan M. Kim, Eugene A. Krejsa, and Abbas Khavaran (Sverdrup Technology, Inc., Brook Park, OH.) Jan. 1993 11 p Presented at the 31st Aerospace Sciences Meeting and Exhibit, Reno, NV, 11-14 Jan. 1993; Sponsored by AIAA

(RTOP 537-02-23)

(NASA-TM-105961; E-7481; NAS 1.15:105961; AIAA Paper 93-0735)

Avail: CASI HC A03/MF A01

The turbulent mixing noise of supersonic jet under imperfectly expanded conditions is calculated for convergent and convergent-divergent (CD) axisymmetric nozzle geometries. The noise prediction incorporates CFD solution of Navier-Stokes equations. The effect of grid resolution on shock structure computation is demonstrated. Mixing noise spectra predicted from fine and coarse grid solutions exhibit little sensitivity to the grid resolution. A proper grid resolution, however, results in a significant improvement in shock capturing capability and helps predictions agree favorably with experimental data. Good agreement between predicted noise spectra and data shows that the CFD-incorporated noise prediction scheme, which was demonstrated for shock-free conditions, works as well for shock-containing flow conditions. Author

N93-15575*# National Aeronautics and Space Administration. Lewis Research Center, Cleveland, OH.

PROPAGATION OF HIGH FREQUENCY JET NOISE USING GEOMETRIC ACOUSTICS

A. Khavaran (Sverdrup Technology, Inc., Brook Park, OH.) and E. A. Krejsa Jan. 1993 18 p Presented at the 31st Aerospace Sciences Meeting and Exhibit, Reno, NV, 11-14 Jan. 1993; sponsored by AIAA

(RTOP 537-02-23)

(NASA-TM-105950; E-7471; NAS 1.15:105950; AIAA Paper 93-0147)

Avail: CASI HC A03/MF A01

Spherical directivity of noise radiated from a convecting quadrupole source embedded in an arbitrary spreading jet is obtained by ray-tracing methods of geometrical acoustics. The six propagation equations are solved in their general form in a rectangular coordinate system. The noise directivity in the far field is calculated by applying an iteration scheme that finds the required radiation angles at the source resulting in propagation through a given observer point. Factors influencing the zone of silence are investigated. The caustics of geometrical acoustics and the exact locations where it forms is demonstrated by studying the variation in ray tube area obtained from transport equation. For a ring source convecting along the center-axis of an axisymmetric jet, the polar directivity of the radiated noise is obtained by an integration with respect to azimuthal directivity of compact quadrupole sources distributed on the ring. The Doppler factor is shown to vary slightly from point to point on the ring. Finally the scaling of the directivity pattern with power -3 of Doppler factor is investigated and compared with experimental data. Author

N93-15647# CDM Federal Programs Corp., Fairfax, VA.

ACOUSTIC LOCATION OF LEAKS IN PRESSURIZED UNDERGROUND PETROLEUM PIPELINES Report, 23 Jan. 1991 - 31 Oct. 1991

Eric G. Eckert (Vista Research Corp., Mountain View, CA.) and Joseph W. Maresca, Jr. (Vista Research Corp., Mountain View, CA.) Aug. 1992 58 p

(Contract EPA-68-03-3409)

(PB92-207687; EPA/600/R-92/143) Avail: CASI HC A04/MF A01

The objective of the work was to make an estimate of the accuracy of locating a leak in a pressurized petroleum pipeline, by means of passive acoustic sensors mounted on the outside wall of the pipeline, as a function of leak rate and distance between acoustic sensors. While there are regulatory standards for detection of leaks in underground pressurized pipelines, there are no standards for leak location. For rapid remediation, it would be highly desirable if the leak could be located within 10 percent

of the length of the pipeline in the case of a line longer than 30.5 m (100 ft), or within 3.0 m (10 ft) in the case of a line shorter than 30.5 m (100 ft). This limits the excavation to only a small fraction of the line. As will be shown below, theoretical estimates suggest that the accuracy of the proposed technique should be better than 25 cm. These theoretical estimates, however, assume that the leak signal is large compared to the noise. GRA

72 ATOMIC AND MOLECULAR PHYSICS

Includes atomic structure, electron properties, and molecular spectra.

N93-14283# California Univ., Berkeley. Dept. of Chemistry.
ELECTRONICALLY EXCITED MOLECULES: REACTION KINETICS AND EMISSION OF LIGHT: NANOSECOND INFRARED SPECTROSCOPY, ELECTRONIC EMISSION FROM CHEMICAL REACTIONS Final Report, 1 Nov. 1986 - 15 Apr. 1991
C. B. Moore 24 Feb. 1992 7 p
(Grant AF-AFOSR-0054-86)
(AD-A255642; AFOSR-92-0829TR) Avail: CASI HC A02/MF A01

A time-resolved IR absorption spectrometer capable of detecting chemical transients on the nanosecond timescale was designed, constructed, and successfully implemented. The spectrometer was used to characterize the vibrational relaxation of an open shell radical species, CF3, produced with excess energy from the photolysis of the parent CF3I compound. The effects of vibrational excitation in the CF3 radical on the reaction CF3 + Br2 yields CF3Br + Br were measured. Broadband data collection techniques were used to monitor the reactive and relaxation pathways simultaneously. The energetic radicals react no faster than the thermalized CF3 and may actually have a lower cross section for reaction. The spectrometer was also used to detect the gas phase absorption spectra of the polyatomic radicals. A thorough investigation into ozone-olefin reactions in a cryogenic matrix environment was completed. It was possible to complex ozone with various olefinic partners through careful control of the matrix deposition process, despite the very low (1-5 kcal/mole) activation energies for the ozonolysis reactions. The ground state complexes were observed to form a charge-transfer (CT) complex upon excitation. GRA

N93-14411# Princeton Univ., NJ. Dept. of Chemistry.
GAS-SOLID DYNAMICS AT DISORDERED AND ADSORBATE COVERED SURFACES Final Report, 1 Apr. 1987 - 30 Sep. 1991
Herschel Rabitz 2 Sep. 1992 27 p
(Contract F49620-87-C-0045)
(AD-A255981; AFOSR-92-0855TR) Avail: CASI HC A03/MF A01

Research carried out over the period of the grant is covered. Two areas of activities were pursued: (1) gas-surface dynamics, and (2) optimal control of molecular motion. In the first category, research was carried out to develop hybrid discrete-continuum techniques to study energy transfer and reactivity of surfaces, including bulk dynamics and surface defects. The second aspect of the research into quantum control theory laid the foundation for the rigorous introduction of theoretical tools capable of designing external optical fields for manipulating molecular scale events. A general formulation of the theory was developed, for treating rotational, vibrational, and electronic degrees of freedom. Both aspects of the research involve the development of formal theoretical techniques, as well as their numerical implementation on a variety of applications. GRA

N93-14424# California Univ., Santa Barbara. Dept. of Chemistry.
FINAL REPORT, 1 NOVEMBER 1988 - 31 OCTOBER 1991
H. Metiu 31 Aug. 1992 12 p
(Grant AF-AFOSR-0132-89)
(AD-A255979; AFOSR-92-0863TR) Avail: CASI HC A02/MF A01

We have achieved two objectives: (1) We developed the theory of electron scattering by adsorbed molecule and used it to demonstrate that electron scattering is a good probe of the orientation of a chemisorbed molecule. (2) We developed the theory of photodissociation with ultrashort pulses, analyzed existing experiments and showed that coherence and interference play a central role in the dissociation process. By using numerical simulations we proposed and documented new types of experiments which can increase the amount of information regarding dynamics of dissociation. GRA

N93-14433# Maryland Univ., College Park.
ELECTRON-PHONON INTERACTION, TRANSPORT AND ULTRAFAST PROCESSES IN SEMICONDUCTOR MICROSTRUCTURES Final Report, 1989 - 1992
Sankar D. Sarma 14 Aug. 1992 12 p
(Contract DAAL03-89-K-0026)
(AD-A255723; ARO-26278-EL) Avail: CASI HC A03/MF A01

We have fulfilled our contract obligations completely by doing theoretical research on electron-phonon interaction and transport properties in submicron semiconductor structures with the emphasis on ultrafast processes and many-body effects. Fifty-five papers have been published based on our research during the contract period. GRA

N93-14438# Texas A&M Univ., College Station. Knowledge Based Systems Lab.
INFORMATION SYSTEM CONSTRAINT LANGUAGE (ISyCL) Final Report, Jan. 1990 - Mar. 1991
Louis P. Decker and Richard J. Mayer Sep. 1992 114 p
(AD-A256268; KBSL-89-1002; AL-TP-1992-0019) Avail: CASI HC A06/MF A02

This paper describes a constraint language designed to serve as a Neutral Information Representation Scheme (NIRS) tying together model languages, procedural programming languages, database languages, transaction and process languages, as well as knowledge representation and reasoning control languages for information system specification. In one of its primary roles, the Information System Constraint Language (ISyCL) serves to augment the expressive power of existing systems engineering methods supported by a graphical languages. ISyCL is designed to be both powerful as a constraint language for completed information systems specification and easy to use by the various classes of users involved in information systems development. Expressive power is imparted to the language through the use of first-order predicate logic and set-theoretic constructs which provide the theoretical foundations of the language. Ease of use is promoted by providing layers within the language, ranging from natural language expressions to precise programming constructs, which shield users form unnecessary detail and complexity as dictated by their role in systems development. GRA

N93-14513# Pennsylvania State Univ., University Park. Dept. of Physics.
EXCITATION OF NUCLEI BY ANTIPROTON ANNIHILATION AT REST Final Report, 15 Jun. 1991 - 14 Jun. 1992
Gerald Smith 14 Jun. 1992 66 p
(Grant AF-AFOSR-0302-91)
(AD-A255447; PSU-LIPS/92-08) Avail: CASI HC A04/MF A01

Research leading to the detailed characterization of antiproton annihilation in nuclei has resulted in three publications during the past year. We have reported on neutron yields and angular distributions from annihilation in uranium. This work is important to our SHIVA Star subcritical microfission measurements currently in progress at the Phillips Laboratory, Kirtland AFB. Proton spectra indicate the presence of multinucleon annihilation in carbon and uranium targets. This is important in determining the pre-fission yield of nucleons in annihilation on uranium. The existence of rare hypernuclei formed in antiproton annihilation on uranium and bismuth was observed. These states live a fraction of a nanosecond and are of considerable interest to theorists trying to understand the binding of particles in heavy nuclei. GRA

N93-14662# Naval Research Lab., Washington, DC.
CURRENT NEUTRALIZATION IN BALLISTIC TRANSPORT OF LIGHT ION BEAMS Interim Report
Richard F. Hubbard, Steven P. Slinker, Martin Lampe, Glenn Joyce, and Paul Ottinger 6 Oct. 1992 48 p
(Contract DE-AC04-76DP-00789)
(AD-A256070; NRL/MR/4790-92-7112) Avail: CASI HC A03/MF A01

Intense light icn beams arc being considered as drivers to ignite fusion targets in the Laboratory Micro-fusion Facility (LMF). Ballistic transport of these beams from the diode to the target is possible only if the beam current is almost completely neutralized by plasma currents. This paper

summarizes related work on relativistic electron beam and heavy ion beam propagation and describes a simple simulation model (DYNAPROP) which has been modified to treat light ion beam propagation. DYNAPROP uses an envelope equation to treat beam dynamics and uses rate equations to describe plasma and conductivity generation. The model has been applied both to the high current, 30 MeV Li-3 beams for LMF as well as low current, 1.2 MeV proton beams which are currently being studied on GAMBLE 2 at the Naval Research Laboratory. The predicted ratio of net currents to beam current is approximately 0.1 to 0.2 for the GAMBLE experiment and approximately 0.01 for LMF. The implications of these results for LMF and the GAMBLE experiments are discussed in some detail. The simple resistive model in DYNAPROP has well-known limitations in the 1 torr regime which arise primarily from the neglect of plasma electron transport. Alternative methods for treating the plasma response are discussed. GRA

N93-15054# Army Lab. Command, White Sands Missile Range, NM. Atmospheric Sciences Lab.

AN ANALYTIC PHASE FUNCTION FOR CYLINDRICAL PARTICLES Final Report

Patti Gillespie Aug. 1992 52 p

(AD-A255750; ASL-TR-0318) Avail: CASI HC A04/MF A01

In this report an analytic phase function for cylindrical particles is developed based on considerations used to develop the Henyey-Greenstein phase function and functions based on electromagnetic theory calculations. The phase function developed in this report is compared to other phase functions and its usefulness is demonstrated. An annotated bibliography on the subject of phase functions for cylindrical particles is included. GRA

N93-15062# Oregon State Univ., Corvallis.

A CLOUDY QUARK BAG MODEL OF S, P, AND D WAVE INTERACTIONS FOR THE COUPLED CHANNEL ANTIKAON-NUCLEON SYSTEM Ph.D. Thesis

Guangliang He 15 May 1992 149 p

(Contract DE-FG06-86ER-40283)

(DE92-040149; DOE/ER-40283/12) Avail: CASI HC A07/MF A02

The Cloudy Quark Bag Model is extended from S-wave to P- and D-wave. The parameters of the model are determined by K(sup -)p scattering cross section data, K(sup -)p yields Sigma pi pi pi production data, K(sup -)p threshold branching ratio data, and K(sup -)p yields Lambda pi pi pi production data. The resonance structure of the Lambda(1405), Sigma(1385), and Lambda(1520) are studied in the model. The shift and width of kaonic hydrogen are calculated using the model. DOE

N93-15279# Washington Univ., Seattle. Dept. of Physics.

LOW ENERGY THEOREMS IN PION PRODUCTION

B. R. Holstein (Massachusetts Univ., Amherst.) 1992 20 p Presented at the Physics With Internal Targets and the Blast Detector, Tempe, AZ, 19-21 Mar. 1992

(Contract DE-FG06-90ER-40561)

(DE92-040071; DOE/ER-40561/67; CONF-9203150-3) Avail: CASI HC A03/MF A01

Considerable activity, both theoretical and experimental, has recently taken place involving the threshold and near threshold of pion photo- and electroproduction. This activity is herein summarized and a program for future work is outlined. DOE

N93-15326# Rochester Univ., NY. Dept. of Chemistry.

STUDIES OF HEAVY-ION REACTIONS AND TRANSURANIC NUCLEI

W. U. Schroeder Aug. 1992 14 p

(Contract DE-FG02-88ER-40414)

(DE92-040457; DOE/ER-40414/5) Avail: CASI HC A03/MF A01

Developments around the fictitious phenomenon of 'cold' deuterium fusion are summarized. Investigations of the decay of Dy composite systems formed in S-32-induced fusion reactions provide no evidence for entrance-channel memory effects. Experimental and theoretical studies of excitation energy division in dissipative reactions are reviewed. Exclusive measurements of neutrons, light charged particles, and massive fragments conducted for the very-heavy-ion reactions Bi-209+Xe-136 and Au-197+Pb-208 at Fermi energies have yielded several new observations. They affirm the effectiveness of the associated-neutron multiplicity as an indicator of dissipated energy and impact parameter. In spite of the elevated incident energies, both reactions are demonstrated to have a binary dissipative character leading to two primary fragments which subsequently decay, for peripheral as well as for central collisions. Atomic-number distributions of the primary fragments reconstructed from the decay products show evidence for multi-nucleon exchange, ruling out participant-spectator reaction scenarios. Correlations observed between deflection angle and dissipated energy in the Bi-209+Xe-136 reaction indicate the onset of orbiting. Intermediate-mass fragments are emitted mostly sequentially but also in a process reminiscent of neck rupture. In each of the very-heavy-ion-reactions studied, only a fraction of the initial kinetic energy is dissipated. The development of the new, highly efficient Super Ball neutron calorimeter is discussed. DOE

N93-15377# Northwestern Univ., Evanston, IL. Dept. of Physics and Astronomy.

STRONG INTERACTIONS STUDIES WITH MEDIUM ENERGY PROBES

K. K. Seth Aug. 1992 51 p

(Contract DE-FG02-87ER-40344)

(DE92-040460; DOE/ER-40344/6) Avail: CASI HC A04/MF A01

This report discusses work on: charmonium spectroscopy; proton form-factor in the time-like region; proton-antiproton forward scattering; QCD scaling laws; light quark spectroscopy; high resolutions electron scattering; quasi-free electron scattering; and low energy pion double charge exchange. DOE

N93-15378# Florida Univ., Gainesville. Dept. of Physics.

STAGGERED FERMIONS AND CHIRAL SYMMETRY BREAKING IN TRANSVERSE LATTICE REGULATED QED

P. A. Griffin Jul. 1992 30 p

(Contract DE-FG05-86ER-40272)

(DE92-040505; DOE/ER-40272/169; UFIFT-HEP-92-19) Avail: CASI HC A03/MF A01

Staggered fermions are constructed for the transverse lattice regularization scheme. The weak perturbation theory of transverse lattice non-compact QED is developed in light-cone gauge, and we argue that for fixed lattice spacing this theory is ultraviolet finite, order by order in perturbation theory. However, by calculating the anomalous scaling dimension of the link fields, we find that the interaction Hamiltonian becomes non-renormalizable for g(sup 2)(a) greater than 4(pi), where g(a) is the bare (lattice) QED coupling constant. We conjecture that this is the critical point of the chiral symmetry breaking phase transition in QED. Non-perturbative chiral symmetry breaking is then studied in the strong coupling limit. The discrete remnant of chiral symmetry that remains on the lattice is spontaneously broken, and the ground state to lowest order in the strong coupling expansion corresponds to the classical ground state of the two-dimensional spin one-half Heisenberg antiferromagnet. DOE

N93-15448# Purdue Univ., West Lafayette, IN. Dept. of Chemistry.

MOLECULAR CAPACITANCE: SEQUENTIAL ELECTRON-TRANSFER ENERGETICS FOR SOLUTION-PHASE METALLIC CLUSTERS IN RELATION TO GAS-PHASE CLUSTERS AND ANALOGOUS INTERFACES

Michael J. Weaver and Xiaoping Gao Oct. 1992 34 p

(Contract N00014-91-J-1409)

(AD-A257057; TR-134) Avail: CASI HC A03/MF A01

A simple electrostatic treatment of the energetics of sequential solution-phase electron transfers involving metallic clusters and other large solutes is outlined and related to the conventional description for charging of gas-phase clusters with the objective of linking these phenomena and assessing phenomenologically the role of solvation in the former class of systems. The common occurrence of electron transfer sequencies for solution-phase solutes suggests the concept of 'molecular capacitance', denoting the dependence of the surface charge density upon the electrode potential; the present treatment is related to conventional descriptions of the capacitance of metal electrode-solution interfaces. The notion of the 'potential of zero charge', E(sub pzc), for cluster solutes, which also emerges from the electrostatic treatment, is related to the corresponding quantities for both metal-solution and metal-vacuum interfaces. The analysis therefore provides an instructive link between the charging energetics of spherical clusters and planar surfaces in solution versus gas-phase environments. GRA

N93-15468# Stanford Research Inst., Menlo Park, CA. Linear Accelerator Center.

PRODUCTION OF RELATIVISTIC ANTI-HYDROGEN ATOMS BY PAIR PRODUCTION WITH POSITRON CAPTURE AND MEASUREMENT OF THE LAMB SHIFT

C. T. Munger (Stanford Univ., CA.), S. J. Brodsky (Stanford Univ., CA.), and I. Schmidt (Universidad Tecnica Federico Santa Maria, Valparaiso, Chile) Sep. 1992 6 p Presented at the Hyperfine Interactions of the Anti-Hydrogen Workshop, Munich (Germany), 30-31 Jul. 1992

(Contract DE-AC03-76SF-00515)

(DE93-001767; SLAC-Pub-5939; CONF-9207149-2) Avail: CASI HC A02/MF A01

A beam of relativistic antihydrogen atoms - the bound state (bar-p)e(+) - can be created by circulating the beam of an antiproton storage ring through an internal gas target. An antiproton which passes through the Coulomb field of a nucleus will create e(+)e(-) pairs, and antihydrogen will form when a positron is created in a bound instead of continuum state about the antiproton. The cross section for this process is roughly 1 Z(exp 2) pb for antiproton momenta above 6 GeV/c. A sample of 200 antihydrogen atoms in a low-emittance, neutral beam will be made in 1994 as an accidental byproduct of Fermilab experiment E760. We describe a simple experiment, Fermilab Proposal P862, which can detect this beam, and outline how a sample of a few 10(exp 4) atoms can be used to measure the antihydrogen Lamb shift to 1 percent. DOE

N93-15486# Stanford Research Inst., Menlo Park, CA. Linear Accelerator Center.

WEAK-ELECTROMAGNETIC INTERFERENCE IN POLARIZED eD SCATTERING

C. Y. Prescott Sep. 1992 15 p Presented at the Third International Symposium on the History of Particle Physics: The Rise of the Standard Model, Stanford, CA, 24-27 Jun. 1992

(Contract DE-AC03-76SF-00515)

(DE93-001763; SLAC-Pub-5910; CONF-9206131-1) Avail: CASI HC A03/MF A01

Observation of parity non-conservation in deep-inelastic scattering of polarized electrons from deuterium was reported in an experiment at SLAC in 1978. The events at SLAC and elsewhere leading to the successful search for parity non-conservation in the electromagnetic processes are described. DOE

N93-15654# Argonne National Lab., IL.

C60 INTERACTIONS WITH SURFACES, GASEOUS SPECIES AND PHOTONS: AN OVERVIEW

D. M. Gruen 1992 18 p Presented at the Workshop on Inelastic Ion Surface Collisions, Aussois (France), 14-18 Sep. 1992

(Contract W-31-109-eng-38)

(DE92-040738; ANL/CP-77000; CONF-920945-1) Avail: CASI HC A03/MF A01

The behavior of C60 in collisions with surfaces, with other gaseous species, and with photons is discussed. The focus is on the processes leading to fragmentation of the molecule, the identification of fragmentation products, and the mechanism of fragmentation. The nature of the fragmentation process of C60 is of considerable interest in itself and needs to be understood in detail if C60 cluster ion beams are to be fully exploited technologically. In addition, one may anticipate that an understanding of C60 fragmentation will contribute mutatis mutandis to an elucidation of the elementary steps leading to the assembly of C60 from smaller carbon clusters. DOE

N93-15657# Argonne National Lab., IL.

SCHWINGER DYSON EQUATIONS: DYNAMICAL CHIRAL SYMMETRY BREAKING AND CONFINEMENT

C. D. Roberts 1992 10 p Presented at the Workshop on QCD Vacuum Structure, Paris (France), 1-5 Jun. 1992

(Contract W-31-109-eng-38)

(DE92-040717; ANL/CP-77129; CONF-9206280-1) Avail: CASI HC A02/MF A01

A representative but not exhaustive review of the Schwinger-Dyson equation (SDE) approach to the nonperturbative study of QCD is presented. The main focus is the SDE for the quark self energy but studies of the gluon propagator and quark-gluon vertex are also discussed insofar as they are important to the quark SDE. The scope of this article is the application of these equations to the study of dynamical chiral symmetry breaking, quark confinement and the phenomenology of the spectrum and dynamics of QCD. DOE

73 NUCLEAR AND HIGH-ENERGY PHYSICS

Includes elementary and nuclear particles; and reactor theory. For space radiation see *93 Space Radiation.*

N93-14127# Naval Research Lab., Washington, DC.

CONDITIONING ELECTRON BEAMS IN THE ION-FOCUSED REGIME

R. F. Fernsler, R. F. Hubbard, and S. P. Slinker 17 Sep. 1992 53 p

(ARPA Order 7781)

(AD-A255635; NRL/MR/4790-92-7110) Avail: CASI HC A04/MF A01

Relativistic electron beams propagating through dense gas are subject to the resistive hose instability, a virulent kink instability that restricts the effective range of high-current beams. Previous studies have shown that the instability can be suppressed by centering the beam and tailoring its emittance prior to injection into the gas. One means of centering and tailoring a beam is to use short 'conditioning' cells that operate in the low pressure, ion-focused regime. In this paper, analytic models are developed to understand and assess the performance of such cells. GRA

N93-14570# Naval Research Lab., Washington, DC.

NUMERICAL MODELLING OF INTENSE ELECTRON BEAM TRANSPORT IN THE SPIRAL LINE INDUCTION ACCELERATOR Interim Report

J. Krall, S. Slinker, M. Lampe, and G. Joyce 28 Aug. 1992 61 p

(ARPA Order 7781)

(AD-A255545; NRL/MR/4790-92-6996) Avail: CASI HC A04/MF A01

Computer simulation is used to study issues of intense electron beam transport arising in the context of the spiral line induction accelerator (SLIA), a device in which the beam is transported along an open-ended beam pipe, making multiple passes through each accelerating cavity and traversing a 180 deg achromatic bend between passes. In the straight sections, the beam is transported on a solenoidal field; in the bends, the beam is subject to a vertical bending field and strong focusing stellarator fields, in addition to the solenoidal field. We show that the self-fields of the beam change the optimum vertical field in the bend but do not significantly affect the achromaticity of the bend. We find that magnetic matching elements are required, at the entrance and exit of each stellarator section, to minimize oscillations of the beam envelope and concomitant emittance growth. We show that matching can be accomplished satisfactorily with a single thick quadrupole lens. We determine the frequency and damping rate of envelope oscillations that result from mismatches, and resulting emittance growth. These are found to be sensitive functions of the beam radial profile. Simulation results are found to be in excellent agreement with experiments conducted recently at Pulse Sciences, Inc. GRA

N93-15277# Sandia National Labs., Albuquerque, NM.

GENERATION, CONTROL, AND TRANSPORT OF A 19-MeV, 700-kA PULSED ELECTRON BEAM

T. W. L. Sanford, P. J. Skogmo, J. A. Halbleib, J. W. Poukey, K. A. Mikkelson, R. C. Mock (Ktech Corp., Albuquerque, NM.), and D. R. Welch (Mission Research Corp., Albuquerque, NM.) Jun. 1992 16 p Presented at the 9th International Conference on High Power Particle Beams, Washington, DC, 25-29 May 1992

(Contract DE-AC04-76DP-00789)

(DE92-019803; SAND-92-1047; CONF-920515-7) Avail: CASI HC A03/MF A01

We show experimentally and theoretically that the generation of the 13-TV Hermes 3 electron beam can be accurately monitored, and that the beam can be accurately directed onto a high-Z target to produce a wide variety of bremsstrahlung patterns. This control allows the study of radiation effects induced by gamma rays to be extended into new parameter regimes. Finally, we show that the beam can be stably transported in low-pressure gas cells. DOE

N93-15362# Aerospace Corp., El Segundo, CA. Space and Environmental Technology Center.
BEVALAC ION BEAM CHARACTERIZATIONS FOR SINGLE EVENT PHENOMENA
R. Koga, N. Katz, S. D. Pinkerton, W. A. Kolasinski, and D. L. Oberg 16 Jul. 1992 23 p
(Contract F04701-88-C-0089)
(AD-A257033; TR-0090(5940-05)-4; SMC-TR-92-30) Avail: CASI HC A03/MF A01

Linear Energy Transfer (LET) distributions of Bevalac ion beams were measured. Subsequent analysis has called into question the standard assumption of a monoenergetic, single-species beam at Bevalac. Both high LET contaminants in the primary beam and very broad LET peaks in degraded beams were observed. High energy ion beams at other accelerators may possess similar characteristics. The existence of beam impurities may have important ramifications for the interpretation of single-event phenomena observed at high energy accelerator sites. GRA

N93-15482*# Institute for Computer Applications in Science and Engineering, Hampton, VA.
HOMOGENEOUS QUANTUM ELECTRODYNAMIC TURBULENCE
John V. Shebalin Oct. 1992 29 p
(RTOP 505-90-52-01)
(NASA-TM-107686; NAS 1.15:107686; ICASE-92-50) Avail: CASI HC A03/MF A01

The electromagnetic field equations and Dirac equations for oppositely charged wave functions are numerically time-integrated using a spatial Fourier method. The numerical approach used, a spectral transform technique, is based on a continuum representation of physical space. The coupled classical field equations contain a dimensionless parameter which sets the strength of the nonlinear interaction (as the parameter increases, interaction volume decreases). For a parameter value of unity, highly nonlinear behavior in the time-evolution of an individual wave function, analogous to ideal fluid turbulence, is observed. In the truncated Fourier representation which is numerically implemented here, the quantum turbulence is homogeneous but anisotropic and manifests itself in the nonlinear evolution of equilibrium modal spatial spectra for the probability density of each particle and also for the electromagnetic energy density. The results show that nonlinearly interacting fermionic wave functions quickly approach a multi-mode, dynamic equilibrium state, and that this state can be determined by numerical means. Author

74 OPTICS

Includes light phenomena; and optical devices.
For lasers see *36 Lasers and Masers.*

N93-14124 Heriot-Watt Univ., Edinburgh (Scotland).
NONLINEAR DYNAMICS OF OPTICAL SYSTEMS Ph.D. Thesis
Weiping Lu 1991 221 p
Avail: Univ. Microfilms Order No. BRDX95729

The general principle of dynamics and chaos are reviewed in the first chapter. In chapter 2 special effort has been given to the development of a generalized presentation of light-material interaction and its subsequent reduction to various low dimensional dynamic systems; notably two level lasers, nonlinear counterpropagating wave interaction and transverse spatial pattern forming systems. In chapter 3 and 4 original theoretical investigations of nonlinear dynamic and chaotic behavior of Raman laser systems is presented. A new theoretical model of a single-mode, homogeneously broadened Raman laser is established using the semi-classical laser theory. Bistable features of the Raman emission and its operating condition are determined from steady state analysis. Linear instability analysis shows that dynamics exists over a broad range of parameter space and for broad cavity detuning to the low frequency side of the Raman gain where bistable emission also prevails, the threshold for the dynamics being as low as the first laser threshold. The analysis of the gain and dispersion characteristics in steady state other with the dynamic side mode analysis establish, that the laser and pump field induced distortion and displacement of dispersion profile associated with the laser gain are responsible for the asymmetric steady and dynamical features and also for a low second laser threshold. Oscillatory behavior and period doubling routes to chaos in both intensity and phase of the Raman emission are found to occur for both good and bad cavity conditions, the dynamics of the phase revealing more complicated oscillatory behavior to that of intensity. Comparisons of these theoretical results with experimental findings are also made. In general, a good qualitative agreement between them have been established in regard to steady state and bistable features, dependence of instabilities on the operating parameters and dynamic and chaotic formations in unstable regions. In chapter 5 and 6 a general theoretical model of stimulated scattering incorporating the integral effect of nonlinear refraction is originated. Our analysis establishes that nonlinear dynamics is generic to and can be a prevalent feature of stimulated scattering phenomena. Finally Appendix A provides an original contribution on absoptive bistability in coherently pumped three-level laser. This work, which completes much of the earlier work of the group on three-level systems, is incorporated as an appendix since it deals with steady state rather than dynamic aspects of behavior. Dissert. Abstr.

N93-14140 Arizona Univ., Tucson.
CHARACTERIZATION OF MAGNETO-OPTICAL RECORDING MEDIA Ph.D. Thesis
Roger Antoine Hajjar 1992 307 p
Avail: Univ. Microfilms Order No. DA9225191

The optical, magnetic and transport properties of magneto-optical recording media are discussed. The various custom-made and off-the-shelf instrumentation used include: a Vibrating Sample Magnetometer (VSM); a modified polarization microscope; a polar Kerr effect loop tracer; a variable angle of incidence ellipsometer; and magnetoresistance/Hall effect/resistivity probes. Most of the samples studied were analyzed for determination of their composition and thickness by Rutherford Back Scattering (RPS) and X Ray Fluorescence (XRF). The samples studied were manufactured in several industrial and academic laboratories under different deposition conditions. The optical properties measured include Kerr rotation angle and ellipticity, Fresnel reflectivity coefficients, and calculation of the dielectric tensor. The magnetic properties include measurements of saturation magnetization, coercivity, anisotropy field, calculations of exchange energy parameters, domain wall, and anisotropy energy densities from experimental observations. The transport properties include measurements of magnetoresistance and Hall effect with three different geometries and calculation of the resistivity tensor. The modeling work consisted of modeling the optical path for various instruments, the current distribution in magnetic films, and the calculation of the demagnetizing energy using the fast Fourier transform technique. Dissert. Abstr.

N93-14152# ERG Systems, Inc., Saint James, NY.
FULL SURFACE TESTING OF GRAZING INCIDENCE MIRRORS Final Report, 12 Sep. 1990 - 12 Sep. 1992
John L. Remo 12 Sep. 1992 175 p
(Contract N00014-90-C-0246)
(AD-A255644) Avail: CASI HC A08/MF A02

The objective was to design, construct, and test a prototype interferometer system (FSIS) for the purpose of testing cylindrical-like mirrors such as those used in grazing incidence X-ray imaging applications. Existing instruments are based on a shearing interferometry, dual laser beam scanning approach, measuring the slope or curvature functions along a single long trace in the long direction of the cylindrical mirror. While these instruments are characterized by a high measuring accuracy, they are very slow and environmentally sensitive. An even slower and more complex two-dimensional scan must be implemented if the full surface measurement is required. Our approach is also based on interferometric slope measurement in the direction of the long side of the mirror, using a grating shearing interferometer head. A full-width beam covering an extended subaperture of the mirror is canned in discrete steps in the direction of the long side of the mirror, so that a single scan allows coverage of the whole mirror surface. By least square fitting the series of subaperture measurements, the system yields parallel measurement of a multiplicity of long traces in the direction of scan. GRA

N93-14165 Alabama Univ., Birmingham.
A DIFFERENTIAL EQUATION DESIGN METHOD FOR FINITE-CONJUGATE, MULTI-MIRROR IMAGING SYSTEMS Ph.D. Thesis
Cheng Wang 1992 131 p
Avail: Univ. Microfilms Order No. DA9223846

Soft-x-rays with wavelengths less than 200 nm are being used for many applications in astronomy, microscopy and lithography. The rapid development of the computer industry requires more advanced fabrication technologies for manufacturing higher-density silicon chips. Soft-X-ray projection lithography (SXPL) has been proposed to achieve tenth or sub-tenth of micron feature size. The specific requirements such as near diffraction-limited performance, a large image field, and very low distortion for SXPL systems, are very difficult to achieve. Soft-x-ray imaging microscopy is developing as a technique to study the structure of macromolecules within living cells. It would be desirable to construct a reflective imaging microscope operating within the water window (23.3 to 43.6 A) to achieve a 100 A resolution for potential studies of the structures of DNA and RNA molecules. All reflective, soft x-ray imaging systems with near diffraction-limited performance with a modest numerical aperture (NA) over a large image field or with a large NA over a modest image field have confronted optical designers with new challenges. In order to address the challenges of the new soft-x-ray applications, alternative optical design techniques are considered. Based on the conditions of aplanatism, a differential equation design method (DEDM) has been developed for design and optimization of finite-conjugate, multi-mirror imaging systems for soft-x-ray applications. The basic theory, numerical calculations, layout design, system optimization and surface fitting process for DEDM will be described. Applications of DEDM to several three- and four-mirror soft-x-ray projection lithography systems have demonstrated the ability of this design technique to improve the performance of the original systems. Also, a number of two-aspherical-mirror microscopes have been designed by using DEDM based on Schwarzschild configurations. Near diffraction-limited performances have been predicted for a numerical aperture of 0.4 while operating with soft-x-ray radiation with wavelength ranging from 40 A to 130 A. These results of the application of DEDM to the design of soft-x-ray imaging systems indicate that DEDM is a very promising design and optimization technique for finite-conjugate, multi-mirror imaging systems. Particular strengths of DEDM have been identified by comparing the performance of optical systems designed by this method to that obtained via conventional optical design methods. Some future directions for extending DEDM will also be discussed. Dissert. Abstr.

N93-14167 Maryland Univ., College Park.
GENERATION OF BROADLY TUNABLE, NARROW BANDWIDTH, AND INTENSE COHERENT VACUUM ULTRAVIOLET RADIATION IN RARE GASES Ph.D. Thesis
Xiaoxiong Xiong 1991 179 p
Avail: Univ. Microfilms Order No. DA9222787

Generation of broadly tunable, narrow bandwidth, and intense coherent vacuum (VUV) radiation in rare gases was investigated using third-order sum-difference frequency mixing processes. VUV radiation in the region between 1180 A and 1240 A was efficiently generated by a resonance enhanced mixing process, omega(sub VUV) = 2(omega sub UV) - omega(sub IR) with near and on the two-photon resonant intermediate states in rare gases, and by phase matching enhancement with gases of oppositely dispersive properties. The input tunable ultraviolet (UV) radiation at frequency omega(sub UV) was produced by a tunable pulsed dye laser pumped by the second harmonic of a Nd:YAG laser. In one scheme, the dye laser radiation near 5440 A was doubled to 2720 A, and then mixed with the YAG fundamental at 1.06 microns to yield the UV radiation at 2167 A (Kr4p(exp 6) yields 4p(exp 5)5p(5/2,2) two-photon resonance wavelength). In another scheme, the tunable UV radiation near 2150 A was obtained by two successive doubling of the dye laser radiation near 8600 A. The input infrared (IR) at frequency omega(sub IR) was chosen from either the dye laser radiation or the YAG fundamental radiation. The generation system presented here was constructed with the capability of accurately monitoring the wavelength, linewidth, and intensity of generated VUV radiation, and was suitable for high resolution spectroscopic applications. Also of great practical interest, radiation of 1202.8 A (helium 1s(exp 2) + 2h(nu) yields 1s2s(sup S-1 transition), and 1215.6 A (hydrogen 1s + h(nu) yields 2p Lyman-alpha) was included in the generation region and studied by using different schemes. UV to VUV power conversion efficiencies as high as 2 x 10(exp -3) for resonant case, and 4 x 10(exp -4) for non-resonant case were achieved. Experimental results of the power dependence of the generated VUV on the input UV and IR, and the nonlinear dispersion of the media demonstrated good agreements with the theoretical analysis and calculation. Operating near, but not on, intermediate resonances allows an efficient, tunable system with only one tunable dye laser. The use of phase matching with a mixture of rare gases raises the off resonance conversion efficiency to within an order of magnitude of the saturated on resonance value. Dissert. Abstr.

N93-14168 Arizona Univ., Tucson.
OPTICAL INSTRUMENTATION AND CHARACTERIZATION FOR MAGNETO-OPTICAL RECORDING MEDIA Ph.D. Thesis
Andy Fenglei Zhou 1992 183 p
Avail: Univ. Microfilms Order No. DA9225184

This dissertation presents instrumentation developed for the optical characterizations of magneto-optic (M-O) recording media and explores the magneto-optic Kerr effect in optical recording applications. We developed an accurate method to measure the wavelength dependencies of the magneto-optic Kerr rotation angle theta(k), ellipticity epsilon(k) and reflectivity R and applied it to the characterization of TbFe and TbFeCo rare earth-transition metal (RE-TM) samples and Co/Pt and Co/Pd superlattice thin films. A variable-angle photometric ellipsometer system is developed for the dielectric tensor characterization of the M-O media. A series of Co/Pd samples with different thicknesses are studied for the understanding of M-O Kerr effect. The composition dependencies of the dielectric tensor for both Co/Pt and Co/Pd superlattice samples are measured, and the enhancement of the magneto-optic Kerr effect for these samples is studied. We also characterized many RE-TM samples and some non-magnetic dielectric, organic, sol-gel and metallic thin films. A semiclassical theory is proposed to describe the wavelength dependence of the magneto-optical Kerr effect. The theory takes into account the effects of the spin-orbit interaction, the band structure of the magnetic electrons and the phenomenological elements of the classical Drude model for the dielectric constant. Analytical formulas for the dielectric constants demonstrate explicitly how the Kerr rotation, the ellipticity and the reflectivity are related to the spin-orbit interaction, the band structure and several phenomenological parameters, such as the number density and relaxation timed of the free electrons. This model is applied to the bulk Co materials and the physics of the magneto-optic Kerr effect in these media is studied. Then we apply the theory to our measurements of the wavelength dependence of theta(k), epsilon(k) and R in a series of multilayered Co/Pt and Co/Pd thin films, covering the range of the 1.2-3.6 eV. With several adjustable parameters we have obtained a satisfactory match between the theory and the experimental data. Dissert. Abstr.

N93-14169 City Univ. of New York, NY.
DIFFUSING WAVE SPECTROSCOPY Ph.D. Thesis
Jixiang Zhu 1992 173 p
Avail: Univ. Microfilms Order No. DA9224870

The development of diffusing-wave spectroscopy (DWS) and the applications of DWS to study concentrated colloidal suspensions is presented. DWS is an extension of the traditional photon correlation spectroscopy to the multiple scattering limit. It is a unique tool for studying the dynamics and the structures of optically opaque materials and thus it opens up for study a new class of systems. An important feature is that DWS probes the motion of scatterers at very short length scale. To utilize DWS, one must account for the effects of internal reflection which results from the index of refraction mismatch at the boundaries between the scattering medium and its surroundings. We develop a model which accounts for the internal reflection by amending the boundary conditions for the diffusion equation for the propagating light. We show that static angular correlation functions can be used to measure the effect of internal reflection. After doing a series of experiments, we find that the theory is in excellent agreement with the experiments. As an important application of DWS, we study the effect of hydrodynamic interactions on the short time non-diffusive motion of Brownian particles suspended in a fluid. We measure the mean square displacement, (delta(r(exp 2)(tau))), for concentrated suspensions at times too short to observe the retarded nature of hydrodynamic interactions. A power-law decay of the velocity autocorrelation function, R(tau) is approximately tau(exp 3/2), is observed for all concentrations. A remarkable scaling behavior of the time dependent diffusion coefficient, D(sub s)(tau) = (delta(r(exp 2)(tau)))/6(tau), with particle volume fraction is observed: if D(sub s)(tau) is scaled by its asymptotic value and if time is scaled by a viscous time constant inversely proportional to the shear viscosity of the suspension, all the data fall onto a single universal curve. Using DWS in

backscattering, we find that light backscattered from an optically dense random medium exhibits a pronounced polarization dependence. An unexpected memory of the incident circular polarization of multiply scattered light arises because the wave's helicity is randomized less rapidly than is its direction. We develop a simple model to account for the observed polarization dependence of the intensity and temporal correlation of the intensity fluctuations of backscattered light. Dissert. Abstr.

N93-14204 Dundee Univ. (Scotland).
OPTICAL INFORMATION PROCESSING USING PHOTOREFRACTIVE BSO Ph.D. Thesis
Colin Soutar 1991 141 p
Avail: Univ. Microfilms Order No. BRDX96676

Several optical processing tasks are implemented using photorefractive BSO as a dynamic holographic medium. The physical basis for the mechanism which allows the implementation of these devices is studied. The properties of BSO which make it particularly attractive as a processing medium are highlighted, and experimental results are presented to demonstrate its practical limitations. An extensive study is presented of the influence of optical bias on the grating formation characteristics. This leads to a documentation of the optimum conditions for transient enhancement of a beam diffracted from such a grating. This transient enhancement can be controlled to provide ideal characteristics for the implementation of transient devices such as novelty filter. A novelty filter utilizing this transient enhancement is subsequently demonstrated. It exhibits good temporal discrimination through the choice of suitable external optical conditions, and the use of digital thresholding. The overall device operates at T.V. frame rates. Results are also presented of various optical correlators using BSO. These include the optical intensity correlator. The unique properties of the intensity correlator are stressed by practical demonstration. Specifically, the relative intolerance of the intensity correlator (compared with coherent correlators) to the position of the various components is demonstrated. Also, the spatially incoherent readout light allows the use of a low-optical quality liquid crystal television (LCTV) as a low-cost spatial light modulator. Output results are then presented from the correlator using the LCTV as a dynamic readout device. This provides an updateable hologram as the reference of the correlator which is interrogated at frame rates by the LCTV. Finally, the temporal discrimination of the novelty filter is combined with the character recognition ability of the intensity correlator. This produces an optical processor which will recognize a particular object but will only register it at the output stage when it is moving.
Dissert. Abstr.

N93-14286# Naval Postgraduate School, Monterey, CA.
DESIGN, DEVELOPMENT, AND TESTING OF A PROTOTYPE OPTICAL SYSTEM FOR A NEXT GENERATION MULTIPLEXED IMAGER M.S. Thesis
Blake D. Huguenin Jun. 1992 104 p
(AD-A256538) Avail: CASI HC A06/MF A02

A proof-of-concept experimental validation of a proposed idea for a prototype optical system was conducted. This system will be incorporated into a new type of infrared, optically multiplexed imaging and multispectral imaging system. This system will use two-sided, transmitting-reflecting encoding Walsh masks to form a two-dimensional optical Kronecker product. First, a ray tracing design was made to model the optical system. Then the optical system was prototyped and ronchigrams were photographed to document the aberrations present in the optical system. It was shown that spherical mirrors could be used to accurately reimage an object onto the encoding masks without significantly affecting the optical accuracy of the image. The geometric aberrations resulting from this design did not significantly effect the overall ability to produce the Kronecker product.
GRA

N93-14403# Arnold Engineering Development Center, Arnold AFS, TN.
EFFECTS OF CRYOCONTAMINANTS ON CRYOGENIC SUPERPOLISHED MIRROR AND SUPERPOLISHED QUARTZ CRYSTAL MICROBALANCE Final Report, Mar. - Dec. 1991
B. L. Seiber, R. J. Bryson, R. P. Young, Sr., and B. E. Wood Sep. 1992 65 p
(AD-A255972; AEDC-TR-92-5) Avail: CASI HC A04/MF A01

Effects of contaminants on optical surfaces is a concern for space-based systems. Many systems contain cryogenic optical systems that operate at temperatures where gases such as nitrogen, oxygen, carbon dioxide, and water will condense. This study presents experimental results of the effects of these gases condensed on highly polished (superpolished) mirror surfaces cooled, under vacuum, to temperatures as low as 15 K. Using these gases as contaminants, the bidirectional reflectance distribution function (BRDF) was obtained at a wavelength of 0.6328 um for various contaminant film thicknesses up to 8 um. Most of the data were obtained using the superpolished sense crystal of a previously developed quartz crystal microbalance (SPQCM) as the mirror surface. The SPQM allowed the mass of the actual contaminant layer to be measured directly. This program has been sponsored by Rome Laboratory and Johns Hopkins University Applied Physics Laboratory. GRA

N93-14404*# National Aeronautics and Space Administration. Pasadena Office, CA.
REAL-TIME EDGE-ENHANCED OPTICAL CORRELATOR Patent Application
Mazen M. Shihabi, inventor (to NASA) (Jet Propulsion Lab., California Inst. of Tech., Pasadena.), Sami M. Hinedi, inventor (to NASA) (Jet Propulsion Lab., California Inst. of Tech., Pasadena.), and Biren N. Shah, inventor (to NASA) (Jet Propulsion Lab., California Inst. of Tech., Pasadena.) 4 Aug. 1992 50 p
(Contract NAS7-918)
(NASA-Case-NPO-18521-1-CU; NAS 1.71:NPO-18521-1-CU; US-Patent-Appl-SN-934078) Avail: CASI HC A03/MF A01

The performance of five symbol lock detectors are compared. They are the square-law detector with overlapping (SQOD) and non-overlapping (SQNOD) integrators, the absolute value detectors with overlapping and non-overlapping (AVNOD) integrators and the signal power estimator detector (SPED). The analysis considers various scenarios when the observation interval is much larger or equal to the symbol synchronizer loop bandwidth, which has not been considered in previous analyses. Also, the case of threshold setting in the absence of signal is considered. It is shown that the SQOD outperforms all others when the threshold is set in the presence of signal, independent of the relationship between loop bandwidth and observation period. On the other hand, the SPED outperforms all others when the threshold is set in the presence of noise only. NASA

N93-14407# Naval Command, Control and Ocean Surveillance Center, San Diego, CA. RDT and E Div.
OPTICAL FIBERS FOR LONG-HAUL TRANSMISSION IN SEVERE-BENDING APPLICATIONS Final Report
N. T. Kamikawa Apr. 1992 19 p
(AD-A255964; NRAD-TR-1490) Avail: CASI HC A02/MF A01

An optical-fiber technique is investigated that allows data transmission through 200 km of dual-mode optical fibers wound onto a bobbin for payout from a tethered missile. The study shows that the dual-mode fibers can be used over longer distances than conventional single-mode fibers and can meet the goal for 200-km transmission. The design of the dual-mode fibers is discussed, and test data are presented on their bending loss. Results from modal-noise and modal-dispersion tests are also given, showing that modal-noise and modal-dispersion effects are negligible, if the second-order mode is loosely bound. GRA

N93-14506# Optical Society of America, Washington, DC.
INTEGRATED PHOTONICS RESEARCH TECHNICAL DIGEST SERIES. VOLUME 10: CONFERENCE EDITION: SUMMARIES OF PAPERS PRESENTED AT THE INTEGRATED PHOTONICS RESEARCH TOPICAL MEETING Quarterly Report
16 Apr. 1992 485 p Meeting held in New Orleans, LA, 13-16 Apr. 1992
(Contract F49620-92-J-0264)
(AD-A255423; AFOSR-92-0739TR) Avail: CASI HC A21/MF A04

This symposium includes sessions on the following topics: (1) Quantum confinement and vertical cavity devices; (2) Acousto-optic and magnetic-optic devices; (3) Spatial solitons and planar waveguides; (4) Optoelectronic integrated circuits; (5) Optical fiber solitons; (6) Dielectric waveguides and devices; (7) Electro-optic devices; (8) Novel materials and processing; (9) Beam propagation methods; (10) Special purpose glasses and fiber amplifiers; (11) Lasers; (12) Nonlinear fiber phenomena; (13) All-optical switching; and (14) Semiconductor waveguides and devices. GRA

N93-14507# Stanford Univ., CA. Optical Communications Research Lab.
ADVANCED OPTICAL FIBER COMMUNICATION SYSTEMS Status Report, 1 Mar. - 31 Aug. 1992
Leonid Kazovsky 28 Aug. 1992 244 p LIMITED REPRODUCIBILITY: Availability: Document partially illegible
(AD-A255424) Avail: CASI HC A11/MF A03

Our research is focused on three aspects of advanced optical fiber communication systems: dynamic wavelength division multiplexing (WDM) networks, linewidth insensitive coherent optical analog links, and impact of fiber nonlinearities on optical communication systems. During the reporting period, we were working in all three fields, as follows. In the area of WDM networks, we investigated, designed, and are currently implementing an experimental coherent WDM optical network with a throughput of 3 Gb/s/node. In the study of coherent optical analog links, we analyzed two linewidth-insensitive schemes that could overcome the impact of phase noise of semiconductor laser diodes. In the area of fiber nonlinearities, we evaluated the performance of optical WDM systems in the presence of four-wave mixing, and are analyzing the impact of stimulated Brillouin scattering on such systems. In addition, we have experimentally observed fiber-induced parasitic phase modulation, investigated its properties, and are beginning to investigate its impact on optical communication systems. GRA

N93-14578# University of Southern California, Los Angeles. Optical Materials and Devices Lab.
PHOTONIC MATERIALS AND DEVICES FOR OPTICAL INFORMATION PROCESSING AND COMPUTING APPLICATIONS Final Report, 15 May 1987 - 14 Sep. 1991
Armand R. Tanguay, Jr. 14 Sep. 1991 338 p
(Contract F49620-87-C-0056; DARPA Order 6015)
(AD-A256047) Avail: CASI HC A15/MF A03

The research program described in this report addresses several generic avenues of opportunity in the advancement of a sophisticated component technology base for applications in optical signal processing, optical information processing, and optical computing. As such, the research program is multifaceted as well as highly interdisciplinary, spanning activities from material growth, processing, and characterization through device invention and evaluation to preliminary system level integration. GRA

N93-14582# Rochester Univ., NY. Dept. of Computer Science.
REAL-TIME GAZE HOLDING IN BINOCULAR ROBOT VISION Ph.D. Thesis
David J. Coombs Jun. 1992 165 p
(Contract N00014-82-K-0193)
(AD-A256226; TR-415) Avail: CASI HC A08/MF A02

Using a binocular, maneuverable visual system, a robot that holds its gaze on a visual target can enjoy improved visual perception and performance in interacting with the world. This dissertation examines the problem of holding gaze on a moving object from a moving platform, without requiring the ability to recognize the target. A novel aspect of the approach taken is the use of controlled camera movements to simplify the visual processing necessary to keep the cameras locked on the target. A gaze holding system on the Rochester robot's binocular head demonstrates this approach. Even while the robot is moving, the cameras are able to track an object that rotates and moves in three dimensions. GRA

N93-14711* National Aeronautics and Space Administration. Marshall Space Flight Center, Huntsville, AL.
X-RAY MONOCHROMATOR Patent
Richard B. Hoover, inventor (to NASA) 22 Dec. 1992 5 p
(NASA-Case-MFS-28392-1; US-Patent-5,173,930;
US-Patent-Appl-SN-803268; US-Patent-Class-378-85;
US-Patent-Class-378-145; Int-Patent-Class-G21K-1/06) Avail: US Patent and Trademark Office

An x-ray monochromator is described, wherin a housing supports a plurality of mirrors forming a plurality of opposed mirror faces in parallel with each other and having thereon multilayer coatings, with each of said pairs of mirror faces being provided with identical coatings which are different from the coatings on the other pairs of mirror faces such that each pair of mirror faces has a peak x-ray reflection at a different wavelength regime. The housing is moveable to bring into a polychromatic x-ray beam that pair of mirror faces having the best x-ray reflection for the desired wavelength, with the mirrors being pivotable to move the mirror faces to that angle of incidence at which the peak reflectivity of the desired wavelength x-rays occurs.
Official Gazette of the U.S. Patent and Trademark Office

N93-14784# Electronics Research Lab., Adelaide (Australia).
A PRELIMINARY DESIGN OF THE Ti:LiNbO3 OPTICAL CHANNEL WAVEGUIDE
Yat Choi Mar. 1992 17 p
(AD-A255443; ERL-0607-RN; DODA-AR-006-940) Avail: CASI HC A03/MF A01

One of the goals of technology-based activities within the Electronic Warfare Division is to facilitate the development within Australia, of facilities and a capability to manufacture sophisticated, highspeed electro-optic devices, in particular, the integrated optical amplitude modulator and integrated optical switch, for use in microwave and millimetre-wave systems for the Australian Defense Force (ADF). An initial step towards this goal would be to produce a low-loss and single-mode propagation optical channel waveguide using titanium-indiffused lithium niobate (Ti:LiNbO3). As no dimensions and fabrication parameters have yet been optimized, this technical report provides preliminary design data which optimizes these parameters. GRA

N93-14800 Department of the Navy, Washington, DC.
INTERFEROMETER WITH TWO PHASE-CONJUGATE MIRRORS Patent
Louis Sica, Jr., inventor (to Navy) 9 Jun. 1992 8 p Filed 21 Dec. 1990
(AD-D015420; US-Patent-5,120,133; US-Patent-Appl-SN-632198;
US-Patent-Class-356-360) Avail: CASI HC A02/MF A01

In an interferometer apparatus used for monitoring an object surface, the apparatus has a source of coherent light, a beam splitter for dividing the coherent light into a reference beam and an object beam, another beam splitter for dividing the object beam into two separate portions, and a light detector for detecting light interference, comprising an externally-pumped phase-conjugate mirror working in conjunction with a self-pumped phase-conjugate mirror. The externally-pumped phase-conjugate mirror receives the reference beam, receives one portion of the object beam, and reflects the received portion of the object beam to the detector as a first phase-conjugate beam. The self-pumped phase conjugate mirror receives a second portion of the object beam and reflects the received portion of the object beam to the detector as a second phase-conjugate beam. The first and second phase-conjugate beams interfere at the detector, and the interference produced thereby is representative of changes in longitudinal distance between the object surface irrespective of roughness and the phase-conjugate mirrors. GRA

N93-14880# Department of the Navy, Washington, DC.
TWO-STAGE TARGET TRACKING SYSTEM AND METHOD Patent Application
Ali T. Alounia, inventor (to Navy) 17 Jun. 1992 19 p
(AD-D015412; US-Patent-Appl-SN-899803) Avail: CASI HC A03/MF A01

An apparatus and method for tracking maneuvering and non-maneuvering targets in the presence of stochastic acceleration are provided. The apparatus and method utilize a two-stage Kalman estimator, the first stage of which is a bias-free filter providing target position and velocity estimates, and the second stage of which is a bias filter providing estimates of target acceleration. These two filters act together to provide parallel processing calculations thereby achieving high speed target state determination. During target maneuvers, the output of the second stage is used to correct the output of the first stage. In the absence of maneuver, the second stage is turned off and the first stage provides the target position and velocity estimates. GRA

N93-15116*# United Technologies Research Center, East Hartford, CT.
ELECTRO-OPTIC ARCHITECTURE (EOA) FOR SENSORS AND ACTUATORS IN AIRCRAFT PROPULSION SYSTEMS Final Report, Apr. 1988 - Jan. 1989
W. L. Glomb, Jr. Jun. 1989 250 p
(Contract NAS3-25343)

(NASA-CR-182270; UTRC-R89-927889; NAS 1.26:182270) Avail: CASI HC A11/MF A03

Results of a study to design an optimal architecture for electro-optical sensing and control in advanced aircraft and space systems are described. The propulsion full authority digital Electronic Engine Control (EEC) was the focus for the study. The recommended architecture is an on-engine EEC which contains electro-optic interface circuits for fiber-optic sensors on the engine. Size and weight are reduced by multiplexing arrays of functionally similar sensors on a pair of optical fibers to common electro-optical interfaces. The architecture contains common, multiplex interfaces to seven sensor groups: (1) self luminous sensors; (2) high temperatures; (3) low temperatures; (4) speeds and flows; (5) vibration; (6) pressures; and (7) mechanical positions. Nine distinct fiber-optic sensor types were found to provide these sensing functions: (1) continuous wave (CW) intensity modulators; (2) time division multiplexing (TDM) digital optic codeplates; (3) time division multiplexing (TDM) analog self-referenced sensors; (4) wavelength division multiplexing (WDM) digital optic code plates; (5) wavelength division multiplexing (WDM) analog self-referenced intensity modulators; (6) analog optical spectral shifters; (7) self-luminous bodies; (8) coherent optical interferometers; and (9) remote electrical sensors. The report includes the results of a trade study including engine sensor requirements, environment, the basic sensor types, and relevant evaluation criteria. These figures of merit for the candidate interface types were calculated from the data supplied by leading manufacturers of fiber-optic sensors. Author

N93-15197# Arizona Univ., Tucson. Optical Sciences Center.
NONUNIFORMITY EFFECTS IN A HYBRID PLATINUM SILICIDE IMAGING DEVICE Final Report, Feb. 1988 - Jul. 1991
Eustace L. Dereniak and David L. Perry May 1992 243 p
(Contract F19623-88-K-0009)
(AD-A256339; RL-TR-92-30) Avail: CASI HC A11/MF A03

The objective of this project was twofold. The first objective was to characterize the Hughes Aircraft Company CRC-365 platinum silicide imaging device in a starting infrared sensor system. The CRC-365 is a hybrid 256 x 256 IR focal plane array that operates in the 3-5 micrometer thermal infrared band. A complete sensor and computer interface were built for these tests, using, plans provided by the Rome Laboratory at Hanscom AFB. Testing of the device revealed largely satisfactory performance, with notable exception in the areas of temporal response, temporal noise, and electrical crosstalk. The second objective of this research was to advance the understanding of how detector nonuniformity effects reduce the performance of sensors of this type. Notable accomplishments in this area included a complete linear analysis of corrected thermal imaging in platinum silicide sensors, a nonlinear analysis of the CRC-365's expected performance, analysis of its actual performance when operated with nonuniformity correction, and the development of a new figure of merit. It was demonstrated that the CRC-365 is capable of maintaining background-noise-limited performance over at least a 40 K target temperature range, when operated with two-point nonuniformity correction. GRA

N93-15223# Sandia National Labs., Albuquerque, NM.
A TEMPERATURE TRACKING SPICE2G.6 MACROMODEL OF THE 6N134 OPTOCOUPLER
Christopher Helms and Glenn Perry (Alliance Technologies Corp., Albuquerque, NM.) 1992 13 p Presented at the 35th Midwest Symposium on Circuits and Systems, Washington, DC, 12 Aug. 1992
(Contract DE-AC04-76DP-00789)
(DE92-040093; SAND-92-0669C; CONF-9208119-3) Avail: CASI HC A03/MF A01

The popular circuit simulator platform SPICE2G.6 was chosen for the development of an advanced macromodel for the 6N134 optocoupler. The subcircuit model presented properly simulates DC and transient characteristics over the temperature range -55 to 125 C using a single parameter set and the .TEMP statement available within SPICE. The model's limitations and predictive accuracy relative to measured data are described. DOE

N93-15230# Sandia National Labs., Albuquerque, NM.
PRELIMINARY LIGHTNING TESTS: OPTICAL FIBER PENETRATION OF AN EXCLUSION REGION BARRIER
Michael A. Dinallo (Quatro Corp., Albuquerque, NM.) and Richard J. Fisher Aug. 1992 62 p
(Contract DE-AC04-76DP-00789)
(DE92-019804; SAND-92-1767) Avail: CASI HC A04/MF A01

As part of the Direct Optical Initiation (DOI) program, an assessment of the possibility of introducing lightning energy into an exclusion region via an Optical Barrier Feedthrough (OBF) is being carried out. One postulated penetration mechanism is the tracking of current past the OBF on the surface of the dielectric optical fiber itself. During September and October of 1991, a series of tests was conducted on a closed metallic cylindrical test object representing the electrical exclusion region of a weapon. Median-level (30 kA) and severe (200 kA) simulated lightning return strokes, singly, doubly, and in combination with a moderate continuing current, were attached directly to the exterior portion of a fiber optic cable, which penetrated through a hole of controlled size into the interior of the exclusion region. The thickness of the barrier surrounding the hole was 0.06 in. Attempts were made to measure any conducted current flowing on the fiber at distances of 1 and 4 inches from the interior surface of the stainless steel top of the cylinder. Test parameter variations included diameter of the penetration hole (475 and 500 microns), length of the exterior portion of the cable and whether or not its jacket was present, and the applied test currents. It is concluded that no signal above measurement noise was recorded on any of the data shots that made up the test series. Measurement resolution was of the order of several amperes. Based on the highest recorded response of 8.5 A, corresponding to a 200 kA input, the OBF can be characterized by a direct-strike lightning attenuation factor of approx. 5 x 10(exp -5) or better. Based on the more typically observed noise level of a few amps, the attenuation is commensurately greater. DOE

N93-15241# EIC, Inc., Norwood, MA.
REMOTE FIBER OPTIC SENSOR FOR GASEOUS AND LIQUID ENVIRONMENTS, PHASE 2 Final Report, 1 Sep. 1988 - 30 Nov. 1990
Michael M. Carrabba, R. D. Rauh, K. M. Spencer, and R. B. Edmonds 28 Sep. 1992 8 p
(Contract N00014-88-C-0661)
(AD-A256224) Avail: CASI HC A02/MF A01

The goal of this program was to develop techniques and instrumentation for the implementation of Raman spectroscopy as a chemical sensor for both gas and liquid phase samples. Surface enhanced Raman techniques have been employed for low level detection. Novel SERS substrates have been demonstrated which enable complexation and preconcentration of gas phase species, a new development since SERS had previously been associated only with the liquid phase. The substrates were demonstrated for Raman sensing of hydrazine, ethanol, dimethyl methylphosphonate (DMMP), and other vapor species. In order to conduct remote sensing using Raman, a fiber optic probe, was developed. The probe permits the excitation and collection of Raman spectra over greater than 50 m of optical fiber without interference from scattering originating within the fibers themselves, previously a serious problem with this approach. Spectral analysis has been conducted with small spectrographs, some of them palm-sized. Special Raman filters based on holographic optical elements were developed for this purpose, removing all vestiges of the primary Raman excitation light before introducing the scattered Raman light into the spectrograph. Several spectrograph configurations were examined, including a novel Echelle design which enables better than 1 cm-1 spectral resolution in a compact package (e.g., approximately 10(exp 3) cu cm, including CCD detector). GRA

N93-15255# Foster-Miller Associates, Inc., Waltham, MA.
NEW NONLINEAR OPTICAL FILM PROCESSING Final Report, Aug. 1987 - Dec. 1990
K. Blizard and M. A. Druy 15 Jan. 1992 41 p
(Contract F33615-87-C-5240)
(AD-A256011; AFW-5240-FM-8784-461; WL-TR-91-4123) Avail: CASI HC A03/MF A01

This program concerned improving the linear optical properties (i.e., transparency) of ordered polymers. These materials have demonstrated high values of X(3) but are not useful for NLO applications because their poor optical quality restricts their use as optical waveguides. Optical quality is defined as transparency and surface flatness, the specific goals of which are reduction in optical loss to less than 1 dB/cm and a reduction in the surface roughness to an optically flat surface of less than 1/4

wavelength. Our approach to introducing these desired improvements in film quality has been to modify the film processing conditions. This program has examined many of the process steps involved in the fabrication of ordered polymer films to determine their effect on the film's optical quality, hence, nonlinear optical performance. Initial efforts focused on poly p-phenylene benzobisthiazole (PBZT), as this is the most technically advanced ordered polymer and it is with this particular ordered polymer Foster-Miller has had its most extensive film processing experience. More recent efforts have involved poly p-phenylene benzobisoxazole (PBO). Over the course of the program, the optical loss, alpha, decreased from 1064 to about 660 cm(exp -1). While significant, these losses are still prohibitive for NLO materials. Our processing changes have also led to 3-fold modulus improvements and nearly 60 percent strength improvements, to 13.9 GPa and 157 MPa, respectively, in biaxial PBO film. GRA

N93-15350# California Univ., Berkeley. Lawrence Berkeley Lab.
CENTER FOR X RAY OPTICS, 1991
Mar. 1992 14 p
(Contract DE-AC03-76SF-00098)
(DE93-001543; LBL-31521) Avail: CASI HC A03/MF A01

This report discusses soft-x-ray imaging with zone-plate lenses, multilayer reflective optics, and spectroscopy with x-rays. DOE

N93-15371# ERG Systems, Inc., Saint James, NY.
FULL SURFACE TESTING OF GRAZING INCIDENCE MIRRORS Final Quarterly Report No. 8
John L. Remo 12 Sep. 1992 40 p
(Contract N00014-90-C-0246)
(AD-A255798) Avail: CASI HC A03/MF A01

In the present report, we present the work done during the period of August 12 to September, 1992. The work includes the implementation of the final testing program for the FSIS prototype system using the latest software package. It also included work on the final report. The custom T.W.O. cylindrical mirror was used for testing. The scan is made of 5 subapertures, two inches each with one inch overlap area between subapertures. GRA

N93-15458# Massachusetts Inst. of Tech., Cambridge. Research Lab. of Electronics.
INTERFEROMETRIC MEASUREMENT WITH SQUEEZED LIGHT Annual Report
Hermann A. Haus 8 Oct. 1992 6 p
(Contract N00014-92-J-1302)
(AD-A257065) Avail: CASI HC A02/MF A01

Squeezed vacuum injected into the 'unused' port of a phase measurement interferometer reduces the noise of the sensor below the shot noise level. Ever since our proposal to generate squeezed vacuum in an optical fiber ring using optical pulses for enhanced Kerr nonlinearity, while saving the pump power for local oscillator, we have been pursuing the goal of utilizing such radiation in a dependable way for improvements in the signal to noise ratio of optical measurements. The research calls for advances in the quantum theory of radiation. The ultimate goal is to use solitons for squeezing, because they offer a higher degree of shot-noise reduction. Thus the quantum theory of solitons needs attention. Further, the use of pulses may lead to nonlinear effects in the sensor utilizing the squeezed radiation. This calls for an investigation of such effects. Guided Acoustic Wave Brillouin Scattering (GAWBS) discovered by the IBM group can introduce sufficient classical noise to destroy the squeezing and thus deserves special attention. This GAWBS noise is convolved into the measurement frequency-window by the (square law) optical detector. GRA

N93-15505*# Arizona Univ., Tucson.
RESEARCH STUDIES ON ADVANCED OPTICAL MODULE/HEAD DESIGNS FOR OPTICAL DATA STORAGE Annual Report, period ending 15 Mar. 1992
15 Mar. 1992 265 p
(Grant NAG5-1346)
(NASA-CR-191307; NAS 1.26:191307) Avail: CASI HC A12/MF A03

Preprints are presented from the recent 1992 Optical Data Storage meeting in San Jose. The papers are divided into the following topical areas: Magneto-optical media (Modeling/design and fabrication/characterization/testing); Optical heads (holographic optical elements); and Optical heads (integrated optics). Some representative titles are as follow: Diffraction analysis and evaluation of several focus and track error detection schemes for magneto-optical disk systems; Proposal for massively parallel data storage system; Transfer function characteristics of super resolving systems; Modeling and measurement of a micro-optic beam deflector; Oxidation processes in magneto-optic and related materials; and A modal analysis of lamellar diffraction gratings in conical mountings. For individual titles, see N93-15506 through N93-15520.

N93-15506*# Arizona Univ., Tucson.
DIFFRACTION ANALYSIS AND EVALUATION OF SEVERAL FOCUS- AND TRACK-ERROR DETECTION SCHEMES FOR MAGNETO-OPTICAL DISK SYSTEMS
Bruce E. Bernacki and M. Mansuripur *In its* Research Studies on Advanced Optical Module/Head Designs for Optical Data Storage 15 Mar. 1992 p 39-46 (For primary document see N93-15505 04-74)
Avail: CASI HC A02/MF A03

A commonly used tracking method on pre-grooved magneto-optical (MO) media is the push-pull technique, and the astigmatic method is a popular focus-error detection approach. These two methods are analyzed using DIFFRACT, a general-purpose scalar diffraction modeling program, to observe the effects on the error signals due to focusing lens misalignment, Seidel aberrations, and optical crosstalk (feedthrough) between the focusing and tracking servos. Using the results of the astigmatic/push-pull system as a basis for comparison, a novel focus/track-error detection technique that utilizes a ring toric lens is evaluated as well as the obscuration method (focus error detection only). Author

N93-15507*# Arizona Univ., Tucson.
IMPROVED ASTIGMATIC FOCUS ERROR DETECTION METHOD
Bruce E. Bernacki *In its* Research Studies on Advanced Optical Module/Head Designs for Optical Data Storage 15 Mar. 1992 p 49-51 (For primary document see N93-15505 04-74)
Avail: CASI HC A01/MF A03

All easy-to-implement focus- and track-error detection methods presently used in magneto-optical (MO) disk drives using pre-grooved media suffer from a side effect known as feedthrough. Feedthrough is the unwanted focus error signal (FES) produced when the optical head is seeking a new track, and light refracted from the pre-grooved disk produces an erroneous FES. Some focus and track-error detection methods are more resistant to feedthrough, but tend to be complicated and/or difficult to keep in alignment as a result of environmental insults. The astigmatic focus/push-pull tracking method is an elegant, easy-to-align focus- and track-error detection method. Unfortunately, it is also highly susceptible to feedthrough when astigmatism is present, with the worst effects caused by astigmatism oriented such that the tangential and sagittal foci are at 45 deg to the track direction. This disclosure outlines a method to nearly completely eliminate the worst-case form of feedthrough due to astigmatism oriented 45 deg to the track direction. Feedthrough due to other primary aberrations is not improved, but performance is identical to the unimproved astigmatic method. Author

N93-15508*# Arizona Univ., Tucson.
INSTRUMENTATION OF THE VARIABLE-ANGLE MAGNETO-OPTIC ELLIPSOMETER AND ITS APPLICATION TO M-O MEDIA AND OTHER NON-MAGNETIC FILMS
Andy F. Zhou, J. Kevin Erwin, and M. Mansuripur *In its* Research Studies on Advanced Optical Module/Head Designs for Optical Data Storage 15 Mar. 1992 p 53-75 (For primary document see N93-15505 04-74)
Avail: CASI HC A03/MF A03

A new and comprehensive dielectric tensor characterization instrument is presented for characterization of magneto-optical recording media and non-magnetic thin films. Random and systematic errors of the system are studied. A series of TbFe, TbFeCo, and Co/Pt samples with different composition and thicknesses are characterized for their optical and magneto-optical properties. The optical properties of several non-magnetic films are also measured. Author

N93-15509*# Arizona Univ., Tucson.
MEASUREMENT OF THE MAGNETIC ANISOTROPY ENERGY CONSTANTS FOR MAGNETO-OPTICAL RECORDING MEDIA

R. A. Hajjar, T. H. Wu, and M. Mansuripur *In its* Research Studies on Advanced Optical Module/Head Designs for Optical Data Storage 15 Mar. 1992 p 79-85 (For primary document see N93-15505 04-74)
Avail: CASI HC A02/MF A03

Measurement of the magneto-optical polar Kerr effect is performed on rare earth-transition metal (RE-TM) amorphous films using in-plane fields. From this measurement and the measurement of the saturation magnetization using a vibrating sample magnetometer (VSM), the magnetic anisotropy constants are determined. The temperature dependence is presented of the magnetic anisotropy in the range of -175 to 175 C. The results show a dip in the anisotropy near magnetic compensation. This anomaly is explained based on the finite exchange coupling between the rare earth and transition metal subnetworks. Author

N93-15510*# Arizona Univ., Tucson.
PROPOSAL FOR MASSIVELY PARALLEL DATA STORAGE SYSTEM **c62**

M. Mansuripur *In its* Research Studies on Advanced Optical Module/Head Designs for Optical Data Storage 15 Mar. 1992 p 89-103 (For primary document see N93-15505 04-74)
Avail: CASI HC A03/MF A03

An architecture for integrating large numbers of data storage units (drives) to form a distributed mass storage system is proposed. The network of interconnected units consists of nodes and links. At each node there resides a controller board, a data storage unit and, possibly, a local/remote user-terminal. The links (twisted-pair wires, coax cables, or fiber-optic channels) provide the communications backbone of the network. There is no central controller for the system as a whole; all decisions regarding allocation of resources, routing of messages and data-blocks, creation and distribution of redundant data-blocks throughout the system (for protection against possible failures), frequency of backup operations, etc., are made locally at individual nodes. The system can handle as many user-terminals as there are nodes in the network. Various users compete for resources, by sending their requests to the local controller-board and receiving allocations of time and storage space. In principle, each user can have access to the entire system, and all drives can be running in parallel to service the requests for one or more users. The system is expandable up to a maximum number of nodes, determined by the number of routing-buffers built into the controller boards. Additional drives, controller-boards, user-terminals, and links can be simply plugged into an existing system in order to expand its capacity. Author

N93-15511*# Arizona Univ., Tucson.
COMBINING RAY-TRACE AND DIFFRACTION ANALYSIS: A DESIGN EXAMPLE

Tom D. Milster and Jeffrey P. Treptau (Cray Research, Inc., Chippewa Falls, WI.) *In its* Research Studies on Advanced Optical Module/Head Designs for Optical Data Storage 15 Mar. 1992 p 107-111 (For primary document see N93-15505 04-74)
Avail: CASI HC A01/MF A03

An example is presented of using a combined ray trace and diffraction modeling code to simulate effects of objective-lens tilt in an optical data storage device. In some cases, neither ray-trace analysis nor diffraction analysis can give an adequate description of an optical system. The designer that is faced with the problem of analyzing such a system is forced to use a ray-trace program to determine aberrations in the exit pupil and then introduce aberration coefficients into a diffraction model that simulate the propagation. This approach was found rather awkward, especially if complicated aberrations are present. Our approach is to integrate a diffraction analysis and a ray-trace description of an optical path into one program. Our design is taken from a data storage application, where we must analyze the effects of objective-lens tilt. Author

N93-15512*# Arizona Univ., Tucson.
TRANSFER FUNCTION CHARACTERISTICS OF SUPER RESOLVING SYSTEMS

Tom D. Milster and Craig H. Curtis *In its* Research Studies on Advanced Optical Module/Head Designs for Optical Data Storage 15 Mar. 1992 p 115-118 (For primary document see N93-15505 04-74)
Avail: CASI HC A01/MF A03

Signal quality in an optical storage device greatly depends on the optical system transfer function used to write and read data patterns. The problem is similar to analysis of scanning optical microscopes. Hopkins and Braat have analyzed write-once-read-many (WORM) optical data storage devices. Herein, transfer function analysis of magnetooptic (MO) data storage devices is discussed with respect to improving transfer-function characteristics. Several authors have described improving the transfer function as super resolution. However, none have thoroughly analyzed the MO optical system and effects of the medium. Both the optical system transfer function and effects of the medium of this development are discussed. Author

N93-15513*# IBM Watson Research Center, Yorktown Heights, NY.
THE 3D MODELING OF HIGH NUMERICAL APERTURE IMAGING IN THIN FILMS

D. G. Flagello and Tom Milster (Arizona Univ., Tucson.) *In* Arizona Univ., Research Studies on Advanced Optical Module/Head Designs for Optical Data Storage 15 Mar. 1992 p 121-136 (For primary document see N93-15505 04-74)
Avail: CASI HC A03/MF A03

A modelling technique is described which is used to explore three dimensional (3D) image irradiance distributions formed by high numerical aperture (NA is greater than 0.5) lenses in homogeneous, linear films. This work uses a 3D modelling approach that is based on a plane-wave decomposition in the exit pupil. Each plane wave component is weighted by factors due to polarization, aberration, and input amplitude and phase terms. This is combined with a modified thin-film matrix technique to derive the total field amplitude at each point in a film by a coherent vector sum over all plane waves. Then the total irradiance is calculated. The model is used to show how asymmetries present in the polarized image change with the influence of a thin film through varying degrees of focus. Author

N93-15514*# Arizona Univ., Tucson.
MODELING AND MEASUREMENT OF A MICRO-OPTIC BEAM DEFLECTOR

Tom D. Milster and J. Nan Wong (Lawrence Livermore National Lab., CA.) *In its* Research Studies on Advanced Optical Module/Head Designs for Optical Data Storage 15 Mar. 1992 p 139-144 (For primary document see N93-15505 04-74)
Avail: CASI HC A02/MF A03

The use is studied of a unity-magnification micro-optic beam deflector. The defelector consists of two arrays of positively powered lenslets. The lenslets on each array are arranged in a square grid. Design criteria are based on usefulness in optical data storage devices. The deflector is designed to operate over a + or - 1.6 range of deflection angles. Modeling results are compared with interferometric analysis of the wavefront from a single lenslet pair. The results indicate that the device is nearly diffraction limited, but there are substantial wavefront errors at the edges and corners of the lenslets. Author

N93-15515*# Arizona Univ., Tucson.
EFFECTS OF HIGHER ORDER ABERRATIONS ON BEAM SHAPE IN AN OPTICAL RECORDING SYSTEM

Mark S. Wang and Tom D. Milster *In its* Research Studies on Advanced Optical Module/Head Designs for Optical Data Storage 15 Mar. 1992 p 147-173 (For primary document see N93-15505 04-74)
Avail: CASI HC A03/MF A03

An unexpected irradiance pattern in the detector plane of an optical data storage system was observed. Through wavefront measurement and scalar diffraction modeling, it was discovered that the energy redistribution is due to residual third-order and fifth-order spherical aberration of the objective lens and cover-plate assembly. The amount of residual aberration is small, and the beam focused on the disk would be considered diffraction limited by several criteria. Since the detector is not in the focal plane, even this small amount of aberration has a significant effect on the energy distribution. We show that the energy redistribution can adversely affect focus error signals, which are responsible for maintaining sub-micron spot diameters on the spinning disk. Author

N93-15516*# Arizona Univ., Tucson.
OXIDATION PROCESSES IN MAGNETO-OPTIC AND RELATED MATERIALS **c76**

Paul A. Lee, Neal R. Armstrong, James L. Danzinger, and Craig D. England *In its* Research Studies on Advanced Optical Module/Head

Designs for Optical Data Storage 15 Mar. 1992 p 177-186 (For primary document see N93-15505 04-74)
Avail: CASI HC A02/MF A03

The surface oxidation processes of thin films of magneto-optic materials, such as the rare-earth transition metal alloys have been studied, starting in ultrahigh vacuum environments, using surface analysis techniques, as a way of modeling the oxidation processes which occur at the base of a defect in an overcoated material, at the instant of exposure to ambient environments. Materials examined have included FeTbCo alloys, as well as those same materials with low percentages of added elements, such a Ta, and their reactivities to both O2 and H2O compared with materials such as thin Fe films coated with ultrathin adlayers of Ti. The surface oxidation pathways for these materials is reviewed, and XPS data presented which indicates the type of oxides formed, and a critical region of Ta concentration which provides optimum protection. Author

N93-15517*# Arizona Univ., Tucson. Optical Sciences Center.
INTEGRATED DEVICE WITH DIFFRACTIVE POLARIZATION COMPONENTS FOR A MAGNETO-OPTICAL DISK HEAD
Charles W. Haggans, Teruo Fujita, and Raymond K. Kostuk *In its* Research Studies on Advanced Optical Module/Head Designs for Optical Data Storage 15 Mar. 1992 p 189-200 (For primary document see N93-15505 04-74)
Avail: CASI HC A03/MF A03

The optical components in the detection train of a conventional magneto-optical (MO) disk head include a half-wave plate and a polarization beamsplitter. These polarization components are bulky and require specialized mounting hardware. In order to realize a more compact head, we propose that these elements be replaced by an integrated device composed of cascaded volume and surface-relief gratings. Herein, the proposed system is described in detail for the individual elements, theoretical and prototype element performance are compared, and the operational tolerances of these elements are discussed. Author

N93-15518*# Arizona Univ., Tucson. Optical Sciences Center.
THE DESIGN AND FABRICATION OF A SINGLE LEAKAGE-CHANNEL GRATING COUPLER
Ronald L. Roncone, Lifeng Li, Keith A. Bates, James J. Burke, Lori Weisenbach, and Brian J. J. Zelinski *In its* Research Studies on Advanced Optical Module/Head Designs for Optical Data Storage 15 Mar. 1992 p 203-232 (For primary document see N93-15505 04-74)
Avail: CASI HC A03/MF A03

The modeling and fabrication is described of waveguide grating couplers with out-coupling efficiencies into a single diffracted order nearing 100 pct. Termed Single Leakage Channel Grating Couplers (SLCGCs), these devices use a high reflectivity dielectric stack to reflect the out-coupled beam diffracted toward the substrate, back up into the air region where it constructively adds with the beam diffracted into the air region. Computer modeling shows that the branching ratio and the leakage rate can be independently controlled, and that the branching ratio is independent of grating depth and grating period. A SLCGC with a branching ratio of 97.1 pct. was fabricated using a combination of vacuum evaporation and wet chemical techniques. Author

N93-15519*# Arizona Univ., Tucson.
A MODAL ANALYSIS OF LAMELLAR DIFFRACTION GRATINGS IN CONICAL MOUNTINGS
Lifeng Li *In its* Research Studies on Advanced Optical Module/Head Designs for Optical Data Storage 15 Mar. 1992 p 235-281 (For primary document see N93-15505 04-74)
Avail: CASI HC A03/MF A03

A rigorous modal analysis of lamellar grating, i.e., gratings having rectangular grooves, in conical mountings is presented. It is an extension of the analysis of Botten et al. which considered non-conical mountings. A key step in the extension is a decomposition of the electromagnetic field in the grating region into two orthogonal components. A computer program implementing this extended modal analysis is capable of dealing with plane wave diffraction by dielectric and metallic gratings with deep grooves, at arbitrary angles of incidence, and having arbitrary incident polarizations. Some numerical examples are included. Author

N93-15520*# Arizona Univ., Tucson.
ON THE CONVERGENCE OF THE COUPLED-WAVE APPROACH FOR LAMELLAR DIFFRACTION GRATINGS
Lifeng Li and Charles W. Haggans *In its* Research Studies on Advanced Optical Module/Head Designs for Optical Data Storage 15 Mar. 1992 p 285-287 (For primary document see N93-15505 04-74)
Avail: CASI HC A01/MF A03

Among the many existing rigorous methods for analyzing diffraction of electromagnetic waves by diffraction gratings, the coupled-wave approach stands out because of its versatility and simplicity. It can be applied to volume gratings and surface relief gratings, and its numerical implementation is much simpler than others. In addition, its predictions were experimentally validated in several cases. These facts explain the popularity of the coupled-wave approach among many optical engineers in the field of diffractive optics. However, a comprehensive analysis of the convergence of the model predictions has never been presented, although several authors have recently reported convergence difficulties with the model when it is used for metallic gratings in TM polarization. Herein, three points are made: (1) in the TM case, the coupled-wave approach converges much slower than the modal approach of Botten et al; (2) the slow convergence is caused by the use of Fourier expansions for the permittivity and the fields in the grating region; and (3) is manifested by the slow convergence of the eigenvalues and the associated modal fields. The reader is assumed to be familiar with the mathematical formulations of the coupled-wave approach and the modal approach. Author

N93-15648# RAND Corp., Santa Monica, CA.
A STRUCTURAL APPROACH TO THE PHOTONIC PROCESSOR
Deborah Jackson 1991 44 p
(N-3399-RC) Avail: CASI HC A03/MF A01

In the early 1990, photonics, the confluence of electronics, and optics technologies to improve net processing efficiency was advanced to the highest priority ranking on the DoD critical technologies list. Currently, photonics is considered a high-leverage technology because it is believed that photonic processors could potentially circumvent the serial processor limitation, or von Neuman bottleneck, which limits the throughput capacity of most electronic processors. Indeed, the realtime solutions to currently military problems, such as high-accurate missile guidance, sensor fusion, automatic target recognition, automated guidance of remotely piloted vehicles, etc., are consistently crippled by information processing bottlenecks. Such bottlenecks are particularly endemic to image-formatted data bases. An image-formatted data base is defined as a data base where, besides the information contained in each pixel, there is also information imparted by the spatial relationship among the data in the pixels. Thus, in image data, variations in grey scale are used to define edges and corners. To extract the spatially imparted information, it is often necessary to compare N x N pixels in the input image with the N x N pixels in a model image; this process takes N exp 4 comparison calculations. As the demand for higher resolution imagery increases and N gets larger, it becomes increasingly more difficult to make the image comparisons in realtime. Currently, digital electronic processor designs are optimized for numerical processing, which is an intrinsically serial operation. It is this serial nature that causes the limitation; the photonic processor, which can be designed with a more parallel architecture, has potential for circumventing this bottleneck. It is, therefore, anticipated that the intrinsic parallelism of optics will enable the photonic processor to solve problems in realtime that were previously considered unsolvable or only marginally solvable. Author

N93-14948# Spar Aerospace Ltd., Weston (Ontario).
VISION DEVELOPMENT TEST BED: THE CRADLE OF THE MSS ARTIFICIAL VISION SYSTEM
Leon Zucherman and John Stovman *In* Canadian Space Agency, Proceedings of the Sixth CASI Conference on Astronautics 1990 9 p Previously announced in IAA as A91-34954 (For primary document see N93-14920 04-12)
Avail: Canadian Aeronautics and Space Inst., 222 Somerset St. W., Suite 601, Ottawa, Ontario K2P 0J1 Canada

75 PLASMA PHYSICS

Includes magnetohydrodynamics and plasma fusion.

For ionospheric plasmas see *46 Geophysics*. For space plasmas see *90 Astrophysics*.

N93-14120 City Univ. of New York, NY.
TURBULENT MAGNETIZED PLASMAS FROM IONIZING SHOCK WAVES Ph.D. Thesis
Zuohua Liang 1992 128 p
Avail: Univ. Microfilms Order No. DA9224832

Turbulent argon plasmas produced behind hypersonic shock waves (10 less than M less than 60) are studied in the presence of weak magnetic fields at various strengths between 0 and 600 gauss, parallel and antiparallel to the shock tube's axis. The experiment is performed in a cylindrical arc discharge shock tube of 5 cm diameter and 210 cm overall length. Laser induced fluorescence and an electric probe are used as diagnostics of the ion density. Turbulent fluctuations behind the shock front are observed which persist for a time in the order of 10 msec. Using standard turbulent and chaotic analytical procedures, the influence of the magnetic field on the characterizing parameters is determined under circumstances of changing Mach number and pressure. These parameters include spectral index, correlation time scales, turbulent intensity and chaotic dimensionality. The parameters of turbulence obtained from the two diagnostics are quite consistent. Fluctuation power spectra follow a P approx. f(sup -n) behavior with 1.3 less than n less than 2.8; this agrees with theoretical predictions as well as the results of other investigators. An increasing magnetic field increases the characterizing correlation time, the turbulent intensity, and the chaotic dimension but decreases the small correlation time. Therefore the magnetic field decreases the order (increases the dimensionality) in the turbulent plasma, independent of the direction of the field parallel or antiparallel to the direction of the shock wave. A turbulent velocity-field-coupling model is proposed. A dispersion relation shows that, in the presence of an external magnetic field, varieties of new modes in a turbulent plasma are generated. The model predicts an increasing complexity of the turbulent system with increasing strength of the field and is in very good qualitative agreement with our experiment results.
Dissert. Abstr.

N93-14122 Texas Univ., Austin.
RESISTIVE MAGNETOHYDRODYNAMIC STUDIES OF TEARING MODE INSTABILITY WITH EQUILIBRIUM SHEAR FLOW AND MAGNETIC RECONNECTION Ph.D. Thesis
Leon Ofman 1992 135 p
Avail: Univ. Microfilms Order No. DA9225692

Magnetic reconnection and tearing can play an important role in fusion experiments and in space plasmas. The magnetohydrodynamic (MHD) study of the linear and nonlinear evolution of the resistive tearing mode instability in the presence of equilibrium shear flow, and the reconnection of an x-point magnetic field configuration are discussed. Numerical solutions of the linearized time-dependent MHD equations and growth rate scaling are obtained. The results of the computations are compared to previous work, and the computed growth rate scalings agree with analytical predictions. The introduction of viscosity and small equilibrium shear flow alters the growth rate scaling considerably. When the shear flow is large, the growth rate behaves in a more complex way, and Kelvin-Helmholtz instability effects are present. The linear evolution of the double tearing mode with equilibrium shear flow and viscosity is investigated numerically. The dispersion relation for the growth rate of the double tearing instability is generalized to include flow. Relatively small shear flow at the resonant surfaces has a stabilizing effect on the double tearing mode. For Reynolds number comparable or larger than the magnetic Reynolds number a stabilizing effect is found. The nonlinear evolution of the tearing mode instability with equilibrium shear flow is investigated via numerical solutions of the resistive incompressible two dimensional MHD equations. The simulations are initiated with solutions of the linearized MHD equations. Magnetic energy release decreases, and the saturation time increases with shear flow. The validity of the numerical solutions is tested by verifying that the total energy and helicity are conserved. The reconnection of two-dimensional stressed x-type neutral point magnetic fields is studied via solution of the nonlinear incompressible and compressible resistive MHD equations. Solutions of the linear eigenvalue problem are obtained and compared to the MHD simulations. It is found that with conducting boundary condition, the fields relax to the force-free x-type neutral point at a rate close to that predicted by linear theory. When flow through the boundaries is present, the x-point evolves into a current sheet.
Dissert. Abstr.

N93-14129 Georgia Inst. of Tech., Atlanta.
ANALYSIS OF ROTATION EXPERIMENTS IN TFTR Ph.D. Thesis
Gabriella Pautasso 1992 221 p
Avail: Univ. Microfilms Order No. DA9223791

The study of momentum confinement is a valuable means of studying the mechanisms governing confinement in tokamak plasmas. A dedicated rotation experiment was conducted in TFTR, in September 1988, using the recently installed CHERS diagnostic. Shots at different values of plasma current, magnetic field, injected beam power and injected direction were made, to study the parametric dependence of local fluxes of momentum and energy. A study of momentum confinement is presented. Its purposes are to analyze the data of the TFTR rotation experiment, to document the results and to compare the experimental results with the predictions of neoclassical and anomalous momentum transport theories. Particular attention is devoted to the evaluation of the magnitude of the poloidal variation of densities and rotation frequencies that determine the magnitude of the gyroviscous momentum flux. We find that: (1) Ware's cold ions theory underpredicts the observed viscosity by a few orders of magnitude; (2) each of the anomalous theories considered predicted torque flows which show magnitudes, radial profiles and parametric dependencies on plasma parameters different from those of the experimental torque flow; (3) up-down poloidal asymmetries of density and rotation frequency, evaluated with a model which neglects heat flux and includes the effect of anomalous particle fluxes, are found to be much smaller than epsilon; and (4) the gyroviscous torque is at least one order of magnitude smaller than the experimental torque flow.
Dissert. Abstr.

N93-14137 Idaho Univ., Moscow.
LINESHAPE ANALYSIS OF LASER LIGHT SCATTERED BY AN ARGON THERMAL PLASMA JET Ph.D. Thesis
Stuart Cody Snyder 1992 182 p
Avail: Univ. Microfilms Order No. DA9222942

Radial gas temperature and velocity profiles in the exit plane of an atmospheric pressure argon thermal plasma jet were determined from high resolution lineshape analysis of elastically scattered laser light. Unlike emission spectroscopy, lineshape analysis of scattered laser light does not rely on assumptions of local thermodynamic equilibrium (LTE) or specific non-LTE models to measure gas or kinetic temperature, and has a high degree of spatial resolution. At atmospheric pressure, if electron densities are greater than 10(exp 22) m(exp -3), coherent Thomson scattering dominates, while at lower electron densities, Rayleigh scattering dominates. Using a frequency doubled injection-seeded Nd:YAG laser and a scanning tandem Fabry-Perot interferometer, high quality lineshapes were measured in the exit plane of a commercial subsonic plasma torch at several radial positions with torch operating currents ranging from 300 to 900 A. The experimental lineshapes were fitted by the lineshape theory and the gas temperatures determined. The scattered wavevector had a component along the flow axis of the jet resulting in a Doppler shift of the frequency of scattered light relative to the frequency of the incident laser. From this Doppler shift the gas velocity was calculated. Maximum centerline temperature and velocity values observed were 13350 K plus or minus 7 percent and 100 m/s plus or minus 3 percent. The fitting errors for the centerline lineshape data were 2-3 percent for all operating currents. The minimum velocity measured in the fringe of the jet was 45 m/s plus or minus 45 percent. Comparison of temperature profiles calculated from the lineshape data with temperatures determined from LTE emission spectroscopy shows a severe departure from LTE in the outer regions of the jet. Centerline temperature and velocity values determined from lineshape analysis of scattered light increase with torch operating current to about 600 A after which they remain essentially constant. However, spectroscopic measurements show that the electron temperature and density continue to increase with current. This indicates that increasing the electrical power dissipated by the torch drives the plasma away from LTE. Measured radial velocity profiles are very nearly parabolic and differ significantly from velocity profiles assumed by computational modelers as boundary conditions for models of the plasma jet.
Dissert. Abstr.

N93-14138 Auburn Univ., AL.
EXPERIMENTAL OBSERVATIONS OF THE PLASMA PROPERTIES OF A HIGH-DENSITY, LOW-TEMPERATURE ACCELERATED ARC Ph.D. Thesis
Keith Allen Thomas 1991 150 p
Avail: Univ. Microfilms Order No. DA9224058

The existence of an absorbing layer, or buffer zone, of weakly ionized gas between the rear of the projectile and the front of the plasma arc armature in a plasma accelerator was demonstrated. A technique was developed to accurately determine the position of the projectile as it accelerates along the bore of the device. The projectile position is compared to that of the plasma arc as measured by magnetic field probes. These measurements provide the basis for a description of the in-bore motion of the projectile with respect to the plasma arc. Observations of this motion in plasma accelerators of 0.6 and 2.4 m lengths show the buffer zone can be as large as 50 times the bore diameter. In-bore measurements of the broadband light emission and pressure of both the buffer region and the plasma arc armature are correlated with the known projectile position to determine the characteristics of both the buffer zone and the plasma arc. Time-integrated spectral measurements of the emission taken through both the side insulators and the electrodes indicate the existence of a nonuniform plasma temperature and of turbulence in the plasma. The presence of molecular species is attributed with the ablation of the side insulator material. Dissert. Abstr.

N93-14139 California Univ., Los Angeles.
INTERACTIONS OF RELATIVISTIC ELECTRONS WITH RELATIVISTIC PLASMA WAVES Ph.D. Thesis
Ronald Leslie Williams 1992 181 p
Univ. Microfilms Order No. DA9224136

The interactions of relativistic electrons with relativistic plasma waves are studied by examining three novel applications: a high gradient particle accelerator; an electron beam diagnostic of relativistic plasma waves; and an undulator for producing short wavelength radiation. The focusing of a high energy particle beam in a ramped density, continuously focusing, plasma lens for use in future high energy e(-)e(+) colliders is also examined. The trapping threshold, energy gain, phase evolution, beam focusing and energy spectrum are found for particles accelerated in the laser plasma beatwave accelerator, plasma wakefield accelerator, and laser wakefield accelerator schemes in which accelerating gradients on the order of 10's to 100's of Giga Volts per meter may exist. The limits due to beam emittance and plasma wave width are found for the measurement of relativistic plasma wave amplitude and wavelength using a relativistic electron beam as a diagnostic. The short wavelength (approx. 1 mu) spontaneous radiation, particle bunching, stimulated radiation, and radiation gain are found for modest energy electrons (approx. 4 MeV) injected into a 1 cm long, 100 micron period, plasma wave undulator which is shown to behave similarly to a free electron laser undulator. The compression of high energy beams to very small spot sizes in the ramped density plasma lens is found to be sensitive to beam and lens matching which is determined by adjusting the Courant-Snyder accelerator parameters. Dissert. Abstr.

N93-14579# Naval Research Lab., Washington, DC.
OPACITY, EQUATION OF STATE, AND RADIATION TRANSPORT MODEL FOR MODERATE DENSITY, eV-TEMPERATURE PLASMAS Interim Report
John P. Apruzese, John L. Giuliani, Jr., and Paul C. Kepple 22 Sep. 1992 19 p
(AD-A256056; NRL/MR/4721-92-7124) Avail: CASI HC A03/MF A01

We present a model suitable for calculating opacity and radiation transport in eV-temperature plasmas such as those encountered in electromagnetic launchers, arcjets, and some types of plasma processing. Using a detailed multilevel, atomic model, the opacity at about 1400 frequency points is calculated for a grid of temperature and electron densities using either the LTE or CRE approximation. This detailed grid is further simplified to 15-20 energy bins within each of which the Planck mean opacity is calculated and stored for use by a radiation transport code. This radiation transport model is a quasi-two-dimensional ray trace at each of these bins suitable for rapid calculation of approximate radiative cooling (heating) for use in conjunction with a hydrodynamics model. GRA

N93-14813# Institute of Plasma Physics, Prague (Czechoslovakia). Academy of Sciences.
TRANSFORMATION OF ENERGY AND MOMENTUM DUE TO LANDAU DAMPING IN TIME
J. Lacina Jan. 1992 24 p
(IPPCZ-316) Avail: CASI HC A03/MF A01

The transformation of energy and momentum due to Landau damping in time, together with the physical mechanism of this process is presented. Unlike the well-known models, the presented theory is not limited to a small ratio of the decrement to the wave frequency, and artificial assumptions together with discrepancies involved in these models are removed. It is shown that the perturbation of particle velocities, caused by the self-consistent electric field, is formed by a superposition of coherent free and forced oscillations propagating in space. The transformation of energy and momentum is a process of the phase interference between the coherent free and forced oscillations, in which the evolution of the forced oscillations is governed by the energy and momentum balance equations. Author

N93-15327# Texas Univ., Austin. Fusion Research Center.
PLASMA CONFINEMENT THEORY AND TRANSPORT SIMULATION
D. W. Ross Apr. 1992 8 p
(Contract DE-FG05-88ER-53266)
(DE92-040523; DOE/ER-53266/40) Avail: CASI HC A02/MF A01

The objectives are: (1) to advance the transport studies of tokamaks, including development and maintenance of the Magnetic Fusion Energy Database; and (2) to provide theoretical interpretation, modeling and equilibrium, and stability studies for TEXT-Upgrade. Recent reports, publications, and conference presentations of the Fusion Research Center are listed. DOE

N93-15349# Yale Univ., New Haven, CT.
THEORETICAL AND NUMERICAL STUDIES IN MAGNETIC FUSION
1992 6 p
(Contract DE-FG02-86ER-53240)
(DE92-040674; DOE/ER-53240/T2) Avail: CASI HC A02/MF A01

The gyrokinetic equation is employed to derive the transport theory for any topologically toroidal device possessing well-defined magnetic surfaces; thus, the theory appropriate for a Tokamak with rotation as well as that for the Stellarator is included. The method does not require a detour via moment equations, and allows for finite mean flows. As an illustration, the technique is applied to the transport of density. An analysis to determine the correct boundary conditions to apply to the transport equations is underway, and a start has been made on the rough characterization and parametric dependence of the neoclassical transport coefficients. The general equations governing the ensemble average field quantities are being analyzed. DOE

N93-15418# Los Alamos National Lab., NM.
ACCURATE METHODS FOR CALCULATING ATOMIC PROCESSES IN HIGH TEMPERATURE PLASMAS
J. J. Keady, J. A. Abdallah, Jr., and R. E. H. Clark 1992 6 p Presented at the 14th International Conference on Plasma Physics and Controlled Nuclear Fusion Research, Wuerzburg, Germany, 30 Sep. - 7 Oct. 1992
(Contract W-7405-eng-36)
(DE92-040215; LA-UR-92-2791; CONF-920913-13) Avail: CASI HC A02/MF A01

A technique for computing monochromatic X-ray absorption is described and compared to experimental data. Calculations of power loss from carbon plasmas with comprehensive new datasets confirm that the direct inclusion of metastable states can noticeably decrease the calculated power loss. DOE

N93-15419# Los Alamos National Lab., NM.
EXACT ANALYTICAL SOLUTION OF THE TOROIDAL SINGULAR MODE EQUATIONS
A. H. Glasser 1992 7 p Presented at the Joint Varenna-Lausanne International Workshop on Theory of Fusion Plasmas, Varenna, Italy, 24-28 Aug. 1992
(Contract W-7405-eng-36)
(DE92-040223; LA-UR-92-2756; CONF-920813-1) Avail: CASI HC A02/MF A01

A subset of the complete fluid equations governing the inner region of

low-eta singular modes in toroidal geometry is solved exactly and analytically. The subset includes toroidal curvature as well as ion and electron diamagnetic and E x B drifts, but not viscosity or thermal conductivity. The Fourier-transformed equations are reduced to a second-order ODE with singular points at 0 and infinity. Exact solutions are found in terms of confluent hypergeometric functions. A dispersion relation Delta' = Delta(Q) is derived from the matching condition between inner and outer solutions in configuration space, with Delta' the ratio of small to large asymptotic coefficients in the ideal outer region and Delta(Q) a complicated function of the scaled growth rate Q obtained from the inner region analysis. DOE

N93-15422# Los Alamos National Lab., NM.
PROGRESS ON THE DEVELOPMENT OF A 2-D PIC/MONTE CARLO MODEL OF GLOW DISCHARGES
A. E. Greene, R. J. Faehl, R. K. Keinigs, T. A. Oliphant, Jr., and W. R. Shanahan 1992 9 p Presented at the Industrial Applications of Plasma Physics Workshop, Varenna, Italy, 2-12 Sep. 1992
(Contract W-7405-eng-36)
(DE92-040226; LA-UR-92-2740; CONF-9209189-2) Avail: CASI HC A02/MF A01

There are several computational approaches that have been and are being implemented for the investigation of plasma processing discharges. One-dimensional electrostatic PIC calculations have proven useful in modeling the bulk properties of discharges far from the edges and have yielded good agreement with experiment for ion distributions in the sheath region. The value of PIC methods is that they follow the evolution of an N-body system unconstrained by equilibrium requirements. Gaseous discharges are in general far from equilibrium. Electrons in the bulk region and ions in the sheath can have energies greatly exceeding the neutral gas temperature and can be distributed in a highly non-Maxwellian fashion. One dimensional models are incapable of treating flow and transport of reactants in reactors properly. Geometrical features are also neglected. Modeling the more recently developed high density reactors, such as the Hitachi ECRH source, requires at least two-dimensional and possibly three-dimensional electromagnetic models. Therefore, at Los Alamos we have chosen to address these problems with the MERLIN code. In this paper we will discuss our progress toward developing this code. We will describe, briefly the physics that we are including in this model. We will discuss a test problem that is being used to exercise most of the new features that have recently been added to MERLIN. Finally, we will discuss our future efforts. DOE

N93-15436# Los Alamos National Lab., NM.
ELECTRICAL RESISTIVITY AND EQUATION OF STATE MEASUREMENTS OF A DENSE ALUMINUM PLASMA
J. F. Benage, Jr. and W. R. Shanahan 1992 6 p Presented at the International Conference on the Physics of Strongly Coupled Plasmas, Rochester, NY, 17-21 Aug. 1992
(Contract W-7405-eng-36)
(DE92-040352; LA-UR-92-2648; CONF-9208135-1) Avail: CASI HC A02/MF A01

In this paper we report results of experiments to measure the electrical resistivity and equation of state for a dense strongly coupled aluminum plasma. These plasmas are near solid density and have temperatures in the 15 - 20 eV range with Gamma = 2 - 3. Our initial results indicate a significant reduction in pressure below the ideal gas law value and initial resistivity measurements agree with a model by Rinker within error bars. DOE

76 SOLID-STATE PHYSICS

Includes superconductivity.

For related information, see also *33 Electronics and Electrical Engineering* and *36 Lasers and Masers*.

N93-14133# National Inst. of Standards and Technology, Gaithersburg, MD. Ceramics Div.
TWIN QUINTUPLETS IN CVD DIAMOND Interim Report
D. Shechtman, A. Feldman, and J. L. Hutchison 26 Aug. 1992 12 p
(Contract N00014-90-F-0011; DA Proj. IRM-T-025)
(AD-A255862; NIST-TR-15) Avail: CASI HC A03/MF A01

The atomic structure of twin quintuplets in a chemical vapor deposited (CVD) diamond film was - investigated by high resolution transmission electron microscopy (HRTEM). We conclude that the twin quintuplets have two main morphologies. The first consists of four Sigma = 3 twin boundaries and one Sigma = 81 twin boundary. The Sigma = 81 twin boundary contains the dislocations needed to accommodate a 7.35 deg misfit angle between a set of (111) planes on opposite sides of the boundary. In the second case, the 7.35 deg misfit angle is accommodated by two or more grain boundaries that are tilted slightly more than the 70.53 deg tilt of a Sigma = 3 boundary. These grain boundaries and the conventional diamond lattice twin boundaries are the only types of boundaries that we have observed in CVD diamond. GRA

N93-14171 Warwick Univ., Coventry (England).
REMOTE TECHNIQUES FOR TIME-OF-FLIGHT FLAW CHARACTERISATION Ph.D. Thesis
Stephen James Davies 1991 335 p
Avail: Univ. Microfilms Order No. BRD-96546

The investigations conducted into the characterization of various defects within solids using laser-generation and interferometric detection of ultrasound are described. Laser-generated ultrasound has advantages over the more commonly used piezoelectric transducers in that it is a reproducible, wide bandwidth, non-contact source which, by using appropriate optics, can be focussed to a point or line source and easily scanned over a surface. Used in association with an interferometric detector enables the possibility of a remote inspection system which would be useful for some applications. The properties of such a system for the characterization of both bulk and surface-breaking defects are ascertained. Part of the research project has been concerned with determining the properties of the ultrasound produced in various solids by different pulse profiles. The results obtained indicate that the risetime of the ultrasonic compression wave decreases with decreasing incident laser pulse risetime. However, the mechanical and thermal properties of the irradiated solid also affects the risetime of the ultrasound. Modelling of the laser-solid interaction was undertaken to understand this phenomenon in more detail. The wide bandwidth nature of laser-generated ultrasound was used in the characterization of bulk defects. This has involved determining the phase change, using a fast Fourier transformation (FFT) algorithm, which occurs when laser-generated ultrasound is scattered from such defects. The aim of the investigation was to assess whether a particular type of defect has a unique phase change which will enable it to be classified. The experimental results obtained compared favorably with the results from theoretical modelling of ultrasonic scattering by defects. Finally the interaction of laser-generated Rayleigh (surface) waves with surface-breaking defects was considered. Various techniques for the characterization of surface-breaking defects by analysis of data in the time and frequency domain were utilized. One such technique involved measurement of the reflection and transmission coefficients of various surface discontinuities. The phase change of the scattered Rayleigh wave was determined and compared to the theoretical data available. Also, a technique was established whereby certain features on the waveforms recorded on transmission of a Rayleigh wave through a surface-breaking defect could be used to determine the depth of the defect. Dissert. Abstr.

N93-14172 Illinois Univ., Chicago.
ELECTRONIC STRUCTURE STUDIES OF HIGH-T(SUB c) SUPERCONDUCTORS BY PHOTOEMISSION AND X RAY ABSORPTION Ph.D. Thesis
Mohamed M. Faiz 1992 200 p
Avail: Univ. Microfilms Order No. DA9226236

Understanding the normal state of the fascinating high-Tc superconductors seems to be a prerequisite to understanding its superconducting state. At present, there are mainly two extreme theoretical points of view for the normal-state-electronic structure of these materials. Therefore, a detailed experimental work on this subject is essential to arrive at a correct theory. In this work we used photoemission and x-ray absorption spectroscopies in order to obtain the electronic structure of these materials. In our angle-resolved photoemission work on Y123, we have mapped the Fermi surfaces and searched for the superconducting energy gap with 25 meV energy resolution. Our findings reveal a sharp Fermi edge, large band dispersions near the Fermi level, and all of the Fermi surfaces predicted by the band structure calculations using local

density approximation (LDA). We have exploited linear polarization of the synchrotron radiation in our x-ray absorption experiments to study the symmetry of holes at the oxygen sites in Y123, Bi2212, and Tl2223 comparatively. Our results suggest that the O 2p holes in Y123, Bi2212, and Tl2223 appear to be of sigma-symmetry in all the Cu-O bonds. None of these materials shows a simple (cos(theta))(sup 2) variation as one might expect, if only the Cu-O layers contribute to the holes at the oxygen sites. The O 2p holes in the Cu-O planes of Y123 remain mostly unaffected as oxygen is lost from the sample surface which indicates having O 2p holes in a material is not a sufficient condition for superconductivity in that material. We have also seen evidence for Cu(3+) state in our XANES measurements on T12223 at the Cu L absorption edge which suggests that the doped holes are shared among O and Cu. All of these findings are in favor of predictions of LDA band structure calculations, and in contradiction with split band descriptions of Hubbard type for the normal-state electronic structure of the high-Tc cuprates. Dissert. Abstr.

N93-14183 Exeter Univ. (England).
TIME-RESOLVED OPTICAL STUDIES OF 3-5 SEMICONDUCTORS Ph.D. Thesis
Andrew Gregory 1991 192 p
Avail: Univ. Microfilms Order No. BRDX96603

This study uses the technique of sub-picosecond time-resolved luminescence spectroscopy in order to investigate the relaxation of hot photo-excited charge carriers in III-V semiconductors. A review is provided of the physical background to the area, along with a discussion of the knowledge already obtained. The luminescence upconversion technique is used which enables measurements to be made with a time-resolution that is primarily limited by the laser pulse length. Photo-excited electrons and holes quickly (approximately 1 ps) establish quasi-equilibrium distributions in their respective bands via carrier-carrier interactions and these processes occur in combination with the emission of optical and acoustic phonons. Carrier temperatures may then be associated with the distributions which are hundreds of Kelvin, well above the lattice temperature of 4 K. Modelling of transient spectra from bulk In(0.53)Ga(0.47)As has yielded carrier cooling curves and produced evidence for the scattering of the excited electrons to satellite conduction band valleys. Modelling of the cooling process has been done and it has been found that to fit the data, the polar-optical phonon energy-loss rate must be adjusted by a time-dependent reduction factor indicating the significance of the hot phonon effect. The measurement of the time evolution of luminescence at fixed photon energies has enabled rise times and decay constants to be obtained. The formation of highly degenerate carrier distributions is observed in the rise times. In addition these provide confirmatory evidence for significant inter-valley scattering. The luminescence decays have exhibited the interesting characteristic of being describable with two decay constants at certain energies. This is explained with recourse to Auger recombination and the evolution of the electron population around the quasi-Fermi energy. Processes associated with the change from bulk material to quasi-two-dimensional structures are observed and new and unexpected features have been found which have been explained principally in terms of the real-space transfer of carrier. Even though much insight has been gained into energy relaxation mechanisms many questions remain in this area--indeed a number are raised by this work--and these are discussed. Dissert. Abstr.

N93-14184 Yale Univ., New Haven, CT.
SENSITIVITY OF QUANTUM ELECTRON CONDUCTANCE TO ELASTIC SCATTERERS AND TO SPIN-ORBIT SCATTERING IN GALLIUM ARSENIDE HETEROSTRUCTURES Ph.D. Thesis
Steven Judson Klepper 1991 245 p
Avail: Univ. Microfilms Order No. DA9224356

'Universal' Conductance Fluctuations (UCF) are studied by measuring electron magnetoconductance in micron-size wires fabricated from GaAs/AlGaAs heterostructures. These aperiodic fluctuations in conductance arise from the complex quantum phase-coherent scattering of conduction electrons from the particular impurity configuration of a sample. Two experiments have been performed: one to study the sensitivity of UCF to individual elastic scatterers, and the second to examine the effect of electron spin-orbit scattering on UCF. In the first experiment, elastic scatterers are introduced at a controlled rate into heterostructure devices by infrared photoionization of DX centers in the doped AlGaAs. Ionized DX centers are elastic scatterers of electrons in the two-dimensional electron gas. A novel technique of UCF difference traces allows the quantitative study of changes in the characteristic magnetoconductance fluctuations of a sample. These changes arise from adding a small number of scatterers to a device. The amplitude and temperature dependence of these conductance changes agree well with theory. For comparison, the effect of changing the electrochemical potential in mesoscopic gated devices was examined. The UCF decorrelation associated with changing gate voltage differs markedly from that caused by elastic scatterer addition, allowing changes in the electrochemical potential to be distinguished from those in the random scattering potential. One can also resolve switching events in the device conductance due to the addition of individual elastic scatterers. A second experiment studied the temperature dependence of magnetoconductance, for fixed impurity configuration, from T = 60 mK to 7 K. Weak localization data show that the spin-orbit (SO) scattering rate exceeds the phase-breaking rate below T = 2 K. A significant reduction in the conductance fluctuation amplitude is observed, also below 2 K, as compared to that extrapolated from higher temperatures. This reduction is due to SO scattering. The amplitude and functional form of the UCF reduction factor for the transition from the weak (high-T) to the strong (low-T) SO scattering regimes agree well with theory. SO scattering also influences the magnetic correlation field for the UCF. Dissert. Abstr.

N93-14260# Naval Postgraduate School, Monterey, CA.
EXPERIMENTAL CONSIDERATIONS OF HIGHER ORDER PARAMETRIC X RAYS FROM SILICON CRYSTALS OF VARYING THICKNESSES M.S. Thesis
Scott R. Evertson Jun. 1992 72 p
(AD-A256082) Avail: CASI HC A04/MF A01

Generation of parametric x-radiation (PXR) may be described as the Bragg scattering of virtual photons to produce real x-rays which satisfy the Bragg condition n lambda = 2d sin(theta sub B) where theta sub B is the angle between the electron beam and the crystal plane. Enhanced higher order parametric s-radiation from the (220) and the (111) planes of silicon crystals of varying thicknesses were observed. Production of PXR of order n=1 for both planes of a 20 micron thick crystal and orders n=1, and n=2 of the (220) and the n=1, n=3, and n=4 of the (111) planes of the 44 microns and 320 microns crystals were observed. Exploiting the formation and attenuation lengths of silicon crystals of varying thicknesses, higher order x-ray production is enhanced relative to the lower energy first order x ray. Photons of 4.5 to 21 keV have been observed. GRA

N93-14413# Princeton Univ., NJ. Dept. of Mathematics.
MACROSCOPIC PROPERTIES OF RANDOM AND QUASIPERIODIC MEDIA Final Report, 1 Apr. 1990 - 31 Jul. 1992
Kenneth Golden 31 Jul. 1992 13 p
(Grant AF-AFOSR-0203-90)
(AD-A255984; AFOSR-92-0859TR) Avail: CASI HC A02/MF A01

New fundamental rigorous results about the critical behavior of percolation models were proven. In the discrete case, for a hierarchical model of the conducting backbone, we have proven inequalities on the critical exponent t for the conductivity of the random resistor network. Our inequality t is less than or equal to 2 in three dimensions rules out roughly one fourth of the numerical estimates published over the last 25 years. GRA

N93-14422# Institute for Defense Analyses, Alexandria, VA.
SDIO WORKSHOP ON PIEZOELECTRIC CERAMIC ACTUATORS FOR SPACE APPLICATIONS Final Report, Jan. - May 1992
Janet Sater Jun. 1992 283 p Workshop held in Alexandria, VA, 25 Feb. 1992
(Contract MDA903-89-C-0003)
(AD-A255959; IDA-D-1189; IDA/HQ-92-41982; AD-E501566) Avail: CASI HC A13/MF A03

A workshop on piezoceramic actuators for space applications is discussed. Its purpose was threefold: to promote communications among the appropriate groups; to focus and prioritize issues for near-team improvements in actuator performance; and to identify and suggest research plans to obtain such improvements. Presentations were given by representatives from each of three invited groups: end users/designers; materials researchers; and materials/device manufacturers. Issues identified in the workshop seemed to fall into three major categories: (1) piezoceramic material performance limitations; (2) distribution of properties of vendor-supplied materials; and (3) actuator applications. Performance

limitation issues include, for example, d31 vs. d33 performance, displacement/volt, fatigue life at high strains, and tensile strain-to-failure. Property distribution issues include composition, capacitance, and surface finish. Actuator application issues include ceramic material/actuator fabrication, material handling, application of electrodes to actuator, and post-composite fabrication actuator performance. GRA

N93-14429# Brown Univ., Providence, RI. Div. of Engineering.
THE PROPERTIES OF THERMALLY PASSIVATED Si(1-x) He(x) PRODUCED USING HIGH PRESSURE TECHNIQUES (AND RELATED AUGMENTATION AWARDS) End of Fiscal Year Summary Report
D. C. Paine 30 Sep. 1992 6 p
(Contract N00014-91-J-1837)
(AD-A255961) Avail: CASI HC A02/MF A01

Since the 1 Jul. 1991 start date of this work, research was pursued on the use of ultra high pressure oxidation for the growth of electronic quality MOS oxides on Si(1-x)Ge(x). High pressure, low temperature oxidation allows the formation of compositionally congruent oxides from Si(1-x)Ge(x) and eliminates the interfacial enrichment of Ge that is seen during conventional oxidation processes. Specific studies of the congruent Si(1-x)Ge(x)O2 grown from Si(1-x)Ge(x) that were carried out over the past year include the following: (1) oxidation kinetic studies; (2) optical characterization (Raman and FTIR); (3) MOS C-V measurements; and (4) high resolution TEM. During this work a second important direction was initiated, in which high pressure oxides of Si(1-x)Ge(x)O2 were used for the synthesis of nanocrystalline Ge. GRA

N93-14439# Lehigh Univ., Bethlehem, PA. Materials Research Center.
LONG TERM STABILITY IN THIN FILM FERROELECTRIC MEMORIES Report, 1 Apr. 1991 - 31 Mar. 1992
D. M. Smyth and M. P. Harmer 29 Sep. 1992 36 p
(Contract N00014-91-J-1755)
(AD-A256290; Rept-533644) Avail: CASI HC A03/MF A01

The mechanism and control of the fatigue of remanent polarization in thin film ferroelectric memories is being investigated. The predicted detrimental effect of acceptor-dopants and beneficial effect of donor-dopants has been confirmed in thinned samples of BaTiO3. A similar but reduced effect has been observed in thin films of PZT, and the possible effect of PbO-loss on reducing the beneficial effect of donor dopants is being investigated. It has become apparent that under high temperature equilibration conditions for perovskite titanates, the concentration of trapped holes exceeds that of free holes, contrary to earlier expectations. This means that the amount of nonstoichiometry and of trapped charge is considerably higher than previously thought. This is being explored with bulk samples of PZT. Reported problems with retention of polarization in PZT films integrated into circuits, i.e., the nonvolatile feature of the memories, has led to a new program to determine the conditions to which PZT films can be exposed without loss of essential properties. Direct observation of the motion of ferroelectric domains by transmission electron microscopy has been achieved, and a new field stage is being designed. Thin films of Pb(MnI/3Nb2/3)O3-PbTiO3 (90 percent PMN) have been prepared with greater than 99 percent perovskite phase. GRA

N93-14485# International Centre for Theoretical Physics, Trieste (Italy).
MEASUREMENT AND ANALYSIS OF EXCITATION FUNCTIONS IN (ALPHA,np) REACTIONS ON (128, 130)Te
B. P. Singh (Aligarh Muslim Univ., India), M. G. V. Sankaracharyulu (Aligarh Muslim Univ., India), M. A. Ansari (Aligarh Muslim Univ., India), R. Prasad, an512388 (Aligarh Muslim Univ., India), and H. D. Bhardwaj (Dharma Samaj National Coll., Unao, India) Feb. 1992 22 p
(DE92-630358; IC-92/29) Avail: CASI HC A03/MF A01

Excitation functions for the reactions Te(alpha,np)-128(I-130), Te(alpha,np)-130(I-132), and Te(alpha,np)-130(I-132m) have been measured using stacked foil technique and have also been calculated using statistical model with and without the inclusion of pre-equilibrium emission. As expected, inclusion of pre-equilibrium emission in compound nucleus calculations agree well with the experimental excitation functions. The pre-equilibrium fraction has been found to be energy and target mass number dependent. DOE

N93-14518# Ballistic Research Labs., Aberdeen Proving Ground, MD.
DETERMINATION OF OPERABLE DEFORMATION MECHANISMS DURING BALLISTIC IMPACT IN TUNGSTEN SINGLE CRYSTALS, UTILIZING TRANSMISSION ELECTRON MICROSCOPY Final Report, 30 Mar. - 15 May 1991
R. A. Herring Aug. 1992 41 p
(AD-A255351; BRL-TR-3385) Avail: CASI HC A03/MF A01

The performance of tungsten single crystals in ballistic impact varies strongly as a function of crystallographic orientation. The deformation structure of recovered single crystal rods fired in ballistic environments has been characterized by optical microscopy, SEM and TEM, and x-ray diffraction. The observed microstructures are varied and provide substantial insights into the factors governing the penetration and flow behavior under ballistic conditions. Crystallographic orientation influences the potential for developing shear which enhances material flow, and this enhancement ultimately maximizes the energy available for target penetration. Microstructural analysis elucidates the various mechanisms occurring during the flow process for single crystals of high-symmetry orientations, and suggests possible analogies between the penetration behavior of the tungsten single crystals and other materials. GRA

N93-14521# Illinois Univ., Urbana-Champaign. Coordinated Science Lab.
THE 3 TO 5 HETEROJUNCTION STRUCTURES AND HIGH SPEED DEVICES Final Report, 1 Jan. 1989 - 31 Dec. 1991
Hadis Morkoc 2 Mar. 1992 43 p
(Grant AF-AFOSR-0239-89)
(AD-A250399; AFOSR-92-0274TR) Avail: NTIS HC A03/MF A01

Growth conditions have been established for GaAs, InGaAs, InP, and InGaP using the newly installed gas source molecular beam epitaxy apparatus. A study was conducted on the pseudomorphic epitaxy of Si on GaAs. MIS structures were pursued through various SiN (x) and SiGe (x) interlayers. Author (GRA)

N93-14537# Naval Postgraduate School, Monterey, CA.
MONTE CARLO ANALYSIS OF ENERGY DEPOSITION IN SOLID STATE MATERIALS BY 400 AND 200 MeV ELECTRONS M.S. Thesis
Richard N. Yaw Jun. 1992 129 p
(AD-A255335) Avail: CASI HC A07/MF A02

Radiation dose distribution measurements have been carried out by the Naval Surface Warfare Center (NSWC) using 200 and 391 MeV electron beams completely penetrating layers of Aluminum, Lead and Aluminum, Polymethyl Melthacrylate (PMMA), and PMMA sandwiching an air gap. For the case of 391 MeV electrons, the results have been compared previously to the corresponding distributions predicted by the Monte Carlo simulation codes EGS3 and ACCEPT. Those measurements/predictions for 391 MeV are here compared to predictions by the CYLTRAN electron/photon transport code, and the 200 MeV measurements done by NSWC are compared to CYLTRAN calculations. The CYLTRAN code predictions agree well with measurements at 391 MeV. Comparison of CYLTRAN calculations with the NSWC results for 200 MeV indicates possible saturation of the detectors used to take the measurements. The distribution of energy dose within the target has a large dependence on the location of the air gap. The variation in dose distribution is caused by the change in target geometry resulting from insertion of the air gap. GRA

N93-14560# Arizona State Univ., Tempe.
RELIABILITY OF SOL-GEL DERIVED FERROELECTRIC MEMORIES Final Progress Report, 1 Jul. 1989 - 30 Jun. 1992
Sandwip K. Dey Jul. 1992 8 p
(Contract DAAL03-89-K-0104)
(AD-A255358; ARO-26827.7-PH) Avail: CASI HC A02/MF A01

A process was developed to prepare PZT(52/48) precursor solutions. Five spin-on depositions of this solution (0.5M) were necessary to grow 0.5 microns thin films of polycrystalline PZT onto PT passivated silicon wafers. An addition of 15 percent excess PbO aided the densification process. Films derived from 1.5M solutions resulted in PZT films of equivalent thickness in only two depositions. Dielectric constant and tan(sigma) were 800 and 2 percent respectively, at 1 kHz. Remnant and saturation polarizations were 12 and 25 microC/cm2, respectively. Coercive fields of 36-48 kV/cm were measured. From retention experiments, a polarization loss of 11.2 percent after 3.2 years was estimated (i.e., the switched charge would diminish from 5.8 to 5.2 microC/cm2). High frequency pulse

fatigue data on Nb and Sn modified PZT showed a reduction of the switched charge of 26 percent after 4x10(exp 12) polarization reversals.
GRA

N93-14576# Massachusetts Inst. of Tech., Lexington.
SOLID STATE RESEARCH Quarterly Technical Report, 1 Aug. - 31 Oct. 1991
Alan L. McWhorter 15 Nov. 1991 104 p
(Contract F19628-90-C-0002)
(AD-A256019; Rept-1991; Rept-4; ESD-TR-91-260) Avail: CASI HC A06/MF A02

This report covers in detail the research work of the Solid State Division at Lincoln Laboratory for the period 1 August through 31 October 1991. The topics covered are optoelectronic devices, quantum electronics, materials research, submicrometer technology, high speed electronics, microelectronics, and analog device technology. Funding is provided primarily by the Air Force, with additional support provided by the Army, DARPA, Navy, SDIO, NASA, and DOE. GRA

N93-14643# Texas Univ., Austin. Dept. of Electrical and Computer Engineering.
A SIMPLE CONTROLLER FOR REPETITIVE CYCLES IN ATOMIC LAYER EPITAXY
D. Kinosky, A. Mahajan, R. Qian, S. Thomas, and S. Banerjee 3 Jun. 1992 3 p
(Contract N00014-91-J-1513)
(AD-A255497; TR-2) Avail: CASI HC A01/MF A01

A simple controller system was designed and added to an existing deposition system in order to implement deposition of silicon by Atomic Layer Epitaxy (ALE). A Remote Plasma-enhanced Chemical Vapor Deposition (RPCVD) system was modified for automatic control of repetitive cycles of disilane dosing and hydrogen desorption via low energy ion bombardment. The simple configuration of the input/output modules and ease of programming allowed efficient debugging of the installation and a large degree of flexibility in in situ cleaning and in both ALE and CVD experiments. GRA

N93-14670# Emory Univ., Atlanta, GA. Dept. of Chemistry.
THERMAL STABILITY OF TRIMETHYL INDIUM ON Si(100)-2 X 1 AS STUDIED WITH HREELS, UPS, AND XPS: A COMPARISON WITH THE RESULTS FROM Si(111)-7 X 7 AND Si(110) STUDIES
Jason C. Chu, Y. Bu, and M. C. Lin 1992 21 p
(Contract N00014-89-J-1235)
(AD-A255242; TR-12) Avail: CASI HC A03/MF A01

The stability of trimethyl indium on the surface of a Si(100)-2x1 single crystal has been investigated with UPS, XPS and HREELS. The Si dangling bonds on Si(100)-2x1 was found to play an important role in the adsorption of TMIn, probably through the interaction with In 5 pz orbitals and thus causing a distortion and possibly slight dissociation of the In-C bonds. However, the In-C bond breaking occurred to a much smaller extent on the (100) surface, if there is any, than on Si(110) and Si(111)7x7. In the case of the (111) surface, TMIn attacks the adatoms before the rest-atoms. When 1L-dosed samples were annealed at 520 K, the In-C stretching vibration mode at 62 meV could still be observed in HREELS for TMIn on Si(100)-2x1, but not on the other two surfaces. Above 520 K, the In-C bond cracking was completed. Meanwhile C-H bond breaking also began to occur on the surface, which continued as the sample was further annealed at higher temperatures. At 950 K, only C species left on the surface following the decomposition of TMIn and the desorption of the In and H species. GRA

N93-14707* National Aeronautics and Space Administration. Marshall Space Flight Center, Huntsville, AL.
CRYSTAL GROWTH IN A MICROGRAVITY ENVIRONMENT Patent
Roger L. Kroes, inventor (to NASA), Donald A. Reiss, inventor (to NASA), and Sandor L. Lehoczky, inventor (to NASA) 22 Dec. 1992 6 p Filed 19 Jun. 1991 Supersedes N91-26968 (29 - 18, p 3071)
(NASA-Case-MFS-28473-1; US-Patent-5,173,087;
US-Patent-Appl-SN-717447; US-Patent-Class-23-295R;
US-Patent-Class-23-300; US-Patent-Class-156-DIG.62;
Int-Patent-Class-B01D-9/02) Avail: US Patent and Trademark Office

Gravitational phenomena, including convection, sedimentation, and interactions of materials with their containers all affect the crystal growth process. If they are not taken into consideration they can have adverse effects on the quantity and quality of crystals produced. As a practical matter, convection, and sedimentation can be completely eliminated only under conditions of low gravity attained during orbital flight. There is, then, an advantage to effecting crystallization in space. In the absence of convection in a microgravity environment cooling proceeds by thermal diffusion from the walls to the center of the solution chamber. This renders control of nucleation difficult. Accordingly, there is a need for a new improved nucleation process in space. Crystals are nucleated by creating a small localized region of high relative supersaturation in a host solution at a lower degree of supersaturation.
Official Gazette of the U.S. Patent and Trademark Office

N93-14741# Optical Society of America, Washington, DC.
PHYSICS OF X RAY MULTILAYER STRUCTURES: SUMMARIES OF PAPERS PRESENTED AT THE PHYSICS OF X RAY MULTILAYER STRUCTURES TOPICAL MEETING, TECHNICAL DIGEST SERIES, 1992, VOLUME 7
Mar. 1992 213 p Meeting held in Jackson Hole, WY, 2-5 Mar. 1992
(Contract F49620-92-J-0264)
(AD-A255383; AFOSR-92-0737TR) Avail: CASI HC A10/MF A03

The present state-of-the-art of multilayer optics is reviewed. Different theories to model the performance of multilayer structures are compared and the influence of imperfections are discussed. Optimized coating designs for the XUV are compared to perfect crystals, as used in x-ray diffraction and laser mirrors, as used for visible light. Practically all deposition methods were used for the fabrication of x-ray multilayer structures, and we summarize their strengths and weaknesses. Material combinations for a specific application are first selected by the optical constants at a specific wavelength and the by the requirement that the materials chosen must form atomically abrupt, smooth, and stable boundaries. Only a handful of combinations are in practical use. The limit on the performance of multilayer structures is given by absorption and by the roughness of the boundaries. The shortest practically useful multilayer period is limited by boundary roughness and a drastic improvement at shorter periods can only be expected if we learn to place atoms by a nonrandom process. Multilayer structures have permitted the extension of classical optics into the soft x ray range. The shorter wavelength should make it possible to build instruments with a resolution that is 100 times better than that of similar instruments for visible light. However, this goal can only be reached with 100 times tighter fabrication tolerances. It appears that recent progress in metrology will make such a performance available during the next decade. Multilayer structures have been used in x-ray astronomy, microscopy, spectroscopy, and plasma plasma diagnostics and have been proposed for the fabrication of integrated circuits. These applications are discussed, and examples of first results are presented. GRA

N93-14795# Aerospace Corp., El Segundo, CA. Engineering and Technology Group.
CHARACTERIZATION OF PZT FILMS FATIGUED AT LOW FREQUENCY
R. A. Lipeles, B. A. Morgan, and Martin S. Leung 30 Oct. 1992 13 p Repr. from ISIF-91 Proceedings of the 3rd International Symposium on Integrated Ferroelectrics
(AEROSPACE-ATR-91(8308)-2) Avail: CASI HC A03/MF A01

We report a method using Scanning Electron Microscopy (SEM), Energy Dispersive X-ray (EDX) Analysis, Scanning Ion Microscopy (SIM), and polarization-voltage hysteresis data to investigate changes that occur in lead zirconate titanate (PZT) thin films fatigued using low (below 100 kHz) frequency square waves. Fatigue in PZT capacitors can limit the lifetime of destructive readout ferroelectric memories. Identification of physical and electronic changes that occur during fatigue will lead to understanding fatigue mechanisms and the development of improved electrode-ferroelectric interfaces. Author

N93-14812# Michigan State Univ., East Lansing. Dept. of Metallurgy, Mechanics and Material Science.
HIGH TEMPERATURE STABILITY, INTERFACE BONDING, AND MECHANICAL BEHAVIOR IN (BETA)-NiAl AND Ni3Al MATRIX COMPOSITES WITH REINFORCEMENTS MODIFIED BY ION BEAM ENHANCED DEPOSITION

D. S. Grummon 22 Jan. 1992 5 p
(Contract DE-FG02-85ER-45205)
(DE92-014399; DOE/ER-45205/7) Avail: CASI HC A01/MF A01

In preparation for experiments with surface modified Al2O3 reinforcements in (beta)NiAl, diffusion bonding experiments were conducted. FP alumina fibers were prepared with ion sputtered surface films (Al2O3, Al, Ni) and then composited with (beta)NiAl slabs and hot pressed. After 70 thermal cycles, interfacial shear strength was measured. A roughness mechanism is proposed for the observed increased strength of the coated fibers. Creep in Ni3Al was studied. DOE

N93-14820 Department of the Navy, Washington, DC.
DUAL ACTIVE LAYER PHOTOCONDUCTOR Patent
Phillip E. Thompson, inventor (to Navy), Nicolas A. Papanicolaou, inventor (to Navy), and J. B. Boos, inventor (to Navy) 7 Apr. 1992 5 p Filed 29 Jun. 1988
(AD-D015423; US-Patent-5,103,280; US-Patent-Appl-SN-212841; US-Patent-Class-357-30) Avail: CASI HC A01/MF A01

A photoconductive semiconductor device having a source, a drain, and a photo-sensitive channel is presented. The channel has a surface layer that is highly doped with respect to the remainder of the channel, compensating at least in part for the channel's surface depletion layer. In this manner, the photosensitivity of the device is increased without disproportionately increasing wasted dark current. In a preferred embodiment, the additional doping of the channel's surface layer is done by ion implantation, and the device is a monolith formed of gallium arsenide. GRA

N93-14838 Syracuse Univ., NY.
SHEAR FATIGUE CRACK GROWTH ANALYSIS IN LARGE-GRAIN POLYCRYSTALS Ph.D. Thesis
Qi Chen 1992 269 p
Avail: Univ. Microfilms Order No. DA9229661

Fatigue cracks are often nucleated as small shear cracks. The propagation of such a crack often results in a crack plane that is inclined to the loading axis in such a manner to induce a mixed Mode I, Mode II, and Mode III crack-tip field. Fatigue crack growth is known as primarily caused by shear decohesion due to dislocation motion in the crack-tip region. The resolved shear stress, which drives dislocations in a crystal, is strongly orientation dependent and, hence, the cyclic plastic deformation of the shear decohesion process is highly anisotropic. For these reasons, the analysis of the growth of a shear crack can not be properly done solely based on Mode I stress intensity factor I(sub I). To better understand the behavior of shear crack growth and to develop a proper technique of analyzing shear crack growth rates, fatigue crack growth study was conducted using a large-grain Al 7029 aluminum alloy. The crack growth rates of both Mode II and Mode III shear cracks as well as Mode I cracks were measured. The crack-tip stress fields were analyzed with the finite element method and the values of K(sub I), K(sub II), and K(sub III) were determined. The calculated crack-tip stress field and the crystal orientation of the grain at the crack-tip were used to compute the resolved shear stress intensity coefficient, K(sub RSS), at each slip system. The result of this study shows that the parameter K(sub RSS) is capable of both characterizing the shear decohesion process of crack growth and explaining the morphological features of a crack surface. The highest delta-K(sub RSS) found at the most active slip system of the grain at the crack-tip correlates much better than delta-K(sub I) with the crack growth rates of both Mode II and Mode III shear cracks. Based on the morphological study and K(sub RSS) analysis, it is suggested that dislocation cross-slip is the leading mechanism of shear crack growth. The effect of grain boundary on crack growth rate was also studied. Experimental results clearly show that the misorientation between neighboring grains is the cause of crack growth retardation, and grain boundary is the main factor responsible for the microstructural effect of small crack growth. Dissert. Abstr.

N93-14909# Minnesota Univ., Minneapolis. Dept. of Chemical Engineering and Materials Science.
THEORY OF THE ELECTRONIC AND STRUCTURAL PROPERTIES OF SOLID STATE OXIDES
J. R. Chelikowsky 1992 37 p
(Contract DE-FG02-89ER-45391)
(DE92-040499; DOE/ER-45391/3) Avail: CASI HC A03/MF A01

This work has concentrated on the electronic and structural properties of solid state oxides. Emphasis has been on the electronic materials: silica, ruthenia, titania and mixed oxides. These are important materials in terms of their technological applications which range from the packaging of electronic devices to catalytic substrates. Fundamental interest has centered on the nature of the micro-structure of such solids in the amorphous, or glassy, state. New theoretical techniques have been implemented to examine such issues. The techniques outlined within this report are based on ab initio pseudopotential methods, and interatomic potentials. Some areas examined under this project are: (1) The nature of the amorphization process of quartz under pressure. (2) The equations of state of crystalline silica polymorphs. (3) The behavior of the optical and electronic properties of quartz under pressure. (4) Elastic anomalies in silica. (5) The optical and structural properties of titania, ruthenia and mixed oxides. (6) New theoretical approaches to understand covalent bonds in oxides and small clusters. DOE

N93-15008# Texas Univ., Austin. Microelectronics Research Center.
Si ATOMIC LAYER EPITAXY USING REMOTE PLASMA ASSISTED HYDROGEN DESORPTION AND DISILANE AS A PRECURSOR
A. Mahajan, D. Kinosky, R. Qian, S. Thomas, and S. Banerjee 4 Jun. 1992 3 p
(Contract N00014-91-J-1513)
(AD-A255606; TR-3) Avail: CASI HC A01/MF A01

We have demonstrated silicon Atomic Layer Epitaxy (ALE) using ions from an rf-excited helium plasma glow discharge which held remote from the substrate in a Remote Plasma Enhanced Chemical Vapor Deposition (RPCVD) system to minimize surface damage. The starting surface was a combination of dihydride and monohydride termination. The ALE experiment cycle consisted of bombarding the substrate with He ions from the plasma for 1-3 min. to desorb it followed by dosing the surface with disilane in a range of partial pressures(10(exp -7) Torr to 1.67 mTorr), temperatures (250 C - 400 C) and times (20 sec to 3min.) without plasma excitation to adsorb Si2H6 on the bare surface Si atoms created by the bombardment as to silyl (SiH3) species in a self-limiting manner which results in a hydrogen terminated surface. The maximum growth obtained was 0.44 monolayers per cycle for a 3 minute bombardment cycle. The growth per cycle decreases as the bombardment cycle time is decreased, indicating that the percentage of hydrogen removed decreases with the bombardment time. GRA

N93-15055# Texas Univ., Austin. Microelectronics Research Center.
Si ATOMIC LAYER EPITAXY BASED ON Si2H6 AND REMOTE He PLASMA BOMBARDMENT
A. Mahajan, J. Irby, D. Kinosky, R. Qian, and S. Thomas 10 Jun. 1992 19 p
(Contract N00014-91-J-1513)
(AD-A255763; TR-4) Avail: CASI HC A03/MF A01

Atomic Layer Epitaxy (ALE) of Si has been demonstrated by using remote He plasma low energy ion bombardment to desorb H from a H-passivated Si (100) surface at low temperatures and subsequently chemisorbing Si2H6 on the surface in a self-limiting fashion. Si substrates were prepared using an RCA clean followed by a dilute HF dip to provide a clean, dihydride-terminated (1 x I) surface, and were loaded into a Remote Plasma Chemical Vapor Deposition (RPCVD) system in which the substrate is downstream from an r-f noble gas (He or Ar) glow discharge in order to minimize plasma damage. An in situ remote H plasma clean at 250 C for 45 min was used to remove surface O and C and provide an alternating monohydride and dihydride termination, as evidenced by a (3x1) RHEED pattern. It was found necessary to desorb the H from the Si surface to create adsorption sites for Si bearing species such as Si2H6. Remote He plasma bombardment for 1-3 min. was investigated over a range of temperatures (250 - 410 C), pressures (50 - 400 mTorr) and r-f powers(6 - 30 W) in order to desorb the H and convert the (3x1) RHEED pattern to a (2 x 1) pattern which is characteristic of either a monohydride termination or a bare Si surface. GRA

N93-15151*# National Aeronautics and Space Administration. Pasadena Office, CA.

EPITAXIAL HETEROJUNCTIONS OF OXIDE SEMICONDUCTORS AND METALS ON HIGH TEMPERATURE SUPERCONDUCTORS Patent Application

Richard P. Vasquez, inventor (to NASA), Brian D. Hunt, inventor (to NASA), and Marc C. Foote, inventor (to NASA) 11 Mar. 1992 19 p

(Contract NAS7-918)

(NASA-Case-NPO-18483-1-CU; NAS 1.71:NPO-18483-1-CU; US-Patent-Appl-SN-852620) Avail: CASI HC A03/MF A01

Epitaxial heterojunctions formed between high temperature superconductors and metallic or semiconducting oxide barrier layers are provided. Metallic perovskites such as LaTiO3, CaVO3, and SrVO3 are grown on electron-type high temperature superconductors such as Nd(1.85)Ce(0.15)CuO(4-x). Alternatively, transition metal bronzes of the form A(x)MO(3) are epitaxially grown on electron-type high temperature superconductors. Also, semiconducting oxides of perovskite-related crystal structures such as WO3 are grown on either hole-type or electron-type high temperature superconductors. NASA

N93-15190# Wright Lab., Wright-Patterson AFB, OH.

CHARACTERIZATION OF CHOLESTERIC CYCLIC SILOXANE LIQUID CRYSTALLINE MATERIALS Interim Report, Jul. 1989 - Jun. 1991

Timothy J. Bunning, Herbert E. Klei, Edward T. Samulski, W. W. Adams, and R. L. Crane Nov. 1991 80 p

(AD-A256128; WL-TR-91-4089) Avail: CASI HC A05/MF A01

The preliminary investigation of a new type of a liquid crystalline material is described. These cyclic cholesteric siloxanes exhibit selective reflection which can be varied from the UV to the NIR by changing composition. DSC, TGA, SEK, TEM, UV-VIS-NIR spectroscopy, and polarized optical microscopy (POM) were used to obtain preliminary information on the thermal, optical, and macroscopic packing behavior as it related to possible optical applications of these materials. Considerable effort was also employed in examining the wide-angle and small-angle X-ray scattering (WAXS and SAXS) patterns obtained from these materials in a variety of forms including film, fiber, and powder samples. GRA

N93-15191# North Carolina State Univ., Raleigh. Dept. of Electrical and Computer Engineering.

A THEORETICAL SEARCH FOR SUPERVELOCITY SEMICONDUCTORS Annual Technical Report, 1 Jan. - 31 Dec. 1992

M. A. Littlejohn and K. W. Kim 31 Dec. 1992 67 p

(Contract N00014-90-J-1553)

(AD-A256325) Avail: CASI HC A04/MF A01

This document presents an annual report to the Office of Naval Research for a research program entitled A Theoretical Search For Supervelocity Semiconductors. This program has been funded by ONR since 1974 in the Department of Electrical and Computer Engineering at N.C. State University. The research has resulted in more than 80 refereed publications and numerous conference presentations from its inception. Major contributions to the field of hot electron transport and semiconductor device modeling have been achieved, new computational methods have been developed (e.g., path integral Monte Carlo techniques), and the work has helped stimulate commercial ventures in the applications of quaternary semiconductor materials to electronic and optical devices. In addition, there have been twenty eight Ph.D. and M.S. students who have received degrees at N.C. State University with this research support. Three visiting faculty members from Japan came to the university to work with the faculty investigators supported under this ONR contract during the 1979-1983 time period. A visiting professor from the French CNRS Microstructure and Microelectronics Laboratory in Bagneux (near Paris) spent a sabbatical year at N.C. State during 1988-89, and he devoted full-time working on this program at no cost to ONR. During the current funding period, a visiting scholar from China is a member of our group working on projects which directly impact this ONR program. This researcher will be appointed as a Visiting Assistant Professor in August, 1992, and will spend approximately 50 percent of his time working on this project. His work will be devoted to advanced device simulation and physics. GRA

N93-15221# M-C Power Corp., Burr Ridge, IL.

IMPACT OF PROTECTIVE OXIDES ON CATHODE-SIDE RESISTANCES IN MCFCS

R. J. Remick, T. G. Benjamin, and T. L. Osif 1992 10 p Presented at the US Department of Energy Contractors Review Meeting on Fuel Cells, Morgantown, WV, 14-15 Jul. 1992

(Contract DE-AC21-90MC-27394)

(DE92-019973; DOE/MC-27394/92/C0050; CONF-920748-10) Avail: CASI HC A02/MF A01

The objective of this work is to evaluate methods for forming protective chromium oxide and lithium ferrite layers ex-situ on the cathode-side stainless steel hardware of a molten carbonate fuel cell prior to cell/stack assembly. It is expected that once these ex-situ processes are identified it will also be possible to dope these protective oxide layers and achieve higher electrical conductivity and lower contact resistances than are experienced with the protective oxide layers which form in-situ when the cell/stack is first heated to operating temperature. DOE

N93-15233# Pittsburgh Univ., PA. Dept. of Chemistry.

SILICON NITRIDE THIN FILM PRODUCTION ON Si(111)

M. L. Colaianni, P. J. Chen, N. Nagashima, and John T. Yates, Jr. 27 Aug. 1992 22 p

(Contract N00014-82-K-0280)

(AD-A256036; TR-51) Avail: CASI HC A03/MF A01

The production of silicon nitride films by ammonia decomposition on Si(111)-(7x7) has been studied by high-resolution electron energy loss spectroscopy (HREELS), Auger electron spectroscopy (AES) and low-energy electron diffraction (LEED). Silicon nitride films of less than 1 monolayer thickness exhibit a characteristic four mode vibrational spectrum after annealing to 1200 K, while multilayer films produce three vibrational modes at 495, 720 and 1020 cm(exp -1). Upon continued heating of the submonolayer and multilayer nitride films, identical vibrational spectra are obtained, suggesting that both layers form Si3N4. These results are in excellent agreement with the vibrational spectra reported in the literature for Si3N4 layers grown using N atoms on the heated Si(111)-(7x7) surface, signifying that identical nitride films can be grown using ammonia. Si3N4 films grown on Si(111) are able to chemisorb ammonia at 300 K, showing that coordinatively unsaturated silicon sites are probably present on the film surface. This is in agreement with other studies which indicate that the growth mechanism for these silicon nitride films involves silicon enrichment at the film/vacuum interface. GRA

N93-15244# North Carolina State Univ., Raleigh.

GROWTH, CHARACTERIZATION AND DEVICE DEVELOPMENT IN MONOCRYSTALLINE DIAMOND FILMS Quarterly Report, 1 Jul. - 30 Sep. 1992

Robert F. Davis Sep. 1992 71 p

(Contract N00014-90-J-1604)

(AD-A256283) Avail: CASI HC A04/MF A01

Ordered diamond films have been deposited on single crystal Si(100) substrates via in-situ carburization followed by bias-enhanced nucleation. Photoluminescence and Raman spectroscopy have been employed to determine the time evolution of defect formation in these CVD diamond films for stages of growth spanning nucleation to continuous film formation. Analysis of the 1332/cm diamond feature showed two rates of diamond growth with a transition at the thickness where nearly complete coverage was obtained. Investigation of the various defects in the films led to the conclusions that Si atoms most likely caused the 1.68 eV optical centers at the initial stages of growth. Luminescence associated with sp squared bonding defects appeared only after a continuous film was formed. The CVD growth of diamond films on Si(100) have also been studied using scanning tunneling spectroscopy. The surface of the diamond film possessed electronic structure similar to single crystal diamond. By contrast the initial growth surface showed evidence of Beta-SiC and graphite electronic structures. The microwave performance of p-type diamond MESFET's is also under investigation. The surface breakdown model has been further refined and an activation model has been included so that free charge density as a function of temperature could be determined. Research is also underway to simulate the performance of the Kobe p-channel MESFET. A pn junction gate model is also being formulated so that the operation of a diamond JFET can be investigated. GRA

N93-15297# David Sarnoff Research Center, Princeton, NJ.

HIGH PERFORMANCE YBCO FILMS Research and Development Status Report, 1 May - 31 Jul. 1992

Edgar J. Denlinger 31 Jul. 1992 33 p
(Contract N00014-91-C-0216; DARPA Order 8100)
(AD-A255439) Avail: CASI HC A03/MF A01

The objective of this program is to identify suitable low loss, low dielectric constant substrates and develop and optimize deposition processes for high quality YBCO films including the necessary buffer layers. Ultimate goals are large area substrates having a double-sided High Temperature Superconducter (HTS) coating with a surface resistance ten times lower than copper at 40 GHz. High quality HTS films on low dielectric constant substrates are expected to find widespread use in advanced millimeter wave components, in extending the power handling capability of microwave and millimeter wave circuitry, and in facilitating high speed computer interconnects. Sample demonstration circuits will be built toward the end of the program. The following progress report begins by describing our latest results with the development of both HTS film and substrate characterization methods. In cooperation with Cryo Industries we have completed the design of a three-axis positioning system for the dielectric resonator thin film test apparatus. This will allow us to efficiently probe a large wafer for surface resistance. A dielectrometer for measuring the dielectric constant of unmetallized substrates was received from Kent Laboratories and was used successfully at room temperatures. Calibrations at liquid nitrogen temperatures will be made soon. We continued investigating the cause of a low frequency roll-off in Q values for self-resonant HTS spirals. Various new ground place configurations did not give us better results. GRA

N93-15309*# Clarkson Univ., Potsdam, NY.
MODELLING DIRECTIONAL SOLIDIFICATION Progress Report, 1 May 1991 - 31 Oct. 1992
William R. Wilcox, Liya L. Regel, Jian Zhou, and Weijun Yuan 31 Oct. 1992 55 p
(NAG8-831)
(NASA-CR-191301; NAS 1.26:191301) Avail: CASI HC A04/MF A01

The long range goal of this program has been to develop an improved understanding of phenomena of importance to directional solidification, in order to enable explanation and prediction of differences in behavior between solidification on Earth and in space. Current emphasis is on determining the influence of perturbations on directional solidification. For individual titles, see N93-15310 through N93-15312.

N93-15310*# Clarkson Univ., Potsdam, NY.
SOLIDIFICATION OF InSb-GaSb ALLOY AND InSb WITH VIBRATION
Weijun Yuan *In its* Modelling Directional Solidification 31 Oct. 1992 p 18-34 (For primary document see N93-15309 04-76)
Avail: CASI HC A03/MF A01

The objective of this project is to determine the influence of vibration on the composition homogeneity and microstructure of alloy semiconductors solidified with the Vertical Bridgman-Stockbarger (VBS) technique. InSb-GaSb and InSb were directionally solidified in a VBS apparatus with axial vibration of the ampoule. Author

N93-15311*# Clarkson Univ., Potsdam, NY.
AN EXPERIMENTAL APPROACH TO DETERMINE THE HEAT TRANSFER COEFFICIENT IN DIRECTIONAL SOLIDIFICATION FURNACES
Mohsen Banan, Ross T. Gray, and William R. Wilcox *In its* Modelling Directional Solidification 31 Oct. 1992 p 557-565 (For primary document see N93-15309 04-76)
Avail: CASI HC A02/MF A01

The heat transfer coefficient between a molten charge and its surroundings in a Bridgman furnace was experimentally determined using in-situ temperature measurement. The ampoule containing an isothermal melt was suddenly moved from a higher temperature zone to a lower temperature zone. The temperature-time history was used in a lumped-capacity cooling model to evaluate the heat transfer coefficient between the charge and the furnace. The experimentally determined heat transfer coefficient was of the same order of magnitude as the theoretical value estimated by standard heat transfer calculations. Author

N93-15312*# Clarkson Univ., Potsdam, NY.
EXPERIMENTAL OBSERVATION OF THE INFLUENCE OF FURNACE TEMPERATURE PROFILE ON CONVECTION AND SEGREGATION IN THE VERTICAL BRIDGMAN CRYSTAL GROWTH TECHNIQUE
G. T. Neugebauer and William R. Wilcox *In its* Modelling Directional Solidification 31 Oct. 1992 p 357-362 (For primary document see N93-15309 04-76)
Avail: CASI HC A02/MF A01

Azulene-doped naphthalene was directionally solidified during the vertical Bridgman-Stockbarger technique. Doping homogeneity and convection were determined as a function of the temperature profile in the furnace and the freezing rate. Convection velocities were two orders of magnitude lower when the temperature increased with height. Rarely was the convection pattern axisymmetric, even though the temperature varied less than 0.1 K around the circumference of the growth ampoule. Correspondingly the cross sectional variation in azulene concentration tended to be asymmetric, especially when the temperature increased with height. This cross sectional variation changed dramatically along the ingot, reflecting changes in convection presumably due to the decreasing height of the melt. Although there was large scatter and irreproducibility in the cross sectional variation in doping, this variation tended to be least when the growth rate was low and the convection was vigorous. It is expected that compositional variations would also be small at high growth rates with weak convection and flat interfaces, although this was not investigated in the present experiments. Neither rotation of the ampoule nor deliberate introduction of thermal asymmetries during solidification had a significant influence on cross sectional variations in doping. It is predicted that slow directional solidification under microgravity conditions could produce greater inhomogeneities than on Earth. Combined use of microgravity and magnetic fields would be required to achieve homogeneity when it is necessary to freeze slowly in order to avoid constitutional supercooling. Author

N93-15321# Los Alamos National Lab., NM.
NORMAL STATE RESISTIVITY AND THE PHASE DIAGRAM OF U(1-x)Th(x)Be13
E. A. Knetsch (Leiden Univ., Netherlands), G. J. Nieuwenhuys (Leiden Univ., Netherlands), J. A. Mydosh (Leiden Univ., Netherlands), R. H. Heffner, and J. L. Smith 1992 13 p Presented at the International Conference on Strongly Correlated Electron Systems, Sendai, Japan, 7-11 Sep. 1992
(Contract W-7405-eng-36)
(DE92-040236; LA-UR-92-2713; CONF-9209202-1) Avail: CASI HC A03/MF A01

Resistivity measurements as a function of temperature (0.4 to 300 K) and field (0 to 7 T) for the heavy-fermion superconductor U(1-x)Th(x)Be13 with 0.00 less than or = chi less than or = 0.06 were analyzed using a sample with x = 0.06 as a reference compound. We show that the low T resistivity maximum, which moves to higher temperatures upon applying a field, shifts below T(sub c), at the kink in the T(sub c) - x phase diagram and is not observed for higher thorium concentrations, not even in a field of 7T. These observations shed new light on the nonmonotonic dependence of T(sub c), on thorium concentration and the occurrence of a second transition. DOE

N93-15351# Ohio State Univ., Columbus. Dept. of Physics.
DYNAMICAL PROPERTIES OF JOSEPHSON JUNCTIONS ARRAYS Final Report, 15 Sep. 1989 - 14 Sep. 1991
C. A. Ebner and C. Jayaprakash Jul. 1992 25 p
(Grant AF-AFOSR-0527-89)
(AD-A255464; AFOSR-92-0848TR) Avail: CASI HC A03/MF A01

Current and recent work in our group on Josephson junction arrays has been focused on two particular types of dynamical states, namely chaotic states and 'chain' states. We summarize briefly the issues addressed and the significant results obtained for each type of state. GRA

N93-15365# Rockwell International Science Center, Thousand Oaks, CA.
SELECTED AREA EPITAXIAL GROWTH FOR COMPLEMENTARY HBT APPLICATIONS Final Report, 1 May 1989 - 30 Apr. 1992
C. W. Farley 17 Aug. 1992 41 p
(Contract DAAL03-89-C-0014)
(AD-A257047; SC71008.FR; ARO-26484.1-EL) Avail: CASI HC A03/MF A01

This report describes the development of a complementary AlGaAs/GaAs heterojunction bipolar transistor (HBT) technology with a highly merged process that simplifies device fabrication without altering or compromising device design. Selected areas molecular beam epitaxy (MBE) was used to monolithically integrate Npn and Pnp devices. These devices show performance levels comparable to separately processed devices. For the first time, microwave frequency integrated circuits were fabricated from both types of devices on the same water. A digital mask set and the Rockwell baseline digital HBT process were modified to develop a merged process. This process includes the use of a light field emitter to provide passivation which reduces surface recombination at the base-emitter junction. This is the first time that edge passivation, which results in increased gain in Npn devices, has been demonstrated to increase gain in Pnp structures. The merged digital process was designed to maximize the number of steps in which both devices could be processed simultaneously, and the resulting process has only two more mask levels (Pnp base and collector metallization) than the baseline process. GRA

N93-15443# State Univ. of New York, Buffalo. Dept. of Chemistry.
GALLIUM AND INDIUM COMPOUNDS CONTAINING THREE DIFFERENT SUBSTITUENTS. CRYSTAL AND MOLECULAR STRUCTURE OF ((Me3 CCH2)ClGaPPh2)3
O. T. Beachley, Jr., John D. Maloney, and Robin D. Rogers 28 Oct. 1992 28 p
(Contract N00014-90-J-1530)
(AD-A257049; TR-35) Avail: CASI HC A03/MF A01

Three new heavier group 13 element compounds containing three different substituents, (Me3CCH2)ClGaPPh2, (Me3CCH2)BrGaPPh2 and (Me3CCH2)ClInPPh2, were prepared and characterized. All compounds were characterized by partial elemental analysis, cryoscopic molecular weight studies in benzene solution, and NMR and IR spectroscopic data. All three compounds exist as trimeric molecules in solution. NMR spectral data were consistent with the presence of multiple isomers of the trimers. The compound ((Me3CCH2)ClGaPPh2)3 crystallizes in the acentric space group Pn2la with a = 17.741(9) A, b = 13.942(6) A, and c = 21.574(8) A. Diffraction data were collected on an Enraf-Nonius CAD-4 diffractometer, and the structure was refined to R = 4.6 percent and wR = 6.0 percent for those 2971 reflections with (F(sub o) greater than or equal to 5(sigma)(F(sub o)). GRA

N93-15444# Lincoln Univ., PA. Dept. of Physics.
FAR INFRARED, MAGNETIC, AND ELECTRONIC STUDIES OF HIGH T(SUB c) SUPERCONDUCTING MATERIALS
Stanley Tsai, Jin T. Wong, and Willie Williams 30 Sep. 1992 23 p
(Contract N00014-89-J-3237)
(AD-A257050) Avail: CASI HC A03/MF A01

Most of the studies of flux motion inside the superconductor are concentrated on the magnetization decay in the zero field cooled condition. We investigated the time dependence of the isothermal magnetization in the field cooled condition. We found that when the temperature is lower than 35K, the isothermal magnetization decreases with time for every temperature at which the isothermal magnetization measurements were carried out. In contrast, when the temperature is higher then 35K, the isothermal magnetization increases at some temperatures but decreases at others during the measurement period (15-20 hours). We discuss the mechanism of the discovered time-dependence of the isothermal magnetization based upon the thermal activation theory. GRA

N93-15446# Colorado Univ., Boulder.
FERROELECTRICS VOLUME 122, NUMBERS 1-4, 1991. PROCEEDINGS OF THE 3RD INTERNATIONAL CONFERENCE ON FERROELECTRIC LIQUID CRYSTALS, PART 2 Final Report, 1 Jun. 1991 - 31 May 1992
Noel A. Clark, David M. Walba, Mark A. Handschy, and Garret Moddel 1992 313 p Conference held in Boulder, CO, 23-28 Jun. 1991
(Contract DAAL03-91-G-0208)
(AD-A257053; ARO-29180.2-PH-CF-Pt-2) Avail: CASI HC A14/MF A03

The present volumes form the proceedings of the Third International Conference on Ferroelectric Liquid Crystals, held in Boulder, Colorado, USA 23-28 June 1991. These volumes continue the publication of this conference series, the proceedings of the first conference (1987) held at Bordeaux/Arcachon appearing in Volumes 84 and 85, and the proceedings of the second conference (1989) held at Goteborg appearing in Volumes 113 and 114. As for the two preceding conferences, FLC-91 provided a broad forum for the exchange of information on FLCs, with most of the groups working in the field well represented. Exciting developments were reported in all FLC areas. The worldwide effort at developing new FLC materials continues apace, with the report of an FLC material possessing a spontaneous polarization nearly equal to the sum of all transverse molecular dipoles, and new thrusts in polymer FLCs and FLCs for electronic nonlinear optical applications. The conference saw many new developments in FLC basic and device physics, including the use of dielectric spectroscopy copy as a tool for studying the molecular origins of the polarization in FLCs. Particularly exciting were the FLC device developments with the emergence of sophisticated FLC devices for opto-electronic computing, display, and other light control applications, including a demonstration of a flexible polymer FLC display. GRA

N93-15447# Colorado Univ., Boulder.
FERROELECTRICS VOLUME 121, NUMBERS 1-4, 1991. PROCEEDINGS OF THE 3RD INTERNATIONAL CONFERENCEON FER ROELECTRIC LIQUID CRYSTALS, PART 1 Final Report, 1 Jun. 1991 - 31 May 1992
Noel A. Clark, David M. Walba, Mark A. Handschy, and Garret Moddel 1992 390 p Conference held in Boulder, CO, 23-28 Jun. 1991
(Contract DAAL03-91-G-0208)
(AD-A257054; ARO-29180.1-PH-CF-Pt-1) Avail: CASI HC A17/MF A04

The present volumes form the proceedings of the Third International Conference on Ferroelectric Liquid Crystals, held in Boulder, Colorado, USA 23-28 June 1991. These volumes continue the publication of this conference series, the proceedings of the first conference (1987) held at Bordeaux/Arcachon appearing in Volumes 84 and 85, and the proceedings of the second conference (1989) held at Goteborg appearing in Volumes 113 and 114. As for the two preceding conferences, FLC-91 provided a broad forum for the exchange of information on FLCs, with most of the groups working in the field well represented. Exciting developments were reported in all FLC areas. The worldwide effort at developing new FLC materials continues apace, with the report of an FLC material possessing a spontaneous polarization nearly equal to the sum of all transverse molecular dipoles, and new thrusts in polymer FLCs and FLCs for electronic nonlinear optical applications. The conference saw many new developments in FLC basic and device physics, including the use of dielectric spectroscopy as a tool for studying the molecular origins of the polarization in FLCs. Particularly exciting were the FLC device developments with the emergence of sophisticated FLC devices for opto-electronic computing, display, and other light control applications including a demonstration of a flexible polymer FLC display. GRA

N93-15449# Florida Univ., Gainesville. Dept. of Materials Science and Engineering.
THE 17TH ANNUAL CONFERENCE ON THE PHYSICS AND CHEMISTRY OF SEMICONDUCTOR INTERFACES Final Report
Paul H. Holloway 12 Oct. 1992 32 p Conference held in Clearwater Beach, FL, 31 Jan. - 2 Feb. 1990
(Contract N00014-90-J-1134)
(AD-A257061) Avail: CASI HC A03/MF A01

The seventeenth annual conference on the Physics and Chemistry of Semiconductor Interfaces (PCSI-17) was held at Clearwater Beach, FL on 31 Jan. - 2 Feb. 1990. The organizing and program committee membership is shown in Appendix 1. In addition, the local arrangements committee is also shown in Appendix 1. The program and meeting was quite successful, with presentation of seventy three papers from the US and nine foreign countries, as shown in Appendix 2. The meeting was attended by 132 scientists as shown in Appendix 3. Finally the papers from the meeting were published in the Journal of Vacuum Science and Technology, Volume B4, July/August, 1990, as shown in Appendix 4. In summary, the meeting was quite successful and served its intended purpose. The organizers are grateful for the support of the office of Naval Research. GRA

N93-15465# Pennsylvania State Univ., University Park. Dept. of Physics.
INNOVATIVE TECHNIQUES FOR STUDYING NEW MATERIALS AND NEW DEVELOPMENTS IN SOLID STATE PHYSICS Annual Summary Report, 1 Nov. 1991 - 31 Oct. 1992
Julian D. Maynard 14 Sep. 1992 21 p

(Contract N00014-92-J-1186)
(AD-A256394) Avail: CASI HC A03/MF A01

The goals of this project involve the use of innovative acoustic techniques to study new materials and new developments in solid state physics, such as effects in mesoscopic electronic systems. Major accomplishments include (1) the publication of a number of major papers, (2) the determination of the anisotropy of an aluminum alloy quasicrystal, (3) the completion of ultrasound measurements on ceramic beads with varying heat treatment, (4) preparation of a diamond substitute material, TiB2, for determination of the elastic constants, (5) the development of a new transduction method for measuring optical absorption in highly transparent materials, (6) the determination of the effects of nonlinearity on Anderson localization, and (7) the use of an acoustic analog to explain the discrepancy between theory and experiment for normal electron persistent currents in a mesoscopic system. GRA

N93-15500*# National Aeronautics and Space Administration. Marshall Space Flight Center, Huntsville, AL.
STUDY OF THE GLASS FORMATION OF HIGH TEMPERATURE SUPERCONDUCTORS
Edwin C. Ethridge, William F. Kaukler (Alabama Univ., Huntsville.), and Terry Rolin (Alabama Univ., Huntsville.) Dec. 1992 25 p
(Proj. 89-04)
(NASA-TM-108389; NAS 1.26:108389) Avail: CASI HC A03/MF A01

A number of compositions of ceramic oxide high T(sub c) superconductors were elevated for their glass formation ability by means of rapid thermal analysis during quenching, optical, and electron microscopy of the quenched samples, and with subsequent DSC measurements. Correlations between experimental measurements and the methodical composition changes identified the formulations of superconductors that can easily form glass. The superconducting material was first formed as a glass; then, with subsequent devitrification, it was formed into a bulk crystalline superconductor by a series of processing methods. Author

N93-15587*# Christopher Newport Coll., Newport News, VA.
A COMPARISON OF SUPERCONDUCTOR AND MANGANIN TECHNOLOGY FOR ELECTRONIC LINKS USED IN SPACE MISSION APPLICATIONS
R. Caton, R. Selim, and A. M. Buoncristiani Washington National Aeronautics and Space Administration Dec. 1992 17 p
(Grant NAG1-1242; RTOP 142-20-14-02)
(NASA-CR-4477; NAS 1.26:4477) Avail: CASI HC A03/MF A01

The electronic link connecting cryogenically cooled radiation detectors to data acquisition and signal processing electronics at higher temperatures contributes significantly to the total heat load on spacecraft cooling systems that use combined mechanical and cryogenic liquid cooling. Using high transition temperature superconductors for this link has been proposed to increase the lifetime of space missions. Herein, several YBCO (YBa2Cu3O7) superconductor-substrate combinations were examined and total heat loads were compared to manganin wire technology in current use. Using numerical solutions to the heat-flow equations, it is shown that replacing manganin technology with YBCO thick film technology can extend a 7-year mission by up to 1 year. Author

N93-15649# Sandia National Labs., Albuquerque, NM.
ENERGY DISTRIBUTION OF TRAPPED HOLES IN IRRADIATED SiO2
D. M. Fleetwood and S. L. Miller 1992 3 p Presented at the 1992 IEEE Semiconductor Interface Specialists Conference, San Diego, CA, 9-13 Dec. 1992
(Contract DE-AC04-76DP-00789)
(DE92-040979; SAND-92-1878C; CONF-921226-2) Avail: CASI HC A01/MF A01

There is a discrepancy between literature estimates of trapped-hole energies in irradiated SiO2 obtained via thermal and optical methods (0.6-1.4 eV and 3 eV, respectively). A method has been developed for obtaining an improved estimate of the energy distribution of trapped holes in irradiated SiO2, which brings thermal and optical estimates into much closer agreement. Experimental and theoretical TSC (thermally stimulated current) spectra are shown for a soft MOS capacitor with a 350-nm oxide cycled through 4 irradiations (10 keV x rays) and TSC measurements. Four trap-energy distributions were also independently derived from TSC at different ramp rates for a 45-nm radiation-hardened oxide. The trap distributions inferred from TSC for the 45-nm hard oxide agree with each other and with that inferred for the soft 350-nm oxide. DOE

N93-15651# Sandia National Labs., Albuquerque, NM.
REVISED NOMENCLATURE FOR DEFECTS AT OR NEAR THE Si/SiO2 INTERFACE
D. M. Fleetwood 1992 3 p Presented at the 1992 IEEE Semiconductor Interface Specialists Conference, San Diego, CA, 9-13 Dec. 1992
(Contract DE-AC04-76DP-00789)
(DE92-040975; SAND-92-1877C; CONF-921226-3) Avail: CASI HC A01/MF A01

A revised nomenclature for defects in MOS devices is described which clearly distinguishes the language used to describe the physical location of defects from that used to describe their electrical response. 'Oxide traps' are simply defects in the SiO2 layer, and 'interface traps' are defects at the Si/SiO2 interface; nothing is presumed about how either communicates with the underlying Si. 'Fixed states' are defined electrically as trap levels that do not communicate with the Si on the time scale, but 'switching states' can exchange charge with the Si. Fixed states presumably are oxide traps, but switching states can either be interface traps or near-interfacial oxide traps that can communicate with the Si, i.e. 'border traps'. Thus the term 'traps' is reserved for defect location, and the term 'states' for electrical response. This defect picture is used to provide new insight into the response of MOS capacitors with 45-nm radiation-hardened oxides to electrical stress and annealing; capacitance-voltage and thermally-stimulated-current measurements are used. DOE

N93-15516*# Arizona Univ., Tucson.
OXIDATION PROCESSES IN MAGNETO-OPTIC AND RELATED MATERIALS
Paul A. Lee, Neal R. Armstrong, James L. Danzinger, and Craig D. England *In its* Research Studies on Advanced Optical Module/Head Designs for Optical Data Storage 15 Mar. 1992 p 177-186 (For primary document see N93-15505 04-74)
Avail: CASI HC A02/MF A03

77 THERMODYNAMICS AND STATISTICAL PHYSICS

Includes quantum mechanics; theoretical physics; and Bose and Fermi statistics.

For related information see also *25 Inorganic and Physical Chemistry* and *34 Fluid Mechanics and Heat Transfer.*

N93-14116 Oxford Univ. (England).
THE LOW-ENERGY STRUCTURE OF COMPACTIFIED SUPERSTRING MODELS Ph.D. Thesis
Myriam Mondragon Ceballos 1991 129 p
Avail: Univ. Microfilms Order No. BRD-95139

The low energy structure is studied of models coming from superstring compactification, as a way of looking for generic features of the superstring vacua. A method is presented for reducing the number of string vacua candidates for generating Standard Model that come from orbifold compactifications. This consists of applying a set of equivalence relations and Weyl reflections to the shift and Wilson lines of the models, showing that many of them are equivalent. The method is very general and can be applied to any Z sub N orbifold, in particular it is applied to the Z sub 3 and Z sub 7 orbifolds. The construction is studied of (0,2) superstring compactifications built by tensoring of N = 2 minimal superconformal models. These models are obtained by embedding discrete symmetries of the superconformal theories into the gauge degrees of freedom. Some of the new models are shown to correspond to orbifold vacua, and some of them can be understood as the addition of Wilson lines in a (2,2) background. The construction is applicable to any model obtained through tensoring of N + 2 superconformal theories, and allows the generalization of well known orbifold techniques, through which it is possible to break the gauge group at the same time as reducing the number of generations. The supersymmetry breaking effects generated by gaugino condensates is studied in the low-energy Lagrangians coming from superstring theories. The case

is considered in which the hidden sector consists of three separate sectors, each sector having a gaugino condensate. The effects are incorporated of the one-loop radiative corrections coming from the massless scalars of the theory and from the Kaluza-Klein modes. It is shown how in some models it is possible to break supersymmetry at a scale which is reasonable for phenomenology, providing an explanation for the large hierarchy problem, and selecting among different vacua. Dissert. Abstr.

N93-14143 Maryland Univ., College Park.
TYPE 2 SUPERSTRINGS IN CURVED D = 10 SPACE-TIME: DYNAMICS OF THEIR MASSLESS FIELDS AND COVARIANT QUANTIZATION Ph.D. Thesis
Branislav Radak 1991 119 p
Avail: Univ. Microfilms Order No. DA9222755

The 2A and 2B superstrings are analyzed as nonlinear sigma-models. These models represent closed strings in 10 dimensions with properties which make them promising candidates for the unification of all known interactions. It is known that their spectra are entirely free from tachyons and ghosts and that they reduce to N = 8 supergravity after a six-torus compactification. The dynamics of the background fields is presented--for type 2A up to level 1 and fully for type 2B. New supergeometries are tailored to simplify calculations of the one-loop quantum corrections of these nonlinear sigma-models. Equations of motion for the massless superstring models are found for 2B theory by imposing constraints on superfield variables and solving Bianchi identities. In order to quantize this system it is necessary to analyze in detail the gauge algebra of all the symmetries which occur in this formulation. The complete gauge algebras for 2A and 2B models in the presence of arbitrary backgrounds are given. The Batalin-Vilkovisky procedure of quantization is then applied to 2A theory. It is also found that in this covariant procedure one-loop Lorentz-violating divergent terms disappear. Finally, Siegel's modification of the Green-Schwarz string is analyzed in some detail. It is shown that this mode is kappa invariant only in flat space-time. The presence of this invariance in an arbitrary curved background necessarily requires a modification of this minimal extension. Dissert. Abstr.

N93-14590 State Univ. of New York, Albany.
SEMI-CLASSICAL QUANTIZATION RULES IN SUPERSYMMETRIC QUANTUM MECHANICS Ph.D. Thesis
Suparmi 1992 146 p
Avail: Univ. Microfilms Order No. DA9230032

Supersymmetry (SUSY) is a symmetry of a system which consists of fermions and bosons and remains invariant under transformations of fermions into bosons and bosons into fermions. Semiclassical quantization rules in supersymmetric quantum mechanics are investigated. First, to understand the role of supersymmetric quantum mechanics in nonrelativistic quantum mechanics, several shape invariant potentials are studied algebraically and semiclassically within the scheme of supersymmetric quantum mechanics. Secondly, the SUSY semiclassical formula is examined in relation with the standard WKB semiclassical formula. A semi-classical WKB-like quantization formula recently proposed for a SUSY system by Comtet, Bandrauk, and Campbell is amazingly successful in evaluating the energy spectrum of a one-dimensional system despite its obscure origin. A prescription for converting the standard WKB formula to the SUSY semiclassical formula is presented for the shape invariant class of potentials. Thirdly, the broken SUSY quantization formula is analyzed. The SUSY formula of Comtet, Bandrauk, and Campbell has been derived from Feynman's path integral for a supersymmetric system. As a by-product, a broken SUSY formula has been obtained. It is shown that the broken SUSY formula can reproduce exact results for certain quantum potential problems. The broken SUSY formula is also applied to another system which is not exactly solvable. It is found that the broken SUSY formula provides approximate energies which are always greater than the correct values, while the standard WKB formula always gives values smaller than the exact ones. Dissert. Abstr.

N93-14905# Los Alamos National Lab., NM.
THERMODYNAMICS AND TRANSPORT IN Ce3Bi4Pt3 AND RELATED COMPOUNDS
J. D. Thompson, P. C. Canfield, Z. Fisk, M. F. Hundley, G. H. Kwei, A. Lacerda, and W. P. Beyermann 1992 26 p Presented at the Transport and Thermal Properties of F Electron Systems, Hiroshima, Japan, 30 Aug. - 2 Sep. 1992
(Contract W-7405-eng-36)
(DE92-040377; LA-UR-92-2800; CONF-9208141-1) Avail: CASI HC A03/MF A01

The transport and thermodynamic properties of the small-gap semiconductor Ce3Bi4Pt3 are reviewed and discussed in relation to other Kondo insulators and metals. The data are consistent with the small-gap semiconductors being Kondo-like metals at temperatures T greater than or = E(sub g)/k(sub B). Kondo insulators appear to be an unusually simple realization of the Anderson Lattice Hamiltonian in which the lower hybridization band is exactly filled, or in Kondo language, the Abrikosov-Suhl resonance exactly fills a Brillouin zone. DOE

N93-15333# Arizona State Univ., Tempe. Dept. of Mathematics.
SPATIO-TEMPORAL COMPLEXITY AND LARGE-SCALE STRUCTURES IN PROBLEMS OF CONTINUUM MECHANICS Final Report, 1 Sep. 1989 - 31 Aug. 1992
Basil Nicolaenko, Dieter Armbruster, Alp Eden, and Eric Kostelich 31 Aug. 1992 19 p
(Grant AF-AFOSR-0507-89)
(AD-A256410; AFOSR-92-0902TR) Avail: CASI HC A03/MF A01

We have studied some difficulties in estimating dynamics from time-delay embeddings of experimental data that can be characterized as low-dimensional. A new procedure is developed to reduce noise by exploiting the properties of saddle periodic orbits on the reconstructed attractor. Most of these methods involve the estimation of a derivative form the data or in some way require a least squares estimate of the location of some portion of the attractor. Some of the inherent problems are addressed in the estimation-of dynamics from data, regardless of the type of model used to approximate the dynamics. These difficulties may arise from the fractal structure of the attractor and errors in all the observations. The problems persist regardless of the amount of available data and affect one's ability to determine an accurate local Model of the dynamics, even when an accurate model should be obtainable in principle. Many of these problems can be circumvented by using as much dynamical information as possible in the formulation of the statistical relationship between the observations. Our attempt to do this involves the use of recurrent orbits to derive an accurate linear model of the dynamics in the vicinity of saddle periodic orbits, on the attractor. We have applied our method to two experimental data sets from Taylor-Couette flows. GRA

N93-15469# Stanford Research Inst., Menlo Park, CA. Linear Accelerator Center.
ANTI-HYDROGEN: THE CUSP BETWEEN QUANTUM MECHANICS AND GENERAL RELATIVITY
H. P. Noyes Sep. 1992 4 p Presented at the Hyperfine Interactions of the Anti-Hydrogen Workshop, Munich (Germany), 30-31 Jul. 1992
(Contract DE-AC03-76SF-00515)
(DE93-001807; SLAC-Pub-5856; CONF-9207149-1) Avail: CASI HC A01/MF A01

We argue that the crossing (CPT) symmetry of relativistic quantum mechanics requires that both the Coulombic and the Newtonian force between pairs of particles will reverse when one is replaced by its anti-particle. For consistency, this requires a theory in which both the equivalence principles and gauge invariance are abandoned. Thus whether anti-hydrogen 'falls' up or down will provide an 'experiment crusis' separating general relativity and gauge invariance from this version of quantum mechanics. DOE

80 SOCIAL SCIENCES (GENERAL)

Includes educational matters.

N93-14417# California Univ., Santa Barbara. Center for Quantized Electronic Structures.
THE CHANGING CULTURE OF SCIENCE: BRINGING IT INTO BALANCE
Fiona Goodchild, Bernard Sadoulet, Rose Sergeant, and Kate Metropolis Aug. 1992 28 p Conference held in Berkeley, CA, 21-23 Jul. 1992
(Contract N00014-92-J-1511)
(AD-A255993) Avail: CASI HC A03/MF A01

The Conference on Changing Culture of Science: Bringing it into Balance,

held June 21-23, 1992 in Berkeley, California assembled a broad spectrum of people dedicated to science to explore attitudes, practices, and policies long woven into the fabric of our working culture of science.This discussion confronted three fears: the fear that many people who want to become scientists are being thwarted by the scientific community's current expectations of what paths must be followed, what choices must be made, as they progress; the fear that the scientific community is not interacting with the rest of society in a positive way; and the fear that the scientific community cannot accommodate people who do not fit the traditional picture of a scientist without lowering the quality of science. Recommendations were made on: how to build an inclusive, heterogeneous scientific community without compromising scientific excellence; how the scientific culture can affirm that child raising, elder care, and mentoring of students and colleagues are valued and respected activities; how to address the under-representation of women and minorities in administrative and management positions in the scientific community; how to make the first year in the scientific community more supportive and welcoming to people from all backgrounds; and how to increase interest in and understanding of science among the general population and among all students. GRA

N93-14526# Navy Personnel Research and Development Center, San Diego, CA.
LONG TERM MEMORY FOR DIFFERENT TYPES OF CLASSROOM KNOWLEDGE Final Report, Sep. 1989 - Oct. 1991
George B. Semb, John A. Ellis, and John Araujo Aug. 1992 22 p
(AD-A255235; NPRDC-TR-92-18) Avail: CASI HC A03/MF A01

Two studies examined students' long-term retention of knowledge learned in college courses. In Experiment 1 retention for four different types of tasks was measured 4 and 11 months after the term ended. Overall students retained a great deal of what they originally learned. Retention for the recognition, recall, comprehension, and mental skill learning tasks differed only for the recall task which was significantly lower than the others. Experiment 2 analyzed knowledge retention in student tutors. Tutors retained more knowledge after four months than did the students they tutored. This suggests that tutoring, a type of overlearning, has positive effects that are maintained over time. GRA

N93-14720# National Science Foundation, Washington, DC.
A PLANNING WORKSHOP: TO STRENGTHEN AMERICAN COGNITIVE SCIENCE FOR THE TWENTY-FIRST CENTURY
1992 16 p
(NSF-92-4) Avail: CASI HC A03/MF A01

Cognitive science's major accomplishments have been analyses of cognition by individual agents, including language, problem solving, representations of knowledge in memory, perception, and decision making. Prospects for continued progress on these important problems are excellent. At the same time, the field is on the threshold of building new integrative understanding in two important directions. One involves understanding individual cognitive agents as participants in larger social and physical systems. This involves integrating the study of individual cognition with research about social practices and about systems in which natural resources and technology contribute to cognitive functioning. The other integrative direction involves connecting the study of cognitive processes with the growing body of research results in neuroscience. The participants decided to prepare brief descriptions of research accomplishments and prospects in four topical areas, rather than trying to survey all important areas of research in cognitive science. The report, therefore, presents overviews of current and prospective research about four general topics: (1) language, (2) conceptual knowledge, (3) abstract neural networks, and (4) analyses of cognitive activity in social and physical environments. Author

N93-14937# Impact Group (Canada).
SPACE EDUCATION: A SELF-PERSERVATION STRATEGY FOR THE CANADIAN SPACE INDUSTRY
Ron Freedman *In* Canadian Space Agency, Proceedings of the Sixth CASI Conference on Astronautics 1990 16 p Previously announced in IAA as A91-34943 (For primary document see N93-14920 04-12)
Avail: Canadian Aeronautics and Space Inst., 222 Somerset St. W., Suite 601, Ottawa, Ontario K2P 0J1 Canada

N93-14938# York Univ. (Ontario). Center for Research in Experimental Space Science.
INTERNATIONAL SPACE UNIVERSITY
J. Bird *In* Canadian Space Agency, Proceedings of the Sixth CASI Conference on Astronautics 1990 14 p Previously announced in IAA as A91-34944 (For primary document see N93-14920 04-12)
Avail: Canadian Aeronautics and Space Inst., 222 Somerset St. W., Suite 601, Ottawa, Ontario K2P 0J1 Canada

81 ADMINISTRATION AND MANAGEMENT

Includes management planning and research.

N93-15118# Aerospatiale, Cannes (France). Artificial Intelligence Dept.
PEX: A REACTIVE PROCEDURE BASED DECISION MAKER
J. C. Chautard and C. Honnorat 1992 5 p
(Rept-921-440-105; ETN-92-92358) Avail: CASI HC A01/MF A01

A reactive planner system called PEX (Procedure Expert) is presented. When confronted with a difficult industrial sized problem, it is revealed to be adequate on the reactivity viewpoint and on the knowledge representation side. In the space domain, controlling dynamic systems, such as spacecraft, is a common problem. Difficulty comes from the complexity of the systems and the uncertainty of their environment. The old classical approach stating a clear distinction between plan construction and plan execution is not satisfactory; the solution is to be found in reactive planning. A procedure based process control system is presented. The purpose of the procedural decision maker is to make the physical system reach a given objective. It exploits a procedural model which maps objectives and behavioral information for deciding in real time what commands should be emitted and when. The concept of integrity context is introduced as a procedure relevance criterion to increase reactivity. This system is applied to satellite control; a prototype is connected to a satellite flight simulator and controls a critical orbit correction maneuver. ESA

82 DOCUMENTATION AND INFORMATION SCIENCE

Includes information management; information storage and retrieval technology; technical writing; graphic arts; and micrography.

For computer documentation see *61 Computer Programming and Software*.

N93-14106# Defense Technical Information Center, Alexandria, VA.
DROLS WORKBOOK Final Report
Christian M. Cupp, Keith L. Thompson, Richard J. Wayman, Karen V. Fox, and Charles E. Reed Jan. 1992 62 p
(AD-A255850; DTIC/TR-92-4) Avail: CASI HC A04/MF A01

This workbook provides practical exercises to assist users in learning the Defense RDT and E Online System (DROLS). It is intended to be used in conjunction with DTICH 4185.4, DROLS Handbook. Basic and advanced search exercises are provided to assist the user in creating the best strategy for getting the desired results. Answers to exercises and problem sets are in Appendix 3. GRA

N93-14130# California Univ., Berkeley. School of Education.
KNOWLEDGE AND PROCESSES IN DESIGN Final Report, Dec. 1987 - Aug. 1992
Peter Pirolli 3 Sep. 1992 173 p
(Contract N00014-88-K-0233; NR Proj. RR0-4206)
(AD-A255663) Avail: CASI HC A08/MF A02

Our project concerned information processing characterizations of the knowledge and processes involved in design. Design is a complex ill-structured task. By their very nature, such ill-structured tasks involve processes of finding, representing, refining, and reformulating goals and constraints, generating appropriate problem spaces to work in, retrieving, integrating, and evaluating information from long-term memory or external sources, and managing complex assemblies of past and current decisions. In classic theories of problem solving in psychology, a problem solver is faced with a problem situation and develops a representation for the problem

(problem structuring). In classical terms, this representation may include information about the current state of the problem situation, a goal, and possible sets of problem solving actions (operators) that may be relevant to changing the current state to conform to the desired goal. A particular goal, a set of states, and a set of operators defines a problem space. Problem solving is characterized as a search process in a problem space, in which the problem solver proposes and decides upon possible operators and sequences of operators that will transform the current state into a goal state. Much of the research on the psychology of problem solving has focused on understanding the knowledge and processes involved in solving well-structured, but semantically impoverished, puzzle tasks. GRA

N93-14182# Colorado Univ., Boulder. Cooperative Inst. for Research in Environmental Science.

DATA MANAGEMENT FOR THE COORDINATED EASTERN ARCTIC EXPERIMENT Final Report, 1 Apr. 1990 - 30 Sep. 1992

Roger G. Barry and Claire S. Hanson 30 Sep. 1992 8 p

(Contract N00014-90-J-1852)

(AD-A255648) Avail: CASI HC A02/MF A01

To assure long-term availability of data sets collected during the Coordinated Eastern Arctic Experiment (CEAREX), and other relevant Eastern Arctic data, a CD-ROM has been prepared and is available for distribution. Titled 'Eastern Arctic Ice, Ocean and Atmosphere Data, Volume 1, CEAREX-I' , the disc contains meteorology, hydrography (CTDs), biophysical sampling, bathymetry, sea ice acceleration, sea ice stress, sea ice deformation, and ambient noise/acoustics samples. The disc is the first in a planned series that will contain CEAREX, MIZEX (Marginal Ice Zone Experiment), and other related data. Distribution began in December 1991. GRA

N93-14205 Drexel Univ., Philadelphia, PA.

THE EFFECT OF A HIERARCHICAL TASK-SPECIFIC EXTERNAL CONCEPTUAL MODEL ON THE LEARNABILITY AND USABILITY OF MICROCOMPUTER APPLICATIONS BY NOVICES Ph.D. Thesis

Yvonne Lederer Antonucci 1992 126 p

Avail: Univ. Microfilms Order No. DA9227948

The study focuses on how an external conceptual model of a microcomputer system could be constructed which would match problem-solving processes of novice users. The study's premise was that this conceptual model would aid novice users in forming initial mental models, as defined by Norman (1983), that guide them in using and understanding the system. Research findings indicate that the problem-solving process depends upon previously developed mental models of similar systems which novice users lack. Furthermore, the absence of these mental models hinders performance (the ability to use a system and accomplish a task). Researchers have agreed that a hierarchical structure is the basic form of the human problem-solving process. This study investigated the effectiveness of a hierarchically organized external conceptual model of a microcomputer system on novice users' ability to use and understand that system. Two external conceptual models were developed for the study and examined through a laboratory study which compared their effectiveness in aiding novice users to use and understand a database system. The reference manual followed traditional manual design considerations. The hierarchical model was developed using characteristics identified in novice user problem-solving. The results indicated that the hierarchical model group performed better and had a higher understanding of the system than the reference model group. The hierarchical model group was able to complete more of the assigned database tasks, with fewer errors, and spent less time with the model than the reference manual group. Although, no statistically significant result was detected in the amount of time to complete the combined tasks, the hierarchical model group was able to complete the first task faster. No evidence was indicated that the perceived difficulty of the system between the two groups was different. The findings suggest that a hierarchical external conceptual model improves the match between the human problem-solving process among novice users and the representation of microcomputer system. They contribute to a better understanding of external conceptual model representation for novice users in assisting them to initiate the problem-solving process necessary for mental model formation of microcomputer systems.

Dissert. Abstr.

N93-14206 California Univ., Berkeley.

INFORMATION-SEEKING BEHAVIOR DURING THE DECISION-MAKING PROCESS: A CASE STUDY Ph.D. Thesis

Samia Benidir 1991 286 p

Avail: Univ. Microfilms Order No. DA9228571

People cannot know everything first hand for themselves. They must, in practice, depend on the knowledge of others: 'second-hand knowledge'. People are influenced in their decisions by peers, friends, family, acquaintances, salesmen, and so on. However, little is known about how much influence these sources have in decision making processes, on what sort of individuals, and how it happens. Following P. Wilson, Second-hand Knowledge (1983), we use the term 'cognitive authority' to denote the respect attributed and the influence allowed to sources of information. This study investigates information seeking behavior and information use in decision making, especially the perceived influence of cognitive authority, among the Berkeley campus population when selecting a personal computer. The researcher worked as a participant observer, administered a questionnaire, and conducted interviews. Questionnaire data were analyzed by Log-linear modelling. A typology of styles of information use was developed. The results of this research illustrate the different information seeking behavior of different consumers for the same decision making. The findings of this study show that the information sources available serve individuals and groups differently. Status and sex directly affect the information seeking behavior of decision makers, including the attribution of cognitive authority and the use of cognitive authorities. Age, discipline, and speaking English as a foreign language are also influential. Interaction, especially informal communication, is important in information use. Libraries were not consulted for this type of information use. The significance of this research is that it aimed at clarifying the complicated process of information seeking and information use for decision making by attempting to isolate the factors that distinguish social groups. Dissert. Abstr.

N93-14208 California Univ., Berkeley.

MAPPING THOUGHTS: VISUAL INTERFACES FOR INFORMATION RETRIEVAL Ph.D. Thesis

Thomas Kevin Gillespie 1991 254 p

Avail: Univ. Microfilms Order No. DA9228661

This dissertation examines interface design for information retrieval systems from the perspective of visual thinking. In the first section I begin by arguing that we have a history of visual thinking which extends back as far as the caves of Altamira and continues in an unbroken line through mythology, the development of writing, and the fine arts to the modern development of television, video games, and cyberspace. I support my argument with cognitive theories of the mind, and empirical research from the fields of cognitive psychology and human factors which demonstrates the usefulness of visual information to aid visual recall land learning. I finish by discussing the history of humankind as a history of visual thinking which argues for an integration of test and graphics to aid the user in searching for information. From this point of view, I next examine traditional information systems such as pictograms, maps, and cataloging systems, and then computerized information systems such as online public access catalogs, spreadsheets, the Desktop Metaphor, and Geographic Information Systems. I then illustrate and comment on five visual interface projects which demonstrate the range of approaches being taken in the design of graphical interfaces for information retrieval. In the second half of this dissertation I develop a detailed prototype model of a visual interface for an online line public access catalog. In this section I begin with a discussion of the strengths and weaknesses of the University of California online public access catalog, MELVYL. In the final section I develop a prototype model of a visual interface to the MELVYL system which I call VisualMELVYL. This model is based upon the history of visual thinking, information retrieval, current graphical design work, and research on visual recall and learning from text and pictures. VisualMELVYL demonstrates a visual interface to an online public access catalog, and potentially to any information resource connected to a wide area network such as the Internet. Dissert. Abstr.

N93-14209 Brandeis Univ., Waltham, MA.

INFORMATION FOR MANAGEMENT, PLANNING, AND DECISION-MAKING IN NONPROFIT ORGANIZATIONS: TOWARD A COMPREHENSIVE MODEL Ph.D. Thesis

Carolyn Margaret Gray 1992 231 p

Avail: Univ. Microfilms Order No. DA9227594

The major thesis of this work is that the collection, organization, and utilization of critical information can help nonprofits become more effective in management, planning, and decision making. Increasing the capacity of nonprofit organizations to collect, organize, and utilize information offers the potential benefit of improving their capacity to deliver human services more effectively. This research is concerned with how nonprofit organizations collect, organize, and use information. The research incorporates a descriptive survey with responses from 230 nonprofit human service organizations in Massachusetts, retrospective analysis of the use of marketing information in home health care organizations, a case study of a large nonprofit organization, and a prescriptive model with practical tools for information management in nonprofit organizations. Since information utilization involves locating, analyzing, and applying information, the main concern of this work is to create a model that will inform practice and help managers understand the important dimensions of information management to improve organizational effectiveness. The model provides a conceptual framework by which the nonprofit manager can apply conclusions from this research while working with information in their own unique environment. The research builds upon theoretical and practical research in nonprofit theory, management, organizational theory, information theory, knowledge utilization, and evaluation research. After a review of the historical and sociological roots of nonprofits, a series of propositions are developed from the literature for examination and discussion. The prescriptive element of the research draws conclusions from research activities and describes actions determined useful to nonprofit organizations in their management, planning, and decision making efforts. The model serves as a practical guide for professionals, management, and boards in assessing organization information management and includes suggestions for increasing organizational information management capacity. The model includes descriptive, analytical, and prescriptive elements, which are: (1) a typology of information including sources and ways information is helpful or not helpful; (2) an anaytical tool for assessing organizational 'readiness' to use information; and (3) successful methods and procedures for utilization of information. The model is designed with indices which can be used to evaluate the 'information health' of an organization. Dissert. Abstr.

N93-14216 Kent Univ., Canterbury (England).
INFORMATION RESOURCE UTILISATION: ACCESSIBILITY BASED ON CONCERNS Ph.D. Thesis
Richard Rolfe 1991 307 p
Avail: Univ. Microfilms Order No. BRDX96897

The utilization of the information resource is a key requirement of an effective information system within the organization. With computing technology generating increasingly complex applications but with an increasing spread of computing contactability through the organization, an inherent conflict is presented which can only worsen as hypermedia and multimedia applications are brought to the organization. This work identified user participation as the key ingredient in improving information resource utilization. A two pronged approach was taken: initially a field based investigation of the utilization of a complex information system within a large organization and secondly the development of a user interface environment to tackle the issues raised. The fieldwork provided evidence to suggest the level of accessibility to Health Service information left wide scope for development. Several variables were identified as having a key relationship with information resource utilization. Of these complexity predominated, both in terms of the database structures in the application and the functionality provided through the interface itself. The prototype focused on this complexity issue directly, providing a user driven interpretative environment in which both user and organization based information can be combined to form a dynamic, user based semantic model. Such a graphical representation evolves in parallel with user requirements, enabling the user to manipulate his/her own view of the application for the expression of database queries. The basis for this interpretation is the generalized conceptual model which is captured from the data modeller during the initial application data modelling process. This view forms the basis for user accessibility, acting as an initial interpretation which the user tailors towards a personal interpretation using 'concerns'. The provision of such an environment promotes user accessibility and hence utilization, being personalized by the individual to the task at hand. Dissert. Abstr.

N93-14218 Ohio State Univ., Columbus.
QUERY PROCESSING IN DISTRIBUTED DATABASE SYSTEMS Ph.D. Thesis
Vasundhara Unnava 1992 128 p
Avail: Univ. Microfilms Order No. DA9227393

During the last decade distributed database management systems (DDBMS) have become important information processing systems supporting business activities of geographically decentralized organizations. Since data files are distributed at several locations in a DDBMS, user queries that reference remote files introduce substantial data communication delays. The efficiency of a DDBMS is determined by the speed with which these queries are processed. This dissertation deals with the optimization of query processing in a relational DDBMS. Our objective is to develop a methodological approach to the design of query processing optimizers. The algorithms developed in this dissertation will be valuable tools in the design of a DDBMS. The first chapter of the dissertation describes a distributed database environment and the importance of query processing in such an environment. The second chapter presents a detailed literature survey. In the third chapter, a special case of queries, star queries, is defined. The requirement for new algorithms to improve system efficiency is demonstrated. Heuristic procedures using greedy approach and a branch and bound solution procedure are proposed. An efficient lower bounding technique is implemented in the branch and bound procedure. The results of extensive computational experiments indicate that the proposed procedures star queries effectively. Also, the greedy algorithm proves to be insensitive to errors in the selectivity estimation procedures. The fourth chapter concentrates on the problem of a generalized star query. The problem, an extension of star query, is significantly harder than the star query problem because its optimization model includes an additional operation of joining files. Heuristic and branch and bound solution methods are developed. Extensive computational testing supports the practical feasibility of the solution methods. Also, rigorous analysis of the generalized star query algorithm in a dynamic mode exhibits that the static version is robust to changes in the procedures used to estimate selectivity. The fifth chapter investigates the use of heuristics in the general query processing problem. Algorithms for the problem of general query processing, which consider various methods of selecting a semijoin in producing a query processing strategy are proposed. Computational experiments are designed to assess the performance of the proposed algorithms relative to existing algorithms. The analyses show that the proposed algorithms outperform the existing algorithms. Chapter six summarizes our work and also discusses future research directions in the field of query processing in DDBMS.
Dissert. Abstr.

N93-14265# Defense Technical Information Center, Alexandria, VA.
SOURCE HIERARCHY LIST. VOLUME 1: A THROUGH D Report, Sep. 1990 - Oct. 1992
Claudine S. Long Oct. 1992 978 p Supersedes DTIC/TR-90/4-Vol-1, dated Dec. 1990, AD-A231100. See also Volume 2, AD-A256101
(AD-A256100; DTIC/TR-92/6-Vol-1; DTIC/TR-90/4-Vol-1) Avail: CASI HC A99/MF A10

This is the first of three volumes of an alphabetical listing of corporate authors as used for announcement of reports received in the Defense Technical Information Center (DTIC). Former names of organizations are included and displayed below the current source name used by DTIC. Cross references direct the user from sub-element organizations to the major source level entry where they are also displayed. Major and sub-hierarchies are preceded and ended by a row of asterisks. This list is used in conjunction with and is not a replacement for DTIC's Source Header List, Volume 1, AD-A256000, and Volume 2, AD-A256001. It displays only those source names from the Source Header List which hierarchical linkages are pertinent. GRA

N93-14524# Army Construction Engineering Research Lab., Champaign, IL.
GEOGRAPHIC RESOURCES ANALYSIS SUPPORT SYSTEM (GRASS) VERSION 4.0 USER'S REFERENCE MANUAL Final Report
James D. Westervelt, Michael Shapiro, William D. Goran, and David P. Gerdes Jun. 1992 543 p Revised
(AD-A255218; CERL-ADP-N-87/22-Rev) Avail: CASI HC A23/MF A04

The Geographic Resources Analysis Support System (GRASS) is a geographic information and image-processing system originally designed to

serve land managers and environmental planners at Army installations. GRASS is an integrated set of programs that provide digitizing, image processing, map production, and geographic information system capabilities to its users. GRASS is written in C and is ported to computers running the UNIX operating system. Since its initial development, GRASS has been developed for many applications on a number of different hardware configurations. GRASS Version 4.0 includes significant additions and modifications to system libraries and programming code. This manual contains a program-by-program description of each program's capabilities and uses; a summary of command-line options; and lists of associated or related programs. GRA

N93-14650# Army Engineer Waterways Experiment Station, Vicksburg, MS. Information Technology Lab.

VENDOR INFORMATION SYSTEM (VIS) SYSTEMS MANUAL Final Report

Patti S. Duett and Monique F. Harrison Aug. 1992 163 p

(AD-A256174; WES/TR/ITL-92-5) Avail: CASI HC A08/MF A02

This manual provides the necessary support documentation to the personnel responsible for either maintenance or support of the Vendor Information System (VIS). The manual consists of documentation for the menu system and individual programs plus a complete data base dictionary. GRA

N93-14719*# National Aeronautics and Space Administration, Washington, DC.

STREAMLINED ACQUISITION HANDBOOK

16 Feb. 1990 18 p

(NASA-TM-108133; NAS 1.15:108133) Avail: CASI HC A03/MF A01

NASA has always placed great emphasis on the acquisition process, recognizing it as among its most important activities. This handbook is intended to facilitate the application of streamlined acquisition procedures. The development of these procedures reflects the efforts of an action group composed of NASA Headquarters and center acquisition professionals. It is the intent to accomplish the real change in the acquisition process as a result of this effort. An important part of streamlining the acquisition process is a commitment by the people involved in the process to accomplishing acquisition activities quickly and with high quality. Too often we continue to accomplish work in 'the same old way' without considering available alternatives which would require no changes to regulations, approvals from Headquarters, or waivers of required practice. Similarly, we must be sensitive to schedule opportunities throughout the acquisition cycle, not just once the purchase request arrives at the procurement office. Techniques that have been identified as ways of reducing acquisition lead time while maintaining high quality in our acquisition process are presented. Author

N93-14771*# National Aeronautics and Space Administration. Goddard Space Flight Center, Greenbelt, MD.

NSSDC CONFERENCE ON MASS STORAGE SYSTEMS AND TECHNOLOGIES FOR SPACE AND EARTH SCIENCE APPLICATIONS, VOLUME 3

Ben Kobler, ed., P. C. Hariharan, ed. (Hughes STX, Inc., Lanham, MD.), and L. G. Blasso, ed. (Hughes STX, Inc., Lanham, MD.) Washington Sep. 1992 283 p Conference held in Greenbelt, MD, 23-25 Jul. 1991 (RTOP 656-80-02-26)

(NASA-CP-3165-Vol-3; Rept-92B00093-Vol-3; NAS 1.55:3165-Vol-3) Avail: CASI HC A13/MF A03

This report contains copies of nearly all of the technical papers and viewgraphs presented at the National Space Science Data Center (NSSDC) Conference on Mass Storage Systems and Technologies for Space and Earth Science Applications. This conference served as a broad forum for the discussion of a number of important issues in the field of mass storage systems. Topics include magnetic disk and tape technologies, optical disk and tape, software storage and file management systems, and experiences with the use of a large, distributed storage system. The technical presentations describe, among other things, integrated mass storage systems that are expected to be available commercially. Also included is a series of presentations from Federal Government organizations and research institutions covering their mass storage requirements for the 1990s. For individual titles, see N93-14772 through N93-14781.

N93-14772*# Ohio State Univ., Columbus. Computer Microtribology and Contamination Lab.

TRIBOLOGY OF MAGNETIC STORAGE SYSTEMS

Bharat Bhushan *In* NASA. Goddard Space Flight Center, NSSDC Conference on Mass Storage Systems and Technologies for Space and Earth Science Applications, Volume 3 Sep. 1992 70 p Submitted for publication (For primary document see N93-14771 04-82)

Avail: CASI HC A04/MF A03

The construction and the materials used in different magnetic storage devices are defined. The theories of friction and adhesion, interface temperatures, wear, and solid-liquid lubrication relevant to magnetic storage systems are presented. Experimental data are presented wherever possible to support the relevant theories advanced. Author

N93-14773*# Ultra Network Technologies, Inc., San Jose, CA.

NETWORK ISSUES FOR LARGE MASS STORAGE REQUIREMENTS

James Perdue *In* NASA. Goddard Space Flight Center, NSSDC Conference on Mass Storage Systems and Technologies for Space and Earth Science Applications, Volume 3 Sep. 1992 24 p Submitted for publication (For primary document see N93-14771 04-82)

Avail: CASI HC A03/MF A03

File Servers and Supercomputing environments need high performance networks to balance the I/O requirements seen in today's demanding computing scenarios. UltraNet is one solution which permits both high aggregate transfer rates and high task-to-task transfer rates as demonstrated in actual tests. UltraNet provides this capability as both a Server-to-Server and Server-to-Client access network giving the supercomputing center the following advantages highest performance Transport Level connections (to 40 MBytes/sec effective rates); matches the throughput of the emerging high performance disk technologies, such as RAID, parallel head transfer devices and software striping; supports standard network and file system applications using SOCKET's based application program interface such as FTP, rcp, rdump, etc.; supports access to the Network File System (NFS) and LARGE aggregate bandwidth for large NFS usage; provides access to a distributed, hierarchical data server capability using DISCOS UniTree product; supports file server solutions available from multiple vendors, including Cray, Convex, Alliant, FPS, IBM, and others. Author

N93-14774*# Network Systems Corp., Vienna, VA.

THE ROLE OF HiPPI SWITCHES IN MASS STORAGE SYSTEMS: A FIVE YEAR PROSPECTIVE

T. A. Gilbert *In* NASA. Goddard Space Flight Center, NSSDC Conference on Mass Storage Systems and Technologies for Space and Earth Science Applications, Volume 3 Sep. 1992 29 p (For primary document see N93-14771 04-82)

Avail: CASI HC A03/MF A03

New standards are evolving which provide the foundation for novel multi-gigabit per second data communication structures. The lowest layer protocols are so generalized that they encourage a wide range of application. Specifically, the ANSI High Performance Parallel Interface (HiPPI) is being applied to computer peripheral attachment as well as general data communication networks. This paper introduces the HiPPI standards suite and technology products which incorporate the standards. The use of simple HiPPI crosspoint switches to build potentially complex extended 'fabrics' is discussed in detail. Several near term applications of the HiPPI technology are briefly described with additional attention to storage systems. Finally, some related standards are mentioned which may further expand the concepts above. Author

N93-14775*# National Aeronautics and Space Administration. Goddard Space Flight Center, Greenbelt, MD.

THE NATIONAL SPACE SCIENCE DATA CENTER: AN OPERATIONAL PERSPECTIVE

Ronald Blitstein (ST Systems Corp., Greenbelt, MD.) and James L. Green *In its* NSSDC Conference on Mass Storage Systems and Technologies for Space and Earth Science Applications, Volume 3 Sep. 1992 13 p (For primary document see N93-14771 04-82)

Avail: CASI HC A03/MF A03

The National Space Science Data Center (NSSDC) manages over 110,000 data tapes with over 4,000 data sets. The size of the digital archive is approximately 6,000 GBytes and is expected to grow to more than 28,000 GBytes by 1995. The NSSDC is involved in several initiatives

to better serve the scientific community and improve the management of current and future data holdings. These initiatives address the need to manage data to ensure ready access by the user and manage the media to ensure continuing accessibility and integrity of the data. This paper will present an operational view of the NSSDC, outlining current policies and procedures that were implemented to ensure the effective use of available resources to support service and mission goals, and maintain compliance with prescribed data management directives. Author

N93-14776*# National Aeronautics and Space Administration. Goddard Space Flight Center, Greenbelt, MD.

EOSDIS/DADS REQUIREMENTS

John Berbert and Ben Kobler *In its* NSSDC Conference on Mass Storage Systems and Technologies for Space and Earth Science Applications, Volume 3 Sep. 1992 10 p (For primary document see N93-14771 04-82)

Avail: CASI HC A02/MF A03

A brief summary of the Earth Observing System Data and Information System (EOSDIS) Core System (ECS) Data Archive and Distribution System (DADS) requirements is given. Among the requirements are the following: the ECS relationship to EOSDIS Version-0; phased implementation of ECS; and data ingest, archive, and distribution daily data volumes anticipated at each of the 7 Distributed Active Archive Centers (DAAC's). Author

N93-14777*# Geological Survey, Sioux Falls, SD. Earth Observing System Data Center.

THE PRESERVATION OF LANDSAT DATA BY THE NATIONAL LAND REMOTE SENSING ARCHIVE

John E. Boyd *In* NASA. Goddard Space Flight Center, NSSDC Conference on Mass Storage Systems and Technologies for Space and Earth Science Applications, Volume 3 9 p(SEE N93-14771 04-82) Sep. 1992 (For primary document see N93-14771 04-82)

Avail: CASI HC A02/MF A03

Digital data, acquired by the National Landsat Remote Sensing Program, document nearly two decades of global agricultural, environmental, and sociological change. The data were widely applied and continue to be essential to a variety of geologic, hydrologic, agronomic, and strategic programs and studies by governmental, academic, and commercial researchers. Landsat data were acquired by five observatories that use primarily two digital sensor systems. The Multispectral Scanner (MSS) was onboard all five Landsats, which have orbited over 19 years; the higher resolution Thematic Mapper (TM) sensor acquired data for the last 9 years on Landsats 4 and 5 only. The National Land Remote Sensing Archive preserves the 800,000 scenes, which total more than 60 terabytes of data, on master tapes that are steadily deteriorating. Data are stored at two terabytes of data, on master tapes that are steadily deteriorating. Data are stored at two locations (Sioux Falls, South Dakota and Landover, Maryland), in three archive formats. The U.S. Geological Survey's EROS Data Center has initiated a project to consolidate and convert, over the next 4 years, two of the archive formats from antiquated instrumentation tape to rotary-recorded cassette magnetic tape. The third archive format, consisting of 300,000 scenes of MSS data acquired from 1972 through 1978, will not be converted because of budgetary constraints. This data preservation project augments EDC's experience in data archiving and information management, expertise that is critical to EDC's role as a Distributed Active Archive Center for the Earth Observing System, a new and much larger national earth science program. Author

N93-14778*# National Inst. of Standards and Technology, Gaithersburg, MD. Computer Systems Lab.

STATUS OF EMERGING STANDARDS FOR REMOVABLE COMPUTER STORAGE MEDIA AND RELATED CONTRIBUTIONS OF NIST

Fernando L. Podio *In* NASA. Goddard Space Flight Center, NSSDC Conference on Mass Storage Systems and Technologies for Space and Earth Science Applications, Volume 3 Sep. 1992 25 p (For primary document see N93-14771 04-82)

Avail: CASI HC A03/MF A03

Standards for removable computer storage media are needed so that users may reliably interchange data both within and among various computer installations. Furthermore, media interchange standards support competition in industry and prevent sole-source lock-in. NIST participates in magnetic tape and optical disk standards development through Technical Committees X3B5, Digital Magnetic Tapes, X3B11, Optical Digital Data Disk, and the Joint Technical Commission on Data Permanence. NIST also participates in other relevant national and international standards committees for removable computer storage media. Industry standards for digital magnetic tapes require the use of Standard Reference Materials (SRM's) developed and maintained by NIST. In addition, NIST has been studying care and handling procedures required for digital magnetic tapes. NIST has developed a methodology for determining the life expectancy of optical disks. NIST is developing care and handling procedures for optical digital data disks and is involved in a program to investigate error reporting capabilities of optical disk drives. This presentation reflects the status of emerging magnetic tape and optical disk standards, as well as NIST's contributions in support of these standards. Author

N93-14779*# National Oceanic and Atmospheric Administration, Suitland, MD. Office of Systems Development.

DATA MANAGEMENT IN NOAA

William M. Callicott *In* NASA. Goddard Space Flight Center, NSSDC Conference on Mass Storage Systems and Technologies for Space and Earth Science Applications, Volume 3 Sep. 1992 20 p (For primary document see N93-14771 04-82)

Avail: CASI HC A03/MF A03

NOAA has 11 terabytes of digital data stored on 240,000 computer tapes. There are an additional 100 terabytes (TB) of geostationary satellite data stored in digital form on specially configured SONY U-Matic video tapes at the University of Wisconsin. There are over 90,000,000 non-digital form records in manuscript, film, printed, and chart form which are not easily accessible. The three NOAA Data Centers service 6,000 requests per year and publish 5,000 bulletins which are distributed to 40,000 subscribers. Seventeen CD-ROM's have been produced. Thirty thousand computer tapes containing polar satellite data are being copied to 12 inch WORM optical disks for research applications. The present annual data accumulation rate of 10 TB will grow to 30 TB in 1994 and to 100 TB by the year 2000. The present storage and distribution technologies with their attendant support systems will be overwhelmed by these increases if not improved. Increased user sophistication coupled with more precise measurement technologies will demand better quality control mechanisms, especially for those data maintained in an indefinite archive. There is optimism that the future will offer improved media technologies to accommodate the volumes of data. With the advanced technologies, storage and performance monitoring tools will be pivotal to the successful long-term management of data and information. Author

N93-14780*# Lawrence Livermore National Lab., CA.

STORAGE NEEDS IN FUTURE SUPERCOMPUTER ENVIRONMENTS

Sam Coleman *In* NASA. Goddard Space Flight Center, NSSDC Conference on Mass Storage Systems and Technologies for Space and Earth Science Applications, Volume 3 Sep. 1992 13 p (For primary document see N93-14771 04-82)

Avail: CASI HC A03/MF A03

The Lawrence Livermore National Laboratory (LLNL) is a Department of Energy contractor, managed by the University of California since 1952. Major projects at the Laboratory include the Strategic Defense Initiative, nuclear weapon design, magnetic and laser fusion, laser isotope separation, and weather modeling. The Laboratory employs about 8,000 people. There are two major computer centers: The Livermore Computer Center and the National Energy Research Supercomputer Center. As we increase the computing capacity of LLNL systems and develop new applications, the need for archival capacity will increase. Rather than quantify that increase, I will discuss the hardware and software architectures that we will need to support advanced applications. Author

N93-14781*# Sandia National Labs., Albuquerque, NM.

REQUIREMENTS FOR A NETWORK STORAGE SERVICE

Suzanne M. Kelly and Rena A. Haynes *In* NASA. Goddard Space Flight Center, NSSDC Conference on Mass Storage Systems and Technologies for Space and Earth Science Applications, Volume 3 Sep. 1992 11 p (For primary document see N93-14771 04-82)

(Contract DE-AC04-76DP-00789)

Avail: CASI HC A03/MF A03

Sandia National Laboratories provides a high performance classified computer network as a core capability in support of its mission of nuclear

weapons design and engineering, physical sciences research, and energy research and development. The network, locally known as the Internal Secure Network (ISN), was designed in 1989 and comprises multiple distributed local area networks (LAN's) residing in Albuquerque, New Mexico and Livermore, California. The TCP/IP protocol suite is used for inner-node communications. Scientific workstations and mid-range computers, running UNIX-based operating systems, compose most LAN's. One LAN, operated by the Sandia Corporate Computing Directorate, is a general purpose resource providing a supercomputer and a file server to the entire ISN. The current file server on the supercomputer LAN is an implementation of the Common File System (CFS) developed by Los Alamos National Laboratory. Subsequent to the design of the ISN, Sandia reviewed its mass storage requirements and chose to enter into a competitive procurement to replace the existing file server with one more adaptable to a UNIX/TCP/IP environment. The requirements study for the network was the starting point for the requirements study for the new file server. The file server is called the Network Storage Services (NSS) and is requirements are described in this paper. The next section gives an application or functional description of the NSS. The final section adds performance, capacity, and access constraints to the requirements. Author

N93-14785# Sparta, Inc., Lexington, MA.
ULTRA-DENSE OPTICAL MASS STORAGE Final Report, 1 Sep. 1991 - 31 Jul. 1992
30 Jul. 1992 34 p
(Contract F49620-91-C-0071)
(AD-A255463; LTR92-013) Avail: CASI HC A03/MF A01

This report summarizes the results obtained and the work performed during the first nine months of an eighteen month program to develop a new ultra dense optical mass storage memory system based on spectral hole burning (SHB) media. The goals of this particular program were as follows: (1) investigate the fundamental properties of a Frequency Channel concept which holds promise for enhancing the resistance to erasure of data recorded in SHB media; (2) investigate the fundamental and practical aspects of the data erasure in SHB media; and (3) to build and test a laboratory demonstration system which has all the key characteristics vital to the operation of this memory system as a digital computer memory system. The experimental aspects of the program were found to be most efficiently performed by addressing all of the above tasks in parallel, so at present the results obtained are preliminary. The work is in progressing well and is expected to be completed on time. GRA

N93-14796*# National Aeronautics and Space Administration. Lewis Research Center, Cleveland, OH.
BIBLIOGRAPHY OF LEWIS RESEARCH CENTER TECHNICAL PUBLICATIONS ANNOUNCED IN 1991
Oct. 1992 401 p
(NASA-TM-105595; E-6928; NAS 1.15:105595) Avail: CASI HC A18/MF A04

This compilation of abstracts describes and indexes the technical reporting that resulted from the scientific engineering work performed and managed by the Lewis Research Center in 1991. All the publications were announced in the 1991 issues of STAR (Scientific and Technical Aerospace Reports) and/or IAA (International Aerospace Abstracts). Included are research reports, journal articles, conference presentations, patents and patent applications, and theses. Author

N93-15027*# National Aeronautics and Space Administration. Goddard Space Flight Center, Greenbelt, MD.
PROCEEDINGS OF THE NSSDC CONFERENCE ON MASS STORAGE SYSTEMS AND TECHNOLOGIES FOR SPACE AND EARTH SCIENCE APPLICATIONS
Kim Blackwell (ST Systems Corp., Lanham, MD.), Len Blasso, ed. (ST Systems Corp., Lanham, MD.), and Ann Lipscomb, ed. (ST Systems Corp., Lanham, MD.) 1991 309 p Conference held in Greenbelt, MD, 23-25 Jul. 1991
(NASA-TM-107989; NSSDC-WDA-A-R/S-91-18; NAS 1.15:107989) Avail: CASI HC A14/MF A03

The proceedings of the National Space Science Data Center Conference on Mass Storage Systems and Technologies for Space and Earth Science Applications held July 23 through 25, 1991 at the NASA/Goddard Space Flight Center are presented. The program includes a keynote address, invited technical papers, and selected technical presentations to provide a broad forum for the discussion of a number of important issues in the field of mass storage systems. Topics include magnetic disk and tape technologies, optical disk and tape, software storage and file management systems, and experiences with the use of a large, distributed storage system. The technical presentations describe integrated mass storage systems that are expected to be available commercially. Also included is a series of presentations from Federal Government organizations and research institutions covering their mass storage requirements for the 1990's. For individual titles, see N93-15028 through N93-15048.

N93-15028*# Storage Technology Corp., Louisville, CO. Strategic Planning Div.
ENTERPRISE STORAGE REPORT FOR THE 1990'S
Fred Moore *In* NASA. Goddard Space Flight Center, Proceedings of the NSSDC Conference on Mass Storage Systems and Technologies for Space and Earth Science Applications 1991 p 1-29 (For primary document see N93-15027 04-82)
Avail: CASI HC A03/MF A03

Data processing has become an increasingly vital function, if not the most vital function, in most businesses today. No longer only a mainframe domain, the data processing enterprise also includes the midrange and workstation platforms, either local or remote. This expanded view of the enterprise has encouraged more and more businesses to take a strategic, long-range view of information management rather than the short-term tactical approaches of the past. Some of the significant aspects of data storage in the enterprise for the 1990's are highlighted. Author

N93-15029*# Mallinson Magnetics, Inc., Carlsbad, CA.
MAGNETIC DISK
John C. Mallinson *In* NASA. Goddard Space Flight Center, Proceedings of the NSSDC Conference on Mass Storage Systems and Technologies for Space and Earth Science Applications 1991 p 31-36 (For primary document see N93-15027 04-82)
Avail: CASI HC A02/MF A03

Magnetic disk recording was invented in 1953 and has undergone intensive development ever since. As a result of this 38 years of development, the cost per byte and the areal density has halved and doubled, respectively every 2 to 2 1/2 years. Today, the cost per byte is lower than 10(exp -6) dollars per byte and area densities exceed 100 x 10(exp 6) bits per square inch. The recent achievements in magnetic disk recording will first be surveyed briefly. Then the principal areas of current technical development will be outlined. Finally, some comments will be made about the future of magnetic disk recording. Author

N93-15030*# San Diego Supercomputer Center, CA.
FILE SERVERS, NETWORKING, AND SUPERCOMPUTERS
Reagan W. Moore *In* NASA. Goddard Space Flight Center, Proceedings of the NSSDC Conference on Mass Storage Systems and Technologies for Space and Earth Science Applications 1991 p 37-65 (For primary document see N93-15027 04-82)
(Grants NSF ASC-84-14524; NSF ASC-90-20416)
Avail: CASI HC A03/MF A03

One of the major tasks of a supercomputer center is managing the massive amount of data generated by application codes. A data flow analysis of the San Diego Supercomputer Center is presented that illustrates the hierarchical data buffering/caching capacity requirements and the associated I/O throughput requirements needed to sustain file service and archival storage. Usage paradigms are examined for both tightly-coupled and loosely-coupled file servers linked to the supercomputer by high-speed networks. Author

N93-15031*# National Archives and Records Service, Washington, DC. Center for Electronic Records.
THE LONG HOLD: STORING DATA AT THE NATIONAL ARCHIVES
Kenneth Thibodeau *In* NASA. Goddard Space Flight Center, Proceedings of the NSSDC Conference on Mass Storage Systems and Technologies for Space and Earth Science Applications 1991 p 67-72 (For primary document see N93-15027 04-82)
Avail: CASI HC A02/MF A03

A description of the information collection and storage needs of the National Archives and Records Administration (NARA) is presented. The

unique situation of NARA is detailed. Two aspects which make the issue of obsolescence especially complex and costly are dealing with incoherent data and satisfying unknown and unknowable requirements. The data is incoherent because it comes from a wide range of independent sources, covers unrelated subjects, and is organized and encoded in ways that are not only not controlled but often unknown until received. NARA's mission to preserve and provide access to records with enduring value makes NARA, in effect, the agent of future generations. NARA's responsibility to the future places itself is a perpetual quandary of devotion to serving needs which are unknown. L.R.R.

N93-15032*# Shell Development Co., Houston, TX.
STEWARDSHIP OF VERY LARGE DIGITAL DATA ARCHIVES
Patric Savage *In* NASA. Goddard Space Flight Center, Proceedings of the NSSDC Conference on Mass Storage Systems and Technologies for Space and Earth Science Applications 1991 p 73-77 (For primary document see N93-15027 04-82)
Avail: CASI HC A01/MF A03

An archive is a permanent store. There are relatively few very large digital data archives in existence. Most business records are expired within five or ten years. Many kinds of business records that do have long lives are embedded in data bases that are continually updated and re-issued cyclically. Also, a great deal of permanent business records are actually archived as microfilm, fiche, or optical disk images - their digital version being an operational convenience rather than an archive. The problems forseen in stewarding the very large digital data archives that will accumulate during the mission of the Earth Observing System (EOS) are addressed. It focuses on the function of shepherding archived digital data into an endless future. Stewardship entails storing and protecting the archive and providing meaningful service to the community of users. The steward will (1) provide against loss due to physical phenomena; (2) assure that data is not lost due to storage technology obsolescence; and (3) maintain data in a current formatting methodology. L.R.R.

N93-15033*# E-Systems, Inc., Dallas, TX. Garland Div.
EMASS (TRADEMARK): AN EXPANDABLE SOLUTION FOR NASA SPACE DATA STORAGE NEEDS
Anthony L. Peterson and P. Larry Cardwell *In* NASA. Goddard Space Flight Center, Proceedings of the NSSDC Conference on Mass Storage Systems and Technologies for Space and Earth Science Applications 1991 p 79-92 (For primary document see N93-15027 04-82)
Avail: CASI HC A03/MF A03

The data acquisition, distribution, processing, and archiving requirements of NASA and other U.S. Government data centers present significant data management challenges that must be met in the 1990's. The Earth Observing System (EOS) project alone is expected to generate daily data volumes greater than 2 Terabytes (2 x 10(exp 12) Bytes). As the scientific community makes use of this data, their work will result in larger, increasingly complex data sets to be further exploited and managed. The challenge for data storage systems is to satisfy the initial data management requirements with cost effective solutions that provide for planned growth. The expendable architecture of the E-Systems Modular Automated Storage System (EMASS(TM)), a mass storage system which is designed to support NASA's data capture, storage, distribution, and management requirements into the 21st century is described. Author

N93-15034*# Mitre Corp., Bedford, MA.
DATA STORAGE AND RETRIEVAL SYSTEM
Glen Nakamoto *In* NASA. Goddard Space Flight Center, Proceedings of the NSSDC Conference on Mass Storage Systems and Technologies for Space and Earth Science Applications 1991 p 93-116 (For primary document see N93-15027 04-82)
Avail: CASI HC A03/MF A03

The Data Storage and Retrieval System (DSRS) consists of off-the-shelf system components integrated as a file server supporting very large files. These files are on the order of one gigabyte of data per file, although smaller files on the order of one megabyte can be accommodated as well. For instance, one gigabyte of data occupies approximately six 9 track tape reels (recorded at 6250 bpi). Due to this large volume of media, it was desirable to shrink the size of the proposed media to a single portable cassette. In addition to large size, a key requirement was that the data needs to be transferred to a (VME based) workstation at very high data rates. One gigabyte (GB) of data needed to be transferred from an archiveable media on a file server to a workstation in less than 5 minutes. Equivalent size, on-line data needed to be transferred in less than 3 minutes. These requirements imply effective transfer rates on the order of four to eight megabytes per second (4-8 MB/s). The DSRS also needed to be able to send and receive data from a variety of other sources accessible from an Ethernet local area network. L.R.R.

N93-15035*# Mesa Archival Systems, Inc., Boulder, CO.
DATA ARCHIVING
David Pitts *In* NASA. Goddard Space Flight Center, Proceedings of the NSSDC Conference on Mass Storage Systems and Technologies for Space and Earth Science Applications 1991 p 117-133 (For primary document see N93-15027 04-82)
Avail: CASI HC A03/MF A03

The viewgraphs of a discussion on data archiving presented at the National Space Science Data Center (NSSDC) Mass Storage Workshop is included. The mass storage system at the National Center for Atmospheric Research (NCAR) is described. Topics covered in the presentation include product goals, data library systems (DLS), client system commands, networks, archival devices, DLS features, client application systems, multiple mass storage devices, and system growth. L.R.R.

N93-15036*# Metrum Information Storage, Hunt Valley, MD.
NETWORK ACCESSIBLE MULTI-TERABYTE ARCHIVE
Fred Rybczynski *In* NASA. Goddard Space Flight Center, Proceedings of the NSSDC Conference on Mass Storage Systems and Technologies for Space and Earth Science Applications 1991 p 134-144 (For primary document see N93-15027 04-82)
Avail: CASI HC A03/MF A03

The viewgraphs of a discussion on Network Accessible Multi-terabyte Archive presented at the National Space Science Data Center (NSSDC) Mass Storage Workshop is included. Topics covered in the presentation include the rotary storage system (RSS) including RSS data access, data management, administration, and hardware and software architecture. L.R.R.

N93-15037*# Imperial Chemical Industries Ltd., Runcorn (England).
ICI OPTICAL DATA STORAGE TAPE
Robert A. McLean and Joseph F. Duffy *In* NASA. Goddard Space Flight Center, Proceedings of the NSSDC Conference on Mass Storage Systems and Technologies for Space and Earth Science Applications 1991 p 145-156 (For primary document see N93-15027 04-82)
Avail: CASI HC A03/MF A03

Optical data storage tape is now a commercial reality. The world's first successful development of a digital optical tape system is complete. This is based on the Creo 1003 optical tape recorder with ICI 1012 write-once optical tape media. Several other optical tape drive development programs are underway, including one using the IBM 3480 style cartridge at LaserTape Systems. In order to understand the significance and potential of this step change in recording technology, it is useful to review the historical progress of optical storage. This has been slow to encroach on magnetic storage, and has not made any serious dent on the world's mountains of paper and microfilm. Some of the reasons for this are the long time needed for applications developers, systems integrators, and end users to take advantage of the potential storage capacity; access time and data transfer rate have traditionally been too slow for high-performance applications; and optical disk media has been expensive compared with magnetic tape. ICI's strategy in response to these concerns was to concentrate its efforts on flexible optical media; in particular optical tape. The manufacturing achievements, media characteristics, and media lifetime of optical media are discussed. L.R.R.

N93-15038*# Odetics, Inc., Anaheim, CA. Automated Tape Library Products Div.
ATL PRODUCTS DIVISION'S ENTRIES INTO THE COMPUTER MASS STORAGE MARKETPLACE
Fred Zeiler *In* NASA. Goddard Space Flight Center, Proceedings of the NSSDC Conference on Mass Storage Systems and Technologies for Space and Earth Science Applications 1991 p 157-172 (For primary document see N93-15027 04-82)
Avail: CASI HC A03/MF A03

The viewgraphs of a discussion on ATL Products Division's entries into the computer mass storage marketplace presented at the National Space Science Data Center (NSSDC) Mass Storage Workshop is included. Topics covered are product evolution including robotics; aperture storage module library; Broadcast Division's TCS2000 Video Cart and TCS90 Videocart System; high density systems business product lines; and storage and library management. L.R.R.

N93-15039*# Advanced Development Corp., Burlington, MA.
CORROSION OF METAL PARTICLE AND METAL EVAPORATED TAPES **c35**

Dennis E. Speliotis *In* NASA. Goddard Space Flight Center, Proceedings of the NSSDC Conference on Mass Storage Systems and Technologies for Space and Earth Science Applications 1991 p 173-185 (For primary document see N93-15027 04-82)
Avail: CASI HC A03/MF A03

Very high coercivity metal particle (MP) and metal evaporated (ME) tapes are being used in 8mm video and digital audio tape applications, and more recently in digital data recording applications. In view of the inherent susceptibility of such media to environmental corrosion, a number of recent studies have addressed their long term stability and archivability. These studies have used an accelerated corrosion test based either on elevated temperature-humidity or polluting gas atmospheres known as Battelle tests. A comparison of the Battelle test results performed at different laboratories reveals a large variation from one location to another, presumably due to incorrect replication of the Battelle condition. Furthermore, when the Battelle tests are performed on enclosed cartridges, it is quite possible that diffusion limits the penetration of the extremely low concentration polluting gaseous species to the inner layers of the tapes during the short time of the accelerated test, whereas in real life these diffusion limitations may not apply. To avoid this uncertainty, the corrosion behavior of commercial 8mm MP and ME tapes when cassettes without their external plastic cases were exposed to 50 deg C and 80 percent RH for 7.5 weeks is investigated. L.R.R.

N93-15040*# Ampex Corp., Redwood City, CA.
A SYSTEM APPROACH TO ARCHIVAL STORAGE

John W. Corcoran *In* NASA. Goddard Space Flight Center, Proceedings of the NSSDC Conference on Mass Storage Systems and Technologies for Space and Earth Science Applications 1991 p 186-203 (For primary document see N93-15027 04-82)
Avail: CASI HC A03/MF A03

The introduction and viewgraphs of a discussion on a system approach to archival storage presented at the National Space Science Data Center (NSSDC) Mass Storage Workshop is included. The use of D-2 iron particles for archival storage is discussed along with how acceleration factors relating short-term tests to archival life times can be justified. Ampex Recording Systems is transferring D-2 video technology to data storage applications, and encountering concerns about corrosion. To protect the D-2 standard, Battelle tests were done on all four tapes in the Class 2 environment. Error rates were measured before and after the test on both exposed and control groups. L.R.R.

N93-15041*# National Media Lab., Saint Paul, MN.
STABILITY OF Co-GAMMA-Fe2O3 TAPE

Darlene M. Carlson *In* NASA. Goddard Space Flight Center, Proceedings of the NSSDC Conference on Mass Storage Systems and Technologies for Space and Earth Science Applications 1991 p 204-214 (For primary document see N93-15027 04-82)
Avail: CASI HC A03/MF A03

The viewgraphs of a discussion on the stability of recording media presented at the National Space Science Data Center (NSSDC) Mass Storage Workshop is included. An overview of archival stability of recording media is presented. Co-gamma-Fe2O3 tape is discussed. Other topics covered are magnetic tape components, dimensional stability and crossply, acetone extraction, coercivity, and phi R percent change. L.R.R.

N93-15042*# Ampex Corp., Redwood City, CA.
THE 19 mm DATE RECORDERS: SIMILARITIES AND DIFFERENCES **c35**

Steve Atkinson *In* NASA. Goddard Space Flight Center, Proceedings of the NSSDC Conference on Mass Storage Systems and Technologies for Space and Earth Science Applications 1991 p 215-219 (For primary document see N93-15027 04-82)
Avail: CASI HC A01/MF A03

Confusion over the use of non-video 19 mm data recorders is becoming more pronounced in the world of high performance computing. The following issues are addressed: (1) the difference between ID-1, ID-2, MIL-STD-2179, and DD-2; (2) the proper machine for the necessary application; and (3) integrating the machine into an existing environment. Also, an attempt is made to clear up any misconceptions there might be about 19 mm tape recorders. L.R.R.

N93-15043*# Ampex Corp., Redwood City, CA.
AN EMPIRICAL APPROACH TO PREDICTING LONG TERM BEHAVIOR OF METAL PARTICLE BASED RECORDING MEDIA **c35**

Allan S. Hadad *In* NASA. Goddard Space Flight Center, Proceedings of the NSSDC Conference on Mass Storage Systems and Technologies for Space and Earth Science Applications 1991 p 220-236 (For primary document see N93-15027 04-82)
Avail: CASI HC A03/MF A03

Alpha iron particles used for magnetic recording are prepared through a series of dehydration and reduction steps of alpha-Fe2O3-H2O resulting in acicular, polycrystalline, body centered cubic (bcc) alpha-Fe particles that are single magnetic domains. Since fine iron particles are pyrophoric by nature, stabilization processes had to be developed in order for iron particles to be considered as a viable recording medium for long term archival (i.e., 25+ years) information storage. The primary means of establishing stability is through passivation or controlled oxidation of the iron particle's surface. Since iron particles used for magnetic recording are small, additional oxidation has a direct impact on performance especially where archival storage of recorded information for long periods of time is important. Further stabilization chemistry/processes had to be developed to guarantee that iron particles could be considered as a viable long term recording medium. In an effort to retard the diffusion of iron ions through the oxide layer, other elements such as silicon, aluminum, and chromium have been added to the base iron to promote more dense scale formation or to alleviate some of the non-stoichiometric behavior of the oxide or both. The presence of water vapor has been shown to disrupt the passive layer, subsequently increasing the oxidation rate of the iron. A study was undertaken to examine the degradation in magnetic properties as a function of both temperature and humidity on silicon-containing iron particles between 50-120 deg C and 3-89 percent relative humidity. The methodology to which experimental data was collected and analyzed leading to predictive capability is discussed. L.R.R.

N93-15044*# Network Systems Corp., Vienna, VA.
THE ROLE OF HiPPI SWITCHES IN MASS STORAGE SYSTEMS: A FIVE YEAR PROSPECTIVE

T. A. Gilbert *In* NASA. Goddard Space Flight Center, Proceedings of the NSSDC Conference on Mass Storage Systems and Technologies for Space and Earth Science Applications 1991 p 237-250 (For primary document see N93-15027 04-82)
Avail: CASI HC A03/MF A03

New standards are evolving which provide the foundation for multi-gigabit per second data communication structures. The lowest layer protocols are so generalized that they encourage a wide range of application. Specifically, the ANSI High Performance Parallel Interface (HiPPI) is being applied to computer peripheral attachment as well as general data communication networks. The HiPPI Standards suite and technology products which incorporate the standards are introduced. The use of simple HiPPI crosspoint switches to build potentially complex extended 'fabrics' is discussed in detail. Several near term applications of the HiPPI technology are briefly described with additional attention to storage systems. Finally, some related standards are mentioned which may further expand the concepts above.
Author

N93-15045*# National Aeronautics and Space Administration. Goddard Space Flight Center, Greenbelt, MD.
THE NATIONAL SPACE SCIENCE DATA CENTER: AN OPERATIONAL PERSPECTIVE

Ronald Blitstein (ST Systems Corp., Greenbelt, MD.) and James L. Green *In its* Proceedings of the NSSDC Conference on Mass Storage Systems

and Technologies for Space and Earth Science Applications 1991 p 251-256 (For primary document see N93-15027 04-82)
Avail: CASI HC A02/MF A03

The National Space Science Data Center (NSSDC) manages over 110,000 data tapes with over 4,000 data sets. The size of the digital archive is approximately 6,000 GBytes and is expected to grow to more than 28,000 GBytes by 1995. The NSSDC is involved in several initiatives to better serve the scientific community and improve the management of current and future data holdings. These initiatives address the need to manage data to ensure ready access by the user and manage the media to ensure continuing accessibility and integrity of the data. An operational view of the NSSDC, outlining current policies and procedures that have been implemented to ensure the effective use of available resources to support service and mission goals, and maintain compliance with prescribed data management directives is presented. Author

N93-15046*# National Center for Atmospheric Research, Boulder, CO. Scientific Computing Div.
MASS STORAGE SYSTEM EXPERIENCES AND FUTURE NEEDS AT THE NATIONAL CENTER FOR ATMOSPHERIC RESEARCH
Bernard T. OLear *In* NASA. Goddard Space Flight Center, Proceedings of the NSSDC Conference on Mass Storage Systems and Technologies for Space and Earth Science Applications 1991 p 257-275 Sponsored by NSF (For primary document see N93-15027 04-82)
Avail: CASI HC A03/MF A03

A summary and viewgraphs of a discussion presented at the National Space Science Data Center (NSSDC) Mass Storage Workshop is included. Some of the experiences of the Scientific Computing Division at the National Center for Atmospheric Research (NCAR) dealing the the 'data problem' are discussed. A brief history and a development of some basic mass storage system (MSS) principles are given. An attempt is made to show how these principles apply to the integration of various components into NCAR's MSS. Future MSS needs for future computing environments is discussed. L.R.R.

N93-15047*# Lawrence Livermore National Lab., CA.
STORAGE NEEDS IN FUTURE SUPERCOMPUTER ENVIRONMENTS
Sam Coleman *In* NASA. Goddard Space Flight Center, Proceedings of the NSSDC Conference on Mass Storage Systems and Technologies for Space and Earth Science Applications 1991 p 276-295 Sponsored by DOE (For primary document see N93-15027 04-82)
Avail: CASI HC A03/MF A03

As the computing capacity of the Lawrence Livermore National Laboratory (LLNL) systems is increased and new applications are developed, the need for archival capacity will increase. The hardware and software architectures that will be needed to support advanced applications are discussed. Viewgraphs are included. L.R.R.

N93-15048*# Sandia National Labs., Albuquerque, NM.
REQUIREMENTS FOR A NETWORK STORAGE SERVICE
Suzanne M. Kelly and Rena A. Haynes *In* NASA. Goddard Space Flight Center, Proceedings of the NSSDC Conference on Mass Storage Systems and Technologies for Space and Earth Science Applications 1991 p 296-306 (For primary document see N93-15027 04-82)
(Contract DE-AC04-76DP-00789)
Avail: CASI HC A03/MF A03

Sandia National Laboratories provides a high performance classified computer network as a core capability in support of its mission of nuclear weapons design and engineering, physical sciences research, and energy research and development. The network, locally known as the Internal Secure Network (ISN), comprises multiple distributed local area networks (LAN's) residing in New Mexico and California. The TCP/IP protocol suite is used for inter-node communications. Scientific workstations and mid-range computers, running UNIX-based operating systems, compose most LAN's. One LAN, operated by the Sandia Corporate Computing Computing Directorate, is a general purpose resource providing a supercomputer and a file server to the entire ISN. The current file server on the supercomputer LAN is an implementation of the Common File Server (CFS). Subsequent to the design of the ISN, Sandia reviewed its mass storage requirements and chose to enter into a competitive procurement to replace the existing file server with one more adaptable to a UNIX/TCP/IP environment. The requirements study for the network was the starting point for the requirements study for the new file server. The file server is called the Network Storage Service (NSS) and its requirements are described. An application or functional description of the NSS is given. The final section adds performance, capacity, and access constraints to the requirements. L.R.R.

N93-15050# Logistics Management Inst., Bethesda, MD.
EDI PLANNING AND IMPLEMENTATION GUIDE Final Report
Thomas P. Hardcastle Jun. 1992 122 p
(Contract MDA903-90-C-0006)
(AD-A255737; LMI-DL203RD1) Avail: CASI HC A06/MF A02

This document presents a methodology that permits DoD activities to develop electronic data interchange (EDI) business plans. It uses structured worksheets to walk the user through the process of identifying EDI opportunities, performing an economic analysis of those opportunities, and developing rational EDI implementation plans. It also contains educational material on EDI legal and security issues, EDI transactions sets and message standards, and procedures for submitting EDI projects to both Executive Agent and the Office of Defense Information for funding. GRA

N93-15051# Logistics Management Inst., Bethesda, MD.
A GUIDE TO EDI TRANSLATION SOFTWARE Final Report
Harold L. Frohman 1992 153 p Revised
(Contract MDA903-90-C-0006)
(AD-A255739; LMI-PL205RD1) Avail: CASI HC A08/MF A02

This guide identifies and provides details on 110 commercially available electronic data interchange (EDI) translation software packages. It was developed for use by the Military Departments and Defense agencies as they procure EDI translation software packages in support of the Department of Defense's (DoD's) EDI program for transportation. However, other DoD entities with an EDI program should find this guide useful. This guide assesses the key features of each package, details a list of functions available in a particular software package, and highlights those features required to meet the EDI needs of Defense transportation in specific operating environments. GRA

N93-15112# Defense Technical Information Center, Alexandria, VA.
SOURCE HEADER LIST. VOLUME 2: K THROUGH Z Report, Sep. 1990 - Sep. 1992
Loretta Brown Sep. 1992 627 p Supersedes DTIC/TR-90/3-Vol-2, dated Sep. 1990, AD-A231001. See also Volume 1, AD-A256000
(AD-A256001; DTIC/TR-92/5-Vol-2; DTIC/TR-90/3-Vol-2) Avail: CASI HC A99/MF A06

This publication is the second of two volumes of an alphabetically arranged, compilation of corporation author names used by the Defense Technical Information Center in the DTIC database system. Each source name is assigned a 6-digit numeric code for computer input and retrieval purposes plus 4-digit alphanumeric geopolitical code and an alphanumeric type code. Source names displayed are included as data elements in the Technical Report, Work Unit Information System and Independent Research and Development databases maintained by DTIC. GRA

N93-15137# Wisconsin Univ., Whitewater. Innovation Service Center.
WISCONSIN INVENTORS' NETWORK DATABASE Final Report
Dec. 1991 63 p
(Contract DE-FG02-90CE-15981)
(DE92-018394; DOE/CE-15981/4) Avail: CASI HC A04/MF A01

The Wisconsin Innovation Service Center at UW-Whitewater received a DOE grant to create an Inventor's Network Database to assist independent inventors and entrepreneurs with new product development. Since 1980, the Wisconsin Innovation Service Center (WISC) at the University of Wisconsin-Whitewater has assisted independent and small business inventors in estimating the marketability of their new product ideas and inventions. The purpose of the WISC as an economic development entity is to encourage inventors who appear to have commercially viable inventions, based on preliminary market research, to invest in the next stages of development, perhaps investigating prototype development, legal protection, or more in-depth market research. To address inventor's information needs, WISC developed on electronic database with search capabilities by geographic region and by product category/industry. It targets both public and private resources capable of, and interested in, working with individual and small business inventors. At present, the project includes resources in Wisconsin only. DOE

N93-15229# Science Applications International Corp., Las Vegas, NV.
TECHNICAL DATA MANAGEMENT AT THE YUCCA MOUNTAIN SITE CHARACTERIZATION PROJECT
Jan Statler, Claudia M. Newbury (Department of Energy, Las Vegas, NV.), and Gail W. Heitland (Science Applications International Corp., Golden, CO.) 1992 12 p Presented at the 16th Annual Nuclear Information and Records Management Association Symposium: Shared Information - Golden Gateway to Progress, San Francisco, CA, 30 Aug. - 2 Sep. 1992
(Contract DE-AC08-87NV-10576)
(DE92-018115; CONF-920849-1) Avail: CASI HC A03/MF A01

The Department of Energy/Office of Civilian Radioactive Waste Management (DOE/OCRWM) is responsible for the characterization of Yucca Mountain, Nevada, to determine its potential as a site of a high-level radioactive waste repository. The characterization of Yucca Mountain encompasses many diverse investigations, both onsite and in laboratories across the country. Investigations are being conducted of the geology, hydrology, mineralogy, paleoclimate, geotechnical properties, and archeology of the area, to name a few. Effective program management requires that data from site investigations be processed, interpreted and disseminated in a timely manner to support model development and validation, repository design, and performance assessment. The program must also meet regulatory requirements for making the technical data accessible to a variety of external users throughout the life of the project. Finally, the DOE/OCRWM must make available the data or its description and access location available for use in support of the license application and supporting documentation. To accomplish these objectives, scientific and engineering data, generated by site characterization activities, and technical data, generated by environmental and socioeconomic impact assessment activities, must be systematically identified, cataloged, stored and disseminated in a controlled manner. DOE

N93-15254# Rutgers - The State Univ., Piscataway, NJ. Dept. of Electrical and Computer Engineering.
QUERY OPTIMIZATION AND PLANNING IN OBJECT-ORIENTED KNOWLEDGE BASES Final Report, 1 Oct. 1989 - 31 Dec. 1991
Phillip Sheu Aug. 1992 77 p
(Grant AF-AFOSR-0004-90)
(AD-A256006; AFOSR-92-0858TR) Avail: CASI HC A05/MF A01

The purpose of the project entitled 'Query Planning and Optimization in Object-oriented Knowledge Bases' sponsored by AFOSR-90-0004 is to extend a deductive object base with knowledge-based problem solving and planning, which is intended to realize the concept of very-high level programming in a database system. The input to such a system is a specification of the problem to be solved (as a set of goals) and the output is a solution of the problem, where the knowledge-based problem solving system deals with problems that do not change the state of a database and the planning system processes goals that require some state changes in the database. In our approach, the knowledge-based problem solving system stores a set of problem models (such as graph problems) so that an input problem can be matched through an object-oriented specialization/generalization process. If no problem models can be matched by a given problem, the user should be provided with a high-level programming system that allows a top-down problem solving process be carried out until some matches can be found at detailed implementation stages. For the planning system, we have realized that most of the conventional approaches based on the formulation of operations-preconditions-postconditions have been proven to be inefficient. We have classified general planning problems into several classes so that each class can be solved individually and efficiently. With this approach, each class of planning problems can be constructed as a problem model and included in the general problem solving system. GRA

N93-15275# Westinghouse Hanford Co., Richland, WA.
THE INFORMATION AGE AS A WORK IN PROGRESS: IMPLICATIONS FOR TECHNICAL COMMUNICATORS
B. L. Preecs Jul. 1992 8 p Presented at the Society for Technical Communication Region 7 Conference, Denver, CO, 15-17 Oct. 1992
(Contract DE-AC06-87RL-10930)
(DE92-019780; WHC-SA-1502; CONF-9210155-1) Avail: CASI HC A02/MF A01

The commercial media system in the United States is in the midst of radical, even revolutionary changes. Cable television companies are vying with telephone companies to provide advanced communications and information services to both homes and businesses. Recent decisions by the Federal Communications Commission to allow television networks to buy cable television systems create the possibility of bypassing local television stations. Computer companies are planning joint ventures with entertainment companies. The publishing, broadcasting, advertising, communications, and information-services businesses are converging into one universal, digital, interactive industry with annual revenues exceeding $120 billion. The same technology-driven changes also affect government. State and local governments are experimenting with delivering some government services electronically. While early experiments focus on easily delivered services, such as auto licenses, more complex applications are underway, such as creating information networks for economic development or converting property and utility records into computerized maps. The Information Age has arrived, and the implications for Society for Technical Communication (STC) members can hardly be overstated. Technical communicators will face changes in the way they work and how their work is distributed. DOE

N93-15315# Air Force Inst. of Tech., Wright-Patterson AFB, OH. School of Engineering.
AN ECLECTIC METHOD FOR OBJECT ORIENTED DATABASE DESIGN
Douglas E. Dyer 9 Sep. 1992 25 p
(AD-A256439; AFIT/EN-TR-92-4) Avail: CASI HC A03/MF A01

No dominant methodology has emerged for designing object-oriented databases. In this paper, we identify characteristics for a good design methodology and review the literature of supporting models and approaches. Semantic data models and object-oriented methods are presented. We then take an extended look at Harel's higraph notation and use it to extend the entity relationship model for object-oriented database design. GRA

N93-15335# Defense Technical Information Center, Alexandria, VA.
USER'S GUIDE FOR SEARCHMAESTRO Final Report
Karen V. Fox, Keith L. Thompson, Barbara Lesser, and Christian M. Cupp Jan. 1992 36 p
(AD-A256422; DTIC/TR-92-3) Avail: CASI HC A03/MF A01

This user's guide was developed to provide end users with easy access to information. SearchMAESTRO users are not required to learn commands and procedures for numerous databases and online human help is provided in addition to help menus. One of the major benefits of this system is that users receive one bill and do not have to register with each vendor. Users also have unclassified access to DROLS. GRA

N93-15393# Naval Research Lab., Washington, DC.
CONVERSION OF IRAMMP DATA TO HDF FORMAT Interim Report
R. G. Priest, U. R. Obeysekare, and C. J. Williams 9 Oct. 1992 9 p
(AD-A256515; NRL/MR/6522-92-7151) Avail: CASI HC A02/MF A01

In the last few years the HDF standard format for the storage of scientific data, images, and auxiliary information has gained popular acceptance. The HDF format is an attractive alternative to the NATO format for the storage of IRAMMP data for several reasons. It is the purpose of this report to describe the implementation of HDF for IRAMMP data developed at the Naval Research Laboratory. The report also provides information on how to acquire the public-domain programs XImage and XDS from NCSA via the Internet. GRA

N93-15409# California Inst. of Tech., Pasadena.
PARALLEL READOUT OF OPTICAL DISKS Final Report, 15 Jun. 1989 - 14 Jun. 1992
Demetri Psaltis 31 Aug. 1992 81 p
(Contract DAAL03-89-K-0114)
(AD-A256625; ARO-26676.15-PH) Avail: CASI HC A05/MF A01

Optical disks can be utilized in a variety of systems that take advantage of the inherent parallel accessibility to the stored data. We experimentally demonstrate the use of parallel access to data stored on optical disks in digital optical computing, several types of neural networks including optical and optoelectronic neural networks, image classifiers, and image correlators. GRA

N93-15492# Universiteit Twente, Enschede (Netherlands). Dept. of Computer Science.

PHYSICAL DESIGN FOR NETWORK DATABASES

Sunil Choenni, Henk M. Blanken, and Thiel Chang (Gemeenschappelijk Administratiekantoor, Amsterdam, Netherlands) Mar. 1992 30 p

(Memo-INF-92-26; ETN-92-92440) Copyright Avail: CASI HC A03/MF A01

Physical database design is an important step in the whole design process of databases. If bad choices are made for the physical design, this will result in poor performance of the whole database system. One of the choices which have to be made is that of storage configurations. There is a lot of attention paid to this subject, resulting in several approaches for the selection of storage configurations. A stock taking of these approaches concerning network databases is presented and the strong points and limitations of each approach are signaled. The strong points of the approaches are combined together with some other ideas to construct a powerful tool which can assist the database administrator in the selection of storage configurations. ESA

N93-15627# Army Construction Engineering Research Lab., Champaign, IL.

PREDICTING DATABASE REQUIREMENTS FOR GEOGRAPHIC INFORMATION SYSTEMS IN THE YEAR 2000: LONG-TERM DESIGN ISSUES FOR GRASS Final Report

Kurt A. Buehler, Michael Shapiro, and James D. Westervelt Aug. 1992 43 p

(DA Proj. 4A1-61102-AT-23)

(AD-A256862; CERL-TR-EC-92/01) Avail: CASI HC A03/MF A01

The Environmental Compliance Modeling and Simulation Division of the U.S. Army Construction Engineering Research Laboratories is responsible for continuing development of the geographic information system (GIS) known as GRASS--the Geographic Resources Analysis Support System. As the use of GRASS has increased, several significant limitations in the system have been identified. At the same time, advances in hardware and software technology have occurred that might help to address some of these limitations. This report presents the results of a preliminary investigation into the software capabilities and implementation strategies involved in revising the GRASS GIS. The research showed that one promising way to enhance GRASS would be to use an extended relational database management system or an object-oriented database management system as the core of the new GIS. GRA

N93-15637# Naval Postgraduate School, Monterey, CA.

UPGRADE AND EXTENSION OF THE DATA ACQUISITION SYSTEM FOR PROPULSION AND GAS DYNAMIC LABORATORIES M.S. Thesis

Richard A. Wendland Jun. 1992 207 p

(AD-A256836) Avail: CASI HC A10/MF A03

The goal of the present work was to upgrade the data acquisition system (DAS) in the high-speed building of the Turbopropulsion Laboratory (TPL) and to develop a high speed acquisition capability for pressure measurements for both TPL and the new Gas Dynamics Laboratory (GDL). Using the Hewlett Packard HP9000 Series 300 Computer as the system controller, a 96-channel high-speed pressure DAS was developed using Scanivalve ZOC-14 modules and a CALSYS2000 calibrator. The system allowed acquisition times for current wind-tunnel experiments to be revised from four minutes to eleven seconds. Also, new software was written to acquire data from existing rotary pneumatic Scanivalves and HP-IB compatible instrumentation so that all other existing acquisition capabilities were maintained in both laboratories. GRA

N93-15639# Massachusetts Inst. of Tech., Cambridge. Lab. for Computer Science.

A DISTRIBUTED DATA-BALANCED DICTIONARY BASED ON THE B-LINK TREE

T. Johnson and A. Colbrook Feb. 1992 23 p

(Contract N00014-89-J-1988)

(AD-A256841; MIT/LCS/TR-530) Avail: CASI HC A03/MF A01

Many concurrent dictionary data structures have been proposed, but usually in the context of shared memory multiprocessors. In this paper, we present an algorithm for a concurrent distributed B-tree that can be implemented on message passing parallel computers. Our distributed B-tree (the db-tree) replicates the interior nodes in order to improve parallelism and reduce message passing. We show how the db-tree algorithm can be used to build an efficient, highly parallel, data-balanced distributed dictionary, the dE-tree. GRA

N93-15641# Army Construction Engineering Research Lab., Champaign, IL.

RECOMMENDATIONS FOR ENHANCEMENT OF THE DESIGN CRITERIA INFORMATION SYSTEM (DCIS) Final Report

William H. Flickinger, Jane L. Solon-Wetmore, and Sandra Kappes Aug. 1992 23 p

(AD-A256857; CERL-TR-FF-92/06) Avail: CASI HC A03/MF A01

Architectural and Engineering Instructions (AEI's) comprise a large, complex body of mandatory design criteria and guidance for U.S. Army Corps of Engineers facility designers, engineers, and contractors. The unabridged set of AEI's is often out of date because AEI's are revised much more frequently than updates are published. Furthermore, to hold down printing and distribution costs, the unabridged body of AEI's receives very narrow distribution. Consequently, hard copies of the latest AEI's are difficult to obtain on a timely basis. The Design Criteria Information System (DCIS) was developed to make current AEI's accessible worldwide to any authorized user with a microcomputer and a modem. DCIS, which resides on the Corps' Programming, Administration, and Execution (PAX) mainframe system, has solved the fundamental problem of distributing current AEI's online. However, DCIS cannot distribute drawings or graphics online, its text-retrieval functions are limited, and the mainframe's supporting technology makes the system cumbersome to use. This report surveys technologies that could be exploited to enhance DCIS, outlines three general alternatives for enhancement, and assesses the advantages and disadvantages of each. Development of a minicomputer-based system employing CD-ROM (compact disc-read only memory) technology, and accessible via microcomputer and telecommunications, is recommended. GRA

N93-15642# Army Construction Engineering Research Lab., Champaign, IL.

GRASS 4.0 MAP DIGITIZING USER'S MANUAL: V. DIGIT Final Report

Craig A. Neidig, David P. Gerdes, and Chester Kos Jul. 1992 56 p

(AD-A256859; CERL-ADP-EGI-92/01) Avail: CASI HC A04/MF A01

The Geographic Resources Analysis Support System (GRASS) is an image-processing and geographic information system (GIS) originally designed to serve land managers and environmental planners at Army installations, but now used by a wide variety of public and private users. Map data are useful for building a GIS data base. Within the GRASS system, map development entails the production of vector, raster, and support files to represent map features. One way analog map data are entered and converted into digital form is by tracing relevant map features with an electronic instrument called a digitizer. In GRASS version 4.0, the program used to conduct this conversion is called v.digit. This manual discusses v.digit options. The v.digit program is an interactive, menu-driven vector digitizing, labeling, and editing package. The samples in this manual require use of a workstation minimally consisting of a graphics monitor and keyboard, a pointing device (mouse), and a digitizing tablet. Drivers for v.digit exist for Altek, Calcomp, GeoGraphics, Hitachi, Kurta, Numonics, and SummaGraphics digitizers. V.digit also operates in an X Windows environment. GRA

N93-15644# Communications General International, Inc., Saint Louis, MO.

FEASIBILITY STUDY FOR AN INTEGRATED DATA PROCESSING SYSTEM

Oct. 1991 191 p Prepared in cooperation with Chelsea International, Inc., Washington, DC and Graphic and Data Solutions, Inc., Saint Louis, MO Prepared for Instituto National de Telecommunicaciones, Panama City

(PB92-214287) Avail: CASI HC A09/MF A02

The U.S. Trade and Development Program (TDP) agreed to fund a feasibility study covering the modernization and integration of the data processing systems at INTEL, the telecommunications administration of Panama. The agreement was reached following a definitional mission in July 1991, which recommended that the study, having met TDP approval criteria, be undertaken. The objective of the study is to review the present INTEL operations and their relationships with data processing services. This is followed by the development of a plan for the introduction of a

modern, integrated data processing system to serve operations, together with financial and technical sub-systems, for all national and international services. The project includes the identification of systems that need to be replaced or upgraded, the type of replacement equipment that would be purchased, the extent that existing hardware could continue to be used, and the methods to be used to bring about the changes. GRA

N93-15655# Argonne National Lab., IL.
HOW SCIENTIFIC MUST TECHNICAL EDITORS BE?
C. M. Caruthers 28 Jul. 1992 5 p Presented at the IEEE International Professional Communications Conference: Crossing Frontiers, Santa Fe, NM, 30 Sep. 1992
(Contract W-31-109-eng-38)
(DE92-040741; ANL/CP-76976; CONF-9209142-7) Avail: CASI HC A01/MF A01

As a senior technical editor in the Computing and Telecommunications Division at Argonne National Laboratory. I am responsible for a small technical editing group including regular staff, temporary editors, and interns. I have supervised some 22 technical communications interns over the past ten years. Previously, I taught at the university level for 21 years. These experiences have led me to believe that while scientific knowledge in the technical editing process is valuable, it is not essential, but a thorough awareness of verbal structure and intended audience is essential. As I composed this paper, I found myself staring at the posted description of an editing job available in another division at Argonne, prominently requiring 'thorough grounding in the basic sciences, including mathematics and physics'. This popular assumption--that successful editors of scientific documents must have some expertise in the scientific field to which the documents relate--is, in my judgment, often magnified out of proportion. DOE

N93-15170# Ministry of Defence, London (England). Procurement Executive.
ROYAL AIR FORCE EXPERIENCE OF THE HARRIER INFORMATION MANAGEMENT SYSTEM [ERFAHRUNGEN DER ROYAL AIR FORCE MIT DEM INFORMATIONS-MANAGEMENT-SYSTEM DES HARRIER-FLUGZEUGES]
R. P. Bookham *In* DLR, Proceedings of the 16th Symposium on Aircraft Integrated Monitoring Systems Jan. 1992 p 341-360 (For primary document see N93-15152 04-06)
(Contract AE12A/159)
Avail: CASI HC A03/MF A06; DLR, Wissenschaftliches Berichtswesen, Postfach 90 60 58, Cologne, Germany, HC

83 ECONOMICS AND COST ANALYSIS

Includes cost effectiveness studies.

N93-14249# Naval Postgraduate School, Monterey, CA.
EVALUATION OF THE COST EFFECTIVENESS ANALYSIS MODEL BEING DEVELOPED FOR THE COMPONENT IMPROVEMENT PROGRAMS OF THE AIR FORCE AND THE NAVY M.S. Thesis
Gerald L. Crowder Jun. 1992 61 p
(AD-A256132) Avail: CASI HC A04/MF A01

This thesis examines the Cost Effectiveness Analysis (CEA) model used by the Air Force to assist with the decision making process of their Cost Improvement Program (CIP). The emphasis was on studying the model for its use in the Naval Component Improvement Program. With an example provided by General Electric, a sensitivity analysis was performed to determine the cost drivers of the model. For the example, the major cost drivers were found to be the Incorporation Style, Kit Hardware Cost, and the Spare Part Factor. Next a simple simulation was conducted to determine how random component failures affect the life cycle cost variability of the CEA model. The author concluded that additional simulation studies should be conducted for other causes of variation. A detailed analysis of the model formulas and assumptions are needed as part of a users' manual. GRA

84 LAW, POLITICAL SCIENCE AND SPACE POLICY

Includes NASA appropriation hearings; aviation law; space law and policy; international law; international cooperation; and patent policy.

No abstracts in this category.

85 URBAN TECHNOLOGY AND TRANSPORTATION

Includes applications of space technology to urban problems; technology transfer; technology assessment; and surface and mass transportation.

For related information see also *03 Air Transportation and Safety, 16 Space Transportation,* and *44 Energy Production and Conversion.*

No abstracts in this category.

88 SPACE SCIENCES (GENERAL)

No abstracts in this category.

89 ASTRONOMY

Includes radio, gamma-ray, and infrared astronomy, and astrometry.

N93-14195 Harvard Univ., Cambridge, MA.
STUDY OF TIDAL INTERACTIONS IN M81-M82-NGC3077 SYSTEM Ph.D. Thesis
Min Su Yun 1992 226 p
Avail: Univ. Microfilms Order No. DA9228314

A nearby system of interacting galaxies M81-M82-NGC3077 triplet has been studied using a combined effort of detailed multi-wavelength observations and numerical simulations to obtain a comprehensive understanding on the dynamics and the consequences of tidal interactions in a group environment. The VLA 12-field mosaic HI observations of 2 x 1.5 deg region have revealed a vast array of HI filaments that suggests the severity and extent of tidal disruptions far exceeding the previous estimates. A tidal remnant of the former HI disk of M82 extending up to 30 kpc in projection is identified for the first time through the new VLA observations, and the pervasive effects of the tidal disruption are traced into the inner disk both by optical and CO observations, including a kinematic trace of a large scale bar potential. The HI disk of M81 is traced out to 40 kpc in radius, and a large scale (I approx. 20 kpc) velocity anomaly ('High Velocity Trough'), which may be a remnant of gaseous collision, is found within the disk of M81. The large HI bridge between M81 and NGC3077 (van der Hulst 1979) is also found to extend greater than approx. 50 kpc beyond NGC3077, toward M82. The total HI detected in this experiment, 5.6 x 10(exp 9) solar magnitude, represents the majority of the single-dish flux and suggests that the bulk of HI found in the region belongs to the three galaxies and the tidal filaments. The impact and details of tidal interactions have been further examined through the use of numerical techniques. The 'restricted 3-body' approach successfully simulates the observed tidal bridges, and it correctly predicts the gas kinematics. While the South Tidal Bridge is identified as a tidal arm originating

from M81, the best model stipulates that the North Tidal Bridge between NGC3077 and M82 is tidally disrupted HI disk (approx. 10(exp 9) solar magnitude) of NGC3077, which currently appears as a gas-poor early type galaxy. The time scale for the tidal interactions is quite short, 3 x 10(exp 8) yrs. The high degree of success achieved by the restricted 3-body calculations suggests that the role of self-gravity in tidal interaction may be over-estimated by previous full N-body studies such as Barnes (1988). A full N-body/SPH model has been developed to incorporate self-gravity and hydrodynamics, but it suffers from various shortcomings. In particular, (3-5) x 10(exp 3) particles used in the simulation are insufficient for modeling a stable self-consistent galaxy, and the King model halo used here is too dissipative in nature to model non-merging cases of tidal interactions. Further investigations of the tidal interactions using the restricted 3-body approach are suggested in order to scrutinize the role of self-gravity in tidal interactions. Dissert. Abstr.

N93-14228 Michigan Univ., Ann Arbor.
A SEARCH FOR DEAD QSO'S AMONG NEARBY LUMINOUS GALAXIES Ph.D. Thesis
Gary Allen Bower 1992 166 p
Avail: Univ. Microfilms Order No. DA9226854

Quasi-stellar objects (QSO's) and active galactic nuclei (AGN's) with luminosities greater than or equal to 10(exp 12) solar luminosity are generally presumed to be powered by accretion of matter onto a black hole with mass of greater than or equal to 10(exp 9) solar mass. When the host galaxy is exhausted of matter capable of feeding the central black hole, the energy output rapidly decreases leaving behind a dead QSO engine. Confirmation of this model would then be provided by the identification or dead engines in nearby galaxies. The observed stellar kinematics in the nuclei of the galaxies, when combined with dynamical models, indicate whether unseen central masses are present. This dissertation describes the first results of an extensive project to analyze high spatial resolution observations of the nuclei of nearby galaxies with similar morphological properties as QSO host galaxies. Long slit optical spectra of spiral galaxies NGC2613, NGC4699, NGC5746, and NGC7331 are analyzed with a cross correlation method to measure the stellar kinematics. Using the observations in conjunction with a maximum entropy method to model the dynamics shows that unseen masses in the nuclei of these four galaxies are not required in order to explain the observations. The upper limit of possible black hole masses are 7 x 10(exp 8) solar mass for NGC7331 and few x 10(exp 9) solar mass for the other three galaxies. In addition, long slit optical spectroscopy of many of the candidate galaxies show weak nuclear emission lines. The ratios of the emission lines indicate that most of the galaxies harbor low-luminosity AGN's or LINER's (Low-Ionization Nuclear Emission Line Regions). Determining the local space density of approximately 10(exp 9) solar mass black holes provides a constraint on evolution scenarios of the QSO population because this space density should be a measure of the rate of the evolution from large redshifts to the present epoch.
Dissert. Abstr.

N93-14231 Southampton Univ. (England).
THE EFFECTS OF MIS-ALIGNMENT AND BACKGROUND NOISE IN A LOW ENERGY GAMMA RAY TELESCOPE Ph.D. Thesis
Peter John Knight 1990 250 p
Avail: Univ. Microfilms Order No. BRDX96932

As a consequence of the nature of gamma-ray interactions with matter, telescopes operating in the low energy gamma-ray region of the spectrum tend to be massive, bulky instruments, and require a platform at or above the top of the atmosphere. This situation can lead to mechanical distortion of the structure, causing a translational or rotational mis-alignment between the various components of the telescope. Such distortion can lead to systematic errors in the reconstructed source position and a decrease in the significance of the source detection. The ZEBRA telescope is a balloon-borne coded aperture instrument designed to operate in the energy range 0.2-10 MeV. Its mechanical structure is such that the distortions described above can cause significant aberration in the images produced by the telescope. The results of simulations written to investigate the effects of mis-alignment on the image quality are presented, and a set of mechanical tolerances is derived. A system of deflection measuring devices was used on the ZEBRA platform during its first flight in May 1989 to enable the quantification of distortions to be carried out in real time. These devices, their calibration, and the associated software written to perform the data analysis are described in detail, together with the results obtained during the flight. The use of such a system on a future flight is discussed, as are some alternative methods. The reduction of background noise in gamma-ray telescopes is of paramount importance due to the inherently low source of background ratio found in their operating environments. A study of the various background contributions is presented, with particular emphasis placed upon the reduction of background noise in actively shielded germanium spectrometers. The results of simulations are presented, and overall conclusions are reached concerning the optimisation of the shielding and orbit with regard to the background level in such instruments. A brief outline of the proposed INTEGRAL satellite is presented, with emphasis placed upon the relevance of this work to the design of the instrument. Dissert. Abstr.

N93-14593 Virginia Univ., Charlottesville.
ULTRAVIOLET SPECTRA OF STARS AND STELLAR SYSTEMS Ph.D. Thesis
Michael Nicholas Fanelli 1991 236 p
Avail: Univ. Microfilms Order No. DA9221062

Ultraviolet spectra are most sensitive to the hottest stellar components in composite systems, greatly facilitating determination of their star formation history. We have characterized the ultraviolet (lambda 1200-3200) spectral morphology of common stars through the use of narrow-band spectral line and continuum indices. The stellar content and formation history of composite populations is explored using a library of UV spectral energy distributions (SED's). Using a dataset of 218 IUE spectra (types O-K), new line and continuum indices are defined and their usefulness as temperature, luminosity, and metallicity diagnostics is discussed. We find modest luminosity discrimination among dwarfs, subgiants, and giants; supergiants form a more distinct sequence in most of the indices. We have constructed a library of 56 mean stellar SED's from the IUE Ultraviolet Spectral Atlas and our Cool Star Extension, including 6 metal-poor and 3 metal-enhanced groups. Indices characterizing the continuum and strong absorption features are examinded as temperature, luminosity and abundance diagnostics. Ultraviolet SED's of synthetic populations (0.005 plus or minus t plus or minus 30 Gyr) have been derived using the library. Due to the great sensitivity of the structure and amplitude of spectral features to the hottest stellar components, dating of stellar populations is most easily accomplished with UV data. We have explored the stellar content of 4 blue, star-forming systems and M32, a quiescent elliptical galaxy, employing an optimizing synthesis approach on spectra obtained with IEU. In the blue galaxies, we find evidence for discrete star formation episodes, a significant blue supergiant component, and modesst continuum extinction. One object displays an unusually strong lambda 2200 extinction feature, apparently the strongest such feature yet observed in a composite extra-galactic system. Dissert. Abstr.

N93-14611 Columbia Univ., New York, NY.
MULTIWAVELENGTH SPECTROSCOPY OF ACTIVE GALACTIC NUCLEI Ph.D. Thesis
Michiel Kolman 1992 157 p
Avail: Univ. Microfilms Order No. DA9232033

Extensive observational studies of two active galactic nuclei, the bright QSO H1821 + 643 and the Seyfert 1 galaxy NGC 3516, are presented. We report on the first simultaneous spectroscopy of the nearby (z = 0.297) QSO H1821 + 643 in the optical, UV, and X-ray band, in addition to optical, X-ray, and radio mapping. This QSO, which had not been detected at radio frequencies before, exhibits a detailed radio structure in which two separate components are distinguished. In the soft X-ray observations we separated (both spectroscopically and spatially) the emission originating in H1821 + 643 from the nearby hot white dwarf K1-16, thus isolating the intrinsic soft X-ray excess in the QSO. In the coadded UV spectrum we detected a Lyman alpha absorption line at z = 0.225 which we identify with a foreground galaxy. The combined spectroscopy shows a strong optical/UV bump with a flat slope in the UV (alpha is approximately -0.96, f(sub nu) varies as nu(sup alpha)) and a steep excess (alpha is approximately -4) in the soft X-ray band in addition to a typical hard slope of alpha is approximately -0.8 between 0.5 and 10 keV. Standard accretion disk models can account for the observed optical/UV emission, but fail to fit both the soft X-ray excess and the optical/UV bump. Also, we report on the first simultaneous UV and hard X-ray observations of the Seyfert 1 galaxy NGC 3516, which were carried out to investigate the connection between the

exceptionally strong and variable absorption in the X-ray and ultraviolet bands. The X-ray spectrum is complex and can be fitted satisfactorily with a warm absorber model, a partial covering model, or a cold reflector model. Lower limits on the column densities of the X-ray and UV absorbers are established at approximately 4 x 10(exp 22) cm(exp -2) and approximately 2 x 10(exp 19) cm (exp -2), respectively. Assuming that the variability in the C IV lambda 1550 absorption is due to changes in ionization level, the UV absorbers should be located closer than 9 pc from the ionizing source for log N(sub H) is approximately 20, and at smaller distances for higher column densities, thus excluding the narrow line region. Although the absence of short-term variability in absorption during the simultaneous X-ray and UV observations preempted a direct test of the common origin of the UV and X-ray absorption, indirect arguments lead to the conclusion that these absorptions probably do not arise in the same location. Dissert. Abstr.

N93-14628 California Inst. of Tech., Pasadena.
GAMMA-RAY IMAGING OBSERVATIONS OF SUPERNOVA 1987A Ph.D. Thesis
David Michael Palmer 1992 222 p
Avail: Univ. Microfilms Order No. DA9232214

The Caltech imaging gamma-ray telescope has made four balloon flights from Alice Springs, Australia, to observe the hard x-ray and gamma-ray emission from Supernova 1987A as it evolved between 1987 May and 1989 April. We have detected gamma-rays with the time behavior and spectral signature expected from freshly-synthesized radioisotopes embedded in cloud ejecta. In particular, we detect the 847 and 1238 keV gamma-ray lines produced by the decay of Co-56, and the continuum spectrum expected from Compton scattering of these gamma-rays. The results of these observations are compared with other measurements and with theoretical models of supernovae, and it is found that our results are consistent with core-collapse models for SN 1987A in which the centrally-produced radioisotopes have propagated outwards to mix with the ejecta. Dissert. Abstr.

N93-14629 Victoria Univ. (British Columbia).
A FAINT SPECTROSCOPIC QUASAR SURVEY Ph.D. Thesis
David Joseph Schade 1990 163 p
Avail: Univ. Microfilms Order No. DANN68135

A very faint spectroscopic quasar survey was undertaken in order to define the statistical behavior of the low luminosity portion of the quasar population at high redshift and to search for evidence of a decline in space density. Both slitless and multi-aperture spectroscopic observations were obtained for approximately 750 objects with B magnitudes in the range 20 less than B less than 24. The total number of emission line candidates found was approximately 50 and there are 5 excellent quasar candidates, 3 very probable at high redshift. In addition to the quasar candidates a number of emission line galaxies have been identified. Dissert. Abstr.

N93-14759*# Smithsonian Astrophysical Observatory, Cambridge, MA.
THE EVOLUTION OF THE QUASAR CONTINUUM Semiannual Report Nos. 1-3, 1 Jul. 1990 - 31 Dec. 1991
M. Elvis Aug. 1992 54 p
(Grant NAGw-2201)
(NASA-CR-191673; NAS 1.26:191673) Avail: CASI HC A04/MF A01

We now have in hand a large data base of Roentgen Satellite (ROSAT), optical, and IR complementary data. We are in the process of obtaining a large amount of the International Ultraviolet Explorer (IUE) data for the same quasar sample. For our complementary sample at high redshifts, where the UV was redshifted into the optical, we have just had approved large amounts of observing time to cover the quasar continuum in the near-IR using the new Near-Infrared Camera and Multi-Object Spectrometer (NICMOS) array spectrographs. Ten micron, optical, and VLA radio, data also have approved time. An ISO US key program was approved to extend this work into the far-IR, and the launch of ASTRO-D (early in 1993) promises to extend it to higher energy X-rays. For individual title, see N93-14760.

N93-14760*# Texas Univ., Austin. Dept. of Astronomy.
QUASAR X-RAY SPECTRA REVISITED
P. Shastri, B. J. Wilkes (Smithsonian Astrophysical Observatory, Cambridge, MA.), M. Elvis (Smithsonian Astrophysical Observatory, Cambridge, MA.), and J. McDowell (Smithsonian Astrophysical Observatory, Cambridge, MA.) *In* Smithsonian Astrophysical Observatory, The Evolution of the Quasar Continuum Aug. 1992 19 p Submitted for publication (For primary document see N93-14759 04-89)
Avail: CASI HC A03/MF A01

A sample of 45 quasars observed by the Imaging Proportional Counter (IPC) on the Einstein satellite is used to re-examine the relationship between the soft (0.2-3.5 keV) X-ray energy index and radio-loudness. We found the following: (1) the tendency for radio-loud quasars to have systematically flatter X-ray slopes than radio-quiet quasars (RQQ's) is confirmed with the soft X-ray excess having negligible effect; (2) there is a tendency for the flatness of the X-ray slope to correlate with radio core-dominance for radio-loud quasars, suggesting that a component of the X-ray emission is relativistically beamed; (3) for the RQQ's the soft X-ray slopes, with a mean of approximately 1.0, are consistent with the slopes found at higher energies (2-10 keV) although steeper than those observed for Seyfert 1 galaxies (also 2-10 keV) where the reflection model gives a good fit to the data; (4) the correlation of FeII emission line strength with X-ray energy index is confirmed for radio-quiet quasars using a subset of 18 quasars. The radio-loud quasars show no evidence for a correlation. This relation suggests a connection between the ionizing continuum and the line emission from the broad emission line region (BELR) of radio-quiet quasars, but in the opposite sense to that predicted by current photoionization models; and (5) the correlations of X-ray slope with radio core dominance and FeII equivalent width within the radio-loud and radio-quiet sub-classes respectively imply that the observed wide range of X-ray spectral slopes is real rather than due to the large measuring uncertainties for individual objects.

Author

N93-14761*# Ohio State Univ., Columbus. Dept. of Astronomy.
ATOMIC DATA AND SPECTRAL ANALYSIS OF CARBON, NITROGEN, OXYGEN AND SILICON IONS OBSERVED WITH THE INTERNATIONAL ULTRAVIOLET EXPLORER Progress Report
Anil K. Pradhan Nov. 1992 55 p
(Grant NAG5-1644; RF Proj. 769157/724904)
(NASA-CR-191302; NAS 1.26:191302) Avail: CASI HC A04/MF A01

According to the plan presented in the original proposal we have now completed most of the atomic calculations involving collision strengths and rate coefficients for electron impact excitation of C II, N III, and O IV ions. These have been reported in the first two publications appended with this report. We have now moved into the applications phase of the project with the new data being used to analyze the International Ultraviolet Explorer (IUE) observations of a variety of objects, as described in the third publication recently submitted (also appended). The analysis and interpretation of archival data will continue well into the next year with several collaborators that the PI and Co-PI are involved with. In addition, the atomic calculations on Si II have been started. For individual title, see N93-14762.

N93-14762*# National Aeronautics and Space Administration. Goddard Space Flight Center, Greenbelt, MD.
ELECTRON DENSITY DIAGNOSTICS FOR GASEOUS NEBULAE INVOLVING THE O 4 INTERCOMBINATION LINES NEAR 1400 A
F. P. Keenan (Queens Univ., Belfast, Northern Ireland), E. S. Conlon (Queens Univ., Belfast, Northern Ireland), D. A. Bowden (Queens Univ., Belfast, Northern Ireland), W. A. Feibelman, and Anil K. Pradhan (Ohio State Univ., Columbus.) *In* Ohio State Univ., Atomic Data and Spectral Analysis of Carbon, Nitrogen, Oxygen and Silicons Observed with the International Ultraviolet Explorer Nov. 1992 19 p Sponsored in cooperation with ESA, the Science and Engineering Research Council of the United Kingdom, and NATO (For primary document see N93-14761 04-89)
Avail: CASI HC A03/MF A01

Theoretical O IV electron density sensitive emission line ratios, determined using electron impact excitation rates calculated with the R-matrix code, are presented for R(sub 1) = I(1407.4 A)/I(1401.2 A), R(sub 2) = I(1404.8 A)/I(1401.2A), R(sub 3) = I(1399.8 A)/(1401.2 A), and R(sub 4) = I(1397.2 A)/I(1401.2 A). The observed values of R(sub 1)-R(sub 4), measured from high resolution spectra obtained with the International Ultraviolet Explorer (IUE) satellite, lead to electron densities that are compatible, and which are also in good agreement with those deduced from line ratios in other

species. This provides observational support for the accuracy of the atomic data adopted in the present calculations. Author

N93-14860 California Inst. of Tech., Pasadena.
QSO ABSORPTION LINES AND THE IONIZING FIELD AT HIGH REDSHIFTS Ph.D. Thesis
Lin Zuo 1992 206 p
Avail: Univ. Microfilms Order No. DA9232248

In this thesis we explore the relationship between the quasar (QSO) absorption line system and the metagalactic ionizing field at high z. In the first introductory chapter we describe the recent development in the field of QSO absorption lines and the ionizing radiation background. In the second chapter we discuss the absorptions produced QSO absorption line systems. We demonstrate that the spectrum of ionizing background is very different from the intrinsic source spectrum. We calculate the QSO contributions to J(nu sub L) (z sub obs). We show that it is very hard to find a 'clear' line of sight to conduct the HeII Gunn-Peterson test. We also show that dust grains in the damped Ly-alpha systems produce a marginally significant obscuration for QSO's: the count reduction factor is 1/1.7 at z = 3. The reddening in a flux limited QSO sample is small. In the following two chapters we discuss fluctuations and intensity correlation in the ionizing field. Absorptions by QSO absorption line systems reduce the total number of sources involved in producing the ionizing background and therefore enhance fluctuation significantly. We have calculated the intensity correlation function Xi(sub J) for randomly distributed QSO's. The Ly-alpha clouds can be used as intensity indicators to reveal Xi(sub J) at high z. We have measured the equivalent width correlation function Xi(sub 1)/W for several selected QSOs and have found, in some cases, strong correlation signals at small separations. If such signals are caused by the enhanced ionizing field near QSOs then J(nu sub L) is less than 10(exp -21) ergs s(exp -1) cm(exp -2) Hz(exp -1) sr(exp -1) at z approximately 3.5. The last two chapters deal with the ionization structure of Ly-alpha clouds. We solved the coupled ionization balance and radiation transfer problem for non-uniform spherical absorbing clouds and calculate the HI column density distribution f(N). We show that with an appropriate density gradient in the clouds we can reproduce the observed overall power law distribution and the apparent excess of absorption systems with N is less than or equal to 2 x 10(exp 20) cm(exp -2). We explore the variation of HeI and HeII distributions under different input ionizing spectra and discuss how to get a self-consistent spectral shape for the ionizing background. Dissert. Abstr.

N93-15203*# National Aeronautics and Space Administration. Marshall Space Flight Center, Huntsville, AL.
IMAGING THE SUN IN HARD X RAYS USING FOURIER TELESCOPES
J. W. Campbell Jan. 1993 277 p
(NASA-TM-108390; NAS 1.15:108390) Avail: CASI HC A13/MF A03

For several years, solar flares have been observed with a variety of instruments confirming that tremendous amounts of energy are locally stored in the solar magnetic field and then rapidly released during the life of the flare. In concert with observations, theorists have attempted to describe the means by which these energetic events occur and evolve. Two competing theories have emerged and have stood the test of time. One theory describes the flare in terms of nonthermal, electron beam injection into a thick target while the other uses a thermal approach. Both theories provide results which are reasonably consistent with current observations; but to date, none have been able to provide conclusive evidence as to the validity of either model. Imaging on short time scales (1 s) and/or small size scales (1 arc s) should give definitive answers to these questions. In order to test whether a realistic telescope can indeed discriminate between models, we construct model sources based upon the thermal and the nonthermal models and calculate the emission as a function of time and energy in the range from 10 to 100 keV. In addition, we construct model telescopes representing both the spatial modulation collimator (SMC) and the rotating modulation collimator (RMC) techniques of observation using random photon counting statistics. With these two types of telescopes we numerically simulate the instrument response to the above two model flares to see if there are distinct x-ray signatures which may be discernable. We find that theoretical descriptions of the primary models of solar flares do indeed predict different hard x-ray signatures for 1 sec time scales and at 1-5 arc sec spatial resolution. However, these distinguishing signatures can best be observed early in the impulsive phase and from a position perpendicular to the plane of the loop. Furthermore, we find that Fourier telescopes with reasonable and currently attainable design characteristics can image these signatures and that the same sensitive areas and short temporal integration times relative to source evolution (i.e., 1 s), the RMC and the SMC will both provide about the same performance. Author

N93-15340*# Smithsonian Institution, Cambridge, MA. Astrophysical Observatory.
ROSAT ALL-SKY SURVEY ON THE EINSTEIN EMSS SAMPLE Final Report, 1 Oct. 1990 - 30 Sep. 1992
Tomasso Maccacaro Nov. 1992 7 p
(Grant NAG5-1428)
(NASA-CR-191627; NAS 1.26:191627) Avail: CASI HC A02/MF A01

The cosmological evolution and the luminosity function (XLF) of X ray selected Active Galactic Nuclei (AGN's) are discussed. The sample used is extracted from the Einstein Observatory Extended Medium Sensitivity Surveys (EMSS) and consists of more than 420 objects. Preliminary results from the ROSAT All-Sky Survey data confirm the correctness of the optical identification of the EMSS sources, thus giving confidence to the results obtained from the analysis of the AGN's sample. The XLF observed at different redshifts (up to z approx. 2) gives direct evidence of cosmological evolution. Data have been analyzed within the framework of luminosity evolution models and the two most common evolutionary forms, L sub x(Z) = L sub x(0) x e(sup Cr) and L sub x(Z) = L sub x(0) x (1 + z)(exp C), have been considered. Luminosity dependent evolution is required if the evolution function has the exponential form, whereas the simpler pure luminosity evolution model is still acceptable if the evolution function has the power law form. Using the whole sample of objects the number-counts and the de-evolved (z = 0) XLF have been derived. A comparison of the EMSS data with preliminary ROSAT results presented at this meeting indicates an overall agreement. Author

N93-15425# Department of Energy, Washington, DC. Assistant Secretary for Defense Programs.
ENVIRONMENTAL ASSESSMENT FOR THE LASER GUIDE STAR EXPERIMENT AT LAWRENCE LIVERMORE NATIONAL LABORATORY
Mar. 1992 19 p
(DE92-040316; DOE/EA-0591) Avail: CASI HC A03/MF A01

Lawrence Livermore National Laboratory proposes to conduct a scientific project over a three to four year period, aimed at dramatically improving the quality of astronomical images obtainable by ground based telescopes. If successful, the research would demonstrate a technology for overcoming the atmospheric distortion that has traditionally limited ground-based astronomical observations, and would produce telescopic images as high in resolution as if the telescopes were located in space. The proposed project would provide an opportunity for a collaboration involving scientists from LLNL, three University of California campuses, and two major observatories. One major problem in attempting to interpret astronomical light images propagated through the atmosphere is to compensate for atmospheric turbulence. The approach for eliminating the effects of atmospheric distortion or turbulence on astronomical images is to precisely measure the effects of distortion on a single star or other constant point light source and compensate for the distortion effects by rapidly altering the shape of a deformable mirror in the observation system. For the proposed action at LLNL, the key environmental consideration is protection of pilots and passengers of aircraft that stray into the vicinity of LLNL while the laser beam is being directed toward the sky. To that end, laser operations would occur during off hours midnight to 4 a.m. and at a low frequency, 2 - 3 times per week, in addition to utilizing a Livermore area safety system based on successful safety programs developed by the Air Force and other organizations while conducting similar atmospheric research using lasers. This safety system will contain surveillance wide area, scanning and boresight static and narrow cone angle centered on the beam radars designed to detect intrusion by aircraft within the area of the laser beam, coupled with an interlock system that will shut down the beam automatically if such intrusions occur. DOE

N93-15589*# Columbia Univ., New York, NY. Dept. of Astronomy and Physics.
DEVELOPMENT OF A HIGH RESOLUTION LIQUID XENON IMAGING TELESCOPE FOR MEDIUM ENERGY GAMMA RAY ASTROPHYSICS Annual Status Report, 1 Jan. - 31 Dec. 1992

Elena Aprile Dec. 1992 31 p
(Grant NAGw-2013)
(NASA-CR-191781; NAS 1.26:191781) Avail: CASI HC A03/MF A01

In the third year of the research project, we have (1) tested a 3.5 liter prototype of the Liquid Xenon Time Projection Chamber, (2) used a prototype having a 4.4 cm drift gap to study the charge and energy resolution response of the 3.5 liter chamber, (3) obtained an energy resolution as good as that previously measured by us using chambers with drift gaps of the order of millimeters, (4) observed the induction signals produced by MeV gamma rays, (4) used the 20 hybrid charge sensitive preamplifiers for a nondestructive readout of the electron image on the induction wires, (5) performed extensive Monte Carlo simulations to obtain results on efficiency, background rejection capability, and source flux sensitivity, and (6) developed a reconstruction algorithm for events with multiple interaction points. For individual titles, see N93-15590 through N93-15592.

N93-15590*# Columbia Univ., New York, NY. Dept. of Physics and Astronomy.

A MONTE CARLO ANALYSIS OF THE LIQUID XENON TPC AS GAMMA RAY TELESCOPE

E. Aprile, A. Bolotnikov, D. Chen, and R. Mukherjee *In its* Development of a High Resolution Liquid Xenon Imaging Telescope for Medium Energy Gamma Ray Astrophysics Dec. 1992 6 p Presented at the International Conference on Liquid Detectors, Tokyo, Japan, 7-10 Apr. 1992 (For primary document see N93-15589 04-89)
(Grant NAGw-2013)
Avail: CASI HC A02/MF A01

Extensive Monte Carlo modeling of a coded aperture x ray telescope based on a high resolution liquid xenon TPC has been performed. Results on efficiency, background reduction capability and source flux sensitivity are presented. We discuss in particular the development of a reconstruction algorithm for events with multiple interaction points. From the energy and spatial information, the kinematics of Compton scattering is used to identify and reduce background events, as well as to improve the detector response in the few MeV region. Assuming a spatial resolution of 1 mm RMS and an energy resolution of 4.5 percent FWHM at 1 MeV, the algorithm is capable of reducing by an order of magnitude the background rate expected at balloon altitude, thus significantly improving the telescope sensitivity. Author

N93-15591*# Columbia Univ., New York, NY. Dept. of Physics and Astronomy.

A LIQUID XENON IMAGING TELESCOPE FOR GAMMA RAY ASTROPHYSICS: DESIGN AND EXPECTED PERFORMANCE

E. Aprile, R. Mukherjee, D. Chen, and A. Bolotnikov *In its* Development of a High Resolution Liquid Xenon Imaging Telescope for Medium Energy Gamma Ray Astrophysics Dec. 1992 9 p Presented at the 3rd International Conference on Advanced Technology and Particle Physics, Como, Italy, 22-26 Jun. 1992 (For primary document see N93-15589 04-89)
(Grant NAGw-2013)
Avail: CASI HC A02/MF A01

A high resolution telescope for imaging cosmic x ray sources in the MeV region, with an angular resolution better than 0.5 deg is being developed as balloon-borne payload. The instrument consists of a 3-D liquid xenon TPC as x ray detector, coupled with a coded aperture at a distance of 1 meter. A study of the actual source distribution of the 1.809 MeV line from the decay of Al-26 and the 511 keV positron-electron annihilation line is among the scientific objectives, along with a search for new x ray sources. The telescope design parameters and expected minimum flux sensitivity to line and continuum radiation are presented. The unique capablity of the LXe-TPC as a Compton Polarimeter is also discussed. Author

N93-15592*# Columbia Univ., New York, NY. Dept. of Physics and Astronomy.

LIQUID XENON TIME PROJECTION CHAMBER FOR GAMMA RAYS IN THE MeV REGION: DEVELOPMENT STATUS

E. Aprile, A. Bolotnikov, D. Chen, and R. Mukherjee *In its* Development of a High Resolution Liquid Xenon Imaging Telescope for Medium Energy Gamma Ray Astrophysics Dec. 1992 13 p Presented at the Gamma Ray Detectors Conference of the SPIE's International Symposium on Optical Engineering, 19-24 Jul. 1992 (For primary document see N93-15589 04-89)
(Grants NAGw-2013; NSF PHY-91-09937)
Avail: CASI HC A03/MF A01

The feasibility of a large volume Liquid Xenon Time Projection Chamber (LXe-TPC) for three dimensional imaging and spectroscopy of cosmic gamma ray sources, was tested with a 3.5 liter prototype. The observation of induction signals produced by MeV gamma rays in liquid xenon is reported, with a good signal-to-noise ratio. The results represent the first experimental demonstration with a liquid xenon ionization chamber of a nondestructive readout of the electron image produced by point-like charges, using a sense wire configuration of the type originally proposed in 1970 by Gatti et al. An energy resolution as good as that previously measured by the millimeter size chambers, was achieved with the large prototype of 4.4 cm drift gap. Author

90 ASTROPHYSICS

Includes cosmology; celestial mechanics; space plasmas; and interstellar and interplanetary gases and dust.

For related information see also *75 Plasma Physics*.

N93-14112 Illinois Univ. at Urbana-Champaign, Savoy.

DYNAMICS IN NEUTRON STARS AND THE EARLY UNIVERSE Ph.D. Thesis

Bennett Karl Link 1991 123 p
Avail: Univ. Microfilms Order No. DA9210897

Observations of pulsar timing suggest that glitches and post-glitch behavior are due to variable coupling between the superfluid and normal components in neutron stars. A rotating superfluid is threaded by quantized vortex lines which, in the inner crust of a neutron star, can pin to the nuclear lattice that coexists with the superfluid. The dynamics of the superfluid is described by the motion of these lines. Vortices overcome their pinning barriers through thermal activation or quantum tunneling, and 'creep' slowing outward under forces created by the superfluid flow. To the extent that vortices remain pinned, the superfluid retains its angular momentum as the crust slows through interactions with its environment. Catastrophic unpinning of vortices could lead to sudden dissipative coupling between the superfluid and the crust thus creating glitches, while post-glitch relaxation is likely due to the recovery of the vortex creep rate to the steady state. To explore this model, we develop a microscopic quantum theory for vortex unpinning and creep based on first principles. In considering a range of vortex pinning parameters obtained theoretically, we estimate the vortex creep rate throughout the inner crust. We make predictions for the form and time scales of post-gitch response, and compare with timing data from the Vela and Crab pulsars. In the second part of the thesis, we study the quark-hadron phase transition in the early universe assuming the transition in first order. First order phase is nucleated which expands at the expense of the old phase. Using relativistic hydrodynamics, we study the propagation of hadron bubbles with surface tension. We demonstrate the hydrodynamic instability of deflagration processes, and discuss possible consequences for baryon concentration effects relevant in later nucleosynthesis. Dissert. Abstr.

N93-14113 Edinburgh Univ. (Scotland).

THE STRUCTURE AND DYNAMICS OF AN ENVIRONMENT FORMING HIGH-MASS STARS Ph.D. Thesis

Toby John Terry Moore 1989 183 p
Avail: Univ. Microfilms Order No. BRD-93943

A detailed investigation is presented of the physical environment associated with high mass star formation. This is carried out by means of an in-depth multi-wavelength study of one such region in W75N. An analysis is made of the nature of the major embedded luminosity sources and the cloud core from which they have recently formed, from the hot dust very close to each object to the cold dust and molecular gas surrounding them. The dynamical relationship between the large molecular outflow and the ambient cloud is studied with regard to limitations that might be placed on plausible flow generation mechanisms. A recently formed stellar cluster was found, associated with the known signs of high mass star formation in W75N. The main heating source and origin of the molecular outflow is identified and found to be very deeply embedded. Very small scale (few X100 A.U.) disk-like formations may exist and play an important dynamical

role. The large molecular outflow in W75N is found to be unable to overcome the gravitational binding force of the large surrounding core unless the flow is initially highly collimated. The lobes of high velocity gas possess a large degree of collimation, probably induced through confinement by the ambient material, but the outflow as a whole is irregular and possibly multipolar and appears to be intrinsically largely isotropic. Of the two reflection nebulae in the region the largest and brightest is associated with the blue-shifted molecular outflow lobe. Features in the nebula, similar to those in other such objects, are consistent with scattering from large grains which produce diffraction-affected and strongly forward-biased scattering patterns. It is shown that large grains should dominate the scattering in the near-infrared, regardless of the detailed grain size distribution. The ubiquitous suppression of backward-directed reflection lobes in bipolar sources may be caused by forward scattering and not by large obscuring disks. Dissert. Abstr.

N93-14134# Texas Univ., Austin.
PERTURBATIONS OF THE ROBERTSON-WALKER SPACE Ph.D. Thesis
Jai Chan Hwang 1992 396 p
Avail: Univ. Microfilms Order No. DA9225611

This dissertation contains three parts consisting of thirteen chapters. Each chapter is self-contained, and can be read independently. In chapter 1, we have presented a complete set of cosmological perturbation equations using the covariant equations. We also present an explicit solution for the evolution of large scale cosmological density perturbations assuming a perfect fluid. In chapter 2, two independent gauge-invariant variables are derived which are continuous at any transition where there is a discontinuous change in pressure. In chapter 3, we present a Newtonian counterpart to the general relativistic covariant approach to cosmological perturbations. In chapter 4, we present a simple way of deriving cosmological perturbation equations in generalized gravity theories which accounts for metric perturbations in gauge-invariant way. We apply this approach to the f(phi,R)-omega(phi)phi, (sub c)phi(sup ;c) Lagrangian. In chapter 5, we have derived second order differential equations for cosmological perturbations in a Robertson-Walker space, for each of the following gravity theories: f(R) gravity, generalized scalar-tensor gravity, gravity with non-minimally coupled scalar field, and induced gravity. Asymptotic solutions are derived for the large and small scale limits. In chapter 6, classical evolution of density perturbations in the large scale limit is clarified in the generalized gravity theories. In chapter 7, we apply our method to a theory with the Lagrangian L approximately f(R) + gamma RR(sup ;c)(sub ;c). In chapter 8, T(M)(sup ab)(sub ;b) equals 0 is shown in a general ground. In chapter 9, the origin of the Friedmann-like behavior of the perturbed model in the large scale limit is clarified in a comoving gauge. Thus, when the imperfect fluid contributions are negligible, the large scale perturbations in a nearly flat background evolve like separate Friedmann models. In chapter 10, we generalize the perturbation equations applicable to a class of generalized gravity theories with multi-component fluids and fields as sources. In chapter 11, comparisons are made with the synchronous gauge results. In chapter 12, we present the solutions of cosmological perturbations for ideal-fluid medium with constant pressure (p) to density (mu) relation in flat Robertson-Walker background model. Both exact and asymptotic solutions are shown in tabular forms. In chapter 13, a heuristic derivation of the perturbation solution, by simply perturbing the Friedman equation, is shown to be fully grounded. As a consequence, the existence of a large scale conserved quantity is explained in a heuristic way without losing any rigor. This conserved quantity is explained in a heuristic way without losing any rigor. This conserved quantity also implies a separate Friedmann-like evolution of each perturbed part of the universe in the large scale limit. Dissert. Abstr.

N93-14136 Columbia Univ., New York, NY.
A STUDY OF THE ABUNDANCE DISTRIBUTIONS ALONG THE MINOR AXIS OF THE GALACTIC BULGE Ph.D. Thesis
Neil DeGrasse Tyson 1992 369 p
Avail: Univ. Microfilms Order No. DA9221224

I present abundance distribution functions for fields along the minor axis of the Galactic bulge based on CCD photometric observations toward seven windows of low extinction. Abundance distribution functions are the most useful form of data to constrain models of the star formation and the chemical enrichment of the bulge. By using the recently-calibrated Washington photometric filter system, the distribution function in (Fe/H) is determined for each field, and consequently I derive the abundance gradient for the bulge. To supplement these observations I analyzed, from medium dispersion spectra, line strengths of the 33 known bulge carbon stars. The radial velocities of these carbon stars and of 39 bulge RR Lyrae variables is also presented. Within 8 degrees of the Galactic center (approximately 1 kpc) there appears to be no appreciable gradient in the distribution of (Fe/H), which is consistent with a dissipationless collapse, and/or sufficient mixing during the star-forming epoch when Fe was produced in the bulge. The mean abundance over this region is between two and five times solar. The form of these distributions is well-fitted by the simple (closed box) model of chemical evolution where the bulge is self-enriched by processing its original gas content to completion. This result carries two direct implications: (1) the inner bulge was not significantly enriched by infall (of any heavy element abundance) from the halo or the disk, and (2) the inner bulge underwent no catastrophic mass-loss from supernova-driven winds or any other mechanism. These scenarios would produce a different signature in the abundance distributions. Beyond 8 degrees from the Galactic center, the mean of the abundance distribution drops precipitously with an abundance gradient of -0.2 dex/degree in (Fe/H). This is consistent with the notion that the inner bulge is chemically distinct from the halo while the transition region is a blending of the two. It may be possible to use kinematics to disentangle the two populations via a radial velocity survey. Dissert. Abstr.

N93-14147 Arizona Univ., Tucson.
THE THEORY AND NUMERICAL SIMULATION OF NON-LOCAL MIXING-LENGTH CONVECTION Ph.D. Thesis
Scott Alan Grossman 1992 357 p
Avail: Univ. Microfilms Order No. DA9225182

Local convection theory makes the unphysical prediction that turbulent mixing terminates at the Schwarzschild stability boundary, and existing non-local convection theories have been criticized by Renzini (1987). Since the size of convecting cores bears upon stellar structures and evolution, a self-consistent treatment of non-local convection is needed. We have developed a theory of non-local mixing-length convection based upon a Boltzman transport theory for subsonic, turbulent fluid elements. The momentum and thermal energy excesses of fluid elements are dissipated on the scale of a mixing length. The distribution function, f(t,z,v,T), which is the mass density per velocity-temperature phase space volume, evolves according to the Boltzman equation. The minimal non-local theory is obtained by taking moments of the Boltzman equation, up to third order. The local limit of the moment equations reduces to standard mixing-length theory. We extend this moment method to local convection in a composition stratified fluid by considering the evolution of the distribution function, f(t,z,v,T,mu), in velocity-temperature-molecular weight phase space. The stability criteria for convection, semiconvection, and salt-finger instability are derived. To determine closure approximations and evaluated the validity of the moment theory, we have developed an algorithm called Generalized Smooth Particle Hydrodynamics (GSPH) that numerically simulates convection. The vertical structure of the background fluid is calculated by SPH averaging of particles on a grid. Forces on particles are calculated from the background grid and from the local deviations between particles and grid. Particles move vertically only, but the local deviation forces, which account for turbulent losses of momentum and energy, arise from horizontal interactions. GSPH simulations show that the fourth moments are approximately proportional to squares of the second moments in unstable regions, with a proportionality constant between 2 and 4. With this closure approximation, we show that solutions of the moment equations agree well with GSPH results. The closure relations lead to nearly correct second moments, even in overshooting regions where the closure approximations are poor. GSPH simulations of convections of convective overshooting in plane parallel and spherical geometry typically give overshooting distances in the range d(sub over) approximately equal to 1-2 l(sub M). We discuss improvements that we would like to make to the GSPH code and to the analytic work to obtain more precise answers that are directly relevant to realistic stars. Dissert. Abstr.

N93-14148 Texas Univ., Austin.
THE BLACK HOLE CANDIDATE BINARY A0620-00 Ph.D. Thesis
Carole Ann Haswell 1992 332 p
Avail: Univ. Microfilms Order No. DA9225593

The compact object in A0620-00 was previously established as a

leading black hole candidate by observations implying a minimum compact object mass, M sub 1 approx. = 3M solar magnitude. To exclude the possibility of a neutron star primary, the constraints on M sub 1 need to be improved. Two avenues of investigation were pursued. The mass ratio of the system, q = M sub 1/M sub 2, was determined by observations of the radial velocity variations of the H(alpha) emission from the accretion disk around the compact object. If the wavelength shifts give an unbiased estimate of the orbital motion of the compact object, q = 10.6 + or - 2.0. However contamination by nonaxisymmetric disk emission is indicated, so q is more uncertain than the reported formal errors. The orbital inclination of the system was examined by modelling of multicolor orbital light curves, which exhibit ellipsoidal variations. The ellipsoidal amplitudes imply a spectra type of K3-K4 for the mass donor. Light curves obtained in 1986/1987 exhibit a grazing eclipse of the mass donor star by the accretion disk, providing tight constraints on the orbital inclination and the radius of the accretion disk. The accretion disk radius is comparable to the tidal radius. Limits on the orbital inclination were derived which lead to limits on the mass of the compact object: 5.50 + or - 0.15 less than or + = M sub 1 less than or = 6.26 + or - 0.17 for q = 5.0; 4.28 + or - 0.12 less than or = M sub 1 less than or = 4.86 + or - 0.13 for q = 10.6; 3.79 + or - 0.10 less than or = M sub 1 less than or = 4.68 + or - 0.13 for q = 15.0. A lower limit on the mass ratio, q greater than 6.47, is established by demanding that M sub 2 less than or = 0.85 M solar magnitude, the mass of a Roche lobe-filling main sequence star. The spectral type of the mass donor implies that q is greater than 10.6 is unlikely. Hence the results imply M sub 1 greater than or = 4.28 + or - 0.12, which is well above the upper limit on the mass of a neutron star. This is compelling evidence in favor of a black hole primary in A0620-00. Dissert. Abstr.

N93-14149 Texas Univ., Austin.
SUBMILLIMETER AND INFRARED SPECTROSCOPY OF MOLECULAR CLOUDS NEAR O AND B STARS Ph.D. Thesis
John Edward Howe, Jr. 1992 136 p
Avail: Univ. Microfilms Order No. DA9225605

The structure and physical properties of molecular cloud boundaries illuminated by ultraviolet radiation from nearby or embedded O and B stars are investigated by observing atomic and molecular emission lines. The selected lines are sensitive to the local gas conditions and to the distribution of the UV field. Since the excitation of interstellar gas by UV photons extends to depths comparable to all but the highest column densities of gas in clouds illuminated by nearby OB stars, it is necessary to learn the physical conditions in the UV-illuminated gas if we are to understand the properties of the bulk of the mass of the interstellar medium. We mapped the spatial distribution of the 158 micron (C II) fine-structure line in the star-forming region W3, the ionization front NGC 1977, and the reflection nebula NGC 2023 to investigate the outer atomic layers of the UV-illuminated molecular gas. The (C II) emission arises from warm (100-300 K), dense (n(sub H) greater than 10(exp 4) cm(exp -3)) photodissociation regions extending over parsec scales or greater. Clumpy or filamentary clouds with a density contrast of 100 or more can explain the distribution and intensity of the emission by allowing deep penetration of carbon-ionizing UV photons into the clouds. We observed near-IR H2 rovibrational lines in NGC 2023 to examine the properties of the outermost molecular gas layers. The density is high (n(sub H2)) approx. greater than 10(exp 5) cm(exp -3) right to the boundary of the molecular gas. The UV field dominates the heating and drives the temperature as high as approximately 500 K. At these temperatures and densities, collisional excitation becomes important in determining the H2 level populations. We mapped the distribution of emission from the J = 7 to 6 transition of CO in Orion to study the properties and structure of regions further into the UV-dominated molecular layers. We observe quiescent emission from gas with temperatures greater than 40 K extending over 2 pc. The temperature peaks to greater than 160 K at the position of Ori theta(exp 1)C, more than twice the dust temperature. Multiple velocity components in the CO (7 to 6) lines suggest that the emission arises from photodissociation regions on the surfaces of several clumps or filaments embedded with the cloud. Dissert. Abstr.

N93-14154 Texas Univ., Austin.
GRAVITATIONAL INSTABILITIES IN A PROTOPLANETARY DISK Ph.D. Thesis
Hye-Rim Noh 1992 105 p
Avail: Univ. Microfilms Order No. DA9225688

Motivated by current observational evidence for circumstellar disks associated with young stellar objects and pre-main sequence stars, we investigate the gravitational instability of a thin, Keplerian protoplanetary disk without a magnetic field (ch 2) and including magnetic field effects (ch 3). The disk is a two fluid system, consisting of gas and dust (ch 2), or a three fluid system, consisting of neutral gas, ionized gas, and neutral dust (ch 3), coupled by gravity and friction. The growth rates and the eigenfunctions are calculated numerically using non-axisymmetric linear perturbation methods. In both cases, we find that for the usual values of input parameters (e.g., mass of disk) the disk is unstable to non-axisymmetric perturbations for some range of azimuthal wavenumber m in addition to m equals 1. The growth rate has a well defined maximum in m and the number of radial nodes. The inclusion of magnetic fields generally reduces the growth rates for each m, and the values of m where the maximum instability occurs. We also study the effect of different boundary conditions (reflecting and transmitting) on the growth rates. The boundary conditions affect the instability only for small m modes. We also present the effect of various properties of dust on the instability and the change of the growth rate due to the change of parameters. In particular, the effect of the ionization abundance on the growth rates is examined for disks including a magnetic field. The inclusion of dust usually enhances the instability, although dust is a small component in mass and the gravitational potential is usually dominated by the gas component. Our study is also concentrated on the stability of the m equals 1 mode (ch 4). We find that different physical mechanisms affect the m equals 1 instability for high disk mass and for low disk mass. For high disk mass, the growth rates are mainly determined by the sling amplification which is associated with the indirect potential. For low disk mass, the swing amplification and the coupling between the swing and sling mechanisms are important in driving the instability. The sensitivity of the swing amplification to Toomre's stability parameter Q is somewhat reduced by the decreasing distance between the corotation and the outer disk edge as the disk mass decreases. Dissert. Abstr.

N93-14194 California Univ., Berkeley.
CALIBRATION OF THE CCD TULLY-FISHER RELATION WITH APPLICATION TO THE PERSEUS-PISCES SUPERCLUSTER Ph.D. Thesis
Jeffrey Alan Willick 1991 433 p
Avail: Univ. Microfilms Order No. DA9228913

Tau band CCD photometric data for a sample of over 500 spiral galaxies is presented. These data were obtained from CCD images acquired at the Lick Observatory 40 inch Nickel Telescope. All of the galaxies in the sample have quality 21 cm (HI) redshift and linewidth data, which I have obtained from the published literature. I use the CCD photometric and HI data for a subsample of 156 cluster galaxies to study the properties of the luminosity-rotation velocity ('Tully-Fisher') relation for spirals. I show how the imaging character of the CCD photometry permits the definition of highly accurate total apparent magnitudes and ellipticites for the galaxies, which in turn lead to a Tully-Fisher relation with small scatter (sigma approximately equals 0.30 mag). My analysis also produces a calibration of the Tully-Fisher relation. This calibration entails zeropointing the Tully-Fisher relation at the distance of the Coma cluster, and measuring the expansion rate of the Universe in units of velocity/(distance to Coma). I apply the calibrated Tully-Fisher relation to another subsample of 330 field galaxies in the Perseus-Pisces Supercluster region. My results indicate that the highly overdense filament, or 'main ridge', of the Perseus-Pisces concentration is moving toward the Local Group with a peculiar velocity of amplitude approximately 350 km s(exp -1). I note that this motion, in combination with other streaming motions previously detected in the local Universe, argues for the presence of a very long wavelength component of the peculiar velocity field. I place great emphasis on the critical role played by statistical biases in the analysis of Tully-Fisher data sets. I distinguish, and examine in quantitative detail, two kinds of bias: one which affects predicted apparent magnitudes when galaxy distances are given by a physical model, such as the redshift-distance relationship; and another which affects redshift-independent distances inferred directly from the Tully-Fisher data. My analysis leads to accurate mathematical formulae for bias correction. I apply these formulae to the data in both my calibration of the Tully-Fisher relation, and my study of peculiar velocities in Perseus-Pisces. Dissert. Abstr.

N93-14230 Johns Hopkins Univ., Baltimore, MD.
PHYSICAL AND CHEMICAL PROCESSES OF THE INNER COMA OBSERVED IN MID-ULTRAVIOLET COMETARY SPECTRA Ph.D. Thesis
Scott Alan Budzien 1992 227 p
Avail: Univ. Microfilms Order No. DA9229300

Accurate measurement of cometary H2O is essential for comparing the compositions and understanding the properties of cometary nuclei. Water production rates Q sub H2O are easily derived from observations of OH solar resonance fluorescence with the International Ultraviolet Explorer (IUE) satellite. Variable solar activity and several inner coma processes affect the estimates of Q sub H2O using IUE. Water photodissociation by solar Lyman-alpha radiation creates OH(A(exp 2)Sigma(+) radicals, which quickly decay to OH(X)sup2 II) through spontaneous emission. This 'prompt' emission can provide a direct measure of Q sub H2O, if observed at sufficiently high spatial resolution. Spectral observations of comets IRAS-Araki-Alcock (1983 VII) and Tuttle (1980 XIII), differing only in effective spatial resolution, show evidence for OH prompt emission in IRAS-Araki-Alcock. The scale length of the short-lived molecule S2 is re-evaluated from IUE spectra of Comet IRAS-ARAKI-Alcock. Spectra of other comets are analyzed to determine S2 abundances relative to H2O and reveal no other detections of S2, but upper limits comparable to values observed in IRAS-Araki-Alcock. The sole exception is significant: the upper limit on S2/H2O in Comet Austin (1989c1) indicates true variation in the relative S2 abundance between comets. Solar resonance fluorescence can create a population inversion of the Lambda states of the OH molecule, but ions collisionally quench the inversion to affect both the UV fluorescence and the 18 cm maser emissions. Previous models of the quenching of OH radio emission do not account for both kinds of observations simultaneously, and do not include solar variability or a Swings effect. A quenching model based upon Giotto observations of Comet P/Haley appropriate for IUE observations is developed and compared to results from high resolution IUE spectra. The solar UV flux determines the photodestruction rates of H2O and OH and affects their spatial density distributions. Lifetimes appropriate to varying levels of solar activity are calculated from cross section measurements and a solar UV flux model. Spatial mapping by IUE of the OH comae of several comets observed at different epochs of solar activity are matched by modeled density distributions. The evolution of Q sub H2O with respect to heliocentric distance of comets Bradfield (1979X) and Austin (1989c1) is determined. Dissert. Abstr.

N93-14243 Michigan Univ., Ann Arbor.
OPTICAL SIGNATURES OF COOLING FLOWS IN ISOLATED EARLY-TYPE GALAXIES Ph.D. Thesis
Susana Elizabeth Deustua 1992 142 p
Avail: Univ. Microfilms Order No. DA9226884

This thesis examines the expected consequences of cooling flows in individual early-type galaxies by studying whether the structure of the cool interstellar medium is related to the hot gas. In a cooling flow the hot gas is expected to cool and produce cold gas at the astrophysically interesting rate of 0.1 to 10 solar mass per year. In order to test these expectations, an observing program to search for optical emission was developed. The observing program consists of long-slit spectroscopy and imaging of a sample of 40 early-type galaxies with a range of X-ray luminosities and hot gas masses. The observations cover the wavelength range of 4500-5200 and 5900-7100 where the strongest lines are H-beta, (OIII) 4959,5007, (OI) 6300, (NII) 6548,6584, H-alpha and (SII) 6715,6731. The data were processed and analyzed using standard techniques. In order to remove the stellar component, the galaxy spectra were subtracted by a template. We fail to find the expected relationship between the cooling rate of the hot gas and the luminosity of the 10(exp 4) K gas, or between the hot gas cooling time and emission line luminosity. We find evidence that supports an intrinsic origin for the 10(exp 4) K gas. The 10(exp 4) K gas has masses of 10(exp 3) to 10(exp 7) solar mass, electron densities of n(sub e) less than 10 cm(exp -3) to n(sub e) = 1.5 X 10(exp 3 cm(exp -3), and electron pressures of P/k = 10(exp 4)cm(exp -3)K to 10(exp 7) cm(exp -3)K. The pressure of this 10(exp 4) K gas is comparable and often greater than the pressure in the surrounding hot gas. The line emission detection rate of 60 percent is consistent with the result of other surveys of early-type galaxies. We find a relationship between dust emission of 60 microns and 100 microns and the 10(exp 4) K gas, suggesting a common ionization and heating source for the dust and optical gas. Photoionization from post asymptotic giant branch stars is the most likely source of ionization for the gas, vitiating collisional ionization or an active galactic nucleus. We concluded that if optical signatures of cooling flow are present, they are masked by other processes. Dissert. Abstr.

N93-14444 Johns Hopkins Univ., Baltimore, MD.
ULTRAVIOLET SPECTROSCOPY OF COMET AUSTIN (1989c1) USING A TWO-DIMENSIONAL DIODE ARRAY DETECTOR Ph.D. Thesis
David James Sahnow 1992 203 p
Avail: Univ. Microfilms Order No. DA9229401

A two-dimensional, photon-counting intensified photodiode array detector has been constructed and successfully tested in the laboratory and on a spectrograph in three sounding rocket flights. The detector is an extension of the one-dimensional intensified diode array detector used in the Hopkins Ultraviolet Telescope. Extensive laboratory measurements have shown that it can successfully centroid with sub-diode resolution, and can be used in place of ranicon detectors to measure the spectra of faint objects. The instrument successfully obtained long slit far-ultraviolet spectra (1250-1850 A) of Comet Austin (1989 c1) on 21 April 1990. Emissions of OI, CI, SI and CO were detected during the 270 seconds of data acquisition. The spectral resolution was 5.5 A, while the spatial resolution was limited by pointing jitter to approximately 30 arcseconds. The spatial profiles of the carbon and oxygen emissions show narrow enhancements which are suggestive of a cometary outburst which occurred 15-20 hours before the observation. The overall shape of the atomic carbon profile is similar to those measured during two observations of Comet Halley (1986 III), and is similarly incompatible with photodissociation of CO as its primary source, as determined by model calculations. The CO profile, however, is consistent with that of a parent molecule evaporating directly from the nucleus, with a production rate of 4 plus or minus 1 x 10(exp 27) molecules s(exp -1). The O I lambda 1304 emission, also similar in spatial shape to that detected in Halley, includes a contribution due to Bowen fluorescence induced by solar HI Lyman-beta, and its profile can be understood as that due to the photodissociation of H2O, with a production rate of 6.2 plus or minus 0.3 x 10(exp 28) molecules s(exp -1), giving an abundance of CO relative to water of 6.5 percent. Spatial profiles of SI lambda 1814 were also obtained, with profiles attributable to that of a daughter product of short-lived species such as CS2 and H2S. Dissert. Abstr.

N93-14460 Oxford Univ. (England).
DISC STRUCTURE AND VARIABILITY IN DWARF NOVAE Ph.D. Thesis
Emilios Theofanus Harlaftis 1991 270 p
Avail: Univ. Microfilms Order No. BRD-96776

An introduction is given to dwarf novae reviewing the current research status in the field. We present IUE observations of Z Cha which support the mass transfer instability as the cause of the superoutbursts observed in SU UMa type dwarf novae. Comparison between the superoutburst and a normal outburst of Z Cha shows that the disc is flatter and has significantly less azimuthal structure than during superoutburst. Z Cha exhibits a soft x-ray deficit during superoutburst compared to OY Car. We find that the secondary star of Z Cha contributes approximately 30 percent of the infrared flux at peak of outburst. The second part of the thesis presents results from the 1988 International Time Project at the Observatorio del Roque de los Muchachos. Investigation of the behavior of SU UMa and YZ Cnc is carried out through the outburst cycle. The secular changes of the equivalent widths of both systems shows an increasing trend even during quiescence and are caused by the continuum decrease. Both systems show a low-velocity emission component which contaminates the wings of the H(alpha) profile. In addition to doppler broadening, the Stark effect is found to cause significant broadening to the line profile. The radial dependence of the emission lines is discussed in relation to other cataclysmic variables. H(alpha) emission from the secondary star of YZ Cnc is found during superoutburst, during outburst and during quiescence after outburst. Photometry during late decline of outburst shows a sinusoidal, weak variation peaking at 0.5 orbital phase and which is related to heating of the red star or to a transient disc event. During quiescence, the flickering is found to be caused by the bright spot. This modulation increases with time and is maximum before the outburst. Doppler tomography of IP Peg during quiescence reveals an emission line distribution not consistent to the standard model. We find Balmer emission from the secondary star, at a level of only 2.5 percent of the total flux during quiescence. Simultaneously to this, line emission from the outer disc decreases by approximately 70

percent 5 days before an outburst. Finally, the main findings of this thesis are summarized and resulting constraints for the outburst mechanism are discussed. Dissert. Abstr.

N93-14461 California Univ., Berkeley.
PHYSICAL PROPERTIES OF EXTENDED EMISSION-LINE REGIONS IN ACTIVE AND COOLING-FLOW GALAXIES Ph.D. Thesis
Joseph Charles Shields 1991 227 p
Avail: Univ. Microfilms Order No. DA9228854

This dissertation utilizes primarily optical observations of extended emission-line regions in active and cooling-flow galaxies to clarify the nature of this nebulosity and its underlying sources of energy. In particular, I employ case studies of Seyfert galaxies in order to elucidate nuclear properties as seen in light that is apparently scattered into our line of sight, and to provide direct measurements of emission-line intensity ratios resulting from a radially diluted photoionizing continuum for comparison with theory. The apparent Seyfert 2 galaxy NGC 4388 displays weak, spatially extended broad-line emission that is most readily understood as scattered light from a hidden Seyfert 1 nucleus. 1C 5135 exhibits both Seyfert 2 and starburst activity in its nucleus, and the influence of both can be traced in nuclear emission-line profiles as well as line intensity ratios of spatially resolved nebulosity. I also report results bearing on star formation and the rate of mass accretion in the cluster cooling-flow galaxy NGC 1275, as revealed from spectroscopy of the nebular filaments in this system. While preferential low mass star formation has been invoked to reconcile high x-ray-inferred accretion rates in cooling flows with a paucity of apparent cooled matter, data reported here reveal a site of high mass star formation in material believed to arise from the flow. Detailed scrutiny of this region suggests, moreover, that the initial mass function of star formation in this locale is unlikely to be unusually biased toward low mass star formation. These results provide additional evidence that the true rate of mass deposition may be less than implied by a simple interpretation of the x-ray data. The same data set is used to derive improved upper limits to the coronal emission features (Fe X) lambda 6374, which is expected to scale with the true rate of mass cooling to low temperatures. The ability of these measurements to constrain the accretion rate is limited by exclusion of the galaxy center, which is host to a Seyfert nucleus. Finally, I present results of a narrow-band imaging survey of x-ray-selected, early-type galaxies that are examined for evidence linking nebulosity in these sources to cooling-flow or weak Seyfert phenomena. The results suggest that optical nebulosity in these systems probably bears a multiparameter relationship to cooling flows, active nuclei, and accretion from external sources.
Dissert. Abstr.

N93-14584 Universitaire Instelling Antwerpen, Wilrijk (Belgium).
STABILITY OF DIFFERENTIALLY ROTATING STARS Ph.D. Thesis
Patrick Luyten 1992 195 p
Avail: Univ. Microfilms Order No. DA9231867

The instabilities, created by differential rotation, in rotating self-gravitating masses are investigated. We use a normal mode and analysis and consider primarily long-wavelength disturbances affecting the global structure of the mass. There exist three types of instabilities. The first one only occurs within a restricted part along the sequence which in the limit of uniform rotation reduces to a bifurcation point of the Maclaurin sequence. For the lowest order (m = 2) harmonic we show that this instability enforces an evolution towards a uniformly rotating stable Jacobi ellipsoid. Contrary to previous studies of shear instabilities, the unstable mode is not always situated inside the corotation spectrum. The second type is a short-wavelength instability created by an infinite discrete spectrum of unstable modes located inside the corotation spectrum. By making the disk approximation we show that the source of this instability is the wave-overreflection mechanism. The third type only occurs for disturbances which have a component along the rotation axis. They resemble the first type although the origin of the instability seems unclear. Possible applications to the structure of main-sequence stars and white dwarfs are discussed. We formulate also a new version of the fission theory. Dissert. Abstr.

N93-14592 Sussex Univ., Brighton (England).
COSMOLOGICAL MODELS IN HIGHER-ORDER GRAVITY Ph.D. Thesis
Spiros Cotsakis 1990 139 p
Avail: Univ. Microfilms Order No. BRDX96993

This thesis is divided into two parts. The first part deals with the conformal structure, inflationary regimes, and singularity theorems in the context of higher-order gravity theories. The second part focuses on the question of the nature of cosmological singularities and in particular on the occurrence of chaotic behavior in the framework of these theories. We begin part one by formulating and proving what we call the conformal equivalence theorem which states that higher order gravity theories which are derived from a lagrangian density that is an analytic function of the scalar curvature are conformally equivalent to general relativity plus a scalar field matter source with a particular self-interaction potential. The solution space of higher-order gravity theories is examined and the weak field limit of these theories is calculated. The role of conformal non-invariance and the associated particle production in these theories is discussed. Several interpretative issues concerning the physical equivalence of these theories to general relativity with scalar field matter source are given and the physical reality of the conformally related metric tensors is examined in detail. The existence and stability conditions of the de Sitter space in the context of these theories are established and several examples which lead to successful inflation are presented. Effective potentials are drawn for certain classes of these theories. Singularity theorems are proved in the context of higher-order gravity theories and the status of the cosmic no-hair conjectures in these theories is critically presented. In the second part we start by reviewing certain useful and powerful methods for the study of chaotic behavior near cosmological singularities in general relativity. Recent numerical evidence that concerns the genericity of such oscillatory solutions is critically presented and commented upon. A new method based on the analytic theory of ordinary differential equations is presented which provides a direct test for deciding about the existence or non-existence of chaotic behavior in a very large class of physical systems. We apply this test to the Yang-Mills system and to the Bianchi IX spacetime in the context of general relativity. We briefly discuss what is presently known about the chaotic behavior of Kaluza-Klein theories. Finally, by using most of the available methods we examine the chaotic properties of higher-order gravity theories. The results obtained indicate that, contrary to what happens in general relativity, chaotic oscillations near the singularity disappear in diagonal models in these theories and another non-chaotic, monotonic evolution of the universe takes place. However, this chaotic behavior is reestablished in more general, non-diagonal models in higher-order gravity theories. A Hamiltonian interpretation of these results is given.
Dissert. Abstr.

N93-14594 California Inst. of Tech., Pasadena.
COMPACT OBJECTS IN THE DISK AND GLOBULAR CLUSTERS Ph.D. Thesis
Helen Margaret Johnston 1992 192 p
Avail: Univ. Microfilms Order No. DA9232189

A multi-wavelength study of compact objects in globular clusters and in the disk is presented. It is divided into two sections, and contains seven independent chapters, linked by the general theme of the study of the evolution and distribution of recycled pulsars and low mass x-ray binaries. Part 1 deals with pulsars in globular clusters. In Chapter 2, the smearing of a pulsar signal in a binary orbit is analyzed numerically, and empirical relations between the observing time and the parameters of detectable binaries are presented. In Chapter 3, sensitive VLA images of four clusters are presented. No emission is detected from the dense cluster Liller 1, which suggests that the pulsar population of a cluster is not dependent only on its density. Seven unidentified sources are detected in or near the cores of three clusters. In Chapter 4, the ultra-short period binary 4U 1820-30 in NGC 6624 is detected at 1.4 GHz. The source is confirmed to be several arc seconds away from the cluster core, implying its negative period derivative cannot be due to acceleration by the cluster. It is suggested that identification of cluster x-ray sources via their radio emission is a potentially powerful tool. In Chapter 5, a statistical analysis of all previous pulsar surveys, as well as new VLA and Westerbork observations, is used to derive the cluster pulsar luminosity function and the cluster density weighting function. The derived luminosity function is very similar to that of disk pulsars, and the density weighting function scales significantly less steeply than predicted by the tidal capture model. Part 2 presents optical spectroscopy of a variety of compact binaries in the disk. Chapter 6 presents observations of the x-ray nova A0620-00. The mass of the compact object is confirmed to be above the maximum allowed mass for a neutron star, and therefore must be a black hole. Chapter 7 presents spectroscopy of

the recurrent nova U Scorpii. From analysis of the absorption lines, an upper limit is placed on the mass of the white dwarf: M is approximately less than 0.9(solar mass)(3sigma). Hydrogen is also detected in absorption, suggesting that the observed high helium abundance in the emission lines is not due to the nature of the companion. In Chapter 8, radial velocities of disk LMXB's are presented. These are considered in the light of the direct formation model for LMXB's. With the inclusion of a random kick at the birth of the neutron star, the observations are found to be consistent with this model. Dissert. Abstr.

N93-14633 Harvard Univ., Cambridge, MA.
HYDRODYNAMICS OF SUPERNOVA 1987 A Ph.D. Thesis
Marc Herant 1992 117 p
Avail: Univ. Microfilms Order No. DA9228212

This is a study of the hydrodynamics of supernova 1987A and, by extension, of Type 2 and Type 1b supernovae in general. I demonstrate that hydrodynamical instabilities which are intrinsically multidimensional have shaped every stage of the explosion of SN 1987A and the resulting observable display. During the initiation of the explosion by the 'delayed mechanism,' neutrinos deposit some of the energy liberated by the collapse of the core at the bottom of the stellar envelope. This leads to large scale, violent convective motions which are crucial to maintain the energy and matter supply to the outgoing shock and prevent a failure of the explosion. Minutes to hours after the beginning of explosion, as the blast-wave propagates through the envelope, Rayleigh-Taylor instabilities develop at the interfaces separating the hydrogen, helium, and carbon-oxygen shells. These instabilities generate sizable extrusions of heavy elements into the outer shells. Finally, in the days which follow, the nickel produced by explosive nucleosynthesis in the first seconds of the explosion decays to cobalt and iron releasing mostly locally its radioactive energy in the form of heat. As a result, a huge, low-density cavity forms in the center of the expanding remnant. I establish that each round of instabilities significantly affects the subsequent phases of the explosion. This is confirmed by observations of SN 1987A, such as the detection of high-velocity nickel, which can only be interpreted within the context of extensive mixing of the ejecta. Further, I show that these results have profound implications on topics ranging from the structure of the Crab Nebula to neutron star peculiar velocities. Dissert. Abstr.

N93-14636 Wyoming Univ., Laramie.
SPATIALLY RESOLVED 10 MICRON SPECTRA OF CIRCUMSTELLAR MATERIAL AROUND EVOLVED STARS Ph.D. Thesis
Gregory Clayton Sloan 1992 121 p
Avail: Univ. Microfilms Order No. DA9231181

Using a long-slit 10 micron spectrometer and new data analysis techniques, I have resolved and studied the circumstellar emission from two evolved stars, alpha Orionis and HD 44179. By fitting a profile to the spatial data at each wavelength, the width of an object as a function of wavelength can be determined. Applying this method to alpha Ori and HD 44179 shows that both objects are extended. To gain as much spatial information as possible on these objects, I have also developed maximum entropy reconstruction techniques for application to long-slit spectroscopic images. Maximum entropy reconstruction of alpha Ori reveals that emission from the object arises from two sources, a central, unresolved photosphere and an extended region of silicate dust emission. The lack of silicate emission in the line of sight directly toward the star constrains the geometry of the circumstellar dust shell. Further analysis indicates that variations of the emissive properties of the dust with distance from the central star may exist. Maximum entropy reconstructions of HD 44179 resolve it into a cool central continuum source embedded within an extended region emitting the unidentified infrared (UIR) emission features at 7.7, 8.6, 11.3, and 12.7 microns. The peak wavelength of the 7.7 microns feature shifts from 7.9 microns close to the central source to roughly 7.4 microns further away. The intensity of the 11.3 microns feature behaves differently with distance from the central source than the other three features, showing a secondary maximum in the emission roughly 1.5 arcsec from the central source. The lack of UIR emission in the center of the nebula and the variations of the character of the emission with distance from the central star indicate that these observations have resolved the formation and evolution of the carrier of the UIR emission features. These results demonstrate the power of long-slit spectroscopy at 10 microns when used in conjunction with maximum entropy reconstruction techniques. Dissert. Abstr.

N93-14637 Kent Univ., Canterbury (England).
CHARACTERISATION AND DYNAMIC MODELLING OF THE NEAR-EARTH SPACE PARTICULATE ENVIRONMENT Ph.D. Thesis
Kenneth Sullivan 1992 227 p
Avail: Univ. Microfilms Order No. BRDX97012

This dissertation is a study of the near-Earth space microparticulate environment from an analysis of the data from the National Aeronautics and Space Administration's satellite the Long Duration Exposure Facility (LDEF). Existing interplanetary and man-made orbital debris measurements and models are initially reviewed. An analysis of hitherto unexamined hypervelocity impact data is then undertaken to define a new particulate penetration limit of thin films and this new formula is then utilized in re-calibrating these pre-LDEF impact experiments. A three dimensional isotropic, single velocity model of the unbound interplanetary micrometeoroid environment as encountered by LDEF is then presented. The relative interplanetary geometry conversions, and impact velocities, for each of LDEF's 14 oriented faces can then be calculated, depending upon an initial mean geocentric particle velocity. Using this dynamic model, coupled with a methodology of flux transformations, it is shown how the LDEF data set can be decomposed into interplanetary and orbital populations, by making simple assumptions about them, and utilizing LDEF's unique gravity gradient stabilized orbital attitude. From this modelling the LDEF interplanetary flux distribution at one astronomical unit from the Sun, along with the mean geocentric particle velocity, can be defined. This flux and velocity are then seen to compare favorably with pre-LDEF models, re-calibrated with the new penetration formula, and optical detection measurements of meteors. The orbital particulate component can then also be defined by comparing the modelled interplanetary fluxes with the actual LDEF impact record, and incorporating similar dynamic modelling and flux transformations. This is also observed to compare well with pre-existing orbital debris measurements, if again, these are re-calibrated with the new formula. Dissert. Abstr.

N93-14638 Washington Univ., Seattle.
FAINT HIGH-LATITUDE CARBON STARS Ph.D. Thesis
Paul Jonathan Green 1992 200 p
Avail: Univ. Microfilms Order No. DA9230370

We have undertaken a wide area survey to search for faint high latitude carbon (FHLC) stars. Carbon giants are ideal for study of the structure and kinematics of the outer galactic halo. We use two color photometric selection with large format charge-coupled devices (CCD's) to cover 52 deg(exp 2) of sky to a depth of about V = 18. Below this limit, we find good (approximately less than 20 percent) agreement between our object counts as a function of magnitude and the galactic models of Bahcall and Soneira at a variety of latitudes and longitudes. Our spectroscopic followup began with low-resolution spectra of 19 unconfirmed C star candidates from the Case objective-prism photographic survey of Sanduleak and Pesch. Four of these we find to be M stars. The 15 C stars we classify on the two-parameter Keenan-Morgan system as warm (color class less than 3). Of 94 faint C star candidates from our own CCD survey, one highly ranked V = 17 candidate was found to have strong carbon and CN bands. We estimate that to a depth of V = 18, the surface density FHLC stars is 0.019(sup +0.044)(sub -.016) deg(exp -2). We identify two FHLC stars with previously catalogued high proper motion objects. These objects are thus inferred to be dwarf carbon (dC) stars, supplementing the one previously known case, G77-61. Not all dC stars will have detectable proper motions, so other luminosity/distance indicators are needed: we find that C dwarfs all have similar JHK colors, and possibly an unusually strong lambda-6191 bandhead of carbon. By comparing positions in the HST Guide Star Catalog and the original Palomar Observatory Sky Survey, we detect proper motions in two additional FHLC stars. Our proper motion survey, spanning a 30 year baseline, thus identifies two new dC's, and provides proper motion upper limits for another 44 FHLC stars. Kinematic simulations suggest that virtually all Population 2 dC's will have detectable proper motions in a survey as sensitive as our own, and that to a limit of V approximately equals 18, at least 10 percent of FHLC stars are dwarfs. The local space density of dC stars may thus substantially exceed that of luminous C stars, so that the automatic assumption of giant luminosities for C stars is no longer valid. Dissert. Abstr.

N93-14686# Nationaal Inst. voor Kernfysica en Hoge Energiefysica, Amsterdam (Netherlands).

QUASARS, GALAXIES, AND PSEUDO-VACUUM DROPLETS

F. R. Klinkhamer and M. Veltman (Michigan Univ., Ann Arbor.) 30 Aug. 1991 9 p Sponsored in part by Royal Netherlands Academy of Arts and Sciences

(Contract DE-AC02-76ER-01112)

(NIKHEF-H/91-20; ETN-92-91618) Avail: CASI HC A02/MF A01

An alternative explanation for the power house of quasars and active galactic nuclei is presented which is associated with energy production and outflow rather than the more accepted theory of matter infall. The basic idea is that quasars and Active Galactic Nuclei (AGN) are small regions (droplets) of pseudovacuum, possibly containing matter, that decay into real vacuum and ordinary matter. These droplets may have strong electromagnetic fields on their boundaries that tend to stabilize them, but ultimately they decay and release their huge energy content (partially in the form of accelerated particles). In other words, it is suggested that the basic energy of quasars and AGN comes from inside the objects themselves. The present limited understanding of the structure of the vacuum is sketched and the possible role of pseudovacuum droplets in cosmology is presented. ESA

N93-14814*# Michigan Univ., Ann Arbor. Space Physics Research Lab.

ANALYSIS OF CCD IMAGES OF THE COMA OF COMET P/HALLEY Final Report

Michael R. Combi Dec. 1992 33 p

(Grant NAGw-1908)

(NASA-CR-191384; NAS 1.26:191384) Avail: CASI HC A03/MF A01

The modeling analysis objective of this project is to make use of the skill acquired in the development of Monte Carlo particle trajectory models for the distributions of gas species in cometary comae as a basis for a new dust coma model. This model will include a self-consistent picture of the time-dependent dusty-gas dynamics of the inner coma and the three-dimensional time-dependent trajectories of the dust particles under the influence of solar gravity and solar radiation pressure in the outer coma. Our purpose is to use this model as a tool to analyze selected images from two sets of data of the comet P/Halley with the hope that we can help to understand the effects of a number of important processes on the spatial morphology of the observed dust coma. The study will proceed much in the same way as our study of the spatially extended hydrogen coma where we were able to understand the spatial morphology of the Lyman-alpha coma in terms of the partial thermalization of the hot H atoms produced by the photodissociation of cometary H2O and OH. The processes of importance to the observed dust coma include: (1) the dust particle size distribution function; (2) the terminal velocities of various sized dust particles in the inner coma; (3) the radiation scattering properties of dust particles, which are important both in terms of the observed scattered radiation and the radiation pressure acceleration on dust particles; (4) the fragmentation and/or vaporization of dust particles; (5) the relative importance of CHON and silicate dust particles as they contribute both to the dusty-gas dynamics in the inner coma (that produce the dust particle terminal velocities) and to the observed spatial morphology of the outer dust coma; and (6) the time and direction dependence of the source of dust. Author

N93-14866 California Inst. of Tech., Pasadena.

ISOTOPIC COMPOSITION OF GALACTIC COSMIC RAY BORON, CARBON, NITROGEN, AND OXYGEN Ph.D. Thesis

Peyton Stinson Gibner 1992 235 p

Avail: Univ. Microfilms Order No. DA9232180

Relative abundances of the isotopes of galactic cosmic ray B, C, N, and O nuclei have been measured using the balloon-borne High Energy Isotope Spectrometer Telescope (HEIST). Analysis of data collected during the 1988 HEIST flight from Prince Albert, Saskatchewan, has resulted in mass histograms containing approximately 890 boron, approximately 3100 carbon, approximately 910 nitrogen, and approximately 3300 oxygen nuclei. Masses were derived using both the Cerenkov-Energy and delta E-E' techniques, achieving a resulting rms mass resolution of approximately 0.26 amu. These isotopic composition measurements correspond to energy intervals at the top of the atmosphere of approximately 400-650 MeV/nucleon for boron, 430-670 MeV/nucleon for carbon, 440-680 MeV/nucleon for nitrogen, and 450-780 MeV/nucleon for oxygen, higher than previous direct isotope measurements for these elements. The abundance ratios at the top of the atmosphere have been interpreted using an interstellar propagation model that includes improved fragmentation cross sections and uses boron as a 'secondary tracer.' The resulting abundance ratios for cosmic ray source material include N-14/O = 0.0042 plus or minus 0.0014 and N-15/O less than or equal to 0.040, favoring no N-15 at the source. The carbon and oxygen isotopes at the cosmic ray source are C-13/C-12 = 0.005 plus or minus 0.11 and O-18/O-16 = 0.0115 plus or minus .0038, compared to solar system values of C-13/C-12 = 0.011 and O-18/O-16 = 0.0020. The derived cosmic ray source abundances show a possible enhancement of O-18/O-16 over the solar system value and a C-13/C-12 ratio consistent with solar system material. Taking a weighted average of our result with previous high resolution measurements of oxygen results in O-18/O-16 = 0.0075 plus or minus 0.0024, an enhancement in O-18 of 3.75 times the solar system value. Current isotope results are compared with models of cosmic ray origin. The Wolf-Rayet model fits many of the currently observed isotopic excesses in cosmic rays, but the predictions for O-18/O-16 and the elemental N/O ratio are still in question. We conclude that although further refinements in the Wolf-Rayet model may explain O-18 and N/O, none of the presently available models account quantitatively for all of the observed differences in composition between cosmic rays and solar system material. Dissert. Abstr.

N93-14867 New Mexico State Univ., University Park.

ORBITAL COPLANARITY IN SOLAR-TYPE BINARY SYSTEMS: IMPLICATIONS FOR PLANETARY SYSTEM FORMATION AND DETECTION Ph.D. Thesis

Alan Hale 1992 236 p

Avail. Univ. Microfilms Order No. DA9232437

The equatorial inclinations of solar-type stars within visual binary systems are computed by combining upsilon sin i measurements with rotational period measurements, or with expected rotational velocities based upon the age of the star in question. These inclinations are then compared with the orbital inclinations of the systems to test the alignment between the equatorial and orbital planes, and how the tendency for or against coplanarity varies as a function of parameters such as spectral type, separation, eccentricity. The results are extended to planetary systems in order to determine the appropriateness of basing planetary search strategies upon a parent star's equatorial inclination, and to address issues in planetary system formation and evolution, including the stability of planetary orbits within binary systems. During the course of this project new or improved upsilon sin i measurements are made for over 30 solar-type stars within binary systems, and provisional orbits are calculated for 13 binary systems. The results suggest that approximate coplanarity between the equatorial and orbital planes exists for solar-type binary systems with separations less than 30-40 AU. The coplanarity tendency, as well as this 'critical separation,' are not significantly affected by most of the other parameters studied. The one significant exception occurs with hierarchical multiple systems, where noncoplanarity may exist at relatively small separations. Assuming planetary distances in our solar system are typical, the results suggest there is no reason to expect planets to orbit in planes significantly different from that of the parent star's equator, in turn suggesting that planetary formation models and search strategies dependent upon this assumption are valid from this standpoint. The results also suggest that noncoplanarity between the components of a binary system is not a significant issue in addressing the stability of planetary orbits within the system. As an application of these results, the equatorial inclination of HD 114762 is measured in order to determine the nature of the low-mass companion reported by Latham et al. (1989), a candidate brown dwarf. Although no definitive statements can be made, the analysis supports the view that the companion is a low-mass M star. Dissert. Abstr.

N93-14869 Colorado Univ., Boulder.

WOLF-RAYET STARS IN THE MILKY WAY, THE LARGE MAGELLANIC CLOUD, AND EMISSION-LINE GALAXIES Ph.D. Thesis

William Donald Vacca 1992 221 p

Avail: Univ. Microfilms Order No. DA9232739

Wolf-Rayet (W-R) stars are the short-lived endpoints of massive star evolution. Recent studies have identified a set of blue emission-line 'starburst' galaxies whose integrated spectra reveal broad emission features due to the presence of 10(exp 2)-10(exp 5) such stars. We have performed a

systematic study of the properties of a sample of such 'W-R galaxies'. The properties of W-R stars in the Galaxy and the Large Magellanic Cloud (LMC) provide the foundation for this analysis. Using a relation between the size of continuum discontinuities and the intrinsic (b - v)0 color found from model atmospheres of WN stars, we derive a formula for calculating the color excesses of such stars. We then calculate color excesses for nearly all WN stars in the Galaxy and the LMC. Our results are in good agreement with previous determinations of the color excesses for WN stars. Next, we derive average intrinsic He II 4686 and C IV 5808 emission line luminosities from the spectra of LMC WN and WC stars, respectively. Models of WN atmospheres are used to calculate effective temperatures, radii, luminosities, and Lyman continuum fluxes of LMC WNL stars. We have obtained a spatially integrated spectrum of the central 8 x 8 min. region of the giant H II region 30 Doradus in the LMC. From the observed line strengths and our average emission line and Lyman continuum luminosities we estimate the numbers of W-R and O stars present. Our results are in excellent agreement with direct star counts in the region. Finally we have obtained moderate resolution optical spectra of ten W-R galaxies and four comparison starburst galaxies. From the strong nebular emission lines, we determine the internal extinctions, densities, temperatures, oxygen abundances, and the Lyman continuum luminosity in these galaxies. From the strength of the broad He II 4686 feature, the number of W-R stars and the ratio of the number of W-R to O stars present are determined. Contrary to model predictions, we find no correlation of the number of W-R stars or the W-R/O number ratio with oxygen abundance. We calculate W-R/O number ratios that are an order of magnitude larger than predicted by current models of starburst regions. Dissert. Abstr.

N93-15079*# Washington Univ., Saint Louis, MO.
CASSINI ATMOSPHERIC CHEMISTRY MAPPER. VOLUME 1. INVESTIGATION AND TECHNICAL PLAN
William Hayden Smith, Kevin Hays Baines (Jet Propulsion Lab., California Inst. of Tech., Pasadena.), Pierre Drossart (Observatoire de Paris-Meudon, France), Bruce Fegley (Max-Planck-Inst. fuer Chemie, Mainz, Germany), Glenn Orton (Jet Propulsion Lab., California Inst. of Tech., Pasadena.), Keith Noll (Arizona Univ., Tucson.), Harold Reitsema (Ball Aerospace Systems Div., Boulder, CO.), and Gordon L. Bjoraker (National Aeronautics and Space Administration. Goddard Space Flight Center, Greenbelt, MD.) 5 Feb. 1990 104 p
(Grant NAGw-1801)
(NASA-CR-190947; NAS 1.26:190947) Avail: CASI HC A06/MF A02

The Cassini Atmospheric Chemistry Mapper (ACM) enables a broad range of atmospheric science investigations for Saturn and Titan by providing high spectral and spatial resolution mapping and occultation capabilities at 3 and 5 microns. ACM can directly address the major atmospheric science objectives for Saturn and for Titan, as defined by the Announcement of Opportunity, with pivotal diagnostic measurements not accessible to any other proposed Cassini instrument. ACM determines mixing ratios for atmospheric molecules from spectral line profiles for an important and extensive volume of the atmosphere of Saturn (and Jupiter). Spatial and vertical profiles of disequilibrium species abundances define Saturn's deep atmosphere, its chemistry, and its vertical transport phenomena. ACM spectral maps provide a unique means to interpret atmospheric conditions in the deep (approximately 1000 bar) atmosphere of Saturn. Deep chemistry and vertical transport is inferred from the vertical and horizontal distribution of a series of disequilibrium species. Solar occultations provide a method to bridge the altitude range in Saturn's (and Titan's) atmosphere that is not accessible to radio science, thermal infrared, and UV spectroscopy with temperature measurements to plus or minus 2K from the analysis of molecular line ratios and to attain an high sensitivity for low-abundance chemical species in the very large column densities that may be achieved during occultations for Saturn. For Titan, ACM solar occultations yield very well resolved (1/6 scale height) vertical mixing ratios column abundances for atmospheric molecular constituents. Occultations also provide for detecting abundant species very high in the upper atmosphere, while at greater depths, detecting the isotopes of C and O, constraining the production mechanisms, and/or sources for the above species. ACM measures the vertical and horizontal distribution of aerosols via their opacity at 3 microns and, particularly, at 5 microns. ACM recovers spatially-resolved atmospheric temperatures in Titan's troposphere via 3- and 5-microns spectral transitions. Together, the mixing ratio profiles and the aerosol distributions are utilized to investigate the photochemistry of the stratosphere and consequent formation processes for aerosols. Finally, ring opacities, observed during solar occultations and in reflected sunlight, provide a measurement of the particle size and distribution of ring material. ACM will be the first high spectral resolution mapping spectrometer on an outer planet mission for atmospheric studies while retaining a high resolution spatial mapping capability. ACM, thus, opens an entirely new range of orbital scientific studies of the origin, physio-chemical evolution and structure of the Saturn and Titan atmospheres. ACM provides high angular resolution spectral maps, viewing nadir and near-limb thermal radiation and reflected sunlight; sounds planetary limbs, spatially resolving vertical profiles to several atmospheric scale heights; and measures solar occultations, mapping both atmospheres and rings. ACM's high spectral and spatial resolution mapping capability is achieved with a simplified Fourier Transform spectrometer with a no-moving parts, physically compact design. ACM's simplicity guarantees an inherent stability essential for reliable performance throughout the lengthy Cassini Orbiter mission. Author

N93-15086 Princeton Univ., NJ.
THE FORMATION OF GIANT MOLECULAR CLOUDS Ph.D. Thesis
Charles Forbes Gammie 1992 169 p
Avail: Univ. Microfilms Order No. DA9230627

Chapter 1 reviews the observational status of gravitationally bound interstellar gas clouds of mass M greater than 10(exp 4) solar mass. It critically reviews theories of cloud formation and discusses observational constraints. Chapter 2 considers the linear stability and responsiveness of a local, two-dimensional model of a mixed star and gas disk. We find that: (1) The combined system is always less stable than either the gas or stars in isolation. (2) The presence of the gas makes it possible for a density wave to cross the Lindblad resonance. (3) The gain of the corotation amplifier can be either raised or lowered over the gain of the corotation amplifer in the stars or gas alone. Chapter 3 considers the nonlinear development of gravitational instability in a local model of a galaxy disk. Simulations of an unstable, isothermal disk are carried out using the smoothed-particle hydrodynamics code TREESPH of Hernquist and Katz. The simulations produce objects that have a mass similar to that of giant molecular clouds in the solar neighborhood on a timescale of approximately less than 10(exp 7) yr. The evolution of an initially azimuthal field is followed in the limit that the field is weak. Collapse always occurs perpendicular to the field lines, so that the magnetic pressure varies as rho(sup 2). Chapter 4 considers the rotation of giant molecular clouds. We calculate the expected rotation frequency in several models of cloud formation. Gravitational instability produces rapid rotation, and this can be understood in terms of the conservation of potential vorticity. Magnetic field torque the cloud in a retrograde sense and can de-spin a cloud in a fraction of an epicyclic time. The rotation of giant molecular clouds is unlikely to provide a strong constraint on cloud formation theories until the magnetic field can be self-consistently included. Dissert. Abstr.

N93-15284 Max-Planck-Inst. fuer Physik und Astrophysik, Garching (Germany). Inst. fuer Extraterrestrische Physik.
SUPERVISED SELECTION OF GALAXY CANDIDATES FROM THE IRAS PSC: THE QUALITY OF THE SELECTION AND THE INFRARED PROPERTIES OF THE GALAXY CANDIDATES
T. Boller (Academy of Sciences, Potsdam, German D.R.), E. J. A. Meurs, and H.-M. Adorf (European Southern Observatory, Garching, Germany) Jan. 1992 32 p Submitted for publication
(MPE-Preprint-216; ETN-92-92287) Copyright Avail: MPI fuer Physik und Astrophysik, 8046 Garching bei Muenchen

A galaxy sample was prepared from the IRAS Point Source Catalog (PSC) for subsequent study in the Rosat X-ray band. The methodology of the trainable statistical classifier of Meurs et al. (1988), which was applied to select extragalactic sources from the IRAS PSC, is summarized. The classifiers performance is assessed using Wolstencroft et al.'s (1986) and Legget at al.'s (1987) identifications of IRAS objects in selected fields and by cross correlating the galaxy sample with the SIMBAD catalog. The selected sample is less than 6 percent contaminated by galactic sources, allowing to undertake a study of statistical correlations with X-ray properties determined from the Rosat all sky survey. The mean infrared colors of the IRAS galaxy sample are compared with those derived from the two selected fields as an additional indicator of the quality of the selection. ESA

N93-15324# Los Alamos National Lab., NM.
HIGH-ENERGY EMISSIONS FROM YOUNG PULSARS: PERSPECTIVE FROM THE OUTER GAP MODEL
Cheng Ho 1992 9 p Presented at the Physics of Isolated Pulsars Workshop, Taos, NM, 23-28 Feb. 1992
(Contract W-7405-eng-36)
(DE92-040365; LA-UR-92-2843; CONF-9202117-5) Avail: CASI HC A02/MF A01

Young pulsars such as the Crab and Vela pulsars are the most prominent gamma-ray sources in the Galaxy, powered by the neutron star's rotational energy and the spinning magnetic field. Since the late 1960's, a large amount of data has been amassed for these pulsars. With the recent launches of ROSAT, Compton Gamma-Ray Observatory, and other new instruments, many exciting new results have been reported. In this Workshop, we learned the weak and soft pulsed emission from the Vela pulsar, the possible detection of spectral turn-over at approximately 30 MeV, the detection of gamma-ray emission from PSR1509-58, and observation of pulse profile variability from the Crab pulsar. Soon after the workshop, the discovery of gamma-ray pulsations from PSR1706-44 and Geminga were reported. All of these contribute to the large pool of hints that theorists need in order to explain the origin of these powerful emission. In this paper, we discuss results from the outer gap model and comparisons to observations. Section 2 gives a brief overview of the outer gap model. Section 3 discusses the high-energy spectrum from the Crab, PSR0540-693, and Vela. In Section 4, we discuss the pulse profile for pulsars with Crab-like parameters. Section 5 discusses outer gap evolution. DOE

N93-15346# Florida Univ., Gainesville. Inst. for Fundamental Theory.
DARK MATTER AXIONS
P. Sikivie 1992 20 p Presented at the Inst. for Fundamental Theory Workshop on Dark Matter, Gainesville, FL, 14-16 Feb. 1992
(Contract DE-FG05-86ER-40272)
(DE92-040501; DOE/ER-40272/171; UFIFT-HEP-92-25; CONF-9202135-1)
Avail: CASI HC A03/MF A01

The physics of axions is briefly reviewed theoretically, and various constraints on the axion mass are recounted. Then the two main contributions to the present cosmological axion energy density, that due to the realignment of the vacuum during the QCD phase transition and that from axions radiated by cosmic axion strings, are discussed. Next, two detection schemes for axions that are sensitive to different mass ranges, an electromagnetic cavity permeated by a strong magnetic field and a system of superconducting wires embedded in a material transparent to microwave radiation, are described. Finally, the phase space structure of cold dark matter galactic halos is considered. DOE

91 LUNAR AND PLANETARY EXPLORATION

Includes planetology; and manned and unmanned flights.

For spacecraft design or space stations see *18 Spacecraft Design, Testing and Performance.*

N93-14146 State Univ. of New York, Stony Brook.
INVESTIGATIONS OF TITAN'S TROPOSPHERE AND SURFACE AND JUPITER'S GREAT RED SPOT WITH INFRARED OBSERVATIONS Ph.D. Thesis
Caitlin Ann Griffith 1991 140 p
Avail: Univ. Microfilms Order No. DA9219313

Titan's lower atmosphere and surface, and the visible region of Jupiter's great red spot (GRS) are analyzed. The large CH4 column abundance and haze opacity of Titan's atmosphere prevent observations of Titan's surface in the visible and infrared wavelengths. Constraints on Titan's haze and cloud optical depths, and surface albedo are determined from an analysis of Titan's near-infrared spectrum. Observations of Titan made at the NASA Infrared Telescope Facility (IRTF) are analyzed using a radiative transfer calculation. The depth in Titan's atmosphere penetrated by near-IR solar radiation depends on the strength of CH4 absorption, which varies considerably with wavelength. This allows us to separate the effects resulting from haze, clouds, and the surface albedo, since these components reside at different atmospheric levels. The results suggest the CH4 clouds exist; however they are optically thin or patchy and allow solar radiation to penetrate to the surface. The most plausible interpretation of Titan's albedo at 7700, 6250 and 4900 cm(exp -1) suggests a surface dominated by 'dirty' water ice. To investigate the chemistry and dynamics of Jupiter's great red spot (GRS), the tropospheric abundances of NH3 and PH3 in the GRS are determined and compared to those of the surrounding region, the South Tropical Zone (STZ). These gases are possible sources of chromophores, and their distributions are sensitive to the rate of vertical transport in the upper troposphere and lower stratosphere. Three groups of Voyagers IRIS spectra are analyzed, two of the STZ and one of the GRS. The two groups of STZ spectra are defined on the basis of their radiances. Variations in the abundances of NH3 and PH3 are determined within the STZ, as a background for our studies of the GRS. Within the uncertainty of our measurements the PH3 mixing ratio at 600 mbar is 3 x 10(exp -7), the same for all three selections. The NH3 mixing ratio profile in the pressure region between 300 and 600 mbar is the same for both STZ selections. In the GRS, however, NH3 is significantly depleted at 300 mbar, with an abundance of 25 percent that derived for the STZ selections. Dissert. Abstr.

N93-14156 Wisconsin Univ., Madison.
THE SULFUR EMISSION AND PERIODICITY OF THE JUPITER PLASMA TORUS IN 1988 Ph.D. Thesis
Roland Carey Woodward, Jr. 1992 177 p
Avail: Univ. Microfilms Order No. DA9218376

In November and December 1988, observations were made of (S II) lambda 6716, 6731 and (S III) 9531 emissions from the Io plasma torus at Kitt Peak National Observatory with a Fabry-Perot interferometer. A total of 231 line spectra, 6 broadband images, and 3 spectrally resolved image sequences, or 'datacubes', were obtained during a six week period. A thorough periodogram analysis of the scan intensities revealed a strong periodicity in intensity fluctuations at 10.14 plus or minus 0.03 (1-sigma) hours, the most precise determination of subcorotational periodicity in the Io plasma torus to date. If the corotational lag is attributed to 'mass-loading', it can be inferred that approximately 55 percent of the torus' mass is injected by charge exchange, and therefore that the total mass injection rate is approximately 2.3 x 10(exp 30) AMU/s. A weak second periodicity at 9.925 hours (Jupiter's rotation period) cannot be excluded, but is not statistically compelling. The proposed 'System IV' period of 10.225 hours has been excluded. An extension of the Lomb-Scargle periodogram that permits the use of unequally weighted data was developed for this analysis. Average S(+) ion temperatures, determined from line widths, were never less than 10(exp 5) K, and were usually three to seven times that amount. No correlation with intensity was found. Using a datacube, ion temperatures were determined both parallel and perpendicular to the Jovian magnetic field simultaneously, and were found to be the same. From the intensity ratio of the (S II) doublet, the electron density was determined to be 1500 plus or minus 400 cm(exp -3); it varied little throughout the run. A determination and measurement of differential rotation between parts of the torus was attempted with the datacubes: an indication of slower rotation beyond 6 R4 was found, but it was not statistically significant. An intensity asymmetry in (S II) lambda 6731 between west and east ansae of 1.18 plus or minus 0.07 was found; no such symmetry existed in ion temperature. All six broadband images, including the three in (S III) lambda 9531, showed the majority of the emission originating from inside Io's orbit.
Dissert. Abstr.

N93-14179 York Univ. (Ontario).
A STUDY OF THE LOW AND MID-LATITUDE UPPER IONOSPHERES OF JUPITER AND SATURN Ph.D. Thesis
Tariq Majeed 1990 260 p
Avail: Univ. Microfilms Order No. DANN66029

A one-dimensional chemical diffusive model has been developed, in conjunction with the measured neural atmospheric structure, to analyze the Voyager RSS ingress and egress electron density, n(sub e), profiles for the ionosphere of Jupiter and Saturn. The model assumes solar EUV radiation as the only source of ionization and solves coupled continuity and flow equations to obtain vertical density distribution for each ion and neutral self-consistently by employing generalized Newton's method. Assuming the condition of charge neutrality of the plasma (i.e., Sigma n sub i = n sub e) the simple ionospheric model finds serious difficulties in explaining the measured n sub e profiles regarding both the magnitude and the location of the ionospheric peak. The model calculates an H+ ionosphere both for Jupiter and Saturn with a peak n sub e of approx. 10

x the measured peak n sub e at an altitude which is approx. 900 to 1000 km lower than the altitude of a peak in the measured electron densities. The simple ionospheric model has been modified to explain the behavior of the measured n sub e profiles by including the effects of vibrational temperatures, T sub v, estimated for a specified value of the rate coefficient, k sub 2, for the reaction H(+) + H2(v greater than or = 4) and the transport of ions via vertical drifts, w sub D, likely being induced by meridional winds in the neutral atmospheres or external electric fields. The combination of T sub v and w sub D enhances the electron loss in an ion-molecule reaction of H(+) + H2(v greater than or = 4) for a given value of k sub 2 and raises the peak of n sub e to higher altitudes through large vertical distances due to long radiative recombination time constants. The values of T sub v and w sub D required to fit the measured n sub e profiles are found to be not excessively large for the thermospheres of Jupiter and Saturn. For the ionosphere of Saturn, the electron densities are affected by an influx of H2O molecules, Phi sub H2O, from the rings. To produce a n sub e peak at the altitude of the measured n sub e peak, an influx of Phi sub H2O approx. 2 x 10(exp 7) molecules/cm/s is required by the model without invoking T sub v via k sub 2. To maintain the model n sub e peak at the measured altitude, an adequate size of w sub D is required. Attempts have also been made to explain the measurements of Saturn's diurnal variation of the peak electron densities based on parameters T sub v, Phi sub H2O, and w sub D. The density distribution of vibrationally excited H2 and associated vibrational temperatures as a function of altitude have also been calculated for the thermospheric regions of Jupiter and Saturn. The photon-induced resonance fluorescence as a source of H2 vibrational excitation, based on the analysis of the Voyager limb observations of H2 band emission, is found to be a very important source for the levels with v greater than or = 4. The vibrational population of these levels are sufficiently increased by flourescence source to the extent that the chemical sink for the ionization is enhanced and, as a result, the electron densities are reduced. The calculated T sub v for the levels with v greater than or = 4 is compared with the estimated T sub v for a given value of k sub 2.

Dissert. Abstr.

N93-14212 Michigan Univ., Ann Arbor.

ETHANE ICE HAZE IN THE UPPER ATMOSPHERE OF URANUS Ph.D. Thesis

Teresa Maria Schulz 1992 256 p

Avail: Univ. Microfilms Order No. DA9226994

A one-dimensional model is developed to study the effect of a tropospheric vapor sink on the formation and evolution of ethane ice haze in the stratosphere of Uranus. The microphysical processes modelled are nucleation of ethane vapor to neutral ice spheres, growth by vapor deposition and Brownian coagulation, and loss by sedimentation and sublimation. The vapor processes are mixing by eddy diffusion and destruction by a sink, which is a highly parameterized representation of cosmic ray induced ion chemistry. The sink is defined by the product of the mixing ratio and a Gaussian distribution with a center z(0), a maximum A and a width b. It is hypothesized that high energy cosmic rays, which penetrate deep into the troposphere, convert simple hydrocarbons into large ion clusters, and that further irradiation of these clusters leads to the formation of complex, involatile aerosol polymers. Numerous experiments were run without particles to determine the relationship between diffusion and destruction as the sink parameters were varied over a wide range of values. The results of these experiments were used to run 21 full model experiments, which included particles. The primary purpose of these experiments was to bracket the cosmic ray sink parameters that resulted in haze distributions most congruous with observations. The most plausible cases examined so far are those for which z(0) = -100 to -200 km relative to the tropopause (3.4 to 9.1 bars), b = 60 to 90 km, and A is large enough to deplete the ethane mixing ratio profile below the tropopause. These sinks predict stratospheric ice hazes containing 10(exp -15) g cm(exp -3) of frozen ethane in submicron particles numbering about 21 cm(exp -3). These hazes typically form at 40-43 km altitude (17 mb) and extend downward about 20-30 km. Mass and number column densities are on the order of 10(exp -10) g cm(exp -2) and 10(exp -7) cm(exp -2) respectively. The most developed hazes have modal radii of 0.13 plus or minus 0.02 microns at 39 km (20 mb), where the number densities are between 0.2 and 0.8 cm(exp -3). These results agree well with observations and suggest that a vapor sink of this nature is not only plausible but may play a key role in the stability and vertical development of the hazes in the upper atmosphere of Uranus.

Dissert. Abstr.

N93-14288*# Lunar and Planetary Inst., Houston, TX.

PAPERS PRESENTED TO THE INTERNATIONAL COLLOQUIUM ON VENUS

1992 150 p Colloquium held in Pasadena, CA, 10-12 Aug. 1992; sponsored by NASA, JPL, Lunar and Planetary Inst., Russian Academy of Sciences, International Union of Geological Sciences, and International Space Year

(Contract NASw-4574)

(NASA-CR-190676; NAS 1.26:190676; LPI-Contrib-789) Avail: CASI HC A07/MF A02

This volume contains short papers that have been accepted for the International Colloquium on Venus, August 10-12, Pasadena, California. The Program Committee consisted of Stephen Saunders (Jet Propulsion Laboratory) and Sean C. Solomon (Massachusetts Institute of Technology). Chairmen: Raymond Arvison (Washington University); Vassily Moroz (Institute for Space Research); Donald B. Campbell (Cornell University); Thomas Donahue (University of Michigan); James W. Head III (Brown University); Pamela Jones (Lunar and Planetary Institute); Mona Jasnow, Andrew Morrison, Timothy Pardker, Jeffrey Plaut, Ellen Stofan, Tommy Thompson, Cathy Weitz (Jet Propulsion Laboratory); Gordon Pettengil (Massachusetts Institute of Technology); and Janet Luhmann (University of California, Los Angeles). For individual titles, see N93-14289 through N93-14398.

N93-14289*# Academy of Sciences (USSR), Moscow. Inst. of Applied Mathematics.

VENUS RADAR MAPPING FROM THE VENERA 15 AND 16 SPACECRAFTS: RESULTS AND RESTRICTIONS Abstract Only

E. L. Akim, A. I. Zakharov, and A. P. Krivtsov *In* Lunar and Planetary Inst., Papers Presented to the International Colloquium on Venus 1992 p 1 (For primary document see N93-14288 04-91)

Avail: CASI HC A01/MF A02

A description of the results of the Venus northern hemisphere radar survey in 1983-1984 from the Venera 15 and 16 spacecrafts is presented. In addition, we discuss some peculiarities in the function of the radar equipment that defined the technology of SAR data processing. Among these peculiarities are insufficient calibration of SAR and radar altimeter and erroneous automatic gain control data transmission from the spacecrafts. As a result, the procedure of image synthesis and mosaicking contained multistage image brightness corrections. This led to the fact that the average image brightness in a spot 100 km in diameter was constant everywhere in the mosaics. Twenty-seven radar mosaics in the Lambert-Hauss conic projection with 1-2 km spatial resolution covering 25 percent of the surface of Venus have been produced. A Venus surface roughness map was constructed by joint processing of SAR and altimeter data. The mutual calibration of the SAR and altimeter was made in the special radar session when the SAR and altimeter were declined from the local vertical at the same angle. The possibility of estimating relative variations in surface reflection properties over a tens-of-kilometers interval from Venera images is still being considered. Joint analysis of the coordinates of small features of the Venera and Magellan images is one more approach being used to refine the period of rotation for Venus. Author

N93-14290*# Colorado Univ., Boulder. Lab. for Atmospheric and Space Physics.

LOCAL-TIME ASYMMETRIES IN THE VENUS THERMOSPHERE

M. J. Alexander, A. I. F. Stewart, and S. W. Bougher (Arizona Univ., Tucson.) *In* Lunar and Planetary Inst., Papers Presented to the International Colloquium on Venus 1992 p 1-2 (For primary document see N93-14288 04-91)

Avail: CASI HC A01/MF A02

Our current understanding of the global structure and dynamics of the Venus thermosphere is embodied in models such as the Venus Thermospheric General Circulation Model (VTGCM) and empirical composition models such as VIRA and VTS3. We have completed an analysis of ultraviolet images of Venus at 130 nm acquired by the Pioneer Venus Orbiter Ultraviolet Spectrometer (PVOUVS). We have examined 97 images spanning the 10-year period between 1980 and 1990, and have developed a technique for global radiative transfer modeling with which we

create synthetic models of each image analyzed. We have developed a hypothesis for understanding the persistent local-time asymmetry observed as a signature of vertically propagating internal gravity waves interacting with the thermospheric SS-AS circulation. This hypothesis is presented.

Author

N93-14291*# Washington Univ., Saint Louis, MO. Dept. of Earth and Planetary Sciences.

RINGED IMPACT CRATERS ON VENUS: AN ANALYSIS FROM MAGELLAN IMAGES

Jim S. Alexopoulos and William B. McKinnon *In* Lunar and Planetary Inst., Papers Presented to the International Colloquium on Venus 1992 p 2-4 (For primary document see N93-14288 04-91)

Avail: CASI HC A01/MF A02

We have analyzed cycle 1 Magellan images covering approximately 90 percent of the venusian surface and have identified 55 unequivocal peak-ring craters and multiringed impact basins. This comprehensive study (52 peak-ring craters and at least 3 multiringed impact basins) complements our earlier independent analysis of Arecibo and Venera images and initial Magellan data and that of the Magellan team. Author

N93-14292*# McGill Univ., Montreal (Quebec). Dept. of Geological Sciences.

IS ISHTAR TERRA A THICKENED BASALTIC CRUST?

Jafar Arkani-Hamed *In* Lunar and Planetary Inst., Papers Presented to the International Colloquium on Venus 1992 p 4-5 (For primary document see N93-14288 04-91)

Avail: CASI HC A01/MF A02

The mountain belts of Ishtar Terra and the surrounding tesserae are interpreted as compressional regions. The gravity and surface topography of western Ishtar Terra suggest a thick crust of 60-110 km that results from crustal thickening through tectonic processes. Underthrusting was proposed for the regions along Danu Montes and Itzpapalotl Tessera. Crustal thickening was suggested for the entire Ishtar Terra. In this study, three lithospheric models with total thicknesses of 40.75 and 120 km and initial crustal thicknesses of 3.9 and 18 km are examined. These models could be produced by partial melting and chemical differentiation in the upper mantle of a colder, an Earth-like, and a hotter Venus having temperatures of respectively 1300 C, 1400 C, and 1500 C at the base of their thermal boundary layers associated with mantle convection. The effects of basalt-granulite-eclogite transformation (BGET) on the surface topography of a thickening basaltic crust is investigated adopting the experimental phase diagram and density variations through the phase transformation.

Author

N93-14293*# McGill Univ., Montreal (Quebec). Dept. of Geological Sciences.

CONSTRAINTS ON THE THERMAL EVOLUTION OF VENUS INFERRED FROM MAGELLAN DATA

Jafar Arkani-Hamed, G. G. Schaber (Arizona Univ., Tucson.), and R. G. Strom (Arizona Univ., Tucson.) *In* Lunar and Planetary Inst., Papers Presented to the International Colloquium on Venus 1992 p 5-6 (For primary document see N93-14288 04-91)

Avail: CASI HC A01/MF A02

The impact craters with diameters from 1.5 to 280 km compiled from Magellan observations indicate that the crater population on Venus has a completely spatially random distribution and the size/density distribution of craters with diameters greater than or equal to 35 km is consistent with a 'production' population with an age of 500 plus or minus 250 m.y. The similarity in size distribution from area to area indicates that the crater distribution is independent of crater size. Also, the forms of the modified craters are virtually identical to those of the pristine craters. These observations imply that Venus reset its cratering record by global resurfacing 500 m.y. ago, and resurfacing declined relatively fast. The fact that less than 40 percent of all craters have been modified and that the few volcanically embayed craters are located on localized tectonic regions indicate that only minor and localized volcanism and tectonism have occurred since the latest vigorous resurfacing event approximately 500 m.y. ago and the interior of Venus has been solid and possibly colder than Earth's. This is because the high-temperature lithosphere of Venus would facilitate upward ascending of mantle plumes and result in extensive volcanism if the venusian upper mantle were as hot as or hotter than Earth's. Therefore, the present surface morphology of Venus may provide useful constraints on the pattern of that vigorous convection, and possibly on the thermal state of the venusian mantle. We examine this possibility through numerical calculations of three-dimensional thermal convection models in a spherical shell with temperature- and pressure-dependent Newtonian viscosity, temperature-dependent thermal diffusivity, pressure-dependent thermal expansion coefficient, and time-dependent internal heat production rate solar magnitude.

Author

N93-14294*# Washington Univ., Saint Louis, MO. Center for Space Sciences.

SURFACE PROCESSES ON VENUS

R. E. Arvidson *In* Lunar and Planetary Inst., Papers Presented to the International Colloquium on Venus 1992 p 6-7 (For primary document see N93-14288 04-91)

Avail: CASI HC A01/MF A02

Magellan synthetic aperture radar (SAR) and altimetry data were analyzed to determine the nature and extent of surface modification for venusian plains in the Sedna Planitia, Alpha Regio, and western Ovda Regio areas. Specific cross sections derived from the SAR data were also compared to similar data for dry terrestrial basaltic lava flows (Lunar Crater and Cima volcanic fields) and playas (Lunar and Lavic Lakes) for which microtopographic profiles (i.e., quantitative roughness information) were available.

Author

N93-14295*# Brown Univ., Providence, RI. Dept. of Geological Sciences.

SHIELD FIELDS: CONCENTRATIONS OF SMALL VOLCANIC EDIFICES ON VENUS

J. C. Aubele and L. S. Crumpler *In* Lunar and Planetary Inst., Papers Presented to the International Colloquium on Venus 1992 p 7-8 (For primary document see N93-14288 04-91)

Avail: CASI HC A01/MF A02

Pre-Magellan analysis of the Venera 15/16 data indicated the existence of abundant small volcanic edifices, each less than or equal to 20 km diameter, interpreted to be predominantly shield volcanoes and occurring throughout the plains terrain, most common in equidimensional clusters. With the analysis of Magellan data, these clusters of greater than average concentration of small volcanic edifices have been called 'shield fields'. Although individual small shields can and do occur almost everywhere on the plains terrain of Venus, they most commonly occur in fields that are well-defined, predominantly equant, clusters of edifices. Major questions include why the edifices are concentrated in this way, how they relate to the source of the eruptive material, and what the possible relationship of shield fields to plains terrain is. There are three possible models for the origin of fields and small shields: (1) a field represents an 'island' of higher topography subsequently surrounded by later plains material; and (2) a field represents the area of magma reservoir.

Author

N93-14296*# Academy of Sciences (USSR), Moscow. Inst. of Geochemistry and Analytical Chemistry.

THE GEOLOGY OF THE VENERA/VEGA LANDING SITES

A. T. Basilevsky and C. M. Weitz (Jet Propulsion Lab., California Inst. of Tech., Pasadena.) *In* Lunar and Planetary Inst., Papers Presented to the International Colloquium on Venus 1992 p 8-10 (For primary document see N93-14288 04-91)

Avail: CASI HC A01/MF A02

We have performed a photogeological analysis of the Venera Vega landing sites using Magellan radar images. These seven sites are the only places on Venus where geochemistry measurements were taken. In this study, the updated coordinates of the landing sites are used and the landing circle has a radius with an admissible error of about 150 km.

Author

N93-14297*# Princeton Univ., NJ. Dept. of Geological and Geophysical Sciences.

GLOBAL DEFORMATION ON THE SURFACE OF VENUS

Frank Bilotti, Chris Connors, and John Suppe *In* Lunar and Planetary Inst., Papers Presented to the International Colloquium on Venus 1992 p 10-12 (For primary document see N93-14288 04-91)

Avail: CASI HC A01/MF A02

Large-scale mapping of tectonic structures on Venus shows that there

is an organized global distribution to deformation. The structures we emphasize are linear compressive mountain belts, extensional rafted zones, and the small-scale but widely distributed wrinkle ridges. Ninety percent of the area of the planet's compressive mountain belts are concentrated in the northern hemisphere whereas the southern hemisphere is dominated by extension and small-scale compression. We propose that this striking concentration of fold belts in the northern hemisphere, along with the globe-encircling equatorial rift system, represents a global organization to deformation on Venus. Author

N93-14298*# California Univ., Los Angeles. Dept. of Earth and Space Sciences.

COLDSPOTS OR HOTSPOTS? THE ORIGIN OF PLATEAU-SHAPED HIGHLANDS ON VENUS

D. L. Bindschadler *In* Lunar and Planetary Inst., Papers Presented to the International Colloquium on Venus 1992 p 12-13 (For primary document see N93-14288 04-91)

Avail: CASI HC A01/MF A02

A compelling question for the terrestrial planets is the origin of the highland regions on Venus. Data on the topography, gravity signature, and surface morphology returned by the Pioneer Venus, Venera 15/16, and Magellan spacecraft represent a basis for dividing these highlands into two distinct groups: volcanic rises and plateau-shaped highlands. Volcanic rises are generally thought to be due to mantle upwellings in the form of large mantle plumes and are thus similar in origin to terrestrial hotspots. There is less agreement as to the origin of plateau-shaped highlands (PSH). Coldspot mantle downwelling can lead to the formation of a highland region under Venus conditions, and previous to Magellan some PSH (particularly W. Ishtar Terra and Ovda and Thetis Regiones) were suggested to be compressionally deformed regions of thickened crust created by mantle downwelling. A hotspot model proposes that such regions are formed by magmatism and tectonism related to the near-surface ascent of either the diapir-shaped large mantle plume or a solitary disturbance propagating up a plume conduit. The characteristics of both volcanic rises and plateau-shaped highlands on Venus and the models for their formation are briefly reviewed, and tests that may help to make clear which model best explains the plateau-shaped highlands are considered. Author

N93-14299*# Colorado Univ., Boulder. Lab. for Atmospheric and Space Physics.

MONTE CARLO MODELING OF THE RESURFACING OF VENUS

M. A. Bullock, David H. Grinspoon, and James W. Head, III (Brown Univ., Providence, RI.) *In* Lunar and Planetary Inst., Papers Presented to the International Colloquium on Venus 1992 p 14 (For primary document see N93-14288 04-91)

Avail: CASI HC A01/MF A02

We have developed a three-dimensional model of venusian resurfacing that employs Monte Carlo simulations of both impact cratering and volcanism. The model simulates the production of craters on Venus by using the observed mass distributions of Earth- and Venus-crossing asteroids and comets. Lava flows are modeled by an energy minimization technique to simulate the effects of local topography on the shape and extent of flows. The model is run under a wide range of assumptions regarding the scale and time evolution of volcanism on Venus. Regions of the parameter space that result in impact crater distributions and modifications that are currently observed will be explored to place limits on the possible volcanic resurfacing history of Venus. Author

N93-14300*# London Univ. Observatory (England).

DEBRIS AVALANCHES AND SLUMPS ON THE MARGINS OF VOLCANIC DOMES ON VENUS: CHARACTERISTICS OF DEPOSITS

M. H. Bulmer, J. E. Guest, K. Beretan (Jet Propulsion Lab., California Inst. of Tech., Pasadena.), Gregory A. Michaels (Jet Propulsion Lab., California Inst. of Tech., Pasadena.), and R. Stephen Saunders (Jet Propulsion Lab., California Inst. of Tech., Pasadena.) *In* Lunar and Planetary Inst., Papers Presented to the International Colloquium on Venus 1992 p 14-15 (For primary document see N93-14288 04-91)

Avail: CASI HC A01/MF A02

Modified volcanic domes, referred to as collapsed margin domes, have diameters greater than those of terrestrial domes and were therefore thought to have no suitable terrestrial analogue. Comparison of the collapsed debris using the Magellan SAR images with volcanic debris avalanches on Earth has revealed morphological similarities. Some volcanic features identified on the seafloor from sonar images have diameters similar to those on Venus and also display scalloped margins, indicating modification by collapse. Examination of the SAR images of collapsed dome features reveals a number of distinct morphologies to the collapsed masses. Ten examples of collapsed margin domes displaying a range of differing morphologies and collapsed masses have been selected and examined. Author

N93-14301*# Massachusetts Inst. of Tech., Cambridge. Dept. of Earth, Atmospheric and Planetary Sciences.

MIXED-VALENCE IRON MINERALS ON VENUS: Fe(2+)-Fe(3+) OXIDES AND OXY-SILICATES FORMED BY SURFACE-ATMOSPHERE INTERACTIONS

Roger G. Burns and DArcy W. Straub *In* Lunar and Planetary Inst., Papers Presented to the International Colloquium on Venus 1992 p 15-17 (For primary document see N93-14288 04-91)

(Grant NAGw-2049)

Avail: CASI HC A01/MF A02

Inferences from these investigations are that Fe(3+)-bearing minerals such as hematite magnesioferrite, acmite, and epidote are thermodynamically unstable, and that magnetite is the predominant mixed-valence iron oxide mineral on venus. Recently, the Fe(2+)-Fe(3+) silicate mineral laihunite was proposed to be a reaction product of olivine with the venusian atmosphere. This possibility is discussed further here. We suggest that other mixed-valence Fe(2+)-Fe(3+)-Oz-OH(-) silicates could also result from surface-atmosphere interactions on Venus. Topics discussed include the following: (1) conversion of hematite to magnetite; (2) stability of laihunite; (3) the possible existence of oxy-amphiboles and oxy-micas on Venus; and (4) other mixed-valence Fe(2+)-Fe(3+) silicates likely to exist on Venus. Author

N93-14302*# Brown Univ., Providence, RI. Dept. of Geological Sciences.

THERMAL BUOYANCY ON VENUS: PRELIMINARY RESULTS OF FINITE ELEMENT MODELING

J. D. Burt and James W. Head, III *In* Lunar and Planetary Inst., Papers Presented to the International Colloquium on Venus 1992 p 17-18 (For primary document see N93-14288 04-91)

Avail: CASI HC A01/MF A02

Enhanced surface temperatures and a thinner lithosphere on Venus relative to Earth have been cited as leading to increased lithospheric buoyancy. This would limit or prevent subduction on Venus and favor the construction of thickened crust through underthrusting. In order to evaluate the conditions distinguishing between underthrusting and subduction, we have modeled the thermal and buoyancy consequences of the subduction end member. This study considers the fate of a slab from the time it starts to subduct, but bypasses the question of subduction initiation. Thermal changes in slabs subducting into a mantle having a range of initial geotherms are used to predict density changes and thus their overall buoyancy. Finite element modeling is then applied in a first approximation of the assessment of the relative rates of subduction as compared to the buoyant rise of the slab through a viscous mantle. Author

N93-14303*# London Univ. Observatory (England).

EROSION VERSUS CONSTRUCTION: THE ORIGIN OF VENUSIAN CHANNELS

D. B. J. Bussey and J. E. Guest *In* Lunar and Planetary Inst., Papers Presented to the International Colloquium on Venus 1992 p 18-19 (For primary document see N93-14288 04-91)

Avail: CASI HC A01/MF A02

Lava channels are a common feature in the volcanic regions of the Moon, and have now been observed on Venus. There has been much debate about the origin of lunar channels as to whether they are the result of erosional (either thermal or mechanical) or constructional processes. It is necessary to determine the criteria to distinguish between the different types of channels. The clearest evidence is that the presence of levees indicates that the channel experienced a constructional phase for a period. One example of a channel of this type in the southeast region of Aphrodite Terra appears to show both erosional and constructional characteristics. It is approximately 700 km long with an average width of about 1 km. It drops a distance of 700 m from beginning to end, which means that the average slope is 0.06 degrees. Its source may have been a graben situated

at the northwest end of the channel. It appears to have different origins along its length. The lack of levees near the source suggests that the channel is erosional in this region. The presence of levees indicates that a constructional phase has occurred. These are formed by lava repeatedly splashing over the channel sides and solidifying. Evidence of levees is seen further away from the source. However, the presence of levees does not mean that the lava was not also eroding and deepening the channel. Thus, in conclusion, our example channel is very sinuous and there is evidence of erosion. There may also have been overflow here. In its middle reaches it roofs over and has the characteristics of a lava tube. In the lower reaches there is strong evidence for the presence of levees indicating construction. On Earth, limited amounts of erosion may occur in basaltic lava channels, although not nearly on the same scale as on the planets just mentioned. For lava erosion on Earth to occur to a comparable extent, excessive eruption times are required. However, low-viscosity komatiite lava may erode to a larger extent and there is direct evidence that carbonatite lava erodes when the underlying strata is also carbonatite. Previously, it has always been assumed that for thermal erosion to occur the flow must be turbulent. Recent findings indicate that this may be a false assumption and that laminar flow may be effective in eroding the substrate. Author

N93-14304*# Cornell Univ., Ithaca, NY. Dept. of Astronomy.
POLARIZATION PROPERTIES AND EARTH-BASED RADAR MEASUREMENTS OF VENUS IN THE POST-MAGELLAN ERA
D. B. Campbell *In* Lunar and Planetary Inst., Papers Presented to the International Colloquium on Venus 1992 p 19-20 (For primary document see N93-14288 04-91)
Avail: CASI HC A01/MF A02

Studies of the polarization properties of reflected radar signals provide information about wavelength-scale surface and subsurface irregularities and can place constraints on the scattering models used to explain anomalously high backscatter cross sections, such as those measured for the surfaces of the icy Galilean satellites. The JPL aircraft-mounted synthetic aperture radars (SAR) provide cross-section and polarization information for terrestrial terrain types. Comparison of these measurements with results from the Magellan mission is helping to relate volcanic flow types on Venus to terrestrial equivalents. Unfortunately, the Magellan SAR transmits and receives a single linear polarization so that information concerning the polarization properties is dependent on past and future observations from the Earth, primarily with the 12.6-cm wavelength (the same as Magellan) radar system on the Arecibo telescope. Author

N93-14305*# Geological Survey, Flagstaff, AZ.
BRIGHT CRATER OUTFLOWS: POSSIBLE EMPLACEMENT MECHANISMS
D. John Chadwick, Gerald G. Schaber, Robert G. Strom (Arizona Univ., Tucson.), and Darla M. Duval (North Dakota Univ., Grand Forks.) *In* Lunar and Planetary Inst., Papers Presented to the International Colloquium on Venus 1992 p 20-21 (For primary document see N93-14288 04-91)
Avail: CASI HC A01/MF A02

Lobate features with a strong backscatter are associated with 43 percent of the impact craters cataloged in Magellan's cycle 1. Their apparent thinness and great lengths are consistent with a low-viscosity material. The longest outflow yet identified is about 600 km in length and flows from the 90-km-diameter crater Addams. There is strong evidence that the outflows are largely composed of impact melt, although the mechanisms of their emplacement are not clearly understood. High temperatures and pressures of target rocks on Venus allow for more melt to be produced than on other terrestrial planets because lower shock pressures are required for melting. The percentage of impact craters with outflows increases with increasing crater diameter. The mean diameter of craters without outflows is 14.4 km, compared with 27.8 km for craters with outflows. No craters smaller than 3 km, 43 percent of craters in the 10- to 30-km-diameter range, and 90 percent in the 80- to 100-km-diameter range have associated bright outflows. More melt is produced in the more energetic impact events that produce larger craters. However, three of the four largest craters have no outflows. We present four possible mechanisms for the emplacement of bright outflows. We believe this 'shotgun' approach is justified because all four mechanisms may indeed have operated to some degree. Author

N93-14306*# Jet Propulsion Lab., California Inst. of Tech., Pasadena.
IMAGE PROCESSING AND PRODUCTS FOR THE MAGELLAN MISSION TO VENUS
Jerry Clark, Doug Alexander, Paul Andres, Scott Lewicki, and Myche McAuley *In* Lunar and Planetary Inst., Papers Presented to the International Colloquium on Venus 1992 p 22 (For primary document see N93-14288 04-91)
Avail: CASI HC A01/MF A02

The Magellan mission to Venus is providing planetary scientists with massive amounts of new data about the surface geology of Venus. Digital image processing is an integral part of the ground data system that provides data products to the investigators. The mosaicking of synthetic aperture radar (SAR) image data from the spacecraft is being performed at JPL's Multimission Image Processing Laboratory (MIPL). MIPL hosts and supports the Image Data Processing Subsystem (IDPS), which was developed in a VAXcluster environment of hardware and software that includes optical disk jukeboxes and the TAE-VICAR (Transportable Applications Executive-Video Image Communication and Retrieval) system. The IDPS is being used by processing analysts of the Image Data Processing Team to produce the Magellan image data products. Various aspects of the image processing procedure are discussed. Author

N93-14307*# Kansas Univ., Lawrence. Dept. of Physics and Astronomy.
THE THERMOSPHERE AND IONOSPHERE OF VENUS
T. E. Cravens *In* Lunar and Planetary Inst., Papers Presented to the International Colloquium on Venus 1992 p 22-23 (For primary document see N93-14288 04-91)
Avail: CASI HC A01/MF A02

Our knowledge of the upper atmosphere and ionosphere of Venus and its interaction with the solar wind has advanced dramatically over the last decade, largely due to the data obtained during the Pioneer Venus mission and to the theoretical work that was motivated by this data. Most of this information was obtained during the period 1978 through 1981, when the periapsis of the Pioneer Venus Orbiter (PVO) was still in the measurable atmosphere. However, solar gravitational perturbations will again lower the PVO periapsis into the upper atmosphere in September 1992, prior to the destruction of the spacecraft toward the end of this year. The physics and chemistry of the thermosphere and ionosphere of Venus are reviewed. Author

N93-14308*# Jet Propulsion Lab., California Inst. of Tech., Pasadena.
NEAR-INFRARED OXYGEN AIRGLOW FROM THE VENUS NIGHTSIDE
D. Crisp, V. S. Meadows (Sydney Univ., Australia), D. A. Allen (Anglo-Australian Observatory, Sydney.), B. Bezard (Observatoire de Paris-Meudon, France), C. DeBergh (Observatoire de Paris-Meudon, France), and J.-P. Maillard (Institut d'Astrophysique, Paris, France) *In* Lunar and Planetary Inst., Papers Presented to the International Colloquium on Venus 1992 p 23-24 (For primary document see N93-14288 04-91)
Avail: CASI HC A01/MF A02

Groundbased imaging and spectroscopic observations of Venus reveal intense near-infrared oxygen airglow emission from the upper atmosphere and provide new constraints on the oxygen photochemistry and dynamics near the mesopause (approximately 100 km). Atomic oxygen is produced by the Photolysis of CO2 on the dayside of Venus. These atoms are transported by the general circulation, and eventually recombine to form molecular oxygen. Because this recombination reaction is exothermic, many of these molecules are created in an excited state known as O2(delta-1). The airglow is produced as these molecules emit a photon and return to their ground state. New imaging and spectroscopic observations acquired during the summer and fall of 1991 show unexpected spatial and temporal variations in the O2(delta-1) airglow. The implications of these observations for the composition and general circulation of the upper venusian atmosphere are not yet understood but they provide important new constraints on comprehensive dynamical and chemical models of the upper mesosphere and lower thermosphere of Venus. Author

N93-14309*# Brown Univ., Providence, RI. Dept. of Geological Sciences.
GLOBAL CORRELATION OF VOLCANIC CENTERS ON VENUS WITH UPLANDS AND WITH EXTENSION: INFLUENCE OF MANTLE CONVECTION AND ALTITUDE

L. S. Crumpler, James W. Head, III, and J. C. Aubele *In* Lunar and Planetary Inst., Papers Presented to the International Colloquium on Venus 1992 p 25-27 (For primary document see N93-14288 04-91)
Avail: CASI HC A01/MF A02

The observed distribution of volcanism on Venus and its associations with geologic and tectonic characteristics are examined for significant global-scale tectonic, mantle, and volcanic influences. We find that volcanic centers are correlated geologically with zones of extension, infrequent in lowland regions, and infrequent in regions with evidence for tectonic shortening. In addition, volcanic centers are significantly concentrated in a broad region at least 10,000 km in diameter between Beta, Alta, and Themis Regiones. This area is nearly hemispheric in scale and coincides spatially with the area of greatest concentration of extensional characteristics. Our analysis suggests that the observed distribution patterns of volcanic centers reflect the regional patterns of extension, the origin of the extension and volcanism are closely related, and the hemispheric scale of both patterns implies a deep-seated origin such as large-scale interior mantle dynamic patterns. However, altitude-dependent effects on both the formation and preservation of volcanic centers could also strongly influence the observed distribution pattern. Author

N93-14310*# RAND Corp., Santa Monica, CA.
THE SPIN VECTOR OF VENUS DETERMINED FROM MAGELLAN DATA
M. E. Davies, T. R. Colvin, P. G. Rogers, P. W. Chodas (Jet Propulsion Lab., California Inst. of Tech., Pasadena.), and W. L. Sjogren (Jet Propulsion Lab., California Inst. of Tech., Pasadena.) *In* Lunar and Planetary Inst., Papers Presented to the International Colloquium on Venus 1992 p 27 (For primary document see N93-14288 04-91)
Avail: CASI HC A01/MF A02

A control network of the north polar region of Venus has been established by selecting and measuring control points on full-resolution radar strips. The measurements were incorporated into a least-squares adjustment program that improved initial estimates of the coordinates of the control points, pole direction, and rotation rate of Venus. The current dataset contains 4206 measurements of 606 points on 619 radar strips. The accuracy of the determination is driven by spacecraft ephemeris errors. An accurate estimate of the rotation period of Venus was obtained by applying an ephemeris improvement technique. The second cycle closure orbits improved ephemeris solutions for 40 orbits (376-384, 520-528, 588-592, 658-668, 1002-1010, 1408-1412, 1746-1764, and 2166-2170) are included and fixed in the geodetic control computations, thus trying the network to the J2000 coordinate system. Author

N93-14311*# Arizona Univ., Tucson.
MONTE CARLO COMPUTER SIMULATIONS OF VENUS EQUILIBRIUM AND GLOBAL RESURFACING MODELS
D. D. Dawson, R. G. Strom, and G. G. Schaber (Geological Survey, Flagstaff, AZ.) *In* Lunar and Planetary Inst., Papers Presented to the International Colloquium on Venus 1992 p 27-29 (For primary document see N93-14288 04-91)
Avail: CASI HC A01/MF A02

Two models have been proposed for the resurfacing history of Venus: (1) equilibrium resurfacing and (2) global resurfacing. The equilibrium model consists of two cases: in case 1, areas less than or equal to 0.03 percent of the planet are spatially randomly resurfaced at intervals of less than or greater than 150,000 yr to produce the observed spatially random distribution of impact craters and average surface age of about 500 m.y.; and in case 2, areas greater than or equal to 10 percent of the planet are resurfaced at intervals of greater than or equal to 50 m.y. The global resurfacing model proposes that the entire planet was resurfaced about 500 m.y. ago, destroying the preexisting crater population and followed by significantly reduced volcanism and tectonism. The present crater population has accumulated since then with only 4 percent of the observed craters having been embayed by more recent lavas. To test the equilibrium resurfacing model we have run several Monte Carlo computer simulations for the two proposed cases. It is shown that the equilibrium resurfacing model is not a valid model for an explanation of the observed crater population characteristics or Venus' resurfacing history. The global resurfacing model is the most likely explanation for the characteristics of Venus' cratering record. The amount of resurfacing since that event, some 500 m.y. ago, can be estimated by a different type of Monte Carolo simulation. To date, our initial simulation has only considered the easiest case to implement. In this case, the volcanic events are randomly distributed across the entire planet and, therefore, contrary to observation, the flooded craters are also randomly distributed across the planet. Author

N93-14312*# Michigan Univ., Ann Arbor.
METHANE MEASUREMENT BY THE PIONEER VENUS LARGE PROBE NEUTRAL MASS SPECTROMETER
T. M. Donahue and R. R. Hodges, Jr. (Texas Univ. at Dallas, Richardson.) *In* Lunar and Planetary Inst., Papers Presented to the International Colloquium on Venus 1992 p 29 (For primary document see N93-14288 04-91)
Avail: CASI HC A01/MF A02

The Pioneer Venus Large Probe Mass Spectrometer detected a large quantity of methane as it descended below 20 km in the atmosphere of Venus. Terrestrial methane and Xe-136, both originating in the same container and flowing through the same plumbing, were deliberately released inside the mass spectrometer for instrumental reasons. However, the Xe-136 did not exhibit behavior similar to methane during Venus entry, nor did CH4 in laboratory simulations. The CH4 was deuterium poor compared to Venus water and hydrogen. While the inlet to the mass spectrometer was clogged with sulfuric acid droplets, significant deuteration of CH4 and its H2 progeny was observed. Since the only source of deuterium identifiable was water from sulfuric acid, we have concluded that we should correct the HDO/H2O ratio in Venus water from 3.2 x 10(exp -2) to (5 plus or minus 0.7) x 10(exp -2). When the probe was in the lower atmosphere, transfer of deuterium from Venus HDO and HD to CH4 can account quantitatively for the deficiencies recorded in HDO and HD below 10 km, and consequently, the mysterious gradients in water vapor and hydrogen mixing ratios we have reported. The revision in the D/H ratio reduces the mixing ratio of water vapor (and H2) reported previously by a factor of 3.2/5. We are not yet able to say whether the methane detected was atmospheric or an instrumental artifact. If it was atmospheric, its release must have been episodic and highly localized. Otherwise, the large D/H ratio in Venus water and hydrogen could not be maintained. Author

N93-14313*# Washington Univ., Saint Louis, MO. Dept. of Earth and Planetary Science.
VISOELASTIC RELAXATION OF VENUSIAN CORONAE AND MOUNTAIN BELTS: CONSTRAINTS ON GLOBAL HEAT FLOW AND TECTONISM
I. Duncan and A. Leith *In* Lunar and Planetary Inst., Papers Presented to the International Colloquium on Venus 1992 p 29-30 (For primary document see N93-14288 04-91)
Avail: CASI HC A01/MF A02

Venus differs from Earth in that water is essentially absent and its surface temperatures are about 470 K higher. The competing effects of high surface temperature and dry lithologies on the long-term history of surface topography have been studied using the finite-element method. The relaxation history of surface topographic features, such as coronae and mountain belts, is a function of thermal gradient, crustal thickness and lithology, regional stresses, and basal tractions applied to the lithosphere. In this study, we have examined the relative effects of these factors over a period of 500 Ma (presumed to be the mean age of the venusian surface). Author

N93-14314*# Massachusetts Inst. of Tech., Cambridge. Dept. of Earth, Atmospheric, and Planetary Sciences.
FLEXURAL ANALYSIS OF UPLIFTED RIFT FLANKS ON VENUS
Susan A. Evans, Mark Simons, and Sean C. Solomon *In* Lunar and Planetary Inst., Papers Presented to the International Colloquium on Venus 1992 p 30-32 (For primary document see N93-14288 04-91)
Avail: CASI HC A01/MF A02

Knowledge of the thermal structure of a planet is vital to a thorough understanding of its general scheme of tectonics. Since no direct measurements of heat flow or thermal gradient are available for Venus, most estimates have been derived from theoretical considerations or by analog with the Earth. The flexural response of the lithosphere to applied loads is sensitive to regional thermal structure. Under the assumption that the yield strength as a function of depth can be specified, the temperature gradient can be inferred from the effective elastic plate thickness. Previous estimates of the effective elastic plate thickness of Venus range from 11-18 km for the foredeep north of Uorsar Rupes to 30-60 km for the

annular troughs around several coronae. Thermal gradients inferred for these regions are 14-23 K km(exp -1) and 4-9 K km(exp -1) respectively. In this study, we apply the same techniques to investigate the uplifted flanks of an extensional rift. Hypotheses for the origin of uplifted rift flanks on Earth include lateral transport of heat from the center of the rift, vertical transport of heat by small-scale convection, differential thinning of the lithosphere, dynamical uplift, and isostatic response to mechanical uploading of the lithosphere. The 1st hypothesis is considered the dominant contributor to terrestrial rift flanks lacking evidence for volcanic activity, particularly for rift structures that are no longer active. In this study, we model the uplifted flanks of a venusian rift as the flexural response to a vertical end load. Author

N93-14315*# Georgia Inst. of Tech., Atlanta. School of Electrical Engineering.

UNDERSTANDING THE VARIATION IN THE MILLIMETER-WAVE EMISSION OF VENUS

Antoine K. Fahd and Paul G. Steffes *In* Lunar and Planetary Inst., Papers Presented to the International Colloquium on Venus 1992 p 32-34 (For primary document see N93-14288 04-91)

Avail: CASI HC A01/MF A02

Recent observations of the millimeter-wave emission from Venus at 112 GHz (2.6 mm) have shown significant variations in the continuum flux emission that may be attributed to the variability in the abundances of absorbing constituents in the Venus atmosphere. Such constituents include gaseous H2SO4, SO2, and liquid sulfuric acid (cloud condensates). Recently, Fahd and Steffes have shown that the effects of liquid H, SO4, and gaseous SO2 cannot completely account for this measured variability in the millimeter-wave emission of Venus. Thus, it is necessary to study the effect of gaseous H2SO4 on the millimeter-wave emission of Venus. This requires knowledge of the millimeter-wavelength (MMW) opacity of gaseous H2SO4, which unfortunately has never been determined for Venus-like conditions. We have measured the opacity of gaseous H2SO4 in a CO2 atmosphere at 550, 570, and 590 K, at 1 and 2 atm total pressure, and at a frequency of 94.1 GHz. Our results, in addition to previous centimeter-wavelength results are used to verify a modeling formalism for calculating the expected opacity of this gaseous mixture at other frequencies. This formalism is incorporated into a radiative transfer model to study the effect of gaseous H2SO4 on the MMW emission of Venus. Author

N93-14316*# Massachusetts Inst. of Tech., Cambridge. Center for Space Research.

RADAR SCATTERING PROPERTIES OF PANCAKELIKE DOMES ON VENUS

P. G. Ford and G. H. Pettengill *In* Lunar and Planetary Inst., Papers Presented to the International Colloquium on Venus 1992 p 34 (For primary document see N93-14288 04-91)

Avail: CASI HC A01/MF A02

Magellan radar images have disclosed the presence of a large number of almost perfectly circular domes, presumably of volcanic origin, in many regions of Venus several with diameters of 30 km or more. Their high degree of symmetry has permitted measurements of their shape, as determined by the Magellan altimeter to be compared with models of dome production from the eruption of high-viscosity magmas. In this work, we examine in detail the radar images of domes in Rusalka Planitia (2.8 deg S, 150.9 deg E) and Tinatin Planitia (12.2 deg N, 7.5 deg E), selected for their circular symmetry and apparent absence of modification due to large-scale slumping or tectonic rifting. Author

N93-14317*# Brown Univ., Providence, RI. Dept. of Geological Sciences.

SEQUENTIAL DEFORMATION OF PLAINS ALONG TESSERA BOUNDARIES ON VENUS: EVIDENCE FROM ALPHA REGIO

M. S. Gilmore and James W. Head, III *In* Lunar and Planetary Inst., Papers Presented to the International Colloquium on Venus 1992 p 34-36 (For primary document see N93-14288 04-91)

Avail: CASI HC A01/MF A02

Tesserae are regions of elevated terrain characterized by two or more sets of ridges and grooves that intersect orthogonally. Tesserae comprise 15-20 percent of the surface of Venus, but the nature of their formation and evolution is not well understood; processes proposed to account for their characteristics are many and varied. Two types of tessera boundaries have been described: type 1 are generally embayed by plains; and type 2 boundaries are characterized by being linear at the 100-km scale and often associated with steep scarps or tectonic features. Margins such as the western edge of Alpha have been described as type 2. Some of the tessera have boundaries that display deformation of both the edge of the tessera and the adjoining plains. This study focuses on the western edge of Alpha Regio in an effort to characterize on occurrence of this type of boundary and assess the implications of the style in general. Using Magellan SAR imagery, lineament lengths, orientations, and spacing were measured for ten 50 x 60 km areas spanning 500 km of the western boundary. Structural characteristics and orientations were compared to stratigraphic units in order to assess the sequence and style of deformation. Author

N93-14318*# Colorado Univ., Boulder. Lab. for Atmospheric and Space Physics.

VENUSIAN HYDROLOGY: STEADY STATE RECONSIDERED

David H. Grinspoon *In* Lunar and Planetary Inst., Papers Presented to the International Colloquium on Venus 1992 p 36-37 (For primary document see N93-14288 04-91)

Avail: CASI HC A01/MF A02

In 1987, Grinspoon proposed that the data on hydrogen abundance, isotopic composition, and escape rate were consistent with the hypothesis that water on Venus might be in steady state rather than monotonic decline since the dawn of time. This conclusion was partially based on a derived water lifetime against nonthermal escape of approximately 10(exp 8) yr. De Bergh et al., preferring the earlier Pioneer Venus value of 200 ppm water to the significantly lower value detected by Bezard et al., found H2O lifetimes of greater than 10(exp 9) yr. Donahue and Hodges derived H2O lifetimes of 0.4-5 x 10 (exp 9) yr. Both these analyses used estimates of H escape flux between 0.4 x 10(exp 7) and 1 x 10(exp 7) cm(exp -2)s(exp -1) from Rodriguez et al. Yet in more recent Monte Carlo modeling, Hodges and Tinsley found an escape flux due to charge exchange with hot H(+) of 2.8 x 10(exp 7) cm(exp -2)s(exp -1). McElroy et al. estimated an escape flux of 8 x 10(exp 6) cm(exp -2)s(exp -1) from collisions with hot O produced by dissociative recombination of O2(+). Brace et al. estimated an escape flux of 5 x 10(exp 6) cm(exp -2)s(exp -1) from ion escape from the ionotail of Venus. The combined estimated escape flux from all these processes is approximately 4 x 10(exp 7) cm(exp -2)s(exp -1). The most sophisticated analysis to date of near-IR radiation from Venus' nightside reveals a water mixing ratio of approximately 30 ppm, suggesting a lifetime against escape for water of less than 10(exp 8) yr. Large uncertainties remain in these quantities, yet the data point toward a steady state. Further evaluation of these uncertainties, and new evolutionary modeling incorporating estimates of the outgassing rate from post-Magellan estimates of the volcanic resurfacing rate are presented. Author

N93-14319*# Brown Univ., Providence, RI. Dept. of Geological Sciences.

DETERMINING STRESS STATES USING DIKE SWARMS: THE LAUMA DORSA EXAMPLE

Eric B. Grosfils and James W. Head, III *In* Lunar and Planetary Inst., Papers Presented to the International Colloquium on Venus 1992 p 37-38 (For primary document see N93-14288 04-91)

Avail: CASI HC A01/MF A02

Initial examination of the Magellan coverage of Venus has revealed between 150 and 300 large, radially lineated landforms distributed across the planet's surface. Where the lineaments have been examined in detail, the majority fail to exhibit signatures indicative of relief at or above the resolution of the radar; however, when the sense of topographic relief may be ascertained, the lineaments commonly appear as fissures or flat-floored trenches interpreted as graben. Individual lineaments can display graben, fissure, and zero relief behavior along their length, suggesting either that these differences are a function of the resolution of the radar, or that the morphological distinctions are real but somehow genetically linked. In many instances, radial lineaments exhibiting these characteristics are directly associated with surface volcanism, including flanking and terminal flows, superimposed shield domes and pit chains, and central, calderalike topographic lows. These observable characteristics, as well as theoretical studies and comparison with similar terrestrial features, have led to the working hypothesis that many of the radial fracture systems on Venus are the surface manifestation of subsurface dikes propagating laterally from a central magma source. If this interpretation is correct, studies of terrestrial

dikes suggest that the lineament directions, with localized exceptions and barring subsequent deformation, should be perpendicular to the orientation of the least compressive stress at the time of their formation. To test this hypothesis, we briefly examine a radial fracture system (63.7 degrees N, 195 degrees E) located between two deformation belts in Vinmara Planitia, and verify that the lineaments to the east behave in the expected manner. We have also chosen this feature, however, because of its proximity to Lauma Dorsa to the west. On the basis of Venera 15/16 data, both compressional and extensional origins for this deformation belt have been proposed. By examining the stratigraphy and applying our interpretation that the fracture system is linked to the presence of subsurface dikes, we present an independent evaluation of the stress state associated with Lauma Dorsa, and thus contribute to the assessment of its origin. Author

N93-14320*# National Aeronautics and Space Administration. Goddard Space Flight Center, Greenbelt, MD.

VENUS MESOSPHERIC WINDS AND THE CARBON MONOXIDE BULGE

Mark A. Gurwell (California Inst. of Tech., Pasadena.), Duane O. Muhleman (California Inst. of Tech., Pasadena.), and Kathryn Pierce Shah *In* Lunar and Planetary Inst., Papers presented to the International Colloquium on Venus 1992 p 39-40 (For primary document see N93-14288 04-91)
Avail: CASI HC A01/MF A02

Recently, our group mapped the CO absorption lines on the disk of Venus in 1988 using the synthetic aperture array at the Owens Valley Radio Observatory. Observations were make in the (0-1) rotational transition of CO at 115 GHz, or a wavelength of 2.6 mm. Systematic variations in the Doppler shifts of the lines (particularly near the limbs) enable the group to directly map the wind field at 100 plus or minus 10 km, the peak altitude for the experimental weighting functions used. These measurements show that the winds are indeed of the order of a 100 m/s at this altitude. Previously, many had assumed that the vertical wind profile would quickly fall to zero above the cloud tops, due to cyclostrophic breakdown. This work is reviewed. Author

N93-14321*# Southern Methodist Univ., Dallas, TX. Dept. of Geological Sciences.

TECTONICS AND VOLCANISM OF EASTERN APHRODITE TERRA: NO SUBDUCTION, NO SPREADING

Vicki L. Hansen, Myra Keep, Robert R. Herrick, and Roger J. Phillips *In* Lunar and Planetary Inst., Papers Presented to the International Colloquium on Venus 1992 p 40-41 (For primary document see N93-14288 04-91)
Avail: CASI HC A01/MF A02

Eastern Aphrodite Terra is approximately equal in size to the western North American Cordillera, from Mexico to Alaska. Its size and unique landforms make it an important area for understanding the tectonics of Venus, yet models for its formation are diametrically opposed. This region is part of the Equatorial Highlands, which was proposed as a region of lithospheric thinning, isostatic uplift, and attendant volcanism. Eastern Aphrodite Terra is dominated by circular structures within which deformation and volcanism are intimately related. These structures are marked by radial and concentric fractures, and volcanic flows that emanate from a central vent, as well as from concentric fracture sets. Cross-cutting relations between flows and concentric fracture sets indicate that outer concentric fracture sets are younger than inner fracture sets. The circular structures are joined by regional northeast- to east-trending fractures that dominantly postdate formation of the circular structures. We propose that the circular structures 'grow' outward with time. Although these structures probably represent addition of crust to the lithosphere, they do not represent significant lithospheric spreading or convergence, and the region does not mark the boundary between two distinct tectonic plates. This region is not easily explained by analogy with either terrestrial midocean rifts or subduction zones. It is perhaps best explained by upwelling of magma diapirs that blister the surface, but do not cause significant lithospheric spreading. Further study of the structural and volcanic evolution of this region using Magellan altimetry and SAR data should lead to better understanding of the tectonic evolution of this region. Author

N93-14322*# University of Northern Arizona, Flagstaff. Dept. of Geology.

WESTERN APHRODITE TERRA, TECTONICS, GEOLOGY, AND LINE-OF-SIGHT GRAVITY

John E. Hays and Paul Morgan *In* Lunar and Planetary Inst., Papers Presented to the International Colloquium on Venus 1992 p 41-43 (For primary document see N93-14288 04-91)
Avail: CASI HC A01/MF A02

Aphrodite Terra is the largest area of high-standing topography on Venus, and isostatic considerations strongly suggest that this high topography is supported at least in part by thickened crust. Previous studies of line-of-sight gravity data from the Pioneer Venus Orbiter indicate rapidly changing apparent depths of compensation across Aphrodite Terra. Magellan imaging data provide the first detailed images of this region, and we are mapping the region along Pioneer Venus orbit 440 to investigate whether the changing apparent depths of compensation correlate with changes in surficial tectonics. Preliminary mapping of geological features on Magellan images along the path of Pioneer Venus orbit 440 do not indicate a first-order correlation among surface features and changes in the apparent depth of compensation of line-of-sight gravity data. The apparent depth of compensation appears to be most variable in regions dominated by tessera, but not all areas of tessera have distinct gravity signatures. There is a weak correlation among areas in which impact craters are relatively common and areas in which the observed and predicted gravity anomalies are poorly correlated. Author

N93-14323*# Brown Univ., Providence, RI. Dept. of Geological Sciences.

VENUS VOLCANISM: A GLOBAL OVERVIEW FROM MAGELLAN DATA

James W. Head, III, L. S. Crumpler, and J. C. Aubele *In* Lunar and Planetary Inst., Papers Presented to the International Colloquium on Venus 1992 p 43-45 (For primary document see N93-14288 04-91)
Avail: CASI HC A01/MF A02

A preliminary analysis of a global survey of Magellan data covering over 90 percent of the surface and designed to document the characteristics, location, and dimensions of all major volcanic features on Venus has revealed over 1660 landforms and deposits. These include over 550 shield fields (concentrations of small volcanos less than 20 km in diameter), 274 intermediate volcanos between 20 and 100 km diameter with a variety of morphologies, 156 large volcanos in excess of 100 km diameter, 86 calderalike structures independent of those associated with shield volcanos and typically 60-80 km in diameter, 175 coronae (annulus of concentric ridges or fractures), 259 arachnoids (inner concentric and outer radial network pattern of fractures and ridges), 50 novae (focused radial fractures forming stellate patterns), and 53 lava flood-type flow fields, and 50 sinuous lava channels (all of which are in excess of 10(exp 2)-10(exp 3) km in length). The near-global coverage of Magellan data analyzed in this study confirms and extends the results of earlier observations that showed that volcanism is a widespread and significant process on the surface of Venus for the period of time in the presently observed record (less than about the last one billion years). Author

N93-14324*# Brown Univ., Providence, RI. Dept. of Geological Sciences.

CHEMICAL DIFFERENTIATION ON ONE-PLATE PLANETS: PREDICTIONS AND GEOLOGIC OBSERVATIONS FOR VENUS

James W. Head, III, E. M. Parmentier, and P. C. Hess *In* Lunar and Planetary Inst., Papers Presented to the International Colloquium on Venus 1992 p 45-47 (For primary document see N93-14288 04-91)
Avail: CASI HC A01/MF A02

Recent studies have examined the partial melting of planetary interiors on one-plate planets and the implications for the formation and evolution of basaltic crust and the complementary residual mantle layer. In contrast to the Earth, where the crust and residual layer move laterally and are returned to the interior following subduction, one-plate planets such as Venus are characterized by vertical accretion of the crust and residual layer. The residual mantle layer is depleted and compositionally buoyant, being less dense than undepleted mantle due to its reduced Fe/Mg and dense Al-bearing minerals; its melting temperature is also increased. As the crust and depleted mantle layer grow vertically during the thermal evolution of the planet, several stages develop. As a step in the investigation and testing of these theoretical treatments of crustal development on Venus, we investigate the predictions deriving from two of these stages (a stable thick crust and depleted layer, and a thick unstable depleted layer) and compare these to geologic and geophysical observations, speculating on

how these might be interpreted in the context of the vertical crustal accretion models. In each case, we conclude with an outline of further tests and observations of these models. Author

N93-14325*# California Inst. of Tech., Pasadena.
DYNAMICS OF THE VENUS ATMOSPHERE
A. P. Ingersoll *In* Lunar and Planetary Inst., Papers Presented to the International Colloquium on Venus 1992 p 47-48 (For primary document see N93-14288 04-91)
Avail: CASI HC A01/MF A02

The superrotation of the Venus atmosphere is a major unanswered problem in planetary science. At cloud-top levels (65-70 km altitude) the atmosphere rotates with a five-day period, corresponding to an equatorial wind speed of 90 m/s. Angular velocity is roughly constant on spherical shells, and decreases linearly with altitude to zero at the surface. The direction of rotation is the same as that of the solid planet, which is retrograde--opposite to the direction of orbital motion, but the 5-day period is short compared to the 243-day spin period of the solid planet or to the mean solar day, which is 117 Earth-days at the surface. The problem with the superrotation is that shearing stresses tend to transfer angular momentum downward, and would slow the atmosphere until it is spinning with the solid planet. Some organized circulation pattern is counteracting the tendency, but the pattern has not been identified. A simple Hadley-type circulation cannot do it because such a circulation is zonally symmetric and Hide's Theorem states that in an axisymmetric circulation an extremum in angular momentum per unit mass M can exist only at the surface. Venus violates the last condition, having a maximum of retrograde M on the equator at 70-80 km altitude. This leaves waves and eddies to maintain the superrotation but the length scales and forcing mechanisms for these motions need to be specified. Possible forcing mechanisms associated with waves, eddies and tides are discussed. Author

N93-14326*# Academy of Sciences (USSR), Moscow. Inst. of Dynamics of Geospheres.
LARGEST IMPACT CRATERS ON VENUS
B. A. Ivanov, C. M. Weitz (Jet Propulsion Lab., California Inst. of Tech., Pasadena.), and A. T. Basilevsky *In* Lunar and Planetary Inst., Papers Presented to the International Colloquium on Venus 1992 p 48-49 (For primary document see N93-14288 04-91)
Avail: CASI HC A01/MF A02

High-resolution radar images from the Magellan spacecraft have allowed us to perform a detailed study on 25 large impact craters on Venus with diameters from 70 to 280 km. The dimension of these large craters is comparable with the characteristic thickness of the venusian lithosphere and the atmospheric scale height. Some physical parameters for the largest impact craters on Venus (LICV), such as depth, ring/diameter ratio, and range of ballistic ejecta deposits, have been obtained from the SAR images and the altimetry dataset produced by MIT. Data related to each of these parameters is discussed. Author

N93-14327*# Washington Univ., Saint Louis, MO. Center for Space Sciences.
VENUSIAN EXTENDED EJECTA DEPOSITS AS TIME-STRATIGRAPHIC MARKERS
Noam R. Izenberg *In* Lunar and Planetary Inst., Papers Presented to the International Colloquium on Venus 1992 p 49-50 (For primary document see N93-14288 04-91)
Avail: CASI HC A01/MF A02

Use of impact crater ejects at time-stratigraphic markers was established during lunar geologic mapping efforts. The basic premise is that the deposition of impact ejecta, either by itself or mixed with impact-excavated material, is superimposed on a surface. The deposit becomes an observable, mappable unit produced in a single instant in geologic time. Up to two-thirds of Venus craters exhibit extended ejecta deposits. A reconnaissance survey of 336 craters (about 40 percent of the total population) was conducted. About half the craters examined were located in and around the Beta-Atla-Themis region, and half were spread over the western hemisphere of the planet. The survey was conducted using primarily C1-MIDR images. The preliminary survey shows: (1) of the 336 craters, 223 were found to have extended ejecta deposits. This proportion is higher than that found in other Venus crater databases by up to a factor of 2. (2) 53 percent of all extended ejecta craters were unambiguously superimposed on all volcanic and tectonic units. Crater Annia Faustina's associated parabolic ejecta deposit is clearly superimposed on volcanic flows coming from Gula Mons to the west. Parabola material from Faustina has covered the lava flows, smoothing the surface and reducing its specific backscatter cross section. The stratigraphy implies that the parabola material is the youngest observable unit in the region. (3) 12 percent of extended ejecta deposits are superimposed by volcanic materials. Crater Hwangcini has extended ejecta that has been covered by volcanic flows from a dome field to the northwest, implying that the volcanic units were emplaced subsequent to the ejecta deposit and are the youngest units in the locality. (4) It is difficult to determine the stratigraphic relationships of the remaining extended ejecta deposits in SAR at C1-MIDR resolution. Examination of higher resolution images and application of the other Magellan datasets in systematic manner should resolve most of the ambiguous cases. Results from the preliminary survey indicate that extended ejecta deposits are effective time-statigraphic markers for the localities. If stratigraphic relationships between the deposits and surrounding units are studied on a case-by-case basis over the whole planet, they should provide useful constraints on Venus history and development of the surface through time. The continuation of the research will expand the study to include the entire crater population and the Magellan emissivity, altimetry, reflectivity, and rms slope datasets. Author

N93-14328*# National Aeronautics and Space Administration. Ames Research Center, Moffett Field, CA.
LONG-TERM VARIATIONS IN ABUNDANCE AND DISTRIBUTION OF SULFURIC ACID VAPOR IN THE VENUS ATMOSPHERE INFERRED FROM PIONEER VENUS AND MAGELLAN RADIO OCCULTATION STUDIES
J. M. Jenkins and P. G. Steffes (Georgia Inst. of Tech., Atlanta.) *In* Lunar and Planetary Inst., Papers Presented to the International Colloquium on Venus 1992 p 50-51 (For primary document see N93-14288 04-91)
Avail: CASI HC A01/MF A02

Radio occultation experiments have been used to study various properties of planetary atmospheres, including pressure and temperature profiles, and the abundance profiles of absorbing constituents in those planetary atmospheres. However, the reduction of amplitude data from such experiments to determine abundance profiles requires the application of the inverse Abel transform (IAT) and numerical differentiation of experimental data. These two operations preferentially amplify measurement errors above the true signal underlying the data. A new technique for processing radio occultation data has been developed that greatly reduces the errors in the derived absorptivity and abundance profiles. This technique has been applied to datasets acquired from Pioneer Venus Orbiter radio occultation studies and more recently to experiments conducted with the Magellan spacecraft. While primarily designed for radar studies of the Venus surface, the high radiated power (EIRP) from the Magellan spacecraft makes it an ideal transmitter for measuring the refractivity and absorptivity of the Venus atmosphere by such experiments. The longevity of the Pioneer Venus Orbiter has made it possible to study long-term changes in the abundance and distribution of sulfuric acid vapor, H2SO4(g), in the Venus atmosphere between 1979 and 1992. The abundance of H2SO4(g) can be inferred from vertical profiles of 13-cm absorptivity profiles retrieved from radio occultation experiments. Data from 1979 and 1986-87 suggest that the abundance of H2SO4(g) at latitudes northward of 70 deg decreased over this time period. This change may be due to a period of active volcanism in the late 1970s followed by a relative quiescent period, or some other dynamic process in the Venus atmosphere. While the cause is not certain, such changes must be incorporated into dynamic models of the Venus atmosphere. Potentially, the Magellan spacecraft will extend the results of Pioneer Venus Orbiter and allow the continued monitoring of the abundance of distribution of H2SO4(g) in the Venus atmosphere, as well as other interesting atmospheric properties. Without such measurements it will be difficult to address other issues such as the short-term spatial variability of the abundance of H2SO4(g) at similar latitudes in Venus atmosphere, and the identities of particles responsible for large-scale variations observed in NIR images. Author

N93-14329*# Scripps Institution of Oceanography, La Jolla, CA.
VARIATIONS IN LITHOSPHERIC THICKNESS ON VENUS
C. L. Johnson and David T. Sandwell *In* Lunar and Planetary Inst.,

Papers Presented to the International Colloquium on Venus 1992 p 51-52 (For primary document see N93-14288 04-91)
Avail: CASI HC A01/MF A02

Recent analyses of Magellan data have indicated many regions exhibiting topograhic flexure. On Venus, flexure is associated predominantly with coronae and the chasmata with Aphrodite Terra. Modeling of these flexural signatures allows the elastic and mechanical thickness of the lithosphere to be estimated. In areas where the lithosphere is flexed beyond its elastic limit the saturation moment provides information on the strength of the lithosphere. Modeling of 12 flexural features on Venus has indicated lithospheric thicknesses comparable with terrestrial values. This has important implications for the venusian heat budget. Flexure of a thin elastic plate due simultaneously to a line load on a continuous plate and a bending moment applied to the end of a broken plate is considered. The mean radius and regional topographic gradient are also included in the model. Features with a large radius of curvature were selected so that a two-dimensional approximation could be used. Comparisons with an axisymmetric model were made for some features to check the validity of the two-dimensional assumption. The best-fit elastic thickness was found for each profile crossing a given flexural feature. In addition, the surface stress and bending moment at the first zero crossing of each profile were also calculated. Flexural amplitudes and elastic thicknesses obtained for 12 features vary significantly. Three examples of the model fitting procedures are discussed. Author

N93-14330*# Arizona Univ., Tucson. Lunar and Planetary Lab.
IGNEOUS AND TECTONIC EVOLUTION OF VENUSIAN AND TERRESTRIAL CORONAE
J. S. Kargel and G. Komatsu *In* Lunar and Planetary Inst., Papers Presented to the International Colloquium on Venus 1992 p 52-54 (For primary document see N93-14288 04-91)
Avail: CASI HC A01/MF A02

A great variety of tectonic and volcanic features have been documented on Venus. It is widely appreciated that there are close spatial associations among certain types of tectonic structures and some classes of volcanic flows and constructs. Coronae are endowed with a particularly rich variety of volcanism. It is thought that coupled tectonic and volcanic aspects of coronae are cogenetic manifestations of mantle plumes. An outstanding feature of most venusian coronae is their circular or elliptical shape defined by peripheral zones of fracturing and/or folding. Some coronae are composite, consisting of two or more small coronae within a larger enclosing corona, suggesting complex histories of structured diapirism analogous in some ways to salt dome tectonics. Coronae range widely in size, from smaller than 100 km to over 1000 km in diameter. Volcanic features associated with venusian coronae include lunar-like sinuous rilles, thin lava flows, cinder cone-like constructs, shield volcanos, and pancake domes. Several types of volcanic features are often situated within or near a single corona, in many instances including land-forms indicating effusions of both low- and high-viscosity lavas. In some cases stratigraphic evidence brackets emplacement of pancake domes during the period of tectonic development of the corona, thus supporting a close link between the igneous and tectonic histories of coronae. These associations suggest emplacement of huge diapirs and massive magmatic intrusions, thus producing the tectonic deformations defining these structures. Igneous differentiation of the intrusion could yield a range of lava compositions. Head and Wilson suggested a mechanism that would cause development of neutral buoyancy zones in the shallow subsurface of Venus, thereby tending to promote development of massive igneous intrusions. Author

N93-14331*# Pennsylvania State Univ., University Park. Dept. of Geosciences.
VENUS: THE CASE FOR A WET ORIGIN AND A RUNAWAY GREENHOUSE
J. F. Kasting *In* Lunar and Planetary Inst., Papers Presented to the International Colloquium on Venus 1992 p 54-55 (For primary document see N93-14288 04-91)
Avail: CASI HC A01/MF A02

To one interested in atmospheric evolution, the most intriguing aspect of our neighboring planet Venus is its lack of water. Measurements made by Pioneer Venus and by Several Venera spacecraft indicate that the present water abundance in Venus' lower atmosphere is of the order of 20 to 200 ppmv, or 3 x 10(exp -6) to 3 x 10 (exp -5) of the amount of water in Earth's oceans. The exact depletion factor is uncertain, in part because of an unexplained vertical gradient in H2O concentration in the lowest 10 km of the venusian atmosphere, but the general scarcity of water is well established. The interesting question, then, is: Was venus deficient in water when it formed and, if not, where did its water go? The conclusion that Venus was originally wet is consistent with its large endowment of other volatiles and with the enhanced D/H ratio in the present atmosphere. The most likely mechanism by which Venus could have lost its water is by the development of a runaway or moist greenhouse atmosphere followed by photodissociation of water vapor and escape of hydrogen to space. Climate model calculations that neglect cloud albedo feedback predict the existence of two critical transitions in atmospheric behavior at high solar fluxes: (1) at a solar flux of approximately 1.1 times the value at Earth's orbit, S(o), the abundance of stratospheric water vapor increases dramatically, permitting rapid escape of hydrogen to space (termed a moist greenhouse) and (2) at a solar flux of approximately 1.4 S(o), the oceans vaporize entirely, creating a true runaway greenhouse. If cloudiness increases at high surface temperatures, as seems likely, and if the dominant effect of clouds is to cool the planet by reflecting incident solar radiation, the actual solar flux required to create moist or runaway conditions would be higher than the values quoted above. Early in solar system history, solar luminosity was about 25 percent to 30 percent less than today, putting the flux at Venus' orbit in the range of 1.34 S(o) to 1.43 S(o). Thus, it is possible that Venus had liquid water on its surface for several hundred million years following its formation. Paradoxically, this might have facilitated water loss by sequestering atmospheric CO2 in carbonate rocks and by providing an effective medium for surface oxidation. Author

N93-14332*# California Univ., Los Angeles.
VENUS TECTONIC STYLES AND CRUSTAL DIFFERENTIATION
W. M. Kaula and A. Lenardic *In* Lunar and Planetary Inst., Papers Presented to the International Colloquium on Venus 1992 p 55-56 (For primary document see N93-14288 04-91)
Avail: CASI HC A01/MF A02

Two of the most important constraints are known from Pioneer Venus data: the lack of a system of spreading rises, indicating distributed deformation rather than plate tectonics; and the high gravity/topography ratio, indicating the absence of an asthenosphere. In addition, the high depth/diameter ratios of craters on Venus indicate that Venus probably has no more crust than Earth. The problems of the character of tectonics and crustal formation and recycling are closely coupled. Venus appears to lack a recycling mechanism as effective as subduction, but may also have a low rate of crustal differentiation because of a mantle convection pattern that is more distributed, less concentrated, than Earth's. Distributed convection, coupled with the nonlinear dependence of volcanism on heat flow, would lead to much less magmatism, despite only moderately less heat flow, compared to Earth. The plausible reason for this difference in convective style is the absence of water in the upper mantle of Venus. We have applied finite element modeling to problems of the interaction of mantle convection and crust on Venus. The main emphasis has been on the tectonic evolution of Ishtar Terra, as the consequence of convergent mantle flow. The early stage evolution is primarily mechanical, with crust being piled up on the down-stream side. Then the downflow migrates away from the center. In the later stages, after more than 100 m.y., thermal effects develop due to the insulating influence of the thickened crust. An important feature of this modeling is the entrainment of some crustal material in downflows. An important general theme in both convergent and divergent flows is that of mixing vs. stratification. Models of multicomponent solid-state flow obtain that lower-density crustal material can be entrained and recycled, provided that the ration of low-density to high-density material is small enough (as in subducted slabs on Earth). The same considerations should apply in upflows; a small percent of partial melt may be carried along with its matrix and never escape to the surface. Models that assume melt automatically rising to the crust and no entrainment or other mechanism of recycling lower-density material obtain oscillatory behavior, because it takes a long time for heat to build up enough to overcome a Mg-rich low-density residuum. However, these models develop much thicker crust than consistent with estimates from crater depth/diameter ratios. Author

N93-14333*# Brown Univ., Providence, RI. Dept. of Geological Sciences.

LARGE SHIELD VOLCANOS ON VENUS: THE EFFECT OF NEUTRAL BUOYANCY ZONE DEVELOPMENT ON EVOLUTION AND ALTITUDE DISTRIBUTION

S. Keddie and James W. Head, III *In* Lunar and Planetary Inst., Papers Presented to the International Colloquium on Venus 1992 p 56-57 (For primary document see N93-14288 04-91)

Avail: CASI HC A01/MF A02

The Magellan mission to Venus has emphasized the importance of volcanism in shaping the surface of the planet. Volcanic plains make up 80 percent of the terrain and hundreds of regions of localized eruptions have been identified. Large volcanos, defined as edifices with diameters greater than 100 km, are the sites of some of the most voluminous eruptions. Head et al. have identified 158 of these structures. Their spatial distribution is neither random nor arranged in linear chains as on the Earth; large volcanos on Venus are concentrated in two large, near-equatorial clusters that are also the site of many other forms of volcanic activity. The set of conditions that must be met on Venus that controls the change from widespread, distributed volcanism to focused, shield-building volcanism is not well understood. Future studies of transitional features will help to address this problem. It is likely, however, that the formation and evolution of a neutral buoyancy zone (NBZ) plays an important role in both determining the style of the volcanism and the development of the volcanic feature once it has begun to erupt. Head and Wilson have suggested that the high surface pressure on Venus may inhibit volatile exsolution, which may influence the density distribution of the upper crust and hence control the nature and location of a NBZ. The extreme variations in pressure with elevation may result in significantly different characteristics of such a NBZ at different locations on the planet. In order to test these ideas regarding the importance of NBZ development in the evolution of a large shield and to determine the style of volcanism, three large volcanos that occur at different basal elevations were examined and the distribution of large volcanos as a function of altitude was determined. Author

N93-14334*# National Aeronautics and Space Administration. Goddard Space Flight Center, Greenbelt, MD.

MANTLE PLUMES ON VENUS REVISITED

Walter S. Kiefer *In* Lunar and Planetary Inst., Papers Presented to the International Colloquium on Venus 1992 p 57-59 (For primary document see N93-14288 04-91)

Avail: CASI HC A01/MF A02

The Equatorial Highlands of Venus consist of a series of quasicircular regions of high topography, rising up to about 5 km above the mean planetary radius. These highlands are strongly correlated with positive geoid anomalies, with a peak amplitude of 120 m at Atla Regio. Shield volcanism is observed at Beta, Eistla, Bell, and Atla Regiones and in the Hathor Mons-Innini Mons-Ushas Mons region of the southern hemisphere. Volcanos have also been mapped in Phoebe Regio and flood volcanism is observed in Ovda and Thetis Regiones. Extensional tectonism is also observed in Ovda and Thetis Regiones. Extensional tectonism is also observed in many of these regions. It is now widely accepted that at least Beta, Atla, Eistla, and Bell Regiones are the surface expressions of hot, rising mantel plumes. Upwelling plumes are consistent with both the volcanism and the extensional tectonism observed in these regions. The geoid anomalies and topography of these four regions show considerable variation. Peak geoid anomalies exceed 90 m at Beta and Atla, but are only 40 m at Eistla and 24 m at Bell. Similarly, the peak topography is greater at Beta and Atla than at Eistla and Bell. Such a range of values is not surprising because terrestrial hotspot swells also have a side range of geoid anomalies and topographic uplifts. Kiefer and Hager used cylindrical axisymmetric, steady-state convection calculations to show that mantle plumes can quantitatively account for both the amplitude and the shape of the long-wavelength geoid and topography at Beta and Atla. In these models, most of the topography of these highlands is due to uplift by the vertical normal stress associated with the rising plume. Additional topography may also be present due to crustal thickening by volcanism and crustal thinning by rifting. Smrekar and Phillips have also considered the geoid and topography of plumes on Venus, but they restricted themselves to considering only the geoid-topography ratio and did not examine either the geoid and topography amplitudes separately or the shapes of anomalies. Author

N93-14335*# National Aeronautics and Space Administration. Goddard Inst. for Space Studies, New York, NY.

PIONEER VENUS POLARIMETRY AND HAZE OPTICAL THICKNESS

W. J. J. Knibbe (Vrije Univ., Amsterdam, Netherlands), W. M. F. Wauben (Vrije Univ., Amsterdam, Netherlands), L. D. Travis, and J. W. Hovenier (Vrije Univ., Amsterdam, Netherlands) *In* Lunar and Planetary Inst., Papers Presented to the International Colloquium on Venus 1992 p 59 (For primary document see N93-14288 04-91)

Avail: CASI HC A01/MF A02

The Pioneer Venus mission provided us with high-resolution measurements at four wavelengths of the linear polarization of sunlight reflected by the Venus atmosphere. These measurements span the complete phase angle range and cover a period of more than a decade. A first analysis of these data by Kawabata et al. confirmed earlier suggestions of a haze layer above and partially mixed with the cloud layer. They found that the haze exhibits large spatial and temporal variations. The haze optical thickness at a wavelength of 365 nm was about 0.06 at low latitudes, but approximately 0.8 at latitudes from 55 deg poleward. Differences between morning and evening terminator have also been reported by the same authors. Using an existing cloud/haze model of Venus, we study the relationship between the haze optical thickness and the degree of linear polarization. Variations over the visible disk and phase angle dependence are investigated. For that purpose, exact multiple scattering computations are compared with Pioneer Venus measurements. To get an impression of the variations over the visible disk, we have first studied scans of the polarization parallel to the intensity equator. After investigating a small subset of the available data we have the following results. Adopting the haze particle characteristics given by Kawabata et al., we find a thickening of the haze at increasing latitudes. Further, we see a difference in haze optical thickness between the northern and southern hemispheres that is of the same order of magnitude as the longitudinal variation of haze thickness along a scan line. These effects are most pronounced at a wavelength of 935 nm. We must emphasize the tentative nature of the results, because there is still an enormous amount of data to be analyzed. We intend to combine further polarimetric research of Venus with constraints on the haze parameters imposed by physical and chemical processes in the atmosphere. Author

N93-14336*# Knudsen Geophysical Branch, Monte Sereno, CA.

VENUS INTERNAL MAGNETIC FIELD AND ITS INTERACTION WITH THE INTERPLANETARY MAGNETIC FIELD

W. C. Knudsen *In* Lunar and Planetary Inst., Papers Presented to the International Colloquium on Venus 1992 p 60 (For primary document see N93-14288 04-91)

Avail: CASI HC A01/MF A02

In a previous study, Knudsen et al. suggested that Venus has a weak internal magnetic dipole field of the order of 7 x 10 + 20 G cm(exp -3) that is manifested in the form of magnetic flux tubes threading the ionospheric holes in the Venus nightside ionosphere. They pointed out that any internal field of Venus, dipole or multipole, would be weakened in the subsolar region and concentrated in the antisolar region of the planet by the supersonic transterminator convection of the dayside ionosphere into the nightside hemisphere. The inferred magnitude of the dipole field does not violate the upper limit for an internal magnetic field established by the Pioneer Venus magnetometer experiment. The most compelling objection to the model suggested by Knudsen et al. has been the fact that it does not explain the observed interplanetary magnetic field (IMF) control of the polarity of the ionospheric hole flux tubes. In this presentation I suggest that a magnetic reconnection process analogous to that occurring at earth is occurring at Venus between the IMF and a weak internal dipole field. At Venus in the subsolar region, the reconnection occurs within the ionosphere. At Earth it occurs at the magnetopause. Reconnection will occur only when the IMF has an appropriate orientation relative to that of the weak internal field. Thus, reconnection provides a process for the IMF to control the flux tube polarity. The reconnection in the subsolar region takes place in the ionosphere as the barrier magnetic field is transported downward into the lower ionosphere by downward convection of ionospheric plasma and approaches the oppositely directed internal magnetic field that is diffusing upward. The reconnected flux tubes are then transported anti-Sunward by the anti-Sunward convecting ionospheric plasma as well as by the anti-Sunward-flowing solar wind. Reconnection will also occur in the Venus

magnetic tail region, somewhat analogously to the reconnection that occurs in the magnetotail of the Earth. The possibility that reconnection is occurring between the IMF and an internal dipole field may be tested by measuring the orientation of the IMF projected into a plane perpendicular to the solar wind velocity during time intervals for which ionospheric holes are observed. The orientations of the IMV components should fall within a 180 deg angle. Author

N93-14337*# Arizona Univ., Tucson. Lunar and Planetary Lab.
VENUSIAN SINUOUS RILLES
G. Komatsu and V. R. Baker *In* Lunar and Planetary Inst., Papers Presented to the International Colloquium on Venus 1992 p 60-61 (For primary document see N93-14288 04-91)
Avail: CASI HC A01/MF A02

After a preliminary assessment of venusian channels, it now seems to be clear that the channels have distinctive classes, which imply a wide range of formation parameters and formation mechanisms. They include outflow channels mainly formed by mechanical erosion from very high discharge flow, and canali-type channels requiring either constructional process or mechanical erosion by rather exotic low-viscosity lava such as carbonatite or sulfur. Here we focus on venusian sinuous rilles. Venusian sinuous rilles are generally simple, and originate from a collapsed source. They are shallow and narrow downstream. The venusian sinuous rilles are distinct from canali-type channels, which exhibit almost constant morphologies throughout their entire length, and from outflow channels, which are characterized by wide anastomosing reaches. The lunar sinuous rilles could have been formed initially as constructional channels. However, incision was caused by the long flow duration and high temperatures of eruption, along with relatively large discharge rates, possibly assisted by a low viscosity of the channel-forming lava. Channel narrowing and levee formation suggest relatively fast cooling. The venusian channels could have had a similar sequence of formation including rapid cooling. Assuming the substrate is typical tholeiitic lava, the flowing lavas' temperatures have to be higher than the melting temperature of the substrate. The flow should have a low viscosity to cause turbulence and keep a high Reynolds number to sustain efficient thermal erosion. Determining eruption conditions also provide insights to estimate lava composition. Assuming a channel is formed mostly by thermal erosion, the channel's length and longitudinal profile are functions of lava properties. The depth profiles of the channel are measured by radar foreshortening methods and stereo images. Eruption conditions of channel forming lava can be estimated by the methods developed by Hulme. Author

N93-14338*# Hibbing Community Coll., MN.
RADIATION PRESSURE: A POSSIBLE CAUSE FOR THE SUPERROTATION OF THE VENUSIAN ATMOSPHERE
J. L. Krause *In* Lunar and Planetary Inst., Papers Presented to the International Colloquium on Venus 1992 p 61-62 (For primary document see N93-14288 04-91)
Avail: CASI HC A01/MF A02

The superrotation of the venusian atmosphere relative to the planet's surface has long been known. Yet the process by which this vigorous circulation is maintained is poorly understood. The purpose of this report is to show that a mechanism by which the solar radiation interacts with the cloudy atmosphere of Venus could be the principle cause of the superrotation. It has been long known that Venus has a high albedo due to the scattering (similar to the reflection process) of solar radiation by the cloud droplets in its atmosphere. The radiation not scattered, but intercepted by the planet and its atmosphere, is mainly absorbed within the cloud layers. Therefore, momentum (equal, more or less, to that of the solar radiation intercepted) is continually transferred to the venusian atmosphere. The atmospheric system presents a symmetrical surface (same radiation-matter interaction) toward the solar radiation at its morning and evening limbs. If the cross-sectional areas at both limbs were equal, the momentum transfer at the morning limb would decelerate the atmosphere's rotation while at the evening limb the same transfer would accelerate the rotation an equal amount. The net result of this is that the overall rate of rotation would be unchanged. Such a symmetrical configuration is not likely since the atmosphere must be warmed as it rotates across the planet's day hemisphere and cooled as it rotates across the planet's night hemisphere. This warming and cooling must result in a formation of an asymmetrical configuration. It is apparent that the momentum transfer at the evening limb must be greater than that at the morning limb because the atmosphere's greater cross section at the evening limb intercepts a greater amount of solar radiation. It should be noted that very little of the solar radiation is transmitted through the cloud layers, especially at or near the limbs where the atmospheric path length of the radiation is long. This net momentum transfer must be continually added to the angular momentum of the atmospheric system at the same time angular momentum is continually removed from the atmosphere by the frictional drag imposed on the atmosphere by the slowly rotating planet's surface. This completes the description of this mechanism. Author

N93-14339*# London Univ. Observatory (England).
LARGE-VOLUME LAVA FLOW FIELDS ON VENUS: DIMENSIONS AND MORPHOLOGY
M. G. Lancaster, J. E. Guest, K. M. Roberts (Brown Univ., Providence, RI.), and James W. Head, III (Brown Univ., Providence, RI.) *In* Lunar and Planetary Inst., Papers Presented to the International Colloquium on Venus 1992 p 62-64 (For primary document see N93-14288 04-91)
Avail: CASI HC A01/MF A02

Of all the volcanic features identified in Magellan images, by far the most extensive and really important are lava flow fields. Neglecting the widespread lava plains themselves, practically every C1-MIDR produced so far contains several or many discrete lava flow fields. These range in size from a few hundred square kilometers in area (like those fields associated with small volcanic edifices for example), through all sizes up to several hundred thousand square kilometers in extent (such as many rift related fields). Most of these are related to small, intermediate, or large-scale volcanic edifices, coronae, arachnoids, calderas, fields of small shields, and rift zones. An initial survey of 40 well-defined flow fields with areas greater than 50,000 sq km (an arbitrary bound) has been undertaken. Following Columbia River Basalt terminology, these have been termed great flow fields. This represents a working set of flow fields, chosen to cover a variety of morphologies, sources, locations, and characteristics. The initial survey is intended to highlight representative flow fields, and does not represent a statistical set. For each flow field, the location, total area, flow length, flow widths, estimated flow thicknesses, estimated volumes, topographic slope, altitude, backscatter, emissivity, morphology, and source has been noted. The flow fields range from about 50,000 sq km to over 2,500,000 sq km in area, with most being several hundred square kilometers in extent. Flow lengths measure between 140 and 2840 km, with the majority of flows being several hundred kilometers long. A few basic morphological types have been identified. Author

N93-14340*# Massachusetts Univ., Amherst. Dept. of Physics and Astronomy.
DERIVATION OF SURFACE PROPERTIES FROM MAGELLAN ALTIMETRY DATA
Amy J. Lovell, F. Peter Schloerb, and George E. McGill *In* Lunar and Planetary Inst., Papers Presented to the International Colloquium on Venus 1992 p 64-65 (For primary document see N93-14288 04-91)
Avail: CASI HC A01/MF A02

The fit of the Hagfors model to the Magellan altimetry data provides a means to characterize the surface properties of Venus. However, the derived surface properties are only meaningful if the model provides a good representation of the data. The Hagfors model provides a good representation of the data. The Hagfors model is generally a realistic fit to surface scattering properties of a nadir-directed antenna such as the Magellan altimeter; however, some regions of the surface of Venus are poorly described by the existing model, according to the goodness of fit parameter provided on the ARCDR CD-ROMs. Poorly characterized regions need to be identified and fit to new models in order to derive more accurate surface properties for use in inferring the geological processes that affect the surface in those regions. We have compared the goodness of fit of the Hagfors model to the distribution of features across the planet, and preliminary results show a correlation between steep topographic slopes and poor fits to the standard model, as has been noticed by others. In this paper, we investigate possible relations between many classes of features and the ability of the Hagfors model to fit the observed echo profiles. In the regions that are not well characterized by existing models, we calculate new models that compensate for topographic relief in order to derive improved estimates of surface properties. Areas investigated to date span from longitude 315 through 45, at all latitudes covered by

Magellan. A survey of those areas yields preliminary results that suggest that topographically high regions are well suited to the current implementation of the Hagfors model. Striking examples of such large-scale good fits are Alpha Regio, the northern edges of Lada Terra, and the southern edge of Ishtar Terra. Other features that are typically well fit are the rims of coronae such as Heng-O and the peaks of volcanos such as Gula Mons. Surprisingly, topographically low regions, such as the ubiquitous plains areas, are modeled poorly in comparison. However, this generalization has has exceptions: Lakshmi Planum is an elevated region that is not well fit compared to the rest of neighboring Ishtar, while the southern parts of topographically low Guinevere Planitia are characterized quite well by the Hagfors model. Features that are candidates for improved models are impact craters, coronae, ridges of significant scale, complex ridged terrains, moderate-sized mountains, and sharp terrain boundaries. These features are chosen because the goodness of fit is likely to be most affected either by departures from normal incidence angles or by sharp changes in terrain type within a single footprint. Most large features that are elevated with respect to their surroundings will suffer from steep slope effects, and smaller coronae and impact craters will probably suffer due to rapid changes in their appearance within a single footprint (10-20 km). Author

N93-14341*# California Univ., Los Angeles. Inst. of Geophysics and Planetary Physics.

THE SOLAR WIND INTERACTION WITH VENUS

J. G. Luthmann *In* Lunar and Planetary Inst., Papers Presented to the International Colloquium on Venus 1992 p 65 (For primary document see N93-14288 04-91)

Avail: CASI HC A01/MF A02

The Pioneer Venus Orbiter (PVO) mission has played a key role in establishing the nature of the solar wind interaction with Venus. Although earlier probes had determined that Venus presented an obstacle much smaller than the size of earth's magnetosphere to the solar wind, they did not carry out in situ measurements pertaining to solar wind interaction studies at low enough altitudes to determine why. They also did not provide datasets of sufficient duration to study the variability of the interaction of both short (one day) and long (solar cycle) timescales. The first 600 of the nearly 5000 orbits of PVO magnetometer data have been used to determine a very low upper limit on the intrinsic dipolar magnetic moment of Venus. The consequence of that low magnetic moment is that the solar wind interacts directly with the upper atmosphere and ionosphere. Relative to a dipolar field obstacle, the ionospheric obstacle is rather incompressible. A bow shock is observed to stand in front of the nearly Venus-sized ionospheric obstacle at a comparatively steady subsolar altitude of approximately 1.5 R(v) (Venus radii). This shock decelerates the supersonic solar wind plasma so that it can flow around the obstacle. It was found to change its average position in the terminator plane from about 2.4 R(v) to 2.1 R(v) as the solar cycle progressed from the 1978 orbit insertion near solar maximum through the 1986-87 solar minimum, and back again during the latest solar activity increase. Between the bow shock and the ionosphere proper, the slowed solar wind plasma flow diverges near the subsolar point and makes its way across the terminator where it reaccelerates and continues anti-Sunward. The solar wind magnetic field, which is in effect frozen into the flowing plasma, is distorted in this 'magnetosheath' region so that it appears to hang up or drape over the dayside ionosphere before it slips around with the flow. These features of the solar wind interaction are also seen when the obstacle is a dipole magnetic field, but there are two important distinctions. In the wake of the Venus obstacle one finds an induced magnetic tail composed of varying interplanetary fields rather than the constant fields of intrinsic origin. This magnetotail is further seen to be populated by Heavy (0+) ions that are evidently escaping from the planet at significant (approximately 10(exp -25) s(exp -1)) rates. These heavy ions are also observed in the dayside magnetosheath. The interpretation is that ions are produced by both photoionization and solar wind electron impact ionization of the upper neutral atmosphere that extends into the magnetosheath. Author

N93-14342*# Brown Univ., Providence, RI. Dept. of Geological Sciences.

EXTENSIVE LAVA FLOW FIELDS ON VENUS: PRELIMINARY INVESTIGATION OF SOURCE ELEVATION AND REGIONAL SLOPE VARIATIONS

K. Magee-Roberts, James W. Head, III, and M. G. Lancaster (London Univ. Observatory, England) *In* Lunar and Planetary Inst., Papers Presented to the International Colloquium on Venus 1992 p 65-67 (For primary document see N93-14288 04-91)

Avail: CASI HC A01/MF A02

Large-volume lava flow fields have been identified on Venus, the most areally extensive of which are known as fluctus and have been subdivided into six morphologic types. Sheetlike flow fields (Type 1) lack the numerous, closely spaced, discrete lava flow lobes that characterize digitate flow fields. Transitional flow fields (Type 2) are similar to sheetlike flow fields but contain one or more broad flow lobes. Digitate flow fields are divided further into divergent (Types 3-5) and subparallel (Type 6) classes on the basis of variations in the amount of downstream flow divergence. As a result of our previous analysis of the detailed morphology, stratigraphy, and tectonic associations of Mylitta Fluctus, we have formulated a number of questions to apply to all large flow fields on Venus. In particular, we would like to address the following: (1) eruption conditions and style of flow emplacement (effusion rate, eruption duration), (2) the nature of magma storage zones (presence of neutral buoyancy zones, deep or shallow crustal magma chambers), (3) the origin of melt and possible link to mantle plumes, and (4) the importance of large flow fields in plains evolution. To answer these questions we have begun to examine variations in flow field dimension and morphology; the distribution of large flow fields in terms of elevation above the mean planetary radius; links to regional tectonic or volcanic structures (e.g., associations with large shield edifices, coronae, or rift zones); statigraphic relationships between large flow fields, volcanic plains, shields, and coronae; and various models of flow emplacement in order to estimate eruption parameters. In this particular study, we have examined the proximal elevations and topographic slopes of 16 of the most distinctive flow fields that represent each of the 6 morphologic types. Author

N93-14343*# Massachusetts Univ., Amherst. Dept. of Geology and Geography.

WRINKLE RIDGES ON VENUSIAN PLAINS: INDICATORS OF SHALLOW CRUSTAL STRESS ORIENTATIONS AT LOCAL AND REGIONAL SCALES

George E. McGill *In* Lunar and Planetary Inst., Papers Presented to the International Colloquium on Venus 1992 p 67-68 (For primary document see N93-14288 04-91)

Avail: CASI HC A01/MF A02

The plains regions of Venus exhibit a complex array of structural features, including deformation belts of various types, wrinkle ridges, grabens, and enigmatic radar-bright linears. Probably the most pervasive of these structures are the wrinkle ridges, which appear to be morphologically identical to their counterparts on the Moon and Mars. Almost all workers agree that wrinkle ridges result from horizontal compressive stresses in the crust; they either are explained as flexural fold structures, or alternatively as scarps or folds related to reverse faults. Wrinkle ridges generally are narrow, have small amplitudes, and commonly are closely spaced as well, characteristics that imply a shallow crustal origin. If wrinkle ridges are due to horizontally directed compressive stresses in the shallow crust, as generally has been inferred, then the trends of these features provide a means to map both local and regional orientations of principal stresses in the uppermost part of the venusian crust: maximum compressive stress is normal to the ridges, minimum compressive stress is normal to the topographic surface, and thus the wrinkle ridge trends trace the orientation of the intermediate principal stress. Because there are few plains areas on Venus totally devoid of wrinkle ridges, it should be possible to establish a number of interesting relationships on a near-global scale by mapping the trends of wrinkle ridges wherever they occur. The present study is addressing three questions: (1) Do the trends of wrinkle ridges define domains that are large relative to the sizes of individual plains regions? If so, can these domains be related to large-scale topographic or geologic features? (2) Are regional trends of wrinkle ridges affected by local features such as coronae? If so, is it possible to determine the relative ages of the far-field and local stresses from detailed study of trend inheritance or superposition relationships? (3) What is the relationship between wrinkle ridges and the larger ridges that make up ridge belts? Author

N93-14344*# Massachusetts Inst. of Tech., Cambridge. Dept. of Earth, Atmospheric, and Planetary Sciences.

ESTIMATES OF ELASTIC PLATE THICKNESSES BENEATH LARGE VOLCANOS ON VENUS

Patrick J. McGovern and Sean C. Solomon *In* Lunar and Planetary Inst., Papers Presented to the International Colloquium on Venus 1992 p 68-70 (For primary document see N93-14288 04-91)

Avail: CASI HC A01/MF A02

Megellan radar imaging and topography data are now available for a number of volcanos on Venus greater than 100 km in radius. These data can be examined to reveal evidence of the flexural response of the lithosphere to the volcanic load. On Earth, flexure beneath large hotspot volcanos results in an annual topographic moat that is partially to completely filled in by sedimentation and mass wasting from the volcano's flanks. On Venus, erosion and sediment deposition are considered to be negligible at the resolution of Magellan images. Thus, it may be possible to observe evidence of flexure by the ponding of recent volcanic flows in the moat. We also might expect to find topographic signals from unfilled moats surrounding large volcanos on Venus, although these signals may be partially obscured by regional topography. Also, in the absence of sedimentation, tectonic evidence of deformation around large volcanos should be evident except where buried by very young flows. We use analytic solutions in axisymmetric geometry for deflections and stresses resulting from loading of a plate overlying an inviscid fluid. Solutions for a set of disk loads are superimposed to obtain a solution for a conical volcano. The deflection of the lithosphere produces an annular depression or moat, the extent of which can be estimated by measuring the distance from the volcano's edge to the first zero crossing or to the peak of the flexural arch. Magellan altimetry data records (ARCDRs) from data cycle 1 are processed using the GMT mapping and graphics software to produce topographic contour maps of the volcanos. We then take topographic profiles that cut across the annular and ponded flows seen on the radar images. By comparing the locations of these flows to the predicted moat locations from a range of models, we estimate the elastic plate thickness that best fits the observations, together with the uncertainty in that estimate. Author

N93-14345*# Cambridge Univ. (England). Inst. of Theoretical Geophysics.

PANCAKELIKE DOMES ON VENUS Abstract Only

Dan McKenzie, Peter G. Ford (Massachusetts Inst. of Tech., Cambridge.), Fang Liu (Massachusetts Inst. of Tech., Cambridge.), and Gordon H. Pettengill (Massachusetts Inst. of Tech., Cambridge.) *In* Lunar and Planetary Inst., Papers Presented to the International Colloquium on Venus 1992 p 70 (For primary document see N93-14288 04-91)

Avail: CASI HC A01/MF A02

The shape of seven large domes on the plains of Venus, with volumes between 100 and 1000 cu km, is compared with that of an axisymmetric gravity current spreading over a rigid horizontal surface. Both the altimetric profiles and the horizontal projection of the line of intersection of domes on the SAR images agree well with the theoretical similarity solution for a newtonian fluid, but not with the shape calculated for a rigid-plastic rheology, nor with that for a static model with a strong skin. As a viscous current spreads, it generates an isotropic strain rate tensor whose magnitude is independent of radius. Such a flow can account for the randomly oriented cracks that are uniformly distributed on the surface of the domes. The stress induced by the flow in the plains material below is obtained, and is probably large enough to produce the short radial cracks in the surface of the plains beyond the domes. The viscosity of the domes can be estimated from their thermal time constants if spreading is possible only when the fluid is hot, and lies between 10(exp 14) and 10(exp 17) Pa s. Laboratory experiments show that such viscosities correspond to temperatures of 610 - 690 C in dry rhyolitic magmas. These temperatures agree with laboratory measurements of the solidus temperature of wet rhyolite. These results show that the development of the domes can be understood using simple fluid dynamical ideas, and that the magmas involved can be produced by wet melting at depths below 10 km, followed by eruption and degassing. Author

N93-14346*# Sydney Univ. (Australia).

GROUNDBASED NEAR-IR OBSERVATIONS OF THE SURFACE OF VENUS

V. S. Meadows, D. Crisp (Jet Propulsion Lab., California Inst. of Tech., Pasadena.), and D. A. Allen (Anglo-Australian Observatory, Sydney.) *In* Lunar and Planetary Inst., Papers Presented to the International Colloquium on Venus 1992 p 70-71 (For primary document see N93-14288 04-91)

Avail: CASI HC A01/MF A02

We present images of the nightside of Venus taken in the near-infrared windows at 1.0, 1.1, 1.18, 1.28, 1.31, and 2.3 microns with the new infrared camera/spectrometer IRIS on the Anglo-Australian Telescope. These data were taken in spectral-mapping mode. This technique involves scanning the telescope perpendicular to the slit, while collecting spectra at successive slit positions across the planet. We produce data cubes with one spectral and two spatial dimensions. Images can be extracted over any wavelength regions. Each image has square pixels of 0.8 inch resolution. We reduced the scattered light from the sunlit crescent in images extracted from each window by subtracting images taken on either side of the window, where the Venus atmosphere is opaque. Unlike the short wavelength windows, which reveal thermal contrasts that originate primarily from the surface and deep atmosphere, the emission in the 2.3 microns window is produced at much higher altitudes (30-40 km). Emission contrasts seen near 2.3 microns are associated with horizontal variations in the cloud optical depths, and have rotation periods of about six days. We detect large contrasts in infrared emission (20-40 percent) across the disc of Venus in the 1.0-, 1.1-, 1.18-, 1.28-, and 1.31-micron images. Contrasts at these wavelengths may be due to a combination of variations in the optical depths of the overlying sulfuric acid clouds and differences in surface emission. Comparison with the 2.3-micron images show that the patterns seen in the 1.28- and 1.31-micron windows are consistent with cloud optical depth variations alone and require no contribution from the surface. However, images at 1.0, 1.1, and 1.8 microns from July 1991 show a dark feature having a contrast that increases with decreasing wavelength. This behavior is contrary to that expected of cloud absorption. Images taken on three successive days in October show another dark feature that is stationary with respect to the surface. These regions of lower emission correspond closely to the high-altitude surface regions of Beta Regio and Aphrodite Terra. The images can potentially reveal the near-infrared emissiveity of the surface of Venus, thereby complementing Magellan radar reflectivity and ground based radio emissivity measurements. The contrast ratio between highlands and plains is much smaller than would be expected for blackbody radiation from the surface along. Unlike at radio wavelengths, where the atmosphere is essentially transparent, at near-infrared wavelengths the atmosphere emits, absorbs, and scatters radiation, and can modify the observed topographically induced contrasts. The additional radiation from the atmosphere reduces the contrast, and further modification would be expected if terrain at different altitudes has different emissivities. A fit to our data therefore requires, and may constrain, a model of the lowest scale height of the atmosphere. Author

N93-14347*# Geological Survey, Menlo Park, CA.

MAGELLAN STEREO IMAGES AND VENUSIAN GEOLOGY

H. J. Moore, R. S. Saunders (Jet Propulsion Lab., California Inst. of Tech., Pasadena.), Jeffrey J. Plaut (Jet Propulsion Lab., California Inst. of Tech., Pasadena.), and T. J. Parker (Jet Propulsion Lab., California Inst. of Tech., Pasadena.) *In* Lunar and Planetary Inst., Papers Presented to the International Colloquium on Venus 1992 p 71-72 (For primary document see N93-14288 04-91)

Avail: CASI HC A01/MF A02

Areas of Venus imaged by Magellan radar with multiple viewing conditions provide unique data that will contribute to the solution of venusian geologic problems and provide a basis for quantitative comparison of venusian landforms with those on other planetary bodies. Three sets of images with different viewing conditions have been acquired: (1) left-looking with variable incidence angles (cycle 1 profile), (2) right-looking with nearly constant incidence angles (cycle 2 profile), and (3) left-looking with variable incidence angles that are almost always smaller than those in (1) (cycle 3 profiles). The unique data provided by paired images of the same scene with different incidence angles arises from image displacements caused by the relief of individual landforms at scales comparable to the ground-range and azimuth resolutions of the images. There are two aspects of the data: (1) Stereopsis achieved by simultaneous viewing of paired left-looking images of the same scene permits three-dimensional perception and interpretation of the morphologies of landforms at resolutions much finer than the altimetry

footprints. (2) Measurements of differences of image displacements (parallax) on paired images with known imaging geometries provide quantitative estimates of the relief and shapes of landforms. The potential scientific contributions of the data can be grouped into two interrelated classes: (A) geologic mapping, analysis, and interpretation and (B) topical studies that involve topographic measurements. Stereopsis, without quantitative measurements, enhances geologic mapping, analysis, and interpretation of the rock units of Venus to a degree that cannot be overestimated. In geologic mapping, assemblages of landforms, assessments of backscatter and variations in backscatter, and fine-scale topography are used to define and characterize geologic map units that represent laterally continuous deposits or rock units. Stereopsis adds the important dimension of local relief for characterization of geologic units at a scale that is not possible with Magellan altimetry or products derived from the altimetry. Relative ages of the geologic units are determined using the well-known principles of superposition and intersection. Here, the perception of relief is invaluable because superposition relations among the geological units are more readily and clearly established. The recognition of folds, faults, and fault systems, regardless of their orientations, is facilitated with stereopsis so that sequences of deformation of the geologic units can be determined and structural analyses vastly improved. Shapes of landforms are readily perceived so that they can be properly interpreted. The end result of the mapping, analyses, and interpretations is a geologic history of Venus that includes the sequences of formation and deformation of various geologic units. Measurements of relief at the finest scale possible are necessary for numerous topical studies. Standard altimetry will provide the necessary information on the relief of most large landforms, but it tends to underestimate the relief of small landforms and distorts their shapes. Although special processing of the altimeter echoes improves the estimates of the relief and shapes of some landforms, there are uncertainties in the interpretations of the echoes. Examples of topical studies requiring measurements of relief are given. Author

N93-14348*# California Univ., Los Angeles.

FLEXURAL MODELS OF TRENCH/OUTER RISE TOPOGRAPHY OF CORONAE ON VENUS WITH AXISYMMETRIC SPHERICAL SHELL ELASTIC PLATES

W. Moore, Gerald Schubert, and David T. Sandwell (Scripps Institution of Oceanography, La Jolla, CA.) *In* Lunar and Planetary Inst., Papers Presented to the International Colloquium on Venus 1992 p 72-73 (For primary document see N93-14288 04-91)

Avail: CASI HC A01/MF A02

Magellan altimetry has revealed that many coronae on Venus have trenches or moats around their peripheries and rises outboard of the trenches. This trench/outer rise topographic signature is generally associated with the tectonic annulus of the corona. Sandwell and Schubert have interpreted the trench/outer rise topography and the associated tectonic annulus around coronae to be the result of elastic bending of the Venus lithosphere (though the tectonic structures are consequences of inelastic deformation of the lithosphere). They used two-dimensional elastic plate flexure theory to fit topographic profiles across a number of large coronae and inferred elastic lithosphere thicknesses between about 15 and 40 km, similar to inferred values of elastic thickness for the Earth's lithosphere at subduction zones around the Pacific Ocean. Here, we report the results of using axisymmetric elastic flexure theory for the deformation of thin spherical shell plates to interpret the trench/outer rise topography of the large coronae modeled by Sandwell and Schubert and of coronae as small as 250 km in diameter. In the case of a corona only a few hundred kilometers in diameter, the model accounts for the small planform radius of the moat and the nonradial orientation of altimetric traces across the corona. By fitting the flexural topography of coronae we determine the elastic thickness and loading necessary to account for the observed flexure. We calculate the associated bending moment and determine whether the corona interior topographic load can provide the required moment. We also calculate surface stresses and compare the stress distribution with the location of annular tectonic features. Author

N93-14349*# California Inst. of Tech., Pasadena. Div. of Geological and Planetary Science.

RADAR-ANOMALOUS, HIGH-ALTITUDE FEATURES ON VENUS

Duane O. Muhleman and Bryan J. Butler *In* Lunar and Planetary Inst., Papers Presented to the International Colloquium on Venus 1992 p 73-74 (For primary document see N93-14288 04-91)

Avail: CASI HC A01/MF A02

Over nearly all of the surface of Venus the reflectivity and emissivity at centimeter wavelengths are about 0.15 and 0.85 respectively. These values are consistent with moderately dense soils and rock populations, but the mean reflectivity is about a factor of 2 greater than that for the Moon and other terrestrial planets. Pettingill and Ford, using Pioneer Venus reflectivities and emissivities, found a number of anomalous features on Venus that showed much higher reflectivities and much lower emissivities with both values approaching 0.5. These include Maxwell Montes, a number of high regions in Aphrodite Terra and Beta Regio, and several isolated mountain peaks. Most of the features are at altitudes above the mean radius by 2 to 3 km or more. However, such features have been found in the Magellan data at low altitudes and the anomalies do not exist on all high structures, Maat Mons being the most outstanding example. A number of papers have been written that attempt to explain the phenomena in terms of the geochemistry balance of weathering effects on likely surface minerals. The geochemists have shown that the fundamentally basaltic surface would be stable at the temperatures and pressures of the mean radius in the form of magnetite, but would evolve to pyrite and/or pyrrhotite in the presence of sulfur-bearing compounds such as SO2. Pyrite will be stable at altitudes above 4 or 5 km on Venus. Although the geochemical arguments are rather compelling, it is vitally important to rationally look at other explanations for radar and radio emission measurements such as that presented by Tryka and Muhleman. The radar reflectivity values are retrieved from the raw Magellan backscatter measurements by fitting the Hagfors' radar scattering model in which a surface roughness parameters and a normal incidence electrical reflectivity are estimated. The assumptions of the theory behind the model must be considered carefully before the results can be believed. These include that the surface roughness exists only at horizontal scales large compared to the wavelength, the vertical deviations are gaussianly distributed, there is no shadowing, and that the reflection occurs at the interface of two homogeneous dielectric half-spaces. Probably all these conditions are violated at the anomalous features under discussion. The most important of these is the homogeneity of the near surface of Venus, particularly in highlands. Under the assumptions of the theory, all of the radio energy is reflected by the impedance jump at the very boundary. However, in heterogeneous soil some fraction of the illuminating energy is propagated into the soil and then scattered back out by impedance discontinuities such as rock, voids, and cracks. In light soils, the latter effect can overwhelm the scattering effects of the true surface and greatly enhance the backscatter power, suggesting a much higher value of an effective dielectric constant that would be estimated from Hagfors' model. Author

N93-14350*# Massachusetts Inst. of Tech., Cambridge. Dept. of Earth, Atmospheric, and Planetary Sciences.

THE GABBRO-ECLOGITE PHASE TRANSITION AND THE ELEVATION OF MOUNTAIN BELTS ON VENUS

Noriyuki Namiki and Sean C. Solomon *In* Lunar and Planetary Inst., Papers Presented to the International Colloquium on Venus 1992 p 74-76 (For primary document see N93-14288 04-91)

Avail: CASI HC A01/MF A02

Among the four mountain belts surrounding Lakshmi Planum, Maxwell Montes is the highest and stands up to 11 km above the mean planetary radius and 7 km above Lakshmi Planum. The bulk composition and radioactive heat production of the crust on Venus, where measured, are similar to those of terrestrial tholeiitic basalt. Because the thickness of the low-density crust may be limited by the gabbro-garnet granulite-eclogite phase transitions, the 7-11 km maximum elevation of Maxwell Montes is difficult to understand except in the unlikely situation that the crust contains a large volume of magma. A possible explanation is that the base of the crust is not in phase equilibrium. It has been suggested that under completely dry conditions, the gabbro-eclogite phase transition takes place by solid-state diffusion and may require a geologically significant time to run to completion. Solid-state diffusion is a strongly temperature-dependent process. In this paper we solve the thermal evolution of the mountain belt to attempt to constrain the depth of the gabbro-eclogite transition and thus to assess this hypothesis quantitatively. The one-dimensional heat equation is solved numerically by a finite difference approximation. The deformation of the

horizontally shortening crustal and mantle portions of the thermal boundary layer is assumed to occur by pure shear, and therefore the vertical velocity is given by the product of the horizontal strain rate and depth. Author

N93-14351*# Colorado Univ., Boulder. Cooperative Inst. for Research in Environmental Science.

RESULTS OF A ZONALLY TRUNCATED THREE-DIMENSIONAL MODEL OF THE VENUS MIDDLE ATMOSPHERE

M. Newman *In* Lunar and Planetary Inst., Papers Presented to the International Colloquium on Venus 1992 p 76-77 (For primary document see N93-14288 04-91)

Avail: CASI HC A01/MF A02

Although the equatorial rotational speed of the solid surface of Venus is only 4 m s(exp-1), the atmospheric rotational speed reaches a maximum of approximately 100 m s(exp-1) near the equatorial cloud top level (65 to 70 km). This phenomenon, known as superrotation, is the central dynamical problem of the Venus atmosphere. We report here the results of numerical simulations aimed at clarifying the mechanism for maintaining the equatorial cloud top rotation. Maintenance of an equatorial rotational speed maximum above the surface requires waves or eddies that systematically transport angular momentum against its zonal mean gradient. The zonally symmetric Hadley circulation is driven thermally and acts to reduce the rotational speed at the equatorial cloud top level; thus wave or eddy transport must counter this tendency as well as friction. Planetary waves arising from horizontal shear instability of the zonal flow (barotropic instability) could maintain the equatorial rotation by transporting angular momentum horizontally from midlatitudes toward the equator. Alternatively, vertically propagating waves could provide the required momentum source. The relative motion between the rotating atmosphere and the pattern of solar heating, which as a maximum where solar radiation is absorbed near the cloud tops, drives diurnal and semidiurnal thermal tides that propagate vertically away from the cloud top level. The effect of this wave propagation is to transport momentum toward the cloud top level at low latitudes and accelerate the mean zonal flow there. We employ a semispectral primitive equation model with a zonal mean flow and zonal wavenumbers 1 and 2. These waves correspond to the diurnal and semidiurnal tides, but they can also be excited by barotropic or baroclinic instability. Waves of higher wavenumbers and interactions between the waves are neglected. Symmetry about the equator is assumed, so the model applies to one hemisphere and covers the altitude range 30 to 110 km. Horizontal resolution is 1.5 deg latitude, and vertical resolution is 1.5 km. Solar and thermal infrared heating, based on Venus observations and calculations drive the model flow. Dissipation is accomplished mainly by Rayleigh friction, chosen to produce strong dissipation above 85 km in order to absorb upward propagating waves and limit extreme flow velocities there, yet to give very weak Rayleigh friction below 70 km; results in the cloud layer do not appear to be sensitive to the Rayleigh friction. The model also has weak vertical diffusion, and very weak horizontal diffusion, which has a smoothing effect on the flow only at the two grid points nearest the pole. Author

N93-14352*# California Univ., Los Angeles. Dept. of Earth and Space Sciences.

A MODEL FOR THE FORMATION OF THE EXTENDED PARABOLOIDAL HALOS AROUND SOME IMPACT CRATERS ON VENUS Abstract Only

W. I. Newman, E. M. Jones (Los Alamos National Lab., NM.), D. B. Campbell (Cornell Univ., Ithaca, NY.), and N. J. S. Stacy (Cornell Univ., Ithaca, NY.) *In* Lunar and Planetary Inst., Papers Presented to the International Colloquium on Venus 1992 p 77 (For primary document see N93-14288 04-91)

Avail: CASI HC A01/MF A02

Many parabolic-shaped extended impact crater-related features have been found in Magellan synthetic aperture radar and emissivity data covering much of the surface of Venus. They are oriented east-west with the apex to the east and the impact crater located just west of the apex. A model for the formation of the parabolic features is developed based on the injection of small particles into the upper atmosphere at the time of impact, and their subsequent transport to the west by the east-west zonal winds. Fallout times from 50 km in the Venus atmosphere for particles of this size are about two hours, allowing westerly drifts of several hundred kilometers for zonal winds of 50 to 100 m s(exp -1). Author

N93-14353*# Moscow State Univ. (USSR). Geological Faculty.

VENUS: PRELIMINARY GEOLOGIC MAPPING OF NORTHERN ATLA REGIO Abstract Only

A. M. Nikishin and G. A. Burba (Academy of Sciences, USSR, Moscow) *In* Lunar and Planetary Inst., Papers Presented to the International Colloquium on Venus 1992 p 77-82 (For primary document see N93-14288 04-91)

Avail: CASI HC A02/MF A02

A preliminary geologic map of C1 sheet 15N197 was compiled according to Magellan data. Northern Atla Regio is dominantly a volcanic plain with numerous volcanic features: radar-bright and -dark flows and spots, shield volcanos, volcanic domes and hills with varied morphology, and coronalike constructions. Tesserae are the oldest terrains semiflooded by plain materials. There are many lineated terrains on this territory. They are interpreted as old, partly buried ridge belts. Lineated terrains have intermediate age between young plains and old tesserae. Ozza Mons and Sapas Mons are the high shield volcanos. The prominent structure of northern Atla Regio is Ganis Chasma rift. The rift dissected the volcanic plain and evolved nearly contemporaneously with Ozza Mons shield volcano. Ganis Chasma rift valley is highly fractured and bounded by fault scarps. There are a few relatively young volcanic features in the rift valley. The rift originated due to 5-10 percent crustal extension and crustal subsidence according to analysis of fracturing and rift valley geometry. Ganis Chasma is characterized by rift shoulder uplifts. Geological structures of Alta Regio and Beta Regio are very similar as assumed earlier. Author

N93-14354*# Moscow State Univ. (USSR). Geological Faculty.

VENUS: PRELIMINARY GEOLOGIC MAPPING OF SOUTHERN BETA REGIO-NORTHERN PHOEBE REGIO Abstract Only

A. M. Nikishin and G. A. Burba (Academy of Sciences, USSR, Moscow) *In* Lunar and Planetary Inst., Papers Presented to the International Colloquium on Venus 1992 p 83 (For primary document see N93-14288 04-91)

Avail: CASI HC A01/MF A02

New preliminary geologic maps of C1 sheets 15N283 and 00N283 were compiled according to Magellan data. The oldest terrains are tesserae that have fragmentlike shapes. Its margins are partly buried by younger plain materials. Volcanic plains are the dominant types of terrains. There are many different volcanic features on plains: radar-bright and -dark flows and spots, shield volcanos, volcanic domes and hills with varied morphology, and coronalike constructions. Devana Chasma rift crosses the surface between Beta Regio and Phoebe regio. The rift's normal faults dissect volcanic plains and shield volcanos. The rift valleys are relatively young structures. According to structural analysis of the rift valleys we conclude the rift originated due to 5-10 percent crustal extension and crustal subsidence. Devana Chasma rift is characterized by shoulder uplifts.

Author

N93-14355*# Moscow State Univ. (USSR). Geological Faculty.

VENUS: GEOLOGY OF BETA REGIO RIFT SYSTEM Abstract Only

A. M. Nikishin, V. K. Borozdin (Academy of Sciences, USSR, Moscow), and N. N. Bobina (Academy of Sciences, USSR, Moscow) *In* Lunar and Planetary Inst., Papers Presented to the International Colloquium on Venus 1992 p 83 (For primary document see N93-14288 04-91)

Avail: CASI HC A01/MF A02

Beta Regio is characterized by the existence of rift structures. We compiled new geologic maps of Beta Regio according to Magellan data. There are many large uplifted tesserae on beta upland. These tesserae are partly buried by younger volcanic cover. We can conclude, using these observations, that Beta upland formed mainly due to lithospheric tectonic uplifting and was only partly constructed by volcanism. Theia Mons is the center of the Beta rift system. Many rift belts are distributed radially to Theia Mons. Typical widths of rifts are 40-160 km. Rift valleys are structurally represented by crustal grabens or half-grabens. There are symmetrical and asymmetrical rifts. Many rifts have shoulder uplifts up to 0.5-1 km high and 40-60 km wide. Preliminary analysis for rift valley structural cross sections lead to the conclusion that rifts originated due to 5-10 percent crustal extension. Many rifts traverse Beta upland and spread to the surrounding lowlands. We can assume because of these data that Beta rift system has an active-passive origin. It formed due to regional tectonic lithospheric extension. Rifting was accelerated by upper-mantle hot spot

origination under the center of passive extension (under the Beta Regio).
Author

N93-14356*# Brown Univ., Providence, RI. Dept. of Geological Sciences.

THE ORIGINS OF RADIAL FRACTURE SYSTEMS AND ASSOCIATED LARGE LAVA FLOWS ON VENUS

Elisabeth A. Parfitt, Lionel Wilson (Lancaster Univ., England), and James W. Head, III *In* Lunar and Planetary Inst., Papers Presented to the International Colloquium on Venus 1992 p 83-84 (For primary document see N93-14288 04-91)
Avail: CASI HC A01/MF A02

Magellan images have revealed the existence of systems of radial fractures on venus that are very similar in form to terrestrial dike swarms such as the Mackenzie swarm in Northern Canada. The association of many of the fracture systems with lava flows, calderas, and volcanic edifices further support the idea of a dike emplacement origin. A global survey of the Magellan images has allowed the location of 300 such fracture systems. Two types of fracture systems are defined. A series of models were developed to simulate the emplacement of dikes on Venus. Observations of fracture lengths and widths were then used to constrain the emplacement conditions. The model results show that the great length and relatively large width of the fractures can only be explained if the dikes that produce them were emplaced in high driving pressure (pressure buffered) conditions. Such conditions imply high rates of melt production, which is consistent with the melt being derived directly from a plume head. We have recently modeled the vertical emplacement of a dike from the top of a mantle plume and calculated the eruption rates such a dike would produce on reaching the surface. This modeling shows that eruption rates of approximately 0.1 cu km/hr can readily be generated by such a dike, consistent with the above results. However, the sensitivity of the model to dike width and therefore driving pressure means that eruption rates from dikes emplaced from the base of the crust or the head of a mantle plume could be orders of magnitude higher than this. Clearly, therefore, the model needs to be refined in order to better constrain eruption conditions. However, it is worth noting here that the initial results do show that even for moderate dike widths, eruption rates could be at least on the order of those estimated for terrestrial flood basalts. Author

N93-14357*# Jet Propulsion Lab., California Inst. of Tech., Pasadena.

APPLICATION OF LEFT- AND RIGHT-LOOKING SAR STEREO TO DEPTH MEASUREMENTS OF THE AMMAVARU OUTFLOW CHANNEL, LADA TERRA, VENUS

T. J. Parker *In* Lunar and Planetary Inst., Papers Presented to the International Colloquium on Venus 1992 p 84-85 (For primary document see N93-14288 04-91)
Avail: CASI HC A01/MF A02

Venusian channels are too narrow to be resolved by Magellan's radar altimeter, so they are not visible in the standard topographic data products. Stereo image data, in addition to their benefit to geologic mapping of Venus structures as a whole, are indispensible in measuring the topography across the channels. These measurements can then be used in conjunction with the regional topographic maps based on the altimeter data to produce cross-sectional areas for the channels and estimate the fluid discharge through them. As an example of the application of the stereo image data to venusian channels, a number of test depth and profile measurements were made of the large outflow channel system in Lada Terra, centered at 50 deg S latitude, 21 deg E longitude (F-MIDR 50S021). These measurements were made by viewing the cycle 1 and 2 digital FMIDRs in stereo on a display monitor, so as to minimize the errors in measuring parallax displacement as much as possible. The MIDRs are produced at a scale of 75 m/pixel. This corresponds to a vertical scale of about 17 m/pixel, when calculating the height of a feature from its parallax displacement. An error in placement determination of 1 pixel was assumed to characterize the vertical accuracy as plus or minus 17 m. When this technique was applied to the outflow channel, it was noted that the walls of the collapsed terrain source and 'trough reach' of the channel are laid over in both the cycle 1 and 2 images. This is evident when examining the distance between features on the plateau and the cliff walls in the two images. The layover 'shifts' the features closer to the apparent edge of the wall relative to the oppositely illuminated image. Author

N93-14358*# Brown Univ., Providence, RI. Dept. of Geological Sciences.

CHEMICAL DIFFERENTIATION OF A CONVECTING PLANETARY INTERIOR: CONSEQUENCES FOR A ONE-PLATE PLANET SUCH AS VENUS

E. M. Parmentier and P. C. Hess *In* Lunar and Planetary Inst., Papers Presented to the International Colloquium on Venus 1992 p 85-87 (For primary document see N93-14288 04-91)
Avail: CASI HC A01/MF A02

Chemically depleted mantle forming a buoyant, refractory layer at the top of the mantle can have important implications for the evolution of the interior and surface. On Venus, the large apparent depths of compensation for surface topographic features might be explained if surface topography were supported by variations in the thickness of a 100-200 km thick chemically buoyant mantle layer or by partial melting in the mantle at the base of such a layer. Long volcanic flows seen on the surface may be explained by deep melting that generates low-viscosity MgO-rich magmas. The presence of a shallow refractory mantle layer may also explain the lack of volcanism associated with rifting. As the depleted layer thickens and cools, it becomes denser than the convecting interior and the portion of it that is hot enough to flow can mix with the convecting mantle. Time dependence of the thickness of a depleted layer may create episodic resurfacing events as needed to explain the observed distribution of impact craters on the venusian surface. We consider a planetary structure consisting of a crust, depleted mantle layer, and a thermally and chemically well-mixed convecting mantle. The thermal evolution of the convecting spherical planetary interior is calculated using energy conservation: the time rate of change of thermal energy in the interior is equated to the difference in the rate of radioactive heat production and the rate of heat transfer across the thermal boundary layer. Heat transfer across the thermal boundary layer is parameterized using a standard Nusselt number-Rayleigh number relationship. The radioactive heat production decreases with time corresponding to decay times for the U, Th, and K. The planetary interior cools by the advection of hot mantle at temperature T interior into the thermal boundary layer where it cools conductively. The crust and depleted mantle layers do not convect in our model so that a linear conductive equilibrium temperature distribution is assumed. The rate of melt production is calculated as the product of the volume flux of mantle into the thermal boundary layer and the degree of melting that this mantle undergoes. The volume flux of mantle into the thermal boundary layer is simply the heat flux divided by amount of heat lost in cooling mantle to the average temperature in the thermal boundary layer. The degree of melting is calculated as the temperature difference above the solidus, divided by the latent heat of melting. A maximum degree of melting is prescribed corresponding to the maximum amount of basaltic melt that the mantle can initially generate. As the crust thickens, the pressure at the base of the crust becomes high enough and the temperature remains low enough for basalt to transform to dense eclogite. Author

N93-14359*# Brown Univ., Providence, RI. Dept. of Geological Sciences.

VENUS STEEP-SIDED DOMES: RELATIONSHIPS BETWEEN GEOLOGICAL ASSOCIATIONS AND POSSIBLE PETROGENETIC MODELS

B. Pavri and James W. Head, III *In* Lunar and Planetary Inst., Papers Presented to the International Colloquium on Venus 1992 p 87-88 (For primary document see N93-14288 04-91)
Avail: CASI HC A01/MF A02

Venus domes are characterized by steep sides, a circular shape, and a relatively flat summit area. In addition, they are orders of magnitude larger in volume and have a lower height/diameter ratio than terrestrial silicic lava domes. The morphology of the domes is consistent with formation by lava with a high apparent viscosity. Twenty percent of the domes are located in or near tessera (highly deformed highlands), while most other (62 percent) are located in and near coronae (circular deformational features thought to represent local mantle upwelling). These geological associations provide evidence for mechanisms of petrogenesis and several of these models are found to be plausible: remelting of basaltic or evolved crust, differentiation of basaltic melts, and volatile enhancement and eruption of basaltic foams. Hess and Head have shown that the full range of magma compositions existing on the Earth is plausible under various environmental

conditions on Venus. Most of the Venera and Vego lander compostional data are consistent with tholeiitic basalt; however, evidence for evolved magmas was provided by Venera 8 data consistent with a quartz monzonite composition. Pieters et al. have examined the color of the Venus surface from Venera lander images and interpret the surface there to be oxidized. Preliminary modeling of dome growth has provided some interpretations of lava rheology. Viscosity values obtained from these models range from 10(exp 14) - 10(exp 17) pa*s, and the yield strength has been calculated to be between 10(exp 4) and 10(exp 6) Pa, consistent with terrestrial silicic rocks. The apparent high viscosity of the dome lavas suggests that the domes have a silicic composition or must augment their viscosity with increased visicularity or crystal content. Sixty-two percent of the Venus domes are associated with coronae, circular features that have been proposed as sites of mantle upwelling, and 20 percent of the domes are located near tessera, relatively high areas of complex deformed terrain. We have investigated several models that are consistent with these geologic associations. The first case involves the differentiation of basalt in a magma reservoir in the crust, perhaps produced by partial melting within a mantle plume. The second case is melting at the base of thickened basaltic crust, and the final case is volatile exsolution and enhancement within a basaltic magma reservoir. The association of domes with tessera might be explained by crustal remelting, while the association with coronae may be consistent with chemical differentiation of a magma reservoir or the exsolution and concentration of volatiles in the reservoir before eruption. Author

N93-14360*# Massachusetts Inst. of Tech., Cambridge. Center for Space Research.

DIELECTRIC SURFACE PROPERTIES OF VENUS

G. H. Pettengill, R. J. Wilt, and P. G. Ford *In* Lunar and Planetary Inst., Papers Presented to the International Colloquium on Venus 1992 p 88-89 (For primary document see N93-14288 04-91)

Avail: CASI HC A01/MF A02

It has been known for over a decade that certain high-altitude regions on Venus exhibit bizarre radar-scattering and radiothermal-emission behavior. For example, observed values for normal-incidence power reflection coefficients in these areas can exceed 0.5; enhanced back scatter in some mountainous areas in the Magellan SAR images creates a bright surface with the appearance of snow; and reduced thermal emission in the anomalous areas makes the surface there appear hundreds of degrees cooler than the corresponding physical surface temperatures. The inferred radio emissivity in several of these regions falls to 0.3 for horizontal linear polarization at viewing angles in the range 20 deg - 40 deg. Several explanations have been offered for these linked phenomena. One involves single-surface reflection from a sharp discontinuity separating two media that have extremely disparate values of electromagnetic propagation. The mismatch may occur in either or both the real (associated with propagation velocity) or imaginary (associated with absorption) components of the relevant indices of refraction, and the discontinuity must take place over a distance appreciably shorter than a wavelength. An example of such an interaction of Earth would occur at the surface of a body of water. At radio wavelengths, water has an index of refraction of 9 (dielectric permittivity of about 80), and an associated loss factor that varies strongly with the amount of dissolved salts, but is generally significant. Its single-surface radar reflectivity at normal incidence is about 0.65, and the corresponding emissivity (viewed at the same angle) is therefore 0.35. Both these values are similar to the extremes found on Venus, but in the absence of liquid water, the process on Venus requires a different explanation. Two of the present authors (Pettengill and Ford) have suggested that scattering from a single surface possessing a very high effective dielectric permittivity could explain many of the unusual characteristics displayed by the Venus surface. A second explantion relates to the volume scattering that results from successive interactions with one or more interfaces interior to the planetary surface. If the near-surface material has a moderately low index of refraction (to ensure that a substantial fraction of the radiation incident from outside is not reflected, but rather penetrates into the surface), and a very low internal propagation loss, successive internal reflections can eventually redirect much of the energy back through the surface toward the viewer. The necessary conditions for this process to be effective are a low internal propagation loss coupled with efficient internal reflection. At sufficiently low temperatures, fractured water ice displays both the necessary low loss and near-total internal reflection. The possibility that this mechanism might be acting on Venus has recently been put forward. Author

N93-14361*# Washington Univ., Saint Louis, MO. Center for Space Sciences.

TECTONIC CONNECTIONS TO INTERIOR PROCESSES ON VENUS

R. J. Phillips *In* Lunar and Planetary Inst., Papers Presented to the International Colloquium on Venus 1992 p 89-90 (For primary document see N93-14288 04-91)

Avail: CASI HC A01/MF A02

The ultimate goal of geophysical/geological exploration of Venus is to relate the present tectonic (and volcanic) state of the lithosphere to interior processes, particularly mantle convection, operating both now and in the past. The Magellan mission has provided a spectacular view of the surface, and upcoming gravity measurements, particularly if the Magellan orbit is circularized, will provide significant constraints on the state of the interior. This extended abstract focuses on several controversial issues regarding venusian tectonics and its relationship to geodynamic mechanisms in the planet's interior. The origin of highlands, coronae diapir structures, and trenches and subduction are discussed. Author

N93-14362*# Jet Propulsion Lab., California Inst. of Tech., Pasadena.

PROBLEM FOOTPRINTS IN MAGELLAN ALTIMETRY DATA

Jeffrey J. Plaut *In* Lunar and Planetary Inst., Papers Presented to the International Colloquium on Venus 1992 p 90-92 (For primary document see N93-14288 04-91)

Avail: CASI HC A01/MF A02

The intensity, time-delay, and frequency content of radar echoes from the Magellan altimetry system are reduced to several parameters that are of great use in addressing many geological issues of the surface of Venus. These parameters include planetary radius, power reflection coefficient (reflectivity, both uncorrected and corrected for diffuse scattering), rms slope, and scattering functions (the behavior of backscatter as a function of incidence angle). Because the surface of Venus often reflects radio energy in unpredictable ways, models of radar scattering and their associated algorithms occasionally fail to accurately solve for the above surface parameters. Methods for identifying possible 'problem' altimetry data footprints, and techniques for resolving some key ambiguities are presented. Author

N93-14363*# Jet Propulsion Lab., California Inst. of Tech., Pasadena.

ANOMALOUS SCATTERING BEHAVIOR OF SELECTED IMPACT PARABOLA FEATURES: MAGELLAN CYCLE-TO-CYCLE COMPARISONS

Jeffrey J. Plaut, R. Stephen Saunders, E. R. Stofan, R. L. Kirk (Geological Survey, Flagstaff, AZ.), G. G. Schaber (Geological Survey, Flagstaff, AZ.), L. A. Soderblom (Geological Survey, Flagstaff, AZ.), P. G. Ford (Massachusetts Inst. of Tech., Cambridge.), G. H. Pettengill (Massachusetts Inst. of Tech., Cambridge.), D. B. Campbell (Cornell Univ., Ithaca, NY.), and N. J. S. Stacy (Cornell Univ., Ithaca, NY.) et al *In* Lunar and Planetary Inst., Papers Presented to the International Colloquium on Venus 1992 p 92-93 (For primary document see N93-14288 04-91)

Avail: CASI HC A01/MF A02

Magellan observations indicate that many venusian impact craters have associated surfaces, typically lower in backscatter and emissivity than the surroundings, that extend up to hundreds of kilometers to the west of craters, in parabolic planforms. During Magellan's second mapping cycle, a number of these parabolic features were imaged for a second time, under a different viewing geometry. In some cases, the SAR backscatter appearance of portions of the parabolic features was quite different in the two datasets. We present a description and preliminary interpretations of the anomalous appearance of these features as observed during Magellan's first and second mapping cycles. Author

N93-14364*# Oulu Univ. (Finland). Dept. of Astronomy.

CYTHEREAN CRUSTAL BENDING AT SALME DORSA

J. Raitala and K. Kauhanen *In* Lunar and Planetary Inst., Papers Presented to the International Colloquium on Venus 1992 p 93-94 (For primary document see N93-14288 04-91)

Avail: CASI HC A01/MF A02

The Salme ridge belt can be interpreted as being the leading edge of a venusian crustal unit that moved against the highland foreland unit. It is

indicative of a compressional zone, with a thrust front facing west. The Salme ridge belt with adjoining structures is an evident indication of lateral stresses and adjoining crustal movements on Venus. It supports the idea of southeast compression against and over the foreland planitia, which has bent under the load and/or lateral stress, resulting in trough and bulge formation in front of the ridge belt. The origin of the driving force for the movements remains masked. Laima Tessera is located in the direction from which the thrust is thought to apply but there are no appropriate candidates for a rift zone although a thrust from the southeast would be in good agreement with structures of Laima Tessera. The temperature gradient suggests that the lithosphere is approximately 12 km thick, while its elastic layer is approximately 3 km thick based either on the load-induced flexure model or on the compressional buckling model. Author

N93-14365*# Geological Survey, Flagstaff, AZ.
COMPUTER SIMULATIONS OF COMET- AND ASTEROIDLIKE BODIES PASSING THROUGH THE VENUSIAN ATMOSPHERE: PRELIMINARY RESULTS ON ATMOSPHERIC AND GROUND SHOCK EFFECTS
D. Roddy, D. Hatfield (California Research and Technology, Inc., Chatsworth.), P. Hassig (California Research and Technology, Inc., Chatsworth.), M. Rosenblatt (California Research and Technology, Inc., Chatsworth.), L. Soderblom, and E. DeJong (Jet Propulsion Lab., California Inst. of Tech., Pasadena.) *In* Lunar and Planetary Inst., Papers Presented to the International Colloquium on Venus 1992 p 94-96 (For primary document see N93-14288 04-91)
Avail: CASI HC A01/MF A02

We have completed computer simulations that model shock effects in the venusian atmosphere caused during the passage of two cometlike bodies 100 m and 1000 m in diameter and an asteroidlike body 10 km in diameter. Our objective is to examine hypervelocity-generated shock effects in the venusian atmosphere for bodies of different types and sizes in order to understand the following: (1) their deceleration and depth of penetration through the atmosphere; and (2) the onset of possible ground-surface shock effects such as splotches, craters, and ejecta formations. The three bodies were chosen to include both a range of general conditions applicable to Venus as well as three specific cases of current interest. These calculations use a new multiphase computer code (DICE-MAZ) designed by California Research & Technology for shock-dynamics simulations in complex environments. The code was tested and calibrated in large-scale explosion, cratering, and ejecta research. It treats a wide range of different multiphase conditions, including material types (vapor, melt, solid), particle-size distributions, and shock-induced dynamic changes in velocities, pressures, temperatures (internal energies), densities, and other related parameters, all of which were recorded in our calculations. Author

N93-14366*# Johns Hopkins Univ., Baltimore, MD. Dept. of Earth and Planetary Sciences.
THE EFFECTS OF VENUS' THERMAL STRUCTURE ON BUOYANT MAGMA ASCENT
S. E. H. Sakimoto and M. T. Zuber *In* Lunar and Planetary Inst., Papers Presented to the International Colloquium on Venus 1992 p 96-97 (For primary document see N93-14288 04-91)
Avail: CASI HC A01/MF A02

The recent Magellan images have revealed a broad spatial distribution of surface volcanism on Venus. Previous work in modeling the ascent of magma on both Venus and Earth has indicated that the planetary thermal structure significantly influences the magmatic cooling rates and thus the amount of magma that can be transported to the surface before solidification. In order to understand which aspects of the thermal structure have the greatest influence on the cooling of ascending magma, we have constructed magma cooling curves for both plutonic and crack buoyant ascent mechanisms, and evaluated the curves for variations in the planetary mantle temperature, thermal gradient curvature with depth, surface temperature gradient, and surface temperature. The planetary thermal structure is modeled as T/T(sub 0) = 1-tau(1-Z/Z(sub 0)(exp n), where T is the temperature, T(sub 0) is the source depth temperature, tau = 1-(T(sub s)/T(sub 0)) where T(sub s) is the planetary surface temperature, Z is the depth, Z(sub 0) is the source depth, and n is a constant that controls thermal gradient curvature with depth. The equation is used both for mathematical convenience and flexibility, as well as its fit to the thermal gradients predicted by the cooling half-space models. We assume a constant velocity buoyant ascent, body-averaged magma temperatures and properties, an initially crystal-free magma, and the same liquidus and solidus for both Venus and Earth. Author

N93-14367*# Scripps Institution of Oceanography, La Jolla, CA.
EVIDENCE FOR RETROGRADE LITHOSPHERIC SUBDUCTION ON VENUS
David T. Sandwell and Gerald Schubert (California Univ., Los Angeles.) *In* Lunar and Planetary Inst., Papers Presented to the International Colloquium on Venus 1992 p 97-99 (For primary document see N93-14288 04-91)
Avail: CASI HC A01/MF A02

Though there is no plate tectonics per se on Venus, recent Magellan radar images and topographic profiles of the planet suggest the occurrence of the plate tectonic processes of lithospheric subduction and back-arc spreading. The perimeters of several large coronae (e.g., Latona, Artemis, and Eithinoha) resemble Earth subduction zones in both their planform and topographic profile. The planform of arcuate structures in Eastern Aphrodite were compared with subduction zones of the East Indies. The venusian structures have radii of curvature that are similar to those of terrestrial subduction zones. Moreover, the topography of the venusian ridge/trench structures is highly asymmetric with a ridge on the concave side and a trough on the convex side; Earth subduction zones generally display the same asymmetry. Author

N93-14368*# Jet Propulsion Lab., California Inst. of Tech., Pasadena.
OVERVIEW OF VENUS GEOLOGY: PRELIMINARY DESCRIPTION OF TERRAIN UNITS FOR VENUS GLOBAL GEOLOGICAL MAPPING
R. Stephen Saunders, Ellen R. Stofan, Jeffrey J. Plaut, and Gregory A. Michaels *In* Lunar and Planetary Inst., Papers Presented to the International Colloquium on Venus 1992 p 99 (For primary document see N93-14288 04-91)
Avail: CASI HC A01/MF A02

Venus terrain units can be categorized on the basis of morphology, reflectivity, backscatter, roughness, and emissivity. Morphology can be inferred from Magellan left-looking nominal incidence angle image mosaics, right-looking coverage, and more limited left-looking stereo. The typical resolution is about 300 m down to about 120 m near periapsis in the cycle one nominal coverage. The scale of geologic mapping governs definition of mappable terrain units. Initial global mapping is being compiled at a scale of 1:50 million. At this scale, the smallest individual features that can be mapped are about 125 km. The categories of terrain types are plains, complex ridge terrain, features with morphology suggesting volcanic or volcano-tectonic origin, features interpreted to be tectonic in origin, crater units, and surficial units such as splotches and streaks. Brief descriptions of terrain units are provided. Author

N93-14369*# National Aeronautics and Space Administration, Washington, DC.
IMPACT CRATERS ON VENUS: AN OVERVIEW FROM MAGELLAN OBSERVATIONS
G. G. Schaber (Geological Survey, Flagstaff, AZ.), R. G. Strom (Arizona Univ., Tucson.), H. J. Moore (Geological Survey, Menlo Park, CA.), L. A. Soderblom (Geological Survey, Flagstaff, AZ.), R. L. Kirk (Geological Survey, Flagstaff, AZ.), D. J. Chadwick (Geological Survey, Flagstaff, AZ.), D. D. Dawson (Arizona Univ., Tucson.), L. R. Gaddis (Geological Survey, Flagstaff, AZ.), J. M. Boyce, and J. Russell (Geological Survey, Flagstaff, AZ.) *In* Lunar and Planetary Inst., Papers Presented to the International Colloquium on Venus 1992 p 100-101 (For primary document see N93-14288 04-91)
Avail: CASI HC A01/MF A02

Magellan has revealed an ensemble of impact craters on Venus that is unique in many important ways. We have compiled a database describing 842 craters on 89 percent of the planet's surface mapped through orbit 2578 (the craters range in diameter from 1.5 to 280 km). We have studied the distribution, size-frequency, morphology, and geology of these craters both in aggregate and, for some craters, in more detail. We have found the following: (1) the spatial distribution of craters is highly uniform; (2) the size-density distribution of craters with diameters greater than or equal to 35 km is consistent with a 'production' population having a surprisingly young age of about 0.5 Ga (based on the estimated population of Venus-crossing asteroids); (3) the spectrum of crater modification differs

greatly from that on other planets--62 percent of all craters are pristine, only 4 percent volcanically embayed, and the remainder affected by tectonism, but none are severely and progressively depleted based on size-density distribution extrapolated from larger craters; (4) large craters have a progression of morphologies generally similar to those on other planets, but small craters are typically irregular or multiple rather than bowl shaped; (5) diffuse radar-bright or -dark features surround some craters, and about 370 similar diffuse 'splotches' with no central crater are observed whose size-density distribution is similar to that of small craters; and (6) other features unique to Venus include radar-bright or -dark parabolic arcs opening westward and extensive outflows originating in crater ejecta.

Author

N93-14370*# Brown Univ., Providence, RI. Dept. of Geological Sciences.

ATMOSPHERIC EFFECTS ON CRATER GROWTH ON VENUS

Peter H. Schultz *In* Lunar and Planetary Inst., Papers Presented to the International Colloquium on Venus 1992 p 101-103 (For primary document see N93-14288 04-91)

Avail: CASI HC A01/MF A02

Laboratory experiments allow examining the consequences of complex processes operating over a wide range of scales (both temporal and spatial) and frequently reveal effects that are obvious only in hindsight. Even though all processes may not scale directly, isolation of the controlling variables allows assessing first-order effects through analytical approximations. This approach can be illustrated by the systematic sequence of ballistic ejection, the response of an atmosphere to a strong energy source, the scaling of ejecta thickness, and the role of secondary cratering. Here it is proposed that the effects of atmospheric pressure and density on crater growth (hence, scaling) observed in laboratory experiments has particular relevance for craters on Venus.

Author

N93-14371*# Brown Univ., Providence, RI. Dept. of Geological Sciences.

EFFECT OF IMPACT ANGLE ON CENTRAL-PEAK/PEAK-RING FORMATION AND CRATER COLLAPSE ON VENUS

Peter H. Schultz *In* Lunar and Planetary Inst., Papers Presented to the International Colloquium on Venus 1992 p 103-104 (For primary document see N93-14288 04-91)

Avail: CASI HC A01/MF A02

Although asymmetry in ejecta patterns and craters shape-in-plan are commonly cited as diagnostic features of impact angle, the early-time transfer of energy from impactor to target also creates distinctive asymmetries in crater profile with the greatest depth uprange. In order to simulate gravity-controlled crater-growth, laboratory experiments use loose particulate targets as analogs for low-strength material properties following passage of the shock. As a result, impact crater diameter D in laboratory experiments generally is many times greater than the impactor diameter 2r (factor of 40), and early-time asymmetries in energy transfer from oblique impacts are consumed by subsequent symmetrical crater growth, except at the lowest angles (less than 25 deg). Such asymmetry is evident for oblique (less than 60 deg from horizontal) impacts into aluminum where D/2r is only 2 to 4. Because cratering efficiency decreases with increasing crater size and decreasing impact angle, large scale planetary craters (4080 km) should have transient excavation diameters only 6-10 times larger than the impactor. At basin scales, D/2r is predicted to be only 3-5, i.e., approaching values for impacts into aluminum in laboratory experiments. As a result, evidence for early-time asymmetry in impactor energy transfer should become evident on planetary surfaces, yet craters generally retain a circular outline for all but the lowest impact angles.

Author

N93-14372*# Brown Univ., Providence, RI. Dept. of Geological Sciences.

IMPACT-GENERATED WINDS ON VENUS: CAUSES AND EFFECTS

Pater H. Schultz *In* Lunar and Planetary Inst., Papers Presented to the International Colloquium on Venus 1992 p 104-106 (For primary document see N93-14288 04-91)

Avail: CASI HC A01/MF A02

The pressure of the dense atmosphere of Venus significantly changes the appearance of ejecta deposits relative to craters on the Moon and Mercury. Conversely, specific styles and sequences of ejecta emplacement can be inferred to represent different intensities of atmospheric response winds acting over different timescales. Three characteristic timescales can be inferred from the geologic record: surface scouring and impactor-controlled (angle and direction) initiation of the long fluidized run-out flows; nonballistic emplacement of inner, radar-bright ejecta facies and radar-dark outer facies; and very late reworking of surface materials. These three timescales roughly correspond to processes observed in laboratory experiments that can be scaled to conditions on Venus (with appropriate assumptions): coupling between the atmosphere and earlytime vapor/melt (target and impactor) that produces an intense shock that subsequently evolves into blast/response winds; less energetic dynamic response of the atmosphere to the outward-moving ballistic ejecta curtain that generates nonthermal turbulent eddies; and late recovery of the atmosphere to impact-generated thermal and pressure gradients expressed as low-energy but long-lived winds. These different timescales and processes can be viewed as the atmosphere equivalent of shock melting, material motion, and far-field seismic response in the target. The three processes (early Processes, Atmospheric Processes, and Late Recovery Winds) are discussed at length.

Author

N93-14373*# Jet Propulsion Lab., California Inst. of Tech., Pasadena.

MAGELLAN PROJECT Progress Report

J. F. Scott, D. G. Griffith, J. M. Gunn, R. G. Piereson, J. M. Stewart, A. M. Tavormina, and T. W. Thompson *In* Lunar and Planetary Inst., Papers Presented to the International Colloquium on Venus 1992 p 106-107 (For primary document see N93-14288 04-91)

Avail: CASI HC A01/MF A02

The Magellan spacecraft was placed into orbit around Venus on 10 Aug. 1990 and started radar data acquisition on 15 Sep. 1990. Since then, Magellan has completed mapping over 2.75 rotations of the planet (as of mid-July 1992). Synthetic aperture radar (SAR), altimetry, and radiometry observations have covered 84 percent of the surface during the first mission cycle from mid-Sep. 1990 through mid-May 1991. Operations in the second mission cycle from mid-May 1991 through mid-Jan. 1992 emphasized filling the larger gaps (the south polar region and a superior conjunction) from that first cycle. Planned observations in the fourth mission cycle from mid-Sep. 1992 through mid-May 1993 will emphasize high-resolution gravity observations of the equatorial regions of Venus.

Author

N93-14374*# Brown Univ., Providence, RI. Dept. of Geological Sciences.

ATLA REGIO, VENUS: GEOLOGY AND ORIGIN OF A MAJOR EQUATORIAL VOLCANIC RISE

D. A. Senske and James W. Head, III *In* Lunar and Planetary Inst., Papers Presented to the International Colloquium on Venus 1992 p 107-109 (For primary document see N93-14288 04-91)

Avail: CASI HC A01/MF A02

Regional volcanic rises form a major part of the highlands in the equatorial region of Venus. These broad domical uplands, 1000 to 3000 km across, contain centers of volcanism forming large edifices and are associated with extension and rifting. Two classes of rises are observed: (1) those that are dominated by tectonism, acting as major centers for converging rifts such as Beta Regio and Alta Regio, and are termed tectonic junctions; and (2) those forming uplands characterized primarily by large-scale volcanism forming edifices. Western Eistla Regio and Bell Regio, where zones of extension and rifting are less developed. Within this second class of features the edifices are typically found at the end of a single rift, or are associated with a linear belt of deformation. We examine the geologic characteristics of the tectonic junction at Alta Regio, concentrating on documenting the styles of volcanism and assessing mechanisms for the formation of regional topography.

Author

N93-14375*# Moscow State Univ. (USSR).

THE GEOLOGIC MAPPING OF VENUS USING C-1 FORMAT: SHEETS 75N254, 60N263

I. V. Shalimov *In* Lunar and Planetary Inst., Papers Presented to the International Colloquium on Venus 1992 p 109-110 (For primary document see N93-14288 04-91)

Avail: CASI HC A01/MF A02

The results of geologic mapping of Venus, produced on the base of Magellan images, are presented. We submit two C-1 format geologic maps with the appropriate legend. The mapping territory was taken from Venera

15 and 16 missions and geologic maps were composed. Magellan images allow us to divide some types of the plains units to determine the lava flow direction and to map with better accuracy. Author

N93-14376*# Massachusetts Inst. of Tech., Cambridge. Dept. of Earth, Atmospheric, and Planetary Sciences.

GEOID, TOPOGRAPHY, AND CONVECTION-DRIVEN CRUSTAL DEFORMATION ON VENUS

Mark Simons, Bradford H. Hager, and Sean C. Solomon *In* Lunar and Planetary Inst., Papers Presented to the International Colloquium on Venus 1992 p 110-112 (For primary document see N93-14288 04-91)

Avail: CASI HC A01/MF A02

High-resolution Magellan images and altimetry of Venus reveal a wide range of styles and scales of surface deformation that cannot readily be explained within the classical terrestrial plate tectonic paradigm. The high correlation of long-wavelength topography and gravity and the large apparent depths of compensation suggest that Venus lacks an upper-mantle low-viscosity zone. A key difference between Earth and Venus may be the degree of coupling between the convecting mantle and the overlying lithosphere. Mantle flow should then have recognizable signatures in the relationships between surface topography, crustal deformation, and the observed gravity field. Author

N93-14377*# Jet Propulsion Lab., California Inst. of Tech., Pasadena.

VENUS GRAVITY: SUMMARY AND COMING EVENTS

W. L. Sjogren *In* Lunar and Planetary Inst., Papers Presented to the International Colloquium on Venus 1992 p 112 (For primary document see N93-14288 04-91)

Avail: CASI HC A01/MF A02

The first significant dataset to provide local measures of venusian gravity field variations was that acquired from the Pioneer Venus Orbiter (PVO) during the 1979-1981 period. These observations were S-band Doppler radio signals from the orbiting spacecraft received at Earth-based tracking stations. Early reductions of these data were performed using two quite different techniques. Estimates of the classical spherical harmonics were made to various degrees and orders up to 10. At that time, solutions of much higher degree and order were very difficult due to computer limitations. These reductions, because of low degree and order, revealed only the most prominent features with poor spatial resolution and very reduced peak amplitudes. Author

N93-14378*# Academy of Sciences (USSR), Moscow. Vernadsky Inst.

DIFFERENT TYPES OF SMALL VOLCANOS ON VENUS

E. N. Slyuta, I. V. Shalimov (Moscow State Univ., USSR), and A. M. Nikishin (Moscow State Univ., USSR) *In* Lunar and Planetary Inst., Papers Presented to the International Colloquium on Venus 1992 p 112-114 (For primary document see N93-14288 04-91)

Avail: CASI HC A01/MF A02

One of the studies of volcanic activity on Venus is the comparison of that with the analogous volcanic activity on Earth. The preliminary report of such a comparison and description of a small cluster of small venusian volcanos is represented in detail in this paper. Author

N93-14379*# Massachusetts Inst. of Tech., Cambridge. Dept. of Earth, Atmospheric, and Planetary Sciences.

CONSTRAINTS ON CRUSTAL RHEOLOGY AND AGE OF DEFORMATION FROM MODELS OF GRAVITATIONAL SPREADING IN ISHTAR TERRA, VENUS

Suzanne E. Smrekar and Sean C. Soloman *In* Lunar and Planetary Inst., Papers Presented to the International Colloquium on Venus 1992 p 114-116 (For primary document see N93-14288 04-91)

Avail: CASI HC A01/MF A02

Gravitational spreading is expected to lead to rapid relaxation of high relief due to the high surface temperature and associated weak crust on Venus. In this study, we use new Magellan radar and altimetry data to determine the extent of gravitational relaxation in Ishtar Terra, which contains the highest relief on Venus as well as areas of extremely high topographic slope. Within Ishtar Terra the only mountain belts found on Venus, Akna, Danu, Freyja, and Maxwell Montes, nearly encircle the smooth, high (3-4 km) plateau of Lakshmi Planum. Finite-element models of this process give expected timescales for relaxation of relief and failure at the surface. From these modeling results we attempt to constrain the strength of the crust and timescales of deformation in Ishtar Terra. Below we discuss observational evidence for gravitational spreading in Ishtar Terra, results from the finite-element modeling, independent age constraints, and implications for the rheology and timing of deformation. Author

N93-14380*# Jet Propulsion Lab., California Inst. of Tech., Pasadena.

MULTIRESOLUTION PATTERN RECOGNITION OF SMALL VOLCANOS IN MAGELLAN DATA

P. Smyth, C. H. Anderson, J. C. Aubele (Brown Univ., Providence, RI.), and L. S. Crumpler (Brown Univ., Providence, RI.) *In* Lunar and Planetary Inst., Papers Presented to the International Colloquium on Venus 1992 p 116-117 (For primary document see N93-14288 04-91)

Avail: CASI HC A01/MF A02

The Magellan data is a treasure-trove for scientific analysis of venusian geology, providing far more detail than was previously available from Pioneer Venus, Venera 15/16, or ground-based radar observations. However, at this point, planetary scientists are being overwhelmed by the sheer quantities of data collected--data analysis technology has not kept pace with our ability to collect and store it. In particular, 'small-shield' volcanos (less than 20 km in diameter) are the most abundant visible geologic feature on the planet. It is estimated, based on extrapolating from previous studies and knowledge of the underlying geologic processes, that there should be on the order of 10(exp 5) to 10(exp 6) of these volcanos visible in the Magellan data. Identifying and studying these volcanos is fundamental to a proper understanding of the geologic evolution of Venus. However, locating and parameterizing them in a manual manner is very time-consuming. Hence, we have undertaken the development of techniques to partially automate this task. The goal is not the unrealistic one of total automation, but rather the development of a useful tool to aid the project scientists. The primary constraints for this particular problem are as follows: (1) the method must be reasonably robust; and (2) the method must be reasonably fast. Unlike most geological features, the small volcanos of Venus can be ascribed to a basic process that produces features with a short list of readily defined characteristics differing significantly from other surface features on Venus. For pattern recognition purposes the relevant criteria include the following: (1) a circular planimetric outline; (2) known diameter frequency distribution from preliminary studies; (3) a limited number of basic morphological shapes; and (4) the common occurrence of a single, circular summit pit at the center of the edifice. Author

N93-14381*# California Inst. of Tech., Pasadena. Div. of Geological and Planetary Sciences.

MELTING AND DIFFERENTIATION IN VENUS WITH A COLD START: A MECHANISM OF THE THIN CRUST FORMATION

Viatcheslav S. Solomatov and David J. Stevenson *In* Lunar and Planetary Inst., Papers Presented to the International Colloquium on Venus 1992 p 117-118 (For primary document see N93-14288 04-91)

Avail: CASI HC A01/MF A02

Recent works argue that the venusian crust is thin: less than 10-30 km. However, any convective model of Venus unavoidably predicts melting and a fast growth of the basaltic crust, up to its maximum thickness of about 70 km limited, by the gabbro-eclogite phase transition. The crust is highly buoyant due to both its composition and temperature and it is problematic to find a mechanism providing its effective recycling and thinning in the absence of plate tectonics. There are different ways to solve this contradiction. This study suggests that a thin crust can be produced during the entire evolution of Venus if Venus avoided giant impacts. Author

N93-14382*# Massachusetts Inst. of Tech., Cambridge. Dept. of Earth, Atmospheric, and Planetary Sciences.

THE TECTONICS OF VENUS: AN OVERVIEW

Sean C. Solomon *In* Lunar and Planetary Inst., Papers Presented to the International Colloquium on Venus 1992 p 118-119 (For primary document see N93-14288 04-91)

Avail: CASI HC A01/MF A02

While the Pioneer Venus altimeter, Earth-based radar observatories, and the Venera 15-16 orbital imaging radars provided views of large-scale tectonic features on Venus at ever-increasing resolution, the radar images from Magellan constitute an improvement in resolution of at least an order of magnitude over the best previously available. A summary of early Magellan observations of tectonic features on Venus was published, but data available at that time were restricted to the first month of mapping and represented

only about 15 percent of the surface of the planet. Magellan images and altimetry are now available for more than 95 percent of the Venus surface. Thus a more global perspective may be taken on the styles and distribution of lithospheric deformation on Venus and their implications for the tectonic history of the planet. Author

N93-14383*# Cornell Univ., Ithaca, NY.
THE SPATIAL DISTRIBUTION OF CORONAE ON VENUS
S. W. Squyres, G. Schubert (California Univ., Los Angeles.), D. L. Bindschadler (California Univ., Los Angeles.), D. M. Janes, J. E. Moersch, W. Moore (California Univ., Los Angeles.), P. Olson (Johns Hopkins Univ., Baltimore, MD.), J. T. Ratcliff (California Univ., Los Angeles.), E. R. Stofan (Jet Propulsion Lab., California Inst. of Tech., Pasadena.), and D. L. Turcotte *In* Lunar and Planetary Inst., Papers Presented to the International Colloquium on Venus 1992 p 119-120 (For primary document see N93-14288 04-91)
Avail: CASI HC A01/MF A02

Coronae on Venus are large, generally circular surface features that have distinctive tectonic, volcanic, and topographic expressions. They range in diameter from less than 200 km to at least 1000 km. Data from the Magellan spacecraft have now allowed complete global mapping of the spatial distribution of coronae on the planet. Unlike impact craters, which show a random (i.e., Poisson) spatial distribution, the distribution of coronae appears to be nonrandom. We investigate the distribution here in detail, and explore its implications in terms of mantle convection and surface modification processes. Author

N93-14384*# Cornell Univ., Ithaca, NY. Dept. of Astronomy.
MICROWAVE SCATTERING AND EMISSION PROPERTIES OF LARGE IMPACT CRATERS ON THE SURFACE OF VENUS
N. J. S. Stacy, D. B. Campbell, and C. Devries *In* Lunar and Planetary Inst., Papers Presented to the International Colloquium on Venus 1992 p 120-121 (For primary document see N93-14288 04-91)
Avail: CASI HC A01/MF A02

Many of the impact craters on Venus imaged by the Magellan synthetic aperture radar (SAR) have interior floors with oblique incidence angle backscatter cross sections 2 to 16 times (3 dB to 12 dB) greater than the average scattering properties of the planet's surface. Such high backscatter cross sections are indicative of a high degree of wavelength-scale surface roughness and/or a high intrinsic reflectivity of the material forming the crater floors. Fifty-three of these (radar) bright floored craters are associated with 93 percent of the parabolic-shaped radar-dark features found in the Magellan SAR and emissivity data, features that are thought to be among the youngest on the surface of Venus. It was suggested by Campbell et al. that either the bright floors of the parabolic feature parent craters are indicative of a young impact and the floor properties are modified with time to a lower backscatter cross section or that they result from some property of the surface or subsurface material at the point of impact or from the properties of the impacting object. As a continuation of earlier work we have examined all craters with diameters greater than 30 km (except 6 that were outside the available data) so both the backscatter cross section and emissivity of the crater floors could be estimated from the Magellan data. Author

N93-14385*# Cologne Univ. (Germany). Inst. fuer Geophysik und Meteorologie.
THE EFFECTS OF VENUSIAN MANTLE CONVECTION WITH MULTIPLE PHASE TRANSITIONS
V. Steinbach, D. A. Yuen (Minnesota Univ., Minneapolis.), and U. R. Christensen (Max-Planck-Inst. fuer Chemie, Mainz, Germany) *In* Lunar and Planetary Inst., Papers Presented to the International Colloquium on Venus 1992 p 121-122 (For primary document see N93-14288 04-91)
Avail: CASI HC A01/MF A02

Recently there was a flurry of activities in studying the effects of phase transitions in the Earth's mantle. From petrological and geophysical considerations, phase-transitions would also play an important role in venusian dynamics. The basic differences between the two planets are the surface boundary conditions, both thermally and mechanically. In this vein we have studied time-dependent mantle convection with multiple phase transitions and depth-dependent thermal expansivity (alpha is approximately rho(exp -6)), based on high-pressure and temperature measurements. Both the olivine-spinel and spinel-perovskite transitions were simulated by introducing an effective thermal expansivity, as described. Used together with the extended Boussinesq Approximation this method serves as a powerful tool to examine the effects of phase transitions on convection at relatively low computational costs. Author

N93-14386*# California Univ., Los Angeles. Inst. of Geophysics and Planetary Physics.
EVIDENCE FOR LIGHTNING ON VENUS
R. J. Strangeway *In* Lunar and Planetary Inst., Papers Presented to the International Colloquium on Venus 1992 p 122-123 (For primary document see N93-14288 04-91)
(Grant NAG2-485)
Avail: CASI HC A01/MF A02

Lightning is an interesting phenomenon both for atmospheric and ionospheric science. At the Earth lightning is generated in regions where there is strong convection. Lightning also requires the generation of large charge-separation electric fields. The energy dissipated in a lightning discharge can, for example, result in chemical reactions that would not normally occur. From an ionospheric point of view, lightning generates a broad spectrum of electromagnetic radiation. This radiation can propagate through the ionosphere as whistler mode waves, and at the Earth the waves propagate to high altitudes in the plasmasphere where they can cause energetic particle precipitation. The atmosphere and ionosphere of Venus are quite different from those on the Earth, and the presence of lightning at Venus has important consequences for our knowledge of why lightning occurs and how the energy is dissipated in the atmosphere and ionosphere. As discussed here, it now appears that lightning occurs in the dusk local time sector at Venus. Author

N93-14387*# California Inst. of Tech., Pasadena. Div. of Geological and Planetary Sciences.
VOLCANISM BY MELT-DRIVEN RAYLEIGH-TAYLOR INSTABILITIES AND POSSIBLE CONSEQUENCES OF MELTING FOR ADMITTANCE RATIOS ON VENUS
P. J. Tackley, D. J. Stevenson, and D. R. Scott (University of Southern California, Los Angeles.) *In* Lunar and Planetary Inst., Papers Presented to the International Colloquium on Venus 1992 p 123-124 (For primary document see N93-14288 04-91)
Avail: CASI HC A01/MF A02

A large number of volcanic features exist on Venus, ranging from tens of thousands of small domes to large shields and coronae. It is difficult to reconcile all these with an explanation involving deep mantle plumes, since a number of separate arguments lead to the conclusion that deep mantle plumes reaching the base of the lithosphere must exceed a certain size. In addition, the fraction of basal heating in Venus' mantle may be significantly lower than in Earth's mantle reducing the number of strong plumes from the core-mantle boundary. In three-dimensional convection simulations with mainly internal heating, weak, distributed upwellings are usually observed. We present an alternative mechanism for such volcanism, originally proposed for the Earth and for Venus, involving Rayleigh-Taylor instabilities driven by melt buoyancy, occurring spontaneously in partially or incipiently molten regions. Author

N93-14388*# Geological Survey, Flagstaff, AZ.
CAN A TIME-STRATIGRAPHIC CLASSIFICATION SYSTEM BE DEVELOPED FOR VENUS?
K. L. Tanaka and G. G. Schaber *In* Lunar and Planetary Inst., Papers Presented to the International Colloquium on Venus 1992 p 124-125 (For primary document see N93-14288 04-91)
Avail: CASI HC A01/MF A02

Magellan radar images reveal that Venus' exposed geologic record covers a relatively short and recent time span, as indicated by the low density of impact craters across the planet. Therefore, because impact cratering in itself will not be a useful tool to define geologic ages on Venus, it was questioned whether a useful stratigraphic scheme can be developed for the planet. We believe that a venusian stratigraphy is possible and that it can be based on the following: (1) an examination of the rationale and methods that have been used to develop such schemes for the other planets; and (2) what can be gleaned from Magellan and other datasets of Venus. Author

N93-14389*# Oulu Univ. (Finland). Dept. of Astronomy.
STRUCTURAL CHARACTERISTICS AND TECTONICS OF NORTHEASTERN TELLUS REGIO AND MENI TESSERA
T. Toermaenen *In* Lunar and Planetary Inst., Papers Presented to the International Colloquium on Venus 1992 p 125-127 (For primary document see N93-14288 04-91)
Avail: CASI HC A01/MF A02

The Tellus Regio-Meni Tessera region is an interesting highland area characterized by large areas of complex ridged terrain or tessera terrain. The area was previously studied from the Venera 15/16 data, typical characteristics of complex tessera terrain of Tellus Regio were analyzed, and a formation mechanism was proposed. Apparent depths of compensation of approximately 30-50 km were calculated from Pioneer Venus gravity and topography data. These values indicate predominant Airy compensation for the area. Regional stresses and lithospheric structures were defined from analysis of surface structures, topography, and gravity data. In this work we concentrate on northeastern Tellus Regio and Meni Tessera, which are situated north and west of Tellus Regio. Structural features and relationships are analyzed in order to interpret tectonic history of the area. Study area was divided into three subareas: northeastern Tellus Regio, Meni Tessera, and the deformed plain between them. Author

N93-14390*# Cornell Univ., Ithaca, NY. Dept. of Geological Sciences.
EPISODIC PLATE TECTONICS ON VENUS
Donald Turcotte *In* Lunar and Planetary Inst., Papers Presented to the International Colloquium on Venus 1992 p 127-128 (For primary document see N93-14288 04-91)
Avail: CASI HC A01/MF A02

Studies of impact craters on Venus from the Magellan images have placed important constraints on surface volcanism. Some 840 impact craters have been identified with diameters ranging from 2 to 280 km. Correlations of this impact flux with craters on the Moon, Earth, and Mars indicate a mean surface age of 0.5 +/- 0.3 Ga. Another important observation is that 52 percent of the craters are slightly fractured and only 4.5 percent are embayed by lava flows. These observations led researchers to hypothesize that a pervasive resurfacing event occurred about 500 m.y. ago and that relatively little surface volcanism has occurred since. Other researchers have pointed out that a global resurfacing event that ceased about 500 MYBP is consistent with the results given by a recent study. These authors carried out a series of numerical calculations of mantle convection in Venus yielding thermal evolution results. Their model considered crustal recycling and gave rapid planetary cooling. They, in fact, suggested that prior to 500 MYBP plate tectonics was active in Venus and since 500 MYBP the lithosphere has stabilized and only hot-spot volcanism has reached the surface. We propose an alternative hypothesis for the inferred cessation of surface volcanism on Venus. We hypothesize that plate tectonics on Venus is episodic. Periods of rapid plate tectonics result in high rates of subduction that cool the interior resulting in more sluggish mantle convection. Author

N93-14391*# Stanford Univ., CA. Center for Radar Astronomy.
SCATTERING PROPERTIES OF VENUS' SURFACE
G. L. Tyler, R. A. Simpson, M. J. Maurer, and E. Holmann *In* Lunar and Planetary Inst., Papers Presented to the International Colloquium on Venus 1992 p 128-129 (For primary document see N93-14288 04-91)
Avail: CASI HC A01/MF A02

Radar backscatter functions Sigma-(carat)(sub 0)(phi) for incidence angles between 0 less than or equal to phi less than or equal to 4-10 deg were derived from Magellan altimetry radar echoes. The procedure includes constrained solution of a system of simultaneous equations for which the echo-spectrum and echo time profile are inputs. A practical and workable set of constraints was applied; optimization and improved results are expected as the analysis matures. The scattering functions yield information on small-scale surface structures (tens of centimeters to tens of meters) but averaged over hundreds of sq km. RMS surface slopes derived from fits of analytic functions to the Sigma-(carat)(sub 0)(phi) results were converted to map form and show patterns similar to those reported using other techniques. While all three forms are found on Venus, fit residuals imply that an exponential scattering function matches data better than either the Hagfors or Gaussian form in most areas, although the Hagfors function may be a better descriptor at some sites. Limited study of image data indicates that average backscatter cross section, and possibly its slope, can be derived at oblique angles (17 deg less than or equal to phi less than or equal to 45 deg). Offsets of the echo peak in altimetry spectra are surprisingly common and are loosely correlated with Venus topography, but no cause for this phenomenon was identified. Author

N93-14392*# Jet Propulsion Lab., California Inst. of Tech., Pasadena.
LOW-EMISSIVITY IMPACT CRATERS ON VENUS
C. M. Weitz, C. Elachi, H. J. Moore (Geological Survey, Menlo Park, CA.), A. T. Basilevsky (Academy of Sciences, USSR, Moscow), B. A. Ivanov (Academy of Sciences, USSR, Moscow), and G. G. Schaber (Geological Survey, Flagstaff, AZ.) *In* Lunar and Planetary Inst., Papers Presented to the International Colloquium on Venus 1992 p 129-131 (For primary document see N93-14288 04-91)
Avail: CASI HC A01/MF A02

An analysis of 144 impact craters on Venus has shown that 11 of these have floors with average emissivities lower than 0.8. The remaining craters have emissivities between 0.8 and 0.9, independent of the specific backscatter cross section of the crater floors. These 144 impact craters were chosen from a possible 164 craters with diameters greater than 30 km as identified by researchers for 89 percent of the surface of Venus. We have only looked at craters below 6053.5 km altitude because a mineralogical change causes high reflectivity/low emissivity above the altitude. We have also excluded all craters with diameters smaller than 30 km because the emissivity footprint at periapsis is 16 x 24 km and becomes larger at the poles. Author

N93-14393*# Brown Univ., Providence, RI. Dept. of Geological Sciences.
FLOOR-FRACTURED CRATER MODELS FOR IGNEOUS CRATER MODIFICATION ON VENUS
R. W. Wichman and P. H. Schultz *In* Lunar and Planetary Inst., Papers Presented to the International Colloquium on Venus 1992 p 131-132 (For primary document see N93-14288 04-91)
Avail: CASI HC A01/MF A02

Although crater modification on the Earth, Moon, and Mars results from surface erosion and crater infilling, a significant number of craters on the Moon also exhibit distinctive patterns of crater-centered fracturing and volcanism that can be modeled as the result of igneous crater modification. Here, we consider the possible effects of Venus surface conditions on this model, describe two examples of such crater modification, and then briefly discuss the constraints these craters place on conditions at depth.
Author

N93-14394*# Smithsonian Astrophysical Observatory, Cambridge, MA.
VENUS: GEOCHEMICAL CONCLUSIONS FROM THE MAGELLAN DATA
J. A. Wood *In* Lunar and Planetary Inst., Papers Presented to the International Colloquium on Venus 1992 p 132-133 (For primary document see N93-14288 04-91)
Avail: CASI HC A01/MF A02

Though the Magellan mission was not designed to collect geochemical or petrological information, it has done so nonetheless. Since the time of the Pioneer Venus mission it has been known that high-altitude (greater than 2.5-5 km) mountainous areas on Venus exhibit anomalously low radiothermal emissivity (e less than 0.6). Magellan has greatly refined and extended these observations. The low emissivity requires surface material in the uplands to have a mineralogical composition that gives it a high bulk dielectric constant, greater than 20. The dielectric constant of dry terrestrial volcanic rocks seldom exceeds 7. The high-dielectric character of high-altitude surface material cannot be a primary property of the local volcanic rock, because there is no reason why rock having the required special mineralogy would erupt only at high altitudes. Therefore it is a secondary property; the primary Venus rock has reacted with the atmosphere to form a mineralogically different surface layer, and the secondary minerals formed are controlled by the ambient temperature, which decreases with altitude on Venus. A further investigation of venusian mineralogy is presented. Author

N93-14395*# National Aeronautics and Space Administration. Ames Research Center, Moffett Field, CA.
FINITE AMPLITUDE GRAVITY WAVES IN THE VENUS ATMOSPHERE GENERATED BY SURFACE TOPOGRAPHY
R. E. Young, H. Houben (Space Physics Research Inst., Sunnyvale, CA.),

R. L. Walterscheid (Aerospace Corp., Los Angeles, CA.), and G. Schubert (California Univ., Los Angeles.) *In* Lunar and Planetary Inst., Papers Presented to the International Colloquium on Venus 1992 p 133-134 (For primary document see N93-14288 04-91)
Avail: CASI HC A01/MF A02

A two-dimensional, fully nonlinear, nonhydrostatic, gravity wave model is used to study the evolution of gravity waves generated near the surface of Venus. The model extends from near the surface to well above the cloud layers. Waves are forced by applying a vertical wind at the bottom boundary. The boundary vertical wind is determined by the product of the horizontal wind and the gradient of the surface height. When wave amplitudes are small, the near-surface horizontal wind is the zonally averaged basic-state zonal wind, and the length scales of the forcing that results are characteristic of the surface height variation. When the forcing becomes larger and wave amplitudes affect the near-surface horizontal wind field, the forcing spectrum becomes more complicated, and a spectrum of waves is generated that is not a direct reflection of the spectrum of the surface height variation. Model spatial resolution required depends on the amplitude of forcing; for very nonlinear cases considered, vertical resolution was 250 m, and horizontal resolution was slightly greater than 1 km. For smaller forcing amplitudes, spatial resolution was much coarser, being 1 km in the vertical and about 10 km in the horizontal. Background static stability and mean wind are typical of those observed in the Venus atmosphere. Author

N93-14396*# Academy of Sciences (USSR), Moscow. Space Research Inst.
MIDDLE ATMOSPHERE OF VENUS AND ITS CLOUDS: LATITUDE AND SOLAR TIME VARIATIONS
L. V. Zasova *In* Lunar and Planetary Inst., Papers Presented to the International Colloquium on Venus 1992 p 134 (For primary document see N93-14288 04-91)
Avail: CASI HC A01/MF A02

The structure of the middle atmosphere of Venus and its upper clouds, derived from infrared spectrometry (from 250 to 1650 cm(exp -1)) on Venera 15 are discussed. Poleward increasing of temperature, monotonous on the average, at altitudes h greater than 70 km changes to poleward decreasing at h less than 60 km. Temperature inversion at 85-95 km at low latitudes was observed as a half-day wave with two minima near 9:00 a.m. and 9:00 p.m, with a more pronounced morning feature. At high latitudes the inversion with temperature minimum near 64 km exists. There are several minima depending on solar time, but the most pronounced is one on the dayside, where the depth of inversion may reach more than 40 K (near 10:00 a.m.; we have no observations closer to noon). Another minimum is situated symmetrically on the nightside. Usually in the polar region the temperature inversion is situated deeper in the atmosphere (near 62 km). A jet at latitudes 50-55 deg N divides Venus into two drastically different latitude zones: pretty homogeneous at 56-95 km zone less than 50 deg N with diffuse clouds and daily temperature variations near cloud tops about several degrees, and zones greater than 55 deg N (where such dynamic structures as cold collar and hot dipole were observed) with dense low clouds (with the exceptions of the regions at 55-80 deg N outside the cold collar). We separate Venus into four latitudinal zones with approximate latitude boundaries, where the different IR-features were observed. Author

N93-14397*# Academy of Sciences (USSR), Moscow. Space Research Inst.
SO2 IN THE MIDDLE ATMOSPHERE OF VENUS: IR MEASUREMENTS FROM VENERA 15 AND COMPARISON TO UV
L. V. Zasova, V. I. Moroz, L. W. Esposito (Colorado Univ., Boulder.), and C. Y. Na (Colorado Univ., Boulder.) *In* Lunar and Planetary Inst., Papers Presented to the International Colloquium on Venus 1992 p 134-135 (For primary document see N93-14288 04-91)
Avail: CASI HC A01/MF A02

Two sets of measurements of SO2 bands in the Venus spectra are presented and compared: IR spectra obtained on the USSR Venera 15 orbiter and UV spectra from the American Pioneer Venus orbiter and sounding rockets. The 40-mbar level was chosen as a reference level for comparison. The UV data are referred to this level. There are three SO2 bands in the infrared spectrum: at 519, 1150, and 1360 cm(exp -1). The levels of their formation in the atmosphere may differ significantly, by more than 10 km. Author

N93-14398*# Lamont-Doherty Geological Observatory, Palisades, NY.
OUTGASSING HISTORY OF VENUS AND THE ABSENCE OF WATER ON VENUS
Youxue Zhang (Michigan Univ., Ann Arbor.) and Alan Zindler *In* Lunar and Planetary Inst., Papers Presented to the International Colloquium on Venus 1992 p 135-137 (For primary document see N93-14288 04-91)
Avail: CASI HC A01/MF A02

Similarities in the size and mean density of Earth and Venus encourage the use of Earth-analogue models for the evolution of Venus. However, the amount of water in the present Venus atmosphere is miniscule compared to Earth's oceans. The 'missing' water is thus one of the most significant problems related to the origin and evolution of Venus. Other researchers proposed that Venus accreted with less water, but this was challenged. The high D/H ratio in Venus' atmosphere is consistent with an earlier water mass more than 100 times higher than at present conditions and is often cited to support a 'wet' Venus, but this amounts to only 0.01 to 0.1 percent of the water in terrestrial oceans and the high D/H ratio on Venus could easily reflect cometary injection. Nevertheless, many authors begin with the premise that Venus once had an oceanlike water mass on its surface, and investigate the many possible mechanisms that might account for its loss. In this paper we propose that Venus degassed to lower degree than the Earth and never had an oceanlike surface water mass. Author

N93-14596 Georgia Inst. of Tech., Atlanta.
STUDY AND INTERPRETATION OF THE MILLIMETER-WAVE SPECTRUM OF VENUS Ph.D. Theis
Antoine K. Fahd 1992 176 p
Avail: Univ. Microfilms Order No. DA9231757

The effects of the Venus atmospheric constitutes on its millimeter wavelength emission are investigated. Specifically, this research describes the methodology and the results of laboratory measurements which are used to calculate the opacity of some of the major absorbers in the Venus atmosphere. The pressure-broadened absorption of gaseous SO2/CO2 and gaseous H2SO4/CO2 has been measured at millimeter-wavelengths. We have also developed new formalisms for computing the absorptivities of these gases based on our laboratory work. The complex dielectric constant of liquid sulfuric acid has been measured and the expected opacity from the liquid sulfuric acid cloud layer found in the atmosphere of Venus has been evaluated. The partial pressure of gaseous H2SO4 has been measured which resulted in a more accurate estimate of the dissociation factor of H2SO4. A radiative transfer model has been developed in order to understand how each atmospheric constituent affects the millimeter-wave emission from Venus. Our results from the radiative transfer model are compared with recent observations of the microwave and millimeter-wave emissions from Venus. Our main conclusion from this work is that gaseous H2SO4 is the most likely cause of the variation in the observed emission from Venus at 112 GHz. Dissert. Abstr.

N93-14612 Saskatchewan Univ., Saskatoon.
COMPARISON OF VIKING ULTRAVIOLET IMAGES WITH LOW ALTITUDE PARTICLE PRECIPITATION Ph.D. Thesis
David Patrick Steele 1991 220 p
Avail: Univ. Microfilms Order No. DANN68208

An investigation of global auroral images at far ultraviolet wavelengths from the Viking Ultraviolet Imager (UVI) was carried out to assess their value for remote sensing of auroral electron precipitation. A large number of Viking orbits were searched for images obtained simultaneously with measurements of electron precipitation by low-altitude satellites within the UVI field of view. Sixteen such orbits were identified during April and May of 1986 when both cameras of the UVI were functioning, providing a total of 45 images. The images were corrected for various instrumental and nonauroral background contributions to the camera signal. The pixels in the images corresponding to the auroras excited by the measured low-altitude electron precipitation were determined. The auroral DN in these pixels were converted to equivalent signals for vertical viewing from Viking. The electron data were averaged over the spatial scale size of the image pixels. The linearity of the camera responses was investigated as a function of the average electron energy flux. The mean responses of the two cameras per unit electron energy flux were 11.1 plus or minus 0.9 and

15.2 plus or minus 3.1 DN per erg/cm(exp 2)s, respectively, for Cameras 0 and 1, in the most common gain state. Current models of electron transport, auroral excitation, and radiative transport were used to estimate the camera responses for comparison with selected measurements. Good agreement was obtained with observations for Camera 0, but not with those from Camera 1. Ratios of auroral signal to electron energy flux, termed 'effective sensitivities' and expressed in units of camera DN per erg/cm(exp 2)s, were plotted versus the mean energy of the electron flux to evaluate their dependence on electron energy. The effective sensitivities of both cameras showed large variations about the mean values quoted above, with no clear dependence on electron energy. The camera 0 sensitivites tended to cluster between 6 and 20 DN per erg/cm(exp 2)s, although several much larger values were measured during three orbits on May 2 and 3, 1986. The sensitivities from Camera 1 were mostly between 8 and 17 DN per erg/cm(exp 2)s. Simultaneous images from the two cameras showed little relative difference in signal strength in auroras. It was concluded that the ratio of signals from the two cameras is not very sensitive to the mean electron energy, and is thus not useful for remote sensing of auroral electron energies. Either camera could be used to estimate the distribution of total electron energy flux, within the uncertainties noted above. The Camera 0 images resolve the auroral distribution more accurately. This study is the first to make quantitative comparisons of large numbers of far ultraviolet auroral images with simultaneous measurements of the exciting particle flux. It provides the most extensive calibration of the Viking UVI cameras to date, and confirms the preflight calibration of the longer-lived camera (Camera 0) to within about 30 percent. It illustrates the possibilities and hazards of using images from the UVI to infer the energy flux precipitating into the auroral oval. The UVI obtained global snapshots of the auroral distribution at one-minute time intervals, and the results of this thesis allow more detailed characterization of the global energy input than ever before possible. Dissert. Abstr.

N93-14635 Colorado Univ., Boulder.
SULFUR OXIDES IN THE MIDDLE ATMOSPHERE OF VENUS: OBSERVATIONS BY THE INTERNATIONAL ULTRAVIOLET EXPLORER AND SOUNDING ROCKETS Ph.D. Thesis
Chan Young Na 1992 144 p
Avail: Univ. Microfilms Order No. DA9232716

Spectral observations of the Venus atmosphere between 2000 and 2300 A made by the International Ultraviolet Explorer (IUE) and by a spectrometer built at the Laboratory for Atmospheric and Space Physics (LASP), and flown on sounding rockets, are compared to synthetic spectra to derive the vertical distribution of sulfur dioxide (SO2) above the clouds of Venus. The data show the concentration of sulfur dioxide above the clouds decreased by at least a factor of 3 over the period from 1979 to 1991. The mixing ratio of SO2 at the 40 mbar level decreased from 380 plus or minus 70 ppm in 1979 (IUE) to 120 plus or minus 60 ppb in 1991 (rockets). These values are in good agreement with the observations by Pioneer Venus. The latitudinal distribution of SO2 above the clouds derived from the rocket observation in 1988 shows more SO2 at high latitudes similar to that observed by Venera-15, and these two data sets are compared. The observations by IUE and the LASP sounding rockets have a high spectral resolution which allowed my discovery of sulfur monoxide (SO) molecules above the clouds of Venus. The vertical distribution of SO derived from the 1991 rocket observation agrees with the predictions by the photochemical models. Using the derived vertical distribution of SO in the photochemical calculations, the predicted vertical profile of disulfur monoxide (S2O) molecules is obtained. This result shows that S2O is the most plausible candidate for the unknown ultraviolet absorber which creates the dark markings in the clouds of Venus, whose identity has been a puzzle since the first detailed analysis of Pioneer Venus observations.
Dissert. Abstr.

N93-14833 Cincinnati Univ., OH.
COMPLETE ANALYTICAL THEORY FOR THE SATELLITES OF NEPTUNE Ph.D. Thesis
Alan M. Segerman 1992 92 p
Avail: Univ. Microfilms Order No. DA9232385

A complete analytical theory for the motion of the satellites of Neptune has been constructed. The theory describes the orbits of Triton and Nereid over several hundred years, including all perturbations to an accuracy of 10(exp -8) relative to the two-body potentials. The perturbation solution uses the Lie transform approach advanced by Deprit and is internally consistent with respect to the magnitudes of the disturbing functions. The Lie method avoids infinite series expansion in the inclinations and eccentricities which is essential, since the orbits of Triton and Nereid possess large inclination and eccentricity respectively. The theory of Triton includes the effects of Neptunes's oblateness and Solar point-mass perturbations. The action of Nereid on Triton contributes a higher-order perturbation and is neglected. For Nereid, the effects of oblateness, Triton, and the Sun are included. Third-body disturbances are expressed using Legendre polynomial expansions which are truncated at the appropriate order of magnitude. (Tidal friction is not a significant perturbation over short time intervals and is not considered). The difficulties associated with multiple short-period angles swept out about Netpune are avoided by treating the angles associated with the perturbing bodies as functions of time which are related to the angles of perturbed body via the ratios of the mean motions. The Solar motion is approximated by a constant orbit of Neptune about the Sun. Standard expansions relating short-period angles are not applicable for Nereid, as they assume small eccentricities. Instead, analytical Fourier series involving Bessel coefficients are employed.
Dissert. Abstr.

N93-14863 California Inst. of Tech., Pasadena.
MICROWAVE OBSERVATIONS OF URANUS Ph.D. Thesis
Mark David Hofstadter 1992 188 p
Avail: Univ. Microfilms Order No. DA9232187

This thesis explores the atmosphere of Uranus using microwave observations at wavelengths from 1 to 20 cm, with primary emphasis on high resolution VLA data at wavelengths of 2 and 6 cm. While radio maps of Uranus have been published previously, this is the first detailed analysis and interpretation of such observations. Several features of the data are immediately clear. First, there are strong horizontal and vertical gradients in the atmospheric properties that control the radio brightness. Polar regions are much brighter than lower latitudes, and the deep troposphere appears much dimmer than would be expected based on the upper troposphere. Second, the intrinsic latitudinal brightness variations at 2 cm and 6 cm are highly correlated with each other and with Voyager infrared measurements, suggesting a common cause. Because these data sets probe different altitudes between 50 and 0.1 bar, the cause must be acting over this altitude range of about 250 km. Finally, the observed radio brightness features have not changed significantly in the 8 years between 1981 and 1989. Since radio brightness is a function of temperature and composition, the observations can be used to map these properties as a function of latitude and height. compositional changes are used as a tracer to infer the general circulation and some of the chemical processes of there atmosphere. The most likely interpretation of the data is that the Southern Hemisphere is dominated by a single meridional circulation cell, with an upwelling centered near -25 deg latitude that brings absorber rich air parcels from 50 bars up to the 0.1 bar region. As parcels rise, the absorber mixing ratio drops by a factor of about 100 between 25 and 10 bars, and then a further factor of 2 at higher altitudes. These depletions are probably due to condensation. The absorber depleted parcels then move poleward and descend, dominating the atmospheric composition over the pole down to 50 bars, but not deeper. This circulation is consistent with the zonal winds and upper atmospheric temperatures observed by Voyager in the context of a simple, linear, dynamical model. Dissert. Abstr.

N93-14865 California Inst. of Tech., Pasadena.
NUMERICAL SIMULATION OF BAROCLINIC JOVIAN VORTICES Ph.D. Thesis
Richard Karl Achterberg 1992 216 p
Avail: Univ. Microfilms Order No. DA9232158

We propose a non-linear, quasi-geostrophic, baroclinic model of Jovian atmospheric dynamics, in which vertical variations of velocity are represented by a truncated sum of orthogonal functions obtained by separation of variables on the linearized quasi-geostrophic potential vorticity equation. A set of equations for the time variation of the mode amplitutes in the non-linear case is then derived. We show that for a planet with a neutrally stable, fluid interior, the barotropic mode represents motions in the interior, and is not affected by the baroclinic modes. We also show that for motions in Jupiter's low troposphere, the stratosphere behaves nearly as a grid lid, so that the normal-mode model is applicable to Jupiter. We test the accuracy of the normal-mode model for Jupiter using two simple problems: forced,

vertically propagating Rossby waves and baroclinic instability. We find that the normal-mode model provides qualitatively correct results, even with only a very limited number of vertical degrees of freedom. We then examine the evolution of baroclinic vortices in a time dependent, nonlinear numerical model of Jupiter's atmosphere, using the normal-mode expansion in the vertical, with the barotropic and first two baroclinic modes. Our results for the stability of baroclinic vortices of an f-plane in the absence of a mean zonal flow are consistent with previous results in the literature. The presence of a mean zonal shear flow is found to stabilize vortices against instability, significantly modify the finite amplitude form of baroclinic instabilities, and when combined with internal barotropic instability produce periodic oscillations in the latitude and longitude of the vortex. This instability may explain some observations of longitudinal oscillations of vortices on the outer planets. Meridional propagation and decay of vortices on a beta-plane is found to be inhibited by the presence of a mean zonal flow. The direction of propagation of a vortex relative to the mean zonal flow depends upon the sign of the meridional potential vorticity gradient; combined with observations of vortex drift rates, this may provide a constaint on model assumption for the flow in the deep interior of Jupiter. Dissert. Abstr.

N93-14868 California Inst. of Tech., Pasadena.
MARTIAN WATER FROST: CONTROL OF GLOBAL DISTRIBUTION BY SMALL-SCALE PROCESSES Ph.D. Thesis
Tomas Svitek 1992 168 p
Avail: Univ. Microfilms Order No. DA9232233

This thesis analyzes the small-scale physical processes occurring in the Martian water polar frosts. The small-scale processes are considered from the point of view of how they control the global distribution and behavior of water on Mars. The analysis of the small-scale properties of the surface frost is essential in efforts to find solutions for some outstanding, contradictory observations, to interpret correctly remote sensing observations, to model the surface-frost thermal balance, and to implement the boundary conditions and parameterizations used in the global models of the volatiles' behavior on Mars. Two different problems are investigated in this thesis: The effect of surface roughness on frost temperature and morphology is studied in Chapter 2 and 3. The investigation of the temperature/roughness feedback leads to the following suggestion: There is a natural tendency of volatile surfaces to develop spontaneously small-scale roughness in a sublimation-dominated environment. The evidence for this claim consists of the model of a rough-surface thermal balance, and of the terrestrial analogs of differential sublimation structures. Such a phenomenon can be tested by the Mars Observer and has important implications for the behavior of water frost on Mars. Viking Lander 2 winter-frost observations are described in Chapter 4. This study suggests that winter water frost occurred there in two forms: (a) thin, almost continuous, early frost, and (b) much thicker, patchy, later frost with local cold-trapping of water vapor playing the crucial role. This conclusion is based on the correlation of multiple data sets (from both Viking Orbiter and Lander) and on the combined models of the physical processes occurring on a small scale--below the resolution of remote sensing. The evidence consists of the frost-surface coverage and color transitions, and of the calculation of the vertical and horizontal water-vapor transport near the surface. Again, this phenomenon can be confirmed or rejected by a set of observations from the Mars Observer. The inherent rough-surface morphology and the frost cold-trapping must be a general property of at least some forms of the seasonal and residual frost. Both effects must be considered in order to understand the global observations of the Martian frost and the surface environment of Mars in general. Dissert. Abstr.

N93-14918 California Inst. of Tech., Pasadena.
INTERFEROMETRIC OBSERVATIONS OF THE J(0,1) CO LINE ON VENUS: UPPER MESOSPHERIC WINDS AND CO ABUNDANCE Ph.D. Thesis
Kathryn Pierce Shah 1992 235 p
Avail: Univ. Microfilms Order No. DA9232224

In 1988, we observed Venus with the millimeter interferometer at the Owens Valley Radio Astronomy Observatory at 115.2712 GHz, the first rotational transition of CO-12. The 33.4 inches diameter disk was spatially resolved by a synthesized beam having a full-width-half-maximum of 2.8 inches. Local time ranged from afternoon on the eastern limb, 2 PM, to just past midnight on the western limb, 12:30 AM. The CO absorption line was finely resolved in frequency by two 32-channel filterbanks having channel widths of 50 kHz and 1 MHz. The 1 MHz and 50 kHz filterbank data were merged to examine the entire CO line. These spectra show a decided local time dependency, becoming progressively deeper from the afternoon to the evening hours. A constrained least-squares inversion algorithm was used to solve for local CO mixing ratio profiles. The resultant profiles appear constant with height at several 10(exp -5) in the late afternoon hours but increase from 10(exp -4) at 80 km to 10(exp -3) at 100 km in the night hours. The highest CO abundances occurred after local 10 PM and centered about the equator between 40 deg N and 40 deg S. This CO distribution fulfills predictions from research based on disk-average CO spectra and photochemical models. Only the late afternoon profiles are surprising, showing small CO abundances rather than expected moderate CO abundances via dayside photodissociation of CO2. The 50 KHz filterbank resolved the inner core of the CO absorption line. This yielded the first measurement of Doppler shifts across Venus caused by strong winds in the upper mesosphere. Calculated weighting functions showed sampling of the mesosphere over a 12 km layer centered at roughly 99 km. The Doppler shifts have a signature which matches that of westward, horizontal winds--being strongly 'blue' on the east/dayside limb, zero near the center, and strongly 'red' on the west/nightside limb of the planet disk. Smoothed wind measurements were best fitted in a least squares sense for a mean zonal flow of 132 plus or minus 10 ms(exp -1). A smaller (less than or equal to 40 ms(exp -1) subsolar-to-antisolar flow may have been superimposed on the dominant zonal flow in 1988. These measurements indicate either a reversal of the mesospheric cyclostrophic breakdown inferred by Pioneer Venus or the influence of uninvestigated dynamical forces. Dissert. Abstr.

N93-15081*# Georgia Inst. of Tech., Atlanta. School of Electrical Engineering.
LABORATORY EVALUATION AND APPLICATION OF MICROWAVE ABSORPTION PROPERTIES UNDER SIMULATED CONDITIONS FOR PLANETARY ATMOSPHERES Semiannual Status Report No. 18, 1 May - 31 Oct. 1992
Paul G. Steffes Oct. 1992 37 p
(Grant NAGw-533)
(NASA-CR-191298; NAS 1.26:191298) Avail: CASI HC A03/MF A01

Radio absorptivity data for planetary atmospheres obtained from spacecraft radio occultation experiments and earth-based radio astronomical observations can be used to infer abundances of microwave absorbing atmospheric constituents in those atmospheres, as long as reliable information regarding the microwave absorbing properties of potential constituents is available. The use of theoretically-derived microwave absorption properties for such atmospheric constituents, or using laboratory measurements of such properties under environmental conditions which are significantly different than those of the planetary atmosphere being studied, often leads to significant misinterpretation of available opacity data. For example, laboratory measurements performed by Fahd and Steffes have shown that the opacity from gaseous SO2 under simulated Venus conditions can be well described by the Van Vleck-Weisskopf lineshape at wavelengths shortward of 2 cm, but that the opacity of wavelengths greater than 2 cm is best described by a different lineshape that was previously used in theoretical predictions. The recognition of the need to make such laboratory measurements of simulated planetary atmospheres over a range of temperatures and pressures which correspond to the altitudes probed by both radio occultation experiments and radio astronomical observations, and over a range of frequencies which correspond to those used in both radio occultation experiments and radio astronomical observations, has led to the development of a facility at Georgia Tech which is capable of making such measurements. It has been the goal of this investigation to conduct such measurements and to apply the results to a wide range of planetary observations, both spacecraft and earth-based, in order to determine the identity and abundance profiles of constituents in those planetary atmospheres. Author

N93-14922# Deputy Assistant Secretary of Defense (Environmental Quality), Washington, DC.
HUMAN EXPLORATION: MOON/MARS MISSION
Douglas A. OHandley *In* Canadian Space Agency, Proceedings of the Sixth CASI Conference on Astronautics 1990 9 p (For primary document see N93-14920 04-12)

Avail: Canadian Aeronautics and Space Inst., 222 Somerset St. W., Suite 601, Ottawa, Ontario K2P 0J1 Canada

N93-14929# Spar Aerospace Ltd., Weston (Ontario).
IN-SITU LUNAR OXYGEN EXTRACTION
Mark Lozowski *In* Canadian Space Agency, Proceedings of the Sixth CASI Conference on Astronautics 1990 6 p Previously announced in IAA as A91-34935 (For primary document see N93-14920 04-12)
Avail: Canadian Aeronautics and Space Inst., 222 Somerset St. W., Suite 601, Ottawa, Ontario K2P 0J1 Canada

N93-14944# Spar Aerospace Ltd., Weston (Ontario). Advanced Technology Systems Div.
MISSION AND TECHNOLOGY ASSESSMENT OF HUMAN EXPLORATION TO THE MOON AND MARS
Moses Wong *In* Canadian Space Agency, Proceedings of the Sixth CASI Conference on Astronautics 1990 11 p Previously announced in IAA as A91-34950 (For primary document see N93-14920 04-12)
Avail: Canadian Aeronautics and Space Inst., 222 Somerset St. W., Suite 601, Ottawa, Ontario K2P 0J1 Canada

N93-14947# Spar Aerospace Ltd., Weston (Ontario). Advanced Technology Systems Div.
THE EVALUATION OF A CONCEPT FOR A CANADIAN-MADE AUTOMATED MULTIPURPOSE MATERIALS EXTRACTION FACILITY
H. Kleinberg *In* Canadian Space Agency, Proceedings of the Sixth CASI Conference on Astronautics 1990 9 p Previously announced in IAA as A91-34953 (For primary document see N93-14920 04-12)
Avail: Canadian Aeronautics and Space Inst., 222 Somerset St. W., Suite 601, Ottawa, Ontario K2P 0J1 Canada

92 SOLAR PHYSICS

Includes solar activity, solar flares, solar radiation and sunspots. For related information see *93 Space Radiation.*

N93-14135 Maryland Univ., College Park.
A SURVEY OF SOLAR FLARE ENERGETIC PARTICLE ABUNDANCES AND ENERGY SPECTRA Ph.D. Thesis
Joseph Edward Mazur 1991 328 p
Avail: Univ. Microfilms Order No. DA9222730

Previous surveys of the relative abundances of energetic particles accelerated in large solar flare events averaged the ionic composition in a single, summary energy interval. The study presents the time-integrated energy spectral of H, He, O, and Fe measured in ten large flare events observed at 1 AU over the energy range of approximately 0.3-80 MeV/Nucleon. Combined measurements from the University of Maryland/Max Planck Institute sensors on the ISEE-1 spacecraft and Goddard Space Flight Center instrumentation on IMP-8 extended the energy range beyond that measured with any single instrument of this study. The spectra showed consistent patterns in the abundances relative to oxygen and helium as functions of energy: particles with larger mean charge-to-mass ratios were generally less abundant at higher energies. In contrast to previous surveys made near 1 MeV/Nucleon and near 10 MeV/Nucleon, we found that these trends with energy remained in an average across many events. We compared abundances integrated over 0.3-100 MeV/Nucleon and 4.94-22.5 MeV/Nucleon with other solar system abundances: the lower energy flare composition was more similar to the solar wind composition and showed a factor of 4 enrichment in Fe/O compared to the photospheric abundances. A model of stochastic particle acceleration with rigidity dependent diffusion coefficients gave the best overall fits to the energy spectra, a quantitative explanation of the observed energy dependences of the abundances, and a means of interpolating small portions of the energy spectra which the instrumentation did not measure. Dissert. Abstr.

N93-14157 New Hampshire Univ., Durham.
RESONANCE ABSORPTION OF MHD SURFACE WAVES WITH APPLICATIONS TO THE SOLAR ATMOSPHERE Ph.D. Thesis
Guang Yang 1992 162 p
Avail: Univ. Microfilms Order No. DA9225269

This thesis studies the physics of resonance absorption of MHD surface waves and examines the effects of velocity shear on the rate of resonance absorption. Theoretical analyses and numerical calculations demonstrate that resonance absorption of MHD surface waves is a viable mechanism for heating of the solar corona. It is shown that resonance absorption has a very simple physical interpretation in terms of driven harmonic oscillators. This insight greatly simplifies the mathematics and allows a thorough discussion of the solar coronal heating. It is found that resonance absorption of MHD surface waves can occur rapidly enough to heat the solar coronal active region loops, which have the largest heating requirements, consistent with the observation that the surface brightness of the loops is roughly independent of loop size. It is suggested that the large velocity shears near the resonant field line could drive a Kelvin-Helmholz instability which would in turn lead to an effective eddy viscosity and ultimately to dissipation into heat. The effects of three different forms of viscosity on the Alfven resonance are considered. Only classical shear viscosity is able to absorb the energy which is pumped into the thin resonant layer. In the steady state, the net heating rate is independent of the viscosity coefficient, if the heating occurs in a thin layer. The effects of velocity shear on the rate of resonance absorption are investigated for both incompressible and compressible MHD surface waves. Velocity shear can either increase or decrease the rate of resonance absorption. It is very interesting to discover that resonance can lead to an instability at values of velocity shear below the threshold for the Kelvin-Helmholz instability. The numerical results reveal these effects are not dramatic for very sub-Alfvenic field-aligned flow in the solar corona, but may play an important role in the super-Alfvenic solar wind streams. Dissert. Abstr.

N93-14591 Alabama Univ., Huntsville.
IMAGING THE SUN IN HARD X-RAYS USING FOURIER TELESCOPES Ph.D. Thesis
Jonathan Wesley Campbell 1992 284 p
Avail: Univ. Microfilms Order No. DA9229498

For several years, solar flares have been observed with a variety of instruments confirming that tremendous amounts of energy are locally stored in the solar magnetic field and then rapidly released during the life of the flare. In order to test whether a Fourier telescope can discriminate solar brightness distributions, we construct sources based upon the thermal and the non-thermal hard x-ray theoretical models and calculate the emission as a function of time and energy in the range from 10 to 100 keV. In addition, using random photon counting statistics, we construct model telescopes representing both the Spatial Modulation Collimator (SMC) and the Rotating Modulation Collimator (RMC). With these two types of telescopes we numerically 'view' the two aforementioned model flares to see if there are distinct x-ray signatures which may be discernable. First, we find that these x-ray models do indeed predict different hard x-ray signatures in the specified energy range for 1 second time scales and at 1-5 arc seconds spatial resolution. Furthermore, we find that Fourier telescopes with reasonable and currently attainable design characteristics can image these signatures. In summary, Fourier telescopes are found to be promising approaches for hard x-ray imaging of the sun and revealing the physical processes at work in flares. Dissert. Abstr.

N93-14859 New Hampshire Univ., Durham.
SOLAR FLARES: THE ONSET OF MAGNETIC RECONNECTION AND THE STRUCTURE OF RADIATIVE SLOW-MODE SHOCKS Ph.D. Thesis
Peng Xu 1992 179 p
Avail: Univ. Microfilms Order No. DA9225268

This is a theoretical study of two magnetohydrodynamic (MHD) processes associated with magnetic reconnection in large solar flares and other related eruptive phenomena. The first process determines the effect of magnetic reconnection in the corona upon the loss of equilibrium triggered by the slow evolution of the field lines mapping to the region in the photosphere where the flare occurs. The quasi-static MHD equations are solved for a magnetic field configuration which satisfies line-tied boundary conditions during the eruption of the flare. Such boundary conditions occur because the inertial mass of the photosphere plasma is much greater than that of the corona. The effect of magnetic reconnection is investigated by assuming three distinct characteristic time scales, namely the convective time scale T(p) (days) for motion in the photosphere, the reconnection time scale T(r) (hours) for reconnection in the corona, and the Alfven time scale T(A) (minutes) for wave propagation in the corona. Magnetic energy can be

gradually stored in the corona in a time period of T(p) as the system evolves through a series of equilibria until it reaches a point where no nearby equilibria are available. The second process is the magnetic energy conversion occurring in slow-mode MHD shocks in a plasma where both radiation and thermal conduction are important. Standing slow shocks actually convert magnetic energy into heat and kinetic energy. In a radiative and conducting plasma a slow shock dissociates into an extended foreshock, an isothermal subshock, and a downstream radiative cooling region. The research reported here shows that for typical flare conditions, about 2/3 of the magnetic energy conversion in the slow shocks occurs in the subshock while the remaining 1/3 occurs in the foreshock. It is also shown that no stable, steady-state solutions exist for radiative slow shocks in a coronal like environment unless the temperature in the radiative region downstream of the subshock falls below 10(exp 5) K. Dissert. Abstr.

N93-15085*# New Hampshire Univ., Durham. Space Science Center.
THEORETICAL STUDIES OF THE PHYSICS OF THE SOLAR ATMOSPHERE Final Report
Joseph V. Hollweg 12 Nov. 1992 13 p
(Grant NsG-7411)
(NASA-CR-191357; NAS 1.26:191357) Avail: CASI HC A03/MF A01

Significant advances in our theoretical basis for understanding several physical processes related to dynamical phenomena on the sun were achieved. We have advanced a new model for spicules and fibrils. We have provided a simple physical view of resonance absorption of MHD surface waves; this allowed an approximate mathematical procedure for obtaining a wealth of new analytical results which we applied to coronal heating and p-mode absorption at magnetic regions. We provided the first comprehensive models for the heating and acceleration of the transition region, corona, and solar wind. We provided a new view of viscosity under coronal conditions. We provided new insights into Alfven wave propagation in the solar atmosphere. And recently we have begun work in a new direction: parametric instabilities of Alfven waves. Author

N93-15318# Aerospace Corp., El Segundo, CA. Electronics Technology Center.
SOLAR PROTON EVENTS OF 1989: EFFECTS ON SPACECRAFT SOLAR ARRAYS
D. C. Marvin and D. J. Gorney 24 Jul. 1992 28 p
(Contract F04701-88-C-0089)
(AD-A256457; TR-0091(6945-01)-2; SMC-TR-92-43) Avail: CASI HC A03/MF A01

Three energetic solar proton events occurred in August to October 1989. The energetic (1 to 10 MeV proton) fluence from these events was among the highest fluence levels observed during the space age. The solar proton events were of sufficient magnitude to produce easily observable (several percent), irreversible losses in solar array output on geosynchronous and polar low earth orbiting satellites. The degradation of solar array output was measured on the GOES-5, GOES-6, and GOES-7 satellites and on two other U.S. Government satellites in geosynchronous orbit. The observed solar array degradation was compared with that computed based on knowledge of the solar cell type, cover glass thickness, the operational mode of the array, the observed proton spectrum, and the length of time on orbit for each satellite. In each case, good agreement was obtained between the observed and the computed results. GRA

N93-15532*# National Aeronautics and Space Administration. Marshall Space Flight Center, Huntsville, AL.
ON THE VARIATION OF THE NIMBUS 7 TOTAL SOLAR IRRADIANCE
Robert M. Wilson Washington Dec. 1992 17 p
(NASA-TP-3316; M-707; NAS 1.60:3316) Avail: CASI HC A03/MF A01

For the interval December 1978 to April 1991, the value of the mean total solar irradiance, as measured by the Nimbus-7 Earth Radiation Budget Experiment channel 10C, was 1,372.02 Wm(exp -2), having a standard deviation of 0.65 Wm(exp -2), a coefficient of variation (mean divided by the standard deviation) of 0.047 percent, and a normal deviate z (a measure of the randomness of the data) of -8.019 (inferring a highly significant non-random variation in the solar irradiance measurements, presumably related to the action of the solar cycle). Comparison of the 12-month moving average (also called the 13-month running mean) of solar irradiance to those of the usual descriptors of the solar cycle (i.e., sunspot number, 10.7-cm solar radio flux, and total corrected sunspot area) suggests possibly significant temporal differences. For example, solar irradiance is found to have been greatest on or before mid 1979 (leading solar maximum for cycle 21), lowest in early 1987 (lagging solar minimum for cycle 22), and was rising again through late 1990 (thus, lagging solar maximum for cycle 22), having last reported values below those that were seen in 1979 (even though cycles 21 and 22 were of comparable strength). Presuming a genuine correlation between solar irradiance and the solar cycle (in particular, sunspot number) one infers that the correlation is weak (having a coefficient of correlation r less than 0.84) and that major excursions (both as 'excesses' and 'deficits') have occurred (about every 2 to 3 years, perhaps suggesting a pulsating Sun). Author

N93-15634*# Stanford Univ., CA. Dept. of Physics
THE DETECTION AND CHARACTERIZATION OF HIGH FREQUENCY AND HIGH WAVENUMBER SOLAR OSCILLATIONS Ph.D. Thesis
David Neil Fernandes Jun. 1992 130 p
(Contracts NAS8-32805; NAS5-26813; NAS5-30386; NGR-559; N00014-89-J-1024; NSF ATM-90-22249)
(NASA-CR-191622; NAS 1.26:191622) Copyright Avail: CASI HC A07/MF A02

Doppler shift measurements of the Na D(sub 1) absorption line have revealed solar oscillations in a new regime of frequency and wavenumber. Oscillations of vertical velocities in the temperature minimum and low chromosphere of the Sun are observed with frequencies ranging up to 9.5 mHz. There is no evidence for chromospheric modes of 3 minute period. This indicates that the chromosphere does not form a good cavity for acoustic waves. The fundamental-modes appear with wavenumbers up to 5.57 M per m (equivalent spherical harmonic degree, 3877). The frequencies lie below the predicted values at wavenumbers above 1 M per m. The values are in agreement with previous measurements that exist for wavenumbers up to 2.67 M per m. Spatial maps of velocity power show that high wavenumber oscillations are suppressed in active regions. The shape of the power depression indicates that wave motion is affected in the layer of atmosphere where the measurement is made. The f-modes are suppressed in the same way as p-modes, indicating that the mechanism for wave suppression affects velocity fluctuations. Mode frequencies are not affected by the magnetic fields by more than 50 micro Hz, the precision of the measurement. Author

93 SPACE RADIATION

Includes cosmic radiation; and inner and outer earth's radiation belts.

For biological effects of radiation see *52 Aerospace Medicine*. For theory see *73 Nuclear and High-Energy Physics*.

N93-14176 Indiana Univ., Bloomington.
EXTRACTING X RAYS, GAMMA RAYS, AND ELECTRON-POSITRON PAIRS FROM SUPERMASSIVE KERR BLACK HOLES USING THE PENROSE MECHANISM Ph.D. Thesis
Reva Kay D. Williams 1991 198 p
Avail: Univ. Microfilms Order No. DA9217429

Monte Carlo computer simulations are presented of Compton scattering and electron-positron (e-e+) pair production processes in the ergosphere of a supermassive rotating black hole. Particles from an accretion disk surrounding the black hole fall into the ergosphere and scatter off particles that are in bound orbits. The equations that govern the orbital trajectory of a particle about a Kerr (rotating) black hole (KBH) are solved to determine the conserved energy and angular momentum of materials and massless particles that have orbits not confined to the equatorial plane. The escape conditions to determine whether or not a particle escapes from the potential well of the KBH are applied to the scatter particles. The Penrose mechanism allows rotational energy of a KBH to be extracted by scattered particles escaping from the ergosphere to large distances from the black hole. The results of these model calculations show that the Penrose mechanism is capable of producing the astronomically observed high energy particles emitted by quasars and other active galactic nuclei (AGN's). This mechanism, as applied in the models, can extract hard X ray/gamma ray photons from the inverse Compton scatterings of initially low energy UV/soft X ray photons by target orbiting electrons in the ergosphere. Such low energy infalling photons are consistent with photons emitted by of a classical thin accretion

disk. These model calculations also allow relativistic e-e+ pairs to be produced by infalling low energy photons interacting with target photons in bound orbits inside the ergosphere. This process may be the origin of the relativistic electrons inferred from observations to emerge from the cores of AGN's. Dissert. Abstr.

N93-14229 Brandeis Univ., Waltham, MA.
THE EVOLUTION OF THE VLBI POLARIZATION OF SUPERLUMINAL RADIO SOURCE 3C345 Ph.D. Thesis
Leslie F. Brown 1992 212 p
Avail: Univ. Microfilms Order No. DA9229453

Very Long Baseline Interferometric techniques for measuring the linear polarization of radio sources are described. These techniques are used to make observations of the radio-bright, core-dominated quasar 3C 345. The polarization structure of this source was observed over six epochs, spanning almost ten years, allowing us to follow the evolution of the magnetic field structure in the core and the jet on parsec scales. In 3C 345 most of the polarized flux is associated with the moving components in a jet a few milliarcseconds in length. New components emerge with a small degree of polarization that increases as the components separate from the core. The most highly polarized part of the jet has m approximately equal to 11 percent. The magnetic field alignment along the jet varies in a complicated fashion in both position and time. Near the core, where components were observed to change their direction, the electric vectors also change rapidly. In the gently-curving part of the jet the electric vectors are very nearly orthogonal to the local jet axis, suggesting a longitudinal magnetic field. At the outermost knot visible at this resolution, the electric vectors swing so as to produce a B-field which is offset to the jet axis and appears to be perpendicular to the component boundary. These data are interpreted in the framework of a relativistic jet model in which the magnetic field consists of a combination of random and ordered components. The field, and hence the polarized radiation, in this picture is enhanced by compression produced when plane shock waves traverse the jet. Further observations capable of unambiguous measurement of the inter-knot polarization will test this mode; observations at multiple wavelengths will enable us to study the narrow-line emission gas through the Faraday effect.
Dissert. Abstr.

N93-14242 Johns Hopkins Univ., Baltimore, MD.
NONTHERMAL RADIO, X RAY AND GAMMA RAY EMISSIONS FROM CHAOTIC WINDS OF EARLY-TYPE, MASSIVE STARS Ph.D. Thesis
Wan Chen 1992 252 p
Avail: Univ. Microfilms Order No. DA9229306

A quantitative multiwavelength theoretical study of the winds of massive stars conducted in this thesis is shown to be a powerful new technique for our understanding of the structure of the chaotic winds and the massive stars themselves. The instability of the fully ionized, line-driven winds of hot stars leads to the formation of strong shocks at the base of the winds. These shocks not only emit thermal X-rays, but also accelerate a small fraction of the thermal electrons and ions to relativistic energies. Synchrotron radiation from the energetic electrons provides the only physical interpretation to date for the non-thermal radio emission observed from some massive stars by VLA and VLBI. Inverse Compton up-scattering of the stellar UV photons by these electrons can also explain the hard X-rays detected in the Einstein Observatory X-ray spectra. Furthermore, the inverse Compton scattering can actually boost the stellar UV photons to MeV energies and the relativistic ions in the winds can interact with thermal ions to generate pi(0)'s which then decay into gamma-rays up to a few GeV. Our calculations indicate that these gamma-rays should be detectable by GRO. The basic picture for the shock structure in the winds is based on Lucy's model. We extend it to large radii in the winds using a simple leaky snow-plough model for the shock propagation. We adopt Bell's single particle approach to develop an analytical method to calculate the non-thermal particle spectra accelerated by shocks which can accommodate the strong electron radiative cooling and repeated acceleration by multiple shocks in winds. Non-thermal particle spectra at different radii are calculated according to their acceleration and cooling history in the winds. These particle spectra are then employed to calculate the inverse Compton, pi(0)-decay and synchrotron radiation emissivities in the winds. Our final result, a broadband electromagnetic spectrum from a chaotic massive stellar wind extending from radio to high energy gamma-rays, is a powerful diagnostic of the shock energy flux and particle acceleration efficiency by the shocks in the winds, and it also places a strong limit on the stellar surface magnetic field strength. Dissert. Abstr.

N93-14244 California Univ., Berkeley.
A SEARCH FOR ANISOTROPY IN THE COSMIC BACKGROUND RADIATION AT MILLIMETER WAVELENGTHS ON ANGULAR SCALES FROM 0.3 TO 3 DEGREES Ph.D. Thesis
Marc Laurenz Fischer 1991 100 p
Avail: Univ. Microfilms Order No. DA9228649

This thesis describes an experiment to measure anisotropy in the cosmic microwave background (CMB) at millimeter wavelengths on angular scales from 0.3 to 3 degrees. The instrument which was developed for these measurements combines an existing 1 meter primary mirror and a pointed balloon gondola with new multimode feed optics and a bolometric receiver. The receiver contains a (3)He-cooled bolometric photometer with passbands centered at frequencies of 3 (90), 6 (180), 9 (270), and 12 (360) cm(exp -1) (GHz). During the first flight in November 1989, a search was made for CMB anisotropy at thirteen points centered near the north celestial pole (NCP). These data set an upper limit on CMB anisotropy of delta T/T less than or equal to 6.2 x 10(exp -5) at the 95 percent confidence level for Gaussian correlation functions with a correlation length of 0.6 degrees. The spectrum of the brightness of the galactic plane at a galactic longitude of 1(II) = 24 degrees was measured to be consistent with thermal emission from interstellar dust with a temperature near 20 K and an emissivity epsilon varies as nu(n), where nu is the frequency and n = 1.5-2. In July 1990 the telescope was flown with improved bolometric detectors. The 3 cm(exp -1) band was removed in order to increase the optical efficiency of the remaining bands. The data gathered in the 6 cm(exp -1) band during a seven point search for CMB anisotropy lasting 1.3 hr have 30 micro-K statistical errors. The data contain a 3-sigma detection of spatial structure with a spectrum that is consistent with an anisotropy in the CMB (Alsop et al. 1991). The possibility that radio frequency interference or earthshine may have been responsible for this anisotropic signature required that we reexamine the region of sky that was observed. In June 1991 the instrument was flown a third time with the same receiver. Data analysis from the third flight is in progress. Future plans for the project are discussed briefly. These plans include the development of a new receiver and new telescope optics which have the potential to search for CMB anisotropy at the delta T/T approximately equal to or approximately equals 10(exp -6) level. Dissert. Abstr.

N93-14634 California Univ., Riverside.
SEARCH FOR PULSED GAMMA RAY EMISSION FROM SN1987A AND THE VELA PULSAR Ph.D. Thesis
Alan Davinson Kerrick 1992 170 p
Avail: Univ. Microfilms Order No. DA9231931

Compton telescope data of 1-30 MeV is analyzed for pulsed gamma-rays from SN1987A and the Vela pulsar on 15 Apr. 1988, and for the Crab pulsar on 30 Sep. 1989. No evidence for pulsations was seen in a fast Fourier transform search on SN1987A. Flux limits are F(sub p)(1.1-30 MeV) less than 3.6(10)(exp -3) cm(exp -2)s(exp -1) for frequencies below 453.6 Hz, and F(sub p)(greater than 0.85 MeV) less than 2.3(10)(exp -3) cm(exp -2) s(exp -1) for frequencies below 97.656 Hz. The Crab pulsar is seen at flux levels consistent with previously published results. The Vela pulsar is possibly seen between 2.5 and 5 MeV, where the telescope effective area is maximum. The possible pulsed flux is consistent with that reported by earlier researchers. No evidence for Vela is seen in the energy bands 1.1-2.5 MeV, 5-10 MeV, and 10-30 MeV. Dissert. Abstr.

N93-14639 Hawaii Univ., Honolulu.
USING THE HALEAKALA BARREL EXTENSIVE AIR SHOWER ARRAY TO STUDY SELECTED U.H.E. GAMMA RAY POINT SOURCES Ph.D. Thesis
Jacob Victor Hudson, Jr. 1992 309 p
Avail: Univ. Microfilms Order No. DA9230487

The Haleakala Gamma Ray Observatory (HGRO) was designed to search for astrophysical gamma ray point sources by employing the atmospheric Cerenkov technique, in the energy region around 1 TeV. A number of prior observations have hinted that the (claimed) point sources detected, did not have the characteristics expected of such high energy photons. A simple array of 32 particle counters surrounding the already

existing Air Cerenkov telescope were employed to search for an unexpected accompaniment of the Cerenkov signals; this anomalous accompaniment would imply non-gamma ray origins of the point sources particles. By setting the individual particle counter rates to the background muon rate, and 'slaving' the array to the air cerenkov telescope, any D.C. excess detected would cast doubt on the present day understanding of cosmic ray phenomenology. Three sources were examined; 81 hours of data from Cygnus X-3 binary system, 132 hours of data from the Crab supernova remnant, and 33.5 hours of data from the 4U0155 binary system was obtained. After performing several layers of off-line cuts, no evidence of an anomalous accompaniment, for any of the observed sources, was found. Dissert. Abstr.

N93-14917 Minnesota Univ., Minneapolis.
THE GAMMA RAY SPECTRUM RESULTING FROM pp INTERACTIONS IN QUASARS Ph.D. Thesis
Murray Eldon Dixson 1992 141 p
Avail: Univ. Microfilms Order No. DA9231027

A simple first order model is developed to explore the hypothesis that the extended multifrequency continuum of 3C273 may be attributed to processes related to production of secondary electrons via inelastic pp interactions. Many features of the observed continuum can be explained in this way. However, problems are apparent in explaining both the high energy X-ray continuum and that at gamma-ray energies. Further studies of variations on this general idea are required. Dissert. Abstr.

N93-15580*# National Inst. of Standards and Technology, Gaithersburg, MD. Ionizing Radiation Div.
PREDICTIONS OF DOSE FROM ELECTRONS IN SPACE Technical Progress Report
Stephen M. Seltzer Dec. 1992 81 p
(NASA Order T-9311-R)
(NASA-CR-191617; NAS 1.26:191617) Avail: CASI HC A05/MF A01

The objective of the project is to develop a general-purpose, user-friendly computerized database and code package, for the PC as well as larger computers, which can be used for the routine prediction of the absorbed dose from incident electrons and their secondary bremsstrahlung (and from incident protons) as functions of the thickness of aluminum shielding in space. The assumption of homogeneous aluminum shields and of isotropic incident fluxes (at least in a time-averaged sense) allows for the rather reliable conversion of doses in slabs to those in other simple bodies, such as spherical and cylindrical solids and shells. On such a basis, depth-dose data for monoenergetic incident radiation can be generated once-and-for-all from accurate transport calculations, and this database can then be used repeatedly in rapid dose predictions for arbitrary radiation spectra and for a variety of spacecraft sizes and shapes, without recourse to the very time-consuming Monte Carlo calculations. This project entails a thorough updating, extension, and refinement of our earlier SHIELDOSE package, with the goal of a more reliable, fool-proof, and general system. Author

N93-14959# Thomson and Nielsen Electronics, Ottawa (Ontario).
RADIATION MONITORING FOR LONG DURATION SPACE FLIGHTS
I. Thomson and G. Mackay *In* Canadian Space Agency, Proceedings of the Sixth CASI Conference on Astronautics 1990 12 p Previously announced in IAA as A91-34965 (For primary document see N93-14920 04-12)
Avail: Canadian Aeronautics and Space Inst., 222 Somerset St. W., Suite 601, Ottawa, Ontario K2P 0J1 Canada

99 GENERAL

N93-14523# Air Force Office of Scientific Research, Bolling AFB, Washington, DC.
AIR FORCE OFFICE OF SCIENTIFIC RESEARCH Quarterly Report, Oct. - Dec. 1991
Debra L. Tyrrell 1991 170 p
(AD-A255331; AFOSR-92-0845TR) Avail: CASI HC A08/MF A02

The Air Force Office of Scientific Research (AFOSR) Technical Report Summaries are published quarterly of each calendar year. They consist of a brief summary of each AFOSR technical report received in the Technical Information Division and submitted to the Defense Technical Information Center for that quarter. GRA

N93-14657# Naval Biodynamics Lab., New Orleans, LA.
BIBLIOGRAPHY OF SCIENTIFIC PUBLICATIONS OF THE NAVAL BIODYNAMICS LABORATORY Interim Report, 1980 - 1991
Jun. 1992 32 p
(AD-A255952; NBDL-92R003) Avail: CASI HC A03/MF A01

This report lists all research reports, special reports, monographs, technical memoranda, joint reports, research information bulletin, journal articles, and conference proceedings published by the Naval Biodynamics Laboratory between January 1980 and December 1991. GRA

N93-14673# Air Force Office of Scientific Research, Bolling AFB, Washington, DC.
AIR FORCE OFFICE OF SCIENTIFIC RESEARCH Quarterly Report, Apr. - Jun. 1992
Debra L. Tyrrell Jun. 1992 396 p
(AD-A255361; AFOSR-TR-92-0843) Avail: CASI HC A17/MF A04

The AFOSR Technical Report Summaries are published quarterly of each calendar year. They consist of a brief summary of each AFOSR technical report received in the Technical Information Division and submitted to the Defense Technical Information Center for that quarter. GRA

N93-14674# Air Force Office of Scientific Research, Bolling AFB, Washington, DC.
AIR FORCE OFFICE OF SCIENTIFIC RESEARCH Quarterly Report, Jul. - Sep. 1991
Debra L. Tyrrell Sep. 1991 199 p
(AD-A255370; AFOSR-TR-92-0813) Avail: CASI HC A09/MF A03

The AFOSR Technical Report Summaries are published quarterly of each calendar year. They consist of a brief summary of each AFOSR technical report received in the Technical Information Division and submitted to the Defense Technical Information Center for that quarter. GRA

N93-15060# Sandia National Labs., Albuquerque, NM.
A DISTRIBUTED VISUALIZATION ENVIRONMENT FOR ENGINEERING SCIENCES
C. J. Pavlakos, L. A. Schoof, and J. F. Mareda 1992 8 p Presented at the Visualization 1992, Boston, MA, 19-23 Oct. 1992
(Contract DE-AC04-76DP-00789)
(DE92-012629; SAND-92-0778C; CONF-921079-1) Avail: CASI HC A02/MF A01

As a multiprogram engineering laboratory, Sandia National Laboratories (SNL) has major research and development responsibilities for nuclear weapons, arms control, energy, environment, and other areas of strategic importance to national security. To accomplish this diversified mission, analysts within the Engineering Sciences Directorate support the entire laboratory using finite element and finite difference solution schemes to solve problems in fluid dynamics (steady state and transient, compressible and incompressible), thermodynamics (heat transfer), hydrodynamics (impact physics, penetration mechanics), solid mechanics (structural/thermal analysis, fracture mechanics, ground subsidence, impact modeling) and structural dynamics. To assist these analysts in performing these analyses most efficiently, the Applied Visualization Group was formed and tasked to develop a 'production scientific visualization environment.' In this paper, we characterize a visualization environment that has been designed and prototyped for a large community of scientists and engineers. The proposed environment makes use of a visualization server concept to provide effective, interactive visualization to the user's desktop. Benefits of using the visualization server approach are discussed. Some thoughts regarding desirable features for visualization server hardware architectures are also addressed. A brief discussion of the software environment is included. The paper concludes by summarizing certain observations which we have made regarding the implementation of such visualization environments. DOE

Typical Subject Index Listing

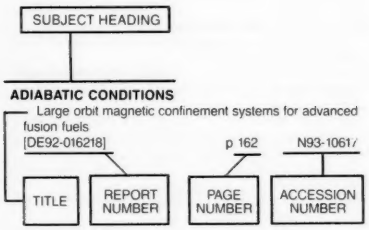

The subject heading is a key to the subject content of the document. Titles, report numbers, and accession numbers of pertinent documents are provided under each subject heading. When the title is insufficiently descriptive of the document content, a title extension has been added, separated from the title by three hyphens. The report number helps to indicate the type of document cited (e.g., NASA report, NASA translation, NASA contractor report). The accession number is the number by which the document abstracts are arranged in this journal and by which the document is sold or requested. The page number helps you locate the the citation in the abstract section. The titles, with title extensions if present, are arranged under each subject heading in ascending accession number order. The subject headings have been selected from the latest revision of the *NASA Thesaurus*.

A

A-7 AIRCRAFT
Software requirements for the A-7E aircraft
| AD-A255746 | p 946 N93-15052

ABERRATION
The 3D modeling of high numerical aperture imaging in thin films p 985 N93-15513
Effects of higher order aberrations on beam shape in an optical recording system p 985 N93-15515

ABILITIES
Identifying ability requirements for operators of future automated air traffic control systems
| AD-A256615 | p 789 N93-14276

ABRASION
Degradation of radiator performance on Mars due to dust p 823 N93-15616

ABSORPTION
Operational strategies for contamination control of composite materials p 822 N93-15614

ABSORPTION CROSS SECTIONS
High resolution absolute absorption cross sections of NO2 at 295, 573, and 673 K at visible wavelengths: Comprehensive data tables
| AD-A255261 | p 839 N93-14530

ABSORPTION SPECTRA
QSO absorption lines and the ionizing field at high redshifts p 1013 N93-14860

ABSORPTIVITY
Optics for diode array transverse pumped laser rod
| AD-D015436 | p 885 N93-14722
Abstracts booklet
| AD-A256115 | p 869 N93-15188

ABSTRACTS
Large space structures and systems in the space station era: A bibliography with indexes (supplement 04)
| NASA-SP-7085(04) | p 817 N93-14606
Abstracts booklet
| AD-A256115 | p 869 N93-15188
LDEF: A bibliography with abstracts
| NASA-TM-107705 | p 813 N93-15646

ACCELERATED LIFE TESTS
Reanalysis of multiple-wheel landing gear traffic tests
| AD-A256593 | p 804 N93-14238
Corrosion of metal particle and metal evaporated tapes p 883 N93-15039
Liquid flow reactor and method of using
| AD-D015392 | p 893 N93-15232

ACCELEROMETERS
Technology development for non-contact measurement in modal testing of large space structures p 809 N93-14942

ACCESS CONTROL
A deadlock-free communication system for a transputer network
| AD-A256473 | p 959 N93-15319

ACCRETION DISKS
The black hole candidate binary A0620-00 p 1015 N93-14148
Extracting x rays, gamma rays, and electron-positron pairs from supermassive Kerr black holes using the Penrose mechanism p 1049 N93-14176
Multiwavelength spectroscopy of active galactic nuclei p 1011 N93-14611

ACCURACY
Optimum pose measurements for kinematic parameters identification
| AD-A256307 | p 970 N93-14443
Establishment of a test course for high accuracy dynamic positioning systems
| AD-A255407 | p 789 N93-14501
Arc digital raster imagery evaluation
| AD-A255403 | p 817 N93-14565

ACOUSTIC ATTENUATION
Co-channel speaker separation
| AD-A256443 | p 861 N93-15317

ACOUSTIC FREQUENCIES
Boundary element analysis of low frequency cavity acoustical problems
| MATHS-REPT-A-158 | p 974 N93-15073

ACOUSTIC MEASUREMENT
Development of a TDS measurement system. Application to acoustic propagation measurement in a non anechoic environment
| ONERA-RT-18/3641-PY | p 975 N93-15130
Acoustic mode measurements in the inlet of a model turbofan using a continuously rotating rake: Data collection/analysis techniques
| NASA-TM-105936 | p 801 N93-15403
Acoustic resonance techniques for quality control
| DE92-040150 | p 895 N93-15413
Innovative techniques for studying new materials and new developments in solid state physics
| AD-A256394 | p 996 N93-15465

ACOUSTIC PROPAGATION
Scattering of sound by sound: Nonlinear interaction of collinear and noncollinear sound beams p 973 N93-14145
Problems in nonlinear acoustics: Rayleigh waves, pulsed sound beams, reflection of focused beams, waveguides, cooperative radiation of sound by buggles, acoustic streaming effects in standing waves, and spark-source lithotripter pulses
| AD-A256289 | p 974 N93-14458
Acoustic propagation loss predictions for a site on the Bermuda Rise at low and very low frequencies
| AD-A255445 | p 925 N93-14512
Development of a TDS measurement system. Application to acoustic propagation measurement in a non anechoic environment
| ONERA-RT-18/3641-PY | p 975 N93-15130

ACOUSTIC PROPERTIES
An analysis of the effect of acoustic non-linearities in wide bandwidth acousto-optic bragg cells
| AD-A256579 | p 973 N93-14269

ACOUSTIC SCATTERING
Scattering of sound by sound: Nonlinear interaction of collinear and noncollinear sound beams p 973 N93-14145
Problems in nonlinear acoustics: Rayleigh waves, pulsed sound beams, reflection of focused beams, waveguides, cooperative radiation of sound by buggles, acoustic streaming effects in standing waves, and spark-source lithotripter pulses
| AD-A256289 | p 974 N93-14458
Experimental investigation of scattering from randomly rough plastic cylinders
| AD-A256018 | p 975 N93-15259

ACOUSTICAL HOLOGRAPHY
A time-domain study of the relationship between drive force time bandwidth and farfield acoustic radiation
| AD-A255616 | p 973 N93-14159

ACOUSTICS
Problems in nonlinear acoustics: Rayleigh waves, pulsed sound beams, reflection of focused beams, waveguides, cooperative radiation of sound by buggles, acoustic streaming effects in standing waves, and spark-source lithotripter pulses
| AD-A256289 | p 974 N93-14458
Program auralization: Sound enhancements to the programming environment p 953 N93-15539
Vibration and acoustic testing of TOPEX/Poseidon satellite p 820 N93-15599
Acoustic and thermal testing of the Titan/Centaur upper stage p 814 N93-15621
Acoustic location of leaks in pressurized underground petroleum pipelines
| PB92-207687 | p 975 N93-15647

ACOUSTO-OPTICS
An analysis of the effect of acoustic non-linearities in wide bandwidth acousto-optic bragg cells
| AD-A256579 | p 973 N93-14269
Integrated photonics research technical digest series. Volume 10: Conference edition: Summaries of papers presented at the Integrated Photonics Research Topical Meeting
| AD-A255423 | p 981 N93-14506

ACQUISITION
Streamlined acquisition handbook
| NASA-TM-108133 | p 1002 N93-14719

ACRYLATES
Spirobislactone acrylate polymers
| AD-D015443 | p 850 N93-14802

ACRYLIC RESINS
Application of gel-silica optics to laser technology and optical element fabrication
| AD-A255666 | p 883 N93-14131
Spirobislactone acrylate polymers
| AD-D015443 | p 850 N93-14802

ACRYLONITRILES
Radical ion formation in polymers as a mechanism for laser eye protection
| AD-A255992 | p 850 N93-15111

ACTIVATION ENERGY
Comments on 'Kinetic Study on the Hexacelsian-Celsian Phase Transformation'
| NASA-TM-105917 | p 850 N93-14886

ACTIVE CONTROL
Active control of combustion instability in a ramjet using large-eddy simulations
| AD-A255226 | p 798 N93-14111
Digital active material processing platform effort (DAMPER), SBIR phase 2
| NASA-CR-190798 | p 856 N93-15353
Vibration isolation technology: An executive summary of systems development and demonstration
| NASA-TM-105937 | p 778 N93-15573

ACTIVE GALACTIC NUCLEI
Extracting x rays, gamma rays, and electron-positron pairs from supermassive Kerr black holes using the Penrose mechanism p 1049 N93-14176
A search for dead QSO's among nearby luminous galaxies p 1011 N93-14228
Multiwavelength spectroscopy of active galactic nuclei p 1011 N93-14611
Quasars, galaxies, and pseudo-vacuum droplets
| NIKHEF-H/91-20 | p 1020 N93-14686
ROSAT all-sky survey on the Einstein EMSS sample
| NASA-CR-191627 | p 1013 N93-15340

ACTIVE GALAXIES
Physical properties of extended emission-line regions in active and cooling-flow galaxies p 1018 N93-14461
Supervised selection of galaxy candidates from the IRAS PSC: The quality of the selection and the infrared properties of the galaxy candidates
[MPE-PREPRINT-216] p 1021 N93-15284
ACTUATORS
SDIO Workshop on Piezoelectric Ceramic Actuators for Space Applications
[AD-A255959] p 990 N93-14422
Smart materials for Army structures
[AD-A254925] p 836 N93-15218
Jointed assembly actuated by fluid pressure
[AD-D015383] p 893 N93-15248
Digital active material processing platform effort (DAMPER), SBIR phase 2
[NASA-CR-190798] p 856 N93-15353
Three position power cylinder
[AD-D015393] p 894 N93-15461
ADA (PROGRAMMING LANGUAGE)
Ada-based multitasking terminal I/O
[AD-A255656] p 942 N93-14164
The 1992 Summer SIGAda AIWG Workshop applications experiences and lessons learned panel message from the panel chair
[AD-A256188] p 962 N93-14519
Autonomous power system brassboard
[NASA-CR-189115] p 867 N93-14798
User manual for the Software Technology for Adaptable, Reliable Systems (STARS). PCTE Browser Tool (PBT) version 0.1 SunOS implementation
[AD-A257064] p 951 N93-15457
ADAPTIVE CONTROL
Adaptive control of nonlinear nonminimum phase systems p 961 N93-14470
Airborne radar simulation with adaptive antenna techniques
[AD-A255460] p 859 N93-14488
Multiple model adaptive estimation applied to the ViSTA F-16 with actuator and sensor failures
[AD-A256444] p 802 N93-14608
Adaptive active noise control using multiple-model approaches
[ISVR-TR-210] p 974 N93-14734
Learning position and force control for mechanical manipulators p 963 N93-15147
Robust control design for uncertain nonlinear dynamic systems p 964 N93-15148
Adaptive control of a manipulator in cartesian space
[F-4-2] p 950 N93-15308
ADAPTIVE OPTICS
Vertical path atmospheric turbulence: Temporal spectra and differential image motion measurements p 914 N93-14641
ADDITIVES
Cesium iodide alloys
[DE92-019818] p 845 N93-14717
ADHESION
Biofilm ecology of bioluminescent bacteria
[AD-A255282] p 932 N93-14532
Tribology of magnetic storage systems p 1002 N93-14772
ADHESION TESTS
Testing and analysis of modified HMMWV front lift provisions
[MTL-TR-92-31] p 891 N93-14735
ADHESIVE BONDING
Preliminary design of composite joints
[DLR-MITT-92-05] p 835 N93-15076
The influence of steel surface chemistry on the bonding of lubricant films
[AD-A256231] p 851 N93-15242
Development of adherent ceramic coatings to reduce contact stress damage of ceramics
[DE92-041373] p 852 N93-15437
ADIABATIC FLOW
Adiabatic two-phase flow in a test section with partial flow blockages
[DE92-016360] p 877 N93-14816
ADJUSTING
Variable speed rotary compressor and adjustable speed drive efficiencies measured in the laboratory
[DE92-040026] p 893 N93-15278
ADSORBENTS
Adsorption and diffusion of fluids in well-characterized adsorbent materials
[DE92-040160] p 843 N93-15414
ADSORPTION
Final Report, 1 November 1988 - 31 October 1991 --- spectroscopy of adsorbed and photodissociated molecules
[AD-A255979] p 976 N93-14424
Absorption of propellant vapors into polymer films
[AD-A255274] p 849 N93-14531
Adsorption and diffusion of fluids in well-characterized adsorbent materials
[DE92-040160] p 843 N93-15414
ADVANCED VERY HIGH RESOLUTION RADIOMETER
SeaWiFS Technical Report Series. Cloud screening for polar orbiting visible and infrared (IR) satellite sensors, volume 7
[NASA-TM-104566] p 932 N93-15645
ADVECTION
Synoptic/planetary-scale interactions and blocking over the North Atlantic Ocean
[NASA-CR-191376] p 925 N93-14769
Fitting microphysical observations to a numerical model through an optimal control theory technique p 924 N93-15100
AERIAL PHOTOGRAPHY
Using digital scanned aerial photography for wetlands delineation
[AD-A255392] p 905 N93-14676
AEROACOUSTICS
A time-domain study of the relationship between drive force time bandwidth and farfield acoustic radiation
[AD-A255616] p 973 N93-14159
Investigations of detail design issues for the high speed acoustic wind tunnel using a 60th scale model tunnel. Part 1: Tests with open circuits
[NASA-CR-191671] p 780 N93-14737
Investigations of detail design issues for the high speed acoustic wind tunnel using a 60th scale model tunnel. Part 2: Tests with the closed circuit
[NASA-CR-191672] p 780 N93-14738
Tiltrotor aircraft noise: A summary of the presentations and discussions at the 1991 FAA/Georgia Tech Workshop
[DOT/FAA/RD-91/23] p 974 N93-14912
AEROASSIST
Development of engineering methods for nonequilibrium radiative phenomena about aeroassisted entry vehicles p 817 N93-14632
AERODYNAMIC CHARACTERISTICS
Application of an aeroelastic analysis method for aerodynamic improvement of fighter wings at maneuver flight conditions p 791 N93-14832
The Applicaiton of CFD to rotary wing flow problems
[NASA-TM-102803] p 782 N93-15483
AERODYNAMIC COEFFICIENTS
Program for calculation of aileron rolling moment and yawing moment coefficients at subsonic speeds
[ESDU-88040] p 779 N93-14514
AERODYNAMIC CONFIGURATIONS
Flight termination systems commonality standard
[AD-A255349] p 789 N93-14517
Computational analysis of hypersonic flows past elliptic-cone waveriders
[NASA-CR-191304] p 781 N93-14767
AERODYNAMIC HEATING
A finite element model for analysis of thermoviscoplastic behavior of hypersonic leading edge structures subject to intense aerothermal heating p 780 N93-14631
AERODYNAMIC LOADS
Multi-disciplinary optimization of aeroservoelastic systems
[NASA-CR-191255] p 901 N93-14766
AERODYNAMIC STABILITY
Program for calculation of aileron rolling moment and yawing moment coefficients at subsonic speeds
[ESDU-88040] p 779 N93-14514
Wing rock prediction method for a high performance fighter aircraft
[AD-A256438] p 792 N93-15314
AERODYNAMIC STALLING
Estimation of unsteady lift on a pitching airfoil from wake velocity surveys
[NASA-TM-105947] p 781 N93-14791
The Applicaiton of CFD to rotary wing flow problems
[NASA-TM-102803] p 782 N93-15483
AERODYNAMICS
Aeronautical engineering: A continuing bibliography with indexes (supplement 282)
[NASA-SP-7037(282)] p 777 N93-14604
Aeronautical engineering: A continuing bibliography with indexes (supplement 284)
[NASA-SP-7037(284)] p 777 N93-14605
Flight testing: Past, present, and future p 777 N93-14615
Subsonic aerodynamic research laboratory
[AD-A256060] p 780 N93-14661
Aeronautical engineering: A continuing bibliography with indexes (supplement 283)
[NASA-SP-7037(283)] p 778 N93-14732
L.D.V. measurements of unsteady flow fields in radial turbine
[AD-A255728] p 878 N93-15065
Analysis of in-flight structural failures of P-3C wing leading edge segments
[AD-A256212] p 792 N93-15238
Flight dynamics system software development environment (FDS/SDE) tutorial
[NASA-TM-108580] p 952 N93-15502
AEROELASTICITY
A compilation of the mathematics leading to the doublet lattice method
[AD-A256304] p 779 N93-14441
The effect of wake dynamics on rotor eigenvalues in forward flight p 780 N93-14595
Multi-disciplinary optimization of aeroservoelastic systems
[NASA-CR-191255] p 901 N93-14766
Finite-state inflow applied to aeroelastic flutter of fixed and rotating wings p 802 N93-14830
Application of an aeroelastic analysis method for aerodynamic improvement of fighter wings at maneuver flight conditions p 791 N93-14832
AERONAUTICAL ENGINEERING
Aeronautical engineering: A continuing bibliography with indexes (supplement 282)
[NASA-SP-7037(282)] p 777 N93-14604
Aeronautical engineering: A continuing bibliography with indexes (supplement 284)
[NASA-SP-7037(284)] p 777 N93-14605
Aeronautical engineering: A continuing bibliography with indexes (supplement 283)
[NASA-SP-7037(283)] p 778 N93-14732
AERONAUTICS
Aeronautical engineering: A continuing bibliography with indexes (supplement 282)
[NASA-SP-7037(282)] p 777 N93-14604
Aeronautical engineering: A continuing bibliography with indexes (supplement 284)
[NASA-SP-7037(284)] p 777 N93-14605
AEROSOLS
Ethane ice haze in the upper atmosphere of Uranus p 1023 N93-14212
Satellite detection of complex aerosols over the Arabian Peninsula/Gulf
[AD-A256085] p 909 N93-14261
Effects of water vapor and anisotropic scattering on aerosol optical depth retrieval
[AD-A256087] p 904 N93-14262
Improved aerosol optical depth and particle size index from satellite detected radiance
[AD-A256089] p 904 N93-14263
Optimization of a Counterflow Virtual Impactor (CVI) for studying aerosol effects on cloud droplet number p 914 N93-14861
On the role of water growth in atmospheric aerosol p 922 N93-14875
Evaluation of a soil fixative to retard particle entrainment: A laboratory study
[UCRL-LR-109806] p 915 N93-14877
An analytic phase function for cylindrical particles
[AD-A255750] p 977 N93-15054
Alpha migration through air filters: A numerical simulation
[UCRL-LR-109866] p 878 N93-15285
AEROSPACE ENGINEERING
Bibliography of Lewis Research Center Technical Publications announced in 1991
[NASA-TM-105595] p 1004 N93-14796
Proceedings of the Sixth CASI Conference on Astronautics
[CTN-92-60336] p 804 N93-14920
A comparison of superconductor and manganin technology for electronic links used in space mission applications
[NASA-CR-4477] p 997 N93-15587
AEROSPACE ENVIRONMENTS
Manned testing in a simulated space environment p 820 N93-15602
Hypervelocity impact simulations of Whipple shields p 821 N93-15604
AEROSPACE INDUSTRY
Proceedings of the Sixth CASI Conference on Astronautics
[CTN-92-60336] p 804 N93-14920
Space education: A self-perservation strategy for the Canadian space industry p 808 N93-14937
AEROSPACE MEDICINE
Test and evaluation report of the Physio Control Defibrillator/Monitor, Model LifePak(tm) 6s
[AD-A255691] p 933 N93-14103
Test and evaluation report of the Catalyst Research Oxygen Monitor, Model Miniox 3
[AD-A255849] p 881 N93-14105
Aerospace medicine and biology: A continuing bibliography with indexes (supplement 368)
[NASA-SP-7011(368)] p 934 N93-14603
Aerospace medicine and biology: A continuing bibliography with indexes (supplement 369)
[NASA-SP-7011(369)] p 935 N93-14731

Publications of the Space Physiology and Countermeasures Program, Neuroscience Discipline: 1980-1990
|NASA-CR-4476| p 936 N93-15583

AEROSPACE PLANES
Robust nonlinear feedback guidance for an aerospace plane: A geometric approach p 803 N93-14835

AEROSPACE SCIENCES
Bibliography of Lewis Research Center Technical Publications announced in 1991
|NASA-TM-105595| p 1004 N93-14796
International Space University p 808 N93-14938

AEROSPACE SYSTEMS
Electro-optic architecture (EOA) for sensors and actuators in aircraft propulsion systems
|NASA-CR-182270| p 982 N93-15116

AEROSPACE VEHICLES
Development of engineering methods for nonequilibrium radiative phenomena about aeroassisted entry vehicles p 817 N93-14632

AEROTHERMODYNAMICS
A finite element model for analysis of thermoviscoplastic behavior of hypersonic leading edge structures subject to intense aerothermal heating p 780 N93-14631
Development of engineering methods for nonequilibrium radiative phenomena about aeroassisted entry vehicles p 817 N93-14632
Results of a FRSI material test under Space Shuttle ascent conditions in the Ames Research Center 9x7 foot supersonic wind tunnel (OS13). Space Shuttle aerothermodynamic data report
|NASA-CR-167699| p 816 N93-15475
Aerothermodynamic flow phenomena of the airframe-integrated supersonic combustion ramjet
|NASA-TM-4376| p 827 N93-15528
Investigation of the aerothermodynamics of hypervelocity reacting flows in the ram accelerator
|NASA-CR-191715| p 783 N93-15588

AFRICA
South African TOPEX/Poseidon altimeter experiment p 928 N93-14976

AGING (MATERIALS)
Effect of thermomechanical treatments on the aging response of centrifugally cast silicon carbide/aluminum composites
|AD-A256204| p 836 N93-15236

AGRICULTURE
Integrating satellite imagery into a geographic information system for monitoring the downstream impacts of dam construction on floodplain agriculture in Sokoto State, Nigeria p 905 N93-14823

AILERONS
Program for calculation of aileron rolling moment and yawing moment coefficients at subsonic speeds
|ESDU-88040| p 779 N93-14514

AIR
The production and use of aeroponically grown inocula of VAM fungi in the native plant nursery
|PB92-204973| p 933 N93-15208

AIR DATA SYSTEMS
Discussion for the ideal AIMS p 793 N93-15153
Software flexibility and configuration control for the A340/A330 Aircraft Condition Monitoring System (ACMS) p 793 N93-15154
FDAMS: An extendable and reconfigurable solution for avionics data management systems p 794 N93-15157

AIR DEFENSE
Air Force Office of Scientific Research
|AD-A255331| p 1051 N93-14523

AIR FILTERS
Alpha migration through air filters: A numerical simulation
|UCRL-LR-109866| p 878 N93-15285

AIR JETS
Optimization of circular orifice jets mixing into a heated cross flow in a cylindrical duct
|NASA-TM-105984| p 800 N93-15359

AIR POLLUTION
Multiscale modeling of the long-range transport and fate of pollutants emitted from urban areas p 909 N93-14118
Performing wind-tunnel modeling for better management of near-field risks
|DE92-040205| p 910 N93-15063
A correlated k-distribution model of the atmospheric heating rates for overlapping spectra of CH4 and N2O
|DE93-000890| p 911 N93-15281
Geographical distribution and seasonal variation of surface emissions and deposition velocities of atmospheric trace gases
|AERONOMICA-ACTA-A-361-1991| p 911 N93-15460
Modelling global methane emissions from livestock: Biological and nutritional controls
|NASA-CR-191354| p 911 N93-15480

AIR QUALITY
Multiscale modeling of the long-range transport and fate of pollutants emitted from urban areas p 909 N93-14118

AIR SAMPLING
Parametric study of air sampling cyclones p 779 N93-14173

AIR TRAFFIC
Terminal area forecasts FY 1992 - 2005
|AD-A255797| p 788 N93-15390

AIR TRAFFIC CONTROL
Identifying ability requirements for operators of future automated air traffic control systems
|AD-A256615| p 789 N93-14276
Information systems for airport operations
|TT-9202| p 789 N93-14729
Terminal area forecasts FY 1992 - 2005
|AD-A255797| p 788 N93-15390

AIR TRAFFIC CONTROLLERS (PERSONNEL)
Performance of color-dependent tasks of air traffic control specialists as a function of type and degree of color vision deficiency
|AD-A256614| p 788 N93-14275
Identifying ability requirements for operators of future automated air traffic control systems
|AD-A256615| p 789 N93-14276

AIR TRANSPORTATION
Terminal area forecasts FY 1992 - 2005
|AD-A255797| p 788 N93-15390

AIR WATER INTERACTIONS
Wind stress analysis over the Western Equatorial Pacific and North Atlantic Oceans based on ECMWF operational wind products, 1985-1989
|AD-A256147| p 920 N93-14256
Sensitivity of the Yoshida jet to the parameterization of vertical mixing: Do easterly winds imply equatorial upwelling? p 922 N93-14864
Sea level response to wind forcing in the tropical Atlantic p 928 N93-14977
Evaluation of methods for estimating wind wave growth on narrow irregular fetches
|AD-A256002| p 932 N93-15113

AIRBORNE EQUIPMENT
Airborne Wind Shear Detection and Warning Systems. Fourth Combined Manufacturers' and Technologists' Conference, part 2
|NASA-CP-10105-PT-2| p 783 N93-14844
Two micron laser development for atmospheric remote sensing at NASA Langley Research Center p 784 N93-14845
NASA/LMSC coherent LIDAR airborne shear sensor: System capabilities and flight test plans p 784 N93-14847
Development of the Advance Warning Airborne System(AWAS) p 784 N93-14849
Systems issues in airborne Doppler radar/LIDAR certification p 785 N93-14855

AIRBORNE RADAR
Airborne radar simulation with adaptive antenna techniques
|AD-A255460| p 859 N93-14488

AIRBORNE/SPACEBORNE COMPUTERS
Rewritable optical disk: Application to flight recording p 794 N93-15160
DAR-2: On-board data acquisition system for aircraft engines p 795 N93-15166
Monitoring of powerplants in advanced commercial aircraft p 795 N93-15171
Output data formatter for the Electronically Scanned Thinned Array Radiometer (ESTAR) instrument
|NASA-TM-4432| p 871 N93-15529

AIRCRAFT ACCIDENT INVESTIGATION
Special investigation report: Piper Aircraft Corporation PA-46 Malibu/Mirage Accidents/Incident, 31 May 1989 - 17 March 1991
|PB92-917007| p 788 N93-15577

AIRCRAFT ACCIDENTS
Aviation accidents, incidents, and violations: Psychological predictors among US pilots p 783 N93-14693
Trans-cockpit authority gradient in Navy/Marine aircraft mishaps p 786 N93-15016
Taxonomy of flight variables p 787 N93-15022
Embedded ADM reduces helicopter human error accidents p 787 N93-15024
Special investigation report: Piper Aircraft Corporation PA-46 Malibu/Mirage Accidents/Incident, 31 May 1989 - 17 March 1991
|PB92-917007| p 788 N93-15577

AIRCRAFT ANTENNAS
Modeling and control of a trailing wire antenna towed by an orbiting aircraft
|AD-A256450| p 859 N93-14610

AIRCRAFT COMPARTMENTS
Effects of seating configuration and number of type 3 exits on emergency aircraft evacuation
|AD-A256616| p 783 N93-14277

AIRCRAFT CONFIGURATIONS
DESAID (the development of an expert system for aircraft initial design) p 790 N93-14448
The 3D Navier-Stokes flow analysis for shared and distributed memory MIMD computers
|AD-A256038| p 878 N93-15187

AIRCRAFT CONSTRUCTION MATERIALS
Stress corrosion susceptibility of ultra-high strength steels for Naval aircraft applications
|AD-A256126| p 846 N93-15189
Fiber reinforced composites: A new class of glass and glass ceramic materials for thermomechanical applications
|REPT-921-430-104| p 838 N93-15490

AIRCRAFT CONTROL
An examination of wing rock for the F-15
|AD-A256613| p 802 N93-14252
Unmanned aerial vehicles: More testing needed before production of short-range system
|AD-A256296| p 790 N93-14440
Adaptive control of nonlinear nonminimum phase systems p 961 N93-14470
Multiple model adaptive estimation applied to the ViSTA F-16 with actuator and sensor failures
|AD-A256444| p 802 N93-14608
Multi-disciplinary optimization of aeroservoelastic systems
|NASA-CR-191255| p 901 N93-14766
Advanced aeroservoelastic stabilization techniques for hypersonic flight vehicles
|NASA-CR-189702| p 802 N93-14811
F/A-18 controls released departure recovery flight test evaluation
|AD-A256522| p 803 N93-15396
Propulsion system performance resulting from an integrated flight/propulsion control design
|NASA-TM-105874| p 801 N93-15525

AIRCRAFT DESIGN
An examination of wing rock for the F-15
|AD-A256613| p 802 N93-14252
DESAID (the development of an expert system for aircraft initial design) p 790 N93-14448
Application of an aeroelastic analysis method for aerodynamic improvement of fighter wings at maneuver flight conditions p 791 N93-14832

AIRCRAFT ENGINES
SAPNEW: Parallel finite element code for thin shell structures on the Alliant FX-80
|NASA-CR-189212| p 901 N93-14799
Electro-optic architecture (EOA) for sensors and actuators in aircraft propulsion systems
|NASA-CR-182270| p 982 N93-15116
Integrated engine control and monitoring with experiences derived from OLMOS p 795 N93-15168
Monitoring of powerplants in advanced commercial aircraft p 795 N93-15171
EJ 200 engine monitoring system: On- and off-board data capture, analysis, and management system p 796 N93-15172
RB199 engine oil system failure diagnostics by comparison of measured and calculated oil consumption using the OLMOS on-board monitoring system p 796 N93-15173
A philosophy for integrated monitoring system design p 796 N93-15174
Modelling the engine temperature distribution between shut down and restart for life usage monitoring p 796 N93-15177

AIRCRAFT EQUIPMENT
F/FB-111 avionics test station and component specialist/technician. Automatic test stations manual and electronic warfare test stations. Training requirements analysis (451X6), volume 2
|AD-A252121| p 793 N93-14110
Definition study PHARUS
|AD-A256560| p 860 N93-14805

AIRCRAFT GUIDANCE
Estimation of rate of climb
|ESDU-92019| p 791 N93-14541

AIRCRAFT ICING
Results of low power deicer tests on a swept inlet component in the NASA Lewis icing research tunnel
|NASA-TM-105968| p 781 N93-14911
Surface roughness due to residual ice in the use of low power deicing systems
|NASA-TM-105971| p 782 N93-15338
Numerical modeling of anti-icing systems and comparison to test results on a NASA 0012 airfoil
|NASA-TM-105975| p 787 N93-15345
Ice accretion and performance degradation calculations with LEWICE/NS
|NASA-TM-105972| p 787 N93-15354

Close-up analysis of aircraft ice accretion
[NASA-TM-105952] p 787 N93-15360
Advancements in the LEWICE ice accretion model
[NASA-CR-191019] p 879 N93-15402
An overview of shed ice impact in the NASA Lewis Icing Research Tunnel
[NASA-TM-105969] p 782 N93-15404
Ice accretion prediction for a typical commercial transport aircraft
[NASA-TM-105976] p 788 N93-15522

AIRCRAFT MAINTENANCE
F/FB-111 avionics test station and component specialist/technician. Automatic test stations manual and electronic warfare test stations. Training requirements analysis (451X6), volume 2
[AD-A252121] p 793 N93-14110
Bearing servicing tool
[NASA-CASE-MSC-21881-1] p 891 N93-14871
Proceedings of the 16th Symposium on Aircraft Integrated Monitoring Systems
[DLR-MITT-92-01] p 793 N93-15152
The Teledyne controls aircraft condition monitoring system p 793 N93-15155
Ground Support Equipment (GSE) for Aircraft Condition Monitoring System (ACMS) p 778 N93-15158
Detection of technical states with aircraft p 794 N93-15159
Monitoring of powerplants in advanced commercial aircraft p 795 N93-15171
Failure diagnostic with MAINTEX based on AIMS at Swissair p 778 N93-15181
Onboard System Evaluation of Rotors Vibration, Engines (OBSERVE) monitoring system
[AD-A255366] p 792 N93-15227

AIRCRAFT MANEUVERS
Application of an aeroelastic analysis method for aerodynamic improvement of fighter wings at maneuver flight conditions p 791 N93-14832

AIRCRAFT MODELS
Sensor fault detection using nonlinear observer and polynomial classifier p 797 N93-15182

AIRCRAFT NOISE
Evaluation of three models used for predicting noise propagated long distances overground
[AD-A255963] p 973 N93-14406
Air Force procedure for predicting noise around airbases: Noise exposure model (Noisemap)
[AD-A255769] p 910 N93-14655
Tiltrotor aircraft noise: A summary of the presentations and discussions at the 1991 FAA/Georgia Tech Workshop
[DOT/FAA/RD-91/23] p 974 N93-14912

AIRCRAFT PERFORMANCE
Application of an aeroelastic analysis method for aerodynamic improvement of fighter wings at maneuver flight conditions p 791 N93-14832
Czechoslovak development and experience in flight data recorder readout and analysis p 794 N93-15162
Real-time in-flight engine performance and health monitoring techniques for flight research application p 795 N93-15169

AIRCRAFT PILOTS
Development of measures of crew coordination
[AD-A255384] p 939 N93-14651
Cockpit decision making p 786 N93-15015
Trans-cockpit authority gradient in Navy/Marine aircraft mishaps p 786 N93-15016

AIRCRAFT RELIABILITY
Embedded ADM reduces helicopter human error accidents p 787 N93-15024
Helicopter flight data recorder and health and usage monitoring system p 797 N93-15178
Helicopter health monitoring: Current practice and future trends p 797 N93-15179
Airbus Industrie TCAS experience p 789 N93-15186

AIRCRAFT SAFETY
Effects of seating configuration and number of type 3 exits on emergency aircraft evacuation
[AD-A256616] p 783 N93-14277
Measuring risk in single-engine and twin-engine helicopters p 787 N93-15025
The FAIR (Flight Animated and Interactive Reconstruction) tool p 788 N93-15164
Special investigation report: Piper Aircraft Corporation PA-46 Malibu/Mirage Accidents/Incident, 31 May 1989 - 17 March 1991
[PB92-917007] p 788 N93-15577

AIRCRAFT STABILITY
Program for calculation of aileron rolling moment and yawing moment coefficients at subsonic speeds
[ESDU-88040] p 779 N93-14514
Icing effects on aircraft stability and control determined from flight data: Preliminary results
[NASA-TM-105977] p 803 N93-14831

AIRCRAFT STRUCTURES
Stress corrosion susceptibility of ultra-high strength steels for Naval aircraft applications
[AD-A256126] p 846 N93-15189

AIRCRAFT WAKES
Estimation of unsteady lift on a pitching airfoil from wake velocity surveys
[NASA-TM-105947] p 781 N93-14791

AIRFOIL OSCILLATIONS
Estimation of unsteady lift on a pitching airfoil from wake velocity surveys
[NASA-TM-105947] p 781 N93-14791

AIRFOILS
Multi-point inverse design of isolated airfoils and airfoils in cascade in incompressible flow p 790 N93-14462
Direct prediction of a separation boundary for aerofoils using a viscous-coupled calculation method
[ESDU-92008] p 780 N93-14516
Estimation of unsteady lift on a pitching airfoil from wake velocity surveys
[NASA-TM-105947] p 781 N93-14791
Numerical modeling of anti-icing systems and comparison to test results on a NASA 0012 airfoil
[NASA-TM-105975] p 787 N93-15345

AIRFRAME MATERIALS
Fiber reinforced composites: A new class of glass and glass ceramic materials for thermomechanical applications
[REPT-921-430-104] p 838 N93-15490

AIRFRAMES
Experimental and analytical investigation of the vibration characteristics of a remotely piloted helicopter
[AD-A256131] p 790 N93-14248
Proceedings of the USAF Structural Integrity Program
[AD-A255379] p 777 N93-14549
Icing effects on aircraft stability and control determined from flight data: Preliminary results
[NASA-TM-105977] p 803 N93-14831
A neural network prototype for predicting F-14B strains at the B.L. 10 longeron
[AD-A255272] p 792 N93-15004
Aeroplane crashes on the runway: Validation and final evaluation of the method of modeling an airframe structure
[IMFL-91-32] p 792 N93-15126
An overview of shed ice impact in the NASA Lewis Icing Research Tunnel
[NASA-TM-105969] p 782 N93-15404

AIRGLOW
Near-infrared oxygen airglow from the Venus nightside p 1026 N93-14308
A study of mid-latitude 5577A CI dayglow emissions
[AD-A255444] p 914 N93-14511

AIRLINE OPERATIONS
In-service evaluation of wind shear systems p 785 N93-14857

AIRPORT TOWERS
Terminal area forecasts FY 1992 - 2005
[AD-A255797] p 788 N93-15390

AIRPORTS
In situ material characterization for pavement evaluation by the Spectral-Analysis-of-Surface-Waves (SASW) method
[AD-A255660] p 804 N93-14128
Terminal Doppler weather radar/low-level wind shear alert system integration algorithm specification, version 1.1
[AD-A255319] p 920 N93-14547
Information systems for airport operations
[TT-9202] p 789 N93-14729
Terminal area forecasts FY 1992 - 2005
[AD-A255797] p 788 N93-15390

AIRSPEED
Development of the Advance Warning Airborne System(AWAS) p 784 N93-14849

ALBEDO
Precision radiation force modeling for the TOPEX/Poseidon mission p 817 N93-14586

ALGEBRA
Type 2 superstrings in curved D = 10 space-time: Dynamics of their massless fields and covariant quantization p 998 N93-14143
Trace algebra for automatic verification of real-time concurrent systems
[AD-A256199] p 968 N93-14492
From data structure to process structure
[MEMO-INF-91-38] p 946 N93-15077
Graph rewriting using a single pushout; a comparison
[MEMO-INF-92-28] p 968 N93-15121
Algorithms for intersecting parametric and algebraic curves p 956 N93-15560

ALGORITHMS
A general purpose radiative transfer model for application to remote sensing in multidimensional systems p 904 N93-14174
Application of partition matrix methods to solve large eigenproblems in structural dynamics p 896 N93-14188
Manipulation strategies for redundant manipulators p 960 N93-14203
Goals versus algorithms
[AD-A256106] p 942 N93-14237
Parallelization of the Navy Space Surveillance Center (NAVSPASUR) satellite model
[AD-A256133] p 816 N93-14253
Iterative algorithms for integral equations of the first kind with applications to statistics
[AD-A256529] p 942 N93-14285
Terminal Doppler weather radar/low-level wind shear alert system integration algorithm specification, version 1.1
[AD-A255319] p 920 N93-14547
An iconic position estimator for a 2-D laser rangefinder
[AD-A255523] p 885 N93-14568
Implementation of the pure pursuit path tracking algorithm
[AD-A255524] p 944 N93-14569
Engineering of massively interconnected computer systems
[AD-A255501] p 958 N93-14645
A probabilistic approach to anytime algorithm for intelligent real-time problem solving
[AD-A255709] p 945 N93-14654
Using an interior point cutting plane method to solve integer programming problems
[AD-A256041] p 945 N93-14659
The perception of articulated motion: Recognizing moving light displays
[AD-A256046] p 937 N93-14660
Adaptive active noise control using multiple-model approaches
[ISVR-TR-210] p 974 N93-14734
Formal verification of an oral messages algorithm for interactive consistency
[NASA-CR-189704] p 958 N93-14808
Modified fast frequency acquisition via adaptive least squares algorithm
[NASA-CASE-NPO-17845-2-CU] p 945 N93-14882
Optimized design of a 5 kW constant frequency series resonant converter for pulsed load space applications p 807 N93-14935
Processor controlpath microarchitecture synthesis based on the A(asterisk) algorithm
[MEMO-INF-92-10] p 963 N93-15083
A non-deterministic recogniser generator
[MEMO-INF-92-21] p 946 N93-15091
A para-functional version of Warshall's algorithm
[MEMO-INF-92-23] p 947 N93-15092
Off-axis conoscopic holography: Optical and digital reconstruction
[TELECOM-PARIS-90-E-023] p 882 N93-15096
Data fragmentation for parallel transitive closure strategies
[MEMO-INF-92-17] p 959 N93-15142
Modelling the engine temperature distribution between shut down and restart for life usage monitoring p 796 N93-15177
Sensor fault detection using nonlinear observer and polynomial classifier p 797 N93-15182
Transcutaneous Analyte Measuring Methods (TAMM), phase 2
[AD-A256327] p 936 N93-15192
Work efficient hashing on parallel and vector computers
[AD-A256355] p 959 N93-15205
Grammatical trigrams: A probabilistic model of link grammar
[AD-A256365] p 947 N93-15206
Implementing the multiprefix operation on parallel and vector computers
[AD-A256367] p 959 N93-15207
Undetermined coefficient problems for quasi-linear parabolic equations
[AD-A256012] p 969 N93-15256
Synthesis and simulation with VHDL (VHSIC hardware description language)
[VHI-5] p 948 N93-15266
Adaptive control of a manipulator in cartesian space
[F-4-2] p 950 N93-15308
New methods for nonlinear tracking and nonlinear chaotic signal processing
[AD-A256421] p 862 N93-15334
Implementation and analysis of NP-complete algorithms on a distributed memory computer
[AD-A256564] p 951 N93-15405
Parallel simulation today
[NASA-CR-189733] p 951 N93-15432
Mathematical software under UNICOS at LCC
[DE93-001828] p 952 N93-15493

Proceedings: Graphics Interface 1992
[ISBN-0-9695338-1-0] p 952 N93-15533
An implementation of multivariate B-spline surfaces over arbitrary triangulations p 952 N93-15534
Fast algorithms for rendering cubic curves p 953 N93-15536
Parameterization in finite precision p 953 N93-15537
An extended cuberille model for identification and display of 3D objects from 3D gray value data p 953 N93-15542
Algorithms for the detection and elimination of specular aliasing p 954 N93-15544
Performing in-place affine transformations in constant space p 954 N93-15546
A data parallel algorithm for raytracing of heterogeneous databases p 955 N93-15553
Object space temporal coherence for ray tracing p 955 N93-15554
Parametric height field ray tracing p 955 N93-15556
Partitioning tree image representation and generation from 3D geometric models p 955 N93-15557
Algorithms for intersecting parametric and algebraic curves p 956 N93-15560
Matrix animation and polar decomposition p 956 N93-15563
Beyond keyframing: An algorithmic approach to animation p 957 N93-15565
Non-uniform patch luminance for global illumination p 957 N93-15569
A two-pass physics-based global lighting model p 957 N93-15570
Development of a High Resolution Liquid Xenon Imaging Telescope for Medium Energy Gamma Ray Astrophysics
[NASA-CR-191781] p 1013 N93-15589
A Monte Carlo analysis of the liquid xenon TPC as gamma ray telescope p 1014 N93-15590

ALIGNMENT
The effects of mis-alignment and background noise in a low energy gamma ray telescope p 1011 N93-14231
Apparatus for checking threaded hole perpendicularity
[NASA-CASE-LEW-15444-1] p 882 N93-14840

ALKENES
Thermal conductivity of liquid aliphatic hydrocarbons. Part 2: Alkenes, dienes and trienes
[ESDU-92025] p 839 N93-14542

ALOUETTE SATELLITES
Canada's role in pushing back the frontiers of space p 806 N93-14928

ALPHA PARTICLES
Alpha migration through air filters: A numerical simulation
[UCRL-LR-109866] p 878 N93-15285

ALPHANUMERIC CHARACTERS
Source header list. Volume 2: K through Z
[AD-A256001] p 1007 N93-15112

ALTERNATING CURRENT
Modeling limits of the EMV analysis program CONCEPT by example of the influence of a helicopter structure on a frame antenna
[MBB-UD-0614-92-PUB] p 863 N93-15487

ALTERNATIVES
Enhanced Aeronautical Resource Management training alternatives p 786 N93-15019

ALTIMETRY
Derivation of surface properties from Magellan altimetry data p 1033 N93-14340
Problem footprints in Magellan altimetry data p 1039 N93-14362
Scattering properties of Venus' surface p 1044 N93-14391

ALUMINIDES
HIP consolidation of aluminum-rich intermetallic alloys and their composites
[NAWCADWAR-92003-60] p 845 N93-14726

ALUMINUM
Method of forming a multiple layer dielectric and a hot film sensor therewith
[NASA-CASE-LAR-13678-3] p 881 N93-14714
The stress development during filament winding of thick cylinders
[AD-A255765] p 901 N93-15066
Characterization of impact-limiting material
[DE92-016767] p 902 N93-15210
Effect of thermomechanical treatments on the aging response of centrifugally cast silicon carbide/aluminum composites
[AD-A256204] p 836 N93-15236
Electrical resistivity and equation of state measurements of a dense aluminum plasma
[DE92-040352] p 989 N93-15436

ALUMINUM ALLOYS
A study of the relationship between macroscopic measures and physical processes occurring during crack closure
[AD-A256587] p 898 N93-14272
Fatigue strength of cruciform and other fillet welded joints in aluminum alloys
[ESDU-92017] p 900 N93-14553
Evaluation of corrosion protection methods for aluminum metal matrix composites
[AD-A255375] p 832 N93-14675
High temperature stability, interface bonding, and mechanical behavior in (beta)-NiAl and Ni3Al matrix composites with reinforcements modified by ion beam enhanced deposition
[DE92-014399] p 992 N93-14812
Shear fatigue crack growth analysis in large-grain polycrystals p 993 N93-14838
Analysis of OSPREY processes and conventional power aluminum alloys
[AD-A255764] p 846 N93-15056
Multifilamentary superconducting cable and a method of manufacturing it
[AD-D015391] p 846 N93-15231
Effects of high thermal neutron fluences on Type 6061 aluminum
[DE92-040569] p 846 N93-15348
Application of the square root diffusivity analysis to measuring the diffusivity of multicomponent alloys
[DE92-040978] p 847 N93-15382
Exceptionally high-strength (approximately 3 GPa) aluminum alloys demonstrated by oxygen ion implantation
[DE92-040980] p 847 N93-15383

ALUMINUM CHLORIDES
Studies of components for thermally regenerative electrochemical systems
[AD-A256124] p 842 N93-14664

ALUMINUM COATINGS
A study for the development of practices to protectively coat and join fibre epoxy composites for use in the Space Station Programme
[CTN-93-60626] p 835 N93-15145

ALUMINUM GALLIUM ARSENIDES
Sensitivity of quantum electron conductance to elastic scatterers and to spin-orbit scattering in gallium arsenide heterostructures p 990 N93-14184
Fast optoelectronic switching processes in surface-emitting semiconductor lasers and nonlinear etalons
[AD-A255802] p 886 N93-15069

ALUMINUM OXIDES
Fabrication of high temperature materials by exothermic synthesis and subsequent dynamic consolidation
[DE92-019836] p 834 N93-14819
Tribology of improved transformation-toughened ceramics-heat engine test
[DE92-041385] p 851 N93-15295
Compaction of submicron and nanocrystalline Al2O3-ZrO2 ceramics
[DE92-040233] p 852 N93-15320
Exceptionally high-strength (approximately 3 GPa) aluminum alloys demonstrated by oxygen ion implantation
[DE92-040980] p 847 N93-15383
Processing of sinterable transformation toughened ceramics for application in ceramic technology for advanced heat engines project
[DE92-041372] p 853 N93-15453

AMAZON REGION (SOUTH AMERICA)
Extreme climatic events in the Amazon Basin and their associations with the circulation of the global tropics p 918 N93-14115
Simulations of the Amazon Basin circulation using the Pennsylvania State University/National Center for Atmospheric Research mesoscale model p 919 N93-14197

AMBIENT TEMPERATURE
Venus: Geochemical conclusions from the Magellan data p 1044 N93-14394
Studies of components for thermally regenerative electrochemical systems
[AD-A256124] p 842 N93-14664

AMMUNITION
Mechanical shielding for electric primer
[AD-D015417] p 860 N93-14889

AMORPHOUS MATERIALS
Theory of the electronic and structural properties of solid state oxides
[DE92-040499] p 993 N93-14909
Infrared laboratory spectra and composition changes of synthetic amorphous silicate grains
[DE92-040211] p 843 N93-15283
Compaction of submicron and nanocrystalline Al2O3-ZrO2 ceramics
[DE92-040233] p 852 N93-15320
Morphological analysis of ionomers
[DE92-040162] p 852 N93-15415

AMORPHOUS SILICON
Design and hardware implementation of neural systems
[AD-A256040] p 866 N93-14577

AMPLITUDE MODULATION
A preliminary design of the Ti:LiNbO3 optical channel waveguide
[AD-A255443] p 982 N93-14784

AMPLITUDES
SCRUNCHER phase and amplitude control
[DE92-040225] p 870 N93-15421

ANALOG CIRCUITS
Dynamics of analog electronic neural networks
[AD-A257019] p 966 N93-15352

ANALYTIC FUNCTIONS
An analytic phase function for cylindrical particles
[AD-A255750] p 977 N93-15054

ANEMOMETERS
Boundary layer transition measurements by optical anemometry p 874 N93-14477

ANGLE OF ATTACK
Pressure drag and lift contributions for blunted forebodies of fineness ratio 2.0 in transonic flow (M infinity less than or equal to 1.4)
[ESDU-89033] p 779 N93-14515
Icing effects on aircraft stability and control determined from flight data: Preliminary results
[NASA-TM-105977] p 803 N93-14831
Flowfield study of a close-coupled canard configuration
[AD-A256311] p 782 N93-15245

ANGLES (GEOMETRY)
Effect of impact angle on central-peak/peak-ring formation and crater collapse on Venus p 1041 N93-14371

ANGULAR ACCELERATION
Finite element analysis of elastic fracture under unsteady translational and rotational loading p 899 N93-14469

ANGULAR DISTRIBUTION
Excitation of nuclei by antiproton annihilation at rest
[AD-A255447] p 976 N93-14513

ANIK SATELLITES
Canada's role in pushing back the frontiers of space p 806 N93-14928
Anik E spacecraft integration and test p 808 N93-14939

ANISOTROPIC MEDIA
Optics for diode array transverse pumped laser rod
[AD-D015436] p 885 N93-14722

ANISOTROPIC SHELLS
Analysis and optimal design of pressurized, imperfect, anisotropic ring-stiffened cylinders p 897 N93-14251

ANISOTROPY
A search for anisotropy in the cosmic background radiation at millimeter wavelengths on angular scales from 0.3 to 3 degrees p 1050 N93-14244
Efficient asymptotic closed form approximation for dyadic green's function for anisotropic substrates, phase 1
[AD-A256258] p 830 N93-14436
High speed magneto-resistive random access memory
[NASA-CASE-NPO-17954-1-CU] p 940 N93-14704
Elastic wave propagation in laminated composites
[ITN-93-85186] p 835 N93-15144
Measurement of the magnetic anisotropy energy constants for magneto-optical recording media p 984 N93-15509

ANNEALING
The III-V semiconductor quantum well lasers and related optoelectronic devices (on silicon). Oxide-defined semiconductor quantum well lasers and optoelectronic devices: Al-based III-V nativeoxide s
[AD-A255239] p 885 N93-14667
Processing and microstructure of Nb-1 percent Zr-0.1 percent C alloy sheet
[NASA-TM-105921] p 847 N93-15524

ANNIHILATION REACTIONS
Excitation of nuclei by antiproton annihilation at rest
[AD-A255447] p 976 N93-14513

ANNOTATIONS
A para-functional version of Warshall's algorithm
[MEMO-INF-92-23] p 947 N93-15092

ANNUAL VARIATIONS
Low-frequency oscillations in radiative-convective models
[DE92-018779] p 922 N93-14901
TOPEX/Poseidon science investigations plan
[NASA-CR-190616] p 925 N93-14964
The western Mediterranean Sea: An area for a regional validation for TOPEX/Poseidon and a field for geophysical and oceanographic studies p 926 N93-14965
Ocean transport and variability studies of the South Pacific, Southern, and Indian Oceans p 927 N93-14971

Sea level response to wind forcing in the tropical Atlantic p 928 N93-14977
Low-frequency variability of sea level as related to the heat balance of global oceans p 928 N93-14979
Ocean circulation using altimetry p 929 N93-14984
Ocean circulation modeling by use of radar altimeter data p 929 N93-14986
General circulation of the South Atlantic between 5 deg N and 35 deg S p 929 N93-14987
Ocean dynamics in the Nordic Seas using satellite altimetry p 930 N93-14988
Application of TOPEX/Poseidon altimetry measurements to observational and modeling studies of the low-frequency upper ocean mass and heat circulation in the tropical Pacific p 930 N93-14989
Equatorial and eastern boundary current variability in the North and South Pacific Oceans p 931 N93-14994
An integrated research program for TOPEX/Poseidon with emphasis on the Pacific Ocean p 931 N93-14995
Analysis of altimeter data jointly with seafloor electric data (vertically integrated velocity) and VCTD-yoyo data (detailed profiles of VCTD) p 931 N93-14998
Geographical distribution and seasonal variation of surface emissions and deposition velocities of atmospheric trace gases
[AERONOMICA-ACTA-A-361-1991] p 911 N93-15460

ANNULAR FLOW
Time-dependent predictions and analysis of turbine cascade data in the transonic flow region
[PNR-90957] p 782 N93-15489
Prediction of turbine cascade flows with a quasi-three-dimensional rotor viscous code and the extension of the algebraic turbulence model
[AD-A256831] p 880 N93-15635

ANODES
Microwave processing of tantalum capacitor anodes
[DE92-017829] p 869 N93-15214
Results from a pilot cell test of cermet anodes
[DE92-041357] p 871 N93-15479

ANODIZING
Studies of components for thermally regenerative electrochemical systems
[AD-A256124] p 842 N93-14664
Evaluation of corrosion protection methods for aluminum metal matrix composites
[AD-A255375] p 832 N93-14675

ANTARCTIC OCEAN
Ocean transport and variability studies of the South Pacific, Southern, and Indian Oceans p 927 N93-14971
Antarctic news clips - 1992
[NSF-92-83] p 916 N93-15080

ANTARCTIC REGIONS
Antarctic news clips - 1992
[NSF-92-83] p 916 N93-15080

ANTENNA ARRAYS
A multiple-aperture multiple-beam EHF antenna for satellite communications
[AD-A256020] p 858 N93-14426
Efficient asymptotic closed form approximation for dyadic green's function for anisotropic substrates, phase 1
[AD-A256258] p 830 N93-14436
Layered parallel interface for an active antenna array
[AD-D015411] p 860 N93-14879
A power compensation system for phased operation of the JET A2 antenna arrays
[DE92-041020] p 863 N93-15440

ANTENNA COMPONENTS
Layered parallel interface for an active antenna array
[AD-D015411] p 860 N93-14879
JSEP fellowship --- Transient radiation from antenna structures
[AD-A257021] p 863 N93-15470

ANTENNA DESIGN
Investigation of antenna pattern constraints for passive geosynchronous microwave imaging radiometers
[NASA-CR-189728] p 905 N93-14792
L-band antenna design for MSAT mission p 812 N93-14961
Ku-band antenna design for MSAT mission p 813 N93-14963
JSEP fellowship --- Transient radiation from antenna structures
[AD-A257021] p 863 N93-15470

ANTENNA RADIATION PATTERNS
JSEP fellowship --- Transient radiation from antenna structures
[AD-A257021] p 863 N93-15470

ANTENNAS
Modeling limits of the EMV analysis program CONCEPT by example of the influence of a helicopter structure on a frame antenna
[MBB-UD-0614-92-PUB] p 863 N93-15487

ANTICONVULSANTS
Autoradiographic distribution and applied pharmacological characteristics of dextromethorphan and related antitissue/anticonvulsant drugs and novel analogs
[AD-A255607] p 935 N93-15009

ANTICYCLONES
Synoptic/planetary-scale interactions and blocking over the North Atlantic Ocean
[NASA-CR-191376] p 925 N93-14769

ANTIFOULING
Biofilm ecology of bioluminescent bacteria
[AD-A255282] p 932 N93-14532

ANTIMATTER
Production of relativistic anti-hydrogen atoms by pair production with positron capture and measurement of the Lamb shift
[DE93-001767] p 978 N93-15468
Anti-hydrogen: The cusp between quantum mechanics and general relativity
[DE93-001807] p 998 N93-15469

ANTIMISSILE DEFENSE
The detection and correlation modeling of Rayleigh distributed radar signals
[AD-A256612] p 858 N93-14250

ANTIPROTONS
Excitation of nuclei by antiproton annihilation at rest
[AD-A255447] p 976 N93-14513
Strong interactions studies with medium energy probes
[DE92-040460] p 977 N93-15377
Production of relativistic anti-hydrogen atoms by pair production with positron capture and measurement of the Lamb shift
[DE93-001767] p 978 N93-15468

ANTIREFLECTION COATINGS
Effects of cryocontaminants on cryogenic superpolished mirror and superpolished quartz crystal microbalance
[AD-A255972] p 981 N93-14403
A high intensity solar cell invention: The edge-illuminated Vertical Multi-Junction (VMJ) solar cell
[DE92-019015] p 907 N93-15224

APERTURES
The 3D modeling of high numerical aperture imaging in thin films p 985 N93-15513

APPLICATION SPECIFIC INTEGRATED CIRCUITS
VHDL (VHSIC hardware description language) use in the US defense procurement process
[VH-2] p 948 N93-15263

APPLICATIONS PROGRAMS (COMPUTERS)
Development of a MATLAB toolbox for image processing
[AD-A256130] p 942 N93-14247
A methodology for the evaluation of structural design software for DOS-based microcomputers
[AD-A255421] p 943 N93-14505
Program for calculation of aileron rolling moment and yawing moment coefficients at subsonic speeds
[ESDU-88040] p 779 N93-14514
Data management and processing plan, Department of Applied Geodesy
[DE93-000774] p 905 N93-14522
Air Force procedure for predicting noise around airbases: Noise exposure model (Noisemap)
[AD-A255769] p 910 N93-14655
Interplanetary Program to Optimize Simulated Trajectories (IPOST). Volume 1: User's guide
[NASA-CR-189653-VOL-1-REV] p 815 N93-14794
BLSTA: A boundary layer code for stability analysis
[NASA-CR-4481] p 877 N93-14797
SAPNEW: Parallel finite element code for thin shell structures on the Alliant FX-80
[NASA-CR-189212] p 901 N93-14799
A guide to EDI translation software
[AD-A255739] p 1007 N93-15051
Workstation tools for feature extraction and classification for nonstationary and transient signals
[AD-A255389] p 947 N93-15228
Validation of an automated torsional and warping stress analysis program
[AD-A256035] p 902 N93-15260
Full surface testing of grazing incidence mirrors
[AD-A255798] p 984 N93-15371
Automated Estimated System (AES) standard value and guidelines programs user's manual
[DE92-041243] p 951 N93-15450
User's guide for a large signal computer model of the helical traveling wave tube
[NASA-TP-3251] p 871 N93-15531

APPROXIMATION
Efficient asymptotic closed form approximation for dyadic green's function for anisotropic substrates, phase 1
[AD-A256258] p 830 N93-14436
Approximate performability analysis using generalized stochastic Petri nets
[MEMO-INF-92-11] p 971 N93-15119
Multiresolution analysis by infinitely differentiable compactly supported functions
[AD-A256526] p 969 N93-15398
An integral equation solution for multistage turbomachinery design calculations
[NASA-TM-105970] p 801 N93-15521

AQUEOUS SOLUTIONS
Softening of rigid polyvinyl chloride by high concentrations of aqueous solutions of methylene chloride
[AD-A255453] p 848 N93-14486

AQUIFERS
Anaerobic microbial transformation of aromatic hydrocarbons and mixtures of aromatic hydrocarbons and halogenated solvents
[AD-A255696] p 932 N93-14557

ARC HEATING
Arc-cathode interaction study
[NASA-CR-191356] p 867 N93-14721

ARC JET ENGINES
Numerical modeling of a vortex stabilized arcjet
[NASA-CR-190797] p 826 N93-14883

ARC WELDING
Mechanisms of forming intergranular microcracks and microscopic surface discontinuities in welds
[AD-A255371] p 845 N93-14740

ARCHES
Weight optimum arch structures
[AD-A256080] p 897 N93-14236
Nonlinear dynamic response of shallow arches to harmonic forcing p 898 N93-14282

ARCHITECTURE
Recommendations for enhancement of the Design Criteria Information System (DCIS)
[AD-A256857] p 1009 N93-15641

ARCHITECTURE (COMPUTERS)
A complete-time approach for chaining and execution control in the AN/UYS-2 parallel signal processor
[AD-A256306] p 859 N93-14442
A specification of the Soar cognitive architecture in Z
[AD-A256198] p 940 N93-14491
The 1992 Summer SIGAda AIWG Workshop applications experiences and lessons learned panel message from the panel chair
[AD-A256188] p 962 N93-14519
Development of neural network architectures for self-organizing pattern recognition and robotics
[AD-A255433] p 962 N93-14551
Computer-aided design package for designers of digital optical computers
[AD-A255381] p 944 N93-14564
The perception of articulated motion: Recognizing moving light displays
[AD-A256046] p 937 N93-14660
Enterprise storage report for the 1990's p 1004 N93-15028
EMASS (trademark): An expandable solution for NASA space data storage needs p 1005 N93-15033
Data storage and retrieval system p 1005 N93-15034
Network accessible multi-terabyte archive p 1005 N93-15036
Storage needs in future supercomputer environments p 1007 N93-15047
Processor controlpath microarchitecture synthesis based on the A(asterisk) algorithm
[MEMO-INF-92-10] p 963 N93-15083
Architecture of low cost, large scale neural networks
[MEMO-INF-92-16] p 941 N93-15089
Progammable connection parallel architecture: Design and routing
[ETN-92-92676] p 958 N93-15124
PRISMA/DB: A parallel, main-memory relational DBMS
[MEMO-INF-92-12] p 959 N93-15141
Personal computer based test- and emulation equipment for maintenance and ground support p 778 N93-15185
Design for tactical situation awareness display
[AD-A256194] p 798 N93-15235
Experience with a course on architectures for software systems. Part 1: Course description
[AD-A256221] p 941 N93-15239
Neural network architectures for general image recognition
[AD-A256017] p 964 N93-15258
VHDL (VHSIC hardware description language): Origins, status, capabilities, and world environment
[VH-1] p 947 N93-15262
Coordinated motion control of a two-hand assembly system
[F-2-8] p 949 N93-15301

CMU common lisp user's manual
[AD-A256431] p 950 N93-15336
Analog Very Large Scale Integration (VLSI) implementations of artificial neural networks
[AD-A256621] p 966 N93-15408
Proposal for massively parallel data storage system p 960 N93-15510
A linear constraint technology for interactive graphic systems p 957 N93-15568
Aspects of a parallel-architecture simulator
[AD-A256872] p 941 N93-15628
A structural approach to the photonic processor
[N-3399-RC] p 986 N93-15648

ARCTIC REGIONS
Data management for the coordinated Eastern Arctic experiment
[AD-A255648] p 1000 N93-14182

ARGON
A global potential energy surface for ArH2
[NASA-CR-190741] p 843 N93-15358

ARGON PLASMA
Turbulent magnetized plasmas from ionizing shock waves p 987 N93-14120
Lineshape analysis of laser light scattered by an argon thermal plasma jet p 987 N93-14137

ARGOS SYSTEM
Control of on-orbit contamination for the Argos (P91-1) satellite p 823 N93-15617

ARITHMETIC
An interval refinement technique for surface intersection p 956 N93-15561

ARM (ANATOMY)
Bar-holding prosthetic limb
[NASA-CASE-MFS-28481-1] p 939 N93-14870

ARMATURES
Validation of the flux loop diagnostic for the measurement of launch package motion during electromagnetic launch
[AD-A256547] p 814 N93-14266

ARMED FORCES (UNITED STATES)
Evaluation of the cost effectiveness analysis model being developed for the component improvement programs of the Air Force and the Navy
[AD-A256132] p 1010 N93-14249
Air Force Office of Scientific Research
[AD-A255331] p 1051 N93-14523
Smart battery controller for lithium sulfur dioxide batteries
[AD-A255490] p 867 N93-14642
Crew requirements definition system user's guide
[AD-A257052] p 951 N93-15445

ARMOR
Strain-rate effects in replica scale model penetration experiments
[AD-A255426] p 844 N93-14508
A progressive resistance weight training program designed to improve the armor crewman's strength
[AD-A255553] p 934 N93-14556

ARRAYS
Organic/IR-Semiconductor heterojunctions for low-cost, high temperature IR arrays
[AD-A255971] p 868 N93-15108

ARTIFICIAL INTELLIGENCE
Decision-making for intelligent control of dual-arm robotic operations p 960 N93-14201
A specification of the Soar cognitive architecture in Z
[AD-A256198] p 940 N93-14491
The 1992 Summer SIGAda AIWG Workshop applications experiences and lessons learned panel message from the panel chair
[AD-A256188] p 962 N93-14519
The human-electronic crew: Is the team maturing? The 2nd Joint GAF/RAF/USAF Workshop on Human-Electronic Crew Teamwork
[AD-A256192] p 939 N93-14520
Machine intelligence, a foreword: The brain as electronic circuitry; electronic circuitry as a brain
[AD-A255283] p 962 N93-14533
A voyage to Mars: A challenge to collaboration between man and machines p 777 N93-14614
A probabilistic approach to anytime algorithm for intelligent real-time problem solving
[AD-A255709] p 945 N93-14654
Analysis of symbolic models of cognition project (ASPM-Pitt)
[AD-A255929] p 962 N93-14656
A planning workshop: To strengthen American cognitive science for the twenty-first century
[NSF-92-4] p 999 N93-14720
Probabilistic inference
[AD-A255471] p 963 N93-14786
Multiple fault diagnosis of spacecraft electrical power systems p 806 N93-14927
A monitoring and control system for complex man-machine systems: Preliminary design p 810 N93-14951
Minimizing conflicts: A heuristic repair method for constraint-satisfaction and scheduling problems
[NASA-TM-108121] p 964 N93-15286
Learning to improve iterative repair scheduling
[NASA-TM-108118] p 965 N93-15289
A beginner's guide to belief revision and truth maintenance systems
[NASA-TM-108117] p 965 N93-15290
An application of artificial intelligence to automatic telescopes
[NASA-TM-108115] p 965 N93-15291
Knowledge and regularity in planning
[NASA-TM-108113] p 965 N93-15293
Automated interpretation of topographic maps
[AD-A257040] p 906 N93-15364
Design of an artificial neural network based tactile sensor for the UTAH/MIT dexterous hand
[AD-A256565] p 966 N93-15406

ARTIFICIAL SATELLITES
Global optimum path planning for a redundant space robot
[AD-A255316] p 889 N93-14545
Comparative study of stability of flexible satellites with and without guy-wire constraints p 817 N93-14585

ASCENT TRAJECTORIES
Results of a FRSI material test under Space Shuttle ascent conditions in the Ames Research Center 9x7 foot supersonic wind tunnel (OS13). Space Shuttle aerothermodynamic data report
[NASA-CR-167699] p 816 N93-15475

ASSEMBLING
Coordinated motion control of a two-hand assembly system
[F-2-8] p 949 N93-15301

ASSIMILATION
Convective scale 4-D data assimilation using simulated single-Doppler radar observations p 921 N93-14683

ASSOCIATIVE PROCESSING (COMPUTERS)
Dynamics of analog electronic neural networks
[AD-A257019] p 966 N93-15352

ASSUMPTIONS
A beginner's guide to belief revision and truth maintenance systems
[NASA-TM-108117] p 965 N93-15290

ASTEROIDS
Computer simulations of comet- and asteroidlike bodies passing through the Venusian atmosphere: Preliminary results on atmospheric and ground shock effects p 1040 N93-14365

ASTIGMATISM
Improved astigmatic focus error detection method p 984 N93-15507

ASTRONOMICAL CATALOGS
Faint high-latitude carbon stars p 1019 N93-14638
Supervised selection of galaxy candidates from the IRAS PSC: The quality of the selection and the infrared properties of the galaxy candidates
[MPE-PREPRINT-216] p 1021 N93-15284

ASTRONOMICAL MODELS
Cosmological models in higher-order gravity p 1018 N93-14592
Faint high-latitude carbon stars p 1019 N93-14638
Quasars, galaxies, and pseudo-vacuum droplets
[NIKHEF-H/91-20] p 1020 N93-14686
Analysis of CCD images of the coma of comet P/Halley
[NASA-CR-191384] p 1020 N93-14814
The gamma ray spectrum resulting from pp interactions in quasars p 1051 N93-14917

ASTRONOMICAL PHOTOGRAPHY
Faint high-latitude carbon stars p 1019 N93-14638

ASTRONOMICAL PHOTOMETRY
Faint high-latitude carbon stars p 1019 N93-14638

ASTRONOMICAL SPECTROSCOPY
A faint spectroscopic quasar survey p 1012 N93-14629
Spatially resolved 10 micron spectra of circumstellar material around evolved stars p 1019 N93-14636
Faint high-latitude carbon stars p 1019 N93-14638

ASTRONOMY
Environmental assessment for the laser guide star experiment at Lawrence Livermore National Laboratory
[DE92-040316] p 1013 N93-15425

ASTROPHYSICS
The theory and numerical simulation of non-local mixing-length convection p 1015 N93-14147

ASYMMETRY
Local-time asymmetries in the Venus thermosphere p 1023 N93-14290
Control of asymmetric jet
[AD-A255967] p 873 N93-14400
Recent advances in numerical simulation and control of asymmetric flows around slender bodies
[PAPER-W.1.2] p 875 N93-14688
Numerical simulation of steady and unsteady asymmetric vortical flow p 876 N93-14691
Passive control of supersonic asymmetric vortical flows around cones p 876 N93-14692

ASYMPTOTIC METHODS
Development of an environment for software reliability model selection
[AD-A256609] p 942 N93-14241
Efficient asymptotic closed form approximation for dyadic green's function for anisotropic substrates, phase 1
[AD-A256258] p 830 N93-14436

ATLANTIC OCEAN
Report of the International Ice Patrol in the North Atlantic, bulletin no. 77
[AD-A256162] p 925 N93-14452
Synoptic/planetary-scale interactions and blocking over the North Atlantic Ocean
[NASA-CR-191376] p 925 N93-14769
Studies of the intermediate and deep circulation in the western equatorial Atlantic p 927 N93-14973
Study of mass and heat transport of the tropical Atlantic Ocean using models and altimeter data p 929 N93-14983
General circulation of the South Atlantic between 5 deg N and 35 deg S p 929 N93-14987

ATMOSPHERIC ATTENUATION
Evaluation of three models used for predicting noise propagated long distances overground
[AD-A255963] p 973 N93-14406

ATMOSPHERIC BOUNDARY LAYER
Super-micro computer weather prediction model
[AD-A255668] p 918 N93-14153
Wave drag in the atmospheric boundary layer p 915 N93-14873

ATMOSPHERIC CHEMISTRY
An investigation of transient atmospheric inorganic peroxides: A theoretical and experimental study p 912 N93-14117
The isotopes of carbon monoxide in the free troposphere and their implications to atmospheric chemistry p 913 N93-14207
Mixed-valence iron minerals on Venus: Fe(2+)-Fe(3+) oxides and oxy-silicates formed by surface-atmosphere interactions p 1025 N93-14301
Near-infrared oxygen airglow from the Venus nightside p 1026 N93-14308
Understanding the variation in the millimeter-wave emission of Venus p 1028 N93-14315
On the role of water growth in atmospheric aerosol p 922 N93-14875
LISA: A limb imaging spectrograph for airglow p 811 N93-14952
Cassini atmospheric chemistry mapper. Volume 1. Investigation and technical plan
[NASA-CR-190947] p 1021 N93-15079

ATMOSPHERIC CIRCULATION
Super-micro computer weather prediction model
[AD-A255668] p 918 N93-14153
Simulations of the Amazon Basin circulation using the Pennsylvania State University/National Center for Atmospheric Research mesoscale model p 919 N93-14197
Revelations of a stratospheric circulation: The dynamical transport of hydrocarbons in the stratosphere of Uranus p 913 N93-14211
The preferred latitudes of the Intertropical Convergence Zone: Observations and theory p 920 N93-14213
Local-time asymmetries in the Venus thermosphere p 1023 N93-14290
Dynamics of the Venus atmosphere p 1030 N93-14325
Radiation pressure: A possible cause for the superrotation of the Venusian atmosphere p 1033 N93-14338
Results of a zonally truncated three-dimensional model of the Venus middle atmosphere p 1037 N93-14351
Impact-generated winds on Venus: Causes and effects p 1041 N93-14372
An observational and theoretical study of squall line evolution p 921 N93-14682
Microwave observations of Uranus p 1046 N93-14863
Low-frequency oscillations in radiative-convective models p 915 N93-14874
Interferometric observations of the J(0,1) CO line on Venus: Upper mesospheric winds and CO abundance p 1047 N93-14918

ATMOSPHERIC COMPOSITION
Investigations of Titan's troposphere and surface and Jupiter's great red spot with infrared observations p 1022 N93-14146
The isotopes of carbon monoxide in the free troposphere and their implications to atmospheric chemistry p 913 N93-14207
Revelations of a stratospheric circulation: The dynamical transport of hydrocarbons in the stratosphere of Uranus p 913 N93-14211

Methane measurement by the Pioneer Venus large probe neutral mass spectrometer p 1027 N93-14312
Understanding the variation in the millimeter-wave emission of Venus p 1028 N93-14315
Long-term variations in abundance and distribution of sulfuric acid vapor in the Venus atmosphere inferred from Pioneer Venus and Magellan radio occultation studies p 1030 N93-14328
Venus: The case for a wet origin and a runaway greenhouse p 1031 N93-14331
Pioneer Venus polarimetry and haze optical thickness p 1032 N93-14335
Outgassing history of Venus and the absence of water on Venus p 1045 N93-14398
Study and interpretation of the millimeter-wave spectrum of Venus p 1045 N93-14596
Method for detecting chemical vapors using a lasing dye sensor
[AD-D015424] p 885 N93-14821
On the role of water growth in atmospheric aerosol p 922 N93-14875
Interferometric observations of the J(0,1) CO line on Venus: Upper mesospheric winds and CO abundance p 1047 N93-14918
Cassini atmospheric chemistry mapper. Volume 1. Investigation and technical plan
[NASA-CR-190947] p 1021 N93-15079
Laboratory evaluation and application of microwave absorption properties under simulated conditions for planetary atmospheres
[NASA-CR-191298] p 1047 N93-15081
Spatial and temporal patterns of biotic exchanges of CO2 between the atmosphere and tropical landscapes and their role in the global carbon balance
[DE92-019170] p 911 N93-15272
A correlated k-distribution model of the heating rates for CO2 and O3 in the atmosphere between 0 and 60 km
[DE93-000889] p 911 N93-15280
A correlated k-distribution model of the atmospheric heating rates for overlapping spectra of CH4 and N2O
[DE93-000890] p 911 N93-15281

ATMOSPHERIC EFFECTS
Atmospheric effects on crater growth on Venus p 1041 N93-14370
Impact-generated winds on Venus: Causes and effects p 1041 N93-14372

ATMOSPHERIC ENTRY
Computer simulations of comet- and asteroidlike bodies passing through the Venusian atmosphere: Preliminary results on atmospheric and ground shock effects p 1040 N93-14365
Shape-stable reentry body nose tip
[AD-D015437] p 817 N93-14725
Interplanetary program to optimize simulated trajectories (IPOST). Volume 4: Sample cases
[NASA-CR-189653-VOL-4] p 815 N93-14768

ATMOSPHERIC GENERAL CIRCULATION MODELS
Extreme climatic events in the Amazon Basin and their associations with the circulation of the global tropics p 918 N93-14115
Carbon dioxide induced ocean climatic change and tracer experiment with an atmosphere-ocean general circulation model p 912 N93-14178
Local-time asymmetries in the Venus thermosphere p 1023 N93-14290
A numerical study of the middle atmosphere response to tropical and subtropical tropospheric heat sources p 920 N93-14640
Geophysical validation of TOPEX/Poseidon altimetry products p 918 N93-14982

ATMOSPHERIC HEATING
Carbon dioxide induced ocean climatic change and tracer experiment with an atmosphere-ocean general circulation model p 912 N93-14178
Infrared radiative properties of clouds p 919 N93-14196
The preferred latitudes of the Intertropical Convergence Zone: Observations and theory p 920 N93-14213
A correlated k-distribution model of the heating rates for CO2 and O3 in the atmosphere between 0 and 60 km
[DE93-000889] p 911 N93-15280
A correlated k-distribution model of the atmospheric heating rates for overlapping spectra of CH4 and N2O
[DE93-000890] p 911 N93-15281

ATMOSPHERIC LASERS
Two micron laser development for atmospheric remote sensing at NASA Langley Research Center p 784 N93-14845

ATMOSPHERIC MODELS
Super-micro computer weather prediction model
[AD-A255668] p 918 N93-14153
Infrared radiative properties of clouds p 919 N93-14196
Four-dimensional data assimilation of GALE data using a multivariate analysis scheme and a mesoscale model with diabatic initialization p 919 N93-14198
The use of chaos metrics to analyze Lagrangian particle diffusion models
[AD-A256142] p 967 N93-14255
Local-time asymmetries in the Venus thermosphere p 1023 N93-14290
Thermal buoyancy on Venus: Preliminary results of finite element modeling p 1025 N93-14302
Understanding the variation in the millimeter-wave emission of Venus p 1028 N93-14315
Venusian hydrology: Steady state reconsidered p 1028 N93-14318
Results of a zonally truncated three-dimensional model of the Venus middle atmosphere p 1037 N93-14351
Four-dimensional data assimilation of gale data using a multivariate analysis scheme and a mesoscale model with diabatic initialization
[AD-A256063] p 921 N93-14680
An observational and theoretical study of squall line evolution p 921 N93-14682
Numerical simulation of baroclinic Jovian vortices p 1046 N93-14865
Wave drag in the atmospheric boundary layer p 915 N93-14873
Low-frequency oscillations in radiative-convective models p 915 N93-14874
Low-frequency oscillations in radiative-convective models
[DE92-018779] p 922 N93-14901
Fitting microphysical observations to a numerical model through an optimal control theory technique p 924 N93-15100
A numerical model of ionospheric convection derived from field-alignment currents and the corresponding conductivity
[TRITA-EPP-91-03-REV] p 916 N93-15252
Spatial and temporal patterns of biotic exchanges of CO2 between the atmosphere and tropical landscapes and their role in the global carbon balance
[DE92-019170] p 911 N93-15272
A correlated k-distribution model of the heating rates for CO2 and O3 in the atmosphere between 0 and 60 km
[DE93-000889] p 911 N93-15280
A correlated k-distribution model of the atmospheric heating rates for overlapping spectra of CH4 and N2O
[DE93-000890] p 911 N93-15281

ATMOSPHERIC MOISTURE
Effects of water vapor and anisotropic scattering on aerosol optical depth retrieval
[AD-A256087] p 904 N93-14262
Improved aerosol optical depth and particle size index from satellite detected radiance
[AD-A256089] p 904 N93-14263
Venus: The case for a wet origin and a runaway greenhouse p 1031 N93-14331
On the role of water growth in atmospheric aerosol p 922 N93-14875

ATMOSPHERIC PHYSICS
Near-infrared oxygen airglow from the Venus nightside p 1026 N93-14308
Sulfur oxides in the middle atmosphere of Venus: Observations by the International Ultraviolet Explorer and sounding rockets p 1046 N93-14635
Cassini atmospheric chemistry mapper. Volume 1. Investigation and technical plan
[NASA-CR-190947] p 1021 N93-15079
Theoretical studies of the physics of the solar atmosphere
[NASA-CR-191357] p 1049 N93-15085

ATMOSPHERIC PRESSURE
Atmospheric effects on crater growth on Venus p 1041 N93-14370

ATMOSPHERIC RADIATION
Near-infrared oxygen airglow from the Venus nightside p 1026 N93-14308
On the variation of the Nimbus 7 total solar irradiance
[NASA-TP-3316] p 1049 N93-15532

ATMOSPHERIC REFRACTION
Evaluation of three models used for predicting noise propagated long distances overground
[AD-A255963] p 973 N93-14406

ATMOSPHERIC SOUNDING
NASA/LMSC instrument design and fabrication --- coherent lidar airborne shear sensor p 784 N93-14846
Cloud fraction, layer, and direction of movement results from sky cameras during the FIRE IFO, Coffeyville, Kansas, experiment for the period Nov. 12 through Dec. 9, 1991
[NASA-TM-107647] p 924 N93-15501

ATMOSPHERIC TEMPERATURE
Middle atmosphere of Venus and its clouds: Latitude and solar time variations p 1045 N93-14396
A numerical study of the middle atmosphere response to tropical and subtropical tropospheric heat sources p 920 N93-14640

ATMOSPHERIC TURBULENCE
A simulation model of atmospheric turbulence for rotorcraft applications p 920 N93-14588
Vertical path atmospheric turbulence: Temporal spectra and differential image motion measurements p 914 N93-14641
Wave drag in the atmospheric boundary layer p 915 N93-14873
Environmental assessment for the laser guide star experiment at Lawrence Livermore National Laboratory
[DE92-040316] p 1013 N93-15425

ATOMIC BEAMS
Advances in laser cooling
[AD-A255969] p 884 N93-14402

ATOMIC CLOCKS
Determining optimum C-field settings that minimize output frequency variations in cesium atomic frequency standards
[AD-A255902] p 971 N93-14108
The effects of acceleration on precision frequency sources
[AD-A255465] p 972 N93-14496
Frequency shifts in a rubidium frequency standard due to coupling to another standard
[AD-A256232] p 972 N93-15243
Introduction to quartz frequency standards, revision 1
[AD-A256373] p 870 N93-15330

ATOMIC EXCITATIONS
A study of mid-latitude 5577 A OI dayglow emissions p 913 N93-14199
Measurement and analysis of excitation functions in (alpha,np) reactions on (128, 130)Te
[DE92-630358] p 991 N93-14485

ATOMIC PHYSICS
Advances in laser cooling
[AD-A255969] p 884 N93-14402
Accurate methods for calculating atomic processes in high temperature plasmas
[DE92-040215] p 988 N93-15418

ATOMIC STRUCTURE
Twin quintuplets in CVD diamond
[AD-A255862] p 989 N93-14133
Electronic structure studies of high-T(sub c) superconductors by photoemission and x ray absorption p 989 N93-14172
Electronically active cyclocarborane-metal-arene assemblies
[AD-A256288] p 865 N93-14457
Theory of the electronic and structural properties of solid state oxides
[DE92-040499] p 993 N93-14909
A global potential energy surface for ArH2
[NASA-CR-190741] p 843 N93-15358

ATOMS
Opacity, equation of state, and radiation transport model for moderate density, eV-temperature plasmas
[AD-A256056] p 988 N93-14579

ATTITUDE (INCLINATION)
A minimum-slip attitude control method for the erebus walking robot
[NASA-CR-191646] p 890 N93-14567
ARCBALL: A user interface for specifying three-dimensional orientation using a mouse p 955 N93-15551

ATTITUDE CONTROL
A minimum-slip attitude control method for the erebus walking robot
[NASA-CR-191646] p 890 N93-14567
Thermal elastic shock and its effect on spacecraft attitude control p 818 N93-14837
Reusable Reentry Satellite (RRS) system design study. Phase B, appendix E: Attitude control system study
[NASA-CR-188578] p 825 N93-15633

AUDIO FREQUENCIES
Audio detection algorithms
[AD-A256076] p 973 N93-14234

AUDIO SIGNALS
Audio detection algorithms
[AD-A256076] p 973 N93-14234

AUDIO TAPES
Corrosion of metal particle and metal evaporated tapes p 883 N93-15039

AUDITORY PERCEPTION
Psychophysical analyses of perceptual representations
[AD-A255432] p 936 N93-14510
Neuromagnetic investigations of cortical regions underlying short-term memory
[AD-A255788] p 937 N93-14646
Demodulation processes in auditory perception
[AD-A255748] p 935 N93-15053
Multimodal interactions in sensory-motor processing
[AD-A255780] p 938 N93-15067

Program auralization: Sound enhancements to the programming environment p 953 N93-15539

AUGER SPECTROSCOPY
Silicon nitride thin film production on Si(111)
[AD-A256036] p 994 N93-15233

AUGMENTATION
Program auralization: Sound enhancements to the programming environment p 953 N93-15539
Recommendations for enhancement of the Design Criteria Information System (DCIS)
[AD-A256857] p 1009 N93-15641

AURORAL ZONES
The effects of magnetic storm phases on F-layer irregularities from auroral to equatorial latitudes
[AD-A256520] p 917 N93-15395

AURORAS
Fine structure of auroral particle acceleration p 912 N93-14121
An analysis of the SCEX 3 ionospheric electron beam injection experiment p 912 N93-14177
A study of mid-latitude 5577A OI dayglow emissions
[AD-A255444] p 914 N93-14511
Comparison of Viking Ultraviolet images with low altitude particle precipitation p 1045 N93-14612

AUSTIN COMET
Ultraviolet spectroscopy of Comet Austin (1989c1) using a two-dimensional diode array detector p 1017 N93-14444

AUTOMATA THEORY
A non-deterministic recogniser generator
[MEMO-INF-92-21] p 946 N93-15091

AUTOMATIC CONTROL
Unmanned aerial vehicles: More testing needed before production of short-range system
[AD-A256296] p 790 N93-14440
Trace algebra for automatic verification of real-time concurrent systems
[AD-A256199] p 968 N93-14492
A simple controller for repetitive cycles in atomic layer epitaxy
[AD-A255497] p 992 N93-14643
Autonomous power system brassboard
[NASA-CR-189115] p 867 N93-14798
An application of artificial intelligence to automatic telescopes
[NASA-TM-108115] p 965 N93-15291
A plan for spacecraft automated rendezvous
[NASA-TM-108385] p 813 N93-15392

AUTOMATION
Identifying ability requirements for operators of future automated air traffic control systems
[AD-A256615] p 789 N93-14276

AUTOMOBILES
Sensor-based driving of a car with fuzzy inferencing VLSI chips and boards
[DE92-017819] p 963 N93-14818
S/EV 1991: Solar and Electric Vehicle Symposium, Car and Trade Show
[DE92-019890] p 869 N93-15226

AUTONOMOUS NAVIGATION
An iconic position estimator for a 2-D laser rangefinder
[AD-A255523] p 885 N93-14568

AUTONOMY
A concurrent real-time autonomous mobile robot programming system p 960 N93-14281

AUTORADIOGRAPHY
Autoradiographic distribution and applied pharmacological characteristics of dextromethorphan and related antitissue/anticonvulsant drugs and novel analogs
[AD-A255607] p 935 N93-15009

AVAILABILITY
Sensitivity and uncertainty analysis in performability modelling
[MEMO-INF-92-18] p 941 N93-15090

AVERAGE
Turbulent fluid motion IV-averages, Reynolds decomposition, and the closure problem
[NASA-TM-105822] p 880 N93-15585

AVIONICS
F/FB-111 avionics test station and component specialist/technician. Automatic test stations manual and electronic warfare test stations. Training requirements analysis (451X6), volume 2
[AD-A252121] p 793 N93-14110
MIL-STD-1760 application guidelines
[AD-A255714] p 790 N93-14432
FDAMS: An extendable and reconfigurable solution for avionics data management systems p 794 N93-15157
Personal computer based test- and emulation equipment for maintenance and ground support p 778 N93-15185

AVOIDANCE
Airbus Industrie TCAS experience p 789 N93-15186

AXIAL LOADS
Failure of composite plates under static biaxial planar loading
[NASA-CR-191391] p 903 N93-15653

AXISYMMETRIC FLOW
BLSTA: A boundary layer code for stability analysis
[NASA-CR-4481] p 877 N93-14797

AXONS
Nerves and tissue repair
[AD-A255299] p 934 N93-14535
Extrathalmic modulation of cortical function
[AD-A255440] p 935 N93-14782
Biophysical and biochemical mechanisms in synaptic transmitter release
[AD-A256340] p 936 N93-15198

B

B STARS
Submillimeter and infrared spectroscopy of molecular clouds near O and B stars p 1016 N93-14149

BACKGROUND NOISE
The effects of mis-alignment and background noise in a low energy gamma ray telescope p 1011 N93-14231

BACKGROUND RADIATION
A general purpose radiative transfer model for application to remote sensing in multidimensional systems p 904 N93-14174
A search for anisotropy in the cosmic background radiation at millimeter wavelengths on angular scales from 0.3 to 3 degrees p 1050 N93-14244
QSO absorption lines and the ionizing field at high redshifts p 1013 N93-14860

BACKSCATTERING
Diffusing wave spectroscopy p 980 N93-14169
Bright crater outflows: Possible emplacement mechanisms p 1026 N93-14305
Radar-anomalous, high-altitude features on Venus p 1036 N93-14349
Problem footprints in Magellan altimetry data p 1039 N93-14362
Anomalous scattering behavior of selected impact parabola features: Magellan cycle-to-cycle comparisons p 1039 N93-14363
Scattering properties of Venus' surface p 1044 N93-14391
Low-emissivity impact craters on Venus p 1044 N93-14392
Experimental investigation of scattering from randomly rough plastic cylinders
[AD-A256018] p 975 N93-15259

BACKWARD FACING STEPS
Preconditioned conjugate-gradient methods for low-speed flow calculations
[NASA-TM-105929] p 877 N93-14885

BACTERIA
Biofilm ecology of bioluminescent bacteria
[AD-A255282] p 932 N93-14532

BALLISTICS
Current neutralization in ballistic transport of light ion beams
[AD-A256070] p 976 N93-14662

BALLOON-BORNE INSTRUMENTS
The effects of mis-alignment and background noise in a low energy gamma ray telescope p 1011 N93-14231

BAND STRUCTURE OF SOLIDS
The 17th Annual Conference on the Physics and Chemistry of Semiconductor Interfaces
[AD-A257061] p 996 N93-15449

BANDWIDTH
On the performance of Trellis coded modulation with octal phase shift keying over the TDRSS channel
[NASA-CR-191366] p 857 N93-14155
A time-domain study of the relationship between drive force time bandwidth and farfield acoustic radiation
[AD-A255616] p 973 N93-14159
Network issues for large mass storage requirements p 1002 N93-14773

BARIUM OXIDES
Method of making substantially single phase superconducting oxide ceramics having a TC above 85 degrees
[AD-D015422] p 850 N93-14743

BAROCLINIC INSTABILITY
Numerical simulation of baroclinic Jovian vortices p 1046 N93-14865
The influence of baroclinic processes on tropical cyclone motion p 923 N93-15099

BARRIER LAYERS
Epitaxial heterojunctions of oxide semiconductors and metals on high temperature superconductors
[NASA-CASE-NPO-18483-1-CU] p 994 N93-15151

BARS
Bar-holding prosthetic limb
[NASA-CASE-MFS-28481-1] p 939 N93-14870

BARYONS
A Cloudy Quark Bag Model of S, P, and D wave interactions for the coupled channel antikaon-nucleon system
[DE92-040149] p 977 N93-15062

BASALT
Is Ishtar Terra a thickened basaltic crust? p 1024 N93-14292

BATHYTHERMOGRAPHS
Altimeter and oceanographic in situ measurements in the area of the Greenland-Iceland-Norwegian Sea, 1987-1988
[AD-A256598] p 960 N93-14239

BAYES THEOREM
A proof of convergence of the Markov chain simulation method
[AD-A255456] p 970 N93-14487
Nonparametric bayesian bioassay including ordered polytomous response
[AD-A255990] p 970 N93-15109
An iterative Monte Carlo method for nonconjugate bayesian analysis
[AD-A255991] p 971 N93-15110

BEACONS
An iconic position estimator for a 2-D laser rangefinder
[AD-A255523] p 885 N93-14568

BEAM INJECTION
An analysis of the SCEX 3 ionospheric electron beam injection experiment p 912 N93-14177
Beam trapping in a modified betatron with a localized bipolar electric field pulse
[AD-A255414] p 866 N93-14504
High-brightness linac for the Advanced Free-Electron Laser Initiative at Los Alamos
[DE92-040213] p 887 N93-15417

BEAM SPLITTERS
Interferometer with two phase-conjugate mirrors
[AD-D015420] p 982 N93-14800
Integrated device with diffractive polarization components for a magneto-optical disk head p 986 N93-15517

BEAMFORMING
Layered parallel interface for an active antenna array
[AD-D015411] p 860 N93-14879

BEAMS (RADIATION)
Scattering of sound by sound: Nonlinear interaction of collinear and noncollinear sound beams p 973 N93-14145
High-brightness linac for the Advanced Free-Electron Laser Initiative at Los Alamos
[DE92-040213] p 887 N93-15417

BEARINGS
Bearing servicing tool
[NASA-CASE-MSC-21881-1] p 891 N93-14871
Summary of the NASA Lewis component technology program for Stirling power converters
[NASA-TM-105640] p 827 N93-15526

BENDING
A geometrically nonlinear stress-deflection relation for thin film/substrate systems p 848 N93-14287
Cytherean crustal bending at Salme Dorsa p 1039 N93-14364
Optical fibers for long-haul transmission in severe-bending applications
[AD-A255964] p 981 N93-14407
Finite element analysis of elastic fracture under unsteady translational and rotational loading p 899 N93-14469
Thermal elastic shock and its effect on spacecraft attitude control p 818 N93-14837
Validation of an automated torsional and warping stress analysis program
[AD-A256035] p 902 N93-15260

BENZENE
Anaerobic microbial transformation of aromatic hydrocarbons and mixtures of aromatic hydrocarbons and halogenated solvents
[AD-A255696] p 932 N93-14557

BERMUDA
Acoustic propagation loss predictions for a site on the Bermuda Rise at low and very low frequencies
[AD-A255445] p 925 N93-14512

BERYLLIUM COMPOUNDS
Normal state resistivity and the phase diagram of U(1-x)Th(x)Be13
[DE92-040236] p 995 N93-15321

BETATRONS
Beam trapping in a modified betatron with a localized bipolar electric field pulse
[AD-A255414] p 866 N93-14504

Simple formulae for the optimization of the FEL gain length including the effects of emittance, betatron oscillations, and energy spread
| DE92-040378 | p 887 N93-15325

BIAS
Simultaneous DIF amplification and cancellation: Shealy-Stout test for DIF
| AD-A256284 | p 970 N93-14455
Implementation issues concerning injection simulation. Part 1: The backbone implementation
| MEMO-INF-91-57-PT-1 | p 946 N93-15078

BIBLIOGRAPHIES
Aerospace medicine and biology: A continuing bibliography with indexes (supplement 368)
| NASA-SP-7011(368) | p 934 N93-14603
Aeronautical engineering: A continuing bibliography with indexes (supplement 282)
| NASA-SP-7037(282) | p 777 N93-14604
Aeronautical engineering: A continuing bibliography with indexes (supplement 284)
| NASA-SP-7037(284) | p 777 N93-14605
Large space structures and systems in the space station era: A bibliography with indexes (supplement 04)
| NASA-SP-7085(04) | p 817 N93-14606
Bibliography of scientific publications of the Naval Biodynamics Laboratory
| AD-A255952 | p 1051 N93-14657
Bibliography of Lewis Research Center Technical Publications announced in 1991
| NASA-TM-105595 | p 1004 N93-14796
NREL photovoltaic subcontract reports: Abstracts and document control information
| DE92-016408 | p 907 N93-14817
Publications of the Space Physiology and Countermeasures Program, Neuroscience Discipline: 1980-1990
| NASA-CR-4476 | p 936 N93-15583
LDEF: A bibliography with abstracts
| NASA-TM-107705 | p 813 N93-15646

BIDIRECTIONAL REFLECTANCE
Effects of cryocontaminants on cryogenic superpolished mirror and superpolished quartz crystal microbalance
| AD-A255972 | p 981 N93-14403

BINARY CODES
High-speed architecture for the decoding of trellis-coded modulation
| NASA-CR-191374 | p 941 N93-14770

BINARY DATA
Representation and manipulation of inductive boolean functions
| AD-A256078 | p 967 N93-14235

BINARY MIXTURES
Compaction of submicron and nanocrystalline Al2O3-ZrO2 ceramics
| DE92-040233 | p 852 N93-15320

BINARY STARS
The black hole candidate binary A0620-00 p 1015 N93-14148
Orbital coplanarity in solar-type binary systems: Implications for planetary system formation and detection p 1020 N93-14867

BINARY SYSTEMS (MATERIALS)
An investigation of crack growth at interfaces in bimaterials and composites using a consistent shear-lag model p 896 N93-14187

BINDERS (MATERIALS)
Waterborne polyurethane binder resins for compliant aircraft coatings
| AD-A256246 | p 849 N93-14573

BINOCULAR VISION
Real-time gaze holding in binocular robot vision
| AD-A256226 | p 982 N93-14582

BIOASSAY
Nonparametric bayesian bioassay including ordered polytomous response
| AD-A255990 | p 970 N93-15109

BIOASTRONAUTICS
Aerospace medicine and biology: A continuing bibliography with indexes (supplement 368)
| NASA-SP-7011(368) | p 934 N93-14603

BIOCHEMISTRY
Biophysical and biochemical mechanisms in synaptic transmitter release
| AD-A256340 | p 936 N93-15198

BIODYNAMICS
Bibliography of scientific publications of the Naval Biodynamics Laboratory
| AD-A255952 | p 1051 N93-14657

BIOLOGICAL EFFECTS
Aerospace medicine and biology: A continuing bibliography with indexes (supplement 368)
| NASA-SP-7011(368) | p 934 N93-14603
Aerospace medicine and biology: A continuing bibliography with indexes (supplement 369)
| NASA-SP-7011(369) | p 935 N93-14731
Radiation monitoring for long duration space flights p 812 N93-14959
Joint HVAC transmission EMF environmental study
| DE92-017863 | p 933 N93-15211
Research for electric energy systems
| DE92-040076 | p 870 N93-15412

BIOLOGICAL MODELS (MATHEMATICS)
Neural network retinal model real time implementation
| AD-A255652 | p 934 N93-14210
Modelling global methane emissions from livestock: Biological and nutritional controls
| NASA-CR-191354 | p 911 N93-15480

BIOLUMINESCENCE
Biofilm ecology of bioluminescent bacteria
| AD-A255282 | p 932 N93-14532

BIOMAGNETISM
Neuromagnetic investigations of cortical regions underlying short-term memory
| AD-A255788 | p 937 N93-14646

BIOPHYSICS
Biophysical and biochemical mechanisms in synaptic transmitter release
| AD-A256340 | p 936 N93-15198

BIPOLAR TRANSISTORS
The 3 to 5 heterojunction structures and high speed devices
| AD-A250399 | p 991 N93-14521
Selected area epitaxial growth for complementary HBT applications
| AD-A257047 | p 995 N93-15365

BIPOLARITY
Beam trapping in a modified betatron with a localized bipolar electric field pulse
| AD-A255414 | p 866 N93-14504

BIREFRINGENCE
Off-axis conoscopic holography: Optical and digital reconstruction
| TELECOM-PARIS-90-E-023 | p 882 N93-15096

BISMALEIMIDE
Degradation and failure modes of carbon/bismaleimide laminates subjected to a tropical exposure
| AD-A256328 | p 836 N93-15193

BISMUTH ALLOYS
Thermodynamics and transport in Ce3Bi4Pt3 and related compounds
| DE92-040377 | p 998 N93-14905

BISMUTH COMPOUNDS
Optical information processing using photorefractive BSO p 981 N93-14204

BIT ERROR RATE
A low bit rate FSK technique for SCPC satellite communication systems p 811 N93-14954

BLACK HOLES (ASTRONOMY)
The black hole candidate binary A0620-00 p 1015 N93-14148
Extracting x rays, gamma rays, and electron-positron pairs from supermassive Kerr black holes using the Penrose mechanism p 1049 N93-14176
A search for dead QSO's among nearby luminous galaxies p 1011 N93-14228

BLACKOUT (PHYSIOLOGY)
Statistical analysis of the human strangulation experiments: Comparison to +Gz-induced loss of consciousness
| AD-A255485 | p 935 N93-14789

BLADE TIPS
An experimental and analytical study of TIP clearance effects in axial flow compressors
| AD-A256434 | p 800 N93-15337

BLADE-VORTEX INTERACTION
The Applicaiton of CFD to rotary wing flow problems
| NASA-TM-102803 | p 782 N93-15483

BLEEDING
An experimental investigation of base bleed effect on the wake turbulent structure behind a two-dimensional blunt model
| MPIS-9/1991 | p 781 N93-15131

BLOWING
Modeling variable blowing on a slender cone in hypersonic flow p 781 N93-14836
Evaluation of methods for estimating wind wave growth on narrow irregular fetches
| AD-A256002 | p 932 N93-15113

BLUFF BODIES
Wake similarity and vortex formation for two-dimensional bluff bodies p 781 N93-15101

BLUNT TRAILING EDGES
An experimental investigation of base bleed effect on the wake turbulent structure behind a two-dimensional blunt model
| MPIS-9/1991 | p 781 N93-15131

BODY SIZE (BIOLOGY)
Body composition and physical performance
| AD-A255627 | p 938 N93-14161

BODY WEIGHT
Body composition and physical performance
| AD-A255627 | p 938 N93-14161

BOLTS
RB 199 high pressure compressor stage 3 spin pit tests p 799 N93-14893
RB211-524B disc and drive cones hot cyclic spinning test p 799 N93-14895
F100 second stage fan disk bolthole crack propagation ferris wheel test p 800 N93-14897

BOLTZMANN TRANSPORT EQUATION
A quasi-equilibrium kinetic model of HF air breakdown
| AD-A256240 | p 859 N93-14453

BOMBARDMENT
Si atomic layer epitaxy based on Si2H6 and remote He plasma bombardment
| AD-A255763 | p 993 N93-15055

BOMBER AIRCRAFT
Reanalysis of multiple-wheel landing gear traffic tests
| AD-A256593 | p 804 N93-14238

BONDING
Core design for use with precision composite reflectors
| NASA-CASE-NPO-17858-1-CU | p 832 N93-14700
Comments on 'Kinetic Study on the Hexacelsian-Celsian Phase Transformation'
| NASA-TM-105917 | p 850 N93-14886
A global potential energy surface for ArH2
| NASA-CR-190741 | p 843 N93-15358

BONES
Training, muscle fatigue and stress fractures
| AD-A255277 | p 935 N93-15006

BOOLEAN ALGEBRA
Representation and manipulation of inductive boolean functions
| AD-A256078 | p 967 N93-14235

BOOLEAN FUNCTIONS
Representation and manipulation of inductive boolean functions
| AD-A256078 | p 967 N93-14235

BOOMS (EQUIPMENT)
On-orbit deployment anamolies: What can be done? p 821 N93-15603

BORON ISOTOPES
Isotopic composition of galactic cosmic ray boron, carbon, nitrogen, and oxygen p 1020 N93-14866

BORON REINFORCED MATERIALS
Composite materials in space: Results from the LDEF satellite p 811 N93-14955

BOSONS
Semi-classical quantization rules in supersymmetric quantum mechanics p 998 N93-14590
Dark matter axions
| DE92-040501 | p 1022 N93-15346

BOUNDARY CONDITIONS
Investigation of the on-surface boundary operators for electromagnetic scattering by conducting object p 857 N93-14189

BOUNDARY ELEMENT METHOD
On the development and application of a modified boundary element method for the analysis of three dimensional elastostatic problems in thick plates p 901 N93-14587
Boundary element analysis of low frequency cavity acoustical problems
| MATHS-REPT-A-158 | p 974 N93-15073

BOUNDARY INTEGRAL METHOD
The numerical stability of nonlinear floating body calculations p 873 N93-14278

BOUNDARY LAYER CONTROL
Wall layers
| AD-A256152 | p 872 N93-14257
Feedback control of flow separation and transition to turbulence in unsteady boundary layers p 873 N93-14464

BOUNDARY LAYER EQUATIONS
Feedback control of flow separation and transition to turbulence in unsteady boundary layers p 873 N93-14464
Combustion in supersonic flows p 841 N93-14627

BOUNDARY LAYER FLOW
Multi-point inverse design of isolated airfoils and airfoils in cascade in incompressible flow p 790 N93-14462
Feedback control of flow separation and transition to turbulence in unsteady boundary layers p 873 N93-14464
Supersonic boundary-layer flow turbulence modeling
| NASA-TM-105893 | p 877 N93-14758
BLSTA: A boundary layer code for stability analysis
| NASA-CR-4481 | p 877 N93-14797
Use of surface heat transfer measurements as a flow separation diagnostic in a two dimensional reflected oblique shock/turbulent boundary layer interaction
| NASA-TM-105981 | p 879 N93-15355

BOUNDARY LAYER SEPARATION
Feedback control of flow separation and transition to turbulence in unsteady boundary layers
p 873 N93-14464
Direct prediction of a separation boundary for aerofoils using a viscous-coupled calculation method
[ESDU-92008] p 780 N93-14516
A plume-induced boundary layer separation experiment
[AD-A255397] p 875 N93-14677
Investigations of detail design issues for the high speed acoustic wind tunnel using a 60th scale model tunnel. Part 1: Tests with open circuits
[NASA-CR-191671] p 780 N93-14737
Study of optical techniques for the Ames unitary wind tunnel. Part 5: Infrared imagery
[NASA-CR-191385] p 804 N93-14809
Use of surface heat transfer measurements as a flow separation diagnostic in a two dimensional reflected oblique shock/turbulent boundary layer interaction
[NASA-TM-105981] p 879 N93-15355
BOUNDARY LAYER STABILITY
Super-micro computer weather prediction model
[AD-A255668] p 918 N93-14153
BLSTA: A boundary layer code for stability analysis
[NASA-CR-4481] p 877 N93-14797
BOUNDARY LAYER TRANSITION
Feedback control of flow separation and transition to turbulence in unsteady boundary layers
p 873 N93-14464
Boundary layer transition measurements by optical anemometry p 874 N93-14477
Study of optical techniques for the Ames unitary wind tunnel. Part 5: Infrared imagery
[NASA-CR-191385] p 804 N93-14809
BOUNDARY LAYERS
Energetic and magnetosheath energy particle signatures of the low-latitude boundary layer at low altitudes near noon
[NASA-CR-191388] p 917 N93-15574
BOUNDARY VALUE PROBLEMS
Applications of a constitutive equation for microstructural change in polymers p 848 N93-14222
Direct simulation of turbulent combustion
p 840 N93-14622
Convective scale 4-D data assimilation using simulated single-Doppler radar observations p 921 N93-14683
Diffusion problems in bonded nonhomogeneous materials with an interface cut
[AD-A256470] p 836 N93-15373
BOW WAVES
Computational analysis of hypersonic flows past elliptic-cone waveriders
[NASA-CR-191304] p 781 N93-14767
BRAGG ANGLE
Experimental considerations of higher order parametric x rays from silicon crystals of varying thicknesses
[AD-A256082] p 990 N93-14260
BRAGG CELLS
An analysis of the effect of acoustic non-linearities in wide bandwidth acousto-optic bragg cells
[AD-A256579] p 973 N93-14269
BRAIDED COMPOSITES
Advances in 3-dimensional braiding
p 833 N93-14748
Development of generalized 3-D braiding machines for composite preforms p 833 N93-14749
Tensile properties of textile composites
p 834 N93-14754
Modeling of Euclidean braided fiber architectures to optimize composite properties p 834 N93-14755
Microstructure-failure mode correlations in braided composites p 834 N93-14756
BRAIN
Neuromagnetic investigations of cortical regions underlying short-term memory
[AD-A255788] p 937 N93-14646
Cognition and the brain
[AD-A255483] p 937 N93-14788
BRANCHING (MATHEMATICS)
An examination of wing rock for the F-15
[AD-A256613] p 802 N93-14252
Using an interior point cutting plane method to solve integer programming problems
[AD-A256041] p 945 N93-14659
BRAYTON CYCLE
Closed Brayton Cycle power system with a high temperature pellet bed reactor heat source for NEP applications
[NASA-TM-105933] p 826 N93-14482
BRAZIL
The regional land use of Paraiba Valley and the North Coast of Sao Paulo State, Brazil p 905 N93-14450
BREADBOARD MODELS
Autonomous power system brassboard
[NASA-CR-189115] p 867 N93-14798
BREAKDOWN
Microstack insulator for flashover inhibition, phase 2
[AD-A256338] p 869 N93-15196
BREMSSTRAHLUNG
Generation, control, and transport of a 19-MeV, 700-kA pulsed electron beam
[DE92-019803] p 978 N93-15277
Predictions of dose from electrons in space
[NASA-CR-191617] p 1051 N93-15580
BRIDGMAN METHOD
Solidification of InSb-GaSb alloy and InSb with vibration p 995 N93-15310
An experimental approach to determine the heat transfer coefficient in directional solidification furnaces
p 995 N93-15311
Experimental observation of the influence of furnace temperature profile on convection and segregation in the vertical Bridgman crystal growth technique
p 995 N93-15312
BRIGHTNESS DISTRIBUTION
Imaging the sun in hard x-rays using Fourier telescopes p 1048 N93-14591
Imaging the sun in hard x rays using Fourier telescopes
[NASA-TM-108390] p 1013 N93-15203
BRIGHTNESS TEMPERATURE
Satellite detection of complex aerosols over the Arabian Peninsula/Gulf
[AD-A256085] p 909 N93-14261
BRILLOUIN EFFECT
Advanced optical fiber communication systems
[AD-A255424] p 982 N93-14507
BRITTLENESS
The mechanics of dislocation nucleation at a crack tip
p 896 N93-14214
BROADBAND
On the detection of ultrawideband radar signals
[AD-A256075] p 858 N93-14233
The evolution of signalling from ISDN to B-ISDN
[MEMO-INF-92-30] p 860 N93-15095
Integration of satellite links into an ATM mode broadband ISDN
[TELECOM-PARIS-91-E-022] p 861 N93-15097
Broadband vibroacoustic frequency control via piezoelectric films
[ONERA-RT-8/3654-RY-010-R] p 974 N93-15129
BROKEN SYMMETRY
The low-energy structure of compactified superstring models p 997 N93-14116
The dynamics of spatially extended lasers
p 883 N93-14123
Staggered fermions and chiral symmetry breaking in transverse lattice regulated QED
[DE92-040505] p 977 N93-15378
Weak-electromagnetic interference in polarized eD scattering
[DE93-001763] p 978 N93-15486
Schwinger Dyson equations: Dynamical chiral symmetry breaking and confinement
[DE92-040717] p 978 N93-15657
BUBBLES
Numerical and experimental study of bubble growth in highly viscous fluids p 874 N93-14465
Nucleate pool boiling in the long duration low gravity environment of the Space Shuttle
[NASA-TM-105973] p 855 N93-15420
BUCKLING
Analysis and optimal design of pressurized, imperfect, anisotropic ring-stiffened cylinders p 897 N93-14251
Nonlinear dynamic response of shallow arches to harmonic forcing p 898 N93-14282
Cytherean crustal bending at Salme Dorsa
p 1039 N93-14364
Reliability of stiffened structural panels: Two examples
[NASA-TM-107687] p 900 N93-14483
The effect of geometry and prescribed delaminations on the postbuckling behaviour of laminated carbon-fibre reinforced plastic panels p 831 N93-14597
The stress development during filament winding of thick cylinders
[AD-A255765] p 901 N93-15066
BUFFER STORAGE
Proposal for massively parallel data storage system
p 960 N93-15510
BULGING
Venus mesospheric winds and the carbon monoxide bulge p 1029 N93-14320
BULKHEADS
Investigation of the use of surface electrical currents for short-range shipboard data communications
[AD-A256197] p 859 N93-14490
BUOYANCY
Thermal buoyancy on Venus: Preliminary results of finite element modeling p 1025 N93-14302
Large shield volcanos on Venus: The effect of neutral buoyancy zone development on evolution and altitude distribution p 1032 N93-14333
Second order closure modeling of turbulent buoyant wall plumes
[NASA-TM-105956] p 877 N93-14829
Numerical study of mixing of two fluids under low gravity
[NASA-TM-105865] p 878 N93-14914
BUOYS
Evaluation of methods for estimating wind wave growth on narrow irregular fetches
[AD-A256002] p 932 N93-15113
BURNING RATE
Calculation of chemical reaction rates in turbulent combustion p 841 N93-14625
BURNS (INJURIES)
The effect of pain on task performance: A review of the literature
[AD-A254336] p 938 N93-15216

C

CABLE TELEVISION
The information age as a work in progress: Implications for technical communicators
[DE92-019780] p 1008 N93-15275
CABLES (ROPES)
Cable-line shortening device
[AD-D015427] p 891 N93-14822
CADASTRAL MAPPING
Measurement-based multipurpose cadastral systems
p 904 N93-14220
CADMIUM TELLURIDES
Electrical conductivity measurements in evaporated cadmium telluride thin films p 865 N93-14191
CALCULUS
A proof of the Church-Rosser theorem and its representation in a logical framework
[AD-A256574] p 942 N93-14268
From data structure to process structure
[MEMO-INF-91-38] p 946 N93-15077
CALDERAS
The origins of radial fracture systems and associated large lava flows on Venus p 1038 N93-14356
CALIBRATING
Calibration of the CCD Tully-Fisher relation with application to the Perseus-Pisces supercluster
p 1016 N93-14194
Optimum pose measurements for kinematic parameters identification
[AD-A256307] p 970 N93-14443
CAMERAS
Real-time gaze holding in binocular robot vision
[AD-A256226] p 982 N93-14582
Cloud fraction, layer, and direction of movement results from sky cameras during the FIRE IFO, Coffeyville, Kansas, experiment for the period Nov. 12 through Dec. 9, 1991
[NASA-TM-107647] p 924 N93-15501
CANADA
Space education: A self-perservation strategy for the Canadian space industry p 808 N93-14937
CANADIAN SPACE PROGRAM
Proceedings of the Sixth CASI Conference on Astronautics
[CTN-92-60336] p 804 N93-14920
Canada's role in pushing back the frontiers of space
p 806 N93-14928
Space education: A self-perservation strategy for the Canadian space industry p 808 N93-14937
Applications of the mobile servicing system to the space exploration initiative p 809 N93-14946
Earth environment space initiative
p 811 N93-14953
CANADIAN SPACECRAFT
The Canadian Solar Sail Project p 804 N93-14921
CANARD CONFIGURATIONS
Flowfield study of a close-coupled canard configuration
[AD-A256311] p 782 N93-15245
CANONICAL FORMS
A linear constraint technology for interactive graphic systems p 957 N93-15568
CAPACITANCE
Electrical conductivity measurements in evaporated cadmium telluride thin films p 865 N93-14191
SDIO Workshop on Piezoelectric Ceramic Actuators for Space Applications
[AD-A255959] p 990 N93-14422
Driven shielding capacitive proximity sensor
[NASA-CASE-GSC-13377-1] p 962 N93-14701
Molecular capacitance: Sequential electron-transfer energetics for solution-phase metallic clusters in relation to gas-phase clusters and analogous interfaces
[AD-A257057] p 977 N93-15448

CAPACITORS
Reliability of sol-gel derived ferroelectric memories
| AD-A255358 | p 991 N93-14560
Characterization of PZT films fatigued at low frequency
| AEROSPACE-ATR-91(8308)-2 | p 992 N93-14795
Microwave processing of tantalum capacitor anodes
| DE92-017829 | p 869 N93-15214
Energy distribution of trapped holes in irradiated SiO2
| DE92-040979 | p 997 N93-15649

CAPILLARY FLOW
Control of thermocapillary convection in a two-layer liquid system p 809 N93-14945

CAPILLARY TUBES
Calculation methods for externally pressurised (hydrostatic) journal bearings with capillary restrictor control
| ESDU-92026 | p 889 N93-14543

CARBIDES
Method for fabricating ohmic contacts on semiconducting diamond
| AD-D015432 | p 850 N93-14825

CARBON
Atomic data and spectral analysis of carbon, nitrogen, oxygen and silicon ions observed with the International Ultraviolet Explorer
| NASA-CR-191302 | p 1012 N93-14761
Accurate methods for calculating atomic processes in high temperature plasmas
| DE92-040215 | p 988 N93-15418

CARBON DIOXIDE
Carbon dioxide induced ocean climatic change and tracer experiment with an atmosphere-ocean general circulation model p 912 N93-14178
Method of making substantially single phase superconducting oxide ceramics having a TC above 85 degrees
| AD-D015422 | p 850 N93-14743
Interferometric observations of the J(0,1) CO line on Venus: Upper mesospheric winds and CO abundance p 1047 N93-14918
Spatial and temporal patterns of biotic exchanges of CO2 between the atmosphere and tropical landscapes and their role in the global carbon balance
| DE92-019170 | p 911 N93-15272
A correlated k-distribution model of the heating rates for CO2 and O3 in the atmosphere between 0 and 60 km
| DE93-000889 | p 911 N93-15280

CARBON DIOXIDE LASERS
The dynamics of spatially extended lasers p 883 N93-14123
Compact high PRF CO2 transmitter
| AD-A255985 | p 884 N93-14414

CARBON FIBER REINFORCED PLASTICS
The effect of geometry and prescribed delaminations on the postbuckling behaviour of laminated carbon-fibre reinforced plastic panels p 831 N93-14597
Composite materials in space: Results from the LDEF satellite p 811 N93-14955
Fracture/damage mechanics of composites: Static and fatigue properties
| DLR-MITT-92-03 | p 835 N93-15075

CARBON FIBERS
Polymer infiltration studies
| NASA-CR-191652 | p 852 N93-15431

CARBON ISOTOPES
Isotopic composition of galactic cosmic ray boron, carbon, nitrogen, and oxygen p 1020 N93-14866

CARBON MONOXIDE
The isotopes of carbon monoxide in the free troposphere and their implications to atmospheric chemistry p 913 N93-14207
Venus mesospheric winds and the carbon monoxide bulge p 1029 N93-14320

CARBON STARS
A study of the abundance distributions along the minor axis of the Galactic bulge p 1015 N93-14136
Faint high-latitude carbon stars p 1019 N93-14638

CARBON TETRACHLORIDE
Anaerobic microbial transformation of aromatic hydrocarbons and mixtures of aromatic hydrocarbons and halogenated solvents
| AD-A255696 | p 932 N93-14557

CARBON-CARBON COMPOSITES
Emittance measurements of Space Shuttle orbiter reinforced carbon-carbon
| NASA-TP-3293 | p 903 N93-15530

CARBORANE
Electronically active cyclocarborane-metal-arene assemblies
| AD-A256288 | p 865 N93-14457

CARBOXYLATION
Morphological analysis of ionomers
| DE92-040162 | p 852 N93-15415

CARBURIZING
Growth, characterization and device development in monocrystalline diamond films
| AD-A256283 | p 994 N93-15244

CARRIER TRANSPORT (SOLID STATE)
Transport in heterostructures and device in microwave and millimeter wave regimes
| AD-A255975 | p 858 N93-14408

CARTESIAN COORDINATES
Simulation of unsteady inviscid flow on an adaptively refined Cartesian grid p 873 N93-14273
Adaptive control of a manipulator in cartesian space
| F-4-2 | p 950 N93-15308

CARTRIDGES
Mechanical shielding for electric primer
| AD-D015417 | p 860 N93-14889

CASCADE FLOW
An algebraic turbulence model for three-dimensional viscous flows
| NASA-TM-105931 | p 777 N93-14102
Multi-point inverse design of isolated airfoils and airfoils in cascade in incompressible flow p 790 N93-14462
Time-dependent predictions and analysis of turbine cascade data in the transonic flow region
| PNR-90957 | p 782 N93-15489
Prediction of turbine cascade flows with a quasi-three-dimensional rotor viscous code and the extension of the algebraic turbulence model
| AD-A256831 | p 880 N93-15635

CAST ALLOYS
The response of dispersion-strengthened copper alloys to high fluence neutron irradiation at 415 C
| DE92-019434 | p 846 N93-15138
Analytical and experimental evaluation of joining ceramic oxides to ceramic oxides and ceramic oxides to metal for advanced heat engine applications
| DE92-041383 | p 851 N93-15294

CATACLYSMIC VARIABLES
Disc structure and variability in dwarf novae p 1017 N93-14460

CATALOGS (PUBLICATIONS)
Facilities and capabilities catalog for landing and escape systems
| NASA-RP-1282 | p 814 N93-14495
Source header list. Volume 2: K through Z
| AD-A256001 | p 1007 N93-15112

CATEGORIES
Compactness and Loewenheim-Skolem properties in pre-institution categories
| MEMO-INF-92-27 | p 968 N93-15094

CATHODES
Lithium rechargeable cell with a poly 3-methylthiophene cathode
| AD-A255436 | p 866 N93-14552
Arc-cathode interaction study
| NASA-CR-191356 | p 867 N93-14721
Impact of protective oxides on cathode-side resistances in MCFCs
| DE92-019973 | p 994 N93-15221

CATHODOLUMINESCENCE
Method and apparatus for a high resolution, flat panel cathodoluminescent display screen
| AD-D015400 | p 868 N93-15107

CAUCHY PROBLEM
Multiply connected spacetimes and closed timelike curves in semiclassical gravity p 915 N93-14884

CAVITIES
Transonic flow calculations for a cavity with and without a store
| AD-A255954 | p 873 N93-14421
Boundary element analysis of low frequency cavity acoustical problems
| MATHS-REPT-A-158 | p 974 N93-15073
Calculation of mechanical vibration frequencies of stiffened superconducting cavities
| DE92-040228 | p 903 N93-15423
Design features of a seven-cell high-gradient superconducting cavity
| DE92-040229 | p 870 N93-15424

CAVITY RESONATORS
Determining optimum C-field settings that minimize output frequency variations in cesium atomic frequency standards
| AD-A255902 | p 971 N93-14108
Processing and characterization of electrophoretically deposited holmium barium copper oxide superconductor films
| AD-A256329 | p 869 N93-15194
SCRUNCHER phase and amplitude control
| DE92-040225 | p 870 N93-15421
Design features of a seven-cell high-gradient superconducting cavity
| DE92-040229 | p 870 N93-15424

CD-ROM
Data management for the coordinated Eastern Arctic experiment
| AD-A255648 | p 1000 N93-14182

CELL ANODES
Results from a pilot cell test of cermet anodes
| DE92-041357 | p 871 N93-15479

CELL DIVISION
Nerves and tissue repair
| AD-A255299 | p 934 N93-14535

CELLS (BIOLOGY)
Nerves and tissue repair
| AD-A255299 | p 934 N93-14535
Mechanisms of microwave induced damage in biologic materials
| AD-A255799 | p 933 N93-14648

CENTAUR LAUNCH VEHICLE
Acoustic and thermal testing of the Titan/Centaur upper stage p 814 N93-15621

CENTERBODIES
Numerical modeling of a vortex stabilized arcjet
| NASA-CR-190797 | p 826 N93-14883

CENTRIFUGAL CASTING
Effect of thermomechanical treatments on the aging response of centrifugally cast silicon carbide/aluminum composites
| AD-A256204 | p 836 N93-15236

CENTRIFUGAL FORCE
Finite element analysis of elastic fracture under unsteady translational and rotational loading p 899 N93-14469

CENTRIFUGES
Parametric study of air sampling cyclones p 779 N93-14173

CERAMIC BONDING
Analytical and experimental evaluation of joining silicon carbide to silicon carbide and silicon nitride to silicon nitride for heat engine applications
| DE92-041376 | p 837 N93-15454

CERAMIC COATINGS
The mixed mode crack problem in a nonhomogeneous elastic plane
| AD-A256469 | p 902 N93-15372
Development of adherent ceramic coatings to reduce contact stress damage of ceramics
| DE92-041373 | p 852 N93-15437
Development of wear-resistant ceramic coatings for diesel engine components
| DE92-041382 | p 853 N93-15439

CERAMIC FIBERS
Properties of textile grade ceramic fibers p 833 N93-14751

CERAMIC MATRIX COMPOSITES
Effect of interfacial thermal conductance and fiber orientation on the thermal diffusivity/conductivity of unidirectional fiber-reinforced ceramic matrix composites p 864 N93-14190
Damage and rupture of ceramic composites
| ETN-92-92722 | p 851 N93-15127
The mixed mode crack problem in a nonhomogeneous elastic plane
| AD-A256469 | p 902 N93-15372
Development of ceramic matrix composites for application in ceramic technology for advanced heat engines project, phase 2
| DE92-041379 | p 836 N93-15387
Development of ceramic matrix composites for application in the ceramic technology for advanced heat engines project. Phase 2A: Development of in-situ toughened silicon nitride
| DE92-041371 | p 853 N93-15452
Processing of sinterable transformation toughened ceramics for application in ceramic technology for advanced heat engines project
| DE92-041372 | p 853 N93-15453
Development of ceramic matrix composites for application in the ceramic technology for advanced heat engines project
| DE92-041378 | p 837 N93-15455
Fiber reinforced composites: A new class of glass and glass ceramic materials for thermomechanical applications
| REPT-921-430-104 | p 838 N93-15490

CERAMICS
Method of applying a thermal barrier coating system to a substrate
| NASA-CASE-LEW-15020-2 | p 832 N93-14706
Method of making substantially single phase superconducting oxide ceramics having a TC above 85 degrees
| AD-D015422 | p 850 N93-14743
Hyperfine experimental investigation of zirconia ceramics
| DE92-040301 | p 850 N93-14903
A fundamental understanding of the effects of ceramic processing on product microstructure
| AD-A255729 | p 850 N93-15049

Three-dimensional nuclear magnetic resonance imaging of green-state ceramics
[DE93-000930] p 851 N93-15282
Analytical and experimental evaluation of joining ceramic oxides to ceramic oxides and ceramic oxides to metal for advanced heat engine applications
[DE92-041383] p 851 N93-15294
Tribology of improved transformation-toughened ceramics-heat engine test
[DE92-041385] p 851 N93-15295
Compaction of submicron and nanocrystalline Al2O3-ZrO2 ceramics
[DE92-040233] p 852 N93-15320
The mixed mode crack problem in a nonhomogeneous elastic plane
[AD-A256469] p 902 N93-15372
Development of ceramic matrix composites for application in ceramic technology for advanced heat engines project, phase 2
[DE92-041379] p 836 N93-15387
An investigation of the processing, high temperature deformation and fracture characteristics of superplastic ceramics
[AD-A256519] p 852 N93-15394
Development of low-expansion ceramics for diesel engine applications
[DE92-041380] p 853 N93-15438
Development of ceramic matrix composites for application in the ceramic technology for advanced heat engines project. Phase 2A: Development of in-situ toughened silicon nitride
[DE92-041371] p 853 N93-15452
Processing of sinterable transformation toughened ceramics for application in ceramic technology for advanced heat engines project
[DE92-041372] p 853 N93-15453
Analytical and experimental evaluation of joining silicon carbide to silicon carbide and silicon nitride to silicon nitride for heat engine applications
[DE92-041376] p 837 N93-15454
Development of ceramic matrix composites for application in the ceramic technology for advanced heat engines project
[DE92-041378] p 837 N93-15455
Innovative techniques for studying new materials and new developments in solid state physics
[AD-A256394] p 996 N93-15465
Study of the glass formation of high temperature superconductors
[NASA-TM-108389] p 997 N93-15500

CEREBRAL CORTEX
Cognition and the brain
[AD-A255483] p 937 N93-14788

CEREBRUM
Statistical analysis of the human strangulation experiments: Comparison to +Gz-induced loss of consciousness
[AD-A255485] p 935 N93-14789

CERENKOV COUNTERS
Using the Haleakala barrel extensive air shower array to study selected U.H.E. gamma ray point sources
p 1050 N93-14639

CERIUM
Thermodynamics and transport in Ce3Bi4Pt3 and related compounds
[DE92-040377] p 998 N93-14905

CERIUM OXIDES
Hyperfine experimental investigation of zirconia ceramics
[DE92-040301] p 850 N93-14903
Tribology of improved transformation-toughened ceramics-heat engine test
[DE92-041385] p 851 N93-15295

CERMETS
Results from a pilot cell test of cermet anodes
[DE92-041357] p 871 N93-15479

CESIUM ALLOYS
Cesium iodide alloys
[DE92-019818] p 845 N93-14717

CESIUM IODIDES
Cesium iodide alloys
[DE92-019818] p 845 N93-14717

CH-47 HELICOPTER
Onboard System Evaluation of Rotors Vibration, Engines (OBSERVE) monitoring system
[AD-A255366] p 792 N93-15227

CHANNEL CAPACITY
NPR and intermodulation in mobile satellite systems
p 806 N93-14931

CHANNEL FLOW
Erosion versus construction: The origin of Venusian channels
p 1025 N93-14303

CHANNELS
Erosion versus construction: The origin of Venusian channels
p 1025 N93-14303
Application of left- and right-looking SAR stereo to depth measurements of the Ammavaru outflow channel, Lada Terra, Venus
p 1038 N93-14357

CHANNELS (DATA TRANSMISSION)
The role of HiPPI switches in mass storage systems: A five year prospective
p 1002 N93-14774
Storage needs in future supercomputer environments
p 1003 N93-14780
Requirements for a network storage service
p 1003 N93-14781
A preliminary design of the Ti:LiNbO3 optical channel waveguide
[AD-A255443] p 982 N93-14784
The role of HiPPI switches in mass storage systems: A five year prospective
p 1006 N93-15044
Co-channel speaker separation
[AD-A256443] p 861 N93-15317

CHAOS
Nonlinear dynamics of optical systems
p 979 N93-14124
Turbulence and chaos in classical and quantum systems
p 972 N93-14144
The use of chaos metrics to analyze Lagrangian particle diffusion models
[AD-A256142] p 967 N93-14255
New methods for nonlinear tracking and nonlinear chaotic signal processing
[AD-A256421] p 862 N93-15334

CHARACTERIZATION
In situ material characterization for pavement evaluation by the Spectral-Analysis-of-Surface-Waves (SASW) method
[AD-A255660] p 804 N93-14128
Method of characterizing residual stress in ferromagnetic materials using a pulse histogram of acoustic emission signals
[NASA-CASE-LAR-14239-1] p 845 N93-14705
Workshop on noninvasive geophysical site characterization
[LA-12311-C] p 914 N93-14724
A fundamental understanding of the effects of ceramic processing on product microstructure
[AD-A255729] p 850 N93-15049
Offloading techniques for large deployable space structures
p 821 N93-15605

CHARGE CARRIERS
Time-resolved optical studies of 3-5 semiconductors
p 990 N93-14183

CHARGE COUPLED DEVICES
Calibration of the CCD Tully-Fisher relation with application to the Perseus-Pisces supercluster
p 1016 N93-14194
Using digital scanned aerial photography for wetlands delineation
[AD-A255392] p 905 N93-14676
Analysis of CCD images of the coma of comet P/Halley
[NASA-CR-191384] p 1020 N93-14814
Performance characteristics of STIS detectors
[NASA-CR-191636] p 868 N93-14915

CHARGED PARTICLES
Measurement and analysis of excitation functions in (alpha,np) reactions on (128, 130)Te
[DE92-630358] p 991 N93-14485
Beam trapping in a modified betatron with a localized bipolar electric field pulse
[AD-A255414] p 866 N93-14504

CHARM (PARTICLE PHYSICS)
Strong interactions studies with medium energy probes
[DE92-040460] p 977 N93-15377

CHECKOUT
A framework for describing and implementing software visualization systems
p 953 N93-15540

CHEMICAL ANALYSIS
On the role of water growth in atmospheric aerosol
p 922 N93-14875
Gallium and indium compounds containing three different substituents. Crystal and molecular structure of ((Me3 CCH2)ClGaPPh2)3
[AD-A257049] p 996 N93-15443

CHEMICAL CLEANING
Cleaning of a thermal vacuum chamber with shrouds in place
p 814 N93-15612

CHEMICAL COMPOSITION
Application of Fourier Transform-infrared spectroscopy (FT-IR) for materials analysis
[AD-A255727] p 838 N93-14435
Photoelectrochemistry of electronic and electro-optical materials
[AD-A256239] p 866 N93-14583
Method of making substantially single phase superconducting oxide ceramics having a TC above 85 degrees
[AD-D015422] p 850 N93-14743
Infrared laboratory spectra and composition changes of synthetic amorphous silicate grains
[DE92-040211] p 843 N93-15283
The effect of processing and compositional changes on the tribology of PM212 in air
[NASA-TM-105945] p 828 N93-15576

CHEMICAL ENGINEERING
Acoustic resonance techniques for quality control
[DE92-040150] p 895 N93-15413

CHEMICAL EXPLOSIONS
Plutonium pyrophoricity
[RFP-4517] p 845 N93-14723

CHEMICAL PROPERTIES
Preliminary investigations of metal liquid-like films and coatings derived from them
[AD-A255477] p 849 N93-14489

CHEMICAL REACTIONS
Electronically excited molecules: Reaction kinetics and emission of light: Nanosecond infrared spectroscopy, electronic emission from chemical reactions
[AD-A255642] p 976 N93-14283
Transport phenomena and interfacial kinetics in multiphase combustion systems.
[AD-A255999] p 838 N93-14418
A study of mid-latitude 5577A Cl dayglow emissions
[AD-A255444] p 914 N93-14511
Method for detecting chemical vapors using a lasing dye sensor
[AD-D015424] p 885 N93-14821
Variational transition state theory
[DE92-040498] p 842 N93-14908
Computed potential energy surfaces for chemical reactions
[NASA-CR-190741] p 843 N93-15356
Theoretical characterization of the potential energy surface for NH + NO
[NASA-CR-190741] p 843 N93-15357
A global potential energy surface for ArH2
[NASA-CR-190741] p 843 N93-15358
Simplified jet-A kinetic mechanism for combustor application
[NASA-TM-105940] p 844 N93-15504

CHIPS (ELECTRONICS)
Neural network retinal model real time implementation
[AD-A255652] p 934 N93-14210
Testability design rating system: Testability handbook, volume 1
[RL-TR-92-12-VOL-1] p 867 N93-14699

CHIRAL DYNAMICS
Staggered fermions and chiral symmetry breaking in transverse lattice regulated QED
[DE92-040505] p 977 N93-15378
Schwinger Dyson equations: Dynamical chiral symmetry breaking and confinement
[DE92-040717] p 978 N93-15657

CHLORIDES
Predicting polymer properties by computational methods 2: A comparison of semi-empirical methods
[AD-A256856] p 854 N93-15640

CHLOROCARBONS
Softening of rigid polyvinyl chloride by high concentrations of aqueous solutions of methylene chloride
[AD-A255453] p 848 N93-14486

CHLOROFLUOROCARBONS
Carbon dioxide induced ocean climatic change and tracer experiment with an atmosphere-ocean general circulation model
p 912 N93-14178

CHOLESTEROL
Characterization of cholesteric cyclic siloxane liquid crystalline materials
[AD-A256128] p 994 N93-15190

CHROMIUM ALLOYS
Application of the square root diffusivity analysis to measuring the diffusivity of multicomponent alloys
[DE92-040978] p 847 N93-15382

CHROMIUM CARBIDES
The effect of processing and compositional changes on the tribology of PM212 in air
[NASA-TM-105945] p 828 N93-15576

CHROMIUM OXIDES
Impact of protective oxides on cathode-side resistances in MCFCs
[DE92-019973] p 994 N93-15221

CHROMOSPHERE
The detection and characterization of high frequency and high wavenumber solar oscillations
[NASA-CR-191622] p 1049 N93-15634

CIRCADIAN RHYTHMS
Sleep inertia: Is there a worst time to wake up?
[AD-A256602] p 934 N93-14240

CIRCUITS
Representation and manipulation of inductive boolean functions
[AD-A256078] p 967 N93-14235

Machine intelligence, a foreword: The brain as electronic circuitry; electronic circuitry as a brain
[AD-A255283] p 962 N93-14533
Computer-aided design package for designers of digital optical computers
[AD-A255381] p 944 N93-14564
A novel, high energy-density electrical storage device for electric weapons
[AD-A255205] p 867 N93-14666
A new multiplier-free structure for DFT based on delta modulation
[AD-A255927] p 861 N93-15106

CIRCULAR CONES
Passive control of supersonic asymmetric vortical flows around cones p 876 N93-14692

CIRCULAR ORBITS
Modeling and control of a trailing wire antenna towed by an orbiting aircraft
[AD-A256450] p 859 N93-14610

CIRCULAR POLARIZATION
High power millimetre-wave polarizers
[AD-A256558] p 867 N93-14803

CIRCULATION
Simulation of vapor compression heat pumps with solution circuits p 872 N93-14200
Management and minimization of photographic wastes at Pantex Plant
[MHSMP-92-01] p 910 N93-14739

CITIES
Multiscale modeling of the long-range transport and fate of pollutants emitted from urban areas p 909 N93-14118

CIVIL AVIATION
Aviation accidents, incidents, and violations: Psychological predictors among US pilots p 783 N93-14693

CLADDING
Characteristics of the Nova laser disk edge cladding epoxy
[DE92-041046] p 853 N93-15462

CLASSICAL MECHANICS
The trajectory analysis of bevel planetary gear trains
[DE92-040898] p 893 N93-15380

CLASSIFICATIONS
Source hierarchy list. Volume 1: A through D
[AD-A256100] p 1001 N93-14265
Can a time-stratigraphic classification system be developed for Venus? p 1043 N93-14388

CLASSIFIERS
A mixed excitation vocoder with fuzzy logic classifier
[AD-A256834] p 864 N93-15636

CLEANING
Ultraviolet-ozone cleaning of semiconductor surfaces, revision 1
[AD-A256158] p 842 N93-14678

CLEAR AIR TURBULENCE
Development and application of a time-space conversion technique for analysis of weather systems passing over the Kennedy Space Center
[NASA-CR-4474] p 924 N93-15581

CLEARANCES
An experimental and analytical study of TIP clearance effects in axial flow compressors
[AD-A256434] p 800 N93-15337

CLIMATE CHANGE
Carbon dioxide induced ocean climatic change and tracer experiment with an atmosphere-ocean general circulation model p 912 N93-14178

CLIMATOLOGY
Extreme climatic events in the Amazon Basin and their associations with the circulation of the global tropics p 918 N93-14115
Cloud fraction, layer, and direction of movement results from sky cameras during the FIRE IFO, Coffeyville, Kansas, experiment for the period Nov. 12 through Dec. 9, 1991
[NASA-TM-107647] p 924 N93-15501

CLIMBING FLIGHT
Estimation of rate of climb
[ESDU-92019] p 791 N93-14541

CLOSED CYCLES
Analytical and experimental investigation of closed-cycle sorption cooling systems p 874 N93-14476
Closed Brayton Cycle power system with a high temperature pellet bed reactor heat source for NEP applications
[NASA-TM-105933] p 826 N93-14482

CLOSURE LAW
Turbulent fluid motion IV-averages, Reynolds decomposition, and the closure problem
[NASA-TM-105822] p 880 N93-15585

CLOTHING
Modeling clothed figures
[AD-A257037] p 940 N93-15363

CLOUD CHAMBERS
Explaining cloud chamber tracks
[DE92-040502] p 972 N93-15057

CLOUD COVER
Cloud-radiative feedbacks in tropical convection p 919 N93-14180
Pioneer Venus polarimetry and haze optical thickness p 1032 N93-14335
Finite amplitude gravity waves in the Venus atmosphere generated by surface topography p 1044 N93-14395
Cloud fraction, layer, and direction of movement results from sky cameras during the FIRE IFO, Coffeyville, Kansas, experiment for the period Nov. 12 through Dec. 9, 1991
[NASA-TM-107647] p 924 N93-15501

CLOUD HEIGHT INDICATORS
Venus mesospheric winds and the carbon monoxide bulge p 1029 N93-14320

CLOUD PHYSICS
Modern methods in meteorological and oceanographic data analysis
[AD-A257080] p 903 N93-15496

CLOUDS (METEOROLOGY)
Infrared radiative properties of clouds p 919 N93-14196
Optimization of a Counterflow Virtual Impactor (CVI) for studying aerosol effects on cloud droplet number p 914 N93-14861
Global survey of effective particle size in liquid water clouds by satellite observations p 921 N93-14862
An investigation into the role of moist, vertical drafts in the rotational development of storms p 923 N93-15087
Cloud fraction, layer, and direction of movement results from sky cameras during the FIRE IFO, Coffeyville, Kansas, experiment for the period Nov. 12 through Dec. 9, 1991
[NASA-TM-107647] p 924 N93-15501

CLUSTER ANALYSIS
Compact objects in the disk and globular clusters p 1018 N93-14594

CLUSTERS
Photodissociation dynamics of cluster ions
[AD-A256375] p 917 N93-15463
C60 interactions with surfaces, gaseous species and photons: An overview
[DE92-040738] p 978 N93-15654

CLUTTER
On the detection of ultrawideband radar signals
[AD-A256075] p 858 N93-14233
Airborne radar simulation with adaptive antenna techniques
[AD-A255460] p 859 N93-14488

COAL GASIFICATION
Contaminant effects in solid oxide fuel cells
[DE92-040255] p 908 N93-15323

COASTAL ZONE COLOR SCANNER
SeaWiFS Technical Report Series. Cloud screening for polar orbiting visible and infrared (IR) satellite sensors, volume 7
[NASA-TM-104566] p 932 N93-15645

COATING
Surface preparation of stainless steel prior to painting
[AD-A256253] p 838 N93-14454
Preliminary investigations of metal liquid-like films and coatings derived from them
[AD-A255477] p 849 N93-14489
Evaluation of corrosion protection methods for aluminum metal matrix composites
[AD-A255375] p 832 N93-14675
Multifilamentary superconducting cable and a method of manufacturing it
[AD-D015391] p 846 N93-15231
Thermal analysis of magnetron sputtering designs
[DE93-000348] p 870 N93-15389
Sputter deposition and characterization of MoSi2/SiC composite coatings
[DE92-040326] p 837 N93-15426

COBALT ALLOYS
Thin-film permanent magnets for integrated electromagnetic components
[AD-A256175] p 972 N93-14679

COBALT 60
Improvement and analysis of the radiation response of RADFET dosimeters
[AD-A254115] p 869 N93-15133

COCKPITS
Development of measures of crew coordination
[AD-A255384] p 939 N93-14651
Does cockpit management training reduce aircrew error? p 785 N93-15014
Cockpit decision making p 786 N93-15015
Trans-cockpit authority gradient in Navy/Marine aircraft mishaps p 786 N93-15016
Simulator evaluation of displays for a revised takeoff performance monitoring system
[NASA-TP-3270] p 803 N93-15366

CODING
Stability and adaptation of neural networks
[AD-A256227] p 962 N93-14598

COEFFICIENTS
Undetermined coefficient problems for quasi-linear parabolic equations
[AD-A256012] p 969 N93-15256

COERCIVITY
Corrosion of metal particle and metal evaporated tapes p 883 N93-15039

COGNITION
Analysis of symbolic models of cognition project (ASPM-Pitt)
[AD-A255929] p 962 N93-14656
A planning workshop: To strengthen American cognitive science for the twenty-first century
[NSF-92-4] p 999 N93-14720
Cognition and the brain
[AD-A255483] p 937 N93-14788
Enhanced Aeronautical Resource Management training alternatives p 786 N93-15019
A cognitive model for training decision making in aircrews p 786 N93-15020
Elements of a theory of natural decision making p 786 N93-15021

COGNITIVE PSYCHOLOGY
A psychometrically sound cognitive diagnostic model: Effect of remediation as empirical validity
[AD-A255926] p 933 N93-14109
Knowledge and processes in design
[AD-A255663] p 999 N93-14130
Information-seeking behavior during the decision-making process: A case study p 1000 N93-14206
A planning workshop: To strengthen American cognitive science for the twenty-first century
[NSF-92-4] p 999 N93-14720
How expert pilots think p 786 N93-15017

COHERENT LIGHT
Interferometer with two phase-conjugate mirrors
[AD-D015420] p 982 N93-14800

COHERENT RADAR
Solid-state coherent laser radar wind shear measuring systems p 784 N93-14848

COHERENT RADIATION
The dynamics of spatially extended lasers p 883 N93-14123
Generation of broadly tunable, narrow bandwidth, and intense coherent vacuum ultraviolet radiation in rare gases p 980 N93-14167

COHERENT SCATTERING
Lineshape analysis of laser light scattered by an argon thermal plasma jet p 987 N93-14137

COLD FRONTS
Structure and propagation of fronts east of the Rocky Mountains and their relationship to precipitation p 921 N93-14827

COLD ROLLING
Processing and microstructure of Nb-1 percent Zr-0.1 percent C alloy sheet
[NASA-TM-105921] p 847 N93-15524

COLLIMATORS
Imaging the sun in hard x rays using Fourier telescopes
[NASA-TM-108390] p 1013 N93-15203

COLLISION PARAMETERS
Modeling clothed figures
[AD-A257037] p 940 N93-15363

COLLISION RATES
Atomic data and spectral analysis of carbon, nitrogen, oxygen and silicon ions observed with the International Ultraviolet Explorer
[NASA-CR-191302] p 1012 N93-14761
Electron density diagnostics for gaseous nebulae involving the O 4 intercombination lines near 1400 A p 1012 N93-14762

COLLISIONS
Airbus Industrie TCAS experience p 789 N93-15186

COLLOCATION
Interplanetary Program to Optimize Simulated Trajectories (IPOST). Volume 1: User's guide
[NASA-CR-189653-VOL-1-REV] p 815 N93-14794

COLLOIDS
Diffusing wave spectroscopy p 980 N93-14169

COLOR
Method and apparatus for a high resolution, flat panel cathodoluminescent display screen
[AD-D015400] p 868 N93-15107

COLOR CENTERS
Color center laser with transverse auxiliary illumination
[AD-D015387] p 887 N93-15250

COLOR VISION
Performance of color-dependent tasks of air traffic control specialists as a function of type and degree of color vision deficiency
[AD-A256614] p 788 N93-14275
Adaptive mesh in visualization of terrain elevation data
[AD-A255481] p 906 N93-15007

Higher order mechanisms of color vision
[AD-A256369] p 938 N93-15329

COMBAT
Walter Reed Army Institute of Research biannual report
[AD-A255630] p 933 N93-14162
Audio detection algorithms
[AD-A256076] p 973 N93-14234

COMBINATORIAL ANALYSIS
A massively distributed parallel genetic algorithm
[AD-A256617] p 959 N93-15407

COMBUSTIBLE FLOW
Transport phenomena and interfacial kinetics in multiphase combustion systems.
[AD-A255999] p 838 N93-14418
Combustion in supersonic flows p 841 N93-14627
Chemical reactions in turbulent mixing flows
[AD-A256004] p 842 N93-15114

COMBUSTION CHAMBERS
Simplified jet-A kinetic mechanism for combustor application
[NASA-TM-105940] p 844 N93-15504

COMBUSTION CHEMISTRY
Transport phenomena and interfacial kinetics in multiphase combustion systems.
[AD-A255999] p 838 N93-14418
Modeling of Combustion and Turbulence
[VKI-LS-1992-03] p 839 N93-14617
Chemical kinetics for combustion p 840 N93-14619
Calculation of chemical reaction rates in turbulent combustion p 841 N93-14625

COMBUSTION CONTROL
Active control of combustion instability in a ramjet using large-eddy simulations
[AD-A255226] p 798 N93-14111

COMBUSTION PHYSICS
Modeling of Combustion and Turbulence
[VKI-LS-1992-03] p 839 N93-14617
Fundamentals of combustion of premixed gases p 840 N93-14618
Chemical kinetics for combustion p 840 N93-14619
Turbulence modeling for combustion flows p 840 N93-14620
Radiative heat transfer in combustion systems p 840 N93-14621
Direct simulation of turbulent combustion p 840 N93-14622
PDF transport modelling p 840 N93-14623
Introduction to spray combustion modelling p 841 N93-14626
Combustion in supersonic flows p 841 N93-14627
Investigation of the aerothermodynamics of hypervelocity reacting flows in the ram accelerator
[NASA-CR-191715] p 783 N93-15588

COMBUSTION PRODUCTS
Absorption of propellant vapors into polymer films
[AD-A255274] p 849 N93-14531

COMBUSTION STABILITY
Active control of combustion instability in a ramjet using large-eddy simulations
[AD-A255226] p 798 N93-14111
Fundamentals of combustion of premixed gases p 840 N93-14618

COMET NUCLEI
Physical and chemical processes of the inner coma observed in mid-ultraviolet cometary spectra p 1017 N93-14230

COMETARY ATMOSPHERES
Analysis of CCD images of the coma of comet P/Halley
[NASA-CR-191384] p 1020 N93-14814

COMETS
Computer simulations of comet- and asteroidlike bodies passing through the Venusian atmosphere: Preliminary results on atmospheric and ground shock effects p 1040 N93-14365

COMMAND AND CONTROL
Military space operations: Satellite control system improved, but serious problems remain
[AD-A256809] p 971 N93-15626

COMMAND GUIDANCE
Digital bank-to-turn control and guidance p 802 N93-14447

COMMERCE
EDI planning and implementation guide
[AD-A255737] p 1007 N93-15050
The information age as a work in progress: Implications for technical communicators
[DE92-019780] p 1008 N93-15275

COMMERCIAL AIRCRAFT
Development of the Advance Warning Airborne System(AWAS) p 784 N93-14849
Monitoring of powerplants in advanced commercial aircraft p 795 N93-15171
Ice accretion prediction for a typical commercial transport aircraft
[NASA-TM-105976] p 788 N93-15522

COMMUNICATING
The changing culture of science: Bringing it into balance
[AD-A255993] p 998 N93-14417

COMMUNICATION
Implementation issues concerning injection simulation. Part 1: The backbone implementation
[MEMO-INF-91-57-PT-1] p 946 N93-15078
The information age as a work in progress: Implications for technical communicators
[DE92-019780] p 1008 N93-15275
A queue model relating synchronous and asynchronous communication
[MEMO-INF-92-04] p 966 N93-15491

COMMUNICATION NETWORKS
Multi-access strategies for voice/data integration in heterogeneous mixed-media packet radio networks
[AD-A255636] p 857 N93-14181
Engineering of massively interconnected computer systems
[AD-A255501] p 958 N93-14645
Next generation satellite communications networks p 812 N93-14962
The role of HiPPI switches in mass storage systems: A five year prospective p 1006 N93-15044
The evolution of signalling from ISDN to B-ISDN
[MEMO-INF-92-30] p 860 N93-15095
Integration of satellite links into an ATM mode broadband ISDN
[TELECOM-PARIS-91-E-022] p 861 N93-15097
Telepresence: Integrating shared task and person spaces p 954 N93-15548

COMMUNICATION SATELLITES
A low bit rate FSK technique for SCPC satellite communication systems p 811 N93-14954
Progress toward a full scale mobile satellite system for Canada p 812 N93-14960
Next generation satellite communications networks p 812 N93-14962
On-orbit deployment anamolies: What can be done? p 821 N93-15603

COMMUNICATION THEORY
On the theory of coded modulation systems for high output digital transmission
[TELECOM-PARIS-92-E-001] p 861 N93-15098

COMPACTING
Deformation characterization of powdered metals in compaction and application of the finite element method to compaction processes p 844 N93-14472
Compaction of submicron and nanocrystalline Al2O3-ZrO2 ceramics
[DE92-040233] p 852 N93-15320

COMPARISON
Different types of small volcanos on Venus p 1042 N93-14378

COMPENSATORS
A power compensation system for phased operation of the JET A2 antenna arrays
[DE92-041020] p 863 N93-15440

COMPILERS
Design and implementation of practical constraint logic programming systems
[AD-A256191] p 943 N93-14558
A non-deterministic recogniser generator
[MEMO-INF-92-21] p 946 N93-15091
Optimal synthesis methods for silicon compilers
[ETN-92-92677] p 947 N93-15125

COMPLEX SYSTEMS
A monitoring and control system for complex man-machine systems: Preliminary design p 810 N93-14951
Automated coding and intersecting cube theory
[ETN-92-92675] p 941 N93-15123

COMPONENT RELIABILITY
Electronics reliability fracture mechanics. Volume 1: Causes of failures of shop replaceable units and hybrid microcircuits
[AD-A255836] p 894 N93-14104
Electronics reliability fracture mechanics. Volume 2: Fracture mechanics
[AD-A256200] p 900 N93-14498
Reliability techniques for combined hardware and software systems
[AD-A256347] p 895 N93-15204

COMPOSITE MATERIALS
Application of gel-silica optics to laser technology and optical element fabrication
[AD-A255666] p 883 N93-14131
Modeling of the thermal elasto-plastic behavior for composite materials using the homogenization method p 830 N93-14466
Proceedings of the USAF Structural Integrity Program
[AD-A255379] p 777 N93-14549
Core design for use with precision composite reflectors
[NASA-CASE-NPO-17858-1-CU] p 832 N93-14700
Fabrication of high temperature materials by exothermic synthesis and subsequent dynamic consolidation
[DE92-019836] p 834 N93-14819
Thermal, mechanical, and electroelastic behavior of composite materials p 835 N93-15146
Material development in the Si3N4 system using glass encapsulated HIP'ing
[DE92-041381] p 837 N93-15388
The effect of processing and compositional changes on the tribology of PM212 in air
[NASA-TM-105945] p 828 N93-15576
Operational strategies for contamination control of composite materials p 822 N93-15614

COMPOSITE STRUCTURES
Analysis of advanced thin-walled composite structures p 895 N93-14158
Modal interactions in the dynamic response of isotropic and composite plates p 829 N93-14221
Fracture mechanisms and fracture control in composite structures p 899 N93-14474
Reliability of stiffened structural panels: Two examples
[NASA-TM-107687] p 900 N93-14483
FIBER-TEX 1991: The Fifth Conference on Advanced Engineering Fibers and Textile Structures for Composites
[NASA-CP-3176] p 832 N93-14744
Progress toward a tungsten alloy wire/high temperature alloy composite turbine blade
[NASA-TM-105901] p 847 N93-15586

COMPRESSIBILITY
Fracture mechanisms and fracture control in composite structures p 899 N93-14474

COMPRESSIBLE FLOW
Three-dimensional computational study of asymmetric flows using Navier-Stokes equations
[ISBN-90-5410-029-X] p 875 N93-14690
An integral equation solution for multistage turbomachinery design calculations
[NASA-TM-105970] p 801 N93-15521

COMPRESSING
Simulation of vapor compression heat pumps with solution circuits p 872 N93-14200

COMPRESSION LOADS
Analysis and optimal design of pressurized, imperfect, anisotropic ring-stiffened cylinders p 897 N93-14251
Kind-band failure analysis of thick composites in compression
[AD-A255431] p 831 N93-14509
The stress development during filament winding of thick cylinders
[AD-A255765] p 901 N93-15066

COMPRESSION WAVES
Remote techniques for time-of-flight flaw characterisation p 989 N93-14171

COMPRESSIVE STRENGTH
Reanalysis of multiple-wheel landing gear traffic tests
[AD-A256593] p 804 N93-14238
Kind-band failure analysis of thick composites in compression
[AD-A255431] p 831 N93-14509

COMPRESSOR EFFICIENCY
Variable speed rotary compressor and adjustable speed drive efficiencies measured in the laboratory
[DE92-040026] p 893 N93-15278

COMPRESSOR ROTORS
Propulsion and Energetics Panel Working Group 20 on Test Cases for Engine Life Assessment Technology
[AGARD-AR-308] p 798 N93-14890
Introduction to test cases for engine life assessment technology p 799 N93-14891
CF6-6 high pressure compressor stage 5 locking slot crack propagation spin pit test p 799 N93-14894
F100 second stage fan disk bolthole crack propagation ferris wheel test p 800 N93-14897

COMPRESSORS
RB 199 high pressure compressor stage 3 spin pit tests p 799 N93-14893
Engine life assessment test case TF41 LP compressor shaft torsional fatigue p 799 N93-14896
Variable speed rotary compressor and adjustable speed drive efficiencies measured in the laboratory
[DE92-040026] p 893 N93-15278

COMPTON EFFECT
A liquid xenon imaging telescope for gamma ray astrophysics: Design and expected performance p 1014 N93-15591

COMPUTATION
Goals versus algorithms
[AD-A256106] p 942 N93-14237
Calculation methods for externally pressurised (hydrostatic) journal bearings with capillary restrictor control
[ESDU-92026] p 889 N93-14543

COMPUTATIONAL CHEMISTRY
An investigation of transient atmospheric inorganic peroxides: A theoretical and experimental study p 912 N93-14117
Computed potential energy surfaces for chemical reactions
[NASA-CR-190741] p 843 N93-15356
Theoretical characterization of the potential energy surface for NH + NO
[NASA-CR-190741] p 843 N93-15357
Predicting polymer properties by computational methods 2: A comparison of semi-empirical methods
[AD-A256856] p 854 N93-15640

COMPUTATIONAL FLUID DYNAMICS
An algebraic turbulence model for three-dimensional viscous flows
[NASA-TM-105931] p 777 N93-14102
Active control of combustion instability in a ramjet using large-eddy simulations
[AD-A255226] p 798 N93-14111
A study of viscous interaction effects on hypersonic waveriders p 778 N93-14160
Simulation of unsteady inviscid flow on an adaptively refined Cartesian grid p 873 N93-14273
Transonic flow calculations for a cavity with and without a store
[AD-A255954] p 873 N93-14421
Feedback control of flow separation and transition to turbulence in unsteady boundary layers p 873 N93-14464
Pressure drag and lift contributions for blunted forebodies of fineness ratio 2.0 in transonic flow (M infinity less than or equal to 1.4)
[ESDU-89033] p 779 N93-14515
Direct prediction of a separation boundary for aerofoils using a viscous-coupled calculation method
[ESDU-92008] p 780 N93-14516
Modeling of Combustion and Turbulence
[VKI-LS-1992-03] p 839 N93-14617
Direct simulation of turbulent combustion p 840 N93-14622
Applications of PDF turbulent combustion models to real non premixed flame calculations p 841 N93-14624
Recent advances in numerical simulation and control of asymmetric flows around slender bodies
[PAPER-W.1.2] p 875 N93-14688
Shock/vortex interaction and vortex-breakdown modes
[PAPER-T.1.3] p 875 N93-14689
Three-dimensional computational study of asymmetric flows using Navier-Stokes equations
[ISBN-90-5410-029-X] p 875 N93-14690
Numerical simulation of steady and unsteady asymmetric vortical flow p 876 N93-14691
Passive control of supersonic asymmetric vortical flows around cones p 876 N93-14692
An investigation of genuinely multidimensional schemes for the Euler equations p 876 N93-14694
Supersonic boundary-layer flow turbulence modeling
[NASA-TM-105893] p 877 N93-14758
Preconditioned conjugate-gradient methods for low-speed flow calculations
[NASA-TM-105929] p 877 N93-14885
Dynamics systems applied to Navier-Stokes equations for the study of turbulence
[ETN-92-92553] p 878 N93-15122
The 3D Navier-Stokes flow analysis for shared and distributed memory MIMD computers
[AD-A256038] p 878 N93-15187
The Applicaiton of CFD to rotary wing flow problems
[NASA-TM-102803] p 782 N93-15483
Numerical modeling tools for chemical vapor deposition
[NASA-CR-4480] p 880 N93-15643

COMPUTATIONAL GEOMETRY
Interactive solid geometry via partitioning trees p 952 N93-15535
Parameterization in finite precision p 953 N93-15537

COMPUTATIONAL GRIDS
Simulation of unsteady inviscid flow on an adaptively refined Cartesian grid p 873 N93-14273
Transonic flow calculations for a cavity with and without a store
[AD-A255954] p 873 N93-14421
Adaptive mesh in visualization of terrain elevation data
[AD-A255481] p 906 N93-15007
A multigrid approach to embedded-grid solvers
[AD-A256405] p 879 N93-15332

COMPUTER AIDED DESIGN
Weight optimum arch structures
[AD-A256080] p 897 N93-14236
DESAID (the development of an expert system for aircraft initial design) p 790 N93-14448
An integrated optimization environment for structural configuration design p 855 N93-14467
A methodology for the evaluation of structural design software for DOS-based microcomputers
[AD-A255421] p 943 N93-14505
Computer based satellite design
[AD-A255315] p 816 N93-14536
Computer-aided design package for designers of digital optical computers
[AD-A255381] p 944 N93-14564
Optimal synthesis methods for silicon compilers
[ETN-92-92677] p 947 N93-15125
Proceedings of the International Conference on CAD/CAM and AMT. Volume 4: VHDL (VHSIC Hardware Description Language) Seminar
[ITN-92-85130] p 947 N93-15261
VHDL (VHSIC hardware description language): Origins, status, capabilities, and world environment
[VH-1] p 947 N93-15262
VHDL (VHSIC hardware description language) use in the US defense procurement process
[VH-2] p 948 N93-15263
The extended VHDL (VHSIC hardware description language) design environment: An unique integrated system and hardware design environment
[VH-3] p 948 N93-15264
System design in a large corporation, using VHDL (VHSIC hardware description language)
[VH-4] p 948 N93-15265
Synthesis and simulation with VHDL (VHSIC hardware description language)
[VH-5] p 948 N93-15266
VHDL (VHSIC hardware description language) in the test environment
[VH-6] p 948 N93-15267
Integrating VHDL (VHSIC hardware description language) with existing EDA tools
[VH-8] p 948 N93-15268
Proceedings of the International Conference on CAD/CAM and AMT. Volume 3: IFIP (International Federation of Information Processing)/Robotics: International Sessions on Robots and Assembly
[ITN-92-85129] p 949 N93-15298
Development of an analog MIMO Quantitative Feedback Theory (QFT) CAD package
[AD-A256435] p 950 N93-15313
A method of representating dimensions and tolerances in solid based freeform surfaces
[PNR-90998] p 951 N93-15386

COMPUTER AIDED MANUFACTURING
Proceedings of the International Conference on CAD/CAM and AMT. Volume 3: IFIP (International Federation of Information Processing)/Robotics: International Sessions on Robots and Assembly
[ITN-92-85129] p 949 N93-15298
CAD-based off-line programming and sensor signal processing in robotics
[F-2-2] p 949 N93-15299
Methodology for robot capability and performance characterization: The basis for robot task planningg
[F-2-3] p 949 N93-15300
Off-line generation of error-free robot/NC (numerical control) code using simulation and automatic programming techniques
[F-3-1] p 949 N93-15302

COMPUTER AIDED MAPPING
Terrain visualization for the portable all-source analysis work station
[AD-A255708] p 905 N93-14430

COMPUTER AIDED TOMOGRAPHY
Personal computer based computed tomography system
[KCP-613-4806] p 945 N93-14876

COMPUTER ANIMATION
Software for flight recorder data evaluation developed by Lufthansa p 794 N93-15163
The FAIR (Flight Animated and Interactive Reconstruction) tool p 788 N93-15164
CAD-based off-line programming and sensor signal processing in robotics
[F-2-2] p 949 N93-15299
A framework for describing and implementing software visualization systems p 953 N93-15540
Object space temporal coherence for ray tracing p 955 N93-15554
Physically-based methods for polygonization of implicit surfaces p 956 N93-15562
Matrix animation and polar decomposition p 956 N93-15563
Generating natural-looking motion for computer animation p 956 N93-15564
Beyond keyframing: An algorithmic approach to animation p 957 N93-15565

COMPUTER ASSISTED INSTRUCTION
Development of a MATLAB toolbox for image processing
[AD-A256130] p 942 N93-14247

COMPUTER COMPONENTS
Synthesis and simulation with VHDL (VHSIC hardware description language)
[VH-5] p 948 N93-15266

COMPUTER DESIGN
An examination of wing rock for the F-15
[AD-A256613] p 802 N93-14252
Processor controlpath microarchitecture synthesis based on the A(asterisk) algorithm
[MEMO-INF-92-10] p 963 N93-15083

COMPUTER GRAPHICS
Mapping thoughts: Visual interfaces for information retrieval p 1000 N93-14208
Data management and processing plan, Department of Applied Geodesy
[DE93-000774] p 905 N93-14522
A distributed visualization environment for engineering sciences
[DE92-012629] p 1051 N93-15060
Modeling clothed figures
[AD-A257037] p 940 N93-15363
Simulator evaluation of displays for a revised takeoff performance monitoring system
[NASA-TP-3270] p 803 N93-15366
Proceedings: Graphics Interface 1992
[ISBN-0-9695338-1-0] p 952 N93-15533
An implementation of multivariate B-spline surfaces over arbitrary triangulations p 952 N93-15534
Interactive solid geometry via partitioning trees p 952 N93-15535
Fast algorithms for rendering cubic curves p 953 N93-15536
Hyper-rendering p 953 N93-15538
A framework for describing and implementing software visualization systems p 953 N93-15540
Volume rendering using the Fourier projection-slice theorem p 953 N93-15541
An extended cuberille model for identification and display of 3D objects from 3D gray value data p 953 N93-15542
Algorithms for the detection and elimination of specular aliasing p 954 N93-15544
Hierarchical Poisson disk sampling distributions p 954 N93-15545
Performing in-place affine transformations in constant space p 954 N93-15546
Working together, virtually p 954 N93-15547
Telepresence: Integrating shared task and person spaces p 954 N93-15548
ARCBALL: A user interface for specifying three-dimensional orientation using a mouse p 955 N93-15551
A data parallel algorithm for raytracing of heterogeneous databases p 955 N93-15553
Object space temporal coherence for ray tracing p 955 N93-15554
Ray tracing polygons using spatial subdivision p 955 N93-15555
Parametric height field ray tracing p 955 N93-15556
Partitioning tree image representation and generation from 3D geometric models p 955 N93-15557
Escape-time visualization method for language-restricted iterated function systems p 956 N93-15558
The object instancing paradigm for linear fractal modeling p 956 N93-15559
Algorithms for intersecting parametric and algebraic curves p 956 N93-15560
An interval refinement technique for surface intersection p 956 N93-15561
Physically-based methods for polygonization of implicit surfaces p 956 N93-15562
Matrix animation and polar decomposition p 956 N93-15563
Generating natural-looking motion for computer animation p 956 N93-15564
Beyond keyframing: An algorithmic approach to animation p 957 N93-15565
A minimalist global user interface p 957 N93-15566
A multi-layer graphic model for building interactive graphical applications p 957 N93-15567
A linear constraint technology for interactive graphic systems p 957 N93-15568
Non-uniform patch luminance for global illumination p 957 N93-15569
A two-pass physics-based global lighting model p 957 N93-15570

COMPUTER NETWORKS
Application of partition matrix methods to solve large eigenproblems in structural dynamics p 896 N93-14188
Network issues for large mass storage requirements p 1002 N93-14773
The role of HiPPI switches in mass storage systems: A five year prospective p 1002 N93-14774

Storage needs in future supercomputer environments p 1003 N93-14780
File servers, networking, and supercomputers p 1004 N93-15030
Network accessible multi-terabyte archive p 1005 N93-15036
The role of HiPPI switches in mass storage systems: A five year prospective p 1006 N93-15044
Requirements for a network storage service p 1007 N93-15048
A distributed visualization environment for engineering sciences
[DE92-012629] p 1051 N93-15060
A deadlock-free communication system for a transputer network
[AD-A256473] p 959 N93-15319
User manual for the Software Technology for Adaptable, Reliable Systems (STARS). PCTE Browser Tool (PBT) version 0.1 SunOS implementation
[AD-A257064] p 951 N93-15457
Physical design for network databases
[MEMO-INF-92-26] p 1009 N93-15492
Proposal for massively parallel data storage system p 960 N93-15510
Telepresence: Integrating shared task and person spaces p 954 N93-15548

COMPUTER PROGRAM INTEGRITY

Development of an environment for software reliability model selection
[AD-A256609] p 942 N93-14241
Software reliability, measurement, and testing software reliability and test integration, volume 1
[AD-A256242] p 944 N93-14572
Software reliability, measurement, and testing. Volume 2: Guidebook for software reliability measurement and testing
[AD-A256164] p 944 N93-14581

COMPUTER PROGRAMMING

Ada-based multitasking terminal I/O
[AD-A255656] p 942 N93-14164
Development of a MATLAB toolbox for image processing
[AD-A256130] p 942 N93-14247
A concurrent real-time autonomous mobile robot programming system p 960 N93-14281
Software Technology for Adaptable, Reliable Systems (STARS) program. Software process tools and techniques evaluation report, version 1.0. Task IS15: Software process management
[AD-A255945] p 942 N93-14405
Iterative software testing
[AD-A255953] p 943 N93-14420
The 1992 Summer SIGAda AIWG Workshop applications experiences and lessons learned panel message from the panel chair
[AD-A256188] p 962 N93-14519
Computer based satellite design
[AD-A255315] p 816 N93-14536
Design and implementation of practical constraint logic programming systems
[AD-A256191] p 943 N93-14558
VANTAGE: A frame-based geometric modeling system programmer/user's manual, V2.0
[AD-A255434] p 944 N93-14566
Using an interior point cutting plane method to solve integer programming problems
[AD-A256041] p 945 N93-14659
Software requirements for the A-7E aircraft
[AD-A255746] p 946 N93-15052
From data structure to process structure
[MEMO-INF-91-38] p 946 N93-15077
Research in programming languages and software engineering
[AD-A256341] p 947 N93-15199
Reliability techniques for combined hardware and software systems
[AD-A256347] p 895 N93-15204
Work efficient hashing on parallel and vector computers
[AD-A256355] p 959 N93-15205
Experience with a course on architectures for software systems. Part 1: Course description
[AD-A256221] p 941 N93-15239
Query optimization and planning in object-oriented knowledge bases
[AD-A256006] p 1008 N93-15254
Off-line generation of error-free robot/NC (numerical control) code using simulation and automatic programming techniques
[F-3-1] p 949 N93-15302
Proceedings of the REXX Symposium for Developers and Users
[DE92-041359] p 951 N93-15451
Flight dynamics system software development environment (FDS/SDE) tutorial
[NASA-TM-108580] p 952 N93-15502
Hyper-rendering p 953 N93-15538
Program auralization: Sound enhancements to the programming environment p 953 N93-15539
A framework for describing and implementing software visualization systems p 953 N93-15540
A minimalist global user interface p 957 N93-15566
Software Management Environment (SME) installation guide
[NASA-TM-108578] p 957 N93-15578
Data collection procedures for the Software Engineering Laboratory (SEL) database
[NASA-TM-108579] p 957 N93-15579

COMPUTER PROGRAMS

Development of an environment for software reliability model selection
[AD-A256609] p 942 N93-14241
Extended surface heat sinks for electronic components: A computer optimization
[AD-A256134] p 865 N93-14254
Software Technology for Adaptable, Reliable Systems (STARS) program. Software process tools and techniques evaluation report, version 1.0. Task IS15: Software process management
[AD-A255945] p 942 N93-14405
Iterative software testing
[AD-A255953] p 943 N93-14420
A specification of the Soar cognitive architecture in Z
[AD-A256198] p 940 N93-14491
The human-electronic crew: Is the team maturing? The 2nd Joint GAF/RAF/USAF Workshop on Human-Electronic Crew Teamwork
[AD-A256192] p 939 N93-14520
Geographic Resources Analysis Support System (GRASS) version 4.0 user's reference manual
[AD-A255218] p 1001 N93-14524
Computer based satellite design
[AD-A255315] p 816 N93-14536
Software reliability, measurement, and testing software reliability and test integration, volume 1
[AD-A256242] p 944 N93-14572
Software reliability, measurement, and testing. Volume 2: Guidebook for software reliability measurement and testing
[AD-A256164] p 944 N93-14581
Spectral analysis of the shuttle glow: AIS science support
[PL-TR-92-2172] p 815 N93-14698
Information systems for airport operations
[TT-9202] p 789 N93-14729
NSSDC Conference on Mass Storage Systems and Technologies for Space and Earth Science Applications, volume 3
[NASA-CP-3165-VOL-3] p 1002 N93-14771
Autonomous power system brassboard
[NASA-CR-189115] p 867 N93-14798
SAFSIM: A computer program for engineering simulations of space reactor system performance
[DE92-016328] p 826 N93-14815
Energy loss analysis of an integrated space power distribution system
[NASA-TM-105772] p 854 N93-14834
Advances in TMG p 811 N93-14956
Automated Estimating System (AES), version 5.1. User's manual
[DE93-000380] p 946 N93-15003
Adaptive mesh in visualization of terrain elevation data
[AD-A255481] p 906 N93-15007
Advanced development active model: A users guide
[AD-A255614] p 974 N93-15012
Storage needs in future supercomputer environments p 1007 N93-15047
Software requirements for the A-7E aircraft
[AD-A255746] p 946 N93-15052
SIDR Relative Weighted Product (RWP) assignment process
[AD-A255801] p 946 N93-15068
Sonar processing on CESAR
[FFI-92/7007] p 974 N93-15074
Evaluation of methods for estimating wind wave growth on narrow irregular fetches
[AD-A256002] p 932 N93-15113
Software flexibility and configuration control for the A340/A330 Aircraft Condition Monitoring System (ACMS) p 793 N93-15154
Software for flight recorder data evaluation developed by Lufthansa p 794 N93-15163
Reliability techniques for combined hardware and software systems
[AD-A256347] p 895 N93-15204
A temperature tracking SPICE2G.6 macromodel of the 6N134 optocoupler
[DE92-040093] p 983 N93-15223
Independent validation testing of the FLAME computer code, version 1.0
[DE92-019691] p 948 N93-15274
Development of an analog MIMO Quantitative Feedback Theory (QFT) CAD package
[AD-A256435] p 950 N93-15313
Root damage analysis of aircraft engine blade subject to ice impact
[NASA-TM-105779] p 902 N93-15343
Numerical modeling of anti-icing systems and comparison to test results on a NASA 0012 airfoil
[NASA-TM-105975] p 787 N93-15345
Ice accretion and performance degradation calculations with LEWICE/NS
[NASA-TM-105972] p 787 N93-15354
High-resolution contrast control on a video display: Method and calibration
[AD-A256552] p 938 N93-15400
Advancements in the LEWICE ice accretion model
[NASA-CR-191019] p 879 N93-15402
Progress on the development of a 2-D PIC/Monte Carlo model of glow discharges
[DE92-040226] p 989 N93-15422
Deterministic transfer function for transionospheric propagation
[DE92-040327] p 862 N93-15427
Development of NASA/DOE NTP system performance models
[NASA-TM-105982] p 827 N93-15428
Finite-difference solution for laminar or turbulent boundary layer flow over axisymmetric bodies with ideal gas, CF4, or equilibrium air chemistry
[NASA-TP-3271] p 879 N93-15434
Software Technology for Adaptable, Reliable Systems (STARS)
[AD-A257022] p 952 N93-15471
Modeling limits of the EMV analysis program CONCEPT by example of the influence of a helicopter structure on a frame antenna
[MBB-UD-0614-92-PUB] p 863 N93-15487
Mathematical software under UNICOS at LCC
[DE93-001828] p 952 N93-15493
A modal analysis of lamellar diffraction gratings in conical mountings p 986 N93-15519
Ice accretion prediction for a typical commercial transport aircraft
[NASA-TM-105976] p 788 N93-15522
A framework for describing and implementing software visualization systems p 953 N93-15540
Numerical modeling tools for chemical vapor deposition
[NASA-CR-4480] p 880 N93-15643

COMPUTER STORAGE DEVICES

Long term stability in thin film ferroelectric memories
[AD-A256290] p 991 N93-14439
High speed magneto-resistive random access memory
[NASA-CASE-NPO-17954-1-CU] p 940 N93-14704
Network issues for large mass storage requirements p 1002 N93-14773
The role of HiPPI switches in mass storage systems: A five year prospective p 1002 N93-14774
Status of emerging standards for removable computer storage media and related contributions of NIST p 1003 N93-14778
Storage needs in future supercomputer environments p 1003 N93-14780
Ultra-dense optical mass storage
[AD-A255463] p 1004 N93-14785
Stewardship of very large digital data archives p 1005 N93-15032
Storage needs in future supercomputer environments p 1007 N93-15047
Transactional distributed shared memory
[AD-A256222] p 941 N93-15240

COMPUTER SYSTEMS DESIGN

The evolution of artificial intelligence and expert computer systems in the Army
[AD-A255221] p 962 N93-14525
Fault tolerant systems practitioner's workshop
[AD-A255376] p 944 N93-14563
Computer-aided design package for designers of digital optical computers
[AD-A255381] p 944 N93-14564
Design and hardware implementation of neural systems
[AD-A256040] p 866 N93-14577
An active tactile perception system p 805 N93-14926
Vision development test bed: The cradle of the MSS artificial vision system p 810 N93-14948
Requirements for a network storage service p 1007 N93-15048
PRISMA/DB: A parallel, main-memory relational DBMS
[MEMO-INF-92-12] p 959 N93-15141
Continuing engineering education for software engineering professionals
[DE92-019888] p 947 N93-15225

System design in a large corporation, using VHDL (VHSIC hardware description language)
[VH-4] p 948 N93-15265
An eclectic method for object oriented database design
[AD-A256439] p 1008 N93-15315
Physical design for network databases
[MEMO-INF-92-26] p 1009 N93-15492
A minimalist global user interface p 957 N93-15566
A new approach for data acquisition at the JPL space simulators p 821 N93-15606

COMPUTER SYSTEMS PERFORMANCE
Development of an environment for software reliability model selection
[AD-A256609] p 942 N93-14241
Upgrade the University of Wisconsin volume imaging lidar
[AD-A255476] p 885 N93-14497
Implementation issues concerning injection simulation. Part 1: The backbone implementation
[MEMO-INF-91-57-PT-1] p 946 N93-15078
Sensitivity and uncertainty analysis in performability modelling
[MEMO-INF-92-18] p 941 N93-15090
Parallelism in a main-memory DBMS: The performance of PRISMA/DB
[MEMO-INF-92-25] p 958 N93-15093
Approximate performability analysis using generalized stochastic Petri nets
[MEMO-INF-92-11] p 971 N93-15119

COMPUTER SYSTEMS PROGRAMS
Hyper-rendering p 953 N93-15538

COMPUTER SYSTEMS SIMULATION
Proceedings of the International Conference on CAD/CAM and AMT. Volume 4: VHDL (VHSIC Hardware Description Language) Seminar
[ITN-92-85130] p 947 N93-15261
Synthesis and simulation with VHDL (VHSIC hardware description language)
[VH-5] p 948 N93-15266

COMPUTER TECHNIQUES
The evolution of artificial intelligence and expert computer systems in the Army
[AD-A255221] p 962 N93-14525
The relationship between computer scoring and safety-pilot grading of flight performance
[AD-A256245] p 937 N93-14600
Mission critical system development: Design views and their integration
[AD-A255498] p 940 N93-14644
SIDR Relative Weighted Product (RWP) assignment process
[AD-A255801] p 946 N93-15068
MATE: The multi-agent test environment
[NASA-TM-108114] p 965 N93-15292

COMPUTER VISION
Neural network retinal model real time implementation
[AD-A255652] p 934 N93-14210
Geometric invariants and object recognition
[AD-A255317] p 943 N93-14546
VANTAGE: A frame-based geometric modeling system programmer/user's manual, V2.0
[AD-A255434] p 944 N93-14566
Design and hardware implementation of neural systems
[AD-A256040] p 866 N93-14577
Parametric study of diffusion-enhancement networks for spatiotemporal grouping in real-time artificial vision
[AD-A256059] p 937 N93-14580
Real-time gaze holding in binocular robot vision
[AD-A256226] p 982 N93-14582
The perception of articulated motion: Recognizing moving light displays
[AD-A256046] p 937 N93-14660
Vision system requirements and concept for the Special Purpose Dexterous Manipulator system (SPDM) p 805 N93-14924
Vision development test bed: The cradle of the MSS artificial vision system p 810 N93-14948
Neural network architectures for general image recognition
[AD-A256017] p 964 N93-15258

COMPUTERIZED SIMULATION
Technology reconciliation in the remote sensing era of US civilian weather forcasting: 1957 - 1987 p 918 N93-14114
Super-micro computer weather prediction model
[AD-A255668] p 918 N93-14153
Simulation of vapor compression heat pumps with solution circuits p 872 N93-14200
Robust control of a flexible link robot and rigid link robot: Theory, simulation, and experiment p 888 N93-14202
Audio detection algorithms
[AD-A256076] p 973 N93-14234
An examination of wing rock for the F-15
[AD-A256613] p 802 N93-14252
Monte Carlo computer simulations of Venus equilibrium and global resurfacing models p 1027 N93-14311
Computer simulations of comet- and asteroidlike bodies passing through the Venusian atmosphere: Preliminary results on atmospheric and ground shock effects p 1040 N93-14365
Optimum pose measurements for kinematic parameters identification
[AD-A256307] p 970 N93-14443
Airborne radar simulation with adaptive antenna techniques
[AD-A255460] p 859 N93-14488
Strain-rate effects in replica scale model penetration experiments
[AD-A255426] p 844 N93-14508
VANTAGE: A frame-based geometric modeling system programmer/user's manual, V2.0
[AD-A255434] p 944 N93-14566
Numerical modelling of intense electron beam transport in the spiral line induction accelerator
[AD-A255545] p 978 N93-14570
Design and hardware implementation of neural systems
[AD-A256040] p 866 N93-14577
Modeling and control of a trailing wire antenna towed by an orbiting aircraft
[AD-A256450] p 859 N93-14610
Current neutralization in ballistic transport of light ion beams
[AD-A256070] p 976 N93-14662
Four-dimensional data assimilation of gale data using a multivariate analysis scheme and a mesoscale model with diabatic initialization
[AD-A256063] p 921 N93-14680
Development of an integrated package of physics models for scene simulation studies to support smart weapons design studies
[LTR92-004] p 945 N93-14696
Interplanetary Program to Optimize Simulated Trajectories (IPOST). Volume 3: Programmer's manual
[NASA-CR-189653-VOL-3-REV] p 815 N93-14730
Adaptive active noise control using multiple-model approaches
[ISVR-TR-210] p 974 N93-14734
Purposive discovery of operations
[NASA-TM-108116] p 963 N93-14765
Interplanetary program to optimize simulated trajectories (IPOST). Volume 4: Sample cases
[NASA-CR-189653-VOL-4] p 815 N93-14768
Interplanetary Program to Optimize Simulated Trajectories (IPOST). Volume 1: User's guide
[NASA-CR-189653-VOL-1-REV] p 815 N93-14794
SAFSIM: A computer program for engineering simulations of space reactor system performance
[DE92-016328] p 826 N93-14815
Propulsion and Energetics Panel Working Group 20 on Test Cases for Engine Life Assessment Technology
[AGARD-AR-308] p 798 N93-14890
Introduction to test cases for engine life assessment technology p 799 N93-14891
Implementation issues concerning injection simulation. Part 1: The backbone implementation
[MEMO-INF-91-57-PT-1] p 946 N93-15078
Addressing earthquake strong ground motion issues at the Idaho National Engineering Laboratory
[DE92-017841] p 916 N93-15136
Experimental determination of magnetohydrodynamic seawater thruster performance in a two Tesla test facility
[DE92-019042] p 826 N93-15215
A temperature tracking SPICE2G.6 macromodel of the 6N134 optocoupler
[DE92-040093] p 983 N93-15223
Plasma confinement theory and transport simulation
[DE92-040523] p 988 N93-15327
Accurate methods for calculating atomic processes in high temperature plasmas
[DE92-040215] p 988 N93-15418
Progress on the development of a 2-D PIC/Monte Carlo model of glow discharges
[DE92-040226] p 989 N93-15422
Parallel simulation today
[NASA-CR-189733] p 951 N93-15432
Modeling limits of the EMV analysis program CONCEPT by example of the influence of a helicopter structure on a frame antenna
[MBB-UD-0614-92-PUB] p 863 N93-15487
Simplified jet-A kinetic mechanism for combustor application
[NASA-TM-105940] p 844 N93-15504
User's guide for a large signal computer model of the helical traveling wave tube
[NASA-TP-3251] p 871 N93-15531
Volume rendering using the Fourier projection-slice theorem p 953 N93-15541
Physically-based methods for polygonization of implicit surfaces p 956 N93-15562
Generating natural-looking motion for computer animation p 956 N93-15564
Beyond keyframing: An algorithmic approach to animation p 957 N93-15565
Aspects of a parallel-architecture simulator
[AD-A256872] p 941 N93-15628
Numerical modeling tools for chemical vapor deposition
[NASA-CR-4480] p 880 N93-15643
The spatial correlation function approach to response surface emission
[DE92-040875] p 969 N93-15656

CONCENTRATION (COMPOSITION)
Infrared laboratory spectra and composition changes of synthetic amorphous silicate grains
[DE92-040211] p 843 N93-15283

CONCENTRIC CYLINDERS
Turbulent drag and transport in high Reynolds number Couette-Taylor flow p 872 N93-14119

CONCURRENT PROCESSING
A portable multiprocessor interface for standard ML of New Jersey
[AD-A255639] p 958 N93-14151
Trace algebra for automatic verification of real-time concurrent systems
[AD-A256199] p 968 N93-14492
Multiple robot programming using concurrent logic language
[F-3-3] p 950 N93-15304

CONDENSATES
The low-energy structure of compactified superstring models p 997 N93-14116

CONDENSATION
Super-micro computer weather prediction model
[AD-A255668] p 918 N93-14153

CONDENSATION NUCLEI
CCN spectra measurements as an active tracer of stratocumulus mechanisms
[AD-A255678] p 920 N93-14258

CONDENSED MATTER PHYSICS
Condensed matter research using the UCSB FEL
[DE92-040560] p 887 N93-15347

CONDUCTING POLYMERS
Electronic, vibrational, and transport properties of conducting polymers p 847 N93-14170
Oriented electro/optical polymers through in-situ chemistry during gel processing: A research opportunity
[AD-A255968] p 848 N93-14401
Solid polymer electrolytes for rechargeable batteries
[DE93-001603] p 871 N93-15485

CONDUCTION ELECTRONS
Sensitivity of quantum electron conductance to elastic scatterers and to spin-orbit scattering in gallium arsenide heterostructures p 990 N93-14184

CONDUCTIVE HEAT TRANSFER
Effect of interfacial thermal conductance and fiber orientation on the thermal diffusivity/conductivity of unidirectional fiber-reinforced ceramic matrix composites p 864 N93-14190

CONDUCTIVITY
Macroscopic properties of random and quasiperiodic media
[AD-A255984] p 990 N93-14413

CONDUCTORS
Modeling limits of the EMV analysis program CONCEPT by example of the influence of a helicopter structure on a frame antenna
[MBB-UD-0614-92-PUB] p 863 N93-15487

CONES (VOLCANOES)
Debris avalanches and slumps on the margins of volcanic domes on Venus: Characteristics of deposits p 1025 N93-14300

CONFERENCES
Organization of workshop on emerging technologies for in-situ processing
[AD-A255977] p 865 N93-14410
The changing culture of science: Bringing it into balance
[AD-A255993] p 998 N93-14417
Proceedings of the data assimilation in coupled air-sea nowcast/forecast systems workshop
[AD-A255409] p 925 N93-14503
Integrated photonics research technical digest series. Volume 10: Conference edition: Summaries of papers presented at the Integrated Photonics Research Topical Meeting
[AD-A255423] p 981 N93-14506
Symposium on the occasion of the farewell of Prof. Dr. Ir. O. H. Gerlach as Chairman of the Board of the Foundation National Aerospace Laboratory NLR, The Netherlands
[ETN-92-92168] p 777 N93-14613
FIBER-TEX 1991: The Fifth Conference on Advanced Engineering Fibers and Textile Structures for Composites
[NASA-CP-3176] p 832 N93-14744

NSSDC Conference on Mass Storage Systems and Technologies for Space and Earth Science Applications, volume 3
[NASA-CP-3165-VOL-3] p 1002 N93-14771
Core support of the board on mathematical sciences
[AD-A255482] p 968 N93-14787
Tiltrotor aircraft noise: A summary of the presentations and discussions at the 1991 FAA/Georgia Tech Workshop
[DOT/FAA/RD-91/23] p 974 N93-14912
Proceedings of the Sixth CASI Conference on Astronautics
[CTN-92-60336] p 804 N93-14920
Proceedings of the NSSDC Conference on Mass Storage Systems and Technologies for Space and Earth Science Applications
[NASA-TM-107989] p 1004 N93-15027
Proceedings of the International Conference on CAD/CAM and AMT. Volume 4: VHDL (VHSIC Hardware Description Language) Seminar
[ITN-92-85130] p 947 N93-15261
Proceedings of the International Conference on CAD/CAM and AMT. Volume 3: IFIP (International Federation of Information Processing)/Robotics: International Sessions on Robots and Assembly
[ITN-92-85129] p 949 N93-15298
Ferroelectrics volume 122, numbers 1-4, 1991. Proceedings of the 3rd International Conference on Ferroelectric Liquid Crystals, part 2
[AD-A257053] p 996 N93-15446
Ferroelectrics volume 121, numbers 1-4, 1991. Proceedings of the 3rd International Conferenceon Fer roelectric Liquid Crystals, part 1
[AD-A257054] p 996 N93-15447
The 17th Annual Conference on the Physics and Chemistry of Semiconductor Interfaces
[AD-A257061] p 996 N93-15449
Proceedings of the REXX Symposium for Developers and Users
[DE92-041359] p 951 N93-15451
Proceedings: Graphics Interface 1992
[ISBN-0-9695338-1-0] p 952 N93-15533
The Seventeenth Space Simulation Conference. Terrestrial Test for Space Success
[NASA-CP-3181] p 819 N93-15593

CONFIGURATION INTERACTION
Theoretical characterization of the potential energy surface for NH + NO
[NASA-CR-190741] p 843 N93-15357

CONFIGURATION MANAGEMENT
Software flexibility and configuration control for the A340/A330 Aircraft Condition Monitoring System (ACMS) p 793 N93-15154

CONFINEMENT
Fluids, gels, and glasses under extreme conditions of pressure and temperature
[AD-A255675] p 847 N93-14166

CONICAL FLOW
BLSTA: A boundary layer code for stability analysis
[NASA-CR-4481] p 877 N93-14797

CONJUGATES
Preconditioned conjugate-gradient methods for low-speed flow calculations
[NASA-TM-105929] p 877 N93-14885

CONJUGATION
Oriented electro/optical polymers through in-situ chemistry during gel processing: A research opportunity
[AD-A255968] p 848 N93-14401

CONNECTION MACHINE
A data parallel algorithm for raytracing of heterogeneous databases p 955 N93-15553

CONNECTORS
Work attachment mechanism/work attachment fixture
[NASA-CASE-GSC-13430-1] p 890 N93-14712
Preliminary lightning tests: Optical fiber penetration of an exclusion region barrier
[DE92-019804] p 983 N93-15230

CONSOLIDATION
HIP consolidation of aluminum-rich intermetallic alloys and their composites
[NAWCADWAR-92003-60] p 845 N93-14726
Fabrication of high temperature materials by exothermic synthesis and subsequent dynamic consolidation
[DE92-019836] p 834 N93-14819

CONSTITUTIVE EQUATIONS
Applications of a constitutive equation for microstructural change in polymers p 848 N93-14222
On the structure of nonlinear constitutive equations for fiber reinforced composites
[NASA-CR-191024] p 830 N93-14484

CONSTRAINTS
Use of kinematic constraint in tracking constant speed maneuvering targets
[AD-A255988] p 858 N93-14415
Design and implementation of practical constraint logic programming systems
[AD-A256191] p 943 N93-14558
A linear constraint technology for interactive graphic systems p 957 N93-15568

CONSTRUCTION
Subsonic aerodynamic research laboratory
[AD-A256060] p 780 N93-14661
Tribology of magnetic storage systems p 1002 N93-14772

CONTAMINANTS
Multiscale modeling of the long-range transport and fate of pollutants emitted from urban areas p 909 N93-14118
Effects of cryocontaminants on cryogenic superpolished mirror and superpolished quartz crystal microbalance
[AD-A255972] p 981 N93-14403
Ultraviolet-ozone cleaning of semiconductor surfaces, revision 1
[AD-A256158] p 842 N93-14678
Performing wind-tunnel modeling for better management of near-field risks
[DE92-040205] p 910 N93-15063
Liquid flow reactor and method of using
[AD-D015392] p 893 N93-15232
Contaminant effects in solid oxide fuel cells
[DE92-040255] p 908 N93-15323
Bevalac ion beam characterizations for single event phenomena
[AD-A257033] p 979 N93-15362

CONTAMINATION
Surface evaluation of UV-degraded contamination
[NASA-CR-184500] p 910 N93-14764
Operational strategies for contamination control of composite materials p 822 N93-15614
A new approach for performing contamination control bakeouts in JPL thermal vacuum test chambers p 823 N93-15618
Mass spectrometer use in a large chamber p 823 N93-15619

CONTEXT
From data structure to process structure
[MEMO-INF-91-38] p 946 N93-15077

CONTEXT FREE LANGUAGES
Grammatical trigrams: A probabilistic model of link grammar
[AD-A256365] p 947 N93-15206

CONTINUUM MECHANICS
Spatio-temporal complexity and large-scale structures in problems of continuum mechanics
[AD-A256410] p 998 N93-15333

CONTINUUM MODELING
Elastic wave propagation in laminated composites
[ITN-93-85186] p 835 N93-15144

CONTINUUMS
The evolution of the quasar continuum
[NASA-CR-191673] p 1012 N93-14759
Partitioning tree image representation and generation from 3D geometric models p 955 N93-15557

CONTOUR SENSORS
An active tactile perception system p 805 N93-14926

CONTOURS
Integration and processing of high-resolution moire-interferometry data p 895 N93-14185
Automated interpretation of topographic maps
[AD-A257040] p 906 N93-15364

CONTRACTORS
Recommendations for enhancement of the Design Criteria Information System (DCIS)
[AD-A256857] p 1009 N93-15641

CONTRAST
High-resolution contrast control on a video display: Method and calibration
[AD-A256552] p 938 N93-15400

CONTROL
Multi-axis transient vibration testing of space objects: Test philosophy, test facility, and control strategy p 820 N93-15598
Application of programmable logic controllers to space simulation p 821 N93-15608
Control of on-orbit contamination for the Argos (P91-1) satellite p 823 N93-15617

CONTROL EQUIPMENT
Autonomous power system brassboard
[NASA-CR-189115] p 867 N93-14798
Design and implementation of a DC-based magnetic field controller with electronic temperature stabilized Hall generator
[DE92-019796] p 870 N93-15276
SMART: A modular architecture for robotics and teleoperation
[DE92-040985] p 966 N93-15385

CONTROL SIMULATION
Multiple model adaptive estimation applied to the ViSTA F-16 with actuator and sensor failures
[AD-A256444] p 802 N93-14608

CONTROL STABILITY
Robust control of a flexible link robot and rigid link robot: Theory, simulation, and experiment p 888 N93-14202
An examination of wing rock for the F-15
[AD-A256613] p 802 N93-14252
Sampled-data control and robust control for discrete-time systems p 964 N93-15149

CONTROL STICKS
F/A-18 controls released departure recovery flight test evaluation
[AD-A256522] p 803 N93-15396

CONTROL SYSTEMS DESIGN
Robust control of a flexible link robot and rigid link robot: Theory, simulation, and experiment p 888 N93-14202
L2 and L-infinity multiobjective control for linear systems p 961 N93-14399
Multiobjective control/structure design optimization in the presence of practical constraints p 898 N93-14446
Online vibration control of a flexible rotor/bearing system p 899 N93-14468
Real-time gaze holding in binocular robot vision
[AD-A256226] p 982 N93-14582
Autonomous power system brassboard
[NASA-CR-189115] p 867 N93-14798
Cooperative control of multiple space manipulators p 805 N93-14923
MOVE: A neutral network paradigm for robotic control p 805 N93-14925
A robotic planning system p 810 N93-14949
A concept for a supervised autonomous robot p 810 N93-14950
A monitoring and control system for complex man-machine systems: Preliminary design p 810 N93-14951
Position and vibration control of flexible space robots p 892 N93-15102
Learning position and force control for mechanical manipulators p 963 N93-15147
Robust control design for uncertain nonlinear dynamic systems p 964 N93-15148
Sampled-data control and robust control for discrete-time systems p 964 N93-15149
Dynamics and control of flexible arm robots
[ISBN-0-315-69011-9] p 892 N93-15150
Optimal active vibration absorber: Design and experimental results
[NASA-TM-107709] p 902 N93-15202
Design and implementation of a DC-based magnetic field controller with electronic temperature stabilized Hall generator
[DE92-019796] p 870 N93-15276
Generating natural-looking motion for computer animation p 956 N93-15564
An alternate method for achieving temperature control in the -130 C to 75 C range p 821 N93-15609
Unsteady flow distortion past blades: Sources of noise generation in rotating flows
[AD-A255496] p 880 N93-15652

CONTROL THEORY
Gas-solid dynamics at disordered and adsorbate covered surfaces
[AD-A255981] p 976 N93-14411
Generating natural-looking motion for computer animation p 956 N93-15564
Beyond keyframing: An algorithmic approach to animation p 957 N93-15565

CONTROL VALVES
High-temperature, high-pressure oxygen metering valve
[NASA-CASE-MSC-21823-1] p 891 N93-14843

CONTROLLED FUSION
Current neutralization in ballistic transport of light ion beams
[AD-A256070] p 976 N93-14662

CONTROLLERS
Robust control of a flexible link robot and rigid link robot: Theory, simulation, and experiment p 888 N93-14202
L2 and L-infinity multiobjective control for linear systems p 961 N93-14399
Utilizing sensed incipient slip signals for grasp force control
[AD-A255725] p 888 N93-14434
Multiobjective control/structure design optimization in the presence of practical constraints p 898 N93-14446
Digital bank-to-turn control and guidance p 802 N93-14447
Online vibration control of a flexible rotor/bearing system p 899 N93-14468

Force and position control of robot manipulators: Learning and repetitive control approach p 888 N93-14473
Smart battery controller for lithium sulfur dioxide batteries [AD-A255490] p 867 N93-14642
A simple controller for repetitive cycles in atomic layer epitaxy [AD-A255497] p 992 N93-14643
Learning position and force control for mechanical manipulators p 963 N93-15147
Robust control design for uncertain nonlinear dynamic systems p 964 N93-15148
Sampled-data control and robust control for discrete-time systems p 964 N93-15149
Dynamics and control of flexible arm robots [ISBN-0-315-69011-9] p 892 N93-15150
Optimal active vibration absorber: Design and experimental results [NASA-TM-107709] p 902 N93-15202
Remote vehicle controller [AD-D015389] p 893 N93-15251
Generation, control, and transport of a 19-MeV, 700-kA pulsed electron beam [DE92-019803] p 978 N93-15277
Propulsion system performance resulting from an integrated flight/propulsion control design [NASA-TM-105874] p 801 N93-15525
ARCBALL: A user interface for specifying three-dimensional orientation using a mouse p 955 N93-15551
Beyond keyframing: An algorithmic approach to animation p 957 N93-15565
Application of programmable logic controllers to space simulation p 821 N93-15608
An alternate method for achieving temperature control in the -130 C to 75 C range p 821 N93-15609
Reusable Reentry Satellite (RRS) system design study. Phase B, appendix E: Attitude control system study [NASA-CR-188578] p 825 N93-15633
Upgrade and extension of the data acquisition system for propulsion and gas dynamic laboratories [AD-A256836] p 1009 N93-15637

CONVECTION
The theory and numerical simulation of non-local mixing-length convection p 1015 N93-14147
Extended surface heat sinks for electronic components: A computer optimization [AD-A256134] p 865 N93-14254
The effects of Venusian mantle convection with multiple phase transitions p 1043 N93-14385
Crystal growth in a microgravity environment [NASA-CASE-MFS-28473-1] p 992 N93-14707
Low-frequency oscillations in radiative-convective models [DE92-018779] p 922 N93-14901

CONVECTION-DIFFUSION EQUATION
Diffusing wave spectroscopy p 980 N93-14169

CONVECTIVE FLOW
Cloud-radiative feedbacks in tropical convection p 919 N93-14180
Volcanism by melt-driven Rayleigh-Taylor instabilities and possible consequences of melting for admittance ratios on Venus p 1043 N93-14387
Control of thermocapillary convection in a two-layer liquid system p 809 N93-14945

CONVECTIVE HEAT TRANSFER
Extended surface heat sinks for electronic components: A computer optimization [AD-A256134] p 865 N93-14254
Constraints on the thermal evolution of Venus inferred from Magellan data p 1024 N93-14293
Global correlation of volcanic centers on Venus with uplands and with extension: Influence of mantle convection and altitude p 1026 N93-14309
Flexural analysis of uplifted rift flanks on Venus p 1027 N93-14314
Analytical and experimental investigation of closed-cycle sorption cooling systems p 874 N93-14476
Experimental observation of the influence of furnace temperature profile on convection and segregation in the vertical Bridgman crystal growth technique p 995 N93-15312

CONVERGENCE
Iterative algorithms for integral equations of the first kind with applications to statistics [AD-A256529] p 942 N93-14285
A proof of convergence of the Markov chain simulation method [AD-A255456] p 970 N93-14487
On the convergence of the coupled-wave approach for lamellar diffraction gratings p 986 N93-15520

CONVERGENT-DIVERGENT NOZZLES
Numerical modeling of a vortex stabilized arcjet [NASA-CR-190797] p 826 N93-14883
Computation of supersonic jet noise under imperfectly expanded conditions [NASA-TM-105961] p 975 N93-15430
Nuclear thermal rocket nozzle testing and evaluation program [NASA-TM-105962] p 827 N93-15571

CONVOLUTION INTEGRALS
Comparison of synchronization techniques for the AFIT direct sequence spread spectrum system [AD-A256440] p 861 N93-15316

COOLING
Advances in laser cooling [AD-A255969] p 884 N93-14402
Crystal growth in a microgravity environment [NASA-CASE-MFS-28473-1] p 992 N93-14707

COOLING FINS
The use of a novel manufacturing process for high performance titanium plate fin heat exchangers [PNR-90934] p 879 N93-15473

COOLING FLOWS (ASTROPHYSICS)
Optical signatures of cooling flows in isolated early-type galaxies p 1017 N93-14243
Physical properties of extended emission-line regions in active and cooling-flow galaxies p 1018 N93-14461

COOLING SYSTEMS
Analytical and experimental investigation of closed-cycle sorption cooling systems p 874 N93-14476

COORDINATION
Development of measures of crew coordination [AD-A255384] p 939 N93-14651
Working together, virtually p 954 N93-15547

COPLANARITY
Orbital coplanarity in solar-type binary systems: Implications for planetary system formation and detection p 1020 N93-14867

COPOLYMERS
Waterborne polyurethane binder resins for compliant aircraft coatings [AD-A256246] p 849 N93-14573

COPPER ALLOYS
The response of dispersion-strengthened copper alloys to high fluence neutron irradiation at 415 C [DE92-019434] p 846 N93-15138

COPPER OXIDES
Method of making substantially single phase superconducting oxide ceramics having a TC above 85 degrees [AD-D015422] p 850 N93-14743

CORES
Core design for use with precision composite reflectors [NASA-CASE-NPO-17858-1-CU] p 832 N93-14700

CORONAS
Visoelastic relaxation of Venusian coronae and mountain belts: Constraints on global heat flow and tectonism p 1027 N93-14313
Flexural analysis of uplifted rift flanks on Venus p 1027 N93-14314
The spatial distribution of coronae on Venus p 1043 N93-14383

CORRELATION
Cognition and the brain [AD-A255483] p 937 N93-14788
The spatial correlation function approach to response surface emission [DE92-040875] p 969 N93-15656

CORROSION
Composite materials in space: Results from the LDEF satellite p 811 N93-14955
Corrosion of metal particle and metal evaporated tapes p 883 N93-15039
Results from a pilot cell test of cermet anodes [DE92-041357] p 871 N93-15479

CORROSION PREVENTION
Evaluation of corrosion protection methods for aluminum metal matrix composites [AD-A255375] p 832 N93-14675

CORROSION RESISTANCE
Surface preparation of stainless steel prior to painting [AD-A256253] p 838 N93-14454
Fe3Al-type iron aluminides: Aqueous corrosion properties in a range of electrolytes and slow-strain rate ductilities during aqueous corrosion [DE92-040520] p 846 N93-15059
Dual role of nickel in sodium/nickel chloride batteries [DE92-041102] p 870 N93-15441

CORROSION TESTS
Corrosion of metal particle and metal evaporated tapes p 883 N93-15039
A system approach to archival storage p 1006 N93-15040
Fe3Al-type iron aluminides: Aqueous corrosion properties in a range of electrolytes and slow-strain rate ductilities during aqueous corrosion [DE92-040520] p 846 N93-15059
Stress corrosion susceptibility of ultra-high strength steels for Naval aircraft applications [AD-A256126] p 846 N93-15189
Results from a pilot cell test of cermet anodes [DE92-041357] p 871 N93-15479

COSMIC DUST
The structure and dynamics of an environment forming high-mass stars p 1014 N93-14113
Infrared laboratory spectra and composition changes of synthetic amorphous silicate grains [DE92-040211] p 843 N93-15283

COSMIC GASES
Electron density diagnostics for gaseous nebulae involving the O 4 intercombination lines near 1400 A p 1012 N93-14762

COSMIC RAY SHOWERS
Using the Haleakala barrel extensive air shower array to study selected U.H.E. gamma ray point sources p 1050 N93-14639

COSMIC RAYS
High-energy emissions from young pulsars: Perspective from the outer gap model [DE92-040365] p 1022 N93-15324

COSMOCHEMISTRY
Infrared laboratory spectra and composition changes of synthetic amorphous silicate grains [DE92-040211] p 843 N93-15283

COSMOLOGY
Perturbations of the Robertson-Walker space p 1015 N93-14134
Cosmological models in higher-order gravity p 1018 N93-14592
Dark matter axions [DE92-040501] p 1022 N93-15346

COST ANALYSIS
Evaluation of the cost effectiveness analysis model being developed for the component improvement programs of the Air Force and the Navy [AD-A256132] p 1010 N93-14249
Reusable Reentry Satellite (RRS) system design study: System cost estimates document [NASA-CR-188480] p 818 N93-14872
Technology commercialization cost model and component case study [DE92-001280] p 907 N93-15213
Automated Estimated System (AES) standard value and guidelines programs user's manual [DE92-041243] p 951 N93-15450

COST EFFECTIVENESS
Evaluation of the cost effectiveness analysis model being developed for the component improvement programs of the Air Force and the Navy [AD-A256132] p 1010 N93-14249
Reusable Reentry Satellite (RRS) system design study [NASA-CR-187897] p 817 N93-14733
Crew requirements definition system user's guide [AD-A257052] p 951 N93-15445

COST ESTIMATES
Reusable Reentry Satellite (RRS) system design study: System cost estimates document [NASA-CR-188480] p 818 N93-14872
Automated Estimating System (AES), version 5.1. User's manual [DE93-000380] p 946 N93-15003
Automated Estimated System (AES) standard value and guidelines programs user's manual [DE92-041243] p 951 N93-15450

COST REDUCTION
Software requirements for the A-7E aircraft [AD-A255746] p 946 N93-15052
A new multiplier-free structure for DFT based on delta modulation [AD-A255927] p 861 N93-15106

COUETTE FLOW
Turbulent drag and transport in high Reynolds number Couette-Taylor flow p 872 N93-14119
Spatio-temporal complexity and large-scale structures in problems of continuum mechanics [AD-A256410] p 998 N93-15333

COUPLERS
The design and fabrication of a single leakage-channel grating coupler p 986 N93-15518

COUPLINGS
Work attachment mechanism/work attachment fixture [NASA-CASE-GSC-13430-1] p 890 N93-14712
Frequency shifts in a rubidium frequency standard due to coupling to another standard [AD-A256232] p 972 N93-15243

COVARIANCE
Type 2 superstrings in curved D = 10 space-time: Dynamics of their massless fields and covariant quantization p 998 N93-14143
L2 and L-infinity multiobjective control for linear systems p 961 N93-14399

The covariance matrix of derived quantities and their combination
[DE92-019066] p 969 N93-15212

CRACK CLOSURE
A study of the relationship between macroscopic measures and physical processes occurring during crack closure
[AD-A256587] p 898 N93-14272

CRACK INITIATION
The influence of geometrical constraint on cyclic, elastoplastic, notch root behavior, and fatigue microcrack initiation p 900 N93-14480
Delamination growth behavior in cross-ply laminated composites due to transverse concentrated loading
[AD-A255974] p 830 N93-14493
Propulsion and Energetics Panel Working Group 20 on Test Cases for Engine Life Assessment Technology
[AGARD-AR-308] p 798 N93-14890
Introduction to test cases for engine life assessment technology p 799 N93-14891
LARZAC HP turbine disk crack initiation and propagation spin pit test p 799 N93-14892
CF6-6 high pressure compressor stage 5 locking slot crack propagation spin pit test p 799 N93-14894
Engine life assessment test case TF41 LP compressor shaft torsional fatigue p 799 N93-14896

CRACK OPENING DISPLACEMENT
A study of the relationship between macroscopic measures and physical processes occurring during crack closure
[AD-A256587] p 898 N93-14272
Closed form expressions for crack mouth displacements and stress intensity factors for chevron notched short bar and short rod specimens based on experimental compliance measurements
[NASA-TM-83796] p 902 N93-15369
The mixed mode crack problem in a nonhomogeneous elastic plane
[AD-A256469] p 902 N93-15372

CRACK PROPAGATION
An investigation of crack growth at interfaces in bimaterials and composites using a consistent shear-lag model p 896 N93-14187
Fracture mechanisms and fracture control in composite structures p 899 N93-14474
Delamination growth behavior in cross-ply laminated composites due to transverse concentrated loading
[AD-A255974] p 830 N93-14493
Shear fatigue crack growth analysis in large-grain polycrystals p 993 N93-14838
Propulsion and Energetics Panel Working Group 20 on Test Cases for Engine Life Assessment Technology
[AGARD-AR-308] p 798 N93-14890
Introduction to test cases for engine life assessment technology p 799 N93-14891
LARZAC HP turbine disk crack initiation and propagation spin pit test p 799 N93-14892
CF6-6 high pressure compressor stage 5 locking slot crack propagation spin pit test p 799 N93-14894
Engine life assessment test case TF41 LP compressor shaft torsional fatigue p 799 N93-14896
F100 second stage fan disk bolthole crack propagation ferris wheel test p 800 N93-14897
In-service considerations affecting component life p 800 N93-14898

CRACK TIPS
The mechanics of dislocation nucleation at a crack tip p 896 N93-14214
Closed form expressions for crack mouth displacements and stress intensity factors for chevron notched short bar and short rod specimens based on experimental compliance measurements
[NASA-TM-83796] p 902 N93-15369
The mixed mode crack problem in a nonhomogeneous elastic plane
[AD-A256469] p 902 N93-15372

CRACKS
Elastic wave scattering by partially debonded or partially coated fibers p 829 N93-14224
Diffusion problems in bonded nonhomogeneous materials with an interface cut
[AD-A256470] p 836 N93-15373
The crack problem for an orthotropic half plane stiffened by elastic films
[AD-A256471] p 903 N93-15374

CRANES
Structurally adaptive space crane concept for assembling space systems on orbit
[NASA-TP-3307] p 818 N93-15368

CRASH LANDING
Aeroplane crashes on the runway: Validation and final evaluation of the method of modeling an airframe structure
[IMFL-91-32] p 792 N93-15126

CRATERING
Monte Carlo modeling of the resurfacing of Venus p 1025 N93-14299
Monte Carlo computer simulations of Venus equilibrium and global resurfacing models p 1027 N93-14311
A model for the formation of the extended paraboloidal halos around some impact craters on Venus p 1037 N93-14352

CRATERS
Episodic plate tectonics on Venus p 1044 N93-14390

CREEP PROPERTIES
The effect of the interphase/interface region on creep and creep rupture of thermoplastic composites p 829 N93-14193
In-service considerations affecting component life p 800 N93-14898
Thermal, mechanical, and electroelastic behavior of composite materials p 835 N93-15146

CREEP RUPTURE STRENGTH
The effect of the interphase/interface region on creep and creep rupture of thermoplastic composites p 829 N93-14193

CREWS
A progressive resistance weight training program designed to improve the armor crewman's strength
[AD-A255553] p 934 N93-14556

CRITICAL LOADING
Analysis of advanced thin-walled composite structures p 895 N93-14158

CRITICAL PATH METHOD
Processor controlpath microarchitecture synthesis based on the A(asterisk) algorithm
[MEMO-INF-92-10] p 963 N93-15083

CRITICAL TEMPERATURE
Viscosity of liquids. Halogenated methanes
[ESDU-92028] p 839 N93-14539

CROSS FLOW
Wake similarity and vortex formation for two-dimensional bluff bodies p 781 N93-15101
Optimization of circular orifice jets mixing into a heated cross flow in a cylindrical duct
[NASA-TM-105984] p 800 N93-15359

CROSSINGS
A numerical investigation of the interaction between crossing oblique shocks and a turbulent boundary layer p 876 N93-14695

CROSSLINKING
Spirobislactone acrylate polymers
[AD-D015443] p 850 N93-14802

CRUDE OIL
Acoustic location of leaks in pressurized underground petroleum pipelines
[PB92-207687] p 975 N93-15647

CRUSTAL FRACTURES
Geoid, topography, and convection-driven crustal deformation on Venus p 1042 N93-14376

CRYOGENIC COOLING
A comparison of superconductor and manganin technology for electronic links used in space mission applications
[NASA-CR-4477] p 997 N93-15587

CRYOGENIC TEMPERATURE
Effects of cryocontaminants on cryogenic superpolished mirror and superpolished quartz crystal microbalance
[AD-A255972] p 981 N93-14403
ISOCAM experiment cryogenic test results
[REPT-921-440-104] p 825 N93-15140

CRYOGENICS
Effects of cryocontaminants on cryogenic superpolished mirror and superpolished quartz crystal microbalance
[AD-A255972] p 981 N93-14403

CRYOPUMPING
From diffusion pumps to cryopumps: The conversion of GSFC's space environment simulator p 814 N93-15611

CRYOSTATS
Level-mixing assisted tunability of nuclear resonance linewidths for gamma ray lasers
[AD-A255791] p 885 N93-14647

CRYPTOGRAPHY
Software stamping
[NPL-DITC-198/92] p 946 N93-15072

CRYSTAL DEFECTS
Long term stability in thin film ferroelectric memories
[AD-A256290] p 991 N93-14439
Revised nomenclature for defects at or near the Si/SiO2 interface
[DE92-040975] p 997 N93-15651

CRYSTAL DISLOCATIONS
The mechanics of dislocation nucleation at a crack tip p 896 N93-14214

CRYSTAL GROWTH
Twin quintuplets in CVD diamond
[AD-A255862] p 989 N93-14133
Organization of workshop on emerging technologies for in-situ processing
[AD-A255977] p 865 N93-14410
Crystal growth in a microgravity environment
[NASA-CASE-MFS-28473-1] p 992 N93-14707
Method of making substantially single phase superconducting oxide ceramics having a TC above 85 degrees
[AD-D015422] p 850 N93-14743
Study of Fluid Experiment System (FES)/CAST/Holographic Ground System (HGS)
[NASA-CR-184483] p 855 N93-14793
Modelling Directional Solidification
[NASA-CR-191301] p 995 N93-15309
Solidification of InSb-GaSb alloy and InSb with vibration p 995 N93-15310
Experimental observation of the influence of furnace temperature profile on convection and segregation in the vertical Bridgman crystal growth technique p 995 N93-15312
The 17th Annual Conference on the Physics and Chemistry of Semiconductor Interfaces
[AD-A257061] p 996 N93-15449

CRYSTAL OPTICS
Optical information processing using photorefractive BSO p 981 N93-14204
Off-axis conoscopic holography: Optical and digital reconstruction
[TELECOM-PARIS-90-E-023] p 882 N93-15096

CRYSTAL OSCILLATORS
The effects of acceleration on precision frequency sources
[AD-A255465] p 972 N93-14496
Introduction to quartz frequency standards, revision 1
[AD-A256373] p 870 N93-15330

CRYSTAL STRUCTURE
Gallium and indium compounds containing three different substituents. Crystal and molecular structure of ((Me3 CCH2)ClGaPPh2)3
[AD-A257049] p 996 N93-15443
Processing and microstructure of Nb-1 percent Zr-0.1 percent C alloy sheet
[NASA-TM-105921] p 847 N93-15524

CRYSTAL SURFACES
Spectroscopy and reactions of hydrazoic acid on silicon single crystal surfaces (III). HN3 and DN3 on Si(111)-7 x 7
[AD-A255241] p 842 N93-14669

CRYSTALLINITY
Electrical conductivity measurements in evaporated cadmium telluride thin films p 865 N93-14191
An investigation of the processing, high temperature deformation and fracture characteristics of superplastic ceramics
[AD-A256519] p 852 N93-15394

CRYSTALLIZATION
Comments on 'Kinetic Study on the Hexacelsian-Celsian Phase Transformation'
[NASA-TM-105917] p 850 N93-14886
Study of the glass formation of high temperature superconductors
[NASA-TM-108389] p 997 N93-15500

CRYSTALLOGRAPHY
Determination of operable deformation mechanisms during ballistic impact in tungsten single crystals, utilizing transmission electron microscopy
[AD-A255351] p 991 N93-14518

CRYSTALS
The mechanics of dislocation nucleation at a crack tip p 896 N93-14214
Experimental considerations of higher order parametric x rays from silicon crystals of varying thicknesses
[AD-A256082] p 990 N93-14260
Crystal growth in a microgravity environment
[NASA-CASE-MFS-28473-1] p 992 N93-14707
Innovative techniques for studying new materials and new developments in solid state physics
[AD-A256394] p 996 N93-15465

CUBIC EQUATIONS
Fast algorithms for rendering cubic curves p 953 N93-15536

CUFFS
Bar-holding prosthetic limb
[NASA-CASE-MFS-28481-1] p 939 N93-14870

CUMULUS CLOUDS
Low-frequency oscillations in radiative-convective models p 915 N93-14874

CURING
Core design for use with precision composite reflectors
[NASA-CASE-NPO-17858-1-CU] p 832 N93-14700

CURRENT CONVERTERS (AC TO DC)
Power conversion system modification to permit use of DC power source
[AD-D015409] p 868 N93-14887

CURRENT REGULATORS
A power compensation system for phased operation of the JET A2 antenna arrays
| DE92-041020 | p 863 N93-15440
CURVATURE
Full surface testing of grazing incidence mirrors
| AD-A255644 | p 979 N93-14152
CURVES (GEOMETRY)
An implementation of multivariate B-spline surfaces over arbitrary triangulations p 952 N93-15534
Fast algorithms for rendering cubic curves p 953 N93-15536
Parameterization in finite precision p 953 N93-15537
Algorithms for intersecting parametric and algebraic curves p 956 N93-15560
CUTTING
Using an interior point cutting plane method to solve integer programming problems
| AD-A256041 | p 945 N93-14659
Core design for use with precision composite reflectors
| NASA-CASE-NPO-17858-1-CU | p 832 N93-14700
Diffusion problems in bonded nonhomogeneous materials with an interface cut
| AD-A256470 | p 836 N93-15373
CYCLES
A simple controller for repetitive cycles in atomic layer epitaxy
| AD-A255497 | p 992 N93-14643
CYCLIC COMPOUNDS
Electronically active cyclocarborane-metal-arene assemblies
| AD-A256288 | p 865 N93-14457
CYCLIC LOADS
Determination of stresses on laminated aircraft transparencies by the strain gage-hole drilling and sectioning method
| AD-A255548 | p 791 N93-14571
RB211-524B disc and drive cones hot cyclic spinning test p 799 N93-14895
Frequency-domain synthesis of the fatigue load spectrum for the NPS 100-kW wind turbine
| DE92-040984 | p 908 N93-15384
CYCLONES
Synoptic/planetary-scale interactions and blocking over the North Atlantic Ocean
| NASA-CR-191376 | p 925 N93-14769
The influence of baroclinic processes on tropical cyclone motion p 923 N93-15099
CYLINDRICAL BODIES
Full surface testing of grazing incidence mirrors
| AD-A255644 | p 979 N93-14152
An analytic phase function for cylindrical particles
| AD-A255750 | p 977 N93-15054
The stress development during filament winding of thick cylinders
| AD-A255765 | p 901 N93-15066
Wake similarity and vortex formation for two-dimensional bluff bodies p 781 N93-15101
CYLINDRICAL SHELLS
A time-domain study of the relationship between drive force time bandwidth and farfield acoustic radiation
| AD-A255616 | p 973 N93-14159
Analysis and optimal design of pressurized, imperfect, anisotropic ring-stiffened cylinders p 897 N93-14251

D

DAMAGE
Nondestructive evaluation of damage in SiC/Al metal matrix composite using x ray tomographic microscopy p 829 N93-14192
Damage location and model refinement for large flexible space structures using a sensitivity-based eigenstructure assignment method p 816 N93-14274
Method and devices for the in situ repair of damaged threads
| AD-D015416 | p 891 N93-14881
Damage and rupture of ceramic composites
| ETN-92-92722 | p 851 N93-15127
Development of adherent ceramic coatings to reduce contact stress damage of ceramics
| DE92-041373 | p 852 N93-15437
DAMAGE ASSESSMENT
Results of a FRSI material test under Space Shuttle ascent conditions in the Ames Research Center 9x7 foot supersonic wind tunnel (OS13). Space Shuttle aerothermodynamic data report
| NASA-CR-167699 | p 816 N93-15475
DAMS
Integrating satellite imagery into a geographic information system for monitoring the downstream impacts of dam construction on floodplain agriculture in Sokoto State, Nigeria p 905 N93-14823
DARK MATTER
Dark matter axions
| DE92-040501 | p 1022 N93-15346
DATA ACQUISITION
Magellan project p 1041 N93-14373
Investigation of the use of surface electrical currents for short-range shipboard data communications
| AD-A256197 | p 859 N93-14490
Upgrade the University of Wisconsin volume imaging lidar
| AD-A255476 | p 885 N93-14497
System for memorizing maximum values
| NASA-CASE-MSC-21922-1 | p 882 N93-14841
Results of in-service evaluation of wind shear systems p 785 N93-14856
Personal computer based computed tomography system
| KCP-613-4806 | p 945 N93-14876
FDAMS: An extendable and reconfigurable solution for avionics data management systems p 794 N93-15157
DAR-2: On-board data acquisition system for aircraft engines p 795 N93-15166
Data collection procedures for the Software Engineering Laboratory (SEL) database
| NASA-TM-108579 | p 957 N93-15579
A new approach for data acquisition at the JPL space simulators p 821 N93-15606
Acoustic and thermal testing of the Titan/Centaur upper stage p 814 N93-15621
Upgrade and extension of the data acquisition system for propulsion and gas dynamic laboratories
| AD-A256836 | p 1009 N93-15637
DATA BASE MANAGEMENT SYSTEMS
Data management for the coordinated Eastern Arctic experiment
| AD-A255648 | p 1000 N93-14182
Query processing in distributed database systems p 1001 N93-14218
Data management and processing plan, Department of Applied Geodesy
| DE93-000774 | p 905 N93-14522
The National Space Science Data Center: An operational perspective p 1006 N93-15045
Parallelism in a main-memory DBMS: The performance of PRISMA/DB
| MEMO-INF-92-25 | p 958 N93-15093
Wisconsin Inventors' Network Database
| DE92-018394 | p 1007 N93-15137
PRISMA/DB: A parallel, main-memory relational DBMS
| MEMO-INF-92-12 | p 959 N93-15141
Technical data management at the Yucca Mountain Site Characterization Project
| DE92-018115 | p 1008 N93-15229
Query optimization and planning in object-oriented knowledge bases
| AD-A256006 | p 1008 N93-15254
Information technologies for global resources management and environmental assessment
| DE92-041107 | p 906 N93-15442
Physical design for network databases
| MEMO-INF-92-26 | p 1009 N93-15492
Predicting database requirements for geographic information systems in the year 2000: Long-term design issues for GRASS
| AD-A256862 | p 1009 N93-15627
DATA BASES
Data management for the coordinated Eastern Arctic experiment
| AD-A255648 | p 1000 N93-14182
Information system constraint language (ISyCL)
| AD-A256268 | p 976 N93-14438
The preliminary Long Duration Exposure Facility (LDEF) materials data base
| NASA-TM-107692 | p 828 N93-14459
Vendor Information System (VIS) systems manual
| AD-A256174 | p 1002 N93-14650
The evolution of the quasar continuum
| NASA-CR-191673 | p 1012 N93-14759
The National Space Science Data Center: An operational perspective p 1002 N93-14775
Stewardship of very large digital data archives p 1005 N93-15032
EMASS (trademark): An expandable solution for NASA space data storage needs p 1005 N93-15033
The National Space Science Data Center: An operational perspective p 1006 N93-15045
Mass storage system experiences and future needs at the National Center for Atmospheric Research p 1007 N93-15046
Source header list. Volume 2: K through Z
| AD-A256001 | p 1007 N93-15112
Wisconsin Inventors' Network Database
| DE92-018394 | p 1007 N93-15137
An eclectic method for object oriented database design
| AD-A256439 | p 1008 N93-15315
User's guide for SearchMAESTRO
| AD-A256422 | p 1008 N93-15335
Physical design for network databases
| MEMO-INF-92-26 | p 1009 N93-15492
CSCW - WCSC: Computer-supported cooperative work. What changes for the science of computing p 954 N93-15549
A data parallel algorithm for raytracing of heterogeneous databases p 955 N93-15553
Data collection procedures for the Software Engineering Laboratory (SEL) database
| NASA-TM-108579 | p 957 N93-15579
Predictions of dose from electrons in space
| NASA-CR-191617 | p 1051 N93-15580
Predicting database requirements for geographic information systems in the year 2000: Long-term design issues for GRASS
| AD-A256862 | p 1009 N93-15627
GRASS 4.0 map digitizing user's manual: V. Digit
| AD-A256859 | p 1009 N93-15642
A structural approach to the photonic processor
| N-3399-RC | p 986 N93-15648
DATA COMPRESSION
Wavelet methods for curve estimation
| AD-A255357 | p 970 N93-14538
A very efficient RCS data compression and reconstruction technique, volume 4
| NASA-CR-191378-VOL-4 | p 945 N93-14807
DATA CORRELATION
The detection and correlation modeling of Rayleigh distributed radar signals
| AD-A256612 | p 858 N93-14250
DATA FLOW ANALYSIS
File servers, networking, and supercomputers p 1004 N93-15030
DATA LINKS
On the performance of Trellis coded modulation with octal phase shift keying over the TDRSS channel
| NASA-CR-191366 | p 857 N93-14155
Multi-access strategies for voice/data integration in heterogeneous mixed-media packet radio networks
| AD-A255636 | p 857 N93-14181
Investigation of the use of surface electrical currents for short-range shipboard data communications
| AD-A256197 | p 859 N93-14490
Progress toward a full scale mobile satellite system for Canada p 812 N93-14960
Tactical line-of-sight path reliability: Improved MSE system procedures
| AD-A256504 | p 862 N93-15376
DATA MANAGEMENT
Proceedings of the data assimilation in coupled air-sea nowcast/forecast systems workshop
| AD-A255409 | p 925 N93-14503
Data management and processing plan, Department of Applied Geodesy
| DE93-000774 | p 905 N93-14522
Data management in NOAA p 1003 N93-14779
EMASS (trademark): An expandable solution for NASA space data storage needs p 1005 N93-15033
Data archiving p 1005 N93-15035
Network accessible multi-terabyte archive p 1005 N93-15036
The National Space Science Data Center: An operational perspective p 1006 N93-15045
Mass storage system experiences and future needs at the National Center for Atmospheric Research p 1007 N93-15046
Requirements for a network storage service p 1007 N93-15048
Data fragmentation for parallel transitive closure strategies
| MEMO-INF-92-17 | p 959 N93-15142
The Teledyne controls aircraft condition monitoring system p 793 N93-15155
Flight data and flight safety in SAS p 793 N93-15156
FDAMS: An extendable and reconfigurable solution for avionics data management systems p 794 N93-15157
Ground Support Equipment (GSE) for Aircraft Condition Monitoring System (ACMS) p 778 N93-15158
Monitoring of powerplants in advanced commercial aircraft p 795 N93-15171
EJ 200 engine monitoring system: On- and off-board data capture, analysis, and management system p 796 N93-15172
Conversion of IRAMMP data to HDF format
| AD-A256515 | p 1008 N93-15393
Space Station Freedom data management system growth and evolution report
| NASA-TM-103869 | p 816 N93-15477
A new approach for data acquisition at the JPL space simulators p 821 N93-15606

DATA PROCESSING
Knowledge and processes in design
[AD-A255663] p 999 N93-14130
Venus radar mapping from the Venera 15 and 16 spacecrafts: Results and restrictions
p 1023 N93-14289
Multiresolution pattern recognition of small volcanos in Magellan data p 1042 N93-14380
Upgrade the University of Wisconsin volume imaging lidar
[AD-A255476] p 885 N93-14497
Convective scale 4-D data assimilation using simulated single-Doppler radar observations p 921 N93-14683
Enterprise storage report for the 1990's
p 1004 N93-15028
From data structure to process structure
[MEMO-INF-91-38] p 946 N93-15077
A non-deterministic recogniser generator
[MEMO-INF-92-21] p 946 N93-15091
Data fragmentation for parallel transitive closure strategies
[MEMO-INF-92-17] p 959 N93-15142
Indian experience in flight data readout and analysis
p 794 N93-15161
Czechoslovak development and experience in flight data recorder readout and analysis p 794 N93-15162
Software for flight recorder data evaluation developed by Lufthansa p 794 N93-15163
The FAIR (Flight Animated and Interactive Reconstruction) tool p 788 N93-15164
The SIROM flight data recorder and evaluation system
p 795 N93-15165
Design for tactical situation awareness display
[AD-A256194] p 798 N93-15235
Radar data processing using a distributed computational system
[AD-A256209] p 861 N93-15237
Data analysis and interpretation for environmental surveillance
[DE92-019009] p 910 N93-15270
Application of programmable logic controllers to space simulation p 821 N93-15608
Feasibility study for an integrated data processing system
[PB92-214287] p 1009 N93-15644

DATA PROCESSING EQUIPMENT
Image processing and products for the Magellan mission to Venus p 1026 N93-14306
A complete-time approach for chaining and execution control in the AN/UYS-2 parallel signal processor
[AD-A256306] p 859 N93-14442
Method and apparatus for increasing a radar's range with improved scan-to-scan integration of Doppler filtered signals
[AD-D015421] p 860 N93-14742
Feasibility study for an integrated data processing system
[PB92-214287] p 1009 N93-15644

DATA RECORDERS
The 19 mm date recorders: Similarities and differences p 883 N93-15042
The SIROM flight data recorder and evaluation system
p 795 N93-15165
Solid state flight data recorder with rapid data access
p 795 N93-15167
Integrated engine control and monitoring with experiences derived from OLMOS p 795 N93-15168

DATA RECORDING
Magnetic disk p 1004 N93-15029
ICI optical data storage tape p 1005 N93-15037
Mass storage system experiences and future needs at the National Center for Atmospheric Research
p 1007 N93-15046

DATA REDUCTION
Convective scale 4-D data assimilation using simulated single-Doppler radar observations p 921 N93-14683
Transcutaneous Analyte Measuring Methods (TAMM), phase 2
[AD-A256327] p 936 N93-15192
Data analysis and interpretation for environmental surveillance
[DE92-019009] p 910 N93-15270

DATA RETRIEVAL
A very efficient RCS data compression and reconstruction technique, volume 4
[NASA-CR-191378-VOL-4] p 945 N93-14807
Proceedings of the NSSDC Conference on Mass Storage Systems and Technologies for Space and Earth Science Applications
[NASA-TM-107989] p 1004 N93-15027
Data storage and retrieval system
p 1005 N93-15034
The 19 mm date recorders: Similarities and differences p 883 N93-15042
Requirements for a network storage service
p 1007 N93-15048
Flight data and flight safety in SAS
p 793 N93-15156
Solid state flight data recorder with rapid data access
p 795 N93-15167
Royal Air Force experience of the Harrier information management system p 795 N93-15170
EJ 200 engine monitoring system: On- and off-board data capture, analysis, and management system
p 796 N93-15172
Work efficient hashing on parallel and vector computers
[AD-A256355] p 959 N93-15205

DATA SMOOTHING
Integration and processing of high-resolution moire-interferometry data p 895 N93-14185
Wavelet methods for curve estimation
[AD-A255357] p 970 N93-14538

DATA STORAGE
Method and apparatus for increasing a radar's range with improved scan-to-scan integration of Doppler filtered signals
[AD-D015421] p 860 N93-14742
NSSDC Conference on Mass Storage Systems and Technologies for Space and Earth Science Applications, volume 3
[NASA-CP-3165-VOL-3] p 1002 N93-14771
Network issues for large mass storage requirements
p 1002 N93-14773
The role of HiPPI switches in mass storage systems: A five year prospective p 1002 N93-14774
The National Space Science Data Center: An operational perspective p 1002 N93-14775
EOSDIS/DADS requirements p 1003 N93-14776
Status of emerging standards for removable computer storage media and related contributions of NIST
p 1003 N93-14778
Data management in NOAA p 1003 N93-14779
Storage needs in future supercomputer environments
p 1003 N93-14780
Requirements for a network storage service
p 1003 N93-14781
Ultra-dense optical mass storage
[AD-A255463] p 1004 N93-14785
System for memorizing maximum values
[NASA-CASE-MSC-21922-1] p 882 N93-14841
Proceedings of the NSSDC Conference on Mass Storage Systems and Technologies for Space and Earth Science Applications
[NASA-TM-107989] p 1004 N93-15027
Enterprise storage report for the 1990's
p 1004 N93-15028
Magnetic disk p 1004 N93-15029
File servers, networking, and supercomputers
p 1004 N93-15030
The long hold: Storing data at the National Archives
p 1004 N93-15031
Stewardship of very large digital data archives
p 1005 N93-15032
EMASS (trademark): An expandable solution for NASA space data storage needs p 1005 N93-15033
Data storage and retrieval system
p 1005 N93-15034
Data archiving p 1005 N93-15035
Network accessible multi-terabyte archive
p 1005 N93-15036
ICI optical data storage tape p 1005 N93-15037
ATL Products Division's entries into the computer mass storage marketplace p 1005 N93-15038
A system approach to archival storage
p 1006 N93-15040
Stability of Co-gamma-Fe2O3 tape
p 1006 N93-15041
The 19 mm date recorders: Similarities and differences p 883 N93-15042
An empirical approach to predicting long term behavior of metal particle based recording media
p 883 N93-15043
Mass storage system experiences and future needs at the National Center for Atmospheric Research
p 1007 N93-15046
Storage needs in future supercomputer environments
p 1007 N93-15047
Requirements for a network storage service
p 1007 N93-15048
Data fragmentation for parallel transitive closure strategies
[MEMO-INF-92-17] p 959 N93-15142
Rewritable optical disk: Application to flight recording
p 794 N93-15160
Solid state flight data recorder with rapid data access
p 795 N93-15167
Conversion of IRAMMP data to HDF format
[AD-A256515] p 1008 N93-15393
Research Studies on Advanced Optical Module/Head Designs for Optical Data Storage
[NASA-CR-191307] p 984 N93-15505
Combining ray-trace and diffraction analysis: A design example p 985 N93-15511
Modeling and measurement of a micro-optic beam deflector p 985 N93-15514
Effects of higher order aberrations on beam shape in an optical recording system p 985 N93-15515

DATA STRUCTURES
From data structure to process structure
[MEMO-INF-91-38] p 946 N93-15077
Work efficient hashing on parallel and vector computers
[AD-A256355] p 959 N93-15205
Experience with a course on architectures for software systems. Part 1: Course description
[AD-A256221] p 941 N93-15239
A two-pass physics-based global lighting model
p 957 N93-15570
A distributed data-balanced dictionary based on the b-link tree
[AD-A256841] p 1009 N93-15639

DATA SYSTEMS
EOSDIS/DADS requirements p 1003 N93-14776
Data archiving p 1005 N93-15035
The National Space Science Data Center: An operational perspective p 1006 N93-15045
The SIROM flight data recorder and evaluation system
p 795 N93-15165

DATA TRANSFER (COMPUTERS)
Network issues for large mass storage requirements
p 1002 N93-14773
The role of HiPPI switches in mass storage systems: A five year prospective p 1002 N93-14774
Storage needs in future supercomputer environments
p 1003 N93-14780
Requirements for a network storage service
p 1003 N93-14781
Data storage and retrieval system
p 1005 N93-15034
Indian experience in flight data readout and analysis
p 794 N93-15161

DATA TRANSMISSION
Venus radar mapping from the Venera 15 and 16 spacecrafts: Results and restrictions
p 1023 N93-14289
Optical fibers for long-haul transmission in severe-bending applications
[AD-A255964] p 981 N93-14407
Investigation of the use of surface electrical currents for short-range shipboard data communications
[AD-A256197] p 859 N93-14490
Engineering of massively interconnected computer systems
[AD-A255501] p 958 N93-14645
System design and development of a low data rate voice (1200 bps) rate converter
[AD-A256071] p 859 N93-14663
Storage needs in future supercomputer environments
p 1003 N93-14780
The role of HiPPI switches in mass storage systems: A five year prospective p 1006 N93-15044
EDI planning and implementation guide
[AD-A255737] p 1007 N93-15050
The evolution of signalling from ISDN to B-ISDN
[MEMO-INF-92-30] p 860 N93-15095
On the theory of coded modulation systems for high output digital transmission
[TELECOM-PARIS-92-E-001] p 861 N93-15098
Tactical line-of-sight path reliability: Improved MSE system procedures
[AD-A256504] p 862 N93-15376

DAYGLOW
A study of mid-latitude 5577 A OI dayglow emissions
p 913 N93-14199
A study of mid-latitude 5577A CI dayglow emissions
[AD-A255444] p 914 N93-14511

DECELERATION
Computer simulations of comet- and asteroidlike bodies passing through the Venusian atmosphere: Preliminary results on atmospheric and ground shock effects
p 1040 N93-14365

DECISION MAKING
Decision-making for intelligent control of dual-arm robotic operations p 960 N93-14201
Information-seeking behavior during the decision-making process: A case study
p 1000 N93-14206
Information for management, planning, and decision-making in nonprofit organizations: Toward a comprehensive model p 1000 N93-14209
Evaluation of the cost effectiveness analysis model being developed for the component improvement programs of the Air Force and the Navy
[AD-A256132] p 1010 N93-14249
Intelligent path prediction for vehicular travel
p 961 N93-14445

Decision making in a dynamic task environment: The effect of time pressure
[AD-A256557] p 937 N93-14602
Workshop on Aeronautical Decision Making (ADM). Volume 2: Plenary Session With Presentations and Proposed Action Plan
[DOT/FAA/RD-92/14-VOL-2] p 785 N93-15013
Does cockpit management training reduce aircrew error? p 785 N93-15014
Cockpit decision making p 786 N93-15015
How expert pilots think p 786 N93-15017
Methodology for studying and training expertise p 786 N93-15018
A cognitive model for training decision making in aircrews p 786 N93-15020
Elements of a theory of natural decision making p 786 N93-15021
Shared mental models and crew decision making p 787 N93-15023
Measuring risk in single-engine and twin-engine helicopters p 787 N93-15025
Proposed action plan to improve ADM effectiveness, part 3: Developing a new ADM paradigm on which to build advanced or expert decision making training p 787 N93-15026
PEX: A reactive procedure based decision maker
[REPT-921-440-105] p 999 N93-15118
Data analysis and interpretation for environmental surveillance
[DE92-019009] p 910 N93-15270
Radar scene generation for tactical decision aids
[AD-A257069] p 863 N93-15495
Telepresence: Integrating shared task and person spaces p 954 N93-15548
CSCW - WCSC: Computer-supported cooperative work. What changes for the science of computing p 954 N93-15549

DECISION THEORY
Wait-free consensus
[AD-A255978] p 943 N93-14423
Probabilistic inference
[AD-A255471] p 963 N93-14786

DECODERS
High-speed architecture for the decoding of trellis-coded modulation
[NASA-CR-191374] p 941 N93-14770

DECODING
High-speed architecture for the decoding of trellis-coded modulation
[NASA-CR-191374] p 941 N93-14770

DECOMPOSITION
Transonic flow calculations for a cavity with and without a store
[AD-A255954] p 873 N93-14421
Computed potential energy surfaces for chemical reactions
[NASA-CR-190741] p 843 N93-15356
Matrix animation and polar decomposition p 956 N93-15563
C60 interactions with surfaces, gaseous species and photons: An overview
[DE92-040738] p 978 N93-15654

DEDUCTION
A proof of the Church-Rosser theorem and its representation in a logical framework
[AD-A256574] p 942 N93-14268

DEFECTS
A proposal to apply Taguchi-inspired methods to the reduction of machining variance
[AD-A256129] p 856 N93-15234

DEFENSE INDUSTRY
The use of International Standards Organization ISO 9000 quality assurance standards in place of military standards
[AD-A256203] p 894 N93-14500

DEFENSE PROGRAM
Unmanned aerial vehicles: More testing needed before production of short-range system
[AD-A256296] p 790 N93-14440
Air Force Office of Scientific Research
[AD-A255361] p 1051 N93-14673
Air Force Office of Scientific Research
[AD-A255370] p 1051 N93-14674
SIDR Relative Weighted Product (RWP) assignment process
[AD-A255801] p 946 N93-15068

DEFLECTION
A geometrically nonlinear stress-deflection relation for thin film/substrate systems p 848 N93-14287

DEFLECTORS
Modeling and measurement of a micro-optic beam deflector p 985 N93-15514

DEFORMATION
Applications of a constitutive equation for microstructural change in polymers p 848 N93-14222
Global deformation on the surface of Venus p 1024 N93-14297
Geoid, topography, and convection-driven crustal deformation on Venus p 1042 N93-14376
Deformation characterization of powdered metals in compaction and application of the finite element method to compaction processes p 844 N93-14472
Mechanics of composite materials for spacecraft
[AD-A255380] p 831 N93-14550
Precise measurements made from a distance of local deformations independent of small object movements
[ETN-92-92723] p 886 N93-15128
Thermal, mechanical, and electroelastic behavior of composite materials p 835 N93-15146
Structural study of thermohardening matrices: Deformation of composite matrices in relation to their molecular structure
[ONERA-RT-12/3521-M] p 836 N93-15253

DEGASSING
A new approach for performing contamination control bakeouts in JPL thermal vacuum test chambers p 823 N93-15618

DEGREES OF FREEDOM
Interplanetary program to optimize simulated trajectories (IPOST). Volume 4: Sample cases
[NASA-CR-189653-VOL-4] p 815 N93-14768
Multiply connected spacetimes and closed timelike curves in semiclassical gravity p 915 N93-14884
Theory and applications of hyper-redundant robotic manipulators p 892 N93-15104

DEHYDROGENATION
Physics of hydrogen storage in metal-hydrides p 854 N93-14630

DEICERS
Results of low power deicer tests on a swept inlet component in the NASA Lewis icing research tunnel
[NASA-TM-105968] p 781 N93-14911
Surface roughness due to residual ice in the use of low power deicing systems
[NASA-TM-105971] p 782 N93-15338
Numerical modeling of anti-icing systems and comparison to test results on a NASA 0012 airfoil
[NASA-TM-105975] p 787 N93-15345

DEICING
Results of low power deicer tests on a swept inlet component in the NASA Lewis icing research tunnel
[NASA-TM-105968] p 781 N93-14911

DELAMINATING
The effect of the interphase/interface region on creep and creep rupture of thermoplastic composites p 829 N93-14193
Elastic wave scattering by partially debonded or partially coated fibers p 829 N93-14224
A preliminary investigation of dual mode fracture sustained by graphite/epoxy laminates impacted by high-velocity spherical metallic projectiles
[AD-A255790] p 898 N93-14419
Fracture mechanisms and fracture control in composite structures p 899 N93-14474
Delamination growth behavior in cross-ply laminated composites due to transverse concentrated loading
[AD-A255974] p 830 N93-14493
The effect of geometry and prescribed delaminations on the postbuckling behaviour of laminated carbon-fibre reinforced plastic panels p 831 N93-14597
Characterizing longitudinal splitting and delamination fracture toughness of composites p 831 N93-14607

DELINEATION
Using digital scanned aerial photography for wetlands delineation
[AD-A255392] p 905 N93-14676

DELTA MODULATION
A new multiplier-free structure for DFT based on delta modulation
[AD-A255927] p 861 N93-15106

DELTA WINGS
Flowfield study of a close-coupled canard configuration
[AD-A256311] p 782 N93-15245

DEMODULATION
Demodulation processes in auditory perception
[AD-A255748] p 935 N93-15053

DEMOGRAPHY
Aviation accidents, incidents, and violations: Psychological predictors among US pilots p 783 N93-14693

DENSE PLASMAS
Electrical resistivity and equation of state measurements of a dense aluminum plasma
[DE92-040352] p 989 N93-15436

DENSITY (MASS/VOLUME)
Orthobaric densities and molar volumes of liquids. Halogenated ethylenes
[ESDU-92018] p 839 N93-14540

DENSITY (NUMBER/VOLUME)
Molecular capacitance: Sequential electron-transfer energetics for solution-phase metallic clusters in relation to gas-phase clusters and analogous interfaces
[AD-A257057] p 977 N93-15448

DEPLOYMENT
On some kinematic and mass characteristics of foldable solar arrays p 812 N93-14957
On-orbit deployment anamolies: What can be done? p 821 N93-15603
Offloading techniques for large deployable space structures p 821 N93-15605

DEPOSITION
Reliability of sol-gel derived ferroelectric memories
[AD-A255240] p 849 N93-14668
Thin-film permanent magnets for integrated electromagnetic components
[AD-A256175] p 972 N93-14679
Method of forming a multiple layer dielectric and a hot film sensor therewith
[NASA-CASE-LAR-13678-3] p 881 N93-14714
Method for fabricating ohmic contacts on semiconducting diamond
[AD-D015432] p 850 N93-14825
Sputter deposition and characterization of MoSi2/SiC composite coatings
[DE92-040326] p 837 N93-15426

DEPOSITS
Venusian extended ejecta deposits as time-stratigraphic markers p 1030 N93-14327

DEPTH MEASUREMENT
Application of left- and right-looking SAR stereo to depth measurements of the Ammavaru outflow channel, Lada Terra, Venus p 1038 N93-14357

DESALINIZATION
Apparatus and process for desalination of seawater
[AD-D015428] p 842 N93-14824

DESCRIPTIVE GEOMETRY
Interactive solid geometry via partitioning trees p 952 N93-15535

DESIGN
Knowledge and processes in design
[AD-A255663] p 999 N93-14130

DESIGN ANALYSIS
Reanalysis of multiple-wheel landing gear traffic tests
[AD-A256593] p 804 N93-14238
Analysis and optimal design of pressurized, imperfect, anisotropic ring-stiffened cylinders p 897 N93-14251
Multiobjective control/structure design optimization in the presence of practical constraints p 898 N93-14446
Multi-point inverse design of isolated airfoils and airfoils in cascade in incompressible flow p 790 N93-14462
Testability design rating system: Testability handbook, volume 1
[RL-TR-92-12-VOL-1] p 867 N93-14699
Aeronautical engineering: A continuing bibliography with indexes (supplement 283)
[NASA-SP-7037(283)] p 778 N93-14732
Advanced aeroservoelastic stabilization techniques for hypersonic flight vehicles
[NASA-CR-189702] p 802 N93-14811
NASA/LMSC instrument design and fabrication --- coherent lidar airborne shear sensor p 784 N93-14846
Experimental evaluation of candidate graphical microburst alert displays p 785 N93-14853
A robotic planning system p 810 N93-14949
Obstacles in object-oriented software development
[MEMO-INF-92-15] p 946 N93-15084
Analysis of in-flight structural failures of P-3C wing leading edge segments
[AD-A256212] p 792 N93-15238
High-brightness linac for the Advanced Free-Electron Laser Initiative at Los Alamos
[DE92-040213] p 887 N93-15417

DESORPTION
Absorption of propellant vapors into polymer films
[AD-A255274] p 849 N93-14531
Si atomic layer epitaxy using remote plasma assisted hydrogen desorption and disilane as a precursor
[AD-A255606] p 993 N93-15008
Operational strategies for contamination control of composite materials p 822 N93-15614

DETECTION
Improved astigmatic focus error detection method p 984 N93-15507
Acoustic location of leaks in pressurized underground petroleum pipelines
[PB92-207687] p 975 N93-15647

DETECTORS
Operational strategies for contamination control of composite materials p 822 N93-15614

DETERIORATION
The preservation of LANDSAT data by the National Land Remote Sensing Archive p 1003 N93-14777

Composite materials in space: Results from the LDEF satellite p 811 N93-14955

DETERMINANTS
Algorithms for intersecting parametric and algebraic curves p 956 N93-15560

DETONATION WAVES
Hydrodynamics of supernova 1987 A p 1019 N93-14633

DIAMOND FILMS
Twin quintuplets in CVD diamond
[AD-A255862] p 989 N93-14133
Growth, characterization and device development in monocrystalline diamond films
[AD-A256283] p 994 N93-15244

DIAMONDS
Twin quintuplets in CVD diamond
[AD-A255862] p 989 N93-14133
Method for fabricating ohmic contacts on semiconducting diamond
[AD-D015432] p 850 N93-14825

DICHLORIDES
Softening of rigid polyvinyl chloride by high concentrations of aqueous solutions of methylene chloride
[AD-A255453] p 848 N93-14486

DICTIONARIES
A distributed data-balanced dictionary based on the b-link tree
[AD-A256841] p 1009 N93-15639

DIELECTRIC PROPERTIES
Dielectric surface properties of Venus p 1039 N93-14360

DIELECTRICS
Efficient asymptotic closed form approximation for dyadic green's function for anisotropic substrates, phase 1
[AD-A256258] p 830 N93-14436
High temperature polymer dielectric film insulation
[AD-A255243] p 849 N93-14527
Method of forming a multiple layer dielectric and a hot film sensor therewith
[NASA-CASE-LAR-13678-3] p 881 N93-14714
Microstack insulator for flashover inhibition, phase 2
[AD-A256338] p 869 N93-15196
Ferroelectrics volume 122, numbers 1-4, 1991. Proceedings of the 3rd International Conference on Ferroelectric Liquid Crystals, part 2
[AD-A257053] p 996 N93-15446
Ferroelectrics volume 121, numbers 1-4, 1991. Proceedings of the 3rd International Conferenceon Ferroelectric Liquid Crystals, part 1
[AD-A257054] p 996 N93-15447

DIENES
Thermal conductivity of liquid aliphatic hydrocarbons. Part 2: Alkenes, dienes and trienes
[ESDU-92025] p 839 N93-14542

DIESEL ENGINES
Development of low-expansion ceramics for diesel engine applications
[DE92-041380] p 853 N93-15438
Development of wear-resistant ceramic coatings for diesel engine components
[DE92-041382] p 853 N93-15439

DIETS
Modelling global methane emissions from livestock: Biological and nutritional controls
[NASA-CR-191354] p 911 N93-15480

DIFFERENCE EQUATIONS
The use of chaos metrics to analyze Lagrangian particle diffusion models
[AD-A256142] p 967 N93-14255

DIFFERENTIAL EQUATIONS
A differential equation design method for finite-conjugate, multi-mirror imaging systems p 979 N93-14165
The center for nonlinear phenomena and magnetic materials
[AD-A255983] p 967 N93-14412
Eno-Osher schemes for Euler equations
[NASA-TM-105928] p 969 N93-15341
Schwinger Dyson equations: Dynamical chiral symmetry breaking and confinement
[DE92-040717] p 978 N93-15657

DIFFERENTIAL GEOMETRY
Robust nonlinear feedback guidance for an aerospace plane: A geometric approach p 803 N93-14835

DIFFRACTION
Research Studies on Advanced Optical Module/Head Designs for Optical Data Storage
[NASA-CR-191307] p 984 N93-15505
Diffraction analysis and evaluation of several focus- and track-error detection schemes for magneto-optical disk systems p 984 N93-15506
Combining ray-trace and diffraction analysis: A design example p 985 N93-15511
Integrated device with diffractive polarization components for a magneto-optical disk head p 986 N93-15517
The design and fabrication of a single leakage-channel grating coupler p 986 N93-15518
On the convergence of the coupled-wave approach for lamellar diffraction gratings p 986 N93-15520

DIFFRACTION PATTERNS
Precise measurements made from a distance of local deformations independent of small object movements
[ETN-92-92723] p 886 N93-15128

DIFFUSERS
Investigations of detail design issues for the high speed acoustic wind tunnel using a 60th scale model tunnel. Part 1: Tests with open circuits
[NASA-CR-191671] p 780 N93-14737

DIFFUSION
Characterization of fiber reinforced phenolic composites p 828 N93-14142
Diffusion problems in bonded nonhomogeneous materials with an interface cut
[AD-A256470] p 836 N93-15373
Adsorption and diffusion of fluids in well-characterized adsorbent materials
[DE92-040160] p 843 N93-15414

DIFFUSION FLAMES
Transport phenomena and interfacial kinetics in multiphase combustion systems.
[AD-A255999] p 838 N93-14418
Dynamic behavior of a dense spray diffusion flame in a potential vortex p 839 N93-14463

DIFFUSION PUMPS
From diffusion pumps to cryopumps: The conversion of GSFC's space environment simulator p 814 N93-15611

DIFFUSION WAVES
Diffusing wave spectroscopy p 980 N93-14169

DIFFUSION WELDING
Method of bonding molybdenum to steel
[AD-D015410] p 845 N93-14888
Diffusion problems in bonded nonhomogeneous materials with an interface cut
[AD-A256470] p 836 N93-15373
The use of a novel manufacturing process for high performance titanium plate fin heat exchangers
[PNR-90934] p 879 N93-15473
High performance titanium plate fin heat exchanger using a novel manufacturing process
[PNR-90933] p 880 N93-15488
Summary of the NASA Lewis component technology program for Stirling power converters
[NASA-TM-105640] p 827 N93-15526

DIFFUSIVITY
Application of the square root diffusivity analysis to measuring the diffusivity of multicomponent alloys
[DE92-040978] p 847 N93-15382

DIGITAL COMPUTERS
Computer-aided design package for designers of digital optical computers
[AD-A255381] p 944 N93-14564

DIGITAL DATA
Method and apparatus for increasing a radar's range with improved scan-to-scan integration of Doppler filtered signals
[AD-D015421] p 860 N93-14742
NSSDC Conference on Mass Storage Systems and Technologies for Space and Earth Science Applications, volume 3
[NASA-CP-3165-VOL-3] p 1002 N93-14771
The preservation of LANDSAT data by the National Land Remote Sensing Archive p 1003 N93-14777
Data management in NOAA p 1003 N93-14779
Stewardship of very large digital data archives p 1005 N93-15032
Tactical line-of-sight path reliability: Improved MSE system procedures
[AD-A256504] p 862 N93-15376

DIGITAL ELECTRONICS
The extended VHDL (VHSIC hardware description language) design environment: An unique integrated system and hardware design environment
[VH-3] p 948 N93-15264
Synthesis and simulation with VHDL (VHSIC hardware description language)
[VH-5] p 948 N93-15266

DIGITAL FILTERS
Algorithms for the detection and elimination of specular aliasing p 954 N93-15544

DIGITAL SYSTEMS
A complete-time approach for chaining and execution control in the AN/UYS-2 parallel signal processor
[AD-A256306] p 859 N93-14442
Digital bank-to-turn control and guidance p 802 N93-14447
Arc digital raster imagery evaluation
[AD-A255403] p 817 N93-14565
The evolution of signalling from ISDN to B-ISDN
[MEMO-INF-92-30] p 860 N93-15095
Integration of satellite links into an ATM mode broadband ISDN
[TELECOM-PARIS-91-E-022] p 861 N93-15097
The extended VHDL (VHSIC hardware description language) design environment: An unique integrated system and hardware design environment
[VH-3] p 948 N93-15264
Digital active material processing platform effort (DAMPER), SBIR phase 2
[NASA-CR-190798] p 856 N93-15353
Tactical line-of-sight path reliability: Improved MSE system procedures
[AD-A256504] p 862 N93-15376
Multi-axis transient vibration testing of space objects: Test philosophy, test facility, and control strategy p 820 N93-15598

DIGITAL TECHNIQUES
Altimeter and oceanographic in situ measurements in the area of the Greenland-Iceland-Norwegian Sea, 1987-1988
[AD-A256598] p 960 N93-14239
Method and apparatus for increasing a radar's range with improved scan-to-scan integration of Doppler filtered signals
[AD-D015421] p 860 N93-14742
Off-axis conoscopic holography: Optical and digital reconstruction
[TELECOM-PARIS-90-E-023] p 882 N93-15096

DIMENSIONAL STABILITY
Composite materials in space: Results from the LDEF satellite p 811 N93-14955

DIRECT CURRENT
A novel, high energy-density electrical storage device for electric weapons
[AD-A255205] p 867 N93-14666
Power conversion system modification to permit use of DC power source
[AD-D015409] p 868 N93-14887

DIRECTIONAL CONTROL
PEX: A reactive procedure based decision maker
[REPT-921-440-105] p 999 N93-15118

DIRECTIONAL SOLIDIFICATION (CRYSTALS)
Modelling Directional Solidification
[NASA-CR-191301] p 995 N93-15309
Solidification of InSb-GaSb alloy and InSb with vibration p 995 N93-15310
An experimental approach to determine the heat transfer coefficient in directional solidification furnaces p 995 N93-15311
Experimental observation of the influence of furnace temperature profile on convection and segregation in the vertical Bridgman crystal growth technique p 995 N93-15312

DIRECTORIES
Directory of research projects: Planetary geology and geophysics program
[NASA-TM-4428] p 864 N93-15638

DISABILITIES
Compliant walker
[NASA-CASE-GSC-13348-2] p 934 N93-14708

DISK GALAXIES
Study of tidal interactions in M81-M82-NGC3077 system p 1010 N93-14195

DISK OPERATING SYSTEM (DOS)
A methodology for the evaluation of structural design software for DOS-based microcomputers
[AD-A255421] p 943 N93-14505

DISPLACEMENT
The mechanics of dislocation nucleation at a crack tip p 896 N93-14214

DISPLAY DEVICES
A spurious pop-out in visual search
[AD-A256548] p 936 N93-14267
Advantages of using a projected head-up display in a flight simulator
[AD-A255332] p 804 N93-14559
VANTAGE: A frame-based geometric modeling system programmer/user's manual, V2.0
[AD-A255434] p 944 N93-14566
Experimental evaluation of candidate graphical microburst alert displays p 785 N93-14853
A distributed visualization environment for engineering sciences
[DE92-012629] p 1051 N93-15060
Method and apparatus for a high resolution, flat panel cathodoluminescent display screen
[AD-D015400] p 868 N93-15107
Design for tactical situation awareness display
[AD-A256194] p 798 N93-15235
Simulator evaluation of displays for a revised takeoff performance monitoring system
[NASA-TP-3270] p 803 N93-15366

High-resolution contrast control on a video display: Method and calibration
[AD-A256552] p 938 N93-15400
A multi-layer graphic model for building interactive graphical applications p 957 N93-15567

DISTILLATION
Apparatus and process for desalination of seawater
[AD-D015428] p 842 N93-14824

DISTILLATION EQUIPMENT
Apparatus and process for desalination of seawater
[AD-D015428] p 842 N93-14824

DISTRIBUTED FEEDBACK LASERS
Multiperiod-grating surface-emitting lasers
[NASA-CASE-NPO-17763-1-CU] p 885 N93-14703

DISTRIBUTED PARAMETER SYSTEMS
Computation and communication constraints for distributed estimation systems
[AD-A256287] p 970 N93-14456
Feedback control of flow separation and transition to turbulence in unsteady boundary layers p 873 N93-14464

DISTRIBUTED PROCESSING
Wait-free consensus
[AD-A255978] p 943 N93-14423
Network issues for large mass storage requirements p 1002 N93-14773
Radar data processing using a distributed computational system
[AD-A256209] p 861 N93-15237
Transactional distributed shared memory
[AD-A256222] p 941 N93-15240
MATE: The multi-agent test environment
[NASA-TM-108114] p 965 N93-15292
Implementation and analysis of NP-complete algorithms on a distributed memory computer
[AD-A256564] p 951 N93-15405
A massively distributed parallel genetic algorithm
[AD-A256617] p 959 N93-15407
CSCW - WCSC: Computer-supported cooperative work. What changes for the science of computing p 954 N93-15549

DISTRIBUTION FUNCTIONS
Effects of cryocontaminants on cryogenic superpolished mirror and superpolished quartz crystal microbalance
[AD-A255972] p 981 N93-14403

DIURNAL VARIATIONS
Cloud-radiative feedbacks in tropical convection p 919 N93-14180
Middle atmosphere of Venus and its clouds: Latitude and solar time variations p 1045 N93-14396
Synoptic scale structure of summertime wet and dry spells in northeastern Kansas p 923 N93-14919
Global ocean tide mapping using TOPEX/Poseidon altimetry p 930 N93-14991

DOCUMENT STORAGE
File servers, networking, and supercomputers p 1004 N93-15030
The long hold: Storing data at the National Archives p 1004 N93-15031

DOCUMENTATION
Bibliography of Lewis Research Center Technical Publications announced in 1991
[NASA-TM-105595] p 1004 N93-14796

DOMES (GEOLOGY)
Radar scattering properties of pancakelike domes on Venus p 1028 N93-14316
Igneous and tectonic evolution of Venusian and terrestrial coronae p 1031 N93-14330
Pancakelike domes on Venus p 1035 N93-14345
Venus steep-sided domes: Relationships between geological associations and possible petrogenetic models p 1038 N93-14359

DOORS
Effects of seating configuration and number of type 3 exits on emergency aircraft evacuation
[AD-A256616] p 783 N93-14277

DOPED CRYSTALS
Electronic, vibrational, and transport properties of conducting polymers p 847 N93-14170
Dual active layer photoconductor
[AD-D015423] p 993 N93-14820

DOPPLER EFFECT
Advances in laser cooling
[AD-A255969] p 884 N93-14402
The detection and characterization of high frequency and high wavenumber solar oscillations
[NASA-CR-191622] p 1049 N93-15634

DOPPLER RADAR
Terminal Doppler weather radar/low-level wind shear alert system integration algorithm specification, version 1.1
[AD-A255319] p 920 N93-14547
An observational and theoretical study of squall line evolution p 921 N93-14682
Convective scale 4-D data assimilation using simulated single-Doppler radar observations p 921 N93-14683
Method and apparatus for increasing a radar's range with improved scan-to-scan integration of Doppler filtered signals
[AD-D015421] p 860 N93-14742
NASA/LMSC coherent LIDAR airborne shear sensor: System capabilities and flight test plans p 784 N93-14847
The Orlando TDWR testbed and airborne wind shear date comparison results p 784 N93-14851
TDWR 1991 Program Review p 785 N93-14852
Systems issues in airborne Doppler radar/LIDAR certification p 785 N93-14855

DOSAGE
Predictions of dose from electrons in space
[NASA-CR-191617] p 1051 N93-15580

DOSIMETERS
Improvement and analysis of the radiation response of RADFET dosimeters
[AD-A254115] p 869 N93-15133

DRAFT (GAS FLOW)
An investigation into the role of moist, vertical drafts in the rotational development of storms p 923 N93-15087

DRAG
Turbulent drag and transport in high Reynolds number Couette-Taylor flow p 872 N93-14119

DRAG REDUCTION
Wall layers
[AD-A256152] p 872 N93-14257
An experimental investigation of base bleed effect on the wake turbulent structure behind a two-dimensional blunt model
[MPIS-9/1991] p 781 N93-15131

DRILL BITS
Retractable tool bit having slider type catch mechanism
[NASA-CASE-GSC-13358-1] p 890 N93-14710

DRILLING
Determination of stresses on laminated aircraft transparencies by the strain gage-hole drilling and sectioning method
[AD-A255548] p 791 N93-14571

DROP SIZE
Optimization of a Counterflow Virtual Impactor (CVI) for studying aerosol effects on cloud droplet number p 914 N93-14861
Global survey of effective particle size in liquid water clouds by satellite observations p 921 N93-14862
An investigation into the role of moist, vertical drafts in the rotational development of storms p 923 N93-15087

DROPS (LIQUIDS)
Introduction to spray combustion modelling p 841 N93-14626
Quasars, galaxies, and pseudo-vacuum droplets
[NIKHEF-H/91-20] p 1020 N93-14686
Optimization of a Counterflow Virtual Impactor (CVI) for studying aerosol effects on cloud droplet number p 914 N93-14861

DRYING
Ultrastructure processing and environmental stability of advanced structural and electronic materials
[AD-A256153] p 831 N93-14665

DUCTED FLOW
Optimization of circular orifice jets mixing into a heated cross flow in a cylindrical duct
[NASA-TM-105984] p 800 N93-15359

DUCTILITY
The mechanics of dislocation nucleation at a crack tip p 896 N93-14214
Fe3Al-type iron aluminides: Aqueous corrosion properties in a range of electrolytes and slow-strain rate ductilities during aqueous corrosion
[DE92-040520] p 846 N93-15059
Progress toward a tungsten alloy wire/high temperature alloy composite turbine blade
[NASA-TM-105901] p 847 N93-15586

DUMP COMBUSTORS
Control of asymmetric jet
[AD-A255967] p 873 N93-14400

DUST
Satellite detection of complex aerosols over the Arabian Peninsula/Gulf
[AD-A256085] p 909 N93-14261

DUST STORMS
Degradation of radiator performance on Mars due to dust p 823 N93-15616

DWARF NOVAE
Disc structure and variability in dwarf novae p 1017 N93-14460

DYE LASERS
Method for detecting chemical vapors using a lasing dye sensor
[AD-D015424] p 885 N93-14821

DYNAMIC CHARACTERISTICS
Nonlinear dynamics of optical systems p 979 N93-14124
Dynamic behavior of a dense spray diffusion flame in a potential vortex p 839 N93-14463
Wind shear related research at Princeton University p 785 N93-14854
Theoretical studies of the physics of the solar atmosphere
[NASA-CR-191357] p 1049 N93-15085
Methodology for robot capability and performance characterization: The basis for robot task planningg
[F-2-3] p 949 N93-15300

DYNAMIC CONTROL
Online vibration control of a flexible rotor/bearing system p 899 N93-14468
Dynamics and control of a rigid/flexible manipulator p 890 N93-14684
Dynamics and control of flexible arm robots
[ISBN-0-315-69011-9] p 892 N93-15150

DYNAMIC LOADS
Root damage analysis of aircraft engine blade subject to ice impact
[NASA-TM-105779] p 902 N93-15343

DYNAMIC MODELS
Nonlinear modeling of gated range tracker dynamics with application to radar range resolution, phase 1
[AD-A256074] p 858 N93-14259
Model reduction of flexible manipulators
[AD-A255251] p 889 N93-14528
Modeling and control of a trailing wire antenna towed by an orbiting aircraft
[AD-A256450] p 859 N93-14610
Development of engineering methods for nonequilibrium radiative phenomena about aeroassisted entry vehicles p 817 N93-14632
Advanced aeroservoelastic stabilization techniques for hypersonic flight vehicles
[NASA-CR-189702] p 802 N93-14811

DYNAMIC PRESSURE
Results of a FRSI material test under Space Shuttle ascent conditions in the Ames Research Center 9x7 foot supersonic wind tunnel (OS13). Space Shuttle aerothermodynamic data report
[NASA-CR-167699] p 816 N93-15475
User manual for NASA Lewis 10 by 10 foot supersonic wind tunnel
[NASA-TM-105626] p 804 N93-15498

DYNAMIC RESPONSE
Modal interactions in the dynamic response of isotropic and composite plates p 829 N93-14221
Nonlinear dynamic response of shallow arches to harmonic forcing p 898 N93-14282
Impact-generated winds on Venus: Causes and effects p 1041 N93-14372
Evaluation and estimation of handling qualities via statistical modeling of pilot response data
[AD-A255324] p 939 N93-14548
Multi-disciplinary optimization of aeroservoelastic systems
[NASA-CR-191255] p 901 N93-14766
USACE geotechnical earthquake engineering software, report 1 WESHAKE for personal computers (version 1.0)
[AD-A257068] p 917 N93-15459

DYNAMIC STABILITY
Comparative study of stability of flexible satellites with and without guy-wire constraints p 817 N93-14585
Stability of elastically tailored rotor blades p 791 N93-14828

DYNAMIC STRUCTURAL ANALYSIS
Modal interactions in the dynamic response of isotropic and composite plates p 829 N93-14221
Experimental and analytical investigation of the vibration characteristics of a remotely piloted helicopter
[AD-A256131] p 790 N93-14248
Nonlinear free vibration analysis of strings by the Galerkin method p 972 N93-14280
Nonlinear dynamic response of shallow arches to harmonic forcing p 898 N93-14282
Advanced aeroservoelastic stabilization techniques for hypersonic flight vehicles
[NASA-CR-189702] p 802 N93-14811
Vibration and acoustic testing of TOPEX/Poseidon satellite p 820 N93-15599

DYNAMIC TESTS
Space craft verification at the David Florida Laboratory p 809 N93-14943
Multi-axis transient vibration testing of space objects: Test philosophy, test facility, and control strategy p 820 N93-15598

DYNAMICAL SYSTEMS
Wall layers
[AD-A256152] p 872 N93-14257
Fitting microphysical observations to a numerical model through an optimal control theory technique p 924 N93-15100

Dynamics systems applied to Navier-Stokes equations for the study of turbulence
[ETN-92-92553] p 878 N93-15122
Robust control design for uncertain nonlinear dynamic systems p 964 N93-15148

E

E GLASS
Fiber pulling apparatus modification
[NASA-CR-184498] p 891 N93-14763
EARLY STARS
Nonthermal radio, x ray and gamma ray emissions from chaotic winds of early-type, massive stars
p 1050 N93-14242
EARTH ATMOSPHERE
Method for detecting chemical vapors using a lasing dye sensor
[AD-D015424] p 885 N93-14821
A correlated k-distribution model of the atmospheric heating rates for overlapping spectra of CH4 and N2O
[DE93-000890] p 911 N93-15281
EARTH GRAVITATION
Application of precise altimetry to the study of precise leveling of the sea surface, the Earth's gravity field, and the rotation of the Earth p 907 N93-14992
EARTH IONOSPHERE
Thunderstorm coupling to the magnetosphere and associated ionospheric effects
[NASA-CR-191383] p 922 N93-14910
Deterministic transfer function for transionospheric propagation
[DE92-040327] p 862 N93-15427
Satellite measurement of ionospheric-induced VHF distortion
[DE92-040328] p 862 N93-15435
EARTH MAGNETOSPHERE
Thunderstorm coupling to the magnetosphere and associated ionospheric effects
[NASA-CR-191383] p 922 N93-14910
EARTH MANTLE
Imaging Earth's interior: Tomographic inversions for mantle P-wave velocity structure p 913 N93-14225
The effects of Venusian mantle convection with multiple phase transitions p 1043 N93-14385
EARTH MOVEMENTS
Addressing earthquake strong ground motion issues at the Idaho National Engineering Laboratory
[DE92-017841] p 916 N93-15136
USACE geotechnical earthquake engineering software, report 1 WESHAKE for personal computers (version 1.0)
[AD-A257068] p 917 N93-15459
EARTH OBSERVATIONS (FROM SPACE)
Earth environment space initiative
p 811 N93-14953
EARTH OBSERVING SYSTEM (EOS)
EOSDIS/DADS requirements p 1003 N93-14776
EARTH ORBITAL ENVIRONMENTS
Characterisation and dynamic modelling of the near-earth space particulate environment
p 1019 N93-14637
Spectral analysis of the shuttle glow. SPA II/IBSS Mission: AIS hardware
[PL-TR-92-2148] p 814 N93-14697
Low Earth orbit atomic oxygen simulation for durability evaluation of solar reflector surfaces
p 819 N93-15594
Simulation of the synergistic low Earth orbit effects of vacuum thermal cycling, vacuum UV radiation, and atomic oxygen p 819 N93-15595
The use of plasma ashers and Monte Carlo modeling for the projection of atomic oxygen durability of protected polymers in low Earth orbit p 819 N93-15596
Leveling coatings for reducing the atomic oxygen defect density in protected graphite fiber epoxy composites
p 819 N93-15597
Accelerated simulation of near-Earth-orbit polymer degradation p 823 N93-15615
LDEF: A bibliography with abstracts
[NASA-TM-107705] p 813 N93-15646
EARTH ORBITS
Reusable Reentry Satellite (RRS) system design study: System cost estimates document
[NASA-CR-188480] p 818 N93-14872
Reusable Reentry Satellite (RRS): Telemetry, Tracking, and Command (TT/C) coverage tradeoff study
[NASA-CR-188583] p 824 N93-15629
EARTH ROTATION
A feasibility study of space VLBI for geodesy and geodynamics p 904 N93-14223
A TOPEX/Poseidon study of oceanic effects on observations of the Earth's interior p 918 N93-14999
EARTH SCIENCES
NSSDC Conference on Mass Storage Systems and Technologies for Space and Earth Science Applications, volume 3
[NASA-CP-3165-VOL-3] p 1002 N93-14771
Proceedings of the NSSDC Conference on Mass Storage Systems and Technologies for Space and Earth Science Applications
[NASA-TM-107989] p 1004 N93-15027
EARTH SURFACE
Igneous and tectonic evolution of Venusian and terrestrial coronae p 1031 N93-14330
EARTH TIDES
A TOPEX/Poseidon study of oceanic effects on observations of the Earth's interior p 918 N93-14999
EARTHQUAKES
Addressing earthquake strong ground motion issues at the Idaho National Engineering Laboratory
[DE92-017841] p 916 N93-15136
USACE geotechnical earthquake engineering software, report 1 WESHAKE for personal computers (version 1.0)
[AD-A257068] p 917 N93-15459
ECOLOGY
Biofilm ecology of bioluminescent bacteria
[AD-A255282] p 932 N93-14532
ECONOMIC ANALYSIS
In-situ lunar oxygen extraction p 806 N93-14929
EDI planning and implementation guide
[AD-A255737] p 1007 N93-15050
Technology commercialization cost model and component case study
[DE92-001280] p 907 N93-15213
ECONOMIC DEVELOPMENT
The CPG 5-kW(e) Dish-Stirling Development Program
[DE92-017050] p 907 N93-15134
Wisconsin Inventors' Network Database
[DE92-018394] p 1007 N93-15137
Technology commercialization cost model and component case study
[DE92-001280] p 907 N93-15213
High temperature tubular solid oxide fuel cell development
[DE92-040253] p 908 N93-15322
ECOSYSTEMS
The production and use of aeroponically grown inocula of VAM fungi in the native plant nursery
[PB92-204973] p 933 N93-15208
Ecological implications of landscape fragmentation
[DE92-019186] p 911 N93-15273
EDDY CURRENTS
Active control of combustion instability in a ramjet using large-eddy simulations
[AD-A255226] p 798 N93-14111
EDDY VISCOSITY
A numerical investigation of the interaction between crossing oblique shocks and a turbulent boundary layer
p 876 N93-14695
Second order closure modeling of turbulent buoyant wall plumes
[NASA-TM-105956] p 877 N93-14829
EDGE DETECTION
Development of a MATLAB toolbox for image processing
[AD-A256130] p 942 N93-14247
EDGES
An extended cuberille model for identification and display of 3D objects from 3D gray value data
p 953 N93-15542
EDITING
GRASS 4.0 map digitizing user's manual: V. Digit
[AD-A256859] p 1009 N93-15642
How scientific must technical editors be?
[DE92-040741] p 1010 N93-15655
EDUCATION
A psychometrically sound cognitive diagnostic model: Effect of remediation as empirical validity
[AD-A255926] p 933 N93-14109
Body composition and physical performance
[AD-A255627] p 938 N93-14161
A progressive resistance weight training program designed to improve the armor crewman's strength
[AD-A255553] p 934 N93-14556
Core support of the board on mathematical sciences
[AD-A255482] p 968 N93-14787
Proceedings of the Sixth CASI Conference on Astronautics
[CTN-92-60336] p 804 N93-14920
Space education: A self-perservation strategy for the Canadian space industry p 808 N93-14937
Training, muscle fatigue and stress fractures
[AD-A255277] p 935 N93-15006
Proposed action plan to improve ADM effectiveness, part 3: Developing a new ADM paradigm on which to build advanced or expert decision making training
p 787 N93-15026
Continuing engineering education for software engineering professionals
[DE92-019888] p 947 N93-15225
Experience with a course on architectures for software systems. Part 1: Course description
[AD-A256221] p 941 N93-15239
EFFICIENCY
Variable speed rotary compressor and adjustable speed drive efficiencies measured in the laboratory
[DE92-040026] p 893 N93-15278
EGRESS
Effects of seating configuration and number of type 3 exits on emergency aircraft evacuation
[AD-A256616] p 783 N93-14277
EIGENVALUES
Application of partition matrix methods to solve large eigenproblems in structural dynamics
p 896 N93-14188
The effect of wake dynamics on rotor eigenvalues in forward flight p 780 N93-14595
On the convergence of the coupled-wave approach for lamellar diffraction gratings p 986 N93-15520
EIGENVECTORS
Application of partition matrix methods to solve large eigenproblems in structural dynamics
p 896 N93-14188
Damage location and model refinement for large flexible space structures using a sensitivity-based eigenstructure assignment method p 816 N93-14274
EJECTA
Venusian extended ejecta deposits as time-stratigraphic markers p 1030 N93-14327
Effect of impact angle on central-peak/peak-ring formation and crater collapse on Venus
p 1041 N93-14371
Impact-generated winds on Venus: Causes and effects p 1041 N93-14372
Gamma-ray imaging observations of Supernova 1987A
p 1012 N93-14628
ELASTIC BENDING
Flexural models of trench/outer rise topography of coronae on Venus with axisymmetric spherical shell elastic plates p 1036 N93-14348
ELASTIC BODIES
Finite element analysis of elastic fracture under unsteady translational and rotational loading p 899 N93-14469
ELASTIC CYLINDERS
Experimental investigation of scattering from randomly rough plastic cylinders
[AD-A256018] p 975 N93-15259
ELASTIC DEFORMATION
On the structure of nonlinear constitutive equations for fiber reinforced composites
[NASA-CR-191024] p 830 N93-14484
Aeroplane crashes on the runway: Validation and final evaluation of the method of modeling an airframe structure
[IMFL-91-32] p 792 N93-15126
ELASTIC MEDIA
The mixed mode crack problem in a nonhomogeneous elastic plane
[AD-A256469] p 902 N93-15372
Diffusion problems in bonded nonhomogeneous materials with an interface cut
[AD-A256470] p 836 N93-15373
ELASTIC PLATES
Estimates of elastic plate thicknesses beneath large volcanos on Venus p 1035 N93-14344
Flexural models of trench/outer rise topography of coronae on Venus with axisymmetric spherical shell elastic plates p 1036 N93-14348
ELASTIC PROPERTIES
Applications of a constitutive equation for microstructural change in polymers p 848 N93-14222
Waterborne polyurethane binder resins for compliant aircraft coatings
[AD-A256246] p 849 N93-14573
On the development and application of a modified boundary element method for the analysis of three dimensional elastostatic problems in thick plates
p 901 N93-14587
Thermal fatigue analysis of metal matrix composite with spherical reinforcements
[AD-A255313] p 831 N93-14672
The crack problem for an orthotropic half plane stiffened by elastic films
[AD-A256471] p 903 N93-15374
ELASTIC WAVES
Some theoretical and experimental aspects of the generation of guided elastic waves using finite sources
p 897 N93-14219
Elastic wave scattering by partially debonded or partially coated fibers p 829 N93-14224
Elastic wave propagation in laminated composites
[ITN-93-85186] p 835 N93-15144

ELASTOMERS
NMR imaging of elastomeric materials
[AD-A256034] p 841 N93-14658
ELASTOPLASTICITY
Modeling of the thermal elasto-plastic behavior for composite materials using the homogenization method
p 830 N93-14466
The influence of geometrical constraint on cyclic, elastoplastic, notch root behavior, and fatigue microcrack initiation p 900 N93-14480
Inelastic deformation of metal matrix composites: Plasticity and damage mechanisms, part 2
[NASA-CR-189096-PT-2] p 837 N93-15401
ELASTOSTATICS
On the development and application of a modified boundary element method for the analysis of three dimensional elastostatic problems in thick plates
p 901 N93-14587
ELECTRIC BATTERIES
S/EV 1991: Solar and Electric Vehicle Symposium, Car and Trade Show
[DE92-019890] p 869 N93-15226
Dual-Shaft Electric Propulsion (DSEP) Technology Development Program
[DE92-040189] p 894 N93-15416
Dual role of nickel in sodium/nickel chloride batteries
[DE92-041102] p 870 N93-15441
Exploratory technology research program for electrochemical energy storage
[DE93-001595] p 909 N93-15484
Solid polymer electrolytes for rechargeable batteries
[DE93-001603] p 871 N93-15485
ELECTRIC CONNECTORS
MIL-STD-1760 application guidelines
[AD-A255714] p 790 N93-14432
ELECTRIC CONTACTS
Method for fabricating ohmic contacts on semiconducting diamond
[AD-D015432] p 850 N93-14825
Preliminary lightning tests: Optical fiber penetration of an exclusion region barrier
[DE92-019804] p 983 N93-15230
ELECTRIC CURRENT
Investigation of the use of surface electrical currents for short-range shipboard data communications
[AD-A256197] p 859 N93-14490
ELECTRIC ENERGY STORAGE
Exploratory technology research program for electrochemical energy storage
[DE93-001595] p 909 N93-15484
ELECTRIC FIELDS
Beam trapping in a modified betatron with a localized bipolar electric field pulse
[AD-A255414] p 866 N93-14504
Measurements of electric and magnetic fields in the Waianae, Hawaii area
[DE92-019891] p 861 N93-15220
Electron acceleration by longitudinal electric field of a Gaussian laser beam
[DE92-526947] p 887 N93-15296
ELECTRIC GENERATORS
Power conversion system modification to permit use of DC power source
[AD-D015409] p 868 N93-14887
ELECTRIC MOTOR VEHICLES
S/EV 1991: Solar and Electric Vehicle Symposium, Car and Trade Show
[DE92-019890] p 869 N93-15226
Dual-Shaft Electric Propulsion (DSEP) Technology Development Program
[DE92-040189] p 894 N93-15416
ELECTRIC MOTORS
Dual-Shaft Electric Propulsion (DSEP) Technology Development Program
[DE92-040189] p 894 N93-15416
ELECTRIC POTENTIAL
Driven shielding capacitive proximity sensor
[NASA-CASE-GSC-13377-1] p 962 N93-14701
High speed magneto-resistive random access memory
[NASA-CASE-NPO-17954-1-CU] p 940 N93-14704
Energy loss analysis of an integrated space power distribution system
[NASA-TM-105772] p 854 N93-14834
A high intensity solar cell invention: The edge-illuminated Vertical Multi-Junction (VMJ) solar cell
[DE92-019015] p 907 N93-15224
ELECTRIC POWER
Power conversion system modification to permit use of DC power source
[AD-D015409] p 868 N93-14887
Overview of environmental test plans for Space Station Freedom work package 4 p 824 N93-15623
ELECTRIC POWER PLANTS
Research for electric energy systems
[DE92-040076] p 870 N93-15412
ELECTRIC POWER SUPPLIES
Photovoltaic power system for a lunar base
p 806 N93-14930
ELECTRIC POWER TRANSMISSION
Measurements of electric and magnetic fields in the Waianae, Hawaii area
[DE92-019891] p 861 N93-15220
ELECTRIC PROPULSION
Numerical study of cathode emission constraints on cylindrical self-field MPD thruster performance
[NASA-CR-190795] p 826 N93-15370
Dual-Shaft Electric Propulsion (DSEP) Technology Development Program
[DE92-040189] p 894 N93-15416
Ion thruster development at NASA Lewis Research Center
[NASA-TM-105983] p 827 N93-15429
ELECTRIC PULSES
High performance pulse generator
[AD-D015378] p 869 N93-15269
ELECTRIC SWITCHES
Internal grounding arrangement in a switching power converter
[AD-D015435] p 868 N93-14826
ELECTRIC WIRE
Electronics reliability fracture mechanics. Volume 2: Fracture mechanics
[AD-A256200] p 900 N93-14498
Multifilamentary superconducting cable and a method of manufacturing it
[AD-D015391] p 846 N93-15231
ELECTRICAL ENGINEERING
A theoretical search for supervelocity semiconductors
[AD-A256325] p 994 N93-15191
Basic research in electronics (JSEP)
[AD-A256016] p 869 N93-15257
ELECTRICAL FAULTS
Multiple fault diagnosis of spacecraft electrical power systems p 806 N93-14927
Microstack insulator for flashover inhibition, phase 2
[AD-A256338] p 869 N93-15196
ELECTRICAL GROUNDING
Internal grounding arrangement in a switching power converter
[AD-D015435] p 868 N93-14826
ELECTRICAL INSULATION
Preliminary investigations of metal liquid-like films and coatings derived from them
[AD-A255477] p 849 N93-14489
High temperature polymer dielectric film insulation
[AD-A255243] p 849 N93-14527
Microstack insulator for flashover inhibition, phase 2
[AD-A256338] p 869 N93-15196
ELECTRICAL MEASUREMENT
Experimental attempt to metallize hydrogen at very high pressures
[AD-A257086] p 843 N93-15497
ELECTRICAL PROPERTIES
Oriented electro/optical polymers through in-situ chemistry during gel processing: A research opportunity
[AD-A255968] p 848 N93-14401
Photoelectrochemistry of electronic and electro-optical materials
[AD-A256239] p 866 N93-14583
Properties of textile grade ceramic fibers
p 833 N93-14751
Theory of the electronic and structural properties of solid state oxides
[DE92-040499] p 993 N93-14909
Dynamical properties of Josephson Junctions arrays
[AD-A255464] p 995 N93-15351
ELECTRICAL RESISTIVITY
Electrical conductivity measurements in evaporated cadmium telluride thin films p 865 N93-14191
High speed magneto-resistive random access memory
[NASA-CASE-NPO-17954-1-CU] p 940 N93-14704
Thermodynamics and transport in Ce3Bi4Pt3 and related compounds
[DE92-040377] p 998 N93-14905
A high intensity solar cell invention: The edge-illuminated Vertical Multi-Junction (VMJ) solar cell
[DE92-019015] p 907 N93-15224
Normal state resistivity and the phase diagram of U(1-x)Th(x)Be13
[DE92-040236] p 995 N93-15321
Electrical resistivity and equation of state measurements of a dense aluminum plasma
[DE92-040352] p 989 N93-15436
Experimental attempt to metallize hydrogen at very high pressures
[AD-A257086] p 843 N93-15497
ELECTRO-OPTICAL EFFECT
Research for electric energy systems
[DE92-040076] p 870 N93-15412
ELECTRO-OPTICS
Oriented electro/optical polymers through in-situ chemistry during gel processing: A research opportunity
[AD-A255968] p 848 N93-14401
Integrated photonics research technical digest series. Volume 10: Conference edition: Summaries of papers presented at the Integrated Photonics Research Topical Meeting
[AD-A255423] p 981 N93-14506
Solid state research
[AD-A256019] p 992 N93-14576
Photoelectrochemistry of electronic and electro-optical materials
[AD-A256239] p 866 N93-14583
Optoelectronics material center: A collaborative program including center for high technology materials of the University of New Mexico, Stanford University, California Institute of Technology
[AD-A256005] p 886 N93-15115
Electro-optic architecture (EOA) for sensors and actuators in aircraft propulsion systems
[NASA-CR-182270] p 982 N93-15116
A structural approach to the photonic processor
[N-3399-RC] p 986 N93-15648
ELECTROCARDIOGRAPHY
Test and evaluation report of the Physio Control Defibrillator/Monitor, Model LifePak(tm) 6s
[AD-A255691] p 933 N93-14103
ELECTROCATALYSTS
Components and materials issues in polymer electrolyte fuel cells for transportation applications
[DE92-013384] p 907 N93-15061
ELECTROCHEMICAL CELLS
Electrochemical oxidation of organic materials
[DE92-019822] p 828 N93-14718
Exploratory technology research program for electrochemical energy storage
[DE93-001595] p 909 N93-15484
ELECTROCHEMICAL CORROSION
The effect of a seawater environment on the galvanic corrosion behavior of graphite/epoxy composites coupled to metals
[AD-A256072] p 830 N93-14232
Fe3Al-type iron aluminides: Aqueous corrosion properties in a range of electrolytes and slow-strain rate ductilities during aqueous corrosion
[DE92-040520] p 846 N93-15059
Dual role of nickel in sodium/nickel chloride batteries
[DE92-041102] p 870 N93-15441
ELECTROCHEMICAL OXIDATION
Electrochemical oxidation of organic materials
[DE92-019822] p 828 N93-14718
ELECTROCHEMISTRY
Studies of components for thermally regenerative electrochemical systems
[AD-A256124] p 842 N93-14664
ELECTRODE MATERIALS
Arc-cathode interaction study
[NASA-CR-191356] p 867 N93-14721
Results from a pilot cell test of cermet anodes
[DE92-041357] p 871 N93-15479
ELECTRODES
SDIO Workshop on Piezoelectric Ceramic Actuators for Space Applications
[AD-A255959] p 990 N93-14422
Gate-all-around device
[AD-A255287] p 866 N93-14534
Microstack insulator for flashover inhibition, phase 2
[AD-A256338] p 869 N93-15196
Numerical study of cathode emission constraints on cylindrical self-field MPD thruster performance
[NASA-CR-190795] p 826 N93-15370
Design of an artificial neural network based tactile sensor for the UTAH/MIT dexterous hand
[AD-A256565] p 966 N93-15406
Dual role of nickel in sodium/nickel chloride batteries
[DE92-041102] p 870 N93-15441
Molecular capacitance: Sequential electron-transfer energetics for solution-phase metallic clusters in relation to gas-phase clusters and analogous interfaces
[AD-A257057] p 977 N93-15448
ELECTROENCEPHALOGRAPHY
Extrathalmic modulation of cortical function
[AD-A255440] p 935 N93-14782
Cognition and the brain
[AD-A255483] p 937 N93-14788
ELECTROEPITAXY
Study of the mathematical modelling and computer simulation of crystal growth from liquid phase under microgravity conditions
[CTN-93-60619] p 855 N93-15201
ELECTROFORMING
Mach 5 electroformed nickel nozzle refurbishment FNAS investigation of ultra-smooth surfaces
[NASA-CR-191416] p 826 N93-14681

ELECTROLYTIC CELLS
Components and materials issues in polymer electrolyte fuel cells for transportation applications
| DE92-013384 | p 907 N93-15061
ELECTROMAGNETIC ABSORPTION
Electrical conductivity measurements in evaporated cadmium telluride thin films p 865 N93-14191
ELECTROMAGNETIC ACCELERATION
Validation of the flux loop diagnostic for the measurement of launch package motion during electromagnetic launch
| AD-A256547 | p 814 N93-14266
ELECTROMAGNETIC COMPATIBILITY
Test and evaluation report of the Physio Control Defibrillator/Monitor, Model LifePak(tm) 6s
| AD-A255691 | p 933 N93-14103
Test and evaluation report of the Catalyst Research Oxygen Monitor, Model Miniox 3
| AD-A255849 | p 881 N93-14105
Modeling limits of the EMV analysis program CONCEPT by example of the influence of a helicopter structure on a frame antenna
| MBB-UD-0614-92-PUB | p 863 N93-15487
ELECTROMAGNETIC COUPLING
A quasi-equilibrium kinetic model of HF air breakdown
| AD-A256240 | p 859 N93-14453
Mechanical shielding for electric primer
| AD-D015417 | p 860 N93-14889
Thunderstorm coupling to the magnetosphere and associated ionospheric effects
| NASA-CR-191383 | p 922 N93-14910
ELECTROMAGNETIC FIELDS
Relativistic dynamics of a charged sphere: Updating the Lorentz-Abraham model
| AD-A256107 | p 971 N93-14245
Mechanisms of microwave induced damage in biologic materials
| AD-A255799 | p 933 N93-14648
Basic research in electronics (JSEP)
| AD-A256016 | p 869 N93-15257
Homogeneous quantum electrodynamic turbulence
| NASA-TM-107686 | p 979 N93-15482
A modal analysis of lamellar diffraction gratings in conical mountings p 986 N93-15519
ELECTROMAGNETIC INTERACTIONS
Investigation of the on-surface boundary operators for electromagnetic scattering by conducting object p 857 N93-14189
Low energy theorems in pion production
| DE92-040071 | p 977 N93-15279
Weak-electromagnetic interference in polarized eD scattering
| DE93-001763 | p 978 N93-15486
ELECTROMAGNETIC INTERFERENCE
Test and evaluation report of the Physio Control Defibrillator/Monitor, Model LifePak(tm) 6s
| AD-A255691 | p 933 N93-14103
Test and evaluation report of the Catalyst Research Oxygen Monitor, Model Miniox 3
| AD-A255849 | p 881 N93-14105
ELECTROMAGNETIC PROPULSION
Opacity, equation of state, and radiation transport model for moderate density, eV-temperature plasmas
| AD-A256056 | p 988 N93-14579
ELECTROMAGNETIC PULSES
A quasi-equilibrium kinetic model of HF air breakdown
| AD-A256240 | p 859 N93-14453
Interferometric measurement with squeezed light
| AD-A257065 | p 984 N93-15458
EMTP based stability analysis of space station electric power system in a test bed environment
| NASA-TM-105845 | p 871 N93-15503
ELECTROMAGNETIC RADIATION
Evidence for lightning on Venus p 1043 N93-14386
Mechanical shielding for electric primer
| AD-D015417 | p 860 N93-14889
Joint HVAC transmission EMF environmental study
| DE92-017863 | p 933 N93-15211
Basic research in electronics (JSEP)
| AD-A256016 | p 869 N93-15257
On the convergence of the coupled-wave approach for lamellar diffraction gratings p 986 N93-15520
ELECTROMAGNETIC SCATTERING
Investigation of the on-surface boundary operators for electromagnetic scattering by conducting object p 857 N93-14189
Effects of water vapor and anisotropic scattering on aerosol optical depth retrieval
| AD-A256087 | p 904 N93-14262
Theory and applications of the 3-dimensional finite-difference time-domain method
| AD-A256559 | p 968 N93-14804
Analytical characterization of bistatic scattering from rough surfaces: Dependence on surface correlation function
| AD-A256525 | p 862 N93-15397
Radar scene generation for tactical decision aids
| AD-A257069 | p 863 N93-15495
ELECTROMAGNETIC SHIELDING
Mechanical shielding for electric primer
| AD-D015417 | p 860 N93-14889
ELECTROMAGNETIC WAVE TRANSMISSION
Efficient asymptotic closed form approximation for dyadic green's function for anisotropic substrates, phase 1
| AD-A256258 | p 830 N93-14436
Deterministic transfer function for transionospheric propagation
| DE92-040327 | p 862 N93-15427
ELECTROMAGNETISM
Basic research in electronics (JSEP)
| AD-A256016 | p 869 N93-15257
ELECTROMAGNETS
Design and implementation of a DC-based magnetic field controller with electronic temperature stabilized Hall generator
| DE92-019796 | p 870 N93-15276
ELECTROMECHANICS
Thermal, mechanical, and electroelastic behavior of composite materials p 835 N93-15146
ELECTRON ACCELERATION
Electron acceleration by longitudinal electric field of a Gaussian laser beam
| DE92-526947 | p 887 N93-15296
Energetic and magnetosheath energy particle signatures of the low-latitude boundary layer at low altitudes near noon
| NASA-CR-191388 | p 917 N93-15574
ELECTRON ACCELERATORS
Numerical modelling of intense electron beam transport in the spiral line induction accelerator
| AD-A255545 | p 978 N93-14570
Generation, control, and transport of a 19-MeV, 700-kA pulsed electron beam
| DE92-019803 | p 978 N93-15277
ELECTRON BEAM WELDING
Mechanisms of forming intergranular microcracks and microscopic surface discontinuities in welds
| AD-A255371 | p 845 N93-14740
ELECTRON BEAMS
An analysis of the SCEX 3 ionospheric electron beam injection experiment p 912 N93-14177
Beam trapping in a modified betatron with a localized bipolar electric field pulse
| AD-A255414 | p 866 N93-14504
Monte Carlo analysis of energy deposition in solid state materials by 400 and 200 MeV electrons
| AD-A255335 | p 991 N93-14537
Numerical modelling of intense electron beam transport in the spiral line induction accelerator
| AD-A255545 | p 978 N93-14570
Imaging the sun in hard x rays using Fourier telescopes
| NASA-TM-108390 | p 1013 N93-15203
Generation, control, and transport of a 19-MeV, 700-kA pulsed electron beam
| DE92-019803 | p 978 N93-15277
Simple formulae for the optimization of the FEL gain length including the effects of emittance, betatron oscillations, and energy spread
| DE92-040378 | p 887 N93-15325
ELECTRON DENSITY (CONCENTRATION)
Electron density diagnostics for gaseous nebulae involving the O 4 intercombination lines near 1400 A p 1012 N93-14762
The effects of magnetic storm phases on F-layer irregularities from auroral to equatorial latitudes
| AD-A256520 | p 917 N93-15395
ELECTRON DENSITY PROFILES
A study of the low and mid-latitude upper ionospheres of Jupiter and Saturn p 1022 N93-14179
ELECTRON DIFFRACTION
Silicon nitride thin film production on Si(111)
| AD-A256036 | p 994 N93-15233
ELECTRON DISTRIBUTION
Relativistic dynamics of a charged sphere: Updating the Lorentz-Abraham model
| AD-A256107 | p 971 N93-14245
Radiation belt dynamic and quasi-static modeling based on CRRES data: Outer-belt short-term response data base
| AD-A256483 | p 916 N93-14899
ELECTRON EMISSION
A study of mid-latitude 5577A CI dayglow emissions
| AD-A255444 | p 914 N93-14511
ELECTRON ENERGY
Fine structure of auroral particle acceleration p 912 N93-14121
Threshold photodetachment spectroscopy
| AD-A255278 | p 842 N93-14671
Silicon nitride thin film production on Si(111)
| AD-A256036 | p 994 N93-15233
ELECTRON FLUX DENSITY
Comparison of Viking Ultraviolet images with low altitude particle precipitation p 1045 N93-14612
ELECTRON IMPACT
Electron density diagnostics for gaseous nebulae involving the O 4 intercombination lines near 1400 A p 1012 N93-14762
ELECTRON MICROSCOPY
Characterization of cholesteric cyclic siloxane liquid crystalline materials
| AD-A256128 | p 994 N93-15190
ELECTRON OSCILLATIONS
Simple formulae for the optimization of the FEL gain length including the effects of emittance, betatron oscillations, and energy spread
| DE92-040378 | p 887 N93-15325
ELECTRON PHONON INTERACTIONS
Electron-phonon interaction, transport and ultrafast processes in semiconductor microstructures
| AD-A255723 | p 976 N93-14433
ELECTRON PLASMA
An analysis of the SCEX 3 ionospheric electron beam injection experiment p 912 N93-14177
ELECTRON PRECIPITATION
Comparison of Viking Ultraviolet images with low altitude particle precipitation p 1045 N93-14612
ELECTRON SCATTERING
Electronic, vibrational, and transport properties of conducting polymers p 847 N93-14170
Extracting x rays, gamma rays, and electron-positron pairs from supermassive Kerr black holes using the Penrose mechanism p 1049 N93-14176
Sensitivity of quantum electron conductance to elastic scatterers and to spin-orbit scattering in gallium arsenide heterostructures p 990 N93-14184
Final Report, 1 November 1988 - 31 October 1991 --- spectroscopy of adsorbed and photodissociated molecules
| AD-A255979 | p 976 N93-14424
Electron-phonon interaction, transport and ultrafast processes in semiconductor microstructures
| AD-A255723 | p 976 N93-14433
A Monte Carlo analysis of the liquid xenon TPC as gamma ray telescope p 1014 N93-15590
ELECTRON SPECTROSCOPY
Silicon nitride thin film production on Si(111)
| AD-A256036 | p 994 N93-15233
ELECTRON TRANSFER
Conditioning electron beams in the ion-focused regime
| AD-A255635 | p 978 N93-14127
Electron-phonon interaction, transport and ultrafast processes in semiconductor microstructures
| AD-A255723 | p 976 N93-14433
Monte Carlo analysis of energy deposition in solid state materials by 400 and 200 MeV electrons
| AD-A255335 | p 991 N93-14537
Molecular capacitance: Sequential electron-transfer energetics for solution-phase metallic clusters in relation to gas-phase clusters and analogous interfaces
| AD-A257057 | p 977 N93-15448
ELECTRON TRANSITIONS
A study of an optically pumped free-jet molecular iodine laser operating in the visible spectrum p 884 N93-14141
ELECTRON-POSITRON PAIRS
Extracting x rays, gamma rays, and electron-positron pairs from supermassive Kerr black holes using the Penrose mechanism p 1049 N93-14176
ELECTRONIC CONTROL
Electro-optic architecture (EOA) for sensors and actuators in aircraft propulsion systems
| NASA-CR-182270 | p 382 N93-15116
ELECTRONIC COUNTERMEASURES
Airborne radar simulation with adaptive antenna techniques
| AD-A255460 | p 859 N93-14488
ELECTRONIC EQUIPMENT
Electronics reliability fracture mechanics. Volume 1: Causes of failures of shop replaceable units and hybrid microcircuits
| AD-A255836 | p 894 N93-14104
Extended surface heat sinks for electronic components: A computer optimization
| AD-A256134 | p 865 N93-14254
Solid state research
| AD-A256019 | p 992 N93-14576
Radiation monitoring for long duration space flights p 812 N93-14959
ELECTRONIC EQUIPMENT TESTS
Thermal fixture for testing an integrated circuit
| AD-D015380 | p 882 N93-15247
Proceedings of the International Conference on CAD/CAM and AMT. Volume 4: VHDL (VHSIC Hardware Description Language) Seminar
| ITN-92-85130 | p 947 N93-15261

VHDL (VHSIC hardware description language) in the test environment
[VH-6] p 948 N93-15267
ELECTRONIC MAIL
EDI planning and implementation guide
[AD-A255737] p 1007 N93-15050
ELECTRONIC PACKAGING
Thermal, mechanical, and electroelastic behavior of composite materials p 835 N93-15146
ELECTRONS
A quasi-equilibrium kinetic model of HF air breakdown
[AD-A256240] p 859 N93-14453
Predictions of dose from electrons in space
[NASA-CR-191617] p 1051 N93-15580
ELECTROPHORESIS
Processing and characterization of electrophoretically deposited holmium barium copper oxide superconductor films
[AD-A256329] p 869 N93-15194
ELECTRORHEOLOGICAL FLUIDS
Smart materials for Army structures
[AD-A254925] p 836 N93-15218
ELECTROSTATIC CHARGE
The sensitivity of energetic materials to friction, impact, and electrostatic stimuli
[DE92-041227] p 855 N93-15478
ELECTROSTATICS
Molecular capacitance: Sequential electron-transfer energetics for solution-phase metallic clusters in relation to gas-phase clusters and analogous interfaces
[AD-A257057] p 977 N93-15448
ELEVATION
Extensive lava flow fields on Venus: Preliminary investigation of source elevation and regional slope variations p 1034 N93-14342
The gabbro-eclogite phase transition and the elevation of mountain belts on Venus p 1036 N93-14350
Adaptive mesh in visualization of terrain elevation data
[AD-A255481] p 906 N93-15007
ELLIPSOMETERS
Instrumentation of the variable-angle magneto-optic ellipsometer and its application to M-O media and other non-magnetic films p 984 N93-15508
ELLIPTIC DIFFERENTIAL EQUATIONS
Undetermined coefficient problems for quasi-linear parabolic equations
[AD-A256012] p 969 N93-15256
ELLIPTICAL ORBITS
Optimal impulsive trajectories for orbital rendezvous between elliptic orbits p 813 N93-15103
EMBEDDED COMPUTER SYSTEMS
Autonomous power system brassboard
[NASA-CR-189115] p 867 N93-14798
EMERGENCIES
Effects of seating configuration and number of type 3 exits on emergency aircraft evacuation
[AD-A256616] p 783 N93-14277
EMISSION
Geographical distribution and seasonal variation of surface emissions and deposition velocities of atmospheric trace gases
[AERONOMICA-ACTA-A-361-1991] p 911 N93-15460
Modelling global methane emissions from livestock: Biological and nutritional controls
[NASA-CR-191354] p 911 N93-15480
EMISSION SPECTRA
Understanding the variation in the millimeter-wave emission of Venus p 1028 N93-14315
Physical properties of extended emission-line regions in active and cooling-flow galaxies p 1018 N93-14461
Study and interpretation of the millimeter-wave spectrum of Venus p 1045 N93-14596
Electron density diagnostics for gaseous nebulae involving the O 4 intercombination lines near 1400 A p 1012 N93-14762
Method for detecting chemical vapors using a lasing dye sensor
[AD-D015424] p 885 N93-14821
Wolf-Rayet stars in the Milky Way, the Large Magellanic Cloud, and emission-line galaxies p 1020 N93-14869
LISA: A limb imaging spectrograph for airglow p 811 N93-14952
High-energy emissions from young pulsars: Perspective from the outer gap model
[DE92-040365] p 1022 N93-15324
A liquid xenon imaging telescope for gamma ray astrophysics: Design and expected performance p 1014 N93-15591
EMISSIVITY
Current status of liquid sheet radiator research
[NASA-TM-105764] p 872 N93-14150
Overview of Venus geology: Preliminary description of terrain units for Venus global geological mapping p 1040 N93-14368
Microwave scattering and emission properties of large impact craters on the surface of Venus p 1043 N93-14384
Low-emissivity impact craters on Venus p 1044 N93-14392
Venus: Geochemical conclusions from the Magellan data p 1044 N93-14394
EMITTANCE
Simple formulae for the optimization of the FEL gain length including the effects of emittance, betatron oscillations, and energy spread
[DE92-040378] p 887 N93-15325
Emittance measurements of Space Shuttle orbiter reinforced carbon-carbon
[NASA-TP-3293] p 903 N93-15530
EMPLOYEE RELATIONS
The changing culture of science: Bringing it into balance
[AD-A255993] p 998 N93-14417
ENCAPSULATING
Material development in the Si3N4 system using glass encapsulated HIP'ing
[DE92-041381] p 837 N93-15388
END EFFECTORS
Utilizing sensed incipient slip signals for grasp force control
[AD-A255725] p 888 N93-14434
Force and position control of robot manipulators: Learning and repetitive control approach p 888 N93-14473
Retractable tool bit having slider type catch mechanism
[NASA-CASE-GSC-13358-1] p 890 N93-14710
Bar-holding prosthetic limb
[NASA-CASE-MFS-28481-1] p 939 N93-14870
Redundancy control of robots by constrained optimization
[F-3-7] p 950 N93-15307
ENDOCRINE GLANDS
Joint HVAC transmission EMF environmental study
[DE92-017863] p 933 N93-15211
ENDOCRINOLOGY
Transcutaneous Analyte Measuring Methods (TAMM), phase 2
[AD-A256327] p 936 N93-15192
ENERGETIC PARTICLES
A survey of solar flare energetic particle abundances and energy spectra p 1048 N93-14135
Energetic and magnetosheath energy particle signatures of the low-latitude boundary layer at low altitudes near noon
[NASA-CR-191388] p 917 N93-15574
ENERGY BUDGETS
Transformation of energy and momentum due to Landau damping in time
[IPPCZ-316] p 988 N93-14813
On the variation of the Nimbus 7 total solar irradiance
[NASA-TP-3316] p 1049 N93-15532
ENERGY CONSERVATION
World energy: Building a sustainable future
[DE93-001598] p 909 N93-15467
ENERGY CONSUMPTION
World energy: Building a sustainable future
[DE93-001598] p 909 N93-15467
ENERGY DISSIPATION
Quasars, galaxies, and pseudo-vacuum droplets
[NIKHEF-H/91-20] p 1020 N93-14686
Energy loss analysis of an integrated space power distribution system
[NASA-TM-105772] p 854 N93-14834
Silicon nitride thin film production on Si(111)
[AD-A256036] p 994 N93-15233
Accurate methods for calculating atomic processes in high temperature plasmas
[DE92-040215] p 988 N93-15418
ENERGY DISTRIBUTION
Fine structure of auroral particle acceleration p 912 N93-14121
An energy analysis of the pseudo Wigner-Ville distribution in support of machinery monitoring and diagnostics
[AD-A256202] p 889 N93-14499
Simple formulae for the optimization of the FEL gain length including the effects of emittance, betatron oscillations, and energy spread
[DE92-040378] p 887 N93-15325
ENERGY GAPS (SOLID STATE)
Electronic structure studies of high-T(sub c) superconductors by photoemission and x ray absorption p 989 N93-14172
ENERGY POLICY
World energy: Building a sustainable future
[DE93-001598] p 909 N93-15467
ENERGY SPECTRA
A survey of solar flare energetic particle abundances and energy spectra p 1048 N93-14135
Radiative heat transfer in combustion systems p 840 N93-14621
Homogeneous quantum electrodynamic turbulence
[NASA-TM-107686] p 979 N93-15482
ENERGY STORAGE
A novel, high energy-density electrical storage device for electric weapons
[AD-A255205] p 867 N93-14666
Latent heat thermal energy storage for lunar oxygen production
[DE92-017817] p 907 N93-15219
ENERGY TECHNOLOGY
Storage needs in future supercomputer environments p 1003 N93-14780
ENERGY TRANSFER
Electronically excited molecules: Reaction kinetics and emission of light: Nanosecond infrared spectroscopy, electronic emission from chemical reactions
[AD-A255642] p 976 N93-14283
Effect of impact angle on central-peak/peak-ring formation and crater collapse on Venus p 1041 N93-14371
Monte Carlo analysis of energy deposition in solid state materials by 400 and 200 MeV electrons
[AD-A255335] p 991 N93-14537
Modelling the engine temperature distribution between shut down and restart for life usage monitoring p 796 N93-15177
ENGINE AIRFRAME INTEGRATION
Aerothermodynamic flow phenomena of the airframe-integrated supersonic combustion ramjet
[NASA-TM-4376] p 827 N93-15528
ENGINE CONTROL
Electro-optic architecture (EOA) for sensors and actuators in aircraft propulsion systems
[NASA-CR-182270] p 982 N93-15116
Integrated engine control and monitoring with experiences derived from OLMOS p 795 N93-15168
Real-time in-flight engine performance and health monitoring techniques for flight research application p 795 N93-15169
ENGINE DESIGN
Engine technologies for future spaceplanes
[ETN-92-92732] p 800 N93-15143
ENGINE FAILURE
Real-time in-flight engine performance and health monitoring techniques for flight research application p 795 N93-15169
RB199 engine oil system failure diagnostics by comparison of measured and calculated oil consumption using the OLMOS on-board monitoring system p 796 N93-15173
Experimental analysis of steady-state and dynamic monitoring of power shaft turbines p 796 N93-15176
ENGINE INLETS
Results of low power deicer tests on a swept inlet component in the NASA Lewis icing research tunnel
[NASA-TM-105968] p 781 N93-14911
ENGINE MONITORING INSTRUMENTS
Proceedings of the 16th Symposium on Aircraft Integrated Monitoring Systems
[DLR-MITT-92-01] p 793 N93-15152
DAR-2: On-board data acquisition system for aircraft engines p 795 N93-15166
Integrated engine control and monitoring with experiences derived from OLMOS p 795 N93-15168
Royal Air Force experience of the Harrier information management system p 795 N93-15170
Monitoring of powerplants in advanced commercial aircraft p 795 N93-15171
EJ 200 engine monitoring system: On- and off-board data capture, analysis, and management system p 796 N93-15172
A philosophy for integrated monitoring system design p 796 N93-15174
Experimental analysis of steady-state and dynamic monitoring of power shaft turbines p 796 N93-15176
ENGINE NOISE
Air Force procedure for predicting noise around airbases: Noise exposure model (Noisemap)
[AD-A255769] p 910 N93-14655
ENGINE PARTS
Results of low power deicer tests on a swept inlet component in the NASA Lewis icing research tunnel
[NASA-TM-105968] p 781 N93-14911
Development of wear-resistant ceramic coatings for diesel engine components
[DE92-041382] p 853 N93-15439
ENGINE TESTS
Propulsion and Energetics Panel Working Group 20 on Test Cases for Engine Life Assessment Technology
[AGARD-AR-308] p 798 N93-14890
Introduction to test cases for engine life assessment technology p 799 N93-14891
Engine life assessment test case TF41 LP compressor shaft torsional fatigue p 799 N93-14896

Tribology of improved transformation-toughened ceramics-heat engine test
| DE92-041385 | p 851 N93-15295
Unsteady pressure loads in a generic high speed engine model
| NASA-TP-3189 | p 975 N93-15391

ENGINEERING
Core support for the Board on Mathematical Sciences
| AD-A256333 | p 968 N93-15195

ENGINEERING DRAWINGS
A method of representating dimensions and tolerances in solid based freeform surfaces
| PNR-90998 | p 951 N93-15386

ENGINEERS
Recommendations for enhancement of the Design Criteria Information System (DCIS)
| AD-A256857 | p 1009 N93-15641

ENRICHMENT
The properties of thermally passivated Si(1-x) He(x) produced using high pressure techniques (and related augmentation awards)
| AD-A255961 | p 991 N93-14429

ENTHALPY
Thermophysical properties of nitric oxide
| ESDU-92027 | p 839 N93-14544

ENTRAINMENT
Mixed-layer parameterization in models of the Indian Ocean
| AD-A255937 | p 925 N93-14428
Evaluation of a soil fixative to retard particle entrainment: A laboratory study
| UCRL-LR-109806 | p 915 N93-14877

ENVIRONMENT EFFECTS
Plutonium pyrophoricity
| RFP-4517 | p 845 N93-14723
Workshop on noninvasive geophysical site characterization
| LA-12311-C | p 914 N93-14724
Environmental assessment: OMEGA upgrade project at the Laboratory for Laser Energetics, University of Rochester
| DE92-040410 | p 886 N93-14907
Addressing earthquake strong ground motion issues at the Idaho National Engineering Laboratory
| DE92-017841 | p 916 N93-15136
Data analysis and interpretation for environmental surveillance
| DE92-019009 | p 910 N93-15270
Spatial and temporal patterns of biotic exchanges of CO2 between the atmosphere and tropical landscapes and their role in the global carbon balance
| DE92-019170 | p 911 N93-15272
Independent validation testing of the FLAME computer code, version 1.0
| DE92-019691 | p 948 N93-15274
Environmental assessment for the laser guide star experiment at Lawrence Livermore National Laboratory
| DE92-040316 | p 1013 N93-15425
World energy: Building a sustainable future
| DE93-001598 | p 909 N93-15467
The Seventeenth Space Simulation Conference. Terrestrial Test for Space Success
| NASA-CP-3181 | p 819 N93-15593
Simulation of the synergistic low Earth orbit effects of vacuum thermal cycling, vacuum UV radiation, and atomic oxygen p 819 N93-15595

ENVIRONMENT MANAGEMENT
Using digital scanned aerial photography for wetlands delineation
| AD-A255392 | p 905 N93-14676

ENVIRONMENT MODELS
Multiscale modeling of the long-range transport and fate of pollutants emitted from urban areas
p 909 N93-14118

ENVIRONMENT SIMULATION
Low Earth orbit atomic oxygen simulation for durability evaluation of solar reflector surfaces
p 819 N93-15594
Simulation of the synergistic low Earth orbit effects of vacuum thermal cycling, vacuum UV radiation, and atomic oxygen p 819 N93-15595
The use of plasma ashers and Monte Carlo modeling for the projection of atomic oxygen durability of protected polymers in low Earth orbit p 819 N93-15596

ENVIRONMENTAL MONITORING
Earth environment space initiative
p 811 N93-14953

ENVIRONMENTAL TESTS
The effect of a seawater environment on the galvanic corrosion behavior of graphite/epoxy composites coupled to metals
| AD-A256072 | p 830 N93-14232
Environmental qualification testing of the prototype pool boiling experiment
| NASA-CR-190774 | p 895 N93-15582
An environmental testing facility for Space Station Freedom power management and distribution hardware
p 820 N93-15601
Acoustic and thermal testing of the Titan/Centaur upper stage p 814 N93-15621
Overview of environmental test plans for Space Station Freedom work package 4 p 824 N93-15623
LDEF: A bibliography with abstracts
| NASA-TM-107705 | p 813 N93-15646

EPHEMERIDES
The spin vector of Venus determined from Magellan data p 1027 N93-14310
Terrestrial reference systems related to the TOPEX/Poseidon project p 906 N93-14967

EPITAXY
Novel engineered compound semiconductor heterostructures for advanced electronics applications
| AD-A255363 | p 866 N93-14562
A simple controller for repetitive cycles in atomic layer epitaxy
| AD-A255497 | p 992 N93-14643
Si atomic layer epitaxy using remote plasma assisted hydrogen desorption and disilane as a precursor
| AD-A255606 | p 993 N93-15008
Si atomic layer epitaxy based on Si2H6 and remote He plasma bombardment
| AD-A255763 | p 993 N93-15055
Epitaxial heterojunctions of oxide semiconductors and metals on high temperature superconductors
| NASA-CASE-NPO-18483-1-CU | p 994 N93-15151
Growth, characterization and device development in monocrystalline diamond films
| AD-A256283 | p 994 N93-15244

EPOXY MATRIX COMPOSITES
Microstructure-failure mode correlations in braided composites p 834 N93-14756
Composite materials in space: Results from the LDEF satellite p 811 N93-14955
A study for the development of practices to protectively coat and join fibre epoxy composites for use in the Space Station Programme
| CTN-93-60626 | p 835 N93-15145
Degradation and failure modes of carbon/bismaleimide laminates subjected to a tropical exposure
| AD-A256328 | p 836 N93-15193
Leveling coatings for reducing the atomic oxygen defect density in protected graphite fiber epoxy composites
| NASA-TM-105732 | p 852 N93-15344
Leveling coatings for reducing the atomic oxygen defect density in protected graphite fiber epoxy composites
p 819 N93-15597

EPOXY RESINS
An evaluation of composites fabricated from powder epoxy towpreg p 832 N93-14745
Characteristics of the Nova laser disk edge cladding epoxy
| DE92-041046 | p 853 N93-15462

EQUATIONS OF MOTION
Relativistic dynamics of a charged sphere: Updating the Lorentz-Abraham model
| AD-A256107 | p 971 N93-14245
Nonlinear free vibration analysis of strings by the Galerkin method p 972 N93-14280
Multiply connected spacetimes and closed timelike curves in semiclassical gravity p 915 N93-14884
Position and vibration control of flexible space robots
p 892 N93-15102
Elastic wave propagation in laminated composites
| ITN-93-85186 | p 835 N93-15144
The sine-Gordon model and the small (kappa)(sup +) region of light-cone perturbation theory
| DE92-040506 | p 969 N93-15379
Turbulent fluid motion IV-averages, Reynolds decomposition, and the closure problem
| NASA-TM-105822 | p 880 N93-15585

EQUATIONS OF STATE
Opacity, equation of state, and radiation transport model for moderate density, eV-temperature plasmas
| AD-A256056 | p 988 N93-14579
Electrical resistivity and equation of state measurements of a dense aluminum plasma
| DE92-040352 | p 989 N93-15436

EQUATORIAL ATMOSPHERE
Results of a zonally truncated three-dimensional model of the Venus middle atmosphere p 1037 N93-14351
Equatorial and eastern boundary current variability in the North and South Pacific Oceans
p 931 N93-14994
Global zones of particle precipitation as observed by EXOS-C
| AD-A256397 | p 917 N93-15466

EQUATORIAL REGIONS
The preferred latitudes of the Intertropical Convergence Zone: Observations and theory p 920 N93-14213

EQUILIBRIUM FLOW
Resistive magnetohydrodynamic studies of tearing mode instability with equilibrium shear flow and magnetic reconnection p 987 N93-14122

EQUIVALENCE
The low-energy structure of compactified superstring models p 997 N93-14116
A queue model relating synchronous and asynchronous communication
| MEMO-INF-92-04 | p 966 N93-15491

ERGODIC PROCESS
A proof of convergence of the Markov chain simulation method
| AD-A255456 | p 970 N93-14487

EROSION
Floor-fractured crater models for igneous crater modification on Venus p 1044 N93-14393

ERROR ANALYSIS
A psychometrically sound cognitive diagnostic model: Effect of remediation as empirical validity
| AD-A255926 | p 933 N93-14109
The spin vector of Venus determined from Magellan data p 1027 N93-14310
Arc digital raster imagery evaluation
| AD-A255403 | p 817 N93-14565
A general observation matrix for attitude error estimation with an offset GPS antenna
| AD-A255214 | p 789 N93-14574
Software reliability, measurement, and testing. Volume 2: Guidebook for software reliability measurement and testing
| AD-A256164 | p 944 N93-14581
A system approach to archival storage
p 1006 N93-15040
Improved astigmatic focus error detection method
p 984 N93-15507

ERROR CORRECTING CODES
Off-line generation of error-free robot/NC (numerical control) code using simulation and automatic programming techniques
| F-3-1 | p 949 N93-15302

ERROR SIGNALS
Modified fast frequency acquisition via adaptive least squares algorithm
| NASA-CASE-NPO-17845-2-CU | p 945 N93-14882
Improved astigmatic focus error detection method
p 984 N93-15507
Effects of higher order aberrations on beam shape in an optical recording system p 985 N93-15515

ERRORS
Methodology for robot capability and performance characterization: The basis for robot task planningg
| F-2-3 | p 949 N93-15300

ESCAPE SYSTEMS
Facilities and capabilities catalog for landing and escape systems
| NASA-RP-1282 | p 814 N93-14495

ESCARPMENTS
Sequential deformation of plains along Tessera boundaries on Venus: Evidence from Alpha Regio
p 1028 N93-14317

ESSENTIALLY NON-OSCILLATORY SCHEMES
Eno-Osher schemes for Euler equations
| NASA-TM-105928 | p 969 N93-15341

ESTIMATES
The spin vector of Venus determined from Magellan data p 1027 N93-14310

ESTIMATING
Computation and communication constraints for distributed estimation systems
| AD-A256287 | p 970 N93-14456
Estimation of rate of climb
| ESDU-92019 | p 791 N93-14541
An iconic position estimator for a 2-D laser rangefinder
| AD-A255523 | p 885 N93-14568
Two-stage target tracking system and method
| AD-D015412 | p 982 N93-14880
Modified fast frequency acquisition via adaptive least squares algorithm
| NASA-CASE-NPO-17845-2-CU | p 945 N93-14882
Automated Estimating System (AES), version 5.1. User's manual
| DE93-000380 | p 946 N93-15003
Evaluation of methods for estimating wind wave growth on narrow irregular fetches
| AD-A256002 | p 932 N93-15113
Automated Estimated System (AES) standard value and guidelines programs user's manual
| DE92-041243 | p 951 N93-15450

ETALONS
Fast optoelectronic switching processes in surface-emitting semiconductor lasers and nonlinear etalons
| AD-A255802 | p 886 N93-15069

ETHANE
Ethane ice haze in the upper atmosphere of Uranus p 1023 N93-14212

ETHYLENE
Orthobaric densities and molar volumes of liquids. Halogenated ethylenes
[ESDU-92018] p 839 N93-14540

ETIOLOGY
Training, muscle fatigue and stress fractures
[AD-A255277] p 935 N93-15006

EULER EQUATIONS OF MOTION
Simulation of unsteady inviscid flow on an adaptively refined Cartesian grid p 873 N93-14273
An investigation of genuinely multidimensional schemes for the Euler equations p 876 N93-14694
Eno-Osher schemes for Euler equations
[NASA-TM-105928] p 969 N93-15341

EUROPEAN AIRBUS
Monitoring of powerplants in advanced commercial aircraft p 795 N93-15171
Airbus Industrie TCAS experience p 789 N93-15186

EUROPEAN COMMUNICATIONS SATELLITE
Regional satellites: The European experience with Eutelsat for TV, voice, data and mobile transmissions
[REPT-921-440-106] p 818 N93-15071

EUROPEAN SPACE AGENCY
The design concept of the 6-degree-of-freedom hydraulic shaker at ESTEC p 820 N93-15600

EUTECTICS
Compaction of submicron and nanocrystalline Al2O3-ZrO2 ceramics
[DE92-040233] p 852 N93-15320

EVACUATING (TRANSPORTATION)
Effects of seating configuration and number of type 3 exits on emergency aircraft evacuation
[AD-A256616] p 783 N93-14277

EVALUATION
Iterative software testing
[AD-A255953] p 943 N93-14420
Establishment of a test course for high accuracy dynamic positioning systems
[AD-A255407] p 789 N93-14501
Evaluation and estimation of handling qualities via statistical modeling of pilot response data
[AD-A255324] p 939 N93-14548
Testability design rating system: Testability handbook, volume 1
[RL-TR-92-12-VOL-1] p 867 N93-14699
Experimental evaluation of candidate graphical microburst alert displays p 785 N93-14853
Results of in-service evaluation of wind shear systems p 785 N93-14856
In-service evaluation of wind shear systems p 785 N93-14857
Proposed action plan to improve ADM effectiveness, part 3: Developing a new ADM paradigm on which to build advanced or expert decision making training p 787 N93-15026
Data analysis and interpretation for environmental surveillance
[DE92-019009] p 910 N93-15270
How scientific must technical editors be?
[DE92-040741] p 1010 N93-15655

EVAPORATION
Electrical conductivity measurements in evaporated cadmium telluride thin films p 865 N93-14191

EVOLUTION
The formation of giant molecular clouds p 1021 N93-15086

EXCIMER LASERS
Excimer laser irradiation of metal surfaces p 884 N93-14175

EXCITATION
Some theoretical and experimental aspects of the generation of guided elastic waves using finite sources p 897 N93-14219
Excitation of nuclei by antiproton annihilation at rest
[AD-A255447] p 976 N93-14513
Experimental and theoretical investigation of surface chemistry induced by direct and indirect electronic excitation
[AD-A256342] p 843 N93-15200
A mixed excitation vocoder with fuzzy logic classifier
[AD-A256834] p 864 N93-15636

EXHAUST EMISSION
Multiscale modeling of the long-range transport and fate of pollutants emitted from urban areas p 909 N93-14118

EXHAUST NOZZLES
Supersonic investigation of two dimensional hypersonic exhaust nozzles
[NASA-TM-105687] p 800 N93-15342

EXOBIOLOGY
Aerospace medicine and biology: A continuing bibliography with indexes (supplement 368)
[NASA-SP-7011(368)] p 934 N93-14603
Aerospace medicine and biology: A continuing bibliography with indexes (supplement 369)
[NASA-SP-7011(369)] p 935 N93-14731

EXOTHERMIC REACTIONS
Fabrication of high temperature materials by exothermic synthesis and subsequent dynamic consolidation
[DE92-019836] p 834 N93-14819

EXPANSION
On some kinematic and mass characteristics of foldable solar arrays p 812 N93-14957

EXPERIMENT DESIGN
A proposal to apply Taguchi-inspired methods to the reduction of machining variance
[AD-A256129] p 856 N93-15234
MATE: The multi-agent test environment
[NASA-TM-108114] p 965 N93-15292
Space Station Freedom user's guide
[NASA-TM-108105] p 825 N93-15650

EXPERT SYSTEMS
DESAID (the development of an expert system for aircraft initial design) p 790 N93-14448
A specification of the Soar cognitive architecture in Z
[AD-A256198] p 940 N93-14491
The evolution of artificial intelligence and expert computer systems in the Army
[AD-A255221] p 962 N93-14525
Autonomous power system brassboard
[NASA-CR-189115] p 867 N93-14798
Multiple fault diagnosis of spacecraft electrical power systems p 806 N93-14927
A robotic planning system p 810 N93-14949
PEX: A reactive procedure based decision maker
[REPT-921-440-105] p 999 N93-15118
Failure diagnostic with MAINTEX based on AIMS at Swissair p 778 N93-15181
Design for tactical situation awareness display
[AD-A256194] p 798 N93-15235
Query optimization and planning in object-oriented knowledge bases
[AD-A256006] p 1008 N93-15254
Coordinated motion control of a two-hand assembly system
[F-2-8] p 949 N93-15301
A single-station forecasting model
[AD-A256403] p 924 N93-15331

EXPLORER 50 SATELLITE
A survey of solar flare energetic particle abundances and energy spectra p 1048 N93-14135

EXPLOSIVE FORMING
Fabrication of high temperature materials by exothermic synthesis and subsequent dynamic consolidation
[DE92-019836] p 834 N93-14819

EXPLOSIVES
The sensitivity of energetic materials to friction, impact, and electrostatic stimuli
[DE92-041227] p 855 N93-15478

EXPONENTIAL FUNCTIONS
Analytical characterization of bistatic scattering from rough surfaces: Dependence on surface correlation function
[AD-A256525] p 862 N93-15397

EXPOSURE
Analysis of retinal function following laser irradiation
[AD-A255649] p 933 N93-14163
The preliminary Long Duration Exposure Facility (LDEF) materials data base
[NASA-TM-107692] p 828 N93-14459

EXTERNAL STORES
MIL-STD-1760 application guidelines
[AD-A255714] p 790 N93-14432

EXTRACTION
The evaluation of a concept for a Canadian-made automated multipurpose materials extraction facility p 810 N93-14947
Removal of THD from painted test panels by liquid systems
[AD-A255624] p 850 N93-15064

EXTRATERRESTRIAL RADIATION
A search for anisotropy in the cosmic background radiation at millimeter wavelengths on angular scales from 0.3 to 3 degrees p 1050 N93-14244
Predictions of dose from electrons in space
[NASA-CR-191617] p 1051 N93-15580

EXTRAVEHICULAR ACTIVITY
Extra-vehicular activity translation tool
[NASA-CASE-MSC-21955-1] p 891 N93-14842

EXTRUDING
Effect of thermomechanical treatments on the aging response of centrifugally cast silicon carbide/aluminum composites
[AD-A256204] p 836 N93-15236

EYE PROTECTION
Radical ion formation in polymers as a mechanism for laser eye protection
[AD-A255992] p 850 N93-15111

F

F REGION
A study of mid-latitude 5577 A OI dayglow emissions p 913 N93-14199
The effects of magnetic storm phases on F-layer irregularities from auroral to equatorial latitudes
[AD-A256520] p 917 N93-15395

F-117A AIRCRAFT
A very efficient RCS data compression and reconstruction technique, volume 4
[NASA-CR-191378-VOL-4] p 945 N93-14807

F-14 AIRCRAFT
A neural network prototype for predicting F-14B strains at the B.L. 10 longeron
[AD-A255272] p 792 N93-15004

F-15 AIRCRAFT
An examination of wing rock for the F-15
[AD-A256613] p 802 N93-14252
Wing rock prediction method for a high performance fighter aircraft
[AD-A256438] p 792 N93-15314

F-16 AIRCRAFT
Determination of stresses on laminated aircraft transparencies by the strain gage-hole drilling and sectioning method
[AD-A255548] p 791 N93-14571
Multiple model adaptive estimation applied to the ViSTA F-16 with actuator and sensor failures
[AD-A256444] p 802 N93-14608

FABRICATION
Application of gel-silica optics to laser technology and optical element fabrication
[AD-A255666] p 883 N93-14131
Processing, fabrication, and demonstration of HTS integrated microwave circuits
[AD-A256109] p 865 N93-14246
Organization of workshop on emerging technologies for in-situ processing
[AD-A255977] p 865 N93-14410
Advanced laser chemical processing for microelectronics and integrated optics
[AD-A255980] p 865 N93-14425
Direct optical to microwave conversion
[RL-TR-91-375] p 859 N93-14728
An evaluation of composites fabricated from powder epoxy towpreg p 832 N93-14745
Advanced stitching technology p 832 N93-14746
Flow behavior in liquid molding p 833 N93-14747
Advances in 3-dimensional braiding p 833 N93-14748
Development of generalized 3-D braiding machines for composite preforms p 833 N93-14749
Mechanical response of composite materials with through-the-thickness reinforcement p 834 N93-14753
Fabrication of high temperature materials by exothermic synthesis and subsequent dynamic consolidation
[DE92-019836] p 834 N93-14819
NASA/LMSC instrument design and fabrication --- coherent lidar airborne shear sensor p 784 N93-14846
Multifilamentary superconducting cable and a method of manufacturing it
[AD-D015391] p 846 N93-15231
Superstrength metal composite material and process for making the same
[AD-D015379] p 836 N93-15246
New nonlinear optical film processing
[AD-A256011] p 983 N93-15255
Selected area epitaxial growth for complementary HBT applications
[AD-A257047] p 995 N93-15365
Development of low-expansion ceramics for diesel engine applications
[DE92-041380] p 853 N93-15438
Development of ceramic matrix composites for application in the ceramic technology for advanced heat engines project
[DE92-041378] p 837 N93-15455

FABRICS
FIBER-TEX 1991: The Fifth Conference on Advanced Engineering Fibers and Textile Structures for Composites
[NASA-CP-3176] p 832 N93-14744
Advanced stitching technology p 832 N93-14746
Industrial applications of multiaxial warp knit composites p 833 N93-14750

Improved inhomogeneous finite elements for fabric reinforced composite mechanics analysis
p 834 N93-14757

FACTORIAL DESIGN
A proposal to apply Taguchi-inspired methods to the reduction of machining variance
| AD-A256129 | p 856 N93-15234

FADING
Tactical line-of-sight path reliability: Improved MSE system procedures
| AD-A256504 | p 862 N93-15376

FAILURE
Failure of composite plates under static biaxial planar loading
| NASA-CR-191391 | p 903 N93-15653

FAILURE ANALYSIS
Electronics reliability fracture mechanics. Volume 1: Causes of failures of shop replaceable units and hybrid microcircuits
| AD-A255836 | p 894 N93-14104
Analysis of advanced thin-walled composite structures
p 895 N93-14158
Reanalysis of multiple-wheel landing gear traffic tests
| AD-A256593 | p 804 N93-14238
Development of an environment for software reliability model selection
| AD-A256609 | p 942 N93-14241
Evaluation of the cost effectiveness analysis model being developed for the component improvement programs of the Air Force and the Navy
| AD-A256132 | p 1010 N93-14249
Reliability of stiffened structural panels: Two examples
| NASA-TM-107687 | p 900 N93-14483
Electronics reliability fracture mechanics. Volume 2: Fracture mechanics
| AD-A256200 | p 900 N93-14498
Kind-band failure analysis of thick composites in compression
| AD-A255431 | p 831 N93-14509
Characterization of PZT films fatigued at low frequency
| AEROSPACE-ATR-91(8308)-2 | p 992 N93-14795
Multiple fault diagnosis of spacecraft electrical power systems p 806 N93-14927
Fracture/damage mechanics of composites: Static and fatigue properties
| DLR-MITT-92-03 | p 835 N93-15075
Reliability modelling for non-electronic systems
| REPT-921-440-103 | p 894 N93-15139
Sensor fault detection using nonlinear observer and polynomial classifier p 797 N93-15182
Neural network based condition monitoring
p 797 N93-15183
Stress corrosion susceptibility of ultra-high strength steels for Naval aircraft applications
| AD-A256126 | p 846 N93-15189
Microstack insulator for flashover inhibition, phase 2
| AD-A256338 | p 869 N93-15196
Analytical and experimental evaluation of joining ceramic oxides to ceramic oxides and ceramic oxides to metal for advanced heat engine applications
| DE92-041383 | p 851 N93-15294

FAILURE MODES
Analysis of advanced thin-walled composite structures
p 895 N93-14158
Characterizing longitudinal splitting and delamination fracture toughness of composites p 831 N93-14607
Microstructure-failure mode correlations in braided composites p 834 N93-14756
Degradation and failure modes of carbon/bismaleimide laminates subjected to a tropical exposure
| AD-A256328 | p 836 N93-15193

FAINT OBJECTS
A faint spectroscopic quasar survey
p 1012 N93-14629

FAIRINGS
Close-up analysis of aircraft ice accretion
| NASA-TM-105952 | p 787 N93-15360

FALLOUT
A model for the formation of the extended paraboloidal halos around some impact craters on Venus
p 1037 N93-14352

FANS
Rotating stall inception in fans of low hub-tip ratio
p 779 N93-14479

FAR INFRARED RADIATION
New electronic materials
| AD-A255612 | p 868 N93-15010
Far infrared, magnetic, and electronic studies of high T(sub c) superconducting materials
| AD-A257050 | p 996 N93-15444

FAR ULTRAVIOLET RADIATION
Generation of broadly tunable, narrow bandwidth, and intense coherent vacuum ultraviolet radiation in rare gases p 980 N93-14167

FASTENERS
Work attachment mechanism/work attachment fixture
| NASA-CASE-GSC-13430-1 | p 890 N93-14712

FATIGUE (MATERIALS)
The influence of geometrical constraint on cyclic, elastoplastic, notch root behavior, and fatigue microcrack initiation p 900 N93-14480
Shear fatigue crack growth analysis in large-grain polycrystals p 993 N93-14838
LARZAC HP turbine disk crack initiation and propagation spin pit test p 799 N93-14892
In-service considerations affecting component life
p 800 N93-14898
Training, muscle fatigue and stress fractures
| AD-A255277 | p 935 N93-15006
Fracture/damage mechanics of composites: Static and fatigue properties
| DLR-MITT-92-03 | p 835 N93-15075
Frequency-domain synthesis of the fatigue load spectrum for the NPS 100-kW wind turbine
| DE92-040984 | p 908 N93-15384

FATIGUE LIFE
SDIO Workshop on Piezoelectric Ceramic Actuators for Space Applications
| AD-A255959 | p 990 N93-14422
Thermal fatigue analysis of metal matrix composite with spherical reinforcements
| AD-A255313 | p 831 N93-14672
Engine life assessment test case TF41 LP compressor shaft torsional fatigue p 799 N93-14896

FATIGUE TESTS
Fatigue strength of cruciform and other fillet welded joints in aluminum alloys
| ESDU-92017 | p 900 N93-14553
Testing and analysis of modified HMMWV front lift provisions
| MTL-TR-92-31 | p 891 N93-14735

FAULT TOLERANCE
Fault tolerant systems practitioner's workshop
| AD-A255376 | p 944 N93-14563
Formal verification of an oral messages algorithm for interactive consistency
| NASA-CR-189704 | p 958 N93-14808
Implementation issues concerning injection simulation. Part 1: The backbone implementation
| MEMO-INF-91-57-PT-1 | p 946 N93-15078
Nonblocking and orphan free message logging protocols
| NASA-CR-191631 | p 862 N93-15339

FEASIBILITY
Feasibility study for an integrated data processing system
| PB92-214287 | p 1009 N93-15644

FEASIBILITY ANALYSIS
A feasibility study of space VLBI for geodesy and geodynamics p 904 N93-14223
A feasibility assessment of magnetic bearings for free-piston Stirling space power converters
| NASA-CR-189135 | p 891 N93-14916

FEEDBACK CIRCUITS
Robot learning of contact tasks
| F-3-2 | p 949 N93-15303

FEEDBACK CONTROL
Utilizing sensed incipient slip signals for grasp force control
| AD-A255725 | p 888 N93-14434
Feedback control of flow separation and transition to turbulence in unsteady boundary layers
p 873 N93-14464
Dynamics and control of a rigid/flexible manipulator
p 890 N93-14684
Optimal and robust control of robot manipulators
p 890 N93-14685
Robust nonlinear feedback guidance for an aerospace plane: A geometric approach p 803 N93-14835
MOVE: A neutral network paradigm for robotic control
p 805 N93-14925
Position and vibration control of flexible space robots
p 892 N93-15102
Robust control design for uncertain nonlinear dynamic systems p 964 N93-15148
Sampled-data control and robust control for discrete-time systems p 964 N93-15149
Optimal active vibration absorber: Design and experimental results
| NASA-TM-107709 | p 902 N93-15202
Development of an analog MIMO Quantitative Feedback Theory (QFT) CAD package
| AD-A256435 | p 950 N93-15313
Propulsion system performance resulting from an integrated flight/propulsion control design
| NASA-TM-105874 | p 801 N93-15525
An alternate method for achieving temperature control in the -130 C to 75 C range p 821 N93-15609

FEEDFORWARD CONTROL
Position and vibration control of flexible space robots
p 892 N93-15102

FERMI SURFACES
Electronic structure studies of high-T(sub c) superconductors by photoemission and x ray absorption
p 989 N93-14172

FERMIONS
Semi-classical quantization rules in supersymmetric quantum mechanics p 998 N93-14590
Staggered fermions and chiral symmetry breaking in transverse lattice regulated QED
| DE92-040505 | p 977 N93-15378
Homogeneous quantum electrodynamic turbulence
| NASA-TM-107686 | p 979 N93-15482

FERRITES
Impact of protective oxides on cathode-side resistances in MCFCs
| DE92-019973 | p 994 N93-15221

FERROELECTRICITY
Long term stability in thin film ferroelectric memories
| AD-A256290 | p 991 N93-14439
Reliability of sol-gel derived ferroelectric memories
| AD-A255358 | p 991 N93-14560
Characterization of PZT films fatigued at low frequency
| AEROSPACE-ATR-91(8308)-2 | p 992 N93-14795
Ferroelectrics volume 122, numbers 1-4, 1991. Proceedings of the 3rd International Conference on Ferroelectric Liquid Crystals, part 2
| AD-A257053 | p 996 N93-15446
Ferroelectrics volume 121, numbers 1-4, 1991. Proceedings of the 3rd International Conferenceon Fer roelectric Liquid Crystals, part 1
| AD-A257054 | p 996 N93-15447

FERROMAGNETIC FILMS
High speed magneto-resistive random access memory
| NASA-CASE-NPO-17954-1-CU | p 940 N93-14704

FERROMAGNETIC MATERIALS
Method of characterizing residual stress in ferromagnetic materials using a pulse histogram of acoustic emission signals
| NASA-CASE-LAR-14239-1 | p 845 N93-14705

FERROMAGNETISM
The center for nonlinear phenomena and magnetic materials
| AD-A255983 | p 967 N93-14412
Instrumentation of the variable-angle magneto-optic ellipsometer and its application to M-O media and other non-magnetic films p 984 N93-15508

FEYNMAN DIAGRAMS
The sine-Gordon model and the small (kappa)(sup -) region of light-cone perturbation theory
| DE92-040506 | p 969 N93-15379

FIBER COMPOSITES
Analysis of advanced thin-walled composite structures
p 895 N93-14158
An investigation of crack growth at interfaces in bimaterials and composites using a consistent shear-lag model p 896 N93-14187
Effect of interfacial thermal conductance and fiber orientation on the thermal diffusivity/conductivity of unidirectional fiber-reinforced ceramic matrix composites
p 864 N93-14190
The effect of the interphase/interface region on creep and creep rupture of thermoplastic composites
p 829 N93-14193
Elastic wave scattering by partially debonded or partially coated fibers p 829 N93-14224
The effect of a seawater environment on the galvanic corrosion behavior of graphite/epoxy composites coupled to metals
| AD-A256072 | p 830 N93-14232
On the structure of nonlinear constitutive equations for fiber reinforced composites
| NASA-CR-191024 | p 830 N93-14484
Proceedings of the USAF Structural Integrity Program
| AD-A255379 | p 777 N93-14549
Characterizing longitudinal splitting and delamination fracture toughness of composites p 831 N93-14607
FIBER-TEX 1991: The Fifth Conference on Advanced Engineering Fibers and Textile Structures for Composites
| NASA-CP-3176 | p 832 N93-14744
An evaluation of composites fabricated from powder epoxy towpreg p 832 N93-14745
Advanced stitching technology p 832 N93-14746
Industrial applications of multiaxial warp knit composites p 833 N93-14750
The optimal fiber volume fraction and fiber-matrix property compatibility in fiber reinforced composites
p 833 N93-14752
Mechanical response of composite materials with through-the-thickness reinforcement
p 834 N93-14753

Improved inhomogeneous finite elements for fabric reinforced composite mechanics analysis p 834 N93-14757
The stress development during filament winding of thick cylinders
[AD-A255765] p 901 N93-15066
Preliminary design of composite joints
[DLR-MITT-92-05] p 835 N93-15076
Damage and rupture of ceramic composites
[ETN-92-92722] p 851 N93-15127
A study for the development of practices to protectively coat and join fibre epoxy composites for use in the Space Station Programme
[CTN-93-60626] p 835 N93-15145
Jointed assembly actuated by fluid pressure
[AD-D015383] p 893 N93-15248
Leveling coatings for reducing the atomic oxygen defect density in protected graphite fiber epoxy composites
[NASA-TM-105732] p 852 N93-15344
Polymer infiltration studies
[NASA-CR-191652] p 852 N93-15431
Emittance measurements of Space Shuttle orbiter reinforced carbon-carbon
[NASA-TP-3293] p 903 N93-15530
Nonlinear finite element analysis of metals and metal matrix composites: A local-global investigation
[AD-A256782] p 838 N93-15625

FIBER OPTICS
Optical fibers for long-haul transmission in severe-bending applications
[AD-A255964] p 981 N93-14407
Variable path length spectrophotometric probe
[DE92-019834] p 881 N93-14716
Development of a fiber optic high temperature strain sensor
[NASA-CR-191316] p 882 N93-14810
Layered parallel interface for an active antenna array
[AD-D015411] p 860 N93-14879
Electro-optic architecture (EOA) for sensors and actuators in aircraft propulsion systems
[NASA-CR-182270] p 982 N93-15116
Development of advanced seal verification
[NASA-CR-184502] p 892 N93-15117
Smart materials for Army structures
[AD-A254925] p 836 N93-15218
Remote fiber optic sensor for gaseous and liquid environments, phase 2
[AD-A256224] p 983 N93-15241
Proposal for massively parallel data storage system p 960 N93-15510

FIBER ORIENTATION
Effect of interfacial thermal conductance and fiber orientation on the thermal diffusivity/conductivity of unidirectional fiber-reinforced ceramic matrix composites p 864 N93-14190
Advanced stitching technology p 832 N93-14746
The optimal fiber volume fraction and fiber-matrix property compatibility in fiber reinforced composites p 833 N93-14752
Mechanical response of composite materials with through-the-thickness reinforcement p 834 N93-14753
Failure of composite plates under static biaxial planar loading
[NASA-CR-191391] p 903 N93-15653

FIBER VOLUME FRACTION
The optimal fiber volume fraction and fiber-matrix property compatibility in fiber reinforced composites p 833 N93-14752

FIELD ALIGNED CURRENTS
A numerical model of ionospheric convection derived from field-alignment currents and the corresponding conductivity
[TRITA-EPP-91-03-REV] p 916 N93-15252

FIELD EFFECT TRANSISTORS
The 3 to 5 heterojunction structures and high speed devices
[AD-A250399] p 991 N93-14521
Gate-all-around device
[AD-A255287] p 866 N93-14534
A new device to aid in the conception and optimization of monolithic millimeter circuits: A distributed and nonliner model of a field effect transistor p 807 N93-14932
Conceptualization of a GaAs field effect transistor frequency tripler (2.5-7.5 GHz) for load use in communication satellites p 807 N93-14934
Simulation and nonlinear modelling of microwave transistors p 807 N93-14936
Improvement and analysis of the radiation response of RADFET dosimeters
[AD-A254115] p 869 N93-15133

FIELD STRENGTH
Measurements of electric and magnetic fields in the Waianae, Hawaii area
[DE92-019891] p 861 N93-15220

FIELD THEORY (PHYSICS)
Type 2 superstrings in curved D = 10 space-time: Dynamics of their massless fields and covariant quantization p 998 N93-14143
Relativistic dynamics of a charged sphere: Updating the Lorentz-Abraham model
[AD-A256107] p 971 N93-14245
Cosmological models in higher-order gravity p 1018 N93-14592
The sine-Gordon model and the small (kappa)(sup +) region of light-cone perturbation theory
[DE92-040506] p 969 N93-15379

FIGHTER AIRCRAFT
Pressure distribution for the wing of the YAV-8B airplane; with and without pylons
[NASA-TM-4429] p 779 N93-14451
The human-electronic crew: Is the team maturing? The 2nd Joint GAF/RAF/USAF Workshop on Human-Electronic Crew Teamwork
[AD-A256192] p 939 N93-14520
Application of an aeroelastic analysis method for aerodynamic improvement of fighter wings at maneuver flight conditions p 791 N93-14832
Standardization of precipitation static test methods and equipment for the Navy
[AD-A257025] p 792 N93-15361
F/A-18 controls released departure recovery flight test evaluation
[AD-A256522] p 803 N93-15396

FILAMENT WINDING
The stress development during filament winding of thick cylinders
[AD-A255765] p 901 N93-15066

FILLERS
Fatigue strength of cruciform and other fillet welded joints in aluminum alloys
[ESDU-92017] p 900 N93-14553

FILLETS
Fatigue strength of cruciform and other fillet welded joints in aluminum alloys
[ESDU-92017] p 900 N93-14553

FILM THICKNESS
Effects of cryocontaminants on cryogenic superpolished mirror and superpolished quartz crystal microbalance
[AD-A255972] p 981 N93-14403
Instrumentation of the variable-angle magneto-optic ellipsometer and its application to M-O media and other non-magnetic films p 984 N93-15508

FILTRATION
Alpha migration through air filters: A numerical simulation
[UCRL-LR-109866] p 878 N93-15285

FINE STRUCTURE
Fine structure of auroral particle acceleration p 912 N93-14121

FINGERS
Utilizing sensed incipient slip signals for grasp force control
[AD-A255725] p 888 N93-14434

FINITE DIFFERENCE THEORY
Theoretical and experimental analysis of residual stress formation after implant resistance welding of polycarbonate p 898 N93-14279
The center for nonlinear phenomena and magnetic materials
[AD-A255983] p 967 N93-14412
BLSTA: A boundary layer code for stability analysis
[NASA-CR-4481] p 877 N93-14797
Theory and applications of the 3-dimensional finite-difference time-domain method
[AD-A256559] p 968 N93-14804
Finite-difference solution for laminar or turbulent boundary layer flow over axisymmetric bodies with ideal gas, CF4, or equilibrium air chemistry
[NASA-TP-3271] p 879 N93-15434
JSEP fellowship --- Transient radiation from antenna structures
[AD-A257021] p 863 N93-15470

FINITE ELEMENT METHOD
Integration and processing of high-resolution moire-interferometry data p 895 N93-14185
Non-linear analysis of wave progagation using transform methods and plates and shells using integral equations p 896 N93-14186
Finite element models of laser welding p 888 N93-14226
Weight optimum arch structures
[AD-A256080] p 897 N93-14236
Experimental and analytical investigation of the vibration characteristics of a remotely piloted helicopter
[AD-A256131] p 790 N93-14248
Theoretical and experimental analysis of residual stress formation after implant resistance welding of polycarbonate p 898 N93-14279
Thermal buoyancy on Venus: Preliminary results of finite element modeling p 1025 N93-14302
Viscoelastic relaxation of Venusian coronae and mountain belts: Constraints on global heat flow and tectonism p 1027 N93-14313
Constraints on crustal rheology and age of deformation from models of gravitational spreading in Ishtar Terra, Venus p 1042 N93-14379
Finite element analysis of elastic fracture under unsteady translational and rotational loading p 899 N93-14469
Large plastic deformations by sequential limit analysis: A finite element approach with applications in metal forming p 899 N93-14471
Deformation characterization of powdered metals in compaction and application of the finite element method to compaction processes p 844 N93-14472
Mechanics of composite materials for spacecraft
[AD-A255380] p 831 N93-14550
A finite element model for analysis of thermoviscoplastic behavior of hypersonic leading edge structures subject to intense aerothermal heating p 780 N93-14631
Testing and analysis of modified HMMWV front lift provisions
[MTL-TR-92-31] p 891 N93-14735
Improved inhomogeneous finite elements for fabric reinforced composite mechanics analysis p 834 N93-14757
Use of the thin-walled torsion specimen
[AD-A255593] p 901 N93-14790
SAPNEW: Parallel finite element code for thin shell structures on the Alliant FX-80
[NASA-CR-189212] p 901 N93-14799
Stability of elastically tailored rotor blades p 791 N93-14828
Dynamics systems applied to Navier-Stokes equations for the study of turbulence
[ETN-92-92553] p 878 N93-15122
Calculation of mechanical vibration frequencies of stiffened superconducting cavities
[DE92-040228] p 903 N93-15423
Time-dependent predictions and analysis of turbine cascade data in the transonic flow region
[PNR-90957] p 782 N93-15489
Nonlinear finite element analysis of metals and metal matrix composites: A local-global investigation
[AD-A256782] p 838 N93-15625

FINNED BODIES
High performance titanium plate fin heat exchanger using a novel manufacturing process
[PNR-90933] p 880 N93-15488

FINS
Extended surface heat sinks for electronic components: A computer optimization
[AD-A256134] p 865 N93-14254

FISSION
Stability of differentially rotating stars p 1018 N93-14584

FIXED WINGS
Finite-state inflow applied to aeroelastic flutter of fixed and rotating wings p 802 N93-14830

FIXTURES
Work attachment mechanism/work attachment fixture
[NASA-CASE-GSC-13430-1] p 890 N93-14712

FLAME PROPAGATION
Modeling of Combustion and Turbulence
[VKI-LS-1992-03] p 839 N93-14617
Fundamentals of combustion of premixed gases p 840 N93-14618
Chemical kinetics for combustion p 840 N93-14619
Turbulence modeling for combustion flows p 840 N93-14620
Radiative heat transfer in combustion systems p 840 N93-14621
Direct simulation of turbulent combustion p 840 N93-14622
Applications of PDF turbulent combustion models to real non premixed flame calculations p 841 N93-14624
Introduction to spray combustion modelling p 841 N93-14626

FLAMES
Independent validation testing of the FLAME computer code, version 1.0
[DE92-019691] p 948 N93-15274

FLASHOVER
Microstack insulator for flashover inhibition, phase 2
[AD-A256338] p 869 N93-15196

FLAT PLATES
Exploiting similarity in turbulent shear flows for turbulence modeling
[NASA-CR-191621] p 875 N93-14481
A numerical investigation of the interaction between crossing oblique shocks and a turbulent boundary layer p 876 N93-14695
A multigrid approach to embedded-grid solvers
[AD-A256405] p 879 N93-15332

FLEXIBLE BODIES
Damage location and model refinement for large flexible space structures using a sensitivity-based eigenstructure assignment method p 816 N93-14274
Dynamics and control of a rigid/flexible manipulator p 890 N93-14684
Position and vibration control of flexible space robots p 892 N93-15102
Dynamics and control of flexible arm robots
|ISBN-0-315-69011-9| p 892 N93-15150
Optimal active vibration absorber: Design and experimental results
|NASA-TM-107709| p 902 N93-15202

FLEXIBLE SPACECRAFT
Comparative study of stability of flexible satellites with and without guy-wire constraints p 817 N93-14585
Advanced aeroservoelastic stabilization techniques for hypersonic flight vehicles
|NASA-CR-189702| p 802 N93-14811

FLEXING
Cytherean crustal bending at Salme Dorsa p 1039 N93-14364

FLIGHT ALTITUDE
A study of viscous interaction effects on hypersonic waveriders p 778 N93-14160

FLIGHT CHARACTERISTICS
A simulation model of atmospheric turbulence for rotorcraft applications p 920 N93-14588
The relationship between computer scoring and safety-pilot grading of flight performance
|AD-A256245| p 937 N93-14600

FLIGHT CONDITIONS
Special investigation report: Piper Aircraft Corporation PA-46 Malibu/Mirage Accidents/Incident, 31 May 1989 - 17 March 1991
|PB92-917007| p 788 N93-15577

FLIGHT CONTROL
Advanced aeroservoelastic stabilization techniques for hypersonic flight vehicles
|NASA-CR-189702| p 802 N93-14811
Robust nonlinear feedback guidance for an aerospace plane: A geometric approach p 803 N93-14835
Taxonomy of flight variables p 787 N93-15022
F/A-18 controls released departure recovery flight test evaluation
|AD-A256522| p 803 N93-15396

FLIGHT CREWS
The human-electronic crew: Is the team maturing? The 2nd Joint GAF/RAF/USAF Workshop on Human-Electronic Crew Teamwork
|AD-A256192| p 939 N93-14520
Development of measures of crew coordination
|AD-A255384| p 939 N93-14651
Does cockpit management training reduce aircrew error? p 785 N93-15014
Trans-cockpit authority gradient in Navy/Marine aircraft mishaps p 786 N93-15016
A cognitive model for training decision making in aircrews p 786 N93-15020
Taxonomy of flight variables p 787 N93-15022
Shared mental models and crew decision making p 787 N93-15023

FLIGHT ENVELOPES
Icing effects on aircraft stability and control determined from flight data: Preliminary results
|NASA-TM-105977| p 803 N93-14831

FLIGHT HAZARDS
The Orlando TDWR testbed and airborne wind shear date comparison results p 784 N93-14851

FLIGHT INSTRUMENTS
Proceedings of the 16th Symposium on Aircraft Integrated Monitoring Systems
|DLR-MITT-92-01| p 793 N93-15152
Sensor fault detection using nonlinear observer and polynomial classifier p 797 N93-15182

FLIGHT OPERATIONS
In-service evaluation of wind shear systems p 785 N93-14857
Proceedings of the 16th Symposium on Aircraft Integrated Monitoring Systems
|DLR-MITT-92-01| p 793 N93-15152
New rotor trim and balance system for helicopter usage monitoring p 797 N93-15180
Terminal area forecasts FY 1992 - 2005
|AD-A255797| p 788 N93-15390

FLIGHT PLANS
Spectral analysis of the shuttle glow: AIS science support
|PL-TR-92-2172| p 815 N93-14698

FLIGHT RECORDERS
Proceedings of the 16th Symposium on Aircraft Integrated Monitoring Systems
|DLR-MITT-92-01| p 793 N93-15152
Discussion for the ideal AIMS p 793 N93-15153
Flight data and flight safety in SAS p 793 N93-15156
Detection of technical states with aircraft p 794 N93-15159
Rewritable optical disk. Application to flight recording p 794 N93-15160
Indian experience in flight data readout and analysis p 794 N93-15161
Czechoslovak development and experience in flight data recorder readout and analysis p 794 N93-15162
Software for flight recorder data evaluation developed by Lufthansa p 794 N93-15163
The FAIR (Flight Animated and Interactive Reconstruction) tool p 788 N93-15164
The SIROM flight data recorder and evaluation system p 795 N93-15165
Solid state flight data recorder with rapid data access p 795 N93-15167
EJ 200 engine monitoring system: On- and off-board data capture, analysis, and management system p 796 N93-15172
Helicopter flight data recorder and health and usage monitoring system p 797 N93-15178
Helicopter health monitoring: Current practice and future trends p 797 N93-15179

FLIGHT SAFETY
Aviation accidents, incidents, and violations: Psychological predictors among US pilots p 783 N93-14693
Trans-cockpit authority gradient in Navy/Marine aircraft mishaps p 786 N93-15016
Embedded ADM reduces helicopter human error accidents p 787 N93-15024
Flight data and flight safety in SAS p 793 N93-15156
The FAIR (Flight Animated and Interactive Reconstruction) tool p 788 N93-15164
Sensor fault detection using nonlinear observer and polynomial classifier p 797 N93-15182
Neural network based condition monitoring p 797 N93-15183
Airbus Industrie TCAS experience p 789 N93-15186
Special investigation report: Piper Aircraft Corporation PA-46 Malibu/Mirage Accidents/Incident, 31 May 1989 - 17 March 1991
|PB92-917007| p 788 N93-15577

FLIGHT SIMULATION
Evaluation and estimation of handling qualities via statistical modeling of pilot response data
|AD-A255324| p 939 N93-14548
Advantages of using a projected head-up display in a flight simulator
|AD-A255332| p 804 N93-14559
The relationship between computer scoring and safety-pilot grading of flight performance
|AD-A256245| p 937 N93-14600
Flight testing: Past, present, and future p 777 N93-14615
Flight simulation leaves the ground p 778 N93-14616

FLIGHT SIMULATORS
Advantages of using a projected head-up display in a flight simulator
|AD-A255332| p 804 N93-14559
Symposium on the occasion of the farewell of Prof. Dr. Ir. O. H. Gerlach as Chairman of the Board of the Foundation National Aerospace Laboratory NLR, The Netherlands
|ETN-92-92168| p 777 N93-14613
Flight simulation leaves the ground p 778 N93-14616

FLIGHT TESTS
Pressure distribution for the wing of the YAV-8B airplane; with and without pylons
|NASA-TM-4429| p 779 N93-14451
Flight termination systems commonality standard
|AD-A255349| p 789 N93-14517
Evaluation and estimation of handling qualities via statistical modeling of pilot response data
|AD-A255324| p 939 N93-14548
Symposium on the occasion of the farewell of Prof. Dr. Ir. O. H. Gerlach as Chairman of the Board of the Foundation National Aerospace Laboratory NLR, The Netherlands
|ETN-92-92168| p 777 N93-14613
Flight testing: Past, present, and future p 777 N93-14615
Icing effects on aircraft stability and control determined from flight data: Preliminary results
|NASA-TM-105977| p 803 N93-14831
NASA/LMSC coherent LIDAR airborne shear sensor: System capabilities and flight test plans p 784 N93-14847
A neural network prototype for predicting F-14B strains at the B.L. 10 longeron
|AD-A255272| p 792 N93-15004
Wing rock prediction method for a high performance fighter aircraft
|AD-A256438| p 792 N93-15314
The use of ultrasonics for oleo compression measurements on a S-70B-2 (Seahawk) helicopter
|AD-A256315| p 792 N93-15328
F/A-18 controls released departure recovery flight test evaluation
|AD-A256522| p 803 N93-15396

FLIGHT TRAINING
Development of measures of crew coordination
|AD-A255384| p 939 N93-14651
F/A-18 controls released departure recovery flight test evaluation
|AD-A256522| p 803 N93-15396

FLOATING
The numerical stability of nonlinear floating body calculations p 873 N93-14278

FLOATS
The numerical stability of nonlinear floating body calculations p 873 N93-14278

FLOOD PLAINS
Integrating satellite imagery into a geographic information system for monitoring the downstream impacts of dam construction on floodplain agriculture in Sokoto State, Nigeria p 905 N93-14823

FLOW CHARACTERISTICS
Parametric study of air sampling cyclones p 779 N93-14173
Pressure distribution for the wing of the YAV-8B airplane; with and without pylons
|NASA-TM-4429| p 779 N93-14451
Control of low-speed turbulent separated flow over a backward-facing ramp p 874 N93-14475
Flow behavior in liquid molding p 833 N93-14747
Wake similarity and vortex formation for two-dimensional bluff bodies p 781 N93-15101

FLOW DISTORTION
Unsteady flow distortion past blades: Sources of noise generation in rotating flows
|AD-A255496| p 880 N93-15652

FLOW DISTRIBUTION
Extensive lava flow fields on Venus: Preliminary investigation of source elevation and regional slope variations p 1034 N93-14342
Direct prediction of a separation boundary for aerofoils using a viscous-coupled calculation method
|ESDU-92008| p 780 N93-14516
Development of engineering methods for nonequilibrium radiative phenomena about aeroassisted entry vehicles p 817 N93-14632
An investigation of genuinely multidimensional schemes for the Euler equations p 876 N93-14694
Comparison between irregularity motion and bulk plasma drifts at high latitudes
|PL-TR-91-2292| p 914 N93-14727
Investigations of detail design issues for the high speed acoustic wind tunnel using a 60th scale model tunnel. Part 2: Tests with the closed circuit
|NASA-CR-191672| p 780 N93-14738
Supersonic boundary-layer flow turbulence modeling
|NASA-TM-105893| p 877 N93-14758
Estimation of unsteady lift on a pitching airfoil from wake velocity surveys
|NASA-TM-105947| p 781 N93-14791
L.D.V. measurements of unsteady flow fields in radial turbine
|AD-A255728| p 878 N93-15065
An experimental investigation of base bleed effect on the wake turbulent structure behind a two-dimensional blunt model
|MPIS-9/1991| p 781 N93-15131
Flowfield study of a close-coupled canard configuration
|AD-A256311| p 782 N93-15245
An experimental and analytical study of TIP clearance effects in axial flow compressors
|AD-A256434| p 800 N93-15337
Ice accretion and performance degradation calculations with LEWICE/NS
|NASA-TM-105972| p 787 N93-15354
Use of surface heat transfer measurements as a flow separation diagnostic in a two dimensional reflected oblique shock/turbulent boundary layer interaction
|NASA-TM-105981| p 879 N93-15355
An integral equation solution for multistage turbomachinery design calculations
|NASA-TM-105970| p 801 N93-15521
Unsteady shear disturbances within a two dimensional stratified flow
|NASA-CR-189121| p 880 N93-15527
Investigation of the aerothermodynamics of hypervelocity reacting flows in the ram accelerator
|NASA-CR-191715| p 783 N93-15588

Numerical modeling tools for chemical vapor deposition
[NASA-CR-4480] p 880 N93-15643
FLOW EQUATIONS
Turbulence modeling for combustion flows p 840 N93-14620
PDF transport modelling p 840 N93-14623
Time-dependent predictions and analysis of turbine cascade data in the transonic flow region
[PNR-90957] p 782 N93-15489
An integral equation solution for multistage turbomachinery design calculations
[NASA-TM-105970] p 801 N93-15521
FLOW GEOMETRY
A numerical investigation of the interaction between crossing oblique shocks and a turbulent boundary layer p 876 N93-14695
FLOW MEASUREMENT
Boundary layer transition measurements by optical anemometry p 874 N93-14477
Optical monitor for observing turbulent flow
[DE92-019831] p 876 N93-14715
Advanced research in instrumentation and diagnostics technology
[DE92-041121] p 883 N93-15411
FLOW STABILITY
Preconditioned conjugate-gradient methods for low-speed flow calculations
[NASA-TM-105929] p 877 N93-14885
On the nonlinear three dimensional instability of Stokes layers and other shear layers to pairs of oblique waves
[NASA-TM-105918] p 880 N93-15499
FLOW VELOCITY
Parametric study of air sampling cyclones p 779 N93-14173
Development of braided rope seals for hypersonic engine applications: Flow modeling
[NASA-TM-105942] p 888 N93-14478
A multigrid approach to embedded-grid solvers
[AD-A256405] p 879 N93-15332
FLOW VISUALIZATION
Subsonic aerodynamic research laboratory
[AD-A256060] p 780 N93-14661
Advanced research in instrumentation and diagnostics technology
[DE92-041121] p 883 N93-15411
FLUENCE
The response of dispersion-strengthened copper alloys to high fluence neutron irradiation at 415 C
[DE92-019434] p 846 N93-15138
Solar proton events of 1989: Effects on spacecraft solar arrays
[AD-A256457] p 1049 N93-15318
FLUID DYNAMICS
A plume-induced boundary layer separation experiment
[AD-A255397] p 875 N93-14677
Control of thermocapillary convection in a two-layer liquid system p 809 N93-14945
FLUID FLOW
Finite element models of laser welding p 888 N93-14226
Development of braided rope seals for hypersonic engine applications: Flow modeling
[NASA-TM-105942] p 888 N93-14478
Study of Fluid Experiment System (FES)/CAST/Holographic Ground System (HGS)
[NASA-CR-184483] p 855 N93-14793
Preconditioned conjugate-gradient methods for low-speed flow calculations
[NASA-TM-105929] p 877 N93-14885
Advanced research in instrumentation and diagnostics technology
[DE92-041121] p 883 N93-15411
Exact analytical solution of the toroidal singular mode equations
[DE92-040223] p 988 N93-15419
FLUID MECHANICS
Current status of liquid sheet radiator research
[NASA-TM-105764] p 872 N93-14150
FLUID PRESSURE
Jointed assembly actuated by fluid pressure
[AD-D015383] p 893 N93-15248
FLUORESCENCE
Biofilm ecology of bioluminescent bacteria
[AD-A255282] p 932 N93-14532
FLUTTER
A compilation of the mathematics leading to the doublet lattice method
[AD-A256304] p 779 N93-14441
Multi-disciplinary optimization of aeroservoelastic systems
[NASA-CR-191255] p 901 N93-14766
Finite-state inflow applied to aeroelastic flutter of fixed and rotating wings p 802 N93-14830
FLUTTER ANALYSIS
Multi-disciplinary optimization of aeroservoelastic systems
[NASA-CR-191255] p 901 N93-14766
FLUX DENSITY
Energetic and magnetosheath energy particle signatures of the low-latitude boundary layer at low altitudes near noon
[NASA-CR-191388] p 917 N93-15574
FLUX PINNING
Dynamics in neutron stars and the early universe p 1014 N93-14112
FLY BY WIRE CONTROL
Multiple model adaptive estimation applied to the ViSTA F-16 with actuator and sensor failures
[AD-A256444] p 802 N93-14608
FOAMS
Characterization of impact-limiting material
[DE92-016767] p 902 N93-15210
FOCAL PLANE DEVICES
Nonuniformity effects in a hybrid platinum silicide imaging device
[AD-A256339] p 983 N93-15197
FOLDING STRUCTURES
On some kinematic and mass characteristics of foldable solar arrays p 812 N93-14957
FOOTPRINTS
Problem footprints in Magellan altimetry data p 1039 N93-14362
FORCED VIBRATION
Transformation of energy and momentum due to Landau damping in time
[IPPCZ-316] p 988 N93-14813
Transient response of a viscous liquid bridge of finite length and anchored edges
[LRT-WE-9-FB-25-1991] p 878 N93-15132
FORECASTING
Terminal area forecasts FY 1992 - 2005
[AD-A255797] p 788 N93-15390
FORGING
Analytical and experimental evaluation of joining ceramic oxides to ceramic oxides and ceramic oxides to metal for advanced heat engine applications
[DE92-041383] p 851 N93-15294
FORMALISM
Mission critical system development: Design views and their integration
[AD-A255498] p 940 N93-14644
Formal verification of an oral messages algorithm for interactive consistency
[NASA-CR-189704] p 958 N93-14808
From data structure to process structure
[MEMO-INF-91-38] p 946 N93-15077
Grammatical trigrams: A probabilistic model of link grammar
[AD-A256365] p 947 N93-15206
FORMAT
Conversion of IRAMMP data to HDF format
[AD-A256515] p 1008 N93-15393
Output data formatter for the Electronically Scanned Thinned Array Radiometer (ESTAR) instrument
[NASA-TM-4432] p 871 N93-15529
FORMING TECHNIQUES
Large plastic deformations by sequential limit analysis: A finite element approach with applications in metal forming p 899 N93-14471
FOUR-WAVE MIXING
Advanced optical fiber communication systems
[AD-A255424] p 982 N93-14507
FOURIER ANALYSIS
Homogeneous quantum electrodynamic turbulence
[NASA-TM-107686] p 979 N93-15482
FOURIER SERIES
Ocean wave detection using satellite altimetry p 906 N93-14839
FOURIER TRANSFORMATION
Application of Fourier Transform-infrared spectroscopy (FT-IR) for materials analysis
[AD-A255727] p 838 N93-14435
Precise measurements made from a distance of local deformations independent of small object movements
[ETN-92-92723] p 886 N93-15128
Volume rendering using the Fourier projection-slice theorem p 953 N93-15541
FOVEA
Analysis of retinal function following laser irradiation
[AD-A255649] p 933 N93-14163
FRACTALS
The use of chaos metrics to analyze Lagrangian particle diffusion models
[AD-A256142] p 967 N93-14255
Escape-time visualization method for language-restricted iterated function systems p 956 N93-15558
The object instancing paradigm for linear fractal modeling p 956 N93-15559
FRACTURE MECHANICS
Electronics reliability fracture mechanics. Volume 1: Causes of failures of shop replaceable units and hybrid microcircuits
[AD-A255836] p 894 N93-14104
Fatigue in single crystal nickel superalloys
[AD-A256095] p 844 N93-14264
A study of the relationship between macroscopic measures and physical processes occurring during crack closure
[AD-A256587] p 898 N93-14272
A preliminary investigation of dual mode fracture sustained by graphite/epoxy laminates impacted by high-velocity spherical metallic projectiles
[AD-A255790] p 898 N93-14419
Fracture mechanisms and fracture control in composite structures p 899 N93-14474
Electronics reliability fracture mechanics. Volume 2: Fracture mechanics
[AD-A256200] p 900 N93-14498
Damage and rupture of ceramic composites
[ETN-92-92722] p 851 N93-15127
Degradation and failure modes of carbon/bismaleimide laminates subjected to a tropical exposure
[AD-A256328] p 836 N93-15193
Closed form expressions for crack mouth displacements and stress intensity factors for chevron notched short bar and short rod specimens based on experimental compliance measurements
[NASA-TM-83796] p 902 N93-15369
The mixed mode crack problem in a nonhomogeneous elastic plane
[AD-A256469] p 902 N93-15372
Diffusion problems in bonded nonhomogeneous materials with an interface cut
[AD-A256470] p 836 N93-15373
The crack problem for an orthotropic half plane stiffened by elastic films
[AD-A256471] p 903 N93-15374
Frequency-domain synthesis of the fatigue load spectrum for the NPS 100-kW wind turbine
[DE92-040984] p 908 N93-15384
Nonlinear finite element analysis of metals and metal matrix composites: A local-global investigation
[AD-A256782] p 838 N93-15625
FRACTURE STRENGTH
Fracture analyses of thin films, interfaces, and joints p 897 N93-14215
Reanalysis of multiple-wheel landing gear traffic tests
[AD-A256593] p 804 N93-14238
Characterizing longitudinal splitting and delamination fracture toughness of composites p 831 N93-14607
Microstructure-failure mode correlations in braided composites p 834 N93-14756
Analytical and experimental evaluation of joining ceramic oxides to ceramic oxides and ceramic oxides to metal for advanced heat engine applications
[DE92-041383] p 851 N93-15294
FRACTURES (MATERIALS)
Characterizing longitudinal splitting and delamination fracture toughness of composites p 831 N93-14607
Microstructure-failure mode correlations in braided composites p 834 N93-14756
Training, muscle fatigue and stress fractures
[AD-A255277] p 935 N93-15006
FRACTURING
Fracture analyses of thin films, interfaces, and joints p 897 N93-14215
Floor-fractured crater models for igneous crater modification on Venus p 1044 N93-14393
A preliminary investigation of dual mode fracture sustained by graphite/epoxy laminates impacted by high-velocity spherical metallic projectiles
[AD-A255790] p 898 N93-14419
Finite element analysis of elastic fracture under unsteady translational and rotational loading p 899 N93-14469
Fracture mechanisms and fracture control in composite structures p 899 N93-14474
FRAGMENTATION
Data fragmentation for parallel transitive closure strategies
[MEMO-INF-92-17] p 959 N93-15142
Ecological implications of landscape fragmentation
[DE92-019186] p 911 N93-15273
FREE CONVECTION
Constraints on the thermal evolution of Venus inferred from Magellan data p 1024 N93-14293
Convective scale 4-D data assimilation using simulated single-Doppler radar observations p 921 N93-14683
FREE ELECTRON LASERS
Three-dimensional guiding effects in a free-electron laser p 883 N93-14125
Compact free electron laser for medical applications
[AD-A256236] p 885 N93-14599
Abstracts booklet
[AD-A256115] p 869 N93-15188

Electron acceleration by longitudinal electric field of a Gaussian laser beam
[DE92-526947] p 887 N93-15296
Simple formulae for the optimization of the FEL gain length including the effects of emittance, betatron oscillations, and energy spread
[DE92-040378] p 887 N93-15325
Condensed matter research using the UCSB FEL
[DE92-040560] p 887 N93-15347
High-brightness linac for the Advanced Free-Electron Laser Initiative at Los Alamos
[DE92-040213] p 887 N93-15417

FREE JETS
A study of an optically pumped free-jet molecular iodine laser operating in the visible spectrum
p 884 N93-14141
Second order closure modeling of turbulent buoyant wall plumes
[NASA-TM-105956] p 877 N93-14829

FREE RADICALS
An investigation of transient atmospheric inorganic peroxides: A theoretical and experimental study
p 912 N93-14117

FREE VIBRATION
Modal interactions in the dynamic response of isotropic and composite plates p 829 N93-14221
Experimental and analytical investigation of the vibration characteristics of a remotely piloted helicopter
[AD-A256131] p 790 N93-14248
Nonlinear free vibration analysis of strings by the Galerkin method p 972 N93-14280
Transformation of energy and momentum due to Landau damping in time
[IPPCZ-316] p 988 N93-14813

FREE-PISTON ENGINES
A feasibility assessment of magnetic bearings for free-piston Stirling space power converters
[NASA-CR-189135] p 891 N93-14916

FREQUENCIES
Modified fast frequency acquisition via adaptive least squares algorithm
[NASA-CASE-NPO-17845-2-CU] p 945 N93-14882

FREQUENCY CONTROL
Broadband vibroacoustic frequency control via piezoelectric films
[ONERA-RT-8/3654-RY-010-R] p 974 N93-15129

FREQUENCY CONVERTERS
Direct optical to microwave conversion
[RL-TR-91-375] p 859 N93-14728

FREQUENCY DISTRIBUTION
New methods for nonlinear tracking and nonlinear chaotic signal processing
[AD-A256421] p 862 N93-15334

FREQUENCY MULTIPLIERS
Conceptualization of a GaAs field effect transistor frequency tripler (2.5-7.5 GHz) for load use in communication satellites p 807 N93-14934

FREQUENCY SHIFT
Frequency shifts in a rubidium frequency standard due to coupling to another standard
[AD-A256232] p 972 N93-15243
The detection and characterization of high frequency and high wavenumber solar oscillations
[NASA-CR-191622] p 1049 N93-15634

FREQUENCY SHIFT KEYING
A low bit rate FSK technique for SCPC satellite communication systems p 811 N93-14954

FREQUENCY STABILITY
Asymmetric natural damped frequencies of a rotating infinitely long viscous liquid column
[LRT-WE-9-FB-23-1991] p 878 N93-15120
Frequency shifts in a rubidium frequency standard due to coupling to another standard
[AD-A256232] p 972 N93-15243
Introduction to quartz frequency standards, revision 1
[AD-A256373] p 870 N93-15330

FREQUENCY STANDARDS
Determining optimum C-field settings that minimize output frequency variations in cesium atomic frequency standards
[AD-A255902] p 971 N93-14108
Frequency shifts in a rubidium frequency standard due to coupling to another standard
[AD-A256232] p 972 N93-15243
Introduction to quartz frequency standards, revision 1
[AD-A256373] p 870 N93-15330

FRESNEL REFLECTORS
Optics for diode array transverse pumped laser rod
[AD-D015436] p 885 N93-14722

FRICTION
Characterization of fiber reinforced phenolic composites p 828 N93-14142
Tribology of magnetic storage systems
p 1002 N93-14772
Exceptionally high-strength (approximately 3 GPa) aluminum alloys demonstrated by oxygen ion implantation
[DE92-040980] p 847 N93-15383
The sensitivity of energetic materials to friction, impact, and electrostatic stimuli
[DE92-041227] p 855 N93-15478

FRONTS (METEOROLOGY)
Structure and propagation of fronts east of the Rocky Mountains and their relationship to precipitation
p 921 N93-14827

FROST
Martian water frost: Control of global distribution by small-scale processes p 1047 N93-14868

FUEL CELLS
Components and materials issues in polymer electrolyte fuel cells for transportation applications
[DE92-013384] p 907 N93-15061
Technology commercialization cost model and component case study
[DE92-001280] p 907 N93-15213
Impact of protective oxides on cathode-side resistances in MCFCs
[DE92-019973] p 994 N93-15221
Jet vapor deposition of thin films for solid oxide and other fuel cell applications
[DE92-019980] p 851 N93-15222
S/EV 1991: Solar and Electric Vehicle Symposium, Car and Trade Show
[DE92-019890] p 869 N93-15226
High temperature tubular solid oxide fuel cell development
[DE92-040253] p 908 N93-15322
Contaminant effects in solid oxide fuel cells
[DE92-040255] p 908 N93-15323
Exploratory technology research program for electrochemical energy storage
[DE93-001595] p 909 N93-15484

FUEL CONSUMPTION
RB199 engine oil system failure diagnostics by comparison of measured and calculated oil consumption using the OLMOS on-board monitoring system
p 796 N93-15173

FUEL FLOW
Propulsion system performance resulting from an integrated flight/propulsion control design
[NASA-TM-105874] p 801 N93-15525

FUEL SPRAYS
Dynamic behavior of a dense spray diffusion flame in a potential vortex p 839 N93-14463

FUEL SYSTEMS
RB199 engine oil system failure diagnostics by comparison of measured and calculated oil consumption using the OLMOS on-board monitoring system
p 796 N93-15173

FUEL TESTS
Liquid flow reactor and method of using
[AD-D015392] p 893 N93-15232

FUEL VALVES
High-temperature, high-pressure oxygen metering valve
[NASA-CASE-MSC-21823-1] p 891 N93-14843

FUEL-AIR RATIO
Simplified jet-A kinetic mechanism for combustor application
[NASA-TM-105940] p 844 N93-15504

FULL SCALE TESTS
Space based radar: Test of large space structures
p 808 N93-14941

FUNCTIONAL DESIGN SPECIFICATIONS
Representation and manipulation of inductive boolean functions
[AD-A256078] p 967 N93-14235
Designing video annotation and analysis systems
p 955 N93-15552

FUNCTIONS (MATHEMATICS)
Representation and manipulation of inductive boolean functions
[AD-A256078] p 967 N93-14235
Measurement and analysis of excitation functions in (alpha,np) reactions on (128, 130)Te
[DE92-630358] p 991 N93-14485
The covariance matrix of derived quantities and their combination
[DE92-019066] p 969 N93-15212
Multiresolution analysis by infinitely differentiable compactly supported functions
[AD-A256526] p 969 N93-15398
Characterizations of linear independence and stability of the shifts of a univariate refinable function in terms of its refinement mask
[AD-A256527] p 969 N93-15399
Escape-time visualization method for language-restricted iterated function systems
p 956 N93-15558
The object instancing paradigm for linear fractal modeling p 956 N93-15559
The spatial correlation function approach to response surface emission
[DE92-040875] p 969 N93-15656

FUNGI
The production and use of aeroponically grown inocula of VAM fungi in the native plant nursery
[PB92-204973] p 933 N93-15208

FURNACES
An experimental approach to determine the heat transfer coefficient in directional solidification furnaces
p 995 N93-15311
Experimental observation of the influence of furnace temperature profile on convection and segregation in the vertical Bridgman crystal growth technique
p 995 N93-15312

FUSION REACTORS
Analysis of rotation experiments in TFTR --- tokamak fusion test reactor p 987 N93-14129

FUZZY SYSTEMS
Stability and adaptation of neural networks
[AD-A256227] p 962 N93-14598
Sensor-based driving of a car with fuzzy inferencing VLSI chips and boards
[DE92-017819] p 963 N93-14818
A mixed excitation vocoder with fuzzy logic classifier
[AD-A256834] p 864 N93-15636

G

GABBRO
The gabbro-eclogite phase transition and the elevation of mountain belts on Venus p 1036 N93-14350

GALACTIC BULGE
A study of the abundance distributions along the minor axis of the Galactic bulge p 1015 N93-14136

GALACTIC CLUSTERS
Calibration of the CCD Tully-Fisher relation with application to the Perseus-Pisces supercluster
p 1016 N93-14194

GALACTIC COSMIC RAYS
Isotopic composition of galactic cosmic ray boron, carbon, nitrogen, and oxygen p 1020 N93-14866

GALACTIC EVOLUTION
Study of tidal interactions in M81-M82-NGC3077 system p 1010 N93-14195
A search for dead QSO's among nearby luminous galaxies p 1011 N93-14228

GALACTIC HALOS
Dark matter axions
[DE92-040501] p 1022 N93-15346

GALACTIC MASS
A search for dead QSO's among nearby luminous galaxies p 1011 N93-14228

GALACTIC RADIATION
Physical properties of extended emission-line regions in active and cooling-flow galaxies p 1018 N93-14461

GALAXIES
Optical signatures of cooling flows in isolated early-type galaxies p 1017 N93-14243
Faint high-latitude carbon stars p 1019 N93-14638
Quasars, galaxies, and pseudo-vacuum droplets
[NIKHEF-H/91-20] p 1020 N93-14686
Supervised selection of galaxy candidates from the IRAS PSC: The quality of the selection and the infrared properties of the galaxy candidates
[MPE-PREPRINT-216] p 1021 N93-15284

GALERKIN METHOD
Nonlinear free vibration analysis of strings by the Galerkin method p 972 N93-14280
The center for nonlinear phenomena and magnetic materials
[AD-A255983] p 967 N93-14412
Dynamics systems applied to Navier-Stokes equations for the study of turbulence
[ETN-92-92553] p 878 N93-15122

GALILEAN SATELLITES
Polarization properties and Earth-based radar measurements of Venus in the post-Magellan era
p 1026 N93-14304

GALLIUM ANTIMONIDES
Solidification of InSb-GaSb alloy and InSb with vibration p 995 N93-15310

GALLIUM ARSENIDES
Sensitivity of quantum electron conductance to elastic scatterers and to spin-orbit scattering in gallium arsenide heterostructures p 990 N93-14184
Advanced laser chemical processing for microelectronics and integrated optics
[AD-A255980] p 865 N93-14425
SETA support for the DARPA microelectronics technology insertion program of the Microelectronics Technology Office
[AD-A255551] p 866 N93-14555

Photoelectrochemistry of electronic and electro-optical materials
[AD-A256239] p 866 N93-14583
Direct optical to microwave conversion
[RL-TR-91-375] p 859 N93-14728
Dual active layer photoconductor
[AD-D015423] p 993 N93-14820
Conceptualization of a GaAs field effect transistor frequency tripler (2.5-7.5 GHz) for load use in communication satellites p 807 N93-14934
Fast optoelectronic switching processes in surface-emitting semiconductor lasers and nonlinear etalons
[AD-A255802] p 886 N93-15069
Study of the mathematical modelling and computer simulation of crystal growth from liquid phase under microgravity conditions
[CTN-93-60619] p 855 N93-15201

GALLIUM PHOSPHIDES
Gallium and indium compounds containing three different substituents. Crystal and molecular structure of ((Me3 CCH2)ClGaPPh2)3
[AD-A257049] p 996 N93-15443

GAMMA RAY ASTRONOMY
Search for pulsed gamma ray emission from SN1987A and the Vela pulsar p 1050 N93-14634
The gamma ray spectrum resulting from pp interactions in quasars p 1051 N93-14917

GAMMA RAY LASERS
Level-mixing assisted tunability of nuclear resonance linewidths for gamma ray lasers
[AD-A255791] p 885 N93-14647

GAMMA RAY OBSERVATORY
Using the Haleakala barrel extensive air shower array to study selected U.H.E. gamma ray point sources p 1050 N93-14639

GAMMA RAY SPECTRA
The gamma ray spectrum resulting from pp interactions in quasars p 1051 N93-14917

GAMMA RAY TELESCOPES
The effects of mis-alignment and background noise in a low energy gamma ray telescope p 1011 N93-14231
Gamma-ray imaging observations of Supernova 1987A p 1012 N93-14628
Search for pulsed gamma ray emission from SN1987A and the Vela pulsar p 1050 N93-14634
Using the Haleakala barrel extensive air shower array to study selected U.H.E. gamma ray point sources p 1050 N93-14639
Development of a High Resolution Liquid Xenon Imaging Telescope for Medium Energy Gamma Ray Astrophysics
[NASA-CR-191781] p 1013 N93-15589
A Monte Carlo analysis of the liquid xenon TPC as gamma ray telescope p 1014 N93-15590
A liquid xenon imaging telescope for gamma ray astrophysics: Design and expected performance p 1014 N93-15591

GAMMA RAYS
Extracting x rays, gamma rays, and electron-positron pairs from supermassive Kerr black holes using the Penrose mechanism p 1049 N93-14176
Nonthermal radio, x ray and gamma ray emissions from chaotic winds of early-type, massive stars p 1050 N93-14242
Gamma-ray imaging observations of Supernova 1987A p 1012 N93-14628
Search for pulsed gamma ray emission from SN1987A and the Vela pulsar p 1050 N93-14634
Using the Haleakala barrel extensive air shower array to study selected U.H.E. gamma ray point sources p 1050 N93-14639
Improvement and analysis of the radiation response of RADFET dosimeters
[AD-A254115] p 869 N93-15133
High-energy emissions from young pulsars: Perspective from the outer gap model
[DE92-040365] p 1022 N93-15324
Liquid xenon time projection chamber for gamma rays in the MeV region: Development status p 1014 N93-15592

GARMENTS
Modeling clothed figures
[AD-A257037] p 940 N93-15363

GAS ANALYSIS
Parametric study of air sampling cyclones p 779 N93-14173

GAS BEARINGS
Digital active material processing platform effort (DAMPER), SBIR phase 2
[NASA-CR-190798] p 856 N93-15353

GAS COMPOSITION
Analysis of CCD images of the coma of comet P/Halley
[NASA-CR-191384] p 1020 N93-14814
C60 interactions with surfaces, gaseous species and photons: An overview
[DE92-040738] p 978 N93-15654

GAS DETECTORS
Methane measurement by the Pioneer Venus large probe neutral mass spectrometer p 1027 N93-14312

GAS DYNAMICS
Upgrade and extension of the data acquisition system for propulsion and gas dynamic laboratories
[AD-A256836] p 1009 N93-15637

GAS FLOW
Control of asymmetric jet
[AD-A255967] p 873 N93-14400

GAS GENERATORS
Propellant grain assembly for a gas generator
[AD-D015439] p 854 N93-14801

GAS IONIZATION
Conditioning electron beams in the ion-focused regime
[AD-A255635] p 978 N93-14127

GAS MIXTURES
Understanding the variation in the millimeter-wave emission of Venus p 1028 N93-14315
Fundamentals of combustion of premixed gases p 840 N93-14618

GAS PATH ANALYSIS
A philosophy for integrated monitoring system design p 796 N93-15174
Some experiments and ideas on GPA before reaching steady state of engine p 796 N93-15175

GAS TUNGSTEN ARC WELDING
Fatigue strength of cruciform and other fillet welded joints in aluminum alloys
[ESDU-92017] p 900 N93-14553
Mechanisms of forming intergranular microcracks and microscopic surface discontinuities in welds
[AD-A255371] p 845 N93-14740

GAS TURBINE ENGINES
Propulsion and Energetics Panel Working Group 20 on Test Cases for Engine Life Assessment Technology
[AGARD-AR-308] p 798 N93-14890
Introduction to test cases for engine life assessment technology p 799 N93-14891
LARZAC HP turbine disk crack initiation and propagation spin pit test p 799 N93-14892
RB 199 high pressure compressor stage 3 spin pit tests p 799 N93-14893
CF6-6 high pressure compressor stage 5 locking slot crack propagation spin pit test p 799 N93-14894
RB211-524B disc and drive cones hot cyclic spinning test p 799 N93-14895
F100 second stage fan disk bolthole crack propagation ferris wheel test p 800 N93-14897
In-service considerations affecting component life p 800 N93-14898
Some experiments and ideas on GPA before reaching steady state of engine p 796 N93-15175
Experimental analysis of steady-state and dynamic monitoring of power shaft turbines p 796 N93-15176

GAS TURBINES
Closed Brayton Cycle power system with a high temperature pellet bed reactor heat source for NEP applications
[NASA-TM-105933] p 826 N93-14482

GAS-SOLID INTERACTIONS
Gas-solid dynamics at disordered and adsorbate covered surfaces
[AD-A255981] p 976 N93-14411
Gas-surface interactions
[AD-A255390] p 841 N93-14652

GASES
Variational transition state theory
[DE92-040498] p 842 N93-14908
C60 interactions with surfaces, gaseous species and photons: An overview
[DE92-040738] p 978 N93-15654

GATES (CIRCUITS)
Gate-all-around device
[AD-A255287] p 866 N93-14534
Computer-aided design package for designers of digital optical computers
[AD-A255381] p 944 N93-14564

GEARS
The trajectory analysis of bevel planetary gear trains
[DE92-040898] p 893 N93-15380

GELS
Fluids, gels, and glasses under extreme conditions of pressure and temperature
[AD-A255675] p 847 N93-14166
Oriented electro/optical polymers through in-situ chemistry during gel processing: A research opportunity
[AD-A255968] p 848 N93-14401

GENERAL AVIATION AIRCRAFT
Terminal area forecasts FY 1992 - 2005
[AD-A255797] p 788 N93-15390

GENETIC ALGORITHMS
A massively distributed parallel genetic algorithm
[AD-A256617] p 959 N93-15407

GEOCHEMISTRY
The geology of the Venera/Vega landing sites p 1024 N93-14296
Mixed-valence iron minerals on Venus: Fe(2+)-Fe(3+) oxides and oxy-silicates formed by surface-atmosphere interactions p 1025 N93-14301
Radar-anomalous, high-altitude features on Venus p 1036 N93-14349
Chemical differentiation of a convecting planetary interior: Consequences for a one-plate planet such as Venus p 1038 N93-14358
Venus: Geochemical conclusions from the Magellan data p 1044 N93-14394

GEOCHRONOLOGY
Venusian extended ejecta deposits as time-stratigraphic markers p 1030 N93-14327

GEODESY
A feasibility study of space VLBI for geodesy and geodynamics p 904 N93-14223

GEODETIC SURVEYS
Plate tectonics from VLBI and SLR global data
[NASA-CR-191319] p 916 N93-14913

GEODYNAMICS
A feasibility study of space VLBI for geodesy and geodynamics p 904 N93-14223
Constraints on crustal rheology and age of deformation from models of gravitational spreading in Ishtar Terra, Venus p 1042 N93-14379
The determination and interpretation of ocean surface topography using TOPEX/Poseidon altimeter data p 931 N93-14997

GEOGRAPHIC INFORMATION SYSTEMS
Geographic Resources Analysis Support System (GRASS) version 4.0 user's reference manual
[AD-A255218] p 1001 N93-14524
Integrating satellite imagery into a geographic information system for monitoring the downstream impacts of dam construction on floodplain agriculture in Sokoto State, Nigeria p 905 N93-14823
Predicting database requirements for geographic information systems in the year 2000: Long-term design issues for GRASS
[AD-A256862] p 1009 N93-15627
GRASS 4.0 map digitizing user's manual: V. Digit
[AD-A256859] p 1009 N93-15642

GEOGRAPHY
GRASS 4.0 map digitizing user's manual: V. Digit
[AD-A256859] p 1009 N93-15642

GEOIDS
Mantle plumes on Venus revisited p 1032 N93-14334
Geoid, topography, and convection-driven crustal deformation on Venus p 1042 N93-14376
Ocean topography mapping, improvement of the marine geoid, and global permanent ocean circulation studies from TOPEX/Poseidon altimeter data p 928 N93-14981

GEOLOGICAL FAULTS
Global deformation on the surface of Venus p 1024 N93-14297
Flexural analysis of uplifted rift flanks on Venus p 1027 N93-14314
Radar scattering properties of pancakelike domes on Venus p 1028 N93-14316
Determining stress states using dike swarms: The Lauma Dorsa example p 1028 N93-14319
Tectonics and volcanism of Eastern Aphrodite Terra: No subduction, no spreading p 1029 N93-14321
Venus: Preliminary geologic mapping of northern Atla Regio p 1037 N93-14353
Venus: Preliminary geologic mapping of southern Beta Regio-northern Phoebe Regio p 1037 N93-14354
Venus: Geology of Beta Regio rift system p 1037 N93-14355
Atla Regio, Venus: Geology and origin of a major equatorial volcanic rise p 1041 N93-14374
Addressing earthquake strong ground motion issues at the Idaho National Engineering Laboratory
[DE92-017841] p 916 N93-15136

GEOLOGICAL SURVEYS
Venus: Preliminary geologic mapping of northern Atla Regio p 1037 N93-14353
Venus: Preliminary geologic mapping of southern Beta Regio-northern Phoebe Regio p 1037 N93-14354
Overview of Venus geology: Preliminary description of terrain units for Venus global geological mapping p 1040 N93-14368
The geologic mapping of Venus using C-1 format: Sheets 75N254, 60N263 p 1041 N93-14375

GEOLOGY
Problem footprints in Magellan altimetry data p 1039 N93-14362

Application of precise altimetry to the study of precise leveling of the sea surface, the Earth's gravity field, and the rotation of the Earth p 907 N93-14992

GEOMAGNETIC LATITUDE
The effects of magnetic storm phases on F-layer irregularities from auroral to equatorial latitudes
[AD-A256520] p 917 N93-15395

GEOMETRICAL ACOUSTICS
Propagation of high frequency jet noise using geometric acoustics
[NASA-TM-105950] p 975 N93-15575

GEOMETRICAL OPTICS
Radar scene generation for tactical decision aids
[AD-A257069] p 863 N93-15495

GEOMORPHOLOGY
Overview of Venus geology: Preliminary description of terrain units for Venus global geological mapping p 1040 N93-14368
Impact craters on Venus: An overview from Magellan observations p 1040 N93-14369
Different types of small volcanos on Venus p 1042 N93-14378
Can a time-stratigraphic classification system be developed for Venus? p 1043 N93-14388

GEOPHYSICS
The effects of Venusian mantle convection with multiple phase transitions p 1043 N93-14385
Workshop on noninvasive geophysical site characterization
[LA-12311-C] p 914 N93-14724
TOPEX/Poseidon science investigations plan
[NASA-CR-190616] p 925 N93-14964
The western Mediterranean Sea: An area for a regional validation for TOPEX/Poseidon and a field for geophysical and oceanographic studies p 926 N93-14965
Geophysical investigations with TOPEX/Poseidon altimetry data p 918 N93-14969
Studies of the intermediate and deep circulation in the western equatorial Atlantic p 927 N93-14973
Application of TOPEX/Poseidon altimetry to ocean dynamics and geophysics p 927 N93-14974
Geophysical validation of TOPEX/Poseidon altimetry products p 918 N93-14982
Application of precise altimetry to the study of precise leveling of the sea surface, the Earth's gravity field, and the rotation of the Earth p 907 N93-14992
The determination and interpretation of ocean surface topography using TOPEX/Poseidon altimeter data p 931 N93-14997
A TOPEX/Poseidon study of oceanic effects on observations of the Earth's interior p 918 N93-14999
Precise orbit computation and sea surface modeling p 813 N93-15000
Directory of research projects: Planetary geology and geophysics program
[NASA-TM-4428] p 864 N93-15638

GEOPOTENTIAL HEIGHT
Parametric height field ray tracing p 955 N93-15556

GEOSAT SATELLITES
Geophysical investigations with TOPEX/Poseidon altimetry data p 918 N93-14969
Mesoscale and large-scale variability of the Antarctic circumpolar current p 926 N93-14970
Assimilation of altimeter topography into oceanic models p 927 N93-14972
Application of TOPEX/Poseidon altimetry to ocean dynamics and geophysics p 927 N93-14974

GEOSTROPHIC WIND
Assimilation of altimeter topography into oceanic models p 927 N93-14972

GEOSYNCHRONOUS ORBITS
Data management in NOAA p 1003 N93-14779

GEOTECHNICAL ENGINEERING
USACE geotechnical earthquake engineering software, report 1 WESHAKE for personal computers (version 1.0)
[AD-A257068] p 917 N93-15459

GEOTHERMAL ENERGY UTILIZATION
Geothermal Energy and the Utility Market: The Opportunities and Challenges for Expanding Geothermal Energy in a Competitive Supply Market: Proceedings
[DE92-019090] p 908 N93-15271

GERMANIUM ALLOYS
The properties of thermally passivated Si(1-x) He(x) produced using high pressure techniques (and related augmentation awards)
[AD-A255961] p 991 N93-14429

GESTALT THEORY
The perception of articulated motion: Recognizing moving light displays
[AD-A256046] p 937 N93-14660

GET AWAY SPECIALS (STS)
Environmental qualification testing of the prototype pool boiling experiment
[NASA-CR-190774] p 895 N93-15582

GIANT STARS
Faint high-latitude carbon stars p 1019 N93-14638

GLASS
Optical glasses for high-peak-power laser applications
[DE92-040403] p 886 N93-14906
Material development in the Si3N4 system using glass encapsulated HIP'ing
[DE92-041381] p 837 N93-15388
Study of the glass formation of high temperature superconductors
[NASA-TM-108389] p 997 N93-15500

GLASS FIBER REINFORCED PLASTICS
Characterization of fiber reinforced phenolic composites p 828 N93-14142

GLASS FIBERS
Characterization of fiber reinforced phenolic composites p 828 N93-14142
Fiber pulling apparatus modification
[NASA-CR-184498] p 891 N93-14763
The stress development during filament winding of thick cylinders
[AD-A255765] p 901 N93-15066

GLOBAL POSITIONING SYSTEM
Establishment of a test course for high accuracy dynamic positioning systems
[AD-A255407] p 789 N93-14501
A general observation matrix for attitude error estimation with an offset GPS antenna
[AD-A255214] p 789 N93-14574
Terrestrial reference systems related to the TOPEX/Poseidon project p 906 N93-14967
Proposed revisions to RTCM SC-104 recommended standards for differential NAVSTAR/GPS service for carrier phase applications
[AD-A255276] p 789 N93-15005

GLOBULAR CLUSTERS
Compact objects in the disk and globular clusters p 1018 N93-14594

GLOW DISCHARGES
Si atomic layer epitaxy using remote plasma assisted hydrogen desorption and disilane as a precursor
[AD-A255606] p 993 N93-15008
Si atomic layer epitaxy based on Si2H6 and remote He plasma bombardment
[AD-A255763] p 993 N93-15055
Progress on the development of a 2-D PIC/Monte Carlo model of glow discharges
[DE92-040226] p 989 N93-15422

GOGGLES
Evaluation of Night Vision Goggles (NVG) for maritime search and rescue (joint Canadian/US Coast Guard experiment)
[AD-A255525] p 939 N93-14554

GOVERNMENT PROCUREMENT
Streamlined acquisition handbook
[NASA-TM-108133] p 1002 N93-14719

GRADIENTS
Theoretical characterization of the potential energy surface for NH + NO
[NASA-CR-190741] p 843 N93-15357
Design features of a seven-cell high-gradient superconducting cavity
[DE92-040229] p 870 N93-15424

GRAIN BOUNDARIES
Shear fatigue crack growth analysis in large-grain polycrystals p 993 N93-14838
Modelling Directional Solidification
[NASA-CR-191301] p 995 N93-15309

GRAINS
Infrared laboratory spectra and composition changes of synthetic amorphous silicate grains
[DE92-040211] p 843 N93-15283

GRAMMARS
Parallel on-line parsing in constant time
[MEMO-INF-91-64] p 958 N93-15082
Grammatical trigrams: A probabilistic model of link grammar
[AD-A256365] p 947 N93-15206

GRAPH THEORY
Graph rewriting using a single pushout; a comparison
[MEMO-INF-92-28] p 968 N93-15121

GRAPHIC ARTS
Mapping thoughts: Visual interfaces for information retrieval p 1000 N93-14208

GRAPHITE-EPOXY COMPOSITES
The effect of a seawater environment on the galvanic corrosion behavior of graphite/epoxy composites coupled to metals
[AD-A256072] p 830 N93-14232
A preliminary investigation of dual mode fracture sustained by graphite/epoxy laminates impacted by high-velocity spherical metallic projectiles
[AD-A255790] p 898 N93-14419
Reliability of stiffened structural panels: Two examples
[NASA-TM-107687] p 900 N93-14483
Delamination growth behavior in cross-ply laminated composites due to transverse concentrated loading
[AD-A255974] p 830 N93-14493
Characterizing longitudinal splitting and delamination fracture toughness of composites p 831 N93-14607
Leveling coatings for reducing the atomic oxygen defect density in protected graphite fiber epoxy composites
[NASA-TM-105732] p 852 N93-15344
Leveling coatings for reducing the atomic oxygen defect density in protected graphite fiber epoxy composites p 819 N93-15597
Failure of composite plates under static biaxial planar loading
[NASA-CR-191391] p 903 N93-15653

GRAPHITIZATION
NMR imaging of elastomeric materials
[AD-A256034] p 841 N93-14658

GRAPHS (CHARTS)
Graph rewriting using a single pushout; a comparison
[MEMO-INF-92-28] p 968 N93-15121

GRATINGS (SPECTRA)
Research Studies on Advanced Optical Module/Head Designs for Optical Data Storage
[NASA-CR-191307] p 984 N93-15505
A modal analysis of lamellar diffraction gratings in conical mountings p 986 N93-15519
On the convergence of the coupled-wave approach for lamellar diffraction gratings p 986 N93-15520

GRAVIMETERS
Precision tests of gravitation: Liquid-supported torsion balance experiments and a tower experiment p 914 N93-14589

GRAVITATION
Precision tests of gravitation: Liquid-supported torsion balance experiments and a tower experiment p 914 N93-14589
Cosmological models in higher-order gravity p 1018 N93-14592
Multiply connected spacetimes and closed timelike curves in semiclassical gravity p 915 N93-14884
Anti-hydrogen: The cusp between quantum mechanics and general relativity
[DE93-001807] p 998 N93-15469

GRAVITATION THEORY
Perturbations of the Robertson-Walker space p 1015 N93-14134

GRAVITATIONAL EFFECTS
An active Z gravity compensation system
[AD-A255258] p 889 N93-14529
Fiber pulling apparatus modification
[NASA-CR-184498] p 891 N93-14763
Aspects of parking orbit selection in a manned Mars mission
[NASA-TP-3256] p 813 N93-15367
Nucleate pool boiling in the long duration low gravity environment of the Space Shuttle
[NASA-TM-105973] p 855 N93-15420
Vibration isolation technology: An executive summary of systems development and demonstration
[NASA-TM-105937] p 778 N93-15573
Vehicle/payload interface specification for the reusable reentry satellite
[NASA-CR-187883] p 824 N93-15631

GRAVITATIONAL FIELDS
Gravitational instabilities in a protoplanetary disk p 1016 N93-14154
Geoid, topography, and convection-driven crustal deformation on Venus p 1042 N93-14376
Venus gravity: Summary and coming events p 1042 N93-14377
An active Z gravity compensation system
[AD-A255258] p 889 N93-14529
Precision tests of gravitation: Liquid-supported torsion balance experiments and a tower experiment p 914 N93-14589
Mean sea surface and gravity investigations using TOPEX/Poseidon altimeter data p 930 N93-14990

GRAVITY ANOMALIES
Western Aphrodite Terra, tectonics, geology, and line-of-sight gravity p 1029 N93-14322

GRAVITY WAVES
Finite amplitude gravity waves in the Venus atmosphere generated by surface topography p 1044 N93-14395
A numerical study of the middle atmosphere response to tropical and subtropical tropospheric heat sources p 920 N93-14640
Wave drag in the atmospheric boundary layer p 915 N93-14873
Surface gravity waves and ambient microseismic noise
[AD-A256498] p 916 N93-15375

GRAY SCALE
An extended cuberille model for identification and display of 3D objects from 3D gray value data p 953 N93-15542

GRAZING INCIDENCE
Full surface testing of grazing incidence mirrors
[AD-A255644] p 979 N93-14152
Full surface testing of grazing incidence mirrors
[AD-A255798] p 984 N93-15371

GREEN'S FUNCTIONS
Efficient asymptotic closed form approximation for dyadic green's function for anisotropic substrates, phase 1
[AD-A256258] p 830 N93-14436
The sine-Gordon model and the small (kappa)(sup +) region of light-cone perturbation theory
[DE92-040506] p 969 N93-15379
GREENHOUSE EFFECT
Venus: The case for a wet origin and a runaway greenhouse p 1031 N93-14331
A correlated k-distribution model of the heating rates for CO2 and O3 in the atmosphere between 0 and 60 km
[DE93-000889] p 911 N93-15280
A correlated k-distribution model of the atmospheric heating rates for overlapping spectra of CH4 and N2O
[DE93-000890] p 911 N93-15281
GRID GENERATION (MATHEMATICS)
Simulation of unsteady inviscid flow on an adaptively refined Cartesian grid p 873 N93-14273
A multigrid approach to embedded-grid solvers
[AD-A256405] p 879 N93-15332
Ice accretion and performance degradation calculations with LEWICE/NS
[NASA-TM-105972] p 787 N93-15354
GROUND EFFECT (COMMUNICATIONS)
Systems issues in airborne Doppler radar/LIDAR certification p 785 N93-14855
GROUND STATE
A study of mid-latitude 5577A CI dayglow emissions
[AD-A255444] p 914 N93-14511
GROUND SUPPORT EQUIPMENT
Waterborne polyurethane binder resins for compliant aircraft coatings
[AD-A256246] p 849 N93-14573
The Teledyne controls aircraft condition monitoring system p 793 N93-15155
Ground Support Equipment (GSE) for Aircraft Condition Monitoring System (ACMS) p 778 N93-15158
GROUND SUPPORT SYSTEMS
Study of Fluid Experiment System (FES)/CAST/Holographic Ground System (HGS)
[NASA-CR-184483] p 855 N93-14793
Failure diagnostic with MAINTEX based on AIMS at Swissair p 778 N93-15181
Personal computer based test- and emulation equipment for maintenance and ground support p 778 N93-15185
GROUND TESTS
Study of Fluid Experiment System (FES)/CAST/Holographic Ground System (HGS)
[NASA-CR-184483] p 855 N93-14793
Space based radar: Test of large space structures p 808 N93-14941
GROUND WATER
Anaerobic microbial transformation of aromatic hydrocarbons and mixtures of aromatic hydrocarbons and halogenated solvents
[AD-A255696] p 932 N93-14557
GROUP THEORY
The dynamics of spatially extended lasers p 883 N93-14123
GUIDE VANES
L.D.V. measurements of unsteady flow fields in radial turbine
[AD-A255728] p 878 N93-15065
GULF STREAM
The dynamics and energetics of midlatitude western boundary currents: A comparison of the Kuroshio Extension and the Gulf Stream p 929 N93-14985
GUNS (ORDNANCE)
Method of bonding molybdenum to steel
[AD-D015410] p 845 N93-14888
GUSTS
Multi-disciplinary optimization of aeroservoelastic systems
[NASA-CR-191255] p 901 N93-14766
Evaluation of a soil fixative to retard particle entrainment: A laboratory study
[UCRL-LR-109806] p 915 N93-14877
GUY WIRES
Comparative study of stability of flexible satellites with and without guy-wire constraints p 817 N93-14585
GYRES
The use of satellite altimetry in the study of weakly defined and variable oceanic gyres p 926 N93-14966
Circulation of the gyres of the world ocean: Observation modeling using TOPEX/Poseidon altimeter data p 927 N93-14975
South African TOPEX/Poseidon altimeter experiment p 928 N93-14976

H

HABITATS
Ecological implications of landscape fragmentation
[DE92-019186] p 911 N93-15273
HALF PLANES
The crack problem for an orthotropic half plane stiffened by elastic films
[AD-A256471] p 903 N93-15374
HALL EFFECT
Characterization of magneto-optical recording media p 979 N93-14140
HALL GENERATORS
Design and implementation of a DC-based magnetic field controller with electronic temperature stabilized Hall generator
[DE92-019796] p 870 N93-15276
HALLEY'S COMET
Analysis of CCD images of the coma of comet P/Halley
[NASA-CR-191384] p 1020 N93-14814
HALOGEN COMPOUNDS
Viscosity of liquids. Halogenated methanes
[ESDU-92028] p 839 N93-14539
Orthobaric densities and molar volumes of liquids. Halogenated ethylenes
[ESDU-92018] p 839 N93-14540
Anaerobic microbial transformation of aromatic hydrocarbons and mixtures of aromatic hydrocarbons and halogenated solvents
[AD-A255696] p 932 N93-14557
HAMILTONIAN FUNCTIONS
Staggered fermions and chiral symmetry breaking in transverse lattice regulated QED
[DE92-040505] p 977 N93-15378
HAND (ANATOMY)
Bar-holding prosthetic limb
[NASA-CASE-MFS-28481-1] p 939 N93-14870
HANDBOOKS
DROLS workbook
[AD-A255850] p 999 N93-14106
HANDLES
Extra-vehicular activity translation tool
[NASA-CASE-MSC-21955-1] p 891 N93-14842
HARDENING (MATERIALS)
Structural study of thermohardening matrices: Deformation of composite matrices in relation to their molecular structure
[ONERA-RT-12/3521-M] p 836 N93-15253
HARDNESS
Sputter deposition and characterization of MoSi2/SiC composite coatings
[DE92-040326] p 837 N93-15426
HARDWARE
Data storage and retrieval system p 1005 N93-15034
Storage needs in future supercomputer environments p 1007 N93-15047
HARMONIC CONTROL
Experimental and analytical investigation of the vibration characteristics of a remotely piloted helicopter
[AD-A256131] p 790 N93-14248
HARMONIC EXCITATION
Nonlinear dynamic response of shallow arches to harmonic forcing p 898 N93-14282
Transient response of a viscous liquid bridge of finite length and anchored edges
[LRT-WE-9-FB-25-1991] p 878 N93-15132
HARMONIC OSCILLATION
Elastic wave propagation in laminated composites
[ITN-93-85186] p 835 N93-15144
HARMONICS
Scattering of sound by sound: Nonlinear interaction of collinear and noncollinear sound beams p 973 N93-14145
HARRIER AIRCRAFT
Pressure distribution for the wing of the YAV-8B airplane; with and without pylons
[NASA-TM-4429] p 779 N93-14451
Royal Air Force experience of the Harrier information management system p 795 N93-15170
HATCHES
Space Shuttle Orbiter Crew Hatch Jettison Test using a 0.0405-scale model (16-0) in the Texas A/M low speed wind tunnel (OA362). Space Shuttle aerothermodynamic data report
[NASA-CR-167698] p 815 N93-15474
HAZARDS
The Orlando TDWR testbed and airborne wind shear date comparison results p 784 N93-14851
USACE geotechnical earthquake engineering software, report 1 WESHAKE for personal computers (version 1.0)
[AD-A257068] p 917 N93-15459
HAZE
Ethane ice haze in the upper atmosphere of Uranus p 1023 N93-14212
Pioneer Venus polarimetry and haze optical thickness p 1032 N93-14335
HEAD (ANATOMY)
Improved head support stand adjustable by compoundturnbuckle
[AD-D015384] p 936 N93-15249
HEAD-UP DISPLAYS
Application of gel-silica optics to laser technology and optical element fabrication
[AD-A255666] p 883 N93-14131
Advantages of using a projected head-up display in a flight simulator
[AD-A255332] p 804 N93-14559
Simulator evaluation of displays for a revised takeoff performance monitoring system
[NASA-TP-3270] p 803 N93-15366
Annotating the real world with knowledge-based graphics on a see-through head-mounted display p 954 N93-15543
HEALTH PHYSICS
Transcutaneous Analyte Measuring Methods (TAMM), phase 2
[AD-A256327] p 936 N93-15192
HEAT AFFECTED ZONE
Mechanisms of forming intergranular microcracks and microscopic surface discontinuities in welds
[AD-A255371] p 845 N93-14740
HEAT BALANCE
Low-frequency variability of sea level as related to the heat balance of global oceans p 928 N93-14979
HEAT ENGINES
Tribology of improved transformation-toughened ceramics-heat engine test
[DE92-041385] p 851 N93-15295
Development of ceramic matrix composites for application in ceramic technology for advanced heat engines project, phase 2
[DE92-041379] p 836 N93-15387
Development of ceramic matrix composites for application in the ceramic technology for advanced heat engines project. Phase 2A: Development of in-situ toughened silicon nitride
[DE92-041371] p 853 N93-15452
Processing of sinterable transformation toughened ceramics for application in ceramic technology for advanced heat engines project
[DE92-041372] p 853 N93-15453
Analytical and experimental evaluation of joining silicon carbide to silicon carbide and silicon nitride to silicon nitride for heat engine applications
[DE92-041376] p 837 N93-15454
Development of ceramic matrix composites for application in the ceramic technology for advanced heat engines project
[DE92-041378] p 837 N93-15455
HEAT EXCHANGERS
The use of a novel manufacturing process for high performance titanium plate fin heat exchangers
[PNR-90934] p 879 N93-15473
High performance titanium plate fin heat exchanger using a novel manufacturing process
[PNR-90933] p 880 N93-15488
Summary of the NASA Lewis component technology program for Stirling power converters
[NASA-TM-105640] p 827 N93-15526
HEAT FLUX
Radiative heat transfer in combustion systems p 840 N93-14621
A numerical study of the middle atmosphere response to tropical and subtropical tropospheric heat sources p 920 N93-14640
A correlated k-distribution model of the heating rates for CO2 and O3 in the atmosphere between 0 and 60 km
[DE93-000889] p 911 N93-15280
A correlated k-distribution model of the atmospheric heating rates for overlapping spectra of CH4 and N2O
[DE93-000890] p 911 N93-15281
HEAT MEASUREMENT
Study of optical techniques for the Ames unitary wind tunnel. Part 5: Infrared imagery
[NASA-CR-191385] p 804 N93-14809
HEAT PIPES
Summary of the NASA Lewis component technology program for Stirling power converters
[NASA-TM-105640] p 827 N93-15526
HEAT PUMPS
Simulation of vapor compression heat pumps with solution circuits p 872 N93-14200
Variable speed rotary compressor and adjustable speed drive efficiencies measured in the laboratory
[DE92-040026] p 893 N93-15278

HEAT RESISTANT ALLOYS
Fatigue in single crystal nickel superalloys
[AD-A256095] p 844 N93-14264
HIP consolidation of aluminum-rich intermetallic alloys and their composites
[NAWCADWAR-92003-60] p 845 N93-14726
Fiber reinforced composites: A new class of glass and glass ceramic materials for thermomechanical applications
[REPT-921-430-104] p 838 N93-15490
HEAT SINKS
Extended surface heat sinks for electronic components: A computer optimization
[AD-A256134] p 865 N93-14254
HEAT SOURCES
Closed Brayton Cycle power system with a high temperature pellet bed reactor heat source for NEP applications
[NASA-TM-105933] p 826 N93-14482
HEAT TRANSFER
An algebraic turbulence model for three-dimensional viscous flows
[NASA-TM-105931] p 777 N93-14102
Finite element models of laser welding
p 888 N93-14226
Advances in TMG p 811 N93-14956
Study of mass and heat transport of the tropical Atlantic Ocean using models and altimeter data
p 929 N93-14983
Application of TOPEX/Poseidon altimetry measurements to observational and modeling studies of the low-frequency upper ocean mass and heat circulation in the tropical Pacific p 930 N93-14989
Oceanic transports of mass, heat, and salt in the western North Pacific p 931 N93-14996
Latent heat thermal energy storage for lunar oxygen production
[DE92-017817] p 907 N93-15219
Use of surface heat transfer measurements as a flow separation diagnostic in a two dimensional reflected oblique shock/turbulent boundary layer interaction
[NASA-TM-105981] p 879 N93-15355
Close-up analysis of aircraft ice accretion
[NASA-TM-105952] p 787 N93-15360
Finite-difference solution for laminar or turbulent boundary layer flow over axisymmetric bodies with ideal gas, CF4, or equilibrium air chemistry
[NASA-TP-3271] p 879 N93-15434
HEAT TRANSFER COEFFICIENTS
Analytical and experimental investigation of closed-cycle sorption cooling systems p 874 N93-14476
An experimental approach to determine the heat transfer coefficient in directional solidification furnaces
p 995 N93-15311
Advancements in the LEWICE ice accretion model
[NASA-CR-191019] p 879 N93-15402
HEAT TRANSMISSION
Flexural analysis of uplifted rift flanks on Venus
p 1027 N93-14314
HEAT TREATMENT
Low toxicity high temperature PMR polyimide
[NASA-CASE-LAR-14639-1] p 849 N93-14709
HEAVY IONS
Studies of heavy-ion reactions and transuranic nuclei
[DE92-040457] p 977 N93-15326
Bevalac ion beam characterizations for single event phenomena
[AD-A257033] p 979 N93-15362
HEAVY NUCLEI
Studies of heavy-ion reactions and transuranic nuclei
[DE92-040457] p 977 N93-15326
HEIGHT
Evaluation of methods for estimating wind wave growth on narrow irregular fetches
[AD-A256002] p 932 N93-15113
HELICOPTER ENGINES
Measuring risk in single-engine and twin-engine helicopters p 787 N93-15025
Onboard System Evaluation of Rotors Vibration, Engines (OBSERVE) monitoring system
[AD-A255366] p 792 N93-15227
HELICOPTER PERFORMANCE
The relationship between computer scoring and safety-pilot grading of flight performance
[AD-A256245] p 937 N93-14600
Helicopter health monitoring: Current practice and future trends p 797 N93-15179
New rotor trim and balance system for helicopter usage monitoring p 797 N93-15180
The use of ultrasonics for oleo compression measurements on a S-70B-2 (Seahawk) helicopter
[AD-A256315] p 792 N93-15328
HELICOPTER WAKES
The Applicaiton of CFD to rotary wing flow problems
[NASA-TM-102803] p 782 N93-15483
HELICOPTERS
Experimental and analytical investigation of the vibration characteristics of a remotely piloted helicopter
[AD-A256131] p 790 N93-14248
Workshop on Aeronautical Decision Making (ADM). Volume 2: Plenary Session With Presentations and Proposed Action Plan
[DOT/FAA/RD-92/14-VOL-2] p 785 N93-15013
Embedded ADM reduces helicopter human error accidents p 787 N93-15024
Measuring risk in single-engine and twin-engine helicopters p 787 N93-15025
Helicopter flight data recorder and health and usage monitoring system p 797 N93-15178
Modeling limits of the EMV analysis program CONCEPT by example of the influence of a helicopter structure on a frame antenna
[MBB-UD-0614-92-PUB] p 863 N93-15487
HELIUM
Generation of broadly tunable, narrow bandwidth, and intense coherent vacuum ultraviolet radiation in rare gases p 980 N93-14167
Closed Brayton Cycle power system with a high temperature pellet bed reactor heat source for NEP applications
[NASA-TM-105933] p 826 N93-14482
HELIUM PLASMA
Si atomic layer epitaxy based on Si2H6 and remote He plasma bombardment
[AD-A255763] p 993 N93-15055
HELMET MOUNTED DISPLAYS
Annotating the real world with knowledge-based graphics on a see-through head-mounted display
p 954 N93-15543
HETEROGENEITY
A data parallel algorithm for raytracing of heterogeneous databases p 955 N93-15553
HETEROJUNCTIONS
The 3 to 5 heterojunction structures and high speed devices
[AD-A250399] p 991 N93-14521
Novel engineered compound semiconductor heterostructures for advanced electronics applications
[AD-A255363] p 866 N93-14562
Organic/IR-Semiconductor heterojunctions for low-cost, high temperature IR arrays
[AD-A255971] p 868 N93-15108
Epitaxial heterojunctions of oxide semiconductors and metals on high temperature superconductors
[NASA-CASE-NPO-18483-1-CU] p 994 N93-15151
Selected area epitaxial growth for complementary HBT applications
[AD-A257047] p 995 N93-15365
HEURISTIC METHODS
Query processing in distributed database systems
p 1001 N93-14218
Intelligent path prediction for vehicular travel
p 961 N93-14445
Minimizing conflicts: A heuristic repair method for constraint-satisfaction and scheduling problems
[NASA-TM-108121] p 964 N93-15286
Learning to improve iterative repair scheduling
[NASA-TM-108118] p 965 N93-15289
A massively distributed parallel genetic algorithm
[AD-A256617] p 959 N93-15407
A minimalist global user interface p 957 N93-15566
HIERARCHIES
The effect of a hierarchical task-specific external conceptual model on the learnability and usability of microcomputer applications by novices
p 1000 N93-14205
HIGH ENERGY ELECTRONS
Interactions of relativistic electrons with relativistic plasma waves p 988 N93-14139
Radiation belt dynamic and quasi-static modeling based on CRRES data: Outer-belt short-term response data base
[AD-A256483] p 916 N93-14899
HIGH ENERGY INTERACTIONS
A Cloudy Quark Bag Model of S, P, and D wave interactions for the coupled channel antikaon-nucleon system
[DE92-040149] p 977 N93-15062
Electron acceleration by longitudinal electric field of a Gaussian laser beam
[DE92-526947] p 887 N93-15296
HIGH LEVEL LANGUAGES
Program verification using higher order logic
[AD-A255408] p 943 N93-14502
HIGH POWER LASERS
Environmental assessment: OMEGA upgrade project at the Laboratory for Laser Energetics, University of Rochester
[DE92-040410] p 886 N93-14907
HIGH PRESSURE
The properties of thermally passivated Si(1-x) He(x) produced using high pressure techniques (and related augmentation awards)
[AD-A255961] p 991 N93-14429
High-temperature, high-pressure oxygen metering valve
[NASA-CASE-MSC-21823-1] p 891 N93-14843
CF6-6 high pressure compressor stage 5 locking slot crack propagation spin pit test p 799 N93-14894
Experimental attempt to metallize hydrogen at very high pressures
[AD-A257086] p 843 N93-15497
HIGH RESOLUTION
Integration and processing of high-resolution moire-interferometry data p 895 N93-14185
Threshold photodetachment spectroscopy
[AD-A255278] p 842 N93-14671
Method and apparatus for a high resolution, flat panel cathodoluminescent display screen
[AD-D015400] p 868 N93-15107
Silicon nitride thin film production on Si(111)
[AD-A256036] p 994 N93-15233
HIGH REYNOLDS NUMBER
Turbulent drag and transport in high Reynolds number Couette-Taylor flow p 872 N93-14119
On the nonlinear three dimensional instability of Stokes layers and other shear layers to pairs of oblique waves
[NASA-TM-105918] p 880 N93-15499
HIGH SPEED
High speed magneto-resistive random access memory
[NASA-CASE-NPO-17954-1-CU] p 940 N93-14704
Upgrade and extension of the data acquisition system for propulsion and gas dynamic laboratories
[AD-A256836] p 1009 N93-15637
HIGH STRENGTH ALLOYS
Exceptionally high-strength (approximately 3 GPa) aluminum alloys demonstrated by oxygen ion implantation
[DE92-040980] p 847 N93-15383
HIGH STRENGTH STEELS
Method of bonding molybdenum to steel
[AD-D015410] p 845 N93-14888
Stress corrosion susceptibility of ultra-high strength steels for Naval aircraft applications
[AD-A256126] p 846 N93-15189
HIGH TEMPERATURE
Low toxicity high temperature PMR polyimide
[NASA-CASE-LAR-14639-1] p 849 N93-14709
Organic/IR-Semiconductor heterojunctions for low-cost, high temperature IR arrays
[AD-A255971] p 868 N93-15108
High temperature tubular solid oxide fuel cell development
[DE92-040253] p 908 N93-15322
HIGH TEMPERATURE ENVIRONMENTS
RB211-524B disc and drive cones hot cyclic spinning test p 799 N93-14895
HIGH TEMPERATURE GAS COOLED REACTORS
Closed Brayton Cycle power system with a high temperature pellet bed reactor heat source for NEP applications
[NASA-TM-105933] p 826 N93-14482
HIGH TEMPERATURE GASES
High-temperature, high-pressure oxygen metering valve
[NASA-CASE-MSC-21823-1] p 891 N93-14843
HIGH TEMPERATURE PLASMAS
Transformation of energy and momentum due to Landau damping in time
[IPPCZ-316] p 988 N93-14813
Accurate methods for calculating atomic processes in high temperature plasmas
[DE92-040215] p 988 N93-15418
HIGH TEMPERATURE RESEARCH
Development of a fiber optic high temperature strain sensor
[NASA-CR-191316] p 882 N93-14810
HIGH TEMPERATURE SUPERCONDUCTORS
Electronic structure studies of high-T(sub c) superconductors by photoemission and x ray absorption
p 989 N93-14172
Processing, fabrication, and demonstration of HTS integrated microwave circuits
[AD-A256109] p 865 N93-14246
Transport in heterostructures and device in microwave and millimeter wave regimes
[AD-A255975] p 858 N93-14408
Method of making substantially single phase superconducting oxide ceramics having a TC above 85 degrees
[AD-D015422] p 850 N93-14743
Epitaxial heterojunctions of oxide semiconductors and metals on high temperature superconductors
[NASA-CASE-NPO-18483-1-CU] p 994 N93-15151

Processing and characterization of electrophoretically deposited holmium barium copper oxide superconductor films
[AD-A256329] p 869 N93-15194
Far infrared, magnetic, and electronic studies of high T(sub c) superconducting materials
[AD-A257050] p 996 N93-15444
Study of the glass formation of high temperature superconductors
[NASA-TM-108389] p 997 N93-15500
A comparison of superconductor and manganin technology for electronic links used in space mission applications
[NASA-CR-4477] p 997 N93-15587

HIGH TEMPERATURE TESTS
Development of a fiber optic high temperature strain sensor
[NASA-CR-191316] p 882 N93-14810

HIGH VOLTAGES
High performance pulse generator
[AD-D015378] p 869 N93-15269

HIGHLANDS
Coldspots or hotspots? The origin of plateau-shaped highlands on Venus p 1025 N93-14298
Tectonics and volcanism of Eastern Aphrodite Terra: No subduction, no spreading p 1029 N93-14321
Mantle plumes on Venus revisited p 1032 N93-14334
Radar-anomalous, high-altitude features on Venus p 1036 N93-14349
Dielectric surface properties of Venus p 1039 N93-14360
Cytherean crustal bending at Salme Dorsa p 1039 N93-14364
Structural characteristics and tectonics of northeastern Tellus Regio and Meni Tessera p 1044 N93-14389

HIPPOCAMPUS
Extrathalmic modulation of cortical function
[AD-A255440] p 935 N93-14782

HISTORIES
The V-22 Osprey: A case analysis
[AD-A256445] p 791 N93-14601
Canada's role in pushing back the frontiers of space p 806 N93-14928

HMX
Thermal decomposition of HNIW and HNIW-Based formulations
[AD-A255613] p 854 N93-15011

HOLE BURNING
Ultra-dense optical mass storage
[AD-A255463] p 1004 N93-14785

HOLE GEOMETRY (MECHANICS)
On the development and application of a modified boundary element method for the analysis of three dimensional elastostatic problems in thick plates p 901 N93-14587
Apparatus for checking threaded hole perpendicularity
[NASA-CASE-LEW-15444-1] p 882 N93-14840
RB211-524B disc and drive cones hot cyclic spinning test p 799 N93-14895

HOLE MOBILITY
The III-V semiconductor quantum well lasers and related optoelectronic devices (on silicon). Oxide-defined semiconductor quantum well lasers and optoelectronic devices: Al-based III-V nativeoxide s
[AD-A255239] p 885 N93-14667

HOLES (ELECTRON DEFICIENCIES)
Electronic structure studies of high-T(sub c) superconductors by photoemission and x ray absorption p 989 N93-14172
Energy distribution of trapped holes in irradiated SiO2
[DE92-040979] p 997 N93-15649

HOLES (MECHANICS)
Reliability of stiffened structural panels: Two examples
[NASA-TM-107687] p 900 N93-14483
RB 199 high pressure compressor stage 3 spin pit tests p 799 N93-14893
F100 second stage fan disk bolthole crack propagation ferris wheel test p 800 N93-14897
Failure of composite plates under static biaxial planar loading
[NASA-CR-191391] p 903 N93-15653

HOLMIUM
Processing and characterization of electrophoretically deposited holmium barium copper oxide superconductor films
[AD-A256329] p 869 N93-15194

HOLOGRAMMETRY
Off-axis conoscopic holography: Optical and digital reconstruction
[TELECOM-PARIS-90-E-023] p 882 N93-15096

HOLOGRAPHY
Optical information processing using photorefractive BSO p 981 N93-14204
Ultra-dense optical mass storage
[AD-A255463] p 1004 N93-14785
Study of Fluid Experiment System (FES)/CAST/Holographic Ground System (HGS)
[NASA-CR-184483] p 855 N93-14793
Off-axis conoscopic holography: Optical and digital reconstruction
[TELECOM-PARIS-90-E-023] p 882 N93-15096

HOMOGENEITY
Experimental observation of the influence of furnace temperature profile on convection and segregation in the vertical Bridgman crystal growth technique p 995 N93-15312

HOMOGENEOUS TURBULENCE
Exploiting similarity in turbulent shear flows for turbulence modeling
[NASA-CR-191621] p 875 N93-14481
Homogeneous quantum electrodynamic turbulence
[NASA-TM-107686] p 979 N93-15482

HONEYCOMB STRUCTURES
Characterization of impact-limiting material
[DE92-016767] p 902 N93-15210

HORIZONTAL FLIGHT
The effect of wake dynamics on rotor eigenvalues in forward flight p 780 N93-14595
The Applicaiton of CFD to rotary wing flow problems
[NASA-TM-102803] p 782 N93-15483

HOT ISOSTATIC PRESSING
HIP consolidation of aluminum-rich intermetallic alloys and their composites
[NAWCADWAR-92003-60] p 845 N93-14726
Superstrength metal composite material and process for making the same
[AD-D015379] p 836 N93-15246

HOT PRESSING
Material development in the Si3N4 system using glass encapsulated HIP'ing
[DE92-041381] p 837 N93-15388
Development of adherent ceramic coatings to reduce contact stress damage of ceramics
[DE92-041373] p 852 N93-15437

HOT STARS
Nonthermal radio, x ray and gamma ray emissions from chaotic winds of early-type, massive stars p 1050 N93-14242

HOT WORKING
Analytical and experimental evaluation of joining ceramic oxides to ceramic oxides and ceramic oxides to metal for advanced heat engine applications
[DE92-041383] p 851 N93-15294

HOVERING
Stability of elastically tailored rotor blades p 791 N93-14828
Finite-state inflow applied to aeroelastic flutter of fixed and rotating wings p 802 N93-14830
The Applicaiton of CFD to rotary wing flow problems
[NASA-TM-102803] p 782 N93-15483

HUBBLE SPACE TELESCOPE
Performance characteristics of STIS detectors
[NASA-CR-191636] p 868 N93-14915

HUMAN BEHAVIOR
Information-seeking behavior during the decision-making process: A case study p 1000 N93-14206

HUMAN BODY
Body composition and physical performance
[AD-A255627] p 938 N93-14161
Modeling clothed figures
[AD-A257037] p 940 N93-15363
Generating natural-looking motion for computer animation p 956 N93-15564
Beyond keyframing: An algorithmic approach to animation p 957 N93-15565

HUMAN FACTORS ENGINEERING
The effect of a hierarchical task-specific external conceptual model on the learnability and usability of microcomputer applications by novices p 1000 N93-14205
Mapping thoughts: Visual interfaces for information retrieval p 1000 N93-14208
Institute for the Study of Human Capabilities
[AD-A256091] p 938 N93-14427
A voyage to Mars: A challenge to collaboration between man and machines p 777 N93-14614
Bibliography of scientific publications of the Naval Biodynamics Laboratory
[AD-A255952] p 1051 N93-14657
Compliant walker
[NASA-CASE-GSC-13348-2] p 934 N93-14708
Workshop on Aeronautical Decision Making (ADM). Volume 2: Plenary Session With Presentations and Proposed Action Plan
[DOT/FAA/RD-92/14-VOL-2] p 785 N93-15013
Does cockpit management training reduce aircrew error? p 785 N93-15014
Cockpit decision making p 786 N93-15015
Trans-cockpit authority gradient in Navy/Marine aircraft mishaps p 786 N93-15016
A cognitive model for training decision making in aircrews p 786 N93-15020
Elements of a theory of natural decision making p 786 N93-15021
Taxonomy of flight variables p 787 N93-15022
Shared mental models and crew decision making p 787 N93-15023
Embedded ADM reduces helicopter human error accidents p 787 N93-15024
Proposed action plan to improve ADM effectiveness, part 3: Developing a new ADM paradigm on which to build advanced or expert decision making training p 787 N93-15026
Movement time prediction in human-computer interfaces p 955 N93-15550
ARCBALL: A user interface for specifying three-dimensional orientation using a mouse p 955 N93-15551
Designing video annotation and analysis systems p 955 N93-15552

HUMAN PERFORMANCE
Body composition and physical performance
[AD-A255627] p 938 N93-14161
Sleep inertia: Is there a worst time to wake up?
[AD-A256602] p 934 N93-14240
Performance of color-dependent tasks of air traffic control specialists as a function of type and degree of color vision deficiency
[AD-A256614] p 788 N93-14275
Institute for the Study of Human Capabilities
[AD-A256091] p 938 N93-14427
Decision making in a dynamic task environment: The effect of time pressure
[AD-A256557] p 937 N93-14602
Elements of a theory of natural decision making p 786 N93-15021
Proposed action plan to improve ADM effectiveness, part 3: Developing a new ADM paradigm on which to build advanced or expert decision making training p 787 N93-15026
The effect of pain on task performance: A review of the literature
[AD-A254336] p 938 N93-15216
Crew requirements definition system user's guide
[AD-A257052] p 951 N93-15445
Movement time prediction in human-computer interfaces p 955 N93-15550
Generating natural-looking motion for computer animation p 956 N93-15564

HUMAN REACTIONS
Movement time prediction in human-computer interfaces p 955 N93-15550

HUMAN RELATIONS
The changing culture of science: Bringing it into balance
[AD-A255993] p 998 N93-14417

HUMAN RESOURCES
The changing culture of science: Bringing it into balance
[AD-A255993] p 998 N93-14417
Proceedings of the Sixth CASI Conference on Astronautics
[CTN-92-60336] p 804 N93-14920
Space education: A self-perservation strategy for the Canadian space industry p 808 N93-14937

HYBRID PROPULSION
Engine technologies for future spaceplanes
[ETN-92-92732] p 800 N93-15143

HYDRAULIC EQUIPMENT
Jointed assembly actuated by fluid pressure
[AD-D015383] p 893 N93-15248
Three position power cylinder
[AD-D015393] p 894 N93-15461
The design concept of the 6-degree-of-freedom hydraulic shaker at ESTEC p 820 N93-15600

HYDRAZOIC ACID
Spectroscopy and reactions of hydrazoic acid on silicon single crystal surfaces (III). HN3 and DN3 on Si(111)-7 x 7
[AD-A255241] p 842 N93-14669

HYDROCARBON FUELS
Liquid flow reactor and method of using
[AD-D015392] p 893 N93-15232

HYDROCARBONS
Revelations of a stratospheric circulation: The dynamical transport of hydrocarbons in the stratosphere of Uranus p 913 N93-14211
Computed potential energy surfaces for chemical reactions
[NASA-CR-190741] p 843 N93-15356

HYDRODYNAMICS
Dynamics in neutron stars and the early universe p 1014 N93-14112
Diffusing wave spectroscopy p 980 N93-14169
Hydrodynamics of supernova 1987 A p 1019 N93-14633

Global ocean tides through assimilation of oceanographic and altimeter satellite data in a hydrodynamic model p 928 N93-14978

HYDROGEN

Generation of broadly tunable, narrow bandwidth, and intense coherent vacuum ultraviolet radiation in rare gases p 980 N93-14167

Si atomic layer epitaxy using remote plasma assisted hydrogen desorption and disilane as a precursor [AD-A255606] p 993 N93-15008

HYDROGEN ATOMS

A global potential energy surface for ArH2 [NASA-CR-190741] p 843 N93-15358

HYDROGENATION

Physics of hydrogen storage in metal-hydrides p 854 N93-14630

HYDROGRAPHY

An integrated research program for TOPEX/Poseidon with emphasis on the Pacific Ocean p 931 N93-14995

Oceanic transports of mass, heat, and salt in the western North Pacific p 931 N93-14996

HYDROLOGY

Venusian hydrology: Steady state reconsidered p 1028 N93-14318

Geothermal Energy and the Utility Market: The Opportunities and Challenges for Expanding Geothermal Energy in a Competitive Supply Market: Proceedings [DE92-019090] p 908 N93-15271

Independent validation testing of the FLAME computer code, version 1.0 [DE92-019691] p 948 N93-15274

HYDROMETEOROLOGY

Extreme climatic events in the Amazon Basin and their associations with the circulation of the global tropics p 918 N93-14115

HYDROPHONES

Statistically calibrated transducer [AD-D015408] p 882 N93-14878

HYDROSTATICS

Calculation methods for externally pressurised (hydrostatic) journal bearings with capillary restrictor control [ESDU-92026] p 889 N93-14543

HYPERBOLIC DIFFERENTIAL EQUATIONS

Undetermined coefficient problems for quasi-linear parabolic equations [AD-A256012] p 969 N93-15256

HYPERCUBE MULTIPROCESSORS

Parallelization of the Navy Space Surveillance Center (NAVSPASUR) satellite model [AD-A256133] p 816 N93-14253

Automated coding and intersecting cube theory [ETN-92-92675] p 941 N93-15123

Implementation and analysis of NP-complete algorithms on a distributed memory computer [AD-A256564] p 951 N93-15405

HYPERFINE STRUCTURE

Hyperfine experimental investigation of zirconia ceramics [DE92-040301] p 850 N93-14903

HYPERGEOMETRIC FUNCTIONS

Introduction to real orthogonal polynomials [AD-A256448] p 968 N93-14609

HYPERNUCLEI

Excitation of nuclei by antiproton annihilation at rest [AD-A255447] p 976 N93-14513

HYPERSONIC BOUNDARY LAYER

Modeling variable blowing on a slender cone in hypersonic flow p 781 N93-14836

HYPERSONIC FLIGHT

Engine technologies for future spaceplanes [ETN-92-92732] p 800 N93-15143

HYPERSONIC FLOW

Computational analysis of hypersonic flows past elliptic-cone waveriders [NASA-CR-191304] p 781 N93-14767

Modeling variable blowing on a slender cone in hypersonic flow p 781 N93-14836

HYPERSONIC NOZZLES

Mach 5 electroformed nickel nozzle refurbishment FNAS investigation of ultra-smooth surfaces [NASA-CR-191416] p 826 N93-14681

Supersonic investigation of two dimensional hypersonic exhaust nozzles [NASA-TM-105687] p 800 N93-15342

HYPERSONIC SHOCK

Turbulent magnetized plasmas from ionizing shock waves p 987 N93-14120

HYPERSONIC SPEED

Supersonic investigation of two dimensional hypersonic exhaust nozzles [NASA-TM-105687] p 800 N93-15342

HYPERSONIC VEHICLES

A study of viscous interaction effects on hypersonic waveriders p 778 N93-14160

Development of braided rope seals for hypersonic engine applications: Flow modeling [NASA-TM-105942] p 888 N93-14478

Advanced aeroservoelastic stabilization techniques for hypersonic flight vehicles [NASA-CR-189702] p 802 N93-14811

HYPERVELOCITY FLOW

Investigation of the aerothermodynamics of hypervelocity reacting flows in the ram accelerator [NASA-CR-191715] p 783 N93-15588

HYPERVELOCITY IMPACT

Characterisation and dynamic modelling of the near-earth space particulate environment p 1019 N93-14637

Hypervelocity impact simulations of Whipple shields p 821 N93-15604

HYPERVELOCITY LAUNCHERS

Opacity, equation of state, and radiation transport model for moderate density, eV-temperature plasmas [AD-A256056] p 988 N93-14579

HYPERVELOCITY PROJECTILES

Investigation of the aerothermodynamics of hypervelocity reacting flows in the ram accelerator [NASA-CR-191715] p 783 N93-15588

I

ICE

Ethane ice haze in the upper atmosphere of Uranus p 1023 N93-14212

Root damage analysis of aircraft engine blade subject to ice impact [NASA-TM-105779] p 902 N93-15343

ICE CLOUDS

Sierra Nevada winter storms: A study using microwave radiometry, ice crystal, and isotopic analysis technique p 923 N93-15088

ICE ENVIRONMENTS

Data management for the coordinated Eastern Arctic experiment [AD-A255648] p 1000 N93-14182

Antarctic news clips - 1992 [NSF-92-83] p 916 N93-15080

ICE FORMATION

Icing effects on aircraft stability and control determined from flight data: Preliminary results [NASA-TM-105977] p 803 N93-14831

Ice accretion and performance degradation calculations with LEWICE/NS [NASA-TM-105972] p 787 N93-15354

Close-up analysis of aircraft ice accretion [NASA-TM-105952] p 787 N93-15360

Advancements in the LEWICE ice accretion model [NASA-CR-191019] p 879 N93-15402

An overview of shed ice impact in the NASA Lewis Icing Research Tunnel [NASA-TM-105969] p 782 N93-15404

Ice accretion prediction for a typical commercial transport aircraft [NASA-TM-105976] p 788 N93-15522

ICE MAPPING

Report of the International Ice Patrol in the North Atlantic, bulletin no. 77 [AD-A256162] p 925 N93-14452

ICE PREVENTION

Results of low power deicer tests on a swept inlet component in the NASA Lewis icing research tunnel [NASA-TM-105968] p 781 N93-14911

Surface roughness due to residual ice in the use of low power deicing systems [NASA-TM-105971] p 782 N93-15338

Numerical modeling of anti-icing systems and comparison to test results on a NASA 0012 airfoil [NASA-TM-105975] p 787 N93-15345

ICE REPORTING

Report of the International Ice Patrol in the North Atlantic, bulletin no. 77 [AD-A256162] p 925 N93-14452

ICY SATELLITES

Polarization properties and Earth-based radar measurements of Venus in the post-Magellan era p 1026 N93-14304

IDENTIFYING

Software stamping [NPL-DITC-198/92] p 946 N93-15072

IGNEOUS ROCKS

Venus: Geochemical conclusions from the Magellan data p 1044 N93-14394

IGNITION

Plutonium pyrophoricity [RFP-4517] p 845 N93-14723

ILLUMINATING

A two-pass physics-based global lighting model p 957 N93-15570

ILMENITE

In-situ lunar oxygen extraction p 806 N93-14929

IMAGE ANALYSIS

Altimeter and oceanographic in situ measurements in the area of the Greenland-Iceland-Norwegian Sea, 1987-1988 [AD-A256598] p 960 N93-14239

Ringed impact craters on Venus: An analysis from Magellan images p 1024 N93-14291

The geology of the Venera/Vega landing sites p 1024 N93-14296

Neural nets for scene analysis [AD-A255976] p 961 N93-14409

Wavelet methods for curve estimation [AD-A255357] p 970 N93-14538

Neural network architectures for general image recognition [AD-A256017] p 964 N93-15258

IMAGE MOTION COMPENSATION

Vertical path atmospheric turbulence: Temporal spectra and differential image motion measurements p 914 N93-14641

IMAGE PROCESSING

Neural network retinal model real time implementation [AD-A255652] p 934 N93-14210

Development of a MATLAB toolbox for image processing [AD-A256130] p 942 N93-14247

Design, development, and testing of a prototype optical system for a next generation multiplexed imager [AD-A256538] p 981 N93-14286

Image processing and products for the Magellan mission to Venus p 1026 N93-14306

Geographic Resources Analysis Support System (GRASS) version 4.0 user's reference manual [AD-A255218] p 1001 N93-14524

Real-time gaze holding in binocular robot vision [AD-A256226] p 982 N93-14582

Using digital scanned aerial photography for wetlands delineation [AD-A255392] p 905 N93-14676

Optical monitor for observing turbulent flow [DE92-019831] p 876 N93-14715

Vision development test bed: The cradle of the MSS artificial vision system p 810 N93-14948

Dynamics of analog electronic neural networks [AD-A257019] p 966 N93-15352

Advanced research in instrumentation and diagnostics technology [DE92-041121] p 883 N93-15411

Information technologies for global resources management and environmental assessment [DE92-041107] p 906 N93-15442

An extended cuberille model for identification and display of 3D objects from 3D gray value data p 953 N93-15542

Algorithms for the detection and elimination of specular aliasing p 954 N93-15544

Performing in-place affine transformations in constant space p 954 N93-15546

Partitioning tree image representation and generation from 3D geometric models p 955 N93-15557

A structural approach to the photonic processor [N-3399-RC] p 986 N93-15648

IMAGE RECONSTRUCTION

Design, development, and testing of a prototype optical system for a next generation multiplexed imager [AD-A256538] p 981 N93-14286

Off-axis conoscopic holography: Optical and digital reconstruction [TELECOM-PARIS-90-E-023] p 882 N93-15096

Advanced research in instrumentation and diagnostics technology [DE92-041121] p 883 N93-15411

Volume rendering using the Fourier projection-slice theorem p 953 N93-15541

Algorithms for the detection and elimination of specular aliasing p 954 N93-15544

IMAGE RESOLUTION

Wavelet methods for curve estimation [AD-A255357] p 970 N93-14538

Multiresolution analysis by infinitely differentiable compactly supported functions [AD-A256526] p 969 N93-15398

High-resolution contrast control on a video display: Method and calibration [AD-A256552] p 938 N93-15400

Transfer function characteristics of super resolving systems p 985 N93-15512

The 3D modeling of high numerical aperture imaging in thin films p 985 N93-15513

IMAGERY

Arc digital raster imagery evaluation [AD-A255403] p 817 N93-14565

Parametric study of diffusion-enhancement networks for spatiotemporal grouping in real-time artificial vision
[AD-A256059] p 937 N93-14580

IMAGING RADAR

Scatterer modeling/calibration study
[AD-A255855] p 856 N93-14107
Upgrade the University of Wisconsin volume imaging lidar
[AD-A255476] p 885 N93-14497

IMAGING SPECTROMETERS

Spectral analysis of the shuttle glow: AIS science support
[PL-TR-92-2172] p 815 N93-14698
Performance characteristics of STIS detectors
[NASA-CR-191636] p 868 N93-14915
LISA: A limb imaging spectrograph for airglow
p 811 N93-14952
SeaWiFS Technical Report Series. Cloud screening for polar orbiting visible and infrared (IR) satellite sensors, volume 7
[NASA-TM-104566] p 932 N93-15645

IMAGING TECHNIQUES

A differential equation design method for finite-conjugate, multi-mirror imaging systems
p 979 N93-14165
Imaging Earth's interior: Tomographic inversions for mantle P-wave velocity structure p 913 N93-14225
Western Aphrodite Terra, tectonics, geology, and line-of-sight gravity p 1029 N93-14322
Magellan stereo images and Venusian geology
p 1035 N93-14347
Evaluation of Night Vision Goggles (NVG) for maritime search and rescue (joint Canadian/US Coast Guard experiment)
[AD-A255525] p 939 N93-14554
Imaging the sun in hard x-rays using Fourier telescopes p 1048 N93-14591
Gamma-ray imaging observations of Supernova 1987A
p 1012 N93-14628
NMR imaging of elastomeric materials
[AD-A256034] p 841 N93-14658
Quasar x-ray spectra revisited p 1012 N93-14760
LISA: A limb imaging spectrograph for airglow
p 811 N93-14952
Nonuniformity effects in a hybrid platinum silicide imaging device
[AD-A256339] p 983 N93-15197
Imaging the sun in hard x rays using Fourier telescopes
[NASA-TM-108390] p 1013 N93-15203
Three-dimensional nuclear magnetic resonance imaging of green-state ceramics
[DE93-000930] p 851 N93-15282
High speed imaging for flash radiography using PIN diodes
[DE92-040959] p 882 N93-15381
The 3D modeling of high numerical aperture imaging in thin films p 985 N93-15513
Proceedings: Graphics Interface 1992
[ISBN-0-9695338-1-0] p 952 N93-15533
Volume rendering using the Fourier projection-slice theorem p 953 N93-15541
Object space temporal coherence for ray tracing
p 955 N93-15554
Ray tracing polygons using spatial subdivision
p 955 N93-15555
Non-uniform patch luminance for global illumination
p 957 N93-15569

IMPACT

Impact-generated winds on Venus: Causes and effects p 1041 N93-14372

IMPACT DAMAGE

Ringed impact craters on Venus: An analysis from Magellan images p 1024 N93-14291
Effect of impact angle on central-peak/peak-ring formation and crater collapse on Venus
p 1041 N93-14371
Hypervelocity impact simulations of Whipple shields
p 821 N93-15604

IMPACT LOADS

The sensitivity of energetic materials to friction, impact, and electrostatic stimuli
[DE92-041227] p 855 N93-15478

IMPACT MELTS

Bright crater outflows: Possible emplacement mechanisms p 1026 N93-14305

IMPACT RESISTANCE

Microwave scattering and emission properties of large impact craters on the surface of Venus
p 1043 N93-14384

IMPACT STRENGTH

Microwave scattering and emission properties of large impact craters on the surface of Venus
p 1043 N93-14384
A preliminary investigation of dual mode fracture sustained by graphite/epoxy laminates impacted by high-velocity spherical metallic projectiles
[AD-A255790] p 898 N93-14419
Characterization of impact-limiting material
[DE92-016767] p 902 N93-15210
Effects of high thermal neutron fluences on Type 6061 aluminum
[DE92-040569] p 846 N93-15348

IMPACT TESTS

An overview of shed ice impact in the NASA Lewis Icing Research Tunnel
[NASA-TM-105969] p 782 N93-15404
Hypervelocity impact simulations of Whipple shields
p 821 N93-15604

IMPEDANCE MATCHING

Optical signal distribution schemes for millimeter phased array radar
[AD-A256262] p 858 N93-14437

IMPINGEMENT

An investigation of crack growth at interfaces in bimaterials and composites using a consistent shear-lag model p 896 N93-14187

IN SITU MEASUREMENT

In situ material characterization for pavement evaluation by the Spectral-Analysis-of-Surface-Waves (SASW) method
[AD-A255660] p 804 N93-14128
Altimeter and oceanographic in situ measurements in the area of the Greenland-Iceland-Norwegian Sea, 1987-1988
[AD-A256598] p 960 N93-14239
Accelerated simulation of near-Earth-orbit polymer degradation p 823 N93-15615

IN-FLIGHT MONITORING

Proceedings of the 16th Symposium on Aircraft Integrated Monitoring Systems
[DLR-MITT-92-01] p 793 N93-15152
Discussion for the ideal AIMS p 793 N93-15153
Software flexibility and configuration control for the A340/A330 Aircraft Condition Monitoring System (ACMS) p 793 N93-15154
The Teledyne controls aircraft condition monitoring system p 793 N93-15155
Flight data and flight safety in SAS
p 793 N93-15156
Detection of technical states with aircraft
p 794 N93-15159
Integrated engine control and monitoring with experiences derived from OLMOS p 795 N93-15168
Real-time in-flight engine performance and health monitoring techniques for flight research application
p 795 N93-15169
Monitoring of powerplants in advanced commercial aircraft p 795 N93-15171
EJ 200 engine monitoring system: On- and off-board data capture, analysis, and management system
p 796 N93-15172
RB199 engine oil system failure diagnostics by comparison of measured and calculated oil consumption using the OLMOS on-board monitoring system
p 796 N93-15173
A philosophy for integrated monitoring system design
p 796 N93-15174
Modelling the engine temperature distribution between shut down and restart for life usage monitoring
p 796 N93-15177
Helicopter flight data recorder and health and usage monitoring system p 797 N93-15178
Helicopter health monitoring: Current practice and future trends p 797 N93-15179
New rotor trim and balance system for helicopter usage monitoring p 797 N93-15180
Failure diagnostic with MAINTEX based on AIMS at Swissair p 778 N93-15181
Neural network based condition monitoring
p 797 N93-15183
Monitoring of pilot actions as part of a knowledge-based system for pilot assistance p 797 N93-15184
Personal computer based test- and emulation equipment for maintenance and ground support
p 778 N93-15185
Airbus Industrie TCAS experience
p 789 N93-15186

INCIDENT RADIATION

Precision radiation force modeling for the TOPEX/Poseidon mission p 817 N93-14586

INCOHERENT SCATTER RADAR

Comparison between irregularity motion and bulk plasma drifts at high latitudes
[PL-TR-91-2292] p 914 N93-14727

INCOMPRESSIBLE FLOW

Multi-point inverse design of isolated airfoils and airfoils in cascade in incompressible flow p 790 N93-14462
Unsteady shear disturbances within a two dimensional stratified flow
[NASA-CR-189121] p 880 N93-15527

INDEXES (DOCUMENTATION)

Aeronautical engineering: A continuing bibliography with indexes (supplement 282)
[NASA-SP-7037(282)] p 777 N93-14604
Aeronautical engineering: A continuing bibliography with indexes (supplement 284)
[NASA-SP-7037(284)] p 777 N93-14605
Bibliography of Lewis Research Center Technical Publications announced in 1991
[NASA-TM-105595] p 1004 N93-14796
Source header list. Volume 2: K through Z
[AD-A256001] p 1007 N93-15112

INDIAN OCEAN

Mixed-layer parameterization in models of the Indian Ocean
[AD-A255937] p 925 N93-14428
Ocean transport and variability studies of the South Pacific, Southern, and Indian Oceans
p 927 N93-14971

INDIUM ANTIMONIDES

Solidification of InSb-GaSb alloy and InSb with vibration p 995 N93-15310

INDIUM COMPOUNDS

Thermal stability of trimethyl indium on Si(100)-2 x 1 as studied with HREELS, UPS, and XPS: A comparison with the results from Si(111)-7 x 7 and Si(110) studies
[AD-A255242] p 992 N93-14670
Gallium and indium compounds containing three different substituents. Crystal and molecular structure of ((Me3 CCH2)ClGaPPh2)3
[AD-A257049] p 996 N93-15443

INDIUM GALLIUM ARSENIDES

Time-resolved optical studies of 3-5 semiconductors
p 990 N93-14183

INDUSTRIAL WASTES

Electrochemical oxidation of organic materials
[DE92-019822] p 828 N93-14718
Workshop on noninvasive geophysical site characterization
[LA-12311-C] p 914 N93-14724
Management and minimization of photographic wastes at Pantex Plant
[MHSMP-92-01] p 910 N93-14739

INDUSTRIES

Acoustic resonance techniques for quality control
[DE92-040150] p 895 N93-15413

INELASTIC SCATTERING

Weak-electromagnetic interference in polarized eD scattering
[DE93-001763] p 978 N93-15486

INERTIA

Vibration isolation technology: An executive summary of systems development and demonstration
[NASA-TM-105937] p 778 N93-15573

INERTIAL CONFINEMENT FUSION

Analysis of rotation experiments in TFTR --- tokamak fusion test reactor p 987 N93-14129

INERTIAL NAVIGATION

A general observation matrix for attitude error estimation with an offset GPS antenna
[AD-A255214] p 789 N93-14574

INFERENCE

Probabilistic inference
[AD-A255471] p 963 N93-14786

INFILTRATION

Polymer infiltration studies
[NASA-CR-191652] p 852 N93-15431

INFORMATION

Information-seeking behavior during the decision-making process: A case study
p 1000 N93-14206
How scientific must technical editors be?
[DE92-040741] p 1010 N93-15655

INFORMATION DISSEMINATION

The 7th World Conference on Titanium
[AD-A255674] p 844 N93-14132
The National Space Science Data Center: An operational perspective p 1002 N93-14775
The information age as a work in progress: Implications for technical communicators
[DE92-019780] p 1008 N93-15275

INFORMATION FLOW

Fault tolerant systems practitioner's workshop
[AD-A255376] p 944 N93-14563
Engineering of massively interconnected computer systems
[AD-A255501] p 958 N93-14645
Information systems for airport operations
[TT-9202] p 789 N93-14729

INFORMATION MANAGEMENT

Information for management, planning, and decision-making in nonprofit organizations: Toward a comprehensive model p 1000 N93-14209

Source hierarchy list. Volume 1: A through D
[AD-A256100] p 1001 N93-14265
EOSDIS/DADS requirements p 1003 N93-14776
Enterprise storage report for the 1990's p 1004 N93-15028
The long hold: Storing data at the National Archives p 1004 N93-15031
The National Space Science Data Center: An operational perspective p 1006 N93-15045
Royal Air Force experience of the Harrier information management system p 795 N93-15170
Design for tactical situation awareness display
[AD-A256194] p 798 N93-15235
Information technologies for global resources management and environmental assessment
[DE92-041107] p 906 N93-15442
Software Technology for Adaptable, Reliable Systems (STARS)
[AD-A257022] p 952 N93-15471
A multi-layer graphic model for building interactive graphical applications p 957 N93-15567

INFORMATION PROCESSING (BIOLOGY)
Knowledge and processes in design
[AD-A255663] p 999 N93-14130
Psychophysical analyses of perceptual representations
[AD-A255432] p 936 N93-14510
Decision making in a dynamic task environment: The effect of time pressure
[AD-A256557] p 937 N93-14602
A planning workshop: To strengthen American cognitive science for the twenty-first century
[NSF-92-4] p 999 N93-14720

INFORMATION RETRIEVAL
DROLS workbook
[AD-A255850] p 999 N93-14106
Knowledge and processes in design
[AD-A255663] p 999 N93-14130
Mapping thoughts: Visual interfaces for information retrieval p 1000 N93-14208
Information resource utilisation: Accessibility based on concerns p 1001 N93-14216
Query processing in distributed database systems p 1001 N93-14218
The National Space Science Data Center: An operational perspective p 1002 N93-14775
Source header list. Volume 2: K through Z
[AD-A256001] p 1007 N93-15112
User's guide for SearchMAESTRO
[AD-A256422] p 1008 N93-15335

INFORMATION SYSTEMS
Information resource utilisation: Accessibility based on concerns p 1001 N93-14216
Information system constraint language (ISyCL)
[AD-A256268] p 976 N93-14438
The preliminary Long Duration Exposure Facility (LDEF) materials data base
[NASA-TM-107692] p 828 N93-14459
Vendor Information System (VIS) systems manual
[AD-A256174] p 1002 N93-14650
Air Force Office of Scientific Research
[AD-A255361] p 1051 N93-14673
Air Force Office of Scientific Research
[AD-A255370] p 1051 N93-14674
Information systems for airport operations
[TT-9202] p 789 N93-14729
The National Space Science Data Center: An operational perspective p 1002 N93-14775
EOSDIS/DADS requirements p 1003 N93-14776
Data management in NOAA p 1003 N93-14779
EMASS (trademark): An expandable solution for NASA space data storage needs p 1005 N93-15033
SIDR Relative Weighted Product (RWP) assignment process
[AD-A255801] p 946 N93-15068
Source header list. Volume 2: K through Z
[AD-A256001] p 1007 N93-15112
Wisconsin Inventors' Network Database
[DE92-018394] p 1007 N93-15137
Royal Air Force experience of the Harrier information management system p 795 N93-15170
Technical data management at the Yucca Mountain Site Characterization Project
[DE92-018115] p 1008 N93-15229
Information technologies for global resources management and environmental assessment
[DE92-041107] p 906 N93-15442
Software Technology for Adaptable, Reliable Systems (STARS)
[AD-A257022] p 952 N93-15471
CSCW - WCSC: Computer-supported cooperative work. What changes for the science of computing p 954 N93-15549
Feasibility study for an integrated data processing system
[PB92-214287] p 1009 N93-15644

INFORMATION THEORY
Knowledge and processes in design
[AD-A255663] p 999 N93-14130
Computation and communication constraints for distributed estimation systems
[AD-A256287] p 970 N93-14456
How scientific must technical editors be?
[DE92-040741] p 1010 N93-15655

INFRARED ASTRONOMY
Investigations of Titan's troposphere and surface and Jupiter's great red spot with infrared observations p 1022 N93-14146
Submillimeter and infrared spectroscopy of molecular clouds near O and B stars p 1016 N93-14149
Groundbased near-IR observations of the surface of Venus p 1035 N93-14346

INFRARED DETECTORS
Organic/IR-Semiconductor heterojunctions for low-cost, high temperature IR arrays
[AD-A255971] p 868 N93-15108
ISOCAM experiment cryogenic test results
[REPT-921-440-104] p 825 N93-15140
Nonuniformity effects in a hybrid platinum silicide imaging device
[AD-A256339] p 983 N93-15197
SeaWiFS Technical Report Series. Cloud screening for polar orbiting visible and infrared (IR) satellite sensors, volume 7
[NASA-TM-104566] p 932 N93-15645

INFRARED IMAGERY
Altimeter and oceanographic in situ measurements in the area of the Greenland-Iceland-Norwegian Sea, 1987-1988
[AD-A256598] p 960 N93-14239
Design, development, and testing of a prototype optical system for a next generation multiplexed imager
[AD-A256538] p 981 N93-14286
Groundbased near-IR observations of the surface of Venus p 1035 N93-14346
Study of optical techniques for the Ames unitary wind tunnel. Part 5: Infrared imagery
[NASA-CR-191385] p 804 N93-14809

INFRARED INSTRUMENTS
Advanced technology wind shear prediction system evaluation p 785 N93-14858

INFRARED RADIATION
Generation of broadly tunable, narrow bandwidth, and intense coherent vacuum ultraviolet radiation in rare gases p 980 N93-14167
Infrared radiative properties of clouds p 919 N93-14196
Cesium iodide alloys
[DE92-019818] p 845 N93-14717
Two micron laser development for atmospheric remote sensing at NASA Langley Research Center p 784 N93-14845
Spacecraft thermal design verification in Canada p 808 N93-14940
New electronic materials
[AD-A255612] p 868 N93-15010
Supervised selection of galaxy candidates from the IRAS PSC: The quality of the selection and the infrared properties of the galaxy candidates
[MPE-PREPRINT-216] p 1021 N93-15284
SeaWiFS Technical Report Series. Cloud screening for polar orbiting visible and infrared (IR) satellite sensors, volume 7
[NASA-TM-104566] p 932 N93-15645

INFRARED SOURCES (ASTRONOMY)
Supervised selection of galaxy candidates from the IRAS PSC: The quality of the selection and the infrared properties of the galaxy candidates
[MPE-PREPRINT-216] p 1021 N93-15284

INFRARED SPACE OBSERVATORY (ISO)
ISOCAM experiment cryogenic test results
[REPT-921-440-104] p 825 N93-15140

INFRARED SPECTRA
Investigations of Titan's troposphere and surface and Jupiter's great red spot with infrared observations p 1022 N93-14146
Submillimeter and infrared spectroscopy of molecular clouds near O and B stars p 1016 N93-14149
Electronic, vibrational, and transport properties of conducting polymers p 847 N93-14170
SO2 in the middle atmosphere of Venus: IR measurements from Venera 15 and comparison to UV p 1045 N93-14397
Absorption of propellant vapors into polymer films
[AD-A255274] p 849 N93-14531
Infrared laboratory spectra and composition changes of synthetic amorphous silicate grains
[DE92-040211] p 843 N93-15283

INFRARED SPECTROMETERS
Electronically excited molecules: Reaction kinetics and emission of light: Nanosecond infrared spectroscopy, electronic emission from chemical reactions
[AD-A255642] p 976 N93-14283
Cassini atmospheric chemistry mapper. Volume 1. Investigation and technical plan
[NASA-CR-190947] p 1021 N93-15079

INFRARED SPECTROSCOPY
Application of Fourier Transform-infrared spectroscopy (FT-IR) for materials analysis
[AD-A255727] p 838 N93-14435
Characterization of cholesteric cyclic siloxane liquid crystalline materials
[AD-A256128] p 994 N93-15190

INHOMOGENEITY
Diffusion problems in bonded nonhomogeneous materials with an interface cut
[AD-A256470] p 836 N93-15373

INJECTION
Investigation of the use of surface electrical currents for short-range shipboard data communications
[AD-A256197] p 859 N93-14490
Biophysical and biochemical mechanisms in synaptic transmitter release
[AD-A256340] p 936 N93-15198

INJECTION MOLDING
Flow behavior in liquid molding p 833 N93-14747

INORGANIC PEROXIDES
An investigation of transient atmospheric inorganic peroxides: A theoretical and experimental study p 912 N93-14117

INPUT
Ada-based multitasking terminal I/O
[AD-A255656] p 942 N93-14164

INSULATORS
Experimental observations of the plasma properties of a high-density, low-temperature accelerated arc p 988 N93-14138
Microstack insulator for flashover inhibition, phase 2
[AD-A256338] p 869 N93-15196

INTEGERS
Using an interior point cutting plane method to solve integer programming problems
[AD-A256041] p 945 N93-14659
Characterizations of linear independence and stability of the shifts of a univariate refinable function in terms of its refinement mask
[AD-A256527] p 969 N93-15399
Fast algorithms for rendering cubic curves p 953 N93-15536

INTEGRAL EQUATIONS
Iterative algorithms for integral equations of the first kind with applications to statistics
[AD-A256529] p 942 N93-14285
An integral equation solution for multistage turbomachinery design calculations
[NASA-TM-105970] p 801 N93-15521

INTEGRATED CIRCUITS
Neural network retinal model real time implementation
[AD-A255652] p 934 N93-14210
Processing, fabrication, and demonstration of HTS integrated microwave circuits
[AD-A256109] p 865 N93-14246
Long term stability in thin film ferroelectric memories
[AD-A256290] p 991 N93-14439
Novel engineered compound semiconductor heterostructures for advanced electronics applications
[AD-A255363] p 866 N93-14562
Design and hardware implementation of neural systems
[AD-A256040] p 866 N93-14577
Physics of x ray multilayer structures: Summaries of papers presented at the physics of x ray multilayer structures topical meeting, technical digest series, 1992, volume 7
[AD-A255383] p 992 N93-14741
A new device to aid in the conception and optimization of monolithic millimeter circuits: A distributed and nonliner model of a field effect transistor p 807 N93-14932
A temperature tracking SPICE2G.6 macromodel of the 6N134 optocoupler
[DE92-040093] p 983 N93-15223
Thermal fixture for testing an integrated circuit
[AD-D015380] p 882 N93-15247
Selected area epitaxial growth for complementary HBT applications
[AD-A257047] p 995 N93-15365

INTEGRATED ENERGY SYSTEMS
Discussion for the ideal AIMS p 793 N93-15153

INTEGRATED LIBRARY SYSTEMS
Data archiving p 1005 N93-15035
ATL Products Division's entries into the computer mass storage marketplace p 1005 N93-15038

INTEGRATED OPTICS
Advanced laser chemical processing for microelectronics and integrated optics
[AD-A255980] p 865 N93-14425
Architecture of low cost, large scale neural networks
[MEMO-INF-92-16] p 941 N93-15089
Research Studies on Advanced Optical Module/Head Designs for Optical Data Storage
[NASA-CR-191307] p 984 N93-15505
The design and fabrication of a single leakage-channel grating coupler p 986 N93-15518
INTELLIGIBILITY
The intelligibility of words, sentences, and continuous discourse using the articulation index
[AD-A256781] p 863 N93-15624
INTERACTING GALAXIES
Study of tidal interactions in M81-M82-NGC3077 system p 1010 N93-14195
INTERACTIONAL AERODYNAMICS
A study of viscous interaction effects on hypersonic waveriders p 778 N93-14160
Pressure distribution for the wing of the YAV-8B airplane; with and without pylons
[NASA-TM-4429] p 779 N93-14451
INTERFACES
A portable multiprocessor interface for standard ML of New Jersey
[AD-A255639] p 958 N93-14151
Revised nomenclature for defects at or near the Si/SiO2 interface
[DE92-040975] p 997 N93-15651
INTERFACIAL TENSION
Transient response of a viscous liquid bridge of finite length and anchored edges
[LRT-WE-9-FB-25-1991] p 878 N93-15132
INTERFEROMETERS
Full surface testing of grazing incidence mirrors
[AD-A255644] p 979 N93-14152
Interferometer with two phase-conjugate mirrors
[AD-D015420] p 982 N93-14800
Preview of Blackbeard interferometry
[DE92-040329] p 818 N93-14904
Full surface testing of grazing incidence mirrors
[AD-A255798] p 984 N93-15371
Interferometric measurement with squeezed light
[AD-A257065] p 984 N93-15458
INTERFEROMETRY
Full surface testing of grazing incidence mirrors
[AD-A255644] p 979 N93-14152
Preview of Blackbeard interferometry
[DE92-040329] p 818 N93-14904
Interferometric measurement with squeezed light
[AD-A257065] p 984 N93-15458
Modeling and measurement of a micro-optic beam deflector p 985 N93-15514
INTERLAYERS
An investigation of crack growth at interfaces in bimaterials and composites using a consistent shear-lag model p 896 N93-14187
INTERMETALLICS
HIP consolidation of aluminum-rich intermetallic alloys and their composites
[NAWCADWAR-92003-60] p 845 N93-14726
Thermodynamics and transport in Ce3Bi4Pt3 and related compounds
[DE92-040377] p 998 N93-14905
Fe3Al-type iron aluminides: Aqueous corrosion properties in a range of electrolytes and slow-strain rate ductilities during aqueous corrosion
[DE92-040520] p 846 N93-15059
INTERMODULATION
NPR and intermodulation in mobile satellite systems p 806 N93-14931
INTERNAL ENERGY
Cooperative control of multiple space manipulators p 805 N93-14923
INTERNAL PRESSURE
Analysis and optimal design of pressurized, imperfect, anisotropic ring-stiffened cylinders p 897 N93-14251
INTERNATIONAL COOPERATION
The 7th World Conference on Titanium
[AD-A255674] p 844 N93-14132
The use of International Standards Organization ISO 9000 quality assurance standards in place of military standards
[AD-A256203] p 894 N93-14500
International Space University p 808 N93-14938
World energy: Building a sustainable future
[DE93-001598] p 909 N93-15467
INTERNATIONAL SUN EARTH EXPLORER 1
A survey of solar flare energetic particle abundances and energy spectra p 1048 N93-14135
INTERPLANETARY MAGNETIC FIELDS
Venus internal magnetic field and its interaction with the interplanetary magnetic field p 1032 N93-14336
INTERPLANETARY SPACE
Interplanetary Program to Optimize Simulated Trajectories (IPOST). Volume 3: Programmer's manual
[NASA-CR-189653-VOL-3-REV] p 815 N93-14730
Interplanetary program to optimize simulated trajectories (IPOST). Volume 4: Sample cases
[NASA-CR-189653-VOL-4] p 815 N93-14768
INTERPLANETARY SPACECRAFT
Combined high and low thrust propulsion for fast piloted Mars missions
[NASA-CR-190788] p 828 N93-15584
INTERPROCESSOR COMMUNICATION
Progammable connection parallel architecture: Design and routing
[ETN-92-92676] p 958 N93-15124
A distributed data-balanced dictionary based on the b-link tree
[AD-A256841] p 1009 N93-15639
INTERSECTIONS
Ray tracing polygons using spatial subdivision p 955 N93-15555
Parametric height field ray tracing p 955 N93-15556
Algorithms for intersecting parametric and algebraic curves p 956 N93-15560
An interval refinement technique for surface intersection p 956 N93-15561
INTERSTELLAR GAS
Submillimeter and infrared spectroscopy of molecular clouds near O and B stars p 1016 N93-14149
The formation of giant molecular clouds p 1021 N93-15086
INTERSTELLAR MATTER
Optical signatures of cooling flows in isolated early-type galaxies p 1017 N93-14243
INTERVALS
An interval refinement technique for surface intersection p 956 N93-15561
INVARIANCE
Geometric invariants and object recognition
[AD-A255317] p 943 N93-14546
INVENTIONS
Wisconsin Inventors' Network Database
[DE92-018394] p 1007 N93-15137
INVERSE KINEMATICS
Manipulation strategies for redundant manipulators p 960 N93-14203
INVISCID FLOW
Simulation of unsteady inviscid flow on an adaptively refined Cartesian grid p 873 N93-14273
Pressure drag and lift contributions for blunted forebodies of fineness ratio 2.0 in transonic flow (M infinity less than or equal to 1.4)
[ESDU-89033] p 779 N93-14515
Computational analysis of hypersonic flows past elliptic-cone waveriders
[NASA-CR-191304] p 781 N93-14767
A multigrid approach to embedded-grid solvers
[AD-A256405] p 879 N93-15332
An integral equation solution for multistage turbomachinery design calculations
[NASA-TM-105970] p 801 N93-15521
Unsteady shear disturbances within a two dimensional stratified flow
[NASA-CR-189121] p 880 N93-15527
IO
The sulfur emission and periodicity of the Jupiter plasma torus in 1988 p 1022 N93-14156
IODIDES
Experimental and theoretical investigation of surface chemistry induced by direct and indirect electronic excitation
[AD-A256342] p 843 N93-15200
IODINE ISOTOPES
Measurement and analysis of excitation functions in (alpha,np) reactions on (128, 130)Te
[DE92-630358] p 991 N93-14485
IODINE LASERS
A study of an optically pumped free-jet molecular iodine laser operating in the visible spectrum p 884 N93-14141
ION ACCELERATORS
Bevalac ion beam characterizations for single event phenomena
[AD-A257033] p 979 N93-15362
ION BEAMS
Current neutralization in ballistic transport of light ion beams
[AD-A256070] p 976 N93-14662
High temperature stability, interface bonding, and mechanical behavior in (beta)-NiAl and Ni3Al matrix composites with reinforcements modified by ion beam enhanced deposition
[DE92-014399] p 992 N93-14812
Bevalac ion beam characterizations for single event phenomena
[AD-A257033] p 979 N93-15362
Exceptionally high-strength (approximately 3 GPa) aluminum alloys demonstrated by oxygen ion implantation
[DE92-040980] p 847 N93-15383
ION CONCENTRATION
On the role of water growth in atmospheric aerosol p 922 N93-14875
ION CYCLOTRON RADIATION
A power compensation system for phased operation of the JET A2 antenna arrays
[DE92-041020] p 863 N93-15440
ION DENSITY (CONCENTRATION)
Turbulent magnetized plasmas from ionizing shock waves p 987 N93-14120
ION IMPLANTATION
Exceptionally high-strength (approximately 3 GPa) aluminum alloys demonstrated by oxygen ion implantation
[DE92-040980] p 847 N93-15383
ION PROPULSION
Ion thruster development at NASA Lewis Research Center
[NASA-TM-105983] p 827 N93-15429
ION TRAPS (INSTRUMENTATION)
Laser-based studies with an ion-trap mass spectrometer: Ion tomography and analytical applications
[DE92-017529] p 887 N93-15135
IONIZATION CHAMBERS
Explaining cloud chamber tracks
[DE92-040502] p 972 N93-15057
Liquid xenon time projection chamber for gamma rays in the MeV region: Development status p 1014 N93-15592
IONIZED GASES
Experimental observations of the plasma properties of a high-density, low-temperature accelerated arc p 988 N93-14138
IONOSPHERIC CONDUCTIVITY
A numerical model of ionospheric convection derived from field-alignment currents and the corresponding conductivity
[TRITA-EPP-91-03-REV] p 916 N93-15252
IONOSPHERIC CURRENTS
A numerical model of ionospheric convection derived from field-alignment currents and the corresponding conductivity
[TRITA-EPP-91-03-REV] p 916 N93-15252
IONOSPHERIC DISTURBANCES
Preview of Blackbeard interferometry
[DE92-040329] p 818 N93-14904
IONOSPHERIC DRIFT
Comparison between irregularity motion and bulk plasma drifts at high latitudes
[PL-TR-91-2292] p 914 N93-14727
IONOSPHERIC PROPAGATION
Preview of Blackbeard interferometry
[DE92-040329] p 818 N93-14904
IONS
Photodissociation dynamics of cluster ions
[AD-A256375] p 917 N93-15463
IRON
Mixed-valence iron minerals on Venus: Fe(2+)-Fe(3+) oxides and oxy-silicates formed by surface-atmosphere interactions p 1025 N93-14301
A system approach to archival storage p 1006 N93-15040
IRON ALLOYS
Fe3Al-type iron aluminides: Aqueous corrosion properties in a range of electrolytes and slow-strain rate ductilities during aqueous corrosion
[DE92-040520] p 846 N93-15059
Analytical and experimental evaluation of joining ceramic oxides to ceramic oxides and ceramic oxides to metal for advanced heat engine applications
[DE92-041383] p 851 N93-15294
IRON COMPOUNDS
Fe3Al-type iron aluminides: Aqueous corrosion properties in a range of electrolytes and slow-strain rate ductilities during aqueous corrosion
[DE92-040520] p 846 N93-15059
IRON OXIDES
Mixed-valence iron minerals on Venus: Fe(2+)-Fe(3+) oxides and oxy-silicates formed by surface-atmosphere interactions p 1025 N93-14301
IRRADIANCE
Effects of higher order aberrations on beam shape in an optical recording system p 985 N93-15515
Accelerated simulation of near-Earth-orbit polymer degradation p 823 N93-15615
IRRADIATION
Analysis of retinal function following laser irradiation
[AD-A255649] p 933 N93-14163
Excimer laser irradiation of metal surfaces p 884 N93-14175
Surface evaluation of UV-degraded contamination
[NASA-CR-184500] p 910 N93-14764

Improvement and analysis of the radiation response of RADFET dosimeters
[AD-A254115] p 869 N93-15133

ISCHEMIA
Statistical analysis of the human strangulation experiments: Comparison to +Gz-induced loss of consciousness
[AD-A255485] p 935 N93-14789

ISENTROPIC PROCESSES
Adiabatic two-phase flow in a test section with partial flow blockages
[DE92-016360] p 877 N93-14816

ISING MODEL
The method of minimal representations in 2D Ising model calculations
[AD-A256581] p 967 N93-14270
Analysis of projections of the transfer matrix in 2D Ising models
[AD-A256583] p 967 N93-14271

ISIS SATELLITES
Full surface testing of grazing incidence mirrors
[AD-A255798] p 984 N93-15371

ISOMERS
An investigation of transient atmospheric inorganic peroxides: A theoretical and experimental study
p 912 N93-14117
Gallium and indium compounds containing three different substituents. Crystal and molecular structure of ((Me3 CCH2)ClGaPPh2)3
[AD-A257049] p 996 N93-15443

ITALIAN SPACE PROGRAM
System test approach for the SAX satellite
p 824 N93-15622

ITERATION
Application of partition matrix methods to solve large eigenproblems in structural dynamics
p 896 N93-14188
Manipulation strategies for redundant manipulators
p 960 N93-14203
Iterative software testing
[AD-A255953] p 943 N93-14420
Scheduling and rescheduling with iterative repair
[NASA-TM-108120] p 965 N93-15287
Rescheduling with iterative repair
[NASA-TM-108119] p 965 N93-15288
Learning to improve iterative repair scheduling
[NASA-TM-108118] p 965 N93-15289
Escape-time visualization method for language-restricted iterated function systems
p 956 N93-15558
The object instancing paradigm for linear fractal modeling p 956 N93-15559
Propagation of high frequency jet noise using geometric acoustics
[NASA-TM-105950] p 975 N93-15575

ITERATIVE SOLUTION
Iterative algorithms for integral equations of the first kind with applications to statistics
[AD-A256529] p 942 N93-14285
The covariance matrix of derived quantities and their combination
[DE92-019066] p 969 N93-15212

IUE
Ultraviolet spectra of stars and stellar systems
p 1011 N93-14593
The evolution of the quasar continuum
[NASA-CR-191673] p 1012 N93-14759
Atomic data and spectral analysis of carbon, nitrogen, oxygen and silicon ions observed with the International Ultraviolet Explorer
[NASA-CR-191302] p 1012 N93-14761

J

J INTEGRAL
Fracture mechanisms and fracture control in composite structures p 899 N93-14474

JACOBI MATRIX METHOD
Optimum pose measurements for kinematic parameters identification
[AD-A256307] p 970 N93-14443

JAMMING
Airborne radar simulation with adaptive antenna techniques
[AD-A255460] p 859 N93-14488

JET AIRCRAFT
Estimation of rate of climb
[ESDU-92019] p 791 N93-14541

JET AIRCRAFT NOISE
Computation of supersonic jet noise under imperfectly expanded conditions
[NASA-TM-105961] p 975 N93-15430
Propagation of high frequency jet noise using geometric acoustics
[NASA-TM-105950] p 975 N93-15575

JET ENGINE FUELS
Simplified jet-A kinetic mechanism for combustor application
[NASA-TM-105940] p 844 N93-15504

JET FLOW
Control of asymmetric jet
[AD-A255967] p 873 N93-14400

JET MIXING FLOW
Control of asymmetric jet
[AD-A255967] p 873 N93-14400
Optimization of circular orifice jets mixing into a heated cross flow in a cylindrical duct
[NASA-TM-105984] p 800 N93-15359

JET NOZZLES
Control of asymmetric jet
[AD-A255967] p 873 N93-14400

JETTISONING
Space Shuttle Orbiter Crew Hatch Jettison Test using a 0.0405-scale model (16-0) in the Texas A/M low speed wind tunnel (OA362). Space Shuttle aerothermodynamic data report
[NASA-CR-167698] p 815 N93-15474

JOINTS (JUNCTIONS)
Fracture analyses of thin films, interfaces, and joints
p 897 N93-14215
Analytical and experimental evaluation of joining ceramic oxides to ceramic oxides and ceramic oxides to metal for advanced heat engine applications
[DE92-041383] p 851 N93-15294

JOSEPHSON JUNCTIONS
Epitaxial heterojunctions of oxide semiconductors and metals on high temperature superconductors
[NASA-CASE-NPO-18483-1-CU] p 994 N93-15151
Dynamical properties of Josephson Junctions arrays
[AD-A255464] p 995 N93-15351

JOURNAL BEARINGS
Online vibration control of a flexible rotor/bearing system p 899 N93-14468
Calculation methods for externally pressurised (hydrostatic) journal bearings with capillary restrictor control
[ESDU-92026] p 889 N93-14543

JUNCTION DIODES
High speed imaging for flash radiography using PIN diodes
[DE92-040959] p 882 N93-15381

JUPITER (PLANET)
The time variability of Jupiter's synchrotron radiation
p 973 N93-14227

JUPITER ATMOSPHERE
A study of the low and mid-latitude upper ionospheres of Jupiter and Saturn p 1022 N93-14179
Numerical simulation of baroclinic Jovian vortices
p 1046 N93-14865
Cassini atmospheric chemistry mapper. Volume 1. Investigation and technical plan
[NASA-CR-190947] p 1021 N93-15079

JUPITER RED SPOT
Investigations of Titan's troposphere and surface and Jupiter's great red spot with infrared observations
p 1022 N93-14146

K

K-EPSILON TURBULENCE MODEL
Exploiting similarity in turbulent shear flows for turbulence modeling
[NASA-CR-191621] p 875 N93-14481
Supersonic boundary-layer flow turbulence modeling
[NASA-TM-105893] p 877 N93-14758

KALMAN FILTERS
Multiple model adaptive estimation applied to the ViSTA F-16 with actuator and sensor failures
[AD-A256444] p 802 N93-14608
Two-stage target tracking system and method
[AD-D015412] p 982 N93-14880
Sampled-data control and robust control for discrete-time systems p 964 N93-15149

KANSAS
Synoptic scale structure of summertime wet and dry spells in northeastern Kansas p 923 N93-14919

KAPTON (TRADEMARK)
High temperature polymer dielectric film insulation
[AD-A255243] p 849 N93-14527

KERNEL FUNCTIONS
Wavelet methods for curve estimation
[AD-A255357] p 970 N93-14538
Mathematical software under UNICOS at LCC
[DE93-001828] p 952 N93-15493
On the nonlinear three dimensional instability of Stokes layers and other shear layers to pairs of oblique waves
[NASA-TM-105918] p 880 N93-15499

KERR MAGNETOOPTICAL EFFECT
Optical instrumentation and characterization for magneto-optical recording media p 980 N93-14168
Measurement of the magnetic anisotropy energy constants for magneto-optical recording media
p 984 N93-15509

KEVLAR (TRADEMARK)
Composite materials in space: Results from the LDEF satellite p 811 N93-14955

KINEMATICS
Use of kinematic constraint in tracking constant speed maneuvering targets
[AD-A255988] p 858 N93-14415
Optimum pose measurements for kinematic parameters identification
[AD-A256307] p 970 N93-14443
On some kinematic and mass characteristics of foldable solar arrays p 812 N93-14957
Modern methods in meteorological and oceanographic data analysis
[AD-A257080] p 903 N93-15496

KINETIC ENERGY
On some kinematic and mass characteristics of foldable solar arrays p 812 N93-14957

KINETIC EQUATIONS
Turbulence and chaos in classical and quantum systems p 972 N93-14144

KNOWLEDGE
Knowledge and regularity in planning
[NASA-TM-108113] p 965 N93-15293

KNOWLEDGE BASES (ARTIFICIAL INTELLIGENCE)
Query optimization and planning in object-oriented knowledge bases
[AD-A256006] p 1008 N93-15254
Annotating the real world with knowledge-based graphics on a see-through head-mounted display
p 954 N93-15543

KNOWLEDGE REPRESENTATION
Information system constraint language (ISyCL)
[AD-A256268] p 976 N93-14438

KONDO EFFECT
Thermodynamics and transport in Ce3Bi4Pt3 and related compounds
[DE92-040377] p 998 N93-14905

L

LABORATORIES
Requirements for a network storage service
p 1003 N93-14781

LACTIC ACID
Autoradiographic distribution and applied pharmacological characteristics of dextromethorphan and related antitissue/anticonvulsant drugs and novel analogs
[AD-A255607] p 935 N93-15009

LAMINAR BOUNDARY LAYER
BLSTA: A boundary layer code for stability analysis
[NASA-CR-4481] p 877 N93-14797

LAMINAR FLOW
Transport phenomena and interfacial kinetics in multiphase combustion systems.
[AD-A255999] p 838 N93-14418
Finite-difference solution for laminar or turbulent boundary layer flow over axisymmetric bodies with ideal gas, CF4, or equilibrium air chemistry
[NASA-TP-3271] p 879 N93-15434

LAMINATES
Modal interactions in the dynamic response of isotropic and composite plates p 829 N93-14221
A preliminary investigation of dual mode fracture sustained by graphite/epoxy laminates impacted by high-velocity spherical metallic projectiles
[AD-A255790] p 898 N93-14419
Fracture mechanisms and fracture control in composite structures p 899 N93-14474
Delamination growth behavior in cross-ply laminated composites due to transverse concentrated loading
[AD-A255974] p 830 N93-14493
Kind-band failure analysis of thick composites in compression
[AD-A255431] p 831 N93-14509
Determination of stresses on laminated aircraft transparencies by the strain gage-hole drilling and sectioning method
[AD-A255548] p 791 N93-14571
The effect of geometry and prescribed delaminations on the postbuckling behaviour of laminated carbon-fibre reinforced plastic panels p 831 N93-14597
Method of forming a multiple layer dielectric and a hot film sensor therewith
[NASA-CASE-LAR-13678-3] p 881 N93-14714
Physics of x ray multilayer structures: Summaries of papers presented at the physics of x ray multilayer structures topical meeting, technical digest series, 1992, volume 7
[AD-A255383] p 992 N93-14741

Mechanical response of composite materials with through-the-thickness reinforcement
p 834 N93-14753
Elastic wave propagation in laminated composites
[ITN-93-85186] p 835 N93-15144
Degradation and failure modes of carbon/bismaleimide laminates subjected to a tropical exposure
[AD-A256328] p 836 N93-15193

LAND MANAGEMENT
The regional land use of Paraiba Valley and the North Coast of Sao Paulo State, Brazil p 905 N93-14450

LAND MOBILE SATELLITE SERVICE
Regional satellites: The European experience with Eutelsat for TV, voice, data and mobile transmissions
[REPT-921-440-106] p 818 N93-15071

LAND USE
The regional land use of Paraiba Valley and the North Coast of Sao Paulo State, Brazil p 905 N93-14450
Integrating satellite imagery into a geographic information system for monitoring the downstream impacts of dam construction on floodplain agriculture in Sokoto State, Nigeria p 905 N93-14823
Spatial and temporal patterns of biotic exchanges of CO_2 between the atmosphere and tropical landscapes and their role in the global carbon balance
[DE92-019170] p 911 N93-15272
Ecological implications of landscape fragmentation
[DE92-019186] p 911 N93-15273

LANDAU DAMPING
Transformation of energy and momentum due to Landau damping in time
[IPPCZ-316] p 988 N93-14813

LANDFORMS
Determining stress states using dike swarms: The Lauma Dorsa example p 1028 N93-14319
Tectonics and volcanism of Eastern Aphrodite Terra: No subduction, no spreading p 1029 N93-14321
Magellan stereo images and Venusian geology
p 1035 N93-14347
Venus: Preliminary geologic mapping of northern Atla Regio p 1037 N93-14353
Venus: Preliminary geologic mapping of southern Beta Regio-northern Phoebe Regio p 1037 N93-14354
Venus: Geology of Beta Regio rift system
p 1037 N93-14355

LANDING AIDS
Facilities and capabilities catalog for landing and escape systems
[NASA-RP-1282] p 814 N93-14495

LANDING GEAR
Reanalysis of multiple-wheel landing gear traffic tests
[AD-A256593] p 804 N93-14238
Stress corrosion susceptibility of ultra-high strength steels for Naval aircraft applications
[AD-A256126] p 846 N93-15189

LANDING SITES
In situ material characterization for pavement evaluation by the Spectral-Analysis-of-Surface-Waves (SASW) method
[AD-A255660] p 804 N93-14128
The geology of the Venera/Vega landing sites
p 1024 N93-14296
Reusable Reentry Satellite (RRS): Recovery tradeoff study
[NASA-CR-186396] p 825 N93-15658

LANDSAT SATELLITES
The preservation of LANDSAT data by the National Land Remote Sensing Archive p 1003 N93-14777

LANGUAGE PROGRAMMING
Information system constraint language (ISyCL)
[AD-A256268] p 976 N93-14438
Program verification using higher order logic
[AD-A255408] p 943 N93-14502

LANGUAGES
Recursively generated networks and dynamical learning
[AD-A255441] p 963 N93-14783

LAPLACE TRANSFORMATION
Non-linear analysis of wave progagation using transform methods and plates and shells using integral equations
p 896 N93-14186

LARGE SCALE INTEGRATION
Anik E spacecraft integration and test
p 808 N93-14939

LARGE SPACE STRUCTURES
Damage location and model refinement for large flexible space structures using a sensitivity-based eigenstructure assignment method p 816 N93-14274
Large space structures and systems in the space station era: A bibliography with indexes (supplement 04)
[NASA-SP-7085(04)] p 817 N93-14606
Investigation of antenna pattern constraints for passive geosynchronous microwave imaging radiometers
[NASA-CR-189728] p 905 N93-14792
Space based radar: Test of large space structures
p 808 N93-14941
Technology development for non-contact measurement in modal testing of large space structures
p 809 N93-14942
Space craft verification at the David Florida Laboratory
p 809 N93-14943
Structurally adaptive space crane concept for assembling space systems on orbit
[NASA-TP-3307] p 818 N93-15368
Offloading techniques for large deployable space structures p 821 N93-15605

LASER ABLATION
Optical probes for laser induced shocks
[AD-A256092] p 884 N93-14284

LASER APPLICATIONS
Application of gel-silica optics to laser technology and optical element fabrication
[AD-A255666] p 883 N93-14131
Lineshape analysis of laser light scattered by an argon thermal plasma jet p 987 N93-14137
Advances in laser cooling
[AD-A255969] p 884 N93-14402
Advanced laser chemical processing for microelectronics and integrated optics
[AD-A255980] p 865 N93-14425
Compact free electron laser for medical applications
[AD-A256236] p 885 N93-14599
Multiperiod-grating surface-emitting lasers
[NASA-CASE-NPO-17763-1-CU] p 885 N93-14703
Precise measurements made from a distance of local deformations independent of small object movements
[ETN-92-92723] p 886 N93-15128
Abstracts booklet
[AD-A256115] p 869 N93-15188

LASER BEAMS
Three-dimensional guiding effects in a free-electron laser p 883 N93-14125
Full surface testing of grazing incidence mirrors
[AD-A255644] p 979 N93-14152
Precise measurements made from a distance of local deformations independent of small object movements
[ETN-92-92723] p 886 N93-15128
Electron acceleration by longitudinal electric field of a Gaussian laser beam
[DE92-526947] p 887 N93-15296
Simple formulae for the optimization of the FEL gain length including the effects of emittance, betatron oscillations, and energy spread
[DE92-040378] p 887 N93-15325
Environmental assessment for the laser guide star experiment at Lawrence Livermore National Laboratory
[DE92-040316] p 1013 N93-15425

LASER DAMAGE
Analysis of retinal function following laser irradiation
[AD-A255649] p 933 N93-14163

LASER DEPOSITION
Advanced laser chemical processing for microelectronics and integrated optics
[AD-A255980] p 865 N93-14425

LASER DOPPLER VELOCIMETERS
NASA/LMSC instrument design and fabrication --- coherent lidar airborne shear sensor
p 784 N93-14846
Technology development for non-contact measurement in modal testing of large space structures
p 809 N93-14942

LASER FUSION
Environmental assessment: OMEGA upgrade project at the Laboratory for Laser Energetics, University of Rochester
[DE92-040410] p 886 N93-14907

LASER GUIDANCE
An iconic position estimator for a 2-D laser rangefinder
[AD-A255523] p 885 N93-14568

LASER INDUCED FLUORESCENCE
Second order closure modeling of turbulent buoyant wall plumes
[NASA-TM-105956] p 877 N93-14829

LASER MATERIALS
Color center laser with transverse auxiliary illumination
[AD-D015387] p 887 N93-15250

LASER MICROSCOPY
Mechanisms of forming intergranular microcracks and microscopic surface discontinuities in welds
[AD-A255371] p 845 N93-14740

LASER OUTPUTS
Nonlinear dynamics of optical systems
p 979 N93-14124
Three-dimensional guiding effects in a free-electron laser p 883 N93-14125
Multiperiod-grating surface-emitting lasers
[NASA-CASE-NPO-17763-1-CU] p 885 N93-14703
Simple formulae for the optimization of the FEL gain length including the effects of emittance, betatron oscillations, and energy spread
[DE92-040378] p 887 N93-15325

LASER PLASMAS
Excimer laser irradiation of metal surfaces
p 884 N93-14175
Accurate methods for calculating atomic processes in high temperature plasmas
[DE92-040215] p 988 N93-15418

LASER SPECTROSCOPY
Time-resolved optical studies of 3-5 semiconductors
p 990 N93-14183
Laser-based studies with an ion-trap mass spectrometer: Ion tomography and analytical applications
[DE92-017529] p 887 N93-15135

LASER TARGET INTERACTIONS
Excimer laser irradiation of metal surfaces
p 884 N93-14175
Finite element models of laser welding
p 888 N93-14226

LASER WELDING
Finite element models of laser welding
p 888 N93-14226
Mechanisms of forming intergranular microcracks and microscopic surface discontinuities in welds
[AD-A255371] p 845 N93-14740

LASERS
Two micron laser development for atmospheric remote sensing at NASA Langley Research Center
p 784 N93-14845
Optical glasses for high-peak-power laser applications
[DE92-040403] p 886 N93-14906
Radical ion formation in polymers as a mechanism for laser eye protection
[AD-A255992] p 850 N93-15111
Color center laser with transverse auxiliary illumination
[AD-D015387] p 887 N93-15250

LASING
Level-mixing assisted tunability of nuclear resonance linewidths for gamma ray lasers
[AD-A255791] p 885 N93-14647

LATCHES
Retractable tool bit having slider type catch mechanism
[NASA-CASE-GSC-13358-1] p 890 N93-14710

LATENT HEAT
Latent heat thermal energy storage for lunar oxygen production
[DE92-017817] p 907 N93-15219

LATITUDE
The preferred latitudes of the Intertropical Convergence Zone: Observations and theory p 920 N93-14213
Middle atmosphere of Venus and its clouds: Latitude and solar time variations p 1045 N93-14396

LATTICE VIBRATIONS
Electronic, vibrational, and transport properties of conducting polymers p 847 N93-14170

LATTICES (MATHEMATICS)
A compilation of the mathematics leading to the doublet lattice method
[AD-A256304] p 779 N93-14441
On the theory of coded modulation systems for high output digital transmission
[TELECOM-PARIS-92-E-001] p 861 N93-15098

LAUNCH VEHICLES
Reusable Reentry Satellite (RRS): Telemetry, Tracking, and Command (TT/C) coverage tradeoff study
[NASA-CR-188583] p 824 N93-15629
Reusable Reentry Satellite (RRS) system design study. Phase B, appendix E: Attitude control system study
[NASA-CR-188578] p 825 N93-15633

LAVA
Erosion versus construction: The origin of Venusian channels p 1025 N93-14303
Igneous and tectonic evolution of Venusian and terrestrial coronae p 1031 N93-14330
Large-volume lava flow fields on Venus: Dimensions and morphology p 1033 N93-14339
Extensive lava flow fields on Venus: Preliminary investigation of source elevation and regional slope variations p 1034 N93-14342
The origins of radial fracture systems and associated large lava flows on Venus p 1038 N93-14356
Episodic plate tectonics on Venus
p 1044 N93-14390

LAW (JURISPRUDENCE)
Comparison of the prevalence index and average wetland values for identification of wetland vegetation
[DE92-016701] p 910 N93-15209

LAYERS
A multi-layer graphic model for building interactive graphical applications p 957 N93-15567

LEAD ZIRCONATE TITANATES
Long term stability in thin film ferroelectric memories
[AD-A256290] p 991 N93-14439
Reliability of sol-gel derived ferroelectric memories
[AD-A255240] p 849 N93-14668

Characterization of PZT films fatigued at low frequency
[AEROSPACE-ATR-91(8308)-2] p 992 N93-14795

LEADING EDGES
A finite element model for analysis of thermoviscoplastic behavior of hypersonic leading edge structures subject to intense aerothermal heating p 780 N93-14631
Computational analysis of hypersonic flows past elliptic-cone waveriders
[NASA-CR-191304] p 781 N93-14767
BLSTA: A boundary layer code for stability analysis
[NASA-CR-4481] p 877 N93-14797
Analysis of in-flight structural failures of P-3C wing leading edge segments
[AD-A256212] p 792 N93-15238
Flowfield study of a close-coupled canard configuration
[AD-A256311] p 782 N93-15245
Root damage analysis of aircraft engine blade subject to ice impact
[NASA-TM-105779] p 902 N93-15343
Emittance measurements of Space Shuttle orbiter reinforced carbon-carbon
[NASA-TP-3293] p 903 N93-15530

LEAKAGE
The design and fabrication of a single leakage-channel grating coupler p 986 N93-15518
Acoustic location of leaks in pressurized underground petroleum pipelines
[PB92-207687] p 975 N93-15647

LEARNING
A psychometrically sound cognitive diagnostic model: Effect of remediation as empirical validity
[AD-A255926] p 933 N93-14109
The effect of a hierarchical task-specific external conceptual model on the learnability and usability of microcomputer applications by novices p 1000 N93-14205
Long term memory for different types of classroom knowledge
[AD-A255235] p 999 N93-14526
Recursively generated networks and dynamical learning
[AD-A255441] p 963 N93-14783

LEAST SQUARES METHOD
Iterative algorithms for integral equations of the first kind with applications to statistics
[AD-A256529] p 942 N93-14285
The spin vector of Venus determined from Magellan data p 1027 N93-14310
Modified fast frequency acquisition via adaptive least squares algorithm
[NASA-CASE-NPO-17845-2-CU] p 945 N93-14882

LENS ANTENNAS
A multiple-aperture multiple-beam EHF antenna for satellite communications
[AD-A256020] p 858 N93-14426

LENSES
Optical glasses for high-peak-power laser applications
[DE92-040403] p 886 N93-14906
Color center laser with transverse auxiliary illumination
[AD-D015387] p 887 N93-15250
Center for x ray optics, 1991
[DE93-001543] p 984 N93-15350
Diffraction analysis and evaluation of several focus- and track-error detection schemes for magneto-optical disk systems p 984 N93-15506
The 3D modeling of high numerical aperture imaging in thin films p 985 N93-15513
Modeling and measurement of a micro-optic beam deflector p 985 N93-15514
Effects of higher order aberrations on beam shape in an optical recording system p 985 N93-15515

LEVELING
Leveling coatings for reducing the atomic oxygen defect density in protected graphite fiber epoxy composites
[NASA-TM-105732] p 852 N93-15344

LIBRARIES
Ultraviolet spectra of stars and stellar systems p 1011 N93-14593
Software Technology for Adaptable, Reliable Systems (STARS)
[AD-A257022] p 952 N93-15471
Mathematical software under UNICOS at LCC
[DE93-001828] p 952 N93-15493

LICENSING
Wisconsin Inventors' Network Database
[DE92-018394] p 1007 N93-15137

LIFE (DURABILITY)
Electronics reliability fracture mechanics. Volume 2: Fracture mechanics
[AD-A256200] p 900 N93-14498
Propulsion and Energetics Panel Working Group 20 on Test Cases for Engine Life Assessment Technology
[AGARD-AR-308] p 798 N93-14890
Introduction to test cases for engine life assessment technology p 799 N93-14891
LARZAC HP turbine disk crack initiation and propagation spin pit test p 799 N93-14892
RB 199 high pressure compressor stage 3 spin pit tests p 799 N93-14893
CF6-6 high pressure compressor stage 5 locking slot crack propagation spin pit test p 799 N93-14894
F100 second stage fan disk bolthole crack propagation ferris wheel test p 800 N93-14897
In-service considerations affecting component life p 800 N93-14898
ICI optical data storage tape p 1005 N93-15037

LIFE CYCLE COSTS
Evaluation of the cost effectiveness analysis model being developed for the component improvement programs of the Air Force and the Navy
[AD-A256132] p 1010 N93-14249
Reusable Reentry Satellite (RRS) system design study: System cost estimates document
[NASA-CR-188480] p 818 N93-14872

LIFE SCIENCES
Advanced sensors technology survey
[NASA-CR-185691] p 881 N93-14494
Aerospace medicine and biology: A continuing bibliography with indexes (supplement 368)
[NASA-SP-7011(368)] p 934 N93-14603
Aerospace medicine and biology: A continuing bibliography with indexes (supplement 369)
[NASA-SP-7011(369)] p 935 N93-14731
Publications of the Space Physiology and Countermeasures Program, Neuroscience Discipline: 1980-1990
[NASA-CR-4476] p 936 N93-15583

LIFE SUPPORT SYSTEMS
Aerospace medicine and biology: A continuing bibliography with indexes (supplement 369)
[NASA-SP-7011(369)] p 935 N93-14731
Segment specification for the payload segment of the reusable reentry satellite: Rodent module version
[NASA-CR-187884] p 824 N93-15630

LIFT
Pressure drag and lift contributions for blunted forebodies of fineness ratio 2.0 in transonic flow (M infinity less than or equal to 1.4)
[ESDU-89033] p 779 N93-14515
Testing and analysis of modified HMMWV front lift provisions
[MTL-TR-92-31] p 891 N93-14735
Estimation of unsteady lift on a pitching airfoil from wake velocity surveys
[NASA-TM-105947] p 781 N93-14791

LIGHT (VISIBLE RADIATION)
SeaWiFS Technical Report Series. Cloud screening for polar orbiting visible and infrared (IR) satellite sensors, volume 7
[NASA-TM-104566] p 932 N93-15645

LIGHT BEAMS
Interferometer with two phase-conjugate mirrors
[AD-D015420] p 982 N93-14800

LIGHT CURVE
The black hole candidate binary A0620-00 p 1015 N93-14148

LIGHT EMISSION
Electronically excited molecules: Reaction kinetics and emission of light: Nanosecond infrared spectroscopy, electronic emission from chemical reactions
[AD-A255642] p 976 N93-14283

LIGHT IONS
Current neutralization in ballistic transport of light ion beams
[AD-A256070] p 976 N93-14662

LIGHT MODULATION
Optical signal distribution schemes for millimeter phased array radar
[AD-A256262] p 858 N93-14437
A preliminary design of the Ti:LiNbO3 optical channel waveguide
[AD-A255443] p 982 N93-14784

LIGHT SCATTERING
Quantum fluctuations in stimulated Raman scattering p 857 N93-14126
Lineshape analysis of laser light scattered by an argon thermal plasma jet p 987 N93-14137
Diffusing wave spectroscopy p 980 N93-14169

LIGHT SOURCES
Vision development test bed: The cradle of the MSS artificial vision system p 810 N93-14948
Environmental assessment for the laser guide star experiment at Lawrence Livermore National Laboratory
[DE92-040316] p 1013 N93-15425

LIGHT TRANSMISSION
Vertical path atmospheric turbulence: Temporal spectra and differential image motion measurements p 914 N93-14641

LIGHTNING
Evidence for lightning on Venus p 1043 N93-14386
Thunderstorm coupling to the magnetosphere and associated ionospheric effects
[NASA-CR-191383] p 922 N93-14910
Preliminary lightning tests: Optical fiber penetration of an exclusion region barrier
[DE92-019804] p 983 N93-15230

LINE OF SIGHT
Western Aphrodite Terra, tectonics, geology, and line-of-sight gravity p 1029 N93-14322
Digital bank-to-turn control and guidance p 802 N93-14447

LINE OF SIGHT COMMUNICATION
Tactical line-of-sight path reliability: Improved MSE system procedures
[AD-A256504] p 862 N93-15376

LINE SPECTRA
Ultraviolet spectra of stars and stellar systems p 1011 N93-14593
QSO absorption lines and the ionizing field at high redshifts p 1013 N93-14860
Interferometric observations of the J(0,1) CO line on Venus: Upper mesospheric winds and CO abundance p 1047 N93-14918

LINEAR ACCELERATORS
Numerical modelling of intense electron beam transport in the spiral line induction accelerator
[AD-A255545] p 978 N93-14570
High-brightness linac for the Advanced Free-Electron Laser Initiative at Los Alamos
[DE92-040213] p 887 N93-15417
SCRUNCHER phase and amplitude control
[DE92-040225] p 870 N93-15421
Calculation of mechanical vibration frequencies of stiffened superconducting cavities
[DE92-040228] p 903 N93-15423
Design features of a seven-cell high-gradient superconducting cavity
[DE92-040229] p 870 N93-15424

LINEAR ENERGY TRANSFER (LET)
Bevalac ion beam characterizations for single event phenomena
[AD-A257033] p 979 N93-15362

LINEAR POLARIZATION
The evolution of the VLBI polarization of superluminal radio source 3C345 p 1050 N93-14229
Polarization properties and Earth-based radar measurements of Venus in the post-Magellan era p 1026 N93-14304
Pioneer Venus polarimetry and haze optical thickness p 1032 N93-14335

LINEAR PREDICTION
A mixed excitation vocoder with fuzzy logic classifier
[AD-A256834] p 864 N93-15636

LINEAR QUADRATIC GAUSSIAN CONTROL
Sampled-data control and robust control for discrete-time systems p 964 N93-15149

LINEAR QUADRATIC REGULATOR
Position and vibration control of flexible space robots p 892 N93-15102

LINEAR SYSTEMS
Non-linear analysis of wave progagation using transform methods and plates and shells using integral equations p 896 N93-14186
L2 and L-infinity multiobjective control for linear systems p 961 N93-14399

LINEAR VIBRATION
Modal interactions in the dynamic response of isotropic and composite plates p 829 N93-14221

LINES OF FORCE
Cooperative control of multiple space manipulators p 805 N93-14923

LIOUVILLE EQUATIONS
Turbulence and chaos in classical and quantum systems p 972 N93-14144

LIQUEFACTION
USACE geotechnical earthquake engineering software, report 1 WESHAKE for personal computers (version 1.0)
[AD-A257068] p 917 N93-15459

LIQUEFIED GASES
Development of a High Resolution Liquid Xenon Imaging Telescope for Medium Energy Gamma Ray Astrophysics
[NASA-CR-191781] p 1013 N93-15589
A Monte Carlo analysis of the liquid xenon TPC as gamma ray telescope p 1014 N93-15590
A liquid xenon imaging telescope for gamma ray astrophysics: Design and expected performance p 1014 N93-15591
Liquid xenon time projection chamber for gamma rays in the MeV region: Development status p 1014 N93-15592

LIQUID CRYSTALS
Optical information processing using photorefractive BSO p 981 N93-14204

Characterization of cholesteric cyclic siloxane liquid crystalline materials
[AD-A256128] p 994 N93-15190
Ferroelectrics volume 122, numbers 1-4, 1991. Proceedings of the 3rd International Conference on Ferroelectric Liquid Crystals, part 2
[AD-A257053] p 996 N93-15446
Ferroelectrics volume 121, numbers 1-4, 1991. Proceedings of the 3rd International Conferenceon Ferroelectric Liquid Crystals, part 1
[AD-A257054] p 996 N93-15447

LIQUID FLOW
Current status of liquid sheet radiator research
[NASA-TM-105764] p 872 N93-14150

LIQUID FUELS
Liquid flow reactor and method of using
[AD-D015392] p 893 N93-15232

LIQUID METALS
Preliminary investigations of metal liquid-like films and coatings derived from them
[AD-A255477] p 849 N93-14489

LIQUID NITROGEN
High performance YBCO films
[AD-A255439] p 994 N93-15297
The evolution of space simulation
p 814 N93-15610

LIQUID PHASE EPITAXY
Study of the mathematical modelling and computer simulation of crystal growth from liquid phase under microgravity conditions
[CTN-93-60619] p 855 N93-15201

LIQUID PHASES
Remote fiber optic sensor for gaseous and liquid environments, phase 2
[AD-A256224] p 983 N93-15241

LIQUID ROCKET PROPELLANTS
Low thrust chemical rocket technology
[NASA-TM-105927] p 827 N93-15572

LIQUID-GAS MIXTURES
An alternate method for achieving temperature control in the -130 C to 75 C range p 821 N93-15609

LIQUID-LIQUID INTERFACES
Control of thermocapillary convection in a two-layer liquid system p 809 N93-14945
Transient response of a viscous liquid bridge of finite length and anchored edges
[LRT-WE-9-FB-25-1991] p 878 N93-15132

LIQUID-SOLID INTERFACES
Technology evaluation report: The Carver-Greenfield process, Dehydro-Tech Corporation
[PB92-217462] p 910 N93-15217

LIQUIDS
Fluids, gels, and glasses under extreme conditions of pressure and temperature
[AD-A255675] p 847 N93-14166
Viscosity of liquids. Halogenated methanes
[ESDU-92028] p 839 N93-14539
Removal of THD from painted test panels by liquid systems
[AD-A255624] p 850 N93-15064
Adsorption and diffusion of fluids in well-characterized adsorbent materials
[DE92-040160] p 843 N93-15414

LISP (PROGRAMMING LANGUAGE)
CMU common lisp user's manual
[AD-A256431] p 950 N93-15336

LISTS
Source hierarchy list. Volume 1: A through D
[AD-A256100] p 1001 N93-14265
Source header list. Volume 2: K through Z
[AD-A256001] p 1007 N93-15112

LITHIUM COMPOUNDS
Impact of protective oxides on cathode-side resistances in MCFCs
[DE92-019973] p 994 N93-15221

LITHIUM SULFUR BATTERIES
Lithium rechargeable cell with a poly 3-methylthiophene cathode
[AD-A255436] p 866 N93-14552
Smart battery controller for lithium sulfur dioxide batteries
[AD-A255490] p 867 N93-14642

LITHOGRAPHY
A differential equation design method for finite-conjugate, multi-mirror imaging systems
p 979 N93-14165

LITHOLOGY
Visoelastic relaxation of Venusian coronae and mountain belts: Constraints on global heat flow and tectonism
p 1027 N93-14313

LITHOSPHERE
Is Ishtar Terra a thickened basaltic crust?
p 1024 N93-14292
Variations in lithospheric thickness on Venus
p 1030 N93-14329
Igneous and tectonic evolution of Venusian and terrestrial coronae p 1031 N93-14330
Estimates of elastic plate thicknesses beneath large volcanos on Venus p 1035 N93-14344
Flexural models of trench/outer rise topography of coronae on Venus with axisymmetric spherical shell elastic plates p 1036 N93-14348
Tectonic connections to interior processes on Venus
p 1039 N93-14361
Cytherean crustal bending at Salme Dorsa
p 1039 N93-14364
Evidence for retrograde lithospheric subduction on Venus p 1040 N93-14367
Geoid, topography, and convection-driven crustal deformation on Venus p 1042 N93-14376
The tectonics of Venus: An overview
p 1042 N93-14382
Volcanism by melt-driven Rayleigh-Taylor instabilities and possible consequences of melting for admittance ratios on Venus p 1043 N93-14387
Structural characteristics and tectonics of northeastern Tellus Regio and Meni Tessera p 1044 N93-14389

LIVESTOCK
Modelling global methane emissions from livestock: Biological and nutritional controls
[NASA-CR-191354] p 911 N93-15480

LOAD CARRYING CAPACITY
Modeling of Euclidean braided fiber architectures to optimize composite properties p 834 N93-14755

LOAD DISTRIBUTION (FORCES)
Nonlinear dynamic response of shallow arches to harmonic forcing p 898 N93-14282

LOAD TESTS
Analytical and experimental evaluation of joining ceramic oxides to ceramic oxides and ceramic oxides to metal for advanced heat engine applications
[DE92-041383] p 851 N93-15294

LOADING
Offloading techniques for large deployable space structures p 821 N93-15605

LOADS (FORCES)
Weight optimum arch structures
[AD-A256080] p 897 N93-14236
Reanalysis of multiple-wheel landing gear traffic tests
[AD-A256593] p 804 N93-14238
On the structure of nonlinear constitutive equations for fiber reinforced composites
[NASA-CR-191024] p 830 N93-14484
Testing and analysis of modified HMMWV front lift provisions
[MTL-TR-92-31] p 891 N93-14735
Energy loss analysis of an integrated space power distribution system
[NASA-TM-105772] p 854 N93-14834
Unsteady pressure loads in a generic high speed engine model
[NASA-TP-3189] p 975 N93-15391

LOCAL AREA NETWORKS
Requirements for a network storage service
p 1003 N93-14781

LOGIC CIRCUITS
High-speed architecture for the decoding of trellis-coded modulation
[NASA-CR-191374] p 941 N93-14770
Optimal synthesis methods for silicon compilers
[ETN-92-92677] p 947 N93-15125

LOGIC DESIGN
Design and implementation of practical constraint logic programming systems
[AD-A256191] p 943 N93-14558
Processor controlpath microarchitecture synthesis based on the A(asterisk) algorithm
[MEMO-INF-92-10] p 963 N93-15083

LOGIC PROGRAMMING
A proof of the Church-Rosser theorem and its representation in a logical framework
[AD-A256574] p 942 N93-14268
Proof of theorems in Z
[AD-A255711] p 968 N93-14431
Program verification using higher order logic
[AD-A255408] p 943 N93-14502
Design and implementation of practical constraint logic programming systems
[AD-A256191] p 943 N93-14558

LONG DURATION EXPOSURE FACILITY
The preliminary Long Duration Exposure Facility (LDEF) materials data base
[NASA-TM-107692] p 828 N93-14459
Characterisation and dynamic modelling of the near-earth space particulate environment
p 1019 N93-14637
Composite materials in space: Results from the LDEF satellite p 811 N93-14955
LDEF: A bibliography with abstracts
[NASA-TM-107705] p 813 N93-15646

LONG DURATION SPACE FLIGHT
Radiation monitoring for long duration space flights
p 812 N93-14959

LONG TERM EFFECTS
Nucleate pool boiling in the long duration low gravity environment of the Space Shuttle
[NASA-TM-105973] p 855 N93-15420

LONGERONS
A neural network prototype for predicting F-14B strains at the B.L. 10 longeron
[AD-A255272] p 792 N93-15004

LORENTZ FORCE
Relativistic dynamics of a charged sphere: Updating the Lorentz-Abraham model
[AD-A256107] p 971 N93-14245

LOW ALTITUDE
Energetic and magnetosheath energy particle signatures of the low-latitude boundary layer at low altitudes near noon
[NASA-CR-191388] p 917 N93-15574

LOW COST
Reusable Reentry Satellite (RRS) system design study: System cost estimates document
[NASA-CR-188480] p 818 N93-14872
Organic/IR-Semiconductor heterojunctions for low-cost, high temperature IR arrays
[AD-A255971] p 868 N93-15108

LOW FREQUENCIES
Acoustic propagation loss predictions for a site on the Bermuda Rise at low and very low frequencies
[AD-A255445] p 925 N93-14512
Characterization of PZT films fatigued at low frequency
[AEROSPACE-ATR-91(8308)-2] p 992 N93-14795
Low-frequency oscillations in radiative-convective models p 915 N93-14874

LOW SPEED
Preconditioned conjugate-gradient methods for low-speed flow calculations
[NASA-TM-105929] p 877 N93-14885

LOW TEMPERATURE ENVIRONMENTS
Operational strategies for contamination control of composite materials p 822 N93-15614

LOW THRUST
Low thrust chemical rocket technology
[NASA-TM-105927] p 827 N93-15572

LOW THRUST PROPULSION
Combined high and low thrust propulsion for fast piloted Mars missions
[NASA-CR-190788] p 828 N93-15584

LOW TURBULENCE
Subsonic aerodynamic research laboratory
[AD-A256060] p 780 N93-14661

LUBRICANTS
Fluids, gels, and glasses under extreme conditions of pressure and temperature
[AD-A255675] p 847 N93-14166
Calculation methods for externally pressurised (hydrostatic) journal bearings with capillary restrictor control
[ESDU-92026] p 889 N93-14543

LUBRICATING OILS
RB199 engine oil system failure diagnostics by comparison of measured and calculated oil consumption using the OLMOS on-board monitoring system
p 796 N93-15173

LUBRICATION
Fluids, gels, and glasses under extreme conditions of pressure and temperature
[AD-A255675] p 847 N93-14166
Tribology of magnetic storage systems
p 1002 N93-14772

LUMINANCE
Effects of spatial luminance nonuniformities on visual-task performance and subjective uniformity
[AD-A255989] p 936 N93-14416
Non-uniform patch luminance for global illumination
p 957 N93-15569

LUMINESCENCE
Time-resolved optical studies of 3-5 semiconductors
p 990 N93-14183

LUMINOSITY
A search for dead QSO's among nearby luminous galaxies p 1011 N93-14228
Optical signatures of cooling flows in isolated early-type galaxies p 1017 N93-14243

LUNAR BASES
In-situ lunar oxygen extraction p 806 N93-14929
Photovoltaic power system for a lunar base
p 806 N93-14930
Mission and technology assessment of human exploration to the Moon and Mars p 809 N93-14944
Power requirements for the first lunar outpost (FLO)
[NASA-TM-105925] p 909 N93-15523

LUNAR EXPLORATION
Mission and technology assessment of human exploration to the Moon and Mars p 809 N93-14944
LUNAR PROGRAMS
In-situ lunar oxygen extraction p 806 N93-14929
LUNAR ROCKS
Latent heat thermal energy storage for lunar oxygen production
[DE92-017817] p 907 N93-15219
LUNAR SOIL
Fiber pulling apparatus modification
[NASA-CR-184498] p 891 N93-14763
LYMAN ALPHA RADIATION
Physical and chemical processes of the inner coma observed in mid-ultraviolet cometary spectra p 1017 N93-14230
LYRA CONSTELLATION
A study of the abundance distributions along the minor axis of the Galactic bulge p 1015 N93-14136

M

MACH NUMBER
A study of viscous interaction effects on hypersonic waveriders p 778 N93-14160
Transonic flow calculations for a cavity with and without a store
[AD-A255954] p 873 N93-14421
Pressure drag and lift contributions for blunted forebodies of fineness ratio 2.0 in transonic flow (M infinity less than or equal to 1.4)
[ESDU-89033] p 779 N93-14515
Results of a FRSI material test under Space Shuttle ascent conditions in the Ames Research Center 9x7 foot supersonic wind tunnel (OS13). Space Shuttle aerothermodynamic data report
[NASA-CR-167699] p 816 N93-15475
User manual for NASA Lewis 10 by 10 foot supersonic wind tunnel
[NASA-TM-105626] p 804 N93-15498
MACHINE LEARNING
Force and position control of robot manipulators: Learning and repetitive control approach p 888 N93-14473
A specification of the Soar cognitive architecture in Z
[AD-A256198] p 940 N93-14491
Machine intelligence, a foreword: The brain as electronic circuitry; electronic circuitry as a brain
[AD-A255283] p 962 N93-14533
Learning position and force control for mechanical manipulators p 963 N93-15147
Learning to improve iterative repair scheduling
[NASA-TM-108118] p 965 N93-15289
MACHINE TOOLS
A proposal to apply Taguchi-inspired methods to the reduction of machining variance
[AD-A256129] p 856 N93-15234
MACHINERY
An energy analysis of the pseudo Wigner-Ville distribution in support of machinery monitoring and diagnostics
[AD-A256202] p 889 N93-14499
Development of generalized 3-D braiding machines for composite preforms p 833 N93-14749
MACHINING
A proposal to apply Taguchi-inspired methods to the reduction of machining variance
[AD-A256129] p 856 N93-15234
MAGELLAN PROJECT (NASA)
Surface processes on Venus p 1024 N93-14294
Image processing and products for the Magellan mission to Venus p 1026 N93-14306
Venus volcanism: A global overview from Magellan data p 1029 N93-14323
Magellan project p 1041 N93-14373
Venus: Geochemical conclusions from the Magellan data p 1044 N93-14394
MAGELLAN SPACECRAFT (NASA)
Anomalous scattering behavior of selected impact parabola features: Magellan cycle-to-cycle comparisons p 1039 N93-14363
Evidence for retrograde lithospheric subduction on Venus p 1040 N93-14367
Impact craters on Venus: An overview from Magellan observations p 1040 N93-14369
Magellan project p 1041 N93-14373
The geologic mapping of Venus using C-1 format: Sheets 75N254, 60N263 p 1041 N93-14375
Constraints on crustal rheology and age of deformation from models of gravitational spreading in Ishtar Terra, Venus p 1042 N93-14379
Multiresolution pattern recognition of small volcanos in Magellan data p 1042 N93-14380
The tectonics of Venus: An overview p 1042 N93-14382
Scattering properties of Venus' surface p 1044 N93-14391
MAGELLANIC CLOUDS
Wolf-Rayet stars in the Milky Way, the Large Magellanic Cloud, and emission-line galaxies p 1020 N93-14869
MAGMA
Igneous and tectonic evolution of Venusian and terrestrial coronae p 1031 N93-14330
Venus steep-sided domes: Relationships between geological associations and possible petrogenetic models p 1038 N93-14359
The effects of Venus' thermal structure on buoyant magma ascent p 1040 N93-14366
MAGNESIUM COMPOUNDS
Physics of hydrogen storage in metal-hydrides p 854 N93-14630
MAGNESIUM OXIDES
Analytical and experimental evaluation of joining ceramic oxides to ceramic oxides and ceramic oxides to metal for advanced heat engine applications
[DE92-041383] p 851 N93-15294
MAGNETIC BEARINGS
A feasibility assessment of magnetic bearings for free-piston Stirling space power converters
[NASA-CR-189135] p 891 N93-14916
MAGNETIC CONTROL
Reusable Reentry Satellite (RRS) system design study. Phase B, appendix E: Attitude control system study
[NASA-CR-188578] p 825 N93-15633
MAGNETIC DIPOLES
Level-mixing assisted tunability of nuclear resonance linewidths for gamma ray lasers
[AD-A255791] p 885 N93-14647
MAGNETIC DISKS
Magnetic disk p 1004 N93-15029
Diffraction analysis and evaluation of several focus- and track-error detection schemes for magneto-optical disk systems p 984 N93-15506
Improved astigmatic focus error detection method p 984 N93-15507
Instrumentation of the variable-angle magneto-optic ellipsometer and its application to M-O media and other non-magnetic films p 984 N93-15508
Proposal for massively parallel data storage system p 960 N93-15510
Combining ray-trace and diffraction analysis: A design example p 985 N93-15511
Transfer function characteristics of super resolving systems p 985 N93-15512
Modeling and measurement of a micro-optic beam deflector p 985 N93-15514
Effects of higher order aberrations on beam shape in an optical recording system p 985 N93-15515
Oxidation processes in magneto-optic and related materials p 985 N93-15516
Integrated device with diffractive polarization components for a magneto-optical disk head p 986 N93-15517
MAGNETIC EFFECTS
Gravitational instabilities in a protoplanetary disk p 1016 N93-14154
MAGNETIC EQUATOR
Global zones of particle precipitation as observed by EXOS-C
[AD-A256397] p 917 N93-15466
MAGNETIC FIELD CONFIGURATIONS
Resistive magnetohydrodynamic studies of tearing mode instability with equilibrium shear flow and magnetic reconnection p 987 N93-14122
The evolution of the VLBI polarization of superluminal radio source 3C345 p 1050 N93-14229
MAGNETIC FIELD RECONNECTION
Resistive magnetohydrodynamic studies of tearing mode instability with equilibrium shear flow and magnetic reconnection p 987 N93-14122
Venus internal magnetic field and its interaction with the interplanetary magnetic field p 1032 N93-14336
Solar flares: The onset of magnetic reconnection and the structure of radiative slow-mode shocks p 1048 N93-14859
MAGNETIC FIELDS
Turbulent magnetized plasmas from ionizing shock waves p 987 N93-14120
Analysis of rotation experiments in TFTR --- tokamak fusion test reactor p 987 N93-14129
Experimental observations of the plasma properties of a high-density, low-temperature accelerated arc p 988 N93-14138
An analysis of the SCEX 3 ionospheric electron beam injection experiment p 912 N93-14177
Compact free electron laser for medical applications
[AD-A256236] p 885 N93-14599
Neuromagnetic investigations of cortical regions underlying short-term memory
[AD-A255788] p 937 N93-14646
Thin-film permanent magnets for integrated electromagnetic components
[AD-A256175] p 972 N93-14679
Cognition and the brain
[AD-A255483] p 937 N93-14788
Measurements of electric and magnetic fields in the Waianae, Hawaii area
[DE92-019891] p 861 N93-15220
Research for electric energy systems
[DE92-040076] p 870 N93-15412
The detection and characterization of high frequency and high wavenumber solar oscillations
[NASA-CR-191622] p 1049 N93-15634
MAGNETIC FILMS
Characterization of magneto-optical recording media p 979 N93-14140
Measurement of the magnetic anisotropy energy constants for magneto-optical recording media p 984 N93-15509
MAGNETIC INDUCTION
Numerical modelling of intense electron beam transport in the spiral line induction accelerator
[AD-A255545] p 978 N93-14570
MAGNETIC MOMENTS
Far infrared, magnetic, and electronic studies of high T(sub c) superconducting materials
[AD-A257050] p 996 N93-15444
MAGNETIC PROPERTIES
An empirical approach to predicting long term behavior of metal particle based recording media p 883 N93-15043
MAGNETIC RECORDING
Characterization of magneto-optical recording media p 979 N93-14140
Magnetic disk p 1004 N93-15029
Stability of Co-gamma-Fe2O3 tape p 1006 N93-15041
An empirical approach to predicting long term behavior of metal particle based recording media p 883 N93-15043
MAGNETIC STORAGE
Tribology of magnetic storage systems p 1002 N93-14772
Stability of Co-gamma-Fe2O3 tape p 1006 N93-15041
MAGNETIC STORMS
Radiation belt dynamic and quasi-static modeling based on CRRES data: Outer-belt short-term response data base
[AD-A256483] p 916 N93-14899
The effects of magnetic storm phases on F-layer irregularities from auroral to equatorial latitudes
[AD-A256520] p 917 N93-15395
MAGNETIC SUSPENSION
Vibration isolation technology: An executive summary of systems development and demonstration
[NASA-TM-105937] p 778 N93-15573
MAGNETIC TAPES
The preservation of LANDSAT data by the National Land Remote Sensing Archive p 1003 N93-14777
Status of emerging standards for removable computer storage media and related contributions of NIST p 1003 N93-14778
Stability of Co-gamma-Fe2O3 tape p 1006 N93-15041
The 19 mm date recorders: Similarities and differences p 883 N93-15042
MAGNETIZATION
Thin-film permanent magnets for integrated electromagnetic components
[AD-A256175] p 972 N93-14679
Far infrared, magnetic, and electronic studies of high T(sub c) superconducting materials
[AD-A257050] p 996 N93-15444
MAGNETO-OPTICS
Characterization of magneto-optical recording media p 979 N93-14140
Optical instrumentation and characterization for magneto-optical recording media p 980 N93-14168
Research Studies on Advanced Optical Module/Head Designs for Optical Data Storage
[NASA-CR-191307] p 984 N93-15505
Diffraction analysis and evaluation of several focus- and track-error detection schemes for magneto-optical disk systems p 984 N93-15506
Instrumentation of the variable-angle magneto-optic ellipsometer and its application to M-O media and other non-magnetic films p 984 N93-15508
Measurement of the magnetic anisotropy energy constants for magneto-optical recording media p 984 N93-15509
Combining ray-trace and diffraction analysis: A design example p 985 N93-15511
Transfer function characteristics of super resolving systems p 985 N93-15512

Oxidation processes in magneto-optic and related materials p 985 N93-15516
Integrated device with diffractive polarization components for a magneto-optical disk head p 986 N93-15517

MAGNETOACOUSTICS
Method of characterizing residual stress in ferromagnetic materials using a pulse histogram of acoustic emission signals
[NASA-CASE-LAR-14239-1] p 845 N93-14705

MAGNETOHYDRODYNAMIC FLOW
Comparison between irregularity motion and bulk plasma drifts at high latitudes
[PL-TR-91-2292] p 914 N93-14727

MAGNETOHYDRODYNAMIC GENERATORS
Design and implementation of a DC-based magnetic field controller with electronic temperature stabilized Hall generator
[DE92-019796] p 870 N93-15276

MAGNETOHYDRODYNAMIC STABILITY
Exact analytical solution of the toroidal singular mode equations
[DE92-040223] p 988 N93-15419

MAGNETOHYDRODYNAMIC WAVES
Resonance absorption of MHD surface waves with applications to the solar atmosphere p 1048 N93-14157
Theoretical studies of the physics of the solar atmosphere
[NASA-CR-191357] p 1049 N93-15085

MAGNETOHYDRODYNAMICS
Resistive magnetohydrodynamic studies of tearing mode instability with equilibrium shear flow and magnetic reconnection p 987 N93-14122
Solar flares: The onset of magnetic reconnection and the structure of radiative slow-mode shocks p 1048 N93-14859
Experimental determination of magnetohydrodynamic seawater thruster performance in a two Tesla test facility
[DE92-019042] p 826 N93-15215

MAGNETOMETERS
Characterization of magneto-optical recording media p 979 N93-14140

MAGNETOPLASMADYNAMICS
Numerical study of cathode emission constraints on cylindrical self-field MPD thruster performance
[NASA-CR-190795] p 826 N93-15370

MAGNETORESISTIVITY
Characterization of magneto-optical recording media p 979 N93-14140

MAGNETOSHEATH
Energetic and magnetosheath energy particle signatures of the low-latitude boundary layer at low altitudes near noon
[NASA-CR-191388] p 917 N93-15574

MAGNETOSPHERE-IONOSPHERE COUPLING
A numerical model of ionospheric convection derived from field-alignment currents and the corresponding conductivity
[TRITA-EPP-91-03-REV] p 916 N93-15252

MAGNETRON SPUTTERING
Thermal analysis of magnetron sputtering designs
[DE93-000348] p 870 N93-15389

MAIN SEQUENCE STARS
Stability of differentially rotating stars p 1018 N93-14584

MAINTENANCE
Global optimum path planning for a redundant space robot
[AD-A255316] p 889 N93-14545
Proceedings of the USAF Structural Integrity Program
[AD-A255379] p 777 N93-14549
Method and devices for the in situ repair of damaged threads
[AD-D015416] p 891 N93-14881
Annotating the real world with knowledge-based graphics on a see-through head-mounted display p 954 N93-15543

MAINTENANCE TRAINING
F/FB-111 avionics test station and component specialist/technician. Automatic test stations manual and electronic warfare test stations. Training requirements analysis (451X6), volume 2
[AD-A252121] p 793 N93-14110

MALAYSIA
Spatial and temporal patterns of biotic exchanges of CO2 between the atmosphere and tropical landscapes and their role in the global carbon balance
[DE92-019170] p 911 N93-15272

MAN MACHINE SYSTEMS
The human-electronic crew: Is the team maturing? The 2nd Joint GAF/RAF/USAF Workshop on Human-Electronic Crew Teamwork
[AD-A256192] p 939 N93-14520
Symposium on the occasion of the farewell of Prof. Dr. Ir. O. H. Gerlach as Chairman of the Board of the Foundation National Aerospace Laboratory NLR, The Netherlands
[ETN-92-92168] p 777 N93-14613
A voyage to Mars: A challenge to collaboration between man and machines p 777 N93-14614
Compliant walker
[NASA-CASE-GSC-13348-2] p 934 N93-14708
Aerospace medicine and biology: A continuing bibliography with indexes (supplement 369)
[NASA-SP-7011(369)] p 935 N93-14731
A concept for a supervised autonomous robot p 810 N93-14950
A monitoring and control system for complex man-machine systems: Preliminary design p 810 N93-14951

MAN-COMPUTER INTERFACE
Mapping thoughts: Visual interfaces for information retrieval p 1000 N93-14208
Information resource utilisation: Accessibility based on concerns p 1001 N93-14216
A distributed visualization environment for engineering sciences
[DE92-012629] p 1051 N93-15060
A single-station forecasting model
[AD-A256403] p 924 N93-15331
Proceedings: Graphics Interface 1992
[ISBN-0-9695338-1-0] p 952 N93-15533
Hyper-rendering p 953 N93-15538
Program auralization: Sound enhancements to the programming environment p 953 N93-15539
A framework for describing and implementing software visualization systems p 953 N93-15540
Annotating the real world with knowledge-based graphics on a see-through head-mounted display p 954 N93-15543
Working together, virtually p 954 N93-15547
Telepresence: Integrating shared task and person spaces p 954 N93-15548
CSCW - WCSC: Computer-supported cooperative work. What changes for the science of computing p 954 N93-15549
Movement time prediction in human-computer interfaces p 955 N93-15550
ARCBALL: A user interface for specifying three-dimensional orientation using a mouse p 955 N93-15551
Designing video annotation and analysis systems p 955 N93-15552
A minimalist global user interface p 957 N93-15566
A multi-layer graphic model for building interactive graphical applications p 957 N93-15567
A linear constraint technology for interactive graphic systems p 957 N93-15568

MANAGEMENT INFORMATION SYSTEMS
Information for management, planning, and decision-making in nonprofit organizations: Toward a comprehensive model p 1000 N93-14209
Geographic Resources Analysis Support System (GRASS) version 4.0 user's reference manual
[AD-A255218] p 1001 N93-14524
Vendor Information System (VIS) systems manual
[AD-A256174] p 1002 N93-14650
Proceedings of the NSSDC Conference on Mass Storage Systems and Technologies for Space and Earth Science Applications
[NASA-TM-107989] p 1004 N93-15027
Recommendations for enhancement of the Design Criteria Information System (DCIS)
[AD-A256857] p 1009 N93-15641
GRASS 4.0 map digitizing user's manual: V. Digit
[AD-A256859] p 1009 N93-15642

MANAGEMENT METHODS
Telepresence: Integrating shared task and person spaces p 954 N93-15548

MANAGEMENT PLANNING
Software Technology for Adaptable, Reliable Systems (STARS) program. Software process tools and techniques evaluation report, version 1.0. Task IS15: Software process management
[AD-A255945] p 942 N93-14405
Data management and processing plan, Department of Applied Geodesy
[DE93-000774] p 905 N93-14522
TQM in a test environment p 823 N93-15620

MANAGEMENT SYSTEMS
Software Technology for Adaptable, Reliable Systems (STARS) program. Software process tools and techniques evaluation report, version 1.0. Task IS15: Software process management
[AD-A255945] p 942 N93-14405
Space Station Freedom data management system growth and evolution report
[NASA-TM-103869] p 816 N93-15477

MANDRELS
The stress development during filament winding of thick cylinders
[AD-A255765] p 901 N93-15066

MANEUVERS
Use of kinematic constraint in tracking constant speed maneuvering targets
[AD-A255988] p 858 N93-14415

MANGANIN (TRADEMARK)
A comparison of superconductor and manganin technology for electronic links used in space mission applications
[NASA-CR-4477] p 997 N93-15587

MANIFOLDS (MATHEMATICS)
The center for nonlinear phenomena and magnetic materials
[AD-A255983] p 967 N93-14412
Physically-based methods for polygonization of implicit surfaces p 956 N93-15562

MANIPULATORS
Decision-making for intelligent control of dual-arm robotic operations p 960 N93-14201
Manipulation strategies for redundant manipulators p 960 N93-14203
Utilizing sensed incipient slip signals for grasp force control
[AD-A255725] p 888 N93-14434
Optimum pose measurements for kinematic parameters identification
[AD-A256307] p 970 N93-14443
Force and position control of robot manipulators: Learning and repetitive control approach p 888 N93-14473
Model reduction of flexible manipulators
[AD-A255251] p 889 N93-14528
Global optimum path planning for a redundant space robot
[AD-A255316] p 889 N93-14545
Dynamics and control of a rigid/flexible manipulator p 890 N93-14684
Optimal and robust control of robot manipulators p 890 N93-14685
Position and vibration control of flexible space robots p 892 N93-15102
Theory and applications of hyper-redundant robotic manipulators p 892 N93-15104
Learning position and force control for mechanical manipulators p 963 N93-15147
Robust control design for uncertain nonlinear dynamic systems p 964 N93-15148
Dynamics and control of flexible arm robots
[ISBN-0-315-69011-9] p 892 N93-15150
Coordinated motion control of a two-hand assembly system
[F-2-8] p 949 N93-15301
Robot learning of contact tasks
[F-3-2] p 949 N93-15303
Planning of continuous path robotic motions by discrete time optimization
[F-3-5] p 950 N93-15305
Time-optimization of point-to-point robotic motions
[F-3-6] p 950 N93-15306
Redundancy control of robots by constrained optimization
[F-3-7] p 950 N93-15307
Adaptive control of a manipulator in cartesian space
[F-4-2] p 950 N93-15308

MANNED MARS MISSIONS
Symposium on the occasion of the farewell of Prof. Dr. Ir. O. H. Gerlach as Chairman of the Board of the Foundation National Aerospace Laboratory NLR, The Netherlands
[ETN-92-92168] p 777 N93-14613
A voyage to Mars: A challenge to collaboration between man and machines p 777 N93-14614
Mission and technology assessment of human exploration to the Moon and Mars p 809 N93-14944
Aspects of parking orbit selection in a manned Mars mission
[NASA-TP-3256] p 813 N93-15367
Combined high and low thrust propulsion for fast piloted Mars missions
[NASA-CR-190788] p 828 N93-15584

MANNED SPACECRAFT
Manned testing in a simulated space environment p 820 N93-15602

MANUALS
DROLS workbook
[AD-A255850] p 999 N93-14106
Ultrashort-pulse laser system: Theory of operation and operating procedures
[AD-A257023] p 887 N93-15472
User manual for NASA Lewis 10 by 10 foot supersonic wind tunnel
[NASA-TM-105626] p 804 N93-15498

Flight dynamics system software development environment (FDS/SDE) tutorial
[NASA-TM-108580] p 952 N93-15502

MANUFACTURING
Organization of workshop on emerging technologies for in-situ processing
[AD-A255977] p 865 N93-14410
SETA support for the DARPA microelectronics technology insertion program of the Microelectronics Technology Office
[AD-A255551] p 866 N93-14555
Core design for use with precision composite reflectors
[NASA-CASE-NPO-17858-1-CU] p 832 N93-14700
Flow behavior in liquid molding p 833 N93-14747
Advances in 3-dimensional braiding p 833 N93-14748
In-situ lunar oxygen extraction p 806 N93-14929
A fundamental understanding of the effects of ceramic processing on product microstructure
[AD-A255729] p 850 N93-15049
Acoustic resonance techniques for quality control
[DE92-040150] p 895 N93-15413
The use of a novel manufacturing process for high performance titanium plate fin heat exchangers
[PNR-90934] p 879 N93-15473
High performance titanium plate fin heat exchanger using a novel manufacturing process
[PNR-90933] p 880 N93-15488

MAPPING
GRASS 4.0 map digitizing user's manual: V. Digit
[AD-A256859] p 1009 N93-15642

MAPS
Terrain visualization for the portable all-source analysis work station
[AD-A255708] p 905 N93-14430
The regional land use of Paraiba Valley and the North Coast of Sao Paulo State, Brazil p 905 N93-14450
Geographical distribution and seasonal variation of surface emissions and deposition velocities of atmospheric trace gases
[AERONOMICA-ACTA-A-361-1991] p 911 N93-15460

MARINE BIOLOGY
Comparison of the prevalence index and average wetland values for identification of wetland vegetation
[DE92-016701] p 910 N93-15209

MARKET RESEARCH
Wisconsin Inventors' Network Database
[DE92-018394] p 1007 N93-15137

MARKETING
Wisconsin Inventors' Network Database
[DE92-018394] p 1007 N93-15137
Technology commercialization cost model and component case study
[DE92-001280] p 907 N93-15213
High temperature tubular solid oxide fuel cell development
[DE92-040253] p 908 N93-15322

MARKING
Software stamping
[NPL-DITC-198/92] p 946 N93-15072

MARKOV CHAINS
A proof of convergence of the Markov chain simulation method
[AD-A255456] p 970 N93-14487
Sensitivity and uncertainty analysis in performability modelling
[MEMO-INF-92-18] p 941 N93-15090
Approximate performability analysis using generalized stochastic Petri nets
[MEMO-INF-92-11] p 971 N93-15119

MARS ENVIRONMENT
Degradation of radiator performance on Mars due to dust p 823 N93-15616

MARS LANDING
Power requirements for the first lunar outpost (FLO)
[NASA-TM-105925] p 909 N93-15523

MARS SURFACE
Martian water frost: Control of global distribution by small-scale processes p 1047 N93-14868
Degradation of radiator performance on Mars due to dust p 823 N93-15616

MASS SPECTROMETERS
Methane measurement by the Pioneer Venus large probe neutral mass spectrometer p 1027 N93-14312
Laser-based studies with an ion-trap mass spectrometer: Ion tomography and analytical applications
[DE92-017529] p 887 N93-15135
Mass spectrometer use in a large chamber p 823 N93-15619

MASS SPECTROSCOPY
Methane measurement by the Pioneer Venus large probe neutral mass spectrometer p 1027 N93-14312
Development of laser-ion beam photodissociation methods
[DE92-040512] p 886 N93-15058
Laser-based studies with an ion-trap mass spectrometer: Ion tomography and analytical applications
[DE92-017529] p 887 N93-15135
Mass spectrometer use in a large chamber p 823 N93-15619

MASS TRANSFER
Transport phenomena and interfacial kinetics in multiphase combustion systems.
[AD-A255999] p 838 N93-14418
Study of mass and heat transport of the tropical Atlantic Ocean using models and altimeter data p 929 N93-14983
Application of TOPEX/Poseidon altimetry measurements to observational and modeling studies of the low-frequency upper ocean mass and heat circulation in the tropical Pacific p 930 N93-14989
Oceanic transports of mass, heat, and salt in the western North Pacific p 931 N93-14996

MASSIVE STARS
Nonthermal radio, x ray and gamma ray emissions from chaotic winds of early-type, massive stars p 1050 N93-14242
Wolf-Rayet stars in the Milky Way, the Large Magellanic Cloud, and emission-line galaxies p 1020 N93-14869

MASSIVELY PARALLEL PROCESSORS
Engineering of massively interconnected computer systems
[AD-A255501] p 958 N93-14645
A massively distributed parallel genetic algorithm
[AD-A256617] p 959 N93-15407
Analog Very Large Scale Integration (VLSI) implementations of artificial neural networks
[AD-A256621] p 966 N93-15408
Research Studies on Advanced Optical Module/Head Designs for Optical Data Storage
[NASA-CR-191307] p 984 N93-15505
Proposal for massively parallel data storage system p 960 N93-15510

MATCHED FILTERS
Sonar processing on CESAR
[FFI-92/7007] p 974 N93-15074
Comparison of synchronization techniques for the AFIT direct sequence spread spectrum system
[AD-A256440] p 861 N93-15316

MATERIALS RECOVERY
The evaluation of a concept for a Canadian-made automated multipurpose materials extraction facility p 810 N93-14947

MATERIALS TESTS
Fiber pulling apparatus modification
[NASA-CR-184498] p 891 N93-14763

MATHEMATICAL LOGIC
Compactness and Loewenheim-Skolem properties in pre-institution categories
[MEMO-INF-92-27] p 968 N93-15094

MATHEMATICAL MODELS
Diffusing wave spectroscopy p 980 N93-14169
A study of the low and mid-latitude upper ionospheres of Jupiter and Saturn p 1022 N93-14179
Evaluation of the cost effectiveness analysis model being developed for the component improvement programs of the Air Force and the Navy
[AD-A256132] p 1010 N93-14249
The detection and correlation modeling of Rayleigh distributed radar signals
[AD-A256612] p 858 N93-14250
The numerical stability of nonlinear floating body calculations p 873 N93-14278
Venusian hydrology: Steady state reconsidered p 1028 N93-14318
Variations in lithospheric thickness on Venus p 1030 N93-14329
Flexural models of trench/outer rise topography of coronae on Venus with axisymmetric spherical shell elastic plates p 1036 N93-14348
The gabbro-eclogite phase transition and the elevation of mountain belts on Venus p 1036 N93-14350
A model for the formation of the extended paraboloidal halos around some impact craters on Venus p 1037 N93-14352
Evaluation of three models used for predicting noise propagated long distances overground
[AD-A255963] p 973 N93-14406
Macroscopic properties of random and quasiperiodic media
[AD-A255984] p 990 N93-14413
A compilation of the mathematics leading to the doublet lattice method
[AD-A256304] p 779 N93-14441
Development of braided rope seals for hypersonic engine applications: Flow modeling
[NASA-TM-105942] p 888 N93-14478
On the structure of nonlinear constitutive equations for fiber reinforced composites
[NASA-CR-191024] p 830 N93-14484
Trace algebra for automatic verification of real-time concurrent systems
[AD-A256199] p 968 N93-14492
Delamination growth behavior in cross-ply laminated composites due to transverse concentrated loading
[AD-A255974] p 830 N93-14493
A general observation matrix for attitude error estimation with an offset GPS antenna
[AD-A255214] p 789 N93-14574
Systems modeling
[AD-A255215] p 944 N93-14575
Introduction to spray combustion modelling p 841 N93-14626
A finite element model for analysis of thermoviscoplastic behavior of hypersonic leading edge structures subject to intense aerothermal heating p 780 N93-14631
An investigation of genuinely multidimensional schemes for the Euler equations p 876 N93-14694
Modeling of Euclidean braided fiber architectures to optimize composite properties p 834 N93-14755
Improved inhomogeneous finite elements for fabric reinforced composite mechanics analysis p 834 N93-14757
Recursively generated networks and dynamical learning
[AD-A255441] p 963 N93-14783
Finite-state inflow applied to aeroelastic flutter of fixed and rotating wings p 802 N93-14830
Modeling variable blowing on a slender cone in hypersonic flow p 781 N93-14836
Numerical modeling of a vortex stabilized arcjet
[NASA-CR-190797] p 826 N93-14883
A new device to aid in the conception and optimization of monolithic millimeter circuits: A distributed and nonliner model of a field effect transistor p 807 N93-14932
Simulation and nonlinear modelling of microwave transistors p 807 N93-14936
Advances in TMG p 811 N93-14956
Advanced development active model: A users guide
[AD-A255614] p 974 N93-15012
The influence of baroclinic processes on tropical cyclone motion p 923 N93-15099
Fitting microphysical observations to a numerical model through an optimal control theory technique p 924 N93-15100
Evaluation of methods for estimating wind wave growth on narrow irregular fetches
[AD-A256002] p 932 N93-15113
Development of advanced seal verification
[NASA-CR-184502] p 892 N93-15117
Asymmetric natural damped frequencies of a rotating infinitely long viscous liquid column
[LRT-WE-9-FB-23-1991] p 878 N93-15120
Aeroplane crashes on the runway: Validation and final evaluation of the method of modeling an airframe structure
[IMFL-91-32] p 792 N93-15126
Addressing earthquake strong ground motion issues at the Idaho National Engineering Laboratory
[DE92-017841] p 916 N93-15136
Reliability modelling for non-electronic systems
[REPT-921-440-103] p 894 N93-15139
Abstracts booklet
[AD-A256115] p 869 N93-15188
Study of the mathematical modelling and computer simulation of crystal growth from liquid phase under microgravity conditions
[CTN-93-60619] p 855 N93-15201
Technology commercialization cost model and component case study
[DE92-001280] p 907 N93-15213
VHDL (VHSIC hardware description language) in the test environment
[VH-6] p 948 N93-15267
Alpha migration through air filters: A numerical simulation
[UCRL-LR-109866] p 878 N93-15285
Plasma confinement theory and transport simulation
[DE92-040523] p 988 N93-15327
The use of ultrasonics for oleo compression measurements on a S-70B-2 (Seahawk) helicopter
[AD-A256315] p 792 N93-15328
Numerical modeling of anti-icing systems and comparison to test results on a NASA 0012 airfoil
[NASA-TM-105975] p 787 N93-15345
The sine-Gordon model and the small (kappa)(sup +) region of light-cone perturbation theory
[DE92-040506] p 969 N93-15379
A method of representating dimensions and tolerances in solid based freeform surfaces
[PNR-90998] p 951 N93-15386
A queue model relating synchronous and asynchronous communication
[MEMO-INF-92-04] p 966 N93-15491

Ice accretion prediction for a typical commercial transport aircraft
[NASA-TM-105976] p 788 N93-15522
Non-uniform patch luminance for global illumination p 957 N93-15569
The use of plasma ashers and Monte Carlo modeling for the projection of atomic oxygen durability of protected polymers in low Earth orbit p 819 N93-15596
Hypervelocity impact simulations of Whipple shields p 821 N93-15604
Numerical modeling tools for chemical vapor deposition
[NASA-CR-4480] p 880 N93-15643

MATHEMATICAL PROGRAMMING
Compactness and Loewenheim-Skolem properties in pre-institution categories
[MEMO-INF-92-27] p 968 N93-15094

MATHEMATICS
Purposive discovery of operations
[NASA-TM-108116] p 963 N93-14765
Core support of the board on mathematical sciences
[AD-A255482] p 968 N93-14787
Core support for the Board on Mathematical Sciences
[AD-A256333] p 968 N93-15195

MATRICES (CIRCUITS)
High speed magneto-resistive random access memory
[NASA-CASE-NPO-17954-1-CU] p 940 N93-14704

MATRICES (MATHEMATICS)
Application of partition matrix methods to solve large eigenproblems in structural dynamics p 896 N93-14188
Analysis of projections of the transfer matrix in 2D Ising models
[AD-A256583] p 967 N93-14271
Implementing the multiprefix operation on parallel and vector computers
[AD-A256367] p 959 N93-15207
The covariance matrix of derived quantities and their combination
[DE92-019066] p 969 N93-15212
Matrix animation and polar decomposition p 956 N93-15563

MATRIX MATERIALS
Low toxicity high temperature PMR polyimide
[NASA-CASE-LAR-14639-1] p 849 N93-14709
An evaluation of composites fabricated from powder epoxy towpreg p 832 N93-14745
Structural study of thermohardening matrices: Deformation of composite matrices in relation to their molecular structure
[ONERA-RT-12/3521-M] p 836 N93-15253
Material development in the Si3N4 system using glass encapsulated HIP'ing
[DE92-041381] p 837 N93-15388
Development of ceramic matrix composites for application in the ceramic technology for advanced heat engines project. Phase 2A: Development of in-situ toughened silicon nitride
[DE92-041371] p 853 N93-15452

MATRIX METHODS
Application of partition matrix methods to solve large eigenproblems in structural dynamics p 896 N93-14188

MAXIMUM ENTROPY METHOD
Spatially resolved 10 micron spectra of circumstellar material around evolved stars p 1019 N93-14636

MEAN SQUARE VALUES
Hierarchical Poisson disk sampling distributions p 954 N93-15545

MEASURE AND INTEGRATION
The dynamics of spatially extended lasers p 883 N93-14123

MEASURING INSTRUMENTS
Variable path length spectrophotometric probe
[DE92-019834] p 881 N93-14716
Sensor fault detection using nonlinear observer and polynomial classifier p 797 N93-15182
Transcutaneous Analyte Measuring Methods (TAMM), phase 2
[AD-A256327] p 936 N93-15192

MECHANICAL DEVICES
Cable-line shortening device
[AD-D015427] p 891 N93-14822

MECHANICAL DRIVES
Retractable tool bit having slider type catch mechanism
[NASA-CASE-GSC-13358-1] p 890 N93-14710
Variable speed rotary compressor and adjustable speed drive efficiencies measured in the laboratory
[DE92-040026] p 893 N93-15278
The trajectory analysis of bevel planetary gear trains
[DE92-040898] p 893 N93-15380

MECHANICAL ENGINEERING
Design features of a seven-cell high-gradient superconducting cavity
[DE92-040229] p 870 N93-15424

MECHANICAL MEASUREMENT
Apparatus for checking threaded hole perpendicularity
[NASA-CASE-LEW-15444-1] p 882 N93-14840

MECHANICAL PROPERTIES
Oriented electro/optical polymers through in-situ chemistry during gel processing: A research opportunity
[AD-A255968] p 848 N93-14401
The preliminary Long Duration Exposure Facility (LDEF) materials data base
[NASA-TM-107692] p 828 N93-14459
Proceedings of the USAF Structural Integrity Program
[AD-A255379] p 777 N93-14549
Industrial applications of multiaxial warp knit composites p 833 N93-14750
Properties of textile grade ceramic fibers p 833 N93-14751
Mechanical response of composite materials with through-the-thickness reinforcement p 834 N93-14753
Tensile properties of textile composites p 834 N93-14754
Development of ceramic matrix composites for application in ceramic technology for advanced heat engines project, phase 2
[DE92-041379] p 836 N93-15387
Morphological analysis of ionomers
[DE92-040162] p 852 N93-15415
Dual role of nickel in sodium/nickel chloride batteries
[DE92-041102] p 870 N93-15441

MEDICAL EQUIPMENT
Test and evaluation report of the Physio Control Defibrillator/Monitor, Model LifePak(tm) 6s
[AD-A255691] p 933 N93-14103
Test and evaluation report of the Catalyst Research Oxygen Monitor, Model Miniox 3
[AD-A255849] p 881 N93-14105
Compact free electron laser for medical applications
[AD-A256236] p 885 N93-14599
Improved head support stand adjustable by compoundturnbuckle
[AD-D015384] p 936 N93-15249

MEDICAL SCIENCE
Walter Reed Army Institute of Research biannual report
[AD-A255630] p 933 N93-14162
Transcutaneous Analyte Measuring Methods (TAMM), phase 2
[AD-A256327] p 936 N93-15192

MEDICAL SERVICES
Walter Reed Army Institute of Research biannual report
[AD-A255630] p 933 N93-14162

MEDITERRANEAN SEA
The western Mediterranean Sea: An area for a regional validation for TOPEX/Poseidon and a field for geophysical and oceanographic studies p 926 N93-14965

MELTING
Melting and differentiation in Venus with a cold start: A mechanism of the thin crust formation p 1042 N93-14381
Volcanism by melt-driven Rayleigh-Taylor instabilities and possible consequences of melting for admittance ratios on Venus p 1043 N93-14387

MELTS (CRYSTAL GROWTH)
An experimental approach to determine the heat transfer coefficient in directional solidification furnaces p 995 N93-15311

MEMBRANE STRUCTURES
Apparatus and process for desalination of seawater
[AD-D015428] p 842 N93-14824

MEMBRANES
The crack problem for an orthotropic half plane stiffened by elastic films
[AD-A256471] p 903 N93-15374

MEMORY
Knowledge and processes in design
[AD-A255663] p 999 N93-14130
Long term memory for different types of classroom knowledge
[AD-A255235] p 999 N93-14526
Neuromagnetic investigations of cortical regions underlying short-term memory
[AD-A255788] p 937 N93-14646

MEMORY (COMPUTERS)
Long term stability in thin film ferroelectric memories
[AD-A256290] p 991 N93-14439
A specification of the Soar cognitive architecture in Z
[AD-A256198] p 940 N93-14491
NSSDC Conference on Mass Storage Systems and Technologies for Space and Earth Science Applications, volume 3
[NASA-CP-3165-VOL-3] p 1002 N93-14771
Network issues for large mass storage requirements p 1002 N93-14773
Enterprise storage report for the 1990's p 1004 N93-15028
The 3D Navier-Stokes flow analysis for shared and distributed memory MIMD computers
[AD-A256038] p 878 N93-15187
Radar data processing using a distributed computational system
[AD-A256209] p 861 N93-15237
Transactional distributed shared memory
[AD-A256222] p 941 N93-15240
Dynamics of analog electronic neural networks
[AD-A257019] p 966 N93-15352
Implementation and analysis of NP-complete algorithms on a distributed memory computer
[AD-A256564] p 951 N93-15405
Parallel simulation today
[NASA-CR-189733] p 951 N93-15432

MENTAL PERFORMANCE
A psychometrically sound cognitive diagnostic model: Effect of remediation as empirical validity
[AD-A255926] p 933 N93-14109
Sleep inertia: Is there a worst time to wake up?
[AD-A256602] p 934 N93-14240
Long term memory for different types of classroom knowledge
[AD-A255235] p 999 N93-14526
Shared mental models and crew decision making p 787 N93-15023

MESOSCALE PHENOMENA
Super-micro computer weather prediction model
[AD-A255668] p 918 N93-14153
Simulations of the Amazon Basin circulation using the Pennsylvania State University/National Center for Atmospheric Research mesoscale model p 919 N93-14197
Four-dimensional data assimilation of GALE data using a multivariate analysis scheme and a mesoscale model with diabatic initialization p 919 N93-14198
Four-dimensional data assimilation of gale data using a multivariate analysis scheme and a mesoscale model with diabatic initialization
[AD-A256063] p 921 N93-14680
Mesoscale and large-scale variability of the Antarctic circumpolar current p 926 N93-14970
Ocean dynamics in the Nordic Seas using satellite altimetry p 930 N93-14988
Equatorial and eastern boundary current variability in the North and South Pacific Oceans p 931 N93-14994
Sierra Nevada winter storms: A study using microwave radiometry, ice crystal, and isotopic analysis technique p 923 N93-15088
Development and application of a time-space conversion technique for analysis of weather systems passing over the Kennedy Space Center
[NASA-CR-4474] p 924 N93-15581

MESOSPHERE
A numerical study of the middle atmosphere response to tropical and subtropical tropospheric heat sources p 920 N93-14640

MESSAGE PROCESSING
Formal verification of an oral messages algorithm for interactive consistency
[NASA-CR-189704] p 958 N93-14808
Progammable connection parallel architecture: Design and routing
[ETN-92-92676] p 958 N93-15124
Nonblocking and orphan free message logging protocols
[NASA-CR-191631] p 862 N93-15339
A distributed data-balanced dictionary based on the b-link tree
[AD-A256841] p 1009 N93-15639

MESSAGES
The intelligibility of words, sentences, and continuous discourse using the articulation index
[AD-A256781] p 863 N93-15624

METAL BONDING
Diffusion problems in bonded nonhomogeneous materials with an interface cut
[AD-A256470] p 836 N93-15373

METAL COATINGS
Preliminary investigations of metal liquid-like films and coatings derived from them
[AD-A255477] p 849 N93-14489
Multifilamentary superconducting cable and a method of manufacturing it
[AD-D015391] p 846 N93-15231

METAL FATIGUE
Fatigue in single crystal nickel superalloys
[AD-A256095] p 844 N93-14264

METAL FILMS
Preliminary investigations of metal liquid-like films and coatings derived from them
[AD-A255477] p 849 N93-14489
Method of forming a multiple layer dielectric and a hot film sensor therewith
[NASA-CASE-LAR-13678-3] p 881 N93-14714

A study for the development of practices to protectively coat and join fibre epoxy composites for use in the Space Station Programme
[CTN-93-60626] p 835 N93-15145

METAL HYDRIDES
Physics of hydrogen storage in metal-hydrides
p 854 N93-14630

METAL MATRIX COMPOSITES
Nondestructive evaluation of damage in SiC/Al metal matrix composite using x ray tomographic microscopy
p 829 N93-14192
On the structure of nonlinear constitutive equations for fiber reinforced composites
[NASA-CR-191024] p 830 N93-14484
Thermal fatigue analysis of metal matrix composite with spherical reinforcements
[AD-A255313] p 831 N93-14672
Evaluation of corrosion protection methods for aluminum metal matrix composites
[AD-A255375] p 832 N93-14675
High temperature stability, interface bonding, and mechanical behavior in (beta)-NiAl and Ni3Al matrix composites with reinforcements modified by ion beam enhanced deposition
[DE92-014399] p 992 N93-14812
Analysis of OSPREY processes and conventional power aluminum alloys
[AD-A255764] p 846 N93-15056
Effect of thermomechanical treatments on the aging response of centrifugally cast silicon carbide/aluminum composites
[AD-A256204] p 836 N93-15236
Superstrength metal composite material and process for making the same
[AD-D015379] p 836 N93-15246
The mixed mode crack problem in a nonhomogeneous elastic plane
[AD-A256469] p 902 N93-15372
Inelastic deformation of metal matrix composites: Plasticity and damage mechanisms, part 2
[NASA-CR-189096-PT-2] p 837 N93-15401
Nonlinear finite element analysis of metals and metal matrix composites: A local-global investigation
[AD-A256782] p 838 N93-15625

METAL OXIDE SEMICONDUCTORS
The properties of thermally passivated Si(1-x) He(x) produced using high pressure techniques (and related augmentation awards)
[AD-A255961] p 991 N93-14429
Gate-all-around device
[AD-A255287] p 866 N93-14534
Energy distribution of trapped holes in irradiated SiO2
[DE92-040979] p 997 N93-15649

METAL OXIDES
Theory of the electronic and structural properties of solid state oxides
[DE92-040499] p 993 N93-14909
Epitaxial heterojunctions of oxide semiconductors and metals on high temperature superconductors
[NASA-CASE-NPO-18483-1-CU] p 994 N93-15151
Oxidation processes in magneto-optic and related materials p 985 N93-15516

METAL PARTICLES
Corrosion of metal particle and metal evaporated tapes p 883 N93-15039
A system approach to archival storage
p 1006 N93-15040
An empirical approach to predicting long term behavior of metal particle based recording media
p 883 N93-15043

METAL PLATES
The use of a novel manufacturing process for high performance titanium plate fin heat exchangers
[PNR-90934] p 879 N93-15473

METAL POWDER
Deformation characterization of powdered metals in compaction and application of the finite element method to compaction processes p 844 N93-14472
Analysis of OSPREY processes and conventional power aluminum alloys
[AD-A255764] p 846 N93-15056

METAL SHEETS
Processing and microstructure of Nb-1 percent Zr-0.1 percent C alloy sheet
[NASA-TM-105921] p 847 N93-15524

METAL STRIPS
Method and devices for the in situ repair of damaged threads
[AD-D015416] p 891 N93-14881

METAL SURFACES
Excimer laser irradiation of metal surfaces
p 884 N93-14175
Surface preparation of stainless steel prior to painting
[AD-A256253] p 838 N93-14454
Physics of hydrogen storage in metal-hydrides
p 854 N93-14630
Mach 5 electroformed nickel nozzle refurbishment FNAS investigation of ultra-smooth surfaces
[NASA-CR-191416] p 826 N93-14681
Method of bonding molybdenum to steel
[AD-D015410] p 845 N93-14888
The influence of steel surface chemistry on the bonding of lubricant films
[AD-A256231] p 851 N93-15242

METAL WORKING
Large plastic deformations by sequential limit analysis: A finite element approach with applications in metal forming p 899 N93-14471

METAL-METAL BONDING
Method of bonding molybdenum to steel
[AD-D015410] p 845 N93-14888

METALLIC HYDROGEN
Experimental attempt to metallize hydrogen at very high pressures
[AD-A257086] p 843 N93-15497

METALLIC PLASMAS
Electrical resistivity and equation of state measurements of a dense aluminum plasma
[DE92-040352] p 989 N93-15436

METALLIZING
Experimental attempt to metallize hydrogen at very high pressures
[AD-A257086] p 843 N93-15497

METALS
Nonlinear finite element analysis of metals and metal matrix composites: A local-global investigation
[AD-A256782] p 838 N93-15625

METASTABLE STATE
A study of mid-latitude 5577A CI dayglow emissions
[AD-A255444] p 914 N93-14511

METEORITE CRATERS
Impact craters on Venus: An overview from Magellan observations p 1040 N93-14369
Effect of impact angle on central-peak/peak-ring formation and crater collapse on Venus
p 1041 N93-14371
Impact-generated winds on Venus: Causes and effects p 1041 N93-14372
Microwave scattering and emission properties of large impact craters on the surface of Venus
p 1043 N93-14384
Can a time-stratigraphic classification system be developed for Venus? p 1043 N93-14388
Low-emissivity impact craters on Venus
p 1044 N93-14392
Floor-fractured crater models for igneous crater modification on Venus p 1044 N93-14393

METEOROLOGICAL CHARTS
Technology reconciliation in the remote sensing era of US civilian weather forcasting: 1957 - 1987
p 918 N93-14114

METEOROLOGICAL INSTRUMENTS
Optimization of a Counterflow Virtual Impactor (CVI) for studying aerosol effects on cloud droplet number
p 914 N93-14861

METEOROLOGICAL PARAMETERS
Synoptic scale structure of summertime wet and dry spells in northeastern Kansas p 923 N93-14919
Modern methods in meteorological and oceanographic data analysis
[AD-A257080] p 903 N93-15496

METEOROLOGICAL RADAR
Terminal Doppler weather radar/low-level wind shear alert system integration algorithm specification, version 1.1
[AD-A255319] p 920 N93-14547
An observational and theoretical study of squall line evolution p 921 N93-14682
NASA/LMSC coherent LIDAR airborne shear sensor: System capabilities and flight test plans
p 784 N93-14847
Solid-state coherent laser radar wind shear measuring systems p 784 N93-14848
The Orlando TDWR testbed and airborne wind shear date comparison results p 784 N93-14851
TDWR 1991 Program Review p 785 N93-14852
Systems issues in airborne Doppler radar/LIDAR certification p 785 N93-14855

METHANE
Methane measurement by the Pioneer Venus large probe neutral mass spectrometer p 1027 N93-14312
Viscosity of liquids. Halogenated methanes
[ESDU-92028] p 839 N93-14539
A correlated k-distribution model of the atmospheric heating rates for overlapping spectra of CH4 and N2O
[DE93-000890] p 911 N93-15281
Geographical distribution and seasonal variation of surface emissions and deposition velocities of atmospheric trace gases
[AERONOMICA-ACTA-A-361-1991] p 911 N93-15460
Modelling global methane emissions from livestock: Biological and nutritional controls
[NASA-CR-191354] p 911 N93-15480

METHYL COMPOUNDS
Softening of rigid polyvinyl chloride by high concentrations of aqueous solutions of methylene chloride
[AD-A255453] p 848 N93-14486
Lithium rechargeable cell with a poly 3-methylthiophene cathode
[AD-A255436] p 866 N93-14552
Experimental and theoretical investigation of surface chemistry induced by direct and indirect electronic excitation
[AD-A256342] p 843 N93-15200

METHYL POLYSILOXANES
The role of entanglements in the swelling of poly(dimethylsiloxane) networks
[AD-A255359] p 849 N93-14561

METROLOGY
Physics of x ray multilayer structures: Summaries of papers presented at the physics of x ray multilayer structures topical meeting, technical digest series, 1992, volume 7
[AD-A255383] p 992 N93-14741

MICROBALANCES
Effects of cryocontaminants on cryogenic superpolished mirror and superpolished quartz crystal microbalance
[AD-A255972] p 981 N93-14403

MICROBURSTS (METEOROLOGY)
Development of the Advance Warning Airborne System(AWAS) p 784 N93-14849
A millimeter-wave radiometer for detecting microbursts
p 784 N93-14850
The Orlando TDWR testbed and airborne wind shear date comparison results p 784 N93-14851
Experimental evaluation of candidate graphical microburst alert displays p 785 N93-14853

MICROCOMPUTERS
Super-micro computer weather prediction model
[AD-A255668] p 918 N93-14153
The effect of a hierarchical task-specific external conceptual model on the learnability and usability of microcomputer applications by novices
p 1000 N93-14205
A methodology for the evaluation of structural design software for DOS-based microcomputers
[AD-A255421] p 943 N93-14505
Recommendations for enhancement of the Design Criteria Information System (DCIS)
[AD-A256857] p 1009 N93-15641

MICROCRACKS
The influence of geometrical constraint on cyclic, elastoplastic, notch root behavior, and fatigue microcrack initiation p 900 N93-14480
Mechanisms of forming intergranular microcracks and microscopic surface discontinuities in welds
[AD-A255371] p 845 N93-14740

MICROELECTRONICS
Electronics reliability fracture mechanics. Volume 1: Causes of failures of shop replaceable units and hybrid microcircuits
[AD-A255836] p 894 N93-14104
Advanced laser chemical processing for microelectronics and integrated optics
[AD-A255980] p 865 N93-14425
Electronics reliability fracture mechanics. Volume 2: Fracture mechanics
[AD-A256200] p 900 N93-14498
SETA support for the DARPA microelectronics technology insertion program of the Microelectronics Technology Office
[AD-A255551] p 866 N93-14555
Solid state research
[AD-A256019] p 992 N93-14576
A theoretical search for supervelocity semiconductors
[AD-A256325] p 994 N93-15191

MICROGRAVITY APPLICATIONS
Study of Fluid Experiment System (FES)/CAST/Holographic Ground System (HGS)
[NASA-CR-184483] p 855 N93-14793

MICROMETEOROIDS
Characterisation and dynamic modelling of the near-earth space particulate environment
p 1019 N93-14637

MICROORGANISMS
Anaerobic microbial transformation of aromatic hydrocarbons and mixtures of aromatic hydrocarbons and halogenated solvents
[AD-A255696] p 932 N93-14557

MICROPHONES
Acoustic mode measurements in the inlet of a model turbofan using a continuously rotating rake: Data collection/analysis techniques
[NASA-TM-105936] p 801 N93-15403

MICROPROCESSORS
Processor controlpath microarchitecture synthesis based on the A(asterisk) algorithm
[MEMO-INF-92-10] p 963 N93-15083
MICROSCOPY
A differential equation design method for finite-conjugate, multi-mirror imaging systems p 979 N93-14165
Nondestructive evaluation of damage in SiC/Al metal matrix composite using x ray tomographic microscopy p 829 N93-14192
Physics of x ray multilayer structures: Summaries of papers presented at the physics of x ray multilayer structures topical meeting, technical digest series, 1992, volume 7
[AD-A255383] p 992 N93-14741
MICROSTRIP ANTENNAS
Efficient asymptotic closed form approximation for dyadic green's function for anisotropic substrates, phase 1
[AD-A256258] p 830 N93-14436
Optical signal distribution schemes for millimeter phased array radar
[AD-A256262] p 858 N93-14437
MICROSTRIP TRANSMISSION LINES
Processing, fabrication, and demonstration of HTS integrated microwave circuits
[AD-A256109] p 865 N93-14246
MICROSTRUCTURE
Applications of a constitutive equation for microstructural change in polymers p 848 N93-14222
Electron-phonon interaction, transport and ultrafast processes in semiconductor microstructures
[AD-A255723] p 976 N93-14433
Mechanisms of forming intergranular microcracks and microscopic surface discontinuities in welds
[AD-A255371] p 845 N93-14740
Microstructure-failure mode correlations in braided composites p 834 N93-14756
In-service considerations affecting component life p 800 N93-14898
Hyperfine experimental investigation of zirconia ceramics
[DE92-040301] p 850 N93-14903
Theory of the electronic and structural properties of solid state oxides
[DE92-040499] p 993 N93-14909
A fundamental understanding of the effects of ceramic processing on product microstructure
[AD-A255729] p 850 N93-15049
Analysis of OSPREY processes and conventional power aluminum alloys
[AD-A255764] p 846 N93-15056
A theoretical search for supervelocity semiconductors
[AD-A256325] p 994 N93-15191
Modelling Directional Solidification
[NASA-CR-191301] p 995 N93-15309
Solidification of InSb-GaSb alloy and InSb with vibration p 995 N93-15310
An investigation of the processing, high temperature deformation and fracture characteristics of superplastic ceramics
[AD-A256519] p 852 N93-15394
Inelastic deformation of metal matrix composites: Plasticity and damage mechanisms, part 2
[NASA-CR-189096-PT-2] p 837 N93-15401
Processing and microstructure of Nb-1 percent Zr-0.1 percent C alloy sheet
[NASA-TM-105921] p 847 N93-15524
MICROWAVE ABSORPTION
Laboratory evaluation and application of microwave absorption properties under simulated conditions for planetary atmospheres
[NASA-CR-191298] p 1047 N93-15081
MICROWAVE ANTENNAS
Investigation of antenna pattern constraints for passive geosynchronous microwave imaging radiometers
[NASA-CR-189728] p 905 N93-14792
MICROWAVE CIRCUITS
Processing, fabrication, and demonstration of HTS integrated microwave circuits
[AD-A256109] p 865 N93-14246
Simulation and nonlinear modelling of microwave transistors p 807 N93-14936
MICROWAVE EMISSION
Microwave scattering and emission properties of large impact craters on the surface of Venus p 1043 N93-14384
Study and interpretation of the millimeter-wave spectrum of Venus p 1045 N93-14596
MICROWAVE EQUIPMENT
Transport in heterostructures and device in microwave and millimeter wave regimes
[AD-A255975] p 858 N93-14408
Definition study PHARUS
[AD-A256560] p 860 N93-14805
MICROWAVE FILTERS
Processing, fabrication, and demonstration of HTS integrated microwave circuits
[AD-A256109] p 865 N93-14246
MICROWAVE FREQUENCIES
Direct optical to microwave conversion
[RL-TR-91-375] p 859 N93-14728
Microwave observations of Uranus p 1046 N93-14863
Selected area epitaxial growth for complementary HBT applications
[AD-A257047] p 995 N93-15365
MICROWAVE IMAGERY
Investigation of antenna pattern constraints for passive geosynchronous microwave imaging radiometers
[NASA-CR-189728] p 905 N93-14792
MICROWAVE INTERFEROMETERS
Interferometric observations of the J(0,1) CO line on Venus: Upper mesospheric winds and CO abundance p 1047 N93-14918
MICROWAVE RADIOMETERS
Investigation of antenna pattern constraints for passive geosynchronous microwave imaging radiometers
[NASA-CR-189728] p 905 N93-14792
A millimeter-wave radiometer for detecting microbursts p 784 N93-14850
MICROWAVE SCATTERING
Microwave scattering and emission properties of large impact craters on the surface of Venus p 1043 N93-14384
MICROWAVE TUBES
Determining optimum C-field settings that minimize output frequency variations in cesium atomic frequency standards
[AD-A255902] p 971 N93-14108
MICROWAVES
A search for anisotropy in the cosmic background radiation at millimeter wavelengths on angular scales from 0.3 to 3 degrees p 1050 N93-14244
Mechanisms of microwave induced damage in biologic materials
[AD-A255799] p 933 N93-14648
Microwave processing of tantalum capacitor anodes
[DE92-017829] p 869 N93-15214
MIDDLE ATMOSPHERE
Results of a zonally truncated three-dimensional model of the Venus middle atmosphere p 1037 N93-14351
Middle atmosphere of Venus and its clouds: Latitude and solar time variations p 1045 N93-14396
SO2 in the middle atmosphere of Venus: IR measurements from Venera 15 and comparison to UV p 1045 N93-14397
Sulfur oxides in the middle atmosphere of Venus: Observations by the International Ultraviolet Explorer and sounding rockets p 1046 N93-14635
A numerical study of the middle atmosphere response to tropical and subtropical tropospheric heat sources p 920 N93-14640
MIGRATION
Sea level response to wind forcing in the tropical Atlantic p 928 N93-14977
Independent validation testing of the FLAME computer code, version 1.0
[DE92-019691] p 948 N93-15274
MILITARY AIRCRAFT
MIL-STD-1760 application guidelines
[AD-A255714] p 790 N93-14432
Unmanned aerial vehicles: More testing needed before production of short-range system
[AD-A256296] p 790 N93-14440
Waterborne polyurethane binder resins for compliant aircraft coatings
[AD-A256246] p 849 N93-14573
MILITARY HELICOPTERS
Unmanned aerial vehicles: More testing needed before production of short-range system
[AD-A256296] p 790 N93-14440
MILITARY OPERATIONS
Walter Reed Army Institute of Research biannual report
[AD-A255630] p 933 N93-14162
Testing and analysis of modified HMMWV front lift provisions
[MTL-TR-92-31] p 891 N93-14735
Military space operations: Satellite control system improved, but serious problems remain
[AD-A256809] p 971 N93-15626
MILITARY SPACECRAFT
Military space operations: Satellite control system improved, but serious problems remain
[AD-A256809] p 971 N93-15626
MILITARY TECHNOLOGY
Air Force Office of Scientific Research
[AD-A255331] p 1051 N93-14523
The evolution of artificial intelligence and expert computer systems in the Army
[AD-A255221] p 962 N93-14525
Development of an integrated package of physics models for scene simulation studies to support smart weapons design studies
[LTR92-004] p 945 N93-14696
A preliminary design of the Ti:LiNbO3 optical channel waveguide
[AD-A255443] p 982 N93-14784
MILKY WAY GALAXY
Wolf-Rayet stars in the Milky Way, the Large Magellanic Cloud, and emission-line galaxies p 1020 N93-14869
MILLIMETER WAVES
A search for anisotropy in the cosmic background radiation at millimeter wavelengths on angular scales from 0.3 to 3 degrees p 1050 N93-14244
Understanding the variation in the millimeter-wave emission of Venus p 1028 N93-14315
Transport in heterostructures and device in microwave and millimeter wave regimes
[AD-A255975] p 858 N93-14408
Optical signal distribution schemes for millimeter phased array radar
[AD-A256262] p 858 N93-14437
Study and interpretation of the millimeter-wave spectrum of Venus p 1045 N93-14596
High power millimetre-wave polarizers
[AD-A256558] p 867 N93-14803
A millimeter-wave radiometer for detecting microbursts p 784 N93-14850
High performance YBCO films
[AD-A255439] p 994 N93-15297
MIMD (COMPUTERS)
The 3D Navier-Stokes flow analysis for shared and distributed memory MIMD computers
[AD-A256038] p 878 N93-15187
Aspects of a parallel-architecture simulator
[AD-A256872] p 941 N93-15628
MIMO (CONTROL SYSTEMS)
Adaptive control of nonlinear nonminimum phase systems p 961 N93-14470
Development of an analog MIMO Quantitative Feedback Theory (QFT) CAD package
[AD-A256435] p 950 N93-15313
MINERAL DEPOSITS
Mixed-valence iron minerals on Venus: Fe(2+)-Fe(3+) oxides and oxy-silicates formed by surface-atmosphere interactions p 1025 N93-14301
MINERALOGY
Venus: Geochemical conclusions from the Magellan data p 1044 N93-14394
MINERALS
Mixed-valence iron minerals on Venus: Fe(2+)-Fe(3+) oxides and oxy-silicates formed by surface-atmosphere interactions p 1025 N93-14301
Radar-anomalous, high-altitude features on Venus p 1036 N93-14349
The evaluation of a concept for a Canadian-made automated multipurpose materials extraction facility p 810 N93-14947
MIRRORS
Full surface testing of grazing incidence mirrors
[AD-A255644] p 979 N93-14152
Design, development, and testing of a prototype optical system for a next generation multiplexed imager
[AD-A256538] p 981 N93-14286
Effects of cryocontaminants on cryogenic superpolished mirror and superpolished quartz crystal microbalance
[AD-A255972] p 981 N93-14403
Physics of x ray multilayer structures: Summaries of papers presented at the physics of x ray multilayer structures topical meeting, technical digest series, 1992, volume 7
[AD-A255383] p 992 N93-14741
Surface evaluation of UV-degraded contamination
[NASA-CR-184500] p 910 N93-14764
Interferometer with two phase-conjugate mirrors
[AD-D015420] p 982 N93-14800
Full surface testing of grazing incidence mirrors
[AD-A255798] p 984 N93-15371
MIS (SEMICONDUCTORS)
The 3 to 5 heterojunction structures and high speed devices
[AD-A250399] p 991 N93-14521
MISALIGNMENT
Kind-band failure analysis of thick composites in compression
[AD-A255431] p 831 N93-14509
MISSILE CONTROL
Optical fibers for long-haul transmission in severe-bending applications
[AD-A255964] p 981 N93-14407
Digital bank-to-turn control and guidance p 802 N93-14447

MISSILE DETECTION
The detection and correlation modeling of Rayleigh distributed radar signals
[AD-A256612] p 858 N93-14250
MISSILES
Optical fibers for long-haul transmission in severe-bending applications
[AD-A255964] p 981 N93-14407
MISSION PLANNING
Mission critical system development: Design views and their integration
[AD-A255498] p 940 N93-14644
Human exploration: Moon/Mars mission p 805 N93-14922
Mission and technology assessment of human exploration to the Moon and Mars p 809 N93-14944
Earth environment space initiative p 811 N93-14953
Combined high and low thrust propulsion for fast piloted Mars missions
[NASA-CR-190788] p 828 N93-15584
MIXED OXIDES
Theory of the electronic and structural properties of solid state oxides
[DE92-040499] p 993 N93-14909
MIXERS
An alternate method for achieving temperature control in the -130 C to 75 C range p 821 N93-15609
MIXING
Numerical study of mixing of two fluids under low gravity
[NASA-TM-105865] p 878 N93-14914
MIXING LENGTH FLOW THEORY
The theory and numerical simulation of non-local mixing-length convection p 1015 N93-14147
MOBILE COMMUNICATION SYSTEMS
NPR and intermodulation in mobile satellite systems p 806 N93-14931
A low bit rate FSK technique for SCPC satellite communication systems p 811 N93-14954
Progress toward a full scale mobile satellite system for Canada p 812 N93-14960
L-band antenna design for MSAT mission p 812 N93-14961
Next generation satellite communications networks p 812 N93-14962
MODAL RESPONSE
Modal interactions in the dynamic response of isotropic and composite plates p 829 N93-14221
MODEL REFERENCE ADAPTIVE CONTROL
Model reduction of flexible manipulators
[AD-A255251] p 889 N93-14528
MODELS
The effect of a hierarchical task-specific external conceptual model on the learnability and usability of microcomputer applications by novices p 1000 N93-14205
Development of an integrated package of physics models for scene simulation studies to support smart weapons design studies
[LTR92-004] p 945 N93-14696
MODEMS
Recommendations for enhancement of the Design Criteria Information System (DCIS)
[AD-A256857] p 1009 N93-15641
MODULATION
High-speed architecture for the decoding of trellis-coded modulation
[NASA-CR-191374] p 941 N93-14770
MODULATORS
Development of a 500 GHz optoelectronic modulator using superconducting transmission lines
[AD-A257062] p 871 N93-15456
MODULUS OF ELASTICITY
In situ material characterization for pavement evaluation by the Spectral-Analysis-of-Surface-Waves (SASW) method
[AD-A255660] p 804 N93-14128
Characterization of fiber reinforced phenolic composites p 828 N93-14142
An investigation of crack growth at interfaces in bimaterials and composites using a consistent shear-lag model p 896 N93-14187
Reanalysis of multiple-wheel landing gear traffic tests
[AD-A256593] p 804 N93-14238
MOIRE FRINGES
Technology development for non-contact measurement in modal testing of large space structures p 809 N93-14942
MOIRE INTERFEROMETRY
Integration and processing of high-resolution moire-interferometry data p 895 N93-14185
MOISTURE CONTENT
Global survey of effective particle size in liquid water clouds by satellite observations p 921 N93-14862
MOLECULAR BEAM EPITAXY
The 3 to 5 heterojunction structures and high speed devices
[AD-A250399] p 991 N93-14521
Selected area epitaxial growth for complementary HBT applications
[AD-A257047] p 995 N93-15365
MOLECULAR BEAMS
Gas-surface interactions
[AD-A255390] p 841 N93-14652
MOLECULAR CHAINS
The role of entanglements in the swelling of poly(dimethylsiloxane) networks
[AD-A255359] p 849 N93-14561
MOLECULAR CLOUDS
Submillimeter and infrared spectroscopy of molecular clouds near O and B stars p 1016 N93-14149
The formation of giant molecular clouds p 1021 N93-15086
MOLECULAR EXCITATION
Electronically excited molecules: Reaction kinetics and emission of light: Nanosecond infrared spectroscopy, electronic emission from chemical reactions
[AD-A255642] p 976 N93-14283
MOLECULAR GASES
The structure and dynamics of an environment forming high-mass stars p 1014 N93-14113
MOLECULAR RELAXATION
Electronically excited molecules: Reaction kinetics and emission of light: Nanosecond infrared spectroscopy, electronic emission from chemical reactions
[AD-A255642] p 976 N93-14283
MOLECULAR SPECTROSCOPY
Final Report, 1 November 1988 - 31 October 1991 --- spectroscopy of adsorbed and photodissociated molecules
[AD-A255979] p 976 N93-14424
MOLECULAR STRUCTURE
Final Report, 1 November 1988 - 31 October 1991 --- spectroscopy of adsorbed and photodissociated molecules
[AD-A255979] p 976 N93-14424
Electronically active cyclocarborane-metal-arene assemblies
[AD-A256288] p 865 N93-14457
The role of entanglements in the swelling of poly(dimethylsiloxane) networks
[AD-A255359] p 849 N93-14561
Gallium and indium compounds containing three different substituents. Crystal and molecular structure of ((Me3 CCH2)ClGaPPh2)3
[AD-A257049] p 996 N93-15443
MOLECULAR THEORY
Gas-solid dynamics at disordered and adsorbate covered surfaces
[AD-A255981] p 976 N93-14411
The role of entanglements in the swelling of poly(dimethylsiloxane) networks
[AD-A255359] p 849 N93-14561
MOLECULAR WEIGHT
Gallium and indium compounds containing three different substituents. Crystal and molecular structure of ((Me3 CCH2)ClGaPPh2)3
[AD-A257049] p 996 N93-15443
MOLECULES
Predicting polymer properties by computational methods 2: A comparison of semi-empirical methods
[AD-A256856] p 854 N93-15640
MOLYBDENUM
Method of bonding molybdenum to steel
[AD-D015410] p 845 N93-14888
MOLYBDENUM ALLOYS
Application of the square root diffusivity analysis to measuring the diffusivity of multicomponent alloys
[DE92-040978] p 847 N93-15382
MOLYBDENUM COMPOUNDS
Sputter deposition and characterization of MoSi2/SiC composite coatings
[DE92-040326] p 837 N93-15426
MOMENTS OF INERTIA
On some kinematic and mass characteristics of foldable solar arrays p 812 N93-14957
MOMENTUM
Optimization of circular orifice jets mixing into a heated cross flow in a cylindrical duct
[NASA-TM-105984] p 800 N93-15359
MOMENTUM THEORY
Transformation of energy and momentum due to Landau damping in time
[IPPCZ-316] p 988 N93-14813
MOMENTUM TRANSFER
Analysis of rotation experiments in TFTR --- tokamak fusion test reactor p 987 N93-14129
Radiation pressure: A possible cause for the superrotation of the Venusian atmosphere p 1033 N93-14338
Second order closure modeling of turbulent buoyant wall plumes
[NASA-TM-105956] p 877 N93-14829
Root damage analysis of aircraft engine blade subject to ice impact
[NASA-TM-105779] p 902 N93-15343
Digital active material processing platform effort (DAMPER), SBIR phase 2
[NASA-CR-190798] p 856 N93-15353
MONITORS
Test and evaluation report of the Physio Control Defibrillator/Monitor, Model LifePak(tm) 6s
[AD-A255691] p 933 N93-14103
Test and evaluation report of the Catalyst Research Oxygen Monitor, Model Miniox 3
[AD-A255849] p 881 N93-14105
An energy analysis of the pseudo Wigner-Ville distribution in support of machinery monitoring and diagnostics
[AD-A256202] p 889 N93-14499
Optical monitor for observing turbulent flow
[DE92-019831] p 876 N93-14715
Discussion for the ideal AIMS p 793 N93-15153
Royal Air Force experience of the Harrier information management system p 795 N93-15170
Generation, control, and transport of a 19-MeV, 700-kA pulsed electron beam
[DE92-019803] p 978 N93-15277
MONKEYS
Extrathalmic modulation of cortical function
[AD-A255440] p 935 N93-14782
MONOCHROMATORS
X-ray monochromator
[NASA-CASE-MFS-28392-1] p 982 N93-14711
MONTE CARLO METHOD
Extracting x rays, gamma rays, and electron-positron pairs from supermassive Kerr black holes using the Penrose mechanism p 1049 N93-14176
Monte Carlo modeling of the resurfacing of Venus p 1025 N93-14299
Monte Carlo computer simulations of Venus equilibrium and global resurfacing models p 1027 N93-14311
Monte Carlo analysis of energy deposition in solid state materials by 400 and 200 MeV electrons
[AD-A255335] p 991 N93-14537
Analysis of CCD images of the coma of comet P/Halley
[NASA-CR-191384] p 1020 N93-14814
An iterative Monte Carlo method for nonconjugate bayesian analysis
[AD-A255991] p 971 N93-15110
A theoretical search for supervelocity semiconductors
[AD-A256325] p 994 N93-15191
Progress on the development of a 2-D PIC/Monte Carlo model of glow discharges
[DE92-040226] p 989 N93-15422
A Monte Carlo analysis of the liquid xenon TPC as gamma ray telescope p 1014 N93-15590
The use of plasma ashers and Monte Carlo modeling for the projection of atomic oxygen durability of protected polymers in low Earth orbit p 819 N93-15596
MORPHOLOGY
Twin quintuplets in CVD diamond
[AD-A255862] p 989 N93-14133
Analysis of retinal function following laser irradiation
[AD-A255649] p 933 N93-14163
Large-volume lava flow fields on Venus: Dimensions and morphology p 1033 N93-14339
Morphological analysis of ionomers
[DE92-040162] p 852 N93-15415
MOSSBAUER EFFECT
Level-mixing assisted tunability of nuclear resonance linewidths for gamma ray lasers
[AD-A255791] p 885 N93-14647
MOTION SIMULATION
CAD-based off-line programming and sensor signal processing in robotics
[F-2-2] p 949 N93-15299
Beyond keyframing: An algorithmic approach to animation p 957 N93-15565
MOTION SIMULATORS
Generating natural-looking motion for computer animation p 956 N93-15564
MOUNTAINS
Is Ishtar Terra a thickened basaltic crust? p 1024 N93-14292
Visoelastic relaxation of Venusian coronae and mountain belts: Constraints on global heat flow and tectonism p 1027 N93-14313
The gabbro-eclogite phase transition and the elevation of mountain belts on Venus p 1036 N93-14350
MOVING TARGET INDICATORS
On the detection of ultrawideband radar signals
[AD-A256075] p 858 N93-14233

MSAT
Progress toward a full scale mobile satellite system for Canada p 812 N93-14960
L-band antenna design for MSAT mission p 812 N93-14961
Ku-band antenna design for MSAT mission p 813 N93-14963

MUD
Technology evaluation report: The Carver-Greenfield process, Dehydro-Tech Corporation
| PB92-217462 | p 910 N93-15217

MULTIBEAM ANTENNAS
A multiple-aperture multiple-beam EHF antenna for satellite communications
| AD-A256020 | p 858 N93-14426
L-band antenna design for MSAT mission p 812 N93-14961

MULTIPHASE FLOW
Transport phenomena and interfacial kinetics in multiphase combustion systems.
| AD-A255999 | p 838 N93-14418
Optimization of circular orifice jets mixing into a heated cross flow in a cylindrical duct
| NASA-TM-105984 | p 800 N93-15359

MULTIPLE ACCESS
Multi-access strategies for voice/data integration in heterogeneous mixed-media packet radio networks
| AD-A255636 | p 857 N93-14181
Computation and communication constraints for distributed estimation systems
| AD-A256287 | p 970 N93-14456
Integration of satellite links into an ATM mode broadband ISDN
| TELECOM-PARIS-91-E-022 | p 861 N93-15097

MULTIPLE TARGET TRACKING
Radar data processing using a distributed computational system
| AD-A256209 | p 861 N93-15237

MULTIPLEXING
Electro-optic architecture (EOA) for sensors and actuators in aircraft propulsion systems
| NASA-CR-182270 | p 982 N93-15116

MULTIPLICATION
Purposive discovery of operations
| NASA-TM-108116 | p 963 N93-14765

MULTIPROCESSING (COMPUTERS)
A portable multiprocessor interface for standard ML of New Jersey
| AD-A255639 | p 958 N93-14151
Ada-based multitasking terminal I/O
| AD-A255656 | p 942 N93-14164
PRISMA/DB: A parallel, main-memory relational DBMS
| MEMO-INF-92-12 | p 959 N93-15141
A data parallel algorithm for raytracing of heterogeneous databases p 955 N93-15553
Aspects of a parallel-architecture simulator
| AD-A256872 | p 941 N93-15628
A distributed data-balanced dictionary based on the b-link tree
| AD-A256841 | p 1009 N93-15639

MULTISENSOR APPLICATIONS
Design for tactical situation awareness display
| AD-A256194 | p 798 N93-15235

MULTISPECTRAL BAND SCANNERS
The preservation of LANDSAT data by the National Land Remote Sensing Archive p 1003 N93-14777

MULTIVARIATE STATISTICAL ANALYSIS
Four-dimensional data assimilation of GALE data using a multivariate analysis scheme and a mesoscale model with diabatic initialization p 919 N93-14198
Four-dimensional data assimilation of gale data using a multivariate analysis scheme and a mesoscale model with diabatic initialization
| AD-A256063 | p 921 N93-14680

MUSCLES
Training, muscle fatigue and stress fractures
| AD-A255277 | p 935 N93-15006

MUSIC
Demodulation processes in auditory perception
| AD-A255748 | p 935 N93-15053

N

NASA PROGRAMS
Streamlined acquisition handbook
| NASA-TM-108133 | p 1002 N93-14719
Bibliography of Lewis Research Center Technical Publications announced in 1991
| NASA-TM-105595 | p 1004 N93-14796

NASA SPACE PROGRAMS
Human exploration: Moon/Mars mission p 805 N93-14922

NATURAL GAS
High temperature tubular solid oxide fuel cell development
| DE92-040253 | p 908 N93-15322
Geographical distribution and seasonal variation of surface emissions and deposition velocities of atmospheric trace gases
| AERONOMICA-ACTA-A-361-1991 | p 911 N93-15460

NATURAL LANGUAGE (COMPUTERS)
Information system constraint language (ISyCL)
| AD-A256268 | p 976 N93-14438
Grammatical trigrams: A probabilistic model of link grammar
| AD-A256365 | p 947 N93-15206

NAVIER-STOKES EQUATION
An algebraic turbulence model for three-dimensional viscous flows
| NASA-TM-105931 | p 777 N93-14102
Recent advances in numerical simulation and control of asymmetric flows around slender bodies
| PAPER-W.1.2 | p 875 N93-14688
Three-dimensional computational study of asymmetric flows using Navier-Stokes equations
| ISBN-90-5410-029-X | p 875 N93-14690
Numerical simulation of steady and unsteady asymmetric vortical flow p 876 N93-14691
Passive control of supersonic asymmetric vortical flows around cones p 876 N93-14692
Supersonic boundary-layer flow turbulence modeling
| NASA-TM-105893 | p 877 N93-14758
Application of an aeroelastic analysis method for aerodynamic improvement of fighter wings at maneuver flight conditions p 791 N93-14832
Dynamics systems applied to Navier-Stokes equations for the study of turbulence
| ETN-92-92553 | p 878 N93-15122
The 3D Navier-Stokes flow analysis for shared and distributed memory MIMD computers
| AD-A256038 | p 878 N93-15187
Ice accretion and performance degradation calculations with LEWICE/NS
| NASA-TM-105972 | p 787 N93-15354
Low thrust chemical rocket technology
| NASA-TM-105927 | p 827 N93-15572

NAVSTAR SATELLITES
Proposed revisions to RTCM SC-104 recommended standards for differential NAVSTAR/GPS service for carrier phase applications
| AD-A255276 | p 789 N93-15005

NAVY
Parallelization of the Navy Space Surveillance Center (NAVSPASUR) satellite model
| AD-A256133 | p 816 N93-14253
Proceedings of the data assimilation in coupled air-sea nowcast/forecast systems workshop
| AD-A255409 | p 925 N93-14503
Standardization of precipitation static test methods and equipment for the Navy
| AD-A257025 | p 792 N93-15361

NEAR FIELDS
Investigation of the on-surface boundary operators for electromagnetic scattering by conducting object p 857 N93-14189
Performing wind-tunnel modeling for better management of near-field risks
| DE92-040205 | p 910 N93-15063

NEAR INFRARED RADIATION
Investigations of Titan's troposphere and surface and Jupiter's great red spot with infrared observations p 1022 N93-14146
Near-infrared oxygen airglow from the Venus nightside p 1026 N93-14308

NEBULAE
Spatially resolved 10 micron spectra of circumstellar material around evolved stars p 1019 N93-14636

NEODYMIUM LASERS
Ultrashort-pulse laser system: Theory of operation and operating procedures
| AD-A257023 | p 887 N93-15472

NEREID
Complete analytical theory for the satellites of Neptune p 1046 N93-14833

NERVOUS SYSTEM
Biophysical and biochemical mechanisms in synaptic transmitter release
| AD-A256340 | p 936 N93-15198

NETWORK CONTROL
Military space operations: Satellite control system improved, but serious problems remain
| AD-A256809 | p 971 N93-15626

NETWORK SYNTHESIS
Synthesis and simulation with VHDL (VHSIC hardware description language)
| VH-5 | p 948 N93-15266

NEUMANN PROBLEM
A structural approach to the photonic processor
| N-3399-RC | p 986 N93-15648

NEURAL NETS
Neural network retinal model real time implementation
| AD-A255652 | p 934 N93-14210
Neural nets for scene analysis
| AD-A255976 | p 961 N93-14409
Machine intelligence, a foreword: The brain as electronic circuitry; electronic circuitry as a brain
| AD-A255283 | p 962 N93-14533
Development of neural network architectures for self-organizing pattern recognition and robotics
| AD-A255433 | p 962 N93-14551
SETA support for the DARPA microelectronics technology insertion program of the Microelectronics Technology Office
| AD-A255551 | p 866 N93-14555
Design and hardware implementation of neural systems
| AD-A256040 | p 866 N93-14577
Stability and adaptation of neural networks
| AD-A256227 | p 962 N93-14598
Recursively generated networks and dynamical learning
| AD-A255441 | p 963 N93-14783
MOVE: A neutral network paradigm for robotic control p 805 N93-14925
A neural network prototype for predicting F-14B strains at the B.L. 10 longeron
| AD-A255272 | p 792 N93-15004
Architecture of low cost, large scale neural networks
| MEMO-INF-92-16 | p 941 N93-15089
Neural network based condition monitoring p 797 N93-15183
Neural network architectures for general image recognition
| AD-A256017 | p 964 N93-15258
Dynamics of analog electronic neural networks
| AD-A257019 | p 966 N93-15352
Design of an artificial neural network based tactile sensor for the UTAH/MIT dexterous hand
| AD-A256565 | p 966 N93-15406
Analog Very Large Scale Integration (VLSI) implementations of artificial neural networks
| AD-A256621 | p 966 N93-15408

NEUROLOGY
Publications of the Space Physiology and Countermeasures Program, Neuroscience Discipline: 1980-1990
| NASA-CR-4476 | p 936 N93-15583

NEURONS
Extrathalmic modulation of cortical function
| AD-A255440 | p 935 N93-14782
Architecture of low cost, large scale neural networks
| MEMO-INF-92-16 | p 941 N93-15089

NEUROPHYSIOLOGY
Neuromagnetic investigations of cortical regions underlying short-term memory
| AD-A255788 | p 937 N93-14646
Extrathalmic modulation of cortical function
| AD-A255440 | p 935 N93-14782
Cognition and the brain
| AD-A255483 | p 937 N93-14788
Statistical analysis of the human strangulation experiments: Comparison to +Gz-induced loss of consciousness
| AD-A255485 | p 935 N93-14789
Publications of the Space Physiology and Countermeasures Program, Neuroscience Discipline: 1980-1990
| NASA-CR-4476 | p 936 N93-15583

NEUTRAL ATMOSPHERES
A study of the low and mid-latitude upper ionospheres of Jupiter and Saturn p 1022 N93-14179

NEUTRAL ATOMS
Advances in laser cooling
| AD-A255969 | p 884 N93-14402

NEUTRINOS
Hydrodynamics of supernova 1987 A p 1019 N93-14633

NEUTRON DIFFRACTION
Morphological analysis of ionomers
| DE92-040162 | p 852 N93-15415

NEUTRON DISTRIBUTION
Excitation of nuclei by antiproton annihilation at rest
| AD-A255447 | p 976 N93-14513

NEUTRON IRRADIATION
The response of dispersion-strengthened copper alloys to high fluence neutron irradiation at 415 C
| DE92-019434 | p 846 N93-15138

NEUTRON STARS
The black hole candidate binary A0620-00 p 1015 N93-14148
Hydrodynamics of supernova 1987 A p 1019 N93-14633

NEUTRONS
The response of dispersion-strengthened copper alloys to high fluence neutron irradiation at 415 C
[DE92-019434] p 846 N93-15138
Studies of heavy-ion reactions and transuranic nuclei
[DE92-040457] p 977 N93-15326
NEWS MEDIA
Antarctic news clips - 1992
[NSF-92-83] p 916 N93-15080
NEWTONIAN FLUIDS
Numerical and experimental study of bubble growth in highly viscous fluids p 874 N93-14465
NICKEL
Dual role of nickel in sodium/nickel chloride batteries
[DE92-041102] p 870 N93-15441
NICKEL ALLOYS
Fatigue in single crystal nickel superalloys
[AD-A256095] p 844 N93-14264
Mach 5 electroformed nickel nozzle refurbishment FNAS investigation of ultra-smooth surfaces
[NASA-CR-191416] p 826 N93-14681
High temperature stability, interface bonding, and mechanical behavior in (beta)-NiAl and Ni3Al matrix composites with reinforcements modified by ion beam enhanced deposition
[DE92-014399] p 992 N93-14812
Application of the square root diffusivity analysis to measuring the diffusivity of multicomponent alloys
[DE92-040978] p 847 N93-15382
NIGERIA
Integrating satellite imagery into a geographic information system for monitoring the downstream impacts of dam construction on floodplain agriculture in Sokoto State, Nigeria p 905 N93-14823
NIGHT VISION
Evaluation of Night Vision Goggles (NVG) for maritime search and rescue (joint Canadian/US Coast Guard experiment)
[AD-A255525] p 939 N93-14554
NIGHTGLOW
LISA: A limb imaging spectrograph for airglow p 811 N93-14952
NIMBUS 7 SATELLITE
On the variation of the Nimbus 7 total solar irradiance
[NASA-TP-3316] p 1049 N93-15532
NIOBIUM ALLOYS
Processing and microstructure of Nb-1 percent Zr-0.1 percent C alloy sheet
[NASA-TM-105921] p 847 N93-15524
NIOBIUM CARBIDES
Processing and microstructure of Nb-1 percent Zr-0.1 percent C alloy sheet
[NASA-TM-105921] p 847 N93-15524
NITRIC OXIDE
Thermophysical properties of nitric oxide
[ESDU-92027] p 839 N93-14544
NITROBENZENES
Absorption of propellant vapors into polymer films
[AD-A255274] p 849 N93-14531
NITROGEN DIOXIDE
High resolution absolute absorption cross sections of NO2 at 295, 573, and 673 K at visible wavelengths: Comprehensive data tables
[AD-A255261] p 839 N93-14530
NITROGEN IONS
Atomic data and spectral analysis of carbon, nitrogen, oxygen and silicon ions observed with the International Ultraviolet Explorer
[NASA-CR-191302] p 1012 N93-14761
NITROGEN ISOTOPES
Isotopic composition of galactic cosmic ray boron, carbon, nitrogen, and oxygen p 1020 N93-14866
NITROUS OXIDES
A correlated k-distribution model of the atmospheric heating rates for overlapping spectra of CH4 and N2O
[DE93-000890] p 911 N93-15281
NOISE (SOUND)
Broadband vibroacoustic frequency control via piezoelectric films
[ONERA-RT-8/3654-RY-010-R] p 974 N93-15129
Surface gravity waves and ambient microseismic noise
[AD-A256498] p 916 N93-15375
NOISE GENERATORS
Unsteady flow distortion past blades: Sources of noise generation in rotating flows
[AD-A255496] p 880 N93-15652
NOISE MEASUREMENT
Evaluation of three models used for predicting noise propagated long distances overground
[AD-A255963] p 973 N93-14406
NOISE POLLUTION
Air Force procedure for predicting noise around airbases: Noise exposure model (Noisemap)
[AD-A255769] p 910 N93-14655
NOISE PREDICTION
Evaluation of three models used for predicting noise propagated long distances overground
[AD-A255963] p 973 N93-14406
Computation of supersonic jet noise under imperfectly expanded conditions
[NASA-TM-105961] p 975 N93-15430
NOISE PREDICTION (AIRCRAFT)
Air Force procedure for predicting noise around airbases: Noise exposure model (Noisemap)
[AD-A255769] p 910 N93-14655
Tiltrotor aircraft noise: A summary of the presentations and discussions at the 1991 FAA/Georgia Tech Workshop
[DOT/FAA/RD-91/23] p 974 N93-14912
NOISE PROPAGATION
Evaluation of three models used for predicting noise propagated long distances overground
[AD-A255963] p 973 N93-14406
Propagation of high frequency jet noise using geometric acoustics
[NASA-TM-105950] p 975 N93-15575
NOISE REDUCTION
Evaluation of three models used for predicting noise propagated long distances overground
[AD-A255963] p 973 N93-14406
Adaptive active noise control using multiple-model approaches
[ISVR-TR-210] p 974 N93-14734
Tiltrotor aircraft noise: A summary of the presentations and discussions at the 1991 FAA/Georgia Tech Workshop
[DOT/FAA/RD-91/23] p 974 N93-14912
A low bit rate FSK technique for SCPC satellite communication systems p 811 N93-14954
NOMENCLATURES
Revised nomenclature for defects at or near the Si/SiO2 interface
[DE92-040975] p 997 N93-15651
NONAQUEOUS ELECTROLYTES
Lithium rechargeable cell with a poly 3-methylthiophene cathode
[AD-A255436] p 866 N93-14552
NONDESTRUCTIVE TESTS
In situ material characterization for pavement evaluation by the Spectral-Analysis-of-Surface-Waves (SASW) method
[AD-A255660] p 804 N93-14128
Nondestructive evaluation of damage in SiC/Al metal matrix composite using x ray tomographic microscopy p 829 N93-14192
Elastic wave scattering by partially debonded or partially coated fibers p 829 N93-14224
Proceedings of the USAF Structural Integrity Program
[AD-A255379] p 777 N93-14549
Testing and analysis of modified HMMWV front lift provisions
[MTL-TR-92-31] p 891 N93-14735
Three-dimensional nuclear magnetic resonance imaging of green-state ceramics
[DE93-000930] p 851 N93-15282
Acoustic resonance techniques for quality control
[DE92-040150] p 895 N93-15413
NONEQUILIBRIUM CONDITIONS
Development of engineering methods for nonequilibrium radiative phenomena about aeroassisted entry vehicles p 817 N93-14632
NONEQUILIBRIUM IONIZATION
A quasi-equilibrium kinetic model of HF air breakdown
[AD-A256240] p 859 N93-14453
NONLINEAR EQUATIONS
Turbulence and chaos in classical and quantum systems p 972 N93-14144
Nonlinear free vibration analysis of strings by the Galerkin method p 972 N93-14280
Iterative algorithms for integral equations of the first kind with applications to statistics
[AD-A256529] p 942 N93-14285
The center for nonlinear phenomena and magnetic materials
[AD-A255983] p 967 N93-14412
On the structure of nonlinear constitutive equations for fiber reinforced composites
[NASA-CR-191024] p 830 N93-14484
Dynamics systems applied to Navier-Stokes equations for the study of turbulence
[ETN-92-92553] p 878 N93-15122
NONLINEAR FEEDBACK
Robust nonlinear feedback guidance for an aerospace plane: A geometric approach p 803 N93-14835
NONLINEAR OPTICS
Oriented electro/optical polymers through in-situ chemistry during gel processing: A research opportunity
[AD-A255968] p 848 N93-14401
Characterization of cholesteric cyclic siloxane liquid crystalline materials
[AD-A256128] p 994 N93-15190
New nonlinear optical film processing
[AD-A256011] p 983 N93-15255
Ferroelectrics volume 122, numbers 1-4, 1991. Proceedings of the 3rd International Conference on Ferroelectric Liquid Crystals, part 2
[AD-A257053] p 996 N93-15446
Ferroelectrics volume 121, numbers 1-4, 1991. Proceedings of the 3rd International Conferenceon Fer roelectric Liquid Crystals, part 1
[AD-A257054] p 996 N93-15447
NONLINEAR SYSTEMS
Active control of combustion instability in a ramjet using large-eddy simulations
[AD-A255226] p 798 N93-14111
Nonlinear dynamics of optical systems p 979 N93-14124
Non-linear analysis of wave progagation using transform methods and plates and shells using integral equations p 896 N93-14186
Nonlinear modeling of gated range tracker dynamics with application to radar range resolution, phase 1
[AD-A256074] p 858 N93-14259
The numerical stability of nonlinear floating body calculations p 873 N93-14278
Nonlinear free vibration analysis of strings by the Galerkin method p 972 N93-14280
Nonlinear dynamic response of shallow arches to harmonic forcing p 898 N93-14282
A geometrically nonlinear stress-deflection relation for thin film/substrate systems p 848 N93-14287
Problems in nonlinear acoustics: Rayleigh waves, pulsed sound beams, reflection of focused beams, waveguides, cooperative radiation of sound by buggies, acoustic streaming effects in standing waves, and spark-source lithotripter pulses
[AD-A256289] p 974 N93-14458
Adaptive control of nonlinear nonminimum phase systems p 961 N93-14470
A new device to aid in the conception and optimization of monolithic millimeter circuits: A distributed and nonliner model of a field effect transistor p 807 N93-14932
Simulation and nonlinear modelling of microwave transistors p 807 N93-14936
Learning position and force control for mechanical manipulators p 963 N93-15147
Robust control design for uncertain nonlinear dynamic systems p 964 N93-15148
Dynamics and control of flexible arm robots
[ISBN-0-315-69011-9] p 892 N93-15150
Wing rock prediction method for a high performance fighter aircraft
[AD-A256438] p 792 N93-15314
NONLINEARITY
An analysis of the effect of acoustic non-linearities in wide bandwidth acousto-optic bragg cells
[AD-A256579] p 973 N93-14269
Finite amplitude gravity waves in the Venus atmosphere generated by surface topography p 1044 N93-14395
The covariance matrix of derived quantities and their combination
[DE92-019066] p 969 N93-15212
Surface gravity waves and ambient microseismic noise
[AD-A256498] p 916 N93-15375
Nonlinear finite element analysis of metals and metal matrix composites: A local-global investigation
[AD-A256782] p 838 N93-15625
NONTHERMAL RADIATION
Nonthermal radio, x ray and gamma ray emissions from chaotic winds of early-type, massive stars p 1050 N93-14242
NONUNIFORMITY
Nonuniformity effects in a hybrid platinum silicide imaging device
[AD-A256339] p 983 N93-15197
Non-uniform patch luminance for global illumination p 957 N93-15569
NOON
Energetic and magnetosheath energy particle signatures of the low-latitude boundary layer at low altitudes near noon
[NASA-CR-191388] p 917 N93-15574
NOREPINEPHRINE
Extrathalmic modulation of cortical function
[AD-A255440] p 935 N93-14782
NORMAL DENSITY FUNCTIONS
Electron acceleration by longitudinal electric field of a Gaussian laser beam
[DE92-526947] p 887 N93-15296
NORTHERN HEMISPHERE
The use of satellite altimetry in the study of weakly defined and variable oceanic gyres p 926 N93-14966

NOSE CONES
Emittance measurements of Space Shuttle orbiter reinforced carbon-carbon
[NASA-TP-3293] p 903 N93-15530
NOSE TIPS
Shape-stable reentry body nose tip
[AD-D015437] p 817 N93-14725
NOSES (FOREBODIES)
Shape-stable reentry body nose tip
[AD-D015437] p 817 N93-14725
NOTCH TESTS
Closed form expressions for crack mouth displacements and stress intensity factors for chevron notched short bar and short rod specimens based on experimental compliance measurements
[NASA-TM-83796] p 902 N93-15369
NOTCHES
The influence of geometrical constraint on cyclic, elastoplastic, notch root behavior, and fatigue microcrack initiation p 900 N93-14480
NOVA LASER SYSTEM
Characteristics of the Nova laser disk edge cladding epoxy
[DE92-041046] p 853 N93-15462
NOWCASTING
Proceedings of the data assimilation in coupled air-sea nowcast/forecast systems workshop
[AD-A255409] p 925 N93-14503
NOZZLE FLOW
Control of asymmetric jet
[AD-A255967] p 873 N93-14400
NOZZLE GEOMETRY
Supersonic investigation of two dimensional hypersonic exhaust nozzles
[NASA-TM-105687] p 800 N93-15342
Computation of supersonic jet noise under imperfectly expanded conditions
[NASA-TM-105961] p 975 N93-15430
NOZZLE WALLS
Numerical modeling of a vortex stabilized arcjet
[NASA-CR-190797] p 826 N93-14883
NOZZLES
Investigations of detail design issues for the high speed acoustic wind tunnel using a 60th scale model tunnel. Part 1: Tests with open circuits
[NASA-CR-191671] p 780 N93-14737
NUCLEAR CAPTURE
Electron acceleration by longitudinal electric field of a Gaussian laser beam
[DE92-526947] p 887 N93-15296
Production of relativistic anti-hydrogen atoms by pair production with positron capture and measurement of the Lamb shift
[DE93-001767] p 978 N93-15468
NUCLEAR ELECTRIC PROPULSION
Combined high and low thrust propulsion for fast piloted Mars missions
[NASA-CR-190788] p 828 N93-15584
NUCLEAR EXPLOSIONS
High speed imaging for flash radiography using PIN diodes
[DE92-040959] p 882 N93-15381
NUCLEAR FUEL REPROCESSING
Design and implementation of a DC-based magnetic field controller with electronic temperature stabilized Hall generator
[DE92-019796] p 870 N93-15276
NUCLEAR FUSION
Hydrodynamics of supernova 1987 A
p 1019 N93-14633
Theoretical and numerical studies in magnetic fusion
[DE92-040674] p 988 N93-15349
NUCLEAR MAGNETIC RESONANCE
NMR imaging of elastomeric materials
[AD-A256034] p 841 N93-14658
Three-dimensional nuclear magnetic resonance imaging of green-state ceramics
[DE93-000930] p 851 N93-15282
NUCLEAR MODELS
Opacity, equation of state, and radiation transport model for moderate density, eV-temperature plasmas
[AD-A256056] p 988 N93-14579
NUCLEAR PROPULSION
SAFSIM: A computer program for engineering simulations of space reactor system performance
[DE92-016328] p 826 N93-14815
Development of NASA/DOE NTP system performance models
[NASA-TM-105982] p 827 N93-15428
Nuclear thermal rocket nozzle testing and evaluation program
[NASA-TM-105962] p 827 N93-15571
Combined high and low thrust propulsion for fast piloted Mars missions
[NASA-CR-190788] p 828 N93-15584
NUCLEAR REACTIONS
Measurement and analysis of excitation functions in (alpha,np) reactions on (128, 130)Te
[DE92-630358] p 991 N93-14485
Studies of heavy-ion reactions and transuranic nuclei
[DE92-040457] p 977 N93-15326
Strong interactions studies with medium energy probes
[DE92-040460] p 977 N93-15377
NUCLEAR REACTORS
The response of dispersion-strengthened copper alloys to high fluence neutron irradiation at 415 C
[DE92-019434] p 846 N93-15138
NUCLEAR RESEARCH
Addressing earthquake strong ground motion issues at the Idaho National Engineering Laboratory
[DE92-017841] p 916 N93-15136
NUCLEAR ROCKET ENGINES
Combined high and low thrust propulsion for fast piloted Mars missions
[NASA-CR-190788] p 828 N93-15584
NUCLEATE BOILING
Nucleate pool boiling in the long duration low gravity environment of the Space Shuttle
[NASA-TM-105973] p 855 N93-15420
Environmental qualification testing of the prototype pool boiling experiment
[NASA-CR-190774] p 895 N93-15582
NUCLEATION
The mechanics of dislocation nucleation at a crack tip
p 896 N93-14214
Crystal growth in a microgravity environment
[NASA-CASE-MFS-28473-1] p 992 N93-14707
Growth, characterization and device development in monocrystalline diamond films
[AD-A256283] p 994 N93-15244
NUCLEONS
A Cloudy Quark Bag Model of S, P, and D wave interactions for the coupled channel antikaon-nucleon system
[DE92-040149] p 977 N93-15062
NUMERICAL ANALYSIS
Resistive magnetohydrodynamic studies of tearing mode instability with equilibrium shear flow and magnetic reconnection p 987 N93-14122
Measurement and analysis of excitation functions in (alpha,np) reactions on (128, 130)Te
[DE92-630358] p 991 N93-14485
NUMERICAL CONTROL
Off-line generation of error-free robot/NC (numerical control) code using simulation and automatic programming techniques
[F-3-1] p 949 N93-15302
SCRUNCHER phase and amplitude control
[DE92-040225] p 870 N93-15421
NUMERICAL INTEGRATION
The dynamics of spatially extended lasers
p 883 N93-14123
NUMERICAL STABILITY
The numerical stability of nonlinear floating body calculations p 873 N93-14278
Stability and adaptation of neural networks
[AD-A256227] p 962 N93-14598
Characterizations of linear independence and stability of the shifts of a univariate refinable function in terms of its refinement mask
[AD-A256527] p 969 N93-15399
Algorithms for intersecting parametric and algebraic curves p 956 N93-15560
NUMERICAL WEATHER FORECASTING
Super-micro computer weather prediction model
[AD-A255668] p 918 N93-14153
NUTRIENTS
Modelling global methane emissions from livestock: Biological and nutritional controls
[NASA-CR-191354] p 911 N93-15480
NUTRITION
Modelling global methane emissions from livestock: Biological and nutritional controls
[NASA-CR-191354] p 911 N93-15480
NUTRITIONAL REQUIREMENTS
Body composition and physical performance
[AD-A255627] p 938 N93-14161

O

O RING SEALS
Development of advanced seal verification
[NASA-CR-184502] p 892 N93-15117
O STARS
Submillimeter and infrared spectroscopy of molecular clouds near O and B stars p 1016 N93-14149
OBJECT PROGRAMS
Obstacles in object-oriented software development
[MEMO-INF-92-15] p 946 N93-15084
OBJECT-ORIENTED PROGRAMMING
Obstacles in object-oriented software development
[MEMO-INF-92-15] p 946 N93-15084
An eclectic method for object oriented database design
[AD-A256439] p 1008 N93-15315
Predicting database requirements for geographic information systems in the year 2000: Long-term design issues for GRASS
[AD-A256862] p 1009 N93-15627
OBLIQUE SHOCK WAVES
A plume-induced boundary layer separation experiment
[AD-A255397] p 875 N93-14677
A numerical investigation of the interaction between crossing oblique shocks and a turbulent boundary layer
p 876 N93-14695
OBSTACLE AVOIDANCE
A concurrent real-time autonomous mobile robot programming system p 960 N93-14281
Theory and applications of hyper-redundant robotic manipulators p 892 N93-15104
OCCLUSION
Volume rendering using the Fourier projection-slice theorem p 953 N93-15541
OCEAN BOTTOM
Surface gravity waves and ambient microseismic noise
[AD-A256498] p 916 N93-15375
OCEAN CURRENTS
Wind stress analysis over the Western Equatorial Pacific and North Atlantic Oceans based on ECMWF operational wind products, 1985-1989
[AD-A256147] p 920 N93-14256
Sensitivity of the Yoshida jet to the parameterization of vertical mixing: Do easterly winds imply equatorial upwelling? p 922 N93-14864
The use of satellite altimetry in the study of weakly defined and variable oceanic gyres p 926 N93-14966
North-Australian tropical seas circulation study
p 926 N93-14968
Circulation of the gyres of the world ocean: Observation modeling using TOPEX/Poseidon altimeter data
p 927 N93-14975
South African TOPEX/Poseidon altimeter experiment
p 928 N93-14976
Sea level response to wind forcing in the tropical Atlantic p 928 N93-14977
Ocean topography mapping, improvement of the marine geoid, and global permanent ocean circulation studies from TOPEX/Poseidon altimeter data p 928 N93-14981
Ocean circulation using altimetry p 929 N93-14984
Ocean circulation modeling by use of radar altimeter data p 929 N93-14986
General circulation of the South Atlantic between 5 deg N and 35 deg S p 929 N93-14987
Equatorial and eastern boundary current variability in the North and South Pacific Oceans
p 931 N93-14994
An integrated research program for TOPEX/Poseidon with emphasis on the Pacific Ocean
p 931 N93-14995
Oceanic transports of mass, heat, and salt in the western North Pacific p 931 N93-14996
Global ocean circulation by altimetry
p 932 N93-15002
OCEAN DYNAMICS
Sensitivity of the Yoshida jet to the parameterization of vertical mixing: Do easterly winds imply equatorial upwelling? p 922 N93-14864
Mesoscale and large-scale variability of the Antarctic circumpolar current p 926 N93-14970
Ocean transport and variability studies of the South Pacific, Southern, and Indian Oceans
p 927 N93-14971
Studies of the intermediate and deep circulation in the western equatorial Atlantic p 927 N93-14973
Application of TOPEX/Poseidon altimetry to ocean dynamics and geophysics p 927 N93-14974
South African TOPEX/Poseidon altimeter experiment
p 928 N93-14976
Sea level response to wind forcing in the tropical Atlantic p 928 N93-14977
Low-frequency variability of sea level as related to the heat balance of global oceans p 928 N93-14979
Studies of tropical ocean dynamics using the TOPEX/Poseidon altimeter-derived sea surface topography p 928 N93-14980
Ocean topography mapping, improvement of the marine geoid, and global permanent ocean circulation studies from TOPEX/Poseidon altimeter data p 928 N93-14981
Study of mass and heat transport of the tropical Atlantic Ocean using models and altimeter data
p 929 N93-14983
Ocean circulation using altimetry p 929 N93-14984

The dynamics and energetics of midlatitude western boundary currents: A comparison of the Kuroshio Extension and the Gulf Stream p 929 N93-14985
Ocean circulation modeling by use of radar altimeter data p 929 N93-14986
General circulation of the South Atlantic between 5 deg N and 35 deg S p 929 N93-14987
Ocean dynamics in the Nordic Seas using satellite altimetry p 930 N93-14988
Application of TOPEX/Poseidon altimetry measurements to observational and modeling studies of the low-frequency upper ocean mass and heat circulation in the tropical Pacific p 930 N93-14989
Mean sea surface and gravity investigations using TOPEX/Poseidon altimeter data p 930 N93-14990
Global ocean tide mapping using TOPEX/Poseidon altimetry p 930 N93-14991
Equatorial and eastern boundary current variability in the North and South Pacific Oceans p 931 N93-14994
Oceanic transports of mass, heat, and salt in the western North Pacific p 931 N93-14996
A TOPEX/Poseidon study of oceanic effects on observations of the Earth's interior p 918 N93-14999
Global ocean circulation by altimetry p 932 N93-15002

OCEAN MODELS
Carbon dioxide induced ocean climatic change and tracer experiment with an atmosphere-ocean general circulation model p 912 N93-14178
Mixed-layer parameterization in models of the Indian Ocean
[AD-A255937] p 925 N93-14428
Proceedings of the data assimilation in coupled air-sea nowcast/forecast systems workshop
[AD-A255409] p 925 N93-14503
Global ocean tides through assimilation of oceanographic and altimeter satellite data in a hydrodynamic model p 928 N93-14978
Ocean circulation modeling by use of radar altimeter data p 929 N93-14986
Precise orbit computation and sea surface modeling p 813 N93-15000
Fitting microphysical observations to a numerical model through an optimal control theory technique p 924 N93-15100

OCEAN SURFACE
Wind stress analysis over the Western Equatorial Pacific and North Atlantic Oceans based on ECMWF operational wind products, 1985-1989
[AD-A256147] p 920 N93-14256
Synoptic/planetary-scale interactions and blocking over the North Atlantic Ocean
[NASA-CR-191376] p 925 N93-14769
Ocean wave detection using satellite altimetry p 906 N93-14839
South African TOPEX/Poseidon altimeter experiment p 928 N93-14976
Studies of tropical ocean dynamics using the TOPEX/Poseidon altimeter-derived sea surface topography p 928 N93-14980
Ocean dynamics in the Nordic Seas using satellite altimetry p 930 N93-14988
Mean sea surface and gravity investigations using TOPEX/Poseidon altimeter data p 930 N93-14990
Application of precise altimetry to the study of precise leveling of the sea surface, the Earth's gravity field, and the rotation of the Earth p 907 N93-14992
The determination and interpretation of ocean surface topography using TOPEX/Poseidon altimeter data p 931 N93-14997
Precise orbit computation and sea surface modeling p 813 N93-15000
Surface gravity waves and ambient microseismic noise
[AD-A256498] p 916 N93-15375

OCEANOGRAPHIC PARAMETERS
Altimeter and oceanographic in situ measurements in the area of the Greenland-Iceland-Norwegian Sea, 1987-1988
[AD-A256598] p 960 N93-14239

OCEANOGRAPHY
Altimeter and oceanographic in situ measurements in the area of the Greenland-Iceland-Norwegian Sea, 1987-1988
[AD-A256598] p 960 N93-14239
Proceedings of the data assimilation in coupled air-sea nowcast/forecast systems workshop
[AD-A255409] p 925 N93-14503
TOPEX/Poseidon science investigations plan
[NASA-CR-190616] p 925 N93-14964
The western Mediterranean Sea: An area for a regional validation for TOPEX/Poseidon and a field for geophysical and oceanographic studies p 926 N93-14965
The use of satellite altimetry in the study of weakly defined and variable oceanic gyres p 926 N93-14966
Global ocean tides through assimilation of oceanographic and altimeter satellite data in a hydrodynamic model p 928 N93-14978
Mean sea surface and gravity investigations using TOPEX/Poseidon altimeter data p 930 N93-14990
Global ocean tide mapping using TOPEX/Poseidon altimetry p 930 N93-14991
Oceanic transports of mass, heat, and salt in the western North Pacific p 931 N93-14996
The determination and interpretation of ocean surface topography using TOPEX/Poseidon altimeter data p 931 N93-14997
Marine research using data from TOPEX/Poseidon p 932 N93-15001
Global ocean circulation by altimetry p 932 N93-15002
Advanced development active model: A users guide
[AD-A255614] p 974 N93-15012
Modern methods in meteorological and oceanographic data analysis
[AD-A257080] p 903 N93-15496

OILS
Technology evaluation report: The Carver-Greenfield process, Dehydro-Tech Corporation
[PB92-217462] p 910 N93-15217

OLIVINE
Infrared laboratory spectra and composition changes of synthetic amorphous silicate grains
[DE92-040211] p 843 N93-15283

ON-LINE SYSTEMS
DROLS workbook
[AD-A255850] p 999 N93-14106
Online vibration control of a flexible rotor/bearing system p 899 N93-14468
Parallel on-line parsing in constant time
[MEMO-INF-91-64] p 958 N93-15082
User's guide for SearchMAESTRO
[AD-A256422] p 1008 N93-15335
Telepresence: Integrating shared task and person spaces p 954 N93-15548
CSCW - WCSC: Computer-supported cooperative work. What changes for the science of computing p 954 N93-15549

ONBOARD DATA PROCESSING
Software flexibility and configuration control for the A340/A330 Aircraft Condition Monitoring System (ACMS) p 793 N93-15154
Flight data and flight safety in SAS p 793 N93-15156
The SIROM flight data recorder and evaluation system p 795 N93-15165
DAR-2: On-board data acquisition system for aircraft engines p 795 N93-15166
EJ 200 engine monitoring system: On- and off-board data capture, analysis, and management system p 796 N93-15172
RB199 engine oil system failure diagnostics by comparison of measured and calculated oil consumption using the OLMOS on-board monitoring system p 796 N93-15173

ONBOARD EQUIPMENT
DAR-2: On-board data acquisition system for aircraft engines p 795 N93-15166
Integrated engine control and monitoring with experiences derived from OLMOS p 795 N93-15168
Royal Air Force experience of the Harrier information management system p 795 N93-15170
EJ 200 engine monitoring system: On- and off-board data capture, analysis, and management system p 796 N93-15172

OPALESCENCE
Diffusing wave spectroscopy p 980 N93-14169

OPERATING SYSTEMS (COMPUTERS)
A portable multiprocessor interface for standard ML of New Jersey
[AD-A255639] p 958 N93-14151

OPERATING TEMPERATURE
Modelling the engine temperature distribution between shut down and restart for life usage monitoring p 796 N93-15177

OPERATIONS RESEARCH
Automated coding and intersecting cube theory
[ETN-92-92675] p 941 N93-15123

OPERATOR PERFORMANCE
Effects of spatial luminance nonuniformities on visual-task performance and subjective uniformity
[AD-A255989] p 936 N93-14416

OPERATORS (MATHEMATICS)
Purposive discovery of operations
[NASA-TM-108116] p 963 N93-14765

OPTICAL COMMUNICATION
Advanced optical fiber communication systems
[AD-A255424] p 982 N93-14507
Development of a 500 GHz optoelectronic modulator using superconducting transmission lines
[AD-A257062] p 871 N93-15456

OPTICAL COMPUTERS
SETA support for the DARPA microelectronics technology insertion program of the Microelectronics Technology Office
[AD-A255551] p 866 N93-14555
Computer-aided design package for designers of digital optical computers
[AD-A255381] p 944 N93-14564
Parallel readout of optical disks
[AD-A256625] p 1008 N93-15409

OPTICAL CORRELATORS
Optical information processing using photorefractive BSO p 981 N93-14204
Real-time edge-enhanced optical correlator
[NASA-CASE-NPO-18521-1-CU] p 981 N93-14404

OPTICAL DATA PROCESSING
Optical information processing using photorefractive BSO p 981 N93-14204
Photonic materials and devices for optical information processing and computing applications
[AD-A256047] p 982 N93-14578
Parallel readout of optical disks
[AD-A256625] p 1008 N93-15409

OPTICAL DATA STORAGE MATERIALS
Optical instrumentation and characterization for magneto-optical recording media p 980 N93-14168
Ultra-dense optical mass storage
[AD-A255463] p 1004 N93-14785
ICI optical data storage tape p 1005 N93-15037
Diffraction analysis and evaluation of several focus- and track-error detection schemes for magneto-optical disk systems p 984 N93-15506
Improved astigmatic focus error detection method p 984 N93-15507
Measurement of the magnetic anisotropy energy constants for magneto-optical recording media p 984 N93-15509
Proposal for massively parallel data storage system p 960 N93-15510
Modeling and measurement of a micro-optic beam deflector p 985 N93-15514
Oxidation processes in magneto-optic and related materials p 985 N93-15516

OPTICAL DISKS
Status of emerging standards for removable computer storage media and related contributions of NIST p 1003 N93-14778
ICI optical data storage tape p 1005 N93-15037
Rewritable optical disk: Application to flight recording p 794 N93-15160
Parallel readout of optical disks
[AD-A256625] p 1008 N93-15409

OPTICAL EQUIPMENT
A theoretical search for supervelocity semiconductors
[AD-A256325] p 994 N93-15191
Ferroelectrics volume 122, numbers 1-4, 1991. Proceedings of the 3rd International Conference on Ferroelectric Liquid Crystals, part 2
[AD-A257053] p 996 N93-15446
Ferroelectrics volume 121, numbers 1-4, 1991. Proceedings of the 3rd International Conferenceon Ferroelectric Liquid Crystals, part 1
[AD-A257054] p 996 N93-15447
A new approach for performing contamination control bakeouts in JPL thermal vacuum test chambers p 823 N93-15618

OPTICAL FIBERS
Optical fibers for long-haul transmission in severe-bending applications
[AD-A255964] p 981 N93-14407
Integrated photonics research technical digest series. Volume 10: Conference edition: Summaries of papers presented at the Integrated Photonics Research Topical Meeting
[AD-A255423] p 981 N93-14506
Advanced optical fiber communication systems
[AD-A255424] p 982 N93-14507
Variable path length spectrophotometric probe
[DE92-019834] p 881 N93-14716
Development of a fiber optic high temperature strain sensor
[NASA-CR-191316] p 882 N93-14810
Electro-optic architecture (EOA) for sensors and actuators in aircraft propulsion systems
[NASA-CR-182270] p 982 N93-15116
Development of advanced seal verification
[NASA-CR-184502] p 892 N93-15117
Preliminary lightning tests: Optical fiber penetration of an exclusion region barrier
[DE92-019804] p 983 N93-15230
Interferometric measurement with squeezed light
[AD-A257065] p 984 N93-15458

OPTICAL FILTERS
Optical monitor for observing turbulent flow
[DE92-019831] p 876 N93-14715

OPTICAL MATERIALS
Application of gel-silica optics to laser technology and optical element fabrication
[AD-A255666] p 883 N93-14131
Oriented electro/optical polymers through in-situ chemistry during gel processing: A research opportunity
[AD-A255968] p 848 N93-14401
Effects of cryocontaminants on cryogenic superpolished mirror and superpolished quartz crystal microbalance
[AD-A255972] p 981 N93-14403
Photonic materials and devices for optical information processing and computing applications
[AD-A256047] p 982 N93-14578
Photoelectrochemistry of electronic and electro-optical materials
[AD-A256239] p 866 N93-14583
Ultrastructure processing and environmental stability of advanced structural and electronic materials
[AD-A256153] p 831 N93-14665
Optical glasses for high-peak-power laser applications
[DE92-040403] p 886 N93-14906
New nonlinear optical film processing
[AD-A256011] p 983 N93-15255

OPTICAL MEASUREMENT
Optical probes for laser induced shocks
[AD-A256092] p 884 N93-14284
Boundary layer transition measurements by optical anemometry p 874 N93-14477
Precise measurements made from a distance of local deformations independent of small object movements
[ETN-92-92723] p 886 N93-15128
Interferometric measurement with squeezed light
[AD-A257065] p 984 N93-15458

OPTICAL MEASURING INSTRUMENTS
Optical monitor for observing turbulent flow
[DE92-019831] p 876 N93-14715
A temperature tracking SPICE2G.6 macromodel of the 6N134 optocoupler
[DE92-040093] p 983 N93-15223

OPTICAL MEMORY (DATA STORAGE)
Ultra-dense optical mass storage
[AD-A255463] p 1004 N93-14785
Parallel readout of optical disks
[AD-A256625] p 1008 N93-15409
Transfer function characteristics of super resolving systems p 985 N93-15512

OPTICAL PATHS
Application of gel-silica optics to laser technology and optical element fabrication
[AD-A255666] p 883 N93-14131
Characterization of magneto-optical recording media p 979 N93-14140
Combining ray-trace and diffraction analysis: A design example p 985 N93-15511

OPTICAL POLARIZATION
Optics for diode array transverse pumped laser rod
[AD-D015436] p 885 N93-14722

OPTICAL PROPERTIES
Electronic, vibrational, and transport properties of conducting polymers p 847 N93-14170
Oriented electro/optical polymers through in-situ chemistry during gel processing: A research opportunity
[AD-A255968] p 848 N93-14401
The preliminary Long Duration Exposure Facility (LDEF) materials data base
[NASA-TM-107692] p 828 N93-14459

OPTICAL PUMPING
Advances in laser cooling
[AD-A255969] p 884 N93-14402

OPTICAL RADAR
Optical signal distribution schemes for millimeter phased array radar
[AD-A256262] p 858 N93-14437
Upgrade the University of Wisconsin volume imaging lidar
[AD-A255476] p 885 N93-14497

OPTICAL RESONATORS
Three-dimensional guiding effects in a free-electron laser p 883 N93-14125
A study of an optically pumped free-jet molecular iodine laser operating in the visible spectrum p 884 N93-14141

OPTICAL SWITCHING
Integrated photonics research technical digest series. Volume 10: Conference edition: Summaries of papers presented at the Integrated Photonics Research Topical Meeting
[AD-A255423] p 981 N93-14506
A preliminary design of the Ti:LiNbO3 optical channel waveguide
[AD-A255443] p 982 N93-14784
Fast optoelectronic switching processes in surface-emitting semiconductor lasers and nonlinear etalons
[AD-A255802] p 886 N93-15069

OPTICAL THICKNESS
Effects of water vapor and anisotropic scattering on aerosol optical depth retrieval
[AD-A256087] p 904 N93-14262
Improved aerosol optical depth and particle size index from satellite detected radiance
[AD-A256089] p 904 N93-14263
Pioneer Venus polarimetry and haze optical thickness p 1032 N93-14335

OPTICAL TRACKING
Precise orbit computation and sea surface modeling p 813 N93-15000

OPTICAL TRANSFER FUNCTION
Transfer function characteristics of super resolving systems p 985 N93-15512

OPTICAL WAVEGUIDES
Integrated photonics research technical digest series. Volume 10: Conference edition: Summaries of papers presented at the Integrated Photonics Research Topical Meeting
[AD-A255423] p 981 N93-14506
New nonlinear optical film processing
[AD-A256011] p 983 N93-15255
The design and fabrication of a single leakage-channel grating coupler p 986 N93-15518

OPTIMAL CONTROL
Gas-solid dynamics at disordered and adsorbate covered surfaces
[AD-A255981] p 976 N93-14411
Digital bank-to-turn control and guidance p 802 N93-14447
Optimal and robust control of robot manipulators p 890 N93-14685
Fitting microphysical observations to a numerical model through an optimal control theory technique p 924 N93-15100
Sampled-data control and robust control for discrete-time systems p 964 N93-15149

OPTIMIZATION
Query processing in distributed database systems p 1001 N93-14218
Weight optimum arch structures
[AD-A256080] p 897 N93-14236
Multiobjective control/structure design optimization in the presence of practical constraints p 898 N93-14446
An integrated optimization environment for structural configuration design p 855 N93-14467
Interplanetary program to optimize simulated trajectories (IPOST). Volume 4: Sample cases
[NASA-CR-189653-VOL-4] p 815 N93-14768
Recursively generated networks and dynamical learning
[AD-A255441] p 963 N93-14783
Cooperative control of multiple space manipulators p 805 N93-14923
Optimized design of a 5 kW constant frequency series resonant converter for pulsed load space applications p 807 N93-14935
A para-functional version of Warshall's algorithm
[MEMO-INF-92-23] p 947 N93-15092
Automated coding and intersecting cube theory
[ETN-92-92675] p 941 N93-15123
Optimal synthesis methods for silicon compilers
[ETN-92-92677] p 947 N93-15125
Minimizing conflicts: A heuristic repair method for constraint-satisfaction and scheduling problems
[NASA-TM-108121] p 964 N93-15286
Simple formulae for the optimization of the FEL gain length including the effects of emittance, betatron oscillations, and energy spread
[DE92-040378] p 887 N93-15325
The spatial correlation function approach to response surface emission
[DE92-040875] p 969 N93-15656

OPTOELECTRONIC DEVICES
Advanced laser chemical processing for microelectronics and integrated optics
[AD-A255980] p 865 N93-14425
Integrated photonics research technical digest series. Volume 10: Conference edition: Summaries of papers presented at the Integrated Photonics Research Topical Meeting
[AD-A255423] p 981 N93-14506
Solid state research
[AD-A256019] p 992 N93-14576
Photonic materials and devices for optical information processing and computing applications
[AD-A256047] p 982 N93-14578
The III-V semiconductor quantum well lasers and related optoelectronic devices (on silicon). Oxide-defined semiconductor quantum well lasers and optoelectronic devices: Al-based III-V nativeoxide s
[AD-A255239] p 885 N93-14667
A preliminary design of the Ti:LiNbO3 optical channel waveguide
[AD-A255443] p 982 N93-14784
Optoelectronics material center: A collaborative program including center for high technology materials of the University of New Mexico, Stanford University, California Institute of Technology
[AD-A256005] p 886 N93-15115

ORBIT CALCULATION
Parallelization of the Navy Space Surveillance Center (NAVSPASUR) satellite model
[AD-A256133] p 816 N93-14253
Complete analytical theory for the satellites of Neptune p 1046 N93-14833
Present-day plate motions: Retrieval from the TOPEX/Poseidon orbitography network (DORIS system) p 918 N93-14993
Precise orbit computation and sea surface modeling p 813 N93-15000

ORBIT PERTURBATION
Precision radiation force modeling for the TOPEX/Poseidon mission p 817 N93-14586

ORBITAL ASSEMBLY
Structurally adaptive space crane concept for assembling space systems on orbit
[NASA-TP-3307] p 818 N93-15368

ORBITAL MANEUVERS
Interplanetary program to optimize simulated trajectories (IPOST). Volume 4: Sample cases
[NASA-CR-189653-VOL-4] p 815 N93-14768

ORBITAL MECHANICS
Complete analytical theory for the satellites of Neptune p 1046 N93-14833

ORBITAL RENDEZVOUS
Optimal impulsive trajectories for orbital rendezvous between elliptic orbits p 813 N93-15103

ORBITAL SERVICING
A concept for a supervised autonomous robot p 810 N93-14950

ORGANIC COMPOUNDS
Application of Fourier Transform-infrared spectroscopy (FT-IR) for materials analysis
[AD-A255727] p 838 N93-14435

ORGANIC MATERIALS
Electrochemical oxidation of organic materials
[DE92-019822] p 828 N93-14718

ORGANIC SEMICONDUCTORS
Organic/IR-Semiconductor heterojunctions for low-cost, high temperature IR arrays
[AD-A255971] p 868 N93-15108

ORGANIZATIONS
Information for management, planning, and decision-making in nonprofit organizations: Toward a comprehensive model p 1000 N93-14209
Source hierarchy list. Volume 1: A through D
[AD-A256100] p 1001 N93-14265
Core support of the board on mathematical sciences
[AD-A255482] p 968 N93-14787
Core support for the Board on Mathematical Sciences
[AD-A256333] p 968 N93-15195

ORGANOMETALLIC COMPOUNDS
Electronically active cyclocarborane-metal-arene assemblies
[AD-A256288] p 865 N93-14457

ORGANOMETALLIC POLYMERS
Electronically active cyclocarborane-metal-arene assemblies
[AD-A256288] p 865 N93-14457

ORIENTATION
Apparatus for checking threaded hole perpendicularity
[NASA-CASE-LEW-15444-1] p 882 N93-14840

ORION CONSTELLATION
Spatially resolved 10 micron spectra of circumstellar material around evolved stars p 1019 N93-14636

OROGRAPHY
Sierra Nevada winter storms: A study using microwave radiometry, ice crystal, and isotopic analysis technique p 923 N93-15088

ORTHOGONAL FUNCTIONS
Introduction to real orthogonal polynomials
[AD-A256448] p 968 N93-14609

ORTHOGONAL MULTIPLEXING THEORY
Design, development, and testing of a prototype optical system for a next generation multiplexed imager
[AD-A256538] p 981 N93-14286

ORTHOGONALITY
Introduction to real orthogonal polynomials
[AD-A256448] p 968 N93-14609

OSCILLATIONS
Low-frequency oscillations in radiative-convective models p 915 N93-14874
Low-frequency oscillations in radiative-convective models
[DE92-018779] p 922 N93-14901

Frequency shifts in a rubidium frequency standard due to coupling to another standard
| AD-A256232 | p 972 N93-15243

OSCILLATORS
A novel, high energy-density electrical storage device for electric weapons
| AD-A255205 | p 867 N93-14666

OUTER RADIATION BELT
Radiation belt dynamic and quasi-static modeling based on CRRES data: Outer-belt short-term response data base
| AD-A256483 | p 916 N93-14899

OUTGASSING
Outgassing history of Venus and the absence of water on Venus p 1045 N93-14398

OUTPUT
Ada-based multitasking terminal I/O
| AD-A255656 | p 942 N93-14164

OXIDATION
The isotopes of carbon monoxide in the free troposphere and their implications to atmospheric chemistry p 913 N93-14207
The properties of thermally passivated Si(1-x) He(x) produced using high pressure techniques (and related augmentation awards)
| AD-A255961 | p 991 N93-14429
Oxidation processes in magneto-optic and related materials p 985 N93-15516

OXIDE FILMS
New electronic materials
| AD-A255612 | p 868 N93-15010

OXIDES
High temperature tubular solid oxide fuel cell development
| DE92-040253 | p 908 N93-15322

OXIDIZERS
Electrochemical oxidation of organic materials
| DE92-019822 | p 828 N93-14718

OXYGEN
Near-infrared oxygen airglow from the Venus nightside p 1026 N93-14308
High-temperature, high-pressure oxygen metering valve
| NASA-CASE-MSC-21823-1 | p 891 N93-14843

OXYGEN ANALYZERS
Test and evaluation report of the Catalyst Research Oxygen Monitor, Model Miniox 3
| AD-A255849 | p 881 N93-14105

OXYGEN ATOMS
A study of mid-latitude 5577 A OI dayglow emissions p 913 N93-14199
The preliminary Long Duration Exposure Facility (LDEF) materials data base
| NASA-TM-107692 | p 828 N93-14459
Leveling coatings for reducing the atomic oxygen defect density in protected graphite fiber epoxy composites
| NASA-TM-105732 | p 852 N93-15344
Low Earth orbit atomic oxygen simulation for durability evaluation of solar reflector surfaces p 819 N93-15594
Simulation of the synergistic low Earth orbit effects of vacuum thermal cycling, vacuum UV radiation, and atomic oxygen p 819 N93-15595
The use of plasma ashers and Monte Carlo modeling for the projection of atomic oxygen durability of protected polymers in low Earth orbit p 819 N93-15596

OXYGEN IONS
Atomic data and spectral analysis of carbon, nitrogen, oxygen and silicon ions observed with the International Ultraviolet Explorer
| NASA-CR-191302 | p 1012 N93-14761
Exceptionally high-strength (approximately 3 GPa) aluminum alloys demonstrated by oxygen ion implantation
| DE92-040980 | p 847 N93-15383

OXYGEN ISOTOPES
Isotopic composition of galactic cosmic ray boron, carbon, nitrogen, and oxygen p 1020 N93-14866

OXYGEN PLASMA
Leveling coatings for reducing the atomic oxygen defect density in protected graphite fiber epoxy composites
| NASA-TM-105732 | p 852 N93-15344
Leveling coatings for reducing the atomic oxygen defect density in protected graphite fiber epoxy composites p 819 N93-15597

OXYGEN PRODUCTION
In-situ lunar oxygen extraction p 806 N93-14929
Latent heat thermal energy storage for lunar oxygen production
| DE92-017817 | p 907 N93-15219

OXYGENATION
Biophysical and biochemical mechanisms in synaptic transmitter release
| AD-A256340 | p 936 N93-15198

OZONE
Ultraviolet-ozone cleaning of semiconductor surfaces, revision 1
| AD-A256158 | p 842 N93-14678
A correlated k-distribution model of the heating rates for CO2 and O3 in the atmosphere between 0 and 60 km
| DE93-000889 | p 911 N93-15280

P

P WAVES
Imaging Earth's interior: Tomographic inversions for mantle P-wave velocity structure p 913 N93-14225
A Cloudy Quark Bag Model of S, P, and D wave interactions for the coupled channel antikaon-nucleon system
| DE92-040149 | p 977 N93-15062

P-I-N JUNCTIONS
High speed imaging for flash radiography using PIN diodes
| DE92-040959 | p 882 N93-15381

P-3 AIRCRAFT
Analysis of in-flight structural failures of P-3C wing leading edge segments
| AD-A256212 | p 792 N93-15238

PACIFIC OCEAN
Ocean transport and variability studies of the South Pacific, Southern, and Indian Oceans p 927 N93-14971
Application of TOPEX/Poseidon altimetry measurements to observational and modeling studies of the low-frequency upper ocean mass and heat circulation in the tropical Pacific p 930 N93-14989
An integrated research program for TOPEX/Poseidon with emphasis on the Pacific Ocean p 931 N93-14995

PACKET SWITCHING
Tactical line-of-sight path reliability: Improved MSE system procedures
| AD-A256504 | p 862 N93-15376

PACKING DENSITY
Development of braided rope seals for hypersonic engine applications: Flow modeling
| NASA-TM-105942 | p 888 N93-14478

PAIN
The effect of pain on task performance: A review of the literature
| AD-A254336 | p 938 N93-15216

PAINTS
Surface preparation of stainless steel prior to painting
| AD-A256253 | p 838 N93-14454
Removal of THD from painted test panels by liquid systems
| AD-A255624 | p 850 N93-15064

PAIR PRODUCTION
Extracting x rays, gamma rays, and electron-positron pairs from supermassive Kerr black holes using the Penrose mechanism p 1049 N93-14176
Production of relativistic anti-hydrogen atoms by pair production with positron capture and measurement of the Lamb shift
| DE93-001767 | p 978 N93-15468

PANELS
The effect of geometry and prescribed delaminations on the postbuckling behaviour of laminated carbon-fibre reinforced plastic panels p 831 N93-14597
Removal of THD from painted test panels by liquid systems
| AD-A255624 | p 850 N93-15064

PANT PROGRAM
Shape-stable reentry body nose tip
| AD-D015437 | p 817 N93-14725

PARABOLAS
Anomalous scattering behavior of selected impact parabola features: Magellan cycle-to-cycle comparisons p 1039 N93-14363

PARABOLIC DIFFERENTIAL EQUATIONS
Undetermined coefficient problems for quasi-linear parabolic equations
| AD-A256012 | p 969 N93-15256

PARALLEL COMPUTERS
A para-functional version of Warshall's algorithm
| MEMO-INF-92-23 | p 947 N93-15092
Parallelism in a main-memory DBMS: The performance of PRISMA/DB
| MEMO-INF-92-25 | p 958 N93-15093
Progammable connection parallel architecture: Design and routing
| ETN-92-92676 | p 958 N93-15124
PRISMA/DB: A parallel, main-memory relational DBMS
| MEMO-INF-92-12 | p 959 N93-15141
The 3D Navier-Stokes flow analysis for shared and distributed memory MIMD computers
| AD-A256038 | p 878 N93-15187
Work efficient hashing on parallel and vector computers
| AD-A256355 | p 959 N93-15205
Implementing the multiprefix operation on parallel and vector computers
| AD-A256367 | p 959 N93-15207
A distributed data-balanced dictionary based on the b-link tree
| AD-A256841 | p 1009 N93-15639

PARALLEL PROCESSING (COMPUTERS)
Parallelization of the Navy Space Surveillance Center (NAVSPASUR) satellite model
| AD-A256133 | p 816 N93-14253
A complete-time approach for chaining and execution control in the AN/UYS-2 parallel signal processor
| AD-A256306 | p 859 N93-14442
Engineering of massively interconnected computer systems
| AD-A255501 | p 958 N93-14645
SAPNEW: Parallel finite element code for thin shell structures on the Alliant FX-80
| NASA-CR-189212 | p 901 N93-14799
Two-stage target tracking system and method
| AD-D015412 | p 982 N93-14880
MOVE: A neutral network paradigm for robotic control p 805 N93-14925
The role of HiPPI switches in mass storage systems: A five year prospective p 1006 N93-15044
Sonar processing on CESAR
| FFI-92/7007 | p 974 N93-15074
Parallelism in a main-memory DBMS: The performance of PRISMA/DB
| MEMO-INF-92-25 | p 958 N93-15093
Progammable connection parallel architecture: Design and routing
| ETN-92-92676 | p 958 N93-15124
Work efficient hashing on parallel and vector computers
| AD-A256355 | p 959 N93-15205
Implementing the multiprefix operation on parallel and vector computers
| AD-A256367 | p 959 N93-15207
Transactional distributed shared memory
| AD-A256222 | p 941 N93-15240
Implementation and analysis of NP-complete algorithms on a distributed memory computer
| AD-A256564 | p 951 N93-15405
A massively distributed parallel genetic algorithm
| AD-A256617 | p 959 N93-15407
Analog Very Large Scale Integration (VLSI) implementations of artificial neural networks
| AD-A256621 | p 966 N93-15408
Parallel simulation today
| NASA-CR-189733 | p 951 N93-15432
Research Studies on Advanced Optical Module/Head Designs for Optical Data Storage
| NASA-CR-191307 | p 984 N93-15505
A data parallel algorithm for raytracing of heterogeneous databases p 955 N93-15553
Aspects of a parallel-architecture simulator
| AD-A256872 | p 941 N93-15628
A structural approach to the photonic processor
| N-3399-RC | p 986 N93-15648

PARALLEL PROGRAMMING
Parallel on-line parsing in constant time
| MEMO-INF-91-64 | p 958 N93-15082
A para-functional version of Warshall's algorithm
| MEMO-INF-92-23 | p 947 N93-15092
PRISMA/DB: A parallel, main-memory relational DBMS
| MEMO-INF-92-12 | p 959 N93-15141
Data fragmentation for parallel transitive closure strategies
| MEMO-INF-92-17 | p 959 N93-15142
An axiomatic treatment of partial correctness and deadlock in a shared variable parallel language
| AD-A256234 | p 960 N93-15494

PARAMETER IDENTIFICATION
Optimum pose measurements for kinematic parameters identification
| AD-A256307 | p 970 N93-14443
Flight testing: Past, present, and future p 777 N93-14615
Icing effects on aircraft stability and control determined from flight data: Preliminary results
| NASA-TM-105977 | p 803 N93-14831

PARAMETERIZATION
Mixed-layer parameterization in models of the Indian Ocean
| AD-A255937 | p 925 N93-14428
Parameterization in finite precision p 953 N93-15537

PARITY
Weak-electromagnetic interference in polarized eD scattering
[DE93-001763] p 978 N93-15486
PARKING ORBITS
Aspects of parking orbit selection in a manned Mars mission
[NASA-TP-3256] p 813 N93-15367
PARSING ALGORITHMS
Parallel on-line parsing in constant time
[MEMO-INF-91-64] p 958 N93-15082
PARTIAL DIFFERENTIAL EQUATIONS
Nonlinear free vibration analysis of strings by the Galerkin method p 972 N93-14280
PARTICLE ACCELERATION
Fine structure of auroral particle acceleration
p 912 N93-14121
PARTICLE ACCELERATOR TARGETS
Measurement and analysis of excitation functions in (alpha,np) reactions on (128, 130)Te
[DE92-630358] p 991 N93-14485
PARTICLE ACCELERATORS
Interactions of relativistic electrons with relativistic plasma waves p 988 N93-14139
PARTICLE BEAMS
Production of relativistic anti-hydrogen atoms by pair production with positron capture and measurement of the Lamb shift
[DE93-001767] p 978 N93-15468
PARTICLE DIFFUSION
The use of chaos metrics to analyze Lagrangian particle diffusion models
[AD-A256142] p 967 N93-14255
Transport phenomena and interfacial kinetics in multiphase combustion systems.
[AD-A255999] p 838 N93-14418
PARTICLE ENERGY
A survey of solar flare energetic particle abundances and energy spectra p 1048 N93-14135
PARTICLE INTERACTIONS
Interactions of relativistic electrons with relativistic plasma waves p 988 N93-14139
Low energy theorems in pion production
[DE92-040071] p 977 N93-15279
PARTICLE MOTION
Evaluation of a soil fixative to retard particle entrainment: A laboratory study
[UCRL-LR-109806] p 915 N93-14877
PARTICLE PRECIPITATION
Global zones of particle precipitation as observed by EXOS-C
[AD-A256397] p 917 N93-15466
PARTICLE SIZE DISTRIBUTION
Improved aerosol optical depth and particle size index from satellite detected radiance
[AD-A256089] p 904 N93-14263
Global survey of effective particle size in liquid water clouds by satellite observations p 921 N93-14862
PARTICLE TRACKS
Explaining cloud chamber tracks
[DE92-040502] p 972 N93-15057
PARTICLE TRAJECTORIES
Analysis of CCD images of the coma of comet P/Halley
[NASA-CR-191384] p 1020 N93-14814
PARTICLES
Liquid flow reactor and method of using
[AD-D015392] p 893 N93-15232
PARTICULATE REINFORCED COMPOSITES
Superstrength metal composite material and process for making the same
[AD-D015379] p 836 N93-15246
PARTICULATES
Characterisation and dynamic modelling of the near-earth space particulate environment
p 1019 N93-14637
PARTITIONS (MATHEMATICS)
Partitioning tree image representation and generation from 3D geometric models p 955 N93-15557
PASSENGER AIRCRAFT
Effects of seating configuration and number of type 3 exits on emergency aircraft evacuation
[AD-A256616] p 783 N93-14277
PASSIVITY
Surface preparation of stainless steel prior to painting
[AD-A256253] p 838 N93-14454
PATHOLOGY
Training, muscle fatigue and stress fractures
[AD-A255277] p 935 N93-15006
PATHS
Global optimum path planning for a redundant space robot
[AD-A255316] p 889 N93-14545
Implementation of the pure pursuit path tracking algorithm
[AD-A255524] p 944 N93-14569
PATTERN RECOGNITION
Multiresolution pattern recognition of small volcanos in Magellan data p 1042 N93-14380
Neural nets for scene analysis
[AD-A255976] p 961 N93-14409
Psychophysical analyses of perceptual representations
[AD-A255432] p 936 N93-14510
Geometric invariants and object recognition
[AD-A255317] p 943 N93-14546
Development of neural network architectures for self-organizing pattern recognition and robotics
[AD-A255433] p 962 N93-14551
Design and hardware implementation of neural systems
[AD-A256040] p 866 N93-14577
Vision development test bed: The cradle of the MSS artificial vision system p 810 N93-14948
A non-deterministic recogniser generator
[MEMO-INF-92-21] p 946 N93-15091
Workstation tools for feature extraction and classification for nonstationary and transient signals
[AD-A255389] p 947 N93-15228
Neural network architectures for general image recognition
[AD-A256017] p 964 N93-15258
Design of an artificial neural network based tactile sensor for the UTAH/MIT dexterous hand
[AD-A256565] p 966 N93-15406
PAVEMENTS
In situ material characterization for pavement evaluation by the Spectral-Analysis-of-Surface-Waves (SASW) method
[AD-A255660] p 804 N93-14128
Reanalysis of multiple-wheel landing gear traffic tests
[AD-A256593] p 804 N93-14238
PAYLOAD INTEGRATION
Vehicle/payload interface specification for the reusable reentry satellite
[NASA-CR-187883] p 824 N93-15631
Space Station Freedom user's guide
[NASA-TM-108105] p 825 N93-15650
PAYLOADS
Segment specification for the payload segment of the reusable reentry satellite: Rodent module version
[NASA-CR-187884] p 824 N93-15630
PELLETS
Closed Brayton Cycle power system with a high temperature pellet bed reactor heat source for NEP applications
[NASA-TM-105933] p 826 N93-14482
PENETRATION
Strain-rate effects in replica scale model penetration experiments
[AD-A255426] p 844 N93-14508
Characterisation and dynamic modelling of the near-earth space particulate environment
p 1019 N93-14637
PERCOLATION
Macroscopic properties of random and quasiperiodic media
[AD-A255984] p 990 N93-14413
PERFORMANCE PREDICTION
Advanced development active model: A users guide
[AD-A255614] p 974 N93-15012
Parallelism in a main-memory DBMS: The performance of PRISMA/DB
[MEMO-INF-92-25] p 958 N93-15093
Approximate performability analysis using generalized stochastic Petri nets
[MEMO-INF-92-11] p 971 N93-15119
Development of NASA/DOE NTP system performance models
[NASA-TM-105982] p 827 N93-15428
PERFORMANCE TESTS
Simulation of vapor compression heat pumps with solution circuits p 872 N93-14200
Facilities and capabilities catalog for landing and escape systems
[NASA-RP-1282] p 814 N93-14495
Flight termination systems commonality standard
[AD-A255349] p 789 N93-14517
Evaluation and estimation of handling qualities via statistical modeling of pilot response data
[AD-A255324] p 939 N93-14548
Precision tests of gravitation: Liquid-supported torsion balance experiments and a tower experiment
p 914 N93-14589
Development of an expendable particle sensor
[AD-A255702] p 881 N93-14653
The Orlando TDWR testbed and airborne wind shear date comparison results p 784 N93-14851
High temperature tubular solid oxide fuel cell development
[DE92-040253] p 908 N93-15322
Contaminant effects in solid oxide fuel cells
[DE92-040255] p 908 N93-15323
Dual-Shaft Electric Propulsion (DSEP) Technology Development Program
[DE92-040189] p 894 N93-15416
Overview of environmental test plans for Space Station Freedom work package 4 p 824 N93-15623
PERIODIC VARIATIONS
The sulfur emission and periodicity of the Jupiter plasma torus in 1988 p 1022 N93-14156
The time variability of Jupiter's synchrotron radiation
p 973 N93-14227
PERIPHERAL NERVOUS SYSTEM
Nerves and tissue repair
[AD-A255299] p 934 N93-14535
PERMANENT MAGNETS
Thin-film permanent magnets for integrated electromagnetic components
[AD-A256175] p 972 N93-14679
PERMEABILITY
Development of braided rope seals for hypersonic engine applications: Flow modeling
[NASA-TM-105942] p 888 N93-14478
PERMITTIVITY
Electrical conductivity measurements in evaporated cadmium telluride thin films p 865 N93-14191
Thermal, mechanical, and electroelastic behavior of composite materials p 835 N93-15146
High performance YBCO films
[AD-A255439] p 994 N93-15297
PEROVSKITES
Long term stability in thin film ferroelectric memories
[AD-A256290] p 991 N93-14439
PERSHING MISSILE
Evaluation of three models used for predicting noise propagated long distances overground
[AD-A255963] p 973 N93-14406
PERSIAN GULF
Satellite detection of complex aerosols over the Arabian Peninsula/Gulf
[AD-A256085] p 909 N93-14261
PERSONAL COMPUTERS
Personal computer based computed tomography system
[KCP-613-4806] p 945 N93-14876
Automated Estimating System (AES), version 5.1. User's manual
[DE93-000380] p 946 N93-15003
Personal computer based test- and emulation equipment for maintenance and ground support
p 778 N93-15185
USACE geotechnical earthquake engineering software, report 1 WESHAKE for personal computers (version 1.0)
[AD-A257068] p 917 N93-15459
PERSONNEL
Body composition and physical performance
[AD-A255627] p 938 N93-14161
Walter Reed Army Institute of Research biannual report
[AD-A255630] p 933 N93-14162
Crew requirements definition system user's guide
[AD-A257052] p 951 N93-15445
Working together, virtually p 954 N93-15547
PERSONNEL DEVELOPMENT
F/FB-111 avionics test station and component specialist/technician. Automatic test stations manual and electronic warfare test stations. Training requirements analysis (451X6), volume 2
[AD-A252121] p 793 N93-14110
The changing culture of science: Bringing it into balance
[AD-A255993] p 998 N93-14417
PERSONNEL SELECTION
Identifying ability requirements for operators of future automated air traffic control systems
[AD-A256615] p 789 N93-14276
PERTURBATION
Perturbations of the Robertson-Walker space
p 1015 N93-14134
Modelling Directional Solidification
[NASA-CR-191301] p 995 N93-15309
PERTURBATION THEORY
Staggered fermions and chiral symmetry breaking in transverse lattice regulated QED
[DE92-040505] p 977 N93-15378
The sine-Gordon model and the small (kappa)(sup +) region of light-cone perturbation theory
[DE92-040506] p 969 N93-15379
PETRI NETS
Approximate performability analysis using generalized stochastic Petri nets
[MEMO-INF-92-11] p 971 N93-15119
PETROLOGY
Venus steep-sided domes: Relationships between geological associations and possible petrogenetic models p 1038 N93-14359
The effects of Venusian mantle convection with multiple phase transitions p 1043 N93-14385

Venus: Geochemical conclusions from the Magellan data p 1044 N93-14394

PHARMACOLOGY
Autoradiographic distribution and applied pharmacological characteristics of dextromethorphan and related antitissue/anticonvulsant drugs and novel analogs
| AD-A255607 | p 935 N93-15009

PHASE CHANGE MATERIALS
Latent heat thermal energy storage for lunar oxygen production
| DE92-017817 | p 907 N93-15219

PHASE CONJUGATION
Interferometer with two phase-conjugate mirrors
| AD-D015420 | p 982 N93-14800

PHASE CONTROL
SCRUNCHER phase and amplitude control
| DE92-040225 | p 870 N93-15421

PHASE DIAGRAMS
Analysis of OSPREY processes and conventional power aluminum alloys
| AD-A255764 | p 846 N93-15056
Normal state resistivity and the phase diagram of U(1-x)Th(x)Be13
| DE92-040236 | p 995 N93-15321

PHASE ERROR
Modified fast frequency acquisition via adaptive least squares algorithm
| NASA-CASE-NPO-17845-2-CU | p 945 N93-14882

PHASE LOCKED SYSTEMS
Real-time edge-enhanced optical correlator
| NASA-CASE-NPO-18521-1-CU | p 981 N93-14404

PHASE MATCHING
Generation of broadly tunable, narrow bandwidth, and intense coherent vacuum ultraviolet radiation in rare gases p 980 N93-14167

PHASE MODULATION
Demodulation processes in auditory perception
| AD-A255748 | p 935 N93-15053

PHASE SHIFT KEYING
On the performance of Trellis coded modulation with octal phase shift keying over the TDRSS channel
| NASA-CR-191366 | p 857 N93-14155

PHASE TRANSFORMATIONS
Is Ishtar Terra a thickened basaltic crust? p 1024 N93-14292
The gabbro-eclogite phase transition and the elevation of mountain belts on Venus p 1036 N93-14350
The effects of Venusian mantle convection with multiple phase transitions p 1043 N93-14385
Comments on 'Kinetic Study on the Hexacelsian-Celsian Phase Transformation'
| NASA-TM-105917 | p 850 N93-14886
Staggered fermions and chiral symmetry breaking in transverse lattice regulated QED
| DE92-040505 | p 977 N93-15378
Experimental attempt to metallize hydrogen at very high pressures
| AD-A257086 | p 843 N93-15497

PHASED ARRAYS
Optical signal distribution schemes for millimeter phased array radar
| AD-A256262 | p 858 N93-14437
Definition study PHARUS
| AD-A256560 | p 860 N93-14805
A power compensation system for phased operation of the JET A2 antenna arrays
| DE92-041020 | p 863 N93-15440

PHENOLIC RESINS
Characterization of fiber reinforced phenolic composites p 828 N93-14142

PHOTOCHEMICAL REACTIONS
Near-infrared oxygen airglow from the Venus nightside p 1026 N93-14308
Experimental and theoretical investigation of surface chemistry induced by direct and indirect electronic excitation
| AD-A256342 | p 843 N93-15200

PHOTOCONDUCTORS
Dual active layer photoconductor
| AD-D015423 | p 993 N93-14820

PHOTODETACHMENT
Threshold photodetachment spectroscopy
| AD-A255278 | p 842 N93-14671

PHOTODIODES
Ultraviolet spectroscopy of Comet Austin (1989c1) using a two-dimensional diode array detector p 1017 N93-14444
Organic/IR-Semiconductor heterojunctions for low-cost, high temperature IR arrays
| AD-A255971 | p 868 N93-15108

PHOTODISSOCIATION
Venus: The case for a wet origin and a runaway greenhouse p 1031 N93-14331
Final Report, 1 November 1988 - 31 October 1991 --- spectroscopy of adsorbed and photodissociated molecules
| AD-A255979 | p 976 N93-14424
Development of laser-ion beam photodissociation methods
| DE92-040512 | p 886 N93-15058
Experimental and theoretical investigation of surface chemistry induced by direct and indirect electronic excitation
| AD-A256342 | p 843 N93-15200
Photodissociation dynamics of cluster ions
| AD-A256375 | p 917 N93-15463

PHOTOELECTROCHEMISTRY
Photoelectrochemistry of electronic and electro-optical materials
| AD-A256239 | p 866 N93-14583

PHOTOELECTRON SPECTROSCOPY
Spectroscopy and reactions of hydrazoic acid on silicon single crystal surfaces (III). HN3 and DN3 on Si(111)-7 x 7
| AD-A255241 | p 842 N93-14669
Threshold photodetachment spectroscopy
| AD-A255278 | p 842 N93-14671

PHOTOELECTRONS
Threshold photodetachment spectroscopy
| AD-A255278 | p 842 N93-14671

PHOTOGEOLOGY
The geology of the Venera/Vega landing sites p 1024 N93-14296

PHOTOGRAMMETRY
Establishment of a test course for high accuracy dynamic positioning systems
| AD-A255407 | p 789 N93-14501

PHOTOGRAPHIC PROCESSING
Management and minimization of photographic wastes at Pantex Plant
| MHSMP-92-01 | p 910 N93-14739

PHOTOLITHOGRAPHY
A differential equation design method for finite-conjugate, multi-mirror imaging systems p 979 N93-14165

PHOTOLYSIS
C60 interactions with surfaces, gaseous species and photons: An overview
| DE92-040738 | p 978 N93-15654

PHOTOMETERS
Direct optical to microwave conversion
| RL-TR-91-375 | p 859 N93-14728
A temperature tracking SPICE2G.6 macromodel of the 6N134 optocoupler
| DE92-040093 | p 983 N93-15223

PHOTOMETRY
Calibration of the CCD Tully-Fisher relation with application to the Perseus-Pisces supercluster p 1016 N93-14194

PHOTONICS
Integrated photonics research technical digest series. Volume 10: Conference edition: Summaries of papers presented at the Integrated Photonics Research Topical Meeting
| AD-A255423 | p 981 N93-14506
Photonic materials and devices for optical information processing and computing applications
| AD-A256047 | p 982 N93-14578
A structural approach to the photonic processor
| N-3399-RC | p 986 N93-15648

PHOTONS
Using the Haleakala barrel extensive air shower array to study selected U.H.E. gamma ray point sources p 1050 N93-14639
High-energy emissions from young pulsars: Perspective from the outer gap model
| DE92-040365 | p 1022 N93-15324
C60 interactions with surfaces, gaseous species and photons: An overview
| DE92-040738 | p 978 N93-15654

PHOTOPLASTICITY
A simulation study of planar swaging deformation
| AD-A255908 | p 902 N93-15070

PHOTOPRODUCTION
Low energy theorems in pion production
| DE92-040071 | p 977 N93-15279

PHOTOSPHERE
Spatially resolved 10 micron spectra of circumstellar material around evolved stars p 1019 N93-14636

PHOTOVOLTAIC CELLS
Photovoltaic power system for a lunar base p 806 N93-14930

PHOTOVOLTAIC CONVERSION
NREL photovoltaic subcontract reports: Abstracts and document control information
| DE92-016408 | p 907 N93-14817
Photovoltaic power system for a lunar base p 806 N93-14930

PHYSICAL EXAMINATIONS
Transcutaneous Analyte Measuring Methods (TAMM), phase 2
| AD-A256327 | p 936 N93-15192
Improved head support stand adjustable by compoundturnbuckle
| AD-D015384 | p 936 N93-15249

PHYSICAL FITNESS
A progressive resistance weight training program designed to improve the armor crewman's strength
| AD-A255553 | p 934 N93-14556
Decision making in a dynamic task environment: The effect of time pressure
| AD-A256557 | p 937 N93-14602

PHYSICAL OPTICS
Radar scene generation for tactical decision aids
| AD-A257069 | p 863 N93-15495

PHYSIOLOGICAL EFFECTS
Bibliography of scientific publications of the Naval Biodynamics Laboratory
| AD-A255952 | p 1051 N93-14657

PICOSECOND PULSES
Three-dimensional guiding effects in a free-electron laser p 883 N93-14125

PIEZOELECTRIC CERAMICS
SDIO Workshop on Piezoelectric Ceramic Actuators for Space Applications
| AD-A255959 | p 990 N93-14422

PIEZOELECTRIC TRANSDUCERS
Reliability of sol-gel derived ferroelectric memories
| AD-A255358 | p 991 N93-14560

PIEZOELECTRICITY
SDIO Workshop on Piezoelectric Ceramic Actuators for Space Applications
| AD-A255959 | p 990 N93-14422
Broadband vibroacoustic frequency control via piezoelectric films
| ONERA-RT-8/3654-RY-010-R | p 974 N93-15129
Smart materials for Army structures
| AD-A254925 | p 836 N93-15218

PILOT PERFORMANCE
Evaluation and estimation of handling qualities via statistical modeling of pilot response data
| AD-A255324 | p 939 N93-14548
The relationship between computer scoring and safety-pilot grading of flight performance
| AD-A256245 | p 937 N93-14600
How expert pilots think p 786 N93-15017
Methodology for studying and training expertise p 786 N93-15018
Monitoring of pilot actions as part of a knowledge-based system for pilot assistance p 797 N93-15184
Simulator evaluation of displays for a revised takeoff performance monitoring system
| NASA-TP-3270 | p 803 N93-15366

PILOT TRAINING
Does cockpit management training reduce aircrew error? p 785 N93-15014
Cockpit decision making p 786 N93-15015
How expert pilots think p 786 N93-15017
Methodology for studying and training expertise p 786 N93-15018
Enhanced Aeronautical Resource Management training alternatives p 786 N93-15019
Embedded ADM reduces helicopter human error accidents p 787 N93-15024
Measuring risk in single-engine and twin-engine helicopters p 787 N93-15025

PILOTLESS AIRCRAFT
Unmanned aerial vehicles: More testing needed before production of short-range system
| AD-A256296 | p 790 N93-14440

PILOTS
Aviation accidents, incidents, and violations: Psychological predictors among US pilots p 783 N93-14693

PION BEAMS
Design features of a seven-cell high-gradient superconducting cavity
| DE92-040229 | p 870 N93-15424

PIONEER VENUS 1 SPACECRAFT
Venus gravity: Summary and coming events p 1042 N93-14377

PIONS
Low energy theorems in pion production
| DE92-040071 | p 977 N93-15279

PIPELINES
Acoustic location of leaks in pressurized underground petroleum pipelines
| PB92-207687 | p 975 N93-15647

PIPER AIRCRAFT
Special investigation report: Piper Aircraft Corporation PA-46 Malibu/Mirage Accidents/Incident, 31 May 1989 - 17 March 1991
| PB92-917007 | p 788 N93-15577

PIPES (TUBES)
Softening of rigid polyvinyl chloride by high concentrations of aqueous solutions of methylene chloride
[AD-A255453] p 848 N93-14486

PISTONS
Three position power cylinder
[AD-D015393] p 894 N93-15461

PITCHING MOMENTS
Multi-point inverse design of isolated airfoils and airfoils in cascade in incompressible flow p 790 N93-14462
Estimation of unsteady lift on a pitching airfoil from wake velocity surveys
[NASA-TM-105947] p 781 N93-14791

PIXELS
Object space temporal coherence for ray tracing p 955 N93-15554

PLAINS
Extensive lava flow fields on Venus: Preliminary investigation of source elevation and regional slope variations p 1034 N93-14342
Wrinkle ridges on Venusian plains: Indicators of shallow crustal stress orientations at local and regional scales p 1034 N93-14343
Venus: Preliminary geologic mapping of southern Beta Regio-northern Phoebe Regio p 1037 N93-14354

PLANAR STRUCTURES
A simulation study of planar swaging deformation
[AD-A255908] p 902 N93-15070
Failure of composite plates under static biaxial planar loading
[NASA-CR-191391] p 903 N93-15653

PLANE STRAIN
Large plastic deformations by sequential limit analysis: A finite element approach with applications in metal forming p 899 N93-14471

PLANE WAVES
Investigation of the on-surface boundary operators for electromagnetic scattering by conducting object p 857 N93-14189
The 3D modeling of high numerical aperture imaging in thin films p 985 N93-15513
A modal analysis of lamellar diffraction gratings in conical mountings p 986 N93-15519

PLANETARY ATMOSPHERES
Computer simulations of comet- and asteroidlike bodies passing through the Venusian atmosphere: Preliminary results on atmospheric and ground shock effects p 1040 N93-14365
Laboratory evaluation and application of microwave absorption properties under simulated conditions for planetary atmospheres
[NASA-CR-191298] p 1047 N93-15081

PLANETARY COMPOSITION
Mixed-valence iron minerals on Venus: Fe(2+)-Fe(3+) oxides and oxy-silicates formed by surface-atmosphere interactions p 1025 N93-14301
Venusian hydrology: Steady state reconsidered p 1028 N93-14318

PLANETARY CORES
Chemical differentiation on one-plate planets: Predictions and geologic observations for Venus p 1029 N93-14324

PLANETARY CRATERS
Ringed impact craters on Venus: An analysis from Magellan images p 1024 N93-14291
Constraints on the thermal evolution of Venus inferred from Magellan data p 1024 N93-14293
Monte Carlo modeling of the resurfacing of Venus p 1025 N93-14299
Bright crater outflows: Possible emplacement mechanisms p 1026 N93-14305
Monte Carlo computer simulations of Venus equilibrium and global resurfacing models p 1027 N93-14311
Western Aphrodite Terra, tectonics, geology, and line-of-sight gravity p 1029 N93-14322
Largest impact craters on Venus p 1030 N93-14326
Venusian extended ejecta deposits as time-stratigraphic markers p 1030 N93-14327
A model for the formation of the extended paraboloidal halos around some impact craters on Venus p 1037 N93-14352
Anomalous scattering behavior of selected impact parabola features: Magellan cycle-to-cycle comparisons p 1039 N93-14363
Impact craters on Venus: An overview from Magellan observations p 1040 N93-14369
Atmospheric effects on crater growth on Venus p 1041 N93-14370
Effect of impact angle on central-peak/peak-ring formation and crater collapse on Venus p 1041 N93-14371

PLANETARY CRUSTS
Is Ishtar Terra a thickened basaltic crust? p 1024 N93-14292
Coldspots or hotspots? The origin of plateau-shaped highlands on Venus p 1025 N93-14298
Thermal buoyancy on Venus: Preliminary results of finite element modeling p 1025 N93-14302
Visoelastic relaxation of Venusian coronae and mountain belts: Constraints on global heat flow and tectonism p 1027 N93-14313
Tectonics and volcanism of Eastern Aphrodite Terra: No subduction, no spreading p 1029 N93-14321
Western Aphrodite Terra, tectonics, geology, and line-of-sight gravity p 1029 N93-14322
Chemical differentiation on one-plate planets: Predictions and geologic observations for Venus p 1029 N93-14324
Venus tectonic styles and crustal differentiation p 1031 N93-14332
Wrinkle ridges on Venusian plains: Indicators of shallow crustal stress orientations at local and regional scales p 1034 N93-14343
Flexural models of trench/outer rise topography of coronae on Venus with axisymmetric spherical shell elastic plates p 1036 N93-14348
The gabbro-eclogite phase transition and the elevation of mountain belts on Venus p 1036 N93-14350
Chemical differentiation of a convecting planetary interior: Consequences for a one-plate planet such as Venus p 1038 N93-14358
Tectonic connections to interior processes on Venus p 1039 N93-14361
Cytherean crustal bending at Salme Dorsa p 1039 N93-14364
Constraints on crustal rheology and age of deformation from models of gravitational spreading in Ishtar Terra, Venus p 1042 N93-14379
Melting and differentiation in Venus with a cold start: A mechanism of the thin crust formation p 1042 N93-14381
Episodic plate tectonics on Venus p 1044 N93-14390

PLANETARY EVOLUTION
Constraints on the thermal evolution of Venus inferred from Magellan data p 1024 N93-14293
Surface processes on Venus p 1024 N93-14294
Global deformation on the surface of Venus p 1024 N93-14297
Monte Carlo modeling of the resurfacing of Venus p 1025 N93-14299
Bright crater outflows: Possible emplacement mechanisms p 1026 N93-14305
Monte Carlo computer simulations of Venus equilibrium and global resurfacing models p 1027 N93-14311
Chemical differentiation on one-plate planets: Predictions and geologic observations for Venus p 1029 N93-14324
Multiresolution pattern recognition of small volcanos in Magellan data p 1042 N93-14380
Melting and differentiation in Venus with a cold start: A mechanism of the thin crust formation p 1042 N93-14381
The effects of Venusian mantle convection with multiple phase transitions p 1043 N93-14385
Can a time-stratigraphic classification system be developed for Venus? p 1043 N93-14388

PLANETARY GEOLOGY
Ringed impact craters on Venus: An analysis from Magellan images p 1024 N93-14291
Is Ishtar Terra a thickened basaltic crust? p 1024 N93-14292
Constraints on the thermal evolution of Venus inferred from Magellan data p 1024 N93-14293
Shield fields: Concentrations of small volcanic edifices on Venus p 1024 N93-14295
The geology of the Venera/Vega landing sites p 1024 N93-14296
Global deformation on the surface of Venus p 1024 N93-14297
Debris avalanches and slumps on the margins of volcanic domes on Venus: Characteristics of deposits p 1025 N93-14300
Erosion versus construction: The origin of Venusian channels p 1025 N93-14303
Bright crater outflows: Possible emplacement mechanisms p 1026 N93-14305
Image processing and products for the Magellan mission to Venus p 1026 N93-14306
Global correlation of volcanic centers on Venus with uplands and with extension: Influence of mantle convection and altitude p 1026 N93-14309
Visoelastic relaxation of Venusian coronae and mountain belts: Constraints on global heat flow and tectonism p 1027 N93-14313
Flexural analysis of uplifted rift flanks on Venus p 1027 N93-14314
Radar scattering properties of pancakelike domes on Venus p 1028 N93-14316
Sequential deformation of plains along Tessera boundaries on Venus: Evidence from Alpha Regio p 1028 N93-14317
Determining stress states using dike swarms: The Lauma Dorsa example p 1028 N93-14319
Tectonics and volcanism of Eastern Aphrodite Terra: No subduction, no spreading p 1029 N93-14321
Western Aphrodite Terra, tectonics, geology, and line-of-sight gravity p 1029 N93-14322
Chemical differentiation on one-plate planets: Predictions and geologic observations for Venus p 1029 N93-14324
Venusian extended ejecta deposits as time-stratigraphic markers p 1030 N93-14327
Variations in lithospheric thickness on Venus p 1030 N93-14329
Igneous and tectonic evolution of Venusian and terrestrial coronae p 1031 N93-14330
Venus tectonic styles and crustal differentiation p 1031 N93-14332
Large shield volcanos on Venus: The effect of neutral buoyancy zone development on evolution and altitude distribution p 1032 N93-14333
Mantle plumes on Venus revisited p 1032 N93-14334
Venusian sinuous rilles p 1033 N93-14337
Large-volume lava flow fields on Venus: Dimensions and morphology p 1033 N93-14339
Derivation of surface properties from Magellan altimetry data p 1033 N93-14340
Extensive lava flow fields on Venus: Preliminary investigation of source elevation and regional slope variations p 1034 N93-14342
Wrinkle ridges on Venusian plains: Indicators of shallow crustal stress orientations at local and regional scales p 1034 N93-14343
Estimates of elastic plate thicknesses beneath large volcanos on Venus p 1035 N93-14344
Pancakelike domes on Venus p 1035 N93-14345
Magellan stereo images and Venusian geology p 1035 N93-14347
Flexural models of trench/outer rise topography of coronae on Venus with axisymmetric spherical shell elastic plates p 1036 N93-14348
Radar-anomalous, high-altitude features on Venus p 1036 N93-14349
The gabbro-eclogite phase transition and the elevation of mountain belts on Venus p 1036 N93-14350
A model for the formation of the extended paraboloidal halos around some impact craters on Venus p 1037 N93-14352
Venus: Preliminary geologic mapping of northern Atla Regio p 1037 N93-14353
Venus: Preliminary geologic mapping of southern Beta Regio-northern Phoebe Regio p 1037 N93-14354
Venus: Geology of Beta Regio rift system p 1037 N93-14355
The origins of radial fracture systems and associated large lava flows on Venus p 1038 N93-14356
Application of left- and right-looking SAR stereo to depth measurements of the Ammavaru outflow channel, Lada Terra, Venus p 1038 N93-14357
Chemical differentiation of a convecting planetary interior: Consequences for a one-plate planet such as Venus p 1038 N93-14358
Venus steep-sided domes: Relationships between geological associations and possible petrogenetic models p 1038 N93-14359
Tectonic connections to interior processes on Venus p 1039 N93-14361
The effects of Venus' thermal structure on buoyant magma ascent p 1040 N93-14366
Evidence for retrograde lithospheric subduction on Venus p 1040 N93-14367
Overview of Venus geology: Preliminary description of terrain units for Venus global geological mapping p 1040 N93-14368
Impact craters on Venus: An overview from Magellan observations p 1040 N93-14369
Atla Regio, Venus: Geology and origin of a major equatorial volcanic rise p 1041 N93-14374
Different types of small volcanos on Venus p 1042 N93-14378
Multiresolution pattern recognition of small volcanos in Magellan data p 1042 N93-14380
The tectonics of Venus: An overview p 1042 N93-14382
The spatial distribution of coronae on Venus p 1043 N93-14383
The effects of Venusian mantle convection with multiple phase transitions p 1043 N93-14385
Can a time-stratigraphic classification system be developed for Venus? p 1043 N93-14388
Directory of research projects: Planetary geology and geophysics program
[NASA-TM-4428] p 864 N93-15638

PLANETARY GRAVITATION
Is Ishtar Terra a thickened basaltic crust? p 1024 N93-14292
Coldspots or hotspots? The origin of plateau-shaped highlands on Venus p 1025 N93-14298
Western Aphrodite Terra, tectonics, geology, and line-of-sight gravity p 1029 N93-14322
Venus gravity: Summary and coming events p 1042 N93-14377
Structural characteristics and tectonics of northeastern Tellus Regio and Meni Tessera p 1044 N93-14389

PLANETARY IONOSPHERES
A study of the low and mid-latitude upper ionospheres of Jupiter and Saturn p 1022 N93-14179
The thermosphere and ionosphere of Venus p 1026 N93-14307
Venus internal magnetic field and its interaction with the interplanetary magnetic field p 1032 N93-14336
Evidence for lightning on Venus p 1043 N93-14386

PLANETARY MAGNETIC FIELDS
Venus internal magnetic field and its interaction with the interplanetary magnetic field p 1032 N93-14336
The solar wind interaction with Venus p 1034 N93-14341

PLANETARY MAGNETOSPHERES
The solar wind interaction with Venus p 1034 N93-14341

PLANETARY MANTLES
Venus tectonic styles and crustal differentiation p 1031 N93-14332
Mantle plumes on Venus revisited p 1032 N93-14334
Chemical differentiation of a convecting planetary interior: Consequences for a one-plate planet such as Venus p 1038 N93-14358
Tectonic connections to interior processes on Venus p 1039 N93-14361
The effects of Venus' thermal structure on buoyant magma ascent p 1040 N93-14366
Volcanism by melt-driven Rayleigh-Taylor instabilities and possible consequences of melting for admittance ratios on Venus p 1043 N93-14387

PLANETARY MAPPING
Venus radar mapping from the Venera 15 and 16 spacecrafts: Results and restrictions p 1023 N93-14289
Global deformation on the surface of Venus p 1024 N93-14297
Venus: Preliminary geologic mapping of northern Atla Regio p 1037 N93-14353
Venus: Preliminary geologic mapping of southern Beta Regio-northern Phoebe Regio p 1037 N93-14354
Venus: Geology of Beta Regio rift system p 1037 N93-14355
Anomalous scattering behavior of selected impact parabola features: Magellan cycle-to-cycle comparisons p 1039 N93-14363
Overview of Venus geology: Preliminary description of terrain units for Venus global geological mapping p 1040 N93-14368
Impact craters on Venus: An overview from Magellan observations p 1040 N93-14369
The geologic mapping of Venus using C-1 format: Sheets 75N254, 60N263 p 1041 N93-14375

PLANETARY METEOROLOGY
Synoptic/planetary-scale interactions and blocking over the North Atlantic Ocean
| NASA-CR-191376 | p 925 N93-14769

PLANETARY NEBULAE
Electron density diagnostics for gaseous nebulae involving the O 4 intercombination lines near 1400 A p 1012 N93-14762

PLANETARY RADIATION
The time variability of Jupiter's synchrotron radiation p 973 N93-14227
Study and interpretation of the millimeter-wave spectrum of Venus p 1045 N93-14596

PLANETARY ROTATION
The spin vector of Venus determined from Magellan data p 1027 N93-14310

PLANETARY STRUCTURE
Chemical differentiation of a convecting planetary interior: Consequences for a one-plate planet such as Venus p 1038 N93-14358
The effects of Venus' thermal structure on buoyant magma ascent p 1040 N93-14366

PLANETARY SURFACES
The tectonics of Venus: An overview p 1042 N93-14382

PLANETARY SYSTEMS
Orbital coplanarity in solar-type binary systems: Implications for planetary system formation and detection p 1020 N93-14867

PLANETARY TEMPERATURE
Constraints on the thermal evolution of Venus inferred from Magellan data p 1024 N93-14293
Flexural analysis of uplifted rift flanks on Venus p 1027 N93-14314

PLANETARY WAVES
A numerical study of the middle atmosphere response to tropical and subtropical tropospheric heat sources p 920 N93-14640

PLANETOLOGY
Martian water frost: Control of global distribution by small-scale processes p 1047 N93-14868

PLANFORMS
Flowfield study of a close-coupled canard configuration
| AD-A256311 | p 782 N93-15245

PLANKTON
Biofilm ecology of bioluminescent bacteria
| AD-A255282 | p 932 N93-14532

PLANNING
Information for management, planning, and decision-making in nonprofit organizations: Toward a comprehensive model p 1000 N93-14209
Scheduling and rescheduling with iterative repair
| NASA-TM-108120 | p 965 N93-15287
Rescheduling with iterative repair
| NASA-TM-108119 | p 965 N93-15288
Learning to improve iterative repair scheduling
| NASA-TM-108118 | p 965 N93-15289
An application of artificial intelligence to automatic telescopes
| NASA-TM-108115 | p 965 N93-15291
Knowledge and regularity in planning
| NASA-TM-108113 | p 965 N93-15293

PLANTS (BOTANY)
Comparison of the prevalence index and average wetland values for identification of wetland vegetation
| DE92-016701 | p 910 N93-15209

PLASMA ACCELERATORS
Experimental observations of the plasma properties of a high-density, low-temperature accelerated arc p 988 N93-14138
Interactions of relativistic electrons with relativistic plasma waves p 988 N93-14139

PLASMA CHEMISTRY
The evaluation of a concept for a Canadian-made automated multipurpose materials extraction facility p 810 N93-14947

PLASMA CONTROL
Plasma confinement theory and transport simulation
| DE92-040523 | p 988 N93-15327
A power compensation system for phased operation of the JET A2 antenna arrays
| DE92-041020 | p 863 N93-15440

PLASMA CURRENTS
Analysis of rotation experiments in TFTR --- tokamak fusion test reactor p 987 N93-14129
Current neutralization in ballistic transport of light ion beams
| AD-A256070 | p 976 N93-14662
A power compensation system for phased operation of the JET A2 antenna arrays
| DE92-041020 | p 863 N93-15440

PLASMA DENSITY
Opacity, equation of state, and radiation transport model for moderate density, eV-temperature plasmas
| AD-A256056 | p 988 N93-14579

PLASMA DIAGNOSTICS
Physics of x ray multilayer structures: Summaries of papers presented at the physics of x ray multilayer structures topical meeting, technical digest series, 1992, volume 7
| AD-A255383 | p 992 N93-14741
Electrical resistivity and equation of state measurements of a dense aluminum plasma
| DE92-040352 | p 989 N93-15436

PLASMA DIFFUSION
Opacity, equation of state, and radiation transport model for moderate density, eV-temperature plasmas
| AD-A256056 | p 988 N93-14579

PLASMA DRIFT
Comparison between irregularity motion and bulk plasma drifts at high latitudes
| PL-TR-91-2292 | p 914 N93-14727

PLASMA DYNAMICS
Plasma confinement theory and transport simulation
| DE92-040523 | p 988 N93-15327

PLASMA EQUILIBRIUM
Exact analytical solution of the toroidal singular mode equations
| DE92-040223 | p 988 N93-15419

PLASMA INTERACTION EXPERIMENT
The use of plasma ashers and Monte Carlo modeling for the projection of atomic oxygen durability of protected polymers in low Earth orbit p 819 N93-15596

PLASMA INTERACTIONS
The solar wind interaction with Venus p 1034 N93-14341
Leveling coatings for reducing the atomic oxygen defect density in protected graphite fiber epoxy composites p 819 N93-15597

PLASMA JETS
Lineshape analysis of laser light scattered by an argon thermal plasma jet p 987 N93-14137
An analysis of the SCEX 3 ionospheric electron beam injection experiment p 912 N93-14177

PLASMA POWER SOURCES
Quasars, galaxies, and pseudo-vacuum droplets
| NIKHEF-H/91-20 | p 1020 N93-14686

PLASMA PROPULSION
Opacity, equation of state, and radiation transport model for moderate density, eV-temperature plasmas
| AD-A256056 | p 988 N93-14579

PLASMA TEMPERATURE
Experimental observations of the plasma properties of a high-density, low-temperature accelerated arc p 988 N93-14138

PLASMA TURBULENCE
Turbulent magnetized plasmas from ionizing shock waves p 987 N93-14120
Experimental observations of the plasma properties of a high-density, low-temperature accelerated arc p 988 N93-14138

PLASMA WAVES
Interactions of relativistic electrons with relativistic plasma waves p 988 N93-14139
An analysis of the SCEX 3 ionospheric electron beam injection experiment p 912 N93-14177

PLASMA-PARTICLE INTERACTIONS
Conditioning electron beams in the ion-focused regime
| AD-A255635 | p 978 N93-14127

PLASMASPHERE
Evidence for lightning on Venus p 1043 N93-14386

PLASTIC DEFORMATION
Large plastic deformations by sequential limit analysis: A finite element approach with applications in metal forming p 899 N93-14471
On the structure of nonlinear constitutive equations for fiber reinforced composites
| NASA-CR-191024 | p 830 N93-14484
Determination of operable deformation mechanisms during ballistic impact in tungsten single crystals, utilizing transmission electron microscopy
| AD-A255351 | p 991 N93-14518
Use of the thin-walled torsion specimen
| AD-A255593 | p 901 N93-14790
A simulation study of planar swaging deformation
| AD-A255908 | p 902 N93-15070
Aeroplane crashes on the runway: Validation and final evaluation of the method of modeling an airframe structure
| IMFL-91-32 | p 792 N93-15126
An investigation of the processing, high temperature deformation and fracture characteristics of superplastic ceramics
| AD-A256519 | p 852 N93-15394

PLASTIC PROPERTIES
Deformation characterization of powdered metals in compaction and application of the finite element method to compaction processes p 844 N93-14472

PLATES (STRUCTURAL MEMBERS)
Non-linear analysis of wave progagation using transform methods and plates and shells using integral equations p 896 N93-14186
Modal interactions in the dynamic response of isotropic and composite plates p 829 N93-14221
Failure of composite plates under static biaxial planar loading
| NASA-CR-191391 | p 903 N93-15653

PLATES (TECTONICS)
Evidence for retrograde lithospheric subduction on Venus p 1040 N93-14367
Geoid, topography, and convection-driven crustal deformation on Venus p 1042 N93-14376
Melting and differentiation in Venus with a cold start: A mechanism of the thin crust formation p 1042 N93-14381
Episodic plate tectonics on Venus p 1044 N93-14390
Plate tectonics from VLBI and SLR global data
| NASA-CR-191319 | p 916 N93-14913

PLATINUM ALLOYS
Thermodynamics and transport in $Ce_3Bi_4Pt_3$ and related compounds
| DE92-040377 | p 998 N93-14905

PLATINUM COMPOUNDS
Nonuniformity effects in a hybrid platinum silicide imaging device
| AD-A256339 | p 983 N93-15197

PLUG NOZZLES
Nuclear thermal rocket nozzle testing and evaluation program
| NASA-TM-105962 | p 827 N93-15571

PLUGS
Thruster sealing system and apparatus
[NASA-CASE-MSC-21898-1] p 890 N93-14702

PLUMES
Satellite detection of complex aerosols over the Arabian Peninsula/Gulf
[AD-A256085] p 909 N93-14261
Mantle plumes on Venus revisited p 1032 N93-14334
A plume-induced boundary layer separation experiment
[AD-A255397] p 875 N93-14677
Second order closure modeling of turbulent buoyant wall plumes
[NASA-TM-105956] p 877 N93-14829
Low thrust chemical rocket technology
[NASA-TM-105927] p 827 N93-15572

PLUTONIUM
Plutonium pyrophoricity
[RFP-4517] p 845 N93-14723

PNEUMATIC EQUIPMENT
Jointed assembly actuated by fluid pressure
[AD-D015383] p 893 N93-15248

POINT SOURCES
Using the Haleakala barrel extensive air shower array to study selected U.H.E. gamma ray point sources p 1050 N93-14639
Development of a TDS measurement system. Application to acoustic propagation measurement in a non anechoic environment
[ONERA-RT-18/3641-PY] p 975 N93-15130

POISSON DENSITY FUNCTIONS
Hierarchical Poisson disk sampling distributions p 954 N93-15545

POISSON RATIO
Tensile properties of textile composites p 834 N93-14754

POLAR REGIONS
Magellan project p 1041 N93-14373
Faint high-latitude carbon stars p 1019 N93-14638
Martian water frost: Control of global distribution by small-scale processes p 1047 N93-14868

POLARIMETRY
Pioneer Venus polarimetry and haze optical thickness p 1032 N93-14335

POLARIZATION (CHARGE SEPARATION)
The effect of a seawater environment on the galvanic corrosion behavior of graphite/epoxy composites coupled to metals
[AD-A256072] p 830 N93-14232
Evidence for lightning on Venus p 1043 N93-14386

POLARIZATION (WAVES)
Conceptualization of a GaAs field effect transistor frequency tripler (2.5-7.5 GHz) for load use in communication satellites p 807 N93-14934
Integrated device with diffractive polarization components for a magneto-optical disk head p 986 N93-15517

POLARIZATION CHARACTERISTICS
Polarization properties and Earth-based radar measurements of Venus in the post-Magellan era p 1026 N93-14304

POLARIZED RADIATION
The evolution of the VLBI polarization of superluminal radio source 3C345 p 1050 N93-14229
Weak-electromagnetic interference in polarized eD scattering
[DE93-001763] p 978 N93-15486

POLARIZERS
High power millimetre-wave polarizers
[AD-A256558] p 867 N93-14803

POLICIES
The National Space Science Data Center: An operational perspective p 1002 N93-14775
Core support of the board on mathematical sciences
[AD-A255482] p 968 N93-14787
Core support for the Board on Mathematical Sciences
[AD-A256333] p 968 N93-15195

POLLUTION CONTROL
The evaluation of a concept for a Canadian-made automated multipurpose materials extraction facility p 810 N93-14947
Performing wind-tunnel modeling for better management of near-field risks
[DE92-040205] p 910 N93-15063
Modelling global methane emissions from livestock: Biological and nutritional controls
[NASA-CR-191354] p 911 N93-15480

POLLUTION TRANSPORT
Multiscale modeling of the long-range transport and fate of pollutants emitted from urban areas p 909 N93-14118
Performing wind-tunnel modeling for better management of near-field risks
[DE92-040205] p 910 N93-15063

POLYACETYLENE
Electronic, vibrational, and transport properties of conducting polymers p 847 N93-14170

POLYCARBONATES
Theoretical and experimental analysis of residual stress formation after implant resistance welding of polycarbonate p 898 N93-14279
A simulation study of planar swaging deformation
[AD-A255908] p 902 N93-15070

POLYCRYSTALS
Shear fatigue crack growth analysis in large-grain polycrystals p 993 N93-14838

POLYETHYLENES
Solid polymer electrolytes for rechargeable batteries
[DE93-001603] p 871 N93-15485

POLYGONIZATION
Physically-based methods for polygonization of implicit surfaces p 956 N93-15562

POLYGONS
Interactive solid geometry via partitioning trees p 952 N93-15535
Ray tracing polygons using spatial subdivision p 955 N93-15555
An interval refinement technique for surface intersection p 956 N93-15561

POLYHEDRONS
Interactive solid geometry via partitioning trees p 952 N93-15535
An extended cuberille model for identification and display of 3D objects from 3D gray value data p 953 N93-15542

POLYIMIDES
High temperature polymer dielectric film insulation
[AD-A255243] p 849 N93-14527
Low toxicity high temperature PMR polyimide
[NASA-CASE-LAR-14639-1] p 849 N93-14709

POLYMER CHEMISTRY
Oriented electro/optical polymers through in-situ chemistry during gel processing: A research opportunity
[AD-A255968] p 848 N93-14401

POLYMER MATRIX COMPOSITES
The effect of the interphase/interface region on creep and creep rupture of thermoplastic composites p 829 N93-14193
NMR imaging of elastomeric materials
[AD-A256034] p 841 N93-14658
Flow behavior in liquid molding p 833 N93-14747
Tensile properties of textile composites p 834 N93-14754

POLYMERIC FILMS
High temperature polymer dielectric film insulation
[AD-A255243] p 849 N93-14527
Waterborne polyurethane binder resins for compliant aircraft coatings
[AD-A256246] p 849 N93-14573
New nonlinear optical film processing
[AD-A256011] p 983 N93-15255

POLYMERIZATION
Oriented electro/optical polymers through in-situ chemistry during gel processing: A research opportunity
[AD-A255968] p 848 N93-14401
Low toxicity high temperature PMR polyimide
[NASA-CASE-LAR-14639-1] p 849 N93-14709
Spirobislactone acrylate polymers
[AD-D015443] p 850 N93-14802

POLYMERS
Applications of a constitutive equation for microstructural change in polymers p 848 N93-14222
Application of Fourier Transform-infrared spectroscopy (FT-IR) for materials analysis
[AD-A255727] p 838 N93-14435

POLYNOMIALS
Orthobaric densities and molar volumes of liquids. Halogenated ethylenes
[ESDU-92018] p 839 N93-14540
Introduction to real orthogonal polynomials
[AD-A256448] p 968 N93-14609
An implementation of multivariate B-spline surfaces over arbitrary triangulations p 952 N93-15534
Algorithms for intersecting parametric and algebraic curves p 956 N93-15560

POLYURETHANE RESINS
Waterborne polyurethane binder resins for compliant aircraft coatings
[AD-A256246] p 849 N93-14573
Characterization of impact-limiting material
[DE92-016767] p 902 N93-15210

POLYVINYL CHLORIDE
Softening of rigid polyvinyl chloride by high concentrations of aqueous solutions of methylene chloride
[AD-A255453] p 848 N93-14486

POROSITY
NMR imaging of elastomeric materials
[AD-A256034] p 841 N93-14658

POROUS MATERIALS
Fluids, gels, and glasses under extreme conditions of pressure and temperature
[AD-A255675] p 847 N93-14166
Development of braided rope seals for hypersonic engine applications: Flow modeling
[NASA-TM-105942] p 888 N93-14478

PORTABLE EQUIPMENT
A portable multiprocessor interface for standard ML of New Jersey
[AD-A255639] p 958 N93-14151

POSEIDON SATELLITE
Precision radiation force modeling for the TOPEX/Poseidon mission p 817 N93-14586
TOPEX/Poseidon science investigations plan
[NASA-CR-190616] p 925 N93-14964
The western Mediterranean Sea: An area for a regional validation for TOPEX/Poseidon and a field for geophysical and oceanographic studies p 926 N93-14965
The use of satellite altimetry in the study of weakly defined and variable oceanic gyres p 926 N93-14966
Terrestrial reference systems related to the TOPEX/Poseidon project p 906 N93-14967
North-Australian tropical seas circulation study p 926 N93-14968
Geophysical investigations with TOPEX/Poseidon altimetry data p 918 N93-14969
Mesoscale and large-scale variability of the Antarctic circumpolar current p 926 N93-14970
Ocean transport and variability studies of the South Pacific, Southern, and Indian Oceans p 927 N93-14971
Assimilation of altimeter topography into oceanic models p 927 N93-14972
Studies of the intermediate and deep circulation in the western equatorial Atlantic p 927 N93-14973
Application of TOPEX/Poseidon altimetry to ocean dynamics and geophysics p 927 N93-14974
Circulation of the gyres of the world ocean: Observation modeling using TOPEX/Poseidon altimeter data p 927 N93-14975
South African TOPEX/Poseidon altimeter experiment p 928 N93-14976
Global ocean tides through assimilation of oceanographic and altimeter satellite data in a hydrodynamic model p 928 N93-14978
Low-frequency variability of sea level as related to the heat balance of global oceans p 928 N93-14979
Studies of tropical ocean dynamics using the TOPEX/Poseidon altimeter-derived sea surface topography p 928 N93-14980
Ocean topography mapping, improvement of the marine geoid, and global permanent ocean circulation studies from TOPEX/Poseidon altimeter data p 928 N93-14981
Geophysical validation of TOPEX/Poseidon altimetry products p 918 N93-14982
Study of mass and heat transport of the tropical Atlantic Ocean using models and altimeter data p 929 N93-14983
Ocean circulation using altimetry p 929 N93-14984
The dynamics and energetics of midlatitude western boundary currents: A comparison of the Kuroshio Extension and the Gulf Stream p 929 N93-14985
General circulation of the South Atlantic between 5 deg N and 35 deg S p 929 N93-14987
Ocean dynamics in the Nordic Seas using satellite altimetry p 930 N93-14988
Application of TOPEX/Poseidon altimetry measurements to observational and modeling studies of the low-frequency upper ocean mass and heat circulation in the tropical Pacific p 930 N93-14989
Mean sea surface and gravity investigations using TOPEX/Poseidon altimeter data p 930 N93-14990
Global ocean tide mapping using TOPEX/Poseidon altimetry p 930 N93-14991
Present-day plate motions: Retrieval from the TOPEX/Poseidon orbitography network (DORIS system) p 918 N93-14993
Equatorial and eastern boundary current variability in the North and South Pacific Oceans p 931 N93-14994
An integrated research program for TOPEX/Poseidon with emphasis on the Pacific Ocean p 931 N93-14995
Oceanic transports of mass, heat, and salt in the western North Pacific p 931 N93-14996
The determination and interpretation of ocean surface topography using TOPEX/Poseidon altimeter data p 931 N93-14997
Analysis of altimeter data jointly with seafloor electric data (vertically integrated velocity) and VCTD-yoyo data (detailed profiles of VCTD) p 931 N93-14998
A TOPEX/Poseidon study of oceanic effects on observations of the Earth's interior p 918 N93-14999
Precise orbit computation and sea surface modeling p 813 N93-15000

Marine research using data from TOPEX/Poseidon
p 932 N93-15001
Global ocean circulation by altimetry
p 932 N93-15002
Vibration and acoustic testing of TOPEX/Poseidon satellite p 820 N93-15599

POSITION (LOCATION)
Workshop on noninvasive geophysical site characterization
[LA-12311-C] p 914 N93-14724
Acoustic location of leaks in pressurized underground petroleum pipelines
[PB92-207687] p 975 N93-15647

POSITION SENSING
Cooperative control of multiple space manipulators
p 805 N93-14923
An active tactile perception system
p 805 N93-14926

POSITIONING
Establishment of a test course for high accuracy dynamic positioning systems
[AD-A255407] p 789 N93-14501
Terrestrial reference systems related to the TOPEX/Poseidon project p 906 N93-14967

POTENTIAL ENERGY
Computed potential energy surfaces for chemical reactions
[NASA-CR-190741] p 843 N93-15356
Theoretical characterization of the potential energy surface for NH + NO
[NASA-CR-190741] p 843 N93-15357
A global potential energy surface for ArH2
[NASA-CR-190741] p 843 N93-15358

POTENTIAL FLOW
A compilation of the mathematics leading to the doublet lattice method
[AD-A256304] p 779 N93-14441

POTENTIOMETRIC ANALYSIS
The effect of a seawater environment on the galvanic corrosion behavior of graphite/epoxy composites coupled to metals
[AD-A256072] p 830 N93-14232

POWDER (PARTICLES)
Method of making substantially single phase superconducting oxide ceramics having a TC above 85 degrees
[AD-D015422] p 850 N93-14743
An evaluation of composites fabricated from powder epoxy towpreg p 832 N93-14745
Polymer infiltration studies
[NASA-CR-191652] p 852 N93-15431

POWDER METALLURGY
The effect of processing and compositional changes on the tribology of PM212 in air
[NASA-TM-105945] p 828 N93-15576

POWER AMPLIFIERS
NPR and intermodulation in mobile satellite systems
p 806 N93-14931

POWER CONDITIONING
Ion thruster development at NASA Lewis Research Center
[NASA-TM-105983] p 827 N93-15429
EMTP based stability analysis of space station electric power system in a test bed environment
[NASA-TM-105845] p 871 N93-15503
Power requirements for the first lunar outpost (FLO)
[NASA-TM-105925] p 909 N93-15523

POWER CONVERTERS
Internal grounding arrangement in a switching power converter
[AD-D015435] p 868 N93-14826
Power conversion system modification to permit use of DC power source
[AD-D015409] p 868 N93-14887
A feasibility assessment of magnetic bearings for free-piston Stirling space power converters
[NASA-CR-189135] p 891 N93-14916
Summary of the NASA Lewis component technology program for Stirling power converters
[NASA-TM-105640] p 827 N93-15526

POWER EFFICIENCY
Cooperative control of multiple space manipulators
p 805 N93-14923

POWER SERIES
Introduction to real orthogonal polynomials
[AD-A256448] p 968 N93-14609

POWER SUPPLIES
Power requirements for the first lunar outpost (FLO)
[NASA-TM-105925] p 909 N93-15523

PREAMPLIFIERS
Development of a High Resolution Liquid Xenon Imaging Telescope for Medium Energy Gamma Ray Astrophysics
[NASA-CR-191781] p 1013 N93-15589

PRECESSION
Aspects of parking orbit selection in a manned Mars mission
[NASA-TP-3256] p 813 N93-15367

PRECIPITATION (METEOROLOGY)
Synoptic scale structure of summertime wet and dry spells in northeastern Kansas p 923 N93-14919

PRECIPITATION HARDENING
Exceptionally high-strength (approximately 3 GPa) aluminum alloys demonstrated by oxygen ion implantation
[DE92-040980] p 847 N93-15383

PRECISION
Integration and processing of high-resolution moire-interferometry data p 895 N93-14185
The effects of acceleration on precision frequency sources
[AD-A255465] p 972 N93-14496
Precision tests of gravitation: Liquid-supported torsion balance experiments and a tower experiment
p 914 N93-14589
Parameterization in finite precision
p 953 N93-15537

PRECONDITIONING
Preconditioned conjugate-gradient methods for low-speed flow calculations
[NASA-TM-105929] p 877 N93-14885

PREDICTION ANALYSIS TECHNIQUES
Resistive magnetohydrodynamic studies of tearing mode instability with equilibrium shear flow and magnetic reconnection p 987 N93-14122
Evaluation of three models used for predicting noise propagated long distances overground
[AD-A255963] p 973 N93-14406
Intelligent path prediction for vehicular travel
p 961 N93-14445
Reliability of stiffened structural panels: Two examples
[NASA-TM-107687] p 900 N93-14483
Advanced technology wind shear prediction system evaluation p 785 N93-14858
LARZAC HP turbine disk crack initiation and propagation spin pit test p 799 N93-14892
Analytical and experimental evaluation of joining ceramic oxides to ceramic oxides and ceramic oxides to metal for advanced heat engine applications
[DE92-041383] p 851 N93-15294
Predicting database requirements for geographic information systems in the year 2000: Long-term design issues for GRASS
[AD-A256862] p 1009 N93-15627

PREDICTIONS
Aviation accidents, incidents, and violations: Psychological predictors among US pilots
p 783 N93-14693
Development of the Advance Warning Airborne System(AWAS) p 784 N93-14849
In-service evaluation of wind shear systems
p 785 N93-14857
Advanced technology wind shear prediction system evaluation p 785 N93-14858
A neural network prototype for predicting F-14B strains at the B.L. 10 longeron
[AD-A255272] p 792 N93-15004
A fundamental understanding of the effects of ceramic processing on product microstructure
[AD-A255729] p 850 N93-15049
Predicting polymer properties by computational methods 2: A comparison of semi-empirical methods
[AD-A256856] p 854 N93-15640

PREFLIGHT OPERATIONS
Scheduling and rescheduling with iterative repair
[NASA-TM-108120] p 965 N93-15287
Rescheduling with iterative repair
[NASA-TM-108119] p 965 N93-15288

PREFORMS
Development of generalized 3-D braiding machines for composite preforms p 833 N93-14749

PREMIXED FLAMES
Fundamentals of combustion of premixed gases
p 840 N93-14618
Direct simulation of turbulent combustion
p 840 N93-14622
Calculation of chemical reaction rates in turbulent combustion p 841 N93-14625

PRESERVING
The preservation of LANDSAT data by the National Land Remote Sensing Archive p 1003 N93-14777

PRESSURE
Time-dependent predictions and analysis of turbine cascade data in the transonic flow region
[PNR-90957] p 782 N93-15489

PRESSURE DISTRIBUTION
Pressure distribution for the wing of the YAV-8B airplane; with and without pylons
[NASA-TM-4429] p 779 N93-14451
Pressure drag and lift contributions for blunted forebodies of fineness ratio 2.0 in transonic flow (M infinity less than or equal to 1.4)
[ESDU-89033] p 779 N93-14515

PRESSURE DRAG
Pressure drag and lift contributions for blunted forebodies of fineness ratio 2.0 in transonic flow (M infinity less than or equal to 1.4)
[ESDU-89033] p 779 N93-14515

PRESSURE EFFECTS
Fluids, gels, and glasses under extreme conditions of pressure and temperature
[AD-A255675] p 847 N93-14166
Atmospheric effects on crater growth on Venus
p 1041 N93-14370

PRESSURE MEASUREMENT
Optical probes for laser induced shocks
[AD-A256092] p 884 N93-14284
Flowfield study of a close-coupled canard configuration
[AD-A256311] p 782 N93-15245
Surface gravity waves and ambient microseismic noise
[AD-A256498] p 916 N93-15375
Upgrade and extension of the data acquisition system for propulsion and gas dynamic laboratories
[AD-A256836] p 1009 N93-15637

PRESSURE OSCILLATIONS
Surface gravity waves and ambient microseismic noise
[AD-A256498] p 916 N93-15375
Unsteady pressure loads in a generic high speed engine model
[NASA-TP-3189] p 975 N93-15391

PRESSURE RATIO
Pressure drag and lift contributions for blunted forebodies of fineness ratio 2.0 in transonic flow (M infinity less than or equal to 1.4)
[ESDU-89033] p 779 N93-14515
Supersonic investigation of two dimensional hypersonic exhaust nozzles
[NASA-TM-105687] p 800 N93-15342

PRESSURE RECOVERY
Investigations of detail design issues for the high speed acoustic wind tunnel using a 60th scale model tunnel. Part 1: Tests with open circuits
[NASA-CR-191671] p 780 N93-14737

PRESSURE SENSORS
Development of advanced seal verification
[NASA-CR-184502] p 892 N93-15117
Surface gravity waves and ambient microseismic noise
[AD-A256498] p 916 N93-15375

PRETREATMENT
Surface preparation of stainless steel prior to painting
[AD-A256253] p 838 N93-14454
A study for the development of practices to protectively coat and join fibre epoxy composites for use in the Space Station Programme
[CTN-93-60626] p 835 N93-15145

PRIMERS
Surface preparation of stainless steel prior to painting
[AD-A256253] p 838 N93-14454

PRIMERS (EXPLOSIVES)
Mechanical shielding for electric primer
[AD-D015417] p 860 N93-14889

PRINTED CIRCUITS
A robotic planning system p 810 N93-14949

PRINTERS (DATA PROCESSING)
A Unix print filter for controlling an HP Laserjet printer
[DE92-041350] p 946 N93-14902

PROBABILITY DISTRIBUTION FUNCTIONS
An energy analysis of the pseudo Wigner-Ville distribution in support of machinery monitoring and diagnostics
[AD-A256202] p 889 N93-14499
PDF transport modelling p 840 N93-14623
Applications of PDF turbulent combustion models to real non premixed flame calculations p 841 N93-14624

PROBABILITY THEORY
Arc digital raster imagery evaluation
[AD-A255403] p 817 N93-14565
A probabilistic approach to anytime algorithm for intelligent real-time problem solving
[AD-A255709] p 945 N93-14654
Probabilistic inference
[AD-A255471] p 963 N93-14786
Modified fast frequency acquisition via adaptive least squares algorithm
[NASA-CASE-NPO-17845-2-CU] p 945 N93-14882
A proposal to apply Taguchi-inspired methods to the reduction of machining variance
[AD-A256129] p 856 N93-15234

PROBLEM SOLVING
Knowledge and processes in design
[AD-A255663] p 999 N93-14130

The effect of a hierarchical task-specific external conceptual model on the learnability and usability of microcomputer applications by novices
p 1000 N93-14205
A probabilistic approach to anytime algorithm for intelligent real-time problem solving
| AD-A255709 | p 945 N93-14654
Undetermined coefficient problems for quasi-linear parabolic equations
| AD-A256012 | p 969 N93-15256
Minimizing conflicts: A heuristic repair method for constraint-satisfaction and scheduling problems
| NASA-TM-108121 | p 964 N93-15286
Scheduling and rescheduling with iterative repair
| NASA-TM-108120 | p 965 N93-15287
Rescheduling with iterative repair
| NASA-TM-108119 | p 965 N93-15288
Learning to improve iterative repair scheduling
| NASA-TM-108118 | p 965 N93-15289
A beginner's guide to belief revision and truth maintenance systems
| NASA-TM-108117 | p 965 N93-15290
MATE: The multi-agent test environment
| NASA-TM-108114 | p 965 N93-15292
Knowledge and regularity in planning
| NASA-TM-108113 | p 965 N93-15293
Exact analytical solution of the toroidal singular mode equations
| DE92-040223 | p 988 N93-15419
Telepresence: Integrating shared task and person spaces p 954 N93-15548
CSCW - WCSC: Computer-supported cooperative work. What changes for the science of computing
p 954 N93-15549

PROCESS CONTROL (INDUSTRY)
Organization of workshop on emerging technologies for in-situ processing
| AD-A255977 | p 865 N93-14410
Flow behavior in liquid molding p 833 N93-14747
PEX: A reactive procedure based decision maker
| REPT-921-440-105 | p 999 N93-15118
Technology evaluation report: The Carver-Greenfield process, Dehydro-Tech Corporation
| PB92-217462 | p 910 N93-15217

PROCUREMENT MANAGEMENT
Streamlined acquisition handbook
| NASA-TM-108133 | p 1002 N93-14719
VHDL (VHSIC hardware description language) use in the US defense procurement process
| VH-2 | p 948 N93-15263

PROCUREMENT POLICY
VHDL (VHSIC hardware description language) use in the US defense procurement process
| VH-2 | p 948 N93-15263

PRODUCT DEVELOPMENT
Software Technology for Adaptable, Reliable Systems (STARS) program. Software process tools and techniques evaluation report, version 1.0. Task IS15: Software process management
| AD-A255945 | p 942 N93-14405
ATL Products Division's entries into the computer mass storage marketplace p 1005 N93-15038
Regional satellites: The European experience with Eutelsat for TV, voice, data and mobile transmissions
| REPT-921-440-106 | p 818 N93-15071
The extended VHDL (VHSIC hardware description language) design environment: An unique integrated system and hardware design environment
| VH-3 | p 948 N93-15264
Integrated support for real-time control systems
| PNR-90994 | p 952 N93-15476

PRODUCTION ENGINEERING
Advances in 3-dimensional braiding
p 833 N93-14748
Development of generalized 3-D braiding machines for composite preforms p 833 N93-14749

PRODUCTION MANAGEMENT
Software Management Environment (SME) installation guide
| NASA-TM-108578 | p 957 N93-15578
TQM in a test environment p 823 N93-15620

PROFILOMETERS
Mach 5 electroformed nickel nozzle refurbishment FNAS investigation of ultra-smooth surfaces
| NASA-CR-191416 | p 826 N93-14681

PROGRAM VERIFICATION (COMPUTERS)
Representation and manipulation of inductive boolean functions
| AD-A256078 | p 967 N93-14235
Iterative software testing
| AD-A255953 | p 943 N93-14420
Trace algebra for automatic verification of real-time concurrent systems
| AD-A256199 | p 968 N93-14492
Program verification using higher order logic
| AD-A255408 | p 943 N93-14502
Software reliability, measurement, and testing software reliability and test integration, volume 1
| AD-A256242 | p 944 N93-14572
Software reliability, measurement, and testing. Volume 2: Guidebook for software reliability measurement and testing
| AD-A256164 | p 944 N93-14581
Formal verification of an oral messages algorithm for interactive consistency
| NASA-CR-189704 | p 958 N93-14808
Research in programming languages and software engineering
| AD-A256341 | p 947 N93-15199
Aspects of a parallel-architecture simulator
| AD-A256872 | p 941 N93-15628

PROGRAMMABLE LOGIC DEVICES
Output data formatter for the Electronically Scanned Thinned Array Radiometer (ESTAR) instrument
| NASA-TM-4432 | p 871 N93-15529
Application of programmable logic controllers to space simulation p 821 N93-15608
From diffusion pumps to cryopumps: The conversion of GSFC's space environment simulator
p 814 N93-15611

PROGRAMMING ENVIRONMENTS
User manual for the Software Technology for Adaptable, Reliable Systems (STARS). PCTE Browser Tool (PBT) version 0.1 SunOS implementation
| AD-A257064 | p 951 N93-15457
Flight dynamics system software development environment (FDS/SDE) tutorial
| NASA-TM-108580 | p 952 N93-15502
Program auralization: Sound enhancements to the programming environment p 953 N93-15539
A minimalist global user interface p 957 N93-15566
Software Management Environment (SME) installation guide
| NASA-TM-108578 | p 957 N93-15578
Data collection procedures for the Software Engineering Laboratory (SEL) database
| NASA-TM-108579 | p 957 N93-15579

PROGRAMMING LANGUAGES
Proof of theorems in Z
| AD-A255711 | p 968 N93-14431
Information system constraint language (ISyCL)
| AD-A256268 | p 976 N93-14438
Obstacles in object-oriented software development
| MEMO-INF-92-15 | p 946 N93-15084
Research in programming languages and software engineering
| AD-A256341 | p 947 N93-15199
Proceedings of the International Conference on CAD/CAM and AMT. Volume 4: VHDL (VHSIC Hardware Description Language) Seminar
| ITN-92-85130 | p 947 N93-15261
VHDL (VHSIC hardware description language): Origins, status, capabilities, and world environment
| VH-1 | p 947 N93-15262
VHDL (VHSIC hardware description language) use in the US defense procurement process
| VH-2 | p 948 N93-15263
System design in a large corporation, using VHDL (VHSIC hardware description language)
| VH-4 | p 948 N93-15265
Integrating VHDL (VHSIC hardware description language) with existing EDA tools
| VH-8 | p 948 N93-15268
Proceedings of the REXX Symposium for Developers and Users
| DE92-041359 | p 951 N93-15451
An axiomatic treatment of partial correctness and deadlock in a shared variable parallel language
| AD-A256234 | p 960 N93-15494
Escape-time visualization method for language-restricted iterated function systems
p 956 N93-15558

PROJECT MANAGEMENT
The V-22 Osprey: A case analysis
| AD-A256445 | p 791 N93-14601
EDI planning and implementation guide
| AD-A255737 | p 1007 N93-15050
Center for Advanced Propulsion Systems (Research)
| AD-A256628 | p 893 N93-15410

PROJECT PLANNING
Earth environment space initiative
p 811 N93-14953
The CPG 5-kW(e) Dish-Stirling Development Program
| DE92-017050 | p 907 N93-15134
Query optimization and planning in object-oriented knowledge bases
| AD-A256006 | p 1008 N93-15254
Space Station Freedom user's guide
| NASA-TM-108105 | p 825 N93-15650

PROJECTILE CRATERING
Atmospheric effects on crater growth on Venus
p 1041 N93-14370
Effect of impact angle on central-peak/peak-ring formation and crater collapse on Venus
p 1041 N93-14371

PROJECTILES
Experimental observations of the plasma properties of a high-density, low-temperature accelerated arc
p 988 N93-14138
A preliminary investigation of dual mode fracture sustained by graphite/epoxy laminates impacted by high-velocity spherical metallic projectiles
| AD-A255790 | p 898 N93-14419
Strain-rate effects in replica scale model penetration experiments
| AD-A255426 | p 844 N93-14508

PROJECTORS
Advantages of using a projected head-up display in a flight simulator
| AD-A255332 | p 804 N93-14559

PROLOG (PROGRAMMING LANGUAGE)
Design and implementation of practical constraint logic programming systems
| AD-A256191 | p 943 N93-14558
Multiple robot programming using concurrent logic language
| F-3-3 | p 950 N93-15304

PROPAGATION
Conditioning electron beams in the ion-focused regime
| AD-A255635 | p 978 N93-14127

PROPAGATION VELOCITY
Imaging Earth's interior: Tomographic inversions for mantle P-wave velocity structure p 913 N93-14225

PROPELLANT COMBUSTION
Introduction to spray combustion modelling
p 841 N93-14626
Combustion in supersonic flows p 841 N93-14627
Investigation of the aerothermodynamics of hypervelocity reacting flows in the ram accelerator
| NASA-CR-191715 | p 783 N93-15588

PROPELLANT GRAINS
Propellant grain assembly for a gas generator
| AD-D015439 | p 854 N93-14801

PROPELLANT SPRAYS
Introduction to spray combustion modelling
p 841 N93-14626

PROPELLANTS
Absorption of propellant vapors into polymer films
| AD-A255274 | p 849 N93-14531

PROPELLER BLADES
Root damage analysis of aircraft engine blade subject to ice impact
| NASA-TM-105779 | p 902 N93-15343

PROPELLERS
Estimation of rate of climb
| ESDU-92019 | p 791 N93-14541

PROPORTIONAL COUNTERS
Quasar x-ray spectra revisited p 1012 N93-14760
Explaining cloud chamber tracks
| DE92-040502 | p 972 N93-15057

PROPOSALS
Directory of research projects: Planetary geology and geophysics program
| NASA-TM-4428 | p 864 N93-15638

PROPRIOCEPTION
Cooperative control of multiple space manipulators
p 805 N93-14923

PROPRIOCEPTORS
An active tactile perception system
p 805 N93-14926

PROPULSION SYSTEM CONFIGURATIONS
Experimental determination of magnetohydrodynamic seawater thruster performance in a two Tesla test facility
| DE92-019042 | p 826 N93-15215
Center for Advanced Propulsion Systems (Research)
| AD-A256628 | p 893 N93-15410
Dual-Shaft Electric Propulsion (DSEP) Technology Development Program
| DE92-040189 | p 894 N93-15416
Development of NASA/DOE NTP system performance models
| NASA-TM-105982 | p 827 N93-15428
Nuclear thermal rocket nozzle testing and evaluation program
| NASA-TM-105962 | p 827 N93-15571
Combined high and low thrust propulsion for fast piloted Mars missions
| NASA-CR-190788 | p 828 N93-15584

PROPULSION SYSTEM PERFORMANCE
Experimental determination of magnetohydrodynamic seawater thruster performance in a two Tesla test facility
| DE92-019042 | p 826 N93-15215
Center for Advanced Propulsion Systems (Research)
| AD-A256628 | p 893 N93-15410
Dual-Shaft Electric Propulsion (DSEP) Technology Development Program
| DE92-040189 | p 894 N93-15416

Development of NASA/DOE NTP system performance models
| NASA-TM-105982 | p 827 N93-15428
Ion thruster development at NASA Lewis Research Center
| NASA-TM-105983 | p 827 N93-15429
Propulsion system performance resulting from an integrated flight/propulsion control design
| NASA-TM-105874 | p 801 N93-15525
Nuclear thermal rocket nozzle testing and evaluation program
| NASA-TM-105962 | p 827 N93-15571
Upgrade and extension of the data acquisition system for propulsion and gas dynamic laboratories
| AD-A256836 | p 1009 N93-15637

PROSTHETIC DEVICES
Bar-holding prosthetic limb
| NASA-CASE-MFS-28481-1 | p 939 N93-14870

PROTECTIVE CLOTHING
Aerospace medicine and biology: A continuing bibliography with indexes (supplement 369)
| NASA-SP-7011(369) | p 935 N93-14731

PROTECTIVE COATINGS
Biofilm ecology of bioluminescent bacteria
| AD-A255282 | p 932 N93-14532
Waterborne polyurethane binder resins for compliant aircraft coatings
| AD-A256246 | p 849 N93-14573
A study for the development of practices to protectively coat and join fibre epoxy composites for use in the Space Station Programme
| CTN-93-60626 | p 835 N93-15145
Impact of protective oxides on cathode-side resistances in MCFCs
| DE92-019973 | p 994 N93-15221
Leveling coatings for reducing the atomic oxygen defect density in protected graphite fiber epoxy composites
| NASA-TM-105732 | p 852 N93-15344
Leveling coatings for reducing the atomic oxygen defect density in protected graphite fiber epoxy composites
p 819 N93-15597

PROTEINS
Nerves and tissue repair
| AD-A255299 | p 934 N93-14535
Biophysical and biochemical mechanisms in synaptic transmitter release
| AD-A256340 | p 936 N93-15198

PROTOCOL (COMPUTERS)
Wait-free consensus
| AD-A255978 | p 943 N93-14423
The role of HiPPI switches in mass storage systems: A five year prospective p 1002 N93-14774
Requirements for a network storage service
p 1003 N93-14781
Nonblocking and orphan free message logging protocols
| NASA-CR-191631 | p 862 N93-15339
Parallel simulation today
| NASA-CR-189733 | p 951 N93-15432

PROTON-PROTON REACTIONS
The gamma ray spectrum resulting from pp interactions in quasars p 1051 N93-14917

PROTONS
Excitation of nuclei by antiproton annihilation at rest
| AD-A255447 | p 976 N93-14513
Strong interactions studies with medium energy probes
| DE92-040460 | p 977 N93-15377
Global zones of particle precipitation as observed by EXOS-C
| AD-A256397 | p 917 N93-15466

PROTOTYPES
Full surface testing of grazing incidence mirrors
| AD-A255644 | p 979 N93-14152
Design, development, and testing of a prototype optical system for a next generation multiplexed imager
| AD-A256538 | p 981 N93-14286
Systems modeling
| AD-A255215 | p 944 N93-14575
A neural network prototype for predicting F-14B strains at the B.L. 10 longeron
| AD-A255272 | p 792 N93-15004

PROVING
Design, development, and testing of a prototype optical system for a next generation multiplexed imager
| AD-A256538 | p 981 N93-14286
Formal verification of an oral messages algorithm for interactive consistency
| NASA-CR-189704 | p 958 N93-14808
Geophysical validation of TOPEX/Poseidon altimetry products p 918 N93-14982
Independent validation testing of the FLAME computer code, version 1.0
| DE92-019691 | p 948 N93-15274
An axiomatic treatment of partial correctness and deadlock in a shared variable parallel language
| AD-A256234 | p 960 N93-15494

PSYCHOLOGICAL TESTS
Simultaneous DIF amplification and cancellation: Shealy-Stout test for DIF
| AD-A256284 | p 970 N93-14455

PSYCHOMETRICS
A psychometrically sound cognitive diagnostic model: Effect of remediation as empirical validity
| AD-A255926 | p 933 N93-14109

PSYCHOMOTOR PERFORMANCE
Publications of the Space Physiology and Countermeasures Program, Neuroscience Discipline: 1980-1990
| NASA-CR-4476 | p 936 N93-15583

PSYCHOPHYSICS
Psychophysical analyses of perceptual representations
| AD-A255432 | p 936 N93-14510
Higher order mechanisms of color vision
| AD-A256369 | p 938 N93-15329
High-resolution contrast control on a video display: Method and calibration
| AD-A256552 | p 938 N93-15400

PSYCHOPHYSIOLOGY
Statistical analysis of the human strangulation experiments: Comparison to +Gz-induced loss of consciousness
| AD-A255485 | p 935 N93-14789

PULLING
Fiber pulling apparatus modification
| NASA-CR-184498 | p 891 N93-14763

PULSARS
Dynamics in neutron stars and the early universe
p 1014 N93-14112
Compact objects in the disk and globular clusters
p 1018 N93-14594
Search for pulsed gamma ray emission from SN1987A and the Vela pulsar p 1050 N93-14634
High-energy emissions from young pulsars: Perspective from the outer gap model
| DE92-040365 | p 1022 N93-15324

PULSE CODE MODULATION
On the theory of coded modulation systems for high output digital transmission
| TELECOM-PARIS-92-E-001 | p 861 N93-15098

PULSE COMMUNICATION
Investigation of the use of surface electrical currents for short-range shipboard data communications
| AD-A256197 | p 859 N93-14490
Integration of satellite links into an ATM mode broadband ISDN
| TELECOM-PARIS-91-E-022 | p 861 N93-15097
On the theory of coded modulation systems for high output digital transmission
| TELECOM-PARIS-92-E-001 | p 861 N93-15098

PULSE DURATION
Compact high PRF CO2 transmitter
| AD-A255985 | p 884 N93-14414

PULSE GENERATORS
Beam trapping in a modified betatron with a localized bipolar electric field pulse
| AD-A255414 | p 866 N93-14504
High performance pulse generator
| AD-D015378 | p 869 N93-15269

PULSE RADAR
The detection and correlation modeling of Rayleigh distributed radar signals
| AD-A256612 | p 858 N93-14250
Method and apparatus for increasing a radar's range with improved scan-to-scan integration of Doppler filtered signals
| AD-D015421 | p 860 N93-14742

PULSE RATE
Compact high PRF CO2 transmitter
| AD-A255985 | p 884 N93-14414

PULSE REPETITION RATE
High performance pulse generator
| AD-D015378 | p 869 N93-15269

PULSED LASERS
Optical probes for laser induced shocks
| AD-A256092 | p 884 N93-14284
Compact high PRF CO2 transmitter
| AD-A255985 | p 884 N93-14414
Ultrashort-pulse laser system: Theory of operation and operating procedures
| AD-A257023 | p 887 N93-15472

PUNCHES
Method of local shaping of thermoplastics
| AD-A255913 | p 856 N93-15105

PURSUIT TRACKING
Implementation of the pure pursuit path tracking algorithm
| AD-A255524 | p 944 N93-14569

PYLONS
Pressure distribution for the wing of the YAV-8B airplane: with and without pylons
| NASA-TM-4429 | p 779 N93-14451

PYROLYSIS
New electronic materials
| AD-A255612 | p 868 N93-15010
Thermal decomposition of HNIW and HNIW-Based formulations
| AD-A255613 | p 854 N93-15011

PYROPHORIC MATERIALS
Plutonium pyrophoricity
| RFP-4517 | p 845 N93-14723

PYROTECHNICS
The sensitivity of energetic materials to friction, impact, and electrostatic stimuli
| DE92-041227 | p 855 N93-15478

Q

Q SWITCHED LASERS
Compact high PRF CO2 transmitter
| AD-A255985 | p 884 N93-14414

QUALITATIVE ANALYSIS
Application of Fourier Transform-infrared spectroscopy (FT-IR) for materials analysis
| AD-A255727 | p 838 N93-14435

QUALITY CONTROL
Development of an environment for software reliability model selection
| AD-A256609 | p 942 N93-14241
The use of International Standards Organization ISO 9000 quality assurance standards in place of military standards
| AD-A256203 | p 894 N93-14500
Data management in NOAA p 1003 N93-14779
SIDR Relative Weighted Product (RWP) assignment process
| AD-A255801 | p 946 N93-15068
Off-line generation of error-free robot/NC (numerical control) code using simulation and automatic programming techniques
| F-3-1 | p 949 N93-15302
Acoustic resonance techniques for quality control
| DE92-040150 | p 895 N93-15413
Characteristics of the Nova laser disk edge cladding epoxy
| DE92-041046 | p 853 N93-15462

QUANTUM CHROMODYNAMICS
Low energy theorems in pion production
| DE92-040071 | p 977 N93-15279
Dark matter axions
| DE92-040501 | p 1022 N93-15346
Strong interactions studies with medium energy probes
| DE92-040460 | p 977 N93-15377
Schwinger Dyson equations: Dynamical chiral symmetry breaking and confinement
| DE92-040717 | p 978 N93-15657

QUANTUM EFFICIENCY
Performance characteristics of STIS detectors
| NASA-CR-191636 | p 868 N93-14915

QUANTUM ELECTRODYNAMICS
Staggered fermions and chiral symmetry breaking in transverse lattice regulated QED
| DE92-040505 | p 977 N93-15378
Homogeneous quantum electrodynamic turbulence
| NASA-TM-107686 | p 979 N93-15482

QUANTUM ELECTRONICS
Solid state research
| AD-A256019 | p 992 N93-14576

QUANTUM MECHANICS
Quantum fluctuations in stimulated Raman scattering
p 857 N93-14126
Gas-solid dynamics at disordered and adsorbate covered surfaces
| AD-A255981 | p 976 N93-14411
Semi-classical quantization rules in supersymmetric quantum mechanics p 998 N93-14590
Anti-hydrogen: The cusp between quantum mechanics and general relativity
| DE93-001807 | p 998 N93-15469

QUANTUM OPTICS
Fast optoelectronic switching processes in surface-emitting semiconductor lasers and nonlinear etalons
| AD-A255802 | p 886 N93-15069

QUANTUM THEORY
Dynamics in neutron stars and the early universe
p 1014 N93-14112
Turbulence and chaos in classical and quantum systems p 972 N93-14144
Gas-solid dynamics at disordered and adsorbate covered surfaces
| AD-A255981 | p 976 N93-14411

Semi-classical quantization rules in supersymmetric quantum mechanics p 998 N93-14590
Multiply connected spacetimes and closed timelike curves in semiclassical gravity p 915 N93-14884
Variational transition state theory
[DE92-040498] p 842 N93-14908
Exact analytical solution of the toroidal singular mode equations
[DE92-040223] p 988 N93-15419

QUANTUM WELLS
Advanced laser chemical processing for microelectronics and integrated optics
[AD-A255980] p 865 N93-14425
The 3 to 5 heterojunction structures and high speed devices
[AD-A250399] p 991 N93-14521
The III-V semiconductor quantum well lasers and related optoelectronic devices (on silicon). Oxide-defined semiconductor quantum well lasers and optoelectronic devices: Al-based III-V nativeoxide s
[AD-A255239] p 885 N93-14667

QUARK MODELS
A Cloudy Quark Bag Model of S, P, and D wave interactions for the coupled channel antikaon-nucleon system
[DE92-040149] p 977 N93-15062

QUARKS
Strong interactions studies with medium energy probes
[DE92-040460] p 977 N93-15377
Schwinger Dyson equations: Dynamical chiral symmetry breaking and confinement
[DE92-040717] p 978 N93-15657

QUARTZ
Theory of the electronic and structural properties of solid state oxides
[DE92-040499] p 993 N93-14909
Introduction to quartz frequency standards, revision 1
[AD-A256373] p 870 N93-15330

QUARTZ CRYSTALS
Effects of cryocontaminants on cryogenic superpolished mirror and superpolished quartz crystal microbalance
[AD-A255972] p 981 N93-14403
The effects of acceleration on precision frequency sources
[AD-A255465] p 972 N93-14496
Introduction to quartz frequency standards, revision 1
[AD-A256373] p 870 N93-15330

QUASARS
A search for dead QSO's among nearby luminous galaxies p 1011 N93-14228
The evolution of the VLBI polarization of superluminal radio source 3C345 p 1050 N93-14229
Multiwavelength spectroscopy of active galactic nuclei p 1011 N93-14611
A faint spectroscopic quasar survey p 1012 N93-14629
Quasars, galaxies, and pseudo-vacuum droplets
[NIKHEF-H/91-20] p 1020 N93-14686
The evolution of the quasar continuum
[NASA-CR-191673] p 1012 N93-14759
Quasar x-ray spectra revisited p 1012 N93-14760
QSO absorption lines and the ionizing field at high redshifts p 1013 N93-14860
The gamma ray spectrum resulting from pp interactions in quasars p 1051 N93-14917

QUATERNARY ALLOYS
Application of the square root diffusivity analysis to measuring the diffusivity of multicomponent alloys
[DE92-040978] p 847 N93-15382

QUENCHING (ATOMIC PHYSICS)
Advances in laser cooling
[AD-A255969] p 884 N93-14402

QUENCHING (COOLING)
Chemical kinetics for combustion p 840 N93-14619

QUERY LANGUAGES
PRISMA/DB: A parallel, main-memory relational DBMS
[MEMO-INF-92-12] p 959 N93-15141
Query optimization and planning in object-oriented knowledge bases
[AD-A256006] p 1008 N93-15254

QUEUEING THEORY
A queue model relating synchronous and asynchronous communication
[MEMO-INF-92-04] p 966 N93-15491

R

RADAR ANTENNAS
Optical signal distribution schemes for millimeter phased array radar
[AD-A256262] p 858 N93-14437
Airborne radar simulation with adaptive antenna techniques
[AD-A255460] p 859 N93-14488

RADAR APPROACH CONTROL
Terminal area forecasts FY 1992 - 2005
[AD-A255797] p 788 N93-15390

RADAR CORNER REFLECTORS
A very efficient RCS data compression and reconstruction technique, volume 4
[NASA-CR-191378-VOL-4] p 945 N93-14807

RADAR CROSS SECTIONS
Polarization properties and Earth-based radar measurements of Venus in the post-Magellan era p 1026 N93-14304
A very efficient RCS data compression and reconstruction technique, volume 4
[NASA-CR-191378-VOL-4] p 945 N93-14807

RADAR DATA
The detection and correlation modeling of Rayleigh distributed radar signals
[AD-A256612] p 858 N93-14250
Anomalous scattering behavior of selected impact parabola features: Magellan cycle-to-cycle comparisons p 1039 N93-14363
Magellan project p 1041 N93-14373
Multiresolution pattern recognition of small volcanos in Magellan data p 1042 N93-14380
Convective scale 4-D data assimilation using simulated single-Doppler radar observations p 921 N93-14683
Method and apparatus for increasing a radar's range with improved scan-to-scan integration of Doppler filtered signals
[AD-D015421] p 860 N93-14742
Radar data processing using a distributed computational system
[AD-A256209] p 861 N93-15237

RADAR DETECTION
On the detection of ultrawideband radar signals
[AD-A256075] p 858 N93-14233
The detection and correlation modeling of Rayleigh distributed radar signals
[AD-A256612] p 858 N93-14250

RADAR ECHOES
Scattering properties of Venus' surface p 1044 N93-14391

RADAR EQUIPMENT
Venus radar mapping from the Venera 15 and 16 spacecrafts: Results and restrictions p 1023 N93-14289

RADAR IMAGERY
The geology of the Venera/Vega landing sites p 1024 N93-14296
Debris avalanches and slumps on the margins of volcanic domes on Venus: Characteristics of deposits p 1025 N93-14300
Image processing and products for the Magellan mission to Venus p 1026 N93-14306
Radar scattering properties of pancakelike domes on Venus p 1028 N93-14316
Sequential deformation of plains along Tessera boundaries on Venus: Evidence from Alpha Regio p 1028 N93-14317
Largest impact craters on Venus p 1030 N93-14326
Magellan stereo images and Venusian geology p 1035 N93-14347
Application of left- and right-looking SAR stereo to depth measurements of the Ammavaru outflow channel, Lada Terra, Venus p 1038 N93-14357
Evidence for retrograde lithospheric subduction on Venus p 1040 N93-14367
Magellan project p 1041 N93-14373
The tectonics of Venus: An overview p 1042 N93-14382
Scattering properties of Venus' surface p 1044 N93-14391
Low-emissivity impact craters on Venus p 1044 N93-14392

RADAR MAPS
Venus radar mapping from the Venera 15 and 16 spacecrafts: Results and restrictions p 1023 N93-14289
Surface processes on Venus p 1024 N93-14294

RADAR MEASUREMENT
Polarization properties and Earth-based radar measurements of Venus in the post-Magellan era p 1026 N93-14304
The spin vector of Venus determined from Magellan data p 1027 N93-14310

RADAR RANGE
Nonlinear modeling of gated range tracker dynamics with application to radar range resolution, phase 1
[AD-A256074] p 858 N93-14259
Method and apparatus for increasing a radar's range with improved scan-to-scan integration of Doppler filtered signals
[AD-D015421] p 860 N93-14742

RADAR RECEIVERS
The detection and correlation modeling of Rayleigh distributed radar signals
[AD-A256612] p 858 N93-14250

RADAR SCATTERING
Scatterer modeling/calibration study
[AD-A255855] p 856 N93-14107
Polarization properties and Earth-based radar measurements of Venus in the post-Magellan era p 1026 N93-14304
Radar scattering properties of pancakelike domes on Venus p 1028 N93-14316
Radar-anomalous, high-altitude features on Venus p 1036 N93-14349
Dielectric surface properties of Venus p 1039 N93-14360
Problem footprints in Magellan altimetry data p 1039 N93-14362
Anomalous scattering behavior of selected impact parabola features: Magellan cycle-to-cycle comparisons p 1039 N93-14363
Scattering properties of Venus' surface p 1044 N93-14391
A very efficient RCS data compression and reconstruction technique, volume 4
[NASA-CR-191378-VOL-4] p 945 N93-14807
Systems issues in airborne Doppler radar/LIDAR certification p 785 N93-14855

RADAR TARGETS
Scatterer modeling/calibration study
[AD-A255855] p 856 N93-14107
On the detection of ultrawideband radar signals
[AD-A256075] p 858 N93-14233
A very efficient RCS data compression and reconstruction technique, volume 4
[NASA-CR-191378-VOL-4] p 945 N93-14807
Radar data processing using a distributed computational system
[AD-A256209] p 861 N93-15237

RADAR TRACKING
Nonlinear modeling of gated range tracker dynamics with application to radar range resolution, phase 1
[AD-A256074] p 858 N93-14259
An observational and theoretical study of squall line evolution p 921 N93-14682

RADARSAT
An overview of RADARSAT payload technologies p 807 N93-14933

RADIANCE
Improved aerosol optical depth and particle size index from satellite detected radiance
[AD-A256089] p 904 N93-14263
A two-pass physics-based global lighting model p 957 N93-15570
Accelerated simulation of near-Earth-orbit polymer degradation p 823 N93-15615

RADIANT HEATING
Radiative heat transfer in combustion systems p 840 N93-14621

RADIATION BELTS
The time variability of Jupiter's synchrotron radiation p 973 N93-14227

RADIATION COUNTERS
Using the Haleakala barrel extensive air shower array to study selected U.H.E. gamma ray point sources p 1050 N93-14639
Studies of heavy-ion reactions and transuranic nuclei
[DE92-040457] p 977 N93-15326

RADIATION DAMAGE
Mechanisms of microwave induced damage in biologic materials
[AD-A255799] p 933 N93-14648
The response of dispersion-strengthened copper alloys to high fluence neutron irradiation at 415 C
[DE92-019434] p 846 N93-15138
Degradation and failure modes of carbon/bismaleimide laminates subjected to a tropical exposure
[AD-A256328] p 836 N93-15193
Joint HVAC transmission EMF environmental study
[DE92-017863] p 933 N93-15211
Accelerated simulation of near-Earth-orbit polymer degradation p 823 N93-15615

RADIATION DETECTORS
Interferometer with two phase-conjugate mirrors
[AD-D015420] p 982 N93-14800
Personal computer based computed tomography system
[KCP-613-4806] p 945 N93-14876
Studies of heavy-ion reactions and transuranic nuclei
[DE92-040457] p 977 N93-15326

Development of a High Resolution Liquid Xenon Imaging Telescope for Medium Energy Gamma Ray Astrophysics
[NASA-CR-191781] p 1013 N93-15589
SeaWiFS Technical Report Series. Cloud screening for polar orbiting visible and infrared (IR) satellite sensors, volume 7
[NASA-TM-104566] p 932 N93-15645

RADIATION DISTRIBUTION
Monte Carlo analysis of energy deposition in solid state materials by 400 and 200 MeV electrons
[AD-A255335] p 991 N93-14537

RADIATION EFFECTS
Precision radiation force modeling for the TOPEX/Poseidon mission p 817 N93-14586
Radiation monitoring for long duration space flights p 812 N93-14959
Improvement and analysis of the radiation response of RADFET dosimeters
[AD-A254115] p 869 N93-15133
The response of dispersion-strengthened copper alloys to high fluence neutron irradiation at 415 C
[DE92-019434] p 846 N93-15138
Solar proton events of 1989: Effects on spacecraft solar arrays
[AD-A256457] p 1049 N93-15318
Effects of high thermal neutron fluences on Type 6061 aluminum
[DE92-040569] p 846 N93-15348
Research for electric energy systems
[DE92-040076] p 870 N93-15412
LDEF: A bibliography with abstracts
[NASA-TM-107705] p 813 N93-15646
Energy distribution of trapped holes in irradiated SiO2
[DE92-040979] p 997 N93-15649

RADIATION HAZARDS
Predictions of dose from electrons in space
[NASA-CR-191617] p 1051 N93-15580

RADIATION MEASUREMENT
Radiation monitoring for long duration space flights p 812 N93-14959
Studies of heavy-ion reactions and transuranic nuclei
[DE92-040457] p 977 N93-15326

RADIATION PRESSURE
Radiation pressure: A possible cause for the superrotation of the Venusian atmosphere p 1033 N93-14338
Precision radiation force modeling for the TOPEX/Poseidon mission p 817 N93-14586

RADIATION PROTECTION
Environmental assessment: OMEGA upgrade project at the Laboratory for Laser Energetics, University of Rochester
[DE92-040410] p 886 N93-14907

RADIATION SOURCES
A general purpose radiative transfer model for application to remote sensing in multidimensional systems p 904 N93-14174
A study of the low and mid-latitude upper ionospheres of Jupiter and Saturn p 1022 N93-14179
Experimental considerations of higher order parametric x rays from silicon crystals of varying thicknesses
[AD-A256082] p 990 N93-14260
High-energy emissions from young pulsars: Perspective from the outer gap model
[DE92-040365] p 1022 N93-15324
Propagation of high frequency jet noise using geometric acoustics
[NASA-TM-105950] p 975 N93-15575
Liquid xenon time projection chamber for gamma rays in the MeV region: Development status p 1014 N93-15592

RADIATION TRANSPORT
Opacity, equation of state, and radiation transport model for moderate density, eV-temperature plasmas
[AD-A256056] p 988 N93-14579
Low-frequency oscillations in radiative-convective models
[DE92-018779] p 922 N93-14901

RADIATIVE HEAT TRANSFER
Opacity, equation of state, and radiation transport model for moderate density, eV-temperature plasmas
[AD-A256056] p 988 N93-14579

RADIATIVE TRANSFER
A general purpose radiative transfer model for application to remote sensing in multidimensional systems p 904 N93-14174
Cloud-radiative feedbacks in tropical convection p 919 N93-14180
Infrared radiative properties of clouds p 919 N93-14196
Understanding the variation in the millimeter-wave emission of Venus p 1028 N93-14315
Non-uniform patch luminance for global illumination p 957 N93-15569

RADIATORS
Degradation of radiator performance on Mars due to dust p 823 N93-15616

RADICALS
Radical ion formation in polymers as a mechanism for laser eye protection
[AD-A255992] p 850 N93-15111

RADIO ALTIMETERS
Venus radar mapping from the Venera 15 and 16 spacecrafts: Results and restrictions p 1023 N93-14289
Surface processes on Venus p 1024 N93-14294
Constraints on crustal rheology and age of deformation from models of gravitational spreading in Ishtar Terra, Venus p 1042 N93-14379
The use of satellite altimetry in the study of weakly defined and variable oceanic gyres p 926 N93-14966
North-Australian tropical seas circulation study p 926 N93-14968
Geophysical investigations with TOPEX/Poseidon altimetry data p 918 N93-14969
Assimilation of altimeter topography into oceanic models p 927 N93-14972
Studies of the intermediate and deep circulation in the western equatorial Atlantic p 927 N93-14973
Application of TOPEX/Poseidon altimetry to ocean dynamics and geophysics p 927 N93-14974
Circulation of the gyres of the world ocean: Observation modeling using TOPEX/Poseidon altimeter data p 927 N93-14975
South African TOPEX/Poseidon altimeter experiment p 928 N93-14976
Global ocean tides through assimilation of oceanographic and altimeter satellite data in a hydrodynamic model p 928 N93-14978
Low-frequency variability of sea level as related to the heat balance of global oceans p 928 N93-14979
Studies of tropical ocean dynamics using the TOPEX/Poseidon altimeter-derived sea surface topography p 928 N93-14980
Geophysical validation of TOPEX/Poseidon altimetry products p 918 N93-14982
Ocean circulation using altimetry p 929 N93-14984
The dynamics and energetics of midlatitude western boundary currents: A comparison of the Kuroshio Extension and the Gulf Stream p 929 N93-14985
Ocean circulation modeling by use of radar altimeter data p 929 N93-14986
General circulation of the South Atlantic between 5 deg N and 35 deg S p 929 N93-14987
Ocean dynamics in the Nordic Seas using satellite altimetry p 930 N93-14988
Application of TOPEX/Poseidon altimetry measurements to observational and modeling studies of the low-frequency upper ocean mass and heat circulation in the tropical Pacific p 930 N93-14989
Mean sea surface and gravity investigations using TOPEX/Poseidon altimeter data p 930 N93-14990
Global ocean tide mapping using TOPEX/Poseidon altimetry p 930 N93-14991
Application of precise altimetry to the study of precise leveling of the sea surface, the Earth's gravity field, and the rotation of the Earth p 907 N93-14992
An integrated research program for TOPEX/Poseidon with emphasis on the Pacific Ocean p 931 N93-14995
Oceanic transports of mass, heat, and salt in the western North Pacific p 931 N93-14996
Analysis of altimeter data jointly with seafloor electric data (vertically integrated velocity) and VCTD-yoyo data (detailed profiles of VCTD) p 931 N93-14998
Marine research using data from TOPEX/Poseidon p 932 N93-15001
Global ocean circulation by altimetry p 932 N93-15002

RADIO ASTRONOMY
The evolution of the VLBI polarization of superluminal radio source 3C345 p 1050 N93-14229
Microwave observations of Uranus p 1046 N93-14863
Laboratory evaluation and application of microwave absorption properties under simulated conditions for planetary atmospheres
[NASA-CR-191298] p 1047 N93-15081

RADIO COMMUNICATION
Multi-access strategies for voice/data integration in heterogeneous mixed-media packet radio networks
[AD-A255636] p 857 N93-14181
Regional satellites: The European experience with Eutelsat for TV, voice, data and mobile transmissions
[REPT-921-440-106] p 818 N93-15071

RADIO EMISSION
Nonthermal radio, x ray and gamma ray emissions from chaotic winds of early-type, massive stars p 1050 N93-14242
Radar-anomalous, high-altitude features on Venus p 1036 N93-14349
Dielectric surface properties of Venus p 1039 N93-14360

RADIO EQUIPMENT
AFIT/AFOSR Workshop on the Role of Wavelets in Signal Processing Applications
[AD-A256172] p 859 N93-14649
Proposed revisions to RTCM SC-104 recommended standards for differential NAVSTAR/GPS service for carrier phase applications
[AD-A255276] p 789 N93-15005
Remote vehicle controller
[AD-D015389] p 893 N93-15251
Comparison of synchronization techniques for the AFIT direct sequence spread spectrum system
[AD-A256440] p 861 N93-15316
Tactical line-of-sight path reliability: Improved MSE system procedures
[AD-A256504] p 862 N93-15376

RADIO FREQUENCIES
Frequency shifts in a rubidium frequency standard due to coupling to another standard
[AD-A256232] p 972 N93-15243

RADIO FREQUENCY DISCHARGE
Si atomic layer epitaxy using remote plasma assisted hydrogen desorption and disilane as a precursor
[AD-A255606] p 993 N93-15008

RADIO OCCULTATION
Long-term variations in abundance and distribution of sulfuric acid vapor in the Venus atmosphere inferred from Pioneer Venus and Magellan radio occultation studies p 1030 N93-14328
Laboratory evaluation and application of microwave absorption properties under simulated conditions for planetary atmospheres
[NASA-CR-191298] p 1047 N93-15081

RADIO RECEIVERS
Real-time edge-enhanced optical correlator
[NASA-CASE-NPO-18521-1-CU] p 981 N93-14404

RADIO SCATTERING
Radar-anomalous, high-altitude features on Venus p 1036 N93-14349

RADIO SPECTROSCOPY
Multiwavelength spectroscopy of active galactic nuclei p 1011 N93-14611

RADIO TRANSMISSION
Short range propagation measurements at 2.4, 4.5, and 11.5 GHz in indoor and outdoor environments
[AD-A256563] p 860 N93-14806

RADIO TRANSMITTERS
Measurements of electric and magnetic fields in the Waianae, Hawaii area
[DE92-019891] p 861 N93-15220

RADIO WAVES
Satellite measurement of ionospheric-induced VHF distortion
[DE92-040328] p 862 N93-15435

RADIOACTIVE CONTAMINANTS
Surface evaluation of UV-degraded contamination
[NASA-CR-184500] p 910 N93-14764

RADIOACTIVE ISOTOPES
Gamma-ray imaging observations of Supernova 1987A p 1012 N93-14628
Alpha migration through air filters: A numerical simulation
[UCRL-LR-109866] p 878 N93-15285

RADIOACTIVE WASTES
Technical data management at the Yucca Mountain Site Characterization Project
[DE92-018115] p 1008 N93-15229

RADIOGRAPHY
High speed imaging for flash radiography using PIN diodes
[DE92-040959] p 882 N93-15381

RADIOMETERS
Output data formatter for the Electronically Scanned Thinned Array Radiometer (ESTAR) instrument
[NASA-TM-4432] p 871 N93-15529
SeaWiFS Technical Report Series. Cloud screening for polar orbiting visible and infrared (IR) satellite sensors, volume 7
[NASA-TM-104566] p 932 N93-15645

RAILGUN ACCELERATORS
Validation of the flux loop diagnostic for the measurement of launch package motion during electromagnetic launch
[AD-A256547] p 814 N93-14266

RAIN
Extreme climatic events in the Amazon Basin and their associations with the circulation of the global tropics p 918 N93-14115
Four-dimensional data assimilation of gale data using a multivariate analysis scheme and a mesoscale model with diabatic initialization
[AD-A256063] p 921 N93-14680

Investigation of antenna pattern constraints for passive geosynchronous microwave imaging radiometers
[NASA-CR-189726] p 905 N93-14792
Development of the Advance Warning Airborne System(AWAS) p 784 N93-14849
Modern methods in meteorological and oceanographic data analysis
[AD-A257080] p 903 N93-15496

RAMAN LASERS
Nonlinear dynamics of optical systems p 979 N93-14124

RAMAN SPECTRA
Quantum fluctuations in stimulated Raman scattering p 857 N93-14126
Low thrust chemical rocket technology
[NASA-TM-105927] p 827 N93-15572

RAMAN SPECTROSCOPY
Remote fiber optic sensor for gaseous and liquid environments, phase 2
[AD-A256224] p 983 N93-15241

RAMJET ENGINES
Active control of combustion instability in a ramjet using large-eddy simulations
[AD-A255226] p 798 N93-14111
Control of asymmetric jet
[AD-A255967] p 873 N93-14400

RAMPS
Control of low-speed turbulent separated flow over a backward-facing ramp p 874 N93-14475

RANDOM ACCESS MEMORY
High speed magneto-resistive random access memory
[NASA-CASE-NPO-17954-1-CU] p 940 N93-14704

RANDOM ERRORS
Instrumentation of the variable-angle magneto-optic ellipsometer and its application to M-O media and other non-magnetic films p 984 N93-15508

RANDOM NOISE
New methods for nonlinear tracking and nonlinear chaotic signal processing
[AD-A256421] p 862 N93-15334

RANDOM VIBRATION
An environmental testing facility for Space Station Freedom power management and distribution hardware p 820 N93-15601

RANDOM WALK
Wait-free consensus
[AD-A255978] p 943 N93-14423

RANGE ERRORS
Nonlinear modeling of gated range tracker dynamics with application to radar range resolution, phase 1
[AD-A256074] p 858 N93-14259

RANKING
Trans-cockpit authority gradient in Navy/Marine aircraft mishaps p 786 N93-15016

RAPID QUENCHING (METALLURGY)
Compaction of submicron and nanocrystalline Al2O3-ZrO2 ceramics
[DE92-040233] p 852 N93-15320

RARE EARTH ALLOYS
Thermodynamics and transport in Ce3Bi4Pt3 and related compounds
[DE92-040377] p 998 N93-14905

RARE EARTH COMPOUNDS
Method of making substantially single phase superconducting oxide ceramics having a TC above 85 degrees
[AD-D015422] p 850 N93-14743

RARE GASES
Generation of broadly tunable, narrow bandwidth, and intense coherent vacuum ultraviolet radiation in rare gases p 980 N93-14167

RASTER SCANNING
Arc digital raster imagery evaluation
[AD-A255403] p 817 N93-14565

RATES (PER TIME)
System design and development of a low data rate voice (1200 bps) rate converter
[AD-A256071] p 859 N93-14663

RATINGS
Testability design rating system: Testability handbook, volume 1
[RL-TR-92-12-VOL-1] p 867 N93-14699

RAY TRACING
Design, development, and testing of a prototype optical system for a next generation multiplexed imager
[AD-A256538] p 981 N93-14286
Combining ray-trace and diffraction analysis: A design example p 985 N93-15511
Hierarchical Poisson disk sampling distributions p 954 N93-15545
A data parallel algorithm for raytracing of heterogeneous databases p 955 N93-15553
Object space temporal coherence for ray tracing p 955 N93-15554
Ray tracing polygons using spatial subdivision p 955 N93-15555
Parametric height field ray tracing p 955 N93-15556
Propagation of high frequency jet noise using geometric acoustics
[NASA-TM-105950] p 975 N93-15575

RAYLEIGH SCATTERING
Lineshape analysis of laser light scattered by an argon thermal plasma jet p 987 N93-14137
Analytical characterization of bistatic scattering from rough surfaces: Dependence on surface correlation function
[AD-A256525] p 862 N93-15397

RAYLEIGH WAVES
Remote techniques for time-of-flight flaw characterisation p 989 N93-14171
The detection and correlation modeling of Rayleigh distributed radar signals
[AD-A256612] p 858 N93-14250
Problems in nonlinear acoustics: Rayleigh waves, pulsed sound beams, reflection of focused beams, waveguides, cooperative radiation of sound by buggles, acoustic streaming effects in standing waves, and spark-source lithotripter pulses
[AD-A256289] p 974 N93-14458

RDX
Thermal decomposition of HNIW and HNIW-Based formulations
[AD-A255613] p 854 N93-15011

REACTING FLOW
Chemical reactions in turbulent mixing flows
[AD-A256004] p 842 N93-15114
Investigation of the aerothermodynamics of hypervelocity reacting flows in the ram accelerator
[NASA-CR-191715] p 783 N93-15588

REACTION KINETICS
Electronically excited molecules: Reaction kinetics and emission of light: Nanosecond infrared spectroscopy, electronic emission from chemical reactions
[AD-A255642] p 976 N93-14283
Transport phenomena and interfacial kinetics in multiphase combustion systems.
[AD-A255999] p 838 N93-14418
Chemical kinetics for combustion p 840 N93-14619
Gas-surface interactions
[AD-A255390] p 841 N93-14652
Comments on 'Kinetic Study on the Hexaelsian-Celsian Phase Transformation'
[NASA-TM-105917] p 850 N93-14886
Variational transition state theory
[DE92-040498] p 842 N93-14908
Studies of heavy-ion reactions and transuranic nuclei
[DE92-040457] p 977 N93-15326
Simplified jet-A kinetic mechanism for combustor application
[NASA-TM-105940] p 844 N93-15504

REACTION TIME
Multimodal interactions in sensory-motor processing
[AD-A255780] p 938 N93-15067
Movement time prediction in human-computer interfaces p 955 N93-15550

REACTOR MATERIALS
The response of dispersion-strengthened copper alloys to high fluence neutron irradiation at 415 C
[DE92-019434] p 846 N93-15138

READING
The intelligibility of words, sentences, and continuous discourse using the articulation index
[AD-A256781] p 863 N93-15624

READOUT
Characterization of PZT films fatigued at low frequency
[AEROSPACE-ATR-91(8308)-2] p 992 N93-14795
Indian experience in flight data readout and analysis p 794 N93-15161
Czechoslovak development and experience in flight data recorder readout and analysis p 794 N93-15162
Solid state flight data recorder with rapid data access p 795 N93-15167
Parallel readout of optical disks
[AD-A256625] p 1008 N93-15409
Transfer function characteristics of super resolving systems p 985 N93-15512

REAL TIME OPERATION
Technology reconciliation in the remote sensing era of US civilian weather forcasting: 1957 - 1987 p 918 N93-14114
Neural network retinal model real time implementation
[AD-A255652] p 934 N93-14210
A concurrent real-time autonomous mobile robot programming system p 960 N93-14281
Real-time edge-enhanced optical correlator
[NASA-CASE-NPO-18521-1-CU] p 981 N93-14404
Trace algebra for automatic verification of real-time concurrent systems
[AD-A256199] p 968 N93-14492
The 1992 Summer SIGAda AIWG Workshop applications experiences and lessons learned panel message from the panel chair
[AD-A256188] p 962 N93-14519
Parametric study of diffusion-enhancement networks for spatiotemporal grouping in real-time artificial vision
[AD-A256059] p 937 N93-14580
Real-time gaze holding in binocular robot vision
[AD-A256226] p 982 N93-14582
A probabilistic approach to anytime algorithm for intelligent real-time problem solving
[AD-A255709] p 945 N93-14654
System design and development of a low data rate voice (1200 bps) rate converter
[AD-A256071] p 859 N93-14663
Wind shear related research at Princeton University p 785 N93-14854
Real-time in-flight engine performance and health monitoring techniques for flight research application p 795 N93-15169
A deadlock-free communication system for a transputer network
[AD-A256473] p 959 N93-15319
A plan for spacecraft automated rendezvous
[NASA-TM-108385] p 813 N93-15392
Integrated support for real-time control systems
[PNR-90994] p 952 N93-15476

RECEIVERS
Development of an expendable particle sensor
[AD-A255702] p 881 N93-14653

RECONNAISSANCE AIRCRAFT
Unmanned aerial vehicles: More testing needed before production of short-range system
[AD-A256296] p 790 N93-14440

RECORDING HEADS
Integrated device with diffractive polarization components for a magneto-optical disk head p 986 N93-15517

RECOVERABLE SPACECRAFT
Segment specification for the payload segment of the reusable reentry satellite: Rodent module version
[NASA-CR-187884] p 824 N93-15630

RED SHIFT
Calibration of the CCD Tully-Fisher relation with application to the Perseus-Pisces supercluster p 1016 N93-14194
A faint spectroscopic quasar survey p 1012 N93-14629
QSO absorption lines and the ionizing field at high redshifts p 1013 N93-14860
ROSAT all-sky survey on the Einstein EMSS sample
[NASA-CR-191627] p 1013 N93-15340

REDUCED GRAVITY
An active Z gravity compensation system
[AD-A255258] p 889 N93-14529
Crystal growth in a microgravity environment
[NASA-CASE-MFS-28473-1] p 992 N93-14707
Passive zero-gravity leg restraint
[NASA-CASE-ARC-11882-1-CU] p 939 N93-14713
Numerical study of mixing of two fluids under low gravity
[NASA-TM-105865] p 878 N93-14914
Digital active material processing platform effort (DAMPER), SBIR phase 2
[NASA-CR-190798] p 856 N93-15353
Nucleate pool boiling in the long duration low gravity environment of the Space Shuttle
[NASA-TM-105973] p 855 N93-15420
Vehicle/payload interface specification for the reusable reentry satellite
[NASA-CR-187883] p 824 N93-15631
System specification for the reusable reentry satellite
[NASA-CR-187882] p 824 N93-15632

REDUNDANCY
Theory and applications of hyper-redundant robotic manipulators p 892 N93-15104
Redundancy control of robots by constrained optimization
[F-3-7] p 950 N93-15307

REDUNDANT COMPONENTS
Global optimum path planning for a redundant space robot
[AD-A255316] p 889 N93-14545

REELS
Cable-line shortening device
[AD-D015427] p 891 N93-14822

REENTRY
System specification for the reusable reentry satellite
[NASA-CR-187882] p 824 N93-15632
Reusable Reentry Satellite (RRS) system design study. Phase B, appendix E: Attitude control system study
[NASA-CR-188578] p 825 N93-15633
Reusable Reentry Satellite (RRS): Recovery tradeoff study
[NASA-CR-186396] p 825 N93-15658

REENTRY VEHICLES
Development of engineering methods for nonequilibrium radiative phenomena about aeroassisted entry vehicles p 817 N93-14632
Shape-stable reentry body nose tip
[AD-D015437] p 817 N93-14725
Reusable Reentry Satellite (RRS) system design study
[NASA-CR-187897] p 817 N93-14733

REFLECTANCE
Characterization of magneto-optical recording media p 979 N93-14140
Radar-anomalous, high-altitude features on Venus p 1036 N93-14349
Problem footprints in Magellan altimetry data p 1039 N93-14362
Surface evaluation of UV-degraded contamination
[NASA-CR-184500] p 910 N93-14764

REFLECTED WAVES
In situ material characterization for pavement evaluation by the Spectral-Analysis-of-Surface-Waves (SASW) method
[AD-A255660] p 804 N93-14128

REFLECTION
A general purpose radiative transfer model for application to remote sensing in multidimensional systems p 904 N93-14174

REFLECTOR ANTENNAS
Ku-band antenna design for MSAT mission p 813 N93-14963

REFLECTORS
Core design for use with precision composite reflectors
[NASA-CASE-NPO-17858-1-CU] p 832 N93-14700
Ku-band antenna design for MSAT mission p 813 N93-14963

REFRACTIVITY
Application of gel-silica optics to laser technology and optical element fabrication
[AD-A255666] p 883 N93-14131
Optical information processing using photorefractive BSO p 981 N93-14204
Vertical path atmospheric turbulence: Temporal spectra and differential image motion measurements p 914 N93-14641

REFRACTORY MATERIALS
Fabrication of high temperature materials by exothermic synthesis and subsequent dynamic consolidation
[DE92-019836] p 834 N93-14819

REGENERATION (PHYSIOLOGY)
Nerves and tissue repair
[AD-A255299] p 934 N93-14535

REGENERATIVE COOLING
Analytical and experimental investigation of closed-cycle sorption cooling systems p 874 N93-14476

REGIONAL PLANNING
The regional land use of Paraiba Valley and the North Coast of Sao Paulo State, Brazil p 905 N93-14450

REGOLITH
In-situ lunar oxygen extraction p 806 N93-14929

REGRESSION ANALYSIS
Goals versus algorithms
[AD-A256106] p 942 N93-14237

REINFORCED PLASTICS
Characterization of fiber reinforced phenolic composites p 828 N93-14142

REINFORCED SHELLS
Analysis and optimal design of pressurized, imperfect, anisotropic ring-stiffened cylinders p 897 N93-14251

REINFORCING FIBERS
Nondestructive evaluation of damage in SiC/Al metal matrix composite using x ray tomographic microscopy p 829 N93-14192
Elastic wave scattering by partially debonded or partially coated fibers p 829 N93-14224
Development of braided rope seals for hypersonic engine applications: Flow modeling
[NASA-TM-105942] p 888 N93-14478
FIBER-TEX 1991: The Fifth Conference on Advanced Engineering Fibers and Textile Structures for Composites
[NASA-CP-3176] p 832 N93-14744
Advances in 3-dimensional braiding p 833 N93-14748
Development of generalized 3-D braiding machines for composite preforms p 833 N93-14749
Industrial applications of multiaxial warp knit composites p 833 N93-14750
Properties of textile grade ceramic fibers p 833 N93-14751
The optimal fiber volume fraction and fiber-matrix property compatibility in fiber reinforced composites p 833 N93-14752
Mechanical response of composite materials with through-the-thickness reinforcement p 834 N93-14753
Modeling of Euclidean braided fiber architectures to optimize composite properties p 834 N93-14755

REINFORCING MATERIALS
Thermal fatigue analysis of metal matrix composite with spherical reinforcements
[AD-A255313] p 831 N93-14672

RELATIVISTIC EFFECTS
Type 2 superstrings in curved D = 10 space-time: Dynamics of their massless fields and covariant quantization p 998 N93-14143

RELATIVISTIC ELECTRON BEAMS
Conditioning electron beams in the ion-focused regime
[AD-A255635] p 978 N93-14127
Current neutralization in ballistic transport of light ion beams
[AD-A256070] p 976 N93-14662
Electron acceleration by longitudinal electric field of a Gaussian laser beam
[DE92-526947] p 887 N93-15296

RELATIVISTIC PARTICLES
Interactions of relativistic electrons with relativistic plasma waves p 988 N93-14139
Radiation belt dynamic and quasi-static modeling based on CRRES data: Outer-belt short-term response data base
[AD-A256483] p 916 N93-14899
Production of relativistic anti-hydrogen atoms by pair production with positron capture and measurement of the Lamb shift
[DE93-001767] p 978 N93-15468

RELATIVISTIC PLASMAS
Interactions of relativistic electrons with relativistic plasma waves p 988 N93-14139

RELATIVISTIC THEORY
Relativistic dynamics of a charged sphere: Updating the Lorentz-Abraham model
[AD-A256107] p 971 N93-14245

RELATIVITY
Anti-hydrogen: The cusp between quantum mechanics and general relativity
[DE93-001807] p 998 N93-15469

RELAY SATELLITES
NPR and intermodulation in mobile satellite systems p 806 N93-14931

RELIABILITY
Reliability of sol-gel derived ferroelectric memories
[AD-A255240] p 849 N93-14668
Sensitivity and uncertainty analysis in performability modelling
[MEMO-INF-92-18] p 941 N93-15090
Reliability modelling for non-electronic systems
[REPT-921-440-103] p 894 N93-15139

RELIABILITY ANALYSIS
Electronics reliability fracture mechanics. Volume 1: Causes of failures of shop replaceable units and hybrid microcircuits
[AD-A255836] p 894 N93-14104
Development of an environment for software reliability model selection
[AD-A256609] p 942 N93-14241
Flight termination systems commonality standard
[AD-A255349] p 789 N93-14517
Software reliability, measurement, and testing software reliability and test integration, volume 1
[AD-A256242] p 944 N93-14572
Software reliability, measurement, and testing. Volume 2: Guidebook for software reliability measurement and testing
[AD-A256164] p 944 N93-14581
Reliability techniques for combined hardware and software systems
[AD-A256347] p 895 N93-15204
An overview of reliability growth models and their potential use for NASA applications
[NASA-TP-3309] p 895 N93-15433

RELIABILITY ENGINEERING
Reliability techniques for combined hardware and software systems
[AD-A256347] p 895 N93-15204
An overview of reliability growth models and their potential use for NASA applications
[NASA-TP-3309] p 895 N93-15433

RELIEF MAPS
Automated interpretation of topographic maps
[AD-A257040] p 906 N93-15364

REMOTE CONTROL
Sensor-based driving of a car with fuzzy inferencing VLSI chips and boards
[DE92-017819] p 963 N93-14818
Remote vehicle controller
[AD-D015389] p 893 N93-15251
SMART: A modular architecture for robotics and teleoperation
[DE92-040985] p 966 N93-15385

REMOTE MANIPULATOR SYSTEM
Cooperative control of multiple space manipulators p 805 N93-14923
Vision system requirements and concept for the Special Purpose Dexterous Manipulator system (SPDM) p 805 N93-14924
MOVE: A neutral network paradigm for robotic control p 805 N93-14925
Applications of the mobile servicing system to the space exploration initiative p 809 N93-14946
Vision development test bed: The cradle of the MSS artificial vision system p 810 N93-14948
A concept for a supervised autonomous robot p 810 N93-14950

REMOTE SENSING
Technology reconciliation in the remote sensing era of US civilian weather forcasting: 1957 - 1987 p 918 N93-14114
Altimeter and oceanographic in situ measurements in the area of the Greenland-Iceland-Norwegian Sea, 1987-1988
[AD-A256598] p 960 N93-14239
Satellite detection of complex aerosols over the Arabian Peninsula/Gulf
[AD-A256085] p 909 N93-14261
Effects of water vapor and anisotropic scattering on aerosol optical depth retrieval
[AD-A256087] p 904 N93-14262
Improved aerosol optical depth and particle size index from satellite detected radiance
[AD-A256089] p 904 N93-14263
The regional land use of Paraiba Valley and the North Coast of Sao Paulo State, Brazil p 905 N93-14450
Comparison of Viking Ultraviolet images with low altitude particle precipitation p 1045 N93-14612
Definition study PHARUS
[AD-A256560] p 860 N93-14805
Integrating satellite imagery into a geographic information system for monitoring the downstream impacts of dam construction on floodplain agriculture in Sokoto State, Nigeria p 905 N93-14823
Ocean wave detection using satellite altimetry p 906 N93-14839
Two micron laser development for atmospheric remote sensing at NASA Langley Research Center p 784 N93-14845
NASA/LMSC instrument design and fabrication --- coherent lidar airborne shear sensor p 784 N93-14846
Solid-state coherent laser radar wind shear measuring systems p 784 N93-14848
Global survey of effective particle size in liquid water clouds by satellite observations p 921 N93-14862
An overview of RADARSAT payload technologies p 807 N93-14933
Earth environment space initiative p 811 N93-14953
Terrestrial reference systems related to the TOPEX/Poseidon project p 906 N93-14967
Geophysical investigations with TOPEX/Poseidon altimetry data p 918 N93-14969
Mesoscale and large-scale variability of the Antarctic circumpolar current p 926 N93-14970
Ocean transport and variability studies of the South Pacific, Southern, and Indian Oceans p 927 N93-14971
Assimilation of altimeter topography into oceanic models p 927 N93-14972
Circulation of the gyres of the world ocean: Observation modeling using TOPEX/Poseidon altimeter data p 927 N93-14975
Low-frequency variability of sea level as related to the heat balance of global oceans p 928 N93-14979
Ocean topography mapping, improvement of the marine geoid, and global permanent ocean circulation studies from TOPEX/Poseidon altimeter data p 928 N93-14981
Ocean circulation using altimetry p 929 N93-14984
The dynamics and energetics of midlatitude western boundary currents: A comparison of the Kuroshio Extension and the Gulf Stream p 929 N93-14985
Application of TOPEX/Poseidon altimetry measurements to observational and modeling studies of the low-frequency upper ocean mass and heat circulation in the tropical Pacific p 930 N93-14989
Precise orbit computation and sea surface modeling p 813 N93-15000
SMART: A modular architecture for robotics and teleoperation
[DE92-040985] p 966 N93-15385
Radar scene generation for tactical decision aids
[AD-A257069] p 863 N93-15495
SeaWiFS Technical Report Series. Cloud screening for polar orbiting visible and infrared (IR) satellite sensors, volume 7
[NASA-TM-104566] p 932 N93-15645

REMOTE SENSORS
Advanced sensors technology survey
[NASA-CR-185691] p 881 N93-14494
NASA/LMSC coherent LIDAR airborne shear sensor: System capabilities and flight test plans
p 784 N93-14847
Development of the Advance Warning Airborne System(AWAS) p 784 N93-14849
Development of advanced seal verification
[NASA-CR-184502] p 892 N93-15117
Remote fiber optic sensor for gaseous and liquid environments, phase 2
[AD-A256224] p 983 N93-15241
Operational strategies for contamination control of composite materials p 822 N93-15614

REMOTELY PILOTED VEHICLES
Experimental and analytical investigation of the vibration characteristics of a remotely piloted helicopter
[AD-A256131] p 790 N93-14248
Unmanned aerial vehicles: More testing needed before production of short-range system
[AD-A256296] p 790 N93-14440
Remote vehicle controller
[AD-D015389] p 893 N93-15251

REMOVAL
Technology evaluation report: The Carver-Greenfield process, Dehydro-Tech Corporation
[PB92-217462] p 910 N93-15217

RENDEZVOUS TRAJECTORIES
Optimal impulsive trajectories for orbital rendezvous between elliptic orbits p 813 N93-15103

RENORMALIZATION GROUP METHODS
Prediction of turbine cascade flows with a quasi-three-dimensional rotor viscous code and the extension of the algebraic turbulence model
[AD-A256831] p 880 N93-15635

REPLACING
Bearing servicing tool
[NASA-CASE-MSC-21881-1] p 891 N93-14871

REPLICAS
Strain-rate effects in replica scale model penetration experiments
[AD-A255426] p 844 N93-14508

REPRODUCTION (BIOLOGY)
Joint HVAC transmission EMF environmental study
[DE92-017863] p 933 N93-15211

REQUIREMENTS
Progress in DND's space-based radar R/D project
p 812 N93-14958
Engine technologies for future spaceplanes
[ETN-92-92732] p 800 N93-15143

RESCUE OPERATIONS
Evaluation of Night Vision Goggles (NVG) for maritime search and rescue (joint Canadian/US Coast Guard experiment)
[AD-A255525] p 939 N93-14554

RESEARCH AIRCRAFT
Icing effects on aircraft stability and control determined from flight data: Preliminary results
[NASA-TM-105977] p 803 N93-14831

RESEARCH AND DEVELOPMENT
Current status of liquid sheet radiator research
[NASA-TM-105764] p 872 N93-14150
Transport phenomena and interfacial kinetics in multiphase combustion systems.
[AD-A255999] p 838 N93-14418
Institute for the Study of Human Capabilities
[AD-A256091] p 938 N93-14427
Advanced sensors technology survey
[NASA-CR-185691] p 881 N93-14494
Fault tolerant systems practitioner's workshop
[AD-A255376] p 944 N93-14563
Solid state research
[AD-A256019] p 992 N93-14576
A planning workshop: To strengthen American cognitive science for the twenty-first century
[NSF-92-4] p 999 N93-14720
Core support for the Board on Mathematical Sciences
[AD-A256333] p 968 N93-15195

RESEARCH FACILITIES
Environmental assessment: OMEGA upgrade project at the Laboratory for Laser Energetics, University of Rochester
[DE92-040410] p 886 N93-14907
Addressing earthquake strong ground motion issues at the Idaho National Engineering Laboratory
[DE92-017841] p 916 N93-15136
Real-time in-flight engine performance and health monitoring techniques for flight research application
p 795 N93-15169
Space Station Freedom user's guide
[NASA-TM-108105] p 825 N93-15650

RESEARCH MANAGEMENT
Air Force Office of Scientific Research
[AD-A255361] p 1051 N93-14673
Air Force Office of Scientific Research
[AD-A255370] p 1051 N93-14674
Geothermal Energy and the Utility Market: The Opportunities and Challenges for Expanding Geothermal Energy in a Competitive Supply Market: Proceedings
[DE92-019090] p 908 N93-15271
Research for electric energy systems
[DE92-040076] p 870 N93-15412

RESEARCH PROJECTS
Air Force Office of Scientific Research
[AD-A255331] p 1051 N93-14523
International Space University p 808 N93-14938
Antarctic news clips - 1992
[NSF-92-83] p 916 N93-15080

RESIDUAL STRESS
Theoretical and experimental analysis of residual stress formation after implant resistance welding of polycarbonate p 898 N93-14279
Method of characterizing residual stress in ferromagnetic materials using a pulse histogram of acoustic emission signals
[NASA-CASE-LAR-14239-1] p 845 N93-14705
F100 second stage fan disk bolthole crack propagation ferris wheel test p 800 N93-14897
The stress development during filament winding of thick cylinders
[AD-A255765] p 901 N93-15066
Development of adherent ceramic coatings to reduce contact stress damage of ceramics
[DE92-041373] p 852 N93-15437

RESIN MATRIX COMPOSITES
Mechanics of composite materials for spacecraft
[AD-A255380] p 831 N93-14550
Low toxicity high temperature PMR polyimide
[NASA-CASE-LAR-14639-1] p 849 N93-14709
An evaluation of composites fabricated from powder epoxy towpreg p 832 N93-14745
Flow behavior in liquid molding p 833 N93-14747
Structural study of thermohardening matrices: Deformation of composite matrices in relation to their molecular structure
[ONERA-RT-12/3521-M] p 836 N93-15253
Polymer infiltration studies
[NASA-CR-191652] p 852 N93-15431

RESIN TRANSFER MOLDING
Flow behavior in liquid molding p 833 N93-14747

RESISTORS
Compact free electron laser for medical applications
[AD-A256236] p 885 N93-14599

RESONANCE
Resonance absorption of MHD surface waves with applications to the solar atmosphere
p 1048 N93-14157
Level-mixing assisted tunability of nuclear resonance linewidths for gamma ray lasers
[AD-A255791] p 885 N93-14647
Acoustic resonance techniques for quality control
[DE92-040150] p 895 N93-15413

RESONANCE FLUORESCENCE
Physical and chemical processes of the inner coma observed in mid-ultraviolet cometary spectra
p 1017 N93-14230

RESONATORS
Introduction to quartz frequency standards, revision 1
[AD-A256373] p 870 N93-15330

RESOURCES MANAGEMENT
Integrating satellite imagery into a geographic information system for monitoring the downstream impacts of dam construction on floodplain agriculture in Sokoto State, Nigeria p 905 N93-14823
Trans-cockpit authority gradient in Navy/Marine aircraft mishaps p 786 N93-15016
Enhanced Aeronautical Resource Management training alternatives p 786 N93-15019
Taxonomy of flight variables p 787 N93-15022
Information technologies for global resources management and environmental assessment
[DE92-041107] p 906 N93-15442

RESPIRATION
The production and use of aeroponically grown inocula of VAM fungi in the native plant nursery
[PB92-204973] p 933 N93-15208

RETENTION (PSYCHOLOGY)
Long term memory for different types of classroom knowledge
[AD-A255235] p 999 N93-14526

RETINA
Analysis of retinal function following laser irradiation
[AD-A255649] p 933 N93-14163
Neural network retinal model real time implementation
[AD-A255652] p 934 N93-14210

RETROREFLECTION
Multiperiod-grating surface-emitting lasers
[NASA-CASE-NPO-17763-1-CU] p 885 N93-14703

REUSABLE HEAT SHIELDING
Results of a FRSI material test under Space Shuttle ascent conditions in the Ames Research Center 9x7 foot supersonic wind tunnel (OS13). Space Shuttle aerothermodynamic data report
[NASA-CR-167699] p 816 N93-15475

REUSABLE SPACECRAFT
Reusable Reentry Satellite (RRS) system design study
[NASA-CR-187897] p 817 N93-14733
Reusable Reentry Satellite (RRS) system design study: System cost estimates document
[NASA-CR-188480] p 818 N93-14872
Reusable Reentry Satellite (RRS): Telemetry, Tracking, and Command (TT/C) coverage tradeoff study
[NASA-CR-188583] p 824 N93-15629
Segment specification for the payload segment of the reusable reentry satellite: Rodent module version
[NASA-CR-187884] p 824 N93-15630
Vehicle/payload interface specification for the reusable reentry satellite
[NASA-CR-187883] p 824 N93-15631
System specification for the reusable reentry satellite
[NASA-CR-187882] p 824 N93-15632
Reusable Reentry Satellite (RRS): Recovery tradeoff study
[NASA-CR-186396] p 825 N93-15658

REVERBERATION
Advanced development active model: A users guide
[AD-A255614] p 974 N93-15012

REYNOLDS NUMBER
Parametric study of air sampling cyclones
p 779 N93-14173
Turbulence modeling for combustion flows
p 840 N93-14620
User manual for NASA Lewis 10 by 10 foot supersonic wind tunnel
[NASA-TM-105626] p 804 N93-15498

REYNOLDS STRESS
Wave drag in the atmospheric boundary layer
p 915 N93-14873

RHENIUM
Low thrust chemical rocket technology
[NASA-TM-105927] p 827 N93-15572

RHEOLOGY
Constraints on crustal rheology and age of deformation from models of gravitational spreading in Ishtar Terra, Venus p 1042 N93-14379
Preliminary investigations of metal liquid-like films and coatings derived from them
[AD-A255477] p 849 N93-14489

RIBBONS
Polymer infiltration studies
[NASA-CR-191652] p 852 N93-15431

RIBONUCLEIC ACIDS
Mechanisms of microwave induced damage in biologic materials
[AD-A255799] p 933 N93-14648

RIDGES
Wrinkle ridges on Venusian plains: Indicators of shallow crustal stress orientations at local and regional scales
p 1034 N93-14343

RIGID ROTORS
Stability of elastically tailored rotor blades
p 791 N93-14828

RIGID STRUCTURES
Dynamics and control of a rigid/flexible manipulator
p 890 N93-14684

RING LASERS
A study of an optically pumped free-jet molecular iodine laser operating in the visible spectrum
p 884 N93-14141

RISK
Aviation accidents, incidents, and violations: Psychological predictors among US pilots
p 783 N93-14693
Measuring risk in single-engine and twin-engine helicopters p 787 N93-15025
Performing wind-tunnel modeling for better management of near-field risks
[DE92-040205] p 910 N93-15063

ROBOT ARMS
Decision-making for intelligent control of dual-arm robotic operations p 960 N93-14201
Optimum pose measurements for kinematic parameters identification
[AD-A256307] p 970 N93-14443
Force and position control of robot manipulators: Learning and repetitive control approach
p 888 N93-14473
Dynamics and control of a rigid/flexible manipulator
p 890 N93-14684
Optimal and robust control of robot manipulators
p 890 N93-14685
Driven shielding capacitive proximity sensor
[NASA-CASE-GSC-13377-1] p 962 N93-14701

Theory and applications of hyper-redundant robotic manipulators p 892 N93-15104
Learning position and force control for mechanical manipulators p 963 N93-15147
Dynamics and control of flexible arm robots
[ISBN-0-315-69011-9] p 892 N93-15150
Jointed assembly actuated by fluid pressure
[AD-D015383] p 893 N93-15248
Redundancy control of robots by constrained optimization
[F-3-7] p 950 N93-15307

ROBOT CONTROL
Decision-making for intelligent control of dual-arm robotic operations p 960 N93-14201
Robust control of a flexible link robot and rigid link robot: Theory, simulation, and experiment p 888 N93-14202
A concurrent real-time autonomous mobile robot programming system p 960 N93-14281
Utilizing sensed incipient slip signals for grasp force control
[AD-A255725] p 888 N93-14434
Optimum pose measurements for kinematic parameters identification
[AD-A256307] p 970 N93-14443
Force and position control of robot manipulators: Learning and repetitive control approach p 888 N93-14473
Real-time gaze holding in binocular robot vision
[AD-A256226] p 982 N93-14582
Dynamics and control of a rigid/flexible manipulator p 890 N93-14684
Optimal and robust control of robot manipulators p 890 N93-14685
Position and vibration control of flexible space robots p 892 N93-15102
Learning position and force control for mechanical manipulators p 963 N93-15147
Robust control design for uncertain nonlinear dynamic systems p 964 N93-15148
Dynamics and control of flexible arm robots
[ISBN-0-315-69011-9] p 892 N93-15150
Proceedings of the International Conference on CAD/CAM and AMT. Volume 3: IFIP (International Federation of Information Processing)/Robotics: International Sessions on Robots and Assembly
[ITN-92-85129] p 949 N93-15298
Coordinated motion control of a two-hand assembly system
[F-2-8] p 949 N93-15301
Off-line generation of error-free robot/NC (numerical control) code using simulation and automatic programming techniques
[F-3-1] p 949 N93-15302
Robot learning of contact tasks
[F-3-2] p 949 N93-15303
Multiple robot programming using concurrent logic language
[F-3-3] p 950 N93-15304
Planning of continuous path robotic motions by discrete time optimization
[F-3-5] p 950 N93-15305
Redundancy control of robots by constrained optimization
[F-3-7] p 950 N93-15307
Adaptive control of a manipulator in cartesian space
[F-4-2] p 950 N93-15308

ROBOT DYNAMICS
Dynamics and control of a rigid/flexible manipulator p 890 N93-14684
Position and vibration control of flexible space robots p 892 N93-15102
Theory and applications of hyper-redundant robotic manipulators p 892 N93-15104
Dynamics and control of flexible arm robots
[ISBN-0-315-69011-9] p 892 N93-15150
Time-optimization of point-to-point robotic motions
[F-3-6] p 950 N93-15306
Redundancy control of robots by constrained optimization
[F-3-7] p 950 N93-15307

ROBOT SENSORS
Utilizing sensed incipient slip signals for grasp force control
[AD-A255725] p 888 N93-14434
Robot learning of contact tasks
[F-3-2] p 949 N93-15303
Design of an artificial neural network based tactile sensor for the UTAH/MIT dexterous hand
[AD-A256565] p 966 N93-15406

ROBOTICS
Optimum pose measurements for kinematic parameters identification
[AD-A256307] p 970 N93-14443
An active Z gravity compensation system
[AD-A255258] p 889 N93-14529
Development of neural network architectures for self-organizing pattern recognition and robotics
[AD-A255433] p 962 N93-14551
A minimum-slip attitude control method for the erebus walking robot
[NASA-CR-191646] p 890 N93-14567
Large space structures and systems in the space station era: A bibliography with indexes (supplement 04)
[NASA-SP-7085(04)] p 817 N93-14606
Work attachment mechanism/work attachment fixture
[NASA-CASE-GSC-13430-1] p 890 N93-14712
Sensor-based driving of a car with fuzzy inferencing VLSI chips and boards
[DE92-017819] p 963 N93-14818
An active tactile perception system p 805 N93-14926
A robotic planning system p 810 N93-14949
A concept for a supervised autonomous robot p 810 N93-14950
Proceedings of the International Conference on CAD/CAM and AMT. Volume 3: IFIP (International Federation of Information Processing)/Robotics: International Sessions on Robots and Assembly
[ITN-92-85129] p 949 N93-15298
CAD-based off-line programming and sensor signal processing in robotics
[F-2-2] p 949 N93-15299
Methodology for robot capability and performance characterization: The basis for robot task planningg
[F-2-3] p 949 N93-15300
Coordinated motion control of a two-hand assembly system
[F-2-8] p 949 N93-15301
Off-line generation of error-free robot/NC (numerical control) code using simulation and automatic programming techniques
[F-3-1] p 949 N93-15302
Robot learning of contact tasks
[F-3-2] p 949 N93-15303
Multiple robot programming using concurrent logic language
[F-3-3] p 950 N93-15304
Planning of continuous path robotic motions by discrete time optimization
[F-3-5] p 950 N93-15305
Time-optimization of point-to-point robotic motions
[F-3-6] p 950 N93-15306
Redundancy control of robots by constrained optimization
[F-3-7] p 950 N93-15307
Adaptive control of a manipulator in cartesian space
[F-4-2] p 950 N93-15308

ROBOTS
Manipulation strategies for redundant manipulators p 960 N93-14203
A concurrent real-time autonomous mobile robot programming system p 960 N93-14281
Global optimum path planning for a redundant space robot
[AD-A255316] p 889 N93-14545
An iconic position estimator for a 2-D laser rangefinder
[AD-A255523] p 885 N93-14568
Real-time gaze holding in binocular robot vision
[AD-A256226] p 982 N93-14582
The perception of articulated motion: Recognizing moving light displays
[AD-A256046] p 937 N93-14660
Position and vibration control of flexible space robots p 892 N93-15102
Proceedings of the International Conference on CAD/CAM and AMT. Volume 3: IFIP (International Federation of Information Processing)/Robotics: International Sessions on Robots and Assembly
[ITN-92-85129] p 949 N93-15298
SMART: A modular architecture for robotics and teleoperation
[DE92-040985] p 966 N93-15385

ROBUSTNESS (MATHEMATICS)
Stability and adaptation of neural networks
[AD-A256227] p 962 N93-14598

ROCK INTRUSIONS
Determining stress states using dike swarms: The Lauma Dorsa example p 1028 N93-14319
The origins of radial fracture systems and associated large lava flows on Venus p 1038 N93-14356

ROCKET ENGINE DESIGN
An overview of reliability growth models and their potential use for NASA applications
[NASA-TP-3309] p 895 N93-15433

ROCKET ENGINES
Experimental determination of magnetohydrodynamic seawater thruster performance in a two Tesla test facility
[DE92-019042] p 826 N93-15215

ROCKET NOZZLES
Thruster sealing system and apparatus
[NASA-CASE-MSC-21898-1] p 890 N93-14702

ROCKET PROPELLANTS
Numerical study of cathode emission constraints on cylindrical self-field MPD thruster performance
[NASA-CR-190795] p 826 N93-15370

ROCKET THRUST
Numerical study of cathode emission constraints on cylindrical self-field MPD thruster performance
[NASA-CR-190795] p 826 N93-15370

ROCKS
Radar-anomalous, high-altitude features on Venus p 1036 N93-14349

RODENTS
Segment specification for the payload segment of the reusable reentry satellite: Rodent module version
[NASA-CR-187884] p 824 N93-15630

RODS
Closed form expressions for crack mouth displacements and stress intensity factors for chevron notched short bar and short rod specimens based on experimental compliance measurements
[NASA-TM-83796] p 902 N93-15369

ROLLING MOMENTS
Program for calculation of aileron rolling moment and yawing moment coefficients at subsonic speeds
[ESDU-88040] p 779 N93-14514

ROOT-MEAN-SQUARE ERRORS
Hierarchical Poisson disk sampling distributions p 954 N93-15545

ROSAT MISSION
The evolution of the quasar continuum
[NASA-CR-191673] p 1012 N93-14759
ROSAT all-sky survey on the Einstein EMSS sample
[NASA-CR-191627] p 1013 N93-15340

ROTARY WING AIRCRAFT
A simulation model of atmospheric turbulence for rotorcraft applications p 920 N93-14588
An overview of shed ice impact in the NASA Lewis Icing Research Tunnel
[NASA-TM-105969] p 782 N93-15404
The Applicaiton of CFD to rotary wing flow problems
[NASA-TM-102803] p 782 N93-15483

ROTARY WINGS
The effect of wake dynamics on rotor eigenvalues in forward flight p 780 N93-14595
Stability of elastically tailored rotor blades p 791 N93-14828
Finite-state inflow applied to aeroelastic flutter of fixed and rotating wings p 802 N93-14830

ROTATING LIQUIDS
Asymmetric natural damped frequencies of a rotating infinitely long viscous liquid column
[LRT-WE-9-FB-23-1991] p 878 N93-15120

ROTATING PLASMAS
Analysis of rotation experiments in TFTR --- tokamak fusion test reactor p 987 N93-14129

ROTATING STALLS
Rotating stall inception in fans of low hub-tip ratio p 779 N93-14479

ROTATION
Finite element analysis of elastic fracture under unsteady translational and rotational loading p 899 N93-14469
The formation of giant molecular clouds p 1021 N93-15086
An investigation into the role of moist, vertical drafts in the rotational development of storms p 923 N93-15087
Acoustic mode measurements in the inlet of a model turbofan using a continuously rotating rake: Data collection/analysis techniques
[NASA-TM-105936] p 801 N93-15403
ARCBALL: A user interface for specifying three-dimensional orientation using a mouse p 955 N93-15551

ROTOR AERODYNAMICS
Rotating stall inception in fans of low hub-tip ratio p 779 N93-14479
The effect of wake dynamics on rotor eigenvalues in forward flight p 780 N93-14595
Finite-state inflow applied to aeroelastic flutter of fixed and rotating wings p 802 N93-14830

ROTOR BLADES (TURBOMACHINERY)
An experimental and analytical study of TIP clearance effects in axial flow compressors
[AD-A256434] p 800 N93-15337
Unsteady flow distortion past blades: Sources of noise generation in rotating flows
[AD-A255496] p 880 N93-15652

ROTOR DYNAMICS
New rotor trim and balance system for helicopter usage monitoring p 797 N93-15180

ROTORS
Online vibration control of a flexible rotor/bearing system p 899 N93-14468

Rotating stall inception in fans of low hub-tip ratio p 779 N93-14479
Onboard System Evaluation of Rotors Vibration, Engines (OBSERVE) monitoring system [AD-A255366] p 792 N93-15227
An experimental and analytical study of TIP clearance effects in axial flow compressors [AD-A256434] p 800 N93-15337
Prediction of turbine cascade flows with a quasi-three-dimensional rotor viscous code and the extension of the algebraic turbulence model [AD-A256831] p 880 N93-15635

RUBIDIUM
Frequency shifts in a rubidium frequency standard due to coupling to another standard [AD-A256232] p 972 N93-15243

RUN TIME (COMPUTERS)
A complete-time approach for chaining and execution control in the AN/UYS-2 parallel signal processor [AD-A256306] p 859 N93-14442
Upgrade the University of Wisconsin volume imaging lidar [AD-A255476] p 885 N93-14497
A massively distributed parallel genetic algorithm [AD-A256617] p 959 N93-15407

RUNGE-KUTTA METHOD
Eno-Osher schemes for Euler equations [NASA-TM-105928] p 969 N93-15341

RUPTURING
Damage and rupture of ceramic composites [ETN-92-92722] p 851 N93-15127

RUTHENIUM COMPOUNDS
Theory of the electronic and structural properties of solid state oxides [DE92-040499] p 993 N93-14909

RUTILE
Experimental and theoretical investigation of surface chemistry induced by direct and indirect electronic excitation [AD-A256342] p 843 N93-15200

S

S WAVES
Acoustic propagation loss predictions for a site on the Bermuda Rise at low and very low frequencies [AD-A255445] p 925 N93-14512
Shock/vortex interaction and vortex-breakdown modes [PAPER-T.1.3] p 875 N93-14689
A Cloudy Quark Bag Model of S, P, and D wave interactions for the coupled channel antikaon-nucleon system [DE92-040149] p 977 N93-15062

SACCADIC EYE MOVEMENTS
Multimodal interactions in sensory-motor processing [AD-A255780] p 938 N93-15067

SAFETY
The relationship between computer scoring and safety-pilot grading of flight performance [AD-A256245] p 937 N93-14600

SALTS
Oceanic transports of mass, heat, and salt in the western North Pacific p 931 N93-14996

SAMARIUM
Thin-film permanent magnets for integrated electromagnetic components [AD-A256175] p 972 N93-14679

SAMPLED DATA SYSTEMS
Sampled-data control and robust control for discrete-time systems p 964 N93-15149

SAMPLERS
An iterative Monte Carlo method for nonconjugate bayesian analysis [AD-A255991] p 971 N93-15110

SAMPLING
Nonparametric bayesian bioassay including ordered polytomous response [AD-A255990] p 970 N93-15109
Algorithms for the detection and elimination of specular aliasing p 954 N93-15544
Hierarchical Poisson disk sampling distributions p 954 N93-15545

SANDWICH STRUCTURES
Core design for use with precision composite reflectors [NASA-CASE-NPO-17858-1-CU] p 832 N93-14700

SATELLITE ALTIMETRY
Altimeter and oceanographic in situ measurements in the area of the Greenland-Iceland-Norwegian Sea, 1987-1988 [AD-A256598] p 960 N93-14239
Ocean wave detection using satellite altimetry p 906 N93-14839
The use of satellite altimetry in the study of weakly defined and variable oceanic gyres p 926 N93-14966
North-Australian tropical seas circulation study p 926 N93-14968
Geophysical investigations with TOPEX/Poseidon altimetry data p 918 N93-14969
Assimilation of altimeter topography into oceanic models p 927 N93-14972
Studies of the intermediate and deep circulation in the western equatorial Atlantic p 927 N93-14973
Application of TOPEX/Poseidon altimetry to ocean dynamics and geophysics p 927 N93-14974
Circulation of the gyres of the world ocean: Observation modeling using TOPEX/Poseidon altimeter data p 927 N93-14975
South African TOPEX/Poseidon altimeter experiment p 928 N93-14976
Global ocean tides through assimilation of oceanographic and altimeter satellite data in a hydrodynamic model p 928 N93-14978
Studies of tropical ocean dynamics using the TOPEX/Poseidon altimeter-derived sea surface topography p 928 N93-14980
Ocean topography mapping, improvement of the marine geoid, and global permanent ocean circulation studies from TOPEX/Poseidon altimeter data p 928 N93-14981
Geophysical validation of TOPEX/Poseidon altimetry products p 918 N93-14982
Study of mass and heat transport of the tropical Atlantic Ocean using models and altimeter data p 929 N93-14983
Ocean circulation using altimetry p 929 N93-14984
The dynamics and energetics of midlatitude western boundary currents: A comparison of the Kuroshio Extension and the Gulf Stream p 929 N93-14985
General circulation of the South Atlantic between 5 deg N and 35 deg S p 929 N93-14987
Ocean dynamics in the Nordic Seas using satellite altimetry p 930 N93-14988
Application of TOPEX/Poseidon altimetry measurements to observational and modeling studies of the low-frequency upper ocean mass and heat circulation in the tropical Pacific p 930 N93-14989
Mean sea surface and gravity investigations using TOPEX/Poseidon altimeter data p 930 N93-14990
Global ocean tide mapping using TOPEX/Poseidon altimetry p 930 N93-14991
Application of precise altimetry to the study of precise leveling of the sea surface, the Earth's gravity field, and the rotation of the Earth p 907 N93-14992
An integrated research program for TOPEX/Poseidon with emphasis on the Pacific Ocean p 931 N93-14995
The determination and interpretation of ocean surface topography using TOPEX/Poseidon altimeter data p 931 N93-14997
Analysis of altimeter data jointly with seafloor electric data (vertically integrated velocity) and VCTD-yoyo data (detailed profiles of VCTD) p 931 N93-14998
Precise orbit computation and sea surface modeling p 813 N93-15000
Marine research using data from TOPEX/Poseidon p 932 N93-15001
Global ocean circulation by altimetry p 932 N93-15002

SATELLITE ANTENNAS
Investigation of antenna pattern constraints for passive geosynchronous microwave imaging radiometers [NASA-CR-189728] p 905 N93-14792
On-orbit deployment anamolies: What can be done? p 821 N93-15603

SATELLITE ATMOSPHERES
Investigations of Titan's troposphere and surface and Jupiter's great red spot with infrared observations p 1022 N93-14146

SATELLITE ATTITUDE CONTROL
Thermal elastic shock and its effect on spacecraft attitude control p 818 N93-14837

SATELLITE COMMUNICATION
Multi-access strategies for voice/data integration in heterogeneous mixed-media packet radio networks [AD-A255636] p 857 N93-14181
A multiple-aperture multiple-beam EHF antenna for satellite communications [AD-A256020] p 858 N93-14426

SATELLITE CONTROL
Military space operations: Satellite control system improved, but serious problems remain [AD-A256809] p 971 N93-15626

SATELLITE DESIGN
Computer based satellite design [AD-A255315] p 816 N93-14536
Comparative study of stability of flexible satellites with and without guy-wire constraints p 817 N93-14585
Reusable Reentry Satellite (RRS) system design study [NASA-CR-187897] p 817 N93-14733
Reusable Reentry Satellite (RRS) system design study: System cost estimates document [NASA-CR-188480] p 818 N93-14872
Anik E spacecraft integration and test p 808 N93-14939
Space based radar: Test of large space structures p 808 N93-14941
Space craft verification at the David Florida Laboratory p 809 N93-14943
Full surface testing of grazing incidence mirrors [AD-A255798] p 984 N93-15371
System test approach for the SAX satellite p 824 N93-15622
Reusable Reentry Satellite (RRS) system design study. Phase B, appendix E: Attitude control system study [NASA-CR-188578] p 825 N93-15633

SATELLITE DOPPLER POSITIONING
Present-day plate motions: Retrieval from the TOPEX/Poseidon orbitography network (DORIS system) p 918 N93-14993

SATELLITE IMAGERY
Altimeter and oceanographic in situ measurements in the area of the Greenland-Iceland-Norwegian Sea, 1987-1988 [AD-A256598] p 960 N93-14239
Comparison of Viking Ultraviolet images with low altitude particle precipitation p 1045 N93-14612
The preservation of LANDSAT data by the National Land Remote Sensing Archive p 1003 N93-14777
Integrating satellite imagery into a geographic information system for monitoring the downstream impacts of dam construction on floodplain agriculture in Sokoto State, Nigeria p 905 N93-14823

SATELLITE INSTRUMENTS
Preview of Blackbeard interferometry [DE92-040329] p 818 N93-14904
Anik E spacecraft integration and test p 808 N93-14939
Full surface testing of grazing incidence mirrors [AD-A255798] p 984 N93-15371
SeaWiFS Technical Report Series. Cloud screening for polar orbiting visible and infrared (IR) satellite sensors, volume 7 [NASA-TM-104566] p 932 N93-15645

SATELLITE LIFETIME
Reusable Reentry Satellite (RRS) system design study: System cost estimates document [NASA-CR-188480] p 818 N93-14872

SATELLITE NAVIGATION SYSTEMS
A general observation matrix for attitude error estimation with an offset GPS antenna [AD-A255214] p 789 N93-14574

SATELLITE NETWORKS
Regional satellites: The European experience with Eutelsat for TV, voice, data and mobile transmissions [REPT-921-440-106] p 818 N93-15071
Integration of satellite links into an ATM mode broadband ISDN [TELECOM-PARIS-91-E-022] p 861 N93-15097
Full surface testing of grazing incidence mirrors [AD-A255798] p 984 N93-15371
Military space operations: Satellite control system improved, but serious problems remain [AD-A256809] p 971 N93-15626

SATELLITE OBSERVATION
Improved aerosol optical depth and particle size index from satellite detected radiance [AD-A256089] p 904 N93-14263
Ocean wave detection using satellite altimetry p 906 N93-14839
Global survey of effective particle size in liquid water clouds by satellite observations p 921 N93-14862
Studies of the intermediate and deep circulation in the western equatorial Atlantic p 927 N93-14973
Low-frequency variability of sea level as related to the heat balance of global oceans p 928 N93-14979
Ocean topography mapping, improvement of the marine geoid, and global permanent ocean circulation studies from TOPEX/Poseidon altimeter data p 928 N93-14981
The dynamics and energetics of midlatitude western boundary currents: A comparison of the Kuroshio Extension and the Gulf Stream p 929 N93-14985
Precise orbit computation and sea surface modeling p 813 N93-15000
Satellite measurement of ionospheric-induced VHF distortion [DE92-040328] p 862 N93-15435
Energetic and magnetosheath energy particle signatures of the low-latitude boundary layer at low altitudes near noon [NASA-CR-191388] p 917 N93-15574
SeaWiFS Technical Report Series. Cloud screening for polar orbiting visible and infrared (IR) satellite sensors, volume 7 [NASA-TM-104566] p 932 N93-15645

SATELLITE ORBITS
Parallelization of the Navy Space Surveillance Center (NAVSPASUR) satellite model
[AD-A256133] p 816 N93-14253
On-orbit deployment anamolies: What can be done? p 821 N93-15603
SATELLITE ORIENTATION
A general observation matrix for attitude error estimation with an offset GPS antenna
[AD-A255214] p 789 N93-14574
SATELLITE SURFACES
The sulfur emission and periodicity of the Jupiter plasma torus in 1988 p 1022 N93-14156
SATELLITE TRACKING
Parallelization of the Navy Space Surveillance Center (NAVSPASUR) satellite model
[AD-A256133] p 816 N93-14253
Global ocean tide mapping using TOPEX/Poseidon altimetry p 930 N93-14991
Reusable Reentry Satellite (RRS): Telemetry, Tracking, and Command (TT/C) coverage tradeoff study
[NASA-CR-188583] p 824 N93-15629
SATELLITE-BORNE INSTRUMENTS
An overview of RADARSAT payload technologies p 807 N93-14933
SATURN ATMOSPHERE
A study of the low and mid-latitude upper ionospheres of Jupiter and Saturn p 1022 N93-14179
Cassini atmospheric chemistry mapper. Volume 1. Investigation and technical plan
[NASA-CR-190947] p 1021 N93-15079
SCALARS
The low-energy structure of compactified superstring models p 997 N93-14116
SCALE MODELS
Strain-rate effects in replica scale model penetration experiments
[AD-A255426] p 844 N93-14508
Investigations of detail design issues for the high speed acoustic wind tunnel using a 60th scale model tunnel. Part 1: Tests with open circuits
[NASA-CR-191671] p 780 N93-14737
Investigations of detail design issues for the high speed acoustic wind tunnel using a 60th scale model tunnel. Part 2: Tests with the closed circuit
[NASA-CR-191672] p 780 N93-14738
SCANNERS
Using digital scanned aerial photography for wetlands delineation
[AD-A255392] p 905 N93-14676
SCANNING ELECTRON MICROSCOPY
Degradation and failure modes of carbon/bismaleimide laminates subjected to a tropical exposure
[AD-A256328] p 836 N93-15193
Compaction of submicron and nanocrystalline Al2O3-ZrO2 ceramics
[DE92-040233] p 852 N93-15320
SCATTERING
Remote techniques for time-of-flight flaw characterisation p 989 N93-14171
An analytic phase function for cylindrical particles
[AD-A255750] p 977 N93-15054
SCATTERING CROSS SECTIONS
A Cloudy Quark Bag Model of S, P, and D wave interactions for the coupled channel antikaon-nucleon system
[DE92-040149] p 977 N93-15062
SCATTERING FUNCTIONS
Scattering properties of Venus' surface p 1044 N93-14391
SCENE ANALYSIS
Neural nets for scene analysis
[AD-A255976] p 961 N93-14409
Development of an integrated package of physics models for scene simulation studies to support smart weapons design studies
[LTR92-004] p 945 N93-14696
SCHEDULES
Streamlined acquisition handbook
[NASA-TM-108133] p 1002 N93-14719
SCHEDULING
Radar data processing using a distributed computational system
[AD-A256209] p 861 N93-15237
Minimizing conflicts: A heuristic repair method for constraint-satisfaction and scheduling problems
[NASA-TM-108121] p 964 N93-15286
Scheduling and rescheduling with iterative repair
[NASA-TM-108120] p 965 N93-15287
Rescheduling with iterative repair
[NASA-TM-108119] p 965 N93-15288
Learning to improve iterative repair scheduling
[NASA-TM-108118] p 965 N93-15289
An application of artificial intelligence to automatic telescopes
[NASA-TM-108115] p 965 N93-15291
SCHLIEREN PHOTOGRAPHY
Study of Fluid Experiment System (FES)/CAST/Holographic Ground System (HGS)
[NASA-CR-184483] p 855 N93-14793
SCIENTIFIC SATELLITES
Preview of Blackbeard interferometry
[DE92-040329] p 818 N93-14904
SCIENTISTS
The changing culture of science: Bringing it into balance
[AD-A255993] p 998 N93-14417
SCINTILLATION
Comparison between irregularity motion and bulk plasma drifts at high latitudes
[PL-TR-91-2292] p 914 N93-14727
The effects of magnetic storm phases on F-layer irregularities from auroral to equatorial latitudes
[AD-A256520] p 917 N93-15395
SCINTILLATION COUNTERS
Personal computer based computed tomography system
[KCP-613-4806] p 945 N93-14876
Studies of heavy-ion reactions and transuranic nuclei
[DE92-040457] p 977 N93-15326
SCORING
The relationship between computer scoring and safety-pilot grading of flight performance
[AD-A256245] p 937 N93-14600
SEA ICE
Report of the International Ice Patrol in the North Atlantic, bulletin no. 77
[AD-A256162] p 925 N93-14452
SEA LEVEL
TOPEX/Poseidon science investigations plan
[NASA-CR-190616] p 925 N93-14964
North-Australian tropical seas circulation study p 926 N93-14968
Mesoscale and large-scale variability of the Antarctic circumpolar current p 926 N93-14970
Application of TOPEX/Poseidon altimetry to ocean dynamics and geophysics p 927 N93-14974
Sea level response to wind forcing in the tropical Atlantic p 928 N93-14977
Low-frequency variability of sea level as related to the heat balance of global oceans p 928 N93-14979
SEA SURFACE TEMPERATURE
The preferred latitudes of the Intertropical Convergence Zone: Observations and theory p 920 N93-14213
Mixed-layer parameterization in models of the Indian Ocean
[AD-A255937] p 925 N93-14428
SEA WATER
The effect of a seawater environment on the galvanic corrosion behavior of graphite/epoxy composites coupled to metals
[AD-A256072] p 830 N93-14232
Apparatus and process for desalination of seawater
[AD-D015428] p 842 N93-14824
SEALING
Thruster sealing system and apparatus
[NASA-CASE-MSC-21898-1] p 890 N93-14702
Method of applying a thermal barrier coating system to a substrate
[NASA-CASE-LEW-15020-2] p 832 N93-14706
SEALS (STOPPERS)
Development of braided rope seals for hypersonic engine applications: Flow modeling
[NASA-TM-105942] p 888 N93-14478
Thruster sealing system and apparatus
[NASA-CASE-MSC-21898-1] p 890 N93-14702
SEARCH RADAR
The detection and correlation modeling of Rayleigh distributed radar signals
[AD-A256612] p 858 N93-14250
SEARCHING
DROLS workbook
[AD-A255850] p 999 N93-14106
Automated interpretation of topographic maps
[AD-A257040] p 906 N93-15364
SEATS
Effects of seating configuration and number of type 3 exits on emergency aircraft evacuation
[AD-A256616] p 783 N93-14277
Passive zero-gravity leg restraint
[NASA-CASE-ARC-11882-1-CU] p 939 N93-14713
SECONDARY EMISSION
Spatially resolved 10 micron spectra of circumstellar material around evolved stars p 1019 N93-14636
SEISMIC WAVES
Addressing earthquake strong ground motion issues at the Idaho National Engineering Laboratory
[DE92-017841] p 916 N93-15136
SEISMOLOGY
Imaging Earth's interior: Tomographic inversions for mantle P-wave velocity structure p 913 N93-14225
SELF CONSISTENT FIELDS
Theoretical characterization of the potential energy surface for NH + NO
[NASA-CR-190741] p 843 N93-15357
SELF LUBRICATION
The effect of processing and compositional changes on the tribology of PM212 in air
[NASA-TM-105945] p 828 N93-15576
SEMANTICS
Program verification using higher order logic
[AD-A255408] p 943 N93-14502
An axiomatic treatment of partial correctness and deadlock in a shared variable parallel language
[AD-A256234] p 960 N93-15494
SEMICONDUCTOR DEVICES
Transport in heterostructures and device in microwave and millimeter wave regimes
[AD-A255975] p 858 N93-14408
Organization of workshop on emerging technologies for in-situ processing
[AD-A255977] p 865 N93-14410
Electron-phonon interaction, transport and ultrafast processes in semiconductor microstructures
[AD-A255723] p 976 N93-14433
Novel engineered compound semiconductor heterostructures for advanced electronics applications
[AD-A255363] p 866 N93-14562
Photoelectrochemistry of electronic and electro-optical materials
[AD-A256239] p 866 N93-14583
Reliability of sol-gel derived ferroelectric memories
[AD-A255240] p 849 N93-14668
Dual active layer photoconductor
[AD-D015423] p 993 N93-14820
A theoretical search for supervelocity semiconductors
[AD-A256325] p 994 N93-15191
SEMICONDUCTOR DIODES
Optics for diode array transverse pumped laser rod
[AD-D015436] p 885 N93-14722
Optoelectronics material center: A collaborative program including center for high technology materials of the University of New Mexico, Stanford University, California Institute of Technology
[AD-A256005] p 886 N93-15115
SEMICONDUCTOR LASERS
Optical signal distribution schemes for millimeter phased array radar
[AD-A256262] p 858 N93-14437
The III-V semiconductor quantum well lasers and related optoelectronic devices (on silicon). Oxide-defined semiconductor quantum well lasers and optoelectronic devices: Al-based III-V nativeoxide s
[AD-A255239] p 885 N93-14667
Fast optoelectronic switching processes in surface-emitting semiconductor lasers and nonlinear etalons
[AD-A255802] p 886 N93-15069
Optoelectronics material center: A collaborative program including center for high technology materials of the University of New Mexico, Stanford University, California Institute of Technology
[AD-A256005] p 886 N93-15115
SEMICONDUCTORS (MATERIALS)
Time-resolved optical studies of 3-5 semiconductors p 990 N93-14183
Organization of workshop on emerging technologies for in-situ processing
[AD-A255977] p 865 N93-14410
Advanced laser chemical processing for microelectronics and integrated optics
[AD-A255980] p 865 N93-14425
Electron-phonon interaction, transport and ultrafast processes in semiconductor microstructures
[AD-A255723] p 976 N93-14433
The 3 to 5 heterojunction structures and high speed devices
[AD-A250399] p 991 N93-14521
Novel engineered compound semiconductor heterostructures for advanced electronics applications
[AD-A255363] p 866 N93-14562
Photoelectrochemistry of electronic and electro-optical materials
[AD-A256239] p 866 N93-14583
Gas-surface interactions
[AD-A255390] p 841 N93-14652
Ultrastructure processing and environmental stability of advanced structural and electronic materials
[AD-A256153] p 831 N93-14665
Ultraviolet-ozone cleaning of semiconductor surfaces, revision 1
[AD-A256158] p 842 N93-14678
Method for fabricating ohmic contacts on semiconducting diamond
[AD-D015432] p 850 N93-14825

Hyperfine experimental investigation of zirconia ceramics
[DE92-040301] p 850 N93-14903
Thermodynamics and transport in Ce3Bi4Pt3 and related compounds
[DE92-040377] p 998 N93-14905
Epitaxial heterojunctions of oxide semiconductors and metals on high temperature superconductors
[NASA-CASE-NPO-18483-1-CU] p 994 N93-15151
A theoretical search for supervelocity semiconductors
[AD-A256325] p 994 N93-15191
Solidification of InSb-GaSb alloy and InSb with vibration p 995 N93-15310
The 17th Annual Conference on the Physics and Chemistry of Semiconductor Interfaces
[AD-A257061] p 996 N93-15449

SENSITIVITY
Sensitivity of quantum electron conductance to elastic scatterers and to spin-orbit scattering in gallium arsenide heterostructures p 990 N93-14184
Sensitivity and uncertainty analysis in performability modelling
[MEMO-INF-92-18] p 941 N93-15090
The sensitivity of energetic materials to friction, impact, and electrostatic stimuli
[DE92-041227] p 855 N93-15478

SENSORIMOTOR PERFORMANCE
Multimodal interactions in sensory-motor processing
[AD-A255780] p 938 N93-15067

SENSORS
Method of forming a multiple layer dielectric and a hot film sensor therewith
[NASA-CASE-LAR-13678-3] p 881 N93-14714
Development of a fiber optic high temperature strain sensor
[NASA-CR-191316] p 882 N93-14810
System for memorizing maximum values
[NASA-CASE-MSC-21922-1] p 882 N93-14841

SENSORY DEPRIVATION
Psychophysical analyses of perceptual representations
[AD-A255432] p 936 N93-14510

SENSORY PERCEPTION
Institute for the Study of Human Capabilities
[AD-A256091] p 938 N93-14427
Design of an artificial neural network based tactile sensor for the UTAH/MIT dexterous hand
[AD-A256565] p 966 N93-15406

SENTENCES
The intelligibility of words, sentences, and continuous discourse using the articulation index
[AD-A256781] p 863 N93-15624

SEPARATED FLOW
Control of low-speed turbulent separated flow over a backward-facing ramp p 874 N93-14475
Investigations of detail design issues for the high speed acoustic wind tunnel using a 60th scale model tunnel. Part 1: Tests with open circuits
[NASA-CR-191671] p 780 N93-14737
Use of surface heat transfer measurements as a flow separation diagnostic in a two dimensional reflected oblique shock/turbulent boundary layer interaction
[NASA-TM-105981] p 879 N93-15355

SEQUENCING
Escape-time visualization method for language-restricted iterated function systems p 956 N93-15558

SERVICE LIFE
Electronics reliability fracture mechanics. Volume 1: Causes of failures of shop replaceable units and hybrid microcircuits
[AD-A255836] p 894 N93-14104
Proceedings of the USAF Structural Integrity Program
[AD-A255379] p 777 N93-14549
Lithium rechargeable cell with a poly 3-methylthiophene cathode
[AD-A255436] p 866 N93-14552
Smart battery controller for lithium sulfur dioxide batteries
[AD-A255490] p 867 N93-14642

SERVICES
Next generation satellite communications networks p 812 N93-14962

SERVOCONTROL
SMART: A modular architecture for robotics and teleoperation
[DE92-040985] p 966 N93-15385

SERVOMECHANISMS
Jointed assembly actuated by fluid pressure
[AD-D015383] p 893 N93-15248

SET THEORY
A queue model relating synchronous and asynchronous communication
[MEMO-INF-92-04] p 966 N93-15491

SEYFERT GALAXIES
Quasar x-ray spectra revisited p 1012 N93-14760

SHADOWGRAPH PHOTOGRAPHY
Boundary layer transition measurements by optical anemometry p 874 N93-14477

SHAFTS (MACHINE ELEMENTS)
Calculation methods for externally pressurised (hydrostatic) journal bearings with capillary restrictor control
[ESDU-92026] p 889 N93-14543
Engine life assessment test case TF41 LP compressor shaft torsional fatigue p 799 N93-14896

SHALLOW SHELLS
Non-linear analysis of wave progagation using transform methods and plates and shells using integral equations p 896 N93-14186

SHALLOW WATER
Advanced development active model: A users guide
[AD-A255614] p 974 N93-15012

SHAPE CONTROL
Ku-band antenna design for MSAT mission p 813 N93-14963

SHAPES
Geometric invariants and object recognition
[AD-A255317] p 943 N93-14546
Computational analysis of hypersonic flows past elliptic-cone waveriders
[NASA-CR-191304] p 781 N93-14767
Modeling clothed figures
[AD-A257037] p 940 N93-15363

SHEAR FLOW
Turbulent drag and transport in high Reynolds number Couette-Taylor flow p 872 N93-14119
Resistive magnetohydrodynamic studies of tearing mode instability with equilibrium shear flow and magnetic reconnection p 987 N93-14122
Exploiting similarity in turbulent shear flows for turbulence modeling
[NASA-CR-191621] p 875 N93-14481

SHEAR LAYERS
Chemical reactions in turbulent mixing flows
[AD-A256004] p 842 N93-15114
On the nonlinear three dimensional instability of Stokes layers and other shear layers to pairs of oblique waves
[NASA-TM-105918] p 880 N93-15499
Unsteady shear disturbances within a two dimensional stratified flow
[NASA-CR-189121] p 880 N93-15527

SHEAR PROPERTIES
An investigation of crack growth at interfaces in bimaterials and composites using a consistent shear-lag model p 896 N93-14187

SHEAR STRESS
Wind stress analysis over the Western Equatorial Pacific and North Atlantic Oceans based on ECMWF operational wind products, 1985-1989
[AD-A256147] p 920 N93-14256
Exploiting similarity in turbulent shear flows for turbulence modeling
[NASA-CR-191621] p 875 N93-14481
Kind-band failure analysis of thick composites in compression
[AD-A255431] p 831 N93-14509
Characterizing longitudinal splitting and delamination fracture toughness of composites p 831 N93-14607
Shear fatigue crack growth analysis in large-grain polycrystals p 993 N93-14838

SHEEP
Joint HVAC transmission EMF environmental study
[DE92-017863] p 933 N93-15211

SHEETS
Current status of liquid sheet radiator research
[NASA-TM-105764] p 872 N93-14150

SHELL STABILITY
Analysis and optimal design of pressurized, imperfect, anisotropic ring-stiffened cylinders p 897 N93-14251

SHIELDING
Driven shielding capacitive proximity sensor
[NASA-CASE-GSC-13377-1] p 962 N93-14701

SHIPS
Investigation of the use of surface electrical currents for short-range shipboard data communications
[AD-A256197] p 859 N93-14490

SHOCK ABSORBERS
Characterization of impact-limiting material
[DE92-016767] p 902 N93-15210

SHOCK LAYERS
Development of engineering methods for nonequilibrium radiative phenomena about aeroassisted entry vehicles p 817 N93-14632

SHOCK TUBES
Turbulent magnetized plasmas from ionizing shock waves p 987 N93-14120
Eno-Osher schemes for Euler equations
[NASA-TM-105928] p 969 N93-15341

SHOCK WAVES
Turbulent magnetized plasmas from ionizing shock waves p 987 N93-14120
Optical probes for laser induced shocks
[AD-A256092] p 884 N93-14284
Computer simulations of comet- and asteroidlike bodies passing through the Venusian atmosphere: Preliminary results on atmospheric and ground shock effects p 1040 N93-14365
Hydrodynamics of supernova 1987 A p 1019 N93-14633
Shock/vortex interaction and vortex-breakdown modes
[PAPER-T.1.3] p 875 N93-14689
Computational analysis of hypersonic flows past elliptic-cone waveriders
[NASA-CR-191304] p 781 N93-14767
Use of surface heat transfer measurements as a flow separation diagnostic in a two dimensional reflected oblique shock/turbulent boundary layer interaction
[NASA-TM-105981] p 879 N93-15355
Time-dependent predictions and analysis of turbine cascade data in the transonic flow region
[PNR-90957] p 782 N93-15489

SHOT NOISE
Computation and communication constraints for distributed estimation systems
[AD-A256287] p 970 N93-14456
Interferometric measurement with squeezed light
[AD-A257065] p 984 N93-15458

SHROUDED PROPELLERS
Acoustic mode measurements in the inlet of a model turbofan using a continuously rotating rake: Data collection/analysis techniques
[NASA-TM-105936] p 801 N93-15403

SHROUDS
Cleaning of a thermal vacuum chamber with shrouds in place p 814 N93-15612

SHUTDOWNS
Modelling the engine temperature distribution between shut down and restart for life usage monitoring p 796 N93-15177

SIDE-LOOKING RADAR
Plate tectonics from VLBI and SLR global data
[NASA-CR-191319] p 916 N93-14913

SIERRA NEVADA MOUNTAINS (CA)
Sierra Nevada winter storms: A study using microwave radiometry, ice crystal, and isotopic analysis technique p 923 N93-15088

SIGNAL ANALYZERS
A complete-time approach for chaining and execution control in the AN/UYS-2 parallel signal processor
[AD-A256306] p 859 N93-14442

SIGNAL DETECTION
On the detection of ultrawideband radar signals
[AD-A256075] p 858 N93-14233
Audio detection algorithms
[AD-A256076] p 973 N93-14234
Statistically calibrated transducer
[AD-D015408] p 882 N93-14878

SIGNAL DISTORTION
Deterministic transfer function for transionospheric propagation
[DE92-040327] p 862 N93-15427
Satellite measurement of ionospheric-induced VHF distortion
[DE92-040328] p 862 N93-15435
Development of a 500 GHz optoelectronic modulator using superconducting transmission lines
[AD-A257062] p 871 N93-15456

SIGNAL PROCESSING
On the detection of ultrawideband radar signals
[AD-A256075] p 858 N93-14233
An analysis of the effect of acoustic non-linearities in wide bandwidth acousto-optic bragg cells
[AD-A256579] p 973 N93-14269
A complete-time approach for chaining and execution control in the AN/UYS-2 parallel signal processor
[AD-A256306] p 859 N93-14442
Advanced sensors technology survey
[NASA-CR-185691] p 881 N93-14494
An energy analysis of the pseudo Wigner-Ville distribution in support of machinery monitoring and diagnostics
[AD-A256202] p 889 N93-14499
Photonic materials and devices for optical information processing and computing applications
[AD-A256047] p 982 N93-14578
AFIT/AFOSR Workshop on the Role of Wavelets in Signal Processing Applications
[AD-A256172] p 859 N93-14649
Method and apparatus for increasing a radar's range with improved scan-to-scan integration of Doppler filtered signals
[AD-D015421] p 860 N93-14742
Modified fast frequency acquisition via adaptive least squares algorithm
[NASA-CASE-NPO-17845-2-CU] p 945 N93-14882

Next generation satellite communications networks
p 812 N93-14962
Sonar processing on CESAR
[FFI-92/7007] p 974 N93-15074
A new multiplier-free structure for DFT based on delta modulation
[AD-A255927] p 861 N93-15106
Co-channel speaker separation
[AD-A256443] p 861 N93-15317
New methods for nonlinear tracking and nonlinear chaotic signal processing
[AD-A256421] p 862 N93-15334

SIGNAL RECEPTION
Layered parallel interface for an active antenna array
[AD-D015411] p 860 N93-14879

SIGNAL TO NOISE RATIOS
NPR and intermodulation in mobile satellite systems
p 806 N93-14931
A low bit rate FSK technique for SCPC satellite communication systems p 811 N93-14954
Co-channel speaker separation
[AD-A256443] p 861 N93-15317
New methods for nonlinear tracking and nonlinear chaotic signal processing
[AD-A256421] p 862 N93-15334
Interferometric measurement with squeezed light
[AD-A257065] p 984 N93-15458

SIGNAL TRANSMISSION
Layered parallel interface for an active antenna array
[AD-D015411] p 860 N93-14879
The evolution of signalling from ISDN to B-ISDN
[MEMO-INF-92-30] p 860 N93-15095

SIGNATURES
Energetic and magnetosheath energy particle signatures of the low-latitude boundary layer at low altitudes near noon
[NASA-CR-191388] p 917 N93-15574

SILANES
Si atomic layer epitaxy using remote plasma assisted hydrogen desorption and disilane as a precursor
[AD-A255606] p 993 N93-15008
Si atomic layer epitaxy based on Si2H6 and remote He plasma bombardment
[AD-A255763] p 993 N93-15055

SILICA GEL
Application of gel-silica optics to laser technology and optical element fabrication
[AD-A255666] p 883 N93-14131
Preliminary investigations of metal liquid-like films and coatings derived from them
[AD-A255477] p 849 N93-14489

SILICA GLASS
Fluids, gels, and glasses under extreme conditions of pressure and temperature
[AD-A255675] p 847 N93-14166

SILICATES
Optical information processing using photorefractive BSO p 981 N93-14204
Mixed-valence iron minerals on Venus: Fe(2+)-Fe(3+) oxides and oxy-silicates formed by surface-atmosphere interactions p 1025 N93-14301
Infrared laboratory spectra and composition changes of synthetic amorphous silicate grains
[DE92-040211] p 843 N93-15283

SILICIDES
Nonuniformity effects in a hybrid platinum silicide imaging device
[AD-A256339] p 983 N93-15197
Sputter deposition and characterization of MoSi2/SiC composite coatings
[DE92-040326] p 837 N93-15426

SILICON
Experimental considerations of higher order parametric x rays from silicon crystals of varying thicknesses
[AD-A256082] p 990 N93-14260
A simple controller for repetitive cycles in atomic layer epitaxy
[AD-A255497] p 992 N93-14643
Spectroscopy and reactions of hydrazoic acid on silicon single crystal surfaces (III). HN3 and DN3 on Si(111)-7 x 7
[AD-A255241] p 842 N93-14669
Thermal stability of trimethyl indium on Si(100)-2 x 1 as studied with HREELS, UPS, and XPS: A comparison with the results from Si(111)-7 x 7 and Si(110) studies
[AD-A255242] p 992 N93-14670
Ultraviolet-ozone cleaning of semiconductor surfaces, revision 1
[AD-A256158] p 842 N93-14678
Atomic data and spectral analysis of carbon, nitrogen, oxygen and silicon ions observed with the International Ultraviolet Explorer
[NASA-CR-191302] p 1012 N93-14761
Si atomic layer epitaxy based on Si2H6 and remote He plasma bombardment
[AD-A255763] p 993 N93-15055
Optimal synthesis methods for silicon compilers
[ETN-92-92677] p 947 N93-15125
Damage and rupture of ceramic composites
[ETN-92-92722] p 851 N93-15127
Study of the mathematical modelling and computer simulation of crystal growth from liquid phase under microgravity conditions
[CTN-93-60619] p 855 N93-15201
Silicon nitride thin film production on Si(111)
[AD-A256036] p 994 N93-15233
Revised nomenclature for defects at or near the Si/SiO2 interface
[DE92-040975] p 997 N93-15651

SILICON ALLOYS
The properties of thermally passivated Si(1-x) He(x) produced using high pressure techniques (and related augmentation awards)
[AD-A255961] p 991 N93-14429

SILICON CARBIDES
Photoelectrochemistry of electronic and electro-optical materials
[AD-A256239] p 866 N93-14583
Effect of thermomechanical treatments on the aging response of centrifugally cast silicon carbide/aluminum composites
[AD-A256204] p 836 N93-15236
Development of ceramic matrix composites for application in ceramic technology for advanced heat engines project, phase 2
[DE92-041379] p 836 N93-15387
Material development in the Si3N4 system using glass encapsulated HIP'ing
[DE92-041381] p 837 N93-15388
Inelastic deformation of metal matrix composites: Plasticity and damage mechanisms, part 2
[NASA-CR-189096-PT-2] p 837 N93-15401
Sputter deposition and characterization of MoSi2/SiC composite coatings
[DE92-040326] p 837 N93-15426
Analytical and experimental evaluation of joining silicon carbide to silicon carbide and silicon nitride to silicon nitride for heat engine applications
[DE92-041376] p 837 N93-15454
Development of ceramic matrix composites for application in the ceramic technology for advanced heat engines project
[DE92-041378] p 837 N93-15455

SILICON DIOXIDE
The properties of thermally passivated Si(1-x) He(x) produced using high pressure techniques (and related augmentation awards)
[AD-A255961] p 991 N93-14429

SILICON NITRIDES
Properties of textile grade ceramic fibers
p 833 N93-14751
Silicon nitride thin film production on Si(111)
[AD-A256036] p 994 N93-15233
Tribology of improved transformation-toughened ceramics-heat engine test
[DE92-041385] p 851 N93-15295
Development of ceramic matrix composites for application in ceramic technology for advanced heat engines project, phase 2
[DE92-041379] p 836 N93-15387
Material development in the Si3N4 system using glass encapsulated HIP'ing
[DE92-041381] p 837 N93-15388
Development of ceramic matrix composites for application in the ceramic technology for advanced heat engines project. Phase 2A: Development of in-situ toughened silicon nitride
[DE92-041371] p 853 N93-15452
Analytical and experimental evaluation of joining silicon carbide to silicon carbide and silicon nitride to silicon nitride for heat engine applications
[DE92-041376] p 837 N93-15454
Development of ceramic matrix composites for application in the ceramic technology for advanced heat engines project
[DE92-041378] p 837 N93-15455

SILICON OXIDES
Optical glasses for high-peak-power laser applications
[DE92-040403] p 886 N93-14906
Theory of the electronic and structural properties of solid state oxides
[DE92-040499] p 993 N93-14909
Energy distribution of trapped holes in irradiated SiO2
[DE92-040979] p 997 N93-15649
Revised nomenclature for defects at or near the Si/SiO2 interface
[DE92-040975] p 997 N93-15651

SILOXANES
Characterization of cholesteric cyclic siloxane liquid crystalline materials
[AD-A256128] p 994 N93-15190

SILVER
Multifilamentary superconducting cable and a method of manufacturing it
[AD-D015391] p 846 N93-15231

SILVER IODIDES
Cesium iodide alloys
[DE92-019818] p 845 N93-14717

SIMPLIFICATION
Method of local shaping of thermoplastics
[AD-A255913] p 856 N93-15105

SIMULATION
A proof of convergence of the Markov chain simulation method
[AD-A255456] p 970 N93-14487
Systems modeling
[AD-A255215] p 944 N93-14575
A simulation model of atmospheric turbulence for rotorcraft applications p 920 N93-14588
Simulation and nonlinear modelling of microwave transistors p 807 N93-14936
Studies of tropical ocean dynamics using the TOPEX/Poseidon altimeter-derived sea surface topography p 928 N93-14980
Performing wind-tunnel modeling for better management of near-field risks
[DE92-040205] p 910 N93-15063
A simulation study of planar swaging deformation
[AD-A255908] p 902 N93-15070
A high intensity solar cell invention: The edge-illuminated Vertical Multi-Junction (VMJ) solar cell
[DE92-019015] p 907 N93-15224
Radar data processing using a distributed computational system
[AD-A256209] p 861 N93-15237
Finite-difference solution for laminar or turbulent boundary layer flow over axisymmetric bodies with ideal gas, CF4, or equilibrium air chemistry
[NASA-TP-3271] p 879 N93-15434

SIMULATORS
Simulator evaluation of displays for a revised takeoff performance monitoring system
[NASA-TP-3270] p 803 N93-15366
Aspects of a parallel-architecture simulator
[AD-A256872] p 941 N93-15628

SINGLE CRYSTALS
Fatigue in single crystal nickel superalloys
[AD-A256095] p 844 N93-14264
Determination of operable deformation mechanisms during ballistic impact in tungsten single crystals, utilizing transmission electron microscopy
[AD-A255351] p 991 N93-14518
Spectroscopy and reactions of hydrazoic acid on silicon single crystal surfaces (III). HN3 and DN3 on Si(111)-7 x 7
[AD-A255241] p 842 N93-14669
Thermal stability of trimethyl indium on Si(100)-2 x 1 as studied with HREELS, UPS, and XPS: A comparison with the results from Si(111)-7 x 7 and Si(110) studies
[AD-A255242] p 992 N93-14670
In-service considerations affecting component life
p 800 N93-14898

SINGLE STAGE TO ORBIT VEHICLES
Robust nonlinear feedback guidance for an aerospace plane: A geometric approach p 803 N93-14835

SINGULAR INTEGRAL EQUATIONS
The crack problem for an orthotropic half plane stiffened by elastic films
[AD-A256471] p 903 N93-15374

SINGULARITY (MATHEMATICS)
Wavelet methods for curve estimation
[AD-A255357] p 970 N93-14538
Cosmological models in higher-order gravity
p 1018 N93-14592

SINTERING
Deformation characterization of powdered metals in compaction and application of the finite element method to compaction processes p 844 N93-14472
Method of making substantially single phase superconducting oxide ceramics having a TC above 85 degrees
[AD-D015422] p 850 N93-14743
A fundamental understanding of the effects of ceramic processing on product microstructure
[AD-A255729] p 850 N93-15049
Microwave processing of tantalum capacitor anodes
[DE92-017829] p 869 N93-15214
Processing of sinterable transformation toughened ceramics for application in ceramic technology for advanced heat engines project
[DE92-041372] p 853 N93-15453
Development of ceramic matrix composites for application in the ceramic technology for advanced heat engines project
[DE92-041378] p 837 N93-15455

SITTING POSITION
Passive zero-gravity leg restraint
[NASA-CASE-ARC-11882-1-CU] p 939 N93-14713
SIZE DISTRIBUTION
A fundamental understanding of the effects of ceramic processing on product microstructure
[AD-A255729] p 850 N93-15049
SKY SURVEYS (ASTRONOMY)
A faint spectroscopic quasar survey
p 1012 N93-14629
SLABS
Efficient asymptotic closed form approximation for dyadic green's function for anisotropic substrates, phase 1
[AD-A256258] p 830 N93-14436
SLEEP
Sleep inertia: Is there a worst time to wake up?
[AD-A256602] p 934 N93-14240
SLEEP DEPRIVATION
Sleep inertia: Is there a worst time to wake up?
[AD-A256602] p 934 N93-14240
SLENDER CONES
Modeling variable blowing on a slender cone in hypersonic flow p 781 N93-14836
SLIDING
Utilizing sensed incipient slip signals for grasp force control
[AD-A255725] p 888 N93-14434
SLIP
A minimum-slip attitude control method for the erebus walking robot
[NASA-CR-191646] p 890 N93-14567
SLIP CASTING
Development of ceramic matrix composites for application in the ceramic technology for advanced heat engines project. Phase 2A: Development of in-situ toughened silicon nitride
[DE92-041371] p 853 N93-15452
SLOPES
Extensive lava flow fields on Venus: Preliminary investigation of source elevation and regional slope variations p 1034 N93-14342
SLOTS
RB 199 high pressure compressor stage 3 spin pit tests p 799 N93-14893
CF6-6 high pressure compressor stage 5 locking slot crack propagation spin pit test p 799 N93-14894
SMALL PERTURBATION FLOW
Wing rock prediction method for a high performance fighter aircraft
[AD-A256438] p 792 N93-15314
SMART STRUCTURES
Smart materials for Army structures
[AD-A254925] p 836 N93-15218
SMOKE
Satellite detection of complex aerosols over the Arabian Peninsula/Gulf
[AD-A256085] p 909 N93-14261
SNOW
Modern methods in meteorological and oceanographic data analysis
[AD-A257080] p 903 N93-15496
SOFT LANDING
Reusable Reentry Satellite (RRS): Telemetry, Tracking, and Command (TT/C) coverage tradeoff study
[NASA-CR-188583] p 824 N93-15629
SOFTENING
Softening of rigid polyvinyl chloride by high concentrations of aqueous solutions of methylene chloride
[AD-A255453] p 848 N93-14486
SOFTWARE ENGINEERING
System design and development of a low data rate voice (1200 bps) rate converter
[AD-A256071] p 859 N93-14663
Software stamping
[NPL-DITC-198/92] p 946 N93-15072
Obstacles in object-oriented software development
[MEMO-INF-92-15] p 946 N93-15084
Software flexibility and configuration control for the A340/A330 Aircraft Condition Monitoring System (ACMS) p 793 N93-15154
A philosophy for integrated monitoring system design
p 796 N93-15174
Continuing engineering education for software engineering professionals
[DE92-019888] p 947 N93-15225
Experience with a course on architectures for software systems. Part 1: Course description
[AD-A256221] p 941 N93-15239
System design in a large corporation, using VHDL (VHSIC hardware description language)
[VH-4] p 948 N93-15265
Integrating VHDL (VHSIC hardware description language) with existing EDA tools
[VH-8] p 948 N93-15268
An eclectic method for object oriented database design
[AD-A256439] p 1008 N93-15315
User manual for the Software Technology for Adaptable, Reliable Systems (STARS). PCTE Browser Tool (PBT) version 0.1 SunOS implementation
[AD-A257064] p 951 N93-15457
Software Technology for Adaptable, Reliable Systems (STARS)
[AD-A257022] p 952 N93-15471
Integrated support for real-time control systems
[PNR-90994] p 952 N93-15476
Data collection procedures for the Software Engineering Laboratory (SEL) database
[NASA-TM-108579] p 957 N93-15579
SOFTWARE RELIABILITY
Reliability techniques for combined hardware and software systems
[AD-A256347] p 895 N93-15204
SOFTWARE REUSE
Software Technology for Adaptable, Reliable Systems (STARS)
[AD-A257022] p 952 N93-15471
SOFTWARE TOOLS
Development of a MATLAB toolbox for image processing
[AD-A256130] p 942 N93-14247
Proof of theorems in Z
[AD-A255711] p 968 N93-14431
A non-deterministic recogniser generator
[MEMO-INF-92-21] p 946 N93-15091
Automated coding and intersecting cube theory
[ETN-92-92675] p 941 N93-15123
Workstation tools for feature extraction and classification for nonstationary and transient signals
[AD-A255389] p 947 N93-15228
VHDL (VHSIC hardware description language): Origins, status, capabilities, and world environment
[VH-1] p 947 N93-15262
System design in a large corporation, using VHDL (VHSIC hardware description language)
[VH-4] p 948 N93-15265
Integrating VHDL (VHSIC hardware description language) with existing EDA tools
[VH-8] p 948 N93-15268
CAD-based off-line programming and sensor signal processing in robotics
[F-2-2] p 949 N93-15299
User manual for the Software Technology for Adaptable, Reliable Systems (STARS). PCTE Browser Tool (PBT) version 0.1 SunOS implementation
[AD-A257064] p 951 N93-15457
Mathematical software under UNICOS at LCC
[DE93-001828] p 952 N93-15493
Flight dynamics system software development environment (FDS/SDE) tutorial
[NASA-TM-108580] p 952 N93-15502
Proceedings: Graphics Interface 1992
[ISBN-0-9695338-1-0] p 952 N93-15533
Hyper-rendering p 953 N93-15538
A framework for describing and implementing software visualization systems p 953 N93-15540
A multi-layer graphic model for building interactive graphical applications p 957 N93-15567
SOI (SEMICONDUCTORS)
Gate-all-around device
[AD-A255287] p 866 N93-14534
SOIL EROSION
Evaluation of a soil fixative to retard particle entrainment: A laboratory study
[UCRL-LR-109806] p 915 N93-14877
SOILS
Radar-anomalous, high-altitude features on Venus
p 1036 N93-14349
Evaluation of a soil fixative to retard particle entrainment: A laboratory study
[UCRL-LR-109806] p 915 N93-14877
SOL-GEL PROCESSES
Fluids, gels, and glasses under extreme conditions of pressure and temperature
[AD-A255675] p 847 N93-14166
Preliminary investigations of metal liquid-like films and coatings derived from them
[AD-A255477] p 849 N93-14489
Reliability of sol-gel derived ferroelectric memories
[AD-A255358] p 991 N93-14560
Ultrastructure processing and environmental stability of advanced structural and electronic materials
[AD-A256153] p 831 N93-14665
Reliability of sol-gel derived ferroelectric memories
[AD-A255240] p 849 N93-14668
SOLAR ACTIVITY
Physical and chemical processes of the inner coma observed in mid-ultraviolet cometary spectra
p 1017 N93-14230
SOLAR ACTIVITY EFFECTS
Global zones of particle precipitation as observed by EXOS-C
[AD-A256397] p 917 N93-15466
On the variation of the Nimbus 7 total solar irradiance
[NASA-TP-3316] p 1049 N93-15532
SOLAR ARRAYS
Photovoltaic power system for a lunar base
p 806 N93-14930
On some kinematic and mass characteristics of foldable solar arrays p 812 N93-14957
Solar proton events of 1989: Effects on spacecraft solar arrays
[AD-A256457] p 1049 N93-15318
The use of plasma ashers and Monte Carlo modeling for the projection of atomic oxygen durability of protected polymers in low Earth orbit p 819 N93-15596
On-orbit deployment anamolies: What can be done?
p 821 N93-15603
SOLAR ATMOSPHERE
Resonance absorption of MHD surface waves with applications to the solar atmosphere
p 1048 N93-14157
Theoretical studies of the physics of the solar atmosphere
[NASA-CR-191357] p 1049 N93-15085
SOLAR CELLS
Computer based satellite design
[AD-A255315] p 816 N93-14536
NREL photovoltaic subcontract reports: Abstracts and document control information
[DE92-016408] p 907 N93-14817
A high intensity solar cell invention: The edge-illuminated Vertical Multi-Junction (VMJ) solar cell
[DE92-019015] p 907 N93-15224
Solar proton events of 1989: Effects on spacecraft solar arrays
[AD-A256457] p 1049 N93-15318
SOLAR COLLECTORS
The CPG 5-kW(e) Dish-Stirling Development Program
[DE92-017050] p 907 N93-15134
SOLAR CORONA
Resonance absorption of MHD surface waves with applications to the solar atmosphere
p 1048 N93-14157
Solar flares: The onset of magnetic reconnection and the structure of radiative slow-mode shocks
p 1048 N93-14859
SOLAR CYCLES
On the variation of the Nimbus 7 total solar irradiance
[NASA-TP-3316] p 1049 N93-15532
SOLAR ELECTRIC PROPULSION
S/EV 1991: Solar and Electric Vehicle Symposium, Car and Trade Show
[DE92-019890] p 869 N93-15226
SOLAR ENERGY
EMTP based stability analysis of space station electric power system in a test bed environment
[NASA-TM-105845] p 871 N93-15503
SOLAR ENERGY CONVERSION
The CPG 5-kW(e) Dish-Stirling Development Program
[DE92-017050] p 907 N93-15134
SOLAR FLARES
A survey of solar flare energetic particle abundances and energy spectra p 1048 N93-14135
Imaging the sun in hard x-rays using Fourier telescopes p 1048 N93-14591
Solar flares: The onset of magnetic reconnection and the structure of radiative slow-mode shocks
p 1048 N93-14859
Imaging the sun in hard x rays using Fourier telescopes
[NASA-TM-108390] p 1013 N93-15203
Solar proton events of 1989: Effects on spacecraft solar arrays
[AD-A256457] p 1049 N93-15318
SOLAR GENERATORS
Energy loss analysis of an integrated space power distribution system
[NASA-TM-105772] p 854 N93-14834
The CPG 5-kW(e) Dish-Stirling Development Program
[DE92-017050] p 907 N93-15134
SOLAR MAGNETIC FIELD
Imaging the sun in hard x-rays using Fourier telescopes p 1048 N93-14591
Solar flares: The onset of magnetic reconnection and the structure of radiative slow-mode shocks
p 1048 N93-14859
SOLAR OSCILLATIONS
The detection and characterization of high frequency and high wavenumber solar oscillations
[NASA-CR-191622] p 1049 N93-15634
SOLAR PLANETARY INTERACTIONS
The time variability of Jupiter's synchrotron radiation
p 973 N93-14227

Radiation pressure: A possible cause for the superrotation of the Venusian atmosphere
p 1033 N93-14338
The solar wind interaction with Venus
p 1034 N93-14341

SOLAR PROTONS
Solar proton events of 1989: Effects on spacecraft solar arrays
[AD-A256457] p 1049 N93-15318

SOLAR RADIATION
Physical and chemical processes of the inner coma observed in mid-ultraviolet cometary spectra
p 1017 N93-14230
Precision radiation force modeling for the TOPEX/Poseidon mission p 817 N93-14586
Degradation and failure modes of carbon/bismaleimide laminates subjected to a tropical exposure
[AD-A256328] p 836 N93-15193
On the variation of the Nimbus 7 total solar irradiance
[NASA-TP-3316] p 1049 N93-15532

SOLAR REFLECTORS
Low Earth orbit atomic oxygen simulation for durability evaluation of solar reflector surfaces
p 819 N93-15594

SOLAR SAILS
The Canadian Solar Sail Project p 804 N93-14921

SOLAR SIMULATION
Spacecraft thermal design verification in Canada
p 808 N93-14940

SOLAR WIND
The thermosphere and ionosphere of Venus
p 1026 N93-14307
The solar wind interaction with Venus
p 1034 N93-14341

SOLDERING
A study for the development of practices to protectively coat and join fibre epoxy composites for use in the Space Station Programme
[CTN-93-60626] p 835 N93-15145

SOLID ELECTROLYTES
Components and materials issues in polymer electrolyte fuel cells for transportation applications
[DE92-013384] p 907 N93-15061
Jet vapor deposition of thin films for solid oxide and other fuel cell applications
[DE92-019980] p 851 N93-15222
High temperature tubular solid oxide fuel cell development
[DE92-040253] p 908 N93-15322
Contaminant effects in solid oxide fuel cells
[DE92-040255] p 908 N93-15323
Solid polymer electrolytes for rechargeable batteries
[DE93-001603] p 871 N93-15485

SOLID LUBRICANTS
The influence of steel surface chemistry on the bonding of lubricant films
[AD-A256231] p 851 N93-15242
The effect of processing and compositional changes on the tribology of PM212 in air
[NASA-TM-105945] p 828 N93-15576

SOLID ROCKET PROPELLANTS
Propellant grain assembly for a gas generator
[AD-D015439] p 854 N93-14801
Thermal decomposition of HNIW and HNIW-Based formulations
[AD-A255613] p 854 N93-15011

SOLID STATE
Basic research in electronics (JSEP)
[AD-A256016] p 869 N93-15257

SOLID STATE DEVICES
Application of gel-silica optics to laser technology and optical element fabrication
[AD-A255666] p 883 N93-14131
Solid state research
[AD-A256019] p 992 N93-14576
Photoelectrochemistry of electronic and electro-optical materials
[AD-A256239] p 866 N93-14583
Solid state flight data recorder with rapid data access
p 795 N93-15167

SOLID STATE LASERS
Optics for diode array transverse pumped laser rod
[AD-D015436] p 885 N93-14722
Solid-state coherent laser radar wind shear measuring systems p 784 N93-14848

SOLID STATE PHYSICS
Innovative techniques for studying new materials and new developments in solid state physics
[AD-A256394] p 996 N93-15465

SOLID-SOLID INTERFACES
Effect of interfacial thermal conductance and fiber orientation on the thermal diffusivity/conductivity of unidirectional fiber-reinforced ceramic matrix composites
p 864 N93-14190
Fracture analyses of thin films, interfaces, and joints
p 897 N93-14215
Preliminary design of composite joints
[DLR-MITT-92-05] p 835 N93-15076
The 17th Annual Conference on the Physics and Chemistry of Semiconductor Interfaces
[AD-A257061] p 996 N93-15449

SOLIDIFICATION
The effects of Venus' thermal structure on buoyant magma ascent p 1040 N93-14366
Study of Fluid Experiment System (FES)/CAST/Holographic Ground System (HGS)
[NASA-CR-184483] p 855 N93-14793

SOLIDIFIED GASES
Experimental attempt to metallize hydrogen at very high pressures
[AD-A257086] p 843 N93-15497

SOLIDS
Remote techniques for time-of-flight flaw characterisation p 989 N93-14171

SOLITARY WAVES
Electronic, vibrational, and transport properties of conducting polymers p 847 N93-14170
Integrated photonics research technical digest series. Volume 10: Conference edition: Summaries of papers presented at the Integrated Photonics Research Topical Meeting
[AD-A255423] p 981 N93-14506
Interferometric measurement with squeezed light
[AD-A257065] p 984 N93-15458

SOLUBILITY
Removal of THD from painted test panels by liquid systems
[AD-A255624] p 850 N93-15064

SOLUTES
Molecular capacitance: Sequential electron-transfer energetics for solution-phase metallic clusters in relation to gas-phase clusters and analogous interfaces
[AD-A257057] p 977 N93-15448

SOLVATION
Molecular capacitance: Sequential electron-transfer energetics for solution-phase metallic clusters in relation to gas-phase clusters and analogous interfaces
[AD-A257057] p 977 N93-15448

SOLVENTS
Characterization of fiber reinforced phenolic composites p 828 N93-14142
Softening of rigid polyvinyl chloride by high concentrations of aqueous solutions of methylene chloride
[AD-A255453] p 848 N93-14486

SONAR
Statistically calibrated transducer
[AD-D015408] p 882 N93-14878
Sonar processing on CESAR
[FFI-92/7007] p 974 N93-15074

SORPTION
Characterization of fiber reinforced phenolic composites p 828 N93-14142
Analytical and experimental investigation of closed-cycle sorption cooling systems p 874 N93-14476

SOUND PRESSURE
Acoustic mode measurements in the inlet of a model turbofan using a continuously rotating rake: Data collection/analysis techniques
[NASA-TM-105936] p 801 N93-15403

SOUND TRANSMISSION
Problems in nonlinear acoustics: Rayleigh waves, pulsed sound beams, reflection of focused beams, waveguides, cooperative radiation of sound by buggles, acoustic streaming effects in standing waves, and spark-source lithotripter pulses
[AD-A256289] p 974 N93-14458

SOUND WAVES
Turbulence and chaos in classical and quantum systems p 972 N93-14144
A time-domain study of the relationship between drive force time bandwidth and farfield acoustic radiation
[AD-A255616] p 973 N93-14159
Statistically calibrated transducer
[AD-D015408] p 882 N93-14878
Boundary element analysis of low frequency cavity acoustical problems
[MATHS-REPT-A-158] p 974 N93-15073
Vibration and acoustic testing of TOPEX/Poseidon satellite p 820 N93-15599
The detection and characterization of high frequency and high wavenumber solar oscillations
[NASA-CR-191622] p 1049 N93-15634

SOUND-SOUND INTERACTIONS
Scattering of sound by sound: Nonlinear interaction of collinear and noncollinear sound beams
p 973 N93-14145

SOUTHERN OSCILLATION
Extreme climatic events in the Amazon Basin and their associations with the circulation of the global tropics
p 918 N93-14115

SPACE BASED RADAR
Space based radar: Test of large space structures
p 808 N93-14941
Progress in DND's space-based radar R/D project
p 812 N93-14958

SPACE DEBRIS
Characterisation and dynamic modelling of the near-earth space particulate environment
p 1019 N93-14637
Hypervelocity impact simulations of Whipple shields
p 821 N93-15604

SPACE ENVIRONMENT SIMULATION
The Seventeenth Space Simulation Conference. Terrestrial Test for Space Success
[NASA-CP-3181] p 819 N93-15593
Manned testing in a simulated space environment
p 820 N93-15602
Hypervelocity impact simulations of Whipple shields
p 821 N93-15604
A new approach for data acquisition at the JPL space simulators p 821 N93-15606
Application of programmable logic controllers to space simulation p 821 N93-15608
INTESPACE's new thermal-vacuum test facility: SIMMER p 814 N93-15613
Accelerated simulation of near-Earth-orbit polymer degradation p 823 N93-15615

SPACE ERECTABLE STRUCTURES
Structurally adaptive space crane concept for assembling space systems on orbit
[NASA-TP-3307] p 818 N93-15368

SPACE EXPLORATION
The Canadian Solar Sail Project p 804 N93-14921
Human exploration: Moon/Mars mission
p 805 N93-14922
Applications of the mobile servicing system to the space exploration initiative p 809 N93-14946
Directory of research projects: Planetary geology and geophysics program
[NASA-TM-4428] p 864 N93-15638

SPACE MISSIONS
Global optimum path planning for a redundant space robot
[AD-A255316] p 889 N93-14545
STS-49: Space shuttle mission report
[NASA-TM-108104] p 815 N93-14736

SPACE NAVIGATION
A plan for spacecraft automated rendezvous
[NASA-TM-108385] p 813 N93-15392

SPACE OBSERVATIONS (FROM EARTH)
Groundbased near-IR observations of the surface of Venus p 1035 N93-14346
An application of artificial intelligence to automatic telescopes
[NASA-TM-108115] p 965 N93-15291

SPACE PERCEPTION
Psychophysical analyses of perceptual representations
[AD-A255432] p 936 N93-14510

SPACE PLASMAS
The sulfur emission and periodicity of the Jupiter plasma torus in 1988 p 1022 N93-14156

SPACE PLATFORMS
Vibration isolation technology: An executive summary of systems development and demonstration
[NASA-TM-105937] p 778 N93-15573

SPACE POWER REACTORS
Closed Brayton Cycle power system with a high temperature pellet bed reactor heat source for NEP applications
[NASA-TM-105933] p 826 N93-14482
SAFSIM: A computer program for engineering simulations of space reactor system performance
[DE92-016328] p 826 N93-14815

SPACE PROCESSING
Study of Fluid Experiment System (FES)/CAST/Holographic Ground System (HGS)
[NASA-CR-184483] p 855 N93-14793
Numerical study of mixing of two fluids under low gravity
[NASA-TM-105865] p 878 N93-14914
Modelling Directional Solidification
[NASA-CR-191301] p 995 N93-15309

SPACE RENDEZVOUS
A plan for spacecraft automated rendezvous
[NASA-TM-108385] p 813 N93-15392

SPACE SHUTTLE MAIN ENGINE
An overview of reliability growth models and their potential use for NASA applications
[NASA-TP-3309] p 895 N93-15433

SPACE SHUTTLE ORBITERS
Extra-vehicular activity translation tool
[NASA-CASE-MSC-21955-1] p 891 N93-14842

Space Shuttle Orbiter Crew Hatch Jettison Test using a 0.0405-scale model (16-0) in the Texas A/M low speed wind tunnel (OA362). Space Shuttle aerothermodynamic data report
[NASA-CR-167698] p 815 N93-15474

SPACE SHUTTLE PAYLOADS
Reusable Reentry Satellite (RRS) system design study
[NASA-CR-187897] p 817 N93-14733

SPACE SHUTTLES
STS-49: Space shuttle mission report
[NASA-TM-108104] p 815 N93-14736
Scheduling and rescheduling with iterative repair
[NASA-TM-108120] p 965 N93-15287
Rescheduling with iterative repair
[NASA-TM-108119] p 965 N93-15288
Learning to improve iterative repair scheduling
[NASA-TM-108118] p 965 N93-15289
Results of a FRSI material test under Space Shuttle ascent conditions in the Ames Research Center 9x7 foot supersonic wind tunnel (OS13). Space Shuttle aerothermodynamic data report
[NASA-CR-167699] p 816 N93-15475

SPACE SIMULATORS
Spacecraft thermal design verification in Canada
p 808 N93-14940
An environmental testing facility for Space Station Freedom power management and distribution hardware
p 820 N93-15601
A new approach for data acquisition at the JPL space simulators p 821 N93-15606
A new thermal vacuum facility at the Martin Marietta Waterton plant p 814 N93-15607
From diffusion pumps to cryopumps: The conversion of GSFC's space environment simulator
p 814 N93-15611
INTESPACE's new thermal-vacuum test facility: SIMMER p 814 N93-15613

SPACE STATION FREEDOM
Damage location and model refinement for large flexible space structures using a sensitivity-based eigenstructure assignment method p 816 N93-14274
Advanced sensors technology survey
[NASA-CR-185691] p 881 N93-14494
Autonomous power system brassboard
[NASA-CR-189115] p 867 N93-14798
A plan for spacecraft automated rendezvous
[NASA-TM-108385] p 813 N93-15392
Space Station Freedom data management system growth and evolution report
[NASA-TM-103869] p 816 N93-15477
An environmental testing facility for Space Station Freedom power management and distribution hardware
p 820 N93-15601
Overview of environmental test plans for Space Station Freedom work package 4 p 824 N93-15623
Space Station Freedom user's guide
[NASA-TM-108105] p 825 N93-15650

SPACE STATION POWER SUPPLIES
EMTP based stability analysis of space station electric power system in a test bed environment
[NASA-TM-105845] p 871 N93-15503

SPACE STATION STRUCTURES
Damage location and model refinement for large flexible space structures using a sensitivity-based eigenstructure assignment method p 816 N93-14274

SPACE STATIONS
Global optimum path planning for a redundant space robot
[AD-A255316] p 889 N93-14545
Large space structures and systems in the space station era: A bibliography with indexes (supplement 04)
[NASA-SP-7085(04)] p 817 N93-14606
Human exploration: Moon/Mars mission
p 805 N93-14922

SPACE TOOLS
Extra-vehicular activity translation tool
[NASA-CASE-MSC-21955-1] p 891 N93-14842

SPACE TRANSPORTATION SYSTEM FLIGHTS
STS-49: Space shuttle mission report
[NASA-TM-108104] p 815 N93-14736

SPACE VEHICLE CHECKOUT PROGRAM
Anik E spacecraft integration and test
p 808 N93-14939
Space based radar: Test of large space structures
p 808 N93-14941
Space craft verification at the David Florida Laboratory
p 809 N93-14943

SPACE-TIME FUNCTIONS
Type 2 superstrings in curved D = 10 space-time: Dynamics of their massless fields and covariant quantization p 998 N93-14143
Multiply connected spacetimes and closed timelike curves in semiclassical gravity p 915 N93-14884
Spatio-temporal complexity and large-scale structures in problems of continuum mechanics
[AD-A256410] p 998 N93-15333
Development and application of a time-space conversion technique for analysis of weather systems passing over the Kennedy Space Center
[NASA-CR-4474] p 924 N93-15581

SPACEBORNE EXPERIMENTS
Spectral analysis of the shuttle glow. SPA II/IBSS Mission: AIS hardware
[PL-TR-92-2148] p 814 N93-14697
Study of Fluid Experiment System (FES)/CAST/Holographic Ground System (HGS)
[NASA-CR-184483] p 855 N93-14793
ISOCAM experiment cryogenic test results
[REPT-921-440-104] p 825 N93-15140
Environmental qualification testing of the prototype pool boiling experiment
[NASA-CR-190774] p 895 N93-15582
Segment specification for the payload segment of the reusable reentry satellite: Rodent module version
[NASA-CR-187884] p 824 N93-15630
LDEF: A bibliography with abstracts
[NASA-TM-107705] p 813 N93-15646

SPACECRAFT CONFIGURATIONS
Computer based satellite design
[AD-A255315] p 816 N93-14536

SPACECRAFT CONSTRUCTION MATERIALS
Mechanics of composite materials for spacecraft
[AD-A255380] p 831 N93-14550
Low Earth orbit atomic oxygen simulation for durability evaluation of solar reflector surfaces
p 819 N93-15594
Simulation of the synergistic low Earth orbit effects of vacuum thermal cycling, vacuum UV radiation, and atomic oxygen p 819 N93-15595
Accelerated simulation of near-Earth-orbit polymer degradation p 823 N93-15615

SPACECRAFT CONTAMINATION
Spectral analysis of the shuttle glow. SPA II/IBSS Mission: AIS hardware
[PL-TR-92-2148] p 814 N93-14697
Control of on-orbit contamination for the Argos (P91-1) satellite p 823 N93-15617

SPACECRAFT CONTROL
Autonomous power system brassboard
[NASA-CR-189115] p 867 N93-14798
Robust nonlinear feedback guidance for an aerospace plane: A geometric approach p 803 N93-14835
Thermal elastic shock and its effect on spacecraft attitude control p 818 N93-14837

SPACECRAFT DESIGN
Interplanetary program to optimize simulated trajectories (IPOST). Volume 4: Sample cases
[NASA-CR-189653-VOL-4] p 815 N93-14768
Proceedings of the Sixth CASI Conference on Astronautics
[CTN-92-60336] p 804 N93-14920
The Canadian Solar Sail Project p 804 N93-14921
Spacecraft thermal design verification in Canada
p 808 N93-14940
Vehicle/payload interface specification for the reusable reentry satellite
[NASA-CR-187883] p 824 N93-15631
System specification for the reusable reentry satellite
[NASA-CR-187882] p 824 N93-15632

SPACECRAFT GLOW
Spectral analysis of the shuttle glow. SPA II/IBSS Mission: AIS hardware
[PL-TR-92-2148] p 814 N93-14697
Spectral analysis of the shuttle glow: AIS science support
[PL-TR-92-2172] p 815 N93-14698

SPACECRAFT GUIDANCE
A plan for spacecraft automated rendezvous
[NASA-TM-108385] p 813 N93-15392

SPACECRAFT LANDING
Reusable Reentry Satellite (RRS): Recovery tradeoff study
[NASA-CR-186396] p 825 N93-15658

SPACECRAFT LAUNCHING
Vibration and acoustic testing of TOPEX/Poseidon satellite p 820 N93-15599

SPACECRAFT MAINTENANCE
Multiple fault diagnosis of spacecraft electrical power systems p 806 N93-14927
A concept for a supervised autonomous robot
p 810 N93-14950
Scheduling and rescheduling with iterative repair
[NASA-TM-108120] p 965 N93-15287
Rescheduling with iterative repair
[NASA-TM-108119] p 965 N93-15288
Learning to improve iterative repair scheduling
[NASA-TM-108118] p 965 N93-15289

SPACECRAFT MODELS
System test approach for the SAX satellite
p 824 N93-15622

SPACECRAFT ORBITS
PEX: A reactive procedure based decision maker
[REPT-921-440-105] p 999 N93-15118
Control of on-orbit contamination for the Argos (P91-1) satellite p 823 N93-15617

SPACECRAFT PERFORMANCE
System specification for the reusable reentry satellite
[NASA-CR-187882] p 824 N93-15632

SPACECRAFT POWER SUPPLIES
Large space structures and systems in the space station era: A bibliography with indexes (supplement 04)
[NASA-SP-7085(04)] p 817 N93-14606
Autonomous power system brassboard
[NASA-CR-189115] p 867 N93-14798
Energy loss analysis of an integrated space power distribution system
[NASA-TM-105772] p 854 N93-14834
A feasibility assessment of magnetic bearings for free-piston Stirling space power converters
[NASA-CR-189135] p 891 N93-14916
Overview of environmental test plans for Space Station Freedom work package 4 p 824 N93-15623

SPACECRAFT PROPULSION
The Canadian Solar Sail Project p 804 N93-14921
Engine technologies for future spaceplanes
[ETN-92-92732] p 800 N93-15143
Low thrust chemical rocket technology
[NASA-TM-105927] p 827 N93-15572

SPACECRAFT RADIATORS
Current status of liquid sheet radiator research
[NASA-TM-105764] p 872 N93-14150

SPACECRAFT RECOVERY
Reusable Reentry Satellite (RRS): Recovery tradeoff study
[NASA-CR-186396] p 825 N93-15658

SPACECRAFT SHIELDING
Results of a FRSI material test under Space Shuttle ascent conditions in the Ames Research Center 9x7 foot supersonic wind tunnel (OS13). Space Shuttle aerothermodynamic data report
[NASA-CR-167699] p 816 N93-15475
Predictions of dose from electrons in space
[NASA-CR-191617] p 1051 N93-15580

SPACECRAFT STRUCTURES
Thermal elastic shock and its effect on spacecraft attitude control p 818 N93-14837
Space Shuttle Orbiter Crew Hatch Jettison Test using a 0.0405-scale model (16-0) in the Texas A/M low speed wind tunnel (OA362). Space Shuttle aerothermodynamic data report
[NASA-CR-167698] p 815 N93-15474
Offloading techniques for large deployable space structures p 821 N93-15605

SPACECRAFT TEMPERATURE
Spacecraft thermal design verification in Canada
p 808 N93-14940

SPACECRAFT TRAJECTORIES
Interplanetary program to optimize simulated trajectories (IPOST). Volume 4: Sample cases
[NASA-CR-189653-VOL-4] p 815 N93-14768
Interplanetary Program to Optimize Simulated Trajectories (IPOST). Volume 1: User's guide
[NASA-CR-189653-VOL-1-REV] p 815 N93-14794
Optimal impulsive trajectories for orbital rendezvous between elliptic orbits p 813 N93-15103

SPACECREWS
Space Shuttle Orbiter Crew Hatch Jettison Test using a 0.0405-scale model (16-0) in the Texas A/M low speed wind tunnel (OA362). Space Shuttle aerothermodynamic data report
[NASA-CR-167698] p 815 N93-15474
Manned testing in a simulated space environment
p 820 N93-15602

SPACERS
In-service considerations affecting component life
p 800 N93-14898

SPATIAL DISTRIBUTION
Impact craters on Venus: An overview from Magellan observations p 1040 N93-14369
Multiresolution pattern recognition of small volcanos in Magellan data p 1042 N93-14380
The spatial distribution of coronae on Venus
p 1043 N93-14383
Effects of spatial luminance nonuniformities on visual-task performance and subjective uniformity
[AD-A255989] p 936 N93-14416
Parametric study of diffusion-enhancement networks for spatiotemporal grouping in real-time artificial vision
[AD-A256059] p 937 N93-14580
Spatial and temporal patterns of biotic exchanges of CO2 between the atmosphere and tropical landscapes and their role in the global carbon balance
[DE92-019170] p 911 N93-15272

SPATIAL RESOLUTION
Venus gravity: Summary and coming events
p 1042 N93-14377

High speed imaging for flash radiography using PIN diodes
[DE92-040959] p 882 N93-15381
SPECIFIC HEAT
Thermophysical properties of nitric oxide
[ESDU-92027] p 839 N93-14544
SPECIFIC IMPULSE
Numerical study of cathode emission constraints on cylindrical self-field MPD thruster performance
[NASA-CR-190795] p 826 N93-15370
SPECIFICATIONS
Flight termination systems commonality standard
[AD-A255349] p 789 N93-14517
VHDL (VHSIC hardware description language) use in the US defense procurement process
[VH-2] p 948 N93-15263
The extended VHDL (VHSIC hardware description language) design environment: An unique integrated system and hardware design environment
[VH-3] p 948 N93-15264
System design in a large corporation, using VHDL (VHSIC hardware description language)
[VH-4] p 948 N93-15265
A queue model relating synchronous and asynchronous communication
[MEMO-INF-92-04] p 966 N93-15491
SPECTRA
Sulfur oxides in the middle atmosphere of Venus: Observations by the International Ultraviolet Explorer and sounding rockets p 1046 N93-14635
Multiresolution analysis by infinitely differentiable compactly supported functions
[AD-A256526] p 969 N93-15398
A two-pass physics-based global lighting model p 957 N93-15570
SPECTRAL BANDS
High resolution absolute absorption cross sections of NO2 at 295, 573, and 673 K at visible wavelengths: Comprehensive data tables
[AD-A255261] p 839 N93-14530
SPECTRAL ENERGY DISTRIBUTION
Homogeneous quantum electrodynamic turbulence
[NASA-TM-107686] p 979 N93-15482
SPECTRAL LINE WIDTH
Advanced optical fiber communication systems
[AD-A255424] p 982 N93-14507
SPECTRAL REFLECTANCE
A two-pass physics-based global lighting model p 957 N93-15570
SPECTRAL SIGNATURES
Optical signatures of cooling flows in isolated early-type galaxies p 1017 N93-14243
SPECTROGRAMS
Analysis of CCD images of the coma of comet P/Halley
[NASA-CR-191384] p 1020 N93-14814
SPECTROGRAPHS
The evolution of the quasar continuum
[NASA-CR-191673] p 1012 N93-14759
LISA: A limb imaging spectrograph for airglow p 811 N93-14952
SPECTROMETERS
Sulfur oxides in the middle atmosphere of Venus: Observations by the International Ultraviolet Explorer and sounding rockets p 1046 N93-14635
The evolution of the quasar continuum
[NASA-CR-191673] p 1012 N93-14759
SPECTROPHOTOMETERS
Variable path length spectrophotometric probe
[DE92-019834] p 881 N93-14716
SPECTROSCOPIC ANALYSIS
The effect of a seawater environment on the galvanic corrosion behavior of graphite/epoxy composites coupled to metals
[AD-A256072] p 830 N93-14232
Methane measurement by the Pioneer Venus large probe neutral mass spectrometer p 1027 N93-14312
SPECTROSCOPY
Diffusing wave spectroscopy p 980 N93-14169
Physics of x ray multilayer structures: Summaries of papers presented at the physics of x ray multilayer structures topical meeting, technical digest series, 1992, volume 7
[AD-A255383] p 992 N93-14741
SPECTRUM ANALYSIS
Application of Fourier Transform-infrared spectroscopy (FT-IR) for materials analysis
[AD-A255727] p 838 N93-14435
Spectral analysis of the shuttle glow. SPA II/IBSS Mission: AIS hardware
[PL-TR-92-2148] p 814 N93-14697
Spectral analysis of the shuttle glow: AIS science support
[PL-TR-92-2172] p 815 N93-14698
Atomic data and spectral analysis of carbon, nitrogen, oxygen and silicon ions observed with the International Ultraviolet Explorer
[NASA-CR-191302] p 1012 N93-14761
SPECULAR REFLECTION
Algorithms for the detection and elimination of specular aliasing p 954 N93-15544
SPEECH RECOGNITION
The intelligibility of words, sentences, and continuous discourse using the articulation index
[AD-A256781] p 863 N93-15624
SPHERES
Relativistic dynamics of a charged sphere: Updating the Lorentz-Abraham model
[AD-A256107] p 971 N93-14245
Thermal fatigue analysis of metal matrix composite with spherical reinforcements
[AD-A255313] p 831 N93-14672
SPHERICAL HARMONICS
Venus gravity: Summary and coming events p 1042 N93-14377
SPHERICAL SHELLS
Flexural models of trench/outer rise topography of coronae on Venus with axisymmetric spherical shell elastic plates p 1036 N93-14348
SPIN TESTS
LARZAC HP turbine disk crack initiation and propagation spin pit test p 799 N93-14892
RB 199 high pressure compressor stage 3 spin pit tests p 799 N93-14893
CF6-6 high pressure compressor stage 5 locking slot crack propagation spin pit test p 799 N93-14894
RB211-524B disc and drive cones hot cyclic spinning test p 799 N93-14895
SPIN-ORBIT INTERACTIONS
Sensitivity of quantum electron conductance to elastic scatterers and to spin-orbit scattering in gallium arsenide heterostructures p 990 N93-14184
SPINAL CORD
Improved head support stand adjustable by compoundturnbuckle
[AD-D015384] p 936 N93-15249
SPIRAL GALAXIES
Calibration of the CCD Tully-Fisher relation with application to the Perseus-Pisces supercluster p 1016 N93-14194
SPLINE FUNCTIONS
An implementation of multivariate B-spline surfaces over arbitrary triangulations p 952 N93-15534
SPONTANEOUS EMISSION
Physical and chemical processes of the inner coma observed in mid-ultraviolet cometary spectra p 1017 N93-14230
SPREAD SPECTRUM TRANSMISSION
Comparison of synchronization techniques for the AFIT direct sequence spread spectrum system
[AD-A256440] p 861 N93-15316
SPREADING
Constraints on crustal rheology and age of deformation from models of gravitational spreading in Ishtar Terra, Venus p 1042 N93-14379
SPUTTERING
Thin-film permanent magnets for integrated electromagnetic components
[AD-A256175] p 972 N93-14679
Sputter deposition and characterization of MoSi2/SiC composite coatings
[DE92-040326] p 837 N93-15426
SQUALLS
An observational and theoretical study of squall line evolution p 921 N93-14682
SQUARE WAVES
Characterization of PZT films fatigued at low frequency
[AEROSPACE-ATR-91(8308)-2] p 992 N93-14795
STABILITY
Long term stability in thin film ferroelectric memories
[AD-A256290] p 991 N93-14439
Electronically active cyclocarborane-metal-arene assemblies
[AD-A256288] p 865 N93-14457
Stability of differentially rotating stars p 1018 N93-14584
Generation, control, and transport of a 19-MeV, 700-kA pulsed electron beam
[DE92-019803] p 978 N93-15277
STABILITY DERIVATIVES
An examination of wing rock for the F-15
[AD-A256613] p 802 N93-14252
STABILITY TESTS
BLSTA: A boundary layer code for stability analysis
[NASA-CR-4481] p 877 N93-14797
STABILIZATION
Advanced aeroservoelastic stabilization techniques for hypersonic flight vehicles
[NASA-CR-189702] p 802 N93-14811
STAINLESS STEELS
Surface preparation of stainless steel prior to painting
[AD-A256253] p 838 N93-14454
Use of the thin-walled torsion specimen
[AD-A255593] p 901 N93-14790
The influence of steel surface chemistry on the bonding of lubricant films
[AD-A256231] p 851 N93-15242
STAMPING
Method of local shaping of thermoplastics
[AD-A255913] p 856 N93-15105
STANDARDIZATION
Standardization of precipitation static test methods and equipment for the Navy
[AD-A257025] p 792 N93-15361
Revised nomenclature for defects at or near the Si/SiO2 interface
[DE92-040975] p 997 N93-15651
STANDARDS
MIL-STD-1760 application guidelines
[AD-A255714] p 790 N93-14432
The use of International Standards Organization ISO 9000 quality assurance standards in place of military standards
[AD-A256203] p 894 N93-14500
Status of emerging standards for removable computer storage media and related contributions of NIST p 1003 N93-14778
Proposed revisions to RTCM SC-104 recommended standards for differential NAVSTAR/GPS service for carrier phase applications
[AD-A255276] p 789 N93-15005
VHDL (VHSIC hardware description language) use in the US defense procurement process
[VH-2] p 948 N93-15263
System design in a large corporation, using VHDL (VHSIC hardware description language)
[VH-4] p 948 N93-15265
VHDL (VHSIC hardware description language) in the test environment
[VH-6] p 948 N93-15267
STAR FORMATION
The structure and dynamics of an environment forming high-mass stars p 1014 N93-14113
A study of the abundance distributions along the minor axis of the Galactic bulge p 1015 N93-14136
STARBURST GALAXIES
Wolf-Rayet stars in the Milky Way, the Large Magellanic Cloud, and emission-line galaxies p 1020 N93-14869
STATIC ELECTRICITY
Standardization of precipitation static test methods and equipment for the Navy
[AD-A257025] p 792 N93-15361
STATIC FRICTION
An active Z gravity compensation system
[AD-A255258] p 889 N93-14529
STATIC LOADS
Failure of composite plates under static biaxial planar loading
[NASA-CR-191391] p 903 N93-15653
STATIC STABILITY
Finite amplitude gravity waves in the Venus atmosphere generated by surface topography p 1044 N93-14395
STATIC TESTS
Fracture/damage mechanics of composites: Static and fatigue properties
[DLR-MITT-92-03] p 835 N93-15075
Standardization of precipitation static test methods and equipment for the Navy
[AD-A257025] p 792 N93-15361
STATISTICAL ANALYSIS
Optimum pose measurements for kinematic parameters identification
[AD-A256307] p 970 N93-14443
Evaluation and estimation of handling qualities via statistical modeling of pilot response data
[AD-A255324] p 939 N93-14548
Statistical analysis of the human strangulation experiments: Comparison to +Gz-induced loss of consciousness
[AD-A255485] p 935 N93-14789
Reliability modelling for non-electronic systems
[REPT-921-440-103] p 894 N93-15139
Core support for the Board on Mathematical Sciences
[AD-A256333] p 968 N93-15195
Predicting polymer properties by computational methods 2: A comparison of semi-empirical methods
[AD-A256856] p 854 N93-15640
STATISTICAL CORRELATION
A correlated k-distribution model of the heating rates for CO2 and O3 in the atmosphere between 0 and 60 km
[DE93-000889] p 911 N93-15280
A correlated k-distribution model of the atmospheric heating rates for overlapping spectra of CH4 and N2O
[DE93-000890] p 911 N93-15281

Spatio-temporal complexity and large-scale structures in problems of continuum mechanics
[AD-A256410] p 998 N93-15333
Analytical characterization of bistatic scattering from rough surfaces: Dependence on surface correlation function
[AD-A256525] p 862 N93-15397

STATISTICAL DISTRIBUTIONS
A correlated k-distribution model of the heating rates for CO2 and O3 in the atmosphere between 0 and 60 km
[DE93-000889] p 911 N93-15280
A correlated k-distribution model of the atmospheric heating rates for overlapping spectra of CH4 and N2O
[DE93-000890] p 911 N93-15281
Analytical characterization of bistatic scattering from rough surfaces: Dependence on surface correlation function
[AD-A256525] p 862 N93-15397

STATISTICAL TESTS
Simultaneous DIF amplification and cancellation: Shealy-Stout test for DIF
[AD-A256284] p 970 N93-14455

STATISTICAL WEATHER FORECASTING
Four-dimensional data assimilation of GALE data using a multivariate analysis scheme and a mesoscale model with diabatic initialization p 919 N93-14198

STEADY FLOW
An integral equation solution for multistage turbomachinery design calculations
[NASA-TM-105970] p 801 N93-15521

STEADY STATE
Venusian hydrology: Steady state reconsidered p 1028 N93-14318
Estimation of rate of climb
[ESDU-92019] p 791 N93-14541
Preconditioned conjugate-gradient methods for low-speed flow calculations
[NASA-TM-105929] p 877 N93-14885
Some experiments and ideas on GPA before reaching steady state of engine p 796 N93-15175

STEELS
The influence of geometrical constraint on cyclic, elastoplastic, notch root behavior, and fatigue microcrack *initiation* p 900 N93-14480
Strain-rate effects in replica scale model penetration experiments
[AD-A255426] *p 844 N93-14508*
Mechanisms of forming intergranular microcracks and microscopic surface discontinuities in welds
[AD-A255371] p 845 N93-14740
The Meta-Lax method of stress reduction in welds
[DE92-018477] p 845 N93-14900
Stress corrosion susceptibility of ultra-high strength steels for Naval aircraft applications
[AD-A256126] p 846 N93-15189
Validation of an automated torsional and warping stress analysis program
[AD-A256035] p 902 N93-15260

STELLAR CORES
The structure and dynamics of an environment forming high-mass stars p 1014 N93-14113

STELLAR ENVELOPES
Gravitational instabilities in a protoplanetary disk p 1016 N93-14154
Hydrodynamics of supernova 1987 A
p 1019 N93-14633
Spatially resolved 10 micron spectra of circumstellar material around evolved stars p 1019 N93-14636

STELLAR EVOLUTION
Compact objects in the disk and globular clusters p 1018 N93-14594
ROSAT all-sky survey on the Einstein EMSS sample
[NASA-CR-191627] p 1013 N93-15340

STELLAR LUMINOSITY
The structure and dynamics of an environment forming high-mass stars p 1014 N93-14113
A faint spectroscopic quasar survey p 1012 N93-14629
ROSAT all-sky survey on the Einstein EMSS sample
[NASA-CR-191627] p 1013 N93-15340

STELLAR MAGNITUDE
Study of tidal interactions in M81-M82-NGC3077 system p 1010 N93-14195

STELLAR MASS
The structure and dynamics of an environment forming high-mass stars p 1014 N93-14113
A search for dead QSO's among nearby luminous galaxies p 1011 N93-14228

STELLAR MASS ACCRETION
A search for dead QSO's among nearby luminous galaxies p 1011 N93-14228

STELLAR MASS EJECTION
Hydrodynamics of supernova 1987 A p 1019 N93-14633

STELLAR MODELS
Theoretical studies of the physics of the solar atmosphere
[NASA-CR-191357] p 1049 N93-15085
High-energy emissions from young pulsars: Perspective from the outer gap model
[DE92-040365] p 1022 N93-15324

STELLAR MOTIONS
Vertical path atmospheric turbulence: Temporal spectra and differential image motion measurements p 914 N93-14641

STELLAR RADIATION
Nonthermal radio, x ray and gamma ray emissions from chaotic winds of early-type, massive stars p 1050 N93-14242
Disc structure and variability in dwarf novae p 1017 N93-14460
High-energy emissions from young pulsars: Perspective from the outer gap model
[DE92-040365] p 1022 N93-15324

STELLAR ROTATION
Stability of differentially rotating stars p 1018 N93-14584

STELLAR SPECTRA
The black hole candidate binary A0620-00 p 1015 N93-14148
Physical and chemical processes of the inner coma *observed in mid-ultraviolet cometary spectra* p 1017 N93-14230
Ultraviolet spectra of stars and stellar systems
p 1011 N93-14593
QSO absorption lines and the ionizing field at high redshifts p 1013 N93-14860
High-energy emissions from young pulsars: Perspective from the outer gap model
[DE92-040365] p 1022 N93-15324

STELLAR STRUCTURE
Disc structure and variability in dwarf novae p 1017 N93-14460

STELLAR SYSTEMS
Ultraviolet spectra of stars and stellar systems p 1011 N93-14593

STELLAR WINDS
Nonthermal radio, x ray and gamma ray emissions from chaotic winds of early-type, massive stars
p 1050 N93-14242

STELLARATORS
Theoretical and numerical studies in magnetic fusion
[DE92-040674] p 988 N93-15349

STEREOSCOPIC VISION
Higher order mechanisms of color vision
[AD-A256369] p 938 N93-15329

STEREOSCOPY
Magellan stereo images and Venusian geology
p 1035 N93-14347
Application of left- and right-looking SAR stereo to depth measurements of the Ammavaru outflow channel, Lada Terra, Venus *p 1038 N93-14357*

STIFFNESS
Multi-disciplinary optimization of aeroservoelastic systems
[NASA-CR-191255] p 901 N93-14766
The crack problem for an orthotropic half plane stiffened by elastic films
[AD-A256471] p 903 N93-15374
Calculation of mechanical vibration frequencies of stiffened superconducting cavities
[DE92-040228] p 903 N93-15423

STIRLING CYCLE
The CPG 5-kW(e) Dish-Stirling Development Program
[DE92-017050] p 907 N93-15134

STIRLING ENGINES
A feasibility assessment of magnetic bearings for *free-piston Stirling space power converters*
[NASA-CR-189135] p 891 N93-14916
Summary of the NASA Lewis component technology program for Stirling power converters
[NASA-TM-105640] p 827 N93-15526

STOCHASTIC PROCESSES
L2 and L-infinity multiobjective control for linear systems p 961 N93-14399
Use of kinematic constraint in tracking constant speed maneuvering targets
[AD-A255988] p 858 N93-14415
A simulation model of atmospheric turbulence for rotorcraft applications p 920 N93-14588
Stability and adaptation of neural networks
[AD-A256227] p 962 N93-14598
AFIT/AFOSR Workshop on the Role of Wavelets in Signal Processing Applications
[AD-A256172] p 859 N93-14649
Approximate performability analysis using generalized stochastic Petri nets
[MEMO-INF-92-11] p 971 N93-15119
Workstation tools for feature extraction and classification for nonstationary and transient signals
[AD-A255389] p 947 N93-15228
Hierarchical Poisson disk sampling distributions p 954 N93-15545

STOKES FLOW
On the nonlinear three dimensional instability of Stokes layers and other shear layers to pairs of oblique waves
[NASA-TM-105918] p 880 N93-15499

STORABLE PROPELLANTS
Low thrust chemical rocket technology
[NASA-TM-105927] p 827 N93-15572

STORAGE BATTERIES
Smart battery controller for lithium sulfur dioxide batteries
[AD-A255490] p 867 N93-14642

STORMS
Synoptic scale structure of summertime wet and dry spells in northeastern Kansas p 923 N93-14919

STORMS (METEOROLOGY)
Four-dimensional data assimilation of GALE data using a multivariate analysis scheme and a mesoscale model with diabatic initialization p 919 N93-14198
Structure and propagation of fronts east of the Rocky Mountains and their relationship to precipitation p 921 N93-14827
An investigation into the role of moist, vertical drafts in the rotational development of storms p 923 N93-15087
Sierra Nevada winter storms: A study using microwave radiometry, ice crystal, and isotopic analysis technique *p 923 N93-15088*

STOVL AIRCRAFT
Propulsion system performance resulting from an *integrated flight/propulsion control design*
[NASA-TM-105874] p 801 N93-15525

STRAIN DISTRIBUTION
Analysis of advanced thin-walled composite structures p 895 N93-14158
Integration and processing of high-resolution *moire-interferometry data* p 895 N93-14185
Reliability of stiffened structural panels: Two examples
[NASA-TM-107687] p 900 N93-14483

STRAIN GAGES
Determination of stresses on laminated aircraft transparencies by the strain gage-hole drilling and sectioning method
[AD-A255548] p 791 N93-14571
Development of a fiber optic high temperature strain sensor
[NASA-CR-191316] p 882 N93-14810

STRAIN MEASUREMENT
Development of a fiber optic high temperature strain sensor
[NASA-CR-191316] p 882 N93-14810
A neural network prototype for predicting F-14B strains *at the B.L. 10 longeron*
[AD-A255272] p 792 N93-15004

STRAIN RATE
Strain-rate effects in replica scale model penetration experiments
[AD-A255426] p 844 N93-14508

STRATIFICATION
Numerical study of mixing of two fluids under low gravity
[NASA-TM-105865] *p 878 N93-14914*

STRATIFIED FLOW
Unsteady shear disturbances within a two dimensional stratified flow
[NASA-CR-189121] p 880 N93-15527

STRATIGRAPHY
Venusian extended ejecta deposits as time-stratigraphic markers p 1030 N93-14327
Can a time-stratigraphic classification system be *developed for Venus?* p 1043 N93-14388

STRATOCUMULUS CLOUDS
CCN spectra measurements as an active tracer of stratocumulus mechanisms
[AD-A255678] p 920 N93-14258

STRATOSPHERE
A numerical study of the middle atmosphere response to tropical and subtropical tropospheric heat sources p 920 N93-14640

STRESS (PHYSIOLOGY)
Decision making in a dynamic task environment: The effect of time pressure
[AD-A256557] p 937 N93-14602
Training, muscle fatigue and stress fractures
[AD-A255277] p 935 N93-15006
The effect of pain on task performance: A review of the literature
[AD-A254336] p 938 N93-15216

STRESS ANALYSIS
Theoretical and experimental analysis of residual stress formation after implant resistance welding of polycarbonate p 898 N93-14279

A geometrically nonlinear stress-deflection relation for thin film/substrate systems p 848 N93-14287
Determining stress states using dike swarms: The Lauma Dorsa example p 1028 N93-14319
On the structure of nonlinear constitutive equations for fiber reinforced composites
[NASA-CR-191024] p 830 N93-14484
Determination of stresses on laminated aircraft transparencies by the strain gage-hole drilling and sectioning method
[AD-A255548] p 791 N93-14571
Method of characterizing residual stress in ferromagnetic materials using a pulse histogram of acoustic emission signals
[NASA-CASE-LAR-14239-1] p 845 N93-14705
Improved inhomogeneous finite elements for fabric reinforced composite mechanics analysis p 834 N93-14757
Use of the thin-walled torsion specimen
[AD-A255593] p 901 N93-14790
RB 199 high pressure compressor stage 3 spin pit tests p 799 N93-14893
CF6-6 high pressure compressor stage 5 locking slot crack propagation spin pit test p 799 N93-14894
RB211-524B disc and drive cones hot cyclic spinning test p 799 N93-14895
Analysis of in-flight structural failures of P-3C wing leading edge segments
[AD-A256212] p 792 N93-15238
Validation of an automated torsional and warping stress analysis program
[AD-A256035] p 902 N93-15260
The mixed mode crack problem in a nonhomogeneous elastic plane
[AD-A256469] p 902 N93-15372
Diffusion problems in bonded nonhomogeneous materials with an interface cut
[AD-A256470] p 836 N93-15373
The crack problem for an orthotropic half plane stiffened by elastic films
[AD-A256471] p 903 N93-15374
Frequency-domain synthesis of the fatigue load spectrum for the NPS 100-kW wind turbine
[DE92-040984] p 908 N93-15384
On explicit algebraic stress models for complex turbulent flows
[NASA-CR-189725] p 879 N93-15481

STRESS CONCENTRATION

RB 199 high pressure compressor stage 3 spin pit tests p 799 N93-14893

STRESS CORROSION

Stress corrosion susceptibility of ultra-high strength steels for Naval aircraft applications
[AD-A256126] p 846 N93-15189
Dual role of nickel in sodium/nickel chloride batteries
[DE92-041102] p 870 N93-15441

STRESS CORROSION CRACKING

Fe3Al-type iron aluminides: Aqueous corrosion properties in a range of electrolytes and slow-strain rate ductilities during aqueous corrosion
[DE92-040520] p 846 N93-15059
Stress corrosion susceptibility of ultra-high strength steels for Naval aircraft applications
[AD-A256126] p 846 N93-15189

STRESS CYCLES

Frequency-domain synthesis of the fatigue load *spectrum for the NPS 100-kW wind turbine*
[DE92-040984] p 908 N93-15384

STRESS DISTRIBUTION

Applications of a constitutive equation for microstructural change in polymers p 848 N93-14222
Theoretical and experimental analysis of residual stress *formation after implant resistance welding of* polycarbonate p 898 N93-14279
Preliminary design of composite joints
[DLR-MITT-92-05] p 835 N93-15076

STRESS FUNCTIONS

Root damage analysis of aircraft engine blade subject to *ice impact*
[NASA-TM-105779] p 902 N93-15343

STRESS INTENSITY FACTORS

Digital caustic investigation of near surface cracks under transient thermal loading p 897 N93-14217
A study of the relationship between macroscopic measures and physical processes occurring during crack closure
[AD-A256587] p 898 N93-14272
Finite element analysis of elastic fracture under unsteady translational and rotational loading p 899 N93-14469
Closed form expressions for crack mouth displacements and stress intensity factors for chevron notched short bar and short rod specimens based on experimental compliance measurements
[NASA-TM-83796] p 902 N93-15369
The mixed mode crack problem in a nonhomogeneous elastic plane
[AD-A256469] p 902 N93-15372
The crack problem for an orthotropic half plane stiffened by elastic films
[AD-A256471] p 903 N93-15374

STRESS RELAXATION

The Meta-Lax method of stress reduction in welds
[DE92-018477] p 845 N93-14900

STRESS-STRAIN RELATIONSHIPS

A preliminary investigation of dual mode fracture sustained by graphite/epoxy laminates impacted by high-velocity spherical metallic projectiles
[AD-A255790] p 898 N93-14419
On the structure of nonlinear constitutive equations for fiber reinforced composites
[NASA-CR-191024] p 830 N93-14484
Preliminary design of composite joints
[DLR-MITT-92-05] p 835 N93-15076

STRING THEORY

The low-energy structure of compactified superstring models p 997 N93-14116
Type 2 superstrings in curved D = 10 space-time: Dynamics of their massless fields and covariant quantization p 998 N93-14143

STRINGS

Nonlinear free vibration analysis of strings by the Galerkin method p 972 N93-14280

STRONG INTERACTIONS (FIELD THEORY)

Strong interactions studies with medium energy probes
[DE92-040460] p 977 N93-15377

STRUCTURAL ANALYSIS

A time-domain study of the relationship between drive force time bandwidth and farfield acoustic radiation
[AD-A255616] p 973 N93-14159
Analysis and optimal design of pressurized, imperfect, anisotropic ring-stiffened cylinders p 897 N93-14251
A methodology for the evaluation of structural design software for DOS-based microcomputers
[AD-A255421] p 943 N93-14505
Proceedings of the USAF Structural Integrity Program
[AD-A255379] p 777 N93-14549
SAPNEW: Parallel finite element code for thin shell structures on the Alliant FX-80
[NASA-CR-189212] p 901 N93-14799
Propulsion and Energetics Panel Working Group 20 on *Test Cases for Engine Life Assessment Technology*
[AGARD-AR-308] p 798 N93-14890
Introduction to test cases for engine life assessment technology p 799 N93-14891
Space based radar: Test of large space structures p 808 N93-14941
Space craft verification at the David Florida Laboratory p 809 N93-14943
Aeroplane crashes on the runway: Validation and final *evaluation of the method of modeling an airframe* structure
[IMFL-91-32] p 792 N93-15126

STRUCTURAL BASINS

Simulations of the Amazon Basin circulation using the Pennsylvania State University/National Center for Atmospheric Research mesoscale model p 919 N93-14197
Ringed impact craters on Venus: An analysis from Magellan images p 1024 N93-14291

STRUCTURAL DESIGN

Weight optimum arch structures
[AD-A256080] p 897 N93-14236
Multiobjective control/structure design optimization in the presence of practical constraints p 898 N93-14446
An integrated optimization environment for structural configuration design p 855 N93-14467
A methodology for the evaluation of structural design software for DOS-based microcomputers
[AD-A255421] p 943 N93-14505
Large space structures and systems in the space station era: A bibliography with indexes (supplement 04)
[NASA-SP-7085(04)] p 817 N93-14606

STRUCTURAL ENGINEERING

A methodology for the evaluation of structural design software for DOS-based microcomputers
[AD-A255421] p 943 N93-14505
Recommendations for enhancement of the Design Criteria Information System (DCIS)
[AD-A256857] p 1009 N93-15641

STRUCTURAL FAILURE

Reliability of stiffened structural panels: Two examples
[NASA-TM-107687] p 900 N93-14483
Analysis of in-flight structural failures of P-3C wing leading edge segments
[AD-A256212] p 792 N93-15238

STRUCTURAL MEMBERS

An integrated optimization environment for structural configuration design p 855 N93-14467
Validation of an automated torsional and warping stress analysis program
[AD-A256035] p 902 N93-15260

STRUCTURAL PROPERTIES (GEOLOGY)

Surface processes on Venus p 1024 N93-14294
Shield fields: Concentrations of small volcanic edifices on Venus p 1024 N93-14295
Debris avalanches and slumps on the margins of volcanic domes on Venus: Characteristics of deposits p 1025 N93-14300
Erosion versus construction: The origin of Venusian channels p 1025 N93-14303
Sequential deformation of plains along Tessera boundaries on Venus: Evidence from Alpha Regio p 1028 N93-14317
Determining stress states using dike swarms: The Lauma Dorsa example p 1028 N93-14319
Venus volcanism: A global overview from Magellan data p 1029 N93-14323
Variations in lithospheric thickness on Venus p 1030 N93-14329
Igneous and tectonic evolution of Venusian and terrestrial coronae p 1031 N93-14330
Large shield volcanos on Venus: The effect of neutral buoyancy zone development on evolution and altitude distribution p 1032 N93-14333
Mantle plumes on Venus revisited p 1032 N93-14334
Venusian sinuous rilles p 1033 N93-14337
Derivation of surface properties from Magellan altimetry data p 1033 N93-14340
Extensive lava flow fields on Venus: Preliminary investigation of source elevation and regional slope variations p 1034 N93-14342
Wrinkle ridges on Venusian plains: Indicators of shallow crustal stress orientations at local and regional scales p 1034 N93-14343
Pancakelike domes on Venus p 1035 N93-14345
The origins of radial fracture systems and associated large lava flows on Venus p 1038 N93-14356
Structural characteristics and tectonics of northeastern Tellus Regio and Meni Tessera p 1044 N93-14389

STRUCTURAL RELIABILITY

Reliability of stiffened structural panels: Two examples
[NASA-TM-107687] p 900 N93-14483

STRUCTURAL STABILITY

Damage location and model refinement for large flexible space structures using a sensitivity-based eigenstructure assignment method p 816 N93-14274
Nonlinear dynamic response of shallow arches to harmonic forcing p 898 N93-14282
Proceedings of the USAF Structural Integrity Program
[AD-A255379] p 777 N93-14549
The effect of geometry and prescribed delaminations on the postbuckling behaviour of laminated carbon-fibre *reinforced plastic panels* p 831 N93-14597
Advanced aeroservoelastic stabilization techniques for hypersonic flight vehicles
[NASA-CR-189702] p 802 N93-14811

STRUCTURAL VIBRATION

Technology development for non-contact measurement in modal testing of large space structures p 809 N93-14942
Optimal active vibration absorber: Design and experimental results
[NASA-TM-107709] p 902 N93-15202
Structurally adaptive space crane concept for assembling space systems on orbit
[NASA-TP-3307] p 818 N93-15368
Multi-axis transient vibration testing of space objects: Test philosophy, test facility, and control strategy p 820 N93-15598

STRUCTURAL WEIGHT

Weight optimum arch structures
[AD-A256080] p 897 N93-14236
Aspects of parking orbit selection in a manned Mars mission
[NASA-TP-3256] p 813 N93-15367

STRUTS

Transonic flow calculations for a cavity with and without a store
[AD-A255954] p 873 N93-14421
Structurally adaptive space crane concept for assembling space systems on orbit
[NASA-TP-3307] p 818 N93-15368

STUDENTS

Development of a MATLAB toolbox for image processing
[AD-A256130] p 942 N93-14247
Long term memory for different types of classroom knowledge
[AD-A255235] p 999 N93-14526

SUBDUCTION (GEOLOGY)

Thermal buoyancy on Venus: Preliminary results of finite element modeling p 1025 N93-14302

Chemical differentiation on one-plate planets: Predictions and geologic observations for Venus p 1029 N93-14324
Tectonic connections to interior processes on Venus p 1039 N93-14361
Evidence for retrograde lithospheric subduction on Venus p 1040 N93-14367
Episodic plate tectonics on Venus p 1044 N93-14390

SUBMILLIMETER WAVES
Submillimeter and infrared spectroscopy of molecular clouds near O and B stars p 1016 N93-14149

SUBSONIC FLOW
Control of asymmetric jet
| AD-A255967 | p 873 N93-14400
A compilation of the mathematics leading to the doublet lattice method
| AD-A256304 | p 779 N93-14441
Chemical reactions in turbulent mixing flows
| AD-A256004 | p 842 N93-15114
Prediction of turbine cascade flows with a quasi-three-dimensional rotor viscous code and the extension of the algebraic turbulence model
| AD-A256831 | p 880 N93-15635

SUBSONIC SPEED
Preconditioned conjugate-gradient methods for low-speed flow calculations
| NASA-TM-105929 | p 877 N93-14885
Acoustic mode measurements in the inlet of a model turbofan using a continuously rotating rake: Data collection/analysis techniques
| NASA-TM-105936 | p 801 N93-15403

SUBSTRATES
A geometrically nonlinear stress-deflection relation for thin film/substrate systems p 848 N93-14287
Method of applying a thermal barrier coating system to a substrate
| NASA-CASE-LEW-15020-2 | p 832 N93-14706
High performance YBCO films
| AD-A255439 | p 994 N93-15297

SULFIDES
New electronic materials
| AD-A255612 | p 868 N93-15010
Removal of THD from painted test panels by liquid systems
| AD-A255624 | p 850 N93-15064

SULFUR
The sulfur emission and periodicity of the Jupiter plasma torus in 1988 p 1022 N93-14156

SULFUR DIOXIDES
SO2 in the middle atmosphere of Venus: IR measurements from Venera 15 and comparison to UV p 1045 N93-14397
Study and interpretation of the millimeter-wave spectrum of Venus p 1045 N93-14596
Smart battery controller for lithium sulfur dioxide batteries
| AD-A255490 | p 867 N93-14642

SULFUR OXIDES
Sulfur oxides in the middle atmosphere of Venus: Observations by the International Ultraviolet Explorer and sounding rockets p 1046 N93-14635

SULFURIC ACID
Long-term variations in abundance and distribution of sulfuric acid vapor in the Venus atmosphere inferred from Pioneer Venus and Magellan radio occultation studies p 1030 N93-14328
Study and interpretation of the millimeter-wave spectrum of Venus p 1045 N93-14596

SUMMER
Synoptic scale structure of summertime wet and dry spells in northeastern Kansas p 923 N93-14919

SUN
Imaging the sun in hard x rays using Fourier telescopes
| NASA-TM-108390 | p 1013 N93-15203

SUNSPOTS
On the variation of the Nimbus 7 total solar irradiance
| NASA-TP-3316 | p 1049 N93-15532

SUPERCOMPUTERS
Storage needs in future supercomputer environments p 1003 N93-14780
File servers, networking, and supercomputers p 1004 N93-15030

SUPERCONDUCTING DEVICES
Epitaxial heterojunctions of oxide semiconductors and metals on high temperature superconductors
| NASA-CASE-NPO-18483-1-CU | p 994 N93-15151

SUPERCONDUCTING FILMS
Processing and characterization of electrophoretically deposited holmium barium copper oxide superconductor films
| AD-A256329 | p 869 N93-15194
High performance YBCO films
| AD-A255439 | p 994 N93-15297

SUPERCONDUCTING SUPER COLLIDER
Data management and processing plan, Department of Applied Geodesy
| DE93-000774 | p 905 N93-14522

SUPERCONDUCTIVITY
Electronic structure studies of high-T(sub c) superconductors by photoemission and x ray absorption p 989 N93-14172
SCRUNCHER phase and amplitude control
| DE92-040225 | p 870 N93-15421
Calculation of mechanical vibration frequencies of stiffened superconducting cavities
| DE92-040228 | p 903 N93-15423
Design features of a seven-cell high-gradient superconducting cavity
| DE92-040229 | p 870 N93-15424
Development of a 500 GHz optoelectronic modulator using superconducting transmission lines
| AD-A257062 | p 871 N93-15456
Study of the glass formation of high temperature superconductors
| NASA-TM-108389 | p 997 N93-15500

SUPERCONDUCTORS
Multifilamentary superconducting cable and a method of manufacturing it
| AD-D015391 | p 846 N93-15231
Normal state resistivity and the phase diagram of U(1-x)Th(x)Be13
| DE92-040236 | p 995 N93-15321

SUPERCOOLING
Experimental observation of the influence of furnace temperature profile on convection and segregation in the vertical Bridgman crystal growth technique p 995 N93-15312

SUPERCRITICAL WINGS
Pressure distribution for the wing of the YAV-8B airplane; with and without pylons
| NASA-TM-4429 | p 779 N93-14451

SUPERFLUIDITY
Dynamics in neutron stars and the early universe p 1014 N93-14112

SUPERGRAVITY
Type 2 superstrings in curved D = 10 space-time: Dynamics of their massless fields and covariant quantization p 998 N93-14143

SUPERHIGH FREQUENCIES
Short range propagation measurements at 2.4, 4.5, and 11.5 GHz in indoor and outdoor environments
| AD-A256563 | p 860 N93-14806

SUPERLATTICES
Optical instrumentation and characterization for magneto-optical recording media p 980 N93-14168

SUPERNOVA 1987A
Gamma-ray imaging observations of Supernova 1987A p 1012 N93-14628
Hydrodynamics of supernova 1987 A p 1019 N93-14633
Search for pulsed gamma ray emission from SN1987A and the Vela pulsar p 1050 N93-14634

SUPERPLASTICITY
An investigation of the processing, high temperature deformation and fracture characteristics of superplastic ceramics
| AD-A256519 | p 852 N93-15394

SUPERROTATION
Dynamics of the Venus atmosphere p 1030 N93-14325
Radiation pressure: A possible cause for the superrotation of the Venusian atmosphere p 1033 N93-14338
Results of a zonally truncated three-dimensional model of the Venus middle atmosphere p 1037 N93-14351

SUPERSATURATION
Crystal growth in a microgravity environment
| NASA-CASE-MFS-28473-1 | p 992 N93-14707

SUPERSONIC COMBUSTION
Combustion in supersonic flows p 841 N93-14627
Aerothermodynamic flow phenomena of the airframe-integrated supersonic combustion ramjet
| NASA-TM-4376 | p 827 N93-15528
Investigation of the aerothermodynamics of hypervelocity reacting flows in the ram accelerator
| NASA-CR-191715 | p 783 N93-15588

SUPERSONIC COMBUSTION RAMJET ENGINES
Unsteady pressure loads in a generic high speed engine model
| NASA-TP-3189 | p 975 N93-15391
Aerothermodynamic flow phenomena of the airframe-integrated supersonic combustion ramjet
| NASA-TM-4376 | p 827 N93-15528

SUPERSONIC FLOW
A plume-induced boundary layer separation experiment
| AD-A255397 | p 875 N93-14677
Analysis and control of asymmetric vortex flows and supersonic vortex breakdown
| NASA-CR-191264 | p 875 N93-14687
Shock/vortex interaction and vortex-breakdown modes
| PAPER-T.1.3 | p 875 N93-14689
Numerical simulation of steady and unsteady asymmetric vortical flow p 876 N93-14691
Passive control of supersonic asymmetric vortical flows around cones p 876 N93-14692
An investigation of genuinely multidimensional schemes for the Euler equations p 876 N93-14694
A numerical investigation of the interaction between crossing oblique shocks and a turbulent boundary layer p 876 N93-14695
Supersonic boundary-layer flow turbulence modeling
| NASA-TM-105893 | p 877 N93-14758
Chemical reactions in turbulent mixing flows
| AD-A256004 | p 842 N93-15114

SUPERSONIC JET FLOW
Combustion in supersonic flows p 841 N93-14627
Computation of supersonic jet noise under imperfectly expanded conditions
| NASA-TM-105961 | p 975 N93-15430

SUPERSONIC SPEED
A multigrid approach to embedded-grid solvers
| AD-A256405 | p 879 N93-15332

SUPERSONIC WIND TUNNELS
A plume-induced boundary layer separation experiment
| AD-A255397 | p 875 N93-14677
User manual for NASA Lewis 10 by 10 foot supersonic wind tunnel
| NASA-TM-105626 | p 804 N93-15498

SUPERSYMMETRY
The low-energy structure of compactified superstring models p 997 N93-14116
Semi-classical quantization rules in supersymmetric quantum mechanics p 998 N93-14590

SUPPORT SYSTEMS
GRASS 4.0 map digitizing user's manual: V. Digit
| AD-A256859 | p 1009 N93-15642

SUPPORTS
Improved head support stand adjustable by compoundturnbuckle
| AD-D015384 | p 936 N93-15249

SURFACE COOLING
Mixed-layer parameterization in models of the Indian Ocean
| AD-A255937 | p 925 N93-14428

SURFACE CRACKS
Digital caustic investigation of near surface cracks under transient thermal loading p 897 N93-14217
Mechanisms of forming intergranular microcracks and microscopic surface discontinuities in welds
| AD-A255371 | p 845 N93-14740

SURFACE DEFECTS
Remote techniques for time-of-flight flaw characterisation p 989 N93-14171
Polarization properties and Earth-based radar measurements of Venus in the post-Magellan era p 1026 N93-14304
Leveling coatings for reducing the atomic oxygen defect density in protected graphite fiber epoxy composites p 819 N93-15597

SURFACE EMITTING LASERS
Fast optoelectronic switching processes in surface-emitting semiconductor lasers and nonlinear etalons
| AD-A255802 | p 886 N93-15069

SURFACE FINISHING
Mach 5 electroformed nickel nozzle refurbishment FNAS investigation of ultra-smooth surfaces
| NASA-CR-191416 | p 826 N93-14681
Exceptionally high-strength (approximately 3 GPa) aluminum alloys demonstrated by oxygen ion implantation
| DE92-040980 | p 847 N93-15383

SURFACE GEOMETRY
An implementation of multivariate B-spline surfaces over arbitrary triangulations p 952 N93-15534
Fast algorithms for rendering cubic curves p 953 N93-15536
Parameterization in finite precision p 953 N93-15537
An interval refinement technique for surface intersection p 956 N93-15561
Physically-based methods for polygonization of implicit surfaces p 956 N93-15562

SURFACE LAYERS
Venus: Geochemical conclusions from the Magellan data p 1044 N93-14394
Mixed-layer parameterization in models of the Indian Ocean
| AD-A255937 | p 925 N93-14428

Dual active layer photoconductor
[AD-D015423] p 993 N93-14820

SURFACE NAVIGATION
Implementation of the pure pursuit path tracking algorithm
[AD-A255524] p 944 N93-14569

SURFACE PROPERTIES
In situ material characterization for pavement evaluation by the Spectral-Analysis-of-Surface-Waves (SASW) method
[AD-A255660] p 804 N93-14128
Surface processes on Venus p 1024 N93-14294
Shield fields: Concentrations of small volcanic edifices on Venus p 1024 N93-14295
Global deformation on the surface of Venus p 1024 N93-14297
Floor-fractured crater models for igneous crater modification on Venus p 1044 N93-14393
Effects of cryocontaminants on cryogenic superpolished mirror and superpolished quartz crystal microbalance
[AD-A255972] p 981 N93-14403
Mechanisms of forming intergranular microcracks and microscopic surface discontinuities in welds
[AD-A255371] p 845 N93-14740
Microstack insulator for flashover inhibition, phase 2
[AD-A256338] p 869 N93-15196
Microwave processing of tantalum capacitor anodes
[DE92-017829] p 869 N93-15214
The 17th Annual Conference on the Physics and Chemistry of Semiconductor Interfaces
[AD-A257061] p 996 N93-15449

SURFACE REACTIONS
Gas-solid dynamics at disordered and adsorbate covered surfaces
[AD-A255981] p 976 N93-14411
Gas-surface interactions
[AD-A255390] p 841 N93-14652
Spectroscopy and reactions of hydrazoic acid on silicon single crystal surfaces (III). HN3 and DN3 on Si(111)-7 x 7
[AD-A255241] p 842 N93-14669
Thermal stability of trimethyl indium on Si(100)-2 x 1 as studied with HREELS, UPS, and XPS: A comparison with the results from Si(111)-7 x 7 and Si(110) studies
[AD-A255242] p 992 N93-14670
Arc-cathode interaction study
[NASA-CR-191356] p 867 N93-14721
Surface evaluation of UV-degraded contamination
[NASA-CR-184500] p 910 N93-14764
Experimental and theoretical investigation of surface chemistry induced by direct and indirect electronic excitation
[AD-A256342] p 843 N93-15200
The influence of steel surface chemistry on the bonding of lubricant films
[AD-A256231] p 851 N93-15242
C60 interactions with surfaces, gaseous species and photons: An overview
[DE92-040738] p 978 N93-15654

SURFACE ROUGHNESS
Excimer laser irradiation of metal surfaces p 884 N93-14175
Overview of Venus geology: Preliminary description of terrain units for Venus global geological mapping p 1040 N93-14368
Surface evaluation of UV-degraded contamination
[NASA-CR-184500] p 910 N93-14764
Interferometer with two phase-conjugate mirrors
[AD-D015420] p 982 N93-14800
Experimental investigation of scattering from randomly rough plastic cylinders
[AD-A256018] p 975 N93-15259
Surface roughness due to residual ice in the use of low power deicing systems
[NASA-TM-105971] p 782 N93-15338
Close-up analysis of aircraft ice accretion
[NASA-TM-105952] p 787 N93-15360
Analytical characterization of bistatic scattering from rough surfaces: Dependence on surface correlation function
[AD-A256525] p 862 N93-15397

SURFACE ROUGHNESS EFFECTS
Martian water frost: Control of global distribution by small-scale processes p 1047 N93-14868
Leveling coatings for reducing the atomic oxygen defect density in protected graphite fiber epoxy composites p 819 N93-15597

SURFACE TEMPERATURE
Thermal buoyancy on Venus: Preliminary results of finite element modeling p 1025 N93-14302
Study of optical techniques for the Ames unitary wind tunnel. Part 5: Infrared imagery
[NASA-CR-191385] p 804 N93-14809

SURFACE TREATMENT
Excimer laser irradiation of metal surfaces p 884 N93-14175
Surface preparation of stainless steel prior to painting
[AD-A256253] p 838 N93-14454
Ultraviolet-ozone cleaning of semiconductor surfaces, revision 1
[AD-A256158] p 842 N93-14678
The influence of steel surface chemistry on the bonding of lubricant films
[AD-A256231] p 851 N93-15242

SURFACE WATER
Outgassing history of Venus and the absence of water on Venus p 1045 N93-14398

SURFACE WAVES
In situ material characterization for pavement evaluation by the Spectral-Analysis-of-Surface-Waves (SASW) method
[AD-A255660] p 804 N93-14128
Resonance absorption of MHD surface waves with applications to the solar atmosphere p 1048 N93-14157
Remote techniques for time-of-flight flaw characterisation p 989 N93-14171
The numerical stability of nonlinear floating body calculations p 873 N93-14278
Surface gravity waves and ambient microseismic noise
[AD-A256498] p 916 N93-15375
The detection and characterization of high frequency and high wavenumber solar oscillations
[NASA-CR-191622] p 1049 N93-15634

SURGES
EMTP based stability analysis of space station electric power system in a test bed environment
[NASA-TM-105845] p 871 N93-15503

SURVEILLANCE
Data analysis and interpretation for environmental surveillance
[DE92-019009] p 910 N93-15270

SURVEILLANCE RADAR
Progress in DND's space-based radar R/D project p 812 N93-14958

SURVEYS
Measurement-based multipurpose cadastral systems p 904 N93-14220
Advanced sensors technology survey
[NASA-CR-185691] p 881 N93-14494
Aviation accidents, incidents, and violations: Psychological predictors among US pilots p 783 N93-14693

SWAGING
A simulation study of planar swaging deformation
[AD-A255908] p 902 N93-15070

SWELLING
The role of entanglements in the swelling of poly(dimethylsiloxane) networks
[AD-A255359] p 849 N93-14561

SWEPT WINGS
BLSTA: A boundary layer code for stability analysis
[NASA-CR-4481] p 877 N93-14797

SWIRLING
Numerical modeling of a vortex stabilized arcjet
[NASA-CR-190797] p 826 N93-14883

SWITCHES
A novel, high energy-density electrical storage device for electric weapons
[AD-A255205] p 867 N93-14666
The role of HiPPI switches in mass storage systems: A five year prospective p 1002 N93-14774
Fast optoelectronic switching processes in surface-emitting semiconductor lasers and nonlinear etalons
[AD-A255802] p 886 N93-15069
High performance pulse generator
[AD-D015378] p 869 N93-15269

SWITCHING
Compact high PRF CO2 transmitter
[AD-A255985] p 884 N93-14414
Development of a 500 GHz optoelectronic modulator using superconducting transmission lines
[AD-A257062] p 871 N93-15456

SWITCHING CIRCUITS
Autonomous power system brassboard
[NASA-CR-189115] p 867 N93-14798
Internal grounding arrangement in a switching power converter
[AD-D015435] p 868 N93-14826

SYMMETRY
Schwinger Dyson equations: Dynamical chiral symmetry breaking and confinement
[DE92-040717] p 978 N93-15657

SYNAPSES
Biophysical and biochemical mechanisms in synaptic transmitter release
[AD-A256340] p 936 N93-15198

SYNCHRONISM
Ada-based multitasking terminal I/O
[AD-A255656] p 942 N93-14164
Wait-free consensus
[AD-A255978] p 943 N93-14423
Integration of satellite links into an ATM mode broadband ISDN
[TELECOM-PARIS-91-E-022] p 861 N93-15097
Comparison of synchronization techniques for the AFIT direct sequence spread spectrum system
[AD-A256440] p 861 N93-15316
A queue model relating synchronous and asynchronous communication
[MEMO-INF-92-04] p 966 N93-15491

SYNCHRONOUS PLATFORMS
Data management in NOAA p 1003 N93-14779

SYNCHRONOUS SATELLITES
Investigation of antenna pattern constraints for passive geosynchronous microwave imaging radiometers
[NASA-CR-189728] p 905 N93-14792

SYNCHROTRON RADIATION
The time variability of Jupiter's synchrotron radiation p 973 N93-14227

SYNOPTIC METEOROLOGY
Synoptic/planetary-scale interactions and blocking over the North Atlantic Ocean
[NASA-CR-191376] p 925 N93-14769
Synoptic scale structure of summertime wet and dry spells in northeastern Kansas p 923 N93-14919
A single-station forecasting model
[AD-A256403] p 924 N93-15331

SYNTAX
Program verification using higher order logic
[AD-A255408] p 943 N93-14502

SYNTHESIS (CHEMISTRY)
Physics of hydrogen storage in metal-hydrides p 854 N93-14630
Fabrication of high temperature materials by exothermic synthesis and subsequent dynamic consolidation
[DE92-019836] p 834 N93-14819
New electronic materials
[AD-A255612] p 868 N93-15010
Radical ion formation in polymers as a mechanism for laser eye protection
[AD-A255992] p 850 N93-15111

SYNTHETIC APERTURE RADAR
Scatterer modeling/calibration study
[AD-A255855] p 856 N93-14107
Surface processes on Venus p 1024 N93-14294
Debris avalanches and slumps on the margins of volcanic domes on Venus: Characteristics of deposits p 1025 N93-14300
Polarization properties and Earth-based radar measurements of Venus in the post-Magellan era p 1026 N93-14304
Image processing and products for the Magellan mission to Venus p 1026 N93-14306
Sequential deformation of plains along Tessera boundaries on Venus: Evidence from Alpha Regio p 1028 N93-14317
Application of left- and right-looking SAR stereo to depth measurements of the Ammavaru outflow channel, Lada Terra, Venus p 1038 N93-14357
Magellan project p 1041 N93-14373
Definition study PHARUS
[AD-A256560] p 860 N93-14805
An overview of RADARSAT payload technologies p 807 N93-14933

SYNTHETIC APERTURES
Venus mesospheric winds and the carbon monoxide bulge p 1029 N93-14320

SYSTEM FAILURES
Development of an environment for software reliability model selection
[AD-A256609] p 942 N93-14241
Multiple model adaptive estimation applied to the ViSTA F-16 with actuator and sensor failures
[AD-A256444] p 802 N93-14608
Detection of technical states with aircraft p 794 N93-15159
Failure diagnostic with MAINTEX based on AIMS at Swissair p 778 N93-15181
On-orbit deployment anamolies: What can be done? p 821 N93-15603

SYSTEMS ANALYSIS
A complete-time approach for chaining and execution control in the AN/UYS-2 parallel signal processor
[AD-A256306] p 859 N93-14442
Systems modeling
[AD-A255215] p 944 N93-14575
Mission critical system development: Design views and their integration
[AD-A255498] p 940 N93-14644
Information systems for airport operations
[TT-9202] p 789 N93-14729
Results of in-service evaluation of wind shear systems p 785 N93-14856
Advanced technology wind shear prediction system evaluation p 785 N93-14858

Multiple fault diagnosis of spacecraft electrical power systems p 806 N93-14927
Obstacles in object-oriented software development [MEMO-INF-92-15] p 946 N93-15084
Sensitivity and uncertainty analysis in performability modelling [MEMO-INF-92-18] p 941 N93-15090
Reliability modelling for non-electronic systems [REPT-921-440-103] p 894 N93-15139
Czechoslovak development and experience in flight data recorder readout and analysis p 794 N93-15162

SYSTEMS ENGINEERING
Systems modeling [AD-A255215] p 944 N93-14575
A voyage to Mars: A challenge to collaboration between man and machines p 777 N93-14614
Flight simulation leaves the ground p 778 N93-14616
Mission critical system development: Design views and their integration [AD-A255498] p 940 N93-14644
System design and development of a low data rate voice (1200 bps) rate converter [AD-A256071] p 859 N93-14663
A robotic planning system p 810 N93-14949
A monitoring and control system for complex man-machine systems: Preliminary design p 810 N93-14951
PEX: A reactive procedure based decision maker [REPT-921-440-105] p 999 N93-15118
Development of a TDS measurement system. Application to acoustic propagation measurement in a non anechoic environment [ONERA-RT-18/3641-PY] p 975 N93-15130
Proceedings of the 16th Symposium on Aircraft Integrated Monitoring Systems [DLR-MITT-92-01] p 793 N93-15152
The Teledyne controls aircraft condition monitoring system p 793 N93-15155
Ground Support Equipment (GSE) for Aircraft Condition Monitoring System (ACMS) p 778 N93-15158
Rewritable optical disk: Application to flight recording p 794 N93-15160
Royal Air Force experience of the Harrier information management system p 795 N93-15170
Helicopter flight data recorder and health and usage monitoring system p 797 N93-15178
Helicopter health monitoring: Current practice and future trends p 797 N93-15179
New rotor trim and balance system for helicopter usage monitoring p 797 N93-15180
Failure diagnostic with MAINTEX based on AIMS at Swissair p 778 N93-15181
Proceedings of the International Conference on CAD/CAM and AMT. Volume 4: VHDL (VHSIC Hardware Description Language) Seminar [ITN-92-85130] p 947 N93-15261

SYSTEMS INTEGRATION
Terminal Doppler weather radar/low-level wind shear alert system integration algorithm specification, version 1.1 [AD-A255319] p 920 N93-14547
Systems modeling [AD-A255215] p 944 N93-14575
Data storage and retrieval system p 1005 N93-15034
Integration of satellite links into an ATM mode broadband ISDN [TELECOM-PARIS-91-E-022] p 861 N93-15097
Proceedings of the 16th Symposium on Aircraft Integrated Monitoring Systems [DLR-MITT-92-01] p 793 N93-15152
Detection of technical states with aircraft p 794 N93-15159
Integrated engine control and monitoring with experiences derived from OLMOS p 795 N93-15168
A philosophy for integrated monitoring system design p 796 N93-15174
Personal computer based test- and emulation equipment for maintenance and ground support p 778 N93-15185
Airbus Industrie TCAS experience p 789 N93-15186
Integrated support for real-time control systems [PNR-90994] p 952 N93-15476

SYSTEMS MANAGEMENT
Software Technology for Adaptable, Reliable Systems (STARS) program. Software process tools and techniques evaluation report, version 1.0. Task IS15: Software process management [AD-A255945] p 942 N93-14405

SYSTEMS SIMULATION
Implementation issues concerning injection simulation. Part 1: The backbone implementation [MEMO-INF-91-57-PT-1] p 946 N93-15078
System test approach for the SAX satellite p 824 N93-15622

T

TABLES (DATA)
Orthobaric densities and molar volumes of liquids. Halogenated ethylenes [ESDU-92018] p 839 N93-14540

TACTICS
Design for tactical situation awareness display [AD-A256194] p 798 N93-15235
Radar scene generation for tactical decision aids [AD-A257069] p 863 N93-15495

TACTILE SENSORS (ROBOTICS)
CAD-based off-line programming and sensor signal processing in robotics [F-2-2] p 949 N93-15299

TAKEOFF
Simulator evaluation of displays for a revised takeoff performance monitoring system [NASA-TP-3270] p 803 N93-15366

TANKS (COMBAT VEHICLES)
A progressive resistance weight training program designed to improve the armor crewman's strength [AD-A255553] p 934 N93-14556

TANKS (CONTAINERS)
Characterization of impact-limiting material [DE92-016767] p 902 N93-15210

TANTALUM
Microwave processing of tantalum capacitor anodes [DE92-017829] p 869 N93-15214

TAPE RECORDERS
The preservation of LANDSAT data by the National Land Remote Sensing Archive p 1003 N93-14777
ICI optical data storage tape p 1005 N93-15037
ATL Products Division's entries into the computer mass storage marketplace p 1005 N93-15038
The 19 mm date recorders: Similarities and differences p 883 N93-15042

TARGET ACQUISITION
Airborne radar simulation with adaptive antenna techniques [AD-A255460] p 859 N93-14488
Real-time gaze holding in binocular robot vision [AD-A256226] p 982 N93-14582

TARGET RECOGNITION
Scatterer modeling/calibration study [AD-A255855] p 856 N93-14107
Evaluation of Night Vision Goggles (NVG) for maritime search and rescue (joint Canadian/US Coast Guard experiment) [AD-A255525] p 939 N93-14554
Vision development test bed: The cradle of the MSS artificial vision system p 810 N93-14948
Multimodal interactions in sensory-motor processing [AD-A255780] p 938 N93-15067

TARGETS
Use of kinematic constraint in tracking constant speed maneuvering targets [AD-A255988] p 858 N93-14415
Two-stage target tracking system and method [AD-D015412] p 982 N93-14880

TASK COMPLEXITY
Movement time prediction in human-computer interfaces p 955 N93-15550

TASK PLANNING (ROBOTICS)
Coordinated motion control of a two-hand assembly system [F-2-8] p 949 N93-15301
Off-line generation of error-free robot/NC (numerical control) code using simulation and automatic programming techniques [F-3-1] p 949 N93-15302
Robot learning of contact tasks [F-3-2] p 949 N93-15303
Multiple robot programming using concurrent logic language [F-3-3] p 950 N93-15304
Redundancy control of robots by constrained optimization [F-3-7] p 950 N93-15307

TASKS
Performance of color-dependent tasks of air traffic control specialists as a function of type and degree of color vision deficiency [AD-A256614] p 788 N93-14275
Identifying ability requirements for operators of future automated air traffic control systems [AD-A256615] p 789 N93-14276
Crew requirements definition system user's guide [AD-A257052] p 951 N93-15445

TAXONOMY
Taxonomy of flight variables p 787 N93-15022

TAYLOR INSTABILITY
Volcanism by melt-driven Rayleigh-Taylor instabilities and possible consequences of melting for admittance ratios on Venus p 1043 N93-14387
Numerical study of mixing of two fluids under low gravity [NASA-TM-105865] p 878 N93-14914

TAYLOR SERIES
Sensitivity and uncertainty analysis in performability modelling [MEMO-INF-92-18] p 941 N93-15090

TDR SATELLITES
On the performance of Trellis coded modulation with octal phase shift keying over the TDRSS channel [NASA-CR-191366] p 857 N93-14155

TEARING MODES (PLASMAS)
Resistive magnetohydrodynamic studies of tearing mode instability with equilibrium shear flow and magnetic reconnection p 987 N93-14122

TECHNICAL WRITING
How scientific must technical editors be? [DE92-040741] p 1010 N93-15655

TECHNOLOGICAL FORECASTING
Next generation satellite communications networks p 812 N93-14962

TECHNOLOGY ASSESSMENT
Organization of workshop on emerging technologies for in-situ processing [AD-A255977] p 865 N93-14410
Advanced sensors technology survey [NASA-CR-185691] p 881 N93-14494
The V-22 Osprey: A case analysis [AD-A256445] p 791 N93-14601
Symposium on the occasion of the farewell of Prof. Dr. Ir. O. H. Gerlach as Chairman of the Board of the Foundation National Aerospace Laboratory NLR, The Netherlands [ETN-92-92168] p 777 N93-14613
Flight simulation leaves the ground p 778 N93-14616
Human exploration: Moon/Mars mission p 805 N93-14922
Mission and technology assessment of human exploration to the Moon and Mars p 809 N93-14944
Progress in DND's space-based radar R/D project p 812 N93-14958
Engine technologies for future spaceplanes [ETN-92-92732] p 800 N93-15143
Technology evaluation report: The Carver-Greenfield process, Dehydro-Tech Corporation [PB92-217462] p 910 N93-15217
The evolution of space simulation p 814 N93-15610

TECHNOLOGY TRANSFER
Fault tolerant systems practitioner's workshop [AD-A255376] p 944 N93-14563
A planning workshop: To strengthen American cognitive science for the twenty-first century [NSF-92-4] p 999 N93-14720
Geothermal Energy and the Utility Market: The Opportunities and Challenges for Expanding Geothermal Energy in a Competitive Supply Market: Proceedings [DE92-019090] p 908 N93-15271

TECHNOLOGY UTILIZATION
SDIO Workshop on Piezoelectric Ceramic Actuators for Space Applications [AD-A255959] p 990 N93-14422
Industrial applications of multiaxial warp knit composites p 833 N93-14750
An overview of RADARSAT payload technologies p 807 N93-14933
Applications of the mobile servicing system to the space exploration initiative p 809 N93-14946
ATL Products Division's entries into the computer mass storage marketplace p 1005 N93-15038
Technology commercialization cost model and component case study [DE92-001280] p 907 N93-15213
Acoustic resonance techniques for quality control [DE92-040150] p 895 N93-15413

TECTONICS
Is Ishtar Terra a thickened basaltic crust? p 1024 N93-14292
Constraints on the thermal evolution of Venus inferred from Magellan data p 1024 N93-14293
Global deformation on the surface of Venus p 1024 N93-14297
Coldspots or hotspots? The origin of plateau-shaped highlands on Venus p 1025 N93-14298
Global correlation of volcanic centers on Venus with uplands and with extension: Influence of mantle convection and altitude p 1026 N93-14309
Monte Carlo computer simulations of Venus equilibrium and global resurfacing models p 1027 N93-14311

Viscoelastic relaxation of Venusian coronae and mountain belts: Constraints on global heat flow and tectonism p 1027 N93-14313
Flexural analysis of uplifted rift flanks on Venus p 1027 N93-14314
Radar scattering properties of pancakelike domes on Venus p 1028 N93-14316
Sequential deformation of plains along Tessera boundaries on Venus: Evidence from Alpha Regio p 1028 N93-14317
Tectonics and volcanism of Eastern Aphrodite Terra: No subduction, no spreading p 1029 N93-14321
Western Aphrodite Terra, tectonics, geology, and line-of-sight gravity p 1029 N93-14322
Chemical differentiation on one-plate planets: Predictions and geologic observations for Venus p 1029 N93-14324
Igneous and tectonic evolution of Venusian and terrestrial coronae p 1031 N93-14330
Venus tectonic styles and crustal differentiation p 1031 N93-14332
Flexural models of trench/outer rise topography of coronae on Venus with axisymmetric spherical shell elastic plates p 1036 N93-14348
Tectonic connections to interior processes on Venus p 1039 N93-14361
Evidence for retrograde lithospheric subduction on Venus p 1040 N93-14367
Atla Regio, Venus: Geology and origin of a major equatorial volcanic rise p 1041 N93-14374
The tectonics of Venus: An overview p 1042 N93-14382
The spatial distribution of coronae on Venus p 1043 N93-14383
Structural characteristics and tectonics of northeastern Tellus Regio and Meni Tessera p 1044 N93-14389
Episodic plate tectonics on Venus p 1044 N93-14390
Plate tectonics from VLBI and SLR global data [NASA-CR-191319] p 916 N93-14913

TELEMETRY
Investigation of the use of surface electrical currents for short-range shipboard data communications [AD-A256197] p 859 N93-14490
Development of an expendable particle sensor [AD-A255702] p 881 N93-14653
SMART: A modular architecture for robotics and teleoperation [DE92-040985] p 966 N93-15385
Reusable Reentry Satellite (RRS): Telemetry, Tracking, and Command (TT/C) coverage tradeoff study [NASA-CR-188583] p 824 N93-15629

TELEOPERATORS
Vision system requirements and concept for the Special Purpose Dexterous Manipulator system (SPDM) p 805 N93-14924
SMART: A modular architecture for robotics and teleoperation [DE92-040985] p 966 N93-15385

TELEROBOTICS
SMART: A modular architecture for robotics and teleoperation [DE92-040985] p 966 N93-15385

TELESCOPES
Imaging the sun in hard x-rays using Fourier telescopes p 1048 N93-14591
An application of artificial intelligence to automatic telescopes [NASA-TM-108115] p 965 N93-15291
Environmental assessment for the laser guide star experiment at Lawrence Livermore National Laboratory [DE92-040316] p 1013 N93-15425

TELEVISION CAMERAS
Vision development test bed: The cradle of the MSS artificial vision system p 810 N93-14948

TELEVISION SYSTEMS
Representation and manipulation of inductive boolean functions [AD-A256078] p 967 N93-14235

TELLURIUM ISOTOPES
Measurement and analysis of excitation functions in (alpha,np) reactions on (128, 130)Te [DE92-630358] p 991 N93-14485

TEMPERATE REGIONS
A study of mid-latitude 5577A CI dayglow emissions [AD-A255444] p 914 N93-14511

TEMPERATURE CONTROL
Thermal fixture for testing an integrated circuit [AD-D015380] p 882 N93-15247
An alternate method for achieving temperature control in the -130 C to 75 C range p 821 N93-15609

TEMPERATURE DEPENDENCE
Orthobaric densities and molar volumes of liquids. Halogenated ethylenes [ESDU-92018] p 839 N93-14540
Thermophysical properties of nitric oxide [ESDU-92027] p 839 N93-14544
Measurement of the magnetic anisotropy energy constants for magneto-optical recording media p 984 N93-15509

TEMPERATURE DISTRIBUTION
Lineshape analysis of laser light scattered by an argon thermal plasma jet p 987 N93-14137
A general purpose radiative transfer model for application to remote sensing in multidimensional systems p 904 N93-14174
The effects of Venus' thermal structure on buoyant magma ascent p 1040 N93-14366
Development of an integrated package of physics models for scene simulation studies to support smart weapons design studies [LTR92-004] p 945 N93-14696
Modelling the engine temperature distribution between shut down and restart for life usage monitoring p 796 N93-15177
Imaging the sun in hard x rays using Fourier telescopes [NASA-TM-108390] p 1013 N93-15203
Thermal analysis of magnetron sputtering designs [DE93-000348] p 870 N93-15389

TEMPERATURE EFFECTS
Digital caustic investigation of near surface cracks under transient thermal loading p 897 N93-14217
High temperature polymer dielectric film insulation [AD-A255243] p 849 N93-14527
Orthobaric densities and molar volumes of liquids. Halogenated ethylenes [ESDU-92018] p 839 N93-14540
Thermal conductivity of liquid aliphatic hydrocarbons. Part 2: Alkenes, dienes and trienes [ESDU-92025] p 839 N93-14542
Thermal elastic shock and its effect on spacecraft attitude control p 818 N93-14837
Characterization of impact-limiting material [DE92-016767] p 902 N93-15210
Thermal fixture for testing an integrated circuit [AD-D015380] p 882 N93-15247
Experimental observation of the influence of furnace temperature profile on convection and segregation in the vertical Bridgman crystal growth technique p 995 N93-15312
An investigation of the processing, high temperature deformation and fracture characteristics of superplastic ceramics [AD-A256519] p 852 N93-15394
Inelastic deformation of metal matrix composites: Plasticity and damage mechanisms, part 2 [NASA-CR-189096-PT-2] p 837 N93-15401
Emittance measurements of Space Shuttle orbiter reinforced carbon-carbon [NASA-TP-3293] p 903 N93-15530
A comparison of superconductor and manganin technology for electronic links used in space mission applications [NASA-CR-4477] p 997 N93-15587

TEMPERATURE GRADIENTS
The effects of Venus' thermal structure on buoyant magma ascent p 1040 N93-14366
Thermal elastic shock and its effect on spacecraft attitude control p 818 N93-14837

TEMPERATURE INVERSIONS
Middle atmosphere of Venus and its clouds: Latitude and solar time variations p 1045 N93-14396

TEMPERATURE MEASUREMENT
Arc-cathode interaction study [NASA-CR-191356] p 867 N93-14721
Study of optical techniques for the Ames unitary wind tunnel. Part 5: Infrared imagery [NASA-CR-191385] p 804 N93-14809
An experimental approach to determine the heat transfer coefficient in directional solidification furnaces p 995 N93-15311

TEMPERATURE PROFILES
Experimental observation of the influence of furnace temperature profile on convection and segregation in the vertical Bridgman crystal growth technique p 995 N93-15312

TEMPORAL DISTRIBUTION
Parametric study of diffusion-enhancement networks for spatiotemporal grouping in real-time artificial vision [AD-A256059] p 937 N93-14580
Spatial and temporal patterns of biotic exchanges of CO2 between the atmosphere and tropical landscapes and their role in the global carbon balance [DE92-019170] p 911 N93-15272
Global zones of particle precipitation as observed by EXOS-C [AD-A256397] p 917 N93-15466

TENSILE DEFORMATION
Inelastic deformation of metal matrix composites: Plasticity and damage mechanisms, part 2 [NASA-CR-189096-PT-2] p 837 N93-15401

TENSILE PROPERTIES
Tensile properties of textile composites p 834 N93-14754

TENSILE STRENGTH
The effect of the interphase/interface region on creep and creep rupture of thermoplastic composites p 829 N93-14193
The response of dispersion-strengthened copper alloys to high fluence neutron irradiation at 415 C [DE92-019434] p 846 N93-15138
Effects of high thermal neutron fluences on Type 6061 aluminum [DE92-040569] p 846 N93-15348

TENSILE TESTS
Progress toward a tungsten alloy wire/high temperature alloy composite turbine blade [NASA-TM-105901] p 847 N93-15586

TERBIUM COMPOUNDS
Optical instrumentation and characterization for magneto-optical recording media p 980 N93-14168

TERMINOLOGY
Revised nomenclature for defects at or near the Si/SiO2 interface [DE92-040975] p 997 N93-15651

TERRAIN
Shield fields: Concentrations of small volcanic edifices on Venus p 1024 N93-14295
Sequential deformation of plains along Tessera boundaries on Venus: Evidence from Alpha Regio p 1028 N93-14317
Venus: Preliminary geologic mapping of northern Atla Regio p 1037 N93-14353
Venus: Preliminary geologic mapping of southern Beta Regio-northern Phoebe Regio p 1037 N93-14354
Overview of Venus geology: Preliminary description of terrain units for Venus global geological mapping p 1040 N93-14368
Structural characteristics and tectonics of northeastern Tellus Regio and Meni Tessera p 1044 N93-14389
Terrain visualization for the portable all-source analysis work station [AD-A255708] p 905 N93-14430
Adaptive mesh in visualization of terrain elevation data [AD-A255481] p 906 N93-15007
Taxonomy of flight variables p 787 N93-15022
Radar scene generation for tactical decision aids [AD-A257069] p 863 N93-15495
Parametric height field ray tracing p 955 N93-15556

TERRAIN ANALYSIS
Terrain visualization for the portable all-source analysis work station [AD-A255708] p 905 N93-14430

TERRESTRIAL PLANETS
Coldspots or hotspots? The origin of plateau-shaped highlands on Venus p 1025 N93-14298
Bright crater outflows: Possible emplacement mechanisms p 1026 N93-14305

TERRESTRIAL RADIATION
Precision radiation force modeling for the TOPEX/Poseidon mission p 817 N93-14586

TEST CHAMBERS
Liquid flow reactor and method of using [AD-D015392] p 893 N93-15232
Environmental qualification testing of the prototype pool boiling experiment [NASA-CR-190774] p 895 N93-15582
A new approach for performing contamination control bakeouts in JPL thermal vacuum test chambers p 823 N93-15618

TEST EQUIPMENT
Parametric study of air sampling cyclones p 779 N93-14173
Establishment of a test course for high accuracy dynamic positioning systems [AD-A255407] p 789 N93-14501
Vision development test bed: The cradle of the MSS artificial vision system p 810 N93-14948
Thermal fixture for testing an integrated circuit [AD-D015380] p 882 N93-15247
An environmental testing facility for Space Station Freedom power management and distribution hardware p 820 N93-15601

TEST FACILITIES
Flight termination systems commonality standard [AD-A255349] p 789 N93-14517
Space based radar: Test of large space structures p 808 N93-14941
Space craft verification at the David Florida Laboratory p 809 N93-14943
Personal computer based test- and emulation equipment for maintenance and ground support p 778 N93-15185

Experimental determination of magnetohydrodynamic seawater thruster performance in a two Tesla test facility
[DE92-019042] p 826 N93-15215
Multi-axis transient vibration testing of space objects: Test philosophy, test facility, and control strategy
p 820 N93-15598
The design concept of the 6-degree-of-freedom hydraulic shaker at ESTEC p 820 N93-15600
An environmental testing facility for Space Station Freedom power management and distribution hardware
p 820 N93-15601
A new thermal vacuum facility at the Martin Marietta Waterton plant p 814 N93-15607
INTESPACE's new thermal-vacuum test facility: SIMMER p 814 N93-15613
TQM in a test environment p 823 N93-15620

TEST RANGES
Establishment of a test course for high accuracy dynamic positioning systems
[AD-A255407] p 789 N93-14501

TEST STANDS
EMTP based stability analysis of space station electric power system in a test bed environment
[NASA-TM-105845] p 871 N93-15503

TETRAETHYL ORTHOSILICATE
Solid polymer electrolytes for rechargeable batteries
[DE93-001603] p 871 N93-15485

TEXTILES
FIBER-TEX 1991: The Fifth Conference on Advanced Engineering Fibers and Textile Structures for Composites
[NASA-CP-3176] p 832 N93-14744
Tensile properties of textile composites
p 834 N93-14754

TEXTS
A minimalist global user interface p 957 N93-15566

THEMATIC MAPPERS (LANDSAT)
The preservation of LANDSAT data by the National Land Remote Sensing Archive p 1003 N93-14777

THEMATIC MAPPING
The regional land use of Paraiba Valley and the North Coast of Sao Paulo State, Brazil p 905 N93-14450

THEOREM PROVING
Proof of theorems in Z
[AD-A255711] p 968 N93-14431

THEOREMS
A proof of the Church-Rosser theorem and its representation in a logical framework
[AD-A256574] p 942 N93-14268
Proof of theorems in Z
[AD-A255711] p 968 N93-14431
Compactness and Loewenheim-Skolem properties in pre-institution categories
[MEMO-INF-92-27] p 968 N93-15094
Low energy theorems in pion production
[DE92-040071] p 977 N93-15279
Volume rendering using the Fourier projection-slice theorem p 953 N93-15541

THEORIES
Elements of a theory of natural decision making
p 786 N93-15021

THERMAL ANALYSIS
Spacecraft thermal design verification in Canada
p 808 N93-14940
Space based radar: Test of large space structures
p 808 N93-14941
Composite materials in space: Results from the LDEF satellite p 811 N93-14955
Advances in TMG p 811 N93-14956
Thermal analysis of magnetron sputtering designs
[DE93-000348] p 870 N93-15389

THERMAL BOUNDARY LAYER
Chemical differentiation of a convecting planetary interior: Consequences for a one-plate planet such as Venus p 1038 N93-14358

THERMAL CONDUCTIVITY
Effect of interfacial thermal conductance and fiber orientation on the thermal diffusivity/conductivity of unidirectional fiber-reinforced ceramic matrix composites
p 864 N93-14190
Modeling of the thermal elasto-plastic behavior for composite materials using the homogenization method
p 830 N93-14466
Thermal conductivity of liquid aliphatic hydrocarbons. Part 2: Alkenes, dienes and trienes
[ESDU-92025] p 839 N93-14542
Thermophysical properties of nitric oxide
[ESDU-92027] p 839 N93-14544
ISOCAM experiment cryogenic test results
[REPT-921-440-104] p 825 N93-15140
Thermal, mechanical, and electroelastic behavior of composite materials p 835 N93-15146
A comparison of superconductor and manganin technology for electronic links used in space mission applications
[NASA-CR-4477] p 997 N93-15587

THERMAL CONTROL COATINGS
Method of applying a thermal barrier coating system to a substrate
[NASA-CASE-LEW-15020-2] p 832 N93-14706

THERMAL CYCLING TESTS
Thermal fatigue analysis of metal matrix composite with spherical reinforcements
[AD-A255313] p 831 N93-14672
Environmental qualification testing of the prototype pool boiling experiment
[NASA-CR-190774] p 895 N93-15582
Simulation of the synergistic low Earth orbit effects of vacuum thermal cycling, vacuum UV radiation, and atomic oxygen p 819 N93-15595

THERMAL DECOMPOSITION
High resolution absolute absorption cross sections of NO2 at 295, 573, and 673 K at visible wavelengths: Comprehensive data tables
[AD-A255261] p 839 N93-14530
Thermal decomposition of HNIW and HNIW-Based formulations
[AD-A255613] p 854 N93-15011

THERMAL DIFFUSION
Crystal growth in a microgravity environment
[NASA-CASE-MFS-28473-1] p 992 N93-14707

THERMAL ENVIRONMENTS
Method for fabricating ohmic contacts on semiconducting diamond
[AD-D015432] p 850 N93-14825
Acoustic and thermal testing of the Titan/Centaur upper stage p 814 N93-15621

THERMAL EXPANSION
Thermal, mechanical, and electroelastic behavior of composite materials p 835 N93-15146
Development of low-expansion ceramics for diesel engine applications
[DE92-041380] p 853 N93-15438

THERMAL FATIGUE
Thermal fatigue analysis of metal matrix composite with spherical reinforcements
[AD-A255313] p 831 N93-14672

THERMAL INSULATION
Results of a FRSI material test under Space Shuttle ascent conditions in the Ames Research Center 9x7 foot supersonic wind tunnel (OS13). Space Shuttle aerothermodynamic data report
[NASA-CR-167699] p 816 N93-15475

THERMAL MAPPING
Study of optical techniques for the Ames unitary wind tunnel. Part 5: Infrared imagery
[NASA-CR-191385] p 804 N93-14809
Nonuniformity effects in a hybrid platinum silicide imaging device
[AD-A256339] p 983 N93-15197

THERMAL NEUTRONS
Effects of high thermal neutron fluences on Type 6061 aluminum
[DE92-040569] p 846 N93-15348

THERMAL PLASMAS
Lineshape analysis of laser light scattered by an argon thermal plasma jet p 987 N93-14137

THERMAL PROTECTION
Emittance measurements of Space Shuttle orbiter reinforced carbon-carbon
[NASA-TP-3293] p 903 N93-15530

THERMAL SHOCK
Thermal elastic shock and its effect on spacecraft attitude control p 818 N93-14837

THERMAL SIMULATION
The Seventeenth Space Simulation Conference. Terrestrial Test for Space Success
[NASA-CP-3181] p 819 N93-15593
A new thermal vacuum facility at the Martin Marietta Waterton plant p 814 N93-15607

THERMAL STABILITY
Spectroscopy and reactions of hydrazoic acid on silicon single crystal surfaces (III). HN3 and DN3 on Si(111)-7 x 7
[AD-A255241] p 842 N93-14669
Thermal stability of trimethyl indium on Si(100)-2 x 1 as studied with HREELS, UPS, and XPS: A comparison with the results from Si(111)-7 x 7 and Si(110) studies
[AD-A255242] p 992 N93-14670
High temperature stability, interface bonding, and mechanical behavior in (beta)-NiAl and Ni3Al matrix composites with reinforcements modified by ion beam enhanced deposition
[DE92-014399] p 992 N93-14812

THERMAL STRESSES
Digital caustic investigation of near surface cracks under transient thermal loading p 897 N93-14217
Theoretical and experimental analysis of residual stress formation after implant resistance welding of polycarbonate p 898 N93-14279
Modeling of the thermal elasto-plastic behavior for composite materials using the homogenization method
p 830 N93-14466

THERMAL VACUUM TESTS
Environmental qualification testing of the prototype pool boiling experiment
[NASA-CR-190774] p 895 N93-15582
Manned testing in a simulated space environment
p 820 N93-15602
A new thermal vacuum facility at the Martin Marietta Waterton plant p 814 N93-15607
INTESPACE's new thermal-vacuum test facility: SIMMER p 814 N93-15613

THERMITES
The sensitivity of energetic materials to friction, impact, and electrostatic stimuli
[DE92-041227] p 855 N93-15478

THERMODYNAMIC PROPERTIES
The preliminary Long Duration Exposure Facility (LDEF) materials data base
[NASA-TM-107692] p 828 N93-14459
Studies of components for thermally regenerative electrochemical systems
[AD-A256124] p 842 N93-14664

THERMODYNAMICS
Mixed-layer parameterization in models of the Indian Ocean
[AD-A255937] p 925 N93-14428
Convective scale 4-D data assimilation using simulated single-Doppler radar observations p 921 N93-14683
Low-frequency oscillations in radiative-convective models p 915 N93-14874
Thermodynamics and transport in Ce3Bi4Pt3 and related compounds
[DE92-040377] p 998 N93-14905
Adsorption and diffusion of fluids in well-characterized adsorbent materials
[DE92-040160] p 843 N93-15414

THERMOELASTICITY
Modeling of the thermal elasto-plastic behavior for composite materials using the homogenization method
p 830 N93-14466

THERMOGRAPHY
Study of optical techniques for the Ames unitary wind tunnel. Part 5: Infrared imagery
[NASA-CR-191385] p 804 N93-14809

THERMOMECHANICAL TREATMENT
Effect of thermomechanical treatments on the aging response of centrifugally cast silicon carbide/aluminum composites
[AD-A256204] p 836 N93-15236

THERMONUCLEAR REACTIONS
Studies of heavy-ion reactions and transuranic nuclei
[DE92-040457] p 977 N93-15326

THERMOPHORESIS
Transport phenomena and interfacial kinetics in multiphase combustion systems.
[AD-A255999] p 838 N93-14418

THERMOPILES
A novel, high energy-density electrical storage device for electric weapons
[AD-A255205] p 867 N93-14666

THERMOPLASTIC RESINS
Mechanics of composite materials for spacecraft
[AD-A255380] p 831 N93-14550
Spirobislactone acrylate polymers
[AD-D015443] p 850 N93-14802
Method of local shaping of thermoplastics
[AD-A255913] p 856 N93-15105

THERMOPLASTICITY
The effect of the interphase/interface region on creep and creep rupture of thermoplastic composites
p 829 N93-14193
Theoretical and experimental analysis of residual stress formation after implant resistance welding of polycarbonate p 898 N93-14279
A finite element model for analysis of thermoviscoplastic behavior of hypersonic leading edge structures subject to intense aerothermal heating p 780 N93-14631

THERMOSETTING RESINS
Structural study of thermohardening matrices: Deformation of composite matrices in relation to their molecular structure
[ONERA-RT-12/3521-M] p 836 N93-15253

THERMOSPHERE
Local-time asymmetries in the Venus thermosphere
p 1023 N93-14290
The thermosphere and ionosphere of Venus
p 1026 N93-14307
LISA: A limb imaging spectrograph for airglow
p 811 N93-14952

THICK FILMS
Thin-film permanent magnets for integrated electromagnetic components
[AD-A256175] p 972 N93-14679

Processing and characterization of electrophoretically deposited holmium barium copper oxide superconductor films
| AD-A256329 | p 869 N93-15194

THICK PLATES
On the development and application of a modified boundary element method for the analysis of three dimensional elastostatic problems in thick plates
p 901 N93-14587

THICKNESS
Kind-band failure analysis of thick composites in compression
| AD-A255431 | p 831 N93-14509

THICKNESS RATIO
Multi-point inverse design of isolated airfoils and airfoils in cascade in incompressible flow p 790 N93-14462

THIN FILMS
Electrical conductivity measurements in evaporated cadmium telluride thin films p 865 N93-14191
Fracture analyses of thin films, interfaces, and joints
p 897 N93-14215
A geometrically nonlinear stress-deflection relation for thin film/substrate systems p 848 N93-14287
Long term stability in thin film ferroelectric memories
| AD-A256290 | p 991 N93-14439
High temperature polymer dielectric film insulation
| AD-A255243 | p 849 N93-14527
Reliability of sol-gel derived ferroelectric memories
| AD-A255358 | p 991 N93-14560
Characterisation and dynamic modelling of the near-earth space particulate environment
p 1019 N93-14637
Reliability of sol-gel derived ferroelectric memories
| AD-A255240 | p 849 N93-14668
Thin-film permanent magnets for integrated electromagnetic components
| AD-A256175 | p 972 N93-14679
Method of forming a multiple layer dielectric and a hot film sensor therewith
| NASA-CASE-LAR-13678-3 | p 881 N93-14714
Characterization of PZT films fatigued at low frequency
| AEROSPACE-ATR-91(8308)-2 | p 992 N93-14795
NREL photovoltaic subcontract reports: Abstracts and document control information
| DE92-016408 | p 907 N93-14817
Control of thermocapillary convection in a two-layer liquid system p 809 N93-14945
New electronic materials
| AD-A255612 | p 868 N93-15010
Jet vapor deposition of thin films for solid oxide and other fuel cell applications
| DE92-019980 | p 851 N93-15222
Silicon nitride thin film production on Si(111)
| AD-A256036 | p 994 N93-15233
Growth, characterization and device development in monocrystalline diamond films
| AD-A256283 | p 994 N93-15244
New nonlinear optical film processing
| AD-A256011 | p 983 N93-15255
The crack problem for an orthotropic half plane stiffened by elastic films
| AD-A256471 | p 903 N93-15374
The 17th Annual Conference on the Physics and Chemistry of Semiconductor Interfaces
| AD-A257061 | p 996 N93-15449
Instrumentation of the variable-angle magneto-optic ellipsometer and its application to M-O media and other non-magnetic films p 984 N93-15508
The 3D modeling of high numerical aperture imaging in thin films p 985 N93-15513
Oxidation processes in magneto-optic and related materials p 985 N93-15516
The design and fabrication of a single leakage-channel grating coupler p 986 N93-15518

THIN PLATES
Broadband vibroacoustic frequency control via piezoelectric films
| ONERA-RT-8/3654-RY-010-R | p 974 N93-15129

THIN WALLED SHELLS
SAPNEW: Parallel finite element code for thin shell structures on the Alliant FX-80
| NASA-CR-189212 | p 901 N93-14799

THIN WALLS
Analysis of advanced thin-walled composite structures
p 895 N93-14158
Use of the thin-walled torsion specimen
| AD-A255593 | p 901 N93-14790

THOMSON SCATTERING
Lineshape analysis of laser light scattered by an argon thermal plasma jet p 987 N93-14137

THORIUM COMPOUNDS
Normal state resistivity and the phase diagram of U(1-x)Th(x)Be13
| DE92-040236 | p 995 N93-15321

THREADS
Method and devices for the in situ repair of damaged threads
| AD-D015416 | p 891 N93-14881

THREE DIMENSIONAL BODIES
On the development and application of a modified boundary element method for the analysis of three dimensional elastostatic problems in thick plates
p 901 N93-14587
Three-dimensional nuclear magnetic resonance imaging of green-state ceramics
| DE93-000930 | p 851 N93-15282

THREE DIMENSIONAL COMPOSITES
Advanced stitching technology p 832 N93-14746
Advances in 3-dimensional braiding
p 833 N93-14748
Development of generalized 3-D braiding machines for composite preforms p 833 N93-14749
Modeling of Euclidean braided fiber architectures to optimize composite properties p 834 N93-14755
Improved inhomogeneous finite elements for fabric reinforced composite mechanics analysis
p 834 N93-14757

THREE DIMENSIONAL FLOW
An algebraic turbulence model for three-dimensional viscous flows
| NASA-TM-105931 | p 777 N93-14102
Recent advances in numerical simulation and control of asymmetric flows around slender bodies
| PAPER-W.1.2 | p 875 N93-14688
Shock/vortex interaction and vortex-breakdown modes
| PAPER-T.1.3 | p 875 N93-14689
Three-dimensional computational study of asymmetric flows using Navier-Stokes equations
| ISBN-90-5410-029-X | p 875 N93-14690
The 3D Navier-Stokes flow analysis for shared and distributed memory MIMD computers
| AD-A256038 | p 878 N93-15187
On explicit algebraic stress models for complex turbulent flows
| NASA-CR-189725 | p 879 N93-15481

THREE DIMENSIONAL MODELS
Monte Carlo modeling of the resurfacing of Venus
p 1025 N93-14299
Results of a zonally truncated three-dimensional model of the Venus middle atmosphere p 1037 N93-14351
VANTAGE: A frame-based geometric modeling system programmer/user's manual, V2.0
| AD-A255434 | p 944 N93-14566
The influence of baroclinic processes on tropical cyclone motion p 923 N93-15099
CAD-based off-line programming and sensor signal processing in robotics
| F-2-2 | p 949 N93-15299
The 3D modeling of high numerical aperture imaging in thin films p 985 N93-15513
Volume rendering using the Fourier projection-slice theorem p 953 N93-15541
Partitioning tree image representation and generation from 3D geometric models p 955 N93-15557
Nonlinear finite element analysis of metals and metal matrix composites: A local-global investigation
| AD-A256782 | p 838 N93-15625

THROATS
Numerical modeling of a vortex stabilized arcjet
| NASA-CR-190797 | p 826 N93-14883

THUNDERSTORMS
Thunderstorm coupling to the magnetosphere and associated ionospheric effects
| NASA-CR-191383 | p 922 N93-14910

TIDES
Study of tidal interactions in M81-M82-NGC3077 system p 1010 N93-14195
Global ocean tides through assimilation of oceanographic and altimeter satellite data in a hydrodynamic model p 928 N93-14978
Global ocean tide mapping using TOPEX/Poseidon altimetry p 930 N93-14991
Application of precise altimetry to the study of precise leveling of the sea surface, the Earth's gravity field, and the rotation of the Earth p 907 N93-14992

TILT ROTOR AIRCRAFT
Tiltrotor aircraft noise: A summary of the presentations and discussions at the 1991 FAA/Georgia Tech Workshop
| DOT/FAA/RD-91/23 | p 974 N93-14912

TIME
Liquid xenon time projection chamber for gamma rays in the MeV region: Development status
p 1014 N93-15592

TIME DEPENDENCE
The dynamics of spatially extended lasers
p 883 N93-14123
Decision making in a dynamic task environment: The effect of time pressure
| AD-A256557 | p 937 N93-14602
Elastic wave propagation in laminated composites
| ITN-93-85186 | p 835 N93-15144
Far infrared, magnetic, and electronic studies of high T(sub c) superconducting materials
| AD-A257050 | p 996 N93-15444
Time-dependent predictions and analysis of turbine cascade data in the transonic flow region
| PNR-90957 | p 782 N93-15489

TIME OF FLIGHT SPECTROMETERS
Development of laser-ion beam photodissociation methods
| DE92-040512 | p 886 N93-15058
Development of a TDS measurement system. Application to acoustic propagation measurement in a non anechoic environment
| ONERA-RT-18/3641-PY | p 975 N93-15130

TIME OPTIMAL CONTROL
Time-optimization of point-to-point robotic motions
| F-3-6 | p 950 N93-15306

TIME SIGNALS
An energy analysis of the pseudo Wigner-Ville distribution in support of machinery monitoring and diagnostics
| AD-A256202 | p 889 N93-14499

TIME TEMPERATURE PARAMETER
An experimental approach to determine the heat transfer coefficient in directional solidification furnaces
p 995 N93-15311
Far infrared, magnetic, and electronic studies of high T(sub c) superconducting materials
| AD-A257050 | p 996 N93-15444

TISSUES (BIOLOGY)
Nerves and tissue repair
| AD-A255299 | p 934 N93-14535
Autoradiographic distribution and applied pharmacological characteristics of dextromethorphan and related antitissue/anticonvulsant drugs and novel analogs
| AD-A255607 | p 935 N93-15009

TITAN
Investigations of Titan's troposphere and surface and Jupiter's great red spot with infrared observations
p 1022 N93-14146
Cassini atmospheric chemistry mapper. Volume 1. Investigation and technical plan
| NASA-CR-190947 | p 1021 N93-15079

TITAN LAUNCH VEHICLES
Acoustic and thermal testing of the Titan/Centaur upper stage p 814 N93-15621

TITANIUM
The 7th World Conference on Titanium
| AD-A255674 | p 844 N93-14132
The use of a novel manufacturing process for high performance titanium plate fin heat exchangers
| PNR-90934 | p 879 N93-15473

TITANIUM ALLOYS
The 7th World Conference on Titanium
| AD-A255674 | p 844 N93-14132
HIP consolidation of aluminum-rich intermetallic alloys and their composites
| NAWCADWAR-92003-60 | p 845 N93-14726

TITANIUM CARBIDES
Fabrication of high temperature materials by exothermic synthesis and subsequent dynamic consolidation
| DE92-019836 | p 834 N93-14819

TITANIUM COMPOUNDS
Inelastic deformation of metal matrix composites: Plasticity and damage mechanisms, part 2
| NASA-CR-189096-PT-2 | p 837 N93-15401

TITANIUM OXIDES
Theory of the electronic and structural properties of solid state oxides
| DE92-040499 | p 993 N93-14909

TOKAMAK DEVICES
Analysis of rotation experiments in TFTR --- tokamak fusion test reactor p 987 N93-14129
Plasma confinement theory and transport simulation
| DE92-040523 | p 988 N93-15327
Theoretical and numerical studies in magnetic fusion
| DE92-040674 | p 988 N93-15349
A power compensation system for phased operation of the JET A2 antenna arrays
| DE92-041020 | p 863 N93-15440

TOLERANCES (MECHANICS)
A method of representating dimensions and tolerances in solid based freeform surfaces
| PNR-90998 | p 951 N93-15386
An overview of shed ice impact in the NASA Lewis Icing Research Tunnel
| NASA-TM-105969 | p 782 N93-15404

TOLUENE
Absorption of propellant vapors into polymer films
| AD-A255274 | p 849 N93-14531

Anaerobic microbial transformation of aromatic hydrocarbons and mixtures of aromatic hydrocarbons and halogenated solvents
[AD-A255696] p 932 N93-14557

TOMOGRAPHY
Nondestructive evaluation of damage in SiC/Al metal matrix composite using x ray tomographic microscopy p 829 N93-14192
Imaging Earth's interior: Tomographic inversions for mantle P-wave velocity structure p 913 N93-14225
A study of the relationship between macroscopic measures and physical processes occurring during crack closure
[AD-A256587] p 898 N93-14272
Studies of the intermediate and deep circulation in the western equatorial Atlantic p 927 N93-14973
Laser-based studies with an ion-trap mass spectrometer: Ion tomography and analytical applications
[DE92-017529] p 887 N93-15135
Advanced research in instrumentation and diagnostics technology
[DE92-041121] p 883 N93-15411

TOOLS
Bearing servicing tool
[NASA-CASE-MSC-21881-1] p 891 N93-14871

TOPEX
Precision radiation force modeling for the TOPEX/Poseidon mission p 817 N93-14586
TOPEX/Poseidon science investigations plan
[NASA-CR-190616] p 925 N93-14964
The western Mediterranean Sea: An area for a regional validation for TOPEX/Poseidon and a field for geophysical and oceanographic studies p 926 N93-14965
The use of satellite altimetry in the study of weakly defined and variable oceanic gyres p 926 N93-14966
Terrestrial reference systems related to the TOPEX/Poseidon project p 906 N93-14967
North-Australian tropical seas circulation study p 926 N93-14968
Geophysical investigations with TOPEX/Poseidon altimetry data p 918 N93-14969
Mesoscale and large-scale variability of the Antarctic circumpolar current p 926 N93-14970
Ocean transport and variability studies of the South Pacific, Southern, and Indian Oceans p 927 N93-14971
Assimilation of altimeter topography into oceanic models p 927 N93-14972
Studies of the intermediate and deep circulation in the western equatorial Atlantic p 927 N93-14973
Application of TOPEX/Poseidon altimetry to ocean dynamics and geophysics p 927 N93-14974
Circulation of the gyres of the world ocean: Observation modeling using TOPEX/Poseidon altimeter data p 927 N93-14975
South African TOPEX/Poseidon altimeter experiment p 928 N93-14976
Global ocean tides through assimilation of oceanographic and altimeter satellite data in a hydrodynamic model p 928 N93-14978
Low-frequency variability of sea level as related to the heat balance of global oceans p 928 N93-14979
Studies of tropical ocean dynamics using the TOPEX/Poseidon altimeter-derived sea surface topography p 928 N93-14980
Ocean topography mapping, improvement of the marine geoid, and global permanent ocean circulation studies from TOPEX/Poseidon altimeter data p 928 N93-14981
Geophysical validation of TOPEX/Poseidon altimetry products p 918 N93-14982
Study of mass and heat transport of the tropical Atlantic Ocean using models and altimeter data p 929 N93-14983
Ocean circulation using altimetry p 929 N93-14984
The dynamics and energetics of midlatitude western boundary currents: A comparison of the Kuroshio Extension and the Gulf Stream p 929 N93-14985
General circulation of the South Atlantic between 5 deg N and 35 deg S p 929 N93-14987
Ocean dynamics in the Nordic Seas using satellite altimetry p 930 N93-14988
Application of TOPEX/Poseidon altimetry measurements to observational and modeling studies of the low-frequency upper ocean mass and heat circulation in the tropical Pacific p 930 N93-14989
Mean sea surface and gravity investigations using TOPEX/Poseidon altimeter data p 930 N93-14990
Global ocean tide mapping using TOPEX/Poseidon altimetry p 930 N93-14991
Application of precise altimetry to the study of precise leveling of the sea surface, the Earth's gravity field, and the rotation of the Earth p 907 N93-14992
Present-day plate motions: Retrieval from the TOPEX/Poseidon orbitography network (DORIS system) p 918 N93-14993
Equatorial and eastern boundary current variability in the North and South Pacific Oceans p 931 N93-14994
An integrated research program for TOPEX/Poseidon with emphasis on the Pacific Ocean p 931 N93-14995
Oceanic transports of mass, heat, and salt in the western North Pacific p 931 N93-14996
The determination and interpretation of ocean surface topography using TOPEX/Poseidon altimeter data p 931 N93-14997
Analysis of altimeter data jointly with seafloor electric data (vertically integrated velocity) and VCTD-yoyo data (detailed profiles of VCTD) p 931 N93-14998
A TOPEX/Poseidon study of oceanic effects on observations of the Earth's interior p 918 N93-14999
Precise orbit computation and sea surface modeling p 813 N93-15000
Marine research using data from TOPEX/Poseidon p 932 N93-15001
Global ocean circulation by altimetry p 932 N93-15002
Vibration and acoustic testing of TOPEX/Poseidon satellite p 820 N93-15599

TOPOGRAPHY
Is Ishtar Terra a thickened basaltic crust? p 1024 N93-14292
Shield fields: Concentrations of small volcanic edifices on Venus p 1024 N93-14295
Coldspots or hotspots? The origin of plateau-shaped highlands on Venus p 1025 N93-14298
Monte Carlo modeling of the resurfacing of Venus p 1025 N93-14299
Determining stress states using dike swarms: The Lauma Dorsa example p 1028 N93-14319
Venusian sinuous rilles p 1033 N93-14337
Derivation of surface properties from Magellan altimetry data p 1033 N93-14340
Wrinkle ridges on Venusian plains: Indicators of shallow crustal stress orientations at local and regional scales p 1034 N93-14343
Magellan stereo images and Venusian geology p 1035 N93-14347
Flexural models of trench/outer rise topography of coronae on Venus with axisymmetric spherical shell elastic plates p 1036 N93-14348
Application of left- and right-looking SAR stereo to depth measurements of the Ammavaru outflow channel, Lada Terra, Venus p 1038 N93-14357
Geoid, topography, and convection-driven crustal deformation on Venus p 1042 N93-14376
The spatial distribution of coronae on Venus p 1043 N93-14383
Structural characteristics and tectonics of northeastern Tellus Regio and Meni Tessera p 1044 N93-14389
Finite amplitude gravity waves in the Venus atmosphere generated by surface topography p 1044 N93-14395
Terrain visualization for the portable all-source analysis work station
[AD-A255708] p 905 N93-14430
Assimilation of altimeter topography into oceanic models p 927 N93-14972
Studies of tropical ocean dynamics using the TOPEX/Poseidon altimeter-derived sea surface topography p 928 N93-14980
Ocean topography mapping, improvement of the marine geoid, and global permanent ocean circulation studies from TOPEX/Poseidon altimeter data p 928 N93-14981
General circulation of the South Atlantic between 5 deg N and 35 deg S p 929 N93-14987
Ocean dynamics in the Nordic Seas using satellite altimetry p 930 N93-14988
An integrated research program for TOPEX/Poseidon with emphasis on the Pacific Ocean p 931 N93-14995
The determination and interpretation of ocean surface topography using TOPEX/Poseidon altimeter data p 931 N93-14997
Adaptive mesh in visualization of terrain elevation data
[AD-A255481] p 906 N93-15007
Automated interpretation of topographic maps
[AD-A257040] p 906 N93-15364

TOPOLOGY
The object instancing paradigm for linear fractal modeling p 956 N93-15559

TOROIDAL PLASMAS
Fine structure of auroral particle acceleration p 912 N93-14121
The sulfur emission and periodicity of the Jupiter plasma torus in 1988 p 1022 N93-14156
Plasma confinement theory and transport simulation
[DE92-040523] p 988 N93-15327
Exact analytical solution of the toroidal singular mode equations
[DE92-040223] p 988 N93-15419

TORQUE
Turbulent drag and transport in high Reynolds number Couette-Taylor flow p 872 N93-14119
Thermal elastic shock and its effect on spacecraft attitude control p 818 N93-14837

TORQUE SENSORS (ROBOTICS)
CAD-based off-line programming and sensor signal processing in robotics
[F-2-2] p 949 N93-15299

TORQUEMETERS
Turbulent drag and transport in high Reynolds number Couette-Taylor flow p 872 N93-14119

TORSION
Finite element analysis of elastic fracture under unsteady translational and rotational loading p 899 N93-14469
Use of the thin-walled torsion specimen
[AD-A255593] p 901 N93-14790
Engine life assessment test case TF41 LP compressor shaft torsional fatigue p 799 N93-14896

TORSIONAL STRESS
Validation of an automated torsional and warping stress analysis program
[AD-A256035] p 902 N93-15260

TOTAL QUALITY MANAGEMENT
TQM in a test environment p 823 N93-15620

TOUCH
An active tactile perception system p 805 N93-14926

TOUGHNESS
Characterizing longitudinal splitting and delamination fracture toughness of composites p 831 N93-14607

TOWED BODIES
Modeling and control of a trailing wire antenna towed by an orbiting aircraft
[AD-A256450] p 859 N93-14610

TOXICITY
Low toxicity high temperature PMR polyimide
[NASA-CASE-LAR-14639-1] p 849 N93-14709

TRACE CONTAMINANTS
Geographical distribution and seasonal variation of surface emissions and deposition velocities of atmospheric trace gases
[AERONOMICA-ACTA-A-361-1991] p 911 N93-15460

TRACKING (POSITION)
Use of kinematic constraint in tracking constant speed maneuvering targets
[AD-A255988] p 858 N93-14415
Intelligent path prediction for vehicular travel p 961 N93-14445
Two-stage target tracking system and method
[AD-D015412] p 982 N93-14880
New methods for nonlinear tracking and nonlinear chaotic signal processing
[AD-A256421] p 862 N93-15334
Diffraction analysis and evaluation of several focus- and track-error detection schemes for magneto-optical disk systems p 984 N93-15506

TRACKING PROBLEM
Optimal and robust control of robot manipulators p 890 N93-14685

TRACKING STATIONS
Terrestrial reference systems related to the TOPEX/Poseidon project p 906 N93-14967
Present-day plate motions: Retrieval from the TOPEX/Poseidon orbitography network (DORIS system) p 918 N93-14993

TRACTION
Damage and rupture of ceramic composites
[ETN-92-92722] p 851 N93-15127

TRAILING EDGES
Direct prediction of a separation boundary for aerofoils using a viscous-coupled calculation method
[ESDU-92008] p 780 N93-14516
Unsteady flow distortion past blades: Sources of noise generation in rotating flows
[AD-A255496] p 880 N93-15652

TRAINING ANALYSIS
F/FB-111 avionics test station and component specialist/technician. Automatic test stations manual and electronic warfare test stations. Training requirements analysis (451X6), volume 2
[AD-A252121] p 793 N93-14110

TRAINING SIMULATORS
Audio detection algorithms
[AD-A256076] p 973 N93-14234

TRAJECTORIES
Interplanetary Program to Optimize Simulated Trajectories (IPOST). Volume 3: Programmer's manual
[NASA-CR-189653-VOL-3-REV] p 815 N93-14730

TRAJECTORY ANALYSIS
Interplanetary program to optimize simulated trajectories (IPOST). Volume 4: Sample cases
[NASA-CR-189653-VOL-4] p 815 N93-14768
Methodology for robot capability and performance characterization: The basis for robot task planningg
[F-2-3] p 949 N93-15300

Planning of continuous path robotic motions by discrete time optimization
[F-3-5] p 950 N93-15305
Time-optimization of point-to-point robotic motions
[F-3-6] p 950 N93-15306
The trajectory analysis of bevel planetary gear trains
[DE92-040898] p 893 N93-15380

TRAJECTORY CONTROL
Theory and applications of hyper-redundant robotic manipulators p 892 N93-15104
Planning of continuous path robotic motions by discrete time optimization
[F-3-5] p 950 N93-15305

TRAJECTORY OPTIMIZATION
Optimal and robust control of robot manipulators p 890 N93-14685
Interplanetary Program to Optimize Simulated Trajectories (IPOST). Volume 1: User's guide
[NASA-CR-189653-VOL-1-REV] p 815 N93-14794
Optimal impulsive trajectories for orbital rendezvous between elliptic orbits p 813 N93-15103
Planning of continuous path robotic motions by discrete time optimization
[F-3-5] p 950 N93-15305
Time-optimization of point-to-point robotic motions
[F-3-6] p 950 N93-15306
Aspects of parking orbit selection in a manned Mars mission
[NASA-TP-3256] p 813 N93-15367

TRAJECTORY PLANNING
Decision-making for intelligent control of dual-arm robotic operations p 960 N93-14201
Robust control of a flexible link robot and rigid link robot: Theory, simulation, and experiment p 888 N93-14202
A concurrent real-time autonomous mobile robot programming system p 960 N93-14281
Global optimum path planning for a redundant space robot
[AD-A255316] p 889 N93-14545
Dynamics and control of a rigid/flexible manipulator p 890 N93-14684
Methodology for robot capability and performance characterization: The basis for robot task planningg
[F-2-3] p 949 N93-15300
Planning of continuous path robotic motions by discrete time optimization
[F-3-5] p 950 N93-15305
Adaptive control of a manipulator in cartesian space
[F-4-2] p 950 N93-15308
A plan for spacecraft automated rendezvous
[NASA-TM-108385] p 813 N93-15392

TRANSFER FUNCTIONS
Deterministic transfer function for transionospheric propagation
[DE92-040327] p 862 N93-15427

TRANSFORMATIONS (MATHEMATICS)
An energy analysis of the pseudo Wigner-Ville distribution in support of machinery monitoring and diagnostics
[AD-A256202] p 889 N93-14499
From data structure to process structure
[MEMO-INF-91-38] p 946 N93-15077
Compactness and Loewenheim-Skolem properties in pre-institution categories
[MEMO-INF-92-27] p 968 N93-15094
Graph rewriting using a single pushout; a comparison
[MEMO-INF-92-28] p 968 N93-15121
Performing in-place affine transformations in constant space p 954 N93-15546

TRANSFORMERS
Extended surface heat sinks for electronic components: A computer optimization
[AD-A256134] p 865 N93-14254

TRANSIENT HEATING
Advances in TMG p 811 N93-14956

TRANSIENT PRESSURES
Unsteady pressure loads in a generic high speed engine model
[NASA-TP-3189] p 975 N93-15391

TRANSIENT RESPONSE
Transient response of a viscous liquid bridge of finite length and anchored edges
[LRT-WE-9-FB-25-1991] p 878 N93-15132

TRANSITION METALS
Electronically active cyclocarborane-metal-arene assemblies
[AD-A256288] p 865 N93-14457

TRANSLATING
A guide to EDI translation software
[AD-A255739] p 1007 N93-15051

TRANSMISSION LINES
Optical fibers for long-haul transmission in severe-bending applications
[AD-A255964] p 981 N93-14407
Development of an expendable particle sensor
[AD-A255702] p 881 N93-14653
Layered parallel interface for an active antenna array
[AD-D015411] p 860 N93-14879
Joint HVAC transmission EMF environmental study
[DE92-017863] p 933 N93-15211
Measurements of electric and magnetic fields in the Waianae, Hawaii area
[DE92-019891] p 861 N93-15220
Research for electric energy systems
[DE92-040076] p 870 N93-15412
Development of a 500 GHz optoelectronic modulator using superconducting transmission lines
[AD-A257062] p 871 N93-15456

TRANSMISSION LOSS
Optical fibers for long-haul transmission in severe-bending applications
[AD-A255964] p 981 N93-14407
Acoustic propagation loss predictions for a site on the Bermuda Rise at low and very low frequencies
[AD-A255445] p 925 N93-14512
Energy loss analysis of an integrated space power distribution system
[NASA-TM-105772] p 854 N93-14834

TRANSMISSIONS (MACHINE ELEMENTS)
The trajectory analysis of bevel planetary gear trains
[DE92-040898] p 893 N93-15380

TRANSMITTANCE
Cesium iodide alloys
[DE92-019818] p 845 N93-14717

TRANSMITTERS
Biophysical and biochemical mechanisms in synaptic transmitter release
[AD-A256340] p 936 N93-15198

TRANSONIC FLIGHT
Pressure distribution for the wing of the YAV-8B airplane; with and without pylons
[NASA-TM-4429] p 779 N93-14451

TRANSONIC FLOW
Transonic flow calculations for a cavity with and without a store
[AD-A255954] p 873 N93-14421
Pressure drag and lift contributions for blunted forebodies of fineness ratio 2.0 in transonic flow (M infinity less than or equal to 1.4)
[ESDU-89033] p 779 N93-14515
Direct prediction of a separation boundary for aerofoils using a viscous-coupled calculation method
[ESDU-92008] p 780 N93-14516
Time-dependent predictions and analysis of turbine cascade data in the transonic flow region
[PNR-90957] p 782 N93-15489

TRANSPARENCE
Determination of stresses on laminated aircraft transparencies by the strain gage-hole drilling and sectioning method
[AD-A255548] p 791 N93-14571
New electronic materials
[AD-A255612] p 868 N93-15010
New nonlinear optical film processing
[AD-A256011] p 983 N93-15255

TRANSPONDERS
On the performance of Trellis coded modulation with octal phase shift keying over the TDRSS channel
[NASA-CR-191366] p 857 N93-14155

TRANSPORT AIRCRAFT
Ice accretion prediction for a typical commercial transport aircraft
[NASA-TM-105976] p 788 N93-15522

TRANSPORT PROPERTIES
Characterization of magneto-optical recording media p 979 N93-14140
Electronic, vibrational, and transport properties of conducting polymers p 847 N93-14170
Macroscopic properties of random and quasiperiodic media
[AD-A255984] p 990 N93-14413
Electron-phonon interaction, transport and ultrafast processes in semiconductor microstructures
[AD-A255723] p 976 N93-14433
A quasi-equilibrium kinetic model of HF air breakdown
[AD-A256240] p 859 N93-14453
Numerical modelling of intense electron beam transport in the spiral line induction accelerator
[AD-A255545] p 978 N93-14570
Current neutralization in ballistic transport of light ion beams
[AD-A256070] p 976 N93-14662
Thermodynamics and transport in Ce3Bi4Pt3 and related compounds
[DE92-040377] p 998 N93-14905

TRANSPORT THEORY
The theory and numerical simulation of non-local mixing-length convection p 1015 N93-14147
PDF transport modelling p 840 N93-14623
Plasma confinement theory and transport simulation
[DE92-040523] p 988 N93-15327
Theoretical and numerical studies in magnetic fusion
[DE92-040674] p 988 N93-15349

TRANSPORTATION
A guide to EDI translation software
[AD-A255739] p 1007 N93-15051

TRANSPUTERS
A deadlock-free communication system for a transputer network
[AD-A256473] p 959 N93-15319

TRANSURANIUM ELEMENTS
Studies of heavy-ion reactions and transuranic nuclei
[DE92-040457] p 977 N93-15326

TRANSVERSE LOADS
Delamination growth behavior in cross-ply laminated composites due to transverse concentrated loading
[AD-A255974] p 830 N93-14493

TRAPPING
Beam trapping in a modified betatron with a localized bipolar electric field pulse
[AD-A255414] p 866 N93-14504
Energy distribution of trapped holes in irradiated SiO2
[DE92-040979] p 997 N93-15649

TRAVELING WAVE TUBES
User's guide for a large signal computer model of the helical traveling wave tube
[NASA-TP-3251] p 871 N93-15531

TRAVELING WAVES
Direct optical to microwave conversion
[RL-TR-91-375] p 859 N93-14728

TREES (MATHEMATICS)
Interactive solid geometry via partitioning trees p 952 N93-15535
Partitioning tree image representation and generation from 3D geometric models p 955 N93-15557
A distributed data-balanced dictionary based on the b-link tree
[AD-A256841] p 1009 N93-15639

TRELLIS CODING
On the performance of Trellis coded modulation with octal phase shift keying over the TDRSS channel
[NASA-CR-191366] p 857 N93-14155
High-speed architecture for the decoding of trellis-coded modulation
[NASA-CR-191374] p 941 N93-14770
On the theory of coded modulation systems for high output digital transmission
[TELECOM-PARIS-92-E-001] p 861 N93-15098

TRIANGULATION
An implementation of multivariate B-spline surfaces over arbitrary triangulations p 952 N93-15534

TRIBOLOGY
Tribology of magnetic storage systems p 1002 N93-14772
Tribology of improved transformation-toughened ceramics-heat engine test
[DE92-041385] p 851 N93-15295
Exceptionally high-strength (approximately 3 GPa) aluminum alloys demonstrated by oxygen ion implantation
[DE92-040980] p 847 N93-15383
Development of wear-resistant ceramic coatings for diesel engine components
[DE92-041382] p 853 N93-15439
The effect of processing and compositional changes on the tribology of PM212 in air
[NASA-TM-105945] p 828 N93-15576

TRIENES
Thermal conductivity of liquid aliphatic hydrocarbons. Part 2: Alkenes, dienes and trienes
[ESDU-92025] p 839 N93-14542

TRIMERS
Gallium and indium compounds containing three different substituents. Crystal and molecular structure of ((Me3 CCH2)ClGaPPh2)3
[AD-A257049] p 996 N93-15443

TRIMETHYL COMPOUNDS
Thermal stability of trimethyl indium on Si(100)-2 x 1 as studied with HREELS, UPS, and XPS: A comparison with the results from Si(111)-7 x 7 and Si(110) studies
[AD-A255242] p 992 N93-14670

TRITON
Complete analytical theory for the satellites of Neptune p 1046 N93-14833

TROPICAL METEOROLOGY
Simulations of the Amazon Basin circulation using the Pennsylvania State University/National Center for Atmospheric Research mesoscale model p 919 N93-14197
The preferred latitudes of the Intertropical Convergence Zone: Observations and theory p 920 N93-14213
Low-frequency oscillations in radiative-convective models
[DE92-018779] p 922 N93-14901

TROPICAL REGIONS
Cloud-radiative feedbacks in tropical convection p 919 N93-14180

A numerical study of the middle atmosphere response to tropical and subtropical tropospheric heat sources p 920 N93-14640
Low-frequency oscillations in radiative-convective models p 915 N93-14874
North-Australian tropical seas circulation study p 926 N93-14968
Sea level response to wind forcing in the tropical Atlantic p 928 N93-14977
Studies of tropical ocean dynamics using the TOPEX/Poseidon altimeter-derived sea surface topography p 928 N93-14980
Study of mass and heat transport of the tropical Atlantic Ocean using models and altimeter data p 929 N93-14983
Application of TOPEX/Poseidon altimetry measurements to observational and modeling studies of the low-frequency upper ocean mass and heat circulation in the tropical Pacific p 930 N93-14989
Degradation and failure modes of carbon/bismaleimide laminates subjected to a tropical exposure [AD-A256328] p 836 N93-15193
Spatial and temporal patterns of biotic exchanges of CO2 between the atmosphere and tropical landscapes and their role in the global carbon balance [DE92-019170] p 911 N93-15272

TROPICAL STORMS
The influence of baroclinic processes on tropical cyclone motion p 923 N93-15099

TROPOSPHERE
The isotopes of carbon monoxide in the free troposphere and their implications to atmospheric chemistry p 913 N93-14207
A numerical study of the middle atmosphere response to tropical and subtropical tropospheric heat sources p 920 N93-14640

TRUSSES
Damage location and model refinement for large flexible space structures using a sensitivity-based eigenstructure assignment method p 816 N93-14274
Model reduction of flexible manipulators [AD-A255251] p 889 N93-14528
Structurally adaptive space crane concept for assembling space systems on orbit [NASA-TP-3307] p 818 N93-15368

TUNABLE LASERS
Compact free electron laser for medical applications [AD-A256236] p 885 N93-14599
Level-mixing assisted tunability of nuclear resonance linewidths for gamma ray lasers [AD-A255791] p 885 N93-14647
Threshold photodetachment spectroscopy [AD-A255278] p 842 N93-14671
Abstracts booklet [AD-A256115] p 869 N93-15188

TUNGSTEN
Determination of operable deformation mechanisms during ballistic impact in tungsten single crystals, utilizing transmission electron microscopy [AD-A255351] p 991 N93-14518

TUNGSTEN ALLOYS
Strain-rate effects in replica scale model penetration experiments [AD-A255426] p 844 N93-14508
Progress toward a tungsten alloy wire/high temperature alloy composite turbine blade [NASA-TM-105901] p 847 N93-15586

TUNING
Compact free electron laser for medical applications [AD-A256236] p 885 N93-14599

TURBINE BLADES
Fatigue in single crystal nickel superalloys [AD-A256095] p 844 N93-14264
Multi-point inverse design of isolated airfoils and airfoils in cascade in incompressible flow p 790 N93-14462
SAPNEW: Parallel finite element code for thin shell structures on the Alliant FX-80 [NASA-CR-189212] p 901 N93-14799
In-service considerations affecting component life p 800 N93-14898
Progress toward a tungsten alloy wire/high temperature alloy composite turbine blade [NASA-TM-105901] p 847 N93-15586
Prediction of turbine cascade flows with a quasi-three-dimensional rotor viscous code and the extension of the algebraic turbulence model [AD-A256831] p 880 N93-15635

TURBINE WHEELS
Propulsion and Energetics Panel Working Group 20 on Test Cases for Engine Life Assessment Technology [AGARD-AR-308] p 798 N93-14890
Introduction to test cases for engine life assessment technology p 799 N93-14891
LARZAC HP turbine disk crack initiation and propagation spin pit test p 799 N93-14892
RB211-524B disc and drive cones hot cyclic spinning test p 799 N93-14895
F100 second stage fan disk bolthole crack propagation ferris wheel test p 800 N93-14897

TURBINES
L.D.V. measurements of unsteady flow fields in radial turbine [AD-A255728] p 878 N93-15065
Prediction of turbine cascade flows with a quasi-three-dimensional rotor viscous code and the extension of the algebraic turbulence model [AD-A256831] p 880 N93-15635

TURBOCOMPRESSORS
An experimental and analytical study of TIP clearance effects in axial flow compressors [AD-A256434] p 800 N93-15337

TURBOFAN ENGINES
SAPNEW: Parallel finite element code for thin shell structures on the Alliant FX-80 [NASA-CR-189212] p 901 N93-14799

TURBOFANS
Investigations of detail design issues for the high speed acoustic wind tunnel using a 60th scale model tunnel. Part 2: Tests with the closed circuit [NASA-CR-191672] p 780 N93-14738
Acoustic mode measurements in the inlet of a model turbofan using a continuously rotating rake: Data collection/analysis techniques [NASA-TM-105936] p 801 N93-15403

TURBOMACHINE BLADES
Time-dependent predictions and analysis of turbine cascade data in the transonic flow region [PNR-90957] p 782 N93-15489

TURBOMACHINERY
SAPNEW: Parallel finite element code for thin shell structures on the Alliant FX-80 [NASA-CR-189212] p 901 N93-14799

TURBOSHAFTS
Experimental analysis of steady-state and dynamic monitoring of power shaft turbines p 796 N93-15176

TURBULENCE
Turbulence and chaos in classical and quantum systems p 972 N93-14144
L.D.V. measurements of unsteady flow fields in radial turbine [AD-A255728] p 878 N93-15065
Dynamics systems applied to Navier-Stokes equations for the study of turbulence [ETN-92-92553] p 878 N93-15122

TURBULENCE EFFECTS
A simulation model of atmospheric turbulence for rotorcraft applications p 920 N93-14588
Second order closure modeling of turbulent buoyant wall plumes [NASA-TM-105956] p 877 N93-14829
Turbulent fluid motion IV-averages, Reynolds decomposition, and the closure problem [NASA-TM-105822] p 880 N93-15585

TURBULENCE MODELS
An algebraic turbulence model for three-dimensional viscous flows [NASA-TM-105931] p 777 N93-14102
Wall layers [AD-A256152] p 872 N93-14257
Modeling of Combustion and Turbulence [VKI-LS-1992-03] p 839 N93-14617
Turbulence modeling for combustion flows p 840 N93-14620
Applications of PDF turbulent combustion models to real non premixed flame calculations p 841 N93-14624
Calculation of chemical reaction rates in turbulent combustion p 841 N93-14625
Wave drag in the atmospheric boundary layer p 915 N93-14873
On explicit algebraic stress models for complex turbulent flows [NASA-CR-189725] p 879 N93-15481
Prediction of turbine cascade flows with a quasi-three-dimensional rotor viscous code and the extension of the algebraic turbulence model [AD-A256831] p 880 N93-15635

TURBULENT BOUNDARY LAYER
Wall layers [AD-A256152] p 872 N93-14257
A numerical investigation of the interaction between crossing oblique shocks and a turbulent boundary layer p 876 N93-14695
Supersonic boundary-layer flow turbulence modeling [NASA-TM-105893] p 877 N93-14758
Modeling variable blowing on a slender cone in hypersonic flow p 781 N93-14836
Unsteady pressure loads in a generic high speed engine model [NASA-TP-3189] p 975 N93-15391
Finite-difference solution for laminar or turbulent boundary layer flow over axisymmetric bodies with ideal gas, CF4, or equilibrium air chemistry [NASA-TP-3271] p 879 N93-15434

TURBULENT FLOW
Turbulent drag and transport in high Reynolds number Couette-Taylor flow p 872 N93-14119
Control of asymmetric jet [AD-A255967] p 873 N93-14400
Feedback control of flow separation and transition to turbulence in unsteady boundary layers p 873 N93-14464
Control of low-speed turbulent separated flow over a backward-facing ramp p 874 N93-14475
Boundary layer transition measurements by optical anemometry p 874 N93-14477
Exploiting similarity in turbulent shear flows for turbulence modeling [NASA-CR-191621] p 875 N93-14481
Turbulence modeling for combustion flows p 840 N93-14620
Direct simulation of turbulent combustion p 840 N93-14622
Calculation of chemical reaction rates in turbulent combustion p 841 N93-14625
Optical monitor for observing turbulent flow [DE92-019831] p 876 N93-14715
Chemical reactions in turbulent mixing flows [AD-A256004] p 842 N93-15114
Dynamics systems applied to Navier-Stokes equations for the study of turbulence [ETN-92-92553] p 878 N93-15122
Spatio-temporal complexity and large-scale structures in problems of continuum mechanics [AD-A256410] p 998 N93-15333
Finite-difference solution for laminar or turbulent boundary layer flow over axisymmetric bodies with ideal gas, CF4, or equilibrium air chemistry [NASA-TP-3271] p 879 N93-15434
On explicit algebraic stress models for complex turbulent flows [NASA-CR-189725] p 879 N93-15481
Turbulent fluid motion IV-averages, Reynolds decomposition, and the closure problem [NASA-TM-105822] p 880 N93-15585

TURBULENT JETS
Chemical reactions in turbulent mixing flows [AD-A256004] p 842 N93-15114

TURBULENT MIXING
The theory and numerical simulation of non-local mixing-length convection p 1015 N93-14147
Chemical reactions in turbulent mixing flows [AD-A256004] p 842 N93-15114
Computation of supersonic jet noise under imperfectly expanded conditions [NASA-TM-105961] p 975 N93-15430

TURBULENT WAKES
An experimental investigation of base bleed effect on the wake turbulent structure behind a two-dimensional blunt model [MPIS-9/1991] p 781 N93-15131

TURING MACHINES
Processor controlpath microarchitecture synthesis based on the A(asterisk) algorithm [MEMO-INF-92-10] p 963 N93-15083
Automated coding and intersecting cube theory [ETN-92-92675] p 941 N93-15123

TVD SCHEMES
Eno-Osher schemes for Euler equations [NASA-TM-105928] p 969 N93-15341

TWO DIMENSIONAL BODIES
Wake similarity and vortex formation for two-dimensional bluff bodies p 781 N93-15101

TWO DIMENSIONAL FLOW
An investigation of genuinely multidimensional schemes for the Euler equations p 876 N93-14694
BLSTA: A boundary layer code for stability analysis [NASA-CR-4481] p 877 N93-14797
Supersonic investigation of two dimensional hypersonic exhaust nozzles [NASA-TM-105687] p 800 N93-15342

TWO DIMENSIONAL MODELS
The method of minimal representations in 2D Ising model calculations [AD-A256581] p 967 N93-14270
Analysis of projections of the transfer matrix in 2D Ising models [AD-A256583] p 967 N93-14271
An investigation into the role of moist, vertical drafts in the rotational development of storms p 923 N93-15087
An experimental investigation of base bleed effect on the wake turbulent structure behind a two-dimensional blunt model [MPIS-9/1991] p 781 N93-15131

Progress on the development of a 2-D PIC/Monte Carlo model of glow discharges
| DE92-040226 | p 989 N93-15422
Nonlinear finite element analysis of metals and metal matrix composites: A local-global investigation
| AD-A256782 | p 838 N93-15625

TWO FLUID MODELS
Numerical study of mixing of two fluids under low gravity
| NASA-TM-105865 | p 878 N93-14914

TWO PHASE FLOW
Adiabatic two-phase flow in a test section with partial flow blockages
| DE92-016360 | p 877 N93-14816

U

UH-60A HELICOPTER
A simulation model of atmospheric turbulence for rotorcraft applications p 920 N93-14588

ULTRASONIC FLAW DETECTION
Remote techniques for time-of-flight flaw characterisation p 989 N93-14171

ULTRASONIC RADIATION
Remote techniques for time-of-flight flaw characterisation p 989 N93-14171

ULTRASONIC TESTS
Elastic wave scattering by partially debonded or partially coated fibers p 829 N93-14224
Advanced research in instrumentation and diagnostics technology
| DE92-041121 | p 883 N93-15411

ULTRASONIC WAVE TRANSDUCERS
The use of ultrasonics for oleo compression measurements on a S-70B-2 (Seahawk) helicopter
| AD-A256315 | p 792 N93-15328

ULTRASONICS
Innovative techniques for studying new materials and new developments in solid state physics
| AD-A256394 | p 996 N93-15465

ULTRAVIOLET ASTRONOMY
Ultraviolet spectra of stars and stellar systems p 1011 N93-14593

ULTRAVIOLET LASERS
Development of laser-ion beam photodissociation methods
| DE92-040512 | p 886 N93-15058

ULTRAVIOLET PHOTOGRAPHY
Comparison of Viking Ultraviolet images with low altitude particle precipitation p 1045 N93-14612

ULTRAVIOLET RADIATION
Generation of broadly tunable, narrow bandwidth, and intense coherent vacuum ultraviolet radiation in rare gases p 980 N93-14167
Ultraviolet-ozone cleaning of semiconductor surfaces, revision 1
| AD-A256158 | p 842 N93-14678
Simulation of the synergistic low Earth orbit effects of vacuum thermal cycling, vacuum UV radiation, and atomic oxygen p 819 N93-15595

ULTRAVIOLET SPECTRA
SO2 in the middle atmosphere of Venus: IR measurements from Venera 15 and comparison to UV p 1045 N93-14397
Ultraviolet spectroscopy of Comet Austin (1989c1) using a two-dimensional diode array detector p 1017 N93-14444
Ultraviolet spectra of stars and stellar systems p 1011 N93-14593

ULTRAVIOLET SPECTROSCOPY
Ultraviolet spectroscopy of Comet Austin (1989c1) using a two-dimensional diode array detector p 1017 N93-14444
Multiwavelength spectroscopy of active galactic nuclei p 1011 N93-14611

UMBRAS
Thermal elastic shock and its effect on spacecraft attitude control p 818 N93-14837

UNCONSCIOUSNESS
Statistical analysis of the human strangulation experiments: Comparison to +Gz-induced loss of consciousness
| AD-A255485 | p 935 N93-14789

UNDERWATER ACOUSTICS
Scattering of sound by sound: Nonlinear interaction of collinear and noncollinear sound beams p 973 N93-14145
Acoustic propagation loss predictions for a site on the Bermuda Rise at low and very low frequencies
| AD-A255445 | p 925 N93-14512
Statistically calibrated transducer
| AD-D015408 | p 882 N93-14878
Experimental investigation of scattering from randomly rough plastic cylinders
| AD-A256018 | p 975 N93-15259
Surface gravity waves and ambient microseismic noise
| AD-A256498 | p 916 N93-15375

UNITED STATES
The use of International Standards Organization ISO 9000 quality assurance standards in place of military standards
| AD-A256203 | p 894 N93-14500

UNIVERSE
Dynamics in neutron stars and the early universe p 1014 N93-14112

UNIVERSITIES
Core support of the board on mathematical sciences
| AD-A255482 | p 968 N93-14787
International Space University p 808 N93-14938

UNIVERSITY PROGRAM
International Space University p 808 N93-14938

UNIX (OPERATING SYSTEM)
Requirements for a network storage service p 1003 N93-14781
A Unix print filter for controlling an HP Laserjet printer
| DE92-041350 | p 946 N93-14902
CMU common lisp user's manual
| AD-A256431 | p 950 N93-15336
Proceedings of the REXX Symposium for Developers and Users
| DE92-041359 | p 951 N93-15451

UNSTEADY AERODYNAMICS
A compilation of the mathematics leading to the doublet lattice method
| AD-A256304 | p 779 N93-14441
The effect of wake dynamics on rotor eigenvalues in forward flight p 780 N93-14595
Multi-disciplinary optimization of aeroservoelastic systems
| NASA-CR-191255 | p 901 N93-14766
Estimation of unsteady lift on a pitching airfoil from wake velocity surveys
| NASA-TM-105947 | p 781 N93-14791
White paper on the AFOSR Supermaneuverability Workshop
| AD-A256385 | p 782 N93-15464

UNSTEADY FLOW
Simulation of unsteady inviscid flow on an adaptively refined Cartesian grid p 873 N93-14273
Transonic flow calculations for a cavity with and without a store
| AD-A255954 | p 873 N93-14421
Feedback control of flow separation and transition to turbulence in unsteady boundary layers p 873 N93-14464
Numerical simulation of steady and unsteady asymmetric vortical flow p 876 N93-14691
L.D.V. measurements of unsteady flow fields in radial turbine
| AD-A255728 | p 878 N93-15065
Unsteady pressure loads in a generic high speed engine model
| NASA-TP-3189 | p 975 N93-15391
White paper on the AFOSR Supermaneuverability Workshop
| AD-A256385 | p 782 N93-15464
Unsteady shear disturbances within a two dimensional stratified flow
| NASA-CR-189121 | p 880 N93-15527
Unsteady flow distortion past blades: Sources of noise generation in rotating flows
| AD-A255496 | p 880 N93-15652

UPGRADING
Application of programmable logic controllers to space simulation p 821 N93-15608

UPWELLING WATER
Sensitivity of the Yoshida jet to the parameterization of vertical mixing: Do easterly winds imply equatorial upwelling? p 922 N93-14864

URANIUM COMPOUNDS
Normal state resistivity and the phase diagram of U(1-x)Th(x)Be13
| DE92-040236 | p 995 N93-15321

URANUS ATMOSPHERE
Revelations of a stratospheric circulation: The dynamical transport of hydrocarbons in the stratosphere of Uranus p 913 N93-14211
Ethane ice haze in the upper atmosphere of Uranus p 1023 N93-14212
Microwave observations of Uranus p 1046 N93-14863

USER MANUALS (COMPUTER PROGRAMS)
Evaluation of the cost effectiveness analysis model being developed for the component improvement programs of the Air Force and the Navy
| AD-A256132 | p 1010 N93-14249
Geographic Resources Analysis Support System (GRASS) version 4.0 user's reference manual
| AD-A255218 | p 1001 N93-14524
Computer based satellite design
| AD-A255315 | p 816 N93-14536
VANTAGE: A frame-based geometric modeling system programmer/user's manual, V2.0
| AD-A255434 | p 944 N93-14566
Vendor Information System (VIS) systems manual
| AD-A256174 | p 1002 N93-14650
Interplanetary Program to Optimize Simulated Trajectories (IPOST). Volume 3: Programmer's manual
| NASA-CR-189653-VOL-3-REV | p 815 N93-14730
Interplanetary Program to Optimize Simulated Trajectories (IPOST). Volume 1: User's guide
| NASA-CR-189653-VOL-1-REV | p 815 N93-14794
BLSTA: A boundary layer code for stability analysis
| NASA-CR-4481 | p 877 N93-14797
Automated Estimating System (AES), version 5.1. User's manual
| DE93-000380 | p 946 N93-15003
Advanced development active model: A users guide
| AD-A255614 | p 974 N93-15012
User's guide for SearchMAESTRO
| AD-A256422 | p 1008 N93-15335
CMU common lisp user's manual
| AD-A256431 | p 950 N93-15336
Automated Estimated System (AES) standard value and guidelines programs user's manual
| DE92-041243 | p 951 N93-15450
User manual for the Software Technology for Adaptable, Reliable Systems (STARS). PCTE Browser Tool (PBT) version 0.1 SunOS implementation
| AD-A257064 | p 951 N93-15457
GRASS 4.0 map digitizing user's manual: V. Digit
| AD-A256859 | p 1009 N93-15642

USER REQUIREMENTS
Information resource utilisation: Accessibility based on concerns p 1001 N93-14216
Vision system requirements and concept for the Special Purpose Dexterous Manipulator system (SPDM) p 805 N93-14924
Progress toward a full scale mobile satellite system for Canada p 812 N93-14960
L-band antenna design for MSAT mission p 812 N93-14961
The evolution of signalling from ISDN to B-ISDN
| MEMO-INF-92-30 | p 860 N93-15095
Crew requirements definition system user's guide
| AD-A257052 | p 951 N93-15445
Working together, virtually p 954 N93-15547
Designing video annotation and analysis systems p 955 N93-15552

V

V-22 AIRCRAFT
The V-22 Osprey: A case analysis
| AD-A256445 | p 791 N93-14601
Tiltrotor aircraft noise: A summary of the presentations and discussions at the 1991 FAA/Georgia Tech Workshop
| DOT/FAA/RD-91/23 | p 974 N93-14912

VACUUM
Quasars, galaxies, and pseudo-vacuum droplets
| NIKHEF-H/91-20 | p 1020 N93-14686
LARZAC HP turbine disk crack initiation and propagation spin pit test p 799 N93-14892
Interferometric measurement with squeezed light
| AD-A257065 | p 984 N93-15458

VACUUM CHAMBERS
A new thermal vacuum facility at the Martin Marietta Waterton plant p 814 N93-15607
The evolution of space simulation p 814 N93-15610
Cleaning of a thermal vacuum chamber with shrouds in place p 814 N93-15612
INTESPACE's new thermal-vacuum test facility: SIMMER p 814 N93-15613
A new approach for performing contamination control bakeouts in JPL thermal vacuum test chambers p 823 N93-15618
Mass spectrometer use in a large chamber p 823 N93-15619

VACUUM EFFECTS
Simulation of the synergistic low Earth orbit effects of vacuum thermal cycling, vacuum UV radiation, and atomic oxygen p 819 N93-15595

VACUUM PUMPS
The evolution of space simulation p 814 N93-15610
From diffusion pumps to cryopumps: The conversion of GSFC's space environment simulator p 814 N93-15611

VACUUM SYSTEMS
Cleaning of a thermal vacuum chamber with shrouds in place p 814 N93-15612

VALLEYS
Venusian sinuous rilles p 1033 N93-14337

VALVES
Thruster sealing system and apparatus
[NASA-CASE-MSC-21898-1] p 890 N93-14702
VAN DER WAALS FORCES
A global potential energy surface for ArH2
[NASA-CR-190741] p 843 N93-15358
VAPOR DEPOSITION
Twin quintuplets in CVD diamond
[AD-A255862] p 989 N93-14133
Organization of workshop on emerging technologies for in-situ processing
[AD-A255977] p 865 N93-14410
Design and hardware implementation of neural systems
[AD-A256040] p 866 N93-14577
A simple controller for repetitive cycles in atomic layer epitaxy
[AD-A255497] p 992 N93-14643
High temperature stability, interface bonding, and mechanical behavior in (beta)-NiAl and Ni3Al matrix composites with reinforcements modified by ion beam enhanced deposition
[DE92-014399] p 992 N93-14812
Si atomic layer epitaxy based on Si2H6 and remote He plasma bombardment
[AD-A255763] p 993 N93-15055
Jet vapor deposition of thin films for solid oxide and other fuel cell applications
[DE92-019980] p 851 N93-15222
Growth, characterization and device development in monocrystalline diamond films
[AD-A256283] p 994 N93-15244
High performance YBCO films
[AD-A255439] p 994 N93-15297
Development of adherent ceramic coatings to reduce contact stress damage of ceramics
[DE92-041373] p 852 N93-15437
Numerical modeling tools for chemical vapor deposition
[NASA-CR-4480] p 880 N93-15643
VAPOR PHASES
Remote fiber optic sensor for gaseous and liquid environments, phase 2
[AD-A256224] p 983 N93-15241
Molecular capacitance: Sequential electron-transfer energetics for solution-phase metallic clusters in relation to gas-phase clusters and analogous interfaces
[AD-A257057] p 977 N93-15448
VAPORIZING
Threshold photodetachment spectroscopy
[AD-A255278] p 842 N93-14671
VAPORS
Simulation of vapor compression heat pumps with solution circuits p 872 N93-14200
Long-term variations in abundance and distribution of sulfuric acid vapor in the Venus atmosphere inferred from Pioneer Venus and Magellan radio occultation studies p 1030 N93-14328
Absorption of propellant vapors into polymer films
[AD-A255274] p 849 N93-14531
VARIABILITY
Understanding the variation in the millimeter-wave emission of Venus p 1028 N93-14315
VARIANCE (STATISTICS)
A proposal to apply Taguchi-inspired methods to the reduction of machining variance
[AD-A256129] p 856 N93-15234
VARIATIONAL PRINCIPLES
Fitting microphysical observations to a numerical model through an optimal control theory technique p 924 N93-15100
The sine-Gordon model and the small (kappa)(sup +) region of light-cone perturbation theory
[DE92-040506] p 969 N93-15379
VECTOR ANALYSIS
Automated interpretation of topographic maps
[AD-A257040] p 906 N93-15364
VECTOR QUANTIZATION
Stability and adaptation of neural networks
[AD-A256227] p 962 N93-14598
VECTORS (MATHEMATICS)
The spin vector of Venus determined from Magellan data p 1027 N93-14310
VEGETATION GROWTH
The production and use of aeroponically grown inocula of VAM fungi in the native plant nursery
[PB92-204973] p 933 N93-15208
Comparison of the prevalence index and average wetland values for identification of wetland vegetation
[DE92-016701] p 910 N93-15209
VEGETATIVE INDEX
Comparison of the prevalence index and average wetland values for identification of wetland vegetation
[DE92-016701] p 910 N93-15209
VEHICLES
Intelligent path prediction for vehicular travel p 961 N93-14445
VELOCITY DISTRIBUTION
Lineshape analysis of laser light scattered by an argon thermal plasma jet p 987 N93-14137
Calibration of the CCD Tully-Fisher relation with application to the Perseus-Pisces supercluster p 1016 N93-14194
Venus mesospheric winds and the carbon monoxide bulge p 1029 N93-14320
Finite amplitude gravity waves in the Venus atmosphere generated by surface topography p 1044 N93-14395
Multi-point inverse design of isolated airfoils and airfoils in cascade in incompressible flow p 790 N93-14462
Unsteady shear disturbances within a two dimensional stratified flow
[NASA-CR-189121] p 880 N93-15527
VELOCITY MEASUREMENT
Boundary layer transition measurements by optical anemometry p 874 N93-14477
Second order closure modeling of turbulent buoyant wall plumes
[NASA-TM-105956] p 877 N93-14829
VENERA SATELLITES
Venus radar mapping from the Venera 15 and 16 spacecrafts: Results and restrictions p 1023 N93-14289
The geology of the Venera/Vega landing sites p 1024 N93-14296
The geologic mapping of Venus using C-1 format: Sheets 75N254, 60N263 p 1041 N93-14375
VENUS (PLANET)
Papers presented to the International Colloquium on Venus
[NASA-CR-190676] p 1023 N93-14288
Venus radar mapping from the Venera 15 and 16 spacecrafts: Results and restrictions p 1023 N93-14289
Ringed impact craters on Venus: An analysis from Magellan images p 1024 N93-14291
Constraints on the thermal evolution of Venus inferred from Magellan data p 1024 N93-14293
Surface processes on Venus p 1024 N93-14294
Shield fields: Concentrations of small volcanic edifices on Venus p 1024 N93-14295
The geology of the Venera/Vega landing sites p 1024 N93-14296
Global deformation on the surface of Venus p 1024 N93-14297
Coldspots or hotspots? The origin of plateau-shaped highlands on Venus p 1025 N93-14298
Monte Carlo modeling of the resurfacing of Venus p 1025 N93-14299
Debris avalanches and slumps on the margins of volcanic domes on Venus: Characteristics of deposits p 1025 N93-14300
Mixed-valence iron minerals on Venus: Fe(2+)-Fe(3+) oxides and oxy-silicates formed by surface-atmosphere interactions p 1025 N93-14301
Thermal buoyancy on Venus: Preliminary results of finite element modeling p 1025 N93-14302
Erosion versus construction: The origin of Venusian channels p 1025 N93-14303
Polarization properties and Earth-based radar measurements of Venus in the post-Magellan era p 1026 N93-14304
Bright crater outflows: Possible emplacement mechanisms p 1026 N93-14305
Image processing and products for the Magellan mission to Venus p 1026 N93-14306
Near-infrared oxygen airglow from the Venus nightside p 1026 N93-14308
Global correlation of volcanic centers on Venus with uplands and with extension: Influence of mantle convection and altitude p 1026 N93-14309
The spin vector of Venus determined from Magellan data p 1027 N93-14310
Monte Carlo computer simulations of Venus equilibrium and global resurfacing models p 1027 N93-14311
Methane measurement by the Pioneer Venus large probe neutral mass spectrometer p 1027 N93-14312
Visoelastic relaxation of Venusian coronae and mountain belts: Constraints on global heat flow and tectonism p 1027 N93-14313
Flexural analysis of uplifted rift flanks on Venus p 1027 N93-14314
Understanding the variation in the millimeter-wave emission of Venus p 1028 N93-14315
Radar scattering properties of pancakelike domes on Venus p 1028 N93-14316
Sequential deformation of plains along Tessera boundaries on Venus: Evidence from Alpha Regio p 1028 N93-14317
Venusian hydrology: Steady state reconsidered p 1028 N93-14318
Determining stress states using dike swarms: The Lauma Dorsa example p 1028 N93-14319
Venus mesospheric winds and the carbon monoxide bulge p 1029 N93-14320
Tectonics and volcanism of Eastern Aphrodite Terra: No subduction, no spreading p 1029 N93-14321
Western Aphrodite Terra, tectonics, geology, and line-of-sight gravity p 1029 N93-14322
Venus volcanism: A global overview from Magellan data p 1029 N93-14323
Chemical differentiation on one-plate planets: Predictions and geologic observations for Venus p 1029 N93-14324
Venus: The case for a wet origin and a runaway greenhouse p 1031 N93-14331
Venus internal magnetic field and its interaction with the interplanetary magnetic field p 1032 N93-14336
The solar wind interaction with Venus p 1034 N93-14341
Estimates of elastic plate thicknesses beneath large volcanos on Venus p 1035 N93-14344
Chemical differentiation of a convecting planetary interior: Consequences for a one-plate planet such as Venus p 1038 N93-14358
Tectonic connections to interior processes on Venus p 1039 N93-14361
The effects of Venus' thermal structure on buoyant magma ascent p 1040 N93-14366
Overview of Venus geology: Preliminary description of terrain units for Venus global geological mapping p 1040 N93-14368
Magellan project p 1041 N93-14373
Atla Regio, Venus: Geology and origin of a major equatorial volcanic rise p 1041 N93-14374
The geologic mapping of Venus using C-1 format: Sheets 75N254, 60N263 p 1041 N93-14375
Venus gravity: Summary and coming events p 1042 N93-14377
Different types of small volcanos on Venus p 1042 N93-14378
Constraints on crustal rheology and age of deformation from models of gravitational spreading in Ishtar Terra, Venus p 1042 N93-14379
Multiresolution pattern recognition of small volcanos in Magellan data p 1042 N93-14380
Melting and differentiation in Venus with a cold start: A mechanism of the thin crust formation p 1042 N93-14381
The tectonics of Venus: An overview p 1042 N93-14382
The spatial distribution of coronae on Venus p 1043 N93-14383
Microwave scattering and emission properties of large impact craters on the surface of Venus p 1043 N93-14384
The effects of Venusian mantle convection with multiple phase transitions p 1043 N93-14385
Evidence for lightning on Venus p 1043 N93-14386
Can a time-stratigraphic classification system be developed for Venus? p 1043 N93-14388
Structural characteristics and tectonics of northeastern Tellus Regio and Meni Tessera p 1044 N93-14389
Episodic plate tectonics on Venus p 1044 N93-14390
Low-emissivity impact craters on Venus p 1044 N93-14392
Floor-fractured crater models for igneous crater modification on Venus p 1044 N93-14393
Venus: Geochemical conclusions from the Magellan data p 1044 N93-14394
Middle atmosphere of Venus and its clouds: Latitude and solar time variations p 1045 N93-14396
SO2 in the middle atmosphere of Venus: IR measurements from Venera 15 and comparison to UV p 1045 N93-14397
Outgassing history of Venus and the absence of water on Venus p 1045 N93-14398
Study and interpretation of the millimeter-wave spectrum of Venus p 1045 N93-14596
Sulfur oxides in the middle atmosphere of Venus: Observations by the International Ultraviolet Explorer and sounding rockets p 1046 N93-14635
Interferometric observations of the J(0,1) CO line on Venus: Upper mesospheric winds and CO abundance p 1047 N93-14918
VENUS ATMOSPHERE
Papers presented to the International Colloquium on Venus
[NASA-CR-190676] p 1023 N93-14288
Local-time asymmetries in the Venus thermosphere p 1023 N93-14290
Mixed-valence iron minerals on Venus: Fe(2+)-Fe(3+) oxides and oxy-silicates formed by surface-atmosphere interactions p 1025 N93-14301
The thermosphere and ionosphere of Venus p 1026 N93-14307

Near-infrared oxygen airglow from the Venus nightside p 1026 N93-14308
Methane measurement by the Pioneer Venus large probe neutral mass spectrometer p 1027 N93-14312
Visoelastic relaxation of Venusian coronae and mountain belts: Constraints on global heat flow and tectonism p 1027 N93-14313
Understanding the variation in the millimeter-wave emission of Venus p 1028 N93-14315
Venus mesospheric winds and the carbon monoxide bulge p 1029 N93-14320
Dynamics of the Venus atmosphere p 1030 N93-14325
Long-term variations in abundance and distribution of sulfuric acid vapor in the Venus atmosphere inferred from Pioneer Venus and Magellan radio occultation studies p 1030 N93-14328
Venus: The case for a wet origin and a runaway greenhouse p 1031 N93-14331
Pioneer Venus polarimetry and haze optical thickness p 1032 N93-14335
Radiation pressure: A possible cause for the superrotation of the Venusian atmosphere p 1033 N93-14338
Groundbased near-IR observations of the surface of Venus p 1035 N93-14346
Results of a zonally truncated three-dimensional model of the Venus middle atmosphere p 1037 N93-14351
Computer simulations of comet- and asteroidlike bodies passing through the Venusian atmosphere: Preliminary results on atmospheric and ground shock effects p 1040 N93-14365
Atmospheric effects on crater growth on Venus p 1041 N93-14370
Impact-generated winds on Venus: Causes and effects p 1041 N93-14372
Evidence for lightning on Venus p 1043 N93-14386
Finite amplitude gravity waves in the Venus atmosphere generated by surface topography p 1044 N93-14395
Middle atmosphere of Venus and its clouds: Latitude and solar time variations p 1045 N93-14396
SO2 in the middle atmosphere of Venus: IR measurements from Venera 15 and comparison to UV p 1045 N93-14397
Outgassing history of Venus and the absence of water on Venus p 1045 N93-14398
Study and interpretation of the millimeter-wave spectrum of Venus p 1045 N93-14596
Sulfur oxides in the middle atmosphere of Venus: Observations by the International Ultraviolet Explorer and sounding rockets p 1046 N93-14635

VENUS CLOUDS

Papers presented to the International Colloquium on Venus
|NASA-CR-190676| p 1023 N93-14288
Study and interpretation of the millimeter-wave spectrum of Venus p 1045 N93-14596
Sulfur oxides in the middle atmosphere of Venus: Observations by the International Ultraviolet Explorer and sounding rockets p 1046 N93-14635

VENUS PROBES

Papers presented to the International Colloquium on Venus
|NASA-CR-190676| p 1023 N93-14288

VENUS SURFACE

Papers presented to the International Colloquium on Venus
|NASA-CR-190676| p 1023 N93-14288
Venus radar mapping from the Venera 15 and 16 spacecrafts: Results and restrictions p 1023 N93-14289
Local-time asymmetries in the Venus thermosphere p 1023 N93-14290
Ringed impact craters on Venus: An analysis from Magellan images p 1024 N93-14291
Is Ishtar Terra a thickened basaltic crust? p 1024 N93-14292
Constraints on the thermal evolution of Venus inferred from Magellan data p 1024 N93-14293
Surface processes on Venus p 1024 N93-14294
Shield fields: Concentrations of small volcanic edifices on Venus p 1024 N93-14295
The geology of the Venera/Vega landing sites p 1024 N93-14296
Global deformation on the surface of Venus p 1024 N93-14297
Coldspots or hotspots? The origin of plateau-shaped highlands on Venus p 1025 N93-14298
Mixed-valence iron minerals on Venus: Fe(2+)-Fe(3+) oxides and oxy-silicates formed by surface-atmosphere interactions p 1025 N93-14301
Thermal buoyancy on Venus: Preliminary results of finite element modeling p 1025 N93-14302
Erosion versus construction: The origin of Venusian channels p 1025 N93-14303
Bright crater outflows: Possible emplacement mechanisms p 1026 N93-14305
Image processing and products for the Magellan mission to Venus p 1026 N93-14306
Monte Carlo computer simulations of Venus equilibrium and global resurfacing models p 1027 N93-14311
Flexural analysis of uplifted rift flanks on Venus p 1027 N93-14314
Radar scattering properties of pancakelike domes on Venus p 1028 N93-14316
Sequential deformation of plains along Tessera boundaries on Venus: Evidence from Alpha Regio p 1028 N93-14317
Tectonics and volcanism of Eastern Aphrodite Terra: No subduction, no spreading p 1029 N93-14321
Western Aphrodite Terra, tectonics, geology, and line-of-sight gravity p 1029 N93-14322
Venus volcanism: A global overview from Magellan data p 1029 N93-14323
Chemical differentiation on one-plate planets: Predictions and geologic observations for Venus p 1029 N93-14324
Largest impact craters on Venus p 1030 N93-14326
Venusian extended ejecta deposits as time-stratigraphic markers p 1030 N93-14327
Variations in lithospheric thickness on Venus p 1030 N93-14329
Igneous and tectonic evolution of Venusian and terrestrial coronae p 1031 N93-14330
Venus tectonic styles and crustal differentiation p 1031 N93-14332
Large shield volcanos on Venus: The effect of neutral buoyancy zone development on evolution and altitude distribution p 1032 N93-14333
Mantle plumes on Venus revisited p 1032 N93-14334
Venusian sinuous rilles p 1033 N93-14337
Large-volume lava flow fields on Venus: Dimensions and morphology p 1033 N93-14339
Derivation of surface properties from Magellan altimetry data p 1033 N93-14340
Extensive lava flow fields on Venus: Preliminary investigation of source elevation and regional slope variations p 1034 N93-14342
Wrinkle ridges on Venusian plains: Indicators of shallow crustal stress orientations at local and regional scales p 1034 N93-14343
Estimates of elastic plate thicknesses beneath large volcanos on Venus p 1035 N93-14344
Pancakelike domes on Venus p 1035 N93-14345
Groundbased near-IR observations of the surface of Venus p 1035 N93-14346
Magellan stereo images and Venusian geology p 1035 N93-14347
Flexural models of trench/outer rise topography of coronae on Venus with axisymmetric spherical shell elastic plates p 1036 N93-14348
Radar-anomalous, high-altitude features on Venus p 1036 N93-14349
The gabbro-eclogite phase transition and the elevation of mountain belts on Venus p 1036 N93-14350
A model for the formation of the extended paraboloidal halos around some impact craters on Venus p 1037 N93-14352
Venus: Preliminary geologic mapping of northern Atla Regio p 1037 N93-14353
Venus: Preliminary geologic mapping of southern Beta Regio-northern Phoebe Regio p 1037 N93-14354
Venus: Geology of Beta Regio rift system p 1037 N93-14355
The origins of radial fracture systems and associated large lava flows on Venus p 1038 N93-14356
Application of left- and right-looking SAR stereo to depth measurements of the Ammavaru outflow channel, Lada Terra, Venus p 1038 N93-14357
Venus steep-sided domes: Relationships between geological associations and possible petrogenetic models p 1038 N93-14359
Dielectric surface properties of Venus p 1039 N93-14360
Tectonic connections to interior processes on Venus p 1039 N93-14361
Problem footprints in Magellan altimetry data p 1039 N93-14362
Anomalous scattering behavior of selected impact parabola features: Magellan cycle-to-cycle comparisons p 1039 N93-14363
Cytherean crustal bending at Salme Dorsa p 1039 N93-14364
Evidence for retrograde lithospheric subduction on Venus p 1040 N93-14367
Overview of Venus geology: Preliminary description of terrain units for Venus global geological mapping p 1040 N93-14368
Impact craters on Venus: An overview from Magellan observations p 1040 N93-14369
Atmospheric effects on crater growth on Venus p 1041 N93-14370
Effect of impact angle on central-peak/peak-ring formation and crater collapse on Venus p 1041 N93-14371
Impact-generated winds on Venus: Causes and effects p 1041 N93-14372
Atla Regio, Venus: Geology and origin of a major equatorial volcanic rise p 1041 N93-14374
Geoid, topography, and convection-driven crustal deformation on Venus p 1042 N93-14376
Constraints on crustal rheology and age of deformation from models of gravitational spreading in Ishtar Terra, Venus p 1042 N93-14379
Melting and differentiation in Venus with a cold start: A mechanism of the thin crust formation p 1042 N93-14381
The tectonics of Venus: An overview p 1042 N93-14382
The spatial distribution of coronae on Venus p 1043 N93-14383
Microwave scattering and emission properties of large impact craters on the surface of Venus p 1043 N93-14384
Volcanism by melt-driven Rayleigh-Taylor instabilities and possible consequences of melting for admittance ratios on Venus p 1043 N93-14387
Can a time-stratigraphic classification system be developed for Venus? p 1043 N93-14388
Episodic plate tectonics on Venus p 1044 N93-14390
Scattering properties of Venus' surface p 1044 N93-14391
Low-emissivity impact craters on Venus p 1044 N93-14392
Floor-fractured crater models for igneous crater modification on Venus p 1044 N93-14393
Finite amplitude gravity waves in the Venus atmosphere generated by surface topography p 1044 N93-14395
Outgassing history of Venus and the absence of water on Venus p 1045 N93-14398

VERBAL COMMUNICATION

The intelligibility of words, sentences, and continuous discourse using the articulation index
|AD-A256781| p 863 N93-15624

VERTICAL DISTRIBUTION

Sulfur oxides in the middle atmosphere of Venus: Observations by the International Ultraviolet Explorer and sounding rockets p 1046 N93-14635

VERY HIGH FREQUENCIES

Satellite measurement of ionospheric-induced VHF distortion
|DE92-040328| p 862 N93-15435

VERY LARGE SCALE INTEGRATION

Design and hardware implementation of neural systems
|AD-A256040| p 866 N93-14577
Parametric study of diffusion-enhancement networks for spatiotemporal grouping in real-time artificial vision
|AD-A256059| p 937 N93-14580
Testability design rating system: Testability handbook, volume 1
|RL-TR-92-12-VOL-1| p 867 N93-14699
Sensor-based driving of a car with fuzzy inferencing VLSI chips and boards
|DE92-017819| p 963 N93-14818
Architecture of low cost, large scale neural networks
|MEMO-INF-92-16| p 941 N93-15089
VHDL (VHSIC hardware description language): Origins, status, capabilities, and world environment
|VH-1| p 947 N93-15262
Analog Very Large Scale Integration (VLSI) implementations of artificial neural networks
|AD-A256621| p 966 N93-15408

VERY LONG BASE INTERFEROMETRY

A feasibility study of space VLBI for geodesy and geodynamics p 904 N93-14223
The evolution of the VLBI polarization of superluminal radio source 3C345 p 1050 N93-14229
Plate tectonics from VLBI and SLR global data
|NASA-CR-191319| p 916 N93-14913

VERY LOW FREQUENCIES

Acoustic propagation loss predictions for a site on the Bermuda Rise at low and very low frequencies
|AD-A255445| p 925 N93-14512
Boundary element analysis of low frequency cavity acoustical problems
|MATHS-REPT-A-158| p 974 N93-15073

VHSIC (CIRCUITS)

Proceedings of the International Conference on CAD/CAM and AMT. Volume 4: VHDL (VHSIC Hardware Description Language) Seminar
|ITN-92-85130| p 947 N93-15261

VHDL (VHSIC hardware description language): Origins, status, capabilities, and world environment
[VH-1] p 947 N93-15262
VHDL (VHSIC hardware description language) use in the US defense procurement process
[VH-2] p 948 N93-15263
The extended VHDL (VHSIC hardware description language) design environment: An unique integrated system and hardware design environment
[VH-3] p 948 N93-15264
System design in a large corporation, using VHDL (VHSIC hardware description language)
[VH-4] p 948 N93-15265
Synthesis and simulation with VHDL (VHSIC hardware description language)
[VH-5] p 948 N93-15266
VHDL (VHSIC hardware description language) in the test environment
[VH-6] p 948 N93-15267
Integrating VHDL (VHSIC hardware description language) with existing EDA tools
[VH-8] p 948 N93-15268

VIBRATION
Addressing earthquake strong ground motion issues at the Idaho National Engineering Laboratory
[DE92-017841] p 916 N93-15136
Modelling Directional Solidification
[NASA-CR-191301] p 995 N93-15309
Solidification of InSb-GaSb alloy and InSb with vibration p 995 N93-15310
Calculation of mechanical vibration frequencies of stiffened superconducting cavities
[DE92-040228] p 903 N93-15423

VIBRATION DAMPING
Robust control of a flexible link robot and rigid link robot: Theory, simulation, and experiment p 888 N93-14202
An examination of wing rock for the F-15
[AD-A256613] p 802 N93-14252
Online vibration control of a flexible rotor/bearing system p 899 N93-14468
Technology development for non-contact measurement in modal testing of large space structures p 809 N93-14942
Position and vibration control of flexible space robots p 892 N93-15102
Optimal active vibration absorber: Design and experimental results
[NASA-TM-107709] p 902 N93-15202
Onboard System Evaluation of Rotors Vibration, Engines (OBSERVE) monitoring system
[AD-A255366] p 792 N93-15227

VIBRATION EFFECTS
The effects of acceleration on precision frequency sources
[AD-A255465] p 972 N93-14496
The Meta-Lax method of stress reduction in welds
[DE92-018477] p 845 N93-14900

VIBRATION ISOLATORS
Digital active material processing platform effort (DAMPER), SBIR phase 2
[NASA-CR-190798] p 856 N93-15353
Vibration isolation technology: An executive summary of systems development and demonstration
[NASA-TM-105937] p 778 N93-15573

VIBRATION MEASUREMENT
New rotor trim and balance system for helicopter usage monitoring p 797 N93-15180

VIBRATION METERS
Technology development for non-contact measurement in modal testing of large space structures p 809 N93-14942

VIBRATION MODE
Model reduction of flexible manipulators
[AD-A255251] p 889 N93-14528

VIBRATION SIMULATORS
The design concept of the 6-degree-of-freedom hydraulic shaker at ESTEC p 820 N93-15600

VIBRATION TESTS
Experimental and analytical investigation of the vibration characteristics of a remotely piloted helicopter
[AD-A256131] p 790 N93-14248
Technology development for non-contact measurement in modal testing of large space structures p 809 N93-14942
Environmental qualification testing of the prototype pool boiling experiment
[NASA-CR-190774] p 895 N93-15582
Multi-axis transient vibration testing of space objects: Test philosophy, test facility, and control strategy p 820 N93-15598
Vibration and acoustic testing of TOPEX/Poseidon satellite p 820 N93-15599

VIBRATIONAL SPECTRA
Silicon nitride thin film production on Si(111)
[AD-A256036] p 994 N93-15233

VIDEO COMMUNICATION
Designing video annotation and analysis systems p 955 N93-15552

VIDEO DATA
A system approach to archival storage p 1006 N93-15040
Designing video annotation and analysis systems p 955 N93-15552

VIDEO SIGNALS
High-resolution contrast control on a video display: Method and calibration
[AD-A256552] p 938 N93-15400

VIDEO TAPES
Corrosion of metal particle and metal evaporated tapes p 883 N93-15039
A system approach to archival storage p 1006 N93-15040

VIEWING
Annotating the real world with knowledge-based graphics on a see-through head-mounted display p 954 N93-15543

VIKING ORBITER SPACECRAFT
Comparison of Viking Ultraviolet images with low altitude particle precipitation p 1045 N93-14612

VIRTUAL MEMORY SYSTEMS
Transactional distributed shared memory
[AD-A256222] p 941 N93-15240
A deadlock-free communication system for a transputer network
[AD-A256473] p 959 N93-15319

VIRTUAL REALITY
Working together, virtually p 954 N93-15547

VISCOELASTICITY
Visoelastic relaxation of Venusian coronae and mountain belts: Constraints on global heat flow and tectonism p 1027 N93-14313
Numerical and experimental study of bubble growth in highly viscous fluids p 874 N93-14465

VISCOPLASTICITY
A finite element model for analysis of thermoviscoplastic behavior of hypersonic leading edge structures subject to intense aerothermal heating p 780 N93-14631

VISCOSITY
Viscosity of liquids. Halogenated methanes
[ESDU-92028] p 839 N93-14539
Thermophysical properties of nitric oxide
[ESDU-92027] p 839 N93-14544

VISCOUS DAMPING
An active Z gravity compensation system
[AD-A255258] p 889 N93-14529
Asymmetric natural damped frequencies of a rotating infinitely long viscous liquid column
[LRT-WE-9-FB-23-1991] p 878 N93-15120

VISCOUS FLOW
An algebraic turbulence model for three-dimensional viscous flows
[NASA-TM-105931] p 777 N93-14102
A study of viscous interaction effects on hypersonic waveriders p 778 N93-14160
Numerical modeling of a vortex stabilized arcjet
[NASA-CR-190797] p 826 N93-14883
On the nonlinear three dimensional instability of Stokes layers and other shear layers to pairs of oblique waves
[NASA-TM-105918] p 880 N93-15499
Prediction of turbine cascade flows with a quasi-three-dimensional rotor viscous code and the extension of the algebraic turbulence model
[AD-A256831] p 880 N93-15635

VISCOUS FLUIDS
Numerical and experimental study of bubble growth in highly viscous fluids p 874 N93-14465
Asymmetric natural damped frequencies of a rotating infinitely long viscous liquid column
[LRT-WE-9-FB-23-1991] p 878 N93-15120
Transient response of a viscous liquid bridge of finite length and anchored edges
[LRT-WE-9-FB-25-1991] p 878 N93-15132

VISIBLE SPECTRUM
A study of an optically pumped free-jet molecular iodine laser operating in the visible spectrum p 884 N93-14141

VISUAL ACUITY
Analysis of retinal function following laser irradiation
[AD-A255649] p 933 N93-14163
Higher order mechanisms of color vision
[AD-A256369] p 938 N93-15329

VISUAL DISCRIMINATION
A spurious pop-out in visual search
[AD-A256548] p 936 N93-14267
Institute for the Study of Human Capabilities
[AD-A256091] p 938 N93-14427
Higher order mechanisms of color vision
[AD-A256369] p 938 N93-15329

VISUAL PERCEPTION
A spurious pop-out in visual search
[AD-A256548] p 936 N93-14267
Effects of spatial luminance nonuniformities on visual-task performance and subjective uniformity
[AD-A255989] p 936 N93-14416
Psychophysical analyses of perceptual representations
[AD-A255432] p 936 N93-14510
Geometric invariants and object recognition
[AD-A255317] p 943 N93-14546
The perception of articulated motion: Recognizing moving light displays
[AD-A256046] p 937 N93-14660

VISUAL STIMULI
The perception of articulated motion: Recognizing moving light displays
[AD-A256046] p 937 N93-14660

VISUAL TASKS
A spurious pop-out in visual search
[AD-A256548] p 936 N93-14267
Effects of spatial luminance nonuniformities on visual-task performance and subjective uniformity
[AD-A255989] p 936 N93-14416

VITERBI DECODERS
High-speed architecture for the decoding of trellis-coded modulation
[NASA-CR-191374] p 941 N93-14770

VOCODERS
A mixed excitation vocoder with fuzzy logic classifier
[AD-A256834] p 864 N93-15636

VOICE COMMUNICATION
Multi-access strategies for voice/data integration in heterogeneous mixed-media packet radio networks
[AD-A255636] p 857 N93-14181
System design and development of a low data rate voice (1200 bps) rate converter
[AD-A256071] p 859 N93-14663
NPR and intermodulation in mobile satellite systems p 806 N93-14931
Progress toward a full scale mobile satellite system for Canada p 812 N93-14960
Co-channel speaker separation
[AD-A256443] p 861 N93-15317

VOICE DATA PROCESSING
Multi-access strategies for voice/data integration in heterogeneous mixed-media packet radio networks
[AD-A255636] p 857 N93-14181
A mixed excitation vocoder with fuzzy logic classifier
[AD-A256834] p 864 N93-15636

VOLCANOES
Surface processes on Venus p 1024 N93-14294
Shield fields: Concentrations of small volcanic edifices on Venus p 1024 N93-14295
Coldspots or hotspots? The origin of plateau-shaped highlands on Venus p 1025 N93-14298
Monte Carlo modeling of the resurfacing of Venus p 1025 N93-14299
Debris avalanches and slumps on the margins of volcanic domes on Venus: Characteristics of deposits p 1025 N93-14300
Erosion versus construction: The origin of Venusian channels p 1025 N93-14303
Polarization properties and Earth-based radar measurements of Venus in the post-Magellan era p 1026 N93-14304
Global correlation of volcanic centers on Venus with uplands and with extension: Influence of mantle convection and altitude p 1026 N93-14309
Monte Carlo computer simulations of Venus equilibrium and global resurfacing models p 1027 N93-14311
Flexural analysis of uplifted rift flanks on Venus p 1027 N93-14314
Radar scattering properties of pancakelike domes on Venus p 1028 N93-14316
Venusian hydrology: Steady state reconsidered p 1028 N93-14318
Tectonics and volcanism of Eastern Aphrodite Terra: No subduction, no spreading p 1029 N93-14321
Venus volcanism: A global overview from Magellan data p 1029 N93-14323
Igneous and tectonic evolution of Venusian and terrestrial coronae p 1031 N93-14330
Large shield volcanos on Venus: The effect of neutral buoyancy zone development on evolution and altitude distribution p 1032 N93-14333
Large-volume lava flow fields on Venus: Dimensions and morphology p 1033 N93-14339
Estimates of elastic plate thicknesses beneath large volcanos on Venus p 1035 N93-14344
Venus: Preliminary geologic mapping of northern Atla Regio p 1037 N93-14353
Venus: Preliminary geologic mapping of southern Beta Regio-northern Phoebe Regio p 1037 N93-14354
The origins of radial fracture systems and associated large lava flows on Venus p 1038 N93-14356
Atla Regio, Venus: Geology and origin of a major equatorial volcanic rise p 1041 N93-14374
Different types of small volcanos on Venus p 1042 N93-14378

Multiresolution pattern recognition of small volcanos in Magellan data p 1042 N93-14380
The spatial distribution of coronae on Venus p 1043 N93-14383
Volcanism by melt-driven Rayleigh-Taylor instabilities and possible consequences of melting for admittance ratios on Venus p 1043 N93-14387

VOLCANOLOGY
Constraints on the thermal evolution of Venus inferred from Magellan data p 1024 N93-14293
Shield fields: Concentrations of small volcanic edifices on Venus p 1024 N93-14295
Monte Carlo modeling of the resurfacing of Venus p 1025 N93-14299
Debris avalanches and slumps on the margins of volcanic domes on Venus: Characteristics of deposits p 1025 N93-14300
Erosion versus construction: The origin of Venusian channels p 1025 N93-14303
Global correlation of volcanic centers on Venus with uplands and with extension: Influence of mantle convection and altitude p 1026 N93-14309
Monte Carlo computer simulations of Venus equilibrium and global resurfacing models p 1027 N93-14311
Flexural analysis of uplifted rift flanks on Venus p 1027 N93-14314
Radar scattering properties of pancakelike domes on Venus p 1028 N93-14316
Determining stress states using dike swarms: The Lauma Dorsa example p 1028 N93-14319
Tectonics and volcanism of Eastern Aphrodite Terra: No subduction, no spreading p 1029 N93-14321
Venus volcanism: A global overview from Magellan data p 1029 N93-14323
Chemical differentiation on one-plate planets: Predictions and geologic observations for Venus p 1029 N93-14324
Large shield volcanos on Venus: The effect of neutral buoyancy zone development on evolution and altitude distribution p 1032 N93-14333
Mantle plumes on Venus revisited p 1032 N93-14334
The effects of Venus' thermal structure on buoyant magma ascent p 1040 N93-14366
Atla Regio, Venus: Geology and origin of a major equatorial volcanic rise p 1041 N93-14374
Different types of small volcanos on Venus p 1042 N93-14378
Volcanism by melt-driven Rayleigh-Taylor instabilities and possible consequences of melting for admittance ratios on Venus p 1043 N93-14387
Episodic plate tectonics on Venus p 1044 N93-14390
Floor-fractured crater models for igneous crater modification on Venus p 1044 N93-14393

VOLTAGE CONVERTERS (DC TO DC)
Optimized design of a 5 kW constant frequency series resonant converter for pulsed load space applications p 807 N93-14935

VOLTAGE REGULATORS
Optimized design of a 5 kW constant frequency series resonant converter for pulsed load space applications p 807 N93-14935

VOLUME
Orthobaric densities and molar volumes of liquids. Halogenated ethylenes
[ESDU-92018] p 839 N93-14540

VORTEX BREAKDOWN
Analysis and control of asymmetric vortex flows and supersonic vortex breakdown
[NASA-CR-191264] p 875 N93-14687
Shock/vortex interaction and vortex-breakdown modes
[PAPER-T.1.3] p 875 N93-14689

VORTEX SHEDDING
Wake similarity and vortex formation for two-dimensional bluff bodies p 781 N93-15101

VORTICES
Dynamics in neutron stars and the early universe p 1014 N93-14112
Dynamic behavior of a dense spray diffusion flame in a potential vortex p 839 N93-14463
Analysis and control of asymmetric vortex flows and supersonic vortex breakdown
[NASA-CR-191264] p 875 N93-14687
Numerical simulation of steady and unsteady asymmetric vortical flow p 876 N93-14691
Passive control of supersonic asymmetric vortical flows around cones p 876 N93-14692
Numerical simulation of baroclinic Jovian vortices p 1046 N93-14865
Numerical modeling of a vortex stabilized arcjet
[NASA-CR-190797] p 826 N93-14883
The influence of baroclinic processes on tropical cyclone motion p 923 N93-15099
Wake similarity and vortex formation for two-dimensional bluff bodies p 781 N93-15101
Flowfield study of a close-coupled canard configuration
[AD-A256311] p 782 N93-15245
Unsteady flow distortion past blades: Sources of noise generation in rotating flows
[AD-A255496] p 880 N93-15652

VORTICITY
The Applicaiton of CFD to rotary wing flow problems
[NASA-TM-102803] p 782 N93-15483
Unsteady shear disturbances within a two dimensional stratified flow
[NASA-CR-189121] p 880 N93-15527
Unsteady flow distortion past blades: Sources of noise generation in rotating flows
[AD-A255496] p 880 N93-15652

VORTICITY EQUATIONS
Numerical simulation of baroclinic Jovian vortices p 1046 N93-14865

W

WAFERS
Architecture of low cost, large scale neural networks
[MEMO-INF-92-16] p 941 N93-15089

WAKES
Exploiting similarity in turbulent shear flows for turbulence modeling
[NASA-CR-191621] p 875 N93-14481
The effect of wake dynamics on rotor eigenvalues in forward flight p 780 N93-14595
Wake similarity and vortex formation for two-dimensional bluff bodies p 781 N93-15101

WALKING
A minimum-slip attitude control method for the erebus walking robot
[NASA-CR-191646] p 890 N93-14567
Compliant walker
[NASA-CASE-GSC-13348-2] p 934 N93-14708

WALKING MACHINES
A minimum-slip attitude control method for the erebus walking robot
[NASA-CR-191646] p 890 N93-14567

WALL FLOW
An experimental and analytical study of TIP clearance effects in axial flow compressors
[AD-A256434] p 800 N93-15337

WALLS
Wall layers
[AD-A256152] p 872 N93-14257
Second order closure modeling of turbulent buoyant wall plumes
[NASA-TM-105956] p 877 N93-14829

WARNING SYSTEMS
Terminal Doppler weather radar/low-level wind shear alert system integration algorithm specification, version 1.1
[AD-A255319] p 920 N93-14547
Airborne Wind Shear Detection and Warning Systems. Fourth Combined Manufacturers' and Technologists' Conference, part 2
[NASA-CP-10105-PT-2] p 783 N93-14844
Development of the Advance Warning Airborne System(AWAS) p 784 N93-14849
A millimeter-wave radiometer for detecting microbursts p 784 N93-14850
Experimental evaluation of candidate graphical microburst alert displays p 785 N93-14853
Wind shear related research at Princeton University p 785 N93-14854
In-service evaluation of wind shear systems p 785 N93-14857
Advanced technology wind shear prediction system evaluation p 785 N93-14858
Proceedings of the 16th Symposium on Aircraft Integrated Monitoring Systems
[DLR-MITT-92-01] p 793 N93-15152
Monitoring of pilot actions as part of a knowledge-based system for pilot assistance p 797 N93-15184

WASTE DISPOSAL
Technical data management at the Yucca Mountain Site Characterization Project
[DE92-018115] p 1008 N93-15229

WASTE TREATMENT
Electrochemical oxidation of organic materials
[DE92-019822] p 828 N93-14718
Technical data management at the Yucca Mountain Site Characterization Project
[DE92-018115] p 1008 N93-15229

WASTE WATER
Management and minimization of photographic wastes at Pantex Plant
[MHSMP-92-01] p 910 N93-14739

WATER
Physical and chemical processes of the inner coma observed in mid-ultraviolet cometary spectra p 1017 N93-14230
Venusian hydrology: Steady state reconsidered p 1028 N93-14318
Venus: The case for a wet origin and a runaway greenhouse p 1031 N93-14331
Martian water frost: Control of global distribution by small-scale processes p 1047 N93-14868
Evaluation of a soil fixative to retard particle entrainment: A laboratory study
[UCRL-LR-109806] p 915 N93-14877
Technology evaluation report: The Carver-Greenfield process, Dehydro-Tech Corporation
[PB92-217462] p 910 N93-15217

WATER LANDING
Reusable Reentry Satellite (RRS): Recovery tradeoff study
[NASA-CR-186396] p 825 N93-15658

WATER LOSS
Venusian hydrology: Steady state reconsidered p 1028 N93-14318

WATER PRESSURE
Surface gravity waves and ambient microseismic noise
[AD-A256498] p 916 N93-15375

WATER RECLAMATION
Management and minimization of photographic wastes at Pantex Plant
[MHSMP-92-01] p 910 N93-14739

WATER RESOURCES
Venusian hydrology: Steady state reconsidered p 1028 N93-14318

WATER TREATMENT
Apparatus and process for desalination of seawater
[AD-D015428] p 842 N93-14824

WATER TUNNEL TESTS
Control of low-speed turbulent separated flow over a backward-facing ramp p 874 N93-14475

WATER VAPOR
Effects of water vapor and anisotropic scattering on aerosol optical depth retrieval
[AD-A256087] p 904 N93-14262
Improved aerosol optical depth and particle size index from satellite detected radiance
[AD-A256089] p 904 N93-14263
Outgassing history of Venus and the absence of water on Venus p 1045 N93-14398
On the role of water growth in atmospheric aerosol p 922 N93-14875

WATER WAVES
Ocean wave detection using satellite altimetry p 906 N93-14839
Evaluation of methods for estimating wind wave growth on narrow irregular fetches
[AD-A256002] p 932 N93-15113
Surface gravity waves and ambient microseismic noise
[AD-A256498] p 916 N93-15375

WAVE DIFFRACTION
A modal analysis of lamellar diffraction gratings in conical mountings p 986 N93-15519

WAVE DISPERSION
Elastic wave propagation in laminated composites
[ITN-93-85186] p 835 N93-15144
Development of a 500 GHz optoelectronic modulator using superconducting transmission lines
[AD-A257062] p 871 N93-15456

WAVE DRAG
Wave drag in the atmospheric boundary layer p 915 N93-14873

WAVE FRONTS
Modeling and measurement of a micro-optic beam deflector p 985 N93-15514
Effects of higher order aberrations on beam shape in an optical recording system p 985 N93-15515

WAVE FUNCTIONS
Homogeneous quantum electrodynamic turbulence
[NASA-TM-107686] p 979 N93-15482

WAVE GENERATION
Some theoretical and experimental aspects of the generation of guided elastic waves using finite sources p 897 N93-14219

WAVE INTERACTION
Nonlinear dynamics of optical systems p 979 N93-14124
A Cloudy Quark Bag Model of S, P, and D wave interactions for the coupled channel antikaon-nucleon system
[DE92-040149] p 977 N93-15062

WAVE PACKETS
AFIT/AFOSR Workshop on the Role of Wavelets in Signal Processing Applications
[AD-A256172] p 859 N93-14649

WAVE PROPAGATION
In situ material characterization for pavement evaluation by the Spectral-Analysis-of-Surface-Waves (SASW) method
[AD-A255660] p 804 N93-14128
Non-linear analysis of wave progagation using transform methods and plates and shells using integral equations p 896 N93-14186
Investigation of the on-surface boundary operators for electromagnetic scattering by conducting object p 857 N93-14189
AFIT/AFOSR Workshop on the Role of Wavelets in Signal Processing Applications
[AD-A256172] p 859 N93-14649
Theory and applications of the 3-dimensional finite-difference time-domain method
[AD-A256559] p 968 N93-14804
Preview of Blackbeard interferometry
[DE92-040329] p 818 N93-14904
Development of a TDS measurement system. Application to acoustic propagation measurement in a non anechoic environment
[ONERA-RT-18/3641-PY] p 975 N93-15130
Elastic wave propagation in laminated composites
[ITN-93-85186] p 835 N93-15144
Deterministic transfer function for transionospheric propagation
[DE92-040327] p 862 N93-15427
WAVE SCATTERING
Investigation of the on-surface boundary operators for electromagnetic scattering by conducting object p 857 N93-14189
Elastic wave scattering by partially debonded or partially coated fibers p 829 N93-14224
WAVEGUIDES
Some theoretical and experimental aspects of the generation of guided elastic waves using finite sources p 897 N93-14219
A preliminary design of the Ti:LiNbO3 optical channel waveguide
[AD-A255443] p 982 N93-14784
WAVELENGTH DIVISION MULTIPLEXING
Advanced optical fiber communication systems
[AD-A255424] p 982 N93-14507
WAVERIDERS
A study of viscous interaction effects on hypersonic waveriders p 778 N93-14160
Computational analysis of hypersonic flows past elliptic-cone waveriders
[NASA-CR-191304] p 781 N93-14767
WEAK ENERGY INTERACTIONS
Weak-electromagnetic interference in polarized eD scattering
[DE93-001763] p 978 N93-15486
WEAPON SYSTEMS
MIL-STD-1760 application guidelines
[AD-A255714] p 790 N93-14432
Development of an integrated package of physics models for scene simulation studies to support smart weapons design studies
[LTR92-004] p 945 N93-14696
WEAPONS DELIVERY
MIL-STD-1760 application guidelines
[AD-A255714] p 790 N93-14432
WEAR
Tribology of magnetic storage systems p 1002 N93-14772
Method and devices for the in situ repair of damaged threads
[AD-D015416] p 891 N93-14881
Exceptionally high-strength (approximately 3 GPa) aluminum alloys demonstrated by oxygen ion implantation
[DE92-040980] p 847 N93-15383
WEAR RESISTANCE
Development of wear-resistant ceramic coatings for diesel engine components
[DE92-041382] p 853 N93-15439
The effect of processing and compositional changes on the tribology of PM212 in air
[NASA-TM-105945] p 828 N93-15576
WEAR TESTS
Tribology of improved transformation-toughened ceramics-heat engine test
[DE92-041385] p 851 N93-15295
Development of wear-resistant ceramic coatings for diesel engine components
[DE92-041382] p 853 N93-15439
WEATHER FORECASTING
Technology reconciliation in the remote sensing era of US civilian weather forcasting: 1957 - 1987 p 918 N93-14114
Wind stress analysis over the Western Equatorial Pacific and North Atlantic Oceans based on ECMWF operational wind products, 1985-1989
[AD-A256147] p 920 N93-14256
Proceedings of the data assimilation in coupled air-sea nowcast/forecast systems workshop
[AD-A255409] p 925 N93-14503
Four-dimensional data assimilation of gale data using a multivariate analysis scheme and a mesoscale model with diabatic initialization
[AD-A256063] p 921 N93-14680
An observational and theoretical study of squall line evolution p 921 N93-14682
A single-station forecasting model
[AD-A256403] p 924 N93-15331
Cloud fraction, layer, and direction of movement results from sky cameras during the FIRE IFO, Coffeyville, Kansas, experiment for the period Nov. 12 through Dec. 9, 1991
[NASA-TM-107647] p 924 N93-15501
Development and application of a time-space conversion technique for analysis of weather systems passing over the Kennedy Space Center
[NASA-CR-4474] p 924 N93-15581
WEATHER STATIONS
A single-station forecasting model
[AD-A256403] p 924 N93-15331
WEIGHT ANALYSIS
Weight optimum arch structures
[AD-A256080] p 897 N93-14236
WEIGHTLESSNESS
An active Z gravity compensation system
[AD-A255258] p 889 N93-14529
Passive zero-gravity leg restraint
[NASA-CASE-ARC-11882-1-CU] p 939 N93-14713
WELDED JOINTS
Theoretical and experimental analysis of residual stress formation after implant resistance welding of polycarbonate p 898 N93-14279
Fatigue strength of cruciform and other fillet welded joints in aluminum alloys
[ESDU-92017] p 900 N93-14553
Mechanisms of forming intergranular microcracks and microscopic surface discontinuities in welds
[AD-A255371] p 845 N93-14740
The Meta-Lax method of stress reduction in welds
[DE92-018477] p 845 N93-14900
WELDING
Theoretical and experimental analysis of residual stress formation after implant resistance welding of polycarbonate p 898 N93-14279
WETLANDS
Using digital scanned aerial photography for wetlands delineation
[AD-A255392] p 905 N93-14676
Comparison of the prevalence index and average wetland values for identification of wetland vegetation
[DE92-016701] p 910 N93-15209
WHEELS
Reanalysis of multiple-wheel landing gear traffic tests
[AD-A256593] p 804 N93-14238
WHISKER COMPOSITES
Development of ceramic matrix composites for application in ceramic technology for advanced heat engines project, phase 2
[DE92-041379] p 836 N93-15387
WHISKERS (CRYSTALS)
Material development in the Si3N4 system using glass encapsulated HIP'ing
[DE92-041381] p 837 N93-15388
WHISTLERS
Evidence for lightning on Venus p 1043 N93-14386
Thunderstorm coupling to the magnetosphere and associated ionospheric effects
[NASA-CR-191383] p 922 N93-14910
WHITE DWARF STARS
Stability of differentially rotating stars p 1018 N93-14584
WIGGLER MAGNETS
Compact free electron laser for medical applications
[AD-A256236] p 885 N93-14599
WIGNER COEFFICIENT
An energy analysis of the pseudo Wigner-Ville distribution in support of machinery monitoring and diagnostics
[AD-A256202] p 889 N93-14499
WIND (METEOROLOGY)
Impact-generated winds on Venus: Causes and effects p 1041 N93-14372
Convective scale 4-D data assimilation using simulated single-Doppler radar observations p 921 N93-14683
Sea level response to wind forcing in the tropical Atlantic p 928 N93-14977
WIND DIRECTION
Evaluation of methods for estimating wind wave growth on narrow irregular fetches
[AD-A256002] p 932 N93-15113
WIND EFFECTS
A model for the formation of the extended paraboloidal halos around some impact craters on Venus p 1037 N93-14352
Sensitivity of the Yoshida jet to the parameterization of vertical mixing: Do easterly winds imply equatorial upwelling? p 922 N93-14864
WIND MEASUREMENT
Venus mesospheric winds and the carbon monoxide bulge p 1029 N93-14320
Solid-state coherent laser radar wind shear measuring systems p 784 N93-14848
WIND PROFILES
Venus mesospheric winds and the carbon monoxide bulge p 1029 N93-14320
Development and application of a time-space conversion technique for analysis of weather systems passing over the Kennedy Space Center
[NASA-CR-4474] p 924 N93-15581
WIND SHEAR
Wind stress analysis over the Western Equatorial Pacific and North Atlantic Oceans based on ECMWF operational wind products, 1985-1989
[AD-A256147] p 920 N93-14256
Terminal Doppler weather radar/low-level wind shear alert system integration algorithm specification, version 1.1
[AD-A255319] p 920 N93-14547
Airborne Wind Shear Detection and Warning Systems. Fourth Combined Manufacturers' and Technologists' Conference, part 2
[NASA-CP-10105-PT-2] p 783 N93-14844
NASA/LMSC coherent LIDAR airborne shear sensor: System capabilities and flight test plans p 784 N93-14847
Solid-state coherent laser radar wind shear measuring systems p 784 N93-14848
Development of the Advance Warning Airborne System(AWAS) p 784 N93-14849
A millimeter-wave radiometer for detecting microbursts p 784 N93-14850
The Orlando TDWR testbed and airborne wind shear date comparison results p 784 N93-14851
TDWR 1991 Program Review p 785 N93-14852
Wind shear related research at Princeton University p 785 N93-14854
Results of in-service evaluation of wind shear systems p 785 N93-14856
In-service evaluation of wind shear systems p 785 N93-14857
Advanced technology wind shear prediction system evaluation p 785 N93-14858
Development and application of a time-space conversion technique for analysis of weather systems passing over the Kennedy Space Center
[NASA-CR-4474] p 924 N93-15581
WIND TUNNEL NOZZLES
Mach 5 electroformed nickel nozzle refurbishment FNAS investigation of ultra-smooth surfaces
[NASA-CR-191416] p 826 N93-14681
WIND TUNNEL TESTS
Control of low-speed turbulent separated flow over a backward-facing ramp p 874 N93-14475
Facilities and capabilities catalog for landing and escape systems
[NASA-RP-1282] p 814 N93-14495
Investigations of detail design issues for the high speed acoustic wind tunnel using a 60th scale model tunnel. Part 1: Tests with open circuits
[NASA-CR-191671] p 780 N93-14737
Investigations of detail design issues for the high speed acoustic wind tunnel using a 60th scale model tunnel. Part 2: Tests with the closed circuit
[NASA-CR-191672] p 780 N93-14738
Evaluation of a soil fixative to retard particle entrainment: A laboratory study
[UCRL-LR-109806] p 915 N93-14877
Results of low power deicer tests on a swept inlet component in the NASA Lewis icing research tunnel
[NASA-TM-105968] p 781 N93-14911
Performing wind-tunnel modeling for better management of near-field risks
[DE92-040205] p 910 N93-15063
Wake similarity and vortex formation for two-dimensional bluff bodies p 781 N93-15101
An overview of shed ice impact in the NASA Lewis Icing Research Tunnel
[NASA-TM-105969] p 782 N93-15404
Space Shuttle Orbiter Crew Hatch Jettison Test using a 0.0405-scale model (16-0) in the Texas A/M low speed wind tunnel (OA362). Space Shuttle aerothermodynamic data report
[NASA-CR-167698] p 815 N93-15474
Results of a FRSI material test under Space Shuttle ascent conditions in the Ames Research Center 9x7 foot supersonic wind tunnel (OS13). Space Shuttle aerothermodynamic data report
[NASA-CR-167699] p 816 N93-15475

User manual for NASA Lewis 10 by 10 foot supersonic wind tunnel
[NASA-TM-105626] p 804 N93-15498
Upgrade and extension of the data acquisition system for propulsion and gas dynamic laboratories
[AD-A256836] p 1009 N93-15637

WIND TUNNELS
Subsonic aerodynamic research laboratory
[AD-A256060] p 780 N93-14661
Close-up analysis of aircraft ice accretion
[NASA-TM-105952] p 787 N93-15360
Upgrade and extension of the data acquisition system for propulsion and gas dynamic laboratories
[AD-A256836] p 1009 N93-15637

WIND TURBINES
Frequency-domain synthesis of the fatigue load spectrum for the NPS 100-kW wind turbine
[DE92-040984] p 908 N93-15384

WIND VELOCITY
Wind stress analysis over the Western Equatorial Pacific and North Atlantic Oceans based on ECMWF operational wind products, 1985-1989
[AD-A256147] p 920 N93-14256
Venus mesospheric winds and the carbon monoxide bulge p 1029 N93-14320
Dynamics of the Venus atmosphere p 1030 N93-14325
Evaluation of a soil fixative to retard particle entrainment: A laboratory study
[UCRL-LR-109806] p 915 N93-14877

WIND VELOCITY MEASUREMENT
NASA/LMSC instrument design and fabrication --- coherent lidar airborne shear sensor p 784 N93-14846

WINDING
Cable-line shortening device
[AD-D015427] p 891 N93-14822

WINDOWS (APERTURES)
Cesium iodide alloys
[DE92-019818] p 845 N93-14717

WING FLAPS
Icing effects on aircraft stability and control determined from flight data: Preliminary results
[NASA-TM-105977] p 803 N93-14831

WING OSCILLATIONS
An examination of wing rock for the F-15
[AD-A256613] p 802 N93-14252
Wing rock prediction method for a high performance fighter aircraft
[AD-A256438] p 792 N93-15314

WING PANELS
Reliability of stiffened structural panels: Two examples
[NASA-TM-107687] p 900 N93-14483

WING SPAN
Analysis of in-flight structural failures of P-3C wing leading edge segments
[AD-A256212] p 792 N93-15238

WINGS
Proceedings of the USAF Structural Integrity Program
[AD-A255379] p 777 N93-14549
Application of an aeroelastic analysis method for aerodynamic improvement of fighter wings at maneuver flight conditions p 791 N93-14832
Analysis of in-flight structural failures of P-3C wing leading edge segments
[AD-A256212] p 792 N93-15238

WINTER
Sierra Nevada winter storms: A study using microwave radiometry, ice crystal, and isotopic analysis technique p 923 N93-15088

WIRE
Sensitivity of quantum electron conductance to elastic scatterers and to spin-orbit scattering in gallium arsenide heterostructures p 990 N93-14184
Modeling and control of a trailing wire antenna towed by an orbiting aircraft
[AD-A256450] p 859 N93-14610
Development of an expendable particle sensor
[AD-A255702] p 881 N93-14653
Progress toward a tungsten alloy wire/high temperature alloy composite turbine blade
[NASA-TM-105901] p 847 N93-15586

WIRELESS COMMUNICATION
Short range propagation measurements at 2.4, 4.5, and 11.5 GHz in indoor and outdoor environments
[AD-A256563] p 860 N93-14806

WISCONSIN
Wisconsin Inventors' Network Database
[DE92-018394] p 1007 N93-15137

WOLF-RAYET STARS
Wolf-Rayet stars in the Milky Way, the Large Magellanic Cloud, and emission-line galaxies p 1020 N93-14869

WORDS (LANGUAGE)
Cognition and the brain
[AD-A255483] p 937 N93-14788
The intelligibility of words, sentences, and continuous discourse using the articulation index
[AD-A256781] p 863 N93-15624

WORK HARDENING
On the structure of nonlinear constitutive equations for fiber reinforced composites
[NASA-CR-191024] p 830 N93-14484

WORKING FLUIDS
Current status of liquid sheet radiator research
[NASA-TM-105764] p 872 N93-14150
Closed Brayton Cycle power system with a high temperature pellet bed reactor heat source for NEP applications
[NASA-TM-105933] p 826 N93-14482

WORKSTATIONS
Terrain visualization for the portable all-source analysis work station
[AD-A255708] p 905 N93-14430
Passive zero-gravity leg restraint
[NASA-CASE-ARC-11882-1-CU] p 939 N93-14713
Workstation tools for feature extraction and classification for nonstationary and transient signals
[AD-A255389] p 947 N93-15228
Development of an analog MIMO Quantitative Feedback Theory (QFT) CAD package
[AD-A256435] p 950 N93-15313

X

X RAY ABSORPTION
Accurate methods for calculating atomic processes in high temperature plasmas
[DE92-040215] p 988 N93-15418

X RAY ANALYSIS
A study of the relationship between macroscopic measures and physical processes occurring during crack closure
[AD-A256587] p 898 N93-14272
Physics of x ray multilayer structures: Summaries of papers presented at the physics of x ray multilayer structures topical meeting, technical digest series, 1992, volume 7
[AD-A255383] p 992 N93-14741
ROSAT all-sky survey on the Einstein EMSS sample
[NASA-CR-191627] p 1013 N93-15340

X RAY APPARATUS
X-ray monochromator
[NASA-CASE-MFS-28392-1] p 982 N93-14711

X RAY ASTRONOMY
Imaging the sun in hard x-rays using Fourier telescopes p 1048 N93-14591
Physics of x ray multilayer structures: Summaries of papers presented at the physics of x ray multilayer structures topical meeting, technical digest series, 1992, volume 7
[AD-A255383] p 992 N93-14741
The evolution of the quasar continuum
[NASA-CR-191673] p 1012 N93-14759
Supervised selection of galaxy candidates from the IRAS PSC: The quality of the selection and the infrared properties of the galaxy candidates
[MPE-PREPRINT-216] p 1021 N93-15284

X RAY BINARIES
Compact objects in the disk and globular clusters p 1018 N93-14594

X RAY DETECTORS
High speed imaging for flash radiography using PIN diodes
[DE92-040959] p 882 N93-15381
A liquid xenon imaging telescope for gamma ray astrophysics: Design and expected performance p 1014 N93-15591

X RAY DIFFRACTION
Physics of x ray multilayer structures: Summaries of papers presented at the physics of x ray multilayer structures topical meeting, technical digest series, 1992, volume 7
[AD-A255383] p 992 N93-14741
Characterization of cholesteric cyclic siloxane liquid crystalline materials
[AD-A256128] p 994 N93-15190

X RAY IMAGERY
Full surface testing of grazing incidence mirrors
[AD-A255644] p 979 N93-14152
Imaging the sun in hard x-rays using Fourier telescopes p 1048 N93-14591
Center for x ray optics, 1991
[DE93-001543] p 984 N93-15350

X RAY INSPECTION
Nondestructive evaluation of damage in SiC/Al metal matrix composite using x ray tomographic microscopy p 829 N93-14192

X RAY LASERS
Physics of x ray multilayer structures: Summaries of papers presented at the physics of x ray multilayer structures topical meeting, technical digest series, 1992, volume 7
[AD-A255383] p 992 N93-14741

X RAY SCATTERING
Characterization of cholesteric cyclic siloxane liquid crystalline materials
[AD-A256128] p 994 N93-15190
Morphological analysis of ionomers
[DE92-040162] p 852 N93-15415

X RAY SOURCES
Personal computer based computed tomography system
[KCP-613-4806] p 945 N93-14876
A liquid xenon imaging telescope for gamma ray astrophysics: Design and expected performance p 1014 N93-15591

X RAY SPECTRA
Quasar x-ray spectra revisited p 1012 N93-14760

X RAY SPECTROSCOPY
Multiwavelength spectroscopy of active galactic nuclei p 1011 N93-14611
Center for x ray optics, 1991
[DE93-001543] p 984 N93-15350

X RAY TELESCOPES
Imaging the sun in hard x rays using Fourier telescopes
[NASA-TM-108390] p 1013 N93-15203

X RAYS
A differential equation design method for finite-conjugate, multi-mirror imaging systems p 979 N93-14165
Extracting x rays, gamma rays, and electron-positron pairs from supermassive Kerr black holes using the Penrose mechanism p 1049 N93-14176
Nonthermal radio, x ray and gamma ray emissions from chaotic winds of early-type, massive stars p 1050 N93-14242
Experimental considerations of higher order parametric x rays from silicon crystals of varying thicknesses
[AD-A256082] p 990 N93-14260
Improvement and analysis of the radiation response of RADFET dosimeters
[AD-A254115] p 869 N93-15133
Imaging the sun in hard x rays using Fourier telescopes
[NASA-TM-108390] p 1013 N93-15203
Center for x ray optics, 1991
[DE93-001543] p 984 N93-15350

XENON
Development of a High Resolution Liquid Xenon Imaging Telescope for Medium Energy Gamma Ray Astrophysics
[NASA-CR-191781] p 1013 N93-15589
A Monte Carlo analysis of the liquid xenon TPC as gamma ray telescope p 1014 N93-15590
A liquid xenon imaging telescope for gamma ray astrophysics: Design and expected performance p 1014 N93-15591
Liquid xenon time projection chamber for gamma rays in the MeV region: Development status p 1014 N93-15592

XV-15 AIRCRAFT
Tiltrotor aircraft noise: A summary of the presentations and discussions at the 1991 FAA/Georgia Tech Workshop
[DOT/FAA/RD-91/23] p 974 N93-14912

Y

YAG LASERS
Ultrashort-pulse laser system: Theory of operation and operating procedures
[AD-A257023] p 887 N93-15472

YAWING MOMENTS
Program for calculation of aileron rolling moment and yawing moment coefficients at subsonic speeds
[ESDU-88040] p 779 N93-14514

YBCO SUPERCONDUCTORS
Processing and characterization of electrophoretically deposited holmium barium copper oxide superconductor films
[AD-A256329] p 869 N93-15194
High performance YBCO films
[AD-A255439] p 994 N93-15297

YIELD STRENGTH
The response of dispersion-strengthened copper alloys to high fluence neutron irradiation at 415 C
[DE92-019434] p 846 N93-15138
Inelastic deformation of metal matrix composites: Plasticity and damage mechanisms, part 2
[NASA-CR-189096-PT-2] p 837 N93-15401

Progress toward a tungsten alloy wire/high temperature alloy composite turbine blade
[NASA-TM-105901] p 847 N93-15586
YTTRIUM OXIDES
Tribology of improved transformation-toughened ceramics-heat engine test
[DE92-041385] p 851 N93-15295
Material development in the Si3N4 system using glass encapsulated HIP'ing
[DE92-041381] p 837 N93-15388
Processing of sinterable transformation toughened ceramics for application in ceramic technology for advanced heat engines project
[DE92-041372] p 853 N93-15453

Z

ZIRCONIUM CARBIDES
Processing and microstructure of Nb-1 percent Zr-0.1 percent C alloy sheet
[NASA-TM-105921] p 847 N93-15524
ZIRCONIUM OXIDES
Hyperfine experimental investigation of zirconia ceramics
[DE92-040301] p 850 N93-14903
Jet vapor deposition of thin films for solid oxide and other fuel cell applications
[DE92-019980] p 851 N93-15222
Analytical and experimental evaluation of joining ceramic oxides to ceramic oxides and ceramic oxides to metal for advanced heat engine applications
[DE92-041383] p 851 N93-15294
Tribology of improved transformation-toughened ceramics-heat engine test
[DE92-041385] p 851 N93-15295
Compaction of submicron and nanocrystalline Al2O3-ZrO2 ceramics
[DE92-040233] p 852 N93-15320
Processing of sinterable transformation toughened ceramics for application in ceramic technology for advanced heat engines project
[DE92-041372] p 853 N93-15453
ZONAL FLOW (METEOROLOGY)
Results of a zonally truncated three-dimensional model of the Venus middle atmosphere p 1037 N93-14351
A model for the formation of the extended paraboloidal halos around some impact craters on Venus
p 1037 N93-14352

Typical Personal Author Index Listing

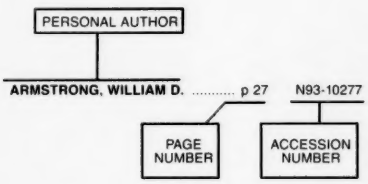

Listings in this index are arranged alphabetically by personal author. The page number helps you locate the citation in the abstract section. The accession number denotes the number by which the citation is identified.

A

AARONS, JULES ..... p 917 N93-15395
ABDALLAH, J. A., JR. ..... p 988 N93-15418
ABDELFATTAH-ZIDAN, RAGAIY .. p 854 N93-14630
ABED, EYAD H. ..... p 858 N93-14259
ABUMERI, G. H. ..... p 902 N93-15343
ABUSHAGUR, MUSTAFA A. ..... p 892 N93-15117
ACHTERBERG, RICHARD KARL p 1046 N93-14865
ADAMOVITS, PETER ..... p 806 N93-14927
ADAMS, CATHERINE A. ..... p 785 N93-15013
ADAMS, KENNETH E. ..... p 854 N93-14801
ADAMS, RICHARD J. ..... p 785 N93-15013
p 786 N93-15017
p 786 N93-15019
ADAMS, W. W. ..... p 994 N93-15190
ADAMSON, H. PATRICK ..... p 784 N93-14849
ADDERLEY, C. I. ..... p 879 N93-15473
p 880 N93-15488
ADELI, HOJJAT ..... p 943 N93-14505
ADIGA, B. S. ..... p 794 N93-15161
ADORF, H.-M. ..... p 1021 N93-15284
AFZAL, ROBERT S. ..... p 887 N93-15250
AGRAWAL, OM P. ..... p 889 N93-14545
AHLVIN, RICHARD G. ..... p 804 N93-14238
AHMAD, J. ..... p 851 N93-15294
AHUJA, K. K. ..... p 974 N93-14912
AJMANI, KUMUD ..... p 877 N93-14885
AKHTER, N. ..... p 856 N93-14107
AKIM, E. L. ..... p 1023 N93-14289
AKIN, O. ..... p 880 N93-15652
AKSIT, MEHMET ..... p 946 N93-15084
AL-KHALIL, KAMEL M. ..... p 787 N93-15345
p 787 N93-15354
ALBRECHT, G. F. ..... p 876 N93-14715
ALCORN, T. R. ..... p 871 N93-15479
ALEXANDER, DON R. ..... p 804 N93-14128
ALEXANDER, DOUG ..... p 1026 N93-14306
ALEXANDER, M. J. ..... p 1023 N93-14290
ALEXANDER, M. L. ..... p 887 N93-15135
ALEXIADES, V. ..... p 907 N93-15219
ALEXOPOULOS, JIM S. ..... p 1024 N93-14291
ALKOV, ROBERT A. ..... p 786 N93-15016
ALLEN, D. A. ..... p 1026 N93-14308
p 1035 N93-14346
ALLEN, JAMES ..... p 945 N93-14654
ALLEN, JOHN A. ..... p 965 N93-15293
ALMON, A. C. ..... p 828 N93-14718
ALOUANI, A. T. ..... p 858 N93-14415
ALOUNIA, ALI T. ..... p 982 N93-14880
ALPERS, W. ..... p 929 N93-14986
ALSPAUGH, THOMAS A. ..... p 946 N93-15052
ALVISI, LORENZO ..... p 862 N93-15339
AMANATIDES, JOHN ..... p 954 N93-15544
AMBROSIUS, B. A. C. ..... p 813 N93-15000
AMLEKAR, PAT ..... p 806 N93-14931
AMRANE, KARIM ..... p 872 N93-14200
AMREIN, BRUCE E. ..... p 936 N93-15249
ANDERSON, C. H. ..... p 1042 N93-14380
ANDERSON, CHARLES E., JR. ..... p 844 N93-14508
ANDERSON, JOHN ..... p 905 N93-14676
ANDERSON, MARK R. ..... p 821 N93-15609
p 823 N93-15618
ANDERSON, R. J. ..... p 966 N93-15385
ANDERSON, SCOTT RICHARD ..... p 873 N93-14464
ANDERSON, THEODORE LYNDE . p 914 N93-14861
ANDERSON, W. E. ..... p 870 N93-15412
ANDRES, PAUL ..... p 1026 N93-14306
ANDREWS, THOMAS S. ..... p 861 N93-15317
ANGELES, J. ..... p 805 N93-14923
ANN, CHARLES ..... p 844 N93-14264
ANSARI, M. A. ..... p 991 N93-14485
ANTOLOVICH, STEPHEN D. ..... p 898 N93-14272
ANTONIADIS, A. ..... p 970 N93-14538
ANTONUCCI, YVONNE LEDERER p 1000 N93-14205
ANTREASIAN, PETER GARO ..... p 817 N93-14586
ANZIC, J. ..... p 852 N93-15344
p 819 N93-15597
APATHY, ISTVAN ..... p 795 N93-15166
APERS, PETER M. G. ..... p 958 N93-15093
p 959 N93-15141
p 959 N93-15142
APRILE, E. ..... p 1014 N93-15590
p 1014 N93-15591
p 1014 N93-15592
APRILE, ELENA ..... p 1013 N93-15589
APRUZESE, JOHN P. ..... p 988 N93-14579
ARAUJO, JOHN ..... p 999 N93-14526
AREFMANESH, ALI ..... p 874 N93-14465
ARGO, P. ..... p 862 N93-15427
ARKANI-HAMED, JAFAR ..... p 1024 N93-14292
p 1024 N93-14293
ARMBRUSTER, DIETER ..... p 998 N93-15333
ARMSTRONG-CARROLL, E. ..... p 834 N93-14755
ARMSTRONG, NEAL R. ..... p 985 N93-15516
ARMSTRONG, W. T. ..... p 862 N93-15435
ARNAULT, S. ..... p 918 N93-14982
p 929 N93-14983
ARVIDSON, R. E. ..... p 1024 N93-14294
ASHFORD, N. J. ..... p 789 N93-14729
ASPNES, JAMES ..... p 943 N93-14423
ATHREYA, KRISHNA B. ..... p 970 N93-14487
ATKINSON, STEVE ..... p 883 N93-15042
ATWATER, TERRILL ..... p 867 N93-14642
AUBELE, J. C. ..... p 1024 N93-14295
p 1026 N93-14309
p 1029 N93-14323
p 1042 N93-14380
AUDOIN, CLAUDE ..... p 972 N93-14496
AUER, BRUCE M. ..... p 819 N93-15596
AVVA, V. SARMA ..... p 834 N93-14754
AYLOR, D. M. ..... p 830 N93-14232
AYLOR, JAMES H. ..... p 948 N93-15264
AZZINARI, STEPHEN M. ..... p 902 N93-15260

B

BABKOFF, HARVEY ..... p 934 N93-14240
BACKES, P. ..... p 900 N93-14498
BADER, ANTON ..... p 778 N93-15185
BADIR, ASHRAF M. ..... p 895 N93-14158
BADLER, NORMAN I. ..... p 940 N93-15363
BAECKER, RONALD M. ..... p 953 N93-15539
p 955 N93-15552
BAINES, KEVIN HAYS ..... p 1021 N93-15079
BAJAJ, CHANDRAJIT ..... p 953 N93-15537
BAKER, STUART W. ..... p 946 N93-15068
BAKER, T. F. ..... p 932 N93-15001
BAKER, V. R. ..... p 1033 N93-14337
BALDWIN, LAWRENCE C. ..... p 939 N93-14548
BALMINO, G. ..... p 926 N93-14965
p 918 N93-14969
p 918 N93-14993
BALUJA, SHUMEET ..... p 959 N93-15407
BANAN, MOHSEN ..... p 995 N93-15311
BANERJEE, S. ..... p 992 N93-14643
p 993 N93-15008
BANKS, BRUCE A. ..... p 819 N93-15594
p 819 N93-15596
BANSAL, NAROTTAM P. ..... p 850 N93-14886
BANURA, GEORGE A. ..... p 868 N93-14826
BARD, ARNOLD ..... p 867 N93-14642
BARKESHLI, SINA ..... p 830 N93-14436
BARLIER, FRANCOIS ..... p 926 N93-14965
p 906 N93-14967
BARNA, P. STEPHEN ..... p 780 N93-14737
p 780 N93-14738
BARNETT, WILLIAM T. ..... p 862 N93-15376
BARRETT, TERENCE W. ..... p 885 N93-14821
BARRY, ROGER G. ..... p 1000 N93-14182
BARSCHDORFF, DIETER ..... p 797 N93-15183
BARTLETT, R. ..... p 816 N93-15477
BARTZ, ROBERT ..... p 881 N93-14653
BASILEVSKY, A. T. ..... p 1024 N93-14296
p 1030 N93-14326
p 1044 N93-14392
BASILI, VICTOR R. ..... p 947 N93-15199
BASS, C. A. ..... p 789 N93-14574
BATES, KEITH A. ..... p 986 N93-15518
BATHOR, MIKLOS ..... p 949 N93-15299
BAUER, HELMUT F. ..... p 878 N93-15120
p 878 N93-15132
BEACHLEY, O. T., JR. ..... p 996 N93-15443
BEAL, ERNA J. ..... p 893 N93-15232
BEAN, J. R. ..... p 907 N93-15134
BECKERDITE, STANLEY M. ..... p 894 N93-14500
BEDNAR, EDWARD A. ..... p 861 N93-15316
BEEBY, MARTIN ..... p 952 N93-15476
BEHI, M. ..... p 853 N93-15452
BEINER, L. ..... p 950 N93-15306
BEITING, EDWARD J. ..... p 839 N93-14530
BEKEFI, GEORGE ..... p 885 N93-14599
BELCHER, JEWELL G. ..... p 939 N93-14870
BELENGER, ROBERT V. ..... p 891 N93-14881
BELL, HAROLD A. ..... p 859 N93-14442
BELTZ, GLENN EDWARD ..... p 896 N93-14214
BEN-ARIEH, D. ..... p 950 N93-15304
BENADY, M. ..... p 949 N93-15303
BENAGE, J. F., JR. ..... p 989 N93-15436
BENIDIR, SAMIA ..... p 1000 N93-14206
BENJAMIN, T. G. ..... p 994 N93-15221
BENNETT, A. F. ..... p 926 N93-14970
BENTON, N. ..... p 918 N93-14999
BENTZ, M. D. ..... p 855 N93-15420
BERBERT, JOHN ..... p 1003 N93-14776
BERETAN, K. ..... p 1025 N93-14300
BERGMANN, HEINRICH W. ..... p 835 N93-15075
BERGMANS, LODEWIJK ..... p 946 N93-15084
BERKE, ANTHONY ..... p 784 N93-14851
BERMAN, J. D. ..... p 933 N93-14162
BERNACKI, BRUCE E. ..... p 984 N93-15506
p 984 N93-15507
BERTENYI, E. ..... p 808 N93-14939
BESSE, DAVID S. ..... p 858 N93-14426
BETHOUX, J. P. ..... p 926 N93-14965
BEUTH, JACK LEE, JR. ..... p 897 N93-14215
BEYERMANN, W. P. ..... p 998 N93-14905
BEZARD, B. ..... p 1026 N93-14308
BHAGAT, R. B. ..... p 838 N93-15625
BHARDWAJ, H. D. ..... p 991 N93-14485
BHATNAGAR, V. ..... p 863 N93-15440
BHATT, HEMANSHU DEVSHANKAR p 864 N93-14190
BHUSHAN, BHARAT ..... p 1002 N93-14772
BIAN, BUMING ..... p 957 N93-15569
BIANCALE, R. ..... p 926 N93-14965
p 918 N93-14969
p 918 N93-14993
BIDAUD, P. ..... p 949 N93-15301
BIDWELL, C. S. ..... p 788 N93-15522
BIEDERMAN, IRVING ..... p 936 N93-14510
BIERMANN, A. ..... p 915 N93-14877
BIERMANN, ARTHUR H. ..... p 878 N93-15285
BILL, ROBERT C. ..... p 799 N93-14891
BILOTTI, FRANK ..... p 1024 N93-14297
BINDSCHADLER, D. L. ..... p 1025 N93-14298
p 1043 N93-14383
BINISMAIL, BAKAR ..... p 865 N93-14191
BIRD, J. ..... p 808 N93-14938
BIRENZVIGE, A. ..... p 854 N93-15640
BISHOP, L. B. ..... p 882 N93-15381
BJORAKER, GORDON L. ..... p 1021 N93-15079
BJORDAL, HALVOR ..... p 974 N93-15074

BLACK, D. p 826 N93-15215
BLACK, S. p 870 N93-15424
BLACK, S. J. p 903 N93-15423
BLACKBURN, JOHN p 856 N93-15353
BLACKWELL, KIM p 1004 N93-15027
BLAIR, KIM BILLY p 898 N93-14282
BLAIR, MAX p 779 N93-14441
BLAIR, W. D. p 858 N93-14415
BLANC, F. p 929 N93-14984
p 929 N93-14987
BLANCO, A. p 843 N93-15283
BLANKEN, HENK M. p 1009 N93-15492
BLASSO, L. G. p 1002 N93-14771
BLASSO, LEN p 1004 N93-15027
BLEVINS, B. p 862 N93-15435
BLITSTEIN, RONALD p 1002 N93-14775
p 1006 N93-15045
BLIZARD, K. p 983 N93-15255
BLOCH, B. p 836 N93-15253
BLOCH, J. J. p 818 N93-15071
BLOCK, JOACHIM p 835 N93-15075
BLOMBERG, L. G. p 916 N93-15252
BLOOMFIELD, JOHN R. p 786 N93-15021
p 787 N93-15022
BOATMAN, DAVE p 820 N93-15599
BOBINA, N. N. p 1037 N93-14355
BODE, L. p 926 N93-14968
BOELCS, A. p 782 N93-15489
BOGDANSKI, MICHAEL S. p 828 N93-15576
BOGNER, S. p 796 N93-15176
BOLLER, T. p 1021 N93-15284
BOLOTNIKOV, A. p 1014 N93-15590
p 1014 N93-15591
p 1014 N93-15592
BOLTON, SCOTT JAY p 973 N93-14227
BOND, THOMAS H. p 781 N93-14911
p 782 N93-15338
p 782 N93-15404
BOND, WILLIAM R. p 814 N93-15612
BONN, JOHN W. p 814 N93-15607
BOOKHAM, R. P. p 795 N93-15170
BOOLCHAND, P. p 885 N93-14647
BOOS, J. B. p 993 N93-14820
BORGHI, R. p 841 N93-14626
BORMAN, G. L. p 893 N93-15410
BORN, GEORGE H. p 926 N93-14966
BOROWSKY, MICHAEL S. p 786 N93-15016
BOROZDIN, V. K. p 1037 N93-14355
BOSIA, G. p 863 N93-15440
BOSISIO, R. G. p 807 N93-14934
BOSISIO, RENATO G. p 807 N93-14932
p 807 N93-14936
BOTT, JULIAN p 795 N93-15168
BOUATOUCH, KADI p 957 N93-15570
BOUCHER, CLAUDE p 926 N93-14965
p 906 N93-14967
p 918 N93-14993
BOUDIN, F. p 949 N93-15301
BOUGHER, S. W. p 1023 N93-14290
BOURCIER, R. J. p 847 N93-15383
BOUSLOG, STANLEY A. p 903 N93-15530
BOUSSUGE, M. p 851 N93-15127
BOWDEN, D. A. p 1012 N93-14762
BOWER, GARY ALLEN p 1011 N93-14228
BOWERS, MICHAEL T. p 917 N93-15463
BOWERY, NORMAN G. p 935 N93-15009
BOWLES, ROLAND L. p 783 N93-14844
BOYCE, J. M. p 1040 N93-14369
BOYCE, REX A. p 891 N93-14871
BOYD, JOHN E. p 1003 N93-14777
BOYLE, R. J. p 777 N93-14102
BOZEK, JOHN M. p 909 N93-15523
BOZEMAN, RICHARD J., JR. p 882 N93-14841
BRADLEY, D. T. p 811 N93-14952
BRADLEY, MICHAEL S. p 849 N93-14489
BRADLEY, S. p 836 N93-15387
p 837 N93-15455
BRADY, ROBERT F. p 850 N93-14802
BRANDT, MADS H. p 793 N93-15156
BRAUN, ROBERT D. p 813 N93-15367
BRAY, K. N. C. p 841 N93-14625
BRESINA, JOHN p 965 N93-15291
BRESINA, JOHN L. p 963 N93-14765
BREUER, KENNETH S. p 787 N93-15360
BREUNIG, THOMAS M. p 829 N93-14192
BREWER, ERIC A. p 941 N93-15628
BRINKLEY, T. J. p 856 N93-14107
BRINKMAN, P. W. p 820 N93-15600
BRINKSMA, ED p 946 N93-15077
BRITTON, KATHRYN H. p 946 N93-15052
BRITTON, RANDALL K. p 782 N93-15404
BROACH, DANA p 789 N93-14276
BROADFOOT, A. L. p 814 N93-14697
p 815 N93-14698
BROADWELL, JAMES E. p 842 N93-15114
BROCKEL, KENNETH H. p 862 N93-15376
BROCKHAUS, R. p 797 N93-15182
BROCKMAN, PHILIP p 784 N93-14845
BRODSKY, S. J. p 978 N93-15468
BROEDE, JURGEN p 799 N93-14893
BROOKES, STEPHEN p 960 N93-15494
BROOKSHIRE, S. P. p 882 N93-14810
BROSSIER, C. p 918 N93-14982
p 929 N93-14984
BROWN, J. J., JR. p 853 N93-15438
BROWN, LESLIE F. p 1050 N93-14229
BROWN, LORETTA p 1007 N93-15112
BROYLES, A. A. p 972 N93-15057
BRUCKART, JAMES E. p 933 N93-14103
p 881 N93-14105
BRUCKNER, A. P. p 783 N93-15588
BRUECK, S. R. p 886 N93-15115
BRYANT, RANDAL E. p 959 N93-15205
BRYSON, R. J. p 981 N93-14403
BU, Y. p 842 N93-14669
p 992 N93-14670
BUBSEY, R. T. p 902 N93-15369
BUCHANAN, R. A. p 846 N93-15059
BUCHHOLZ, J. J. p 797 N93-15182
BUCKLEY, JOHN D. p 832 N93-14744
BUDZIEN, SCOTT ALAN p 1017 N93-14230
BUECHLER, D. p 894 N93-14104
p 900 N93-14498
BUEHLER, KURT A. p 1009 N93-15627
BUELL, JOHN p 952 N93-15502
BUFFINGTON, CHARLES O. p 849 N93-14531
BULLOCK, M. A. p 1025 N93-14299
BULMER, M. H. p 1025 N93-14300
BUNNING, TIMOTHY J. p 994 N93-15190
BUONCRISTIANI, A. M. p 997 N93-15587
BURBA, G. A. p 1037 N93-14353
p 1037 N93-14354
BURCH, JERRY R. p 968 N93-14492
BURKE, JAMES J. p 986 N93-15518
BURNETT, JACK C. p 893 N93-15232
BURNS, ROGER G. p 1025 N93-14301
BURNSIDE, W. D. p 945 N93-14807
BURRAGE, DEREK p 926 N93-14968
BURT, J. D. p 1025 N93-14302
BUSALACCHI, A. J., JR. p 928 N93-14977
p 928 N93-14980
p 930 N93-14989
BUSSEY, D. B. J. p 1025 N93-14303
BUSSOLETTI, E. p 843 N93-15283
BUTERBAUGH, ALAN L. p 858 N93-14250
BUTLER, BRYAN J. p 1036 N93-14349
BUTLER, DANIEL H., JR. p 866 N93-14555
BUXTON, WILLIAM A. A. p 954 N93-15548
BUYONG, TAHER BIN p 904 N93-14220
BYROM, TED GARY p 780 N93-14631

C

CADIEU, F. J. p 972 N93-14679
CAIN, CLARENCE P. p 887 N93-15472
CALDWELL, J. L. p 937 N93-14600
CALDWELL, JOHN A. p 937 N93-14600
CALEF, CHARLES p 914 N93-14724
CALFO, FREDERICK D. p 872 N93-14150
CALLICOTT, WILLIAM M. p 1003 N93-14779
CAMPBELL, A. P. p 906 N93-15442
CAMPBELL, D. B. p 1026 N93-14304
p 1037 N93-14352
p 1039 N93-14363
p 1043 N93-14384
CAMPBELL, J. H. p 886 N93-14906
CAMPBELL, J. W. p 1013 N93-15203
CAMPBELL, JONATHAN WESLEY p 1048 N93-14591
CAMPBELL, STEVEN p 784 N93-14851
CAMPONESCHI, E. T., JR. p 831 N93-14509
CANARD-CARUANA, S. p 975 N93-15130
CANE, M. p 928 N93-14977
CANFIELD, P. C. p 998 N93-14905
CANT, A. p 943 N93-14502
CAPPABIANCA, R. p 915 N93-14877
CARADONNA, F. X. p 782 N93-15483
CARAM, JOSE M. p 903 N93-15530
CARAVAGGIO, LEVINO p 821 N93-15605
CARBONI, JEANNE D. p 800 N93-15342
CARDEN, JAMES R. p 939 N93-14870
CARDEW-HALL, M. J. p 951 N93-15386
CARDWELL, P. LARRY p 1005 N93-15033
CARGILL, A. p 782 N93-15489
CARLIN, BRADLEY P. p 971 N93-15110
CARLSON, DARLENE M. p 1006 N93-15041
CARLSTEN, B. E. p 887 N93-15417
CARPENTER, GAIL A. p 962 N93-14551
CARRABBA, MICHAEL M. p 983 N93-15241
CARROLL, KIERAN A. p 804 N93-14921
CARTER, DAVID J. p 937 N93-14600
CARTER, HAROLD W. p 948 N93-15266
CARTER, M. J. p 818 N93-14904
p 862 N93-15435
CARTON, J. p 928 N93-14977
CARTWRIGHT, D. E. p 930 N93-14991
CARUTHERS, C. M. p 1010 N93-15655
CARY, RON p 814 N93-15611
CASASENT, DAVID p 961 N93-14409
CASSE, V. p 918 N93-14982
CATALDO, ROBERT L. p 909 N93-15523
CATON, R. p 997 N93-15587
CAVALLARO, CHRISTOPHER p 891 N93-14735
CAVALLARO, PAUL V. p 891 N93-14735
CAWLEY, J. p 851 N93-15294
CAZENAVE, ANNY p 918 N93-14969
p 918 N93-14993
CEBALLOS, MYRIAM MONDRAGON p 997 N93-14116
CERVARICH, PETER J. p 789 N93-14501
CHADWICK, D. J. p 1040 N93-14369
CHADWICK, D. JOHN p 1026 N93-14305
CHAI, GIN BOAY p 831 N93-14597
CHALKLEY, JOHN C. p 942 N93-14164
CHALLENOR, P. p 932 N93-15001
CHAMBERS, GARY D. p 823 N93-15620
CHAMIS, C. C. p 902 N93-15343
CHAMPION, M. p 841 N93-14627
CHAN, SAMUEL Y. p 802 N93-14811
CHANEY, KENNETH D. p 862 N93-15376
CHANG, C. L. p 837 N93-15388
CHANG, FU-KUO p 830 N93-14493
CHANG, JINHWA p 778 N93-14160
CHANG, THIEL p 1009 N93-15492
CHANG, YEOU SHIN p 829 N93-14193
CHANG, YUN p 878 N93-15285
CHASE, G. G. p 846 N93-15056
CHAUTARD, J. C. p 999 N93-15118
CHELIKOWSKY, J. R. p 993 N93-14909
CHELTON, DUDLEY B. p 926 N93-14970
CHEN, C. p 809 N93-14945
CHEN, C. S. p 889 N93-14528
CHEN, D. p 1014 N93-15590
p 1014 N93-15591
p 1014 N93-15592
CHEN, HSICHIEH p 831 N93-14607
CHEN, P. J. p 994 N93-15233
CHEN, QI p 993 N93-14838
CHEN, TSAI-LIN p 897 N93-14217
CHEN, WAN p 1050 N93-14242
CHENEY, R. p 927 N93-14974
CHENG, CHAO-HSIEN p 830 N93-14466
CHENG, CHING-WEI p 813 N93-15103
CHENG, PETER Y. p 802 N93-14811
CHEUNG, Y. K. p 875 N93-14690
CHIANG, YU-LIANG p 873 N93-14273
CHILDS, EDWARD P. p 880 N93-15643
CHIMA, R. V. p 777 N93-14102
CHIN, Y. H. p 887 N93-15325
CHIREHDAST, MEHRAN p 855 N93-14467
CHIRIKJIAN, GREGORY SCOTT p 892 N93-15104
CHITTUM, CHARLES B. p 783 N93-14277
CHIU, Y. T. p 916 N93-14899
CHODAS, P. W. p 1027 N93-14310
CHOENNI, SUNIL p 1009 N93-15492
CHOI, DONG p 944 N93-14575
CHOI, YAT p 982 N93-14784
CHOKSHI, ATUL H. p 852 N93-15394
CHOU, Y. T. p 903 N93-15374
CHOUEIRY, E. p 808 N93-14940
CHREN, WILLIAM A., JR. p 871 N93-15529
CHRIST, RICHARD E. p 951 N93-15445
CHRISTENSEN, U. R. p 1043 N93-14385
CHRISTIANSON, ROLLIN C. p 891 N93-14843
CHRYSTALL, KEITH p 810 N93-14949
CHU, JASON C. p 842 N93-14669
p 992 N93-14670
CHUBB, DONALD L. p 872 N93-14150
CHUN, WAN JONG p 857 N93-14189
CHUNG, J. N. p 948 N93-15274
CHURCH, JOHN A. p 927 N93-14971
CHUVALA, TOM p 823 N93-15619
CISPER, M. E. p 887 N93-15135
CLARK, JERRY p 1026 N93-14306
CLARK, NOEL A. p 996 N93-15446
p 996 N93-15447
CLARK, R. E. H. p 988 N93-15418
CLAVIN, PAUL p 840 N93-14618
CLEMENTS, SHAUN p 899 N93-14468
CLIFFORD, MARY B. p 904 N93-14262
CLIFTON, JAMES M. p 859 N93-14610
CLINE, J. P. p 850 N93-15049
COHEN, RICHARD JONATHAN p 847 N93-14170
COLAIANNI, M. L. p 994 N93-15233
COLANGELI, L. p 843 N93-15283
COLBROOK, A. p 1009 N93-15639
COLBY, FRANK P., JR. p 918 N93-14153

COLE, RODNEY E. ..... p 920 N93-14547
COLEMAN, JAMES J. ..... p 866 N93-14562
COLEMAN, R. ..... p 926 N93-14968
p 927 N93-14971
COLEMAN, SAM ..... p 1003 N93-14780
p 1007 N93-15047
COLINGE, J. P. ..... p 866 N93-14534
COLLAUDIN, B. ..... p 825 N93-15140
COLLETTE, J. G. R. ..... p 816 N93-15475
COLOMBO, O. L. ..... p 930 N93-14991
COLVIN, T. R. ..... p 1027 N93-14310
COMBI, MICHAEL R. ..... p 1020 N93-14814
CONLON, E. S. ..... p 1012 N93-14762
CONNATSER, ROBERT ..... p 910 N93-14764
CONNORS, CHRIS ..... p 1024 N93-14297
COOK, R. A. ..... p 972 N93-15243
COOMBS, DAVID J. ..... p 982 N93-14582
COOPER, BARRY ..... p 787 N93-15022
COOPER, THOMAS D. ..... p 777 N93-14549
COOPER, TOMMY G. ..... p 881 N93-14494
CORBIN, N. D. ..... p 837 N93-15388
CORCORAN, JOHN W. ..... p 1006 N93-15040
CORCORAN, TIMOTHY C. ..... p 839 N93-14530
CORTEZ, MAXIMO G. ..... p 821 N93-15609
p 823 N93-15618
CORTINAS, JOHN VICTOR, JR. ... p 923 N93-15087
COSTELLO, DAVID J. ..... p 881 N93-14494
COTARAS, FREDERICK D. ..... p 925 N93-14512
COTSAKIS, SPIROS ..... p 1018 N93-14592
COULTER, R. C. ..... p 944 N93-14569
COURAIN, MARGARET EILEEN ... p 918 N93-14114
COUSSEMENT, R. ..... p 885 N93-14647
COWLEY, STEPHEN J. ..... p 880 N93-15499
COX, DANIEL JOSEPH ..... p 960 N93-14201
CRANE, J. ALLEN ..... p 934 N93-14708
CRANE, R. L. ..... p 994 N93-15190
CRAVENS, T. E. ..... p 1026 N93-14307
CREMER, JAMES F. ..... p 957 N93-15565
CRESSWELL, G. R. ..... p 927 N93-14971
CREUTZBERG, F. ..... p 811 N93-14952
CRISP, D. ..... p 1026 N93-14308
p 1035 N93-14346
CRONIN, T. M. ..... p 906 N93-15364
CROW, S. E. ..... p 799 N93-14895
CROWDER, GERALD L. ..... p 1010 N93-14249
CRUMPLER, L. S. ..... p 1024 N93-14295
p 1026 N93-14309
p 1029 N93-14323
p 1042 N93-14380
CUMMINGS, RICK ..... p 855 N93-14793
CUNNINGHAM, ROBERT K. ..... p 937 N93-14580
CUNNINGTON, GEORGE R., JR. .. p 903 N93-15530
CUPP, CHRISTIAN M. ..... p 999 N93-14106
p 1008 N93-15335
CURTIS, CRAIG H. ..... p 985 N93-15512
CURWEN, PETER W. ..... p 891 N93-14916
CUTKOSKY, M. R. ..... p 888 N93-14434
CUTLER, LEONARD S. ..... p 972 N93-14496
CZAJKOWSKI, C. J. ..... p 846 N93-15348
CZARNECKI, GREGORY J. ..... p 898 N93-14419

D

DAGNINO, A. ..... p 810 N93-14949
DANGELO, C. ..... p 852 N93-15437
DANIEL, JAMES A. ..... p 891 N93-14843
DANIELS, GRAHAME ..... p 797 N93-15178
DANZINGER, JAMES L. ..... p 985 N93-15516
DAROZA, ROBERT A. ..... p 878 N93-15285
DARZI, MICHAEL ..... p 932 N93-15645
DAUN, BRIAN ..... p 965 N93-15287
p 965 N93-15288
DAVIDIAN, KENNETH O. ..... p 827 N93-15571
DAVIES, M. E. ..... p 1027 N93-14310
DAVIES, STEPHEN JAMES ..... p 989 N93-14171
DAVIS, D. DALE, JR. ..... p 900 N93-14483
DAVIS, EUGENE ..... p 965 N93-15287
p 965 N93-15288
p 965 N93-15289
DAVIS, G. ..... p 816 N93-15477
DAVIS, J. ..... p 870 N93-15421
DAVIS, JERRY G. ..... p 881 N93-14494
DAVIS, JOHN M. ..... p 828 N93-14459
DAVIS, LINDA J. ..... p 939 N93-14548
DAVIS, PAUL I. ..... p 947 N93-15225
DAVIS, ROBERT F. ..... p 994 N93-15244
DAVIS, WAYNE ..... p 953 N93-15542
DAVISON, MICHAEL T. ..... p 802 N93-14252
DAWSON, D. D. ..... p 1027 N93-14311
p 1040 N93-14369
DAYYANI, MOHAMMAD BASEL ... p 906 N93-14839
DDOSS, HANI ..... p 970 N93-14487
DEALE, MICHAEL ..... p 965 N93-15287
p 965 N93-15288
DEATON, A. W. ..... p 813 N93-15392
DEBERGH, C. ..... p 1026 N93-14308
DECKER, LOUIS P. ..... p 976 N93-14438
DEFIGUEIREDO, LUIZ HENRIQUE ..... p 956 N93-15562
DEGROH, K. K. ..... p 852 N93-15344
DEGROH, KIM K. ..... p 819 N93-15594
p 819 N93-15595
p 819 N93-15596
p 819 N93-15597
DEHAVEN, R. A. ..... p 870 N93-15421
DEISSLER, ROBERT G. ..... p 880 N93-15585
DEJONG, E. ..... p 1040 N93-14365
DELCROIX, T. ..... p 930 N93-14989
DELETOMBE, E. ..... p 792 N93-15126
DELEUTERIO, GABRIELE M. T. .... p 805 N93-14925
DELFRATE, JOHN H. ..... p 779 N93-14451
DELLACORTE, CHRISTOPHER .... p 828 N93-15576
DELUCA, DANIEL P. ..... p 844 N93-14264
DEMEY, PIERRE ..... p 927 N93-14972
DEMIRANDAGOMES, JONAS ..... p 956 N93-15562
DEMMEL, JAMES ..... p 956 N93-15560
DEMOLLERAT, T. ..... p 894 N93-15139
DEMOZ, BELAY BERHANE ..... p 923 N93-15088
DENCH, P. ..... p 951 N93-15386
DENLINGER, EDGAR J. ..... p 994 N93-15297
DEPAOLIS, R. A. ..... p 863 N93-15624
DEPIERO, N. L. ..... p 945 N93-14696
DERENIAK, EUSTACE L. ..... p 983 N93-15197
DEREUS, A. J. ..... p 938 N93-15400
DEROUIN, C. R. ..... p 907 N93-15061
DERUIJTER, W. P. M. ..... p 813 N93-15000
DESA, L. ..... p 825 N93-15140
DESAI, PRASUN N. ..... p 813 N93-15367
DESAUBIES, YVES ..... p 927 N93-14973
DESHAIES, B. ..... p 841 N93-14627
DESZOEKE, R. A. ..... p 926 N93-14970
DEUSTUA, SUSANA ELIZABETH p 1017 N93-14243
DEUTSCH, BARUCH ..... p 948 N93-15268
DEUTSCH, T. F. ..... p 884 N93-14284
DEVER, JOYCE A. ..... p 819 N93-15595
DEVER, THERESE M. ..... p 819 N93-15595
DEVRIES, C. ..... p 1043 N93-14384
DEY, SANDWIP K. ..... p 991 N93-14560
p 849 N93-14668
DHONDT, G. ..... p 796 N93-15177
DI, Y. ..... p 851 N93-15222
DIALETIS, D. ..... p 866 N93-14504
DIAMENT, M. ..... p 918 N93-14969
DICAPRIO, PAUL N. ..... p 964 N93-15258
DICKINSON, LARRY C. ..... p 834 N93-14753
DICKSON, KATHERINE J. ..... p 936 N93-15583
DIDZIULIS, S. V. ..... p 851 N93-15242
DIECKMAN, S. L. ..... p 851 N93-15282
DIEHL, ALAN E. ..... p 785 N93-15014
p 786 N93-15015
DIGIANO, CHRISTOPHER J. ..... p 953 N93-15539
DIMARCO, J. N. ..... p 870 N93-15424
DIMOTAKIS, PAUL E. ..... p 842 N93-15114
DINALLO, MICHAEL A. ..... p 983 N93-15230
DITRI, JOHN JOSEPH ..... p 897 N93-14219
DIVECHA, AMARNATH P. ..... p 845 N93-14888
p 846 N93-15231
DIVER, R. B. ..... p 907 N93-15134
DIXSON, MURRAY ELDON ..... p 1051 N93-14917
DOBRANICH, D. ..... p 826 N93-14815
DOCHERTY, P. ..... p 840 N93-14621
DOEL, DAVID L. ..... p 796 N93-15174
DOMAS, PAUL A. ..... p 799 N93-14894
DOMINGUE, JOHN ..... p 953 N93-15540
DOMINH, K. ..... p 918 N93-14969
p 918 N93-14993
DONAHUE, T. M. ..... p 1027 N93-14312
DONATO, M. ..... p 808 N93-14940
DONNELLAN, MARY E. ..... p 845 N93-14726
DONZAC, J. M. ..... p 838 N93-15490
DOOLEY, ROBERT B. ..... p 891 N93-14735
DOORENBOS, ROBERT ..... p 940 N93-14491
DORNATH-MOHR, MICHELLE A. ..... p 869 N93-15194
DORSEY, JOHN T. ..... p 818 N93-15368
DOSS, E. ..... p 826 N93-15215
DOST, SADIK ..... p 855 N93-15201
DOUGLAS, BRUCE ..... p 927 N93-14974
DOUGLAS, STEPHANIE A. ..... p 845 N93-14740
DRAVID, NARAYAN V. ..... p 871 N93-15503
DRESHFIELD, R. L. ..... p 847 N93-15586
DRISCOLL, MICHAEL M. ..... p 972 N93-14496
DROSSART, PIERRE ..... p 1021 N93-15079
DROUET, C. ..... p 838 N93-15490
DRUCKER, STEVEN M. ..... p 955 N93-15553
DRUMMOND, CHARLES H., III ..... p 850 N93-14886
DRUMMOND, MARK ..... p 965 N93-15291
DRUY, M. A. ..... p 983 N93-15255
DU, GUANG-WU ..... p 888 N93-14478
DUBOIS, T. ..... p 878 N93-15122
DUDEK, H.-L. ..... p 797 N93-15184
DUECKMAN, J. H. ..... p 809 N93-14946
DUETT, PATTI S. ..... p 1002 N93-14650
DUFF, CHRISTOPHER ..... p 941 N93-15123
DUFF, TOM ..... p 956 N93-15563
DUFFEY, T. A. ..... p 902 N93-15210
DUFFY, JOSEPH F. ..... p 1005 N93-15037
DUFFY, KEVIN ..... p 811 N93-14956
DUFRESNE, ERIC ..... p 882 N93-15096
DUGGER, M. T. ..... p 847 N93-15383
DUNCAN, I. ..... p 1027 N93-14313
DUNCAN, L. ..... p 900 N93-14498
DUNHAM, JANET ..... p 944 N93-14572
p 944 N93-14581
DUNN, MARTIN LEONARD ..... p 835 N93-15146
DUPENHOAT, Y. ..... p 930 N93-14989
DUPRAT, RAYMOND ..... p 814 N93-15613
DUPRE, J. C. ..... p 886 N93-15128
DUTTON, J. C. ..... p 875 N93-14677
DUVAL, DARLA M. ..... p 1026 N93-14305
DUVAL, WALTER M. B. ..... p 878 N93-14914
DVORAK, GEORGE J. ..... p 831 N93-14550
DYER, DOUGLAS E. ..... p 1008 N93-15315
DYN, N. ..... p 969 N93-15398

E

EATOCK, BRIAN C. ..... p 812 N93-14958
EBNER, C. A. ..... p 995 N93-15351
ECKART, DONALD W. ..... p 869 N93-15194
ECKELMANN, H. ..... p 781 N93-15131
ECKERT, ERIC G. ..... p 975 N93-15647
EDEN, ALP ..... p 998 N93-15333
EDENS, ELEANA ..... p 787 N93-15022
EDMONDS, R. B. ..... p 983 N93-15241
EDWARDS, ARTHUR A. ..... p 814 N93-15610
EDWARDS, D. J. ..... p 846 N93-15138
EDWARDS, ELIZABETH A. ..... p 932 N93-14557
EDWARDS, RONALD L. ..... p 970 N93-14443
EERNISSE, ERROL P. ..... p 972 N93-14496
EGGERS, H. ..... p 835 N93-15075
EISENSTADT, MARC ..... p 953 N93-15540
EISSES, KENNETH J. ..... p 932 N93-15113
EKIS, J. W. ..... p 945 N93-14876
EKLUND, WAYNE D. ..... p 934 N93-14708
EL-GENK, MOHAMED S. ..... p 826 N93-14482
EL-SHIEKH, ALY ..... p 833 N93-14748
p 834 N93-14756
ELACHI, C. ..... p 1044 N93-14392
ELEWA, SALAH A. ..... p 942 N93-14241
ELISHAKOFF, ISAAC ..... p 900 N93-14483
ELIZONDO, JUAN M. ..... p 869 N93-15196
ELLINGSON, W. A. ..... p 851 N93-15282
ELLIOTT, S. J. ..... p 974 N93-14734
ELLIS, JOHN A. ..... p 999 N93-14526
ELMORE, KIM ..... p 785 N93-14852
ELORANTA, E. W. ..... p 885 N93-14497
ELVIS, M. ..... p 1012 N93-14759
p 1012 N93-14760
EMERIC, DARIO A. ..... p 838 N93-14454
EMERSON, TERRY ..... p 939 N93-14520
EMERY, W. ..... p 926 N93-14966
EMHARDT, JUERGEN ..... p 953 N93-15538
ENFIELD, D. B. ..... p 931 N93-14994
ENGELHAUPT, DARELL ..... p 826 N93-14681
ENGLAND, CRAIG D. ..... p 985 N93-15516
EPP, D. ..... p 811 N93-14953
ERDOGAN, F. ..... p 902 N93-15372
p 903 N93-15374
ERDOGAN, FAZIL ..... p 836 N93-15373
ERICKSON, J. ..... p 894 N93-14104
ERICSSON, K. ANDERS ..... p 786 N93-15018
ERWIN, J. KEVIN ..... p 984 N93-15508
ESPOSITO, L. W. ..... p 1045 N93-14397
ESTES, R. H. ..... p 930 N93-14991
ETHRIDGE, EDWIN C. ..... p 997 N93-15500
ETT, WILLIAM H. ..... p 942 N93-14405
EVANS, JAMES ..... p 785 N93-14855
EVANS, SUSAN A. ..... p 1027 N93-14314
EVERTSON, SCOTT R. ..... p 990 N93-14260
EXERTIER, P. ..... p 926 N93-14965

F

FAEHL, R. J. ..... p 989 N93-15422
FAHD, ANTOINE K. ..... p 1028 N93-14315
p 1045 N93-14596
FAIRLIE, GREGORY W. ..... p 783 N93-14277
FAIRWEATHER, M. ..... p 840 N93-14621
FAIZ, MOHAMED M. ..... p 989 N93-14172
FAMINI, G. R. ..... p 854 N93-15640
FANELLI, MICHAEL NICHOLAS . p 1011 N93-14593
FARKAS, JANOS ..... p 795 N93-15166
FARLEY, C. W. ..... p 995 N93-15365
FARLEY, GARY L. ..... p 833 N93-14749
p 834 N93-14753
FARLEY, W. W. ..... p 936 N93-14416

FARMER, THOMAS E. p 800 N93-14897
FARRELL, K. p 846 N93-15348
FAULK, STUART R. p 946 N93-15052
FEGLEY, BRUCE p 1021 N93-15079
FEIBELMAN, W. A. p 1012 N93-14762
FEIGHAN, P. p 810 N93-14949
FEINER, STEVEN p 954 N93-15543
FEKETE, JEAN-DANIEL p 957 N93-15567
FELDMAN, A. p 989 N93-14133
FENDER, DONNA L. p 820 N93-15602
FERNANDES, DAVID NEIL p 1049 N93-15634
FERNSLER, R. F. p 978 N93-14127
FERRANDO, WILLIAM A. p 845 N93-14888
p 846 N93-15231
FETH, LAWRENCE L. p 935 N93-15053
FIEDLER, K. p 796 N93-15175
FIFER, ROBERT A. p 854 N93-15011
FIJMA, DUCO p 947 N93-15092
FILATOVS, G. J. p 834 N93-14756
FILLOUX, J. H. p 931 N93-14998
FINNEGAN, ROBERT D. p 869 N93-15194
FIRESTONE, ELAINE R. p 932 N93-15645
FISCHER, MARC LAURENZ p 1050 N93-14244
FISHER, ALLAN L. p 967 N93-14235
FISHER, RICHARD J. p 983 N93-15230
FISHER, TERRY C. p 821 N93-15606
FISHKIN, KEN p 954 N93-15546
FISK, Z. p 998 N93-14905
FIUME, EUGENE p 954 N93-15545
FLAGELLO, D. G. p 985 N93-15513
FLASH, T. p 949 N93-15303
FLATAU, MARIA p 923 N93-15099
FLEETWOOD, D. M. p 997 N93-15649
p 997 N93-15651
FLEISCHAUER, P. D. p 851 N93-15242
FLICKINGER, WILLIAM H. p 1009 N93-15641
FLOKSTRA, JAN p 958 N93-15093
p 959 N93-15141
FLORYAN, J. M. p 809 N93-14945
FOLEY, M. R. p 837 N93-15454
FOLK, EARL W. p 783 N93-14277
FOLLSTAEDT, D. M. p 847 N93-15383
FONG, PHILIP p 952 N93-15534
FONTAINE, D. p 949 N93-15301
FONTI, S. p 843 N93-15283
FOOTE, MARC C. p 994 N93-15151
FOOTE, STEPHEN L. p 935 N93-14782
FORBES, GREGORY S. p 924 N93-15581
FORD, J. M. p 851 N93-15282
FORD, P. G. p 1028 N93-14316
p 1039 N93-14360
p 1039 N93-14363
FORD, PETER G. p 1035 N93-14345
FORKAPA, MARK p 823 N93-15616
FORSTER, ESTRELLE M. p 935 N93-14789
FOWLER, J. O. p 879 N93-15473
p 880 N93-15488
FOX, KAREN V. p 999 N93-14106
p 1008 N93-15335
FOX, ROY G. p 787 N93-15024
p 787 N93-15025
FOYE, R. L. p 834 N93-14757
FRANCIS, PETER N. p 919 N93-14196
FRANCIS, W. E. p 916 N93-14899
FRANK, THOMAS A. p 868 N93-14887
FRANKIGNOUL, C. p 927 N93-14973
FRANSSON, T. p 782 N93-15489
FRAZIER, WILLIAM E. p 845 N93-14726
FREEDMAN, RON p 808 N93-14937
FREEMAN, MICHAEL p 821 N93-15603
FREER, DOROTHY J. p 942 N93-14247
FRETY, N. p 851 N93-15127
FRICKE, ROBERT W. p 815 N93-14736
FRIEDMAN, M. A. p 895 N93-15204
FRITSCH, F. N. p 952 N93-15493
FROES, F. H. p 844 N93-14132
FROHMAN, HAROLD L. p 1007 N93-15051
FRUEHOLZ, R. P. p 972 N93-15243
FU, LEE-LUENG p 926 N93-14970
p 927 N93-14975
FUJIMOTO, RICHARD p 951 N93-15432
FUJITA, TERUO p 986 N93-15517
FULFORD, J. K. p 974 N93-15012
FULTON, DAVID p 925 N93-14964
FULTON, MARK VERNER p 791 N93-14828
FUNK, JOAN G. p 828 N93-14459
FUNKHOUSER, GORDON E. p 783 N93-14277
FUSS, IAN G. p 973 N93-14269
FUSSELL, DONALD S. p 957 N93-15569

G

GADDIS, L. R. p 1040 N93-14369
GAEDKE, M. p 835 N93-15075
GAIER, JAMES R. p 823 N93-15616
GALLIMORE, J. J. p 936 N93-14416
GALLY, THOMAS ANTHONY p 817 N93-14632
GAMACHE, GERALD L. p 938 N93-15216
GAMMIE, CHARLES FORBES p 1021 N93-15086
GANDHI, MUKESH V. p 836 N93-15218
GANEKO, Y. p 907 N93-14992
GANNON, JOHN D. p 947 N93-15199
GANTZ, DONALD T. p 939 N93-14548
GANZ, H. p 789 N93-15186
GAO, XIAOPING p 977 N93-15448
GARDNER, R. H. p 911 N93-15273
GARG, SANJAY p 801 N93-15525
GARLAN, DAVID p 941 N93-15239
GARLAND, P. J. p 812 N93-14962
GARMON, JOEL S. p 951 N93-15405
GARNER, F. A. p 846 N93-15138
GARRETT, S. J. p 843 N93-15200
GASIEWSKI, A. J. p 905 N93-14792
GATSKI, T. B. p 879 N93-15481
GATTINGER, R. L. p 811 N93-14952
GAU, CHUNG-YUN p 899 N93-14469
GAUTHIER, F. p 811 N93-14952
GAUTIER, G. p 930 N93-14989
GAZZANIGA, MICHAEL S. p 938 N93-15067
GEBAUER, LINDA p 819 N93-15596
GEHRINGER, MARK p 814 N93-15621
GEIER, B. p 835 N93-15075
GELFAND, ALAN E. p 970 N93-15109
p 971 N93-15110
GELINAS, F. p 805 N93-14926
GENNERO, M. C. p 929 N93-14984
GENSURE, JOHN R. p 865 N93-14254
GEOFFROY, P. p 792 N93-15126
GERANIOTIS, EVAGGELOS p 857 N93-14181
GERDES, DAVID P. p 1001 N93-14524
p 1009 N93-15642
GERING, GREG p 785 N93-14858
GERSHON, D. p 949 N93-15303
GHANNOUCHI, F. M. p 807 N93-14934
GHANNOUCHI, FADHEL M. p 807 N93-14936
GHIASI, ALI p 858 N93-14437
GHORASHI, BAHMAN p 844 N93-15504
GIBNER, PEYTON STINSON p 1020 N93-14866
GIBSON, CHRIS p 814 N93-15621
GIBSON, J. p 816 N93-15477
GIEL, P. W. p 777 N93-14102
GIESE, P. p 795 N93-15165
GILBERT, T. A. p 1002 N93-14774
p 1006 N93-15044
GILL, TEPPER L. p 967 N93-14412
GILLAND, JAMES H. p 828 N93-15584
GILLESPIE, J. W., JR. p 831 N93-14509
GILLESPIE, PATTI p 977 N93-15054
GILLESPIE, THOMAS KEVIN p 1000 N93-14208
GILLINGWATER, D. p 789 N93-14729
GILMORE, M. S. p 1028 N93-14317
GIORDANO, PIETRO p 824 N93-15622
GIULIANI, JOHN F. p 885 N93-14821
GIULIANI, JOHN L., JR. p 988 N93-14579
GLAD, W. E. p 846 N93-15056
GLASS, R. E. p 902 N93-15210
GLASSER, A. H. p 988 N93-15419
GLEICHER, MICHAEL p 956 N93-15561
GLICKMAN, ALBERT S. p 938 N93-15216
GLOECKLER, FRED p 789 N93-15005
GLOMB, W. L., JR. p 982 N93-15116
GODDARD, NIGEL H. p 937 N93-14660
GODDARD, P. L. p 895 N93-15204
GOERGENS, KURT p 850 N93-15064
GOERKE, ROGER THEODORE p 912 N93-14177
GOETTING, H. C. p 835 N93-15075
GOETZ, RAYMOND J. p 860 N93-14889
GOLDBERG, ALLEN J. p 858 N93-14259
GOLDEN, KENNETH p 990 N93-14413
GOLOB, ALEX p 821 N93-15605
GOLZ, J. W. p 851 N93-15222
GOMES, WENDY M. p 849 N93-14573
GONSALVES, PAUL G. p 798 N93-15235
GONZALEZ, JAVIER p 885 N93-14568
GOODCHILD, FIONA p 998 N93-14417
GOODRICH, J. A. p 792 N93-15227
GOPALSAMI, N. p 851 N93-15282
GOPALSWAMY, SWAMINATHAN p 961 N93-14470
GOPINATH, ANAND p 858 N93-14437
GORAN, WILLIAM D. p 1001 N93-14524
GORNEY, D. J. p 1049 N93-15318
GOTTESFELD, S. p 907 N93-15061
GOUGER, H. GARLAND p 813 N93-15646
GOULDING, R. H. p 863 N93-15440
GOURDEAU, L. p 929 N93-14983
GOVER, ROBERT E. p 858 N93-14259
GOWDY, M. J. p 910 N93-15209
GRABBE, MICHAEL THOMAS p 890 N93-14685
GRAHAM, DARIN P. W. p 805 N93-14925
GRAHAM, W. B. p 809 N93-14942
GRAINGER, JOHN L. p 845 N93-14705
GRANT, K. p 911 N93-15280
GRANT, K. E. p 911 N93-15281
GRANT, T. L. p 816 N93-15477
GRAY, CAROLYN MARGARET p 1000 N93-14209
GRAY, HENRY F. p 868 N93-15107
GRAY, ROSS T. p 995 N93-15311
GRBIC-GALIC, DUNIA p 932 N93-14557
GREEN, CHARLES KENNETH p 883 N93-14123
GREEN, JAMES L. p 1002 N93-14775
p 1006 N93-15045
GREEN, PAUL JONATHAN p 1019 N93-14638
GREEN, SAMANTHA p 946 N93-15072
GREENDYKE, ROBERT B. p 879 N93-15434
GREENE, A. E. p 989 N93-15422
GREENE, HAROLD J. p 832 N93-14675
GREENE, J. J. p 933 N93-14648
GREENE, TIM p 832 N93-14745
GREENSPAN, M. p 805 N93-14926
GREENWELL, E. N. p 871 N93-15479
GREFEN, PAUL W. P. J. p 959 N93-15141
GREGOIRE, G. p 970 N93-14538
GREGORY, ANDREW p 990 N93-14183
GRENIER, T. p 838 N93-15490
GRIFFIN, P. A. p 977 N93-15378
p 969 N93-15379
GRIFFIN, S. R. p 859 N93-14490
GRIFFITH, CAITLIN ANN p 1022 N93-14146
GRIFFITH, CHARLES p 826 N93-14681
GRIFFITH, D. G. p 1041 N93-14373
GRIMES, RUSSELL N. p 865 N93-14457
GRINSPOON, DAVID H. p 1025 N93-14299
p 1028 N93-14318
GRISOGONO, BRANKO p 915 N93-14873
GRODSINSKY, CARLOS M. p 778 N93-15573
GROSFILS, ERIC B. p 1028 N93-14319
GROSSBERG, STEPHEN p 962 N93-14551
GROSSMAN, A. S. p 911 N93-15280
p 911 N93-15281
GROSSMAN, SCOTT ALAN p 1015 N93-14147
GROSZ, F. B. p 859 N93-14490
GROTHAUS, MICHAEL G. p 869 N93-15269
GRUEN, D. M. p 978 N93-15654
GRUENDLINGH, MARTEN L. p 928 N93-14976
GRUMMON, D. S. p 992 N93-14812
GRUMSTRUP-SCOTT, JUDITH p 938 N93-14161
GUBNER, JOHN A. p 970 N93-14456
GUBSER, DONALD U. p 850 N93-14743
GUCKENHEIMER, JOHN p 872 N93-14257
GUEST, J. E. p 1025 N93-14300
p 1025 N93-14303
p 1033 N93-14339
GUGLIELMO, KENNON HARDY p 963 N93-15147
GUILLAUME, A. p 918 N93-14982
GUINOT, J. C. p 949 N93-15301
GUNN, J. M. p 1041 N93-14373
GUPTA, AARTI p 967 N93-14235
GUPTA, G. S. p 812 N93-14961
p 813 N93-14963
GURLEY, JOHN V. p 975 N93-15259
GURWELL, MARK A. p 1029 N93-14320
GUYMER, T. H. p 932 N93-15001
GUZA, R. T. p 916 N93-15375

H

HACKNEY, C. T. p 910 N93-15209
HADAD, ALLAN S. p 883 N93-15043
HADAWAY, JAMES B. p 910 N93-14764
HADIAN, MOHAMMAD JAFAR p 829 N93-14221
HAERI, MITCHELL BEHJAN p 972 N93-14144
HAGER, BRADFORD H. p 1042 N93-14376
HAGGANS, CHARLES W. p 986 N93-15517
p 986 N93-15520
HAGGARD, R. A. p 881 N93-14716
HAGIWARA, Y. p 907 N93-14992
HAHMANN, ANDREA NOEMI p 919 N93-14197
HAHN, H. T. p 901 N93-15066
HAIDVOGEL, D. p 932 N93-15002
HAJJAR, R. A. p 984 N93-15509
HAJJAR, ROGER ANTOINE p 979 N93-14140
HAJJI, RACHED p 807 N93-14936
HALBLEIB, J. A. p 978 N93-15277
HALE, ALAN p 1020 N93-14867
HALL, DAVID G. p 801 N93-15403
HALL, JIM W., JR. p 804 N93-14238
HALLOCK, Z. R. p 929 N93-14985
HALPERN, B. L. p 851 N93-15222
HAMBY, C. p 869 N93-15214
HAMILTON, H. HARRIS, II p 879 N93-15434
HAMILTON, M. L. p 846 N93-15138
HAMILTON, MARK F. p 974 N93-14458
HAMILTON, N. p 811 N93-14953
HAMILTON, VIVIEN p 952 N93-15476
HAMLEY, JOHN A. p 827 N93-15429
HAMMARSTROM, J. L. p 837 N93-15388

HAMMEL, MARK S. ..... p 956 N93-15558
HAN, MYUNG-CHUL ..... p 964 N93-15148
HAN, QINGYUAN ..... p 921 N93-14862
HANDSCHY, MARK A. ..... p 996 N93-15446
p 996 N93-15447
HANSEN, J. S. ..... p 811 N93-14955
p 837 N93-15388
HANSEN, PATRICIA A. ..... p 822 N93-15614
HANSEN, VICKI L. ..... p 1029 N93-14321
HANSMAN, R. JOHN ..... p 785 N93-14853
p 787 N93-15360
HANSON, CLAIRE S. ..... p 1000 N93-14182
HANSON, FRANK ..... p 885 N93-14722
HANSON, RICKEY L. ..... p 962 N93-14525
HARDCASTLE, THOMAS P. ..... p 1007 N93-15050
HARDESTY, LEONARD W. ..... p 869 N93-15269
HARDY, DENNIS R. ..... p 893 N93-15232
HARIHARAN, P. C. ..... p 1002 N93-14771
HARLAFTIS, EMILIOS THEOFANUS
p 1017 N93-14460
HARMER, M. P. ..... p 991 N93-14439
HARMS, DEWEY E. ..... p 921 N93-14680
HARMS, DEWEY ELVIN ..... p 919 N93-14198
HARPER, WILLIAM B., JR. ..... p 826 N93-14482
HARR, RANDOLPH E. ..... p 948 N93-15263
HARRIS, F. R. ..... p 811 N93-14952
HARRIS, JULIUS E. ..... p 875 N93-14481
HARRISON, BEVERLY L. ..... p 955 N93-15552
HARRISON, CHRISTOPHER G. A. ..... p 916 N93-14913
HARRISON, MONIQUE F. ..... p 1002 N93-14650
HART, JOHN C. ..... p 956 N93-15559
HARTJEN, GARY L. ..... p 820 N93-15601
HARTNESS, J. TIMOTHY ..... p 832 N93-14745
HARTUNG, W. ..... p 835 N93-15075
HARTZ, LESLIE S. ..... p 891 N93-14842
HARVEY, ROBERT L. ..... p 964 N93-15258
HASAN, M. M. ..... p 855 N93-15420
HASSAN, H. A. ..... p 875 N93-14481
HASSELMANN, K. ..... p 929 N93-14986
HASSIG, P. ..... p 1040 N93-14365
HASTINGS, ANDREW B. ..... p 941 N93-15240
HASWELL, CAROLE ANN ..... p 1015 N93-14148
HATCH, RONALD R. ..... p 789 N93-15005
HATFIELD, D. ..... p 1040 N93-14365
HAUS, HERMANN A. ..... p 984 N93-15458
HAUSER, D. ..... p 851 N93-15294
HAUSER, J. P. ..... p 859 N93-14663
HAVERKORT, BOUDEWIJN R. ..... p 941 N93-15090
p 971 N93-15119
HAYES, JOHN R., JR. ..... p 943 N93-14505
HAYES, S. P. ..... p 930 N93-14989
HAYNES, RENA A. ..... p 1003 N93-14781
p 1007 N93-15048
HAYS, JOHN E. ..... p 1029 N93-14322
HAZAN, DIDIER ..... p 787 N93-15360
HAZELL, C. R. ..... p 809 N93-14942
HE, GUANGLIANG ..... p 977 N93-15062
HEAD, JAMES W., III ..... p 1025 N93-14299
p 1025 N93-14302
p 1026 N93-14309
p 1028 N93-14317
p 1028 N93-14319
p 1029 N93-14323
p 1029 N93-14324
p 1032 N93-14333
p 1033 N93-14339
p 1034 N93-14342
p 1038 N93-14356
p 1038 N93-14359
p 1041 N93-14374
HEBERLEIN, J. ..... p 867 N93-14721
HEDGES, R. ..... p 816 N93-15477
HEEGER, ALAN J. ..... p 848 N93-14401
HEFFNER, R. H. ..... p 995 N93-15321
HEIDELBERG, LAURENCE ..... p 801 N93-15403
HEIJENK, G. J. ..... p 860 N93-15095
HEIMERDINGER, WALTER L. ..... p 944 N93-14563
HEINEMANN, K. ..... p 843 N93-15356
HEINEMANN, KARL G. ..... p 964 N93-15258
HEITLAND, GAIL W. ..... p 1008 N93-15229
HELLER, GERARD ..... p 957 N93-15579
HELM, RICHARD ..... p 957 N93-15568
HELMS, CHRISTOPHER ..... p 983 N93-15223
HEMBERGER, P. H. ..... p 887 N93-15135
HENAGER, C. H., JR. ..... p 871 N93-15479
HENCH, LARRY L. ..... p 831 N93-14665
HENG, WEE-LIANG ..... p 967 N93-14270
p 967 N93-14271
HERANT, MARC ..... p 1019 N93-14633
HERRICK, ROBERT R. ..... p 1029 N93-14321
HERRING, R. A. ..... p 991 N93-14518
HERSHFELD, DONALD ..... p 820 N93-15599
HERTZBERG, A. ..... p 783 N93-15588
HESS, ELIZABETH ..... p 936 N93-15583
HESS, P. C. ..... p 1029 N93-14324
p 1038 N93-14358
HEVRONI, IRIS ..... p 835 N93-15144
HICKS, JOHN W. ..... p 795 N93-15169
HILTON, M. R. ..... p 851 N93-15242
HINDMAN, EDWARD E. ..... p 903 N93-15496
HINEDI, SAMI M. ..... p 981 N93-14404
HINGST, WARREN R. ..... p 879 N93-15355
HINMAN, MICHAEL L. ..... p 966 N93-15408
HIRVONEN, J.-P. ..... p 837 N93-15426
HO, CHENG ..... p 1022 N93-15324
HO, CHIH-MING ..... p 873 N93-14400
HOANG, NGOCDUNG ..... p 940 N93-14644
HODGES, LARRY F. ..... p 953 N93-15536
HODGES, R. R., JR. ..... p 1027 N93-14312
HODGINS, JESSICA K. ..... p 956 N93-15564
HOFFMAN, D. J. ..... p 863 N93-15440
HOFFMAN, F. M. ..... p 946 N93-14902
HOFFMAN, MARGERY E. ..... p 792 N93-15004
HOFFMAN, R. ..... p 944 N93-14566
HOFSTADTER, MARK DAVID ..... p 1046 N93-14863
HOKE, STEVEN H. ..... p 849 N93-14531
HOLCOMBE, C. E. ..... p 869 N93-15214
HOLDEMAN, J. D. ..... p 800 N93-15359
HOLLAND, C. R. ..... p 859 N93-14490
HOLLAND, W. R. ..... p 927 N93-14975
HOLLOWAY, PAUL H. ..... p 996 N93-15449
HOLLWEG, JOSEPH V. ..... p 1049 N93-15085
HOLMANN, E. ..... p 1044 N93-14391
HOLMES-SIEDLE, ANDREW G. ..... p 869 N93-15133
HOLMES, PHILIP ..... p 872 N93-14257
HOLONYAK, N., JR. ..... p 885 N93-14667
HOLONYAK, NICK, JR. ..... p 866 N93-14562
HOLSTEIN, B. R. ..... p 977 N93-15279
HOLT, HENRY ..... p 864 N93-15638
HONG, P. E. ..... p 815 N93-14730
p 815 N93-14768
p 815 N93-14794
HONNORAT, C. ..... p 999 N93-15118
HOOGEBOOM, P. ..... p 860 N93-14805
HOOKER, STANFORD B. ..... p 932 N93-15645
HOOVER, RICHARD B. ..... p 982 N93-14711
HOOVER, SCOTT M. ..... p 845 N93-14888
HOPPE, BRUCE ..... p 862 N93-15339
HOPPER, A. T. ..... p 851 N93-15294
HOPSON, PURNELL, JR. ..... p 881 N93-14714
HORST, RICHARD L. ..... p 881 N93-14494
HORTON, MICHAEL J. ..... p 951 N93-15457
HORVATH, ISTVAN ..... p 804 N93-14921
HOUBEN, H. ..... p 1044 N93-14395
HOURY, S. ..... p 918 N93-14969
HOUSE, M. B. ..... p 838 N93-15625
HOUTSMA, MAURICE A. W. ..... p 959 N93-15142
HOVENIER, J. W. ..... p 1032 N93-14335
HOWE, JOHN EDWARD, JR. ..... p 1016 N93-14149
HOWELL, STEVE ..... p 944 N93-14575
p 940 N93-14644
HOWELL, STEVEN ..... p 958 N93-14645
HSIEH, K. C. ..... p 885 N93-14667
HU, QI ..... p 915 N93-14874
p 922 N93-14901
HUANG, HSING-HSIN ..... p 964 N93-15149
HUANG, JU-CHRONG ..... p 910 N93-15063
HUBBARD, R. F. ..... p 978 N93-14127
HUBBARD, RICHARD F. ..... p 976 N93-14662
HUBER, PETER J. ..... p 942 N93-14237
HUCKA, MIKE ..... p 940 N93-14491
HUDSON, JACOB VICTOR, JR. ..... p 1050 N93-14639
HUDSON, JAMES G. ..... p 920 N93-14258
HUEY, CECIL O., JR. ..... p 833 N93-14749
HUFFAKER, R. MILTON ..... p 784 N93-14848
HUGUENIN, BLAKE D. ..... p 981 N93-14286
HUME, EDWARD E., JR. ..... p 914 N93-14511
HUME, EDWARD EUGENE, JR. ..... p 913 N93-14199
HUMMEL, J. R. ..... p 945 N93-14696
HUNDLEY, M. F. ..... p 998 N93-14905
HUNSTON, D. ..... p 833 N93-14747
HUNT, BRIAN D. ..... p 994 N93-15151
HUNTER, J. R. ..... p 927 N93-14971
HUNTLEY, HUGH EDGAR ..... p 848 N93-14222
HURD, HARRY L. ..... p 947 N93-15228
HURLBURT, H. E. ..... p 929 N93-14985
HURRELL, J. P. ..... p 971 N93-14108
HUSSAIN, K. A. ..... p 974 N93-15073
HUTCHISON, J. L. ..... p 989 N93-14133
HUTHNANCE, J. M. ..... p 932 N93-15001
HUYNH, TIEN ..... p 957 N93-15568
HWAN, CHUNG-LI ..... p 899 N93-14471
HWANG, BEONG-BOK ..... p 844 N93-14472
HWANG, JAI CHAN ..... p 1015 N93-14134
HWANG, PHIL ..... p 944 N93-14575

I

IKEUCHI, K. ..... p 944 N93-14566
ILOTT, P. ..... p 813 N93-14963
IMAM, M. A. ..... p 836 N93-15246
IMLAY, SCOTT T. ..... p 878 N93-15187
INAN, UMRAN S. ..... p 922 N93-14910
INGERSOLL, A. P. ..... p 1030 N93-14325
INKSTER, R. ..... p 811 N93-14953
INOUE, M. ..... p 926 N93-14968
INSERRA, JOSEPH R. ..... p 862 N93-15376
IRBY, J. ..... p 993 N93-15055
ISHII, H. ..... p 907 N93-14992
IVANOV, B. A. ..... p 1030 N93-14326
p 1044 N93-14392
IVRISSIMTZIS, L. P. ..... p 856 N93-14107
IZENBERG, NOAM R. ..... p 1030 N93-14327

J

JACKOLA, ARTHUR S. ..... p 820 N93-15601
JACKSON, DEBORAH ..... p 986 N93-15648
JACKSON, KOREY V. ..... p 967 N93-14255
JACKSON, SUZETTE ..... p 916 N93-15136
JACOBS, G. ..... p 907 N93-15219
JACOY, PAUL J. ..... p 832 N93-14700
JADUSZLIWER, B. ..... p 972 N93-15243
JANES, D. M. ..... p 1043 N93-14383
JANES, RON ..... p 814 N93-15621
JANSSEN, G. J. ..... p 860 N93-14806
JANSSON, STEFAN ..... p 830 N93-14484
JARSTFER, AMIEL G. ..... p 933 N93-15208
JASINSKI, THOMAS J. ..... p 880 N93-15643
JASPERSON, WILLIAM H. ..... p 924 N93-15331
JAUBERTEAU, F. ..... p 878 N93-15122
JAWORSKE, D. A. ..... p 852 N93-15344
p 819 N93-15597
JAYAPRAKASH, C. ..... p 995 N93-15351
JELETIC, KELLYANN ..... p 957 N93-15578
JEN, GWANG-SHEN ..... p 902 N93-15[illegible]
JENKINS, J. M. ..... p 1030 N93-14328
JENKINS, LAWRENCE M. ..... p 799 N93-14895
JENKINS, MICHAEL ..... p 958 N93-14645
JEON, DOYOUNG ..... p 888 N93-14473
JERVIS, T. R. ..... p 837 N93-15426
JEVANS, DAVID A. ..... p 955 N93-15554
JIANG, XINGJIAN ..... p 912 N93-14178
JINGCHENG, SIANG ..... p 861 N93-15106
JOHANNESSEN, O. M. ..... p 930 N93-14988
JOHNS, JANET F. ..... p 962 N93-14519
JOHNSON, C. L. ..... p 1030 N93-14329
JOHNSON, D. R. ..... p 929 N93-14985
JOHNSON, DONALD E. ..... p 911 N93-15480
JOHNSON, KENNETH R. ..... p 821 N93-15609
p 823 N93-15618
JOHNSON, M. J. ..... p 816 N93-15477
JOHNSON, MARK ..... p 962 N93-14533
JOHNSON, R. ..... p 870 N93-15421
JOHNSON, RUDY A. ..... p 879 N93-15332
JOHNSON, T. ..... p 1009 N93-15639
JOHNSON, W. A. ..... p 971 N93-14108
JOHNSTON, HELEN MARGARET p 1018 N93-14594
JOHNSTON, MARK ..... p 964 N93-15286
JONAS, J. ..... p 847 N93 14166
JONES, BRIAN ..... p 855 N93-14793
JONES, COLIN E. ..... p 868 N93-15108
JONES, DAVID ..... p 884 N93-14141
JONES, E. M. ..... p 1037 N93-14352
JONES, HEBER D. ..... p 937 N93-14600
JONES, J. R. ..... p 945 N93-14696
JONES, MICHAEL G. ..... p 975 N93-15391
JONES, ROBERT J. ..... p 849 N93-14527
JONES, W. P. ..... p 840 N93-14620
JOOSTEN, STEF ..... p 941 N93-15089
JOYCE, G. ..... p 978 N93-14570
JOYCE, GLENN ..... p 976 N93-14662
JUANG, JER-NAN ..... p 902 N93-15202
JUHASZ, ALBERT J. ..... p 826 N93-14482

K

KACPURA, THOMAS J. ..... p 871 N93-15503
KACYNSKI, KENNETH J. ..... p 827 N93-15571
KAIJUN, TANG ..... p 861 N93-15106
KALAYCIOGLU, S. ..... p 810 N93-14950
KALBE, HELMUT ..... p 793 N93-15154
KALLIS, J. ..... p 894 N93-14104
p 900 N93-14498
KAMAT, MANOHAR P. ..... p 901 N93-14799
KAMIKAWA, N. T. ..... p 981 N93-14407
KANADE, T. ..... p 944 N93-14566
KANDIL, H. A. ..... p 875 N93-14689
KANDIL, OSAMA A. ..... p 875 N93-14687
p 875 N93-14688
p 875 N93-14689
p 875 N93-14690
p 876 N93-14691
p 876 N93-14692
KANG, SANG-WOOK ..... p 870 N93-15389

KANKAM, M. DAVID p 854 N93-14834
KAPETANAKOS, C. A. p 866 N93-14504
KAPPES, SANDRA p 1009 N93-15641
KAPPLER, G. p 796 N93-15176
KAPUSTA, A. A. p 836 N93-15193
KARANGELEN, NICHOLAS p 940 N93-14644
KARASEK, K. p 836 N93-15387
p 837 N93-15455
KARGEL, J. S. p 1031 N93-14330
KARIA, KRIS p 806 N93-14930
KARMARKAR, SUBHASH D. p 845 N93-14888
KARMOKOLIAS, C. p 789 N93-14574
KARPEL, MARDECHAY p 901 N93-14766
KARS, PIM p 946 N93-15077
KARUZA, S. K. p 971 N93-14108
KASE, R. p 929 N93-14986
KASHANGAKI, THOMAS ANTHONY LWANGA
p 816 N93-14274
KASS, MICHAEL p 956 N93-15561
KASSER, M. p 918 N93-14993
KASTING, J. F. p 1031 N93-14331
KATTELUS, H. p 837 N93-15426
KATTI, ROMNEY R. p 940 N93-14704
KATZ, ELI JOEL p 928 N93-14977
KATZ, J. p 852 N93-15320
KATZ, N. p 979 N93-15362
KAUFMAN, L. p 937 N93-14786
KAUFMAN, LLOYD p 937 N93-14646
KAUFMANN, JAMES R. p 833 N93-14750
KAUHANEN, K. p 1039 N93-14364
KAUKLER, WILLIAM F. p 997 N93-15500
KAULA, W. M. p 1031 N93-14332
KAZOVSKY, LEONID p 982 N93-14507
KEADY, J. J. p 988 N93-15418
KEDDIE, S. p 1032 N93-14333
KEENAN, F. P. p 1012 N93-14762
KEEP, MYRA p 1029 N93-14321
KEINIGS, R. K. p 989 N93-15422
KEIZER, W. P. p 860 N93-14805
KELLER, MICHAEL E. p 867 N93-14699
KELLEY, JOSEPH G. p 823 N93-15617
KELLNER, ARTHUR J. p 951 N93-15445
KELLY, SUZANNE M. p 1003 N93-14781
p 1007 N93-15048
KELLY, TAMSIN p 934 N93-14240
KENT, P. D p 815 N93-14768
KENT, P. D. p 815 N93-14730
p 815 N93-14794
KEPPLE, PAUL C. p 988 N93-14579
KERLEY, JAMES J. p 934 N93-14708
KERR, JAMES p 846 N93-15231
KERRICK, ALAN DAVINSON p 1050 N93-14634
KERSTEN, MARTIN L. p 959 N93-15141
KERSTHOLT, J. H. p 937 N93-14602
KHAMSEH, AMIR R. p 903 N93-15653
KHATRI, A. p 789 N93-14574
KHAVARAN, A. p 975 N93-15575
KHAVARAN, ABBAS p 975 N93-15430
KIDD, A. p 808 N93-14939
KIEFER, WALTER S. p 1032 N93-14334
KIM, CHAN M. p 975 N93-15430
KIM, H. J. p 852 N93-15437
KIM, HYOUN-EE p 845 N93-14717
KIM, J. G. p 846 N93-15059
KIM, J. H. p 880 N93-15652
KIM, J. J. p 906 N93-15007
KIM, K. W. p 994 N93-15191
KIM, WONE-CHUL p 899 N93-14474
KIM, YONG WOO p 829 N93-14224
KINDLE, J. C. p 929 N93-14985
KINDLE, JOHN C. p 920 N93-14256
KING, ELIZABETH A. p 823 N93-15620
KINOSHITA, K. p 909 N93-15484
KINOSKY, D. p 992 N93-14643
p 993 N93-15008
p 993 N93-15055
KINSMAN, GRANT p 884 N93-14175
KIRK, R. L. p 1039 N93-14363
p 1040 N93-14369
KIRSCHKE, L. p 835 N93-15075
KISTLER, DAVID p 957 N93-15578
KLEI, HERBERT E. p 994 N93-15190
KLEIMAN, J. p 811 N93-14955
KLEIN, GARY A. p 786 N93-15020
KLEINBERG, H. p 810 N93-14947
KLEPIN, K. M. p 792 N93-15227
KLEPPER, STEVEN JUDSON p 990 N93-14184
KLINKHAMER, F. R. p 1020 N93-14686
KLINKHAMMER, GUNNAR ULRICH
p 915 N93-14884
KLOSKO, S. M. p 928 N93-14981
KLYDE, DAVID H. p 802 N93-14811
KNETSCH, E. A. p 995 N93-15321
KNIBBE, W. J. J. p 1032 N93-14335
KNIGHT, PETER JOHN p 1011 N93-14231
KNOLL, R. H. p 855 N93-15420
KNOWLEN, C. p 783 N93-15588
KNUDSEN, W. C. p 1032 N93-14336
KO, F. K. p 834 N93-14755
KO, FRANK p 888 N93-14478
KOBLER, BEN p 1002 N93-14771
p 1003 N93-14776
KOBLINSKY, C. J. p 928 N93-14981
KOEHAN, FRANCIS L. p 849 N93-14573
KOGA, R. p 979 N93-15362
KOLASINSKI, W. A. p 979 N93-15362
KOLLMANN, W. p 840 N93-14623
KOLMAN, MICHIEL p 1011 N93-14611
KOMATSU, G. p 1031 N93-14330
p 1033 N93-14337
KOMOROSKI, RICHARD A. p 841 N93-14658
KONAK, S. p 880 N93-15652
KONDA, NOBORU p 902 N93-15372
KONG, J. A. p 863 N93-15495
KONNO, KEVIN p 801 N93-15403
KOOMEN, P. J. p 860 N93-14805
KOOPS, M. p 814 N93-14266
KOPP, BRIAN T. p 857 N93-14155
KORTH, G. E. p 834 N93-14819
KOS, CHESTER p 1009 N93-15642
KOSKO, BART p 962 N93-14598
KOSTELICH, ERIC p 998 N93-15333
KOSTEN, SUSAN E. p 892 N93-15117
KOSTUK, RAYMOND K. p 986 N93-15517
KOZAK, J. p 794 N93-15162
KOZOL, JOSEPH p 846 N93-15189
KRAFFT, ROLAND p 799 N93-14892
KRALL, J. p 978 N93-14570
KRAMMER, P. p 800 N93-15143
KRAUSE, D. p 933 N93-14648
KRAUSE, J. L. p 1033 N93-14338
KRAUSKOPF, JOHN p 938 N93-15329
KRAUSS, W. p 929 N93-14986
KREJSA, E. A. p 975 N93-15575
KREJSA, EUGENE A. p 975 N93-15430
KRETZ, D. p 820 N93-15600
KRISHNAMURTHY, THIAGARAJA p 900 N93-14483
KRISHNAN, P. N. p 854 N93-15640
KRIVTSOV, A. P. p 1023 N93-14289
KROES, ROGER L. p 992 N93-14707
KROLL, J. T. p 800 N93-15359
KROZEL, JAMES ALAN p 961 N93-14445
KRUEDENER, MATTHIAS p 794 N93-15163
KUHLMAN, CHRIS J. p 844 N93-14508
KULKARNI, MADHAV NARAYAN p 904 N93-14223
KUMAR, B. p 944 N93-14566
KUMAR, RAJENDRA p 945 N93-14882
KUNDU, KRISHNA p 844 N93-15504
KUNHARDT, ERICH p 869 N93-15257
KUO, LYNN p 970 N93-15109
KUPER, J. p 968 N93-15121
KURYLA, J. p 880 N93-15652
KUSHNICK, PETER W. p 845 N93-14705
KUTSERUBOV, A. T. p 856 N93-15105
KWEI, G. H. p 998 N93-14905
KYBURG, HENRY E., JR. p 963 N93-14786

L

LABANS, T. p 951 N93-15386
LACERDA, A. p 998 N93-14905
LACHENMAYR, GEORG p 820 N93-15598
LACINA, J. p 988 N93-14813
LACKEY, JAMES B. p 803 N93-15396
LAFFERTY, JOHN p 947 N93-15206
LAGARDE, A. p 886 N93-15128
LAGO, B. p 918 N93-14969
p 918 N93-14982
LAI, MING-CHIA p 877 N93-14829
LAIRD, JOHN p 940 N93-14491
LAIRD, PHIL p 964 N93-15286
LAIZET, J. C. p 836 N93-15253
LAMB, MILTON p 800 N93-15342
LAMINIE, J. p 878 N93-15122
LAMPE, M. p 978 N93-14570
LAMPE, MARTIN p 976 N93-14662
LANCASTER, M. G. p 1033 N93-14339
p 1034 N93-14342
LAND, JAMES E. p 797 N93-15178
LANE, ROBERT W. p 821 N93-15609
p 823 N93-15618
LANG, ROBERT J. p 885 N93-14703
LANGLEY, PAT p 965 N93-15293
LAPOINTE, MICHAEL R. p 826 N93-15370
LARKIN, PAUL p 820 N93-15599
LARNAC, G. p 838 N93-15490
LASHBROOK, DAVID D. p 816 N93-14536
LASSEZ, CATHERINE p 957 N93-15568
LATHROP, DANIEL PERRY p 872 N93-14119
LAU, VICKITT p 810 N93-14951
LAUE, ERIC p 823 N93-15615
LAUF, R. J. p 869 N93-15214
LAUTERBACH, LINDA p 944 N93-14572
p 944 N93-14581
LAWRENCE, DAVID G. p 956 N93-15564
LAWRENCE, STEVEN H. p 850 N93-14743
LAWRENCE, W. P. p 883 N93-15411
LAYTON, JEFFREY BOESE p 898 N93-14446
LE, DI-LUAN p 807 N93-14934
LEAVITT, LAURENCE D. p 800 N93-15342
LEBEN, R. p 926 N93-14966
LEDFORD, J. p 870 N93-15424
LEE-GLAUSER, GINA p 902 N93-15202
LEE, CHI-MING p 844 N93-15504
LEE, EUN U. p 831 N93-14672
LEE, GEORGE p 804 N93-14809
LEE, J. H. W. p 875 N93-14690
LEE, JINHEE p 888 N93-14226
LEE, PAUL A. p 985 N93-15516
LEE, S. S. p 901 N93-15066
LEE, SANG SOO p 880 N93-15499
LEE, SOO HAN p 888 N93-14202
LEETMAA, A. p 927 N93-14974
LEGGE, GORDON E. p 936 N93-14510
LEHOCZKY, SANDOR L. p 992 N93-14707
LEIBOVICH, SIDNEY p 872 N93-14257
LEITH, A. p 1027 N93-14313
LEMOINE, J.-M. p 918 N93-14993
LEMOINE, P. L. p 816 N93-15475
LENARDIC, A. p 1031 N93-14332
LEONARD, ANTHONY p 842 N93-15114
LEPROVOST, CHRISTIAN p 928 N93-14978
LERCH, F. J. p 928 N93-14981
LESPADE, P. p 838 N93-15490
LESSARD, CHARLES S. p 881 N93-14494
LESSER, BARBARA p 1008 N93-15335
LETRAON, L. Y. p 929 N93-14987
LETRAON, P. Y. p 929 N93-14984
LEUNG, A. Y. T. p 875 N93-14690
LEUNG, MARTIN S. p 992 N93-14795
LEVINE, M. D. p 931 N93-14994
LEVIONNOIS, A. p 778 N93-15158
LEVITAN, LEE p 787 N93-15022
LEVOY, MARC p 953 N93-15541
LEWICKI, SCOTT p 1026 N93-14306
LEY, ROBERT PAUL p 897 N93-14251
LI, C. W. p 853 N93-15452
LI, JIN p 954 N93-15547
LI, LIFENG p 986 N93-15518
p 986 N93-15519
p 986 N93-15520
LIANG, LI-NUO p 932 N93-14557
LIANG, ZUOHUA p 987 N93-14120
LIBLONG, BREEN p 810 N93-14951
LICINA, JOSEPH R. p 933 N93-14103
p 881 N93-14105
LIKONEN, J. p 837 N93-15426
LILLEY, E. p 851 N93-15295
p 853 N93-15453
LIM, SEUNGCHUL p 892 N93-15102
LIN, C. S. p 855 N93-15420
LIN, CHEN-CHOU p 893 N93-15380
LIN, JOHN CHING-NIEN p 874 N93-14475
LIN, M. C. p 842 N93-14669
p 992 N93-14670
LIN, SHIH-YUNG p 895 N93-14185
LINCOLN, JOHN W. p 777 N93-14549
LINDSAY, ANTHONY C. p 973 N93-14269
LINK, BENNETT KARL p 1014 N93-14112
LIOU, MENG-SING p 877 N93-14885
LIPELES, R. A. p 992 N93-14795
LIPSCOMB, ANN p 1004 N93-15027
LISKA, D. J. p 870 N93-15424
LITOVITZ, T. A. p 933 N93-14648
LITTLEJOHN, M. A. p 994 N93-15191
LIU, C. H. p 875 N93-14688
p 875 N93-14689
p 875 N93-14690
p 876 N93-14691
p 876 N93-14692
LIU, FANG p 1035 N93-14345
LIU, LIANQUAN p 874 N93-14476
LIU, SHENG p 830 N93-14493
LIU, W. TIMOTHY p 928 N93-14979
LIU, Y. K. p 816 N93-15477
LIVINGSTON, ROBERT C. p 914 N93-14727
LLINAS, RODOLFO R. p 936 N93-15198
LOCHER, ROBERT J. p 862 N93-15376
LOCKE, J. GREG p 910 N93-14739
LOCKWOOD, G. J. p 882 N93-15381
LOGSDON, KIRK A. p 778 N93-15573
LOMAS, J. J. p 813 N93-15392
LONG, CLAUDINE S. p 1001 N93-14265
LONG, G. G. p 850 N93-15049
LONGTIN, D. R. p 945 N93-14696
LOPEZ, CARLOS ALBERTO p 874 N93-14477
LOTT, DENNIS A. p 792 N93-15238

LOUAT, N. P. ..... p 836 N93-15246
LOVELL, AMY J. ..... p 1033 N93-14340
LOWREY, R. ..... p 870 N93-15441
LOZOWSKI, MARK ..... p 806 N93-14929
LU, LINGYUN ..... p 901 N93-14587
LU, WEIPING ..... p 979 N93-14124
LUBNER, MAXINE ESTA ..... p 783 N93-14693
LUBOMSKI, JOSEPH F. ..... p 778 N93-15573
LUCASSEN, M. P. ..... p 936 N93-14267
LUKAS, ROGER ..... p 928 N93-14980
LUM, WILLIAM ..... p 838 N93-14435
LUMLEY, JOHN L. ..... p 872 N93-14257
LUNDBERG, W. R. ..... p 973 N93-14406
LUNDERSTAEDT, R. ..... p 796 N93-15175
LUTHMANN, J. G. ..... p 1034 N93-14341
LUTJEHARMS, J. R. ..... p 928 N93-14976
LUYTEN, PATRICK ..... p 1018 N93-14584
LY, L. N. ..... p 920 N93-14256
LYALL, ELIZABETH A. ..... p 787 N93-15022
LYCOU, PETER P. ..... p 891 N93-14843
LYNCH, KRISTINA ANNE ..... p 912 N93-14121
LYNCH, M. J. ..... p 927 N93-14971
LYON, MALCOLM ..... p 834 N93-14754
LYONS, L. R. ..... p 917 N93-15574

M

MABSON, G. E. ..... p 811 N93-14955
MACCACARO, TOMASSO ..... p 1013 N93-15340
MACIKUNAS, ARUNAS ..... p 807 N93-14933
MACINTYRE, BLAIR ..... p 954 N93-15543
MACKAY, G. ..... p 812 N93-14959
MACKENZIE, I. SCOTT ..... p 955 N93-15550
MACLACHLAN, ROBERT A. ..... p 950 N93-15336
MADALA, RAO V. ..... p 921 N93-14680
MAGALHAESDEOLIVEIRA, HELIO ..... p 861 N93-15098
MAGDALENO, RAYMOND E. ..... p 802 N93-14811
MAGEE-ROBERTS, K. ..... p 1034 N93-14342
MAGUIRE, GREGORY J. ..... p 867 N93-14699
MAHAJAN, A. ..... p 992 N93-14643
p 993 N93-15008
p 993 N93-15055
MAHAJAN, R. ..... p 903 N93-15374
MAIER-REIMER, E. ..... p 929 N93-14986
MAIER, MATTHEW R. ..... p 792 N93-15361
MAILLARD, J.-P. ..... p 1026 N93-14308
MAIMON, O. ..... p 950 N93-15304
MAISSEL, LEON ..... p 948 N93-15265
MAJEED, TARIQ ..... p 1022 N93-14179
MAJUMDAR, B. ..... p 851 N93-15294
MAJUMDAR, B. S. ..... p 837 N93-15401
MAK, JOHN EUGENE ..... p 913 N93-14207
MAKOWIECKI, D. M. ..... p 870 N93-15389
MALANOTTE-RIZZOLI, P. ..... p 927 N93-14975
MALLINSON, JOHN C. ..... p 1004 N93-15029
MALONE, SHAWN P. ..... p 849 N93-14561
MALONEY, JAMES G. ..... p 863 N93-15470
MALONEY, JOHN D. ..... p 996 N93-15443
MAMEN, ROLF ..... p 809 N93-14943
MANN, J. ADIN ..... p 973 N93-14159
MANNING, CAROL A. ..... p 789 N93-14276
MANOCHA, DINESH ..... p 956 N93-15560
MANSAGER, B. ..... p 973 N93-14234
MANSURIPUR, M. ..... p 984 N93-15506
p 984 N93-15508
p 984 N93-15509
p 960 N93-15510
MANTEI, MARILYN ..... p 954 N93-15547
MANTEI, MARILYN M. ..... p 954 N93-15549
MANTIPLY, EDWIN D. ..... p 861 N93-15220
MANZINI, ELISA ..... p 920 N93-14640
MARCHELLO, JOSEPH M. ..... p 852 N93-15431
MAREDA, J. F. ..... p 1051 N93-15060
MARENGOORSINI, JOSE ANTONIO
p 918 N93-14115
MARESCA, JOSEPH W., JR. ..... p 975 N93-15647
MARHEFKA, R. J. ..... p 856 N93-14107
MARING, LISE D. ..... p 900 N93-14483
MARION, M. ..... p 878 N93-15122
MARKLUND, G. T. ..... p 916 N93-15252
MARRIOTT, BERNADETTE M. ..... p 938 N93-14161
MARRIOTT, KIM ..... p 957 N93-15568
MARSEE, R. L. ..... p 939 N93-14554
MARSH, JAMES G. ..... p 928 N93-14981
MARSH, S. J. ..... p 866 N93-14504
MARTIAN, P. ..... p 948 N93-15274
MARTIN, JONATHAN EDWARD ..... p 921 N93-14827
MARTINO, M. ..... p 843 N93-15283
MARVIN, D. C. ..... p 1049 N93-15318
MARZULLO, KEITH ..... p 862 N93-15339
MASKALISK, N. J. ..... p 908 N93-15323
MASON, CINDY L. ..... p 965 N93-15290
p 965 N93-15292
MASTERS, CHRISTINE BEISLER ..... p 848 N93-14287
MASTERS, MICHAEL W. ..... p 942 N93-14164
MATHEW, J. ..... p 866 N93-14504
MATSUMURA, S. ..... p 931 N93-14996
MATTERN, DUANE ..... p 801 N93-15525
MATTHEWS, MICHAEL ..... p 784 N93-14851
MATTICK, A. T. ..... p 783 N93-15588
MATWIN, STAN ..... p 965 N93-15293
MAURER, M. J. ..... p 1044 N93-14391
MAY, BRADLEY W. ..... p 934 N93-14556
MAY, CHRISTOPHER W. ..... p 836 N93-15236
MAYER, RICHARD J. ..... p 976 N93-14438
MAYNARD, JULIAN D. ..... p 996 N93-15465
MAYR, HERWIG ..... p 949 N93-15302
MAZUR, JOSEPH EDWARD ..... p 1048 N93-14135
MAZZEGA, P. ..... p 906 N93-14967
p 928 N93-14978
p 929 N93-14984
p 918 N93-14993
MAZZOLENI, ANDRE PETER ..... p 817 N93-14585
MCADOO, D. ..... p 927 N93-14974
MCAULEY, MYCHE ..... p 1026 N93-14306
MCCALL, JAMES A. ..... p 944 N93-14572
p 944 N93-14581
MCCARTY, J. E. ..... p 881 N93-14716
MCCOLLUM, T. ..... p 852 N93-15344
p 819 N93-15597
MCCONNEL, P. ..... p 902 N93-15210
MCCONNELL, GEORGE ..... p 802 N93-14447
MCCONNELL, ROBERT L. ..... p 962 N93-14701
MCCOOL, MICHAEL ..... p 954 N93-15545
MCCREADY, MARY C. ..... p 914 N93-14727
MCCREARY, JULIAN P., JR. ..... p 925 N93-14428
MCDOUGALL, T. J. ..... p 927 N93-14971
MCDOWELL, J. ..... p 1012 N93-14760
MCFARLAND, ERIC R. ..... p 801 N93-15521
MCGILL, GEORGE E. ..... p 1033 N93-14340
p 1034 N93-14343
MCGIMPSEY, W. G. ..... p 850 N93-15111
MCGOVERN, PATRICK J. ..... p 1035 N93-14344
MCHUGH, MARTIN PATRICK ..... p 914 N93-14589
MCINERNEY, JOHN G. ..... p 886 N93-15069
MCKEAGUE, I. W. ..... p 970 N93-14538
MCKENZIE, DAN ..... p 1035 N93-14345
MCKINNON, WILLIAM B. ..... p 1024 N93-14291
MCKITTRICK, J. ..... p 852 N93-15320
MCKITTRICK, JOANNA ..... p 852 N93-15394
MCLEAN, GARNET A. ..... p 783 N93-14277
MCLEAN, ROBERT A. ..... p 1005 N93-15037
MCMASTER, MATTHEW S. ..... p 872 N93-14150
MCMATH, W. S. ..... p 805 N93-14926
MCMILLAN, ROBERT ..... p 784 N93-14850
MCMILLAN, WILLIAM WALLACE ..... p 913 N93-14211
MCNESBY, KEVIN L. ..... p 854 N93-15011
MCPHADEN, M. J. ..... p 930 N93-14989
MCRUER, DUANE T. ..... p 802 N93-14811
MCTAVISH, D. J. ..... p 808 N93-14941
MCWHORTER, ALAN L. ..... p 992 N93-14576
MEADOWS, V. S. ..... p 1026 N93-14308
p 1035 N93-14346
MEANS, ROBERT W. ..... p 934 N93-14210
MEEUWISSEN, ADRIANUS M. H. ..... p 941 N93-15090
MEIDINGER, N. ..... p 974 N93-15129
MEILER, P. P. ..... p 959 N93-15319
MEISTER, R. ..... p 933 N93-14648
MELNGAILIS, JOHN ..... p 865 N93-14410
MENARD, YVES ..... p 926 N93-14965
p 927 N93-14972
p 918 N93-14982
p 929 N93-14983
MENDILLO, MICHAEL ..... p 917 N93-15395
MENESSIER, E. ..... p 838 N93-15490
MENKE, TIMOTHY E. ..... p 802 N93-14608
MENNELLA, V. ..... p 843 N93-15283
MENON, S. ..... p 798 N93-14111
MENVIELLE, M. ..... p 931 N93-14998
MERCIER, H. ..... p 929 N93-14987
MERLE, JACQUES ..... p 927 N93-14973
p 918 N93-14982
p 929 N93-14983
MEROLLA, ANTHONY ..... p 867 N93-14798
MERTENS, HENRY W. ..... p 788 N93-14275
MESCHER, ANTHONY L. ..... p 934 N93-14535
MESEROLE, J. S. ..... p 855 N93-15420
MESSIDORO, PIERO ..... p 824 N93-15622
METCALF, HAROLD ..... p 884 N93-14402
METIU, H. ..... p 976 N93-14424
METROPOLIS, KATE ..... p 998 N93-14417
MEURS, E. J. A. ..... p 1021 N93-15284
MEYERS, S. ..... p 909 N93-15467
MEYERSON, ROBERT E. ..... p 814 N93-14495
MIAH, M. A. ..... p 917 N93-15466
MICHAELS, GREGORY A. ..... p 1025 N93-14300
p 1040 N93-14368
MICHALEK, DONNA JEAN ..... p 876 N93-14694
MICHAYLOV, SPIRO ..... p 943 N93-14558
MICHEL, CLAUDE D. ..... p 868 N93-14887
MIDDLETON, DAVID B. ..... p 803 N93-15366
MIKKELSON, K. A. ..... p 978 N93-15277
MILBURN, NELDA J. ..... p 788 N93-14275
MILES, R. T. ..... p 859 N93-14490
MILLER, BRIAN H. ..... p 904 N93-14263
MILLER, CHRISTOPHER E. ..... p 838 N93-14454
MILLER, CHRISTOPHER R. ..... p 939 N93-14713
MILLER, L. ..... p 927 N93-14974
MILLER, R. ..... p 928 N93-14977
MILLER, R. N. ..... p 926 N93-14970
MILLER, ROBERT A. ..... p 832 N93-14706
MILLER, S. L. ..... p 997 N93-15649
MILLER, W. A. ..... p 893 N93-15278
MILLMAN, DANIEL R. ..... p 879 N93-15434
MILSTER, TOM ..... p 985 N93-15513
MILSTER, TOM D. ..... p 985 N93-15511
p 985 N93-15512
p 985 N93-15514
p 985 N93-15515
MINSTER, JEAN-FRANCOIS ..... p 918 N93-14982
p 929 N93-14984
MINTON, STEVE ..... p 964 N93-15286
MITCHELL, A. K. ..... p 809 N93-14942
MITCHELL, C. E. ..... p 815 N93-15474
MITCHELL, JAMES L. ..... p 929 N93-14985
MITCHELL, JOHN E. ..... p 945 N93-14659
MITCHELL, MARK O. ..... p 839 N93-14530
MITCHELL, T. J. ..... p 969 N93-15656
MITCHUM, G. T. ..... p 928 N93-14980
MITTELMAN, MARC W. ..... p 932 N93-14532
MJOLSNESS, ERIC ..... p 963 N93-14783
MOAZED, KHOSROW L. ..... p 850 N93-14825
MOCK, R. C. ..... p 978 N93-15277
MODDEL, GARRET ..... p 996 N93-15446
p 996 N93-15447
MOEHRES, W. ..... p 796 N93-15177
MOENY, WILLIAM M. ..... p 869 N93-15196
MOERSCH, J. E. ..... p 1043 N93-14383
MOGNARD, N. ..... p 918 N93-14982
MOHR, R. K. ..... p 933 N93-14648
MONROE, JOHN W. ..... p 893 N93-15248
MONTARDI, Y. ..... p 838 N93-15490
MOODY, PAUL ..... p 894 N93-15461
MOOIJ, H. A. ..... p 778 N93-14616
MOORE, C. B. ..... p 976 N93-14283
MOORE, FRED ..... p 1004 N93-15028
MOORE, H. J. ..... p 1035 N93-14347
p 1040 N93-14369
p 1044 N93-14392
MOORE, JAMES T. ..... p 864 N93-15636
MOORE, MURRAY EDWARD ..... p 779 N93-14173
MOORE, REAGAN W. ..... p 1004 N93-15030
MOORE, T. R. ..... p 876 N93-14715
MOORE, TOBY JOHN TERRY ..... p 1014 N93-14113
MOORE, W. ..... p 1036 N93-14348
p 1043 N93-14383
MOORE, W. E. ..... p 877 N93-14816
MOORHEAD, A. J. ..... p 845 N93-14717
MORAN, STUART L. ..... p 869 N93-15269
MORGAN, B. A. ..... p 992 N93-14795
MORGAN, J. P. ..... p 870 N93-15276
MORGAN, PAUL ..... p 1029 N93-14322
MORGAN, WILLIAM P. ..... p 909 N93-14261
MORI, T. ..... p 907 N93-14992
p 931 N93-14996
MORISON, W. D. ..... p 811 N93-14955
MORKOC, HADIS ..... p 991 N93-14521
MORLIERE, A. ..... p 929 N93-14983
MOROZ, V. I. ..... p 1045 N93-14397
MORRAL, J. E. ..... p 847 N93-15382
MORRIS, C. L. ..... p 870 N93-15421
MORRIS, JEFFREY B. ..... p 854 N93-15011
MORRIS, M. D. ..... p 969 N93-15656
MORRIS, R. E. ..... p 854 N93-15640
MORRIS, VERNON ROBINSON ..... p 912 N93-14117
MORRIS, W. O. ..... p 877 N93-14816
MORRISETT, J. GREGORY ..... p 958 N93-14151
MOTA, GILBERTO F. ..... p 861 N93-15237
MOULTON, CAREY L. ..... p 910 N93-14655
MOUROU, GERARD ..... p 858 N93-14408
p 871 N93-15456
MOUTON, ANDRE ..... p 814 N93-15613
MOYLE, IAN N. ..... p 800 N93-15337
MUELLER, JEAN-FRANCOIS ..... p 911 N93-15460
MUELLER, PAUL ..... p 866 N93-14577
MUHLEMAN, DUANE O. ..... p 1029 N93-14320
p 1036 N93-14349
MUKHERJEE, R. ..... p 1014 N93-15590
p 1014 N93-15591
p 1014 N93-15592
MULDER, J. A. ..... p 777 N93-14615
MULLIN, SCOTT A. ..... p 844 N93-14508
MULLINS, L. D. ..... p 813 N93-15392
MUNGER, C. T. ..... p 978 N93-15468
MURALIDHAR, S. J. ..... p 794 N93-15161
MURDOCCA, MILES ..... p 944 N93-14564
MURPHY, K. E. ..... p 882 N93-14810

MURPHY, T. ..... p 862 N93-15435
MURR, TODD ..... p 785 N93-14856
MURRAY, J. N. ..... p 830 N93-14232
MURTHY, P. L. N. ..... p 902 N93-15343
MURTY, VENKATAESH V. ..... p 950 N93-15308
MUTHARASAN, RAJAKKANNU ..... p 888 N93-14478
MYDOSH, J. A. ..... p 995 N93-15321
MYERS, PHILIP ..... p 952 N93-15502
MYERS, S. M. ..... p 847 N93-15383
MYERS, THOMAS T. ..... p 802 N93-14811

N

NA, C. Y. ..... p 1045 N93-14397
NA, CHAN YOUNG ..... p 1046 N93-14635
NADKARNY, A. ..... p 846 N93-15138
NAGABHUSHANA, S. ..... p 794 N93-15161
NAGAMATSU, F. ..... p 793 N93-15153
NAGASHIMA, N. ..... p 994 N93-15233
NAGY, PETER V. ..... p 890 N93-14567
NAH, SEUNG-HYEOG ..... p 790 N93-14448
NAHON, M. ..... p 805 N93-14923
NAITOH, PAUL ..... p 934 N93-14240
NAKAGAWA, I. ..... p 907 N93-14992
NAKAMOTO, GLEN ..... p 1005 N93-15034
NAM, H. D. ..... p 974 N93-14734
NAMIKI, NORIYUKI ..... p 1036 N93-14350
NAMKUNG, MIN ..... p 845 N93-14705
NANDAKUMAR, RATNA ..... p 970 N93-14455
NANEY, M. ..... p 907 N93-15219
NAPFEL, HANS F. ..... p 795 N93-15167
NARANG, SUBHASH C. ..... p 871 N93-15485
NARAYAN, SUBRAMANIAM ..... p 828 N93-14142
NARAYANSWAMI, NATRAJ ..... p 876 N93-14695
NASTASI, M. ..... p 837 N93-15426
NAYLOR, BRUCE F. ..... p 952 N93-15535
p 955 N93-15557
NAYLOR, M. G. S. ..... p 853 N93-15439
NEBRES, JOSE LUIS VILLAFRANCA
p 781 N93-15101
NEES, JOHN A. ..... p 871 N93-15456
NEIDIG, CRAIG A. ..... p 1009 N93-15642
NENNIE, F. A. ..... p 867 N93-14803
NEREM, R. S. ..... p 928 N93-14981
NERING, JEFFERY D. ..... p 966 N93-15406
NESSIM, MAHER ..... p 810 N93-14951
NETA, B. ..... p 973 N93-14234
NETZER, V. ..... p 950 N93-15305
NEU, CHARLES E. ..... p 846 N93-15189
NEUGEBAUER, G. T. ..... p 995 N93-15312
NEUMARK, DANIEL M. ..... p 842 N93-14671
NEWAZ, G. M. ..... p 837 N93-15401
NEWBURY, CLAUDIA M. ..... p 1008 N93-15229
NEWKIRK, J. W. ..... p 846 N93-15138
NEWMAN, M. ..... p 1037 N93-14351
NEWMAN, W. I. ..... p 1037 N93-14352
NEWSON, D. ..... p 853 N93-15452
NG, WING-FAI ..... p 877 N93-14885
NGAI, THOMAS T. ..... p 817 N93-14725
NIBBELINK, BRUCE DAVID ..... p 802 N93-14830
NICKEL, JEFFERY D. ..... p 936 N93-15249
NICOL, DAVID ..... p 951 N93-15432
NICOLAENKO, BASIL ..... p 998 N93-15333
NIEMEGEERS, I. G. ..... p 860 N93-15095
NIEUWENHUYS, G. J. ..... p 995 N93-15321
NIGHTINGALE, R. W. ..... p 916 N93-14899
NIILER, P. ..... p 928 N93-14979
NIKISHIN, A. M. ..... p 1037 N93-14353
p 1037 N93-14354
p 1037 N93-14355
p 1042 N93-14378
NILSSON, C. S. ..... p 927 N93-14971
NISHIDA, H. ..... p 931 N93-14996
NOGAR, N. S. ..... p 887 N93-15135
NOH, HYE-RIM ..... p 1016 N93-14154
NOLAN, ROBERT C., II ..... p 792 N93-15314
NOLL, KEITH ..... p 1021 N93-15079
NORRIS, THEODORE ..... p 858 N93-14408
NORTON, WILLIAM E. ..... p 939 N93-14870
NOYES, H. P. ..... p 998 N93-15469
NYMEYER, ALBERT ..... p 946 N93-15091

O

OBERG, D. L. ..... p 979 N93-15362
OBEYSEKARE, U. R. ..... p 1008 N93-15393
OBLAS, D. W. ..... p 852 N93-15437
OBRIEN, MARK A. ..... p 791 N93-14601
OCONNOR, ANDREW M. ..... p 871 N93-15503
ODMAN, MEHMET TALAT ..... p 909 N93-14118
ODONNELL, J. M. ..... p 870 N93-15421
OFMAN, LEON ..... p 987 N93-14122
OHANDLEY, DOUGLAS A. ..... p 805 N93-14922
OKAL, E. B. ..... p 918 N93-14969
OKASAKI, CHRIS ..... p 941 N93-15239
OLAUSSEN, T. I. ..... p 930 N93-14988
OLBERS, DIRK ..... p 929 N93-14986
OLDING, BILL ..... p 933 N93-14103
p 881 N93-14105
OLEAR, BERNARD T. ..... p 1007 N93-15046
OLEARY, JOHN F. ..... p 782 N93-15245
OLESON, KEITH ..... p 823 N93-15620
OLESON, STEVEN R. ..... p 828 N93-15584
OLIPHANT, T. A., JR. ..... p 989 N93-15422
OLLERO, ANIBAL ..... p 885 N93-14568
OLLITRAULT, MICHEL ..... p 929 N93-14987
OLSON, D. W. ..... p 815 N93-14730
p 815 N93-14768
p 815 N93-14794
OLSON, P. ..... p 1043 N93-14383
OLSZEWSKI, M. ..... p 907 N93-15219
ONEILL, R. V. ..... p 911 N93-15273
ONGAREAU, ERIC ..... p 807 N93-14932
ONKEN, R. ..... p 797 N93-15184
OOE, M. ..... p 907 N93-14992
ORANGE, T. W. ..... p 902 N93-15369
ORASANU, JUDITH ..... p 787 N93-15023
OROURKE, P. E. ..... p 881 N93-14716
ORTON, GLENN ..... p 1021 N93-15079
OSAKA, WALTER K. ..... p 817 N93-14725
OSBORNE, F. J. ..... p 812 N93-14962
OSBORNE, WILLIAM P. ..... p 857 N93-14155
p 941 N93-14770
OSGOOD, R. M. ..... p 908 N93-15384
OSGOOD, RICHARD M., JR. ..... p 865 N93-14425
OSIF, T. L. ..... p 994 N93-15221
OSOFSKY, MICHAEL S. ..... p 850 N93-14743
OSTERYOUNG, ROBERT A. ..... p 842 N93-14664
OTTEN, M. P. ..... p 860 N93-14805
OTTIGER, R. ..... p 778 N93-15181
OTTINGER, PAUL ..... p 976 N93-14662
OXLEY, MARK E. ..... p 859 N93-14649
OZTURK, MURAT ..... p 836 N93-15373

P

PABSCH, A. ..... p 835 N93-15075
PACKARD, W. J. ..... p 888 N93-14434
PAGLIERONI, DAVID W. ..... p 955 N93-15556
PAINE, D. C. ..... p 991 N93-14429
PALMER, DAVID MICHAEL ..... p 1012 N93-14628
PALMER, RAYMOND W. ..... p 871 N93-15531
PAN, NING ..... p 833 N93-14752
PANDA, J. ..... p 781 N93-14791
PAPANICOLAOU, NICOLAS A. ..... p 993 N93-14820
PAQUAY, M. H. ..... p 860 N93-14805
PARASHAR, S. ..... p 811 N93-14953
PARFITT, ELISABETH A. ..... p 1038 N93-14356
PARK, E. ..... p 851 N93-15294
PARK, JONG-HWAN ..... p 873 N93-14278
PARK, JOON BOO ..... p 898 N93-14279
PARKER, LOUISE V. ..... p 848 N93-14486
PARKER, R. A. ..... p 946 N93-15052
PARKER, T. J. ..... p 1035 N93-14347
p 1038 N93-14357
PARKER, WILLIAM H. ..... p 799 N93-14896
PARKINSON, J. S. ..... p 952 N93-15476
PARLETT, BERESFORD ..... p 967 N93-14270
PARLIER, M. ..... p 838 N93-15490
PARMENTIER, E. M. ..... p 1029 N93-14324
p 1038 N93-14358
PARNAS, DAVID L. ..... p 946 N93-15052
PARNAS, R. ..... p 833 N93-14747
PARROTT, TONY L. ..... p 975 N93-15391
PARSONS, B. ..... p 918 N93-14969
PASCAL, F. ..... p 878 N93-15122
PASIN, M. ..... p 878 N93-15065
PASSMAN, ROBERT H. ..... p 783 N93-14844
PASTORE, C. ..... p 834 N93-14755
PATCHETT, DAVID B. ..... p 842 N93-14824
PATENAUDE, Y. ..... p 812 N93-14961
PATER, RUTH H. ..... p 849 N93-14709
PATON, NEIL ..... p 844 N93-14132
PATTERSON-HINE, A. ..... p 816 N93-15477
PATTERSON, MICHAEL J. ..... p 827 N93-15429
PATTERSON, PHILIP ..... p 838 N93-14435
PATZERT, W. ..... p 928 N93-14979
PAUTASSO, GABRIELLA ..... p 987 N93-14129
PAVLAKOS, C. J. ..... p 1051 N93-15060
PAVRI, B. ..... p 1038 N93-14359
PAWLAS, GARY E. ..... p 826 N93-14883
PAWLIK, EUGENE A., SR. ..... p 939 N93-14651
PEAT, K. S. ..... p 974 N93-15073
PEEL, H. HERBERT ..... p 881 N93-14494
PELLETIER, P. J. ..... p 851 N93-15295
PELTON, GARRETT ..... p 940 N93-14491
PENROSE, J. ..... p 927 N93-14971
PEPPLER, PHILIPP W. ..... p 804 N93-14559
PERDUE, JAMES ..... p 1002 N93-14773
PERES, P. ..... p 838 N93-15490
PEREY, F. G. ..... p 969 N93-15212
PEREZ-DAVIS, MARLA E. ..... p 823 N93-15616
PERKINS, A. L. ..... p 925 N93-14503
PERRY, DAVID L. ..... p 983 N93-15197
PERRY, GLENN ..... p 983 N93-15223
PERSON, LEE H., JR ..... p 803 N93-15366
PESCE-RODRIGUEZ, ROSE A. ..... p 854 N93-15011
PETERSEN, SIDNEY M. ..... p 955 N93-15556
PETERSON, ANTHONY L. ..... p 1005 N93-15033
PETERSON, MIRIAM R. ..... p 924 N93-15331
PETERSON, TOM J. ..... p 824 N93-15623
PETRIU, E. ..... p 805 N93-14926
PETTENGILL, G. H. ..... p 1028 N93-14316
p 1039 N93-14360
p 1039 N93-14363
PETTENGILL, GORDON H. ..... p 1035 N93-14345
PETTERSSON, LASSE H. ..... p 930 N93-14988
PFENNING, FRANK ..... p 942 N93-14268
PFOERTNER, H. ..... p 796 N93-15173
PHELAN, F. ..... p 833 N93-14747
PHILIPS, ANDREW ..... p 964 N93-15286
PHILLIPS, NICHOLAS J. ..... p 883 N93-14131
PHILLIPS, R. J. ..... p 1039 N93-14361
PHILLIPS, ROGER J. ..... p 1029 N93-14321
PHIPPS, WARREN E., JR. ..... p 816 N93-14253
PICAUT, JOEL ..... p 930 N93-14989
PICOLOGLOU, B. ..... p 826 N93-15215
PIERCE, W. S. ..... p 902 N93-15369
PIERESON, R. G. ..... p 1041 N93-14373
PIERRON, F. ..... p 926 N93-14965
PIKE, ROB ..... p 957 N93-15566
PILANT, MICHAEL S. ..... p 969 N93-15256
PILON, PAUL GILLES ..... p 905 N93-14823
PIN, F. G. ..... p 963 N93-14818
PINARDI, NADIA ..... p 927 N93-14972
PINEDA, JAIME A. ..... p 935 N93-14782
PINKERTON, S. D. ..... p 979 N93-15362
PIPER, T. C. ..... p 870 N93-15276
PIPKINS, DANIEL SCOTT ..... p 896 N93-14186
PIROLLI, PETER ..... p 999 N93-14130
PISTEK, PAVEL ..... p 960 N93-14239
PITCHFORD, MARC LYNN ..... p 922 N93-14875
PITTS, DAVID ..... p 1005 N93-15035
PIZZINO, JOSEPH F. ..... p 842 N93-14824
PLAUT, JEFFREY J. ..... p 1035 N93-14347
p 1039 N93-14362
p 1039 N93-14363
p 1040 N93-14368
PLEY, MICHAEL ..... p 807 N93-14933
PLOURDE, J. V. ..... p 939 N93-14554
PODIO, FERNANDO L. ..... p 1003 N93-14778
PODOJIL, G. ..... p 852 N93-15344
p 819 N93-15597
POINSOT, THIERRY J. ..... p 840 N93-14622
POIROT, FRANCK ..... p 947 N93-15125
POLLINGER, J. ..... p 853 N93-15452
POPEJOY, DAVID BRIAN ..... p 896 N93-14187
PORRO, A. ROBERT ..... p 879 N93-15355
PORTER, CHRISTOPHER C. ..... p 832 N93-14700
POTAPCZUK, MARK G. ..... p 787 N93-15345
p 787 N93-15354
POTENZIANI, ERNEST, II ..... p 869 N93-15194
POUKEY, J. W. ..... p 978 N93-15277
POWELL, I. P. ..... p 811 N93-14952
POWELL, RICHARD W. ..... p 813 N93-15367
POWERS, JANET V. ..... p 936 N93-15583
PRADHAN, ANIL K. ..... p 1012 N93-14761
p 1012 N93-14762
PRAKASH, J. ..... p 870 N93-15441
PRASAD, R. ..... p 991 N93-14485
PRATER, DAVID L. ..... p 803 N93-15396
PREECS, B. L. ..... p 1008 N93-15275
PRESCOTT, C. Y. ..... p 978 N93-15486
PRESS, RONALD ..... p 867 N93-14699
PRICE, BLAINE A. ..... p 953 N93-15540
PRICE, RONALD R. ..... p 868 N93-15107
PRIEST, R. G. ..... p 1008 N93-15393
PRINZ, R. ..... p 835 N93-15075
PROVENZANO, V. ..... p 836 N93-15246
PROVOST, C. ..... p 931 N93-14998
PRUSINKIEWICZ, PRZEMYSLAW ..... p 956 N93-15558
PSALTIS, DEMETRI ..... p 1008 N93-15409
PUDNOS, ERIC ..... p 833 N93-14751
PUJARI, V. K. ..... p 837 N93-15388
PULLIAM, ROBERT JAY ..... p 913 N93-14225
PURGOLD, GERALD C. ..... p 924 N93-15501
PYGAS, J. W. ..... p 811 N93-14952

Q

QIAN, R. ..... p 992 N93-14643
p 993 N93-15008
p 993 N93-15055
QU, XIAOQING ..... p 953 N93-15542

QUADRI, SYED B. ..... p 850 N93-14743
QUATTLEBAUM, MARTIN ..... p 933 N93-14103
p 881 N93-14105

R

RABIN, B. H. ..... p 834 N93-14819
RABINOWICZ, M. ..... p 918 N93-14969
RABITZ, HERSCHEL ..... p 976 N93-14411
RADAK, BRANISLAV ..... p 998 N93-14143
RAIMONDO, GIACOMO ..... p 824 N93-15622
RAINER, F. ..... p 886 N93-14906
RAITALA, J. ..... p 1039 N93-14364
RAMAMONJIARISOA, F. ..... p 918 N93-14982
RAMAMURTHY, SUBRAMANIAM ..... p 836 N93-15218
RAMAN, SETHU ..... p 921 N93-14680
RAMSEY, P. B. ..... p 870 N93-15389
RANAUDO, R. J. ..... p 803 N93-14831
RANDALL, D. A. ..... p 922 N93-14901
RANDELL, WILLIAM ..... p 944 N93-14572
p 944 N93-14581
RANNEY, THOMAS A. ..... p 848 N93-14486
RAO, DANTAM K. ..... p 891 N93-14916
RAPP, RICHARD H. ..... p 930 N93-14990
RAPTIS, A. C. ..... p 851 N93-15282
p 883 N93-15411
RASMUSSEN, ERIK NELS ..... p 921 N93-14682
RASMUSSEN, MAURICE L. ..... p 781 N93-14767
RATCLIFF, J. T. ..... p 1043 N93-14383
RATVASKY, T. P. ..... p 803 N93-14831
RAUH, R. D. ..... p 866 N93-14583
p 983 N93-15241
RAUSCH, E. O. ..... p 882 N93-14810
RAWLIN, VINCENT K. ..... p 827 N93-15429
RAY, E. R. ..... p 908 N93-15322
p 908 N93-15323
RAY, RONALD J. ..... p 795 N93-15169
REBENNE, H. E. ..... p 852 N93-15437
REDDY, E. S. ..... p 902 N93-15343
REDEY, L. ..... p 870 N93-15441
REED, CHARLES E. ..... p 999 N93-14106
REEHORST, ANDREW ..... p 787 N93-15360
REGEL, LIYA L. ..... p 995 N93-15309
REID, RONA ..... p 833 N93-14748
REINECKE, MICHAEL ..... p 939 N93-14520
REISING, JOHN ..... p 939 N93-14520
REISS, DONALD A. ..... p 992 N93-14707
REITSEMA, HAROLD ..... p 1021 N93-15079
REMER, LORRAINE ANN ..... p 919 N93-14180
REMICK, R. J. ..... p 994 N93-15221
REMO, JOHN L. ..... p 979 N93-14152
p 984 N93-15371
REMY, F. ..... p 929 N93-14984
RIAZ, JAMSHED ..... p 920 N93-14588
RIBEIRO, P. F. ..... p 854 N93-14834
RICHMAN, BRUCE ARAM ..... p 883 N93-14125
RICK, H. ..... p 796 N93-15176
RINALDI, M. A. ..... p 916 N93-14899
RISER, DANIEL T. ..... p 939 N93-14651
RISPIN, LAWRENCE W. ..... p 858 N93-14426
RITTER, J. J. ..... p 850 N93-15049
RITZERT, F. J. ..... p 847 N93-15586
RIZO, P. ..... p 851 N93-15282
RIZOS, C. ..... p 927 N93-14971
ROBAUDO, STEFANO ..... p 916 N93-14913
ROBBINS, DAVID O. ..... p 933 N93-14163
ROBE, R. Q. ..... p 939 N93-14554
ROBERT, J. C. ..... p 944 N93-14566
ROBERTS, C. D. ..... p 978 N93-15657
ROBERTS, K. M. ..... p 1033 N93-14339
ROBINSON, DAVID F. ..... p 875 N93-14481
ROBINSON, PAUL ..... p 784 N93-14847
ROBINSON, R. M. ..... p 916 N93-14899
ROCKWELL, D. O. ..... p 880 N93-15652
ROCKWELL, DONALD ..... p 782 N93-15464
RODDY, D. ..... p 1040 N93-14365
RODRIGUEZ, A. E. ..... p 859 N93-14453
RODRIGUEZ, ELVIN ..... p 819 N93-15595
ROEDER, J. L. ..... p 917 N93-15574
ROGERS, BRAD ..... p 817 N93-14565
ROGERS, P. G. ..... p 1027 N93-14310
ROGERS, ROBIN D. ..... p 996 N93-15443
ROHACS, J. ..... p 794 N93-15159
ROLFE, RICHARD ..... p 1001 N93-14216
ROLFE, ROBERT M. ..... p 948 N93-15267
ROLIN, TERRY ..... p 997 N93-15500
ROMIG, A. D., JR. ..... p 847 N93-15382
RON, A. ..... p 969 N93-15398
RON, AMOS ..... p 969 N93-15399
RONCONE, RONALD L. ..... p 986 N93-15518
ROOD, ROBERT ..... p 826 N93-14681
ROOS, MAURITS ..... p 905 N93-14676
ROSBOROUGH, G. ..... p 926 N93-14966
ROSCOE, OREST S. ..... p 812 N93-14960
ROSENBLATT, M. ..... p 1040 N93-14365
ROSENBLOOM, PAUL ..... p 940 N93-14491
ROSENFIELD, A. R. ..... p 851 N93-15294
ROSIER, C. ..... p 878 N93-15122
ROSNER, DANIEL E. ..... p 838 N93-14418
ROSS, D. W. ..... p 988 N93-15327
ROSS, MICHAEL ..... p 857 N93-14155
ROSSI, G. A. ..... p 851 N93-15295
p 837 N93-15388
p 853 N93-15453
p 837 N93-15454
ROUSSEL-DUPRE, R. ..... p 862 N93-15427
p 862 N93-15435
ROWE, IAN H. ..... p 806 N93-14928
ROYAPPA, ANDREW V. ..... p 953 N93-15537
RUBIN, CLINTON T. ..... p 935 N93-15006
RUBINOVITZ, JACOB ..... p 949 N93-15300
RUMBOLD, J. G. ..... p 811 N93-14952
RUMMEL, R. ..... p 813 N93-15000
RUMSEY, C. L. ..... p 781 N93-14791
RUNDELL, WILLIAM ..... p 969 N93-15256
RUSHBY, JOHN ..... p 958 N93-14808
RUSSELL, D. H. ..... p 886 N93-15058
RUSSELL, J. ..... p 1040 N93-14369
RUTLEDGE, SHARON K. ..... p 819 N93-15596
p 823 N93-15616
RYAN, P. M. ..... p 863 N93-15440
RYBCZYNSKI, FRED ..... p 1005 N93-15036

S

SAAD, AHMED MOUSTAFA ..... p 972 N93-14280
SABSAY, CATHERINE M. ..... p 779 N93-14451
SADANANDA, K. ..... p 836 N93-15246
SADLER, ROBERT L. ..... p 834 N93-14754
p 834 N93-14756
SADOULET, BERNARD ..... p 998 N93-14417
SAFIE, F. M. ..... p 895 N93-15433
SAHNOW, DAVID JAMES ..... p 1017 N93-14444
SAIKI, M. ..... p 931 N93-14996
SAKIMOTO, S. E. H. ..... p 1040 N93-14366
SALIBRA, ANTONINO ..... p 968 N93-15094
SALTZMAN, EDWIN J. ..... p 779 N93-14451
SAMAL, P. ..... p 846 N93-15138
SAMUELSEN, G. S. ..... p 800 N93-15359
SAMULSKI, EDWARD T. ..... p 994 N93-15190
SANCHEZ-ALIAS, ALEJO ..... p 904 N93-14174
SANCHEZ, BRAULIO V. ..... p 930 N93-14991
SANDKULLA, D. ..... p 900 N93-14498
SANDWELL, D. T. ..... p 931 N93-14997
SANDWELL, DAVID T. ..... p 1030 N93-14329
p 1036 N93-14348
p 1040 N93-14367
SANFORD, T. W. L. ..... p 978 N93-15277
SANKARACHARYULU, M. G. V. ..... p 991 N93-14485
SARIN, V. K. ..... p 852 N93-15437
SARKAR, SUBHENDRA N. ..... p 841 N93-14658
SARMA, SANKAR D. ..... p 976 N93-14433
SARVER-VERHEY, TIMOTHY R. ..... p 827 N93-15429
SASAKI, M. ..... p 907 N93-14992
SASHEGYI, KEITH D. ..... p 921 N93-14680
SATER, BERNARD L. ..... p 907 N93-15224
SATER, JANET ..... p 990 N93-14422
SATING, RICHARD R. ..... p 950 N93-15313
SAUNDERS, LARRY ..... p 947 N93-15262
SAUNDERS, R. S. ..... p 1035 N93-14347
SAUNDERS, R. STEPHEN ..... p 1025 N93-14300
p 1039 N93-14363
p 1040 N93-14368
SAVAGE, PATRIC ..... p 1005 N93-15032
SAWYER, S. ..... p 915 N93-14877
SCANLON, RAYMOND ..... p 962 N93-14533
SCARDINO, FRANK L. ..... p 832 N93-14746
SCARMOZZINO, ROBERT ..... p 865 N93-14425
SCARPELLI, AUGUST R. ..... p 882 N93-14840
SCHABER, G. G. ..... p 1024 N93-14293
p 1027 N93-14311
p 1039 N93-14363
p 1040 N93-14369
p 1043 N93-14388
p 1044 N93-14392
SCHABER, GERALD G. ..... p 1026 N93-14305
SCHADE, DAVID JOSEPH ..... p 1012 N93-14629
SCHARTON, TERRY ..... p 820 N93-15599
SCHIENLE, J. ..... p 836 N93-15387
p 837 N93-15455
SCHIPPER, GIDEON L. V. ..... p 959 N93-15142
SCHIPPER, L. ..... p 909 N93-15467
SCHLAGER, KENNETH J. ..... p 936 N93-15192
SCHLOERB, F. PETER ..... p 1033 N93-14340
SCHMIDT, I. ..... p 978 N93-15468
SCHMIDT, K.-J. ..... p 796 N93-15175
SCHMITIGAL, WESLEY P. ..... p 832 N93-14700
SCHMITT, J. J. ..... p 851 N93-15222
SCHMITZ, JOHN J. ..... p 893 N93-15251
SCHMITZ, W. J. ..... p 929 N93-14985
SCHNEIDER, IRWIN ..... p 887 N93-15250
SCHNEIDER, NIKLAS ..... p 922 N93-14864
SCHNEIDER, STEVEN J. ..... p 827 N93-15572
SCHNEIDER, WALTER T. ..... p 882 N93-15247
SCHOOF, L. A. ..... p 1051 N93-15060
SCHOPF, P. ..... p 927 N93-14974
SCHROEDER, JON M. ..... p 867 N93-14666
SCHROEDER, MICHAEL A. ..... p 854 N93-15011
SCHROEDER, PETER ..... p 955 N93-15553
SCHROEDER, W. U. ..... p 977 N93-15326
SCHROETER, J. ..... p 927 N93-14972
SCHUBERT, G. ..... p 1043 N93-14383
p 1044 N93-14395
SCHUBERT, GERALD ..... p 1036 N93-14348
p 1040 N93-14367
SCHULTZ, P. H. ..... p 1044 N93-14393
SCHULTZ, PATER H. ..... p 1041 N93-14372
SCHULTZ, PETER H. ..... p 1041 N93-14370
p 1041 N93-14371
SCHULZ, TERESA MARIA ..... p 1023 N93-14212
SCHULZ, UWE ..... p 795 N93-15168
SCHUSTER, DAVID MARTIN ..... p 791 N93-14832
SCHUTZ, B. E. ..... p 931 N93-14997
SCHWAB, R. R. ..... p 800 N93-15143
SCHWARZ, R. K. ..... p 946 N93-15003
p 951 N93-15450
SCHWENKE, DAVID W. ..... p 843 N93-15358
SCHWIDERSKI, E. W. ..... p 927 N93-14974
SCOLLO, GIUSEPPE ..... p 968 N93-15094
SCOTT, CURTIS M. ..... p 941 N93-15239
SCOTT, D. R. ..... p 1043 N93-14387
SCOTT, J. F. ..... p 1041 N93-14373
SEGAWA, J. ..... p 907 N93-14992
SEGERMAN, ALAN M. ..... p 1046 N93-14833
SEGLETES, STEVEN B. ..... p 821 N93-15604
SEIBER, B. L. ..... p 981 N93-14403
SEIDEL, HANS-PETER ..... p 952 N93-15534
SEITTER, KEITH L. ..... p 918 N93-14153
SELIG, MICHAEL SCOTT ..... p 790 N93-14462
SELIGMANN, DOREE ..... p 954 N93-15510
SELIM, R. ..... p 997 N93-15587
SELPH, M. M. ..... p 882 N93-15381
SELTZER, STEPHEN M. ..... p 1051 N93-15580
SEMB, GEORGE B. ..... p 999 N93-14526
SENSKE, D. A. ..... p 1041 N93-14374
SERGEANT, ROSE ..... p 998 N93-14417
SETH, K. K. ..... p 977 N93-15377
SETHURAMAN, JAYARAM ..... p 970 N93-14487
SEXTON, J. ANDREW ..... p 895 N93-15582
SHADER, WILLIAM ..... p 867 N93-14642
SHAH, BIREN N. ..... p 981 N93-14404
SHAH, KATHRYN PIERCE ..... p 1029 N93-14320
p 1047 N93-14918
SHALIMOV, I. V. ..... p 1041 N93-14375
p 1042 N93-14378
SHAMIR, TZILA ..... p 950 N93-15307
SHANAHAN, W. R. ..... p 989 N93-15422
p 989 N93-15436
SHANNON, J. L., JR. ..... p 902 N93-15369
SHANNON, L. V. ..... p 928 N93-14976
SHAPIRO, MICHAEL ..... p 1001 N93-14524
p 1009 N93-15627
SHARAF, HAZEM H. ..... p 875 N93-14688
SHARPE, LISA M. ..... p 862 N93-15397
SHASTRI, P. ..... p 1012 N93-14760
SHAW, MARY ..... p 941 N93-15239
SHAW, RUSSELL J. ..... p 875 N93-14677
SHEBALIN, JOHN V. ..... p 979 N93-15482
SHECHTMAN, D. ..... p 989 N93-14133
SHEEN, S. H. ..... p 883 N93-15411
SHEFFIELD, R. L. ..... p 887 N93-15417
SHEFFLER, THOMAS J. ..... p 959 N93-15205
p 959 N93-15207
SHELTON, J. ..... p 789 N93-14729
SHEM, L. M. ..... p 910 N93-15209
SHEPHARD, MARK S. ..... p 831 N93-14550
SHEU, PHILLIP ..... p 1008 N93-15254
SHIAH, SHEAU-MING ..... p 839 N93-14463
SHIELDS, JOSEPH CHARLES ..... p 1018 N93-14461
SHIH, TSAN-HSING ..... p 877 N93-14829
SHIHABI, MAZEN M. ..... p 981 N93-14404
SHIMEALL, STEPHEN C. ..... p 943 N93-14420
SHIMEALL, TIMOTHY J. ..... p 943 N93-14420
SHIMODA, KOICHI ..... p 887 N93-15296
SHIN, JAIWON ..... p 781 N93-14911
p 782 N93-15338
SHIRCK, SAM ..... p 785 N93-14857
SHOEMAKE, KEN ..... p 955 N93-15551
p 956 N93-15563
SHPILKA, VLADIMIR ..... p 811 N93-14954
SHUM, C. K. ..... p 931 N93-14997
SHUNJI, HUANG ..... p 861 N93-15106
SHUNMUGAM, M. S. ..... p 950 N93-15308
SHYNE, RICKEY J. ..... p 800 N93-15342
SIBENER, STEVEN J. ..... p 841 N93-14652
SICA, LOUIS, JR. ..... p 982 N93-14800

SIEBEIN, K. N. ..... p 837 N93-15388
SIEDLER, G. ..... p 929 N93-14986
SIEGLER, ANDRAS ..... p 949 N93-15299
SIGETY, P. ..... p 836 N93-15253
SIKES, ALLISON M. ..... p 850 N93-14802
SIKES, W. C. ..... p 826 N93-15215
SIKIVIE, P. ..... p 1022 N93-15346
SIKKEL, KLAAS ..... p 958 N93-15082
SILVA, WALTER J. ..... p 916 N93-15136
SILVANO, SILENZI ..... p 788 N93-15164
SILVERA, ISSAC F. ..... p 843 N93-15497
SIMON, ROBERT ..... p 939 N93-14651
SIMONS, MARK ..... p 1027 N93-14314
p 1042 N93-14376
SIMPSON, R. A. ..... p 1044 N93-14391
SIMS, MICHAEL H. ..... p 963 N93-14765
SINCARSIN, G. B. ..... p 808 N93-14941
SINCARSIN, W. G. ..... p 808 N93-14941
SINGH, B. P. ..... p 991 N93-14485
SINGH, TARUN-RAJ ..... p 892 N93-15150
SINGH, VINOD KUMAR ..... p 960 N93-14203
SINHA, D. N. ..... p 895 N93-15413
SJOGREN, W. L. ..... p 1027 N93-14310
p 1042 N93-14377
SKINDLOV, JONATHAN ANDERS ..... p 923 N93-14919
SKOCYPEC, R. ..... p 870 N93-15441
SKOFRONICK, G. M. ..... p 905 N93-14792
SKOGMO, P. J. ..... p 978 N93-15277
SLANE, STEVEN M. ..... p 866 N93-14552
SLEATOR, DANIEL ..... p 947 N93-15206
SLINEY, HAROLD E. ..... p 828 N93-15576
SLINKER, S. ..... p 978 N93-14570
SLINKER, S. P. ..... p 978 N93-14127
SLINKER, STEVEN P. ..... p 976 N93-14662
SLIWA, N. ..... p 816 N93-15477
SLOAN, GREGORY CLAYTON ..... p 1019 N93-14636
SLYUTA, E. N. ..... p 1042 N93-14378
SMEYS, P. ..... p 866 N93-14534
SMITH, A. ..... p 968 N93-14431
SMITH, DENNIS ..... p 856 N93-15353
SMITH, GERALD ..... p 976 N93-14513
SMITH, GUY A. ..... p 891 N93-14763
SMITH, J. L. ..... p 995 N93-15321
SMITH, PAUL ..... p 848 N93-14401
SMITH, PHILLIP J. ..... p 925 N93-14769
SMITH, REGINALD ..... p 835 N93-15145
SMITH, RICHARD P. ..... p 916 N93-15136
SMITH, S. M. ..... p 845 N93-14900
SMITH, WILLIAM HAYDEN ..... p 1021 N93-15079
SMREKAR, SUZANNE E. ..... p 1042 N93-14379
SMYTH, D. M. ..... p 991 N93-14439
SMYTH, P. ..... p 1042 N93-14380
SNYDER, STUART CODY ..... p 987 N93-14137
SODERBLOM, L. ..... p 1040 N93-14365
SODERBLOM, L. A. ..... p 1039 N93-14363
p 1040 N93-14369
SOEDER, RONALD H. ..... p 804 N93-15498
SOETRISNO, MOELJO ..... p 878 N93-15187
SOLIDUM, E. ..... p 836 N93-15387
p 853 N93-15452
p 837 N93-15455
SOLOMAN, SEAN C. ..... p 1042 N93-14379
SOLOMATOV, VIATCHESLAV S. ..... p 1042 N93-14381
SOLOMON, A. D. ..... p 907 N93-15219
SOLOMON, SEAN C. ..... p 1027 N93-14314
p 1035 N93-14344
p 1036 N93-14350
p 1042 N93-14376
p 1042 N93-14382
SOLON-WETMORE, JANE L. ..... p 1009 N93-15641
SON, YOON-HO ..... p 847 N93-15382
SOROUSHNEJAD, MOHSEN ..... p 857 N93-14181
SOUCY, Y. ..... p 808 N93-14941
p 809 N93-14942
SOULES, DAVID BRIAN ..... p 914 N93-14641
SOUNDRANAYAGAM, M. ..... p 779 N93-14479
SOURIAU, ANNIE ..... p 918 N93-14993
SOUTAR, COLIN ..... p 981 N93-14204
SOVEY, JAMES S. ..... p 827 N93-15429
SOWA, W. A. ..... p 800 N93-15359
SOWIZRAL, H. ..... p 816 N93-15477
SPALEK, G. ..... p 903 N93-15423
p 870 N93-15424
SPELIOTIS, DENNIS E. ..... p 883 N93-15039
SPENCER, K. M. ..... p 983 N93-15241
SPEZIALE, C. G. ..... p 879 N93-15481
SPOONER, SCOTT G. ..... p 889 N93-14499
SPRINGER, T. E. ..... p 907 N93-15061
SQUYRES, S. W. ..... p 1043 N93-14383
SRIVATSAN, RAGHAVACHARI ..... p 803 N93-15366
SROKOSZ, M. ..... p 932 N93-15001
STACY, N. J. S. ..... p 1037 N93-14352
p 1039 N93-14363
p 1043 N93-14384
STADLER, HENRY L. ..... p 940 N93-14704
STADLMEIER, P. ..... p 796 N93-15172
STAIR, PETER C. ..... p 843 N93-15200
STAKEBAKE, J. L. ..... p 845 N93-14723
STARK, CATHY L. ..... p 916 N93-15136
STATLER, IRVING C. ..... p 777 N93-14614
STATLER, JAN ..... p 1008 N93-15229
STAUB, T. A. ..... p 797 N93-15180
STECHER, JOSEPH L., III ..... p 819 N93-15593
STEELE, DAVID PATRICK ..... p 1045 N93-14612
STEFFES, P. G. ..... p 1030 N93-14328
STEFFES, PAUL G. ..... p 1028 N93-14315
p 1047 N93-15081
STEINBACH, V. ..... p 1043 N93-14385
STEINER, M. ..... p 858 N93-14233
STEINETZ, BRUCE M. ..... p 888 N93-14478
STELLBRINK, KUNO ..... p 835 N93-15076
STENGEL, ROBERT ..... p 785 N93-14854
STENGER, GREGORY J. ..... p 791 N93-14571
STENTZ, ANTHONY ..... p 885 N93-14568
STEPHENS, J. R. ..... p 843 N93-15283
STERN, ROBERT A. ..... p 868 N93-14915
STEVENS, MARC G. ..... p 803 N93-15396
STEVENSON, D. J. ..... p 1043 N93-14387
STEVENSON, DAVID J. ..... p 1042 N93-14381
STEWART, A. I. F. ..... p 1023 N93-14290
STEWART, A. JAMES ..... p 957 N93-15565
STEWART, J. M. ..... p 1041 N93-14373
STEWART, R. H. ..... p 931 N93-14997
STEWART, R. M. ..... p 797 N93-15179
STEWART, REGINA M. ..... p 849 N93-14573
STIDHAM, CURTIS R. ..... p 819 N93-15595
STIFTER, SABINE ..... p 949 N93-15302
STILLMAN, G. E. ..... p 885 N93-14667
STILLMAN, GREGORY E. ..... p 866 N93-14562
STOCK, STUART R. ..... p 898 N93-14272
STOFAN, E. R. ..... p 1039 N93-14363
p 1043 N93-14383
STOFAN, ELLEN R. ..... p 1040 N93-14368
STONES, A. ..... p 811 N93-14953
STORMSHAK, F. ..... p 933 N93-15211
STOVMAN, JOHN ..... p 810 N93-14948
STRACHAN, D. M. ..... p 871 N93-15479
STRANFORD, G. ..... p 836 N93-15387
p 837 N93-15455
STRANGEWAY, R. J. ..... p 1043 N93-14386
STRAUB, DARCY W. ..... p 1025 N93-14301
STREIFINGER, H. ..... p 796 N93-15173
STRICKLAND, JOHN W. ..... p 828 N93-14459
STROKES, R. ..... p 894 N93-14104
STROM, R. G. ..... p 1024 N93-14293
p 1027 N93-14311
p 1040 N93-14369
STROM, ROBERT G. ..... p 1026 N93-14305
STROTHOTTE, THOMAS ..... p 953 N93-15538
STROUD, W. JEFFERSON ..... p 900 N93-14483
STRUB, P. TED ..... p 931 N93-14994
STUEBER, THOMAS J. ..... p 819 N93-15595
STURDIVAN, L. M. ..... p 854 N93-15640
SU, GWANG-HUEI ..... p 902 N93-15070
SUDDHOO, A. ..... p 782 N93-15489
SUGIHARA, RYO ..... p 887 N93-15296
SUHS, N. E. ..... p 873 N93-14421
SULLA, JEFFREY L. ..... p 902 N93-15202
SULLIVAN, EDMUND J. ..... p 882 N93-14878
SULLIVAN, KENNETH ..... p 1019 N93-14637
SUN, JUANZHEN ..... p 921 N93-14683
SUNDBERG, G. J. ..... p 837 N93-15388
p 837 N93-15454
SUNI, I. ..... p 837 N93-15426
SUPARMI ..... p 998 N93-14590
SUPPE, JOHN ..... p 1024 N93-14297
SURESHBABU, B. N. ..... p 859 N93-14488
SUSHON, JANET ..... p 821 N93-15608
SUTER, BRUCE W. ..... p 859 N93-14649
SUTHERLAND, H. J. ..... p 908 N93-15384
SUTHERLAND, LYNN ..... p 810 N93-14951
SUTTER, THOMAS R. ..... p 818 N93-15368
SVEJKOVSKY, PAUL A. ..... p 890 N93-14702
SVITEK, TOMAS ..... p 1047 N93-14868
SWANSON, KEITH ..... p 965 N93-15291
SWANSON, RAND CURTIS ..... p 857 N93-14126
SWARTZ, S. L. ..... p 851 N93-15294
SWEC, DIANE M. ..... p 827 N93-15526
SWEENEY, PAULA K. ..... p 956 N93-15564
SWONGER, ROY F. ..... p 941 N93-15239
SYKA, J. E. P. ..... p 887 N93-15135
SYKORA, DAVID W. ..... p 917 N93-15459
SYLVIA, DAVID M. ..... p 933 N93-15208
SYMOLON, P. D. ..... p 877 N93-14816
SZEMEREY, ISTVAN ..... p 795 N93-15166
SZENDRO, SANDOR ..... p 795 N93-15166
SZIRTES, THOMAS ..... p 812 N93-14957

T

TABAKOFF, W. ..... p 878 N93-15065
TACKLEY, P. J. ..... p 1043 N93-14387
TAI, CHANG-KOU ..... p 931 N93-14995
TAIRA, K. ..... p 931 N93-14996
TAKEUCHI, SATOSHI ..... p 887 N93-15296
TANAKA, K. L. ..... p 1043 N93-14388
TANEJA, V. S. ..... p 895 N93-15433
TANGUAY, ARMAND R., JR. ..... p 982 N93-14578
TANJU, MEHMET CELAL ..... p 807 N93-14935
TAO, XIAOMING ..... p 888 N93-14478
TAPLEY, BYRON D. ..... p 931 N93-14997
TARG, RUSSEL ..... p 784 N93-14846
TARITS, PASCAL D. ..... p 931 N93-14998
TATSUOKA, KIKUMI K. ..... p 933 N93-14109
TATSUOKA, MAURICE M. ..... p 933 N93-14109
TAUBER, WOLFGANG ..... p 863 N93-15487
TAVORMINA, A. M. ..... p 1041 N93-14373
TAYLOR, DANIEL M. ..... p 823 N93-15618
TAYLOR, HENRY F. ..... p 859 N93-14728
TAYLOR, JOHN G. ..... p 800 N93-15342
TAYLOR, PETER R. ..... p 843 N93-15358
TAYLOR, ROBERT ..... p 939 N93-14520
TAYLOR, SUSAN ..... p 848 N93-14486
TEACHOUT, DUANE A. ..... p 794 N93-15160
TEAGUE, W. J. ..... p 929 N93-14985
TELLIER, PIERRE ..... p 957 N93-15570
TEMAM, R. ..... p 878 N93-15122
TEMPERLEY, DAVY ..... p 947 N93-15206
TENBERG, A. J. W. M. ..... p 963 N93-15083
TENCATE, JAMES ALAN ..... p 973 N93-14145
TENENBERG, JOSH ..... p 945 N93-14654
TENNYSON, R. C. ..... p 811 N93-14955
TERLEP, JUDITH A. ..... p 819 N93-15595
TERZOPOULOS, DEMETRI ..... p 956 N93-15562
TESTA, BRUCE ..... p 867 N93-14642
THAMBURAJ, RAJ ..... p 800 N93-14898
THAXTON, CIRRELIA ..... p 833 N93-14748
THEEUWES, J. ..... p 936 N93-14267
THERIAULT, JAMES A. ..... p 925 N93-14512
THIBODEAU, KENNETH ..... p 1004 N93-15031
THIEME, LANNY G. ..... p 827 N93-15526
THOMAS, KEITH ALLEN ..... p 988 N93-14138
THOMAS, S. ..... p 992 N93-14643
p 993 N93-15008
p 993 N93-15055
THOMAS, WILLIAM H., III ..... p 968 N93-14609
THOMPSON, BRIAN S. ..... p 836 N93-15218
THOMPSON, D. ..... p 811 N93-14953
THOMPSON, J. ..... p 933 N93-15211
THOMPSON, J. D. ..... p 920 N93-14256
p 998 N93-14905
p 929 N93-14985
THOMPSON, KEITH L. ..... p 999 N93-14106
p 1008 N93-15335
THOMPSON, M. S. ..... p 847 N93-15382
THOMPSON, PHILLIP E. ..... p 993 N93-14820
THOMPSON, T. W. ..... p 1041 N93-14373
THOMSON, I. ..... p 812 N93-14959
THURLOW, ERNIE M. ..... p 975 N93-15391
TITRAN, ROBERT H. ..... p 847 N93-15524
TOERMAENEN, T. ..... p 1044 N93-14389
TOLLIVER, ROBERT ..... p 881 N93-14494
TOLMACH, ANDREW ..... p 958 N93-14151
TORRES, J. A. ..... p 859 N93-14488
TOTH, LOUIS E. ..... p 850 N93-14743
TRAINER, WILLIAM T. ..... p 790 N93-14248
TRAN, P. Y. ..... p 895 N93-15204
TRAN, SANG Q. ..... p 881 N93-14714
TRAVIS, L. D. ..... p 1032 N93-14335
TREGONING, ROBERT LEE ..... p 900 N93-14480
TREMBLAY, M. R. ..... p 888 N93-14434
TREPTAU, JEFFREY P. ..... p 985 N93-15511
TRETMANS, JAN ..... p 966 N93-15491
TRIETSCH, DAN ..... p 856 N93-15234
TROEDSON, SHAUN C. ..... p 973 N93-14269
TRUHLAR, D. G. ..... p 842 N93-14908
TSAI, LUNG-WEN ..... p 893 N93-15380
TSAI, STANLEY ..... p 996 N93-15444
TSENG, N. Y. ..... p 945 N93-14807
TSEYLER, V. I. ..... p 856 N93-15105
TUNABOYLU, B. ..... p 852 N93-15320
TURCOTTE, D. L. ..... p 1043 N93-14383
TURCOTTE, DONALD ..... p 1044 N93-14390
TURCOTTE, LOUIS HARVIE ..... p 896 N93-14188
TURNER, M. G. ..... p 911 N93-15273
TYC, G. ..... p 811 N93-14953
TYLER, G. L. ..... p 1044 N93-14391
TYRRELL, DEBRA L. ..... p 1051 N93-14523
p 1051 N93-14673
p 1051 N93-14674
TYSON, NEIL DEGRASSE ..... p 1015 N93-14136

U

UNDERWOOD, J. H. ..... p 836 N93-15193
UNNAVA, VASUNDHARA ..... p 1001 N93-14218

URIBE, F. A. p 907 N93-15061
UYTHOVEN, A. p 793 N93-15155
UZ, MEHMET p 847 N93-15524

V

VACCA, WILLIAM DONALD p 1020 N93-14869
VALERIO, J. A. p 907 N93-15061
VALETON, J. M. p 938 N93-15400
VALETT, JON p 957 N93-15579
VALISENA, N. p 894 N93-15139
VALLADO, C. A. p 815 N93-14730
p 815 N93-14768
p 815 N93-14794
VANBUREN, MARKUS ANTONIUS p 803 N93-14835
VANDENBERG, CAREL A. p 959 N93-15141
VANDENBROEK, P. M. p 968 N93-15121
VANDERMADE, J. W. p 813 N93-15000
VANDERVEGT, JACOBUS J. p 969 N93-15341
VANDIERENDONCK, A. J. p 789 N93-15005
VANDYKE, G. D. p 910 N93-15209
VANEECKHOUT, EDWARD p 914 N93-14724
VANGEL, MARK p 942 N93-14285
VANGENNIP, G. J. p 968 N93-14804
VANLEHN, KURT p 962 N93-14656
VANMOORSEL, AAD P. A. p 946 N93-15078
VANNET, M. D. p 855 N93-15478
VANOSDOL, JOHN GARY p 781 N93-14836
VARGAS, MARIO p 787 N93-15360
VASQUEZ, RICHARD P. p 994 N93-15151
VASSIE, J. M. p 932 N93-15001
VELAZQUEZ, MATTHEW T. p 787 N93-15354
VELHO, LUIZ p 956 N93-15562
VELTMAN, M. p 1020 N93-14686
VENNE, DAVID E. p 924 N93-15331
VENTRES, C. S. p 797 N93-15180
VENTURA, SUSANNA C. p 871 N93-15485
VERHAARD, LOUIS p 966 N93-15491
VERLINDE, JOHANNES p 924 N93-15100
VERMAAT, E. p 813 N93-15000
VERRON, J. p 927 N93-14972
VERSTRAETE, J. M. p 929 N93-14983
VERVISCH, L. p 841 N93-14624
VEST, THOMAS W. p 939 N93-14870
VICROY, DAN D. p 783 N93-14844
VIEILLARD, ANTOINE p 795 N93-15171
VIEROW, W. F. p 869 N93-15214
VIG, JOHN R. p 972 N93-14496
p 842 N93-14678
p 870 N93-15330
VINCENT, P. p 926 N93-14965
p 928 N93-14978
VISSERS, D. p 870 N93-15441
VOELLMER, GEORGE M. p 890 N93-14710
VOGELER, K. p 782 N93-15489
VOIT, F. J. p 971 N93-14108
VRANISH, JOHN M. p 962 N93-14701
p 890 N93-14712

W

WAAS, ANTHONY M. p 903 N93-15653
WADE, J. A. p 837 N93-15454
WADE, T. J. p 863 N93-15440
WAGNER, G. R. p 865 N93-14246
WAHL, RONALD E. p 917 N93-15459
WAHR, JOHN p 918 N93-14999
WAILLE, PHILIPPE p 958 N93-15124
WAKKER, KAREL F. p 813 N93-15000
WALBA, DAVID M. p 996 N93-15446
p 996 N93-15447
WALCH, STEPHEN P. p 843 N93-15356
p 843 N93-15357
p 843 N93-15358
WALISER, DUANE EDWARD p 920 N93-14213
WALKER, CHARLES W., JR. p 866 N93-14552
WALLACE-ROBINSON, JANICE p 936 N93-15583
WALLACE, DAVID C. p 917 N93-15459
WALTERSCHEID, R. L. p 1044 N93-14395
WALTON, JAMES T. p 827 N93-15428
p 827 N93-15528
WANG, CHENG p 979 N93-14165
WANG, CHI-RONG p 877 N93-14758
WANG, CHUN-WEI p 880 N93-15635
WANG, HUA p 906 N93-15442
WANG, MARK S. p 985 N93-15515
WANG, YI-REN p 780 N93-14595
WANKE, CRAIG p 785 N93-14853
WARHOLA, GREGORY T. p 859 N93-14649
WARNATZ, J. p 840 N93-14619
WASILENKO, MICHAEL p 817 N93-14565
WATANABE, Y. p 963 N93-14818
WATERS, WILLIAM M. p 860 N93-14742
p 860 N93-14879
WATSON, BENJAMIN p 953 N93-15536
WATSON, BRIAN C. p 901 N93-14799
WATSON, CHARLES S. p 938 N93-14427
WATSON, G. A. p 858 N93-14415
WATSON, ROBERT N. p 814 N93-15607
WAUBEN, W. M. F. p 1032 N93-14335
WAUGH, FREDERICK R. p 966 N93-15352
WAXMAN, ALLEN M. p 937 N93-14580
WAXMAN, RONALD p 947 N93-15262
p 948 N93-15264
WAYMAN, RICHARD J. p 999 N93-14106
WEAVER, MICHAEL J. p 977 N93-15448
WEBB, D. J. p 932 N93-15001
WEBER, A. H. p 910 N93-15063
WEEKS, J. R. p 846 N93-15348
WEHRLE, VICTOR A. p 804 N93-14920
WEIGHT, KRISTEN D. p 891 N93-14735
WEININGER, S. J. p 850 N93-15111
WEINSTOCK, CHARLES B. p 944 N93-14563
WEISENBACH, LORI p 986 N93-15518
WEISS, ISAAC p 943 N93-14546
WEITZ, C. M. p 1024 N93-14296
p 1030 N93-14326
p 1044 N93-14392
WEITZ, ERIC p 843 N93-15200
WELCH, D. R. p 978 N93-15277
WENDLAND, RICHARD A. p 1009 N93-15637
WERETA, ANTHONY, JR. p 817 N93-14725
WEST, G. p 951 N93-15386
WESTERHUYZEN, D. V. p 894 N93-14104
WESTERVELT, JAMES D. p 1001 N93-14524
p 1009 N93-15627
WHALEN, P. p 853 N93-15452
WHEELER, ROBERT J. p 924 N93-15501
WHINNERY, JAMES E. p 935 N93-14789
WHITAKER, JOHN p 858 N93-14408
WHITE, CHARLES S. p 901 N93-14790
WHITE, DAVID C. p 932 N93-14532
WHITE, GREG p 889 N93-14529
WHITE, M. G. p 859 N93-14453
WHITE, W. B. p 931 N93-14995
WHITLOCK, CHARLES H. p 924 N93-15501
WHITNEY, THOMAS J. p 791 N93-14571
WICHMAN, KEITH D. p 795 N93-15169
WICHMAN, R. W. p 1044 N93-14393
WIE, YONG-SUN p 877 N93-14797
WILBER, WILLIAM p 869 N93-15194
WILCOSKI, JAMES p 943 N93-14505
WILCOX, WILLIAM R. p 995 N93-15309
p 995 N93-15311
p 995 N93-15312
WILD, MARY p 957 N93-15579
WILKES, B. J. p 1012 N93-14760
WILKINS, D. J. p 831 N93-14509
WILLEBRAND, J. p 929 N93-14986
WILLIAMS, ANDREW p 804 N93-14921
WILLIAMS, C. J. p 1008 N93-15393
WILLIAMS, FIONA p 946 N93-15072
WILLIAMS, J. D. p 887 N93-15135
WILLIAMS, REVA KAY D. p 1049 N93-14176
WILLIAMS, RONALD LESLIE p 988 N93-14139
WILLIAMS, WILLIE p 996 N93-15444
WILLIAMSON, DANA W. p 786 N93-15016
WILLIAMSON, R. G. p 928 N93-14981
p 930 N93-14991
WILLIAMSON, R. L. p 834 N93-14819
WILLIAMSON, S. J. p 937 N93-14788
WILLIAMSON, SAMUEL J. p 937 N93-14646
WILLIAMSON, STEVEN L. p 871 N93-15456
WILLIAMSON, THOMAS J. p 897 N93-14236
WILLICK, JEFFREY ALAN p 1016 N93-14194
WILLIS, P. p 926 N93-14965
p 906 N93-14967
p 918 N93-14993
WILLKENS, C. A. p 837 N93-15388
WILMOT, STEPHEN B. p 794 N93-15157
WILSCHUT, ANNITA N. p 958 N93-15093
p 959 N93-15141
WILSON, DONALD R. p 891 N93-14916
WILSON, LIONEL p 1038 N93-14356
WILSON, M. S. p 907 N93-15061
WILSON, ROBERT M. p 1049 N93-15532
WILT, R. J. p 1039 N93-14360
WINDISCH, C. F., JR. p 871 N93-15479
WITTELS, NORMAN p 957 N93-15569
WITTIG, T. p 797 N93-15184
WOLCOTT, TED J. p 857 N93-14155
WOLD, AARON p 868 N93-15010
WOLFE, C. R. p 853 N93-15462
WONG, IVAN G. p 916 N93-15136
WONG, J. NAN p 985 N93-15514
WONG, JIN T. p 996 N93-15444
WONG, MOSES p 809 N93-14944
WONG, TIN-CHEE p 875 N93-14688
p 875 N93-14690
p 876 N93-14691
p 876 N93-14692
WOO, ANDREW p 955 N93-15555
WOOD, B. E. p 981 N93-14403
WOOD, J. A. p 1044 N93-14394
WOODWARD, ROLAND CAREY, JR. p 1022 N93-14156
WOODWORTH, PHILIP L. p 932 N93-15001
WOOTEN, E. W. p 841 N93-14658
WORKMAN, GARY L. p 891 N93-14763
p 855 N93-14793
p 892 N93-15117
WRIGHT, JON A. p 862 N93-15334
WRIGHT, R. N. p 834 N93-14819
WRIGHT, WARD F. p 849 N93-14527
WRIGHT, WILLIAM B. p 879 N93-15402
WU, F. J. p 837 N93-15454
WU, JIIN-CHUAN p 940 N93-14704
WU, K. CHAUNCEY p 818 N93-15368
WU, T. H. p 984 N93-15509
WU, XUESONG p 880 N93-15499
WUDL, FRED p 848 N93-14401
WUNSCH, CARL p 932 N93-15002
WYRTKI, K. p 928 N93-14980
WYSK, RICHARD A. p 949 N93-15300

X

XIONG, XIAOXIONG p 980 N93-14167
XU, PENG p 1048 N93-14859
XU, YANGSHENG p 889 N93-14528
p 889 N93-14529
p 889 N93-14545

Y

YACAVONE, DAVID W. p 786 N93-15016
YAGHJIAN, ARTHUR D. p 971 N93-14245
YAMANIS, J. p 853 N93-15452
YANG, GUANG p 1048 N93-14157
YANG, JIE p 889 N93-14528
YANG, YU-CHU p 850 N93-15064
YARGER, JILL M. p 779 N93-14451
YATES, JOHN T., JR. p 994 N93-15233
YAW, RICHARD N. p 991 N93-14537
YEH, CHARLES p 958 N93-14645
YEH, CHUN-TIEN p 890 N93-14684
YEH, H. p 836 N93-15387
p 853 N93-15452
p 837 N93-15455
YEUNG, S. K. p 805 N93-14926
YOKOTA, JEFFREY W. p 880 N93-15527
YOON, BOK-HYUN p 781 N93-14767
YOST, WILLIAM T. p 845 N93-14705
YOUNG, J. D. p 856 N93-14107
YOUNG, L. M. p 887 N93-15417
YOUNG, MICHAEL B. p 891 N93-14822
YOUNG, R. E. p 1044 N93-14395
YOUNG, R. P., SR. p 981 N93-14403
YOUNGBLOOD, JANET p 944 N93-14575
YOUTSEY, WESLEY J. p 920 N93-14256
YU, HUIMING p 960 N93-14281
YUAN, WEIJUN p 995 N93-15309
p 995 N93-15310
YUEN, D. A. p 1043 N93-14385
YUHAS, D. p 836 N93-15387
p 837 N93-15455
YUN, MIN SU p 1010 N93-14195

Z

ZACHARIAS, GREG L. p 798 N93-15235
ZAHEL, W. p 929 N93-14986
ZAKHAROV, A. I. p 1023 N93-14289
ZAMAN, K. B. M. Q. p 781 N93-14791
ZASOVA, L. V. p 1045 N93-14396
p 1045 N93-14397
ZAWODZINSKI, T. A. p 907 N93-15061
ZEIDLER, JAMES R. p 850 N93-14825
ZEILER, FRED p 1005 N93-15038
ZEINALABEDEEN, TARIF p 861 N93-15097
ZELINSKI, BRIAN J. J. p 986 N93-15518
ZELKOWITZ, MARVIN V. p 947 N93-15199
ZHANG, CHENG-GEN p 902 N93-15070
ZHANG, YOUXUE p 1045 N93-14398
ZHAO, Z. p 969 N93-15212
ZHDANOV, V. L. p 781 N93-15131
ZHOU, ANDY F. p 984 N93-15508
ZHOU, ANDY FENGLEI p 980 N93-14168
ZHOU, JIAN p 995 N93-15309
ZHOU, X. p 867 N93-14721
ZHU, GANG p 877 N93-14829
ZHU, GUOMING p 961 N93-14399
ZHU, JIXIANG p 980 N93-14169
ZILLMER, MANFRED p 850 N93-15064
ZIMBELMAN, DARRELL FRANK p 818 N93-14837

ZIMMERMAN, J. T. F. p 813 N93-15000
ZIMMERMAN, R. E. p 910 N93-15209
ZINDLER, ALAN p 1045 N93-14398
ZLOTNICKI, V. p 927 N93-14975
ZUBER, M. T. p 1040 N93-14366
ZUCHERMAN, LEON p 805 N93-14924
p 810 N93-14948
ZUKAS, JONAS A. p 821 N93-15604
ZUO, LIN p 1013 N93-14860
ZWEBEN, MONTE p 965 N93-15287
p 965 N93-15288
p 965 N93-15289
ZWICK, H. H. p 811 N93-14953

CORPORATE SOURCE INDEX

Typical Corporate Source Index Listing

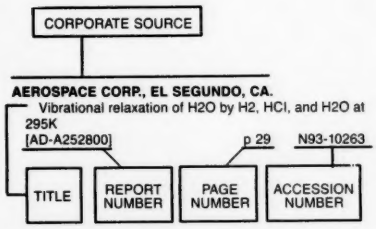

Listings in this index are arranged alphabetically by corporate source. The title of the document provides the user with a brief description of the subject matter. The report number helps to indicate the type of document cited (e.g., NASA report, translation, NASA contractor report). The accession number denotes the number by which the citation is identified. The page number helps you locate the citation in the abstract section. The titles are arranged under each corporate source in ascending accession number order.

A

ACADEMY OF SCIENCES (USSR), MOSCOW.
Venus radar mapping from the Venera 15 and 16 spacecrafts: Results and restrictions
p 1023 N93-14289
The geology of the Venera/Vega landing sites
p 1024 N93-14296
Largest impact craters on Venus
p 1030 N93-14326
Different types of small volcanos on Venus
p 1042 N93-14378
Middle atmosphere of Venus and its clouds: Latitude and solar time variations
p 1045 N93-14396
SO2 in the middle atmosphere of Venus: IR measurements from Venera 15 and comparison to UV
p 1045 N93-14397

ADVANCED AVIATION CONCEPTS, JUPITER, FL.
Workshop on Aeronautical Decision Making (ADM). Volume 2: Plenary Session With Presentations and Proposed Action Plan
[DOT/FAA/RD-92/14-VOL-2] p 785 N93-15013
How expert pilots think
p 786 N93-15017
Enhanced Aeronautical Resource Management training alternatives
p 786 N93-15019
Proposed action plan to improve ADM effectiveness, part 3: Developing a new ADM paradigm on which to build advanced or expert decision making training
p 787 N93-15026

ADVANCED DEVELOPMENT CORP., BURLINGTON, MA.
Corrosion of metal particle and metal evaporated tapes
p 883 N93-15039

ADVISORY GROUP FOR AEROSPACE RESEARCH AND DEVELOPMENT, NEUILLY-SUR-SEINE (FRANCE).
Propulsion and Energetics Panel Working Group 20 on Test Cases for Engine Life Assessment Technology
[AGARD-AR-308] p 798 N93-14890

AERITALIA S.P.A., NAPLES (ITALY).
The FAIR (Flight Animated and Interactive Reconstruction) tool
p 788 N93-15164

AERONAUTICAL RESEARCH LABS., MELBOURNE (AUSTRALIA).
The use of ultrasonics for oleo compression measurements on a S-70B-2 (Seahawk) helicopter
[AD-A256315] p 792 N93-15328

AEROSPACE CORP., EL SEGUNDO, CA.
Determining optimum C-field settings that minimize output frequency variations in cesium atomic frequency standards
[AD-A255902] p 971 N93-14108
High resolution absolute absorption cross sections of NO2 at 295, 573, and 673 K at visible wavelengths: Comprehensive data tables
[AD-A255261] p 839 N93-14530
Characterization of PZT films fatigued at low frequency
[AEROSPACE-ATR-91(8308)-2] p 992 N93-14795
The influence of steel surface chemistry on the bonding of lubricant films
[AD-A256231] p 851 N93-15242
Frequency shifts in a rubidium frequency standard due to coupling to another standard
[AD-A256232] p 972 N93-15243
Solar proton events of 1989: Effects on spacecraft solar arrays
[AD-A256457] p 1049 N93-15318
Bevalac ion beam characterizations for single event phenomena
[AD-A257033] p 979 N93-15362
Energetic and magnetosheath energy particle signatures of the low-latitude boundary layer at low altitudes near noon
[NASA-CR-191388] p 917 N93-15574

AEROSPACE MEDICAL RESEARCH LABS., BROOKS AFB, TX.
Advantages of using a projected head-up display in a flight simulator
[AD-A255332] p 804 N93-14559

AEROSPACE MEDICAL RESEARCH LABS., WRIGHT-PATTERSON AFB, OH.
Evaluation of three models used for predicting noise propagated long distances overground
[AD-A255963] p 973 N93-14406

AEROSPATIALE, CANNES (FRANCE).
Regional satellites: The European experience with Eutelsat for TV, voice, data and mobile transmissions
[REPT-921-440-106] p 818 N93-15071
PEX: A reactive procedure based decision maker
[REPT-921-440-105] p 999 N93-15118
Reliability modelling for non-electronic systems
[REPT-921-440-103] p 894 N93-15139
ISOCAM experiment cryogenic test results
[REPT-921-440-104] p 825 N93-15140

AEROSPATIALE AQUITAINE, SAINT-MEDARD EN JALLES (FRANCE).
Fiber reinforced composites: A new class of glass and glass ceramic materials for thermomechanical applications
[REPT-921-430-104] p 838 N93-15490

AIR FORCE INSPECTION AND SAFETY CENTER, NORTON AFB, CA.
Does cockpit management training reduce aircrew error?
p 785 N93-15014
Cockpit decision making
p 786 N93-15015

AIR FORCE INST. OF TECH., WRIGHT-PATTERSON AFB, OH.
Development of an environment for software reliability model selection
[AD-A256609] p 942 N93-14241
The detection and correlation modeling of Rayleigh distributed radar signals
[AD-A256612] p 858 N93-14250
An examination of wing rock for the F-15
[AD-A256613] p 802 N93-14252
A study of mid-latitude 5577A Cl dayglow emissions
[AD-A255444] p 914 N93-14511
Multiple model adaptive estimation applied to the ViSTA F-16 with actuator and sensor failures
[AD-A256444] p 802 N93-14608
AFIT/AFOSR Workshop on the Role of Wavelets in Signal Processing Applications
[AD-A256172] p 859 N93-14649
A simulation study of planar swaging deformation
[AD-A255908] p 902 N93-15070
Method of local shaping of thermoplastics
[AD-A255913] p 856 N93-15105
A new multiplier-free structure for DFT based on delta modulation
[AD-A255927] p 861 N93-15106
Development of an analog MIMO Quantitative Feedback Theory (QFT) CAD package
[AD-A256435] p 950 N93-15313
Wing rock prediction method for a high performance fighter aircraft
[AD-A256438] p 792 N93-15314
An eclectic method for object oriented database design
[AD-A256439] p 1008 N93-15315
Comparison of synchronization techniques for the AFIT direct sequence spread spectrum system
[AD-A256440] p 861 N93-15316
Co-channel speaker separation
[AD-A256443] p 861 N93-15317
Implementation and analysis of NP-complete algorithms on a distributed memory computer
[AD-A256564] p 951 N93-15405
Design of an artificial neural network based tactile sensor for the UTAH/MIT dexterous hand
[AD-A256565] p 966 N93-15406

AIR FORCE OCCUPATIONAL MEASUREMENT CENTER, RANDOLPH AFB, TX.
F/FB-111 avionics test station and component specialist/technician. Automatic test stations manual and electronic warfare test stations. Training requirements analysis (451X6), volume 2
[AD-A252121] p 793 N93-14110

AIR FORCE OFFICE OF SCIENTIFIC RESEARCH, BOLLING AFB, WASHINGTON, DC.
Air Force Office of Scientific Research
[AD-A255331] p 1051 N93-14523
Air Force Office of Scientific Research
[AD-A255361] p 1051 N93-14673
Air Force Office of Scientific Research
[AD-A255370] p 1051 N93-14674

AIRBUS INDUSTRIE, BLAGNAC (FRANCE).
Monitoring of powerplants in advanced commercial aircraft
p 795 N93-15171

AIRBUS INDUSTRIE, TOULOUSE (FRANCE).
Airbus Industrie TCAS experience
p 789 N93-15186

ALABAMA UNIV., BIRMINGHAM.
A differential equation design method for finite-conjugate, multi-mirror imaging systems
p 979 N93-14165

ALABAMA UNIV., HUNTSVILLE.
Imaging the sun in hard x-rays using Fourier telescopes
p 1048 N93-14591
Mach 5 electroformed nickel nozzle refurbishment FNAS investigation of ultra-smooth surfaces
[NASA-CR-191416] p 826 N93-14681
Fiber pulling apparatus modification
[NASA-CR-184498] p 891 N93-14763
Surface evaluation of UV-degraded contamination
[NASA-CR-184500] p 910 N93-14764
Study of Fluid Experiment System (FES)/CAST/Holographic Ground System (HGS)
[NASA-CR-184483] p 855 N93-14793
Development of advanced seal verification
[NASA-CR-184502] p 892 N93-15117

ALABAMA UNIV., UNIVERSITY.
Application of partition matrix methods to solve large eigenproblems in structural dynamics
p 896 N93-14188

ALBERTA RESEARCH COUNCIL, CALGARY.
A robotic planning system
p 810 N93-14949

ALBERTA RESEARCH COUNCIL, EDMONTON.
A monitoring and control system for complex man-machine systems: Preliminary design
p 810 N93-14951

ALBERTA UNIV., EDMONTON.
An extended cuberille model for identification and display of 3D objects from 3D gray value data
p 953 N93-15542

ALENIA SPAZIO S.P.A., TURIN (ITALY).
System test approach for the SAX satellite
p 824 N93-15622
ALFRED-WEGENER-INST. FOR POLAR RESEARCH, BREMERHAVEN (GERMANY).
Ocean circulation modeling by use of radar altimeter data
p 929 N93-14986
ALIAS RESEARCH CORP., TORONTO (ONTARIO).
Ray tracing polygons using spatial subdivision
p 955 N93-15555
ALLIED-SIGNAL AEROSPACE CO., KANSAS CITY, MO.
Personal computer based computed tomography system
[KCP-613-4806] p 945 N93-14876
ALLIED-SIGNAL AEROSPACE CO., TORRANCE, CA.
Development of ceramic matrix composites for application in ceramic technology for advanced heat engines project, phase 2
[DE92-041379] p 836 N93-15387
Development of ceramic matrix composites for application in the ceramic technology for advanced heat engines project. Phase 2A: Development of in-situ toughened silicon nitride
[DE92-041371] p 853 N93-15452
Development of ceramic matrix composites for application in the ceramic technology for advanced heat engines project
[DE92-041378] p 837 N93-15455
AMERICAN AIRLINES FLIGHT ACADEMY, FORT WORTH, TX.
Advanced technology wind shear prediction system evaluation
p 785 N93-14858
AMPEX CORP., REDWOOD CITY, CA.
A system approach to archival storage
p 1006 N93-15040
The 19 mm date recorders: Similarities and differences
p 883 N93-15042
An empirical approach to predicting long term behavior of metal particle based recording media
p 883 N93-15043
AMTEC ENGINEERING, INC., BELLEVUE, WA.
The 3D Navier-Stokes flow analysis for shared and distributed memory MIMD computers
[AD-A256038] p 878 N93-15187
ANALYSIS AND TECHNOLOGY, INC., NEW LONDON, CT.
Evaluation of Night Vision Goggles (NVG) for maritime search and rescue (joint Canadian/US Coast Guard experiment)
[AD-A255525] p 939 N93-14554
APPLE COMPUTER, INC., CUPERTINO, CA.
Object space temporal coherence for ray tracing
p 955 N93-15554
APPLIED TECHNOLOGY ASSOCIATES, INC., ALBUQUERQUE, NM.
Digital active material processing platform effort (DAMPER), SBIR phase 2
[NASA-CR-190798] p 856 N93-15353
ARGONNE NATIONAL LAB., IL.
Comparison of the prevalence index and average wetland values for identification of wetland vegetation
[DE92-016701] p 910 N93-15209
Experimental determination of magnetohydrodynamic seawater thruster performance in a two Tesla test facility
[DE92-019042] p 826 N93-15215
Three-dimensional nuclear magnetic resonance imaging of green-state ceramics
[DE93-000930] p 851 N93-15282
Advanced research in instrumentation and diagnostics technology
[DE92-041121] p 883 N93-15411
Dual role of nickel in sodium/nickel chloride batteries
[DE92-041102] p 870 N93-15441
Information technologies for global resources management and environmental assessment
[DE92-041107] p 906 N93-15442
C60 interactions with surfaces, gaseous species and photons: An overview
[DE92-040738] p 978 N93-15654
How scientific must technical editors be?
[DE92-040741] p 1010 N93-15655
Schwinger Dyson equations: Dynamical chiral symmetry breaking and confinement
[DE92-040717] p 978 N93-15657
ARIZONA STATE UNIV., TEMPE.
Reliability of sol-gel derived ferroelectric memories
[AD-A255358] p 991 N93-14560
Reliability of sol-gel derived ferroelectric memories
[AD-A255240] p 849 N93-14668
Spatio-temporal complexity and large-scale structures in problems of continuum mechanics
[AD-A256410] p 998 N93-15333
ARIZONA UNIV., PHOENIX.
Spectral analysis of the shuttle glow: AIS science support
[PL-TR-92-2172] p 815 N93-14698
ARIZONA UNIV., TUCSON.
Characterization of magneto-optical recording media
p 979 N93-14140
The theory and numerical simulation of non-local mixing-length convection
p 1015 N93-14147
Optical instrumentation and characterization for magneto-optical recording media
p 980 N93-14168
Monte Carlo computer simulations of Venus equilibrium and global resurfacing models
p 1027 N93-14311
Igneous and tectonic evolution of Venusian and terrestrial coronae
p 1031 N93-14330
Venusian sinuous rilles
p 1033 N93-14337
Spectral analysis of the shuttle glow. SPA II/IBSS Mission: AIS hardware
[PL-TR-92-2148] p 814 N93-14697
Nonuniformity effects in a hybrid platinum silicide imaging device
[AD-A256339] p 983 N93-15197
Research Studies on Advanced Optical Module/Head Designs for Optical Data Storage
[NASA-CR-191307] p 984 N93-15505
Diffraction analysis and evaluation of several focus- and track-error detection schemes for magneto-optical disk systems
p 984 N93-15506
Improved astigmatic focus error detection method
p 984 N93-15507
Instrumentation of the variable-angle magneto-optic ellipsometer and its application to M-O media and other non-magnetic films
p 984 N93-15508
Measurement of the magnetic anisotropy energy constants for magneto-optical recording media
p 984 N93-15509
Proposal for massively parallel data storage system
p 960 N93-15510
Combining ray-trace and diffraction analysis: A design example
p 985 N93-15511
Transfer function characteristics of super resolving systems
p 985 N93-15512
Modeling and measurement of a micro-optic beam deflector
p 985 N93-15514
Effects of higher order aberrations on beam shape in an optical recording system
p 985 N93-15515
Oxidation processes in magneto-optic and related materials
p 985 N93-15516
Integrated device with diffractive polarization components for a magneto-optical disk head
p 986 N93-15517
The design and fabrication of a single leakage-channel grating coupler
p 986 N93-15518
A modal analysis of lamellar diffraction gratings in conical mountings
p 986 N93-15519
On the convergence of the coupled-wave approach for lamellar diffraction gratings
p 986 N93-15520
ARKANSAS UNIV., PINE BLUFF.
Global zones of particle precipitation as observed by EXOS-C
[AD-A256397] p 917 N93-15466
ARKANSAS UNIV. FOR MEDICAL SCIENCES, LITTLE ROCK.
NMR imaging of elastomeric materials
[AD-A256034] p 841 N93-14658
ARMY AEROMEDICAL RESEARCH LAB., FORT RUCKER, AL.
Test and evaluation report of the Physio Control Defibrillator/Monitor, Model LifePak(tm) 6s
[AD-A255691] p 933 N93-14103
Test and evaluation report of the Catalyst Research Oxygen Monitor, Model Miniox 3
[AD-A255849] p 881 N93-14105
The relationship between computer scoring and safety-pilot grading of flight performance
[AD-A256245] p 937 N93-14600
ARMY AEROSTRUCTURES DIRECTORATE, HAMPTON, VA.
Mechanical response of composite materials with through-the-thickness reinforcement
p 834 N93-14753
ARMY ARMAMENT RESEARCH, DEVELOPMENT AND ENGINEERING CENTER, WATERVLIET, NY.
Machine intelligence, a foreword: The brain as electronic circuitry; electronic circuitry as a brain
[AD-A255283] p 962 N93-14533
Degradation and failure modes of carbon/bismaleimide laminates subjected to a tropical exposure
[AD-A256328] p 836 N93-15193
ARMY AVIATION RESEARCH AND DEVELOPMENT COMMAND, MOFFETT FIELD, CA.
The Applicaiton of CFD to rotary wing flow problems
[NASA-TM-102803] p 782 N93-15483
ARMY AVIATION SYSTEMS COMMAND, CLEVELAND, OH.
Introduction to test cases for engine life assessment technology
p 799 N93-14891
ARMY BELVOIR RESEARCH AND DEVELOPMENT CENTER, FORT BELVOIR, VA.
Application of Fourier Transform-infrared spectroscopy (FT-IR) for materials analysis
[AD-A255727] p 838 N93-14435
Surface preparation of stainless steel prior to painting
[AD-A256253] p 838 N93-14454
ARMY BIOMEDICAL RESEARCH AND DEVELOPMENT LAB., FORT DETRICK, MD.
Absorption of propellant vapors into polymer films
[AD-A255274] p 849 N93-14531
ARMY CHEMICAL RESEARCH AND DEVELOPMENT CENTER, ABERDEEN PROVING GROUND, MD.
Thermal decomposition of HNIW and HNIW-Based formulations
[AD-A255613] p 854 N93-15011
ARMY COLD REGIONS RESEARCH AND ENGINEERING LAB., HANOVER, NH.
Softening of rigid polyvinyl chloride by high concentrations of aqueous solutions of methylene chloride
[AD-A255453] p 848 N93-14486
ARMY COMMAND AND GENERAL STAFF COLL., FORT LEAVENWORTH, KS.
The evolution of artificial intelligence and expert computer systems in the Army
[AD-A255221] p 962 N93-14525
A progressive resistance weight training program designed to improve the armor crewman's strength
[AD-A255553] p 934 N93-14556
ARMY COMMUNICATIONS-ELECTRONICS COMMAND, FORT MONMOUTH, NJ.
Tactical line-of-sight path reliability: Improved MSE system procedures
[AD-A256504] p 862 N93-15376
ARMY CONSTRUCTION ENGINEERING RESEARCH LAB., CHAMPAIGN, IL.
A methodology for the evaluation of structural design software for DOS-based microcomputers
[AD-A255421] p 943 N93-14505
Geographic Resources Analysis Support System (GRASS) version 4.0 user's reference manual
[AD-A255218] p 1001 N93-14524
Predicting database requirements for geographic information systems in the year 2000: Long-term design issues for GRASS
[AD-A256862] p 1009 N93-15627
Recommendations for enhancement of the Design Criteria Information System (DCIS)
[AD-A256857] p 1009 N93-15641
GRASS 4.0 map digitizing user's manual: V. Digit
[AD-A256859] p 1009 N93-15642
ARMY ENGINEER STUDIES CENTER, FORT BELVOIR, VA.
Establishment of a test course for high accuracy dynamic positioning systems
[AD-A255407] p 789 N93-14501
ARMY ENGINEER WATERWAYS EXPERIMENT STATION, VICKSBURG, MS.
In situ material characterization for pavement evaluation by the Spectral-Analysis-of-Surface-Waves (SASW) method
[AD-A255660] p 804 N93-14128
Reanalysis of multiple-wheel landing gear traffic tests
[AD-A256593] p 804 N93-14238
Vendor Information System (VIS) systems manual
[AD-A256174] p 1002 N93-14650
USACE geotechnical earthquake engineering software, report 1 WESHAKE for personal computers (version 1.0)
[AD-A257068] p 917 N93-15459
ARMY LAB. COMMAND, FORT MONMOUTH, NJ.
The effects of acceleration on precision frequency sources
[AD-A255465] p 972 N93-14496
Lithium rechargeable cell with a poly 3-methylthiophene cathode
[AD-A255436] p 866 N93-14552
Smart battery controller for lithium sulfur dioxide batteries
[AD-A255490] p 867 N93-14642
Ultraviolet-ozone cleaning of semiconductor surfaces, revision 1
[AD-A256158] p 842 N93-14678
Processing and characterization of electrophoretically deposited holmium barium copper oxide superconductor films
[AD-A256329] p 869 N93-15194
Introduction to quartz frequency standards, revision 1
[AD-A256373] p 870 N93-15330
ARMY LAB. COMMAND, WHITE SANDS MISSILE RANGE, NM.
An analytic phase function for cylindrical particles
[AD-A255750] p 977 N93-15054

ARMY MATERIALS TECHNOLOGY LAB., WATERTOWN, MA.
Testing and analysis of modified HMMWV front lift provisions
[MTL-TR-92-31] p 891 N93-14735
Use of the thin-walled torsion specimen
[AD-A255593] p 901 N93-14790
ARMY SIGNALS WARFARE LAB., VINT HILL FARMS STATION, VA.
Automated interpretation of topographic maps
[AD-A257040] p 906 N93-15364
ARMY TOPOGRAPHIC ENGINEERING CENTER, FORT BELVOIR, VA.
Using digital scanned aerial photography for wetlands delineation
[AD-A255392] p 905 N93-14676
Proposed revisions to RTCM SC-104 recommended standards for differential NAVSTAR/GPS service for carrier phase applications
[AD-A255276] p 789 N93-15005
Adaptive mesh in visualization of terrain elevation data
[AD-A255481] p 906 N93-15007
ARNOLD ENGINEERING DEVELOPMENT CENTER, ARNOLD AFS, TN.
Effects of cryocontaminants on cryogenic superpolished mirror and superpolished quartz crystal microbalance
[AD-A255972] p 981 N93-14403
Transonic flow calculations for a cavity with and without a store
[AD-A255954] p 873 N93-14421
AUBURN UNIV., AL.
Experimental observations of the plasma properties of a high-density, low-temperature accelerated arc
p 988 N93-14138
AUGSBURG COLL., MINNEAPOLIS, MN.
A single-station forecasting model
[AD-A256403] p 924 N93-15331
AUSTRALIAN INST. OF MARINE SCIENCE, QUEENSLAND.
North-Australian tropical seas circulation study
p 926 N93-14968
AVIATRONIC LTD., BUDAPEST (HUNGARY).
The SIROM flight data recorder and evaluation system
p 795 N93-15165

B

BALL AEROSPACE SYSTEMS DIV., BOULDER, CO.
Cassini atmospheric chemistry mapper. Volume 1. Investigation and technical plan
[NASA-CR-190947] p 1021 N93-15079
BALLISTIC RESEARCH LABS., ABERDEEN PROVING GROUND, MD.
Determination of operable deformation mechanisms during ballistic impact in tungsten single crystals, utilizing transmission electron microscopy
[AD-A255351] p 991 N93-14518
BARNA (P. STEPHEN), CONSULTANT, NORFOLK, VA.
Investigations of detail design issues for the high speed acoustic wind tunnel using a 60th scale model tunnel. Part 1: Tests with open circuits
[NASA-CR-191671] p 780 N93-14737
Investigations of detail design issues for the high speed acoustic wind tunnel using a 60th scale model tunnel. Part 2: Tests with the closed circuit
[NASA-CR-191672] p 780 N93-14738
BASF STRUCTURAL MATERIALS, INC., CHARLOTTE, NC.
An evaluation of composites fabricated from powder epoxy towpreg p 832 N93-14745
BATTELLE COLUMBUS LABS., OH.
Analytical and experimental evaluation of joining ceramic oxides to ceramic oxides and ceramic oxides to metal for advanced heat engine applications
[DE92-041383] p 851 N93-15294
Inelastic deformation of metal matrix composites: Plasticity and damage mechanisms, part 2
[NASA-CR-189096-PT-2] p 837 N93-15401
BELL TELEPHONE LABS., INC., MURRAY HILL, NJ.
Interactive solid geometry via partitioning trees
p 952 N93-15535
Partitioning tree image representation and generation from 3D geometric models p 955 N93-15557
A minimalist global user interface p 957 N93-15566
BEN GURION UNIV. OF THE NEGEV, BEERSHEVA (ISRAEL).
Multiple robot programming using concurrent logic language
[F-3-3] p 950 N93-15304
BIOTRONICS TECHNOLOGIES, INC., WAUKESHA, WI.
Transcutaneous Analyte Measuring Methods (TAMM), phase 2
[AD-A256327] p 936 N93-15192
BONNEVILLE POWER ADMINISTRATION, PORTLAND, OR.
Joint HVAC transmission EMF environmental study
[DE92-017863] p 933 N93-15211
BOOZ-ALLEN AND HAMILTON, INC., ARLINGTON, VA.
SETA support for the DARPA microelectronics technology insertion program of the Microelectronics Technology Office
[AD-A255551] p 866 N93-14555
BOOZ-ALLEN AND HAMILTON, INC., BETHESDA, MD.
Technology commercialization cost model and component case study
[DE92-001280] p 907 N93-15213
BOSTON UNIV., MA.
Development of neural network architectures for self-organizing pattern recognition and robotics
[AD-A255433] p 962 N93-14551
The effects of magnetic storm phases on F-layer irregularities from auroral to equatorial latitudes
[AD-A256520] p 917 N93-15395
BRANDEIS UNIV., WALTHAM, MA.
Information for management, planning, and decision-making in nonprofit organizations: Toward a comprehensive model p 1000 N93-14209
The evolution of the VLBI polarization of superluminal radio source 3C345 p 1050 N93-14229
BRITISH GAS CORP., SOLIHULL (ENGLAND).
Radiative heat transfer in combustion systems
p 840 N93-14621
BROOKHAVEN NATIONAL LAB., UPTON, NY.
Effects of high thermal neutron fluences on Type 6061 aluminum
[DE92-040569] p 846 N93-15348
BROWN UNIV., PROVIDENCE, RI.
Shield fields: Concentrations of small volcanic edifices on Venus p 1024 N93-14295
Thermal buoyancy on Venus: Preliminary results of finite element modeling p 1025 N93-14302
Global correlation of volcanic centers on Venus with uplands and with extension: Influence of mantle convection and altitude p 1026 N93-14309
Sequential deformation of plains along Tessera boundaries on Venus: Evidence from Alpha Regio
p 1028 N93-14317
Determining stress states using dike swarms: The Lauma Dorsa example p 1028 N93-14319
Venus volcanism: A global overview from Magellan data p 1029 N93-14323
Chemical differentiation on one-plate planets: Predictions and geologic observations for Venus
p 1029 N93-14324
Large shield volcanos on Venus: The effect of neutral buoyancy zone development on evolution and altitude distribution p 1032 N93-14333
Extensive lava flow fields on Venus: Preliminary investigation of source elevation and regional slope variations p 1034 N93-14342
The origins of radial fracture systems and associated large lava flows on Venus p 1038 N93-14356
Chemical differentiation of a convecting planetary interior: Consequences for a one-plate planet such as Venus p 1038 N93-14358
Venus steep-sided domes: Relationships between geological associations and possible petrogenetic models p 1038 N93-14359
Atmospheric effects on crater growth on Venus
p 1041 N93-14370
Effect of impact angle on central-peak/peak-ring formation and crater collapse on Venus
p 1041 N93-14371
Impact-generated winds on Venus: Causes and effects p 1041 N93-14372
Atla Regio, Venus: Geology and origin of a major equatorial volcanic rise p 1041 N93-14374
Floor-fractured crater models for igneous crater modification on Venus p 1044 N93-14393
The properties of thermally passivated Si(1-x) He(x) produced using high pressure techniques (and related augmentation awards)
[AD-A255961] p 991 N93-14429
New electronic materials
[AD-A255612] p 868 N93-15010

C

CADONOMIST, SAN FRANCISCO, CA.
VHDL (VHSIC hardware description language) use in the US defense procurement process
[VH-2] p 948 N93-15263
CALGARY UNIV. (ALBERTA).
Escape-time visualization method for language-restricted iterated function systems
p 956 N93-15558
CALIFORNIA INST. OF TECH., PASADENA.
Dynamics of the Venus atmosphere
p 1030 N93-14325
Radar-anomalous, high-altitude features on Venus
p 1036 N93-14349
Melting and differentiation in Venus with a cold start: A mechanism of the thin crust formation
p 1042 N93-14381
Volcanism by melt-driven Rayleigh-Taylor instabilities and possible consequences of melting for admittance ratios on Venus p 1043 N93-14387
On the development and application of a modified boundary element method for the analysis of three dimensional elastostatic problems in thick plates
p 901 N93-14587
Compact objects in the disk and globular clusters
p 1018 N93-14594
Gamma-ray imaging observations of Supernova 1987A
p 1012 N93-14628
QSO absorption lines and the ionizing field at high redshifts p 1013 N93-14860
Microwave observations of Uranus
p 1046 N93-14863
Numerical simulation of baroclinic Jovian vortices
p 1046 N93-14865
Isotopic composition of galactic cosmic ray boron, carbon, nitrogen, and oxygen p 1020 N93-14866
Martian water frost: Control of global distribution by small-scale processes p 1047 N93-14868
Multiply connected spacetimes and closed timelike curves in semiclassical gravity p 915 N93-14884
Interferometric observations of the J(0,1) CO line on Venus: Upper mesospheric winds and CO abundance
p 1047 N93-14918
Theory and applications of hyper-redundant robotic manipulators p 892 N93-15104
Chemical reactions in turbulent mixing flows
[AD-A256004] p 842 N93-15114
Parallel readout of optical disks
[AD-A256625] p 1008 N93-15409
CALIFORNIA UNIV., BERKELEY.
Knowledge and processes in design
[AD-A255663] p 999 N93-14130
Calibration of the CCD Tully-Fisher relation with application to the Perseus-Pisces supercluster
p 1016 N93-14194
Information-seeking behavior during the decision-making process: A case study
p 1000 N93-14206
Mapping thoughts: Visual interfaces for information retrieval p 1000 N93-14208
Imaging Earth's interior: Tomographic inversions for mantle P-wave velocity structure p 913 N93-14225
The time variability of Jupiter's synchrotron radiation
p 973 N93-14227
A search for anisotropy in the cosmic background radiation at millimeter wavelengths on angular scales from 0.3 to 3 degrees p 1050 N93-14244
The method of minimal representations in 2D Ising model calculations
[AD-A256581] p 967 N93-14270
Analysis of projections of the transfer matrix in 2D Ising models
[AD-A256583] p 967 N93-14271
Electronically excited molecules: Reaction kinetics and emission of light: Nanosecond infrared spectroscopy, electronic emission from chemical reactions
[AD-A255642] p 976 N93-14283
Physical properties of extended emission-line regions in active and cooling-flow galaxies p 1018 N93-14461
Adaptive control of nonlinear nonminimum phase systems p 961 N93-14470
Deformation characterization of powdered metals in compaction and application of the finite element method to compaction processes p 844 N93-14472
Force and position control of robot manipulators: Learning and repetitive control approach
p 888 N93-14473
Fracture mechanisms and fracture control in composite structures p 899 N93-14474
Threshold photodetachment spectroscopy
[AD-A255278] p 842 N93-14671
Algorithms for intersecting parametric and algebraic curves p 956 N93-15560
CALIFORNIA UNIV., BERKELEY. LAWRENCE BERKELEY LAB.
Simple formulae for the optimization of the FEL gain length including the effects of emittance, betatron oscillations, and energy spread
[DE92-040378] p 887 N93-15325
Center for x ray optics, 1991
[DE93-001543] p 984 N93-15350
World energy: Building a sustainable future
[DE93-001598] p 909 N93-15467

Exploratory technology research program for electrochemical energy storage
| DE93-001595 | p 909 N93-15484
Solid polymer electrolytes for rechargeable batteries
| DE93-001603 | p 871 N93-15485

CALIFORNIA UNIV., DAVIS.
Cloud-radiative feedbacks in tropical convection
p 919 N93-14180
PDF transport modelling p 840 N93-14623
The optimal fiber volume fraction and fiber-matrix property compatibility in fiber reinforced composites
p 833 N93-14752

CALIFORNIA UNIV., LOS ANGELES.
Interactions of relativistic electrons with relativistic plasma waves p 988 N93-14139
Turbulence and chaos in classical and quantum systems p 972 N93-14144
Coldspots or hotspots? The origin of plateau-shaped highlands on Venus p 1025 N93-14298
Venus tectonic styles and crustal differentiation
p 1031 N93-14332
The solar wind interaction with Venus
p 1034 N93-14341
Flexural models of trench/outer rise topography of coronae on Venus with axisymmetric spherical shell elastic plates p 1036 N93-14348
A model for the formation of the extended paraboloidal halos around some impact craters on Venus
p 1037 N93-14352
Evidence for lightning on Venus p 1043 N93-14386

CALIFORNIA UNIV., RIVERSIDE.
Search for pulsed gamma ray emission from SN1987A and the Vela pulsar p 1050 N93-14634

CALIFORNIA UNIV., SAN DIEGO.
The isotopes of carbon monoxide in the free troposphere and their implications to atmospheric chemistry
p 913 N93-14207
The preferred latitudes of the Intertropical Convergence Zone: Observations and theory p 920 N93-14213
An investigation of the processing, high temperature deformation and fracture characteristics of superplastic ceramics
| AD-A256519 | p 852 N93-15394

CALIFORNIA UNIV., SAN DIEGO, LA JOLLA.
Extrathalmic modulation of cortical function
| AD-A255440 | p 935 N93-14782

CALIFORNIA UNIV., SANTA BARBARA.
Oriented electro/optical polymers through in-situ chemistry during gel processing: A research opportunity
| AD-A255968 | p 848 N93-14401
The changing culture of science: Bringing it into balance
| AD-A255993 | p 998 N93-14417
Final Report, 1 November 1988 - 31 October 1991
| AD-A255979 | p 976 N93-14424
On the structure of nonlinear constitutive equations for fiber reinforced composites
| NASA-CR-191024 | p 830 N93-14484
Condensed matter research using the UCSB FEL
| DE92-040560 | p 887 N93-15347
Photodissociation dynamics of cluster ions
| AD-A256375 | p 917 N93-15463

CAMBRIDGE UNIV. (ENGLAND).
Pancakelike domes on Venus p 1035 N93-14345
Calculation of chemical reaction rates in turbulent combustion p 841 N93-14625

CANADIAN ASTRONAUTICS LTD., OTTAWA (ONTARIO).
Optimized design of a 5 kW constant frequency series resonant converter for pulsed load space applications
p 807 N93-14935

CANADIAN HUMAN-COMPUTER COMMUNICATIONS SOCIETY, TORONTO (ONTARIO).
Proceedings: Graphics Interface 1992
| ISBN-0-9695338-1-0 | p 952 N93-15533

CANADIAN SPACE AGENCY, OTTAWA (ONTARIO).
Proceedings of the Sixth CASI Conference on Astronautics
| CTN-92-60336 | p 804 N93-14920
Multiple fault diagnosis of spacecraft electrical power systems p 806 N93-14927
Spacecraft thermal design verification in Canada
p 808 N93-14940
Technology development for non-contact measurement in modal testing of large space structures
p 809 N93-14942
Space craft verification at the David Florida Laboratory
p 809 N93-14943
Earth environment space initiative
p 811 N93-14953

CANADIAN SPACE SOCIETY, DOWNSVIEW (ONTARIO).
The Canadian Solar Sail Project p 804 N93-14921

CAPE COD RESEARCH, BUZZARDS BAY, MA.
Waterborne polyurethane binder resins for compliant aircraft coatings
| AD-A256246 | p 849 N93-14573

CARNEGIE-MELLON UNIV., PITTSBURGH, PA.
Multiscale modeling of the long-range transport and fate of pollutants emitted from urban areas
p 909 N93-14118
A portable multiprocessor interface for standard ML of New Jersey
| AD-A255639 | p 958 N93-14151
Representation and manipulation of inductive boolean functions
| AD-A256078 | p 967 N93-14235
A proof of the Church-Rosser theorem and its representation in a logical framework
| AD-A256574 | p 942 N93-14268
Neural nets for scene analysis
| AD-A255976 | p 961 N93-14409
Wait-free consensus
| AD-A255978 | p 943 N93-14423
A specification of the Soar cognitive architecture in Z
| AD-A256198 | p 940 N93-14491
Trace algebra for automatic verification of real-time concurrent systems
| AD-A256199 | p 968 N93-14492
Model reduction of flexible manipulators
| AD-A255251 | p 889 N93-14528
An active Z gravity compensation system
| AD-A255258 | p 889 N93-14529
Global optimum path planning for a redundant space robot
| AD-A255316 | p 889 N93-14545
Design and implementation of practical constraint logic programming systems
| AD-A256191 | p 943 N93-14558
Fault tolerant systems practitioner's workshop
| AD-A255376 | p 944 N93-14563
VANTAGE: A frame-based geometric modeling system programmer/user's manual, V2.0
| AD-A255434 | p 944 N93-14566
A minimum-slip attitude control method for the erebus walking robot
| NASA-CR-191646 | p 890 N93-14567
An iconic position estimator for a 2-D laser rangefinder
| AD-A255523 | p 885 N93-14568
Implementation of the pure pursuit path tracking algorithm
| AD-A255524 | p 944 N93-14569
Work efficient hashing on parallel and vector computers
| AD-A256355 | p 959 N93-15205
Grammatical trigrams: A probabilistic model of link grammar
| AD-A256365 | p 947 N93-15206
Implementing the multiprefix operation on parallel and vector computers
| AD-A256367 | p 959 N93-15207
Experience with a course on architectures for software systems. Part 1: Course description
| AD-A256221 | p 941 N93-15239
Transactional distributed shared memory
| AD-A256222 | p 941 N93-15240
CMU common lisp user's manual
| AD-A256431 | p 950 N93-15336
A massively distributed parallel genetic algorithm
| AD-A256617 | p 959 N93-15407
An axiomatic treatment of partial correctness and deadlock in a shared variable parallel language
| AD-A256234 | p 960 N93-15494
An interval refinement technique for surface intersection p 956 N93-15561

CASA-RI/SME, TEL AVIV (ISRAEL).
Proceedings of the International Conference on CAD/CAM and AMT. Volume 4: VHDL (VHSIC Hardware Description Language) Seminar
| ITN-92-85130 | p 947 N93-15261
Proceedings of the International Conference on CAD/CAM and AMT. Volume 3: IFIP (International Federation of Information Processing)/Robotics: International Sessions on Robots and Assembly
| ITN-92-85129 | p 949 N93-15298

CATHOLIC UNIV. OF AMERICA, WASHINGTON, DC.
Mechanisms of microwave induced damage in biologic materials
| AD-A255799 | p 933 N93-14648

CDM FEDERAL PROGRAMS CORP., FAIRFAX, VA.
Acoustic location of leaks in pressurized underground petroleum pipelines
| PB92-207687 | p 975 N93-15647

CENTRAL RESEARCH INST. FOR PHYSICS, BUDAPEST (HUNGARY).
DAR-2: On-board data acquisition system for aircraft engines p 795 N93-15166

CENTRE NATIONAL D'ETUDES SPATIALES, TOULOUSE (FRANCE).
Geophysical investigations with TOPEX/Poseidon altimetry data p 918 N93-14969
Assimilation of altimeter topography into oceanic models p 927 N93-14972
Geophysical validation of TOPEX/Poseidon altimetry products p 918 N93-14982
Ocean circulation using altimetry p 929 N93-14984
Present-day plate motions: Retrieval from the TOPEX/Poseidon orbitography network (DORIS system)
p 918 N93-14993

CENTRE NATIONAL DE LA RECHERCHE SCIENTIFIQUE, PARIS (FRANCE).
Direct simulation of turbulent combustion
p 840 N93-14622

CESKOSLOVENSKA AKADEMIE VED, PRAGUE.
Czechoslovak development and experience in flight data recorder readout and analysis p 794 N93-15162

CHARLES RIVER ANALYTICS, INC., CAMBRIDGE, MA.
Design for tactical situation awareness display
| AD-A256194 | p 798 N93-15235

CHELSEA INTERNATIONAL, INC., WASHINGTON, DC.
Feasibility study for an integrated data processing system
| PB92-214287 | p 1009 N93-15644

CHEMICAL RESEARCH AND DEVELOPMENT CENTER, ABERDEEN PROVING GROUND, MD.
Removal of THD from painted test panels by liquid systems
| AD-A255624 | p 850 N93-15064
Predicting polymer properties by computational methods 2: A comparison of semi-empirical methods
| AD-A256856 | p 854 N93-15640

CHICAGO UNIV., IL.
Gas-surface interactions
| AD-A255390 | p 841 N93-14652

CHRISTOPHER NEWPORT COLL., NEWPORT NEWS, VA.
A comparison of superconductor and manganin technology for electronic links used in space mission applications
| NASA-CR-4477 | p 997 N93-15587

CHRYSLER TECHNOLOGIES AIRBORNE SYSTEMS, INC., NEW ORLEANS, LA.
Space Shuttle Orbiter Crew Hatch Jettison Test using a 0.0405-scale model (16-0) in the Texas A/M low speed wind tunnel (OA362). Space Shuttle aerothermodynamic data report
| NASA-CR-167698 | p 815 N93-15474
Results of a FRSI material test under Space Shuttle ascent conditions in the Ames Research Center 9x7 foot supersonic wind tunnel (OS13). Space Shuttle aerothermodynamic data report
| NASA-CR-167699 | p 816 N93-15475

CINCINNATI UNIV., OH.
Level-mixing assisted tunability of nuclear resonance linewidths for gamma ray lasers
| AD-A255791 | p 885 N93-14647
Complete analytical theory for the satellites of Neptune p 1046 N93-14833
L.D.V. measurements of unsteady flow fields in radial turbine
| AD-A255728 | p 878 N93-15065
Optimal impulsive trajectories for orbital rendezvous between elliptic orbits p 813 N93-15103
Synthesis and simulation with VHDL (VHSIC hardware description language)
| VH-5 | p 948 N93-15266

CITY COLL. OF THE CITY UNIV. OF NEW YORK, NY.
Modern methods in meteorological and oceanographic data analysis
| AD-A257080 | p 903 N93-15496

CITY UNIV. OF NEW YORK, NY.
Turbulent magnetized plasmas from ionizing shock waves p 987 N93-14120
Diffusing wave spectroscopy p 980 N93-14169

CLARKSON UNIV., POTSDAM, NY.
Modelling Directional Solidification
| NASA-CR-191301 | p 995 N93-15309
Solidification of InSb-GaSb alloy and InSb with vibration p 995 N93-15310
An experimental approach to determine the heat transfer coefficient in directional solidification furnaces
p 995 N93-15311
Experimental observation of the influence of furnace temperature profile on convection and segregation in the vertical Bridgman crystal growth technique
p 995 N93-15312

CLEMSON UNIV., SC.
Optimal and robust control of robot manipulators
p 890 N93-14685

COAST GUARD, WASHINGTON, DC.
Report of the International Ice Patrol in the North Atlantic, bulletin no. 77
| AD-A256162 | p 925 N93-14452

COAST GUARD RESEARCH AND DEVELOPMENT CENTER, GROTON, CT.
Evaluation of Night Vision Goggles (NVG) for maritime search and rescue (joint Canadian/US Coast Guard experiment)
[AD-A255525] p 939 N93-14554

COASTAL ENGINEERING RESEARCH CENTER, VICKSBURG, MS.
Evaluation of methods for estimating wind wave growth on narrow irregular fetches
[AD-A256002] p 932 N93-15113

COBB (MICHAEL A.) AND CO., AKRON, OH.
Technology commercialization cost model and component case study
[DE92-001280] p 907 N93-15213

COHERENT TECHNOLOGIES, INC., BOULDER, CO.
Solid-state coherent laser radar wind shear measuring systems p 784 N93-14848

COLOGNE UNIV. (GERMANY).
The effects of Venusian mantle convection with multiple phase transitions p 1043 N93-14385

COLORADO STATE UNIV., FORT COLLINS.
Vertical path atmospheric turbulence: Temporal spectra and differential image motion measurements p 914 N93-14641
An observational and theoretical study of squall line evolution p 921 N93-14682
Low-frequency oscillations in radiative-convective models p 915 N93-14874
Low-frequency oscillations in radiative-convective models
[DE92-018779] p 922 N93-14901
The influence of baroclinic processes on tropical cyclone motion p 923 N93-15099
Fitting microphysical observations to a numerical model through an optimal control theory technique p 924 N93-15100
Modelling global methane emissions from livestock: Biological and nutritional controls
[NASA-CR-191354] p 911 N93-15480

COLORADO UNIV., BOULDER.
Data management for the coordinated Eastern Arctic experiment
[AD-A255648] p 1000 N93-14182
Local-time asymmetries in the Venus thermosphere p 1023 N93-14290
Monte Carlo modeling of the resurfacing of Venus p 1025 N93-14299
Venusian hydrology: Steady state reconsidered p 1028 N93-14318
Results of a zonally truncated three-dimensional model of the Venus middle atmosphere p 1037 N93-14351
Precision radiation force modeling for the TOPEX/Poseidon mission p 817 N93-14586
Precision tests of gravitation: Liquid-supported torsion balance experiments and a tower experiment p 914 N93-14589
Sulfur oxides in the middle atmosphere of Venus: Observations by the International Ultraviolet Explorer and sounding rockets p 1046 N93-14635
Thermal elastic shock and its effect on spacecraft attitude control p 818 N93-14837
Ocean wave detection using satellite altimetry p 906 N93-14839
Wolf-Rayet stars in the Milky Way, the Large Magellanic Cloud, and emission-line galaxies p 1020 N93-14869
The use of satellite altimetry in the study of weakly defined and variable oceanic gyres p 926 N93-14966
A TOPEX/Poseidon study of oceanic effects on observations of the Earth's interior p 918 N93-14999
Methodology for studying and training expertise p 786 N93-15018
Ferroelectrics volume 122, numbers 1-4, 1991. Proceedings of the 3rd International Conference on Ferroelectric Liquid Crystals, part 2
[AD-A257053] p 996 N93-15446
Ferroelectrics volume 121, numbers 1-4, 1991. Proceedings of the 3rd International Conferenceon Fer roelectric Liquid Crystals, part 1
[AD-A257054] p 996 N93-15447

COLUMBIA UNIV., NEW YORK, NY.
A study of the abundance distributions along the minor axis of the Galactic bulge p 1015 N93-14136
Advanced laser chemical processing for microelectronics and integrated optics
[AD-A255980] p 865 N93-14425
Multiwavelength spectroscopy of active galactic nuclei p 1011 N93-14611
Aviation accidents, incidents, and violations: Psychological predictors among US pilots p 783 N93-14693
Global survey of effective particle size in liquid water clouds by satellite observations p 921 N93-14862
Annotating the real world with knowledge-based graphics on a see-through head-mounted display p 954 N93-15543
Development of a High Resolution Liquid Xenon Imaging Telescope for Medium Energy Gamma Ray Astrophysics
[NASA-CR-191781] p 1013 N93-15589
A Monte Carlo analysis of the liquid xenon TPC as gamma ray telescope p 1014 N93-15590
A liquid xenon imaging telescope for gamma ray astrophysics: Design and expected performance p 1014 N93-15591
Liquid xenon time projection chamber for gamma rays in the MeV region: Development status p 1014 N93-15592

COM DEV LTD., CAMBRIDGE (ONTARIO).
An overview of RADARSAT payload technologies p 807 N93-14933

COMMONWEALTH SCIENTIFIC AND INDUSTRIAL RESEARCH ORGANIZATION, HOBART (AUSTRALIA).
Ocean transport and variability studies of the South Pacific, Southern, and Indian Oceans p 927 N93-14971

COMMUNICATIONS GENERAL INTERNATIONAL, INC., SAINT LOUIS, MO.
Feasibility study for an integrated data processing system
[PB92-214287] p 1009 N93-15644

COMPUTATIONAL MECHANICS CONSULTANTS, INC., TOWSON, MD.
Hypervelocity impact simulations of Whipple shields p 821 N93-15604

CONNECTICUT UNIV., STORRS.
Preliminary investigations of metal liquid-like films and coatings derived from them
[AD-A255477] p 849 N93-14489

CONTINENTAL AIRLINES, INC., LOS ANGELES, CA.
In-service evaluation of wind shear systems p 785 N93-14857

CONTROL DATA CORP., MINNEAPOLIS, MN.
MIL-STD-1760 application guidelines
[AD-A255714] p 790 N93-14432

CORNELL UNIV., ITHACA, NY.
Wall layers
[AD-A256152] p 872 N93-14257
Polarization properties and Earth-based radar measurements of Venus in the post-Magellan era p 1026 N93-14304
The spatial distribution of coronae on Venus p 1043 N93-14383
Microwave scattering and emission properties of large impact craters on the surface of Venus p 1043 N93-14384
Episodic plate tectonics on Venus p 1044 N93-14390
Nonblocking and orphan free message logging protocols
[NASA-CR-191631] p 862 N93-15339
Adsorption and diffusion of fluids in well-characterized adsorbent materials
[DE92-040160] p 843 N93-15414

CRANFIELD INST. OF TECH., BEDFORD (ENGLAND).
DESAID (the development of an expert system for aircraft initial design) p 790 N93-14448
Rotating stall inception in fans of low hub-tip ratio p 779 N93-14479

CREARE, INC., HANOVER, NH.
Numerical modeling tools for chemical vapor deposition
[NASA-CR-4480] p 880 N93-15643

CUMMINS ENGINE CO., INC., COLUMBUS, IN.
Development of wear-resistant ceramic coatings for diesel engine components
[DE92-041382] p 853 N93-15439

D

DAISY/CADNETIX ISRAEL LTD., HERZLIYA.
integrating VHDL (VHSIC hardware description language) with existing EDA tools
[VH-8] p 948 N93-15268

DARTMOUTH COLL., HANOVER, NH.
Multimodal interactions in sensory-motor processing
[AD-A255780] p 938 N93-15067

DAVID SARNOFF RESEARCH CENTER, PRINCETON, NJ.
High performance YBCO films
[AD-A255439] p 994 N93-15297

DAYTON UNIV., OH.
Direct optical to microwave conversion
[RL-TR-91-375] p 859 N93-14728

DAYTON UNIV. RESEARCH INST., OH.
Determination of stresses on laminated aircraft transparencies by the strain gage-hole drilling and sectioning method
[AD-A255548] p 791 N93-14571

DEFENCE RESEARCH AGENCY, MALVERN (ENGLAND).
Proof of theorems in Z
[AD-A255711] p 968 N93-14431

DEFENCE RESEARCH ESTABLISHMENT ATLANTIC, DARTMOUTH (NOVA SCOTIA).
Acoustic propagation loss predictions for a site on the Bermuda Rise at low and very low frequencies
[AD-A255445] p 925 N93-14512

DEFENCE RESEARCH ESTABLISHMENT, OTTAWA (ONTARIO).
Progress in DND's space-based radar R/D project p 812 N93-14958

DEFENSE TECHNICAL INFORMATION CENTER, ALEXANDRIA, VA.
DROLS workbook
[AD-A255850] p 999 N93-14106
Source hierarchy list. Volume 1: A through D
[AD-A256100] p 1001 N93-14265
Source header list. Volume 2: K through Z
[AD-A256001] p 1007 N93-15112
User's guide for SearchMAESTRO
[AD-A256422] p 1008 N93-15335

DELAWARE UNIV., NEWARK.
Numerical and experimental study of bubble growth in highly viscous fluids p 874 N93-14465
Synoptic scale structure of summertime wet and dry spells in northeastern Kansas p 923 N93-14919

DEPARTMENT OF ENERGY, IDAHO FALLS, ID.
Dual-Shaft Electric Propulsion (DSEP) Technology Development Program
[DE92-040189] p 894 N93-15416

DEPARTMENT OF ENERGY, WASHINGTON, DC.
Environmental assessment: OMEGA upgrade project at the Laboratory for Laser Energetics, University of Rochester
[DE92-040410] p 886 N93-14907
Geothermal Energy and the Utility Market: The Opportunities and Challenges for Expanding Geothermal Energy in a Competitive Supply Market: Proceedings
[DE92-019090] p 908 N93-15271
Environmental assessment for the laser guide star experiment at Lawrence Livermore National Laboratory
[DE92-040316] p 1013 N93-15425

DEPARTMENT OF THE ARMY, WASHINGTON, DC.
Jointed assembly actuated by fluid pressure
[AD-D015383] p 893 N93-15248
Improved head support stand adjustable by compoundturnbuckle
[AD-D015384] p 936 N93-15249
Remote vehicle controller
[AD-D015389] p 893 N93-15251

DEPARTMENT OF THE NAVY, ARLINGTON, VA.
Thermal fixture for testing an integrated circuit
[AD-D015380] p 882 N93-15247
High performance pulse generator
[AD-D015378] p 869 N93-15269

DEPARTMENT OF THE NAVY, WASHINGTON, DC.
Optics for diode array transverse pumped laser rod
[AD-D015436] p 885 N93-14722
Shape-stable reentry body nose tip
[AD-D015437] p 817 N93-14725
Method and apparatus for increasing a radar's range with improved scan-to-scan integration of Doppler filtered signals
[AD-D015421] p 860 N93-14742
Method of making substantially single phase superconducting oxide ceramics having a TC above 85 degrees
[AD-D015422] p 850 N93-14743
Interferometer with two phase-conjugate mirrors
[AD-D015420] p 982 N93-14800
Propellant grain assembly for a gas generator
[AD-D015439] p 854 N93-14801
Spirobislactone acrylate polymers
[AD-D015443] p 850 N93-14802
Dual active layer photoconductor
[AD-D015423] p 993 N93-14820
Method for detecting chemical vapors using a lasing dye sensor
[AD-D015424] p 885 N93-14821
Cable-line shortening device
[AD-D015427] p 891 N93-14822
Apparatus and process for desalination of seawater
[AD-D015428] p 842 N93-14824
Method for fabricating ohmic contacts on semiconducting diamond
[AD-D015432] p 850 N93-14825
Internal grounding arrangement in a switching power converter
[AD-D015435] p 868 N93-14826
Statistically calibrated transducer
[AD-D015408] p 882 N93-14878
Layered parallel interface for an active antenna array
[AD-D015411] p 860 N93-14879

Two-stage target tracking system and method
| AD-D015412 | p 982 N93-14880
Method and devices for the in situ repair of damaged threads
| AD-D015416 | p 891 N93-14881
Power conversion system modification to permit use of DC power source
| AD-D015409 | p 868 N93-14887
Method of bonding molybdenum to steel
| AD-D015410 | p 845 N93-14888
Mechanical shielding for electric primer
| AD-D015417 | p 860 N93-14889
Method and apparatus for a high resolution, flat panel cathodoluminescent display screen
| AD-D015400 | p 868 N93-15107
Multifilamentary superconducting cable and a method of manufacturing it
| AD-D015391 | p 846 N93-15231
Liquid flow reactor and method of using
| AD-D015392 | p 893 N93-15232
Superstrength metal composite material and process for making the same
| AD-D015379 | p 836 N93-15246
Color center laser with transverse auxiliary illumination
| AD-D015387 | p 887 N93-15250
Three position power cylinder
| AD-D015393 | p 894 N93-15461

DEPUTY ASSISTANT SECRETARY OF DEFENSE (ENVIRONMENTAL QUALITY), WASHINGTON, DC.
Human exploration: Moon/Mars mission p 805 N93-14922

DEUTSCHE AIRBUS G.M.B.H., MUNICH (GERMANY).
Software flexibility and configuration control for the A340/A330 Aircraft Condition Monitoring System (ACMS) p 793 N93-15154

DEUTSCHE FORSCHUNGSANSTALT FUER LUFT- UND RAUMFAHRT, BRUNSWICK (GERMANY).
Fracture/damage mechanics of composites: Static and fatigue properties
| DLR-MITT-92-03 | p 835 N93-15075
Proceedings of the 16th Symposium on Aircraft Integrated Monitoring Systems
| DLR-MITT-92-01 | p 793 N93-15152

DEUTSCHE FORSCHUNGSANSTALT FUER LUFT- UND RAUMFAHRT, STUTTGART (GERMANY).
Preliminary design of composite joints
| DLR-MITT-92-05 | p 835 N93-15076

DEUTSCHE LUFTHANSA A.G., FRANKFURT AM MAIN (GERMANY).
Software for flight recorder data evaluation developed by Lufthansa p 794 N93-15163

DIRECTION DES RECHERCHES, ETUDES ET TECHNIQUES, PARIS (FRANCE).
Precise measurements made from a distance of local deformations independent of small object movements
| ETN-92-92723 | p 886 N93-15128

DORNIER SYSTEM G.M.B.H., FRIEDRICHSHAFEN (GERMANY).
Integrated engine control and monitoring with experiences derived from OLMOS p 795 N93-15168

DOW CORNING CORP., MIDLAND, MI.
Properties of textile grade ceramic fibers p 833 N93-14751

DREXEL UNIV., PHILADELPHIA, PA.
The dynamics of spatially extended lasers p 883 N93-14123
The effect of a hierarchical task-specific external conceptual model on the learnability and usability of microcomputer applications by novices p 1000 N93-14205
Some theoretical and experimental aspects of the generation of guided elastic waves using finite sources p 897 N93-14219

DUNDEE UNIV. (SCOTLAND).
Optical information processing using photorefractive BSO p 981 N93-14204

DYNACON ENTERPRISES LTD., DOWNSVIEW (ONTARIO).
Space based radar: Test of large space structures p 808 N93-14941

DYNAMICS RESEARCH CORP., WILMINGTON, MA.
Development of measures of crew coordination
| AD-A255384 | p 939 N93-14651

E

E-SYSTEMS, INC., DALLAS, TX.
EMASS (trademark): An expandable solution for NASA space data storage needs p 1005 N93-15033

ECOLE NATIONALE SUPERIEURE DE MECANIQUE ET D'AERONAUTECHNIQUE, POITIERS (FRANCE).
Combustion in supersonic flows p 841 N93-14627

ECOLE NATIONALE SUPERIEURE DES TELECOMMUNICATIONS, PARIS (FRANCE).
Off-axis conoscopic holography: Optical and digital reconstruction
| TELECOM-PARIS-90-E-023 | p 882 N93-15096
Integration of satellite links into an ATM mode broadband ISDN
| TELECOM-PARIS-91-E-022 | p 861 N93-15097
On the theory of coded modulation systems for high output digital transmission
| TELECOM-PARIS-92-E-001 | p 861 N93-15098

ECOLE NATIONALE SUPERIEURE DU PETROLE ET DES MONTEURS, RUEIL-MALMAISON (FRANCE).
Damage and rupture of ceramic composites
| ETN-92-92722 | p 851 N93-15127

ECOLE POLYTECHNIQUE, MONTREAL (QUEBEC).
A new device to aid in the conception and optimization of monolithic millimeter circuits: A distributed and nonliner model of a field effect transistor p 807 N93-14932
Conceptualization of a GaAs field effect transistor frequency tripler (2.5-7.5 GHz) for load use in communication satellites p 807 N93-14934
Simulation and nonlinear modelling of microwave transistors p 807 N93-14936

EDGERTON, GERMESHAUSEN AND GRIER, INC., IDAHO FALLS, ID.
Independent validation testing of the FLAME computer code, version 1.0
| DE92-019691 | p 948 N93-15274
Dual-Shaft Electric Propulsion (DSEP) Technology Development Program
| DE92-040189 | p 894 N93-15416

EDINBURGH UNIV. (SCOTLAND).
The structure and dynamics of an environment forming high-mass stars p 1014 N93-14113

EDUCATIONAL TESTING SERVICE, PRINCETON, NJ.
A psychometrically sound cognitive diagnostic model: Effect of remediation as empirical validity
| AD-A255926 | p 933 N93-14109

EG AND G ENERGY MEASUREMENTS, INC., IDAHO FALLS.
Fabrication of high temperature materials by exothermic synthesis and subsequent dynamic consolidation
| DE92-019836 | p 834 N93-14819
Addressing earthquake strong ground motion issues at the Idaho National Engineering Laboratory
| DE92-017841 | p 916 N93-15136

EG AND G ROCKY FLATS, INC., GOLDEN, CO.
Plutonium pyrophoricity
| RFP-4517 | p 845 N93-14723

EIC, INC., NORWOOD, MA.
Photoelectrochemistry of electronic and electro-optical materials
| AD-A256239 | p 866 N93-14583
Remote fiber optic sensor for gaseous and liquid environments, phase 2
| AD-A256224 | p 983 N93-15241

ELECTROMAGNETIC SCIENCES, INC., NORCROSS, GA.
On-orbit deployment anamolies: What can be done? p 821 N93-15603

ELECTRONICS RESEARCH LAB., ADELAIDE (AUSTRALIA).
An analysis of the effect of acoustic non-linearities in wide bandwidth acousto-optic bragg cells
| AD-A256579 | p 973 N93-14269
Program verification using higher order logic
| AD-A255408 | p 943 N93-14502
A preliminary design of the Ti:LiNbO3 optical channel waveguide
| AD-A255443 | p 982 N93-14784

ELORET CORP., PALO ALTO, CA.
Theoretical characterization of the potential energy surface for NH + NO
| NASA-CR-190741 | p 843 N93-15357
A global potential energy surface for ArH2
| NASA-CR-190741 | p 843 N93-15358

ELORET CORP., SUNNYVALE, CA.
Computed potential energy surfaces for chemical reactions
| NASA-CR-190741 | p 843 N93-15356

EMORY UNIV., ATLANTA, GA.
Spectroscopy and reactions of hydrazoic acid on silicon single crystal surfaces (III). HN3 and DN3 on Si(111)-7 x 7
| AD-A255241 | p 842 N93-14669
Thermal stability of trimethyl indium on Si(100)-2 x 1 as studied with HREELS, UPS, and XPS: A comparison with the results from Si(111)-7 x 7 and Si(110) studies
| AD-A255242 | p 992 N93-14670

ERG SYSTEMS, INC., SAINT JAMES, NY.
Full surface testing of grazing incidence mirrors
| AD-A255644 | p 979 N93-14152
Full surface testing of grazing incidence mirrors
| AD-A255798 | p 984 N93-15371

ESDU INTERNATIONAL LTD., LONDON (ENGLAND).
Program for calculation of aileron rolling moment and yawing moment coefficients at subsonic speeds
| ESDU-88040 | p 779 N93-14514
Pressure drag and lift contributions for blunted forebodies of fineness ratio 2.0 in transonic flow (M infinity less than or equal to 1.4)
| ESDU-89033 | p 779 N93-14515
Direct prediction of a separation boundary for aerofoils using a viscous-coupled calculation method
| ESDU-92008 | p 780 N93-14516
Viscosity of liquids. Halogenated methanes
| ESDU-92028 | p 839 N93-14539
Orthobaric densities and molar volumes of liquids. Halogenated ethylenes
| ESDU-92018 | p 839 N93-14540
Estimation of rate of climb
| ESDU-92019 | p 791 N93-14541
Thermal conductivity of liquid aliphatic hydrocarbons. Part 2: Alkenes, dienes and trienes
| ESDU-92025 | p 839 N93-14542
Calculation methods for externally pressurised (hydrostatic) journal bearings with capillary restrictor control
| ESDU-92026 | p 889 N93-14543
Thermophysical properties of nitric oxide
| ESDU-92027 | p 839 N93-14544
Fatigue strength of cruciform and other fillet welded joints in aluminum alloys
| ESDU-92017 | p 900 N93-14553

EUROPEAN SPACE AGENCY. EUROPEAN SPACE RESEARCH AND TECHNOLOGY CENTER, ESTEC, NOORDWIJK (NETHERLANDS).
The design concept of the 6-degree-of-freedom hydraulic shaker at ESTEC p 820 N93-15600

EXETER UNIV. (ENGLAND).
Time-resolved optical studies of 3-5 semiconductors p 990 N93-14183

EXOTECH, INC., FREMONT, CA.
An experimental and analytical study of TIP clearance effects in axial flow compressors
| AD-A256434 | p 800 N93-15337

F

FAIRCHILD SPACE CO., GERMANTOWN, MD.
Reusable Reentry Satellite (RRS) system design study
| NASA-CR-187897 | p 817 N93-14733

FEDERAL AVIATION ADMINISTRATION, WASHINGTON, DC.
Performance of color-dependent tasks of air traffic control specialists as a function of type and degree of color vision deficiency
| AD-A256614 | p 788 N93-14275
Identifying ability requirements for operators of future automated air traffic control systems
| AD-A256615 | p 789 N93-14276
Effects of seating configuration and number of type 3 exits on emergency aircraft evacuation
| AD-A256616 | p 783 N93-14277
Airborne Wind Shear Detection and Warning Systems. Fourth Combined Manufacturers' and Technologists' Conference, part 2
| NASA-CP-10105-PT-2 | p 783 N93-14844
Terminal area forecasts FY 1992 - 2005
| AD-A255797 | p 788 N93-15390

FLORIDA INST. OF TECH., MELBOURNE.
Physics of hydrogen storage in metal-hydrides p 854 N93-14630
Sampled-data control and robust control for discrete-time systems p 964 N93-15149

FLORIDA SEA GRANT COLL., GAINESVILLE.
The production and use of aeroponically grown inocula of VAM fungi in the native plant nursery
| PB92-204973 | p 933 N93-15208

FLORIDA STATE UNIV., TALLAHASSEE.
A proof of convergence of the Markov chain simulation method
| AD-A255456 | p 970 N93-14487
Wavelet methods for curve estimation
| AD-A255357 | p 970 N93-14538

FLORIDA UNIV., ALACHUA.
Ultrastructure processing and environmental stability of advanced structural and electronic materials
| AD-A256153 | p 831 N93-14665

FLORIDA UNIV., GAINESVILLE.
Explaining cloud chamber tracks
| DE92-040502 | p 972 N93-15057
Dark matter axions
| DE92-040501 | p 1022 N93-15346
Staggered fermions and chiral symmetry breaking in transverse lattice regulated QED
| DE92-040505 | p 977 N93-15378

The sine-Gordon model and the small (kappa)(sup +) region of light-cone perturbation theory
[DE92-040506] p 969 N93-15379
The 17th Annual Conference on the Physics and Chemistry of Semiconductor Interfaces
[AD-A257061] p 996 N93-15449

FOSTER-MILLER ASSOCIATES, INC., WALTHAM, MA.
New nonlinear optical film processing
[AD-A256011] p 983 N93-15255

FRAMASYS A.G., ZURICH (SWITZERLAND).
Failure diagnostic with MAINTEX based on AIMS at Swissair p 778 N93-15181

FREIE UNIV., BERLIN (GERMANY).
Hyper-rendering p 953 N93-15538

G

GENERAL ACCOUNTING OFFICE, WASHINGTON, DC.
Unmanned aerial vehicles: More testing needed before production of short-range system
[AD-A256296] p 790 N93-14440
Military space operations: Satellite control system improved, but serious problems remain
[AD-A256809] p 971 N93-15626

GENERAL DYNAMICS CORP., SAINT LOUIS, MO.
Acoustic and thermal testing of the Titan/Centaur upper stage p 814 N93-15621

GENERAL ELECTRIC CO., CINCINNATI, OH.
CF6-6 high pressure compressor stage 5 locking slot crack propagation spin pit test p 799 N93-14894
A philosophy for integrated monitoring system design p 796 N93-15174

GENERAL ELECTRIC CO., HOUSTON, TX.
Advanced sensors technology survey
[NASA-CR-185691] p 881 N93-14494

GENERAL ELECTRIC CO., PRINCETON, NJ.
Mass spectrometer use in a large chamber p 823 N93-15619

GENERAL ELECTRIC CO., SCHENECTADY, NY.
Adiabatic two-phase flow in a test section with partial flow blockages
[DE92-016360] p 877 N93-14816

GENERAL MOTORS CORP., INDIANAPOLIS, IN.
Engine life assessment test case TF41 LP compressor shaft torsional fatigue p 799 N93-14896

GEOLOGICAL SURVEY, FLAGSTAFF, AZ.
Bright crater outflows: Possible emplacement mechanisms p 1026 N93-14305
Computer simulations of comet- and asteroidlike bodies passing through the Venusian atmosphere: Preliminary results on atmospheric and ground shock effects p 1040 N93-14365
Can a time-stratigraphic classification system be developed for Venus? p 1043 N93-14388

GEOLOGICAL SURVEY, MENLO PARK, CA.
Magellan stereo images and Venusian geology p 1035 N93-14347

GEOLOGICAL SURVEY, SIOUX FALLS, SD.
The preservation of LANDSAT data by the National Land Remote Sensing Archive p 1003 N93-14777

GEORGE MASON UNIV., FAIRFAX, VA.
Evaluation and estimation of handling qualities via statistical modeling of pilot response data
[AD-A255324] p 939 N93-14548

GEORGE WASHINGTON UNIV., WASHINGTON, DC.
Boundary layer transition measurements by optical anemometry p 874 N93-14477
Publications of the Space Physiology and Countermeasures Program, Neuroscience Discipline: 1980-1990
[NASA-CR-4476] p 936 N93-15583

GEORGIA INST. OF TECH., ATLANTA.
An investigation of transient atmospheric inorganic peroxides: A theoretical and experimental study p 912 N93-14117
Analysis of rotation experiments in TFTR p 987 N93-14129
Analysis of advanced thin-walled composite structures p 895 N93-14158
Non-linear analysis of wave progagation using transform methods and plates and shells using integral equations p 896 N93-14186
Nondestructive evaluation of damage in SiC/Al metal matrix composite using x ray tomographic microscopy p 829 N93-14192
Robust control of a flexible link robot and rigid link robot: Theory, simulation, and experiment p 888 N93-14202
A study of the relationship between macroscopic measures and physical processes occurring during crack closure
[AD-A256587] p 898 N93-14272
Understanding the variation in the millimeter-wave emission of Venus p 1028 N93-14315
A simulation model of atmospheric turbulence for rotorcraft applications p 920 N93-14588
The effect of wake dynamics on rotor eigenvalues in forward flight p 780 N93-14595
Study and interpretation of the millimeter-wave spectrum of Venus p 1045 N93-14596
Investigation of antenna pattern constraints for passive geosynchronous microwave imaging radiometers
[NASA-CR-189728] p 905 N93-14792
SAPNEW: Parallel finite element code for thin shell structures on the Alliant FX-80
[NASA-CR-189212] p 901 N93-14799
Development of a fiber optic high temperature strain sensor
[NASA-CR-191316] p 882 N93-14810
Stability of elastically tailored rotor blades p 791 N93-14828
Finite-state inflow applied to aeroelastic flutter of fixed and rotating wings p 802 N93-14830
Application of an aeroelastic analysis method for aerodynamic improvement of fighter wings at maneuver flight conditions p 791 N93-14832
Laboratory evaluation and application of microwave absorption properties under simulated conditions for planetary atmospheres
[NASA-CR-191298] p 1047 N93-15081
An investigation into the role of moist, vertical drafts in the rotational development of storms p 923 N93-15087
Learning position and force control for mechanical manipulators p 963 N93-15147
Robust control design for uncertain nonlinear dynamic systems p 964 N93-15148
Validation of an automated torsional and warping stress analysis program
[AD-A256035] p 902 N93-15260
JSEP fellowship
[AD-A257021] p 863 N93-15470
Fast algorithms for rendering cubic curves p 953 N93-15536

GEORGIA TECH RESEARCH INST., ATLANTA.
A millimeter-wave radiometer for detecting microbursts p 784 N93-14850

GRAPHIC AND DATA SOLUTIONS, INC., SAINT LOUIS, MO.
Feasibility study for an integrated data processing system
[PB92-214287] p 1009 N93-15644

GROUPE DE RECHERCHE DE GEODESIE SPATIALE, GRASSE (FRANCE).
The western Mediterranean Sea: An area for a regional validation for TOPEX/Poseidon and a field for geophysical and oceanographic studies p 926 N93-14965

GTE LABS., INC., WALTHAM, MA.
Development of adherent ceramic coatings to reduce contact stress damage of ceramics
[DE92-041373] p 852 N93-15437

GUELPH UNIV. (ONTARIO).
Movement time prediction in human-computer interfaces p 955 N93-15550

H

HARVARD UNIV., CAMBRIDGE, MA.
Study of tidal interactions in M81-M82-NGC3077 system p 1010 N93-14195
The mechanics of dislocation nucleation at a crack tip p 896 N93-14214
Fracture analyses of thin films, interfaces, and joints p 897 N93-14215
Iterative algorithms for integral equations of the first kind with applications to statistics
[AD-A256529] p 942 N93-14285
Hydrodynamics of supernova 1987 A p 1019 N93-14633
Dynamics of analog electronic neural networks
[AD-A257019] p 966 N93-15352
Experimental attempt to metallize hydrogen at very high pressures
[AD-A257086] p 843 N93-15497

HAWAII UNIV., HONOLULU.
Using the Haleakala barrel extensive air shower array to study selected U.H.E. gamma ray point sources p 1050 N93-14639
Sensitivity of the Yoshida jet to the parameterization of vertical mixing: Do easterly winds imply equatorial upwelling? p 922 N93-14864

HAWKER SIDDELEY CANADA LTD., TORONTO (ONTARIO).
In-service considerations affecting component life p 800 N93-14898

HECHT-NIELSEN NEUROCOMPUTER CORP., INC., SAN DIEGO, CA.
Neural network retinal model real time implementation
[AD-A255652] p 934 N93-14210

HERIOT-WATT UNIV., EDINBURGH (SCOTLAND).
Nonlinear dynamics of optical systems p 979 N93-14124

HERZBERG INST. OF ASTROPHYSICS, OTTAWA (ONTARIO).
LISA: A limb imaging spectrograph for airglow p 811 N93-14952

HIBBING COMMUNITY COLL., MN.
Radiation pressure: A possible cause for the superrotation of the Venusian atmosphere p 1033 N93-14338

HIGH INTENSITY PHOTOVOLTAICS, INC., OLMSTEAD FALLS, OH.
A high intensity solar cell invention: The edge-illuminated Vertical Multi-Junction (VMJ) solar cell
[DE92-019015] p 907 N93-15224

HIGH TECHNOLOGY CORP., HAMPTON, VA.
BLSTA: A boundary layer code for stability analysis
[NASA-CR-4481] p 877 N93-14797

HOECHST CELANESE CORP., CHARLOTTE, NC.
Industrial applications of multiaxial warp knit composites p 833 N93-14750

HONEYWELL, INC., MINNEAPOLIS, MN.
Elements of a theory of natural decision making p 786 N93-15021
Taxonomy of flight variables p 787 N93-15022

HOWARD UNIV., WASHINGTON, DC.
The center for nonlinear phenomena and magnetic materials
[AD-A255983] p 967 N93-14412

HOWMET TURBINE COMPONENTS CORP., WHITE HALL, MI.
The 7th World Conference on Titanium
[AD-A255674] p 844 N93-14132

HUGHES AIRCRAFT CO., EL SEGUNDO, CA.
Electronics reliability fracture mechanics. Volume 1: Causes of failures of shop replaceable units and hybrid microcircuits
[AD-A255836] p 894 N93-14104
Electronics reliability fracture mechanics. Volume 2: Fracture mechanics
[AD-A256200] p 900 N93-14498

HUGHES AIRCRAFT CO., FULLERTON, CA.
Reliability techniques for combined hardware and software systems
[AD-A256347] p 895 N93-15204

HUMAN ENGINEERING LABS., ABERDEEN PROVING GROUND, MD.
Effects of spatial luminance nonuniformities on visual-task performance and subjective uniformity
[AD-A255989] p 936 N93-14416

HUNGARIAN ACADEMY OF SCIENCES, BUDAPEST.
CAD-based off-line programming and sensor signal processing in robotics
[F-2-2] p 949 N93-15299

HURD (HARRY L.) ASSOCIATES, INC., RALEIGH, NC.
Workstation tools for feature extraction and classification for nonstationary and transient signals
[AD-A255389] p 947 N93-15228

I

IBM FEDERAL SYSTEMS DIV., GAITHERSBURG, MD.
Software Technology for Adaptable, Reliable Systems (STARS) program. Software process tools and techniques evaluation report, version 1.0. Task IS15: Software process management
[AD-A255945] p 942 N93-14405

IBM WATSON RESEARCH CENTER, YORKTOWN HEIGHTS, NY.
The 3D modeling of high numerical aperture imaging in thin films p 985 N93-15513
Generating natural-looking motion for computer animation p 956 N93-15564
A linear constraint technology for interactive graphic systems p 957 N93-15568

IDAHO UNIV., MOSCOW.
Lineshape analysis of laser light scattered by an argon thermal plasma jet p 987 N93-14137

ILLINOIS INST. OF TECH., CHICAGO.
Feedback control of flow separation and transition to turbulence in unsteady boundary layers p 873 N93-14464
Analytical and experimental investigation of closed-cycle sorption cooling systems p 874 N93-14476

ILLINOIS UNIV., CHICAGO.
Electronic structure studies of high-T(sub c) superconductors by photoemission and x ray absorption p 989 N93-14172
Investigation of the on-surface boundary operators for electromagnetic scattering by conducting object p 857 N93-14189
Manipulation strategies for redundant manipulators p 960 N93-14203

The object instancing paradigm for linear fractal modeling p 956 N93-15559

ILLINOIS UNIV., URBANA.

Fluids, gels, and glasses under extreme conditions of pressure and temperature
[AD-A255675] p 847 N93-14166

Simultaneous DIF amplification and cancellation: Shealy-Stout test for DIF
[AD-A256284] p 970 N93-14455

Novel engineered compound semiconductor heterostructures for advanced electronics applications
[AD-A255363] p 866 N93-14562

The III-V semiconductor quantum well lasers and related optoelectronic devices (on silicon). Oxide-defined semiconductor quantum well lasers and optoelectronic devices: Al-based III-V nativeoxide s
[AD-A255239] p 885 N93-14667

A plume-induced boundary layer separation experiment
[AD-A255397] p 875 N93-14677

ILLINOIS UNIV., URBANA-CHAMPAIGN.

The 3 to 5 heterojunction structures and high speed devices
[AD-A250399] p 991 N93-14521

ILLINOIS UNIV. AT URBANA-CHAMPAIGN, SAVOY.

Dynamics in neutron stars and the early universe p 1014 N93-14112

Carbon dioxide induced ocean climatic change and tracer experiment with an atmosphere-ocean general circulation model p 912 N93-14178

IMPACT GROUP (CANADA).

Space education: A self-perservation strategy for the Canadian space industry p 808 N93-14937

IMPERIAL CHEMICAL INDUSTRIES LTD., RUNCORN (ENGLAND).

ICI optical data storage tape p 1005 N93-15037

IMPERIAL COLL. OF SCIENCE AND TECHNOLOGY, LONDON (ENGLAND).

Turbulence modeling for combustion flows p 840 N93-14620

INDIAN INST. OF TECH., MADRAS.

Adaptive control of a manipulator in cartesian space
[F-4-2] p 950 N93-15308

INDIANA UNIV., BLOOMINGTON.

Extracting x rays, gamma rays, and electron-positron pairs from supermassive Kerr black holes using the Penrose mechanism p 1049 N93-14176

Institute for the Study of Human Capabilities
[AD-A256091] p 938 N93-14427

Nerves and tissue repair
[AD-A255299] p 934 N93-14535

INDUSTRIEANLAGEN-BETRIEBSGESELLSCHAFT M.B.H., OTTOBRUNN (GERMANY).

Multi-axis transient vibration testing of space objects: Test philosophy, test facility, and control strategy p 820 N93-15598

INSTITUT D'AERONOMIE SPATIALE DE BELGIQUE, BRUSSELS.

Geographical distribution and seasonal variation of surface emissions and deposition velocities of atmospheric trace gases
[AERONOMICA-ACTA-A-361-1991] p 911 N93-15460

INSTITUT DE MECANIQUE DE GRENOBLE (FRANCE).

Global ocean tides through assimilation of oceanographic and altimeter satellite data in a hydrodynamic model p 928 N93-14978

INSTITUT DE MECANIQUE DES FLUIDES DE LILLE (FRANCE).

Aeroplane crashes on the runway: Validation and final evaluation of the method of modeling an airframe structure
[IMFL-91-32] p 792 N93-15126

INSTITUT DE PHYSIQUE DU GLOBE, PARIS (FRANCE).

Analysis of altimeter data jointly with seafloor electric data (vertically integrated velocity) and VCTD-yoyo data (detailed profiles of VCTD) p 931 N93-14998

INSTITUT DE RECHERCHE EN INFORMATIQUE ET SYSTEMES ALEATOIRES, RENNES (FRANCE).

A two-pass physics-based global lighting model p 957 N93-15570

INSTITUT FRANCAIS DE RECHERCHE POUR L'EXPLOITATION DE LA MER, BREST (FRANCE).

Studies of the intermediate and deep circulation in the western equatorial Atlantic p 927 N93-14973

General circulation of the South Atlantic between 5 deg N and 35 deg S p 929 N93-14987

INSTITUT GEOGRAPHIQUE NATIONAL, PARIS (FRANCE).

Terrestrial reference systems related to the TOPEX/Poseidon project p 906 N93-14967

INSTITUT NATIONAL DES SCIENCES APPLIQUEES, ROUTEN (FRANCE).

Applications of PDF turbulent combustion models to real non premixed flame calculations p 841 N93-14624

INSTITUT NATIONAL POLYTECHNIQUE, GRENOBLE (FRANCE).

Automated coding and intersecting cube theory
[ETN-92-92675] p 941 N93-15123

Progammable connection parallel architecture: Design and routing
[ETN-92-92676] p 958 N93-15124

Optimal synthesis methods for silicon compilers
[ETN-92-92677] p 947 N93-15125

INSTITUTE FOR COMPUTER APPLICATIONS IN SCIENCE AND ENGINEERING, HAMPTON, VA.

Parallel simulation today
[NASA-CR-189733] p 951 N93-15432

Homogeneous quantum electrodynamic turbulence
[NASA-TM-107686] p 979 N93-15482

INSTITUTE FOR DEFENSE ANALYSES, ALEXANDRIA, VA.

SDIO Workshop on Piezoelectric Ceramic Actuators for Space Applications
[AD-A255959] p 990 N93-14422

VHDL (VHSIC hardware description language) in the test environment
[VH-6] p 948 N93-15267

INSTITUTE FOR NAVAL OCEANOGRAPHY, BAY SAINT LOUIS, MS.

Wind stress analysis over the Western Equatorial Pacific and North Atlantic Oceans based on ECMWF operational wind products, 1985-1989
[AD-A256147] p 920 N93-14256

Proceedings of the data assimilation in coupled air-sea nowcast/forecast systems workshop
[AD-A255409] p 925 N93-14503

INSTITUTE FOR PERCEPTION RVO-TNO, SOESTERBERG (NETHERLANDS).

A spurious pop-out in visual search
[AD-A256548] p 936 N93-14267

Decision making in a dynamic task environment: The effect of time pressure
[AD-A256557] p 937 N93-14602

High-resolution contrast control on a video display: Method and calibration
[AD-A256552] p 938 N93-15400

INSTITUTE OF ELECTRICAL AND ELECTRONICS ENGINEERS, NEW YORK, NY.

Proceedings of the International Conference on CAD/CAM and AMT. Volume 4: VHDL (VHSIC Hardware Description Language) Seminar
[ITN-92-85130] p 947 N93-15261

Proceedings of the International Conference on CAD/CAM and AMT. Volume 3: IFIP (International Federation of Information Processing)/Robotics: International Sessions on Robots and Assembly
[ITN-92-85129] p 949 N93-15298

INSTITUTE OF PLASMA PHYSICS, PRAGUE (CZECHOSLOVAKIA).

Transformation of energy and momentum due to Landau damping in time
[IPPCZ-316] p 988 N93-14813

INSTITUTE OF SOUND AND VIBRATION RESEARCH, SOUTHAMPTON (ENGLAND).

Adaptive active noise control using multiple-model approaches
[ISVR-TR-210] p 974 N93-14734

INSTITUTO DE MATEMATICA PURA E APLICADA, RIO DE JANEIRO (BRAZIL).

Physically-based methods for polygonization of implicit surfaces p 956 N93-15562

INSTITUTO DE PESQUISAS ESPACIAIS, SAO JOSE DOS CAMPOS (BRAZIL).

The regional land use of Paraiba Valley and the North Coast of Sao Paulo State, Brazil p 905 N93-14450

INSTITUTO NATIONAL DE TELECOMMUNICACIONES, PANAMA CITY (PANAMA).

Feasibility study for an integrated data processing system
[PB92-214287] p 1009 N93-15644

INTERNATIONAL BUSINESS MACHINES CORP., POUGHKEEPSIE, NY.

System design in a large corporation, using VHDL (VHSIC hardware description language)
[VH-4] p 948 N93-15265

INTERNATIONAL CENTRE FOR THEORETICAL PHYSICS, TRIESTE (ITALY).

Measurement and analysis of excitation functions in (alpha,np) reactions on (128, 130)Te
[DE92-630358] p 991 N93-14485

INTERNATIONAL FEDERATION FOR INFORMATION PROCESSING, GENEVA (SWITZERLAND).

Proceedings of the International Conference on CAD/CAM and AMT. Volume 4: VHDL (VHSIC Hardware Description Language) Seminar
[ITN-92-85130] p 947 N93-15261

Proceedings of the International Conference on CAD/CAM and AMT. Volume 3: IFIP (International Federation of Information Processing)/Robotics: International Sessions on Robots and Assembly
[ITN-92-85129] p 949 N93-15298

INTERNATIONAL FEDERATION OF ASSOCIATIONS OF COMPUTER USERS IN ENGINEERING AND ARCHITECTURE.

Proceedings of the International Conference on CAD/CAM and AMT. Volume 4: VHDL (VHSIC Hardware Description Language) Seminar
[ITN-92-85130] p 947 N93-15261

Proceedings of the International Conference on CAD/CAM and AMT. Volume 3: IFIP (International Federation of Information Processing)/Robotics: International Sessions on Robots and Assembly
[ITN-92-85129] p 949 N93-15298

INTERNATIONAL INST. FOR PRODUCTION ENGINEERING RESEARCH, PARIS (FRANCE).

Proceedings of the International Conference on CAD/CAM and AMT. Volume 4: VHDL (VHSIC Hardware Description Language) Seminar
[ITN-92-85130] p 947 N93-15261

Proceedings of the International Conference on CAD/CAM and AMT. Volume 3: IFIP (International Federation of Information Processing)/Robotics: International Sessions on Robots and Assembly
[ITN-92-85129] p 949 N93-15298

INTERUNIVERSITY MICRO-ELECTRONICS CENTER, LEUVEN (BELGIUM).

Gate-all-around device
[AD-A255287] p 866 N93-14534

INTESPACE, TOULOUSE (FRANCE).

INTESPACE's new thermal-vacuum test facility: SIMMER p 814 N93-15613

IOWA STATE UNIV. OF SCIENCE AND TECHNOLOGY, AMES.

A time-domain study of the relationship between drive force time bandwidth and farfield acoustic radiation
[AD-A255616] p 973 N93-14159

IOWA UNIV., IOWA CITY.

A general purpose radiative transfer model for application to remote sensing in multidimensional systems p 904 N93-14174

ISRAEL SOCIETY FOR CAD/CAM, TEL AVIV.

Proceedings of the International Conference on CAD/CAM and AMT. Volume 4: VHDL (VHSIC Hardware Description Language) Seminar
[ITN-92-85130] p 947 N93-15261

Proceedings of the International Conference on CAD/CAM and AMT. Volume 3: IFIP (International Federation of Information Processing)/Robotics: International Sessions on Robots and Assembly
[ITN-92-85129] p 949 N93-15298

ITHACO, INC., ITHACA, NY.

Reusable Reentry Satellite (RRS) system design study. Phase B, appendix E: Attitude control system study
[NASA-CR-188578] p 825 N93-15633

J

JAPAN AIR LINES CO. LTD., TOKYO.

Discussion for the ideal AIMS p 793 N93-15153

JET PROCESS CORP., NEW HAVEN, CT.

Jet vapor deposition of thin films for solid oxide and other fuel cell applications
[DE92-019980] p 851 N93-15222

JET PROPULSION LAB., CALIFORNIA INST. OF TECH., PASADENA.

Image processing and products for the Magellan mission to Venus p 1026 N93-14306

Near-infrared oxygen airglow from the Venus nightside p 1026 N93-14308

Application of left- and right-looking SAR stereo to depth measurements of the Ammavaru outflow channel, Lada Terra, Venus p 1038 N93-14357

Problem footprints in Magellan altimetry data p 1039 N93-14362

Anomalous scattering behavior of selected impact parabola features: Magellan cycle-to-cycle comparisons p 1039 N93-14363

Overview of Venus geology: Preliminary description of terrain units for Venus global geological mapping p 1040 N93-14368

Magellan project p 1041 N93-14373

Venus gravity: Summary and coming events p 1042 N93-14377

Multiresolution pattern recognition of small volcanos in Magellan data p 1042 N93-14380

Low-emissivity impact craters on Venus p 1044 N93-14392

Real-time edge-enhanced optical correlator
[NASA-CASE-NPO-18521-1-CU] p 981 N93-14404

Core design for use with precision composite reflectors
| NASA-CASE-NPO-17858-1-CU | p 832 N93-14700
Multiperiod-grating surface-emitting lasers
| NASA-CASE-NPO-17763-1-CU | p 885 N93-14703
High speed magneto-resistive random access memory
| NASA-CASE-NPO-17954-1-CU | p 940 N93-14704
TOPEX/Poseidon science investigations plan
| NASA-CR-190616 | p 925 N93-14964
Circulation of the gyres of the world ocean: Observation modeling using TOPEX/Poseidon altimeter data
p 927 N93-14975
Low-frequency variability of sea level as related to the heat balance of global oceans p 928 N93-14979
A new approach for data acquisition at the JPL space simulators p 821 N93-15606
An alternate method for achieving temperature control in the -130 C to 75 C range p 821 N93-15609
Accelerated simulation of near-Earth-orbit polymer degradation p 823 N93-15615
A new approach for performing contamination control bakeouts in JPL thermal vacuum test chambers
p 823 N93-15618

JOHANNES KEPLER UNIV., LINZ (AUSTRIA).
Off-line generation of error-free robot/NC (numerical control) code using simulation and automatic programming techniques
| F-3-1 | p 949 N93-15302

JOHNS HOPKINS UNIV., BALTIMORE, MD.
Revelations of a stratospheric circulation: The dynamical transport of hydrocarbons in the stratosphere of Uranus
p 913 N93-14211
Physical and chemical processes of the inner coma observed in mid-ultraviolet cometary spectra
p 1017 N93-14230
Nonthermal radio, x ray and gamma ray emissions from chaotic winds of early-type, massive stars
p 1050 N93-14242
The effects of Venus' thermal structure on buoyant magma ascent p 1040 N93-14366
Ultraviolet spectroscopy of Comet Austin (1989c1) using a two-dimensional diode array detector
p 1017 N93-14444
The influence of geometrical constraint on cyclic, elastoplastic, notch root behavior, and fatigue microcrack initiation p 900 N93-14480

K

KANSAS UNIV., LAWRENCE.
The thermosphere and ionosphere of Venus
p 1026 N93-14307

KEELE UNIV. (ENGLAND).
A study of an optically pumped free-jet molecular iodine laser operating in the visible spectrum
p 884 N93-14141
Electrical conductivity measurements in evaporated cadmium telluride thin films p 865 N93-14191

KENT UNIV., CANTERBURY (ENGLAND).
Information resource utilisation: Accessibility based on concerns p 1001 N93-14216
Characterisation and dynamic modelling of the near-earth space particulate environment
p 1019 N93-14637

KLEIN ASSOICIATES, INC., FAIRBORN, OH.
A cognitive model for training decision making in aircrews p 786 N93-15020

KNUDSEN GEOPHYSICAL BRANCH, MONTE SERENO, CA.
Venus internal magnetic field and its interaction with the interplanetary magnetic field p 1032 N93-14336

KRUG LIFE SCIENCES, INC., SAN ANTONIO, TX.
Ultrashort-pulse laser system: Theory of operation and operating procedures
| AD-A257023 | p 887 N93-15472

L

LABORATOIRE D'OCEANOGRAPHIE DYNAMIQUE ET DE CLIMATOLOGIE, PARIS (FRANCE).
Study of mass and heat transport of the tropical Atlantic Ocean using models and altimeter data
p 929 N93-14983

LAMONT-DOHERTY GEOLOGICAL OBSERVATORY, PALISADES, NY.
Outgassing history of Venus and the absence of water on Venus p 1045 N93-14398

LAWRENCE LIVERMORE NATIONAL LAB., CA.
Optical monitor for observing turbulent flow
| DE92-019831 | p 876 N93-14715
Storage needs in future supercomputer environments
p 1003 N93-14780
Evaluation of a soil fixative to retard particle entrainment: A laboratory study
| UCRL-LR-109806 | p 915 N93-14877
Optical glasses for high-peak-power laser applications
| DE92-040403 | p 886 N93-14906
Storage needs in future supercomputer environments
p 1007 N93-15047
A correlated k-distribution model of the heating rates for CO2 and O3 in the atmosphere between 0 and 60 km
| DE93-000889 | p 911 N93-15280
A correlated k-distribution model of the atmospheric heating rates for overlapping spectra of CH4 and N2O
| DE93-000890 | p 911 N93-15281
Alpha migration through air filters: A numerical simulation
| UCRL-LR-109866 | p 878 N93-15285
Thermal analysis of magnetron sputtering designs
| DE93-000348 | p 870 N93-15389
Characteristics of the Nova laser disk edge cladding epoxy
| DE92-041046 | p 853 N93-15462
Mathematical software under UNICOS at LCC
| DE93-001828 | p 952 N93-15493

LEHIGH UNIV., BETHLEHEM, PA.
Long term stability in thin film ferroelectric memories
| AD-A256290 | p 991 N93-14439
The mixed mode crack problem in a nonhomogeneous elastic plane
| AD-A256469 | p 902 N93-15372
Diffusion problems in bonded nonhomogeneous materials with an interface cut
| AD-A256470 | p 836 N93-15373
The crack problem for an orthotropic half plane stiffened by elastic films
| AD-A256471 | p 903 N93-15374
White paper on the AFOSR Supermaneuverability Workshop
| AD-A256385 | p 782 N93-15464
Unsteady flow distortion past blades: Sources of noise generation in rotating flows
| AD-A255496 | p 880 N93-15652

LINCOLN UNIV., PA.
Far infrared, magnetic, and electronic studies of high T(sub c) superconducting materials
| AD-A257050 | p 996 N93-15444

LOCKHEED ENGINEERING AND SCIENCES CO., HAMPTON, VA.
Improved inhomogeneous finite elements for fabric reinforced composite mechanics analysis
p 834 N93-14757

LOCKHEED ENGINEERING AND SCIENCES CO., HOUSTON, TX.
STS-49: Space shuttle mission report
| NASA-TM-108104 | p 815 N93-14736

LOCKHEED MISSILES AND SPACE CO., PALO ALTO, CA.
NASA/LMSC instrument design and fabrication
p 784 N93-14846
NASA/LMSC coherent LIDAR airborne shear sensor: System capabilities and flight test plans
p 784 N93-14847
Radiation belt dynamic and quasi-static modeling based on CRRES data: Outer-belt short-term response data base
| AD-A256483 | p 916 N93-14899
Performance characteristics of STIS detectors
| NASA-CR-191636 | p 868 N93-14915

LOGISTICS MANAGEMENT INST., BETHESDA, MD.
EDI planning and implementation guide
| AD-A255737 | p 1007 N93-15050
A guide to EDI translation software
| AD-A255739 | p 1007 N93-15051

LONDON UNIV. (ENGLAND).
Autoradiographic distribution and applied pharmacological characteristics of dextromethorphan and related antitissue/anticonvulsant drugs and novel analogs
| AD-A255607 | p 935 N93-15009

LONDON UNIV. OBSERVATORY (ENGLAND).
Debris avalanches and slumps on the margins of volcanic domes on Venus: Characteristics of deposits
p 1025 N93-14300
Erosion versus construction: The origin of Venusian channels p 1025 N93-14303
Large-volume lava flow fields on Venus: Dimensions and morphology p 1033 N93-14339

LORAL DATA SYSTEMS, SARASOTA, FL.
Solid state flight data recorder with rapid data access
p 795 N93-15167

LORAL DEFENSE SYSTEMS, AKRON, OH.
Terrain visualization for the portable all-source analysis work station
| AD-A255708 | p 905 N93-14430

LORAL WESTERN DEVELOPMENT LABS., SAN JOSE, CA.
Parametric height field ray tracing p 955 N93-15556

LOS ALAMOS NATIONAL LAB., NM.
Workshop on noninvasive geophysical site characterization
| LA-12311-C | p 914 N93-14724
Preview of Blackbeard interferometry
| DE92-040329 | p 818 N93-14904
Thermodynamics and transport in Ce3Bi4Pt3 and related compounds
| DE92-040377 | p 998 N93-14905
Components and materials issues in polymer electrolyte fuel cells for transportation applications
| DE92-013384 | p 907 N93-15061
Laser-based studies with an ion-trap mass spectrometer: Ion tomography and analytical applications
| DE92-017529 | p 887 N93-15135
Infrared laboratory spectra and composition changes of synthetic amorphous silicate grains
| DE92-040211 | p 843 N93-15283
Compaction of submicron and nanocrystalline Al2O3-ZrO2 ceramics
| DE92-040233 | p 852 N93-15320
Normal state resistivity and the phase diagram of U(1-x)Th(x)Be13
| DE92-040236 | p 995 N93-15321
High-energy emissions from young pulsars: Perspective from the outer gap model
| DE92-040365 | p 1022 N93-15324
Acoustic resonance techniques for quality control
| DE92-040150 | p 895 N93-15413
High-brightness linac for the Advanced Free-Electron Laser Initiative at Los Alamos
| DE92-040213 | p 887 N93-15417
Accurate methods for calculating atomic processes in high temperature plasmas
| DE92-040215 | p 988 N93-15418
Exact analytical solution of the toroidal singular mode equations
| DE92-040223 | p 988 N93-15419
SCRUNCHER phase and amplitude control
| DE92-040225 | p 870 N93-15421
Progress on the development of a 2-D PIC/Monte Carlo model of glow discharges
| DE92-040226 | p 989 N93-15422
Calculation of mechanical vibration frequencies of stiffened superconducting cavities
| DE92-040228 | p 903 N93-15423
Design features of a seven-cell high-gradient superconducting cavity
| DE92-040229 | p 870 N93-15424
Sputter deposition and characterization of MoSi2/SiC composite coatings
| DE92-040326 | p 837 N93-15426
Deterministic transfer function for transionospheric propagation
| DE92-040327 | p 862 N93-15427
Satellite measurement of ionospheric-induced VHF distortion
| DE92-040328 | p 862 N93-15435
Electrical resistivity and equation of state measurements of a dense aluminum plasma
| DE92-040352 | p 989 N93-15436

LOUGHBOROUGH UNIV. OF TECHNOLOGY (ENGLAND).
Application of gel-silica optics to laser technology and optical element fabrication
| AD-A255666 | p 883 N93-14131
Boundary element analysis of low frequency cavity acoustical problems
| MATHS-REPT-A-158 | p 974 N93-15073

LOVELACE SCIENTIFIC RESOURCES, INC., ALBUQUERQUE, NM.
Advanced sensors technology survey
| NASA-CR-185691 | p 881 N93-14494

LUNAR AND PLANETARY INST., HOUSTON, TX.
Papers presented to the International Colloquium on Venus
| NASA-CR-190676 | p 1023 N93-14288

M

M-C POWER CORP., BURR RIDGE, IL.
Impact of protective oxides on cathode-side resistances in MCFCs
| DE92-019973 | p 994 N93-15221

MAINE UNIV., ORONO.
Measurement-based multipurpose cadastral systems
p 904 N93-14220

MALLINSON MAGNETICS, INC., CARLSBAD, CA.
Magnetic disk p 1004 N93-15029

MARTIN MARIETTA CORP., DENVER, CO.
Interplanetary Program to Optimize Simulated Trajectories (IPOST). Volume 3: Programmer's manual
[NASA-CR-189653-VOL-3-REV] p 815 N93-14730
Interplanetary program to optimize simulated trajectories (IPOST). Volume 4: Sample cases
[NASA-CR-189653-VOL-4] p 815 N93-14768
Interplanetary Program to Optimize Simulated Trajectories (IPOST). Volume 1: User's guide
[NASA-CR-189653-VOL-1-REV] p 815 N93-14794
TQM in a test environment p 823 N93-15620
MARTIN MARIETTA ENERGY SYSTEMS, INC., OAK RIDGE, TN.
Microwave processing of tantalum capacitor anodes
[DE92-017829] p 869 N93-15214
MARTIN MARIETTA ENERGY SYSTEMS, INC., PIKETON, OH.
Continuing engineering education for software engineering professionals
[DE92-019888] p 947 N93-15225
MARYLAND UNIV., COLLEGE PARK.
A survey of solar flare energetic particle abundances and energy spectra p 1048 N93-14135
Type 2 superstrings in curved D = 10 space-time: Dynamics of their massless fields and covariant quantization p 998 N93-14143
A study of viscous interaction effects on hypersonic waveriders p 778 N93-14160
Generation of broadly tunable, narrow bandwidth, and intense coherent vacuum ultraviolet radiation in rare gases p 980 N93-14167
Electronic, vibrational, and transport properties of conducting polymers p 847 N93-14170
Simulation of vapor compression heat pumps with solution circuits p 872 N93-14200
Electron-phonon interaction, transport and ultrafast processes in semiconductor microstructures
[AD-A255723] p 976 N93-14433
Geometric invariants and object recognition
[AD-A255317] p 943 N93-14546
Research in programming languages and software engineering
[AD-A256341] p 947 N93-15199
The trajectory analysis of bevel planetary gear trains
[DE92-040898] p 893 N93-15380
MASON AND HANGER-SILAS MASON CO., INC., AMARILLO, TX.
Management and minimization of photographic wastes at Pantex Plant
[MHSMP-92-01] p 910 N93-14739
MASSACHUSETTS GENERAL HOSPITAL, BOSTON.
Optical probes for laser induced shocks
[AD-A256092] p 884 N93-14284
MASSACHUSETTS INST. OF TECH., CAMBRIDGE.
Goals versus algorithms
[AD-A256106] p 942 N93-14237
Mixed-valence iron minerals on Venus: Fe(2+)-Fe(3+) oxides and oxy-silicates formed by surface-atmosphere interactions p 1025 N93-14301
Flexural analysis of uplifted rift flanks on Venus p 1027 N93-14314
Radar scattering properties of pancakelike domes on Venus p 1028 N93-14316
Estimates of elastic plate thicknesses beneath large volcanos on Venus p 1035 N93-14344
The gabbro-eclogite phase transition and the elevation of mountain belts on Venus p 1036 N93-14350
Dielectric surface properties of Venus p 1039 N93-14360
Geoid, topography, and convection-driven crustal deformation on Venus p 1042 N93-14376
Constraints on crustal rheology and age of deformation from models of gravitational spreading in Ishtar Terra, Venus p 1042 N93-14379
The tectonics of Venus: An overview p 1042 N93-14382
Organization of workshop on emerging technologies for in-situ processing
[AD-A255977] p 865 N93-14410
Compact free electron laser for medical applications
[AD-A256236] p 885 N93-14599
Mechanisms of forming intergranular microcracks and microscopic surface discontinuities in welds
[AD-A255371] p 845 N93-14740
The Orlando TDWR testbed and airborne wind shear date comparison results p 784 N93-14851
Experimental evaluation of candidate graphical microburst alert displays p 785 N93-14853
Systems issues in airborne Doppler radar/LIDAR certification p 785 N93-14855
Global ocean circulation by altimetry p 932 N93-15002
Interferometric measurement with squeezed light
[AD-A257065] p 984 N93-15458
Radar scene generation for tactical decision aids
[AD-A257069] p 863 N93-15495
Aspects of a parallel-architecture simulator
[AD-A256872] p 941 N93-15628
A distributed data-balanced dictionary based on the b-link tree
[AD-A256841] p 1009 N93-15639
MASSACHUSETTS INST. OF TECH., LEXINGTON.
A multiple-aperture multiple-beam EHF antenna for satellite communications
[AD-A256020] p 858 N93-14426
Terminal Doppler weather radar/low-level wind shear alert system integration algorithm specification, version 1.1
[AD-A255319] p 920 N93-14547
Solid state research
[AD-A256019] p 992 N93-14576
Parametric study of diffusion-enhancement networks for spatiotemporal grouping in real-time artificial vision
[AD-A256059] p 937 N93-14580
Neural network architectures for general image recognition
[AD-A256017] p 964 N93-15258
MASSACHUSETTS UNIV., AMHERST.
Derivation of surface properties from Magellan altimetry data p 1033 N93-14340
Wrinkle ridges on Venusian plains: Indicators of shallow crustal stress orientations at local and regional scales p 1034 N93-14343
MASSACHUSETTS UNIV., LOWELL.
Super-micro computer weather prediction model
[AD-A255668] p 918 N93-14153
MAX-PLANCK-INST. FUER PHYSIK UND ASTROPHYSIK, GARCHING (GERMANY).
Supervised selection of galaxy candidates from the IRAS PSC: The quality of the selection and the infrared properties of the galaxy candidates
[MPE-PREPRINT-216] p 1021 N93-15284
MAX-PLANCK-INST. FUER STROEMUNGSFORSCHUNG, GOETTINGEN (GERMANY).
An experimental investigation of base bleed effect on the wake turbulent structure behind a two-dimensional blunt model
[MPIS-9/1991] p 781 N93-15131
MAYA HEAT TRANSFER TECHNOLOGIES LTD., MONTREAL (QUEBEC).
Advances in TMG p 811 N93-14956
MCAT INST., SAN JOSE, CA.
Study of optical techniques for the Ames unitary wind tunnel. Part 5: Infrared imagery
[NASA-CR-191385] p 804 N93-14809
MCDONNELL AIRCRAFT CO., SAINT LOUIS, MO.
Advanced aeroservoelastic stabilization techniques for hypersonic flight vehicles
[NASA-CR-189702] p 802 N93-14811
MCGILL UNIV., MONTREAL (QUEBEC).
Is Ishtar Terra a thickened basaltic crust? p 1024 N93-14292
Constraints on the thermal evolution of Venus inferred from Magellan data p 1024 N93-14293
MECHANICAL TECHNOLOGY, INC., LATHAM, NY.
A feasibility assessment of magnetic bearings for free-piston Stirling space power converters
[NASA-CR-189135] p 891 N93-14916
MESA ARCHIVAL SYSTEMS, INC., BOULDER, CO.
Data archiving p 1005 N93-15035
MESSERSCHMITT-BOELKOW-BLOHM G.M.B.H., MUNICH (GERMANY).
Modeling limits of the EMV analysis program CONCEPT by example of the influence of a helicopter structure on a frame antenna
[MBB-UD-0614-92-PUB] p 863 N93-15487
METRUM INFORMATION STORAGE, HUNT VALLEY, MD.
Network accessible multi-terabyte archive p 1005 N93-15036
MIAMI UNIV., FL.
Plate tectonics from VLBI and SLR global data
[NASA-CR-191319] p 916 N93-14913
MICHIGAN STATE UNIV., EAST LANSING.
High temperature stability, interface bonding, and mechanical behavior in (beta)-NiAl and Ni3Al matrix composites with reinforcements modified by ion beam enhanced deposition
[DE92-014399] p 992 N93-14812
MICHIGAN UNIV., ANN ARBOR.
A study of mid-latitude 5577 A OI dayglow emissions p 913 N93-14199
Ethane ice haze in the upper atmosphere of Uranus p 1023 N93-14212
Applications of a constitutive equation for microstructural change in polymers p 848 N93-14222
Finite element models of laser welding p 888 N93-14226
A search for dead QSO's among nearby luminous galaxies p 1011 N93-14228
Optical signatures of cooling flows in isolated early-type galaxies p 1017 N93-14243
Simulation of unsteady inviscid flow on an adaptively refined Cartesian grid p 873 N93-14273
Damage location and model refinement for large flexible space structures using a sensitivity-based eigenstructure assignment method p 816 N93-14274
The numerical stability of nonlinear floating body calculations p 873 N93-14278
Methane measurement by the Pioneer Venus large probe neutral mass spectrometer p 1027 N93-14312
Transport in heterostructures and device in microwave and millimeter wave regimes
[AD-A255975] p 858 N93-14408
Dynamic behavior of a dense spray diffusion flame in a potential vortex p 839 N93-14463
Modeling of the thermal elasto-plastic behavior for composite materials using the homogenization method p 830 N93-14466
An integrated optimization environment for structural configuration design p 855 N93-14467
Large plastic deformations by sequential limit analysis: A finite element approach with applications in metal forming p 899 N93-14471
Analysis of CCD images of the coma of comet P/Halley
[NASA-CR-191384] p 1020 N93-14814
Development of a 500 GHz optoelectronic modulator using superconducting transmission lines
[AD-A257062] p 871 N93-15456
Failure of composite plates under static biaxial planar loading
[NASA-CR-191391] p 903 N93-15653
MICRONET, CELLE (GERMANY).
Personal computer based test- and emulation equipment for maintenance and ground support p 778 N93-15185
MIDWEST RESEARCH INST., GOLDEN, CO.
NREL photovoltaic subcontract reports: Abstracts and document control information
[DE92-016408] p 907 N93-14817
MINISTRY OF DEFENCE, LONDON (ENGLAND).
Royal Air Force experience of the Harrier information management system p 795 N93-15170
MINNESOTA UNIV., MINNEAPOLIS.
An analysis of the SCEX 3 ionospheric electron beam injection experiment p 912 N93-14177
Optical signal distribution schemes for millimeter phased array radar
[AD-A256262] p 858 N93-14437
Psychophysical analyses of perceptual representations
[AD-A255432] p 936 N93-14510
Arc-cathode interaction study
[NASA-CR-191356] p 867 N93-14721
Variational transition state theory
[DE92-040498] p 842 N93-14908
Theory of the electronic and structural properties of solid state oxides
[DE92-040499] p 993 N93-14909
The gamma ray spectrum resulting from pp interactions in quasars p 1051 N93-14917
MISSOURI UNIV., ROLLA.
Characterization of fiber reinforced phenolic composites p 828 N93-14142
An investigation of crack growth at interfaces in bimaterials and composites using a consistent shear-lag model p 896 N93-14187
MITRE CORP., BEDFORD, MA.
Airborne radar simulation with adaptive antenna techniques
[AD-A255460] p 859 N93-14488
The 1992 Summer SIGAda AIWG Workshop applications experiences and lessons learned panel message from the panel chair
[AD-A256188] p 962 N93-14519
Data storage and retrieval system p 1005 N93-15034
MONTANA STATE UNIV., BOZEMAN.
Quantum fluctuations in stimulated Raman scattering p 857 N93-14126
MOOIJ AND ASSOCIATES, OEGSTGEEST (NETHERLANDS).
Flight simulation leaves the ground p 778 N93-14616
MOSCOW STATE UNIV. (USSR).
Venus: Preliminary geologic mapping of northern Atla Regio p 1037 N93-14353
Venus: Preliminary geologic mapping of southern Beta Regio-northern Phoebe Regio p 1037 N93-14354
Venus: Geology of Beta Regio rift system p 1037 N93-14355
The geologic mapping of Venus using C-1 format: Sheets 75N254, 60N263 p 1041 N93-14375
MOTOREN- UND TURBINEN-UNION MUENCHEN G.M.B.H. (GERMANY).
RB 199 high pressure compressor stage 3 spin pit tests p 799 N93-14893

Engine technologies for future spaceplanes
| ETN-92-92732 | p 800 N93-15143
EJ 200 engine monitoring system: On- and off-board data capture, analysis, and management system
p 796 N93-15172
RB199 engine oil system failure diagnostics by comparison of measured and calculated oil consumption using the OLMOS on-board monitoring system
p 796 N93-15173
Modelling the engine temperature distribution between shut down and restart for life usage monitoring
p 796 N93-15177

MOUND LAB., MIAMISBURG, OH.
The sensitivity of energetic materials to friction, impact, and electrostatic stimuli
| DE92-041227 | p 855 N93-15478

N

NAGOYA UNIV. (JAPAN).
Electron acceleration by longitudinal electric field of a Gaussian laser beam
| DE92-526947 | p 887 N93-15296

NANSEN OCEAN AND REMOTE SENSING CENTER, SOLHEIMSVIK (NORWAY).
Ocean dynamics in the Nordic Seas using satellite altimetry p 930 N93-14988

NATIONAAL INST. VOOR KERNFYSICA EN HOGE ENERGIEFYSICA, AMSTERDAM (NETHERLANDS).
Quasars, galaxies, and pseudo-vacuum droplets
| NIKHEF-H/91-20 | p 1020 N93-14686

NATIONAL ACADEMY OF SCIENCES - NATIONAL RESEARCH COUNCIL, WASHINGTON, DC.
Body composition and physical performance
| AD-A255627 | p 938 N93-14161
Core support of the board on mathematical sciences
| AD-A255482 | p 968 N93-14787
Core support for the Board on Mathematical Sciences
| AD-A256333 | p 968 N93-15195

NATIONAL AERONAUTICAL LAB., BANGALORE (INDIA).
Indian experience in flight data readout and analysis
p 794 N93-15161

NATIONAL AERONAUTICS AND SPACE ADMINISTRATION, WASHINGTON, DC.
Impact craters on Venus: An overview from Magellan observations p 1040 N93-14369
Aerospace medicine and biology: A continuing bibliography with indexes (supplement 368)
| NASA-SP-7011(368) | p 934 N93-14603
Aeronautical engineering: A continuing bibliography with indexes (supplement 282)
| NASA-SP-7037(282) | p 777 N93-14604
Aeronautical engineering: A continuing bibliography with indexes (supplement 284)
| NASA-SP-7037(284) | p 777 N93-14605
Large space structures and systems in the space station era: A bibliography with indexes (supplement 04)
| NASA-SP-7085(04) | p 817 N93-14606
Work attachment mechanism/work attachment fixture
| NASA-CASE-GSC-13430-1 | p 890 N93-14712
Streamlined acquisition handbook
| NASA-TM-108133 | p 1002 N93-14719
Aerospace medicine and biology: A continuing bibliography with indexes (supplement 369)
| NASA-SP-7011(369) | p 935 N93-14731
Aeronautical engineering: A continuing bibliography with indexes (supplement 283)
| NASA-SP-7037(283) | p 778 N93-14732
Space Station Freedom user's guide
| NASA-TM-108105 | p 825 N93-15650

NATIONAL AERONAUTICS AND SPACE ADMINISTRATION. AMES RESEARCH CENTER, MOFFETT FIELD, CA.
Long-term variations in abundance and distribution of sulfuric acid vapor in the Venus atmosphere inferred from Pioneer Venus and Magellan radio occultation studies
p 1030 N93-14328
Finite amplitude gravity waves in the Venus atmosphere generated by surface topography p 1044 N93-14395
A voyage to Mars: A challenge to collaboration between man and machines p 777 N93-14614
Passive zero-gravity leg restraint
| NASA-CASE-ARC-11882-1-CU | p 939 N93-14713
Purposive discovery of operations
| NASA-TM-108116 | p 963 N93-14765
Shared mental models and crew decision making
p 787 N93-15023
Minimizing conflicts: A heuristic repair method for constraint-satisfaction and scheduling problems
| NASA-TM-108121 | p 964 N93-15286
Scheduling and rescheduling with iterative repair
| NASA-TM-108120 | p 965 N93-15287
Rescheduling with iterative repair
| NASA-TM-108119 | p 965 N93-15288
Learning to improve iterative repair scheduling
| NASA-TM-108118 | p 965 N93-15289
A beginner's guide to belief revision and truth maintenance systems
| NASA-TM-108117 | p 965 N93-15290
An application of artificial intelligence to automatic telescopes
| NASA-TM-108115 | p 965 N93-15291
MATE: The multi-agent test environment
| NASA-TM-108114 | p 965 N93-15292
Knowledge and regularity in planning
| NASA-TM-108113 | p 965 N93-15293
A global potential energy surface for ArH2
| NASA-CR-190741 | p 843 N93-15358
Space Station Freedom data management system growth and evolution report
| NASA-TM-103869 | p 816 N93-15477
The Applicaiton of CFD to rotary wing flow problems
| NASA-TM-102803 | p 782 N93-15483

NATIONAL AERONAUTICS AND SPACE ADMINISTRATION. GODDARD INST. FOR SPACE STUDIES, NEW YORK, NY.
Pioneer Venus polarimetry and haze optical thickness
p 1032 N93-14335

NATIONAL AERONAUTICS AND SPACE ADMINISTRATION. GODDARD SPACE FLIGHT CENTER, GREENBELT, MD.
Venus mesospheric winds and the carbon monoxide bulge p 1029 N93-14320
Mantle plumes on Venus revisited
p 1032 N93-14334
Driven shielding capacitive proximity sensor
| NASA-CASE-GSC-13377-1 | p 962 N93-14701
Compliant walker
| NASA-CASE-GSC-13348-2 | p 934 N93-14708
Retractable tool bit having slider type catch mechanism
| NASA-CASE-GSC-13358-1 | p 890 N93-14710
Electron density diagnostics for gaseous nebulae involving the O 4 intercombination lines near 1400 A
p 1012 N93-14762
NSSDC Conference on Mass Storage Systems and Technologies for Space and Earth Science Applications, volume 3
| NASA-CP-3165-VOL-3 | p 1002 N93-14771
The National Space Science Data Center: An operational perspective p 1002 N93-14775
EOSDIS/DADS requirements p 1003 N93-14776
Application of TOPEX/Poseidon altimetry to ocean dynamics and geophysics p 927 N93-14974
Sea level response to wind forcing in the tropical Atlantic p 928 N93-14977
Studies of tropical ocean dynamics using the TOPEX/Poseidon altimeter-derived sea surface topography p 928 N93-14980
Ocean topography mapping, improvement of the marine geoid, and global permanent ocean circulation studies from TOPEX/Poseidon altimeter data p 928 N93-14981
Application of TOPEX/Poseidon altimetry measurements to observational and modeling studies of the low-frequency upper ocean mass and heat circulation in the tropical Pacific p 930 N93-14989
Global ocean tide mapping using TOPEX/Poseidon altimetry p 930 N93-14991
Proceedings of the NSSDC Conference on Mass Storage Systems and Technologies for Space and Earth Science Applications
| NASA-TM-107989 | p 1004 N93-15027
The National Space Science Data Center: An operational perspective p 1006 N93-15045
Flight dynamics system software development environment (FDS/SDE) tutorial
| NASA-TM-108580 | p 952 N93-15502
Output data formatter for the Electronically Scanned Thinned Array Radiometer (ESTAR) instrument
| NASA-TM-4432 | p 871 N93-15529
Software Management Environment (SME) installation guide
| NASA-TM-108578 | p 957 N93-15578
Data collection procedures for the Software Engineering Laboratory (SEL) database
| NASA-TM-108579 | p 957 N93-15579
The Seventeenth Space Simulation Conference. Terrestrial Test for Space Success
| NASA-CP-3181 | p 819 N93-15593
Vibration and acoustic testing of TOPEX/Poseidon satellite p 820 N93-15599
SeaWiFS Technical Report Series. Cloud screening for polar orbiting visible and infrared (IR) satellite sensors, volume 7
| NASA-TM-104566 | p 932 N93-15645

NATIONAL AERONAUTICS AND SPACE ADMINISTRATION. HUGH L. DRYDEN FLIGHT RESEARCH FACILITY, EDWARDS, CA.
Pressure distribution for the wing of the YAV-8B airplane; with and without pylons
| NASA-TM-4429 | p 779 N93-14451
Real-time in-flight engine performance and health monitoring techniques for flight research application
p 795 N93-15169

NATIONAL AERONAUTICS AND SPACE ADMINISTRATION. JOHN C. STENNIS SPACE CENTER, BAY SAINT LOUIS, MS.
The dynamics and energetics of midlatitude western boundary currents: A comparison of the Kuroshio Extension and the Gulf Stream p 929 N93-14985

NATIONAL AERONAUTICS AND SPACE ADMINISTRATION. LYNDON B. JOHNSON SPACE CENTER, HOUSTON, TX.
Facilities and capabilities catalog for landing and escape systems
| NASA-RP-1282 | p 814 N93-14495
Thruster sealing system and apparatus
| NASA-CASE-MSC-21898-1 | p 890 N93-14702
System for memorizing maximum values
| NASA-CASE-MSC-21922-1 | p 882 N93-14841
Extra-vehicular activity translation tool
| NASA-CASE-MSC-21955-1 | p 891 N93-14842
High-temperature, high-pressure oxygen metering valve
| NASA-CASE-MSC-21823-1 | p 891 N93-14843
Bearing servicing tool
| NASA-CASE-MSC-21881-1 | p 891 N93-14871
Emittance measurements of Space Shuttle orbiter reinforced carbon-carbon
| NASA-TP-3293 | p 903 N93-15530
Manned testing in a simulated space environment
p 820 N93-15602

NATIONAL AERONAUTICS AND SPACE ADMINISTRATION. LANGLEY RESEARCH CENTER, HAMPTON, VA.
The preliminary Long Duration Exposure Facility (LDEF) materials data base
| NASA-TM-107692 | p 828 N93-14459
Reliability of stiffened structural panels: Two examples
| NASA-TM-107687 | p 900 N93-14483
Recent advances in numerical simulation and control of asymmetric flows around slender bodies
| PAPER-W.1.2 | p 875 N93-14688
Shock/vortex interaction and vortex-breakdown modes
| PAPER-T.1.3 | p 875 N93-14689
Three-dimensional computational study of asymmetric flows using Navier-Stokes equations
| ISBN-90-5410-029-X | p 875 N93-14690
Numerical simulation of steady and unsteady asymmetric vortical flow p 876 N93-14691
Passive control of supersonic asymmetric vortical flows around cones p 876 N93-14692
Method of characterizing residual stress in ferromagnetic materials using a pulse histogram of acoustic emission signals
| NASA-CASE-LAR-14239-1 | p 845 N93-14705
Low toxicity high temperature PMR polyimide
| NASA-CASE-LAR-14639-1 | p 849 N93-14709
Method of forming a multiple layer dielectric and a hot film sensor therewith
| NASA-CASE-LAR-13678-3 | p 881 N93-14714
FIBER-TEX 1991: The Fifth Conference on Advanced Engineering Fibers and Textile Structures for Composites
| NASA-CP-3176 | p 832 N93-14744
Development of generalized 3-D braiding machines for composite preforms p 833 N93-14749
Airborne Wind Shear Detection and Warning Systems. Fourth Combined Manufacturers' and Technologists' Conference, part 2
| NASA-CP-10105-PT-2 | p 783 N93-14844
Two micron laser development for atmospheric remote sensing at NASA Langley Research Center
p 784 N93-14845
Optimal active vibration absorber: Design and experimental results
| NASA-TM-107709 | p 902 N93-15202
Simulator evaluation of displays for a revised takeoff performance monitoring system
| NASA-TP-3270 | p 803 N93-15366
Aspects of parking orbit selection in a manned Mars mission
| NASA-TP-3256 | p 813 N93-15367
Structurally adaptive space crane concept for assembling space systems on orbit
| NASA-TP-3307 | p 818 N93-15368
Unsteady pressure loads in a generic high speed engine model
| NASA-TP-3189 | p 975 N93-15391

Finite-difference solution for laminar or turbulent boundary layer flow over axisymmetric bodies with ideal gas, CF4, or equilibrium air chemistry
[NASA-TP-3271] p 879 N93-15434
On explicit algebraic stress models for complex turbulent flows
[NASA-CR-189725] p 879 N93-15481
Cloud fraction, layer, and direction of movement results from sky cameras during the FIRE IFO, Coffeyville, Kansas, experiment for the period Nov. 12 through Dec. 9, 1991
[NASA-TM-107647] p 924 N93-15501
LDEF: A bibliography with abstracts
[NASA-TM-107705] p 813 N93-15646

NATIONAL AERONAUTICS AND SPACE ADMINISTRATION. LEWIS RESEARCH CENTER, CLEVELAND, OH.
An algebraic turbulence model for three-dimensional viscous flows
[NASA-TM-105931] p 777 N93-14102
Current status of liquid sheet radiator research
[NASA-TM-105764] p 872 N93-14150
Development of braided rope seals for hypersonic engine applications: Flow modeling
[NASA-TM-105942] p 888 N93-14478
Closed Brayton Cycle power system with a high temperature pellet bed reactor heat source for NEP applications
[NASA-TM-105933] p 826 N93-14482
Method of applying a thermal barrier coating system to a substrate
[NASA-CASE-LEW-15020-2] p 832 N93-14706
Supersonic boundary-layer flow turbulence modeling
[NASA-TM-105893] p 877 N93-14758
Estimation of unsteady lift on a pitching airfoil from wake velocity surveys
[NASA-TM-105947] p 781 N93-14791
Bibliography of Lewis Research Center Technical Publications announced in 1991
[NASA-TM-105595] p 1004 N93-14796
Second order closure modeling of turbulent buoyant wall plumes
[NASA-TM-105956] p 877 N93-14829
Icing effects on aircraft stability and control determined from flight data: Preliminary results
[NASA-TM-105977] p 803 N93-14831
Energy loss analysis of an integrated space power distribution system
[NASA-TM-105772] p 854 N93-14834
Apparatus for checking threaded hole perpendicularity
[NASA-CASE-LEW-15444-1] p 882 N93-14840
Preconditioned conjugate-gradient methods for low-speed flow calculations
[NASA-TM-105929] p 877 N93-14885
Comments on 'Kinetic Study on the Hexacelsian-Celsian Phase Transformation'
[NASA-TM-105917] p 850 N93-14886
Results of low power deicer tests on a swept inlet component in the NASA Lewis icing research tunnel
[NASA-TM-105968] p 781 N93-14911
Numerical study of mixing of two fluids under low gravity
[NASA-TM-105865] p 878 N93-14914
Surface roughness due to residual ice in the use of low power deicing systems
[NASA-TM-105971] p 782 N93-15338
Eno-Osher schemes for Euler equations
[NASA-TM-105928] p 969 N93-15341
Supersonic investigation of two dimensional hypersonic exhaust nozzles
[NASA-TM-105687] p 800 N93-15342
Root damage analysis of aircraft engine blade subject to ice impact
[NASA-TM-105779] p 902 N93-15343
Leveling coatings for reducing the atomic oxygen defect density in protected graphite fiber epoxy composites
[NASA-TM-105732] p 852 N93-15344
Numerical modeling of anti-icing systems and comparison to test results on a NASA 0012 airfoil
[NASA-TM-105975] p 787 N93-15345
Ice accretion and performance degradation calculations with LEWICE/NS
[NASA-TM-105972] p 787 N93-15354
Use of surface heat transfer measurements as a flow separation diagnostic in a two dimensional reflected oblique shock/turbulent boundary layer interaction
[NASA-TM-105981] p 879 N93-15355
Optimization of circular orifice jets mixing into a heated cross flow in a cylindrical duct
[NASA-TM-105984] p 800 N93-15359
Close-up analysis of aircraft ice accretion
[NASA-TM-105952] p 787 N93-15360
Closed form expressions for crack mouth displacements and stress intensity factors for chevron notched short bar and short rod specimens based on experimental compliance measurements
[NASA-TM-83796] p 902 N93-15369
Acoustic mode measurements in the inlet of a model turbofan using a continuously rotating rake: Data collection/analysis techniques
[NASA-TM-105936] p 801 N93-15403
An overview of shed ice impact in the NASA Lewis Icing Research Tunnel
[NASA-TM-105969] p 782 N93-15404
Nucleate pool boiling in the long duration low gravity environment of the Space Shuttle
[NASA-TM-105973] p 855 N93-15420
Development of NASA/DOE NTP system performance models
[NASA-TM-105982] p 827 N93-15428
Ion thruster development at NASA Lewis Research Center
[NASA-TM-105983] p 827 N93-15429
Computation of supersonic jet noise under imperfectly expanded conditions
[NASA-TM-105961] p 975 N93-15430
User manual for NASA Lewis 10 by 10 foot supersonic wind tunnel
[NASA-TM-105626] p 804 N93-15498
On the nonlinear three dimensional instability of Stokes layers and other shear layers to pairs of oblique waves
[NASA-TM-105918] p 880 N93-15499
EMTP based stability analysis of space station electric power system in a test bed environment
[NASA-TM-105845] p 871 N93-15503
Simplified jet-A kinetic mechanism for combustor application
[NASA-TM-105940] p 844 N93-15504
An integral equation solution for multistage turbomachinery design calculations
[NASA-TM-105970] p 801 N93-15521
Ice accretion prediction for a typical commercial transport aircraft
[NASA-TM-105976] p 788 N93-15522
Power requirements for the first lunar outpost (FLO)
[NASA-TM-105925] p 909 N93-15523
Processing and microstructure of Nb-1 percent Zr-0.1 percent C alloy sheet
[NASA-TM-105921] p 847 N93-15524
Propulsion system performance resulting from an integrated flight/propulsion control design
[NASA-TM-105874] p 801 N93-15525
Summary of the NASA Lewis component technology program for Stirling power converters
[NASA-TM-105640] p 827 N93-15526
Aerothermodynamic flow phenomena of the airframe-integrated supersonic combustion ramjet
[NASA-TM-4376] p 827 N93-15528
User's guide for a large signal computer model of the helical traveling wave tube
[NASA-TP-3251] p 871 N93-15531
Nuclear thermal rocket nozzle testing and evaluation program
[NASA-TM-105962] p 827 N93-15571
Low thrust chemical rocket technology
[NASA-TM-105927] p 827 N93-15572
Vibration isolation technology: An executive summary of systems development and demonstration
[NASA-TM-105937] p 778 N93-15573
Propagation of high frequency jet noise using geometric acoustics
[NASA-TM-105950] p 975 N93-15575
The effect of processing and compositional changes on the tribology of PM212 in air
[NASA-TM-105945] p 828 N93-15576
Turbulent fluid motion IV-averages, Reynolds decomposition, and the closure problem
[NASA-TM-105822] p 880 N93-15585
Progress toward a tungsten alloy wire/high temperature alloy composite turbine blade
[NASA-TM-105901] p 847 N93-15586
Low Earth orbit atomic oxygen simulation for durability evaluation of solar reflector surfaces
p 819 N93-15594
Simulation of the synergistic low Earth orbit effects of vacuum thermal cycling, vacuum UV radiation, and atomic oxygen p 819 N93-15595
The use of plasma ashers and Monte Carlo modeling for the projection of atomic oxygen durability of protected polymers in low Earth orbit p 819 N93-15596
Leveling coatings for reducing the atomic oxygen defect density in protected graphite fiber epoxy composites
p 819 N93-15597
Degradation of radiator performance on Mars due to dust p 823 N93-15616

NATIONAL AERONAUTICS AND SPACE ADMINISTRATION. MARSHALL SPACE FLIGHT CENTER, HUNTSVILLE, AL.
Crystal growth in a microgravity environment
[NASA-CASE-MFS-28473-1] p 992 N93-14707
X-ray monochromator
[NASA-CASE-MFS-28392-1] p 982 N93-14711
Bar-holding prosthetic limb
[NASA-CASE-MFS-28481-1] p 939 N93-14870
Imaging the sun in hard x rays using Fourier telescopes
[NASA-TM-108390] p 1013 N93-15203
A plan for spacecraft automated rendezvous
[NASA-TM-108385] p 813 N93-15392
An overview of reliability growth models and their potential use for NASA applications
[NASA-TP-3309] p 895 N93-15433
Study of the glass formation of high temperature superconductors
[NASA-TM-108389] p 997 N93-15500
On the variation of the Nimbus 7 total solar irradiance
[NASA-TP-3316] p 1049 N93-15532

NATIONAL AERONAUTICS AND SPACE ADMINISTRATION. PASADENA OFFICE, CA.
Real-time edge-enhanced optical correlator
[NASA-CASE-NPO-18521-1-CU] p 981 N93-14404
Core design for use with precision composite reflectors
[NASA-CASE-NPO-17858-1-CU] p 832 N93-14700
Multiperiod-grating surface-emitting lasers
[NASA-CASE-NPO-17763-1-CU] p 885 N93-14703
High speed magneto-resistive random access memory
[NASA-CASE-NPO-17954-1-CU] p 940 N93-14704
Modified fast frequency acquisition via adaptive least squares algorithm
[NASA-CASE-NPO-17845-2-CU] p 945 N93-14882
Epitaxial heterojunctions of oxide semiconductors and metals on high temperature superconductors
[NASA-CASE-NPO-18483-1-CU] p 994 N93-15151

NATIONAL AEROSPACE LAB., AMSTERDAM (NETHERLANDS).
Symposium on the occasion of the farewell of Prof. Dr. Ir. O. H. Gerlach as Chairman of the Board of the Foundation National Aerospace Laboratory NLR, The Netherlands
[ETN-92-92168] p 777 N93-14613

NATIONAL ARCHIVES AND RECORDS SERVICE, WASHINGTON, DC.
The long hold: Storing data at the National Archives
p 1004 N93-15031

NATIONAL CENTER FOR ATMOSPHERIC RESEARCH, BOULDER, CO.
TDWR 1991 Program Review p 785 N93-14852
Mass storage system experiences and future needs at the National Center for Atmospheric Research
p 1007 N93-15046

NATIONAL COMPUTER GRAPHICS ASSOCIATION, FAIRFAX, VA.
Proceedings of the International Conference on CAD/CAM and AMT. Volume 4: VHDL (VHSIC Hardware Description Language) Seminar
[ITN-92-85130] p 947 N93-15261
Proceedings of the International Conference on CAD/CAM and AMT. Volume 3: IFIP (International Federation of Information Processing)/Robotics: International Sessions on Robots and Assembly
[ITN-92-85129] p 949 N93-15298

NATIONAL INST. OF STANDARDS AND TECHNOLOGY, GAITHERSBURG, MD.
Twin quintuplets in CVD diamond
[AD-A255862] p 989 N93-14133
Flow behavior in liquid molding p 833 N93-14747
Status of emerging standards for removable computer storage media and related contributions of NIST
p 1003 N93-14778
A fundamental understanding of the effects of ceramic processing on product microstructure
[AD-A255729] p 850 N93-15049
Research for electric energy systems
[DE92-040076] p 870 N93-15412
Predictions of dose from electrons in space
[NASA-CR-191617] p 1051 N93-15580

NATIONAL MEDIA LAB., SAINT PAUL, MN.
Stability of Co-gamma-Fe2O3 tape
p 1006 N93-15041

NATIONAL OCEANIC AND ATMOSPHERIC ADMINISTRATION, SUITLAND, MD.
Data management in NOAA p 1003 N93-14779

NATIONAL PARACHUTE TECHNOLOGY COUNCIL, ALBUQUERQUE, NM.
Facilities and capabilities catalog for landing and escape systems
[NASA-RP-1282] p 814 N93-14495

NATIONAL PHYSICAL LAB., TEDDINGTON (ENGLAND).
Software stamping
[NPL-DITC-198/92] p 946 N93-15072

NATIONAL RESEARCH INST. FOR OCEANOLOGY, STELLENBOSCH (SOUTH AFRICA).
South African TOPEX/Poseidon altimeter experiment
p 928 N93-14976

NATIONAL SCIENCE FOUNDATION, WASHINGTON, DC.
A planning workshop: To strengthen American cognitive science for the twenty-first century
| NSF-92-4 | p 999 N93-14720
Antarctic news clips - 1992
| NSF-92-83 | p 916 N93-15080

NATIONAL TRANSPORTATION SAFETY BOARD, WASHINGTON, DC.
Special investigation report: Piper Aircraft Corporation PA-46 Malibu/Mirage Accidents/Incident, 31 May 1989 - 17 March 1991
| PB92-917007 | p 788 N93-15577

NATIONAL TSING HUA UNIV., HSINCHU (TAIWAN).
Digital caustic investigation of near surface cracks under transient thermal loading p 897 N93-14217

NAVAL AIR DEVELOPMENT CENTER, WARMINSTER, PA.
Thermal fatigue analysis of metal matrix composite with spherical reinforcements
| AD-A255313 | p 831 N93-14672
Modeling of Euclidean braided fiber architectures to optimize composite properties p 834 N93-14755

NAVAL AIR WARFARE CENTER, PATUXENT RIVER, MD.
Standardization of precipitation static test methods and equipment for the Navy
| AD-A257025 | p 792 N93-15361
F/A-18 controls released departure recovery flight test evaluation
| AD-A256522 | p 803 N93-15396

NAVAL AIR WARFARE CENTER, WARMINSTER, PA.
HIP consolidation of aluminum-rich intermetallic alloys and their composites
| NAWCADWAR-92003-60 | p 845 N93-14726
Statistical analysis of the human strangulation experiments: Comparison to +Gz-induced loss of consciousness
| AD-A255485 | p 935 N93-14789
A neural network prototype for predicting F-14B strains at the B.L. 10 longeron
| AD-A255272 | p 792 N93-15004
Stress corrosion susceptibility of ultra-hi; strength steels for Naval aircraft applications
| AD-A256126 | p 846 N93-15189

NAVAL BIODYNAMICS LAB., NEW ORLEANS, LA.
Bibliography of scientific publications of the Naval Biodynamics Laboratory
| AD-A255952 | p 1051 N93-14657

NAVAL COMMAND, CONTROL AND OCEAN SURVEILLANCE CENTER, SAN DIEGO, CA.
Optical fibers for long-haul transmission in severe-bending applications
| AD-A255964 | p 981 N93-14407
A general observation matrix for attitude error estimation with an offset GPS antenna
| AD-A255214 | p 789 N93-14574
Analysis of OSPREY processes and conventional power aluminum alloys
| AD-A255764 | p 846 N93-15056

NAVAL HEALTH RESEARCH CENTER, SAN DIEGO, CA.
Sleep inertia: Is there a worst time to wake up?
| AD-A256602 | p 934 N93-14240

NAVAL OCEANOGRAPHIC AND ATMOSPHERIC RESEARCH LAB., BAY SAINT LOUIS, MS.
Altimeter and oceanographic in situ measurements in the area of the Greenland-Iceland-Norwegian Sea, 1987-1988
| AD-A256598 | p 960 N93-14239
Investigation of the use of surface electrical currents for short-range shipboard data communications
| AD-A256197 | p 859 N93-14490
Advanced development active model: A users guide
| AD-A255614 | p 974 N93-15012

NAVAL POSTGRADUATE SCHOOL, MONTEREY, CA.
Audio detection algorithms
| AD-A256076 | p 973 N93-14234
Weight optimum arch structures
| AD-A256080 | p 897 N93-14236
Development of a MATLAB toolbox for image processing
| AD-A256130 | p 942 N93-14247
Experimental and analytical investigation of the vibration characteristics of a remotely piloted helicopter
| AD-A256131 | p 790 N93-14248
Evaluation of the cost effectiveness analysis model being developed for the component improvement programs of the Air Force and the Navy
| AD-A256132 | p 1010 N93-14249
Parallelization of the Navy Space Surveillance Center (NAVSPASUR) satellite model
| AD-A256133 | p 816 N93-14253
Extended surface heat sinks for electronic components: A computer optimization
| AD-A256134 | p 865 N93-14254
The use of chaos metrics to analyze Lagrangian particle diffusion models
| AD-A256142 | p 967 N93-14255
Experimental considerations of higher order parametric x rays from silicon crystals of varying thicknesses
| AD-A256082 | p 990 N93-14260
Satellite detection of complex aerosols over the Arabian Peninsula/Gulf
| AD-A256085 | p 909 N93-14261
Effects of water vapor and anisotropic scattering on aerosol optical depth retrieval
| AD-A256087 | p 904 N93-14262
Improved aerosol optical depth and particle size index from satellite detected radiance
| AD-A256089 | p 904 N93-14263
Design, development, and testing of a prototype optical system for a next generation multiplexed imager
| AD-A256538 | p 981 N93-14286
Iterative software testing
| AD-A255953 | p 943 N93-14420
A complete-time approach for chaining and execution control in the AN/UYS-2 parallel signal processor
| AD-A256306 | p 859 N93-14442
Optimum pose measurements for kinematic parameters identification
| AD-A256307 | p 970 N93-14443
An energy analysis of the pseudo Wigner-Ville distribution in support of machinery monitoring and diagnostics
| AD-A256202 | p 889 N93-14499
The use of International Standards Organization ISO 9000 quality assurance standards in place of military standards
| AD-A256203 | p 894 N93-14500
Computer based satellite design
| AD-A255315 | p 816 N93-14536
Monte Carlo analysis of energy deposition in solid state materials by 400 and 200 MeV electrons
| AD-A255335 | p 991 N93-14537
The V-22 Osprey: A case analysis
| AD-A256445 | p 791 N93-14601
Introduction to real orthogonal polynomials
| AD-A256448 | p 968 N93-14609
Modeling and control of a trailing wire antenna towed by an orbiting aircraft
| AD-A256450 | p 859 N93-14610
A proposal to apply Taguchi-inspired methods to the reduction of machining variance
| AD-A256129 | p 856 N93-15234
Effect of thermomechanical treatments on the aging response of centrifugally cast silicon carbide/aluminum composites
| AD-A256204 | p 836 N93-15236
Radar data processing using a distributed computational system
| AD-A256209 | p 861 N93-15237
Analysis of in-flight structural failures of P-3C wing leading edge segments
| AD-A256212 | p 792 N93-15238
Flowfield study of a close-coupled canard configuration
| AD-A256311 | p 782 N93-15245
Prediction of turbine cascade flows with a quasi-three-dimensional rotor viscous code and the extension of the algebraic turbulence model
| AD-A256831 | p 880 N93-15635
A mixed excitation vocoder with fuzzy logic classifier
| AD-A256834 | p 864 N93-15636
Upgrade and extension of the data acquisition system for propulsion and gas dynamic laboratories
| AD-A256836 | p 1009 N93-15637

NAVAL RESEARCH LAB., WASHINGTON, DC.
Conditioning electron beams in the ion-focused regime
| AD-A255635 | p 978 N93-14127
Multi-access strategies for voice/data integration in heterogeneous mixed-media packet radio networks
| AD-A255636 | p 857 N93-14181
On the detection of ultrawideband radar signals
| AD-A256075 | p 858 N93-14233
Nonlinear modeling of gated range tracker dynamics with application to radar range resolution, phase 1
| AD-A256074 | p 858 N93-14259
Beam trapping in a modified betatron with a localized bipolar electric field pulse
| AD-A255414 | p 866 N93-14504
Numerical modelling of intense electron beam transport in the spiral line induction accelerator
| AD-A255545 | p 978 N93-14570
Opacity, equation of state, and radiation transport model for moderate density, eV-temperature plasmas
| AD-A256056 | p 988 N93-14579
Current neutralization in ballistic transport of light ion beams
| AD-A256070 | p 976 N93-14662
System design and development of a low data rate voice (1200 bps) rate converter
| AD-A256071 | p 859 N93-14663
Four-dimensional data assimilation of gale data using a multivariate analysis scheme and a mesoscale model with diabatic initialization
| AD-A256063 | p 921 N93-14680
Software requirements for the A-7E aircraft
| AD-A255746 | p 946 N93-15052
Conversion of IRAMMP data to HDF format
| AD-A256515 | p 1008 N93-15393

NAVAL SAFETY CENTER, NORFOLK, VA.
Trans-cockpit authority gradient in Navy/Marine aircraft mishaps p 786 N93-15016

NAVAL SURFACE WARFARE CENTER, BETHESDA, MD.
The effect of a seawater environment on the galvanic corrosion behavior of graphite/epoxy composites coupled to metals
| AD-A256072 | p 830 N93-14232
Kind-band failure analysis of thick composites in compression
| AD-A255431 | p 831 N93-14509

NAVAL SURFACE WARFARE CENTER, DAHLGREN, VA.
Ada-based multitasking terminal I/O
| AD-A255656 | p 942 N93-14164
Use of kinematic constraint in tracking constant speed maneuvering targets
| AD-A255988 | p 858 N93-14415
Evaluation of corrosion protection methods for aluminum metal matrix composites
| AD-A255375 | p 832 N93-14675

NAVAL SURFACE WARFARE CENTER, SILVER SPRING, MD.
Systems modeling
| AD-A255215 | p 944 N93-14575
Mission critical system development: Design views and their integration
| AD-A255498 | p 940 N93-14644
Engineering of massively interconnected computer systems
| AD-A255501 | p 958 N93-14645

NAVY PERSONNEL RESEARCH AND DEVELOPMENT CENTER, SAN DIEGO, CA.
Long term memory for different types of classroom knowledge
| AD-A255235 | p 999 N93-14526

NETWORK SYSTEMS CORP., VIENNA, VA.
The role of HiPPI switches in mass storage systems: A five year prospective p 1002 N93-14774
The role of HiPPI switches in mass storage systems: A five year prospective p 1006 N93-15044

NEVADA UNIV., RENO.
CCN spectra measurements as an active tracer of stratocumulus mechanisms
| AD-A255678 | p 920 N93-14258
Wave drag in the atmospheric boundary layer p 915 N93-14873
On the role of water growth in atmospheric aerosol p 922 N93-14875
Sierra Nevada winter storms: A study using microwave radiometry, ice crystal, and isotopic analysis technique p 923 N93-15088

NEW HAMPSHIRE UNIV., DURHAM.
Fine structure of auroral particle acceleration p 912 N93-14121
Resonance absorption of MHD surface waves with applications to the solar atmosphere p 1048 N93-14157
Solar flares: The onset of magnetic reconnection and the structure of radiative slow-mode shocks p 1048 N93-14859
Theoretical studies of the physics of the solar atmosphere
| NASA-CR-191357 | p 1049 N93-15085

NEW MEXICO STATE UNIV., LAS CRUCES.
On the performance of Trellis coded modulation with octal phase shift keying over the TDRSS channel
| NASA-CR-191366 | p 857 N93-14155
High-speed architecture for the decoding of trellis-coded modulation
| NASA-CR-191374 | p 941 N93-14770

NEW MEXICO STATE UNIV., UNIVERSITY PARK.
Orbital coplanarity in solar-type binary systems: Implications for planetary system formation and detection p 1020 N93-14867

NEW MEXICO UNIV., ALBUQUERQUE.
Fast optoelectronic switching processes in surface-emitting semiconductor lasers and nonlinear etalons
| AD-A255802 | p 886 N93-15069

Optoelectronics material center: A collaborative program including center for high technology materials of the University of New Mexico, Stanford University, California Institute of Technology
[AD-A256005] p 886 N93-15115

NEW YORK UNIV., NEW YORK.
Neuromagnetic investigations of cortical regions underlying short-term memory
[AD-A255788] p 937 N93-14646
Cognition and the brain
[AD-A255483] p 937 N93-14788
Biophysical and biochemical mechanisms in synaptic transmitter release
[AD-A256340] p 936 N93-15198
Higher order mechanisms of color vision
[AD-A256369] p 938 N93-15329

NORTH CAROLINA AGRICULTURAL AND TECHNICAL STATE UNIV., GREENSBORO.
Tensile properties of textile composites p 834 N93-14754
Microstructure-failure mode correlations in braided composites p 834 N93-14756
Improved inhomogeneous finite elements for fabric reinforced composite mechanics analysis p 834 N93-14757

NORTH CAROLINA STATE UNIV., RALEIGH.
Four-dimensional data assimilation of GALE data using a multivariate analysis scheme and a mesoscale model with diabatic initialization p 919 N93-14198
Exploiting similarity in turbulent shear flows for turbulence modeling
[NASA-CR-191621] p 875 N93-14481
Advances in 3-dimensional braiding p 833 N93-14748
A theoretical search for supervelocity semiconductors
[AD-A256325] p 994 N93-15191
Growth, characterization and device development in monocrystalline diamond films
[AD-A256283] p 994 N93-15244

NORTHEST SUSTAINABLE ENERGY ASSOCIATION, GREENFIELD, MA.
S/EV 1991: Solar and Electric Vehicle Symposium, Car and Trade Show
[DE92-019890] p 869 N93-15226

NORTHWEST AIRLINES, INC., SAINT PAUL, MN.
Results of in-service evaluation of wind shear systems p 785 N93-14856

NORTHWEST RESEARCH ASSOCIATES, INC., BELLEVUE, WA.
New methods for nonlinear tracking and nonlinear chaotic signal processing
[AD-A256421] p 862 N93-15334

NORTHWESTERN UNIV., EVANSTON, IL.
Experimental and theoretical investigation of surface chemistry induced by direct and indirect electronic excitation
[AD-A256342] p 843 N93-15200
Strong interactions studies with medium energy probes
[DE92-040460] p 977 N93-15377

NORTON CO., NORTHBORO, MA.
Tribology of improved transformation-toughened ceramics-heat engine test
[DE92-041385] p 851 N93-15295
Material development in the Si3N4 system using glass encapsulated HIP'ing
[DE92-041381] p 837 N93-15388
Processing of sinterable transformation toughened ceramics for application in ceramic technology for advanced heat engines project
[DE92-041372] p 853 N93-15453
Analytical and experimental evaluation of joining silicon carbide to silicon carbide and silicon nitride to silicon nitride for heat engine applications
[DE92-041376] p 837 N93-15454

NORWEGIAN DEFENCE RESEARCH ESTABLISHMENT, KJELLER.
Sonar processing on CESAR
[FFI-92/7007] p 974 N93-15074

NOTRE DAME UNIV., IN.
Wake similarity and vortex formation for two-dimensional bluff bodies p 781 N93-15101

NOVA UNIV., DANIA, FL.
Mixed-layer parameterization in models of the Indian Ocean
[AD-A255937] p 925 N93-14428

NSI TECHNOLOGY SERVICES CORP., GREENBELT, MD.
Application of programmable logic controllers to space simulation p 821 N93-15608
From diffusion pumps to cryopumps: The conversion of GSFC's space environment simulator p 814 N93-15611
Cleaning of a thermal vacuum chamber with shrouds in place p 814 N93-15612

O

OAK RIDGE K-25 SITE, TN.
Automated Estimating System (AES), version 5.1. User's manual
[DE93-000380] p 946 N93-15003
Automated Estimated System (AES) standard value and guidelines programs user's manual
[DE92-041243] p 951 N93-15450

OAK RIDGE NATIONAL LAB., TN.
Cesium iodide alloys
[DE92-019818] p 845 N93-14717
Sensor-based driving of a car with fuzzy inferencing VLSI chips and boards
[DE92-017819] p 963 N93-14818
A Unix print filter for controlling an HP Laserjet printer
[DE92-041350] p 946 N93-14902
Fe3Al-type iron aluminides: Aqueous corrosion properties in a range of electrolytes and slow-strain rate ductilities during aqueous corrosion
[DE92-040520] p 846 N93-15059
The covariance matrix of derived quantities and their combination
[DE92-019066] p 969 N93-15212
Latent heat thermal energy storage for lunar oxygen production
[DE92-017817] p 907 N93-15219
Data analysis and interpretation for environmental surveillance
[DE92-019009] p 910 N93-15270
Ecological implications of landscape fragmentation
[DE92-019186] p 911 N93-15273
Variable speed rotary compressor and adjustable speed drive efficiencies measured in the laboratory
[DE92-040026] p 893 N93-15278
Analytical and experimental evaluation of joining ceramic oxides to ceramic oxides and ceramic oxides to metal for advanced heat engine applications
[DE92-041383] p 851 N93-15294
Tribology of improved transformation-toughened ceramics-heat engine test
[DE92-041385] p 851 N93-15295
Development of ceramic matrix composites for application in ceramic technology for advanced heat engines project, phase 2
[DE92-041379] p 836 N93-15387
Material development in the Si3N4 system using glass encapsulated HIP'ing
[DE92-041381] p 837 N93-15388
Development of adherent ceramic coatings to reduce contact stress damage of ceramics
[DE92-041373] p 852 N93-15437
Development of low-expansion ceramics for diesel engine applications
[DE92-041380] p 853 N93-15438
Development of wear-resistant ceramic coatings for diesel engine components
[DE92-041382] p 853 N93-15439
A power compensation system for phased operation of the JET A2 antenna arrays
[DE92-041020] p 863 N93-15440
Development of ceramic matrix composites for application in the ceramic technology for advanced heat engines project. Phase 2A: Development of in-situ toughened silicon nitride
[DE92-041371] p 853 N93-15452
Processing of sinterable transformation toughened ceramics for application in ceramic technology for advanced heat engines project
[DE92-041372] p 853 N93-15453
Analytical and experimental evaluation of joining silicon carbide to silicon carbide and silicon nitride to silicon nitride for heat engine applications
[DE92-041376] p 837 N93-15454
Development of ceramic matrix composites for application in the ceramic technology for advanced heat engines project
[DE92-041378] p 837 N93-15455
The spatial correlation function approach to response surface emission
[DE92-040875] p 969 N93-15656

ODETICS, INC., ANAHEIM, CA.
ATL Products Division's entries into the computer mass storage marketplace p 1005 N93-15038

OFFICE NATIONAL D'ETUDES ET DE RECHERCHES AEROSPATIALES, PARIS (FRANCE).
Broadband vibroacoustic frequency control via piezoelectric films
[ONERA-RT-8/3654-RY-010-R] p 974 N93-15129
Development of a TDS measurement system. Application to acoustic propagation measurement in a non anechoic environment
[ONERA-RT-18/3641-PY] p 975 N93-15130
Structural study of thermohardening matrices: Deformation of composite matrices in relation to their molecular structure
[ONERA-RT-12/3521-M] p 836 N93-15253

OFFICE OF RADIATION PROGRAMS, MONTGOMERY, AL.
Measurements of electric and magnetic fields in the Waianae, Hawaii area
[DE92-019891] p 861 N93-15220

OFFICE OF SPACE SCIENCE AND APPLICATIONS, WASHINGTON, DC.
Directory of research projects: Planetary geology and geophysics program
[NASA-TM-4428] p 864 N93-15638

OHIO STATE UNIV., COLUMBUS.
Scatterer modeling/calibration study
[AD-A255855] p 856 N93-14107
Query processing in distributed database systems p 1001 N93-14218
A feasibility study of space VLBI for geodesy and geodynamics p 904 N93-14223
Theoretical and experimental analysis of residual stress formation after implant resistance welding of polycarbonate p 898 N93-14279
Nonlinear free vibration analysis of strings by the Galerkin method p 972 N93-14280
Atomic data and spectral analysis of carbon, nitrogen, oxygen and silicon ions observed with the International Ultraviolet Explorer
[NASA-CR-191302] p 1012 N93-14761
Tribology of magnetic storage systems p 1002 N93-14772
A very efficient RCS data compression and reconstruction technique, volume 4
[NASA-CR-191378-VOL-4] p 945 N93-14807
Mean sea surface and gravity investigations using TOPEX/Poseidon altimeter data p 930 N93-14990
Demodulation processes in auditory perception
[AD-A255748] p 935 N93-15053
Dynamical properties of Josephson Junctions arrays
[AD-A255464] p 995 N93-15351

OHIO WESLEYAN UNIV., DELAWARE.
Analysis of retinal function following laser irradiation
[AD-A255649] p 933 N93-14163

OKLAHOMA UNIV., NORMAN.
Convective scale 4-D data assimilation using simulated single-Doppler radar observations p 921 N93-14683
Computational analysis of hypersonic flows past elliptic-cone waveriders
[NASA-CR-191304] p 781 N93-14767

OLD DOMINION UNIV., NORFOLK, VA.
Control of low-speed turbulent separated flow over a backward-facing ramp p 874 N93-14475
Analysis and control of asymmetric vortex flows and supersonic vortex breakdown
[NASA-CR-191264] p 875 N93-14687
Polymer infiltration studies
[NASA-CR-191652] p 852 N93-15431

OPEN UNIV., MILTON (ENGLAND).
A framework for describing and implementing software visualization systems p 953 N93-15540

OPTICAL SOCIETY OF AMERICA, WASHINGTON, DC.
Integrated photonics research technical digest series. Volume 10: Conference edition: Summaries of papers presented at the Integrated Photonics Research Topical Meeting
[AD-A255423] p 981 N93-14506
Physics of x ray multilayer structures: Summaries of papers presented at the physics of x ray multilayer structures topical meeting, technical digest series, 1992, volume 7
[AD-A255383] p 992 N93-14741

OREGON HEALTH SCIENCES UNIV., PORTLAND.
Joint HVAC transmission EMF environmental study
[DE92-017863] p 933 N93-15211

OREGON REGIONAL PRIMATE RESEARCH CENTER, BEAVERTON.
Joint HVAC transmission EMF environmental study
[DE92-017863] p 933 N93-15211

OREGON STATE UNIV., CORVALLIS.
Hyperfine experimental investigation of zirconia ceramics
[DE92-040301] p 850 N93-14903
Mesoscale and large-scale variability of the Antarctic circumpolar current p 926 N93-14970
Equatorial and eastern boundary current variability in the North and South Pacific Oceans p 931 N93-14994
A Cloudy Quark Bag Model of S, P, and D wave interactions for the coupled channel antikaon-nucleon system
[DE92-040149] p 977 N93-15062

OREGON STATE UNIV., NEWPORT.
Dynamics and control of a rigid/flexible manipulator p 890 N93-14684

OTTAWA UNIV. (ONTARIO).
An active tactile perception system
p 805 N93-14926
OULU UNIV. (FINLAND).
Cytherean crustal bending at Salme Dorsa
p 1039 N93-14364
Structural characteristics and tectonics of northeastern Tellus Regio and Meni Tessera p 1044 N93-14389
OXFORD UNIV. (ENGLAND).
The low-energy structure of compactified superstring models p 997 N93-14116
Infrared radiative properties of clouds
p 919 N93-14196
Disc structure and variability in dwarf novae
p 1017 N93-14460

P

PACIFIC NORTHWEST LAB., RICHLAND, WA.
The response of dispersion-strengthened copper alloys to high fluence neutron irradiation at 415 C
[DE92-019434] p 846 N93-15138
Results from a pilot cell test of cermet anodes
[DE92-041357] p 871 N93-15479
PADERBORN UNIV. (GERMANY).
Neural network based condition monitoring
p 797 N93-15183
PARAMAX SYSTEMS CORP., RESTON, VA.
User manual for the Software Technology for Adaptable, Reliable Systems (STARS). PCTE Browser Tool (PBT) version 0.1 SunOS implementation
[AD-A257064] p 951 N93-15457
Software Technology for Adaptable, Reliable Systems (STARS)
[AD-A257022] p 952 N93-15471
PARIS-SUD UNIV., ORSAY (FRANCE).
Dynamics systems applied to Navier-Stokes equations for the study of turbulence
[ETN-92-92553] p 878 N93-15122
A multi-layer graphic model for building interactive graphical applications p 957 N93-15567
PARIS VI UNIV. (FRANCE).
Coordinated motion control of a two-hand assembly system
[F-2-8] p 949 N93-15301
PENNSYLVANIA STATE UNIV., UNIVERSITY PARK.
Elastic wave scattering by partially debonded or partially coated fibers p 829 N93-14224
A geometrically nonlinear stress-deflection relation for thin film/substrate systems p 848 N93-14287
Venus: The case for a wet origin and a runaway greenhouse p 1031 N93-14331
Multi-point inverse design of isolated airfoils and airfoils in cascade in incompressible flow p 790 N93-14462
Excitation of nuclei by antiproton annihilation at rest
[AD-A255447] p 976 N93-14513
The stress development during filament winding of thick cylinders
[AD-A255765] p 901 N93-15066
Innovative techniques for studying new materials and new developments in solid state physics
[AD-A256394] p 996 N93-15465
Development and application of a time-space conversion technique for analysis of weather systems passing over the Kennedy Space Center
[NASA-CR-4474] p 924 N93-15581
The intelligibility of words, sentences, and continuous discourse using the articulation index
[AD-A256781] p 863 N93-15624
Nonlinear finite element analysis of metals and metal matrix composites: A local-global investigation
[AD-A256782] p 838 N93-15625
PENNSYLVANIA UNIV., PHILADELPHIA.
Design and hardware implementation of neural systems
[AD-A256040] p 866 N93-14577
Modeling clothed figures
[AD-A257037] p 940 N93-15363
ARCBALL: A user interface for specifying three-dimensional orientation using a mouse
p 955 N93-15551
Matrix animation and polar decomposition
p 956 N93-15563
PHILADELPHIA COLL. OF TEXTILES AND SCIENCE, PA.
Advanced stitching technology p 832 N93-14746
PHYSICS AND ELECTRONICS LAB. TNO, THE HAGUE (NETHERLANDS).
High power millimetre-wave polarizers
[AD-A256558] p 867 N93-14803
Theory and applications of the 3-dimensional finite-difference time-domain method
[AD-A256559] p 968 N93-14804
Definition study PHARUS
[AD-A256560] p 860 N93-14805
Short range propagation measurements at 2.4, 4.5, and 11.5 GHz in indoor and outdoor environments
[AD-A256563] p 860 N93-14806
A deadlock-free communication system for a transputer network
[AD-A256473] p 959 N93-15319
PITTSBURGH-DES MOINES STEEL CO., PA.
A new thermal vacuum facility at the Martin Marietta Waterton plant p 814 N93-15607
PITTSBURGH UNIV., PA.
Analysis of symbolic models of cognition project (ASPM-Pitt)
[AD-A255929] p 962 N93-14656
Silicon nitride thin film production on Si(111)
[AD-A256036] p 994 N93-15233
PLANNING RESEARCH CORP., CINCINNATI, OH.
Technology evaluation report: The Carver-Greenfield process, Dehydro-Tech Corporation
[PB92-217462] p 910 N93-15217
POLYTECHNIC INST. OF NEW YORK, FARMINGDALE.
Basic research in electronics (JSEP)
[AD-A256016] p 869 N93-15257
PORTLAND STATE UNIV., OR.
Joint HVAC transmission EMF environmental study
[DE92-017863] p 933 N93-15211
PRATT AND WHITNEY AIRCRAFT, WEST PALM BEACH, FL.
Fatigue in single crystal nickel superalloys
[AD-A256095] p 844 N93-14264
F100 second stage fan disk bolthole crack propagation ferris wheel test p 800 N93-14897
PRINCETON UNIV., NJ.
Global deformation on the surface of Venus
p 1024 N93-14297
Gas-solid dynamics at disordered and adsorbate covered surfaces
[AD-A255981] p 976 N93-14411
Macroscopic properties of random and quasiperiodic media
[AD-A255984] p 990 N93-14413
A numerical study of the middle atmosphere response to tropical and subtropical tropospheric heat sources
p 920 N93-14640
Robust nonlinear feedback guidance for an aerospace plane: A geometric approach p 803 N93-14835
Wind shear related research at Princeton University
p 785 N93-14854
The formation of giant molecular clouds
p 1021 N93-15086
PRINS MAURITS LAB. TNO, RIJSWIJK (NETHERLANDS).
Validation of the flux loop diagnostic for the measurement of launch package motion during electromagnetic launch
[AD-A256547] p 814 N93-14266
PROUDMAN OCEANOGRAPHIC LAB., BIRKENHEAD (ENGLAND).
Marine research using data from TOPEX/Poseidon
p 932 N93-15001
PROVENCE UNIV., MARSEILLE (FRANCE).
Fundamentals of combustion of premixed gases
p 840 N93-14618
PURDUE UNIV., WEST LAFAYETTE, IN.
Nonlinear dynamic response of shallow arches to harmonic forcing p 898 N93-14282
L2 and L-infinity multiobjective control for linear systems p 961 N93-14399
Intelligent path prediction for vehicular travel
p 961 N93-14445
Multiobjective control/structure design optimization in the presence of practical constraints
p 898 N93-14446
Synoptic/planetary-scale interactions and blocking over the North Atlantic Ocean
[NASA-CR-191376] p 925 N93-14769
Molecular capacitance: Sequential electron-transfer energetics for solution-phase metallic clusters in relation to gas-phase clusters and analogous interfaces
[AD-A257057] p 977 N93-15448
Parameterization in finite precision
p 953 N93-15537

Q

Q-SOURCE, INC., EAST HARTFORD, CT.
Compact high PRF CO2 transmitter
[AD-A255985] p 884 N93-14414
QUANTUM CONSULTANTS, INC., EAST LANSING, MI.
Smart materials for Army structures
[AD-A254925] p 836 N93-15218
QUEENS COLL., FLUSHING, NY.
Thin-film permanent magnets for integrated electromagnetic components
[AD-A256175] p 972 N93-14679
QUEENS UNIV., BELFAST (NORTHERN IRELAND).
Digital bank-to-turn control and guidance
p 802 N93-14447
QUEENS UNIV., KINGSTON (ONTARIO).
A study for the development of practices to protectively coat and join fibre epoxy composites for use in the Space Station Programme
[CTN-93-60626] p 835 N93-15145
QUEST INTEGRATED, INC., KENT, WA.
Active control of combustion instability in a ramjet using large-eddy simulations
[AD-A255226] p 798 N93-14111

R

RADIATION EXPERIMENTS AND MONITORS, OXFORD (ENGLAND).
Improvement and analysis of the radiation response of RADFET dosimeters
[AD-A254115] p 869 N93-15133
RAND CORP., SANTA MONICA, CA.
The spin vector of Venus determined from Magellan data p 1027 N93-14310
A structural approach to the photonic processor
[N-3399-RC] p 986 N93-15648
RANGE COMMANDERS COUNCIL, WHITE SANDS MISSILE RANGE, NM.
Flight termination systems commonality standard
[AD-A255349] p 789 N93-14517
RAYTHEON CO., MARLBOROUGH, MA.
Testability design rating system: Testability handbook, volume 1
[RL-TR-92-12-VOL-1] p 867 N93-14699
RENSSELAER POLYTECHNIC INST., TROY, NY.
Mechanics of composite materials for spacecraft
[AD-A255380] p 831 N93-14550
Using an interior point cutting plane method to solve integer programming problems
[AD-A256041] p 945 N93-14659
RESEARCH TRIANGLE INST., RESEARCH TRIANGLE PARK, NC.
Investigation of antenna pattern constraints for passive geosynchronous microwave imaging radiometers
[NASA-CR-189728] p 905 N93-14792
ROCHESTER UNIV., NY.
Real-time gaze holding in binocular robot vision
[AD-A256226] p 982 N93-14582
A probabilistic approach to anytime algorithm for intelligent real-time problem solving
[AD-A255709] p 945 N93-14654
The perception of articulated motion: Recognizing moving light displays
[AD-A256046] p 937 N93-14660
Probabilistic inference
[AD-A255471] p 963 N93-14786
Studies of heavy-ion reactions and transuranic nuclei
[DE92-040457] p 977 N93-15326
ROCKWELL INTERNATIONAL CORP., CANOGA PARK, CA.
An environmental testing facility for Space Station Freedom power management and distribution hardware
p 820 N93-15601
ROCKWELL INTERNATIONAL CORP., PITTSBURGH, PA.
Space Shuttle Orbiter Crew Hatch Jettison Test using a 0.0405-scale model (16-0) in the Texas A/M low speed wind tunnel (OA362). Space Shuttle aerothermodynamic data report
[NASA-CR-167698] p 815 N93-15474
Results of a FRSI material test under Space Shuttle ascent conditions in the Ames Research Center 9x7 foot supersonic wind tunnel (OS13). Space Shuttle aerothermodynamic data report
[NASA-CR-167699] p 816 N93-15475
ROCKWELL INTERNATIONAL CORP., SEAL BEACH, CA.
Control of on-orbit contamination for the Argos (P91-1) satellite p 823 N93-15617
Overview of environmental test plans for Space Station Freedom work package 4 p 824 N93-15623
ROCKWELL INTERNATIONAL SCIENCE CENTER, THOUSAND OAKS, CA.
Selected area epitaxial growth for complementary HBT applications
[AD-A257047] p 995 N93-15365
ROLLS-ROYCE LTD., BRISTOL (ENGLAND).
RB211-524B disc and drive cones hot cyclic spinning test p 799 N93-14895
ROLLS-ROYCE LTD., DERBY (ENGLAND).
A method of representating dimensions and tolerances in solid based freeform surfaces
[PNR-90998] p 951 N93-15386
The use of a novel manufacturing process for high performance titanium plate fin heat exchangers
[PNR-90934] p 879 N93-15473

Integrated support for real-time control systems
[PNR-90994] p 952 N93-15476
High performance titanium plate fin heat exchanger using a novel manufacturing process
[PNR-90933] p 880 N93-15488
Time-dependent predictions and analysis of turbine cascade data in the transonic flow region
[PNR-90957] p 782 N93-15489

ROME LAB., GRIFFISS AFB, NY.
Relativistic dynamics of a charged sphere: Updating the Lorentz-Abraham model
[AD-A256107] p 971 N93-14245
Analog Very Large Scale Integration (VLSI) implementations of artificial neural networks
[AD-A256621] p 966 N93-15408

ROME LAB., HANSCOM AFB, MA.
Analytical characterization of bistatic scattering from rough surfaces: Dependence on surface correlation function
[AD-A256525] p 862 N93-15397

ROUEN UNIV. (FRANCE).
Introduction to spray combustion modelling
p 841 N93-14626

ROYAL INST. OF TECH., STOCKHOLM (SWEDEN).
A numerical model of ionospheric convection derived from field-alignment currents and the corresponding conductivity
[TRITA-EPP-91-03-REV] p 916 N93-15252

RUTGERS - THE STATE UNIV., NEW BRUNSWICK, NJ.
Technology reconciliation in the remote sensing era of US civilian weather forcasting: 1957 - 1987
p 918 N93-14114
Computer-aided design package for designers of digital optical computers
[AD-A255381] p 944 N93-14564
A numerical investigation of the interaction between crossing oblique shocks and a turbulent boundary layer
p 876 N93-14695

RUTGERS - THE STATE UNIV., PISCATAWAY, NJ.
Query optimization and planning in object-oriented knowledge bases
[AD-A256006] p 1008 N93-15254

S

SABBAGH ASSOCIATES, INC., BLOOMINGTON, IN.
Efficient asymptotic closed form approximation for dyadic green's function for anisotropic substrates, phase 1
[AD-A256258] p 830 N93-14436

SAN DIEGO SUPERCOMPUTER CENTER, CA.
File servers, networking, and supercomputers
p 1004 N93-15030

SANDIA NATIONAL LABS., ALBUQUERQUE, NM.
Requirements for a network storage service
p 1003 N93-14781
SAFSIM: A computer program for engineering simulations of space reactor system performance
[DE92-016328] p 826 N93-14815
Requirements for a network storage service
p 1007 N93-15048
A distributed visualization environment for engineering sciences
[DE92-012629] p 1051 N93-15060
The CPG 5-kW(e) Dish-Stirling Development Program
[DE92-017050] p 907 N93-15134
Characterization of impact-limiting material
[DE92-016767] p 902 N93-15210
A temperature tracking SPICE2G.6 macromodel of the 6N134 optocoupler
[DE92-040093] p 983 N93-15223
Preliminary lightning tests: Optical fiber penetration of an exclusion region barrier
[DE92-019804] p 983 N93-15230
Generation, control, and transport of a 19-MeV, 700-kA pulsed electron beam
[DE92-019803] p 978 N93-15277
High speed imaging for flash radiography using PIN diodes
[DE92-040959] p 882 N93-15381
Application of the square root diffusivity analysis to measuring the diffusivity of multicomponent alloys
[DE92-040978] p 847 N93-15382
Exceptionally high-strength (approximately 3 GPa) aluminum alloys demonstrated by oxygen ion implantation
[DE92-040980] p 847 N93-15383
Frequency-domain synthesis of the fatigue load spectrum for the NPS 100-kW wind turbine
[DE92-040984] p 908 N93-15384
SMART: A modular architecture for robotics and teleoperation
[DE92-040985] p 966 N93-15385
Energy distribution of trapped holes in irradiated SiO2
[DE92-040979] p 997 N93-15649
Revised nomenclature for defects at or near the Si/SiO2 interface
[DE92-040975] p 997 N93-15651

SANTA BARBARA FOCALPLANE, GOLETA, CA.
Organic/IR-Semiconductor heterojunctions for low-cost, high temperature IR arrays
[AD-A255971] p 868 N93-15108

SASKATCHEWAN UNIV., SASKATOON.
Comparison of Viking Ultraviolet images with low altitude particle precipitation p 1045 N93-14612

SCANDINAVIAN AIRLINES SYSTEM, STOCKHOLM (SWEDEN).
Flight data and flight safety in SAS
p 793 N93-15156

SCIENCE APPLICATIONS INTERNATIONAL CORP., GLENDORA, CA.
Operational strategies for contamination control of composite materials p 822 N93-15614

SCIENCE APPLICATIONS INTERNATIONAL CORP., LAS VEGAS, NV.
Technical data management at the Yucca Mountain Site Characterization Project
[DE92-018115] p 1008 N93-15229

SCIENCE APPLICATIONS INTERNATIONAL CORP., MCLEAN, VA.
Crew requirements definition system user's guide
[AD-A257052] p 951 N93-15445

SCIENCE APPLICATIONS INTERNATIONAL CORP., SAN DIEGO, CA.
Software reliability, measurement, and testing software reliability and test integration, volume 1
[AD-A256242] p 944 N93-14572
Software reliability, measurement, and testing. Volume 2: Guidebook for software reliability measurement and testing
[AD-A256164] p 944 N93-14581

SCIENCE APPLICATIONS INTERNATIONAL CORP., TORRANCE, CA.
Reusable Reentry Satellite (RRS) system design study
[NASA-CR-187897] p 817 N93-14733
Reusable Reentry Satellite (RRS) system design study: System cost estimates document
[NASA-CR-188480] p 818 N93-14872
Reusable Reentry Satellite (RRS): Telemetry, Tracking, and Command (TT/C) coverage tradeoff study
[NASA-CR-188583] p 824 N93-15629
Segment specification for the payload segment of the reusable reentry satellite: Rodent module version
[NASA-CR-187884] p 824 N93-15630
Vehicle/payload interface specification for the reusable reentry satellite
[NASA-CR-187883] p 824 N93-15631
System specification for the reusable reentry satellite
[NASA-CR-187882] p 824 N93-15632
Reusable Reentry Satellite (RRS) system design study. Phase B, appendix E: Attitude control system study
[NASA-CR-188578] p 825 N93-15633
Reusable Reentry Satellite (RRS): Recovery tradeoff study
[NASA-CR-186396] p 825 N93-15658

SCIENTIFIC-ATLANTIC, INC., SAN DIEGO, CA.
Onboard System Evaluation of Rotors Vibration, Engines (OBSERVE) monitoring system
[AD-A255366] p 792 N93-15227

SCRIPPS INSTITUTION OF OCEANOGRAPHY, LA JOLLA, CA.
Variations in lithospheric thickness on Venus
p 1030 N93-14329
Evidence for retrograde lithospheric subduction on Venus p 1040 N93-14367
An integrated research program for TOPEX/Poseidon with emphasis on the Pacific Ocean
p 931 N93-14995
Surface gravity waves and ambient microseismic noise
[AD-A256498] p 916 N93-15375

SEA TECH, INC., CORVALLIS, OR.
Development of an expendable particle sensor
[AD-A255702] p 881 N93-14653

SHELL DEVELOPMENT CO., HOUSTON, TX.
Stewardship of very large digital data archives
p 1005 N93-15032

SMITHSONIAN ASTROPHYSICAL OBSERVATORY, CAMBRIDGE, MA.
Venus: Geochemical conclusions from the Magellan data p 1044 N93-14394
The evolution of the quasar continuum
[NASA-CR-191673] p 1012 N93-14759

SMITHSONIAN INSTITUTION, CAMBRIDGE, MA.
ROSAT all-sky survey on the Einstein EMSS sample
[NASA-CR-191627] p 1013 N93-15340

SOCIETE FRANCAISE D'INSTRUMENTS DE MESURE, MASSY (FRANCE).
Ground Support Equipment (GSE) for Aircraft Condition Monitoring System (ACMS) p 778 N93-15158

SOCIETE NATIONALE D'ETUDES ET DE CONSTRUCTION DE MOTEURS AERONAUTIQUES, MOISSY-CRAMAYEL (FRANCE).
LARZAC HP turbine disk crack initiation and propagation spin pit test p 799 N93-14892

SOUTHAMPTON UNIV. (ENGLAND).
The effects of mis-alignment and background noise in a low energy gamma ray telescope
p 1011 N93-14231
Abstracts booklet
[AD-A256115] p 869 N93-15188

SOUTHERN CALIFORNIA INST. OF ARCHITECTURE, SANTA MONICA.
Passive zero-gravity leg restraint
[NASA-CASE-ARC-11882-1-CU] p 939 N93-14713

SOUTHERN METHODIST UNIV., DALLAS, TX.
Tectonics and volcanism of Eastern Aphrodite Terra: No subduction, no spreading p 1029 N93-14321

SOUTHWEST RESEARCH INST., SAN ANTONIO, TX.
Strain-rate effects in replica scale model penetration experiments
[AD-A255426] p 844 N93-14508

SPACE SYSTEMS/LORAL, PALO ALTO, CA.
The evolution of space simulation
p 814 N93-15610

SPAR AEROSPACE LTD., OTTAWA (ONTARIO).
Offloading techniques for large deployable space structures p 821 N93-15605

SPAR AEROSPACE LTD., SAINTE-ANNE-DE-BELLEVUE (QUEBEC).
L-band antenna design for MSAT mission
p 812 N93-14961
Ku-band antenna design for MSAT mission
p 813 N93-14963

SPAR AEROSPACE LTD., TORONTO (ONTARIO).
Vision system requirements and concept for the Special Purpose Dexterous Manipulator system (SPDM)
p 805 N93-14924
Next generation satellite communications networks
p 812 N93-14962

SPAR AEROSPACE LTD., WESTON (ONTARIO).
Canada's role in pushing back the frontiers of space
p 806 N93-14928
In-situ lunar oxygen extraction p 806 N93-14929
Photovoltaic power system for a lunar base
p 806 N93-14930
Mission and technology assessment of human exploration to the Moon and Mars p 809 N93-14944
Applications of the mobile servicing system to the space exploration initiative p 809 N93-14946
The evaluation of a concept for a Canadian-made automated multipurpose materials extraction facility
p 810 N93-14947
Vision development test bed: The cradle of the MSS artificial vision system p 810 N93-14948
On some kinematic and mass characteristics of foldable solar arrays p 812 N93-14957

SPARTA, INC., LEXINGTON, MA.
Development of an integrated package of physics models for scene simulation studies to support smart weapons design studies
[LTR92-004] p 945 N93-14696
Ultra-dense optical mass storage
[AD-A255463] p 1004 N93-14785

SRI INTERNATIONAL CORP., MENLO PARK, CA.
Comparison between irregularity motion and bulk plasma drifts at high latitudes
[PL-TR-91-2292] p 914 N93-14727
Formal verification of an oral messages algorithm for interactive consistency
[NASA-CR-189704] p 958 N93-14808
Solid polymer electrolytes for rechargeable batteries
[DE93-001603] p 871 N93-15485

STANFORD LINEAR ACCELERATOR CENTER, CA.
Proceedings of the REXX Symposium for Developers and Users
[DE92-041359] p 951 N93-15451

STANFORD RESEARCH INST., MENLO PARK, CA.
Production of relativistic anti-hydrogen atoms by pair production with positron capture and measurement of the Lamb shift
[DE93-001767] p 978 N93-15468
Anti-hydrogen: The cusp between quantum mechanics and general relativity
[DE93-001807] p 998 N93-15469
Weak-electromagnetic interference in polarized eD scattering
[DE93-001763] p 978 N93-15486

STANFORD UNIV., CA.
Three-dimensional guiding effects in a free-electron laser p 883 N93-14125
Scattering properties of Venus' surface
p 1044 N93-14391
Utilizing sensed incipient slip signals for grasp force control
[AD-A255725] p 888 N93-14434

Delamination growth behavior in cross-ply laminated composites due to transverse concentrated loading
[AD-A255974] p 830 N93-14493
Advanced optical fiber communication systems
[AD-A255424] p 982 N93-14507
Anaerobic microbial transformation cf aromatic hydrocarbons and mixtures of aromatic hydrocarbons and halogenated solvents
[AD-A255696] p 932 N93-14557
Thunderstorm coupling to the magnetosphere and associated ionospheric effects
[NASA-CR-191383] p 922 N93-14910
Nonparametric bayesian bioassay including ordered polytomous response
[AD-A255990] p 970 N93-15109
An iterative Monte Carlo method for nonconjugate bayesian analysis
[AD-A255991] p 971 N93-15110
Volume rendering using the Fourier projection-slice theorem p 953 N93-15541
The detection and characterization of high frequency and high wavenumber solar oscillations
[NASA-CR-191622] p 1049 N93-15634

STATE UNIV. COLL. OF NEW YORK, BUFFALO.
Studies of components for thermally regenerative electrochemical systems
[AD-A256124] p 842 N93-14664

STATE UNIV. OF NEW YORK, ALBANY.
Semi-classical quantization rules in supersymmetric quantum mechanics p 998 N93-14590
Spatial and temporal patterns of biotic exchanges of CO2 between the atmosphere and tropical landscapes and their role in the global carbon balance
[DE92-019170] p 911 N93-15272

STATE UNIV. OF NEW YORK, BUFFALO.
Modeling variable blowing on a slender cone in hypersonic flow p 781 N93-14836
Gallium and indium compounds containing three different substituents. Crystal and molecular structure of ((Me3 CCH2)ClGaPPh2)3
[AD-A257049] p 996 N93-15443

STATE UNIV. OF NEW YORK, STONY BROOK.
Investigations of Titan's troposphere and surface and Jupiter's great red spot with infrared observations p 1022 N93-14146
Advances in laser cooling
[AD-A255969] p 884 N93-14402
Training, muscle fatigue and stress fractures
[AD-A255277] p 935 N93-15006

STEVENS INST. OF TECH., HOBOKEN, NJ.
A concurrent real-time autonomous mobile robot programming system p 960 N93-14281
Finite element analysis of elastic fracture under unsteady translational and rotational loading p 899 N93-14469

STEWART HUGHES LTD., EASTLEIGH (ENGLAND).
Helicopter health monitoring: Current practice and future trends p 797 N93-15179

STORAGE TECHNOLOGY CORP., LOUISVILLE, CO.
Enterprise storage report for the 1990's p 1004 N93-15028

STRATHCLYDE UNIV., GLASGOW (SCOTLAND).
Online vibration control of a flexible rotor/bearing system p 899 N93-14468
The effect of geometry and prescribed delaminations on the postbuckling behaviour of laminated carbon-fibre reinforced plastic panels p 831 N93-14597

STUTTGART UNIV. (GERMANY).
Chemical kinetics for combustion p 840 N93-14619

SUNDSTRAND DATA CONTROL, INC., REDMOND, WA.
FDAMS: An extendable and reconfigurable solution for avionics data management systems p 794 N93-15157
Rewritable optical disk: Application to flight recording p 794 N93-15160

SUPERCONDUCTING SUPER COLLIDER LAB., DALLAS, TX.
Data management and processing plan, Department of Applied Geodesy
[DE93-000774] p 905 N93-14522

SUSSEX UNIV., BRIGHTON (ENGLAND).
Cosmological models in higher-order gravity p 1018 N93-14592

SVERDRUP TECHNOLOGY, INC., BROOK PARK, OH.
Autonomous power system brassboard
[NASA-CR-189115] p 867 N93-14798
Numerical study of cathode emission constraints on cylindrical self-field MPD thruster performance
[NASA-CR-190795] p 826 N93-15370
Advancements in the LEWICE ice accretion model
[NASA-CR-191019] p 879 N93-15402
Unsteady shear disturbances within a two dimensional stratified flow
[NASA-CR-189121] p 880 N93-15527
Environmental qualification testing of the prototype pool boiling experiment
[NASA-CR-190774] p 895 N93-15582
Combined high and low thrust propulsion for fast piloted Mars missions
[NASA-CR-190788] p 828 N93-15584

SYDNEY UNIV. (AUSTRALIA).
Groundbased near-IR observations of the surface of Venus p 1035 N93-14346

SYNECTICS CORP., ROME, NY.
Arc digital raster imagery evaluation
[AD-A255403] p 817 N93-14565

SYRACUSE UNIV., NY.
Shear fatigue crack growth analysis in large-grain polycrystals p 993 N93-14838

SYSTEMS CONTROL TECHNOLOGY, INC., ARLINGTON, VA.
Tiltrotor aircraft noise: A summary of the presentations and discussions at the 1991 FAA/Georgia Tech Workshop
[DOT/FAA/RD-91/23] p 974 N93-14912

T

TECHNICAL UNIV. OF BUDAPEST (HUNGARY).
Detection of technical states with aircraft p 794 N93-15159

TECHNICO SOUTHWEST, INC., LOS ALAMOS, NM.
The effect of pain on task performance: A review of the literature
[AD-A254336] p 938 N93-15216

TECHNION - ISRAEL INST. OF TECH., HAIFA.
Methodology for robot capability and performance characterization: The basis for robot task planningg
[F-2-3] p 949 N93-15300

TECHNION RESEARCH AND DEVELOPMENT FOUNDATION LTD., HAIFA (ISRAEL).
Multi-disciplinary optimization of aeroservoelastic systems
[NASA-CR-191255] p 901 N93-14766

TECHNISCHE UNIV., BRUNSWICK (GERMANY).
Sensor fault detection using nonlinear observer and polynomial classifier p 797 N93-15182

TECHNISCHE UNIV., DELFT (NETHERLANDS).
Flight testing: Past, present, and future p 777 N93-14615
Precise orbit computation and sea surface modeling p 813 N93-15000

TECHNISCHE UNIV., MUNICH (GERMANY).
Experimental analysis of steady-state and dynamic monitoring of power shaft turbines p 796 N93-15176

TEL-AVIV UNIV. (ISRAEL).
Elastic wave propagation in laminated composites
[ITN-93-85186] p 835 N93-15144
Multiple robot programming using concurrent logic language
[F-3-3] p 950 N93-15304
Planning of continuous path robotic motions by discrete time optimization
[F-3-5] p 950 N93-15305
Time-optimization of point-to-point robotic motions
[F-3-6] p 950 N93-15306

TELEDYNE CONTROLS, LOS ANGELES, CA.
The Teledyne controls aircraft condition monitoring system p 793 N93-15155
Helicopter flight data recorder and health and usage monitoring system p 797 N93-15178

TELESAT CANADA, OTTAWA (ONTARIO).
NPR and intermodulation in mobile satellite systems p 806 N93-14931
Anik E spacecraft integration and test p 808 N93-14939
A low bit rate FSK technique for SCPC satellite communication systems p 811 N93-14954

TELESAT MOBILE, INC., OTTAWA (ONTARIO).
Progress toward a full scale mobile satellite system for Canada p 812 N93-14960

TENNESSEE UNIV., KNOXVILLE.
Biofilm ecology of bioluminescent bacteria
[AD-A255282] p 932 N93-14532

TETRA CORP., ALBUQUERQUE, NM.
A quasi-equilibrium kinetic model of HF air breakdown
[AD-A256240] p 859 N93-14453
Microstack insulator for flashover inhibition, phase 2
[AD-A256338] p 869 N93-15196

TEXAS A&M UNIV., COLLEGE STATION.
Parametric study of air sampling cyclones p 779 N93-14173
Information system constraint language (ISyCL)
[AD-A256268] p 976 N93-14438
A finite element model for analysis of thermoviscoplastic behavior of hypersonic leading edge structures subject to intense aerothermal heating p 780 N93-14631
Development of engineering methods for nonequilibrium radiative phenomena about aeroassisted entry vehicles p 817 N93-14632
Development of laser-ion beam photodissociation methods
[DE92-040512] p 886 N93-15058
Undetermined coefficient problems for quasi-linear parabolic equations
[AD-A256012] p 969 N93-15256

TEXAS UNIV., ARLINGTON.
An investigation of genuinely multidimensional schemes for the Euler equations p 876 N93-14694

TEXAS UNIV., AUSTIN.
Turbulent drag and transport in high Reynolds number Couette-Taylor flow p 872 N93-14119
Resistive magnetohydrodynamic studies of tearing mode instability with equilibriurn shear flow and magnetic reconnection p 987 N93-14122
Perturbations of the Robertson-Walker space p 1015 N93-14134
Scattering of sound by sound: Nonlinear interaction of collinear and noncollinear sound beams p 973 N93-14145
The black hole candidate binary A0620-00 p 1015 N93-14148
Submillimeter and infrared spectroscopy of molecular clouds near O and B stars p 1016 N93-14149
Gravitational instabilities in a protoplanetary disk p 1016 N93-14154
Decision-making for intelligent control of dual-arm robotic operations p 960 N93-14201
Problems in nonlinear acoustics: Rayleigh waves, pulsed sound beams, reflection of focused beams, waveguides, cooperative radiation of sound by buggles, acoustic streaming effects in standing waves, and spark-source lithotripter pulses
[AD-A256289] p 974 N93-14458
A simple controller for repetitive cycles in atomic layer epitaxy
[AD-A255497] p 992 N93-14643
Quasar x-ray spectra revisited p 1012 N93-14760
The determination and interpretation of ocean surface topography using TOPEX/Poseidon altimeter data p 931 N93-14997
Si atomic layer epitaxy using remote plasma assisted hydrogen desorption and disilane as a precursor
[AD-A255606] p 993 N93-15008
Si atomic layer epitaxy based on Si2H6 and remote He plasma bombardment
[AD-A255763] p 993 N93-15055
Plasma confinement theory and transport simulation
[DE92-040523] p 988 N93-15327
Non-uniform patch luminance for global illumination p 957 N93-15569

TEXTRON BELL HELICOPTER, FORT WORTH, TX.
Embedded ADM reduces helicopter human error accidents p 787 N93-15024
Measuring risk in single-engine and twin-engine helicopters p 787 N93-15025

THINKING MACHINES CORP., CAMBRIDGE, MA.
A data parallel algorithm for raytracing of heterogeneous databases p 955 N93-15553

THOMSON AND NIELSEN ELECTRONICS, OTTAWA (ONTARIO).
Radiation monitoring for long duration space flights p 812 N93-14959

THOMSON-CSF, OTTAWA (ONTARIO).
A concept for a supervised autonomous robot p 810 N93-14950

TOKYO UNIV. (JAPAN).
Application of precise altimetry to the study of precise leveling of the sea surface, the Earth's gravity field, and the rotation of the Earth p 907 N93-14992
Oceanic transports of mass, heat, and salt in the western North Pacific p 931 N93-14996

TOLEDO UNIV., OH.
Numerical modeling of a vortex stabilized arcjet
[NASA-CR-190797] p 826 N93-14883

TORONTO UNIV. (ONTARIO).
MOVE: A neutral network paradigm for robotic control p 805 N93-14925
Composite materials in space: Results from the LDEF satellite p 811 N93-14955
Program auralization: Sound enhancements to the programming environment p 953 N93-15539
Hierarchical Poisson disk sampling distributions p 954 N93-15545
Working together, virtually p 954 N93-15547
Telepresence: Integrating shared task and person spaces p 954 N93-15548
CSCW - WCSC: Computer-supported cooperative work. What changes for the science of computing p 954 N93-15549
Designing video annotation and analysis systems p 955 N93-15552
Beyond keyframing: An algorithmic approach to animation p 957 N93-15565

TOTAL ARMY PERSONNEL AGENCY (PROVISIONAL), ALEXANDRIA, VA.
The role of entanglements in the swelling of poly(dimethylsiloxane) networks
[AD-A255359] p 849 N93-14561
TRW SPACE AND DEFENSE SECTOR, REDONDO BEACH, CA.
High temperature polymer dielectric film insulation
[AD-A255243] p 849 N93-14527
TRYMER CO., LEANDER, TX.
A novel, high energy-density electrical storage device for electric weapons
[AD-A255205] p 867 N93-14666
TURBULENCE PREDICTION SYSTEMS, BOULDER, CO.
Development of the Advance Warning Airborne System(AWAS) p 784 N93-14849

U

ULTRA NETWORK TECHNOLOGIES, INC., SAN JOSE, CA.
Network issues for large mass storage requirements p 1002 N93-14773
UNITED TECHNOLOGIES RESEARCH CENTER, EAST HARTFORD, CT.
Electro-optic architecture (EOA) for sensors and actuators in aircraft propulsion systems
[NASA-CR-182270] p 982 N93-15116
UNIVERSITAET DER BUNDESWEHR, HAMBURG (GERMANY).
Some experiments and ideas on GPA before reaching steady state of engine p 796 N93-15175
UNIVERSITAET DER BUNDESWEHR MUENCHEN, NEUBIBERG (GERMANY).
Asymmetric natural damped frequencies of a rotating infinitely long viscous liquid column
[LRT-WE-9-FB-23-1991] p 878 N93-15120
Transient response of a viscous liquid bridge of finite length and anchored edges
[LRT-WE-9-FB-25-1991] p 878 N93-15132
Monitoring of pilot actions as part of a knowledge-based system for pilot assistance p 797 N93-15184
UNIVERSITAIRE INSTELLING ANTWERPEN, WILRIJK (BELGIUM).
Stability of differentially rotating stars p 1018 N93-14584
UNIVERSITEIT TWENTE, ENSCHEDE (NETHERLANDS).
From data structure to process structure
[MEMO-INF-91-38] p 946 N93-15077
Implementation issues concerning injection simulation. Part 1: The backbone implementation
[MEMO-INF-91-57-PT-1] p 946 N93-15078
Parallel on-line parsing in constant time
[MEMO-INF-91-64] p 958 N93-15082
Processor controlpath microarchitecture synthesis based on the A(asterisk) algorithm
[MEMO-INF-92-10] p 963 N93-15083
Obstacles in object-oriented software development
[MEMO-INF-92-15] p 946 N93-15084
Architecture of low cost, large scale neural networks
[MEMO-INF-92-16] p 941 N93-15089
Sensitivity and uncertainty analysis in performability modelling
[MEMO-INF-92-18] p 941 N93-15090
A non-deterministic recogniser generator
[MEMO-INF-92-21] p 946 N93-15091
A para-functional version of Warshall's algorithm
[MEMO-INF-92-23] p 947 N93-15092
Parallelism in a main-memory DBMS: The performance of PRISMA/DB
[MEMO-INF-92-25] p 958 N93-15093
Compactness and Loewenheim-Skolem properties in pre-institution categories
[MEMO-INF-92-27] p 968 N93-15094
The evolution of signalling from ISDN to B-ISDN
[MEMO-INF-92-30] p 860 N93-15095
Approximate performability analysis using generalized stochastic Petri nets
[MEMO-INF-92-11] p 971 N93-15119
Graph rewriting using a single pushout; a comparison
[MEMO-INF-92-28] p 968 N93-15121
PRISMA/DB: A parallel, main-memory relational DBMS
[MEMO-INF-92-12] p 959 N93-15141
Data fragmentation for parallel transitive closure strategies
[MEMO-INF-92-17] p 959 N93-15142
A queue model relating synchronous and asynchronous communication
[MEMO-INF-92-04] p 966 N93-15491
Physical design for network databases
[MEMO-INF-92-26] p 1009 N93-15492
UNIVERSITY OF NORTHERN ARIZONA, FLAGSTAFF.
Western Aphrodite Terra, tectonics, geology, and line-of-sight gravity p 1029 N93-14322
UNIVERSITY OF SOUTHERN CALIFORNIA, LOS ANGELES.
Control of asymmetric jet
[AD-A255967] p 873 N93-14400
Photonic materials and devices for optical information processing and computing applications
[AD-A256047] p 982 N93-14578
Stability and adaptation of neural networks
[AD-A256227] p 962 N93-14598
UNIVERSITY OF TECHNOLOGY, LEICESTER (ENGLAND).
Information systems for airport operations
[TT-9202] p 789 N93-14729
UNIVERSITY OF WESTERN ONTARIO, LONDON.
Control of thermocapillary convection in a two-layer liquid system p 809 N93-14945
UTAH UNIV., SALT LAKE CITY.
Simulations of the Amazon Basin circulation using the Pennsylvania State University/National Center for Atmospheric Research mesoscale model p 919 N93-14197
Characterizing longitudinal splitting and delamination fracture toughness of composites p 831 N93-14607

V

VECTOR RESEARCH, INC., ANN ARBOR, MI.
SIDR Relative Weighted Product (RWP) assignment process
[AD-A255801] p 946 N93-15068
VIBRO-METER S.A., FRIBOURG (SWITZERLAND).
New rotor trim and balance system for helicopter usage monitoring p 797 N93-15180
VICTORIA UNIV. (BRITISH COLUMBIA).
A faint spectroscopic quasar survey p 1012 N93-14629
Cooperative control of multiple space manipulators p 805 N93-14923
Study of the mathematical modelling and computer simulation of crystal growth from liquid phase under microgravity conditions
[CTN-93-60619] p 855 N93-15201
VIRGINIA POLYTECHNIC INST. AND STATE UNIV., BLACKSBURG.
Integration and processing of high-resolution moire-interferometry data p 895 N93-14185
Effect of interfacial thermal conductance and fiber orientation on the thermal diffusivity/conductivity of unidirectional fiber-reinforced ceramic matrix composites p 864 N93-14190
The effect of the interphase/interface region on creep and creep rupture of thermoplastic composites p 829 N93-14193
Modal interactions in the dynamic response of isotropic and composite plates p 829 N93-14221
Analysis and optimal design of pressurized, imperfect, anisotropic ring-stiffened cylinders p 897 N93-14251
Position and vibration control of flexible space robots p 892 N93-15102
Development of low-expansion ceramics for diesel engine applications
[DE92-041380] p 853 N93-15438
VIRGINIA UNIV., CHARLOTTESVILLE.
Electronically active cyclocarborane-metal-arene assemblies
[AD-A256288] p 865 N93-14457
Ultraviolet spectra of stars and stellar systems p 1011 N93-14593
VHDL (VHSIC hardware description language): Origins, status, capabilities, and world environment
[VH-1] p 947 N93-15262
The extended VHDL (VHSIC hardware description language) design environment: An unique integrated system and hardware design environment
[VH-3] p 948 N93-15264
VON KARMAN INST. FOR FLUID DYNAMICS, RHODE-SAINT-GENESE (BELGIUM).
Modeling of Combustion and Turbulence
[VKI-LS-1992-03] p 839 N93-14617

W

WALTER REED ARMY INST. OF RESEARCH, WASHINGTON, DC.
Walter Reed Army Institute of Research biannual report
[AD-A255630] p 933 N93-14162
WARWICK UNIV., COVENTRY (ENGLAND).
Remote techniques for time-of-flight flaw characterisation p 989 N93-14171
WASHINGTON STATE UNIV., PULLMAN.
Independent validation testing of the FLAME computer code, version 1.0
[DE92-019691] p 948 N93-15274
WASHINGTON UNIV., SAINT LOUIS, MO.
Ringed impact craters on Venus: An analysis from Magellan images p 1024 N93-14291
Surface processes on Venus p 1024 N93-14294
Visoelastic relaxation of Venusian coronae and mountain belts: Constraints on global heat flow and tectonism p 1027 N93-14313
Venusian extended ejecta deposits as time-stratigraphic markers p 1030 N93-14327
Tectonic connections to interior processes on Venus p 1039 N93-14361
Cassini atmospheric chemistry mapper. Volume 1. Investigation and technical plan
[NASA-CR-190947] p 1021 N93-15079
WASHINGTON UNIV., SEATTLE.
Faint high-latitude carbon stars p 1019 N93-14638
Structure and propagation of fronts east of the Rocky Mountains and their relationship to precipitation p 921 N93-14827
Optimization of a Counterflow Virtual Impactor (CVI) for studying aerosol effects on cloud droplet number p 914 N93-14861
Thermal, mechanical, and electroelastic behavior of composite materials p 835 N93-15146
Low energy theorems in pion production
[DE92-040071] p 977 N93-15279
Investigation of the aerothermodynamics of hypervelocity reacting flows in the ram accelerator
[NASA-CR-191715] p 783 N93-15588
WATERLOO UNIV. (ONTARIO).
Integrating satellite imagery into a geographic information system for monitoring the downstream impacts of dam construction on floodplain agriculture in Sokoto State, Nigeria p 905 N93-14823
Dynamics and control of flexible arm robots
[ISBN-0-315-69011-9] p 892 N93-15150
An implementation of multivariate B-spline surfaces over arbitrary triangulations p 952 N93-15534
WEIZMANN INST. OF SCIENCE, REHOVOTH (ISRAEL).
Robot learning of contact tasks
[F-3-2] p 949 N93-15303
Redundancy control of robots by constrained optimization
[F-3-7] p 950 N93-15307
WELDING CONSULTANTS, INC., COLUMBUS, OH.
The Meta-Lax method of stress reduction in welds
[DE92-018477] p 845 N93-14900
WESTINGHOUSE ELECTRIC CORP., PITTSBURGH, PA.
High temperature tubular solid oxide fuel cell development
[DE92-040253] p 908 N93-15322
Contaminant effects in solid oxide fuel cells
[DE92-040255] p 908 N93-15323
WESTINGHOUSE HANFORD CO., RICHLAND, WA.
The information age as a work in progress: Implications for technical communicators
[DE92-019780] p 1008 N93-15275
WESTINGHOUSE IDAHO NUCLEAR CO., INC., IDAHO FALLS.
Design and implementation of a DC-based magnetic field controller with electronic temperature stabilized Hall generator
[DE92-019796] p 870 N93-15276
WESTINGHOUSE SAVANNAH RIVER CO., AIKEN, SC.
Variable path length spectrophotometric probe
[DE92-019834] p 881 N93-14716
Electrochemical oxidation of organic materials
[DE92-019822] p 828 N93-14718
Performing wind-tunnel modeling for better management of near-field risks
[DE92-040205] p 910 N93-15063
WESTINGHOUSE SCIENCE AND TECHNOLOGY CENTER, PITTSBURGH, PA.
Processing, fabrication, and demonstration of HTS integrated microwave circuits
[AD-A256109] p 865 N93-14246
WISCONSIN UNIV., MADISON.
Extreme climatic events in the Amazon Basin and their associations with the circulation of the global tropics p 918 N93-14115
The sulfur emission and periodicity of the Jupiter plasma torus in 1988 p 1022 N93-14156
Computation and communication constraints for distributed estimation systems
[AD-A256287] p 970 N93-14456
Upgrade the University of Wisconsin volume imaging lidar
[AD-A255476] p 885 N93-14497
Comparative study of stability of flexible satellites with and without guy-wire constraints p 817 N93-14585
Multiresolution analysis by infinitely differentiable compactly supported functions
[AD-A256526] p 969 N93-15398

Characterizations of linear independence and stability of the shifts of a univariate refinable function in terms of its refinement mask
[AD-A256527] p 969 N93-15399
Center for Advanced Propulsion Systems (Research)
[AD-A256628] p 893 N93-15410
Morphological analysis of ionomers
[DE92-040162] p 852 N93-15415

WISCONSIN UNIV., WHITEWATER.
Wisconsin Inventors' Network Database
[DE92-018394] p 1007 N93-15137

WOODS HOLE OCEANOGRAPHIC INST., MA.
Experimental investigation of scattering from randomly rough plastic cylinders
[AD-A256018] p 975 N93-15259

WORCESTER POLYTECHNIC INST., MA.
Radical ion formation in polymers as a mechanism for laser eye protection
[AD-A255992] p 850 N93-15111

WRIGHT LAB., EGLIN AFB, FL.
A multigrid approach to embedded-grid solvers
[AD-A256405] p 879 N93-15332

WRIGHT LAB., WRIGHT-PATTERSON AFB, OH.
A preliminary investigation of dual mode fracture sustained by graphite/epoxy laminates impacted by high-velocity spherical metallic projectiles
[AD-A255790] p 898 N93-14419
A compilation of the mathematics leading to the doublet lattice method
[AD-A256304] p 779 N93-14441
The human-electronic crew: Is the team maturing? The 2nd Joint GAF/RAF/USAF Workshop on Human-Electronic Crew Teamwork
[AD-A256192] p 939 N93-14520
Proceedings of the USAF Structural Integrity Program
[AD-A255379] p 777 N93-14549
Subsonic aerodynamic research laboratory
[AD-A256060] p 780 N93-14661
Characterization of cholesteric cyclic siloxane liquid crystalline materials
[AD-A256128] p 994 N93-15190

WYLE LABS., INC., EL SEGUNDO, CA.
Air Force procedure for predicting noise around airbases: Noise exposure model (Noisemap)
[AD-A255769] p 910 N93-14655

WYOMING UNIV., LARAMIE.
Spatially resolved 10 micron spectra of circumstellar material around evolved stars p 1019 N93-14636

X

XEROX PALO ALTO RESEARCH CENTER, CA.
Performing in-place affine transformations in constant space p 954 N93-15546

Y

YALE UNIV., NEW HAVEN, CT.
Sensitivity of quantum electron conductance to elastic scatterers and to spin-orbit scattering in gallium arsenide heterostructures p 990 N93-14184
Transport phenomena and interfacial kinetics in multiphase combustion systems.
[AD-A255999] p 838 N93-14418
Recursively generated networks and dynamical learning
[AD-A255441] p 963 N93-14783
Theoretical and numerical studies in magnetic fusion
[DE92-040674] p 988 N93-15349

YORK UNIV. (ONTARIO).
Excimer laser irradiation of metal surfaces p 884 N93-14175
A study of the low and mid-latitude upper ionospheres of Jupiter and Saturn p 1022 N93-14179
International Space University p 808 N93-14938
Algorithms for the detection and elimination of specular aliasing p 954 N93-15544

CONTRACT NUMBER INDEX

Typical Contract Number Index Listing

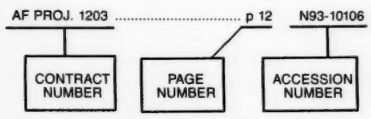

Listings in this index are arranged alphanumerically by contract number. Under each contract number the accession numbers denoting documents that have been produced as a result of research done under that contract are arranged in ascending order. The page number helps to locate the citation in the abstract section. The accession number denotes the number by which the citation is identified.

AE12A/159 ..... p 795 N93-15170
AF PROJ. ST85 ..... p 814 N93-14697
AF PROJ. S321 ..... p 815 N93-14698
AF PROJ. 1123 ..... p 804 N93-14559
AF PROJ. 2305 ..... p 862 N93-15397
AF PROJ. 2338 ..... p 867 N93-14699
AF PROJ. 2401 ..... p 779 N93-14441
AF PROJ. 2402 ..... p 898 N93-14419
AF PROJ. 2403 ..... p 939 N93-14520
AF PROJ. 2404 ..... p 780 N93-14661
AF PROJ. 2418 ..... p 777 N93-14549
AF PROJ. 2567 ..... p 879 N93-15332
AF PROJ. 2853 ..... p 859 N93-14728
AF PROJ. 4594 ..... p 966 N93-15408
AF PROJ. 4643 ..... p 914 N93-14727
AF PROJ. 5321 ..... p 945 N93-14696
AF PROJ. 622-02-F-7231 ..... p 910 N93-14655
AF PROJ. 7321 ..... p 973 N93-14406
AF-AFOSR-0004-90 ..... p 1008 N93-15254
AF-AFOSR-0019-92 ..... p 859 N93-14649
AF-AFOSR-0031-90 ..... p 947 N93-15199
AF-AFOSR-0048-91 ..... p 970 N93-14538
AF-AFOSR-0054-86 ..... p 976 N93-14283
AF-AFOSR-0083-90 ..... p 962 N93-14551
AF-AFOSR-0090-91 ..... p 844 N93-14132
AF-AFOSR-0099-89 ..... p 847 N93-14166
AF-AFOSR-0102-89 ..... p 917 N93-15463
AF-AFOSR-0108-91 ..... p 945 N93-14654
AF-AFOSR-0132-89 ..... p 976 N93-14424
AF-AFOSR-0170-91 ..... p 838 N93-14418
AF-AFOSR-0181-90 ..... p 970 N93-14456
AF-AFOSR-0203-90 ..... p 990 N93-14413
AF-AFOSR-0210-90 ..... p 884 N93-14284
AF-AFOSR-0214-90 ..... p 858 N93-14408
AF-AFOSR-0215-90 ..... p 938 N93-14427
AF-AFOSR-0221-90 ..... p 937 N93-14788
AF-AFOSR-0226-89 ..... p 872 N93-14257
AF-AFOSR-0227-89 ..... p 935 N93-15053
AF-AFOSR-0236-88 ..... p 962 N93-14598
AF-AFOSR-0239-89 ..... p 991 N93-14521
AF-AFOSR-0240-88 ..... p 963 N93-14783
AF-AFOSR-0270-89 ..... p 936 N93-15198
AF-AFOSR-0274-90 ..... p 936 N93-14510
AF-AFOSR-0276-91 ..... p 953 N93-15537
AF-AFOSR-0297-88 ..... p 843 N93-15200
AF-AFOSR-0300-91 ..... p 883 N93-14131
AF-AFOSR-0301-90 ..... p 873 N93-14400
AF-AFOSR-0302-91 ..... p 976 N93-14513
AF-AFOSR-0304-90 ..... p 842 N93-15114
AF-AFOSR-0305-91 ..... p 884 N93-14402
AF-AFOSR-0325-90 ..... p 935 N93-14782
AF-AFOSR-0351-88 ..... p 932 N93-14557
AF-AFOSR-0360-90 ..... p 866 N93-14534
AF-AFOSR-0401-91 ..... p 937 N93-14646
AF-AFOSR-0412-89 ..... p 942 N93-14237
AF-AFOSR-0418-89 ..... p 841 N93-14658
AF-AFOSR-0429-89 ..... p 938 N93-15329
AF-AFOSR-0437-89 ..... p 938 N93-15067
AF-AFOSR-0507-89 ..... p 998 N93-15333
AF-AFOSR-0527-89 ..... p 995 N93-15351
AF-AFOSR-0554-89 ..... p 830 N93-14493
ARPA ORDER 6671 ..... p 961 N93-14409
ARPA ORDER 6685 ..... p 878 N93-15187
ARPA ORDER 7330 ..... p 941 N93-15240
p 950 N93-15336
ARPA ORDER 7526 ..... p 886 N93-15115
ARPA ORDER 7597 ..... p 942 N93-14268
p 940 N93-14491
p 968 N93-14492
p 943 N93-14558
p 959 N93-15205
p 959 N93-15207
ARPA ORDER 7781 ..... p 978 N93-14127
p 978 N93-14570
ARPA ORDER 7932 ..... p 865 N93-14246
ARPA ORDER 8313 ..... p 958 N93-14151
ARPA ORDER 8459 ..... p 943 N93-14546
BWF PROJ. 609.506/1-26/88 ..... p 949 N93-15302
DA PROJ. IRM-T-025 ..... p 989 N93-14133
DA PROJ. RC3-2-A-13 ..... p 859 N93-14663
DA PROJ. RR0-1509 ..... p 857 N93-14181
DA PROJ. R31-030 ..... p 925 N93-14503
DA PROJ. 1L1-61102-AH-43 ..... p 854 N93-15011
DA PROJ. 1L1-61102-AH-47 ..... p 869 N93-15194
DA PROJ. 1L1-61102-BH-57 ..... p 869 N93-15133
DA PROJ. 1L1-62105-AH-84 ..... p 891 N93-14735
DA PROJ. 1L1-62622-A-553 ..... p 854 N93-15640
DA PROJ. 1L1-62705-AH-94 ..... p 842 N93-14678
DA PROJ. 1L1-62716-AH-70 ..... p 936 N93-14416
DA PROJ. 1N4-64806-DF-97 ..... p 850 N93-15064
DA PROJ. 2Q2-63007-A-793 ..... p 951 N93-15445
DA PROJ. 3M1-61102-BS-11 ..... p 935 N93-15009
DA PROJ. 3M1-61102-BS-15 ..... p 938 N93-14161
DA PROJ. 3M1-62787-A-874 ..... p 934 N93-14535
DA PROJ. 3M1-62787-A-878 ..... p 933 N93-14163
DA PROJ. 3M2-63002-F-995 ..... p 937 N93-14600
DA PROJ. 3M4-63807-D-836 ..... p 933 N93-14103
p 881 N93-14105
DA PROJ. 301-61102-BS-15 ..... p 935 N93-15006
DA PROJ. 4A1-61102-AT-23 ..... p 1009 N93-15627
DAAA15-90-C-0019 ..... p 798 N93-15235
DAAB10-86-C-0567 ..... p 963 N93-14786
DAAH01-89-C-0418 ..... p 961 N93-14409
DAAH01-90-C-0373 ..... p 878 N93-15187
DAAH01-91-C-R240 ..... p 934 N93-14210
DAAJ02-91-C-0030 ..... p 792 N93-15227
DAAK60-91-K-0002 ..... p 850 N93-15111
DAAL02-91-C-0020 ..... p 830 N93-14436
DAAL02-91-C-0025 ..... p 859 N93-14453
DAAL03-G-90-0090 ..... p 969 N93-15398
p 969 N93-15399
DAAL03-86-G-0200 ..... p 893 N93-15410
DAAL03-86-K-0174 ..... p 893 N93-15410
DAAL03-89-C-0014 ..... p 995 N93-15365
DAAL03-89-G-0076 ..... p 966 N93-15352
DAAL03-89-G-0078 ..... p 863 N93-15470
DAAL03-89-K-0008 ..... p 885 N93-14667
DAAL03-89-K-0026 ..... p 976 N93-14433
DAAL03-89-K-0071 ..... p 871 N93-15456
DAAL03-89-K-0080 ..... p 866 N93-14562
DAAL03-89-K-0104 ..... p 991 N93-14560
p 849 N93-14668
DAAL03-89-K-0105 ..... p 865 N93-14457
DAAL03-89-K-0114 ..... p 1008 N93-15409
DAAL03-89-K-0145 ..... p 852 N93-15394
DAAL03-90-G-0021 ..... p 875 N93-14677
DAAL03-90-G-0060 ..... p 849 N93-14489
DAAL03-90-G-0103 ..... p 970 N93-14487
p 970 N93-14538
DAAL03-90-G-0129 ..... p 878 N93-15065
DAAL03-90-G-0191 ..... p 940 N93-15363
DAAL03-91-C-0021 ..... p 844 N93-14508
DAAL03-91-G-0208 ..... p 996 N93-15446
p 996 N93-15447
DAAL03-91-G-0222 ..... p 885 N93-14497
DAAL04-91-C-0033 ..... p 836 N93-15218
DACA39-87-K-0022 ..... p 863 N93-15495
DACA76-90-C-0018 ..... p 905 N93-14430
DACA76-92-C-0009 ..... p 943 N93-14546
DAHC35-89-D-0030 ..... p 939 N93-14651
DAJA45-90-C-0042 ..... p 869 N93-15133
DAJA45-92-M-0334 ..... p 869 N93-15188
DAMD17-83-C-3172 ..... p 933 N93-14163
DAMD17-86-C-6260 ..... p 933 N93-14648
DAMD17-88-C-8032 ..... p 933 N93-14163
DAMD17-90-C-0124 ..... p 935 N93-15009
DAMD17-90-Z-0054 ..... p 935 N93-15006
DAMD17-91-Z-1002 ..... p 934 N93-14535
DAMD17-92-J-2003 ..... p 938 N93-14161
DARPA ORDER 6015 ..... p 982 N93-14578
DARPA ORDER 7597 ..... p 967 N93-14235
p 960 N93-15494
DARPA ORDER 8100 ..... p 994 N93-15297
DASG60-90-C-0147 ..... p 951 N93-15432
DASG60-92-C-0049 ..... p 867 N93-14666
DE-AC02-76CH-00016 ..... p 846 N93-15348
DE-AC02-76ER-01112 ..... p 1020 N93-14686
DE-AC02-83CH-10093 ..... p 907 N93-14817
DE-AC03-76SF-00098 ..... p 887 N93-15325
p 984 N93-15350
p 909 N93-15467
p 909 N93-15484
p 871 N93-15485
DE-AC03-76SF-00515 ..... p 951 N93-15451
p 978 N93-15468
p 998 N93-15469
p 978 N93-15486
DE-AC04-76DP-00613 ..... p 945 N93-14876
DE-AC04-76DP-00789 ..... p 976 N93-14662
p 1003 N93-14781
p 826 N93-14815
p 1007 N93-15048
p 1051 N93-15060
p 907 N93-15134
p 902 N93-15210
p 983 N93-15223
p 983 N93-15230
p 978 N93-15277
p 882 N93-15381
p 847 N93-15382
p 847 N93-15383
p 908 N93-15384
p 966 N93-15385
p 997 N93-15649
p 997 N93-15651
DE-AC04-88DP-43495 ..... p 855 N93-15478
DE-AC04-90A1-58770 ..... p 844 N93-14508
DE-AC04-90DE-62349 ..... p 845 N93-14723
DE-AC04-91AL-65030 ..... p 910 N93-14739
DE-AC05-76OR-00001 ..... p 947 N93-15225
DE-AC05-84OR-21400 ..... p 845 N93-14717
p 963 N93-14818
p 946 N93-14902
p 846 N93-15059
p 969 N93-15212
p 869 N93-15214
p 907 N93-15219
p 910 N93-15270
p 911 N93-15273
p 893 N93-15278
p 851 N93-15294
p 851 N93-15295
p 836 N93-15387
p 837 N93-15388
p 852 N93-15437
p 853 N93-15438
p 853 N93-15439
p 863 N93-15440
p 853 N93-15452
p 853 N93-15453
p 837 N93-15454
p 837 N93-15455
p 969 N93-15656
DE-AC05-84OT-21400 ..... p 946 N93-15003
p 951 N93-15450
DE-AC06-76RL-01830 ..... p 846 N93-15138
p 871 N93-15479
DE-AC06-87RL-10930 ..... p 1008 N93-15275
DE-AC07-76ID-01570 ..... p 834 N93-14819
p 916 N93-15136
p 948 N93-15274
DE-AC07-84ID-12435 ..... p 870 N93-15276
DE-AC07-84NV-10366 ..... p 894 N93-15416
DE-AC08-87NV-10576 ..... p 1008 N93-15229
DE-AC09-89SR-18035 ..... p 881 N93-14716
p 828 N93-14718
p 910 N93-15063

DE-AC12-76SN-00052 p 877 N93-14816
DE-AC21-86MC-25104 p 907 N93-15213
DE-AC21-89MC-26355 p 908 N93-15323
DE-AC21-90MC-27394 p 994 N93-15221
DE-AC35-89ER-40486 p 905 N93-14522
DE-AI01-87CE-34011 p 870 N93-15412
DE-AI03-86SF-16310 p 847 N93-15524
DE-BI79-90BP-04293 p 933 N93-15211
DE-FC02-86CH-10311 p 908 N93-15384
DE-FC21-91MC-28055 p 908 N93-15322
DE-FG01-87CE-15337 p 907 N93-15224
DE-FG01-91CE-15978 p 845 N93-14900
DE-FG02-85ER-45205 p 992 N93-14812
DE-FG02-86ER-13579 p 842 N93-14908
DE-FG02-86ER-53240 p 988 N93-15349
DE-FG02-87ER-40344 p 977 N93-15377
DE-FG02-88ER-13974 p 843 N93-15414
DE-FG02-88ER-40414 p 977 N93-15326
DE-FG02-88ER-45370 p 852 N93-15415
DE-FG02-89ER-45391 p 993 N93-14909
DE-FG02-89ER-69027 p 922 N93-14901
DE-FG02-90CE-15981 p 1007 N93-15137
DE-FG02-90ER-61080 p 911 N93-15272
DE-FG03-84ER-45089 p 887 N93-15347
DE-FG05-85ER-13434 p 886 N93-15058
DE-FG05-86ER-40272 p 972 N93-15057
p 1022 N93-15346
p 977 N93-15378
p 969 N93-15379
DE-FG05-88ER-13977 p 893 N93-15380
DE-FG05-88ER-53266 p 988 N93-15327
DE-FG05-91ER-81156 p 851 N93-15222
DE-FG06-85ER-45191 p 850 N93-14903
DE-FG06-86ER-40283 p 977 N93-15062
DE-FG06-90ER-40561 p 977 N93-15279
DNA001-88-C-0207 p 938 N93-15216
DNA001-89-C-0025 p 869 N93-15196
DRET-88-003-01 p 792 N93-15126
DRET-88-164 p 878 N93-15122
DRET-88-34-001-BC-35 p 836 N93-15253
DRET-89-001-218 p 975 N93-15130
DRET-89-34-001 p 974 N93-15129
DRET-90-1625-A000 p 886 N93-15128
DRET/ARMINES-89-250 p 851 N93-15127
DTFA01-87-C-00014 p 974 N93-14912
DTFA01-89-Z-02033 p 920 N93-14547
DTFA01-90-C-00042 p 785 N93-15013
DTFA01-91-C-00040 p 787 N93-15022
EPA-68-CO-0047 p 910 N93-15217
EPA-68-03-3409 p 975 N93-15647
ESTEC-8219/89/NL/PH(SC) p 835 N93-15075
F04611-89-K-0003 p 843 N93-15497
F04701-88-C-0089 p 971 N93-14108
p 839 N93-14530
p 851 N93-15242
p 972 N93-15243
p 1049 N93-15318
p 979 N93-15362
F19623-88-K-0009 p 983 N93-15197
F19628-86-C-0092 p 924 N93-15581
F19628-86-K-0040 p 814 N93-14697
F19628-88-D-0031 p 951 N93-15457
p 952 N93-15471
F19628-88-D-0032 p 942 N93-14405
F19628-88-K-0007 p 858 N93-14437
F19628-88-K-0016 p 918 N93-14153
F19628-88-K-0021 p 972 N93-14679
F19628-88-K-0028 p 815 N93-14698
F19628-88-K-0031 p 914 N93-14727
F19628-89-C-0015 p 924 N93-15331
F19628-89-K-0037 p 886 N93-15069
F19628-90-C-0002 p 920 N93-14547
p 992 N93-14576
p 937 N93-14580
p 964 N93-15258
F19628-90-C-0003 p 944 N93-14563
F19628-90-C-0097 p 916 N93-14899
F19628-90-0002 p 858 N93-14426
F19628-91-C-0093 p 945 N93-14696
F19628-91-C-0168 p 958 N93-14151
F30602-86-C-0269 p 944 N93-14572
p 944 N93-14581
F30602-88-D-0028 p 859 N93-14728
F30602-89-C-0111 p 895 N93-15204
F30602-89-C-0121 p 867 N93-14699
F30602-91-D-0003 p 817 N93-14565
F33615-84-C-3404 p 791 N93-14571
F33615-87-C-3402 p 894 N93-14104
F33615-87-C-3403 p 900 N93-14498
F33615-87-C-5240 p 983 N93-15255
F33615-88-C-0631 p 887 N93-15472
F33615-88-C-1792 p 856 N93-14107
F33615-88-C-2902 p 849 N93-14527
F33615-90-C-1465 p 967 N93-14235
p 942 N93-14268
p 940 N93-14491

F49620-87-C-0045 p 968 N93-14492
F49620-87-C-0056 p 943 N93-14558
F49620-88-C-0073 p 959 N93-15205
F49620-88-C-0138 p 959 N93-15207
F49620-89-C-0071 p 960 N93-15494
F49620-89-C-0079 p 976 N93-14411
F49620-89-C-0088 p 982 N93-14578
F49620-91-C-0071 p 831 N93-14665
F49620-92-C-0014 p 848 N93-14401
F49620-92-J-0065 p 917 N93-15466
F49620-92-J-0233 p 967 N93-14412
F49620-92-J-0264 p 865 N93-14425
p 1004 N93-14785
F49629-88-C-0075 p 868 N93-15108
MDA903-85-C-0440 p 782 N93-15464
MDA903-88-C-0147 p 865 N93-14410
MDA903-89-C-0003 p 981 N93-14506
MDA903-90-C-0006 p 992 N93-14741
p 869 N93-15257
MDA972-90-C-0035 p 951 N93-15445
p 946 N93-15068
MDA972-90-C-0046 p 990 N93-14422
MDA972-92-C-0029 p 1007 N93-15050
MIPR-ARO-137-90 p 1007 N93-15051
MIPR-ARO-145-89 p 941 N93-15240
MIPR-102-90 p 950 N93-15336
MIPR-120-89 p 886 N93-15115
NAGW-1331 p 866 N93-14555
p 968 N93-14787
NAGW-1613 p 968 N93-14787
NAGW-1708 p 850 N93-15049
NAGW-1801 p 850 N93-15049
NAGW-1829 p 875 N93-14481
NAGW-1908 p 834 N93-14754
NAGW-2013 p 834 N93-14756
p 917 N93-15574
p 901 N93-14766
NAGW-2049 p 1021 N93-15079
NAGW-2201 p 911 N93-15480
NAGW-2998 p 1020 N93-14814
NAGW-533 p 1013 N93-15589
NAG1-1040 p 1014 N93-15590
NAG1-1060 p 1014 N93-15591
NAG1-1067 p 1014 N93-15592
NAG1-1242 p 1025 N93-14301
NAG1-886 p 1012 N93-14759
NAG1-994 p 890 N93-14567
p 1047 N93-15081
NAG1-995 p 903 N93-15653
NAG2-485 p 951 N93-15432
NAG2-542 p 852 N93-15431
NAG2-593 p 997 N93-15587
NAG3-1061 p 781 N93-14767
NAG3-1110 p 875 N93-14687
NAG3-1332 p 875 N93-14688
NAG3-666 p 875 N93-14689
NAG3-894 p 875 N93-14690
NAG3-895 p 876 N93-14691
NAG5-1346 p 951 N93-15432
NAG5-1428 p 1043 N93-14386
NAG5-1491 p 945 N93-14807
p 862 N93-15339
NAG5-1549 p 783 N93-15588
NAG5-1644 p 800 N93-15359
NAG5-741 p 867 N93-14721
NAG8-754 p 787 N93-15360
NAG8-764 p 830 N93-14484
NAG8-831 p 901 N93-14799
NAG8-869 p 984 N93-15505
NASA ORDER C-99066-G p 1013 N93-15340
NASA ORDER T-9311-R p 857 N93-14155
NASW-4324 p 941 N93-14770
NASW-4574 p 922 N93-14910
NAS1-18147 p 1012 N93-14761
NAS1-18230 p 916 N93-14913
p 924 N93-15581
NAS1-18584 p 925 N93-14769
p 995 N93-15309
NAS1-18605 p 882 N93-14810
p 969 N93-15341
p 1051 N93-15580
NAS1-18648 p 936 N93-15583
NAS1-18763 p 1023 N93-14288
NAS1-18834 p 815 N93-14730
NAS1-18925 p 815 N93-14768
NAS1-18969 p 815 N93-14794
NAS1-19299 p 876 N93-14691
p 876 N93-14692
p 951 N93-15432
p 879 N93-15481
p 880 N93-15643
p 802 N93-14811
p 832 N93-14745
p 905 N93-14792
p 958 N93-14808
p 877 N93-14797

NAS1-19480 p 951 N93-15432
p 879 N93-15481
NAS3-25266 p 867 N93-14798
p 826 N93-15370
p 879 N93-15402
p 880 N93-15527
p 895 N93-15582
NAS3-25343 p 982 N93-15116
NAS3-26061 p 891 N93-14916
NAS5-26813 p 1049 N93-15634
NAS5-30386 p 1049 N93-15634
NAS5-30435 p 868 N93-14915
NAS7-918 p 981 N93-14404
p 832 N93-14700
p 994 N93-15151
NAS8-32805 p 1049 N93-15634
NAS8-36955 p 910 N93-14764
p 892 N93-15117
NAS8-38609 p 826 N93-14681
p 891 N93-14763
p 855 N93-14793
NAS9-17840 p 815 N93-15474
p 816 N93-15475
NAS9-17884 p 881 N93-14494
NAS9-18202 p 817 N93-14733
p 818 N93-14872
p 824 N93-15629
p 824 N93-15630
p 824 N93-15631
p 824 N93-15632
p 825 N93-15633
p 825 N93-15658
NA89AA-D-SG-053 p 933 N93-15208
NCC1-22 p 875 N93-14481
NCC2-371 p 843 N93-15358
NCC2-478 p 843 N93-15356
p 843 N93-15357
p 843 N93-15358
NCC2-716 p 804 N93-14809
NGL-22-0069-640 p 787 N93-15360
NGR-559 p 1049 N93-15634
NR PROJ. RR0-4204 p 933 N93-14109
NR PROJ. RR0-4206 p 999 N93-14130
NR PROJ. RS3-4-P-11 p 940 N93-14644
p 958 N93-14645
NR PROJ. RS3-4-P-12 p 944 N93-14575
NSF ASC-84-14524 p 1004 N93-15030
NSF ASC-87-15728 p 956 N93-15560
NSF ASC-88-19373 p 951 N93-15432
NSF ASC-90-05933 p 956 N93-15560
NSF ASC-90-20416 p 1004 N93-15030
NSF ATM-86-01405 p 924 N93-15581
NSF ATM-90-22249 p 1049 N93-15634
NSF CCR-87-16884 p 941 N93-15628
NSF CCR-89-02362 p 951 N93-15432
NSF CCR-90-00028 p 953 N93-15537
NSF CCR-92-01195 p 951 N93-15432
NSF CDA-90-22123 p 954 N93-15543
NSF DCR-85-52474 p 956 N93-15560
NSF DMS-90-00053 p 969 N93-15398
p 969 N93-15399
NSF DMS-91-01424 p 953 N93-15537
NSF ECD-88-11111 p 954 N93-15543
NSF PHY-91-09937 p 1014 N93-15592
NSG-7411 p 1049 N93-15085
N00014-09-J-1777 p 903 N93-15496
N00014-82-K-0193 p 982 N93-14582
N00014-82-K-0280 p 994 N93-15233
N00014-84-C-0717 p 924 N93-15581
N00014-85-K-0789 p 842 N93-14664
N00014-86-J-1218 p 845 N93-14740
N00014-86-K-0688 p 924 N93-15581
N00014-87-C-0408 p 866 N93-14583
N00014-87-K-0495 p 842 N93-14671
N00014-88-C-0661 p 983 N93-15241
N00014-88-K-0233 p 999 N93-14130
N00014-88-2035 p 885 N93-14647
N00014-89-C-0310 p 947 N93-15228
N00014-89-C-3188 p 902 N93-15372
p 836 N93-15373
p 903 N93-15374
N00014-89-J-1003 p 974 N93-14458
N00014-89-J-1008 p 969 N93-15256
N00014-89-J-1024 p 1049 N93-15634
N00014-89-J-1061 p 841 N93-14652
N00014-89-J-1235 p 842 N93-14669
p 992 N93-14670
N00014-89-J-1249 p 866 N93-14577
N00014-89-J-1708 p 898 N93-14272
N00014-89-J-1754 p 917 N93-15395
N00014-89-J-1799 p 880 N93-15652
N00014-89-J-1849 p 868 N93-15010
N00014-89-J-1988 p 941 N93-15628
p 1009 N93-15639
N00014-89-J-3146 p 939 N93-14548
N00014-89-J-3237 p 996 N93-15444

N00014-90-C-0089 ..... p 798 N93-14111
N00014-90-C-0123 ..... p 881 N93-14653
N00014-90-C-0246 ..... p 979 N93-14152
p 984 N93-15371
N00014-90-F-0011 ..... p 989 N93-14133
N00014-90-J-1113 ..... p 916 N93-15375
N00014-90-J-1134 ..... p 996 N93-15449
N00014-90-J-1307 ..... p 933 N93-14109
N00014-90-J-1372 ..... p 967 N93-14270
p 967 N93-14271
N00014-90-J-1530 ..... p 996 N93-15443
N00014-90-J-1553 ..... p 994 N93-15191
N00014-90-J-1604 ..... p 994 N93-15244
N00014-90-J-1852 ..... p 1000 N93-14182
N00014-90-J-1940 ..... p 970 N93-14455
N00014-90-J-4014 ..... p 888 N93-14434
N00014-90-J-4018 ..... p 944 N93-14564
N00014-90-J-4130 ..... p 885 N93-14599
N00014-91-C-0112 ..... p 865 N93-14246
N00014-91-C-0124 ..... p 844 N93-14264
N00014-91-C-0154 ..... p 884 N93-14414
N00014-91-C-0190 ..... p 936 N93-15192
N00014-91-C-0216 ..... p 994 N93-15297
N00014-91-J-1005 ..... p 942 N93-14285
N00014-91-J-1222 ..... p 943 N93-14546
N00014-91-J-1409 ..... p 977 N93-15448
N00014-91-J-1513 ..... p 992 N93-14643
p 993 N93-15008
p 993 N93-15055
N00014-91-J-1529 ..... p 962 N93-14656
N00014-91-J-1598 ..... p 932 N93-14532
N00014-91-J-1755 ..... p 991 N93-14439
N00014-91-J-1837 ..... p 991 N93-14429
N00014-91-J-1872 ..... p 954 N93-15543
N00014-91-J-2002 ..... p 973 N93-14159
N00014-91-J-4008 ..... p 925 N93-14428
N00014-91-J-4103 ..... p 901 N93-15066
N00014-91-3-1714 ..... p 945 N93-14659
N00014-92-C-0043 ..... p 862 N93-15334
N00014-92-J-1186 ..... p 996 N93-15465
N00014-92-J-1254 ..... p 970 N93-15109
p 971 N93-15110
N00014-92-J-1302 ..... p 984 N93-15458
N00014-92-J-1511 ..... p 998 N93-14417
N00025-92-J-1264 ..... p 970 N93-15109
p 971 N93-15110
N00038-88-C-0051 ..... p 863 N93-15624
N00039-84-C-0165 ..... p 954 N93-15543
N00039-88-C-0051 ..... p 838 N93-15625
N60530-82-R-0012 ..... p 790 N93-14432
N62269-91-C-0249 ..... p 849 N93-14573
PROJ. IR-90-2 ..... p 933 N93-15208
PROJ. R/C-S-27 ..... p 933 N93-15208
PROJ. 89-04 ..... p 997 N93-15500
RF PROJ. 769157/724904 ..... p 1012 N93-14761
RTOP 142-20-14-02 ..... p 997 N93-15587
RTOP 324-02-00 ..... p 880 N93-15643
RTOP 474-42-10 ..... p 871 N93-15503
RTOP 488-51-01 ..... p 816 N93-15477
RTOP 505-52-62 ..... p 781 N93-14791
RTOP 505-59-10 ..... p 877 N93-14797
RTOP 505-59-53 ..... p 779 N93-14451
RTOP 505-61-51 ..... p 782 N93-15483
RTOP 505-62-0K ..... p 902 N93-15343
RTOP 505-62-21 ..... p 877 N93-14829
p 877 N93-14885
p 969 N93-15341
p 880 N93-15499
RTOP 505-62-50 ..... p 801 N93-15525
RTOP 505-62-52 ..... p 877 N93-14758
p 879 N93-15355
p 801 N93-15521
RTOP 505-62-84 ..... p 804 N93-15498
RTOP 505-63-1B ..... p 901 N93-14799
RTOP 505-63-5A ..... p 828 N93-15576
RTOP 505-63-5B ..... p 888 N93-14478
p 902 N93-15369
RTOP 505-63-50-05 ..... p 832 N93-14744
RTOP 505-63-53-01 ..... p 900 N93-14483
RTOP 505-64-12-01 ..... p 783 N93-14844
RTOP 505-66-01-02 ..... p 803 N93-15366
RTOP 505-68-10 ..... p 803 N93-14831
p 781 N93-14911
p 782 N93-15338
p 787 N93-15345
p 787 N93-15354
p 787 N93-15360
p 879 N93-15402
p 788 N93-15522
RTOP 505-70-64-01 ..... p 802 N93-14811
RTOP 505-90-52-01 ..... p 951 N93-15432
p 879 N93-15481
p 979 N93-15482
RTOP 505-90-53 ..... p 880 N93-15585
RTOP 506-40-91-01 ..... p 879 N93-15434
RTOP 506-41-11 ..... p 872 N93-14150
RTOP 506-41-41 ..... p 854 N93-14834
p 852 N93-15344
RTOP 506-42-31 ..... p 826 N93-14883
p 826 N93-15370
p 827 N93-15429
p 827 N93-15572
RTOP 506-42-72 ..... p 827 N93-15571
RTOP 506-43-41-02 ..... p 818 N93-15368
RTOP 506-48-91 ..... p 828 N93-14459
RTOP 506-49-11-01 ..... p 813 N93-15367
RTOP 506-49-11-02 ..... p 815 N93-14730
p 815 N93-14768
p 815 N93-14794
RTOP 506-49-64-01 ..... p 905 N93-14792
RTOP 506-72-00 ..... p 871 N93-15531
RTOP 510-01-50 ..... p 830 N93-14484
p 850 N93-14886
p 837 N93-15401
RTOP 535-03-10 ..... p 801 N93-15403
RTOP 535-05-10 ..... p 777 N93-14102
RTOP 537-01-11 ..... p 844 N93-15504
RTOP 537-02-20 ..... p 800 N93-15359
RTOP 537-02-23 ..... p 975 N93-15430
p 975 N93-15575
RTOP 539-72-00 ..... p 828 N93-15584
RTOP 578-12-23-70 ..... p 924 N93-15501
RTOP 589-01-2C ..... p 855 N93-15420
RTOP 590-12-33 ..... p 867 N93-14798
RTOP 590-13-11 ..... p 826 N93-14482
p 847 N93-15524
p 827 N93-15526
RTOP 590-14-21-01 ..... p 902 N93-15202
RTOP 590-21-11 ..... p 847 N93-15586
RTOP 590-49-00 ..... p 909 N93-15523
RTOP 593-00-71 ..... p 827 N93-15428
RTOP 656-80-02-26 ..... p 1002 N93-14771
RTOP 674-21-05 ..... p 878 N93-14914
RTOP 694-03-0C ..... p 856 N93-15353
p 778 N93-15573
RTOP 694-03-03 ..... p 895 N93-15582
RTOP 763-01-21 ..... p 800 N93-15342
RTOP 763-01-41-27 ..... p 975 N93-15391
RTOP 906-11-00 ..... p 814 N93-14495
SAIC-11-900286-39 ..... p 825 N93-15633
W-31-109-ENG-38 ..... p 910 N93-15209
p 826 N93-15215
p 851 N93-15282
p 883 N93-15411
p 870 N93-15441
p 906 N93-15442
p 978 N93-15654
p 1010 N93-15655
p 978 N93-15657
W-7405-ENG-36 ..... p 914 N93-14724
p 818 N93-14904
p 998 N93-14905
p 907 N93-15061
p 887 N93-15135
p 843 N93-15283
p 852 N93-15320
p 995 N93-15321
p 1022 N93-15324
p 895 N93-15413
p 887 N93-15417
p 988 N93-15418
p 988 N93-15419
p 870 N93-15421
p 989 N93-15422
p 903 N93-15423
p 870 N93-15424
p 837 N93-15426
p 862 N93-15427
p 862 N93-15435
p 989 N93-15436
W-7405-ENG-48 ..... p 876 N93-14715
p 915 N93-14877
p 886 N93-14906
p 911 N93-15280
p 911 N93-15281
p 878 N93-15285
p 870 N93-15389
p 853 N93-15462
p 952 N93-15493

REPORT NUMBER INDEX

Typical Report Number Index Listing

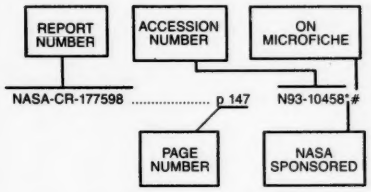

Listings in this index are arranged alphanumerically by report number. The accession number denotes the number by which the citation is identified. The page number helps to locate the citation in the abstract section. An asterisk (*) indicates that the item is a NASA report. A pound sign (#) indicates that the item is available on microfiche.

A-90110 ..... p 782 N93-15483 * #
A-91163 ..... p 816 N93-15477 * #

AARL-92-27 ..... p 933 N93-14103 #
AARL-92-30 ..... p 937 N93-14600 #

AD-A250399 ..... p 991 N93-14521 #
AD-A252121 ..... p 793 N93-14110 #
AD-A254115 ..... p 869 N93-15133 #
AD-A254336 ..... p 938 N93-15216 #
AD-A254925 ..... p 836 N93-15218 #
AD-A255205 ..... p 867 N93-14666 #
AD-A255214 ..... p 789 N93-14574 #
AD-A255215 ..... p 944 N93-14575 #
AD-A255218 ..... p 1001 N93-14524 #
AD-A255221 ..... p 962 N93-14525 #
AD-A255226 ..... p 798 N93-14111 #
AD-A255235 ..... p 999 N93-14526 #
AD-A255239 ..... p 885 N93-14667 #
AD-A255240 ..... p 849 N93-14668 #
AD-A255241 ..... p 842 N93-14669 #
AD-A255242 ..... p 992 N93-14670 #
AD-A255243 ..... p 849 N93-14527 #
AD-A255251 ..... p 889 N93-14528 #
AD-A255258 ..... p 889 N93-14529 #
AD-A255261 ..... p 839 N93-14530 #
AD-A255272 ..... p 792 N93-15004 #
AD-A255274 ..... p 849 N93-14531 #
AD-A255276 ..... p 789 N93-15005 #
AD-A255277 ..... p 935 N93-15006 #
AD-A255278 ..... p 842 N93-14671 #
AD-A255282 ..... p 932 N93-14532 #
AD-A255283 ..... p 962 N93-14533 #
AD-A255287 ..... p 866 N93-14534 #
AD-A255299 ..... p 934 N93-14535 #
AD-A255313 ..... p 831 N93-14672 #
AD-A255315 ..... p 816 N93-14536 #
AD-A255316 ..... p 889 N93-14545 #
AD-A255317 ..... p 943 N93-14546 #
AD-A255319 ..... p 920 N93-14547 #
AD-A255324 ..... p 939 N93-14548 #
AD-A255331 ..... p 1051 N93-14523 #
AD-A255332 ..... p 804 N93-14559 #
AD-A255335 ..... p 991 N93-14537 #
AD-A255349 ..... p 789 N93-14517 #
AD-A255351 ..... p 991 N93-14518 #
AD-A255357 ..... p 970 N93-14538 #
AD-A255358 ..... p 991 N93-14560 #
AD-A255359 ..... p 849 N93-14561 #
AD-A255361 ..... p 1051 N93-14673 #
AD-A255363 ..... p 866 N93-14562 #
AD-A255366 ..... p 792 N93-15227 #
AD-A255370 ..... p 1051 N93-14674 #
AD-A255371 ..... p 845 N93-14740 #
AD-A255375 ..... p 832 N93-14675 #
AD-A255376 ..... p 944 N93-14563 #
AD-A255379 ..... p 777 N93-14549 #
AD-A255380 ..... p 831 N93-14550 #
AD-A255381 ..... p 944 N93-14564 #
AD-A255383 ..... p 992 N93-14741 #
AD-A255384 ..... p 939 N93-14651 #
AD-A255389 ..... p 947 N93-15228 #
AD-A255390 ..... p 841 N93-14652 #
AD-A255392 ..... p 905 N93-14676 #
AD-A255397 ..... p 875 N93-14677 #
AD-A255403 ..... p 817 N93-14565 #
AD-A255407 ..... p 789 N93-14501 #
AD-A255408 ..... p 943 N93-14502 #
AD-A255409 ..... p 925 N93-14503 #
AD-A255414 ..... p 866 N93-14504 #
AD-A255421 ..... p 943 N93-14505 #
AD-A255423 ..... p 981 N93-14506 #
AD-A255424 ..... p 982 N93-14507 #
AD-A255426 ..... p 844 N93-14508 #
AD-A255431 ..... p 831 N93-14509 #
AD-A255432 ..... p 936 N93-14510 #
AD-A255433 ..... p 962 N93-14551 #
AD-A255434 ..... p 944 N93-14566 #
AD-A255436 ..... p 866 N93-14552 #
AD-A255439 ..... p 994 N93-15297 #
AD-A255440 ..... p 935 N93-14782 #
AD-A255441 ..... p 963 N93-14783 #
AD-A255443 ..... p 982 N93-14784 #
AD-A255444 ..... p 914 N93-14511 #
AD-A255445 ..... p 925 N93-14512 #
AD-A255447 ..... p 976 N93-14513 #
AD-A255453 ..... p 848 N93-14486 #
AD-A255456 ..... p 970 N93-14487 #
AD-A255460 ..... p 859 N93-14488 #
AD-A255463 ..... p 1004 N93-14785 #
AD-A255464 ..... p 995 N93-15351 #
AD-A255465 ..... p 972 N93-14496 #
AD-A255471 ..... p 963 N93-14786 #
AD-A255476 ..... p 885 N93-14497 #
AD-A255477 ..... p 849 N93-14489 #
AD-A255481 ..... p 906 N93-15007 #
AD-A255482 ..... p 969 N93-14787 #
AD-A255483 ..... p 937 N93-14788 #
AD-A255485 ..... p 935 N93-14789 #
AD-A255490 ..... p 867 N93-14642 #
AD-A255496 ..... p 880 N93-15652 #
AD-A255497 ..... p 992 N93-14643 #
AD-A255498 ..... p 940 N93-14644 #
AD-A255501 ..... p 958 N93-14645 #
AD-A255522 ..... p 890 N93-14567 * #
AD-A255523 ..... p 885 N93-14568 #
AD-A255524 ..... p 944 N93-14569 #
AD-A255525 ..... p 939 N93-14554 #
AD-A255545 ..... p 978 N93-14570 #
AD-A255548 ..... p 791 N93-14571 #
AD-A255551 ..... p 866 N93-14555 #
AD-A255553 ..... p 934 N93-14556 #
AD-A255593 ..... p 901 N93-14790 #
AD-A255606 ..... p 993 N93-15008 #
AD-A255607 ..... p 935 N93-15009 #
AD-A255612 ..... p 868 N93-15010 #
AD-A255613 ..... p 854 N93-15011 #
AD-A255614 ..... p 974 N93-15012 #
AD-A255616 ..... p 973 N93-14159 #
AD-A255624 ..... p 850 N93-15064 #
AD-A255627 ..... p 938 N93-14161 #
AD-A255630 ..... p 933 N93-14162 #
AD-A255635 ..... p 978 N93-14127 #
AD-A255636 ..... p 857 N93-14181 #
AD-A255639 ..... p 958 N93-14151 #
AD-A255642 ..... p 976 N93-14283 #
AD-A255644 ..... p 979 N93-14152 #
AD-A255648 ..... p 1000 N93-14182 #
AD-A255649 ..... p 933 N93-14163 #
AD-A255652 ..... p 934 N93-14210 #
AD-A255656 ..... p 942 N93-14164 #
AD-A255660 ..... p 804 N93-14128 #
AD-A255663 ..... p 999 N93-14130 #
AD-A255666 ..... p 883 N93-14131 #
AD-A255668 ..... p 918 N93-14153 #
AD-A255674 ..... p 844 N93-14132 #
AD-A255675 ..... p 847 N93-14166 #
AD-A255678 ..... p 920 N93-14258 #
AD-A255691 ..... p 933 N93-14103 #
AD-A255696 ..... p 932 N93-14557 #
AD-A255702 ..... p 881 N93-14653 #
AD-A255708 ..... p 905 N93-14430 #
AD-A255709 ..... p 945 N93-14654 #
AD-A255711 ..... p 968 N93-14431 #
AD-A255714 ..... p 790 N93-14432 #
AD-A255723 ..... p 976 N93-14433 #
AD-A255725 ..... p 888 N93-14434 #
AD-A255727 ..... p 838 N93-14435 #
AD-A255728 ..... p 878 N93-15065 #
AD-A255729 ..... p 850 N93-15049 #
AD-A255737 ..... p 1007 N93-15050 #
AD-A255739 ..... p 1007 N93-15051 #
AD-A255746 ..... p 946 N93-15052 #
AD-A255748 ..... p 935 N93-15053 #
AD-A255750 ..... p 977 N93-15054 #
AD-A255763 ..... p 993 N93-15055 #
AD-A255764 ..... p 846 N93-15056 #
AD-A255765 ..... p 901 N93-15066 #
AD-A255769 ..... p 910 N93-14655 #
AD-A255780 ..... p 938 N93-15067 #
AD-A255786 ..... p 937 N93-14646 #
AD-A255790 ..... p 898 N93-14419 #
AD-A255791 ..... p 885 N93-14647 #
AD-A255797 ..... p 788 N93-15390 #
AD-A255798 ..... p 984 N93-15371 #
AD-A255799 ..... p 933 N93-14648 #
AD-A255801 ..... p 946 N93-15068 #
AD-A255802 ..... p 886 N93-15069 #
AD-A255836 ..... p 894 N93-14104 #
AD-A255849 ..... p 881 N93-14105 #
AD-A255850 ..... p 999 N93-14106 #
AD-A255855 ..... p 856 N93-14107 #
AD-A255862 ..... p 989 N93-14133 #
AD-A255902 ..... p 971 N93-14108 #
AD-A255908 ..... p 902 N93-15070 #
AD-A255913 ..... p 856 N93-15105 #
AD-A255926 ..... p 933 N93-14109 #
AD-A255927 ..... p 861 N93-15106 #
AD-A255929 ..... p 962 N93-14656 #
AD-A255937 ..... p 925 N93-14428 #
AD-A255945 ..... p 942 N93-14405 #
AD-A255952 ..... p 1051 N93-14657 #
AD-A255953 ..... p 943 N93-14420 #
AD-A255954 ..... p 873 N93-14421 #
AD-A255959 ..... p 990 N93-14422 #
AD-A255961 ..... p 991 N93-14429 #
AD-A255963 ..... p 973 N93-14406 #
AD-A255964 ..... p 981 N93-14407 #
AD-A255967 ..... p 873 N93-14400 #
AD-A255968 ..... p 848 N93-14401 #
AD-A255969 ..... p 884 N93-14402 #
AD-A255971 ..... p 868 N93-15108 #
AD-A255972 ..... p 981 N93-14403 #
AD-A255974 ..... p 830 N93-14493 #
AD-A255975 ..... p 858 N93-14408 #
AD-A255976 ..... p 961 N93-14409 #
AD-A255977 ..... p 865 N93-14410 #
AD-A255978 ..... p 943 N93-14423 #
AD-A255979 ..... p 976 N93-14424 #
AD-A255980 ..... p 865 N93-14425 #
AD-A255981 ..... p 976 N93-14411 #
AD-A255983 ..... p 967 N93-14412 #
AD-A255984 ..... p 990 N93-14413 #
AD-A255985 ..... p 884 N93-14414 #
AD-A255988 ..... p 858 N93-14415 #
AD-A255989 ..... p 936 N93-14416 #
AD-A255990 ..... p 970 N93-15109 #
AD-A255991 ..... p 971 N93-15110 #
AD-A255992 ..... p 850 N93-15111 #
AD-A255993 ..... p 998 N93-14417 #
AD-A255999 ..... p 838 N93-14418 #
AD-A256001 ..... p 1007 N93-15112 #
AD-A256002 ..... p 932 N93-15113 #
AD-A256004 ..... p 842 N93-15114 #
AD-A256005 ..... p 886 N93-15115 #
AD-A256006 ..... p 1008 N93-15254 #
AD-A256011 ..... p 983 N93-15255 #
AD-A256012 ..... p 969 N93-15256 #
AD-A256016 ..... p 869 N93-15257 #
AD-A256017 ..... p 964 N93-15258 #
AD-A256018 ..... p 975 N93-15259 #

AD-A256019 ..... p 992 N93-14576 #
AD-A256020 ..... p 858 N93-14426 #
AD-A256034 ..... p 841 N93-14658 #
AD-A256035 ..... p 902 N93-15260 #
AD-A256036 ..... p 994 N93-15233 #
AD-A256038 ..... p 878 N93-15187 #
AD-A256040 ..... p 866 N93-14577 #
AD-A256041 ..... p 945 N93-14659 #
AD-A256046 ..... p 937 N93-14660 #
AD-A256047 ..... p 982 N93-14578 #
AD-A256056 ..... p 988 N93-14579 #
AD-A256059 ..... p 937 N93-14580 #
AD-A256060 ..... p 780 N93-14661 #
AD-A256063 ..... p 921 N93-14680 #
AD-A256070 ..... p 976 N93-14662 #
AD-A256071 ..... p 859 N93-14663 #
AD-A256072 ..... p 830 N93-14232 #
AD-A256074 ..... p 858 N93-14259 #
AD-A256075 ..... p 858 N93-14233 #
AD-A256076 ..... p 973 N93-14234 #
AD-A256078 ..... p 967 N93-14235 #
AD-A256080 ..... p 897 N93-14236 #
AD-A256082 ..... p 990 N93-14260 #
AD-A256085 ..... p 909 N93-14261 #
AD-A256087 ..... p 904 N93-14262 #
AD-A256089 ..... p 904 N93-14263 #
AD-A256091 ..... p 938 N93-14427 #
AD-A256092 ..... p 884 N93-14284 #
AD-A256095 ..... p 844 N93-14264 #
AD-A256100 ..... p 1001 N93-14265 #
AD-A256106 ..... p 942 N93-14237 #
AD-A256107 ..... p 971 N93-14245 #
AD-A256109 ..... p 865 N93-14246 #
AD-A256115 ..... p 869 N93-15188 #
AD-A256124 ..... p 842 N93-14664 #
AD-A256126 ..... p 846 N93-15189 #
AD-A256128 ..... p 994 N93-15190 #
AD-A256129 ..... p 856 N93-15234 #
AD-A256130 ..... p 942 N93-14247 #
AD-A256131 ..... p 790 N93-14248 #
AD-A256132 ..... p 1010 N93-14249 #
AD-A256133 ..... p 816 N93-14253 #
AD-A256134 ..... p 865 N93-14254 #
AD-A256142 ..... p 967 N93-14255 #
AD-A256147 ..... p 920 N93-14256 #
AD-A256152 ..... p 872 N93-14257 #
AD-A256153 ..... p 831 N93-14665 #
AD-A256158 ..... p 842 N93-14678 #
AD-A256162 ..... p 925 N93-14452 #
AD-A256164 ..... p 944 N93-14581 #
AD-A256172 ..... p 859 N93-14649 #
AD-A256174 ..... p 1002 N93-14650 #
AD-A256175 ..... p 972 N93-14679 #
AD-A256188 ..... p 962 N93-14519 #
AD-A256191 ..... p 943 N93-14558 #
AD-A256192 ..... p 939 N93-14520 #
AD-A256194 ..... p 798 N93-15235 #
AD-A256197 ..... p 859 N93-14490 #
AD-A256198 ..... p 940 N93-14491 #
AD-A256199 ..... p 968 N93-14492 #
AD-A256200 ..... p 900 N93-14498 #
AD-A256202 ..... p 889 N93-14499 #
AD-A256203 ..... p 894 N93-14500 #
AD-A256204 ..... p 836 N93-15236 #
AD-A256209 ..... p 861 N93-15237 #
AD-A256212 ..... p 792 N93-15238 #
AD-A256221 ..... p 941 N93-15239 #
AD-A256222 ..... p 941 N93-15240 #
AD-A256224 ..... p 983 N93-15241 #
AD-A256226 ..... p 982 N93-14582 #
AD-A256227 ..... p 962 N93-14598 #
AD-A256231 ..... p 851 N93-15242 #
AD-A256232 ..... p 972 N93-15243 #
AD-A256234 ..... p 960 N93-15494 #
AD-A256236 ..... p 885 N93-14599 #
AD-A256239 ..... p 866 N93-14583 #
AD-A256240 ..... p 859 N93-14453 #
AD-A256242 ..... p 944 N93-14572 #
AD-A256245 ..... p 937 N93-14600 #
AD-A256246 ..... p 849 N93-14573 #
AD-A256253 ..... p 838 N93-14454 #
AD-A256258 ..... p 830 N93-14436 #
AD-A256262 ..... p 858 N93-14437 #
AD-A256268 ..... p 976 N93-14438 #
AD-A256283 ..... p 994 N93-15244 #
AD-A256284 ..... p 970 N93-14455 #
AD-A256287 ..... p 970 N93-14456 #
AD-A256288 ..... p 865 N93-14457 #
AD-A256289 ..... p 974 N93-14458 #
AD-A256290 ..... p 991 N93-14439 #
AD-A256296 ..... p 790 N93-14440 #
AD-A256304 ..... p 779 N93-14441 #
AD-A256306 ..... p 859 N93-14442 #
AD-A256307 ..... p 970 N93-14443 #
AD-A256311 ..... p 782 N93-15245 #
AD-A256315 ..... p 792 N93-15328 #
AD-A256325 ..... p 994 N93-15191 #
AD-A256327 ..... p 936 N93-15192 #
AD-A256328 ..... p 836 N93-15193 #
AD-A256329 ..... p 869 N93-15194 #
AD-A256333 ..... p 968 N93-15195 #
AD-A256338 ..... p 869 N93-15196 #
AD-A256339 ..... p 983 N93-15197 #
AD-A256340 ..... p 936 N93-15198 #
AD-A256341 ..... p 947 N93-15199 #
AD-A256342 ..... p 843 N93-15200 #
AD-A256347 ..... p 895 N93-15204 #
AD-A256355 ..... p 959 N93-15205 #
AD-A256365 ..... p 947 N93-15206 #
AD-A256367 ..... p 959 N93-15207 #
AD-A256369 ..... p 938 N93-15329 #
AD-A256373 ..... p 870 N93-15330 #
AD-A256375 ..... p 917 N93-15463 #
AD-A256385 ..... p 782 N93-15464 #
AD-A256394 ..... p 996 N93-15465 #
AD-A256397 ..... p 917 N93-15466 #
AD-A256403 ..... p 924 N93-15331 #
AD-A256405 ..... p 879 N93-15332 #
AD-A256410 ..... p 998 N93-15333 #
AD-A256421 ..... p 862 N93-15334 #
AD-A256422 ..... p 1008 N93-15335 #
AD-A256431 ..... p 950 N93-15336 #
AD-A256434 ..... p 800 N93-15337 #
AD-A256435 ..... p 950 N93-15313 #
AD-A256438 ..... p 792 N93-15314 #
AD-A256439 ..... p 1008 N93-15315 #
AD-A256440 ..... p 861 N93-15316 #
AD-A256443 ..... p 861 N93-15317 #
AD-A256444 ..... p 802 N93-14608 #
AD-A256445 ..... p 791 N93-14601 #
AD-A256448 ..... p 968 N93-14609 #
AD-A256450 ..... p 859 N93-14610 #
AD-A256457 ..... p 1049 N93-15318 #
AD-A256469 ..... p 902 N93-15372 #
AD-A256470 ..... p 836 N93-15373 #
AD-A256471 ..... p 903 N93-15374 #
AD-A256473 ..... p 959 N93-15319 #
AD-A256483 ..... p 916 N93-14899 #
AD-A256498 ..... p 916 N93-15375 #
AD-A256504 ..... p 862 N93-15376 #
AD-A256515 ..... p 1008 N93-15393 #
AD-A256519 ..... p 852 N93-15394 #
AD-A256520 ..... p 917 N93-15395 #
AD-A256522 ..... p 803 N93-15396 #
AD-A256525 ..... p 862 N93-15397 #
AD-A256526 ..... p 969 N93-15398 #
AD-A256527 ..... p 969 N93-15399 #
AD-A256529 ..... p 942 N93-14285 #
AD-A256538 ..... p 981 N93-14286 #
AD-A256547 ..... p 814 N93-14266 #
AD-A256548 ..... p 936 N93-14267 #
AD-A256552 ..... p 938 N93-15400 #
AD-A256557 ..... p 937 N93-14602 #
AD-A256558 ..... p 867 N93-14803 #
AD-A256559 ..... p 968 N93-14804 #
AD-A256560 ..... p 860 N93-14805 #
AD-A256563 ..... p 860 N93-14806 #
AD-A256564 ..... p 951 N93-15405 #
AD-A256565 ..... p 966 N93-15406 #
AD-A256574 ..... p 942 N93-14268 #
AD-A256579 ..... p 973 N93-14269 #
AD-A256581 ..... p 967 N93-14270 #
AD-A256583 ..... p 967 N93-14271 #
AD-A256587 ..... p 898 N93-14272 #
AD-A256593 ..... p 804 N93-14238 #
AD-A256598 ..... p 960 N93-14239 #
AD-A256602 ..... p 934 N93-14240 #
AD-A256609 ..... p 942 N93-14241 #
AD-A256612 ..... p 858 N93-14250 #
AD-A256613 ..... p 802 N93-14252 #
AD-A256614 ..... p 788 N93-14275 #
AD-A256615 ..... p 789 N93-14276 #
AD-A256616 ..... p 783 N93-14277 #
AD-A256617 ..... p 959 N93-15407 #
AD-A256621 ..... p 966 N93-15408 #
AD-A256625 ..... p 1008 N93-15409 #
AD-A256628 ..... p 893 N93-15410 #
AD-A256781 ..... p 863 N93-15624 #
AD-A256782 ..... p 838 N93-15625 #
AD-A256809 ..... p 971 N93-15626 #
AD-A256831 ..... p 880 N93-15635 #
AD-A256834 ..... p 864 N93-15636 #
AD-A256836 ..... p 1009 N93-15637 #
AD-A256841 ..... p 1009 N93-15639 #
AD-A256856 ..... p 854 N93-15640 #
AD-A256857 ..... p 1009 N93-15641 #
AD-A256859 ..... p 1009 N93-15642 #
AD-A256862 ..... p 1009 N93-15627 #
AD-A256872 ..... p 941 N93-15628 #
AD-A257019 ..... p 966 N93-15352 #
AD-A257021 ..... p 863 N93-15470 #
AD-A257022 ..... p 952 N93-15471 #
AD-A257023 ..... p 887 N93-15472 #
AD-A257025 ..... p 792 N93-15361 #
AD-A257033 ..... p 979 N93-15362 #
AD-A257037 ..... p 940 N93-15363 #
AD-A257040 ..... p 906 N93-15364 #
AD-A257047 ..... p 995 N93-15365 #
AD-A257049 ..... p 996 N93-15443 #
AD-A257050 ..... p 996 N93-15444 #
AD-A257052 ..... p 951 N93-15445 #
AD-A257053 ..... p 996 N93-15446 #
AD-A257054 ..... p 996 N93-15447 #
AD-A257057 ..... p 977 N93-15448 #
AD-A257061 ..... p 996 N93-15449 #
AD-A257062 ..... p 871 N93-15456 #
AD-A257064 ..... p 951 N93-15457 #
AD-A257065 ..... p 984 N93-15458 #
AD-A257068 ..... p 917 N93-15459 #
AD-A257069 ..... p 863 N93-15495 #
AD-A257080 ..... p 903 N93-15496 #
AD-A257086 ..... p 843 N93-15497 #

AD-D015378 ..... p 869 N93-15269 #
AD-D015379 ..... p 836 N93-15246 #
AD-D015380 ..... p 882 N93-15247 #
AD-D015383 ..... p 893 N93-15248 #
AD-D015384 ..... p 936 N93-15249 #
AD-D015387 ..... p 887 N93-15250 #
AD-D015389 ..... p 893 N93-15251 #
AD-D015391 ..... p 846 N93-15231 #
AD-D015392 ..... p 893 N93-15232 #
AD-D015393 ..... p 894 N93-15461 #
AD-D015400 ..... p 868 N93-15107 #
AD-D015408 ..... p 882 N93-14878 #
AD-D015409 ..... p 868 N93-14887 #
AD-D015410 ..... p 845 N93-14888 #
AD-D015411 ..... p 860 N93-14879 #
AD-D015412 ..... p 982 N93-14880 #
AD-D015416 ..... p 891 N93-14881 #
AD-D015417 ..... p 860 N93-14889 #
AD-D015420 ..... p 982 N93-14800
AD-D015421 ..... p 860 N93-14742
AD-D015422 ..... p 850 N93-14743
AD-D015423 ..... p 993 N93-14820
AD-D015424 ..... p 885 N93-14821
AD-D015427 ..... p 891 N93-14822
AD-D015428 ..... p 842 N93-14824
AD-D015432 ..... p 850 N93-14825
AD-D015435 ..... p 868 N93-14826
AD-D015436 ..... p 885 N93-14722
AD-D015437 ..... p 817 N93-14725
AD-D015439 ..... p 854 N93-14801
AD-D015443 ..... p 850 N93-14802 #

AD-E201155 ..... p 918 N93-14153 #
AD-E201186 ..... p 843 N93-15497 #
AD-E201218 ..... p 916 N93-14899 #
AD-E501566 ..... p 990 N93-14422 #

AEDC-TR-92-5 ..... p 981 N93-14403 #

AERONOMICA-ACTA-A-361-1991 p 911 N93-15460

AEROSPACE-ATR-91(8308)-2 ..... p 992 N93-14795 #

AFIT/CI/CIA-92-012D ..... p 914 N93-14511 #

AFIT/DS/ENC/92-1 ..... p 942 N93-14241 #

AFIT/EN-TR-92-3 ..... p 859 N93-14649 #
AFIT/EN-TR-92-4 ..... p 1008 N93-15315 #

AFIT/GA/ENG/92J-01 ..... p 802 N93-14608 #

AFIT/GAE/ENY/92J-02 ..... p 792 N93-15314 #
AFIT/GAE/ENY/92M-01 ..... p 802 N93-14252 #

AFIT/GE/ENG/92-M ..... p 951 N93-15405 #
AFIT/GE/ENG/92J-01 ..... p 861 N93-15316 #
AFIT/GE/ENG/92J-04 ..... p 950 N93-15313 #
AFIT/GE/ENG/92S-03 ..... p 858 N93-14250 #
AFIT/GE/ENG/92S-04 ..... p 966 N93-15406 #
AFIT/GE/ENG/92S-07 ..... p 861 N93-15317 #

AFOSR-TR-92-0813 ..... p 1051 N93-14674 #
AFOSR-TR-92-0843 ..... p 1051 N93-14673 #

AFOSR-92-0274TR ..... p 991 N93-14521 #
AFOSR-92-05446TR ..... p 937 N93-14788 #
AFOSR-92-0737TR ..... p 992 N93-14741 #
AFOSR-92-0739TR ..... p 981 N93-14506 #
AFOSR-92-0828TR ..... p 945 N93-14654 #
AFOSR-92-0829TR ..... p 976 N93-14283 #
AFOSR-92-0831TR ..... p 963 N93-14783 #
AFOSR-92-0834TR ..... p 936 N93-14510 #
AFOSR-92-0835TR ..... p 962 N93-14551 #
AFOSR-92-0837TR ..... p 935 N93-15053 #

AFOSR-92-0845TR ..... p 1051 N93-14523 #
AFOSR-92-0848TR ..... p 995 N93-15351 #
AFOSR-92-0852TR ..... p 938 N93-14427 #
AFOSR-92-0853TR ..... p 831 N93-14665 #
AFOSR-92-0854TR ..... p 967 N93-14412 #
AFOSR-92-0855TR ..... p 976 N93-14411 #
AFOSR-92-0857TR ..... p 872 N93-14257 #
AFOSR-92-0858TR ..... p 1008 N93-15254 #
AFOSR-92-0859TR ..... p 990 N93-14413 #
AFOSR-92-0860TR ..... p 942 N93-14237 #
AFOSR-92-0862TR ..... p 865 N93-14410 #
AFOSR-92-0863TR ..... p 976 N93-14424 #
AFOSR-92-0864TR ..... p 873 N93-14400 #
AFOSR-92-0865TR ..... p 841 N93-14658 #
AFOSR-92-0866TR ..... p 865 N93-14425 #
AFOSR-92-0867TR ..... p 848 N93-14401 #
AFOSR-92-0870TR ..... p 883 N93-14131 #
AFOSR-92-0871TR ..... p 844 N93-14132 #
AFOSR-92-0872TR ..... p 847 N93-14166 #
AFOSR-92-0874TR ..... p 842 N93-15114 #
AFOSR-92-0875TR ..... p 970 N93-14456 #
AFOSR-92-0875TR ..... p 932 N93-14557 #
AFOSR-92-0877TR ..... p 938 N93-15329 #
AFOSR-92-0878TR ..... p 782 N93-15464 #
AFOSR-92-0883TR ..... p 938 N93-15067 #
AFOSR-92-0885TR ..... p 962 N93-14598 #
AFOSR-92-0888TR ..... p 858 N93-14408 #
AFOSR-92-0889TR ..... p 884 N93-14402 #
AFOSR-92-0890TR ..... p 838 N93-14418 #
AFOSR-92-0891TR ..... p 830 N93-14493 #
AFOSR-92-0893TR ..... p 884 N93-14284 #
AFOSR-92-0895TR ..... p 869 N93-15257 #
AFOSR-92-0896TR ..... p 868 N93-15108 #
AFOSR-92-0897TR ..... p 917 N93-15466 #
AFOSR-92-0898TR ..... p 843 N93-15200 #
AFOSR-92-0899TR ..... p 917 N93-15463 #
AFOSR-92-0900TR ..... p 947 N93-15199 #
AFOSR-92-0901TR ..... p 936 N93-15198 #
AFOSR-92-0902TR ..... p 998 N93-15333 #
AFOSR-92-8841TR ..... p 935 N93-14782 #

AFW-5240-FM-8784-461 ..... p 983 N93-15255 #

AGARD-AR-308 ..... p 798 N93-14890 #

AIAA PAPER 92-0335 ..... p 969 N93-15341 * #
AIAA PAPER 93-0021 ..... p 844 N93-15504 * #
AIAA PAPER 93-0029 ..... p 787 N93-15360 * #
AIAA PAPER 93-0031 ..... p 782 N93-15338 * #
AIAA PAPER 93-0032 ..... p 781 N93-14911 * #
AIAA PAPER 93-0147 ..... p 975 N93-15575 * #
AIAA PAPER 93-0170 ..... p 787 N93-15345 * #
AIAA PAPER 93-0171 ..... p 879 N93-15402 * #
AIAA PAPER 93-0173 ..... p 787 N93-15354 * #
AIAA PAPER 93-0174 ..... p 788 N93-15522 * #
AIAA PAPER 93-0249 ..... p 800 N93-15359 * #
AIAA PAPER 93-0301 ..... p 782 N93-15404 * #
AIAA PAPER 93-0398 ..... p 803 N93-14831 * #
AIAA PAPER 93-0465 ..... p 855 N93-15420 * #
AIAA PAPER 93-0599 ..... p 801 N93-15403 * #
AIAA PAPER 93-0735 ..... p 975 N93-15430 * #
AIAA PAPER 93-0775 ..... p 879 N93-15355 * #

AL-TP-1992-0019 ..... p 976 N93-14438 #

AL-TR-1991-0126 ..... p 973 N93-14406 #
AL-TR-1991-0146 ..... p 887 N93-15472 #
AL-TR-1992-0042 ..... p 804 N93-14559 #
AL-TR-1992-0059 ..... p 910 N93-14655 #

ANL-91/39 ..... p 851 N93-15282 #

ANL/CP-75445 ..... p 910 N93-15209 #
ANL/CP-76155 ..... p 870 N93-15441 #
ANL/CP-76576 ..... p 826 N93-15215 #
ANL/CP-76750 ..... p 883 N93-15411 #
ANL/CP-76976 ..... p 1010 N93-15655 #
ANL/CP-77000 ..... p 978 N93-15654 #
ANL/CP-77129 ..... p 978 N93-15657 #
ANL/CP-77152 ..... p 906 N93-15442 #

ARCCB-TR-92030 ..... p 962 N93-14533 #
ARCCB-TR-92036 ..... p 836 N93-15193 #

ARI-RN-92-68 ..... p 939 N93-14651 #

ARI-RP-92-07 ..... p 951 N93-15445 #

ARL-FLIGHT-MECH-TM-456 ..... p 792 N93-15328 #

ARO-D-126 ..... p 970 N93-14538 #

ARO-24623.111-EG-UIR ..... p 893 N93-15410 #
ARO-26278-EL ..... p 976 N93-14433 #
ARO-26484.1-EL ..... p 995 N93-15365 #
ARO-26676.15-PH ..... p 1008 N93-15409 #
ARO-26760.3-EL ..... p 871 N93-15456 #
ARO-26827.7-PH ..... p 991 N93-14560 #
ARO-26827.7-PH ..... p 849 N93-14668 #
ARO-26852.10-MS-A ..... p 852 N93-15394 #
ARO-26923.1-EL-SDI ..... p 866 N93-14562 #
ARO-27006.2-EL-F ..... p 863 N93-15470 #
ARO-27007.8-EL-F ..... p 966 N93-15352 #
ARO-27058.1-MA ..... p 968 N93-14787 #
ARO-27558.9-EG ..... p 875 N93-14677 #
ARO-27759.CH ..... p 849 N93-14489 #
ARO-27868.16-MA ..... p 970 N93-14487 #
ARO-27868.18-MA ..... p 970 N93-14538 #
ARO-28066.1-MA ..... p 940 N93-15363 #
ARO-29180.1-PH-CF-PT-1 ..... p 996 N93-15447 #
ARO-29180.2-PH-CF-PT-2 ..... p 996 N93-15446 #
ARO-29204.3-GS-EQ ..... p 885 N93-14497 #

ASD-TR-91-5009 ..... p 790 N93-14432 #

ASL-TR-0318 ..... p 977 N93-15054 #

ASR-4 ..... p 974 N93-14458 #

ATCOM-TR-92-B-015 ..... p 900 N93-14483 * #

ATEC-R-186 ..... p 789 N93-14501 #

ATR-91(7190)-2 ..... p 917 N93-15574 * #

BNL-46330 ..... p 846 N93-15348 #

BRDEC-TR-2529 ..... p 838 N93-14435 #
BRDEC-TR-2534 ..... p 838 N93-14454 #

BRL-TR-3385 ..... p 991 N93-14518 #
BRL-TR-3402 ..... p 854 N93-15011 #

CAR-TR-632 ..... p 943 N93-14546 #

CARDEROCKDIV-SME-92/29 ..... p 831 N93-14509 #

CECOM-TR-92-1 ..... p 862 N93-15376 #

CERC-TR-92-8 ..... p 932 N93-15113 #

CERL-ADP-EGI-92/01 ..... p 1009 N93-15642 #

CERL-ADP-N-87/22-REV ..... p 1001 N93-14524 #

CERL-TR-EC-92/01 ..... p 1009 N93-15627 #

CERL-TR-FF-92/06 ..... p 1009 N93-15641 #

CERL-TR-FM-92/02 ..... p 943 N93-14505 #

CMOTT-92-10 ..... p 969 N93-15341 * #
CMOTT-92-11 ..... p 877 N93-14829 * #

CMS-TSR-93-3 ..... p 969 N93-15399 #
CMS-TSR-93-4 ..... p 969 N93-15398 #

CMU-CS-92-129 ..... p 967 N93-14235 #
CMU-CS-92-154 ..... p 960 N93-15494 #
CMU-CS-92-155 ..... p 958 N93-14151 #
CMU-CS-92-161 ..... p 950 N93-15336 #
CMU-CS-92-164 ..... p 943 N93-14423 #
CMU-CS-92-167 ..... p 941 N93-15240 #
CMU-CS-92-168 ..... p 943 N93-14558 #
CMU-CS-92-169 ..... p 940 N93-14491 #
CMU-CS-92-172 ..... p 959 N93-15205 #
CMU-CS-92-173 ..... p 959 N93-15207 #
CMU-CS-92-176 ..... p 941 N93-15239 #
CMU-CS-92-179 ..... p 968 N93-14492 #
CMU-CS-92-181 ..... p 947 N93-15206 #
CMU-CS-92-186 ..... p 942 N93-14268 #
CMU-CS-92-196 ..... p 959 N93-15407 #

CMU-RI-TR-91-15 ..... p 889 N93-14545 #
CMU-RI-TR-91-31 ..... p 944 N93-14566 #
CMU-RI-TR-92-01 ..... p 944 N93-14569 #
CMU-RI-TR-92-04 ..... p 885 N93-14568 #
CMU-RI-TR-92-07 ..... p 890 N93-14567 * #
CMU-RI-TR-92-08 ..... p 889 N93-14528 #
CMU-RI-TR-92-09 ..... p 889 N93-14529 #

CMU/SEI-91-SR-13 ..... p 944 N93-14563 #

CONF-9002111 ..... p 910 N93-15270 #
CONF-9105365-1 ..... p 911 N93-15273 #
CONF-910957-4 ..... p 893 N93-15380 #
CONF-9110122-29 ..... p 916 N93-15136 #
CONF-9110161-6 ..... p 922 N93-14901 #
CONF-911094 ..... p 869 N93-15226 #
CONF-9202117-5 ..... p 1022 N93-15324 #
CONF-9202135-1 ..... p 1022 N93-15346 #
CONF-9203150-3 ..... p 977 N93-15279 #
CONF-920378 ..... p 908 N93-15271 #
CONF-920402-45 ..... p 869 N93-15214 #
CONF-9205149 ..... p 951 N93-15451 #
CONF-920515-7 ..... p 978 N93-15277 #
CONF-9205204-2 ..... p 910 N93-15209 #
CONF-920574-10 ..... p 887 N93-15135 #
CONF-9206131-1 ..... p 978 N93-15486 #
CONF-9206267-1 ..... p 947 N93-15225 #
CONF-9206271-1 ..... p 837 N93-15426 #
CONF-9206278-1 ..... p 843 N93-15283 #
CONF-9206280-1 ..... p 978 N93-15657 #
CONF-9206282-1 ..... p 846 N93-15348 #
CONF-920673-9 ..... p 846 N93-15138 #
CONF-9207118-2 ..... p 862 N93-15427 #
CONF-9207118-3 ..... p 862 N93-15435 #
CONF-9207118-4 ..... p 818 N93-14904 #
CONF-9207146-1 ..... p 852 N93-15320 #
CONF-9207149-1 ..... p 998 N93-15469 #
CONF-9207149-2 ..... p 978 N93-15468 #
CONF-920748-10 ..... p 994 N93-15221 #
CONF-920748-18 ..... p 908 N93-15323 #
CONF-920748-20 ..... p 908 N93-15322 #
CONF-920748-6 ..... p 851 N93-15222 #
CONF-920792-31 ..... p 886 N93-14906 #
CONF-920801-16 ..... p 907 N93-15134 #
CONF-920801-22 ..... p 826 N93-15215 #
CONF-920803-11 ..... p 826 N93-14815 #
CONF-920804-23 ..... p 877 N93-14816 #
CONF-9208109-26 ..... p 887 N93-15417 #
CONF-9208109-29 ..... p 870 N93-15421 #
CONF-9208109-31 ..... p 903 N93-15423 #
CONF-9208109-34 ..... p 870 N93-15424 #
CONF-9208117-12 ..... p 910 N93-15063 #
CONF-9208119-3 ..... p 983 N93-15223 #
CONF-920813-1 ..... p 988 N93-15419 #
CONF-9208135-1 ..... p 989 N93-15436 #
CONF-9208141-1 ..... p 998 N93-14905 #
CONF-9208142-1 ..... p 887 N93-15325 #
CONF-920849-1 ..... p 1008 N93-15229 #
CONF-920913-13 ..... p 988 N93-15418 #
CONF-9209142-7 ..... p 1010 N93-15655 #
CONF-9209160-17 ..... p 906 N93-15442 #
CONF-9209179-3 ..... p 847 N93-15382 #
CONF-9209188-3 ..... p 882 N93-15381 #
CONF-9209189-2 ..... p 989 N93-15422 #
CONF-9209202-1 ..... p 995 N93-15321 #
CONF-920930-1 ..... p 863 N93-15440 #
CONF-920945-1 ..... p 978 N93-15654 #
CONF-920951-1 ..... p 883 N93-15411 #
CONF-9210155-1 ..... p 1008 N93-15275 #
CONF-921036-1 ..... p 907 N93-15061 #
CONF-921036-8 ..... p 870 N93-15441 #
CONF-921049-1 ..... p 908 N93-15384 #
CONF-921079-1 ..... p 1051 N93-15060 #
CONF-921110-26 ..... p 893 N93-15278 #
CONF-921110-9 ..... p 907 N93-15219 #
CONF-921181-1 ..... p 963 N93-14818 #
CONF-921181-3 ..... p 966 N93-15385 #
CONF-921183-3 ..... p 847 N93-15383 #
CONF-921199-1 ..... p 895 N93-15413 #
CONF-921219-2 ..... p 969 N93-15656 #
CONF-921226-2 ..... p 997 N93-15649 #
CONF-921226-3 ..... p 997 N93-15651 #

CRDEC-TR-361 ..... p 854 N93-15640 #
CRDEC-TR-392 ..... p 850 N93-15064 #

CRREL-SR-92-12 ..... p 848 N93-14486 #

CS-TR-2942 ..... p 943 N93-14546 #

CSWD-92-TRF-0041 ..... p 906 N93-15364 #
CSWD-92-TRF-0050 ..... p 963 N93-14786 #

CTN-92-60336 ..... p 804 N93-14920 #
CTN-93-60619 ..... p 855 N93-15201 #
CTN-93-60626 ..... p 835 N93-15145 #

C912F ..... p 866 N93-14583 #

DARPA-RD/0992 ..... p 961 N93-14409 #

DE92-001280 ..... p 907 N93-15213 #
DE92-012629 ..... p 1051 N93-15060 #
DE92-013384 ..... p 907 N93-15061 #
DE92-014399 ..... p 992 N93-14812 #
DE92-016328 ..... p 826 N93-14815 #
DE92-016360 ..... p 877 N93-14816 #
DE92-016408 ..... p 907 N93-14817 #
DE92-016701 ..... p 910 N93-15209 #
DE92-016767 ..... p 902 N93-15210 #
DE92-017050 ..... p 907 N93-15134 #
DE92-017529 ..... p 887 N93-15135 #
DE92-017817 ..... p 907 N93-15219 #
DE92-017819 ..... p 963 N93-14818 #
DE92-017829 ..... p 869 N93-15214 #

DE92-017841 ..... p 916 N93-15136 #
DE92-017863 ..... p 933 N93-15211 #
DE92-018115 ..... p 1008 N93-15229 #
DE92-018394 ..... p 1007 N93-15137 #
DE92-018477 ..... p 845 N93-14900 #
DE92-018779 ..... p 922 N93-14901 #
DE92-019009 ..... p 910 N93-15270 #
DE92-019015 ..... p 907 N93-15224 #
DE92-019042 ..... p 826 N93-15215 #
DE92-019066 ..... p 969 N93-15212 #
DE92-019090 ..... p 908 N93-15271 #
DE92-019170 ..... p 911 N93-15272 #
DE92-019186 ..... p 911 N93-15273 #
DE92-019434 ..... p 846 N93-15138 #
DE92-019691 ..... p 948 N93-15274 #
DE92-019780 ..... p 1008 N93-15275 #
DE92-019796 ..... p 870 N93-15276 #
DE92-019803 ..... p 978 N93-15277 #
DE92-019804 ..... p 983 N93-15230 #
DE92-019818 ..... p 845 N93-14717
DE92-019822 ..... p 828 N93-14718
DE92-019831 ..... p 876 N93-14715
DE92-019834 ..... p 881 N93-14716
DE92-019836 ..... p 834 N93-14819
DE92-019888 ..... p 947 N93-15225 #
DE92-019890 ..... p 869 N93-15226 #
DE92-019891 ..... p 861 N93-15220 #
DE92-019973 ..... p 994 N93-15221 #
DE92-019980 ..... p 851 N93-15222 #
DE92-040026 ..... p 893 N93-15278 #
DE92-040071 ..... p 977 N93-15279 #
DE92-040076 ..... p 870 N93-15412 #
DE92-040093 ..... p 983 N93-15223 #
DE92-040149 ..... p 977 N93-15062 #
DE92-040150 ..... p 895 N93-15413 #
DE92-040160 ..... p 843 N93-15414 #
DE92-040162 ..... p 852 N93-15415 #
DE92-040189 ..... p 894 N93-15416 #
DE92-040205 ..... p 910 N93-15063 #
DE92-040211 ..... p 843 N93-15283 #
DE92-040213 ..... p 887 N93-15417 #
DE92-040215 ..... p 988 N93-15418 #
DE92-040223 ..... p 988 N93-15419 #
DE92-040225 ..... p 870 N93-15421 #
DE92-040226 ..... p 989 N93-15422 #
DE92-040228 ..... p 903 N93-15423 #
DE92-040229 ..... p 870 N93-15424 #
DE92-040233 ..... p 852 N93-15320 #
DE92-040236 ..... p 995 N93-15321 #
DE92-040253 ..... p 908 N93-15322 #
DE92-040255 ..... p 908 N93-15323 #
DE92-040301 ..... p 850 N93-14903 #
DE92-040316 ..... p 1013 N93-15425 #
DE92-040326 ..... p 837 N93-15426 #
DE92-040327 ..... p 862 N93-15427 #
DE92-040328 ..... p 862 N93-15435 #
DE92-040329 ..... p 818 N93-14904 #
DE92-040352 ..... p 989 N93-15436 #
DE92-040365 ..... p 1022 N93-15324 #
DE92-040377 ..... p 998 N93-14905 #
DE92-040378 ..... p 887 N93-15325 #
DE92-040403 ..... p 886 N93-14906 #
DE92-040410 ..... p 886 N93-14907 #
DE92-040457 ..... p 977 N93-15326 #
DE92-040460 ..... p 977 N93-15377 #
DE92-040498 ..... p 842 N93-14908 #
DE92-040499 ..... p 993 N93-14909 #
DE92-040501 ..... p 1022 N93-15346 #
DE92-040502 ..... p 972 N93-15057 #
DE92-040505 ..... p 977 N93-15378 #
DE92-040506 ..... p 969 N93-15379 #
DE92-040512 ..... p 886 N93-15058 #
DE92-040520 ..... p 846 N93-15059 #
DE92-040523 ..... p 988 N93-15327 #
DE92-040560 ..... p 887 N93-15347 #
DE92-040569 ..... p 846 N93-15348 #
DE92-040674 ..... p 988 N93-15349 #
DE92-040717 ..... p 978 N93-15657 #
DE92-040738 ..... p 978 N93-15654 #
DE92-040741 ..... p 1010 N93-15655 #
DE92-040875 ..... p 969 N93-15656 #
DE92-040898 ..... p 893 N93-15380 #
DE92-040959 ..... p 882 N93-15381 #
DE92-040975 ..... p 997 N93-15651 #
DE92-040978 ..... p 847 N93-15382 #
DE92-040979 ..... p 997 N93-15649 #
DE92-040980 ..... p 847 N93-15383 #
DE92-040984 ..... p 908 N93-15384 #
DE92-040985 ..... p 966 N93-15385 #
DE92-041020 ..... p 863 N93-15440 #
DE92-041046 ..... p 853 N93-15462 #
DE92-041102 ..... p 870 N93-15441 #
DE92-041107 ..... p 906 N93-15442 #
DE92-041121 ..... p 883 N93-15411 #
DE92-041227 ..... p 855 N93-15478 #
DE92-041243 ..... p 951 N93-15450 #

DE92-041350 ..... p 946 N93-14902 #
DE92-041357 ..... p 871 N93-15479 #
DE92-041359 ..... p 951 N93-15451 #
DE92-041371 ..... p 853 N93-15452 #
DE92-041372 ..... p 853 N93-15453 #
DE92-041373 ..... p 852 N93-15437 #
DE92-041376 ..... p 837 N93-15454 #
DE92-041378 ..... p 837 N93-15455 #
DE92-041379 ..... p 836 N93-15387 #
DE92-041380 ..... p 853 N93-15438 #
DE92-041381 ..... p 837 N93-15388 #
DE92-041382 ..... p 853 N93-15439 #
DE92-041383 ..... p 851 N93-15294 #
DE92-041385 ..... p 851 N93-15295 #
DE92-526947 ..... p 887 N93-15296 #
DE92-630358 ..... p 991 N93-14485 #
DE93-000348 ..... p 870 N93-15389 #
DE93-000380 ..... p 946 N93-15003 #
DE93-000774 ..... p 905 N93-14522 #
DE93-000889 ..... p 911 N93-15280 #
DE93-000890 ..... p 911 N93-15281 #
DE93-000930 ..... p 851 N93-15282 #
DE93-001543 ..... p 984 N93-15350 #
DE93-001595 ..... p 909 N93-15484 #
DE93-001598 ..... p 909 N93-15467 #
DE93-001603 ..... p 871 N93-15485 #
DE93-001763 ..... p 978 N93-15486 #
DE93-001767 ..... p 978 N93-15468 #
DE93-001807 ..... p 998 N93-15469 #
DE93-001828 ..... p 952 N93-15493 #

DLR-MITT-92-01 ..... p 793 N93-15152 #
DLR-MITT-92-03 ..... p 835 N93-15075 #
DLR-MITT-92-05 ..... p 835 N93-15076 #

DMS-DR-2287 ..... p 816 N93-15475 * #
DMS-DR-2541 ..... p 815 N93-15474 * #

DNA-TR-91-178 ..... p 938 N93-15216 #
DNA-TR-91-86 ..... p 869 N93-15196 #

DODA-AR-006-670 ..... p 792 N93-15328 #
DODA-AR-006-933 ..... p 943 N93-14502 #
DODA-AR-006-940 ..... p 982 N93-14784 #
DODA-AR-006-986 ..... p 973 N93-14269 #

DOE/BP-1792 ..... p 933 N93-15211 #

DOE/CE-15337/T15 ..... p 907 N93-15224 #
DOE/CE-15978/T1 ..... p 845 N93-14900 #
DOE/CE-15981/4 ..... p 1007 N93-15137 #

DOE/EA-0548 ..... p 886 N93-14907 #
DOE/EA-0591 ..... p 1013 N93-15425 #

DOE/ER-13434/7 ..... p 886 N93-15058 #
DOE/ER-13579/6 ..... p 842 N93-14908 #
DOE/ER-13974/3 ..... p 843 N93-15414 #
DOE/ER-40272/165 ..... p 969 N93-15379 #
DOE/ER-40272/168 ..... p 972 N93-15057 #
DOE/ER-40272/169 ..... p 977 N93-15378 #
DOE/ER-40272/171 ..... p 1022 N93-15346 #
DOE/ER-40283/12 ..... p 977 N93-15062 #
DOE/ER-40344/6 ..... p 977 N93-15377 #
DOE/ER-40414/5 ..... p 977 N93-15326 #
DOE/ER-40561/67 ..... p 977 N93-15279 #
DOE/ER-45089/T1 ..... p 887 N93-15347 #
DOE/ER-45191/20 ..... p 850 N93-14903 #
DOE/ER-45205/7 ..... p 992 N93-14812 #
DOE/ER-45370/4 ..... p 852 N93-15415 #
DOE/ER-45391/3 ..... p 993 N93-14909 #
DOE/ER-53240/T2 ..... p 988 N93-15349 #
DOE/ER-53266/40 ..... p 988 N93-15327 #
DOE/ER-61080/2 ..... p 911 N93-15272 #
DOE/ER-81156/92/C0059 ..... p 851 N93-15222 #

DOE/MC-25104/3092 ..... p 907 N93-15213 #
DOE/MC-26355/92/C0062 ..... p 908 N93-15323 #
DOE/MC-27394/92/C0050 ..... p 994 N93-15221 #
DOE/MC-28055/92/C0065 ..... p 908 N93-15322 #

DOE/NV-10366/21 ..... p 894 N93-15416 #

DOT/FAA/AM-92/26 ..... p 789 N93-14276 #
DOT/FAA/AM-92/27 ..... p 783 N93-14277 #
DOT/FAA/AM-92/28 ..... p 788 N93-14275 #

DOT/FAA/NR-92/3 ..... p 920 N93-14547 #

DOT/FAA/RD-91/23 ..... p 974 N93-14912 #
DOT/FAA/RD-92/14-VOL-2 ..... p 785 N93-15013 #
DOT/FAA/RD-92/19-PT-2 ..... p 783 N93-14844 * #

DRA-92006 ..... p 968 N93-14431 #

DREA-TM-92/215 ..... p 925 N93-14512 #

DTIC/TR-90/3-VOL-2 ..... p 1007 N93-15112 #
DTIC/TR-90/4-VOL-1 ..... p 1001 N93-14265 #
DTIC/TR-92-3 ..... p 1008 N93-15335 #
DTIC/TR-92-4 ..... p 999 N93-14106 #
DTIC/TR-92/5-VOL-2 ..... p 1007 N93-15112 #
DTIC/TR-92/6-VOL-1 ..... p 1001 N93-14265 #

E-2293 ..... p 902 N93-15369 * #
E-6166-1 ..... p 888 N93-14478 * #
E-6751 ..... p 827 N93-15528 * #
E-6804 ..... p 871 N93-15531 * #
E-6822 ..... p 867 N93-14798 * #
E-6928 ..... p 1004 N93-14796 * #
E-6967 ..... p 804 N93-15498 * #
E-7055 ..... p 854 N93-14834 * #
E-7067 ..... p 800 N93-15342 * #
E-7070-1 ..... p 827 N93-15526 * #
E-7136 ..... p 852 N93-15344 * #
E-7181 ..... p 872 N93-14150 * #
E-7206 ..... p 902 N93-15343 * #
E-7253 ..... p 880 N93-15585 * #
E-7288 ..... p 871 N93-15503 * #
E-7326 ..... p 878 N93-14914 * #
E-7339 ..... p 801 N93-15525 * #
E-7360 ..... p 877 N93-14758 * #
E-7368 ..... p 847 N93-15586 * #
E-7385 ..... p 895 N93-15582 * #
E-7408 ..... p 850 N93-14886 * #
E-7410 ..... p 880 N93-15499 * #
E-7412-PT-2 ..... p 837 N93-15401 * #
E-7414 ..... p 847 N93-15524 * #
E-7416 ..... p 826 N93-15370 * #
E-7419 ..... p 826 N93-14883 * #
E-7421 ..... p 856 N93-15353 * #
E-7422 ..... p 901 N93-14799 * #
E-7423 ..... p 828 N93-15584 * #
E-7427 ..... p 909 N93-15523 * #
E-7434 ..... p 827 N93-15572 * #
E-7435 ..... p 969 N93-15341 * #
E-7438 ..... p 877 N93-14885 * #
E-7440 ..... p 891 N93-14916 * #
E-7442 ..... p 777 N93-14102 * #
E-7446 ..... p 826 N93-14482 * #
E-7452 ..... p 801 N93-15403 * #
E-7454 ..... p 778 N93-15573 * #
E-7457 ..... p 844 N93-15504 * #
E-7461 ..... p 830 N93-14484 * #
E-7462 ..... p 828 N93-15576 * #
E-7465 ..... p 781 N93-14791 * #
E-7471 ..... p 975 N93-15575 * #
E-7473 ..... p 787 N93-15360 * #
E-7476 ..... p 877 N93-14829 * #
E-7481 ..... p 975 N93-15430 * #
E-7482 ..... p 827 N93-15571 * #
E-7485 ..... p 855 N93-15420 * #
E-7492 ..... p 782 N93-15404 * #
E-7493 ..... p 801 N93-15521 * #
E-7494 ..... p 782 N93-15338 * #
E-7495 ..... p 781 N93-14911 * #
E-7497 ..... p 787 N93-15354 * #
E-7498 ..... p 787 N93-15345 * #
E-7499 ..... p 788 N93-15522 * #
E-7500 ..... p 803 N93-14831 * #
E-7505 ..... p 879 N93-15355 * #
E-7506 ..... p 827 N93-15428 * #
E-7507 ..... p 827 N93-15429 * #
E-7508 ..... p 800 N93-15359 * #
E-7523 ..... p 879 N93-15402 * #

EDFG-R-160309-VOL-1 ..... p 894 N93-14104 #

EGG-GEO-10368 ..... p 948 N93-15274 #

EGG-M-91365 ..... p 916 N93-15136 #

EPA-400R-92-009 ..... p 861 N93-15220 #

EPA/450/R-92/002 ..... p 910 N93-15217 #
EPA/600/R-92/143 ..... p 975 N93-15647 #

ERL-0600-RR ..... p 943 N93-14502 #
ERL-0607-RN ..... p 982 N93-14784 #
ERL-0643-RR ..... p 973 N93-14269 #

ESC-TR-92-072 ..... p 858 N93-14426 #
ESC-TR-92-100 ..... p 964 N93-15258 #
ESC-TR-92-121 ..... p 937 N93-14580 #

ESD-TR-91-260 ..... p 992 N93-14576 #

ESDU-88040 ..... p 779 N93-14514
ESDU-89033 ..... p 779 N93-14515
ESDU-92008 ..... p 780 N93-14516
ESDU-92017 ..... p 900 N93-14553
ESDU-92018 ..... p 839 N93-14540
ESDU-92019 ..... p 791 N93-14541

ESDU-92025 ..... p 839 N93-14542
ESDU-92026 ..... p 889 N93-14543
ESDU-92027 ..... p 839 N93-14544
ESDU-92028 ..... p 839 N93-14539

ESG-179 ..... p 887 N93-15325 #

ETN-92-91618 ..... p 1020 N93-14686 #
ETN-92-92109 ..... p 863 N93-15487 #
ETN-92-92162 ..... p 793 N93-15152 #
ETN-92-92168 ..... p 777 N93-14613 #
ETN-92-92213 ..... p 880 N93-15488 #
ETN-92-92214 ..... p 879 N93-15473 #
ETN-92-92230 ..... p 782 N93-15489 #
ETN-92-92250 ..... p 952 N93-15476 #
ETN-92-92252 ..... p 951 N93-15386 #
ETN-92-92269 ..... p 911 N93-15460
ETN-92-92287 ..... p 1021 N93-15284
ETN-92-92352 ..... p 838 N93-15490 #
ETN-92-92356 ..... p 894 N93-15139 #
ETN-92-92357 ..... p 825 N93-15140 #
ETN-92-92358 ..... p 999 N93-15118 #
ETN-92-92359 ..... p 818 N93-15071 #
ETN-92-92360 ..... p 839 N93-14617 #
ETN-92-92376 ..... p 946 N93-15072
ETN-92-92381 ..... p 974 N93-15073 #
ETN-92-92392 ..... p 974 N93-15074 #
ETN-92-92405 ..... p 835 N93-15075 #
ETN-92-92407 ..... p 835 N93-15076 #
ETN-92-92426 ..... p 946 N93-15077 #
ETN-92-92427 ..... p 946 N93-15078 #
ETN-92-92428 ..... p 958 N93-15082 #
ETN-92-92429 ..... p 966 N93-15491 #
ETN-92-92430 ..... p 963 N93-15083 #
ETN-92-92431 ..... p 971 N93-15119 #
ETN-92-92432 ..... p 959 N93-15141 #
ETN-92-92433 ..... p 946 N93-15084 #
ETN-92-92434 ..... p 941 N93-15089 #
ETN-92-92435 ..... p 959 N93-15142 #
ETN-92-92436 ..... p 941 N93-15090 #
ETN-92-92437 ..... p 946 N93-15091 #
ETN-92-92438 ..... p 947 N93-15092 #
ETN-92-92439 ..... p 958 N93-15093 #
ETN-92-92440 ..... p 1009 N93-15492 #
ETN-92-92441 ..... p 968 N93-15094 #
ETN-92-92442 ..... p 968 N93-15121 #
ETN-92-92443 ..... p 860 N93-15095 #
ETN-92-92550 ..... p 882 N93-15096 #
ETN-92-92551 ..... p 861 N93-15097 #
ETN-92-92552 ..... p 861 N93-15098 #
ETN-92-92553 ..... p 878 N93-15122 #
ETN-92-92624 ..... p 916 N93-15252 #
ETN-92-92675 ..... p 941 N93-15123 #
ETN-92-92676 ..... p 958 N93-15124 #
ETN-92-92677 ..... p 947 N93-15125 #
ETN-92-92721 ..... p 792 N93-15126 #
ETN-92-92722 ..... p 851 N93-15127 #
ETN-92-92723 ..... p 886 N93-15128 #
ETN-92-92724 ..... p 974 N93-15129 #
ETN-92-92725 ..... p 836 N93-15253 #
ETN-92-92726 ..... p 975 N93-15130 #
ETN-92-92731 ..... p 781 N93-15131 #
ETN-92-92732 ..... p 800 N93-15143 #
ETN-92-92734 ..... p 878 N93-15120 #
ETN-92-92735 ..... p 878 N93-15132 #

ETS-RR-92-38-0N4 ..... p 933 N93-14109 #

F-2-2 ..... p 949 N93-15299 #
F-2-3 ..... p 949 N93-15300 #
F-2-8 ..... p 949 N93-15301 #
F-3-1 ..... p 949 N93-15302 #
F-3-2 ..... p 949 N93-15303 #
F-3-3 ..... p 950 N93-15304 #
F-3-5 ..... p 950 N93-15305 #
F-3-6 ..... p 950 N93-15306 #
F-3-7 ..... p 950 N93-15307 #
F-4-2 ..... p 950 N93-15308 #

FASTC-ID(RS)T-0571-92 ..... p 856 N93-15105 #
FASTC-ID(RS)T-1060-91 ..... p 861 N93-15106 #
FASTC-ID(RS)T-1065-91 ..... p 902 N93-15070 #

FEL-90-B370 ..... p 959 N93-15319 #
FEL-91-A324 ..... p 867 N93-14803 #
FEL-91-A375 ..... p 860 N93-14805 #
FEL-92-B154 ..... p 860 N93-14806 #
FEL-92-B190 ..... p 968 N93-14804 #

FFI-92/7007 ..... p 974 N93-15074 #

FIA-92-14 ..... p 965 N93-15289 * #
FIA-92-15 ..... p 965 N93-15288 * #
FIA-92-16 ..... p 965 N93-15287 * #
FIA-92-21 ..... p 964 N93-15286 * #
FIA-92-24 ..... p 965 N93-15293 * #
FIA-92-25 ..... p 965 N93-15292 * #
FIA-92-26 ..... p 965 N93-15291 * #
FIA-92-27 ..... p 963 N93-14765 * #
FIA-92-33 ..... p 965 N93-15290 * #

FSU-M-868 ..... p 970 N93-14487 #
FSU-M-869 ..... p 970 N93-14538 #

GAO/IMTEC-92-3 ..... p 971 N93-15626 #

GAO/NSIAD-92-311 ..... p 790 N93-14440 #

H-1708 ..... p 779 N93-14451 * #

HAC/EDSG-R160309 ..... p 900 N93-14498 #

HEL-TM-5-92 ..... p 936 N93-14416 #

HTC-9204 ..... p 877 N93-14797 * #

IAF-92-0669 ..... p 827 N93-15572 * #

IC-92/29 ..... p 991 N93-14485 #

ICASE-92-50 ..... p 979 N93-15482 * #
ICASE-92-58 ..... p 879 N93-15481 * #
ICASE-92-62 ..... p 951 N93-15432 * #

ICOMP-92-20 ..... p 880 N93-15499 * #
ICOMP-92-21 ..... p 969 N93-15341 * #
ICOMP-92-23 ..... p 877 N93-14829 * #

IDA-D-1189 ..... p 990 N93-14422 #

IDA/HQ-92-41982 ..... p 990 N93-14422 #

IMFL-91-32 ..... p 792 N93-15126 #

INO-SP-8 ..... p 925 N93-14503 #

INO-TR-3 ..... p 920 N93-14256 #

INT-PATENT-CLASS-A61F-2/54 . p 939 N93-14870 *

INT-PATENT-CLASS-B01D-9/02 . p 992 N93-14707 *
INT-PATENT-CLASS-B05D-1/02 . p 832 N93-14706 *
INT-PATENT-CLASS-B05D-3/12 . p 832 N93-14706 *
INT-PATENT-CLASS-B23B-31/10 p 890 N93-14710 *
INT-PATENT-CLASS-B23P-19/00 p 891 N93-14871 *
INT-PATENT-CLASS-B62D-51/04 p 934 N93-14708 *
INT-PATENT-CLASS-B64G-1/60 . p 939 N93-14713 *
INT-PATENT-CLASS-B65D-39/12 p 890 N93-14702 *

INT-PATENT-CLASS-F02K-9/96 . p 890 N93-14702 *

INT-PATENT-CLASS-G01B-33/12 p 845 N93-14705 *
INT-PATENT-CLASS-G01B-7/24 . p 845 N93-14705 *
INT-PATENT-CLASS-G08B-13/26 p 962 N93-14701 *
INT-PATENT-CLASS-G08C-19/10 p 962 N93-14701 *
INT-PATENT-CLASS-G11C-11/15 p 940 N93-14704 *
INT-PATENT-CLASS-G21K-1/06 . p 982 N93-14711 *

INT-PATENT-CLASS-H01R-13/54 p 890 N93-14712 *
INT-PATENT-CLASS-H01S-3/19 . p 885 N93-14703 *

IPPCZ-316 ..... p 988 N93-14813 #

ISBN-0-315-69011-9 ..... p 892 N93-15150
ISBN-0-85679-813-4 ..... p 780 N93-14516
ISBN-0-85679-821-5 ..... p 900 N93-14553
ISBN-0-85679-822-3 ..... p 839 N93-14540
ISBN-0-85679-824-X ..... p 791 N93-14541
ISBN-0-85679-830-4 ..... p 839 N93-14542
ISBN-0-85679-831-2 ..... p 889 N93-14543
ISBN-0-85679-832-0 ..... p 779 N93-14514
ISBN-0-85679-833-9 ..... p 839 N93-14544
ISBN-0-85679-834-7 ..... p 839 N93-14539
ISBN-0-85679-850-9 ..... p 779 N93-14515
ISBN-0-904747-37-8 ..... p 789 N93-14729 #
ISBN-0-9695338-1-0 ..... p 952 N93-15533
ISBN-90-5410-029-X ..... p 875 N93-14690 * #
ISBN-92-835-0686-3 ..... p 798 N93-14890 #

ISVR-TR-210 ..... p 974 N93-14734

ITN-92-85129 ..... p 949 N93-15298 #
ITN-92-85130 ..... p 947 N93-15261 #
ITN-93-85186 ..... p 835 N93-15144

IZF-1992-B-1 ..... p 937 N93-14602 #
IZF-1992-B-7 ..... p 938 N93-15400 #
IZF-1992-B-8 ..... p 936 N93-14267 #

JPL-PUBL-91-27 ..... p 925 N93-14964 * #

K/CSD/TM-102 ..... p 951 N93-15450 #
K/CSD/TM-64-REV-4 ..... p 946 N93-15003 #

KAPL-4733 ..... p 877 N93-14816 #

KBSL-89-1002 ..... p 976 N93-14438 #

KCP-613-4806 ..... p 945 N93-14876 #

L-16761 ..... p 803 N93-15366 * #
L-16912 ..... p 975 N93-15391 * #
L-17102 ..... p 879 N93-15434 * #
L-17115 ..... p 813 N93-15367 * #
L-17173 ..... p 832 N93-14744 * #
L-17175 ..... p 818 N93-15368 * #

LA-UR-92-1434 ..... p 907 N93-15061 #
LA-UR-92-1862 ..... p 887 N93-15135 #
LA-UR-92-2477 ..... p 843 N93-15283 #
LA-UR-92-2604 ..... p 837 N93-15426 #
LA-UR-92-2607 ..... p 862 N93-15427 #
LA-UR-92-2608 ..... p 862 N93-15435 #
LA-UR-92-2609 ..... p 818 N93-14904 #
LA-UR-92-2648 ..... p 989 N93-15436 #
LA-UR-92-2713 ..... p 995 N93-15321 #
LA-UR-92-2721 ..... p 852 N93-15320 #
LA-UR-92-2734 ..... p 870 N93-15424 #
LA-UR-92-2735 ..... p 903 N93-15423 #
LA-UR-92-2740 ..... p 989 N93-15422 #
LA-UR-92-2746 ..... p 870 N93-15421 #
LA-UR-92-2756 ..... p 988 N93-15419 #
LA-UR-92-2791 ..... p 988 N93-15418 #
LA-UR-92-2800 ..... p 998 N93-14905 #
LA-UR-92-2804 ..... p 887 N93-15417 #
LA-UR-92-2843 ..... p 1022 N93-15324 #
LA-UR-92-3044 ..... p 895 N93-15413 #

LA-12311-C ..... p 914 N93-14724 #

LBL-31521 ..... p 984 N93-15350 #
LBL-32059 ..... p 871 N93-15485 #
LBL-32212 ..... p 909 N93-15484 #
LBL-32249 ..... p 887 N93-15325 #
LBL-32385 ..... p 909 N93-15467 #

LMI-DL203RD1 ..... p 1007 N93-15050 #

LMI-PL205RD1 ..... p 1007 N93-15051 #

LPI-CONTRIB-789 ..... p 1023 N93-14288 * #

LRT-WE-9-FB-23-1991 ..... p 878 N93-15120 #
LRT-WE-9-FB-25-1991 ..... p 878 N93-15132 #

LTR92-004 ..... p 945 N93-14696 #
LTR92-013 ..... p 1004 N93-14785 #

M-703 ..... p 924 N93-15581 * #
M-705 ..... p 895 N93-15433 * #
M-707 ..... p 1049 N93-15532 * #

MATHS-REPT-A-158 ..... p 974 N93-15073 #

MBB-UD-0614-92-PUB ..... p 863 N93-15487 #

MCAT-92-020 ..... p 804 N93-14809 * #

MEMO-INF-91-38 ..... p 946 N93-15077 #
MEMO-INF-91-57-PT-1 ..... p 946 N93-15078 #
MEMO-INF-91-64 ..... p 958 N93-15082 #
MEMO-INF-92-04 ..... p 966 N93-15491 #
MEMO-INF-92-10 ..... p 963 N93-15083 #
MEMO-INF-92-11 ..... p 971 N93-15119 #
MEMO-INF-92-12 ..... p 959 N93-15141 #
MEMO-INF-92-15 ..... p 946 N93-15084 #
MEMO-INF-92-16 ..... p 941 N93-15089 #
MEMO-INF-92-17 ..... p 959 N93-15142 #
MEMO-INF-92-18 ..... p 941 N93-15090 #
MEMO-INF-92-21 ..... p 946 N93-15091 #
MEMO-INF-92-23 ..... p 947 N93-15092 #
MEMO-INF-92-25 ..... p 958 N93-15093 #
MEMO-INF-92-26 ..... p 1009 N93-15492 #
MEMO-INF-92-27 ..... p 968 N93-15094 #
MEMO-INF-92-28 ..... p 968 N93-15121 #
MEMO-INF-92-30 ..... p 860 N93-15095 #

MHSMP-92-01 ..... p 910 N93-14739 #

MIT-ATC-187 ..... p 920 N93-14547 #

MIT-TR-92-100 ..... p 964 N93-15258 #
MIT-TR-957 ..... p 858 N93-14426 #

MIT/LCS/TR-527 ..... p 941 N93-15628 #
MIT/LCS/TR-530 ..... p 1009 N93-15639 #

MITRE-92-103 ..... p 962 N93-14519 #

MLM-3762 ..... p 855 N93-15478 #

MPE-PREPRINT-216 ..... p 1021 N93-15284

MPIS-9/1991 ..... p 781 N93-15131 #

MTI91-TR-53 ..... p 891 N93-14916 * #

MTL-TR-92-29 ..... p 836 N93-15218 #
MTL-TR-92-31 ..... p 891 N93-14735 #
MTL-TR-92-49 ..... p 901 N93-14790 #

M92B0000083 ..... p 859 N93-14488 #

N-3399-RC ..... p 986 N93-15648 #

NADC-91059-60 ..... p 831 N93-14672 #

NAS 1.15:102803 ..... p 782 N93-15483 * #
NAS 1.15:103869 ..... p 816 N93-15477 * #
NAS 1.15:104566 ..... p 932 N93-15645 * #
NAS 1.15:105595 ..... p 1004 N93-14796 * #
NAS 1.15:105626 ..... p 804 N93-15498 * #
NAS 1.15:105640 ..... p 827 N93-15526 * #
NAS 1.15:105687 ..... p 800 N93-15342 * #
NAS 1.15:105732 ..... p 852 N93-15344 * #
NAS 1.15:105764 ..... p 872 N93-14150 * #
NAS 1.15:105772 ..... p 854 N93-14834 * #
NAS 1.15:105779 ..... p 902 N93-15343 * #
NAS 1.15:105822 ..... p 880 N93-15585 * #
NAS 1.15:105845 ..... p 871 N93-15503 * #
NAS 1.15:105865 ..... p 878 N93-14914 * #
NAS 1.15:105874 ..... p 801 N93-15525 * #
NAS 1.15:105893 ..... p 877 N93-14758 * #
NAS 1.15:105901 ..... p 847 N93-15586 * #
NAS 1.15:105917 ..... p 850 N93-14886 * #
NAS 1.15:105918 ..... p 880 N93-15499 * #
NAS 1.15:105921 ..... p 847 N93-15524 * #
NAS 1.15:105925 ..... p 909 N93-15523 * #
NAS 1.15:105927 ..... p 827 N93-15572 * #
NAS 1.15:105928 ..... p 969 N93-15341 * #
NAS 1.15:105929 ..... p 877 N93-14885 * #
NAS 1.15:105931 ..... p 777 N93-14102 * #
NAS 1.15:105933 ..... p 826 N93-14482 * #
NAS 1.15:105936 ..... p 801 N93-15403 * #
NAS 1.15:105937 ..... p 778 N93-15573 * #
NAS 1.15:105940 ..... p 844 N93-15504 * #
NAS 1.15:105942 ..... p 888 N93-14478 * #
NAS 1.15:105945 ..... p 828 N93-15576 * #
NAS 1.15:105947 ..... p 781 N93-14791 * #
NAS 1.15:105950 ..... p 975 N93-15575 * #
NAS 1.15:105952 ..... p 787 N93-15360 * #
NAS 1.15:105956 ..... p 877 N93-14829 * #
NAS 1.15:105961 ..... p 975 N93-15430 * #
NAS 1.15:105962 ..... p 827 N93-15571 * #
NAS 1.15:105968 ..... p 781 N93-14911 * #
NAS 1.15:105969 ..... p 782 N93-15404 * #
NAS 1.15:105970 ..... p 801 N93-15521 * #
NAS 1.15:105971 ..... p 782 N93-15338 * #
NAS 1.15:105972 ..... p 787 N93-15354 * #
NAS 1.15:105973 ..... p 855 N93-15420 * #
NAS 1.15:105975 ..... p 787 N93-15345 * #
NAS 1.15:105976 ..... p 788 N93-15522 * #
NAS 1.15:105977 ..... p 803 N93-14831 * #
NAS 1.15:105981 ..... p 879 N93-15355 * #
NAS 1.15:105982 ..... p 827 N93-15428 * #
NAS 1.15:105983 ..... p 827 N93-15429 * #
NAS 1.15:105984 ..... p 800 N93-15359 * #
NAS 1.15:107647 ..... p 924 N93-15501 * #
NAS 1.15:107686 ..... p 979 N93-15482 * #
NAS 1.15:107687 ..... p 900 N93-14483 * #
NAS 1.15:107692 ..... p 828 N93-14459 * #
NAS 1.15:107705 ..... p 813 N93-15646 * #
NAS 1.15:107709 ..... p 902 N93-15202 * #
NAS 1.15:107989 ..... p 1004 N93-15027 * #
NAS 1.15:108104 ..... p 815 N93-14736 * #
NAS 1.15:108105 ..... p 825 N93-15650 * #
NAS 1.15:108113 ..... p 965 N93-15293 * #
NAS 1.15:108114 ..... p 965 N93-15292 * #
NAS 1.15:108115 ..... p 965 N93-15291 * #
NAS 1.15:108116 ..... p 963 N93-14765 * #
NAS 1.15:108117 ..... p 965 N93-15290 * #
NAS 1.15:108118 ..... p 965 N93-15289 * #
NAS 1.15:108119 ..... p 965 N93-15288 * #
NAS 1.15:108120 ..... p 965 N93-15287 * #
NAS 1.15:108121 ..... p 964 N93-15286 * #
NAS 1.15:108133 ..... p 1002 N93-14719 * #
NAS 1.15:108385 ..... p 813 N93-15392 * #
NAS 1.15:108390 ..... p 1013 N93-15203 * #
NAS 1.15:108578 ..... p 957 N93-15578 * #
NAS 1.15:108579 ..... p 957 N93-15579 * #
NAS 1.15:108580 ..... p 952 N93-15502 * #
NAS 1.15:3307 ..... p 818 N93-15368 * #
NAS 1.15:4376 ..... p 827 N93-15528 * #
NAS 1.15:4428 ..... p 864 N93-15638 * #
NAS 1.15:4429 ..... p 779 N93-14451 * #
NAS 1.15:4432 ..... p 871 N93-15529 * #
NAS 1.15:83796 ..... p 902 N93-15369 * #
NAS 1.21:7011(368) ..... p 934 N93-14603 *
NAS 1.21:7011(369) ..... p 935 N93-14731 *
NAS 1.21:7037(282) ..... p 777 N93-14604 *
NAS 1.21:7037(283) ..... p 778 N93-14732 *
NAS 1.21:7037(284) ..... p 777 N93-14605 *
NAS 1.21:7085(04) ..... p 817 N93-14606 *
NAS 1.26:108389 ..... p 997 N93-15500 * #
NAS 1.26:167698 ..... p 815 N93-15474 * #
NAS 1.26:167699 ..... p 816 N93-15475 * #
NAS 1.26:182270 ..... p 982 N93-15116 * #
NAS 1.26:184483 ..... p 855 N93-14793 * #
NAS 1.26:184498 ..... p 891 N93-14763 * #
NAS 1.26:184500 ..... p 910 N93-14764 * #
NAS 1.26:184502 ..... p 892 N93-15117 * #
NAS 1.26:185691 ..... p 881 N93-14494 * #
NAS 1.26:186396 ..... p 825 N93-15658 * #
NAS 1.26:187882 ..... p 824 N93-15632 * #
NAS 1.26:187883 ..... p 824 N93-15631 * #
NAS 1.26:187884 ..... p 824 N93-15630 * #
NAS 1.26:187897 ..... p 817 N93-14733 * #
NAS 1.26:188480 ..... p 818 N93-14872 * #
NAS 1.26:188578 ..... p 825 N93-15633 * #
NAS 1.26:188583 ..... p 824 N93-15629 * #
NAS 1.26:189096-PT-2 ..... p 837 N93-15401 * #
NAS 1.26:189115 ..... p 867 N93-14798 * #
NAS 1.26:189121 ..... p 880 N93-15527 * #
NAS 1.26:189135 ..... p 891 N93-14916 * #
NAS 1.26:189212 ..... p 901 N93-14799 * #
NAS 1.26:189653-VOL-1-REV ..... p 815 N93-14794 * #
NAS 1.26:189653-VOL-3-REV ..... p 815 N93-14730 * #
NAS 1.26:189653-VOL-4 ..... p 815 N93-14768 * #
NAS 1.26:189702 ..... p 802 N93-14811 * #
NAS 1.26:189704 ..... p 958 N93-14808 * #
NAS 1.26:189725 ..... p 879 N93-15481 * #
NAS 1.26:189728 ..... p 905 N93-14792 * #
NAS 1.26:189733 ..... p 951 N93-15432 * #
NAS 1.26:190616 ..... p 925 N93-14964 * #
NAS 1.26:190676 ..... p 1023 N93-14288 * #
NAS 1.26:190741 ..... p 843 N93-15356 * #
NAS 1.26:190774 ..... p 895 N93-15582 * #
NAS 1.26:190788 ..... p 828 N93-15584 * #
NAS 1.26:190795 ..... p 826 N93-15370 * #
NAS 1.26:190797 ..... p 826 N93-14883 * #
NAS 1.26:190798 ..... p 856 N93-15353 * #
NAS 1.26:190947 ..... p 1021 N93-15079 * #
NAS 1.26:191019 ..... p 879 N93-15402 * #
NAS 1.26:191024 ..... p 830 N93-14484 * #
NAS 1.26:191255 ..... p 901 N93-14766 * #
NAS 1.26:191264 ..... p 875 N93-14687 * #
NAS 1.26:191298 ..... p 1047 N93-15081 * #
NAS 1.26:191301 ..... p 995 N93-15309 * #
NAS 1.26:191302 ..... p 1012 N93-14761 * #
NAS 1.26:191304 ..... p 781 N93-14767 * #
NAS 1.26:191307 ..... p 984 N93-15505 * #
NAS 1.26:191316 ..... p 882 N93-14810 * #
NAS 1.26:191319 ..... p 916 N93-14913 * #
NAS 1.26:191354 ..... p 911 N93-15480 * #
NAS 1.26:191356 ..... p 867 N93-14721 * #
NAS 1.26:191357 ..... p 1049 N93-15085 * #
NAS 1.26:191366 ..... p 857 N93-14155 * #
NAS 1.26:191374 ..... p 941 N93-14770 * #
NAS 1.26:191376 ..... p 925 N93-14769 * #
NAS 1.26:191378-VOL-4 ..... p 945 N93-14807 * #
NAS 1.26:191383 ..... p 922 N93-14910 * #
NAS 1.26:191384 ..... p 1020 N93-14814 * #
NAS 1.26:191385 ..... p 804 N93-14809 * #
NAS 1.26:191388 ..... p 917 N93-15574 * #
NAS 1.26:191391 ..... p 903 N93-15653 * #
NAS 1.26:191416 ..... p 826 N93-14681 * #
NAS 1.26:191617 ..... p 1051 N93-15580 * #
NAS 1.26:191621 ..... p 875 N93-14481 * #
NAS 1.26:191622 ..... p 1049 N93-15634 * #
NAS 1.26:191627 ..... p 1013 N93-15340 * #
NAS 1.26:191631 ..... p 862 N93-15339 * #
NAS 1.26:191636 ..... p 868 N93-14915 * #
NAS 1.26:191646 ..... p 890 N93-14567 * #
NAS 1.26:191652 ..... p 852 N93-15431 * #
NAS 1.26:191671 ..... p 780 N93-14737 * #
NAS 1.26:191672 ..... p 780 N93-14738 * #
NAS 1.26:191673 ..... p 1012 N93-14759 * #
NAS 1.26:191715 ..... p 783 N93-15588 * #
NAS 1.26:191781 ..... p 1013 N93-15589 * #
NAS 1.26:4474 ..... p 924 N93-15581 * #
NAS 1.26:4476 ..... p 936 N93-15583 * #
NAS 1.26:4477 ..... p 997 N93-15587 * #
NAS 1.26:4480 ..... p 880 N93-15643 * #
NAS 1.26:4481 ..... p 877 N93-14797 * #
NAS 1.55:10105-PT-2 ..... p 783 N93-14844 * #
NAS 1.55:3165-VOL-3 ..... p 1002 N93-14771 * #
NAS 1.55:3176 ..... p 832 N93-14744 * #
NAS 1.55:3181 ..... p 819 N93-15593 * #
NAS 1.60:3189 ..... p 975 N93-15391 * #
NAS 1.60:3251 ..... p 871 N93-15531 * #
NAS 1.60:3256 ..... p 813 N93-15367 * #
NAS 1.60:3270 ..... p 803 N93-15366 * #
NAS 1.60:3271 ..... p 879 N93-15434 * #
NAS 1.60:3293 ..... p 903 N93-15530 * #
NAS 1.60:3309 ..... p 895 N93-15433 * #
NAS 1.60:3316 ..... p 1049 N93-15532 * #
NAS 1.61:1282 ..... p 814 N93-14495 * #
NAS 1.71:NPO-18483-1-CU ..... p 994 N93-15151 * #
NAS 1.71:NPO-18521-1-CU ..... p 981 N93-14404 * #

NASA-CASE-ARC-11882-1-CU .... p 939 N93-14713 *

NASA-CASE-GSC-13348-2 ..... p 934 N93-14708 *
NASA-CASE-GSC-13358-1 ..... p 890 N93-14710 *
NASA-CASE-GSC-13377-1 ..... p 962 N93-14701 *
NASA-CASE-GSC-13430-1 ..... p 890 N93-14712 *

NASA-CASE-LAR-13678-3 ..... p 881 N93-14714 *
NASA-CASE-LAR-14239-1 ..... p 845 N93-14705 *
NASA-CASE-LAR-14639-1 ..... p 849 N93-14709 *

NASA-CASE-LEW-15020-2 ..... p 832 N93-14706 *
NASA-CASE-LEW-15444-1 ..... p 882 N93-14840 * #

NASA-CASE-MFS-28392-1 ..... p 982 N93-14711 *
NASA-CASE-MFS-28473-1 ..... p 992 N93-14707 *
NASA-CASE-MFS-28481-1 ..... p 939 N93-14870 *

NASA-CASE-MSC-21823-1 ..... p 891 N93-14843 * #
NASA-CASE-MSC-21881-1 ..... p 891 N93-14871 *
NASA-CASE-MSC-21898-1 ..... p 890 N93-14702 *
NASA-CASE-MSC-21922-1 ..... p 882 N93-14841 * #
NASA-CASE-MSC-21955-1 ..... p 891 N93-14842 * #

NASA-CASE-NPO-17763-1-CU .... p 885 N93-14703 *
NASA-CASE-NPO-17845-2-CU .... p 945 N93-14882 *
NASA-CASE-NPO-17858-1-CU .... p 832 N93-14700 *
NASA-CASE-NPO-17954-1-CU .... p 940 N93-14704 *
NASA-CASE-NPO-18483-1-CU .... p 994 N93-15151 * #
NASA-CASE-NPO-18521-1-CU .... p 981 N93-14404 * #

NASA-CP-10105-PT-2 ..... p 783 N93-14844 * #
NASA-CP-3165-VOL-3 ..... p 1002 N93-14771 * #
NASA-CP-3176 ..... p 832 N93-14744 * #
NASA-CP-3181 ..... p 819 N93-15593 * #

NASA-CR-167698 ..... p 815 N93-15474 * #
NASA-CR-167699 ..... p 816 N93-15475 * #
NASA-CR-182270 ..... p 982 N93-15116 * #
NASA-CR-184483 ..... p 855 N93-14793 * #
NASA-CR-184498 ..... p 891 N93-14763 * #
NASA-CR-184500 ..... p 910 N93-14764 * #
NASA-CR-184502 ..... p 892 N93-15117 * #
NASA-CR-185691 ..... p 881 N93-14494 * #
NASA-CR-186396 ..... p 825 N93-15658 * #
NASA-CR-187882 ..... p 824 N93-15632 * #
NASA-CR-187883 ..... p 824 N93-15631 * #
NASA-CR-187884 ..... p 824 N93-15630 * #
NASA-CR-187897 ..... p 817 N93-14733 * #
NASA-CR-188480 ..... p 818 N93-14872 * #
NASA-CR-188578 ..... p 825 N93-15633 * #
NASA-CR-188583 ..... p 824 N93-15629 * #
NASA-CR-189096-PT-2 ..... p 837 N93-15401 * #
NASA-CR-189115 ..... p 867 N93-14798 * #
NASA-CR-189121 ..... p 880 N93-15527 * #
NASA-CR-189135 ..... p 891 N93-14916 * #
NASA-CR-189212 ..... p 901 N93-14799 * #
NASA-CR-189653-VOL-1-REV ..... p 815 N93-14794 * #
NASA-CR-189653-VOL-3-REV ..... p 815 N93-14730 * #
NASA-CR-189653-VOL-4 ..... p 815 N93-14768 * #
NASA-CR-189702 ..... p 802 N93-14811 * #
NASA-CR-189704 ..... p 958 N93-14808 * #
NASA-CR-189725 ..... p 879 N93-15481 * #
NASA-CR-189728 ..... p 905 N93-14792 * #
NASA-CR-189733 ..... p 951 N93-15432 * #
NASA-CR-190616 ..... p 925 N93-14964 * #
NASA-CR-190676 ..... p 1023 N93-14288 * #
NASA-CR-190741 ..... p 843 N93-15356 * #
NASA-CR-190741 ..... p 843 N93-15357 * #
NASA-CR-190741 ..... p 843 N93-15358 * #
NASA-CR-190774 ..... p 895 N93-15582 * #
NASA-CR-190788 ..... p 828 N93-15584 * #
NASA-CR-190795 ..... p 826 N93-15370 * #
NASA-CR-190797 ..... p 826 N93-14883 * #
NASA-CR-190798 ..... p 856 N93-15353 * #
NASA-CR-190947 ..... p 1021 N93-15079 * #
NASA-CR-191019 ..... p 879 N93-15402 * #
NASA-CR-191024 ..... p 830 N93-14484 * #
NASA-CR-191255 ..... p 901 N93-14766 * #
NASA-CR-191264 ..... p 875 N93-14687 * #
NASA-CR-191298 ..... p 1047 N93-15081 * #
NASA-CR-191301 ..... p 995 N93-15309 * #
NASA-CR-191302 ..... p 1012 N93-14761 * #
NASA-CR-191304 ..... p 781 N93-14767 * #
NASA-CR-191307 ..... p 984 N93-15505 * #
NASA-CR-191316 ..... p 882 N93-14810 * #
NASA-CR-191319 ..... p 916 N93-14913 * #

NASA-CR-191354 ..... p 911 N93-15480 * #
NASA-CR-191356 ..... p 867 N93-14721 * #
NASA-CR-191357 ..... p 1049 N93-15085 * #
NASA-CR-191366 ..... p 857 N93-14155 * #
NASA-CR-191374 ..... p 941 N93-14770 * #
NASA-CR-191376 ..... p 925 N93-14769 * #
NASA-CR-191378-VOL-4 ..... p 945 N93-14807 * #
NASA-CR-191383 ..... p 922 N93-14910 * #
NASA-CR-191384 ..... p 1020 N93-14814 * #
NASA-CR-191385 ..... p 804 N93-14809 * #
NASA-CR-191388 ..... p 917 N93-15574 * #
NASA-CR-191391 ..... p 903 N93-15653 * #
NASA-CR-191416 ..... p 826 N93-14681 * #
NASA-CR-191617 ..... p 1051 N93-15580 * #
NASA-CR-191621 ..... p 875 N93-14481 * #
NASA-CR-191622 ..... p 1049 N93-15634 * #
NASA-CR-191627 ..... p 1013 N93-15340 * #
NASA-CR-191631 ..... p 862 N93-15339 * #
NASA-CR-191636 ..... p 868 N93-14915 * #
NASA-CR-191646 ..... p 890 N93-14567 * #
NASA-CR-191652 ..... p 852 N93-15431 * #
NASA-CR-191671 ..... p 780 N93-14737 * #
NASA-CR-191672 ..... p 780 N93-14738 * #
NASA-CR-191673 ..... p 1012 N93-14759 * #
NASA-CR-191715 ..... p 783 N93-15588 * #
NASA-CR-191781 ..... p 1013 N93-15589 * #
NASA-CR-4474 ..... p 924 N93-15581 * #
NASA-CR-4476 ..... p 936 N93-15583 * #
NASA-CR-4477 ..... p 997 N93-15587 * #
NASA-CR-4480 ..... p 880 N93-15643 * #
NASA-CR-4481 ..... p 877 N93-14797 * #

NASA-RP-1282 ..... p 814 N93-14495 * #

NASA-SP-7011(368) ..... p 934 N93-14603 *
NASA-SP-7011(369) ..... p 935 N93-14731 *
NASA-SP-7037(282) ..... p 777 N93-14604 *
NASA-SP-7037(283) ..... p 778 N93-14732 *
NASA-SP-7037(284) ..... p 777 N93-14605 *
NASA-SP-7085(04) ..... p 817 N93-14606 *

NASA-TM-102803 ..... p 782 N93-15483 * #
NASA-TM-103869 ..... p 816 N93-15477 * #
NASA-TM-104566 ..... p 932 N93-15645 * #
NASA-TM-105595 ..... p 1004 N93-14796 * #
NASA-TM-105626 ..... p 804 N93-15498 * #
NASA-TM-105640 ..... p 827 N93-15526 * #
NASA-TM-105687 ..... p 800 N93-15342 * #
NASA-TM-105732 ..... p 852 N93-15344 * #
NASA-TM-105764 ..... p 872 N93-14150 * #
NASA-TM-105772 ..... p 854 N93-14834 * #
NASA-TM-105779 ..... p 902 N93-15343 * #
NASA-TM-105822 ..... p 880 N93-15585 * #
NASA-TM-105845 ..... p 871 N93-15503 * #
NASA-TM-105865 ..... p 878 N93-14914 * #
NASA-TM-105874 ..... p 801 N93-15525 * #
NASA-TM-105893 ..... p 877 N93-14758 * #
NASA-TM-105901 ..... p 847 N93-15586 * #
NASA-TM-105917 ..... p 850 N93-14886 * #
NASA-TM-105918 ..... p 880 N93-15499 * #
NASA-TM-105921 ..... p 847 N93-15524 * #
NASA-TM-105925 ..... p 909 N93-15523 * #
NASA-TM-105927 ..... p 827 N93-15572 * #
NASA-TM-105928 ..... p 969 N93-15341 * #
NASA-TM-105929 ..... p 877 N93-14885 * #
NASA-TM-105931 ..... p 777 N93-14102 * #
NASA-TM-105933 ..... p 826 N93-14482 * #
NASA-TM-105936 ..... p 801 N93-15403 * #
NASA-TM-105937 ..... p 778 N93-15573 * #
NASA-TM-105940 ..... p 844 N93-15504 * #
NASA-TM-105942 ..... p 888 N93-14478 * #
NASA-TM-105945 ..... p 828 N93-15576 * #
NASA-TM-105947 ..... p 781 N93-14791 * #
NASA-TM-105950 ..... p 975 N93-15575 * #
NASA-TM-105952 ..... p 787 N93-15360 * #
NASA-TM-105956 ..... p 877 N93-14829 * #
NASA-TM-105961 ..... p 975 N93-15430 * #
NASA-TM-105962 ..... p 827 N93-15571 * #
NASA-TM-105968 ..... p 781 N93-14911 * #
NASA-TM-105969 ..... p 782 N93-15404 * #
NASA-TM-105970 ..... p 801 N93-15521 * #
NASA-TM-105971 ..... p 782 N93-15338 * #
NASA-TM-105972 ..... p 787 N93-15354 * #
NASA-TM-105973 ..... p 855 N93-15420 * #
NASA-TM-105975 ..... p 787 N93-15345 * #
NASA-TM-105976 ..... p 788 N93-15522 * #
NASA-TM-105977 ..... p 803 N93-14831 * #
NASA-TM-105981 ..... p 879 N93-15355 * #
NASA-TM-105982 ..... p 827 N93-15428 * #
NASA-TM-105983 ..... p 827 N93-15429 * #
NASA-TM-105984 ..... p 800 N93-15359 * #
NASA-TM-107647 ..... p 924 N93-15501 * #
NASA-TM-107686 ..... p 979 N93-15482 * #
NASA-TM-107687 ..... p 900 N93-14483 * #
NASA-TM-107692 ..... p 828 N93-14459 * #
NASA-TM-107705 ..... p 813 N93-15646 * #
NASA-TM-107709 ..... p 902 N93-15202 * #
NASA-TM-107989 ..... p 1004 N93-15027 * #
NASA-TM-108104 ..... p 815 N93-14736 * #
NASA-TM-108105 ..... p 825 N93-15650 * #
NASA-TM-108113 ..... p 965 N93-15293 * #
NASA-TM-108114 ..... p 965 N93-15292 * #
NASA-TM-108115 ..... p 965 N93-15291 * #
NASA-TM-108116 ..... p 963 N93-14765 * #
NASA-TM-108117 ..... p 965 N93-15290 * #
NASA-TM-108118 ..... p 965 N93-15289 * #
NASA-TM-108119 ..... p 965 N93-15288 * #
NASA-TM-108120 ..... p 965 N93-15287 * #
NASA-TM-108121 ..... p 964 N93-15286 * #
NASA-TM-108133 ..... p 1002 N93-14719 * #
NASA-TM-108385 ..... p 813 N93-15392 * #
NASA-TM-108389 ..... p 997 N93-15500 * #
NASA-TM-108390 ..... p 1013 N93-15203 * #
NASA-TM-108578 ..... p 957 N93-15578 * #
NASA-TM-108579 ..... p 957 N93-15579 * #
NASA-TM-108580 ..... p 952 N93-15502 * #
NASA-TM-4376 ..... p 827 N93-15528 * #
NASA-TM-4428 ..... p 864 N93-15638 * #
NASA-TM-4429 ..... p 779 N93-14451 * #
NASA-TM-4432 ..... p 871 N93-15529 * #
NASA-TM-83796 ..... p 902 N93-15369 * #

NASA-TP-3189 ..... p 975 N93-15391 * #
NASA-TP-3251 ..... p 871 N93-15531 * #
NASA-TP-3256 ..... p 813 N93-15367 * #
NASA-TP-3270 ..... p 803 N93-15366 * #
NASA-TP-3271 ..... p 879 N93-15434 * #
NASA-TP-3293 ..... p 903 N93-15530 * #
NASA-TP-3307 ..... p 818 N93-15368 * #
NASA-TP-3309 ..... p 895 N93-15433 * #
NASA-TP-3316 ..... p 1049 N93-15532 * #

NAVSWC-TR-91-561 ..... p 858 N93-14415 #
NAVSWC-TR-91-586 ..... p 940 N93-14644 #
NAVSWC-TR-91-588 ..... p 958 N93-14645 #
NAVSWC-TR-91-592 ..... p 944 N93-14575 #
NAVSWC-TR-91-783 ..... p 942 N93-14164 #

NAWCADWAR-92003-60 ..... p 845 N93-14726 #
NAWCADWAR-92018-60 ..... p 846 N93-15189 #
NAWCADWAR-92026-60 ..... p 935 N93-14789 #
NAWCADWAR-92042-60 ..... p 792 N93-15004 #
NAWCADWAR-92060-60 ..... p 849 N93-14573 #

NBDL-92R003 ..... p 1051 N93-14657 #

NHRC-91-45 ..... p 934 N93-14240 #

NIKHEF-H/91-20 ..... p 1020 N93-14686 #

NIST-TR-15 ..... p 989 N93-14133 #

NISTIR-4931 ..... p 870 N93-15412 #

NOARL-TN-268 ..... p 859 N93-14490 #
NOARL-TN-290 ..... p 974 N93-15012 #

NOARL-14 ..... p 960 N93-14239 #

NPL-DITC-198/92 ..... p 946 N93-15072

NPRDC-TR-92-18 ..... p 999 N93-14526 #

NPS-AA-92-001CR ..... p 800 N93-15337 #

NPS-AS-92-021 ..... p 856 N93-15234 #

NPS-MA-92-008 ..... p 973 N93-14234 #

NPSCS-92-008 ..... p 943 N93-14420 #

NRAD-TD-2311 ..... p 789 N93-14574 #

NRAD-TR-1490 ..... p 981 N93-14407 #
NRAD-TR-1500 ..... p 846 N93-15056 #

NREL/TP-410-5008 ..... p 907 N93-14817 #

NRL/FR-4795-92-7114 ..... p 866 N93-14504 #

NRL/FR/5340-92-9517 ..... p 858 N93-14233 #
NRL/FR/5530-92-9194 ..... p 946 N93-15052 #
NRL/FR/5753-92-9371 ..... p 858 N93-14259 #

NRL/MR/4223-92-7147 ..... p 921 N93-14680 #
NRL/MR/4721-92-7124 ..... p 988 N93-14579 #
NRL/MR/4790-92-6996 ..... p 978 N93-14570 #
NRL/MR/4790-92-7110 ..... p 978 N93-14127 #
NRL/MR/4790-92-7112 ..... p 976 N93-14662 #
NRL/MR/4795-92-7114 ..... p 866 N93-14504 #
NRL/MR/5520-92-7136 ..... p 859 N93-14663 #
NRL/MR/5521-92-7107 ..... p 857 N93-14181 #
NRL/MR/6522-92-7151 ..... p 1008 N93-15393 #

NSF-92-4 ..... p 999 N93-14720 #
NSF-92-83 ..... p 916 N93-15080 #

NSSDC-WDA-A-R/S-91-18 ..... p 1004 N93-15027 * #

NSTS-08276 ..... p 815 N93-14736 * #

NTSB/SIR-92/03 ..... p 788 N93-15577 #

ONERA-RT-12/3521-M ..... p 836 N93-15253 #
ONERA-RT-18/3641-PY ..... p 975 N93-15130 #
ONERA-RT-8/3654-RY-010-R ..... p 974 N93-15129 #

OR-SBIR-92-6 ..... p 868 N93-15108 #

ORNL/SUB-85-22008/2 ..... p 837 N93-15455 #
ORNL/SUB-85-22008/3-PHASE-2Ap 853 N93-15452 #
ORNL/SUB-85-22011/2 ..... p 836 N93-15387 #
ORNL/SUB-85-22031/2 ..... p 853 N93-15453 #
ORNL/SUB-86-22049/1 ..... p 853 N93-15438 #
ORNL/SUB-86-95906/2 ..... p 837 N93-15388 #
ORNL/SUB-86-95915/1 ..... p 852 N93-15437 #
ORNL/SUB-87-SA581/1 ..... p 853 N93-15439 #
ORNL/SUB-87-SB045/1 ..... p 837 N93-15454 #
ORNL/SUB-87-SB046/1 ..... p 851 N93-15294 #
ORNL/SUB-88-07685CT92/02 .... p 846 N93-15059 #
ORNL/SUB-90-SG372/1 ..... p 851 N93-15295 #

ORNL/TM-12106 ..... p 969 N93-15212 #
ORNL/TM-12190 ..... p 946 N93-14902 #

OSU-722780-4-SUPPL-2 ..... p 945 N93-14807 * #

OU-AME-91-2 ..... p 781 N93-14767 * #

PAM-545 ..... p 967 N93-14271 #
PAM-549 ..... p 967 N93-14270 #

PAPER-T.1.3 ..... p 875 N93-14689 * #

PAPER-W.1.2 ..... p 875 N93-14688 * #

PATENTS-US-A-7641823 ..... p 828 N93-14718
PATENTS-US-A-7641945 ..... p 834 N93-14819
PATENTS-US-A-7641978 ..... p 881 N93-14716
PATENTS-US-A-7642577 ..... p 876 N93-14715
PATENTS-US-A-7645448 ..... p 845 N93-14717

PB92-204973 ..... p 933 N93-15208 #
PB92-207687 ..... p 975 N93-15647 #
PB92-214287 ..... p 1009 N93-15644 #
PB92-217462 ..... p 910 N93-15217 #
PB92-917007 ..... p 788 N93-15577 #

PHJ-91-2 ..... p 942 N93-14237 #

PL-TR-91-2292 ..... p 914 N93-14727 #
PL-TR-92-2023 ..... p 918 N93-14153 #
PL-TR-92-2081 ..... p 945 N93-14696 #
PL-TR-92-2097 ..... p 924 N93-15331 #
PL-TR-92-2148 ..... p 814 N93-14697 #
PL-TR-92-2160 ..... p 916 N93-14899 #
PL-TR-92-2172 ..... p 815 N93-14698 #
PL-TR-92-3016 ..... p 843 N93-15497 #

PML-1992-42 ..... p 814 N93-14266 #

PNL-SA-19956 ..... p 846 N93-15138 #

PNL-8269 ..... p 871 N93-15479 #

PNR-90933 ..... p 880 N93-15488 #
PNR-90934 ..... p 879 N93-15473 #
PNR-90957 ..... p 782 N93-15489 #
PNR-90994 ..... p 952 N93-15476 #
PNR-90998 ..... p 951 N93-15386 #

POEF-T-3559B ..... p 947 N93-15225 #

POLY-WRI-1600-91 ..... p 869 N93-15257 #

PSC-16 ..... p 887 N93-15296 #

PSU-LIPS/92-08 ..... p 976 N93-14513 #

PWA-FR21998-11 ..... p 844 N93-14264 #

QUEST-TR-575 ..... p 798 N93-14111 #

R/D-6474-CH-01 ..... p 869 N93-15133 #
R/D-6971-EE-02 ..... p 869 N93-15188 #

REM-AR-92-2R ..... p 869 N93-15133 #

REPT-03705-001 ..... p 942 N93-14405 #
REPT-160-573 ..... p 901 N93-14766 * #
REPT-182-80-18 ..... p 790 N93-14432 #
REPT-1991 ..... p 992 N93-14576 #
REPT-33-518 ..... p 843 N93-15497 #
REPT-3405-F-92 ..... p 934 N93-14210 #
REPT-4 ..... p 992 N93-14576 #
REPT-533644 ..... p 991 N93-14439 #
REPT-7415-2 ..... p 843 N93-15497 #
REPT-92-105 ..... p 878 N93-15065 #
REPT-92B00093-VOL-3 ..... p 1002 N93-14771 * #
REPT-92B00118 ..... p 819 N93-15593 * #
REPT-921-430-104 ..... p 838 N93-15490 #
REPT-921-440-103 ..... p 894 N93-15139 #
REPT-921-440-104 ..... p 825 N93-15140 #
REPT-921-440-105 ..... p 999 N93-15118 #
REPT-921-440-106 ..... p 818 N93-15071 #
REPT-93B00007 ..... p 871 N93-15529 * #
REPT-93B00016-VOL-7 ..... p 932 N93-15645 * #
REPT-93851-PHASE-B-APP-E ..... p 825 N93-15633 * #

RFP-4517 ..... p 845 N93-14723 #

RHD-04 ..... p 866 N93-14534 #

RL-TR-91-375 ..... p 859 N93-14728 #
RL-TR-92-104 ..... p 858 N93-14437 #
RL-TR-92-12-VOL-1 ..... p 867 N93-14699 #
RL-TR-92-134 ..... p 862 N93-15397 #
RL-TR-92-149 ..... p 966 N93-15408 #
RL-TR-92-154 ..... p 817 N93-14565 #
RL-TR-92-15 ..... p 895 N93-15204 #
RL-TR-92-184 ..... p 972 N93-14679 #
RL-TR-92-30 ..... p 983 N93-15197 #
RL-TR-92-46 ..... p 971 N93-14245 #
RL-TR-92-50 ..... p 886 N93-15069 #
RL-TR-92-52-VOL-1 ..... p 944 N93-14572 #
RL-TR-92-52-VOL-2 ..... p 944 N93-14581 #

RRS-IFS-101 ..... p 824 N93-15631 * #

RRS-RM-200 ..... p 824 N93-15630 * #

RRS-SS-100 ..... p 824 N93-15632 * #

RRS-022 ..... p 825 N93-15658 * #
RRS-025 ..... p 824 N93-15629 * #
RRS-037-PHASE-B-APP-E ..... p 825 N93-15633 * #
RRS-037 ..... p 817 N93-14733 * #
RRS-046 ..... p 818 N93-14872 * #

RSG-319-92 ..... p 789 N93-14517 #

RTI/4500/017-02F ..... p 905 N93-14792 * #

R89351 ..... p 798 N93-15235 #

S-682 ..... p 814 N93-14495 * #
S-691 ..... p 903 N93-15530 * #

SA/TR-5/91 ..... p 830 N93-14436 #

SAIC-RRS-038 ..... p 824 N93-15632 * #
SAIC-RRS-040 ..... p 824 N93-15630 * #
SAIC-RRS-044 ..... p 824 N93-15631 * #

SAND-91-2813C ..... p 907 N93-15134 #
SAND-92-0213C ..... p 847 N93-15383 #
SAND-92-0611C ..... p 908 N93-15384 #
SAND-92-0669C ..... p 983 N93-15223 #
SAND-92-0746C ..... p 826 N93-14815 #
SAND-92-0773 ..... p 902 N93-15210 #
SAND-92-0778C ..... p 1051 N93-15060 #
SAND-92-1047 ..... p 978 N93-15277 #
SAND-92-1632C ..... p 966 N93-15385 #
SAND-92-1767 ..... p 983 N93-15230 #
SAND-92-1845C ..... p 882 N93-15381 #
SAND-92-1877C ..... p 997 N93-15651 #
SAND-92-1878C ..... p 997 N93-15649 #
SAND-92-2001C ..... p 847 N93-15382 #

SCT-A8924-1 ..... p 974 N93-14912 #

SC71008.FR ..... p 995 N93-15365 #

SEL-86-003 ..... p 952 N93-15502 * #
SEL-92-001 ..... p 957 N93-15578 * #
SEL-92-002 ..... p 957 N93-15579 * #

SESC-UAPB-01-92 ..... p 917 N93-15466 #

SGEB-22 ..... p 933 N93-15208 #

SLAC-PUB-5856 ..... p 998 N93-15469 #
SLAC-PUB-5910 ..... p 978 N93-15486 #
SLAC-PUB-5939 ..... p 978 N93-15468 #

SLCET-TR-91-3-REV-1 ..... p 972 N93-14496 #
SLCET-TR-91-31 ..... p 866 N93-14552 #
SLCET-TR-91-33-REV-1 ..... p 842 N93-14678 #
SLCET-TR-91-36 ..... p 867 N93-14642 #
SLCET-TR-92-1-REV-1 ..... p 870 N93-15330 #
SLCET-TR-92-12 ..... p 869 N93-15194 #

SMC-TR-92-30 ..... p 979 N93-15362 #
SMC-TR-92-38 ..... p 851 N93-15242 #
SMC-TR-92-43 ..... p 1049 N93-15318 #
SMC-TR-92-48 ..... p 972 N93-15243 #
SMC-TR-92-49 ..... p 971 N93-14108 #

SME/92-32 ..... p 830 N93-14232 #

SR-1 ..... p 945 N93-14696 #
SR-2 ..... p 916 N93-14899 #

SSCL-595 ..... p 905 N93-14522 #

SSD-TR-92-26 ..... p 839 N93-14530 #

STARS-AC-04107A/001/00 ..... p 952 N93-15471 #

STARS-TC-04014/003/00 ..... p 951 N93-15457 #

SU-SLAC-401 ..... p 951 N93-15451 #

SU-TR-457-ONR ..... p 971 N93-15110 #

SWRI-3593-002 ..... p 844 N93-14508 #

T-87-109 ..... p 863 N93-15470 #

TDCK-91-3641 ..... p 814 N93-14266 #
TDCK-91-3693 ..... p 867 N93-14803 #
TDCK-91-3982 ..... p 860 N93-14805 #
TDCK-92-0240 ..... p 937 N93-14602 #
TDCK-92-1439 ..... p 860 N93-14806 #
TDCK-92-1762 ..... p 968 N93-14804 #
TDCK-92-2282 ..... p 938 N93-15400 #
TDCK-92-2288 ..... p 936 N93-14267 #

TEC-R-182 ..... p 906 N93-15007 #
TEC-R-187 ..... p 905 N93-14676 #
TEC-R-191 ..... p 789 N93-15005 #

TEC-0011 ..... p 905 N93-14430 #

TELECOM-PARIS-90-E-023 ..... p 882 N93-15096 #
TELECOM-PARIS-91-E-022 ..... p 861 N93-15097 #
TELECOM-PARIS-92-E-001 ..... p 861 N93-15098 #

TETRA-TR91-17 ..... p 859 N93-14453 #

TFL-RR-1992-1 ..... p 966 N93-15491 #

TIOS-91/11 ..... p 946 N93-15077 #
TIOS-91/37-PT-1 ..... p 946 N93-15078 #
TIOS-92/02 ..... p 966 N93-15491 #
TIOS-92/07 ..... p 971 N93-15119 #
TIOS-92/09 ..... p 941 N93-15090 #
TIOS-92/12 ..... p 968 N93-15094 #
TIOS-92/13 ..... p 860 N93-15095 #

TM-1504 ..... p 880 N93-15643 * #

TR-ONR-C-12 ..... p 942 N93-14285 #

TR-0090(5940-05)-4 ..... p 979 N93-15362 #
TR-0091(6470-03)-1 ..... p 972 N93-15243 #
TR-0091(6925-08)-4 ..... p 971 N93-14108 #
TR-0091(6935-18)-1 ..... p 839 N93-14530 #
TR-0091(6945-01)-2 ..... p 1049 N93-15318 #
TR-0091(6945-03)-5 ..... p 851 N93-15242 #
TR-11 ..... p 842 N93-14669 #
TR-12 ..... p 992 N93-14670 #
TR-134 ..... p 977 N93-15448 #
TR-1992-4 ..... p 970 N93-14455 #
TR-1 ..... p 884 N93-14402 #
TR-2 ..... p 992 N93-14643 #
TR-2 ..... p 938 N93-15329 #
TR-35 ..... p 996 N93-15443 #
TR-3 ..... p 993 N93-15008 #
TR-405 ..... p 937 N93-14660 #
TR-415 ..... p 982 N93-14582 #
TR-458-ONR ..... p 970 N93-15109 #
TR-4 ..... p 993 N93-15055 #
TR-51 ..... p 994 N93-15233 #
TR-721198-6 ..... p 856 N93-14107 #
TR-92-01 ..... p 838 N93-15625 #
TR-92-04 ..... p 863 N93-15624 #
TR-92-1317 ..... p 862 N93-15339 * #

TRITA-EPP-88-03-REV ..... p 916 N93-15252 #
TRITA-EPP-91-03-REV ..... p 916 N93-15252 #

TT-9202 ..... p 789 N93-14729 #

TTC-1207 ..... p 902 N93-15210 #

UAH-5-32937 ..... p 826 N93-14681 * #

UC-602 ..... p 910 N93-14739 #
UC-903 ..... p 914 N93-14724 #

UCRL-ID-110831 ..... p 870 N93-15389 #
UCRL-ID-111521 ..... p 853 N93-15462 #
UCRL-ID-111804 ..... p 911 N93-15281 #
UCRL-ID-111805 ..... p 911 N93-15280 #
UCRL-ID-111810 ..... p 952 N93-15493 #

UCRL-JC-109255 ..... p 886 N93-14906 #

UCRL-LR-109806 ..... p 915 N93-14877 #
UCRL-LR-109866 ..... p 878 N93-15285 #

UDR-TR-90-106 ..... p 791 N93-14571 #

UFIFT-HEP-92-17 ..... p 969 N93-15379 #
UFIFT-HEP-92-19 ..... p 977 N93-15378 #
UFIFT-HEP-92-21 ..... p 972 N93-15057 #
UFIFT-HEP-92-25 ..... p 1022 N93-15346 #

US PATENT-CLASS-244-162 ..... p 939 N93-14713 *

US-PATENT-APPL-SN-212841 ..... p 993 N93-14820
US-PATENT-APPL-SN-245421 ..... p 885 N93-14821
US-PATENT-APPL-SN-254052 ..... p 939 N93-14713 *
US-PATENT-APPL-SN-374498 ..... p 850 N93-14825
US-PATENT-APPL-SN-502001 ..... p 885 N93-14722
US-PATENT-APPL-SN-503487 ..... p 832 N93-14700 *
US-PATENT-APPL-SN-541991 ..... p 860 N93-14742
US-PATENT-APPL-SN-545019 ..... p 940 N93-14704 *
US-PATENT-APPL-SN-555864 ..... p 845 N93-14705 *
US-PATENT-APPL-SN-557450 ..... p 891 N93-14822
US-PATENT-APPL-SN-587466 ..... p 850 N93-14743
US-PATENT-APPL-SN-601957 ..... p 832 N93-14706 *
US-PATENT-APPL-SN-607936 ..... p 842 N93-14824
US-PATENT-APPL-SN-618323 ..... p 868 N93-14826
US-PATENT-APPL-SN-621103 ..... p 854 N93-14801
US-PATENT-APPL-SN-632198 ..... p 982 N93-14800
US-PATENT-APPL-SN-641823 ..... p 828 N93-14718
US-PATENT-APPL-SN-641945 ..... p 834 N93-14819
US-PATENT-APPL-SN-641978 ..... p 881 N93-14716
US-PATENT-APPL-SN-642577 ..... p 876 N93-14715
US-PATENT-APPL-SN-645448 ..... p 845 N93-14717
US-PATENT-APPL-SN-651062 ..... p 849 N93-14709 *
US-PATENT-APPL-SN-660214 ..... p 817 N93-14725
US-PATENT-APPL-SN-688361 ..... p 881 N93-14714 *
US-PATENT-APPL-SN-708255 ..... p 832 N93-14706 *
US-PATENT-APPL-SN-710845 ..... p 962 N93-14701 *
US-PATENT-APPL-SN-717447 ..... p 992 N93-14707 *
US-PATENT-APPL-SN-725111 ..... p 934 N93-14708 *
US-PATENT-APPL-SN-765069 ..... p 890 N93-14710 *
US-PATENT-APPL-SN-780512 ..... p 890 N93-14702 *
US-PATENT-APPL-SN-782009 ..... p 885 N93-14703 *
US-PATENT-APPL-SN-785637 ..... p 891 N93-14871 *
US-PATENT-APPL-SN-799857 ..... p 945 N93-14882 *
US-PATENT-APPL-SN-803268 ..... p 982 N93-14711 *
US-PATENT-APPL-SN-824126 ..... p 890 N93-14712 *
US-PATENT-APPL-SN-828630 ..... p 836 N93-15246 #
US-PATENT-APPL-SN-852620 ..... p 994 N93-15151 * #
US-PATENT-APPL-SN-866920 ..... p 882 N93-15247 #
US-PATENT-APPL-SN-868806 ..... p 887 N93-15250 #
US-PATENT-APPL-SN-873931 ..... p 939 N93-14870 *
US-PATENT-APPL-SN-874156 ..... p 860 N93-14889 #
US-PATENT-APPL-SN-875955 ..... p 893 N93-15232 #
US-PATENT-APPL-SN-889885 ..... p 868 N93-15107 #
US-PATENT-APPL-SN-898591 ..... p 869 N93-15269 #
US-PATENT-APPL-SN-899803 ..... p 982 N93-14880 #
US-PATENT-APPL-SN-902166 ..... p 936 N93-15249 #
US-PATENT-APPL-SN-902262 ..... p 894 N93-15461 #
US-PATENT-APPL-SN-902264 ..... p 893 N93-15251 #
US-PATENT-APPL-SN-903316 ..... p 860 N93-14879 #
US-PATENT-APPL-SN-904096 ..... p 850 N93-14802 #
US-PATENT-APPL-SN-905702 ..... p 891 N93-14881 #
US-PATENT-APPL-SN-914669 ..... p 846 N93-15231 #
US-PATENT-APPL-SN-916428 ..... p 845 N93-14888 #
US-PATENT-APPL-SN-924213 ..... p 882 N93-14841 * #
US-PATENT-APPL-SN-925048 ..... p 893 N93-15248 #
US-PATENT-APPL-SN-926112 ..... p 868 N93-14887 #
US-PATENT-APPL-SN-929215 ..... p 882 N93-14878 #
US-PATENT-APPL-SN-929552 ..... p 891 N93-14843 * #
US-PATENT-APPL-SN-931468 ..... p 891 N93-14842 * #
US-PATENT-APPL-SN-934078 ..... p 981 N93-14404 * #
US-PATENT-APPL-SN-947597 ..... p 882 N93-14840 * #

US-PATENT-CLASS-102-290 ..... p 854 N93-14801
US-PATENT-CLASS-156-DIG.62 . p 992 N93-14707 *
US-PATENT-CLASS-210-640 ..... p 842 N93-14824
US-PATENT-CLASS-23-295R ..... p 992 N93-14707 *
US-PATENT-CLASS-23-300 ..... p 992 N93-14707 *

US-PATENT-CLASS-24-71.2 ..... p 891 N93-14822
US-PATENT-CLASS-244-118.5 .... p 939 N93-14713 *
US-PATENT-CLASS-244-158R .... p 939 N93-14713 *
US-PATENT-CLASS-272-145 ..... p 939 N93-14713 *
US-PATENT-CLASS-279-79 ..... p 890 N93-14710 *
US-PATENT-CLASS-279-89 ..... p 890 N93-14710 *
US-PATENT-CLASS-280-1.5 ..... p 934 N93-14708 *
US-PATENT-CLASS-280-290 ..... p 934 N93-14708 *
US-PATENT-CLASS-280-87.051 .. p 934 N93-14708 *
US-PATENT-CLASS-29-263 ..... p 891 N93-14871 *
US-PATENT-CLASS-29-426.5 ..... p 891 N93-14871 *
US-PATENT-CLASS-29-898.01 .... p 891 N93-14871 *
US-PATENT-CLASS-29-898.07 .... p 891 N93-14871 *
US-PATENT-CLASS-29-898.08 .... p 891 N93-14871 *
US-PATENT-CLASS-297-423 ..... p 939 N93-14713 *
US-PATENT-CLASS-323-351 ..... p 868 N93-14826
US-PATENT-CLASS-324-209 ..... p 845 N93-14705 *
US-PATENT-CLASS-324-227 ..... p 845 N93-14705 *
US-PATENT-CLASS-324-232 ..... p 845 N93-14705 *
US-PATENT-CLASS-324-687 ..... p 962 N93-14701 *
US-PATENT-CLASS-324-79D ..... p 945 N93-14882 *
US-PATENT-CLASS-324-79R ..... p 945 N93-14882 *
US-PATENT-CLASS-324-83Q ..... p 945 N93-14882 *
US-PATENT-CLASS-340-562 ..... p 962 N93-14701 *
US-PATENT-CLASS-340-870.37 .. p 962 N93-14701 *
US-PATENT-CLASS-342-100 ..... p 945 N93-14882 *
US-PATENT-CLASS-342-111 ..... p 860 N93-14742
US-PATENT-CLASS-356-360 ..... p 982 N93-14800
US-PATENT-CLASS-357-30 ..... p 993 N93-14820
US-PATENT-CLASS-364-724.06 .. p 945 N93-14882 *
US-PATENT-CLASS-364-724.07 .. p 945 N93-14882 *
US-PATENT-CLASS-364-724.08 .. p 945 N93-14882 *
US-PATENT-CLASS-365-158 ..... p 940 N93-14704 *
US-PATENT-CLASS-365-173 ..... p 940 N93-14704 *
US-PATENT-CLASS-372-108 ..... p 885 N93-14703 *
US-PATENT-CLASS-372-20 ..... p 885 N93-14703 *
US-PATENT-CLASS-372-96 ..... p 885 N93-14703 *
US-PATENT-CLASS-378-145 ..... p 982 N93-14711 *
US-PATENT-CLASS-378-85 ..... p 982 N93-14711 *
US-PATENT-CLASS-408-124 ..... p 890 N93-14710 *
US-PATENT-CLASS-408-239R .... p 890 N93-14710 *
US-PATENT-CLASS-408-241R .... p 890 N93-14710 *
US-PATENT-CLASS-427-248.1 .... p 881 N93-14714 *
US-PATENT-CLASS-427-255.6 .... p 881 N93-14714 *
US-PATENT-CLASS-427-255.7 .... p 881 N93-14714 *
US-PATENT-CLASS-427-255 ..... p 881 N93-14714 *
US-PATENT-CLASS-427-344 ..... p 881 N93-14714 *
US-PATENT-CLASS-427-367 ..... p 832 N93-14706 *
US-PATENT-CLASS-427-404 ..... p 832 N93-14706 *
US-PATENT-CLASS-427-419.2 .... p 832 N93-14706 *
US-PATENT-CLASS-427-456 ..... p 832 N93-14706 *
US-PATENT-CLASS-427-527 ..... p 881 N93-14714 *
US-PATENT-CLASS-427-58 ..... p 881 N93-14714 *
US-PATENT-CLASS-428-105 ..... p 832 N93-14700 *
US-PATENT-CLASS-428-179 ..... p 832 N93-14700 *
US-PATENT-CLASS-428-182 ..... p 832 N93-14700 *
US-PATENT-CLASS-428-184 ..... p 832 N93-14700 *
US-PATENT-CLASS-428-185 ..... p 832 N93-14700 *
US-PATENT-CLASS-428-186 ..... p 832 N93-14700 *
US-PATENT-CLASS-428-213 ..... p 832 N93-14700 *
US-PATENT-CLASS-436-113 ..... p 885 N93-14821
US-PATENT-CLASS-437-188 ..... p 850 N93-14825
US-PATENT-CLASS-439-131 ..... p 890 N93-14712 *
US-PATENT-CLASS-439-139 ..... p 890 N93-14712 *
US-PATENT-CLASS-439-310 ..... p 890 N93-14712 *
US-PATENT-CLASS-482-68 ..... p 934 N93-14708 *
US-PATENT-CLASS-482-69 ..... p 934 N93-14708 *
US-PATENT-CLASS-528-125 ..... p 849 N93-14709 *
US-PATENT-CLASS-528-126 ..... p 849 N93-14709 *
US-PATENT-CLASS-528-128 ..... p 849 N93-14709 *
US-PATENT-CLASS-528-170 ..... p 849 N93-14709 *
US-PATENT-CLASS-528-172 ..... p 849 N93-14709 *
US-PATENT-CLASS-528-173 ..... p 849 N93-14709 *
US-PATENT-CLASS-528-188 ..... p 849 N93-14709 *
US-PATENT-CLASS-60-223 ..... p 890 N93-14702 *
US-PATENT-CLASS-60-259 ..... p 890 N93-14702 *
US-PATENT-CLASS-60-271 ..... p 890 N93-14702 *
US-PATENT-CLASS-60-39.091 .... p 890 N93-14702 *
US-PATENT-CLASS-623-57 ..... p 939 N93-14870 *
US-PATENT-CLASS-623-65 ..... p 939 N93-14870 *
US-PATENT-CLASS-73-598 ..... p 845 N93-14705 *
US-PATENT-CLASS-73-801 ..... p 845 N93-14705 *
US-PATENT-CLASS-901-41 ..... p 890 N93-14710 *

US-PATENT-4,865,270 ..... p 939 N93-14713 *
US-PATENT-5,103,280 ..... p 993 N93-14820
US-PATENT-5,106,829 ..... p 850 N93-14743
US-PATENT-5,107,270 ..... p 860 N93-14742
US-PATENT-5,108,931 ..... p 885 N93-14821
US-PATENT-5,120,133 ..... p 982 N93-14800
US-PATENT-5,158,801 ..... p 881 N93-14714 *
US-PATENT-5,162,143 ..... p 832 N93-14700 *
US-PATENT-5,163,966 ..... p 939 N93-14870 *
US-PATENT-5,164-669 ..... p 845 N93-14705 *
US-PATENT-5,164,956 ..... p 885 N93-14703 *
US-PATENT-5,165,051 ..... p 945 N93-14882 *
US-PATENT-5,165,169 ..... p 891 N93-14871 *
US-PATENT-5,165,229 ..... p 890 N93-14702 *
US-PATENT-5,166,679 ..... p 962 N93-14701 *
US-PATENT-5,169,674 ..... p 832 N93-14706 *
US-PATENT-5,171,822 ..... p 849 N93-14709 *
US-PATENT-5,173,087 ..... p 992 N93-14707 *
US-PATENT-5,173,873 ..... p 940 N93-14704 *
US-PATENT-5,173,930 ..... p 982 N93-14711 *
US-PATENT-5,174,590 ..... p 934 N93-14708 *
US-PATENT-5,174,694 ..... p 890 N93-14710 *
US-PATENT-5,174,772 ..... p 890 N93-14712 *

USAARL-92-29 ..... p 881 N93-14105 #

USAAVSCOM-TR-92-A-004 ..... p 782 N93-15483 * #

USABRDL-TR-9117 ..... p 849 N93-14531 #

USCG-D-13-92 ..... p 939 N93-14554 #

USCG-R&DC-03/92 ..... p 939 N93-14554 #

USCG-188-46 ..... p 925 N93-14452 #

UTRC-R89-927889 ..... p 982 N93-15116 * #

VH-1 ..... p 947 N93-15262 #
VH-2 ..... p 948 N93-15263 #
VH-3 ..... p 948 N93-15264 #
VH-4 ..... p 948 N93-15265 #
VH-5 ..... p 948 N93-15266 #
VH-6 ..... p 948 N93-15267 #
VH-8 ..... p 948 N93-15268 #

VKI-LS-1992-03 ..... p 839 N93-14617 #

VRI-DMIS-2.60-WP92-10 ..... p 946 N93-15068 #

WES/IR/GL-92-4 ..... p 917 N93-15459 #

WES/MP/GL-92-32 ..... p 804 N93-14238 #

WES/TR/GL-92-10 ..... p 804 N93-14128 #

WES/TR/ITL-92-5 ..... p 1002 N93-14650 #

WHC-SA-1502 ..... p 1008 N93-15275 #

WINCO-1100 ..... p 870 N93-15276 #

WL-TR-91-2105 ..... p 849 N93-14527 #
WL-TR-91-3119 ..... p 900 N93-14498 #
WL-TR-91-4089 ..... p 994 N93-15190 #
WL-TR-91-4123 ..... p 983 N93-15255 #
WL-TR-92-1006 ..... p 856 N93-14107 #
WL-TR-92-3015-VOL-1 ..... p 894 N93-14104 #
WL-TR-92-3025 ..... p 791 N93-14571 #
WL-TR-92-3028 ..... p 779 N93-14441 #
WL-TR-92-3053 ..... p 780 N93-14661 #
WL-TR-92-3078 ..... p 939 N93-14520 #
WL-TR-92-3094 ..... p 898 N93-14419 #
WL-TR-92-4045 ..... p 777 N93-14549 #
WL-TR-92-7039 ..... p 879 N93-15332 #

WRAIR-92-001 ..... p 933 N93-14162 #

WSRC-MS-92-211 ..... p 910 N93-15063 #

Appendix

NASA SCIENTIFIC AND TECHNICAL INFORMATION PROGRAM PRODUCTS AND SERVICES

The NASA Scientific and Technical Information (STI) Program provides for the collection and announcement of aerospace-related reports and literature obtained worldwide through agreements and exchanges. The result of the collection is the comprehensive NASA STI Database that covers aeronautics, space, and supporting disciplines.

The STI Database, documents generated or obtained by NASA, and products and services derived from or supporting the database are made available to the NASA research community and to the public. Descriptions and sources of these items are presented in the following pages.

Scientific and Technical Aerospace Reports (*STAR*) is an abstract journal, listing citations with abstracts for aerospace-related reports obtained from worldwide sources. *STAR* is issued on the first of each month, and announces current documents that have been entered into the NASA STI Database during the previous month. The reports are of the following types:

- NASA, NASA contractor, and NASA grantee reports;
- Reports issued by other U.S. Government agencies, domestic and foreign institutions, universities, and private firms;
- Translations in report form;
- NASA-owned patents and patent applications;
- Other U.S. Government agency and foreign patents and patent applications;
- Domestic and foreign dissertations and theses.

Journal, book, and conference literature, journal translations, and certain foreign dissertations having the same subject scope as *STAR* are announced in a companion journal, *International Aerospace Abstracts* (*IAA*). *IAA* is issued on the 1st and 15th of each month and is available from the American Institute of Aeronautics and Astronautics, Technical Information Service, 555 West 57th Street, 12th Floor, New York, NY 10019.

ELIGIBILITY AND REGISTRATION FOR NASA STI PRODUCTS AND SERVICES

Organizations of the type listed below that have registered with NASA can receive products and services.

- NASA offices and installations, contractors, subcontractors, grantees, and consultants;
- Other U.S. Government agencies and their contractors;
- Libraries in the United States that have arrangements with NASA to maintain collections of NASA documents for public reference;
- Other organizations in the United States having a need for NASA documents in work related to aeronautics and space research;
- Organizations abroad that have established reciprocal documents exchange arrangements with NASA.

The central service points — central points of document acquisition and control within qualified organizations — or individuals are eligible to register for NASA STI products and services. Domestic organizations or individuals may be eligible to receive various classes of NASA publications and services and should address their requests for registration or further information to:

ATTN: Registration Services
NASA Center for AeroSpace Information
800 Elkridge Landing Road
Linthicum Heights, MD 21090-2934
301-621-0390

Organizations abroad should direct requests to:

National Aeronautics and Space Administration
Scientific and Technical Information Program (JTT)
International STI Program
Washington, DC 20546-0001
USA
703-271-5640

SUBJECT SCOPE

The subject scope of *STAR* and *IAA* includes all aspects of aeronautics and space research and development, supporting basic and applied research, and applications. Aerospace aspects of Earth resources, energy development, conservation, oceanography, environmental protection, urban transportation, and other topics of high national priority are also covered.

HOW TO USE *STAR* SUBJECT CATEGORIES

Abstracts in *STAR* are categorized by 10 major subject divisions that are divided further into 76 specific subject categories. The subject divisions and categories are listed in the Table of Contents together with a note for each that defines its scope and provides any cross-references. For example:

16 SPACE TRANSPORTATION
Includes passenger and cargo space transportation, e.g., shuttle operations; and space rescue techniques. For related information see also *03 Air Transportation and Safety* and *18 Spacecraft Design, Testing and Performance.* For space suits see *54 Man/System Technology and Life Support.*

CROSS-REFERENCES

Individual *STAR* abstracts are not ordinarily cross-referenced, except for certain conference reports or book translations that have had separate abstracts written for their component papers or chapters. Citations and abstracts of the components follow immediately after those of the parent document. When the subject content of a component differs sufficiently from the general content of the parent, a cross-reference citation also is printed at the end of the category to which it normally would have been assigned if it were independent.

DOCUMENTS ON MICROFICHE

Documents available on microfiche are designated by a pound sign (#) following the accession number.

LIMITED REPRODUCIBILITY

A note of limited reproducibility appears in the citation, if there are factors affecting the reproducibility of more than 20% of the document. These factors include faint or broken type, color photographs, black and white photographs, foldouts, dot matrix print, or some other factor that limits the reproducibility of the document. This notation also appears on the microfiche header.

COLOR COPIES

An increasing number of NASA scientific and technical reports are being produced with color graphs, charts, illustrations, and photographs. An indication that a document has color pages follows the source and pricing (SAP) information in the *STAR* citation.

Registered users of the NASA Scientific and Technical Information Program will receive ordered documents with color at no additional cost, as long as stock copies of the document are available. Otherwise, an additional fee of $2.00 per color page will be charged. The NASA Center for AeroSpace Information staff will contact registered users to determine individual user's needs.

NASA PATENTS AND PATENT APPLICATIONS

Patents and patent applications owned by NASA are announced in *STAR* under appropriate subject categories and are referenced in the *STAR* indexes. In the Report/Accession Number Index, patents are indexed by the NASA Case Number, and the U.S. Patent Class. Patent applications are indexed by the NASA Case Number and the U.S. Patent Application Serial Number.

Printed copies of patents (which are not microfiched) are available for purchase from the U.S. Patent and Trademark Office.

When ordering patents, the U.S. Patent Number should be used, and payment must be remitted in advance, by money order or check payable to the Commissioner of Patents and Trademarks. Prepaid purchase coupons for ordering are also available from the U.S. Patent and Trademark Office.

NASA patent application specifications are sold in both paper copy and microfiche by the NASA Center for AeroSpace Information (CASI). The N accession number should be used in ordering either paper copy or microfiche from CASI.

The patents and patent applications announced in *STAR* are owned by NASA and are available for royalty-free licensing. Requests for licensing terms and further information should be addressed to:

National Aeronautics and Space Administration
Associate General Counsel for Intellectual Property
Code GP
Washington, DC 20546-0001

SOURCES FOR DOCUMENTS

One or more sources from which a document announced in *STAR* is available to the public is given in each citation. The most commonly indicated sources and their acronyms or abbreviations are listed below, and their addresses are listed on page A-6. If the publication is available from a source other than those listed, the publisher and address will be displayed on the availability line or in combination with the corporate source line.

Avail: CASI. Sold by the NASA Center for AeroSpace Information. Prices for hard copy (HC) and microfiche (MF) are indicated by a price code following the letters HC or MF in the *STAR* citation. Current values for the price codes are given in the tables on page A-7.

NOTE ON ORDERING DOCUMENTS: When ordering publications from CASI, use the N accession number or other report number. It is also advisable to cite the title and other bibliographic identification.

Avail: SOD (or GPO). Sold by the Superintendent of Documents, U.S. Government Printing Office, in hard copy.

Avail: BLL (formerly NLL): British Library Lending Division, Boston Spa, Wetherby, Yorkshire, England. Photocopies available from this organization at the price shown. (If none is given, address inquiry to the BLL.)

Avail: DOE Depository Libraries. Organizations in U.S. cities and abroad that maintain collections of Department of Energy reports, usually in microfiche form, are listed in *Energy Research Abstracts*. Services available from the DOE and its depositories are described in a booklet, *DOE Technical Information Center - Its Functions and Services* (TID-4660), which may be obtained without charge from the DOE Technical Information Center.

Avail: ESDU. Pricing information on specific data, computer programs, and details on Engineering Sciences Data Unit (ESDU) topic categories can be obtained from ESDU International Ltd. Requesters in North America should use the Virginia address while all other requesters should use the London address, both of which are on page A-6.

Avail: Fachinformationszentrum, Karlsruhe. Gesellschaft fur wissenschaftlich-technische Information mbH 7514 Eggenstein-Leopoldshafen 2, Germany.

Avail: HMSO. Publications of Her Majesty's Stationery Office are sold in the U.S. by Pendragon House, Inc. (PHI), Redwood City, CA. The U.S. price (including a service and mailing charge) is given, or a conversion table may be obtained from PHI.

Avail: Issuing Activity, or Corporate Author, or no indication of availability. Inquiries as to the availability of these documents should be addressed to the organization shown in the citation as the corporate author of the document.

Avail: NASA Public Document Rooms. Documents so indicated may be examined at or purchased from the National Aeronautics and Space Administration (JBD-4), Public Documents Room (Room 1H23), Washington, DC 20546-0001, or public document rooms located at NASA installations, and the NASA Pasadena Office at the Jet Propulsion Laboratory.

Avail: NTIS. Sold by the National Technical Information Service. Initially distributed microfiche under the NTIS SRIM (Selected Research in Microfiche) are available. For information concerning this service, consult the NTIS Subscription Section, Springfield, VA 22161.

Avail: Univ. Microfilms. Documents so indicated are dissertations selected from *Dissertation Abstracts* and are sold by University Microfilms as xerographic copy (HC) and microfilm. All requests should cite the author and the Order Number as they appear in the citation.

Avail: US Patent and Trademark Office. Sold by Commissioner of Patents and Trademarks, U.S. Patent and Trademark Office, at the standard price of $1.50 each, postage free. (See discussion of NASA patents and patent applications on page A-3.)

Avail: (US Sales Only). These foreign documents are available to users within the United States from the National Technical Information Service (NTIS). They are available to users outside the United States through the International Nuclear Information Service (INIS) representative in their country, or by applying directly to the issuing organization.

Avail: USGS. Originals of many reports from the U.S. Geological Survey, which may contain color illustrations, or otherwise may not have the quality of illustrations preserved in the microfiche or facsimile reproduction, may be examined by the public at the libraries of the USGS field offices whose addresses are listed on page A-6. The libraries may be queried concerning the availability of specific documents and the possible utilization of local copying services, such as color reproduction.

FEDERAL DEPOSITORY LIBRARIES: To provide the general public with greater access to U.S. Government publications, Congress established the Federal Depository Library Program under the Government Printing Office (GPO), with 53 regional depositories responsible for permanent retention of material, inter-library loan, and reference services. (These libraries are not sales outlets.) At least one copy of nearly every NASA and NASA-sponsored publication, either in printed or microfiche format, is received and retained by the 53 regional depositories. A list of the regional GPO libraries, appears on page A-8. A local library can contact a regional depository library to help locate specific reports, or direct contact may be made by an individual.

PUBLIC COLLECTION OF NASA DOCUMENTS

An extensive collection of NASA and NASA-sponsored publications is maintianed by the British Library Lending Divison, Boston Spa, Wetherby, Yorkshire, England, for public access. The British Library Lending Division also has available many of the non-NASA publications cited in *STAR.*

European requesters may purchase facsimile copy or microfiche of NASA and NASA-sponsored documents, those identified by both the symbols # and * from ESA—Information Retrieval Service, European Space Agency, 8-10 rue Mario-Nikis, 75738 Paris CEDEX 15, France.

SUBMITTING DOCUMENTS

All users of this abstract service are urged to forward reports to be considered for announcement in *STAR.* This will aid NASA in its efforts to provide the fullest possible coverage of all scientific and technical publications that might support aeronautics and space research and development. If you have prepared relevant reports (other than those you will transmit to NASA, DOD, or DOE through the usual contract- or grant-reporting channels), please send them for consideration to the NASA Center for AeroSpace Information, 800 Elkridge Landing Road, Linthicum Heights, MD 21090-2934.

Reprints of journal articles, book chapters, and conference papers are also welcome. These will be considered for announcement in *STAR*'s companion journal, *IAA.*

You may specify a particular source to be included in a report announcement if you wish; otherwise the report will be placed on a public sale at the NASA Center for AeroSpace Information. Copyrighted publications will be announced but not distributed or sold.

PURCHASE OF *STAR*

STAR is publicly available on annual subscription from the NASA Center for AeroSpace Information (CASI) at $94.00 domestic, $117.00 foreign. Single copy prices: $33/domestic, $41/foreign.

An annual, cumulative *STAR Index* is also available at $54/domestic and $65/foreign.

STAR is available to registered users on annual subscription from the NASA Center for AeroSpace Information, ATTN: Registration Services, 800 Elkridge Landing Road, Linthicum Heights, MD 21090-2934.

Microfiche of the abstract sections of *STAR* are available, on annual subscription, from CASI. Annual subscription rates are $216.00 North America; $432.00 foreign.

ADDRESSES OF ORGANIZATIONS

American Institute of Aeronautics and Astronautics
Technical Information Service
555 West 57th Street, 12th Floor
New York, New York 10019

British Library Lending Division,
Boston Spa, Wetherby, Yorkshire,
England

Commissioner of Patents and Trademarks
U.S. Patent and Trademark Office
Washington, DC 20231

Department of Energy
Technical Information Center
P.O. Box 62
Oak Ridge, Tennessee 37830

European Space Agency-Information Retrieval Service
ESRIN
Via Galileo Galilei
00044 Frascati (Rome) Italy

Engineering Sciences Data Unit International
P.O. Box 1633
Manassas, Virginia 22110

Engineering Sciences Data Unit International, Ltd.
251-259 Regent Street
London, W1R 7AD, England

Fachinformationszentrum Karlsruhe
Gesellschaft fur wissenschaftlich-technische
Information mbH
7514 Eggenstein-Leopoldshafen 2, Germany

Her Majesty's Stationery Office
P.O. Box 569, S.E. 1
London, England

NASA Center for AeroSpace Information
800 Elkridge Landing Road
Linthicum Heights, MD 21090-2934

National Aeronautics and Space Administration
Scientific and Technical Information Program (JTT)
Washington, DC 20546-0001

National Technical Information Service
5285 Port Royal Road
Springfield, Virginia 22161

Pendragon House, Inc.
899 Broadway Avenue
Redwood City, California 94063

Superintendent of Documents
U.S. Government Printing Office
Washington, DC 20402

University Microfilms
A Xerox Company
300 North Zeeb Road
Ann Arbor, Michigan 48106

University Microfilms, Ltd.
Tylers Green
London, England

U.S. Geological Survey Library National Center
MS 950
12201 Sunrise Valley Drive
Reston, Virginia 22092

U.S. Geological Survey Library
2255 North Gemini Drive
Flagstaff, Arizona 86001

U.S. Geological Survey
345 Middlefield Road
Menlo Park, California 94025

U.S. Geological Survey Library
Box 25046
Denver Federal Center, MS914
Denver, Colorado 80225

CASI PRICE TABLES

(Effective October 1, 1992)

STANDARD PRICE DOCUMENTS

PRICE CODE	NORTH AMERICAN PRICE	FOREIGN PRICE
A01	$ 9.00	$ 18.00
A02	12.50	25.00
A03	17.00	34.00
A04-A05	19.00	38.00
A06-A09	26.00	52.00
A10-A13	35.00	70.00
A14-A17	43.00	86.00
A18-A21	50.00	100.00
A22-A25	59.00	118.00
A99	69.00	138.00

MICROFICHE

PRICE CODE	NORTH AMERICAN PRICE	FOREIGN PRICE
A01	$ 9.00	$ 18.00
A02	12.50	25.00
A03	17.00	34.00
A04	19.00	38.00
A06	26.00	52.00
A10	35.00	70.00

IMPORTANT NOTICE

CASI Shipping and Handling Charges
U.S. — ADD $3.00 per TOTAL ORDER
Canada and Mexico — ADD $3.50 per TOTAL ORDER
All Other Countries — ADD $7.50 per TOTAL ORDER
Does NOT apply to orders
requesting CASI RUSH HANDLING.
Contact CASI for charge.

FEDERAL REGIONAL DEPOSITORY LIBRARIES

ALABAMA

AUBURN UNIV. AT MONTGOMERY LIBRARY
Documents Dept.
7300 University Drive
Montgomery, AL 36117-3596
(205) 244-3650 FAX: (205) 244-0678

UNIV. OF ALABAMA
Amelia Gayle Gorgas Library
Govt. Documents
Box 870266
Tuscaloosa, AL 35487-0266
(205) 348-6046 FAX: (205) 348-8833

ARIZONA

DEPT. OF LIBRARY, ARCHIVES, AND PUBLIC RECORDS
Federal Documents
Third Floor State Capitol
1700 West Washington
Phoenix, AZ 85007
(602) 542-4121 FAX: (602) 542-4400; 542-4500

ARKANSAS

ARKANSAS STATE LIBRARY
State Library Services
One Capitol Mall
Little Rock, AR 72201
(501) 682-2869

CALIFORNIA

CALIFORNIA STATE LIBRARY
Govt. Publications Section
914 Capitol Mall - P.O. Box 942837
Sacramento, CA 94237-0001
(916) 322-4572 FAX: (916) 324-8120

COLORADO

UNIV. OF COLORADO - BOULDER
Norlin Library
Govt. Publications
Campus Box 184
Boulder, CO 80309-0184
(303) 492-8834 FAX: (303) 492-2185

DENVER PUBLIC LIBRARY
Govt. Publications Dept. BS/GPD
1357 Broadway
Denver, CO 80203
(303) 571-2135

CONNECTICUT

CONNECTICUT STATE LIBRARY
231 Capitol Avenue
Hartford, CT 06106
(203) 566-4971 FAX: (203) 566-3322

FLORIDA

UNIV. OF FLORIDA LIBRARIES
Documents Dept.
Library West
Gainesville, FL 32611-2048
(904) 392-0366 FAX: (904) 392-7251

GEORGIA

UNIV. OF GEORGIA LIBRARIES
Govt. Documents Dept.
Jackson Street
Athens, GA 30602
(404) 542-8949 FAX: (404) 542-6522

HAWAII

UNIV. OF HAWAII
Hamilton Library
Govt. Documents Collection
2550 The Mall
Honolulu, HI 96822
(808) 948-8230 FAX: (808) 956-5968

IDAHO

UNIV. OF IDAHO LIBRARY
Documents Section
Moscow, ID 83843
(208) 885-6344 FAX: (208) 885-6817

ILLINOIS

ILLINOIS STATE LIBRARY
Reference Dept.
300 South Second
Springfield, IL 62701-1796
(217) 782-7596 FAX: (217) 524-0041

INDIANA

INDIANA STATE LIBRARY
Serials/Documents Section
140 North Senate Avenue
Indianapolis, IN 46204
(317) 232-3678 FAX: (317) 232-3728

IOWA

UNIV. OF IOWA LIBRARIES
Govt. Publications Dept.
Washington & Madison Streets
Iowa City, IA 52242
(319) 335-5926 FAX: (319) 335-5830

KANSAS

UNIV. OF KANSAS
Govt. Documents & Map Library
6001 Malatt Hall
Lawrence, KS 66045-2800
(913) 864-4660 FAX: (913) 864-5380

KENTUCKY

UNIV. OF KENTUCKY LIBRARIES
Govt. Publications/Maps Dept.
Lexington, KY 40506-0039
(606) 257-3139 FAX: (606) 257-1563; 257-8379

LOUISIANA

LOUISIANA STATE UNIV.
Middleton Library
Govt. Documents Dept.
Baton Rouge, LA 70803
(504) 388-2570 FAX: (504) 388-6992

LOUISIANA TECHNICAL UNIV.
Prescott Memorial Library
Govt. Documents Dept.
305 Wisteria Street
Ruston, LA 71270-9985
(318) 257-4962 FAX: (318) 257-2447

MAINE

TRI-STATE DOCUMENTS DEPOSITORY
Raymond H. Fogler Library
Govt. Documents & Microforms Dept.
Univ. of Maine
Orono, ME 04469
(207) 581-1680

MARYLAND

UNIV. OF MARYLAND
Hornbake Library
Govt. Documents/Maps Unit
College Park, MD 20742
(301) 454-3034 FAX: (301) 454-4985

MASSACHUSETTS

BOSTON PUBLIC LIBRARY
Govt. Documents Dept.
666 Boylston Street
Boston, MA 02117
(617) 536-5400 ext. 226
FAX: (617) 267-8273; 267-8248

MICHIGAN

DETROIT PUBLIC LIBRARY
5201 Woodward Avenue
Detroit, MI 48202-4093
(313) 833-1440; 833-1409
FAX: (313) 833-5039

LIBRARY OF MICHIGAN
Govt. Documents Unit
P.O. Box 30007
Lansing, MI 48909
(517) 373-0640 FAX: (517) 373-3381

MINNESOTA

UNIV. OF MINNESOTA
Wilson Library
Govt. Publications Library
309 19th Avenue South
Minneapolis, MN 55455
(612) 624-5073 FAX: (612) 626-9353

MISSISSIPPI

UNIV. OF MISSISSIPPI
J.D. Williams Library
Federal Documents Dept.
106 Old Gym Bldg.
University, MS 38677
(601) 232-5857 FAX: (601) 232-5453

MISSOURI

UNIV. OF MISSOURI - COLUMBIA
Ellis Library
Govt. Documents
Columbia, MO 65201
(314) 882-6733 FAX: (314) 882-8044

MONTANA

UNIV. OF MONTANA
Maureen & Mike Mansfield Library
Documents Div.
Missoula, MT 59812-1195
(406) 243-6700 FAX: (406) 243-2060

NEBRASKA

UNIV. OF NEBRASKA - LINCOLN
D.L. Love Memorial Library
Documents Dept.
Lincoln, NE 68588
(402) 472-2562

NEVADA

UNIV. OF NEVADA
Reno Library
Govt. Publications Dept.
Reno, NV 89557
(702) 784-6579 FAX: (702) 784-1751

NEW JERSEY

NEWARK PUBLIC LIBRARY
U.S. Documents Div.
5 Washington Street - P.O. Box 630
Newark, NJ 07101-0630
(201) 733-7812 FAX: (201) 733-5648

NEW MEXICO

UNIV. OF NEW MEXICO
General Library
Govt. Publications Dept.
Albuquerque, NM 87131-1466
(505) 277-5441 FAX: (505) 277-6019

NEW MEXICO STATE LIBRARY
325 Don Gaspar Avenue
Santa Fe, NM 87503
(505) 827-3826 FAX: (505) 827-3820

NEW YORK

NEW YORK STATE LIBRARY
Documents/Gift & Exchange Section
Federal Depository Program
Cultural Education Center
Albany, NY 12230
(518) 474-5563 FAX: (518) 474-5786

NORTH CAROLINA

UNIV. OF NORTH CAROLINA - CHAPEL HILL
CB#3912, Davis Library
BA/SS Dept.—Documents
Chapel Hill, NC 27599
(919) 962-1151 FAX: (919) 962-0484

NORTH DAKOTA

NORTH DAKOTA STATE UNIV. LIBRARY
Documents Office
Fargo, ND 58105
(701) 237-8886 FAX: (701) 237-7138
In cooperation with Univ. of North Dakota, Chester Fritz Library
Grand Forks

OHIO

STATE LIBRARY OF OHIO
Documents Dept.
65 South Front Street
Columbus, OH 43266
(614) 644-7051 FAX: (614) 752-9178

OKLAHOMA

OKLAHOMA DEPT. OF LIBRARIES
U.S. Govt. Information Div.
200 NE 18th Street
Oklahoma City, OK 73105-3298
(405) 521-2502, ext. 252, 253
FAX: (405) 525-7804

OKLAHOMA STATE UNIV.
Edmon Low Library
Documents Dept.
Stillwater, OK 74078
(405) 744-6546 FAX: (405) 744-5183

OREGON

PORTLAND STATE UNIV.
Millar Library
934 SW Harrison - P.O. Box 1151
Portland, OR 97207
(503) 725-3673 FAX: (503) 725-4527

PENNSYLVANIA

STATE LIBRARY OF PENN.
Govt. Publications Section
Walnut St. & Commonwealth Ave. - P.O. Box 1601
Harrisburg, PA 17105
(717) 787-3752

SOUTH CAROLINA

CLEMSON UNIV.
Cooper Library
Public Documents Unit
Clemson, SC 29634-3001
(803) 656-5174 FAX: (803) 656-3025
In cooperation with Univ. of South Carolina, Thomas Cooper Library, Columbia

TENNESSEE

MEMPHIS STATE UNIV. LIBRARIES
Govt. Documents
Memphis, TN 38152
(901) 678-2586 FAX: (901) 678-2511

TEXAS

TEXAS STATE LIBRARY
United States Documents
P.O. Box 12927 - 1201 Brazos
Austin, TX 78711
(512) 463-5455 FAX: (512) 463-5436

TEXAS TECH. UNIV. LIBRARY
Documents Dept.
Lubbock, TX 79409
(806) 742-2268 FAX: (806) 742-1920

UTAH

UTAH STATE UNIV.
Merrill Library & Learning Resources Center, UMC-3000
Documents Dept.
Logan, UT 84322-3000
(801) 750-2684 FAX: (801) 750-2677

VIRGINIA

UNIV. OF VIRGINIA
Alderman Library
Govt. Documents
Charlottesville, VA 22903-2498
(804) 924-3133 FAX: (804) 924-4337

WASHINGTON

WASHINGTON STATE LIBRARY
Document Section
MS AJ-11
Olympia, WA 98504-0111
(206) 753-4027 FAX: (206) 753-3546

WEST VIRGINIA

WEST VIRGINIA UNIV. LIBRARY
Govt. Documents Section
P.O. Box 6069
Morgantown, WV 26506
(304) 293-3640

WISCONSIN

ST. HIST. SOC. OF WISCONSIN LIBRARY
Govt. Publications Section
816 State Street
Madison, WI 53706
(608) 262-2781 FAX: (608) 262-4711
In cooperation with Univ. of Wisconsin-Madison, Memorial Library

MILWAUKEE PUBLIC LIBRARY
Documents Div.
814 West Wisconsin Avenue
Milwaukee, WI 53233
(414) 278-2167 FAX: (414) 278-2137

National Aeronautics and
Space Administration
Code JTT
Washington, D.C.
20546-0001

Official Business

Penalty for Private Use, $300

SPECIAL FOURTH-CLASS RATE
POSTAGE & FEES PAID
NASA
PERMIT No. G27

NASA

POSTMASTER: If Undeliverable (Section 158 Postal Manual) Do Not Return

Please circulate this publication to other colleagues within your organization.